Spectrophotometric Determination of Iron in Serum

By Shunji UMEMOTO and Yasuhisa YAMAMOTO

(Received April 13, 1956)

For the determination of iron in serum, various methods have been proposed. They cover photometry or colorimetry applied to the colored solution obtained by adding a color-developing reagent, such as thiocyanate[1-4], *o*-phenanthroline[5-11], α,α'-dipyridyl[12,13] or 4,7-dimethyl-1,10-phenanthroline[14] to the serum after the removal of protein. In ordinary cases the iron content of serum is low and the available amount of serum is small. When the methods mentioned above are applied to a few ml. of serum, the color of the solution is very feeble. Therefore, it is difficult to obtain precise results unless a very sensitive photometer or colorimeter is available. Hence, a method was devised by Jones[2], which is based on light absorption of colored extract obtained by the extraction of iron thiocyanate from the aqueous solution to the solvent immiscible with water. In this method, however, the decolorization of the solution occurs before the extraction is complete, because of the instability of iron thiocyanate in an aqueous medium.

Here the authors propose to apply to serum Torii's method for determination of iron[15,16] which was published recently. The method is based on the comparison of light absorptions of green solutions obtained by the reaction of *o*-nitroso resorcinmonomethylether (hereafter N. R. M. E.) with ferrous iron.

1) K. Brøchner-Mortensen and C. Olsen, *Compt. rend. trav. lab. Carlsberg, ser. chim.*, **23**, 235 (1940).
2) F. Jones, *Anal. Chem.*, **21**, 1216 (1949).
3) A. Sachs, V. E. Levine, A. C. Andersen and A. Schmidt, *J. Lab. Clin. Med.*, **26**, 734 (1941).
4) W. Schotten, *Apoth.-Ztg.*, **62**, 85 (1950).
5) J. C. Dreyfus and G. Schaprira, *Le Sang*, **20**, 374 (1949).
6) G. Graziani, M. Fusco and L. Rossi, *Il Policlinico (Rome), Sez. prat.*, **59**, 1251 (1952).
7) G. Høyer, *Scand. J. Clin. Lab. Invest.*, **2**, 123 (1950).
8) I. Kaldor, *Australian J. Exptl. Biol. Med. Sci.*, **31**, 41 (1953).
9) H. G. Schmidt, *Biochem. Z.*, **305**, 104 (1940).
10) S. L. Tompsett and R. A. Mc Allister, *Analyst*, **74**, 315 (1949).
11) Bo C. Vahlquist, *Acta Paediat*, **28**, *Suppl. V*, 374 (1941).
12) K. Kimura, R. Hara and N. Iijima, *J. Pharm. Soc. Japan*, **72**, 1240 (1952).
13) G. Kitzes, C. A. Elvehjim and H. A. Schuette, *J. Biol. Chem.*, **155**, 653 (1944).
14) R. E. Peterson, *Anal. Chem.*, **25**, 1337 (1953).
15) F. Iimura and T. Torii, *Japan Analyst*, **4**, 177 (1955).
16) T. Torii, *J. Chem. Soc. Japan, Pure Chem. Sec. (Nippon KagakuZassi)*, **76**, 333 (1955).

Reagents

Distilled water.—Redistilled water is obtained by using the water-distilling apparatus made of hard glass.

Standard iron solution.—In 10 ml. of sulfuric acid (1 : 10), 0.1015 gram of analytical-grade iron wire is dissolved for 20 hours' digestion. To the iron solution is added 3 ml. of concentrated nitric acid and the resulting solution is diluted to 500 ml..

6 N hydrochloric acid.—Distilled hydrochloric acid is titrated with alkali, and the hydrochloric acid of a known concentration is diluted to 6 N.

20% trichloroacetic acid.—Twenty grams of trichloroacetic acid is dissolved in 100 ml. of distilled water.

10% hydroxylamine hydrochloride.—Ten grams of hydroxylamine hydrochloride is dissolved in 100 ml. of distilled water.

0.1% p-nitrophenol.—One tenth gram of *p*-nitrophenol is dissolved in 100 ml. of distilled water.

6 N ammonium hydroxide.—Forty ml. of conc. ammonium hydroxide is diluted to 100 ml..

Acetic acid-sodium acetate buffer solution.—In 200 ml. of distilled water, 33.5 grams of sodium acetate is dissolved and the resulting solution is filtered. After addition of 27.2 ml. of distilled acetic acid, it is diluted to 250 ml..

5% sodium thiosulfate solution.—Five grams of sodium thiosulfate is dissolved in 100 ml. of distilled water and the resulting solution is filtered.

Saturated aqueous solution of N. R. M. E..—N. R. M. E. is dissolved in 100 ml. of distilled water andt he insoluble matter is filtered off (solubility: 40.2 mg./100 ml.).

Carbon tetrachloride.—Distilled carbon tetrachloride is obtained using a distilling apparatus made of hard glass.

Procedure and Apparatus

In a centrifuge tube, 2.0 ml. of clear serum is taken, acidified with 0.5 ml. of 6 N hydrochloric acid, and allowed to stand for 10 minutes. To the resulting solution is added 1.0 ml. of 20% trichloroacetic acid†. The mixture is centrifuged and filtered, if necessary. The precipitate is

† When serum is not acidified with hydrochloric acid and is treated only with trichloroacetic acid, the mixture is kept in a water bath for 5 minutes at 100°C.

washed with a mixture of 1.0 ml. of distilled water and 0.5 ml. of 20% trichloroacetic acid. (Filteration and washing are not always necessary when the centrifugation is complete.) The clear filtrate, together with washing solution, is taken in a 10-ml. stoppered measuring cylinder. After addition of 0.5 ml. of 10% hydroxylamine hydrochloride, the solution is kept for at least 15 min. with shaking at certain intervals until the reduction of iron is complete. The mixture is then neutralized with 6 N ammonium hydroxide, the neutralization being indicated by the development of color of 0.1% *p*-nitrophenol (one drop) added to the solution.

For the pH control, 2.0 ml. of acetic acid-sodium acetate buffer solution (pH 4.5) is added. To this mixture are added 0.5 ml. of 5% sodium thiosulfate, and, after 5 minutes, 1.0 ml. of saturated aqueous solution of N. R. M. E.. The volume of the resulting solution was adjusted exactly to 10.0 ml. by adding distilled water. After being allowed to stand for at least 15 minutes†† the, mixture is transferred into a 30-ml. separatory funnel, and shaken with 2 ml. of carbon tetrachloride. Then the N. R. M. E. solution in carbon tetrachloride is discarded. The extraction is repeated three times to remove the excess of N. R. M. E. completely. The aqueous solution is poured into a centrifuge tube and is centrifuged to remove the suspended carbon tetrachloride. The supernatant aqueous solution is transferred to a 20-mm. absorption cell, and its absorption is measured at 700 mμ with Shimadzu's photoelectric spectrophotometer.

Examination

The following experiments were carried out with iron standard solution and serum at room temperature of 27–30°C.

a) To check the possibility of rapid reduction of ferric iron by sodium thiosulfate in the absence of hydroxylamine hydrochloride, the color was developed by the method mentioned above without adding hydroxylamine hydrochloride to iron standard solutions. The result seems to show that one hour is necessary for complete reduction of iron by sodium thiosulfate. (Table I)

TABLE I

ABSORBANCY OF SOLUTION OBTAINED BY THE REDUCTION OF IRON WITH BOTH HYDROXYLAMINE HYDROCHLORIDE AND SODIUM THIOSULFATE OR WITH SODIUM THIOSULFATE ALONE

Time in min.	15	30	60
Hydroxylamine hydrochloride and sodium thiosulfate	0.235	0.234	0.236
	0.184	0.185	0.184
Sodium thiosulfate	0.182	0.220	0.234*
	0.144	0.177	0.185**

* To be compared with 1st line.
** To be compared with 2nd line.

b) After the pH of solution is adjusted to 4.5, hydroxylamine hydrochloride was added to reduce iron in the standard solution. One hour was necessary for complete reduction. (Table II)

TABLE II

ABSORBANCY OF SOLUTION OBTAINED BY THE REDUCTION OF IRON IN STRONG ACIDIC MEDIUM AND pH 4.5

Time in min.	15	30	60
Strong acidic medium	0.208	0.210	0.209
	0.156	0.159	0.158
pH 4.5	0.149	0.183	0.210*
	0.116	0.139	0.158**

* To be compared with 1st line.
** To be compared with 2nd line.

From the results of experiments a) and b), it was found that iron was reduced completely within a short time by hydroxylamine hydrochloride in a strongly acidic medium as was used in the procedure mentioned above.

c) In the presence of 0.5 ml. of 6 N hydrochloric acid, the addition of 1.0 ml. of 20 % trichloroacetic acid to 2.0 ml. of serum is satisfactory to remove protein from serum. It was checked qualitatively by using sulfosalicylic acid. Under this condition, iron is liberated in solution completely by Surgenor et al.[17].

d) To check the effect of hydrochloric acid concentration on the development of color, each 2.0 ml. of serum was treated with 0.5 ml. or 1.0 ml. of 6 N hydrochloric acid. The subsequent treatment was the same as in the procedure mentioned above for each 2.0 ml. of serum. The results are shown in Table III, and no serious difference was found between these two conditions.

TABLE III

ABSORBANCY OF SOLUTION OBTAINED BY ADDING 0.5 ML. AND 1.0 ML. OF HYDROCHLORIC ACID TO SERUM

Serum	I	II	III	IV
0.5 ml. HCl	0.191	0.170	0.124	0.133
1.0 ml. HCl	0.186	0.168	0.126	0.136

e) In the determination of iron by Torii's method, the presence of copper in larger quantities than iron interfere with the determination. In human serum, the copper content is 1–1.5 times as great as that of iron. To see if addition of 5% sodium thiosulfate 0.5 ml. is sufficient for

†† Not for as long a time as two or three days, which was the private suggestion given by T. Torii.

17) D. M. Surgenor, B. A. Koechlin and L. E. Strong, *J. Clin. Investigation*, **28**, 73 (1949).

the prevention from interference of copper. The experimental results are shown in Table IV, and the corresponding absorbancies obtained for these two sets of solution are the same. Therefore it is clear that copper in human serum will not interfere seriously.

TABLE IV

ABSOREANCY OF SOLUTION OBTAINED FROM IRON STANDARD SOLUTIONS CONTAINING AND FREE FROM COPPER

Concentration of iron (γ/100 ml.)	81.2	121.8	162.3	203.0
Iron solution free from copper	0.110	0.160	0.204	0.258
	0.105	0.156	0.210	0.261
	0.100	0.152	0.217	0.264
Iron solution containing copper (300 γ/100 ml. Cu)	0.108	0.161	0.210	0.260
	0.110	0.160	0.214	0.266
	0.112	0.156	0.218	0.272

f) Based on the method proposed here, the standard solutions were used for the preparation of a calibration curve. The experimental results corrected for the blank test (absorbancy, 0.044) are shown in Fig. 1. The curve in Fig. 1 is linear and obeys Beer's law within the range of iron content from 0 to 800 γ per 100 ml.. The method presented here is advantageous over the usual one. The absorptions to be measured in the present method, are from two to three times as strong as those in the usual methods for a given content of iron in solution.

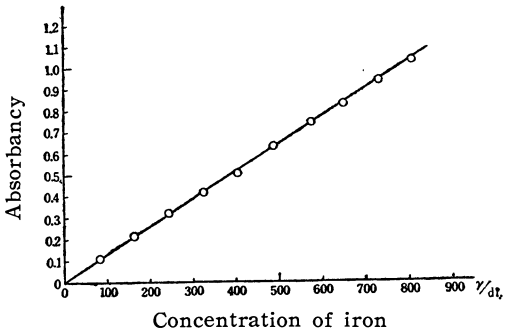

Fig. 1.

g) Recovery experiments were run in which iron was added to four samples of serum. In this set of analysis, a few ml. of a standard iron solution was added to a few ml. of the serum so as to made the total volume 2 ml. and this mixture was then analysed. The results in Table V show quantitative recovery.

TABLE V

RECOVERY OF KNOWN QUANTITY OF IRON ADDED TO SERUM

Serum volume ml.	Iron solution added. concentration γ/100 ml.	Iron solution added. volume ml.	Determined iron γ/100 ml.	Calculated iron from the value of pure serum γ/100 ml.
2.0			71	
1.0	406.0	1.0	235	238
0.6	406.0	1.4	299	305
0.4	406.0	1.6	345	339
2.0			135	
1.0	406.0	1.0	275	270
2.0			95	
1.0	406.0	1.0	128	129
2.0			102	
1.8	162.3	0.2	106	108
1.8	243.6	0.2	116	116
1.8	324.8	0.2	126	124
1.8	406.0	0.2	129	132

Summary

To improve the procedure of photometric determination of iron in human serum, Torii's method recently proposed for the determination of iron was applied to serum. After the removal of protein from serum, the iron in serum is reduced, the pH of the solution is adjusted to 4.5, the color-developing reagent is added, and the excess of the reagent is removed by extraction with carbon tetrachloride. The green solution thus obtained is effective for spectrophotometric determination.

The interference of copper is avoided by the addition of thiosulfate, and the substances other than copper remaining after the removal of protein from serum do not give any appreciable interference.

The authors wish to thank Professor Kenjiro Kimura of the University of Tokyo and Dr. Nobufusa Saito for their kind guidance and encouragement, Dr. Tetsuya Torii for his kind suggestion and supply of *o*-nitrosoresorcinmonomethylether, and Dr. Satoya Sasaki for his helpful suggestions.

Balneological Laboratory, Okayama University, Misasa Hot Springs Tottori Prefecture

The Dimerization of 3-Methyl-3-penten-2-one

By Tatsuo TAKESHIMA, Teruyasu IMASEKI and Sachiko OGATA

(Received August 23, 1957)

In an attempt to prepare an ethynylcarbinol from 3-methyl-3-penten-2-one (I) and acetylene by the action of sodium amide in ethereal solution, we encountered a characteristic crystalline product (II) which proved to be a dimer of I. This reaction is considered to be of the same class as that of acetylcyclohexene which was reported by Jones and Koch[1].

In the present experiment I was treated with sodium amide in ethereal solution in the cold. From the reaction mixture, colorless crystals (II) were obtained in ca. 30% yield in addition to other oily products.

II had no unsaturated nature and the existence of two carbonyl groups in its molecule was presumed on the basis of its diketonic derivatives. Together with analyses and molecular weight determined, a cyclic structure corresponding to a dimer of I was considered for it. Its one carbonyl group seemed to be in the ring and the other in the exocyclic position because of the following facts.

On treatment with hypobromite it gave bromo-derivatives instead of the corresponding acid, and at most, trisubstituted derivative could be obtained though the reagent was applied in great excess. From these bromo-derivatives certain materials having unsaturated nature could easily be formed. Further, II gave positive reaction toward acetyl test[2]. On these evidences, a six-membered ring was proposed and the three hydrogen atoms which are easily replaceable were considered to be in some special positions, perhaps on the two carbon atoms adjacent to the endocyclic carbonyl group.

Thus structure II_a or II_b was proposed for the dimer in question. Structure II_a (4-acetyl-2,3,4,5-tetramethyl-1-cyclohexanone) seems probable, on the basis of the results obtained in the case of acetylcyclohexene[1]. The reaction seems to follow the mode of diene synthesis.

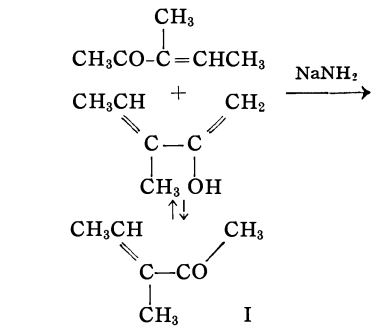

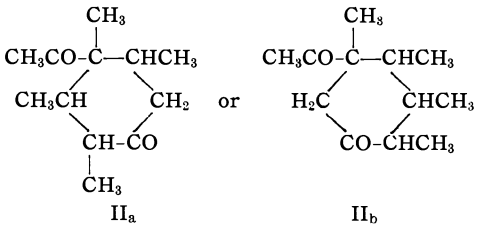

It may be noted that mesityl oxide gave a dimer of different nature when treated with sodium amide in a manner similar to that in the above case. The crystalline substance obtained here had unsaturated nature and its melting point was almost identical with 2-acetyl-1,3,3,5-tetramethyl-5-cyclohexen-1-ol reported by Braude et al.[3] who obtained the compound from mesityl oxide in the presence of lithium.

Experimental

3-Methyl-3-penten-2-one (I).—The preparation followed the method of Hinkel et al.[4] with some modifications. Paraldehyde was used in place of acetaldehyde, and pyridine was substituted for quinoline to eliminate hydrogen chloride in the crude product. B.p. 136~138°.

Dimerization of I.—The yield of the dimer was rather dependent upon the reaction temperature and other trivial conditions. A typical run is described below.

Fifty grams of I was added dropwise to a suspension of 25 g. of powdered sodium amide in 300 cc. of dry ether in a course of ca. 40 min. at −2~6°, and kept stirred for ca. 4 hr. at the same temperature. The reaction mixture was

1) E. R. H. Jones and H. P. Koch, *J. Chem. Soc.*, **1942**, 393.
2) J. Adachi, *J. Chem. Soc. Japan, Pure Chem. Sec.* (*Nippon Kagaku Zassi*), **71**, 566 (1950); *J. Anal. Chem.*, **23**, 1491 (1951).
3) E. A. Braude, B. F. Gofton, G. Lowe and E. S. Waight, *J. Chem. Soc.*, **1956**, 4054.
4) L. E. Hinkel, E. E. Ayling, J. F. J. Dippy and T. H. Angel, ibid., **1931**, 814.

poured onto crushed ice containing acetic acid; the ethereal portion was separated, washed with a solution of potassium carbonate and dried over calcium chloride. Ether was then removed and the residue was distilled under reduced pressure to yield the following fractions: (1) b. p. ca. 50°/30 mmHg, ca. 4.5 g.; (2) b.p. ca. 140~164°/23 mmHg, ca. 26.5 g., somewhat viscous yellowish oil; residue, ca. 5 g., dark resinous material.

Fraction (2) was kept cooled overnight in an ice-box and the colorless crystals(II) separated out were collected, ca. 11 g., yield, ca. 22%.

In another experiment, II was obtained in ca. 30% yield, in which the reaction was held at 2~12° for 6 hr. (after the addition of I) and the whole was allowed to stand for 10 hr. at room temperature.

The crude crystalline product was crystallized twice from methanol; colorless square plates or needles, fairly easily soluble in ethanol, methanol and ether, insoluble in cold water, somewhat soluble in hot water, m. p. 80~81.5°.

Anal. Found: C, 73.56; H, 10.10; mol. wt. (Rast), 192. Calcd. for $C_{12}H_{20}O_2$: C, 73.43; H, 10.27%; mol. wt., 196.3.

II did not decolorize bromine water and gave red coloration on heating with potassium hypobromite solution and pyridine, suggesting the presence of acetyl group[2].

The remaining oil of fraction (2), from which the above crystals were separated, seemed still to contain a fair amount of II or its isomers; this was inferred from the amount of the corresponding semicarbazone obtained from it. Likewise, this oil instantly decolorized bromine water indicating the presence of another unsaturated material.

Derivatives of II. — *Semicarbazone.* — The semicarbazone was prepared in aqueous ethanolic solution and recrystallized from ethanol, colorless long plates, m. p. 217°(with frothing; slowly heated), 240°(with frothing; rapidly heated).

Anal. Found: C, 61.25; H, 8.97; N, 16.45. Calcd. for $C_{13}H_{23}O_2N_3$: C, 61.63; H, 9.15; N, 16.59%.

2,4-Dinitrophenylhydrazone. — The derivative was recrystallized from pyridine; orange-yellow crystals, m.p. 200~201°.

Anal. Found: C, 57.47; H, 6.19; N, 14.83. Calcd. for $C_{18}H_{24}O_5N_4$: C, 57.43; H, 6.43; N, 14.89%.

Bis-2,4-dinitrophenylhydrazone.—An excess of a solution of 2,4-dinitrophenylhydrazine in methanolic sulfuric acid was added to II and refluxed for ca. 30 min. The orange crystals formed, which were sparingly soluble in boiling methanol, were crystallized twice from hot pyridine; orange crystals, m.p. 263~264° (with decomposition; rapidly heated) and 236~237°(with decomposition; slowly heated (ca. 1° per 30 sec.)).

Anal. Found: C, 52.11; H, 5.17; N, 20.15. Calcd. for $C_{24}H_{28}O_8N_8$: C, 51.79; H, 5.07; N, 20.14%.

Phenylhydrazone.—One and a half grams of II was refluxed in a mixture of 3 g. of phenylhydrazine, 5 cc. of ethanol and 1 cc. of water for ca. 20 min., and, after being cooled, the product was collected. Recrystallization from pyridine-ethanol gave almost colorless (faintly pale) plates, m.p. 155~156° (in sealed tube).

Anal. Found: C, 75.36; H, 9.05; N, 9.77. Calcd. for $C_{18}H_{26}ON_2$: C, 75.48; H, 9.15; N, 9.78%.

Bisphenylhydrazone.—A solution of 1.8 g. of II and 2.7 g. of phenylhydrazine in a mixture of ca. 3 cc. of 50 per cent. acetic acid and ca. 4 cc. of methanol was refluxed for ca. 1 hr. The crude product was recrystallized from methanol-pyridine, almost colorless(faintly greenish yellow) needles, m.p. 155~156° (in sealed tube).

Anal. Found: C, 76.24; H, 8.53; N, 14.96. Calcd. for $C_{24}H_{32}N_4$: C, 76.55; H, 8.57; N, 14.88%.

Hydrazone.—Two grams of II was refluxed with a mixture of excessive hydrazine hydrate and 3 cc. of ethanol for several minutes. Colorless long needles (ca. 2 g.) which readily separated out on standing, were crystallized twice from a small amount of ethanol; colorless needles or prisms, somewhat soluble in water and in ether, much more soluble in hot water, easily soluble in ethanol and methanol, m.p. 130~131°.

Anal. Found: C, 68.46; H, 10.54; N, 13.41; mol. wt. (Rast), 202. Calcd. for $C_{12}H_{22}ON_2$: C, 68.53; H, 10.55; N, 13.32%; mol. wt., 210.3.

Bromo-derivatives of II. — An attempt to oxidize II by hypobromite for the purpose of obtaining the corresponding acid resulted in bromination.

Tribromo-derivative (III). — Five grams of II was shaken with hypobromite solution, made from 24 g. of bromine, 28 g. of potassium hydroxide and 250 cc. of water, for ca. 4 hr. at room temperature, and left overnight. The reaction product which weighed ca. 3 g. was separated and recrystallized from ethanol; colorless needles or prisms, m. p. 81° (with partial decomposition), 100~101° (with partial decomposition; rapidly heated).

Anal. Found: C, 33.29; H, 3.94; Br, 54.92; mol. wt. (Rast), 455. Calcd. for $C_{12}H_{17}O_2Br_3$: C, 33.28; H, 3.96; Br, 55.37%; mol. wt., 433.0.

2,4-Dinitrophenylhydrazone of III.—Recrystallization from ethanol-pyridine gave long orange plates, m. p. 145° (with decomposition), 157~158° (with decomposition; rapidly heated).

Anal. Found: C, 35.20; H, 3.43; N, 9.03; Br, 38.97. Calcd. for $C_{18}H_{21}O_5N_4Br_3$: C, 35.26; H, 3.45; N, 9.14; Br, 39.11%.

Dibromo-derivative. — On applying a smaller amount of hypobromite another bromo-derivative containing one bromine atom less was obtained from II together with III. However its rigid separation from III was difficult, its 2,4-dinitrophenylhydrazone being obtained in fairly pure state; orange plates or fine yellowish orange needles from pyridine, m. p. 160° (with decomposition), 174° (with decomposition; rapidly heated).

Anal. Found: C, 40.66; H, 4.11; N, 10.43. Calcd. for $C_{18}H_{22}O_5N_4Br_2$: C, 40.47; H, 4.15; N, 10.49%.

Some Notes on the Bromo-derivatives of

II.—(a) III was warmed with ethanolic potassium hydroxide for ca. 1 hr., the reaction mixture was acidified with sulfuric acid and extracted with ether. After the ether was evaporated, a small amount of yellow needles was formed. A similar substance was obtained from the aqueous portion in the case of the hypobromite reaction mentioned above. In both cases the amount was insufficient for characterization purposes.

(b) When the bromo-derivatives were recrystallized from hot ethanolic acetic acid containing a little water, they turned into an oily material which instantly decolorized bromine water. Further, the bromo-derivatives, on warming with pyridine for ca. 1.5 hr., gave almost colorless crystals which also decolorized bromine water.

Dimerization of Mesityl Oxide.—The reaction was carried out in the same manner as in the case of I. A considerable amount of colorless needles or prisms was obtained, which on recrystallization from ethanol had m. p. 74~75°. It instantly decolorized bromine water and was positive toward acetyl test[2].

Anal. Found: C, 73.31; H, 10.17; mol. wt. (Rast), 184. Calcd. for $C_{12}H_{20}O_2$: C, 73.43; H, 10.27%; mol. wt., 196.3.

Department of Chemistry
Faculty of Science
Ibaraki University, Mito

Ion Exchange in Concentrated Solutions II. Beryllium Chloride-Hydrochloric Acid System*

By Hitoshi OHTAKI and Kazuo YAMASAKI

(Received May 15, 1957)

Although the ion-exchange in concentrated solutions has been applied successfully by several investigators to the separation of transuranic elements from rare earths[1] and the mutual separation of transition metals[2], only a few studies have been reported on ion-exchange equilibria in solutions of large ionic strength[3,4]. We had previously studied the equilibria in sodium chloride-hydrochloric acid and lithium chloride-hydrochloric acid systems[5]. In the present study the equilibrium in beryllium chloride-hydrochloric acid system was investigated.

Experimental

(1) The Resin.—The resin used was Dowex 50-X8 (hydrogen form) of mesh size 30~80 obtained by wet screening. It was dried at 40°C. The amount of water adsorbed on the resin was determined from the weight decrease on drying the resin at 110°C. It was 0.20-0.23 ml. per gram of the resin. The amount of resin used in one batch experiment was 3.6 g., i.e., about 15 milliequivalents.

(2) Reagents.—Commercial beryllium chloride was converted into beryllium basic acetate, and it was purified by recrystallization from hot glacial acetic acid. Purified beryllium basic acetate was decomposed with hot water and beryllium hydroxide was precipitated with ammonia. Beryllium hydroxide thoroughly washed was dissolved in a calculated amount of hydrochloric acid and thus solutions of beryllium chloride were prepared.

(3) Procedure.—A certain amount of the resin (exchange capacity E meq.) was put into a glass-stoppered Erlenmeyer flask containing a known amount (V=30 ml.) of 0.1~5 N $BeCl_2$-HCl mixtures. After shaking for 40 minutes in a thermostat at 25°C, the resin was quickly separated from the solution by suction on a glass filter. An aliquot of the filtered solution (external solution at equilibrium) was titrated with 0.1 N barium hydroxide solution, and the hydrogen ion concentration $(H^+)_S$ was determined using methyl yellow (pH of its color change: 2.9—4.0) as indicator, because beryllium chloride was hydrolized in the higher pH range. After the above procedure the chloride ion concentration of the filtrate, $(Cl^-)_S$, was determined by Fajans' argentometric titration, using fluorescein as indicator.

The separated resin was then poured into a column (20 cm.×1 cm. diameter) with water and washed repeatedly with distilled water. The amount of hydrogen ion in these washings, $[H^+]_Q$, was similarly determined by titration. The amount of beryllium ion in these washings,

* Read at the Annuel Meeting of the Chemical Society of Japan held at Kyoto in April, 1956. The first report was published in *J. Phys. Chem.*, **60**, 36 (1956).

1) K. Street, Jr. and G. T. Seaborg, *J. Am. Chem. Soc.*, **72**, 2790 (1950).
2) K. A. Kraus, et al., ibid., **71**, 3263, 3855 (1949); **72**, 4293, 5792 (1950); **73**, 9, 13, 2900 (1951); **74**, 843 (1952); **75**, 1460, 3273 (1953); **76**, 984, 5916 (1954); **77**, 1383 (1955).
3) K. A. Kraus, F. Nelson and G. W. Smith, *J. Phys. Chem.*, **58**, 11 (1954).
4) R. M. Diamond, *J. Am. Chem. Sec.*, **77**, 2978 (1955).
5) H. Kakihana, N. Maruichi and K. Yamasaki, *J. Phys. Chem.*, **60**, 36 (1956).

$[Be^{++}]_Q$ was determined colorimetrically by 8-hydroxyquinaldine[6].

Then 0.5 N barium nitrate solution was passed through the resin column, and the effluent was titrated with 0.1 N barium hydroxide. The amount of the hydrogen ion which had been retained in the resin, $[H^+]_R$, was thus determined and the amount of the beryllium ion in the effluent, $[Be^{++}]_R$, was determined by the gravimetric method using hydrazine as the precipitating agent.

Relations between the quantities determined above are

$$[Be^{++}]_Q=[Cl^-]_Q-[H^+]_Q$$
$$[Be^{++}]_S=[Be^{++}]_O-[Be^{++}]_R-[Be^{++}]_Q$$
$$(Be^{++})_S=(Cl^-)_S-(H^+)_S,$$

where parentheses and brackets represent concentration (milliequivalents per ml.) and amounts (milliequivalents) of the ions, respectively. Subscripts O, R, S and Q denote the original solution, the resin phase at equilibrium (the perfect exchange phase), the external solution at equilibrium and the quasi-exchange phase, respectively. The last phase, i. e. the quasi-exchange phase, consists of two kinds of solution. One is the solution which adheres to the surface of resin particles and the other is the solution which penetrates into the resin without being exchanged at the time of the exchange equilibrium.

Results and Discussion

(1) Adsorbed Water.—The amount of the water adsorbed by the resin, which is in contact with the external solution, is important in the ion exchange and many authors have tried to determine its amount by various methods[7-10]. However, the methods used by previous investigators in dilute or moderately dilute solutions are considerably complicated. The amount of adsorbed water was, therefore, estimated indirectly by the following calculation as reported in the previous paper[5].

The total amount of hydrogen ion in the solution and the resin is equal to

$$(H^+)_S(V-A')+[H^+]_Q+[H^+]_R, \qquad (1)$$

where A' is the volume of water adsorbed in the resin phase at equilibrium. The first term in (1) denotes the amount of hydrogen ion in the external solution. The total amount of hydrogen ion is also equal to

$$E+[H^+]_O, \qquad (2)$$

where E denotes the total exchange capacity of the resin used. Thus

$$(H^+)_S(V-A')+[H^+]_Q+[H^+]_R=E+[H^+]_O \qquad (3)$$

By arranging the equation,

$$A'=\frac{(H^+)_SV+[H^+]_Q+[H^+]_R-E-[H^+]_O}{(H^+)_S} \qquad (4)$$

As all the terms in (4) are determined experimentally, the amount of adsorbed water A' can be calculated. If the water content of the resin used (weight decrease on drying at 110°C) is denoted by A'', total amount of the water in the resin used (E meq.) at the equilibrium is

$$A=A'+A'' \qquad (5)$$

A part of the data obtained and the amounts of water in the resin thus calculated are given in Tables I and II. Values of A decrease as the concentration of the hydrogen ion increases. These values agree with the data of Pepper et al. and those of Davies et al. determined in hydrochloric acid solution. Quite recently

TABLE I
WATER IN THE RESIN

Total exchange capacity	Original soln.		External soln. at equilibrium		Water in the resin
E meq.	$BeCl_2$ (N)	HCl (N)	$BeCl_2$ (N)	HCl (N)	ml./g. dry resin
16.04	0.1	0.00	0.00_3	0.10	2.21
〃	〃	0.32	0.01	0.43	1.30
〃	〃	0.64	0.01	0.76	1.25
〃	〃	0.96	0.02	1.10	1.15
〃	〃	1.27	0.04	1.40	1.16
15.24	0.5	0.00	0.15	0.30	0.86
〃	〃	0.28	0.18	0.58	1.28
〃	〃	0.57	0.26	0.85	1.28
〃	〃	1.56	0.33	1.76	0.98
〃	〃	2.78	0.45	2.97	0.95
〃	〃	5.21	0.38	5.31	0.67
15.12	1.0	0.00	0.59	0.61	2.62
〃	〃	0.56	0.62	0.93	1.62
〃	〃	1.10	0.65	1.41	1.43
〃	〃	2.28	0.68	2.49	1.00
〃	〃	4.59	0.66	4.80	0.96
〃	〃	7.43	0.83	7.57	0.73
15.12	5.0	1.16	4.27	1.76	2.28
〃	〃	4.17	4.08	4.70	1.40

6) K. Motojima, This Bulletin, **29**, 71 (1956).
7) K. W. Pepper and D. Reichenberg, *Z. Elekteochem.*, **57**, 183 (1953); B. R. Sundheim, M. H. Waxman and H. P. Gregor, *J. Phys. Chem.*, **57**, 974 (1953).
8) K. W. Pepper, D. Reichenberg and D. K. Hale, *J. Chem. Soc.*, **1952**, 3219.
9) H. P. Gregor, K. M. Held and J. Bellin, *Anal. Chem.*, **23**, 620 (1951).
10) C. W. Davies and G. D. Yeoman, *Trans. Faraday Soc.*, **49**, 968, 975 (1953).

Gupta[11] applied our method of determining the adsorbed water to the study of sodium chloride-hydrochloric acid system and found that the ratio of the amount of water in the resin to the concentration of hydrochloric acid used increased linearly with the latter value.

(2) Concentrations of ions in the quasi-exchange phase.—In Fig. 1, the

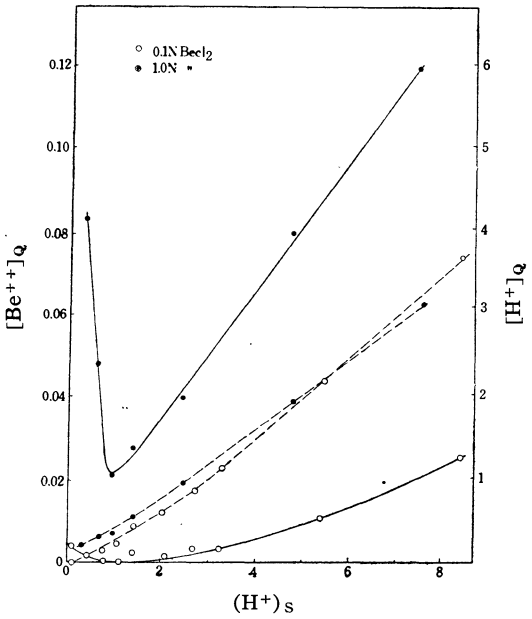

Fig. 1. Amounts of Be and H ions in the quasi-exchange phase. Solid and broken lines denote $[Be^{++}]_Q$ and $[H^+]_Q$, respectively.

amount of the beryllium ion in the quasi-exchange phase, $[Be^{++}]_Q$, and that of hydrogen ion, $[H^+]_Q$, are plotted against hydrogen ion concentration in the solution, $(H^+)_S$. If there is any competition between beryllium and hydrogen ions in the adsorption on the resin, it is expected that the amount of beryllium ion in the quasi-exchange phase, $[Be^{++}]_Q$, will decrease as hydrogen ion concentration in the external solution, $(H^+)_S$, increases. Such a fact is found when $(H^+)_S$ is low. But, when it is higher than 1 N, values of $[Be^{++}]_Q$ show a minimum and then increase as $(H^+)_S$ increases. On the other hand, $[H^+]_Q$ increases always as $(H^+)_S$ increases. This means that some change in the ionic species takes place in the solution. The results of spectrophotometric studies given in (4) reveal formation of complexes in the solution.

11) H. C. Gupta, *Naturwissenschaften*, **43**, 543 (1956).

(3) Apparent equilibrium constant.—Apparent equilibrium constant, K, of the exchange reaction between beryllium and hydrogen ions is given by the following equation:

$$K = \frac{(H^+)_S^2 (Be^{++})_R}{(H^+)_R^2 (Be^{++})_S}$$

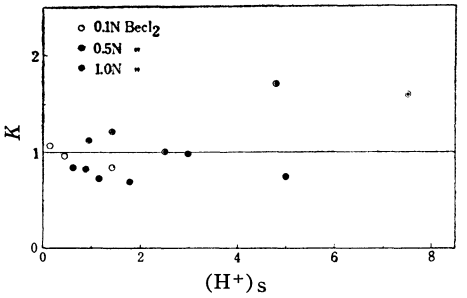

Fig. 2. Relations between apparent equilibrium constant K and the hydrogen ion concentration in the external solution, $(H^+)_S$.

where $(H^+)_R$ and $(Be^{++})_R$ are defined as $[H^+]_R/A$ and $[Be^{++}]_R/A$ respectively[12]. In Fig. 2 values of K are plotted against the concentration of hydrogen ion in the external solution. When the concentration of beryllium ion is low, K is smaller than 1, but when it is 1.0 N or higher, the value of K is greater than unity. This fact can be explained by the formation of cationic complexes which are more easily captured by the resin than the simple beryllium ion. The formation of such a complex is shown by the spectrophotometric experiments.

(4) Ionic species in the solution.—In Table II values found for $[H^+]_R+[Be^{++}]_R$, i. e. sums of amounts of ions in the resin phase are always larger than the total equivelent capacities of the resin. This means that two hydrogen ions do not exchange for one beryllium ion and some complexes are formed in the solution.

The formation of complexes is also shown by spectrophotometric evidence. In the region of higher concentrations of hydrochloric acid, mixed solutions of beryllium chloride and hydrochloric acid have a yellow color. In Fig. 3 spectrophotometric curves of beryllium chloride, hydrochloric acid and their mixture are shown. The mixture absorbs more strongly than the components and new absorption bands appear at 265 and 370 mμ.

12) As the activity coefficients of beryllium and hydrogen ions in the mixtures are not known, neither the rtelaive affinity of the exchange equilibrium of beryllium and hydrogen nor the Donnan equilibrium constant can be calculated.

TABLE II
A PART OF THE DATA OBTAINED
( ): meq./ml., [ ]: meq.

Original soln.		External soln. at equilibrium			Quasi-exchange phase		Resin phase			Total exchange capacity
$(H^+)_o$	$(Be^{++})_o$	$(H^+)_s$	$(Cl^-)_s$	$(Be^{++})_s = (Cl^-)_s - (H^+)_s$	$[H^+]_Q$	$[Be^{++}]_Q$	$[H^+]_R$	$[Be^{++}]_R$	$[H^+]_R + [Be^{++}]_R$	E meq.
1.27	0.10	1.40	1.44	0.04	1.53	0.00_8	15.04	1.14	16.18	16.04
1.56	0.50	1.76	2.09	0.33	1.84	0.00_5	12.18	3.98	16.06	15.24
1.10	1.0	1.41	2.05	0.64	2.11	0.10	9.00	7.63	16.63	15.12
1.16	5.0	1.76	6.03	4.27	4.74	3.10	3.28	13.61	16.89	15.12

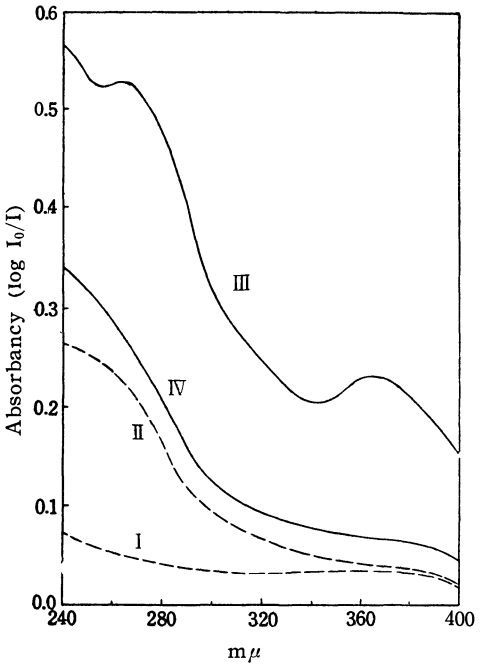

Fig. 3. Absorption curves of beryllium chloride, hydrochloric acid and their mixture.
Curve I: 5 N HCl, II: 3 N $BeCl_2$, III: Mixture of 3 N $BeCl_2$ and 5 N HCl, IV: Sum of I and II.

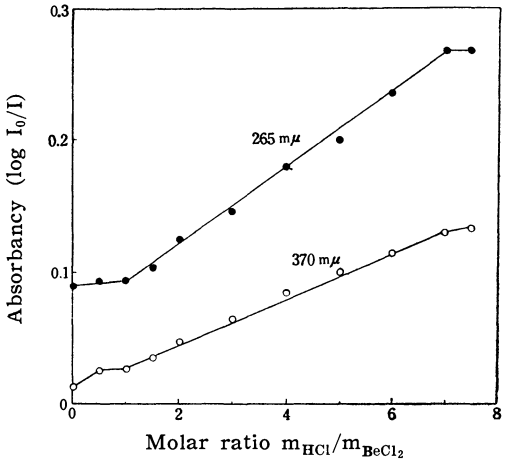

Fig. 4. Relations between absorbancy and molar ratio. Black and white circles denote the absorbancy values at 265 and 370 mμ, respectively.

This supports the view that complexes are formed between beryllium chloride and hydrochloric acid.

An attempt was made to determine the composition of the complexes thus formed by the molar ratio method[13]. The result is shown in Fig. 4. The line has a break at $m_{HCl}/m_{BeCl_2}=1$. This may suggest that the formation of complexes begins at 1 N of hydrochloric acid concentration. Another break seems to be present at $m_{HCl}/m_{BeCl_2}=7$. Since beryllium chloride solution was prepared by dissolving beryllium hydroxide into hydrochloric acid, it was difficult to prepare the mixture of beryllium chloride and hydrochloric acid of larger molar ratio, m_{HCl}/m_{BeCl_2} than 7.5 and to confirm the existence of the second break.

To find out whether the formed complex is cationic or anionic, the solution containing 3 N beryllium chloride and 5 N hydrochloric acid was passed through a column of chloride form of Dowex 1-X8. The ionic species containing beryllium ion was not adsorbed on the resin and the resin and the complex thus formed was found to be cationic.

Kraus et al.[3] reported that the beryllium ion of the tracer scale was not captured by the anion-exchange resin, Dowex 1, in 7 N and 12 N hydrochloric acid. Diamond[4] measured the distribution ratios of the beryllium ion of tracer scale and concluded that the beryllium ion existed as a cationic chloro-complex, probably a polynuclear one. The results of our experiments agree well with their conclusions.

Summary

The ion exchange equilibrium was

13) J. H. Yoe and A. L. Jones, *Ind. Eng. Chem. Anal. Ed.*, **16**, 111 (1944).

studied in the concentrated solutions of beryllium chloride and hydrochloric acid. The amount of water in the resin was calculated from the difference of hydrogen ion concentration before and after the ion exchange equilibrium. A cationic complex containing beryllium was found to be formed in the solution.

The expenses of the present study were defrayed by Grant-in-Aid for Fundamental Scientific Resiarch from the Ministry of Education.

Chemical Institute, Faculty of Science, Nagoya University
Chikusa, Nagoya

Various Alkyl Amines and Ammonium Compounds as Accelerators for Grain Growth of Silver Chloride Suspensions in Aqueous Polyvinyl Alcohol Solution

By Yasushi OH-YAMA and Kiyoshi FUTAKI

(Received June 14, 1957)

The physical ripening of silver chloride polyvinyl alcohol emulsion (i. e. the grain growth of silver chloride suspension in an aqueous polyvinyl alcohol solution) was found able to be accelerated by the addition of some sorts of substance[1,2,3].

Substances already reported as active comprise many sorts of substance, some of them having active sulfur atom, are so-called "sulfur-sensitizers" in photographic chemistry, e. g. inorganic thiosulfates, thiocyanates or organic derivatives of thiourea, rhodanine, or the like[1]. Some without active sulfur are those that contain a nitrogen atom together with some other nitrogen, oxygen or non-active sulfur atom in their molecule, e. g. *N*-alkyl homologues of guanidine, pyrrolidone, pyridone, quinolone or 2-imino-thiazolines[2].

In later experiments much simpler compounds which contain only one heterogeneous atom, sulfur or nitrogen, such as alkyl thiols or alkyl ammonium compounds were active. In the present paper, however, only alkyl amines such as primary, secondary, tertiary amines and some *N*-alkyl quaternary ammonium compounds (both non-cyclic and cyclic) are dealt with. Surface active properties of higher alkyl homologues of these compounds are well known, and a remarkable resemblance of the mechanism of grain growth and that of micelle formation of many of these surface active substances was also reported by one of the present authors[3].

1) Y. Oh-yama: "Science and Application of Photography" (Proceedings of the R. P. S. Centenary Conference, London 1953) 37 (1955).
2) Y. Oh-yama and K. Futaki: This Bulletin, **28**, 243 (1955).
3) Y. Oh-yama, Lectured at "Internat. Konferenz f. Wiss. Phot." Köln, 1956. (*Sci. et Ind. Phot.* [2], **27**, 390 (1956)).

Experimental

To 42 ml. of aqueous solution of an active substance of varying concentrations (10 ml. of this solution may be replaced by ethanol when necessary for sparingly soluble substance), 10 ml. of 6% solutions of polyvinyl alcohol and 4 ml. of 0.6 M sodium chloride solution are added. The mixture is heated to 70°C, and 4 ml. of 0.2 M silver nitrate solution (70°C) is added within 15 seconds.

After drawing out 2 ml. of this suspension of silver chloride at 2, 4, 8 and 16 min. after the addition of silver ions, it is diluted with 20 ml. of cold water and the turbidity is measured.

From the fact[4,5] that the turbidity of the suspension is in linear proportion to the mean diameter of grains in the region of the sizes in question (0.05~0.25 μ in diameter), the grain growth can be traced by the nephelometric method as was previously reported[1,2]. The turbidity measurement usually adopted[1,2] (designated as K-method) was, however, altered in some cases by the method closely resembling Ammann's[6] (designated as A-method). A simpler method which was used in the previous report and designated as Transmission method (or T-method)[2], was used only in a few cases. The suspension remains almost neutral (6~7) without using buffer-solution.

4) H. Ammann-Brass: *Sci. et Ind. Phot.* [2], **23**, 249 (1952).
5) F. Evva: *Z. wiss. Phot.*, **47**, 39 (1952).
6) H. Ammann-Brass: *Kolloid Z.*, **110**, 161 (1948).

Ripening characteristics (graphs plotting turbidities against logarithm of the concentration of added substances) were obtained as usual[1,2]. The critical concentrations for grain growth (C. C. G.) of various compounds were determined as the minimum addition concentration which caused a definite turbidity-increase (10 units above blank in the K-method or total turbidity of 35 units in the A-method after 16 minutes' ripening) on these characteristics. The reciprocal of this concentration (in millimol) defines the activity and is used for the comparison of activities of various compounds.

Results and Discussion

(a) Primary Alkyl and Aralkyl Amines.—Primary amines tested were benzyl, β-phenylethyl, *n*-hexyl, *n*-octyl, *n*-decyl, dodecyl and octadecyl amine. Some of the ripening characteristics obtained are shown in Fig. 1. The critical concentration for grain growth and activity of these compounds are computed from these curves and listed in Table I. The equivalent chain length listed in the 4th column was assumed to be counted with

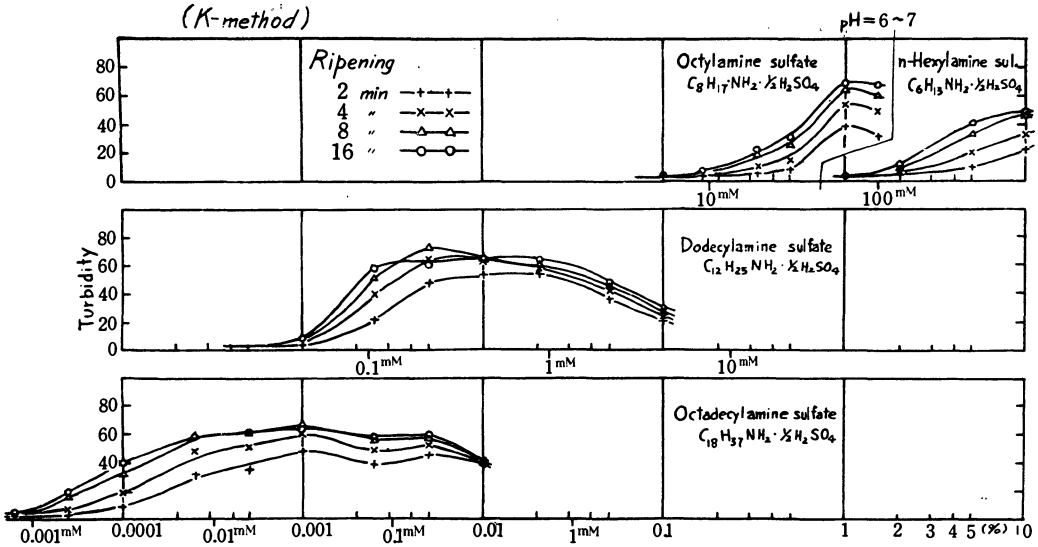

Fig. 1. Some of the ripening characteristics of primary amines.

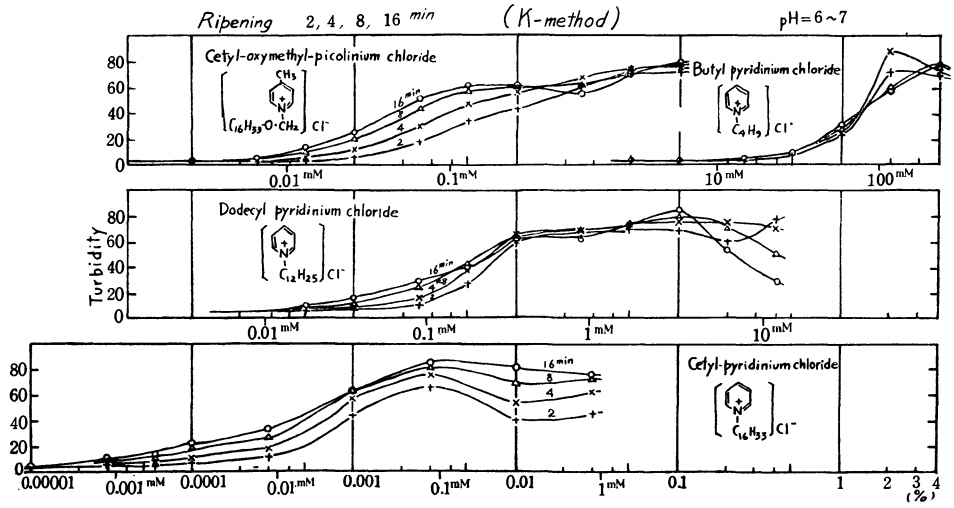

Fig. 2. Some of the ripening characteristics of alkyl pyridinium and pycolinium compounds.

TABLE I

CRITICAL CONCENTRATIONS FOR GRAIN GROWTH AND ACTIVITIES OF PRIMARY AMINES AT pH 6~7

Substances tested	Mol. W.	Equiv. chain length	C. C. G. (mM)	Activity	Method of measuring turbidity	Salt used
Benzyl amine	107	4	700(?)	0.0014(?)	K	sulfate
Phenyl ethyl amine	121	5	132	0.0076	K	〃
n-Hexyl amine	101	6	135	0.0074	K	〃
n-Octyl amine	129	8	13.5	0.074	K	〃
n-Decyl amine	158	10	2.8 2.8	0.357 0.357	A K	〃
Dodecyl amine	185	12	0.0470	21.3	K	〃
Octadecyl amine	269	18	0.00130	770	K	〃

TABLE II

CRITICAL CONCENTRATIONS FOR GRAIN GROWTH AND ACTIVITIES OF *N*-ALKYL PYRIDINIUM AND PYCOLINIUM COMPOUNDS AT pH 6~7

Substances tested	Equiv. W.	Equiv. chain length	C. C. G. (mM)	Activity	Method of measuring turbidity	Salt used
n-Butyl pyridinium ion	136	6	36.0	0.028	K	chloride
n-Octyl 〃 〃	192	10	3.95 4.00	0.253 0.250	A K	〃
n-Decyl 〃 〃	220	12	1.40 1.63	0.714 0.613	A K	〃
Dodecyl 〃 〃	248	14	0.0250	40.0	K	〃
Hexadecyl 〃 〃	304	18	0.00146	685	K	〃
Octadecyl 〃 〃	332	20	0.00106	942	K	bromide
Hexadecyl oxymethyl-pycolinium ion	348	21(?)	0.0125	80	K	chloride

TABLE III

CRITICAL CONCENTRATIONS FOR GRAIN GROWTH AND ACTIVITIES OF *N*-ALKYL QUINOLINIUM COMPOUNDS AT pH 6~7

Substances tested	Equiv. W.	Equiv. chain length	C. C. G. (mM)	Activity	Method of measuring turbidity	Salt used
n-Butyl quinolinium ion	186	10	5.00 4.50	0.200 0.223	A K	chloride
Benzyl quinolinium ion	220	10	3.30 3.50	0.303 0.285	A K	〃
n-Octyl quinolinium ion	242	14	0.222 0.230	4.56 4.35	A K	〃
Decyl quinolinium ion	270	16	0.072 0.074	13.9 13.5	A K	〃
Dodecyl quinolinium ion	298	18	0.0064 0.0063	147 159	A K	〃

their real number of carbon atoms in the simple alkyl amines and phenyl group in benzyl or phenyl-ethyl radicals was counted as 3, and in some other cases it will be discussed later in detail.

(b) *N*-Alkyl Pyridinium, Pycolinium and Quinolinium Compounds.—Some of the ripening characteristics are shown in Fig 2, and all of the substances tested are listed in Tables II and III.

(c) Relations between Activity and Molecular Weight or Chain Length.—The activity increases as a whole with increase in the molecular weight as shown in Fig. 3, yet the relation is not so simple as was in the case with guanidine, pyridone, pyrrolidone or quinolones which was reported before.[2]

(d) The Concept of Equivalent Chain Length.—The fact that the activities are related intrinsically to the chain length of the linear alkyl radical attaching to the nitrogen atom of these amines rather than to the molecular weight itself, was demonstrated in Fig. 4. Although there is a "break" or a sudden rise of activity

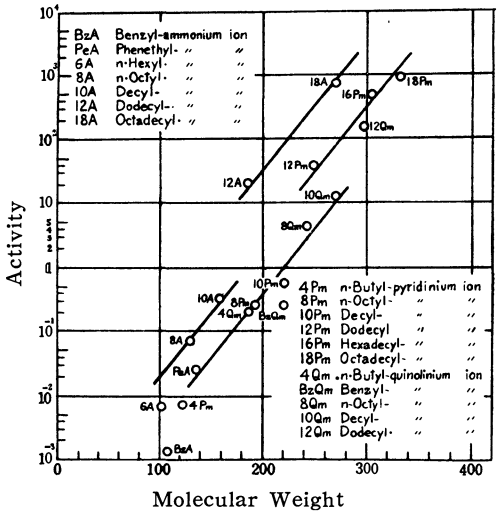

Fig. 3. Relation between activities and molecular weights of primary alkyl amines and *N*-alkyl homologues of pyridinium and quinolinium compounds.

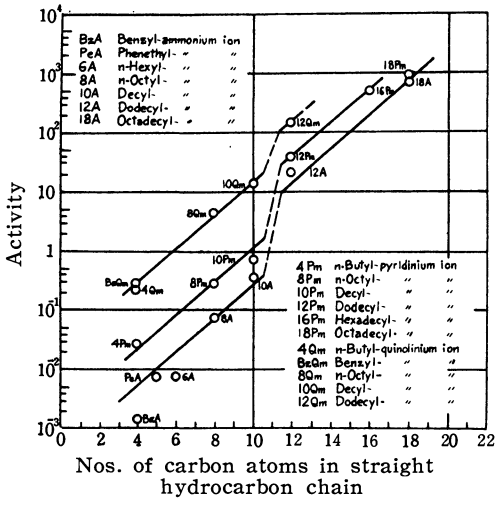

Fig. 4. Relation between activities and alkyl chain-length of primary alkyl amines and *N*-alkyl cyclo-ammonium compounds.

between 10 and 12 carbon atoms, the parallel relation among these three lines is quite clear. It is also clear that the number of carbon atoms of these cyclic hydrocarbon chains of pyridinium or quinolinium nucleus would participate in the activities with the linear alkyl carbon chains.

If we assume an adequate chain length for these cyclic nuclei for example, 1 for pyrrole, 2 for pyridine, 6 for quinoline respectively, and define the equivalent chain length (n_E) of a certain active compound as the sum of the number of carbon atoms of linear alkyl chain and that of the chain length of the nucleus assumed as above, the relation between activity (or the critical concentration of grain growth) and the chain length will be expressed in the following equation as shown in Fig. 5,

$$-\log_{10} C_g = \log_{10} A = \frac{n_E - \beta}{3.50}$$

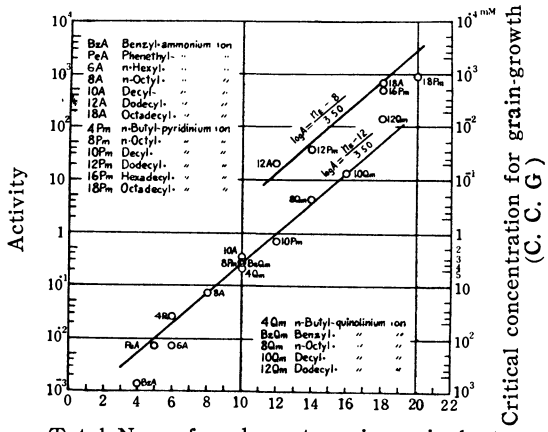

Fig. 5. Relation between activities and equivalent chain lengths of various primary amines and cyclo ammonium compounds.

where C_g is the critical concentration for grain growth (in mM), A the activity and β a constant. Three lines in Fig. 4 now coincide with one another and the sudden increase in activitys between 10 and 12 carbon atoms of linear alkyl chains is now turned to decrease in β from 12 to 8 abruptly.

Assumed chain lengths of these cyclic unclei are only empirical, yet the equivalent chain length of these compounds seems to be able to be calculated according to the following equation,

$$n_E = n_A + (n_C - 3)$$

where n_A is the number of carbon atoms in the alkyl chain attached directly to the central nitrogen atom, and n_C that of carbon atoms in the cyclic nucleus containing the nitrogen atom.

(e) Coincidences of the Relation with that of Guanidine. Pyridone-quinolone, and Imino-pyridine Series.—The concept of equivalent chain length is also held well as shown in Fig. 6 for guanidine and pyridone, quinolone series, whose relations

between activity and molecular weight were already reported[2]. In Fig. 6, the case of imino-pyridines is also included.

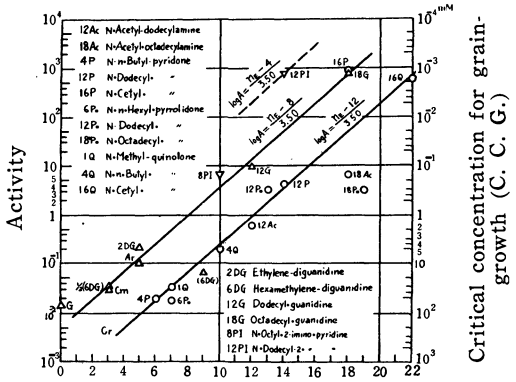

Fig. 6. Relation between activities and equivalent chain lengths of various compounds of guanidine-, pyridone- and quinolone series.

The coincidence of Fig. 5 and Fig. 6 is most striking, considering that they were derived from results of independent experiments. The reason for this coincidence and the intimate relationship between the grain growth of silver halide in this case and the micelle formation of surface active substances was already discussed in another report in connection with the mechanism of these two phenomena[3].

(f) Secondary and Tertiary Amines and Quaternary Ammonium Salts. — These compounds tested are listed in Table IV, and some of the ripening characteristics are shown in Fig. 7. They are also as powerful as primary amines, yet somewhat less powerful when compared on the basis of the molecular weight. It will be easily deduced from the above mentioned results regarding cyclic ammonium compounds, that the concept of equivalent chain length holds well. Because of lack of examples and exactness, the calculating method of the equivalent chain length for them, however, could not be found out from the experimental results.

Fortunately the critical micelle concentration (C. M. C.) of various surface active substances can be determined much more exactly, so the calculation of the equivalent chain length could be easily deduced from these data, and at first the equivalent chain length (n_E) of these compounds is assumed to be expressed by the following equation,

$$n_E = n_1 + \alpha(n_2 + n_3 + n_4)$$

where n_1, n_2, n_3 and n_4 are the numbers of carbon atom in four alkyl chains attached to the central nitrogen atom of these ammonium ions and there exist $n_1 \geq n_2 \geq n_3 \geq n_4$ (of course for tertiary amines $n_4 = 0$, and for secondary amines $n_3 = n_4 = 0$).

The constant α calculated from the data plotted from the curves determined by

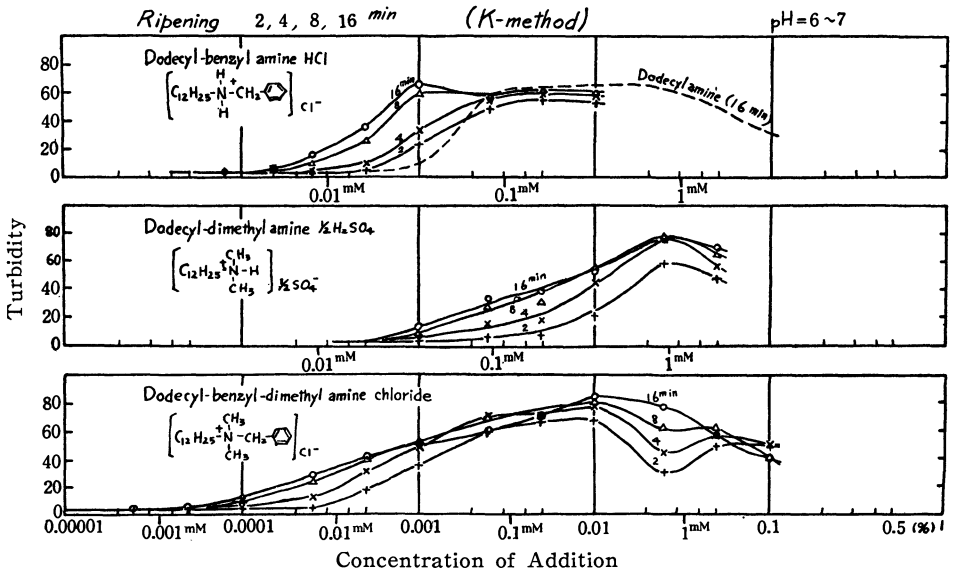

Fig. 7. Some of the ripening characteristics of secondary, tertiary amines and quaternary ammonium salts.

TABLE IV

CRITICAL CONCENTRATIONS FOR GRAIN GROWTH AND ACTIVITIES OF VARIOUS SECONDARY, TERTIARY AND QUATERNARY AMMONIUM SALTS AT pH 6~7

Substances tested	Equiv. W.	Equiv. chain length	C. C. G. (mM)	Activity	Method of measuring turbidity	Salt used
Benzyl diethyl-ammonium ion	164	6.20	56.0 44.0	0.0175 0.0227	A K	chloride
Dodecyl dimethyl-ammonium ion	214	13.10	0.044 0.038	22.7 26.3	T K	sulphate
Dodecyl benzyl-ammonium ion	275	15.85	0.0073	137	K	chloride
Dodecyl benzyl dimethyl-ammonium ion	304	16.95	0.0032	313	K	〃
Hexadecyl trimethyl ammonium ion	284	17.65	0.0035	286	K	bromide
Octadecyl dimethyl-ammonium ion	298	19.10	0.0130 0.0103	77.0 97.0	T K	sulfate
Octadecyl trimethyl-ammonium ion	312	19.65	0.0040	250	K	chloride
Octadecyl benzyl-ammonium ion	359	21.85	0.00102	980	K	〃

TABLE V

ESTIMATION OF THE EQUIVALENT CHAIN LENGTH OF SOME ALIPHATIC QUATERNARY AMMONIUM SALTS

Substances[1]	C.M.C.[2] (mM)	$-\log$ (C.M.C.)	n_E[3]	n_1	$n_2+n_3+n_4$	n_E-n_1	$\frac{n_E-n_1}{n_2+n_3+n_4}$	$n'_E=n_1+0.55(n_2+n_3+n_4)$ Calc.	Deviation
8- 8-1-1-Am	28.3	−1.450	13.42	8	10	5.42	0.542	13.50	−0.08
10-10-1-1-Am	2.16	−0.334	17.33	10	12	7.33	0.611	16.60	+0.73
12- 1-1-1-Am	23.2	−1.365	13.73	12	3	1.73	0.577	13.65	+0.08
12- 8-1-1-Am	1.69	−0.226	17.71	12	10	5.71	0.571	17.50	+0.21
12-12-1-1-Am	0.760	+0.119	18.92	12	14	6.92	0.495	19.70	−0.78
16- 1-1-1-Am	1.77	−0.247	17.63	16	3	1.63	0.543	17.65	−0.02
						mean	0.5565	mean	0.316

(1) Names of substances are abbreviated by the numbers of carbon atoms in alkyl chains, e. g. Di-octyl-dimethyl ammonium ion is shown by 8-8-1-1-Am.

(2) Deta from Ralston et al.[7]

(3) n_E are calculated from the equation; $-\log(\text{C. M. C.}) = \frac{n_E-18.50}{3.50}$

Ralston et al.[7] is 0.55 as shown in Table V. This table would also prove the validity of the above mentioned assumption.

In Table IV, together with the experimental data there also are shown the equivalent chain lengths of compounds tested, calculated by the above mentioned method. The relation between the activity and the equivalent chain-length is plotted in Fig. 8. Two straight lines drawn in the figure are identical with those of Fig. 5.

It is interesting to know that the activity of the compound, whose solubility in water is very great, e. g. dodecylbenzyldimethyl ammonium salt (10% solution is quite clear), is much higher than those scarcely soluble compounds such as decyl- or dodecylamine, and is almost comparable with that of octadecyl amine which is not completely soluble in less than 0.001%.

7) A. W. Ralston, D. N. Eggenberger and P. L. Du. Brow. *J. Am. Chem. Soc.*, **70**, 977 (1948).

Summary

Various alkyl amines and ammonium compounds (non-cyclic and cyclic) were tested as accelerators for the grain growth of silver chloride suspension in aqueous polyvinyl alcohol solution.

The relation previously found between the molecular weight and the grain growth acceleration activity (A) of various organic *N*-derivatives did not exactly hold for these series of compounds.

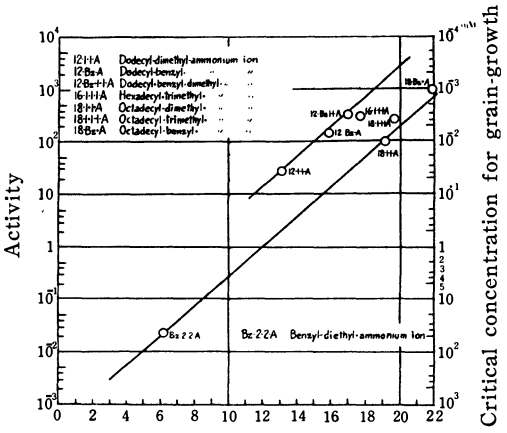

Fig. 8. Relation between activities and equivalent chain lengths of various secondary, tertiary amines and quaternary ammonium salts.

Instead, when the concept of the equivalent chain length is introduced, the data were able to be represented by:
$\log A = -\log C_g = (n_E - \beta)/3.50$, where C_g is the critical concentration for grain growth (in millimol), n_E the equivalent chain length and β 8 or 12.

This equation quite resembles the relation between chain length and critical micelle concentration of many surface active compounds. The fact leads to the author's assumption that the mechanism of grain growth of silver chloride would be intrinsically identical with that of micelle formation and this was discussed in another paper.

The equivalent chain lengths of some of these active substances were able to be derived empirically from the number of carbon atoms in the molecule.

Research Section, Kyoto Factory
Mitsubishi Paper Mills Co.
Kyoto

Studies on the Monodisperse Aerosols. III. The Formation of Sulfur Aerosols

By Susumu KITANI

(Received July 22, 1957)

The formation of monodisperse aerosols of various substances has been frequently investigated with relation to the colloid chemical studies on aerosols. Since the studies of La Mer-Sinclair using their aerosol generator[1,2], the preparation of uniform aerosols has become easy to perform and it has been possible to extend the method to any kind of aerosol.

Ford and La Mer[3] measured the vapor pressure of a supercooled liquid sulfur droplet which was prepared by the La Mer-Sinclair generator with the nuclei of sodium chloride. Kerker and others[4] announced that a sulfur aerosol could be nucleated with sulfuric acid vapor to produce smaller particles, while large particles of sulfur aerosols were prepared by self-nucleation. As a rule, monodisperse aerosols are obtained only when proper nuclei are given homogeneously to a supersaturated vapor. Sinclair[2] mentioned that, in the formation of monodisperse aerosols by the La Mer-Sinclair generator, the condensation nuclei are formed in the ionizer by a high-voltage electric spark, and that the nuclei may be ionized molecules of air and its related compounds.

It was found in this experiment that monodispersed aerosols were obtained by introduction of the nuclei produced by the flaming spark of silver electrodes. We attempted to investigate what nuclei are effective in the formation of sulfur aerosol by the condensation method.

Experimental

The apparatus used for the formation of sulfur aerosols is shown schematically in Fig. 1. The

1) D. Sinclair and V. K. La Mer, *Chem. Rev.*, **44**, 245 (1949).
2) Atomic Energy Commission, "Handbook on Aerosols", Washington, D. C., (1950), p. 77.
3) G. P. Ford and V. K. La Mer, *J. Am. Chem. Soc.*, **72**, 1959 (1950).
4) M. Kerker and others, *J. Colloid Sci.*, **10**, 413 (1950).

sulfur aerosols have been prepared by using a modified La Mer-Sinclair aerosol generator and ion separators A and B. The modification consists in separating the ionizer from the boiler. The

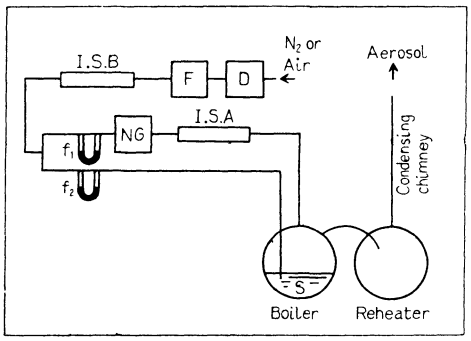

D: Drier
F: Glasswool filter
I. S. A., I. S. B.: Ion separator
NG: Nuclei generator
f_1, f_2: Flow-meter
S: Sulfur

Fig. 1. The apparatus for the formation of sulfur aerosols.

ionizer is called "nuclei generator" in this paper. It consists of a glass tube, 35 mm. in diameter and 90 mm. in length, fitted with the electrodes, made of silver wires (0.5 mm. in diameter) and fixed 6 mm. apart. An electric current of 10 mA. was applied at 11 kV. of A.C. in nitrogen or air. The ion separator A was placed between the boiler and the nuclei generator in order to remove the charged substances resulting from the electric spark; another ion separator B was used to exclude air ions and charged particles of dust. The separators A and B consist of rectangular pipe, 20 cm. in length, made of aluminum plates, 1 cm. in width and 20 cm. in length, set parallel and 1 cm. apart from each other, and other parallel plates are made of bakelite of the same size as the aluminum electrodes and serve as the electric insulator.

The boiler and the reheater were heated electrically and kept at a given temperature by thermoregulators: the former was operated at from 120° to 140°C, and the latter at from 130° to 150°C. In most runs of experiment, the latter was maintained higher by 10°C than the former.

The air, purified by passing through concentrated sulfuric acid, glasswool and the ion separator B, was passed through both of two branches at the rate of 0.25 l./min. into the boiler; one branch served to bubble through liquid sulfur and the other to send condensation nuclei through the ion separator A.

The distribution of particle size was measured by the "Owl"[1,2] and an ultramicroscope. The average radius $\bar{r}$ was calculated by application of the Stokes-Cunningham's equation from the terminal velocity of particles in the cell of the ultramicroscope[5]. The standard deviation σ was evaluated by

$$\sigma=\left\{\frac{\sum_i N_i(r_i-\bar{r})^2}{\sum_i N_i}\right\}^{1/2} \quad (1)$$

where N_i is the number of particles of radius r_i. The fractions of charged particles were also measured from the direction of electrophoresis of particles in the cell of the ultramicroscope. Sulfur, used in this experiment, was purified by recrystallization from carbon disulfide solution.

Results

The condensing chimney of La Mer-Sinclair generator consists of a double tube and, for comparison, the chimney of a single tube was also used in the present work. In both cases, the monodisperse aerosols in the state of supercooled liquid were formed only when the nuclei were given by the flaming spark of silver electrodes. In the case of the absence of nuclei, polydisperse aerosols were produced in the condensing chimney of a single tube but we could hardly get the aerosols in the chimney of the double tube. When the single tube was used, the aerosols might be produced by self-nucleation owing to a rapid cooling.

It is found in Fig. 2 that the higher the temperature of the boiler, the larger the average radius $\bar{r}$. The higher order Tyndall spectra on sulfur aerosols were

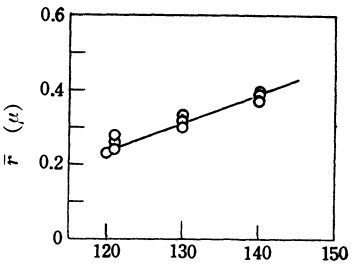

Boiler temperature, °C.

Fig. 2. Dependence of the average radius, $\bar{r}$, as a function of boiler temperature.

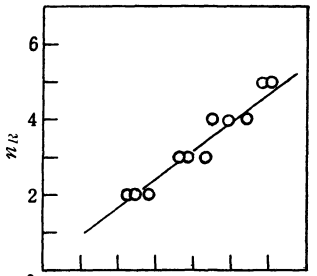

$\bar{r}$ (μ)

Fig. 3. The number of reds, n_R, (the higher order Tyndall spectra) vs. the particle of average radius, $\bar{r}$.

observed by the "Owl". The number of red bands, n_R, is plotted against $\bar{r}$ in Fig. 3. The $\bar{r}$, σ and the fractions of charged particles obtained using the condensing chimney of a single tube and of a double one were plotted as the function of voltage of the ion separator A as shown in Figs. 4, 5 and 6.

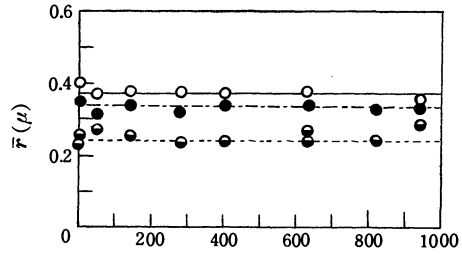

---●---: Boiler temp. 120°C & reheater temp. 130°C. } with the condensing chimney of double tube.

---●---: Boiler temp. 130°C & reheater temp. 140°C. } with the condensing chimney of double tube.

—○—: Boiler temp. 140°C & reheater temp. 150°C. } with the condensing chimney of single tube.

Fig. 4. Dependence of the average radius, $\bar{r}$, as a function of the voltage of the ion separator A.

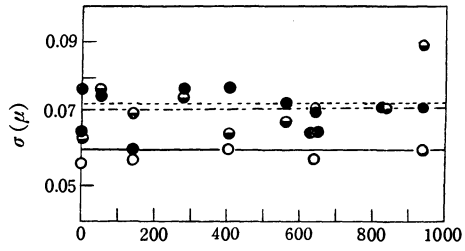

Fig. 5. Dependence of the standard deviation, $\sigma(\mu)$, as a function of the voltage of the ion separator A. (notations are the same as Fig. 4.)

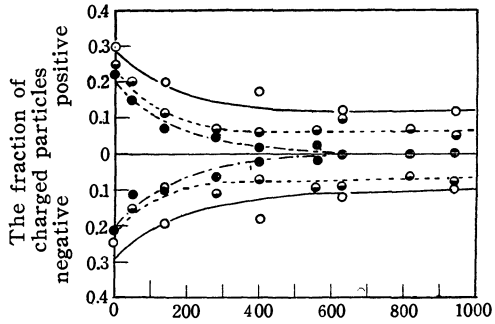

Fig. 6. Dependence of the fraction of charged particles as a function of the voltage of the ion separator A. (notations are the same as Fig. 4.)

It appears that $\bar{r}$ and σ remained almost constant while the fractions of charged particles decreased monotonously with the increase in the voltage of the ion separator A. It was noted that these tendencies were similar in all the other cases.

Discussion

The liquid sulfur aerosols were formed by means of the La Mer-Sinclair generator using the flaming spark of silver electrodes. It seems that silver is vaporized at high temperature in the process of eletric discharge. Particles of silver vapor can coalesce with each other both by condensation and by coagulation to yield minute particles. It appears in this work that the effective nuclei are such silver particles as described below.

If a particle of radius r, having an electric charge of n units, moves in air with velocity v in a uniform electric field E, it holds that

$$nEe=6\pi r\eta v(1+Al/r)^{-1} \qquad (2)$$

where η is the viscosity coefficient of air, A the Cunningham's constant and l the mean free path of air molecules. It is calculated from the flow rate of air that the charged particle moving towards the electrode of opposite sign, with a velocity greater than 0.21 cm., is excluded while it passes through the ion separator. Assuming that

$n=1$, $e=4.8\times10^{-10}$ e. s. u., $\eta=1.8\times10^{-4}$ c. g. s. u., $Al=1.0\times10^{-5}$ cm.

and $Al\gg r$, the relation between E' (the electric field expressed in terms of practical units) and the radius r of the particle to be excluded becomes

$$E'=4.5\times10^{13}\, r^2, \qquad (3)$$

which will be applicable in the range of gas molecules[6]. The equation (3) is plotted in Fig. 7.

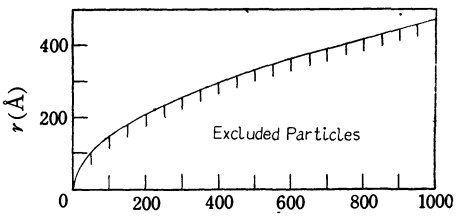

Fig. 7. The particle radius, r, excluded vs. the voltage of the ion separator.

5) R. Whytlaw-Gray and H. S. Patterson, "Smoke", London, (1932), p. 94.

6) J. W. Thomas, *J. Colloid Sci.*, **10**, 25 (1955).

It is seen from equation (3) that ordinary air ions were easily removed under the condition of 0.1 V./cm. through the ion separator A owing to their large mobility. If these air ions were effective nuclei as presumed by Sinclair, both values of $\bar{r}$ and σ of aerosols would be remarkably altered by excluding them. But it is difficult to find such an effect in this experiment (cf. Figs. 4 & 5).

Silver was detected by spectrographic analysis of the flaming spark in the nuclei generator. The silver particles resulting from the electrodes at high temperature were detected in the electron microscopic photograph. Although the particles found in the photograph are large, the nuclei, working in the process of the aerosol formation may be minute; the former particles might have grown by coagulation.

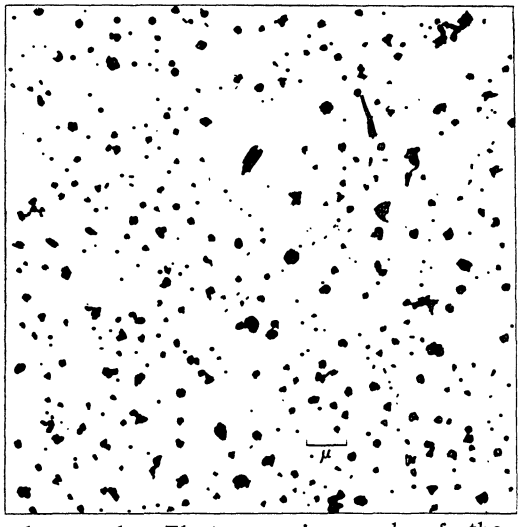

Photograph. Electron micrograph of the silver particles produced from the electrodes in nuclei generator (discharging 2.5 min. and standing 17 hours in nitrogen).

The oxygen compounds such as ozone and nitrogen dioxide which come out from discharge were detected easily. Ozone was detected in the gas passed through the nuclei generator by the iodine-starch reaction, and nitrogen dioxide was collected in a dry ice-alcohol cold trap from the above gas and detected by the change in color coming from the variation of the temperature. However, it is supposed that such substances do not act as the nuclei in the process of the aerosol formation, because the sulfur aerosols were formed equally in both nitrogen and air.

It is permissible from the above arguments to conclude that the minute silver particles are the effective nuclei in the process of aerosol formation, while neither ionized gaseous molecules nor the oxygen compounds such as ozone and nitrogen dioxide act as the nuclei.

The author expresses his thanks to Professor I. Sano and Mr. Y. Fujitani for their helpful suggestion during this work.

Department of Chemistry
Faculty of Science
Nagoya University
Chikusa, Nagoya

Heats of Dilution of Polystyrene Solutions. II

By Kazuo AMAYA and Ryoichi FUJISHIRO*

(Received June 24, 1957)

The measurement of heat of dilution of polymer solutions is very significant for investigating the interaction power between polymer and solvent molecules. In the previous paper[1] we reported the heats of dilution in the solutions of polystyrene in toluene, ethylbenzene and chloroform. In this paper we shall report the heats of dilution in the systems of polystyrene-benzene, and polystyrene-cyclohexane. In both systems the heats have been directly measured by a few authors and in particular the results obtained in the former system seem not to be consistent with each other.

* Present address: Institute of Polytechnics, Osaka City University, Kitaku, Osaka.

1) K. Amaya and R. Fujishiro, This Bulletin, **29**, 270 (1956).

Experimentals

Apparatus—The calorimeter used has been described in the previous paper[1].

Materials—A sample of polystyrene was the same as that used in the previous paper[1] and its degree of polymerisation was 275. The solvents were purified according to the method described in the literature and finally distilled.

Result and Discussion

The heat of dilution was measured by adding 5 cc. of solvent to the polymer solution having a definite concentration. The measurement was made at 25°C in the benzene system and at 30°C in the cyclohexane one, since at 25°C homogeneous solution could not be obtained for the latter.

The results obtained are shown in Table I. Both systems, solutions of polystyrene-benzene and polystyrene-cyclohexane, were endothermic. Assuming that the heat of mixing is represented by the formula of van Laar's type, and making a simple treatment described in the previous paper, the integral heat of dilution ΔH_0 from the volume fraction of polymer v_r to v_r' can be represented by

$$\Delta H_0 = \alpha(Vv_r - V'v'_r) \qquad (1)$$

TABLE I

HEAT OF DILUTION OF POLYMER SOLUTION

Before dilution		After dilution		Heat absorbed	α
V cc.	v	V'	v'	cal.	cal/cc.
1. Polystyrene-benzene system at 25°C.					
4.75	0.185	9.75	0.090	0.052	0.62
4.85	0.185	9.85	0.091	0.061	0.72
3.73	0.185	8.73	0.079	0.067	0.92
4.82	0.153	9.82	0.075	0.048	0.82
4.79	0.153	9.79	0.075	0.034	0.59
2. Polystyrene-cyclohexane system at 30°C.					
4.90	0.108	9.90	0.053	0.142	4.9
9.90	0.053	14.90	0.036	0.118	12
14.90	0.036	19.90	0.027	0.099	21
4.95	0.108	9.95	0.054	0.154	5.3
9.95	0.054	14.95	0.036	0.127	13
14.95	0.036	19.95	0.027	0.089	19

where α is the interaction parameter between polymer and solvent, and V and V' are the volume of solutions before or after the dilution, respectively.

By the use of (1), the values of α can be calculated for both systems. They are shown in the last column of Table I. From Table I, it will be found that the values of α for the polystyrene-benzene system fluctuate considerably and those for the polystyrene-cyclohexane system increase anomally as the concentration of polymer decreases.

Considerable fluctuation of the values of α in the former case may be probably due to the experimental errors arising from stirring of the viscous solution on mixing, though the correction owing to stirring is made in each operation.

This could be understood, if it is considered that as the volume fractions of polystyrene are about two times higher in benzene than in cyclohexane and benzene is a better solvent than cyclohexane for polystyrene, the benzene solution is considerably more viscous than the cyclohexane solution and the former required much longer duration of stirring than the latter to make the solution homogeneous.

Even taking these experimental errors into consideration, the value of α in the benzene solution seems to be positive and is in the neighborhood of +0.7.

For the cyclohexane-polystyrene system, anormal increase of the values of α with the decrease of polymer concentration is difficult to explain. A tentative explanation may be as follows. Cyclohexane is a bad solvent for polystyrene and the critical temperature for the cyclohexane solution of polystyrene is in the neighborhood of 27°C**, though it is dependent on the molecular weight of polystyrene. The temperature at which the measurements were made is 30°C, being slightly higher than the critical temperature. Hence, it may be reasonable to suppose that in the solution at 30°C there will remain more or less the same aggregations of polymer as in the solution below the critical temperature. On dilution of such a solution it will be presumed that unusual heats are absorbed for separating these aggregations in the range of lower concentrations of polymer.

For the sake of comparison with the data for polymer solution, the heat of mixing and of dilution of ethylbenzene (which may be regarded as a monomer unit of polystyrene), with benzene and cyclohexane was also measured. The results are shown in Table II. From these data the values of α were calculated by the same procedure as in the polystyrene solution. These values are shown in the last column of Table II.

As in the previous paper, it will be found that the interaction parameter

** A. R. Shultz and P. J. Flory. *J. Am. Chem. Soc.*, **74**, 4760 (1952).

TABLE II

HEATS OF MIXING AND DILUTION OF ETHYLBENZENE SOLUTION AT 25°C.

1. Ethylbenzene-benzene system

Before dilution		After dilution		Heat absorbed	α
V cc.	v	V cc.	v	cal.	cal./cc.
5	1.000	10	0.500	2.450	0.98
10	0.500	15	0.333	0.792	0.97
15	0·333	20	0.250	0.351	0.96
2. Ethylbenzene-cyclohexane system					
5	1.000	10	0.500	9.04	3.0
10	0.500	15	0.333	1.918	2.8
15	0.333	20	0.250	1.491	2.9
20	0.250	25	0.200	0.824	2.9

between polymer and solvent has the same sign as that between the monomer unit of polymer (ethylbenzene) and the solvent for each system. The interaction parameter in the benzene-polystyrene system is a little smaller than that in the monomer unit-benzene system. This may be easily understood, as it is supposed that there may be more chances of the self-contacts between polymer segments in the polymer solution, as Meares pointed out[2]. On the other hand, the values of α for the polystyrene-cyclohexane system are higher than for the monomer unit-cyclohexane system. This may be explained if it is considered that there remain more or less the aggregations of polymers in the cyclohexane solution as mentioned above.

Our results are compared with the data obtained by other authors. Tompa[3] found that the value of α for the benzene solution was $-0.7\sim-1.6$ cal./cc. from the direct measurement of heats of dilution. (Here the value of α is recalculated from the value of μ obtained by Tompa according to the equation, $\mu=V_0\alpha/kT$, where V_0 is the partial molar volume of benzene in the polymer solution) Tompa's value of α is contradictory to our result in sign.

As for this system there have been no other reports on direct measurement of heat of dilution to be compared with ours. But here we shall discuss, making use of the results of heats of mixing between polystyrene and benzene obtained by Hellfritz[4]. According to Hellfritz, the heat of solution of polystyrene in benzene is -3.69 cal. per gram of polystyrene, which seems to be favorable for explaining Tompa's data.

The measurement of density of polystyrene by Boyer and Streeter[5], however, showed that the specific volume of polystyrene is considerably smaller in the dilute solution than in the solid state and it is constant independent of the concentration in the former state. Hence, the solid state of polymer may be supposed to have a glassy and loose structure containing many vacant holes and to be a metastable state, as Jenckel and Gorke pointed out[6]. The state of polymer having the same specific volume as in the dilute solution will probably be the one in equilibrium.

Thus, the process of solution will be divided into two parts. The one is the transformation of polymer from a glassy state to a stable one or the occupation of many holes in polymer by solvent molecules, and this may be expected to occur in the range of higher concentrations and decrease the specific volume of polymer considerably. The other is the process of normal dilution or of mixing between polymer in equilibrium state and solvents. This will occur in all concentration ranges and is detectable only in the dilution of solution having a lower concentration, because of the dominancy of the first process in the higher concentrations.

Hence, the heat of solution will be given as the sum of the heat of two processes. The heat of the first is calculated as that arising from the condensation of solvent into holes of polymer. As the specific volumes of polystyrene in a solid state and in a dilute solution are 0.956 and 0.905 cc. respectively and the heat of vaporization per cc. of benzene is 80.9 cal., the energy of condensation of benzene in 0.051 cc. (0.956—0.905 cc.) of vacant holes of polystyrene will amount to -4.21 cal.. Combining this value with the heat of solution, we can obtain 0.52 cal. for the value of the heat arising only from infinite dilution of a gram of polystyrene with benzene.

Taking 0.52 cal./g. as the heat of infinite dilution and using Eq. (1) we can obtain the value of α of 0.6 cal./cc., which may be consistent with our result both in sign and in magnitude.

Similar treatments can be applied to other solutions of polystyrene. The values of α thus obtained are shown in Table III. The values of α thus calculated from the heat of solution seems to be consistent

2) P. Meares, *Trans. Faraday Soc.*, **47**, 699 (1951).
3) H. Tompa, *J. Polymer Sci.*, **8**, 51 (1953).
4) H. Hellfritz, *Makromol. Chem.*, **7**, 191 (1951).
5) D. J. Streeter and R. F. Boyer, *Ind. Eng. Chem.*, **43**, 1780 (1951).
6) E. Jenckel and K. Gorke, *Z. Electrochem.*, **60**. 579 (1956).

TABLE III

INTERACTION PARAMETER CALCULATED FROM THE HEATS OF SOLUTION

Solvent	Chloroform	Toluene	Benzene	Cyclohexane
Heat of solution of polymer[4]. cal./g.	−4.4	−3.99	−3.69	0.59
Spec. vol. of polymer in solid[5]. cc.	0.957	0.957	0.957	0.957
Spec. vol. of polymer in dil. soln[5]. cc.	0.908	0.914	0.905	0.933***
Decrease of volume polymer cc.	0.049	0.043	0.052	0.024
Heat of vaporization of solvent[7]. cal/cc.	79.7	74.4	80.9	60.8
Heat of condensation of solvent into vacant sites of polymer. cal./g.	−3.91	−3.20	−4.21	−1.46
Net heat of dilution cal./g.	−0.49	−0.79	0.52	2.05
α cal./cc.	−0.54	−0.86	0.57	2.20
α observed. cal./cc.	−1.1～−1.3	−1.4～−1.5	0.5～0.9	5～20

in sign with our results, though in magnitude some deviations are seen.

Summary

The heats of dilution in the systems of polystyrene - benzene and polystyrene-cyclohexane were measured and the values of interaction parameters were derived. The heat of mixing of ethylbenzene, which may be regarded as the monomer unit of polystyrene, with the same solvents was also measured and it was found that the interaction of polymer solutions has the same sign as those of the corresponding monomer unit solutions.

We would like to express our gratitude to Professor A. Kotera of Tokyo University of Education for his valuable suggestions.

Department of Chemistry
Faculty of Science, Kobe University
Higashinada-ku, Kobe

7) J. H. Hildebrand and R. L. Scott, "Solubility of Non-electrolytes", Reinhold, 1950.

*** Since there is no data in cyclohexane, the value in dioxane which is considered to be similar to cyclohexane, is indicated.

Alkylalkoxypolysiloxanes. VI[1]*. Lower Members of Cyclic Methyl-, and Ethyl-ethoxypolysiloxanes*

By Rokuro ŌKAWARA, Gi-ichi MINAMI and Zensaburo OKU

(Received July 11, 1957)

Lower members of linear methyl-, and ethyl-ethoxypolysiloxanes as indicated by formula L_n have been prepared by the partial hydrolysis of methyltriethoxysilane[2] and by the thermal reaction between ethyltriethoxysilane and partially ethanolyzed ethyltrichlorosilane[3], but of the cyclo-compounds as indicated by formula C_n no report has been presented.

$$L_n: C_2H_5O\left[\begin{array}{c}R\\|\\-SiO-\\|\\OC_2H_5\end{array}\right]_n C_2H_5 \quad (R=CH_3 \text{ and } C_2H_5)$$

$$C_n: \left[\begin{array}{c}R\\|\\-SiO-\\|\\OC_2H_5\end{array}\right]_n \quad (R=CH_3 \text{ and } C_2H_5)$$

Recently, diethoxycyclopolysiloxanes[4] having three to five silicon atoms were prepared by rapid hydrolysis of diethoxydichlorosilane using pyridine as an acid acceptor, and the liberated cyclotrimer, hexaethoxycyclotrisiloxane was found to be an unstable compound.

Here, this process was applied to methylethoxydichlorosilane (I) and ethylethoxydichlorosilane (II), and the first two members of cyclopolysiloxanes, C_3 and C_4

1) Part V of this series, R. Okawara and M. Sakiyama, This Bulletin, **28**, 367 (1955).
2) H. J. Flether and M. J. Hunter, *J. Am. Chem. Soc.*, **71**, 2922 (1949).
3) R. Okawara, This Bulletin, **27**, 428 (1954).
4) R. Okawara, S. Hotta and T. Shimura, ibid., **28**, 541 (1955).

were obtained. As well as the case of diethoxydichlorosilane, these cyclotrimers were formed preferably by the hydrolysis carried out with considerable dropping rate. From the results of the fractionation of the hydrolyzate obtained from I, the boiling point of the cyclotetramer (129°C/10 mm.) was found to be very close to that of the linear trimer (126°C/10 mm.) which was obtained by treating the fractionation residue of the partially ethanolyzed product with sodium bicarbonate. The fractionation of the hydrolyzate of II gave succeeding plateaus of dimer, cyclotrimer, linear trimer and cyclotetramer. In this case, the amount of the cyclotrimer was not so small as in the case of hydrolysis of I, which was carried out under similar conditions. Further fractionation of the hydrolyzates I and II gave some plateaus, but their silicon content was not satisfactory enough to be taken as cyclo compounds.

The refractive index of cyclotrimer, $(CH_3Si(OC_2H_5)O)_3$ gradually increased during storage, but the change was not observed on the other three compounds given in Table II. A similar change has been reported with unstable cyclotrimers, $((CH_3)HSiO)_3$[5], $((C_2H_5O)_2SiO)_3$[4] and $((C_2H_5)HSiO)_3$[6].

Infrared spectra of two cyclotrimers obtained in these experiments showed an absorption band at 1023 cm^{-1}. Recently, the band appearing at 1023 cm^{-1} in the spectra of unstable triethylcyclotrisiloxane[6] was found to decrease in intensity with its increase in refractive index and viscosity on storage. Since with unstable $((CH_3)Si(OC_2H_5)O)_3$ a similar decrease in intensity and an increase in viscosity were also found, it is natural to suppose that this band is a characteristic one associated with the cyclotrisiloxane ring, as the band at 1010—1020 cm^{-1} has been found in the spectra of dialkylcyclotrisiloxanes[7]. If the assumption described above were an appropriate one, the decrease in intensity of 1023 cm^{-1} band should be related to the opening of cyclotrisiloxane ring probably to form a higher polymer.

Experimental

Starting Materials. — Methyltrichlorosilane used in these experiments was prepared by fractionation through a Stedman column of about 20 theoretical plates from "98% methyltrichlorosilane" supplied by the Shin-etsu Chem. Ind. Co. The hydrolyzable chlorine of the sample was 70.8—71.2% (Calcd. for CH_3SiCl_3 : Cl, 71.2%). Methylethoxydichlorosilane was prepared by adding 0.8 mole of absolute ethanol to 1 mole of methyltrichlorosilane with vigorous stirring. After the addition, the mixture was heated gradually to 50°C with stirring. Then the mixture, which contained unreacted methyltrichlorosilane (ca. 30%), methylethoxydichlorosilane (ca. 30%) and further ethanolyzed substances, was fractionated through the same column. The methylethoxydichlorosilane fraction which had a constant boiling point of 100°C, having a chlorine content of 43—44% was collected and redistilled through the same column and the middle portion of the distillate was taken as the starting materials.

Anal. Found: Cl, 44.6%. Calcd. for $C_3H_8OCl_2Si$: Cl, 44.6%.

Ethylethoxydichlorosilane (b. p. 127°C) was prepared by the similar partial ethanolysis of ethyltrichlorosilane which was obtained from the product of silicon-ethylchloride reaction.

Anal. Found: Cl, 41.0%. Calcd. for $C_4H_{10}OCl_2Si$: Cl, 41.0%.

Hydrolysis and Fractionation of the Hydrolyzate.—Hydrolysis was carried out as described in the preceding paper[4]. The product (*P* g.) was simply distilled at 10 mm. by using a Claisen flask. The weight percentage to *P* of the distillate (*D*) which came out up to the indicated temperature is also given in Table I.

In Table I, the results obtained with methylethoxydichlorosilane(I) as starting material are given in Expt. 1 to 4. In these experiments, the distillate (*D*) was rigorously fractionated through a Stedman column of about 20 theoretical plates and the refractive indices of the distillates were measured throughout the distillation. Two plateaus, which were due to cyclotrimer (94°C/10 mm.) and cyclotetramer (129°C/10 mm.) appeared in Expt. 1 to 3, in which the hydrolysis was carried out rapidly. In these three experiments, the refractive index and the silicon content of the plateau of cyclotrimer were n_D^{20} 1.3955—9, and

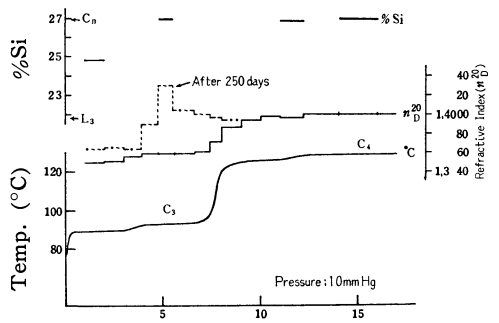

Fig. 1. Distillation curve of methylethoxypolysiloxanes (Expt. 2 of Table I).
L_n: Linear *n*-mer, C_n: Cyclo-*n*-mer

5) S. D. Brewer, *J. Am. Chem. Soc.*, **70**, 3962 (1948).
6) R. Okawara, U. Takahashi and M. Sakiyama, This Bulletin, **30**, 608 (1957).
7) C. W. Young, P. C. Servais, C. C. Currie and M. J. Hunter, *J. Am. Chem. Soc.*, **70**, 3758 (1948).

TABLE I
HYDROLYSIS OF DICHLOROSILANE

Expt. No.		Dichlorosilane g. (mole)	Hydrolysis: Mixture: Benzene g.	Pyridine g. (mole)	H_2O g. (mole)	Highest Temp. attained with mixing °C	Dropping Rate of Chlorosilane g./min.	Product (*P.*): g.	% Theory	Simple Distillation of *P.* at 10mmHg: Temp.** °C	Distillate (*D.*) % to *P.*
1	I*	159 (1.0)	250	175 (2.2)	19 (1.05)	39	14	66	63	180	33
2	I	159 (1.0)	250	175 (2.2)	18 (1.0)	52	32	75	72	175	33
3	I	159 (1.0)	250	175 (2.2)	18 (1.0)	43	24	82	79	171	39
4	I	80 (0.5)	125	87 (1.1)	9 (0.5)	3	1.6	41	79	148	30
5	II*	173 (1.0)	250	160 (1.0)	18 (1.0)	48	25	92	78	198	49
6	II	173 (1.0)	400	160 (1.0)	18 (1.0)	39	35	95	80	200	53

* I: $CH_3(C_2H_5O)SiCl_2$ II: $C_2H_5(C_2H_5O)SiCl_2$
** Distillate was collected up to this temperature (the stil-pot temperature was 250—260°C).

26.86—26.97% (Calcd. for $C_3H_8O_2Si$: Si, 26.96%) respectively. The refractive index of the plateau of cyclotetramer gradually approached to a constant value, n_D^{20} 1.4001, and the silicon content of this portion was also satisfactory to take it as a cyclocompound. For example, the distillation curve of Expt. 2 is shown in Fig. 1.

In Expt. 4, chlorosilane was dropped very slowly to make sure that the presumption that the formation of the cyclotrimer is related to the dropping rate in this case too. Because a half mole of the chlorosilane was used in this run, the distillate (*D*) which could be put to use for fractionation was 12 g. Only 2 cc. of the fraction which distilled out below 120°C/10 mm. was separated into four portions. Though the silicon content of the third portion (0.5 cc.) boiling at 89°—94°C/10 mm. showed the presence of cyclotrimer, its plateaus did not appear.

The residues of the simple distillation under 10 mm. were collected and further distilled simply under 1 mm. To the distillate coming out below 200°C (stil-pot temperature, 260°C), the fractionation residues of (*D*) were added and redistilled rigorously through a high efficient Stedman column of about 50 theoretical plates. Two gradually rising plateaus were found at 114°—118°C/1 mm. and 140°—143°C/1 mm., but the silicon contents of these plateaus were 25.7—24.8% 25.0—24.3% respectively, which shows that these plateaus are not those of pure cyclocompounds. (Calcd. for cyclocompounds; Si, 26.96%).

The data starting with ethylethoxydichlorosilane(II) are given in Expt. 5 and 6 in Table I. The distillate (*D*) was clear oil and the residue was highly viscous oil. The distillate was fractionated through the high efficient Stedman column. A small amount of dimer (n_D^{20} 1.4024, d_4^{20} 0.9500. Reported[3]: n_D^{20} 1.4006, d_4^{20} 0.9473. *Anal.* Found: Si, 18.65%. Calcd. for $C_{12}H_{30}O_5Si_2$: Si, 18.06 %) then the succeeding plateaus of cyclotrimer, linear trimer (n_D^{20} 1.4074, d_4^{20} 0.9764. Reported[3]: n_D^{20} 1.4074, d_4^{20} 0.9750. *Anal.* Found: Si, 19.76%. Calcd. for linear trimer: Si, 19.64 %) and cyclotetramer were obtained as shown in Fig. 2.

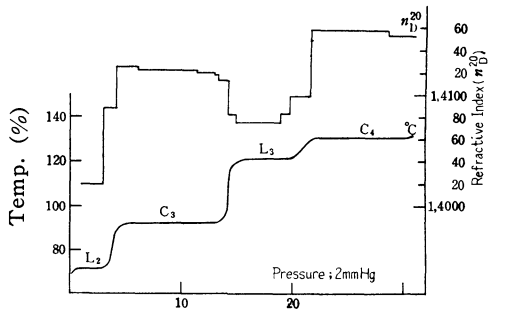

Fig. 2. Distillation curve of ethylethoxypolysiloxanes (Expt. 5. of Table I).
L_n: Linear *n*-mer, C_n: Cyclo-*n*-mer

The residue of each experiment was collected and fractionated through the same column. A small amount of linear tetramer (n_D^{20} 1.4127, d_4^{20} 0.9900. Reported[3]: n_D^{20} 1.4148, d_4^{20} 0.9960. *Anal.* Found: Si, 20.47%. Calcd. for linear tetramer: Si, 20.63%) and impure cyclopentamer (b. p. 147°C/1 mm., n_D^{20} 1.4204. *Anal.* Found: Si, 23.26%. Calcd. for cyclopentamer: Si, 23.76%) were obtained. Properties of the cyclocompounds are given in Table II.

Preparation and Physical Constants of Linear Metylethoxypolysiloxanes.—The fractionation residue of the partially ethanolyzed methyltrichlorosilane (186 g., chlorine content: 20.1%) was treated with 49g. of sodium bicarbonate[8]. Chlorine-free product (107 g.) was rigorously fractionated through a high efficient

8) R. Okawara et al., This Bulletin, **28**, 360, 364, 367 (1955).

TABLE II

CYCLIC METHYL-, AND ETHYL-ETHOXYPOLYSILOXANES

Polymer Size n	Boiling Point °C/mmHg	Refractive Index n_D^{20}	Density d_4^{20}	Molar Refraction Found (Calcd.)*	Molecular Weight Found** (Calcd.)	%Si*** Found (Calcd.)
$(CH_3(C_2H_5O)SiO)_n$						
3	94/10	1.3959	—	— (72.09)	— (313)	26.94 (26.96)
4	129/10	1.4001	1.0462	96.48 (96.12)	417 (417)	26.97 (26.96)
$(C_2H_5(C_2H_5O)SiO)_n$						
3	92/2	1.4125	1.0292	85.86 (85.98)	349 (355)	23.77 (23.76)
4	131/2	1.4158	1.0317	115.0 (114.2)	477 (473)	23.72 (23.76)

* Calculated from bond refractivities by E. L. Warrick, *J. Am. Chem. Soc.*, **68**, 2455 (1946).
** Cryoscopic measurements in benzene.
*** Silicon was determined by decomposing the sample with sulfuric acid.

column. Succeeding to a small amount of ethanol (5%), monomer (15%), dimer (16%), trimer (10%) and tetramer (5%) of the methylethoxypolysiloxanes were obtained. Properties of the linear polymers until trimer accorded well with the values reported by Fletcher and Hunter[2] which are indicated in parentheses.

Monomer: b. p. °C/760 mm. 141 (143), n_D^{20} 1.3834 (1.3835), d_4^{20} 0.8979 (0.8923).

Dimer: b. p. °C/mm. 86 /10(100/20), n_D^{20} 1.3910, n_D^{25} 1.3893 (1.3895), d_4^{20} 0.9547, d_4^{25} 0.9516 (0.9441).

Trimer: b. p. °C/mm. 126/10 (73/0.5), n_D^{20} 1.3960, n_D^{25} 1.3935 (1.3934), d_4^{20} 0.9855, d_4^{25} 0.9840 (0.9744).

Stability of Cyclotrimer. — The measurements of the physical properties of cyclotrimer were carried out immediately after the fractionation. Gradual increase in refractive index and viscocity was found by the samples of $(CH_3Si(OC_2H_5)O)_3$, which were sealed in a soft glass ampulla; though they became very viscous the gelation did not take place after 500 days. The typical results obtained with two samples are shown in Table III.

TABLE III

days	0	80	140	250	500
n_D^{20}	1.3956	1.3986	1.4004	1.4040	—
	1.3959	1.3990	1.3992	1.4030	1.4052

With all the samples which were contaminated by this cyclotrimer, the elevation of the refractive index was also observed. For example, it is shown in Fig. 1 in dotted lines. The other three compounds shown in Table II gave no changes of refractive index within one year.

Infrared absorption spectra were obtained with a Hilger H-800 infrared spectrophotometer with a rock salt prism in the range of 700—1300 cm^{-1}. Samples were observed as solution 2% in carbon disulfide. The position of the strong band which appeared in the range 1000—1120 cm^{-1} is shown in Table IV.

TABLE IV

COMPOUND ABSORPTION SPECTRA (in cm^{-1})

$(CH_3Si(OC_2H_5)O)_3$	1023	1078	1111
〃 after 500 days	(1027)*	1075	1118
$(CH_3Si(OC_2H_5)O)_4$	—	1068	1117
$(C_2H_5Si(OC_2H_5)O)_3$	1023	1083	1112
$(C_2H_5Si(OC_2H_5)O)_4$	—	1070	1120

* very weak.

It is interesting to follow the change of bands of $(CH_3Si(OC_2H_5)O)_3$ with reference to the change of refractive index. The results showed that the three strong bands observed in the spectra did not change remarkable after 140 days, but it was found clearly that that the strongest band at 1023 cm^{-1} became very weak after 500 days.

Summary

1) Methyl- and ethyl-ethoxydichlorosilane were hydrolyzed with considerable dropping rate using pyridine as an acid acceptor.

2) Methyl- and ethyl-ethoxycyclotrisiloxane have been prepared and characterized. The former was found to be an unstable compound.

3) Methyl- and ethyl-ethoxycyclotetrasiloxane have been prepared and characterized.

4) Some brief data of infrared absorption spectra of those compounds have been presented.

Department of Applied Chemistry
Faculty of Engineering
Osaka University, Higashinoda
Miyakojima-ku Osaka

The Crystal Structure of Bromodinitro-triammine-cobalt (III)

By Yoshimichi KOMIYAMA

(Received July 20, 1957)

Bromodinitro-triammine-cobalt(III), $[Co(NH_3)_3(NO_2)_2Br]$, can be prepared by treating chlorodinitro-triammine-cobalt (III), $[Co(NH_3)_3(NO_2)_2Cl]$, with hydrobromic acid[1]. This suggests that the former is formed through a simple replacement reaction of chlorine atom in the latter with bromine atom. Kobayashi and his collaborators measured the absorption spectra of these coordination compounds[2], showing that the absorption curve of the bromo-compound is quite similar to that of the chloro-compound. However, the most interesting and instructive feature of a report is a remark regarding the configuration of these compounds; the presence of the third absorption band in any of them indicates that both of them should have two of the negative ligands in *trans*-position with respect to each other, on the basis of the Shibata and Tsuchida's hypothesis of the *trans* negative radicals[3].

The structure of chlorodinitro-triammine-cobalt(III) has been already analyzed by the present author and his co-workers[4], and it is known that this compound has a *trans*-dinitro-configuration. Taking this result together with the above-mentioned knowledge into consideration, one may assume that the bromo-compound also has the same configuration, i. e., the one illustrated in Fig. 1, (a).

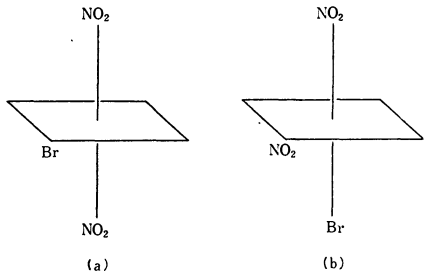

Fig. 1. Two possible forms of $[Co(NH_3)_3(NO_2)_2Br]$, having two negative radicals in *trans*-positions.

However, one can not exclude the possibility of another configuration (b), since there is no evidence that no change in configuration has taken place at any stage of substitution reaction during the course of preparation from the chloro-compound. Therefore, an attempt was made to investigate the crystal structure of the bromo-compound by means of X-ray diffraction, which is the most powerful method in the direct determination of its configuration. Furthermore, the results of absorption measurement on the aqueous solution of this compound will be given, since the absorption curve previously reported was obtained by the photographic method.

Experimental

Bromodinitro-triammine-cobalt(III) $[Co(NH_3)_3(NO_2)_2Br]$ has been prepared by Jörgensen's method. The crystals are monoclinic and dark red in color. Only thin tabular crystals were available. FeK_α radiation was used and a multiple-film technique was employed in taking Weissenberg photographs about the three principal axes.

The unit cell dimensions were calculated from high order reflections of some oscillation photographs taken for this measurement. They are:

$a=12.06\pm0.04$ Å, $b=10.30\pm0.02$ Å,

$c=6.85\pm0.02$ Å and $\beta=105.6\pm3°$.

The observed density is 2.295 g./cc. at 8.5°C, which may be compared with a calculated value of 2.286 g./cc., assuming four formula units in the unit cell. The systematic absence of $(0k0)$ for k odd and $(h0l)$ for h, l odd shows that the space group is $C_{2h}^5-P2_1/n$. All the atoms are on the general positions. The relative intensities of the reflexions were estimated visually by comparison with a standard scale. The usual correction factors were applied by means of the chart given by Cochran[5]. No correction for absorption was made.

A temperature factor and a scale factor for converting the observed values of $|F_{rel.}|$ approximately into the absolute scale were calculated by Wilson's method[6]. The measurement of absorption spectrum of this complex was made over the wavelength range from 220 to 560 mμ

1) S. M. Jörgensen; *Z. anorg. Chem.*, **7**, 315 (1894).
2) M. Kobayashi, A. Hagitani and I. Mita, *J. Chem. Soc. Japan*, **58**, 391 (1937).
3) R. Tsuchida, "Colours and Structures of the Metallic Compounds" (1944), p. 96-113 (in Japanese).
4) Y. Tanito, Y. Saito and H. Kuroya, This Bulletin, **26**, 420 (1953).
5) W. Cochran, *J. Sci. Inst.*, **25**, 253 (1949).
6) A. J. C. Wilson, *Acta Cryst.*, **2**, 318 (1949).

with Beckman Model DU spectro-photometer. Concentrations of aqueous solutions used for measurement were from 10^{-3} to 10^{-5} mol./l. The absorption maxima are:

$\lambda_1(m\mu)$	$\log \varepsilon_1$	$\lambda_2(m\mu)$	$\log \varepsilon_2$
457.5	2.15	334.0	2.59
$\lambda_3(m\mu)$	$\log \varepsilon_3$	$\lambda_3(m\mu)$	$\log \varepsilon_3$
252.0	4.12	237.0	4.16

and the absorption curve is shown in Fig. 2. It is interesting that the third absorption band is split into two maxima just as in the case of chlorodinitro-triammine-cobalt(III), $[Co(NH_3)_3(NO_2)_2Cl]$[7].

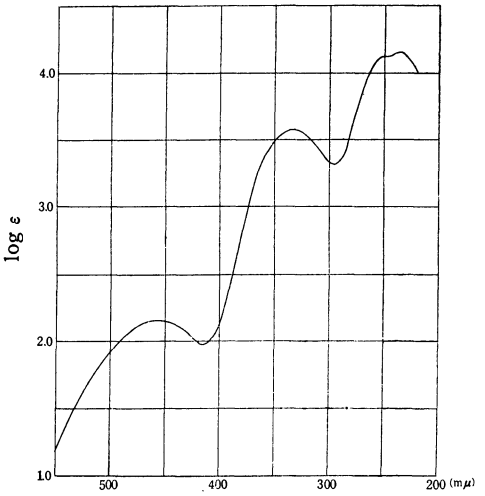

Fig. 2. Absorption spectrum of $[Co(NH_3)_3(NO_2)_2Br]$ in aqueous solution.

Determination of the structure

The Patterson projections $P(X, Y)$, $P(Y, Z)$ and $P(Z, X)$ were evaluated. These served for the purpose of determining the approximate parameters of cobalt and bromine atoms. These atoms were then used to fix the signs of the F values and successive Fourier syntheses were made. Approximate nitrogen positions were indicated in them, and inclusion of these in the preparation of the second synthesis resulted in positions leading to few further changes in sign. Then arranging the positions of oxygen atoms under an assumption that the two nitro-groups are in *trans*-coordination, F values were calculated. In any of such models, however, no good agreement was achieved between the observed and the calculated structure factors. Therefore, a model having a bromine atom and one of the nitro-groups in *trans*-coordination was adopted. This time the process of structure factor calculation and Fourier syntheses went on satisfactorily, thus allowing observed and calculated structure factors to be in comparatively good accord.

All the parameter values were refined by the usual procedure of successive approximations. The final parameters are listed in Table I. A final electron density projection along the c-crystal axis is shown in Fig. 3. The comparison of the observed structure factors with those calculated is given in Table II. The atomic scattering factors used for the calculation of the structure factors were those listed in the International Tables. A temperature factor was used in the form of $\exp -B(\sin\theta/\lambda)^2$, where B had the value 2.5 Å^2.

TABLE I
FINAL PARAMETERS

	x/a	y/b	z/c
Co	0.250	0.063	0
Br	0.124	0.125	0.225
N(1)	0.333	0.230	0.062
N(2)	0.350	0.015	−0.175
NH_3(1)	0.167	−0.104	−0.062
NH_3(2)	0.364	−0.015	0.236
NH_3(3)	0.136	0.141	−0.236
O(1)	0.412	0.246	0.220
O(2)	0.306	0.320	−0.057
O(3)	0.368	0.095	−0.300
O(4)	0.400	−0.092	−0.152

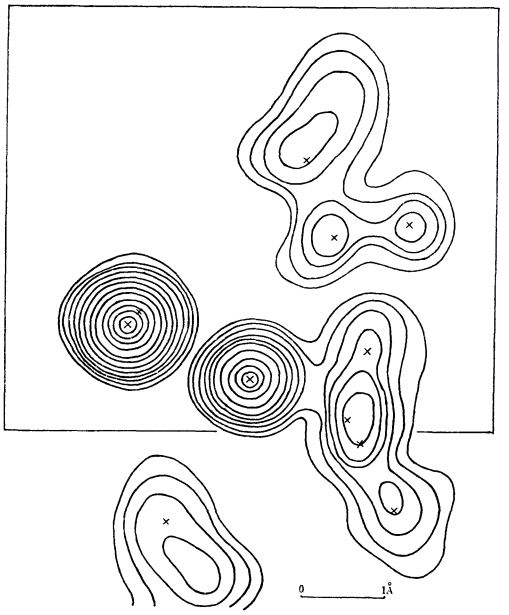

Fig. 3. Electron densities along the c-crystal axis of $[Co(NH_3)_3(NO_2)_2Br]$.
Contours are drawn at 2 e. Å^{-2} intervals, starting at two electron level and after 12 e. Å.$^{-2}$ level at intervals of 4 e. Å^{-2}. Atoms marked by crosses all belong to the same formula unit.

7) Y. Komiyama, This Bulletin, **30**, 13 (1957) Fig. 9.

TABLE II

OBSERVED AND CALCULATED STRUCTURE FACTORS

hkl	F_o	F_c	*hkl*	F_o	F_c	*hkl*	F_o	F_c	*hkl*	F_o	F_c
200	33.5	−34.0	510	2.5	− 1.9	002	17.2	−18.0	101	13.5	−14.5
400	35.7	−34.8	520	10.4	6.6	004	29.1	32.8	10$\bar{1}$	6.7	5.8
600	12.7	− 8.6	530	10.4	12.1	006	—	− I.0	103	8.3	14.2
800	30.6	29.4	540	13.3	−14.2				10$\bar{3}$	20.9	−20.6
1000	6.4	− 8.5	550	4.2	6.1	011	35.0	32.6	105	—	− 1.5
			560	17.2	−17.7	012	17.6	−13.7	10$\bar{5}$	20.7	14.5
020	16.6	16.7	570	7.7	− 8.6	013	6.2	3.9			
040	24.1	−23.8	580	—	− 0.4	014	7.6	10.3	202	33.3	−34.2
060	14.2	−14.2	590	3.2	− 3.9	015	11.9	16.0	20$\bar{2}$	12.9	−16.0
080	10.5	8.9				016	4.6	− 7.5	204	4.4	− 3.8
0100	5.2	− 2.1	610	18.9	18.1				20$\bar{4}$	25.7	−22.4
			620	6.9	− 7.7	021	25.6	−26.7	206	7.8	−10.7
110	4.9	5.3	630	12.5	12.5	022	5.0	5.3	20$\bar{6}$	2.2	− 2.0
120	35.9	−34.6	640	1.7	0.6	023	2.4	− 6.4			
130	22.0	−22.6	650	13.5	−14.2	024	7.1	6.4	301	12.1	−13.3
140	19.3	−18.3	660	8.6	8.4	025	9.2	− 9.7	30$\bar{1}$	15.5	22.8
150	12.1	−10.3	670	6.5	− 5.5	026	4.1	7.5	303	19.4	18.6
160	—	3.3	680	9.2	7.5				30$\bar{3}$	10.1	− 9.3
170	12.1	10.8				031	6.5	8.9	305	12.8	−15.9
180	1.6	0.2	710	3.9	4.6	032	9.7	− 9.5	30$\bar{5}$	7.4	4.8
190	2.7	2.3	720	24.7	24.4	033	12.0	9.7			
1100	3.5	− 3.3	730	11.9	−11.9	034	2.2	6.8	402	43.6	45.6
			740	8.8	9.0	035	4.2	− 1.4	40$\bar{2}$	51.6	52.8
210	9.5	− 7.7	750	9.1	−10.7	036	3.3	− 4.5	404	3.7	− 2.6
220	13.7	−14.6	760	4.0	− 4.6				40$\bar{4}$	1.5	− 2.8
230	23.2	−25.4	770	2.8	5.3	041	5.7	3.7	406	12.4	11.5
240	—	0.8	780	2.2	0.6	042	14.1	17.2			
250	20.2	21.2				043	5.0	0.4	501	3.2	3.5
260	5.3	5.8	810	1.6	3.3	044	10.0	−10.1	50$\bar{1}$	9.5	−10.7
270	10.0	6.8	820	13.9	13.9	045	0.6	2.6	503	4.6	− 6.7
280	12.0	10.1	830	4.8	4.3	046	3.3	4.9	50$\bar{3}$	11.3	10.1
290	7.9	− 8.4	840	11.1	−15.0				505	2.0	0.9
2100	4.1	3.6	850	—	1.5	051	15.5	−12.0	50$\bar{5}$	14.4	−12.4
			860	2.3	− 5.6	052	1.7	0.4			
310	7.5	− 7.4	870	—	− 3.0	053	2.4	− 3.8	602	1.3	− 3.6
320	11.2	− 7.8				054	7.6	− 6.6	60$\bar{2}$	13.7	−13.9
330	25.2	24.8	910	5.9	4.5	055	5.4	− 5.4	604	14.6	−15.6
340	19.5	21.3	920	19.1	−20.2				60$\bar{4}$	—	− 1.7
350	12.2	12.2	930	6.7	− 5.9	061	20.0	16.7	606	11.5	−12.9
360	20.8	20.7	940	9.1	− 8.5	062	10.0	− 8.0			
370	10.0	− 8.7	950	1.3	− 1.3	063	13.2	−12.5	701	18.8	15.8
380	3.0	− 1.0	960	—	3.1	064	5.8	− 5.1	70$\bar{1}$	10.7	− 8.9
390	1.7	− 1.5				065	2.4	5.2	703	12.7	−11.9
3100	9.6	−11.3	1010	9.8	−12.3				70$\bar{3}$	5.2	4.8
			1020	9.7	− 9.2	071	10.6	−10.2	705	1.9	− 2.6
410	11.6	− 8.2	1030	3.1	− 5.5	072	10.7	10.9			
420	6.4	7.0	1040	2.0	− 1.5	073	19.4	−14.0	802	7.7	− 5.3
430	6.7	− 5.9	1050	8.0	− 7.5	074	4.0	− 4.7	80$\bar{2}$	15.7	−12.4
440	17.3	20.6							80$\bar{4}$	18.4	18.2
450	—	1.3	1110	—	− 2.4	081	3.0	3.9	806	2.0	2.5
460	4.5	− 4.9	1120	1.9	− 1.8	082	30.4	−24.9			
470	1.6	− 0.5	1130	5.2	6.1	083	5.1	0.8	901	4.5	− 4.9
480	26.6	−25.2	1140	1.3	5.2	084	3.3	2.7	90$\bar{1}$	6.9	7.0
490	—	2.9							903	3.3	− 0.2
						091	3.7	− 2.4	90$\bar{3}$	8.1	− 6.8
						092	1.7	− 0.6	905	13.9	11.1
						093	8.6	− 8.6			
									1002	9.9	− 9.3
						0101	6.6	− 7.2	100$\bar{2}$	3.2	− 5.0
									100$\bar{4}$	13.1	−15.2
									1101	9.4	− 9.0
									110$\bar{1}$	9.2	4.3
									110$\bar{3}$	4.4	− 3.3
									120$\bar{2}$	18.2	18.3

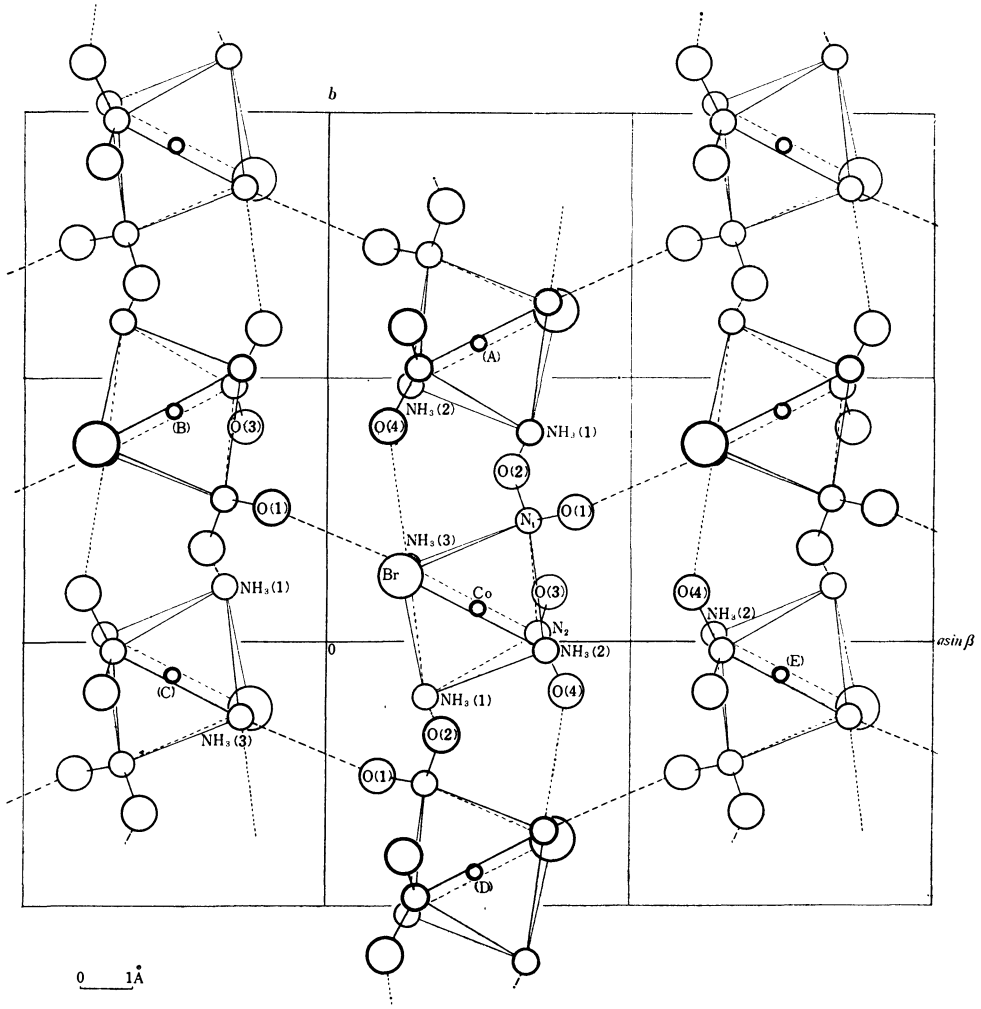

Fig. 4. Projection of the structure upon a plane normal to the *c*-crystal axis.

The reliability factors $R=\sum||F_o|-|F_c||/\sum|F_o|$ are 0.114, 0.198 and 0.133 for (*hk*0), (0*kl*) and (*h*0*l*) respectively. The higher value of R for (0*kl*) may be attributed to the less accurate values due to the absorption. The weighted mean value of R is 0.147 for which only observed reflections up to $\sin\theta/\lambda=0.500$ have been used.

Description of the Structure

The structure projected upon a plane normal to the *c*-crystal axis is shown in Fig. 4, which correspounds to Fig. 3. The crystal consists of bromodinitro-triammine-cobalt(III) $[Co(NH_3)_3(NO_2)_2Br]$ molecules. Two nitro-groups are coordinated to a cobalt atom in *cis*-position and one of them is in *trans*-coordination with respect to the bromine atom, making a remarkable difference from the configuration of the chloro-compound. The six ligands form a distorted octahedron around the central cobalt atom.

The interatomic distances and the interbond angles calculated on the basis of the atomic parameters in Table I are given in Table III. These interatomic distances and the bond angles are in good agreement with those found in the various complexes of cobalt(III), except the cobalt-bromine and other related distances.

The distances of approach between the nitrogen atom of an ammonia molecule and the oxygen atom of the nitro-group of an adjacent molecule are found to be 2.83, 2.86 and 2.88 Å. These short distances suggest the presence of hydrogen bonding between them. By these NH···O bonds, the complex radicals are held together, forming a layer parallel to the *b*-crystal

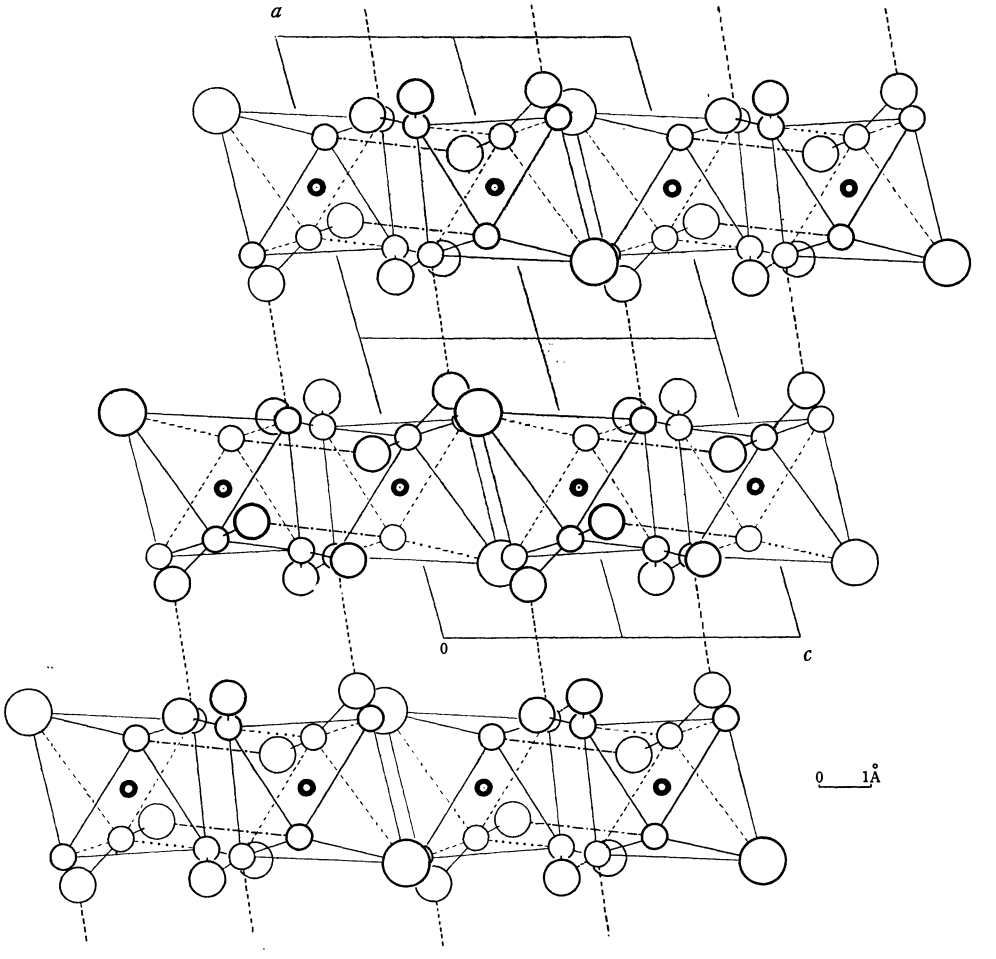

Fig. 5. Structure of $[Co(NH_3)_3(NO_2)_2Br]$, showing layers parallel to the *b*-crystal axis in double sheet.
-·-·-: linkages of 2.83 Å. ------: linkages of 2.86 Å. - - -: linkages of 2.88 Å.

TABLE III
INTERATOMIC DISTANCES AND INTERBOND ANGLES

Co—Br	2.45 Å
—N(1)	1.98 Å
—N(2)	1.98 Å
$—NH_3(1)$	1.98 Å
$—NH_3(2)$	1.99 Å
$—NH_3(3)$	1.99 Å
N(1)—O(1)	1.25 Å
—O(2)	1.22 Å
∠O(1)N(1)O(2)	118°
N(2)—O(3)	1.25 Å
—O(4)	1.24 Å
∠O(3)N(2)O(4)	121°
$NH_3(1)...O(2)$ (D−)	2.83 Å
$NH_3(3)...O(4)$ (A−)	2.86 Å
$NH_3(3)...O(1)$ (B−)	2.88 Å

O(1)	$...NH_3(1)$ (A)	3.16 Å
O(3)	$...NH_3(1)$ (A−)	3.23 Å
O(3)	$...NH_3(2)$ (E)	3.25 Å
O(3)	$...NH_3(2)$ (−)	3.40 Å
O(2)	...O(4) (A−)	2.88 Å
O(1)	...O(4) (E)	2.90 Å
O(4)	...O(4) (E)	3.32 Å
Br	$...NH_3(1)$ (C)	3.39 Å
	$...NH_3(2)$ (A)	3.72 Å
	$...NH_3(1)$ (A)	4.04 Å
	$...NH_3(3)$ (C)	4.18 Å
	...O(3) (+)	3.76 Å
	...O(1) (B−)	3.94 Å
	...O(3) (B)	4.19 Å
	...O(1) (D)	3.95 Å
	...O(2) (D)	3.84 Å
Br	...Br	4.48 Å

axis in double sheet as shown in Fig. 5. The closest approach between the adjacent layers are seen between bromine and nitrogen atoms of ammonia molecules with distances 3.39, 3.72, 4.04 and 4.18 Å. General characteristics of the structure containing such net works were also found in the structure of the cobalt(III) complexes previously reported by us[8].

It is interesting that the configuration of this bromo-complex is entirely different from that expected from the similarity of absorption spectra of the chloro- and bromo-complexes.

Summary

The crystal structure of bromodinitro-triammine-cobalt(III) $[Co(NH_3)_3(NO_2)_2Br]$ is monoclinic, with four formula units in a cell of dimensions; $a=12.06$ Å, $b=10.30$ Å, $c=685$ Å and $\beta=105.6°$. The space group is $C_{2h}^5-P2_1/n$. The determination of atomic parameters was made by Fourier methods.

The configuration of the complex molecule is described. One nitro-group is found to be in *trans*-position with respect to bromine atom and in *cis*-position to the other nitro-group.

The absorption spectrum of this complex was re-examined in aqueous solution.

The author expresses his hearty thanks to Professors H. Kuroya and Y. Saito of this University for encouragement and valuable discussion. Part of the cost of this study has been defrayed from a Grant of the Ministry of Education.

Institute of Polytechnics
Osaka City University
Kita-ku, Osaka

8) Y. Tanito, Y. Saito and H. Kuroya, This Bulletin, **25**, 188, 328 (1952); **26**, 420 (1953). Y. Komiyama, ibid., **29**, 300 (1956); **30**, 13 (1957).

Study of Nickel Oxide-Kieselguhr Catalyst. IV. The Effect of Temperature upon the Initial Rate of Polymerization and the Amount of Initial Adsorption of Propylene[1,2]

By Shinichi KAWAGUCHI

(Received May 10, 1957)

In a previous paper[3] it was reported that the course of catalytic polymerization of propylene over the nickel oxide-kieselguhr catalyst at 0°C obeyed the Zeldowitch type equation[4]

$$-\frac{dP}{dt}=ae^{-\alpha(P_0'-P)} \quad (1)$$

where P is the observed pressure of propylene at time t and a, α and P_0' are empirical constants; "the initial rate" $R_0\equiv a$ was found to vary linearly with the amount v of "the initial adsorption", i. e. the amount of propylene corresponding to the pressure difference P_0-P_0', as

$$R_0=k(v-v_0) \quad (2)$$

where P_0 is the pressure of propylene, which would be observed, if expanded in the dead space at $t=0$ without interaction with the catalyst and k or v_0 is a constant. This initial rate law 2 was established at 0°C irrespective of the catalyst composition, the ineffective amount v_0 increasing almost linearly with the nickel oxide content, and the rate constant k increasing with decreasing nickel oxide.

The present paper reports results obtained in other series of experiments at higher temperatures which were performed to see whether the initial rate law 2 still holds and to determine the activation energy and the heat of initial adsorption respectively from k and v.

Experimental Results

The catalyst employed is a different species from the previous one and contains nickel oxide of about twenty per cent. The course of the over-all reaction was followed by the measure-

1) Presented before the tenth Annual Meeting of the Chemical Society of Japan held at Tokyo, April 1957.

2) Part 3 appeared in *Catalyst*, **12**, 72 (1955) (in Japanese).

3) S. Kawaguchi, *J. Phys. Chem.*, **61**, 394 (1957).

4) H. A. Taylor and N. Thon, *J. Am. Chem. Soc.*, **74**, 4169 (1952); P. T. Landsberg, *J. Chem. Phys.*, **23**, 1079 (1955).

ment of pressure decrease at constant volume. The apparatus and the experimental procedure including the catalyst preparation were previously reported[5]. Experiments were made at 0, 20, 80, 100, 110.6 and 140°C. The higher reaction temperatures were maintained constant by means of vapor baths of benzene, water, toluene and *m*-xylene, respectively.

Eq. 1 was applied to each pressure-time curve. The rate equation can reproduce data for more than four hours at 0 and 20°, but only for the first several ten minutes at higher temperatures. Numerical value of the constant α decreases with increasing initial pressure at all temperatures as shown in Fig. 1, but increases as the temperature rises from 0 to 80°. Usually α decreases with increasing temperature[6] and is considered theoretically to be proportional to the reciprocal of absolute temperature[7]. However such an anomalous temperature dependence as in this case has also been reported in other systems[6]. Data of α at 100, 110.6 and 140° fall on the same curve as those at 80° within the experimental error.

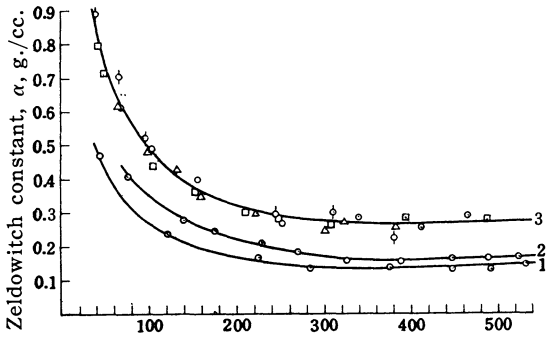

Fig. 1. Dependence of Zeldowitch constant, α, upon the initial pressure, P_0', when applied to the catalytic polymerization of propylene over a nickel oxide-kieselguhr catalyst. Curve 1: 0°, curve 2: 20°, curve 3: 80° (⊙), 100° (△), 110.6° (▣), and 140° (⊙).

The isotherm of the initial adsorption v of propylene at each temperature is shown in Fig. 2. Isotherms at 0 and 20° obey the B. E. T. equation at the higher relative pressure than 0.05, giving monolayer volumes $v_m=11.63$ and 11.57 cc. (STP)/g. cat., and energy factors $c=49$ and 37, respectively. At 80° and higher temperatures, the pressure range examined is lower than the relative pressure 0.05 and the B. E. T. equation does not hold. Langmuir equation can not fit the data, either.

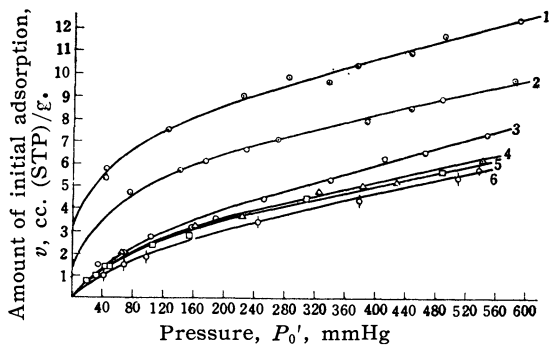

Fig. 2. Isotherm of the initial adsorption of propylene on a nickel oxide-kieselguhr catalyst at 0° (curve 1), 20° (curve 2), 80° (curve 3, ⊙), 100° (curve 4, △), 110.6° (curve 5, ▣), and 140° (curve 6, ⊙).

The pressure dependence of the initial rate R_0 of over-all reaction is plotted in Fig. 3. The initial rate markedly increases as the temperature rises from 0 to 20 and 80°, but curves at higher temperatures lie closely near to that at 80°. Plotting the logarithm of the initial rate against the logarithm of the initial pressure, the following empirical pressure exponents are obtained.

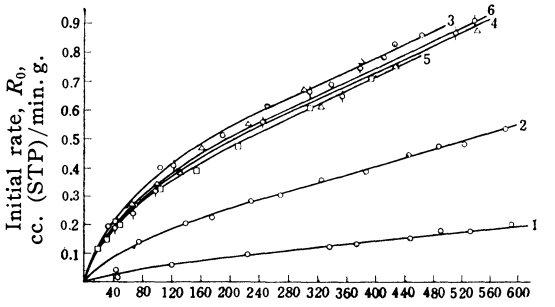

Fig. 3. Pressure dependence of the initial rate of propylene polymerization over a nickel oxide-kieselguhr catalyst at 0° (curve 1), 20° (curve 2), 80° (curve 3, ⊙), 100° (curve 4, △), 110.6° (curve 5, ▣), and 140° (curve 6, ⊙).

$$R_0 = kP^x$$

$x=0.75$ at 0°
0.68 at 20°
0.58 at 80~140°

When initial rates are plotted directly against amounts of initial adsorption, straight lines are obtained as shown in Fig. 4. The rate equation 2 holds too in this case, the constant v_0 however vanishing at temperatures above 20°C in accordance with the rate law as shown in Table I.

Activation energy determined from values of the rate constant, k, at 0 and 20° is 8.7 kcal./mole, and that obtained from the Arrhenius plot (Fig. 5) for data at higher temperatures is 0.86 kcal./mole.

5) S. Kawaguchi and H. Kihara, *J. Inst. Polytech., Osaka City Univ.*, **4C**, 202 (1953).
6) H. A. Taylor and N. Thon, *J. Am. Chem. Soc.*, **74**, 4169 (1952).
7) M. A. Cook and A. G. Oblad, *Ind. Eng. Chem.*, **45**, 1456 (1953); I. Higuchi, T. Ree and H. Eyring, *J. Am. Chem. Soc.*, **77**, 4969 (1955).

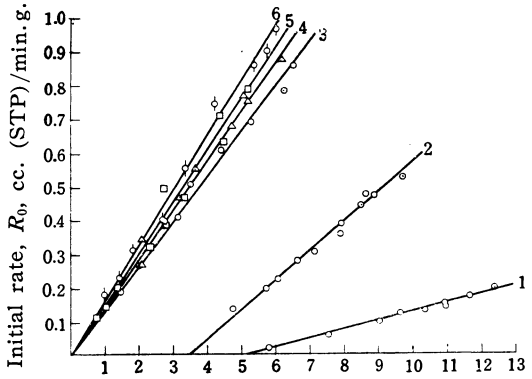

Amount of initial adsorption, v, cc. (STP)/g.

Fig. 4. The initial rate of polymerization vs. the amount of initial adsorption of propylene at 0° (line 1), 20° (line 2), 80° (line 3, ⊙), 100° (line 4, △), 110.6° (line 5, ▣), and 140° (line 6, ⊙).

TABLE I

CONSTANTS OF THE INITIAL RATE LAW, $R_0=k(v-v_0)$

Reaction temp. °C	Rate const., k min.$^{-1}$	Ineffective amt. of adsorpn. v_0, cc. (STP)/g.
0	0.029	5.1
20	0.087	3.4
80	0.133	0
100	0.145	0
110.6	0.149	0
140	0.159	0

From isotherms of the initial adsorption in Fig. 2, the isosteric heat of propylene adsorption was calculated by means of the Clausius-Clapeyron equation, and is illustrated in Fig. 6 as the function of the amount of adsorption. The heat of adsorption obtained between 0 and 20° is 7 to 8 kcal./mole for the range of surface coverage examined, while that obtained at higher temperatures shows a very remarkable drop at low

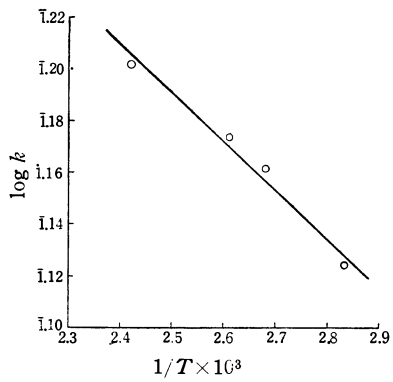

Fig. 5. Arrhenius plot of the first-order rate constant of the initial rate law for the catalytic polymerization of propylene over a nickel oxide-kieselguhr catalyst.

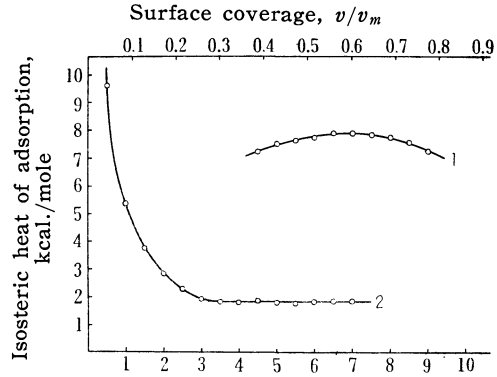

Adsorbed amount, v, cc. (STP)/g.

Fig. 6. Isosteric heat of the initial adsorption of propylene on a nickel oxide-kieselguhr catalyst. Curve 1: 0—20°, curve 2: 80—140°.

surface coverage down to 1.9 kcal./mole at the higher coverage region.

Discussion

The appearance of a distinct break in the Arrhenius plot of the over-all initial rate of propylene polymerization was previously reported[2] upon experimental results performed with similar initial pressure at various temperatures. The difference between activation energies at lower and higher temperature ranges is now clarified by the present systematic investigation. The change of activation energy with temperature has occasionally been reported on various systems, and Ozaki[8] also obtained apparent activation energies of 7 and −2 kcal./mole in the ranges of reaction temperature of −70∼−10° and 40∼150°, respectively, for the near-initial rate of ethylene polymerization over a nickel oxide-acid clay catalyst which was pretreated at 400°.

The change in the activation energy may indicate the change of the elementary step whose velocity is measured as the initial rate of the over-all reaction. The course of the over-all reaction at 0° was previously assumed[3] to correspond primarily to chemisorption of the propylene molecule from van der Waals layer onto the active site. If the chemisorption were so rapid as the physical adsorption at higher temperatures and attains equilibrium in the initial several minutes, the initial rate which is determined by the extrapolation of pressure data beyond ten minutes would correspond to the addition step of pro-

8) A. Ozaki, *Catalyst*, 12, 31 (1955).

pylene. In this case the initial rate could be represented by Eq. 2, if it were assumed that the chemisorbed amount is constant in the pressure range examined and the addition step proceeds between the chemisorbed monomer and the physically adsorbed one. If this were the case, the time course of the over-all reaction at higher temperatures should be represented by a rate law taking into account the superposition of addition steps or desorption of products. However previous theoretical treatment[2] showed that a rate law derived assuming the superposition of monomer chemisorption and dimerization can reproduce the kinetic data from 70 minutes to 6 hours at higher temperatures. Furthermore the fact that the heat of adsorption also changes remarkably with temperature suggests the possibility that the change in the activation energy is merely due to the change in the heat of adsorption.

The value of 7 to 8 kcal./mole appears slightly great as the heat of physical adsorption, however the system of propylene-nickel oxide also shows the isosteric heat of adsorption of 5 to 6 kcal./mole at the similar surface coverage[9]. The large and rapid decrease of the heat of adsorption at low surface coverage as depicted in Fig. 6 seems to indicate the existence of rapid chemisorption at higher temperatures, while the constant value of about 1.9 kcal./mole at the higher coverage suggests the physical adsorption. The remarkable change of the heat value between the two temperature ranges can not be unequivocally interpreted. It may be due to the a priori heterogeneity of the catalyst surface.

9) To be published.

Summary

The catalytic polymerization of propylene over a nickel oxide-kieselguhr catalyst was studied at constant volume and at 0, 20, 80, 100, 110.6 and 140°C. The pressure-time curve was analyzed by means of the Zeldowitch type equation. The initial rate law, $R_0=k(v-v_0)$, can again represent the data at 0 and 20°, but the ineffective amount of initial adsorption, v_0, becomes zero at higher temperatures, resulting in a simple first-order rate law, $R_0=kv$. The activation energies obtained between 0 and 20°, and among higher temperatures are 8.7 and 0.86 kcal./mole, respectively. The isosteric heats of initial adsorption are 7—8 and 1.9 kcal./mole in the respective temperature regions. The elementary process whose initial rate was measured is considered again to be slow chemisorption of propylene from the van der Waals layer onto the active site of the catalyst.

Institute of Polytechnics
Osaka City University
Minami-ogi-machi, Kita-ku, Osaka

*Dielectric Properties of Starch. I. Audio Frequency Region**

By Sôzaburo ONO, Takashi KUGE and Naokazu KOIZUMI**

(Received August 26, 1957)

It is well known that there are two modifications of starch, so-called α-modification (gelatinized starch) and β-modification (native starch) which produce different types of X-ray diffraction pattern, the V for the former and the A, B or C for the latter. They also show quite different behavior towards water.

Dielectric measurements have been an effective method for the studies of the sorbed vapors of polar compounds, particularly water, on the various high polymers[1]. However, there have been few dielectric studies of starch, especially for α-modification, except the report by

* Presented at the 8th Annual Meeting of the Chemical Society of Japan held in Tokyo, April, 1955.

** Institute for Chemical Research, Kyoto University.

1) In connection with the problem of bound water, some attention has been given to dielectric method, for example, see a review by K. Higasi, *Monogr. Res. Inst. Appl. Elec., Hokkaido Univ.*, No. 5, 9 (1955); "Chemistry of Protein" (Edited by S. Mizushima & S. Akabori), Vol. 4, p. 126 (1956) (Japanese), Kyôritsu Shuppan Co. Ltd., Tokyo.

Shikata and Ueda[2] in 1937 and a rather recent one by P. Abadie et al.[3]. Although we have reported briefly[4] on the same problem, it may be desirable to carry out more detailed studies in wider temperature and frequency ranges and to attempt to find some information on the difference in the configuration between the two modifications.

Experimental

Electrical.—The Schering type bridge[5] used in this study was designed to eliminate errors arising from stray capacitance by use of the Wagner earth[6] (Fig. 1). When the bridge is

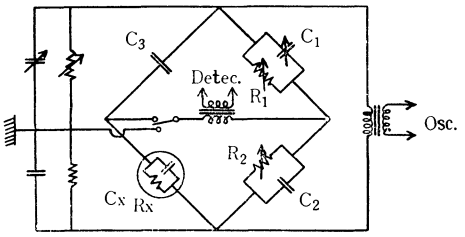

Fig. 1. Schering bridge.

C_x, R_x: equivalent capacitance and resistance of dielectric cell
C_1: maximum 850 $\mu\mu F$, variable air condenser
C_2: 225 $\mu\mu F$, mica condenser
C_3: 350 $\mu\mu F$, air condenser
R_1, R_2: 10–100 kΩ variable resistance

balanced finally, the loss tangent, tan δ, and the capacitance, C_x, of the dielectric cell are related to the other bridge elements through the equations

$$\tan\delta=\frac{1}{\omega C_x R_x}=\left(\frac{C_1R_1}{C_2R_2}-1\right)\Big/\left(\frac{1}{\omega C_2R_2}+\omega C_1R_1\right) \quad (1)$$

$$C_x=\left(\frac{C_3R_1}{R_2}\right)\left(\frac{1}{1+\omega C_1R_1\tan\delta}\right) \quad (2)$$

where ω is 2π times the frequency.

Since we made no attempt to prevent the inductive effects, the upper limit of frequency was about 30 kilocycles per second. The lower limit of frequency was influenced by the character of the detector, and 500 cycles per second was the lower limit in our case. In this frequency range experimental errors of measurements were within $\pm1.0\%$ and $\pm3.5\%$, for capacitance and loss tangent respectively.

Dielectric constant, ε', and loss factor, ε'', are calculated from the value of C_x and tan δ, by the following equations.

$$\varepsilon'=C_x/C_0 \quad (3)$$

$$\varepsilon''=\varepsilon'\tan\delta \quad (4)$$

where C_0 is the capacitance of the empty cell.

Dielectric Cell.—The cell used is shown in Fig. 2. It consisted of two concentric glass

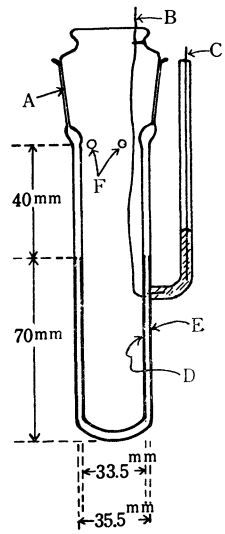

Fig. 2. Dielectric cell.

A is a taper ground-glass joint, D and E are copper electrodes connected to the lead wires B and C respectively through platinum seals, and F is a small orifice made on inner cylinder from which air is removed.

cylinders connected at a taper ground-glass joint. Copper electrodes were made by plating on the silver plates which were deposited on the ground glass walls.

Materials.—Since, as we already reported[4], no remarkable difference has been found between the dielectric properties of various kinds of starch (potato, waxy rice, lily bulb and potato amylose); both modifications of potato starch were only investigated in this study. The β-modification was pharmacopoeial grade. The α-modification was prepared by Onishi Syokuhin Co. Ltd., according to the following method. Gelatinized sol of pharmacopoeial grade starch was dried by heated rolls and ground to fine powder. According to Katzbeck et al.[7], thus prepared α-modification seems amorphous. The liquid paraffin used was the fraction distilled at temperatures between 170°—250°C under 5 mmHg pressure, and was loss free within the experimental error.

Procedures.—Starch was dried in an oven at 100°—105°C until constant weight was reached. The starch conditioned in this way was regarded as dry starch, although a small quantity of water could still remain. The water content of the sample was determined by weighing the increasing weight after the starch was exposed to the

2) M. Shikata and S. Ueda. *J. Electrochem. Assoc. Japan*, **5**, 438 (1937).
3) P. Abadie, R. Charbonnière, A. Gidel, P. Girard and A. Guilbot, *J. Chim. Phys.*, **50**, C46 (1953).
4) N. Koizumi, S. Ono and T. Kuge, *Bull. Inst. Chem. Research, Kyoto Univ.*, **22**, 80 (1950).
5) R. M. Fuoss, *J. Am. Chem. Soc.*, **59**, 1703 (1937).
6) D. Owen, "Alternating Current Measurements", Methuen & Co: Ltd., London (1950) p. 57.
7) W. J. Katzbeck and R. W. Kerr, *J. Am. Chem. Soc.*, **72**, 3208 (1950).

atmospheric moisture. The starch dispersed in liquid paraffin was poured in the sample space of the cell. The cell was then evacuated to remove the air which is contained in the sample. The dielectric measurements were carried out, after the cell had been kept for two days to sedimentate the starch spontaneously to the lower part of the cell where electrodes were placed. The method described above was convenient to keep the water content constant during the measurement, but has the disadvantage that we can not make the volume fraction of the starch between the electrodes a given desired value.

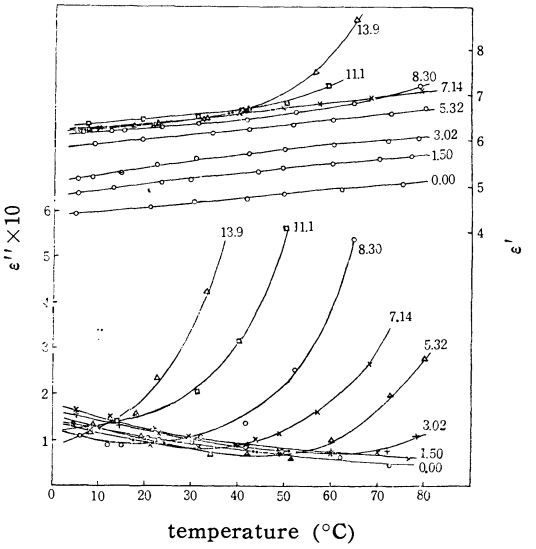

Fig. 3. Variations of ε' and ε'' with temperature at 4 kc. for β-modifications of potato starch containing sorbed water at the inscribed amounts (g./100 g. dry starch).

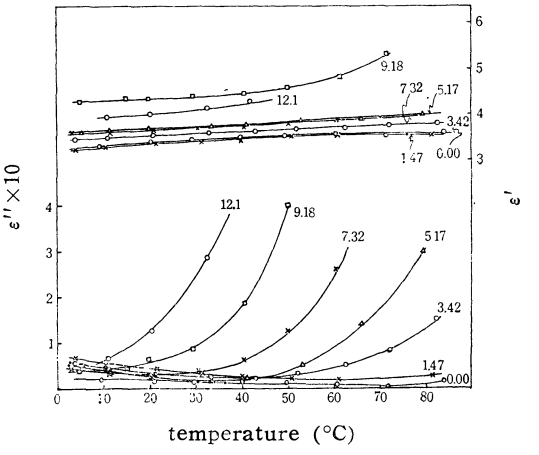

Fig. 4. Variations of ε' and ε'' with temperature at 4 kc. for α-modifications of potato starch containing sorbed water at the inscribed amounts (g./100 g. dry starch).

The volume fraction of each sample was estimated from the sedimentation volume of the starch of a known weight by using a graduated sedimentation tube whose diameter was about 1 cm.

An insulating oil bath fitted with a small electric heater was used to control the temperature during the measurements at temperatures higher than room temperature. At lower temperatures a Dewar flask filled with ethanol was employed as a bath which was cooled by dry ice. The temperature inside the cell was adjusted to the bath temperature within one degree, and all measurements were made as a function of frequency at fixed temperatures.

Results and Discussion

Some typical results of the measurements are shown in Figs. 3—7. Figs. 3 and

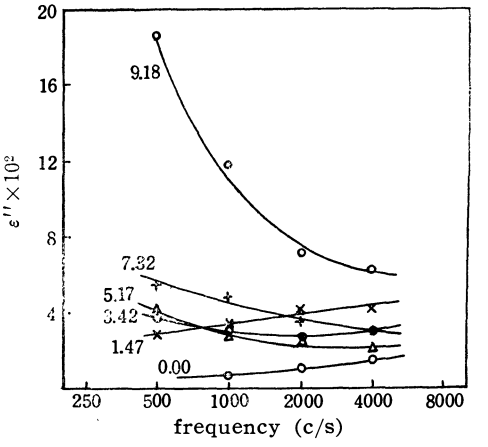

Fig. 5. Frequency dependence of ε'' of α-modifications containing sorbed water at the inscribed amounts (g./100 g. dry starch) at room temperature.

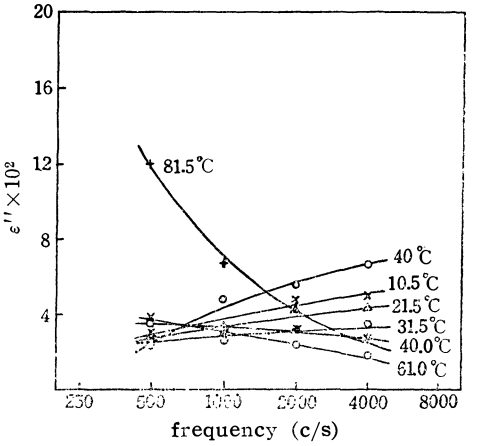

Fig. 6. Frequency dependence of ε'' of α-modification containing 1.47% water (g./100 g. dry starch) at various temperatures.

4 show the results obtained at 4 kc. for β- and α-modification of potato starch respectively which contained various amounts of water. The temperature coefficients of ε' were always positive. The ε'' value of each sample decreased with increasing temperature until a certain temperature was reached, and thereafter began to increase sharply. The more water the sample contained, the lower the temperature became. ε' became larger as the water content was increased. Frequency dependence of ε'' of α-modification is shown in Figs. 5 and 6. The sharp increase of ε'' found in the lower frequency region may be ascribed to the mechanism which causes a similar increase in the higher temperature region as shown in Figs. 3 and 4. We call this loss process "the low frequency loss process of starch". This loss process is affected markedly by the sorption of water. Similar phenomena have been observed in the case of cellulose[8] and wood[9].

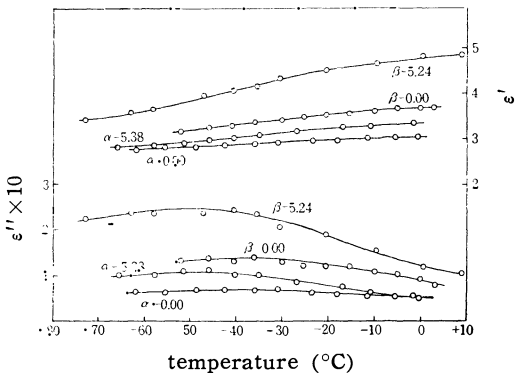

Fig. 7. Variations of ε' and ε'' of potato starch with temperature at 4 kc.

β-0.00 and β-5.24 express β-modifications containing 0.00 and 5.24% water (g./100 g. dry starch) respectively; α-0.00 and α-5.38 express α-modifications containing 0.00 and 5.38% water (g./100g. dry starch) respectively.

Fig. 7 shows the results obtained in the low temperature range, i.e., from room temperature to −70°C at 4 kc. It can be seen from Fig. 7 that each curve of ε'' appears to have a maximum at −40° to −50°C, although the maximum region is broad. In such a temperature region, ε' shows somewhat steep changes with temperature. We call this dielectric dispersion "the high frequency loss process of starch" on which we shall discuss in detail, using results in radio frequency region, in the following paper. This process may be attributed to dipole orientation of hydroxyl group.

On examination of the curves shown in Figs. 3, 4 and 7, it may be concluded that both modifications of starch have qualitatively the similar dielectric properties. Different numerical values of ε' and ε'' between both modifications appear to be caused mostly by the difference between their volume fractions.

It may be difficult to see to what extent the loss due to direct current conduction, interfacial-polarization (Maxwell-Wagner type) or usual dipole orientation (Debye type) contributes to the low frequency loss process. Among these effects, however, direct current conduction, due to inorganic ions adsorbed on the native starch granules, may probably be able to give most of the loss of the low frequency loss process. In order to test this possibility, log ε'' was plotted against log f(f is the frequency.). These plots gave almost straight lines with a slope −0.65 to −0.75 in the region where the low frequency loss process was distinctly observed***. This fact suggests that direct current conduction effect may be associated with an additional alternative current behavior, since the theoretical slope would be −1, if direct current conduction were only the cause of the low frequency loss process. It seems most likely that the Maxwell-Wagner type loss is superposed on the direct current loss in a similar manner to the case of terylene described by Reddish[10]. More detailed discussion on the low frequency loss process is difficult, because direct current and lower frequency measurements are not available in our study. Shikata and Ueda[2] found a maximum loss tangent of starch at frequencies less than 1 kc. and explained it by means of dipole orientation of water sorbed on starch granule. However, according to our interpretations, their results should correspond to the low frequency loss process, so that the larger orientational unit (e.g. glucose, glucose chain etc.) than the one that they proposed should be considered as the cause of the dielectric loss even if Debye type loss is postulated.

8) R. Seidman and S. G. Mason, *Can. J. Chem.*, **32**, 744 (1954).

9) L. Pungs, *Electrotech. Z.*, **A75**, 433 (1954).

*** A. Similar behavior concerning the frequency dependence of ε'' at low frequencies has been found for many other dispersed systems; R. Gotoh, T. Hanai and N. Koizumi (to be published).

10) W. Reddish, *Trans. Farady Soc.*, **46**, 459 (1950).

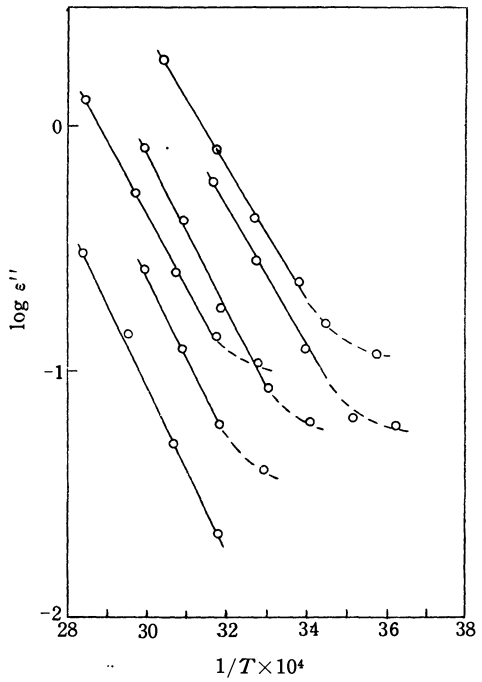

Fig. 8. Plot of log ε'' against $1/T$ at 4 kc. $\alpha-5.17$, $\alpha-7.32$, $\beta-8.30$, $\alpha-9.18$, $\alpha-12.1$ and $\beta-13.9$ in order from left to right.

In Fig. 8 log ε'' was plotted against reciprocal absolute temperature and linear relations were found when the influence of the high frequency loss process was allowed for. The activation energies of conduction in the low frequency loss process were calculated from these plots to be 15–12 kcal./mole, being smaller as the water content is increased. Although physical meanings of these energies are not obvious, it is mentioned that the values of the similar magnitude are obtained for both α- and β-modification.

It is favorable for the investigation of the properties of sorbed water to calculate its polarization. Since dielectric constants and loss factors hitherto described are those of starch-liquid paraffin systems having different volume fractions (Table I), the dielectric constant of starch itself (including sorbed water), ε_a was evaluated from the observed values ε', by using Kamiyoshi's formula[11]. The calculated value of ε_a was inserted into the following Kirkwood's formula[12] in order to obtain the specific polarization, P_a,

$$P_a=\frac{(\varepsilon_a-1)(2\varepsilon_a+1)}{9\varepsilon_a}\frac{1}{d} \qquad (5)$$

11) K. Kamiyoshi, *Sci. Rep. Res. Inst. Tohoku Univ.* **A2**, 180 (1950).
12) J. G. Kirkwood, *J. Chem. Phys.*, **7**, 911 (1939); *Trans. Faraday Soc.*, **42A**, 7 (1946).

where d is the density of starch measured by means of picnometer using toluene as an immersion medium. These values are shown in Table I. Assuming that the additivity of the polarization holds

$$P_a=P_sW_s+\sum P_iW_i \qquad (6)$$

$$W_s+\sum W_i=1 \qquad (7)$$

where P_s and W_s are the specific polarization and the weight fraction of starch alone respectively, P_i and W_i are the specific polarization and the weight fraction of the i th component of the sorbed water. If P and P_i are independent of each other, then from Eqs. (6) and (7)

$$\partial P_a/\partial W_i=P_i-P \qquad (8)$$

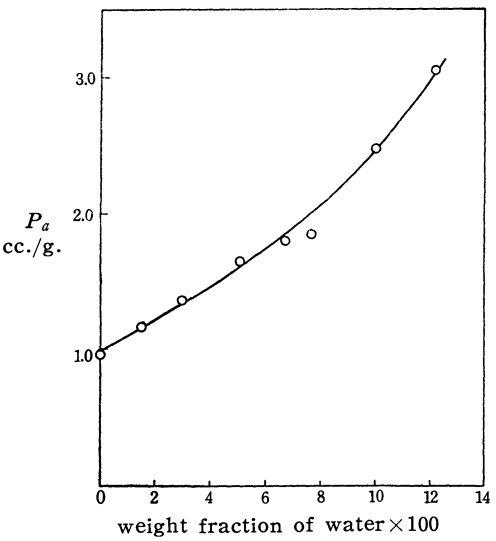

Fig. 9. Relation between the specific polarization and water content of potato starch at 20°C, 4 kc.

TABLE I

WATER CONTENT, DIELECTRIC CONSTANT AND POLARIZATION FOR β-MODIFICATION OF POTATO STARCH CONTAINING SORBED WATER AT SEVERAL DIFFERENT AMOUNTS

frequency: 4 kc., temperature: 20°C

Water content g./100g. dry starch	Volume fraction of starch	d g./cc.	ε'	ε_a	P_a cc./g.	P_i cc./g.
0.00	0.56	1.540	4.53	7.38	0.98	12.1
1.50	0.56	1.540	5.01	8.68	1.17	
3.02	0.55	1.535	5.40	10.0	1.36	
5.32	0.55	1.530	6.00	11.9	1.65	14.9
7.14	0.55	1.524	6.34	13.0	1.82	
8.30	0.54	1.520	6.26	13.1	1.84	
11.1	0.47	1.510	6.42	17.4	2.48	23.2
13.9	0.42	1.490	6.33	21.1	3.06	

Fig. 9 shows the variation of P_i with water content at 20°C and 4 kc. We can calculate P_i (given in Table I) from the slope at each point on the best smooth curve drawn through the experimental points, when the observed value for the dry sample is used as P_s. P_i increases gradually from 12.1 cc./g. for the dry sample to over 23.0 cc./g. for the higher water content so that we can not distinguish the sorbed water in various sorption states, according to the sorbed amount. Windle and Shaw[13] obtained a curve for wool similar to that in the present results and estimated the molar polarizations of the localized and the mobile water separately, using Cassie's results concerning water absorption. On the other hand, in the case of silica gel, Kurosaki[14] found that three different states of sorbed water were separately observed by the bending points of dielectric constant vs. water content curve. These facts seem to show the different ways of the sorptions corresponding to absorption and adsorption respectively. For comparison, polarization of water in various states is given in Table II. At first glance it may seem

TABLE II
SPECIFIC POLARIZATION OF WATER IN VARIOUS STATES

Adsorbent	Frequency and temperature	Specific polarization cc./g. 1	8-15	17.7	22-23
water	static			liquid water	
starch	4 kc. 20°C		0-5% sorbed water		10% sorbed water
wool[13]*	3×10^8 mc. 25°C	bound water	mobile water		
silica gel[14]	5 kc. 25°C	0-1.5% water of 1st sorption	2-8% water of 2nd sorption		10% water of 3rd sorption

* Recalculated from molar polarization. The values at audio frequency should be larger than the above ones.

that water would not be so strongly absorbed on starch as on wool or silica gel, because there is no water having P_i of about unity in our case****. According to the absorption theory[15], however, it seems reasonable that water sorption occurs at various sites distributed throughout starch, and water molecules restricted in different strengths exist simultaneously in any sorption stage. Therefore, P_i should be regarded as the mean polarization of the sorbed water. From the continuous change of P_i, it may be merely concluded that the fraction of the less firmly bound water gradually increases as sorption proceeds. It is unable to estimate the polarizations of localized (bound) and mobile (free) water separately without the knowledge of their fractional numbers. The fact found by Sato[16] that the heat of the water sorption by starch decreases with increasing sorption without discontinuous points, seems to be in good agreement with our observation.

The sorbed water of about 10% or more has a larger polarization value, i.e., 23 cc./g. or more, than that of liquid water. There are two ways in which these large polarizations may be explained. One is to consider a much more highly developed hydrogen bond than that of liquid water, and the other is to consider that P_s is not constant as was assumed in the derivation of Eq. (8), but must increase with increasing water content. The latter may be more plausible for starch, since water molecules seem to penetrate into the starch granule throughout and to loosen the secondary force which is associated with micell formation[15]. In other words, the polar group of starch becomes more polarizable, while the penetrating water loosens the micell structure.

Since the reproducibility of the volume fraction measurement was insufficient in the case of α-modification, calculations of P_i were not performed.

Summary

The results of dielectric measurements for α- and β-modification of potato starch containing 0.0–13.9% sorbed water at audio frequency region are described. At different temperature regions, two different dielectric loss processes are found which we call low frequency loss process and high frequency loss process. Discussions on the low frequency loss process are made. Qualitatively, both modifications of starch have the similar dielectric properties. From the analysis of the

13) J. J. Windle and T. M. Shaw, *J. Chem. Phys.*, **22**, 1752 (1954).
14) S. Kurosaki, *J. Phys. Chem.*, **58**, 320 (1954).
**** Water which still remains after the heating procedure at 105°C is not taken into consideration.
15) N. N. Hellman and E. H. Melvin, *J. Am. Chem. Soc.*, **72**, 5186 (1950); N. N. Hellman, T. F. Boech and E. H. Melvin, ibid., **74**, 348 (1952).
16) H. Sato, *J. Chem. Soc. Japan, Pure Chem. Sec.* (*Nippon Kagaku Zassi*), **72**, 790 (1951).

polarization of the sorbed water, it may be concluded that sorbed waters change their properties gradually as sorption is increased, while they also loosen the micell structure of starch.

This research has been financed partially by the Scientific Research Encouragement Grant of the Ministry of Education, to which the authors' thanks are due.

Laboratory of Biophysical Chemistry
College of Agriculture
University of Osaka Prefecture, Sakai

*Dielectric Properties of Starch. II. High Frequency Loss Process**

By Sôzaburo ONO, Takashi KUGE and Naokazu KOIZUMI**

(Received August 26, 1957)

In Part I[1] of this series the dielectric properties of starch at audio frequency region were discussed. In the present paper, dielectric measurements have been made on the α- and β-modification of potato starch containing various amounts of water in the frequency range from 2kc. to 3mc. Dielectric dispersion, which was called "high frequency loss process" in Part I, was again observed and has been discussed.

Experimental

Dielectric constant, ε', and loss factor, ε'', were measured in the frequency range from 2 to 30 kc. using the Schering bridge described in the previous paper[1], and the radio frequency range from 190 to 3000 kc. was covered by Heathkit Model QM-1 Q-Meter which is shown in Fig. 1. Mica condenser, C_m, having practically

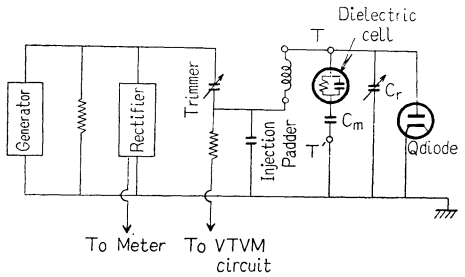

Fig 1. Circuit-diagram of Heathkit Model QM-1 Q-Meter.

pure capacitance of about 5000 $\mu\mu F$, was connected in series with the dielectric cell between the terminals T and T' in order to make the vacuum tube voltmeter circuit operate normally even when the cell had an appreciable loss. The loss tangent, $\tan\delta$, and the capacitance, C_x, of the dielectric cell are readily calculated from

$$\tan\delta = \frac{A+2}{A+1}\frac{C_1(Q_1-Q_2)}{(C_1-C_2)Q_1Q_2}$$

$$C_x = \frac{C_m(C_1-C_2)}{C_m-(C_1-C_2)}$$

$$A = C_m/C_x$$

where C_1 and Q_1 are the value of resonance condenser C_r and the Q value of the circuit, respectively, observed at resonance without the dielectric cell. C_2 and Q_2 are the values observed at resonance with the dielectric cell.

Other experimental procedures were the same as those described in Part I.

Results

The variations of ε' and ε'' with temperature for the β-modification cotaining various amounts of sorbed water at 700 kc. or its neighborhood are shown in Fig. 2. The curve v in this figure represents the one for the starch which was dried for 12 hr. at 80°C under the reduced pressure of 7 mmHg. It can be seen from Fig. 2 that ε'' of each sample has its maximum value ε''_{max}, although the shape of the curve is so flat that the temperature T_m where ε'' passes through a maximum is not determined accurately. The temperature coefficient of ε' of each sample is always positive and seems somewhat greater at the temperature near T_m. An increase in sorbed water produces serious variations in the data; ε' increases as has been observed previously[1], ε''_{max} value increases, and T_m shifts to lower temperatures. The lower values of ε' and ε''_{max} for the sample of 17.5% water content seem to be mostly due to its smaller

* Presented at the Symposium of High Polymer and Water held in Tokyo, November, 1956.

** Institute for Chemical Research, Kyoto University.

1) S. Ono, T. Kuge and N. Koizumi, This Bulletin, **31**, 34 (1958).

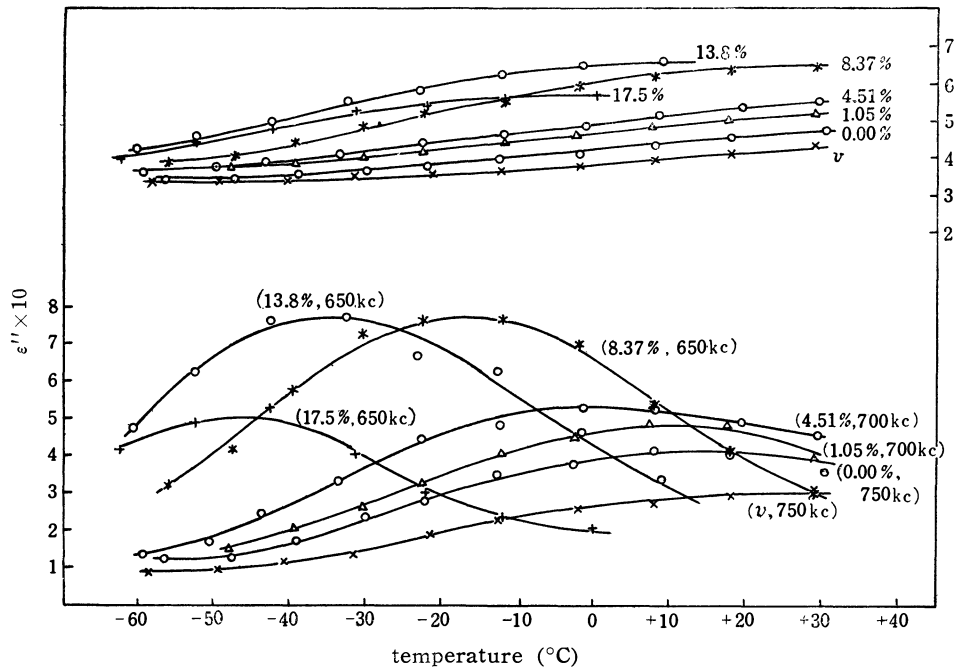

Fig. 2. Temperature dependence of ε' and ε'' of β-modifications of potato starch containing sorbed water at the inscribed amounts (g./100 g. dry starch) and frequencies.

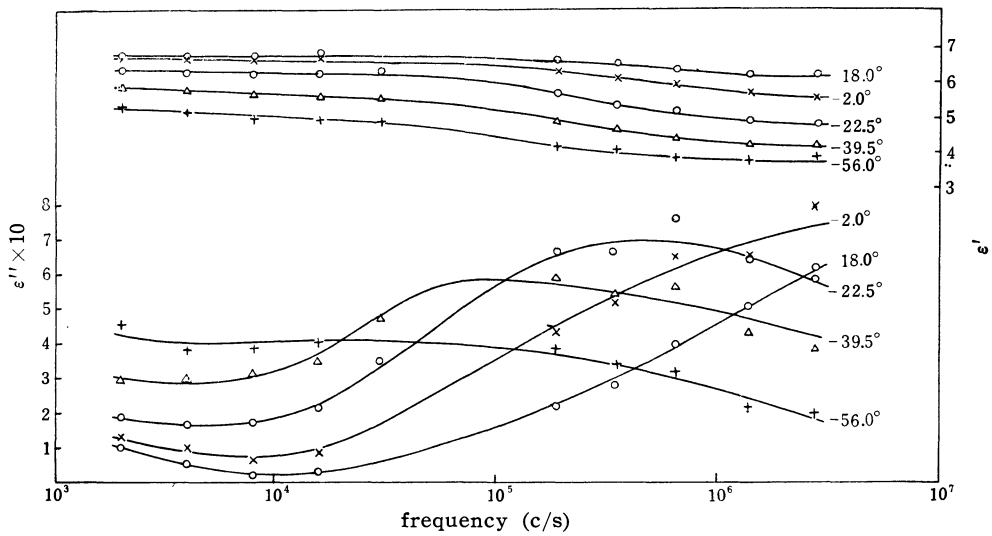

Fig. 3. Frequency dependence of ε' and ε'' of β-modification of potato starch containing 8.37% water (g./100 g. dry starch) at several different temperatures.

volume fraction of starch than that of those of the other samples.

At a given water content, ε' and ε'' are affected remarkably by the frequency and the temperature of measurement. Figs. 3 and 4 show the typical frequency dependences of ε' and ε'' for both modifications. The critical frequency f_m where ε''_{max} occurs shifts to lower frequencies as the temperature is lowered. The relation between f_m and the temperature for each sample is given in Fig. 5. It can be seen that a plot of $\log f_m$ against reciprocal absolute temperature is almost a straight line. Since the data at frequencies 30—190 kc. are lacking in our study, a considerable number of errors might be encountered when the figures showing the frequency dependence of ε'' at a given temperature, e.g. Figs. 3 and 4, were used

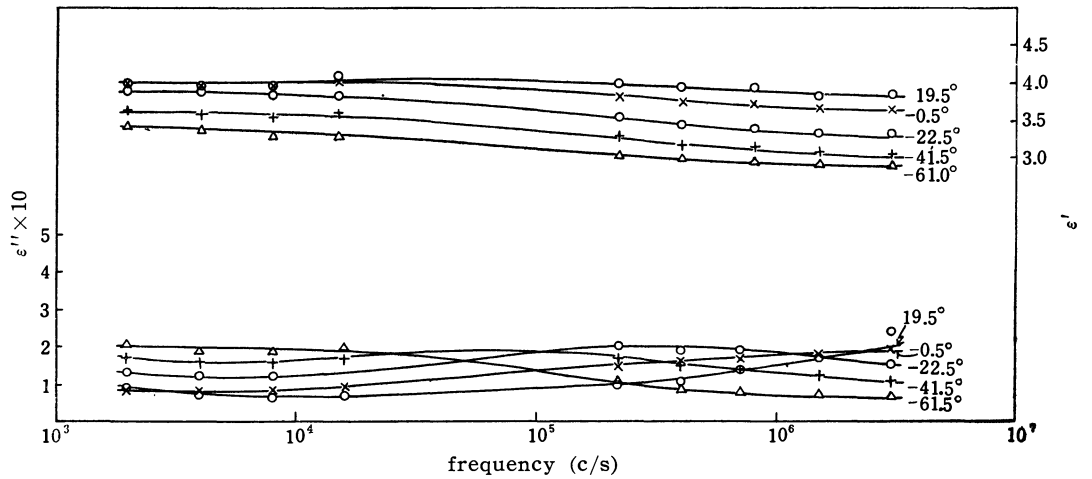

Fig. 4. Frequency dependence of ε' and ε'' of α-modification of potato starch containing 8.84% water (g./100 g. dry starch) at several different temperatures.

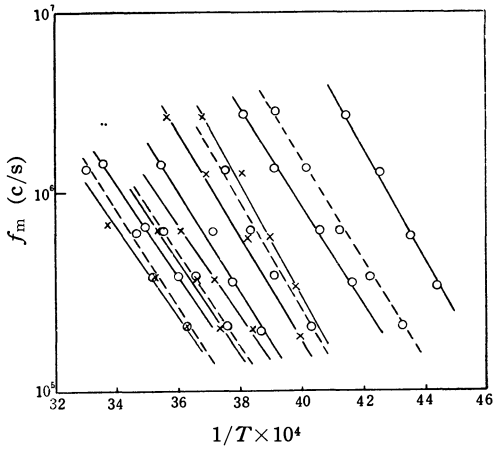

Fig. 5. Relation between critical frequency and temperature for potato starch which contain sorbed water at the inscribed amounts (g./100 g. dry starch).
—— β-modification ---- α-modification

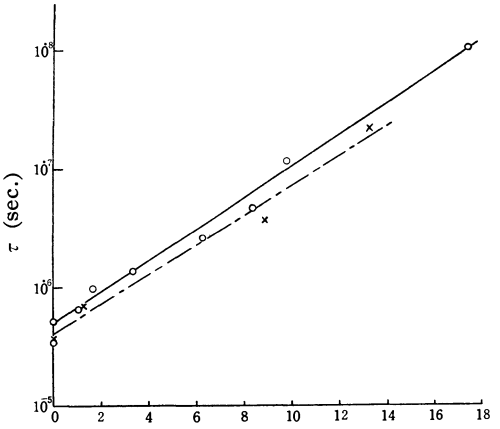

Fig. 6. Relation between the mean relaxation time and water content of potato starch at −15°C.
—○——○— β-modification
-×— - —×- α-modification

in determining the critical frequency. Therefore, T_m was taken at a given frequency from the figures which show the temperature dependence of ε'', e.g. Fig. 2, and now this frequency was regarded as the critical frequency at the temperature T_m. The relation given in Fig. 5 was thus obtained.

The mean relaxation time, $\bar{\tau}$, of the dielectric loss process may be regarded as

$$\bar{\tau}=1/2\pi f_m \qquad (1)$$

The values of $\bar{\tau}$ calculated from f_m which was obtained by interpolation or extrapolation to −15°C in Fig. 5 are listed in Table I. When the $\log \bar{\tau}$ is plotted against the water content, an almost linear relationship is found in the range examined. (Fig. 6)

By the use of the theory of absolute reaction rate developed by Eyring et al.[2], the relaxation time can be expressed by

$$\frac{1}{\bar{\tau}}=\frac{kT}{h}\exp(-\Delta F^{\neq}/RT) \qquad (2)$$

where k and h are Boltzmann's and Planck's constant, respectively, and $\Delta F^{\neq}$ is the free energy of activation for dielectric relaxation. This can be rewritten as

2) S. Glasstone, K. J. Laidler and H. Eyring, "Theory of Rats Processes", McGraw Hill Book Co. Inc., New York (1941), p. 548.

TABLE I
VARIATIONS OF THE THERMODYNAMIC QUANTITIES AND RELAXATION TIME WITH CHANGE IN WATER CONTENT

modification	water content g./100 g. dry starch	$\Delta F^{\neq}$ at −15°C kcal./mole	$\Delta H^{\neq}$ kcal./mole.	$\Delta S^{\neq}$ at −15°C e.u.	$\bar{\tau}$ at −15°C sec.
β	0.00(v)*	8.48	9.80	9.77	2.84×10^{-6}
	0.00	8.27	10·6	10.6	1.87×10^{-6}
	1.05	8.15	10.9	11.0	1.59×10^{-6}
	1.62	7.95	10.3	11.6	1.00×10^{-6}
	3.35	7.78	11.3	12.5	7.24×10^{-7}
	6.24	7.47	11.8	13.7	3.89×10^{-7}
	8.37	6.91	11.9	15.9	2.15×10^{-7}
	9.80	6.67	11.5	16.8	8.40×10^{-8}
	17.5	5.57	12.6	21.0	1.00×10^{-8}
α	0.00	8.45	10.9	9.90	2.69×10^{-6}
	1.16	8.14	10.9	11.1	1.45×10^{-6}
	8.84	7.28	12.2	14.4	2.75×10^{-7}
	13.3	6.38	11.5	17.9	4.55×10^{-8}

* v represents the sample dried under the pressure of 7 mm Hg for 12 hr. at 80°C.

$$\frac{1}{\bar{\tau}}=\frac{kT}{h}\exp(-\Delta H^{\neq}/RT)\exp(\Delta S^{\neq}/R) \quad (3)$$

where $\Delta H^{\neq}$ is the heat of activation and $\Delta S^{\neq}$ is the entropy of activation for dielectric relaxation. From Eqs. (1) and (3)

$$-\Delta H^{\neq}=\frac{R\,\mathrm{d}\ln f_m}{\mathrm{d}(1/T)}+RT \quad (4)$$

Therefore, $\Delta H^{\neq}$ can be obtained from the slope of the curve drawn in Fig. 5. $\Delta S^{\neq}$ may be calculated since $\Delta F^{\neq}$ is now known. These values are presented in Table I.

In considering those quantities as a function of water content, we should take those values at a particular temperature, since they are also functions of temperature. It is seen in appearance that $\Delta H^{\neq}$ increases with increasing water content. However, it may be reasonable to think that all $\Delta H^{\neq}$ would take the similar value of about 11 kcal./mole as a mean, because the errors for the determination of f_m would be appreciable, for the absorption maximum is flat, and the values of $\Delta H^{\neq}$ given in Table I are not ones obtained at a particular temperature. Eleven kcal./mole was used as the value of $\Delta H^{\neq}$ in the calculation of $\Delta S^{\neq}$ for all samples.

Discussion

There are two main theories which have been advanced to account for the dielectric relaxation process. One is the dipolar theory first proposed by Debye, in which the relaxation time of the absorption process depends on the hindrance to free rotation imposed on the dipolar group by the environment, and the other is the inhomogeneity theory proposed by Maxwell and Wagner, in which the relaxation time is governed by the relative dielectric constant and the conductivity values attached to the constituents of the material. Both give similar dependence of the dielectric constant and loss factor on frequency and temperature, so that it is impossible to determine which mechanism is responsible for the process by means of the analysis of the phenomena.

According to the consideration by Sillars[3], the water, which is considered to be present as single molecule or in a small group of molecules throughout the starch granule[4], may not produce serious loss due to Maxwell-Wagner type.

In the previous paper[1] we considered that Maxwell-Wagner type effect would occur in the low frequency loss process. The dielectric dispersion described in this paper, which has been called the high frequency loss process in Part I, may be attributed to the hindered rotation of hydroxyl group from the following reasons. i) The absorption curves for the carbohydrates, such as glucose[5], maltose[5], cellulose[6,7] and starch, are very similar to

3) R. W. Sillars, *J. Inst. Elect. Eng.*, **80**, 378 (1937).
4) N. N. Hellman and E. H. Melvin, *J. Am. Chem. Soc.*, **72**, 5186 (1950); N. N. Hellman, T. F. Boech and E. H. Melvin, ibid., **74**, 348 (1952).
5) P. Abadie, R. Charbonnière, A. Gidel, A. Girard and A. Guilbot, *J. chim. phys.*, **50**. C46 (1953).
6) L. Pungs, *Electrotech. Z.*, **A75**, 433 (1954).
7) R. Seidman and S. G. Mason, *Can. J. Chem.*, **32**, 744 (1954).

each other in respect to the fact that the curve has a very broad maximum in the frequency region of a few to ten megacycles at room temperature. That is, these loss processes have the relaxation time and its distribution of the same order. ii) The value of $\Delta H^{\neq}$ obtained for starch can be compared with those for cellulose (11.7 kcal., for 3.3 % water content)[7], ice (13.3 kcal.)[8] and the hydroxyl group of terylene (12.4 kcal.)[9].

Since the hydroxyl groups of starch and/or the sorbed water cause the high frequency loss process, we should take into consideration the situation of the hydroxyl group in the micell of starch. The effect of the sorbed water on the dielctric relaxation should be considered from the change of the micellar structure due to water penetration into the granule. Considering the large swelling of the starch granule by the sorption of water[4], it is certain that the sorbed water loosens the forces between the starch chains, thus facilitating the movements of the hydroxyl group of the starch. In the previous paper[1], the change of polarization of starch has also been interpreted by the loosening effects of water on the micell structure. An increased moment which orientates to the electric field can result from the water sorption, because the greater part of the sorbed water may be considered to be combined with the hydroxyl group of starch and to rotate together with it. From the above considerations, experimental results that $\Delta F^{\neq}$ decreased, $\bar{\tau}$ became shorter and ε''_{max} increased with increasing sorbed water, are now understood well.

Abadie et al.[5] concluded from the variation of the critical frequency with increasing water content that the water, below a 15—16% water content, was believed to be bound chemically, while the water, above this limit, appeared to be adsorbed physically*. Our results, however, show that such a distinction can not be made, since $\bar{\tau}$ decreases continuously with the sorbed water, as can be seen in Fig. 6.

Comparing the values of $\bar{\tau}$, $\Delta H^{\neq}$, $\Delta F^{\neq}$ and $\Delta S^{\neq}$ of the α-modification with those of the β-modification, we can find no significant difference between them when the accuracy of the estimation of f_m is allowed for, though $\bar{\tau}$ of both modifications lies on the separate two lines in Fig. 6 respectively.

The most interesting feature is the fact that the value of ε''_{max} increases with increasing temperature as is seen in Fig. 3. This is unusual in the Debye type absorption. We have analyzed the data by the Cole-Cole plot method[10]. Fig. 7 shows one

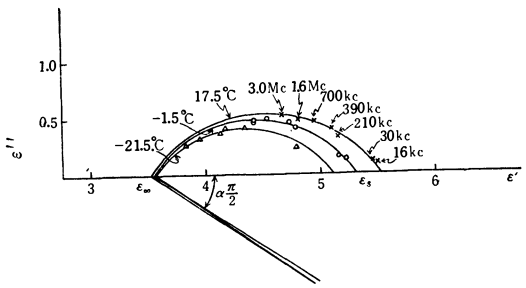

Fig. 7. Cole-Cole plot of the β-modification of starch containing 1.62% water (g./100 g. dry starch).

of these plots indicatig greater value of ε''_{max} for higher temperature. It can also be seen that the static dielectric constant, ε_s increases with increasing temperature and that the parameter α, a measure of the distribution of the relaxation times, is almost independent of temperature. Neither the value of α appreciably varied with water content in our study. The small variation of the optical dielectric constant, ε_∞, with temperature which is seen in Fig. 7 is most likely owing to the increase in the density of the liquid paraffin between the electrodes so that ε_∞ seems to be independent of temperature.

According to Fröhlich[11], for temperatures below the transition point, increased temperature creates some disordered arrangement of dipole in crystalline solid, thus leading to increase in ε_s, which can be expressed as

$$\varepsilon_s - \varepsilon_\infty \propto \exp(-V/kT) \text{ when } V \gg kT \quad (5)$$

where V is the energy difference of a dipole in the two equilibrium directions. If the distribution of relaxation times is independent of temperature, it follows that

$$\varepsilon''_{max} \propto \exp(-V/kT) \quad (6)$$

Although quantitative treatment is not possible without a detailed knowledge of

8) R. P. Auty and R. H. Cole, *J. Chem. Phys.*, **20**, 1309 (1952).

9) W. Reddish, *Trans. Faraday Soc.*, **46**, 459 (1950).

* In spite of their interpretation, it is difficult for us to find any discontinuing behavior of absorption curves given by them, during the sorption of water.

10) K. S. Cole and R. H. Cole, *J. Chem. Phys.*, **9**, 341 (1941).

11) H. Fröhlich, "Theory of Dielectrics" Oxford Press (1949), p. 53-61, 132.

the micell structure, our results are interpreted qualitatively by Fröhlich's theory. One of the equilibrium positions of the hydroxyl group is more stable than the other. In other words, the arrangement of the hydroxyl group is considered to be well-ordered in the micell of starch and to be somewhat disordered with increasing temperature. The fact that the temperature coefficient of ε_s is positive, means that an external field increases the entropy[12]. This indicates also the possibility that in the absence of the field the hydroxyl group in the micell is well-ordered as may be expected in a crystalline solid.

Abadie et al.[13] found also that ε''_{max} of cellulose and starch increases with increasing temperature, and interpreted that these temperature effects were due to the diminution of the action of the environment on the rotation of the hydroxyl groups.

For the α-modification, the relation between the ε' and ε'' was not so satisfactorily represented by the circular arc as for the β-modification and this fact seemed to arise from the relatively large experimental error due to the small volume fraction of the α-modification. Since, however, as can be seen in Fig. 4, the ε''_{max} value for the α-modification remains almost constant regardless of temperature, it seems plausible that the arrangement of the hydroxyl group for the α-modification is not so well-ordered as for the β-modification. The present conclusion coincides with the opinion[14] that the α-modification used here is amorphous.

12) reference 11) p. 9-13.
13) P. Abadie, R. Charbonnière, A. Gidel, P. Girard and A. Guilbot, *Compt. rend.*, **241**, 1137 (1955).

Summary

Dielectric measurements have been made on α- and β-modification of potato starch containing 0.0—17.7% sorbed water in the frequency range from 2 kc. to 3 mc. and temperature range from room temperature to −70°C. The dielectric relaxation process found has been attributed to the hindered rotation of the hydroxyl groups of starch and sorbed water. The heat of activation for this process is about 11 kcal./mole as a mean. The free energy of activation and the mean relaxation time of this process are lowered as the sorbed water is increased. The variation of the dielectric loss curve with the sorbed water has been discussed. Both modifications show similar dielectric behavior qualitatively, except in the case of the temperature dependence of ε''_{max} value. The variation of the ε''_{max} value with temperature for β-modification suggests that the arrangement of the hydroxyl group would be considerably well-ordered in the micell of starch granule.

Laboratory of Biophysical Chemistry
College of Agriculture, University of
Osaka Prefecture, Sakai

14) V. J. Katzbeck and R. W. Kerr, *J. Am. Chem. Soc.*, **72**, 3208 (1950).

Rate of Methanol Synthesis

By Hiroshi UCHIDA and Yoshisada OGINO

(Received June 13, 1957)

Although there have appeared many papers[1-4] dealing with measurements on the methanol synthesis, only the paper by G. Natta and his coworkers[5] provides the experimental data sufficient for kinetic interpretation of the methanol synthesis. On the basis of their experimental results, they have proposed a rate equation of the methanol synthesis, which contains a few constants to be determined by laborious measurements at high pressure.

In the course of our study[6] on catalysts for the methanol synthesis, we desired to

1) W. K. Lewis and P. K. Frolich, *Ind. Eng. Chem.*, **20**, 285 (1928).
2) P. K. Frolich, M. R. Fenske et al., ibid., **20**, 1327 (1928).
3) D. S. Cryder and P. K. Frolich, ibid., **21**, 867 (1929).
4) M. R. Fenske and P. K. Frolich, ibid., **21**, 1052 (1929).
5) G. Natta, P. Pino et al., *La Chimica e L'Industria*, **35**, 705 (1953).
6) H. Uchida and Y. Ogino, This Bulletin, **29**, 587 (1956).

obtain the rate constant from a small number of measurements. In order to obtain a rate equation, which is more convenient for this purpose than that by G. Natta et al., necessary experimental data have been prepared by carrying out measurements on the methanol synthesis in wide ranges of the pressure and the ratio of hydrogen to carbon monoxide.

Experimental Procedure

The synthesis was conducted in a reactor containing 5 cc. of a catalyst of 2—3 mm. size. The gas for the synthesis was introduced into the reactor from a pressure storage; and the decrease in the pressure in the storage served as a measure of the volume of the gas fed. The exit from the reactor was freed from methanol through an ice-cooled condenser, and the volume was determined by means of a gas-meter at atmospheric pressure. By assuming the stoichiometric methanol yield of the gas consumed in the reactor, the methanol concentration in the exit gas just having left the reactor and the conversion into methanol were calculated*1.

Some series of the synthesis were made under different total pressures ranging from 90 to 150 kg./cm^2 at several different temperatures between 300 and 360°C with gases of varying H_2/CO ratios. Moreover, in order to obtain the kinetic data, each series of the experiments at a definite pressure, H_2/CO ratio, and temperature, was made at different space velocities between 1×10^4 and 1×10^5.

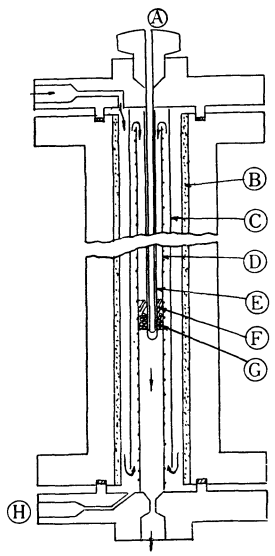

Fig. 1. Reactor.
A, thermocouple well: B, quartz tube: C, D and E, copper tubes: F, copper granules: G, catalyst: H, lead for heater.

*1 The concentration could also be determined from the quantity of methanol actually obtained in the synthesis. The value agreed well with that calculated by the above method.

The reactor is illustrated in Fig. 1. The catalyst (a packed bed of 22 mm. diameter and 17 mm. high) was pretreated for six hours at 350°C with a mixture of the gas (two moles of hydrogen and one mole of carbon monoxide) at atmospheric pressure, and thereafter the reactor was once brought to a lower temperature. At this lower temperature the gas was admitted at a space velocity at a high pressure, and then the temperature was raised gradually up to 330—340°C. After two hours' synthesis at this high temperature, a stationary conversion could be attained, and the temperature was then brought to the desired levels. During the synthesis the temperature difference along the catalyst bed remained less than 1°C.

Quantities of nitrogen such as 7.9% and 2.9% were contained in the feed gases of H_2/CO ratios of 2 and 3,74 respectively. Hydrogen, carbon monoxide and carbon dioxide in the gas after the synthesis were determined by the conventional methods; hardly any methane or olefine were

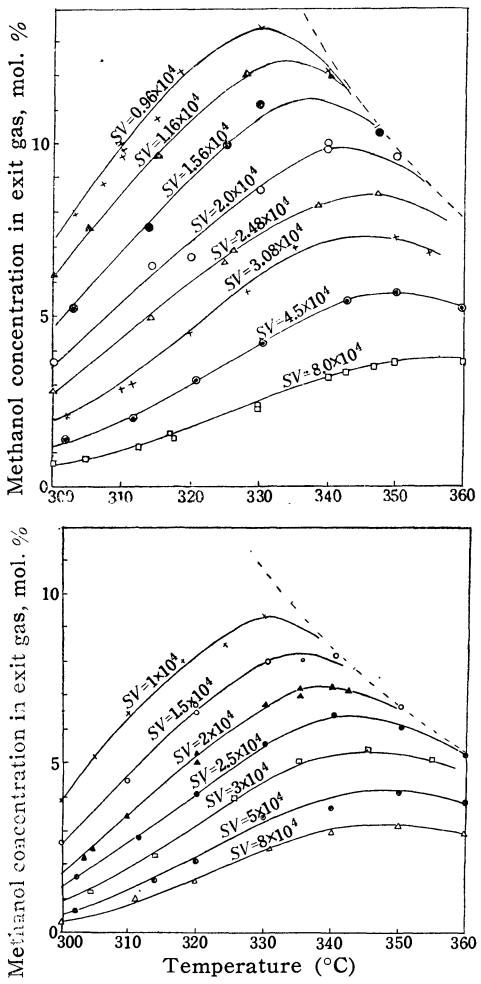

Figs. 2, 3. Methanol concentration as function of reaction temperature at different space velocities. 150 kg./cm^2. Fig. 2, $H_2/CO=2$: Fig. 3, $H_2/CO=6$

detected. The liquid product was analyzed for water by Karl-Fischer's method and for methyl formate and formaldehyde by the procedures described in our previous paper[6].

The catalyst used in this study was a zinc oxide-chromia catalyst which was prepared from an intimate mixture of commercial zinc oxide (grade, pure) and aqueous solution of chromic acid. The mixture was dried in air at room temperature, and the resulting cake was powdered and pressed to tablets. The catalyst contained 19 wt. % chromia.

Results

Methanol Concentration as a Function of Temperature. — A part of the experimental results are shown in Figs. 2 and 3. In the figures, the methanol concentration in the exit gas in the synthesis at 150 kg./cm^2 are plotted as a function of temperature for each space velocity. Fig. 2 refers to the results with the gas of H_2/CO ratio of 2, and Fig. 3 to those with the gas of H_2/CO ratio of 6.

As is seen in Table I, the product contained water, methylformate and formaldehyde as by-products; and a little increase in carbon dioxide was found in the exit gas. However, it may reasonably be expected that the methanol concentration calculated by the above mentioned method is correct, because quantities of the by-products are very small.

TABLE I

IMPURITIES IN PRODUCT AND CARBON DIOXIDE CONTENT IN EXIT GAS

Reaction temperature, °C	By-products, wt. % H_2O	HCO_2CH_3	HCHO	CO_2 in exit gas, vol. %
300	1.07	0.13	0.05	0.4
320	0.55	0.20	0.16	0.4
340	0.75	0.13	0.11	0.4
360	1.04	0.20	0.11	0.6

Every experiment was made at 150 kg./cm^2 at SV_0 of 1×10^4 with the gas of $H_2/CO=2$. The gas contained 0.2 vol. % of CO_2.

Equilibrium Constant for Methanol Synthesis.—The equilibrium constant of the methanol synthesis was determined by many workers,[1,7-14] and the thermodynamical calculation was given by R. H. Ewell[15]. However, there were some discrepancies among the values. In the present study an attempt has been made to obtain the equilibrium constant K by conducting the synthesis at a low space velocity at relatively high temperatures. The results*2 are given in Fig. 4, in comparison with the results reported by the above investigators. The values obtained here are intermediate between Newit's and Ewell's. The values of the equilibrium constant on the straight line drawn through our observed values will be employed in our kinetic interpretation of the experimental data. The line runs parallel to Ewell's.

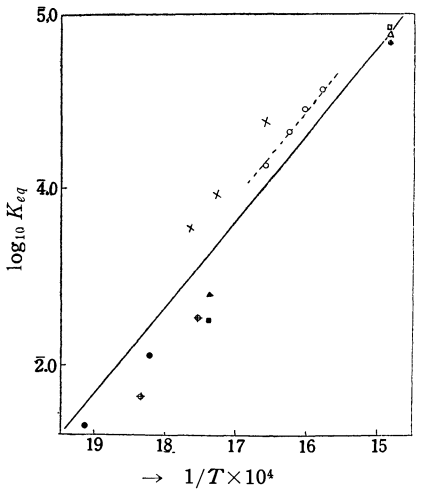

Fig. 4. Equilibrium constant for methanol synthesis.
×, Newit, Byrne and Strong: ○, the present authors: □, Lewis and Frolich: △, Brown and Galloway: ⊙, Audibert and Raineau: ▲, Smith and Hirst: ■, Smith and Branting: ⊕, Wettberg and Dodge: ●, Newton and Dodge: full line, Ewell.

Relations of Total Pressure to Methanol Concentration and Conversion Efficiency.—Changes in the methanol concentration and in the conversion efficiency (actual methanol concentration/equilibrium methanol concentration) with the total pressure are exemplified in Figs. 5 and 6 for the syntheses at 310 and 330°C

7) D. M. Newit, B. J. Byrne et al., *Proc. Roy. Soc.*, **123**, 236 (1929).
8) L. Brown and A. E. Galloway, *Ind. Eng. Chem.*, **20**, 960 (1928).
9) E. Audiert and A. Raineau, ibid., **20**, 1105 (1928).
10) D. F. Smith, L. L. Hirst et al., ibid., **22**, 1037 (1930).
11) D. F. Smith and B. F. Branting, *J. Am. Chem. Soc.*, **51**, 129 (1929).
12) E. F. Wettberg and B. F. Dodge, *Ind. Eng. Chem.*, **22**, 1040, (1930).
13) R. H. Newton and B. F. Dodge, *J. Am. Chem. Soc.*, **56**, 1287 (1934).
14) A. Tomita, *J. Chem. Soc. Japan, Ind. Chem. Sec.* (*Kogyo Kagaku Zassi*), **54**, 504 (1951).
15) R. H. Ewell, *Ind. Eng. Chem.*, **32**, 147 (1940).
*2 Deviation of the pressure-concentration relation from the ideal gas law was corrected by means of the activity coefficient derived from Berthelot's formula (refer to R. H. Ewell[15]).

with a gas-mixture containing two moles of hydrogen and one mole of carbon monoxide. The conversion efficiency tends to change with the total pressure more remarkably at the lower temperature but less so at the higher temperature. At the high temperature of 350°C it becomes nearly constant independent of the total pressure.

Dependence of the Methanol Concentration and the Conversion Efficiency on the Ratio of Hydrogen to Carbon Monoxide. —Figs. 7 and 8 show the plots of methanol concentration and of the conversion efficiency, vs. the ratio H_2/CO, respectively. At high ratios, the methanol concentration remains small, but it increases rapidly, at first, with the decreasing ratio, and then slowly at a ratio less than four. This increasing tendency appears less marked in the synthesis at higher space velocities where the concentration remains far below the equilibrium value. So far as the ratio is limited to a range from 2 to 4, it is expected that in the industrial synthesis, where the space velocity is relatively high

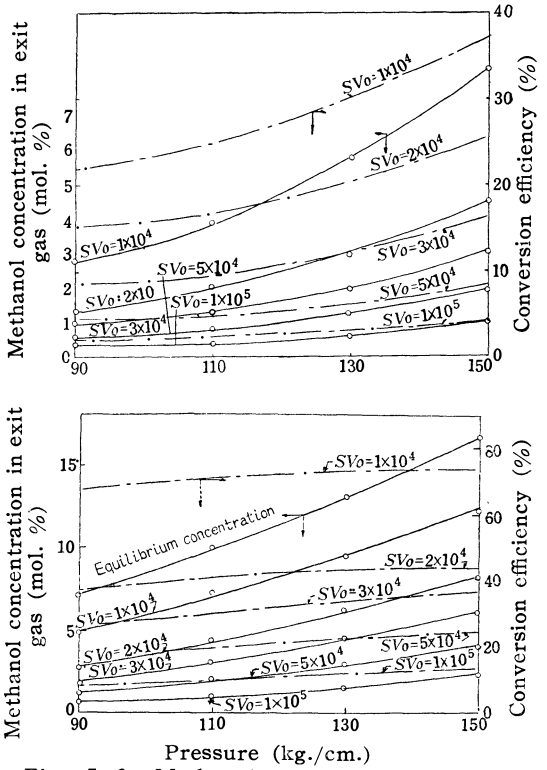

Figs. 5, 6. Methanol concentration and conversion efficiency as function of pressure at different space velocities.
full line, methanol concentration: dotted and dashed line, conversion efficiency.
$H_2/CO=2$, Fig. 5, 310°C: Fig. 6, 330°C

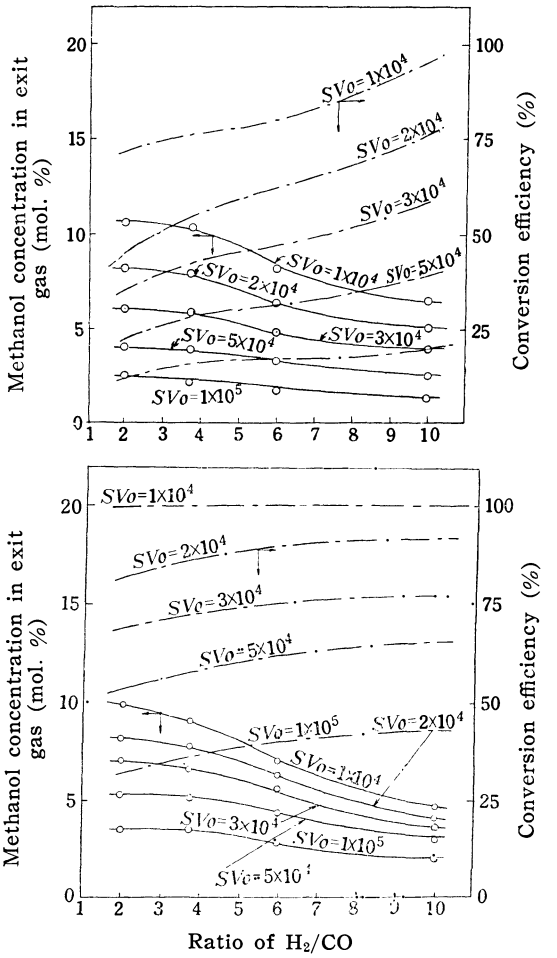

Figs. 7, 8. Methanol concentration and conversion efficiency as function of H_2/CO ratio.
full line, methanol concentration: dotted line, conversion efficiency. Fig. 7, 330°C: Fig. 8, 350°C

and consequently the methanol concentration remains considerably lower than the equilibrium value, the space-time-yield will remain nearly the same, independent of the change in the ratio. At high ratios, the conversion efficiency is high, and tends to decrease monotonously as the ratio lowers to the value of two.

Discussion

Rate Equation of Methanol Synthesis. —In contrast to the rate equation by Natta et al., which was derived on the assumption of Langmuir's adsorption isotherm of the reactants and product on the catalyst, the rate equation presented here has been derived on the assumption of the logarithmic adsorption isotherm. The procedure of the derivation is analogous to that

made by Temkin et al.[16] with their rate equation of the ammonia synthesis. It is assumed, however, that the desorption of methanol is rate determining and that neither the adsorption of hydrogen nor that of carbon monoxide is rate determining*3.

Based on the foregoing assumption, the rate of the methanol synthesis is given by

$$r=V_{des}-V_{ads}=k'_d e^{h\theta}-k'_a p_{CH_3OH} e^{-g\theta} \quad (1)$$

where h and g are constants, θ is the degree of coverage with methanol, and k'_d and k'_a are constants at a definite temperature. On the other hand, it follows from the assumption that the adsorption isotherm must satisfy the equation:

$$\theta=\frac{1}{f}\ln a_0 p_{CH_3OH} \quad (2)$$

where $f(f=g+h)$ is a constant and a_0 is a coefficient dependent only on temperature. To eliminate θ, $p^*_{CH_3OH}$ is introduced by following the manner of Temkin et al.,

$$\theta=\frac{1}{f}\ln a_0 p^*_{CH_3OH} \quad (3)$$

$$p^*_{CH_3OH}=K\cdot p_{CO}p^2_{H_2} \quad (4)$$

where K is the equilibrium constant of reaction and $p^*_{CH_3OH}$ is the fictitious methanol pressure in equilibrium with the degree of coverage θ. Hence the substitution of (3) and (4) in equation (1) gives the rate equation of the methanol synthesis.

$$\begin{aligned} r&=k_d(p_{CO}p^2_{H_2})^{1-\alpha}-k_a p_{CH_3OH}\cdot(p_{CO}p^2_{H_2})^{-\alpha} \\ &=k_d\{(p_{CO}p^2_{H_2})^{1-\alpha} \\ &\quad -p_{CH_3OH}\cdot(p_{CO}p^2_{H_2})^{-\alpha}/K\} \end{aligned} \quad (5)$$

where α is g/f.

The reaction rate of the methanol synthesis in a steady-state flow system through a fixed catalyst bed is usually given by equation (6),

$$r=c\cdot\frac{1}{(1+2z)^2}\cdot\frac{dz}{d(1/SV_0)} \quad (6)$$

in the equation, c is a constant equal to $1/273\cdot R\cdot c_m$, where R is the gas constant and c_m is the mean compressibility coefficient of a gas at normal state, SV_0 is the space velocity based on the inlet side of the reactor, and z is the methanol concentration (mol. %) in the exit gas. The term $1/(1+2z)^2$ comes from the change in number of moles of the components of the system $2H_2+CO\rightleftarrows CH_3OH$.

By combining equation (5) with equation (6) and integrating the resulting equation, equation (7) is obtained,

$$k/SV_0=\int_0^z \frac{dz}{(1+2z)^2\{(p_{CO}p^2_{H_2})^{1-\alpha}-p_{CH_3OH}\cdot(p_{CO}p^2_{H_2})^{-\alpha}/K\}} \quad (7)^*$$

where k, the rate constant, is given by $k=273\cdot R\cdot c_m k_d$. The equation involves a constant α besides k. The constant α is here evaluated by the trial and error procedure as follows: since the integral term in equation (7) can be solved numerically for arbitrary values of z and α, the three values, 0.1, 0.3, and 0.7, were chosen for α and the integration was performed*5. The values of the integral thus obtained are plotted against the reciprocal space velocity which corresponds to the value of z employed in the integration. The equation postulates that whenever a correct value of α is chosen, the plots for the synthesis at a definite temperature at different pressures fall on one straight line passing through the origin. The postulate is well satisfied when the value of α is 0.3, as shown in Fig. 9. When α is 0.1 the plots for different pressures begin to diverge progressively with rising temperature, while when α is 0.7 they do so with lowering temperature. Moreover, the gradient of the straight line ($\alpha=0.3$) gives the rate constant k.

The validity of our rate equation becomes established only when the rate constant is independent of the total pressure, the ratio of H_2/CO, and the space velocity. In Fig. 9 it has already been proved that the rate constant is independent of the total pressure so far as α is 0.3.

16) M. Temkin and V. Pyzhev, *Acta Physicochim., U. S. S. R.*, **12**, 327 (1940).

*3 This is because the premise that the adsorption of reactant is rate determining has proved to lead to a rate equation representing the results less satisfactorily. On the other hand, other steps such as the reaction between the adsorbed hydrogen and the adsorbed carbon monoxide might also be adopted as a rate determining step, but it will not be stated in this case, because the data could be explained by the concept written here.

*4 By introducing into equation (7) the following relations,

$a_{CH_3OH}=\gamma_{CH_3OH}\cdot Pz$, $a_{H_2}=\gamma_{H_2}\cdot 2p\cdot(n/2-z)/(1+n)$, $a_{CO}=\gamma_{CO}p\{1+(1-n)z/(1+n)\}$, where a is the activity, γ is the activity coefficient, and p is the total pressure, the equation is rewritten as

$$K/SV_0=\int_0^z \frac{\left[\gamma_{CO}\gamma^2_{H_2}\frac{4P^3\{1+(1-n)z\}(n/2-z)}{(1+n)^3}\right]^{\alpha}\cdot dz}{(1+2z)^2\left[\gamma_{CO}\gamma^2_{H_2}\frac{4P^3\{1+(1-n)z\}(n/2-z)}{(1+n)^3}-\gamma_{CH_3OH}Pz/K\right]}$$

*5 M. Temkin et al., gave 0.5 for α in their derivation of the rate equation for the ammonia synthesis.

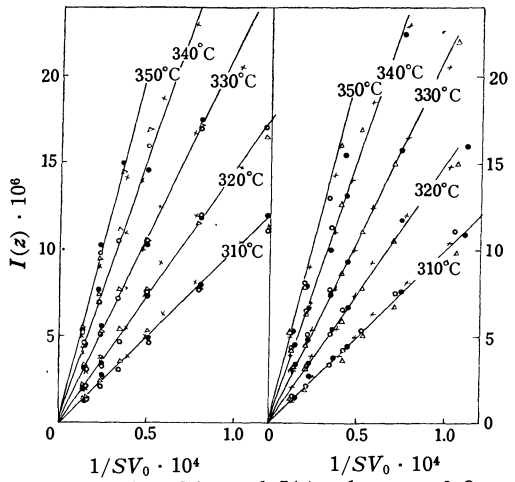

Figs. 9 and 10 Plots of $I(z)$ where $\alpha=0.3$ vs. reciprocal space velocity in the syntheses with gas of $n=2$ at different pressures (Fig. 9) and of different values of n at 150 kg./cm² (Fig. 10). Fig. 9, pressures (kg./cm²): ×, 150: △, 130: ○, 110: ●, 90. Fig. 10, n (H_2/CO): ×, 2.0: ●, 3.74: △, 6: ○, 10.

As shown in Fig. 10, the variation in the ratio of H_2/CO causes hardly any change in the rate constant. Furthermore, the values of z at the different space velocities are calculated by employing a value of k and are plotted against the reciprocal space velocity in Fig. 11 (curves in full line). The curves agree well with the experimental data over a wide range of the space velocity.

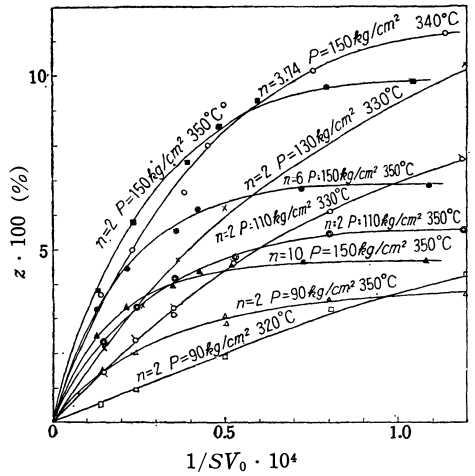

Fig. 11. Verification of the rate equation.

The plot of $\log k$ vs. reciprocal absolute temperature shows a straight line and the slope gives an apparent activation energy, 26.1 kcal./mol.

On the other hand, the rate equation which is the same in formula as equation (5) can also be obtained on the basis of Freundlich's adsorption isotherm (refer to the paper by T. Kwan[17]).

A rate equation of the methanol synthesis has already been proposed by Natta et al. on the basis of their very comprehensive experimental data on the synthesis. Their equation contains four constants, three of which are to be determined from the initial rate in three experiments performed at the same temperature, but at different total pressures and ratios of hydrogen to carbon monoxide. In the present work, however, accurate determination of the initial rate has been difficult, since the results do not contain so many values of the methanol concentration at very high space velocities as are sufficient for the drawing of the plot.

It is probable that by choice of suitable values for the constants, the rate equation by Natta et al. should represent the present experimental results well. However, the choice must be made by the trial and error method, and requires a tedious task of calculation.

Summary

Over a wide range of the total pressure and the ratio of hydrogen to carbon monoxide measurements on the methanol synthesis have been made at different temperatures at different space velocities. Relations of the total pressure to the methanol concentration and the conversion efficiency, and the dependence of the methanol concentration and the conversion efficiency on the ratio of hydrogen to carbon monoxide are presented.

Based on the assumption of the logarithmic adsorption isotherm and of the methanol desorption as the rate determining step, the rate equation for the methanol synthesis has been derived, which follows:

$$r=k_d\{(p_{CO}p^2_{H_2})^{0.7}-p_{CH_3OH}\cdot(p_{CO}p^2_{H_2})^{-0.3}/K\}$$

The equation has proved capable of representing our experimental results satisfactorily over relatively wide ranges of the pressures, the ratio of hydrogen to carbon monoxide and the space velocity.

Government Chemical Industrial Research Institute, Tokyo
Shibuya-ku, Tokyo

17) T. Kwan, *J. Phy. Chem.*, **60**, 1033 (1956).

*Chemical Constitution of Isorenieratene**

By Masaru YAMAGUCHI

(Received September 4, 1957)

The orange-colored sponge "*Reniera japonica*" contains a number of polyene pigments[1,2]. Among them a pigment named renieratene predominates in quantity, while a pigment of m. p. 199° forms a second constituent which amounts to 30~50% of the former. It has been reported that this second constituent is also a hydrocarbon, $C_{40}H_{48}$ or $C_{40}H_{50}$, and exhibits the absorption maxima at 520, 484 and 452 mμ in carbon disulfide[2].

The absorption maxima and the melting point of the pigment closely resemble leprotin ($C_{40}H_{54}$, m. p. 199~200°; absorption maxima in carbon disulfide 517, 478, 447 mμ; 12 double bonds) which has been isolated by Grundmann and Takeda from an acid-resisting bacteria of a leper[3]. However, the pigment differs from leprotin in the molecular formula and in the number of double bonds. These differences seem to afford the evidence to conclude that these pigments are not identical with each other, though it may not be said that leprotin has been thoroughly characterized in these respects. Therefore the name *isorenieratene* is tentatively proposed to the pigment by the author.

The study of the chemical constitution of isorenieratene has been considerably difficult at first because of the small amount of material available (ca. 450 mg.), but as the pigment had fortunately a symmetrical structure which facilitated the isolation of the degradation products, it was possible to elucidate its constitution almost throughly, as will be described below.

The solution of the pigment isomerized by the addition of iodine shows the absorption spectrum with a marked *cis*-peak which can not be observed in the fresh solution (Fig. 1). Therefore isorenieratene seems to have an all-*trans* configuration as to the conjugated double bonds.

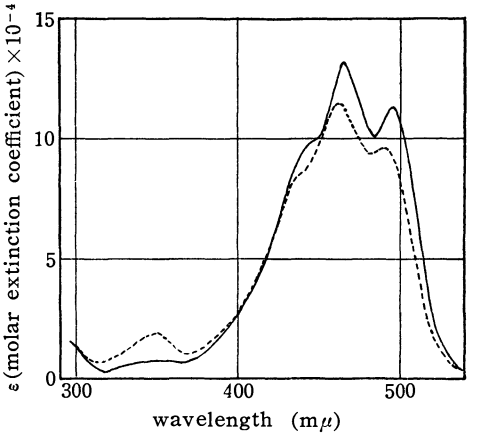

Fig. 1. Absorption curve of isorenieratene (benzene).
—— fresh solution
····· isomerized solution

Isorenieratene absorbs 15 moles of hydrogen on catalytic hydrogenation, which indicates that two rings exist in the molecule of the pigment. On determination of side chain methyl groups, it gives volatile acid corresponding to 7 moles of acetic acid.

The negative result in the determination of isopropylidene group indicates that isorenieratene possesses neither an isopropylidene group, nor an ionone ring. This agrees with the fact that the pigment has no Vitamin A activity.

From the molecular formula, isorenieratene is considered to be an isomer of renieratene which has a molecular formula $C_{40}H_{48}$ and 15 double bonds[4]. The results of the determinations described above are also very similar to those obtained on renieratene. Therefore isorenieratene is considered to have a structurally close relation to renieratene. In the previous paper[4] it has been interpreted that renieratene should have benzene rings in the molecule. The same argument is also valid for isorenieratene, and that the

* "Pigments of Marine Animals", V. IV of this series; This Bulletin, **30**, 979 (1957).

1) T. Tsumaki, M. Yamaguchi and T. Tsumaki, *J. Chem. Soc. Japan, Pure Chem. Sec.* (*Nippon Kagaku Zassi*), **75**, 297 (1954).

2) M. Yamaguchi, This Bulletin, **30**, 111 (1957).

3) C. Grundmann and Y. Takeda, *Naturwiss.*, **25**, 27 (1937); Y. Takeda and T. Ohta, *Z. Physiol. Chem.*, **258**, 6 (1939).

4) M. Yamaguchi, This Bulletin, **30**, 979 (1957).

pigment possesses benzene rings as the terminal groups, is deducible from the following reasons. Though isorenieratene absorbs 15 moles of hydrogen, it exhibits the absorption maxima similar to those of β-carotene which has 11 double bonds. In order to contain fifteen unsaturations, a C_{40}-carotenoid should have nessesarily triple bonds, allenic bonds or ringsystems with benzenoid structure or the like. However, in the infra-red spectrum (Fig. 2) no bands are observed which indicate the presence of triple or allenic bonds, but on the other hand a marked absorption at 810 cm^{-1} is observed, which can be considered to be due to the out-of-plane deformation of two or three adjacent hydrogen atoms attached to the tetra- or tri-substituted benzene ring.

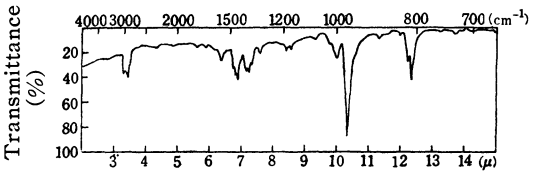

Fig. 2. Infra-red spectrum of isorenieratene.

The direct proof of the presence of benzene ring has been given by chromic acid oxidation and potassium permanganate oxidation. When isorenieratene is weakly oxidized with chromic acid corresponding to five atoms of oxygen per mole of the pigment, crocetin dialdehyde[5] (I) is obtained as a main product. This has established the structure of the middle part of the molecule of the pigment.

When isorenieratene is oxidized with chromic acid corresponding to two atoms of oxygen, a carotenoid aldehyde $C_{30}H_{36}O$ is obtained as a main product. The aldehyde is identical with isorenieral which has been obtained by the oxidation of renieratene[4]. From the fact that while renieratene gives two aldehydes, renieral and isorenieral, isorenieratene gives isorenieral only, it is concluded that isorenieratene has a symmetrical structure. From the colorless part of the chromatogram of the above oxidation product, a small amount of viscous oil is obtained. The oil affords the semicarbazone of m.p. 167°, which is proved to be identical with the semicarbazone of 2,3,6-trimethylbenzaldehyde (IV) described later.

When isorenieratene is oxidized with potassium permanganate, three acidic substances and one neutral product are obtained. One of the acidic products is oxalic acid (VII), which is identified by an elementary analysis and a mixed melting point. The second acidic product is a dibasic acid of m. p. 231°, which has a formula $C_{10}H_{10}O_4$. When the acid is further oxidized with potassium permanganate, it furnishes a tetrabasic acid of m. p. 215~238°, $C_{10}H_6O_8$, which is identified as 1,2,3,4-benzenetetracarboxylic acid (VIII) by an elementary analysis and a mixed melting point with an authentic sample[6]. The dibasic acid of m. p. 231° is also formed synthetically by the moderate oxidation of 2,3,6-trimethylbenzoic acid (V), and it does not show any tendency to form an anhydride at the melting point. Therefore it is obvious that the acid is 2,4-dimethylbenzene-1,3-dicarboxylic acid (VI). As the third acidic substance is considerably difficult to purify because of the small amount of material and its large solubility, it is converted into *p*-phenylazophenacyl ester and purified by means of chromatography. The pure ester thus obtained is identical with the authentic sample of *p*-phenylazophenacyl-2,3,6-trimethylbenzoate (free acid: (V)).

The neutral fraction is a viscous oil and it gives impure semicarbazone, m. p. 149~154°. The semicarbazone is converted into 2,4-dinitrophenylhydrazone, and the chromatographic purification of the latter gives a hydrazone of m. p. 219°. As it has been easily expected that the aldehyde may be 2,3,6-trimethylbenzaldehyde (IV), it has been synthesized from 3-bromopseudocumene by the Grignard reaction in a ca. 64% yield. The synthesized aldehyde gives 2,4-dinitrophenylhydrazone of m. p. 219°, which is not depressed by mixing it with the sample from isorenieratene. The aldehyde gives a semicarbazone of m. p. 167°, which is proved to be identical with the sample obtained by the chromic acid oxidation of isorenieratene described above by the mixed melting point determination.

These results are summerized in Fig. 3, and it is concluded that isorenieratene has a structure of 1,18-bis-(2,3,6-trimethylphenyl)-3,7,12,16-tetramethyl-1,3,5,7,9,11,13,15,17-octadecanonaene (III), and that isorenieral has the structure indicated by the formula (II).

5) O. Isler, H. Gutmann, H. Lindlar, M. Montavon, R. Rüegg, G. Ryser and P. Zeller, *Helv. Chim. Acta*, **39**, 463 (1956).

6) M. Freund and K. Fleischer, *Ann.*, **411**, 14 (1916).

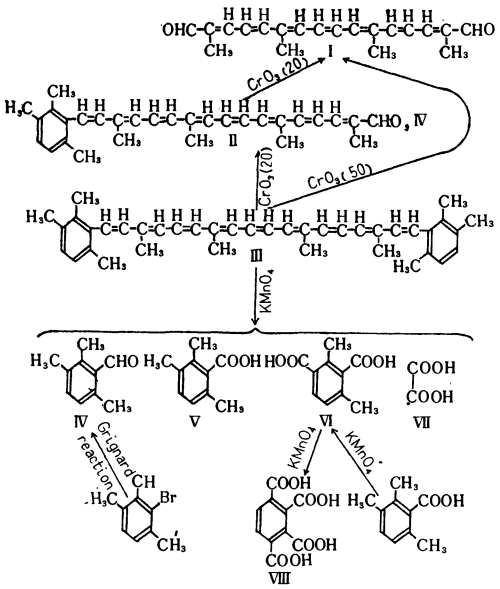

Fig. 3. Oxidation of isorenieratene.

A carotenoid with two non-substituted benzene rings (IX) has been synthesized by Eugster and coworkers[7], and it has been proved to exhibit the absorption maxima at 541, 502, 472 mμ in carbon disulfide. Isorenieratene however shows the absorption maxima at 520, 484, 452 mμ in the same solvent. The difference in

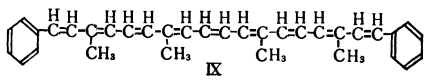

the position of the absorption maxima is considered to be due to the steric hindrance caused by the methyl groups attached to the neighboring positions of the polyene chain in the benzene nucleus of the molecule of the pigment. It is considered that the presence of such methyl groups hinders the uniplanarity between the benzene rings and the polyene chain, and causes subsequent decrease in the degree of conjugation, which resulted in the shift of the absorption maxima to the shorter wavelength location[8].

That the chemical constitution of isorenieral is expressed by the formula (II), lead to the conclusion that renieratene has a partial formula indicated by (X), for it has already been shown that renieratene gives isorenieral besides renieral on oxidation and that it is also the derivative of tetramethyloctadecanonaene.

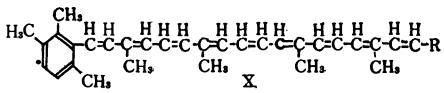

The carotenoids have hitherto been considered to belong exclusively to aliphatic or alicyclic compounds. Therefore it should be emphasized that the presence of a carotenoid containing aromatic structure in nature is established for the first time by the elucidation of the chemical constitution of isorenieratene.

Isorenieratene can be regarded as composed of isoprene unites as indicated in Fig. 4, but it is also possible that the

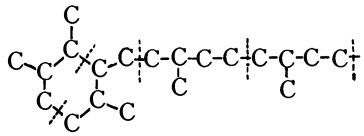

Fig. 4. Isoprene residues in isorenieratene.

pigment is formed from β-carotene by the migration of methyl groups of 1- and 1'-position and following dehydrogenation, such the migration of methyl groups being considered to occur possibly through the process involving the oxidation of 2- and 2'-position, and the retropinacolinic rearrangement. However the clear indication on the mode of formation of the pigment can not easily be given from our knowledge of carotenoid biogenesis.

Experimental

Isorenieratene prepared in the way described in the preceding papers[1,2] was employed. It formed purplish red needles, m. p. 199°. Absorption maxima were 520, 484, 452 mμ in carbon disulfide.

Anal. Found: C, 90.93; H, 9.07 %. Calcd. for $C_{40}H_{48}$: C, 90.85; H, 9.15 %.

The infrared spectrum.—It was taken in a potassium bromide pellet, with a Perkin-Elmer 21 double beam instrument equipped with a potassium bromide prism. It is given Fig. 2.

Catalytic hydrogenation (method of Kuhn and Möller[9]).—Catalyst, platinum dioxide; solvent, decalin-acetic acid (1 : 1); test substance, sorbic acid. Found: 15.17, 15.18 moles of hydrogen.

Isopropylidene group (method of Kuhn and Roth[10]).—On ozonolysis isorenieratene (15.706 mg.) gave acetone (0.081 mg.) after subtraction of blanc value. It corresponded to 0.05 mole of acetone per mole of the pigment.

Side-chain methyl group (method of Kuhn and Roth[11]).—Isorenieratene (4.390 mg. and 4.473 mg.) gave volatile acid corresponding to 5.93 cc.

7) C. H. Eugster, C. Garbers and P. Karrer, *Helv. Chim. Acta*, **35**, 1179 (1952).

8) Such phenomena are, for example, reviewed in, W. Klyne, "Progress in Stereochemistry", Butterworths Scientific Publications, London (1954), p. 126.

9) R. Kuhn and E. E. Möller, *Angew. Chem.*, **47**, 145 (1934).

10) R. Kuhn and H. Roth, *Ber.*, **65**, 1285 (1932).

11) R. Kuhn and H. Roth, ibid., **66**. 1274 (1933).

and 6.20 cc. of 0.01 N sodium hydroxide solution, which corresponded to 7.15 and 6.92 moles of acetic acid.

Vitamine A activity.—Isorenieratene was examined for three groups of rats in daily doses of 5γ, 20γ and 40γ respectively. All the rats of these groups died within 38 days after decreases of 28, 26 and 30 g. in body weight (average on the rats of each group). The rats of the group for the positive control for which 7γ of β-carotene were applied in daily doses, gained 33 g. on the average in body weight in 30 days.

***cis-trans* Isomerization**[12].—The solution of isorenieratene (1.379 mg.) in benzene (25 cc.) was isomerized by exposure to scattered light for 30 minutes after the addition of iodine (ca. 1.5 % of the weight of the pigment), and the solution as well as the fresh solution was determined spectrophotoelectrically. The absorption curves are given by Fig. 1, which shows a marked *cis*-peak at 351 mμ in the isomerized solution.

Chromic acid oxidation.—a) *Isorenieral and 2,3,6-trimethylbenzaldehyde.* Isorenieratene (67 mg.) was dissolved in a mixture of benzene (70 cc.) and acetic acid (70 cc.) and each 10 cc. portion of the solution (containing ca. 5 mg. of the pigment) was oxidized with the mixture of the aqueous chromic acid solution (0.1 N, 0.2 cc.) and acetic acid (2 cc.) for ca. 10 seconds under vigorous stirring. The reaction mixture was poured into water (20 cc.) covered with petroleum ether (10 cc.), and washed with water several times. The combined solution was dried with anhydrous sodium sulfate and chromatographed on alumina (developer; benzene). The main zone (brown red) afforded isorenieral (10.5 mg.), after elution and recrystallization of the residue of the eluate from petroleum ether. Isorenieral, m. p. 125~127°, mixed m. p. with the sample obtained from renieratene[4], 125~127°, gave absorption maxima, 486, 454 mμ in petroleum hexane.

Anal. Found: C, 87.48; H, 8.94 %. Calcd. for $C_{30}H_{36}O$: C, 87.33; H, 8.80 %. Phenylhydrazone melted at 206°. One of the upper minor zones afforded a minute quantity of crocetin dialdehyde.

From the faint colored part of the chromatogram, between the zone of isorenieral and that of unchanged isorenieratene, yellow oily residue with characteristic odor was obtained by the evaporation of the eluate. The residue was dissolved in methanol (5 cc.), and treated with an aqueous solution containing semicarbazide hydrochloride (20 mg.) and sodium acetate (30 mg.). After 24 hours the solution was somewhat concentrated and the precipitate was recrystallized from benzene in colorless prisms (4.4 mg.,) m. p. 167°, mixed m. p. with 2,3,6-trimethylbenzaldehyde semicarbazone (described later), 167°.

b) *Crocetin dialdehyde.* Isorenieratene (40 mg.) was oxidized with chromic acid (0.1 N, 0.5 cc. per 5 mg. of the pigment). The procedure was the same as above except that the reaction time was for ca. one minute. The main zone of the chromatography of the product was orange red and it afforded crocetin dialdehyde, m. p. 189~190°, (3.1 mg.), mixed m. p. with the sample obtained from renieratene, 189~190°. Absorption maxima 458, 430, 407 mμ (hexane). Crocetin dialdehyde was also obtained by the oxidation of isorenieral with chromic acid.

Oxidation with potassium permanganate.—The solution of isorenieratene (69 mg.) in pure benzene (30 cc.) and the solution of potassium permanganate (930 mg.) and sodium carbonate (930 mg.) in water (35 cc.) were mixed under vigorous stirring to form an emulsion at the room temperature and the stirring was continued for 12 hours. An excess of potassium permanganate was decolorized by the addition of the sodium sulfite solution. The mixture was filtered and the precipitate was repeatedly washed with hot water and benzene. In this way totally 183 mg. of the pigment was oxidized. All the filtrates and the washings were combined, and the aqueous layer was separated from the benzene layer (benzene solution A). The aqueous solution was concentrated under diminished pressure to ca. 10 cc., acidified with 20 % sulfuric acid, and extracted with ether. The ether solution was dried with anhydrous sodium sulfate and concentrated, and the partly crystallized residue was extracted with benzene (5 cc.) by refluxing for 5 minutes (benzene solution B). The residue was dissolved in a small quantity of water, and separated by fractional crystallizations into two parts: difficultly soluble colorless needles (15.5 mg.) which melted at 231° without decomposition, and easily soluble colorless plates, m. p. 99° (6 mg.).

The acid of m. p. 99° melted at 188° when dried at 70° under 18 mmHg for one hour. The mixed melting points with hydrated and anhydrous oxalic acid were 99~100° and 188° respectively.

Anal. Found: C, 19.11; H, 5.05 %. Calcd. for $C_2H_2O_4 \cdot 2H_2O$: C, 19.05; H, 4.80 %.

The acid of m. p. 231° is moderately soluble in hot water and difficultly soluble in benzene and in petroleum benzine.

Anal. Found: C, 61.65; H, 5.29 %. Neutralization equivalent, 97.9. Calcd. for $C_{10}H_{10}O_4$: C, 61.85; H, 5.19 %. Neutralization equivalent, 97.1 (dibasic acid).

The dibasic acid (7 mg.) and that recovered from the neutralization experiment (ca. 3 mg.) were heated with potassium permanganate (43 mg.) and sodium carbonate (50 mg.) in water (4 cc.) on a steam bath for 18 hours and then evaporated to ca. 0.5 cc. The mixture was acidified with 20 % sulfuric acid and manganese dioxide was dissolved by the addition of concentrated sodium sulfite solution. The clear solution was then extracted eight times with ether (total 150 cc.) and after drying with anhydrous sodium sulfate, ether was evaporated up. The residue was recrystallized from a small quantity of water

12) L. Zechmeister and P. Tuzson, ibid., **72**, 1340 (1935); L. Zechmeister and A. Polgár, *J. Am. Chem. Soc.*, **65**, 1522 (1943).

using a little active charcoal in colorless prisms (5.2 mg.), m.p. 215~238° (decomposition), which was identified to be 1,2,3,4-benzenetetracarboxylic acid by an analysis and a mixed melting point with the authentic sample[6].

Anal. Found: C, 47.73; H, 2.64 %. Neutralization equivalent, 61.6. Calcd. for $C_{10}H_6O_8$: C, 47.26; H, 2.38 %. Neutralization equivalent, 63.5.

The benzene solution (B) was concentrated under diminished pressure and the oily residue was extracted with petroleum benzine. Evaporation of the solvent of the extract gave a minute quantity of fine needles which was still contaminated by oily substance (the needles showed a m. p. 65~72° after drying on a porous plate). It was neutralized with 0.01 N sodium hydroxyde solution (2.642 cc.) by the use of phenolphthalein, extracted with ether to remove phenolphthalein, evaporated to dryness and treated with *p*-phenylazophenacyl bromide[13] (8.2 mg.) in ethanol for 30 minutes on a steam bath. After evaporation of the solvent, the residue was once recrystallized from methanol and chromatographed on alumina from the benzene solution. The main orange red zone afforded a minute quantity of red needles, m. p. 163°. A mixed m. p. 163° and a mixed chromatography with the authentic sample of *p*-phenylazophenacyl-2, 3, 6-trimethylbenzoate (Red needles, m. p. 163°. *Anal.* Found: C, 74.61; H, 5.84 %. Calcd. for $C_{24}H_{22}O_3N_2$: C, 74.59; H, 5.73 %. The acid was prepared from pseudocumene-3-magnesium bromide by the introduction of carbon dioxide at −7° in 55 % yield[14].) proved their identity.

The benzene solution (A) was evaporated up under reduced pressure and the residue was dissolved in methanol (5 cc.) and treated with the solution of semicarbazide hydrochloride (20 mg.) and sodium acetate (30 mg.) in a little water. The solvent was somewhat concentrated and the precipitate was recrystallized twice from benzene-methanol in colorless prisms, m. p. 149~154° (13 mg.). As it seemed still impure, it was converted into 2, 4-dinitrophenylhydrazone in ethanol containing a little sulfuric acid by the addition of 2, 4-dinitrophenylhydrazine, and chromatographed on alumina from a benzene solution. The main orange zone gave pure 2, 4-dinitrophenylhydrazone, m. p. 219°, (8.5 mg.), in deep red fine needles, when recrystallized from benzene-methanol. From the mother liquor of recrystallization of the above semicarbazone, 3.2 mg. of the hydrazone was further obtained. The mixed m.p. with 2, 3, 6-trimethylbenzaldehyde-2, 4-dinitrophenylhydrazone was 219°.

Anal. Found: C, 58.83; H, 4.99 %. Calcd. for $C_{16}H_{16}O_4N_4$: C, 58.53; H, 4.91 %.

2,4-Dimethylbenzene-1,3-dicarboxylic acid.—2, 3, 6-Trimethylbenzoic acid (165 mg.), potassium permanganate (590 mg.) and sodium carbonate (590 mg.) in water (25 cc.) were vigorously stirred at an ordinary temperature for 10 hours. The mixture was then filtered, and the filtrate, combined with washings, was concentrated to 5 cc. and acidified with 20 % sulfuric acid. The precipitate and the residue of the ether extract of the mother liquor were combined and recrystallized twice from water in colorless needles of m. p. 231° (90 mg.).

Anal. Found: C, 61.69; H, 5.31 %. Neutralization equivalent, 98.1. Calcd. for $C_{10}H_{10}O_4$: C, 61.85; H, 5.19 %. Neutralization equivalent, 97.1. The acid gave 1, 2, 3, 4-benzenetetracarboxylic acid on oxidation with potassium permanganate.

2,3,6-Trimethylbenzaldehyde.—Ethyl orthoformate (12 g.) and the Grignard reagent, prepared from 3-bromopseudocumene (16 g.) and magnesium (2 g.) in ether (80 cc.) was gently boiled for 40 minutes. The ether was then distilled off, and after the violent reaction with foaming [a large flask (500 cc.) was employed to avoid the overflowing] was subsided, which took place when the temperature of the water bath reached to 70~80°, the mixture was heated on a steam bath for further 20 minutes. The product was then decomposed with dilute sulfuric acid, the oil separated was hydrolysed by boiling with 20 % hydrochloric acid and was treated in methanol (50 cc.) with semicarbazide hydrochloride (12 g.) and sodium acetate (20 g.) in water (20 cc.). The precipitate was filtered, washed successively with petroleum ether and with water, and recrystallized from benzene-methanol in colorless plates (10.5 g.), m. p. 167°.

Anal. Found: C, 64.54; H, 7.51 %. Calcd. for $C_{11}H_{15}ON_3$: C, 64.36; H, 7.37 %.

The free aldehyde was obtained by the steam distillation of the semicarbazone with 20 % sulfuric acid. B. p. 137~138° (30 mm Hg); 7 g. 2, 4-Dinitrophenylhydrazone, red needles, m. p. 219°.

Anal. Found: C, 58.86; H, 5.07 %. Calcd. for $C_{16}H_{16}O_4N_4$: C, 58.53; H, 4.91 %.

The author wishes to express his thanks to Professer Tokuichi Tsumaki for his exceedingly kind directions throughout this work. The author also thanks Mr. Kiyoshi Nakamura of Dainippon Pharmaceutical Co. Ltd. for the infrared determination, Mr. Toshihiko Mukai and Mr. Yoichi Demura for their help in the collection of materials, and Mr. Michio Shido and Miss Sachiko Indo for microanalysis. The cost of this work has been partially covered by the Scientific Research Grant of Ministry of Education.

Department of Chemistry, Faculty of Science, Kyushu University
Hakozaki, Fukuoka

13) S. Masuyama, *J. Chem. Soc. Japan, Pure Chem. Sec.* (*Nippon Kagaku Zassi*), **71**, 402 (1950).
14) H. A. Smith and J. A. Stanfield, *J. Am. Chem. Soc.*, **71**, 81 (1949).

The Addition Compounds of Bis-Salicylaldehyde Copper(II) and its Derivatives with Pyridine, and α, α'-Dipyridyl

By Yoneichiro MUTO

(Received June 5, 1957)

Recently, a few compounds have been reported in which the copper(II) atom appears to be five-coordinate[1] or six-coordinate[2] in the solid state, although the copper(II) ion is normally reluctant to raise its coordination number of four. On the other hand, it is well known that inner complexes of four-coordinated nickel (II) add two molecules of pyridine to form six-coordinated nickel(II) complexes[3-5]. For example, bis-pyridine-bis-salicylaldehyde nickel(II) was isolated crystalline from pyridine solution of bis-salicylaldehyde nickel(II)[5]. Therefore, it is interesting to see whether or not inner complexes of four-coordinated copper(II) form addition compounds with pyridine in a similar manner to nickel(II) complexes. Also, α, α'-dipyridyl presumably forms a more stable coordination compound than does pyridine, because chelation greatly enhances coordination. Accordingly, the present writer has undertaken to examine whether bis-salicylaldehyde copper(II) and its derivatives form addition compounds with pyridine or α, α'-dipyridyl. In several instances, it was possible to isolate well-defined crystalline compounds containing two molecules of pyridine or one molecule of α, α'-dipyridyl having formula I.

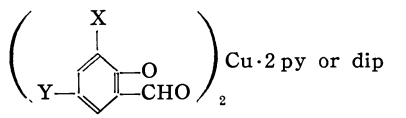

I

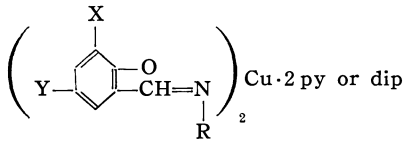

II

(X: H, NO_2; Y: H, Br, NO_2; py: Pyridine; dip: α, α'-Dipyridyl; R: C_6H_5, $CH_3C_6H_4$).

They are soluble in organic solvents and insoluble in water, except α, α'-dipyridyl-3-nitrosalicylaldehyde copper(II). All of the addition compounds with pyridine lost the pyridine on heating in ethanol or in benzene, leading to the precipitation of bis-salicylaldehyde copper(II) or its derivatives, while several addition compounds with α, α'-dipyridyl produced α, α'-dipyridyl-copper(II)-mono-salicylate and its derivatives (formula III) on heating their ethanolic or pyridine solutions. The above result showed that the aldehyde group was oxidized to a carboxyl group.

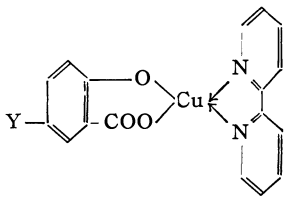

III

(Y: H, Cl, Br, NO_2.)

Further, it was possible to isolate several addition compounds of substituted bis-salicylaldimine complexes of copper(II) with pyridine or α, α'-dipyridyl (formula II). They lost pyridine or α, α'-dipyridyl on heating in organic solvents.

An analogous addition reaction has been reported by Dwyer[6] who found that bis-diazoaminobenzene copper(II) added two molecules of pyridine or one molecule of ethylenediamine. Ley and Wingner[7] found that bis-glycine copper(II) added two molecules of ammonia. These investigators considered that the chelate rings were broken and these addition compounds of copper(II) were four-coordinate[6,8]*.

There are studies by several investigators that copper(II) can form complexes with

1) D. E. C. Corbridge and E. G. Cox, *J. Chem. Soc.*, **1956**, 594.
2) S. Kirschner, *J. Am. Chem. Soc.*, **78**, 2372 (1956).
3) P. Pfeiffer, E. Bucholtz and O. Bauer, *J. prakt. Chem.*, **129**, 63 (1931).
4) F. P. Dwyer and D. P. Meller, *J. Am. Chem. Soc.*, **63**, 81 (1941).
5) F. Basolo and W. R. Matoush, ibid., **75**, 5663 (1953).
6) F. P. Dwyer, ibid. **63**, 78 (1941).
7) H. Ley and G. Wingner, *Z. Electrochemie.*, **11**, 584 (1905).
8) H. Ley, *Ber.*, **42**, 354 (1909).

coordination number higher than four[9]. Recently Kirschner[2] has shown by infrared and rotatory dispersion studies that copper(II) ethylenediaminetetra-acetate and copper(II) bis-aspartate are six-coordinate. Although these addition compounds of copper(II) studied in the present report may be six-coordinate, it seems more likely that they are four-coordinate in view of the comparative rarity of copper(II) complexes with a higher coordination number and the lack of experimental data on these addition compounds by physical means such as infrared spectroscopy.

Experimental

(A) Preparation of bis-salicylaldehyde copper(II) and its derivatives.—These complexes were obtained by the addition of aqueous solution of cupric acetate to the ethanolic solution of salicylaldehyde or its derivatives in the usual way as reported in the literature.

(B) Preparation of addition compounds with pyridine.—They were obtained by dissolving complexes prepared in (A) in cold pyridine and by precipitating with cold water. They were purified by recrystallization from pyridine. Bis-5-chlorosalicylaldehyde copper(II) and bis-5-bromosalicylaldehyde copper(II) did not form addition compounds with pyridine.

1. Bis-pyridine-bis-5-bromo-3-nitrosalicylaldehyde copper(II).—Light green prismatic crystals which loss pyridine at about 110°C.

Anal. Found: C. 40.64; H, 2.52; N, 8.15; Cu, 8.74; pyridine, 22.31. Calcd. for $C_{14}H_6O_8N_2Br_2Cu \cdot 2C_5H_5N$: C, 40.50; H, 2.27; N, 7.87; Cu, 8.93; pyridine 22.23%.

2. Bis-pyridine-bis-3-nitrosalicylaldehyde copper (II). Yellow green prismatic crystals which loss pyridine at about 90°~100°C.

Anal. Found: N, 10.38; Cu, 11.24; pyridine, 28.46. Calcd. for $C_{14}H_8O_8N_2Cu \cdot 2C_5H_5N$: N, 10.12; Cu, 11.47; pyridine, 28.56%.

3. Bis-pyridine-bis-5-nitrosalicylaldehyde copper (II).—Deep green prismatic crystals which loss pyridine slowly at about 40°~50°C.

Anal. Found: N, 10.13; Cu, 11.25; pyridine, 28.15. Calcd. for $C_{14}H_8O_8N_2Cu \cdot 2C_5H_5N$: N, 10.12; Cu, 11.47; pyridine, 28.56%.

4. Bis-pyridine-bis-salicylaldehyde copper (II).—Light green prismatic crystals which loss pyridine slowly at room temperature. Therefore, the analysis was performed without delay after preparation.

Anal. Found: N, 5.93; Cu, 13.72; pyridine, 33.87. Calcd. for $C_{14}H_{10}O_4Cu \cdot 2C_5H_5N$: N, 6.09; Cu, 13.82; pyridine, 34.10%.

5. Bis-pyridine-bis-salicylal-aniline copper (II).—Light green prismatic crystals which lose pyridine slowly at room temperature.

Anal. Found: N, 9.20; Cu, 10.36; pyridine, 25.58. Calcd. for $C_{26}H_{20}O_2N_2Cu \cdot 2C_5H_5N$: N, 9.12; Cu, 10.34; pyridine, 25.76%.

6. Bis-pyridine-bis-5-bromo-3-nitrosalicylal-toluidine copper (II).—Green prismatic crystals.

Anal. Found: N, 9.18; Cu, 7.18; pyridine, 17.67. Calcd. for $C_{28}H_{20}O_6N_4Br_2Cu \cdot 2C_5H_5N$: N, 9.44; Cu, 7.14; pyridine, 17.77%.

(C) Preparation of addition compounds with α, α'-dipyridyl.—The addition compounds with α, α'-dipyridyl were obtained by dissolving the calculated amount of α, α'-dipyridyl and complexes prepared in (A) in cold pyridine or in ethanol and by precipitating with cold water. They were purified by recrystallization from pyridine without heating. Bis-5-chlorosalicylaldehyde copper(II) did not form an addition compound and readily gave an oxidized compound directly.

1. α, α'-Dipyridyl-bis-salicylaldehyde Cu(II).—Brown prismatic crystals. This compound was decomposed with dilute sulfuric acid and then subjected to steam distillation. Salicylaldehyde in the distillate was identified by its 2, 4-dinitrophenylhydrazone which melted at 247°~248°C.

Anal. Found: C, 40.70; H, 2.12; N, 6.03; Cu, 13.81. Calcd. for $C_{14}H_{10}O_4Cu \cdot C_{10}H_8N_2$: C, 40.61; H, 1.99; N, 6.07; Cu, 13.75%.

2. α, α'-Dipyridyl-bis-5-bromosalicylaldehyde copper (II).—Greenish yellow prismatic crystals.

Anal. Found: N, 4.61; Cu, 10.03, Calcd, for $C_{14}H_8O_4Br_2Cu \cdot C_{10}H_8N_2$: N, 4.52; Cu, 10.25%.

3. α, α'-Dipyridyl-bis-5-nitrosalicylaldehyde copper(II).—Light green prismatic crystals.

Anal. Found: N, 10.27; Cu, 11.73. Calcd. for $C_{14}H_8O_8N_2Cu \cdot C_{10}H_8N_2$: N, 10.15; Cu, 11.51%.

4. α, α'-Dipyridyl-bis-5-bromo-3-nitrosalicylaldehyde copper(II).—Yellow-green prismatic crystals. When this complex was decomposed by dilute sulfuric acid and the solution was extracted with ether, light yellow needle crystals of 5-bromo-3-nitrosalicyaldehyde melting at 147°~148°C were obtained.

Anal. Found: N, 8.05, Cu, 8.88. Calcd. for $C_{14}H_6O_8N_2Br_2Cu \cdot C_{10}H_8N_2$: N, 7.90; Cu 8.95%.

5. α, α'-Dipyridyl-bis-3-nitrosalicylaldehyde copper (II).—Yellow-brown crystals. This complex was insoluble in alcohol, but was soluble in cold water to a certain extent. It could not be oxidized.

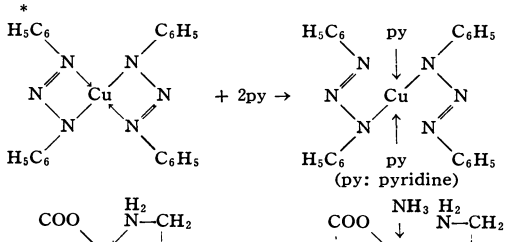

9) F. Rosenblatt, *Z. anorg. Chem.*, **204**, 351 (1932); H. Laitinen, E. Onstott, J. Bailar, Jr., and S. Swann, *J. Am. Chem. Soc.*, **71**, 1550 (1949); F. Basolo, Y. T. Chen and R. K. Murmann, ibid., **76**, 956 (1954); N. R. Davies and F. P. Dwyer, *J. Proc. Roy. Soc. N. S. W.*, **86**, 64 (1954) etc.

Anal. Found: N, 10.16; Cu, 11.36. Calcd. for $C_{14}H_8O_8N_2Cu \cdot C_{10}H_8N_2$: N, 10.15; Cu, 11.51%.

6. α, α'-Dipyridyl-bis-salicylal-aniline copper (II).—Green prismatic crystals.

Anal. Found: N, 9.31; Cu, 10.44. Calcd. for $C_{26}H_{20}O_2N_2Cu \cdot C_{10}H_8N_2$: N, 9.15; Cu, 10.38%.

7. α, α'-Dipyridyl-bis-5-bromo-3-nitrosalicylal-aniline copper (II).—Red-brown prismatic crystals.

Anal. Found: N, 9.67; Cu, 7.52. Calcd. for $C_{16}H_{16}O_6N_4Br_2Cu \cdot C_{10}H_8N_2$: N, 9.77; Cu, 7.39%.

(D) Oxidation of α, α'-dipyridyl complexes.—When the addition compounds with α, α'-dipyridyl were dissolved in ethanol or pyridine, heated on a water bath for about half an hour, and precipitated with water, gray needles of α, α'-dipyridyl copper(II)-monosalicylate and its derivatives were obtained. The pure complexes were obtained by recrystallization from ethanol. When these complexes were decomposed with dilute sulfuric acid and were distilled in steam or extracted with ether, salicylic acid and its derivatives were obtained, and α, α'-dipyridyl-copper (II)-sulfate was isolated from the residue.

1. α, α'-Dipyridyl-copper (II)-monosalicylate.—Gray needles which melt at 262°~263°C with decomposition.

Anal. (the sample obtained by oxidation) Found: C, 53.16; H, 4.06; N, 7.46; Cu, 16.83. Calcd. for $C_7H_4O_3Cu \cdot C_{10}H_8N_2 \cdot 1.5\ H_2O$: C, 53.33; H, 3.95; N, 7.32; Cu, 16.60%.

The complex obtained by heating a calculated amount of copper(II)-monosalicylate and α, α'-dipyridyl in ethanol, showed nearly the same m. p. (262°~263°C) and analytical result as the complex obtained by oxidation of α, α'-dipyridyl-bis-salicylaldehyde copper(II). Therefore, it was concluded that the structure of this compound corresponded to the formula III.

Anal. Found: N, 7.59; Cu, 16.77%.

2. α, α'-Dipyridyl-copper (II)-mono-5-bromo-salicylate.—Green needles.

Anal. Found: N, 5.85; Cu, 13.79; H_2O, 7.48. Calcd. for $C_7H_3O_3BrCu \cdot C_{10}H_8N_2 \cdot 2H_2O$: N, 6.08; Cu, 13.36; H_2O, 7.61%.

3. α, α'-Dipyridyl-copper (II)-mono-5-nitrosalicylate.—Gray needles.

Anal. Found: N, 10.36; Cu, 15.84. Calcd. for $C_7H_3O_5N \cdot Cu \cdot C_{10}H_8N_2$: N, 10.48; Cu, 15.85%.

4. α, α'-Dipyridyl-copper (II)-mono-5-chloro-salicylate.—Gray needles.

Anal. Found: N, 6.88; Cu, 14.76; H_2O, 8.50. Calcd. for $C_7H_3O_3ClCu \cdot C_{10}H_8N_2 \cdot 2H_2O$: N, 6.64; Cu, 14.90; H_2O, 8.41%.

5. Oxidation product of α, α'-dipyridyl-bis-5-bromo-3-nitrosalicylaldehyde copper (II).—When the complex which was obtained by oxidation of α, α'-dipyridyl-bis-5-bromo-3-nitrosalicylaldehyde copper(II) was decomposed with dilute sulfuric acid and the decomposition product was extracted with ether, white needle crystals were obtained. When this compound was recrystallized from dilute sulfuric acid, colorless needle crystals melting at 216.5°~217.5°C were obtained. This compound was not 5-bromo-3-nitrosalicylic acid or its aldehyde, and its constitution is not yet elucidated.

Chemical Laboratory, Faculty of Liberal Arts, Saga University, Saga

Dispersed Structure of Chromia-Zinc Oxide Catalyst System

By Yoshio MATSUNAGA

(Received August 7, 1957)

In the previous paper[1] the author has reported the correlation between the degree of dispersion of chromia which is supported on alumina and its stability towards oxidation at various temperatures. In the extreme case where chromium ions are in two-dimensional infinite dilution, it has been revealed that chromium can be oxidized completely to the hexavalent state, contrary to our knowledge of the thermal decomposition of chromic anhydride. This anomalous stability of the higher oxide on the surface of alumina has been explained nearly quantitatively by the relative importance of surface oxidation of chromia. Therefore, the determination of mean oxidation number of chromium in the oxidized chromia-alumina catalysts might be useful in the same way as the susceptibility isotherm method[2] to deduce the dispersed structure of supported chromia.

The magnetic method developed by Selwood was applied by Shida and his collaborators[3] to the chromia-zinc oxide catalysts prepared by the impregnation method. They found that chromic ions

1) Y. Matsunaga, This Bulletin, **30**, 984 (1957).

2) R. P. Eischens and P. W. Selwood, *J. Am. Chem. Soc.*, **69**, 1590, 2693 (1947).

3) S. Shida et al, Abstracts of the paper presented at the Annual Meeting of the Chemical Society of Japan, April 1954.

are dispersed more highly than in the chromia-alumina system and attributed this distinction to the three-dimensional dispersion of a part of the chromic ions associated with the formation of zinc chromate in the process of impregnation. The form of the susceptibility isotherm is concerned not only with the dispersed structure of chromia on the catalyst surface but also with the three-dimensional dispersion, so it seems to be difficult to deduce the structure of chromia in this catalyst system by the magnetic method alone. On the other hand, however, our chemical method described in the previous paper gives a measure of surface area of chromia; namely, it is concerned with the two-dimensional dispersed structure. Hence for the purpose of elucidating the structure of the chromia-zinc oxide catalyst more fully, the application of these two methods was extended to this catalyst system.

Experimental

Preparation of Catalysts.—Zinc oxide used in this work was prepared by a method similar to that described in our previous work on its diamagnetism[4]. After zinc sulfate solution had been carefully purified, the oxalate was precipitated, filtered and dried at 110°C. Non-sintered zinc oxide was prepared by the calcination of oxalate at 450°C for six hours and a sintered sample was obtained by heating at 850°C for three hours. The magnetic susceptibilitiy of both materials was found to be -0.33×10^{-6} and was independent of magnetic field strength.

Catalyst samples were prepared by the impregnation method in the similar way as in the case where alumina was used as a carrier. Instead of chromic acid solution ammonium bichromate solution was employed for this purpose because Shida et al. claimed that the latter is more suitable for achieving two-dimensional dispersion of chromia on the surface of zinc oxide. The samples with chromium content from about 1 to 17 per cent. were obtained by varying the concentration of the ammonium bichromate solution. The conditions of drying and reduction of the catalysts and the method of determination of the chromium content were the same as those used in the case of the chromia-alumina catalyst system.

Oxygen Treatment.—The reduced catalysts were cooled in a stream of hydrogen, then oxidized with air at room temperature. Further oxidations were carried out in a stream of oxygen for five hours at 250° and 450°C. The oxidation number of chromium in these oxidized catalysts was determined iodometrically.

Magnetic Measurements.—Measurements of the susceptibilities of catalyst samples were made at room temperature using a Gouy balance as previously described[5]. The field was calibrated at two constant current strengths with distilled water, and the field strength dependence of susceptibility was examined. No ferromagnetic effect, however, was found in any sample.

The gram susceptibility of the chromium ion was calculated on the assumption that the magnetic contribution of chromium, zinc, and oxygen ions are additive, and that of the last two is independent of the concentration of any constituent. This assumption seems to be justified by the fact that the change in concentration of lattice defect has no measurable effect on the diamagnetism of zinc oxide[4].

Results

The series in which non-sintered zinc oxide is used as a carrier will be considered at first. In Fig. 1 the mean oxidation number of chromium is plotted against its content. The value in the samples oxidized at room temperature is less than 3.1 in the whole range of chromium content. The degree of oxidation state reached by the treatment at higher temperature is appreciably smaller than that in the chromia-alumina catalyst similarly treated; besides, the forms of curves in these two catalyst systems are quite different.

The susceptibility per gram of chromium derived by direct application of an additivity rule is graphically shown in Fig. 2. In this figure the dissimilarity between the kinds of behavior of chromium in two systems, in which alumina and zinc oxide respectively are used as carrier, is more remarkable. For example, in the samples oxidized at room temperature, the susceptibility of chromium supported on alumina is markedly dependent on its content and the relation between these two variables gives information with regard to the dispersed structure of chromia. But in the case presented in this paper, its magnitude is constant regardless of the content of chromium, and we can not deduce a definite conclusion from these results. The susceptibility of chromium in the series oxidized at higher temperatures decreases as the content of chromium is decreased.

Similar data for the second series, in which sintered zinc oxide is used as the carrier, are shown in Figs. 3 and 4. The susceptibility of chromium in the series oxidized at room temperature shows a

4) Y. Matsunaga, This Bulletin, **30**, 680 (1957).

5) H. Akamatu and Y. Matsunaga, ibid., **26**, 364 (1953).

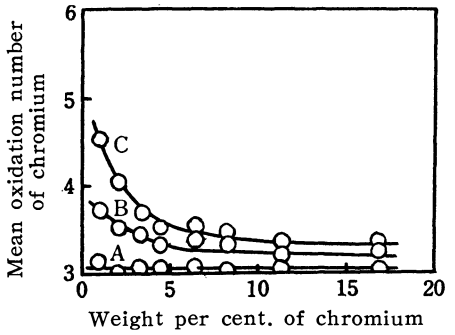

Fig. 1. Relation of oxidation number of chromium supported on non-sintered zinc oxide to its content.
A; oxidized at room temperature,
B; at 250°C, C; at 450°C.

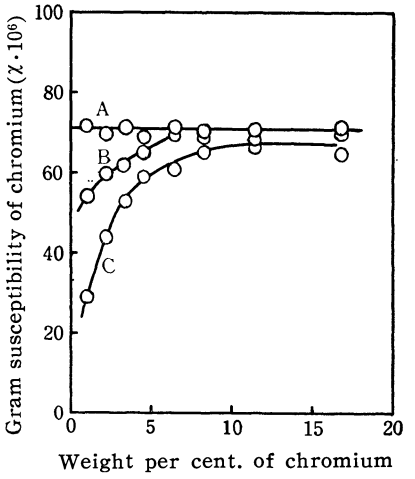

Fig. 2. Susceptibility-composition isotherms of chromia impregnated on non-sintered zinc oxide.
A; oxidized at room temperature,
B; at 250°C, C; at 450°C.

slight increase as its content decreases, and the value extrapolated to infinite dilution of chromia seems to be somewhat greater than that found in the first series. The dependencies of susceptibility and oxidation number in the series treated at higher temperature on the variation of the chromium content are less appreciable than those in the first series.

Discussion

According to the results given by Shida et al., the susceptibility of chromium (χ) in the present oxide-catalyst system follows the Curie-Weiss law expressed by

$$\chi = C/(T+\Delta)$$

where C, Δ are the Curie and the Weiss constants, and T is the absolute temperature. The Curie constant relates to the number of unpaired electrons in a paramagnetic ion, namely the oxidation number of chromium in this case, and the magnitude of the Weiss constant increases in proportional to the number of equidistant neighboring chromium ions as expressed by the formula,

$$\Delta = -2JzS(S+1)/3k,$$

where J is the exchange integral, z the number of equidistant neighboring chromium ions, S the vector sum of spin moments, and k the Boltzmann constant.

The susceptibility and the mean oxidation number of chromium for the samples of the first series oxidized at room temperature are independent of the composition of the catalyst. The moment of chromium ion is 3.8 Bohr magnetons at infinite magnetic dilution and the susceptibility value is about 115×10^{-6} at the temperature of measurement[6]. Therefore, we can conclude that z is appreciably great and constant throughout the measured range of chromium content. It must be nine at the maximum value in massive chromia, and may decrease as the crystallite size of chromia decreases or as the neighboring chromic ion is displaced by a diamagnetic ion. The former case was found in the chromia-alumina catalyst system and discussed in detail by Eischens and Selwood. Furthermore, we have presumed that the anomalous oxidation of supported chromia is in close relation with the value of z and confirmed Selwood and Eischens' conclusion from this standpoint. The magnitude of z in the present catalyst system may be about five to six judging from the susceptibility value of chromium. If we wish to interpret this decrease of z by the shrinkage of the crystal nuclei of chromia, they must be, on the average, about three layers thick, regardless of the content of chromium. The mean oxidation number of chromium in such a case must be +3.6 or more as expressed in our previous paper[1] when the samples are oxidized at higher temperatures. Besides, it must be constant throughout the whole range of chromium content. As shown in Fig. 1, however, such an increase in oxidation number is achieved only in the samples which contain less than four per cent. of chromium.

6) P. W. Selwood, L. Lyon and M. Ellis, *J. Am. Chem. Soc.*, **73**, 2310 (1951).

In the present catalyst system, the displacement of a neighboring chromic ion by a diamagnetic zinc ion must also be considered. It seems highly likely that in the process of impregnation, basic zinc chromate is formed and, after heating and reduction, most of it is converted into zinc chromite and a small proportion of chromic ions are dissolved in the carrier. The estimated value of z seems to be consistent with this model, if the crystal nuclei of zinc chromite are so large that the effect on the magnitude of z of chromic ions situated on the surface can be left out of consideration even in the catalyst which contains only two per cent. chromium. However, such a large crystallite of zinc chromite can not be oxidized appreciably and this model is inconsistent with the apprecible oxidation appearing in the low content range of chromium. Thus it is suggested that the dependence of the oxidation number of chromium on the composition of the catalyst is not explainable without the combination of these two models mentioned above, namely the thin crystal nuclei of supported chromia and the relatively large crystallites of zinc chromite. In the catalyst samples containing a small amount of chromium, the promoter may be mainly in the form of a thin layer of chromia which must be responsible for the high surface oxidation. As the content of chromium is increased, the crystallites of zinc chromite appear and the surface oxidation of the chromia layer becomes less important.

We have shown in the previous paper that the chemical method developed by us gives no more information on the dispersed structure of chromia than that given by the susceptibility isotherm method if the promoter is situated only on the surface of the carrier. However, as described in the above paragraphs these two methods are complementary to each other in the present system so we can clarify more fully the structure of the catalyst by using both methods.

In the second series, the carrier is more or less compact as the result of being heated at higher temperature and may be less reactive than the non-sintered one. Consequently, the reaction between adsorbed chromate ion and zinc oxide becomes rather difficult and the crystal nuclei of chromia grow more easily on the surface of the carrier. The slight decrease in susceptibility of a chromic ion accompanying its increasing concentration in the catalyst must be attributed to this crystal growth. It seems to be consistent with this expectation that the chromic ion in this series is less active towards oxidation.

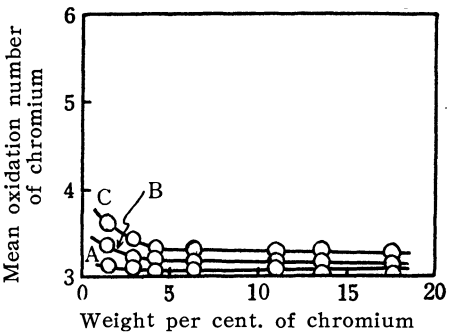

Fig. 3. Relation of oxidation number of chromium supported on sintered zinc oxide to its content.
A; oxidized at room temperature,
B; at 250°C, C; at 450°C.

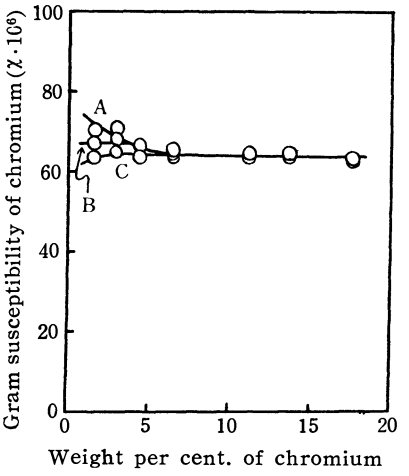

Fig. 4. Susceptibility-composition isotherms of chromia impregnated on sintered zinc oxide.
A; oxidized at room temperature,
B; at 250°C, C; at 450°C.

The cause of discrepancy between the forms of the susceptibility-composition isotherms reported by Shida et al. and by us is not yet accounted for. However, it appears that chromia-zinc oxide catalysts prepared by the impregnation method consist of zinc oxide, relatively large crystallites of zinc chromite, and a thin layer of supported chromia. If the carrier is less reactive than our sintered zinc oxide, the content dependence of susceptibility of chromium will resemble much more that found in the chromia-alumina catalyst system. This is probably due to the

fact that chromia arises from the chromate ion adsorbed on the carrier but not combined with it throughout the processes of preparation, i. e. impregnation, drying, and heat treatment. The reactivity of zinc oxide depends on its state of subdivision and the degree of crystallinity as seen by comparison between our two cases. Moreover, it is expected to depend on the type and the concentration of lattice defects contained in the material because these factors govern the diffusion process by which reaction proceeds. For this reason the effect of impurity in zinc oxide must be one of the important causes which determine the structure of this catalyst system.

Summary

Chromia-zinc oxide catalysts have been prepared by the impregnation method using non-sintered and sintered zinc oxide as carriers. Measurements of magnetic susceptibility have been made for these two series of catalysts of varying composition. The values of gram susceptibility and the mean oxidation number of chromium in the samples oxidized with air at room temperature are nearly independent of the content of chromium. After oxygen-treatment at 250° or 450°C has been carried out, however, the surface oxidation becomes appreciable in the samples of low content of chromium, and the variations in the susceptibility and the mean oxidation number suggest that the dispersed structure of chromia depends on the composition of the catalyst. It appears that chromic ions are distributed in the two compounds, namely the thin layers of chromia on the catalyst surface and the relatively large crystallites of zinc chromite and, as the chromium content is decreased, the former becomes more important. By comparison between the two series examined in the present work, it is suggested that the form of the magnetic susceptibility-composition isotherm is governed by the reactivity of the carrier and the cause of the discrepancy between the results obtained by Shida et al and by us may be due to the difference between the kinds of chemical behavior of the zinc oxides employed as carrier.

The author wishes to express his hearty thanks to Professor H. Akamatu for his kind direction.

Department of Chemistry
Faculty of Science
The University of Tokyo
Hongo, Tokyo

*Irreversible Photobleaching of the Solution of Fluorescent Dyes. V. Photobleaching of Erythrosin**

By Masashi IMAMURA

(Received October 2, 1957)

In the first paper of this series[1], photobleaching of uranin (sodium fluoresceinate) and its halogenated derivatives, eosin and erythrosin, was investigated in the aqueous solutions; further studies were made on the photobleaching of eosin in alcoholic solutions in the presence of air[2] and in vacuo[3,4]. For eosin, its long-lived species (in the excited triplet state) participates in the primary acts: formation of labile complex with oxygen in the presence of air and dehydrogenation from alcohol in vacuo.

Recently, Oster and Adelman[5,6] declared that, in the photoreduction of fluorescein-type dyes with ascorbic acid, these dyes behave similarly. But the data on the effect of oxygen pressure upon the rate of photobleaching in the aqueous solution[1]

* Presented at the 10th Annual Meeting of the Chemical Society of Japan, Tokyo, April 5, 1957.

1) M. Imamura and M. Koizumi, This Bulletin, **28**, 117 (1955); M. Imamura, *J. Inst. Polytech. Osaka City Univ.*, **5C**, 85 (1956).

2) M. Imamura, This Bulletin, **30**, 249 (1957).

3) M. Imamura and M. Koizumi, ibid., **29**, 899 (1956).

4) M. Imamura and M. Koizumi, ibid., **29**, 913 (1956).

5) G. Oster and A. H. Adelman, *J. Am. Chem. Soc.*, **78**, 913 (1956).

6) A. H. Adelman and G. Oster, ibid., **78**, 3977 (1956).

suggests that, although erythrosin exhibits behavior similar to eosin, uranin is not quite similar[7]. This paper comprises a study of photobleaching reactions of erythrosin taking place in the aqueous and in the aqueous alcoholic solutions.

Experimental

Materials.—E. Merck Co. Erythrosin was used as in paper I[1]. Alcohols were purified by the usual methods[8]. Doubly distilled water was used in all mixtures.

Procedures.—The methods and the procedures were almost identical with those described previously[1,3,4]. A reaction cell was a cylindrical one to which an absorption cell (1 cm×1 cm×5 cm) was attached. Cells were made of glass. Dye concentration was determined from the absorption spectra or colorimetrically by using an interference filter or a gelatin filter of a narrow band. Absorption spectra were measured with the Beckman Spectrophotometer DU. Concentration of erythrosin used was 10^{-5} mole/l. throughout the experiments.

Analysis was made on aldehyde with Tollens' reagent and with fuchsin-sulfurous acid[9]. Changes in pH were examined spectrophotometrically by using some usual acid-base indicators. Acetone was examined either spectrophotometrically or with sodium nitroprussate[9].

Results

1. Photobleaching of Aerobic Aqueous Solutions.—All the data on the photobleaching of aerobic aqueous erythrosin solutions were reported in paper I. The quantum yields of photobleaching of erythrosin were much greater than those of eosin. For example, the quantum yield, k, was 3.7×10^{-4} for erythrosin, whereas 1.8×10^{-4} for eosin, at 20°C; the energies of activation were 5 and 6 kcal/mole, respectively.

2. Retarding Effect of Alcohols on the Aerobic Photobleaching.—As in the case of eosin[1,2], methanol, ethanol and isopropanol retarded the aerobic photobleaching of the aqueous erythrosin solutions. The absorption spectrum of erythrosin in the aqueous solution had its maximum optical density at the wavelength of 524 mμ at room temperature. By addition of alcohol to the system, the peak wavelength shifted for the longer wavelengths without appreciable change in the shape of the absorption curve. Limiting peak wavelengths in absolute alcohols were 529, 534 and 542 mμ, for methanol, ethanol and isopropanol, respectively. The rates of photobleaching of the aqueous alcoholic solutions were also expressed by the same equation as the one for eosin[3],

$$-\frac{dc}{dt}=1000\frac{k}{d}I_o(1-e^{-\alpha cd})$$

in which k is the quantum yield. The mean molar absorption coefficient, α, varies with the shift of the peak wavelength following the change in alcohol concentration, so its value was determined for each solution experimentally and/or by calculation with the same method as that described previously[4]. Quantum yields obtained at various alcohol concentrations are listed in Table I.

Table I
Quantum yields of aerobic photobleaching of the aqueous alcoholic solutions
$k\times10^4$ 27°C

Concn. of alcohols in vol. %	0	5	10	15	20	25	30	40	50
MeOH	5.0	3.8	3.1	2.3	1.9	1.3	1.1	0.6	0.4
EtOH	5.0	3.6	2.3	1.9	1.4	0.9	0.8	0.5	0.4
i-PrOH	5.0	3.5	2.3	1.6	1.1	0.7	0.4	0.3	0.3

The experimental formula which had been applied to eosin[1] held well for erythrosin in the low concentration ranges of alcohols (Fig. 1.):

$$\frac{1}{k}=\frac{1}{k^\circ}+K\frac{[RH]}{[H_2O]}$$

k° and k are the quantum yeilds for the pure aqueous solution and for the aqueous alcoholic solution, respectively. RH represents alcohol and K is a constant

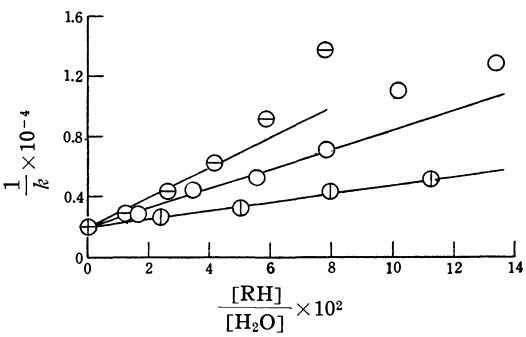

Fig. 1. Retarding effects of alcohols on the photobleaching of aerobic aqueous erythrosin solution at 27°C.
①: methanol; ○: ethanol; ⊖: *iso*-propanol.

7) To be published.
8) A. Weissberger and E. S. Proskauer, "Organic Solvents," Interscience, New York (1955).
9) F. Feigl, "Spot Tests," Vol. II, Elsevier Publ. Co. (1954).

TABLE II
VALUES OF K AND $k°K$. 27°C

	$K\times10^{-5}$	$k°K$
MeOH	0.29	15
EtOH	0.56	28
i-PrOH	0.97	49

experimentally determined. Values of K calculated from the slopes of these straight lines are tabulated in Table II.

With increasing concentration of alcohol, the rate of reaction more and more decreased, but it did not become zero even in absolute alcohol, showing a slight uniform reduction of the absorption curve after irradiation.

3. Photobleaching of the Aqueous Alcoholic Solutions in vacuo.—The rate of photobleaching of aqueous erythrosin solution, below a certain concentration of dissolved oxygen, decreased with decreasing concentration of oxygen[1], and at the complete deaeration photobleaching was not observed within the experimental errors. Addition of alcohol to the aqueous solution caused an increased rate of photobleaching in vacuo (Fig. 2). The rates of the reactions in this system were expressed also by the rate formula described above.

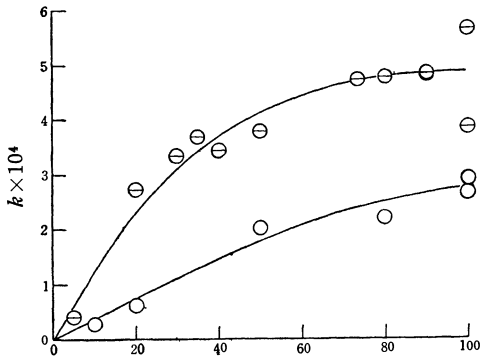

Fig. 2. Variation of the quantum yield with the alcohol concentration in vacuo at 27°C.
○: ethanol; ⊖: isopropanol.

In the case of eosin, when the alcohol concentration was relatively low, a greater part of the dye was converted into uranin by irradiation, which exhibited a strong fluorescence and had the peak wavelength at 490 mμ[4]; in absolute alcohol, however, no formation of uranin was observed[3]. In contrast with eosin, irradiated aqueous alcoholic erythrosin solutions, even at low concentration of alcohol, did not exhibit any detectable shift of the peak wavelength under the present conditions. The result seems to be very interesting at first sight, but it was found later that the formation of uranin from eosin and erythrosin (photochemical dehalogenation) is very sensitive to pH of the irradiating solutions. In the present investigation pH of the solutions was not controlled. In alkaline aqueous alcoholic solutions in vacuo, appreciable formation of uranin from erythrosin has been observed; pH-dependency of this reaction will be reported elsewhere in near future.

Apart from the peak wavelength, the solutions exhibited by irradiation slight increases in the optical densities of the absorption spectra at the wavelengths near 400 mμ, which was outside the spectral range of the incident light used. Photobleached alcoholic dye solutions, after introduction of air to the reaction cell and violent shaking for some minutes, and even after standing in the dark for several days, did not show any detectable changes in the shape of the absorption spectra in the near ultraviolet or in the visible region. Thus, it is concluded that the photobleaching of alcoholic erythrosin solution in vacuo is irreversible under these conditions.

The energy of activation of the photobleaching reaction of erythrosin in the absolute ethanolic solution was determined to be 8±1 kcal./mole, which is much larger than that for eosin (5±1 kcal/mole).

As in the case of eosin, erythrosin in alcoholic solution is believed to be photoreduced by alcohol in vacuo. Qualitative analysis of the irradiated methanolic and ethanolic solutions revealed the formation of aldehyde but not of acid. Acetone could not be detected from the irradiated *iso*-propanolic solution.

4. Influence of a Small Amount of Oxygen upon the Photobleaching of Alcoholic Solutions.—As described in sec. 2, the rate of photobleaching of erythrosin in aerobic absolute alcoholic solution was slight but detectable for each alcohol. When a very small amount of oxygen was added to the completely evacuated absolute *iso*-propanolic solution, an induction period appeared, after which the reaction proceeded at a rate equal to that of the oxygen-free system. The induction period was proportional to the amount of oxygen added. This phenomenon is similar to that observed in the case of ethanolic eosin solutions. During

this induction period, however, a slight decrease in concentration of erythrosin, which was approximately of the same degree as observed in the aerobic system, was observed. Assuming that the oxygen added was exhausted completely during the induction period, the ratio of γ (quantum yield for the photochemical disappearance of oxygen) to k (quantum yield for the photobleaching in vacuo) was obtained to be approximately 5. (3 for eosin in ethanol[3])

In the case of the absolute ethanolic solution, however, results were not reproducible. Though an induction period actually appeared, its duration was not dependent on the amount of oxygen added and the rates of photobleaching proceeded after the induction period were not always constant.

Discussion

Erythrosin is tetraiodo-uranin and a very weak fluorescer in water, while eosin is tetrabromo-derivative and a medium fluorescer: fluorescence yields are 0.02 and 0.15 in water for erythrosin and eosin, respectively[10]. From the results reported in paper I and in this paper, an analogous reaction scheme to that for eosin could be applied to erythrosin as well. This may be suppported by the works of Oster and co-workers[6,11].

Concerning the primary process in aerobic aqueous solution, it has been confirmed, for the case of eosin, that the dye participating in the process is in the long-lived excited state[1]. A similar conclusion is given also in the case of erythrosin as follows. The lifetime of the excited erythrosin attacked by oxygen was estimated in the same way as that for eosin[1] to be of the order of 10^{-7} sec., which is long enough as compared with that of the excited singlet state, 0.08×10^{-9} sec.[12]. The accuracy of the data is not sufficient for the precise value of the lifetime of the excited erythrosin to be obtained. It appears, however, that the lifetime of erythrosin is somewhat shorter than that of eosin from the data in paper I. These results are consistent with the facts that such substances as organic halogen-compounds readily transfer to the triplet levels[13] and that increasing atomic weight of the substituted atoms causes a decrease in the lifetime of the triplet state[14].

Alternative schemes for the primary process in the aerobic aqueous solutions in general were proposed in paper I: namely, $D^t+O_2\rightarrow D\cdots\cdots O_2$ (I) or $D^t+H_2O\rightarrow D\cdots\cdots H_2O$ (II); and in paper IV it was concluded that the process (I) is the correct one for eosin. It will be shown below that this is also true for erythrosin. Photobleaching of the aqueous alcoholic or the absolute alcoholic erythrosin solutions in vacuo should de due to the photoreduction of the dye by alcohol molecules, $D^t+RH\rightarrow DH\cdot+R\cdot$, hence the same equation as eq. 18 in paper IV[2] can be employed,

$$\frac{1}{k}\frac{[RH]}{[H_2O]}=\frac{1}{\varphi_{S\rightarrow T}}\frac{k_1^s}{k_2}+\frac{1}{\varphi_{S\rightarrow T}}\frac{k_2^s}{k_2}\frac{[RH]}{[H_2O]}$$ [15]

Fig. 3 illustrates a plot of $[RH]/k[H_2O]$ vs. $[RH]/[H_2O]$ for *iso*-propanolic solutions. A plot for ethanolic solutions also yielded a straight line. Values obtained from the slopes and the intercepts of the straight lines for ethanolic and *iso*-propanolic solutions are summarized in Table III.

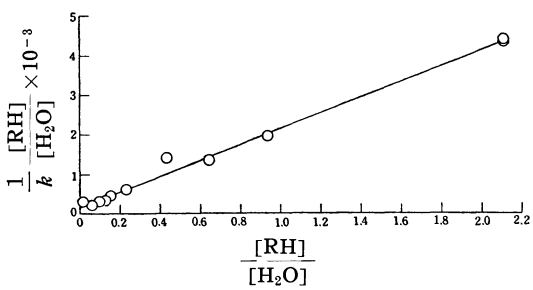

Fig. 3. The dependence of $[RH]/k[H_2O]$ upon $[RH]/[H_2O]$ for the isopropanolic erythrosin solution in vacuo at 27°C.

TABLE III
(at 27°C)

	$\varphi_{S\rightarrow T}\frac{k_2}{k_2^s}\cdot10^4$	$\varphi_{S\rightarrow T}\frac{k_2}{k_1^s}\cdot10^3$	$\frac{k_2^s}{k_1^s}$
EtOH	3	0.9	3
i-PrOH	5	6.7	13

10) P.Pringsheim, "Fluorescence and Phosphorescence." p. 316, Interscience, New York (1949).
11) J. S. Bellin and G. Oster, *J. Am. Chem. Soc.*, **79**, 2461 (1957).
12) E. Gaviola, *Z. Physik*, **42**, 853 (1927).
13) See, for example, E. J. Bowen and F. Workes, "Fluorescence of Solutions," p. 27. Longmans, Green and Co., London, (1953).
14) D. S. McClure, N. W. Blake and P. L. Hanst, *J. Chem. Phys.*, **22**, 255 (1954); D. S. McClure, ibid., **17**, 905 (1949).
15) Here, $\varphi_{S\rightarrow T}$ is the $D^*\rightarrow D^t$ transition probability, and k_1 and k_2 are the specific rates of the reactions D^t+H_2O and D^t+RH, respectively. The superscript s represents the summation of the mere deactivation and the effective process leading to the photobleaching.

On the basis of the similar arguments to those given in paper IV, the following two relations are derived from the schemes (I) and (II). If the primary process of the aerobic photobleaching follows (I),

$$\frac{k_2'^s}{k_1'^s}=k^\circ K, \text{ (eq. 15 in paper IV)}$$

and if it follows (II),

$$\frac{k_2^s}{k_1^s}=k^\circ K. \text{ (eq. 17 in paper IV)}$$

Values of $k^\circ K$ are given in Table II. Comparing these values with those of k_2^s/k_1^s in Table III, it is apparent that the differences between them are far beyond the errors, and the scheme (II) must be rejected. Thus, it can be concluded that the primary process of the photobleaching of erythrosin in the aerobic aqueous solution proceeds via the scheme (I). The values of $k^\circ K$ in Table II therefore are interpreted as those of $k_2'^s/k_1'^s$ for the process (I).

Further, from the data on the effect of oxygen pressure on the rate of the photobleaching of aqueous erythrosin solution given in paper I, the value of $k_1^s/k_{O_2}^s$ at 30°C is calculated as 8×10^{-8}, according to eq. 20 in paper IV:

$$\frac{1}{k}\frac{[O_2]}{[H_2O]}=\frac{1}{k^\circ}\frac{k_1}{k_{O_2}^s}+\frac{1}{k^\circ}\frac{[O_2]}{[H_2O]}$$

A Plot of $[O_2]/k[H_2O]$ against $[O_2]/[H_2O]$ is illustrated in Fig. 4.

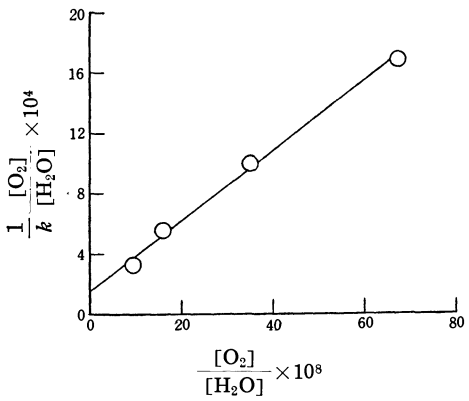

Fig. 4. The dependence of $[O_2]/k[H_2O]$ upon $[O_2]/[H_2O]$ for the aqueous erythrosin solution at 30°C.

The quantum yield, k°, for erythrosin in the aerobic aqueous solution is about twice that for eosin. In the presence of sufficient oxygen, k° is given by

$$k^\circ=\frac{k_{O_2}}{k_{O_2}^s}\frac{k_1'}{k_1'^s}$$

in which k_{O_2} and k_1' are the specific rates of the reaction between D^t and O_2 (dissolved), and between $D\cdots\cdots O_2$ and H_2O, respectively. Assuming that the rate of reaction between peroxy-dye-radical, $D\cdots\cdots O_2$, and H_2O is not so affected by the nature of dyes, k° depends mainly on $\varphi_{S\to T}(k_{O_2}/k_{O_2}^s)$. It seems probable to assume, therefore, that an increase in k° of erythrosin is due to the increases both in $\varphi_{S\to T}$ and in $k_{O_2}/k_{O_2}^s$. On the other hand, values of $\varphi_{S\to T}(k_2/k_2^s)$, $\varphi_{S\to T}(k_2^s/k_1)$ and k_2^s/k_1^s exhibit appreciable differences between eosin and erythrosin, while the values of $k_2'^s/k_1'^s(=k^\circ K)$ are nearly the same for both. It is concluded, therefore, that the reactivity of D^t towards alcohols is relatively smaller for erythrosin than for eosin.

Irregular results observed for the ethanolic erythrosin solutions in the presence of a small amount of oxygen may perhaps be related to the smaller reactivity of this dye towards ethanol. It is seen, from Table III, that *iso*-propanol is more photo-oxidizable than ethanol[16], and a clear-cut result was obtained for this solution.

Summary

Photobleaching of the aqueous alcoholic erythrosin solutions in air and in vacuo was investigated. In general, erythrosin showed behavior similar to eosin. An excited dye molecule which participates in the primary processes is the long-lived species, having a lifetime of the order of 10^{-7} sec. It was concluded that the primary process in aerobic aqueous erythrosin solution proceeds via the process, $D^t+O_2\to D\cdots\cdots O_2$, as in the case of eosin. It was found that excited erythrosin is somewhat more reactive than excited eosin towards dissolved oxygen, while it is less reactive towards alcohols in vacuo. Some quantitative values on the reactivities were given.

The author wishes to express his appreciation to Professor M. Koizumi of the Tohoku University for his support of this work and criticism of this paper.

Institute of Polytechnics,
Osaka City University,
Kita-ku, Osaka

16) It is probably true that $\varphi_{S\to T}$ in ethanol is not so different from that in *iso*-propanol.

The Infrared Spectra of Methylhydropolysiloxanes

By Minoru SAKIYAMA

(Received July 11, 1957)

Infrared spectra of methylpolysiloxanes were studied by Wright and Hunter[1] and their conclusions were ascertained by Richards and Thompson[2]. There are characteristic absorption bands common to all the methylpolysiloxanes at 1260 cm^{-1} (CH_3—Si) and 1000—1100 cm^{-1} (Si—O—Si), and the characteristic bands associated with the structural units were found as follows;

Unit	Absorption Band (cm^{-1})
$(CH_3)_3SiO_{1/2}$	841, 754—6
$(CH_3)_2SiO_{2/2}$	800—14
$CH_3SiO_{3/2}$	800

From these, one can conclude that the assignment of the group frequency to the siloxane unit is satisfactory.

It is interesting to study methylhydropolysiloxanes having hydrogen atoms attached directly to silicon atoms. Recently, methylhydropolysiloxanes[3] involving the units, $H(CH_3)_2SiO_{1/2}$ and $H(CH_3)SiO_{2/2}$, were synthesized. In this paper, the infrared spectra of these compounds will be described and especially it is intended to determine whether the group frequency can be assigned or not to these units.

The following short hand notation will be used to indicate the various polysiloxanes.

Notation	Unit
M'	$H(CH_3)_2SiO_{1/2}$
M	$(CH_3)_3SiO_{1/2}$
D'	$H(CH_3)SiO_{2/2}$
D	$(CH_3)_2SiO_{2/2}$
T	$CH_3SiO_{3/2}$
Q	$SiO_{4/2}$

Experimental

Materials.—The compounds used in this experiment were as follows:

Linear polysiloxanes;

$\mathbf{M'D'_nM'}$	$n=0,1,2,3$
$\mathbf{MD'_nM}$	$n=1,2,3,4,5$
$\mathbf{M'D_nM'}$	$n=1,2$
M'D'DM', MM'	

cyclic polysiloxanes;

$\mathbf{D'_n}$	$n=4,5,6$
$\mathbf{D'_nD_{4-n}}$	$n=1,2,3$

branched polysiloxane;

$\mathbf{M'_3T}$

Measurements.—Spectra were obtained with a Hilger H-800 infrared spectrophotometer with a rock salt prism. Samples were observed as solutions, 2~5% solution in carbon disulfide being used in the range 700 to 1500 cm^{-1} and 3~5% in carbon tetrachloride from 1250 to 5000 cm^{-1}. Pure liquid was also used. No appreciable difference was observed between both cases. The cells were 0.03 mm. thick for solution and less than 0.01 mm. for pure liquid. In order to compare relative intensities approximately, the spectra of the compounds belonging to the same series (such as $\mathbf{M'D'_nM'}$, $n=0-3$) were recorded on a same chart, keeping the conditions as similar as possible. **M'**$_2$, **M'D'M'**, $\mathbf{M'D'_2M'}$, $\mathbf{M'D'_3M'}$ and **M'D'DM'** were measured also with a Perkin-Elmer Model 21 spectrophotometer with a calcium fluoride prism in the range 1500 to 3300 cm^{-1}. The cells were 0.026 and 0.109 mm. thick and the concentration of the solution was 3% in carbon tetrachloride. The spectra and the position of the absorption bands are presented in Fig. 1 and Table I~III respectively.

TABLE I

METHYLHYDROPOLYSILOXANES: POSITIONS OF BANDS (in cm^{-1})

$\mathbf{D'_n}$			$\mathbf{D'_nD_{4-n}}$		
$n=4$	5	6	$\mathbf{D'D_3}$	$\mathbf{D'_2D_2}$	$\mathbf{D'_3D}$
771	769	767	751	755	761
			801	798	795
			818	826	831
880	874	870		867	858
	893	892			884
917	916	919	906	905	903
1085	1086	1082	1070	1078	1081
1258	1258	1258	1256	1256	1258
			1397	1395	1399
1405	1409	1409	1407	1408	1410
2162	2159	2162	2148	2158	2170
2991	2987	2991	2990	2985	2991

1) N. Wright and M. J. Hunter, *J. Am. Chem. Soc.*, **69**, 803 (1947).
2) R. E. Richards and H. W. Thompson, *J. Chem. Soc.*, **1949**, 124.
3) R. Okawara and M. Sakiyama, This Bulletin, **29**, 236, 547 (1956); R. Okawara, U. Takahashi and M. Sakiyama, ibid., **30**, 608 (1957).

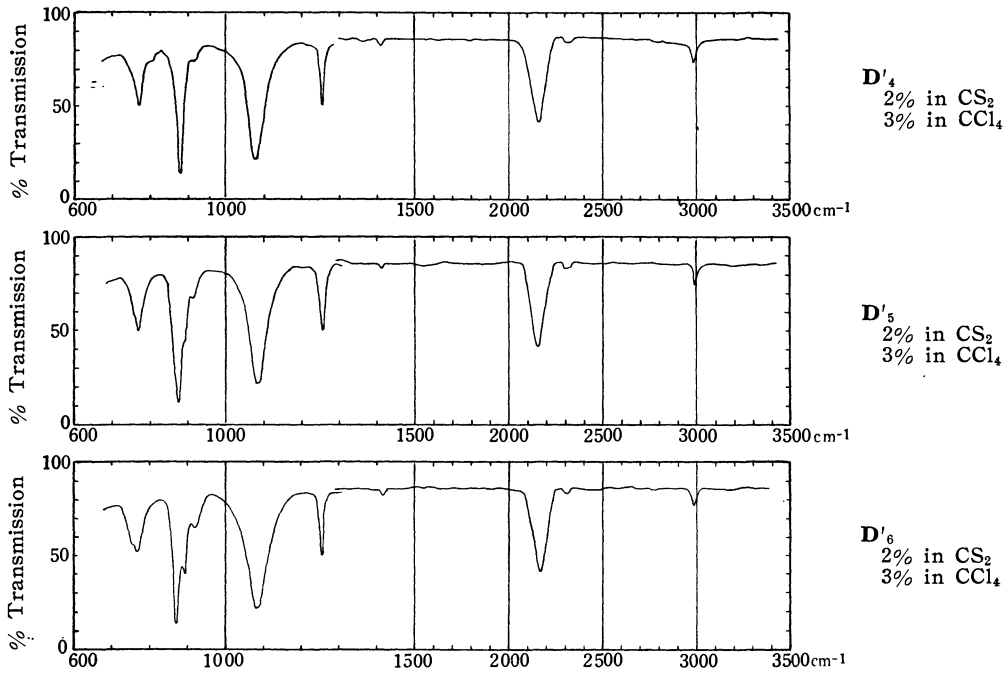
% Transmission
100
50
0
600
1000
1500
2000
2500
3000
3500cm-1
D'4
2% in CS2
3% in CCl4
D'5
2% in CS2
3% in CCl4
D'6
2% in CS2
3% in CCl4

Fig. 1 (1).

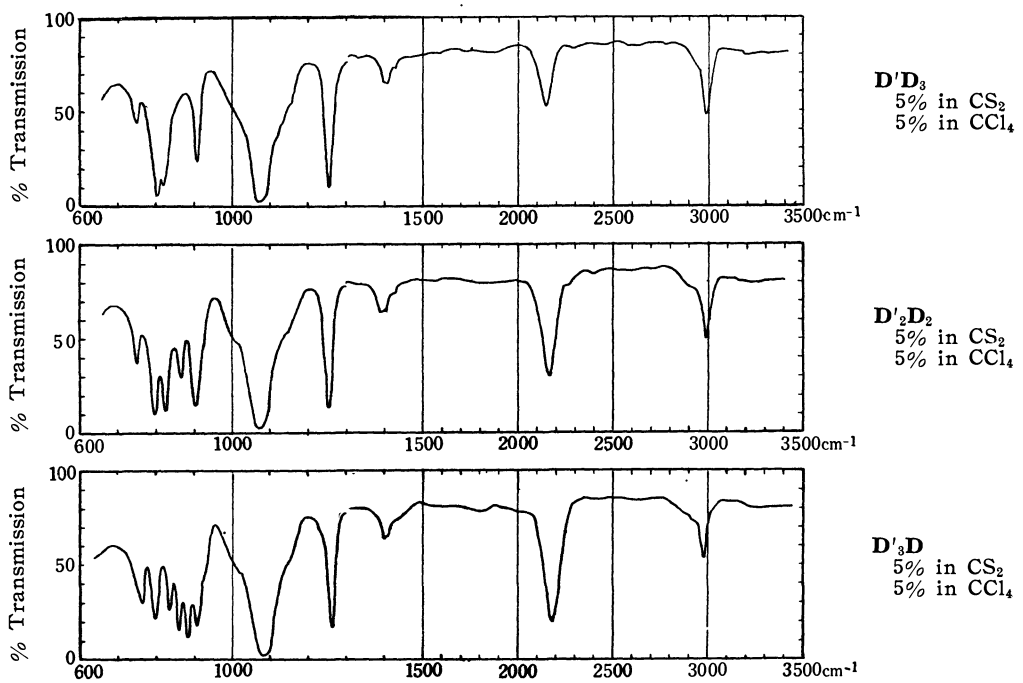
% Transmission
100
50
0
600
1000
1500
2000
2500
3000
3500cm-1
D'D3
5% in CS2
5% in CCl4
D'2D2
5% in CS2
5% in CCl4
D'3D
5% in CS2
5% in CCl4

Fig. 1 (2).

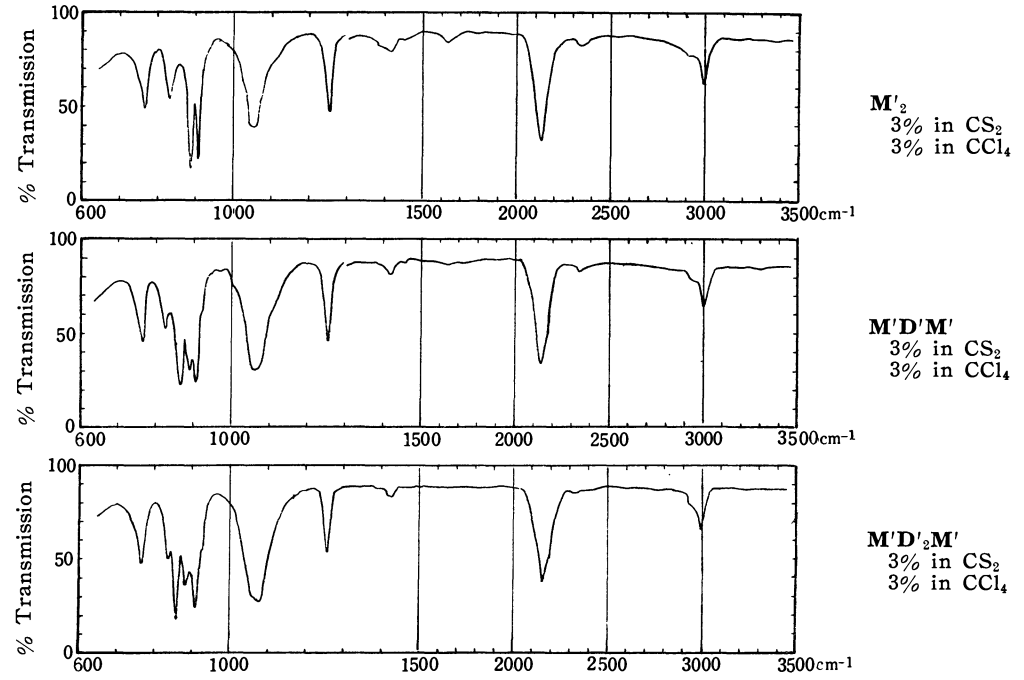
% Transmission
100
50
0
600
1000
1500
2000
2500
3000
3500cm-1
M'2
3% in CS2
3% in CCl4
M'D'M'
3% in CS2
3% in CCl4
M'D'2M'
3% in CS2
3% in CCl4

Fig. 1 (3).

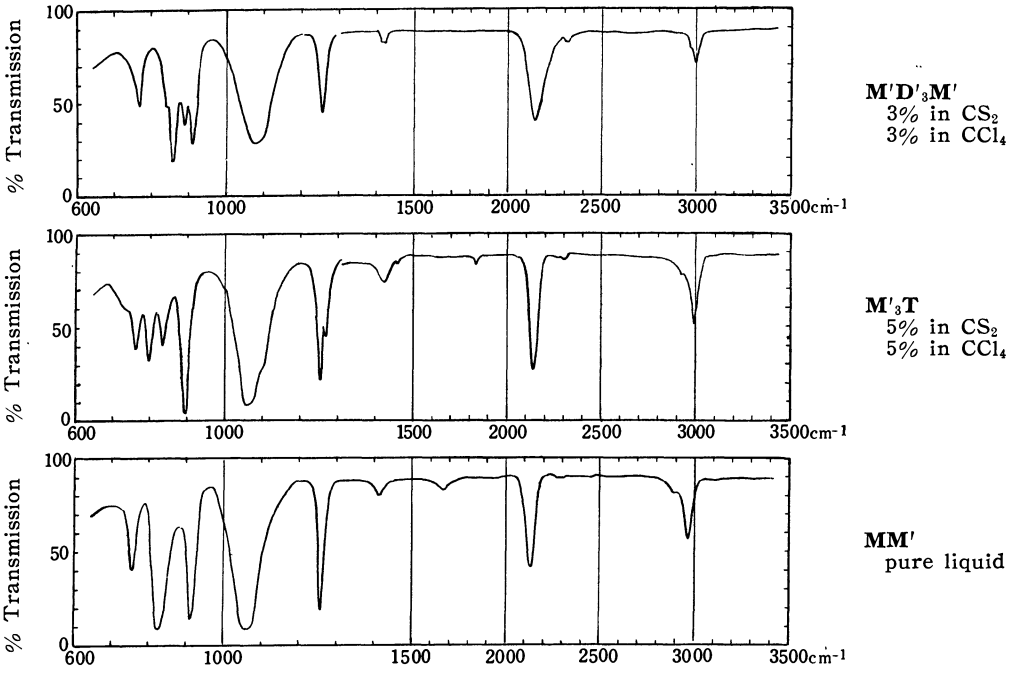
% Transmission
100
50
0
600
1000
1500
2000
2500
3000
3500cm-1
M'D'3M'
3% in CS2
3% in CCl4
M'3T
5% in CS2
5% in CCl4
MM'
pure liquid

Fig. 1 (4).

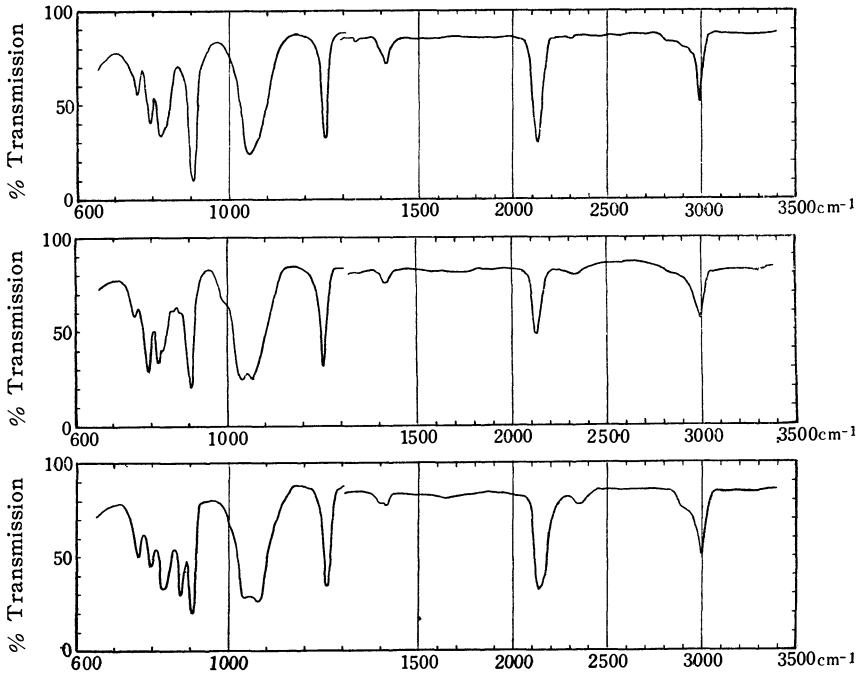
% Transmission
100
50
0
600
1000
1500
2000
2500
3000
3500cm-1
M'DM'
4% in CS2
3% in CCl4
M'D2M'
4% in CS2
3% in CCl4
M'D'DM'
4% in CS2
3% in CCl4

Fig. 1 (5).

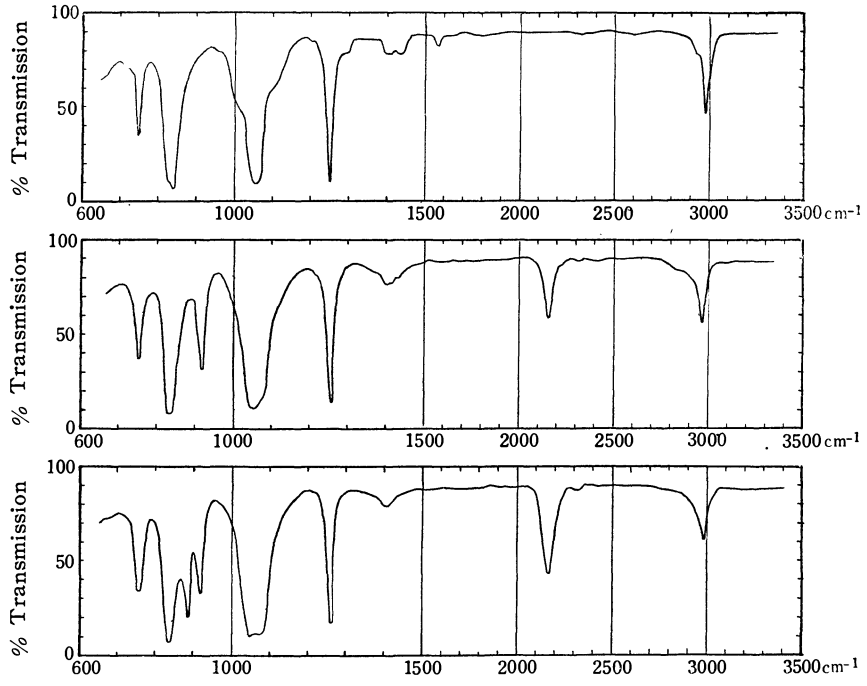
% Transmission
100
50
0
600
1000
1500
2000
2500
3000
3500cm-1
M2
pure liquid
MD'M
pure liquid
MD'2M
pure liquid

Fig. 1 (6).

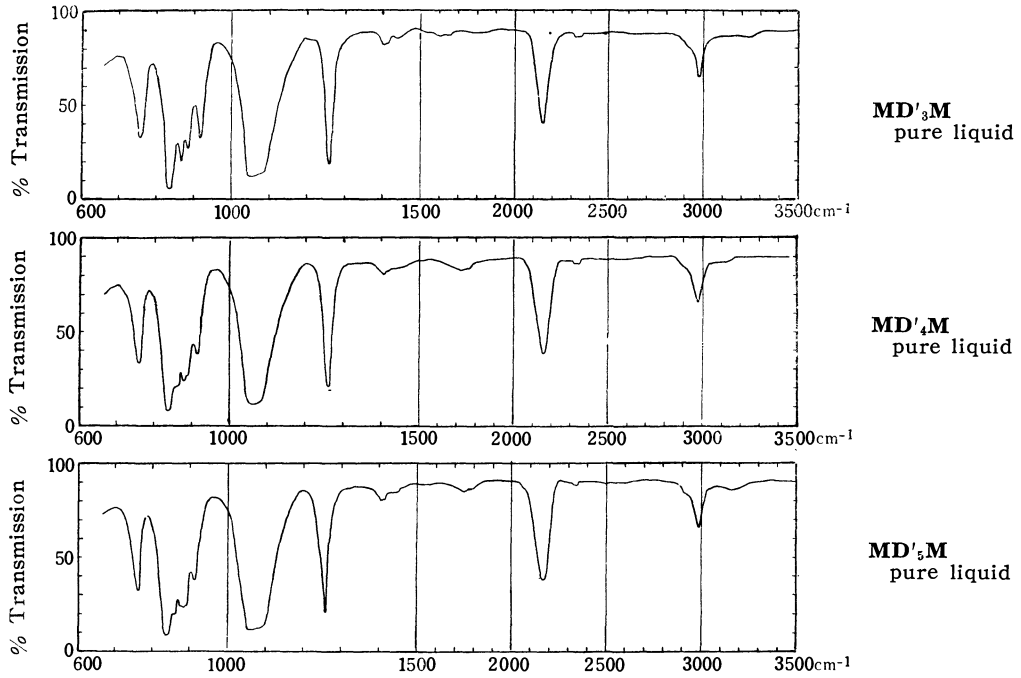

Fig. 1 (7). The infrared spectra of methylhydropolysiloxanes.

TABLE II

METHYLHYDROPOLYSILOXANES: POSITIONS OF BANDS (in cm^{-1})

	M'D'$_n$M'					M'D$_n$M'		
$n=0$	1	2	3	MM'	M'$_3$T	M'DM'	M'D$_2$M'	M'D'DM'
763	764	763	765	755	763	760	759	761
						794	792	791
					798			
832	824	833	834	834	830	820	820	826
	861	856	854					874
878	885	881	884					
906	902	905	907	904	899	906	901	904
1055	1063	1072	1074	1054	1059	1055	1037	1045
							1070	1075
1252	1255	1253	1254	1258	1253	1254	1254	1256
					1262			
1416	1413	1413	1413	1414	1419	1412	1405	1406
2129	2136	2137	2140	2114	2132	2130	2126	2134
	2169	2169	2169					
2931	2931	2920	2922	2912	2924	2920	2924	2905
2990	2993	2988	2988	2968	3004	2983	2983	2983

Discussion of the Results

Si—H Vibration.—The most remarkable difference between the spectra of dimethylpolysiloxanes[1,2] and those discussed in this study, is that a strong band in the 2100 cm^{-1} region is present only in the latter. This band is characteristic of the organosilicon compounds containing an Si—H bond, and has been assigned to the stretching vibration involving an Si—H bond[4]. In this case also, it will be attributable to that vibration because all the compounds contain this bond.

Two kinds of methylhydrosiloxy unit, one chain-forming **D'** unit and the other chain-terminating unit **M'**, are involved in the compounds studied. It is of interest to study whether the position of this band

4) For example, (a): 2135 cm^{-1} in $(C_6H_5)_3SiH$ and 2108 cm^{-1} in $(n\text{-}C_3H_7)_3SiH$ (L. Kaplan, *J. Am. Chem. Soc.*, **76**, 5880 (1954)) and (b): 2258 cm^{-1} in $HSiCl_3$ (J. G. Gibian and D. S. McKinney, ibid., **73**, 1431 (1951)).

TABLE III
METHYLHYDROPOLYSILOXANES: POSITIONS OF BANDS (in cm^{-1})

MD'_nM					
$n=0$*	1	2	3	4	5
749	751	762	762	762	762
826	834	834	834	834	834
840			867	860	858
		879	886	878	875
				890	891
	914	913	913	912	912
1055	1052	1046	1046	1050	1052
1252	1258	1258	1258	1258	1258
1405	1404	1402	1405	1407	1407
	2149	2154	2159	2159	2159
2927	2915	2914	2918	2918	2918
2978	2965	2978	2978	2978	2978

* This spectrum was measured for comparison.

varies in these two units. In M'_2 and D'_4, involving only one kind of unit, this band is found at 2129 cm^{-1} in the former and 2162 cm^{-1} in the latter. But in the compounds having both units, this band is not likely to have two peaks. For example, the relation of the bands of **M'D'M'** and **M'D'$_3$M'** with that of M'_2 is illustrated in Fig. 2.

A similar broadening of the band is also observed in **M'D'$_2$M'**, and **M'D'DM'**. This band was not separated into two peaks although the spectra were abtained with a spectrophotometer with a calcium fluoride prism. The position of this band shifts to the side of less wave number

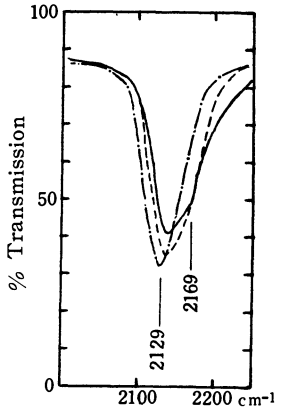

Fig. 2. Si—H stretching vibration bands of **M'D'$_n$M'**
—·—·— M'_2 -------- **M'D'M'**
——— **M'D'$_3$M'**
In **M'D'M'** and **M'D'$_3$M'**, a weak band, which is absent in M'_2 is observed at 2169 cm^{-1}.

when the units, **M**, **D** and **T** are introduced in a molecule. This relation is generally seen. For example, in the series **M'D$_n$M'**, **D'$_n$D$_{4-n}$** and **MD'$_n$M**, in which Si—H content varies systematically along the series, not only the intensity but also the position of this band changes regularly.

Below 1000 cm^{-1}, a common band to all the compounds is observed at 760 cm^{-1}. Of course, **M** may give rise to a band in the same position in **MD'$_n$M** and **MM'**. This band, though more tentative than in the case of the band described above, seems to be able to be assigned to the bending vibration involving an Si—H bond as was suggested by Ulbrich[5] with the Raman spectra of D'_4 and D'_5. The position seems to be the same in both **M'** and **D'** units.

This assignment is consistent with the following facts once studied by other authres: (1) Trisubstituted silanes, $HSiCl_3$[4b] (IR), $HSiBr_3$[6] (Raman) and $(C_6H_5)_3SiH$[4a] (IR) give rise to this band at 798, 767 and 805 cm^{-1} respectively. (2) $H(CH_3)SiCl_2$[5], which gives **D'$_n$** by hydrolysis, has two bands at 753 and 805 cm^{-1} in this region, of which only the former is kept in **D$_n$'**, while its position attributable to such a vibration will not be expected to vary after hydrolysis. (3) In the series **D$_n$'D$_{4-n}$** and **M'D$_n$M'**, a similar relation is observed for the position and the intensity as was observed in the case of Si—H stretching band when **D'** is replaced by **D**, i.e., both intensity and wave number decrease as n increases.

C—H Vibration.—In the region 2900—3000 cm^{-1}, all the compounds show the bands associated with the stretching vibration of C—H linkage. These bands consist of two bands near 2920 and 2980 cm^{-1}. The former is weaker than the latter and may be a combination or overtone band. The latter is also weak as shown in the case of methylpolysiloxane[1]. It is interesting to compare this intensity with that of Si—H stretching vibration bands.

The band near 1410 cm^{-1} will be attributed to the methyl deformation vibration. To a sharp intense band near 1260 cm^{-1} some different assignments have been made. The workers[1] who studied methylpolysiloxanes attributed them to the methyl rocking vibration and others who studied tetramethylsilane to the sym-

5) R. Ulbrich, *Z. Naturforsch.*, **9B**, 380 (1954).
6) J. M. Delfosse and R. G. Ghoovaerts, *Bull. Berg.*, **21**, 410 (1935): F. Francois and H. Buisset, *Compt. rend.*, **230**, 1946 (1950).

metrical deformation mode[7] or γ-(CH) vibration[8] of the methyl group. In this study, it is impossible to determine the assignment of this band, but it has become clearer that this band is related to the CH_3-(Si) group since this band is observed in all the compounds. In a branched polysiloxane $\mathbf{M'_3T}$, this band has two peaks at 1253 and 1262 cm^{-1} and the former is more intense than the latter as was reported[1] in $\mathbf{M_3T}$ and $\mathbf{M_4Q}$.

Si—O Vibration.—The strong absorption band in the region 1000—1100 cm^{-1} is probably associated with Si—O linkage. This band occurs in the range 1070—1085 cm^{-1} in the cyclic compounds, 1045—1060 cm^{-1} in the linear and the branched compounds. In $\mathbf{M'DM'}$, $\mathbf{M'D'DM'}$ and $\mathbf{M'D_2M'}$, this band consists of two peaks.

Characteristic Bands below 1000 cm^{-1}. All the bands which have been assigned to **M**, **D** and **T** in the study of methylpolysiloxanes are found without exception also in the spectra of methylhydropolysiloxanes containing these units. In $\mathbf{D'_nD_{4-n}}$, the intensity of 800 cm^{-1} band of **D** clearly increases as is expected from the increasing group concentration, but the wave number is less than those which were reported and decreases as **D** is replaced by **D'**. At least, within the limits of this study, it may be said that the conclusion of Wright and Richards are confirmed.

There are three bands at 906, 878 and 832 cm^{-1} in $\mathbf{M'_2}$. They are observed also in the other members of $\mathbf{M'D'_nM'}$ and their intensities clearly decrease when n increases. In the compounds having both **M'** and other units (**M**, **D** or **T**), i.e., **MM'**, $\mathbf{M'D_nM'}$, $\mathbf{M'D'DM'}$ and $\mathbf{M'_3T}$, only one band is found instead of the former two bands. Therefore it may probably be considered that one or two bands in the range 870—910 cm^{-1} are characteristic of the unit **M'**. The 832 cm^{-1} band is found at the same position also in other compounds but in **MM'** this band may overlap with the **M** band at 841 cm^{-1}.

A new band occurs at 861 cm^{-1} in $\mathbf{M'D'M'}$, which is absent in $\mathbf{M'_2}$. This band is caused by the introduction of **D'** unit and moves to the side of lower wave number as the group concentration increases in $\mathbf{M'D_n'M'}$. This band is found at 874 cm^{-1} in $\mathbf{M'D'DM'}$. In $\mathbf{MD'_nM}$, the greater the n, the more complex the spectra. All the members of this series ($n \geq 1$) have a band at 914 cm^{-1}. Except this band, $\mathbf{MD'_2M}$ has one band, $\mathbf{M'D'_3M}$ has two bands in this region, and so on. The number of bands in this region seems to increase.

A similar complexity is found also in $\mathbf{D'_nD_{4-n}}$. Wright et al.[1] found that $\mathbf{D_4}$ has two bands at 862(strong) and 880 cm^{-1} (weak). In $\mathbf{D'_nD_{4-n}}$, a common band is found at 900 cm^{-1}. Except this band, $\mathbf{D'D_3}$ has a band at 818 cm^{-1}, $\mathbf{D'_2D_2}$ has two bands at 827 and 867 cm^{-1} and $\mathbf{D'_3D}$ has three bands at 831, 858 and 884 cm^{-1}. On the other hand $\mathbf{D'_4}$ has only one band in this region. It is necessary to point out that $\mathbf{D'_2D_2}$ may be a mixture of two isomers, $\mathbf{|\text{-}DDD'D'\text{-}|}$ and $\mathbf{|\text{-}DD'DD'\text{-}|}$. In spite of this, the complexity of the spectra of the compound containing **D'** unit, either linear or cyclic, shows that this unit is less independent than other units and the group frequency treatment must be disclaimed with this unit.

Summary

1) Infrared spectra of some methylhydropolysiloxanes involving the units, $H(CH_3)_2SiO_{1/2}$ and $H(CH_3)SiO_{2/2}$, were studied. The assignments of Wright and Richards with methylpolysiloxanes were comfirmed in this study.

2) The stretching and the bending band involving an Si—H bond are found in the range 2120—2170 cm^{-1} and 760 cm^{-1}, respectively.

3) Characteristic absorption bands of the unit $H(CH_3)_2SiO_{1/2}$ are observed near 900 cm^{-1} and 830 cm^{-1}, while the unit $H(CH_3)SiO_{2/2}$ does not give the characteristic band and the band related with this unit is different in each compound.

The author wishes to express his sincere thanks to Dr. R. Okawara for encouragement and numerous suggestions throughout this investigation.

Department of Applied Chemistry
Faculty of Engineering
Osaka University
Miyakojima-ku, Osaka

7) C. W. Young, J. S. Koehler and D. S. McKinney, *J. Am. Chem. Soc.*, **69**, 1910 (1947).
8) D. H. Rank, B. D. Saksena and E. R. Shull, *Discuss. Farad. Soc.*, **9**, 187 (1950).

*Stability of Cobalt(III) and Chromium(III) Ammine Complexes in a Strongly Alkaline Solution**

By Hayami YONEDA

(Received June 4, 1957)

It is well known that cobalt(III) and chromium(III) ammine complexes are very stable in an acid solution, whereas they decompose more or less rapidly in an alkaline solution to free ammonia and precipitate metal hydroxides. On the other hand, ammine complexes of bivalent transition metal ions, such as zinc, copper(II), nickel and cobalt(II), can remain in solution only in the presence of an excess of ammonia and ammonium salts. The complexes of the latter type are not sensitive to a slight addition of alkali, but decompose instantaneously on addition of acid. Such a marked difference in the chemical behavior may be naturally attributable to the difference in the degree of covalency of the coordination bond. In the ammine complexes of the latter type, the metal-nitrogen bonding is due largely to the ion-dipole attraction, and the ligand can be exchanged constantly with the outer ammonia or water molecule. For cobalt (III) and chromium(III) ammine complexes, the exchange of a ligand with the outer water molecule is presumed to be difficult, since the coordination bonds involved in these complexes are highly covalent. However, any investigation on the decomposition of these cobalt(III) and chromium(III) ammine complexes in an alkaline solution has hardly ever been reported. In the present investigation, the rate of decomposition of cobalt(III) and chromium(III) hexammine and monoaquopentammine complexes was measured in a concentrated solution of sodium hydroxide. At the same time, infrared absorption spectra of these complexes were measured. From these results, the stability of the complexes has been discussed.

Experimental

Determination of the rate of decomposition.—The complexes used in the measurement were hexammine cobalt(III) chloride $[Co(NH_3)_6]Cl_3$ (I), monoaquopentammine cobalt (III) perchlorate $[Co(NH_3)_5H_2O](ClO_4)_3$ (II), hexaammine chromium(III) chloride $[Cr(NH_3)_6]Cl_3$ (III) and monoaquopentammine chromium(III) perchlorate $[Cr(NH_3)_5H_2O](ClO_4)_3$ (IV). The rate of decomposition of these complexes was measured in 1 M sodium hydroxide** at various temperatures. The initial concentration of the complex was 0.01 M in all of the measurements. The alkaline solution of the complex for the determination of the rate of decomposition was prepared as follows. Equal volumes of 0.02 M solution of the complexes and 2 M solution of sodium hydroxide, which were separately heated to a given temperature, were mixed together. This was carried out in several brown test-tubes having a stopper, which were dipped in a thermostat. At an appropriate time interval, the content of each test-tube was poured into another tube which was dipped in an ice-bath, and quickly cooled. Then the cooled reaction mixture was filtered to remove the precipitate of the metal hydroxide. To prevent further decomposition, 5 cc of the transparent solution thus obtained was poured into another tube containing 2 cc. of 6 N acid. The opitical densities of solutions thus obtained were measured. By comparing them with the optical densities of the standared solution, the concentrations of the complex were determined. A Beckman DU spectrophotometer was used for measurements of optical densities.

Infrared absorption spectra.—Infrared absorption spectra of I, II, III and IV in Nujol mulls were determined with a Perkin-Elmer Model 21 recording spectrophotometer using a sodium chloride prism.

Results

The measurements of optical densities were carried out at several wavelengths near the maximum of the first absorption band of the complex concerned. In every case, no shift of the absorption maximum was observed. This suggests almost conclusively that series of reacting solutions were composed of the initial complexes. The change in the relative concentration of the complex, which was determined

* This is Part III of "Stabilities of Metal Ammine Complexes."

** With a high concentration of alkali and a low concentration of the ammine complex, the ionic strength of the reacting solution is kept practically constant during the whole process; besides, the decomposition of the complex is approximately of the first order with respect to the complex.

from the observed opitcal densities is shown in Figs. 1~4. From the analysis of these curves the decomposition of the complex was found to be a practically first-order reaction. Accordingly the activation energy of the decomposition could be obtained from the rate constants at various temperatures, which were calculated from the half-lives (See Fig. 5.).

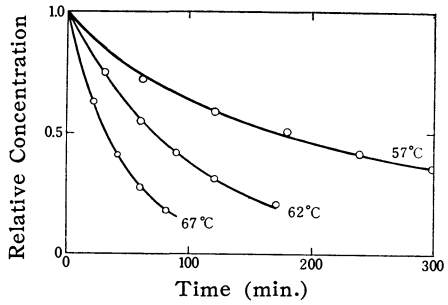

Fig. 1. Decomposition of $[Co(NH_3)_6]Cl_3$ in 1N NaOH.

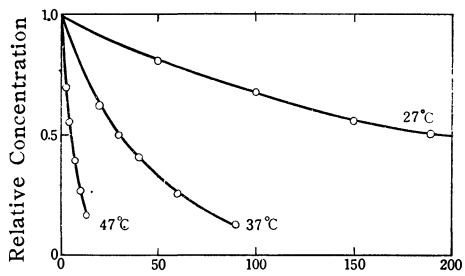

Fig. 2. Decomposition of $[Co(NH_3)_5H_2O](ClO_4)_3$ in 1N NaOH.

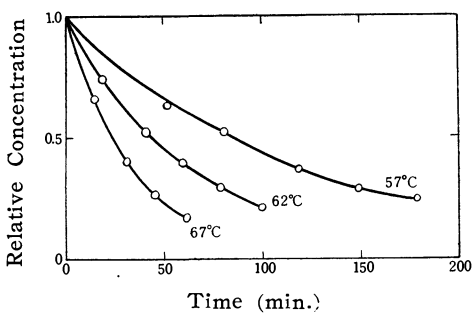

Fig. 3. Decomposition of $[Cr(NH_3)_6]Cl_3$ in 1N NaOH.

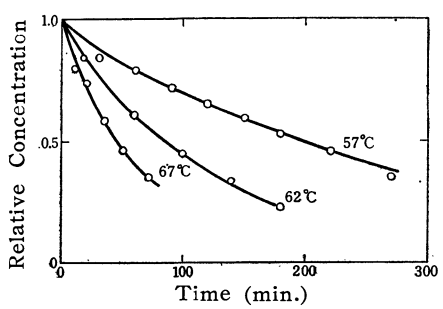

Fig. 4. Decomposition of $[Cr(NH_3)H_2O](ClO_4)_3$ in 1N NaOH.

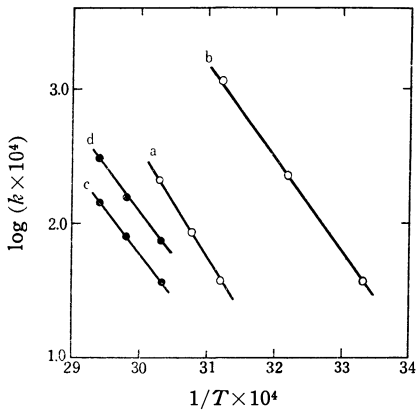

Fig. 5. Determination of the activation energy for the decomposition of cobalt (III) and chromium(III) ammine complexes from plots of $\log k$ against $1/T$.
a) $\log k$ for $[Co(NH_3)_6]Cl_3$
b) $\log k$ for $[Co(NH_3)_5H_2O](ClO_4)_3$
c) $\log k$ for $[Cr(NH_3)_6]Cl_3$
d) $\log k$ for $[Cr(NH_3)_5H_2O](ClO_4)_3$

TABLE I
ACTIVATION ENERGIES OF DECOMPOSITION

$[Co(NH_3)_6]^{3+}$	36 Kcal. mol^{-1}
$[Co(NH_3)_5H_2O]^{3+}$	32 Kcal. mol^{-1}
$[Cr(NH_3)_6]^{3+}$	31 Kcal. mol^{-1}
$[Cr(NH_3)_5H_2O]^{3+}$	31 Kcal. mol^{-1}

Absorption bands, which are regarded as being due to the rocking vibration of ammonia within the complex[1] are shown in Fig. 5. As the hexammine and the monoaquopentammine perchlorates of cobalt (III) and chromium(III) are all isomorphous, we can compare the strengths of the metal-ammonia bonds in these compounds by comparing the frequencies of the rocking vibrations of the coordinated ammonia. As the aquopentammine complex changes into the hydroxopentammine complex in a basic medium, it is more desirable that the strength of the metal-ammonia bond of the hexammine is compared with that of hydroxopentammine. However, as the infrared absorption spectrum is influenced markedly by the change of the symmetry of the crystal structure, the aquopentammine complex was chosen for comparison.

1) S. Mizushima, I. Nakagawa and J. V. Quagliano, *J. Chem. Phys.*, **23**, 1367 (1955).

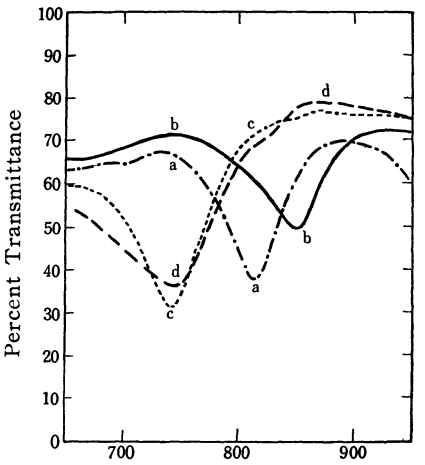

Fig. 6. Infrared absorption spectra of
a) $[Co(NH_3)_6](ClO_4)_3$
b) $[Co(NH_3)_5H_2O](ClO_4)_3$
c) $[Cr(NH_3)_6](ClO_4)_3$
d) $[Cr(NH_3)_5H_2O](ClO_4)_3$

TABLE II
FREQUENCIES OF THE ROCKING VARIATIONS OF THE COORDINATED AMMONIA

$[Co(NH_3)_6](ClO_4)_3$	815 cm^{-1}
$[Co(NH_3)_5H_2O](ClO_4)_3$	853 cm^{-1}
$[Cr(NH_3)_6](ClO_4)_3$	744 cm^{-1}
$[Cr(NH_3)_5H_2O](ClO_4)_3$	747 cm^{-1}

As is easily seen from Table II, the rocking vibration of the coodinated ammonia appears in the shorter wavelength in the cobalt(III) ammine complex than in the chromium(III) ammine complex. This means that the metal-ammonia bond is stronger in the cobalt(III) complex than in the chromium(III) complex. In addition, ammonia in the cobalt(III) pentammine complex combines with the metal ion more firmly than in the hexammine complex. In the chromium(III) complex, a very slight tendency of this kind can be observed. In the chromium(III) complex, the replacement of ammonia with water hardly has any noticeably influence on the other coodination bonds within the complex.

Discussion

From the data of the infrared absorption spectra it was concluded that for the cobalt(III) complexes the metal-ammonia bond is stronger in the pentammine complex than in the hexammine complex. This tendency is observed in the chromium(III) ammine complexes too, although it appears to be much less marked. This tendency can be inferred from the data of the consecutive formation constants of various metal ammine complexes. A part of the data is shown in Table III.

TABLE III
CONSECUTIVE FORMATION CONSTANTS OF THREE HEXAMMINE COMPLEXS[2]

	$\log k_1$	$\log k_2$	$\log k_3$	$\log k_4$	$\log k_5$	$\log k_6$	$\log\left(\frac{k_5}{k_6}\right)$
Ni^{2+}	2.80	2.24	1.78	1.19	0.75	0.03	0.72
Co^{2+}	2.11	1.63	1.05	0.76	0.18	−0.62	0.80
Co^{3+}	7.3	6.7	6.1	5.6	5.5	4.41	0.64

In this table, the values of $\log(k_5/k_6)_{obs.}$ are calculated to be 0.72, 0.80 and 0.64 for nickel(II), cobalt(II) and cobalt(III) ammine complexes respectively. On the other hand, when we take a special case, where the strength of the metal-ammonia bond and the state of aquation of the complex in a solution are almost identical among hexammine, pentammine, tetrammine etc., there is a statistical effect which prevents the successive formation constants from being equal. This was suggested previously by Wegscheider[3] and Adams[4], who gave the following expression;

$$\frac{k_n}{k_{n-1}} = \binom{n-1}{n}\binom{N-n+1}{N-n}$$

where n represents the number of the ligands already attached, except water and N is the coordination number of the complex, and k_n and k_{n+1} are the consecutive formation constants. Thus $\log(k_5/k_6)_{stat.} = 0.38$ is obtained. This value is smaller than any value of $\log(k_5/k_6)_{obs.}$ already described. This indicates that in the actual complex the metal-ammonia bond is stronger in the pentammine complex than in the hexammine complex. In fact, Bjerrum compared $\log(k_n/k_{n+1})_{obs.}$ with $\log(k_n/k_{n+1})_{stat.}$ in various complexes and concluded that the ligand of the complex $[M(ligand)_n(H_2O)_{N-n}]$ is linked to the metal ion more firmly than that of the complex $[M(ligand)_{n+1}(H_2O)_{N-n-1}]$.

Thus, both the data of the infrared absorption spectra and those of the consecutive formation constants suggest that the metal-ammonia bond is stronger in the pentammine complex than in the hexammine complex.

2) J. Bjerrum, "Metal Ammine Formation in Aqueous Solution," P. Haase and Son, Copenhagen (1941), p. 188, 285.
3) Wegscheider, *Monatsh.*, **16**, 75 (1895).
4) Adams, *J. Am. Chem. Soc.*, **33**, 1503 (1916).

In connection with this fact, let us consider the stabilities of I and II in an alkaline solution. The experimental result indicates that II decomposes easily than I. This fact suggests that the decomposition of the cobalt(III) ammine complex in an alkaline solution is not a mere substitution of the coordinated ammonia by hydroxyl ion. As suggested by the fact that ammonia situates ahead of water and hydroxyl ion in the spectrochemical series[5], it is presumed that ammonia combines more firmly with the central cobalt(III) ion than water or hydroxyl ion does.

Therefore, so long as the coordinated ammonia molecule keeps its original form NH_3, it is difficult to think that the ammonia might be expelled from the coordination sphere. This is borne out by the remarkably great stability of the cobalt (III) ammine complex in an acid solution. However, the situation is quite different in an alkaline solution. Here, let us recall the institability of hexahydroxylamine cobalt(III) complex discussed in the previous paper[6]. In this case, both the first and the second absorption band of the complex lie much farther in the shorter wavelength than those of other hexammine cobalt(III) complexes, and a much stronger metal-amine bond is suggested. Nevertheless, this complex is very unstable in an aqueous solution and decomposes fairly rapidly. We attributed this to the proton dissociation of the ligand. That is, a very strong bonding between the metal and nitrogen atoms induces the relaxation of the N–H bond in the ligand, and facilitates the proton dissociation of the ligand. The amide group thus produced combines with the metal ion very weakly and is easily replaced by a hydroxyl ion in the outside of the complex. In the ammonia complex, the bond between the cobalt(III) ion and the nitrogen atom of the ligand must be weaker than in the hydroxylamine complex. Therefore, the proton dissociation from the coordinated ammonia is expected to take place with much greater difficulty. Thus, as the equilibrium

$$[Co(NH_3)_6]^{3+} + H_2O \rightleftarrows [Co(NH_3)_5NH_2]^{2+} + H_3O^+$$

is shifted almost completely to the left side in an acid or neutral solution, the phenomena which suggest the proton dissociation are hardly detectable. However, in an alkaline solution the reverse reaction does not take place, and the effect of the proton dissociation can be observed. Thus, the proton dissociation from the coordinated ammonia takes place first; then the NH_2^- group thus produced is dissociated. This is our mechanism of the decomposition of the cobalt(III) amine complex. In the above discussion, we regarded the proton dissociation from the coordinated ammonia as the rate-determining step in the decomposition of the ammine complex. On this assumption we can understand that the stability of the pentammine complex is greater than that of the hexammine complex. Here the difference in the activation energy between the two complexes can be interpreted as the difference in the energy required to break off a proton from the coordinated ammonia.

The above discussion is based upon the assumption that the ligand which has dissociated a proton is linked to the central cobalt(III) ion less covalently and less firmly than the ligand which keeps a proton. This assumption seems to be in agreement with the fact that hydroxyl ion is behind water in the spectrochemical series, being linked less firmly to the cobalt(III) ion than water. The chemical behavior of the hexahydroxylammine cobalt(III) complex also supports this assumption. In addition, this assumption finds theoretical support in the concept of hybridization of orbitals of the donor atom. As was pointed out by Coulson[7], the non-bonding electrons of water and ammonia do not occupy the pure 2s orbital, but the hybrid orbital which has to some extent the character of the *p* orbital. Consequently, the electronic cloudes of the lone pair have no longer any spherical symmetry, but are pulled out in the direction opposite to the binding hydrogen atoms. The large dipole moments of water and ammonia are mainly due to the so-called atom-dipoles which are produced by such hybridization. However, as a result of hybridization, the bonding electrons also occupy the hybrid orbitals which overlap with the bonding orbitals of the hydrogen atoms to much greater extent than the pure *p* opbitals. Such an increase of the overlapping of the bonding orbitals results in the gain of energy which compensates for the above mensioned loss of

5) R. Tsuchida, This Bulletin, **13**, 388, 436 (1938).
6) H. Yoneda, This Bulletin, **30**, 924 (1957).
7) C. A. Coulson, "Valence" Oxford Press (1953). p. 210.

energy. That is, the tendency to stabilize the bonds by increasing the overlapping of the bonding orbitals and the energy loss due to the pulling out of the non-bonding electrons compete with each other to determine the degree of hybridization. Accordingly, the larger is the number of bonds which are stabilized by hybridization, and the fewer is the number of the non-bonding electrons, the larger would be the degree of hybridization. Thus, the degree of hybridization is greater in water than in hydroxyl ion, and also in ammonia than in amide ion. Therefore, the localization of the lone pair electrons occurs more markedly in water and ammonia than in hydroxyl ion and amide ion. As it is such lone pair electrons that participate in the coordination bond, it is easily understood that the greater degree of hybridization the ligand takes, the more covalent and more stable coordination bond it can form. Previously, Kuroya and Tsuchida[8] found spectrochemically that the affinity of ligands to the metal ion is in the decreasing order of $NH_3 > H_2O > OH^- > F^-$, and asserted that the larger the num ber of the lone pairs of electrons in the donor atom of the ligand, the less firm the coodination bond becomes. This empirical rule can be understood easily by the above mentioned concept of hybridization.

Thus, we have explained the mechanism of the decomposition of the cobalt(III) ammine complex by assuming the process of proton dissociation of the ligand. In the case of the chromium(III) complex, however, the situation is different. In this case, the frequencies of the rocking vibrations of the coodinated ammonia were found to be almost identical in hexammine and aquopentammine complexes. This suggests that the strength of the metal-ammonia bond is almost identical in hexammine and aquopentammine complexes. Consequently, in the case of the chromium (III) ammine complex, it can not be concluded simply whether the decomposition proceeds through the proton dissociation from the coodinated ammonia or through the mere replacement of ammonia by hydroxyl ion. However, from the data of the infrared spectra, the metal-ammonia bond is concluded to be much weaker in the chromimum(III) complex than in the cobalt(III) complex. Therefore, if we take the proces of proton dissociation of the ligand, the activation energy must be much larger than that of the corresponding cobalt(III) ammine complex. This is not the case, and it may be natural to assume that the decomposition of the chromium(III) complex does not go through the proton dissociation of the ligand, but through the direct dissociation of the coordinated ammonia. That is, since the stability of the metal-ammonia bond in the chromium(III) complex is considerably small, the coordination bond itself is broken with a less amount of energy than that required for the proton dissociation. This tendency becomes much more marked in the case of the ammine complexes of bivalent transition metal ions. In this case, the infrared absorption spectra indicate that the metal-ammonia bond becomes weaker. Accordingly, in the solution of these ammine complexes, the exchange of ligands takes place and the complex can exist only in the equilbrium with an excess of ammonia.

Summary

The rate of decomposition of the cobalt (III) and chromium(III) hexammine and monoaquopentammine complexes in an alkaline solution was measured. The activation energies of the decomposition were found to be 36, 32, 31 and 31 Kcal/mole for $[Co(NH_3)_6]^{3+}$, $[Co(NH_3)_5H_2O]^{3+}$, $[Cr(NH_3)_6]^{3+}$ and $[Cr(NH_3)_5H_2O]^{3+}$ respectively. At the same time the infrared absorption spectra of these complexes were also measured. The frequencies of the rocking vibration of the coordinated ammonia were found to be 815, 853, 744 and 747cm^{-1} for $[Co(NH_3)_6]^{3+}$, $[Co(NH_3)_5H_2O]^{3+}$, $[Cr(NH_3)_6]^{3+}$ and $[Cr(NH_3)_5H_2O]^{3+}$ respectively. From these results it was concluded that the decomposition of the cobalt(III) ammine complex was not a mere replacement of the coordinated ammonia by hydroxyl ion, but a reaction through the proton dissociation step as exemplified in the following scheme

$$[Co(NH_3)_6]^{3+} + OH^- \rightarrow [Co(NH_3)_5NH_2]^{2+} + H_2O,$$

while, in the chromium(III) ammine complex, the decomposition was inferred to proceed through a substitution of hydroxyl ion for the coordnated ammonia.

We wish to express our sincere thanks to

8) H. Kuroya and R. Tsuchida, *J. Chem. Soc. Japan, Pure Chem. Sec.* (*Nippon Kagaku Zassi*) **61**, 597 (1940).

9) For example, D. B. Powell and N. Sheppard, *J. Chem. Soc.*, **1956**, 3108.

Professer R. Tsuchida of Osaka University for his kind advice and encouragement during this work. Our appreciation is also expressed to Professor O. Nagai of Wakayama Medical College who gave us a chance to use a Beckman DU spectrophotometer, and to Mr. S. Kida of Wakayama University for his valuable discussions.

Department of Chemistry, Wakayama University, Masago-cho, Wakayama

*Ultraviolet Absorption Spectra and the Electronic Structure of Metallic Complexes. II. Cyanide Complexes**

By Sigeo KIDA, Junnosuke FUJITA, Kazuo NAKAMOTO and Ryutaro TSUCHIDA

(Received August 13, 1957)

In the preceding paper of this series[1], we have calculated the energy levels of the chloroammine cobalt(III) complexes by the semi-empirical moleculer orbital (M. O.) method taking π-orbitals of the ligands into consideration. In those complexes, however, the π-bonding between the metal orbital and the π-orbital of the ligand is relatively weak. On the contrary it is well known that the unsaturated ligands such as CN^- and CO coordinate strongly to the central metal. Recent infrared study of potassium tetracyano platinum (III) trihydrate $K_2[Pt(CN)_4]\cdot 3H_2O$ by Sweeny et al.[2] has shown that the Pt–CN stretching force constant is comparable to that of the usual covalent bonding of organic molecules. Pauling[3] has pointed out that this fact can be explained reasonably by considering the resonance formula containing the double bond between the ligands and the metallic ion. A similar discussion has been made by Williams[4] from the standpoint of the molecular orbital theory. But both of their descriptions are qualitative, and moreover no calculation has been done on these complexes.

In the present study, we calculated the energy levels of hexacyano chromium (III) $[Cr(CN)_6]^{3-}$, hexacyano cobalt(III) $[Co(CN)_6]^{3-}$, tetracyano nickel(II) $[Ni(CN)_4]^{3-}$, tetracyano copper(I) $[Cu(CN)_4]^{2-}$, *trans*-dicyano-diethylene-diamine cobalt(III) *trans*-$[Co\ en_2(CN)_2]^+$ and hexa-ammine cobalt(III) $[Co(NH_3)_6]^{3+}$ ions by the semi-empirical M. O. method, and the stability of the complex ions and the nature of their absorption bands were discussed.

Procedure

The method is the same in principle as that of the preceding paper[1]. The sets of molecular orbitals for each complex are shown in Table I and Fig. 1. The secular equation of the form $|H_{ij}-G_{ij}E|=0$ was solved for each class of the irreducible representation. Here, H_{ij} was approximated by the following equation.

$$H_{ij}=F_x\cdot G_{ij}(H_{ii}+H_{jj})/2$$

The values of F_x is 1.67 for $H_{\sigma\sigma}$ and 2.00 for $H_{\pi\pi}$. G_{ij} are group overlap integrals which can be expressed by the usual overlap integrals.

The values of H_{ii} for metallic ion were selected from the values of Kuroda and Ito[5]. However, they were slightly modified not to contradict the charge distribution obtained from Pauling's neutrality principle, i.e., "the central atom is almost neutralized by the donation of electrons from the ligand". The values of H_{ii} of the ligand were selected from Mulliken's

* Presented at the 10th Annual Meeting of the Chemical Society of Japan, Tokyo, April 6, 1957.

1) K. Nakamoto, J. Fujita, M. Kobayashi and R. Tsuchida. *J. Chem. Phys.*, **27**, 439 (1957).

2) D. M. Sweeny, I. Nakagawa, S. Mizushima and J. V. Quagliano, *J. Am. Chem. Soc.*, **78**, 889 (1956).

3) L. Pauling "The Nature of the Chemical Bond" Cornell University Press, New York (1940).

4) R. J. Williams, *J. Chem. Soc.*, **1956**, 8.

5) Y. Kuroda and K. Ito, *J. Chem. Soc. Japan, Pure. Chem. Sec.* (*Nippon Kagaku Zassi*), **76**, 545, 763 (1955).

TABLE
MOLECULAR ORBITAL

Complex Ion (point group)	Irred. Rep.	Metal orbitals	Ligand orbitals σ_{NH_3}	Ligand orbitals σ_{CN}
$[M(NH_3)_6]$ (O_h)	a_{1g}	$4s$	$\frac{1}{\sqrt{6}}(\sigma_1+\sigma_2+\sigma_3+\sigma_4+\sigma_5+\sigma_6)$	
	e_g	$3d_{z^2}$	$\frac{1}{\sqrt{12}}(\sigma_2+\sigma_3+\sigma_4+\sigma_5-2\sigma_1+2\sigma_6)$	
		$3d_{x^2-y^2}$	$\frac{1}{2}(\sigma_2-\sigma_3+\sigma_4-\sigma_5)$	
	f_{1u}	$4p_x$	$\frac{1}{\sqrt{2}}(\sigma_2-\sigma_4)$	
		$4p_y$	$\frac{1}{\sqrt{2}}(\sigma_3-\sigma_5)$	
		$4p_z$	$\frac{1}{\sqrt{2}}(\sigma_1-\sigma_6)$	
	f_{2g}	$3d_{xy}$ $3d_{yz}$ $3d_{xz}$		
trans $[M\,en_2(CN)_2]^+$ (D_{4h})	a_{1g}	$4s$. $3d_{z^2}$	$\frac{1}{2}(\sigma_2+\sigma_3+\sigma_4+\sigma_5)$	$\frac{1}{\sqrt{2}}(\sigma_1+\sigma_6)$
	b_{1g}	$3d_{x^2-y^2}$	$\frac{1}{2}(\sigma_2-\sigma_3+\sigma_4-\sigma_5)$	
	a_{2u}	$4p_z$		$\frac{1}{\sqrt{2}}(\sigma_1-\sigma_6)$
	e_u	$4p_x$	$\frac{1}{\sqrt{2}}(\sigma_3-\sigma_5)$	
		$4p_y$	$\frac{1}{\sqrt{2}}(\sigma_2-\sigma_4)$	
	e_g	$3d_{xz}$		
		$3d_{yz}$		
	b_{2g}	$3d_{xy}$		
$[M(CN)_6]$ (O_h)	a_{1g}	$4s$		$\frac{1}{\sqrt{6}}(\sigma_1+\sigma_2+\sigma_3+\sigma_4+\sigma_5+\sigma_6)$
	e_g	$3d_{z^2}$		$\frac{1}{\sqrt{12}}(\sigma_2+\sigma_3+\sigma_4+\sigma_5-2\sigma_1-2\sigma_6)$
		$3d_{x^2-y^2}$		$\frac{1}{2}(\sigma_2-\sigma_3+\sigma_4-\sigma_5)$
	f_{1g}			
	f_{1u}	$4p_x$		$\frac{1}{\sqrt{2}}(\sigma_2-\sigma_4)$
		$4p_y$		$\frac{1}{\sqrt{2}}(\sigma_3-\sigma_5)$
		$4p_z$		$\frac{1}{\sqrt{2}}(\sigma_1-\sigma_6)$

I.

COMBINATIONS

π_C	π_N
$\frac{1}{\sqrt{2}}(\pi_{1x}-\pi_{6x})$	$\frac{1}{\sqrt{2}}(\pi_{1x}-\pi_{6x})$
$\frac{1}{\sqrt{2}}(\pi_{1y}-\pi_{6y})$	$\frac{1}{\sqrt{2}}(\pi_{1y}-\pi_{6y})$
$\frac{1}{\sqrt{2}}(\pi_{1x}+\pi_{6x})$	$\frac{1}{\sqrt{2}}(\pi_{1x}+\pi_{6x})$
$\frac{1}{\sqrt{2}}(\pi_{1y}+\pi_{6y})$	$\frac{1}{\sqrt{2}}(\pi_{1y}+\pi_{6y})$
$\frac{1}{2}(\pi_{2z}+\pi_{4z}-\pi_{1x}-\pi_{6x})$	$\frac{1}{2}(\pi_{2z}+\pi_{4z}-\pi_{1x}-\pi_{6x})$
$\frac{1}{2}(\pi_{3z}+\pi_{5z}-\pi_{1y}-\pi_{6y})$	$\frac{1}{2}(\pi_{3z}+\pi_{5z}-\pi_{1y}-\pi_{6y})$
$\frac{1}{2}(\pi_{2y}+\pi_{4y}-\pi_{3x}-\pi_{5x})$	$\frac{1}{2}(\pi_{2y}+\pi_{4y}-\pi_{3x}-\pi_{5x})$
$\frac{1}{2}(\pi_{3x}-\pi_{5x}+\pi_{1x}-\pi_{6x})$	$\frac{1}{2}(\pi_{3x}-\pi_{5x}+\pi_{1x}-\pi_{6x})$
$\frac{1}{2}(\pi_{2y}-\pi_{4y}+\pi_{1y}-\pi_{6y})$	$\frac{1}{2}(\pi_{2y}-\pi_{4y}+\pi_{1y}-\pi_{6y})$
$\frac{1}{2}(\pi_{2z}+\pi_{3z}-\pi_{4z}-\pi_{5z})$	$\frac{1}{2}(\pi_{2z}+\pi_{3z}-\pi_{4z}-\pi_{5z})$

	f_{2g}	$3d_{yx}$ $3d_{yz}$ $3a_{zx}$	
	f_{2u}		
[M(CN)$_4$]Planar (D_{4h})	a_{1g}	$4s$, $3d_{z^2}$	$\frac{1}{2}(\sigma_1+\sigma_2+\sigma_3+\sigma_4)$
	a_{2g}		
	a_{2u}	$4p_z$	
	b_{2g}	$3d_{x^2-y^2}$	$\frac{1}{2}(\sigma_1+\sigma_3-\sigma_2-\sigma_4)$
	b_{2g}	$3d_{xy}$	
	b_{2u}		
	e_g	$3d_{xz}$ $3d_{yz}$	
	e_u	$4p_x$ $4p_y$	$\frac{1}{\sqrt{2}}(\sigma_1-\sigma_3)$ $\frac{1}{\sqrt{2}}(\sigma_2-\sigma_4)$
[M(CN)$_4$] tetrahedral (T_d)	a_1	$4s$	$\frac{1}{2}(\sigma_1+\sigma_2+\sigma_3+\sigma_4)$
	e	$3d_{z^2}$ $3d_{x^2-y^2}$	
	f_2	$4p_x$, $3d_{yz}$ $4p_y$, $3d_{xy}$ $4p_z$, $3d_{xy}$	$\frac{1}{2}(\sigma_1+\sigma_3-\sigma_2-\sigma_4)$ $\frac{1}{2}(\sigma_1+\sigma_2-\sigma_3-\sigma_4)$ $\frac{1}{2}(\sigma_1+\sigma_4-\sigma_2-\sigma_3)$
	f_1		

$\frac{1}{2}(\pi_{2y}+\pi_{3x}+\pi_{4y}+\pi_{5x})$	$\frac{1}{2}(\pi_{2x}+\pi_{4x}+\pi_{1x}+\pi_{6x})$
$\frac{1}{2}(\pi_{2x}+\pi_{4x}+\pi_{1x}+\pi_{6x})$	$\frac{1}{2}(\pi_{2x}+\pi_{4x}+\pi_{1x}+\pi_{6x})$
$\frac{1}{2}(\pi_{3z}+\pi_{5z}+\pi_{1y}+\pi_{6y})$	$\frac{1}{2}(\pi_{3z}+\pi_{5z}+\pi_{1z}+\pi_{6y})$
$\frac{1}{2}(\pi_{3x}-\pi_{5x}-\pi_{1x}+\pi_{6x})$	$\frac{1}{2}(\pi_{3x}-\pi_{5x}-\pi_{1x}+\pi_{6x})$
$\frac{1}{2}(\pi_{2y}-\pi_{4y}-\pi_{1y}+\pi_{6y})$	$\frac{1}{2}(\pi_{2y}-\pi_{4y}-\pi_{1y}+\pi_{6y})$
$\frac{1}{2}(\pi_{2z}-\pi_{4z}-\pi_{3z}+\pi_{5z})$	$\frac{1}{2}(\pi_{2z}-\pi_{4z}-\pi_{3z}+\pi_{5z})$
$\frac{1}{2}(\pi_{1y}-\pi_{2x}+\pi_{3y}-\pi_{4x})$	$\frac{1}{2}(\pi_{1y}-\pi_{2x}+\pi_{3y}-\pi_{4x})$
$\frac{1}{2}(\pi_{1z}+\pi^2{}_z-\pi_{3z}-\pi_{4z})$	$\frac{1}{2}(\pi_{1z}+\pi_{2z}-\pi_{3z}-\pi_{4z})$
$\frac{1}{2}(\pi_{1y}+\pi_{2x}+\pi_{3y}+\pi_{4x})$	$\frac{1}{2}(\pi_{1y}+\pi_{2x}+\pi_{3y}+\pi_{4x})$
$\frac{1}{2}(\pi_{1z}-\pi_{2z}-\pi_{3z}+\pi_{4z})$	$\frac{1}{2}(\pi_{1z}-\pi_{2z}-\pi_{3z}+\pi_{4z})$
$\frac{1}{\sqrt{2}}(\pi_{1z}+\pi_{3z})$	$\frac{1}{\sqrt{2}}(\pi_{1z}+\pi_{3z})$
$\frac{1}{\sqrt{2}}(\pi_{2z}+\pi_{4z})$	$\frac{1}{\sqrt{2}}(\pi_{3z}+\pi_{4z})$
$\frac{1}{\sqrt{2}}(\pi_{2x}-\pi_{4x})$	$\frac{1}{\sqrt{2}}(\pi_{2x}-\pi_{4x})$
$\frac{1}{\sqrt{2}}(\pi_{1y}-\pi_{3y})$	$\frac{1}{\sqrt{2}}(\pi_{1y}-\pi_{3y})$
$\frac{1}{4}\{\pi_{1x}+\pi_{3x}+\pi_{2x}+\pi_{4x}-\sqrt{3}(\pi_{1y}+\pi_{2y}+\pi_{3y}+\pi_{4y})\}$	$\frac{1}{4}\{\pi_{1x}+\pi_{3x}+\pi_{2x}+\pi_{4x}-\sqrt{3}(\pi_{1y}+\pi_{2y}+\pi_{3y}+\pi_{4y})\}$
$\frac{1}{4}\{\pi_{1x}+\pi_{3x}+\pi_{2x}+\pi_{4x}+\sqrt{3}(\pi_{1y}+\pi_{2y}+\pi_{3y}+\pi_{4y})\}$	$\frac{1}{4}\{\pi_{1x}+\pi_{3x}+\pi_{2x}+\pi_{4x}+\sqrt{3}(\pi_{1y}+\pi_{2y}+\pi_{3y}+\pi_{4y})\}$
$\frac{1}{4}\{\pi_{4x}+\pi_{2x}-\pi_{1x}-\pi_{3x}+\sqrt{3}(\pi_{4y}+\pi_{2y}-\pi_{1y}-\pi_{3y})\}$	$\frac{1}{4}\{\pi_{4x}+\pi_{2x}-\pi_{1x}-\pi_{3x}+\sqrt{3}(\pi_{4y}+\pi_{2y}-\pi_{1y}-\pi_{3y})\}$
$\frac{1}{2}(\pi_{1x}+\pi_{2x}-\pi_{3x}-\pi_{4x})$	$\frac{1}{2}(\pi_{1x}+\pi_{2x}-\pi_{3x}-\pi_{4x})$
$\frac{1}{4}\{\pi_{3x}+\pi_{2x}-\pi_{1x}-\pi_{4x}+\sqrt{3}(\pi_{4y}+\pi_{1y}-\pi_{2y}-\pi_{3y})\}$	$\frac{1}{4}\{\pi_{3x}+\pi_{2x}-\pi_{1x}-\pi_{4x}+\sqrt{3}(\pi_{4y}+\pi_{1y}-\pi_{2y}-\pi_{3y})\}$
$\frac{1}{4}\{\pi_{2y}+\pi_{4y}-\pi_{3y}-\pi_{1y}+\sqrt{3}(\pi_{1x}+\pi_{3x}-\pi_{2x}-\pi_{4x})\}$	$\frac{1}{4}\{\pi_{2y}+\pi_{4y}-\pi_{3y}-\pi_{1y}+\sqrt{3}(\pi_{1x}+\pi_{3x}-\pi_{2x}-\pi_{4x})\}$
$\frac{1}{2}(\pi_{1y}+\pi_{2y}-\pi_{3y}-\pi_{4y})$	$\frac{1}{2}(\pi_{1y}+\pi_{2y}-\pi_{3y}-\pi_{4y})$
$\frac{1}{4}\{\pi_{2y}+\pi_{3y}-\pi_{1y}-\pi_{4y}+\sqrt{3}(\pi_{2x}+\pi_{3x}-\pi_{1x}-\pi_{4x})\}$	$\frac{1}{4}\{\pi_{2y}+\pi_{3y}-\pi_{1y}-\pi_{4y}+\sqrt{3}(\pi_{2x}-\pi_{3x}-\pi_{1x}-\pi_{4x})\}$

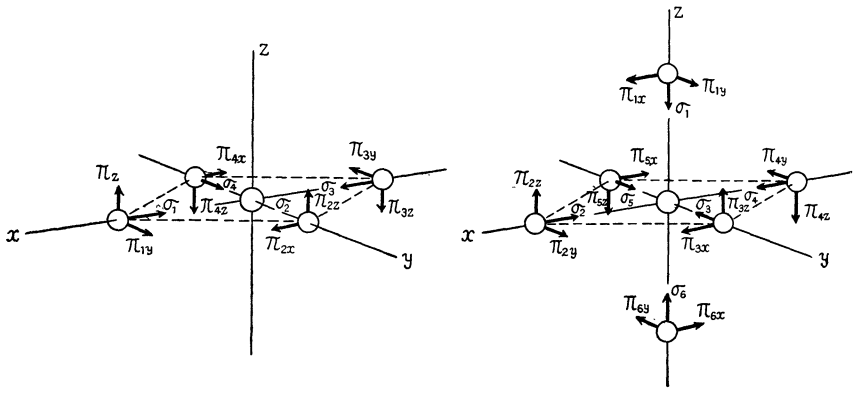

M(CN)$_6$—type (planar) M(CN)$_6$—type (Octahedral)

Fig. 1. Orientation of the orbital.

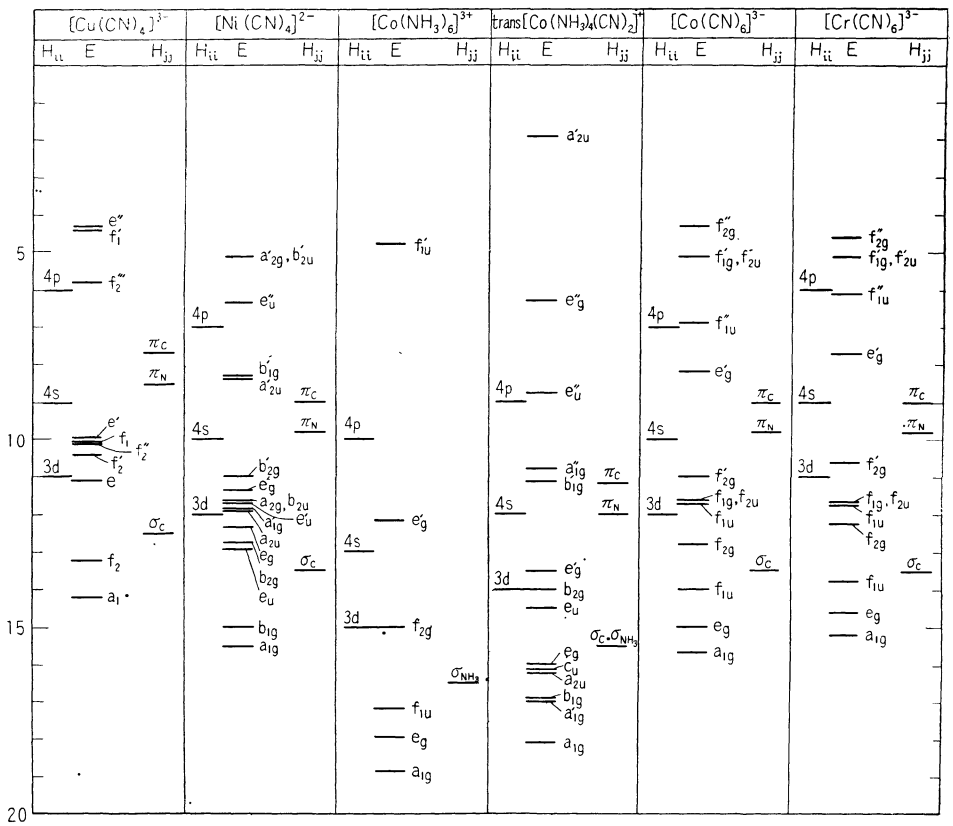

Fig. 2. The orbital energy levels.

ionization potentials[6], according to the charge distribution postulated above. For example, the charge of the individual atom in hexacyano cobalt(III) complex $[Co(CN)_6]^{3-}$, was assumed to be $[Co^{0.20+}(C^{0.22-}N^{0.32-})_6]$. According to this assumption, H_{ii}'s were obtained as shown below:

$$H_{3d3d} = {}_{3d}I_{Co} \times 0.80 + {}_{3d}I_{Co^+} \times 0.20 = 9.0 \times 0.80 + 25.0 \times 0.20 \fallingdotseq 12$$

$$H_{\pi C\pi C} = {}_{2p}I_C \times 0.78\, {}_{2p}I_{C^-} \times 0.22 = 11.17 \times 0.78 + 0.69 \times 0.22 \fallingdotseq 9.0$$

$$H_{\pi N\pi N} = {}_{2p}I_N \times 0.68 + {}_{2p}I_{N^-} \times 0.32 = 13.81 \times 0.68 + 0.99 \times 0.32 \fallingdotseq 9.8$$

$$H_{\sigma\sigma} = \frac{({}_{2p}I_C + {}_{2s}I_C)}{2} \times 0.78$$

6) R. S. Mulliken, *J. Chem. Phys.*, **2**, 792 (1934).

$$+\frac{({}_{2p}I_{C^-}+{}_{2s}I_{C^-})}{2}\times 0.22$$
$$=\frac{(11.17+21.06)}{2}\times 0.78$$
$$+\frac{(8.74+0.69)}{2}\times 0.22\fallingdotseq 13.5$$

Here, ${}_{3d}I_{Co}$ etc. are the ionization potentials of electrons in the orbitals shown by the subscripts. The validity of such a procedure may be doubtful. However, no better method is known at present.

Complete sp hydridization was assumed for σ-orbital of the ligand. Interaction between the ligands have been entirely ignored. The values of the overlap integrals were obtained mostly from the tables of Mulliken, Orloff and Orloff[7], and Jaffé and Doak[8] except $S(3d_\pi/5p_\pi)$ which was calculated from the master formula of Jaffé[8]. The metal–C and C–N distances, 1.92 and 1.16 Å, respectively, were taken from the X-ray analysis on potassium ferrocyanate $K_4[Fe(CN)_6]\cdot 3H_2O$[9].

After the secular equation was solved, the charge distribution was calculated. The result was then compared with the formerly postulated charge distribution. If the calculated result was very different from the formerly postulated one, the calculation was repeated using a new charge distribution until the agreement was satisfactory. The final result of the postulated and the calculated charge distribution is shown in Table II.

TABLE II
CHARGE DISTRIBUTION

	Atom	Postulated	Calculated
$[Cr(CN_6)]^{3-}$	Cr	+0.12	+0.12
	C	−0.21	−0.36
	N	−0.31	−0.16
$[Co(CN)_6]^{3-}$	Co	+0.20	+0.18
	C	−0.22	−0.21
	N	−0.32	−0.32
$[Co(NH_3)_6]^{3+}$	Co	+0.44	+0.60
	NH_3	+0.43	+0.40
$[Ni(CN)_4]^{2-}$	Ni	+0.15	−0.18
	C	−0.22	−0.20
	N	−0.31	0.00
$[Cu(CN)_4]^{3-}$	Cu	0.00	−0.42
	C	−0.32	−0.24
	N	−0.43	−0.41

7) R. S. Mulliken, C. A. Rieke, D. Orloff and H. Orloff, ibid., **17**, 1248 (1949).
8) H. H. Jaffe and D. O. Doak, ibid., **21**, 196 (1953).
9) V. A. Pospelov and G. S. Zhdanov, *J. Phys Chem.* (USSR) **21**, 879 (1947).

Discussion

The orbital energy level diagram obtained by our calculation is shown in Fig. 2. For hexa-ammine cobalt(III) $[Co(NH_3)_6]^{3+}$, dicyano tetra-ammine cobalt(III) $[Co(NH_3)_4(CN)_2]^+$, hexacyano cobalt(III) $[Co(CN)_6]^{3-}$, tetracyano nickel(III) $[Ni(CN)_4]^{2-}$ and tetracyano copper(I) $[Cu(CN)_4]^{3-}$ ions the highest occupied levels—f_{2g}, e'_g, f'_{2g}, b'_{2g} and e', respectively, —are filled up with electrons. This fact explains the diamagnetism of these complexes which was formerly interpreted by Van Vleck[10] and Pauling[3] using the M. O. and the V. B. method, respectively, but both ignored the π-bonding. If one or more electrons are added to these complexes, they must enter into the next higher level which is located far above the ground level. This will make the energy state of the complex much higher than before. Thus, hexacyano cobalt(II) $[Co(CN)_6]^{4-}$ and tetracyano copper(I) $[Cu(CN)_4]^{3-}$ ions (square planar) are less stable than hexacyano cobalt(III) $[Co(CN)_6]^{3-}$ and tetracyano nickel(II) $[Ni(CN)_4]^{2-}$, respectively.

The U. V. absorption spectra of the cyanide complexes were investigated by Kashimoto and Tsuchida[11], and Kuroya and Tsuchida[12]. They concluded that the bands at 24000, 32500 and 39000 cm^{-1} of hexacyano cobalt(III) $[Co(CN)_6]^{3-}$ ion and at 21700, 31700 and 35100~37500 cm^{-1} of tetracyano nickel(II) $[Ni(CN)_4]^{2-}$ were called "the first, the second and the third bands", respectively. However, the first bands of these two complexes are unusually weak compared with the first bands of the other complexes*. This anomaly of the first band has long been a subject of discussion.

Our present calculation clearly indicates that the bands at 32500 and 39000 cm^{-1} in hexacyano cobalt(III) ion $[Co(CN)_6]^{3-}$ are due to $f'_{2g}\rightarrow e'_g$ forbiden transitions which give rise to two electronic states (singlet) F_{1g} and F_{2g}. Therefore these bands correspond to the first and the second bands of cobalt(III) ammine complexes, since Kuroda and Ito[5], and Yamatera[13] have

10) J. H. Van Vleck, *J. Chem. Phys.*, **3**, 807 (1935).
11) M. Kashimoto and R. Tsuchida, *J. Chem. Soc. Japan, Pure Chem. Sec.* (*Nippon Kagaku Zassi*) **60**, 347 (1939).
12) H. Kuroya and R. Tsuchida, ibid. **61**, 597 (1940).
13) H. Yamada, Presented at the Symposium of Metallic Complexes. Tokyo, October, (1954).
* In $[Ni(CN)_4]^{2-}$, $\log\varepsilon=-0.05$ and in $[Co(CN)_6]^{3-}$, $\log\varepsilon=-0.28$, but these values are not strictly reproducible.

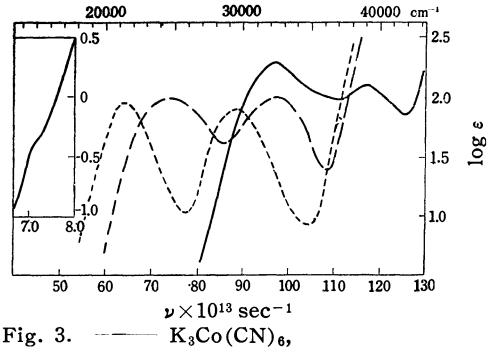

Fig. 3. ——— $K_3Co(CN)_6$,
- - - - $[Co\ en_3](ClO_4)_3$
— — — $[Co\ en_2(CN)_2]_2SO_4 \cdot 3H_2O$

shown that the first and the second band of hexa-ammine cobalt ion $[Co(NH_3)_6]^{3+}$ were attributable to $f_{2g} \rightarrow e'_g$ transitions. Fig. 3 indicates the correlation of the absorption bands between hexacyano cobalt (III) ions $[Co(CN)_6]^{3-}$, dicyanodiethylenediamine cobalt(III) $[Coen_2(CN)_2]^+$ and trisethylenediamine cobalt(III) $[Co\ en_3]^{3+}$ ions**. It is seen that the absorption bands of trisethylenediamine cobalt(III) $[Co\ en_3]^{3+}$ shift to the shorter wave length as the ethylenediamine is replaced by cyanide. Furthermore, the magnitude of the shift has a linear relation with the number of cyanide, as is generally seen in the absorption spectra of the mixed complex[14,15]. This fact also suggests that these two absorption bands of hexacyano cobalt(III) ion $[Co(CN)_6]^{3-}$ are of similar character to the first and the second band of hexa-ammine cobalt(III) $[Co(NH_3)_6]^{3+}$ ion. Thus we conclude that the weak shoulder at 24000 cm^{-1} may be attributable to the singlet-triplet transition. It should be noted, however, that the f_{2g} orbital of hexacyano cobalt(III) ion $[Co(CN)_6]^{3-}$ consists of 3*d* (cobalt)and 2*p* (ligand) orbitals, whereas th f_{2g} orbital of hexa-ammine cobalt(III) $[Co(NH_3)_6]^{3+}$ includes only non-bonding 3*d* (cobalt)orbital. In dicyanodiethylenediamine cobalt(III) $[Co\ en_2(CN)_2]^+$, the transitions occur from b_{2g} or e'_g to a''_{1g} or b'_{1g} levels according to our calculation. This is not unexpected, because lowering of symmetry from O_h to D_{4h} splits f_{2g} into e_g and b_{2g}, and e_g into a_{1g} and b_{1g}, respectively. Thus, the observed bands at 25000 and 32400 cm^{-1} will be due to these transitions.

As is seen in Fig. 4, the bands at 26300 and 32200 cm^{-1} of hexacyano chromium (III) ion $[Cr(CN)_6]^{3-}$ are also attributable to $f'_{2g} \rightarrow e'_g$ transitions. In this case, our result is in good accord with Tsuchida's former assignment, which ascribed these bands to the first and the second bands.

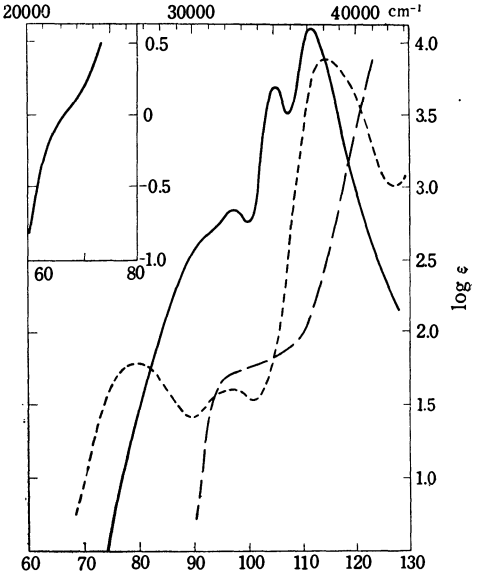

Fig. 4. ——— $K_2[Ni(CN)_4]$
- - - - $K_3[Cr(CN)_6]$[12]
— — — $K_3Cu(CN)_4$[11]

In planar tetracyano nickel(II) $[Ni(CN)_4]^{2-}$ ion, the lowest transition occurs from b'_{2g} or e'_g to b'_{1g} or a'_{2u} level. Of these transitions, $e'_g \rightarrow a'_{2u}$ is allowed, and $b'_{2g} \rightarrow b'_{1g}$, $e'_g \rightarrow b'_{1g}$ and $b'_{2g} \rightarrow a'_{2u}$ are forbidden. The intense bands at 35100 ($\log \varepsilon = 3.67$) and 37500 cm^{-1} ($\log \varepsilon = 4.09$) may be due to $e'_g \rightarrow a'_{2u}$ transitions, which substantially correspond to $f'_{2g} \rightarrow f'''_{1u}$ transition of hexacyano cobalt(III) ion $[Co(CN)_6]^{3-}$. Since $b'_{2g} \rightarrow b'_{1g}$ and $e'_g \rightarrow b'_{1g}$ transitions correspond to $f_{2g} \rightarrow e'_g$ transitions of hexa-ammine cobalt(III) $[Co(NH_3)_6]^{3+}$, the band at 31700 cm^{-1} may be "the first band". The second band may be hidden by the strong "specific band" in the region of 33000~40000 cm^{-1}. The weak shoulder at 21700 cm^{-1} may be due to the singlet-triplet transition.

In tetrahedral tetracyano copper(I) $[Cu(CN)_4]^{3-}$ ion, the lowest transition occurs from e', f_1, f'_2 and f''_2 to f'''_2 which contains allowed transitions. The bands

** Though the calculation was made on *trans*-$[Co(NH_3)_4(CN)_2]^+$, absorption measurement was made on *trans*-$[Co\ en_2\ (CN)_2]^+$, because the former complex has not yet been prepared. It has been well known, however, that absorption spectra of ethylenediamine complexes always bear a close resemblance to that of ammine complexes. Therefore, experimental data of $[Co\ en_2\ (CN)_2]^+$ have been used instead of $[Co(NH_3)_4(CN)_2]^+$.

14) Y. Shimura and R. Tsuchida, This Bulletin, **28**, 572 (1955).

15) S. Kida, ibid., **29**, 805 (1956).

observed at about 32000 cm^{-1} and following higher absorption will be probably due to those transitions. In this case, no band exists corresponding to "the first or the second band" of the octahedral cobalt(III) complexes.

Finally we tabulated the calculated and observed energies of transitions in each complex in Table III. It may be possible to obtain better agreement between these values if the values of the ionization potentials are selected appropriately. However, we did not do so since we thought consideration of the charge distribution obtained from the Pauling's neutrality principle was more important.

TABLE III

COMPARISON OF THE OBSERVED AND THE CALCULATED ENERGIES OF TRASITION IN EV. UNIT

	$[Cr(CN)_6]^{3-}$	$[Co(CN)_6]^{3-}$
	3.25, 3.95*	3.97, 4.80
obs.	(1.76) (1.65)	(2.29) (2.09)
calcd.	2.9(*f*)	2.8(*f*)

	$[Ni(CN)_4]^{2-}$	$[Cu(CN)_4]^{3-}$
	4.00, 4.34, 4.63	4.15, 5.3**
obs.	(2.85) (3.67) (4.09)	(1.67) (4.0)
calcd.	2.6 3.0(*a* & *f*)	4.0 4.3(*a* & *f*)

	$[Co\,en_2(CN)_2]^+$	$[Co(NH_3)_6]^{3+}$	$[Co\,en_3]^{3+}$
	3.09, 4.01	2.61, 3.66***	2.64, 3.66***
obs.	(1.98) (2.00)	(1.78) (1.74)	(1.94) (1.90)
calcd.	2.6 3.2(*f*)	2.8(*f*)	—

Literature of the observed data.

* H. Kuroya and R. Tsuchida, *J. Chem. Soc. Japan, (Nippon Kagaku Zassi)* **61**, 597 (1940).

** M. Kashimoto and R. Tsuchida, ibid. **60** 347 (1939).

*** Y. Shimura and R. Tsuchida, This Bulletin, **29**, 313 (1956).

The number in the bracket in the "obs." column indicates logarithm of the molecular extinction coefficient. (*a*) and (*f*) in the "calcd." column denote "allowed" and "forbidden" transitions, respectively.

Experimental

The absorption measurement was made by the Beckmann DK Spectrophotometer.

Potassium hexacyano cobalt(III)ate $K_3[Co(CN)_6]$ and potassium tetracyano nickel(II)-ate $K_2[Ni(CN)_4]$ were prepared according to the description of "Inorganic Syntheses Vol. II". Dicyano-diethylenediamine cobalt(III) sulfate trihydrate $[Co\,en_2(CN)_2]\,1/2\,SO_4 \cdot 3H_2O$ was prepared by the method of Ray et al.[16]. In the preparation of these complexes, the contamination of other metallic ions was avoided by careful purification of the starting materials, cobaltous chloride and nickel sulfate.

Summary

The energy levels of the cyanide complexes—hexacyano chromium(III) $[Cr(CN)_6]^{3-}$, hexacyno cobalt(III) $[Co(CN)_6]^{3-}$, tetracyano nickel(II) $[Ni(CN)_4]^{2-}$, and tetracyano copper(I) $[Cu(CN)_4]^{3-}$ ions—have been calculated by the semi-emprical M. O. method taking π-orbitals of the ligands into consideration. The ionization potentials used have been determined so that the calculated charge distribution does not contradict that obtained from Pauling's neutrality principle. The stability and the magnetic property of these complexes have been well interpreted by our calculation. The results have revealed that the first and the second bands of hexacyano chromium (III) $[Co(CN)_6]^{3-}$ and hexacyano cobalt (III) $[Co(CN)_6]^{3-}$ are attributable to $f'_{2g} \rightarrow e'_g$ transitions which are of the similar character to the first and the second bands of hexammine cobalt(III) $[Co(NH_3)_6]^{3+}$, although the ground level, f'_{2g} combines strongly with the π-orbitals of the ligands. In tetracyano nickel(II) $[Ni(CN)_4]^{2-}$, the "second band" is hidden by the allowed transition. For tetracyano copper(I) $[Cu(CN)_4]^{3-}$, there is no band corresponding to "the first and the second band".

The authors are very grateful to Dr. K. Ito of Nagoya University and Mr. H. Yamatera of the Osaka City University for their kind advice and helpful discussions during the course of this work.

Department of Chemistry, Wakayama University, Masagocho, Wakayama
Department of Chemistry, Faculty of Science, Osaka University, Kita-ku, Osaka

16) P. Ray and B. Sarma, *J. Indian Chem. Soc.*, **28**, 59 (1951).

Studies on Serine Peptides. IV. Synthesis of L-Seryl-L-histidyl-L-leucyl-L-valyl-L-glutamic Acid with Strepogenin Activity

By Kenji OKAWA

(Received August 12, 1957)

A peptide having strepogenin activity was recently isolated by R. Merrifield and D. Woolley from a partial hydrolysate of beef insulin and its structure was established to be as L-seryl-L-histidyl-L-leucyl-L-valyl-L-glutamic acid[1,2].

In a previous paper[3], the author reported that L-seryl-L-histidyl-L-leucine was synthesized from Cbzo-O-Bz-L-seryl-L-histidine and L-leucine methyl ester in good yields by Sheehan's method[4], followed by the elimination of protecting groups with hydrogen bromide in dioxane.

In the present experiment, the pentapeptide was synthesized by the condensation of Cbzo-O-Bz-L-seryl-L-histidine with L-leucyl-L-valyl-L-glutamic acid diethyl ester, followed by the removal of the protecting groups in the same way as above.

During the course of the present work, Woolley and Merrifield reported[5] that the synthesis of this peptide had the same strepogenin activity as that of the native one. The yields in all coupling reactions of these authors' are less than ours.

The synthetic pentapeptide showed strepogenin activity in the biological test using *L. casei**. By addition of zinc acetate to an aqueous solution of the pentapeptide, an insoluble zinc-complex was readily formed.

The reaction sequences were the following. Cbzo-L-leucyl-L-valine was prepared by coupling Cbzo-L-leucine with L-valine methyl ester, followed by hydrolysis of Cbzo-peptide methyl ester produced. Then the product was coupled with glutamic acid diethyl ester to give Cbzo-L-leucyl-L-valyl-L-glutamic acid diethyl ester. Then the Cbzo-group was removed by dry hydrogen bromide in dioxane and the tripeptide ester hydrobromide was obtained. Cbzo-O-Bz-L-seryl-L-histidine was prepared by the same method as described in the previous paper[4]. This Cbzo-dipeptide was coupled with the above tripeptide ester in chloroform by means of dicyclohexylcarbodiimide to give Cbzo-O-Bz-L-seryl-L-histidyl-L-leucyl-L-valyl-L-glutamic acid diethyl ester in 80% yield. It seems that the good yield of this last stage is due to the high solubility of Cbzo-O-Bz-L-seryl-L-histidine in the organic solvent. The hydrolysis of the ester group by the usual method was unsuccesful, as Woolley pointed out[6], owing to low solubility of this peptide derivative in dioxane or acetone-water system. The desired free pentapeptide was obtained after removal of the protecting groups by treatment of Cbzo-Bz-L-seryl-L-histidyl-L-leucyl-L-valyl-L-glutamic acid diethyl ester with concentrated hydrochloric acid at 37°C for 80 minutes.

Experimental

Cbzo-L-leucyl-L-valine.—L-Valine methyl ester hydrochloride (11.5 g.) in 40 cc. of dry tetrahydrofurane was treated with 43 cc. of 1.66 N-ammonia—chloroform. After removal of ammonium chloride, excess of ammonia and chloroform was evaporated in vacuo at 40°C, and the residue was mixed with dicyclohexylcarbodiimide (14.17 g.) and Cbzo-L-leucine (18.25 g.) in 20 cc. of tetrahydrofurane at room temperature. Immediately after mixing, dicyclohexylurea deposited in the above reaction mixture. After the product being kept overnight at room temperature, acetic acid (1 cc.) was added to decompose the unchanged dicyclohexylcarbodiimide. The mixture was allowed to stand at room temperature for an hour and the precipitate produced was filtered off. Then, tetrahydrofurane was replaced by ethyl acetate and the solution was washed with 0.1 N hydrochloric acid, 1% sodium bicarbonate and water successively, dried over anhydrous sodium sulfate and concentrated in vacuo. The syrupy product was saponified with N-sodium hydroxide in dioxane-acetone (about 14 : 1 v/v) solution and Cbzo-L-leucyl-L-valine was extracted twice with ethyl acetate. The extract was dried over anhydrous sodium sulfate and then concentrated in vacuo. Addition of petroleum ether

1) R. B. Merrifield and D. W. Woolley, *Arch. Biochem. Biophys.*, **56**, 265 (1955).
2) R. B. Merrifield and D. W. Woolley, *J. Am. Chem. Soc.*, **78**, 358 (1956).
3) K. Okawa, Part III This Bulletin, **30**, 976 (1957).
4) J. C. Sheehan and G. P. Hess, *J. Am. Chem. Soc.*, **77**, 1067 (1955).
5) R. B. Merrifield and D. W. Woolley, ibid., **78**, 4646 (1956).
* L. casei; (Bioassay).
6) R. B. Merrifield and D. W. Woolley, ibid., **78**, 4646 (1956).

TABLE I

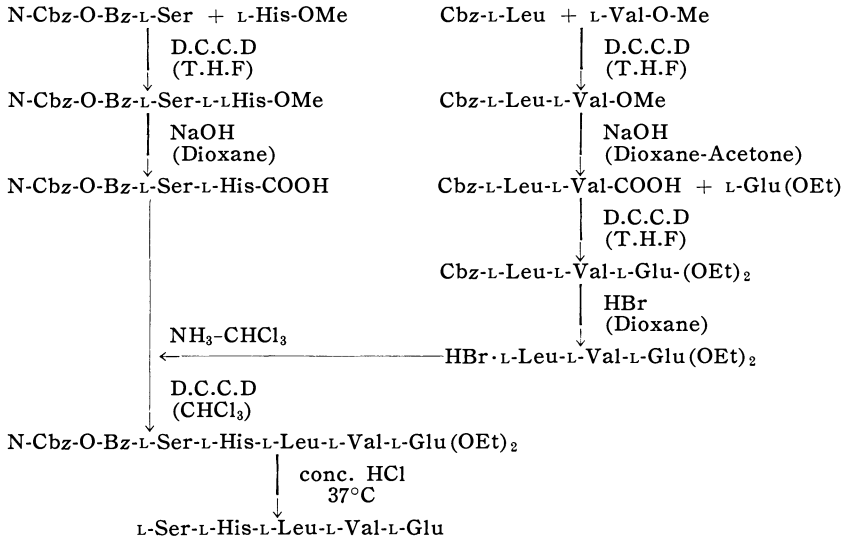

T.H.F; Tetrahydrofurane D.C.C.D; Dicyclohexylcarbodiimide

gave 15 g. (65.2%) of white crystals. The product was recrystallized from ethyl acetate-petroleum ether, yield 13.5 g. (59%), m.p. 107—108°C. $[\alpha]_D^{13} = -18.52$ (10 mg./cc. EtOH)[7].

Anal. Found: C, 62.88; H, 7.38; N, 7.81. Calcd. for $C_{19}H_{28}O_5N_2$: C, 62.60; H, 7.77; N, 7.68%.

Cbzo-L-leucyl-L-valyl-L-glutamic Acid Diethyl Ester.—L-Glutamic acid diethyl ester from L-glutamic acid diethyl ester hydrochloride (4.83 g.) was coupled with Cbzo-L-leucyl-L-valine (6.69 g.) in 20 cc. of tetrahydrofurane by the same procedure as described above. Dicyclohexylurea was precipitated more slowly in this case than in the above. After standing overnight, Cbzo-L-leucyl-L-valyl-L-glutamic acid diethyl ester was precipitated together with dicyclohexylurea since it was difficultly soluble in tetrahydrofurane. Then Cbzo-tripeptide ester was extracted with hot ethyl acetate. After evaporation of ethyl acetate, the precipitate was recrystallized from hot ethylacetate. The yield was 6.5 g. (68%), m. p. 178—179°C. $[\alpha]_D^{13} = -41.1$ (15 mg./cc. acetic acid).

Anal. Found: C, 61.16; H, 7.39; N, 7.85. Calcd. for $C_{28}H_{43}O_8N_3$: C, 61.18; H, 7.70; N, 7.65%.

L-Leucyl-L-valyl-L-glutamic Acid Diethyl Ester-HBr.—Cbzo-tripeptide ester was suspended in dry dioxane (10 g.) into which dry hydrogen bromide was passed through until saturation was completed. After an hour, absolute ether (150 cc.) was added to the reaction mixture and the ether solution was concentrated in vacuo. The residual syrup was dissolved in absolute ethanol and the solvent was distilled off in vacuo. After the white residue was recrystallized from absolute ethanol and absolute ether, 1.7 g. of the hydrobromide was obtained in 90% yield. m. p. 220°C. $[\alpha]_D^{13} = -30.46$ (20 mg./cc. ethanol).

Anal. Found: C, 48.20; H, 7.48; N, 8.70. Calcd. for $C_{20}H_{38}O_6N_3Br$: C, 48.38; H, 7.66; N, 8.46%.

Cbzo-O-Bz-L-seryl-L-histidyl-L-leucyl-L-valyl-L-glutamic Acid Diethyl Ester.—To the solution of Cbzo-O-Bz-L-seryl-L-histidine (1.0 g.) in 25 cc. of dioxane, was added 50 cc. of the dioxane solution of the tripeptide ester which was prepared from the hydrobromide (1.2 g.) using the chloroform-ammonia solution, and dicyclohexylcarbodiimide (0.5 g.). After the solution was left overnight at room temperature, acetic acid (0.2 cc.) was added to the mixture, which was allowed to stand for an hour. The reaction mixture was concentrated in vacuo, the residual precipitate was dissolved in chloroform and the urea derivative produced was filtered off. The filtrate was washed with dilute acid, but the aqueous layer was not separated from the organic layer. After chloroform was distilled off, the precipitate was filtered and washed with aq. solution of sodium bicarbonate. The precipitate was recrystallized from hot ethanol; 1.5 g. of crystals was obtained in 82.3% yield. m. p. 192—3°C. $[\alpha]_D^{13} = -34.5$ (10 mg./cc. acetic acid).

Anal. Found: C, 59.91; H, 6.94; N, 11.25. Calcd. for $C_{44}H_{61}O_{11}N_7$: 61.11; H, 7.06; N. 11.34%.

L-Seryl-L-histidyl-L-leucyl-L-valyl-L-glutamic Acid.—The above Cbzo-peptide ester (0.9 g.) was treated with 50 cc. of 12 N hydrochloric acid at 37°C for 80 min. After thirty min. Cbzo-peptide ester was almost dissolved and slight turbidity appeared. At the end of the reaction period, the solution was dried over sodium hydroxide in a vaccum desiccator. The residual solid was dissolved in 10 cc. of water and the insoluble product was filtered off. The filtrate was treated with triethylamine and brought to pH 6.8. After

7) E. L. Smith, D. H. Spackman and W. J. Polglase, *J. Biol. Chem.*, **199**, 801 (1952).

concentration in vacuo, the residual product was washed with ethanol. The crude pentapeptide (0.4 g.) was obtained, in 70%. The product was dissolved in a small amount of water and 5 times as great an amount of alcohol was added; the mixture was allowed to stand in an ice-box until crystallization was completed. Recrystallization was repeated four times in the same way. Paper chromatography of this synthetic pentapeptide in butanol-acetic acid-water (4 : 1 : 1) gave one spot with R_f 0.53. Paper chromatography of an acid hydrolysate of the synthetic peptide gave approximately equimolecular amounts of five spots corresponding to serine, histidine, valine, leucine and glutamic acid. m. p. 233—5°C. $[\alpha]_D^{13} = -52.3$ (10 mg./cc. water).

Anal. Found: C, 50.88; H, 7.02; N, 16.50. Calcd. for $C_{25}H_{41}O_9N_7$: C, 51.45; H, 7.03; N, 16.80%.

Biological Activity. — The synthetic pentapeptide was shown to have strepogenin activity three times as great as that of the casein hydrolysate. With regard to both the peptides, L-seryl-L-histidine and L-seryl-L-histidyl-L-leucine, activity was detected.

Zinc Complex of Pentapeptide.—A zinc complex was readily formed in an aqueous solution of the pentapeptide by adding equimolecular zinc acetate. The analytical value of this product varied according to the reaction condition, a inly concentration of the solution. One of these data suggests the under signed formula.

Anal. Found: N, 12.78; Zn, 0.81. Calcd. for $C_{29}H_{47}O_{11}N_7Zn$: N, 12.78; Zn, 0.85%.

Summary

L-Seryl-L-histidyl-L-leucyl-L-valyl-L-glutamic acid having strepogenin activity has been synthesized from O-Bz-L-serine as a starting material in a good yield by Sheehan's dicyclohexylcarbodiimide method.

The author wishes to express his appreciation to Professor S. Akabori for his kind guidance during the course of this work and to Professor K. Kitahara, Tokyo University, for his co-operation in the biological test. He also thanks Mr. T. Yamakawa and F. Sakiyama for their assistance.

Department of Chemistry Faculty of Science, Osaka University
Kita-ku, Osaka

Heats of Mixing of Dichloroethane with Non-polar Liquids

By Kazuo AMAYA and Ryoichi FUJISHIRO*

(Received June 24, 1957)

In a number of papers[1] concerning the solutions of non-electrolytes published hitherto, the discussions were made from the standpoint of inter-molecular energy. However, in solutions containing steric isomers due to the internal rotation[2], their intra-molecular energy may be expected to contribute to the thermodynamical effects of solutions and this fact has not been discussed before.

In the following section of this report, we shall derive a simple theory about the excessive enthalpy arising from the internal rotation and compare it with experimental data of the heats of mixing of dichloroethane with cyclohexane, carbon tetrachloride and benzene, where dichloroethane is the typical molecule having isomers owing to the internal rotation.

Solutions of Dichloroethane with Non-polar Solvent.—It is well known that molecules of dichloroethane can exist in the *trans* and the *gauche* form. In the gaseous state, the potential energy of the former is lower than that of the latter by about 1.5 kcal./mole and the molecules of dichloroethane exist predominantly in the *trans* form at room temperature.

In the liquid state, however, the *gauche* form with a large dipole moment is considerably more stabilized than the *trans* one by the reaction field from the surrounding dielectric medium, so that a considerable part of the molecules is in the *gauche* form. When a non-polar solvent of a lower dielectric constant is added to the pure liquid of dichloroethane,

* Present address: Institute of Polytechnics, Osaka City University, Kita-ku, Osaka.

1) A. Münster, *Trans. Faraday Soc.*, **46**, 165 (1950); J. S. Rowlison, ibid., **50**, 1036 (1954); J. Barker, *J. Chem. Phys.*, **20**, 794 (1952); H. Tompa, ibid., **21**, 250 (1953); J. A. Pople, *Discussions Faraday Soc.*, **15**, 35 (1953); etc.

2) S. Mizushima, "Structure of Molecules and Internal Rotation". Academic Press Inc., Publishers. New York, N. Y. (1954).

the dielectric constant of the surrounding medium of the dichloroethane molecules become lower, resulting in transition from the *gauche* form to the *trans*. Owing to this transition, the change in ethalpy which does not appear in ordinary solutions will be expected to occur in these solutions.

We suppose that the solution contains N_d molecules of dichloroethane and N_s molecules of solvent. Of N_d molecules of dichloroethane, N_t molecules are in the *trans* form and N_g in the *gauche*, that is, $N_d=N_t+N_g$.

We further make the following assumptions;

1) Internal partition functions of dichloroethane in the *trans* and in the *gauche* form are the same.

2) A part of inter-molecular energy, arising from dispersion force between both forms and solvent molecules are the same.

3) The part of inter-molecular energy arising from the dipole of the dichloroethane molecule in the *gauche* form are included in the mutual energy between the dipole and the reaction field.

4) The sizes of the dichloroethane and the solvent molecules are nearly equal.

5) On the mixing of the solution, no volume change occurs, that is, the volume of the solution is additive.

Under these assumptions the configurational partition function Z of the solution is represented by the following equation;

$$Z=2^{N_g}\phi_d^{N_t+N_g}\phi_s^{N_s}\frac{(N_t+N_g+N_s)!}{N_t!\ N_g!\ N_s!}\times e^{-Xw/RT}e^{-N_g(\Delta E-\Delta G)/kT} \quad (1)$$

where ϕ_d and ϕ_s are the internal partition functions of the dichloroethane and the solvent molecule, X the number of pairs of the dichloroethane-solvent and $2w$ defined as follows:

$2w=2w_{ds}-w_{dd}-w_{ss}$, where w_{ds}, w_{dd} and w_{ss} are the ordinary interaction energy of dichloroethane-solvent pair, dichloroethane-dichloroethane pair and solvent-solvent pair, respectively. ΔE is the internal potential energy difference between the *trans* and the *gauche* form. ΔG is the stabilization free energy of a dipole arising from the reaction field of surrounding dielectric medium.

Assuming the simplest model in which the dichloroethane molecule is spherical and the dipole is at the center of this sphere, ΔG can be represented as follows[3];

$$\Delta G=(1/2)\mu_g^2R/(1-R\alpha_d),\qquad R=2(\varepsilon-1)/(2\varepsilon+1)a_d^3 \quad (2)$$

where μ_g is the dipole moment of the *gauche* form, a_d is the molecular radius of the dichloroethane molecule assumed to be spherical, α_d is the polarizability of dichloroethane and ε is the dielectric constant of the solution.

Naturally, ε in the formula (2) is dependent on N_g and N_s, and is expressed by the following formula[4];

$$\varepsilon-1=\frac{3\varepsilon}{2\varepsilon+1}\left\{\frac{4\pi\mu_g^2N_g}{3kT}\left(\frac{2\varepsilon+1}{2\varepsilon+n_d^2}\cdot\frac{n_d^2+2}{3}\right)^2+\frac{2\varepsilon+1}{2\varepsilon+n_d^2}(n_d^2-1)\times\frac{4\pi}{3}a_d^3N_d+\frac{2\varepsilon+1}{2\varepsilon+n_s^2}(n_s^2-1)\times\frac{4\pi}{3}a_s^3N_s\right\} \quad (3)$$

where n_d and n_s are the refractive indices of dichloroethane and solvent respectively and a_s is the molecular radius of solvent molecule assumed to be spherical.

To obtain the ratio of N_g to N_t, we shall assume that the chemical potential of the *trans* form is equal to that of the *gauche*, that is,

$$\partial\ln Z/\partial N_g=\partial\ln Z/\partial N_t$$

and then we can derive

$$N_g/N_t=2\exp-\{\Delta E-(\Delta G+N_g\partial\Delta G/\partial N_g)\}/kT \quad (4)$$

Using (4), we now proceed to obtain the excess enthalpy of the solution. Enthalpy of the solution arising only from the internal rotation is expressed as follows;

$$H_i=kT^2(\partial\ln Z/\partial T)-Xw \quad (5)$$

The excess of enthalpy is obtained by subtracting the value of H_{io} of pure liquid of dichloroethane from the above. Thus the excess of enthalpy is

$$\Delta H_i=H_i-H_{io} \quad (6)$$

where H_{io} is the enthalpy of dichloroethane in the pure lipuid state.

We shall apply this treatment to the actual systems. In the measurement of heats of mixing, cyclohexane, carbon tetrachloride and benzene were used as non-polar solvents, but here in the calculation we shall take up only the dichloroethane-carbon tetrachloride system. Other two systems may be expected to show only a small deviation from the carbon tetrachloride system, because the refractive indices of benzene and cyclohexane are

3) C. G. Böttcher, "Theory of Electric Polarization," Elsevier, Houston, p. 139.

4) H. Fröhlich, "Theory of Dielectrics", Oxford, London, p. 47.

little different from that of carbon tetrachloride. The values of refractive index n and molar volume of dichloroethane and carbon tetrachloride in the pure liquid used in the calculations are as follows;

	n^2		Molar volume (ml.)	
	20°C	25°C	20°C	25°C
Dichloroethane	2.0861	2.0702	79.03	79.88
Carbon tetrachloride	2.1316	2.1220	96.49	97.08

According to Wada and Morino[5], we adopt ΔE=1.27 kcal/mole and μ_g=2.55 D. To obtain the values of N_g/N_t, we have to perform successive approximations using formula (4). The results thus obtained are plotted against the concentration of dichloroethane in Fig. 1. It is seen that

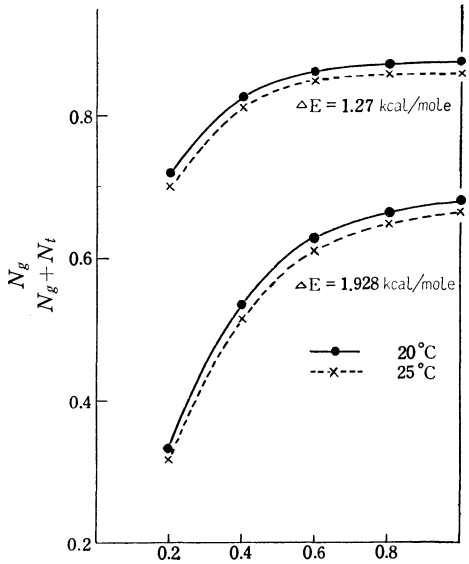

Mole Fraction of Dichloroethane

Fig. 1

the fraction of the *gauche* form decreases appreciably with dilution of dichloroethane by carbon tetrachloride. There have been no reports on systematic experimental data to be compared with the above expectation. Only in the pure liquid of dichloroethane**, it was found from spectroscopic data that the fraction of the *gauche* form is about 2/3, and is somewhat lower than the calculated value. This may be attributed, as Wada[6] pointed out, to the calculation on the oversimplified spherical model of molecule and may be improved by various corrections.

To diminish the overestimation of the energy due to the reaction field, it will be necessary to increase the value of ΔE. We, therefore, adopted a larger value of 1.928 kcal./mole as ΔE, with which the value 2/3 of the fraction of the *gauche* form in pure liquid was obtained. By the use of this value as ΔE, the fraction of the *gauche* form is recalculated and shown in the same figure. Here, it will also be seen that the appreciable decreases in the fraction of the *gauche* form take place with dilution by carbon tetrachloride. Hence we may use both values of ΔE in the later calculation.

Knowing the values of $N_g/(N_g+N_t)$ and using Eqs. (5) and (6), we can calculate the values of the excess of enthalpies of the solution. As in the formula (5), $N_g/(N_g+N_t)$, ε and n are all dependent on temperature, the explicit derivation of (5) is complicated. Consequently the following formula may be used instead of (5).

$$H_i = -k\{(\ln Z_1 - \ln Z_2)/(1/T_1 - 1/T_2)\} - xw$$

where Z_1 and Z_2 are the partition functions at the different temperatures T_1 and T_2, and here as T_1 and T_2 the values of 298.16 and 293.16°K will be used respectively.

The excess of enthalpies of the solution calculated is shown in Fig. 2. From this figure it will be seen that a fairly large amount of heat, in particular when the value of ΔE=1.27 kcal./mole is used, is to be absorbed when dichloroethane and carbon tetrachloride are mixed.

Experimental

In order to compare these theoretical results with the experiment, we measured the heat of mixing of dichloroethane with cyclohexane, carbon tetrachloride and benzene at 25°C.

These four materials were purified according to the method described in the literature and finally distilled by a long column of about thirty theoretical plates and the fractions having the boiling point range of 0.1°C were taken. The apparatus used for the measurement was already described elsewhere[7] and in this experiment it was improved in some points. The temperature sensitivity of the apparatus was 1.5×10^{-5}°C, which corresponds to the heat sensitivity of 10^{-3} cal.

Results and Discussion

The results obtained for the three systems are shown in Tables I, II and III, respectively. Heats of mixing per mole

5) A. Wada and Y. Morino, *J. Chem. Phys.*, **22**, 1276 (1954).

** Private communication from Mr. I. Miyagawa.

6) A. Wada, *J. Chem. Phys.*, **22**, 198 (1954).

7) K. Amaya and R. Fujishiro, This Bulletin, **29**, 270 (1956).

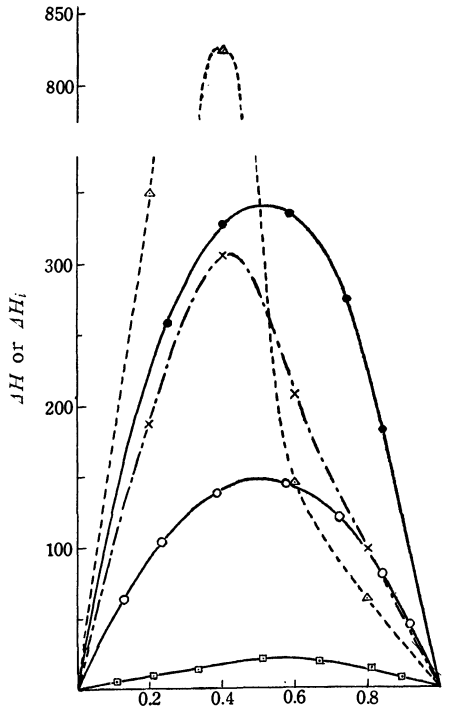

Fig. 2.

Expt.
—●— *DE*-cyclohexane
—○— *DE*-carbon tetrachloride
—⊡— *DE*-benzene
Calcd.
---△--- ΔE=1.27 kcal./mole
–·×·– ΔE=1.928 kcal./mole

TABLE I

HEAT OF MIXING FOR DICHLOROETHANE-CYCLOHEXANE SYSTEM (25°C)

Mole fraction of dichloroethane	ΔH/mole of sol. cal.
0.2551	260.9
0.4065	326.5
0.5781	330.8
0.5781	329.8
0.7326	271.8
0.8457	186.0

TABLE II

HEAT OF MIXING FOR DICHLOROETHANE-CARBON TETRACHLORIDE SYSTEM

Mole fraction of dichloroethane	ΔH/mole of sol. cal.
0.1284	64.2
0.2324	104.1
0.3992	141.6
0.5695	146.8
0.5535	155.6
0.7219	124.8
0.8423	81.8
0.9139	48.0

TABLE III

HEAT OF MIXING FOR DICHLOROETHANE-BENZENE SYSTEM

Mole fraction of dichloroethane	ΔH/mole of sol. cal.
0.1114	6.66
0.2026	11.5
0.3340	17.6
0.5084	22.6
0.5138	19.1
0.6740	20.2
0.8043	16.6
0.8938	10.9

of mixtures are plotted in Fig. 2, in which the theoretical curves are also shown.

Since the observed heats of mixing contain not only the contribution from the dipolar energy but also that from the dispersion energy, we have to estimate the part of the contribution from the latter and derive that from the former to compare it with the theory. A molecule of *trans*-dichloroethylene is nearly isoelectric with that of dichloroethane and has a dipole moment of zero; it seems to be reasonable to assume that the contribution of the dispersion energy is nearly the same for both molecules.

So we took the molecule of dichloroethylene as an imaginary molecule of dichloroethane with zero dipole moment and estimated the part of the contribution from dispersion forces for dichloroethane, using the data for *trans*-dichloroethylene. Expected heat of mixing of dichloroethylene with three solvents was calculated for equimolar mixture of dichloroethylene and three solvents according to the Scatchard formula*** for three equimolar mixtures of dichloroethylene: 23 cal./mole for cyclohexane, 18 cal./mole for carbon tetrachloride and nearly zero for benzene.

These corrections seem to be relatively small for each case, so we did not make any corrections of the observed heats of mixing. Since these non-polar liquids used as solvents have nearly equal values of dielectric constant, it is not unreasonable to expect from the theory that the values of ΔH_i for these systems are nearly equal to one another. However, the observed values of heats of mixing, which may be taken as values of ΔH_i disregarding the minor corrections mentioned above, do not coincide with one another; the maximum values of the heats of mixing per

*** Joel H. Hildebrand and Robert L. Scott, "The solubility of nonelectrolytes". Reinhold Publishing Co., New York (1948). p. 124.

mole of mixture are 330 cal., 150 cal. and 20 cal., for the systems of cyclohexane-dichloroethane, carbon tetrachloride-dichloroethane and benzene-dichloroethane, respectively.

These discrepancies seem to show that the simple assumption of taking dichloroethylene as an imaginary dichloroethane of zero dipole moment can not be necessarily applied to these systems to estimate the contribution from dispersion forces.

As for the comparison with the theoretical value, the value of ΔH_i obtained by the use of the value of 1.27 kcal./mole for ΔE is much greater than the observed value and this may be due to the overestimation of the reaction field in the simple Onsager model.

By the use of the higher value of 1.928 kcal./mole for ΔE to diminish the overestimation of the reaction field, rather good agreements between the theory and the experiment were obtained for the systems of cyclohexane-dichloroethane and carbon tetrachloride-dichloroethane. But such a higher value of ΔE seems to be inconsistent with the experimental fact, so that these discrepancies may have to be explained by considering two dipoles in the dichloroethane molecule with proper angles between them, as was done by Wada[6], or by some other more refined theory of dielectrics.

For the benzene-dichloroethane system, the agreement is very poor and the deviation is negative. This will suggest that the specific interactions occur between these two kinds of molecule. More quantitative discussions for these systems will be impossible until more data concerning various physical properties are accumulated.

Summary

For three solutions of dichloroethane which is regarded as a typical molecule having internal rotation isomers, the excessive enthalpies arising from the internal rotation were calculated according to a simple theory derived from the Onsager model, and were compared with the results obtained from the measurements of heats of mixing for these solutions. The agreement was not very good and it seems to owe to the overestimation of the reaction field based on the simple molecular model in the Onsager model. Especially for the dichloroethane-benzene system, special interactions may be expected to exist between dichloroethane and benzene.

We would like to express our gratitude to Professor Y. Morino of Tokyo University for his valuable suggestions.

Department of Chemistry, Faculty of Science, Kobe University
Higashinada-ku, Kobe

Phase Transition of Li_2O—Fe_2O_3 System. I. Thermal and Electric Properties of Lithium Ferrite $LiFeO_2$

By Eizo KATO

(Received September 2, 1957)

In 1931, Posnjak and Barth[1] interpreted an X-ray diffraction pattern obtained from an isometric modification of lithium ferrite, and found that its crystal structure is of sodium chloride type, O_h^5-*Fm3m*, in which cations, lithium and ferric ions, are randomly distributed among the equivalent points. This crystal has variate atom equipoint structure. At the same time they observed that lithium ferrite has an anisotropic modification below about 600°, but did not explain the relation between these two modifications. For the cubic modification Kordes[2], Hoffmann[3] and Collongues and Chaudron[4] gave the lattice constants.

In 1944, Barblan et al.[5] showed that unknown anisotropic modification is tetragonal, D_{4h}^{19}-*I4/amd*, in which lithium and ferric ions are arranged in the different equivalent positions, and that the phase transition between these modifications is an order-disorder one. In addition, they stated that the modifications sluggishly transform within 570–670°. Recently Collongues[6] found that another orderd modification exists at the temperature range below the preceding ordered phase. These investigations were made only by X-ray diffraction method and the transition temperature was vague.

The author was interested in the correlation between the crystal structure and

1) E. Posnjak and T. F. W. Barth, *Phys. Rev.*, **38**, 2234 (1931).
2) E. Kordes, *Z. Kryst.*, **92**, 139 (1935).
3) A. Hoffmann, *Naturwiss.*, **26**, 431 (1938).
4) R. Collongues and G. Chaudron, *Compt. rend.*, **231**, 143 (1950).
5) F. Barblan, E, Brandenberger and P. Niggli, *Helv. Chim. Acta*, **27**, 88 (1944).
6) R. Collongues, *Compt. rend.*, **241**, 1577 (1955); *Bull. soc., chim. France*, **1957**, 261.

the physico-chemical properties in the course of transition, and measured the the thermal electric properties of lithium ferrite.

Experimental

i) Specimens.—Ferrous oxalate and lithium corbonate were mixed in wet condition and heated in an open furnace at ca. 800° for a day. In order to complete the reaction, the above procedure was repeated with an excess of lithium carbonate, which was removed by cold dilute acetic acid.

Anal. Found: Li_2O, 15.73 %; Fe_2O_3, 82.00 %; insoluble, 0.33 %. Calcd. for $LiFeO_2$: Li_2O, 15.76 %; Fe_2O_3, 84.24 %.

Ceramic specimens to be tested were prepared according to Weisz[7], i. e., fine-ground powder of the products was mixed with a little quantity of triethanolamine stearate and of *Carbowax 3000* as binder and lubricant, and then moulded with a pressure of 100 kg./cm². After being sintered at ca. 1000° for two hours, they were further given appropriate heat treatments; ordered specimens were annealed at ca. 570° for more than fifty hours, and disordered specimens were quenched by rapid cooling, either by immersion into water or exclusion of the air.

The specimen for dilatometry was rod-shaped, 7 mm. in diameter and 5 cm. in length. For electric measurement a pellet was prepared, 1 cm. in diameter and 2～5 mm. in thickness. Both sides of the pellet were polished with emery powder.

For the identification of these specimens, X-ray powder diffraction method was taken with FeKα radiation. The observed lattice constants showed the following values and agreed with former investigators',

ordered phase: $a=4.034$ Å, $c=8.71$ Å;
disordered phase: $a=4.145$ Å.

ii) Apparatus and Procedures.—Sudo's apparatus[8] was used for differential thermal analysis, which was made by Mitamura & Co. Ltd. The nickel vessel has three holes; the outside one was packed with alumina powder as standard and the opposite one by fine-powdered probe. The temperature difference between these two materials was measured by means of an inserted platinum-platinum rhodium themocouple connected to a galvanometer. The mid hole contained alumina, in which another thermocouple was inserted to measure the temperature of the whole assembly. The ascending rate of temperature in the furnace was manually controlled. The apparatus was not appropriate for a sluggish transition, because it was constructed for a mineralogical investigation for a comparatively rapid rate of temperature rises so that the measurement at slower rate than 0.4°/min. was impossible.

7) R. S. Weisz, *Ceram. Ind.*, **58**, No. 4, 130, 133; No. 5, 76 (1952).
8) Toshio Sudo, "The Clay Minerals (Nendo-kobutsu)", Iwanami Shoten, Tokyo, 1953, p. 49.

The schematic diagram of dilatometer is shown in Fig. 1. The difference of thermal expansion between the specimen and a quartz glass was observed by mirror-telescope-scale system. The temperature was measured with a Chromel-Alumel thermocouple, which was inserted near the specimen and connected to a Potentiometer Type K-2 Shimadzu Seisakusho Ltd. The reading of elongation had an accuracy of ca. 7×10^{-6} cm. and the reading of temperature of ±0.1°. To adjust the heating rate, the temperature of the furnace was controlled with a Potentiometer-type

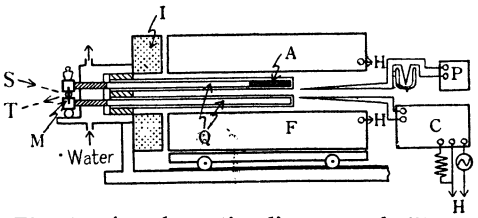

Fig. 1. A schematic diagram of dilatometer.
A: specimen to be tested;
C; temperature controller;
F: furnace;
I: heat-insulating ceramics, "Isolite N-4";
M: mirror;
P: potentiometer;
Q: quartz glass rod;
S: scale;
T: telescope.

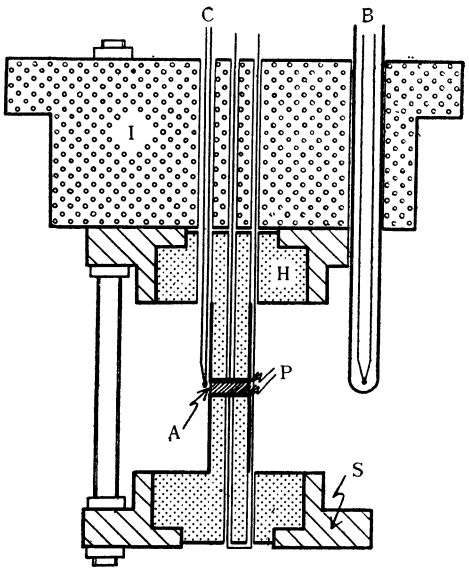

Fig. 2. Electrode assembly.
A: pellet to be tested;
B: Pt-PtRh thermocouple;
C: Chromel-Alumel thermocouple;
H: sillimanite holder;
I: heat-insulating ceramics, "Isolite N-4";
P: Pt foil;
S: heat-resistant steel.

Controller Chino Works Ltd., which permits the fluctuation of ±1°.

D. C. resistance was measured with a D. C. Bridge Type BR-7A Shimadzu Seisakusho Ltd. Electrode assembly* is shown in Fig. 2. The pellet was placed between two discs of platinum foils to which lead wires were attached. The platinum foils and the pellet were tightly fitted by steel holders to ensure a good contact. All the assembly except the upper-insulating part was inserted in a vertical furnace, and the resistance was measured as a function of temperature.

The bridge was connected to two volt d. c. source, thus the pellet was placed in a constant electric field during the measurements. The resistance at room temperature was measured with Megger Type L-4 Yokogawa Electric Works Ltd., because it was too large to be measured with a bridge. Determination and control of temperature were by the same method as in the case of the dilatometry.

Results and Discussion

Differential Thermal Analysis. — In general, there is a change in specific heat with phase transition. For an exact study of the transition, it is desirable to measure the specific heat at various temperatures. However, for the sake of simplicity, the differential thermal analysis was adopted to see the transition.

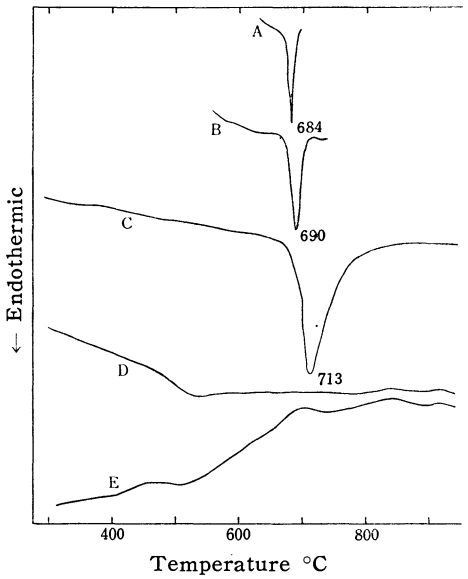

Fig. 3. Differential thermal analysis of $LiFeO_2$.
A: annealed at 570° for 50 hr., repeated twice: 0.4°/min.;
B: annealed at 570° for 60 hr.: 1.6°/min.;
C: same as B: 10°/min.:
D: annealed at intervals of 100° from 1000° to 500° for 12 hr. at each temperature: 10°/min.;
E: quenched from 1000° in the air: 10°/min.

Since it is obvious that the transition velocity is very sluggish, a series of thermal analyses under various conditions were performed. The deflection of the galvanometer as a function of temperature is shown in Fig. 3. The curves A and B are registered with a different scale from the curves C, D and E, for the deflection of the former is smaller than that of the latter owing to the slow rise of temperature.

The curves, measured under various rates of heating for ordered specimens, are A, B and C. The endothermic reaction evidently appears in each case, and the corresponding temperatures are 684°, 690° and 713° for the curves A, B and C, respectively. It is well known that the endothermic reaction appears by the phase transition between the stable modifications. To verify this phenomenon, the curve E was taken using a disordered specimen. In the commenting temperature range no reaction is observed on the curve. Undoubtedly this reaction can be attributed to the order-disorder transition.

Considering the following two points, it is confirmed that the transition velocity is very sluggish. First, it is difficult to obtain perfect ordered specimens, in spite of annealing for a considerably long time, as is obvious in the specimen for curve D. Secondly, difference in endothermic temperatures is caused by the difference in heating rate among the curves A, B and C. If it were measured at a slower rate than 0.4°/min., it could be expected to settle down to a definite temperature which is somewhat lower than 684°; this is impossible with our apparatus.

Dilatometry.—By measurement of the linear coefficients of thermal expansion with a heating rates both for annealed and quenched specimens, Fig. 4 was obtained.

The expansion coefficient is remains unchanged at 300° to 750°C (1.80×10^{-5}), for the ordered specimen at a heating rate of 30°/hr. The same result is obtained at as rate 5°/hr. The anomaly of expansion distingushably appears when the heating rate is brought down to 2°/hr. For the purpose of verifying the behavior around the transition temperature, the expansion curve measured at rate of 1°/hr. is shown

* The author was referred to Parravano's apparatus; G. Parravano, *J. Chem. Phys.*, **23**, 5 (1955).

in Fig. 5, where the expansion coefficient becomes maximum at 660±2°. The increment caused by the anomalous expansion for this case is 0.12 %.

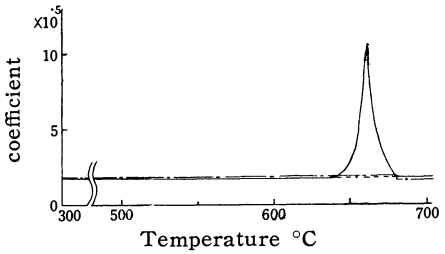

Fig. 4. Curves of expansion coefficient *vs.* temperature of $LiFeO_2$.
——: ordered specimen: 1°/hr. above 550°, 30°/hr. below 550°;
- - -: above specimen at 30°/hr. within the anomalous range;
—·-: disordered specimen: 80°/hr.

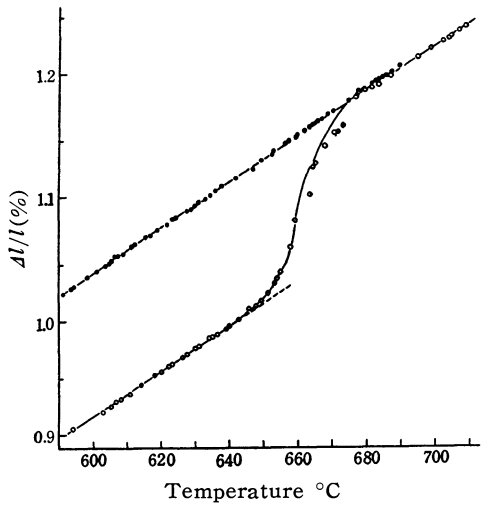

Fig. 5. Expansion curves of ordered specimen around the transition temperature.
○: ascending;
●: descending.

The descending curve is measured down to 550° with the same specimen at a rate of 1°/hr. and a constant coefficient 1.85×10^{-5} is obtained. Although it shows an irreversible process as in a monotropic transition, this is due to the long time required by this transition. The same sort of measurement was carried out for the quenched disordered specimens. Their coefficients were 1.88×10^{-5} below and 1.61×10^{-5} above 680°C at considerably rapid ascending rate. From these results, the transition temperature is determined to 660±2°, inferred to the results of differential thermal analysis.

Electric Resistance Measurement.— Electric properties in relation to the phase transition are generally studied by the measurement of dielectric constant and dielectric loss. The electric resistance of our pellets is not great enough at higher temperatures, to enable their measurement. It may be natural that a strict reproducibility can not be expected for the measurement of electric resistance of a semiconductor. It is, therefore, necessary to repeat the same sort of measurement. In fact, it is quite difficult not only to make each resistance-temperature curve coincide, but also to determine the transition temperature in which the anomalies appear. From more than twenty measurements, some significiant examples are shown in Fig. 6. Generally, the curves similar to A are observed at a rapid heating rate (30°/hr.), and the curves similar to D, at a slower rate (2°/hr.). The tangent of ρ versus $1/T$ steadily decreases in the former, while the change of the tangent is found within 660–680° in the latter. A peculiar example is the curve B, in which a negative tangent is observed in the above temperature range. The pellet was placed in a steady electric field during the measurement; electrolysis was indicated on the pellet surface. The circuit was kept closed for as short a time as possible to obtain a reading of the curve C, in order to minimize the influence of electrolytic polarization. An anomaly of electric resistance is recognised within 660–680° from these results.

A semiconducting feature is expressed by

$$\rho=\rho_0\exp(-\phi/kT),$$

where ρ : electric resistance
ρ_0: constant
ϕ : activation energy
k : Boltzmann constant
T: absolute temperature

From the above results, the values of activation energy are 0.65~0.9 eV for ordered specimen (200~400°), 0.3 eV for disordered specimen (100~300°) and 1.2~1.4 eV for each specimen (680~710°). The net resistance at room temperature has the order of magnitude 1000 MΩ for ordered specimens and several MΩ for disordered ones.

When the current has flowed for a long time, color change is observed on the surface; the cathode side is white and the opposite is brown, At the same time, white materials which contain lithium adhere to platinum cathode. Those color

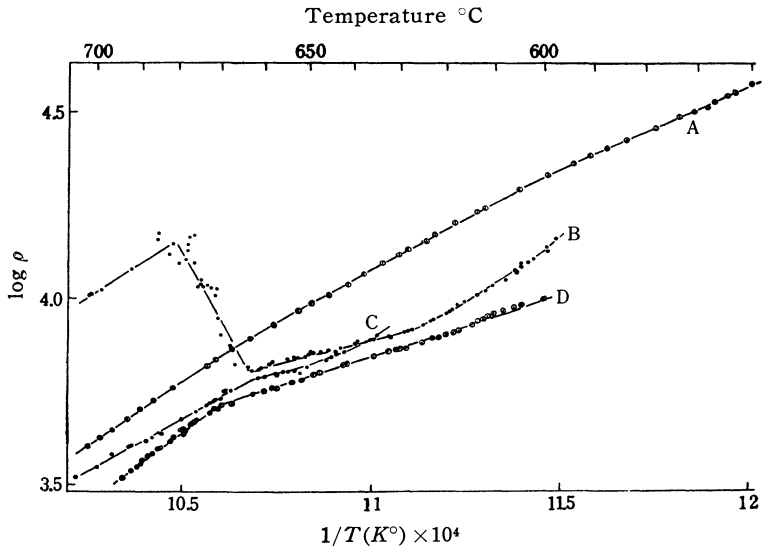

Fig. 6. D.C. resistance curves of $LiFeO_2$.

changes are hard to find below 300°, and become more evident with increasing temperature. For the materials having the order-disorder transition such as AgI and Ag_2HgI_4, it is known that the conduction is electrolytic, owing to the vacant points in the lattice. The conduction mechanism is also electronic for the material containing iron such as magnetite. From the above simple experiment, considering the influence of excess of Li_2O, it is assumed that the electrolytic conduction takes place within the temperature range of transition.

Summary

The measurements of differential thermal analysis, thermal expansion and d.c. electric resistance for lithium ferrite were performed in relation to the order-disorder transition. Conclusions are described as follows;

(1) The endothermic reaction and the anomalous expantion take place during the transition.

(2) The value of the transition temperature is determined as 660±2°C. by means of dilatometry.

(3) The existence of electrolytic conduction is qualitatively recognized.

(4) It is verified that the transition is very sluggish.

The author wishes to express his sincere thanks to Professor S. Nagaura of Osaka City University for his kind advice and encouragement during this work.

The Institute of Polytechnics
Osaka City University
Kita-ku, Osaka

*Phase Transition of Li_2O—Fe_2O_3 System. II. Thermal and Electric Properties of Lithium Ferrospinel $LiFe_5O_8$**

By Eizo KATO

(Received September 2, 1957)

Lithium ferrospinel has been used as magnetic material for high frequency field because of its ferromagnetic properties. The ferrimagnetism for lithium ferrospinel and other ferrites was widely studied; Weisz[1] gave a detailed review concerning its practical uses.

In 1938, Hoffmann[2] studied the crystal structure of lithium ferrospinel by means of X-ray diffraction method. He found that its crystal structure is spinel-type, O_h^7-$Fd3m$. After Hoffmann's work Barblan[3], Collongues[4] and Kordes[5] investigated the same problem and determined the lattice constant. All of these investigators confirmed the structure of disordered modification, that is, the lithium and the ferric ions in octahedral positions are distributed at random.

In 1949, Braun[6] investigated the extra-line of lithium ferrospinel, which could not be explained by spinel structure, and determined the space group of its ordered modification, O^6—$P4_32$, in which lithium and ferric ions in octahedral positions are arranged in different positions. The transition was observed at 735° to 755°C. Verwey et al.[7] calculated the contribution of long-range ordering to lattice energy using the above-mentioned structures. It is worth mentioning that Behar[8] clarified the mechanism of the order-disorder transition of lithium ferrospinel by metallurgical technique.

In the following sections of this paper the thermal and the electric properties of lithium ferrospinel will be described from the viewpoint of order-disorder transition, and the correlation between lithium ferrite and lithium ferrospinel will also be discussed.

Experimentals

Specimens.—Lithium ferrospinel was prepared by a similar method to that for lithium ferrite; only heat treatments will be described here. An ordered specimen can be satisfactorily obtained by annealing in a furnace from ca. 800° to the room temperature, while a disordered specimen by rapid cooling, immersed into water from 1000°. The lithium content in the specimens was analysed by means of flame photometry; Found: 3.09%, Calcd. for $LiFe_5O_8$: 3.61%.

For the identification of the above specimens, X-ray diffraction was carefully applied by the back-reflection method, and the following observed values of lattice constant agreed with former investigators';

ordered phase; $a=8.329_6\pm0.000_5$ Å,
disordered phase; $a=8.332_6\pm0.000_5$ Å.

Apparatus and Procedure.—The apparatus used for differential thermal anlysis, dilatometry and d.c. electric resistance measurements are all the same as were described in the previous paper; no further description will be given.

Results

Differential Thermal Analysis.—A series of differential thermal analyses under various heating rates were performed, to obtain preliminaly knowledge for further measurements concerning the transition temperature and the transition velocity. The resultant curves are shown in Fig. 1, where the curves A and B are registered with a different scale from that of other curves, corresponding to the different heating rate, to exaggerate the relatively small effect. Some features of these curves are as follows:

(a) For the ordered specimens well-annealed, the apparent temperatures of endothermic reaction seem to converge from 766° to 745.5° according as the rate is slower. No wide spreading of apparent

* *Lithium ferrospinel* stands for $LiFe_5O_8$, to avoid confusin with $LiFeO_2$ of sodium chloride structure.

1) R. S. Weisz, *Ceram. Ind.*, **58**, No. 4, 130, 133; No. 5, 76 (1952).
2) A. Hoffmann, *Naturwiss.*, **26**, 431 (1938).
3) F. Barblan, E. Brandenberger and P. Niggli, *Helv. Chim. Acta*, **27**, 88 (1944).
4) R. Collongues and G. Chaudron, *Compt. rend.*, **231**, 143 (1950).
5) E. Kordes and E. Röttig, *Z. anorg. allgem. Chem.*, **264**, 34 (1951).
6) P. B. Braun, Paper at ASXRED meeting, Itheca, 1949; *Nature*, **170**, 1123 (1952).
7) F. de Boer, J. H. van Santen and E. J. W. Verwey *J. Chem. Phys.*, **18**, 1032 (1950); E. J. W. Verwey, P. B. Braun, E. W. Gorter, F. C. Romijn and J. H. van Santen, *Z. Phys. Chem.*, **198**, 6 (1951).
8) I. Behar, *Compt. rend.*, **242**, 2465 (1956).

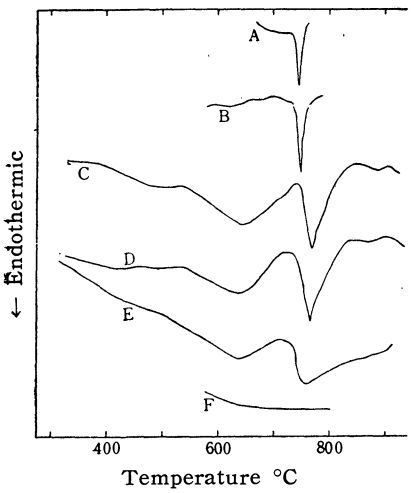

Fig. 1. Differential thermal analysis of $LiFe_5O_8$.
A: annealed in a furnace after being cooled from 850° to 580° at 30°/hr.: 0.5°/min.;
B: same as A: 1.5°/min.;
C: annealed at intervals of 100° from 1000° to 500° for 12 hrs. at each temperature: 10°/min.;
D: quenched from 1000° in the air: 10°/min.;
E: quenched from 1000° in water: 10°/min.;
F: quenched from 1000° in water most rapidly: 1.5°/min.

transition temperatures, as in the case of $LiFeO_2$, was obtained (Curves A, B and C).

(b) The curve F is that for a disordered specimen, quenched as rapidly as possible, and shows no reaction at 700—800° different from other. It may be concluded that the endothermic reaction around 745.5° is due to the order-disorder transition.

(c) Another endothermic valley is found at 635—638° (Curves C, D and E).

(d) The curves change from A to F, as the specimen transfers from ordered to disordered form. By comparison of the curves D, E and F, it is seen that the quenching must be completed within 1~2 seconds for the preparation of the disordered specimen. As for the curve E for the semi-ordered specimen, the endothermic deflection due to the transition is somewhat smaller than that of the ordered specimen.

Dilatometry. — Thermal expansion of ordered and disordered specimens was measured, in order to confirm the transition temperature taken from the differential thermal analysis and to know the volume change caused by the transition. Linear expansion coefficients as a function of the temperature are shown in Fig. 2. Since the transition velocity gets extremely low around the transition temperature, at the lower temperature range it is not the case, the measurements at different temperature ranges were undertaken under different ascending rates, e.g. 100°/hr. for 400—570°, 30°/hr. for 570—680° and 5°/hr. for above 680°. The curve of a quenched specimen which was obtained at the rate of 100°/hr. has much complexity. It is not only difficult but seems meaningless to make a detailed analysis of the curve. The negative coefficient at 700—800°, however, is probably due to the ordering from disordered phase. From these curves, it is seen that the transition occurs at

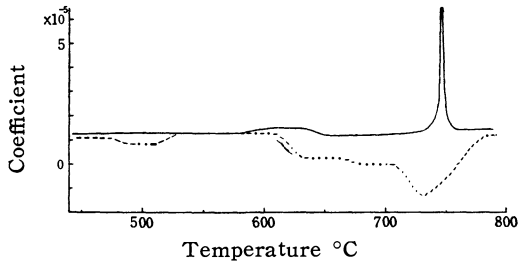

Fig. 2. Curves of expansion coefficient vs. temperature of $LiFe_5O_8$.
———: ordered specimen;
------: disordered specimen.

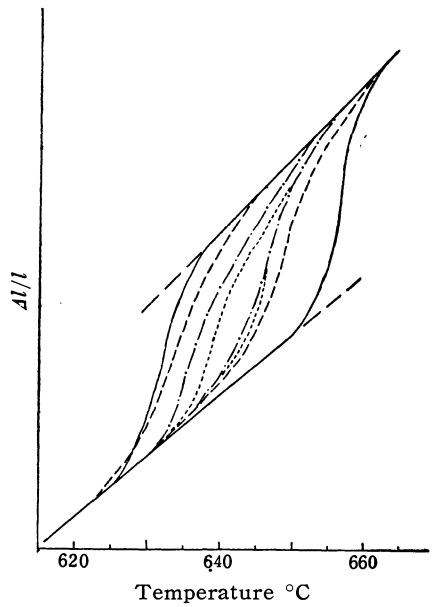

Fig. 3. Expansion curves of ordered specimen around the transition temperature.
———: 100°/hr.; — — —: 30°/hr.;
— · —: 5°/hr.; ------: 1°/hr.

745±1° and an anomalous expansion due to the transition is evident.

Detailed measurements were repeatedly made for the ordered specimem at various rates and the resultant hysteresis curves are shown in Fig. 3*. The slower the ascending or the descending rate of temperature, the lower the temperature at which the anomaly takes place. The dilatometric values determined from these curves are as follows;

transition temperature: 745±1°C.,
expansion gap caused by anomaly: $(32\pm2)10^{-3}$%,
coefficient before transition: $(1.20\pm0.03)\times10^{-5}$,
coefficient after transition: $(1.44\pm0.04)\times10^{-5}$.

Electric Resistance Measurement.— The specific resistance of ordered and disordered pellets of the ferrospinel at the room temperature have the values of 100 MΩ and 2~3 KΩ, respectively. They are more conductive compared with lithium ferrite; especially this phenomenon is remarkable for disordered pellets. The observed d. c. resistance is shown in Fig.

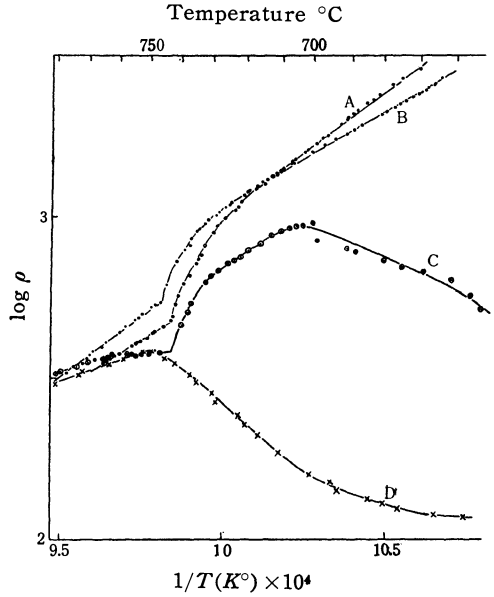

Fig. 4. D. C. resistance curves of $LiFe_5O_8$.
A: ordered specimen; heating rate: 5°/hr.;
B: same as A; heating rate: 30°/hr.;
C: disordered specimen; heating rate: 30°/hr.;
D: same as C; heating rate: 600°/hr.

4. In the curve A and B, the value of resistance shows a constant tangent at a lower temperature. Near the transition temperature, resistance decreases anomalously and again shows a linear tangent at a higher region. Although measurements were made not only at different heating rates but also with specimens different in crystal phase, every curve shows a distinct change in conductance at a nearly definite temperature. Compared with the thermal changes, this temperature is concluded to be the transition one. The difference in tangent at the temperature range of the anomaly seems to be related to the different transition velocity corresponding to the heating rate.

On the other hand, the curves of a quenched pellet give a negative tangent, which seems to be under the influence of transition to the ordered state of equilibrium from disordered phase at a higher temperature. The temperature range of negative tangent is affected by the heating rate. The values of activation energy are as follows:

0.60 eV: ordered specimen within 200~500°,
0.20 eV: disordered specimen within 130~500°,
1.2~1.4 eV: each specimen after transition.

When the pellets were kept in a stationary d. c. field during the measurements, a color change was observed on the surface as was previously reported for lithium ferrite.

Discussion

It may be convenient to discuss the present results referring to that of lithium ferrite. These compounds take the same kind of transition, i.e. order-disorder transition, but the relative number of the existing two kinds of cation, the same number of lithium and ferric ion, contribute to the transition. For lithium ferrospinel, however, some portions of cations, lithium ions and three times their magnitude of ferric ions at octahedral position, contribute to the transition. Oxygen ions of the ferrite or ferric ions in tetrahedral position and oxygen ions of the ferrospinel, scarcely vary the lattice points by the transition. Regarding only the numbers of migrating ions, the relation between the ferrite and the ferrospinel is analogous to that between β-CuZn and Cu_3Au in binary alloys.

* As J. B. Austin (*J. Am. Ceram. Soc.*; **35**, 243 (1952).) suggested, the descending curve does not coincide with the ascending one, but it is unavoidable for aggregated specimens used in the present experiments.

Anomalous Expansion.—Anomalous expansions around the transition temperature were observed in the ferrite and the ferrospinel as in the case of other crystals which show the order-disorder transition. The curve of the expansion coefficient of non-stoichiometric compound shows symmetrical form, but that of stoichiometric one shows abrupt λ form. The anomalous gap of expansion was compared with the value calculated from the lattice constant and the numerical results are shown in Table I, where the values obtained by the two methods coincide well.

TABLE I

Compound	% Contraction on Ordering	
	from Lattice Constant	from Expansion Gap
$LiFeO_2$	0.14	0.12
$LiFe_5O_8$	0.036	0.032

Hysteresis and Transition Velocity.—Lithium ferrospinel makes a dilatometric hysteresis curve around the transition temperature, which is shown in Fig. 3. The temperature interval of the hysteresis has about 25° at the rapid rate (100°/hr.). Naturally, the slower the rate, the narrower the interval. The ascending curve at the rate of 1°/hr. is almost the same with that at 5°/hr., but the descending curve of the former is nearer its ascending curve than that of the latter. Under an equilibrated condition, it may be expected that the descending curve will agree with the ascending one and the hysteresis loop vanishes.

Though the transition velocities were not directly measured in the present work, it is of much interest to elaborate the the measurement of the transition velocity with respect to the transition mechanism. The difference in the transition velocities in the ferrite and the ferrospinel can be probably correlated with each crystal structure. This subject should be considered from a crystallographic aspect and also from a diffusion process caused by lattice defect.

Thermal Properties at the Magnetic Curie Point.—There should be a discontinuity in specific heat as ferromagnetic material passes through the Curie point, so that its effect should also appear in the thermal analysis* and dilatometry. As mentioned already, the endothermic reaction around 635° and the increase in expansion coefficient at 590—640° were examined. As for the Curie point, the following data were reported by many authors up to date; 637° (Hilpert et al.[9]), 635° (Kordes and Röttig[4]), 620±2° (Collongues and Chaudron[3]) and 590° (Weisz[7]). From these data, ca. 635° seems to be the ferromagnetic Curie point. Further discussion of the magnetic properties of these materials lies outside of this work.

Transition Temperature and the Composition.—The specimens used in the preceding measurements have the analytical composition $LiFe_{5.86}O_8$. It is necessary to deal with the specimen which has stoichiometric ratio $LiFe_5O_8$, for the purpose of the determination of accurate transition temperature. Several specimens having nearly the stoichiometric composition were prepared and heat-treated under th same condition. The dilatometry was carried out at the rate of 5°/hr. The values of the transition with respect to the composition are shown in Table II.

TABLE II

Composition	Transition Temperature, °C
$LiFe_{4.44}O_8$	749
$LiFe_{4.71}O_8$	751
$LiFe_{4.87}O_8$	749.5
$LiFe_{5.14}O_8$	750
$LiFe_{5.38}O_8$	749
$LiFe_{5.86}O_8$*	745

* The condition of preparation and heat treatment of this specimen is distinguished from others.

In binary alloys, where the homogeneous specimen can be easily prepared, it is well known that the specimen composition affects apparently the transition temperature[10]. On the contrary, in ceramics, it is almost impossible to obtain a homogeneous specimen either in composition or in grain size. This might be the reason why the change in average composition does not affect so appreciably the transition temperature as in the case of alloys. Considering these arguments, the transition temperature of lithium ferrospinel is determined to be 750±1°C.

* Using differential thermal analysis, Blum et al.. (*Am. Ceram. Sac. Bull.*, **36**, 175 (1957).) detected the Curie point of ferromagnetic and ferroelectric materials.

9) R. Hilpert, A. Hoffmann and F. Huch, *Ber.*, **72B**, 848 (1939).

10) F. C. Nix and D. MacNair, *Rev. Sci. Inst.*, **12**, 66 (1941).

Summary

The measurements of differential thermal analysis, thermal expansion and d. c. electric resistance for lithium ferrospinel were performed ; the results were discussed in relation to these for the lithium ferrite. Conclusions are as follows ;

(1) Anomalous changes in the thermal and the electric properties take place during the transition and the hysteresis loops are observed.

(2) The transition temperature for $LiFe_{5.86}O_8$, 745±1°C., is obtained from both thermal and electric measurements. The true transition temperature is determined to be 750±1°C. for the stoichiometric specimen.

(3) It is verified that the transition velocity is more rapid than that of lithium ferrite.

(4) The thermal properties change at the magnetic Curie point, ca. 635°C.

The author wishes to express his sincere thanks to Professor S. Nagaura of Osaka City University for his kind advice and encouragement during this work.

The Institute of Polytechnics
Osaka City University
Kita-ku, Osaka

On the Relation between Viscosity and Critical Micelle Concentration of Detergent Solutions. III. Relations between Micellar Molecular Weight, Viscosity and Critical Micelle Concentration of Detergent Solutions

By Kiyoshi TYUZYO*

(Received September 7, 1957)

Various methods are proposed for measuring micellar molecular weight (M_m) in detergent solutions; namely, X-ray diffraction[1,2], diffusion[3,4], osmotic coefficent[5] and light scatering[6,7]. Each method has its own characteristic and M_m obtained from various methods are quite different from each other[5]. However, recently, several light scattering investigations were made and accurate M_m values were obtained. This method seems to be the only one that has sure theoretical background.

It is shown in this paper that a kind of empirical relation is established between critical micelle concentration (CMC) and and association number (n) measured by the light scattering method. Using this relation, new empirical equations are proposed which hold between micellar molecular weight (M_m) and two kinds of intrinsic viscosity ($[\eta_1]$ and $[\eta_2]$) proposed in the first paper of this series. Further, some discussions are made concerning the characteristic behavior of viscosity in the range of low concentration of detergent solutions.

Relation between Association Number (n) and Critical Micelle Concentration (CMC)

In Table I are summarized the values of M_m*, association number (n) measured by the light scattering method and CMC (C_c). As both n and C_c are expected to be dependent mainly upon affinity of detergent molecules for solvent, n is plotted against $\log(1/C_c)$. The result is shown

* Present address: Research Laboratory, Dai-Nippon Celluloid Co., Sakai, Osaka.

1) R. W. Matoon, R. S. Stearns and W. D. Harkins, *J. Chem. Phys.*, **16**, 644 (1948).
2) D. E. Andersen and G. B. Carpenter, *J. Am. Chem. Soc.*, **75**, 850 (1953).
3) R. J. Vetter, *J. Phys. Colloid Chem.*, **51**, 262 (1947).
4) H. Okuyama and K. Tyuzyo, This Bulletin., **27**, 259 (1954)
5) W. Phillippoff, *Trans. Faraday Soc.*, Discussion, No. 11, 96 (1951).
6) P. Debye, *J. Phys. Colloid Chem.*, **53**, 1 (1949).
7) P. Debye and E. W. Anacker, ibid., **55**, 644 (1951).

* Whether M_m is independent of detergent concentration or not is not clear at present. (K. Sasaki, S. Saito and H. Okuyama, This Bulletin., **29**, 186 (1957)) M_m obtained from light scattering is the value at C_c and so M_m which appears in our discussion also means the one at CMC.

TABLE I
ASSOCIATION NUMBER, MICELLAR MOLECULAR WEIGHT AND CMC

Number	Substance	Temperature	Solvent	n	M_m	$C_c \times 10^3$ (mol./l.)	Literature
1	Na-Octane-sulfonate	23	water	25.4	5500	155	8)
2	Na-Decane-sulfonate	30	water	40	9900	38	〃
3	Na-Dodecane-sulfonate	40	water	54	14700	11	〃
4	Na-Tetradecane-sulfonate	60	water	80	24000	3.3	〃
5	Na-Decyl-sulfate	23	water	50	13000	31	〃
6	Na-Dodecyl-sulfate	23	water	71	20500	8	〃
7	Na-Tetradecyl-sulfate	23	0.01 M NaCl	138	43500	1.9	〃
8	Dodecyl trimethyl ammonium-Br	23	water	50	15400	14.4	〃
9	Dodecyl trimethyl ammonium sulfate	23	water	65	17900	16.6	〃
10	Mg-Octane-sulfate	23	water	51	10400	110	〃
11	Mg-Decane-sulfate	60	water	103	24000	20	〃
12	Mg-Dodecane-sulfate	60	water	107	28500	3.3	〃
13	Didodecyl dimethyl ammonium-Cl	60	0.003 M NaCl	206	43000	0.1	〃
14	Triton X-100	—	water	139	90000	0.9	9)
15	Dodecylamine-HCl	—	water	59	12300	14.0	6)
16	Dodecylamine-HCl	—	0.016 M NaCl	99	20500	11.6	〃
17	Dodecylamine-HCl	—	0.046 M NaCl	152	31400	8.2	〃
18	Decyl trimethyl ammonium-Br	—	water	36	10080	70	〃
19	Decyl trimethyl ammonium-Br	—	0.013 M KBr	38	10600	67.2	〃
20	Dodecyl trimethyl ammonium-Br	—	water	50	15400	15.1	〃
21	Dodecyl trimethyl ammonium-Br	—	0.013 M KBr	56	17200	10.5	〃
22	Tetradecyl trimethyl ammonium-Br	—	water	75	25200	3.4	〃
23	Tetradecyl trimethyl ammonium-Br	—	0.013 M KBr	95	31900	1.76	〃
24	Hexadecyl trimethyl ammonium-Br	—	0.013 M KBr	170	61700	—	〃

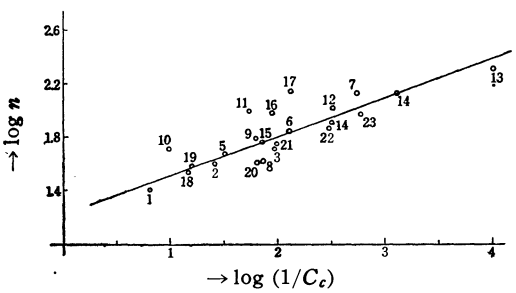

Fig. 1. Relation between log n and log $(1/C_c)$.

in Fig. 1. In this case it is necessary to use mol./l. as unit of CMC. The number in the figure corresponds to that of Table I.

1) A linear relationship between n and log $(1/C_c)$ approximately holds, independent of the presence of added electrolytes.

2) The linear relationship between n and log $(1/C_c)$ is especially satisfactory in the case where the counter ion is univalent, independent of the sign of charge of the detergent ion, with the exception of No. 16 and 17. That relation does not seem to hold when the counter ion is bivalent. (e.g., No. 10, 11, 12)

3) A definite conclusion can not be given as to non-ionic detergent because of the lack of available data. But, Triton-100 (No. 14) follows the linear relationship satisfactorily. When M_m instead of n is plotted against log $(1/C_c)$, deviation is quite large. The fact that the linear relation holds only for n vs. C_c plot and not for M_m vs. C_c one, seems to show that the direct measure of interaction between detergent molecules and solvent is not M_m but n.

The micelle formation of non-ionic detergent is different from that of ionic detergent in many respects. Especially, CMC is not clear because of polymolecularity of the monomer. Therefore, the linear relationship observed in the case of ionic detergent may not always be applicable to non-ionic detergent[10,11]. Further investigation is necessary in order to clarify the applicability of a similar relation to non-ionic detergent.

4) The linear relationship between n

8) H. V. Tartar and A. L. M. LeLong, *J. Phys. Chem.*, **59**, 1185 (1955).
9) L. M. Kushner and W. D. Hubbard, ibid., **58**, 1163 (1954).
10) R. Goto, N. Koizumi, N. Hayama and T. Sugano, *J. Chem. Soc. Japan, Pure Chem. Sec.* (*Nippon Kagaku Zassi*), **74**, 994 (1953) (in Japanese).
11) S. Kuroiwa, K. Shimizu and Y. Yano, *J. Chem. Soc. Japan., Ind. Chem. Sec.* (*Kogyo Kagaku Zassi*), **58**, 859 (1956) (in Japanese).

and $\log(1/C_c)$ is satisfactorily expressed by the following equation.

$$n=\beta_1\times(1/C_c)^{\alpha_1} \quad (1)$$

where $\alpha_1=0.29$, $\beta_1=17.0$

The Eq. (1) is shown graphically in Fig. 1. Approximate values of n and M_m can be obtained from C_c using Eq. (1).

5) It is well known that a linear relationship holds between $\log C_c$ and the number of carbon atoms (N) in a hydrogen chain of a detergent molecule for each homologue[12,13]. Namely,

$$\log C_c=-\alpha_2 N+\beta_2 \quad (2)$$

where α_2, β_2 are characteristic constants for a given homologue.

As seen in Eqs. (1) and (2), a linear relationship may hold between $\log n$ and N for each homologue. Fig. 2 shows a relation

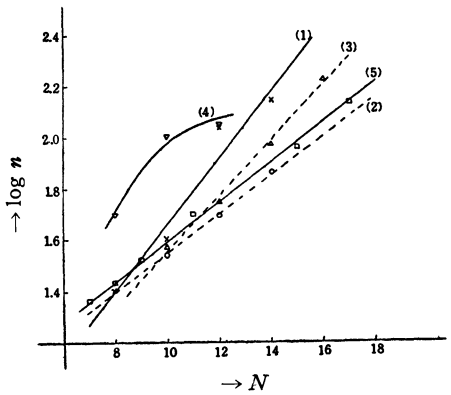

Fig. 1. Relation between $\log n$ and N.
(1) Na-alkylsulfonate in water[8]
(2) Alkyl trimethyl ammonium bromide in water[6]
(3) Alkyl trimethyl ammonium bromide in 0.0130 M KBr[6]
(4) Mg-alkylsulfonate in water[8]
(5) Na-alkyl carboxylate in water*

between $\log n$ and N. A linear relationship between them is clear from the figure. That is,

$$\log n=-\alpha_3 N+\beta_3 \quad (3)$$

where $\alpha_3=0.29\alpha_2$, $\beta_3=17.0-0.29\beta_2$. It can be noted that α_1 and β_1 in Eq. (1) are common constants for all homologues, on the contrary that α_2, α_3, β_2 and β_3 in Eq. (2) and (3) are characteristic constants for each homologue.

6) Several theoretical approaches have been made concerning CMC[6,14], but a satisfactory result has not been obtained yet. CMC can be given by Eq. (4), according to Ooshika's recent treatment[15].

$$kT\log C_c=Z\sqrt{w_e w_s}-w_m \quad (4)$$

where w_e, w_s and w_m are constants for each detergent, and are related with Coulombic repulsive energy, van der Waals' attractive energy and surface energy, respectively.

However, as the relation w_e, w_s, w_m and n is not clear, Eq. (1) can not be derived from Eq. (4). Recently, Hutchinson et al.[16] regarded micelle formation as phase change and obtained Eq. (5) using Clausius-Clapeyron relation.

$$\log C_c=-H_m/RT+A \quad (5)$$

where A and H_m are constants and H_m is the heat of micelle formation.

Therefore, an equation similar to Eq. (1) could be obtained, if H_m were linearly related with $\log n$. However, log CMC vs. $1/T$ is not linear even in a narrow range of temperature but generally convex upwards[17], and Eq. (5) can not be applied satisfactorily. Theoretical explanation of general empirical equation (1) should be made in future.

Relation between Micellar Molecular Weight (M_m) and Intrinsic Viscosity

A simple method for determining C_c from solution viscosity was proposed by the present author[18]. This method was also confirmed to be applicable to non-ionic detergent, recently[10,11,19].

Moreover, the authors presumed the possibility of the existence of some relationships between M_m and two kinds of intrinsic viscosity, $[\eta_1]$ and $[\eta_2]$ determined from solution viscosity[18]. Now it is possible to compute the approximate value of M_m from C^0 using Eq. (1). Therefore, the above relationships can be tested.

According to the first paper of this series, $[\eta_1]$ and $[\eta_2]$ are defined by the following equations,

$$\eta^0_{sp}/C^0=\frac{(\eta_r/\eta_{r\,\min})-1}{C-C_1} \quad (6)$$

12) H. B. Klevens, *J. Phys. Colloid Chem.*, **52**, 130 (1948).
13) M. E. L. McBain and E. Hutchinson, "Solubilization" Academic Press Inc., New York, p. 40 (1955).
* calculated from CMC using Eq. (1)
14) M. Nakagaki, *J. Chem. Soc. Japan, Pure Chem. Sec.* (*Nippon Kagaku Zassi*), **72**, 113 (1950); **73**, 801 (1951) (in Japanese).
15) Y. Ooshika, *J. Colloid Sci.*, **9**, 254 (1954).
16) E. Hutchinson et al., *Z. phys. Chem.*, Neue Folge **5**, 450 (1955).
17) Ref. No. 12) may be refered for temperature variation of CMC.
18) N. Sata and K. Tyuzyo, This Bulletin, **26**, 177, (1953).
19) H. Okuyama and K. Tyuzyo, ibid., **27**, 259 (1954).

TABLE INTRINSIC VISCOSITY AND

Number	Substance	Temperature	$[\eta_1]$	$[\eta_2]$	$C_c \times 10^3$ (mol./l.)
1	Na-Caprylate	20	0.65	0.87	360
2	Na-Nonylate	20	0.81	1.28	220
3	Na-Caprate	20	1.19	—	100
4	K-Caprate	20	0.87	—	100
5	Na-Laurate	20	1.18	(2.2)	25
6	K-Laurate	20	—	2.6	20
7	K-Myristate	20	—	3.3	8
8	Na-Palmitate	60	—	2.0	3
9	Na-Stearate	60	—	2.5	0.8
10	Na-Dodecyl-sulfate	40	2.23	2.65	10
11	Na-Dodecyl-sulfate	70	1.94	2.57	12
12	Dodecylamine hydrochloride	20	1.08	2.0	13
13	Dodecylamine-hydrochloride	30	1.05	1.9	13
14	Na-Oleate	20	1.35	3.81	1
15	Aerosol MA	25	1.73	1.84	27
16	Hexanolamine-caprylate	25	1.13	—	260
17	Emasol 1112	30	2.59	5.17	3.5
18	Emasol 1115	30	1.00	5.20	3.0
19	Emasol 1120	30	—	6.71	6.2
20	Emosol 1130	30	—	9.13	3.1
21	Emulgen 120	30	—	7.25	2.9

(1) Literature 18) may be refered for $[\eta_1]$, $[\eta_2]$ of No. 1～No. 16.
(2) Literature 19) may be refered for $[\eta_1]$, $[\eta_2]$ of No. 17～No. 21.

$$[\eta_1] = \lim_{C^0 \to 0} (\eta_{sp}{}^0/C^0) \tag{7}$$

$$[\eta_2] = \lim_{C^0 \to C^0{}_2} (\eta^0{}_{sp}/C^0) \tag{8}$$

were C_c is CMC and η_r is relative viscosity at CMC. They are shown in Fig. 3. The unit of concentration should neither be weight per cent. nor volume per cent. but mol./l.

In Table II are shown $[\eta_1]$, $[\eta_2]$ obtained by the above method, n and M_m being computed from Eq. (1), $n[\eta_1]$ and $n[\eta_2]$.

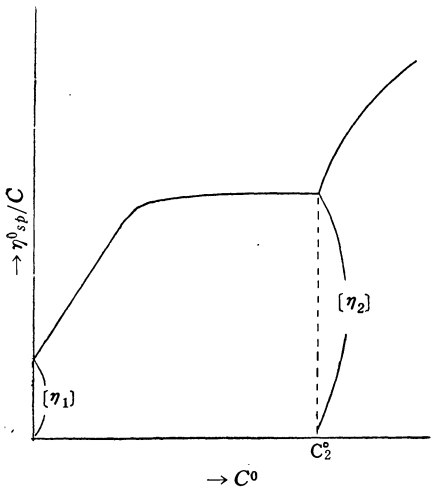

Fig. 3. Determination of C_2, $[\eta_1]$ and $[\eta_2]$.

When M_m is plotted against $[\eta_1]$ and $[\eta_2]$, definite relations can not be found but when M_m is plotted against $n[\eta_1]$ and $n[\eta_2]$, smooth curves can be obtained, regardless of their cationic, anionic and non-ionic nature*. To multiply $[\eta_1]$ and $[\eta_2]$ with n is equivalent to transform the unit of concentration from mol. of monomer/l. to mol. of micelle/l. Neither $\log M_m$ vs. $n[\eta]$ nor M_m vs. $\log n[\eta]$ is linear, but the following eqations apply between $\log M_m$ and $\log n[\eta]$.

$$\log M_m = 0.41\{\log n[\eta_1]\}^2 - 0.39\{\log n[\eta_1]\} + 3.47 \tag{9}$$

$$\log M_m = 0.45\{\log n[\eta_2]\}^2 - 0.91\{\log n[\eta_2]\} + 4.04 \tag{10}$$

M_m-value, $M_{m\,\mathrm{calc}}/M_m$ calculated from Eqs. (9) and (10) are shown in Table II. Experimental values and curves expressed by Eqs. (9) and (10) are shown in Fig. 4. Experimental and calculated values coincide fairly well with each other with a few exceptions. Therefore, n and M_m can be calculated from $[\eta_1]$ and $[\eta_2]$, using Eqs. (9) and (10). It is very remarkable that the above relationships are generally applicable, regardless of their cationic, anionic

* CMC obtained by different methods fluctuates cosiderably in the case of non-ionic detergent. The concentration where η_{sp}/C becomes minimum is adopted as CMC in this paper.

II

MICELLAR MOLECULAR WEIGHT

n	M_m	$n[\eta_1]$	$n[\eta_2]$	$M^1{}_m$ from $[\eta]$	$M^2{}_m$ from $[\eta]$	$M^1{}_{m\,\text{calc}}/M_m$	$M^2{}_{m\,\text{calc}}/M_m$
23.2	3900	15.1	22.0	3800	4370	0.97	1.12
26.9	4900	21.8	27.9	4900	4580	1.00	0.94
33.4	6500	39.7	—	7940	—	1.22	—
33.4	7000	29.0	—	6030	—	0.86	—
50	11000	59.0	110	11800	11500	1.07	1.04
53	12600	—	138	—	14500	—	1.15
69	18400	—	228	—	25200	—	1.37
92	25700	—	184	—	20000	—	0.78
135	41400	—	338	—	41700	—	1.01
65	19600	145	172	35500	18200	1.81	0.93
62	18700	120	159	27600	16600	1.48	0.89
60	13300	65	120	12900	12600	0.97	0.95
60	13300	63	114	12600	11750	0.95	0.89
126	38300	170	480	44700	69200	1.17	1.80
49	19000	85	90	17800	9600	0.94	0.50
26	5600	29.4	—	6200	—	1.10	—
89	71800	231	461	69200	64600	0.96	0.90
91	90600	—	473	—	66200	—	0.73
74	90000	—	496	—	74200	—	0.83
91	151000	—	831	—	166000	—	1.10
93	99200	—	674	—	117500	—	1.18

(3) Solvent is water in all cases.

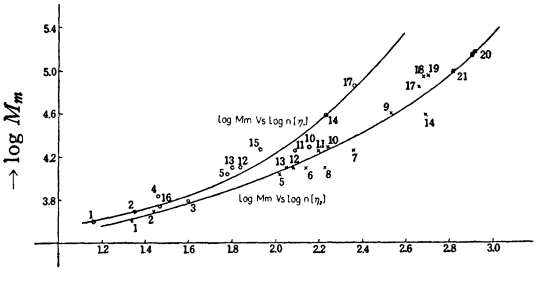

Fig. 4. Relation between log M_m and log $n[\eta_1]$, log $n[\eta_2]$.

and non-ionic nature. $n[\eta]$ is related with the degree of solvation, shape and size of micelle and electro-viscous effect. Theoretical explanationof Eqs. (9) and (10) may be quite difficult, because of uncertainty of the relation between above factors and M_m*.

On the Remarks for the Characteristic Behavior of Viscosity at CMC

We have shown that η_{sp}/C becomes minimum at CMC when η_{sp}/C of the detergent solution is plotted against concentration as is shown in Fig. 5—a and b[18,19]. The complete explanation for this phenomenon has never been performed until now, but it is natural that this is due to adsorption of detergent molecules to the wall of viscometer, if we consider the following terms.

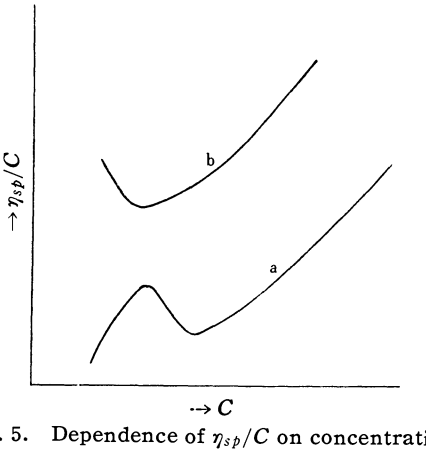

Fig. 5. Dependence of η_{sp}/C on concentration.

1) This phenomenon always appears, for both ionic- and non-ionic detergent. Therefore, it is different from the abnormality of viscosity in dilute solutions of polyelectrolytes which is due to

* K. J. Mysels[20] discussed charge effect for determining M_m from light scattering, but data are too few and the correlation can not fundamentlly influence the above results. Therefore, charge effect was neglected in this paper.

20) K. J. Mysels, *J. Colloid Sci.*, **10**, 507 (1955).

the result of electric repulsion and high polymer characteristics.

2) The phenomena are recently often found that η_{sp}/C becomes minimum at some concentration in the case of extremly dilute solutions of non-electrclytic high polymers[21]. It is generally recognized that this phenomenon is due to the result of adsorption of polymer molecules to the wall of viscometer[22].

3) In general, detergent molecules have high adsorbability to the interface as is evident from their nature. Moreover, the action of lowering interfacial tension is especially remarkable in dilute solutions and interfacial tension becomes almost constant, passing through CMC[23]. These phenomena seem to indicate that monomers of a detergent have a great adsorbability but micelles of a detergent have quite small.

Then, it is expected that characteristic minimum of η_{sp}/C at CMC can be explained from the above view-point of adsorption on the wall of viscometer but further details of explanation cannot be given in the present situation.

21) R. F. Boyer and D. J. Streeter, *J. Poly. Sci.*, **16**, 5 (1954); H. Umstätter, *Makromol. Chem.*, **12**, 94 (1954).
22) H. G. Fendler, H. Rohlender and H. A. Stuart, *Makromol. Chem.*, **18/19**, 385 (1956); O. E. Öhrn, *J. Poly. Sci.*, **17**, 137 (1955).
23) J. Powney and C. C. Addison; *Trans. Faraday Soc.*, **34**, 372 (1938); L. Schedlovsky and L. Ross, Jr., C. W. Jakob, *J. Colloid Sci.*, **4**, 25 (1949).

Summary

1) The following equation is found between association number (n) and critical micelle concentration (C_c in mol./l.) in detergent solutions

$$n=17.0\times(1/C_c)^{0.29}$$

This relation holds, independent of anionic and cationic detergents and added electrolytes.

2) The following equations are found between micellar weight (M_m) and two kinds of intrinsic viscosity ($[\eta_1]$ and $[\eta_2]$) already reported in the previous paper.

$$\log M_m=0.41\{\log n[\eta_1]\}^2-0.39\{\log n[\eta_1]\}+3.47$$

$$\log M_m=0.45\{\log n[\eta_2]\}^2-0.91\{\log n[\eta_2]\}+4.04$$

These relations are applicable, not only to ionic- but also to non-ionic detergents.

3) Discussions are made on the cause of characteristic behavior of viscosity at CMC. This phenomenon seems to be due to adsorption of detergent molcules to the wall of viscometer.

The author wishes to express his sincere thanks to Professor Dr. N. Sata and Assistant Professor H. Okuyama of Osaka University for their helpful discussions.

Department of Chemistry, Faculty of Science, Osaka University
Kita-ku, Osaka

Studies on the Denaturation of Lysozyme. III. Comparative Study of Lysozyme Denaturation on Surface and in Solutions

By Kozo HAMAGUCHI

(Received September 17, 1957)

Previously, the author has reported the surface-[1-4], heat-[5], and urea-denaturation[6] of lysozyme. The properties of the monolayers of lysozyme are closely related to the state of the molecules in spreading solutions. Therefore, the studies on the denaturation in solutions throw light on the mechanism of the surface denaturation. In this paper will be shown the correlation between the denaturation of lysozyme on surface and that in solutions.

Experimental

Lysozyme was prepared from hens' egg white by direct crystallization method, recrystallized four times and finally lyophilized.

Surface pressure was measured by the hanging plate method of Wilhelmy type. Simultaneously surface potential was measured by the vibrating electrode method. Surface viscosity was measured by the damping of the oscillatory rotation of a disc on the surface covered with monolayers.

The precipitation method to investigate the heat denaturation was as follows: a lysozyme solution in a test-tube was heated in a constant-temperature bath. After each time-interval the test-tube was taken out from the bath. When borate buffer of pH 11.0 (i.e., the isoelectric point of lysozyme) was added, the denatured protein was precipitated. The amounts of the precipitates thus formed were measured by micro-Kjeldahl method. The viscosity of lysozyme solutions was measured by means of Ostwald viscometer. The other experimental details should be consulted for the previous papers[1-6].

Results and Discussion

Surface Chemical Method to Investigate Protein Denaturation[1] — Bull[7] reported that the monolayer of lysozyme is not formed on water surface. However, it was found that the stable monolayers are formed on the substrate of which pH lies near its isoelectric point. When lysozyme was spread from 0.001 N hydrochloric acid solution, the surface pressure-area (F-A) curve had much smaller limiting area than that of the usual proteins, such as ovalbumin. However, the F-A curves obtained with the films spread from 8 or 10 M urea solutions began to develop from the area of about 14.5 Å²/residue. This value was also found with the films of other proteins or synthetic polypeptides.

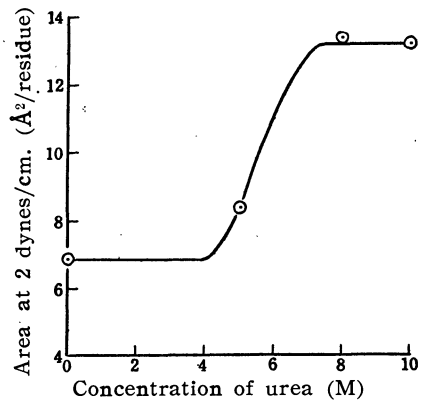

Fig. 1. Relationship between areas at 2 dynes/cm. and urea concentrations in spreading solutions.

Fig. 1 shows the relation between the areas at 2 dynes/cm. and the urea concentrations in the spreading solutions. From Fig. 1 it was expected that the expansion of lysozyme monolayers may reflect the degree of denaturation in urea solutions. This fact means that the denaturation of lysozyme in solutions can be investigated by the surface chemical method.

"Surface Heat Denaturation" of Lysozyme[2]—As described above, the F-A curve of lysozyme monolayer was affected by the kind of spreading solution. On the other hand, it was found that the properties of lysozyme monolayers were also affected by the temperature of the substrate. The effect of temperature of the substrate on the area at 2 dynes/cm. is shown in Fig. 2. As shown in this figure the area became larger with the rise of temperature of the substrate.

1) K. Hamaguchi, *J. Biochem.*, **42**, 449 (1955).
2) K. Hamaguchi, ibid., **42**, 705 (1955).
3) K. Hamaguchi, ibid., **43**, 83 (1956).
4) K. Hamaguchi, ibid., **43**, 355 (1956).
5) K. Hamaguchi, ibid., **44**, 695 (1957).
6) K. Hamaguchi, ibid., **45**, No. 2 (1958).
7) H. B. Bull, *J. Biol. Chem.*, **185**, 27 (1950).

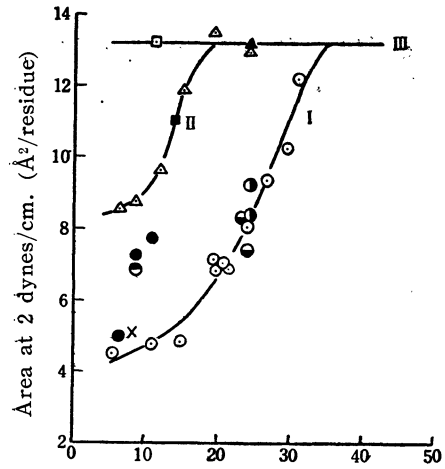

Fig. 2. Relationship between areas at 2 dynes/cm. and temperatures of substrate. Spreading solutions: ⊙, 0.001 N hydrochloric acid (fresh); ◒, 5 M urea solution; ◑, 0.001 N hydrochloric acid heated at 65° for two hours prior to spreading; ◬, 8 M urea solution; ◙, 8 M urea solution heated at 55° for two hours prior to spreading; ▲, 10 M urea solution; ■, 0.02 N sodium hydroxide (old); ●, 0.001 N hydrochloric acid (old); ◓, 0.04 N sodium hydroxide; ×, 0.02 N sodium hydroxide (fresh).

Curve I in Fig. 2 was obtained for the films spread from 0.001 N hydrochloric acid. The films spread from 5 M urea solution and from 0.001 N hydrochloric acid solution which was heated to 65°C. for two hours beforehand, occupied the areas on this curve. This fact shows that lysozyme molecules are not denatured in these solutions.

Curve II was obtained for the films spread from 8 M urea solution. Although curve II shifted to larger areas than curve I, the dependence of the areas on the temperature was also observed. The films spread from strong alkaline solutions also belong to this curve. These facts show that lysozyme is denatured in these solutions.

When the temperature of the substrate was sufficiently high, the films occupied the areas on curve III, irrespective of spreading solutions. That is, curves I and II tend to approach this straight line above 35° and 18°, respectively. The areas occupied by the films spread from 10 M urea solution also fall on curve III. Therefore, this straight line represents the maximum expansion beyond which the films of lysozyme do not expand.

The facts described above should be designated as "the surface heat denaturation" of lysozyme. Such a phenomenon has not yet been observed. It is generally believed that the temperature coefficient is unity for surface denaturation[8]. The direct examination of the denaturation in solutions can clarify the dependence of the monolayer properties on the spreading solutions and further can make our surface chemical method to investigate the denaturation more certain, details of which will be described in the later part of this paper.

Mechanism of Surface Denaturation of Lysozyme[2]—In order to analyze the results shown in Fig. 2, we make the following two assumptions: (a) The maximum expansion represented by curve III in Fig. 2 corresponds to that of the films which consist of the completely unfolded molecules of lysozyme and the films having smaller areas than this maximum expansion consist of two different kinds of molecular configuration, one of which is in a state of complete surface denaturation and the other, globular or partially altered configuration. (b) The latter configuration was assumed by the molecules existing in the adsorbed layer and would contribute neither to surface pressure nor to surface potential.

These assumptions were confirmed by the fact that the surface potential of the films spread from various solutions was a function of surface pressure and not of the area[4]. By these assumptions, C_n in Eq. (1) represents the concentration of the "globular" molecules in adsorbed layer.

$$\frac{1}{A}-\frac{1}{A_d}=C_n \qquad (1),$$

where A is the area at any given expansion and A_d the area represented by curve III in Fig. 2. The globular molecules present in adsorbed layer gradually suffer surface denaturation with time, giving rise to completely unfolded films. Because the curves shown in Fig. 2 were obtained for the films all of which were stood for 30 minutes before measurements, the relations indicate that the amounts of reactant, suffered surface denaturation, are different according to the temperature of substrate.

Therefore, the rate constant of surface denaturation must be obtained, when the F-A curves of the films are measured on the substrate at a given temperature at

8) H. B. Bull and H. Neurath, ibid., **125**, 113 (1938).

different ages after spreading. In fact, the F-A curves on the substrate at a given temperature shifted to larger areas with time after spreading.

The logarithms of the concentrations of "globular" molecules in adsorbed layer, C_n, which are calculated from Eq. (1) by the use of the areas at 2 dynes/cm., are plotted against time in Fig. 3 and linear relations are obtained.

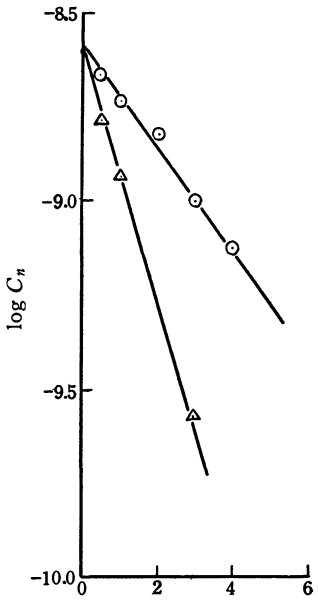

Fig. 3. Relationship between log C_n and elapsed time. Temperature of substrate: ⊙, 11°; △, 21°C.

This is the indication that the surface denaturation obeys the first order kinetics. Therefore, the first order rate constant can be calculated. By means of Arrhenius equation the apparent activation energy can be calculated from the rate constants at 11° and 21°C. and is found to be 15 kcal./mole.

From these considerations, it is found that the activation energy of 15 kcal./mole is necessary in order to obtain the monolayers consisting of completely unfolded molecules when native lysozyme is spread at an air-water interface. This is the reason why the F-A curves of lysozyme films are profoundly affected by the temperature of substrate. When the proteins such as ovalbumin and serum albumin, which have been so far investigated in detail, are spread as monolayers, the activation energy to pass from globular molecules to completely unfolded ones would be very low and then the completely unfolded films are formed instantaneously. Therefore, in the case of these protein films, neither the effect of temperature nor the time effect has been observed. The mechanism of surface denaturation can be clarified by using the proteins such as lysozyme which are very difficult to be denatured by surface.

The free energy, enthalpy and entropy activation, which are calculated from the methods according to Eyring and Stearn, are as follows: $\Delta F^*=22.4$ kcal./mole, $\Delta H^*=14.4$ kcal./mole, and $\Delta S^*=-28$ e. u. at 11°. With protein denaturation, in general, there are great increases in entropy and heat during the activation process. In this case, however, there is a decrease in entropy and a small increase in heat. The reason for this is not clear. There are two possibilities to explain the negative value of entropy: (a) that involved in a decrease in degree of freedom at interfaces compared with that in solutions and (b) that involved in freezing water molecules to the protein molecules.

Urea Denaturation of Lysozyme[6]—As described above, the properties of lysozyme monolayers depend on the concentration of urea in the spreading solutions. It was expected that this fact would reflect the denaturation in urea solutions and so the denaturation can be examined by the surface chemical method. It is an interesting problem whether the results obtained by a direct examination of the behavior of lysozyme in urea solutions

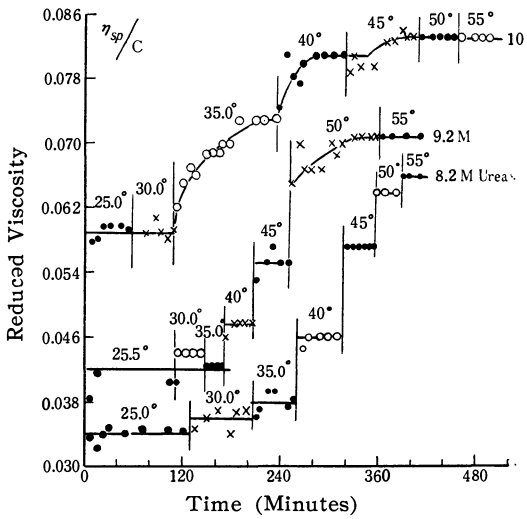

Fig. 4. Change with time of reduced viscosities of lysozyme in urea solutions. Concentration of lysozyme: 0.41 g./100 ml. pH 5.4-5.8.

correspond to those by the surface chemical method or not. Furthermore, the mechanism of surface denaturation will be made more clear when the denaturation in solutions is studied by other physicochemical methods. The urea denaturation of lysozyme was examined by viscosity measurements. The change with time of the reduced viscosity of lysozyme in the solutions at various urea concentrations over a rather wide temperature range are shown in Fig. 4.

It is very remarkable that the reduced viscosity was increased instantaneously with the rise of temperature and did not change with time at each temperature. Most of the proteins show the time effect on the viscosity in urea solution. In the case of lysozyme, however, the time effect was only observed in 9.2 and 10 M urea. Fig. 5 shows the maximum values of the reduced viscosities at each temperature.

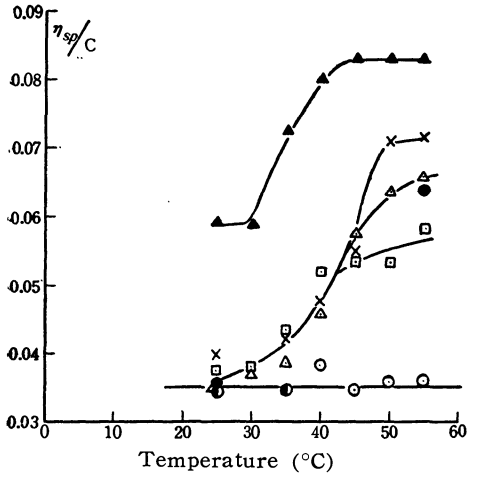

Fig. 5. Relationship between maximum reduced viscosities and temperatures. ◐, 0 M; ⊙, 4.2 M; ◙, 6.3 M; ●, 7.4 M; △, 8.2 M; ×, 9.2 M; ▲, 10 M urea.

It was found that the reduced viscosity in 4.2 M urea did not change between 25° and 55°C. and was the same as that of native lysozyme. In above 6.3 M urea solution the reduced viscosity increased from about 30° and tends to approach the constant value from 45°. Although the viscosity-temperature curves for 6.3, 8.2 and 9.2 M urea were almost the same at lower temperatures, the viscosity became greater with the increase in concentration of urea at higher temperatures. The reduced viscosity in 10 M urea was greater than that in 9.2 M urea even at 25°. In this case the viscosity was also increased from 30° and became constant from 45°. In order to examine the reversibility of the urea denaturation, after the lysozyme solutions once heated up to 55° had been kept at room temperature overnight, the viscosity was measured again at 25°. In 10 M urea, the reduced viscosity thus obtained was the same as that at 55°. The viscosity in 9.2 M urea returned to a smaller extent and the reversibility was nearly complete in 8.2 M urea.

With urea denaturation of proteins, in general, the reversibility is studied on the solutions after removal of urea by dialysis. In the case of lysozyme, however, the reversibility was observed merely by the lowering of temperature. This is a very remarkable fact. It might be more appropriate to term these phenomena as the "heat denaturation of lysozyme in urea solutions" rather than "urea denaturation". From the facts described above, it is assumed that at each temperature native lysozyme molecules are in equilibrium with those of another modification which are stable above 50° in 8 M urea. The equilibrium constant (K) at each temperature may be calculated from Eq. (2).

$$K = \frac{\eta - \eta_0}{\eta_\infty - \eta} \qquad (2),$$

where η_0 is the reduced viscosity of native lysozyme and η_∞ the viscosity above 50°.

When the logarithms of the equilibrium

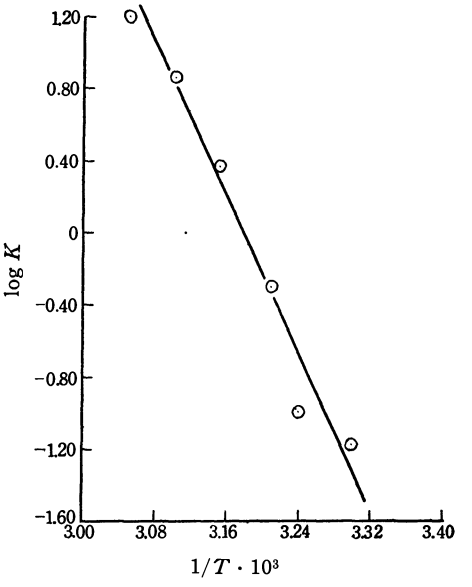

Fig. 6. Relationship between logarithms of equilibrium constants (K) and reciprocals of absolute temperatures.

constants are plotted against the reciprocals of absolute temperatures, a straight line is obtained as shown in Fig. 6. Therefore, the change in enthalpy ($\Delta H°$) can be evaluated from van't Hoff's equation. The change in standard free energy ($\Delta F°$) and entropy ($\Delta S°$) can be also obtained by the usual thermodynamic calculations. These thermodynamic parameters are as follows: $\Delta F° = -530$ cal./mole, $\Delta H° = 4{,}950$ cal./mole, and $\Delta S° = 17.2$ e. u. at 45°. The values of $\Delta H°$ and $\Delta S°$ are much smaller than those generally accepted for protein denaturation. This fact suggests that the structural change of lysozyme molecules in 8 M urea is only minor.

The investigations on urea denaturation have been mainly concerned with the structural change of protein molecules by urea and not with the interaction of urea with protein molecules. The interaction is inferred easily by monolayer technique[3]. Because urea is not a surface active substance, protein monolayers should not be profoundly affected unless urea molecules interact with protein monolayers. The F-A curves of lysozyme monolayers were shifted to larger areas with the increase in urea concentration in the substrate. The increase in area proceeded stepwise with the increase in urea concentration and was smaller at lower temperatures. These phenomena could be explained by the cleavage of bonds by urea attack which remain intact by spreading and by the adsorption of urea on the bonds emerged by the cleavage. It was also inferred from these experiments that urea molecules are scarcely adsorbed on lysozyme molecules in urea solutions.

Relationship between Monolayer and Bulk Properties of Lysozyme — The concern, here, is with the comparison of the results on the urea denaturation obtained by the surface chemical method with those by viscosity measurements. The behavior of lysozyme monolayer spread from 5 M urea solution was the same as that of native lysozyme. In 4 M urea the reduced viscosity did not change between 25° and 55° and was the same as that of native lysozyme. It is concluded, therefore, that lysozyme is not denatured in the urea solutions of which concentrations are below 4 or 5 M. The area of lysozyme monolayer was increased from 5 M urea (Fig. 1). The reduced viscosity also became sensitive to the temperature from the same urea concentration.

The expansion of lysozyme monolayer spread from 10 M urea was maximum and the areas scarcely depend on the temperature of the substrate. The reduced viscosity in 10 M urea was greater than that in 9.2 M urea. In addition, the effect of time on the reduced viscosity was observed and the viscosity did not reverse to the original value by cooling. These facts suggest that the secondary structure of lysozyme molecules may be destroyed in 10 M urea.

While the areas occupied by the lysozyme monolayers spread from 8 M urea was greater than that spread from native lysozyme, the temperature dependence of the expansion was the same as that of native lysozyme. On the other hand, it was found from the viscosity measurements that there exists an equilibrium between native and reversibly denatured molecules in 8 M urea. Therefore, the facts shown in Fig. 2 will be well convinced when the latter molecules are considered to be easily denatured by surface owing to a decrease in the activation energy for surface denaturation. The denaturation in 8 M urea may be caused by a rather slight change in the tertiary structure of the lysozyme molecule. The foregoing considerations show the remarkable correspondence between monolayer and bulk properties of lysozyme.

Heat Denaturation of Lysozyme[5] — In this section will be described the heat denaturation of lysozyme. As a matter of course, the heat denaturation in

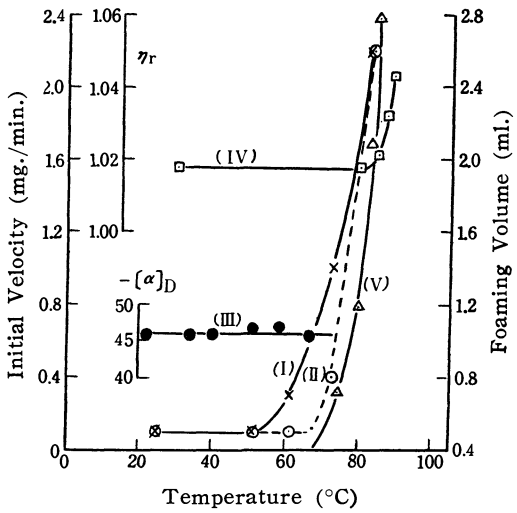

Fig. 7. Foaming volume (curves I and II), optical rotation (curve III), relative viscosity (curve IV) and initial velocity (curve V) as a function of temperature.

solutions is detected at much higher temperatures than "the heat denaturation on surface" owing to the absence of interface.

The temperature where lysozyme begins to be denatured by heat depends on the method to be used. This temperature was determined by the measurements of foaminess, optical rotation, viscosity, and of solubility. The results are shown in Fig. 7. It is evident that a change appears in foaming volume at the lowest temperature, 50°. Curve I was obtained for the solutions immediately after heating for a quarter of an hour at each temperature. This fact suggests that lysozyme molecules are slightly denatured and changed to a state susceptible to surface denaturation by vigorous shaking. As described above, native lysozyme is not easily denatured by surface, but readily undergoes surface denaturation when the protein is denatured in solutions beforehand. The foaming volume, however, decreased reversibly by standing at room temperature after heating (curve II). The surface chemical method could not distinguish the behavior of the monolayers spread from a solution of native lysozyme and those spread from a solution heated at 65° beforehand. These facts suggest that lysozyme might be reversibly denatured in the vicinity of 50°. The optical rotation did not change up to about 70° (curve III). This is the indication that the reversible denaturation might not result from a greater change in the secondary structure but from a change in the tertiary structure. It is interesting that the optimum temperature of the enzymatic activity of lysozyme (55°)[9] corresponds to the temperature from which the foaminess increases. That is, the enzymatic activity may be decreased by a minor change in the tertiary structure.

The viscosity began to increase from about 85° (curve VI). The increase in viscosity, however, accompanied the increase in turbidity. Therefore, this is not due to the effect of the unfolding of each lysozyme molecule. The solubility at the isoelectric point began to change from 70°. That is, the denaturation could be detected by the precipitation method, nevertheless the viscosity did not change. Therefore, the heat denaturation of lysozyme might be caused by the aggregation of the molecules rather than by the unfolding.

The effects of temperature, lysozyme concentration, and of pH on the heat denaturation were determined by the precipitation method in detail. Increase in the concentration of lysozyme had the effect of speeding up the rate of its denaturation. The reaction order of the heat denaturation was determined by the differential, integral, and half-life method. As a result, the initial velocity of the heat denaturation (v_0) was expressed approximately by the following equation:

$$v_0 = k\frac{[P_0]^2}{[H^+]} \qquad (3),$$

where $[P_0]$ is the initial concentration of lysozyme and $[H^+]$ the hydrogen ion concentration. However, the reaction order increases as the reaction proceeds.

The apparent activation energy calculated from Arrhenius equation using the initial velocities was found to be 50.3 kcal./mole, which was independent of the initial concentration.

Role of Disulfide Bonds in Denaturation of Lysozyme[4,6].—One of the most striking structural features of lysozyme molecule is that five intrapeptide disulfide bridges exist within its rather small molecule. Accordingly, it is important to investigate the role played by these disulfide bridges. Sodium sulfite was used as a splitting agent for these bonds. In Fig. 8 is shown the effect of sodium sulfite (0.03 M) on the reduced viscosity of lysozyme in different urea concentrations[6].

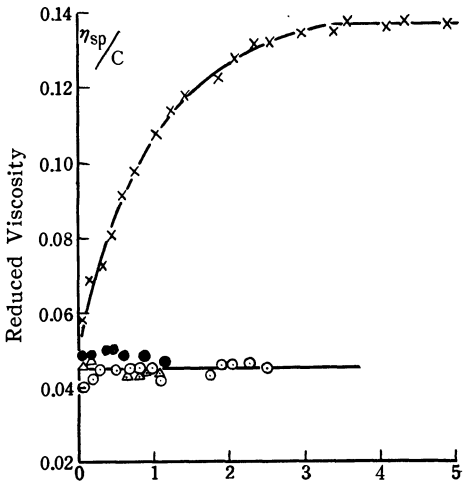

Fig. 8. Effect of sodium sulfite (0.03 M) on reduced viscosity at different urea concentrations. (30.0°, pH 9.6). ●, 6.3 M urea; ⊙, 6.3 M urea, 0.03 M Na_2SO_3; △, 8.2 M urea; ×, 8.2 M urea, 0.03 M Na_2SO_3.

9) C. Fromageot, *Bull. soc. chim. biol.* Supple. **11-12**, 63 (1948).

Fig. 8 clearly shows that the effect of sodium sulfite was not observed in 6.3 M urea but was very striking in 8.2 M urea. In the absence of sulfite, however, the reduced viscosity was almost the same irrespective of the urea concentration. In 8.2 M urea at pH 9.6 containing 0.03 M sodium sulfite, the reduced viscosity was increased rapidly with time and the final value was much higher than that in the absence of sodium sulfite at 30°. These facts show that the disulfide bridges might be masked in the interior of the molecules and that the degree of denaturation in 6.3 M urea is so small that the disulfide bonds can not react with sulfite. Thus,

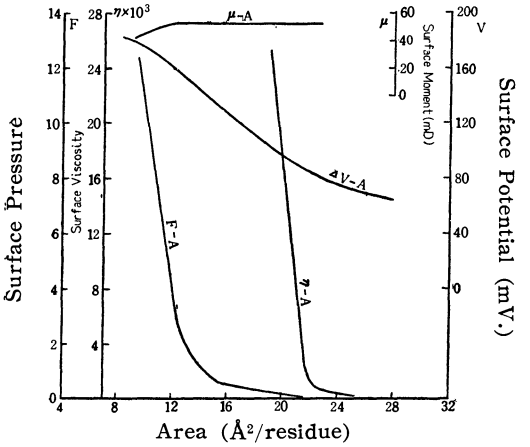

Fig. 9. F-A, η-A, ΔV-A and μ-A curves of lysozyme monolayer spread from 8 M urea solution. Substrate, 10^{-2} M potassium carbonate (pH 10.5), 19°.

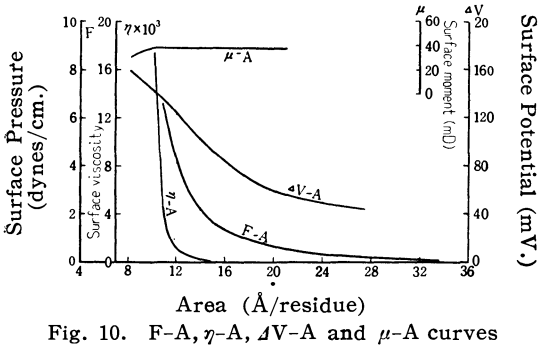

Fig. 10. F-A, η-A, ΔV-A and μ-A curves of lysozyme monolayer spread from 8 M urea solution. Substrate, 10^{-2} M K_2CO_3 $+10^{-2}$ M Na_2SO_3.

the easiness of the splitting of the disulfide bonds gives a measure of denaturation by urea. The marked increase in viscosity by the splitting of disulfide bonds in 8 M urea suggests that the five intrapeptide bonds of lysozyme must be incorporated into widely separated parts of polypeptide chains and they do not neighbor with each other along the chain.

Fig. 9 shows the surface pressure-area, surface viscosity-area (η-A), surface potential-area (ΔV-A) and surface moment-area (μ-A) curves of lysozyme monolayers spread from 8 M urea[4].

In Fig. 10 are shown the effect of sodium sulfite in the substrate on the properties of the monolayer spread from 8 M urea[4]. From the comparison of the results shown in Figs. 9 and 10, it was found that the F-A, η-A and ΔV-A curves are greatly changed by the presence of sulfite in the substrate. The changes are explained by the increase in ionizable groups due to splitting of disulfide bonds.

Summary

In order to clarify the correlation between the denaturation of lysozyme on surface and that in solutions, the surface-, heat-, and urea-denaturation which were so far reported by the author were summarized.

The properties of lysozyme monolayers depend not only on the temperature of substrate but also on the state of lysozyme molecules in spreading solutions. The mechanism of the formation of the protein monolayer was clarified by the examination of the denaturation in solutions. Because of the very high content of disulfide bonds in lysozyme molecules, the role played by these bridges in the denaturation on surface and in solutions was also examined and its significance was made clear.

The author expresses his hearty thanks to Professor T. Isemura for his kind guidance throughout the present work.

Department of Biology
Faculty of Science
Osaka University, Kita-ku, Osaka

An Electron Diffraction Investigation on the Molecular Structures of Sulfur Monochloride and Monobromide

By Eizi HIROTA

(Received September 24, 1957)

In 1934 Penney and Sutherland[1] predicted the so-called right-angle model for the molecular structure of hydrogen peroxide on the basis that lone-pair electrons of oxygen atoms hinder the rotation about the oxygen to oxygen axis. Giguère and his collaborators[2] studied the structure of the molecule by various methods and confirmed the prediction of Penney and Sutherland. The molecules of this type are of interest, because they are so simple that precise treatment can be applied to get information on internal rotation. Sulfur monohalide, S_2X_2, belongs probably to the same category. Many researches were carried out on the structure of sulfur monochloride. Morino and Mizushima[3] rejected either the $S=SCl_2$ structure or the *trans* configuration by measuring both the dipole moment and the Raman effect, but they did not distinguish between the two possibilities of the right-angle model and of freely rotating one. Gerding and Westrik[4] observed the depolarization degree of the Raman lines in the liquid state. They considered the depolarized line at 106 cm^{-1} as one of the fundamentals, which rejected the C_2 model and preferred the C_{2v} structure (the *cis* form). Some progress in the assignment of an infrared spectrum was made by Bernstein and Powling[5], who resolved the line centered at 440 cm^{-1} into two lines of 438 cm^{-1} and 448 cm^{-1} and found that the spectral data were not inconsistent with a C_2 structure if the line at 106 cm^{-1} in the Raman spectrum was taken as weakly polarized rather than as depolarized and was considered to be due to the torsional oscillation. Recently Luft and Todhunter[6] proposed an idea to interpret the line at 106 cm^{-1} as the first overtone of the torsional mode. It can be expected that the mean square amplitude of a pair of chlorine atoms, if measured accurately, will make a choice between them, because the mean amplitude depends strongly upon the frequency of the torsional mode. The S-S stretching mode has been assigned to one of the two lines resolved by Bernstein and Powling, but when the spectrum of sulfur monochloride is compared with those of monobromide and of monofluoride, it is clear that this assignment is by no means final.

Ackermann and Mayer[7] and Palmer[8] studied the molecular structure of sulfur monochloride by the visual method of electron diffraction, but they did not obtain any precise information about internal rotation. Guthrie[9] arrived by electron diffraction measurement at the result that this molecule has the *cis* configuration, but no precise report has been published. As for physico-chemical investigation on sulfur monobromide, we have only two reports of the Raman effect by Stammreich et al[10,11].

In this paper there is described the result of electron diffraction investigation by the sector-microphotometer method, mainly to see whether the configuration of these molecules is really of the right-angle form or not, and further to determine the potential barrier restricting the internal rotation.

1) W. G. Penney and G. B. B. M. Sutherland, *J. Chem. Phys.* **2**, 492 (1934).
2) L. R. Zumwalt and P. A. Giguère, ibid., **9**, 458 (1941); P. A. Giguère, ibid., **18**, 88 (1950); P. A. Giguère and O. Bain, *J. Phys. Chem.* **56**, 340 (1952); P. A. Giguère, I. D. Liu, J. S. Dugdale, and J. A. Morrison, *Can. J. Chem.* **32**, 117 (1954); O. Bain and P. A. Giguère, ibid., **33**, 527 (1955).
3) Y. Morino and S. Mizushima, *Sci. Papers Inst. Phys. Chem. Research* (Tokyo), **32**, 220 (1937).
4) H. Gerding and R. Westrik, *Rec. trav. chim. Pays-bas*, **60**, 702 (1941).
5) H. J. Bernstein and J. Powling, *J. Chem. Phys.*, **18**, 1018 (1950).
6) N. W. Luft and K. H. Todhunter, ibid., **21**, 2225 (1953).
7) P. G. Ackermann and J. E. Mayer, ibid., **4**, 377 (1936).
8) K. J. Palmer, *J. Am. Chem. Soc.*, **60**, 2360 (1938).
9) G. B. Guthrie, quoted by P. W. Allen and L. E. Sutton, *Acta Cryst.* **3**, 46 (1950).
10) H. Stammreich, R. Forneris and K. Sone, *J. Chem. Phys.*, **23**, 972 (1955).
11) H. Stammreich and R. Forneris, *Spectrochim. Acta* **8**, 46 (1956).

TABLE I
EXPERIMENTAL CONDITIONS

Compound	Camera length (cm.)	Wave length of the electron beam (Å)	Sector	Stopper	Index of resolution	Measured range of q value
S_2Cl_2	11.82	0.057	r^2	without	0.73	15-83
	27.91	0.069	r^2	without	0.73	5-27
S_2Br_2	11.82	0.057	r^3	with	about 1	18-95
	27.91	0.056	r^2	with	about 1	6-31

Experimental

Sulfur monochloride obtained from a commercial source was purified by vacuum distillation over dry purified sulfur and activated charcoal. Sulfur monobromide was synthesized from equimolar mixture of purified sulfur and bromine according to the method described by Brauer[12].

The apparatus of electron diffraction and the procedure taken are the same as those previously reported[13]. Two kinds of sector, r^2 and r^3 type, were used. In addition to the of a camera shorter length (11.82 cm.), a longer one with 27.91 cm. length was also used, which was particularly suitable for the study of internal rotation. The experimental conditions are given in Table I.

Analysis

a) Modified Radial Distribution Function.—*Sulfur Monochloride.*—According to the procedure developed by Karle and Karle[14] the molecular intensity curves $sM(s)$ were obtained as shown in Fig. 1.

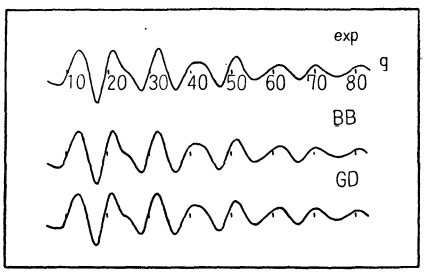

Fig. 1. The molecular intensity curves for sulfur monochloride.

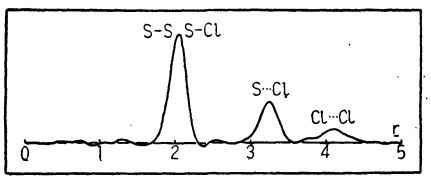

Fig. 2. The modified radial distribution curve for sulfur monochloride.

The radial distribution curve was obtained by Fourier transformation of the molecular intensity curve, in which the intensity from $q=0$ to q_{min} was spliced by a curve calculated for an assumed model. The curve thus obtained (Fig. 2) consists of three peaks: (S-S, S-Cl), (S···Cl)*, and (Cl···Cl). Although the radial distribution function of the Cl···Cl pair reflects directly the behavior of the internal rotation, it is influenced strongly by the intensity at small q region; when the modified radial distribution function is calculated by supplementing the observed intensity from $q=0$ to 18 with the intensity of the right-angle model or that of the *trans* one, quite different curves are obtained for the Cl···Cl region as seen in Fig. 3.

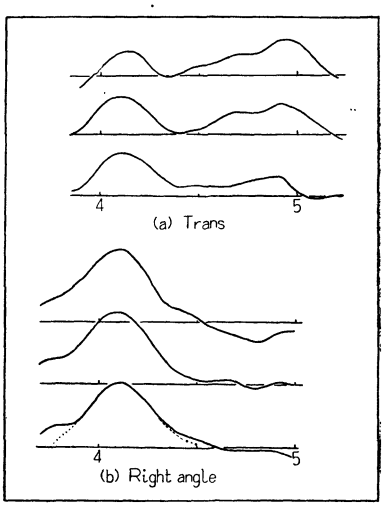

Fig. 3. The modified radial distribution curve for Cl···Cl pair of sulfur monochloride.
(a) interation started from the *trans* form;
(b) it started from the right angle model.

Of course the Fourier transformation must be repeated until the resultant radial distribution function becomes consistent with the assumed model. If the

12) G. Brauer, "Handbuch der präparativen anorganischen Chemie" Ferdinand Enke Verlag, Stuttgart (1954), p. 290. See also O. Ruff and G. Winterfeld, *Ber.* **36**, 2437 (1903).
13) Y. Morino and E. Hirota, *J. Chem. Phys.* (in press).
14) J. Karle and I. L. Karle, ibid., **18**, 957 (1950).

* S-Cl denotes the directly bonded sulfur-chlorine atom pair and S···Cl the non-bonded atom pair separated by another sulfur atom.

trans model is first assumed, the rate of convergence is quite slow, and the shape of the third peak (Fig. 3a) is different from that of the pure *trans* form and rather like that of the right-angle model with a wide amplitude of torsional oscillation. Under the assumption of the right-angle model a consistent model is readily obtained (Fig. 3b).

The first (S-S, S-Cl) and the second peak (S···Cl) are independent of the assumption about the internal rotation, and hence one can easily get parameters for these atom pairs. However, a difficulty remains in separating two atom pairs, S-S and S-Cl, because these two peaks overlap each other heavily. As shown in Fig. 4 and in Table II, any of three

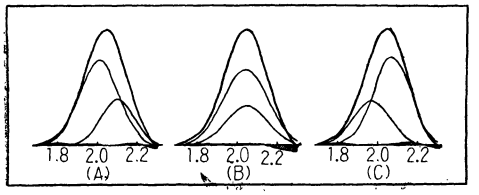

Fig. 4. The compound modified radial distribution curves of S-S and S-Cl pairs of sulfur monochloride, explained by three distinct sets of parameters. (Cf. Table II)

TABLE II
RESULTS OF ANALYSIS OF MRD FOR S_2Cl_2*

	A		B		C	
	r	$\langle\Delta r^2\rangle^{1/2}$	r	$\langle\Delta r^2\rangle^{1/2}$	r	$\langle\Delta r^2\rangle^{1/2}$
S-Cl	2.01	0.06	2.04	0.08	2.07	0.05
S-S	2.10	0.03	2.04_5	0.06_5	1.97	0.05
S···Cl			3.24_5	0.08_7		
Cl···Cl			4.10_7	0.12_5–0.15_5		

* The first number denotes the equilibrium distance and the second the rms amplitude of vibration.

distinct sets of parameters can explain the observed curve equally well. There was no difficulty about the analysis of S···Cl. The results of analysis of the modified radial distribution curve are summarized in Table II, where the peak of Cl···Cl was also assumed to be Gaussian.

The unmodified radial distribution function[13] may be useful to resolve further this compound peak of S-S and S-Cl, but the error included in the present experiment did not allow any higher resolution. (Compare the reliability factor[13] given in the later section).

Sulfur Monobromide.—As described above it was difficult to obtain accurate values of the S-S and the S-Cl bond distance in a sulfur monochloride molecule. It seems that the length of S-S can be obtained from the analysis of the curve of sulfur monobromide. The modified radial distribution curve is shown in Fig. 6. For calculating this curve, the observed

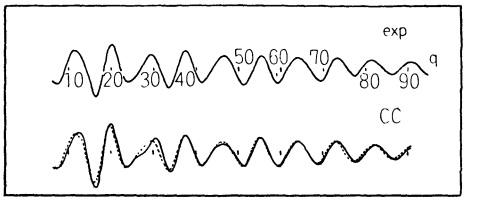

Fig. 5. The molecular intensity curves for sulfur monobromide. The dotted curve is for the case where the bromine is added to about 30%.

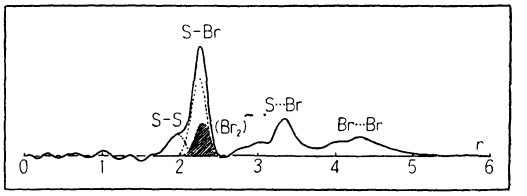

Fig. 6. The modified radial distribution curve for sulfur monobromide. The contamination of bromine is taken into consideration by the shaded area.

molecular intensity at q larger than 8 (Fig. 5) was corrected for the effect of diffraction by electron cloud[15] and was spliced with the theoretically calculated one in the region from $q=0$ to 8. The S-S and the S-Br pair give two distinct peaks: the lower peak, corresponding to S-S, appears at the short-distance side of the higher peak and is clearly separated from that of the latter. The peak of Br···Br is flatter than that of Cl···Cl and shows considerable deviation from the Gaussian shape. About two thirds of the upper part of the S···Br peak stands clearly above the level of the ghost, but its area amounts to only about 75% of the theoretical one. This difference may be explained by assuming a contamination of bromine. Since the vapor pressure of bromine is far greater than that of sulfur monobromide, we can expect that bromine gas which was first included in the sample was removed by pumping off the gas before the exposure, but sulfur

15) L. S. Bartell, L. O. Brockway and R. H. Schwendeman, ibid., **23**, 1854 (1955).

monobromide is readily decomposed into sulfur and bromine, for example, by radiation of the electron beam or by contact with the metal surface of the apparatus. In fact, if one assumes the mixing of bromine gas, the ratio of areas of S-Br and S···Br peaks can be well explained, because the atomic distance in bromine molecule is about 2.28 Å, comparable with the length of S-Br, so that the presence of bromine vapor will make the area of S-Br pair large. In Fig. 6 the abundance of bromine was tentatively assumed to be about 30%, then the equilibrium distance of S-Br pair must be reduced 0.01 or 0.02 Å from that of the peak (about 2.25 Å). The result of analysis of the modified radial distribution curve is given in Table III.

TABLE III
RESULTS OF ANALYSIS OF MRD FOR S_2Br_2

	r	$\langle\Delta r^2\rangle^{1/2}$
S-S	$\sim$ 1.97	—
S-Br*	2.24	0.05_3**
S···Br	3.35	0.09_8**
Br···Br	$\sim$ 4.26	$\sim$ 0.31

* When bromine is added, the peak has the parameters $r=2.25$ Å and $\langle\Delta r^2\rangle^{1/2}=0.04_7$ Å.
** The correction for the Born approximation was carried out by the procedure given in ref. 15.

b) The Correlation Method. — *Sulfur Monochloride.*—It is reasonable to determine first the parameters of S-S and S-Cl by examining the intensity curve in the region of $q\geqq 50$, since the result of analysis of the radial distribution curve showed that the temperature factors of S···Cl and Cl···Cl were definitely large and hence their intensities damped out in this region. Since an atom pair has two parameters to be determined, an equilibrium distance and a temperature factor, four parameters must be taken into consideration. These parameters are strongly dependent on each other, as seen from the three sets given in Table II. The parameter chart of the temperature factor was projected on that of the equilibrium length, the axes of the latter chart being the bond lengths of S-S and S-Cl (Fig. 7). Reasonable models fall on a line connecting three models A, B and C, which were obtained from the analysis of the radial distribution function, whereby temperature factors were taken tentatively for each model. There was found a rough relation between the sum of temperature factors of S-S and S-Cl, M. A., and the difference between their equilibrium distances, Δr:

$$\text{M. A.}=0.15-0.5\,\Delta r,$$

which holds in the range of $\Delta r<0.3$. The atom pair S···Cl influences, in particular, the shape of the maximum at $q=40$ to 45: when the distance is short, the shoulder of the peak at the short-distance side becomes prominent, and the long-distance side falls off rapidly, and when the distance becomes long, the contrary is the case. The best values of this distance are inscribed in Fig. 7 for seven models on the line from A to C. The most satisfactory models are BB and GD, while the model DD is unsatisfactory. The mean amplitude of S···Cl, 0.08_7 Å, is concluded to be reliable within 0.02 Å by the calculation with the model BB.

The reliability factors of BB and GD were 10.9% and 10.7%, while the random error of the experiment was 13.2% in the region of $q=18$ to 83. Thus both models agree with the observed intensity within the error. For sulfur monochloride it can not be determined by the analysis which of the models, BB or GD, is better, but the model GD seems to be preferable, for the S-S distance of sulfur monobromide was found to be 1.97 Å. The intensity curves of the models are compared with the experimental one in Fig. 1.

Sulfur Monobromide.—The comparison of the calculated intensity with the observed one was carried out only in the region of $q\geqq 30$, where the intensity of Br···Br was excluded from the calculation, for its amplitude damped out in this region. By taking the length of S-Br to be 2.25 Å two ratios of the atomic distances, (S-S)/(S-Br) and (S···Br)/(S-Br), were varied as the

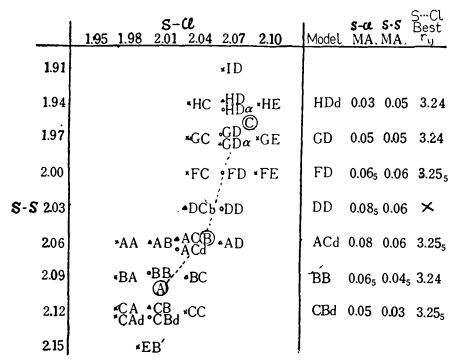

Fig. 7. The parameter chart for sulfur monochloride.

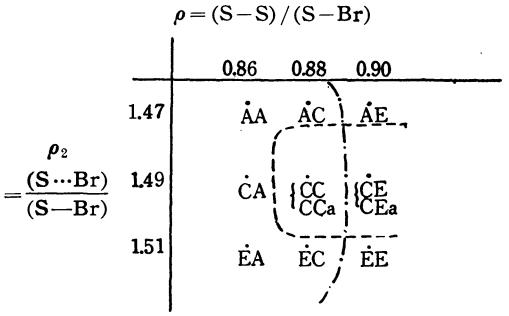

Fig. 8. The parameter chart for sulfur monobromide.
----: acceptable region obtained from the comparison of q_c/q_0
-·-·-: acceptable region concluded from the intensity checking

parameters to be determined. The temperature factors were assumed to be 0.06 Å for S-Br, 0.05 Å for S-S and 0.11 Å for S···Br (these values were mainly taken from the observed values obtained with the radial distribution function, and the correction for the Born approximation was excluded), but later the temperature factor of S-Br was varied and found to be reliable within 0.015 Å. The models were examined referring to the two criteria: the ordinary mean deviation of q_c/q_0 and the amplitude of intensity, the latter being, for simplicity, taken as the intensity from peak to valley; because this definition is free from inadequate drawing of the background line. The parameter chart and the acceptable region are indicated in Fig. 8. The results are:

$$\text{S-Br} = 2.25_9 \text{ Å},$$
$$\text{S-S} = 1.98_8 \text{ Å},$$
and
$$\text{S···Br} = 3.36_3 \text{ Å}.$$

q_c/q_0 of the CC model is 1.004 ± 0.004, and its reliability factor is calculated to be 28.7%, in comparison with the random error of the experiment, 29.4%. The reliability factor can be reduced to 24.9% if it is assumed that the gas contains bromine molecules of 30% in molecular ratio. The dotted line of the model CC in Fig. 5 indicates the effect of bromine mixing. Thus the presence of bromine molecules is again expected in this respect.

The large reliability factor of sulfur monobromide may be explained by the fact that the mixing ratio of bromine gas varied case by case, and the two independent observations did not coincide with each other. In addition to this, the intensity factors of sulfur monobromide are definitely smaller than those of monochloride, owing to the large atomic number of bromine (see Table IV): the ratio of the $sM(s)$ of the two molecules amounts to 2 : 3 or even near 1 : 2.

TABLE IV
INTENSITY FACTORS OF S_2Cl_2 AND S_2Br_2

	S_2Cl_2	S_2Br_2
S-S	72	27
S-X	144	102
S···X	92	70
X···X	39	59

c) Small-Angle Scattering. — *Sulfur Monochloride.*—For further detailed study of internal rotation it is desirable to observe the intensity at a small angle. The principle and the procedure applied were already described in the previous paper[13]. It was the Cl···Cl atom pair to which attention was called. By using the values of parameters: $r=2.09$ Å, $\langle \Delta r^2 \rangle^{1/2}=0.045$ Å for S-S, $r=2.01$ Å, $\langle \Delta r^2 \rangle^{1/2}=0.065$ Å for S-Cl and $r=3.24$ Å, $\langle \Delta r^2 \rangle^{1/2}=0.09$ Å for S···Cl, which correspond approximately to the model A of the modified radial distribution function or to the model BB in the correlation method. The theoretical background functions were calculated for four cases: the *cis*, the *trans*, the freely rotating, and the right-angle configuration**. The curves shown in Fig. 9 clearly indicate that the smoothest one is that of the right-angle model. Thus it can be concluded that the most probable

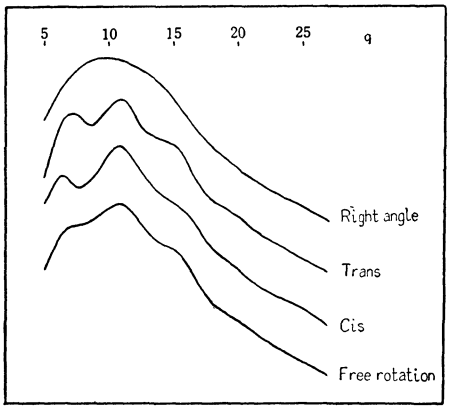

Fig. 9. The background functions for sulfur monochloride.

** The atom form factor used were calculated by Viervoll and Ögrim, *Acta Cryst.*, **2**, 277 (1949) and the inelastic scattering terms were given by Bewilogua, *Physik. Zeits.*, **32**, 743 (1931).

configuration of this molecule is the right-angle type structure.

Sulfur Monobromide.—The background function for S_2Br_2 was calculated by the same procedure: the potential for the internal rotation was taken as $V=\frac{1}{2}V_0(1-\cos 2\phi)$, where three values of $V_0=0$, $4\,kT$ (2.5 kcal/mole), and $8\,kT$ (4.8 kcal/mole) were assumed. A glance at Fig. 10 shows that $V_0=0$ is unsatisfactory

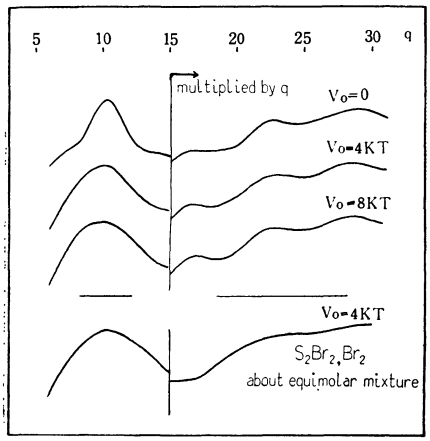

Fig. 10. The background functions for sulfur monobromide.

in the region of $q=6$ to 13, and V_0 must be larger than $4\,kT$. In the region of $q>13$ none of the three curves are smooth, probably owing to the contamination of bromine. In fact the mixing of bromine molecules of 50% smooths out sufficiently the background function. Thus here is another evidence that the gas was contaminated by bromine, the amounts being 30 to 50%. But the precise value of the potential barrier V_0 could not be obtained because of the contamination of bromine.

Calculation of Mean Square Amplitudes

Six fundamental frequencis have been observed for sulfur monochloride by the Raman effect and by the infrared adsorption spectra: their wave numbers are 102, 206, 240, 436, 449, and 540 cm^{-1}.*** According to the assignment given hitherto the lines of 240 and 540 cm^{-1} have been considered to belong to the B class and the other four lines to the A class, but if one compares them with the Raman lines of sulfur monobromide, i.e., with the five lines of 66, 172, 200, 356, and 529 cm^{-1}, then one would recognize that the line 540 cm^{-1} of monochloride and the line 529 cm^{-1} of monobromide are assigned reasonably to the S-S stretching mode. In addition to this, the frequency of the S-S stretching mode of sulfur monofluoride was reported by Barceló and Oteró[16] as 526 cm^{-1}. Thus the correct assignment of sulfur monochloride is taken to be as follows: the four lines, 102, 206, 436 (or 449), and 540 cm^{-1}, belongs to the A type and the remaining two, 240 and 449 (or 436) cm^{-1}, to the B type vibration. Since the measurement of depolarization is very difficult, in particular, for a weak line such as 540 cm^{-1} and for overlapping lines such as 436 or 449 cm^{-1}, the result of the measurement of depolarization can not be considered very serious. In the present type of molecules two S-X stretching modes are likely to have the same frequencies, so that the line 356 cm^{-1} reported for sulfur monobromide included probably the other S-Br stretching vibration just as in monochloride. A weak line at 302 cm^{-1}, omitted first and then reported later by Stammreich et al, can be interpreted to be a combination or difference band, or a band due to impurity. The final assignments are given in Tables V and VI for sulfur monochloride and monobromide, respectively.

In order to obtain the force constants, normal coordinate treatment was carried out, based on the Urey-Bradley type of force fields:

$$\begin{aligned}2V=&K_{SS}(\Delta R)^2+K_{SX}\{(\Delta r_1)^2+(\Delta r_2)^2\}\\&+H_{SSX}\{(r\Delta\alpha_1)^2+(r\Delta\alpha_2)^2\}\\&+F_{SX}\{(\Delta q_1)^2+(\Delta q_2)^2\}+\Phi(r\Delta\phi)^2\\&+2K'_{SS}R\Delta R+2K'_{SX}(r\Delta r_1+r\Delta r_2)\\&+2H'_{SSX}(r^2\Delta\alpha_1+r^2\Delta\alpha_2)\\&+2F'_{SX}(q\Delta q_1+q\Delta q_2)+2\Phi' r^2\Delta\phi,\end{aligned}$$

where R denotes the equilibrium distance of the S-S atom pair, r_1 and r_2 denote those of the S-X atom pairs, q_1 and q_2 those of the S···X atom pairs, α_1 and α_1 the equilibrium values of ∠S-S-X, and ϕ stands for that of the torsional angle; Δ indicates a displacement from the equilibrium value. The equilibrium value of ϕ is assumed to be 90°. Among the five constants K'_{SS}, K'_{SX},

*** These values were cited from the reference 11; other workers gave essentially the same results.

16) J. R. Barceló and C. Otero, *Anal. Real. Soc. Espan. Fis. Quim.* **B51**, 223 (1955).

TABLE V
VIBRATIONAL FREQUENCIES AND FORCE CONSTANTS FOR S_2Cl_2

Symmetry	Observed frequency (cm^{-1})	Assignment	Calculated frequencies I (cm^{-1})	Calculated frequencies II (cm^{-1})	Force constant (md/Å)
A	540	ν(S-S)	536	536	K_{SS} =2.46
	436	ν(S-Cl)	440	439	K_{SCl} =1.87
	206	δ(SSCl)	212	199	H_{SSCl}=0.21
	102 or 55	torsion	105	56	F_{SCl} =0.19
					ϕ =0.065(I)
					=0.016(II)
B	449	ν(S-Cl)	446	446	$F'_{SCl}=-0.1\,F_{SCl}$
	240	δ(SSCl)	242	242	

TABLE VI
VIBRATIONAL FREQUENCIES AND FORCE CONSTANTS FOR S_2Br_2

Symmetry	Observed frequency (cm^{-1})	Assignment	Calculated frequency (cm^{-1})	Force constant (md/Å)
A	529	ν(S-S)	531	K_{SS} =2.46
	356	ν(S-Br)	354	K_{SBr} =1.56
	172	δ(SSBr)	174	H_{SSBr}=0.15
	66	torsion	63.7	F_{SBr} =0.16
				ϕ =0.046$_3$
B	356	ν(S-Br)	357	$F'_{SBr}=-0.1\,F_{SBr}$
	200	δ(SSBr)	201	

H'_{SSX}, F'_{SX}, and Φ', there exist four relations to express the balancing of the forces at the equilibrium configuration. Therefore the constants K'_{SS}, K'_{SX}, H'_{SSX}, and Φ' can be expressed as functions of F'_{SX}. In total, the potential function here assumed has six adjustable parameters for six observed frequencies.

For sulfur monochloride two cases were considered, in one of which the line 102 cm^{-1} was taken the fundamental torsional mode (set I) and in the other of which it was taken the first overtone of this mode (set II). Force constants given in Tables V and VI give the frequencies in very satisfactory agreement with the observed data.

It is easy to calculate the rms amplitudes of vibration from this force fields: they are given by the formula[17]

$$\langle \Delta q^2 \rangle = kT\mathbf{A}\mathbf{U}'\mathbf{F}^{-1}\mathbf{U}\mathbf{A}' + (h^2/64\pi^2 kT)(\mu+\mu')$$

where **A** is a matrix which expresses, in terms of the internal coordinates, the displacement of the distance whose mean amplitude is to be calculated, **U** the transformation matrix between the internal and the symmetry coordinates, $\mathbf{F}^{-1}$ the inverse matrix of **F** expressed in the symmetry coordinates, and μ and μ' stand for the reciprocals of the masses of the atoms located at both ends of the distance. The calculated values are compared with the observed in Tables VII and VIII. Agreement is very satisfactory

TABLE VII
MEAN AMPLITUDES OF S_2Cl_2

	Calculated (Å)	Observed (Å) A	Observed (Å) C
S-Cl	0.054	0.06±0.01	0.05±0.01
S-S	0.048	0.03±0.03	0.05±0.03
S···Cl	0.087	0.08_7 ± 0.02	
Cl···Cl			
(I)	0.158	0.14 ± 0.07	
(II)	0.257		

TABLE VIII
MEAN AMPLITUDES OF S_2Br_2

	Calculated (Å) 25°C	Calculated (Å) 100°C	Observed (Å)
S-Br	0.055	0.060	0.05_3±0.015*
S-S	0.048	0.051	0.05 (ass.)
S···Br	0.092	0.101	0.09_8±0.02*
Br···Br	0.189	0.211	~0.31

* Corrected for the Born approximation. (See ref. 15).

for S-S, S-X, and S···X atom pairs. The rms amplitude of the Cl···Cl pair in sulfur monochloride was observed to be 0.14± 0.07 Å, in close agreement with the calculated value, 0.15_8 Å, which was based upon the assignment that the line 102 cm^{-1} is the fundamental. For the Br···Br pair of sulfur monobromide such an agreement

17) Y. Morino, K. Kuchitsu, and T. Shimanouchi, *J. Chem. Phys.*, **20**, 726 (1952); Y. Morino, K. Kuchitsu, A. Takahashi, and K. Maeda, ibid., **21**, 1927 (1953); Y. Morino and E. Hirota, ibid., **23**, 737 (1955).

was not obtained: a rough estimate of the rms amplitude of the Br···Br atom pair gave 0.31 Å, definitely larger than the calculated value of 0.19 to 0.21 Å. This disagreement could be understood by taking into consideration the mixing of bromine discussed above.

The correction for the Born approximation was carried out for S-Br and S···Br atom pairs, by using an approximate formula proposed by Bartell et al.[15].

It may be noted that, if the calculated rms amplitude of S-S and S-Cl are added, they amount to about 0.10 Å. This sum gives, with the relation derived in IIIb, the following two sets of parameters for S-S and S-Cl atom pairs on a line Å to C in Fig. 7 (a) if $r_{SCl}-r_{SS}=0.10$ Å, then $r_{SCl}=2.07$ Å and $r_{SS}=1.97$ Å, and (b) if $r_{SS}-r_{SCl}=0.10$ Å, then $r_{SCl}=2.00$ Å and $r_{SS}=2.10$ Å. The set (a) corresponds to the model GD and the set (b) approximately to the model BB.

Discussion

The four distances observed for sulfur monochloride indicate clearly that this molecule does not have the thionyl chloride type structure; because in the latter the length of the Cl···Cl pair must be shorter than 2(S-Cl) sin α (α equals to the angle of S-S-Cl). The observed values of the three atom pairs, S-S, S-Cl and S···Cl, give 3.96 Å for 2(S-Cl) sin α. It is significantly shorter than the observed 4.11 Å, and the discrepancy is definitely beyond the experimental error. Thionyl chloride has a pyramidal structure in which the two OSCl planes are not coplanar, hence in this structure Cl···Cl atom pair would have to be further shorter than 3.96 Å. This holds also for sulfur monobromide: 2(S-Br) sin α (α equals to the angle of S-S-Br) is calculated to be 4.33 Å, which is comparable in magnitude with the observed 4.26 Å, but a definitely shorter distance than 4.33 Å must be given for Br···Br distance of the presumed thionyl chloride type structure. Thus it is concluded that both molecules have the structure containing S-S bond, and the angles of the internal rotation ϕ (the angle between two SSX planes, the position of $\phi=0$ being at the *cis* one) are nearly equal to 90°: precisely speaking, 82.5° for S_2Cl_2, and 83.5° for S_2Br_2.

The bond length of S-S was found to be 1.97 to 1.98 Å from the data of sulfur monobromide, which is somewhat shorter than the usual single bond distance, such as 2.05 Å in H_2S_2[18], 2.05$_3$ Å in $(CF_3)_2S_2$[19], 2.06$_5$ Å in $(CF_3)_2S_3$[20], or 2.04 Å in $(CH_3)_2S_2$[20], but longer than the double bond 1.89 Å in S_2[21]. It is to be noted that the S-S stretching modes of sulfur monohalides are about 530 cm^{-1}, higher by about 20 cm^{-1} than those of usual single S-S bond. The length of S-Cl of sulfur monochloride, 2.07Å is close to S-Cl=2.07 Å in thionyl chloride, but longer than S-Cl=2.01 Å in SCl_2. The frequencies of S-Cl stretching modes in SCl_2 were observed to be 514 cm^{-1} and 534 cm^{-1}, but the corresponding values of sulfur monochloride are 436 cm^{-1} and 449 cm^{-1}. Thus it is likely that there is a parallelism between the vibrational frequencies and the bond lengths. The bond length of S-Br in sulfur monobromide 2.24 Å is also approximately equal to S-Br=2.27 Å in thionyl bromide.

The observed rms amplitude of the Cl···Cl pair of sulfur monochloride indicates that the line 102 cm^{-1} is the fundamental of the torsional oscillation. If the potential energy for this mode, $\frac{1}{2}\Phi(r\Delta\phi)^2$, is set equal to $V=\frac{1}{2}V_0(1-\cos 2\Delta\phi)\cong V_0(\Delta\phi)^2$, then V_0 is found to be about 17 kcal/mole. This potential barrier seems to be high in comparison with that of hydrogen peroxide; for the latter the height of the barrier of 0.3[22] to 4.5[2] kcal/mole was reported. Though the accurate evaluation of the interaction between the lone-pair electrons of oxygen atoms is very difficult, its estimation would be possible by calculating the overlap integral of $p\pi$ electrons. For the O-O bond length of 1.48 Å the overlap integral of $2p\pi$ electrons is 0.069 and for the S-S bond length of 1.97 Å $3p\pi$ electrons have the overlap integral of 0.152. The ratio of squares of these two integrals, which are considered to be a measure of the interaction of $p\pi$ electrons, is about 1 : 4.8. Hence a higher barrier is expected for the sulfur compound, in agreement with the observation. A similar discussion

18) M. K. Wilson and R. M. Badger, ibid., **17**, 1232 (1949).
19) H. J. M. Bowen, *Trans. Faraday Soc.*, **50**, 452 (1954).
20) P. W. Allen and L. E. Sutton, *Acta Cryst.*, **3**, 46 (1950).
21) G. Herzberg, "Molecular Spectra and Molecular Structure," Vol. II. D. van Nostrand Co., New York, (1945).
22) J. T. Massey and D. R. Bianco, *J. Chem. Phys.*, **22**, 442 (1954).
23) R. S. Mulliken, C. A. Rieke, D. Orloff and H. Orloff, ibid., **17**, 1248 (1949).

for sulfur monobromide was limited by the contamination of bromine.

As mentioned already, the rms amplitude of Br···Br was observed considerably larger than the calculated. The reason may be attributed to the anharmonicity of the torsional oscillation. Since the frequency of the torsional mode of sulfur monobromide is 66 cm^{-1}, there must be many molecules in the first, the second, and the third excited torsional state, and all these molecules can make transitions of the torsional oscillation (a kind of hot band), then anharmonicity of this mode would be greater. It is, however, difficult to know the real shape of the potential barrier through the data available at present.

Conclusion

By the sector and microphotometer method the molecular structures of sulfur monochloride and monobromide were obtained as follows:

sulfur monochloride:

S-Cl: $r=2.07\pm0.01$ Å,
$\langle\Delta r^2\rangle^{1/2}=0.05\pm0.01$ Å,

S-S: $r=1.97\pm0.03$ Å,
$\langle\Delta r^2\rangle^{1/2}=0.05\pm0.03$ Å,

S···Cl: $r=3.24_5\pm0.02$ Å,
$\langle\Delta r^2\rangle^{1/2}=0.08_7\pm0.02$ Å,

Cl···Cl: $r=4.11\pm0.05$ Å,
$\langle\Delta r^2\rangle^{1/2}=0.14\pm0.07$ Å,

$\angle$S-S-Cl$=107°\pm2.5°$,
$\phi=82.5°\pm12°$ ($\phi=0$ at the cis).

sulfur monobromide:

S-Br: $r=2.24\pm0.02$ Å,
$\langle\Delta r^2\rangle^{1/2}=0.05\pm0.02$ Å,

S-S: $r=1.98\pm0.04$ Å,
$\langle\Delta r^2\rangle^{1/2}=0.05$ Å (assumed),

S···Br: $r=3.35\pm0.02$ Å,
$\langle\Delta r^2\rangle^{1/2}=0.09_8\pm0.02$ Å,

Br···Br: $r=4.26\pm0.08$ Å,
$\langle\Delta r^2\rangle^{1/2}=0.31$ Å,

$\angle$S-S-Br$=105°\pm3°$,
$\phi=83.5°\pm11°$ ($\phi=0$ at the ***cis***).

Both molecules have the right angle structure of hydrogen peroxide type.

The lowest band 102 cm^{-1} of sulfur monochloride was concluded from the observed mean amplitude of Cl···Cl to be the fundamental of the torsional mode, contrary to the proposal by Luft and Todhunter. Sulfur monobromide is easily decomposed, and bromine molecule thus evolved obscured the intensity of sulfur monobromide, but free rotation was definitely denied and torsional oscillation about the right angle position was clearly concluded.

The author wishes to express his gratitude to Professor Yonezo Morino for his kind guidance and encouragement throughout the course of this research, to Mr. S. Shibata and to Mr. H. Morimoto, Nagoya University, for their kind help in the measurement of microphotometer tracing, and to Mr. R. Tsunoda and to Mr. Y. Suzuki, Division of Health and Welfare Statistics, for the use of Punched Card Machine. His thanks are also due to Mr. I. Nakagawa and to Mr. T. Oka for their advice and help in the calculation of the rms amplitudes. The expenses of this research were defrayed from the Scientific Research Encouragement Grant of the Ministry of Education to which the author's thanks are also due.

Department of Chemistry
Faculty of Science
The University of Tokyo
Hongo, Tokyo

SHORT COMMUNICATIONS

State of Aggregation of Primary Particles in Colloidal Silica

By Takeshi Okura, Katsumi Goto, and Tsuyoshi Komatsu

(Received October 14, 1957)

It has been shown in our previous reports[1,2] that the rate of polymerization of silicic acid increases with pH, and larger particles of colloidal silica are formed at higher pH values.

On the other hand, measurements carried out by many investigators of gelation time have shown that silicic acid gels most rapidly in a slightly acidic medium[3]. The fact seems to be an indication of the most rapid polymerization in a slightly acidic medium.

The present investigation was undertaken to reconcile the above two contrasting results, as well as to show that, as has already been suggested by Goto[4], different types of colloidal silica are formed at different pH values.

For these purposes, measurements were made of the relative viscosity and the dissolution time (i.e., the time required for the complete dissolution of colloidal silica particles in a proper medium) at various aging times.

Experimental

Preparation of Silicic Acid.—Silicic acid solutions containing 8 g./l. of SiO_2 were prepared from sodium metasilicate by ion exchange, and the pH was adjusted by adding appropriate amounts of sodium metasilicate solution. The aging of silicic acid solutions were carried out at room temperature.

Measurement of Dissolution Time (τ).—The method used for the determination of dissolution time was similar to that reported in the previous papers[1,2] with the following exceptions:

a) Instead of a solution of sodium carbonate, a solution containing sodium fluoride (300 mg. F^-/l.) and hydrochloric acid (0.1 N) was used for the dissolution of colloidal silica.

b) Aluminum chloride was employed to stop the dissolution reaction and to reduce the interference of the fluoride ion in the colorimetric determination of molecularly dispersed silica. The temperature was kept constant at 25°C during the measurement of dissolution time. Full descriptions of the method of measurement will be reported later.

Measurement of Relative Viscosity.—The viscosity was measured with the usual Ostwald viscosimeter.

Results and Discussion

The results are summarised in Table 1. The volume, V, immobilized by 1 g. of SiO_2 in water was estimated on the basis of the well known Einstein's formula, by using the equation

$$V = \frac{\eta_{rel} - 1}{0.0025\,C}$$

where η_{rel} is the relative viscosity, C, the concentration of silica in g./l., and V is expressed in cc. The effect of the charge was ignored in the calculation. The results were also shown in Table I.

It is clearly shown in this Table that at pH values slightly below 7, V increases

Table I

Changes in τ, η_{rel}, and V with aging time

Initial pH		Aging time (Day) 1	4	14	63
2.4	τ(min.)	<1	<1	1	2.0
	η_{rel}	1.009	1.010	1.018	1.070
	V(cc.)	0.45	0.50	0.90	3.5
3.7	τ(min.)	<1	1.4	2.1	3.7
	η_{rel}	1.009	1.035	1.062	1.140
	V(cc.)	0.45	1.8	3.1	7.0
5.2	τ(min.)	3.2	6.8	12.8	29.6
	η_{rel}	1.095	1.125	1.150	1.135
	V(cc.)	4.8	6.3	7.5	6.8
6.6	τ(min.)	10.3	17.3	29.3	40.0
	η_{rel}	1.060	1.060	1.060	1.070
	V(cc.)	3.0	3.0	3.0	3.5
8.2	τ(min.)	14.2	24.7	38.5	50.0
	η_{rel}	1.012	1.020	1.012	1.010
	V(cc.)	0.6	1.0	0.6	0.5

1) K. Goto, *J. Chem. Soc. Japan, Pure Chem. Sec.*, (*Nippon Kagaku Zassi*) **77**, 958 (1956).
2) K. Goto, *J. Phys. Chem.*, **60**, 1007 (1956).
3) R. C. Merrill and R. W. Spencer, *J. Phys. & Coll. Chem.*, **54**, 806 (1950); I. A. Heald, K. B. Coates and J. E. Edwards, *J. Appl. Chem.*, **5**, 425 (1955); M. F. Bechtold, *J. Phys. Chem.*, **59**, 532 (1955); Also see R. K. Iler, "The Colloid Chemistry of Silica and Silicates," Cornell Univ. Press (1955), p. 45.
4) K. Goto, *J. Chem. Soc. Japan, Pure Chem. Sec.*, (*Nippon Kagaku Zassi*) **76**, 729 (1955).

considerably with aging time, while the dissolution time remains very small. At higher pH values, V remains very low, even when the dissolution time has acquired a very high value.

There are two possible forms of colloidal silica, as has been suggested by Iler[5]:

a) particles of colloidal silica which are aggregates of many smaller primary particles as schematically shown in Fig. 1 a.

b) dense, descrete particles as shown in Fig. 1 b.

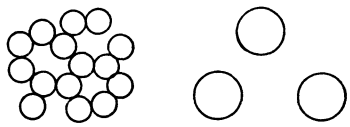

a b

Fig. 1

Since dissolution time, which is theoretically proportional to the radius of particles, may be influenced mainly by the size of primary particles, it may be reasonable, to take the dissolution time as a measure of the size of primary particles. On the other hand, the viscosity and the value of V may be a measure of the looseness with which primary particles are associated together, or the packing density of primary particles.

It is thus suggested from the above results that the aging in slightly acidic media leads to the formation of aggregates of very fine primary particles, while a tendency towards the formation of larger, descrete particles becomes marked as the pH increases.

The authors wish to express their thanks to Professors Y. Uzumasa, G. Okamoto, and I. Kayama for their valuable advice and encouragement. In addition, it would have been impossible to carry out the work with out the assistance of the Asahi Glass Foundation for the Promotion of Researches in Chemical Industries.

Faculty of Engineering
Hokkaido University, Sapporo

5) R. K. Iler, "The Colloid Chemistry of Silica and Silicates," Cornell Univ. Press (1955), p. 96.

Crystal Structure of Bayerite

By Goro YAMAGUCHI and
Kenichi SAKAMOTO

(Received September 19, 1957)

Bayerite, one of aluminumtrihydroxides, was identified by Fricke[1] as a new crystal which has a composition of $Al(OH)_3$ or $Al_2O_3 \cdot 3H_2O$. Montoro[2] reported for the first time that bayerite has a hexagonal lattice with $c=4.76$ kX and $a=5.01$ kX. Later Milligan[3] reported that Montoro's lattice was not correct. We have examined the structure of bayerite and found that Montoro's lattice was essentially correct (See Table 1). Assuming that the structure is analogous to that of brucite, $Mg(OH)_2$, from which one third of columns of the metallic ions are taken out, we have arrived at a satisfactory atomic arrangement based upon the space group D'_3 d. The calculated and the observed values of spacings and intensities are shown in Table II. As can be seen from this table, calculated values are in good accord with observed values. As a result, bayerite has the following structure.

TABLE I

Crystal Class	Hexagonal (Trigonal)
Unit Cell	$a=5.047$ Å $c=4.730$ Å
Space Group	D^1_{3d}
Atomic Coordinates	Al : 2 (c)
	O : 6 (k) :0.340 :0.210

The structure is shown in Fig. 1 and this structure can be said to be the idealized monolayer structure of hydrargillite[4].

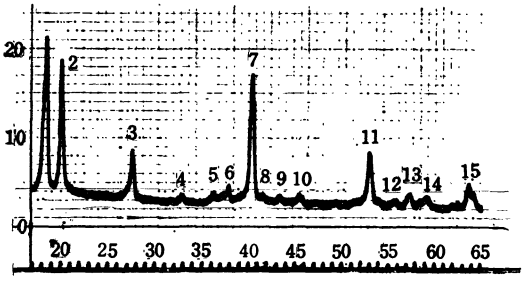

Fig. 1. Diffraction Pattern of Bayerite

1) R. Fricke, *Z. anorg. allg. Chem.* **175**, 249 (1928).
2) V. Montoro, *Ricerca Sci.* **13**, 565 (1942).
3) W. O. Milligan, *J. Phys. Colloid Chem.* **55**, 497 (1951).
4) H. Megow, *Z. Krist.* **87**, 185 (1934).

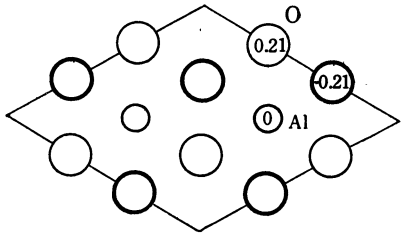

Fig. 2. Crystal Structure of Bayerite.

TABLE II
SPACINGS AND INTENSITIES OF DIFFRACTION LINES

No.	h k l	Spacings		Intensities	
		obs.	calcd.	obs.	calcd.
1	0 0 1	4.753	4.730	100	100
2	1 0 0	4.385	4.371	60	30
3	1 0 1	3.220	3.210	34	25
4*		2.705			
5*		2.468			
6	0 0 2	2.368	2.365	7	2
7	1 1 1	2.227	2.226	90	99
8	2 0 0	2.171	2.186	2	3
9	1 0 2	2.079	2.080	3	6
10	2 0 1	1.987	1.984	4	6
11	1 1 2	1.725	1.726	45	51
12	1 2 0	1.653	1.653	3	3
13	2 0 2	1.604	1.605	10	6
14	1 2 1	1.560	1.561	15	6
15	3 0 0	1.460	1.457	25	26
16	3 0 1	1.394	1.392	8	14
17	1 1 3	1.333	1.337	21	18
18	2 2 1	1.216	1.219	15	8

* Impurity lines, presumably due to polytype layer structure of bayerite (to be published later).

Department of Applid Chemistry
Faculty of Eng. Tokyo University
Hongo Tokyo

Catalysis on an Organic Semi-Conductor

By Kenzi TAMARU and Takeo SHIMADA

(Received October 22, 1957)

Mostly because of the elaborate works of Akamatu and his co-workers[1], it is generally recognized that the condensed polycyclic aromatic hydrocarbons and their related quinones are organic semi-conductors and their fundamental properties such as semi- and photo-conductivity and its temperature dependency have been elucidated.

In the field of catalysis many investigations have been made on the relation between the electronic properties of solid and its catalytic activity, and the theory of semi-conductor has successfully been applied to the problem of heterogeneous catalysis[2].

It is of interest to examine whether the organic semi-conductor would catalyze the exchange reaction between hydrogen and deuterium, as it would be a new type of catalytic reaction on a molecular crystal. It can also be noted on this problem that the ortho-para hydrogen conversion can be catalyzed by charcoal which is thought, from the X-ray diffraction analysis, to consist of many crystallites of graphitic carbon, in other words, large condensed polycyclic aromatic hydrocarbons.

The polycyclic aromatic compounds can react with bromine or iodine, the halogen atoms penetrating between the layers of the net planes. The halogen atoms thus chemisorbed might react with hydrogen to form hydrogen halide, the organic compound acting as a catalyst.

In order to obtain informations on these points the exchange reaction of hydrogen and deuterium in addition to the reaction between hydrogen and iodine has been studied in a static method in the presence of violanthrone, one of the organic semiconductors.

The gas, H_2, HD and D_2, prepared from heavy water (47.5% D content) and sodium metal[3] was added to hydrogen to such an amount that the ratio of hydrogen deuteride to hydrogen was 0.326. The gas mixture was conducted to a reaction vessel at 18°C which contains 0.80 g. of violanthrone. The gas pressure was 307 mmHg. The reaction vessel was then heated up to 100° for 13 hours and a part of the gas mixture was taken out for mass spectrometric analysis, which showed no exchange reaction within the experimental error. From the statistical mechanical calculation, the activation energy for the exchange reaction could roughly be estimated as higher than 50 kcal. per mole.

Violanthrone (2.14 g.) was mixed with

1) H. Akamatu and H. Inokuchi, *J. Chem. Phys.*, **18**, 810 (1950); **20**, 1481 (1952): H. Inokuchi, This Bulletin, **29**, 131 (1956) etc.

2) K. Hauffe, Advances in Catalysis, Vol. VII, Academic Press. Inc., N. Y. p. 213 (1955).

3) A. Farkas and H. W. Melville, "Experimental Methods in Gas Reactions." Macmillan, London, 1939.

20.26 g. of iodine in a mortar, and 6.8 g. of the mixture was put in a reaction vessel, into which 402 mm. of hydrogen was introduced at 100°C. The reaction vessel was kept at 100° for nine hours, then at 130° for four hours and finally at 150° for four hours. No pressure change, however, could be observed other than that from the temperature change.

In short, the catalytic reaction neither between hydrogen and deuterium nor between hydrogen and iodine could be observed.

The assistance of Professor T. Titani and Professor S. Horibe of the Tokyo Metropolitan University in the mass spectrometric analysis is gratefully acknowledged. The authors are also indebted to Professor H. Akamatu of the University of Tokyo for his valuable suggestions and assistance.

Department of Chemical Industry
Faculty of Engineering, Yokohama
National University, Minami-ku
Yokohama

by one of the present authors and others[1], using three-dimensional Fourier series. The published data showed that there were two close contacts between the nitrogen atom and the oxygen atoms. Recently the present authors checked the data given in the previous paper, and found that another type of close contact should be added. This is between the nitrogen atom and the O_2' atom, O_2' being in the molecule related to the original one by the screw axis. The N···O distances and the C_α—N···O angles for the all types of close contacts are given in the figures.

The above distances and angles strongly suggest that there are three N(H)···O hydrogen bonds in this structure as in the cases of other amino acids of which crystal structures have been investigated.

Thus it can be said of the structure that the molecules are tied into infinite sheets approximately parallel to the (010) by the two different types of the N(H)···O hydrogen bonds, and these sheets are tied together in the other direction by the third type of the hydrogen bonds.

Department of Chemistry, Defence Academy, Yokosuka

1) S. Hirokawa, S. Kuribayashi and I. Nitta, This Bulletin, **25**, 192 (1952).

A Remark on the Crystal Structure of α-Amino-isobutyric Acid

By Sakutaro Hirokawa and Tamaichi Ashida

(Received September 9, 1957)

The crystal structure of α-amino-isobutyric acid has previously been analysed

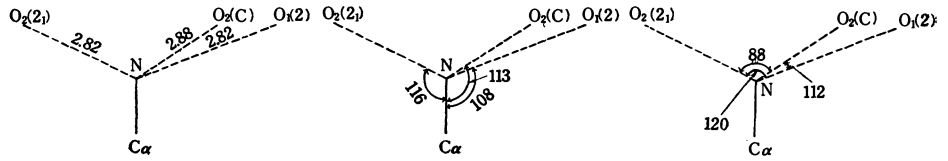

Figures showing hydrogen-bond distances and bond angles around the nitrogen atom. Symbols in brackets show symmetry elements.

TABLE I
PHYSICAL PROPERTIES OF HYDROCARBONS USED FOR THE DETERMINATIONS

Name	b. p., °C		d_4^{20}		n_D^{20}		Remarks
	Obs.	Lit.[10]	Obs.	Lit.[10]	Obs.	Lit.[10]	
n-Hexane	68.7	68.740	0.6594	0.65937	1.3749	1.37486	a
n-Heptane	98.3	98.427	0.6838	0.68376	1.3878	1.38764	b[8,9]
n-Octane	125.4	125.665	0.7026	0.70252	1.3976	1.39743	a
2, 2, 4-Trimethylpentane	99.2	99.238	0.6919	0.69192	1.3916	1.39145	b
n-Cetane	286.6	286.793	0.7749	0.77344	1.4350	1.43453	c, m. p. 17.2 Lit. 18.165
Cyclohexane	80.5-81.0	80.738	0.7788	0.77855	1.4263	1.42623	d[11], m. p. 6.32 Lit. 6.554
Methylcyclohexane	100.9	100.934	0.7686	0.76939	1.4231	1.42312	c
Decalin *cis*	189-190	195.69	0.8859	0.8965	1.4750	1.4810	c[12]
Decalin *trans*		187.25		0.8699		1.4695	
Cyclohexene	82.8	82.979	0.8096	0.81096	1.4465	1.44654	c, Br. No. 194.6 Theor. 194.58
1-Octene	122.6	121.280	0.7161	0.71492	1.4086	1.40870	a[11], Br. No. 142.2 Theor. 142.7
Styrene	48/24.1	145.2	0.9059	0.90600	1.5468	1.54682	c[1], Br. No. 151.2 Theor. 153.5
Toluene	110.5	110.625	0.8660	0.86694	1.4961	1.49693	c[8,9]
Ethylbenzene	136.0	136.186	0.8670	0.86702	1.4959	1.49588	a[1]
o-Xylene	144.2	144.414	0.8805	0.88020	1.5045	1.50545	a, m. p. −25.3 Lit. −25.182
m-Xylene	139.1	139.103	0.8636	0.86417	1.4971	1.49722	d, m. p. −47.9 Lit. −47.872
p-Xylene	138.4	138.351	0.8605	0.86105	1.4957	1.49582	a, m. p. 13.2 Lit. 13.263
Propylbenzene	159.2	159.217	0.8619	0.86204	1.4920	1.49202	a
iso-Propylbenzene	152.4	152.392	0.8618	0.86179	1.4912	1.49145	a[13]
Mesitylene	164.7	164.715	0.8647	0.86518	1.4993	1.49937	a[14]
1-Methylnaphthalene	244.4	244.642	1.0200	1.02015	1.6174	1.6174	a
Tetralin	207	207.57	0.9702	0.9702	1.5414	1.54135	d[12]

a) This material was synthesized.
b) This material is the reference fuel for Octane Number determination.
c) Commercially available product was purified according to the ordinary method.
d) Commercially available product was purified according to the description in the literature.

methylation of toluene, and purified by the conversion in to the sulfonate which melted at 86°C after three recrystallizations from water.

Mesitylene was synthesized by sulfuric acid condensation of acetone[14]. 1-Methylnaphthalene was synthesized by the reduction of 1-chloromethylnaphthalene which was obtained by the chloromethylation of naphthalene, and purified by applying chromatographic cleavage of the picrate whose melting point was 141—141.5°C. Methods of purifying for the other materials have been described in the previous paper[8,11,12].

Results

Mutual solubility data of liquid ammonia and paraffins, naphthenes and olefins are given in Table II.

Values for *n*-heptane[9], cyclohexane[1], decalin[12] and purified commercial hexane which is used for the extraction of vegetable oils[1,11] are also given in Table II for convenience of comparison.

As will be clear from Table II, it is observed for liquid ammonia-saturated hydrocarbons systems that within the experimental range, naphthenic hydrocarbons are more soluble in liquid ammonia at a given temperature than paraffins which have the same number of carbon atoms, whereas the quantities of ammonia dissolved in hydrocarbon rich phase are greater in paraffins; it is also observed that solubilities decrease as the molecular weight increases. For binary systems of aliphatic hydrocarbons and liquid ammonia, it is observed that logarithms of solubilities of paraffins in each phase are almost proportional to those of vapor pressures of these hydrocarbons at a given temperature, and that their solubilities are small compared with those of olefins.

The experimental data for aromatic

TABLE II

MUTUAL SOLUBILITY DATA FOR PARAFFINS, NAPHTHENES AND OLEFINS WITH LIQUID AMMONIA, Wt. % OF NH_3

Material	Phase	Temperature, °C					
		30	20	10	0	−7.5	−15
Purified Hexane Used for Vegetable Oil Extraction	Upper		94.4				
	Lower		6.1				
n-Hexane	Upper		94.9_4		97.4_1		
	Lower		5.7_8		3.0_2		
n-Heptane	Upper		96.9_2		98.1_6	98.4_9	98.8_0
	Lower		4.8_5		2.7_3	2.2_3	1.7_1
n-Octane	Upper		97.7_5		98.5_6		
	Lower		4.1_3		2.2_9		
2, 2, 4-Trimethylpentane	Upper		96.8_9		98.5_1		
	Lower		5.0_8		2.7_3		
n-Cetane	Upper	98.5_7	99.4_4				
	Lower	3.0_8	2.4_3				
Cyclohexane	Upper		94.2_2		96.7_8		
	Lower		3.9_9		2.1_2		
Methylcyclohexane	Upper		94.7_2		97.8_8		
	Lower		4.1_5		2.2_0		
Decalin	Upper		97.8_4		98.3_5		
	Lower		2.2_8		1.4_0		
1-Octene	Upper		93.6_9		96.8_3		
	Lower		7.8_8		4.0_9		
Cyclohexene	Upper	72.6_4	82.1_9	88.0_0	91.6_1		
	Lower	15.2_2	9.3_9	6.3_7	4.5_5		

TABLE III

SOLUBILITY OF AROMATICS IN LIQUID AMMONIA, Wt. % of NH_3

Material	Temperature, °C								
	30	25	20	15	10	5	0	−5	−15.5
Ethylbenzene		miscible			57.0_1	71.4_7	78.1_1	82.2_5	87.0_2
o-Xylene		miscible			61.8_3	72.6_3	78.8_2	82.9_6	
m-Xylene		miscible			69.5_0	76.7_2	81.0_2	84.2_0	
p-Xylene		miscible			64.9_2	74.4_7	79.9_4	83.7_5	
Propylbenzene	miscible		68.5_0	77.3_5	82.8_2	86.4_6	88.8_8		
iso-Propylbenzene	miscible		C.S.T.	70.8_2	78.9_2	83.3_1	86.7_2		
Mesitylene	67.6_7	76.2_0	81.0_9	84.8_5	87.5_7	89.9_2	91.4_4		
1-Methylnaphthalene		64.3_7	71.7_8	77.1_6	81.1_2	83.9_4	85.9_4		
Tetralin			86.3_9				93.7_2		

Temperature, °C (±0.1°)	−10	−15	−20	−25	−30
Material					
Toluene	64.4_4	73.1_8	78.5_9		
Styrene			68.7_6	76.3_4	79.8_8

hydrocarbons are given in Tables III and IV. *p*-Xylene is present as crystals at the experimental temperatures, but the mixture with liquid ammonia was liquid over the experimental temperature range above 5°C. *p*-Xylene-rich layer stayed in a supercooled liquid state at the temperatures of 0° and −5°C, and it was difficult to cause it to crystallize by mere agitation. Occasionally, *p*-xylene-rich layer was caused to crystallize by the stimulation such as the release of a portion of the solution from the bottle containing the system, which closed the reducing valve and made it impossible to continue the experiment. The data for *p*-xylene at the temperatures of 0° and −5°C given in Table IV are values in a supercooled condition. In Tables III and IV, the data for tetralin[12] and toluene[9] are also adopted for comparison from the previous paper.

In Table V are given the results of the determinations of compositions and cloud points for the binary systems of aromatics and liquid ammonia at temperatures near the critical solution temperature. The critical solution temperatures and their compositions estimated graphically from

TABLE IV

SOLUBILITY OF LIQUID AMMONIA IN AROMATIC HYDROCARBONS, Wt. % OF NH_3

Material	Temperature, °C								
	30	25	20	15	10	5	0	−5	−15.5
Ethylbenzene		miscible			30.7_6	18.9_0	14.1_3	11.3_1	8.0_0
o-Xylene		miscible			24.3_2	16.9_5	13.0_7	10.8_3	
m-Xylene		miscible			20.2_5	15.0_3	11.8_7	9.6_7	
p-Xylene		miscible			22.1_3	16.1_2	12.7_8	10.3_3	
Propylbenzene	miscible		22.5_4	16.5_5	13.1_7	10.8_9	9.1_5		
iso-Propylbenzene	miscible		C.S.T.	20.5_7	15.2_6	12.2_3	10.0_1		
Mesitylene	21.0_4	15.5_2	12.5_7	10.3_6	8.6_2	7.2_6	6.2_9		
1-Methylnaphthalene		22.2_4	17.3_6	14.3_0	12.1_9	10.4_3	9.1_2		
Tetralin			8.0_9				4.7_1		

Temperature, °C (±0.1°)	−10	−15	−20	−25	−30
Material					
Toluene	20.2_2	15.3_4	12.4_1		
Styrene			20.7_5	14.6_6	11.9_5

TABLE V

CLOUD POINTS AND THEIR COMPOSITION FOR AROMATICS WITH LIQUID AMMONIA

Cloud Pt., °C	NH_3 Wt. %	Cloud Pt., °C	NH_3 Wt. %	Cloud Pt., °C	NH_3 Wt. %
Styrene		*o*-Xylene		*p*-Xylene	
−16.8	27.6_5	11.5	34.3_8	12.3	29.9_3
−16.3	30.2_5	11.9	41.9_7	12.8	42.9_0
−15.85	32.1_1	11.9	45.3_4	12.6	48.0_9
−15.7	34.7_1	11.8	47.9_3	12.6	48.2_2
−15.5	40.3_8	11.5	54.5_5	12.5	52.0_0
−15.5	42.4_4	11.3	56.6_8	11.7	58.0_3
−15.5	43.9_1	11.2	57.0_6	11.6	58.9_9
−15.8	50.2_2	11.1	57.6_2	10.2	64.0_9
−17.8	62.5_3	10.6	60.2_6	12.8*	40.5**
−15.5*	43.9**	11.9*	43.3**		
Ethylbenzene		*m*-Xylene		Propylbenzene	
9.0	26.2_1	14.1	31.6_3	21.3	24.9_3
10.2	32.1_1	14.6	42.1_0	23.6	36.0_4
10.5	36.0_7	14.4	46.5_1	23.9	40.2_3
10.6	37.2_2	13.9	54.0_9	23.9	41.8_7
10.7	44.2_4	13.8	54.9_4	23.0_5	56.7_4
10.4	51.7_7	13.5	56.7_5	22.6	58.8_5
10.1	55.4_4	11.6	65.0_7	22.4_5	59.5_9
0.0	62.2_0	14.6*	41.5**	23.9*	44.7**
10.7*	43.4**				
iso-Propylbenzene		Mesitylene		1-Methylnaphthalene	
18.0	25.2_7	32.6	26.8_2	26.0	23.7_3
19.0_5	28.5_0	33.8	36.5_1	27.4	27.4_1
19.8	34.2_3	33.9	39.6_2	27.4_5	27.4_8
20.0	42.5_7	33.9	41.8_3	28.6	36.1_7
19.9	48.5_8	33.9	45.0_2	28.8	42.3_4
19.7	52.7_4	33.9	45.4_7	28.8	44.4_7
19.6	54.3_4	33.8_5	48.7_2	28.7_5	47.6_7
19.3	56.7_8	33.7	52.7_8	28.7	48.8_3
18.0	63.7_5	33.6	53.0_7	28.5	50.9_8
20.0*	71.7**	33.5_5	53.6_1	28.2	53.5_2
		32.9	59.5_6	27.0	59.2_6
		32.4_5	61.1_8	28.8*	42.6**
		33.9*	42.9**		

* Critical solution Temperature.
** Critical Composition.

the data given in Tables III, IV and V are also given in Table V.

The critical solution temperatures for toluene[9] and *iso*-propylbenzene with liquid ammonia in the present investigation, −7.4° and 20.0°C, are lower than those given in the literature[6], −5° and 25°C, respectively. But, the value for *m*-xylene, 14.6°C, agrees with that obtained by Kraus, et al.[4], 14.7°C, which is believed to be accurate. The critical composition for this system is 81.5 mole per cent. of ammonia and compared with the Kraus' value of 81.4 mole per cent. ammonia. The critical solution temperature for 1-methylnaphthalene with liquid ammonia is 28.8°C by the present determination, compared with the Francis' value of 28°C[6].

In the case of all these systems, it will be clear from Tables II, III and IV that solubilities in both phases are smaller at lower temperatures exhibiting positive deviations from Raoult's law, and roughly symmetrical on the basis of weight fraction. However, as the molecular weight of ammonia is considerably small compared with that of any other component, the solubility curves lean to the ammonia side on the basis of mole fraction expressing unsymmetrical form, as shown in Fig. 1. The mole fractions of ammonia in hydrocarbon-rich phase are greater than those of oils in liquid ammonia rich phase. Solubilities of these hydrocarbons in liquid ammonia are less than 10 mole per cent., except for the cases in the neighborhood of the critical solution temperature, and the solubility change in ammonia-rich phase due to temperature variation is small compared with that in the hydrocarbon-rich phase.

In Fig. 1, in addition to the mutual solubilities of aromatic hydrocarbons and liquid ammonia, the concentrations of ammonia in hydrocarbon-rich phase for other representative hydrocarbons are shown on the basis of mole fraction. The values of Kraus, et al. for *m*-xylene are also given for comparison. Solubility curves for paraffins, naphthenes and olefins in liquid ammonia-rich phase are omitted in the figure except for *n*-heptane, because they are so nearly of the same order that the curves for them can not be expressed clearly without overlapping.

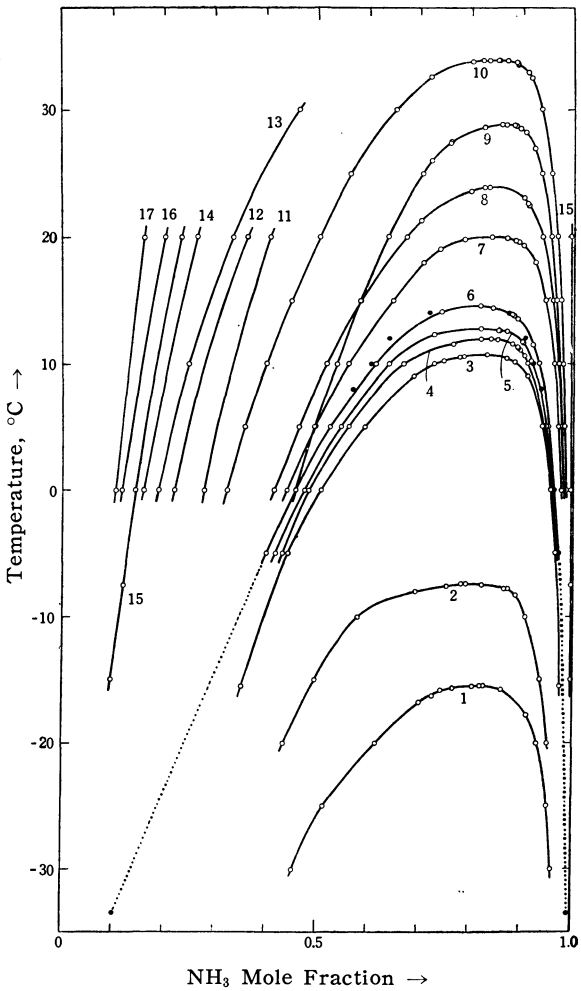

Fig. 1. Solubility curves for some hydrocarbons and liquid ammonia.

1. Styrene
2. Toluene
3. Ethylbenzene
4. *o*-Xylene
5. *p*-Xylene
6. *m*-Xylene (• Kraus value)
7. *iso*-Propylbenzene
8. Propylbenzene
9. 1-Methylnaphthalene
10. Mesitylene
11. Tetralin
12. 1-Octene
13. Cyclohexene
14. 2,2,4-Trimethylpentane
15. *n*-Heptane
16. Methylcyclohexane
17. Decalin

Summary

In order to obtain the quantitative knowledge on the solubility relations for liquid ammonia systems, mutual solubilities of aromatic hydrocarbons and liquid ammonia were determined at the several temperatures near the critical

solution temperature, and data for other hydrocarbons were mainly obtained at 20° and 0°C. These results were presented in tables and a figure.

The Chemical Research Institute of Non-Aqueous Solutions
Tohoku University
Katabira-cho, Sendai

Mutual Solubilities of Some Hydrocarbon Oils and Liquid Ammonia. II. Application of the Solubility Parameter Theory

By Kiyoharu ISHIDA

(Received September 13, 1957)

The simple expression according to solubility parameter theory which has been developed by Hildebrand[1,2] and Scatchard[3] about nonpolar components, or its variant with the Flory-Huggins configurational term, has proved useful in interpreting qualitatively and often semi-quantitatively a wide variety of nonelectrolyte solutions including those of high polymers, especially when solubility phenomena are involved and when components are nonpolar. Liquid ammonia has not only a rather high dielectric constant and a dipole moment, but also hydrogen bonding capacity, although weaker than that of water or hydrogen fluoride. However, it has been observed that this theory interprets satisfactorily the solubility relationships even for the case including polar components such as water and aniline; for the systems of hydrocarbons and aniline, hydrocarbons and water, etc., values for solubility parameter of polar component, obtained from the solubility using the expression according to solubility parameter theory, are almost identical with values calculated from the vaporization energy[2]. It is interesting to study what relations are obtained for liquid ammonia systems. And also, some knowledge of the special interaction induced by polarity might be given from the differences between the theory and the experiment, which are obtained by applying the solubility data for liquid ammonia and hydrocarbon oils to the solubility parameter theory.

1) J. H. Hildebrand, *J. Am. Chem. Soc.*, **38**, 1452 (1916); **41**, 1067 (1919); **42**, 2180 (1920); **51**, 66 (1929); **57**, 866 (1935). J. H. Hildebrand and S. E. Wood, *J. Chem. Phys.*, **1**, 817 (1933).

2) J. H. Hildebrand and R. L. Scott, "The Solubility of Nonelectrolytes", 3rd. Ed., Reinhold Pub. Corp., New York, 1950.

3) G. Scatchard, *Chem. Revs.*, **8**, 321 (1931); *Trans. Faraday Soc.*, **33**, 160 (1937).

Expressions according to the Solubility Parameter Theory

Solubility parameter theory, which is derived under the assumption that in a mixture of two nonpolar molecules having spherical symmetry, the partial molal free energy of a component is the sum of a term from the entropy of mixing which is assumed to be ideal, and one from the heat of mixing which is derived from the London theory of dispersion forces neglecting the difference between arithmetic and geometric means, may be expressed in its simplest form as follows:

$$RT \ln \gamma_1 = V_1 \varphi_2^2 (\delta_1 - \delta_2)^2 \qquad (1a)$$

$$RT \ln \gamma_2 = V_2 \varphi_1^2 (\delta_1 - \delta_2)^2 \qquad (1b)$$

where γ_1 and γ_2 are the respective activity coefficients, V_1 and V_2 are the molal volumes of the pure components, φ_1 and φ_2 are the volume fractions, and δ_1 and δ_2 are solubility parameters defined as

$$\delta = (\Delta E^v / V)^{1/2} \qquad (2)$$

where ΔE^v is the energy of vaporization of the pure component and V its molal volume, all at the temperature T. $\Delta E^v/V$ is of course the "internal pressure" or "cohesive energy density". Equations (1a) and (1b) are exactly equivalent to equations of the form given by van Laar,[4] equations (3a, b) and (12).

Further complications are introduced if the effect of volume change on mixing or difference in molecular size is taken into consideration. Solutions which exhibit positive deviations from Raoult's law are formed from their constituents with an absorption of heat and volume expansion, although effect on volume change is fairly small. Effect of differences in molecular

4) J. J. van Laar, *Z. physik. Chem.*, **72**, 723 (1910).

size upon the entropy of mixing can not be disregarded when molecular volumes are considerably different, and exhibit negative deviations from the ideal entropy ($-\boldsymbol{R}\ln x$). However, it has recently been confident[5] that since expansion of volume on mixing increases both the entropy and the enthalpy, free energy or isothermal solubility may be treated without serious error by the equations (1a, b) in which the entropy of mixing is assumed to be ideal and volume changes on mixing are neglected, despite the fact that both the actual entropy and the enthalpy are far from ideal.

When the volumes V_1 and V_2 in equations (1a, b) are replaced by empirical parameters q_1 and q_2 which may be related to the "effective volumes" of molecules of different shapes, and the term of intermolecular energy on mixing is represented by the more generalized form of D included also the contributions due to polarity instead of $\left\{\left(\frac{\Delta E_1^v}{q_1}\right)^{1/2}-\left(\frac{\Delta E_2^v}{q_2}\right)^{1/2}\right\}^2$, extensive empirical use of the van Laar equation may be possible even in the case of containing polar components, as well as nonpolar components. Then, equations (1a, b) may lead to

$$\log\gamma_1=A_{12}\Big/\left(1+\frac{x_1A_{12}}{x_2A_{21}}\right)^2 \tag{3a}$$

$$\log\gamma_2=A_{21}\Big/\left(1+\frac{x_2A_{21}}{x_1A_{12}}\right)^2 \tag{3b}$$

and

$$A_{12}=q_1D/2.303\,\boldsymbol{RT} \tag{4a}$$

$$A_{21}=q_2D/2.303\,\boldsymbol{RT} \tag{4b}$$

where x_1 and x_2 are the respective mole fractions, and A_{12} and A_{21} the van Laar constants.

Critical solution temperature, T_c, and the critical composition, x', are obtained by applying the following conditions to both components:

$$\partial a/\partial x=0, \qquad \partial^2 a/\partial x^2=0$$

where a is the activity.

When activity coefficients are expressed by Eqs. (1a, b), the followings are obtained:

$$\boldsymbol{RT}_c=\frac{2x_1'x_2'V_1^2V_2^2}{(x_1'V_1+x_2'V_2)^3}(\delta_1-\delta_2)^2 \tag{5}$$

and at T_c,

$$x_1'=1-x_2'=\frac{(V_1^2+V_2^2-V_1V_2)^{1/2}-V_1}{V_2-V_1} \tag{6}$$

If the molal volumes of two components are noticeably unequal and the Flory-Huggins equation[6] is applicable to the athermal mixing of liquids, and the relation of activity follows to equations of the form (7),

$$\ln\gamma_1=\ln V_1-\ln(x_1V_1+x_2V_2)+\varphi_2\left(1-\frac{V_1}{V_2}\right)+V_1\varphi_2^2D/\boldsymbol{RT} \tag{7}$$

then, T_c and x' may be obtained from the equations (8) and (9), respectively:

$$\boldsymbol{RT}_c=\frac{2\varphi_1\varphi_2V_1V_2}{V_1\varphi_1+V_2\varphi_2}D \tag{8}$$

and at T_c,

$$\varphi_1=\frac{V_2-(V_1V_2)^{1/2}}{V_2-V_1}, \qquad x_1'=\frac{V_2^{3/2}}{V_1^{3/2}+V_2^{3/2}} \tag{9}$$

TABLE I

COMPARISON OF D CALCULATED FROM CRITICAL DATA WITH $(\delta_1-\delta_2)^2$.
Suffix 1 and 2 represent hydrocarbon and liquid ammonia, respectively

Component, 1	T_c, °K	Eq. (10) δ_1	Eq. (10) δ_2	$(\delta_1-\delta_2)^2$	D, Eq. (5): using obs. value for x_1'	D, Eq. (5): using calcd. value by Eq. (6) for x_1'	obs. x_1'	Eq. (6) x_1'
Toluene	265.8	9.36	13.40	16.32	16.23	15.14	0.200	0.134
Styrene	257.7	9.65	13.68	16.24	14.50	13.79	0.173	0.122
Ethylbenzene	283.9	8.93	12.70	14.21	14.92	14.07	0.173	0.119
o-Xylene	285.1	9.12	12.66	12.53	15.04	14.13	0.174	0.120
m-Xylene	287.8	8.94	12.56	13.10	15.29	14.07	0.184	0.118
p-Xylene	286.0	8.91	12.63	13.84	15.43	13.97	0.191	0.117$_5$
Propylbenzene	297.1	8.64	12.16	12.39	13.49	12.83	0.149	0.105
iso-Propylbenzene	293.2	8.62	12.34	13.84	13.86	12.72	0.165	0.104
Mesitylene	307.1	8.66	11.73	9.43	14.02	13.17	0.159	0.107
1-Methylnaphthalene	302.0	10.0*	11.96	3.84	13.38	13.00	0.139	0.106

* Calculated by the equation[10], $\Delta H^v_{298}=-2950+23.7\,Tb+0.020\,Tb^2$.

5) L. W. Reeves and J. H. Hildebrand, *J. Phys. Chem.*, **60**, 949 (1956).

6) M. L. Huggins, *J. Chem. Phys.*, **9**, 449 (1941); P. J. Flory, ibid., **9**, 660 (1941); **10**, 51 (1942).

TABLE II

COMPARISON OF ACTIVITY COEFFICIENTS AT INFINITE DILUTION

Suffiix 1 and 2 represent hydrocarbon and liquid ammonia, respectively

Component, 1	Temp. °C	V_1 ml./mole	δ_1 (cal./ml.)$^{1/2}$	$\frac{V_1(\delta_1-\delta_2)^2}{2.303RT}$	A_{12}	$\frac{V_2(\delta_1-\delta_2)^2}{2.303RT}$	A_{21}	$\frac{A_{12}}{A_{21}}/\frac{V_1}{V_2}$
n-Hexane	20	130.6	7.42	2.36	1.991	0.50	0.782	0.544
	0	127.2	7.61	3.10	2.282	0.65	0.986	0.485
n-Heptane	20	146.5	7.54	2.52	2.244	0.48	0.773	0.553
	0	142.9	7.76	3·30	2.481	0.62	0.959	0.483
n-Octane	20	162.8	7.59	2.74	2.424	0.47	0.773	0.538
	0	159.2	7.90	3.48	2.638	0.58	0.969	0.456
n-Cetane	20	292.3	7.64[a]	4.81	3.276	0.46	0.691	0.452
2,2,4-Trimethyl-pentane	20	165.1	6.92	3.62	2.280	0.61	0.713	0.540
	0	161.5[b]	7.17	4.59	2.616	0.76	0.907	0.476
Cyclohexane	20	108.0	8.34	1.29	1.944	0.33	0.919	0.546
	0	105.5[f]	8.89	1.52	2.193	0.38	1.127	0.492
Methylcyclohexane	20	127.6	7.90	1.88	2.031	0.41	0.848	0.524
	0	124.7[b]	8.15	2.47	2.422	0.53	1.047	0.495
1-Octene	20	157.0	7.49[c]	2.75	1.968	0.49	0.605	0.579
	0	153.7[d]	7.79[c]	3.51	2.280	0.61	0.791	0.500
Cyclohexene	20	101.3	8.50[e]	1.11	1.492	0.31	0.710	0.579
	0	98.8[b]	8.84[e]	1.45	1.787	0.39	0.898	0.537
Ethylbenzene	0	119.1	9.01	1.62	1.478	0.36	0.529	0.625
o-Xylene	0	118.2	9.24	1.43	1.491	0.32	0.547	0.615
m-Xylene	0	120.3	9.09	1.57	1.532	0.35	0.565	0.601
p-Xylene[f]	0	120.7	9.04	1.62	1.511	0.36	0.549	0.608
Propylbenzene	20	139.4	8.68	1.39	1.376	0.28	0.413	0.666
	0	136.9	8.82[a]	2.03	1.767	0.40	0.566	0.609
iso-Propylbenzene	0	136.7[b]	8.75	2.10	1.697	0.41	0.550	0.602
Mesitylene	20	138.9	8.85	1.26	1.561	0.25	0.511	0.613
	0	136.5[g]	9.09[a]	1.78	1.888	0.35	0.664	0.555
1-Methylnaphthalene	20	139.4	10.05[c]	0.54	1.449	0.11	0.417	0.695
	0	137.6[g]	10.30[c]	0.88	1.725	0.17	0.528	0.633
Decalin	20	156.0[g]	7.85[h]	2.34	2.540	0.42	0.909	0.500
	0	153.4[h]	8.08[a,h]	3.13	2.670	0.54	1.079	0.430
Tetralin	20	136.1	9.50[a]	0.82	1.726	0.17	0.583	0.606
	0	133.8[i]	9.73[a]	1.24	2.053	0.25	0.711	0.576

Liquid ammonia, at 20°C, $V_2=27.90$, $\delta_2=12.34$; at 0°C, $V_2=26.67$, $\delta_2=13.13$

a) ΔH^v was estimated by extrapolation.
b) Calculated from Geist and Cannon's data[12].
c) Calculated from the equation[13], $\delta=4.1(\gamma/V^{1/3})^{0.43}$. Surface tension for 1-methylnaphthalene was estimated from parachor[19] neglecting vapor density.
d) Estimated from surface tension[14] and density at 20°C assuming that the dependency of parachor upon temperature and vapor density are negligible.
e) ΔH was estimated from vapor pressure-temperature relations according to Lister[15].
f) Values in the supercooled condition.
g) Observed value.
h) Calculated value as a mixture of 60% *cis* form and 40% *trans* form. Seyer's data[16] for density were used in calculation.
i) Estimated by extrapolation from the data in reference[17].

In equations (6) and (9) the composition at the critical solution temperature is expressed in terms of molal volumes only.

Comparison of Solubility Data with Theory

The values for the term of intermolecular energy on mixing, D, calculated from Eq. (5) using the data on the critical point for some aromatic hydrocarbons with liquid ammonia reported in Part I are shown in Table I, compared with the values obtained from heat of vaporization at each of critical solution temperature. The values of critical compositions calculated from Eq. (6) are also given in Table I, and compared with the values which are obtained graphically from the solubility data in the neighborhood of the critical solution temperature. The solubility parameter of hydrocarbons, δ_1, and

TABLE III

COMPARISON OF VAN LAAR CONSTANTS FROM MUTUAL SOLUBILITIES WITH THOSE FROM EQUATION (12)

Suffix 1 and 2 represent hydrocarbon and liquid ammonia, respectively

	Temp. °C	P[19]	ΔE^v kcal./mole	A_{12}		A_{21}	
				Eq.	obs.	Eq.	obs.
n-Heptane	20	311.3	8.34	0.325	2.244	0.110	0.773
2, 2, 4-Trimethylpentane	20	343.7	7.92	0.542	2.280	0.171	0.713
Methylcyclohexane	20	281.6	7.95	0.279	2.031	0.101	0.848
1-Octene	20	339.6[a]	8.80[b]	0.349	1.968	0.111	0.605
Cyclohexene	20	230	7.32[c]	0.188	1.492	0.078	0.710
m-Xylene	0	284.2	9.94	0.151	1.532	0.054	0.565
Propylbenzene	0	323.1	10.66	0.182	1.767	0.060	0.566
Decalin	20	369.4	9.60	0.321	2.540	0.097	0.909
Tetralin	20	335.9	12.29	0.013	1.726	0.0042	0.583
1-Methylnaphthalene	20	353.8	14.08[b]	0.002	1.449	0.0006	0.417
Liquid ammonia	20	61.1[d]	4.25				
	0	60.8[d]	4.60				

a) Estimated from surface tension[14] and liquid density neglecting vapor density.
b) Cf. Table II, c. Estimated from δ.
c) Cf. Table II, e.
d) Calculated value. Values according to King[20] were used for surface tension and densities for liquid and vapor were taken from "International Critical Tables", Vol. III, p. 235.

of liquid ammonia, δ_2, were estimated from the equation[2]

$$\delta=\left(\frac{\Delta H^v-RT}{V}\right)^{1/2} \qquad (10)$$

where ΔH^v is the heat of vaporization at temperature T. Heats of vaporization for hydrocarbons at T_c were evaluated from the slopes of the vapor pressure—temperature curves[7]. Heat of vaporization for liquid ammonia[8] and most of densities[9] used in calculating molal volumes were taken from tabulations. The critical compositions derived from the equation (6) agree with the experimental values qualitatively, but not quantitatively. However, except for two systems of mesitylene-liquid ammonia and 1-methylnaphthalene-liquid ammonia, the values for D or solubility parameter of ammonia, δ_2, calculated from Eq. (5) are, surprisingly enough, practically identical with that obtained from the heat of vaporization and the molal volume at the critical solution temperature, as in the cases of hydrocarbon-aniline system and hydrocarbon-water system. But, this agreement should be regarded as sheer good luck, owing to a compensation of disturbing factors.

As the solubility parameter of ammonia obtained from the data for the critical point is almost identical with the value calculated from the heat of vaporization as stated above, it seems that this agreement is held at other temperatures. Namely, the following equation may be written approximately;

$$D=(\delta_1-\delta_2)^2 \qquad (11)$$

In Table II, logarithms of activity coefficients at infinite dilution at the temperatures 0° and 20°C which are calculated according to equations (1a, b) or (4a, b) assumed $q=V$ and (11) are given, compared with the experimental values for the van Laar constants which are obtained from the mutual solubility data in Part I according to the equations derived by Carlson and Colburn[11]. A_{12} and A_{21} are logarithums of activity coefficients at infinite dilution of hydrocarbons in liquid ammonia-rich layer and of liquid ammonia in hydrocarbon-rich layer, respectively.

Although the experimental error and uncertainty of the numerical values for

7) D. R. Stull, *Ind. Eng. Chem.*, **39**, 517 (1947).
8) "International Critical Tables", McGraw-Hill Book Company Inc., New York, 1928, Vol. V, p. 138.
9) Ibid., Vol. III, p. 27.
10) Cf. ref. 2, p. 427.
11) H. C. Carlson and A. P. Colburn, *Ind. Eng. Chem.*, **34**, 581 (1942).
12) J. M. Geist and M. R. Cannon, *Ind. Eng. Chem. Anal. Ed.*, **18**, 611 (1946).
13) Cf. ref. 2, p. 431.
14) J. J. Jasper and E. R. Kerr, *J. Am. Chem. Soc.*, **76**, 2659 (1954).
15) M. W. Lister, ibid., **63**, 143 (1941).
16) W. F. Seyer and C. H. Davenport, ibid., **63**, 2425 (1941).
17) S. Doldi, *Ann. chim. applicata*, **28**, 454 (1938); *Chem. Abst.*, **33**, 5250[5] (1939).

TABLE IV

COMPARISON OF D AND CRITICAL COMPOSITION ASSUMING DIMERIZATION OF AMMONIA WITH THOSE NOT ASSUMING DIMERIZATION

Suffix 1 and 2 represent hydrocarbon and liquid ammonia, respectively

Component, 1		Assuming $V_1=q_1$, $V_2=q_2$			Assuming $V_1=q_1$, $2V_2=q_2$				
		D	x_1'	x_1'	D		x_1'		
	$(\delta_1-\delta_2)^2$	Eq. (8)	obs.	Eq. (9)	Eq. (8)	Eq. (5)	obs.	Eq. (9)	Eq. (6)
Toluene	16.32	22.75	0.200	0.114	14.79	13.22	0.334	0.266	0.272
Styrene	16.24	21.74	0.173	0.101	13.99	12.19	0.295	0.241	0.249
Ethylbenzene	14.21	22.50	0.173	0.097	14.46	12.47	0.295	0.234	0.243
o-Xylene	12.53	22.61	0.174	0.099	14.54	12.57	0.296	0.237	0.245
m-Xylene	13.10	22.57	0.184	0.097	14.50	12.49	0.312	0.232	0.241
p-Xylene	13.84	22.48	0.191	0.096	14.43	12.41	0.320	0.231	0.240
Propylbenzene	12.39	21.97	0.149	0.083	13.98	11.53	0.260	0.203	0.215
iso-Propylbenzene	13.84	21.86	0.165	0.082	13.91	11.44	0.284	0.202	0.214
Mesitylene	9.43	22.28	0.159	0.085	14.20	11.81	0.274	0.208	0.220
1-Methylnaphthalene	3.84	22.13	0.139	0.084	14.10	11.67	0.244	0.206	0.217

TABLE V

COMPARISON OF VAN LAAR CONSTANTS ASSUMING DIMERIZATION OF AMMONIA WITH THOSE NOT ASSUMING DIMERIZATION

Component, 1	Temp. °C	Assuming NH_3				Assuming $(NH_3)_2$					
		A_{12}		A_{21}		A_{12}			A_{21}		
		Eq. (7)	obs.	Eq. (7)	obs.	obs.	Eq. (7)	Eq. (1)	obs.	Eq. (7)	Eq. (1)
n-Heptane	20	1.39	2.244	0.11	0.773	2.003	2.23	2.52	1.020	0.81	0.96
2,2,4-Trimethylpentane	20	2.26	2.280	0.20	0.713	2.045	3.24	3.62	0.956	1.04	1.22
Methylcyclohexane	20	0.98	2.031	0.09	0.848	1.787	1.68	1.88	1.099	0.71	0.82
1-Octene	20	1.28	1.968	0.09_6	0.605	1.975	2.42	2.75	0.941	0.81	0.98
Cyclohexene	20	0.53	1.492	0.06	0.710	1.282	1.02	1.11	0.943	0.55	0.61
m-Xylene	0	0.70	1.532	0.03	0.565	1.343	1.38	1.57	0.789	0.58	0.70
Propylbenzene	0	0.95	1.767	0.03_6	0.566	1.569	1.76	2.03	0.793	0.65	0.79
Decalin	20	0.30	2.540	−0.11	0.909	2.280	1.22	1.55	1.166	0.39	0.55
Tetralin	20	−0.18	1.726	−0.18	0.583	1.526	0.58	0.82	0.811	0.20	0.34
1-Methylnaphthalene	20	−0.49	1.449	−0.24	0.417	1.295	0.29	0.54	0.623	0.08	0.22

solubility parameters used in the calculation should be taken into account, values of A_{12} according to equations (1a, b), $V_1(\delta_1-\delta_2)^2/2.303RT$, are generally similar to those calculated from the mutual solubility data but A_{21}'s are smaller. It may be shown from this result that the effective volumes, q's, are not exactly identical with molal volumes and they are related not only to molecular volumes, but also to their shapes and surfaces.

The semi-empirical expression proposed by Erdos[18] for calculating the constants of van Laar equations from the properties of pure components, which may be considered as a modification replaced the molal volumes in equations (1a, b) by the surface areas in terms of parachors, may be written as follows:

$$A_{12}=\frac{P_1^{2/3}}{2.303RT}\left\{\left(\frac{\Delta E_1}{P_1^{2/3}}\right)^{1/2}-\left(\frac{\Delta E_2}{P_2^{2/3}}\right)^{1/2}\right\}^2 \tag{12}$$

where P_1 and P_2 are the parachors of the pure components 1 and 2.

The values for some representative compounds calculated from equation (12) are shown in Table III, compared with the experimental values. The ratios of effective volumes, A_{12}/A_{21}, almost agree with the experimental values, but values for each van Laar constant calculated according to equation (12) are considerably smaller than the experimental values, and the disagreement between these values is greater when compared with that obtained

18) E. Erdös, *Chem. Listy*, **50**, 503 (1956); *Chem. Abst.* **50**, 11752g (1956).

by equations (1a, b), or equations (4a, b) assuming $q=V$ and equation (11). It may be considered from the results shown in Table III that the effective volumes related to the difference in molecular shape or effective surface can not be expressed with only the surface areas in terms of parachors.

As the molal volumes of ammonia and hydrocarbons are considerably different, it may be impossible to expect the entropy of mixing to be ideal. The critical compositions for aromatic hydrocarbons with liquid ammonia obtained by equation (9) which is derived under the assumption that the entropy of mixing is expressed by the Flory-Huggins equation, are shown in the left half column of Table IV. Values for D which are calculated by equation (8) using the calculated values for critical compositions by equation (9) are also shown in Table IV. Calculated values for D by equation (8) are considerably greater and for compositions by equation (9) are smaller, and the disagreement is larger than the result shown in Table I, the reason being that the Flory-Huggins equation may be almost an over-correction for the size effect[5].

Ratio of van Laar constants, A_{12}/A_{21}, namely, the ratio of effective volumes corresponds to molal volume ratio in equations (1a, b), V_1/V_2. The ratios of effective volumes to those of molal volumes are given in the last column in Table II. For every case of the long chain molecule such as *n*-paraffin, the plain molecule of aromatic hydrocarbon and the semi-spherical one of *iso*-octane, values for V_1/V_2 are larger than A_{12}/A_{21}, and the ratios of the latter to the former are about 0.5 in all systems of hydrocarbon oils and liquid ammonia which have been studied. Morever, this ratio at lower temperature for a binary mixture is less than that at higher temperature; namely, it shows that effective volume for liquid ammonia derived from the solubility data is larger at lower temperature. Ratios for styrene and toluene at low temperatures, which are given in Table II, show also the same result. It will be seen from these results that though the different shape and surface of molecule may be related to the effective volume, they are not large factors for these ammonia systems, and that when V_2 is roughly doubled the ratios of molal volumes are almost similar to those of effective volumes. The change for molal volume of liquid ammonia, V_2, results in the change of mole fraction and so van Laar constants. But it may be clear that unless V_2 becomes larger, theoretical values are too far apart from the experimental.

In the case of water having strong hydrogen bonding capacity, the presence of the association states of 2, 4, and 8 molecules has been considered in addition to H_2O[21]. Also in the case of ammonia, the dimerization of ammonia has been known even in the gaseous state[22], and the molecular weight of liquid ammonia has been found to be 24.5 from the surface tension determination[20]. It is probable that a different kind of association may occur in various rates in liquid ammonia and its solution. If ammonia is assumed to form double molecules in liquid state on the average, for the sake of simplicity, the apparent mole fraction will be different from that for single molecule, but the value for solubility parameter calculated by equation (10) would be scarecely different from δ_2 used in the preceding calculations, since the dimerization of ammonia in vapor phase is almost negligible[22] and the heat of vaporization per gram is identical for both NH_3 and $(NH_3)_2$.

Values for D and for the critical composition, x', by equations (8) and (9) or (5) and (6) assuming the dimerization of ammonia are given in the right half column of Table IV, where the agreement with the experimental values is improved compared with those of the left half column calculated for the case of not assuming the association. Table V shows the comparison of the observed van Laar constants for representative compounds with values calculated from equation (7) assuming no association of ammonia and with values obtained by equations (7) and (1a, b); in both cases ammonia is assumed to form double molecules in liquid.

The result obtained by assuming the dimerization of ammonia may exhibit a far closer agreement than that the dimerization is not assumed, in view of all the approximations involved.

Summary

The result of the comparison of experi mental data for the critical compositions

19) O. R. Quayle, *Chem. Revs.*, **53**, 439 (1953).
20) H. H. King, J. L. Hall and G. C. Ware, *J. Am. Chem. Soc.*, **52**, 5128 (1930).
21) A. Eucken, *Nachr. Akad. Wiss. Göttingen, Math.-physik. Klasse*, 38 (1946); *Chem. Abst.*, **43**, 7283 d (1949); *Z. Elektrochem.*, **52**, 255 (1948); **53**, 102 (1949).
22) J. D. Lambert and E. D. T. Strong, *Proc. Roy. Soc.*, **A, 200**, 565 (1960).

and the logarithms of activity coefficients at infinite dilution for binary systems of some hydrocarbon oils and liquid ammonia with those expected from the solubility parameter theory, is that the solubility relations may be more satisfactorily interpreted by the theory by assuming that ammonia is associated nearly to dimerized form in the liquid state.

The author is greatly indebted to Professor T. Toriumi for his interest and encouragement during this investigation.

The Chemical Research Institute of Non-Aqueous Solutions, Tohoku University, Katabira-cho, Sendai

The Infrared Spectra of Ethoxy- and Methylethoxy-polysiloxanes

By Rokuro ŌKAWARA

(Received August 26, 1957)

In this report, the studies of infrared spectra of three types of methylethoxy-polysiloxanes represented by A, B and C, and linear and cyclic ethoxypolysiloxanes D and E will be described, of which the spectra of A_1[1], B_1[1] and D_1[2] have already been reported briefly.

A_n $C_2H_5O((CH_3)_2SiO)_nC_2H_5$ $n=1,2,3,4$
B_n $C_2H_5O((CH_3)Si(OC_2H_5)O)_nC_2H_5$ $n=1,2,3,4,5$
C_n $((CH_3)Si(OC_2H_5)O)_n$ $n=3,4$
D_n $C_2H_5O(Si(OC_2H_5)_2O)_nC_2H_5$ $n=1,2,3$
E_n $(Si(OC_2H_5)_2O)_n$ $n=4,5$

One of the objects of this study is to find characteristic absorption bands associated with the group $(Si)OC_2H_5$*. The spectra of methylpolysiloxanes F and G, which were discussed by Wright[3] and Richards[1], are used to explain the spectra obtained in this study.

F $CH_3((CH_3)_2SiO)_nSi(CH_3)_3$
G $((CH_3)_2SiO)_n$

Experimental

Materials.—The preparation and the properties of the members of B, C and E used in this experiment have already been reported[4,5]. Authentic samples were used for the measurement of the spectra of A and D.

Measurements.—Spectra were obtained with a Hilger H-800 infrared spectrophotometer with a rock salt prism. Samples were used both as pure liquid and as solutions, 2—5% in carbon disulfide for 700 to 1500 cm^{-1}, and 5—10% in carbon tetrachloride for 1250 to 3500 cm^{-1}. No appreciable difference was observed between the two cases. The cells were 0.03 mm. thick for the solution and less than 0.01 mm. for pure liquid. In order to compare relative intensity, the absorption of the compounds belonging to the same series was recorded on the same chart, keeping the conditions as much alike as possible.

TABLE I

INFRARED SPECTRA OF METHYLETHOXYPOLYSILOXANES : POSITIONS OF BANDS (in cm^{-1})

A_n					B_n						C_n	
$n=1$*	$n=1$	$n=2$	$n=3$	$n=4$	$n=1$*	$n=1$	$n=2$	$n=3$	$n=4$	$n=5$	$n=3$	$n=4$
798	785	797	798	803	732		759	760	760	762	755	761
841	835	841	838	844	780	775	779	785	784		791	
846					806		794	799		791	809	801
953	949	955	953	952	820	818						
		1059	1043	1034	831	824	820	821	820	827	843	
1078	1075	1080	1080	1078	960	956	959	958	960	959	960	957
1105	1102	1111	1109	1111			1060	1056	1060	1056	1023	1068
1166	1160	1162	1156	1162	1078	1074	1073	1071	1071	1070	1078	1087
1260	1254	1256	1256	1256	1100	1098	1099	1096	1096	1096		
					1120		1116	1114	1117	1114	1111	1117
					1166	1164	1163	1162	1162	1158	1160	1159
					1266	1259	1260	1260	1259	1262	1260	1262

* R. E. Richards and H. W. Thompson, *loc. cit.*[1]

1) R. E. Richards and H. W. Thompson, *J. Chem. Soc.*, **1949**, 124.
2) I. Šimon and H. O. McMahon, *J. Chem. Phys.*, **20**, 905 (1952).
3) N. Wright and M. J. Hunter, *J. Am. Chem. Soc.*, **69**, 803 (1947).

* $(Si)OC_2H_5$ indicates an ethoxy group attached to silicon atom.
4) R. Ōkawara, S. Hotta and T. Shimura, This Bulletin, **28**, 541 (1955).
5) R. Ōkawara, G. Minami and Z. Oku, ibid., **31**, (1958).

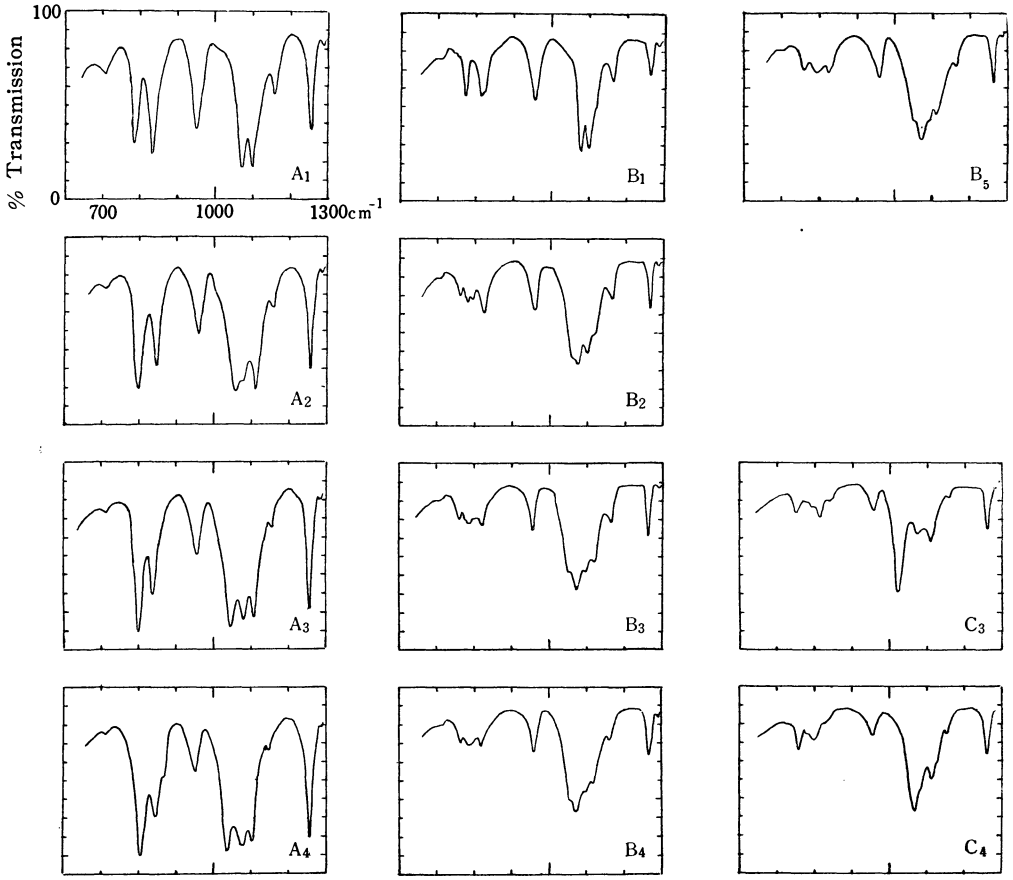

Fig. 1. Infrared spectra of methylethoxypolysiloxanes.

A_n: $C_2H_5O((CH_3)_2SiO)_nC_2H_5$, 5% in CS_2
B_n: $C_2H_5O((CH_3)Si(OC_2H_5)O)_nC_2H_5$, 3% in CS_2
C_n: $((CH_3)Si(OC_2H_5)O)_n$, 2% in CS_2

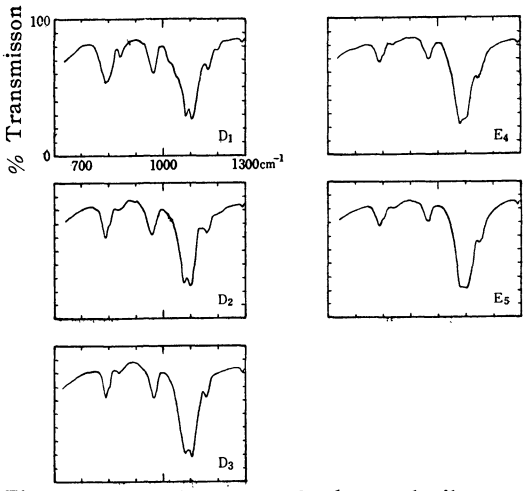

Fig. 2. Infrared spectra of ethoxypolysiloxanes.
D_n: $C_2H_5O(Si(OC_2H_5)_2O)_nC_2H_5$, 2% in CS_2
E_n: $(Si(OC_2H_5)_2O)_n$, 2% in CS_2

TABLE II
INFRARED SPECTRA OF ETHOXYPOLYSILOXANES: POSITIONS OF BANDS (in cm^{-1})

D_n			E_n	
$n=1$	$n=2$	$n=3$	$n=4$	$n=5$
790	790	788	791	790
846	847	848		
962	966	968	968	968
1081	1079	1080	1078	1079
1104	1102	1102	1101	1099
1163	1162	1160	1163	1163

The spectra of A, B and C, and those of D and E are shown in Fig. 1 and Fig. 2, respectively. The positions of the bands up to 1300 cm^{-1} are given in Table I and II.

Discussion of the Results

In the region 750—1000 cm^{-1}, there are some strong bands. Among them the one

near 960 cm^{-1} has an approximately constant wave number and no neighboring absorption band in any of the compounds investigated. Since this band does not appear in F and G, it seems certain that the band is associated with the grouping $(Si)OC_3H_5$. This presumption is further supported by comparing the relative intensity of the band of each member belonging to the same series. For example in A and B, the intensity of this band decreases as n increases. A similar band appears at 960 cm^{-1} in the compounds having $(Si)CH_2CH_3$ grouping[6]; accordingly it is probably possible to attribute those to the vibration in ethyl group, probably to that of the stretching of C—C bond.

In A, there are two common bands near 800 cm^{-1} and 840 cm^{-1}. The intensity of the former becomes stronger and that of the latter becomes weaker, as n increases. It may be concluded that the former corresponds to 800 cm^{-1} band characteristic of $(CH_3)_2SiO$[1,3] unit in F and G, and the latter is connected with the OC_2H_5 group in $(CH_3)_2Si(OC_2H_5)O_{1/2}$ unit. In B and C, there are overlap bands near 800 cm^{-1}, and their shape is so complex that they may be considered to consist of many bands. In D and E, a band is observed near 790 cm^{-1}, which may be thought to be a characteristic band of ethoxypolysiloxanes.

The absorption bands in 1000—1200 cm^{-1} are probably associated with Si—O—Si and Si—O—C linkages. Since the absorption band, though not very strong in intensity, appeared at constant wave number of 1160 cm^{-1} in all the compounds, and the intensity decreases clearly with increasing polymer size in A, it seems certain that this band is associated with $(Si)OC_2H_5$ grouping. Though quite tentative, this band would be connected with the stretching vibration of C—O bond, because this band is not found in the spectra of the compounds containing $(Si)CH_2CH_3$ group[6]. In A and B, common strong bands occur at 1080 cm^{-1} and 1110 cm^{-1} which may be connected with the Si—O—C linkage and are attributed probably to the stretching of Si—O bond. In A_n except A_1, another band of comparative intensity is observed near 1050 cm^{-1}, which decreases in wave number as n increases. Since Wright and Hunter have assigned 1050 cm^{-1} band in F and G to the stretching mode of Si—O vibration and have pointed out their shift to a smaller wave number with increasing polymer size, it seems possible to connect this band with Si—O stretching mode of Si—O—Si linkage. B_1 has only two bands at 1070 and 1098 cm^{-1} in this region, while in the higher members of this series another two bands are observed, of which the one found at 1060—1056 cm^{-1} would correspond to the band at 1050 cm^{-1} in A. It has been known[7] that stable cyclotrisiloxanes of the type $(RR'SiO)_3$ (R, R'= alkyl or aryl group) have their Si—O(—Si) stretching band in the region 1000—1020 cm^{-1}. As already reported[5], this band appears also in the spectra of unstable C_3 as well as $(C_2H_5Si(OC_2H_5)O)_3$ at 1023 cm^{-1}. With samples of the former reserved in a glass ampule, this band decreased in intensity after 500 days, while the refractive index and the viscosity increased. As in the case of unstable $((C_2H_5)HSiO)_3$[8], this band will be associated with the stretching vibration of Si—O bond of cyclotrisiloxane ring, and the 1068 cm^{-1} band of C_4 will be attributed to the same vibration of cyclotetrasiloxane ring.

A fairly successful explanation of the spectra of this region from the similarity of the structure to dimethylpolysiloxanes may be made only in the case of A, and it becomes difficult in the case of D and E. All the members of series D and E appear to have only two bands. It is likely that the bands associated with Si—O—Si and Si—O—C linkages cover each other.

To a sharp intense band near 1265 cm^{-1}, some different assignments[9] have been

TABLE III

INFRARED SPECTRA OF POLYSILOXANES IN 1300—1500 CM^{-1} REGION:

POSITIONS OF BANDS (in cm^{-1})

A, B, C	D, E	F*	G**
1295	1295	—	1300
1365	1365	—	—
1390	1390	—	—
1410	—	1410	1405
			1417
1440	1442	1442	1446
1485	1483	—	—

* N. Wright and M. J. Hunter, *loc. cit.*[3]

** R. E. Richards and H. W. Thompson, *loc. cit.*[1]

6) M. Sakiyama, *J. Chem. Soc. Japan, Ind. Chem. Sec.* (*Kogyo Kagaku Zassi*), **60**, 1385 (1957).

7) C. W. Young, P. C. Servais, C. C. Currie and M. J. Hunter, *J. Am. Chem. Soc.*, **70**, 3758 (1948).

8) R. Ōkawara, U. Takahashi and M. Sakiyama, This Bulletin, **30**, 608 (1957).

9) C. W. Young, J. S. Koheler and D. S. McKinney, *J. Am. Chem. Soc.*, **69**, 1410 (1947); D. H. Rank, B. D. Saksena and E. R. Shull, *Discuss. Farad. Soc.*, **9**, 187 (1950).

made. In this study, it has become clear that this band is related to the $(Si)CH_3$ group since this band is observed in A, B and C.

In 1300—1500 cm^{-1} region, six weak bands are observed. For comparison the absorption bands in this region are presented in Table III together with those of F and G.

From Table III, 1295, 1365, 1390, 1440 and 1485 cm^{-1} bands are supposed to be associated with $(Si)OC_2H_5$ group.

Summary

1) The infrared spectra of the lower members of ethoxy-, and methylethoxypolysiloxanes measured in the rock salt region are discussed.

2) Up to 1200 cm^{-1}, the common bands near 960 and 1160 cm^{-1} are certainly to be connected with the grouping $(Si)OC_2H_5$.

3) Moreover, characteristic bands of $(Si)OC_2H_5$ group appear near 840 cm^{-1} in ethoxy end-blocked dimethylpolysiloxanes and near 790 cm^{-1} in ethoxypolysiloxanes.

The author wishes to express his hearty thanks to Mr. M. Sakiyama and Dr. T. Matsuura for their helpful discussion.

Department of Applied Chemistry
Faculty of Engineering
Osaka University
Miyakojima-ku, Osaka

Studies on the Effect of Substituents on the Spectra of Quinoline Derivatives

By Tadashi SATO and Masaki OHTA

(Received September 3, 1957)

For interpreting the effect of substituents on the spectra of triphenylmethyl ions and other dyes, Lewis et al.[1] took account of the orientation of the molecule in the electric field and designated the absorption bands as *x*-bands or *y*-bands on the assumption that they were associated with electric moments directed along mutually perpendicular axes in the main plane of the molecule. Later, this assumption was extended to the other types of molecules and treated theoretically by some physical chemists.

In 1949, Klevens and Platt[2], using the free electron model, classified the spectra of cata-condensed hydrocarbons and gave them a systematic nomenclature: with naphthalene, they designated its absorption bands as Lb-, La- and Bb-bands in the order of decreasing wave length. The polarization diagrams were represented in Fig. 1. They stated that the Lb-band showed a red shift with increasing chain length and was therefore longitudinally polarized along an axis of molecular

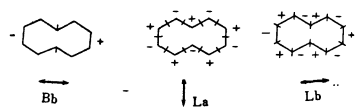

Fig. 1.

length, and that the La-band exhibited a bathochromic shift as molecular width increased. This band was, therefore, transversely polarized. A similar phenomenon was observed by Jones[3] with anthracene derivatives.

Ewing et al.[4], without referring to the above discussion, reported on the spectra of naphthols, naphthylamines, hydroxy- and aminoquinolines. These spectra showed the properties corresponding to the above discussion: in molecules of β-type, the Lb-bands were bathochromically shifted and the intensities increased, indicating the existence of three clearly distinguishable bands, whereas in α-type, the La-bands were so much bathochromically shifted that the weak Lb-bands were almost covered.

1) G. N. Lewis and M. Calvin, *Chem. Rev.*, **25**, 273 (1939); G. N. Lewis and J. Bigeleisen, *J. Am. Chem. Soc.*, **65**, 520, 2120, 2107 (1943).
2) H. B. Klevens and J. R. Platt, *J. Chem. Phys.*, **17**, 486 (1949).
3) R. N. Jones, *Chem. Rev.*, **41**, 353 (1947).
4) G. W. Ewing and E. A. Steck, *J. Am. Chem. Soc.*, **68**, 2181 (1943); **70**, 3397 (1948).

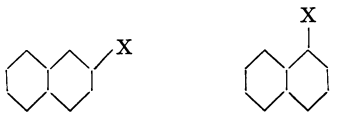

β-type* α-type

Knight et al.[5] classified the spectra of bromoquinolines along this consideration and observed the same regularity as described above. All studies so far reported have dealt with the simple monosubstituted molecules. In our synthetic study of furoquinoline alkaloid, it was necessary to determine where the nitro group would enter when methoxy-dihydrofuroquinoline derivative II was subjected to nitration. With the intention of predicting its position spectroscopically, we investigated whether the regularity existing between the displacement of bands and the position of the substituents could be observed in these rather complicated molecules.

The spectra of four compounds (I—IV) are compared in Fig. 2.** As can be noted from the comparison of the spectrum of IV

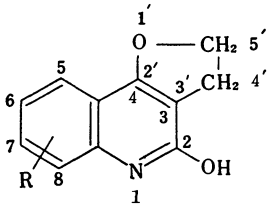

I R=H
II R=8-OCH_3
III R=7-OCH_3
IV R=6-OCH_3

with that of I, introduction of the methoxyl group in 6-position displaces the Lb-band to the red, while the La-band remains almost unchanged. In the other two cases (II and III), λ_{max} is hardly affected at all, while the intensities are much affected; as for 7-isomer, the Lb-band increases with the depression of the La-band, and with 8-isomer, the circumstance is the reverse. As noted from these data, there are two modes of exerting the effect, namely on the wave length

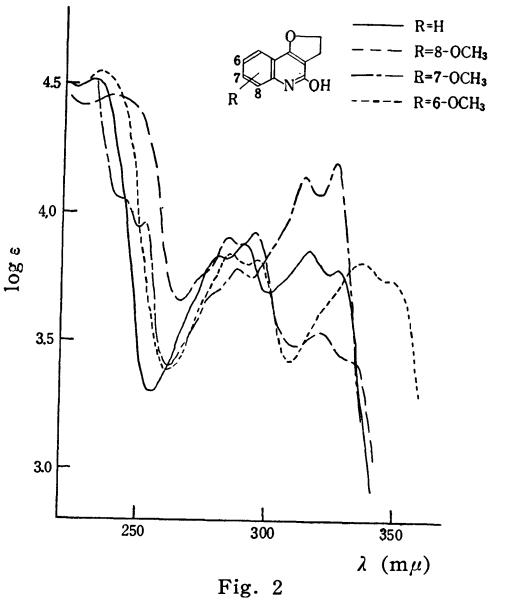

Fig. 2

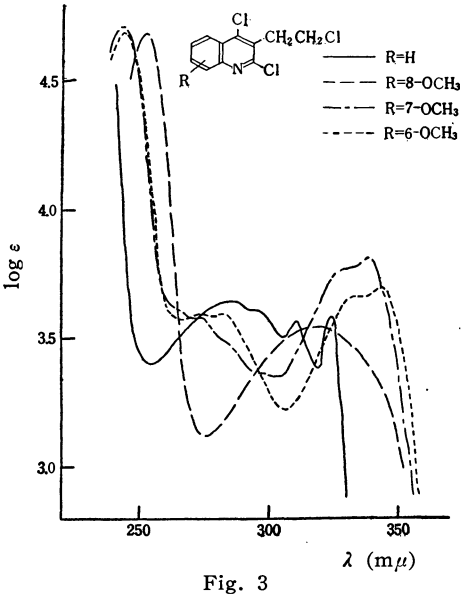

Fig. 3

in one case, and on the intensity in the other. Though we can not find a satisfactory explanation to this difference, a generalization can be observed that the substitution which increases the molecular length (6- and 7-position) acts so as to displace the Lb-band bathochromically or to increase the intensity, while substitution perpendicular to this direction exerts the same influence on La-band.

In Fig. 3, the spectra of another series of molecules (V—VIII) are shown. Here, the spectra of 6- and 7-isomer are similar. In both cases, Lb-bands are bathochromically shifted, while La-bands are shifted

* Here, the diagram represents the naphthalene and the quinoline nucleus.

5) S. B. Knight et al., ibid., **76**, 3780 (1954).

** We prepared these compounds by the condensation of appropriate aromatic amines and diethyl β-methoxyethylmalonate[6]. As for the condensation product from *m*-anisidine, two isomers are possible (i and ii). We proved the product as to be 7-methoxy derivative (i), by converting it into evolitrine (iii). See the following paper: T. Sato and M. Ohta, This Bulletin, **31**, 161 (1958).

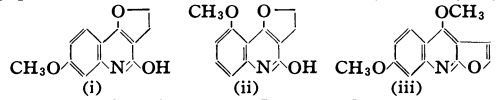

(i) (ii) (iii)

6) M. F. Grundon et al., *J. Chem. Soc.*, **1955**, 4284; T. Sato and M. Ohta, This Bulletin, **30**, 708 (1957).

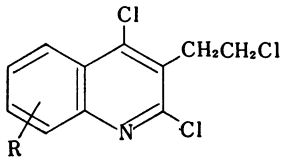

V R=H
VI R=8-OCH_3
VII R=7-OCH_3
VIII R=6-OCH_3

in the opposite direction. As for 8-isomer, the La-band is so much bathochromically shifted as to cover the Lb-band completely.

From these data, we can undoubtedly say that the electronic transition responsible for the Lb-band is of the type of polarization along the axis of molecular length, while that for La-band is of the type perpendicular to this axis, and that even in these rather complicated molecules, the regularity found in the simpler molecules can also be observed.

Nitration of III gave a nitro derivative IX. Reduction of the nitro derivative with stannous chloride gave the amino

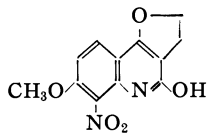

IX

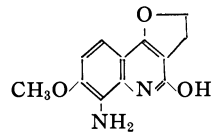

X

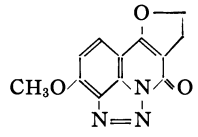

XI

derivative X, from which the triazol derivative XI was derived by the reaction with nitrous acid[7]. From this fact the position of the nitro group in IX could definitely be decided.

Comparing the spectrum of this nitro derivative IX with that of III (Fig. 4), we can see that, in accordance with the above observation, the introduction of the nitro group causes the La-band to displace bathochromically and hyperchromically. Though a little bathochromic shift is also observed with Lb-band, the extent is far smaller than that for La-band. When the spectrum of the amino derivative X is compared with that of III (Fig. 4), it is obvious that the La-band is more influenced than Lb-band.

As we could thus extend this consideration to somewhat complicated molecule, it

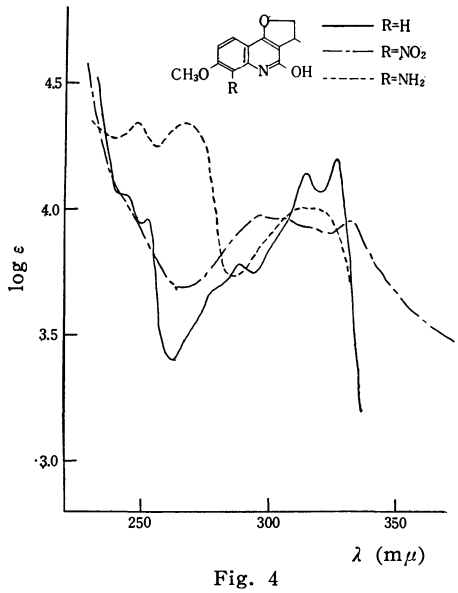

Fig. 4

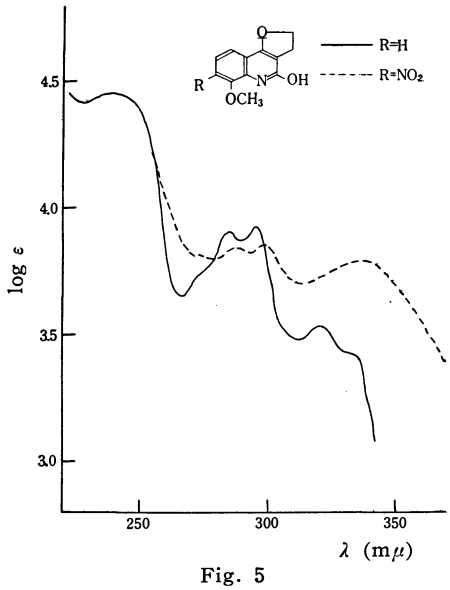

Fig. 5

is now possible to determine which of the two possible products XII and XIII was produced by the nitration of II. The fact that the spectrum of this nitro derivative suffers much bathochromic and hyperchromic shift on the Lb-band when compared with that of II, as shown in Fig. 5, seems to show that it would probably be 7-isomer XII.

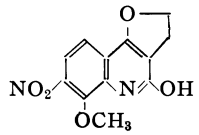

XII

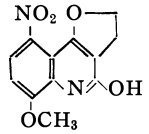

XIII

7) S. E. Krahler and A. Burger, *J. Am. Chem. Soc.*, **64**, 2417 (1942).

Experimental

Absorption Spectra — All spectra were measured in methanol with Beckman Quartz Spectrophotometer, Model DU.

2-Hydroxy-4′, 5′-dihydrofuro (3′ : 2′—3 : 4) quinoline (I),* 2-hydroxy-8-methoxy-4′, 5′-dihydrofuro (3′ : 2′—3 : 4) quinoline (II), 2, 4-dichloro-3-(β-chloroethyl) quinoline (V), and 2, 4-dichloro-3-(β-chloroethyl)-8-methoxyquinoline (VI).**—These compounds were prepared according to the methods reported by Grundon and by us[6] All were identified by their melting points and nitrogen analyses.

2-Hydroxy-7-methoxy-4′, 5′-dihydrofuro (3′ : 2′—3 : 4) quinoline (III) — A solution of *m*-anisidine (12 g.) and diethyl β-methoxyethylmalonate (25 g.) in diphenyl ether (35 cc.) was heated under reflux for 3 hours. After cooling, the product was recrystallized from nitrobenzene. m. p. 250°. A pure sample resulting from the recrystullization from dilute acetic acid. m. p. 252°.

Anal. Found: C, 66.15; H, 5.55; N, 6.69. Calcd. for $C_{12}H_{11}O_3N$: C, 66.35; H, 5.10; N, 6.45%.

Addition of petroleum ether to the diphenyl ether mother liquor gave a solid from which a small amount of unidentified crystals was obtained, in addition to III, by repeated recrystallization from acetic acid. m. p. 334°.

2-Hydroxy-6-methoxy-4′, 5′-dihydrofuro (3′ : 2′—3 : 4) quinoline (IV)—This was prepared from *p*-anisidine in a manner similar to that used for 7-isomer (III). A pure sample was recrystallized from ethyl "Cellosolve". m. p. 277°.

Anal. Found: N, 6.31. Calcd. for $C_{12}H_{11}O_3N$: N, 6.45%.

2, 4-Dichloro-3-(β-chloroethyl)-7-methoxyquinoline (VII)—A mixture of III (0.5 g.) and phosphorus oxychloride (5 cc.) was heated under reflux for 1.5 hours. Decomposition of the excessive phosphorus oxychloride with ice gave a solid which was recrystallized from dilute methanol. m. p. 121°.

Anal. Found: N, 4.79. Calcd. for $C_{12}H_{10}ONCl_3$: N, 4.82%.

2, 4-Dichloro-3-(β-chloroethyl)-6-methoxyquinoline (VIII) — This was prepared in the same way as described for 7-isomer (VII). Recrystallization from dilute methanol gave a pure sample. m. p. 118°.

Anal. Found: N, 4.95. Calcd. for $C_{12}H_{10}ONCl_3$: N, 4.82%.

2-Hydroxy-7-methoxy-8-nitro-4′,5′-dihydrofuro (3′ : 2′—3 : 4) quinoline (IX)—To a solution of methoxy-dihydrofuroquinoline derivative III (0.4 g.) in concentrated sulfuric acid (3 cc.) was added powdered potassium nitrate (0.2 g.) in portions with occational cooling. After being kept at 100° for 30 min., the solution was poured into crushed ice. The precipitates were recrystallized from dilute acetic acid. The nitro derivative contained one mole of acetic acid of crystallization. m. p. 256—60° (decomp.).

Anal. Found: C, 51.45; H, 4.47; N, 8.94. Calcd. for $C_{14}H_{14}O_7N_2$: C, 52.17; H, 4.38; N, 8.69%.

The solvent-free sample was obtained by drying over phosphorus pentoxide in vacuo at 100° for 3 hours. m. p. 260° (decomp.).

Anal. Found: C, 54.51; H, 3.76; N, 10.87. Calcd. for $C_{12}H_{10}O_5N_2$: C, 54.96; H, 3.84; N, 10.68%.

2-Hydroxy-7-methoxy-8-amino-4′, 5′-dihydrofuro (3′ : 2′—3 : 4) quinoline (X)—To a solution of dihydrated stannous chloride (1.2 g.) in concentrated hydrochloric acid (4 cc.) was slowly added powdered nitro derivative IX (0.3g.) with occational cooling. The mixture was kept at 50—60° for 20 min., and then bolied gently for 30 min. The solution was made alkaline with 10% sodium hydroxide and the solid was recrystallized from ethyl "Cellosolve". m. p. 312° (decomp.).

Anal. Found: C, 61.80; H, 5.40; N, 11.85. Calcd. for $C_{12}H_{12}O_3N_2$: C, 62.06; H, 5.21; N, 12.06%.

2-Oxo-1, 2, 4′, 5′-tetrahydrofuro (3′ : 2′—3 : 4) quinoline-1, 8-diazoimide (XI)—To a solution of the amino derivative X (0.3 g) in 20% sulfuric acid (6 cc.) was added water (4 cc.), and then 7.5% aqueous solution of sodium nitrite (2 cc.) with constant stirring and cooling with ice-water. The mixture was kept at room temperature for 30 min., and the yellow product was recrystallized from "Cellosolve ethyl." m. p. 226—8° (decomp.). This was a monohydrate.

Anal. Found: N, 16.31. Calcd. for $C_{12}H_{11}O_4N_3$: N, 16.08%.

The anhydrate was obtained by drying over phosphorus pentoxide in vacuo at 100° for 2 hours. m. p. 228° (decomp.).

Anal. Found: N, 17.26. Calcd. for $C_{12}H_9O_3N_3$: N, 17.28%.

2-Hydroxy-7-nitro-8-methoxy-4′,5′-dihydrofuro (3′ : 2′—3 : 4) quinoline (XII) — To a suspension of methoxy-dihydrofuroquinoline derivative II (1 g.) in acetic anhydride (40 cc.) was added a mixture of 60% nitric acid (1 cc.) and glacial acetic acid (4 cc.) under external cooling. The solid went into solution immediately, but soon after, new crystals began to deposit. After 2 hours' standing at room temperature, they were recrystallized from acetic acid. m. p. 260° (decomp.). The sample contained one mole of acetic acid of crystallization.

Anal. Found: C, 52.22; H, 4.51; N, 9.02. Calcd. for $C_{14}H_{14}O_7N_2$: C, 52.17; H, 4.38; N, 8.69%.

The solvent-free sample was obtained by drying over phosphorus pentoxide in vacuo at 100° for 3 hours. m. p. 260° (decomp.).

Anal. Found: C, 54.47; H, 3.92; N, 10.62. Calcd. for $C_{12}H_{10}O_5N_2$: C, 54.96; H, 3.84; N, 10.68%.

The authors are indebted to Mr. A. Kondo for the microanalyses.

Laboratory of Organic Chemistry
Tokyo Institute of Technology
Meguro-ku, Tokyo

*** The furoquinoline derivatives were named as indicated in order to make the numbering accord with that for quinoline derivatives.

Synthesis of Evolitrine, an Alkaloid of Evodia littoralis

By Tadashi SATO and Masaki OHTA

(Received September 3, 1957)

The structure of evolitrine was determined by Cook et al.[1] to be 7-methoxydictamnine (I). The position of the extra methoxyl group was unambigously determined by comparing the degration product II with the product obtained from the

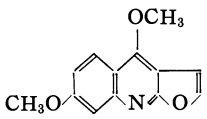

I

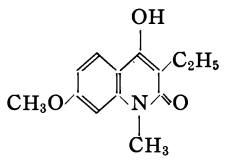

II

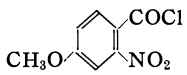

III

reaction between 4-methoxy-2-nitrobenzoyl chloride III and diethyl ethoxymagnesiumethylmalonate, followed by the reduction of nitro group, cyclization and *N*-methylation.

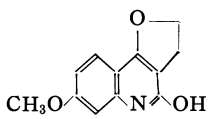

IV

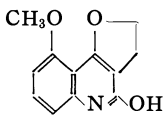

V

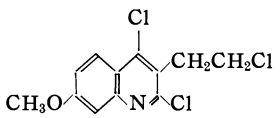

VI

In connection with our spectroscopic study of quinoline derivatives[2], we were obliged to determine which of the two possible products IV or V resulted in fact from the condensation of *m*-anisidine and diethyl β-methoxyethylmalonate. By synthesizing evolitrine starting with this condensation product[3,4] we identified it as IV, thus affirming the structure of evolitrine.

When *m*-anisidine and diethyl β-methoxyethylmalonate were refluxed in diphenyl ether IV was obtained. In search of another possible isomer V, the mother liquor was subjected to repeated purification, but the substance isolated was a small amount of white crystals which had a different and unidentified structure. Treatment of the compound IV with phosphorus oxychloride gave the trichloro derivative VI gave a white solid which was supposed to be a mixture of 2-hydroxy derivative VII and dihydrofuroquinoline derivative VIII in view of the experience gained from our dictamnine synthesis[3]. This mixture afforded the dihydrofuroquinoline derivative VIII on treatment with alkali. When

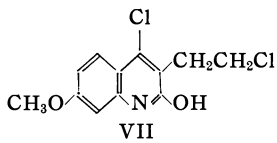

VII

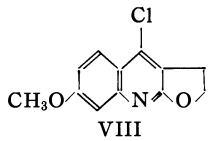

VIII

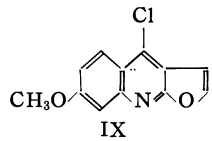

IX

the trichloro derivative VI was hydrolysed with acid according to the method of Grundon[4], the intermediate product VII was isolated, which was also cyclized to VIII by alkali. Treatment of VIII with *N*-bromosuccinimide in the presence of a small amount of benzoyl peroxide, and successive treatment with dimethylaniline afforded the chloro-furoquinoline derivative IX. This was converted by sodium methoxide into evolitrine I. The synthetic evolitrine was shown to be identical with the natural product by comparing their melting points, ultraviolet spectra and melting points of their picrates.

Experimental

2-Hydroxy-3-(β-chloroethyl)-4-chloro-7-methoxyquinoline (VII).—A mixture of trichloro derivative VI[2] (0.28 g.), 6N-hydrochloric acid (8 cc.) and dioxane (6.5 cc) was heated under reflux for 3 hours. Additon of water gave a white solid which was recrystallized from dilute methanol. m. p. 193°.

1) R. G. Cook and H. F. Hyne, *Austral. J. Chem.*, **7**, 273 (1954).
2) T. Sato and M. Ohta, This Bulletin, **31**, 157 (1958).
3) T. Sato and M. Ohta, ibid, **30**, 708 (1957).
4) M. F. Grundon et al., *J. Chem. Soc.*, **1957**, 2177.

Anal. Found: N, 5.24, Calcd. for $C_{12}H_{11}O_2NCl_2$: N, 5.15%.

4-Chloro-7-methoxy-2,3-dihydrofuro[2,3-b]quinoline (VIII)—a) To a solution of VII (0.3 g.) of methanol (2 cc.) was added 10% methanolic sodium hydroxide and the solution was kept at 50—60° for 30 min. Addition of water gave a white solid which was recrystallized from dilute methanol m. p. 158°.

Anal. Found: C, 60.63; H, 4.61; N, 5.86. Calcd. for $C_{12}H_{10}O_2NCl$: C, 61.01; H, 4.23; N, 5.94%.

b) A solution of trichloro derivative VI (0.3 g) in glacial acetic acid (3 cc.) was heated under reflux for 1.5 hours. Addition of water gave a white solid which was treated with methanolic sodium hydroxide in the same way as described in a). m. p. and mixed m. p. 158°.

4-Chloro-7-methoxyfuro[2,3-b]quinoline (IX).—A mixture of dihydrofuroquinoline derivative VIII (0.45 g.), N-bromosuccinimide, (0.45 g) a trace of benzoyl peroxide and carbon tetrachloride (15 cc.) was heated under reflux for 2 hours. Succinimide was filtered off and carbon tetrachloride evaporated in vacuo. The resulting residual oil, after dilution with dimethylaniline (4.5 cc.) was heated under reflux for 3 hours. After cooling the mixture was added to 3N-hydrochloric acid (45 cc.). The solid thus formed was collected, and recrystallized from dilute methanol. m. p. 169°. The compound was a semihydrate.

Anal. Found: C, 59.72; H, 3.71; N, 6.04. Calcd. for $C_{24}H_{18}O_5N_2Cl_2$: C, 59.32; H, 3.71; N, 5.77%.

Evolitrine (I).—To the chloro derivative IX (0.1 g) was added methanolic sodium methoxide (5 cc.), containing sodium (0.15 g). The mixture was heated under reflux for 3 hours, and allowed to stand overnight. Sodium chloride was filtered off and the filtrate, after partial evaporation of methanol, was treated with water. Recrystallization from dilute methanol gave pure evolitrine. m. p. 114°.

Anal. Found: C, 67.70; H, 5.22; N, 6.30. Calcd. for $C_{13}H_{11}O_3N$: C, 68.11; H, 4.84; N, 6.11%.

The ultraviolet spectrum in ethanol was also identical with the reported one. The picrate was prepared and recrystallized from methanol. m. p. 192—4°.

Anal. Found: N, 12.50. Calcd. for $C_{19}H_{14}O_{10}N_4$: N, 12.23%.

The authors are indebted to Mr. A. Kondo for the microanalyses.

Laboratory of Organic Chemistry, Tokyo Institute of Technology
Meguro-ku, Tokyo

Studies on the Separation of Alkaline Earth Elements. IV. Coprecipitation of Barium in the Induced Precipitate of Lead Sulfate

By Mutsuaki SHINAGAWA and Toshifumi MURATA

(Received September 16, 1957)

In the preceding paper[1] the precipitation of lead sulfate induced[2] by the barium ion was studied by means of turbidimetry, and it was shown experimentally that there were several relations among the quantities of substances involved. The present paper reports the ratio of coprecipitation of barium measured radiometrically by use of ^{140}Ba as a tracer, and the amount of induced precipitate of lead sulfate measured amperometrically[3]. Freundlich's equation of adsorption isotherm[4] was found to be applicable to the experimental results obtained. It is understood that this induced precipitation furnishes a method of concentration of small amounts of barium in the presence of large amounts of lead.

1) M. Shinagawa and T. Murata, *J. Science Hiroshima Univ., Series A*, **18**, 429 (1955).
2) F. Feigl. "Spot Tests", Vol. 1. Elsevier Publishing Co., (1954), p. 204.
3) I. M. Kolthoff and J. J. Lingane, "Polarography", Interscience Publishers, Inc., New York, N. Y. (1952), p. 913.
4) H. Freundlich, *Z. physik. Chem.*, **57**, 385 (1907).

Experimental

Reagents. — Lead nitrate, guaranteed grade, 0.482 M, aqueous solution.

Barium chloride, 0.005 M/l; Aqueous solution of guaranteed grade salt was mixed with a suitable amount of a hydrochloric acid solution of carrier free $^{140}BaCl_2$.

Ammonium acetate, 10.23 M/l (pH=6.22); prepared from ammonia water and acetic acid, both of which were of guaranteed grade.

Apparatus. — SHIMADZU pen — recording polarograph for amperometry.

SHIMADZU glass electrode pH meter for pH measurement.

KOBE KOGYO End Window G. M. Counter (131 Type. Thickness of the mica window was 3.1 mg./cm^2.) and stainless steel cupped planchets with 2.5 cm. diameter were used for the radioactivity measurements.

Procedure and Results.

1) Determination of the amounts of precipitated barium and lead.—In order to know the quantity of coprecipitated barium with lanthanum fluoride, Gest et al. reported the dilution method[5], while the authors prefered the following method. The specific activity of β-ray of the remaining barium labeled with ^{140}Ba in the supernatant solution was measured and compared with that of the standard solution. Two ml. of either solution was almost evaporated in a cupped planchet under an infrared lamp and less than 0.8 ml. of 0.5 M sulfuric acid was added to make the lead sulfate layer uniform which had a thickness of 18 mg./cm.^{2} This way of preparation facilitated good reproducibility of the counting. Since the solutions labeled with ^{140}Ba usually contain the daughter, ^{140}La, they had been kept more than 20 days after their preparation before the specific activities were measured.

The quantity of precipitated lead ions was also determined indirectly, measuring the lead ions in the supernatant solution by the amperometric titration with potassium chromate solution at -1.0 V of fixed potential.

2) The amount of coprecipitated barium as a function of aging time.—Into a stoppered Erlenmeyer flask, 500 ml. of a mixed solution (pH 5.50) containing 0.096 M lead nitrate, 2.07 M ammonium acetate (The molar ratio of ammonium acetate to the lead ion was chosen as in the previous paper[1].), and 2×10^{-4} M barium chloride, was placed and stirred well after the addition of 7.50 ml. or 12.5 ml. of 0.5 M sulfuric acid. The flask was kept in a 20 ± 0.05°C thermostat.

At regular intervals 5 ml. batches of solution were taken out of it and centrifuged. The specific activities of the supernatant solution told the amount of the precipitated barium removed at intervals as shown in Fig. 1. It was found that the percentage of coprecipitation remarkably increased within the first half an hour and remained almost constant thereafter.

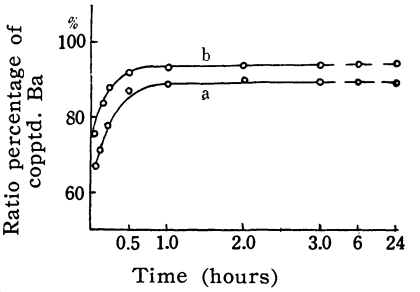

Fig. 1. The amount of coprecipitated barium as a function of aging time.
Solution: $Pb(NO_3)_2$ 0.096 M.
CH_3COONH_4 2.07 M.
Ba^{++} 1×10^{-4} M.
To 500 ml. of the solution 7.50 ml. (Curve (a)) or 12.50 ml. (Curve (b)) of 0.5 M H_2SO_4 was added, aged at 20°C.

3) The precipitations as a function of the amount of sulfuric acid added.—As mentioned in section 2, 40 ml. of the mixed solution was taken into a 100 ml. stoppered Erlenmeyer flask, and 0.50—5.00 ml. of 0.5 M sulfuric acid was added at a rate of 7—8 sec./ml.

It was stirred well and kept being aged at 20°C. After 2 hours it was centrifuged and analysed. Fig. 2 illustrates the results when the coexisting barium concentrations were 0 M, 1×10^{-4} M and 2×10^{-4} M Ba^{++}. Table 1 (A) shows the data of the last case.

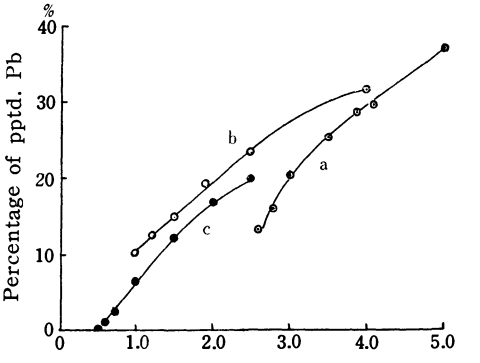

a: Ba^{++} none
b: 〃 1×10^{-4} M
c: 〃 2×10^{-4} M

Fig. 2. Precipitation ratio of lead as a function of the amounts of sulfuric acid added.
Solution: Pb^{++} 800 mg 40 ml., CH_3COONH_4 2.07 M, pH 5.50. 0.5 M H_2SO_4 was added. Aged for 2 hours at 20°C.

TABLE I (A)
AMOUNTS OF SULFURIC ACID AND THE PRECIPITATES

Solution: 800 mg. Pb^{++} and 1098 γ Ba^{++} in 40 ml of 2.07 M CH_3COONH_4. 0.5 M H_2SO_4 was added, aged for 2 hours at 20°C.

H_2SO_4 added ml.	Ba copptd. γ	Ba copptd. %	Pb pptd. mg.	Pb pptd. %	ratio of pptd. (Ba)/(Pb) γ/mg.
0.50	94_3	$85._9$	$3._2$	0.4	236
0.60	94_9	$86._4$	$4._8$	0.6	198
0.80	103_6	$94._4$	$18._4$	2.3	57
1.00	104_2	$94._9$	$40._8$	5.1	26
1.50	105_3	$95._9$	$96._0$	12.0	11
2.00	106_4	$96._8$	$130._4$	16.3	8
2.50	106_8	$97._3$	$156._0$	19.5	7

(Mean values of three data.)

5) H. Gest, N. F. Ballov, B. M. Abraham and C. D. Coryell, "Radiochemical Studies; Fission Products", McGraw-Hill Book Co., Inc., New York, Paper **12**, 145 (1951).

TABLE I (B)

Solution: 1600 mg. Pb^{++} and 1098 γ Ba^{++} in 40 ml of 4.14 M CH_3COONH_4, 0.5 M H_2SO_4 was added, aged for 2 hours at 20°C.

H_2SO_4 added ml.	Ba copptd. γ	Ba copptd. %	Pb pptd. mg.	Pb pptd. %	ratio of pptd. (Ba)/(Pb) γ/mg.
1.50	101_3	92.3	52.8	3.3	192
2.00	103_4	94.2	52.8	3.3	195
3.00	104_3	95.0	147.2	9.2	71
4.00	105_3	95.9	241.6	15.1	43
5.00	106_0	96.5	320.0	20.0	33
7.00	108_5	98.8	320.0	20.0	34
10.00	109_6	99.8	588.8	36.8	19

(Mean values of three data.)

As can be seen from Fig. 2, when barium was absent lead ions were not precipitated until 2.60 ml. of sulfuric acid was added, because of the masking effect of acetic acid radical. Since in the presence of barium the precipitate appeared by the addition of less than 2.60 ml. of sulfuric acid, it was possible to regard this as induced precipitation owing to the presence of barium.

In the case of Table 1 (A), 86—96% of barium was coprecipitated with 20% of lead precipitate, while 92—99% of barium with less than 20% of lead in the case of double concentrations of lead ions and ammonium acetate as shown in Table I (B). In this case lead sulfate was not precipitated until 7.50 ml. of sulfuric acid was added, in the absence of barium. Therefore, the more concentrate the lead ion, the greater the readiness with which lead sulfate was induced to precipitate. The amount of coprecipitated barium increased significantly with the increase in lead sulfate precipitate, while the ratio of barium to lead in the precipitate decreased noticeably.

Results

1) The precipitation as a function of the initial concentration of barium. — A mixed solution as prepared in section 2 was used, having several concentrations between 6.86 and 68.6 mg. barium per liter. To each 40 ml. batch of these solutions were added 1.00 and 1.30 ml. of sulfuric acid as the representing amounts of the acid necessary for the induced precipitation taken by the preliminary experiments shown in Fig. 2 curve a and c, and it was then let stand for 30 min. in a thermostat to equilibriate the precipitate as in section 2. Table II (A) and (B) show the data of the experiments.

From Table II where the amount of sulfuric acid is constant, it can be seen that in the presence of more barium ions, more lead sulfate precipitates, while the percentage of coprecipitation of barium is unchanged with the initial concentration of

TABLE II (A)

INITIAL CONCENTRATIONS OF BARIUM AND THE PRECIPITATES

Solution: 800 mg. Pb^{++} in 40 ml. of 2.07 M CH_3COONH_4. 1 ml. of 0.5 M H_2SO_4 was added, aged for 30 min. at 20°C.

Initial Ba γ	copptd. Ba γ	copptd. Ba %	pptd. Pb mg.	pptd. Pb %	ratio of pptd. (Ba)/(Pb) γ/mg.
279	24_4	87.9	28.8	3.6	8.4
549	48_7	88.7	35.2	4.4	13.8
1098	97_3	88.6	42.4	5.3	22.9
1647	145_4	88.3	50.4	6.3	28.8
2196	198_1	90.2	58.4	7.3	33.9
2745	249_0	90.7	72.8	9.1	34.2

(Mean values of three data.)

TABLE II (B)

The same conditions as in (A), but 1.30 ml. of H_2SO_4

Initial Ba γ	copptd. Ba γ	copptd. Ba %	pptd. Pb mg.	pptd. Pb %	ratio of pptd. (Ba)/(Pb) γ/mg.
279	25_3	92.1	87.2	10.9	2.9
549	50_6	92.2	92.8	11.6	5.4
1098	98_6	89.5	100.8	12.6	9.7
1647	146_0	88.7	112.8	14.1	12.9
2196	198_3	90.3	138.4	17.3	14.3
2745	250_3	91.2	146.4	18.3	17.0

(Mean values of three data.)

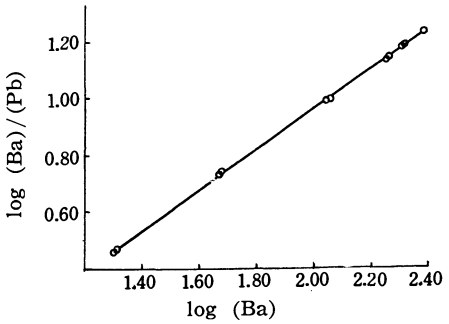

Fig. 3 (A) Logarithmic relation between ppt. ratio and final barium concentration.
Solution: Pb^{++} 800 mg./40 ml., CH_3COONH_4 2.07 M.
1.00 ml. of 0.5 M H_2SO_4 was added, aged for 30 min. at 20°C.

barium in the solution; i.e. 89—90% in the case of (A) and 89—92% in (B).

In Fig. 3 (A) and (B), linear relationship between the logarithmic value of precipitation ratio ((Ba)/(Pb) in γ/mg., in Tables II (A) and (B)) and that of the concentration of barium in the final solution equilibriated with the precipitate (C in γ/40 ml.). Therefore, these relations

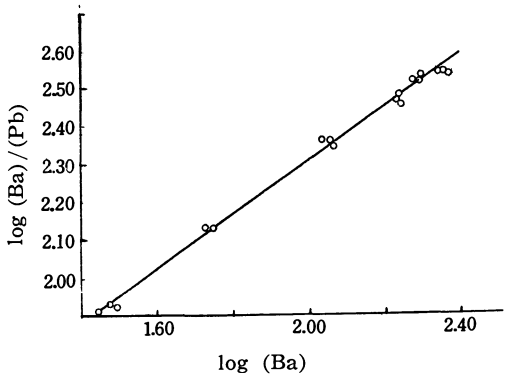

Fig. 3 (B) Conditions were the same as (A), but 1.30 ml. of H_2SO_4 was added.

are expressed by the Freundlich's adsorption isotherm,

$$(Ba)/(Pb) = aC^{1/n}$$

Where a and n are the constants which can be calculated from the intercepts and the inclination of the linear relations; $a=2.63$ and $n=1.38$ in (A) while $a=0.30$ and $n=1.38$ in (B). The value of a is larger in (A) than in (B), indicating that the adsorbability of barium is greater in (A) than in (B); in other words the smaller the amount of sulfuric acid added, the relatively larger the amount of coprecipitated barium. The n values in both cases are identical, indicating that the natures of the adsorption phenomena are of the same quality.

TABLE III

THE PRECIPITATIONS WITHOUT INDUCTION

Solution: 800 mg. Pb^{++} and 549 γ Ba^{++} in 40 ml., 1.5 ml. of 0.5 M H_2SO_4 was added, aged for 30 min. at 20°C.

copptd. Ba		pptd. Pb		ratio of pptd. (Ba)/(Pb)
γ	%	mg.	%	γ/mg.
17_0	$31._7$	$8._0$	1.0	42.5
18_4	$33._5$	$20._0$	2.5	9.2
21_1	$38._5$	$40._0$	5.0	5.3
22_0	$40._0$	$60._0$	7.5	3.6
24_0	$43._8$	$80._0$	10.0	3.0
26_6	$48._4$	$100._0$	12.5	2.7

(Mean values of three data.)

2) Precipitations from the solution without ammonium acetate.—When there was no ammonium acetate, the masking agent for lead ions, the ordinary lead sulfate precipitation was observed. It was not regarded as a precipitation induced by barium sulfate. The experimental results can be seen in Table III.

It was found from Table III that the percentage of the coprecipitated barium without induced lead sulfate was about 32—48%, which was much lower than that with the induced precipitate, i.e. about 85—99%.

Conclusion

On adding 0.5 M sulfuric acid, 0.096 M lead in 2.07 M ammonium acetate solution is precipitated inductively in the presence of $0.5—5\times10^{-4}$ M barium ion.

The amount of the coprecipitating barium follows the Freundlich's adsorption isotherm. The adsorption equilibrium is obtained within 30 min. after the addition of sulfuric acid. The adsorption percentage is greater as the amount of sulfuric acid added decreases in the range of possible amount of producing the lead sulfate.

The amount of coprecipitating barium is not the function of the amount of lead sulfate precipitate; it is almost constant, (85—99%) being much greater than that in the absence of ammonium acetate.

Further investigations with more elaborated experimental conditions are expected to get an excellent method of separation of a small amount of barium from a large amount of lead.

Department of Chemistry
Faculty of Science
Hiroshima University
Hiroshima

Studies on the Separation of Alkaline Earth Elements. V. Coprecipitation of Radium in the Induced Precipitate of Lead Sulfate

By Mutsuaki SHINAGAWA and Toshifumi MURATA

(Received September 16, 1957)

In the former papers[1,2] the authors reported on the lead sulfate precipitation induced by barium, and on its usefulness as a method of separation of a small amount of barium from a large amount of lead. In the present paper an analogous method of accumulation of radium is reported by coprecipitation with inductively precipitated lead sulfate by means of barium. In this case barium plays a role of the inducer for lead sulfate and at the same time that of the carrier for radium.

Experimental

Reagents.—The solutions of lead nitrate, barium chloride and ammonium acetate were the same as those prepared in the preceding paper[2]. Radium chloride solution 100 μC/100 ml. was the officially approved article, N. B. S. (U. S. Department of Commerce).

Apparatus.—RIKEN Lauritsen electrometer was used to measure the radioactivity of radium in the sample in a stainless steel cupped planchet with 2.5 cm. diameter.

SHIMADZU Pen-recording Polarograph was used for the amperometric titration, and SHIMADZU glass electrode pH-meter for the measurement of hydrogen ion concentration.

Procedures.—*1) Experimental conditions.* Into a stoppered Erlenmeyer flask was put 40 ml. of a solution of pH 5.50 containing 0.096 M lead nitrate, 2.07 M ammonium acetate, and 2×10^{-4} M barium chloride as their final concentration. The optimum molar ratio of ammonium sulfate to lead for this induced precipitation is $\approx$20[1]. After the temperature of the mixture was adjusted to 20$\pm$0.05°C, a suitable amount of 0.5 M sulfuric acid was added at a rate of 7—8 sec. per ml. The precipitate obtained in the solution was stirred, kept standing for 2 hr. at 20°C and centrifuged. The supernatant solution was analysed for radium and lead content.

2) The measurement of radioactivity of radium. To determine how much radium is coprecipitated with lead sulfate, it is easier to analyse radium in the supernatant solution than in the precipitate. According to Tompkins et al.[3], when lead is thoroughly precipitated as lead sulfate, radium will be completely coprecipitated with it, and all the disintegrated products will be included without any appreciable loss. For this reason, the following procedure is preferred; 1 ml. of the supernatant sample solution or the standard solution is taken into a stainless steel cupped planchet, and concentrated under an infrared lamp to half of its original volume. Then to it 0.4 ml. of 0.5 M sulfuric acid is added to obtain the lead sulfate precipitate, which is dried up carefully and kept in a calcium chloride desiccator for eight days till it reaches 3/4 of the secular equilibrium for radium, and the radioactivity was measured by Tompkins' alpha-ray method[3].

This procedure was checked as follows; the standard solution was prepared as the supernatant sample solution mentioned above, except that a known amount of radium was added. The drying condition of lead sulfate in the cupped planchet and the amount of sulfuric acid added had a very subtle effect upon the alpha activity. Amount of sulfuric acid (0.2 to 0.6 ml.) was examined and the use of 0.4 ml. was found to be the best, permitting the determination of 1×10^{-3} μC radium with $\pm$4% average deviation, provided that the drying of the planchet was complete. The calibration curve thus obtained is shown in Fig. 1., and serves as the standard measure of the activity.

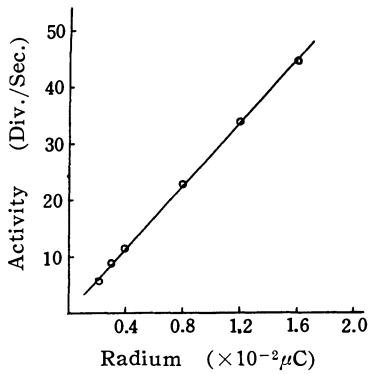

Fig. 1. The calibration curve of radium.

The absorption of alpha rays of radium by lead sulfate was examined and the results were

1) M. Shinagawa and T. Murata, *J. Science Hiroshima Univ.*, A, **18**, 429 (1955).
2) M. Shinagawa and T. Murata, This Bulletin, **31**, 162 (1958).
3) P. C. Tompkins, W. P. Norris, L. Wish and R. D. Finkle, *MDDC.*, 699 (1946).

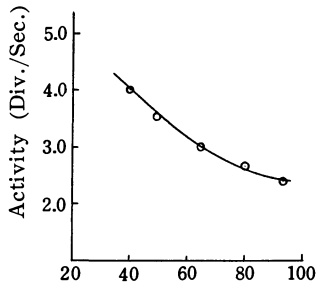

Fig. 2. The absorption of alpha rays by lead sulfate.

obtained as shown in Fig. 2., by which the self-absorption of the sample was calibrated.

3) Measurement of the amount of lead sulfate precipitated. The procedure for amperometric titration was the same as that mentioned in the previous paper[2].

Results

1) The coprecipitation ratio of radium and the induced precipitation ratio of lead as a function of the amount of sulfuric acid added. The solution mixture used had the same composition as in section 1, except 1×10^{-4} M of barium chloride and 40 μC of radium chloride per liter. Forty ml. of this solution was taken and 1.00—3.00 ml. of 0.5 M sulfuric acid was added and aged for 2 hours at 20°C. The analyses of lead and radium were carried out regularly, giving the results as shown in Fig. 3. The amount of lead sulfate precipitate increased as the amount of sulfuric

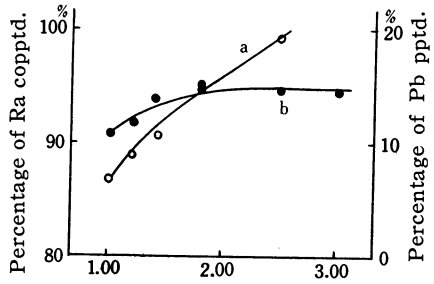

Fig. 3. Results of induced precipitation as a function of the amount of sulfuric acid added.
Curve a: Induced precipitation of lead.
Curve b: Coprecipitation of radium.

acid added increased, while the amount of coprecipitated radium remained constant on the addition of more than 1.40 ml. of sulfuric acid, where ca. 9% of lead precipitated with ca. 90% of radium. The ratio (Ra)/(Pb) in the precipitate decreased significantly thereafter, just as in the case of coprecipitation of barium[2].

2) As a function of the amount of barium present. To each 40 ml. of the mixed solution (see Procedure section 1) which had been mixed with 0.80 μC of radium and a varying amount of barium, 1.20 ml. of 0.5 M sulfuric acid was added. The analyses of radium and lead in these solution gave the results as shown in Table I.

TABLE I
RESULTS OF THE COPRECIPITATION AS A FUNCTION OF THE AMOUNT OF THE BARIUM PRESENT
Solution: 800 mg. Pb^{++} and 0.8 μC $RaCl_2$ in 40 ml. of 2.07 M CH_3COONH_4; 1.20ml. of 0.5 M H_2SO_4 added, aged for 2 hours at 20°C.

Ba added	Ra copptd.		Pb pptd.	
mg.	μC	%	mg.	%
0.549	0.74_9	$93._6$	$66._4$	8.3
1.098	0.76_0	$95._0$	$73._6$	9.2
1.647	0.76_6	$95._8$	$87._2$	10.9
2.196	0.77_2	$96._6$	$98._4$	12.3
2.745	—	—	$113._6$	14.2

It is seen that when a sufficient amount of sulfuric acid, i.e. 1.20 ml. is added in the presence of more barium ions, more lead sulfate precipitates. The percentage of coprecipitation of radium appears to remain constant, although it has an overall trend to increase slightly.

3) As a function of initial concentration of radium. To each 40 ml. of the mixed solution (Procedure section 1), radium was added from 0.2 to 1.6 μC. After the addition of 1.20 ml. of sulfuric acid, the samples were analysed to find the amount of coprecipitated radium. Table II shows the results. In this case, too, the amount of lead sulfate induced was constant (9.2 %), while the amount of coprecipitated

TABLE II
COPRECIPITATION RATIO OF RADIUM AS A FUNCTION OF ITS INITIAL CONCENTRATION
Solution: 800 mg. Pb^{++} and 1.098 mg. Ba^{++} in 40 ml. of 2.07 M CH_3COONH_4. 1.20 ml. of 0.5 M H_2SO_4 was added, aged for 2 hours at 20°C, 9.2% of Pb (73.6 mg.) was precipitated.

Initial Ra	Ra copptd.		pptn. ratio (Ra)/(Pb)
μC	μC	%	$\times10^3$
0.200	0.18_7	$93._6$	2.5
0.400	0.38_2	$95._4$	5.2
0.800	0.76_4	$95._5$	10.4
1.200	1.15_0	$95._9$	15.6
1.600	1.53_0	$96._1$	20.8

radium increased as the initial concentration of radium increased according to Freundlich's adsorption isotherm as in the case of barium in the previous report[2].

4) In the absence of barium. The mixed solution mentioned in Procedure section 1, but without barium was used. To obtain the same amount of lead sulfate much more sulfuric acid was required than when barium was present. The experimental results are shown in Table III.

TABLE III
COPRECIPITATION IN THE ABSENCE OF BARIUM
Solution: 800 mg. Pb^{++} and 0.80 μC Ra^{++} in 40 ml., 2.07 M of CH_3COONH_4, 0.5 M H_2SO_4 was added, aged for 2 hours at 20°C.

H_2SO_4 added	Ra copptd.		Pb pptd.		pptn. ratio (Ra)/(Pb)
ml.	μC	%	mg.	%	$\times 10^3$
2.80	0.77_6	$97._0$	$92._0$	11.5	8.4
3.00	0.77_4	$96._7$	$139._0$	17.4	5.6
3.40	0.77_4	$96._8$	$174._0$	21.7	4.4
3.80	0.77_3	$96._6$	$191._0$	23.9	4.0

It can be understood that even when the amount of lead precipitate increases to a large extent, the coprecipitation ratio for radium remains constant and the precipitation ratio (Ra)/(Pb) decreases accordingly.

5) In the absence of acetate. The solution mixture containing 0.096 M lead nitrate and 20 μC/*l* radium chloride was used. To 40 ml. of this solution, an equivalent amount of sulfuric acid to the measured quantity of lead sulfate precipitate was added. The results of analyses are shown in Fig. 4, curve a. Curve b was derived from the same data shown in Fig. 3, curve b for comparison. In Fig. 4, curve b shows clearly that a small amount of induced precipitate of lead sulfate carries off radium from solution as efficiently as a relatively large amount of it does (curve a). While the ordinary precipitate of lead sulfate catches radium in an almost proportional amount to itself.

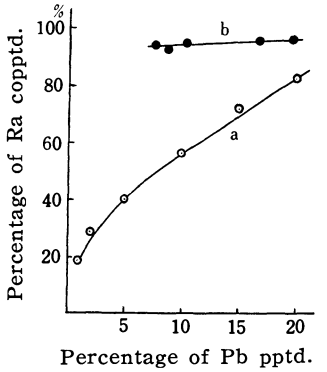

Fig. 4. Comparison of coprecipitation of radium.
Curve a: Ordinary precipitation of lead sulfate.
Curve b: Induced precipitation of lead sulfate in the presence of barium.

Summary

A solution of pH 5.50 composed of 0.096 M lead nitrate, 2.07 M ammonium acetate, $1-5\times10^{-4}$ M barium and 5—50 μC radium per liter, produces an induced precipitate of lead sulfate in proportion to the amount of 0.5 M sulfuric acid added. Under the same conditions, in the absence of barium, a lead sulfate precipitate is obtained in proportion to the amount of sulfuric acid added. But the required amount of sulfuric acid to obtain the same amount of precipitate is larger in this case than that in the case of induction by barium.

In both of the above cases, the ratio of the amount of the radium coprecipitated to the original amount of radium in sample solution is almost constant, i.e. 92—97%, irrespective of the amount of lead sulfate precipitate or of sulfuric acid added. This tendency is the same as in the case of coprecipitation of barium with the induced precipitate of lead sulfate as shown in the previous paper. More than 90% of radium is carried down by a precipitate of lead sulfate of 8—20% of lead. Such an extent was not found in the case of the ordinary precipitation of lead sulfate, i.e. in the absence of the masking agent, ammonium acetate for lead ions.

In conclusion, the induced precipitation of lead sulfate by barium can be made use of as an efficient method of separation or concentration of radium. For a practical usage of this method, more detailed examination according to each sample should be conducted.

Department of Chemistry
Faculty of Science
Hiroshima University
Hiroshima

Hydrogen Bonding Effect on the Electronic Absorption Spectrum of p-Hydroxyazobenzene

By Hiroaki BABA

(Received October 7, 1957)

When the effect of hydrogen bonding on the electronic absorption spectra of organic compounds came to be noticed, attention was drawn to the anomalies of the effects of the solvents on the spectra. It was then pointed out that the hydrogen bonding effect could serve as a new method for the study of the nature of hydrogen bonding itself[1]. Indeed some thermochemical quantities, such as free energy, entropy and enthalpy changes in hydrogen bonds, have been determined for a number of compounds, e. g. phenol[1-5], cresols[6,7], naphthols[7], pyridine *N*-oxide[8] etc. In all these studies the influence of hydrogen bonding on an electronic absorption was made clear by the use of a three-component system: an inert solvent, a solute of a chromophore, and a substance which forms hydrogen bond with the solute molecule. It may be added that this method of three-component system which was originally used in the study of the ultraviolet absorption of phenol[1,2] has recently been utilized by Brealey and Kasha in demonstrating the role of hydrogen bonding in the $n\rightarrow\pi^*$ blue shift phenomenon[9]. Further, it has been applied to the study of the fluorescence of some organic compounds[10].

The present article will suggest that there is another promising application of the studies concerning the hydrogen bonding effect, that is: a new clue to the nature of the absorption bands of a given molecule is to be provided from the spectral changes at the time of formation of a hydrogen bond. For this purpose, however, some additional information is required on the relation between the type of an electronic transition and the change in its corresponding spectrum accompanied by the hydrogen bonding.

With this point in mind, the hydrogen bonding effect on the absorption spectrum of *p*-hydroxyazobenzene has been newly investigated. This substance is provided with features fitted for the present purpose. It has a proton-donating hydroxyl group, and has several absorption bands of different types. Moreover, there is no ambiguity regarding its structure in solution. It is known that *p*-hydroxyazobenzene exists only in the azo-form in any common solvent, and further for this molecule one need not consider the formation of an intramolecular hydrogen bond such as occurs in *o*-hydroxyazobenzene[11].

Azobenzene and its derivatives, including *p*-hydroxyazobenzene, have three absorption bands in the visible and the near ultraviolet regions[12,13]. The band situated in the visible region has been assigned by McConnell[14] to an $n\rightarrow\pi^*$ transition, while the other two bands appearing in the ultraviolet region are considered to be due to $\pi\rightarrow\pi^*$ transitions[13]. In the following, it will be shown that the changes in $n\rightarrow\pi^*$ and $\pi\rightarrow\pi^*$ absorptions caused by the hydrogen bond between *p*-hydroxyazobenzene and ether or pyridine are of entirely different nature.

Experimental

Materials.—*p-Hydroxyazobenzene* (Kanto Chemical Co., Inc., guaranteed) was purified chromatographically through an alumina column by

1) H. Baba and S. Nagakura, *J. Chem. Soc. Japan, Pure Chem. Sect.* (*Nippon Kagaku Zassi*), **72**, 3 (1951).
2) S. Nagakura and H. Baba, *J. Am. Chem. Soc.*, **74**, 5693 (1952).
3) H. Tsubomura, *J. Chem. Soc. Japan, Pure Chem. Sec.* (*Nippon Kagaku Zassi*), **73**, 920 (1952).
4) S. Nagakura, ibid., **74**, 153 (1953); *J. Am. Chem. Soc.*, **76**, 3070 (1954).
5) S. Mizushima, M. Tsuboi, T. Shimanouchi and Y. Tsuda, *Spectrochim. Acta*, **7**, 100 (1955).
6) H. Baba, *Monogr. Res. Inst. Appl. Elec.*, Hokkaido Univ., No. 4, 61 (1954).
7) S. Nagakura, *J. Chem. Soc. Japan, Pure Chem. Sec.* (*Nippon Kagaku Zassi*), **75**, 734 (1954).
8) T. Kubota, *J. Pharm. Soc. Japan*, **74**, 831 (1954); **75**, 1540 (1955).
9) G. J. Brealey and M. Kasha, *J. Am. Chem. Soc.*, **77**, 4462 (1955).
10) N. Mataga, Y. Kaifu and M. Koizumi, *Nature*, **175**, 731 (1955); This Bulletin, **29**, 115 (1956).
11) See, for instance, H. Shingu, *J. Chem. Soc. Japan, Pure Chem. Sec.* (*Nippon Kagaku Zassi*), **60**, 542 (1939).
12) A. Burawoy and J. T. Chamberlain, *J. Chem. Soc.*, **1952**, 3734.
13) P. P. Birnbaum, J. H. Linford and D. W. G. Style, *Trans. Faraday Soc.*, **49**, 735 (1953).
14) H. McConnell, *J. Chem. Phys.*, **20**, 700 (1952).
15) W. R. Brode, *J. Phys. Chem.*, **30**, 56 (1926).

developing with benzene: m. p. 154°C (literature 152°C corrected[15], 155—156°C corrected[16]).

Iso-octane (2, 2, 4-trimethylpentane; Enjay Co., Inc., U. S. A.) was purified using the purification method for hexane[17]: b. p. 99°C, $n_D^{20}=1.3910$.

Ethyl ether (Kanto, guaranteed) was treated with mercury to eliminate peroxides and distilled: b. p. 34.5°C.

Pyridine was added to a solution of oxalic acid in acetone, and from the resulting precipitate of oxalate it was obtained in pure form[18]: b. p. 115—116°C, $n_D^{21}=1.5087$.

Method and Results. — Absorption spectra were obtained with a Beckman Quartz Spectrophotometer Model DU. A set of spectra were measured for the following solutions:

Solution 1, *p*-hydroxyazobenzene in *iso*-octane;
Solution 2, *p*-hydroxyazobenzene in *iso*-octane containing a small quantity of a proton-accepting substance;
Solution 3, *p*-hydroxyazobenzene in *iso*-octane containing a proton-accepting substance, the amount of which is about five times that in solution 2.

Ether and pyridine were used as the proton-accepting substance. The reference liquids adopted in measuring absorbances were *iso*-octane for solution 1, and *iso*-octane-ether or -pyridine mixtures for solutions 2 and 3 in which the concentrations of the latter substance were the same as in solutions 2 and 3, respectively. The concentrations of *p*-hydroxyazobenzene were about 5×10^{-5} mole/*l* in all cases. At such a low concentration one may expect that no association occurs among the *p*-hydroxyazobenzene molecules[19].

Measurements were made at room temperatures: 20°C for ether series, and 15°C for pyridine series. The observed spectra are given as curves 1, 2 and 3 in Figs. 1 and 2.

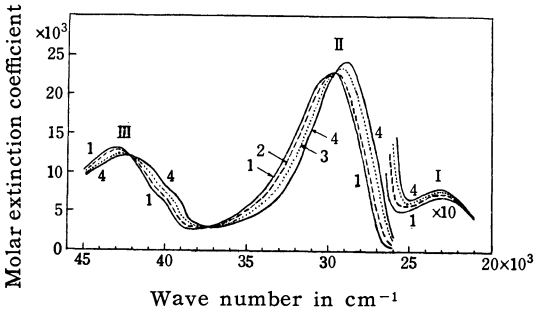

Fig. 1. The absorption spectrum of *p*-hydroxyazobenzene in *iso*-octane solution, and changes therein due to the addition of ether. The concentrations of ether: curve 1, zero; curve 2, 0.0152 mole/*l*; curve 3, 0.0797 mole/*l*. Curve 4 represents the absorption spectrum of the hydrogen bonded *p*-hydroxyazobenzene.

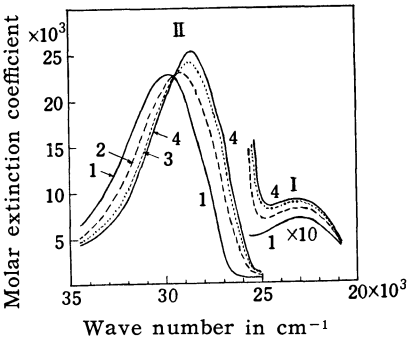

Fig. 2. The absorption spectrum of *p*-hydroxyazobenzene in *iso*-octane solution, and changes therein due to the addition of pyridine. The concentration of pyridine: curve 1, zero; curve 2, 0.00271 mole/*l*; curve 3, 0.0135 mole/*l*. Curve 4 represents the absorption spectrum of the hydrogen bonded *p*-hydroxyazobenzene.

The transitions are referred to as I, II and III in the order of increasing wave number. A remarkable spectral change occurs in the presence of a very small amount of ether or pyridine. Let it be assumed that the change is solely due to the formation of a hydrogen bond between *p*-hydroxyazobenzene and ether or pyridine.

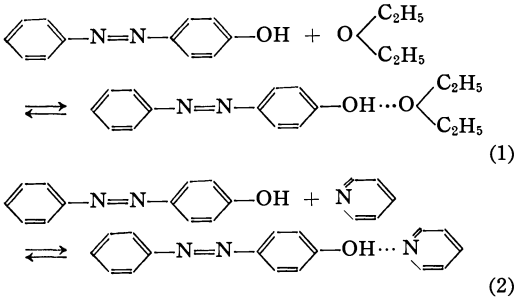

Then the curves 2 and 3 will be interpreted as the superposition of two kinds of absorption; one is due to the free *p*-hydroxyazobenzene, and the other due to the hydrogen bonded *p*-hydroxyazobenzene. This view is substantiated by the existence of several isosbestic points in Figs. 1 and 2.

The equilibrium constant K for equilibriums (1) and (2) can be obtained according to the usual manner[4,6]. Let the total concentrations of the proton-accepting substance in solutions 2 and 3 be C and C', respectively. Then it follows that

$$K = \frac{\varepsilon-\varepsilon_f}{\varepsilon'-\varepsilon}\frac{1}{C} - \frac{\varepsilon'-\varepsilon_f}{\varepsilon'-\varepsilon}\frac{1}{C'}, \qquad (3)$$

16) A. Pongratz, G. Markgraf and E. Mayer-Pitsch, *Ber.*, **71B**, 1287 (1938).
17) T. Kuwada, "Solvents", p. 117, Maruzen, Tokyo (1953).
18) E. L. Whitford, *J. Am. Chem. Soc.*, **47**, 2934 (1925).
19) M. Tsuboi, *Kagaku-no-Ryoiki*, **7**, 611 (1953).

where ε_f is the molar extinction coefficient of free *p*-hydroxyazobenzene (see curve 1), and ε and ε' are apparent coefficients of *p*-hydroxyazobenzene in solutions 2 and 3, respectively (see curves 2 and 3). All these coefficients refer to a given wave number. Using the above K value, the molar extinction coefficient ε_b of the hydrogen-bonded *p*-hydroxyazobenzene is calculated as

$$\varepsilon_b = \varepsilon' + \frac{\varepsilon' - \varepsilon_f}{KC'}. \qquad (4)$$

The values of K obtained from the spectral data are 25 and 450, respectively, for equilibriums (1) and (2). By the relation $\Delta F = -RT \ln K$, these K values lead to the free energy changes of −1.9 kcal./mole and −3.5 kcal./mole, respectively. The calculated molar extinction coefficients of the hydrogen-bonded complexes are indicated as curves 4 in Figs. 1 and 2.

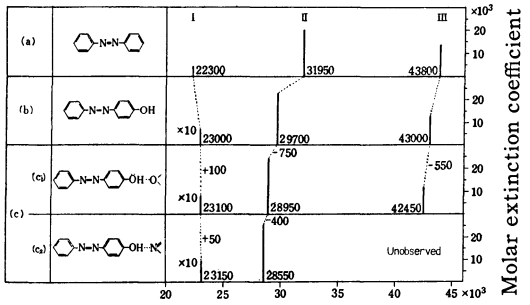

Fig. 3. The location and intensity of the absorption maxima of *p*-hydroxyazobenzene and its related substances.

Fig. 3 shows graphically the location and the intensity of the absorption maxima of both the free and the hydrogen-bonded *p*-hydroxyazobenzene, and also the wave number shifts arising from the hydrogen bond formation. The data for the parent compound, azobenzene[13,20], are given for the sake of comparison.

Discussion

Solvent effects in electronic spectra depend upon a number of factors, among which the dispersion and the polarity of solvents have been regarded as two important factors. The measure of the former is the refractive indices for the visible light and that of the latter is the dipole moments or sometimes the dielectric constants of the solvents. It is generally accepted that when the solvent has no dipole moment, the effect is largely determined by its refractive index, irrespective of whether the solute is polar or non-polar. On the other hand, when both the solvent and the solute are polar the solvent effect is determined by the magnitude of the dipole moment as well as the refractive index of the solvent[21,22].

In the present experiments the solute, *p*-hydroxyazobenzene, is polar and the solvent, *iso*-octane, is non-polar. In the case of solutions 2 or 3 there is an additional polar substance, ether or pyridine. Since the concentration of the last substance amounts to only 1% or less in mole ratio of the main solvent, *iso*-octane, one may expect that both the refractive index and the dielectric constant of the solvent remain almost unchanged with the addition of the polar substance. Therefore it may be reasonable to ascribe the spectral changes, which are observed when passing from *iso*-octane to *iso*-octane-ether or -pyridine mixture, to specific interaction of hydrogen bonding.

The spectral changes due to the hydrogen bonding are not independent of the type of the transition concerned. As is seen from Fig. 3, $n \rightarrow \pi^*$ transition I slightly shifts to the shorter wavelengths in the sequence (a) to (c), while $\pi \rightarrow \pi^*$ transitions II and III shift to the longer wavelengths in the same order. For the interpretation of the above phenomena it will be useful to refer to the fact pointed out by several authors[23] that introduction of an electron-repelling substituent such as OR or NR_2 into a chromophore often results in a red-shift of a $\pi \rightarrow \pi^*$ transition and a blue-shift of an $n \rightarrow \pi^*$ transition.

Let us consider $n \rightarrow \pi^*$ transition I. This transition corresponds to the jump of an electron from the non-bonding orbital of nitrogen atoms of the azo group to the lowest vacant π-orbital. The effect of substitution with an electron-repelling group upon an $n \rightarrow \pi^*$ transition was discussed by the present writer[24,25], and the following conclusions were drawn: (i) The

20) A. Burawoy, *J. Chem. Soc.*, **1937**, 1865.

21) N. S. Bayliss, *J. Chem. Phys.*, **18**, 292 (1950); N. S. Bayliss and E. G. McRae, *J. Phys. Chem.*, **58**, 1002 (1954).

22) Y. Ooshika, *Bull. Kobayashi Inst. Phys. Research*, **2**, 99 (1952); *J. Phys. Soc. Japan*, **9**, 594 (1954).

23) See, for instance, A. E. Gillam, E. S. Stern and E. R. H. Jones, "An Introduction to Electronic Absorption Spectroscopy in Organic Chemistry", Chap. 8, Edward Arnold (1954).

24) H. Baba, *J. Chem. Soc. Japan, Pure Chem. Sec.* (*Nippon Kagaku Zassi*), **72**, 74 (1951).

25) H. Baba, ibid., **72**, 341 (1951).

rate of the electron migration, hence the stabilization energy due to the electron migration, is smaller in the excited state than in the ground state of a substituted molecule. (ii) As a result, the $n\rightarrow\pi^*$ transition energy increases in comparison with that of the parent molecule. (iii) Such an effect will become larger with decreasing ionization potential of the non-bonding electron belonging to the substituent.

From (ii) the increase of the $n\rightarrow\pi^*$ absorption frequency from (a) to (b) may be understood. If the hydrogen bonds expressed in equilibriums (1) and (2) are formed, the ionization potential of the non-bonding electron of the hydroxyl group will decrease. Then from (iii) it follows that the absorption frequency is increased by the formation of the hydrogen bonds (see (b) and (c) of Fig. 3).

According to (i) the electronegativity of the oxygen atom of the hydroxyl group is expected to be lowered as a result of the $n\rightarrow\pi^*$ transition. Therefore the O—H···O< or O—H···N< hydrogen bonding energy will be smaller in the excited state than in the ground state. This fact will also contribute to the increase of the $n\rightarrow\pi^*$ absorption frequency†.

The situation is entirely different for the $\pi\rightarrow\pi^*$ transitions. In the excited state for a $\pi\rightarrow\pi^*$ transition of a substituted molecule the rate of electron migration is in general larger than in the ground state[24,26]. This illustrates the reduction of the absorption frequency in the order (a) to (c) as contrasted with the case of the $n\rightarrow\pi^*$ transition. This behavior of the $\pi\rightarrow\pi^*$ absorption bands of the *p*-hydroxyazobenzene is quite similar to that of $\pi\rightarrow\pi^*$ bands of other molecules reported in the literature[1-7].

Lastly let consideration be given to the difference between the effects of O—H···O< and O—H···N< hydrogen bonds. The present experiments have revealed that both the equilibrium constant and the frequency shift for the O—H···N< bond are larger than those for the O—H···O< bond (see (c_1) and (c_2) of Fig. 3). It is then suggested that the proton-accepting power of the nitrogen atom is stronger than that of the oxygen atom. This is in accord with Tsuboi's conclusion derived from infrared spectroscopy[19].

26) K. F. Herzfeld, *Chem. Revs.*, **41**, 233 (1947).

† As is seen from Figs. 1 and 2, $n\rightarrow\pi^*$ absorption band I is superposed on the tail of $\pi\rightarrow\pi^*$ band II which is of high intensity and is displaced to the red by the hydrogen bonds. This fact may be responsible to some extent for the observed blue-shift of the $n\rightarrow\pi^*$ band.

Summary

The electronic absorption spectra of *p*-hydroxyazobenzene in *iso*-octane and also in the mixtures of *iso*-octane-ether and *iso*-octane-pyridine were measured. The spectral change observed when addition was made of a small amount of ether or pyridine to a solution of *p*-hydroxyazobenzene in pure *iso*-octane was satisfactorily interpreted as due to the formation of a hydrogen bond between the solute molecule and ether or pyridine. The equilibrium constants for the hydrogen bonds and the absorption curves of the hydrogen-bonded complexes were determined from the spectral data.

It is made clear that the effects of hydrogen bonding on the absorption bands are dependent upon the type of the electronic transitions from which the bands originate. The $\pi\rightarrow\pi^*$ bands situated in the ultraviolet region are markedly displaced to the red, while the $n\rightarrow\pi^*$ band in the visible region slightly to the blue. A theoretical explanation for the above phenomena is offered.

The author wishes to express his sincere thanks to Professor K. Higasi for his encouragement and for reading the manuscript. Thanks are also due to Dr. S. Nagakura for his help in carrying out the experiments.

Research Institute of Applied Electricity
Hokkaido University, Sapporo

Studies on the Cobalt(III) Complexes Containing Only One Chelate Ring. I. Syntheses of $[Co(NH_3)_4\,gly]X_2$ *and* $[Co(NH_3)_4\,alan]X_2$[1].

By Yoichi SHIMURA

(Received November 13, 1957)

Limited number of cobalt(III) complexes which contain only one chelate ring are known, in contrast with the numerous series of those containing two chelate rings. The most familiar examples of such "mono-chelate cobalt(III) complexes" hitherto known are monocarbonato-tetrammine and monoxalato-tetrammine complexes. Mono(amino-acido)-tetrammine or monoethylenediamine-tetrammine cobalt(III) complexes were not known heretofore. Recently, Kuebler and Bailar[2] reported that the attempted replacement of the chloride ion or the sulfono group[3], respectively, in $[Co(NH_3)_4Cl_2]^+$ and $[Co(NH_3)_4(SO_3)_2]^-$ by *N*, *N*-diethylglycine was unsuccessful.

In the present paper, the syntheses of monoglycinato-tetrammine and mono-alaninato-tetrammine Co(III) complexes will be reported. Furthermore, the visible and ultraviolet absorption spectra of the (amino-acido)-ammine series of Co(III) complexes will be discussed mainly in relation to the geometrical structures of the complex ions.

Results and Discussion

Method of Syntheses.—For the first place, the reactions between sodium glycinate and $[Co(NH_3)_4(OH_2)_2]^{3+}$ or $[Co(NH_3)_4(OH_2)Cl]^{2+}$ were investigated. Evidences for the formation of some glycinato complexes were obtained, but the complexes were not isolated in pure state. Next, the use of decolorizing charcoal as catalyst[4] was examined. However, in the presence of charcoal glycinate radical gradually expelled the co-ordinated ammonia molecules and consequently the desired tetrammine complexes were not obtained.

Lastly, therefore, the reaction of $[Co(NH_3)_4(OH_2)Cl]SO_4$ with sodium glycinate was examined in the presence of decolorizing charcoal and of aqueous ammonia (see experimental part). This procedure produces a mixture of three or more species of the complex ions which belong to the glycinato-ammine series. From the mixture, $[Co(NH_3)_6]^{3+}$ was removed as the sparingly soluble chloride-sulfate, $[Co(NH_3)_6]Cl\cdot SO_4\cdot 3H_2O$, and the desired complex $[Co(NH_3)_4\,gly]^{2+}$ was separated as sulfate from the mother liquor*. The yield did not exceed 30%. As a by-product, $[Co(NH_3)_2\,gly_2]Cl$ was also obtained in a small yield.

The reaction between sodium alaninate and $[Co(NH_3)_4(OH_2)Cl]SO_4$ proceeds in a similar way. In this case an amount of tris-alaninato cobalt(III) complex also yielded.

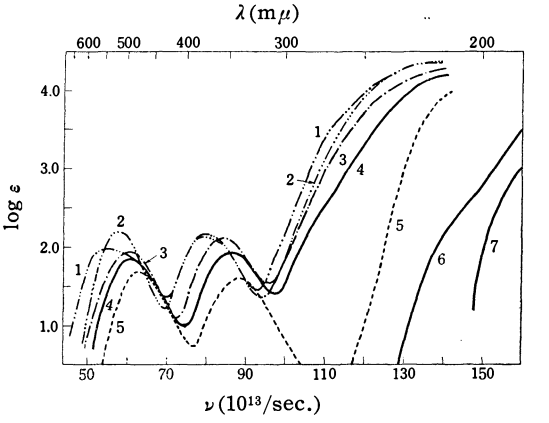

Fig. 1. Absorption curves of $[Co(NH_3)_{6-2x}(gly)_x]$ series.

1. *trans-cis*-$[Co\ gly_3]\cdot 2H_2O$
2. *cis-cis*-$[Co\ gly_3]\cdot H_2O$
3. $[Co(NH_3)_2\,gly_2]Cl$
4. $[Co(NH_3)_4\,gly]SO_4\cdot H_2O$
5. $[Co(NH_3)_6](ClO_4)_3$
6. $NH_2CH_2CO_2Na$[5]
7. NH_3[5]

1) Partly presented at the Symposium on Co-ordination Compounds, Tokyo, October 28, 1956.

2) J. R. Kuebler, Jr. and J. C. Bailar, Jr., *J. Am. Chem. Soc.*, **74**, 3535 (1952).

3) The "sulfono group" is $SO_3^=$ radical bound to the central metal ion by the sulfur atom: See Y. Shimura, This Bulletin, **25**, 46 (1952).

4) J. C. Bailar, Jr. and J. B. Work, *J. Am. Chem. Soc.*, **67**, 176 (1945).

* The following abbreviations are used: am, amino-acid radical in general; gly, $NH_2\cdot CH_2\cdot CO_2^-$; alan, $NH_2\cdot CH(CH_3)\cdot CO_2^-$.

TABLE I

ABSORPTION DATA OF $[Co(NH_3)_{6-2x}(gly)_x]$ AND $[Co(NH_3)_{6-2x}(alan)_x]$ SERIES.

Complex ion	First absorption band				Second absorption band				$\Delta(\nu_{max})$[e]	$(\log \varepsilon_{max})$[f]
	ν_{max} (10^{13}/sec.)	$\log \varepsilon_{max}$	l[b] (10^{13}/sec.)	δ[c] (10^{13}/sec.)	ν_{max} (10^{13}/sec.)	$\log \varepsilon_{max}$	l[b] (10^{13}/sec.)	δ[c] (10^{13}/sec.)		
$[Co(NH_3)_6]^{3+}$	62.9	1.68	10.3	0.5	88.3	1.60	12.5	0.35	25.4	−0.08
$[Co(NH_3)_4gly]^{2+}$	60.8	1.86	11.3	0.55	86.4	1.93	12.3	0.35	25.6	+0.07
$[Co(NH_3)_2gly_2]^{+}$	60.4	1.94	11.3	0.25	84.3	2.11	11.8	0.5	23.9	+0.17
cis-cis-$[Co\ gly_3]$[d]	57.7	2.20	9.1	0.55	80.2	2.14	12.7	0.6	22.5	−0.06
trans-cis-$[Co\ gly_3]$	55.2[a]	1.99	—	—	80.4	2.16	12.1	0.35	—	—
$[Co(NH_3)_4alan]^{2+}$	61.5	1.87	11.0	0.6	86.7	1.90	12.8	0.4	25.2	+0.03
cis-cis-$[Co\ alan_3]$[d]	57.9	2.27	9.0	0.6	80.3	2.21	11.7	0.7	22.4	−0.06
trans-cis-$[Co\ alan_3]$[d]	55.6[a]	2.00	—	—	80.9	2.18	12.3	0.5	—	—

a: This band splits into two or more components (see Figs. 1 and 2).
b: l=half-value width. This corresponds to $\{\delta(+)+\delta(-)\}$ in Jørgensen's notation[6].
c: δ=inclination parameter[7] or Inklination (in German)[8]. This parameter corresponds to $\frac{1}{2}\{\delta(+)-\delta(-)\}$ in Jørgensen's notation[6], and is defined by the equation $\delta=\frac{1}{2}\{\nu_k+\nu_l\}-\nu_{max}$, where ν_k and ν_l are the two frequencies where the formal extinction coefficients are equal to the half of ε_{max}.
d: Measured in 60% perchloric acid.
e: Frequency difference between the maxima of the second and the first absorption band.
f: Difference between $\log \varepsilon_{max}$'s of the second and the first band.

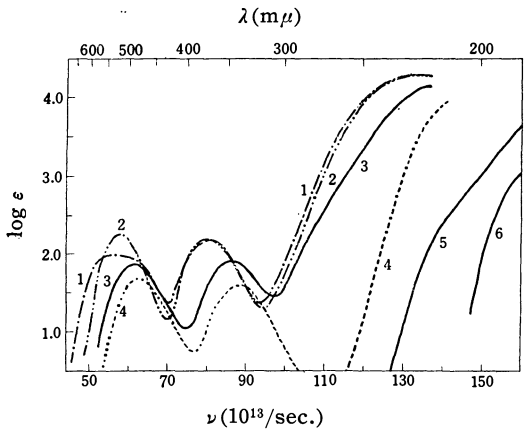

Fig. 2. Absorption curves of $[Co(NH_3)_{6-2x}(alan)_x]$ series.
1. *trans-cis*-$[Co\ alan_3]$
2. *cis-cis*-$[Co\ alan_3]$
3. $[Co(NH_3)_4alan]SO_4$
4. $[Co(NH_3)_6](ClO_4)_3$
5. $NH_2CH(CH_3)CO_2Na$[5]
6. NH_3[5]

The aqueous solutions of the $[Co(NH_3)_4\ am]X_2$-type complexes are rather unstable. These complexes can be recrystallized from warm water, but hot water decomposes the complexes.

Absorption Spectra.—The absorption curves of the cobalt(III) complexes which belong to the glycinato-ammine and the alaninato-ammine series are shown in Figs. 1 and 2. The numerical data of the first and the second absorption bands of these complexes are summarized in Table I.

As is seen in the figures and the table, the successive substitution of ammonia ligands in those complexes by the glycinate or the alaninate ions causes the regular red-shifts of the band maxima and the regular increase in the absorption intensities. The alaninate ion has a slightly higher position in the spectrochemical series[9,10] than the glycinate ion.

The two isomers, α(violet) and β(red), are known for the complexes of $[Co^{III}am_3]$type. The two forms correspond to the geometrical isomers, *cis-cis* and *trans-cis* forms (Fig. 3). As will be seen

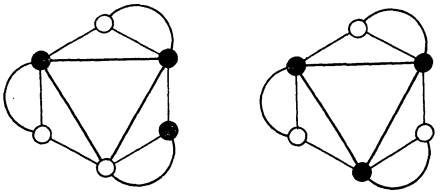

α(*trans-cis*, violet) β(*cis-cis*, red)

Fig. 3. Two geometrical isomers of $[Co^{III}am_3]$. (white circle, oxygen atom; black circle, nitrogen atom)

5) H. Ley and B. Arends, *Z. physik. Chem.*, **B 17**, 117 (1932).

6) C. K. Jørgensen, *Acta Chem. Scand.*, **8**, 1495 (1954).
7) Y. Shimura and R. Tsuchida, This Bulletin, **28**, 572 (1955).
8) H. Siebert and M. Linhard, *Z. physik. Chem., N. F.*, **11**, 318 (1957).
9) R. Tsuchida, This Bulletin, **13**, 388, 436 (1938).
10) Y. Shimura and R. Tsuchida, ibid., **29**, 311 (1956).

in Figs. 1 and 2, the main difference between the absorption curves of the two isomers occurred in the first absorption bands. Thus the first band of the β-isomer has a normal pseudo-parabolic form, while that of the α-form distinctly shows an indication of splitting. This splitting may be considered as a proof of the *trans-cis* structure of the α-form, since a similar splitting was reported for the first band of *trans* isomer of $[Co(NH_3)_4(OCOCH_3)_2]ClO_4$ and not for that of the corresponding *cis* isomer[11]. The above conclusion was reported briefly in a previous report[10]. Independently, Basolo et al.[12] came to the same conclusion. The assignment is also supported by the semi-empirical molecular orbital calculations by Nakamoto et al.[13] and by Yamatera[14].

Five geometrical isomers are possible for the complex ion, $[Co(NH_3)_2\,gly_2]^{2+}$ (Fig. 4). In the present study only one species was obtained. Since the first band of the species has no indication of splitting, it has probably a *cis* structure concerning the two oxygen atoms of the two glycinate ligands, i.e., one of (a), (c) or (d) in Fig. 4.

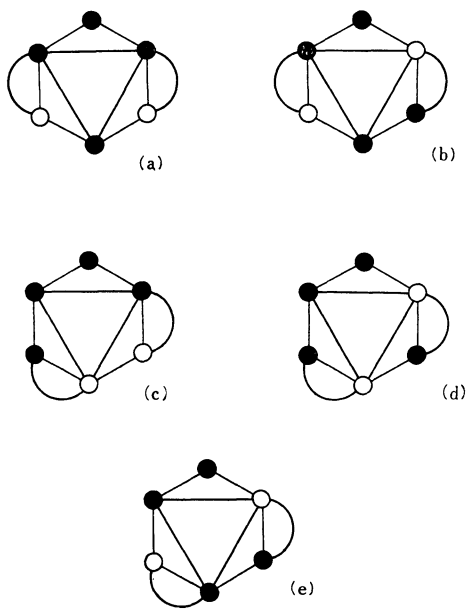

Fig. 4. The possible five geometrical isomers of $[Co(NH_3)_2\,gly_2]^{2+}$. (white circle, oxygen atom; black circle, nitrogen atom)

11) M. Linhard and M. Weigel, *Z. anorg. Chem.*, **264**, 321 (1951).
12) F. Basolo, C. J. Ballhausen and J. Bjerrum, *Acta Chem. Scand.*, **9**, 810 (1955).
13) K. Nakamoto, J. Fujita, M. Kobayashi and R. Tsuchida, *J. Chem. Phys.*, **27**, 439 (1957).
14) H. Yamatera, presented at the Symposium on Coordination Compounds, Osaka, October 30, 1955.

Experimental

Glycinato-tetrammine cobalt(III) sulfate monohydrate, $[Co(NH_3)_4\,gly]SO_4\cdot H_2O$ — Two grams of glycine and one gram of Na_2CO_3 were dissolved in 6 ml. of warm water. To this solution were added 7.4 g. of $[Co(NH_3)_4(OH_2)Cl]SO_4$[15], 0.5 g. of decolorizing charcoal and 0.5 ml. of aqueous ammonia (28 %). The resulting mixture was evaporated on a water bath almost to dryness. The residue was treated with about 60 ml. of warm water and any sparingly soluble materials were filtered off by suction. Upon cooling, some amount of $[Co(NH_3)_6]SO_4\cdot Cl\cdot 3H_2O$* separated from the filtrate in orange-yellow crystals. After removal of the orange-yellow crystals by filtration, a large amount of 95 % ethanol was added to the filtrate. The desired complex separated as the orange precipitate. This was separated by filtration from the red-colored mother liquor. (This mother liquor contains $[Co(NH_3)_2\,gly_2]Cl$.) The crude product was much contaminated by the orange-yellow crystals above mentioned. Therefore it was recrystallized from warm water or by the addition of ethanol to the cold aqueous solution. Three or more recrystallizations were necessary to obtain the pure products. The pure crystals are orange-red plates and effloresced on exposure to the air. The freshly dried crystals were analyzed for water of crystallization.

Anal. Found: H_2O, 5.27 %. Calcd. for $[Co(NH_3)_4\,gly]SO_4\cdot H_2O$: H_2O, 5.72 %.

The analyses for the following components were performed by use of the salts dehydrated at 90–100°C.

Anal. Found: Co, 19.4; C, 8.40; H, 5.50; SO_4^{--}, 32.18 %; Calcd. for $[Co(NH_3)_4(NH_2CH_2Co_2)]SO_4$: Co, 19.83; C, 8.08; H, 5.43; SO_4^{--}, 32.32 %.

Bisglycinato-diammine cobalt(III) chloride, $[Co(NH_3)_2\,gly_2]Cl$—The red colored mother liquor above mentioned was evaporated in vacuo over sulfuric acid at room temperature. The separated red precipitates were dissolved in hot water and filtered. After cooling, 99 % ethanol was added to the filtrate. The pure product was precipitated as red crystals.

Anal. Found: C, 17.45; H, 4.96; Cl, 12.4 %. Calcd. for $[Co(NH_3)_2(C_2H_4O_2N)_2]Cl$: C, 17.37; H, 5.10; Cl, 12.82 %.

Alaninato-tetrammine cobalt(III) sulfate, $[Co(NH_3)_4\,alan]SO_4$—One gram of sodium carbonate and 2.4 g. of *dl*-α-alanine were dissolved in 6 ml. of warm water. To this solution were added 7.4 g. of $[Co(NH_3)_4(OH_2)Cl]SO_4$[15], 0.5 g. of decolorizing charcoal and 0.4 ml. of aqueous ammonia (30 %). The resulting mixture was evaporated on a water bath almost to dryness. The residue was treated with about 100 ml. of

15) S. M. Jørgensen, *J. prakt. Chem.*, **42**, 211 (1890).
* *Anal.* Found: Co, 17.4; H_2O, 15.85%. Calcd. for $[Co(NH_3)_6]SO_4\cdot Cl\cdot 3H_2O$: Co, 17.00; H_2O, 15.53%.

warm water and any sparingly soluble materials** were filtered off by suction. When the filtrate was cooled, some amount of orange-yellow crystals, $[Co(NH_3)_6]SO_4 \cdot Cl \cdot 3H_2O$, separated. After removal of the orange-yellow crystals by filtration, a large amount of 95% ethanol was added to the filtrate. The crude complex was obtained as orange precipitate. This was separated by filtration from the red mother liquor. The product was much contaminated by the orange-yellow crystals above mentioned. Therefore, this was dissolved in warm water and fractionally precipitated by addition of ethanol. The contaminants were concentrated in the first fraction. The second and the following fractions were put together and precipitated twice more by the same manner. The orange red crystals obtained were washed with 95% ethanol and dried in air. The crystals dried in air contained 1—1.5 moles of water of hydration. This was completely dehydrated by heating at about 100°C.

Anal. Found: SO_4^{--}, 31.30%. Calcd. for $[Co(NH_3)_4(C_3H_5O_2N)]SO_4$: SO_4^{--}, 30.87%.

By evaporation of the red mother liquor above mentioned, a small amount of red crystals separates, and this is probably $[Co(NH_3)_2 alan_2]Cl$. Further studies were not intended for this complex, since only a small amount of the sample was available.

trans-cis-[Co gly_3]$\cdot 2H_2O$, *cis-cis*-[Co gly_3]$\cdot H_2O$, *trans-cis*-[Co $alan_3$] and *cis-cis*-[Co $alan_3$] were prepared by the method of Ley and Winkler[16] with reference to the report of Holtzclaw and Sheetz[17]. $[Co(NH_3)_6](ClO_4)_3$ was prepared by the method of Linhard[18].

Absorption Measurement.—The absorption spectra of *cis-cis*-[Co gly_3] and the two isomers of [Co $alan_3$] were measured in 60% perchloric acid. The aqueous solutions were used for the other complexes. The concentrations of the solutions varied from 1.0×10^{-2} to 0.5×10^{-4} gram complex-ion per liter. The absorption measurements were made by a Beckman DU spectrophotometer at room temperature.

Summary

The three new complexes, $[Co^{III}(NH_3)_4 gly]SO_4 \cdot H_2O$, $[Co^{III}(NH_3)_4 alan]SO_4$ and $[Co^{III}(NH_3)_2 gly_2]Cl$, have been synthesized by the reaction of $[Co(NH_3)_4(OH_2)Cl]SO_4$ with the amino-acid radicals in the presence of ammonia and decolorizing charcoal.

The visible and the ultraviolet absorption spectra of the glycinato-ammine and alaninato-ammine series of cobalt(III) complexes have been measured and discussed in relation to the geometrical structures of the complex ions.

The author wishes to thank Professor R. Tsuchida for his kind guidance throughout this work.

Department of Chemistry, Faculty of Science, Osaka University
Kita-ku, Osaka

** This is a mixture of decolorizing charcoal and the two isomers of $[Co^{III} alan_3]$.

16) H. Ley and H. Winkler, *Ber.*, **42**, 3894 (1909).

17) H. F. Holtzclaw, Jr. and D. P. Sheetz, *J. Am. Chem. Soc.*, **75**, 3053 (1953).

18) M. Linhard, *Z. Elektrochem.*, **50**, 224 (1944).

Some Remarks on the Spreading of Protein Monolayers (Dynamic Studies on Monolayer. I)

By Maresuke KASHIWAGI

(Received October 16, 1957)

The monolayer of low molecular compounds such as fatty acids has been extensively studied[1]. These molecules dissolve often in benzene and usually they can be spread from the benzene solution, leaving a stable monolayer in the air-water interface after the evaporation of the solvent. In such a case, the spreading process itself does not present any difficulty and much more important are the physico-chemical investigations on the spread monolayer.

Proteins, on the other hand, are quite different from these compounds in respect to surface chemical behavior owing to their unique mloecular structure. Water-soluble protein can not be expected to spread on water substrate. In fact, most proteins fail to spread on pure water.

1) W. D. Harkins, "The Physical Chemistry of Surface Films", Reinhold, New York (1954).

Thus the spreading process becomes important and this spreading is known to be dependent largely on sub strate and other experimental conditions. Many pioneer chemists have emphasized the importance of those experimental conditions since those are rather fundamental for the protein monolayer. Certain proteins may spread immediately on some good substrate, but may take a considerable time to reach equilibrium state on the other substrate. This time effect was attributed mainly to the unfolding of a large complex structure of protein, by Bull and Neurath[2], and also by Jonxis[3].

The author also demonstrated[4] this effect, using one of the largest proteins, myosin. A theoretical equation was derived which was found to fit the experiments quite well. Attempts were made to examine other types of protein (i. e., relatively low molecular weight) in this respect. The spreading of ovalbumin is found to be complete within the first 5 minutes on 20% ammonium sulfate substrate at its isoelectric point and the spreading was not disturbed by different rates of compression. But a partial collapse is observed on 0.1 N hydrochloric acid substrate. Hemoglobin appears to take considerable time to come to equilibrium on account of physical or chemical changes in molecular structure. These results will be discussed on the basis of protein structure in the surface film.

Experimental

Apparatus.—The surface balance used for the present investigation is a vertical plate type of the size $60\times15\times2$ cm. The sensitivity is 0.02 dyn./cm. The whole apparatus is installed in a glass cabinet to avoid accidental contamination during the measurement. The use of such an apparatus is made possible by the courtesy of Professor T. Tachibana of Ochanomizu Women's University. All normal precautions, namely those described by Adam[5] were taken.

Protein.—Ovalbumin is extracted from fresh egg by the usual method[6] and recrystallized three times from saturated sodium sulfate solution. Bovine serum Hemoglobin is purchased from Pentex Corp., Kankakee, Illinois and used without further purification.

To examine the extent of spreading of protein monolayer, surface pressure change is observed with time and the constant value of surface pressure is considered to be that at equilibrium. The measurement is carried out at room temperature, but the temperature remained practically constant during each time of operation.

Experimental procedure.—Protein is spread in the air-water interface from its aqueous solution and the concentration is determined by drying a solution to constant weight. General spreading conditions are as follows: a known amount of protein solution is spread by means of a calibrated micropipet over a very large area (2.5 m^2/mg) and the film is kept there for exactly 5 minutes before the start of compression. The moving barrier is compressed gently to the desired area. The measurement is begun immediately when the barrier is adjusted to the area.

Theoretical Consideration

When a stable monolayer formation is not completed, the film is still in an unstable state. The system therefore will endeavor to reach lower free energy state and such a transitional process may involve change in surface pressure at a constant area, if the area is smaller than that in the gaseous state. Absence of such phenomena would indicate that the monolayer is at equilibrium under that condition. This equilibrium will be achieved quickly only on a good substrate. These structural changes in the film may be grouped, excluding surface interaction phenomena, as follows;

a) *Surface pressure increase with time* ($\Delta F>0$): This increase would mean that a configurational change of molecules in the film is occurring to reach a state of lower free energy. It may include, in a special case, dissociation of molecules.

b) *Surface pressure decrease with time* ($\Delta F<0$): Owing to a strong hydrophilic attraction between protein and water, some molecules in the film are dissolving into the water underneath them. Or else, some proteins are aggregating in the film.

c) *Constant surface pressure* ($\Delta F=0$): This means that all molecules in the film are in a state of the lowest free energy under that experimental condition. The film is thermodynamically in a stable equilibrium.

Results

Table I is a summary of measured values of surface pressure change ΔF as a function of time t at various areas under an identical condition.

2) H. B. Bull and H. Neurath, *Chem. Revs.*, **23**, 391 (1938); *J. Biol. Chem.*, **118**, 163 (1937).
3) J. H. P. Jonxis, *Biochem. J.*, **33**, (1943).
4) K. Kashiwagi and B. Rabinowitch, *J. Phys. Chem.*, **59**, 498 (1955).
5) N. K. Adam, "The Physics and Chemistry of Surfaces", 3rd ed. p. 27-31, Oxford Univ. Press, London (1944).
6) R. A. Kekwick and R. K. Cannon, *Biochem.*, **30**, 227 (1936).

TABLE I

SURFACE PRESSURE CHANGE OF OVALBUMIN AT CONSTANT AREA

Time Allowed For After Spreading, 5 min.
Substrate is 20% Ammonium Sulfate at pH 4.8.

Const. Area $m^2/mg.$	Temp. °C	Rate of compression cm./min.	ΔF dyn./cm.				
			1 min.	5	15	30	60
0.75	26	15	0	−0.12	−0.12	−0.12	0
0.76	26	100	0	0	0	0	0
0.81	26	12	0	0	0	0	0
0.82	26	90	0	0	0	0	0
0.85	26	80	0	0	0	0.12	0.12
0.90	28	76	0	0	0	0.12	0.12
0.99	30	92	0	0	0	0	−0.12
1.10	26	12	0	0	0	0	0

It is clear that surface pressure is constant over the whole period of experiment and that it is independent of the rate of compression. These facts can be taken as a direct indication that albumin spreading is complete within the first 5 minutes. Concentrated ammonium sulfate solution at isoelectric point is therefore a good substrate. Some proteins are known to spread on strong acid substrate. Whether this is true or not may be tested in the same way.

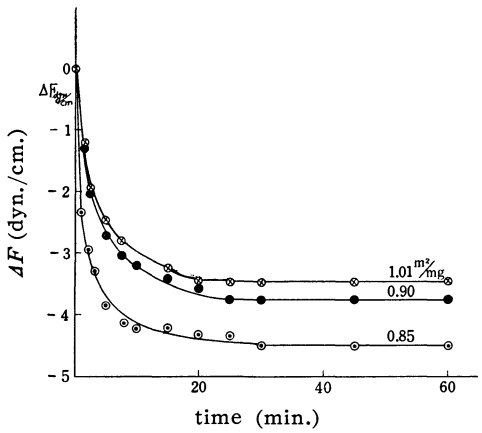

Fig. 1. Surface pressure change of ovalbumin (substrate 0.1 N HCl, 31°C).

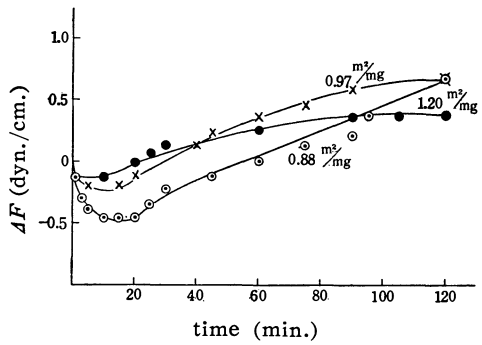

Fig. 2. Surface pressure change of Hemoglobin (substrate 20 % $(NH_4)_2SO_4$, pH 4.2, temp. 31°C).

Fig. 1 shows surface pressure change of ovalbumin on 0.1 N hydrochloric acid at various areas. ΔF decreases with time, in all cases, on 0.1 N hydrochloric acid. It reaches, however, a final pressure after a certain lapse of time. Fig. 2 shows ΔF–t curves of Hemoglobin on 20 % ammonium sulfate at pH 4.2. ΔF decreases with time in the initial stage and, after reaching a definite minimum, increases again. If the main cause for pressure change is attributed to molecular movements in very limited space in the film, those time effects and the values of final pressure will be related to the compressibility, which is expressed as $-I\,dA/A\,dF$.

One convenient way of calculation may be an adoptation of the following approximation.

$$-\frac{I}{A}\frac{dA}{dF} \fallingdotseq -\frac{I}{A}\frac{\Delta A}{\Delta F} \fallingdotseq \frac{I}{\frac{A_1+A_2}{2}}\frac{A_2-A_1}{F_1-F_2}, \quad (1)$$

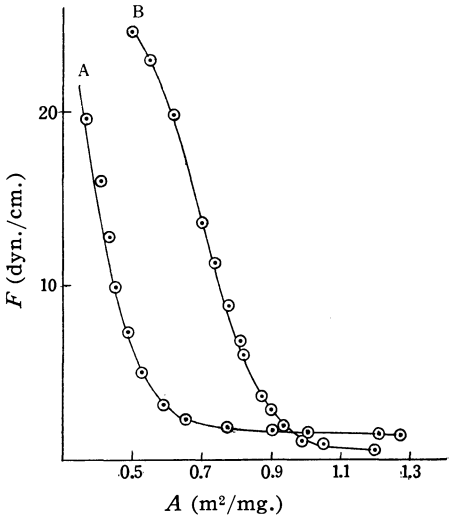

Fig. 3. Surface pressure of protein (time for spreading 20 min.).
A Albumin on 0.1 N HCl, 22°C
B Hemoglobin on 20 % $(NH_4)_2SO_4$, 31°C

where subscripts 1 and 2 refer to specified points close to each other on F–A curve. The F–A curves of albumin on 0.1 N hydrochloric acid and Hemoglobin on 20% ammonium sulfate are shown in Fig. 3.

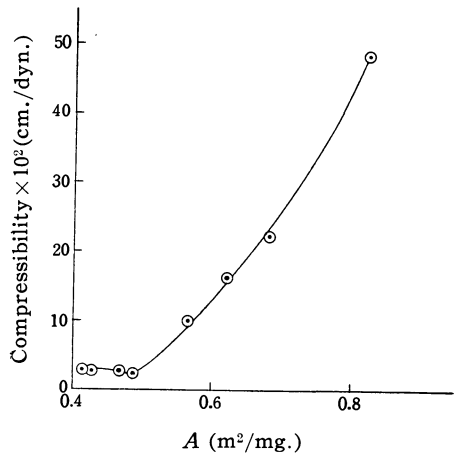

Fig. 4A. Compressibility of Albumin.

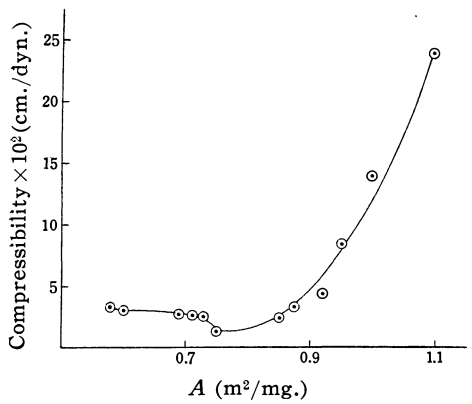

Fig. 4B. Compressibility of Hemoglobin.

Calculated values of compressibility are indicated in Fig. 4. In the region of low compressibility partially unfolded protein will be pushed downward more strongly by the surrounding molecules or will take more time to reach equilibrium. Both surface pressure change and the time needed for complete spreading are thus connected with compressibility.

Discussion

Neurath[7] considered that the unfolding of the protein molecule is a main cause for the time dependence of spreading. In fact, it will readily be thought that polypeptide chains in protein would need considerable time to orient and unfold themselves in the very viscous surface film into positions which yield minimum free energy. The author finds close analogy between behaviors of protein in bulk and in surface film. There seem to be plentiful evidences to prove that protein can take different configurations under different conditions[8,9].

According to Kauzmann et al.[10], the denaturation of protein in bulk may be illustrated as follows (Fig. 5). Stage 1

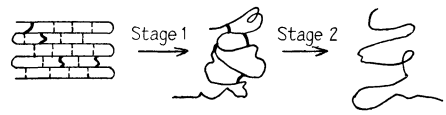

Fig. 5. Possible stages in the denaturation of a protein according to Kauzmann.

represents the initial unfolding reaction caused by rupture of many weak linkages and stage 2 the subsequent loop opening caused by rupture of relatively strong few intramolecular cross links. These ideas lead Kashiwagi and Rabinowitch[3] to the following expression

$$\frac{I}{(F_e+F^0)^2}\ln\frac{(F_e-F_0)(F+F^0)}{(F_e-F)(F_0+F^0)} + \frac{I}{(F_e+F^0)}\left\{\frac{I}{(F_0+F^0)}-\frac{I}{(F+F^0)}\right\} = kt/c, \qquad (2)$$

where F^0, a parameter, F_0, the surface pressure at zero time, F_e, the final equilibrium pressure, and F, the measured surface pressure at time t.

The derivation of this equation involves one assumption that the rate of increase in area occupied by the unfolding molecules at time t is proportional to the pressure under which the film finds itself, that is,

$$dA_0/dt = k(F_e-F) \qquad (3)$$

Although equation (2) fits myosin very well[4], it appears to fail for albumin. The reason for this seems clear, because on 20% ammonium sulfate at pH 4.8 spreading was complete in the first 5 minutes. There should be no increase in surface pressure after 5 minutes. Decrease in surface pressure on 0.1 N hydrochloric acid may indicate that some molecules

7) H. Neurath, *J. Phys. Chem.*, **40**, 361 (1936).

8) J. T. Yang and P. Doty, *J. Am. Chem. Soc.*, **79**. 761 (1957).

9) A. Elliott and B. R. Malcolm, *Biochim. et Biophys. Acta*, **21**, 466 (1956).

10) H. K. Frensdorff, M. T. Watson and W. Kauzmann, *J. Am. Chem., Soc.*, **75**, 5157 (1953).

which failed to unfold completely at the time of delivery tend to dissolve slowly into substrate. A once-unfolded molecule in low free-energy state will not dissolve again. These become evident when consideration is given to the difference in molecular structure as shown in Table II.

TABLE II
DIFFERENCE IN MOLECULAR STRUCTURE

	Myosin[11]	Albumin
Mol. Wt.	1,000,000	45,000
Solubility	insoluble	very soluble
Shape	flexible rod-like	globular

Concerning the complicated surface behavior of Hemoglobin, it is difficult to distinguish whether the pressure rise after the initial decrease with time is due to dissociation of molecule and/or chemisorption of oxygen and carbon dioxide from the air.

The author wishes to express deep thanks to Professor T. Tachibana without whom this research would not have been possible. Thanks are also due to Miss E. Hirano and Miss N. Hayashi for their assistance.

Mitsuwa Chemical Laboratory
Marumiya Co. Ltd.
Terajima-machi, Sumida-ku, Tokyo

11) A. Szent-Ggörgyi, "Chemistry of Muscular Contraction," Academic Press, New York (1951).

*Isotopic Exchange Reaction between Cyclohexane and Deuterium on Evaporated Molybdenum Films**

By Teruo HAYAKAWA and Toshio SUGIURA

(Received October 16, 1957)

Catalytic exchange reactions between cyclic hydrocarbons and deuterium have been the subject of recent investigations. The exchange reaction between cyclohexane and deuterium on evaporated metal films has been studied by Anderson and Kemball[1]. Their results on rhodium and palladium clearly indicated that half of the hydrogen atoms were readily exchanged. For the remaining six hydrogen atoms to be exchanged, they proposed the mechanism in which the adsorbed radical turns over on the surface by second-point adsorption. Although their multiple exchange mechanism is very efficient, the discordance between the experiments and the theoretical calculations based on this mechanism for the initial product distributions was considerably predominant.

The exchange reaction between cyclohexane and deuterium over various nickel catalysts have also been reported by Burwell et al[2,3]. According to their results, no discontinuities which separate the concentrations of $C_6H_6D_6$ and $C_6H_5D_7$ appeared at 160–200°C when evaporated nickel films or reduced nickel oxide were used. In recent years we have also investigated the isotopic exchange reaction between cyclohexane and deuterium on evaporated metal films, since it was of interest to clarify the mechanism of this exchange and the contribution of the deuterium isotope effect.

Experimental

Materials.—Wako Chemicals Pure Grade *cyclohexane* was purified by several fractionations and dissolved gases were removed by pumping under vacuum while chilled. *Deuterated hydrogen* was prepared from complete decomposition of heavy water over pure metallic sodium preliminary outgassed and distilled in vacuo; it was purified by passing through traps cooled in liquid nitrogen under the reduced pressure and then by passing through a sodium-gettered glass tube.

* A part of this paper was read before the 9th Annual Meeting of the Chemical Society of Japan held in Kyoto, April, 1956. Another part of this paper was also presented before the "Symposium on the Catalytic Reactions" held in Tokyo, April, 1957.

1) J. R. Anderson and C. Kemball, *Proc, Roy. Soc.* (London), **A226**, 472 (1954).

2) H. C. Rowlinson, R. L. Burwell, Jr. and R. H. Tuxworth, *J. Phys. Chem.*, **59**, 225 (1955).

3) R. L. Burwell, Jr. and R. H. Tuxworth, ibid., **60**, 1043 (1956).

The mass spectrometric analyses revealed that the deuterium content of this sample was 36.1 atomic %.

Evaporated Molybdenum Films.—Evaporated molybdenum films were prepared by customary procedures including careful degassing at elevated temperatures. The reaction vessel was a cylindrical glass tube (inside diameter 30 mm., length about 20 cm.) and between 5.1 and 10.9 mg. of molybdenum was evaporated onto the inner surface of this tube while the tube was cooled in ice water. After each experiment the weight of evaporated films was determined by the usual volumetric analysis.

Apparatus and Procedure.—The principal diagram of the apparatus is shown in Fig. 1.

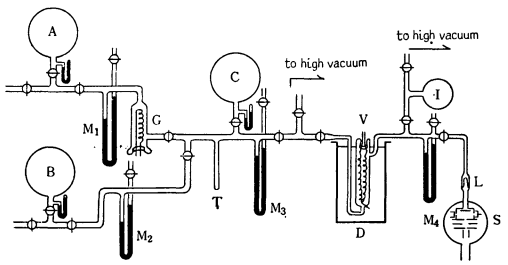

Fig. 1. Principal diagram of the apparatus.

Reservoir A containing purified deuterated hydrogen was connected to a sodium-gettered valve G by which the trace quantity of oxygen or water vapor was removed. The bulb B shows a reservoir of purified cyclohexane vapors, M_1 and M_2 auxiliary mercury manometers. T shows a trap cooled in liquid nitrogen, by which cyclohexane vapors were chilled before mixing. The sample gases were premixed and introduced into the storage bulb C, and the composition of each gas mixture was determined by means of the mercury manometer M_3.

Before commencing each experiment, the reaction vessel V was thoroughly evacuated for several hours and molybdenum was evaporated onto the inner surface of this vessel (the high vacuum was measured by means of the ionization gauge I). Then the reaction vessel was heated and controlled to the required temperature by means of the oil-bath thermostat D; the sample gases were admitted into the reaction vessel and the pressure was measured by means of the mercury manometer M_4. The oil-bath thermostat was operated by the usual electrical relay circuit; the temperature variation recorded by this thermostat was never greater than ± 0.1°C. After a given time, the gases were introduced, through the gas leak L, into the ion source S of a mass spectrometer and the product-compositions were determined. Since the orifice diameter of the gas leak was very small (i. e. smaller than 0.01 mm.), the pressure in the reaction vessel was practically unchanged.

In the present experiments, mass spectrometric analyses were performed on a modified Hitachi RMC mass spectrometer (90° sector type, the radius of curvature of the ion path and the maximum mass resolution were 135 mm. and about 150, respectively). The recording time required for magnetic scanning in the mass range between $m/e=83$ and 96 was about one minute, and other details of this instrument were already given[4]. For cyclohexane, 30 V. electrons were used for ionization, and at this ionizing voltage only a small fragmentation correction was required owing to the production of 6 % of the ion formed by the loss of one hydrogen atom. Corrections for fragmentation were made by assuming that the probability of ionization in the mass spectrometer was independent of isotopic content. Corrections were also made for deuterium and heavy carbon (C^{13}) occurring naturally in cyclohexane.

Results

The experimental conditions are shown in Table I, where the run numbers

TABLE I
DETAILS OF ISOTOPIC EXCHANGE RUNS

Run	Temp. (°C)	Partial pressure (mmHg) cyclohexane	deuterated hydrogen
7	111	15.4	15.4
8	75	15.5	15.5
9	97	19.6	19.6
11	56	11.4	11.4
12	102	10.1	10.1
13	86.5	14.8	14.8
14	75	6.8	6.8
15	106	9.0	9.0
16	102	6.9	6.9
17	87	6.7	6.7
18	86.5	6.8	6.8
21	75	20.4	5.1
22	94	3.0	2.0
23	102.5	1.5	1.0
24	97	7.5	7.5
28	97	6.5	6.5
29	97	12.8	6.4
30	97	18.9	6.3
31	97	24.3	6.1

indicate the chronological order of the experiments. Figs. 2-6 show some typical results on the variation in the percentage of the various cyclohexane molecules with time. In these figures, the notation d_i has been used in place of cyclohexane-d_i ($C_6H_{12-i}D_i$) to facilitate presentation. Typical results on the initial product distributions obtained from measuring the initial slopes of these curves are also listed in Table II.

4) T. Hayakawa and T. Sugiura, *Bull. Naniwa Univ., Series A*, **3**, 193 (1955).

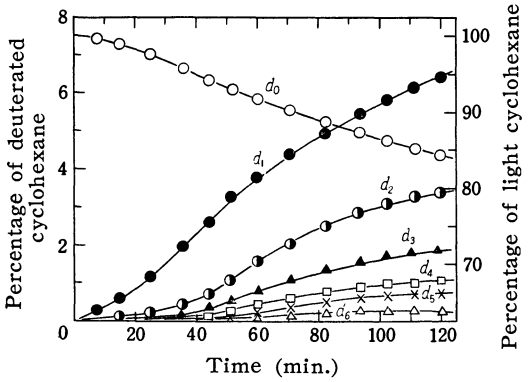

Fig. 2. The exchange of cyclohexane on 6.8 mg. of molybdenum at 75°C (run 14).

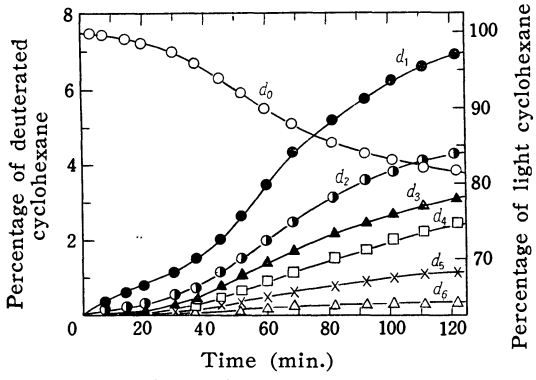

Fig. 3. The exchange of cyclohexane on 6.7 mg. of molybdenum at 86.5°C (run 18).

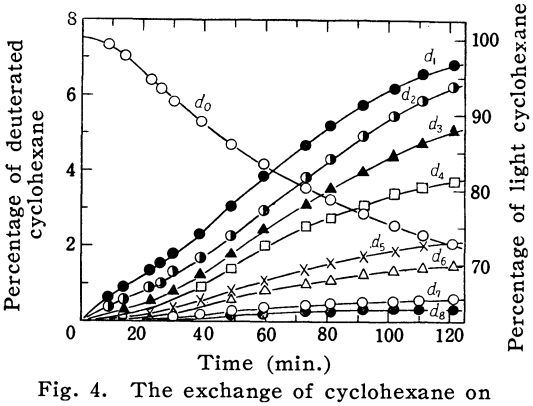

Fig. 4. The exchange of cyclohexane on 8.1 mg. of molybdenum at 102°C (run 16).

As described in the works of Anderson and Kemball[1,5], two different rates were determined from each experiment. The variation in the percentage (n) of light cyclohexane with time followed the equation

5) J. R. Anderson and C. Kemball, *Proc. Roy. Soc.* (London), **A223**, 361 (1954).

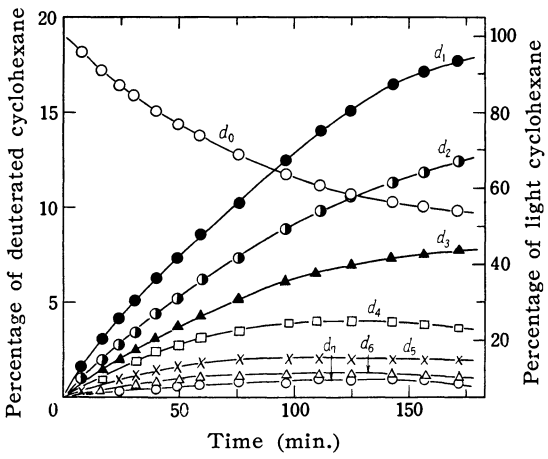

Fig. 5. The exchange of cyclohexane on 9.9 mg. of molybdenum at 97°C (run 29).

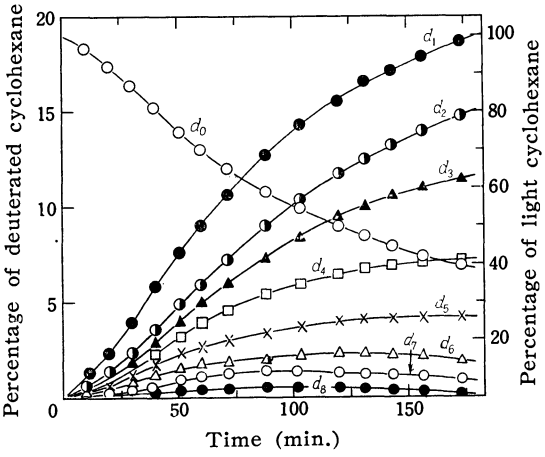

Fig. 6. The exchange of cyclohexane on 5.0 mg. of molybdenum at 97°C (run 31).

TABLE II
PERCENTAGE DISTRIBUTION OF INITIAL PRODUCTS
(Equimolecular mixtures)

Initial rate	Temperature (°C) 75 (run 14)	86.5 (run 18)	97 (run 28)	102 (run 16)
$d(C_6H_{11}D)/dt$	41.0	32.4	30.4	26.2
$d(C_6H_{10}D_2)/dt$	26.4	24.8	24.1	22.2
$d(C_6H_9D_3)/dt$	15.8	20.2	17.4	20.2
$d(C_6H_8D_4)/dt$	10.5	12.1	12.5	15.7
$d(C_6H_7D_5)/dt$	4.2	6.5	7.9	7.0
$d(C_6H_6D_6)/dt$	2.1	4.0	5.3	4.9
$d(C_6H_5D_7)/dt$	—	—	2.4	3.8

$$-\log(n-n_\infty) = \frac{k_H t}{2.303(100-n_\infty)} + \text{constant}, \quad (1)$$

where n_∞ represents the equilibrium value of n and k_H the initial rate of disappear-

ance of light cyclohexane in percent. per unit time. For cyclohexane ϕ was defined

$$\phi = \sum_i i \times N_i, \qquad (2)$$

where N_i denotes the percentage of cyclohexane-d_i ($C_6H_{12-i}D_i$, $i=1\sim12$) at the given time. The variation of ϕ with time also followed the equation

$$-\log(\phi_\infty - \phi) = \frac{k_D t}{2.303\phi_\infty} + \text{constant}, \qquad (3)$$

where ϕ_∞ was the equilibrium value of ϕ and k_D the initial rate of entry of deuterium atoms into cyclohexane expressed as the number of deuterium atoms entering 100 cyclohexane molecules in unit time.

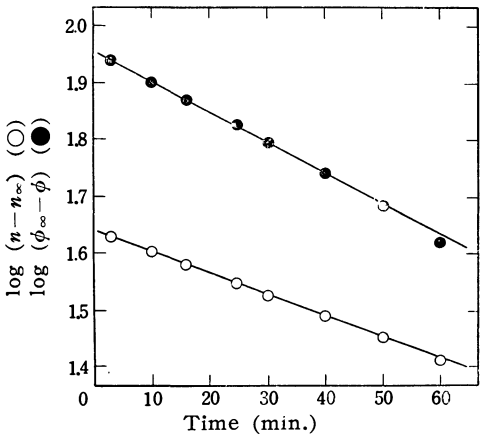

Fig. 7. The exchange of cyclohexane on 5.7 mg. of molybdenum at 97°C plotted according to the rate law expressions (run 28).

TABLE III
INITIAL RATES
(Equimolecular mixtures)

	Temperature (°C)			
	75 (run 14)	86.5 (run 18)	97 (run 28)	102 (run 16)
k_D(%/min.10mg.)	0.705	1.077	1.545	1.922
k_H(%/min.10mg.)	0.309	0.387	0.501	0.556
k_D/k_H	2.28	2.78	3.17	3.46

Fig. 7 shows typical results plotted according to Eqs. (1) and (3). The values of k_H and k_D at various temperatures are summarized in Table III in which the weight of evaporated films was normalized to 10 mg. Arrhenius plots are given in Fig. 8 and the apparent activation energies and the frequency factors in Table IV.

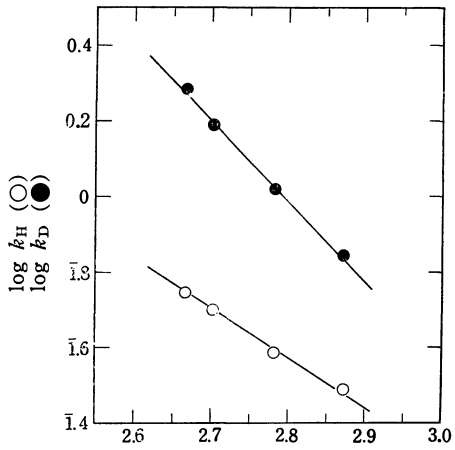

Fig. 8. The effect of temperature on the initial rates of exchange of cyclohexane on molybdenum. k_H and k_D in %/min.10 mg.

TABLE IV
APPARENT ACTIVATION ENERGIES (E) AND FREQUENCY FACTORS (A)

	E(kcal./mol.)	A(mol./min. 10 mg.)	Temp. range(°C)
k_D plot	9.8	7.05×10^{10}	75 to 102
(k_H plot)	(6.2)	(1.10×10^{8})	(75 to 102)

Discussion

Distributions of the Exchange Products.—Considering the fact that the deuterium content of hydrogen in our experiments was only 36.1 atomic %, the production of considerable amounts of highly deuterated products, as seen in Figs. 2–6 and Table II, requires a process of multiple exchange. Anderson and Kemball[1] have reported that isotopic exchange between cyclohexane and deuterium on evaporated films of rhodium (−48 and −28°C) and palladium (18.5°C) leads to distribution patterns in which marked discontinuities separate the concentrations of $C_6H_6D_6$ and $C_6H_5D_7$. On the other hand, Burwell and Tuxworth[3] have reported that at 160–200°C no such discontinuities between $C_6H_6D_6$ and $C_6H_5D_7$ appeared when evaporated nickel films or reduced nickel oxide were used. As seen in Figs. 2–6 and Table II, the present results clearly indicate that at 75–102°C one can observe no discontinuities between $C_6H_6D_6$ and $C_6H_5D_7$ for molybdenum films.

It is well known that both in the liquid and the vapor all cyclohexane molecules are practically present in the chair form,

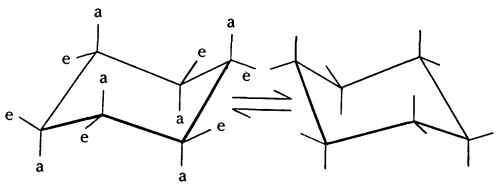

Fig. 9. The chair conformation of cyclohexane. The axial and equatorial bonds are marked (a) and (e) respectively.

as shown in Fig. 9, in which the twelve C–H bonds may be divided into two geometrically different groups of six equatorial (e) and six axial (a)[6]. Furthermore, owing to the flexibility of this chair conformation the two planes (i.e. each plane contains three carbon atoms) may interchange their positions, and all C–H bonds which were axial in the former chair form will be equatorial in the latter, and vice versa[7]. Based on this chair conformation mentioned above, a suggestion has been made by Anderson and Kemball that the reaction easily proceeds by exchanging alternately axial and equatorial hydrogen atoms in one group of three axial and three equatorial and that, for the remaining six hydrogen atoms to be exchanged, the adsorbed radical must turn over on the surface by second-point adsorption. Marked discontinuities between $C_6H_6D_6$ and $C_6H_5D_7$ found by them over evaporated films of rhodium and palladium were attributed to the small probability of this turning over of the adsorbed radicals.

Their explanations, however, contain some uncertainties, since dissociative adsorption of desorbed cyclohexane molecules ($C_6H_{12-i}D_i$, $i<7$) may take place with the same probability of the rupture of a C–H bond on either side of the carbon ring. Moreover, when an adsorbed radical takes an inclined position towards the surface, exchange may proceed between adjacent equatorial hydrogen atoms within different groups and the radical may easily turn over on the surface. Considering the matter from these facts, it seems rather reasonable to consider that there are no definite reasons to support the appearance of a marked discontinuity which separates the concentrations of $C_6H_6D_6$ and $C_6H_5D_7$.

Pressure-Dependence of Reaction Rate.—According to the present experiments, the initial rates of this exchange were found to follow

$$k_D(\text{or } k_H) \propto p(C_6H_{12})^{1.0} \cdot p(\text{d.h.})^{-0.6}, \quad (4)$$

where p(d.h.) denotes the partial pressure of deuterated hydrogen. The uncertainty in the exponents amounts to about 0.1.

The non-activated chemisorption of hydrogen on various metal films has been reported by many investigators[8]; then one can easily deduce the following kinetic relation by assuming that the coverage of the mobile layer of the adsorbed radicals is considerably smaller than that of chemisorbed hydrogen atoms and that the initial rate (k) of this exchange is proportional to the amount of the adsorbed radicals.

$$k \propto \frac{p(C_6H_{12})}{\sqrt{b}\, p(\text{d.h.})^{0.5} + b\, p(\text{d.h.})^{1.0}}, \quad (5)$$

where b indicates the constant which characterizes adsorption and desorption of hydrogen, and p(d.h.) the partial pressure of deuterated hydrogen. Since Eq. (5) indicates that the initial rate is proportional to p(deuterated hydrogen)$^{-1.0\sim-0.5}$, the present results shown in Eq. (4) and those obtained by Anderson and Kemball* approximately coincide with Eq. (5). It may, therefore, be considered probable that the rate-determining step of this exchange is desorption of the adsorbed radicals. On account of the fact that the deuterium content in our experiments was considerably small, the apparent activation energy derived from Arrhenius plot of k_D values is significant. Hence the value of 9.8 kcal./mol. shown in Table IV would imply the activation energy of dissociative adsorption of cyclohexane.

Deuterium Isotope Effect.—In order to examine the influence of the deuterium isotope effect, the compositions in equilibrated mixtures were determined both for the gas phase and for the gases newly desorbed from the surface after rapid evacuation. Typical results are summarized in Table V. Since only a minute quantity of the gases was newly desorbed, the present analytical results on the minor components in newly desorbed gases inevitably contain considerable uncertainties. Considering the problem from this fact, it seems reasonable to consider that, so far as the present experiments

6) O. Hassel, *Quart. Rev.*, **7**, 221 (1953).

7) W. G. Dauben and K. S. Pitzer, "Steric Effects in Organic Chemistry", John Wiley & Sons, Inc., New York (1956), p. 17.

8) M. W. Trapnell, "Chemisorption", Butterworths Scientific Publications, London (1955), p. 60.

* The pressure-dependence for this exchange over evaporated palladium films was found by them to follow $k_H \propto p(C_6H_{12})^{0.8} \cdot p(D_2)^{-1.0}$.

TABLE V
PERCENTAGE COMPOSITIONS OF EQUILIBRATED MIXTURES

Temp. (°C)	Sample	C_6H_{12}	$C_6H_{11}D$	$C_6H_{10}D_2$	$C_6H_9D_3$	$C_6H_8D_4$	$C_6H_7D_5$	$C_6H_6D_6$
94	Gas phase	60.9	28.7	7.5	1.7	0.8	0.4	—
	Newly desorbed gases	61.3	28.8	7.2	1.5	0.9	0.3	—
102	Gas phase	58.1	26.1	9.9	3.6	1.5	0.6	0.2
	Newly desorbed gases	57.4	26.4	9.8	3.8	1.7	0.6	0.3
111	Gas phase	54.7	22.9	12.2	6.1	2.7	0.9	0.5
	Newly desorbed gases	55.1	21.8	12.7	6.5	2.4	1.1	0.4

were concerned, the deuterium isotope effect gives no significant influence upon the overall reaction of this exchange.

Summary

Isotopic exchange reaction between cyclohexane and deuterium over evaporated molybdenum films has been studied mass-spectrometrically at the temperature range 56–111°C. The present results were compared either with Anderson and Kemball's or Burwell and Tuxworth's, and summarized as follows;

1) Since the deuterium content in our experiments was considerably low the production of considerable amounts of highly deuterated products requires a process of multiple exchange.

2) The present results clearly indicate that one can observe no discontinuities which separate the concentrations of $C_6H_6D_6$ and $C_6H_5D_7$.

3) The pressure-dependence was studied for this exchange and the initial rate (k) was found to be expressed as $k \propto p(C_6H_{12})^{1.0} \cdot p(\text{deuterated hydrogen})^{-0.6}$.

4) According to the present kinetic evidence, the rate-determining step of this exchange is probably the desorption of the cyclohexyl radicals.

5) So far as the present experiments were concerned, it seems reasonable to consider that the deuterium isotope effect gives no significant influence upon the present exchange reaction.

The authors wish to express their grateful thanks to Professor N. Sasaki of Kyoto University, Professor T. Titani of Tokyo Metropolitan University and Professor O. Toyama of Osaka Prefectural University for their kind encouragement and discussion. The expense has been defrayed in part from a grant given by the Ministry of Education to which the authors' thanks are due.

Departments of Pure and Applied Chemistry
College of General Education and
Faculty of Engineering
Osaka Prefectural
University, Sakai

*Isotopic Exchange Reaction between Cyclohexane and Deuterium on Evaporated Tungsten Films**

By Teruo HAYAKAWA and Toshio SUGIURA

(Received October 16, 1957)

In the previous communication[1], the authors studied the isotopic exchange reaction between cyclohexane and deuterium over evaporated molybdenum films. It was found that the initial production of highly deuterated products required a process of multiple exchange. No discontinuites which separate the concentrations of $C_6H_6D_6$ and $C_6H_5D_7$ appeared at 56—111°C and the deuterium isotope effect practically gave no significant influence upon the exchange reaction. The pressure-dependence for this exchange and simple kinetic consideration revealed that the rate-determining step may be attributed to desorption of the chemisorbed radicals and hence that the apparent activation energy experimentally found would imply the activation energy of dissociative adsorption of cyclohexane.

It was therefore of interest in the present work to study the same exchange reaction over evaporated tungsten films, since this permits a comparison of the catalytic activities of these metal films.

Experimental

Materials.—The method of preparation and purification of the sample gases was already given in a previous communication[1]. Evaporated tungsten films were prepared by customary procedures including careful degassing at elevated temperatures. Between 7.9 and 16.4 mg. of evaporated film was used in the subsequent experiments.

Apparatus and Procedure.—The apparatus and the procedure were described in the previous communication[1].

Results

The experimental conditions are summarized in Table I, where the run numbers indicate the chronological order of the experiments. Figs. 1, 2 and 3 show some typical results on the variation in the percentages of the various cyclohexane molecules with time. In these figures the notation d_i has been used in place of cyclohexane-d_i

TABLE I
DETAILS OF ISOTOPIC EXCHANGE RUNS

Run	Temp. (°C)	Partial pressures (mmHg) cyclohexane	deuterated hydrogen
2	94	2.0	2.0
5	111	2.0	2.0
6	98.5	2.2	2.2
8	80	2.7	2.7
9	86	1.9	1.9
10	102	2.1	2.1
12	79	1.5	1.5
15	84	2.2	2.2

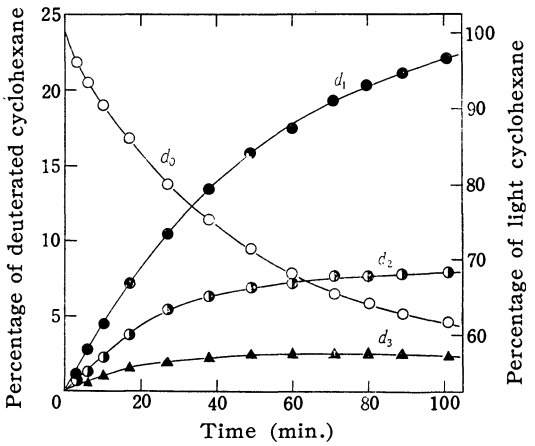

Fig. 1 (a). The exchange of cyclohexane on 12.4 mg. of tungsten at 84°C (run 15, major components).

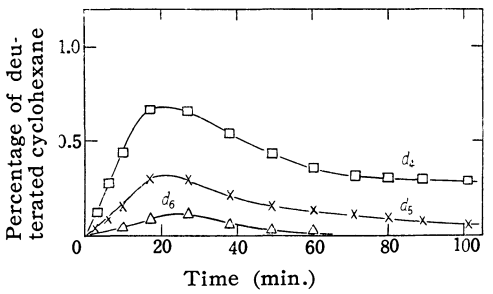

Fig. 1 (b). The exchange of cyclohexane on 12.4 mg. of tungsten at 84°C (run 15, minor components).

* Part of this paper was read before the 10th Annual Meeting of the Chemical Society of Japan held in Tokyo, April, 1957. Another part of this paper was also presented before the Symposium on the Catalytic Reactions held in Tokyo, April, 1957.

1) T. Hayakawa and T. Sugiura, This Bulletin, **31**, 180 (1958).

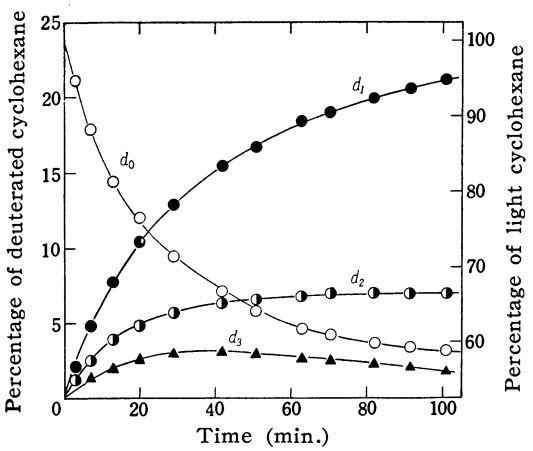

Fig. 2 (a). The exchange of cyclohexane on 16.4 mg. of tungsten at 94°C (run 2, major components).

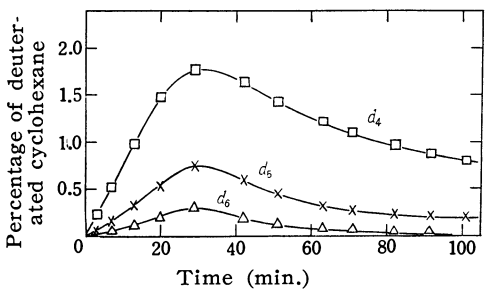

Fig. 2 (b). The exchange of cyclohexane on 16.4 mg. of tungsten at 94°C (run 2, minor components).

TABLE II
PERCENTAGE DISTRIBUTIONS OF INITIAL PRODUCTS

	Temperature (°C)			
Initial rate	84	94	102	111
$d(C_6H_{11}D)/dt$	57.2	51.7	40.6	36.3
$d(C_6H_{10}D_2)/dt$	25.3	27.0	26.0	26.9
$d(C_6H_9D_3)/dt$	9.2	11.9	19.6	18.2
$d(C_6H_8D_4)/dt$	5.8	6.0	7.8	11.8
$d(C_6H_7D_5)/dt$	1.9	2.4	4.5	5.1
$d(C_6H_6D_6)/dt$	0.6	1.0	1.2	1.3
$d(C_6H_5D_7)/dt$	—	—	0.3	0.4

TABLE III
INITIAL RATES
(Equimolecular mixtures)

	Temperature (°C)			
	84	94	102	111
k_D(%/min. 10 mg.)	1.175	1.682	2.281	3.116
k_H(%/min. 10 mg.)	0.742	1.006	1.208	1.611
k_D/k_H	1.58	1.68	1.89	1.93

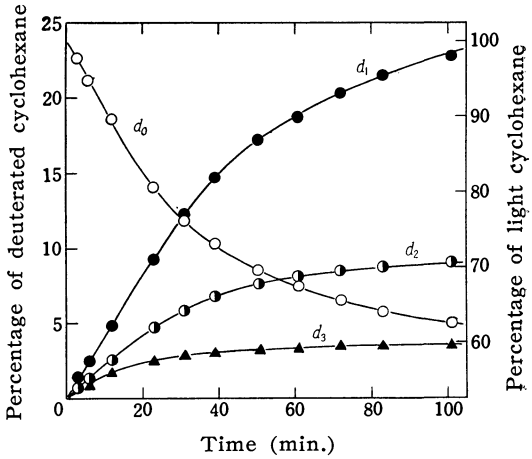

Fig. 3 (a). The exchange of cyclohexane on 9.9 mg. of tungsten at 102°C (run 10, major components).

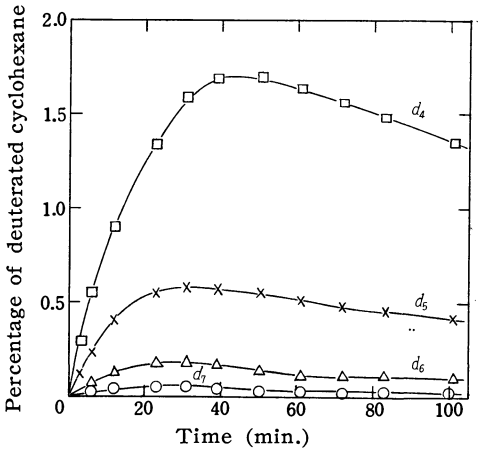

Fig. 3 (b). The exchange of cyclohexane on 9.9 mg. of tungsten at 102°C (run 10, minor components).

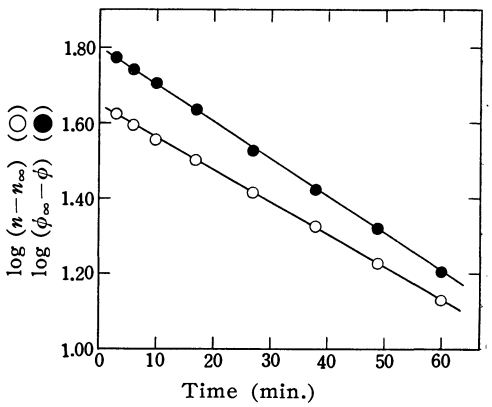

Fig. 4. The exchange of cyclohexane on 12.4 mg. of tungsten at 84°C plotted according to the rate law expressions (run 15).

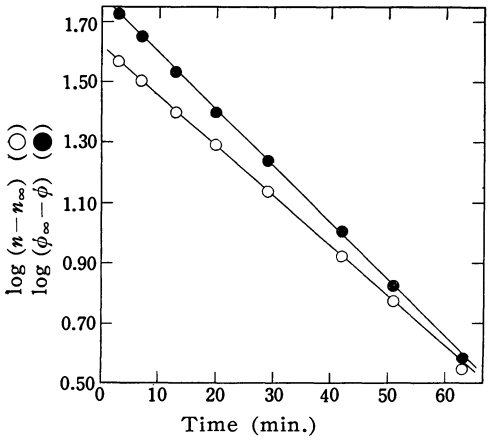

Fig. 5. The exchange of cyclohexane on 16.4 mg. of tungsten at 94°C plotted according to the rate law expressions (run 2).

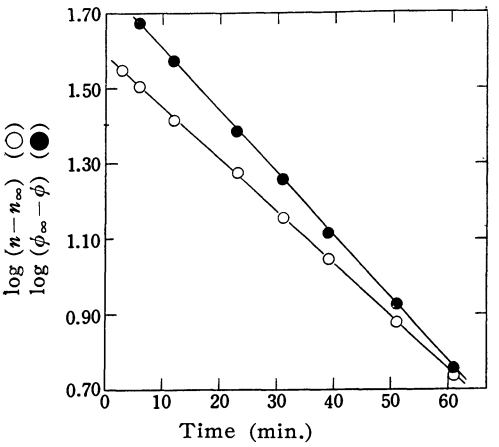

Fig. 6. The exchange of cyclohexane on 9.9 mg. of tungsten at 102°C plotted according to the rate law expressions (run 10).

($C_6H_{12-i}D_i$) to facilitate presentation. Typical results on the initial product distributions obtained from measuring the initial slopes of these curves are summarized in Table II. Two different rates, i. e. the initial rate of disappearance of light cyclohexane (k_H) and the initial rate of entry of deuterium atoms into cyclohexane (k_D), were calculated from the plot of the rate law expressions reported in the preceding paper[1]. Figs. 4, 5 and 6 show typical results plotted according to these expressions. The values of two different rates at various temperatures are summarized in Table III in which the weight of evaporated films was normalized to 10 mg. Arrhenius plots are given in Fig. 7 and the apparent activation energies and frequency factors in Table IV, together with the values obtained by Anderson and Kemball[2].

2) J. R. Anderson and C. Kemball, *Proc. Roy. Soc.* (London), **A226**, 472 (1954).

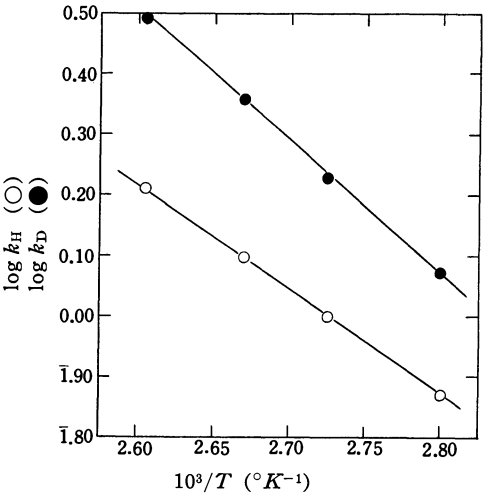

Fig. 7. The effect of temperature on the initial rates of exchange of cyclohexane on tungsten. k_H and k_D in %/min. 10 mg.

TABLE IV
APPARENT ACTIVATION ENERGIES (E) AND FREQUENCY FACTORS (A)

	E (kcal./mol.)	A (mol./min. 10 mg.)	Temp. range (°C)
k_D plot	10.3	7.43×10^{11}	84 to 111
(k_H plot)	(7.9)	(8.80×10^{9})	(84 to 111)
Anderson and Kemball* (k_H plot)	11	4.76×10^{28}	−69 to −48

* The initial deuterium content was 99.7%.

Discussion

Distributions of the Exchange Products.—As seen in Figs. 1~3, considerable amounts of highly deuterated products appeared in the early stage of this reaction. Since the deuterium content of hydrogen in our experiments was only 36.1 atomic %, it is quite reasonable to consider that the process of multiple exchange plays a significant role in the present exchange reaction. These figures clearly indicate that increased temperature results in a marked increase in extensive multiple exchange. Comparing the present product distributions shown in Table II with those already reported in the preceding paper[1], it is obvious that the multiple exchange is more extensive on molybdenum films than on tungsten films.

As seen in Figs. 1~3 and Table II, although decreased temperature results in the decline in concentrations of highly deuterated products, at 84—111°C one can observe no discontinuity which separates the concentrations of $C_6H_6D_6$ and $C_6H_5D_7$.

TABLE V
PERCENTAGE COMPOSITIONS OF EQUILIBRATED MIXTURES

Temp. (°C)	Sample	C_6H_{12}	$C_6H_{11}D$	$C_6H_{10}D_2$	$C_6H_9D_3$	$C_6H_8D_4$	$C_6H_7D_5$
84	Gas phase	60.1	29.6	8.2	1.8	0.3	—
	Newly desorbed gases	60.7	29.4	7.9	1.5	0.5	—
94	Gas phase	56.9	30.9	8.7	2.7	0.8	—
	Newly desorbed gases	57.4	30.6	8.2	2.8	1.0	—
102	Gas phase	58.1	25.8	10.9	3.5	1.3	0.4
	Newly desorbed gases	56.2	26.7	10.9	4.1	1.5	0.6

These results closely resemble those already found for evaporated molybdenum films. Moreover, no such discontinuities between $C_6H_6D_6$ and $C_6H_5D_7$ have been observed either by Anderson and Kemball[2] for evaporated films of platinum (at 0°C) and tungsten (at −69°C) nor by Burwell and Tuxworth[3] for evaporated nickel films (at 160—200°C). From these facts, it seems reasonable for the present authors to consider that marked discontinuities between $C_6H_6D_6$ and $C_6H_5D_7$ observed by Anderson and Kemball[2] for evaporated films of rhodium (at −48 and −28°C) and palladium (at 18.5°C) must not be attributed to the characteristic chair conformation of the cyclohexane molecule.

Apparent Activation Energy.—Since the deuterium content of hydrogen in the present experiments was only 36.1 atomic %, the apparent activation energy derived from k_D plot is of significance. As seen in Table IV, the agreement between the present value and that obtained by Anderson and Kemball is well maintained. Although the pressure-dependence of this exchange over evaporated tungsten films was not further studied, the kinetic consideration discussed in the preceding paper may equally fit the present results. Hence the apparent activation energy experimentally found (10.3 kcal./mol.) would imply the activation energy of chemisorption of cyclohexane.

Deuterium Isotope Effect.—The deuterium isotope effect for the exchange of cyclohexane on evaporated tungsten films was studied by conducting additional experiments. After the usual determination of the gas phase compositions in equilibrated mixtures, the reaction vessel was rapidly evacuated and the gases newly desorbed from the surface were collected and analysed. Typical results are summarized in Table V. As seen in Table V, at 102°C the present exchange reaction might be influenced to some extent by the deuterium isotope effect. However, the present analytical results on the newly desorbed gases shown in Table V inevitably contain some uncertainties, since only a minute quantity of gases was newly desorbed from the surface. From this fact, it seems rather reasonable, so far as the present experiments were concerned, to consider that the deuterium isotope effect gives no significant influence upon the present exchange reaction.

3) R. L. Burwell, Jr., and R. H. Tuxworth, *J. Phys. Chem.*, **60**, 1043 (1956).

Summary

Isotopic exchange reaction between cyclohexane and deuterium over evaporated tungsten films has been studied mass-spectrometrically at the temperature range 79~111°C. The present results are summarized as follows;

1) The production of highly deuterated products in the initial stage of this exchange requires a process of multiple exchange.

2) Evaporated tungsten films showed, however, little tendency for multiple exchange, while evaporated molybdenum films promoted multiple exchange to a large extent.

3) One can observe no discontinuities which separate the concentrations of $C_6H_6D_6$ and $C_6H_5D_7$.

4) It seems reasonable to consider that marked discontinuities between $C_6H_6D_6$ and $C_6H_5D_7$ observed by Anderson and Kemball for evaporated films of rhodium and palladium must not be attributed to the characteristic chair conformation of the cyclohexane molecule.

5) The deuterium isotope effect gives no significant influence upon the overall reaction of this exchange.

The authors wish to express their grateful thanks to Professor N. Sasaki of Kyoto University, Professor T. Titani of Tokyo Metropolitan University and Professor O. Toyama of Osaka Prefectural University

for their kind encouragement and discussion. The expense has been defrayed in part from a grant given by the Ministry of Education to which the authors' thanks are due.

Departments of Pure and Applied Chemistry, College of General Edcation and Faculty of Engineering, Osaka Prefectural University, Sakai

*The Mechanism of the Isotopic Exchange Reaction between Cyclohexane and Deuterium on Evaporated Metal Films**

By Teruo HAYAKAWA and Toshio SUGIURA

(Received October 16, 1957)

In recent years many improved theoretical treatments have been carried out to determine the mechanism of the catalytic hydrogenation and the exchange reaction of various olefinic and paraffinic hydrocarbons[1-6]. Refined theoretical treatments of the catalytic exchange reactions between cyclic hydrocarbons and deuterium on evaporated metal films have also been carried out by Anderson and Kemball[7]. In that work the probabilities of two kinds of multiple exchange were statistically calculated. In the case of cyclohexane, the first was the probability of exchanging alternately axial and equatorial hydrogen atoms in one group (i.e. three axial and three equatorial), and the second was the probability of turning over of the adsorbed radical by second-point adsorption. However, the discordance between the experimental and the calculated values of the initial product distributions was, in general, considerably predominant.

In the former papers[8,9] the authors have investigated the isotopic exchange reaction between cyclohexane and deuterium on evaporated films of molybdenum and tungsten. It was therefore of interest to study the theoretical treatments of this exchange reaction.

Outline of Theoretical Calculation

According to the experimental results and the kinetic consideration already reported in the former papers, it may be considered probable that the isotopic exchange reaction between cyclohexane and deuterium over evaporated films of molybdenum and tungsten proceeds with the following processes.

(1) Dissociative adsorption of deuterated hydrogen takes place on the metal surface. Adsorption and desorption of hydrogen lie in an equilibrium.

(2) Dissociative adsorption of cyclohexane also takes place on the metal surface. Adsorption and desorption of cyclohexane also lie in an equilibrium.

(3) The adsorbed "cyclohexyl" radical may be desorbed to the gas phase as "cyclohexane" (i.e. the single exchange process).

(4) Either by exchanging adjacent hydrogen atoms in one group or by turning over on the surface, the adsorbed "cyclohexyl" radical further migrates over the surface (i.e. the multiple exchange process).

According to Anderson and Kemball, the last process (4) may be termed a "trip". However, as already discussed in the former papers[8,9], there is no definite experimental and geometrical reason to support the appearance of a marked discontinuity which separates the concentrations of $C_6H_6D_6$ and $C_6H_5D_7$. It matters little, therefore, for the present authors to distinguish the multiple exchange among adjacent hydrogen atoms

* Part of this paper was read before the 9th Annual Meeting of the Chemical Society of Japan held in Kyoto, April, 1956. Another part of this paper was presented before the "Symposium on the Catalytic Reactions" held in Tokyo, April, 1957.

1) C. D. Wagner, J. N. Wilson, J. W. Ötvos and D. P. Stevenson, *J. Chem. Phys.*, **20**, 338; 1331 (1952).
2) T. Keii, ibid., **22**, 144 (1954); **23**, 210 (1955); **25**, 364 (1956).
3) C. Kemball, *J. Chem. Soc.*, **1956**, 735.
4) J. R. Anderson and C. Kemball, *Proc. Roy. Soc.* (London), **A223**, 361 (1954).
5) C. Kemball, ibid., **A223**, 377 (1954).
6) K. Miyahara, *J. Res. Inst. Catalysis*, **4**, 143 (1956).
7) J. R. Anderson and C. Kemball, *Proc. Roy. Soc.* (London), **A226**, 472 (1954).
8) T. Hayakawa and T. Sugiura, This Bulletin, **31**, 180 (1958).
9) T. Hayakawa and T. Sugiura, This Bulletin, **31**, 186 (1958).

in one group from that accompanied by the turning over of the adsorbed cyclohexyl radical on the surface.

From the reasons mentioned above, the present authors support the following reaction scheme, in which downward dotted lines, upward broken lines, and sideward full lines represent adsorption, desorption (i.e. the single exchange process) and tripping (i.e. the multiple exchange process) respectively.

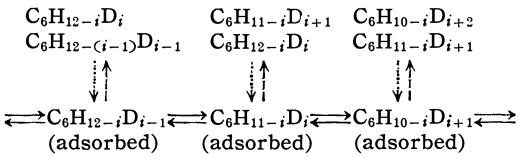

In the present theoretical calculation, the following assumptions were made:

(1) At the initial stage of this exchange, the deuterium content of the adsorbed hydrogen atoms equals to that in the gas phase (i.e. hydrogen lies in an isotopic equilibrium).

(2) The adsorbed hydrogen atoms are randomly distributed on the metal surface.

(3) The deuterium isotope effect is negligible for each process shown in the reaction scheme.

Let V, the overall tripping rate of adsorbed cyclohexyl radicals, V', the overall rate of desorption (or dissociative adsorption) of cyclohexane, C_i, the surface concentration of the cyclohexyl-d_i ($i=0\sim11$) radical, C_i', the concentration of cyclohexane-d_i ($i=0\sim12$) in the gas phase, Q_i, the concentration ratio of the cyclohexyl-d_i radical to total cyclohexyl radicals on the surface, Q_i', the concentration ratio of cyclohexane-d_i to total cyclohexane molecules in the gas phase, and Ω, the ratio of the fraction covered by deuterium atoms to that by total hydrogen atoms.

The increasing rate of the surface concentration of the cyclohexyl-d_i radical and the gas phase concentration of cyclohexane-d_i are then given by the following Eqs. (1) to (4).

$$\mathrm{d}C_i/\mathrm{d}t = V'\left(\frac{12-i}{12}Q_i' + \frac{i+1}{12}Q'_{i+1}\right) - V'Q_i + V\left\{\frac{12-i}{11}\Omega Q_{i-1} - \frac{(11-i)\Omega+i(1-\Omega)}{11}Q_i + \frac{i+1}{11}(1-\Omega)Q_{i+1}\right\}, \quad i=1\sim10, \tag{1}$$

$$\mathrm{d}C_{11}/\mathrm{d}t = V'\left(\frac{1}{12}Q'_{11} + Q'_{12}\right) - V'Q_{11} + V\left\{\frac{1}{11}\Omega Q_{10} - (1-\Omega)Q_{11}\right\}, \tag{2}$$

$$\mathrm{d}C_i'/\mathrm{d}t = V'\{(1-\Omega)Q_i + \Omega Q_{i-1} - Q_i'\}, \quad i=1\sim11, \tag{3}$$

$$\mathrm{d}C'_{12}/\mathrm{d}t = V'(\Omega Q_{11} - Q'_{12}). \tag{4}$$

As reported in the work of Anderson and Kemball[7], the extent of multiple exchange may be defined in terms of a parameter P, the ratio of V to V'. At the steady state of this exchange reaction all $\mathrm{d}C_i/\mathrm{d}t$ ($i=1\sim11$) values tend to zero and at the initial stage of this exchange all Q'_i($i=1\sim12$) values may be negligible, so that Eqs. (1)$\sim$(4) become respectively

$$P\left\{\frac{(12-i)\Omega}{11}\cdot\frac{Q_{i-1}}{Q_0} - \frac{(11-i)\Omega+i(1-\Omega)}{11}\cdot\frac{Q_i}{Q_0} + \frac{(i+1)(1-\Omega)}{11}\cdot\frac{Q_{i+1}}{Q_0}\right\} - \frac{Q_i}{Q_0} = 0, \quad i=1\sim10, \tag{5}$$

$$P\left\{\frac{\Omega}{11}\cdot\frac{Q_{10}}{Q_0} - (1-\Omega)\frac{Q_{11}}{Q_0}\right\} - \frac{Q_{11}}{Q_0} = 0, \tag{6}$$

$$\mathrm{d}C_i'/\mathrm{d}t = V'Q_0\left\{(1-\Omega)\frac{Q_i}{Q_0} + \Omega\frac{Q_{i-1}}{Q_0}\right\}, \quad i=1\sim11, \tag{7}$$

$$\mathrm{d}C'_{12}/\mathrm{d}t = V'Q_0\cdot\Omega\frac{Q_{11}}{Q_0}. \tag{8}$$

Since assumption (1) indicates that at the initial stage of this exchange Ω stays in a constant value*, one can obtain each Q_i/Q_0($i=1\sim11$) value for each given value of P by solving Eqs. (5)$\sim$(6). Then, by inserting each Q_i/Q_0 value thus obtained in Eqs. (7)$\sim$(8), one can calculate the relative values of $\mathrm{d}C_i'/\mathrm{d}t$($i=1\sim12$) at the initial stage of this exchange.

Results

The present results on the theoretical distributions of the initial products as functions of $\log P$ are shown in Fig. 1. The theoretical values of the percentage distributions of the initial products at various temperatures over evaporated films of molybdenum and tungsten are

* As already reported in the former papers[8,9], the experimental value of Ω was 0.361. In the present theoretical calculation, however, the value of Ω was taken as 1/3 to facilitate calculations.

TABLE I
PERCENTAGE DISTRIBUTIONS OF INITIAL PRODUCTS ON EVAPORATED MOLYBDENUM FILMS

Temp. (°C)	P		$d(C_6H_{12-i}D_i)/dt$ $i=1$	2	3	4	5	6	7	8
75	6	calcd.	40.2	27.8	17.1	9.0	4.1	1.4	0.4	—
		obsd.	41.0	26.4	15.8	10.5	4.2	2.1	—	—
86.5	9	calcd.	32.3	26.6	19.3	12.2	6.3	2.5	0.8	—
		obsd.	32.4	24.8	20.2	12.1	6.5	4.0	—	—
97	10.5	calcd.	30.1	25.8	20.1	12.1	7.2	3.4	1.2	0.1
		obsd.	30.4	24.1	17.4	12.5	7.9	5.3	2.4	—
102	13	calcd.	26.5	24.6	20.8	14.6	8.3	3.6	1.3	0.3
		obsd.	26.2	22.2	20.2	15.7	7.0	4.9	3.8	—

TABLE II
PERCENTAGE DISTRIBUTIONS OF INITIAL PRODCUTS ON EVAPORATED TUNGSTEN FILMS

Temp. (°C)	P		$d(C_6H_{12-i}D_i)/dt$ $i=1$	2	3	4	5	6	7
84	2.8	calcd.	56.3	26.5	11.2	4.2	1.4	0.4	—
		obsd.	57.2	25.3	9.2	5.8	1.9	0.6	—
94	3.8	calcd.	50.2	27.6	13.6	5.8	2.1	0.7	—
		obsd.	51.7	27.0	11.9	6.0	2.4	1.0	—
102	5.8	calcd.	40.6	28.2	17.0	8.7	3.8	1.4	0.3
		obsd.	40.6	26.0	19.6	7.8	4.5	1.2	0.3
111	7.4	calcd.	36.3	27.5	18.4	10.6	4.9	1.8	0.5
		obsd.	36.3	26.9	18.2	11.8	5.1	1.3	0.4

TABLE III
ACTIVATION ENERGY DIFFERENCES AND FREQUENCY FACTOR RATIOS

Catalyst	E(tripping) $-E$(desorption) (kcal./mol.)	A(tripping) / A(desorption)	Temp. range (°C)
Molybdenum films	6.8	1.15×10^5	75 to 102
Tungsten films	9.7	2.43×10^6	84 to 111

TABLE IV
ACTIVATION ENERGIES

Catalyst	E(desorption) (kcal./mol.)	E(tripping) (kcal./mol.)	Temp. range (°C)
Molybdenum films	$9.8+(-\Delta H)$	$16.6+(-\Delta H)$	75 to 102
Tungsten films	$10.3+(-\Delta H)$	$20.0+(-\Delta H)$	84 to 111

summarized in Tables I and II, together with the observed values by the present authors[8,9]. Arrhenius plots of P values are given in Fig. 2. The differences between the activation energy of tripping and that of desorption (or chemisorption) for these evaporated films are listed in Table III, together with the ratios of the frequency factor of tripping to that of desorption (or chemisorption).

Discussion

Initial Product Distributions.—In spite of the fact that the value of Ω used in the present theoretical calculations was slightly different from that experimentally found, the agreements between the theoretical and the experimental values of the initial product distributions for these metal films shown in Tables I and II are well maintained. This is attributed to the fact that the theoretical distributions shown in Fig. 1 were practically unchanged by a slight difference in the value of Ω. Refined statistical calculations of the initial product distributions for the same exchange reaction have been carried out by Anderson and Kemball[7]. However, the discrepancies between the theoretical and the experimental values were considerably predominant except for the results on palladium films at 44°C. The incompleteness of their theoretical treatments may be mainly attributed to the fact that the steady state conditions were not taken into consideration.

Mechanism of the Present Exchange

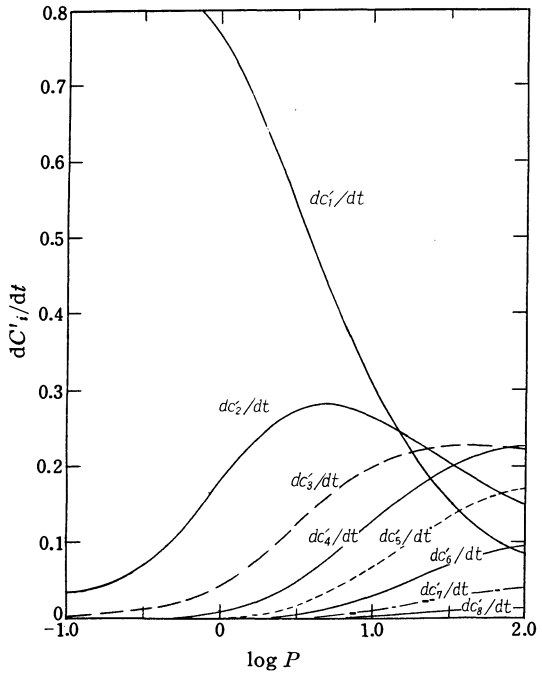

Fig. 1. Theoretical distributions of initial products as functions of log P. dC'_i/dt is fraction of initial rate of increase of cyclohexane-d_i.

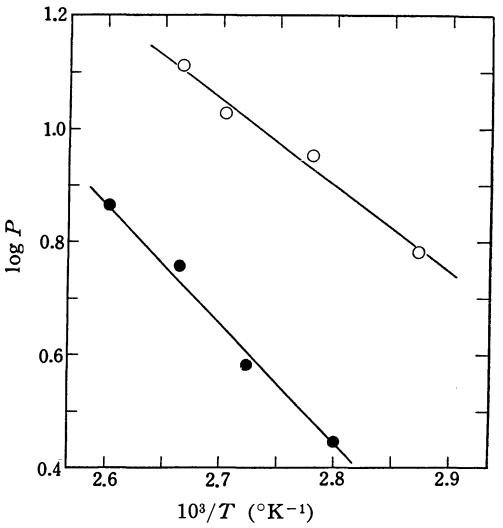

Fig. 2. Arrhenius plot of P values.
—○—○—, on evaporated molybdenum films;
—●—●—, on evaporated tungsten films.

Reaction. — As already discussed in a preceding paper[8], the rate-determining step of this exchange reaction may be the desorption of the cyclohexyl radicals. This coincides well with the fact that, as seen in Tables I and II, the theoretical values of P at various temperatures are considerably greater than unity. Since, as described in a preceding paper[8], the apparent activation energy experimentally found for this exchange would imply the activation energy of chemisorption of cyclohexane, one can obtain the activation energy for each process by combining the present theoretical calculations with the experimental results already reported in the fomer papers[8,9]. The present results on these activation energies are summarized in Table IV, where $(-\Delta H)$ denotes the heat of chemisorption of cyclohexane.

Summary

The theoretical treatments of the isotopic exchange reaction between cyclohexane and deuterium over evaporated metal films have been studied. The present results of the theoretical calculations were compared with the experimental results already obtained by the present authors for evaporated films of molybdenum and tungsten. The present results are summarized as follows:

1) The agreements between the theoretical and the experimental values of the initial product distributions for these metal films are well maintained.

2) The initial rate of tripping of the adsorbed radicals on evaporated films of molybdenum or tungsten at each temperature is considerably greater than that of desorption (or chemisorption) of cyclohexane. This coincides well with the experimental fact that the rate-determining step of this exchange reaction may be attributed to desorption of the adsorbed radicals.

3) The differences between the activation energy of tripping of the adsorbed radicals and that of desorption for evaporated films of molybdenum and tungsten amount to 6.8 and 9.7 kcal./mol. respectively.

The authors wish to express their sincere thanks to Professor N. Sasaki of Kyoto University, Professor T. Titani of Tokyo Metropolitan University and Professor O. Toyama of Osaka Prefectural University for their encouragement and discussion. The expense has been defrayed in part from a grant given by the Ministry of Education to which the authors' thanks are due.

Departments of Pure and Applied Chemistry College of General Education and Faculty of Engineering, Osaka Prefectural University, Sakai

Alkylalkoxypolysiloxanes. VII.[1] *Lower Members of tert-Butoxy End-blocked Dimethylpolysiloxanes with One to Four Silicon Atoms*

By Rokuro ŌKAWARA and Shōhei IMAEDA

(Received November 14, 1957)

Ethoxy end-blocked dimethylpolysiloxanes[2] have been prepared by the partial hydrolysis of dimethyldiethoxysilane. Also, the lower members of methoxy[3] and isopropoxy[4] end-blocked dimethylpolysiloxanes have been prepared by the sodium bicarbonate treatment of partially methanolyzed and *iso*-propanolyzed dimethyldichlorosilane respectively. In this paper, we wish to report on the preparation and properties of *tert*-butoxy end-blocked dimethylpolysiloxanes as indicated by formula T_n.

$$T_n: \quad (CH_3)_3CO\left[\begin{array}{c} CH_3 \\ | \\ -Si-O- \\ | \\ CH_3 \end{array}\right]_n C(CH_3)_3 \quad (n=1-4)$$

The higher members of the series T_n may be synthesized by the partial hydrolysis of dimethyldi-*tert*-butoxysilane. In this paper, two other routes of preparation will be reported. It has been known that *tert*-butanol does not react with chlorosilanes without an acid acceptor to form *tert*-butoxysilanes. Accordingly, an equivalent amount of pyridine to chlorosilane was used as an acid acceptor in these experiments. In the first route, dimethyldichlorosilane was added to the mixture of aqueous *tert*-butanol, pyridine and benzene. After refluxing, the pyridine hydrochloride was dissolved with an excessive amount of water and the separated organic layer was fractionated. In this route, the water in the reaction medium reacted with dimethyldichlorosilane more rapidly and there was obtained a relatively large amount of dimethylcyclopolysiloxanes (D_n) in the product. D_n distilled out between the plateaus of linear polymers, T_{n-3} and T_{n-2}, and the lower members of these polymers were not difficult to separate, but the separation was supposed to become difficult with the increasing polymer size. In a hope of obtaining the linear polymers with the formation of as small an amount of cyclopolymers as possible, the following second route was carried out.

In the second route, dimethyldichlorosilane was added to the mixture of pyridine, benzene and various insufficient amounts of *tert*-butanol and refluxed to complete the alcoholysis. By adding excess of water to the product, dissolving of the pyridine hydrochloride and hydrolysis of the remaining Si—Cl were carried out at the same time. Fractionation gave a small amount of crystalline solid with the fraction of T_2. This crystalline solid was confirmed to be tetramethyldisiloxane-1,3-diol. It is interesting to note that an unstable diol is obtained through the distillation. The higher diols were also supposed to be present at the fore part of the plateaus of T_n ($n=3,4$ and 5), considering from the higher refractive index at this part, but they could not be isolated. The amount of this crystalline diol was decreased by redistillation or by refluxing the partially alcoholyzed product with a slight excess of water to convert the remaining Si—Cl into Si—O. Properties of T_n are shown in Table I.

Experimental

Starting Materials.— Dimethyldichlorosilane supplied by Shin-etsu Chem. Ind. Co. and *tert*-butanol of Shell Chemicals were used without further purification.

Reaction of Dimethyldichlorosilane with Aqueous *tert*-Butanol.—A mixture of pyridine (0.4 mole), benzene (50 g.), *tert*-butanol ($x^*=2$ to 1) and water ($0.2\times(2-x)/2$ mole) was placed in a 300 cc. three-necked flask equipped with an efficient stirrer, a dropping funnel and a reflux condenser. Dimethyldichlorosilane (0.2 mole) was added drop by drop with vigorous

1) Part VI of this series, R. Ōkawara, G. Minami and Z. Oku, This Bulletin, **31**, 22 (1958).
2) H. J. Fletcher and M. J. Hunter, *J. Am. Chem. Soc.*, **71**, 2918 (1949).
3) T. Tanaka and R. Ōkawara, This Bulletin, **28**, 364 (1955).
4) R. Ōkawara, T. Ando and K. Ayama, *Technol. Repts. Osaka Univ.*, **8**, 171 (1958).

* x indicates molar ratios: *tert*-butanol/ dimethyldichlorosilane

TABLE I

tert-BUTOXY END-BLOCKED DIMETHYLPOLYSILOXANES:

$$(CH_3)_3CO\left[\begin{array}{c}CH_3\\|\\-SiO-\\|\\CH_3\end{array}\right]_n C(CH_3)_3$$

Polymer Size	Boiling Point	Density	Refractive Index	Molar Refraction Found (Calcd.)*	Molecular Weight Found** (Calcd.)	%Si Found (Calcd.)
$n=$	°C/mm Hg	d_4^{20}	n_D^{20}			
1	50.5/15	0.8295	1.3970	59.34 (59.58)	202 (204.39)	13.72 (13.74)
2	85/15	0.8666	1.4001	77.94 (78.22)	276 (278.55)	20.20 (20.17)
3	115/15	0.8936	1.4010	95.90 (96.86)	353 (352.71)	23.98 (23.89)
4	95/1	0.9178	1.4025	113.37 (115.50)	430 (426.87)	26.10 (26.32)

* Calculated from bond refractivities by E. L. Warrick, *J. Am. Chem. Soc.*, **68**, 2455 (1946).

** Cryoscopic measurements in benzene.

stirring to the mixture which was cooled with an ice-bath. After the addition the mixture was refluxed for one hour with stirring. An excessive amount of water was added to the mixture which was cooled with a water-bath to dissolve the precipitated pyridine hydrochloride. The separated benzene layer was thoroughly washed with 50 cc. water over five times to separate the dissolved chloride completely. The organic layer was dehydrated with sodium sulfate and simply distilled to drive off benzene, *tert*-butanol and pyridine. The composition of the oily product (Yield: ca. 45—60%) was determined by fractionation through a Stedman column of about 30 theoretical plates. The crystalline hexamethylcyclotrisiloxane (D_3) distilled out at first, the amount of which increased with decreasing x, and then the fraction of monomer (T_1) distilled out, the amount of which decreased from 90 to 55% of the product as x became 2 to 1. All the fractions higher than T_1 and residues thus obtained were united and distilled through the same column. Succeeding to the plateau of T_1, there was found a small plateau of octamethylcyclotetrasiloxane (D_4) at the boiling point of 82°—83°C/35 mm. n_D^{20} 1.3961 (Reported[5]: b. p. 175°C, n_D^{20} 1.3968)

Hydrolysis of Partially *tert*-Butanolyzed Dimethyldichlorosilane.—An insufficient amount of *tert*-butanol (x=1.6, 1.2 and 0.8) without water was caused to react with dimethyldichlorosilane (0.2 mole) under the same conditions as described above. By adding water, hydrolysis and dissolving of pyridine hydrochloride were carried out at the same time. Crystals of D_3 were not found in the product of experiments when x is 1.6 or 1.2, but they were found when x is 0.8. When x is 1.2, a portion having a slightly higher refractive index was found at the fore part of the plateau of T_2, and when x is 0.8, a small amount of a crystalline solid was found in that part and the portion which dissolved the crystals showed a higher refractive index than T_2.

To obtain a sufficient amount to characterize this crystalline solid, the alcoholysis was carried out with the same conditions by the use of a larger amount of the starting materials, i. e. 1 mole of dimethyldichlorosilane and 1.2 moles of *tert*-butanol (x=1.2). To the mixture, water (9 g.) was added and refluxed for ten minutes with stirring. Fractionation of the product (Yield: 45%) gave a large amount of solid with T_2. The recrystallized solid from benzene-ether mixture having m. p. 63°~65°C and specific gravity 1.118 at 16°C, which was determined by flotation method in the mixture of carbon tetrachloride and benzene, was identified to be tetramethyldisiloxane-1, 3-diol (Reported[6]: m. p. 67°~68°C).

Anal. Found: C, 29.41; H, 8.66%. Calcd. for $C_4H_{14}O_3Si_2$: C, 28.91; H, 8.49%.

Further fractionation gave T_3, but no plateaus higher than this could be obtained. Accordingly, starting with 1 mole of dimethyldichlorosilane and 1 mole of *tert*-butanol, refluxing was carried out after addition of water (11 g.) for thirty minutes to condense diol. Fractionation of the product (Yield: 50%) gave plateaus of T_1 and then D_4. The refractive indices of T_1 and D_4 are nearly the same but the boiling points are so different that T_1 may be separated from D_4 by distillation. Also, a small plateau succeeding to the fraction of T_2 would be assigned to that of D_5. Above T_2, the portion having the higher refractive index was found at the fore part of the plateau, which was supposed to be caused by a contamination of dimethylpolysiloxane-α,ω-diol. As to T_4 (in Table I) and T_5 (b. p. 113°C/1 mm., d_4^{20} 0.9311, n_D^{20} 1.4055. *Anal.* Found: Si, 28.31%. Calcd. for T_5: Si, 28.03%), though small in amount, they were separated but the amount was not enough to be taken as pure compounds,

5) W. I. Patnode and D. F. Wilcock, *J. Am. Chem. Soc.*, **68**, 358 (1946).

6) G. R. Lucas and R. W. Martin, ibid., **74**, 5225 (1952).

in view of the question from the increment of refractive index and analysis of silicon.

Analysis of Silicon.—Samples were weighed in gelatin capsule[7] and decomposed by concentrated sulfuric acid.

Summary

1) *tert*-Butoxy end-blocked dimethylpolysiloxanes were prepared from dimethyldichlorosilane, *tert*-butanol and water by the use of pyridine as an acid acceptor.

2) The lower members of those polysiloxanes having one to four silicon atoms were characterized.

Department of Applied Chemistry
Faculty of Engineering
Osaka University
Higashinoda, Miyakojima-ku, Osaka

7) T. Tanaka and R. Ōkawara, This Bulletin, **28**, 364 (1955).

TABLE I
CONDITIONS OF PREPARATION AND MOLE. RATIOS OF THE PRODUCTS

Sample	Reagent	Temp. (°C)	pH	Time of Adding	CaO/P_2O_5 Added	Mole. Ratios Products
SS-1	$Na_2HPO_4+CaCl_2$	65	7.2—8.0	3.5 hr.	3.00	3.08
SS-2	〃	60	6.8—7.6	〃	〃	2.95
SS-3	〃	50	6.2—6.8	〃	〃	2.69
SS-4	〃	65	〃	〃	〃	2.84
HSS	$CaCl_2+Na_2HPO_4$	70	7.6—8.2	〃	3.33	3.22
SA-2	$(NH_4)_2HPO_4+Ca(NO_3)_2$	65	7.0—7.6	2.5 hr.	3.00	3.04
SA-3	〃	60	〃	〃	〃	2.98
SA-4	〃	〃	6.8—7.4	〃	〃	2.95
SA-6	〃	45	7.4—7.8	〃	〃	2.91
SA-7	〃	25	〃	〃	〃	2.90
HSA-1	$Ca(NO_3)_2+(NH_4)_2HPO_4$	70	8.0—8.6	〃	3.33	3.33
HSA-2	〃	65	8.0—8.4	〃	〃	3.25
QS-1	$Ca(NO_3)_2+(NH_4)_2HPO_4$	20	10	5 sec.	3.00	3.11
QA-2	〃	25	8.2	〃	〃	2.87
QA-3	〃	〃	9.0	〃	〃	2.97
PQA-1	〃	〃	8.9	〃	〃	2.95
PQA-2	〃	〃	9.2	〃	〃	2.96

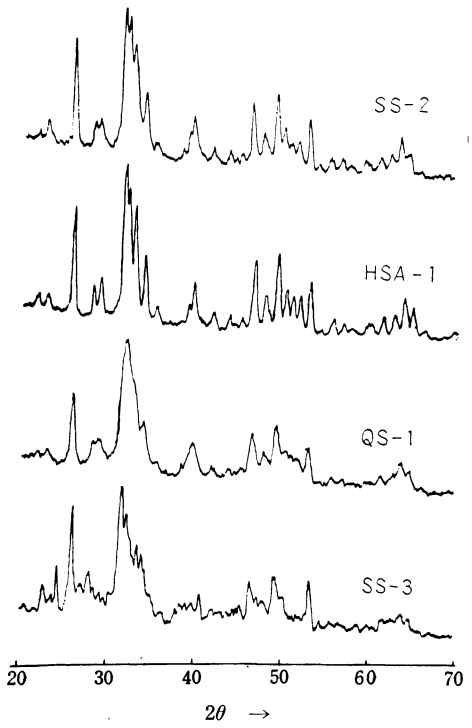

Fig. 1. X-ray diffraction patterns of the samples by Geiger-counter spectrometer. (Cu K_α, Ni Filter)

the while. Others (QS-1, QA-2 etc.) were prepared by quick addition of the reagents in order to obtain colloidal products. In this case, ammonia was added previously to the phosphate solution to adjust pH of the solution after the reaction. The amount of products, after being filtered, washed with water and then dried at 90°C, was 10—15 g., and the amount of the total solution was 1.5—2 liters for each preparation. These products were tested by electron microscope, X-ray diffraction and chemical analysis as shown in the Photographs, Fig. 1, and Table I.

Structure of both samples, SS-2 and QS-1, CaO/P_2O_5 ratio of which are 2.97 and 3.11 respectively, is the same as that of hydroxy apatite HSA-1 with the ratio 3.33, though the state of crystallization differs. Sample SS-3 with the ratio 2.69 consists of hydroxy apatite and dicalcium phosphate; the latter forms larger, thin crystals as shown in the photograph. These results confirm the modern view that tricalcium phosphate hydrate with a definite structure may not be formed but hydroxy apatite with excessive phosphoric acid may be formed.

(II) Variation by Heating—This precipitated apatite contains about 5% zeolitic water which is gradually evaporated by heating under 700°C. Then the hydroxy apatite with excessive phosphoric acid varies to form β-tricalcium phosphate between 700—800°C (Figs. 2 and 3) and solubility of the phosphate increases (Figs. 4 and 5). However, if the CaO/P_2O_5 ratio of the phosphate is slightly more than 3.0, a considerable amount of hydroxy apatite remains above 800°C, which gradually loses water of crystallization (OH) above 1100°C but scarcely ever decomposes even at 1450°C in air. Above 1500°C it is almost decomposed to form α-tricalcium phosphate

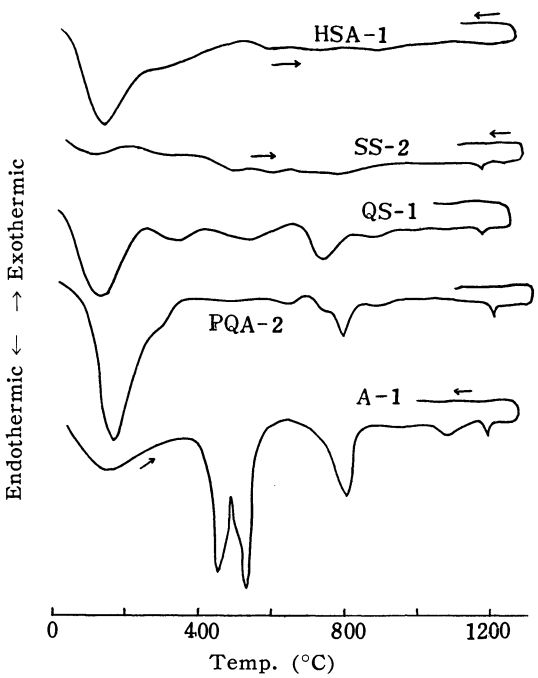

Fig. 2. Differential thermal analysis of phosphates.

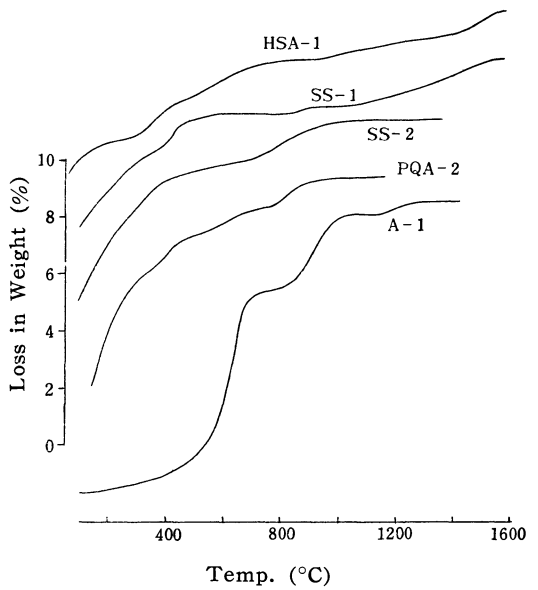

Fig. 3. Weight loss by heating.

and tetracalcium phosphate which are both soluble in citric acid. Calcined samples with CaO/P_2O_5 ratio less than 3.0 is mixed with pyrophosphate.

Sample A-1, prepared by adding phosphoric acid to refined lime by the ratio of 3 mol. CaO to 1 mol. P_2O_5, consists mainly of γ-pyrophosphate at 700°C, the ratio varies above 800°C on reaction with lime to form β-tricalcium phosphate (Figs. 2, 3, and 4). Then β-tricalcium phosphate thus formed inverts to α modification at 1180°C by endothermic reaction (Fig. 2). This inversion point coincides exactly with that described by Bredig[3]. α modification thus formed inverts to β modification slowly, by more than several hours heating at 1100°C. This $\alpha \rightarrow \beta$ inversion is somewhat promoted by the presence of a slight excess of P_2O_5.

On the other hand, β-tricalcium phosphate prepared with samples of Table I inverts to α modification not exactly at 1180°C but between 1160 and 1200°C, and moreover, inverts from α to β modification easily by slow cooling. It seems that these were caused by a small amount of impurity such as Na_2O or MgO derived from the reagents.

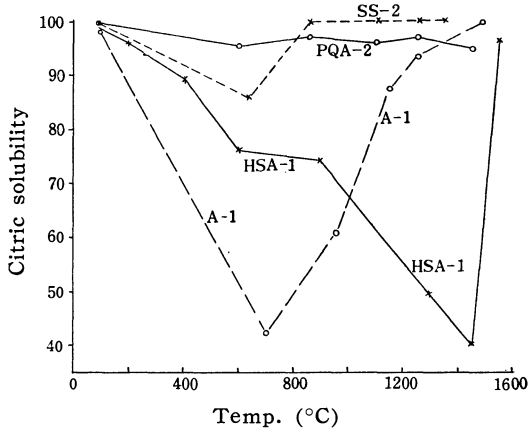

Fig. 4. Citric solubility of phosphates tested by the Japanese official method (150 ml. method).

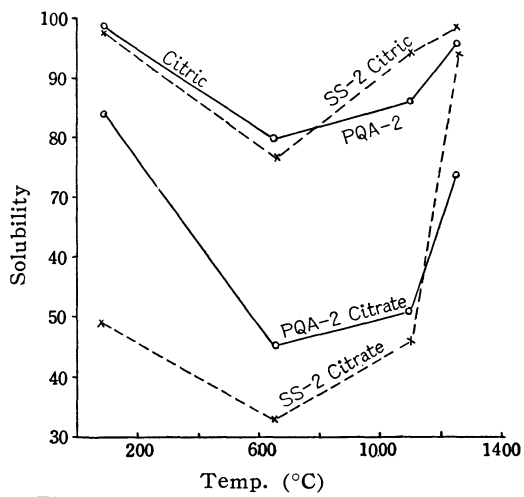

Fig. 5. Citric solubility by the 100 ml. method and citrate solubility by the American official method.

TABLE II

TYPE OF MODIFICATIONS OF TRICALCIUM PHOSPHATE COOLED QUICKLY IN AIR FROM VARIOUS TEMPERATURES (°C)

(C=CaO, P=P_2O_5, A=Al_2O_3, F=Fe_2O_3, M=MgO, B=BaO, N=Na_2O, S=SiO_2)

Samples	Chemical Composition (Mol. Ratios)	Type of Modifications			
		1100	1250	1350	1450
a	3C·P	β	α	α	α
b	3C·P·0.1A	β	β	β	$\alpha+\beta$
c	3C·P·0.1F	β	β	$\alpha+\beta$	α
d	2.9C·0.1M·P	β	β	β	β
e	2.7C·0.3M·P	β	β	β	β
f	2.9C·0.1B·P	$\alpha+\beta$	α	α	α
g	2.9C·0.1N·P	β	$\beta+\alpha$	$\beta+\alpha$	$\beta+\alpha$
h	2.8C·0.2N·P·0.1A	—	β	$\alpha+\beta$	—
i	2.7C·0.2N·0.1M·P	β	β	β	—
j	2.8C·0.2B·P·0.1A	—	$\alpha+\beta$	α	—
k	2.7C·0.2B·0.1M·P	β	$\beta+\alpha$	$\alpha+\beta$	—
l	a+0.35(2C·S)	—	—	α	α
m	b+0.35(2C·S)	—	—	α	—
n	d+0.35(2C.S)	—	—	$\alpha+\beta$	—

(III) Solubility of Phosphates—Solubility was tested by the Japanese official method (150 ml. method), [150 ml. of 2% citric acid for 1 g. of sample ground to pass 100 meshes/inch sieve; shaking for 1 hour (Fig. 4)], by an other method (100 ml. method) which is being practised in other countries, [100 ml. of 2% citric acid for 1 g. of sample ; shaking for half an hour], and also by the American official method with neutral ammonium citrate (Fig. 5).

It was found that hydroxy apatite could be dissolved in 2% citric acid to an extent of 1.1 g./100 ml. ultimately at room temperature, and tricalcium phosphate could be dissolved furthermore, so that citric solubility of these compounds was a matter of velocity of dissolution which relates to the grain size, the structure and the state of crystallization of the phosphates.

Precipitated hydroxy apatite HSA-1 is almost soluble in citric acid by the 100 ml. method because of its fineness, though citrate solubility is about 50%. Other samples with less lime are more soluble than the sample HSA-1.

Solubility of these phosphates decreases gradually by heating below 700°C. By this heating zeolitic water contained in the apatite lattice is lost and the distance between the lattice planes becomes slightly smaller.

Contrary to many other reports, it was found that β-tricalcium phosphate was fairly soluble in citric acid. Citric solubility of the phosphate with moderate grain size (mostly 120~40 μ) is 90~95% by the 150 ml. method and 80~90% by the 100 ml. method, and citrate solubility is about 40~50%. The solubility decreases when the phosphate contains a small amount of impurity as described below.

α-Tricalcium phosphate is completely soluble by the 150 ml. method and 95~100% soluble by the 100 ml. method. Though usually a small amount of insoluble residue remains in testing the citric solubility of the phosphate calcined at 1200~1500°C, the residue is not tricalcium phosphate but hydroxy apatite or pyrophosphate or β-tricalcium phosphate stabilized by a small amount of impurities.

Citrate solubility of α-tricalcium phosphate is much higher than that of β-tricalcium phosphate, but it does not reach 90% when the grains of the sample are not fine enough to pass 170 meshes/inch sieve (−88 μ).

(IV) Crystalline Solutions with other Ingredients — Phosphate rocks usually contain small amounts of silica, alumina, iron oxide, and sometimes magnesia. Moreover, in the manufacture of phosphate fertilizers, other materials are added to the phosphate rocks. So, it is thought that tricalcium phosphate in fertilizers is a crystalline solution with other ingredients. In order to clarify the effect of these ingredients upon the structure and the solubility of tricalcium phosphate, many samples with various compositions (Table 2) were prepared with calcium oxalate, phosphoric acid, hydroxides of alumina, iron and magnesium, sodium and barium carbonate and colloidal silica, all

of which were refined in the laboratory. These were first mixed like a paste, dried with frequent mixing, heated at 1000°C, ground to pass 100 meshes/inch sieve, and again heated in a platinum crucible for half an hour at various temperatures as indicated in Table II. Then the products, after being cooled quickly in air, were tested by X-ray diffraction and chemical analysis. Citric and citrate solubility were tested after the products were ground to pass 100 meshes/inch sieve again. Solubility of sample (a) in Table II calcined at 1100°C (β-tricalcium phosphate) was 93.2% by the 150 ml. method, 84.2% by the 100 ml. method, and 45.1% by the citrate method.

It was found that β-tricalcium phosphate was stabilized by the addition of small amounts of alumina, ferric oxide or magnesia. β-Tricalcium phosphate with alumina hardly ever inverts to α modification at 1250°C, moreover it is less soluble in citric acid and especially in citrate. At a higher temperature, α-modification is formed to some extent and the solubility becomes higher (Table II and Fig. 6).

The effect of ferric oxide to stabilize β modification diminishes at 1450°C. The effect of magnesia which substitutes for lime is most remarkable. Containing 0.1 mol. MgO, the distance between crystal planes of the β modification becomes apparently smaller, solubility decreases, and does not invert to α modification even at 1450°C.

On the contrary, it was found that barium, the larger cation, stabilizes α modification. Tricalcium phosphate with 0.1 mol. BaO (sample f) inverts from β to α modification at 1100°C. This temperature is 80°C lower than the inversion temperature of pure tricalcium phosphate.

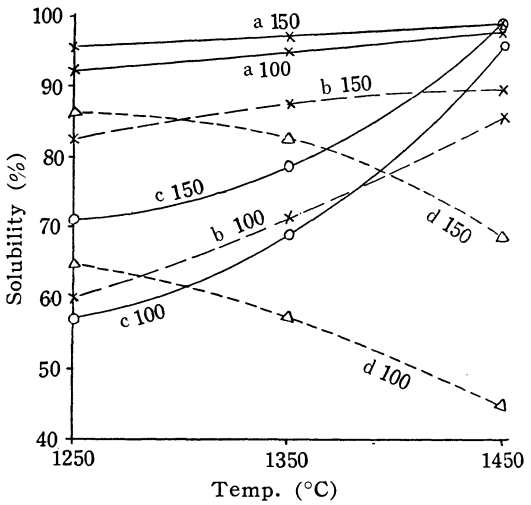

Fig. 6. Citric solubility of samples in Table II tested by 150 ml. and 100 ml. method.

Sodium oxide affects variously according to the ratio of substitution for lime. The inversion of tricalcium phosphate from α to β is so much quickened by replacing a small amount of Na_2O for CaO that α modification almost inverts to β modification even when quenched from a high temperature (Sample g). When more than 0.2 mol. of Na_2O to 1 mol. P_2O_5 is introduced into phosphate α-rhenanite type crystalline solution is formed.

By addition of small amounts of alumina, ferric oxide, magnesia, or silica, inversion of tricalcium phosphate from α to β is somewhat quickened.

Addition of 0.2 mol. Na_2O or BaO or 0.35 mol. $2CaO \cdot SiO_2$ to the tricalcium phosphate with alumina favors the formation of α modification (Samples h, j and m). Citric solubility of samples h, j and m calcined at 1350°C and air-quenched was 99.1%, 92.7%, and 98.5% respectively, by 150 ml. method showing considerable increase compared with the solubility of the sample b. The effect of magnesia to stabilize β modification is so intense that solubility of the phosphate with magnesia is hardly ever raised by adding these materials (Samples i, k and n).

Discussion

As is illustrated by the above results, magnesia reacts most remarkably to stabilize β modification of tricalcium phosphate and to depress the solubility. This explains why satisfactory results could not be obtained in the manufacture of calcined phosphate with a Swedish phosphate rock (with about 5% MgO)[6], and also why addition of serpentine to raw materials of calcined phosphate was unfavorable[7].

Alumina and iron oxide usually contained in phosphate rocks also react to prevent the formation of α-tricalcium phosphate. In calcined phosphate produced by calcining phosphate rock with silica in steam, the effect of alumina and iron oxide is not manifested very much, because excessive lime and silica react with

6) J. A. Hedvall, H. O. Gernandt and Y. Akesson, *Transactions of Chalmers Univ. of Tech.* Göteborg, Sweden, Nr. 100 (1950).

7) S. Nagai and J. Ando, *J. Chem. Soc. Japan, Ind. Chem. Sec.* (*Kogyo Kagaku Zassi*), **57**, 707 (1954).

these oxides to depress the effect. However, in calcined phosphate, produced by calcining phosphate rock with a small amount of phosphoric acid to promote defluorination, alumina and iron oxide affect remarkably to stabilize β modification, because excess of lime is combined with phosphoric acid to form tricalcium phosphate[8]. The phosphate obtained by such a method consists of β-tricalcium phosphate even when cooled quickly from 1350°C. The addition of a small amount of barium to the phosphate causes partial formation of α modification at 1300°C, but solubility of the phosphate is not easily raised because evaporation of fluorine in the phosphate is interrupted to some extent. Addition of 0.1 mol. Na_2O to 1 mol. P_2O_5 of the phosphate is unfavorable but more than 0.2 mol. of Na_2O favors the formation of soluble phosphate[8].

It is often said that tricalcium phosphate hydrate is formed in reverting superphosphate by adding ammonia or serpentine or by using other basic materials. However, as is illustrated by the above results, hydroxy apatite or fluor apatite must be formed instead of tricalcium phosphate. Under such conditions as in the reversion of superphosphate, the state of apatite thus formed is colloidal or crystalline. Such hydroxy apatite is almost entirely soluble in 2% citric acid and even fluor apatite can be dissolved in 2% citric acid to the extent of 0.5 g./100 cc.

8) J. Ando, ibid., **60**, 542 (1957).

Summary

Properties of tricalcium phosphate and effects of many other ingredients upon the structure and solubility of the phosphate were investigated. By the reaction of calcium salts with phosphates in aqueous solution, tricalcium phosphate hydrate with a definite structure is not formed but hydroxy apatite with an excess of phosphoric acid is formed, which varies to β-tricalcium phosphate by heating between 700—800°C. Contrary to many other reports, it was found that β-tricalcium phosphate was fairly soluble in citric acid. The solubility is reduced remarkably by a small amount of admixtures, especially of magnesia. Magnesia stabilizes the β modification and prevents $\beta \rightarrow \alpha$ inversion of the phosphate. The effect of alumina and ferric oxide is similar but not so intense as magnesia. On the contrary, barium oxide stabilizes the α modification. Sodium oxide affects variously according to the ratio of substitution for lime. Constitution and solubility of phosphate fertilizers were discussed in relation to these results.

Department of Industrial Chemistry
Faculty of Engineering
Chuo University
Bunkyo-ku, Tokyo

Phase Diagrams of $Ca_3(PO_4)_2$-$Mg_3(PO_4)_2$ and $Ca_3(PO_4)_2$-$CaNaPO_4$ Systems

By Jumpei ANDO

(Received September 24, 1957)

$Ca_3(PO_4)_2$-$Mg_3(PO_4)_2$ system is important for a fundamental study of fused phosphate fertilizers such as calcium magnesium phosphate (serpentine fused) or defluorinated tricalcium phosphate with magnesia. However little information is found in literature on phases of this system except in the case of tricalcium phosphate.

On the other hand, $Ca_3(PO_4)_2$—$CaNaPO_4$ system is important for the study on calcined phosphate fertilizer, especially on low-alkali phosphate as was produced in England under the name of silicophosphate or as has been produced in Japan for these several years. Among the phases of this system, $CaNaPO_4$ is well known as rhenanite which is a principal constituent of Rhenania phosphate in Germany, and the structure of a phosphate with a composition $Ca_4Na(PO_4)_3$ was stated by Klement[1].

1) R. Klement and F. Steckenreiter, *Z. anorg. allg. Chem.*, **245**, 236-243 (1940).

In the present work, phase systems were investigated systematically by means of differential thermal analysis, X-ray diffraction, microscopy and chemical analysis.

Experimental and Results

(I) $Ca_3(PO_4)_2$-$Mg_3(PO_4)_2$ System Samples were prepared by calcining or fusing the mixture of refined calcium oxalate, magnesium hydroxide and phosphoric acid, and were tested by thermal analysis in a small platinum vessel during fusion and cooling at a rate of 5°C/min.

Fig. 1 illustrates the results of thermal analysis. Within the range from 3 $CaO \cdot P_2O_5$ to 1.5 $CaO \cdot 1.5\,MgO \cdot P_2O_5$ tricalcium phosphate first crystallizes from the melt. In this range the liquidus temperature was not detected clearly by thermal analysis and was determined by quenching the melt from various temperatures and examining it with microscope and X-rays.

It was found that the phase diagram of this system was of peritectic type and that a new compound $Ca_3Mg_3(PO_4)_4$ was formed below 1175°C (Fig. 1, 2 and 4).

Samples with more than 1.5 mol. MgO to 1 mol. P_2O_5 consist of trimagnesium phosphate and $Ca_3Mg_3(PO_4)_4$. Even in samples with more than 1.5 mol. CaO to 1 mol. P_2O_5, formation of trimagnesium phosphate was detected by thermal analysis. This shows that the reaction of tricalcium phosphate and the melt to form $Ca_3Mg_3(PO_4)_4$ is not accomplished under such a cooling condition.

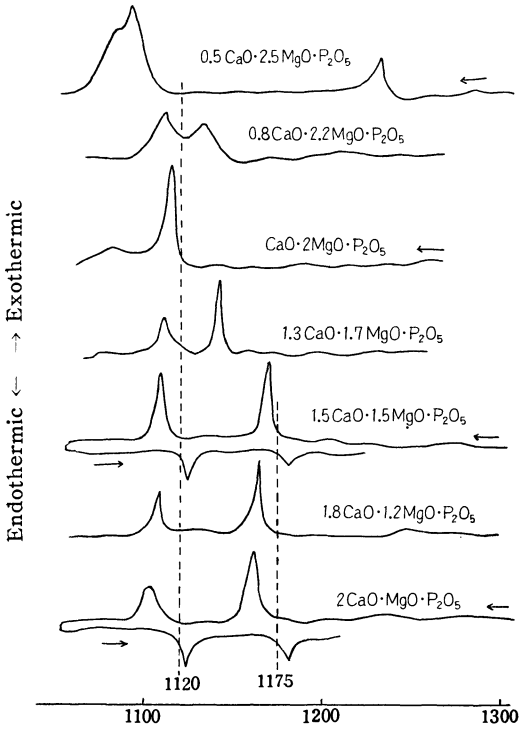

Fig. 1. Differential thermal analysis of samples.

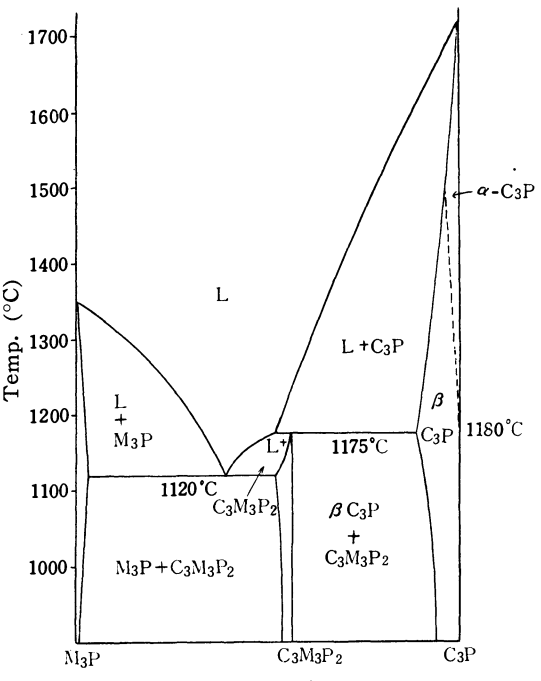

Fig. 2. Phase diagram [$C_3P = Ca_3(PO_4)_2$, $M_3P = Mg_3(PO_4)_2$, $C_3M_3P_2 = Ca_3Mg_3(PO)_4)_4$].

Fig. 3 illustrates the solubility of samples treated in various ways. Samples with the mark A were prepared by calcining at 1100°C. Samples with the mark B

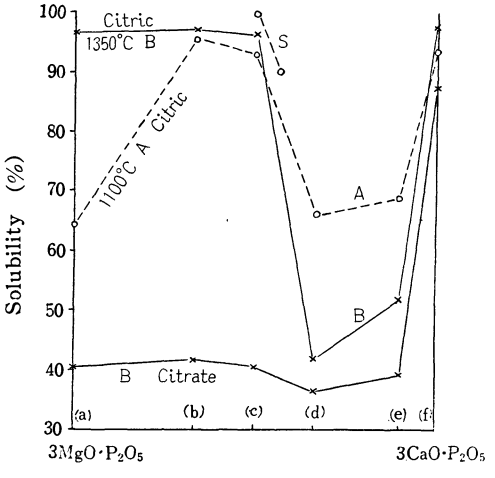

Fig. 3. Solubility of samples.

were heated in a platinum crucible at 1350°C and then cooled quickly in air. 'Citric' means the solubility tested by the Japanese official method, (150 ml. of 2% citric acid to 1 g. of sample pulverized to pass 100 meshes per inch sieve; shaking for an hour). 'Citrate' means the solubility tested by the American official method with neutral ammonium citrate solution.

Samples with less than 1 mol. MgO to 1 mol P_2O_5 consist mainly of tricalcium phosphate. By substitution of magnesia for lime β modification of tricalcium phosphate is stabilized. The distance between the crystal planes becomes smaller and the solubility of the phosphate is reduced remarkably.

The fused product with the composition of $1.5CaO \cdot 1.5MgO \cdot P_2O_5$ consists mostly of the compound $Ca_3Mg_3(PO_4)_4$; however as mentioned above, small amounts of unchanged β-tricalcium phosphate and trimagnesium phosphate are mixed. The melt of this sample was quenched, powdered and then sintered at 1140°C for 5 hours; thus pure $Ca_3Mg_3(PO_4)_4$ was obtained. Samples prepared by such a procedure are indicated in Fig. 3 by the mark S.

The compound $Ca_3Mg_3(PO_4)_4$ is completely soluble in citric acid by the Japanese official method. Citric solubility of the compound, tested by the method with 100 ml. of 2% citric acid for 1 g. of sample (shaking for half an hour), was 91%. However the compound is less soluble in citrate by the American official method. Also the sample with more magnesia is soluble in citric acid but less soluble in citrate.

X-ray diffraction pattern of $Ca_3Mg_3(PO_4)_4$ resembles that of α-tricalcium phosphate (Fig. 4 and Table I). Possibly these two compounds are isomorphous but can hardly form a crystalline solution with each other because of the difference of axial ratio.

Formation of trimagnesium phosphate was not accomplished by calcining the sample with the composition of $3MgO \cdot P_2O_5$ at 1100°C but a considerable amount of insoluble magnesium pyrophosphate was mixed. By fusing the sample at 1350°C pure trimagnesium phosphate was obtained. Also trimagnesium phosphate is soluble in citric acid but less soluble in citrate.

Fused trimagnesium phosphate with an excess of P_2O_5 is mixed with magnesium pyrophosphate, and the fused product with excessive magnesia is mixed with crystals of MgO.

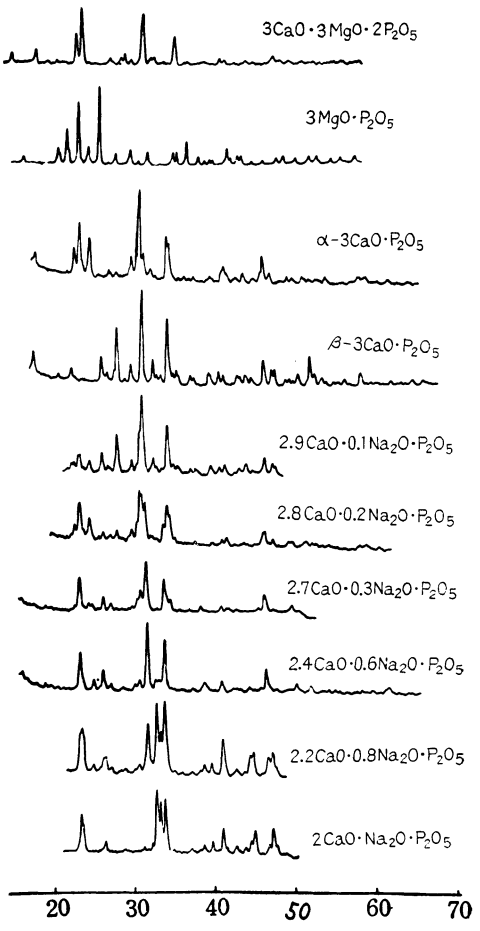

Fig. 4. X-ray diffraction patterns by Geiger-counter spectrometer. (Cu, Kα, Ni Filter)

(II) $Ca_3(PO_4)_2$-$CaNaPO_4$ Systems Samples of this system were prepared by calcining the mixture of refined calcium oxalate, sodium carbonate and phosphoric acid for half an hour at 1300°C. X-ray diffraction patterns of samples, cooled quickly in air after calcination, are shown in Fig. 4 and Table I.

$CaNaPO_4$ has β-rhenanite structure, low-temperature modification of rhenanite $CaNaPO_4$. Inversion of this compound from α (high temperature) to β modification occurs so quickly that α modification can not be obtained at room temperature even if the phosphate is cooled quickly from a high temperature as was described by Bredig[2]. Reversible $\alpha \rightleftarrows \beta$ inversion was observed at 660°C by thermal analysis. X-ray diffraction patterns of the sample $2.4CaO \cdot 0.6Na_2O \cdot P_2O_5$ coincides with that

2) M. A. Bredig, *J. Phys. Chem.*, **46**, 478 (1942).

TABLE I
RESULTS OF X-RAY ANALYSIS OF SAMPLES

$Ca_3Mg_3(PO_4)_4$		$Mg_3(PO_4)_2$		α-$Ca_3(PO_4)_2$		2.4 CaO·0.6 Na_2O·P_2O_5	
d	*I*	*d*	*I*	*d*	*I*	*d*	*I*
8.42	w w	5.61	w w	7.31	w w		
6.11	w w	4.35	w	5.18	w w	4.79	w w
5.01	w	4.12	m	4.02	m		
3.87	m	3.85	s	3.90	m s	3.90	m s
3.75	s	3.66	w	3.69	m	3.60	w
3.25	w w	3.45	s			3.44	m w
3.11	w w	3.20	w			3.31	w w
3.05	w	3.00	w	2.91	s	2.93	w
2.82	s	2.79	w	2.87	w	2.85	s
2.75	w w	2.54	w	2.63	m s	2.67	s
2.71	w w	2.50	w	2.60	m s		
2.51	m s	2.42	m	2.25	w w	2.32	w
2.17	w w	2.13	m w	2.17	m w	2.20	m w
2.14	w w	2.07	w	2.405	w	2.03	w w
2.02	w w	2.045	w	1.943	m	1.94	m
1.877	w	1.831	w	1.907	w	1.80	w
1.807	w w	1.725	w	1.821	w w		
1.629	w w	1.692	w	1.800	w w		
1.605	w w	1.563	w	1.759	w w	1.743	w
				1.670	w	1.490	w

of α modification of rhenanite tested by a high-temperature X-ray camera. Also the sample 2.6 CaO·0.4 Na_2O·P_2O_5 shows the same pattern. Samples with 0.3 or 0.2 mol. Na_2O consist of α-rhenanite and α-tricalcium phosphate. The sample with 0.8 mol. Na_2O consists of both α and β modification of rhenanite.

Thermal analysis of samples with 0.5~0.8 mol. Na_2O shows endothermic reaction on heating and exothermic reaction on cooling between 615~620°C, corresponding to the $\alpha \rightleftarrows \beta$ inversion of rhenanite. This illustrates the fact that by partial substitution of lime for Na_2O of rhenanite, high-temperature modification of rhenanite is stabilized and can easily be obtained at room temperature. The α-rhenanite type crystalline solution is most stable when nearly half of Na_2O is replaced by CaO. Inversion of these crystalline solutions is not reversible. By repeated cooling and heating of the sample, the inversion temperature detected by thermal analysis gradually approaches that of $CaNaPO_4$, the crystalline solution being decomposed to β-rhenanit and β-tricalcium phosphate. Samples with 0.2 or 0.3 mol. Na_2O do not show any distinct peak of reaction between 600~700°C. These samples are easily decomposed to β-tricalcium phosphate and β-rhenanite by slow cooling.

Thermal analysis of the sample with 0.1 mol. Na_2O gives distinct peaks of endothermic reaction on heating and exothermic reaction on cooling between 1130~1180°C. $\alpha \rightarrow \beta$ inversion of tricalcium phosphate is so much quickened by substituting a small amount of Na_2O for CaO that the phosphate almost inverts to β modification even if cooled quickly from high temperature.

Solubility of these samples is illustrated in Fig. 5. The sample with 0.1 mol. Na_2O is less soluble because this consists mainly of β-tricalcium phosphate. α-Rhenanite type crystalline solution is highly soluble in both citric acid and neutral ammonium citrate. The solubility is reduced when the crystalline solution is cooled slowly and decomposed to β-tricalcium phosphate and β-rhenanite.

The α-rhenanite type crystalline solution is furthermore stabilized by the addition of calcium orthosilicate. A sample with a composition of 2.9 CaO·0.1 Na_2O·P_2O_5+0.35 (2 CaO·SiO_2), calcined at 1350°C and cooled quickly, consists of a mixture of α-rhenanite, α-tricalcium phosphate and β-tricalcium phospate. A sample with a composition of 2.8 CaO·0.2 Na_2O·P_2O_5+0.35 (2CaO · SiO_2) treated in the same way consists of α-rhenanite type crystalline solution and a small amount of α-tricalcium phosphate.

However, the sample 2.8 CaO·0.2 Na_2O·

P_2O_5+0.7 (CaO·SiO) treated in the same way consists mainly of α-tricalcium phosphate, illustrating that Na_2O is combined

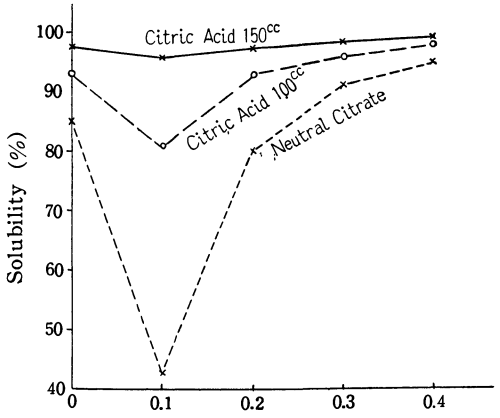

Fig. 5. Solubility of samples cooled quickly from 1300°C.

with excess of silica and does not react with calcium phosphate, so that in the manufacture of low-alkali calcined phosphate, addition of excessive silica must be avoided.

Discussion

Magnesia in fused phosphate fertilizers affects seriously the constitution and the solubility of the phosphate. In order to render the phosphate soluble, magnesia content in the phosphate which usually contains 20—30% of silica must be kept less than 5% so that the formation of α-tricalcium phosphate is not prevented; otherwise it must be kept around more than 12% so that the melting point of the phosphate is lowered and the phosphate can easily be rendered to a glass state by quenching with water[3].

In a usual fused phosphate fertilizer, the compound $Ca_3Mg_3(PO_4)_4$ is not easily formed because magnesia combines with silica to form Mg_2SiO_4, $MgSiO_3$ and $CaMg(SiO_3)_2$[4].

The compound $Ca_3Mg_3(PO_4)_4$ as well as the serpentine fused phosphate fertilizer is less soluble in neutral citrate or in Petermann's citrate, though these are highly soluble in citric acid. It seems that the low solubility of these phosphates in these citrate solutions is attributable to the low solubility of magnesium phosphate in neutral or alkaline solution with much ammonia. For testing the solubility of phosphate fertilizer with much magnesia neither the neutral nor the alkaline ammonium citrate method is suitable, but citric acid or acidic citrate method is preferable. On the other hand, calcium sodium phosphate is soluble in both citric acid and citrate. On the calcination of low-alkali phosphate fertilizer with 0.2—0.6 mol. Na_2O to 1 mol. P_2O_5, Na_2O reacts with phosphate rock to promote decomposition and defluorination of apatite, to depress the effect of alumina and iron oxide which stabilize β-tricalcium phosphate and to form a soluble crystalline solution of α-rhenanite structure.

Summary

The small amount of magnesia contained in tricalcium phosphate replacing lime stabilizes β modification of the phosphate. However, a new compound $Ca_3Mg_3(PO_4)_4$ is formed below 1175°C when more than 0.6 mol. of MgO to 1 mol. of P_2O_5 is introduced into the phosphate. This compound is soluble in citric acid but less soluble in neutral ammonium citrate similarly as is serpentine-fused phosphate fertilizer.

In $Ca_3(PO_4)_2$-$CaNaPO_4$ system, a crystalline solution with α-rhenanite structure is easily formed within the range of 2.6 CaO·0.4 Na_2O·P_2O_5—2.4 CaO·0.6 Na_2O·P_2O_5, and is furthermore stabilized by the admixture of calcium orthosilicate. This crystalline solution is highly soluble in both citric acid and citrate, composing a principal part of low-alkali calcined phosphate fertilizers.

Department of Industrial Chemistry
Faculty of Engineering
Chuo University
Bunkyo-ku, Tokyo

3) J. Ando, *J. Chem. Soc. Japan, Ind. Chem. Sect.* (*Kogyo Kagaku Zassi*) **59**, 1112 (1956).
4) J. Ando, ibid, **60**, 1101 (1957).

The Scattering of Beams of Alkali Atoms in Various Gases. I. Sodium and Argon

By Kumasaburo KODERA and Teijiro TAMURA

(Received November 7, 1957)

The collision between gaseous molecules is the fundamental process in various phenomena which occur in the gas phase. By means of the molecular beam, it is possible to observe directly the process, which enables us to evaluate the effective collision radii and to get information about the mutual interaction between the molecules.

When the atoms in a molecular beam are scattered by an atom which is at rest in the co-ordinate system, the scattering cross-section Q is expressed by

$$Q=2\pi\int_0^\pi I(\theta)\sin\theta\mathrm{d}\theta \qquad (1)$$

where $I(\theta)$ is the scattering intensity per unit solid angle of the beam atoms scattered through the angle θ from the direction of the incident beam. From the classical kinetic theory, it is easy to show, for a hard sphere model, that $I(\theta)$ is independent of θ and expressed as

$$I(\theta)=\frac{1}{4}\sigma^2, \qquad (2)$$

where σ is the sum of the radii of colliding molecules; hence Q is equal to $\pi\sigma^2$. On the other hand, from the quantum mechanical calculation for the hard sphere model, $I(\theta)$ is approximately given by the curve A in Fig. 1[1]. The curve shows that $I(\theta)$ becomes larger than the classical value when θ is smaller than $\theta_0=\pi/k\sigma$.

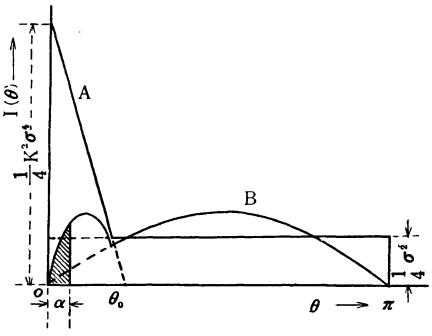

Fig. 1.

In this case, the collision cross-section given by equation (1) is equal to the area between the curve B and the abscissa multiplied by 2π, and therefore, is larger than the classical value. Q varies with $k\sigma$ in such a way that it becomes $2\pi\sigma^2$ when $k\sigma$ is very large, and approaches $4\pi\sigma^2$ when $k\sigma$ is zero. k is equal to $2\pi/\lambda$, where λ is the de Broglie wave length $\lambda=\hbar/\mu v_r$, $\mu=m_A m_G/(m_A+m_G)$ is the reduced mass, and v_r is the relative velocity of the colliding molecules.

Since in actual experiments, both the molecular beam and its detector have definite widths, e. g., α in Fig. 1, the atoms scattered inside this region, i. e., the shaded region, are counted as unscattered, hence giving smaller Q. To minimize this error the resolving power of the apparatus should be increased by making α much smaller than θ_0.

The existence of van der Waals' force should be considered between the actual molecules. In this case, the classical kinetic theory predicts also the marked increase of $I(\theta)$ in the region of small θ, and gives infinite cross-section Q. On the other hand, quantum mechanical treatment with molecules having intermolecular potential of the type

$$V(r)=-Cr^{-s} \qquad (3)$$

gives a finite $I(\theta)$ at θ equal to zero, provided that s is larger than 3, thus giving a finite Q. Therefore, it is necessary to make the widths of the beam and its detector small compared with θ_0. If it were not the case, i. e., if the resolving power of the apparatus were small, the measured cross-section and hence the collision radius would be too small. This can be ascertained from the values presented by several authors. For instance, Mais[2] with the apparatus which excludes the atoms scattered more than 4.5′, obtained the collision radius of 6.91 Å for potassium and helium, Rosin and Rabi[3] with the angle of exclusion 1.7′, gave the values

1) H. S. M. Massey and C. B. O. Mohr, *Proc. Roy. Soc.*, **A141**, 454 (1933).

2) W. H. Mais, *Phys. Rev.*, **45**, 773 (1933).

3) S. Rosin and I. I. Rabi, ibid., **48**, 373 (1935).

7.25 Å for the same pair and 7.18 Å for cesium and helium. Estermann, Foner and Stern[4] obtained the value 12.5 Å for cesium and helium by reducing the angle to 5′. Further, Jawstusch, Schuster and Jaeckel[5], using potassium beams, have shown that the collision radii increase markedly with the resolving power of the apparatus. Since in these instances angles of exclusion α were very small compared with θ_0, it was inferred that an appreciable interaction exists between colliding atoms, and the increase in $I(\theta)$ is greater than for hard spheres. Therefore, in order to measure the effective collision radii, it is essential to make the resolving power of the apparatus as great as possible, and the comparision of the values for various molecules should be done with the apparatus of the same dimensions.

In the works cited above, the collision radii of alkali atoms with, mainly, rare gases were measured to verify the quantum mechanical collision theory. One of the present authors[6] carried out the experiments with potassium beam and various gases including chlorine. In the experiments described below, the apparatus was improved and, in addition to simpler molecules, more complex ones were measured, giving information of chemical interest. In this report, the details of the apparatus and the result with sodium and argon will be mentioned.

Apparatus

The methods to measure the scattering of a molecular beam by gases are roughly classified into the following two. In the first method, the scattering gas is confined in a small region in the path of the beam, while in the second, the gas fills the whole region behind the collimating slit. The former method was employed by Rosin and Rabi, Estermann, Foner and Stern; the crossing beam method of Jawtusch, Schuster and Jaeckel can also be classified into this type. In this method, the angle of scattering of beam atoms and their angular distribution can definitely be determined; since the beam path in the scattering region is short, it is possible to make use of a high pressure, which makes the measurement easier and more accurate. On the other hand, the accuracy in the measurement of the length of the scattering region decreases and the effect of escaping gas molecules from the region increases.

Mais and one of the present authors employed the second method. Although the apparatus can be simplified by this method, the beam detector placed in the scattering gas detects atoms scattered in large angles from points directly in front of it, making the overall resolving power decrease. The determination of the pressure of scattering gas, in this case, is rather difficult because the pressure must be kept low to avoid multiple collisions. These points being considered, in the experiments described below, the first method was employed to raise the resolving power, but a rather large region of scattering gas was taken to facilitate precise determination of its length. The pressure of the scattering gas, which should be low in this case, was measured by a sensitive Pirani gauge calibrated carefully by a McLeod gauge.

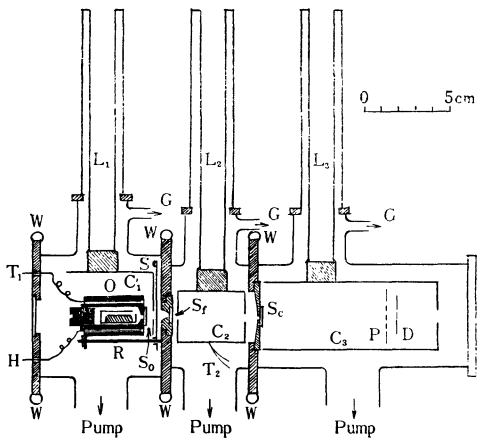

Fig. 2. Apparatus.
O, oven; S_o, oven slit; S_f, fore slit; S_e, collimating slit, S, shutter; D, detector; P, ion collector; T_1 T_2, thermocouples; H, heater; L_1 L_2 L_3, traps; C_1 C_2 C_3, cooling plates; G, to Pirani gauge; W, cooling water; R, supporting rod.

The vertical section of the apparatus is shown in Fig. 2. It consists of three chambers, i.e., the oven chamber I, the scattering gas chamber II and the detector chamber III. The source of the beam was the small oven O made of a single piece of nickel-chromium steel. It had six holes inside the side wall, in five of which were inserted tungsten heater filaments coated with alumina; the last hole contained a copper-constantan thermocouple. The junction was placed near the front wall of the oven to measure the temperature near the oven slit. The oven was joined by three thin iron rods R to the wall separating I and II. S shows a magnetically operated shutter to screen the beam. The beam path was surrounded by plates C_1, C_2 and C_3 which were cooled by liquid air or carbon dioxide snow contained in traps, L_1, L_2 and L_3, respectively. The temperature of C_2 was

4) J. Estermann, S. N. Foner and O. Stern, ibid., **71**, 250 (1949).
5) W. Jawstusch, G. Schuster and R. Jaeckel, *Z. Physik*, **141**, 146 (1955).
6) K. Kodera, *J. Chem. Soc. Japan, Pure Chem. Sect.*, (*Nippon Kagaku Zassi*), **65**, 645 (1944); **66**, 52 (1945); **67**, 80 (1946); N. Sasaki and K. Kodera, *Mem. Col. Science, Univ. Kyoto*, A, **25**, 83 (1949).

measured by a copper-constantan thermocouple T_2 fastened to it.

The beam was formed by an oven slit S_o, a fore slit S_f and a collimating slit S_c. The widths of the slits were 0.019 mm., 0.5 mm. and 0.015 mm., for the oven slit, fore slit and collimating slit, respectively; all of them were 3 mm. high and the fore slit had a thickness of 1.5 mm. to form a canal. The length of the beam was 1.55 cm. in the chamber I, 5.06 cm. in II of which 4.10 cm. was inside C_2, and 7.91 cm. in III. The beam atoms (sodium) were detected by a Langmuir Taylor surface ionization gauge[7], D, made of a tungsten filament of a diameter 0.016 mm. The filament could be moved across the beam from outside by a screw device. Sodium ions emitted from the filament were collected on a negatively charged plate P and measured by a Lindemann electrometer connected to it. The detector filament subtended an angle 2.0×10^{-4} radian $= 41''$ at the collimating slit. This angle was low compared with θ_0, which was estimated to be about 2° for sodium and argon under the experimental conditions.

The chambers I, II and III were separately evacuated by three Hickman oil diffusion pumps, which in turn were connected to a one stage mercury diffusion pump and then to a mechanical fore pump. The scattering gas was introduced into the chamber II from a reservoir through a glass capillary tube. The inlet of the gas was provided on the evacuation tube of the chamber II and during the introduction of the gas the pump was kept working. After the pressure in the chamber reached a stationary value, the measurements were carried out.

The sodium which was used was melted in vacuo to remove oxide coating, distilled three times and poured into a glass tube in high vacuum. Just before the experiment, it was cut into a suitable length and put into a stainless steel sheath and introduced into the oven; then, the apparatus was evacuated as fast as possible. Argon (99.9 %) was purchased on the market.

Experimental Procedure

As described above, it is necessary to measure the beam intensity in vacuo I_0 and the weakened intensity in the scattering gas I, along with the pressure and temperature. The experimental procedure was as follows:

The apparatus was evacuated until the McLeod gauge registered "sticking" for both the scattering and the detector chamber. The trap L_1 was cooled by a mixture of carbon dioxide snow and ethanol, L_2 and L_3 by liquid oxygen. The oven was heated to about 250°C by a constant current supplied through a current stabilizer. The detector was then traversed across the beam and its intensity distribution was measured to find the position of maximum intensity. All the measurements described below were carried out with the detector fixed at that position. The intensity in vacuo I_0 was measured, then the scattering gas, argon, was introduced into the scattering chamber. After the pressure of the gas reached the stationary value, the weakened intensity I and the pressure were measured. The vacuum intensity I_0 was measured again and this value was averaged with the former I_0 and taken as the beam intensity at the instant of measurement of I. These processes were repeated for different pressures of the scattering gas.

Since the pressure range was below about 10^{-4}mmHg, its precise measurement was rather difficult. The McLeod gauge could not be used as it showed a rather large margin of error in this pressure range. For this purpose, a Pirani gauge improved by Yoshida[8] was employed. Since the deflections of the gauge were linear with respect to the pressures below 2×10^{-2}mmHg, it was calibrated by the McLeod gauge at relatively high pressures where high precisions were expected. The sensitivity was tested every time after the measurement to confirm its constancy. It was found that in certain cases a slight change in sensitivity did occur at long intervals but not during the measurements.

The probability that a beam atom will pass 1 cm. through the scattering gas without collision is given by the equation,

$$P=\exp(-l/\lambda) \tag{3}$$

where λ is the mean free path of the atom. If the scattering gas were confined within the chamber II, and the temperature of the gas were homogeneous, then l would be equal to 5.06 cm. In practice, however, some of the scattering gas would flow out of the chamber through the slits S_f and S_c into the chambers I and III, respectively. Moreover, the temperature of the gas in II was low inside C_2 and high outside it. From the pressure and the widths of the slits, the flows could be assumed as molecular effusions. The collision of the beam atoms with the effusing molecules might be ignored, as the density of the effusing molecules just outside the slit is half that inside and decreases rapidly with the distance. But these effusing molecules, although they were evacuated continuously, produced certain stationary pressures in the chambers so that the scattering of the beam atoms could not be ignored. Taking into consideration these effects, equation (3) can be written as follows;

$$P=\exp\left\{-\left(\frac{l_1}{\lambda_1}+\frac{l}{\lambda}+\frac{l_2}{\lambda_2}+\frac{l_3}{\lambda_3}\right)\right\} \tag{4}$$

where λ and l are mean free path and beam length inside C_2, respectively, and λ_2 and l_2 those outside C_2 in the chamber II. Suffixes 1 and 3 show the corresponding values in the chamber I and III, respectively. When the distribution of the pressure and temperature for each chamber is assumed to be independent of the pressure introduced into II, the equation (4) can be rewritten by using an effective path length l_e, as follows:

7) J. B. Taylor, *Z. Physik*, **57**, 242 (1929).

8) S. Yoshida, *J. Chem. Soc. Japan, Pure Chem. Sect.*, (*Nippon Kagaku Zassi*), **63**, 383, 391, 520, 527 (1942).

$$P=\exp -l_e/\lambda \tag{5}$$

where l_e can be evaluated from the knowledge of the pressure and temperature distribution in each chamber. If the beam atoms experienced no multiple collision, P should be equal to I/I_0, where I_0 and I are the beam intensities in vacuo and with scattering gas, respectively. Then,

$$I/I_0=\exp -l_e/\lambda \tag{6}$$

Therefore,

$$\lambda=l_e/\ln(I_0/I) \tag{7}$$

From the λ obtained by Eq. (7) the collision radius can be calculated by the equation of Taits' mean free path[9], i. e.,

$$\left.\begin{aligned}\lambda&=\frac{2}{\pi^{1/2}\nu_G\sigma^2}\left(\frac{T_GM_A}{T_AM_G}\right)^2\\&\int_0^\infty\frac{x^5e^{-(T_GM_A/T_AM_G)x^2}dx}{\psi(x)}\\\psi(x)&=xe^{-x^2}+(2x^2+1)\int_0^\infty e^{-y^2}dy\end{aligned}\right\}\tag{8}$$

where ν_G is the number of scattering molecules per cc., T_A, T_G, M_A and M_G are the temperatures and molecular weights of beam atoms and scattering molecules. x is equal to v/α_G, in which v is the velocity of beam atoms and $\alpha_G=\sqrt{2RT_G/M_G}$, Numerical values of $\psi(x)$ have already been calculated by Rosin and Rabi.

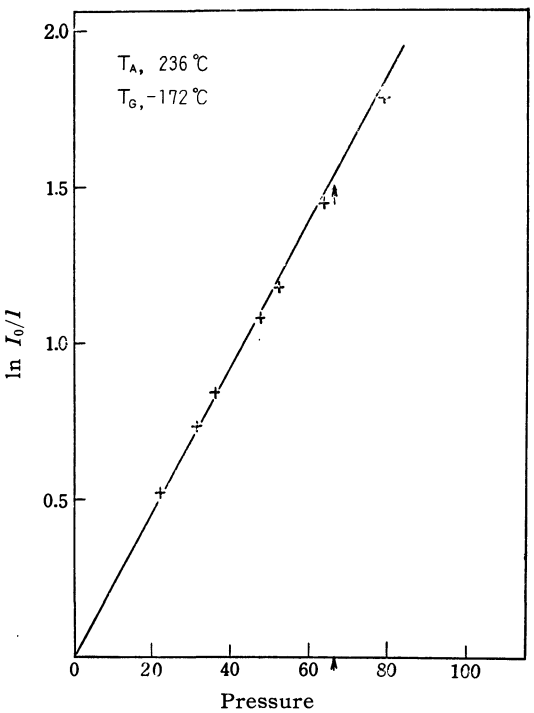

Fig. 3. Weakening of sodium beam scattered by argon.

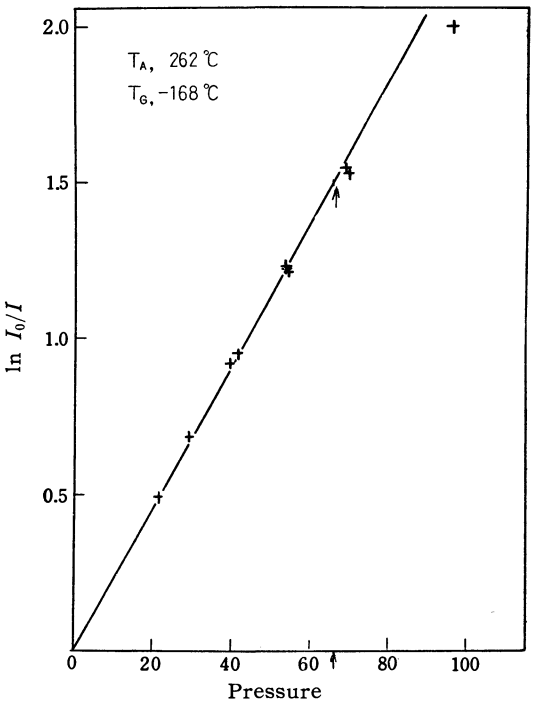

Fig. 4. Weakening of sodium beam scattered by argon.

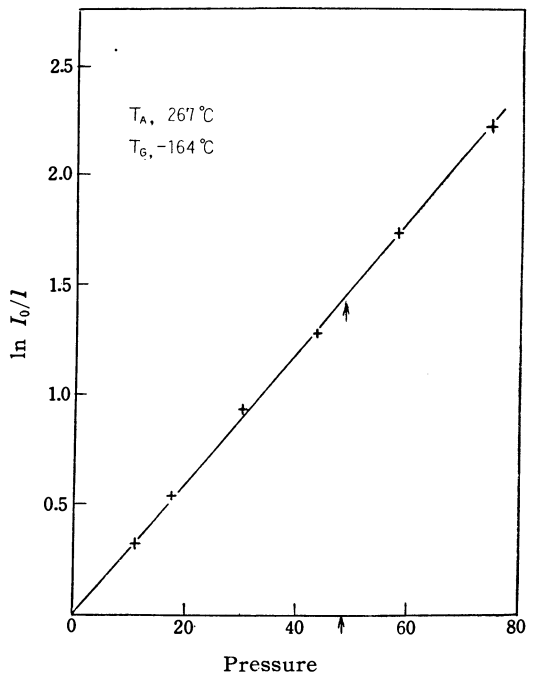

Fig. 5. Weakening of sodium beam scattered by argon.

It should be remarked here that the Pirani gauge was kept at 0°C but the temperature of the chamber whose pressure had to be known differed from 0°C, so that the effect of the thermal transpiration must be taken into account to evaluate the true pressure.

9) J. H. Jeans, "Dynamical Theory of Gases", Combridge, 4th ed. (1916) p. 255; N. F. Ramsey, "Molecular Beams", Oxford, (1956), p. 24.

Results

Three series of measurements were carried out on different days and the results are shown in Figs. 3, 4 and 5. In these figures the values of $\ln I_0/I$ are plotted against the pressure of the scattering gas. The pressure are shown by the readings of the Pirani gauge, and arrows in the figures show the pressure in the unit of 10^{-4}mmHg in the gauge. The plots coincide with straight lines below 10^{-4}mmHg, which show that Eq. (6) is satisfied in this pressure region. For higher pressures, trends are seen to deviate downwards from the straight lines; this fact may be explained by the multiple collisions experienced by the beam atoms.

The measured pressure distribution of the scattering gas in each chamber, collected with the thermal transpiration effect was as follows:

$$p : p_1 : p_3 = 1 : 0.34 : 0.013$$

where p, p_1 and p_3 represent the pressure in the chamber II, I and III, respectively. From these values, together with the temperature distribution in the scattering chamber and the beam length in each chamber, the effective beam length l_e was evaluated as 5.06 cm., i. e., the same value as the beam length in the scattering chamber. It means that the scattering in chambers I and III was compensated by its decrease in the low density region in chamber II outside C_2, where the temperature of the gas was higher than that inside of C_2.

Results calculated from Figs. 3 to 5 are listed in Table I. λ is the mean free path of the beam atoms when the Pirani gauge registered 10^{-4}mmHg. σ is the collision radius between sodium and argon.

TABLE I

COLLISION RADIUS BETWEEN SODIUM AND ARGON

T_A	T_G	λ	σ
236°C	−172°C	3.36 cm.	$12.4^7\times10^{-8}$ cm.
262	−168	3.36	$12.3^8\times10^{-8}$
267	−164	3.47	$12.3^6\times10^{-8}$
	average		12.4×10^{-8} cm.

Discussion

As mentioned above, the quantum mechanical theory for the collision of hard spheres without interaction predicts that $I(\theta)$ increases in the region of small θ; hence, when $k\sigma$ is large, cross-section Q assumes the value twice as great as the classical theory value, consequently σ becomes $\sqrt{2}$ times the classical value. When $k\sigma$ approaches zero, i.e., the relative velocity of colliding particles approaches zero, Q increases four times and σ twice the classical value. In the present experiment σ should be about $\sqrt{2}$ times that of classical theory. When the classical theory radius of argon is assumed to be 1.8×10^{-8}cm. as evaluated from the viscosity of the gas[10], and the radius of sodium in the gas phase to be 3.0×10^{-8}cm.*, the collision radius will be evaluated to be 4.8×10^{-8} cm. The measured value 12.4×10^{-8}cm. is 2.6 times as great as this value, thus much greater than the value given by multiplying 4.8×10^{-8}cm. by $\sqrt{2}$. This discrepancy can be ascribed to the presence of an appreciable van der Waals' force between the colliding particles.

The value 11.3×10^{-8}cm. presented by Rosin and Rabi for sodium and argon is slightly lower than the present value. The difference may be attributed to the smaller resolving power in the former case, i. e., 1.7′ in the former whereas 41″ in the latter. That is, the shaded area in Fig. 1 seems to be appreciable in these small regions of θ. This is also explained by the attractive force between coolliding particles.

The authors take this opportunity to thank Professor N. Sasaki of Kyoto University for permitting them to use the Lindemann electrometer in his laboratory.

Department of Chemistry, Faculty of Industrial Arts, Kyoto Technical University, Sakyo-ku, Kyoto

10) E. H. Kennard, "Kinetic Theory of Gases", McGraw-Hill, (1938), p. 149.

* This value is assumed by the similar consideration as Mais. See also Ref. 6.

Diamagnetism of Azeotropic Binary Liquid Mixtures

By K. VENKATESWARLU and S. SRIRAMAN

(Received October 29, 1957)

A large amount of work has been reported on the diamagnetism of organic liquid mixtures. Ranganathan[1] investigated the mixtures benzene-carbon tetrachloride, acetone-chloroform, acetone-water, and ethanol-water and found small deviations from additivity, the deviations being least in mixtures of two non-polar liquids. Molecular deformation by dipole-dipole interaction and compound formation was invoked to explain the deviation. Rao and his collaborators[2-6] studied a large number of mixtures of liquids having large electric moments and having molecules of different shapes and concluded that in the cases studied there were no variations from additive law. Kido[7] reported that in all the mixtures investigated by him there were no departures from the additive law. Broersma[8] from his study of a few organic liquid mixtures concluded that the departures from the additive law are not appreciable. The work of Farquharson[9] and Angus and Hill[10] suggests a method of explaining small deviations from additivity observed by some authors, on the basis of hydrogen bond formation.

Though a large amount of work has been done on the subject, the reports published so far regarding the behavior of such mixtures from the point of view of the additive law have not been unanimous. Probably more accurate data on a larger number of liquids may help to arrive at some definite conclusions. It was with this object the present investigations were undertaken. All the mixtures chosen for study are azeotropic mixtures. None of the previous workers have chosen binary mixtures from this point of view though a few mixtures studied might come under this category. The results obtained regarding the magnetic measurements in the case of the mixtures studied are reported in this paper.

1) Ranganathan, *Indian J. Physics*, **6**, 421 (1931).
2) Rao and Sivaramakrishnan, ibid., **6**, 509 (1932).
3) Rao, ibid., **8**, 483 (1934).
4) Rao and Varadachari, *Proc. Indian Acad. Sci.*, **1A**, 77 (1934).
5) Rao and Narayanaswamy, ibid., **9A**, 35 (1939).
6) Rao and Sriraman, *J. Annamalai Univ.*, **7**, 187 (1938).
7) Kido, *Sci. Rep. Tohoku Imp. Univ.*, **21**, 385 (1932).
8) Broersma, *J. Chem. Phys.*, **17**, 873 (1949).
9) Farquharson, *Trans. Faraday Soc.*, **32**, 219 (1933).
10) Angus and Hill, ibid., **36**, 923 (1940).

Experimental

Thorough purification of the liquids studied and the adoption of a magnetic method which could give reliable and consistant results were the chief guiding features of this investigation. The procedure adopted for the purification of the liquids was generally based upon Weissberger, 'Organic Solvents', Interscience, New York, 1956.

The determination of the specific susceptibility was made by a perfected form of Gouy method. The pole faces of the large PYE electromagnet used were 3 cm. in diameter and the air gap had a width of 1.2 cm.

Measurements were made with two ground glass stoppered tubes of slightly different cross-sections and at different field strengths ranging from 12 to 15 kilogauss. The experimental tube which was about 30 cm. long and 0.8 cm. in diameter was suspended from one arm of a sensitive balance and was arranged to be vertical with the liquid meniscus symmetrically situated between the pole faces. The field at the lower end of the liquid column was negligible. By a preliminary experiment the position of exact compensation for the glass tube was determined. Pure benzene was taken as the standard.

Assuming the influence of the vapor of the liquid to be negligible, the susceptibility values have been corrected for the residual air in the space above the liquid in the manner described by Rao and Narayanaswamy[5]. The refractive indices of the mixtures were measured with an Abbe refractometer made by Hilger's firm. The densities of the mixtures were found with a special type of stoppered specific gravity bottle.

Results

The mixtures were prepared by weight and due care was taken to minimise any possible change in concentration by evaporation. In Table I are given the values of the density, refractive index and specific susceptibility of the pure liquids and of the mixtures studied at various concentrations. The observed values of the density, refractive index, and magnetic susceptibility of the pure liquids are in good agreement with the previously

TABLE I

ρ, μ AND χ FOR THE PURE LIQUIDS AND MIXTURES

Component A	Component B	wt. % of A	$\rho_{4^\circ}^{32^\circ}$	μ	χ_1 Observed	χ_2 Calcd.	$\chi_2-\chi_1$
Ethanol	Benzene	100.0	0.782	1.3545	0.727		
		80.0	0.800	1.3810	0.721	0.722	+0.001
		60.0	0.813	1.4053	0.718	0.717	−0.001
		40.0	0.830	1.4330	0.712	0.712	0.000
		32.4	0.835	1.4431	0.711	0.710	−0.001
		20.0	0.845	1.4621	0.706	0.707	+0.001
		0.0	0.870	1.4925	0.702		
	Carbon tetrachloride	80.0	0.872	1.3610	0.667	0.669	+0.002
		60.0	0.980	1.3792	0.610	0.611	+0.001
		40.0	1.121	1.3923	0.553	0.552	−0.001
		20.0	1.311	1.4205	0.495	0.494	−0.001
		15.8	1.353	1.4263	0.481	0.482	+0.001
		0.0	1.577	1.4540	0.436		
	Ethyl acetate	80.0	0.800	1.3590	0.702	0.705	+0.003
		60.0	0.812	1.3609	0.677	0.683	+0.006
		40.0	0.838	1.3629	0.656	0.660	+0.004
		30.8	0.851	1.3638	0.648	0.650	+0.002
		20.0	0.863	1.3650	0.636	0.638	+0.002
		0.0	0.889	1.3777	0.616		
	n-propyl bromide	80.0	0.864	1.3668	0.687	0.688	+0.001
		60.0	0.940	1.3751	0.647	0.649	+0.002
		40.0	1.037	1.3889	0.610	0.611	+0.001
		20.5	1.147	1.4012	0.574	0.573	−0.001
		0.0	1.310	1.4257	0.533		
	Chloroform	80.0	0.880	1.3670	0.679	0.681	+0.002
		60.0	0.974	1.3788	0.634	0.635	+0.001
		40.0	1.095	1.3927	0.587	0.589	+0.002
		20.0	1.269	1.4142	0.544	0.543	−0.001
		7.0	1.393	1.4302	0.511	0.513	+0.002
		0.0	1.473	1.4393	0.497		
Methanol	Chloroform	100.0	0.791	1.3285	0.686		
		80.0	0.870	1.3386	0·648	0.648	0.000
		60.0	0.995	1.3505	0.609	0.610	+0.001
		40.0	1.097	1.3695	0.574	0.573	−0.001
		20.0	1.256	1.4042	0.533	0.535	+0.002
		12.6	1.325	1.4165	0.520	0.521	+0.001
		0.0	1.473	1.4393	0.497		
	Carbon tetrachloride	80.0	0.879	1.3340	0.637	0.636	−0.001
		60.0	0.982	1.3460	0.587	0.586	−0.001
		40.0	1.127	1.3790	0.534	0.536	+0.002
		20.6	1.304	1.4110	0.485	0.486	+0.001
		0.0	1.577	1.4540	0.436		
	Benzene	80.0	0.805	1.3475	0.688	0.689	+0.001
		60.0	0.820	1.3663	0.693	0.692	−0.001
		39.6	0.837	1.4215	0.695	0.696	+0.001
		20.0	0.854	1.4601	0.698	0.699	+0.001
		0.0	0.870	1.4945	0.702		

Component A	Component B	wt. % of A	$\rho_{4^\circ}^{32^\circ}$,	μ	χ_1 Observed	χ_2 Calcd.	$\chi_2-\chi_1$
Methanol	Acetone	80.0	0.789	1.3337	0.666	0.665	−0.001
		60.0	0.787	1.3394	0.643	0.644	+0.001
		40.0	0.785	1.3454	0.626	0.624	−0.002
		20.0	0.783	1.3509	0.602	0.603	+0.001
		12.1	0.783	1.3524	0.593	0.595	+0.002
		0.0	0.782	1.3534	0.582		
n-propanol	Acetal	100.0	0.797	1.3815	0.750		
		80.0	0.800	1.3811	0.739	0.738	−0.001
		60.0	0.807	1.3806	0.725	0.725	0.000
		37.0	0.813	1.3793	0.712	0.711	−0.001
		20.0	0.816	1.3781	0.702	0.700	−0.002
		0.0	0.819	1.3761	0.688		
	Toluene	80.0	0.812	1.4019	0.746	0.745	−0.001
		60.0	0.823	1.4218	0.739	0.740	+0.001
		52.5	0.827	1.4298	0.737	0.738	+0.001
		40.0	0.834	1.4440	0.734	0.735	+0.001
		20.0	0.847	1.4662	0.731	0.730	−0.001
		0.0	0.856	1.4908	0.725		
Acetic acid	Toluene	100.0	1.041	1.3648	0.525		
		80.0	0.990	1.3937	0.567	0.565	−0.002
		60.0	0.950	1.4171	0.603	0.605	+0.002
		40.0	0.914	1.4417	0.644	0.645	+0.001
		34.0	0.905	1.4491	0.656	0.657	+0.001
		20.0	0.885	1.4666	0.686	0.685	−0.001
		0.0	0.856	1.4908	0.725		
	Chlorobenzene	80.0	1.048	1.3951	0.542	0.544	+0.002
		58.5	1.054	1.4253	0.563	0.564	+0.001
		40.0	1.067	1.4530	0.583	0.581	−0.002
		20.0	1.081	1.4849	0.600	0.600	0.000
		0.0	1.099	1.5198	0.618		
	Ethylene bromide	80.0	1.157	1.3843	0.502	0.504	+0.002
		60.0	1.302	1.4038	0.484	0.484	0.000
		55.0	1.340	1.4092	0.478	0.479	+0.001
		40.0	1.495	1.4312	0.465	0.463	−0.002
		20.0	1.761	1.4700	0.442	0.443	+0.001
		0.0	2.157	1.5332	0.422		
Formic acid	Diethyl ketone	100.0	1.206	1.3686	0.435		
		80.0	1.092	1.3722	0.482	0.482	0.000
		60.0	1.003	1.3770	0.531	0.530	−0.001
		33.0	0.904	1.3830	0.596	0.595	−0.001
		20.0	0.865	1.3855	0.624	0.625	+0.001
		0.0	0.811	1.3887	0.672		
	Methyl *n*-propyl ketone	80.0	1.091	1.3720	0.484	0.482	−0.002
		60.0	1.003	1.3761	0.528	0.529	+0.001
		40.0	0.922	1.3808	0.578	0.577	−0.001
		32.0	0.892	1.3821	0.594	0.595	+0.001
		20.0	0.859	1.3842	0.623	0.624	+0.001
		0.0	0.800	1.3871	0.671		
Acetone	Chloroform	100.0	0.782	1.3534	0.582		
		80.0	0.864	1.3639	0.564	0.565	+0.001
		60.0	0.964	1.3764	0.547	0.548	+0.001
		40.0	1.089	1.3922	0.532	0.531	−0.001
		20.4	1.247	1.4124	0.514	0.514	0.000
		0.0	1.473	1.4393	0.497		

recorded values. In the case of mixtures the values of χ calculated on the basis of additive law are also given for comparison. The values of the azeotropic concentrations are underlined.

Discussion

All the mixtures with an alcohol as one of the components, except ethanol-ethyl acetate show practically little or no deviation from the additive law, with regard to magnetic susceptibilities. However, in all the cases departures from additive law were observed in their densities and refractive indices. The Raman spectra of ethanol benzene mixture have been studied by Cennamo and Vitale[11] and Sundara Rao[12]. The former authors found evidence of the existence of association in the mixture and the results of the latter indicated no such association. Ethanol-ethyl acetate and methanol-acetone mixtures are cases of two polar liquids for the mixtures. The magnetic data for ethanol-ethyl acetate mixture show slight departures from additive law. The observed χ values are lower than the additive values, the maximum deviation being nearly 1% at a concentration of 60% of alcohol. Ethyl acetate is an electron donor with a strong anionoid center C=O. When this is mixed with ethanol, the two types of molecules may associate through a hydrogen bond, lowering the anionoid power of C=O. The variation of χ from additive values might be due to the formation of hydrogen bonds between ethanol and ester molecules as represented below.

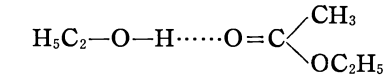

Murthy and Seshadri[13] found from Raman spectra of this mixture a diffuseness in the C=O frequency towards the shorter wavelength and they have taken this as evidence for the formation of hydrogen bonds as shown above.

The Raman spectra of methanol-acetone have been studied by Koteswaram[14], Joerges and Nikuradse[15] and Murthy and Seshadri[16]. From a study of the infrared spectra of this mixture Gordy[17] reported a shift of the C=O frequency of acetone. Koteswaram[14] observed a perceptible shift of C=O line at 1712 cm.$^{-1}$ towards shorter frequency. In 1:1 mixture, the C=O line was found to have a structure with two peaks. Also he reported a shift of C—C line towards higher frequency. These he attributed to the formation of association complexes. Joerges and Nikuradse[15] have also suggested the possibility of the formation of complexes by hydrogen bonding.

Acetone has a strong anionoid C=O center and hence it is normal to expect the formation of such complexes in this mixture. Any large change in the C=O bond strength will normally manifest itself in a susceptibility change. But the magnetic data do not show any such change from additive law. Murthy and Seshadri[16] studied the Raman spectra of this mixture but did not find any shift in the C=O line of acetone at 1710, thus indicating no evidence for the formation of hydrogen bonds. They distinguished between an ordinary hydrogen bond and a true hydrogen bond by postulating that a true hydrogen bond is one where both the cationoid and the anionoid center (OH and CO group) are affected. In the weaker type the OH group only will be affected. Quite possibly this mixture belongs to the case where the weaker type of hydrogen bond is formed and hence no deviation from additive law is observed.

The case of *n*-propanol acetal mixture is similar to methanol acetone mixture. Acetal has two anionoid centers. Because of this, one can expect the formation of associated complexes through a hydrogen bond. But the negative charge on the oxygen atom is very weak and the hydrogen bond that might be formed will consequently be weak. That this might be the case is evidenced by the magnetic data which show that the mixture obeys additive law.

The magnetic data of all the five mixtures having for one of their components a fatty acid, either acetic or formic, show fairly good agreement with additive values. Both acetic and formic acid are known to exist as associated molecules.

From a study of Raman spectra of some liquid mixtures Koteswaram[14] has observed that certain general changes might be expected when a fatty acid is mixed with a polar solvent. According to him the

11) Cennamo and Vitale, *Nuovo Cemento*, **13**, 465, (1936).
12) Sundara Rao, *J. Indian Chem. Soc.*, **22**, 260 (1945).
13) Murthy and Seshadri, *Proc. Indian Acad. Sci.*, **14A**, 593 (1941).
14) Koteswaram, *Indian J. Physics*, **14**, 341 (1940).
15) Joerges and Nikuradse, *Naturforsch*, **5A**, 25 (1950).
16) Murthy and Seshadri, *Proc. Indian Acad. Sci.*, **15A**, 154 (1942).
17) Gordy, *Phy. Rev.*, **50**, 1151 (1936).

changes expected are (i) breaking up of associated molecules into simpler ones and (ii) the formation of complexes between the solvent molecule and the monomeric molecule. Hence in such a mixture the possibilities are three fold.

1) The associated molecules are not affected by the presence of the solvent. If this is the case the magnetic susceptibility will be additive. 2) Depolymerisation may take place. This by itself will to some extent affect the susceptibility. 3) These simpler molecules may associate with the solvent molecules forming 'addition compounds'. This again may result in a change in the value in the reverse direction.

As all these five mixtures obey additive law, it might be inferred that the solvents used with these acids act merely as diluents without affecting the association in the acid molecules. If the association in the acid molecules is broken and the monomers form complexes with the solvent molecules, the two competing processes may compensate each other. But exact compensation is a remote possibility. Hence it may be taken that association between the acid molecules is not affected when the two acids are dissolved in the solvent used.

The acetone-chloroform mixture is of special interest. Its magnetic susceptibility, Raman spectrum and infrared spectrum have been studied by several workers. But the conclusions arrived at from these studies are not in agreement with one another. In view of the divergent views expressed regarding this mixture, the magnetic study has been repeated several times for each concentration. The data obtained show that the maximum departure from additive law is only about 0.2%. Even this small variation is not progressive. Hence the results may be taken to indicate that this mixture obeys additive law in conformity with the observations of Rao and his collaborators[2-4] and contrary to those made by Trifonov[18], Trew and Spencer[19], Buchner[20], Ranganathan[1] and Sibaiya and Venkataramiah[21].

Gordy[22] from a study of infrared spectra of this mixture has reported a shift of C=O absorption towards longer frequency in chloroform solution. A new absorption frequency at $4\mu(\Delta\nu=2500)$ was found and is attributed to a hydrogen bond between oxygen in C=O and hydrogen in C—H in chloroform as represented below.

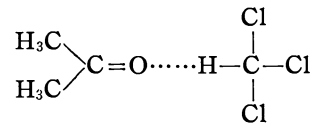

This he claimed[23] to be the first discovery of the direct spectrum of the hydrogen bond, all other evidences being indirectly based upon the changes in frequency.

Koteswaram[14] studied the Raman spectra of this mixture and found that even prolonged exposures did not give any trace of a line or band at $\Delta\nu=2500$. Even assuming that the band excited by the hydrogen bond is only infrared active, there must be a pronounced effect on the C=O frequency in acetone. No such effect was observed.

Murty and Seshadri[16] found no shift or diffuseness in the C=O line either. In the case of methanol-acetone and chloroform-acetone mixtures they found that the C=O frequency is not affected. If hydrogen bond existed, it should only be a weak one which could not affect the C=O group. If this group is affected, then it would produce a change from additivity. But these mixtures obey additive low. Hence in these mixtures either no hydrogen bonds are formed or the hydrogen bonds formed are so weak that the C=O group is not affected.

Though azeotropic mixtures have been specially chosen for this investigation, it has been found that the magnetic data in general seem to be unaffected even at the azeotropic concentrations. Hence any peculiarity that might be characteristic of the mixtures at the azeotropic concentrations could not be detected by the magnetic investigations.

From the present study and from previous literatures available, it may be concluded that, in general, binary organic liquid mixtures obey very closely additive law unless the bonds linked to the carbon atoms are affected.

Summary

An exhaustive study of the diamagnetic susceptibilities of the two types of azeotropic binary mixtures has been made

18) Trifonov, *Ins. Anal, Physico-Chem. Leningrad*, **3**, 434 (1925).
19) Trew and Spencer, *Proc. Roy. Soc.*, **131A**, 209 (1931).
20) Buchner, *Z. Physik*, **72**, 344 (1931).
21) Sibaiya and Venkatramiah, *Indian J. Physics*, **7**, 393 (1932).
22) Gordy, *J. Am. Chem. Soc.*, **60**, 605 (1938).
23) Gordy, *Nature*, **142**, 831 (1938).

with a view to find out any correlation between the magnetic data and the azeotropic behavior of the mixtures. The results obtained in the case of seventeen mixtures show that in almost all the cases additive law is obeyed even at the azeotropic concentrations. The small deviation from additivity observed in the case of ethanol-ethyl acetate mixture is explained on the basis of the formation of hydrogen bonds. The magnetic data are not affected by the azeotropic nature of the mixtures.

Department of Physics, Annamalai University, Annamalainagar South India

Activation Analysis of Manganese in Ferromanganese Alloy Using Radium-Beryllium Neutron Source

By Yuzuru KUSAKA

(Received April 26, 1957)

The method of analysis using slow neutron activation was early suggested by Hevesy and Levi[1], who used a 200 to 300 mc radium-emanation beryllium source in their determination of certain rare-earth elements possessing high neutron activation cross sections. More recently Boyd etc.[2] have reviewed the principles of radioactivation analysis, and a large number of papers have been published on their applications to various problems.

In 1953 Meinke and Anderson[3] explored the possibility of using low level neutron sources, 25 mg. radium-beryllium source, for activation analysis of rhodium, silver and indium.

The thermal neutron activation with a low-level neutron source has one major advantage over activation with higher sources; only those isotopes with a very high activation cross section and a short half-life are detected after a short irradiation. The profusion of neutron-induced activity obtained when a mixture of elements is irradiated in a nuclear reactor is eliminated. Thus it is possible to perform activation analysis without subsequent chemical separation; therefore analysis for favorable elements can be completed rapidly. Morever the amount of activity formed in the irradiation is so small and decays out so rapidly that the sample used for the irradiations is unchanged at the end of the analysis.

Recently, the writer reported the fundamental studies on activation analysis of manganese[4]. This paper describes some results of activation analysis of manganese in ferromanganese alloy using a low-level neutron source, 50 mg. radium-beryllium with a thermal neutron flux of about 10^2 —10^3 neutrons/cm^2/sec.

Nuclear Data for the Elements under Consideration

The radioactive isotopes and other nuclear data for the elements considered in this work are listed in Table I[5].

From Table I, one can expect that, an irradiation of eighteen hours will practically lead to the saturation activity of ^{56}Mn, whereas the activities of ^{55}Fe and ^{59}Fe will be negligible owing to their long half-lives, small cross sections and low abundance.

Experimental

The activation source consisted of a mixture of 84.2 mg. of radium bromide (49.3 mg. as radium element) with beryllium, which was sealed in a platinum tube, length 40.0 mm., diameter 5.0 mm., wall-thickness 0.5 mm., and certificated by the State Radiological Institute of the Czchoslovak Republic in 1938. The source was surrounded by paraffin to moderate the fast neutrons to thermal velocities. At the distance of 3.0 cm. around of the source, eight samples were arranged in the paraffin block of a 26.5×24.0×24.0 cm. cube; and the weight of each sample was 6.000 g. of granular powders (being sifted through a 100 mesh screen), which were put in the polyethylene tubes (inner diameter : 0.8 cm.,

1) G. V. Hevesy and H. Levi, *Kgl. Danske Videnskab. Math-Fys. Medd.*, **14**, 5 (1936); **15**, 11 (1938).
2) G. E. Boyd, *Anal. Chem.*, **21**, 335 (1949); J. V. Jakovlev, International Conference on Peaceful Uses of Atomic Energy, Geneva, Paper 632 (1955); A. A. Smales, ibid., Paper 770 (1955); M. P. Lévêque, ibid., paper 342 (1955): N. Saito, *Japan Analyst (Bunseki Kagaku)*, **4**, 254 (1955).
3) W. W. Meinke and R. E. Anderson, *Anal. Chem.*, **25**, 778 (1953).
4) Y. Kusaka., Radioisotopes, **6**, 1 (1957), (In Japanese).

height: 5.4 cm.) with cork stoppers. The standard samples were prepared by mixing metallic iron and manganese powders in an appropriate ratio.

The irradiated time was about eighteen hours. After irradiation, the specimens and the standards were spread into the copper counting cup (diameter: 2.9 cm., height: 0.6 cm.) and their induced radioactivities were directly measured for 5 minutes by means of an end window type G. M. tube (thickness of mica window: 1.96 mg./cm^2) in the same geometrical position. These measured values of radio-activity were corrected to the value at the end of the irradiation. A comparision of the activity of the unknown and the standard makes possible an estimate of the amount of manganese in the unknown sample.

Results and Discussion

Induced Radioactivity.—An example of the decay curve of the induced radioactivity of the ferromanganese sample (Mn content: 80.1%) is shown in Fig. 1. The measured value of half-life was 2.6 hours, being in good agreement with that of ^{56}Mn. The same results were obtained in every sample. From these results, it was recongnized that in those experiments all induced radioactivities were due to ^{56}Mn only.

Self-shadowing Effect for Neutrons.—The radioactivity strength produced by this method were approximately proportional to the manganese content in the samples. Concerning the specific activity of the samples of a higher manganese content, a significant decreasing effect was recognized, to a greater extent for 6 g. of the sample than for 1 g. of the sample, as shown in Fig. 2.

This phenomenon will be based upon the self-shadowing effect for the neutrons used for activation of manganese. The

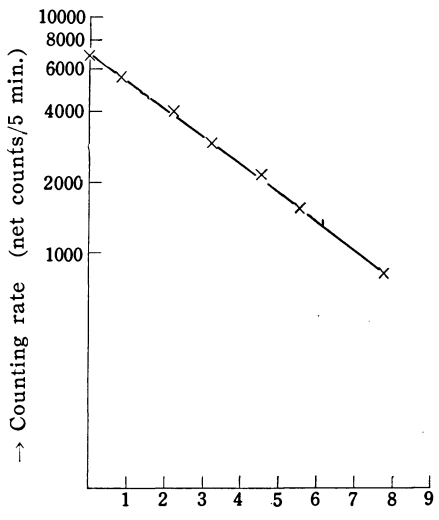

Fig. 1. Decay curve of irradiated ferromanganese.

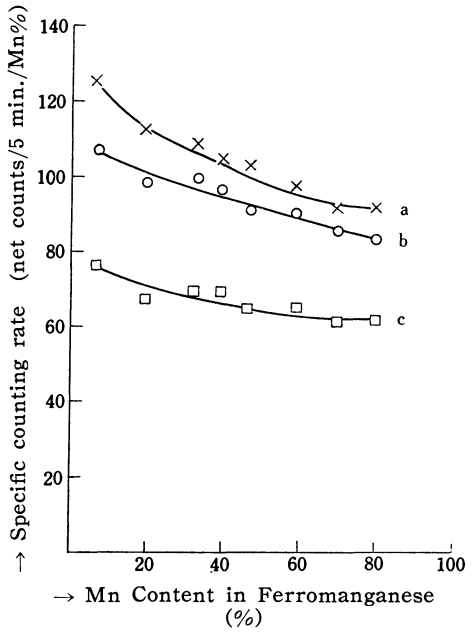

Fig. 2. Specific counting rate formed as a function of Mn content of ferromanganese.
(a)……sample weights 6 g.
(b)……sample weights 3 g.
(c)……sample weights 1 g.

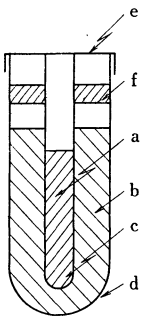

Fig. 3. Irradiation sample for self-shadowing experiments.
(a): manganese powder (2 g.)
(b): ferromanganese powder (15 g.)
(c): glass tube (inner diameter: 0.5 cm., thickness: 0.1 cm, height: 5.0 cm.)
(d): polyethylene tube (inner diameter: 1.7 cm., thickness: 0.1 cm., height: 5.4 cm.)
(e): polyethylene cup
(f): cork stopper

5) D. J. Hughes and J. A. Harvey, "Neutron Cross Sections", BNL 325 (1955).

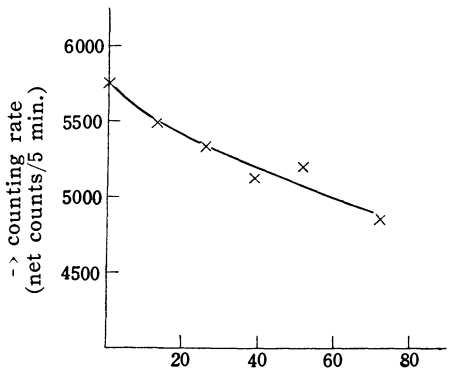

Fig. 4. Radioactivity formed in manganese powders.

manganese atoms in the samples did not encounter identical neutron flux during the irradiation, —that is, the flux for the inner part of the sample may be entirely different from that for the skin of the specimen. The next experiment was designed to investigate the flux depression caused by increasing manganese content. Two grams of manganese powder and 15 g. of ferromanganese powder of various manganese contents were separately put in a polyethylene tube as shown in Fig. 3 and irradiated in the paraffin block, at a distance of 3.0 cm. from the source. After irrradiation under the same condition, the radioactivity induced in 2 g. manganese powder was measured. In Fig. 4 the radioactivity strength was plotted against the content of manganese in ferromanganese.

Fig. 4 shows that under the experimental conditions the flux at the center of the 80% ferromanganese is about 0.85 of the flux without manganese and with iron.

Radioactivation Analysis of Manganese in Ferromanganese.—Manganese content of ferromanganese alloy is in 70—80% as manganese metal. In this region of

TABLE I

NUCLEAR CHARACTERISTICS OF THE ELEMENTS DETERMINED

Element	Isotope	Abundance (%)	Thermal Neutron Cross Section (barn) σ abs.	σ act.	Radioactive Nuclide Formed	Half -life	Radiations (Energy, Mev)
Mn	^{55}Mn	100	13.2 ±0.4	13.4±0.3	^{56}Mn	2.58 hr.	β^-(2.81), γ
Fe			2.53±0.06				
	^{54}Fe	5.84	2.2 ±0.2	2.2±0.5	^{55}Fe	3.0 yr.	k
	^{56}Fe	91.68	2.6 ±0.2				
	^{57}Fe	2.17	2.4 ±0.2				
	^{58}Fe	0.31	2.5 ±2.0	0.9±0.2	^{59}Fe	45.1 d	β^-(0.46), γ

TABLE II

ONE EXAMPLE OF EXPERIMENTAL RESULTS

Sample	Mn Content (%)	Measurment Time* (minutes)	Counting rate (net counts/5 min.) Obtained	St. Dev. (%)	Activity at the end of irradiation	Mean
ferromanganese	unknown	43— 48	5013	1.4	6157	6137
		67— 72	4484	1.5	6117	
ferromanganese	unknown	19— 24	5624	1.3	6193	6136
		92— 97	3982	1.6	6079	
standard	78.7	7— 12	6301	1.3	6577	6240
		105—110	3648	1.8	5903	
standard	78.7	31— 36	5497	1.3	6384	6331
		80— 85	4338	1.5	6278	
standard	73.8	37— 42	5046	1.4	6036	5983
		73— 78	4228	1.5	5930	
standard	73.8	25— 30	5171	1.4	5850	5874
		86— 91	3970	1.6	5899	
standard	68.9	13— 18	5383	1.4	5770	5576
		98—103	3434	1.7	5382	
standard	68.9	49— 54	4395	1.5	5535	5519
		61— 66	4144	1.5	5503	

* The time after the end of irradiation.

TABLE III

EXPERIMENTAL RESULTS OF MANGANESE ANALYSIS IN FERROMANGANESE

Exp. No.	Manganese Content (%) Radioactivation Method						Mean	Chemical Method
1.	78.4	78.1	76.1	77·9	77.8		77.7	77.4
2.	76.6	76.6	74.6	74.2	79.5	76.6	76.5	78.7
	77.1	77.8	77.3	76.7	74.0			
3.	74.0	74.6	78.0	76.3			75.7	78.2
4.	75.0	75.3	77.3	71.1	73.2	72.3	74.0	77.1

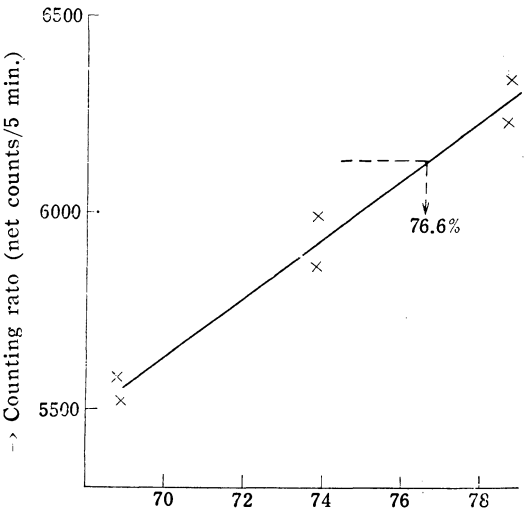

Fig. 5. Calibration curve in radioactivation analysis of Mn in ferromanganese.

manganese content, within experimental error it is possible to assume that the specific counting rate has a definite value. In these experiments, the manganese contents of the standard samples were 68.9%, 73.8% and 78.7%. A pair of samples, one a standard sample and the other, an unknown sample, were irradiated at the same time. One example of experimental results is shown in Table II.

From Table II, the manganese content of an unknown sample was graphically determined as shown in Fig. 5.

The experimental results of manganese analysis in various ferromanganese alloys by this method and comparison with the chemical analysis by the bismuthate method[6] are summarized in Table III.

Summary

A method was developed to determine macro-amounts of manganese in ferromanganese by radioactivation, using 50 mg. radium - beryllium as thermal neutron source. By activation of a sample (6 g.) for 18 hours and directly counting the activity with an end-window G. M. counter, the induced radioactivity was found to be entirely due to the 154.8 min. ^{56}Mn radioisotope. The amount of radioactivity was approximately proportional to the manganese content, but with samples of higher manganese content the self-shadowing phenomenon was recognized. By this method, it was possible to determine the manganese content in ferromanganese with a mean error of 2.5% without chemical procedures.

The writer wishes to express his hearty thanks to President Bunsaku Arakatsu and other members of the Chemical and Physical Laboratory of Konan University and to Professor Masayoshi Ishibashi of Kyoto University for their kind guidance and valuable advice through this study, and to Itsuo Araki of Kobe Seiko Co. for furnishing samples. A part of the expense for this study was defrayed from the Scientific Research Grant from the Ministry of Education, to which the author's thanks are due.

Department of Chemistry, Faculty of Science, Konan University
Higashinada-ku, Kobe

6) Treadwell-Hall, "Analytical Chemistry", Vol. II, p. 551 (ninth edition).

*The Electrolytic Separation Factor of Hydrogen Isotopes on Metal Electrodes**

By Yōichi TAKAHASHI, Shumpei OKA and Mitsuru OIKAWA

(Received October 10, 1957)

The electrolytic separation factor of hydrogen isotopes (α) usually represents the ratio between the evolution velocities of light hydrogen and heavy hydrogen under the same condition, viz;

$$\alpha = d\frac{(H/D)\ gas}{(H/D)\ liq.}$$

So we can get a competent side view for the study of the hydrogen evolution reaction from the measurement of α.

Some investigations were done previously on the problems of how α depends upon the sort of electrode materials, current density and other conditions. According to Horiuti and Okamoto[1], and Walton and Wolfenden[2], α does not vary much with the change of current density, but depends mainly upon the cathode materials. They pointed out that α of many metals were either about 3 or about 6, and that these two groups of α correspond respectively to two different hydrogen electrode mechanisms. Assuming that these two mechanisms exist, Horiuti, Okamoto and Hirota[3] calculated the values of α, and showed the correspondence between the measured value and the theoretical one.

On the other hand, however, these data are lacking in reproducibility. This poor reproducibility may be caused, firstly, by the difficulty in the micro-isotope analysis of hydrogen. Moreover, it is considered that the electrode process of hydrogen evolution reaction is very sensitive to changes of conditions, such as the state of electrode surface or of electrolyte.

Therefore, in order to discuss the mechanisms of hydrogen electrode reaction from the value of α, more extensive works are needed on the point of getting reproducible data. Rome and Hiskey[4] have investigated the separation factor on mercury cathode making use of a mass spectrometer for isotope analysis. Concurrently with Rome and Hiskey, the authors have investigated the separation factor on the various electrodes making use of mass spectrometer, and found some interesting facts about the electrolytic separation factor.

Experimental

Apparatus.—The apparatus used is illustrated in Fig. 1. The capacity of the cell was about 70 cc.

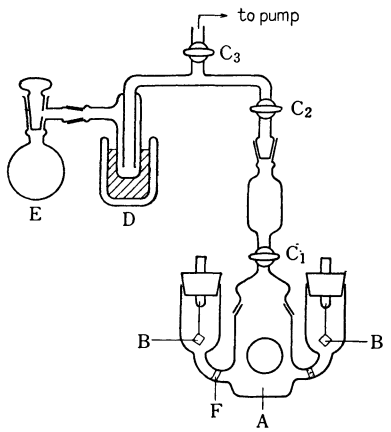

Fig. 1. Schematic diagram of the cell used.
A: Cell
B: Anode
C1, C2, C3: Stop cocks
D: Cold trap
E: Sample bulb
F: Sintered glass disc

As shown in Fig. 1, the cell was divided into three sections separated from each other by a pair of sintered glass discs. Attention was paid to avoid the contamination of electrolyte and electrode surfaces with tap grease.

The cathode part was inserted into the cathode compartment using a glass joint, for which no grease was used. As shown in Fig. 2, the cathode holder was specially devised so that

* Part of this paper was read at the discussion meeting of the Electrochemical Society of Japan on November 5, 1956.

1) Horiuti and Okamoto, *Sci. Pap. Inst. Phys. Chem. Res. Tokyo*, **28**, 231 (1936).

2) Walton and Wolfenden, *Trans. Faraday Soc.*, **34**, 436 (1938).

3) Horiuti, Okamoto and Hirota, *Sci. Pap. Inst. Phys. Chem. Res. Tokyo*, **29**, 223 (1936).

4) Rome and Hiskey, *J. Am. Chem. Soc.*, **76**, 5207 (1954).

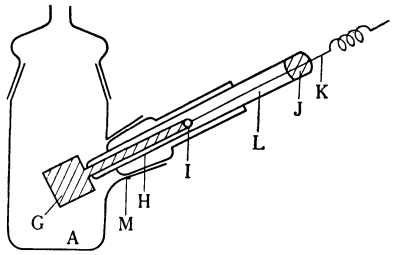

Fig. 2. The cathode and its setting device.

A: Cell	J: Paraffin
G: Cathode metal	K: Lead wire
H: Glass tube	L: Closed air
I: Solder	M: Glass joint

metal parts except cathode might not come into contact with electrolyte.

When mercury was used as the cathode it was put in a little glass vessel which was laid on the bottom of the cell; and a platinum-wire sealed in the glass tube, as in the cases of other cathode materials, was inserted into the mercury without coming into contact with the electrolyte. The surface area of the cathode was in all cases 2 cm^2.

Electrode and Solution—The separation factor was measured on such cathodes as platinum, gold, silver, nickel, iron, lead, copper, tin and mercury.

The mercury used was purified by electrolysis after distillation. The electrode plates were carefully polished, just before use, with emery paper and washed with distilled water. These electrodes were used repeatedly, being given the same treatment before each experiment. In the cases of iron, nickel, silver and tin, two specimens were used for each metal, but no difference was found between these specimens. The platinum electrode was cleaned, in some cases, by dipping it in concentrated hydrochloric acid at 100°C for an hour, and it was washed with distilled water.

The anodes, two small plates of platinum, had the total surface area of 2 cm^2.

The electrolyte of 0.2 N sulfuric acid solution was prepared from the re-distilled water containing as much deuterium as 0.2 atomic per cent. and guaranteed concentrated sulfuric acid. The solution was then purified by pre-electrolysis for about 15 hours at 0.5 mA/cm^2, and for an hour at 40 mA/cm^2.

Just before the experiment, tank-hydrogen was bubbled into the solution for an hour to saturate the solution with hydrogen and to remove dissolved air.

Procedure.—After setting the electrode to the cell, the hydrogen-saturated solution was poured into the anode compartment. Then it was sucked into the cathode compartment by evacuating this compartment through the cock 1 in Fig. 1.

The cathodic current density was 10 mA/cm^2. It was impossible to prevent entirely the oxygen, evolved by anode reaction, from coming through the glass discs into the cathode compartment, but according to Bockris[5], under such a high current density as in the present experiment, the depolarization effect of oxygen is so small as to be ignored.

The hydrogen gas evolved during the first 15 minutes, being contaminated with the pre-saturated tank-hydrogen, was purged by evacuation. Then, the hydrogen gas evolved during the next 30 minutes was introduced into the evacuated sample bulb, after drying the gas by passing it through a cold trap cooled with a mixture of solid-carbon dioxide and ethanol.

In order to measure the time variation of the value of α, sampling was performed every 30 or 15 minutes as mentioned above. The electrolytic current was never cut off during the run of an experiment. The hydrogen gas gathered in the sample bulb was then analysed on the mass spectrometer, the type of CEC 21—103 A.

For isotope analysis of the solution, the exchange equilibrium method[6] was used. The tank-hydrogen, led to the isotopical equilibrium with the solution at 25°C (equilibrium constant 3.87) by making use of Adams' catalyst for five hours, was analysed similarly on the mass spectrometer.

Results

The data of the electrolytic separation factor are shown in Table I. The values of the separation factor were derived from the following equation;

$$\alpha = 3.87 \frac{(D/H)_{evol.}}{(D/H)_{equil.}}$$

where the subscripts evol. and equil. designate the hydrogen evolved and the hydrogen equilibrated with the solution, respectively, and the factor 3.87 is the equilibrium constant of the following reaction

TABLE I

THE ELECTROLYTIC SEPARATION FACTOR OF HYDROGEN ISOTOPES ON SEVERAL METALS

0.2 N H_2SO_4 solution containing 0.2 atomic per cent. deuterium.

current density at 10 mA/cm^2

metal	α						average
Fe	6.7	6.9	6.6				6.7
Cu	7.0	6.9	7.1	5.2	5.4	6.4	6.3
Ni	5.7	5.5	6.7	5.4	4.9		5.6
Ag	4.6	4.2	4.6				4.5
Pt	4.4	4.8	4.4	4.3	4.4		4.5
Au	4.1	4.3	5.2	4.1			4.4
Pb	3.7	3.6					3.7
Hg	3.7	3.7	3.8				3.7
Sn	2.6	2.2					2.4

5) Bockris, *Chem. Rev.*, **43**, 547 (1948).

6) Kirshenbaum, "Physical Properties and Analysis of Heavy Water", (McGraw-Hill, 1951) p. 205.

$$(H_2O)_{liq.} + (HD)_{gas} \rightleftarrows (HDO)_{liq.} + (H_2)_{gas}$$

at 25°C.

The values listed above refer to the sample gas evolved during 30 minutes after purging initial gas evolved during first 15 minutes of electrolysis.

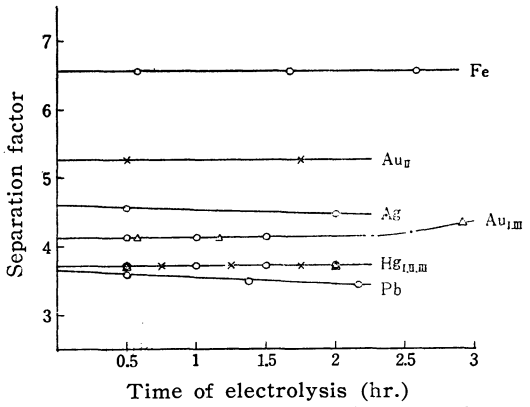

Fig. 3. Time variation of separation factors on several metal cathodes (I). ○, ×, △ designates 1st, 2nd and 3rd run, respectively, on the same metals.

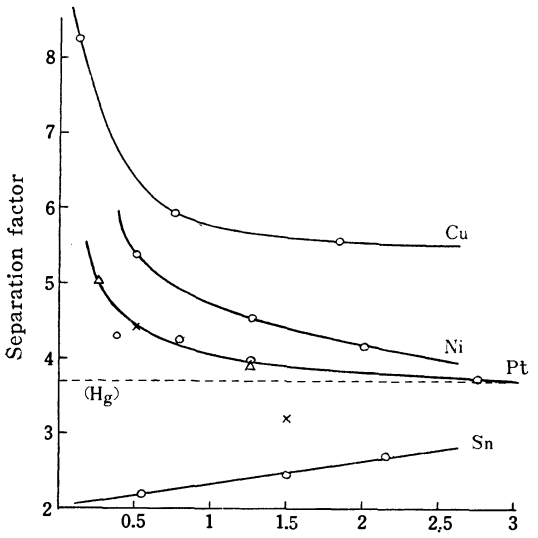

Fig. 4. Time variation of separation factors on several metal cathodes (II). ○, ×, △ designates 1st, 2nd and 3rd run, respectively, on platinum cathode. (Except platinum, typical curves are shown to avoid confusion.)

The time variation of α is shown in Fig. 3 and Fig. 4. In the cases of mercury, iron and gold, values of α were nearly constant in the lapse of time (Fig. 3). As to mercury, values of α obtained in three runs of the experiment coincided within the limit of experimental error, not only in an individual run, but also in all runs of the experiment. On the other hand, for platinum, nickel and copper α decreased with the duration of electrolysis. These decreasing curves of α were lacking in reproducibility, as shown in Fig. 4, but the three runs of the experiments on platinum showed undoubtedly the decrease of α with time. On the contrary, α on tin increased with time (Fig. 4).

Discussion

Time variation of separation factor.— Rome and Hiskey[7] found out that, on mercury cathode, the separation factor decreased markedly when the solution was contaminated with tap grease. Thus, if the cause of the time variation of separation factor in our experiment were imputed to the impurities in the solution, such as dissolved oxygen, tap grease etc., α on mercury, iron and gold must also vary with time. But the fact that not only on mercury but also on iron and gold, the separation factor did not vary with time indicates that the time variation of the separation factor on platinum, nickel etc. was not caused by the effect of impurities.

Apart from this, it may be considered that, since platinum, nickel and copper are all effective catalysts for hydrogen-exchange reaction[8], the secondary exchange reaction of evolved hydrogen gas with the solution may occur at the electrode surface, and as the result of this effect α approaches 3.87, the equilibrium value, with the lapse of time. But in this experiment, evolved hydrogen gas was taken into the sample bulb successively at the same intervals; hence, if decrease of α owes to the secondary exchange reaction, the catalytic activity of electrode surface must increase with time. This increase in catalytic activity with time is also unlikely.

For these reasons, and moreover from the fact that on platinum or nickel the hydrogen over-potential continues to increase for a much longer time than on the other metals[9-11] it may be presumed.

7) Rome and Hiskey, *J. Am. Chem. Soc.*, **76**, 5209 (1954).
8) Hirota and Horiuti, *Sci. Pap. Inst. Phys. Chem. Res. Tokyo*, **30**, 151 (1936).
9) Hickling and Salt, *Trans. Faraday Soc.*, **36**, 1226 (1940).
10) Bockris and Azzam, ibid., **48**, 153 (1952).
11) Cousens, Ives and Swaroopa, *J. Chem. Soc.*, **1955**, 3482.

that the time variation of the separation factor is chiefly caused by the hydrogen electrode process itself.

Separation factor and mechanisms of hydrogen evolution reaction.— Horiuti and Okamoto[1] found out that the separation factors of several metals fell into two groups, viz. ca. 3 and 6, and discussed the fact that these experimental results set forth the mechanisms of the hydrogen evolution reaction, namely the catalytic mechanism for which α was about 6 and the electrochemical mechanism for which α was about 3 at room temperature. Walton and Wolfenden supported this theory, mainly because they found out that the temperature coefficient of α of these two groups showed clearly different tendencies.

However, the measured values of α in our experiment are rather distributed in the range from 2 to 7 at room temperature. For example, α on platinum, silver and gold shows an intermediate value, namely about 4.5. This tendency of distribution can be seen also in the Walton and Wolfenden's results. In their experiments, the separation factors at very low current density (0.03 mA/cm^2) at 15–20°C are as follows[12]:

Ni : 7.8_5, Ag : 6.8, Pt : 5.0,
Hg : 3.5_5, Sn : 3.5_5.

The fact that the values of α are distributed between 2 and 7 as mentioned above may be explained as follows. The path of hydrogen evolution reaction may not be only one, but probably two or more. If on a cathode metal the evolution of hydrogen took only one reaction path, or at least very predominantly one, separation factors of many metals could be classified according to the mechanisms of hydrogen evolution. This situation was adopted by Horiuti et al. But it is surely possible that on some metals the intermediate state may exist on which the evolution of hydrogen takes several paths in parallel. Supposing this, it is likely that the separation factor has an intermediate value. In addition to this, the value of α will be very sensitive to the condition of the electrode and the solution.

This sensitivity also can be seen, in the case of platinum especially. In our experimental condition α on platinum decreased with the lapse of time, and in addition to this, some preliminary experiments showed that the value of α on the platinum electrode, without any re-treatment after using it once for a run, was ca. 3.6 (the three runs of experiments showed the same results), and that after anodic pre-polarization α had the value higher than before as already reported by Eucken and Bratzler[13].

Moreover, it must be pointed out that, although, in general, good agreement is seen between the values of α obtained by Walton and Wolfenden and those obtained by Horiuti and Okamoto, in the case of platinum a remarkable discrepancy is found between the two.

These facts may indicate, at least on platinum electrode, that under some conditions the evolution of hydrogen has the possibility of taking several reaction paths in parallel, and that the state of the hydrogen evolution changes with the change of condition of the electrode surface—for example, changes due to pre-treatment of electrode, or to hydrogen saturation of electrode surface with the duration of electrolysis.

Conclusion

According to our experimental data, the values of electrolytic separation factor of hydrogen isotopes on various metals were distributed in the range from 2 to 7. On platinum, nickel and copper, a remarkable time variation of the separation factor was observed. These results do not coincide with the theory of Horiuti and Okamoto, in which two different mechanisms of hydrogen evolution reaction were assumed. The intermediate values of α and the noticeable sensitivity of α on several metals suggest us that it seems rather likely that the hydrogen evolution reaction may take several parallel paths. The time dependence of α may indicate the change of reaction process which follows the change of surface conditions of electrode, probably caused by the electrode process itself.

Considering the above discussion, the measurement of the electrolytic separation factor of hydrogen isotopes will be very useful for the study of hydrogen evolution reaction, though it involves still a complicated aspect. The theory of electrode process at hydrogen evolution is at present yet incomplete, especially in regard to

12) Walton and Wolfenden, *Trans. Faraday Soc.*, **34**, 444 (1938).

13) Eucken and Bratzler, *Z. phys. Chem.*, **A174**, 273 (1935).

the relation between the reaction and the state of electrode.

From this standpoint, the authors are now studying in more detail the nature of the electrolytic separation factor, especially the relation between the change of over-potential with conditions of electrode and that of the separation factor.

The authors wish to express their sincere gratitude to Assistant Professor S. Araki, Tokyo University, for affording us the convenience of using a mass spectrometer.

Labolatory of Applied Electrochemistry and Photochemistry, Faculty of Engineering, University, of Tokyo, Hongo, Tokyo

Ultraviolet Absorption Spectra of Three Isomeric Pyridinemethanols and Their N-Oxides

By Norisuke HATA

(Received June 27, 1957)

In recent years, the ultraviolet absorption spectra of pyridine derivatives were investigated by various workers[1-3], and several studies were also made for pyridine *N*-oxides[4-6]. However, the ultraviolet absorption spectra of hydroxymethyl, aldehyde, and carboxyl derivatives of pyridine were not studied in detail, although these compounds are important in the fields of organic and biological chemistry.

In the present investigation, the author measured the ultraviolet absorption spectra of three isomeric pyridinemethanols and their *N*-oxides in various solvents, and discussed the solvent effects on their spectra and also the effects of introduction of a hydroxymethyl group on the absorption spectra of pyridine and pyridine *N*-oxide.

Experimental

The synthesis of 2-, 3- and 4-pyridinemethanols were carried out by methods given in the literature and these compounds were purified several times by recrystallization or vacuum distillation.

2-Pyridinemethanol[7]: b. p. 100°~3°C/5 mmHg.
3-Pyridinemethanol[8]: b. p. 144°~5°C/20 mmHg.
4-Pyridinemethanol[7]: m. p. 176°~7°C (from butanol).

The syntheses of 2-, 3- and 4-pyridinemethanol *N*-oxides were done by treating the corresponding pyridinemethanol with aqueous hydrogen peroxide in glacial acetic acid and they were purified by recrystallization from ethyl acetate several times[9].

2-Pyridinemethanol *N*-oxide: m. p. 141°C. 3-Pyridinemethanol *N*-oxide: m. p. 93°~4°C. 4-Pyridinemethanol *N*-oxide: m. p. 125°C.

Solvents used in the spectral measurements were purified[10] *n*-hexane, carbon tetrachloride, ethanol and water.

The ultraviolet absorption spectra were measured with a SHIMADZU Quartz Spectrophotometer Type QB-50, using a fused quartz cell of 1 cm. thickness.

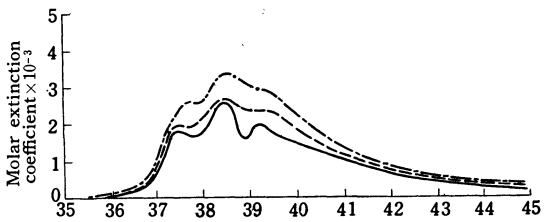

Fig. 1. Absorption curves of 2-pyridinemethanol.
——— *n*-Hexane.
—·—·— Ethanol.
– – – – Water.

1) H. Sponer and H. Stückeln, *J. Chem. Phys.*, **14**, 101 (1946); J. H. Rush and H. Sponer, ibid., **20**, 1847 (1952); W. K. Miller et al., *J. Am. Chem. Soc.*, **72**, 1629 (1950).
2) R. J. L. Andon et al., *Trans. Faraday Soc.*, **50**, 918 (1954); N. Ikekawa et al., *Pharm. Bull.*, **2**. 209 (1954).
3) H. P. Stephenson, *J. Chem. Phys.*, **22**, 1077 (1954).
4) H. Hirayama and T. Kubota, *Annual Reports of Shionogi Research Laboratory*, **2**, 47 (1952); T. Kubota, *J. Pharm. Soc. Japan* (*Yakugaku Zassi*), **73**, 140 (1953); **74**, 831 (1954); H. H. Jaffe, *J. Am. Chem. Soc.*, **77**, 4451 (1955).
5) N. Ikekawa and Y. Sato, *Pharm. Bull.*, **2**, 400 (1954).
6) M. Ito and N. Hata, This Bulletin, **28**, 260 (1955); N. Hata, ibid., **29**, 82 (1956).
7) V. Boekelheide and W. Linn, *J. Am. Chem. Soc.*, **76**, 1286 (1954).
8) R. G. Jones and E. C. Kornfeld, ibid., **73**, 107 (1951).
9) The synthesis was performed by Mr. S. Furukawa of our laboratory, to whom the author's thanks are due. For the details, see S. Furukawa, *J. Pharm. Soc. Japan* (*Yakugaku Zassi*), in press.
10) A. Weissberger and E. S. Proskauer, "Organic Solvents", 2nd, Ed. (1955).

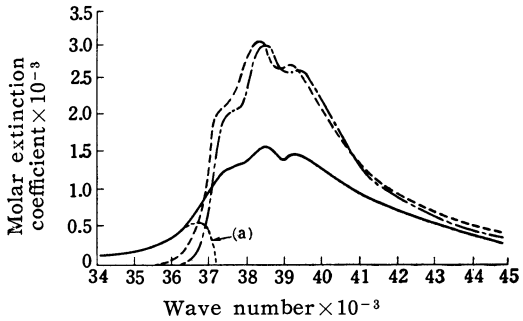

Fig. 2. Absorption curves of 3-pyridinemethanol.
——— *n*-Hexane.
— — — Ethanol.
— · — · — Water.
(a)··· *n*-π^* Absorption curve separated by peak analysis. (c.f., refs. 3 and 6).

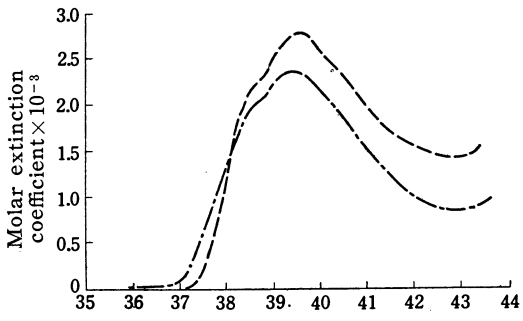

Fig. 3. Absorption curves of 4-pyridinemethanol.
— — — Ethanol.
— · — · — Water.

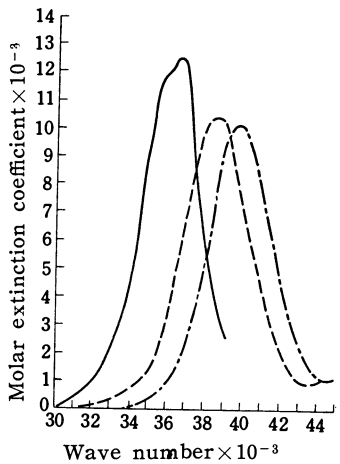

Fig. 4. Absorption curves of 2-pyridinemethanol *N*-oxide.
— · — · — Carbon tetrachloride.
— — — Ethanol.
— · — · — Water.

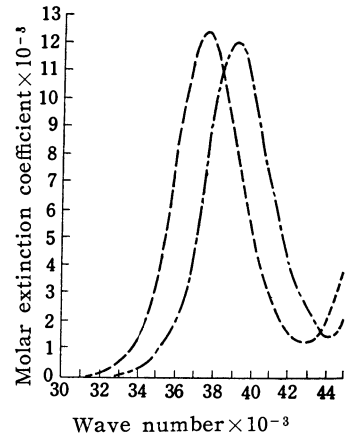

Fig. 5. Absorption curves of 3-pyridinemethanol *N*-oxide.
— — — Ethanol.
— · — · — Water.

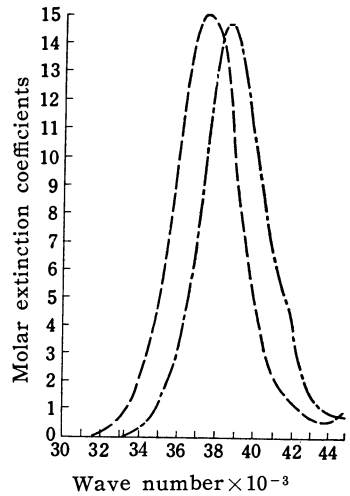

Fig. 6. Absorption curves of 4-pyridinemethanol *N*-oxide.
— — — Ethanol.
— · — · — Water.

Results and Discussion

Figs. 1 to 6 show the absorption curves of three isomeric pyridinemethanols and their *N*-oxides in various solvents. The observed values of maximum wavelength, wave number, molar extinction coefficient, and oscillator sterength[11] are listed in Table I.

(1) Effect of Solvent *a) Pyridinemethanols.* — These compounds show the absorption bands (ε=2000~5000) with some vibrational structure in the region between 35000 cm.$^{-1}$ and 44000 cm.$^{-1}$ like correspond-

11) The calculations of the oscillator strengths were made according to the method described in Stephenson, *J. Chem. Phys.*, **22**, 1077 (1954).

ing three isomeric picolines. On account of the wavelength of the absorption region, the absorption intensity, and the solvent effect, this absorption is regarded to be due to a $\pi-\pi^*$ transition corresponding to an A_1-B_1 type in pyridine.

In 2-pyridinemethanol, the absorption maximum at about 38450 cm.$^{-1}$ does not essentially shift in solvents such as *n*-hexane, ethanol and water, but the intensity increases in the above order of solvents. $n-\pi^*$ Absorption due to the excitation of a non-bonding electron localized on the nitrogen atom as observed in 2-picoline was not observed in this compound.

The absorption spectrum of 3-pyridinemethanol shows a solvent effect similar to that of 2-pyridinemethanol, but when *n*-hexane is used as solvent, a shoulder absorption is observed near 36400 cm.$^{-1}$. This is regarded to be due to an $n-\pi^*$ transition like that observed in 3-picoline. This assignment is supported by the facts that when ethanol or water, acting as a proton donor to the nitrogen atom of a pyridine nucleus, is used as solvent, this absorption completely disappears and the ratio of oscillator strength between this absorption and the $\pi-\pi^*$ absorption near 39100 cm.$^{-1}$ is in the order of 10^{-2}. In ethanolic or aqueous solution, however, the intensity of the $\pi-\pi^*$ absorption increases remarkably. This fact may be considered to be due to the overlap with the $n-\pi^*$ absorption displaced to shorter wavelength as a result of the hydrogen bond formation between the nitrogen atom of ethanol or water, since the non-bonding electron of nitrogen is largely stabilized in energy as a result of such a hydrogen bond formation.

The solvent effect for 4-pyridinemethanol absorption differs somewhat from other pyridine derivatives and is similar to that of pyridine. That is, $\pi-\pi^*$ absorption of 4-pyridinemethanol shifts to red and the intensity dereases by changing the solvent from ethanol to water.

In the spectra of 2-, 3- and 4-pyridinemethanols mentioned above, the $n-\pi^*$ absorption is observed only for 3-pyridine methanol in *n*-hexane. The explanation for this fact is qualitatively given as follows. If a hydrogen atom of the methyl group were replaced by a hydroxyl group, the inductive effect of methyl group would decrease to some extent. Therefore, the binding energy of a non-bonding electron localized on the nitrogen atom in 2-pyridinemethanol would increase compared with that of 2-picoline. Such an increase in binding energy causes the $n-\pi^*$ absorption shift to the spectral region of the $\pi-\pi^*$ transition or further. On the other hand, the inductive effect of of hydroxymethyl group for the nitrogen atom of 3-pyridinemethanol is negligible. Consequently, the $n-\pi^*$ absorption is observed in *n*-hexane solution as a shoulder absorption like pyridine. However, the $n-\pi^*$ absorption is not observed in ethanolic or aqueous solution, because the $n-\pi^*$ absorption which is displaced to shorter wavelength by the hydrogen bonding between the solute and the solvent falls in the spectral region of $\pi-\pi^*$ transition.

In 4-pyridinemethanol, it is presumed that the $n-\pi^*$ absorption occurs in the region at about 34500cm.$^{-1}$, because this compound is insoluble in non-polar solvents.

b) Pyridinemethanol N-oxides.—The solvent effects for the strong absorption bands of pyridinemethanol *N*-oxides appearing at 31000 cm.$^{-1}$ to 43000 cm.$^{-1}$ are noticeably different from those of pyridinemethanols mentioned above. As is seen from Figs. 4~6, the absorption of these compounds shows a greater blue shift when the solvent is changed from carbon tetrachloride to ethanol and water, just as does the absorption of pyridine *N*-oxide[4,6]. This phenomenon is considered to be due to the formation of a hydrogen bond between N—O group and R—OH of the solvent acting as a proton donor, a phenomenon similar to that found in pyridine *N*-oxide.

(2) Effect of Hydroxymethyl Group.—Since several pyridinemethanols and their *N*-oxides are insoluble in non-polar solvents, the effect of hydroxymethyl substitution on pyridine or pyridine *N*-oxide absorption is discussed in relation to the spectra in ethanolic solution.

As seen from Table I and Fig. 7, the absorption at about 38900 cm.$^{-1}$ of pyridine shifts to the shorter wavelength in 4-pyridinemethanol and to the longer wavelength in 2- or 3-pyridinemethanol. This tendency is similar to those in picoline[2] or monohalogeno-pyridines[3]. Such a shift of absorption maxima caused by substituting a group for hydrogen of pyridine nucleus is in agreement with the results of the molecular orbital calculations by Tsubomura[12] who discussed the electron migration effect from the substituent to the conjugated system of pyridine ring. The

12) H. Tsubomura, *J. Chem. Soc. Japan, Pure Chem. Sec.*, (*Nippon Kagaku Zassi*), **78**, 293 (1957).

Table I

WAVE LENGTH, WAVE NUMBER, MOLAR EXTINCTION COEFFICIENT, AND OSCILLATOR STRENGTH OF THREE ISOMERIC PYRIDINEMETHANOLS AND THEIR *N*-OXIDES

Compound	Solvent	Wave length (mμ)	Wave number (cm.$^{-1}$)	Molar extinction coefficient	Oscillator strength
2-Pyridinemethanol	*n*-Hexane	267	37430	1850	0.032
		260	38450	2600	
		255.5	39100	1950	
	Ethanol	266.5	37500	1850	0.046
		260	38450	2700	
	Water	265	37700	2600	0.056
		259.5	38500	3400	
3-Pyridinemethanol	*n*-Hexane	260	38400	1650	0.0043
		255.5	39100	1500	
		275s†	36350	400	0.00036
	Ethanol	261	38350	3000	0.0056
		256	39100	2700	
	Water	259.5	38500	2980	
		254	39300	2700	0.0050
4-Pyridinemethanol	Ethanol	253	39570	2760	0.040
	Water	253.5	39450	2340	0.035
2-Pyridinemethanol	CCl_4	276	36240	12600	0.210
N-oxide	Ethanol	259	38580	10500	0.204
	Water	252	39600	10300	0.201
3-Pyridinemethanol	Ethanol	264	37800	12400	0.239
N-oxide	Water	254	39300	12000	0.234
4-Pyridinemethanol	Ethanol	266	37600	15000	0.285
N-oxide	Water	257	38800	14800	0.279

† denotes the shoulder absorption ($n-\pi^*$)

smaller shift of absorption maximum to the shorter wavelength in 2-, 3- and 4-pyridinemethanols compared with the corresponding picolines may be considered to be due to the decrease in hyperconjugative power of the methyl group. The decrease in shift is caused by the replacement of a hydrogen atom in the methyl introdution group with a hydroxyl group.

In pyridinemethanol *N*-oxides, the absorption at 38000 cm.$^{-1}$ shifts to the longer wavelength by the substitution of hydroxymethyl group at 3- or 4-position and to the shorter wavelength by substitution at 2-position. A similar tendency of shift is found in picoline *N*-oxides[5]. Previously, Ikekawa and Sato[5] have reported that the absorption maximum of pyridine *N*-oxide shifted to blue by the introduction of 2-methyl group. For the cause of this shift they attributed the formation of a weak intramolecular hydrogen bond between the oxygen atom of N—O group and the hydrogen atom of 2-methyl group as shown in (A), which hindered the

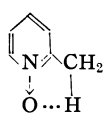

(A)

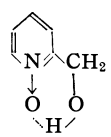

(B)

resonance of pyridine *N*-oxide. In the present work the blue shift caused by the introduction of 2-hydroxymethyl group was also observed. If the formation of a weak intramolecular hydrogen bond is assumed to 2-pyridinemethanol *N*-oxide as one of the main factors for such a blue shift phenomenon, the electron migration from the oxygen atom of N—O group to the pyridine ring may be prevented by the increase in its electronegativity caused by the formation of the intramolecular hydrogen bond as shown in (B). Therefore, the maximum wavelength of 2-pyridinemethanol *N*-oxide may be close to that of pyridine. As is seen from Fig. 7 and Table I, the ethanol solution of 2-pyridinemethanol *N*-oxide has a similar

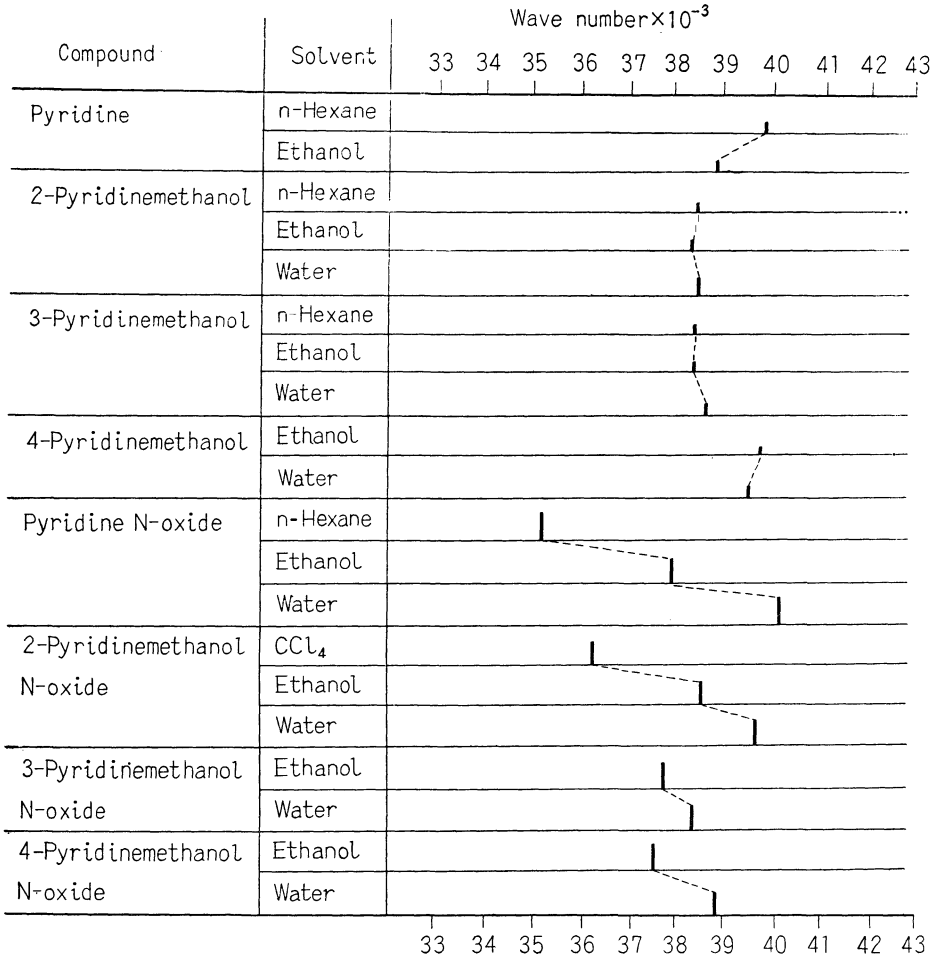

Fig. 7. Schematic expression of absorption spectra of three isomeric pyridinemethanols and their *N*-oxides.

value of the maximum wavelength with pyridine, while in 3- or 4-pyridinemethanol *N*-oxide its maximum wavelength differs remarkably from that of pyridine. These facts also support the intramolecular hydrogen bond formation in 2-pyridinemethanol.

Summary

The ultraviolet absorption spectra of three isomeric pyridinemethanols and their *N*-oxides were measured in various solvents. $n-\pi^*$ Absorption was observed as the shoulder absorption only in *n*-hexane solution of 3-pyridinemethanol, for which a qualitative discussion was made.

It was also found that the substituiton of a hydroxymethyl group in 4-position of pyridine or 2-position of pyridine *N*-oxide caused the blue shift. To explain this fact the presence of a weak intramolecular hydrogen bond in 2-pyridinemethanol *N*-oxide was assumed.

In conclusion, the author wishes to express his hearty thanks to Professor S. Imanishi of Kyushu University for his kind guidance and encouragement. Thanks are also due to Dr. E. Suenaga of Nagasaki University for his helpful advice.

Faculty of Pharmacy, Nagasaki University, Nagasaki

Polymerization of Olefins with Trialkylboron Catalysts. I. Polymerization of Vinylchloride and Acrylonitrile

By Nobuyuki ASHIKARI

(Received September 20, 1957)

Since the discovery of Ziegler's catalyst, organometallic compounds have been studied by many investigators. Recently, Kolesnikov[1] studied the polymerization of acrylonitrile with a mixed catalyst of tributylboron and borontrifluoride. However, there are few studies on the polymerization with trialkylboron catalyst only.

The author studied the polymerization of olefins with trialkylborons, and found that they are excellent catalysts to some olefins such as acrylonitrile, vinylchloride, vinylacetate and styrene.

Reaction mechanism of trialkylalminium catalyst to ethylene has been considered as[2],

$$\mathrm{Ral}+n(\mathrm{CH_2}=\mathrm{CH_2}) \rightarrow \mathrm{R}(\mathrm{CH_2}-\mathrm{CH_2})_n-\mathrm{al}$$

where, $\mathrm{al}=1/3\mathrm{Al}$

Similarly, in the case of trialkylboron catalyst, an anionic reaction can be considered in some cases. But in other cases, a radical reaction also can be considered.

Experimental and Results

1. On some trialkylborons. — There are several methods of preparation of trialkylboron, and the author adopted the common method, i.e., the reaction of Grignard reagent and borontrifluoride-etherate in ether.

The catalysts prepared in this experiment are triethyl-, tri-*iso*-propyl-, and tri-*iso*-butylboron. Triethylboron was prepared by dropping borontrifluoride-etherate into cooled ether solution of ethylmagnesiumbromide. After the reaction was over, the ether solution was distilled.

Thus, from the Grignard reagent prepared with 24 g. (1 mol.) of magnesium and 40 g. (0.28 mol.) of borontrifluoride-etherate, 22 g. of triethylboron was obtained. The yield to magnesium used was 67%.

Similarly, tri-*iso*-propyl- and tri-*iso*-butylboron were prepared from borontrifluoride-etherate and the corresponding alkylmagnesiumbromide.

Tri-*iso*-butylboron (b. p. 188°C) is very stable even in water, so that it can be used in the emulsion system. Tri-*iso*-propylboron (b. p. 150°C) fumes but does not flame in the air. Triethylboron is very flamable in the air so that it was diluted with hexane or toluene when it was used.

2. Polymerization of vinylchloride.— Vinylchloride has large polarity, and it can be polymerized very easily. The reaction proceeded slowly at −60°C, and rapidly at room temperature. Usually, the product was colorless except in cases when the reaction was carried out in tetrahydrofuran or cyclohexanon.

2.1 Bulk polymerization of vinylchloride.—Since the rate of reaction in the beginning of the polymerization was very great it was easy to obtain up to about 50 per cent. conversion. However, it was fairly difficult to obtain more than 50 per cent. conversion, because the rate of polymerization dropped.

The monomer whose amount is shown in Table I, with 0.1225 g. of triethylboron was sealed in a glass tube under a nitrogen stream. The reaction was carried out at 50°C for five hours. The solution became to solidify within three hours after the reaction occurred. After five hours the sealed tube was opened and the polymer was poured into ethanol, filtered, dried under reduced pressure at 50°C, and weighed. The results are shown in Table I.

TABLE I

BULK POLYMERIZATION OF VINYLCHLORIDE

exp. No.	monomer (g.)	polymer (g.)	Yield (%)
VCB-1	10	2.8795	28.80
VCB-2	15	4.7273	31.52
VCB-3	20	6.9894	34.95
VCB-4	25	8.6975	34.79
VCB-5	30	10.8695	36.23
VCB-6	35	16.8486	48.14

2.2 Solution polymerization.—To look over the rate of polymerization of vinylchloride in alcohol solvent, the author did the following experiment.

Vinylchloride (10 g., 0.16 mol.) was polymerized with 0.148 g. (0.00075 mol.) of tri-*iso*-butylboron catalyst in 30 cc. of ethanol. The reaction was carried out in a sealed tube at 35°C. Each sealed

1) G. S. Kolesnikov and L. S. Fedorova, *Izv. An. USSR*, No. 2, 236 (1957).

2) K. Ziegler and E. Holzkamp, *Angew. Chem.*, **67**, 543 (1955).

tube was opened after a certain time, and the polymer was separated by filtration. Then, the polymer was dried and weighed. The results are shown in Fig. 1.

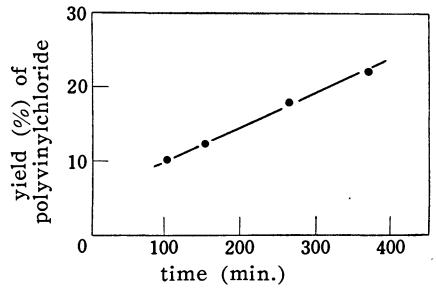

Fig. 1. Relation between the yield and the reaction time.

Vinylchloride also polymerized in tetrahydrofuran or cyclohexanon. In these solvents the product was colored. On account of the reaction system being homogenious, in tetrahydrofuran, the reaction proceeded smoothly.

The monomer (25 g.) was polymerized with 0.1225 g. of triethylboron in 25 g. of tetrahydrofuran at 50°C, for eight hours, and 12.444 g. of the polymer was obtained. The yield was 49.78%.

2.3 Emulsion polymerization.—In emulsion polymerization of vinylchloride the reaction proceeded rapidly. Of course, the rate of polymerization is varied by the concentration of catalyst. Fig. 2 represents the relation between the yield and the concentration of catalyst.

In this experiment, the monomer (20 g.) was polymerized with a certain weight of tri-*iso*-butylboron catalyst in 20 g. of aqueous solution containing 1 g. of emulsifier at 40°C in a sealed tube. After four hours, each sealed tube was opened and the solution was treated with five per cent. aqueous sodium chloride solution. Then the polymer was separated, filtered, washed throughly with water, dried and weighed.

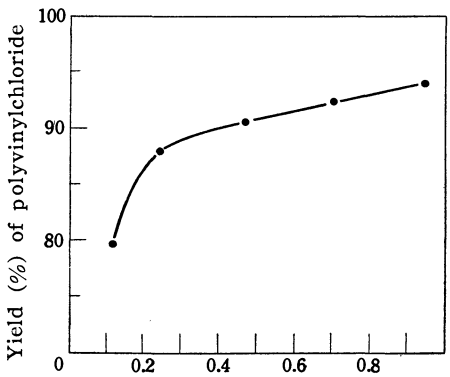

Fig. 2. Relation between the yield and the concentration of catalyst.

2.4 Influence of addition of titaniumtetrachloride.—As is well known, in the polymerization of ethylen, the mixed catalyst of trialkylaluminum and titaniumtetrachloride is used.

Similarly, an experiment using the mixted catalyst of trialkylboron and titaniumtetrachloride for the polymerization of vinylchloride was done, i.e., the monomer (20 g.) and the mixed catalyst consisting of 0.07 g. of tri-*iso*-butylboron and 0.05 g. of titaniumtetrachloride were sealed and maintained at 30°C. After one month, only 7.4 g. of polymer was obtained. Therefore, it is considered that the addition of titaniumtetrachloride to trialkylboron drops the rate of polymerization.

2.5 Measurement of molecular weight of polyvinylchloride.—Each sample got in the experiments of Table I was dissolved in cyclohexanon and the viscosity was measured at 30°C with Ubbelohde viscometer. The specific viscosity by concentration (η_{sp}/C) is represented in Fig. 3.

From Fig. 3, the intrinsic viscosity is 0.275–0.620. Therefore, the weight-average molecular weight calculated from Nakajima's equation[3] $M=313\times10^2\left(\log^{-1}\frac{[\eta]}{2}-1\right)$

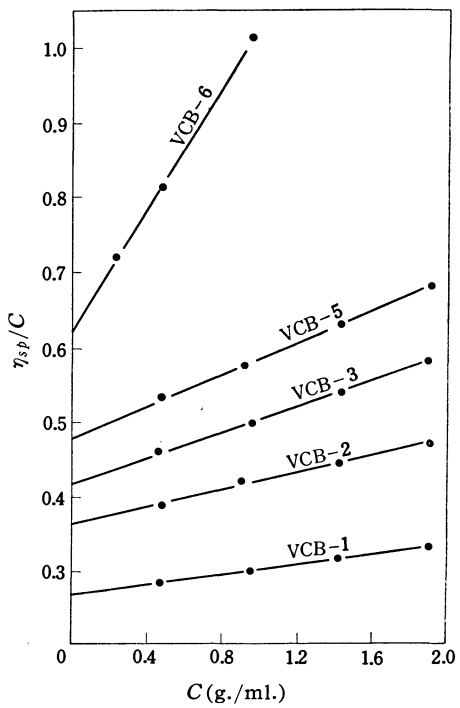

Fig. 3. Intrinsic viscosity of polyvinylchloride.

3) A. Nakajima, *Chemistry of High Polymers, Japan, Kōbunshi Kagaku*, **7**, 309 (1950).

is 11675-32615. The molecular weight of the polymer prepared in emulsion system, is 40500 (exp. No. VCH-4).

The condition of polymerization of exp. No. VCH-4 is as follows: monomer, 20 g.; aqueous solution containing five per cent. sodium lauryl sulfate, 20 g.; tri-*iso*-butylboron, 0.148 g.; temperature, 40°C; reaction time, four hours.

3 Polymerization of acrylonitrile.—Acrylonitrile was very easily polymerized by trialkylboron catalyst. Generally, a white polymer was obtained except for such case as those in which the reaction was very vigorous or polymerization proceeds in dimethylformamide.

3.1 Relation between the yield and the reaction time.—Each sealed tube which contained 12 g. of monomer, 20 cc. of *n*-hexane, and 0.693 g. of triethylboron, was set at 50°C. After certain intervals of time, the polymer was taken out from the sealed tube, treated with ethanol, dried, and weighed. The yield is shown in Table II.

TABLE II
RELATION BETWEEN THE YIELD AND THE REACTION TIME

exp. No.	time (hr.)	polymer (g.)	yield (%)
A-1	1	1.6757	13.8
A-2	3	5.7621	48.0
A-3	5	10.2811	85.0
A-4	7	10.6320	88.6

Proceeding of polymerization in ethanol with tri-*iso*-butylboron catalyst was slower than that of polymerization in hexane, and usually a white product was obtained. For example, when the polymerization of 20 g. of monomer was carried out with 0.396 g. (0.0015 mol.) of tri-*iso*-butylboron, in 25 cc. of ethanol, at 50°C for seven hours, 13.674 g. of polymer was obtained. The yield is 70%.

3.2 Influence of concentration of catalyst on the yield of polymer.—The result of polymerization that was carried out at 50°C, for five hours, with triethylboron catalyst is shown in Table III. In this case, the amount of catalyst is constant (0.0693 g.), and that of monomer is varied.

TABLE III
RELATION BETWEEN THE YIELD AND THE CONCENTRATION OF CATALYST

exp. No.	monomer (g.)	catalyst*	polymer (g.)	yield (%)
B-1	8.06	0.4602	7.66	94
B-2	12.09	0.3068	11.49	95
B-3	16.16	0.2301	15.12	94
B-4	20.15	0.1841	19.14	90
B-5	24.18	0.1534	20.55	85

* catalyst/monomer, mol. %

3.3 Relation between the intrinsic viscosity and the concentration of catalyst.—The same sample in Table III was dissolved in dimethylformamide and the viscosity measured at 25°C. The intrinsic viscosity was calculated from specific viscosity by the following equation;

$$[\eta] = [(1-4k'\eta_{sp})^{1/2}-1]/2k'C \quad (1)$$

where, $k' = 0.33$[4].

The relation between $[\eta]$ and the concentration of catalyst is represented in Fig. 4.

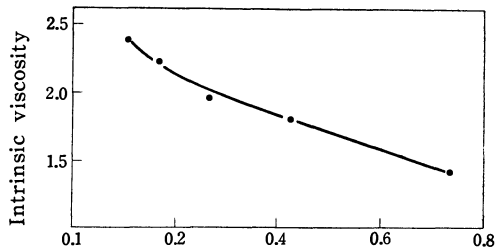

Fig. 4. Relation between the intrinsic viscosity and concentration of catalyst (triethylboron).

3.4 The molecular weight of polyacrylonitrile.—The value of intrinsic viscosity calculated from equation (1) is slightly greater than that extrapolated in Fig. 5. The molecular weight calculated from Stockmayer's equation[5], $[\eta] = 2.43 \times 10^{-4} M^{0.75}$, is 100,000—200,000.

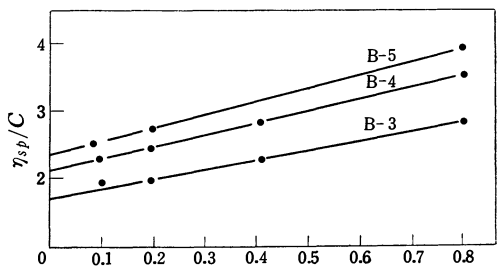

Fig. 5. Intrinsic viscosity of polyacrylonitrile.

Summary

It was found that trialkylboron is an excellent catalyst for the polymerization to some olefins which have comparatively large polarities. Vinylchloride and acrylonitrile were polymerized with this catalyst at a comparatively low temperature, and

4) R. Clealand and W. Stockmayer, *J. Polymer Sci.*, **17**, 473 (1955).
5) B. Cleland and W. Stockmayer, ibid., **17**, 476 (1955).

white polymers were usually obtained.

Vinylchloride was polymerized in bulk-, solution- and emulsion-system, and the rate of polymerization or the relation between the yield and the concentration of catalyst was investigated. Generally, the molecular weight of the polyvinylchloride was small (less than 50,000).

The polymerization of acrylonitrile was studied chiefly in a solution system. Usually, the molecular weight of polyacrylonitrile was fairly large.

Electrical Communication Laboratory
Nippon Telegraph and Telephone
Public Corporation, Musashino
Tokyo

The Ignition of Methane-Oxygen Mixture by Shock Wave

By Momotaro SUZUKI, Hajime MIYAMA and Shiro FUJIMOTO

(Received June 28, 1957)

The ignition of detonable gaseous mixtures by shock wave has been investigated by several authors. In many of those investigations the shock tube was used for the measurement of the ignition temperature of gaseous mixtures. Most of the authors[1-3] claimed the ignition temperature generated by shock waves is essentially lower than that obtained by any other means. Recently, however, Steinberg et al.[4] reported that they could not find any appreciable difference in temperatures between the various methods. Shepherd[2] has made similar investigations on the methane-oxygen mixture under ordinary pressure, for the purpose of measuring the ignition temperature. The present investigations dealing with a variety of pressures and gaseous compositions determined the minimum ignition pressure under these various experimental conditions.

Experimental

The brief scheme of the measuring system is given in Fig. 1. As shown in Fig. 2, the shock tube made of mild steel of 2.5 cm. internal diameter and 214.7 cm. length is divided into two sections, the reservoir chamber of 51.3 cm. length and the ignition test chamber of 163.4 cm. length, respectively. Furthermore, the test chamber can be divided into two; the first portion or buffer chamber, which is adjacent to the reservoir, has a length of 57.2 cm. and can be separated with a

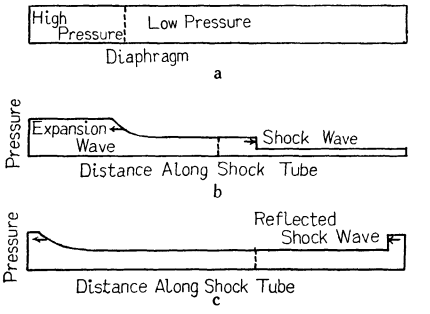

Fig. 1. Shematic of shock tube (a) and pressure distributions in shock tube (b and c).

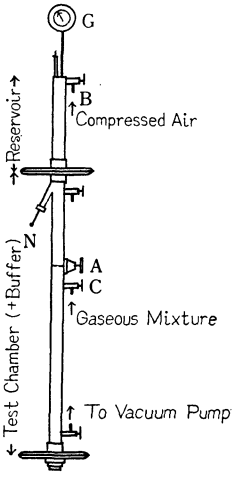

Fig. 2. Diagram of shock tube.

A; Sluice valve
B, C; Needle valve
N; Needle
G; Pressure gauge

1) J. A. Fay, "Fourth Symposium on Combustion", p. 501, Baltimore, The Williams and Wilkins Co. (1953).
2) W. C. F. Shepherd, "Third Symposium on Combustion" p. 302, ibid. (1949).
3) D. J. Berets, E. F. Greene and G. B. Kistiakowsky, *J. Am. Chem. Soc.*, **72**, 1080 (1950).
4) M. Steinberg and W. E. Kaskan, "Fifth Symposium on Combustion", p. 664 (1955).

sluice valve A from the second or remaining part of the test chamber on necessary occasions. The second portion then serves as the actual test chamber. The reservoir and the test chamber are separated by suitable sheets of cellophane films of 0.040 and 0.027 mm. thickness. The number of sheets of cellophane films is so chosen that it barely withstands the pressure difference between the two chambers without rupturing before the start of the experiment.

To carry on the measurement, compressed air is first sent into the reservoir chamber and this air pressure acts as firing pressure for the gaseous mixture. The test chamber is filled with a detonable gaseous mixture of desired composition of methane and oxygen. After valve B is closed, the diaphragm is punctured by the needle N through a side tube attached obliquely to the shock tube.

When the buffer chamber is used, it is filled with air of the same pressure as that of the detonable gaseous mixture in the test chamber after the two chambers are separated by closing the sluice valve A. The reservoir chamber is filled with compressed air in the same way as described above. After the sluice valve A is opened, the diaphragm is broken with the help of a hand-operated needle N.

As shown in Fig. 1, the air in the reservoir spurts out and generates a shock wave. The gaseous mixture will be ignited by the direct shock wave or by the wave reflected from the bottom of the tube and superposed on the direct shock wave. At the ignition, the sound of detonation is clearly audible. On opening the tube after the experiment, the cellophane diaphragm is found to be discolored, and white smoke drifts out from the interior of the shock tube. As the bottom of the tube, the plane end plate is mainly used but, on necessary occasions, the conical bottom of the vertical angle 90° as shown in Fig. 3 is used, so as to cause the reflected shock wave to converge at a certain distance from the bottom on the center axis of the tube and thus produce a high temperature and high pressure region locally.

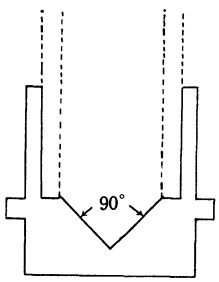

Fig. 3. Conical end of shock tube.

As to the experimental materials, commercial oxygen and methane in cylinders were used. For the experiment, both gases, through a sodium hydroxide tube to eliminate the carbon dioxide, are mixed to the desired composition and the mixture was kept in a tank over 24 hours. The methane in the cylinder consists usually of 87.8% methane, 9.7% nitogen, 0.3% carbon dioxide and 0.2% oxygen.

The buffer chamber serves to eliminate the effect of puncturing the diaphragm. As both sluice valve A and the needle N are operated by hand, the opening of the valve and puncture of the diaphragm can not possively be carried out at the same moment. Especially the fact that the opening of the valve has taken time, seems to cause the diffusion of the gases of the buffer and test chambers. Also the experimental result with the buffer chamber often shows poor reproducibility. At the puncture of the separating films the fragments of these will be scattered all about in the ignition mixture and these may cause some error in the experiment. To avoid the effect, some authors used a trap device such as metal coil or gauze to catch the fragments. In the experiment of Shepherd[2], he found some effect of fragments of copper film on the pressure value under which ignition occurs but in case of using cellophane films he could not find any of these effect. Accordingly, we eliminated the trap, as we used cellophane films only.

Results and Discussion

We have carried out a series of experiments of ignition by shock waves with various pressures in the reservoir against a certain gaseous mixture with definite composition and definite pressure. With a pressure in the reservoir lower than a certain limiting value, the ignition does not take place. The lowest pressure value necessary for the ignition is called minimum ignition pressure P_1 for the gaseous mixture of definite composition and definite pressure P_0. In Fig. 4, the ratio P_1/P_0 is plotted against various compositions of methane and oxygen. The values of P_1/P_0 correspond to the temperature of ignition for the mixtures of pressure P_0.

Owing to the mechanical strength of the shock tube used, the maximum pressure of the reservoir was limited to 30 kg./cm^2. Up to this value it was not possible to find any pressure values above which ignition does not occur. Such upper limiting pressure values for the ignition of gaseous mixtures of various compositions were reported by Shepherd[2]. In his case a higher pressure in the reservoir could be attained than is possible for us. As will be seen from Fig. 4, the minimum values of P_1/P_0 tends to decrease with the increase of P_0, and at the same time the minimum point drifts to the methane rich side. The limit concentration for the explosion of this gaseous mixture lies between 3 to 42% methane,

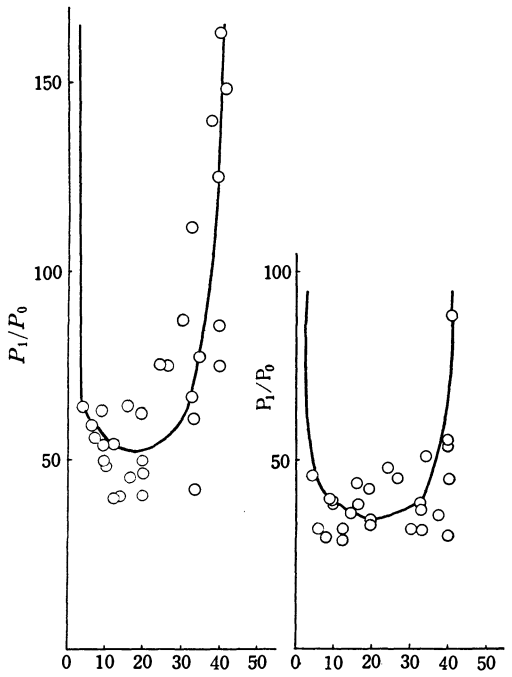

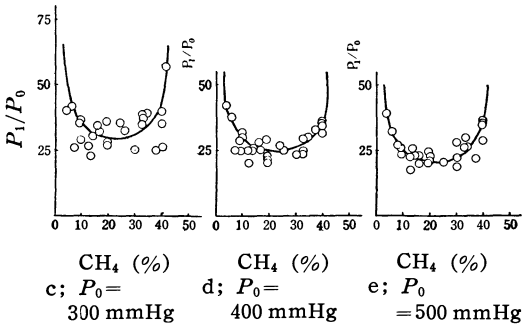

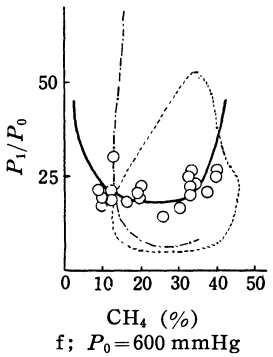

------ Shepherd's data with trap at 760 mmHg

-·-·- Shepherds's data without trap at 760 mmHg

Fig. 4. Variation of P_1/P_0 with concentration of CH_4.

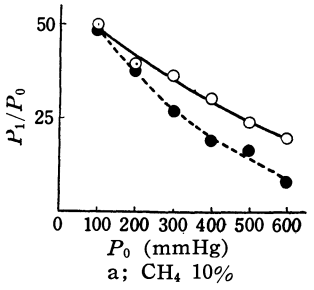

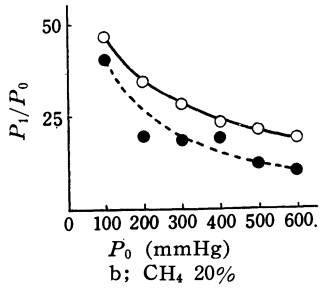

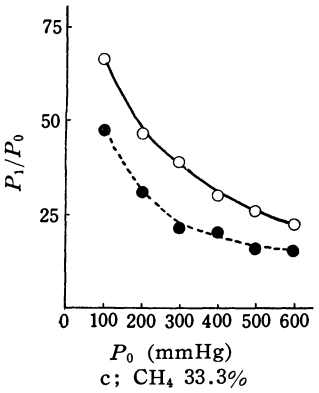

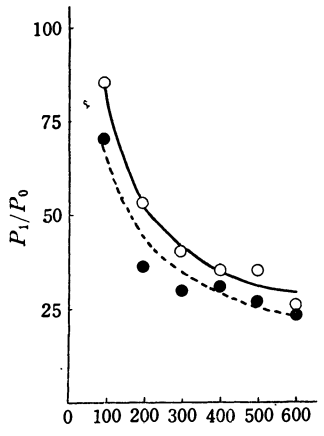

Fig. 5. Variation of P_1/P_0 with pressure of gaseous mixture.

○; with plane end

●; with conical end

and is entirely independent of the gaseous pressure. The minimum ignition point observed is at the gaseous mixture of about 20—25% methane.

As seen from Fig. 5, P_1/P_0 values decrease in accordance with the increasing value of P_0, which means that the higher the pressure of gaseous mixture, the easier to detonate the gas under the same conditions. The curves in thick lines in Fig. 5 denote the values using the plane bottom, and the dotted lines the conical bottom of the shock tube, respectively. The values obtained using the buffer chamber were found not to be sufficiently reproducible, probably for the reasons described above. We have selected some reliable values of both cases, with and without buffer which are tabulated in Table I. Though it seems that the ignition with buffer is easier than without buffer, the differences are by no means remarkable.

TABLE I

COMPARISON OF P_1/P_0 BETWEEN WITH AND WITHOUT BUFFER

P_0 (mmHg)	P_1/P_0	
	with buffer	without buffer
200	46.1	52.4
300	32.8	34.4
400	25.8	27.6

The ignition limits in Fig. 4f manifest some difference from those obtained by Shepherd. The discrepancies may be attributed to the fact that, in our experiment, a shock tube with closed end was used and in his case open tube was employed. Accordingly, in his experiment the gaseous mixture in the ignition chamber may have been diluted by the air diffused through open end. In spite of these differences, the concordance of the results from both investigations manifest themselves to be satisfactory.

In our experimental conditions the ignition temperatures could not be determined directly. But they may be estimated indirectly and theoretically with help of the equation[5]

$$[yP_0/P_1]^{(\gamma_1-1)/2\gamma_1} = 1-C_0(\gamma_1-1)(y-1)/C_1[2\gamma_0\{(\gamma_0-1)+(\gamma_0+1)y\}]^{1/2} \quad (1)$$

where P is the pressure of the shock wave; C_1 and C_0 are each the sound velocity in the reservoir and the test chamber respectively; γ_1 and γ_0 are the ratio of specific heat at constant volume and at constant pressure of both gases in two chambers cited above; and $y=P/P_0$. The gases are all assumed to be perfect gases. In taking $\gamma_0=\gamma_1=1.4$, $C_1=C_0$ and $T_1=T_0$ where T_0 is the temperature of the gas in reservoir and T_1 that of the test chamber, we have

$$P_1/P_0=y[1-\{(y-1)/(7+42y)^{1/2}\}]^{-7} \quad (2)$$

The values of y or the values of P can be determined by substituting the experimental values in the equation (2). Furthermore the temperature T of the direct shock wave and T_r of the reflected one can be expressed as follows[5];

$$T/T_0=(P/P_0)(1+\mu^2 P/P_0)/(P/P_0+\mu^2) \quad (3)$$

$$T_r/T_0=\{(2\mu^2+1)P/P_0-\mu^2\}\{2\mu^2P/P_0-(\mu^2-1)\}/\{(P/P_0+\mu^2)(\mu^2+1)\} \quad (4)$$

where $\mu^2=(\gamma_0-1)/(\gamma_0+1)$.

Using the expressions (2), (3) and (4) the values of T and T_r can be estimated approximately. In spite of those simplifications used above, the values obtained may serve as an orientation of the ignition temperature. In Fig. 6 we have shown the temperature values of T and T_r with plane end shock tube together with the

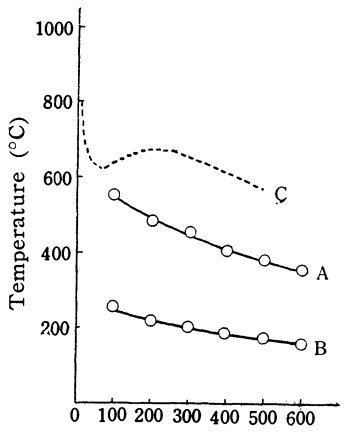

Fig. 6. Variation of ignition temperature with pressure of gaseous mixture CH_4+2O_2.
A; Reflected shock ignition
B; Direct shock ignition
C; Thermal ignition

5) W. Bleakney, *Rev. Mod. Phys.*, **21**, 584 (1949); I. I. Glass, W. Martin and G. N. Patterson, *UTIA Report* No. 2 (1953); R. N. Hollyer, Jr., "Engineering Research Institute Report", Univ. of Michigan, July (1953).

6) N. Semenoff, "Chemical Kinetics and Chain Reaction", p. 308, Oxford at the Clarendon Press. (1955).

results of thermal ignition[6]. In the respective cases, the higher the pressure of the detonable gaseous mixture, the easier the ignition. The peninsula-shaped region which is seen in thermal ignition is lacking in both direct and reflected shock wave detonation. Ignition in the shock tube with conical bottom is more easily produced by the reflected shock wave, than it is with the plane bottom. In general the temperatures of shock wave ignition are essentially lower than those of thermal ignition.

All these estimations however are indirect. They should be determined in a more direct way, and we are now preparing to take up such further investigations.

Summary

Using the shock tube, the authors measured the minimum ignition pressure P_1 of the reservoir for the methane-oxygen mixture of various pressure P_0 and various compositions, and obtained the following results.

1) The higher the value of P_0, the easier the ignition.

2) The concentration range of methane in the gaseous mixture for shock ignition is 3—42%, and the minimum value of P_1/P_0 or the ignition temperature, was found at a gaseous mixture of about 20—25% methane.

3) The ignition easier is by the use of the shock tube with conical end rather than with the plane end.

4) Shock ignition temperatures estimated indirectly were found to be remarkably lower than the thermal ignition temperature.

Department of Chemistry
Defense Academy
Yokosuka, Kanagawa

*On the Mechanism of the Coalescence of Drops at an Oil-Water Interface**

By Takehiko WATANABE and Makoto KUSUI

(Received May 16, 1957)

In regard to the stability of emulsions[1], the following three phenomena should be considered; (1) concentration of the dispersed droplets towards the top or the bottom of the emulsion, on account of a difference in density between the liquids, which is known as "creaming" or "settling", (2) flocculation or clumping of the dispersed droplets to form larger aggregates, without the droplets actually losing their identity, (3) coalescence of droplets to form larger ones and eventually bulk liquid.

Of these phenomena, only the third represents instability in the sense of the reverse process of dispersion. Therefore, the third phenomenon may be the most important clue in order to discuss the stability of emulsions. From this point of view, coalescence of drops at an oil-water interface has been studied. A more reasonable mechanism of the coalescence of drops at the oil-water interface than ever previously accepted is proposed.

Experimental

Materials.—The following surfactants were used as the emulsifier.

Anionic surfactant—Sodium dodecyl sulfate (SDS), (purity, 98.9 %), was offered by the Kaō Sekken Co.

Cationic surfactant—Cetyl-oxymethyl-trimethyl-ammonium chloride (CEA), purity, $\simeq$100 %, was kindly offered by Professor Nirō Murata of our University.

Non-ionic surfactant—Emulgen 120 (polyoxyethylene-lauryl ether), HLB, 15.5; Emulgen 220 (polyoxyethylene-cetyl ether), HLB, 14.0; Emulgen 408 (polyoxyethylene-oleyl ether), HLB, 9.0; Emasol 320 (sorbitan di-stearate), HLB, 2.7; Emasol 410 (sorbitan mono-oleate), HLB, 5.9, were offered by the Kaō Sekken Co.

Cholesterol was a product from Wakō Pure Chemicals Ltd.

* Presented in part at the Symposium on Colloid Chemistry of the Chemical Society of Japan, held at Nagoya, in November 6, 1955 and at the 9th Annual Meeting of the Chemical Society of Japan, Kyoto, April 3, 1956.

1) C. G. Sumner, "Clayton's the Theory of Emulsions and their Technical Treatment", J. & A. Churchill Ltd., London (1954), p, 198.

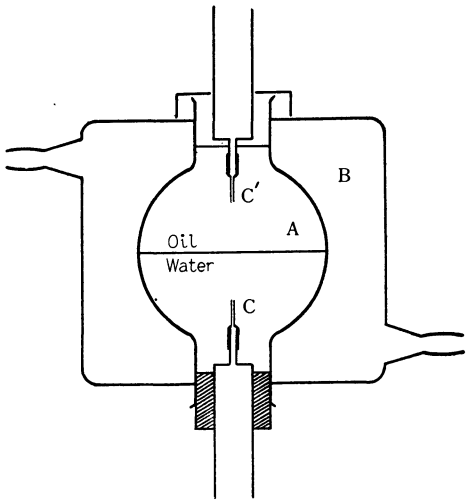

Fig. 1. Apparatus for determining the life-time of drops.

Apparatus and Procedure.—To measure the stability or persistency of water or oil drops at the oil-water interface, an apparatus shown in Fig. 1, similar to that of Cockbain and McRoberts[2] was used. It consists of a spherical part A (its diameter, 5 cm.) in which the oil-water interface is made, a thermostatted water jacket B, and tips, C and C' to form oil or water drops respectively. Both C and C' consist of three parts, a syringe (capacity, 2 cc.), a syringe needle with flattened tip, and a micrometer which was modified to push the syringe piston and at the same time to measure the distance travelled by the piston. A drop which was detached from the top of C or C', will ascend or descend in the vessel A and come into contact with a plane oil-water interface and then will coalesce after a certain time. The time of coalescence, life-time of drop, was measured with a stop watch and was taken as the interval in which one drop appears to be in contact with the interface and coalesces. In some cases, the drop did not completely coalesce in a single stage with the bulk liquid phase; partial coalescence occurred leaving a smaller drop, which also partially coalesced after some longer time than in the case of the parent drop, leaving still a smaller drop. In such cases, the time required for the first stage was taken as the life-time of the drop. Each drop was separately formed and its life-time was measured. Drops used for one experiment were 30 to 40.

Results

The life-time of drops at the interface.—The experiment has been made with benzene-water system, in which the surfactant was dissolved in either liquid as an emulsifier. In the given system, the life-times of individual drops were not constant. When N the number of drops whose life-time$\geqq$time t, were plotted in logarithmic scale against t, it was observed that most plots were found to be linear, as shown AB in Fig. 2, in agreement with the results obtained by Cockbain et al.[2].

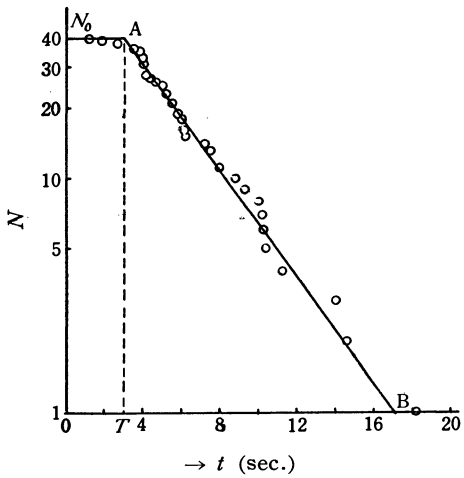

Fig. 2. Typical relationship between N (in logarithmic scale) and t; water phase—pure water, oil phase—2.0 g. cholesterol/100 cc. benzene, drop—pure water drop, temperature—25°C.

Then, the value T was estimated as the time of the intersection (A) of the AB with the straight line drawn parallel to the t axis through N_0, which is the total number of drops experimented. The experimental values are given in Table I. T_O and T_W are the values of T, for oil and water drops respectively.

Behavior of drop at the interface.—Two series of experiments on the behavior of water drop at the oil-water interface were made. First, in order to observe the behavior of the water drop in detail, the drop was colored with various dyes or colored inorganic salts. The experiments were made in the combinations of a drop and an oil-water interface with equal or different interfacial tension to the drop. The behavior of the colored drop is schematically shown in Fig. 3. When a drop comes into contact with an oil-water interface, the interface is deformed and consequently a concave surface is formed around the drop [(I) of Fig. 3]. After a while, coalescence of the drop occurs. If the interfacial tension around the drop (σ_d) is lower than that of the oil-water interface (σ_s), the process of coalescence will proceed as follows.

2) E. G. Cockbain and T. S. McRoberts, *J. Colloid Sci.*, **8**, 440 (1953).

TABLE I

T_W AND T_O OBTAINED WITH BENZENE-WATER SYSTEMS USING VARIOUS SURFACTANTS AS THE EMULSIFIER

Surfactant (dissolved phase)	Concn. of surfactant (g./100 cc.)	Water drop		Oil drop		Temp. (°C)
		Drop volume (cc.)	T_W (sec.)	Drop volume (cc.)	T_O (sec.)	
None	—	0.03	2	0.02	3	20
SDS	1.0	0.003	3	0.004	3×10^2	15
(water)	1.0	0.003	4	0.004	1×10^2	25
	0.1	0.009	1	0.01	2×10	15
	0.1	0.008	1	0.01	2×10	25
	0.01	0.02	1	0.03	5	15
	0.01	0.03	1	0.03	5	25
Emulgen 120	0.02	0.02	3	0.03	2×10	15
(water)	0.02	0.02	1	0.03	1×10	25
Emulgen 220	0.02	0.02	1	0.02	2	15
(water)	0.02	0.02	1	0.02	2	25
Emulgen 408	0.02	0.03	0.5	0.03	3	15
(benzene)	0.02	0.03	0.4	0.03	3	25
Emasol 320	0.02	0.03	0.6	0.03	2	15
(benzene)	0.02	0.04	1	0.04	4	25
Emasol 410	0.02	0.02	2×10	0.02	8	15
(benzene)	0.02	0.02	3	0.02	2	25
Cholesterol	2.0	0.02	3	0.03	2	15
(benzene)	2.0	0.02	3	0.03	1	25
	0.5	0.03	2	0.04	3	15
	0.5	0.03	1	0.04	3	25

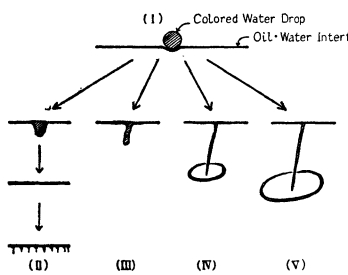

Fig. 3. Schematic presentation of the behavior of water drop at the interface.

Although the interface which is in contact with the drop, is deformed momentarily, the colored liquid can not penetrate into the bulk water phase through the interface. The momentarily deformed portion of the interface is restored to the original flat state and at the same time the colored liquid spreads along the interface, as if it soaked into the interface, and a layer of colored liquid is formed. After the formation of the colored layer, the colored liquid diffuses into the bulk water phase as illustrated in (II) of Fig. 3. If σ_d is approximately equal to σ_s or higher than it, the most part of the colored liquid penetrates into the bulk water phase through the interface, and the rest spreads along the interface as shown in (III) or (IV) of Fig. 3. The rate of penetration of the colored liquid increases with rise of the value, σ_d. The behavior of a colored liquid, having the greater rate of penetration at the moment of coalescence is shown in (IV) and (V) of Fig. 3. The formation of a ring of the colored liquid is observed around the straight penetrating stream of the same colored liquid. The last case (V) illustrated in Fig. 3 is the extreme one of the (IV), where $\sigma_d \gg \sigma_s$, and the spreading of the colored liquid along the oil-water interface is hardly ever observed.

From the above observations, it may be concluded that the main process of the coalescence of a drop at an oil-water interface, is the formation of a defect in the emulsifier layer around the drop at the portion in contact with the interface, and it is followed by the flowing out of the liquid of the drop through the defective portion. If the flowing liquid can make a hole in an oil-water interface owing to the pressure of flowing, the liquid will

penetrate into the bulk liquid phase of the same kind. If not, the liquid will spread along the oil-water interface. Here it is supposed that the main factor which may determine the life-time of a drop at an oil-water interface would be the characteristics of the layer of emulsifier around the drop.

The second series of experiments have been carried out in order to investigate the mechanism of the coalescence of a drop from another standpoint. Pure benzene and distilled water or bentonite suspension were used as the oil and the aqueous phase respectively. A drop (volume $\fallingdotseq$0.002 cc.) of 10^{-4} mol./l. solution of CEA was made to flow out from C′ in Fig. 1. When distilled water was used as the aqueous phase, the gradual increase in the life-time of the drop was observed as dropping proceeded, but this regular increase was only until nearly the tenth drop. On the contrary, when bentonite suspension was used as the aqueous phase, the same phenomenon could not be observed.

In these experiments, σ_d is lower than σ_s. Therefore, according to the results obtained with the colored drop mentioned above, it may be concluded that the liquid of the drop spreads along an oil-water interface and thereafter diffuses into the bulk aqueous phase as shown in (II) of Fig. 3. It may be assumed that, compared with the time required for a series of experiments, the diffusion rate of the liquid which forms the drop into the bulk aqueous phase may be slow, so that the marked decrease in the interfacial tension of an oil-water interface may be induced with the successive coalescence of the drop at the interface at least in the initial period of the experiment. The conclusion may be further developed that the lower the interfacial tension of an oil-water interface, the longer the life-time of the drop being in contact with that interface, provided that the interfacial tension around the drop remains constant. The reason why the life-time does not increase as dropping proceeds with bentonite suspension, may be as follows. The cationic surfactant, CEA dissolved in the drop solution may be fixed on the bentonite particles owing to the cationic exchange reaction or adsorption, so that the decrease in the interfacial tension of an oil-water interface may be reduced considerably compared with the above case without bentonite.

Discussion

On the experimental method.—Both Cockbain et al.[2] and Gillespie and Rideal[3] found with benzene-water system that the stability of the drops was markedly increased by putting a cover on A (Fig. 1). The latter authors found that the drops become more stable when the whole apparatus is further surrounded by an air bath whose temperature is approximately the same as that of the water jacket B. These effects were attributed to the elimination of convection currents at the interface. In the present experiments, similar phenomena were also observed when measurements were made under a tightly-fitting cover. However, in the present investigation, where the value of T is simply taken to discuss the observed data and also the singular significant figure is taken to represent the magnitude of the value T, the influence of the above operation on the experimental results can be neglected.

Cockbain et al. observed that the stability of the drops had not been markedly affected by volume in the range 0.0005$\sim$0.01 cc., whereas below 0.0005 cc. the stability had increased rapidly with decreasing volume. On the other hand, Gillespie et al. reported that in the absence of surfactant the stability of the drops had increased with increasing volume in the range 0.014$\sim$0.38 cc. (drop radius; 0.15$\sim$0.45 cm.). In the present experiments, the value of T was not markedly affected by the change of the drop volume as shown in Table I. where singular significant figure was taken to represent the magnitude of the value of T.

In order to obtain a clean oil-water interface in the vessel A, the method by Cockbain et al. was employed. But our experiences showed that it is not necessary to be extremely careful for the cleanliness of the interface to obtain well reproducible values of T. In the present experiments the reproducibility was satisfactory with T in any case.

On the process of the coalescence of a drop.—Cockbain et al. have suggested that the life-times of the drops are determined by two distinct processes, viz., drainage of the continuous phase from the space between the drop and the plane oil-water interface, followed by rupture of the adsorbed film of surfactant. They

3) T. Gillespie and E. K. Rideal, *Trans. Faraday Soc.*, **52**, 173 (1956).

concluded that the main factor determining stability is the resistance to wetting of segments of the adsorbed film by the discontinuous phase. But it was not substantiated whether both the films, viz. the film around the drop and that of the plane oil-water interface, must be wetted by the discontinuous phase simultaneously or only one of them.

According to Gillespie et al., the coalescence of a drop at an oil-water interface is very unlikely until the film formed between the drop and the interface has been drained to a certain thickness for which it takes a certain time. The coalescence of a drop will occur owing to the rupture of the film which will be brought about by thermal and possibly mechanical disturbances.

In contrast to the processes proposed by Gillespie et al., the present experiments showed that the main process of the coalescence of a drop at an oil-water interface is the formation of a defect in the emulsifier layer around the drop at the portion in contact with the interface. It is consequently concluded that though the initial process, the drainage of the continuous phase from between the drop and the interface, will occur in the same manner as proposed by them, the final process which includes the main process as mentioned above, will proceed in the following manner.

When a defect has been formed in the emulsifier layer around the drop at the portion in contact with the plane oil-water interface, the local disturbance will be induced at that portion and this will be promoted by thermal or mechanical disturbances such as convection currents etc. Consequently the liquid of the drop will flow out through the defective portion owing to the internal pressure due to the interfacial tension around the drop itself. At the same time, since the interfacial tension of the defective portion becomes higher than that of the other portion of the same drop which is surrounded by the emulsifier layer, the transference of the emulsifier to the defect from the other portion of the drop interface will take place to repair the defect with the new emulsifier layer. In this case, so far as the repairing of the defect with new emulsifier layer has been completed before the arrival of the flowing liquid at the oil-water interface, the coalescence of the drop will not occur. If not, the reformation of emulsifier layer around the drop becomes impossible and the liquid of the drop will flow out through the defective portion progressively and the interface will be exposed to the pressure of the flowing liquid. At this stage if the flowing liquid can make a hole in an oil-water interface owing to the pressure of flow, the liquid will penetrate into the bulk liquid phase of the same kind. If not, the liquid will come into direct contact with the bulk liquid phase of the same kind. As seen from our experimental data using a drop of colored solution, the latter phenomenon can be observed only in the case where σ_d is less than σ_s. Therefore, when the liquid of the drop comes into direct contact with the bulk liquid, it may be considered that the interfacial tension between the former and the latter liquid would be nearly null. In the present case, the interfacial tension between the liquid of the drop and the original continuous phase liquid (σ_d) is lower than that of the oil-water interface (σ_s), so that the liquid of the drop spreads along the oil-water interface and produces the new oil-water interface between the spreading liquid and the original continuous phase liquid, resulting in the disappearance of the original interface.

However, also in the present experiments, it can be still expected that the probability of coalescence will be small until the continuous phase between a drop and an interface has been drained to a certain thickness. Therefore, the values of T may also depend on a factor which is influenced by the rate of drainage of the continuous phase.

On the treatment of the experimental data.—Cockbain et al. have found that after a time t_D (drainage time), $\ln N = -kt + \text{constant}$ holds. The quantity t_D corresponds to T in the present experiments. The constant k (rate constant for the film rupture) will be obtained from the slope of AB in Fig. 2. These authors have discussed the stability of drop using both the values t_D and k. Gillespie et al. have further discussed the probable effect of electric double layer forces, electroviscosity and other factors on the values t_D and k. In the present report, however, an attempt was made to discuss the stability or persistency of drops only referring to the values of T, from the following reasons.

(1) The well-reproducible values of T can be readily obtained, as shown in the above discussion, while the values

of k are readily influenced even by the slight differences in the experimental conditions. Therefore, in order to obtain the significant values of k, the experimental conditions must be more strictly controlled and moreover, according to Gillespie et al., the measurements of the life-time must be made with from 100 to 200 drops.

(2) T denotes, as will be stated later, the time during which most drops can exist without coalescence, while k is a rate constant for the coalescence after time T. Consequently, the stability or persistency of drops may be primarily defined by the value of T and the contribution of k to the same problem is by far less important.

On the life-time of drops.—From the results mentioned above, it is concluded that the values of T are determined by two factors, viz., drainage of the continuous phase from between the drop and the plane oil-water interface, and formation of a defect in the emulsifier layer around the drop.

Now let us consider the latter factor, irrespective of the former one. In the present experiments it was assessed from 30 to 40 drops to obtain the value of T. The number of drops which coalesced within the time T was from 1 to 5 drops. Hence, it may be said that the value of T is the life-time at which the probability of coalescence is about 0.1.

Subsequently, the factors which affect the coalescence of drops will be considered. When a drop comes into contact with an oil-water interface, the interface will be deformed and consequently a concave surface will be formed around the drop as illustrated in (I) of Fig. 3. In this case, it is assumed that the drop remains on the interface at equilibrium position without deformation and the radius of curvature of the concave surface (a) is equal to the radius of the drop (r) itself. The area of the concave surface at the interface which comes into contact with the drop is A. For small drops it may be supposed that this contact portion is a plane surface, since the contact portion itself must be quite small. Then, the following relation is given, since a equals to r

$$\frac{4}{3}\pi d g r^3 \fallingdotseq \frac{2\sigma_s}{a}\cdot A = \frac{2\sigma_s}{r}\cdot A \qquad (1)$$

where d is the difference in the density between the drop and the surrounding medium and g the gravity constant. We see that the contact area A is proportional to r^4.

Next, the probability of the formation of a defect in the emulsifier layer around the drop will be considered. It may be assumed that this probability is constant anywhere around the surface of the drop, since no deformation of the drop is considered. So that the probability of forming the defect at the portion of the drop in contact with the interface will be proportional to A/B, where B is the total surface area of the drop and proportional to r^2. Therefore, the probability of forming a defect at the contact portion of the drop and the interface should be proportional to r^2. However, it may be suggested that the above condition is strictly satisfied only when the diameter of the drop is smaller than 1 mm., which can be deduced from the data obtained by Cockbain et al. or by the present investigation on the effect of the drop volume and also by the calculated values of A using relation (1) with the substitution of appropriate values for σ_s and r.

The experimental results reported in page 239 that if σ_d is smaller than σ_s and at the same time σ_d and the drop volume are constant, the lower the interfacial tension of an oil-water interface, the longer the life-time of the drop being in contact with the interface may be explained as follows.

From the relation (1), it may be expected that the higher the σ_s, the smaller the A; consequently the life-time of a drop would increase. The experimental result is, however, contrary to the above expectation. This inconsistency may be caused by the assumption, viz. $a=r$, and this assumption will not be satisfied under the present experimental conditions. Here it should be expected that a changes with the change of σ_s and consequently a is not equal to r. Therefore, if the value of σ_s is higher, the value of a also becomes greater and consequently variation of the value A with the variation of σ_s will be smaller than that given by the relation (1).

If the area A is constant, the deformation of the drop corresponding to the change of a must be expected. Consequently the strain will be induced on the emulsifier layer of the drop at the contact portion. Under these conditions, the higher the σ_s, the larger the difference between a and r and the larger the strain induced on the emulsifier layer. On the other hand, it is expected that a defect on the emulsifier layer will be more

readily formed at the portion on which the strain is induced. As a conclusion, it is expected that when the drop volume and σ_d are constant and σ_d is less than σ_s, the lower the value of σ_s, the longer the life-time of the drop in accordance with the present experimental results.

The above discussion has been presented without the consideration on the drainage process of the continuous phase from between the drop and the plane oil-water interface. However, the time necessary for this drainage process is also included in the values of T, so that it must also be taken into consideration, when the meaning of the value T is strictly discussed. On the other hand, it is hard to say that the values t_D obtained by Cockbain et al. and also probably by Gillespie et al. are determined only by the drainage process. Therefore, the extent of the contribution of the drainage process to the value T, may be estimated from the minimum value of the life-time assessed with a number of drops. Since the life-time of each drop is short in the system without surfactant, the time necessary for the net drainage will be obtained from the data assessed from 100 to 200 drops in each experiment such as in the case carried out by Gillespie et al.

According to Gillespie et al. the time required for drainage process t_D decreases with the decrease in the drop volume. On the other hand, from the results obtained by Cockbain et al. and also by the present authors, it was shown that if the diameter of the drop is about 1 mm. or less, the stability or the life-time increases rapidly with the decrease of the volume. From these results, it is concluded that the time required for drainage with such droplets as in ordinary emulsions whose diameters are in the range of a few μ, will be practically negligible, compared with their whole life-times.

Cockbain et al. have reported that the stability of the drops was not markedly affected by volume in a fairly wide range, whereas below a certain volume the stability increased rapidly with decreasing volume. From the above results, it is concluded that in the range of the volume at which the stability of the drops is nearly constant, the factor increasing the life-time will be compensated by that decreasing it. Therefore, it may be said that one can estimate the life-time of a drop less than 1 mm. in diameter by using the value of T in the present investigation or t_D obtained by Cockbain et al., regarding it as the one which does not include any contribution from the factor of the drainage process. Now, if it can be assumed that the life-time of the drops is determined only by the value of A/B, it may be suggested that when the experiments are made with the drops of 1 μ in diameter under the same condition as the present investigations, the values of T will be about 10^6 times greater than those listed on Table I.

From the discussions mentioned above, the main process of the coalescence of a drop at an oil-water interface may be said to be the formation of a defect in the emulsifier layer around the drop at the portion in contact with the interface. Consequently, the more readily the emulsifier (surfactant) escapes from the oil-water interface around the drop, the more readily the defect on the emulsifier layer will be formed and also the shorter the life-time of the drop will be.

To consider the stability or persistency of the droplets in the ordinary emulsions (droplet diameter=a few μ) referring to that of the drops as discussed above, it must be first examined whether the escaping tendency of the emulsifier from the oil-water interface of the former small droplets is the same as that of the latter. This can be studied by the following Kelvin-Gibbs relation[4,5], where the electric double-layer effect can be neglected;

$$\ln\frac{S_r}{S}=\frac{2\sigma M}{dR\Theta r} \qquad (2)$$

where

S_r=escaping tendency of emulsifier molecule from interface of radius r (r is negative for concave interface).
S=escaping tendency from plane interface.
σ=interfacial tension.
M=molecular weight of emulsifier (surfactant).
d=density of emulsifier molecule at the interface.
R=gas constant.
Θ=absolute temperature.

After the examination with relation (2), having substituted the appropriate values into (2), it was found that the variation of S_r/S with r becomes appreciable only when r is less than $10^{-4}\sim10^{-5}$ cm. So that, it

4) R. M. Wiley, *J. Colloid Sci.*, **9**, 427 (1954).
5) E. A. Guggenheim, "Thermodynamics, an Advanced Treatment for Chemists and Physicists", Interscience Publishers Inc., New York, (1950), p. 41.

is concluded that the escaping tendency of emulsifier from the interface of the large drops investigated in the present experiments, is practically the same as that of the small droplets with the diameter of a few μ. Referring to effects of the electric double layer on the solubility[6], the effects of the electric double layer on the escaping tendency of the emulsifier from the oil-water interface may be neglected under the present experimental conditions.

According to the relation (2), the escaping tendency of the emulsifier from the interface to the water or oil phase is independent of the state of the interface, whether it is convex or concave. Therefore it can not be determined by the relation (2) which more stable or persistent, the oil drop or the water drop is. However, if it is assumed that the escaping of the emulsifier molecule into the continuous phase is likely to be hindered by the close juxtaposition of the interfaces, the probability to form a defect will be determined by the escaping tendency of the emulsifier into the aqueous phase or the oil phase, in the case of water drops or oil drops respectively. The difference of the life-time between the aqueous and oil drops, as can be seen in Table I, may clearly be explained with the above assumption.

The type of the emulsion produced with the combination of oil, water and emulsifier will be determined by several factors, including volume ratio of oil to water, characteristics of the emulsifier used and mechanical conditions such as stirring, shaking etc. Therefore, it can not be foretold from the difference of the values T_O and T_W, whether the O/W type emulsions will be produced or W/O type. However, in the system in which the difference in viscosity between oil and water is small such as benzene and water, it may be said that O/W type emulsion is more stable or persistent if T_O is greater than T_W and, W/O type, if T_O is less than T_W, as the emulsions produced using a given emulsifier.

It is not easy to estimate the stability of emulsions according to the values of T. However, it may be said qualitatively that the system having the value of T at least a few times greater than ten seconds must be used in order to obtain the emulsions in which the breaking of emulsions is not observed after a month or more.

6) A. E. Alexander and P. Johnson, "Colloid Science", Oxford University Press, London (1949) p. 37.

Summary

The stability or persistency of drops at an oil-water interface in the presence of emulsifier has been studied. The behavior of drops at an oil-water interface has been observed using colored drops to interpret the process of the coalescence.

A mechanism, which explains the coalescence of drops at an oil-water interface more reasonably, was proposed as follows: the main process of the coalescence of drops at an oil-water interface is the formation of a defect in the emulsifier layer around the drops at the portion in contact with the plane interface.

The stability or persistency of emulsions may be estimated qualitatively by the values of T obtained in the present investigations.

The authors would like to express their gratitude to Professor Sôzaburo Ono for his kind guidance and discussion throughout this work. The cost of the present research has been partly defrayed from the Scientific Research Grant from the Ministry of Education.

Laboratory of Biophysical Chemistry
College of Agriculture, University of
Osaka Prefecture, Sakai

SHORT COMMUNICATIONS

Synthesis of L-Pyroglutamyl-L-glutaminyl-L-glutamine

By Tetsuo SHIBA, Shigeo IMAI and Takeo KANEKO

(Received January 6, 1958)

The synthesis of eisenine[1] isolated from a brown marine alga *Eisenia bicyclis* Setchell had been recently performed by us[2]. Eisenine is a tripeptide having the structure L-pyroglutamyl-L-glutaminyl-L-alanine. In 1949 a tripeptide fastigiatine* was isolated by J. S. Fruton and his collaborators[3] from American brown alga *Pelvetia fastigiata*. In the present investigation L-pyroglutamyl-L-glutaminyl-L-glutamine proposed by J. S. Fruton for the structure of fastigiatine was synthesized according to the following scheme similar to the synthetic route of eisenine.

A mixed anhydride from γ-methyl-carbobenzyloxy-L-glutamate (I) and ethyl chloroformate was coupled with L-glutamine to yield carbobenzyloxy-L-(γ-methyl ester)-glutamyl-L-glutamine (II) (37%), $C_{19}H_{25}O_8N_3 \cdot 2H_2O$, m.p. 184.5—185°C**. Compound (II) was converted by methanolic ammonia into amide ammonium salt (III) (77%), m.p. 195—196°C (dec.), which was heated at 100°C over phosphorous pentoxide in vacuo to give carbobenzyloxy-L-glutaminyl-L-glutamine (IV), m.p. 177—178°C. Carbobenzyloxy diamide (IV) was

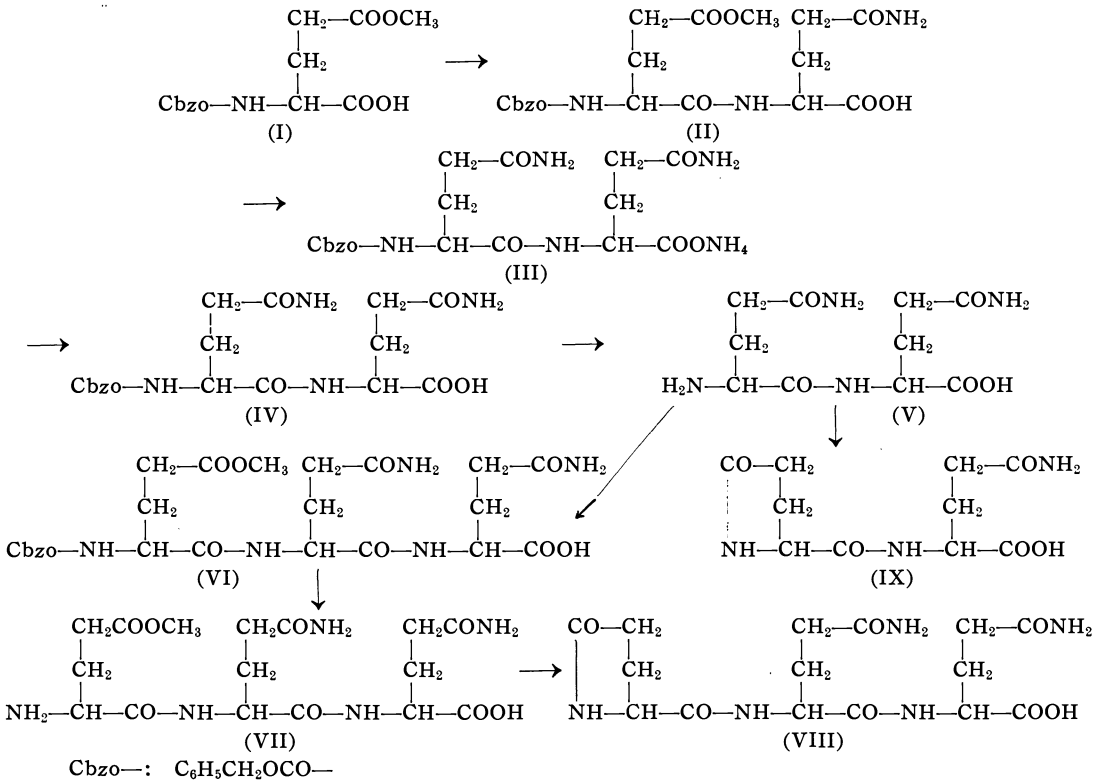

1) T. Ohira, *J. Agr. Chem. Soc. Japan* (*Nogei Kakaku Zassi*) **15**, 370 (1939).
2) T. Kaneko, T. Shiba, S. Watarai, S. Imai, T. Shimada and K. Ueno, *Chem. & Ind.* (London), **1957**, 986.
3) C. A. Dekker, D. Stone and J. S. Fruton, *J. Biol. Chem.*, **181**, 719 (1949).
4) A. Meister, "Biochemistry of the Amino Acids", Academic Press Inc., Publishers, N. Y. (1957), p. 56.

* For this tripeptide, J. S. Fruton has expressed in the term of "peptide from *Pelvetia fastigiata*". While the name "pelvetine" was used by us early, A. Meister[4] employed the nomenclature "fastigiatine". Now, we use fastigiatine instead of pelvetine to avoid the confusion of these nomenclatures.

** All melting points were uncorrected.

hydrogenated using palladium charcoal to L-glutaminyl-L-glutamine (V) (78%), $C_{10}H_{18}O_5N_4\ 1\frac{1}{2}H_2O$, m. p. 208—209°C (dec.). $[\alpha]_D^{29}$ +24.54° (*c*, 1.74, in H_2O). Furthermore diamide (V) and γ-methylcarbobenzyloxy-L-glutamate (I) were combined through the mixed anhydride method as described above, to yield carbobenzyloxy tripeptide derivative (VI) (53%), m. p. 175—180°C (dec.), which was hydrogenated to compound (VII) (61.3%), m. p. 221°C (dec.). Compound (VII) was cyclized in absolute methanol saturated with ammonia, followed by treatment with Dowex 50 to obtain L-pyroglutamyl-L-glutaminyl-L-glutamine (VIII)*** (80%), m. p. 203—204°C (dec.), $[\alpha]_D^{28}$ −36.24° (*c*, 2.02, in H_2O), pK_a' 3.5.

Anal. Found: C, 46.75; H, 5.81; N, 18.47; equiv. 427. Calcd. for $C_{15}H_{23}O_7N_5$: C, 46.75; H, 6.02; N, 18.17%; equiv. 385.

While this substance failed to give a color with ninhydrin, it gave a strong biuret reaction. From the results obtained above, however, it is not necessarily concluded that this synthetic product was identical with natural fastigiatine, since the latter has m. p. 190—195°C and $[\alpha]_D$ −43.7∼−46.5° (in H_2O).

The cyclization of a γ-amide to a pyroglutamyl derivative can also be successfully produced by boiling the aqueous solution of the former. For example, L-glutaminyl-L-glutamine (IV) was converted by this procedure into L-pyroglutamyl-L-glutamine (IX) (73%), m. p. 178—180°C (dec.), $[\alpha]_D^{15}$ −22.14° (*c*, 1.65 in H_2O).

Department of Chemistry, Faculty of Science, Osaka University
Kita-ku, Osaka

*** After this synthesis had been accomplished, a private communication from Professor J. Rudinger to Professor S. Akabori indicated that Professor Rudinger and his collaborators have also succeeded in the synthesis of the same peptide independently of ours.

On the Volatility of Polonium Compounds

By Hisao MABUCHI

(Received January 14, 1958)

As reported before[1], polonium dithizonate sublimes at about 120°C under atmospheric pressure. In order to confirm whether or not such a low-temperature sublimation is characteristic of dithizonate, the volatility of other polonium compounds was studied. The compounds investigated were those which are extractable with organic solvents. They are divided into two groups according to their chemical species.

Group I: The compounds resulting from the interaction of polonium with organic reagents. The organic reagents used for this study are as follows: 8-hydroxyquinoline, sodium diethyl-dithiocarbamate, thenoyltrifluoroacetone, thiourea, *sym*-diphenylthiourea, thiosemicarbazide, 1-phenylthiosemicarbazide, diphenylcarbazone, diphenylcarbazide, diphenylthiocarbazone and di-β-naphthylthiocarbazone.

Group II: The polonium compounds which are extracted in the absence of organic reagents;

(a) polonium compound which is extracted with *iso*-propyl ether from an aqueous solution of 0.5 M potassium iodide and 3 N hydrochloric acid[2].

(b) polonium compound which is extracted with methyl *iso*-butyl ketone from an aqueous solution of 0.5 M potassium iodide and 1.5 N hydrochloric acid[2].

The samples were mounted in stainless steel dishes and the heating was carried out on a hot plate. The measurement of polonium activity was made with a Lauritsen electroscope.

The results of the experiment are summarized below;

1) All polonium compounds of Group I sublime below 160°C/1 atm., while no sublimation is observed even at 200°C/1 atm. for the compounds of Group II.

(2) The volatility of the polonium compounds with organic reagents of a similar type tends to decrease in the following order.

thiourea > *sym*-diphenylthiourea.

diphenylcarbazone, diphenylcarbazide > diphenylthiocarbazone > di-β-naphthylthiocarbazone.

(3) The volatility is remarkable for the compounds with diphenylcarbazone, diphenylcarbazide and diphenylthiocarbazone. Above all, the compounds with the first two reagents sublime below 100°C/1 atm.

From the results mentioned above, it follows that the low-temperature sublima-

1) K. Kimura and H. Mabuchi, This Bulletin, **28**, 535, (1955).

2) K. Kimura, N. Saito, Y. Koda and K. Tanaka, paper presented before the 9th Annual Meeting of the Chemical Society of Japan (1956).

tion is not characteristic of polonium dithizonate, but common to many organo-compounds of polonium.

As an application of this property of polonium organo-compounds to radiochemical analysis, the carrier-free separation of radium-F (polonium) from radium-D (lead) and radium-E (bismuth) was carried out by distillation of polonium compounds with diphenylcarbazide. The most effective procedure for distillation is as follows.

Fifty milliliters of nitric acid solution of radium-D, -E, -F mixture is taken in an all-glass distilling apparatus. The acidity of the solution should be adjusted between 0.1 and 0.5 N in nitric acid. To this solution is added 30 mg. of diphenylcarbazide. Then the distillation is carried out until one half of the initial volume of the solution is distilled. Radiochemically pure radium-F is found in the distillate. Moreover, this aqueous distillate is almost free from the excess of the organic reagent. The presence of strong oxidizing agents and the chloride ion in the initial solution decreases the efficiency of separation.

The detail of these studies will be reported in a separate paper.

The author would like to express his sincere thanks to Professors N. Saito and Y. Yokoyama of this laboratory and to Dr. K. Kimura of Japan Atomic Energy Research Institute for their valuable advice and helpful discussion.

Department of Chemistry, Faculty of Science, The University of Tokyo
Hongo, Tokyo

Rate Equation for the Chemisorption of Nitrogen on Ammonia Synthesis Catalysts

By Takao KWAN

(Received December 26, 1957)

The present author put forward a power rate law[1] expressed by

$$-\frac{dp}{dt}=kp\theta^{-\alpha} \qquad (1)$$

to describe adequately the rate of the chemisorption of nitrogen on a promoted iron catalyst. Zwietering and Roukens[2] also investigated the same system and applied their data to the Elovich type equation of the form

$$-\frac{dp}{dt}=kpe^{-g\theta} \qquad (2)$$

Recently Scholten and Zwietering[3] expressed their view that the experimental data due to Kwan are well subscribed in the Eq. (2) rather than (1). Whether or not experiments conform to these equations can be demonstrated viz., power rate law should give a linear relation in the logarithmic plot of $-1/p\cdot dp/dt$ against θ while the Elovich equation a linear semi-log plot. The purpose of the present note is to show a semi-log plot on the data already published by this author and discuss the consequences.

Rate data at 300 and 400C given in Table II of the previous paper[4] are far below equilibrium and permit ignoring the desorption of nitrogen. They are reproduced in Fig. 1 in a semi-log scale. Apparently experimental plots are curved convexly against θ-axis. Such curvilinear plots in a semilog scale were reproducible with respect to any $p-t$ run measured in a constant volume on the re-reduced catalyst, hence throwing doubt on the validity of the Elovich equation.

Experimental data obtained repeatedly on a re-reduced catalyst were found however to shift more or less in relation each other with each run, probably due to different surface states. Thus, if one plot several runs in a semi-log scale, than an approximate linear relation may appear within the experimental accuracy. A straight line of this kind has been demonstrated by Scholten and Zwietering[3].

If, on the other hand, one plot the experimental data for any single run in a logarithmic scale, a good linear relation holds with a break near $\theta=0.08$. Such a plot has been preferred by this author and presented together with those of other runs in the previous paper[4]. Unfortunately the measurements were only within a small range of coverage. Further works are needed to confirm the linearity of the latter kind at a higher coverage.

Assuming that the linear portion extends far beyond $\theta=0.08$, activation energies for

1) T. Kwan, *J. Res. Inst. Catalysis*, **3**, 16 (1953); This Bulletin, **27**, 70 (1954).

2) P. Zwietering and J. J. Roukens, *Trans. Faraday Soc.*, **49**, 543 (1954).

3) J. J. F. Sholten and P. Zwietering, ibid., **53**, 1363 (1957).

4) T. Kwan, *J. Res. Inst. Catalysis*, **3**, 109 (1955).

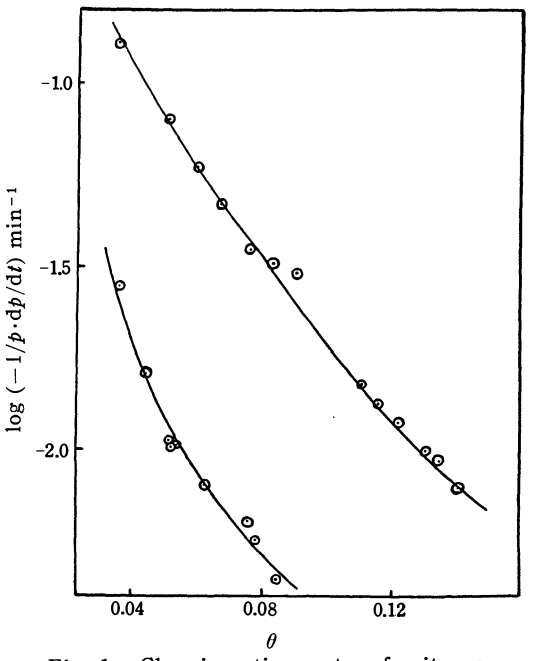

Fig. 1. Chemisorption rate of nitrogen as a function of coverage θ constructed from a single $p-t$ run obtained by Kwan[4]. T: 300° and 400°C.

the chemisorption of nitrogen were given by[4]

$$E=11\log\theta+23\ \text{kcal./mole}$$

Apart from the numerical value, this functional form for E seems compatible with the result of Zwietering and Roukens that the experimental E is not linear but concave against θ-axis at higher coverage of their measurements. Such a curved portion, when plotted against $\log\theta$, gives a linear portion in accordance with the above function—a family of power rate law.

Such an argument has been a frequent problem in adsorption—for instance the shape of adsorption isotherm and the corresponding heat curve. The author expressed his view elsewhere[5] that the Langmuir type isotherm is useful at lower coverage only, whereas the Freundlich equation provides an excellent validity at higher coverage. As a consequence, the isothermal heat curve appears to be somewhat reverse-s-shaped or linear against $\log\theta$ at higher coverage, e.g., hydrogen on a reduced nickel powder[6]. Schuit et al. observed adsorpiton isotherms for hydrogen on nickel-on-silica and derived a linear heat decrease with θ. On closer inspection, the heat-coverage relation is, according to them[7], slightly sigmoidal in character. It is the opinion of this author that different viewpoints expressed by Zwietering et al. and the author mentioned above may lie in a situation such was revealed in the adsorption of hydrogen on a nickel sample.

Research Institute for Catalysis and Chemistry Department, Hokkaido University, Sapporo

5) T. Kwan, *Advances in Catalysis*, **6**, 67 (1954).
6) S. Ohkoshi and T. Kwan, *J. Res. Inst. Catalysis*, **4**, 199 (1957).
7) G. C. A. Schuit et al., "Chemisorption" edited by Garner, 39 (1957) Butterworths Scientific Pub. London.

X-ray Determination of the Molecular Weight of Luteoskyrin

By Hiroshi Okuto*, Yoshio Sasada and Kiichi Sakurai

(Received January 6, 1958)

A chemical study on luteoskyrin, one of the toxic components produced by penicillium islandicum, has been carried out by T. Yamamoto, Y. Yamamoto, Kanatomo, Tanimichi and Kikui[1]. According to their results, this substance exists in two different crystal forms; one is needle-like and the other cube-shaped. The former is obtained by recrystallization from an ethanolic solution, and the latter from a mixed solvent of aceton, petroleum benzine and water (2:1:1). Both forms of crystals have the same composition, $C_{2.45}H_{2.05}O_1$.

Since ordinary methods failed to give a reliable value for the molecular weight, we applied the single crystal X-ray diffraction method to its determination. The samples used in this study were supplied by the above-mentioned authors.

The unit-cell dimensions of each form were determined from oscillation and Sauter-Schiebold photographs about the *c* axis taken with Cu K_α radiation. The length of the *c* axis was measured from layer-line spacings. The other two axial lengths were first estimated roughly from Sauter-Schiebold photographs and accurately determined using the spectra on a set of oscillation photographs which were

* Present address: Research Laboratories, Takeda Pharmaceutical Industries, Ltd.

1) Y. Yamamoto, T. Yamamoto, S. Kanatomo, K. Tanimichi and H. Kikui, *J. Pharm. Soc. Japan, (Yakugaku Zassi)* **76**, 670, (1956).

completely indexed by the graphical method.

The densities were measured by the floatation and the pyknometer methods** at 20°C. In the former method, aqueous solution of zinc chloride was used as floatation liquid. The results are tabulated in Table I.

TABLE I
CRYSTAL DATA

Crystal form	needle-like	cube-shaped
Crystal system & lattice type	orthorhombic primitive lattice	monoclinic primitive lattice
Lattice constants		
a	14.8_4 Å	15.1_7 Å
b	15.0_3	12.6_4
c	12.5_0	21.5_0
α	90°	90°
β	90°	135°***
γ	90°	90°
Volume of cell	2.79×10^3 Å^3	2.91×10^3 Å^3
Density	1.48 g.cm^{-3}.	1.47 g.cm.$^{-3}$

From the volume of the unit cell V and the density ρ, the molecular weight M can be calculated according to the formula

$$M=\rho VN/Z,$$

where N is the Avogadro number and Z the number of molecules in the unit cell, which is necessary to calculate M. From symmetry consideration, Z should be 2^n. However, the value of Z greater than eight can be excluded on account of the fact that the molecular weight of this substance has been supposed to be of the order of several hundreds[2], and this is also supported by its high melting point (273°C decomp.). It is highly improbable that Z equals to unity. The value of Z is four or two, the former being more probable.

When Z is assumed to be four, the molecular weight is found to be 621±30 for needle-like crystals and 644±20 for cube-shaped.

The difference, if it is significant, between these two values may be due to the fact that one or both forms crystallize with solvent molecules, but this can not be concluded from this experiment alone.

Faculty of Science, Osaka University
Kita-ku, Osaka

** In order to lower interfacial tension, a small amount of surface-active substance was added.

*** This value was estimated using layer-line reflections on the oscillation photographs.

2) T. Yamamoto, Private communication.

*On the Ring Opening Reaction of ε-Caprolactam Derivatives**

By Hirosuke YUMOTO, Kenzaburoh IDA and Naoya OGATA

(Received October 14, 1957)

It must be considered for the condensation polymerization whether ring-monomer and -oligomers are stable or not; if |–A–| or |–A–A–| is considerably stable in comparison with –A– or –A–A–, such a large quantity of the ring-monomer or -dimer may be produced that the polymer molecule can not be found in the reaction product. δ-Aminovaleric acid or δ-valerolactam is an instance of the former case and α-amino-acid dimer or diketopiperazine is that of the latter case. Thus the ring-chain equilibrium is not only interesting in the structural chemistry but also important for the purpose of polymer manufacturing. It is the object of this paper to study experimentally the influence of side chains on ε-caprolactam polymerization.

Results

Monomethyl-ε-caprolactam. — Methyl cyclohexanone (b. p. 160~170°C) was obtained from cresol (b. p. 190~200°C) through methyl cyclohexanol (b. p. 165~175°C) by the usual method. Methyl-ε-caprolactam (b. p. 123~124°C/5mmHg) was prepared from methyl cyclohexanone with a yield of 75 % by Schmidt's method using sodium azide[1]. This monosubstituted caprolactam, which was a mixture of α, β, γ, δ and ε-derivative, was used for the polymerization experiment; the melting point of the polymer is 164~166°C. Methyl-ε-aminocaproic acid was prepared by the hydrolysis of methyl-ε-caprolactam.

About 3 g. of monomethyl-ε-caprolactams was previously polymerized, with 0.1~0.05 g. of monomethyl-ε-aminocaproic acid as the catalyst, by heating in a glass tube at 230°C for 100 hr. Then, after the tube was sealed, heating was continued at 280°C for 15 hr., at 257°C for 25 hr., at 215°C for 30 hr. or at 182°C for 30 hr. to reach the equilibrium at each temperature. The quantities of lactam-monomer and -oligomers were measured by the same procedure with that for the unsubstituted polycapramide[2]. The intrinsic viscosity of polymerized contents was also measured in the cresol solution at 25°C. The obtained results are shown in Table I.

TABLE I

ANALYTICAL VALUES OF POLY-MONOMETHYL-ε-CAPRAMIDE

($L_1°$ or $L_2°$ = mole of lactam-monomer or -oligomers in the product in the case that 1 mol. of monomer is initially used for polymerization)

Temp. of polymerization °C	$L_1°$ mol.	$L_2°$ mol.	$[\eta]^{25°C}_{cresol}$
280	0.198	0.022	0.56
257	0.164	0.023	0.57
230	0.150	0.021	0.64
205	0.129	0.021	0.69
182	0.119	0.018	0.74

The equilibrium of the reactions concerning lactam-monomer,

$$\mathrm{NH\cdot CO\cdot C_5H_9(CH_3)} + [\text{——}\mathrm{NH_3^+}] \underset{\kappa}{\overset{k}{\rightleftarrows}} [\text{——}\mathrm{NH\cdot CO\cdot C_5H_9(CH_3)\cdot NH_3^+}] \quad (1)$$

can be expressed by the following equation for the high polymeric system[2];

$$L_1° = A\kappa/k = AK \quad (2)$$

where $L_1°$ is the mole number of lactam-monomer at equilibrium, A the whole mole number of the average unit of the Brownian motion in the reaction phase, k the rate constant of ring-opening reaction, κ that of ring-closuring one and K the chain-ring equilibrium constant.

The values of A were determined by the experiment which follows. Monomethyl-ε-caprolactam was diluted with thymol at various ratios and polymerized at 230°C for 100 hr.; analytical results for products are given in Table II. The following equation can be applied to the increase of $L_1°$ with dilution as shown in the previous paper[3];

$$L_1°/(1-L_1°) = \kappa/k\{(S+L_1°)/(1-L_1°)\} + (\kappa/k)\alpha \quad (3)$$

where the mole number of the diluent per 1 mol. of the initial lactam-monomer is denoted by S and, on assuming that 1 mol. of lactam polymerizes completely into a chain molecule, the mole number

* Presented at the Annual Meeting of the Chemical Society of Japan at Kyoto, April 3, 1956.

1) T. Hoshino, Y. Iwakura and H. Iwasaki, *J. Polymer Chem. (Japan)*, **2**, 280 (1945).

2) H. Yumoto, This Bulletin, **28**, 94 (1955).

3) H. Yumoto, ibid., **28**, 101 (1955).

of the average unit of the Brownian motion by α. The data in Table II are used for Fig. 1, which satisfy the equation 3. From Fig. 1, α is estimated to be ca. 0.6 and consequently the average unit of the Brownian motion of chain macromolecules corresponds to 1.66(=1/0.6) structure units, i.e. 13.3(=8×1.66) skeleton atoms or 11.6(=7×1.66) ring-forming atoms. This value is smaller than 19 skeleton atoms for the unsubstituted one[3]; it means that the side chain such as methyl group makes the chain-molecules more kinky and activities of reaction components larger.

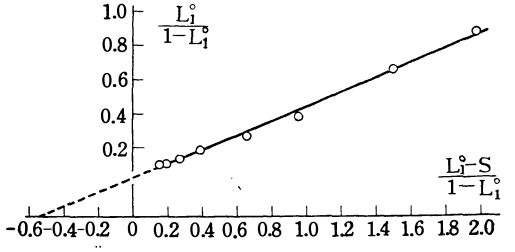

Fig. 1. The effect of dilution on the polymerization of monomethyl-ε-caprolactam.

TABLE II

ANALYTICAL VALUES OF PRODUCTS IN THE CASE THAT MONOMETHYL-ε-CAPROLACTAM IS POLYMERIZED UNDER THE DILUTION IN THYMOL AT 230°C

Initial Monomer mol.	Thymol mol.	L_1° mol.	L_2° mol.	$[\eta]^{25°C}_{cresol}$
1.00	0.846	0.349	0.027	—
〃	0.675	0.297	0.029	0.35
〃	0.507	0.229	0.027	0.39
〃	0.338	0.189	0.025	0.41
〃	0.169	0.155	0.023	0.51
〃	0.085	0.141	0.022	0.60
〃	0.043	0.132	0.021	0.65
〃	0.000	0.133	0.021	0.59

When there is no diluent,

$$A = L_1^\circ + (1 - L_1^\circ)\alpha \qquad (4)$$

The value of α for unsubstituted poly-ε-capramide is hardly changed at all with the temperature in the range from 200 to 250°C[3]. On the assumption that α is 0.6, equilibrium constants $K(=\kappa/k)$ can be found by equations 4 and 2; they were calculated as given in Table III. The relation between K and the absolute temperature T in Fig. 2 is expressed as follows:

$$\log K = 0.39 - 500/T \qquad (5)$$

Then the heat of the ring-opening reaction was estimated to be 2.3 kcal/mol., which is smaller than the value 3.5 kcal/mol. for the unsubstituted one[3].

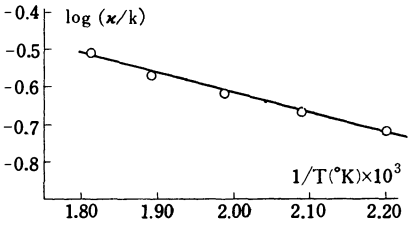

Fig. 2. The effect of temperature on the polymerization of monomethyl-ε-caprolactam.

TABLE III

EQUILIBRIUM CONSTANTS ON RING-CHAIN EQUILIBRIA AT VARIOUS TEMPERATURES FOR MONOMETHYL-ε-CAPROLACTAM

Temp. °C	L_1° mol.	A mol.	K
280	0.198	0.639	0.310
257	0.164	0.624	0.263
230	0.150	0.617	0.237
205	0.129	0.608	0.212
182	0.119	0.603	0.197

(1 mol. of lactam monomer is used for polymerization)

The relation between the intrinsic viscosities in the cresol solution ($[\eta]$) and the number average degrees of polymerization ($\overline{P}$), which were calculated from the numbers of the carboxyl end-group, is shown in Fig. 3. The following equation can be derived approximately,

$$\overline{P} = K_m[\eta]^a$$

where K_m is 214 and a is 1.67; these are

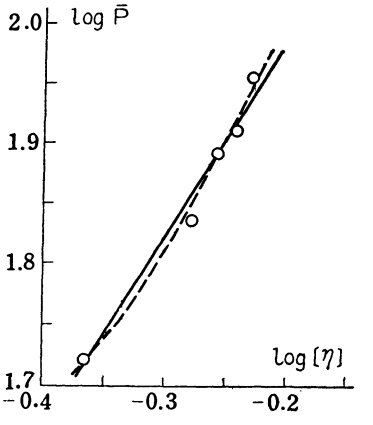

Fig. 3. The relation between the degree of polymerization of poly-monomethyl-ε-capramide and its intrinsic viscosity in cresol solution at 25°C.

TABLE IV
ANALYTICAL VALUES FOR POLY-MONOMETHYL-ε-CAPRAMIDE USING ACETIC ACID TO CONTROL THE DEGREE OF POLYMERIZATION

Acetic acid mol./1mol. of lactam monomer	-COOH mol./127 g of polymer	$-NH_2$ mol./127 g of polymer	$[\eta]^{25°C}_{cresol}$
0.0200	1.89×10^{-2}	0.27×10^{-2}	0.431
0.0100	1.44 〃	0.45 〃	0.526
0.0066	1.30 〃	0.51 〃	0.554
0.0050	1.21 〃	0.53 〃	0.569
0.0033	1.11 〃	0.60 〃	0.584

greater than the values of K_m(=127) and a(=1.44) for the unsubstituted one.[4]

N-Methyl-ε-caprolactam. — N-methyl-ε-caprolactam (b. p. = 124°C/123 mmHg and $n_D^{25} = 1.428$) was prepared from ε-caprolactam by dimethyl sulfuric acid[5], and N-methyl-ε-aminocaproic acid containing 2 moles of the water of crystallization (m. p. 69°C) was obtained by the acid hydrolysis of N-methyl-ε-caprolactam[5]. On heating N-methyl-ε-caprolactam at 230°C with water, water and benzoic acid, or water and ε-aminocaproic acid, no polymer molecules were obtained. N-methyl-ε-aminocaproic acid transformed into N-methyl-ε-caprolactam on heating at 230°C. N-methylol-ε-caprolactam, prepared from ε-caprolactam and formladehyde[5], did not polymerize, either.

These results agree with J. Prochazka's, that N-substituted caprolactam does not polymerize[6]. Poly-N-methyl-ω-hendecanamid or -undecanamid has been known[7]. Then the reason, why N-derivatives of ε-caprolactam can not polymerize, seems to be ascribed to their small ring size.

Dimethyl-ε-caprolactam.—The mixture of α, δ and β, ε-dimethyl ε-caprolactam (m. p. 95~98°C, b. p. 110~115°C/5 mmHg) was prepared from p-xylenol through p-dimethyl cyclohexanol (b. p. 179°C), p-dimethyl cyclohexanone (b.p. 80°C/25 mmHg) and its oxime (m. p. 97°C) by a process similar to that for the caprolactam manufacturing. Dimethyl-ε-aminocaproic acid (m. p. 173~175°C) was obtained by the hydrolysis of dimethyl ε-caprolactam.

Dimethyl ε-caprolactam was heated with catalysts at 230°C for five hours but did not polymerize at all. When dimethyl ε-aminocaproic acid was heated at 230°C for five hours, it only transformed into dimethyl ε-caprolactam and no polymer was obtained.

It is suggested, therefore, when two hydrogen atoms on the different carbon atoms in ε-caprolactam ring are replaced by methyl groups, the ring-chain equilibrium shifts extremely to the ring-form. Even by the use of amino acid for the starting material, it changes into lactam ring by the intramolecular condensation; the contribution of the intermolecular condensation is too small to give the polymer molecule.

Hoshino has already published in 1941[8] the experiment that menton isoxime (methyl isopropyl ε-caprolactam) does not polymerize at all.

Conclusion

The experimental results on the ring-chain equilibria for monomethyl ε-caprolactam can be analyzed through the same procedure with that for the unsubstituted one; the substitution shifts the equilibrium to the ring-form. The heat of reaction, i. e. the energy difference between the chain and the ring form for the monomethyl derivative is 2.3 kcal/mol., which is smaller than 3.5 kcal/mol. for the unsubstituted one.

For dimethyl and N-methyl or -methylol derivatives the equilibria shift too much in favor of the ring-form to give polymer molecules at high temperatures. When amino acids, which are prepared from these lactams by hydrolysis, are heated, they transform into lactam. The theoretical interpretation on these behaviors can be made by the intramolecular rotational isomers[9], which will be reported subsequently. The average unit of the Brownian motion of chain molecules, i. e. the segment, for the monomethyl derivative is 13.3 skeleton atoms which is smaller than 19 skeleton atoms for the unsubstituted polycapramide; the substitution makes it easier for chain molecules to be kinky.

Summary

The ring-chain equilibria,

$$-CO-R-NH- \rightleftharpoons \underset{|}{CO}-R-\underset{|}{NH}$$

were investigated experimentally for ε-caprolactam derivatives and their results

4) O. Fukumoto, *J. Polymer Sci.*, **22**, 263 (1956).
5) R. E. Benson and T. L. Cairns, *J. Am. Chem. Soc.*, **70**, 2115 (1948).
6) J. Procházka, *Chem. Listy.*, **37**, 202 (1943); *Chem. Abst.*, **40**, 2113 (1946).
7) G. Champetier and R. Aelion, *Bull. soc. chim. France*, 683 (1948); *Chem. Abst.*, **42**, 7099 (1948).
8) K. Hoshino, *J. Chem. Soc. Japan Pure Chem. Sec.* (*Nippon Kagaku Zassi*), **63**, 1184 (1942).
9) H. Yumoto, Presented at the Symposium on the Structural Chemistry of the Chemical Society of Japan in Nagoya, October 16, 1956.

could be analyzed by the method similar to that for ε-caprolactam. For the monomethyl derivative the equilibrium shifts to the ring-form and ΔH has been estimated to be 2.3 kcal/mol. which is smaller than ΔH(=3.5 kcal/mol.) for the unsubstituted. For dimethyl and *N*-methyl or -methylol derivatives equilibria shift too much to the ring-form to give polymers at high temperatures. The average unit of the Brownian motion of polymer chain molecules, i. e. the segment, for the monomethyl derivative is 13.3 skeleton atoms which is smaller than 19 skeleton atoms for unsubstituted polycapramide; the substitution makes it easier for chain molecules to be kinky.

The authors wish to thank Drs. K. Hoshino and H. Kobayashi who instructed them and permitted the publication.

Nylon Laboratory, Research Department
Toyo Rayon Co., Ltd.
Minato-ku, Nagoya

Studies on the Antitubercular Compounds. XIII. Preparation of Some Derivatives of Benzimidazole and 2, 1, 3-Benzothiadiazole***

By Isao SEKIKAWA

(Received November 11, 1957)

In the foregoing paper[1], several kinds of 2-substituted benzimidazole compound were prepared and their antibacterial activities in vitro were examined. As a result 2-mercaptomethylbenzimidazole was found to be most effective against Mycobacterium tuberculosis.

Brown et al.[2] and Kushner et al.[3], who studied the tuberculostatic action of alkylmercapto derivatives, found that structural modification, which increased its ability to release ethylmercaptan, increased the antitubercular activity. Therefore, a series of alkylthioether was prepared for comparative studies as indicated in Table I. A compound which was formed by condensation of *o*-phenylenediamine with alkylthioglycolic acid in the presence of dilute hydrochloric acid was identical with that obtained by condensation of mercaptomethylbenzimidazole with alkyl bromide, thus confirming the fact that *S*-alkylation occurred.

Benzimidazole derivatives having substituents at the phenyl nucleus are shown in Table II. Condensation of 3, 4-diaminophenetole with formic acid in the presence of dilute hydrochloric acid gave 5-ethoxybenzimidazole, which was converted into VI by the acid cleavage of ether group. VII was obtained by amination of the corresponding acid chloride. VIII was

TABLE I

2-ALKYLMERCAPTOMETHYLBENZIMIDAZOLE DERIVATIVES

No.	R	Method of prepn.	Yield (%)	m. p. (°C)	Appearance	Formula	Analysis (%) Calcd. C	Calcd. H	Found C	Found H
I	CH_3	b	90	156—157	Pale yellow needles	$C_9H_{10}N_2S$	60.64	5.60	60.37	5.96
II	C_2H_5	b	60	136—137	White needles	$C_{10}H_{12}N_2S$	62.46	6.29	62.57	6.69
III	*n*-C_3H_7	b	80	122—124	〃	$C_{11}H_{14}N_2S$	64.04	6.34	63.67	7.01
IV	*n*-C_4H_9	a b	68 95	143—144	〃	$C_{12}H_{16}N_2S$	65.41	7.31	65.10	7.45

* This constitutes a part of a series entitled "Studies on the Antitubercular Compounds" by S. Kakimoto.

** A part of this study was presented at the Annual Meeting of the Chemical Society of Japan in Tokyo in April 6, 1957. Paper XII, S. Kakimoto and K. Yamamoto: *Kekkaku no Kenkyu* (Annual Report of the Research Institute for Tuberculosis, Hokkaido University), **6**, 1 (1956).

1) S. Kakimoto and I. Sekikawa, *J. Chem. Soc. Japan, Pure Chem. Sec.*, (*Nippon Kagaku Zassi*), **77**, 78 (1955).

2) H. D. Brown, M. Solotorvsky and I. H. Quastel, *J. Am. Chem. Soc.*, **76**, 3860 (1954).

3) S. Kushner, H. Dalalian and L. Bach, ibid., **77**, 1152 (1955).

TABLE II
BENZIMIDAZOLE DERIVATIVES

V	5-NO_2[4]
VI	5-OH
VII	5-$CONH_2$
VIII	5-$CONHNH_2$

TABLE III
2,1,3-BENZOTHIADIAZOLE DERIVATIVES

IX	5-NO_2[5]
X	5-OH[6]
XI	4-NO_2[7]
XII	4-$NHCOCH_3$[8]

prepared by the usual method.

2,1,3-Benzothiadiazole derivatives, which were formed by replacing the carbon atom of 2-position in benzimidazole molecule with sulfur atom, are shown in Table III. Reduction of XI with tin or stannous chloride in the presence of hydrochloric acid gave the parent *o*-phenylenediamine and sulfur. Vigorous reduction produced hydrogen sulfide[9]. Khaletskiĭ et al.[10] obtained a 4-amino compound by reduction of the nitro compound with acetic acid and iron powder. However, the present author found that the compound was very readily obtained by reducing the nitro compound with sodium chloride and iron powder in the presence of a minute amount of hexachloroplatinic acid.

Recently, Huebner et al.[11] reported a relation between chemical structure and antibacterial activity in the case of over three hundred compounds of *N,N'*-disubstituted thiourea derivatives and Konopka et al.[12] found that 4-ethoxy-4'-*iso*-butoxythiocarbanilide and 4-*n*-butoxy-4'-dimethylaminothiocarbanilide were the most effective in vivo.

A series of *N*-(Benzothiadiazolyl-4)-*N'*-(*p*-alkoxyphenyl)-thiourea, indicated in Table IV, was prepared. XIII, XIV, XV, XVI and XVII were derived from 4-aminobenzothiadiazole and phenyl-, *p*-methoxyphenyl-, *p*-ethoxyphenyl-, *p*-*n*-propoxyphenyl- and *p*-*n*-butoxyphenyl-isothiocyanate by the usual method.

Upon oxidation of 5-methylbenzothiadiazole with potassium permanganate by the usual procedure, the corresponding 5-benzothiadiazolecarboxylic acid was not obtained; an unknown acidic substance of m.p. 281°C (decomp.) was, on the other hand, formed. The investigation of the structure of this compound is now in progress.

The antitubercular activities of all derivatives described above were examined in vitro, and found less active than 2-mercaptomethyl-benzimidazole[1].

Experimental

IV. (a) A mixture of 2 g. of *o*-phenylenediamine, 3 g. of *n*-butylmercaptoacetic acid, 10 ml. of concentrated hydrochloric acid, and 10 ml. of water was refluxed for 12 hr., and the solution was concentrated under reduced pressure. The residue was dissolved in 10 ml. of water, and the solution was poured slowly into 20 ml. of cold concentrated ammonium hydroxide. The solid thus formed was recrystallized from 70 % ethanol to give 3 g. (68%) of white needles m.p. 145°.

V. (b) To a solution of 0.5 g. sodium metal in 30 ml. of *n*-butanol, 3.3g. of 2-mercaptomethylbenzimidazol was added, with stirring. The mixture was cooled and 2.7 g. of *n*-butylbromide in 10 ml. of *n*-butanol was added in small portions during 10 min. The mixture was then stirred for another 15 min., and then refluxed for 5 hr. After removal of the *n*-butanol, 70 ml. of water was added and allowed to stand overnight in an ice box. The solidified product was recrystallized from 70% ethanol to give 4.3 g. (95%) of

TABLE IV
N-(BENZOTHIADIAZOLYL-4)-*N'*-SUBSTITUTED THIOUREA DERIVATIVES

No.	Substituent	Yield (%)	m. p. (°C)	Appearance	Formula	Analysis (%) Calcd. C	Calcd. H	Found C	Found H
XIII	C_6H_5-	73	154—155	Yellow needles	$C_{13}H_{10}N_4S_2$	54.52	3.52	54.40	3.93
XIV	*p*-CH_3O-C_6H_4-	65	161—162	〃	$C_{14}H_{12}ON_4S_2$	53.14	3.82	53.14	4.10
XV	*p*-C_2H_5O-C_6H_4-	70	173—174	〃	$C_{15}H_{14}ON_4S_2$	54.52	4.27	54.56	4.56
XVI	*p*-C_3H_7O-C_6H_4-	54	146—148	〃	$C_{16}H_{16}ON_4S_2$	55.79	4.68	55.83	4.83
XVII	*p*-C_4H_9O-C_6H_4-	57	139—141	〃	$C_{17}H_{18}ON_4S_2$	56.96	5.06	57.32	5.30

4) G. M. van der Want, *Rec. trav. chim.*, **67**, 45 (1948).
5) A. M. Khaletskiĭ and V. G. Pesin, *Zhur. Obshcheĭ Khim.*, **24**, 133 (1954); *Chem. Abst.*, **49**, 3170 (1955).
6) Heineman, *Friedländer*, **11**, 1126 (1915).
7) L. S. Efros and R. N. Levit, *Zhur. Obshchei Khim.*, **23**, 1552 (1953); *Chem. Abst.*, **48**, 1209 (1956).
8) L. S. Efros and R. N. Levit, ibid **25**, 199 (1955); *Chem. Abst.*, **50**, 1783 (1954).
9) Bayer and Co., *Friedländer*, **2**, 534 (1891).
10) A. M. Khaletskiĭ and V. G. Pesin, *Zhur. Obshcheĭ Khim.*, **20**, 1914 (1950); *Chem. Abst.*, **46**, 106 (1952).
11) C. F. Huebner, J. L. Marsh, P. H. Mizzoni, R. P. Mull, D. C. Schroeder, H. A. Trovell and C. R. Scholz, *J. Am. Chem. Soc.*, **75**, 2274 (1953).
12) E. A. Konopka, P. C. Eisman, R. L. Mayer, F. Paker and S. L. Pobbins, *Amm. Rev. Tuberc.*, **70**, 130 (1954).

white needles, m.p. 143~144°C, showing no depression on admixture with the above-mentioned sample (a).

Anal. Found: C, 65.10; H, 7.45. Calcd. for $C_{12}H_{16}N_2S$: C, 65.41; H, 7.31%.

VI. A mixture of 7.5 g. of 3, 4-diaminophenetole dihydrochloride, 10 ml. of 80% formic acid, 5 ml. of concentrated hydrochloric acid, and 30 ml. of water was refluxed for 8 hr. The mixture was evaporated under a reduced pressure and the residue was poured into 30 ml. of concentrated ammonium hydroxide. The solid thus formed was recrystallized from ethanol to give 4.6 g. (85%) of 5-ethoxybenzimidazole, m.p. 118~119°C.

Anal. Found: C, 66.64; H, 6.18. Calcd. for $C_9H_{10}ON_2$: C, 66.65; H, 6.15%.

The hydrolysis was carried out by gently refluxing a mixture of 1.2 g. of 5-ethoxybenzimidazole and 4 ml. of hydriodic acid (d=1.7) for 7hr. After removal of the excess of hydriodic acid in vacuo, the residue was dissolved in 5 ml. of water and neutralized with sodium hydrogen carbonate. The product deposited was recrystallized from water to give 0.8 g. (80%) of white needles, m.p. 216~217°.

Anal. Found: C, 62.98; H, 4.84. Calcd. for $C_7H_6ON_2$: C, 62.68; H, 4.51%.

VII. Upon oxidation of 8.5g. of 5-methylbenzimidazole with 35 g. of potassium permanganate by the usual procedure, 5-benzimidazolecarboxylic acid was obtained; the crude product was dissolved in aqueous ammonia solution, and treated with active carbon. Precipitation with acetic acid gave 7 g. (70%) of white needles, m.p. 325°C (decomp.).

Anal. Found: C, 59.05; H, 3.95. Calcd. for $C_8H_6O_2N_2$: C, 59.26; H, 3.73%.

A mixture of 1.2 g. of 5-benzimidazolcarboxylic acid and 12 ml. of thionyl chloride was refluxed for 5 hr. Excessive thionyl chloride was removed and dried off in a vacuum desiccator. The residue was poured slowly, with stirring, into 15 ml. of cold concentrated ammonia water. The solid was recrystallized from water to give 0.6 g. (50%) of white prisms, m. p. 247~248°C (monohydrate).

Anal. Found: C, 53.70; H, 5.43; H_2O 10.13. Calcd. for $C_8H_7ON_3 \cdot H_2O$: C, 53.62; H, 5.62; H_2O 10.05%.

VIII. A mixture of 5 g. of 5-benzimidazolecarboxylic acid, 100 ml. of absolute ethanol, and 3 ml. of concentrated sulfuric acid was refluxed for 10 hr. After removal of the excess of ethanol in vacuo, the residue was treated with 20 ml. of water and neutralized with sodium hydrogen carbonate. A white crystalline precipitate was immediately formed. After standing for several hours at 0°C, the solid was collected and recrystallized from ethanol to give 4.1 g. (70%) of ester, m.p. 101~103°C.

A mixture of 5.3 g. of ester, 2.5 ml. of hydrazinhydrate (80%), and 10 ml. of ethanol was heated on a water bath for 10 hr. After removing the ethanol, the solidified residue was recrystallized from ethanol, affording 4 g. (82%) of acid hydrazide in the form of white needles, m.p. 240°, 248°C (decamp.).

Anal. Found: C, 54.71; H, 4.73. Calcd. for $C_8H_8ON_4$: C, 54.54; H, 4.58%.

Reduction of 4-nitrobenzothiadiazole.—To a suspension of 10 g. of 4-nitrobenzothiadiazole in 100 ml. of 10% sodium chloride solution, 0.3 ml. of 0.5% hexachloroplatinic acid solution was added and stirred in a hot water bath. When 4-nitro derivative was melted, 30 g. of iron powder was added in one portion. The mixture was heated and stirred for an additional 1 hr., cooled, and extracted with 50 ml. of benzene (twice). The benzene layer was dried and distilled. The residue was recrystallized from water to give 4 g. of yellow needles, m.p. 67—68°C[13].

The acetylation was carried out by gently refluxing a mixture of 0.7 g. of 4-amino compound, 4 ml. of acetic acid, and 0.7 ml. of acetic anhydride for 1 hr. Recrystallization from water gave 0.5 g. of white needles, m.p. 152°C[14].

XIII. A mixture of 3 g. of 4-aminobenzothiadiazole, 2.7 g. of phenylisothiocyanate, and 5 ml. of alcohol was refluxed for 1 hr. to give 4.2 g. (73%) of the desired product melting at 150°C. The crude material was recrystallized from ethanol to yield a pure substance melting at 154~155°.

Anal. Found: C, 54.40; H, 3.93. Calcd. for $C_{13}H_{10}N_4S_2$: C, 54.52; H, 3.52%.

The author wishes to express his gratitude to Professor S. Kakimoto of Hokkaido University for his kind encouragement and advice.

The Research Institute for Tuberculosis
Hokkaido University, Sapporo

13) m. p. 68°C[8]
14) m. p. 152.5°C[8]

Ultraviolet Absorption Spectra of Three Isomeric Pyridine Monocarboxylic Acids and Their N-Oxides

By Norisuke HATA

(Received October 15, 1957)

In a previous paper[1], the author has reported the effect of hydroxymethyl group on the absorption spectra of pyridine and pyridine *N*-oxide. In order to obtain the knowledge on the effect of an electron-attracting substituent, the present author measured the ultraviolet absorption spectra of three isomeric pyridine monocarboxylic acids and their *N*-oxides in various solvents, and discussed the solvent effects on their spectra and also the effect of a carboxyl group on the absorption spectra of pyridine and pyridine *N*-oxide. The results of these spectral measurements were shown to be interpreted under the assumption of the intramolecular hydrogen bond formation or the steric interaction in picolinic acid and its *N*-oxide.

Experimental

Commercial picolinic, nicotinic, and isonicotinic acid were purified by recrystallization from ethanol several times.

Picolinic acid: m. p., 135°~7°C; nicotinic acid: m. p., 232°C; isonicotinic acid: m. p., 315°C.

Picolinic[2] and isonicotinic acid *N*-oxide[3] were synthesized by the method given in all kinds of literature, and nicotinic acid *N*-oxide was synthesized by treating the nicotinic acid with aqueous hydrogen peroxide in glacial acetic acid in a similar way as for isonicotinic acid *N*-oxide, all of which were purified by recrystallisation from ethanol or methanol several times.

Picolinic acid *N*-oxide: m. p., 160°C, (from ethanol); nicotinic acid *N*-oxide: m. p., 247°~8°C, decomp., (from methanol); isonicotinic acid *N*-oxide: m. p., 260°C, (from methanol).

Solvents used in the spectral measurements were dioxane, ethanol and water which were purified according to the directions described in "Organic Solvents"[4]. The ultraviolet absorption spectra were measured with a Shimadzu Quartz Spectrophotometer Type QB-50, using a fused quartz cell of 1 cm. thickness.

Results and Discussion

Figs. 1 to 6 show the absorption curves of three isomeric pyridine monocarboxylic acids and their *N*-oxides in various solvents, and the schematic spectra of these compounds are given in Fig. 7. The observed values of maximum wavelength, wave number, and molar extinction coefficient are listed in Table I.

(1) Pyridine monocarboxylic acids:— From the spectral measurements of these compounds, the following results were obtained for the absorption appearing in the region between 35000 cm^{-1} and 40000 cm^{-1}.

a) The absorption maximum of picolinic acid does not essentially shift in solvents such as dioxane, ethanol and water, but that of nicotinic or isonicotinic acid shifts to the shorter wavelength in the above order of solvents.

b) The absorption maxima of all these compounds occur in the shorter wavelength than that of benzoic acid[5].

c) The absorption at about 38900 cm^{-1} (257 mμ) of pyridine in ethanol shifts to longer wavelength by the introduction of a carboxyl group to the pyridine nucleus[8].

The 38500 cm^{-1} (260 mμ) absorption of benzene shifts to the longer wavelength by substituting a carboxyl group into the benzene nucleus. This shift is regarded as mainly due to the electron migration effect from the benzene ring to the carboxyl group[9]. Moreover, it may be

1) N. Hata, This Bulletin, in press.
2) R. Adams and S. Miyano, *J. Am. Chem. Soc.*, **76**, 3168 (1954).
3) E. Chigi, *Ber.*, **75**, 1318 (1942).
4) A. Weissberger and E. S. Proskauer, "Organic Solvents" 2nd. Ed., (1955).
5) The absorption maximum of benzoic acid occurs in 36750 cm^{-1} (272 mμ) in dioxane or ethanol[6] and 36890 cm^{-1} (271 mμ) in water[7], where the value of absorption maximum in various solvents shows that of the greatest intensity in the fine structures of this band.
6) H. E. Ungnade and R. W. Lamb, *J. Am. Chem. Soc.*, **74**, 3789 (1952).
7) C. Moser and A. I. Kohlenberg, *J. Chem. Soc.*, **1950**, 804.
8) In this paper, the effects of a carboxyl group on the absorption spectra of pyridine and pyridine *N*-oxide are discussed in relation to the spectra of ethanol solution, since the compounds used in this experiment are insoluble in non-polar solvents.
9) About the effect of the substituent on the electronic absorption spectrum of benzene, see, for example, W. West, "Chemical Applications of Spectroscopy", Chapter V, New York, (1956).

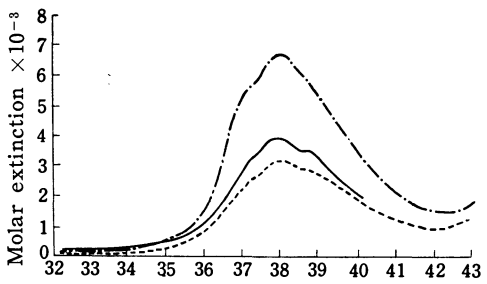

Fig. 1. Absorption curve of picolinic acid.
—— Dioxane. - - - Ethanol. -·-·- Water.

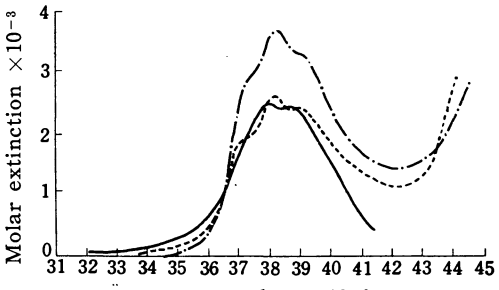

Fig. 2. Absorption curve of nicotinic acid.
—— Dioxane. - - - Ethanol. -·-·- Water.

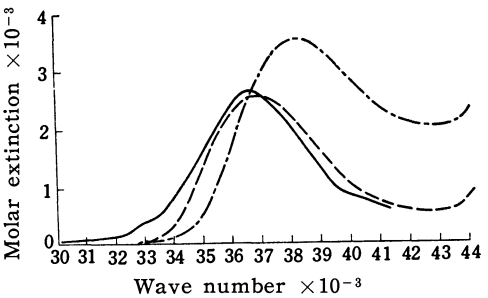

Fig. 3. Absorption curve of isonicotinic acid.
—— Dioxane. - - - Ethanol. -·-·- Water.

expected that there exists a qualitatively parallel relationship between the wavelength shift and the magnitude of the electron migration. If one of the C—H groups of benzene is replaced by a nitrogen atom, the electron migration possibly decreases to some extent compared with the case of benzoic acid, since the electron attracting power of the nitrogen atom of pyridine nucleus competes with that of the carboxyl group. Thus, pyridine monocarboxylic acid absorbs the shorter wavelength light than benzoic acid does. Here, since the competetive resonance interaction between the nitrogen atom and the carboxyl group is the greatest in nicotinic acid, its absorption spectrum appears in the region of the shorter wavelength than that of the other two acids.

It is of interest to know that the absorption maximum of pyridine shifts to longer wavelength by the introduction of a carboxyl group upon the pyridine nucleus. Particularly in the case of 2-carboxyl substitution, the absorption maximum locates at the shorter wavelength than that of 4-carboxyl substitution. These facts are remarkably different from the effect of substitution of an electron-repelling group(e.g., methyl, amino, halogen etc.). In this case, the absorption maximum of 2-substituted derivatives occurs in the longer wavelength than that of 4-substituted ones[1,10]. To explain such a displacement toward shorter wavelength of the absorption band of picolinic acid (when compared with the absorption band of isonicotinic acid), we assumed the formation of the intramolecular hydrogen bond as shown in (A) for

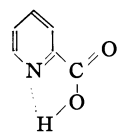

(A)

picolinic acid. This assumption leads to the conclusion that the electron migration from the pyridine ring to the carboxyl group in picolinic acid should be somewhat prevented by the increase in the electronegativity of the nitrogen atom caused by the formation of such an intramolecular hydrogen bond, from which the hindrance of resonance of this molecule may result. Consequently, the absorption spectrum of picolinic acid appears in the shorter wavelength than that of isonicotinic acid in which the intramolecular hydrogen bond does not occur.

Moreover, it seems to be accepted as an additional evidence for such an intramolecular hydrogen bond formation that the absorption maximum in dioxane solution of picolinic acid does not shift in solvents such as ethanol and water acting as a proton donor to the nitrogen atom of pyridine nucleus.

(2) Pyridine monocarboxylic acid *N*-oxides:—From the spectral measurements of these compounds, the following results are obtained for the absorption appearing in the region between 30000 and 41000 cm^{-1}.

a) The absorption maxima of these

10) H. Tsubomura, *J. Chem. Soc. Japan, Pure Chem. Sec.*, (*Nippon Kagaku Zassi*), **78**, 293 (1957).

compounds show a greater blue shift with the change of the solvents from dioxane to ethanol and water[11]. However, the extent of the shift in picolinic acid *N*-oxide is smaller than that in nicotinic or isonicotinic acid *N*-oxide.

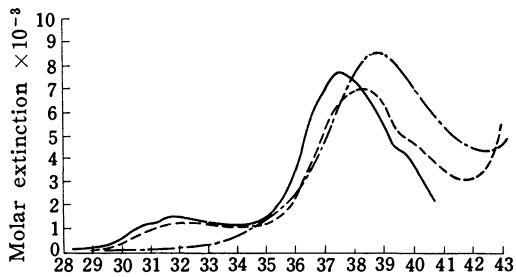

Fig. 4. Absorption curve of picolinic acid *N*-oxide.
—— Dioxane. - - - Ethanol. -·-·- Water.

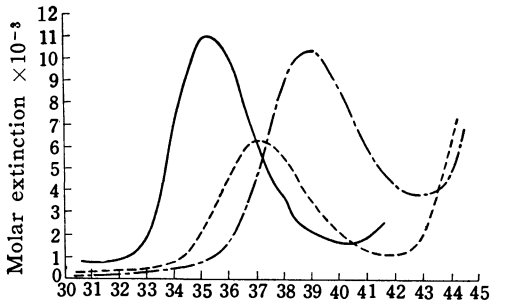

Fig. 5. Absorption curve of nicotinic acid *N*-oxide.
—— Dioxane. - - - Ethanol. -·-·- Water.

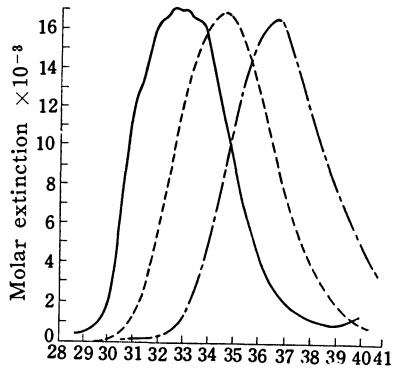

Fig. 6. Absorption curve of isonicotinic acid *N*-oxide.
—— Dioxane. - - - Ethanol. -·-·- Water.

b) The absorption spectrum of picolinic acid *N*-oxide shows considerable similarity to that of picolinic acid in the value of maximum wavelength. On the other hand, for nicotinic or isonicotinic acid *N*-oxide, the maximum wavelength is noticeably different from that of the corresponding acid.

c) The maximum wavelength of isonicotinic acid *N*-oxide in water is nearly the same value with that of isonicotinic acid in dioxane, while the maximum wavelength of picolinic acid *N*-oxide in water locates at the shorter wavelength than that of the corresponding acid in dioxane.

d) The absorption at about 37700 cm^{-1} (265 mμ) of pyridine *N*-oxide in ethanol shifts to the longer wavelength by the substitution of a carboxyl group at 3- or 4-position and to the shorter wavelength by that at 2-position.

It is infarred from the value of dipole moment[13] and the chemical reactivity[14] of pyridine *N*-oxide that the electron migration both into the pyridine ring from the N—O group, and in the opposite direction, is possible. From the studies of dipole moments of 4-substituted pyridine *N*-oxides by Katritzky et al.[15], however, it was shown that the N—O group behaves as an electron-attracting group when 4-substituent (Z) is an electron-repelling group as shown in (B). On the other hand, the N—O group shows a character acting as

(B) ($Z=CH_3$, Cl, $N(CH_3)_2$, etc.)

(C) ($Z=NO_2$, $COOC_2H_5$ etc.)

an electron repelling group when 4-substituent (Z) is an electron attracting group as shown in (C). Therefore, if one assumes the N—O group as an electron-repelling group in pyridine monocarboxylic acid *N*-oxides, the following qualitative discussions are made for their spectra.

The absorption spectrum of pyridine monocarboxylic acid *N*-oxide is expected

11) Such a greater blue shift is probably due to the hydrogen bonding effect between the oxygen atom of N-O group and R-OH of solvent like other pyridine *N*-oxides[1,12].

12) T. Kubota, *J. Pharm. Soc. Japan* (*Yakugaku Zassi*), **74**, 831 (1954). M. Ito and N. Hata, This Bulletin, **28**, 260 (1955). N. Hata, ibid., **29**, 82 (1956).

13) E. P. Linton, *J. Am. Chem. Soc.*, **62**, 1945 (1940).

14) E. Ochiai, *J. Org. Chem.*, **18**, 534 (1953).

15) A. R. Katritzky et al., *J. Chem. Soc.*, **1957**, 1769.

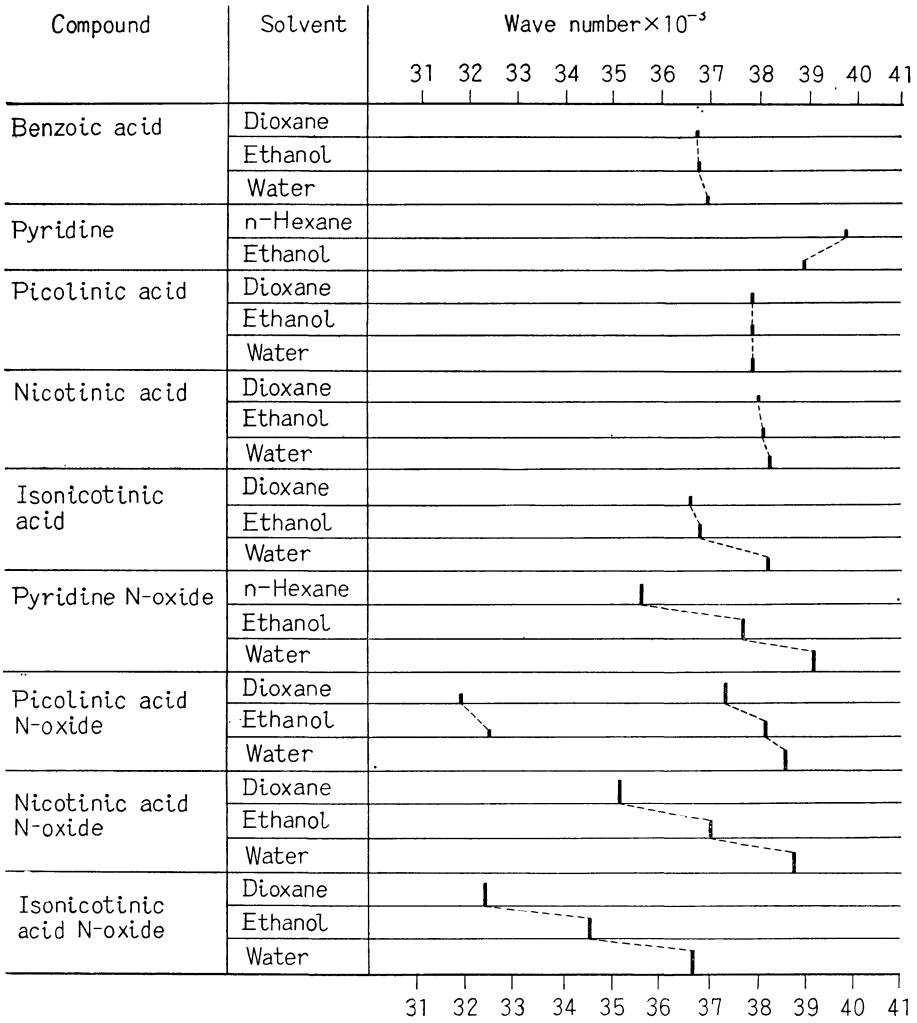

Fig. 7. Schematic spectra of three isomeric pyridine monocarboxylic acids and their *N*-oxides.

to occur in the region of the longer wavelength than that of pyridine *N*-oxide or benzoic acid, because the electron migration from the ring to the carboxyl group is facilitated by the N—O group acting as an electron-repelling group. Here, since the resonance interaction between N—O and carboxyl group is the greatest in picolinic and isonicotinic acid *N*-oxides, it is presumed that the absorption spectra of these two *N*-oxides occur in the longer wavelength than that of nicotinic acid *N*-oxide. Although nicotinic or isonicotinic acid *N*-oxide shows an effect expected above, picolinic acid *N*-oxide shows a blue-shift with a decreased intensity like other 2-substituted pyridine *N*-oxides[1,16]. To explain these facts, the author attributed the formation of the intramolecular hydrogen bond and the steric interaction in picolinic acid *N*-oxide, both of which prevented the resonance of this molecule.

Firstly,if one assumes the intramolecular hydrogen bond as shown in (D) for picolinic acid *N*-oxide, the electron migration

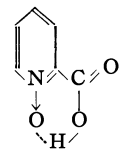

(D)

from the oxygen atom of N—O group to the pyridine ring may be somewhat pre-

16) N. Ikekawa and Y. Sato, *Pharm. Bull.*, **2**, 400 (1954).

TABLE I

WAVE LENGTHS, WAVE NUMBERS, AND MOLAR EXTINCTION COEFFICIENTS OF THREE ISOMERIC PYRIDINE MONOCARBOXYLIC ACIDS AND THEIR *N*-OXIDES

Compound	Solvent	Wave length (mμ)	Wave Number (cm^{-1})	Molar extinction coefficient
Picolinic acid	Dioxane	264	37900	3980
	Ethanol	264	37900	3240
	Water	264	37900	6750
Nicotinic acid	Dioxane	263	38000	2500
		259	38600	2460
	Ethanol	262	38100	2640
		257	38900	2430
	Water	261.5	38200	3660
Isonicotinic acid	Dioxane	273	36600	2670
	Ethanol	271.5	36800	2580
	Water	261.5	38200	3520
Picolinic acid *N*-oxide	Dioxane	313	31900	1500
		268	37350	7700
	Ethanol	307.5	32500	1250
		261.5	38200	7000
	Water	259	38600	8600
Nicotinic acid *N*-oxide	Dioxane	284	35200	11000
	Ethanol	269.5	37100	6300
	Water	258	38800	10300
Isonicotinic acid *N*-oxide	Dioxane	308.5	32400	17000
	Ethanol	289	34600	16700
	Water	272	36700	16300

vented owing to the increase in its electronegativity caused by this intramolecular hydrogen bond. Therefore, the maximum wavelength of picolinic acid *N*-oxide may be close to that of picolinic acid. Such an intramolecular hydrogen bond will also decrease the effect of the solvent acting as a proton donor to the oxygen atom of N—O group on the absorption spectrum of picolinic acid *N*-oxide. The above expectations are in good agreement with the experimental results a) and b).

Secondly, it is also necessary to consider the steric or the electrostatic interaction between the N—O group and the carboxyl group. As is seen from Table I, the maximum wavelength lies in the order of 4-> 3-> 2-isomer and the intensity decreases remarkably in the same order. These facts are partly regarded to be due to the obstruction of the coplanarity of this molecule caused by the steric or the electrostatic interaction between N—O group and carboxyl group, just as in the spectra of ortho-substituted benzoic acids[7], by which the conjugation between the ring and the carboxyl group becomes weakened[17]. Such interactions are the greatest in picolinic acid *N*-oxide and the small electrostatic interaction may also arise from the polarities of N—O group and carboxyl group in nicotinic acid *N*-oxide. This consideration is in agreement with the spectral behavior of these compounds.

It seems probable that the experimental results c) are accounted for by the weakening of the conjugation between the ring and the carboxyl group in picolinic acid *N*-oxide, (when compared with that of corresponding acid) resulting from the steric or the electrostatic effect mentioned above. If the conjugation between the ring and the carboxyl group of pyridine monocarboxylic acid *N*-oxide were nearly identical with that of the corresponding acid, an increase in the electronegativity of the oxygen atom caused by the hydrogen bond formation between the

17) About the steric effect in the electronic absorption spectra see, for example, E. A. Braude and E. S. Waight, "Progress in Spectrochemistry. I." (edited by W. Klyne), London, p. 136, (1954).

oxygen atom of N—O group and the hydrogen atom of water should result in the fact that the wevelength of the absorption maximum observed with the *N*-oxide molecule might be similar to that of the corresponding acid.

In the case of picolinic acid *N*-oxide, in addition to the strong absorption band near 37350 cm^{-1} (268 mμ), a small one at about 31900 cm^{-1} (313 mμ) is observed in dioxane, which shows a blue shift in ethanol and apparently disappears in water. This disappearance is possibly due to the overlap with the strong absorption band at the shorter wavelength. This absorption may be regarded as due to an n–π^* transition like other pyridine *N*-oxides.

Summary

The ultraviolet absorption spectra of 2-, 3- and 4-pyridine monocarboxylic acid and their *N*-oxides were measured in various solvents. The absorption spectra of these compounds with the exception of picolinic acid show the blue shift with the change of the solvent from dioxane to ethanol and water.

The absorption band of picolinic acid occurs in the region of the shorter wavelength than that of isonicotinic acid; this fact may be caused by the formation of the intramolecular hydrogen bond, which prevents the resonance of this molecule. The absorption band of picolinic acid *N*-oxide occurs in the region of the shorter wevelength than that of nicotinic or isonicotinic acid *N*-oxide, for which the present author attributed the formation of the intramolecular hydrogen bond and the steric interaction in picolinic acid *N*-oxide.

We also observed the n–π^* absorption in picolinic acid *N*-oxide.

The author wishes to express his hearty thanks to Professor S. Imanishi of Kyushu University for his kind guidance and encouragement. Thanks are also due to Dr. E. Suenaga of Nagasaki University for his support throughout this work.

Faculty of Pharmacy, Nagasaki University, Nagasaki

Some Studies of the Inductive Effect

By Shiro MAEDA

(Received October 12, 1957)

Inductive effect has long been recognized as a useful idea in organic chemistry, particularly in relation to chemical reactivity problems. We can see the occurrence of this effect among the values of electric dipole moment of various molecules, most remarkably in some chain homologues.

In most cases, it is relatively a simple matter to take this effect qualitatively into consideration, but rather difficult quantitatively. In recent years, some developments were brought about on the latter point. Morino, Miyagawa and Oiwa[1] have established an empirical rule successfully applicable to the electric moments of various haloalkanes. Smith, Ree, Magee and Eyring[2] have developed a semi-classical theory advantageous for the application to chemical reactivity problems. Cahill and Mueller[3] have treated the effect of carboxylic group on the adjacent C-C bond quantum-mechanically.

For all these and previous studies, however, the theoretical basis of inductive effect can not yet be considered to be well established enough for quantitative applications. Now, in this paper, an approximate method will be developped to

1) Y. Morino, I. Miyagawa and J. Oiwa, *Botyu-kagaku*, **15**, 181 (1950). I. Miyagawa, *J. Chem. Soc. Japan, Pure Chem. Sec.* (*Nippon Kagaku Zassi*), **75**, 1061 (1954).

2) R. P. Smith, T. Ree, J. L. Magee and H. Eyring, *J. Am. Chem. Soc.*, **73**, 2263 (1951).

3) J.M. Cahill and C.R. Mueller, *J. Chem. Phys.*, **24** 513 (1956).

estimate the details of induced electric moment in non-conjugate systems, with some illustrative applications to haloalkane molecules.

An Approximate Expression of the Polarity of Bond

The object of the present work is the description of saturated systems such as substituted paraffin compounds. It is a conclusion of chemical experiences that the bonding electron pair of each separate bond in such a molecule can be regarded as fairly well localized. For such systems, the treatment based on bond orbital wave functions may be a fairly good approximation.

The bond orbital ϕ_i of the i-th bond A-B may be approximated by the localized molecular orbital as given by Eq. 1,

$$\phi_i(1)=a_i\chi_{Ai}(1)+b_i\chi_{Bi}(1) \tag{1}$$

where χ_{Ai} and χ_{Bi} are the valence atomic orbitals of both atoms. Each ϕ_i is subjected to the normalization condition, Eq. 2.

$$\int\phi_i^*(1)\phi_i(1)d\tau_1=a_i^2+2a_ib_iS_i+b_i^2=1 \tag{2}$$

$$S_i=\int\chi_{Ai}^*(1)\chi_{Bi}(1)d\tau_1$$

A quantity Q_i is also used as defined in Eq. 3, named "bond charge" by Mulliken[4], in the present formulation as the principal parameter.

$$Q_i=a_i^2-b_i^2=(a_i^2+a_ib_iS_i)-(b_i^2+a_ib_iS_i) \tag{3}$$

Now, when the complete localization of bond obitals were assumed, the electronic energy of a molecule may be approximately expressed by Eq. 4, the basic elucidation for which is given in appendix.

$$E=2\sum H_i+\sum_{i,j}(2-\delta_{ij})J_{ij} \tag{4}$$

$$H_i=\int\phi_i^*(1)h_1\phi_i(1)d\tau_1 \tag{5}$$

$$J_{ij}=\int\phi_i^*(1)\phi_j^*(2)(e^2/r_{12})\phi_i(1)\phi_j(2)d\tau_1d\tau_2 \tag{6}$$

In Eq. 4, H_i and J_{ij} are the bare-nuclear field orbital energy and the coulomb integral as given in Eqs. 5 and 6 respectively, where h_1 is the bare nuclear field energy Hamiltonian, r_{12} the interelectronic distance, and $\delta_{ij}=1$ or 0 for $i=j$ or $\neq j$.

With the ϕ_i given in Eq. 1, H_i can be written as Eq. 7 taking Eq. 2 into consideration.

$$H_i=(1/2)(\alpha_A^i+\alpha_B^i)+(1/2)Q_i(\alpha_A^i-\alpha_B^i)+2a_ib_i\beta_i \tag{7}$$

$$\left.\begin{aligned}\alpha_A^i&=\int\chi_{Ai}^*(1)h_1\chi_{Ai}(1)d\tau_1,\\ \alpha_B^i&=\int\chi_{Bi}^*(1)h_1\chi_{Bi}(1)d\tau_1\\ \beta_i&=\int\chi_{Ai}^*(1)h_1\chi_{Bi}(1)d\tau_1\\ &\quad-(1/2)S_i(\alpha_A^i+\alpha_B^i)\end{aligned}\right\} \tag{8}$$

Further, it is transformed to Eq. 9 by expanding $2a_ib_i$ into a power series of Q_i.

$$H_i=(1/2)(\alpha_A^i+\alpha_B^i)+(\beta_i/1+S_i)-(1/2)(\alpha_A^i-\alpha_B^i)Q_i-(1/2)\beta_iQ_i^2-(1/8)(1-S_i^2)\beta_iQ_i^4\cdots\cdots \tag{9}$$

In order to express J_{ij} by a simple function of Q_i's, we shall adopt the approximate equation (10)[4].

$$\phi_i^*\phi_i\approx(1+Q_i)\chi_{Ai}^*\chi_{Ai}+(1-Q_i)\chi_{Bi}^*\chi_{Bi} \tag{10}$$

Then Eq. 11 is obtained, where the coefficients C^{ij}'s take the form of Eq. 12.

$$J_{ij}=C_0^{ij}+C_i^{ij}Q_i+C_j^{ij}Q_j+C_{ij}^{ij}Q_iQ_j \tag{11}$$

$$\left.\begin{aligned}C_0^{ij}&=(1/4)[(ii/jj)+(ii/j'j')+(i'i'/jj)+(i'i'/j'j')]\\ C_i^{ij}&=(1/4)[(ii/jj)+(ii/j'j')-(i'i'/jj)-(i'i'/j'j')]\\ C_j^{ij}&=(1/4)[(ii/jj)-(ii/j'j')+(i'i'/jj)-(i'i'/j'j')]\\ C_{ij}^{ij}&=(1/4)[(ii/jj)-(ii/j'j')-(i'i'/jj)+(i'i'/j'j')]\end{aligned}\right\} \tag{12}$$

$$(pq/rs)=\int p^*(1)s^*(2)(e^2/r_{12})q(1)r(2)d\tau_1d\tau_2,$$

(i, i', j, j' represent χ_{Ai}, χ_{Bi}, $\chi_{A'j}$, $\chi_{B'j}$, respectively).

Consequently, the total energy E is approximately given by Eq. 13.

$$E=\sum_i\{(\alpha_A^i+\alpha_B^i)+(2\beta_i/1+S_i)+\sum_j(2-\delta_{ij})C_0^{ij}+Q_i[(\alpha_A^i-\alpha_B^i)+2\sum_j(2-\delta_{ij})C_i^{ij}]-(\beta_i-C_{ij}^{ij})Q_i^2+\sum_{j\neq i}2C_{ij}^{ij}Q_iQ_j-(1/4)(1-S_i^2)\beta_iQ_i^4\cdots\cdots\} \tag{13}$$

Now, in Eq. 13, each Q_i has to take the value so as to minimize E, according to the variation principle; that is, Eq. 14 must be fulfiled by all Q_n's.

$$\partial E/\partial Q_n=0 \tag{14}$$

This equation takes the form of an infinite series in Q's in the present formulation. But, the Q's appearing in the

4) R. S. Mulliken, *J. chim. phys.*, **46**, 497, 675 (1949).

systems in which we are interested are supposed to be fairly small against unity, and the approximate equation 15 may serve the purpose, where the quadratic and successive higher terms were neglected, and $\gamma_n=-\beta_n+C_{nn}^{nn}$.

$$[(\alpha_A^n-\alpha_B^n)+\sum_i 2(2-\delta_{ni})C_n^{ni}]$$
$$+2\gamma_n Q_n+4\sum_{i\neq n} C_{ni}^{ni}Q_i=0 \qquad (15)$$

If we could solve the simultaneous equations resulting from Eq. 15, approximate Q's for all separate bonds might be determined. But it seems hardly possible, at present, because of the difficulty in fixing the values of necessary integrals, especially α and γ. In the present calculation, however, we do not look for the Q_i's themselves, but their changes due to some change in molecular constitution.

Now, we shall consider about the changes of Q of residual C-H or C-C bonds, due to subsitution by some polar group. In such a case, a hydrocarbon molecule before the substitution is taken as the reference constitution, for which Eq. 15 is written as Eq. 16; where Q_i^0 represents the magnitude in the reference constitution.

$$[(\alpha_A^n-\alpha_B^n)+\sum_i 2(2-\delta_{ni})C_n^{ni}]$$
$$+2\gamma_n Q_n^0+4\sum_{i\neq n} C_{ni}^{ni}Q_i^0=0 \qquad (16)$$

When m C-H bonds corresponding to 1-st to m-th in reference constitution were replaced by other kind of polar bond, e. g. $CX_1\cdots\cdots CX_m$, then Eq. 15 is written as Eq. 17 for each C-H or C-C bond in substituted constitution;

$$[(\bar{\alpha}_A^n-\bar{\alpha}_B^n)+\sum_{i=1}^{m}4\bar{C}_n^{ni}+\sum_{i=m+1}^{z}2(2-\delta_{ni})C_n^{ni}]$$
$$+2\gamma_n Q_n+4\sum_{i\neq n}^{z=m+1} C_{ni}^{ni}Q_i+4\sum_{i=1}^{m}\bar{C}_{ni}^{ni}Q_i=0 \qquad (17)$$

(z: the final number of bonds).

where the bar above some quantities implies the change due to substituion. It is to be noted, here, that β (and consequently γ) may be taken as fairly invariable at the substitution[4]. Subtracting Eq. 16 from Eq. 17, Eq. 18 is obtained.

$$[(\bar{\alpha}_A^n-\alpha_A^n)-(\bar{\alpha}_B^n-\alpha_B^n)+4\sum_{i=1}^{m}(\bar{C}_n^{ni}-C_n^{ni})]$$
$$+2\gamma_n(Q_n-Q_n^0)+4\sum_{i=1}^{m}(\bar{C}_{ni}^{ni}Q_i-C_{ni}^{ni}Q_i^0)$$
$$+4\sum_{i\neq n}^{z=m+1} C_{ni}^{ni}(Q_i-Q_i^0)=0 \qquad (18)$$

In this equation, the braced term, which represents the change of penetration energy due to the substitution (cf. Eq. 12), may well be neglected as fairly small. Thus, Eq. 18 may be simplified as follows:

$$\gamma_n(Q_n-Q_n^0)+2\sum_{i=1}^{m}(\bar{C}_{ni}^{ni}Q_i-C_{ni}^{ni}Q_i^0)$$
$$+2\sum_{i\neq n}^{z=m+1} C_{ni}^{ni}(Q_i-Q_i^0)=0 \qquad (19)$$

(for every unsubstituted bond, n).

On the other hand, for change of Q of the substituent bond C-X, the simplest molecule CH_3X is taken as the reference constitution. Then the similar procedure as above gives Eq. 20 finally.

$$\gamma_n(Q_n-Q_n^0)+2\sum_{i\neq n}^{z=1}(\bar{C}_{ni}^{ni}Q_i-C_{ni}^{ni}Q_i^0)=0 \qquad (20)$$

(for every substituted bond, n).

In the following calculation, Eqs. 19 and 20 shall be used together to calculate the approximate magnitudes of induced polarity ($Q_n-Q_n^0$).

Some Reference to Molecular Polarizability

Now, it is helpful for the present study to treat the molecular polarizability from the same point of view as above. The polarizability along one of the principal axes y of a molecule is given by Eq. 21, where f is a homogeneous electric field parallel to y-axis.

$$\alpha_y=-(d^2E/df^2)_{f=0} \qquad (21)$$

The total energy E under the field is written as Eq. 22 which includes several f-dependent terms in addition to Eq. 13.

$$E=\sum_i\{(\alpha_A^i+\alpha_B^i)+(2\beta_i/1+S_i)$$
$$+\sum_j(2-\delta_{ij})C_0^{ij}-f(y_A^i+y_B^i)$$
$$+Q_i[(\alpha_A^i-\alpha_B^i)+\sum_j 2(2-\delta_{ij})C_i^{ij}-f(y_A^i-y_B^i)]$$
$$+\gamma_i Q_i^2+\sum_{j\neq i}2C_{ij}^{ij}Q_iQ_j-(1/4)(1-S_i^2)\beta_i Q_i^4\cdots\} \qquad (22)$$

where y_A^i and y_B^i denote the average positions of electrons as given by

$$y_A^i=\int\chi_{Ai}^*(1)y_1\chi_{Ai}(1)d\tau_1,$$

and

$$y_B^i=\int\chi_{Bi}^*(1)y_1\chi_{Bi}(1)d\tau_1 \qquad (23)$$

where y_1 is the y-coordinate of electron 1. Then, Eq. 24 results from Eqs. 21 and 22.

$$\alpha_y=\sum_i\{2Q_i(y_A^i-y_B^i-2\sum_{j\neq i}C_{ij}^{ij}\dot{Q}_j)$$

$$+\dot{Q}_i^2[-2\gamma_i+3(1-S_i^2)\beta_i Q_i^2+\cdots]$$
$$-\ddot{Q}_i[\alpha_A^i-\alpha_B^i+2\sum_j(2-\delta_{ij})C_i^{ij}+2\gamma_i Q_i$$
$$+4\sum_{j\neq i}C_{ij}^{ij}Q_j-(1-S_i^2)\beta_i Q_i^3+\cdots]\}_{f=0} \quad (24)$$

$$\dot{Q}=(dQ_i/df)_{f=0},\quad \ddot{Q}_i=(d^2Q_i/df^2)_{f=0} \quad (25)$$

On the other hand, all $Q's$ have to satisfy Eq. 26 which corresponds to Eq. 14 in the last section.

$$\partial E/\partial Q_i=\alpha_A^i-\alpha_B^i+\sum_j 2(2-\delta_{ij})C_i^{ij}-f(y_A^i-y_B^i)$$
$$+2\gamma_i Q_i+\sum_{j\neq i}4C_{ij}^{ij}Q_j-(1-S_i^2)\beta_i Q_i^3+\cdots=0 \quad (26)$$

Since this equation should hold for arbitrary value of f, Eq. 27 is available also.

$$[d(\partial E/\partial Q_i)/df]_{f=0}=-(y_A^i-y_B^i)+2\gamma_i\dot{Q}_i$$
$$+\sum_{j\neq i}4C_{ij}^{ij}\dot{Q}_j-3(1-S_i^2)\beta_i(Q_i)_{f=0}^2\dot{Q}_i+\cdots=0 \quad (27)$$

Thus, Eq. 28 is obtained finally from the combination of Eqs. 24 and 27. It shows also that the approximation employed thus far is consistent with the expression of bond moment given by Eq. 29.

$$\alpha_y=\sum_i\dot{Q}_i(y_A^i-y_B^i) \quad (28)$$

$$m_i=Q_i(y_A^i-y_B^i) \quad (29)$$

The values of γ_i, which is essential to carry out the calculation formally given in the last section, can be determined by solving Eq. 28 simultaneously with Eq. 27′,

$$(y_A^i-y_B^i)-2\gamma_i\dot{Q}_i-\sum_{j\neq i}4C_{ij}^{ij}\dot{Q}_j=0 \quad (27')$$

where the fourth and further terms in Eq. 27 have been neglected. It must be noticed here, however, that the α_y in Eq. 28 represents only longitudinal contributions of bond polarizabilities dismissing the transverse; that is, as to methane, for example, $\alpha_y=(4/3)\alpha_{L(CH)}$, where $\alpha_{L(CH)}$ is the longitudinal bond polarizability determined empirically for CH bond. We solve Eqs. 28 and 27′ with such an α_y and theoretically calculated C_{ij}^{ij} and $(y_A^i-y_B^i)$, giving γ_{CH}. Next, γ_{CC} can be determined by similar calculation for ethane molecule, where γ_{CH} obtained above be available. In this way, the values of γ_i for several bonds were evaluated presuming that they are actually definite by bond species, and given in Table I.

TABLE I

Bond A-B	C-H	C-C	C-Cl	C-Br	unit
γ_{AB}	0.396	0.309	0.368	0.388	e^2/a_0
$\alpha_L(AB)$	7.9*	18.8*	36.7*	50.4*	10^{-25} cc.
$y_A^{AB}-y_B^{AB}$	1.291	1.372	2.461	2.915	a_0**

* H. A. Stuart, "Die Struktur des freien Molekuls" pp. 449, Springer, (1952).
** Bohr radius.

Illustrative Examples

Some examples of the calculation for the systems of the simplest type will be shown. Throughout them, Q_{CH}^0 and Q_{CC}^0 have presumably been taken equal to zero, and, necessary integrals such as $C_{ij}^{ij}(i\neq j)$, y_A^i and y_B^i were computed with Slater atomic orbitals[5] assuming sp^3 tetrahedral hybridization for carbon, except C_{ij}^{ij} of non-neighbors which were approximated by point charge model.

Example I. CH_3X (cf. Fig. 1)

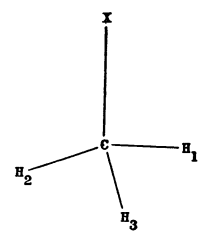

Fig. 1

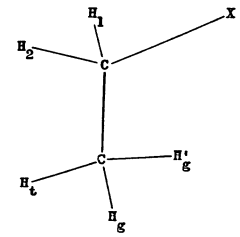

Fig. 2

For the CH bond of this type of molecule, Eq. 19 is written as Eq. i,

$$\gamma_{CH}Q_{CH}+2(C_{CH,CX}Q_{CX}+2C_{1,2}Q_{CH})=0 \quad (i)$$

where the superscripts in C_{ij}^{ij} were dropped. On the other hand, this type is taken as the reference constitution for all other X-substituted systems in the sense stated under Eq. 19. Therefore, Q_{CX} is taken so as the electric moment to be in accord with observed value. That is, Eq. ii is adopted as the second condition,

$$M_{exp}(CH_3X)=M_{cal}(CH_3X)=m_{CX}^{\rightarrow}+m_{CH}^{\leftarrow} \quad (ii)$$

where each bond moment is given by Eqs. iii and iv.

$$m_{CH}^{\leftarrow}=(1+Q_{CH})y_C^{CH}+(1-Q_{CH})y_H^{CH} \quad (iii)$$

5) J. C. Slater, *Phys. Rev.* **36**, 57 (1930).

$$m_{CX}^{\rightarrow}=(1-Q_{CX})y_C^{CX}+(1+Q_{CX})y_X^{CX} \quad \text{(iv)}$$

Then, Q_{CH} and Q_{CX} can be determined from these equations, and induced bond moment is given by Eq. v.

$$\Delta m_{CH}=Q_{CH}(y_C^{CH}-y_H^{CH}) \quad \text{(v)}$$

Example II. C_2H_5X (cf. Fig. 2)

The staggered form is assumed in this case. Then, Eq. 19 is written down as Eqs. iv~ix for the adjacent, *trans*, and *gauche* C-H bonds as to C-X bond respectively.

$$\gamma_{CH}Q_{CH}+C_{1,CX}Q_{CX}+C_{1,2}Q_{CH}+C_{CH,CC}Q_{CC}+C_{1,g}(Q_{CHg}+Q_{CHt})+C_{1,t}Q_{CHg}=0 \quad \text{(vi)}$$

$$\gamma_{CH}Q_{CHg}+C_{g,CX}Q_{CX}+(C_{1,g}+C_{1,t})Q_{CH}-C_{CH,CC}Q_{CC}+C_{1,2}(Q_{CHg}+Q_{CHt})=0 \quad \text{(vii)}$$

$$\gamma_{CH}Q_{CHt}+C_{t,CX}Q_{CX}+2C_{1,g}Q_{CH}-C_{CH,CC}Q_{CC}+2C_{1,2}Q_{CHg}=0 \quad \text{(viii)}$$

$$\gamma_{CC}Q_{CC}+C_{CC,CH}Q_{CX}+C_{CH,CC}(2Q_{CH}-2Q_{CHg}-Q_{CHt})=0 \quad \text{(ix)}$$

On the other hand, Eq. 20 is written as Eq. x for CX bond,

$$\gamma_{CX}(Q_{CX}-Q'_{CX})+2C_{1,CX}(Q_{CH}-Q'_{CH})+C_{CC,CX}Q_{CC}-C_{1,CX}Q'_{CH}+2C_{t,CX}Q_{CHg}+C_{t,CX}Q_{CHt}=0 \quad \text{(x)}$$

where the primed quantities represent the corresponding values in reference constitution CH_3X. In this way, all Q values can be determined.

For the other type of molecules, a similar procedure can be applied.

Results and Discussion

The theory has really been applied to the inductive effect occurring in some haloalkane molecules, the results of which are given in Table II and Fig. 3. For the present time, we have dealt with chloro- and bromo derivatives for which reliable experimental data could be obtained.

Looking at the Table II, the correspondence between the calculated and the experimental electric moments may be called fairly good in spite of several shortcomings in this treatment as mentioned below. Therefore, it may be permissible to

TABLE II

Molecule	Δm_{CH}	m^*_{CX}	M_{cal}	M_{exp}	Reference
CH_3Cl	0.186 D.	1.674 D.	(1.86) D.	1.86, 1.87 D.	1) 2), 3)
CH_3Br	0.167	1.623	(1.79)	1.78, 1.79, 1.80	4), 5), 3)
CH_2Cl_2	0.299	1.148	1.671	1.57, 1.62	1), 6)
CH_2Br_2	0.252	1.044	1.496	1.43	7)
$CHCl_3$	0.377	0.797	1.174	1.01, 1.15	1), 8)
$CHBr_3$	0.313	0.700	1.013	0.90, 0.99, 1.3	8), 9), 10)
C_2H_5Cl		1.773	2.029	1.98, 2.00, 2.02, 2.03	11), 12), 2), 4)
C_2H_5Br		1.739	1.966	1.92, 1.99, 2.01	4), 12), 5)
i-C_3H_7Cl		1.853	2.131	2.15	5)
n-C_3H_7Cl $\begin{cases}t\\g\end{cases}$		1.794 1.825	2.178 1.974 } 2.044**	2.03, 2.04	7), 12)

* The value subtracted by the atomic dipole of carbon tetrahedral orbital.

** Mean value for the abundance ratio *gauche*/*trans*=2/1[13].

References:

1) G. A. Barclay and R. J. W. LeFevre, *J. Chem. Soc.*, **1950**, 556.
2) R. Sanger, O. Steiger and K. Gachter, *Helv. Phys. Acta*, **5**, 200 (1932).
3) R. G. Shulman, C. H. Townes and B. D. Dailey, *Phys. Rev.*, **78**, 145 (1950).
4) C. P. Smyth and K. B. Mcalpine, *J. Chem. Phys.*, **2**, 499 (1934).
5) L. G. Groves and S. Sugden, *J. Chem. Soc.*, **1937**, 158.
6) P. C. Mahanti and D. N. Sen-Gupta, *J. Indian Chem. Soc.*, **5**, 673 (1928).
7) H. A. Stuart, "Die Struktur des freien Molekuls" pp. 290, Springer (1952).
8) B. Timm and R. Mecke, *Z. Physik*, **98**, 363 (1936).
9) Y. K. Syrkin and M. E. Dyatkina, "Structure of Molecules and the Chemical Bond" Intersci. Publ., New York: (1950).
10) *Trans. Faraday Soc.*, **30**, Appendix (1934).
11) J. G. Gelatis, *J. Appl. Phys.*, **19**, 419 (1948).
12) P. C. Mahanti, *Phil. Mag.*, (7) **20**, 274 (1935).
13) C. Komaki, I. Ichishima, K. Kuratani, T. Miyazawa, T. Shimanouchi and S. Mizushima, This Bulletin, **28**, 330 (1955).

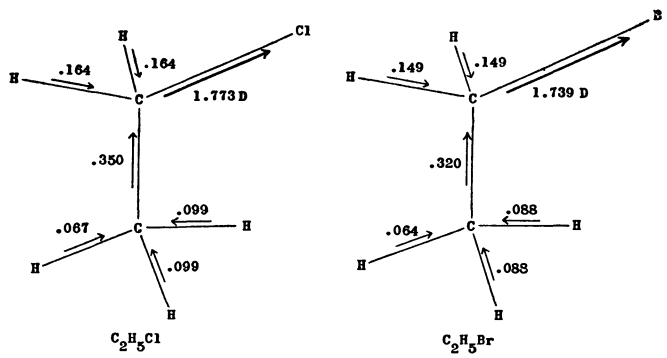

Fig. 3 (a)

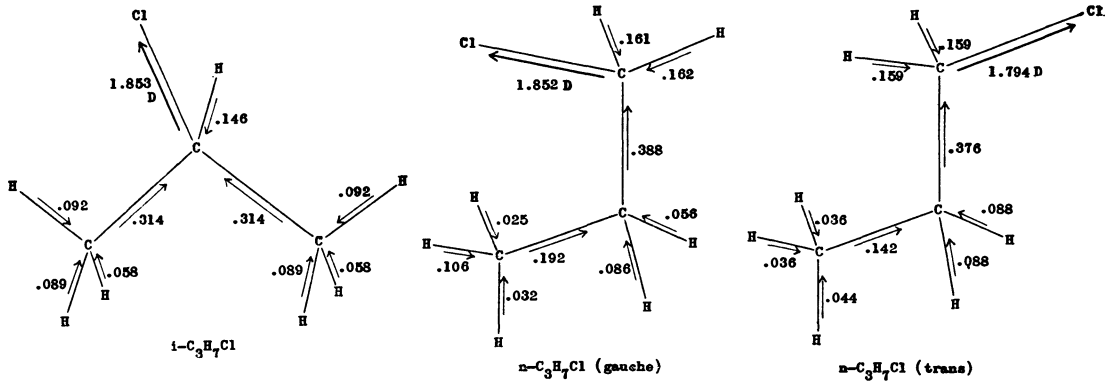

Fig. 3 (b)

discuss the detailed features of inductive effect somewhat quantitatively through the present treatment. It is also noticeable that Table II and Fig. 3 show fairly good agreement, in principal parts, with the preceding works[1,2]. In the present calculation, however, all inductive interaction terms have been included, and then, any change in the relative arrangement of bonds is reflected upon the whole results more or less, as can be observed at the difference between the *trans* and *gauche* forms of n-C_3H_7Cl in Fig. 3. The larger moment induced on γ-CH parallel to C-X than the β-C-H's may be understood as the marked consequence of direct effect. It must be noticed also that the *trans* form gives somewhat greater value of total moment than the *gauche* form in which actual induction is stronger than the *trans*. This means that the observed value of dipole moment can not always be taken as the measure of inductive effect without consideration about the abundance ratio of rotational isomers.

For the present calculation, we have assumed $Q^0_{CH}=0$ somewhat arbitrarily. It can readily be shown, however, that the different choice of Q^0_{CH}, which is smaller enough than Q_{CX} anyway, does not affect the results very much. Now, there may arise a question as to whether the inductive effect can be properly described with such a simple LCAO wave function as one which includes no polarization of atomic orbitals. This difficulty has essentially been avoided in the above treatment by employing the γ values determined from experimental bond polarizabilities, which are closely related phenomenally with the inductive effect. But yet, it is doubtful whether the bond polarizability data corresponding to vanishing field strength be efficient to estimate finite magnitudes of polarization. At present, little comment can be given on this problem. But the numerical results seem to permit the adoption of the data.

There still remains, however, an important problem; that is, the neglect of the possibility of transverse polarization. Considerable explanation against it might be found in the situation that the greater portion of general inductive effect is still attributable to the electronegativity change of end atoms; that is, the inductive effect

in the narrower sense, which causes mainly longitudinal polarization. However, the datails of the affair are yet an open question.

In practice of calculation, we must be concerned with the valence electronic configuration of substituent atoms. The present calculation has been carried out for $(ns)^2(np\sigma)(np\pi)^2(np\pi')^2$ configuration of halogen atoms. However, the possibility of mixing $(ns)(np\sigma)^2(np\pi)^2(np\pi')^2$ can not be ignored as has often been pointed out. After the mixing, the C-X bond moment becomes able to comprise the contribution from σ-type lone pair dipole in addition to the one from bonding pair expressed by Eq. ii, where the value of y_X^{CX} also changes with the mixing. This modification changes the formal expression of γ_{CX} and $C_{Xi}'s$ in Eqs. 19 and 20. The formal change in γ_{CX} is not very significant, because it is determined empirically in practical calculations, as if it were a simple empirical parameter. The change in $C_{Xi}'s$, however, may possibly lead to markedly different results. There is no doubt that this effect might be most obvious on the neighboring bonds, and, the test-calculation has been carried out for methyl chloride and bromide. The result given in Fig. 4 shows that the effect seems not very serious.

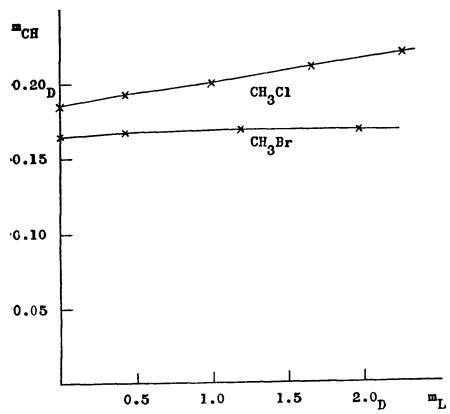

Fig. 4. The calculation has been carried out by the same procedure as in Example I, except that the lone pair dipole of X-atom, m_L, was added to M_{cal}. The bonding and lone pair orbitals of X-atom have been taken to be orthogonal with each other.

m_L can exceed the values of m_{CX} in Table II, because the latter is subtracted by the atomic dipole of carbon tetrahedral orbital.

Appendix

In SCF MO theory, the electronic energy of a molecule in closed shell state is expressed by Eq. I[4], where H_i, J_{ij}, and K_{ij} are bare nuclear field orbital energy, coulomb integral, and exchange integral

$$E=2\sum_i H_i+\sum_{i,j}(2J_{ij}-K_{ij}) \quad \text{(I)}$$

$$H_i=\int\phi_i^*(1)\,h_1\phi_i(1)\,d\tau_1 \quad \text{(II)}$$

$$J_{ij}=\int\phi_i^*(1)\phi_j^*(2)\,(e^2/r_{12})\,\phi_i(1)\,\phi_j(2)\,d\tau_1 d\tau_2 \quad \text{(III)}$$

$$K_{ij}=\int\phi_i^*(1)\phi_j^*(2)\,(e^2/r_{12})\,\phi_i(2)\,\phi_j(1)\,d\tau_1 d\tau_2 \quad \text{(IV)}$$

as given by Eqs. II~IV respectively. Now, an SCF MO ϕ_i may approximately be expressed by the linear combination of bond orbitals localized at each bond, as given by Eq. V.

$$\phi_i=\sum_r c_{ir}\phi_r \quad \text{(V)}$$

Then, we assume two approximate conditions as follows:

(1) There exists little overlapping between two different $\phi_r's$, and therefore those integrals which include the product $\phi_r^*\phi_s$ $(r\neq s)$ such as S_{rs}, H_{rs}, and electronic interaction energy integrals other than coulomb type may be neglected. Then, Eq. VI may be taken as an approximate orthonormality condition.

$$\sum_r c_{ir}^* c_{jr}=\delta_{ij} \quad \text{(VI)}$$

(2) The electron density at each bond orbital and the bond order* between different bond orbitals remain constantly equal to 2 and 0 respectively, as expressed by Eq. VII.

$$\sum_i c_{ir}^* c_{is}=\delta_{rs} \quad \text{(VII)}$$

Under these assumptions, Eqs. II~IV can be written as follows:

$$H_i=\sum_r\sum_s c_{ir}^* c_{is}H_{rs}=\sum_r c_{ir}^2 H_{rr} \quad \text{(VIII)}$$

$$J_{ij}=\sum_r\sum_s\sum_t\sum_u c_{ir}^* c_{js}^* c_{it}c_{ju}(rt/su)$$

$$=\sum_r\sum_s c_{ir}^2 c_{js}^2(rr/ss) \quad \text{(IX)}$$

$$K_{ij}=\sum_r\sum_s\sum_t\sum_u c_{ir}^* c_{js}^* c_{it}c_{ju}(ru/st)$$

$$=\sum_r\sum_s c_{ir}^* c_{js}^* c_{is}c_{jr}(rr/ss) \quad \text{(X)}$$

where

$$H_{rs}=\int\phi_r^*(1)\,h_1\phi_s(1)\,d\tau_1 \quad \text{(XI)}$$

$$(rt/su)=\int\phi_r^*(1)\,\phi_s^*(2)\,(e^2/r_{12})\,\phi_t(1)\,\phi_u(2)\,d\tau_1 d\tau_2\,. \quad \text{(XII)}$$

Then, the total energy E can be given by Eq. XIII taking Eqs. VI and VII into consideration.

$$E=2\sum_i\sum_r c_{ir}^2 H_{rr}+\sum_i\sum_j\sum_r\sum_s(2c_{ir}^2 c_{js}^2$$

$$-c_{ir}^* c_{js}^* c_{is}c_{jr})\,(rr/ss)$$

$$=2\sum_r H_{rr}+\sum_r\sum_s(2-\delta_{rs})\,(rr/ss). \quad \text{(XIII)}$$

* Similarly defined as in LCAO approximation.

The author wishes to thank Professor K. Kozima of Tokyo Institute of Technology for his valuable advice and encouragement, and Dr. S. Nagakura of Tokyo University for his helpful discussion.

Department of Chemistry, National Deffence Academy, Yokosuka

Synthesen und Konfigurationsermittlung in Rotenoid-Reihe. I. Ein Beitrag zur Synthese der Toxicarsäure

von Masateru MIYANO und Masanao MATSUI

(Eingegangen am 15 Oktober, 1957)

Die Strukturformel des auf Fische und Insekten giftig wirkenden Rotenons (I) ist gleichzeitig von Takei[1], von Butenandt[2] und von LaForge[3] aufgestellt worden. Seither von verschiedenen Arbeitsgruppen u. a. von Robertson und Mitarbb. sind viele Abbauprodukte der Rotenoide synthetisch dargestellt worden. Es bleibt heute die Aufgabe übrig, erstens die Konfigurationen des C_{12}- und C_{13}-Atoms aufzuschliessen, zweitens die natürlichen Rotenoide (Rotenon, Deguelin (II, R=H), Toxicarol (II, R=OH) usw.) zu synthetisieren.

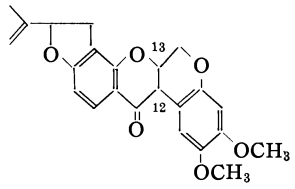

(I)

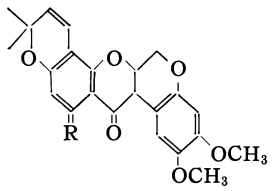

(II)

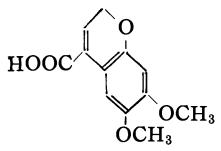

(III)

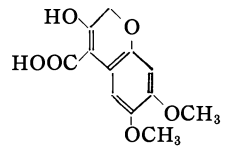

(IV)

In der vorliegenden Arbeit werden die verbesserten Synthesen der Toxicarsäure (6,7-Dimethoxy-Δ^3-chromen-4-carbonsäure) (III) berichtet.

Es entspricht die Toxicarsäure bzw. Oxynetorsäure (3-Oxy-6,7-dimethoxy-chroman-4-carbonsäure) (IV) dem halben Grundgerüst aller Rotenoide, daher scheint uns diese beiden Säuren die Schlüsselverbindungen für die gesamte Synthese von Rotenoiden zu sein. Die Toxicarsäure, welche von Butenandt[4] bei der Oxydation von *dl*-Toxicarol mit alkalischem Perhydrol und von Clark[5] auch bei der gleichen Oxydation von *dl*-Apotoxicarol(V) isoliert worden war, wurde durch sehr geschickte Reaktionsreihe von Robertson und Mitarbb[6~8]. synthetisch dargestellt. Am Anfang wollten wir diese Säure auf dem durch das Schema 1 dargestellten Wege erhalten, aber es war Essig damit, weil unter der gewöhnlichen Bedingung 6,7-Dimethoxy-chromanon (VI) die Blausäure nicht aufnimmt. Wir haben dann den anderen Weg gewählt. Ausgehend vom Robertsons Zwischenprodukt d. h. 6,7-Dimethoxy-chroman-3-keto-4-carbonsäure-äthylester (VII) durch die neuen

(1)

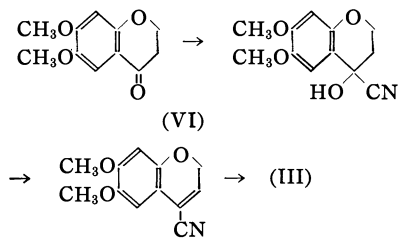

(VI)

(III)

1) S. Takei, S. Miyajima und M. Ohno, *Ber.*, **65**, 1041 (1932).
2) A. Butenandt und W. McCartney, *Ann.*, **494**, 17 (1932).
3) F. B. LaForge, *J. Am. Chem. Soc.*, **54**, 3377 (1932).
4) A. Butenandt und G. Hilgetag, *Ann.*, **495**, 172 (1932).
5) E. P. Clark, *J. Am. Chem. Soc.*, **54**, 2537 (1932).
6) A. Robertson, *J. Chem. Soc.*, **1930**, 2440.
7) A. Robertson, ebenda, **1932**, 1380.
8) A. Robertson und G. L. Rusby, ebenda, **1936**, 212.

(2) 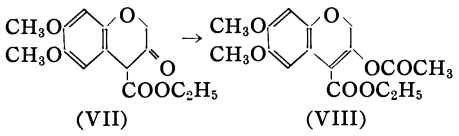

(VII) (VIII)

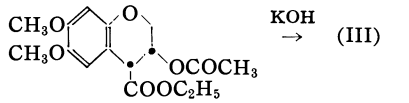

(IX)

(3) (VII) → 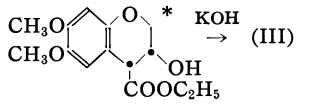 (III)

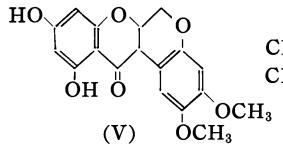

(V)

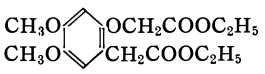

(XI)

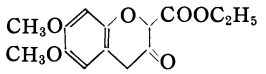

(XII)

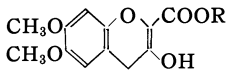

(XIII)

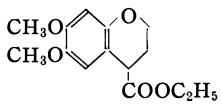

(XIV)

Reaktionen 2 und 3 haben wir die Toxicarsäure erhalten. Bei der intramolekulare Kondensation des Derrsäure-diäthylesters (XI) unter Einwirkung von Natrium hat Robertson[8] nur den 6,7-Dimethoxy-chroman-3-keto-4-carbonsäure-äthylester (VI) isoliert, dagegen haben wir neben dem letzteren den bisher noch nicht beschriebenen 6,7-Dimethoxy-chroman-3-keto-2-carbonsäure-äthylester (XII) erhalten, welcher bei der anschliessenden katalytischen Hydrierung 3-Oxy-6,7-dimethoxy-chroman-2-carbonsäure-äthylester (XIII, R=C_2H_5) liefert. Durch Versetzung vom Ketoester (VII) mit Acetanhydrid in Pyridin haben wir das entsprechende Enolacetat (VIII) dargestellt. Obwohl sich unser Enolacetat um 12～3°C niedriger Schmp. (71～2°C) als Literatur (84°C) zeigt, machen das IR- und UV-Spektrum sowie die Analysenzahlen sicher, dass unserem Enolacetat die in der Formel VIII angegebene Struktur zukommt. Bei der katalytischen Hydrierung mit Palladium-Kohle in Äthanol geht das Enolacetat in den noch nicht bekannten *dl-cis*-Acetoxynetorsäure-äthylester (3-Acetoxy-6,7-dimethoxy-chroman-4-carbonsäure-äthylester) (IX) über, der durch Behandlung mit alkoholischer Kalilauge oder Natriumcarbonat die Toxicarsäure liefert. Hingegen hat Robertson berichtet, dass sein Enolacetat (Schmp. 84°C) bei der katalytischen Hydrierung mit Platinoxyd Netorsäure-äthylester (XIV) lieferte. Auf Grund der guten Gesamtausbeute und sehr leicht verlaufenden Hydrierung scheint uns die Reaktionsfolge (2) der beste Weg zur Darstellung der Toxicarsäure zu sein. Andererseits haben wir die Robertsons Hydrierungsbedingung vom Schritt (VII) →(X) verbessert. Behandelt man den Ester (X) mit siedender alkoholischer Kalilauge, so geht es in die Toxicarsäure über. Dieser Weg ist auch das Beste zur Synthese der Toxicarsäure.

* Bestimmung dieser Konfiguration wird in der nachfolgenden Mitteilung berichtet werden.

Beschreibung der Versuche

Alle Schmpp. sind unkorrigiert.

6,7-Dimethoxy-chroman-3-keto-4-carbonsäure-äthylester (VII) und 6,7-Dimethoxy-chroman-3-keto-2-carbonsäure-äthylester (XII)—Eine Lösung von 68 g Derrsäure-diäthylester (XI) in 350 ccm Toluol und 50 ccm Xylol wird mit 8 g Natrium versetzt und 4 Stunden auf 110°C erhitzt. Nach dem Erkalten und der Zersetzung des zurückbleibenden Natriums durch Zutropfen von 40 ccm Eisessig, wird die Toluol-lösung mit Wasser gewaschen, über Natriumsulfat getrocknet und unter vermindertem Druck eingedampft. Die so erhaltenen rohen Kristalle werden in 250 ccm heissem Äthanol aufgenommen, unter Aktivkohlezusatz abfiltriert, und das Filtrat lässt sich bei Zimmertemperatur stehen. Die ausgeschiedenen Nadeln werden abgenutscht, und mit kaltem Alkohol gewaschen. Schmp. 103～5°C, Ausbeute 45 g. Beim Konzentrieren und bei der Behandlung mit Aktivkohle erhält man weitere Menge von Kristallnadeln (3 g). Obgleich diese Kristalle reinigenug zu sein scheinen, sind es zwar ein Gemisch von zwei isomeren Estern. Durch zweimalige Umkristallisation aus Alkohol werden 27.5 g reinen 6,7-Dimethoxy-chroman-3-keto-4-carbonsäure-äthylester vom Schmp. 109°C isoliert.

Anal. Gef. C, 59.9; H, 5.7. Ber. für $C_{14}H_{16}O_6$: C, 60.0; H, 5.75%.

$\lambda_{max}^{Isopropanol}$ 247 mμ (ε 18800)

λ_{max} 6.01 (C=O), 6.17 (C=C) μ

6,7-Dimethoxy-chroman-3-keto-2-carbonsäure-äthylester vom Schmp. 95°C wird aus der Mutterlauge isoliert.

Anal. Gef. C, 60.0; H, 5.8. Ber. für $C_{14}H_{16}O_6$: C, 60.0; H, 5.75%.

$\lambda_{max}^{Isopropanol}$ 295 mμ (ε 5210)

λ_{max} 6.11 (C=O), 6.21 (C=C) μ

dl-cis-3-Oxy-6,7-dimethoxy-chroman-4-carbonsäure-äthylester (dl-cis-Oxynetorsäure-äthylester) (X)* — a) Der Ketoester (VII) (10 g) in 150ccm Essigester wird mit 4 g 10 proz. Palladium-Kohle

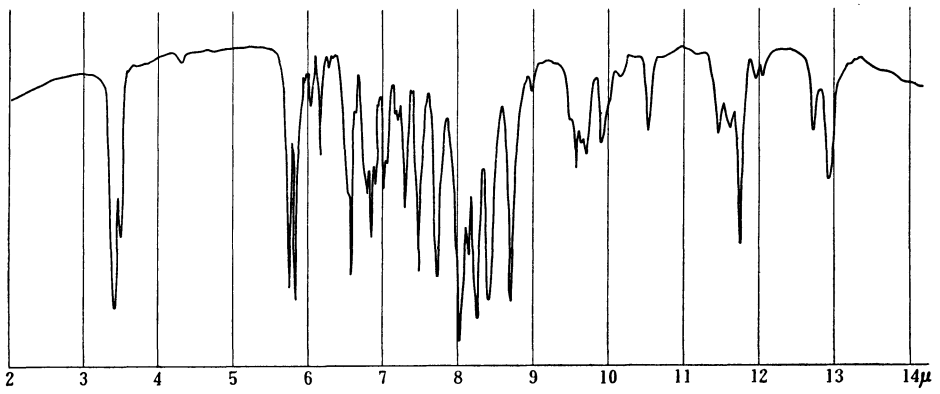

Abb. 1. IR-Spektrum des Enolacetats (XIII) in Nujol
5.75 μ(Acetat C=O), 5.84 μ(Ester C=O), 6.04 μ(konjg. C=C), 8.25 μ(Enolacetat C−C)

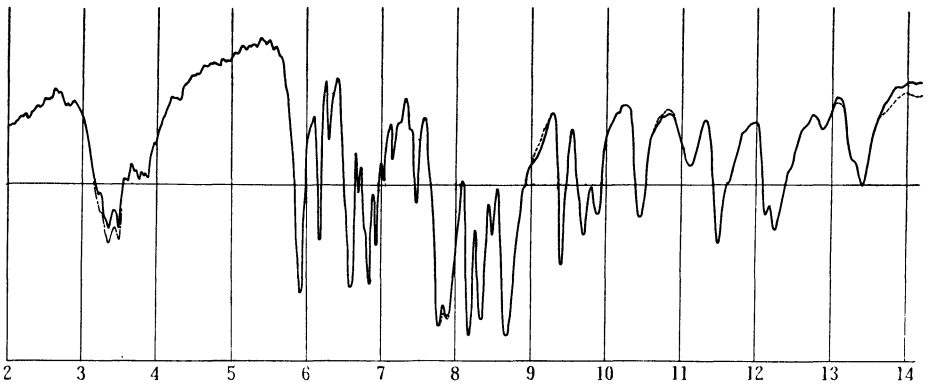

Abb. 2. IR-Spektrum der Toxicarsäure (Kaliumbromid-Presslinge)
—— Authentische Probe
------ Verseifung und Deacetylierung von Acetoxyester (s. Beschreibung der Versuche a))
-·-·- Verseifung und Dehydratisierung von Oxynetorsäureäthylester (s. Beschreibung der Versuche b))

unter Wasserstoffström geschüttelt. Die Reaktion kommt nach Verbrauch von 1 Mol. Wasserstoff zum Stillstand. Die abfiltrierte Lösung wird in Vakuum konzentriert, mit 5 ccm Benzol aufgenommen und durch Zutropfen von 20 ccm Cyclohexan kristallisiert. Farblose Nädelchen werden abgesaugt, mit Äther gewaschen. Schmp. 108°C, Ausbeute 8.6 g.

Anal. Gef. C, 59.6; H, 6.4. Ber. für $C_{14}H_{18}O_6$: C, 59.6; H 6.5%.

Beim Eindampfen des Filtrats wird eine weitere Menge von Kristallen gewonnen (0.6 g, Schmp. 102~3°C).

b) In analoger Weise werden 10 g des Ketoesters (VII) in 50 ccm Essigster mit 1.0 g Platinoxyd unter Wasserstoffström geschüttelt. Der Oxyester (7.5 g) vom Schmp. 108°C wird erhalten.

c) Der Ketoester (VII) (5 g) nimmt 1 Mol. Wasserstoff auf beim Schütteln in 80 ccm Essigester in Gegenwart von 0.5 g Platinoxyd unter Zugabe von 1 ccm Morpholin. Die von Katalysator abgetrennte Lösung wird nach Waschen mit verd. Salzsäure, Bicarbonat-lösung und Wasser, über Natriumsulfat getrocknet, und das Lösungsmittel wird verdampft. Beim Versetzen von Äther und Cyclohexan und Stehen bei Zimmertemperatur erhält man 4.2 g von farblosen Nädelchen vom Schmp. 102~3°C. IR-Spektren der durch a), b) und c) gewonnenen drei Oxyester, die in Nujol Paste aufgenommen werden, sind ganz gleich.

dl-3-Oxy-6,7-dimethoxy-chroman-2-carbonsäure (XIII, R=H) und sein Äthylester (XII, R=C_2H_5) —6,7-Dimethoxy-chroman-3-keto-2-carbonsäureäthylester (XII) wird in Essigester in Gegenwart von Platinoxyd reduziert. Das Hydrierungsprodukt wird vom Katalysator und Essigester befreit und gereinigt durch Umlösen aus Benzol. Schmp. 141°C.

Anal. Gef. C, 59.6; H, 6.4. Ber. für $C_{14}H_{18}O_6$: C, 59.5; H, 6.4%.

Der Oxyester wird beim 3stundigen Rückfliessen in 10 proz. alkoholischer Kalilauge zur freien Säure verseift. Schmp. 222~3°C (Umkristallisation aus Wasser).

Anal. Gef. C, 56.7; H, 5.5. Ber. für $C_{12}H_{14}O_6$: C, 5.67; H, 5.55%.

6,7-Dimethoxy-3-acetoxy-Δ^3-chromen-4-carbon-

säure-äthylester (*VIII*)—Der Ketoester (VII) (9.0 g) wird mit 90 ccm Acetanhydrid und 45 ccm Pyridin versetzt, und die Mischung wird eine Stunde auf einem siedenden Wasserbad erhitzt, dann lässt sich bei Zimmertemperatur über Nacht stehen. Zu dieser Lösung wird 45 ccm Äthanol gegeben, und nach dem Erkalten wird das Produkt mit Äther aufgenommen. Nach Neutralwaschen der ätherischen Lösung mit verd. Salzsäure, Wasser, Bicarbonat und schliesslich mit Wasser, wird es über Natriumsulfat getrocknet und das Lösungsmittel wird verdampft. Nach der Umkristallisation aus Benzol—Cylcohexan erhält man 8.0 g des Enolacetats vom Schmp. 71～2°C (Literatur 84°C).

Anal. Gef. C, 59.6; H, 5.6. Ber. für $C_{16}H_{18}O_7$: C, 59.6; H, 5.6%.

$\lambda_{max}^{Isopropanol}$ 326 mμ (ε 4090)

Weitere Mengen (1.5 g) des Esters werden beim Eindampfen der Mutterlauge isoliert.

dl-cis-6,7-Dimethoxy-3-acetoxy-chroman-4-carbonsäure-äthylester (*IX*)

1.9 g des Enolacetats (VIII) werden in Äthanol mit 0.3 g 10 proz. Palladium-Kohle geschüttelt. Nach der raschen Aufnahme (2～3 Min) des Wasserstoffs (170 ccm, 1.2 Mol.) hörte die Reaktion plötzlich auf. Die alkoholische Lösung wird von Katalysator befreit und dann eingeengt. Das Rohprodukt kann ohne weitere Reinigung in die nachfolgende Reaktion übergeführt werden, nur ein Teil des Produktes wurde durch Chromatographie (vorläufig mit Säure behandelte Alumina, Benzol als Lösungsmittel) gereinigt für Elementaranalyse.

Anal. Gef. C, 59.2; H, 6.4. Ber. für $C_{16}H_{20}O_7$: C, 59.3; H, 6.2%.

$n_D^{23.5}$ 1.5250

Toxicarsäure (*6,7-Dimethoxy-Δ^3-chromen-4-carbonsäure*) (*III*) — a) Verseifung und Deacetylierung des Acetoxyesters (IX). Eine halbe Menge des rohen Acetoxyesters, der wie oben gezeigt aus den 1.9 g Enolacetaten (VIII) dargestellt wird, wird mit 15 ccm 10 proz. alkoholischer Kalilauge versetzt, und lässt sich 2 Tage bei Zimmertemperatur stehen. Zu dieser Lösung wird 50 ccm verd. Salzsäure zugegeben. Nach 2-tägigem Stehen in Eisschrank, werden die ausgeschiedenen braunen Kristallnadeln abgesaugt, mit Wasser gewaschen. So erhält man 0.7 g der fast reinen Toxicarsäure vom Schmp. 209°C (zersetz.).

Anal. Gef. C, 61.0; H, 5.1. Ber. für $C_{12}H_{12}O_5$: C, 61.0; H, 5.1.

$\lambda_{max}^{Isopropanol}$ 330 mμ (ε 4070)

Diese Säure stimmt an allen Eigenschaften mit der authentischen Toxicarsäure überein.

Die andere Hälfte des rohen Acetoxyesters wird in einer Lösung von 20 ccm 5 proz. Kaliumcarbonat und 20 ccm Äthanol gelöst. Nach 9-tägigem Stehen bei Zimmertemperatur wird die entstandene Toxicarsäure (0.6 g) analogerweise isoliert.

b) Verseifung und Dehydratisierung von Oxynetorsäure-äthylester (X)—4.0 g des *dl-cis*-Oxynetorsäure-äthylesters werden 3 Stunden in 35 ccm 10 proz. alkoholischer Kalilauge unter Rückfluss gekocht. Nach dem Erkalten werden 190 ccm Wasser und 10 ccm konz. Salzsäure zugegeben. Die ausgeschiedenen gelbbraunen Kristallnadeln werden abfiltriert, mit Wasser gewaschen. 2.7 g (80% der Theorie) des Toxicarsäure vom Schmp. 210°C (zersetz.) werden erhalten.

Anal. Gef. C, 61.0; H, 5.3. Ber. für $C_{12}H_{12}O_5$: C, 61.0; H, 5.1%.

Herren Professor Dr. R. Yamamoto und Professor Dr. Y. Sumiki danken wir herzlich für die Unterstützung und Förderung dieser Arbeit. Wir danken Herrn K. Aizawa für die Aufnahme des IR-Spektrums; Frau K. Satô, Fräulein M. Suzuki und Fräulein I. Isobe für Mikroanalysen. Herrn Dr. S. Tamura möchten wir auch an dieser Stelle für seine entgegenkommende Unterstützung danken.

Organisch-Chemisches Laboratorium,
Agrikulturlich-Chemisches
Departement, Universität
zu Tokyo, Hongo, Tokyo

Synthesen und Konfigurationsermittlung in Rotenoid-Reihe. II. Zur Synthese und Konfiguration der dl-cis- und dl-trans-Oxynetorsäure

Von Masateru MIYANO und Masanao MATSUI

(Eingegangen am 15. Oktober, 1957)

Eine Oxynetorsäure vom Schmp. 189°C neben Toxicarsäure (II) ist von Clark[1] bei der Oxydation von *dl*-Apotoxicarol (III) mit alkalischem Perhydrol isoliert worden, dazu kommt die in der Formel (I, R=H) angegebene Struktur. Ein Oxynetorsäure-äthylester (I, $R=C_2H_5$) ist von Robertson[2] durch die katalytische Hydrierung des zugehörigen Ketoesters (IV) dargestellt worden, aber er hat weder über die freie Säure noch seine Konfiguration beschrieben.

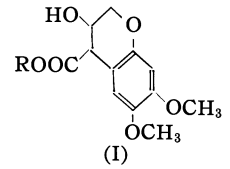

(I)

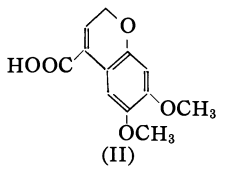

(II)

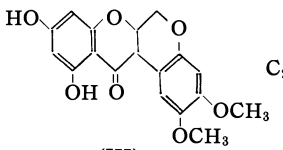

(III)

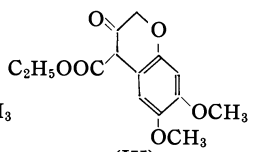

(IV)

Kürzlich haben wir[3] 3-Acetoxy-6,7-dimethoxy-chroman-4-carbonsäure-äthylester (3-Acetoxynetorsäure-äthylester) (VI) durch die katalytische Hydrierung von Enolacetat (V) dargestellt. Demjenigen Ester (VI) muss die *cis*(erythro)-Konfiguration zukommen, weil bei der katalytischen Hydrierung der einfachen Doppelbindung gewöhnlich das *cis*-Addukt erhalten wird.

Wie schon von uns berichtet[3], geht der Oxynetorsäure-äthylester beim Rückfluss mit alkoholischer Kalilauge in die Toxicarsäure über. Behandelt man mit alkoholischer Kalilauge bei Zimmertemperatur, ist der Ester dagegen zu einem Stereoisomerengemisch der entsprechenden Säuren verseift worden, welches zu rund 90% aus eine Oxynetorsäure vom Schmp. 161°C und zu rund 10% aus der alternativen Oxynetorsäure vom Schmp. 156~7°C besteht. Wir dürfen diese Oxynetorsäure als Schlüsselverbindung gebrauchen, um die Konfigurationen des C_{12}- und C_{13}-Atoms des Rotenons aufzuschliessen. Diese besondere Bedeutung hat uns veranlassen dies eingehend zu untersuchen. Aus der theoretischen Überlegung kann man die entstandene Konfiguration nicht folgern. Aus der von K. von Auwers[4] und Skita[5], neuerdings von Barton[6] angegebenen Regel dürfen wir die Entstehung der *trans*(threo)-Form (X) bei der katalytischen Hydrierung von cyclischem Keton in neutraler bzw. basischer Lösung mit Platinoxyd erwarten. Wird der Ketoester (IV) durch die Enolform reduziert, dagegen soll die *cis*-Form (VII) entstehen. Infrarot-bzw. ultraviolett-Spektrum des Ketoesters bezeigen, dass derjenige Ester als Kristall oder *iso*-Propanol-lösung ganz die Enolform sei (s. Beschreibung d. Versuche). Aber in diesem Fall ist es uns unbegreiflich, dass das Enolacetat (V) ungefähr 60-malig schneller als die Enolform des Ketoesters (IV) hydriert wird, während die letztere sterisch weniger verhindert.

Um dies näher nachzuweisen, ist der Acetoxyester (VI) einerseits schonend verseift worden, damit wir *dl-cis*-Oxynetorsäure erwerben könnten. Aber, wie schon in der 1. Mitteilung erörtert, bei dieser Hydrolyse ist nur die Toxicarsäure als einziges Produkt isoliert worden. Auf der anderen Seite ist *dl*-Oxynetorsäure-äthylester (VII) mit Acetanhydrid und Pyridin versetzt worden und nach der chromatographischen Reinigung haben wir fast farbloses Öl erhalten, dessen IR-Spektrum mit demjenigen des chromatographisch gereinigten Acetoxyesters (VI) fast übereinstimmt.

Daher handelt es sich eine *dl*-Oxynetorsäure vom Schmp. 161°C um die *cis*-Form

1) E. P. Clark, *J. Am. Chem. Soc.*, **54**, 2537 (1932).
2) A. Robertson und G. L. Rusby, *J. Chem. Soc.*, **1934**, 212.
3) M. Miyano und M. Matsui, Dieses Bulletin, **31**, 267 (1958).
4) K. von Auwers, *Ann.*, **420**, 91 (1921).
5) A. Skita und W. Faust, *Ber.*, **64**, 2878 (1931).
6) D. H. R. Barton, *J. Chem. Soc.*, **1953**, 1027.

und die andere vom Schmp. 156~7°C um die *trans*-Form.

Die Oxynetorsäure vom Schmp. 161°C ist in einen Methylester vom Schmp. 74~5° und die andere Oxynetorsäure vom Schmp. 156~7°C in einen Methylester vom Schmp. 72~3°C übergegangen. Obgleich die beiden Methylester sehr ähnliche IR-Spektren aufweisen, zeigt der erste, wie der Äthylester (VII) eine starke Absorption bei 8.81 μ, während der letztere nicht.

Um die oben erwähnte Konfiguration ferner zu bestätigen, haben wir zunächst die höher schmelzende Säure mit Alkali zu isomerisieren untersucht. Wir haben die *dl-trans*-Oxynetorsäure vom Schmp. 156~7°C neben der Toxicarsäure erhalten, obwohl die Ausbeute schlecht war.

Endlich haben wir den Ketoester (IV)

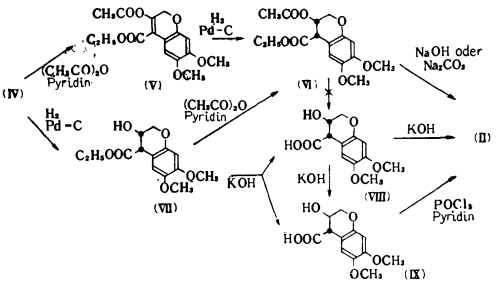

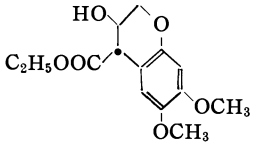

(X)

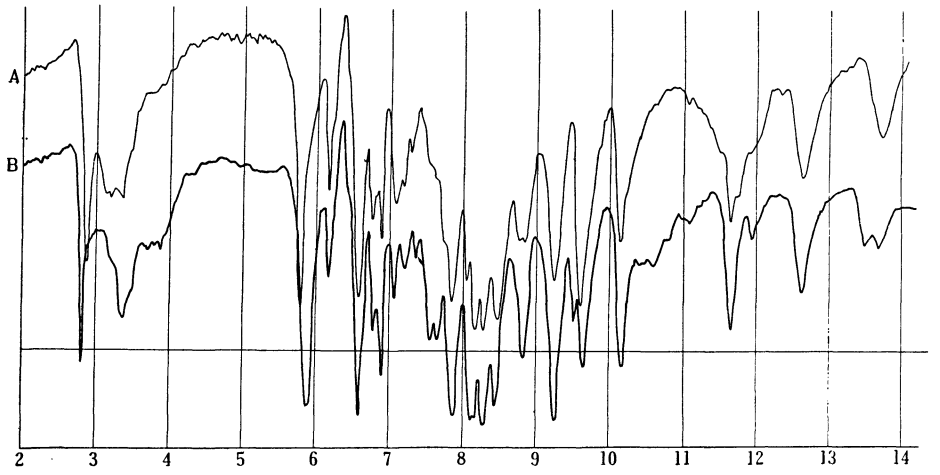

Abb. 1. IR-Spektrum der *dl-cis*-Oxynetorsäure (fest in KBr gepresst) ····· (A)
2.88(OH), 5.79(C=O) μ.
IR-Spektrum der *dl-trans*-Oxynetorsäure (fest in KBr gepresst) ····· (B)
2.80(OH), 5.87(C=O) μ.

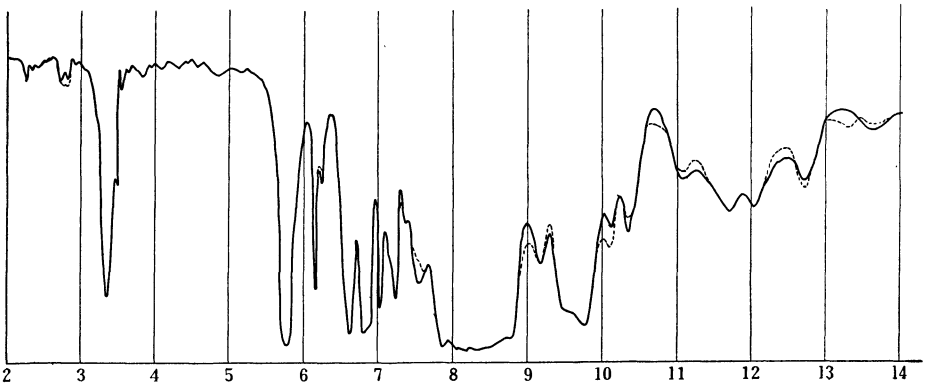

Abb. 2. IR-Spektrum des *dl-cis*-3-Acetoxy-6,7-dimethoxy-chroman-4-carbonsäure-äthylesters (flüssig).
—— Hydrierung von Enolester
------ Acetylierung von *dl-cis*-Oxynetorsäure-äthylester

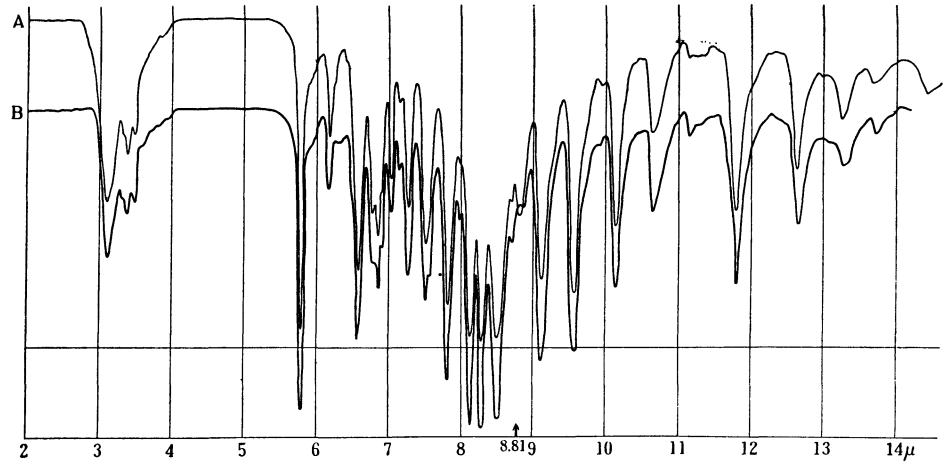

Abb. 3. IR-Spektrum des *dl-cis*-Oxynetorsäure-methylesters ·····(A)
IR-Spektrum des *dl-trans*-Oxynetorsäure-methylesters ·····(B)
(fest in KBr gepresst)

mit Natriumborohydrid reduziert, mit der Erwartung, den thermodynamisch stabileren *trans*-Ester (X) als Hauptprodukt zu erwerben. Obgleich keine reine Oxynetorsäure isoliert worden ist, wurde die Toxicarsäure nach der Dehydratisierung vom Rohprodukt mit Phosphoroxychlorid in Pyridin in geringer Ausbeute isoliert.

Unserer Erwartung zuwider, stimmt die von Clark isolierte Oxynetorsäure mit den in der vorliegenden Arbeit beschriebenen beiden Oxynetorsäuren nicht überein.

Beschreibung der Versuche

Alle Schmp. sind unkorrigiert.

dl-cis-3-Oxy-6,7-dimethoxy-chroman-4-carbonsäure (*dl-cis-Oxynetorsäure*) (*VIII*) *und dl-trans-3-Oxy-6,7-dimethoxy-chroman-4-carbonsäure* (*dl-trans-Oxynetorsäure*) (*IX*).—Zehn Gramme des Äthylesters (VII)[3] werden in 150 ccm 10proz. alkoholischer Kalilauge gelöst und die Lösung wird 24 Stunden bei Zimmertemperatur aufbewahrt, dann neutralisiert mit verd. Salzsäure (Congorot). Das Lösungsmittel wird abdestilliert und die zurückbleibende organische Säure in siedendem Aceton aufgenommen. Nach dem Eindampfen der Acetonlösung ist ein Rohprodukt geblieben, woraus bei der zweimaligen Umkristallisation aus 50 ccm heissem Wasser unter Aktivkohlezusatz 7.0 g der *dl-cis*-Oxynetorsäure vom Schmp. 161°C isoliert werden.

Anal. Gef.: C, 56.4; H, 5.5. Ber. für $C_{12}H_{14}O_6$: C, 56.7; H, 5.55%. λ_{max} 2.88(OH), 5.79(C=O) μ.

Aus der Mutterlauge, nach Konzentration und Behandlung mit Kohle erhält man 0.6 g von *dl-trans*-Oxynetorsäure vom Schmp. 156~7°C.

Anal. Gef.: C, 56.4; H, 5.5. Ber. für $C_{12}H_{14}O_6$: C, 56.7; H, 5.55%. λ_{max} 2.80(OH), 5.87(C=O) μ.

3-Acetoxy-6,7-dimethoxy-chroman-4-carbonsäure-äthylester (*3-Acetoxy-netorsäure-äthylester*) (*VI*).—Ein Gramm des *dl-cis*-Oxynetorsäure-äthylesters wird mit 3 ccm Acetanhydrid und 10 ccm Pyridin versetzt und 24 Stunden bei Zimmertemperatur aufbewahrt. Nach dem Eingiessen in verd. Salzsäure und Eis, wird das Produkt mit Äther extrahiert, mit Wasser, Bicarbonat, dann mit Wasser gewaschen, und über Natriumsulfat getrocknet. Beim Eindampfen des Lösungsmittels erhält man gelbliches Öl, welches hauptsächlich aus dem Acetoxyester besteht, doch mit geringer Menge der Toxicarsäure begleitet ist. Durch chromatographische Reinigung (Alumina, Benzol) erhält man den reinen Acetoxyester, dessen IR-Spektrum mit dem des in 1. Mitteilung beschriebenen *dl-cis*-Esters fast übereinstimmt (s. Abb. 2).

Anal. Gef.: C, 59.3; H, 6.2. Ber. für $C_{16}H_{20}O_7$: C, 59.3; H, 6.2%. $n_D^{23.5}$ 1.5260.

Toxicarsäure (*II*).—a) 1.0 g der *dl-cis*-Oxynetorsäure wird 3 Stunden in 10 ccm 10proz. alkoholischer Kalilauge unter Rückfluss gekocht. Nach dem Erkalten werden 50 ccm Wasser und 2.5 ccm konz. Salzsäure versetzt. Man erhält 0.83 g der Toxicarsäure vom Schmp. 206°C (zersetz.). Nach dem Umlösen aus wässerigem Aceton, Schmp. 209~210°C (zersetz.).

Anal. Gef.: C, 60.8; H, 5.3. Ber. für $C_{12}H_{12}O_5$: C, 61.0; H, 5.1%.

b) *Natriumborohydrid Reduktion und anschliessende Dehydratisierung.*—Mit einer auf 10° gekühlten Suspension von 1.4 g Ketoester in 100 ccm Methanol wird 1 g von Natriumborohydrid versetzt. Nach 2tägigem Stehen bei Zimmertemperatur wird das Reaktionsgemisch in verd. Salzsäure eingegossen, dann in Essigester aufgenommen, mit Wasser gewaschen, und über Natriumsulfat getrocknet. Nach dem Eindampfen des Lösungsmittels versetzt man das bleibende Öl mit 30 ccm Kollidin und 1.5 ccm Phosphoroxychlorid und erhitzt die Mischung eine Stunde auf 100°C. Die so erhaltene fast farblose Lösung wird in verd. Salzsäure eingegossen, mit Essigester extrahiert. Nach dem Neutralwaschen und Eindampfen der Essigester-lösung kocht man das zurückbleibende Öl in 15 ccm alkoholischer

Kalilauge unter Rückfluss. Die bei der Wasserzugabe ausgeschiedenen Kristalle werden abfiltriert und das Filtrat wird konzentriert, und dann angesäuert mit verd. Salzsäure. Beim Stehen über Nacht scheiden die gelbbraune Kristallnadeln (ca. 6 mg) vom Schmp. 200° (zersetz.) aus.

Anal. Gef.: C, 60,2; H, 5,3. Ber. für $C_{12}H_{12}O_5$: C, 61,0; H, 5,1%.

IR-Spektrum stimmt mit dem der authentischen Probe überein.

dl-cis-3-Oxy-6,7-dimethoxy-chroman-4-carbonsäure-methylester (dl-cis-Oxynetorsäure-methylester).—Zu 0,5 gr der fein gepulverten *dl-cis*-Oxynetorsäure in 50 ccm Essigester gibt man Diazomethan in Äther zu. Nach 1-stündigem Stehen bei Zimmertemperatur zersetzt man überschüssiges Diazomethan mit Essigsäure, wäscht mit Bicarbonatlösung und Wasser, und trocknet über Natriumsulfat. Beim Eindampfen des Lösungsmittels und Umlösen aus Äther erhält man 0,45 gr des Methylesters vom Schmp. 74~5°.

Anal. Gef.: C, 58,2; H, 6,2. Ber. für $C_{13}H_{16}O_6$: C, 58,2; H, 6,0%.

Der Methylester (0,5 g) wird mit 10 proz. alkoholischer Kalilauge (20 ccm) versetzt und lässt sich 2 Tage beim Zimmertemperatur stehen. Nach dem Neutralisieren mit wässeriger Salzsäure und Eindampfen des Lösungsmittels unter vermindertem Druck wird die organische Substanz in heissem Aceton aufgenommen. Das Aceton wird dann abdestilliert und das zurückbleibende Produkt wird aus heissem Wasser (Aktivkohle) umkristallisiert. Schmp. und Mischschmp. 157~161°. λ_{max} 2,88(OH), 5,79(C=O) μ.

dl-trans-3-Oxy-6,7-dimethoxy-chroman-4-carbonsäure-methylester (dl-trans-Oxynetorsäure-methylester). — Analogerweise ergibt sich die *dl-trans*-Oxynetorsäure den Methylester vom Schmp. 72~3° (Umkristallisation aus Äther), der bei der Verseifung die *dl-trans*-Oxynetorsäure liefert.

Anal. Gef.: C, 58,4; H, 6,0. Ber. für $C_{13}H_{16}O_6$: C, 58,2; H, 6,0%.

Isomerisierung von d-lcis-Oxynetorsäure.—Ein g der *dl-cis*-Oxynetorsäure wird mit 20 ccm 10 proz. alkoholischer Kalilauge und 20 ccm Wasser versetzt und während 10 Tagen bei Zimmertemperatur aufbewahrt, und des Gemisch wird mit verd. Salzsäure angesäuert (Congorot) und unter vermindertem Druck eingedampft. Die organische Substanz wird mit siedendem Aceton extrahiert. Nach dem Vertreiben des Acetons wird der Rückstand aus 20 ccm heissem Wasser unter Aktivkohlezusatz umkristallisiert. Die sofort ausgeschiedenen gelben Kristalle der Toxicarsäure (ca. 0,1 g) wird abgesaugt und die Mutterlauge liefert *dl-cis*-Oxynetorsäure (0,6 g) beim Stehen in Kühlschrank. Die letzte Mutterlauge wird zu etwa 5 ccm eingeengt und mit Aktivkohle behandelt. Die isomerisierte *dl-trans*-Oxynetorsäure wird isoliert, ca. 0,15 g.

Herren Professor Dr. R. Yamamoto und Professor Dr. Y. Sumiki danken wir an dieser Stelle für die Unterstützung und Förderung dieser und nachfolgender Arbeiten. Herren Dr. Y. Chen, Taipei (Formosa) und Dr. W. F. Barthel, Agricultural Research Service (U. S. A.) für ihr Interesse und Überlassung von einigen Proben sind wir zu bestem Dank verpflichtet. Die Mikroanalysen wurden im analytischen Laboratorium unseres Departements ausgeführt; IR-Spektren wurden mit IR-Spektrophotometer Ôyô-Kôken, Modell DS 301 aufgenommen, wofür wir insbesondere Herrn. K. Aizawa bestens danken.

Organisch-Chemisches Laboratorium,
Agrikulturlich-Chemisches
Departement, Universität
zu Tokyo, Hongo, Tokyo

Structural Variations of Kaolin Minerals

By Hiroshi TAKAHASHI

(Received December 12, 1957)

Kaolin minerals are made of stacking of aluminosilicate unit layers in their crystal structure. However, there are a continuous gradation in the manner of stacking from kaolinite which has a perfectly ordered sequence of layers to halloysite which has a throughly disordered sequence of layers.[1)]

In the results given by Murray, the degree of crystallinity determined by using the X-ray powder diffraction data does not agree with that based on the differential thermal analysis curve of halloysite.[2)] When one say the degree of crystallinity, however, there are two kinds of structural imperfection. One is the imperfections within the crystallographic unit layer and the other is the stacking disorder of the unit layers. As the definition of the crystallinity, both kinds of imperfection should be considered.

The purpose of this study is to determine the degree of crystallinity for all kaolin minerals through X-ray, thermal and other experimental methods, and to get some fundamental information for the relationship between structural characteristics and physico-chemical properties.

Results and Discussion

Samples.—The following kaolin minerals were investigated: Kaolinite from Mesa Alta, N.M., U.S.A., Kaolinite from Drybranch, Geor., U.S.A. The both materials are the API Standard Clay Minerals. Kibushi-clay from Shidare, Gifu, Japan which is a kaolin of fireclay type. Halloysite from Spruce Pine, N.C., U.S.A. which is the API Standard Clay Mineral and is considered to have the highest degree of crystallinity from the result of study through electron diffraction[3)]. Halloysite from Bedford, Ind., U.S.A. which is the API Standard Clay Mineral. Halloysite from Tintic, Utah, U.S.A. which is the API Standard Clay Mineral. Shichinoe-clay from Shichinoe, Aomori, Japan which is known to have a considerably low degree of crystallinity among halloysites[4)].

X-Ray Diffraction Studies.—From the investigation made by Brindley and Robinson, it was clarified that kaolin minerals are characterized by the stacking randomness in their structure. Their X-ray diagrams indicate the structural variations in kaolin minerals. To determine the relative degreee of crystallinity of kaolin minerals, in the present study, the criteria used by Brindley and Robinson, and some additional features found by Murray were used.

X-ray powder diffraction diagrams of kaolin minerals were obtained by X-ray diffractometer (Geigerflex). Halloysites were treated at 110°C in order to dry up the inter-layer water, this might result to have approximately the same basal spacing as in kaolinites. All specimens were ground, dried, and then sieved through 300 mesh. Experimental conditions were as follows: Filtered Cu radiation (Cu $K\alpha$: 1.5418 Å) is used at 35 kV and 15 mA, scanning speed is 1° or 1/4° 2θ per minute, time constant is 4 seconds, receiving slit is 0.2 mm or 0.1 mm, angular aperture is 1° or 1/2°.

To determine the degree of crystallinity in the X-ray diagram, the following major differences were used as criteria.

(1) Sharpness of the reflections.
(2) Number of reflections.
(3) Slight change in the basal spacing.
(4) Resolution between closely spaced reflections.
(5) Absence of certain reflections.

X-ray diffractometer traces of kaolin minerals are shown in Fig. 1. The X-ray reflections of kaolinites are sharp and distinct, and those of Spruce Pine halloysite are considerably sharp. For all other kaolin minerals, X-ray reflections are relatively broad and diffuse. These diffractometer records were made carefully by repeating the X-ray traces of specimens. It is also observable that the sharpness of reflections is dependent on particle size and orientation.

In the experiments, the specimens were prepared not to be oriented and particles of almost the same size were used, accordingly the effects of these factors might be

1) G. W. Brindley and K. Robinson, *Trans. Farad. Soc.*, **42B**, 198 (1946); S. Iwai, *Min. J.*, **1**, 233 (1955).
2) H. H. Murray, *Am. Mineral.*, **39**, 97 (1954).
3) G. Honjo and K. Mihama, *Acta Cryst.*, **7**, 511 (1954).
4) T. Sudo and H. Takahashi, "Proc. Fourth Conference on Clay and Clay Minerals". National Academy of Science-National Research Council, 1956, p, 67.

TABLE I

POWDER DATA OF KAOLIN MINERALS (in Å)

Brindley and Robinson			Kaolinite								Halloysite					
			Mesa Alta, N.M.		Drybranch, Geor.		Kibushi-Clay Shidare, Gifu		Spruce Pine, N.C.		Bedford, Ind		Tintic, Utah		Shichinoe, Aomori	
d	*I*	*hkl*	*d*	*I*	*d*	*I*	*d*	*I*	*d*	*I*	*d*	*I*	*d*	*I*	*d*	*I*
7.15	10+	001	7.14	VS	7.15	VS	7.20	S	7.15	VS	7.25	S	7.30	S	7.40	M
4.45	4	020	4.46	M	4.45	S	4.45	MS br	4.44	S	4.45	S	4.46	S	4.47	S
4.35	6	$1\bar{1}0$	4.35	S	4.36	M	4.33	W								
4.17	6	$11\bar{1}$	4.18	S	4.17	M										
4.12	3	$1\bar{1}\bar{1}$	4.13	W												
3.837	4	$0\bar{2}1$	3.84	M	3.86	W										
3.734	2	021	3.73	W	3.74	WV										
3.566	10+	002	3.57	VS	3.58	VS	3.58	S	3.57	VS	3.63	MS	3.64	MS	3.66	M
3.365	4	111	3.37	M	3.37	W										
3.138	2	$11\bar{2}$	3.14	W												
3.091	2	$1\bar{1}\bar{2}$	3.09	W												
2.748	2	022	2.75	W	2.74	W										
2.553	8	$20\bar{1}, 1\bar{3}0, 130$	2.55	MS	2.56	MS	2.56	M br	2.56	M	2.57	W br	2.57	W br	2.57	W br
2.521	4	$13\bar{1}, 1\bar{1}2$	2.53	M	2.53	W	2.53	W br	2.53	W						
2.486	9	$1\bar{3}\bar{1}, 200, 112$	2.49	S	2.49	MS	2.50	VW br	2.49	M						
2.374	7	003	2.37	M	2.38	M	2.38	M br	2.38	M						
2.331	10	$20\bar{2}, 1\bar{3}1, 11\bar{3}$	2.33	S	2.34	S	2.34	VW br	2.33	M	(2.37	W br)	(2.37	W br)	(2.38	W br)
2.284	9	$1\bar{1}\bar{3}, 131$	2.29	MS	2.29	M			2.29	W						
2.243	1	$13\bar{2}, 040$	2.24	W	2.24	VW										
2.182	3	$13\bar{2}, 220$	2.18	W	2.18	W	2.20	VW	2.20	W						
2.127	2	$02\bar{3}, 041$	2.13	W												
2.057	1	$2\bar{2}\bar{2}$	2.06	W												
1.985	7	$20\bar{3}, 1\bar{3}2$	1.992	S	1.990	S	1.992	M	1.997	MS						
1.935	4	132, 221	1.941	M	1.936	M	1.90	W br								
1.892	2	$13\bar{3}$	1.902	W	1.898	W										
1.865	1	042	1.862	W												
1.835	4	$1\bar{3}\bar{3}, 202, 22\bar{3}$	1.840	M	1.840	W										
1.805	1	$11\bar{4}, 2\bar{2}\bar{3}$	1.810	W												
1.778	5	004	1.782	M	1.790	M	1.79	W br			1.80	W br			1.78	W br
1.704	1	$2\bar{2}2$	1.702	W												
1.682	2	$1\bar{5}0, 24\bar{1}, 31\bar{1}, 3\bar{1}\bar{1}, 222$	1.684	W	1.688	W										
1.659	8	$2\bar{4}0, 1\bar{5}\bar{1}, 20\bar{4}, 1\bar{3}3$	1.664	S	1.668	S	1.65	M br	1.670	MS	1.68	W br	1.68	W br	1.67	W br

Key to abbreviation: VS: very strong, S: strong, MS: medium strong, M: medium, W: weak, br: broad.

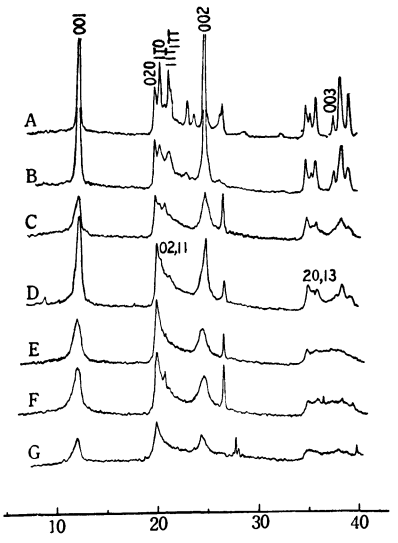

Fig. 1. X-ray diffractometer traces of kaolin minerals.
A, kaolinite, Mesa Alta, N.M., U.S.A.
B, kaolinite, Drybranch, Geor., U.S.A.
C, Kibushi-clay, Shidare, Gifu, Japan
D, halloysite, Spruce Pine, N.C., U.S.A.
E, halloysite, Bedford, Ind., U.S.A.
F, halloysite, Tintic, Utah, U.S.A.
G, halloysite, Shichinoe, Aomori, Japan

little. Among the specimens of halloysite, Spruce Pine halloysite has the largest number of reflections. The number of X-ray reflections which appear in the diagram indicates the relative degree of crystallinity.

Table I shows powder data for the kaolin minerals used in this study obtained from the X-ray diagram in Fig. 1.

The basal spacings were measured precisely. Slight changes of the basal spacings were detected for samples from Mesa Alta kaolinite to Shichinoe-clay. The basal spacing indicates a measure for the relative degree of crystallinity. The basal spacing in halloysite with lower degree of crystallinity is generally greater than that in kaolinite with higher degree of crystallinity. The slight change in the basal spacing can be attributed to the following reasons: (a) the presence of water layer between neighboring unit layers in kaolin minerals with lower degree of crystallinity, and/or (b) the disorderliness in the unit layer and looseness of the packing or stacking variations of the kaolin unit layers which should be greater in the specimens with lower degree of crystallinity.

The resolution between the closely spaced reflections in an X-ray diagram can be used as an indicator of the relative degree of crystallinity. The closely spaced reflections in an X-ray diagram of kaolinite with a considerable high degree of crystallinity are well resolved as exemplified by the reflections adjacent to the (020) and the (003) reflections of Fig. 1. These closely spaced reflections become hazy and indistinct in the diagrams of Kibushi-clay and Spruce Pine halloysite, and are completely merged in the diagrams of Bedford halloysite, Tintic halloysite and Shichinoe-clay.

The number of reflections closely related to the randomness of the stacking of kaolin unit layers. Reflections are not so many in the X-ray diagrams of kaolin minerals with lower degree of crystallinity. It is well known that the (OH) groups in the kaolin layers are arranged regular intervals along the b-axis, this distance being equall to $b_0/3$. This means that if one of two adjacent layers is displaced along the b-axis by an integral multiple of $b_0/3$, the two sheets will still be each oriented with same relationship to each other. If the displacement is not an integral multiple of $b_0/3$, then all reflections are cut out except those with a k index of $0, 3, 6, \cdots\cdots$. And if one of two adjacent layers is rotated by $n2\pi/3$, that is, random displacement is taken, all reflections indexed as (hkl) completely disappear. As the displacement in the kaolin layer remarkably increases and becomes irregular, the total number of reflections decreases and reflections become broad and diffuse.

As shown in Fig. 1 and Table I, Mesa Alta kaolinite has the highest degree of crystallinity and Shichinoe-clay has the lowest degree of crystallinity among the samples in this study.

Differential Thermal Analysis.—The crystallinity of kaolinite is indicated by differential thermal analysis curves..[5] Differential thermal analysis curves were made by using the same kaolin minerals as were used in the X-ray studies. The results obtained by using the differential thermal analysis curves are compared with the results of the X-ray data.

The specimens is the same as that described by Sudo et al[6]. Care was taken to place the sample into the sample block

5) R. E. Grim and W.F. Bradley, *Am, Mineral.*, **32**, 493 (1947).
6) T. Sudo et al., *J. Geol. Soc. Japan*, (*Chishitsu Gaku Zasshi*) **58**, 115 (1952).

as being packed homogeneously and keeping nearly constant weight. The mean heating rate was 12.5° per minute. It is known that the temperature of the peak of the endothermic reaction is correlated with the degree of crystallinity of kaolin minerals. However, general criteria based on differential thermal analysis curves which can be used for all kaolin minerals to determine the relative degree of crystallinity are yet to be found. In this study, the criteria used by Murray and some additional features were used to determine the relative degrees of crystallinity of the kaolin minerals.

The following measurements can be used as criteria to determine the relative degree of crystallinity:

(1) The peak temperature, the peak height and the area of the first endothermic reaction (E_{n1}) associated with the loss of the adsorbed or inter-layer water. The area is measured by a planimeter from the basal line.

(2) The peak temperature, the peak height and the area of the second endothermic reaction (E_{n2}) associated with the loss of the lattice water.

(3) The peak temperature, the peak height, the area and the breadth of the exothermic reaction (E_x) associated with the transformation to the new phase from the original mineral. The breadth is measured at the half value of the exothermic peak.

Differential thermal analysis cuves and data are shown in Fig. 2 and Table II respectively. The peak temperature of the second endothermic reaction indicates the degree of crystallinity, as the lattice water should be more tightly bonded in the kaolin with higher degree of crystallinity than the one with lower degree of crystallinity. As a large amount of energy is needed to break the bonds holding the lattice water, the peak temperature, and its peak height become higher and its area becomes larger as the degree of crystallinity becomes higher. From the data of Table II, it is clearly seen that the peak temperature, the peak height and the area of the reaction are correlated to the relative degree of crystallinity of kaolinite group based on X-ray data. This relation is also maintained in the halloysite group. However, as shown in Table II, the peak temperature, the peak height and the area of halloysite with higher degree of crystallinity are greater than those of Kibushi-clay. The

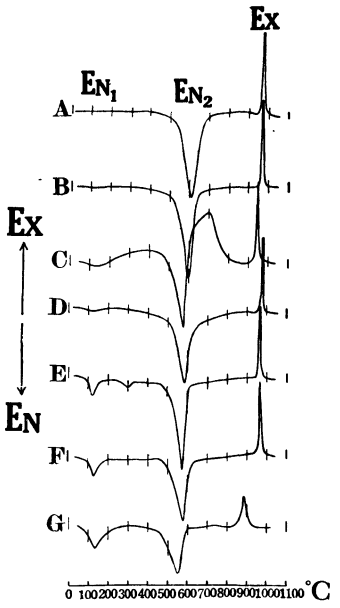

Fig. 2. Differential thermal analysis curves of kaolin minerals.
A, kaolinite, Mesa Alta, N.M., U.S.A.
B, kaolinite, Drybranch, Geor., U.S.A.
C, Kibushi-clay, Shidare, Gifu, Japan
D, halloysite, Spruce Pine, N.C, U.S.A.
E, halloysite, Bedford, Ind., U.S.A.
F, halloysite, Tintic, Utah, U.S.A.
G, halloysite, Shichinoe, Aomori, Japan

data in Table II show that in addition to those values the breadth of the exothermic reaction is also correlated to the relative degree of crystallinity. The breadth of peak of the exothermic reaction is expressed as the breadth at a half of peak height, since the expression of the breadth as the difference in temperature between the points at which the reaction begins and ends is indistinct in the measurement of those points. In Mesa Alta kaolinite and Drybranch kaolinite, the peak breadths are small, the peak temperatures are high and the heights are large. In spite of the degree of crystallinity based on X-ray data for Spruce Pine halloysite being low as compared with that of kaolinite, a higher degree of crystallinity is suggested from the character of the exothermic peak. In Kibushi-clay and halloysite excepting Spruce Pine halloysite, the degree of crystallinity is lower than that of kaolinite and Spruce Pine halloysite in the data of the final exothermic reaction. The smallness of the value of breadth of a kaolin mineral with a high degree of crystallinity confirms that the structure of the new phase

formed by exothermic reaction is correlated to the structure of original kaolin mineral, and that the more regular is the original structure, the faster is the transformation of the kaolin structure. In general, the peak temperature of the exothermic reaction of the kaolinites with a high degree of crystallinity is high, for more energy is needed in transformation to a new phase when the mother structure is stronger.

It is proved by the differential thermal analysis that Mesa Alta kaolinite, Drybranch kaolinite and Spruce Pine halloysite among the halloysite group have higher degree of crystallinity and that their crystallinity is higher than that of a kaolin of fireclay type like Kibushi-clay. Therefore, it is noteworthy that the degree of crystallinity of kaolinite determined by using a differential thermal analysis has the different meaning from that of halloysite determined by the same method.

Relationship between X-Ray and Thermal Data—The degree of crystallinity determined from the X-ray diffraction data is consistent with that from the thermal data in the series from kaolinite to kaolin of fireclay type, but not in the halloysite series.

When the inter-layer water is removed from the hydrated halloysite, it is considered that the unit layer which is structurally similar to the kaolinite layer may be the same as in a well-crystallized kaolinite. But the configuration of aluminum atoms may not be in the same manner as they are in a well-crystallized kaolinite. The possible variation in the configuration of aluminum atoms in each succesive layer is considered as a cause of broad reflections which are characteristic of the X-ray pattern of halloysite.

From the data of the X-ray diffraction, it seems that there is a continuous gradation of the structure from a kaolinite with a high degree of crystallinity to a halloysite with a low degree of crystallinity such as Shichinoe-clay. The differential thermal analysis made it clear that Spruce Pine halloysite has a high degree of crystallinity. This fact gives a valuable suggestion to the definition of the degree of crystallinity of kaolin minerals. This means that the degree of crystallinity of kaolin minerals involves two elements, that is, internal orderliness and stacking orderliness. The X-ray and thermal data suggest that X-ray reflections reveal both internal structural disorder and random stacking of the unit layers, whereas differential thermal analysis curves indicate internal structural disorder of the unit layers. Differential thermal analysis curves indicate the energy changes which a structure breaks down or a new phase forms. As shown by the thermal data, Spruce Pine halloysite has considerably perfect unit layers, however, as shown by X-ray data, the unit layers orientate with each other in a completely random manner with respect to to the *a*- and *b*-axis. In Kibushi-clay which is in a considerably low degree of crystallinity, there is a random displacement of $nb_0/3$ in different layers but not in a random orientation.

From these facts, it is considered that there are four typical variations in kaolin minerals when crystallinity is concerned.

(I) The mineral with the highest degree of crystallinity is estimated by using both X-ray and thermal method.

(II) The kaolin mineral with the lowest degree of crystallinity, estimated by using both methods.

(III) The kaolin mineral with the highest degree of crystallinity which is estimated by using X-ray method, but with the lowest degree of crystallinity by using thermal method.

(IV) The kaolin mineral with the highest degree of crystallinity estimated by using thermal method, but with lowest degree of crystallinity by using X-ray method.

These four ideal forms are related to the sizes and shapes of crystallites, physico-chemical properties and other forms.

Base Exchange Capacity.—A comparison of the relative degree of crystallinity of kaolin mineral used in this study with their base exchange capacity was made. It is well known that the base exchange capacity in kaolin mineral is attributed primarily to broken bonds[7], and possibly to negative charges of the lattice due to vacancies of alumina or silica positions in kaolin with the lower degree of crystallinity.

The base exchange capacity was determined by the titration method. The clay was treated with hydrochloric acid, to convert it into "hydrogen clay", then it was washed with water and titrated with sodium hydroxide solution. The base capacity was expressed as the number of

7) S. Speil, *J. Am. Ceram. Soc.*, **23**, 33 (1940).

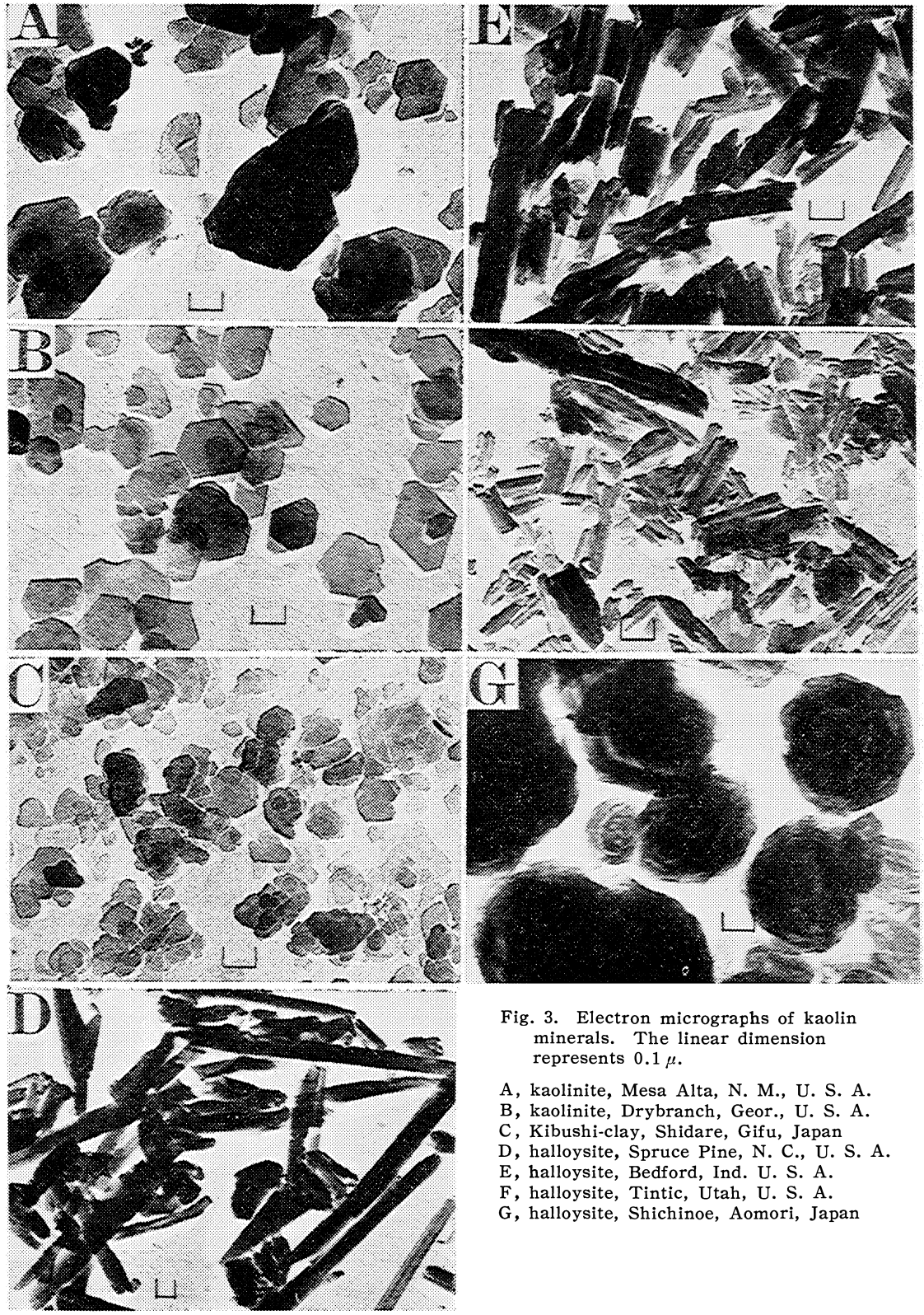

Fig. 3. Electron micrographs of kaolin minerals. The linear dimension represents 0.1 μ.

A, kaolinite, Mesa Alta, N. M., U. S. A.
B, kaolinite, Drybranch, Geor., U. S. A.
C, Kibushi-clay, Shidare, Gifu, Japan
D, halloysite, Spruce Pine, N. C., U. S. A.
E, halloysite, Bedford, Ind. U. S. A.
F, halloysite, Tintic, Utah, U. S. A.
G, halloysite, Shichinoe, Aomori, Japan

TABLE II
THERMAL DATA OF KAOLIN MINERALS
(all temp. are degrees centigrade)

Specimen	E_{n1}			E_{n2}			E_x			
	Temp.	Height	Area	Temp.	Height	Area	Temp.	Height	Area	Breadth
Kaolinite (Mesa Alta, N.M.)	—	—	—	604°	16	1080	966°	39	220	5.1°
Kaolinite (Drybranch, Geor.)	—	—	—	592	20	1280	964	41	250	4.8
Kibushi-Clay (Shidare, Gifu)	130°	1	140	574	14	740	945	13	140	10.5
Halloysite (Spruce Pine, N.C.)	125	1	70	583	17	1380	973	41	220	4.0
Halloysite (Bedford, Ind.)	125	2	110	574	16	720	970	34	170	4.5
Halloysite Tintic, Utah)	130	4	170	571	12	680	999	16	170	9.4
Halloysite (Shichinoe, Aomori)	129	6	480	550	12	660	885	7	130	23.4

TABLE III
BASE EXCHANGE CAPACITY OF KAOLIN MINERALS AT THE DRIED STATE

Specimen		Base exchange capacity (meq./100 g.)
Kaolinite	Mesa Alta, N.M., U.S.A.	1.0
	Drybranch, Geor., U.S.A.	1.4
Kibushi-clay (fireclay type)	Shidare, Gifu, Japan	7.3
Halloysite	Spruce Pine, N.C., U.S.A.	0.8
	Bedford, Ind., U.S.A.	4.0
	Tintic, Utah, U.S.A.	6.0
	Shichinoe, Aomori, Japan	12.5

TABLE IV
DENSITY OF KAOLIN MINERALS AT THE DRIED STATE

Specimen		Density (g./cc)
Kaolinite	Mesa Alta, N.M., U.S.A.	2.622
	Drybranch, Geor., U.S.A.	2.606
Kibushi-clay (fireclay type)	Shidare, Gifu, Japan	2.489
Halloysite	Spruce Pine, N.C., U.S.A.	2.561
	Bedford, Ind., U.S.A.	2.516
	Tintic, Utah, U.S.A.	2.464
	Shichinoe, Aomori, Japan	2.339

milli-equivalents of cations, per 100 g. of clay, required to bring the pH to 7.

Table III shows the base exchange capacity of kaolin samples. These results indicate that kaolin mineral with a lower degree of crystallinity has a higher base exchange capacity. Consequently, it can be concluded that the base exchange capacity is correlated to the internal randomness of structure.

Density—Another property which is considered to indicate the degree of crystallinity of kaolin minerals is their density. The density was determined with a pycnometer in carbon tetrachloride. The density of kaolin minerals used in this study are shown in Table IV. These values indicate that the density is correlated to the relative degree of crystallinity in the internal and stacking variations. The kaolinite with a higher degree of crystallinity has a larger density, and halloysite with a lower degree of crystallinity has a smaller density, with the exception of Kibushi-clay which contains organic matter as seen in the differential thermal analysis curve.

Electron Microscopic Studies.—Electron micrographs were obtained by the Hitachi HU-10A Type Electron Microscope.

Electron micrographs of kaolin minerals used in this study are shown in Fig. 3. The two kaolinites have platty particles, and the particles of Mesa Alta kaolinite has a sharp but irregular shape and the particles of Drybranch kaolinite has a hexagonal shape. The electron micrographs of halloysite samples with the exception of Shichinoe-clay have tubular particle. Bates et al. have indicated a structure that explains the tubular arrangement of halloysite.[8] That is, when the bonding forces of atoms in kaolin unit layer are very much stronger than the inter-layer forces, a particle takes tubular shape due to the characteristic of the unit layer lattice of the kaolin mineral. This means that the shape of the particle of the kaolin mineral is correlated to the disorderliness of the crystallographic unit layer and the disorderliness of the stacking of kaolin unit layer.

The X-ray data indicate that the degree of crystallinity of the Kibushi-clay is higher than that of the Spruce Pine halloysite while the thermal data indicate the opposite. This means that the kaolin layers in Kibushi-clay orient with respect to each other in relatively regular manner, but the layers themselves are less perfect than in Spruce Pine halloysite. As shown in the micrograph of Kibushi-clay, its crystal has a far finer size than the two kaolinites. The shape of Kibushi-clay is hexagonal and platty. This leads to assumption that the degree of crystallinity is the higher, the larger is the size of a crystal whose shape is platty.

Shichinoe-clay has the lowest degree of crystallinity among kaolin minerals used in this study by X-ray, thermal and other methods. As shown in a micrograph (Fig. 3-G), the shape of Shichinoe-clay is a round grain, which is well-defined and many of the grains have polyhedral outlines. The interiors of the polyhedral grains were observed in detail. It was found then that polyhedral grains are composed entirely of polyhedral crust like a cabbage. As to the shape of halloysite like the Shichinoe-clay, they were reported in previous papers.[4,9]

It is supposed that a schematic diagram for all the shapes of kaolin minerals could be drawn with respect to the degree of crystallinity in the internal randomness of the unit layer and the degree of crystallinity in the stacking randomness of kaolin layers. An ideal schematic diagram is shown in Fig. 4.

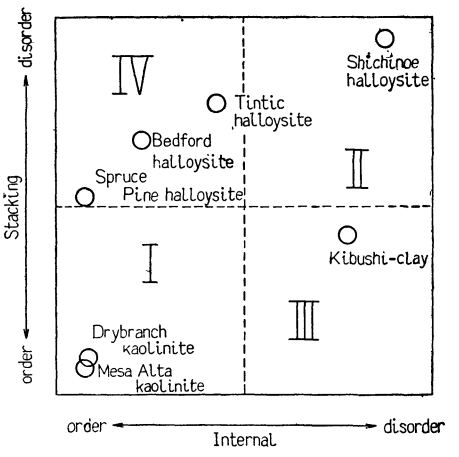

Fig. 4. A schematic diagram for the shapes of kaolin minerals with respect to two elements of the degree of crystallinity.

I : hexagonal, platty and large particle
II : fibrous, lath, cabbage like particle or rounded grain composed of fiber and lath
III : hexagonal, platty and fine particle
IV : tubular particle

All kaolin minerals are composed of kaolin unit layers, and kaolin minerals have various shapes. These facts are particularly remarkable in the hydrated halloysite clays altered from Japanese glassy tuff in the course of weathering. But the various shapes of kaolin minerals as above-mentioned can be readily understood by reference to the two elements of the randomness.

Summary

(1) The degree of crystallinity of kaolin minerals must be defined in relation to the degree of crystallinity in the internal randomness of the kaolin unit layer and that of the stacking randomness of kaolin unit layers. The X-ray diffraction data seem to reflect both internal and stacking variations.

(2) The relative degrees of crystallinity determined by the X-ray data and thermal data are consistent with each other in the series from kaolinite to fireclay. This holds also in the halloysite series. There is a continuous variation in the series from kaolinite to fireclay and also in the

8) T. F. Bates, F. A. Hildebrand and A. Swineford, *Am. Mineral.*, 35, 463 (1950).
9) H. Takahashi, *J. Electron Microscopy*, (*Denshi-Kenbikyo*), 4, 269 (1955).

halloysite series. The X-ray data indicate that some of halloysites have a low degree of crystallinity, but the thermal data show a high degree of crystallinity. This means that in most cases the displacement in the series from kaolinite to fireclay is a one-dimensional displacement with respect to the *b*-axis, while the displacement in halloysite is a rotational displacement, that is, a two-dimensional displacement.

(3) The values of the base exchange capacity of kaolinite, fireclay and halloysite are correlated to the internal disorderliness of kaolin structure.

(4) The values of density of kaolin mineral samples nearly correspond to the degrees of the crystallinity with the exception of Kibushi-clay.

(5) The variety of shapes of kaolin minerals are determined in the relation of the two elements of the internal variation and the stacking variation.

The author wishes to express his hearty thanks to Professor H. Akamatu for his continuous advice and encouragement. Thanks are due to Professor T. Sudo of the Tokyo University of Education for his valuable suggestion and discussion. The writer is also indepted to Mr. S. Sakata for the electron micrographs.

Department of Chemistry, Faculty of Science, the University of Tokyo, Hongo, Tokyo

The Kinetics of Displacement Reactions Involving Metal Complexes. I. Reaction between Copper(II) and Lead-Ethylenediaminetetraacetate Complexes in Aqueous Solutions

By Nobuyuki TANAKA, Kiyoko KATO and Reita TAMAMUSHI

(Received October 28, 1957)

There has been an increasing interest in the kinetics of the displacement reactions involving metal complexes of ethylenediaminetetraacetate (EDTA). Ackermann and Schwarzenbach[1] studied the kinetics of the reaction,

$$Cu^{2+}+CdY^{2-} \rightleftarrows CuY^{2-}+Cd^{2+},$$

and found that this seemingly simple reaction proceeds actually via four different paths. Bril, Bril and Krumholz[2] extended the study to the displacement reaction between lead and zinc-EDTA complexes, when they justified the "quasi-equilibrium hypothesis" which Ackermann and Schwarzenbach assumed for the reaction,

$$CdHY^{-} \rightleftarrows CdY^{2-}+H^{+} \rightleftarrows Cd^{2+}+HY^{3-}$$
$$\qquad\qquad\quad \vdash +2H^{+} \rightleftarrows Cd^{2+}+H_2Y^{2-}.$$

As it seemed worth while to know the reaction rate of the displacement reactions involving EDTA-complexes of other metal ions, we applied Bril et al.'s method to the reactions between copper and lead-EDTA complex,

$$Cu^{2+}+PbY^{2-} \rightleftarrows Pb^{2+}+CuY^{2-}. \qquad (1)$$

Experimental

Reagents.—The standard solution of cupric nitrate was prepared by dissolving a known amount of pure copper metal in a reagent-grade nitric acid. The solution of disodium ethylenediaminetetraacetate was standardized against the standard copper solution by the amperometric titration using a dropping mercury electrode as an indicator electrode[3]. The standard solution of lead nitrate was prepared from the commercial guaranteed grade reagent and standardized amperometrically against the standardized EDTA solution[3].

Apparatus and Procedure.—The rate of the reaction between the copper and lead-EDTA complex was followed by measuring the change of the polarographic diffusion current of the cupric ion with time. The current-time curves were obtained with a Shimadzu RP-II pen-recording polarograph using a dropping mercury electrode, which had an m value of 1.27 mg./sec. and

1) H. Ackermann and G. Schwarzenbach, *Helv. Chim. Acta*, **35**, 485 (1952).
2) K. Bril, S. Bril and P. Krumholz, *J. Phys. Chem.*, **59**, 596 (1955); **60**, 251 (1956).
3) N. Tanaka, M. Kodama, M. Sasaki and M. Sugino, *Japan Analyst (Bunseki Kagaku)*, **6**, 86 (1957).

a drop time of 3.69 sec., measured in an air-free solution of 0.1 M potassium chloride at 25°C in open-circuit.

Measurements were made in acetate buffers of pH 4.5 to 5.7 which contained 0.1 M of sodium acetate. The ionic strength was adjusted to be 0.2 with potassium nitrate. Gelatin was added as a maximum suppressor by 0.01% in concentration. The pH of the solution was measured with a Hitachi Model EHP-1 pH meter, immediately after the measurement of current-time curves, within the accuracy of 0.02 pH unit.

The reaction was initiated by adding a known amount of cupric nitrate solution into the deaerated reaction mixture with the aid of a 1 ml. syringe within one second. The solution was thoroughly stirred by bubbling nitrogen gas rapidly for 5 seconds. With this technique, reproducible current-time curves could be obtained from 15 seconds after the initiation of the reaction.

In the preliminary experiment, we observed a white salt-like compound precipitating from the solution which contained lead and EDTA ions. This compound contained lead and EDTA at the mole ratio of 2 to 1, being analyzed by the polarographic method, and was considered to be identical with that prepared by Brintzinger, Thiele and Müller[4]. Although they gave the formula $Pb_2\begin{pmatrix}(OOCCH_2)_2NCH_2\\ |\\ (OOCCH_2)_2NCH_2\end{pmatrix}$ to their compound, our experimental results suggested that the compound would have the formula Pb[PbY]. This was supported by the observations of other researchers[5,6] in which some metal-EDTA complex ions, such as CoY^- and HgY^{2-}, were found to react with excess of metal ions to form salt-like compounds, $Co[CoY]_2$, $Hg_2[HgY]$ and Hg[HgY]. The solubility product ($[Pb^{2+}]\times[PbY^{2-}]$) was measured in an acetate buffer of pH 5.0 and determined to be 3.4×10^{-5} at 15°C and 4.8×10^{-5} at 25°C*. The concentrations of lead and ethylenediaminetetraacetate in the reaction mixture were adjusted not to exceed the solubility product.

Results

The overall exchange reaction of the copper(II) and the lead-EDTA system is represented by equation (1).

$$Cu^{2+}+PbY^{2-} \rightleftarrows Pb^{2+}+CuY^{2-} \qquad (1)$$

Under the condition that lead ions and lead-EDTA complexes are present in a large excess over cupric ions, the reaction (1) can be simplified to,

$$Cu^{2+} \underset{k^-}{\overset{k^+}{\rightleftarrows}} CuY^{2-}, \qquad (2)$$

whose reaction rate is given by

$$-\frac{d[Cu^{2+}]}{dt}=k^+[Cu^{2+}]-k^-[CuY^{2-}]. \qquad (3)$$

Integrating eq. (3), we obtain,

$$\ln\{[Cu^{2+}]-[Cu^{2+}]_e\}=-(k^++k^-)t+\ln\{[Cu^{2+}]_0-[Cu^{2+}]_e\},$$

where $[Cu^{2+}]_0$ and $[Cu^{2+}]_e$ mean the initial concentration of copper ions and the concentration at equilibrium, respectively. At the equilibrium of the reaction the relation,

$$\frac{k^+}{k^-}=\frac{[CuY^{2-}]_e}{[Cu^{2+}]_e}\fallingdotseq K\frac{[PbY^{2-}]_0}{[Pb^{2+}]_0},$$

may be satisfied, where K represents the equilibrium constant of the reaction (1), expressed as,

$$K=\frac{[CuY^{2-}]_e[Pb^{2+}]_e}{[Cu^{2+}]_e[PbY^{2-}]_e}.$$

The values of K were determined polarographically to be 9.3 at 15°C, 12.3 at 25°C and 15.6 at 35°C in an acetate buffer of pH 5.2 at ionic strength of 0.2.

Those values were compared with the value of 5.8 which was calculated from the formation constants of PbY^{2-} and CuY^{2-} both determined by Schwarzenbach and his coworkers[7] at ionic strength 0.1 and at 20°C.

The apparent rate constants of the forward reaction (1), $k^+/[PbY^{2-}]_0$, were found independent of the initial concentration of cupric ions and that of lead-EDTA complexes, provided that the other conditions were kept the same. This is clearly shown in Table I.

TABLE I

$k^+/[PbY^{2-}]_0$ VALUES AT VARIOUS INITIAL CONCENTRATIONS (25°C, IONIC STRENGTH 0.2)

$[Cu^{2+}]_0$ M×10⁴	$[PbY^{2-}]_0$ M×10³	$[Pb^{2+}]_0$ M×10³	pH	$k^+/[PbY^{2-}]_0$ l.mole⁻¹sec.⁻¹
1.86	5.07	4.92	5.25	1.10
3.72	5.07	4.92	5.22	1.07
1.86	4.05	3.95	5.09	1.18
1.86	8.10	3.90	5.09	1.15

The apparent rate constant, $k^+/[PbY^{2-}]_0$, was obtained at varied pH's with two different concentrations of lead ions at 25°C, keeping the concentrations of other species constant. The resulting values are plotted against the hydrogen ion activity as given in Fig. 1, which clearly

4) H. Brintzinger, H. Thiele and U. Müller, *Z. anorg. allgem. Chem.*, **251**, 285 (1943).
5) G. Schwarzenbach, *Helv. Chim. Acta*, **32**, 839 (1949).
6) R. W. Schmid and C. N. Reilley, *J. Am. Chem. Soc.*, **78**, 5513 (1956).
* The details of the study will be reported elsewhere.

indicates that a linear relation exists between $k^+/[PbY^{2-}]_0$ and a_{H^+}. The same results were obtained at 15° and 35°C.

The values of $k^+/[PbY^{2-}]_0$ were also measured with different concentrations of lead at the same pH. The results obtained at 25°C are given in Fig. 2, in which the values of $k^+/[PbY^{2-}]_0$ is plotted against $1/[Pb^{2+}]_0$. Fig. 2 shows that $k^+/[PbY^{2-}]_0$ is inversely proportional to the lead concentration and that the values of $k^+/[PbY^{2-}]_0$ at $1/[Pb^{2+}]_0=0$, which were obtained by extrapolation, are dependent on the hydrogen ion activity of the solution.

Similar relations were obtained for the reverse reaction of reaction (1), which are shown in Figs. 3 and 4.

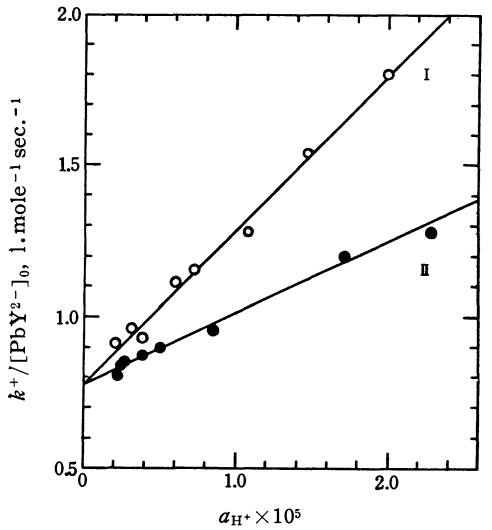

Fig. 1. $k^+/[PbY^{2-}]_0$ as a function of the hydrogen ion activity in acetate buffer-potassium nitrate solutions of ionic strength 0.2 at 25°C. Initial concentrations are: $[Cu^{2+}]_0=1.86\times10^{-4}$ M; $[PbY^{2-}]_0=4.05\times10^{-3}$ M; $[Pb^{2+}]_0=3.95\times10^{-3}$ M (curve I), 9.97×10^{-3} M (curve II).

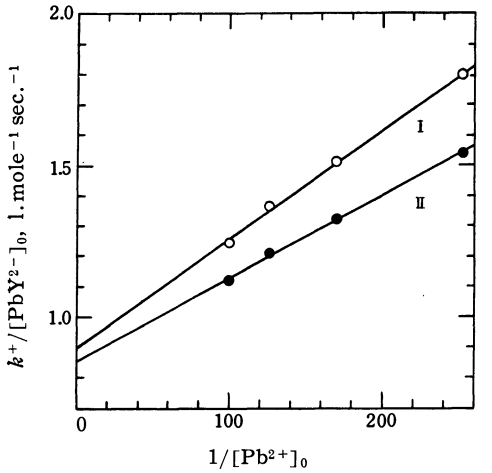

Fig. 2. $k^+/[PbY^{2-}]_0$ as a function of the reciprocal lead concentration in acetate buffer-potassium nitrate solutions of ionic strength 0.2 at 25°C. Initial concentrations are: $[Cu^{2+}]_0=1.86\times10^{-4}$ M; $[PbY^{2-}]_0=4.05\times10^{-3}$ M; pH 4.70 (curve I), 4.83 (curve II).

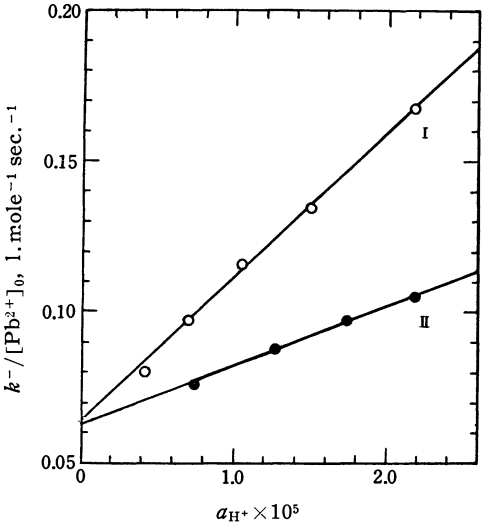

Fig. 3. $k^-/[Pb^{2+}]_0$ as a function of the hydrogen ion activity in acetate buffer-potassium nitrate solutions of ionic strength 0.2 at 25°C. Initial concentrations are: $[CuY^{2-}]_0=4.65\times10^{-4}$ M; $[PbY^{2-}]_0=4.05\times10^{-3}$ M; $[Pb^{2+}]_0=3.95\times10^{-3}$ M (curve I), 9.97×10^{-3} M (curve II).

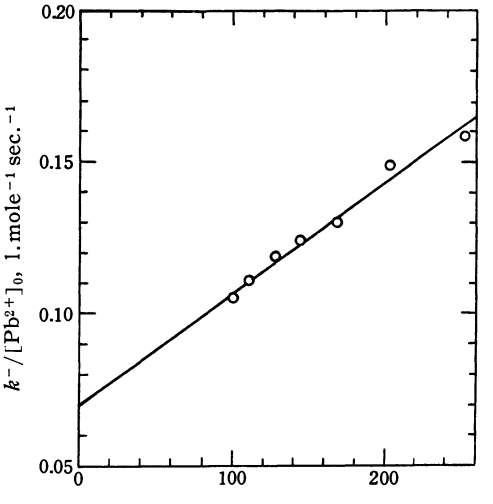

Fig. 4. $k^-/[Pb^{2+}]_0$ as a function of the reciprocal lead concentration in acetate buffer-potassium nitrate solutions of ionic strength 0.2 at 25°C. Initial concentrations are: $[CuY^{2-}]_0=4.65\times10^{-4}$ M; $[PbY^{2-}]_0=4.05\times10^{-3}$ M; pH 4.68.

Discussion

According to Bril et al.[2], who studied the forward and the reverse reaction between lead(II) and zinc-EDTA complexes and found that the overall reaction proceeds through three simultaneous reaction paths, the following mechanism was set down for the reaction (1).

$$\text{(i)}\quad Cu^{2+}+PbY^{2-} \underset{k_1^-}{\overset{k_1^+}{\rightleftarrows}} CuY^{2-}+Pb^{2+} \qquad (4)$$

$$\text{(ii)}\quad PbY^{2-}+H^+ \rightleftarrows PbHY^- \qquad (5a)$$

$$Cu^{2+}+PbHY^- \underset{k_{II}^-}{\overset{k_{II}^+}{\rightleftarrows}} CuHY^-+Pb^{2+} \qquad (5b)$$

$$CuHY^- \rightleftarrows CuY^{2-}+H^+ \qquad (5c)$$

$$\text{(iii)}\quad PbY^{2-}+H^+ \underset{k_a^-}{\overset{k_a^+}{\rightleftarrows}} Pb^{2+}+HY^{3-} \qquad (6a)$$

$$Cu^{2+}+HY^{3-} \underset{k_{II}^-}{\overset{k_{II}^+}{\rightleftarrows}} CuY^{2-}+H^+ \qquad (6b)$$

The overall reaction rate for reaction (1) is expressed by

$$-\frac{d[Cu^{2+}]}{dt}=\left\{k_1^+ +k_2^+[H^+] +k_3^+\frac{[H^+]}{[Pb^{2+}]}\right\}[Cu^{2+}][PbY^{2-}] -\left\{k_1^- +k_2^-[H^+] +k_3^-\frac{[H^+]}{[Pb^{2+}]}\right\}[Pb^{2+}][CuY^{2-}], \qquad (7)$$

and the relations,

$$k_2^+=k_{II}^+K^H_{PbHY},\quad k_2^-=k_{II}^-K^H_{CuHY} \qquad (8)$$
$$k_3^+=k_{II}^+/(K_{PbY}K_{HY}),\quad k_3^-=k_{II}^-$$

are obtained, where K^H_{PbHY} and K^H_{CuHY} represent the equilibrium constants of the reaction (5a) and the reverse reaction of eq. (5c), respectively. K_{PbY} means the formation constant of PbY^{2-} and K_{HY}, the fourth dissociation constant of ethylenediaminetetraacetic acid.

The values obtained experimentally for $k^+/[PbY^{2-}]_0$ and $k^-/[Pb^{2+}]_0$ correspond to $\left\{k_1^+ +k_2^+[H^+] +k_3^+\frac{[H^+]}{[Pb^{2+}]}\right\}$ and $\left\{k_1^- +k_2^-[H^+] +k_3^-\frac{[H^+]}{[Pb^{2+}]}\right\}$ in eq. (7), respectively. The confirmation of this was attained in comparison of the observed relations at various pH's and at various concentrations of the lead ions as seen in Figs. 1 to 4, which consequently justified the reaction mechanism given in eqs. (4) to (6b).

The rate constants in eq. (7) were calculated from the plots of $k^+/[PbY^{2-}]_0$ (or $k^-/[Pb^{2+}]_0$) against hydrogen ion activity, which are tabulated in Table II. The activity coefficient of hydrogen ion at ionic strength of 0.2 was assumed to be 0.80.

TABLE II
RATE CONSTANTS IN EQUATION (7) OBTAINED EXPERIMENTALLY AT IONIC STRENGTH 0.2 AT VARIOUS TEMPERATURES

Temperature, °C	Rate constant, l.mole^{-1} sec.$^{-1}$					
	k_1^+	k_2^+	k_3^+	k_1^-	k_2^-	k_3^-
15	0.27	9×10^2	0.53×10^2			
25	0.78	4×10^3	1.5×10^2	0.064	2×10^2	14
35	2.2	2×10^4	3.1×10^2			

From eq. (7), the relation,

$$k_1^+/k_1^- = k_2^+/k_2^- = k_3^+/k_3^- = K \qquad (9)$$

is expected. The experimental results indicate that k_1^+/k_1^- and k_3^+/k_3^- agree with this prediction, but k_2^+/k_2^- does not. This may be due to the uncertainty which was involved in the procedure for determining the values of k_2^+ and k_2^-.

In the third process (iii), the concentration of HY^{3-} is given by

$$[HY^{3-}]=\frac{k_a^+[PbY^{2-}]+k_{II}^-[CuY^{2-}]}{k_a^-[Pb^{2+}]+k_{II}^+[Cu^{2+}]}[H^+]. \qquad (10)$$

The rate of this process, therefore, is expressed as

$$v_3=\frac{k_a^+k_{II}^+[PbY^{2-}][Cu^{2+}]-k_a^-k_{II}^-[CuY^{2-}][Pb^{2+}]}{k_a^-[Pb^{2+}]+k_{II}^+[Cu^{2+}]}\times[H^+]. \qquad (11)$$

Assuming the condition,

$$k_{II}^+[Cu^{2+}] \ll k_a^-[Pb^{2+}], \qquad (12)$$

eq. (11) can be reduced to a simpler form as given in eq. (7), *i.e.*,

$$v_3=k_3^+\frac{[Cu^{2+}][PbY^{2-}][H^+]}{[Pb^{2+}]} -k_3^-[CuY^{2-}][H^+]. \qquad (13)$$

When the condition given in eq. (12) is not fulfilled, the $k^+/[PbY^{2-}]_0$ (or $k^-/[Pb^{2+}]_0$) can not be plotted linearly against $1/[Pb^{2+}]_0$. This is not the case. The plots of $k^+/[PbY^{2-}]_0$ (or $k^-/[Pb^{2+}]_0$) *vs.* $1/[Pb^{2+}]_0$ gave straight lines and the values of $k^+/[PbY^{2-}]_0$ (or $k^-/[Pb^{2+}]_0$) at $1/[Pb^{2+}]_0=0$, obtained by extrapolation, agreed well with those calculated from the plots of $k^+/[PbY^{2-}]_0$ (or $k^-/[Pb^{2+}]_0$)

against hydrogen ion activity. These apparently confirm the fact that the condition given in eq. (12) was satisfied in the present experiments.

From the relations given in eqs. (8), the rate constants of both elementary reactions (5b) and (6b) can be calculated, provided that the values of K^{H}_{PbHY}, K_{PbY} and K_{HY} at ionic strength 0.2 and at 15°, 25° and 35°C are known. Unfortunately none of those have been reported. Schwarzenbach, Gut and Anderegg[7] determined those values at ionic strength 0.1 and at 20°C. The corrections for ionic strength were made more or less reasonably with the Debye-Hückel equation. The heat of formation of the lead-EDTA complex was reported to be −13.1 kcal./mole,[8] which was employed in the calculation of K_{PbY} at 15°, 25° and 35°C. As for K_{HY}, the values obtained by Schwarzenbach and Ackermann[9] were used after correction for temperature and ionic strength. The temperature coefficient of K_{HY} was evaluated from the values of Carini and Martell[10], who determined the fourth dissociation constant of ethylenediaminetetraacetic acid at 0°C to 30°C and at ionic strength 0.1.

Those values which were used in the calculation are given in Table III and the rate constants obtained of three elementary reactions (4), (5b) and (6b) are summarized in Table IV.

TABLE III
EQUILIBRIUM CONSTANTS AT IONIC STRENGTH 0.2 AT VARIOUS TEMPERATURES

Temperature, °C	$\log K_{PbY}$	pK_{HY}	$\log K^{H}_{PbHY}$
15	17.97	10.20	—
20	—	—	2.7
25	17.63	10.04	—
35	17.31	9.91	—

TABLE IV
RATE CONSTANTS FOR REACTIONS (4), (5b) AND (6b) AT IONIC STRENGTH 0.2 AT VARIOUS TEMPERATURES

Temperature, °C	Rate constant, l.mole^{-1} sec.$^{-1}$		
	k_1^+	k_{II}^+	k_{III}^+
15	0.27	2	3.2×10^9
25	0.78	8	5.8×10^9
35	2.2	40	7.8×10^9

Linear relations were found between $\log k^+$ and $1/T$ for those three elementary reactions, which made it possible to express the rate constants in the form of the Arrhenius equation and to calculate the heat of activation and the entropy of activation. The results are given in Table V. The values for the elementary reaction (5b) are considered less accurate compared with those for the other two elementary reactions.

The authors thank the Ministry of Education for the financial support to this research.

TABLE V
RATE CONSTANTS, HEAT OF ACTIVATION AND ENTROPY OF ACTIVATION FOR REACTIONS (4), (5b) AND (6b)

Reaction	Rate constant, expressed	$\Delta H^{\neq}$ kcal./mole	$\Delta S^{\neq}$ e.u.
$Cu^{2+}+PbY^{2-}\rightarrow CuY^{2-}+Pb^{2+}$	$k_1^+=1.6\times10^{13}\exp(-18,100/RT)$	17.5	~0
$Cu^{2+}+PbHY^{-}\rightarrow CuHY^{-}+Pb^{2+}$	$k_{II}^+=4.3\times10^{20}\exp(-26,800/RT)$	26	34
$Cu^{2+}+HY^{3-}\rightarrow CuY^{2-}+H^{+}$	$k_{III}^+=2.2\times10^{15}\exp(-7,700/RT)$	7.1	9.7

7) G. Schwarzenbach, R. Gut and G. Anderegg, *Helv. Chim. Acta*, **37**, 937 (1954).
8) R. G. Charles, *J. Am. Chem. Soc.*, **76**, 5854 (1954).
9) G. Schwarzenbach and H. Ackermann, *Helv. Chim. Acta*, **30**, 1798 (1947).
10) F. F. Carini and A. E. Martell, *J. Am. Chem. Soc.*, **75**, 4810 (1953).

Department of Chemistry
Faculty of Science
Tohoku University
Katahira-cho, Sendai

Studies on Micelle Formation in Non-polar Solvent by Thermistor

By Ayao KITAHARA

(Received November 30, 1957)

It will be useful for the study of micelle formation to know the aggregation number at varying temperature. The measurement of vapor pressure depression is one of the several methods applicable to this purpose. The accuracy of the measurement has been recently increased, and the operation has become handy by the use of the thermistor which was also used for the study on micelle formation in the aqueous solution[1].

In order to obtain the aggregation number and the critical micelle concentration and to calculate the change in the thermodynamic value for micelle formation of detergents in the non-polar solvent, measurements on the vapor pressure depression and its temperature dependence were carried out using a pair of thermistors.

Experimental

Materials: Dodecylammonium benzoate, dodecylammonium butyrate and dodecylammonium caprylate were used as detergents, the preparation of which was reported already[2,3]. Cyclohexane for spectrophotometric use was employed as the solvent.

Apparatus: The vapor pressure depression was measured by making use of a couple of matched thermistors. The principle of the measurement was similar to those of McBain et al.[1], Müller et al.[4] and Davies et al.[5] Two thermistors used had resistances of 5040 and 4790 Ω at 19.9°C and the equal mean temperature coefficient of 3.7% per degree between 20° and 30°C. A Wheatstone bridge was employed for measuring the resistance change of the thermistors. Two adjacent arms were occupied by both thermistors. A fixed arm was a standard resistor of 1,000 Ω. The balancing arm consisted of a five dial resistor (R_x), variable in 0.1 Ω step. A galvanometer was a lamp-scale type having a sensitivity of 8.22×10^{-10} A per mm. The voltage which was applied potentiometrically was maintained at 0.4 V throughout the whole experiment. The cell containing both thermistors was similar to that of McBain et al.[1] and was kept in a thermostat controlled to ±0.0005°C. The well of the solvent which developed the atomosphere of the saturated vapor had been placed on the bottom of the cell.

Method: First, solvent drops were placed on both thermistors and R_x(solvent~solvent) was measured, the bridge being balanced. Next, a solvent and a solution drop were placed on each thermistor and R_x(solvent~solution) balance was also obtained. The relation between mole fraction of a solute (N) and $\Delta R_x = R_x$(solvent~solvent) $- R_x$(solvent~solution) was obtained with the cyclohexane solution of naphthalene, ranging from 0.0005 to 0.002 of N. This concentration range was chosen, because it will be safely assumed that the solutions are ideal. The result was as follows: $N = k \cdot \Delta R_x$. The values of the proportional constant k were 2.04×10^{-3} and 2.12×10^{-3} ohm^{-1} at 19.7° and 31.1°C, respectively. The measurement carried out with the cyclohexane solutions of diphenyl gave consistent values of k. ΔR_x was then measured for the detergent solutions with a method similar to that mentioned above at 19.7° and 31.1°C. The apparent mean aggregation number (Z) was calculated by the following equation 1:

$$Z = \frac{m}{k \cdot \Delta R_x} \frac{M_s}{1000} \qquad (1)$$

where m and M_s are the molality of the detergent and the molecular weight of the solvent, respectively; $Z = M/M_0$ (M and M_0 are the apparent mean micellar weight measured and the monomeric molecular weight of the detergent, respectively). Hence, Z has been evaluated by involving both monomer and micelle. The measurement of R_x(solvent~solvent) was always carried out before and after that of R_x(solvent~solution) throughout the whole measurement in order to ensure constancy in the thermistor conditions. ΔR_x was measured several times and the average value was adopted for the calculation of Z.

Results and Discussion

Monomer Concentration and Aggregation Number.—The values of Z calculated at 20° and 31°C are given in Table I. The fluctuation in the values of Z was not beyond ten per cent.

1) A. P. Brady, H. Huff and J. W. MeBain, *J. Phys. and Colloid Chem.*, **55**, 304 (1951).
2) A. Kitahara, This Bulletin, **30**, 586 (1957).
3) A. Kitahara, ibid., **28**, 234 (1955).
4) R. H. Müller and H. J. Stolten, *Anal. Chem.*, **25**, 1103 (1953).
5) M. Davies and D. K. Thomas, *J. Phys. Chem.*, **60**, 763, 767 (1956).

TABLE I
THE VALUES OF Z, λ AND C_1

Detergent	Concentration C (millimole/l) 20°	31°	$N\times10^4$ (mole fraction)	Z 20°	31°	Kreuzer's Treatment C_1 (millimole/l) 20°	31°	λ 20°	31°	Least Square Method C_1 (millimole/l) 20°	31°	λ 20°	31°
Dodecylammonium benzoate	22	22	26	3.6	2.9	4.7	5.4	—	10	2	2.3	12	6
	27	27	32	4.8	3.8	4.8	5.2						
	34	—	40	7.0	—	4.6	—						
	37	36	42	7.4	4.2	4.5	5.4						
	44	43	51	8.3	4.4	4.6	5.6						
	55	54	63	9.1	5.3	4.7	6.2						
Dodecylammonium caprylate	22	22	25.4	1.8	1.6	8.8	9.5	7±1	4	10	6	6.5	2.6
	33	32	38	2.1	2.1	9.8	10.2						
	45	44	52.5	3.2	2.3	9.3	11.3						
	66	64	76	3.6	2.2	9.8	14.0						
Dodecylammonium butyrate	23	23	26	2.3	1.55	6.7	10.6	9±1	6±1	8	10	8.5	6
	34	33	39.5	3.1	2.25	6.7	10.8						
	45	44	48	3.5	2.65	7.2	11.3						
	68	66	79	4.4	3.55	7.2	11.9						

TABLE II
CRITICAL MICELLE CONCENTRATION (millimole/l)

	Kreuzer's treatment 20°	30°	Solubilization mothod 20°	30°	Spectral method 20°	30°
Dodecylammonium benzoate	4.6	5.2	12±2	15±2	12±1	12±1
Dodecylammonium caprylate	8.3±0.2	9.1±0.1	16±2	16±2	—	—
Dodecylammonium butyrate	6.3±0.2	10	2±1	2±1	—	—

According to Kreuzer[5,6], the general equation 2 is obtained without making any assumption as to the nature of the associative equilibria involved.

$$\ln(1/\alpha)=(Z-1)/Z+\int_0^N\{(Z-1)/ZN\}dN \quad (2)$$

where α is the fraction of the monomer and N the total concentration of the solute in terms of mole fraction as monomer. The monomer concentration (C_1) at each concentration are obtained from the values of α which are graphically calculated from the above equation. These values of C_1 are tabulated in Table I. They are nearly independent of the concentration of detergents.

It has scarcely ever been subjected to experimental studies whether micelles should be monodisperse or not in the non-polar solvent. It was shown in ultraviolet absorption spectra of cyclohexane solutions of dodecylammonium benzoate that the extinction coefficient of the solute molecule participating in micelle formation is almost constant within a concentration range above the critical micelle concentration (*cmc*)[2]. This fact seems to be an evidence that the micelle is approximately monodisperse within this range. If the aggregation of the monomer to only one species of λ-mer is assumed*, the special relation 3 is deduced:[6,7]

$$Z=\lambda-(\lambda-1)\alpha\cdot Z \quad (3)$$

where λ is the true aggregation number evaluated by subtracting the coexisting monomer. The values of λ are graphically obtained from the plot of Z vs. $\alpha\cdot Z$. They are also shown in Table I. The λ value for dodecylammonium benzoate at 20°C was not successfully obtained because of the scattering of the plots.

The equation 3 is transformed into the following equation, using the molar concentration:

6) J. Kreuzer, *Z. physik. Chem.*, **B53**, 213 (1942).

* If a whole sequence of aggregates occurs with successive stages and the equilibrium constant at each stage is all equal, the equilibrium constant K must be described as $N(Z-1)/Z$. The values of K calculated for each concentration using this formula were not constant. Hence, such process of aggregation was not taken into consideration.

7) I. Prigogine and R. Defay, "Chemical Thermodynamics" p. 422, Longmans Green and Co., London, 1954.

$$C - \lambda C/Z + (\lambda-1)C_1 = 0$$

where C is the analytical concentration of the detergent. The values of λ and C_1 were calculated by the least square method with this equation, assuming that λ and C_1 are constant. The resulting values are given in Table I. The first value of Z was not adopted for the calculation in the case of dodecylammonium benzoate at 20°C. It is seen in Table I that these values of C_1 and λ are properly consistent with those of C_1 and λ which were calculated from the equations 2 and 3. The values of λ are comparable with those of Singleterry et al. in benzene solutions of dinonylnaphthalene sulfonate[8].

The *cmc* is obtained by plotting C_1 obtained from the equation 2 vs. C and by extrapolating to $C_1=C$. They are given in Table II and the *cmc* obtained by other methods are also shown in the table for the comparison. The agreement among these values seems to be satisfactory, when it is considered that they have been obtained by independent methods.

TABLE III
THE VALUES OF SOLUBILIZING POWER

	20°	30°
Dodecylammonium benzoate	4.7	4.0
Dodecylammonium caprylate	3.2	2.5
Dodecylammonium butyrate	20	15

It is seen from Table I that the values of λ decrease with the increase in the temperature. This corresponds qualitatively to the change of the solubilizing power with the temperature which is shown in Table III. No quantitative proportionality between them is found. The solubilizing power is defined as the moles of water solubilized per one mole of a detergent.

Calculation of Changes of Thermodynamic Values.—The *cmc* obtained from the Kreuzer's equation may be safely used for the quantitative treatment, though the C_1 obtained by the least square method is not quantitative. When the micelle is considered as the condensed phase, the following equation is deduced:[9]

$$\frac{d\ln(cmc)}{dT} = -\frac{\Delta H}{RT^2} \qquad (4)$$

where ΔH is the change of heat content associated with micelle formation at the mean temperature (25°C). ΔH was calculated from the equation 4 by the use of the *cmc* in the 2nd and 3rd columns in Table II. ΔH is independently obtained from the temperature dependence of the equilibrium constant for the λ-mer aggregation of the monomer. Thus ΔH was again calculated by the use of the λ and C_1 obtained by the least square method. These vlaues for ΔH and related ΔS are given in Table IV.

TABLE IV
THE VALUES OF ΔH AND ΔS ASSOCIATED WITH MICELLE FORMATION

	ΔH(kcal/mole)		ΔS(cal/deg/mole)	
	from *cmc*	from λ and C_1	from *cmc*	from λ and C_1
Dodecylammonium benzoate	−1.9	−5.9	−6.4	−20
Dodecylammonium caprylate	−1.7±0.5	−5.3	−5.7±1.7	−18
Dodecylammonium butyrate	−7.5±0.5	−7.5	−25±1.7	−25

The values obtained from these separate methods agree roughly with each other; hence they may be accepted as the probable values for micelle formation in the non-polar solvent. The absolute values of the heat change for micelle formation in the non-polar solvent seem to be somewhat greater than those in the aqueous solutions[9,10]. This may be due to the dipolar force or the hydrogen bonding which will participate in micelle formation of these detergents.

Summary

The apparent mean aggregation number (Z) of dodecylammonium carboxylate in cyclohexane was obtained from the vapor pressure depression measurement by the use of a pair of thermistors. The monomer concentration (C_1) was calculated from Kreuzer's equations. The C_1 was nearly independent of the concentration. The true aggregation number (λ) was obtained, assuming that the micelle is monodisperse. The *cmc* extraploated from C_1 agreed approximately with those by other methods.

The change of the heat content associated with micelle formation was calculated from the change of the *cmc* with

8) S. Kaufman and C. R. Singleterry, *J. Colloid Sci.*, **10**, 139 (1955).
9) G. Stainby and A. E. Alexander, *Trans. Faraday Soc.*, **46**, 587 (1950).
10) E. Hutchinson and L. Winslow, *J. Phys. Chem.*, **58**, 1125 (1954). E. D. Goddard and G. C. Benson, *Trans. Faraday Soc.*, **52**, 409 (1956).

the temperature and from the temperature dependence of the equilibrium constant for the λ-mer aggregation. Both agreed roughly with each other.

The author acknowledges the advice on the use of the thermistor given by Mr. Hisao Futaki in the Central Research Institute of Hitachi Manufacturing Co., and thanks Professor Hideo Akamatu for his continuing interest in this study.

Department of Chemistry, Toho University, Narashino, Chiba

Studies on the Synthesis of Metal Complexes. III. Synthesis of Ethylenediamine-carbonato, Ammine-oxalato and Ethylenediamine-oxalato Series of Cobalt(III) Complexes*

By Motoshichi MORI, Muraji SHIBATA, Eishin KYUNO and Koji HOSHIYAMA

(Received December 7, 1957)

In the preceding paper[1] of this series, a systematic method of synthesis for the ammine-carbonato series of cobalt(III) complexes was described. An important feature of the method was that it involved successive substitution of carbonate ions by ammonia groups. This method has now been extended to the synthesis of various complexes belonging to the ethylenediamine-carbonato, the ammine-oxalato and the ethylenediamine-oxalato series. All the attempts were successful; it is most interesting that a blue and a violet variety were found in every member of the present series, too. The two varieties are probably to be regarded as new complexes and also as stereoisomers.

Experimental

Synthesis.—1) *Starting material.*—Through all the procedures described below, a green cold solution of potassium tricarbonatocobaltate(III) was used as starting material. This was prepared from 20 g. of $KHCO_3$ and 10 g. of $CoCl_2 \cdot 6H_2O$—5 ml. of 30% H_2O_2 by the method described in the previous paper[1].

2) *Blue variety of potassium dicarbonatoethylenediaminecobaltate(III)*, Blue-K[Co en$(CO_3)_2$]$\cdot H_2O$.—To the green cold solution obtained in 1), was added 5 g. of ethylenediamine carbonate prepared by passing carbon dioxide into an aqueous solution of 70% ethylenediamine in the cold. The mixture was placed in an icebath until the green color of the solution changed into violetish blue within thirty minutes. When about 20 ml. absolute ethanol was added to the solution, crystals began to appear, but they were appreciably contaminated with other salts. The precipitates, therefore, were filtered off, another 50 ml. of ethanol was added to the filtrate and the solution was left for some time at nearly 0°C. The crystals were collected and purified by dissolving in as little cold water as possible and then by adding absolute ethanol. The product was washed with ethanol and ether in turn. Yield, about 4 g.

3) *Violet variety of potassium dicarbonatoethylenediaminecobaltate(III)*, Violet-K[Co en$(CO_3)_2$]$\cdot H_2O$.—After adding 5 g. of ethylenediamine carbonate to the starting material in the same manner as above, the mixture was allowed to stand at room temperature until a violet solution was obtained (about 20 min.). At the end of this period 20 ml. ethanol was added to the solution and then it was kept overnight in a refrigerator. After repeating reprecipitation three times in the same manner as in 2), the final precipitate was washed with ethanol and ether. Yield, about 6 g.

4) *Carbonato-bis (ethylenediamine) cobalt (III) chloride*, $[Coen_2CO_3]Cl \cdot H_2O$.—This was prepared by adding 10 ml. ethylenediamine (70%) to the green solution, heating the mixture on a water bath until the color of the solution became reddish violet, and further continuing to heat the solution in an evaporating dish. After cooling, the crude product was collected and recrystallized from water by the usual procedure. Yield, about 11 g.

5) *Tris (ethylenediamine) cobalt (III) chloride*, $[Co\ en_3]Cl_3 \cdot 3H_2O$.—Ethylenediamine (70%, 15 ml.), potassium chloride (3 g.) and active charcoal (1 g.) were introduced into the green solution,

* Presented at the Symposium on Co-ordination Compounds, Tokyo, October 27, 1956. For previous paper in this series see M. Mori, M. Shibata, E. Kyuno and H. Nakajima, This Bulletin, **29**, 887 (1956).

1) M. Mori, M. Shibata, E. Kyuno and T. Adachi, This Bulletin, **29**, 883 (1956).

TABLE I
THE FLOW CHART OF SYNTHESIS

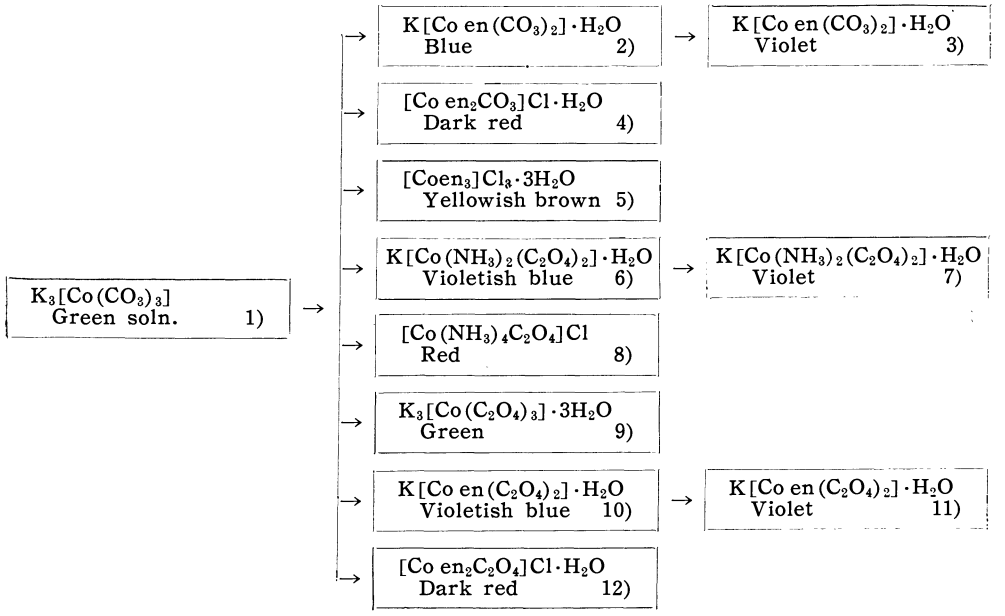

TABLE II
ANALYTICAL RESULTS (amounts in %)

	Co		N		K_2CO_3 or $K_2C_2O_4$		H_2O	
	calcd.	obsd.	calcd.	obsd.	calcd.	obsd.	calcd.	obsd.
Blue-K[Co en$(CO_3)_2$]·H_2O	19.9	19.8	9.5	9.5	23.3	24.5	6.1	5.9
Violet-K[Co en$(CO_3)_2$]·H_2O	19.9	19.6	9.5	9.4	23.3	24.6	6.1	6.2
Blue-K[Co$(NH_3)_2(C_2O_4)_2$]·H_2O	18.4	18.9	8.8	8.9	26.3	25.8	5.7	5.7
Violet-K[Co$(NH_3)_2(C_2O_4)_2$]·H_2O	18.4	18.1	8.8	8.8	26.3	26.5	5.7	5.8
Blue-K[Co en$(C_2O_4)_2$]·H_2O	16.7	16.8	7.7	7.8	23.6	23.4	5.1	5.1
Violet-K[Co en$(C_2O_4)_2$]·H_2O	16.7	16.2	7.7	7.6	23.6	25.6	5.1	5.2

and the mixture was heated on a water bath for about thirty minutes whereby the color of the solution changed into brownish yellow. After removal of the charcoal by filteration while hot, the filtrate was evaporated to about a half of the initial volume and then left to cool. The deposited crystals were washed with ethanol and dried in an oven. Yield, about 12 g.

6) *Blue variety of potassium dioxalatodiamminecobaltate (III)*, Blue-K[Co$(NH_3)_2(C_2O_4)_2$]·H_2O.—The green solution containing 10 g. of powdered ammonium oxalate was warmed on a water-bath at nearly 70°C. As soon as the solution became bluish, the vessel was dipped in an ice bath in order to stop further reaction. When the content was completely cooled, ethanol (50 ml.) was added to it and the whole was allowed to stand about an hour. The crude product was collected and reprecipitated from the cold solution by the addition of ethanol. After repeating this procedure twice, the final precipitate was washed with ethanol and ether in turn. Yield, about 7 g.

7) *Violet variety of potassium dioxalatodiamminecobaltate(III)*, Violet-K[Co$(NH_3)_2(C_2O_4)_2$]·H_2O.—The starting material, to which ammonium oxalate was added as described in the preceding paragraph, was allowed to remain on a water bath until the color turned blue and finally violet. After adding 80 ml. ethanol to the solution, it was kept overnight in a refrigerator. The violet precipitate was collected, dissolved in a small amount of cold water to remove impurities as residues, and then the complex reprecipitated by the addition of ethanol. After repetition of this procedure, the precipitate was washed with ethanol and then with ether. Yield, about 7 g.

8) *Oxalatotetramminecobalt(III) chloride*, [Co$(NH_3)_4C_2O_4$]Cl.—Powdered ammonium oxalate (5 g.) and concentrated aqueous ammonia solution (30 ml.) were added to the green solution and the mixture was warmed on a water bath at nearly 80°C with addition of ammonium chloride (in small portions, about 2 g. altogether), until the color of the mixture became pink. After cooling, about 10 ml. of ethanol was added to it

to precipitate all other salts; thereupon these were removed by filtration and another 20 ml. of ethanol was added in order to obtain the complex salt. Yield, about 6 g.

9) *Potassium trioxalatocobaltate(III)*, $K_3[Co(C_2O_4)_3]\cdot 3H_2O$.—To the cold green solution was added powdered oxalic acid (16 g.) little by little, whereby carbon dioxide was evolved and a bluish green solution was obtained. This was warmed on a water bath at nearly 60°C until no more carbon dioxide appeared. After cooling, the solution was acidified with dil. acetic acid and 50 ml. of ethanol was added to it. The product was purified as usual. Yield, about 12 g.

10) *Blue variety of potassium dioxalatoethylenediaminecobaltate(III)*, Blue-K[Co en$(C_2O_4)_2]\cdot H_2O$.—Potassium oxalate (5 g.) and ethylenediamine oxalate (5 g.) prepared by neutralizing 15 g. of ethylenediamine (70%) with 23 g. of powdered oxalic acid in the cold, were poured upon the cold green solution and the whole was left at room temperature until the color of the solution turned bluish violet, which took about half an hour. At the end of this period the solution was thoroughly cooled, and treated with a small amount of ethanol to remove foreign salts; the filtrate is further mixed with ethanol to precipitate the complex salt. The precipitate was purified from the cold solution by the addition of ethanol, and washed first with ethanol and then with ether. Yield, about 3 g.

11) *Violet variety of potassium dioxatatoethylenediaminecobaltate(III)*, Violet-K[Co en$(C_2O_4)_2]\cdot H_2O$.—This was synthesized in the same way as the blue variety, except for the mixture being heated for an hour instead of being left at room temperature. At the end of the reaction, the color of the solution changed completely to violet. Yield, about 7 g.

12) *Oxalato-bis (ethylenediamine) cobalt(III) chloride*, $[Co\,en_2(C_2O_4)]Cl\cdot H_2O$.—Oxalic acid (6 g.), potassium chloride (2 g.) and 70% ethylenediamine (16 ml.) were added to the green solution and the mixture was allowed to evaporate on a water bath until a crust was formed on the surface. After cooling, the crystals were filtered and washed with ethanol and ether in turn. Yield, about 10 g.

A flow chart of the synthesis of the above-mentioned complexes is given in Table I.

Determination of Chemical Formulae.—This was carried out for the six complexes obtained in 2), 3), 6), 7), 10) and 11), because they were thought to be new compounds. The results of thermal and chemical analysis and spectroscopic measurements were used for determining their chemical formulae in the same manner as that described in the previous paper[1]. Furthermore, coagulation values of ferric oxide sol by the complexes were measured in order to determine the valency of the complex ions. The measurements were carried out with the method used by S. Nakahara, K. Nakamoto and R. Tsuchida[2].

2) S. Nakahara, K. Nakamoto and R. Tsuchida, *J. Chem. Soc. Japan, Pure Chem. Sec.* (*Nippon Kagaku Zassi*), **74**, 488 (1953).

Results and Discussion

Analysis and Coagulation Value.—All the numerical values obtained from the chemical and the thermal analysis are given in Table II. These data seem to justify the assignment of such chemical formulae as are given in the experimental section.

Additional evidence for the validity of these formulae is afforded by the coagulation values given in Table III. Nakahara and co-workers have given 6.6 mF, 0.48 mF and 0.090 mF as the average values for uni-, bi- and tervalent complex anions respectively. In the present experiment, all of the complex species belonging to the blue variety showed coagulation values ranging from 6 mF to 7 mF, and they are consequently regarded as univalent anions. On the other hand, all the species belonging to the violet variety gave values about 3 mF, which are somewhat lower than the average value for a univalent ion, but far too high for a bivalent anion. These species may also be regarded as univalent anions provided that the deviation of their coagulation values from the average is attributed to partial liberation of the carbonate or the oxalate ion out of the complex radical by water molecules;

$$[Co\,en(CO_3)_2]^- + 2H_2O \rightleftarrows [Co\,en(H_2O)_2CO_3]^+ + CO_3^{--}$$

$$[Co(NH_3)_2(C_2O_4)_2]^- + 2H_2O \rightleftarrows [Co(NH_3)_2(H_2O)_2C_2O_4]^+ + C_2O_4^{--}$$

TABLE III

COAGULATION VALUES OF FERRIC OXIDE SOL

Blue-K$[Co(NH_3)_2(CO_3)_2]\cdot H_2O$	ca. 6 mF
Violet-K$[Co(NH_3)_2(CO_3)_2]\cdot H_2O$	ca. 3 〃
Blue-K$[Co\,en(CO_3)_2]\cdot H_2O$	ca. 6 〃
Violet-K$[Co\,en(CO_3)_2]\cdot H_2O$	ca. 3 〃
Blue-K$[Co(NH_3)_2(C_2O_4)_2]\cdot H_2O$	ca. 7 〃
Violet-K$[Co(NH_3)_2(C_2O_4)_2]\cdot H_2O$	ca. 3 〃
Blue-K$[Co\,en(C_2O_4)_2]\cdot H_2O$	ca. 7 〃
Violet-K$[Co\,en(C_2O_4)_2]\cdot H_2O$	ca. 3 〃

Absorption Spectra.—All the absorption data for newly synthesized complexes are given in Figs. 1 and 2 and Table IV together with those for previously synthesized potassium dicarbonatodiamminecobaltate(III).

Fig. 3 is a diagrammatic representation of the absorption maxima of the first band. It is seen from the figure that the frequencies for the blue variety increase in the order of NH_3-CO_3, en-CO_3, NH_3-ox. and en-ox in an arithmetrical progression.

TABLE IV
ABSORPTION MAXIMA AND log ε

	ν_1	log ε_1	ν_2	log ε_2	ν_3	log ε_3
	(10^{13} sec.$^{-1}$)					
Blue-K[Co$(NH_3)_2(CO_3)_2$]	52.2	2.14	76.8	2.40	126.6	4.14
Violet-K[Co$(NH_3)_2(CO_3)_2$]	55.5	1.80	80.2	2.04	128.1	4.30
Blue-K[Co en$(CO_3)_2$]	52.6	2.17	76.9	2.33	125.5	4.46
Violet-K[Co en$(CO_3)_2$]	54.9	1.94	77.3	2.31	129.8	4.29
Blue-K[Co$(NH_3)_2(C_2O_4)_2$]	53.1	2.09	79.4	2.35	129.3	4.56
Violet-K[Co$(NH_3)_2(C_2O_4)_2$]	55.3	2.08	79.3	2.58	130.4	4.06
Blue-K[Co en$(C_2O_4)_2$]	53.5	2.17	78.5	2.30	127.1	4.31
Violet-K[Co en$(C_2O_4)_2$]	54.7	1.98	77.9	2.10	129.8	3.98

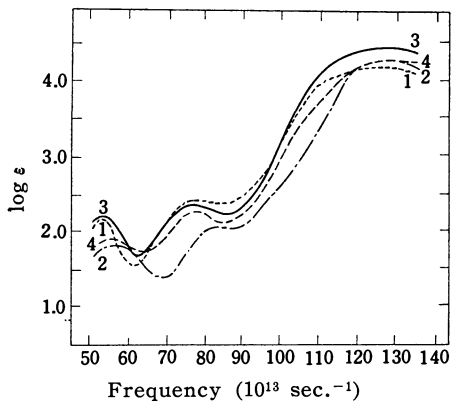

Fig. 1. Absorption spectra of:
1. Blue-K[Co$(NH_3)_2(CO_3)_2$]
2. Violet-K[Co$(NH_3)_2(CO_3)_2$]
3. Blue-K[Co en$(CO_3)_2$]
4. Violet-K[Co en$(CO_3)_2$]

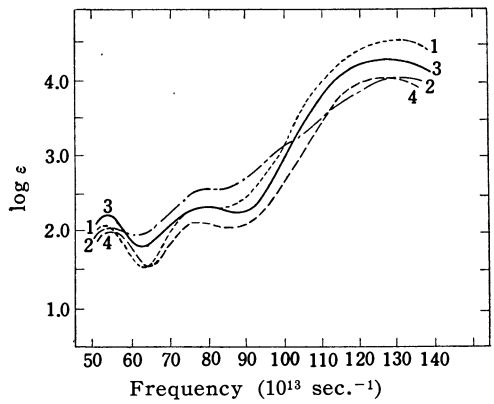

Fig. 2. Absorption spectra of:
1. Blue-K[Co$(NH_3)_2(C_2O_4)_2$]
2. Violet-K[Co$(NH_3)_2(C_2O_4)_2$]
3. Blue-K[Co en$(C_2O_4)_2$]
4. Violet-K[Co en$(C_2O_4)_2$]

(where, NH_3-CO_3 represents carbonato-diamminecobaltate(III) and so forth). These hypsochromic effects of the ligands may be explained by the familiar empirical rule that ethylenediamine is a more hypsochromic ligand than ammonia, and oxalate, than carbonate ion. On the other hand, the values for the violet variety increase in the order of en-ox, en-CO_3, NH_3-ox and NH_3-CO_3. In this case, the hypsochromic effects of the ligands are opposed to those predicted by the familiar rule.

The frequencies for the first and the second bands of the complexes belonging to each series are plotted in Figs. 4 and

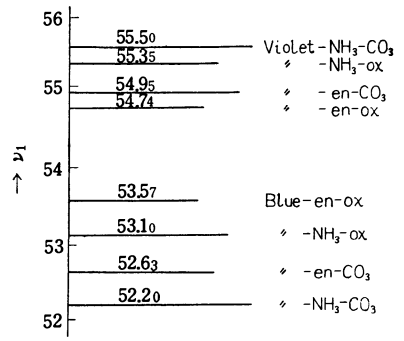

Fig. 3. Diagrammatic representation of absorption maxima.

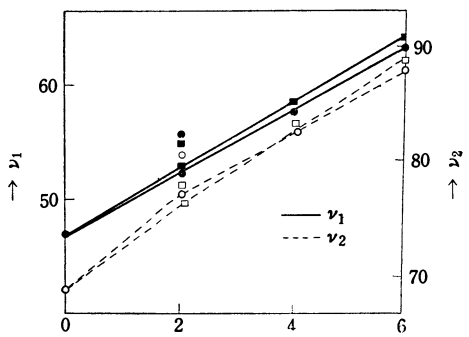

Fig. 4. Frequency position of the absorption bands of the complexes.
●—○ NH_3-CO_3 series
■—□ en-CO_3 series

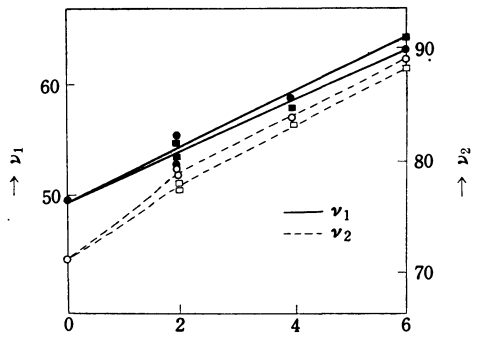

Fig. 5. Frequency position of the complexes.
NH_3-ox series
en-ox series

5, in the same manner as in the preceding paper[1], and the result shows that the same relationship exists in the present case, too.

Configuration.—In the previous paper[1] the authors assumed that the blue variety of $K[Co(NH_3)_2(CO_3)_2]\cdot H_2O$ to be the *cis* isomer and the violet one the *trans* isomer. The two varieties, blue and violet, of the complex salts obtained in the present experiment must also be regarded as stereoisomers because of 1) identity of the chemical composition, 2) equality of the valency and 3) similarity of the absorption spectra.

Assuming this to be true, the authors have attempted to find out which is *cis* and which *trans*. Y. Shimura[3] has generalized that the first band of a *trans*-isomer of a $[Co(NH_3)_4A_2]$- or a $[Co\,en_2A_2]$-type ion (A=unidentate molecule or negative ion) has shorter or longer wave lengths than that of the corresponding *cis*-isomers according as A is ahead of or behind ammonia or ethylenediamine on the spectrochemical series. If such a generalization can be extended to our $[CoX_4(NH_3)_2]$- and $[CoX_4\,en]$-type ions, the blue variety in question must be the *cis*-form and the violet variety, *trans*-form, since ethylenediamine or ammonia is ahead of the bidentate anions, carbonate and oxalate. But there is some doubt as to the legitimacy of such an extention.

There is an additional evidence; it was qualitatively observed that elution of the violet variety from the anion-exchanger column (Cl-form) was faster than that of the corresponding blue variety. The authors have already reported that the *trans*-form of $[Co(NH_3)_4X_2]^+$ or $[Co\,en_2X_2]^+$ is eluted more rapidly than the corresponding *cis*-form, and the stronger affinity of the *cis*-form to the cation exchanger may be attributed to the dipole moment resulting from the existence of acid groups in the *cis*-position[4]. Provided that the same holds in the above case, the blue variety is to be regarded as *cis*-form and the violet one, *trans*-form.

Apart from the adequacy of the above discussion on the assignment of configuration, it is natural that the diammine-type ions should exist in the *cis*- and the *trans*-form. On the other hand, it seems unreasonable to suppose the corresponding (mono) ethylenediamine-type ions exist in both forms, because it is generally agreed that an ethylenediamine is sterically incapable of spanning *trans*-positions in an octahedron. The existence of stereoisomers, however, seems invulnerable at the present stage of investigation. Consequently, further studies must be carried out to solve this problem.

Summary

Three series of cobalt(III) complexes were systematically synthesized from the green solution of potassium tricarbonatocobaltate(III) by means of successive substitution of carbonate by other groups:

i) Blue-$K[Co\,en(CO_3)_2]\cdot H_2O$, Violet-$K[Co\,en(CO_3)_2]\cdot H_2O$, $[Co\,en_2CO_3]Cl\cdot H_2O$, $[Co\,en_3]Cl_3\cdot 3H_2O$

ii) Blue-$K[Co(NH_3)_2(C_2O_4)_2]\cdot H_2O$, Violet-$K[Co(NH_3)_2(C_2O_4)_2]\cdot H_2O$, $[Co(NH_3)_4C_2O_4]Cl$, $K_3[Co(C_2O_4)_3]\cdot 3H_2O$

iii) Blue-$K[Co\,en(C_2O_4)_2]\cdot H_2O$, Violet-$K[Co\,en(C_2O_4)_2]\cdot H_2O$, $[Co\,en_2(C_2O_4)]Cl\cdot H_2O$.

Of these, the blue and the violet varieties are probably to be regarded as new complexes, stereoisomeric with each other.

Department of Chemistry, Faculty of Science, Kanazawa University, Kanazawa

3) Y. Shimura, This Bulletin, **25**, 49 (1952).

4) M. Mori, M. Shibata and M. Nanasawa, ibid., **29**, 947 (1956).

Normal Vibration and Internal Rotation of Ethane-type Molecules

By Eizi HIROTA

(Received December 4, 1957)

Internal rotation is the motion in which one part of a molecule moves relatively to the other parts of the molecule.[1] In some molecules the parts are so tightly bound that their relative motion can be treated as one of the vibrational modes, but in other molecules the groups are connected loosely with each other and are able to rotate almost freely. According to the general discussion given by Born and Oppenheimer[2], the molecular vibration can approximately be treated separately from the rotation, but internal rotation does not allow such a simplified treatment; one must apply a method suitable for each case.

Many researches have been carried out on the coupling of internal rotation with overall rotation. Even in the cases where the energy of internal rotation is small or comparable in magnitude with that of overall rotation, studies have been restricted to particular types of molecules, such as symmetric[3,4] or almost symmetric top[5,6], and main interest has been concerned with the complicated rotational spectra observed by the microwave spectroscopy[7].

The other coupling scheme, the interaction of internal rotation with vibrations, is important when the energy of internal rotation becomes comparable with that of vibrations. Usually internal rotation is ignored in analyzing the normal modes, but the vibrations of low frequencies, such as deformation vibrations, do couple strongly with the internal rotation, and hence the force constants obtained by the usual procedure may sometimes be in considerable error.

At present, data are often insufficient in number to determine the general quadratic force field, and hence it is necessary to assume a particular force field, for instance, valence force field[8]. The most satisfactory field seems to be of the Urey-Bradley type[9]; the characteristic of this force field is the explicit introduction of the repulsive forces between two non-bonded atoms. Usually, however, one takes into consideration only the next nearest interaction, that is, the interaction between the next nearest atom pairs, and in this approximation the internal rotation and accordingly its coupling with the vibration are completely ignored in the analysis of the normal modes. In order to discuss the internal rotation the procedure must be extended to include the atom pairs, whose interaction hinders the internal rotation. In this paper the discussion will be restricted for simplicity to a particular case: the ethane-type molecules and as one of the most typical examples hexachloroethane will be treated in detail.

The analysis of the normal vibrations gives a basis of calculating mean square amplitudes of atom pairs (abbreviated as mean amplitudes) obtained by the recent electron diffraction experiment[10]. The mean amplitudes of some atom pairs relate closely with the internal rotation, and when one compares such observed amplitudes with those calculated on the basis of the normal coordinate analysis, an estimate can be made on the value of the potential barrier restricting the internal

1) S. Mizushima, "Structure of Molecules and Internal Rotation", Academic Press, Inc., New York, 1954.
2) M. Born and J. R. Oppenheimer, *Ann. Physik*, **84**, 457 (1927).
3) H. H. Nielsen, *Phys. Rev.* **40**, 445 (1832).
4) D. Kivelson, *J. Chem. Phys.* **22**, 1733 (1954); **23**, 2230, 2236 (1955).
5) J. S. Koehler and D. M. Dennison, *Phys. Rev.* **57**, 1006 (1940).
6) D. G. Burkhard and D. M. Dennison, ibid. **84**, 408 (1951); E. V. Ivash and D. M. Dennison, *J. Chem. Phys.* **21**, 1804 (1953); E. Bright Wilson, Jr., C. C. Lin and D. R. Lide, ibid. **23**, 136 (1955); K. T. Hecht and D. M. Dennison, ibid. **26**, 31, 48 (1957);, R. W. Kilb, C. C. Lin, and E. B. Wilson, Jr., ibid. **26**, 1695 (1957).
7) See W. Gordy, W. V. Smith and R. F. Trambarulo, "Microwave Spectroscopy", John Wiley & Sons, Inc., New York, 1953. pp 105-106; C. H. Townes and A. L. Schawlow, "Microwave Spectroscopy", McGraw Hill Book Co., Inc., New York, 1955.
8) G. Herzberg, "Molecular Spectra and Molecular Structure", Vol II, D. Van Nostrand Co., Inc., New York, 1944.
9) T. Shimanouchi, *J. Chem. Phys.* **17**, 245, 734, 848 (1949).
10) Y. Morino, K. Kuchitsu, and T. Shimanouchi, ibid. **20**, 726 (1952); Y. Morino, K. Kuchitsu, A. Takahashi, and K. Maeda, ibid. **21**, 1927 (1957); Y. Morino and E. Hirota, ibid. **23**, 737 (1955).

rotation[11]. This method of the determination of the potential barrier is very interesting and important since there are at present no other possible ways of obtaining the barrier height of ethane-type molecules, except the thermodynamic methods.

Analysis of the Normal Modes

The potential energy usually used in the analysis of the normal modes consists of terms which are functions of three kinds of coordinate: the bond lengths, the bond angles, and the distances between the next nearest atoms[12]. As stated previously, in this expression for the potential energy there are no forces restricting the rotation about the central bond ($X-X'$ axis in Fig. 1). Two types of coordinates, the distances such as Y_1-Y_2' and the

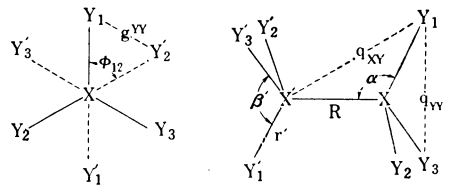

Fig. 1. Schematic diagram of X_2Y_6-type molecule

angles projected along the $X-X'$ axis such as $\phi_{12}=\angle Y_1XY_2'$, may be used to express the interaction between twe XY_3 groups, though the distances such as $Y_1Y'_1$ are so long that the interactions associated with them can be ignored. Four new force constants being added to these coordinates, the Urey-Bradley type expression for potential energy becomes

$$\begin{aligned}2V=&2K'_{XX}R\Delta R+K_{XX}(\Delta R)^2\\&+2K'_{XY}r[\Sigma(\Delta r_i)+\Sigma(\Delta r'_i)]\\&\quad+K_{XY}[\Sigma(\Delta r_i)^2+\Sigma(\Delta r'_i)^2]\\&+2H'_{XXY}r^2[\Sigma(\Delta\alpha_i)+\Sigma(\Delta\alpha'_i)]\\&\quad+H_{XXY}r^2[\Sigma(\Delta\alpha_i)^2+\Sigma(\Delta\alpha'_i)^2]\\&+2H'_{YXY}r^2[\Sigma(\Delta\beta_{ij})+\Sigma(\Delta\beta'_{ij})]\\&\quad+H_{YXY}r^2[\Sigma(\Delta\beta_{ij})^2+\Sigma(\Delta\beta'_{ij})^2]\\&+2F'_{XY}q_{XY}[\Sigma(\Delta q_i)+\Sigma(\Delta q'_i)]\\&\quad+F_{XY}[\Sigma(\Delta q_i)^2+\Sigma(\Delta q'_i)^2]\\&+2F'_{YY}q_{YY}[\Sigma(\Delta q_{ij})+\Sigma(\Delta q'_{ij})]\\&\quad+F_{YY}[\Sigma(\Delta q_{ij})^2+\Sigma(\Delta q'_{ij})^2]\\&+2J'_{YY}g^{YY}\Sigma(\Delta g^{YY}{}_{ij})\\&\quad+J_{YY}\Sigma(\Delta g^{YY}{}_{ij})^2\\&+2\Phi'r^2\Sigma(\Delta\phi_{ij})+\Phi r^2\Sigma(\Delta\phi_{ij})^2\end{aligned}\qquad(1)$$

where the last four terms are newly introduced. R denotes the equilibrium distance of $X-X'$, r that of $X-Y$ or of $X'-Y'$, q_{XY} that of $X'-Y$ or of $X-Y'$, q_{YY} that of $Y-Y$ or of $Y'-Y'$, and g^{YY} that of $Y_i-Y'_j$ with $i\neq j$. Δ indicates a small deviation from the equilibrium value. α's refer to the bond angles such as $\angle X'XY$ or $\angle XX'Y'$ and β's to $\angle YXY$ or $\angle Y'X'Y'$. As seen easily from Fig. 1 the redundant condition is given by

$$\Sigma(\Delta\phi_{ij})=0,\qquad(2)$$

and the four relations

$$\Delta R:\quad K'_{XX}R+6F'_{XY}(R-r\cos\alpha)+6J'_{YY}(R-2r\cos\alpha)=0,\qquad(3a)$$

$$\Delta r:\quad K'_{XY}r+F'_{XY}(r-R\cos\alpha)+2F'_{YY}r(1-\cos\beta)+2J'_{YY}[r(1/2+3/2\cos^2\alpha)-R\cos\alpha]=0,\qquad(3b)$$

$$\Delta\alpha:\quad H'_{XXY}R+3H'_{YXY}r\sin\alpha\cos\alpha/\sin\beta+2J'_{YY}(R\sin\alpha-3/2\,r\sin\alpha\cos\alpha)+F'_{XY}R\sin\alpha+3F'_{YY}r\sin\alpha\cos\alpha=0,\qquad(3c)$$

and

$$\Delta\phi:\quad(\kappa+\Phi')+\sqrt{3}\,H'_{YXY}\sin^2\alpha/\sin\beta+\sqrt{3}F'_{YY}\sin^2\alpha+\sqrt{3}/2J'_{YY}\sin^2\alpha=0\qquad(3d)$$

must be fulfilled to secure the stable equilibrium. These four types of coodinates are taken to be independent; that is, two distances, $X-X'(\Delta R)$ and $X-Y(\Delta r)$, and two angles, $\angle X'XY(\Delta\alpha)$ and $\Delta\phi$. On the other hand angles $\angle YXY(\Delta\beta)$ are dependent coordinates and can be expressed in terms of $\Delta\alpha$ and $\Delta\phi$. It is a quite conspicuous difference to the usual treatment. κ is the Lagrange's multiplication factor which is used to take into consideration the redundant condition of Eq. 2.

There are eight coefficients in the linear terms, but only four of them are independent, owing to the four relations given above. These four independent coefficients and the eight force constants in the quadratic expression are the parameters available for making the calculated frequencies agree with the observed ones.

If the molecule has the staggered configuration, as is usually the case, the

11) Y. Morino and E. Hirota, ibid 28, 185 (1958).
12) See ref. 9. Recently an additional degree of freedom was introduced; that is, the bending about the middle point of the X-X bond, cf. T. Shimanouchi, *J. Chem. Phys.* **26**, 594 (1957).

molecular symmetry is D_{3d} and the normal modes are factored into five groups; three modes belong to A_{1g}, one to A_{1u}, two to A_{2u}, three pairs to E_g, and the last three ones to E_u. The symmetry coordinates are given by

$$\left.\begin{aligned}
&S_1=1/\sqrt{6}\,[\Delta r_1+\Delta r_2+\Delta r_3+\Delta r'_1\\
&\qquad+\Delta r'_2+\Delta r'_3],\\
&S_2=\Delta R,\\
&S_3=r/\sqrt{6}\,[\Delta\alpha_1+\Delta\alpha_2+\Delta\alpha_3+\Delta\alpha'_1\\
&\qquad+\Delta\alpha'_2+\Delta\alpha'_3],\\
&S_{13}=r/\sqrt{6}\,[\Delta\phi_{12}+\Delta\phi_{23}+\Delta\phi_{31}\\
&\qquad+\Delta\phi_{21}+\Delta\phi_{32}+\Delta\phi_{13}],
\end{aligned}\right\}\ A_{1g}\qquad(4a)$$

$$A_{1u}\quad S_4=r/\sqrt{6}\,[\Delta\phi_{12}+\Delta\phi_{23}+\Delta\phi_{31}-\Delta\phi_{21}-\Delta\phi_{32}-\Delta\phi_{13}],\qquad(4b)$$

$$\left.\begin{aligned}
&S_5=1/\sqrt{6}\,[\Delta r_1+\Delta r_2+\Delta r_3\\
&\qquad-\Delta r'_1-\Delta r'_2-\Delta r'_3],\\
&S_6=r/\sqrt{6}\,[\Delta\alpha_1+\Delta\alpha_2+\Delta\alpha_3\\
&\qquad-\Delta\alpha'_1-\Delta\alpha'_2-\Delta\alpha'_3],
\end{aligned}\right\}\ A_{2u}\qquad(4c)$$

$$\left.\begin{aligned}
&S_{7a}=1/2[\Delta r_1-\Delta r_3+\Delta r'_1-\Delta r'_3],\\
&S_{7b}=1/2\sqrt{3}\,[\Delta r_1-2\Delta r_2+\Delta r_3\\
&\qquad+\Delta r'_1-2\Delta r'_2+\Delta r'_3],\\
&S_{8a}=r/2[\Delta\alpha_1-\Delta\alpha_3+\Delta\alpha'_1-\Delta\alpha'_3],\\
&S_{8b}=r/2\sqrt{3}\,[\Delta\alpha_1-2\Delta\alpha_2+\Delta\alpha_3\\
&\qquad+\Delta\alpha'_1-2\Delta\alpha'_2+\Delta\alpha'_3],\\
&S_{9a}=r/2[\Delta\phi_{12}-\Delta\phi_{23}+\Delta\phi_{21}-\Delta\phi_{32}],\\
&S_{9b}=r/2\sqrt{3}\,[-\Delta\phi_{12}-\Delta\phi_{23}+2\Delta\phi_{31}\\
&\qquad-\Delta\phi_{21}-\Delta\phi_{32}+2\Delta\phi_{13}],
\end{aligned}\right\}\ E_g\qquad(4d)$$

$$\left.\begin{aligned}
&S_{10a}=1/2[\Delta r_1-\Delta r_3-\Delta r'_1+\Delta r'_3],\\
&S_{10b}=1/2\sqrt{3}\,[\Delta r_1-2\Delta r_2+\Delta r_3\\
&\qquad-\Delta r'_1+2\Delta r'_2-\Delta r'_3],\\
&S_{11a}=r/2[\Delta\alpha_1-\Delta\alpha_3+\Delta\alpha'_1-\Delta\alpha'_3],\\
&S_{11b}=r/2\sqrt{3}\,[\Delta\alpha_1-2\Delta\alpha_2+\Delta\alpha_3\\
&\qquad-\Delta\alpha'_1+2\Delta\alpha'_2-\Delta\alpha'_3],\\
&S_{12a}=r/2\sqrt{3}\,[\Delta\phi_{12}+\Delta\phi_{23}-2\Delta\phi_{31}\\
&\qquad-\Delta\phi_{21}-\Delta\phi_{32}+2\Delta\phi_{13}],\\
&S_{12b}=r/2[\Delta\phi_{12}-\Delta\phi_{23}-\Delta\phi_{21}+\Delta\phi_{32}].
\end{aligned}\right\}\ E_u\qquad(4e)$$

S_{13} is obviously a redundant coordinate and can be ignored hereafter. S_4 corresponds to the torsional oscillation and is split by the present molecular symmetry from other symmetry coordinates. The torsional coordinate is, in general, not split from others, hence the coupling between the internal rotation and other normal modes becomes more appreciable in molecules of lower symmetry. For the ethane-type molecules the coupling is indirect: as shown in the following discussion the force constants J_{YY} and Φ introduced above enter not only in the F-matrix of A_{1u} but also in the F-matrix of other symmetries.

The unitary transformation given by Eqs. 4 factorizes also the potential energy of Eq. 1 into five parts, which are expressed by the following five F-matrices:

$$\mathrm{F}(A_{1g})=\begin{bmatrix} A+2B+2B' & & \\ \sqrt{6}\,C & A' & \\ D+2D'+2D'' & \sqrt{6}\,D_0 & L+2L'+2L'' \end{bmatrix}\qquad(5a)$$

$$\mathrm{F}(A_{1u})=[N-2N']\qquad(5b)$$

$$\mathrm{F}(A_{2u})=\begin{bmatrix} A+2B-2B' & \\ D+2D'+2D'' & L+2L'-2L'' \end{bmatrix}\qquad(5c)$$

$$\mathrm{F}(E_g)=\begin{bmatrix} A-B-B' & & \\ D-D'-D'' & L-L'-L'' & \\ E-2E' & M-2M' & N-N' \end{bmatrix}\qquad(5d)$$

$$\mathrm{F}(E_u)=\begin{bmatrix} A-B+B' & & \\ D-D'+D'' & L-L'+L'' & \\ \sqrt{3}\,E & \sqrt{3}\,M & N+N' \end{bmatrix}\qquad(5e)$$

where the notations A, B, and so on are given in Fig. 2. The potential energy of the internal rotation in the present type molecule is safely assumed as $V=(V_0/2)(1-\cos 3\phi)$, which, in the high barrier approximation, can be expanded as $(9V_0/4)\phi^2$. The internal coordinate ϕ is expressed in terms of the symmetry coordinate S_4; $\phi=(1/\sqrt{6}r)S_4$, and the expression for the potential energy becomes $(3V_0/8r^2)S_4^2$, which is put equal to $(1/2)F_{44}S_4^2$, thus

$$\begin{aligned}\mathrm{F}(A_{1u})&=(3/4)(V_0/r^2)\\&=\Phi+(3/4)J_{YY}r^2\sin^4\alpha/(g^{YY})^2\\&\quad-(1/2)J'_{YY}[\sin^2\alpha\\&\quad+3r^2\sin^4\alpha/2(g^{YY})^2],\end{aligned}\qquad(6)$$

$\mathrm{F}(A_{1u})$ being equal to F_{44}. It is an important relation giving V_0 in terms of the two force constants J_{YY} and Φ. It is to be noted that the two force constants, J_{YY} and Φ, important for the internal rotation enter also in the F-matrices of A_{1g}, E_g and E_u symmetries. Hence the internal rotation couples indirectly with other normal modes through J_{YY} and Φ.

The kinetic energy matrices are also factorized analogously; tedious calculation gives:

$$A=K_{XY}+F_{XY}(r-R\cos\alpha)^2/q^2_{XY}+2F_{YY}r^2(1-\cos\beta)^2/q^2_{YY}+2J_{YY}[r(1+3\cos^2\alpha)/2 -R\cos\alpha]^2/(g^{YY})^2+F'_{XY}[1-(r-R\cos\alpha)^2/q^2_{XY}]+2F'_{YY}[1-r^2(1-\cos\beta)^2/q^2_{YY}] +2J'_{YY}\{1-[r(1+3\cos^2\alpha)/2-R\cos\alpha]^2/(g^{YY})^2\},$$

$$B=F_{YY}r^2(1-\cos\beta)^2/q^2_{YY}-F'_{YY}[\cos\beta+r^2(1-\cos\beta)^2/q^2_{YY}],$$

$$B'=J_{YY}[r(1+3\cos^2\alpha)/2-R\cos\alpha]^2/(g^{YY})^2+J'_{YY}\{(-1+3\cos^2\alpha)/2-[r(1+3\cos^2\alpha)/2 -R\cos\alpha]^2/(g^{YY})^2\},$$

$$C=F_{XY}(R-r\cos\alpha)(r-R\cos\alpha)/q^2_{XY}+2J_{YY}[r(1+3\cos^2\alpha)/2-R\cos\alpha] \times(R-2r\cos\alpha)/(g^{YY})^2-F'_{XY}[\cos\alpha+(R-r\cos\alpha)(r-R\cos\alpha)/q^2_{XY}]-2J'_{YY}\{\cos\alpha +[r(1+3\cos^2\alpha)/2-R\cos\alpha](R-2r\cos\alpha)/(g^{YY})^2\},$$

$$A'=K_{XY}+6F_{XY}(R-r\cos\alpha)^2/q^2_{XY}+6J_{YY}(R-2r\cos\alpha)^2/(g^{YY})^2 +6F'_{XY}[1-(R-r\cos\alpha)^2/q^2_{XY}]+6J'_{YY}[1-(R-2r\cos\alpha)^2/(g^{YY})^2],$$

$$D=F_{XY}r(r-R\cos\alpha)\sin\alpha/q^2_{XY}+3F_{YY}r^3(1-\cos\beta)\sin\alpha\cos\alpha/Rq^2_{YY}+2J_{YY}(1/R) \times[r(1+3\cos^2\alpha)/2-R\cos\alpha][Rr\sin\alpha-(3/2)r^2\sin\alpha\cos\alpha]/(g^{YY})^2+F'_{XY}[\sin\alpha-r \times(r-R\cos\alpha)\sin\alpha/q^2_{XY}]+3F'_{YY}[(r/R)-r^3(1-\cos\beta)/Rq^2_{YY}]\sin\alpha\cos\alpha+2J'_{YY}(1/R) \times\{R\sin\alpha-(3/2)r\sin\alpha\cos\alpha-[r(1+3\cos^2\alpha)/2-R\cos\alpha] \times[Rr\sin\alpha-(3/2)r^2\sin\alpha\cos\alpha]/(g^{YY})^2\},$$

$$D'=(3/2)F_{YY}r^3(1-\cos\beta)\sin\alpha\cos\alpha/Rq^2_{YY}+(3/2)F'_{YY} \times[(r/R)-r^3(1-\cos\beta)/Rq^2_{YY}]\sin\alpha\cos\alpha,$$

$$D''=J_{YY}(1/R)[r(1+3\cos^2\alpha)/2-R\cos\alpha][Rr\sin\alpha-(3/2)r^2\sin\alpha\cos\alpha]/(g^{YY})^2 -J'_{YY}(1/R)\{(3/2)r\sin\alpha\cos\alpha+[r(1+3\cos^2\alpha)/2-R\cos\alpha] \times[Rr\sin\alpha-(3/2)r^2\sin\alpha\cos\alpha]/(g^{YY})^2,$$

$$D_0=F_{XY}r(R-r\cos\alpha)\sin\alpha/q^2_{XY}+2J_{YY}(1/R)[R-2r\cos\alpha][Rr\sin\alpha-(3/2)r^2\sin\alpha\cos\alpha]/(g^{YY})^2 +F'_{XY}[r\sin\alpha/R-r(R-r\cos\alpha)\sin\alpha/q^2_{XY}]+2J'_{YY}(1/R)\{r\sin\alpha-[R-2r\cos\alpha][Rr\sin\alpha -(3/2)r^2\sin\alpha\cos\alpha]/(g^{YY})^2\},$$

$$L=H_{XXY}+(9/2)H_{YXY}(r/R)^2\sin^2\alpha\cos^2\alpha/\sin^2\beta+F_{XY}r^2\sin^2\alpha/q^2_{XY}+(9/2)F_{YY}(r^2/R)^2 \times\sin^2\alpha\cos^2\alpha/q^2_{YY}+2J_{YY}(1/R)^2[Rr\sin\alpha-(3/2)r^2\sin\alpha\cos\alpha]^2/(g^{YY})^2 +2H'_{YXY}(r/R)^2(\cos\beta/\sin^3\beta)[\sin^2\beta-(9/4)\sin^2\alpha\cos^2\alpha]+F'_{XY}[r\cos\alpha/R-r^2\sin^2\alpha/q^2_{XY}] +2F'_{YY}(r/R)^2[\cos\beta-(9/4)r^2\sin^2\alpha\cos^2\alpha/q^2_{YY}]+2J'_{YY}(1/R^2)\{[Rr\cos\alpha-r^2(-1 +3\cos^2\alpha)/2]-[Rr\sin\alpha-(3/2)r^2\sin\alpha\cos\alpha]^2/(g^{YY})^2\},$$

$$L'=(9/4)H_{YXY}(r/R)^2\sin^2\alpha\cos^2\alpha/\sin^2\beta+(9/4)F_{YY}(r^2/R)^2\sin^2\alpha\cos^2\alpha/q^2_{YY} +H'_{YXY}(r/R)^2(2\sin^2\beta\cos^2\alpha-4\sin^2\beta\sin^2\alpha-9\cos\beta\sin^2\alpha\cos^2\alpha)/4\sin^3\beta +F'_{YY}(r^2/2R^2)[\cos^2\alpha-2\sin^2\alpha-qr^2\sin^2\alpha\cos^2\alpha/2q^2_{YY}],$$

$$L''=J_{YY}(1/R^2)(Rr\sin\alpha-(3/2)r^2\sin\alpha\cos\alpha)^2/(g^{YY})^2+J'_{YY}(1/R^2)\{r^2(\sin^2\alpha-(1/2)\cos^2\alpha) -(Rr\sin\alpha-(3/2)r^2\sin\alpha\cos\alpha)^2/(g^{YY})^2\},$$

$$N=\Phi+(3/2)H_{YXY}\sin^4\alpha/\sin^2\beta+(3/2)F_{YY}r^2\sin^4\alpha/q^2_{YY}+(3/4)J_{YY}r^2\sin^4\alpha/(g^{YY})^2 -H'_{YXY}(3\cos\beta\sin^4\alpha+2\sin^2\beta\sin^2\alpha)/2\sin^3\beta-F'_{YY}\sin^2\alpha(1+3r^2\sin^2\alpha/2q^2_{YY}) -J'_{YY}[\sin^2\alpha/2+3r^2\sin^4\alpha/4(g^{YY})^2],$$

$$N'=(3/4)H_{YXY}\sin^4\alpha/\sin^2\beta+(3/4)F_{YY}r^2\sin^4\alpha/q^2_{YY}-H'_{YXY}(3\cos\beta\sin^4\alpha +2\sin^2\beta\sin^2\alpha)/4\sin^3\beta-(1/2)F'_{YY}\sin^2\alpha(1+3r^2\sin^2\alpha/2q^2_{YY}),$$

$$E=(\sqrt{3}/2)F_{YY}r^2(1-\cos\beta)\sin^2\alpha/q^2_{YY}+(\sqrt{3}/2)J_{YY}r[r(1+3\cos^2\alpha)/2-R\cos\alpha]\sin^2\alpha/(g^{YY})^2 +(\sqrt{3}/2)F'_{YY}[1-r^2(1-\cos\beta)/q^2_{YY}]\sin^2\alpha+(\sqrt{3}/2)J'_{YY}\{1-r[r(1+3\cos^2\alpha)/2 -R\cos\alpha]/(g^{YY})^2\}\sin^2\alpha,$$

$$E'=(\sqrt{3}/2)F_{YY}r^2(1-\cos\beta)\sin^2\alpha/q^2_{YY}+(\sqrt{3}/2)F'_{YY}[1-r^2(1-\cos\beta)/q^2_{YY}]\sin^2\alpha,$$

$$M=(3\sqrt{3}/4)H_{YXY}(r/R)\sin^3\alpha\cos\alpha/\sin^2\beta+(3\sqrt{3}/4)F_{YY}(r^3/R)\sin^3\alpha\cos\alpha/q^2_{YY} +(\sqrt{3}/2)J_{YY}(r^2/R)\sin^2\alpha(Rr\sin\alpha-(3/2)r^2\sin\alpha\cos\alpha)/(g^{YY})^2 +(\sqrt{3}/4)H'_{YXY}(r/R)\sin\alpha\cos\alpha(2\sin^2\beta-3\cos\beta\sin^2\alpha)/\sin^3\beta+(\sqrt{3}/2) \times F'_{YY}(r/R)\sin\alpha\cos\alpha(1-3r^2\sin^2\alpha/2q^2_{YY})+(\sqrt{3}/2)J'_{YY}(r/R)\sin\alpha[\cos\alpha -(Rr\sin\alpha-(1/2)r^2\sin\alpha\cos\alpha)\sin\alpha/(g^{YY})^2],$$

$$M'=(3\sqrt{3}/4)H_{YXY}(r/R)\sin^3\alpha\cos\alpha/\sin^2\beta+(3\sqrt{3}/4)F_{YY}(r^3/R)\sin^3\alpha\cos\alpha/q^2_{YY} +(\sqrt{3}/4)H'_{YXY}(r/R)\sin\alpha\cos\alpha(2\sin^2\beta-3\cos\beta\sin^2\alpha)/\sin^3\beta +(\sqrt{3}/2)F'_{YY}(r/R)\sin\alpha\cos\alpha(1-3r^2\sin^2\alpha/2q^2_{YY})$$

Fig. 2. Notations used for the elements of the F-matrix.

$A=\mu_1+\mu_2$, $B=\mu_1\cos\beta$, $C=\mu_1\cos\alpha$,
$C_0=2\mu_1$, $D=D''=-\mu_1\rho\sin\alpha$,
$D'=-\mu_1[(\rho-\cos\alpha)\cos\beta+(1-\rho\cos\alpha)\cos\alpha]/\sin\alpha$,
$D'''=(1/2)\mu_1\rho\sin\alpha$, $D_0=-\mu_1\sin\alpha$,
$L=\mu_1[2\rho^2-2\rho\cos\alpha+1]+\mu_2$,
$L'=\mu_1[(2\rho^2-2\rho\cos\alpha+\cos^2\alpha)\cos\beta-2(1-\rho\cos\alpha+\rho^2)\cos^2\alpha+1]/\sin^2\alpha$
$L''=2\mu_1\rho(\rho-\cos\alpha)$, $L'''=-\mu_1\rho(\rho-\cos\alpha)$,
$N=2\mu_1[1-3\rho\cos\alpha+3\rho^2\cos^2\alpha]/\sin^2\alpha+2\mu_2[5-9\cos^2\alpha-4\cos\beta]/3\sin^4\alpha$,
$N'=\mu_1[2(1-6\cos^2\alpha)-9\rho\cos\alpha(1-5\cos^2\alpha)+9\rho^2\cos^2\alpha(1-5\cos^2\alpha)+2(5-18\rho\cos\alpha+18\rho^2\cos^2\alpha)\cos\beta]/3\sin^4\alpha$,
$N''=\mu_1[2(4-9\cos^2\alpha)-36\rho\cos\alpha(1-2\cos^2\alpha)+36\rho^2\cos^2\alpha(1-2\cos^2\alpha)+2(5-18\rho\cos\alpha+18\rho^2\cos^2\alpha)\cos\beta]/3\sin^4\alpha$,
$N'''=\mu_1[1-6\cos^2\alpha+18\rho\cos^3\alpha-18\rho^2\cos^4\alpha+(5-18\rho\cos\alpha+18\rho^2\cos^2\alpha)\cos\beta]/3\sin^4\alpha+\mu_2(-1-3\cos^2\alpha+4\cos\beta)/3\sin^4\alpha$,
$E=-(\sqrt{3}/2)\mu_1\rho\cos\alpha$,
$E'=(1/\sqrt{3})(\mu_1/\sin^2\alpha)[(1-3\rho\cos\alpha)\cos\beta-(1-(3/2)\rho\cos\alpha-(3/2)\rho\cos^3\alpha)]$,
$E''=(1/\sqrt{3})(\mu_1/\sin^2\alpha)[(1-3\rho\cos\alpha)\cos\beta+(2-3\cos^2\alpha)-3\rho\cos\alpha(1-2\cos^2\alpha)]$,
$M=-(\sqrt{3}/2)(\mu_1\rho/\sin\alpha)(1+\cos^2\alpha-2\rho\cos\alpha)$,
$M'=(1/\sqrt{3})(\mu_1/\sin^3\alpha)[(\cos\alpha-3\rho-3\rho\cos^2\alpha+6\rho^2\cos\alpha)\cos\beta+(-\cos\alpha+(3/2)\rho+3\rho\cos^2\alpha+(3/2)\rho\cos^4\alpha-3\rho^2\cos\alpha-3\rho^2\cos^3\alpha)]$,
$M''=(1/\sqrt{3})(\mu_1/\sin^3\alpha)[(\cos\alpha-3\rho-3\rho\cos^2\alpha+6\rho^2\cos\alpha)\cos\beta+(2\cos\alpha-3\cos^3\alpha-3\rho+3\rho\cos^2\alpha+6\rho\cos^4\alpha+6\rho^2\cos\alpha-12\rho^2\cos^3\alpha)]$

where

$$\mu_1=1/m_C,\quad \mu_2=1/m_{Cl},\quad \rho=r/R.$$

Fig. 3. Notations used for the elements of the G-matrix.

$$G(A_{1g})=\begin{bmatrix} A+2B & & \\ \sqrt{6}C & C_0 & \\ D+2D'+D''+2D''' & \sqrt{6}D_0 & L+2L'+L''+2L''' \end{bmatrix} \tag{7a}$$

$$G(A_{1u})=[N+2N'-N''-2N'''] \tag{7b}$$

$$G(A_{2u})=\begin{bmatrix} A+2B & \\ D+2D'-D''-2D''' & L+2L'-L''-2L''' \end{bmatrix} \tag{7c}$$

$$G(E_g)=\begin{bmatrix} A-B & & \\ D-D'+D''-D''' & L-L'+L''-L''' & \\ E-2E'+E'' & M-2M'+M'' & N-N'+N''-N''' \end{bmatrix} \tag{7d}$$

$$G(E_u)=\begin{bmatrix} A-B & & \\ D-D'-D''+D''' & L-L'-L''+L''' & \\ \sqrt{3}(E-E'') & \sqrt{3}(M-M'') & N-N'-N''+N''' \end{bmatrix} \tag{7e}$$

where the notations A, B, and so on are given in Fig. 3. Using the **F**-matrices Eqs. 5 and the **G**-matrices Eqs. 7 the frequencies of normal modes can be calculated through the determinant[13]:

$$|\mathbf{GF}-\lambda\mathbf{E}|=0 \tag{8}$$

where **E** denotes the unit matrix.

A Numerical Example; Hexachloroethane

One of the molecules, to which the present treatment can adequately be applied, is hexachloroethane, for a rather large steric repulsion is expected for the large substituents, chlorine atoms, and seems to result in a high hindering potential barrier. In fact, according to an electron diffraction investigation by Morino and Iwasaki[14], the barrier height of 15 kcal/mole was reported, definitely higher than the level of thermal energy of about 600 cal/mole. Hence, the high barrier approximation is expected in this case.

By using Eqs. 5, 7, and 8 with appropriate force constants given in Table

13) E. Bright Wilson, Jr., ibid. **7**, 1047 (1939); **9**, 76 (1941).

14) Y. Morino and M. Iwasaki ibid. **17**, 216 (1949).

TABLE I
FORCE CONSTANTS USED FOR HEXACHLOROETHANE (in 10^5 dynes/cm).

$K_{CC}=2.15$, $F_{CCl}=0.55$, $F'_{CCl}=-0.04$, $H_{CCCl}=0.07$, $K_{Cl}=2.30$, $F_{ClCl}=0.70$, $F'_{ClCl}=-0.035$, $H_{ClCCl}=0.04$, $J_{ClCl}=0.090$, others assumed to be zero

TABLE II
CALCULATED AND OBSERVED FREQUENCIES OF NORMAL VIBRATIONS OF HEXACHLOROETHANE (in cm^{-1}).

		$\tilde{\nu}_{calc}$	$\tilde{\nu}_{obs}$	deviation (%)
	ν_1	969	974	− 0.6
A_{1g}	ν_2	469	431	+ 8.9
	ν_3	189	169	+12.0
A_{1u}	ν_4	62	—	—
	ν_5	671	675	− 0.6
A_{2u}	ν_6	354	—	—
	ν_7	851	853	− 0.3
E_g	ν_8	313	341	− 8.2
	ν_9	200	224	−10.6
	ν_{10}	799	769	+ 3.9
E_u	ν_{11}	249	—	—
	ν_{12}	143	—	—

TABLE III
CALCULATED AND OBSERVED ROOT MEAN SQUARE AMPLITUDES OF HEXACHLOROETHANE (in Å)

atom pair	calc.	obs.
C—C	0.055	—
C—Cl	0.051	0.06_6
C...Cl	0.071	0.06_9
Cl...Cl	0.070	0.06_4
*g*Cl...Cl	(0.136)	0.13_6
*t*Cl...Cl	0.069	0.10_9

I the frequencies of twelve normal vibrations were calculated; the results are summarized in Table II, where the observed data, if available, are given for comparison. It is seen that the discrepancy is somewhat large for ν_3 and ν_9; one is too high (+12.0%) and the other is too low (−10.6%). However, it was found difficult to make better the agreements of both frequencies simultaneously. Apart from this point, the set of force constants is satisfactory, though the low frequency vibrations active in the infrared have not yet been observed. (ν_6 of A_{2u} type and ν_{11} and ν_{12} of E_u type). Unfortunately all these bands are of low frequency and have large contributions to the root mean square amplitudes, so that the accuracies of the calculated root mean square amplitudes are limited.

The force constant J_{YY} was chosen to be $0.090 \cdot 10^5$ dynes/cm, which means the potential barrier of about 10 kcal/mole (see Eq. 6), and the frequency of the torsional mode was calculated to be 62 cm^{-1}. These values are chosen because they are consistent with the result of the recent electron diffraction experiment[11] (see the next section). Another force constant Φ was simply set equal to zero, for the interaction between chlorine atoms was considered to be more important than the C—Cl bond interactions.

The **L**-matrices given by the relation $\mathbf{S}=\mathbf{LQ}$ are important not only for understanding the nature of the normal modes, but also for calculating the mean amplitudes. The following values were obtained for the elements of the **L**-matrices;

$$A_{1g}\begin{bmatrix}+0.179 & +0.154 & +0.011\\ -0.407 & +0.032 & -0.001\\ +0.469 & -0.048 & +0.167\end{bmatrix} \quad (9a)$$

$$A_{1u}\ [+0.356] \quad (9b)$$

$$A_{2u}\begin{bmatrix}+0.232 & -0.047\\ +0.399 & +0.301\end{bmatrix} \quad (9c)$$

$$E_g\begin{bmatrix}+0.369 & +0.054 & +0.018\\ -0.889 & +0.287 & +0.144\\ +1.090 & -0.432 & +0.186\end{bmatrix} \quad (9d)$$

$$E_u\begin{bmatrix}+0.373 & +0.003 & -0.013\\ -0.099 & +0.006 & +0.176\\ -0.335 & +0.239 & +0.054\end{bmatrix} \quad (9e)$$

where the unit is $(\text{a. m. u.})^{-1/2}$. It can be seen that the coupling between the bond stretching modes and the bond angle deformation vibrations is unusually large.

Mean Amplitudes and Determination of the Potential Barrier

The recent improvement in the electron diffraction technique, the sector-microphotometer method, gives us not only the equilibrium distances of atom pairs but also their mean square amplitudes $\langle \Delta r^2_{ij} \rangle_{AV}$[15]. Because Δr_{ij}, the small deviation from the equilibrium distance of atom pair (i, j), is one of the internal coordinates, it can be expressed in terms of the normal coordinates Q_k's:

$$\Delta\mathbf{r}=\mathbf{AULQ} \quad (10)$$

where **U** and **L** are the unitary and the **L**-matrices, as explained above, and **A** is a matrix which transforms the independent internal coordinates to a particular atom distance, for example between the two atom pair (i, j). Thus the mean amplitude $\langle \Delta r^2_{ij} \rangle_{AV}$ is given by

15) I. L. Karle and J. Karle, ibid. **17**, 1052 (1949).

$$\langle \Delta r^2_{ij} \rangle_{AV} = \mathbf{AULQ}^2 \rangle_{AV} \mathbf{L'U'A'} \quad (11)$$

where $\langle \mathbf{Q}^2 \rangle_{AV}$ is the square of the normal coordinate averaged out over its vibrational states and is for the kth vibration given by

$$\langle Q^2_k \rangle_{AV} = (h/8\pi^2\nu_k)\coth(h\nu_k/2kT). \quad (12)$$

For hexachloroethane there are six atom pairs and their mean amplitudes have been observed except for the C—C atom pair which has too low scattering power to be measured accurately. Thus it is very interesting to compare these observed data with the calculated values based upon Eqs. 11 and 12. The agreement between them, though indirectly, indicates the validity of the force field we have applied. As shown in Table III, the agreement is very good when the experimental error and the approximation made for the force field are taken into consideration.

One atom pair, denoted as gCl—Cl in Table III, is particularly important for the determination of the potential barrier. The mean amplitude of the atom pair is also expressed by a sum of the mean square amplitudes of several normal vibrations, including that of the torsional oscillation, Q_4. If the classical approximation of Eq. (12) is applied for the torsional mode*, the mean amplitude of the gCl—Cl atom pair is given by

$$\langle r^2(g\text{Cl—Cl}) \rangle_{AV} = A + B/V_0, \quad (13)$$

where the first term A is the contribution from skeletal vibrations and the second term B/V_0 from the torsional mode, and the constant B is given by

$$B = (2/9)kT(r^4/(g^{ClCl})^2)\sin^4\alpha \sin^2\phi. \quad (14)$$

However, since the electron diffraction experiment gives us only this sum and cannot separate two parts, it is impossible to obtain the value of the potential barrier only by the observation. Now, since a good force field has become available for us, the unknown constant A can be calculated to be $11.53 \cdot 10^{-3}$ Å^2. Thus the observed mean amplitude $\langle r^2(g\text{Cl—Cl}) \rangle_{AV}$ determines the barrier height V_0. A remark must, however, be given to the value of A, which is indirectly a function of V_0, for the force constant J_{ClCl} determining V_0 enters also into the **F**-matrices of skeletal modes. The force constants given in Table I and the value of A shown above are all consistent with the final value of V_0 of about 10.8 kcal/mole. As described above, the force constants were able to reproduce the observed frequencies of normal vibrations with error of 10%, thus the uncertainties of the calculated mean square amplitudes are about 20% or less, and the height of potential barrier is also accurate in the same order of magnitude.

* The frequency of the torsion Q_4 is low, which allows us to treat it classically.

Discussion

The force field developed here is only of an approximate nature, hence the values of individual force constants given in Table I do not reflect exactly the interatomic interactions in molecules; other coupling constants omitted in the present investigation may influence strongly the values of force constants. It is, however, interesting to discuss the force constant J_{ClCl} introduced first in the present paper, for this constant determines the frequency of the torsional oscillation. The torsional mode is the only one belonging to the A_{1u} symmetry, hence the value of J_{ClCl} is relatively independent of the non-diagonal coupling constants in the **F**-matrices. In fact the constant J_{ClCl} plays the main role in the **F**-matrix of the A_{1u} symmetry [cf. Eq. 5b]. As stated above, its value can be determined by the recent electron diffraction experiment accurately enough to make it worth while to discuss further.

The origin of the hindrance of the internal rotation is very complicated; the diversity of the circumstances has already been noted in the Introduction. Lassettre and Dean[16] discussed the effect of the bond quadrupole interaction. In many instances this effect would be appreciable[17], but the steric repulsion is more important in the present example of hexachloroethane; if one considers the cis-configuration of this molecule the distance between the two eclipsed chlorine atoms becomes about 2.72 A, and the exchange force would be very large. Morino and Miyagawa[18] gave a semi-empirical expression for the repulsive potential between two chlorine atoms:

$$V = -1.515 \cdot 10^{-10} r^{-6} + 1.620 \cdot 10^{-7} r^{-12} \text{ erg/molecule}, \quad (15)$$

r being given in unit of Å. It is based

16) E. N. Lassettre and L. B. Dean, Jr., *J. Chem. Phys.* **17**, 317 (1949); L. J. Oosterhoff, *Discussions Faraday Soc.* **10**, 79 (1951).
17) H. S. Gutowsky and E. O. Stejskal, *J. Chem. Phys.* **22**, 937 (1954); D. R. Lide and D. K. Coles, *Phys. Rev.* **80**, 911 (1950) and so on; see also ref. 11.
18) Y. Morino and I. Miyagawa, *J. Chem. Soc. Japan, (Nippon Kagaku Zassi)* **68**, 62 (1947).

upon the potential obtained from the second virial coefficient of chlorine gas. The force constant J_{ClCl} corresponds to the second derivative of this potential at the equilibrium distance of gCl—Cl pair:

$$J_{ClCl}=(\partial^2 V/\partial r^2)_{r=g\mathrm{ClCl}}, \quad (16)$$

which is calculated to be $0.17\cdot10^5$ dynes/cm, which is in the same order of magnitude with but about twice as large as that previously given in Table I.

The high barrier approximation was used through this paper, but the anharmonicity may be appreciable for the internal rotation. It is, however, of the order of magnitude of $(h\nu_4)^2/V_0$, which is very small, and can be neglected in the present discussion. If the barrier height becomes lower, each torsional level splits owing to the symmetry of the two CCl_3 groups; the three states $H^n{}_1$, $H^n{}_2$ and $H^n{}_3$ corresponding to the three minima and degenenerating in the high barrier case, must be replaced by the irreducible representation[3,5]:

$$\Psi^n{}_1=(1/3)^{1/2}\exp(-iK\phi/2)(H^n{}_1+H^n{}_2+H^n{}_3), \quad (17a)$$

$$\Psi^n{}_2=(1/6)^{1/2}\exp(-iK\phi/2)(2H^n{}_1-H^n{}_2-H^n{}_3), \quad (17b)$$

and

$$\Psi^n{}_3=(1/2)^{1/2}\exp(-iK\phi/2)(H^n{}_2-H^n{}_3), \quad (17c)$$

but this splitting due to the tunneling effect is also small and can be ignored in the present case.

The projected angle introduced here may be applied as one of the internal coordinates to other molecules of lower symmetries with the internal rotation of relatively high frequencies; the mathematical complexity involved is not very serious. If the internal rotation is included in this way in the treatment of the normal mode, its important coupling with other normal vibrations of low frequencies will be obtained, and also the more correct force constants for the latter modes.

The author wishes to express his appreciation to Professor Yonezo Morino, under whose guidiance this research was carried out.

Department of Chemistry
Faculty of Science
The University of Tokyo
Hongo, Tokyo

Spectrochemical Study of Microscopic Crystals. XVII[1]. *The Structure of Cupric Salts with Monocarboxylic Fatty Acids*[2]

By Shoichiro YAMADA, Hiroji NAKAMURA and Ryutaro TSUCHIDA

(Received December 18, 1957)

In 1953 van Niekerk and Schoening[3] showed with X-ray that copper acetate monohydrate in the crystalline state consisted of dimeric molecules with a formula of $Cu_2(CH_3COO)_4 \cdot 2H_2O$. It was concluded later from measurements of absorption spectra[1,4] that cupric propionate in organic solvents as well as in the crystalline state had dimeric molecules similar to those of cupric acetate monohydrate, involving a sort of interaction between the copper atoms. This was found to be in agreement with the conclusion derived from the unusual magnetic property of the compound in the crystalline state[5]. In these circumstances, it seemed to be of significance to examine whether cupric salts with higher homologues of monocarboxylic acids would involve the dimeric molecules, or not. About the structure of some of the cupric alkanoates, there have recently appeared a few reports[6,7], dealing mainly with magnetic properties. The present authors also have carried out

1) Part XVI of this series, S. Yamada, H. Nakamura and R. Tsuchida, This Bulletin, **30**, 953 (1957).
2) R. Tsuchida, S. Yamada and H. Nakamura, Presented in part before the Symposium on Co-ordination Compounds, Tokyo, October, 1956.
3) J. N. van Niekerk and F. R. L. Schoening, *Acta Cryst.*, **6**, 227 (1953).
4) R. Tsuchida and S. Yamada, *Nature*, **176**, 1171 (1957).
5) H. Abe, *Phys. Rev.*, **92**, 1572 (1953).
6) R. C. Herron and R. C. Pink, *J. Chem. Soc.*, **1956**, 3948.
7) R. L. Martin and H. Waterman, ibid., **1957**, 2545.

examinations about the structure of cupric butyrate, valerianate, capronate, caprylate, palmitate and stearate mostly on the basis of their polarized absorption spectra[2,8]. A brief report of this study was formerly presented as a communication[8], the detailed account of which is given below.

Experimental

Materials.—Cupric *n*-butyrate was prepared by the method of von Alth[9] from barium *n*-butyrate and cupric sulfate. Recrystallization of the product from water yielded the monohydrate in green crystals. Anhydrous cupric *n*-butyrate was obtained by repeated recrystallization from acetone or chloroform.

Cupric *iso*-butyrate was prepared in a similar way, and obtained in anhydrous crystals when recrystallized from water.

Cupric *n*-valerianate monohydrate was prepared by the same method as that for cupric butyrate[9]. Anhydrous cupric *n*-valerianate was obtained after dehydration of the monohydrate, followed by repeated recrystallization from chloroform.

Cupric *iso*-valerianate was prepared by the same method as in the case of the *n*-valerianate monohydrate. Recrystallization from water always yielded green crystals of the anhydrous *iso*-valerianate.

Cupric *n*-capronate was prepared according to the method of Freund[10] from cupric acetate and *n*-caproic acid. Recrystallization from ethanol gave green crystals of the anhydrous *n*-capronate.

Cupric *n*-caprylate was prepared according to the method of Zincke[11] from sodium *n*-caprylate and cupric sulfate. After recrystallization from ethanol, anhydrous *n*-caprylate was obtained in green crystals. The compound exists only in an anhydrous form.

The crystals of the above-described compounds all show a striking dichroism on their well-developed planes; that is, blue and green.

Cupric *n*-palmitate and *n*-stearate were prepared according to the method of Cady et al.[12] and Heintz[13]. Anhydrous forms of both the compounds were obtained in greenish-blue, powdery microcrystals. The crystals obtained were found to be too small for the dichroism measurement. Therefore, absorption spectra in the visible and the ultraviolet region of the compounds were determined only in solution.

Measurements.—Quantitative dichroism measurements in the visible and the ultraviolet region were carried out at room temperature by the same method as that in the previous papers of this series[14]. The measurements were made with respect to the directions of extinction on one of the well-developed planes which was shown in each figure. The notations refer to the directions shown in the figure.

Absorption spectra of the compounds in ethanol or carbon tetrachloride were determined at room temperature by a Beckman DU spectrophotometer. It was confirmed in every measurement that Beer's law was obeyed in the presence of the free aliphatic carboxylic acid in addition.

Infrared absorption spectra of the cupric compounds in Nujol mulls were determined in the rock salt region by a Hilger H-800 infrared spectrophotometer.

The notations in the present paper are the same as those used in the former papers of this series. Extinction coefficients, ε, are calculated, and referred to a formula weight instead of a molecular weight.

Results and Discussion

Polarized Absorption Spectra of the Cupric Alkanoates in the Crystalline State.—In the preceding paper[1], we have reported about the structure of cupric formate, acetate and propionate on the basis of their polarized absorption spectra. A similar treatment will be made here concerning the structure of cupric salts with higher homologues of monocarboxylic fatty acids. Since some of the results and discussions in the preceding paper are used in the present discussion, it would be appropriate to give a brief account of the conclusions obtained in the former paper.

Cupric acetate and propionate in the crystalline state and in organic solvents show in the visible and the near-ultraviolet region a band at about 80×10^{13}/sec. (band II) besides a band at about 43×10^{13}/sec. (band I), whereas most cupric compounds show in this wave-length region only one band which may be considered as corresponding to the band at 43×10^{13}/sec. For the band I, electric vector is more strongly absorbed along the complex plane than along the *z*-direction of the dimeric molecule. For the band II, electric vector is more strongly absorbed along the *z*-direction; the polarization for this band is the reverse of that for the band I. These facts were considered to show that the compounds involve along the *z*-direction a sort of copper-to-copper interaction characteristic of the dimeric molecule of the cupric carboxylates. The same result

8) R. Tsuchida, S. Yamada and H. Nakamura, *Nature*, **178**, 1192 (1956).
9) T. von Alth, *Ann.*, **91**, 170 (1854).
10) A. Freund, *J. prakt. Chem.*, (2) **3**, 233 (1871).
11) T. Zincke, *Ann.*, **152**, 11 (1869).
12) H. P. Cady and E. J. Baldwin, *J. Am. Chem. Soc.*, **43**, 648 (1921).
13) W. Heintz, *Ann.*, **84**, 299 (1852).
14) R. Tsuchida and M. Kobayashi, "The Colour and the Structure of Metallic Compounds," Zoshindo, Osaka, 1944, p. 180 (in Japanese).

was obtained with cupric propionate, hydrated or anhydrous. Thus the appearance of the band at about 80×10^{13}/sec., combined with the polarization property of the band, may be regarded as showing the existence of the dimeric molecule similar to that of cupric acetate or propionate involving the copper-to-copper interaction.

The results of the present measurements are shown in Figs. 1 to 8. As the components of the cupric compounds in the crystalline state may be under rather weak perturbation owing to the crystalline field, the polarized absorption spectra as determined on a suitable plane are regarded as representing the main features of the dichroism of the components. The exact arrangement of the components in the crystals is unknown for all the cupric compounds reported here. It is easy, however, to see the principal characteristics of the dichroism of the components themselves by comparing their absorption spectra with those of cupric acetate monohydrate whose crystal structure was accurately determined.

The present measurements indicate that cupric butyrate monohydrate in the crystalline state shows an absorption band at about 80×10^{13}/sec. in addition to a band at about 43×10^{13}/sec. Moreover, the polarization for the former band is found to be the reverse of the polarization for the latter (Fig. 1). This relationship, which closely resembles that encountered in the case of the acetate monohydrate, may suggest that cupric butyrate monohydrate in the crystalline state consists

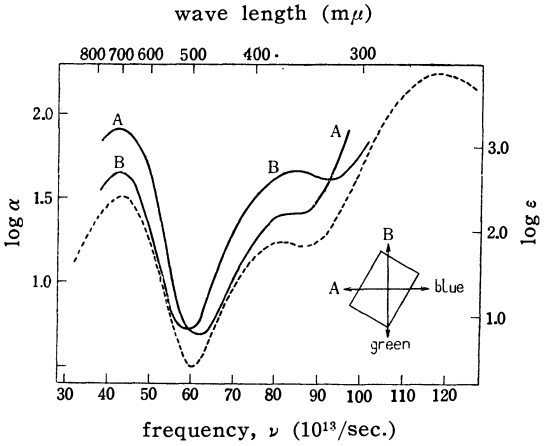

Fig. 1. Absorption spectra of $Cu(n\text{-}C_3H_7COO)_2\cdot H_2O$ in the crystalline state (——) and in ethanol (------).

of the binuclear molecules resembling those of copper acetate monohydrate. The crystal structure was formerly examined by Iball[15], who noted an unusual number of the molecules involved in a unit cell of the compound. This may presumably be related to the dimeric structure of the compound. It is certain that the A- and the B-absorption in Fig. 1 may represent the characteristics of the absorption along and perpendicular to the complex-plane, respectively.

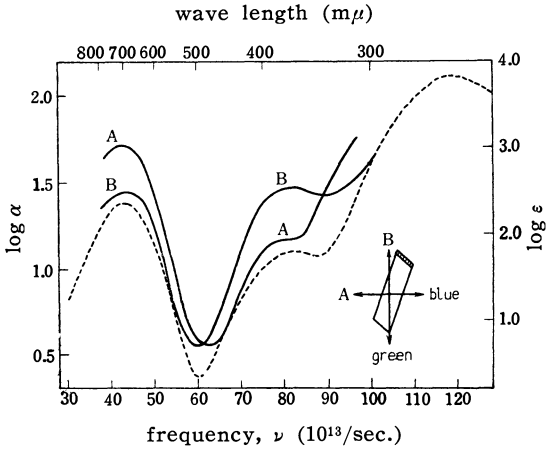

Fig. 2. Absorption spectra of $Cu(n\text{-}C_4H_9COO)_2\cdot H_2O$ in the crystalline state (——) and in ethanol (------).

Cupric valerianate monohydrate is found to show polarized absorption spectra, which are essentially similar to the acetate monohydrate[1], as shown in Fig. 2. Thus the appearance of the band at 80×10^{13}/sec. and the polarization of the band unanimously show, on the basis of the criteria mentioned in the earlier part of this discussion, that the valerianate monohydrate also consists of dimeric molecules.

Cupric *n*-butyrate and *n*-valerianate exist in either a monohydrated or an anhydrous form. Polarized absorption spectra of the anhydrous *n*-butyrate have also been determined in the present work (Fig. 3). It is seen that the anhydrous butyrate exhibits absorption bands at about 43 and 80×10^{13}/sec., the polarization for the latter band being the reverse of the polarization for the former. This relationship bears a close resemblance to that with cupric butyrate, indicating that the anhydrous butyrate contains the dimeric molecule which is fundamentally similar to that of the monohydrate. It may, therefore, be

15) J. Iball, *Nature*, **159**, 95 (1947).

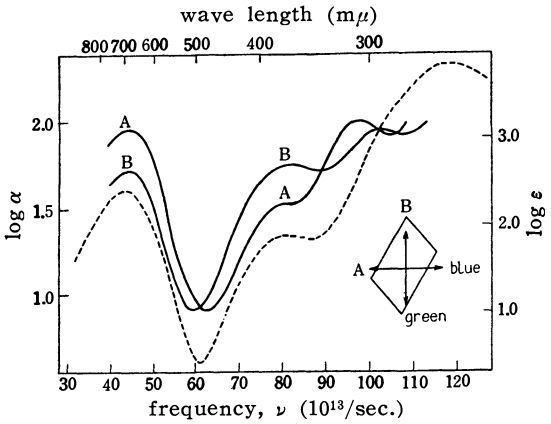

Fig. 3. Absorption spectra of $Cu(n\text{-}C_3H_7COO)_2$ in the crystalline state (——) and in ethanol (------).

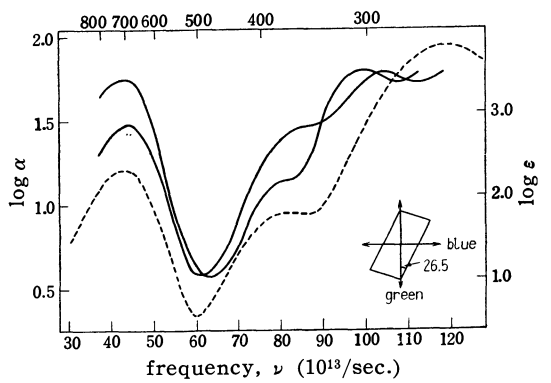

Fig. 4. Absorption spectra of $Cu(n\text{-}C_5H_{11}COO)_2$ in the crystalline state (——) and in ethanol (------).
(The angle 26.5 stands for 26.5°)

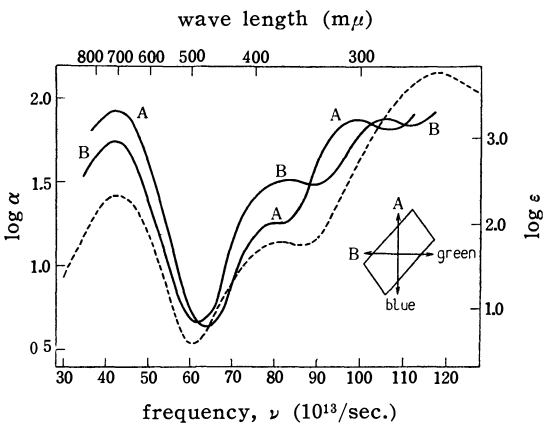

Fig. 5. Absorption spectra of $Cu(n\text{-}C_7H_{15}COO)_2$ in the crystalline state (——) and in ethanol (------).

concluded that both the monohydrated and the anhydrous form of cupric butyrate have the dimeric molecules with the possible interaction between the two copper atoms. Anhydrous cupric valerianate exhibits a similar color to that of the anhydrous butyrate. Although the dichroism has not been measured with the anhydrous valerianate, it may be certain that the anhydrous valerianate also shows polarized absorption spectra with the same characteristics as are observed with the butyrate, having the dimeric molecules of the same type. Note should be taken of the fact that the same relationships were obtained in the case of cupric propionate. It may be suggested that the linkage of the water molecule to the copper atom within the hydrated dimer is not strong.

Cupric capronate and caprylate exist only in an anhydrous form. Polarized absorption spectra of the two compounds have been determined in the crystalline state (Figs. 4 and 5). The crystal structure analysis has not been reported with either of them. It may be admitted, however, that the polarization property as well as the positions of the band maxima are the same as those of the compounds described above. It is most reasonable to assume that both the anhydrous compounds have the dimeric molecule with a general formula, $Cu_2(R\cdot COO)_4$.

In the above part, we have discussed about the cupric salts with normal carboxylic acids. Examination of the steric condition shows that the corresponding *iso*-alkanoates may be able to form the binuclear molecule, since the steric hindrance due to the branching alkyl-radical in the *iso*-series is not so great as to prohibit the formation of the binuclear molecules. Therefore, some of cupric

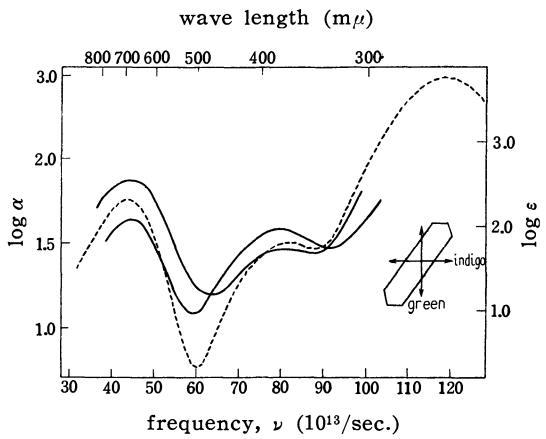

Fig. 6. Absorption spectra of $Cu(iso\text{-}C_3H_7COO)_2$ in the crystalline state (——) and in ethanol (------).

compounds with *iso*-carboxylic acids have been examined by the same method as that applied to the normal alkanoates. The polarized absorption spectra of anhydrous cupric *iso*-butyrate (Fig. 6) are found to be quite similar to those of cupric acetate monohydrate, showing the absorption band at about 80×10^{13}/sec. whose polarization is the reverse of that for the band at about 43×10^{13}/sec.

The same result has been obtained with cupric *iso*-valerianate (Fig. 7). These facts may readily be interpreted as showing, on the basis of the criteria as described above, that both cupric *iso*-butyrate

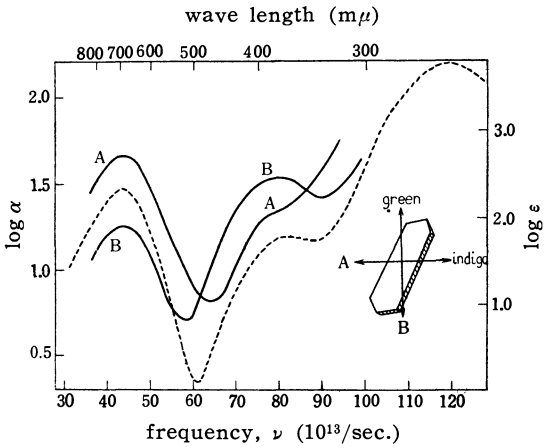

Fig. 7. Absorption spectra of $Cu(iso\text{-}C_4H_9COO)_2$ in the crystalline state (——) and in ethanol (------).

and *iso*-valerianate have the dimeric molecules with a formula of $Cu_2(iso\text{-}R\cdot COO)_4$. It may safely be assumed that the cupric *iso*-alkanoates in general consist of the binuclear molecules similar to the corresponding normal alkanoates.

Absorption Spectra of the Cupric Alkanoates in Solution.—Some of the cupric compounds examined in the present and preceding papers are soluble in water to dissociate into component ions to a great extent. Thus the absorption spectra of the alkanoates in water show the main characteristics of the aquated cupric ion, indicating a considerably great degree of dissociation of the compounds. Absorption spectra, therefore, were measured in organic solvents. When ethanol is used as solvent, it is supposed to form some amount of the ethyl alkanoate with a part of the free ligand which is added in excess. In all the present measurements, however, it was confirmed that Beer's law was obeyed on addition of the free ligand throughout the whole concentration range examined. Without the addition of the free ligand, the cupric alkanoate in solution was found to show deviation from Beer's law in the shorter wave-length region when the solution was much diluted.

It is seen from the measurements (Fig. 8) that all the above compounds in solution show absorption spectra which are closely similar to one another in both the wave-length and the molar extinction coefficients at their absorption maxima. Thus they show absorption bands with maxima at about 43 and 82×10^{13}/sec., and a much more intense absorption band in the shorter wave-length region. It seems to be of significance that the compounds

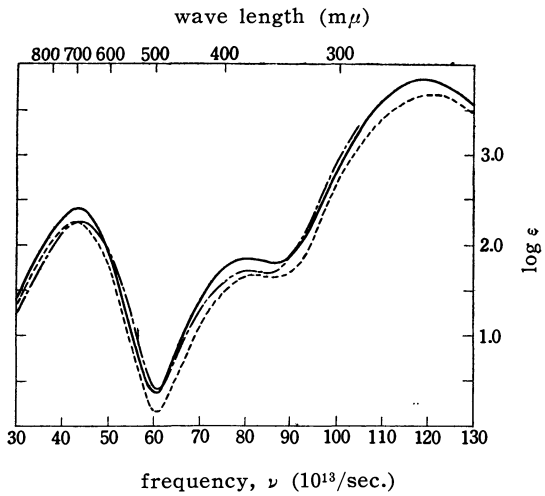

Fig. 8. Absorption spectra of cupric alkanoates: acetate (------) and butyrate (——) in ethyl alcohol, and palmitate (—·—·) in acetic anhydride.

show an absorption band at 82×10^{13}/sec. even in solution. These facts indicate that the cupric alkanoates all have, in organic solvents, molecules of a similar type which may most probably be the binuclear molecule represented by a formula of $Cu_2(R\cdot COO)_4$. This molecule in solution may be solvated; then, this is represented by a molecular formula of $Cu_2(R\cdot COO)_4\cdot 2A$, A being a molecule of the solvent.

Absorption spectra of cupric *n*-palmitate (C 16) and *n*-stearate (C 18) were determined in acetic anhydride, since their solubility in other solvents is not sufficiently high. The absorption curves (Fig. 8 and Table I) are quite similar to those of the other alkanoates in ethanol. It is reasonable to conclude that cupric

TABLE I
VISIBLE AND ULTRAVIOLET ABSORPTION SPECTRA OF CUPRIC MONOCARBOXYLATES WITH AN EMPIRICAL FORMULA OF $Cu(RCOO)_2$*

R	band I		band II		band III	
	ν (10^{13}/sec.)	log ε	ν (10^{13}/sec.)	log ε	ν (10^{13}/sec.)	log ε
CH_3	42.8	2.25	82.0	1.65	120.1	3.68
C_2H_5	43.0	2.27	82.0	1.75	118.9	3.71
n-C_3H_7	43.1	2.42	81.4	1.87	118.4	3.90
iso-C_3H_7	43.4	2.22	81.6	1.71	117.6	3.67
n-C_4H_9	43.1	2.37	82.4	1.82	118.2	3.85
iso-C_4H_9	43.2	2.32	81.7	1.76	118.0	3.75
n-C_5H_{11}	43.0	2.33	81.1	1.80	118.1	3.80
n-C_7H_{15}	43.0	2.33	81.1	1.78	117.7	3.80
n-$C_{15}H_{31}$**	44.2	2.27	82.0	1.71		
n-$C_{17}H_{35}$**	44.2	2.26	82.4	1.72		

* Unless otherwise indicated, the used solvent is ethanol.
** Data in acetic anhydride.

n-palmitate and *n*-stearate in acetic anhydride consist of the dimeric molecules similar to the above described.

Infrared Absorption Spectra.—It is known that the carboxylate ion in general exhibits anti-symmetrical vibrations in the region between 1550 and 1700 cm^{-1}. Anti-symmetrical vibrations due primarily to the carboxylate-group have been examined with the cupric carboxylates in pressed potassium bromide discs and in Nujol mulls. Sodium acetate, which contains carboxylate ions in an ionized form, shows a broad and strong band around 1560 cm^{-1}, and cupric formate, which involves carboxylate-groups coordinated to copper ions in such a way that the dimeric molecule of the cupric salt is not formed, shows a broad and strong band over the region between 1560 and 1600 cm^{-1}. On the other hand, cupric acetate, propionate, butyrate, valerianate, caprylate, capronate, palmitate and stearate show the absorption at about 1595 to 1600 cm^{-1}, which is rather sharp and well-defined. The infrared spectra indicate that the state of the carboxylate ion in the latter group of the cupric compounds differs from that in cupric formate or sodium acetate, being in agreement with the afore-mentioned conclusion that the cupric compounds examined in the present study may involve the binuclear molecules similar to those of cupric acetate or anhydrous cupric propionate. Although such an evidence alone is not to be regarded as decisive, this, combined with other materials, may be confirmatory enough for us to reach the above conclusion of the binuclear structure.

General Discussion

Visible and Ultraviolet Absorption Spectra of the Compounds.—It is seen from the measurements that the cupric alkanoates show in the visible and the ultra violet region absorption bands at about 43 (band I) and 80×10^{13}/sec. (band II) besides a strong absorption band in the region of the shorter wave length. It is most probable that the band I may correspond to the band in the long wavelength region of cupric complexes of an ordinary type, which is usually ascribed to the copper ion under perturbation of the surrounding ligands. On the other hand, the band II is assumed to be closely related with the copper-to-copper interaction. This is borne out by the solvent effect upon these absorption bands. Thus when a solvent is alternated with a more polar one, the band I undergoes red-shift, while the band II shows blue shift. The solvent effect upon the former band agrees with that upon the band at the longer wave length of the cupric ethylenediamine and acetylacetonate complexes, showing that the two bands may be originated from similar electronic transitions. On the contrary, the band II differs in the origin from the absorption bands of the above type. The detailed discussion on the solvent effect will be reported elsewhere.

Although the crystal structure analyses have not been reported with most of the compounds in the present paper, we may make the following generalization about the dichroism of the above compounds.

The band I is polarized along the $Cu(O)_4$-plane, while the band II is polarized along the z-axis of the dimeric molecule, along

which the copper-to-copper interaction is expected to exist.

The relation for the band I is found to be the same as the dichroism for the absorption band at the longer wave length of cupric complexes, being in agreement with the assumption that these two bands correspond to each other.

Reviewing the absorption curves of the cupric alkanoates in organic solvents, we can obtain the following relationships which are valid for the cupric salts consisting of the dimeric molecules.

The compounds show absorption curves which are similar to one another. The wave length and the molar extinction coefficients at the corresponding band maxima are almost equal among the compounds. Moreover, the intensity ratio of the band I to the band II is equally three and a half for all the compounds examined in the present paper. This close similarity seems to be in agreement with the above conclusion that the compounds all have a similar structure, which involves the dimeric molecules.

The intensity of the band I is seen to be nearly ten times as great as that of the corresponding band exhibited by cupric complexes of an ordinary type with all the coordination positions occupied by oxygen atoms. This fact, which indicates a definite difference in the linkage between the present compounds and the compounds of an ordinary type, may be explained on the basis of the copper-to-copper linkage in the dimeric molecules of the cupric alkanoates.

Examination of the data (Table I) reveals that the intensity of the corresponding bands changes in the following order:

acet.<prop.<butyr.<valerian.
>capron.>capryl. (*n*-homologues).

Thus the intensity of the band increases as we go from the acetate to the valerianate, and then decreases as we go further down the series. Clear explanation for this tendency is not available at present.

Structure of the Cupric Alkanoates.— As described in the preceding part of the present paper, *cupric n- and iso-butyrate, n- and iso-valerianate, n-capronate, n-caprylate, n-palmitate and n-stearate, both in organic solvents and in the crystalline state, are considered to have the dimeric molecules with a kind of weak linkage between the two copper atoms.* Thus it is seen that the length or the shape of the alkyl-group causes no great effect upon the linkage of the carboxylate-group with the copper atom. It may be assumed further that cupric salts with higher homologues of *n-* or *iso*-carboxylic acids also contain the dimeric molecules, since increasing the length of the methylene chain or putting an alkyl-branch in the chain would give rise to no great change, sterically or electronically. This assumption is borne out by a recent study on the structure of cupric behenate (C 22) through magnetic measurements[7].

It is worth noting that cupric formate does not involve a dimeric molecule whereas the other cupric alkanoates consist of the dimeric molecules. This conspicuous difference may tentatively be explained from the standpoint of the electronic theory, when we take into account the effect caused upon the linkages around the copper atoms by increasing the number of the carbon atoms. As a radical neighboring the carboxylate-group is replaced by another, the electronic charge on the carbon atom in the carboxylate-group would change to a greater or lesser extent. Since the electronic theory of organic chemistry gives the following order with respect to the electron-attracting capacity: $H > CH_3 > C_2H_5 > C_3H_7 > \cdots\cdots$, the electronic charge on the carbon atom of the carboxylate-group may increase as we go from hydrogen down the series. The more the electronic density on the carbon atom of the carboxylate-group, the more negatively the oxygen atom would be charged, with the result that the electronic cloud on the copper atom would be withdrawn less strongly toward the oxygen atom. If we assume that the increase of the electronic density on the copper atom means increase of the electronic charge available for the additional linkage between the two copper atoms, the copper-to-copper linkage might become stronger as the electronic charge on the copper increases on going from the formate down the series of the homologous alkanoates. The above concept seems to be supported qualitatively by the decrease of acid strength on going from formic acid down the series of the homologous fatty acids.

Our measurements in the present and preceding papers show that a great difference in absorption maxima was not observed among the cupric alkanoates except cupric formate which involves

components of an exceptional sort. This may be interpreted as indicating that the electron-attracting capacity of the alkyl-groups charges only very slightly from one alkyl-group to another. In contrast to the other cupric alkanoates, cupric formate was not found to have a dimeric molecule. The electronic charge of the copper atom in cupric formate is assumed to be withdrawn toward the oxygen atom to such an extent that the linkage could not be formed between the two copper atoms. Thus the striking difference in the structure between cupric formate and acetate may be understandable on the assumption that the line of demarcation with respect to the electronic charge on the oxygen atom could be drawn somewhere between the formate and the acetate.

As was mentioned in the preceding part, cupric *n*-capronate and higher *n*-alkanoates exist only in an anhydrous form, whereas the lower *n*-alkanoates of copper, such as the acetate, propionate, *n*-butyrate and *n*-valerianate, have the dimeric molecules with water molecules bonded to the copper atom[16]. Thus crystals of anhydrous cupric capronate are precipitated on addition of water to an ethanolic solution of the compound. This critical difference between cupric valerianate and capronate may also be understood on the above described assumption. According to the above mentioned concept, we may assume that the positive charge on the copper atom, which seems to be necessary for the combination of a water molecule with the copper atom, should be greater than a threshold value in order that the copper atom may bind a water molecule. Since the positive charge on the copper atom decreases slightly as we go from the formate down the series, the linkage of the water to the copper atom may become weaker in that order. Thus there is good reason for us to suppose that the line of demarcation may be drawn between the valerianate and the capronate, beyond which the copper atom in the dimeric cupric alkanoates may not be able to bind the water molecule with ease. The inductive effect of the alkyl-group, on the basis of which the above discussion has been made, may not be the only factor. However, the explanation, as given above, seems to be qualitatively correct.

The effect of the water molecule upon the copper in the hydrated dimer of the cupric alkanoates is found to be comparatively small, since no great difference between them was observed in the absorption spectra. It is most probable that the linkage of the water to the copper atom is highly ionic.

A definite difference, however, was reported in the exchange interaction, which was estimated from magnetic measurements[17]. Thus the exchange energy between the two copper atoms was found to be greater in cupric stearate than in cupric acetate monohydrate. In this case, two effects may be regarded as responsible for the observed difference. One is the effect of replacing acetate by stearate groups, and the other is the effect of the water molecules. The two effects would compensate each other to a certain extent, but the above result may be assumed to show that the former overshadows the latter in this case.

Nature of the Copper-to-copper Linkage.—It is shown in the preceding part of the present paper that cupric acetate and higher alkanoates may have the dimeric molecules with a sort of linkage between the two copper atoms in a molecule. Although the nature of the copper-to-copper linkage is not completely clarified, the following two models for the extraordinary linkage may be regarded as most probable. One involves the $d_\pi - d_\pi$ bonding. We assume in this model an extreme structure, in which the two copper atoms form octahedral d_2sp_3 hybridization orbitals. Two orbitals of them, each from one of the two copper atoms, over lap each other in the region above or below the complex-plane. It is interesting to note that the two copper atoms in this model have an electronic structure of a rare-gas type, the possible stability of which may be of some importance in this model.

In the second model, the overlap is assumed to take place between the two $3d_{x^2-y^2}$ orbitals, each from either of the two copper atoms in the molecule, since the copper atoms have non-bonding $3d_{x^2-y^2}$ orbitals which spread in the space above and below the complex-plane. This model was proposed by Martin et al.[7], who

16) We are here concerned with normal alkanoates only; cupric *iso*-butyrate and *iso*-valerianate are usually obtained as anhydrous compounds.

17) K. Kido and T. Watanabe, Presented at the Symposium on Co-ordination Compounds, Nagoya, November, 1957.

considered, mostly on grounds of energy, this type of interaction as more probable than the d_z-d_z interaction. The present authors, however, are inclined to consider that the decision between the two models could not be made for the present.

Summary

In order to examine the structure of cupric alkanoates, the dichroism in the visible and the ultra violet region has been determined by the microscopic method with normal butyrate, valerianate, capronate and caprylate of copper(II). Visible and ultra-violet absorption spectra in organic solvents and infrared absorption spectra in Nujol mulls have been determined with the above compounds, along with cupric palmitate and stearate. *Iso*-alkanoates have also been examined in a similar way.

All these compounds in the crystalline state and in organic solvents are found to show similar absorption spectra having the dichroism with characteristics fundamentally similar to those of cupric acetate and propionate which had earlier been reported. From these results, it has been concluded that all the above compounds consist of the dimeric molecules.

The anhydrous forms of the compounds have been shown to consist of the dimeric molecules resembling those of the hydrated form.

All the above compounds show absorption bands at about 43 and 80×10^{13}/sec. The former is polarized along the $Cu(O)_4$-plane and the latter along the direction binding the two copper atoms in a molecule.

The present authors wish to thank the Ministry of Education for a grant.

Department of Chemistry, Faculty of Science, Osaka University, Kita-ku, Osaka

Studies on the Cobalt(III) Complexes Containing Only One Chelate Ring. II.[1] *Syntheses and Properties of Monoethylenediamine-tetrammine-cobalt(III) Complexes,* [*Co en* $(NH_3)_4$]X_3[2]

By Yoichi SHIMURA

(Received December 7, 1957)

No monoethylenediamine-tetrammine cobalt(III) complexes were hitherto known, while all the other members of ammine-ethylenediamine series of cobalt(III) complexes have thoroughly been studied. In the present paper, the syntheses of these missing luteo salts, [Co en $(NH_3)_4$]X_3, will be reported. And the absorption spectra of the cobalt(III) complexes which belong to the ammine-ethylenediamine series will be discussed.

Results and Discussion

Method of Syntheses.—For the syntheses of the monoethylenediamine-tetrammine complexes, after several preliminary attempts, the following scheme was adopted.

$$[\text{Co en } (NH_3)_2\ Cl_2^{(1)}_{(6)}]Cl \xrightarrow[KNCS]{(i)}$$

$$[\text{Co en } (NH_3)_2\ (NCS)_2]^+ \xrightarrow[H_2O_2]{(ii)}$$

$$[\text{Co en } (NH_3)_2\ (NH_3)_2]^{3+} \xrightarrow[H_2SO_4]{(iii)}$$

$$[\text{Co en } (NH_3)_4]_2\ (SO_4)_3$$

The starting material, [Co en $(NH_3)_2$ $Cl_2^{(1)}_{(6)}$]Cl, was prepared from NH_4[Co en $(NH_3)_2(SO_3)_2]\cdot H_2O$ by Bailar and Pappard's method[3]. The possible three geometrical isomers of [Co en $(NH_3)_2$ $(NCS)_2]^+$ may result from the reaction i. The separation of these isomers, however, was not

1) Part I of this series: Y. Shimura, This Bulletin, **31**, 173 (1958).

2) Partly presented at the Symposium on Co-ordination Compounds, Tokyo, October 28, 1956.

3) J. C. Bailar, Jr. and D. F. Peppard, *J. Am. Chem. Soc.*, **62**, 105 (1940).

intended, because it was expected that all these isomers equally produce the desired complex by the reaction ii.

The reaction ii was carried out by a modification of the Werner's method[4], who prepared *trans*- and *cis*-[Co en$_2$ $(NH_3)_2$]X_3 from the corresponding isothiocyanato-complexes by hydrolytic oxidation with chlorine or with hydrogen peroxide. These reactions leave the nitrogen atoms co-ordinated to the cobalt atom; the co-ordinated isothiocyanato-groups are transformed into co-ordinated ammonia molecules.

The crystals of the sulfate or the bromide of [Co en $(NH_3)_4$]$^{3+}$ are orange-colored and indistinguishable by the color from the other members of the ammine-ethylenediamine series. The monoethylenediamine-tetrammine complexes have rather high solubilities in water as compared with hexammine or trisethylenediamine complexes. For this reason, the purification of the chloride, [Co en $(NH_3)_4$]$Cl_3 \cdot xH_2O$, was not practical.

Unsuccessful Attempt on Optical Resolution.—Recently several X-ray[5,6] and infrared[7] studies have shown that the co-ordinated ethylenediamine molecule is not planar but takes so-called *gauche* form. This *gauche* configuration has a mirror image antipode. Therefore, it is very interesting to test the possibilities for the optical resolution of [Co en $(NH_3)_4$]X_3.

Firstly, the chemical resolution by *d*-tartrate was tried. By the double decomposition of [Co en $(NH_3)_4$]$Br_3 \cdot H_2O$ and silver *d*-tartrate(tart), an oily product was obtained, the composition of which is perhaps [Co en $(NH_3)_4$]Br$\cdot$(*d*-tart)$\cdot xH_2O$. The oily product was dissolved in water and fractionally treated with ethanol. But no evidences for the separation of diastereoisomers were obtained. Secondly, the method of asymmetric adsorption on optically-active quartz[8,9] was applied. But the result was also negative. These negative results, however, are not improbable, since the puckered five-membered ethylenediamine-cobalt ring may be easily inverted into its antipode.

The last method tested, though it was also unsuccessful, is an equilibrium method with the aid of rotatory dispersion measurements. Very recently, Kirschner[10] succeeded to demonstrate that K_2[Cu (edta)] is optically active by showing that the mixed aqueous solution of *l*-quinone hydrobromide and the copper complex exhibits an anomalous rotatory dispersion in the vicinity of the absorption band of the complex. This fact indicated that there was a shift in the equilibrium, D-[Cu(edta)]$^=$ $\rightleftarrows$ L-[Cu(edta)]$^=$, under the asymmetric influence of *l*-quinone hydrobromide.

Following the above method, the rotatory dispersion of the mixed aqueous solution of [Co en $(NH_3)_4$]$_2$ $(SO_4)_3 \cdot 4H_2O$ and Rochelle salt was measured. In the region of 600$\sim$300 mμ, scarcely any anomalous rotatory dispersion was observed (Table I.).

TABLE I

OPTICAL ROTATION OF MIXED SOLUTION OF ROCHELLE SALT AND [Co en$(NH_3)_4]_2(SO_4)_3 \cdot 4H_2O$

λ(mμ)	ν(10^{13}/sec.)	α_1	α_2	$\alpha_2-\alpha_1$
577	52.0	0.643°	0.640°	−0.003°
546	54.9	0.723	0.715	−0.008
492	61.0	0.890	0.878	−0.012
436	68.8	1.148	1.142	−0.006
405	74.1	1.328	1.323	−0.005
365	82.2	1.607	1.598	−0.009
312.6	96.0	1.972	1.967	−0.005

α_1: Optical rotation of 0.1 F aq. soln. of $NaKC_4H_4O_6 \cdot 4H_2O$ (1 dm, 28°C).

α_2: Optical rotation of mixed aq. soln. of 0.1F $NaKC_4H_4O_6 \cdot 4H_2O$ and 0.001 F [Co en $(NH_3)_4$] $(SO_4)_{1\frac{1}{2}} \cdot 2H_2O$ (1 dm, 28°C).

This result may be considered to indicate that little of the asymmetric shift of the equilibrium, D-[Co en $(NH_3)_4$]$^{3+}$ $\rightleftarrows$ L-[Co en $(NH_3)_4$]$^{3+}$ occurred, or that the anomalous rotatory dispersion of this complex ion is very small. An alternative explanation is to postulate that the first and the second absorption band of this complex are optically inactive.

Absorption Spectra.—The absorption curves of the cobalt(III) complexes which belong to the ammine-ethylenediamine series are shown in Fig. 1. The numerical data of the first and the second absorption band are tabulated in Table II.

4) A. Werner, *Ann.*, **386**, 1 (1912); A. Werner, F. Bräunlich, E. Rogowina and C. Kreutzer, ibid., **351**, 65 (1907).

5) A. Nakahara, Y. Saito and H. Kuroya, This Bulletin, **25**, 331 (1952); K. Nakatsu, Y. Saito and H. Kuroya, ibid., **29**, 428 (1956) etc.

6) H. Kuroya, Y, Saito, A. Nakahara, Y. Komiyama and K. Nakatsu, *J. Inst. Polytech. Osaka City Univ.*, **5**, C, 1 (1956).

7) J. V. Quagliano and S. Mizushima, *J. Am. Chem. Soc.*, **75**, 6084 (1953); S. Mizushima, I. Ichishima, I. Nakagawa and J. V. Quagliano, *J. Phys. Chem.*, **59**, 293, (1955) etc.

8) R. Tsuchida, M. Kobayashi and A. Nakamura, *J. Chem. Soc. Japan, (Nippon Kagaku Zassi)*, **56**, 1339 (1935).

9) H. Kuroya, S. Aimi and R. Tsuchida, ibid. **64**, 905 (1943).

10) S. Kirschner, *J. Am. Chem. Soc.*, **78**, 2372 (1956).

TABLE II

ABSORPTION DATA OF [Co (en)x $(NH_3)_{6x-2x}]^{3+}$ SERIES

Complex Ion	First Absorption Band				Second Absorption Band				$\Delta(\nu_{max})$***	$\Delta(\log \varepsilon_{max})$****
	ν_{max} (10^{13}/sec.)	$\log \varepsilon_{max}$	l* (10^{13}/sec.)	δ** (10^{13}/sec.)	ν_{max} (10^{13}/sec.)	$\log \varepsilon_{max}$	l* (10^{13}/sec.)	δ** (10^{13}/sec.)		
$[Co(NH_3)_6]^{3+}$	62.9	1.68	10.3	0.45	88.3	1.60	12.5	0.35	25.4	−0.08
$[Co\ en(NH_3)_4]^{3+}$	63.6	1.83	10.7	0.55	88.4	1.76	13.1	0.55	24.8	−0.07
trans-$[Co\ en_2(NH_3)_2]^{3+}$	64.2	1.77	10.8	0.8	89.2	1.73	12.3	0.55	25.0	−0.04
cis-$[Co\ en_2(NH_3)_2]^{3+}$	64.4	1.79	10.7	0.65	89.4	1.74	12.6	0.5	25.0	−0.05
$[Co\ en_3]^{3+}$	63.9	1.94	10.4	0.55	88.4	1.90	12.0	0.4	24.5	−0.04

* l=half-value width. This corresponds to $\{\delta(+)+\delta(-)\}$ in Jørgensen's notation[13].

** δ=inclination parameter[14] or Inklination (in German)[15]. This parameter corresponds to $\frac{1}{2}\{\delta(+)-\delta(-)\}$ in Jørgensen's notation[13], and is defined by the equation $\delta=\frac{1}{2}\{\nu_k+\nu_l\}-\nu_{max}$, where ν_k and ν_l are the two frequencies where the formal extinction coefficients are equal to the half of ε_{max}.

*** Frequency difference between the maxima of the second and the first absorption band.

**** Difference between $\log \varepsilon_{max}$'s of the second and the first band.

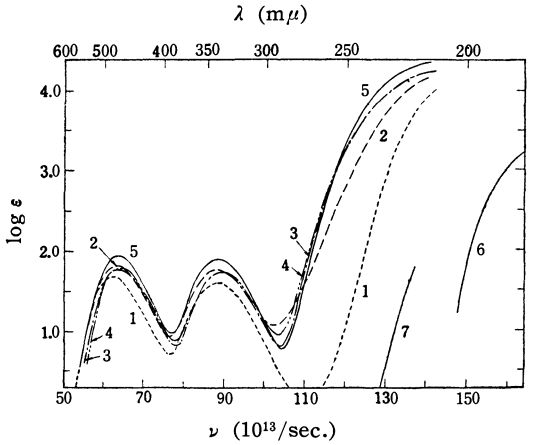

Fig. 1. Absorption curves of:
1, $[Co(NH_3)_6](ClO_4)_3$;
2, $[Co\ en(NH_3)_4](SO_4)_{1\frac{1}{2}}\cdot 2H_2O$;
3, *trans*-$[Co\ en_2(NH_3)_2](ClO_4)_3\cdot H_2O$;
4, *cis*-$[Co\ en_2(NH_3)_2](ClO_4)_3\cdot H_2O$;
5, $[Co\ en_3](ClO_4)_3$;
6, NH_3[11];
7, en[12].

From these data, the following conclusions are drawn.

i) Ethylenediamine has a higher position in the spectrochemical series [16,17] than that of ammonia.

ii) The successive substitution of ammonia molecules by ethylenediamine causes somewhat irregular shifts of band maxima. The change of the intensity by such a substitution is also irregular. Thus, for example, the first band of $[Co\ en(NH_3)_4]^{3+}$ is higher than that of *cis*- and *trans*-$[Co\ en_2(NH_3)_2]^{3+}$.

iii) The first or the second band of *cis*-$[Co\ en_2(NH_3)_2]^{3+}$ are at shorter wave lengths than those of the corresponding *trans* isomer. This fact coincides very well with the general rule which was reported previously by the present author[18].

iv) Generally speaking, the half-value width and the inclination parameter[14] are in the order of

$$trans\text{-}(NH_3)_2 > (NH_3)_4 > cis\text{-}(NH_3)_2 > en_3 > (NH_3)_6 .$$

The larger half-value width and the larger inclination parameter of the first three members in the above series are possibly explained by the slight splitting of the bands owing to the lower symmetry of those ions.

v) For all the complexes studied, the intensity of the second band is lower than that of the first band.

vi) The mean value of the frequency difference between the maxima of the second and the first band, is 24.94×10^{13}/sec.

vii) The intense ultraviolet bands are perhaps due to the co-ordinated ammonia and ethylenediamine molecules. Roughly speaking, an additive nature can be seen in the intensities of these bands. But the quantitative curve analysis was abandoned since only a part of the long wave length side of the band is available.

11) H. Ley and B. Arends, *Z. physik. Chem.*, **B 17**, 177 (1932).
12) M. Linhard, *Z. Elektrochem.*, **50**, 224 (1944).
13) C. K. Jørgensen, *Acta. Chem. Scand.*, **8**, 1495 (1954).
14) Y. Shimura and R. Tsuchida, This Bulletin, **28**, 572 (1955).
15) H. Siebert and M. Linhard, *Z. physik. Chem.* N. F., **11**, 318 (1957).
16) R. Tsuchida, This Bulletin, **13**, 388, 436 (1938).
17) Y. Shimura and R. Tsuchida, This Bulletin, **29**, 311 (1956).
18) Y. Shimura, This Bulletin, **25**, 49 (1952).

Experimental

Ethylenediamine - tetrammine - cobalt(III) Sulfate Tetrahydrate, [Co en $(NH_3)_4]_2$ $(SO_4)_3 \cdot 4H_2O$—Ten grams of *trans*-[Co en $(NH_3)_2$ $Cl_2]Cl \cdot \frac{1}{2}H_2O$[3] is dissolved in 100 ml. of warm water and to this solution 10 g. of potassium thiocyanate in 20 ml. of water is added. The resulting green mixture is heated for 20 min. at 75~80°C on a water bath and for more 3 min. at 85°C. The dark red mixture is allowed to cool and acidified by a few drops of dilute sulfuric acid. Fifty milliliters of 30% hydrogen peroxide is next added drop by drop to the mixture. After being allowed to stand for several hours, the resulting dark orange solution is concentrated to about 75 ml. by evaporation, and cooled. Twenty five milliliters of dilute sulfuric acid and 150 ml. of ethanol is added to the solution. The crude complex separates in voluminous precipitates. The product is treated with a small amount of water and any less soluble materials are filtered off. Ethanol-water mixture is then added to the filtrate. The desired complex precipitates as orange-colored plates. The crystals were washed by ethanol and dried in air. For purification, the salt was recrystallized from ethanol-water mixture. The yield was 7 to 8 g. (about 50~60%). The crystals effloresced on exposure to the air. The crystals freshly dried were analyzed for water of crystallization. The analyses for the other components were performed by making use of the salts dehydrated at 100~110°C.

Anal. Found: H_2O, 9.93%. Calcd. for $[Co(C_2H_8N_2)(NH_3)_4]_2(SO_4)_3 \cdot 4H_2O$: H_2O 9.84%.

Found: Co, 17.7; C, 7.29; H, 6.16; SO_4^{--}, 43.83%. Calcd. for $[Co(C_2H_8N_2)(NH_3)_4]_2(SO_4)_3$: Co, 17.79; C, 7.25; H, 6.09; SO_4^{--}, 43.50%.

Ethylenediamine - tetrammine - cobalt(III) Bromide Monohydrate, [Co en $(NH_3)_4]Br_3 \cdot H_2O$—A solution of the above sulfate is treated with a solution of the equivalent amount of barium chloride and the resulting barium sulfate is filtered off. The filtrate is concentrated by evaporation. To this solution solid ammonium bromide is added. The desired bromide monohydrate separates as orange prismatic crystals. They are recrystallized from water containing a small amount of ethanol, washed with ethanol and dried in air.

Anal. Found: Br, 53.38; H_2O, 3.64%. Calcd. for $[Co(C_2H_8N_2)(NH_3)_4]Br \cdot H_2O$: Br, 53.88; H_2O, 4.05%.

The corresponding chloride, [Co en $(NH_3)_4]Cl_3 \cdot xH_2O$ was also prepared, but its purification was impractical because it is very soluble in water or in water-ethanol mixtures.

Absorption and Rotation Measurements.—The absorption measurements were made in aqueous solutions by a Beckman DU Spectrophotometer at room temperature. The concentration of the solutions varied from 1.0×10^{-2} to 1.0×10^{-4} gram complex-ion per liter. The measurements of optical rotation were made by a Rudolph photoelectric spectropolarimeter, Model 200S-80.

Summary

A new cobalt(III) luteo ion, [Co en $(NH_3)_4]^{3+}$, has been prepared by the hydrolytic oxidation of [Co en $(NH_3)_2$ $(NCS)_2]^+$. The sulfate and the bromide of the new complex ion have been isolated. Several attempts to resolve the ion were unsuccessful.

The visible and the ultraviolet absorption spectra of all the members of the cobalt(III) ammine-ethylenediamine series have been measured and discussed.

The author wishes to thank Professor R. Tsuchida for his kind guidance throughout this work.

Department of Chemistry, Eaculty of Science, Osaka University, Kita-ku, Osaka

Studies on the Cobalt(III) Complexes Containing Only One Chelate Ring. III[1]. *Rotatory Dispersion of Tetrammine-l-leucinato-cobalt(III) Perchlorate,* $[Co(NH_3)_4(l\text{-}leuc)](ClO_4)_2$[2]

By Yoichi SHIMURA

(Received December 10, 1957)

It is well known that optically active complexes of cobalt(III) or chromium(III) exhibit very marked anomalous rotatory dispersion in the vicinity of their first absorption bands. In some cases, the curve of the anomalous rotatory dispersion is typical and has a point-symmetrical shape. In the present paper, such a point-symmetrical dispersion will be named as "inversive dispersion". In other cases, the rotatory dispersion is intricate and "anomalous" in the literal sense of the word. This "anomalous" rotatory dispersion, however, may be analyzed into two or more typical inversive dispersions as will be shown below.

The above results have been obtained mainly from the studies on the complexes of the $[M(AA)_3]$-[3] or $[M(AA)_2BC]$-type[4], in which the asymmetry is around the central metallic ion. As to the complexes, in which the asymmetric center is at the atom in the co-ordinated ligand, the studies of Lifschitz[5] and Pfeiffer et al.[6] have been reported. These authors stated that no anomalous rotatory dispersion occurred in the complexes having the asymmetric center far apart from the central metallic ion and that the anomalous rotatory dispersion might be produced by the so-called "vicinal effect" provided that the asymmetric center and the central metallic ion were so close to interact each other. The experimental evidences for the above claim, however, have scarcely ever been obtained.

In the present paper the rotatory dispersion of $[Co^{III}(NH_3)_4(l\text{-leuc})]^{2+}$* will be studied in the vicinity of its first and second absorption band. In this uni-chelate complex the asymmetric center is only on a carbon atom of the ligand leucinate ion. As a result of the measurements and the analyses of the rotatory dispersion curves, the existence of the "vicinal effect" between the central cobalt atom and the asymmetric carbon atom will be clarified.

Experimental

Tetrammine-*l*-leucinato-cobalt(III) Perchlorate, $[Co(NH_3)_4(l\text{-leuc})](ClO_4)_2$—This new compound was prepared by a modification of the method which was described in the part I of the present series for the syntheeses of the corresponding glycinato or alaninato complexes[7]. One gram of anhydrous sodium carbonate and 3.5 g. of *l*-leucine were dissolved in 60 ml. of hot water. To this solution were added 7.4 g. of $[Co(NH_3)_4(OH_2)Cl]SO_4$[8], 2 g. of decolorizing charcoal and 5 ml. of aqueous ammonia (30%). The resulting mixture was evaporated on a water bath almost to dryness. The residue was treated with about 50 ml. of warm water and insoluble materials** were filtered off by suction. After cooling, a large amount of 95% ethanol was fractionally added to the filtrate. First, about 2 g. of $[Co(NH_3)_6]SO_4 \cdot Cl \cdot 3H_2O$, and then the impure sulfate of the desired complex were precipitated. For purification the impure sulfate was converted into the perchlorate as follows. The impure sulfate was dissolved in a small quantity of water and was treated with an equivalent amount of barium chloride solution and the resulting barium sulfate was filtered off. To the filtrate, sodium perchlorate and ethanol were added and the solution was evaporated in vacuo over sulfuric acid. The desired perchlorate was separated as light red crystals. This was recrystallized from water-ethanol mixture by evaporation over sulfuric acid. The yield was very small (not exceed one g.).

Anal. Found: C, 15.90; H, 5.35; Cl, 15.40%. Calcd. for $C_6H_{24}O_{10}N_5Cl_2Co$: C, 15.80; H, 5.30; Cl, 15.55%.

1) Part II of This series: Y. Shimura, This Bulletin, **31**, 311 (1958).
2) Presented at the Symposium on Co-ordination Compounds, Nagoya, November 16, 1957.
3) J.-P. Mathieu, *J. chim. phys.*, **33**, 78 (1936).
4) J.-P. Mathieu, *Bull. soc. chim. France*, [5] **3**, 476 (1936).
5) I. Lifschitz, *Z, physik. Chem.*, **105**, 27 (1923); **114**, 485 (1925).
6) P. Pfeiffer, W. Christeleit, T. Hesse, H. Pfitzner and H. Thielert, *J. prakt. Chem.*, **150**, 261 (1938).
* The following abbreviations are used: gly, $NH_2CH_2CO_2^-$; alan, $NH_2CH(CH_3)CO_2^-$; leuc, $NH_2CH(CO_2^-)CH_2CH(CH_3)_2$.
7) Y. Shimura, This Bulletin, **31**, 173 (1958).
8) S. M. Jörgensen, *J. prakt. Chem.*, **42**, 211 (1890).
** This is a mixture of decolorizing charcoal and two geometrical isomers (pink and reddish violet) of $[Co^{III}(l\text{-leuc})_3]$.

TABLE
SUMMARY OF

Complexes	Inversive rotatory dispersion		
	Center of inversion[a]	Sign of Cotton effect	Degree of rotation[b]
$[Co(NH_3)_4$ (*l*-leuc)$]^{2+}$	Ia: 59.6 Ib: 65.6	+ −	320° 650°
d-$[Co\ en_2\ (NH_3)Cl]^{2+}$	Ia: 54.6 Ib: 63.4	+ +	580° 390°
d-$[Co\ en_2$ (*l*-leuc)$]^{2+}$	59.5	+	ca. 5000°
d-$[Co\ en_3]^{3+}$	61.2	+	ca. 4000°

a) These values are given by the unit of 10^{13}/sec.

d-$[Co\ en_2$ (*l*-leuc)$]Cl_2$—This was prepared and resolved by the method of Lifschitz[9] with reference to Mathieu's report[10].

d-$[Co\ en_2\ (NH_3)Cl]Br_2$—This was prepared and resolved by Werner and King's method[11].

d-$[Co\ en_3]Br_3 \cdot 2H_2O$—For the resolution Werner's method[12,13] was followed.

Measurements of Rotatory Dispersion and Absorption Spectra.—The rotatory dispersion measurements were made in aqueous solutions by a Rudolph photoelectric spectropolarimeter, Model 200S—80. The concentration of the solution was 1.0×10^{-3} gram complex-ion per liter. The absorption measurements were made by a Beckman DU spectrophotometer. All the measurements were made at room temperature.

Results and Discussion

The rotatory dispersion curve and the absorption curve of $[Co(NH_3)_4$ (*l*-leuc)$](ClO_4)_2$ are shown in Fig. 1. For comparison, similar measurements were also made for *d*-$[Co\ en_2$ (*l*-leuc)$]Cl_2$, *d*-$[Co\ en_2\ (NH_3)Cl]Br_2$ and *d*-$[Co\ en_3]Br_3 \cdot 2H_2O$ (Figs. 2—4). The numerical data for these measurements are summarized in Table I.

From the Figs. 1—4, it is seen that all the four complexes studied exhibit the remarkable change of rotation in the region of the first absorption bands. On the other hand, there have been found few indications of such anomalous rotatory dispersion in the region of their second absorption bands. This fact coincides with the observations reported heretofore by Mathieu[3], Kuhn and Bein[15], Tsuchida[16] and Kobayashi[17] for many cobalt(III) or chromium(III) complexes.

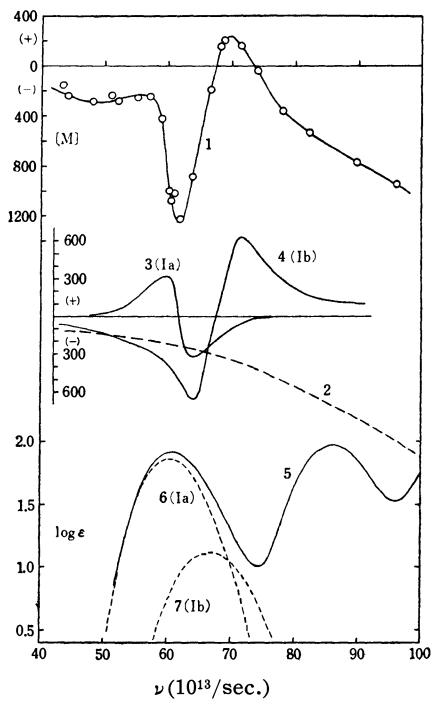

Fig. 1. Rotatory dispersion and absorption of $[Co(NH_3)_4$ (*l*-leuc)$](ClO_4)_2$:
1, rotatory dispersion curve; 2~4, curve analyses of the rotatory dispersion curve; 5, absorption curve; 6~7, curve analyses of the first absorption band.

The shape of the rotatory dispersion curve of $[Co(NH_3)_4$ (*l*-leuc)$]^{2+}$ in its first absorption band suggests that an overlapping of two inversive dispersions occurred. As a result of a tentative curve analysis, it was shown that the experimental dispersion curve (1) was well reproduced by

9) I. Lifschitz, *Rec. trav. chim.*, **58**, 785 (1939).
10) J.-P. Mathieu, *Bull. soc. chim. France*, [5] **6**, 873 (1939).
11) A. Werner and V. L. King, *Ber.*, **44**, 1887 (1911).
12) A. Werner, *Ber.*, **45**, 121 (1912).
13) D. H. Busch, *J. Am. Chem. Soc.*, **77**, 2747 (1955).
14) Y. Shimura and R. Tsuchida, This Bulletin, **28**, 572 (1955).
15) W. Kuhn and K. Bein, *Z. anorg. Chem.*, **216**, 321 (1934).
16) R. Tsuchida, *J. Chem. Soc. Japan* (*Nippon Kagaku Zassi*), **58**, 621 (1937).
17) M. Kobayashi, ibid., **64**, 648 (1934).
18) J.-P. Mathieu, *Bull. soc. chim. France*, [5] **5**, 105 (1938).

I

MEASUREMENTS

First absorption band				Second absorption band			
ν_{max}[a]	log ε_{max}	Half-value width[a]	Inclination parameter[14),a]	ν_{max}[a]	log ε_{max}	Half-value width[a]	Inclination parameter[14),a]
60.8	1.90	11.3	0.55	86.1	1.97	12.5	0.35
Ia: 57.0	1.85	10.2	0.5	82.7	1.90	12.4	0.3
Ib: 65.6	1.38	11.8	0.5				
61.5	2.02	11.3	0.65	86.1	2.06	12.4	0.5
63.9	1.94	10.4	0.55	88.4	1.90	12.0	0.4

b) The difference between the maximum and the minimum value of the partial inversive rotatory dispersion was halved.

TABLE II

ABSORPTION MAXIMUM AND THE CENTER OF INVERSIVE ROTATORY DISPERSION

Complex ion	ν_{rot}	ν_{abs}	$\nu_{abs}-\nu_{rot}$	Ref.
d-[Co en_3]$^{3+}$	61.2	63.9	+2.7	*
l-[Co ox_3**]$^{3-}$	48.8	50.2	+1.4	15
d-[Co en_2 ox]$^{+}$	57.7	60.0	+2.3	4
d-[Co en_2 CO_3]$^{+}$	57.0	59.0	+2.0	4
d-[Co en_2 $(NH_3)_2^{(1)}_{(2)}$]$^{3+}$	60.4	64.4	+4.0	4
l-[Co en_2 gly]$^{2+}$	58.8	61.4	+2.6	10
d-[Co en_2 (*d*-alan)]$^{2+}$	59.2	61.9	+2.7	10
l-[Co en_2 (*l*-phenylalan)]$^{2+}$	59.0	61.7	+2.7	10
d-[Co en_2 (*d*-val***)]$^{2+}$	59.3	61.8	+2.5	10
d-[Co en_2 (*l*-leuc)]$^{2+}$	59.5	61.5	+2.0	*
d-[Co en_2 (NO_2) $(OH_2)^{(1)}_{(2)}$]$^{2+}$	59.0	65.1	+6.1	4
l-[en_2 Co$\langle^{NH_2}_{O_2}\rangle$Co en_2]$^{4+}$	60.9	64.3	+3.4	18
d-[Co en_2 $(NH_3)Cl^{(1)}_{(2)}$]$^{2+}$	Ia: 54.6	57.0	+2.4	*
	Ib: 63.4	65.6	+2.2	*
d-[Cr en_3]$^{3+}$	64.9	65.5	+0.6	3
d-[Cr ox_3]$^{3-}$	54.3	52.6	−1.7	3
d-[Cr en_2 ox]$^{+}$	62.5	63.0	+0.5	4

ν_{rot}: Center of inversive rotatory dispersion (10^{13}/sec.).
ν_{abs}: Absorption maximum (10^{13}/sec.).
* New measurement by the present author. ** ox stands for oxalate ion.
*** val stands for valinate ion.

the overlap of the curves (2), (3) and (4). Thus it was concluded that the first absorption band of this complex showed two inversive dispersions, the one of which had positive Cotton effect and the other negative Cotton effect.

Since the complex ion, [Co$(NH_3)_4$ (*l*-leuc)]$^{2+}$, belongs to the type of [CoN_5O], it is expected that its first absorption band splits into two components, Ia and Ib. Therefore, the two inversive dispersions above obtained probably correspond to the two components of the first absorption band.

A survey of the data for the cobalt(III) or chromium(III) complexes, which are found in literature as well as in the present author's measurements, revealed that the center of inversion of the rotatory dispersion was almost always in the longer wave-length region as compared with the position of the absorption maximum (Table II). Taking this fact into consideration, a tentative curve analysis was made to separate the two components of the first absorption band of [Co$(NH_3)_4$ (*l*-leuc)]$^{2+}$. In the analyses of the absorption curves, the experimental equation was used, which was recently developed by the present author[14]. The results are shown in Fig. 1. The similar curve analyses of the rotatory dispersion curve and the absorption curve were performed for *d*-[Co en_2 $(NH_3)Cl^{(1)}_{(2)}$]$^{2+}$ (Fig. 2). In this case the two inversive dispersions

Ia and Ib have equally the positive sign of the Cotton effect. This coincides very well with the results of direct measurement of the Cotton effect (circular dichroism) by Mathieu[4].

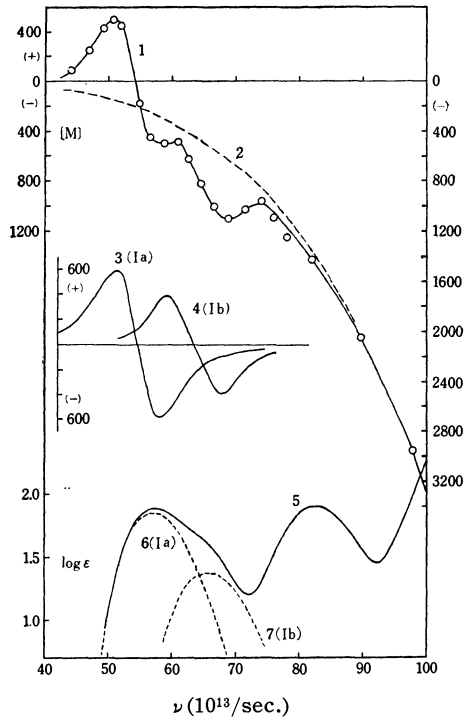

Fig. 2. Rotatory dispersion and absorption of *d*-[Co en$_2$ (NH_3)Cl]Br_2:
1, rotatory dispersion curve: 2~4, curve analyses of the rotatory dispersion curve; 5, absorption curve; 6~7, curve analyses of the first absorption band.

On the basis of the facts above discussed it is concluded that, so far as the first absorption band is concerned, the so-called "vicinal effect" exists between the cobalt atom and the asymmetric carbon atom C* in the structure of

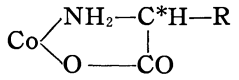

In contrast with $[Co(NH_3)_4$ (*l*-leuc)$]^{2+}$, no evidence was obtained for the overlap of two or more inversive dispersions in *d*-[Co en$_2$ (*l*-leuc)]Cl_2 (Fig. 3). The rotatory dispersion of the latter compound, as well as that of *d*-[Co en$_3$]$^{3+}$ (Fig. 4), has a typical shape of a single inversive dispersion. The reason for this difference between the *bis*-ethylenediamine complex

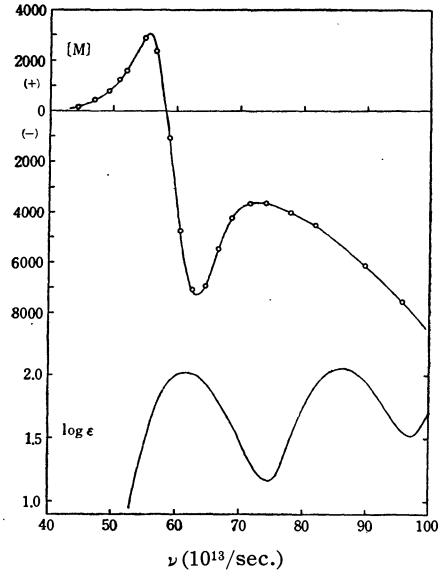

Fig. 3. Rotatory dispersion and absorption of *d*-[Co en$_2$ (*l*-leuc)]Cl_2.

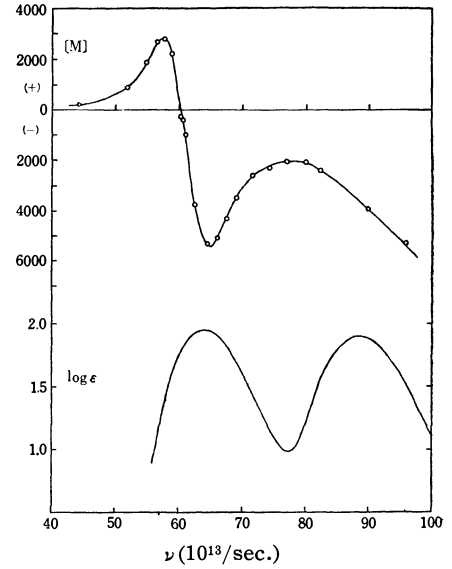

Fig. 4. Rotatory dispersion and absorption of *d*-[Co en$_3$]$Br_3 \cdot 2H_2O$.

and the tetrammine complex is unknown. It should be added, however, that the degree of rotation is extraordinarily greater in the *bis*-ethylenediamine complex than in the tetrammine complex. It is probable that the asymmetry around the central cobalt atom contributes more profoundly to the rotatory power of the region of the first absorption band than the asymmetric carbon atom in the co-ordinated ligand.

Summary

A new complex compound, $[Co^{III}(NH_3)_4(l\text{-leuc})](ClO_4)_2$, has been prepared, in which the asymmetric center is only on a carbon atom of the ligand leucinate ion. From the measurements of the visible and the ultraviolet rotatory dispersion of this compound, it has been concluded that the so-called "vicinal effect" exists between the cobalt atom and the asymmetric carbon atom.

The rotatory dispersion measurements have also been made for *d*-[Co en_2 (*l*-leuc)]Cl_2, *d*-[Co en_2 $(NH_3)Cl^{(1)}_{(2)}$]Br_2 and *d*-[Co en_3]$Br_3 \cdot 2H_2O$. On the basis of these data the relation of the splitting of the first absorption band with the so-called anomalous rotatory dispersion has been discussed. Thus it has been shown that the anomalous rotatory dispersion of $[Co(NH_3)_4(l\text{-leuc})]^{2+}$ or of [Co en_2 (NH_3) $Cl]^{2+}$ is explicable by assuming the overlap of the two inversive dispersions, Ia and Ib, which correspond to the component bands, Ia and Ib, of the split first absorption band.

In agreement with the observations by several previous authors, it has been shown that all the complexes studied scarecely show the anomalous rotatory dispersion in the vicinity of their second absorption bands.

The author wishes to thank Professor R. Tsuchida for his kind guidance throughout this work.

Department of Chemistry, Faculty of Science, Osaka University
Kita-ku, Osaka

The Dielectric Properties of Thiacyclohexane

By Seiichi KONDO and Masaru MATSUMOTO

(Received November 28, 1957)

The thermodynamic properties of thiacyclohexane were studied by J.P. McCullough and others[1] and it was shown that the entropy of fusion of this material is 2.002 e.u. at 292.25°K. They also found three phase transitions at 240.02°K, 207°K and 201.4°K. One of the present writers studied the structure of high crystalline modification of this material by means of X-rays[2]. According to his result, this high modification is in a disordered state in respect to the molecular orientation on the lattice site, and it was suggested that the high thiacyclohexane belongs to the category of the plastic crystals. This material shows a similar thermodynamic behavior and crystal structure with those of high cyclohexane, in spite of the fact that thiacyclohexane has the lower molecular symmetry, C_s, than that of cyclohexane, D_{3d}, and also has the permanent dipole moment of about 1.7 D. The investigation of the dielectric properties of this material will be interesting and may give more information than the study of non-polar compounds can provide, for the purpose of clarifying further details of the structure of high thiacyclohexane and of obtaining the informations of some properties of other phases. From this point of view the authors carried out the dielectric measurement of this material and found some interesting results on the rotational mechanism of the molecule in the crystalline phases of this material.

Experimentals

The electric circuit for the dielectric measurement is an audio-frequency transformer bridge described elsewhere[3]. The frequencies used for the measurement range from 100 to 3×10^4 c.p.s. The electric condenser for the measurement of the sample consists of platinum electrodes sealed in a soft glass cell in order to keep the sample between the electrodes under low pressure without exposure to air, as illustrated in Fig. 1. This cell can keep about 0.5 cc. of the sample and its electric capacity is about 0.2 p.f. in vacuum. It is enclosed in a copper block with the drying agent such as silica gel and is dipped in liquid air or in an oil bath. The dielectric constant

1) J.P. McCullough, et al., *J. Am. Chem. Soc.*, **76**, 261 (1954).

2) S. Kondo, This Bulletin, **29**, 999 (1956).

3) S. Kondo and T. Oda, ibid., **27**, 567 (1954).

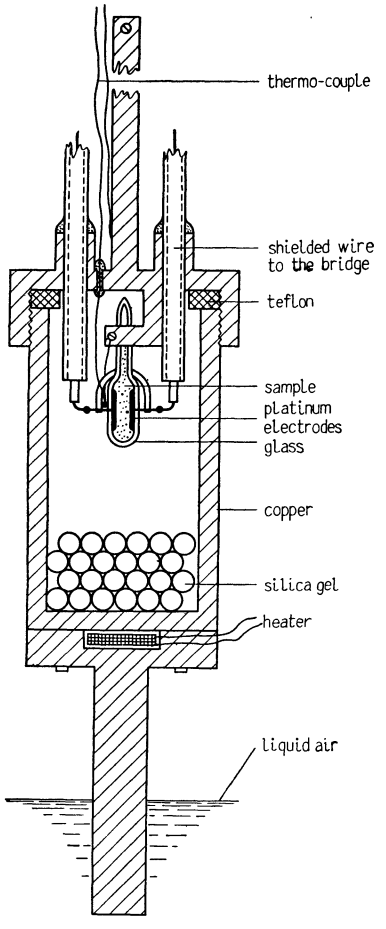

Fig. 1. The cell for the measurement of the dielectric constant of the sample.

of the sample can be determined by the comparison with those of purified benzene, carbon disulphide and ethyl ether. The sample was sent from the U.S. Bureau of Mines[4]. The purity of the sample thus received was stated to be 99.99 per cent. This sample was sublimed and sealed in the cell in Fig. 1. All these procedures were carried out without exposure to air or day light. The liquid in the cell is cooled very slowly at the freezing point, in order to avoid the formation of voids or cracks during the solidification of the sample. The temperature of the sample can be maintained constant within $\pm 0.1°$ for each set of observations with various frequencies. The dielectric constant of thiacyclohexane is shown in Fig. 2. There exist four condensed phases in this figure: liquid, solid phase III, solid phase II, and solid phase I according to the notation by McCullough and

4) This sample of thiacyclohexane was provided by the American Petroleum Institute Research Project 48 on "the production, isolation and purification of sulfur compounds and measurement of their properties" and were prepared and purified at the Petroleum and Oil Shale Experiment Station, U. S. Bureau of Mines, Laramie, Wyoming, U.S.A.

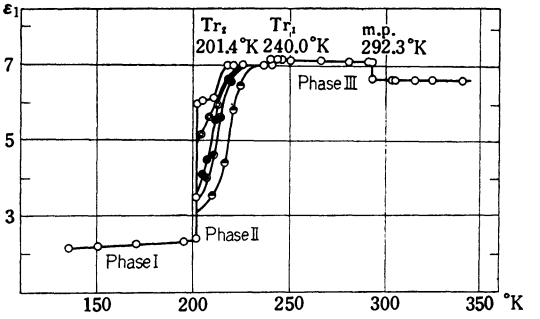

Fig. 2. The static dielectric constant of thiacyclohexane. The frequencies used for the measueement were 30 (◔), 10 (◉), 3 (●), 1 (◎), 0.1 (○) k.c.p.s.

others[1]. The dielectric interpretations of this curve as well as of the dielectric loss data will be made in the following sections.

Results and Discussion

Liquid and Solid Phase III.—The permanent electric dipole moment of thiacyclohexane in the liquid phase can be calculated by using the Onsager equation for pure polar liquid and is equal to 1.7 D. This value is equal to the dipole moment of this molecule estimated with the bond moment C—S, 1.4 D[5], and the valence angle C—S—C, 105°[1]. No dispersion phenomena were observed in the liquid phase.

In the solid phase III which is considered to be plastic, the dielectric constant measured may not include experimental errors which may arise from voids or cracks since the melt is solidified so carefully that repeated solidifications show the same value of the solid dielectric constant and no cracks or voids were assured visually. The dipole moment of thiacyclohexane in the plastic phase can be calculated by using the Onsager equation[6] and will give the same value as that in the liquid phase. This agreement seems to mean that the molecules in phase III behave in a manner roughly similar to those in the liquid phase except the fact that the molecules in the plastic phase are on the regular face-centered cubic lattice site. This dielectric interpretation is in good agreement with the result of thermodynamic[1] and X-ray[2] study of this material in the sense that these investigations revealed the very

5) G.C. Hampson, R.H. Farmer and L.E. Sutton, *Proc. Roy. Soc.* **A143** 147 (1933).

6) S. Kondo, *Memory of Osaka University of Liberal Arts and Education*, No. 6 (1957) (in press).

high disorder of molecular orientation in the phase III. In view of the existence of the relaxation phenomenon in phase II, there seems to be the molecular rotation with possibly smaller relaxation times and higher degree of rotational freedom, although in these two phases (the liquid phase and the phase III), there has been observed no relaxation phenomenon within the present frequency range. The value of dielectic loss, $\tan\delta$, is approximately equal to 3×10^{-4}.

Solid Phase II.—As seen in Fig. 2, The static dielectric constant of thiacyclohexane decreases by small amount from phase III to phase II at the transition point 240°K. The reason for this decrease could be either in the formation of many cracks during the phase transition which might decrease the apparent value of dielectric constant or in the intrinsic decrease of the dielectric constant in this phase II. Since no crystallographic or density data are available, it is impossible to decide which effect is more responsible for the decrease of the observed dielectric constant. However it may be supposed that the dipolar contribution still remains to some extent in this phase II, because the amout of change in the dielectric constant is comparatively small.

The low frequency dielectric dispersion was found in this phase. The Cole-Cole arcs are shown in Fig. 3 at 209.5° and

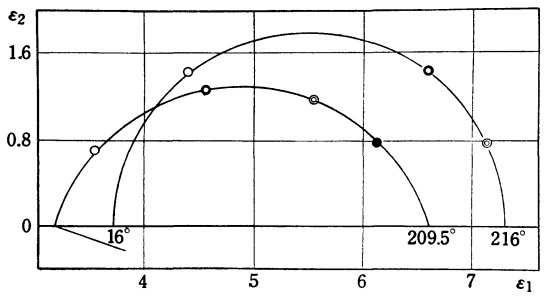

Fig. 3. The Cole-Cole plot of the dielectric relaxation of thiacyclohexane in the solid phase from 201.4°K to 200.02°K. The frequencies used are 30 (○), 10 (○), 3 (◎), and 1 (●) k.c.p.s.

216°K. At a higher temperature, the high frequency side more than 30 k.c.p.s. was not measured and the Cole-Cole arcs were drawn by the extrapolation. The relaxation times τ were obtained from these arcs at various temperatures and these values range from 3×10^{-6} to 6×10^{-5} sec. The $\ln\tau$ vs. reciprocal temperature curve is shown in Fig. 4. The activation energy of this relaxation phenomenon is calculated

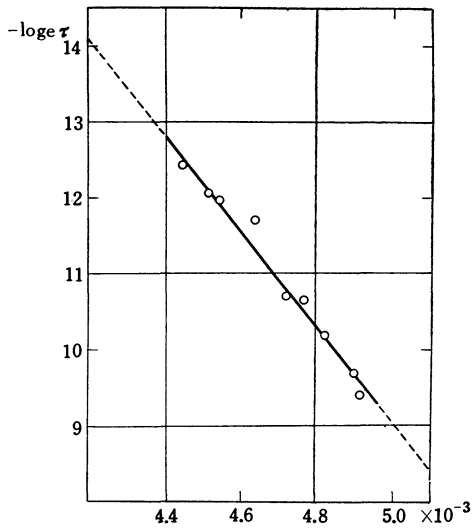

Fig. 4. The relaxation times vs. reciprocal temperature curve of thiacyclohexane.

from this curve to be 13.22 kcal. per mole and $\tau_0=5.75\times10^{-19}$ sec. This value of activation energy seems to be relatively greater than those which were found in such plastic crystals as *d*-camphor[7] and cyclohexane[8], determined by the dielectric and nuclear magnetic resonance experiments respectively, and which are considered to have the origin in the molecular rotations.

The radii of the Cole-Cole arcs seem to increase at higher temperatures. The Onsager equation for pure polar liquid can be modified to the following expression for the mixed case such as one consisting of a rotator component and a non-rotator component of the same one molecular species[9]. That is,

$$N_1=\frac{9kT}{4\pi\mu^2}\frac{(\varepsilon_s-\varepsilon_\infty)(2\varepsilon_s+\varepsilon_\infty)}{\varepsilon_s(\varepsilon_\infty+2)^2},$$

where μ and N_1 are the dipole moment and the number of the rotating molecules per c.c. respectively, k is the Boltzman constant and T is the absolute temperature. If it is assumed that the thiacyclohexane molecules began to rotate with some degree of rotational freedom with the activation energy 13.22 kcal. per mole, whose diople moment was constant, and if the density of this solid phase II were constant in

7) J.G. Powles, *J. Chem. Phys.*, **20**, 148 (1952).
8) E.R. Andrew and R.G. Eades, *Proc. Roy. Soc.*, **A216**, 398 (1953).
9) Refer, for instance, H. Fröhlich, "Theory of Dielectrics", Oxford (1949), p 36.

this dispersion region, the increase of the Cole-Cole arc radii might mean the increase of N_1. Therefore one may think that the number of rotating molecules would increase by temperature elevation and thus there would appear the order-disorder state during the process of the increase of N_1. This dielectric interpretation seems to be in good agreement with the thermal study by McCullough and others[1]. They found the λ type heat anomaly which will be the transition of higher order. The crystal structure analysis of this phase will make these discussions clearer.

Phase I.—The dielectric constant drops to a very small value at the transition point 201.4°K by cooling. There is no dielectric dispersion in the present frequency range in this phase I. The value of the dielectric constant in this phase lies in the range of the square of the optical refractive index and thus there seems to exist only the contribution of atomic and electronic polarizability to the dielectric constant. In other words, there seems to be no dipole rotation or disorder of dipolar orientation of molecules on the lattice sites in this phase.

Summary

1) The molecules are in the rotational states in the solid phases II, III and liquid phase, and not in the phase I.

2) There is an order-disorder transition in phase II which may have its origin in the molecular dipole rotation.

3) The dielectric behavior in phase III is similar to that of other polar plastic crystals.

The writers wish to express their thanks to Dr. John P. McCullough for his useful discussions and also for his kindness to supply pure thiacyclohexane.

Osaka University of Liberal Arts and Education, Tennoji-ku, Osaka

Bond Localization and the Hyperconjugative Effect in the Aromatic Carbonium Ions. I. Absorption Spectra of Benzenium-, Toluenium-, and Mesitylenium- Ions[1]

By Toshifumi MORITA

(Received December 14, 1956)

Reid's measurements of the absorption spectra of methylbenzenes in anhydrous hydrogen fluoride-boron trifluoride indicate that the bands of the longest wave length which Reid attributed to those of carbonium ions of methylbenzenes shift toward violet with the increasing number of methyl substituents[2]. To investigate this phenomenon theoretically seems to be of much interest. In performing the theoretical treatment on these carbonium ions, it should be taken into account, whether the hyperconjugation takes place or not between the aromatic ring and the H_2 group constructed by the attached proton together with the hydrogen atom already present at the position of proton attack in the ring. Under the assumption of localization of the H_2—C bond with respect to the conjugated part of molecules, Gold and Tye[3] have calculated the π-electron energies of the carbonium ions of many hydrocarbons and have suggested the order of base strengths of hydrocarbons[4]. Heilbronner and Simonetta[5] have also carried out similar computations on azulenium- and methyl azulenium- ions from the standpoint of the same hypothesis. In addition, it seems to be reasonable that these carbonium ions correspond to the transition state intermediates in the electrophilic substitution reactions from the fact that in methylbenzenes, a parallel relation exists between the equilibrium constants for the carbonium ion

1) As to the review on the experimental results, see, L. J. Andrews, *Chem. Revs.*, **54**, 713 (1954).
2) C. Reid, *J. Am. Chem. Soc.*, **76**, 3264 (1954).
3) V. Gold and F. L. Tye, *J. Chem. Soc.*, **1952**, 2184.
4) For polymethyl benzenes which are the objects of the present study, calculations have not been carried out.
5) E. Heilbronner and M. Simonetta, *Helv. Chim. Acta*, **35**, 1049 (1952).

formation and the rates of substitution in the electrophilic substitution reactions, with respect to the number of methyl substituents in the aromatics[6], and moreover the bond localization theory has gained much success in the interpretation of chemical reactivities[7-10], so that in the case of the aromatic carbonium ion also, the bond localization hypothesis will have much importance in the consideration of its behavior. On the other hand, Muller, Pickett, and Mulliken[11] have discussed the hyperconjugative effect of the H_2 group, and explained the absorption spectra of the benzenium ion. Generally speaking, it may be desirable to take the hyperconjugative effect of the H_2 quasi-atom into consideration. In the following, consequently, the experimental blue shifts are treated by the theoretical computation for benzenium-, toluenium- and mesitylenium- ions, using the semi-empirical LCAO MO method, from the point of the localization, on the one hand, and of the hyperconjugation, on the other, of the H_2—C bond.

Method of Calculation

Molecular Models. — The molecular models and the numbering in the present calculations are shown in Fig. 1 for the hyperconjugation and in Fig. 2 for the bond localization, in both cases (a), (b), and (c) being benzenium, toluenium, and mesitylenium ions, respectively. The attached proton at position 2 in the ring constructs the quasi-atom H_2 together with the hydrogen atom already present there, which takes part in hyperconjugation

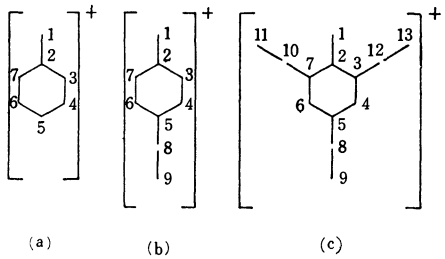

Fig. 1. Molecular models for the hyperconjugation.

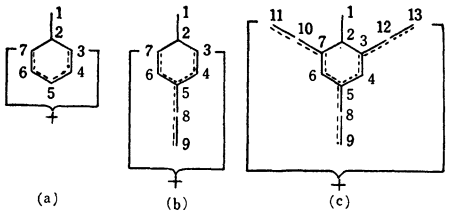

Fig. 2. Molecular models for the bond localization.

with the aromatic ring for the hyperconjugation model, but not for the bond localization one. The symmetry group to which these ions belong is C_{2v}. As for toluenium ion, there are other different models depending on the position at which proton attaches to the ring with respect to the methyl substituent, but only the C_{2v} type is adopted, because the selection rule is not applied to the molecules having attached proton at ortho- or meta-position with regard to the carbon atom linking to the methyl substituent, on account of lack of symmetry; furthermore it seems not bad to adopt the C_{2v} type from the analogy of the *p*- (and *o*-) orienting effect of the methyl substituent in the electrophilic substitution reaction of toluene.

Inclusion of Overlap.—Effects of neglect and inclusion of overlap on the various quantities, such as π-bond order, π-electron density, dipole moment, resonance energy, hyperconjugation energy, and absorption wave length, have been discussed in the numerous hydrocarbons and heteromolecules. As regards bond lengths, dipole moments and resonance energies there are little differences between their magnitudes calculated with and without overlap[12-16]. Mulliken et al.[17] have found that explicit inclusion of overlap improves the agreement of the calculations with the observed hyperconjugation shift in the ultraviolet absorption spectra, and with hyperconjugation energies, whereas for these empirical data the calculations without overlap gain less success[18]. Consequently in the present treatment also, overlap integrals between adjacent atoms are included.

Molecular Orbitals and Secular Equations.—Molecular orbitals used are of the

6) H. C. Brown, and J. D. Brady, *J. Am. Chem. Soc.*, **74**, 3570 (1952).
7) G. W. Wheland, ibid., **64**, 900 (1942).
8) M. J. S. Dewar, *J. Chem. Soc.*, **1949**, 463.
9) C. A. Coulson, *Research*, **4**, 307 (1951).
10) R. D. Brown, *Quart. Rev.*, **6**, 63 (1952).
11) N. Muller, L. W. Pickett and R. S. Mulliken, *J. Chem. Phys.*, **21**, 1400 (1953); *J. Am. Chem. Soc.*, **76**, 477 0 (1954).
12) D. W. Davies, *Trans. Faraday Soc.*, **51**, 449 (1955).
13) T. H. Goodwin and V. Vand, *J. Chem. Soc.*, **1955**, 1683.
14) T. H. Goodwin, ibid., **1955**, 4451.
15) R. H. Knipe, *J. Chem. Phys.*, **23**, 2089 (1955).
16) G. W. Wheland, *J. Am. Chem. Soc.*, **63**, 2025 (1941).
17) R. S. Mulliken and C. A. Rieke, ibid., **63**, 1770 (1941).
18) R. S. Mulliken, C. A. Rieke and W. G. Brown, ibid., **63**, 41 (1941).

LCAO (linear combination of atomic orbitals) type $\psi_j=\sum_\mu x_{j\mu}\phi_\mu$, where ψ_j is the j'th MO (molecular orbital), ϕ_μ the AO (atomic orbital) on the μ'th atom, $x_{j\mu}$ the coefficient of the μ'th AO in the j'th MO, ψ_j. The energies of the π-electron levels are given by the roots of the secular equation[10,19],

$$|\beta_{\mu\nu}+S_{\mu\nu}\lambda_{\mu\nu}|=0,$$

where

$$\beta_{\mu\nu}=\gamma_{\mu\nu}-(1/2)S_{\mu\nu}(\alpha_\mu+\alpha_\nu),$$

$$S_{\mu\nu}=\int\phi_\mu\phi_\nu d\tau,$$

$$\lambda_{\mu\nu}=(1/2)(\alpha_\mu+\alpha_\nu)-\varepsilon_j,$$

and

$$\gamma_{\mu\nu}=\int\phi_\mu H\phi_\nu d\tau, \quad \alpha_\mu=\int\phi_\mu H\phi_\mu d\tau,$$

$$\varepsilon_j=\int\psi_j H\psi_j d\tau.$$

The coefficient of each atomic orbital in the molecular orbital is computed by solving linear equations under the normalization condition of the molecular orbital with the knowledge of the energy of the latter.

Assumptions and Choice of Semi-empirical Parameters. — In the semi-empirical method, appropriate values of the resonance and the Coulomb integrals must be chosen. As for the resonance integrals several authors[6,20,21] have used the assumption of the proportionality of the parameter γ to the overlap integral S. However, in the present work the parameter β introduced for the first time by Mulliken[22] is assumed proportional to S[23]. Values of overlap integrals are obtained from Mulliken et al.[24], and those used in the present calculation are like those in Table I. For the value of the corrected term δ for the Coulomb integral of H_3 or H_2, several authors have used the empirical values of -0.2[4,6,25-28] or -0.5[10,20,21]. The value used in the present work is -0.3 obtained by I'haya[29] through the theoretical calculations.

TABLE I
VALUES OF OVERLAP INTEGRALS USED IN THE PRESENT CALCULATIONS

Bonds	Values of overlap integrals
C—H_2 or C—H_3	0.541[a]
C_{methyl}—C_{arom}[b]	0.203[c]
C—C[d]	0.247

a). See, ref. 21), footnote 27. b). The bond between the methyl carbon and the neighboring carbon atom in the ring. c). The value corresponding to the interatomic distance of 1.51 Å. d). The bond between the adjacent carbon atoms in the benzene ring.

The choice of the auxiliary inductive parameter, δ_{ind}, for the Coulomb integral of the carbon atom with which the H_3 or H_2 quasi-atom binds is considerably arbitrary and its decision is essentially empirical, although Goodman and Shull[30] have pointed out the possibility of finding the reasonable values from the experimental transition- and ionization-energy shifts due to this effect. Various values of this parameter have been used, such as $\delta_{ind}/\delta=1/4\sim1/10$[31], $1/2$[25], $1/5$[20], $1/8$[32,33] and $1/3\sim1/5$[34]. In the present treatment $\delta_{ind}/\delta=1/3$ is used in accordance with many investigators' arguments[35-37]. The use of this parameter is limited to the case of the bond localization calculations.

The Hyperconjugation Energy

The hyperconjugation energy, for example, of benzenium ion, is obtained as follows. (1) The π-electron energies of the hyperconjugation and of the bond localization model are calculated. (2) The vertical hyperconjugation energy is obtained by subtracting the ground state π-electron energy of the hyperconjugation model from that of the bond localization one. (3) The correction of the compressional energies[38] is carried out assuming that the bonds are distorted harmonically, taking the values of force constants,

19) L. Lofthus, ibid., **79**, 24 (1957).
20) C. A. Coulson and V. A. Crawford, *J. Chem. Soc.*, **1953**, 2052.
21) Y. I'haya, This Bulletin, **28**, 376 (1955).
22) R. S. Mulliken, *J. chim. phys.*, **46**, 497 (1949).
23) R. S. Mulliken, ibid., **46**, 675 (1949).
24) R. S. Mulliken, C. A. Rieke, D. Orloff and H. Orloff, *J. Chem. Phys.*, **17**, 1248 (1949).
25) B. Pullman, M. Mayot and G. Berthier, ibid., **18**, 257 (1950).
26) H. C. Longuet-Higgins and R. G. Sowden, *J. Chem. Soc.*, **1952**, 1404.
27) C. A. Coulson, *Proc. Phys. Soc.*, **45**, 933 (1952).
28) H. H. Jaffé, *J. Chem. Phys.*, **20**, 778 (1952).
29) Y. I'haya, ibid, **23**, 1165 (1955).
30) L. Goodman and H. Shull, *J. Chem. Phys.*, **23**, 33 (1955).
31) G. W. Wheland and L. Pauling, *J. Am. Chem. Soc.*, **57**, 2086 (1935).
32) P. O. Löwdin, *J. Chem. Phys.*, **19**, 1323 (1951).
33) H. H. Jaffé, *J. Am. Chem. Soc.*, **76**, 3527 (1954).
34) Y. I'haya, *J. Chem. Soc. Japan, Pure Chem. Sec. (Nippon Kagaku Zassi)*, **77**, 314 (1956).
35) G. E. K. Branch and M. Calvin, "The Theory of Organic Chemistry" Prentice-Hall, Inc., New York, 1941.
36) V. Gold, *Trans. Faraday Soc.*, **46**, 326 (1950).
37) H. H. Jaffé, *J. Chem. Phys.*, **20**, 279, 778, 1554 (1952); **21**, 415 (1953); *J. Am. Chem. Soc.*, **77**, 274 (1955).
38) Lennard-Jones, *Proc. Roy. Soc.*, A **158**. 280 (1937); D. F. Hornig, *J. Am. Chem. Soc.*, **72**, 5772 (1950); C. A. Coulson, and S. L. Altmann, *Trans. Faraday Soc.*, **48**, 293 (1952).

TABLE II

ELECTRIC STATES AND TRANSITION PROCESSES

Carbonium ions	Ground state	Lowest excited state	Transition	Polarization
Benzenium	$(1b_1)^2(2b_1)^2(1a_2)^2$	$(1b_1)^2(2b_1)^2(1a_2)^1(3b_1)^1$	$A_1 \rightarrow B_2$	y
Toluenium	$\cdots\cdots (3b_1)^2(1a_2)^2$	$\cdots\cdots (3b_1)^2(1a_2)^1(4b_1)^1$	$A_1 \rightarrow B_2$	y
Mesitylenium	$\cdots\cdots (4b_1)^2(2a_2)^2$	$\cdots\cdots (1a_2)^2(4b_1)^2(2a_2)^1(5b_1)^1$	$A_1 \rightarrow B_2$	y

TABLE III

THE FIRST TRANSITION ENERGIES CALCULATED FOR TWO MODELS AND EXPERIMENTAL VALUES

Carbonium ions	For hyperconjugation model (unit of $-\beta$)	For bond localization model (unit of $-\beta$)	Absorption wave length observed (A)	Oscillator strength observed
Benzenium	0.87083	0.80193	4170	0.15
Toluenium	0.87902	0.81574	4000	0.15
Mesitylenium	0.81801 0.81445	0.76018	3900	0.27

TABLE IV

THEORETICAL DATA FAITHFUL TO REID'S EXPERIMENTS

Carbonium ions	Model	Singlet-triplet separations assumed (eV)	Longest absorption wave length (A)	Oscillator strength
Benzenium	Bond localization	1.77	4168	0.31
Toluenium	Bond localization	1.95	3999	0.20
Mesitylenium	Hyperconjugation	2.10	3909	0.32

TABLE V

THE SECOND TRANSITIONS CALCULATED FOR TWO MODELS

Carbonium ions	Transition	Polarization	Transition energies for hyperconjugation (unit of $-\beta$)	Transition energies for bond localization (unit of $-\beta$)
Benzenium	$A_1 \rightarrow A_1$ $(2b_1 \rightarrow 3b_1)$	z	1.18005	1.21308
Toluenium	$A_1 \rightarrow A_1$ $(3b_1 \rightarrow 4b_1)$	z	1.09208	1.09131
Mesitylenium	$A_1 \rightarrow A_1$ $(4b_1 \rightarrow 5b_1)$	z	1.09661	0.93919

4.50×10^5, 9.57×10^5, and 4.80×10^5 dyne/cm. for C—C, C=C, and C—H bonds[39], respectively, and calculating π-bond orders by the following relations of Chirgwin and Coulson[40],

$$p_{\mu\nu} = (1/2)\sum_{j=1}^{m} n_j (x_{j\mu} y_{j\nu} + x_{j\nu} y_{j\mu}),$$

$$\nu, \mu = 1, 2, \cdots\cdots n, ; \nu \neq \mu,$$

$$y_{j\mu} = \sum_{\nu=1}^{n} S_{\mu\nu} x_{j\nu},$$

n_j: number of electrons occupying the j'th MO,

m: number of occupied molecular orbitals,

bond lengths being obtained by the correlation between the bond length and the total bond order[41]. Calculations show 10.28 kcal/mole[42] for the hyperconjugation energy.

It will be noticed here that this value is too large for the hyperconjugation energy itself, which is usually of the order of a few kcal./mole. Positive δ values indicate smaller hyperconjugation energies[10], but from the electronegativity consideration of the H_2 quasi-atom compared with the $2p\pi$ carbon negative values of δ will be accepted[10]. The value -0.3

39) G. Herzberg, "Infrared and Raman Spectra of Polyatomic Molecules", B. Van Nostrand, New York, N. Y. 1945, p. 193.

40) B. H. Chirgwin and C. A. Coulson, *Proc. Roy. Soc.*, A **201**, 196 (1950).

41) C. A. Coulson, ibid., A **169**, 413 (1939).

42) Energies are expressed by the unit of β, the resonance integral including overlap between the neighboring carbon atoms in benzene molecule, and in converting those into the unit of kcal. $\beta = -60$ kcal./mole is used. See, C. C. J. Roothaan and R. S. Mulliken, *J. Chem. Phys.*, **16**, 118 (1948).

for δ gives the smaller hyperconjugation energy than the value -0.5 does[10]. However, the difference between both cases is small and, in addition, $\delta=-0.5$ is adequate to account for the dipole moment and the spectral shift as well as the hyperconjugation energy of toluene[20,21]; consequently, it will not be of importance which value of these will have to be chosen. Matters will probably be otherwise; in fact the improved calculations by means of the self-consistent technique by Muller, Pickett, and Mulliken[10] show the smaller hyperconjugation energy, 5.9 kcal./mole. In relation to this, it will be very interesting to carry out the ASMO calculations.

The Spectra

Calculated results on the spectra and comparisons with experiments are indicated in Tables II, III, IV and V.

Table II shows the electronic states and transition processes for the first transitions. For these three aromatic carbonium ions, the manner in which electron transitions occur is the same, namely one electron elevates from the a_2 to the b_1 orbital, transition process being $A_1 \rightarrow B_2$, and polarization is in the y direction which is perpendicular to the molecular axis, z, and lies in the molecular plane.

Table III indicates the experimental values and the calculated transition energies for the first transitions. The experimental values of the absorption wave lengths in the fourth column are taken from the paper of Reid[11] and experimental oscillator strengths in the last column are determined roughly by the author on the basis of the experimental extinction curves by Reid through the following relation[43],

$$f=4.32\times10^{-9}\int\varepsilon_\nu d\nu,$$

where f is the oscillator strength, and ε_ν the extinction coefficient of the observed absorption of frequency ν. The calculated transition energies for the case of the bond localization model are those obtained using $\delta=-0.3$ as well as the auxiliary inductive parameter, $\delta_{\text{ind}}=-0.1$, while those for the hyperconjugation model correspond to the values obtained using only $\delta=-0.3$, except the second value of mesitylenium ion, the calculation of which includes $\delta_{\text{ind}}=-0.1$ also. All these are mean values of the transition energies to the singlet and the triplet excited states; consequently, in order to compare these calculated values with observed ones, an additional factor must be taken into account, e.g. the singlet-triplet separation in the excited state. Here, if it is assumed that the singlet-triplet splittings of these three molecules are not the same in general, but may not differ very much from each other, then it seems safe to let the calculated mean transition energies have the same tendency as the absorption shifts observed among these three substances. According to Table III, and from the view point just mentioned, the calculated mean transition energies for these three ions can explain the experimental "blue-shifts" in terms of neither the hyperconjugation nor the bond localization, although only the "blue-shift" of toluenium relative to benzenium ion is predicted by both models. At this point, if the bond localization rather than the hyperconjugation model is preferably chosen for benzenium and toluenium ion, while the hyperconjugation rather than the bond localization model, for mesitylenium ion, then there will be no contradiction between theories and experiments. However, this remains only to be an arrangement of the calculated results, so as to be faithful to Reid's measurements, and the critical discussion on this point will be performed in the following section.

The theoretical data arranged so as to be faithful to Reid's experiments are indicated in Table IV. When the values of siglet-triplet separations are assumed to be such as those shown in the third column and for the purpose of obtaining only the transition energies to the singlet excited states, a half of those values are added to the mean transition energies; the absorption wave lengths thus calculated may accord with the experimental values (compare the fourth column of Table IV with the fourth column of Table III). The theoretical oscillator strengths in the fifth column are computed by the relation[44],

$$f=1.085\times10^{11}\nu D,$$
$$D=Q^2,$$
$$\vec{Q}=\sqrt{2}\sum_\mu x_{i\mu}x_{j\mu}\vec{r}_\mu,$$

43) J. R. Platt and H. B. Klevens, *Rev. Mod. Phys.*, **16**, 182 (1944).

44) R. S. Mulliken and C. A. Rieke, *Reports on Progress in Physics*, **8**, 231 (1941).

where, ν is the absorption frequency (in cm.$^{-1}$); D, the dipole strength; $x_{i\mu}$, $x_{j\mu}$, coefficients of μ'th atom in the molecular orbitals, i and j, respectively, which are concerned with the electron jump; $\vec{r}_\mu$, the position vector of the μ'th atom with respect to some convenient origin. Oscillator strengths calculated and observed agree satisfactorily with each other.

Calculated results for the second transitions are shown in Table V. One electron concerning this transition elevates from the b_1 to the b_1 molecular orbital, and the polarization is in the direction of the molecular axis, z.

Discussion

In the preceding section the bond localization model is assumed for benzenium- and toluenium- ions and the hyperconjugation one for mesitylenium ion. This assumption is, however, only having put a finger on one possibility of the π-electron structures of these ions, and must be verified also from other criterions, which, however, unfortunately are not available at present.

Our calculation is only very approximate. The more rigorous approximation[11] including the self-consistent technique can not either determine distinctly which of the bond localization and the hyperconjugation model is suitable to benzenium ion, and further complicated factors, besides those pointed out by Coulson and Dewar[45], will have to be taken into account, such as configuration interactions, which are useful in predicting the absorption spectra, and screening effects by the electron distributions enhanced through the existence of the methyl substituents in the aromatic nucleus; it is difficult to carry out calculations including the former factor in the simple LCAO MO treatments on these systems in question[46]; furthermore, reasonable computations including the latter factor are difficult in the present step. Because our calculation is only rough, jumping from one model (bond localization) to the other (hyperconjugation) may be probably open to suspicion. Generally speaking, whenever the H_2 or H_3 group exists in conjugated systems, it may be adequate to assume the presence of its hyperconjugation[47].

In order to avoid these difficulties mentioned above, we assume that the hyperconjugation always occurs but its extent is different in each case of these ions in question; then it may be said that benzenium as well as toluenium is less hyperconjugated than mesitylenium ion, if we admit the simple theory and Reid's experiments. If, as in the preliminary report[48], the eigenfunction Φ of these ions is written by the linear combination of the eigenfunctions Φ_{HCJ} of the perfect hyperconjugation and Φ_{BL} of the bond localization model, Φ is the so-called hybrid and has commonly the lower energy than both models, while now we assume that Φ has the intermediate energy between the two extreme models, namely bond localization and perfect hyperconjugation models. In this respect there have been some confusions in the preliminary report.

There will be an additional way of treating these intermediate systems; that is, the systems having intermediate energies between those of the perfect hyperconjugation and bond localization models. Namely, by attributing different values to the resonance integrals between atoms 2 and 3 (Fig. 1 or Fig. 2) in these three molecules in question, computations on the spectra may be carried out. However, in so far as the approximation made is rough, the calculated results here also remain only to point out one possibility of the π-electron structures of these aromatic carbonium ions.

Recently Kilpatrick and Hyman[49] have measured the absorption spectra of benzene, mesitylene, and hexamethylbenzene in the various acids including anhydrous hydrogen fluoride. They have indicated the loss of fine structure at 260 mμ band of benzene due to the effect of the acidic environment and have been unable to detect the presence of the protonated benzene. They entertain a doubt on the absorption band which Reid attributed to that of benzenium ion[50]. Further Kilpatrick and Hyman have shown that the bands of protonated hexamethylbenzene shifts towards red compared to those of

45) C. A. Coulson and M. J. S. Dewar, *Discussions Faraday Soc.*, **2**, 54 (1947).

46) As regards some alternant hydrocarbons, for example, polyacenes, inclusion of configuration interactions in the simple molecular orbital calculations, is possible. See, W. Moffitt, *J. Chem. Phys.*, **22**, 1820 (1954).

47) The author wishes to express his sincere thanks to Professor R. S. Mulliken (University of Chicago) for his critical advice on these points (private communication to the author).

48) T. Morita, *J. Chem. Phys.*, **25**, 1290 (1956).

49) Private communication to Dr. S. Nagakura.

protonated mesitylene. This fact may suggest that the band of mesitylenium ion shifts towards red compared to that of toluenium ion. If so, our calculations may predict this red shift in terms of both the bond localization and the hyperconjugation models. Unfortunately measurements on toluene in anhydrous hydrogen fluoride have not been shown. Probably protonated toluene (and/or benzene) will occur in the system of anhydrous hydrogen fluoride and toluene (and/or benzene), but on account of its small quantity the absorption band of this carbonium ion seems not to exhibit itself.

Because of these experiments contrary to Reid's and because of the ambiguity of the absorption bands of benzenium and toluenium ions, we reserve making any conclusion about the calculated results. At any rate, at present, experimental facts are scarce, and the performance of experiments from various view points may be desirable.

Summary

The semi-empirical LCAO MO treatment on the spectra of benzenium, toluenium, and mesitylenium ions have been carried out. Neither the localization nor the hyperconjugation of the H_2—C bond with respect to the aromatic ring can explain the blue-shifts of the experimental spectra by Reid with the increasing number of methyl substituents. If, however, benzenium and toluenium ions are assumed to be less hyperconjugated than mesitylenium ion, the spectroscopic behaviors of these aromatic carbonium ions are understandable. However, if the mesitylenium band is assumed to shift towards red compared with toluenium by the analogy of the case of protonated hexamethylbenzene and mesitylenium ion, whose absorption spectra have been measured by Kilpatrick and Hyman, our theoretical calculations will predict well the case of mesitylenium and toluenium ion in terms of both the bond localization and the hyperconjugation models. Unfortunately, however, the measurement on toluene in acid medium have not yet been made. Further the case of benzenium ion is yet open to question. Consequently we reserve making any distinct conclusions on these three aromatic carbonium ions.

The author wishes to thank Professor T. Titani (Tokyo Metropolitan University) for his interest and encouragement, Professor A. Kotera (Tokyo University of Education) for his intuitive guidance, Dr. S. Nagakura (University of Tokyo) for many valuable discussions, and Mr. Y. I'haya (Tokyo University of Education) for his helpful advice.

Department of Chemistry, Tokyo Metropolitan University
Setagaya-ku, Tokyo

50) Here see, H. Luther, and G. Pockels, *Z. Electrochem.*, **59**, 159 (1955). Luther and Pockels' measurements of the absorption spectra of the system, benzene-Al_2Br_6·HBr(or -Al_2Cl_6·HCl) and toluene-Al_2Br_6·HBr(or -Al_2Cl_6·HCl), indicate different absorption wave lengths from those of Reid, and the absorption wave lengths are time-dependent, but the tendency of the blue-shifts of the spectra through the presence of the methyl substituents exists. However, it is questionable whether $[ArH]^+$, where Ar is the aromatic molecule, is responsible for these spectra. See also the paper by E. L. Mackor [*Chem. Weekblad*, **52**, 240 (1956)], who suggested the presence of the more complicated complexes.

Formation and Aging of Precipitates. VI. Morphology of Crystals in Various Vanadium Pentoxide Sols by Electron Microscopy

By Kazuyoshi TAKIYAMA

(Received November 21, 1957)

Since the report of Biltz[1], the formation and aging of vanadium pentoxide sol has been investigated by many scholars. Recently, as the fibrous shape of the crystals contained in the sol which was confirmed distinctly with the electron microscope has attracted the attention of many investigators, morphological and crystallographic investigations have become popular. The crystals in Biltz sol were small fibrils at the outset and they grew like long fibers upon aging. Huber and Zbinden[2], watson, Heller and Wojtowicz[3] and Tamamushi[4] observed the growth of the crystals in Biltz sol with an electron microscope and they found that the fibrous crystals were nearly monodisperse at first, but they became polydisperse upon aging. The present author prepared vanadium pentoxide sols by Biltz', Müller's, and ion exchange method and studied the crystals in these sols by means of the electron microscopy to make a research on the aging process.

Experimental and Results

Formation of Sols.—*Biltz sol.* Two g. of ammonium metavanadate was mixed thoroughly with 6 ml. of 3 N hydrochloric acid in an agate mortar. The brownish red precipitate produced was washed in a glass filter and all the precipitate was dispersed completely in 200 ml. of water, giving a clear reddish brown sol.

Müller sol. Five g. of ammonium metavanadate was fused in a porcelain crucible for about half an hour and the melt was poured into 500 ml. of cold water. The sol formed in this way was dark reddish brown in color.

Ion exchange sol. Ammonium metavanadate solution (0.5%) was passed through a column of hydrogen ion exchange resin (Amberlite IR-120) and the yellow vanadic acid produced was decomposed in boiling water for about half an hour, and a reddish brown sol was formed.

Concentration of Sols and Quantity of Impurities.—The concentration of sols and the quantity of electrolytes in sols were determined as stated below.

Concentration of sols. The total quantity of vanadium pentoxide contained in the sols was determined as follows: a certain quantity of a sol was mixed with a small amount of 6 N sodium hydroxide solution, and the mixture was warmed until the vanadium pentoxide was completely dissolved. After the addition of sulfuric acid, the vanadic acid was titrated potentiometrically with 0.01 N standard ferrous ammonium sulfate.

Dissolved vanadium pentoxide in sols. A certain quantity of the sol was mixed with a suitable amount of potassium chloride solution to coagulate the disperse phase, and the coagulum was filtered and washed with potassium chloride solution. Vanadium pentoxide in the filtrate was determined as described above.

Ammonia in sols. The quantity of ammonia contained in the sol was determined by Kjeldahl's method.

Chloride in sols. The disperse phase of the sol was coagulated with potassium nitrate solution and the coagulum was filtered and washed. The filtrate was titrated with standard silver nitrate solution by potentiometry.

Results of the measurements. The results obtained by the above-mentioned methods are listed in Table I.

TABLE I
CONCENTRATION OF SOLS AND IMPURITIES

No.	Sol	Time of aging	Concn. of sol	Concn. of dissolved V_2O_5	Concn. of NH_3
			g./l.	g./l.	mg./l.
1	Biltz sol	0	7.083	1.052	—
2	〃	2 day	7.057	0.526	218.8
3	〃	6 months	7.120	0.281	—
4	〃	18 months	7.184	0.285	214.5
5	Müller sol	0	6.990	1.090	0.2
6	〃	10 days	6.420	0.325	—
7	Ion excange sol	0	6.094	0.400	0
8	〃	0	6.370	0.298	0

The concentration of every sol was about 7 g. V_2O_5 per liter. The amount of the dissolved vanadium pentoxide in Biltz and Müller sols was about 1 g. per liter (about 15% of the total vanadium pentoxide) in those fresh sols, but it decreased to about 0.28 g. per liter (about 4% of the total vanadium pentoxide) upon aging. In

1) W. Biltz, *Ber.*, **37**, 1095 (1904).
2) H. Huber and H. Zbinden, *Z. anorg. Chem.*, **258**, 188 (1949).
3) J. H. Watson, W. Heller and W. Wojtowicz, *Science*, **109**, 274 (1949).
4) B. Tamamushi, *J. Electron-Microscopy*, **1**, 35 (1950).

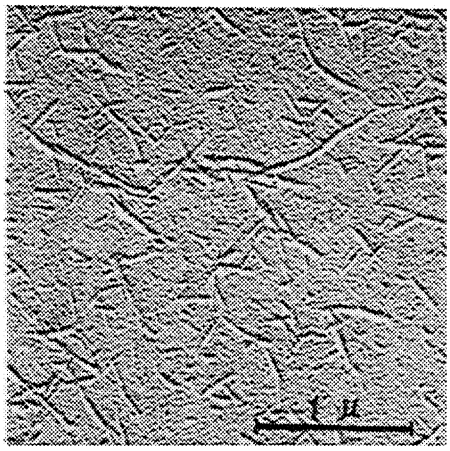

Fig. 1. Crystals in 2 days old Biltz sol. (Cr shadowing) × 20,000

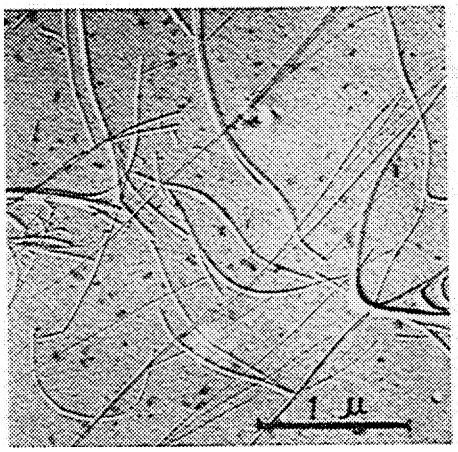

Fig. 2. Crystals in 2 weeks old Biltz sol. (Cr shadowing) × 20,000

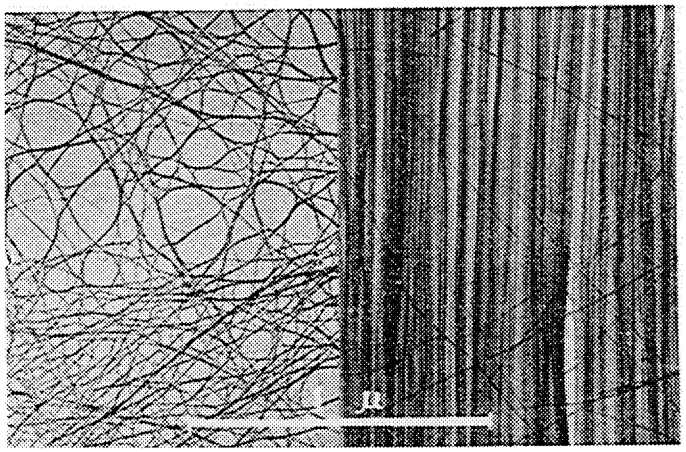

Fig. 3. Crystals in 1 year old Biltz sol. × 40,000

the case of ion exchange sol the amount of the dissolved vanadium pentoxide was less than that in Biltz and Müller sols even in the incipient stage of standing. About 0.2 g. ammonia existed in one liter of Biltz sol, (about 0.013 mole NH_3/l.; $V_2O_5 : NH_3 = 3 : 1$), but only a trace of it was found in Müller sol, and it was not detected at all in the ion exchange sol. Chloride ion was not detected in any of the sols. pH of the sols was 2.5 to 3.0.

Morphology of Crystals in Sols by Electron Microscopy.—Morphological characteristics of crystals in the three kinds of sol described above were observed by means of electron microscopy.

Biltz sol. The crystals in Biltz sol were small fibrils, a few score mμ long and 14 mμ thick, at the outset as shown in Fig. 1, but they grew like long fibers on standing. They grew to about 1 μ in size after a week, about 2 μ after 2 weeks (Fig. 2) and over a few μ after a month, then fibrous crystals got intertwined with one another and their length could not be measured. But a few weeks old Biltz sol contained small fibrils also as seen in Fig. 2. The thickness was, however, about 14 mμ and almost constant. An electron micrograph obtained from a specimen of a year old sol mounted on a specimen holder without supporting film showed a network structure as in Fig. 3 a. The fibrous crystals of various lengths clung together, forming a network structure. Thin films of crystals were formed on the surface of the sol which was aged over a few months. They were floated on the water and were scooped up with specimen holders without supporting films. The electron micrographs of these specimens showed the orientation of fibrous crystals with their long axes parallel to one another as in Fig. 3 b. When a small amount of the old Biltz sol was allowed to flow on the surface of still water and was scooped up with a specimen holder, an electron micrograph similar to that described above was also obtained. This figure was formed by the orientation of fibrous crystals to the direction of the flow. The fibrous crystals in Biltz sol grew markedly extended along their long axes on standing, but the fibrils in the sol dialyzed

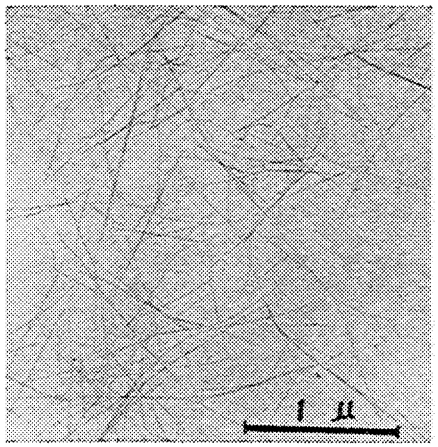

Fig. 4. Crystals in dialyzed Biltz sol. (1 year old sol) × 20,000

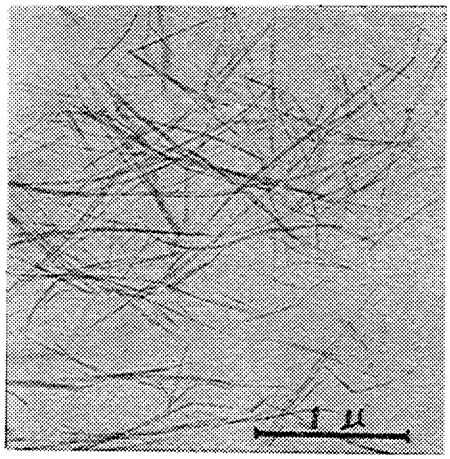

Fig. 5. Crystals in 1 year old Müller sol. × 20,000

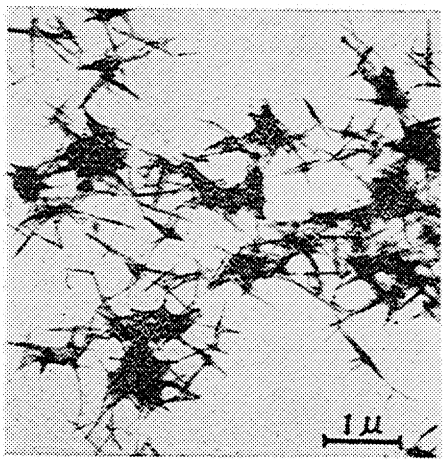

Fig. 6. Crystals in 2 months old ion exchange sol. × 10,000

immediately after preparation hardly grew at all as compared with the original Biltz sol, and an electron micrograph taken for one year old dialyzed sol showed needle crystals, a few μ long, as in Fig. 4.

Müller sol. The crystals in a freshly prepared Müller sol were small fibrils, about 50 mμ long and about 15 mμ thick, similar to those in Biltz sol. After standing for one year, their length was about 400 mμ and after 2 years it was about 1 μ as shown in Fig. 5. That is to say, the fibrous crystals more or less grew like fibers, but the rate of their growth was very small as compared with those of Biltz sol.

Ion exchange sol. The crystals in ion exchange sol were like needles, which were about 1.2 μ long and about 50 mμ thick, as shown in Fig. 6. Many needle crystals crossing at their center are observed in the micrograph. The shape and the size of the crystals are independent of the decomposition time and standing of the sol. A characteristic of the ion exchange sol is that the needle crystals in it do not grow on standing.

The crystals in these three kinds of sol described above were identified as vanadium pentoxide by electron diffraction method, which will de mentioned in the next paper.

Discussion of Results

There are two theories for the growth phenomena of the fibrous crystals in Biltz sol. One is the recrystallization theory and the other is the coagulation theory. Nemtsova[5] found the rapid growth of the crystals in Biltz sol when it was enclosed in a collodion bag and was dipped in saturated vanadium pentoxide solution. Tamamushi[6] reported that the aging of Biltz sol depended upon its adsorption of VO_3^- and H^+ ions on the fibrous crystals. These experiments suggested that the crystal growth in Biltz sol was attributed to the recrystallization. Lukjanovich[7] supported the coagulation theory by his studies of a phenomenon of the adsorption of colloidal silver on the ends of fibrous crystals in Biltz sol. Thiele and Kienast[8] also suggested the coagulation theory. The author will discuss the growth phenomenon by his experimental results as stated below.

The small fibrils in the freshly prepared

5) V. V. Nemtsova, *Doklady Akad. Nauk, USSR*, **79**, 297 (1951); *Chem. Abst.*, **45**, 6013 (1951).

6) B. Tamamushi, *Sci. Paper Coll. Gen. Ed. Univ. Tokyo*, **6**, 37 (1956); cf. H. Tanaka and K. Meguro, *J. Chem. Soc. Japan, Pure Chem. Sec.* (*Nippon Kagaku Zassi*), **74**, 49 (1953).

7) A. V. Bromberg, V. M. Lukjanovich, V. V. Nemtsova, L. V. Radushkevich and K. C. Chemutov, *Doklady Akad. Nauk, USSR*, **79**, 281, 827 (1951); **80**, 615 (1952).

8) H. Thiele and G. Kienast, *Kolloid-Z.*, **127**, 134 (1952).

Biltz sol increase their length during the aging process, but the fibrils in the dialyzed Biltz sol, Müller sol, and ion exchange sol hardly grow at all on standing. As indicated in Table I, the concentrations of every sol are almost the same. The amount of the dissolved vanadium pentoxide in Biltz and Müller sols is somewhat greater than that in ion exchange sol at the outset of the standing, but it gradually decreased to a constant value, which is almost the same as the solubility of vanadium pentoside, 0.29 g. per liter[9]. The supersaturated vanadium pentoxide is deposited on the crystals during the aging, but this phenomenon seems not to be the origin of the growth of the fibrils to the very long fibrous crystals in Biltz sol, because the fibrils in Müller sol hardly grow at all on standing.

The main difference between the Biltz sol and the other sols is that of the amount of ammonia contained in the sols. Biltz sol contains about 219 mg. of ammonia per liter, but the Müller and the ion exchange sols contain little and no ammonia respectively. As the acidity of various sols is in the range of pH 2.5 to 3.0, it seems that the greater part of ammonia contained in Biltz sol combines with dissolved vanadium pentoxide (about 1 g. V_2O_5/l.) as ammonium vanadate at the initial stage of aging, and a part of ammonia is adsorbed by the crystals. The growth of the fibrous crystals in Biltz sol seems to be promoted by ammonium ion contained in the sol. Huber and Zbinden[2] prepared vanadium pentoxide sols from various alkali vanadates and indicated that alkali ions resulted from the preparation which promoted the growth of the fibrous crystals in sols and the effect increased with the increase of the atomic weight and the concentration of alkali ions. They also observed that the effect of the ammonium ion was almost the same as that of the potassium ion. It seemed that the vanadium pentoxide crystals in Biltz sol were apt to form ammonium vanadiate in the presence of ammonium ion and that the crystals of vanadium pentoxide were in equilibrium with dissolved ammonium vanadate and were liable to recrystallize.

By an electron microscopic observation, the small fibrils are found besides the long fibrous crystals in aged Biltz sol as shown in Fig. 2. The small fibrils were observed even in 2 months old Biltz sol and seemed to be formed by dissolution of small fibrous crystals.

The author considered that the growth of the fibrous crystals in Biltz sol was caused by Ostwald's ripening which was promoted by the increase of the solubility of the crystals owing to the presence of the ammonium ion in the sol.

9) M. Kerker, G. L. Jones, J. B. Reed, N. P. Yang and M. D. Schvenberg, *J. Phys. Chem.*, **58**, 1147 (1954).

Summary

Vanadium pentoxide sols were prepared by Biltz', Müller's and ion exchange method, and the crystals in the sols were observed with an electron microscope. The crystals in Biltz sol were small fibrils at first, but they grew into long fibrous crystals upon aging. The crystals in Müller and ion exchange sols were fibrils and needles respectively and hardly grew at all. The growth of the fibrous crystals in Biltz sol is likely to be due to the recrystallization of the fibrils.

The author acknowledges the guidance and discussion of Professor Eiji Suito of Kyoto University. He also particularly wishes to express his hearty thanks to Professor Masayoshi Ishibashi of Kyoto University for his discussions and encouragement throughout this investigation.

Institute for Chemical Research
Kyoto University, Takatsuki
Osaka

Studies on Sarkomycin—Preparation of Optically Active 2-Methylenecyclopentanone-3-carboxylic Acids

By Katsuyuki TOKI

(Received August 2, 1957)

Hooper et al.[1] reported in 1955 that the effective ingredient of the natural sarkomycin is 2-methylenecyclopentanone-3-carboxylic acid. Afterwards, the present author[2] synthesized *dl*-2-methylenecyclopentanone-3-carboxylic acid (I), starting from alkyl cyclopentanone-3-carboxylate. Tatsuoka et al.[3] showed that the naturally occurring sarkomycin is in the levoform.

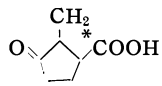

I

In the present paper, the preparation of optically active 2-methylenecyclopentanone-3-carboxylic acids is described.

Since 2-methylenecyclopentanone-3-carboxylic acid is a very unstable compound, and, moreover, is an α,β-unsaturated ketone liable to react with active amines, a direct resolution may be very difficult. As 2-methylenecyclopentanone-3-carboxylic acid has only one asymmetric carbon, preparation from an active intermediate is likely more convenient to obtain it in the optically active form. The use of active cyclopentanone-3-carboxylic acid being suggested, the present author resolved *dl*-cyclopentanone-3-carboxylic acid with brucine which was the best suited for this purpose.

When brucine was combined with *dl*-cyclopentanone-carboxylic acid in aqueous solution, 80% of the expected amount of brucine *d*-cyclopentanone-3-carboxylate was deposited, and the mother liquor gave the nearly pure brucine *l*-cyclopentanone-3-carboxylate on evaporation. Pure salts were obtained in theoretical yields by repeated recystallization from hot water. The active acid and the alkaloid were easily recovered by adding aqueous ammonia or a mineral acid.

When cinchonine was employed, separation of cinchonine *d*- and *l*-cyclopentanone-3-carboxylates required laborious recrystallization. The two optically active 2-methylenecyclopentanone-3-carboxylic acids were synthesized starting from the active cyclopeotanone-3-carboxylic acids by a four-stage process in the same manner as described for the racemic acid. Though ethyl 2-(piperidinomethyl)-cyclopentanone-3-carboxylate (II) from each active cyclopentanone-3-carboxylic acid, the final intermediate prepared by the Mannich reaction, was a mixture of two diastereoisomers, it was used without separation, because separation at this stage was unnecessary for the preparation of active 2-methylenecyclopentanone-3-carboxylic acid.

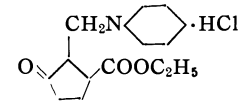

II

The infrared spectra of the synthetic optically active 2-methylene-cyclopentanone-3-carboxylic acids and natural sarkomycin Hooper[1] were essentially identical and exhibited a characteristic peak at 6.1 μ.

Details of the biological studies on the synthetic optically active 2-methylenecyclopentanone-3-carboxylic acid will be published elsewhere.

Experimental

Resolution of Cyclopentanone-3-carboxylic acid with Brucine.—A mixture of 112 g. (0.88 mol.) of racemic cyclopentanone-3-carboxylic acid and 400 g. of brucine-$4H_2O$ was warmed with 2000 ml. of water with stirring to a clear solution. When the solution was allowed to stand overnight in a refrigerator, 580 g. (wet) of silky needles of brucine *d*-cyclopentanone-3-carboxylate, m.p. 110~113°, precipitated. The crude product was recrystallized from hot water several times, m.p. 115~117°, $[\alpha]_D^{25}$ −28.4 (chloroform, C=1.6). Yield 205 g. Further 50 g. of the same substance was obtained on evaporation of the mother liquor and recrystallization. Total yield 255 g.

The combined mother liquor was evaporated to dryness and the residue was recrystallized

* Presented at the meeting of Japan Antibiotic Research Association, at the Institute of Infections Diseases, Tokyo, July 26, 1957.

1) I. R. Hooper et al., *Antibio. & Chem.*, **5**, 588 (1955).
2) K. Toki, This Bulletin, **30**, 450 (1957).
3) S. Tatsuoka et al., *J. Antibio., Ser.* B, **IX** 157 (1956).

from hot water several times to yield 250 g. of brucine *l*-cyclopentanone-3-carboxylate, m.p. 103 ~105°, $[\alpha]_D^{25}$ −38.5 (chloroform, C=1.3).

Brucine *d*-cyclopentanone-3-carboxylate (235 g.) was dissolved in 400 ml. of hot water and then an excess of concentrated aqueous ammonia was added to the solution.

After being cooled overnight in a refrigerator, 200 g. of silky needles of brucine was recovered by filtration. The filtrate was concentrated and acidified with hydrochloric acid. The condensed filtrate was saturated with ammonium sulfate, and extracted with ether. After removal of ether, *d*-cyclopentanone-3-carboxylic acid was distilled at 138~140°/0.2 mm. Yield 55 g. (98.2%), m.p. 66~67°, $[\alpha]_D^{21}$+22.1 (methanol, C=1.9).

Anal. Found: C, 56.20; H, 6.08. Calcd. for $C_6H_8O_3$: C, 56.25; H, 6.25%.

l-Cyclopentanone-3-carboxylate was obtained in the same manner as described above. Yield 53 g. (94.6%) from 250 g. of the brucine salt. b.p. 138~140°/0.2mm., m.p. 65~66°, $[\alpha]_D^{21}$−22.2 (methanol, C=2.0).

Anal. Found: C, 56.23; H, 6.21. Calcd. for $C_6H_8O_3$: C, 56.25; H, 6.25%.

Esterification of *d*- and *l*-Cyclopentanone-3-carboxylic Acids.—A mixture of 55 g. (0.43 mol.) of *d*-cyclopentanone-3-carboxylic acid, 50 g. of absolute ethanol, 80 g. of absolute benzene, and a small amout of *p*-toluenesulfonic acid, was heated on a water bath using a water separater for about eight hours. The reaction mixture was concentrated, poured into ice and aqueous sodium bicarbonate and extracted with ether. After drying over anhydrous sodium sulfate and evaporation, ethyl *d*-cyclopentanone-3-carboxylate was separated by fractional distillation. Yield 55.5 g. (83.7%), b.p. 116~118°/16 mm., n_D^{21} 1.4523, $[\alpha]_D^{21}$+20.0 (methanol, C=1.5).

Anal. Found: C, 61.73; H, 7.66. Calcd. for $C_8H_{12}O_3$: C, 61.54; H, 7.69%.

The 2,4-dinitrophenylhydrazone melted at 172 ~173°.

Anal. Found: C, 49.80; H, 4.93; N, 16.72. Calcd. for $C_{14}H_{16}O_6N_4$: C, 60.00; H, 4.76; N, 16.67%.

Unchanged *d*-cyclopentanone-3-carboxylic acid (6.4 g.) was recovered from the alkaline solution.

A mixture of 53 g. (0.41 mol.) of *l*-cyclopentanone-3-carboxylic acid, 50 g. of absolute ethyl alcohol, 80 g. of absolute benzene, and a small amount of *p*-toluenesulfonic acid, was treated similarly to obtain ethyl *l*-cyclopentanone-3-carboxylate. Yield 56.2 g. (87.80%), b.p. 117°/16 mm, n_D^{24} 1.4510, $[\alpha]_D^{21}$−21.9 (methanol, C=1.6).

Anal. Found: C, 61.49; H, 7.68. Calcd. for $C_8H_{12}O_3$; C, 61.54; H, 7.69%.

The 2,4-dinitrophenylhydrazone melted at 172 −173°.

Anal. Found: C, 49.89; H, 4.98; N, 16.62. Calcd. for $C_{14}H_{16}O_6N_4$: C, 50.00; H, 4.76; N, 16.67%.

Unchanged *l*-cyclopentanone-3-carboxylic acid (4.0 g.) was recovered from the alkaline solution.

Ethyl *d*- and *l*-2-Methylenecyclopentanone-3-carboxylates.—(*a*) *Ethyl d-2-methylenecyclopentanone-3-carboxylate.* A mixture of 10 g. (0.06 mol.) of ethyl *d*-cyclopentanone-3-carboxylate, 7.2 g. (0.06 mol.) of piperidine hydrochloride, and 4.3 g. of 37% formaline, was heated on a water bath at 75~80° with stirring for thirty minutes. After extracting the unchanged ethyl *d*-cyclopentanone-3-carboxylate with ether, the aqueous layer was concentrated to dryness under a reduced pressre. Ethyl 2-(piperidinomethyl)-*d*-cyclopentanone-3-carboxylate hydrochloride was produced in a semi-solid mass. The hydrochloride was purified by recrystallization from methanol for analysis. Yield 9.7 g., m.p. 156° (sinter), $[\alpha]_D^{25}$+37.5 (methanol C=1.6).

Anal. Found: C, 57.86; H, 8.22; N, 4.82. Calcd. for $C_{14}H_{24}O_3NCl$: C, 58.13; H, 8.30; N, 4.84%.

The 2,4-dinitrophenylhdrazone melted at 128 ~130°.

The residual oil separated from the crystals was considered to be a diastereo-isomer of ethyl 2-(piperidinomethyl)-*d*-cyclopentanone-3-carboxylate hydrochloride and could be also used for successing reaction.

The crystalline hydrochloride was disssolved in a amount of water and pH was adjusted to 9~10 with aqueous sodium bicarbonate. The mixture was extracted with ether and the ethereal solution was dried over anhydrous sodium sulfate and evaporated. The residue was distilled under a reduce pressure (90~100°/0.1 mm.).

The distillate was dissolved in ether and the solution was washed with diluted hydrochloric acid to remove piperidine. Thus ethyl *d*-2-methylenecyclopentanone-3-carboxylate was obtained. Yield 1.11 g. (11.0% from ethyl *d*-cyclopentanone-3-carboxylate), $[\alpha]_D^{26}$+15.8 (methanol, C=3.4).

The 2,4-dinitrophenylhydrazone melted at 179 ~180°

Anal. Found: C, 51.70; H, 4.52; N, 16.00. Calcd. for $C_{15}H_{16}O_6N_4$: C, 51.72; H, 4.60; N, 16.09%.

(*b*) *Ethyl l-2-methylenecyclopentanone-3-carboxylate.* A mixture of 10 g. (0.06 mol.) of ethyl *l*-cyclopentanone-3-carboxylate, 7.2 g. (0.06 mol.) of piperidine hydrochloride, and 4.3 g. of 37% formaline, was treated in the same manner as mentioned above. Ethyl 2-(piperidinomethyl)-*l*-cyclopentanone-3-carboxylate hydrochloride was obtained in this way. Yield 9.3 g., m.p. 155° (sinter), $[\alpha]_D^{23}$−37.3 (methanol, C=1.6).

The residual oil separated from the crystals was considered a diastereo-isomer of ethyl 2-(piperidinomethyl)-*l*-cyclopentanone-3-carboxylate hydrochloride and could be used for next reaction.

Anal. Found: C, 57.89; H, 8.19; N, 4.80. Calcd. for $C_{14}H_{24}O_3NCl$: C, 58.13; H, 8.30; N, 4.84%.

The 2,4-dinitrophenylhydrazone melted at 129 ~131°.

Ethyl *l*-2-methylenecyclopentanone-3-carboxylate was obtained by heat decomposition. Yield 0.89 g. (8.8% from ethyl *l*-cyclopentanone-3-carboxylate), $[\alpha]_D^{23}$−15.4 (methanol, C=1.3).

The 2,4-dinitrophenylhydrazone melted at 179 ~180°.

Anal. Found: C, 51.70; H, 4.48; N, 16.07. Calcd. for $C_{15}H_{16}O_6N_4$: C, 51.72; H, 4.60; N, 16.09%.

***d*- and *l*-2-Methylenecyclopentanone-3-carboxylic Acids.**—(*a*) *d-2-Methylenecyclopentanone-*

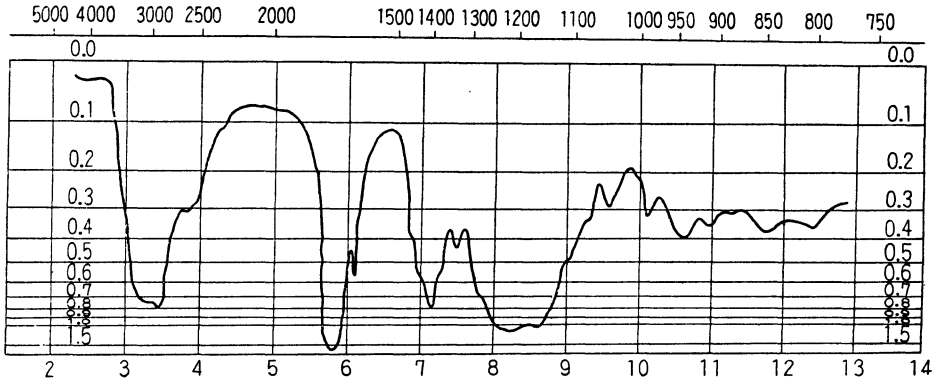

Fig. 1. Infrared spectrum of *d*-2-methylenecyclopentanone-3-carboxylic acid.

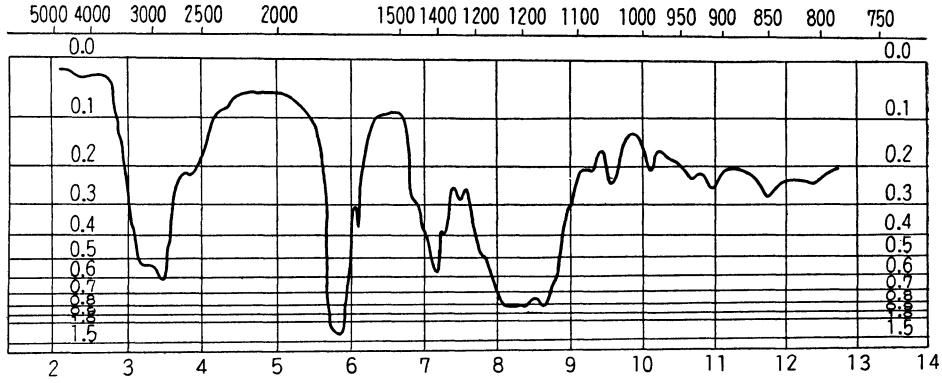

Fig. 2. Infrared spectrum of *l*-2-methylenecyclopentanone-3-carboxylic acid.

3-carboxylic acid. A mixture of 3.5 g. of ethyl *d*-2-methlenecyclopentanone-3-carboxylate and 35 ml. of a 5% acetone solution of the hydrochloride was allowed to stand at 20° for ten hours, and then an equivalent amount of aqueous sodium dicarbonate was added to the mixture with cooling. After removal of acetone under a reduced pressure, the aqueous layer was shaken with ether to recover the unchanged ester. The aqueous layer was then acidified with dilute hydrochloric acid with cooling, saturated with ammonium sulfate, and extracted with ethyl acetate. The ethyl acetate solution was concentrated under a reduced pressure. *d*-2-Methylenecyclentanone - 3 - carboxylic acid was obtained in a pale yellow oil in a yield of 0.85 g. (29.0%), $[\alpha]_D^{23}$+28.9 ** (ethylacetate, C=1.6). The infrared spectrum is shown in Fig. 1.

Anal. Found: C, 59.81; H, 5.43. Calcd. for $C_7H_8O_3$: C, 60.00; H, 5·71%.

(*b*) *l-2-Methylenecyclopentanone - 3 - carboxylic acid.*—*l*-2-Methylenecyclopentanone - 3 - carboxylic acid (2.2 g.) was obtained in the same manner as mentioned above. Yield 0.39 g. (21.5% from 2.2 g. of the corresponding ethyl ester), $[\alpha]_D^{23}$−28.4 **(ethyl acetate, C=1.6). Fig. 2. shows the infrared spectrum of the substance.

Anal. Found: C, 59.62; H, 5.31. Calcd. for $C_7H_8O_3$: C, 60.00; H, 5.71%.

** The values will be flexible becouse of the unstability of 2-methylenecyclopentanone-3-carboxylic acid.

Both *d*- and *l*-2-methylenecyclopentanone-3-carboxylic acid showed essentially identical infrared absorption as natural sarkomycin (Hooper[1]).

Summary

d- and *l*-2-Methylenecyclopentanone-3-carboxylic acid were synthesized starting from optically active cyclopentanone-3-carboxylic acid obtained by resolution of the racemic acid with brucine, and both *d*- and *l*-isomer, thus obtained, showed the same infrared absorption as natural sarkomycin (Hooper).

Thanks are due to Professor Shiro Akabori of Osaka University, Professor Hamao Umezawa of the National Institute of Health of Japan, and Professor Masanao Matsui of Tokyo University for their continous interest and encouragement through this investigation.

The author is also indebted to Mr. Naofumi Ohi and his associates for infrared analyses, to Mr. Noboru Nishimura and his associates for microanalyses, to Mr. Chiharu Saito for biological tests, and to Messrs. Hiroo Wada and Yoshio Suzuki for their helpful collaborations.

Sumitomo Chem. Co. Ltd.
Osaka Works

Reactions of Active Methylene Compounds. I. Alkylation of Cyclohexanone via Ethyl 2-Ketocyclohexylglyoxalate

By Yoshiyuki KAWASE

(Received February 19, 1957)

Alkylations of cyclohexanone derivatives are usually carried out by two methods, A and B shown in Chart I. The procedure of method A involves only one step employing sodium amide or potassium *t*-butoxide, and the ketone is alkylated at the α-carbon atom having less hydrogen according to the extended Saytzeff rule[1], but the product is contaminated with polyalkylated compounds. In the case of method B, the ketone is alkylated in the unsubstituted α-methylene group according to the Hofmann rule and the product is obtained in pure state, but the procedure involves many steps, namely, carbethoxylation (or formylation), alkylation, and hydrolytic decomposition.

A method of alkylation analogous to method B was reported by A. Kötz et al.[2] in 1912, in which substituted ethyl 2-ketocyclohexylglyoxalate was alkylated and the product was decomposed to alkylketone by alkaline hydrolysis. But this method has not often been used hitherto[1a,3].

Here, A. Kötz's method has been studied, and seems to be better than method B when the alkylation according to the Hofmann rule is desired. In this paper, some alkylations of cyclohexanone via ethyl 2-ketocyclohexylglyoxalate, which have not yet been reported, are described.

The sodio compound of ethyl 2-ketocyclohexylglyoxalate (I), prepared from cyclohexanone and ethyl oxalate in absolute ethanol without isolation, was refluxed with an alkylating reagent such as methyl iodide, benzyl bromide, ethyl bromoacetate, and 1-(diethylamino)-3-pentanone methyl iodide. (see Table).

As the alkylated product was obtained together with ethyl oxalate without hydrolysis, it seemed that the intermediate ethyl 1-alkyl-2-ketocyclohexylglyoxalate (II) was liable to cleave to alkylcyclohexanone and ethyl oxalate in ethanol. (see Chart II). In the case of methylation, 2-methylcyclohexanone (III) was purified by alkaline hydrolysis as it was contaminated by ethyl oxalate, and it seemed that the yield of ethyl 2-ketocyclohexylacetate (V) was lowered by secondary condensation of the product.

Experimental[4]

Preparation of 2-Methylcyclohexanone (III). (*a*) *From Cyclohexanone.*—A mixture of 19.6 g. of cyclohexanone and 29.2 g. of ethyl oxalate was slowly added with stirring below 10° to the sodium ethoxide solution (4.5 g. of sodium in 100 ml. of absolute ethanol) according to H.R. Snyder et al.'s method[5], and the mixture was allowed to stand overnight at room temperature. The was mixture heated at 70~80° for six hours with 40 g. of methyl iodide with stirring. After the solvent was evaporated, the cooled residue was diluted with water and extracted with ether. The ethereal solution was washed with water, fully dried on calcium chloride, and evaporated. By distillation of the residue, crude 2-methylcyclohexanone (III) was obtained in colorless oil boiling at 164~177° (mainly at 164~169°)[6]. Yield, 15 g. (68% of the theory from cyclohexanone). It was purified by hydrolysis with 30% aqueous sodium hydroxide, acidification, extraction with ether, drying on calcium chloride and distillation. From the aqueous mother solution of ether extraction, oxalic acid was obtained. The pure III was colorless oil boiling at 162~5°. Yield, 8.5 g. (40% of the theory from cyclohexanone), and gave semicarbazone, m.p. 189.5~190.5° (from ethanol).

Anal. of semicarbazone. Found: C, 56.87; H, 8.87; N, 24.82. Calcd. for $C_8H_{15}ON_3$: C, 56.87; H, 8.94; N, 24.83%.

The m.p. of semicarbazone showed no depression on admixture with an authentic sample, which was prepared in 30.5% yield from cyclohexanone by method B—a. Reported b.p. of III and m.p. of semicarbazone are 165° and 192° (prepared by method B—b)[7] respectively.

(*b*) *From Ethyl 2-Ketocyclohexylglyoxalate.*—

1) a) R. Cornubert et al., *Bull. soc. chim.*, (4) **49**, 1229 (1931); b) H. M. E. Cardwell, *J. Chem. Soc.*, **1951**, 2442.
2) A. Kötz et al., *Ber.*, **45**, 3702 (1912); *J. pr. Chem.*, (ii) **88**, 257 (1913); ibid., **90**, 382 (1914).
3) O. Wallach, *Ann.*, **397**, 197 (1913); ibid., **414**, 219 (1916).
4) Melting and boiling points are uncorrected.
5) H. R. Snyder, L. A. Brookes and S. H. Shapiro, "Org. Synth." Coll. Vol., **II**, 531 (1943).
6) Almost pure III was obtained in 70% yield by distillation under diminished pressure (b. p. 84°/50mm.).
7) H. K. Sen and K. Mondal, *J. Indian Chem. Soc.*, **5**, 621 (1928).

Chart I

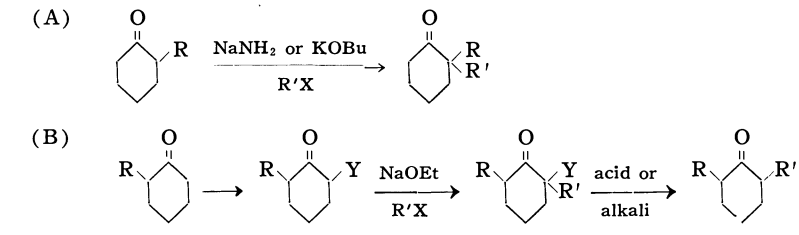

Chart II

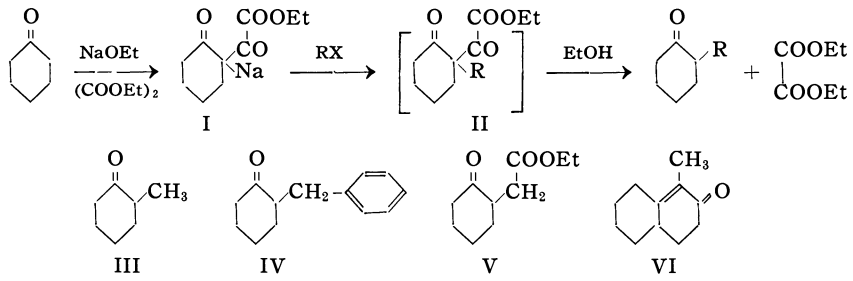

TABLE

Reagent	Reac. temp. (°C) & time (hr.)	Product	b.p.(°C/mm.)	m.p. (°C) of the deriv.[i]	Yield in %[ii]
MeI	70~80; 6	III	162~5	189.4~190.5 Se	40.
MeI	70~80; 6	III	159~161	189 Se	36.[iii]
MeI	method B—a	III	84/50	189 Se	30.5
$PhCH_2Br$	70~80; 7	IV	162~5/16[iv]	165~6 Se	60.
$PhCH_2Cl$	80~90; 8	IV	164~171/17	167~8 Se	37.2
$BrCH_2COOEt$	80~90; 6	V	131~142/17	194~5 Se	13.6
$BrCH_2COOEt$	method A	V	126~135/16	192~192.5 Se	43.
[v]	room tem.; 3 hr. then 80~90°; 2 hr.	VI	140~5/17	216 (dec.) Se 177 Dn	21.
[v]	method B—a	VI	136~140/15	213~4 (dec.) Se 175~7 Dn	16.8

i) Se and Dn mean semicarbazone and 2,4-dinitrophenylhydrazone, respectively.
ii) Yields were calculated from cyclohexanone.
iii) Ethyl 2-ketocyclohexylglyoxalate was isolated.
iv) M.p. was 28~31°.
v) 1-(diethylamino)-3-pentanone methyl iodide.

Ethyl 2-ketocyclohexylglyoxalate[5] (20 g.) was dropped into an absolute ethanol solution of sodium ethoxide (2.3 g. of sodium in 50 ml. of absolute ethanol) and the mixture was heated with 20 g. of methyl iodide at 70~80° for six hours, and treated as usual. Crude III distilled at 160~175° (mainly at 160~5°). Yield, 8.5 g. (75% of the theory). The pure III was obtained by purification in the same way as above, b.p. 159~161°. Yield, 6 g. (55%), and gave semicarbazone, m.p. 189° (from ethanol).

Preparation of 2-Benzylcyclohexanone (IV).—The sodio compound (I), prepared from 9.8 g. of cyclohexanone in the same way, was mixed with 17.1 g. of benzyl bromide, and the mixture was heated at 70~80° for seven hours. After the usual treatment, two fractions were obtained by vacuum distillation, that is fraction (i), b.p. 76~81°/17 mm. (10 g.), and fraction (ii), b.p. 162~177°/17 mm. (mainly 162~7°) (11.5 g.). As fraction i gave oxalic acid by alkaline hydrolysis, it seemed to consist mainly of diethyl oxalate, corresponding to about 60% of the amount initially used. By redistillation of fraction ii, 2-benzylcyclohexanone (IV) was obtained in colorless oil boiling at 162~5°/16 mm., and it crystallized afterwards, m.p. 28~31° (yield, 60% of the theory from cyclohexanone). It gave semicarbazone, m.p. 165~6° (from ethanol).

Anal. of semicarbazone. Found: C. 68.88; H. 7.84; N, 17.72. Calcd. for $C_{14}H_{19}ON_3$: C, 68.54; H, 7.81; N, 17.13%.

The m.p. of semicarbazone showed no depres-

sion on admixture with the authentic sample, prepared by method A[8]. Reported b.p. of IV and m.p. of semicarbazone are 165~6°/18 mm. and 166~7°[8] respectively. When the benzylation was carried out with benzyl chloride, instead of bromide, at 80~90° for eight hours, the yield was 37.2%.

Preparation of Ethyl 2-Ketocyclohexylacetate (V).—To the sodio compound (I) prepared from 9.8 g. of cyclohexanone, 16.7 g. of ethyl bromoacetate was added and the mixture was refluxed for six hours. After a similar treatment as described above, 10 g. (64% recovery) of ethyl oxalate, b.p. 81°/17 mm., and 2.5 g. (13.6% yield) of ethyl 2-ketocyclohexylacetate (V), b.p. 131~142°/17 mm. were obtained, and the latter gave semicarbazone, m.p. 194~5° (from ethanol).

Anal. of semicarbazone. Found: C, 54.83; H, 7.93; N, 17.44. Calcd. for $C_{11}H_{19}O_3N_3$: C, 54.75; H, 7.93; N, 17.41%.

The m.p. of semicarbazone showed no depression on admixture with the authentic sample, prepared by method A as follows: to the sodio compound of cyclohexanone, prepared from 10 g. of cyclohexanone and 4 g. of sodium amide in absolute ether, 17 g. of ethyl bromoacetate was added and the mixture was refluxed for six hours. By the usual treatment, ethyl 2-ketocyclohexylacetate (V) was obtained in colorless oil, boiling at 126~135°/16 mm. (yield, 8 g. or 43%), and gave semicarbazone, m.p. 192~192.5°.

Anal. of semicarbazone. Found: C, 54.85; H, 7.89; N, 17.50. Calcd. for $C_{11}H_{19}O_3N_3$: C, 54.75; H, 7.93; N, 17.41%.

Reported b.p. of V is 131~3°/9.8 mm. (25.4% yield from cyclohexanone by method B—a) and m.p. of semicarbazone is 191~3°[9].

Preparation of 2-Keto-1-methyl-2,3,4,5,6,7,8,10-octahydronaphthalene (VI).—To the sodio compound (I) prepared from 9.8 g. of cyclohexanone, 1-(diethylamino)-3-pentanone methyl iodide (from 15.7 g. of amine and 14.2 g. of methyl iodide in 20 ml. of ethanol) was added and the mixture was allowed to stand at room temperature for three hours, and then refluxed for two hours. The solvent was evaporated, the residue was diluted with water, extracted with ether, the ethereal solution was washed with dilute hydrochloric acid and water, dried and evaporated. After the residue was refluxed with 50 ml. of 40% aqueous potassium hydroxide in 20 ml. of ethanol for fifteen hours, the resulting mixture was diluted with water, extracted with ether, the ethereal solution was washed with water, dried and evaporated. By the distillation of the residue, 3.4 g. (21% yield) of 2-keto-1-methyl-octahydronaphthalene (VI) was obtained in colorless oil boiling at 140~5°/17 mm. and gave 2,4-dinitrophenylhydrazone, m.p. 177° (from ethanol), and semicarbazone, m.p. 216° (decomp.) (from ethanol).

Anal. of 2,4-dinitrophenylhydrazone. Found: C, 59.37; H, 5.57; N, 15.39. Calcd. for $C_{17}H_{20}O_4N_4$: C, 59.29; H, 5.85; N, 16.29%. *Anal.* of semicarbazone. Found: C, 65.14; H, 8.38; N, 18.70. Calcd. for $C_{12}H_{19}ON_3$: C, 65.12; H, 8.65; N, 18.99%.

Their m.p. showed no depression on admixture with the authentic samples, prepared by method B—a according to the method of Robinson[10] as follows: to the sodio compound prepared from 7.4 g. of ethyl 2-ketocyclohexylcarboxylate and sodium ethoxide (from 2.3 g. of sodium) in absolute ethanol, 1-(diethylamino)-3-pentanone methyl iodide (from 6.8 g. of amine and 6.2 g. of methyl iodide) was added and the mixture was allowed to stand at room temperature for three hours and then refluxed for two hours. Then the product was cyclized and hydrolyzed into VI by refluxing with 40% aqueous potassium hydroxide in ethanol for fifteen hours. The product VI was colorless oil boiling at 136~140°/15 mm. (yield, 2 g. or 16.8% from cyclohexanone), and gave 2,4-dinitrophenylhydrazone, m.p. 175~7°, and semicarbazone, m.p. 213~4° (decomp.). Reported b.p. of VI is 125~7°/8 mm. (22% yield from cyclohexanone by the method described in footnote) and m.p. of semicarbazone is 212° (decomp.)[11].

The author wishes to express his hearty thanks to Professor K. Fukui for his helpful advice and encouragement, to Professor Y. Yukawa of Osaka University for his valuable discussion during the course of this work and to the members of Agricultural Department of Kyoto University for microanalyses.

Faculty of Literature and Science
Toyama University, Toyama

8) M. Tiffeneau and M. Porcher, *Bull. soc. chim.*, (4) **31**, 330 (1922).

9) Chang-Kong Chuang and Chi-Ming Ma, *Ber.*, **68B**, 871 (1935).

10) E. C. Du Feu, F. J. McQuillin, and R. Robinson, *J. Chem. Soc.*, **1937**, 53.

11) D. K. Banerjee, S. Chatterjee and S. P. Bhattacharaya, *J. Am. Chem. Soc.*, **77**, 408 (1955).

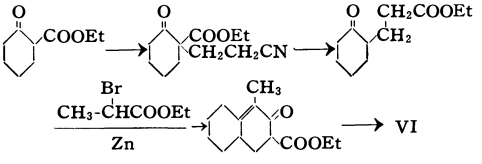

Partial Hydrogenation of 1, 4-Butynediol

By Tosao FUKUDA and Tokishige KUSAMA

(Received October 2, 1957)

For the partial catalytic hydrogenation of acetylenic compounds in the liquid phase, it is necessary to stop the hydrogenation purposely when one molecule of hydrogen has reacted. If we can, however, retard the hydrogenation of ethylenic compounds by some means other than that of acetylenic compounds, the preparation of ethylenic compounds will be simple.

Recently, O. Isler et al.[1] found that the palladium-charcoal catalyst was poisoned by quinoline hydrogenated acetylenic compounds to the corresponding ethylenic compounds, but not to the corresponding saturated compounds. H. Lindler[2] also observed similar phenomena in the hydrogenation of some acetylenic compounds with the palladium calcium-carbonate catalyst poisoned by lead acetate, with the addition of quinoline. W. Oroshnic et al.[3] and B. Elsner et al.[4] found that with the Raney nickel catalyst poisoned by zinc acetate and copper acetate, the hydrogenation of ethylenic compounds was selectively retarded by the addition of piperidine. Since then, some application of these methods have been developed[5].

It was shown that, when the palladium catalyst is poisoned, the hydrogenating activity for acetylenic compounds and that for ethylenic compounds are decreased at different rates[6]. It was also found that, in the case of nitrobenzyl chloride, the hydrogenation takes place selectively when quinoline is added[7]. However, the mechanism of the partial hydrogenation of acetylenic compounds has not clearly been explained.

The present paper describes the experimental results of the hydrogenation of 1, 4-butynediol carried out with the Pd-$CaCO_3$ catalyst poisoned by lead acetate and the poisons, and the partial hydrogenation achieved by using Pd-$CaCO_3$ catalyst with quinoline.

Experimental

Apparatus.—An about 300 cc. usual glass vessel shaken at a constant oscillation was employed.

Materials.—1, 4-Butynediol was recrystallized several times from ethyl acetate. Commercial hydrogen was used. Calcium carbonate was of a commercial extra pure grade (Koso Chemical Co., Tokyo).

Procedures.—Pd-$CaCO_3$ catalyst (Pd-content, 5% by wt.) was prepared from palladium chloride solution according to Lindler[1]. Its poisoning with lead acetate was carried out by adding various amounts of aqueous lead acetate (5g. of $(AcO)_2Pb \cdot 3H_2O$ in 100 cc. of water) to 2 g. of the catalyst. Aqueous 1, 4-butynediol was used. Catalytic hydrogenation was carried out at room temperature (12°~16°C) and at atmospheric pressure, with 250~300 turns oscillation.

Results.—The overall hydrogenation of 1, 4-butynediol proceeded in two distinct steps as shown in Fig. 1. When 30 g. (0.35 mol.) of 1, 4-butynediol in 150 cc. of water was hydrogenated on Pd-$CaCO_3$ catalyst, 8.5 l. (N. T. P.), or 0.38 mol., of hydrogen was absorbed, and the following products were obtained by the distillation of the reaction mixture.

Purified raw material		28 g.
Distillates	i~102°C/3 mmHg	2 g.
	102°~107°C/3 mmHg	19 g.
Decomposed product (found in the trap)		0.7 g.
Residue		5 g.

The product distilling at 102°~107°C/3 mmHg was proved to be a *cis*- and *trans*-1, 4-butenediol mixture by the infrared spectrographic analysis, and found to contain 0.0110 mol. double bond per one gram substance by bromine addition, the theoretical value for pure 1, 4-butenediol being 0.0116 mol.

Fig. 1 shows that the hydrogenation takes place mainly at 1, 4-butynediol in the first step, and then at 1, 4-butenediol. Hydrogenation was carried out with various concentrations of 1, 4-butynediol, 0.3 g. of Pd-$CaCO_3$ being used. The dependency of the initial velocity of the hydrogenation upon the concentration of 1, 4-butynediol is shown in Fig. 2.

1) O. Isler, et al.; *Helv. chim. Acta*, **30**, 1911 (1947).
2) H. Lindler; ibid., **35**, 446 (1952).
3) W. Oroshnik, G. Karmas and A. D. Mcbane: *J. Am. Chem. Soc.*, **74**, 295 (1952).
4) B. B. Elsner and P. F. M. Paul; *J. Chem. Soc.*, **1953**, 3156.
5) a) K. Hofmann and S. M. Sax, *J. Biol. Chem.*, **205**, 55 (1953): see also, L. Luzika and P. Muller, *Helv. chim. Acta*, **22**, 755 (1939): b) J. L. H. Allan, E. R. H. Jones and M. C. Whiting: *J. Chem. Soc.*, **1955**, 1862: c) W. Oroshnic, G. Karmas and A. D. Mcbane, *J. Am. Chem. Soc.*, **74**, 3807 (1952): P. Karrer and J. Kebele, *Helv. chim. Acta*, **35**, 2570 (1952).
6) K. Tamaru, This Bulletin. **23**, 180 (1950).
7) K. W. Rosenmond and F. Zetzsche, *Ber.*, **54**, 425 (1921).

The acivation energies of the hydrogenation were calculated to be 2.7 kcal./mol. for 1,4-butynediol and 5.2 kcal./mol. for 1,4-butenediol, from the hydrogenation experiments at 0°C and 30°C. The results of poisoning of Pd-$CaCO_3$ catalyst by lead acetate are schematically shown in Fig. 3 and Fig. 4. When 0.3 cc. of pyridine, piperidine, or quinoline was added to the reactant, the hydrogenation proceeded as shown in Fig. 5.

When 30 g. (0.35 mol.) of 1,4-butynediol in 150 cc. of water was hydrogenated with Pd-$CaCO_3$ catalyst in the presence of 0.3 cc. of quinoline, 8.21. (N. T. P.), or 0.37 mol. of hydrogen was absorbed, and then the reaction stopped. From the reaction mixture, the following products were obtained.

Puriefied raw material .....29 g.
Distillates { i~102°C/3 mmHg ..... 1 g.
{ 102°~107°C/3 mmHg .....22 g.
Decomposed product
(found in the trap)..... 1 g.
Residue..... 5 g.

The product distilling out at 102°~107°C/3 mmHg was proved to be a mixture of *cis*- and *trans*-1,4-butenediol by the infrared spectrographic analysis, and found to contain 0.0112 mol. double bond per one gram substance by bromine addition.

The Pd-$CaCO_3$ catalyst poisoned by lead acetate was used with 0.3 cc. of pyridine, piperidine or quinoline. The results are schematically shown in Figs. 6~8.

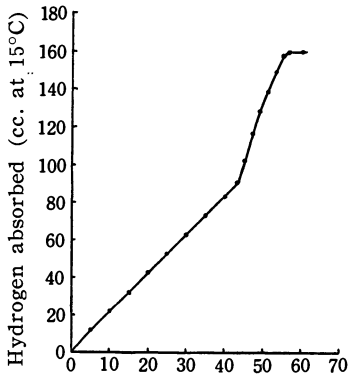

Fig. 1. The hydrogenation rate on Pd-$CaCO_3$ catalyst.
Pd-$CaCO_3$ 0.30 g.
aqueous butynediol 20 cc.
(butynediol, 0.34 g.)
experimental temp. 15°C

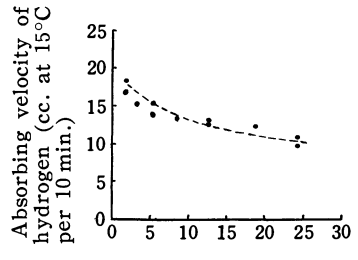

Fig. 2. The effect of the concn. of butynediol on the hydrogenation rate.
Pd-$CaCO_3$ 0.30 g.
aqueous butynediol 20 cc.
experimental temp. 15°C

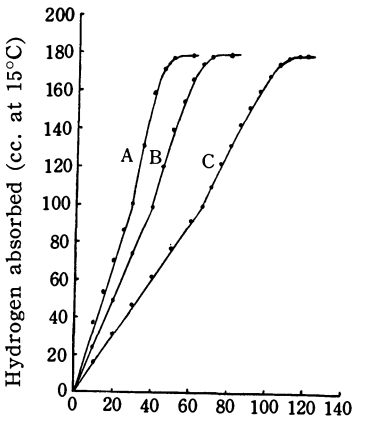

Fig. 3. The effect of lead acetate on the hydrogenating activity of Pd-$CaCO_3$ catalyst.
Pd-$CaCO_3$ poisoned by lead acetate 0.30 g.
aqueous butynediol 20 cc.
(butynediol, 0.34 g.)
experimental temp. 15°C
A: the catalyst poisoned by 0.5 cc. of aqueous lead acetate
B: the catalyst poisoned by 2.0 cc. of aqueous lead acetate
C: the catalyst poisoned by 5.0 cc. of aqueous lead acetate

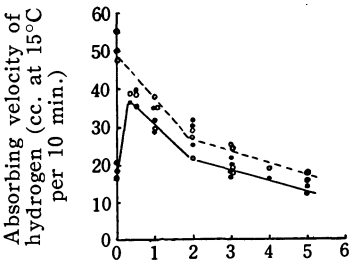

Fig. 4. The effect of lead acetate on the hydrogenating activity of Pd-$CaCO_3$ catalyst.
Pd-$CaCO_3$ poisoned by lead acetate 0.30 g.
aqueous butynediol 20 cc.
(butynediol, 0.34 g.)
experimental temp. 15°C
●: the hydrogenation rate in the 1st step
○: the hydrogenation rate in the 2nd step

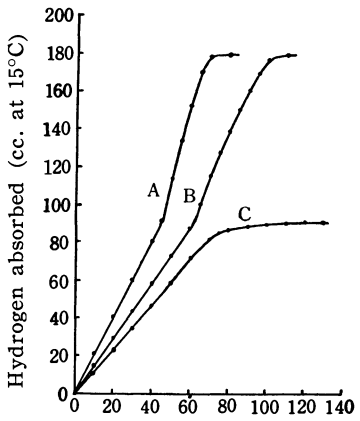

Fig. 5. The effect of poisons on the hydrogenating activity of Pd-$CaCO_3$ catalyst.
Pd-$CaCO_3$ 0.30 g.
aqueous butynediol 20 cc.
(butynediol, 0.34 g.)
experimental temp. 15°C
A: 0.3 cc. of pyridine was added
B: 0.3 cc. of piperidine was added
C: 0.3 cc. of quinoline was added

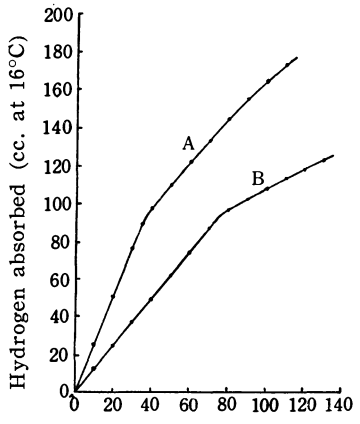

Fig. 6. The effect of pyridine on the hydrogenating activity of the Pd-$CaCO_3$ catalyst poisoned by lead acetate.
Pd-$CaCO_3$ poisoned by lead acetate 0.30 g.
aqueous butynediol 20 cc.
(butynediol, 0.34 g.)
pyridine 0.3 cc.
experimental temp. 16°C
A: the catalyst poisoned by 1.0 cc. of aqueous lead acetate
B: the catalyst poisoned by 5.0 cc. of aqueous lead acetate

Discussion

The hydrogenation of 1,4-butynediol with Pd-$CaCO_3$ catalyst at room temperatures takes place in two distinct steps; the first step is the hydrogenation to 1,4-butenediol, and the second step is its hydrogenation to 1,4-butanediol. The effect of lead acetate and the poisons were

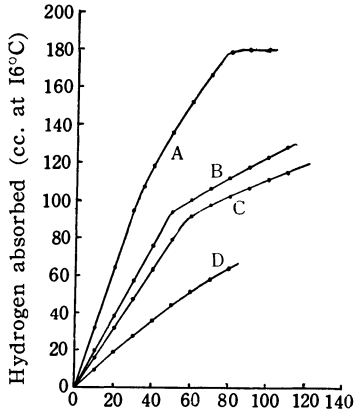

Fig. 7. The effect of piperidine on the hydrogenating activity of the Pd-$CaCO_3$ catalyst poisoned by lead acetate.
Pd-$CaCO_3$ poisoned by lead acetate 0.30 g.
aqueous butynediol 20 cc.
(butynediol, 0.34 g.)
piperidine 0.3 cc.
experimental temp. 16°C
A: the catalyst poisoned by 0.5 cc. of aqueous lead acetate
B: the catalyst poisoned by 0.7 cc. of aqueous lead acetate
C: the catalyst poisoned by 0.9 cc. of aqueous lead acetate
D: the catalyst poisoned by 1.5 cc. of aqueous lead acetate

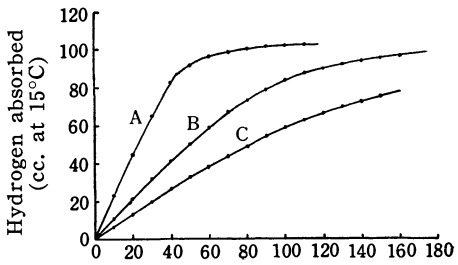

Fig. 8. The effect of quinoline on the hydrogenating activity of the Pd-$CaCO_3$ catalyst poisoned by lead acetate.
Pd-$CaCO_3$ poisoned by lead acetate 0.30 g.
aqueous butynediol 20 cc.
(butynediol, 0.34 g.)
quinoline 0.3 cc.
experimental temp. 15°C
A: the catalyst poisoned by 0.2 cc. of aqueous lead acetate
B: the catalyst poisoned by 0.7 cc. of aqueous lead acetate
C: the catalyst poisoned by 1.0 cc. of aqueous lead acetate

found to be very interesting. When Pd-$CaCO_3$ catalyst is poisoned by increasing amount of lead acetate, the activity for the hydrogenation of 1,4-butynediol increases at first, and then gradually decreases as the poisoning proceeds. On the other hand, that for the hydrogenation of 1,4-butenediol simply decreases with increasing amount of lead acetate. The hydrogenation of 1,4-butynediol is slightly retarded by quinoline, but not by pyridine or piperidine. On the other hand, the hydrogenation of 1,4-butenediol is retarded to some extent by pyridine, more markedly by piperidine and stopped almost completely by quinoline. The effect of these bases is almost the same when they are applied to the Pd-$CaCO_3$ catalyst poisoned by lead acetate. Accordingly, the partial hydrogenation of 1,4-butynediol can be achieved by the use of quinoline.

The reaction velocity in the first step of the hydrogenation is approximated by the following equation, which indicates the retardation of the hydrogenation by 1,4-butynediol,

$$-\frac{dV}{dt}=\frac{k}{1+bC}$$

where V denotes the volume of hydrogen absorbed, t, the time, C, the concentration of 1,4-butynediol, and k and b stand for constants. The retardation may result from the strong adsorption of 1,4-butynediol on the catalyst surface. This theory may be supported by the fact that 1,4-butynediol is adsorbed on the catalyst surface prior to 1,4-butenediol, and the latter is unable to be adsorbed while the former is present. Thus, the hydrogenation may take place in two distinct steps.

The phenomena found on the Pd-$CaCO_3$ catalyst poisoned by lead acetate indicate that the properties of the catalyst are changed by the adsorption of lead acetate. It may be stated that, when pyridine, piperidine, or quinoline is added, these substances are adsorbed on the catalyst surface, even when 1,4-butynediol (or lead acetate and 1,4-butynediol) has been adsorbed previously. The properties of the catalyst surface may also be affected by the adsorption of these bases. Their effect on the palladium catalyst might be different from that of lead acetate. Consequently, the selective hydrogenation may take place as observed.

Summary

1. The effect of lead acetate and the poisons on the Pd-$CaCO_3$ catalyst was studied with the hydrogenation of 1,4-butynediol.

2. The hydrogenation of 1,4-butynediol with the Pd-$CaCO_3$ catalyst at room temperatures takes place in two distinct steps; the first step is the hydrogenation to 1,4-butenediol, and the second is its hydrogenation to 1,4-butanediol.

3. When Pd-$CaCO_3$ catalyst is poisoned by increasing amount of lead acetate, the activity for the hydrogenation of 1,4-butynediol increases at first, and then gradually decreases as the poisoning proceeds. On the other hand, that for the hydrogenation of 1,4-butenediol simply decreases with increasing amount of lead acetate.

4. The hydrogenation of 1,4-butynediol with Pd-$CaCO_3$ catalyst is slightly retarded by quinoline, but not by pyridine or piperidine. On the other hand, the hydrogenation of 1,4-butenediol is retarded to some extent by pyridine, more markedly by piperidine, and stopped almost completely by quinoline. The effect of these bases is almost the same when they are applied to the Pd-$CaCO_3$ catalyst poisoned by lead acetate.

5. The partial hydrogenation of 1,4-butynediol can be achieved by using quinoline, but not by using pyridine or piperidine.

6. The selective hydrogenation may result from the strong adsorption of 1,4-butynediol on the catalyst surface. When the catalyst adsorbs the poisons, the properties of the catalyst surface may be changed. As a result, the selectivity of the catalyst may become very characteristic. Consequently, the selective hydrogenation may take place as observed.

This study was carried out in the Institute of Carbide Chemistry, Yokohama National University, and the cost was defrayed from the Institute. The assistance of Industrial Research Institute of Kanagawa Prefecture, in the infrared spectrographic analysis is gratefully acknowledged. The authors are also indebted to Professor K. Tamaru, for his valuable advice on this study.

Faculty of Engineering
Yokohama National University
Minami-ku, Yokohama

Partial Hydrogenation of 1, 4-Butynediol. II. On the Role of Calcium Carbonate as a Carrier of the Palladium Catalyst

By Tosao FUKUDA

(Received January 20, 1958)

As previously reported[1], when palladium–calcium carbonate catalyst was poisoned by lead acetate, the activity for the hydrogenation of 1,4-butenediol decreased with increasing amount of lead acetate, but was not suppressed completely. When it was poisoned by quinoline, the activity for the hydrogenation of 1,4-butenediol disappeared almost completely, while that for the hydrogenation of 1,4-butynediol decreased only slightly. On the other hand, when Pd-$CaCO_3$ catalyst was poisoned by pyridine or piperidine, the activity for the hydrogenation of 1,4-butenediol decreased only to some extent and did not disappear. When the Pd-$CaCO_3$ catalyst poisoned by lead acetate was poisoned furthermore by quinoline, similar results were obtained. Consequently, it has been shown that the partial hydrogenation of 1,4-butynediol can be achieved by using the Pd-$CaCO_3$ catalyst with quinoline.

However, it is well-known that the properties of a catalyst occasionally depend upon the kind of the carrier on which it is deposited[2]. Accordingly, the selectivity of the catalyst would also be associated with the kind of the carrier. Therefore, the effect of calcium carbonate as a carrier was studied in the hydrogenation of 1,4-butynediol. This paper describes the experimental results and the consideration on the role of calcium carbonate as a carrier of Pd-$CaCO_3$ catalyst.

Experimental

The same apparatus as previously described was employed[1].

1,4-Butynediol was recrystallized several times from ethyl acetate. Commercial hydrogen was used. Calcium carbonate, active charcoal, alumina, silica gel, and Kieselguhr were all obtained from the commercial products. Barium carbonate and barium sulfate were prepared from barium chloride and sodium carbonate and sulfuric acid, respectively.

Various catalysts were prepared from aqueous solutions of palladium (II) chloride by H. Lindler's method[3].

Twenty cc. of an aqueus solution of 0.34 g. of 1,4-butynediol was used. The hydrogenation experiments were carried out at 25°C and at about the atmospheric pressure, with 200 turns oscillation, using 0.3—0.6 g. of the catalyst.

Results and Discussion

With various catalysts the whole hydrogenation of 1,4-butynediol took place in two distinct steps at room temperature. The first step is the hydrogenation of 1,4-butynediol to 1,4-butenediol and the second is that of the latter to 1,4-butanediol, as shown in the previous paper[1].

The absorbing velocity of hydrogen depended upon the kind of the carrier

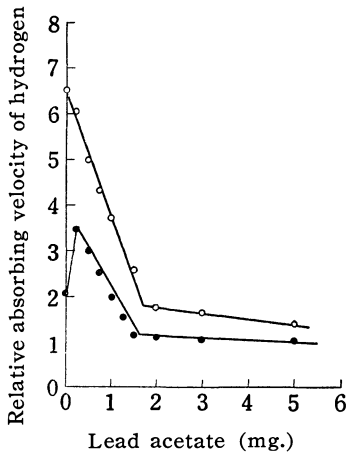

Fig. 1. The poisoning effect of lead acetate on the activities of Pd-$CaCO_3$ catalyst, at 25°C.
Pd-$CaCO_3$ catalyst (Pd, 5%) 0.3 g.
1,4-butynediol solution 20 (1,4-butynediol, 0.34 g.)
●: the effect on the hydrogenation of 1,4-butynediol
○: the effect on the hydrogenation of 1,4-butenediol

1) T. Fukuda and T. Kusama, This Bulletin **31**, 339 (1958).

2) N. D. Zelinsky and A. A. Balandin, *Z. Phys. Chem.*, **126**, 267 (1927); T. Sabalitschka and K. Moses, *Ber.*, B. **60**, 786 (1927); J. T. McCartney, W. K. Hall and L. T. E. Hofer, *Ind. Eng. Chem.*, **39**, 1618 (1947); A. Wheeler, "Catalysis", Vol. 2, p 110 (1950).

3) H. Lindler, *Helv. chim. Acta*, **35**, 446 (1952).

used, as shown in Table I. The activity of Pd-$CaCO_3$ catalyst was not the highest.

When 1.0 cc. each of aqueous solutions of lead acetate, containing various amounts of lead acetate, was added to the reactant prior to hydrogenation, the activity of Pd-$CaCO_3$, Pd-$BaCO_3$, Pd-alumina, and Pd-$BaSO_4$ catalyst decreased with increasing amount of lead acetate, as shown in Figs. 1~4. That is, when Pd-$CaCO_3$ and Pd-$BaCO_3$ catalyst were poisoned by increasing amount of lead acetate, the activity for the hydrogenation of 1,4-butynediol increased at first, and then decreased as the poisoning proceeded. On the other hand, that for 1,4-butenediol monotonously

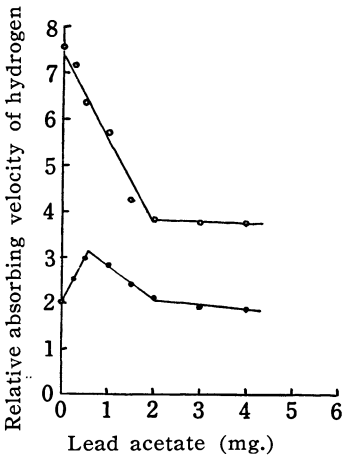

Fig. 2. The poisoning effect of lead acetate on the activities of Pd-$BaCO_3$ catalyst, at 25°C.
Pd-$BaCO_3$ catalyst (Pd, 3%) 0.3 g.
1,4-butynediol solution 20 cc. (1,4-butynediol, 0.34 g.)
●: the effect on the hydrogenation of 1,4-butynediol
○: the effect on the hydrogenation of 1,4-batenediol

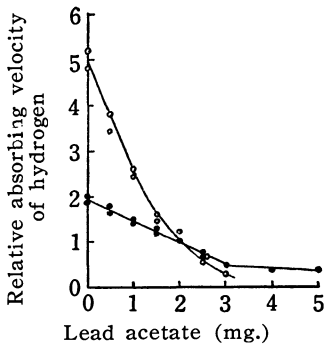

Fig. 3. The poisoning effect of lead acetate on the activities of Pd-alumina catalyst, at 25°C.
Pd-alumina catalyst (Pd, 5%) 0.3 g.
1,4-butynediol solution 20 cc. (1,4-butynediol, 0.34 g.)
●: the effect on the hydrogenation of 1,4-butynediol
○: the effect on the hydrogenation of 1,4-butenediol

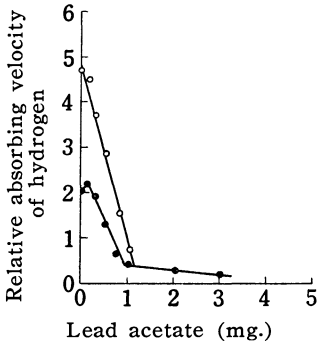

Fig. 4. The poisoning effect of lead acetate on the activities of Pd-$BaSO_4$ catalyst, at 25°C.
Pd-$BaSO_4$ catalyst (Pd, 5%) 0.3 g.
1,4-butynediol solution 20 cc. (1,4-butynediol, 0.34 g.)
●: the effect on the hydrogenation of 1,4-butynediol
○: the effect on the hydrogenation of 1,4-butenediol

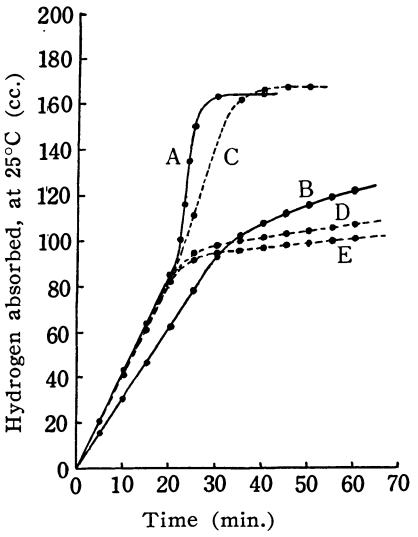

Fig. 5. The poisoning effect of quinoline on the activity of Pd-$BaCO_3$ catalyst, at 25°C.
Pd-$BaCO_3$ catalyst (Pd, 3.5%)
1,4-butynediol solution
A: no poison was added
B: quinoline (0.3 cc.) was added
C: lead acetate (3 mg.) was added
D: lead acetate (3 mg.) and quinoline (0.3 cc.) was added
E: lead acetate (5 mg.) and quinoline (0.3 cc.) was added

TABLE I

THE ABSORBING VELOCITY OF HYDROGEN, AT 25°, IN THE HYDROGENATION OF 1,4-BUTYNEDIOL ON THE VARIOUS CATALYSTS

Catalysts	Pd-content (% by wt.)	Used amt. (g.)	Absorbing velocity of hydrogen, per 10 min. (at 25°C) 1st step (cc., N.T.P.)	2nd step (cc., N.T.P.)
Pd-$CaCO_3$	5	0.3	18~20	46~ 59
〃	2	0.6	17~19	75~ 91
Pd-$BaCO_3$	3.5	0.3	36~37	163~174
〃	2	0.6	32~34	156~169
Pd-Alumina	5	0.3	16~20	35~ 46
〃	2	0.6	12~14	27~ 31
Pd-Charcoal	5	0.3	26~28	92~101
Pd-Kieselguhr	5	0.6	14~16	38~ 39
Pd-$BaSO_4$	5	〃	18~20	38~ 40
〃	3.5	〃	15~16	33~ 35
Pd-Silica-gel	3.5	〃	17~18	35~ 37

TABLE II

THE VOLUME OF HYDROGEN ABSORBED IN THE HYDROGENATION OF 1,4-BUTYNEDIOL ON THE VARIOUS CATALYSTS

Catalysts*	(Pd-content)	Poisons	(amt.)	Absorbing volume of hydrogen per 0.3 g. of 1,4-butynediol, at 25°C 1st step (cc., N.T.P.)	2nd step (cc., N.T.P.)	total volume (cc., N.T.P.)	%**
Pd-$CaCO_3$	(5%)	none	—	83	68	151	85.4
〃	〃	lead-acetate	(1 mg.)	85	83	168	95.0
〃	〃	〃	(5 〃)	〃	〃	〃	〃
〃	〃	piperidine	(0.3 cc.)	〃	〃	〃	〃
〃	〃	quinoline	〃	87	—	—	49.6
Pd-$BaCO_3$	(3.5%)	none	—	84	67	151	85.4
〃	〃	lead-acetate	(1 mg.)	85	69	154	87.0
〃	〃	〃	(5 〃)	〃	〃	〃	〃
〃	〃	piperidine	(0.3 cc.)	87	72	159	89.9
Pd-Charcoal	(5%)	none	—	76	69	145	82.0
〃	〃	lead-acetate	(1 mg.)	78	67	〃	83.1
〃	〃	piperidine	(0.3 cc.)	70	88	158	89.3
Pd-Alumina	(5%)	none	—	82	74	156	88.2
〃	〃	lead-acetate	(1 mg.)	〃	〃	〃	〃
〃	〃	piperidine	(0.3 cc.)	78	90	168	95.0
Pd-$BaSO_4$	(5%)	none	—	84	79	163	92.1
〃	〃	lead-acetate	(1 mg.)	88	82	170	96.0
Pd-Kieselguhr	(5%)	none	—	85	73	158	89.3

* 0.3 g. of the catalyst was used in all the experiments.

** Calculated adsorption (177 cc., N.T.P.) was taken as 100%.

decreased with increasing amount of lead acetate. When Pd-alumina catalyst was poisoned by lead acetate, its catalytic activity for both steps of the hydrogenation decreased monotonously. Pd-charcoal catalyst (Pd, 1~5% by weight) was not affected by lead acetate in the experimental range (1~5 mg. of lead acetate to 0.3 g. of the catalyst).

When 0.3 cc. of piperidine or quinoline was added to the reactant, the hydrogenation proceeded as shown in Figs. 5~7 with Pd-$BaCO_3$, Pd-charcoal, and Pd-alumina catalyst, respectively. The activity of Pd-$CaCO_3$ catalyst was diminished by quinoline, but the effect of quinoline was small for the hydrogenation of 1,4-butynediol and relatively great for that

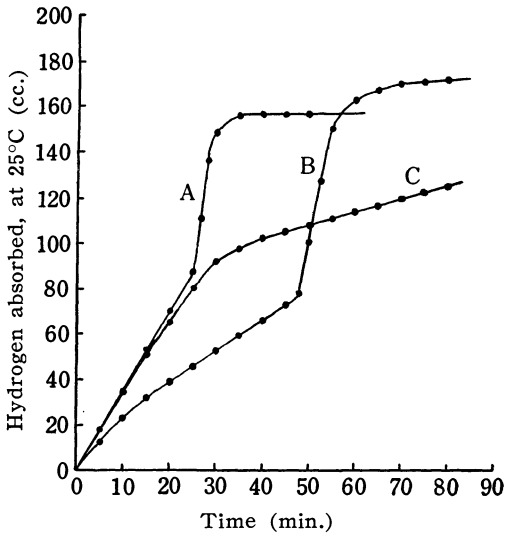

Fig. 6. The poisoning effect of piperidine and quinoline on the activity of Pd-charcoal catalyst, at 25°C.

Pd-charcoal catalyst (Pd, 5%) 0.3 g.
1,4-butynediol solution 20 cc. (1,4-butynediol, 0.34 g.)
A: no poison was added
B: piperidine (0.3 cc.) was added
C: quinoline (0.3 cc.) was added

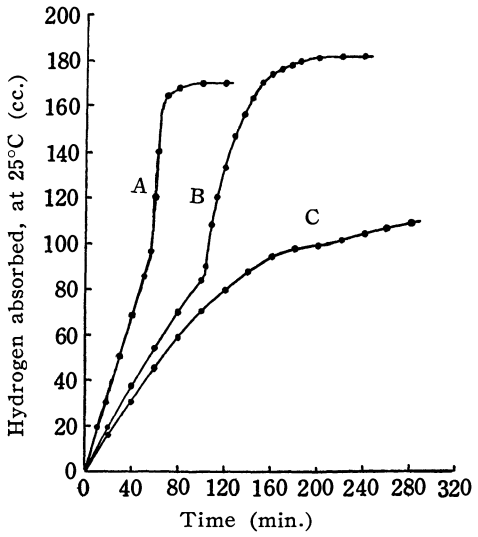

Fig. 7. The poisoning effect of piperidine and quinoline on the activity of Pd-alumina catalyst, at 25°C.

Pd-alumina catalyst (Pd, 5%) 0.3 g.
1,4-butynediol solution 20 cc. (1,4-butynediol, 0.34 g.)
A: no poison was added
B: piperidine (0.3 cc.) was added
C: quinoline (0.3 cc.) was added

of 1,4-butenediol. On the other hand, the activity of Pd-$BaCO_3$ catalyst was not diminished by piperidine. The activity of Pd-alumina catalyst for the hydrogenation of 1,4-butynediol was more markedly diminished by piperidine and by quinoline, and that for the hydrogenation of 1,4-butenediol was markedly diminished, especially by quinoline. When Pd-charcoal catalyst was poisoned by piperidine, the activity for the hydrogenation of 1,4-butynediol markedly decreased, and that for the hydrogenation of 1,4-butenediol remained almost unchanged. When it was poisoned by quinoline, however, the former was not changed much on the contrary, while the latter decreased markedly.

When Pd-$BaCO_3$ catalyst was used with lead acetate and quinoline, the hydrogenation proceeded as shown by dotted lines in Fig. 2. Its activity for the hydrogenation of 1,4-butenediol was suppressed much remarkably than when quinoline alone was used, while that for the hydrogenation of 1,4-butynediol did not change substantially.

As the properties of the catalyst depend upon the kind of the carrier, it is considered that the effect of the poisons varies complicatedly with the kind of the carrier. But it should be noticed that the partial hydrogenation of 1,4-butynediol might also be achieved by using the Pd-$BaCO_3$ catalyst poisoned by both lead acetate and quinoline, though it would not be in the same manner as in the case of Pd-$CaCO_3$ catalyst.

The volume of hydrogen absorbed during the hydrogenation depended upon the kind of the carrier and the poison added to the catalyst. The results are shown in Table II. The volume absorbed was relatively large in the case of the poisoned Pd-$CaCO_3$ catalyst.

According to the previous research, the catalytic hydrogenation of acetylene always causes the acetylene polymerization as its side reaction.[4] The polymerization may be depressed if the catalyst is poisoned[5]. The polymerization may be accompanied with the decrease of the absorbing volume of hydrogen. It is thus considered that 1,4-butynediol also polymerizes during the hydrogenation. Accordingly, the variation of the absorbed volume of hydrogen as observed may be

4) K. Tamaru, This Bulletin, **23**, 64, 180, 184 (1950).
5) M. Sato and N. Ota, *Catalyst*, **12**, 45 (1955); T. Yamanaka: *J. Scientific Research Institute*, **29**, 319 (1948).

attributed to 1,4-butynediol polymerization. It seems that the role of calcium carbonate as a carrier consists in suppressing the polymerization with the poisons, but not in increasing the hydrogenating activity, nor in giving the selectivity for the hydrogenation.

Summary

1. The role of calcium carbonate as carrier of the palladium catalyst was studied in the hydrogenation of 1,4-butynediol.

2. The hydrogenation velocity on Pd-$CaCO_3$ catalyst was not the highest among various palladium catalysts. And the partial hydrogenation of 1,4-butynediol might also be achieved by using the Pd-$BaCO_3$ catalyst poisoned by both lead acetate and quinoline. On the poisoned Pd-$CaCO_3$ catalyst, however, the 1,4-butynediol polimerization, a side reaction of the hydrogenation, was suppressed largely.

3. Consequently, it seems that the role of calcium carbonate as a carrier is to decrease the polymerization as a side reaction of the hydrogenation, but not to increase the activity for the hydrogenation, nor to give the selectivity for the hydrogenation.

This study was carried out in the Institute of Carbide Chemistry, Faculty of Engineering, Yokohama National University, and the cost of this study was defrayed by the Institute. The author is indebted to Professor T. Kusama and Professor K. Tamaru for their valuable advice. The author is also indebted to Mr. H. Kawakami for assistance.

Faculty of Engineering, Yokohama National University, Minami-ku Yokohama

Steroids. XXI[1]*. The Oxidation and Hypobromous Acid Addition of Steroids by Means of Isocyanur Bromide*

By Ken-ichi MORITA

(Received January 9, 1958)

Recently it was shown that isocyanur chloride[2-5] is an effective reagent for oxidation[6] and hypochlorous acid addition[7,8] of steroids. The present investigation aims at elucidating the characteristics of isocyanur bromide, which has not yet been obtained in a pure state, towards oxidation, hypobromous acid addition and allylic bromination of steroids.

The synthesis of isocyanur bromide was attempted by Chattaway and Wadmore[2] about half a century ago. Adding bromine to a solution of cyanuric acid in a cold 5% solution of caustic potash, they obtained a pale yellow substance which rapidly decomposed on exposure to air, evolving bromine. They posturated that the substance was a bromine addition product of a bromoimino derivative of cyanuric acid, in which all the imino-hydrogen atoms of the cyanuric acid were not substituted. The present author added bromine to an alkaline solution of cyanuric acid in the cold with swirling with hand, and obtained a similar substance, while, when bromine was carefully added with vigorous stirring at 0~3°C, a somewhat stable substance was obtained. A better result was obtained when the order of addition was reversed, namely, when the alkaline cyanuric acid solution was added to bromine[9]. It was necessary to remove

1) Part XX: K. Morita, *J. Chem. Soc. Japan, Pure Chem. Sec.* (*Nippon Kagaku Zassi*), **78**, 1705 (1957).

2) F. D. Chattaway and J. M. Wadmore, *J. Chem. Soc.*, **1902**, 191.

3) C. H. G. Hands, F. R. White and J. W. C. Phillips, *J. Soc, Chem. Ind.*, **61**, 66 (1948); Brit. Pat., 634, 801; *Chem. Abst.*, **44**, 7356e (1950).

4) T. Ishii, S. Kanai and T. Ueda, *J. Soc. Org. Synth. Chem. Japan* (*Yuki Gosei Kagaku Kyokaishi*), **15**, 241 (1957).

5) Isocyanur chloride is also a bleaching and sterilizing agent. Cf. *Chem. Trade J.*, **140**, 884 (1957).

6) F. Mukawa, *J. Chem. Soc. Japan, Pure Chem. Sec.* (*Nippon Kagaku Zassi*), **78**, 450 (1957).

7) Idem., ibid., **78**, 452 (1957).

8) S. Mori, K. Morita and F. Mukawa, *Proc. Japan Acad.*, **23**, 535 (1956).

9) Y. Yukawa and U. Suzuki (*Mem. Inst. Sci. Ind. Des. Osaka Univ.*, **10**, 190, (1952) stated that the addition of alkaline succinimide to a mixture of bromine and water was preferable for preparation of *N*-bromosuccinimide.

the moisture in the cake after filtration as fast as possible. The moisture lingering in the product markedly decreased the purity. The percentage of bromine in the product was determined by micro Carius method and by iodometry[4] with well coincident results. The purity of the product was 80~92%. In some cases the isocyanur bromide contained bromine in a percentage as low as 50% (cf. experimental part), but it should be noted that for oxidation and hypobromous acid addition, 50~70% isocyanur bromide was usable as well.

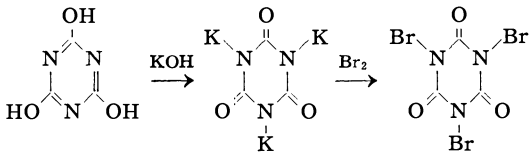

Isocyanur bromide is a white or slightly yellow crystalline powder. It has an odour resembling that of hypobromous acid. It does not melt below 300°C, but decomposes when heated by direct flame. It dissolves to some extent in water and in glacial acetic acid with hydrolysis. When it is added to hydrobromic acid, bromine is liberated. It liberates iodine from hydroiodic acid and from an aqueous solution of potassium iodide. When added to aqueous ammonia, a violent decomposition takes place.

Mukawa[6] reported that the reaction of cholestane-3 β,5 α,6 β-triol (II) with isocyanur chlorid and pyridine in warm benzene furnished cholestane-3 β,5 α-diol-6-one (III) in 80% yield. Under similar conditions the starting material was recovered when isocyanur bromide was used instead of isocyanur chloride, while the oxidation took place smoothly to produce cholestane-3 β,5 α-diol-6-one (III) when *tert*-butanol was used as the solvent. Fieser et al.[10] reported that the oxidation of cholesterol (I) with *N*-bromosuccinimide and acetic acid in aqueous acetone produced cholestane-3 β,5 α-diol-6-one (III) and choleterol dibromide. Under nearly the same conditions except that isocyanur bromide was used in place of *N*-bromosuccinimide cholestane-3 β,5 α,6 β-triol (II) and cholesterol dibromide were obtained but cholestane-3 β,5 α-diol-6-one (III) was not detected. A similar result was reported by Ueno[11], who found that oxidation of cholesterol with *N*,*N*-dibromobenzenesulfonamide gave cholestane-3 β,5 α,6 β-triol (II). It is concluded that isocyanur bromide is an oxidizing agent milder than *N*-bromosuccinimide or isocyanur chloride.

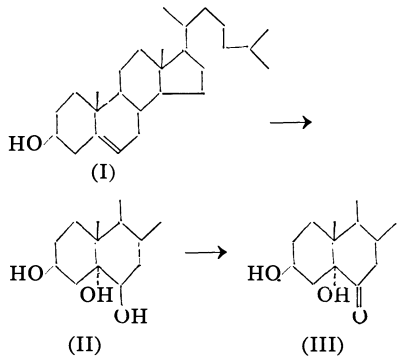

Hypochlorous acid addition of 5-ene-steroids by means of isocyanur chloride and acetic acid in aqueous acetone is known to produce corresponding chlorohydrins in good yields[7,8]. Hypobromous acid addition of cholesteryl acetate (IV) by means of isocyanur bromide and acetic acide in the same solvent furnished 5 α-bromocholestane-3 β,6 β-diol 3-monoacetate (V) and cholesteryl acetate dibromide (VII) only in low yields. Fried and Sado[13] demonstrated that hypobromous acid addition of 4,9(11)-pregnadiene-17 α,21-diol-3,20-dione 21-acetate with *N*-bromoacetamide in dioxane containing dilute sulfuric acid gave 9 α-bromohydrocortisone acetate in only 48% yield, while in dioxane containing dilute perchloric acid, 9 α-bromohydrocortisone acetate was obtained in 80~90% yield[14]. Mori[15] reported that the reaction of cholesteryl acetate (IV) with *N*-bromoacetamide in ether containing dilute sulfuric acid gave no hypobromous acid addition product V, but gave cholesteryl acetate dibromide (VII). The present author obtained the bromohydrin (V) from cholesteryl acetate (IV) in 61% yield with *N*-bromoacetamide and dilute perchloric acid in dioxane and in 49% yield with isocyanur bromide and dilute perchloric acid in the same solvent. Ueno[12] reported

10) L. F. Fieser and S. Rajagopalan, *J. Am. Chem. Soc.*, **71**, 3938 (1949).
11) Y. Ueno, *J. Pham. Soc. Japan* (*Yakugaku Zasshi*), **72**, 1626 (1952).
12) Idem., ibid., **72**, 1622 (1952).
13) J. Fried and E. F. Sabo, *J. Am. Chem. Soc.*, **79**, 1136 (1957).
14) Perchloric acid has been employed on hydroxybromination of 9(11)-ene-steroids (H. B. Henbest et al., *J. Chem. Soc.*, **1955**, 2477; R. H. Lenhars and S. Bernstein, *J. Am. Chem. Soc.*, **77**, 6665 (1955)), of 11-ene-steroids (J. E. Herzig et al., ibid., **78**, 2017 (1956)), and of 5-ene-steroids (B. Ellis and V. Petrow, *J. Chem. Soc.*, **1956**, 4417). Cf. B. Loenken et al., *J. Am. Chem. Soc.*, **78**, 1738 (1956).
15) S. Mori, *J. Chem. Soc. Japan, Pure Chem. Sec.* (*Nippon Kagaku Zassi*), **73**, 505 (1952).

the same hydroxy-bromination reaction with *N*-bromosuccinimide and with *N,N*-dibromobenzenesulfonamide and acetic acid in aqueous acetone, obtaining compound V in 15 and 37% yields, respectively[16]. Proof for the bromohydrin structure was obtained from its coversion into cholesteryl acetate β-oxide (VI) by a reaction with potassium acetate and into 5 α-bromocholestan-3 β-ol-6-one acetate by oxidation with chromic acid in acetic acid.

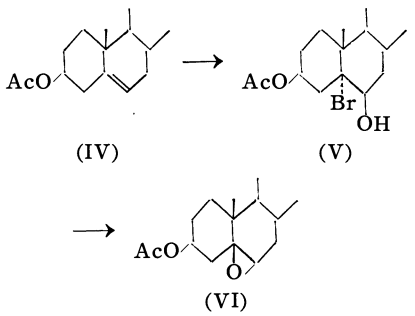

(IV) (V) (VI)

It seemed to be of interest to study the allylic bromination with isocyanur bromide, since Ziegler and his coleagues[17] described the allylic chlorination of cyclohexene with isocyanur chloride. Reaction of cholesteryl acetate (IV), 4-cholesten-3-one and testosterone benzoate with isocyanur bromide in boiling carbon tetrachloride under a strong illumination, however, failed to produce brominated compounds but resulted in the recovery of the starting materials, except only in special case (See experimental part).

Experimental[18]

Isocyanur Bromide.—Ten grams of bromine and 60 ml. of distilled water were mixed and cooled in an ice-salt bath to 0°C. A solution of 2 g. of cyanuric acid (purity 92.5%[4]) and 3 g. of potassium hydroxide in 60 ml. of distilled water was added dropwise to the well-stirred mixture at 0~3°C, caution being taken not to cool down below 0°C. After the addition, the mixture was stirred for further twenty minutes. The solid was collected, washed thoroughly with ice water to neutral reaction, with purified acetone several times and twice with ether, (in order to remove the moisture quickly and stored in a sulfuric acid desiccator. Yield 5.3 g. or 75% of the theoretical.

Anal. Found: Br, 60.38% (micro Carius method; 92.2% of the theoretical); Br, 60.02% (Iodometry[4]); 91.8% of the theoretical). Calcd. for $C_3O_3N_3Br_3$: Br, 65.54%.

The purity was practically unchanged after stored in a sulfuric acid desiccator for three months in the dark. In other runs the percentage of bromine in the product ranged from 80% to 92%, doubtlessly owing to slight changes of washing procedures. When the precipitate was washed with dioxane and then with ether, nearly the same results were obtained. It took about ten days to dry the product completely over sulfuric acid and the purity became about 40~50%. When dried over phosphorous pentoxide under a reduced pressure (5 mmHg) overnight the purity also decreased to 55~60%.

Similar results were obtained when the reaction was carried out under illumination.

Cholestane-3 β, 5 α, 6 β-triol (II).—A suspension of 4.5 g. of cholesterol (I) in 200 ml. of acetone and 25 ml. of water was mixed with 3.3 g. (1.25 equiv.) of 55.1% isocyanur bromide and 2.5 ml. of acetic acid and the mixture was shaken occasionally at room temperature. Soon the mixture became yellow in color. In about one hour the whole solid went into solution and in 2.5 hours from the beginning a new solid appeared. After being kept over night, the suspension was filtered off and extracted with ether, and the extract was washed with water and alkali, dried and concentrated until crystals began to separate. After cooling with ice, the crystalline material was collected. Recrystallization from chloroform gave colorless needles melting at 237~238°C. Yield 1.0 g.

The identity was established by conversion into the diacetate[19], m.p. and mixed m.p. 165~166°C. The product did not produce a phenylhydrazone.

The ethereal mother liquor was evaporated under a reduced pressure and triturated with methanol to give 1.2 g. of a solid with m.p. 107~118°C*. Recrystallization from ethanol gave colorless needles, m.p. 121~122°C, which was identified as cholesterol dibromide by a mixed m.p. determination.

Cholestane-3 β, 5 β-diol-6-one (III).—To a solution of 251 mg. of compound II in 25 ml. of *tert*-butyl alcohol 0.5 ml. of pyridine, 0.5 ml. of water and 99.5 mg. of 83.8% isocyanur bromide were added successively. The mixture was warmed at 65~70°C for 30 minutes. After filtration the filtrate was diluted with ether, washed with a 10% bisulfite solution, aqueous alkali and water, and dried over anhydrous sodium sulfate. The solution was concentrated under a reduced pressure. Careful dilution with water gave needles, m.p. 230~233°C (decomp.), which was not depressed when admixed with an authentic sample[10]. Yield 228 mg.

The substance was further characterized by

16) Ueno obtained a small anount of 6β-bromocholestane-3β, 5α-diol 3-acetate from the mother liquor, but the present author did not attempt to isolate it.

17) K. Ziegler, A. Spath, E. Schauf, W. Schumann and E. Winklman, *Ann.*, **551**, 80 (1942).

18) All melting points are uncorrected. All rotations are measured in chloroform solution. Concentrations (*c*) are expressed in g. per 100 ml. of solution. The author is indebted to Mr. T. Iwama for microanalyses and to Mr. F. Mukawa for the supply of cyanuric acid.

19) V. A. Petrow, *J. Chem. Soc.*, **1937**, 1077.

* All of brominated steroids described in this paper melted with decomposition.

coversion into the phenylhydrazone[20], m.p. 163～164°C and into 3-monoacetate[10], m.p. 232～233°C.

Attempted Oxidation of Cholestane-3β, 5α, 6β-triol (II) with Isocyanur Bromide and Pyridine in Benzene.—A mixture of 0.25 g. of compound II, 20 ml. of benzene, 0.12 g. of 91.8% isocyanur bromide and 0.3 ml. of pyridine was heated under reflux for 15 minutes and treated as described above. The strating material, m.p. 215～225°C, was recovered. (0.19 g.) Recrystallized material melted at 236～238°C.

The identity was established by conversion into the diacetate[19], m.p. and mixed m.p. 165～166°C,

Hypobromous Acid Addition of Cholesteryl Acetate (IV).—(*a*) *Perchloric Acid-Isocyanur Bromide Method.* A solution of 1 g. of compound IV in 50 ml. of dioxane and 7 ml. of water was mixed with 0.6 g. of 84.5% isocyanur bromide and 0.3 ml. of 60% perchloric acid and the mixture was shaken occasionally at room temperature (19°C). After two hours the suspension was diluted with 25 ml. of a 10% sodium bisulfite solution and left to stand in a refrigerater (5°C) for one hour, and the solid was collected by filtration. The material was dried and extracted with a small volume of hot chloroform and the chloroform solution was diluted with petroleum ether. Crystals were collected. Needles, m.p. 160～165°C (0.68 g.). Recrystallization from chloroform-petroleum ether gave fine needles, m.p. 174～175°C, $[\alpha]_D^{21.5}-35$ (c, 0.998). Yield 0.6 g. or 49% of the theoretical. The melting point was not depressed on admixture with authentic 5α-bromocholestane-3β, 6β-diol 3-monoacetate[15]. (Found: Br, 15.42%, Calcd. for $C_{29}H_{49}O_3Br$; Br 15.24%) Reported m.p. 177°C, $[\alpha]_D-37$[21]; m.p. 175°C, $[\alpha]_D-33.8$[12]; m.p. 177～178°C[15].

(*b*) *Perchloric Acid-N-Bromoacetamide Method.* A mixture of 1 g. of compound IV, 50 ml. of dioxane, 7 ml. of water, 0.45 g. of *N*-bromoacetamide and 0.3 ml. of 60% perchloric acid were treated in the same way as described above. Recrystallization from chloroform-petroleum ether gave needles, m.p. 158～161°C (0.9 g.). Further recrystallization yielded the pure substance, m.p. 174～175°C, $[\alpha]_D^{21}-38$ (c, 1.02). Yield 0.75 g. or 61% of the theoretical. The melting point was not depressed on admixture with a specimen from method *a*.

(*c*) *Acetic Acid-Isocyanur Bromide Method.* A mixture of 2.5 g. of compound IV, 1.3 g. of 83.8% isocyanur bromide, 150 ml. of acetone, 10 ml. of water and 4 ml. of acetic acid was refluxed for ten minutes, poured into an excess of water, and extracted with ether. The extract was washed with water, dried over anhydrous sodium sulfate, and evaporated. The oily residue was dissolved in ethyl acetate and methanol was added to produce faint turbidity. Then a small volume of ether was added and the mixture was left to stand in a refrigerator (5°C) for 5 days. Crystals (m.p. 100～158°C) were collected and recrystallized from ether-methanol to produce long needles with m.p. 112～115°C (0.3 g.). The melting point was not depressed on admixture with authentic cholesteryl acetate dibromide.

The mother liquor from the above experiment was concentrated to produce crystals, which were mainly cholesteryl acetate dibromide (0.2 g.). The mother liquor from the above concentrate was again concentrated to produce crystals, which were collected and recrystallized from chloroform-petroleum ether to give needles, m.p. 174～175°C (0.2 g.). This substance did not depress the melting point of 5α-bromocholestane-3β, 6β-diol 3-monoacetate (V).

A solution of the mixture (0.75 g.) of the products from methods *a*, *b* and *c* in acetic acid (26 ml.) and water (7 drops) was oxidized with chromic acid (0.35 g.) to give 5α-bromocholestan-3β-ol-6-one acetate (0.6 g.), m. p. 165～166°C. (Found: Br, 15.18%. Calcd. for $C_{29}H_{47}O_3Br$: Br, 15.26%). Reported m.p. 164～166°C[12], 164～165°C[15], 163°C[22].

Cholesteryl Acetate β-Oxide (VI).—To a suspension of 212 mg. of compound V in 7 ml. of ethanol was added 0.4 g. of sodium acetate (crystalline) and the mixture was refluxed for 1.5 hours. Soon the solid went wholly into solution and a new solid appeared. After cooling, water was added and the solid was collected by filtration. The crystals, after recrystallized from aqueous methanol, gave a negative Beilsterin test, and melted at 111～112°C. Needles (189 mg.). The melting point was not depressed when admixed with authentic cholesteryl acetatate β-oxide[24] (VI). Reported m.p. 111～113°C; $[\alpha]_D-1$[23], 113°C[24].

The product (21.2 mg.) in chloroform (0.5 ml.) was treated with 4 N hydrogen bromide in acetic acid (0.5 ml.) for 10 minutes at room temperature to give needles with m.p. 172～174°C when recrystallized from chloroform-petroleum ether. The melting point was not depressed on admixture with 5α-bromocholestane-3β, 6β-diol 3-monoacetate (V).

Attempted Allylic Bromination of Testosterone Benzoate.—(*a*) *With Isocyanur Bromide washed with Acetone as Described Above.* A mixture of 0.5 g. of testosterone benzonate and 0.25 g. of 91.8% isocyanur bromide in 10 ml. of carbon tetrachloride was refluxed for 30 minutes with exposure to strong light. The starting material was recovered in nearly quantitative yield. Under nearly the same conditions, 4-cholesten-3-one and cholesteryl acetate could not be brominated.

(*b*) *With Isocyanur Bromide not washed with Acetone but left to stand in a Sulfuric Acid Desiccator Overnight.* To a solution of 1 g. of testosterone benzoate in 20 ml. of carbon tetrachloride was added 1.2 g. of the isocyanur bro-

20) R. H. Pickard and J. Yates, ibid., **93**. 1678 (1908).
21) D. R. Jones and C. W. Shoppee, ibid., **1954**, 4224.
22) I. M. Heilbron, E. R. H. Jones and F. S. Spring, ibid., **1937**, 801.
23) P. A. Plattner et al., *Helv. chim. Acta*, **27**, 513 (1944).
24) S. Mori, *J. Chem. Soc. Japan, Pure Chem. Sec.* (*Nippon Kagaku Zassi*), **64**, 981 (1943).

mide and the mixture was refluxed for 30 minutes with exposure to strong light. The solid was removed by filtration and the solution was evaporated to dryness. Recrystallization from acetone-methanol gave needles with m.p. 150~152°C (0.55 g.). After recrystallization from ethyl acetate-methanol, the analytical sample showed m.p. 178°C, $[\alpha]_D^{19}+86$ (c, 0.370), λ_{max} 232 mμ (ε 23,800).

Anal. Found: Br, 17.29%. Calcd. for $C_{26}H_{31}O_3Br$: Br, 16.96%.

Ruzicka et al.[25] reported m.p. 176~177°C for 6ξ-bromotestosterone benzoate. The product may be 6ζ-bromotestosterone benzoate, since the same substance was obtained when testoserone benzoate was brominated with *N*-bromosuccinimide as described below and it is known that reactions of 4-ene-3-ketosteroids and *N*-bromosuccinimide give corresponding 6ξ-bromo-4-ene-3-ketosteroids[26]. But the abnormal shift of the ultraviolet absorption maximum to the shorter wavelength can not be explained[27].

(*c*) *With N-Bromosuccinimide.* One half gram of testosterone benzoate was treated with 0.25 g. of *N*-bromosuccinimide in refluxing 10 ml. of carbon tetrachloride for 30 minutes under the ordinary light. After evaporation under a reduced pressure, the residue was triturated with *n*-hexane to give a colorless solid (0.45 g.), m.p. 143~144°C. The melting point was raised to 177~177.5°C when recrystallized from ethyl acetate-methanol and was not dedressed on admixture with the sample obtained above.

The author is indebted to Professor S. Mori of Tokyo Metropolitan University for his encouragement throughout this work. The author's thanks are also due to Dr. M. Nakamura and Mr. R. Mamine of this Institute for their interest in this investigation.

Sugiyama Chemical Research Institute
Mure, Mitaka, Tokyo

25) R. Ruzicka et al., *Helv. chim. Acta*, **20**, 328 (1937).
26) C. Djerassi et al., *J. Am. Chem. Soc.*, **72**, 4534 (1950); F. Sondheimer et al., ibid., **75**, 4712, 5932 (1953); B. Camerino et al., *Gazz. chim. ital.*, **84**, 301 (1954); *Chem. Abst.*, **49**, 14787b (1955); V. R. Mattox et al., *J. Biol. Chem.*, **197**, 261 (1952).
27) Cf. K. Morita, *J. Chem. Soc. Japan, Pure Chem. Sec.* (*Nippon Kagaku Zassi*), **78**, 1581 (1957).

Benzylation of Acetylene. II. On the Structure and Oxidation of 3-Benzyl-3,4-diphenyl-1-Butyne

By Teisuke ANDO and Niichiro TOKURA

(Received July 24, 1957)

We reported the formation of 3,4-diphenyl-1-butyne (I) and its isomer, 3,4-diphenyl-1,2-butadiene (II), by the reaction of benzyl chloride and sodium or lithium acetylide in liquid ammonia[1], whereas formation of benzylacetylene had been expected[2]. In the present paper, we report the formation and the structure of 3-benzyl-3,4-diphenyl-1-butyne (III).

It is particularly interesting that III was produced in addition to I and II in the reaction using an equimolar ratio of benzyl chloride to a metallic acetylide and that III resisted oxidation.

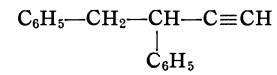

I

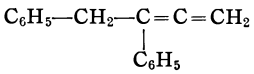

II

III was obtained as a fraction distilling at 207°C (4.5 mmHg) and following the fraction of I and II from the reaction mixture. III was a yellowish, viscous liquid and formed complex salts with silver nitrate and with alkaline mercuric iodide[3,4], showing the presence of an ethynyl group —C≡CH. The presence of the terminal acetylenic bond was reassured by a strong absorption maximum at 3320 cm.$^{-1}$ due to stretching vibration of the bond and a weak one at 2120 cm.$^{-1}$ for a monosubstituted acetylene[5]. The

1) T. Ando and N. Tokura, This Bulletin, **30**, 259 (1957).
2) T. H. Vaughn, G. F. Hennion, R. R. Vogt and J. A. Nieuwland, *J. Org. Chem.*, **2**, 1 (1938).
3) J. R. Johnson and W. L. McEwen, *J. Am. Chem. Soc.*, **48**, 469 (1926).
4) B. B. Elsner and P. F. M. Paul, *J. Chem. Soc.*, **1951**, 893.
5) L. J. Bellamy, "The Infra-red Spectra of Complex Molecules", John Wiley and Sons, Inc., New York (1954), p 49.

ethynyl group of III resisted strongly against oxidizing agents, as compared with a double bond between ordinary aliphatic carbon atoms[6]. Namely, (1) by passing air into a solution of III for many hours at room temperature, III was not oxidized and was completely recovered. (2) When an alkaline aqueous solution of III (a part was dissolved but most part remained as a suspension) was agitated with 30% aqueous hydrogen peroxide and the solution was left to stand for one night, the substance was not oxidized. Even when the alkaline solution was mixed with an excess of hydrogen peroxide and the solution was heated on a water bath, it remained without being oxidized. (3) When 5% ozone was introduced into a solution of III in ethyl acetate for 30 minutes at −10°C, a minute amount of benzoic acid was produced, but the main part remained without being oxidized. The above results well coincided with the experiment of Criegee and Lederer[7] on an ethynyl compound. III was oxidized with potassium permanganate either in neutral, alkaline or acidic solution at room temperature. The oxidation in an acidic medium gave a white crystalline substance (A), m.p. 139~140°C, in a low yield, but the yield was increased to 92% in a neutral solution. The aqueous solution of A was acidic. When a piece of A was dropped into concentrated sulfuric acid, instant vesication was observed, showing A was an α-keto acid. An absorption of carboxyl ion $-COO^-$[8] was observed at 1370 cm.$^{-1}$ in infrared spectrum of A. Absorptions at 1711 cm.$^{-1}$ and 1722 cm.$^{-1}$ showed that the substance was a derivative of pyruvic acid, according to Icherweed[9] and Jones[10]. In addition to the above I.R. spectra, elementary analysis of A corresponded to $C_{23}H_{20}O_3$. This acid (A) is therefore considered to be phenyldibenzylpyruvic acid (IV).

By either decarbonylation by heat or oxidation with hydrogen peroxide or potassium permanganate, IV always gave a white crystalline substance (B), melting at 122~123°C. When III was reduced with hydrogen and palladium carbon, a colorless, slightly viscous oil (C), b.p. 192~194°C (3 mmHg), was produced through absorption of one mole of hydrogen. In C, the absorptions of the ethynyl group (3320 cm.$^{-1}$) disappeared, but stretching vibration of C=C (non-conjugate)[11] newly appeared at 1668 cm^{-1}. Absorption maxima at 1430 cm.$^{-1}$ and 912 cm.$^{-1}$ showed the presence of a vinyl group (—CH=CH_2). C was therefore assumed to be 3-benzyl-3,4-diphenyl-1-butene (V).

Oxidation of V with potassium permanganate gave an acid, m.p. 139~140°C, and no lowering of the melting point of a mixture of this acid and IV was observed. It was supposed that, when gently oxidized with potassium permanganate, III and V gave the same keto-acid owing to the degradation of ethynyl and vinyl group, respectively. When oxidized with ozone, V gave an acid, m.p. 122~123°C, which was identified as B by the mixed melting point.

Treatment of III with sulfuric acid in the presence of mercuric sulfate gave a crystalline substance (VI) in a yield of 78%, b.p. 230~240°C (6 mmHg), m.p. 84~84.5°C. I.R. spectrum of VI showed carbonyl stretching vibration in open chain ketones[11] at 1700 cm.$^{-1}$ and methyl deformation of methyl ketone[12] at 1354 cm.$^{-1}$. From the above I.R. spectral analyses and a positive iodoform reaction, it should have a methyl ketone group, but it has not yet yielded oxime, hydrazone nor semicarbazone. We suppose that this ketone is difficult to react with the carbonyl reagents on account of the steric hindrance by the three phenyl groups.

Furthermore, an attempt to reduce VI by Clemmensen's method failed. When oxidized with hypobromite[13], VI gave an acid of m.p. 122~123°C, which was identified as B by the mixed melting point.

When B was allowed to stand about two months at room temperature, the melting point was raised to 153~154°C from 122~123°C, but I.R. and U.V. spectra did not change. We call the higher melting substance α-form and the lower melting one β-form tentatively.

Hauser and Brasen[14], and Baker[15] reported the benzylation of benzyl cyanide in liquid ammonia. We carried out the same reaction and prepared 2-benzyl-2,3-diphenylpropionitrile (VII). Hydrolysis

6) F. Bohlmann and J. Sinn, *Ber.* **88**, 1869 (1955).
7) R. Criegee and M. Lederer, *Ann.* **583**, 29 (1953).
8) M. st. C. Flett, *J. Chem. Soc.*, **1951**, 962.
9) F. A. Icherweed, *Nature*, **195**, 419 (1955).
10) R. L. Jones, ibid., **173**, 121 (1954).
11) R.B. Barmes, R.C. Gore, U. Lidded and V.Z. Williams, "Infra-red Spectroscopy", Reinhold Publishing Co. (1944).
12) J.A. Anderson and W.D. Seybried, *Anal. Chem.*, **20**, 998 (1948).
13) W. S. Johnson, C. D. Gustsche and R. D. Offenhauer, *J. Am. Chem. Soc.*, **68**, 1648 (1946).
14) C. R. Hauser and W. R. Brasen, ibid., **78**, 494 (1956).
15) R. H. Baker, ibid., **70**, 3857 (1948).

of this nitrile to an acid amide (VIII) by refluxing for four days with sulfuric acid in glacial acetic acid, followed by treatment with sodium nitrite, gave 2-benzyl-2,3-diphenylpropionic acid (IX), m.p. 153~154.5°C, which on admixture with the β-form (m.p. 153~154.5°C) showed no depression of the melting point.

It is also of interest that Hauser's[14] acid, obtained by the same procedure as above, showed the same melting point 124~125°C, as our α-form.

When we compared melting points of nitrile VII, amide VIII and acid IX to those of Hauser's[14] and Baker's[15] substance, respectively (Table I), we found that our values resembled Baker's closely except acid IX.

TABLE I

	Author	Hauser et al.[14]	Baker[15]
Nitrile VII	81~83°C	92~92.5°C	82°C
amide VIII	112.7~114°C	—	111~112°C
acid IX	α 122~123°C	124~125°C	131~132°C
	β 153~154.5°C		

It was observed that nitrile VII affords two forms, m.p. 92°C and 82°C. We concluded the α-form and the β-form are polymorphs of 2-benzyl-2,3-diphenylpropionic acid (IX). Such cases often occur in sterically hindered systems[16].

It appears likely that Baker's acid was a mixture of the α- and the β-form. Table II shows a series of compounds derived from III was described above. Since the structure of IX has been thus decided, the structure of III, IV, V and VI are established, as already assumed, as 3-benzyl-3,4-diphenyl-1-butyne, phenyldibenzylpyruvic acid, 3-benzyl-3,4-diphenyl-1-butene and 3-benzyl-3,4-diphenyl-2-butanone, respectively.

A similar benzylation of allylbenzene in liquid ammonia has given 3-benzyl-3,4-diphenyl-1-butene (V) in a good yield, as will be reported later.

Experimental[17]

3-Benzyl-3,4-diphenyl-1-butyne (III).— Metallic sodium was dissolved in liquid ammonia and to this solution acetylene gas was introduced to form sodium acetylide, and the product was added to an equimolar amount of benzyl chloride in liquid ammonia, for the mixture to be treated as reported in the preceding paper[1]. Following the fraction of I and II, 3-benzyl-3,4-diphenyl-1-butyne (III) distilled at 207°C (4.5 mmHg), a pale yellow oil; yield, 15.3% or 30 g. from 252 g. of benzyl chloride.

Anal. Found: C, 93.48; H, 6.64. Calcd. for $C_{23}H_{20}$: C, 93.20; H, 6.80%. I.R. ν max: 3320 and 2120 cm.$^{-1}$ Mol. wt.: Found, 296; Calcd. for $C_{23}H_{20}$: 296.

A mercuric complex[3] was given as white fine needles from petroleum ether (b.p. 40~60°C), m.p. 159~159.5°C.

Mercury determination of the complex salt: 4.093 mg. of the substance gave 1.0379 mg. or 25.36% of Hg. Calcd. for $C_{46}H_{38}Hg$: Hg, 25.36%.

Oxidation of III with Potassium Permanganate. Phenyldibenzylpyruvic Acid (IV).— (*a*). *Oxidation in a neutral medium.* A three necked flask of two litre capacity equipped with an air-tight agitator and a reflux condenser are used as the reaction vessel. III (4.2 g.) was dissolved in 400 cc. of acetone and to the solution 8 g. of potassium permaganate dissolved in 400 cc. of water was added and the mixture was agitated for 48 hours at room temperature. After distilling off acetone, sulfur dioxide gas cooled with ice

TABLE II

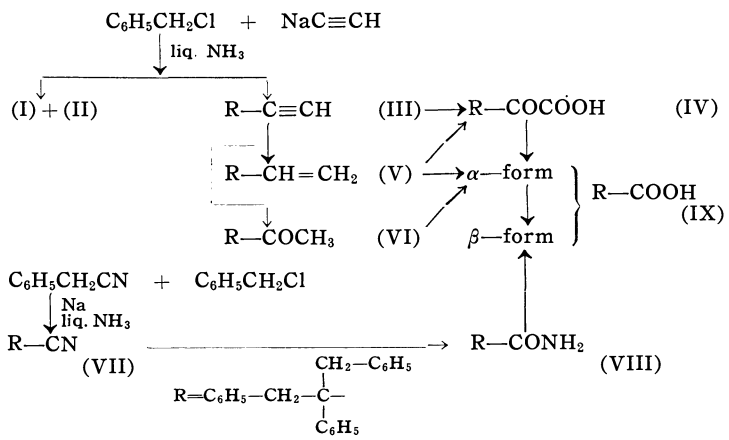

16) W. V. Miller and G. Rohde, *Ber.*, **25**, 2017 (1892).

17) Melting points were not corrected.

was introduced into the residue and then the solution was made basic with dilute aqueous sodium hydroxide. Unchanged neutral part was extracted with ether and the remaining alkaline layer was acidified with hydrochloric acid and extracted with ether. After removal of ether, 4.5 g. of crystals melting at 139.51~40°C were obtained in a yield of 92%.

Anal. Found: C, 80.68; H, 5.92. Calcd. for $C_{23}H_{20}O_3$: C, 80.21; H, 5.85%. I.R. ν max: 1722, 1711, and 1370 cm.$^{-1}$

In other experiments oxidation was carried out for 100 hours at room temperature and 8 hours at boiling water bath temperature, the yields of IV being depressed to 17.2 and 21%, respectively, when the precipitate of manganese dioxide was not decomposed with sulfur dioxide.

(*b*) *Oxidation in an alkaline medium.* One gram of III was vigorously agitated and emulsified with 150 cc. of water and 20 cc. of 2N potassium hydroxide solution. To the emulsion 200 cc. of 1% aqueous potassium permanganate was added and then agitation was continued for 150 hours at room temperature. Then the solution was treated as stated above yielding 0.1 g. (8.6%) of crystals (IV), m.p. 139.5~140°C.

(*c*) *Oxidation in an acidic medium.* Two grams of III was dissolved in 500 cc. of glacial acetic acid, and 300 cc. of 1% aqueous potassium permanganate was added to the solution. By 3 hours agitation, reddish violet color disappeared. When the solution was treated as described above, only a minute amount of an acidic part was obtained.

Partial Hydrogenation, 3-Benzyl-3,4-diphenyl-1-butene (V).—Two grams of III was dissolved in 100 cc. of metanol in a reducing flask. In a Willstätter reducing apparatus III was reduced at 15°C in the presence of 0.5 g. of 5% palladium carbon. In 25 minutes, 160 cc. of hydrogen was absorbed. Then the reaction was discontinued and the solvent was distilled off. The residue was distilled under a reduced pressure, and 1.8 g. of V was obtained, b.p. 192~194°C (3 mmHg).

Anal. Found: C, 92.17; H, 7.61. Calcd. for $C_{23}H_{22}$: C, 92.57; H, 7.43%. I.R. ν max: 1668, 1430, 1002 and 912 cm.$^{-1}$

Oxidation of V with Potassium Permanganate.—Two grams of V was dissolved in 500 cc. of acetone in a three-necked flask of 1 liter capacity and to the solution 100 cc. of a 4.2% potassium permanganate solution was added. The mixture was agitated for 48 hours at room temperature, and then for 15 hours at 45°C. After removal of the solvent, sulfur dioxide gas was introduced under cooling with ice. The residue was made basic with dilute caustic alkali and extracted with ether. The aqueous layer was acidified and extracted with ether. After removal of the solvent from the ethereal solution, 0.5 g. (21%) of white globular crystals were obtained; m.p. 138~140°C. It was confirmed that they were identical with IV by a melting point determination of the mixed crystals after recrystallization.

Hydration of III. 3-Benzyl-3,4-diphenyl-2-butanone (VI).—Ten grams of III was dissolved in 200 cc. of methanol in a three-necked flask equipped with a mechanical agitator and a reflux tube. To the solution a mixture of 1.5 g. of mercuric sulfate, 3 cc. of concentrated sulfuric acid and 10 cc. of water was added and agitated under reflux. After 6 days, the reaction was terminated, the insoluble substances were filtered off and the solvent was distilled off from the filtrate. Then the residue was distilled under a reduced pressure. A reddish brown viscous oil was obtained; b.p. 230~240°C (6 mm Hg). On addition of a small amount of ethanol to the oil, white heavy plates were crystallized, m.p. 84~84.5°C; yield, 8.3 g. (78%).

Anal. Found: C, 87.79; H, 7.13. Calcd. for $C_{23}H_{22}O$: C, 87.86; H, 7.05%. I.R. ν max: 1700, 1354, 1152, 1078 and 1031 cm^{-1}.

The α-Form of 2-Benzyl-2,3-diphenylpropionic Acid (IX).—(*a*) *Heat decarbonylation of IV.* IV (0.5 g.) was taken in a small test tube and gradually heated on a sulfuric acid bath. On elevation of the temperature of the bath above the melting point of IV, 140°C, the evolution of a gas from the substance was observed. When the temperature of the bath reached to 220°C, splitting of carbon monoxide occurred very quickly. While the temperature of the bath was elevated to 260°C for 1 hour, the gas evolution was completed. The colorless fused substance changed orange and then to reddish orange in color. After cooling, the product was crystallized form ligroin (b.p. 80~100°C), yielding white crystals, m.p. 122~122.5°C (α-form); yield, 0.1 g. (21.7%).

(*b*) *Reaction of IV with hydrogen peroxide.*—In a beaker of 200 cc. capacity, 1.5 g. of IV was mixed with 20 cc. of 10% sodium hydroxide solution and 30 cc. of 10% hydrogen peroxide, and the mixture was allowed to stand for one night in an ice box. Then another 10 cc. portion of hydrogen peroxide (10%) was added to the mixture with stirring. After 8 hours, the mixture was acidified and extracted with ether. When the ethereal solution was dried and evaporated, fine scales were afforded, m.p. 115~120°C; yield, 0.4 g. (87%). When recrystallized from ligroin (b.p. 80~100°C), 0.28 g. of white scales were obtained, m.p. 122~123°C (α-form).

(*c*) *Oxidation of IV with potassium permanganate.* IV (0.5 g.) was dissolved in 100 cc. of 2% aqueous sodium hydroxide in a round flask of 300 cc. capacity, and to the solution 50 cc. of 1% aqueous potassium permanganate was added. The mixture was agitated for 8 hours and left to stand for one night. The mixture was neutralized with dilute sulfuric acid, treated with sulfur dioxide gas to dissolve manganese dioxide, and then extracted with ether. When the ether was distilled off, white crystals remained. On recrystallization from ligroin (b.p. 80~100°C), 0.2 g. (43.5%) of white scales were obtained, m.p. 121~122°C (α-form).

(*d*) *Oxidation of V with ozone.* Two grams of V was dissolved in 100 cc. of ethyl acetate,

cooled at −60°C and ozone (0.01 mole/hour) was passed for 50 minutes. The solvent in the reaction mixture was distilled off under a reduced pressure. After decomposition of the ozonide in the residue with ice, 10 cc. of 10% aqueous sodium hydroxide and 5 cc. of 10% hydrogen peroxide were added; the mixture was left to stand for one night, and extracted with ether to remove the neutral part. The residual solution gave 1.5 g. (71%) of an acid, m.p. 119~121°C, on acidification. When the product was recrystallized from ligroin (b.p. 80~100°C), crystals (1.2 g.) m.p. 122~123°C (α-form), were obtained.

(*e*) ***Oxidation of VI with sodium hypobromite.*** To 50 cc. of 1,4-dioxane containing 5 g. of VI, a sodium hypobromite solution (5 cc. of bromine in 50 cc. of ice-cooled alkali solution containing 15 g. of the alkali hydroxide) was added with vigorous agitation and the mixture was left to stand for two days at room temperature. The dioxane layer was separated and concentrated to a greyish white semisolid, which was dissolved in ether and washed with water. From the ether layer 1.6 g. (yield, 32%) of crystals were obtained, m.p. 118~120°C. On recrystallization from petroleum ether, white plates were obtained m.p. 122~123°C (α-form).

Anal. Found: C, 83.51; H, 6.45. Calcd. for $C_{22}H_{20}O_2$: C, 83.51; H, 6.37%. I.R. ν max: 3500, 2200 and 1700 cm.$^{-1}$ U.V. λ max: 258 mμ (log ε: 2.67) and 265 mμ (log ε: 2.56).

The specimens obtained by the above five reactions were confirmed to be the same acid by the melting point determination of mixed crystals.

On standing about two months at room temperature, the melting point of the crystals (IX, α-form) rose to 153~154°C (β-form) from 122 ~123°C (α-form). In I.R. and U.V. spectra of these two forms, no difference was observed.

Benzylation of Benzylcyanide. 2-Benzyl-2,3-diphenylpropionitrile (VII), 2-Benzyl-2,3-diphenylpropioamide (VIII), and the β-Form of 2-Benzyl-2,3-diphenylpropionic Acid (IX).—We carried out the benzylation reaction, as reported by Hauser et al.[14] and Baker[15] to get VII in a fair yield.

The product, 2-benzyl-2,3-diphenylpropionitrile, (VII), m.p. 81~83°C, b.p. 204~205°C (2 mm Hg). was mixed with 70% sulfuric acid in glacial acetic acid and the mixture was refluxed for 4 days to afford 2-benzyl-2,3-diphenylpropioamide (VIII), m.p. 122.7~114°C (Baker[15] reported m.p. 111~ 112°C).

Anal. Found: N, 4.20, Calcd. for $C_{22}H_{21}ON$: N, 4.44%.

When amide VIII was treated with sodium nitrite, 2-benzyl-2,3-diphenylpropionic acid (IX) (β-form) was given, m.p. and mixed m.p. with an authentic specimen of β-form, 153~154.5°C.

Anal. Found: C, 83.51; H, 6.45. Calcd. for $C_{22}H_{20}O_2$: C, 83.51; H, 6.37%. I.R. ν max: 5300, 2200 and 1700 cm^{-1}. U.V. λ max: 258 mμ (log ε: 2.67) and 265 mμ (log ε: 2.56).

Summary

The equimolar reaction between benzyl chloride and sodium acetylide in liquid ammonia resulted in the formation of 3-benzyl-3,4-diphenyl-1-butyne in addition to 3,4-diphenyl-1-butyne and 3,4-diphenyl-1,2-butadiene. This compound resisted various oxidative reagents except potassium permanganate. 2-Benzyl-2,3-diphenylpropionic acid was obtained in two polymorphs.

Infrared absorption sepectra were measured by Professor Kinumaki and his associates of this Institute and the elementary analyses were performed in the Laboratory of Shionogi Drug Manufg. Co., Ltd., to whom the writers are deeply indebted.

Chemical Research Institute of Non-aqueous Solutions, Tohoku University
Katahira-cho, Sendai

Polarographic Investigations of Vitamin C. I. On the Oxidation Waves of L-Ascorbic Acid and the Reduction Wave of Dehydro-L-ascorbic Acid

By Sôzaburo ONO, Masanosuke TAKAGI and Tamotsu WASA

(Received September 24, 1957)

Although the physiological importance of vitamin C (V. C) has been well known since its discovery, there still remain many problems unsolved concerning this vitamin. Namely, very little knowledge has been obtained even for the mechanism of its antiscorbutic processes[1]. The vitamin has been also discussed on its role as a member of the oxidation-reduction systems in both vegetable and animal bodies, and the measurements of the oxidation-reduction potentials of the system have been exhaustively carried out by several investigators[2~4]. In spite of their efforts, the previous knowledge may not seem to be sufficient to interpret the specificity of V. C. There are considerably many related substances of V. C which also possess close oxidation-reduction potentials to those of V. C and still do not show any physiological similitude[5~7].

On the other hand, as to the polarographic investigations of V. C hitherto reported, L-ascorbic acid (A. A.) has been known to be readily oxidizable at the dropping mercury electrode and the half-wave potential of the first wave (at pH= 0) is about 200 mV. more positive than the corresponding standard oxidation-reduction potential measured potentiometrically, while its oxidized form dehydro-L-ascorbic acid (D. A. A.) has been believed to show no reduction wave under the ordinary polarographic conditions[8~12].

In order to interpret these phenomena, many experimental and theoretical studies have been made by several investigators[13~16]. Indeed, the analysis of these disagreements between the polarographic and the potentiometric results would be expected to offer some clue to obtain real knowledge on the specificity of V. C.

It is, however, important to realize that the previous discussions have not been developed on the basis of the sufficient experimental results of both A. A. and D. A. A., and therefore the problem may not be said to have been solved even qualitatively.

In the present experiments, first the reinvestigations of the already known facts on the oxidation waves of A. A. were made and followed by the more careful and detailed experiments in alkaline region than previously known, and further a reduction wave of D. A. A. was obtained.

Although some of the observations concerning this reduction wave of D. A. A. have been already reported by the present authors[17], more detailed results are presented in this paper and discussions are made on the mechanism of the electrode reactions of both A. A. and D. A. A.

Experimental

Materials:—A. A. was a product of Takeda Pharmaceutical Ind. which was used without further purification.

D. A. A. was first prepared by using Pecherer's method[18], but later A. A. in aqueous solution was oxidized to D. A. A. with equimolar amount of iodine or bimolar amount of silver nitrate.

1) A. Szent-Györgyi, "Bioenergetics", Academic New York Press, (1957) p. 49.
2) H. Borsook and G. Keighly, *Proc. Nat. Acad. Sci.*, **19**, 875 (1933).
3) R. Wurmser and J. A. De Loureiro, *J. chim. phys.*, **31**, 419 (1934).
4) E. G. Ball, *J. Biol. Chem.*, **118**, 219 (1937).
5) G. M. Richardson and R. K. Cannan, *Biochem. J.*, **23**, 68 (1929).
6) N. Mayer, *J. chim. phys.*, **34**, 107 (1937).
7) R. Wurmser, N. Mayer and O. Crepy, ibid., **33**, 101 (1936).
8) E. Kodicek and K. Wenig, *Nature*, **142**, 35 (1937).
9) C. Cattaneo and G. Sartori, *Gazz. chim. ital.*, **72**, 351 (1942).
10) Y. Okada, *J. Agr. Chem. Soc. Japan*, (*Nippon Nogei Kagaku Kaishi*), **19**, 749, 955 (1943).
11) D. Nomura, Thesis for the graduation, Kyoto Univ. (1942).
12) C. Go, *J. Ferment. Technol. Japan*, **28**, 165 (1945).
13) Z. Vavrin, *Coll. Czech. Chem. Communs.*, **14**, 367 (1949).
14) R. Brdicka and P. Zuman, ibid., **15**, 766 (1950).
15) D. H. M. Kern, *J. Am. Chem. Soc.*, **76**, 4234 (1954).
16) J. Koutecky, *Coll. Czech. Chem. Communs.*, **20**, 116 (1955).
17) S. Ono, M. Takagi and T. Wasa, *J. Am. Chem. Soc.*, **75**, 4369 (1953).
18) B. Pecherer, ibid., **73**, 3827 (1951).

In order to obtain D. A. A. solutions of relatively high concentrations as purely as possible, the latter method was used preferably. In the case of the oxidation with iodine, iodine was used in an aqueous solution containing about twice mole of potassium iodide, and after the oxidation in a volumetric flask, the resulting solution was partly neutralized with sodium hydroxide or sodium acetate and then filled up to the mark. The solution was used without removing iodide ions. Silver nitrate as an oxidizing reagent was also used in an aqueous solution. After the oxidation of A. A. in a volumetric flask, some amounts of sodium hydroxide or sodium acetate which had been taken to adjust the pH of the solution to the desired value. The solution was filled up to the mark and then the silver precipitate was filtered off. The filtrate was used as D. A. A. solution.

The aqueous solution of D. A. A. was prepared each time freshly, since D. A. A. is fairly unstable even in acidic solution.

Buffer Solutions:—For the acidic range, McIlvaine's buffer solutions (pH 2.2~8.0) and acetate buffer solutions (pH 3.6~5.6) were used. For the alkaline range Kolthoff's buffer solutions (pH 8.0~12.0) and 0.1N sodium hydroxide (pH 13) were used. In the course of experiments, it was sometimes necessary to avoid the use of borate in the electrolytic solutions as will be seen later and in such cases, pH's were adjusted with sodium hydroxide and disodium hydrogen phosphate.

The water for preparing stock solutions of the sample and the buffer solutions was redistilled 3 or 4 times with a glass apparatus, since even the presence of trace of the copper ion is still unfavorable for the stability of A. A.

As maximum suppressor, aqueous solution of gelatin was used whose concentration was about 0.005% in the final electrolytic solution.

Apparatus and Procedure:—A Yanagimoto Polarograph with photographic recorder was used. The maximum sensitivity of the galvanometer was 5.5×10^{-9} A. The characteristics of the capillary used were $m=1.323$ mg./sec. and $t=2.7$ sec./drop in 0.1N potassium chloride solution at open circuit when the height of the mercury reservoir was 60 cm. A normal calomel electrode (N.C.E.) was used as a reference electrode. For the experiments of the oxidation waves of A. A. and D. A. A., the height of the mercury reservoir was usually 60 cm. The electrolytic cells were the most simple and common ones. Although no thermostat was used, the room temperature was roughly controlled at 15°±1°C during the experiments. For the experiments in acidic range, polarograms were taken from +0.3 V. (vs. N. C. E.).

As it is well known, A. A. in aqueous solution is readily oxidized by the atmospheric oxygen, especially in an alkaline medium, even the stock solution, whose pH was usually adjusted to less than 4 with buffer solution or meta phosphoric acid, was freed from oxygen by bubbling nitrogen gas, while a known volume of buffer solution (usually less than 7 ml.) was taken into an electrolytic cell and it was also bubbled with nitrogen gas for twenty minutes. Thereafter, a knwon volume of the stock solution (usually about 1 ml.) was pipetted out and added into the electrolytic cell, bubbling of nitrogen gas being still continued through the buffer solution. The bubbling was stopped after a few minutes and the polarogram was taken immediately. The concentration of the sample was usually 10^{-4} to 10^{-3} mol./l.

For obtaining the reduction wave of D. A. A. experiments were carried out under the following conditions.

Concentration range of D. A. A.:
0.025~0.1 mol./l.
pH range: 2~5
Temperature range:
10~50°C at 5°C intervals.

For the temperature control, the electrolytic cell fitted with a jacket was used, through which water of a constant temperature was circulated. The accuracy of the temperature control was ±0.05°C. Nitrogen was used for the removal of oxygen from the electrolytic solution.

Controlled Potential Electrolysis:—In order to know whether the electroreduction product of D. A. A. is A. A. or not, a manually controlled potential electrolysis, modifying Lingane's method[19], was employed. To omit the procedure to take up some portion of the electrolytic solution each time after the electro-reduction at the mercury pool, the electrolytic cell as shown in Fig. 1 was used; after the electrolysis for a given time at a fixed potential (a), the capillary is dipped into the same cell and polarograms are taken, using a calomel electrode as the outer reference electrode (b). For the salt bridge potassium nitrate was used in stead of potassium

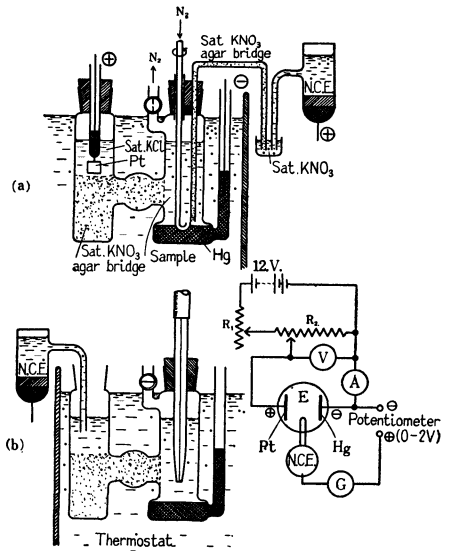

Fig. 1. Controlled potential electrolysis.
V—Voltometer A—Ammeter
E—Electrolytic cell G—Galvanometer

19) J. J. Lingane, *Discussions Faraday Soc.*, **1**, 203(1947).

chloride, since the anodic wave of A. A. is masked by that of the chloride ion. The preparation of D. A. A. by oxidation with iodine was not used for this electrolysis, since the presence of the iodide ion is not favorable in the same meaning as above.

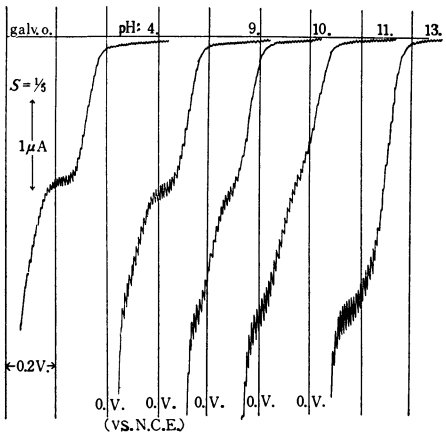

Fig. 2. Polarograms of A. A. in various pH. concn. of A. A. = 2.3×10^{-4} mol./l.

Results and Discussion

Oxidation Waves of A. A.—As is seen in Fig. 2, A. A. shows one oxidation wave at pH less than 8 and two at pH more than 8. Both the first and the second waves have almost an equal height. Since two-electron transfer has been known with the first wave[8~16] the second wave should also involve another two-electron transfer. This total four-electron transfer for the oxidation of A. A. in alkaline range coincides with the observation by Euler and Hasselquist[20,21] who studied the oxidation of A. A. by means of the titration with 2, 6-dichlorophenol indophenol. Concerning the presence of the second wave, Müller and Phillips[22] have already stated it briefly, but they did not present its polarograms and, since then, there has been no other report which confirms even the presence of the wave. The second wave should not be overlooked, since there is certain possibility that it might be confused with the first one.

The relation between the half-wave potential of the first wave and pH was not so much different from those reported by other authors[9~14], but it was remarked that above pH 12 the measurement of the potential becomes difficult because of the superimposing of the first wave with the second.

The instability of A. A. should be also taken into consideration to obtain reliable data with A. A., especially in alkaline range. Fig. 3 shows an example of the change of the waves with time. The rate of the decrease of the wave height strongly depends on pH.

In Fig. 3 the first wave seems to decrease more quickly than the second. Considering only this phenomenon, it was first

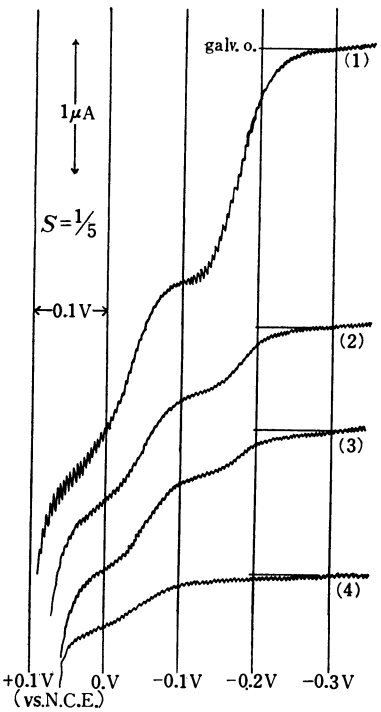

Fig. 3. Decrease of wave heights of A. A. due to the air-oxidation. pH=10.27, borate-NaOH buffer solution.
(1) concn. of A. A.=2.3×10^{-4} mol./l. without airation. (2) after 20 min. airation. (3) after 30 min. airation. (4) after standing for 24 hr. without airation.

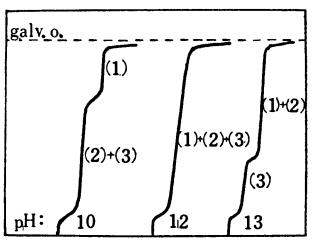

Fig. 4. Schematic polarograms of A. A. containing its decomposition product in alkaline buffer solution. (1) 1st wave (2) 2nd wave (3) 3rd wave

20) H. v. Euler and H. Hasselquist, *Arkiv Kemi*, **4**, 169 (1952).
21) H. Hasselquist, ibid., **4**, 370 (1952).
22) O. H. Müller and R. A Phillips, *Am. J. Physiol.*, **129**, 426 (1940).

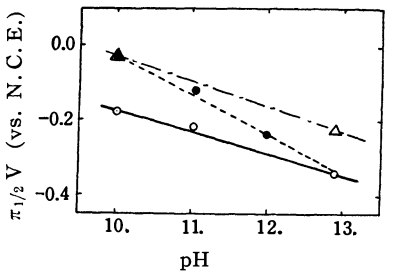

Fig. 5. pH dependence of the three waves of A. A.
○ 1st wave ●, 2nd wave, △ 3rd wave; $\pi_{1/2}$ of the large drawn wave at pH 12 was taken as the value of the 2nd wave at the pH.

supposed that the first oxidation product of A. A. in bulk alkaline solution would be identical with the electro-oxidation product corresponding to the first wave. But it was soon revealed that the above supposition was not adequate; it is readily seen when the same kind of experiment as shown in Fig. 3 is carried out at higher pH's. Fig. 4 schematically shows three different waves in alkaline range after partial oxidation of A. A. Here A. A. was first partially oxidized in alkaline solution and reacidified by metaphosphoric acid to pH 4 and used as stock solution. The experimental values of the half-wave potential of the three waves are presented in Fig. 5. From Figs. 4 and 5, it is apparent that the third wave which appeared after oxidation should be distinguished from the other two which have been initially present. At present it is, however, still difficult to predict to which stage of the oxidation processes of A. A. this third wave corresponds.

D. A. A. was also examined, in order to know its behavior in alkaline solution, in comparison with the above described three waves of A. A.; D. A. A. does not show any oxidation wave in the buffer solutions which contain more or less borate, though the three waves of A. A. were observed in the same buffer solutions. D. A. A. or 2, 3-diketogulonic acid (D. G. A.) seems to combine with the borate ion to a product which may be no more oxidizable at the dropping mercury electrode. This coincides with Militzer's observation[23] that the oxidation of D. A. A. or D. G. A. with methylene blue or the copper ion was completely hindered by the borate ion in alkaline solution. The present results may be also referred to Pasternak's report[24] that the disappearance of the polarographic reduction wave of benzil was caused by the reaction of its carbonyl group with the borate ion.

However, when buffer solutions were prepared only with sodium hydroxide and disodium hydrogen phosphate, D. A. A. showed very unstable and complicated oxidation waves. They were much less

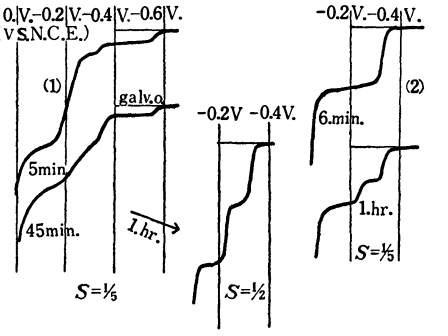

Fig. 6. Change of oxidation waves of A. A. and D. A. A. in alkaline solution (pH=12.9). (1) started with D. A. A. of 4.3×10^{-4} mol./l. (2) started with A. A. of 7.5×10^{-5} mol./l.

stable than those of A. A. and under the present experimental conditions they decreased quickly with time, even if the electrolytic solutions were kept from oxygen as free as possible. Fig. 6 shows an example of the change of the waves with time; starting with D. A. A. the waves were first considerably different from those of A. A., but after a certain time they seemed to show quite a similar character to each other. Above all, when the solution was reacidified, the polarogram of the former showed a wave which had the same $\pi_{1/2}$ as that of A. A. at the given pH. From these observations, though the possibility of reduction of D. A. A. to A. A. in alkaline solutions seems not to be denied, it may be more reasonable to consider the formation of some endiol compound which has a similar $\pi_{1/2}$ to that of A. A., e. g., triose-reductone[14].

The fact that D. A. A. or its decomposition products showed complicated oxidation waves may indicate that there must be several alkaline decomposition products of D. A. A., each of which has an endiol group or some other functional group as readily oxidizable as an endiol, as Petuely and Künssberg[25] have widely investigated with many of the related substances.

23) W. E. Militzer, *J. Biol. Chem.*, **158**, 247 (1945).

24) R. Pasternak, *Helv. Chim. Acta*, **30**, 1984 (1947).
25) F. Petuely and U. Künssberg, *Monatsh.*, **83**, 80 (1952).

Also the fact that some endiol compounds are formed during the decomposition process of D. A. A. in alkaline solution has been known by Euler and Hasselquist[26]. On the other hand, Trnka[27] found three different anodic waves during the decomposition process of glucose in alkaline solution from which he predicted three kinds of endiol compound. Taking into account the possibility of some common processes between the decomposition of glucose and that of A. A., it would be expected to find some common endiols, and further investigations of this kind may seem to be interesting to continue. For that purpose, however, not only polarography but some other more direct methods should be used. At present, therefore, no further discussion is made.

In consideration of the present results together with the previous knowledge on endiol compounds obtained by Euler et al.[28,29] and Petuely et al.[25], the stepwise electrode reactions of A. A. in alkaline solution may be expressed in one way as follows.

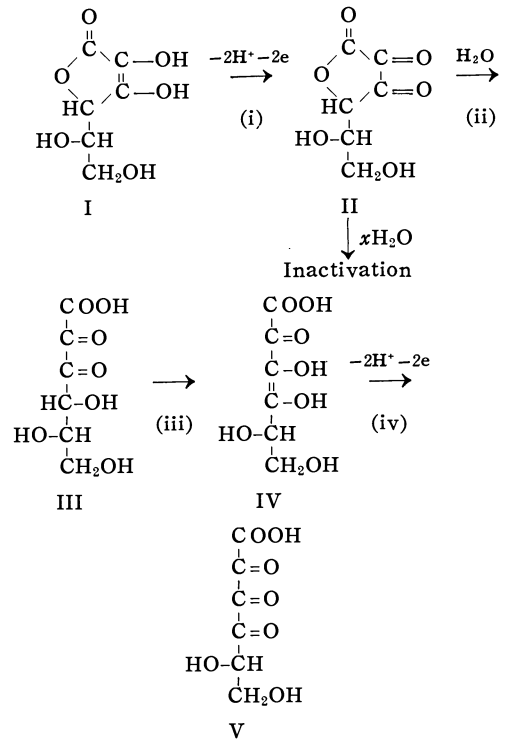

In the above diagram, i) is the reaction corresponding to the first wave of A. A. and iv) to the second. Here it is supposed that D. A. A. which has been produced by the reaction i) opens its lactone ring (ii) and further it is converted into an endiol by the rearrangement iii). The endiol is further oxidized at the dropping mercury electrode (iv). In this case the rate of reaction of both ii) and iii) must be by all means enough rapid, compared with the diffusion process. Since it has been found that D. A. A. or D. G. A. reacts with the borate ion to an electroinactive substance, the rate of both ii) and iii) must be also sufficiently rapid than that of the above inactivation reaction. Further it may be supposed that the substances IV and V can be decomposed in the bulk solution. Above all, the fact that though D. A. A. or D. G. A. reacts with the borate ion to produce an inactive substance, A. A. showed an oxidation wave of its decomposition product after standing of the solution even in the presence of the borate ion, may suggest the possibility of the direct opening of the lactone ring.

Reduction Wave of D. A. A.—D. A. A. shows a small reduction wave at the potential between −0.3 and −0.5 V. (vs. N. C. E.) in pH 2~5, when polarograms are taken at room temperature with D. A. A. of relatively high concentrations (0.025 ~0.1 mol./l.).

The reduction wave of D. A. A. at 25°C corresponds to about 1/1000 of its expected diffusion current which can be approximately estimated from the oxidation wave of A. A. The shape of the wave of D. A. A. and its inclination differ considerably from those of A. A. Also the reduction wave of D. A. A. shows all the typical characteristics of a kinetic current: constancy of the wave height, independency of the height of the mercury reservoir (Fig. 7) and its great temperature coefficient, which was 7~8%/degree (Fig. 8).

At a given temperature, the wave height

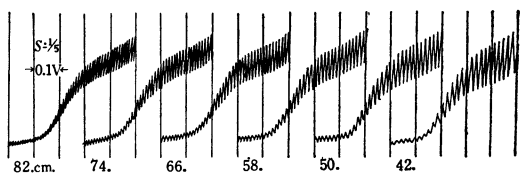

Fig. 7. Constancy of the wave height of D. A. A., independent of the height of the mercury reservoir. Concn. of D. A. A.=0.1 mol./l. in McIlvaine buffer, pH 2.8, 25°C.

26) H. v. Euler and H. Hasselquist, *Arkiv Kemi*, **8**, 67 (1955).
27) J. Trnka, *Proc. I. Intern. Polarogr. Congr. Prag* **III**, 518 (1951).
28) H. v. Euler and H. Hasselquist, "Die Reduktone", Stuttgart, Enke (1950).
29) H. v. Euler and H. Hasselquist, *Arkiv Kemi*, **5**, 49 (1952).

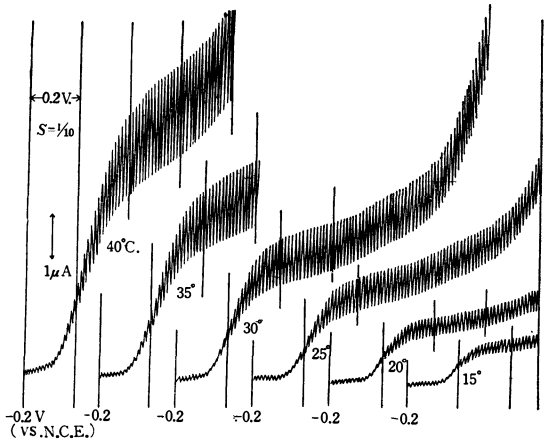

Fig. 8. Increase of wave height of D. A. A. with increasing temperature. Concn. of D. A. A.=0.1 mol./l. in McIlvaine buffer solution, pH 2.8.

of D. A. A. was roughly proportional to its concentration and was not appreciably changed with pH and it was also the case even in the neighborhood of pH 0.

TABLE I
HALF-WAVE POTENTIALS OF D. A. A. IN MCILVAINE BUFFER SOLUTION AT 25°C.
Conc. of D. A. A.=0.025 mol./l.

pH	2.20	2.66	2.96	3.48
$\pi_{1/2}$(vs. N.C.E.)	−0.350	−0.372	−0.392	−0.410
pH	3.80	4.22	4.63	5.04
$\pi_{1/2}$(vs. N.C.E.)	−0.432	−0.450	−0.462	−0.480

The half-wave potential of the reduction wave is presented in Table I. Whether the half-wave potential, the wave height or the shape of the wave can be influenced by the components of the buffer or the manner of preparation of D. A. A. was examined and no appreciable change has been observed except for the D. A. A. prepared by the oxidation with iodine in aqueous solution, in which the presence of the iodide ion caused the shift of the half-wave potential of D. A. A. toward a little more negative value.

On plot of the logarithms of the wave heights of D. A. A. against reciprocal absolute temperature, a linear relationship has been obtained and its inclination was found to be independent of pH and the concentration of D. A. A. as seen in Fig. 9.

Above pH 5 the rate of decomposition of D. A. A. increases abruptly and besides the reduction wave of D. A. A., another reduction wave begins to grow up which may be due to one of the decomposition products of D. A. A. whose $\pi_{1/2}$ is slightly more negative than that of D. A. A. Consequently it becomes difficult to take reproducible polarograms of D. A. A. and in the present studies further experiments in pH more than 5 have not been made.

As stated in the experimental part, gelatin, an ordinary maximum suppressor, was not used for obtaining well defined polarograms, since gelatin markedly influenced the shape of the reduction wave of D. A. A. Fig. 10 shows the effect of gelatin on the reduction wave of D. A. A. On addition of only 1 drop of 0.5% gelatin

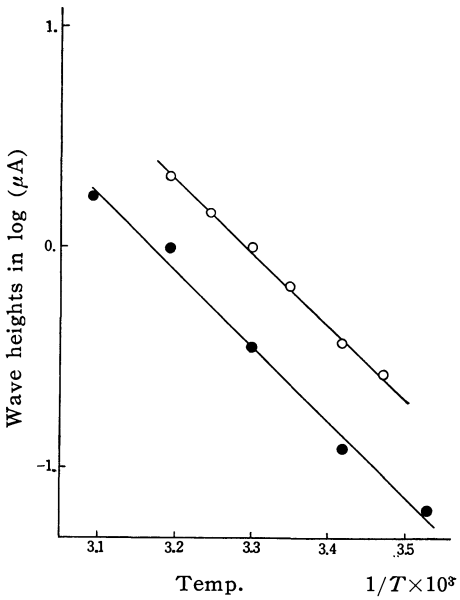

Fig. 9. Relationship between the logarithm of the height of the reduction wave of D. A. A. and reciprocal absolute temperature.
○ Concn. of D.A.A.=0.1 mol./l. at pH 2.8
● Concn. of D.A.A.=0.05 mol./l. at pH 2.7

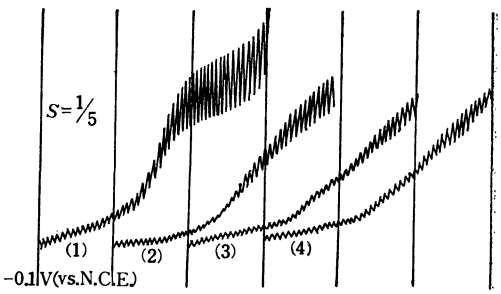

Fig. 10. Influence of gelatin on the reduction wave of D. A. A. Concn. of D. A. A.=0.1 mol./l., pH 2.8, 30°C.
(1) without gelatin
(2) 1 drop of 0.5% gelatin to 10 ml. of the soln. (1)
(3) 2 drops of 0.5% gelatin
(4) 3 drops of 0.5% gelatin

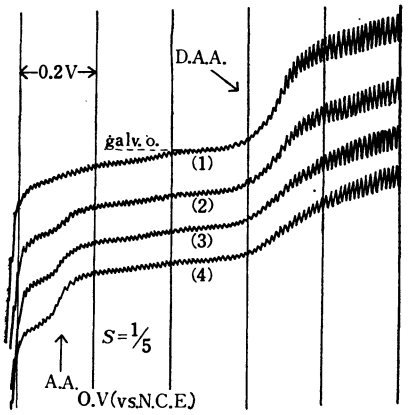

Fig. 11. Controlled potential electrolysis of D. A. A. at −0.7 V. (vs. N. C. E.), Concn. of D. A. A.=0.1 mol./l., pH 3.5, 25°C
(1) before electrolysis (2) after 20 min. (3) 40 min. (4) 60 min.

aqueous solution into 10 ml. of the electrolytic solution, the wave was strongly deformed; with three drops of the same gelatin solution, the wave became completely drawn out. Though no further experiments have been carried out concerning this problem, the above phenomena may indicate that a reaction which proceeds before the electrode reaction is retarded by the presence of the surface active substance such as gelatin.

Fig. 11 shows that the growth of the anodic wave of A. A. can be observed as the electrolysis proceeds. In this case, it may be easily understood that the anodic wave of A. A. increases with increasing time, while the cathodic wave of D. A. A. remains almost unchanged, since the former has the character of a normal diffusion current and the latter that of a typical kinetic one. During the electrolysis it was found that the reduction wave of D. A. A. was gradually deformed with time. It may be considered to owe to a surface active property of the agar-agar which was dissolved from the salt bridge into the electrolytic solution.

From the above series of experiments on D. A. A., it has been seen that the reduction wave of D. A. A. is a typical kinetic current and its reduction product is A. A. Then, the attention should be turned to the inactive form of D. A. A. in the follow ingsystem in which the inactiavtion reaction of D. A. A. must be reversible.

$$\text{Inactive form of D. A. A.} \rightleftarrows \text{D. A. A.} \underset{-2H^+-2e}{\overset{+2H^++2e}{\rightleftarrows}} \text{A. A.} \quad (1)$$

The inactive form of D. A. A. may be most probably its hydrated form. What D. A. A. may react with water to produce a hydrated product, has long since been suggested by Herbert et al.[30], and also Vavrin[13] supposed the hydration when he interpreted the discrepancy between the $\pi_{1/2}$ of the anodic wave of A. A. and its potentiometrically obtained π_0. However, any detail of the hydration itself has not been discussed. It may be partly because no reduction wave of D. A. A. has been obtained.

The hydrated form of D. A. A. which is proposed as the most probable one by the present authors, is II′ of the following two configurations.

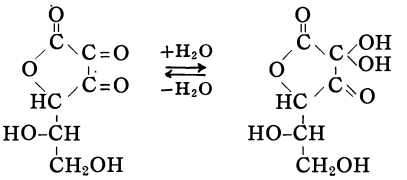

D. A. A. II — Hydrated D. A. A. II′

The high reducibility of D. A. A. (II) at the dropping mercury electrode is readily understood since three carbonyl groups are conjugated, while the hydrate (II′) seems difficult to be reduced since the conjugation of II is here completely hindered by the hydration at the central carbonyl group of the three. The most feasible hydration at the central carbonyl group among the three may be inferred from the electronic effect caused with two other carbonyl groups on the central.

As for the similar type of hydration of carbonyl group, it is seen in the investigations of some aldehydes, especially of formaldehyde[31~34] and acetaldehyde[35~37].

On the other hand, there must be certain possibility of hydration not only at the central carbonyl group but also at either one of the other two or both. Let us, however, assume, for convenience'

30) R. W. Herbert, E. L. Hirst, E. G. V. Parcival, R., J. W. Reynolds and F. Smith, *J. Chem. Soc.*, **1933**, 1270.
31) K. Vesely and R. Brdicka, *Coll. Czech. Chem. Communs.*, **12**, 313 (1947).
32) R. Bieber and G. Trümpler, *Helv. Chim. Acta*, **30**, 706 (1947).
33) R. Brdicka, *Coll. Czech. Chem. Communs.*, **20**, 387 (1955).
34) J. Koutecky, ibid., **21**, 652 (1956).
35) R. Bieber and G. Trümpler, *Helv. Chim. Acta*, **30**, 2000 (1947).
36) R. P. Bell and J. C. Clunie, *Trans. Faraday Soc.*, **48**, 439 (1952).
37) R. P. Bell and J. C. Clunie, *Proc. Roy. Soc.*, (*London*), **212A**, 33 (1952).

sake, only one hydrated form of D. A. A., namely II'. Since the reduction wave of D. A. A. is much smaller than its expected diffusion current and possesses all the typical characteristics of the kinetic current, the equation derived by Koutecky[16,38,39] may be applied to the present problem.

$$\text{Hydrated D. A. A.} \underset{k_2}{\overset{k_1}{\rightleftarrows}} \text{D. A. A.} \underset{\text{Electrode reaction}}{\rightleftarrows} \text{A. A.} \quad (1')$$

$$k_1 = [i_k/(i_d - i_k)]^2 1.31 K_h/t \quad (2)$$

where k_1 and k_2 are the rate constants of the dehydration and hydration, respectively, and i_d and i_k are the expected diffusion current and actual kinetic current, respectively. K_h is the hydration constant and equal to k_2/k_1 and t, the drop time. If the diffusion constant of D. A. A. is assumed to be approximately equal to that of A. A., i_d may be calculated with the latter which is readily known from the anodic diffusion current of A. A. However, in order to obtain k_1 and k_2 from the kinetic current of D. A. A. by using the above equation, the hydration constant K_h should be known. It seems scarcely possible to obtain its reliable value even by the spectrophotometric method as it was applied by Bieber and Trümpler[32] to measure the hydration constant of formaldehyde, since the equilibrium between D. A. A. and its hydrated form seems much shifted toward the hydrated form and also D. A. A. is unstable in an aqueous solution.

Reversibility of the A. A. and D. A. A. System:— Aside from the question how the problem is related to the biological meaning, it must have some value to consider the reversibility of the system from the electrochemical standpoint.

Compared with the fact that an impression as if the reduction wave of D. A. A. were in any way unobtainable has been hitherto maintained among polarographists, the results of the present investigations may be said to have ascertained at least that D. A. A. can be reduced to A. A. at the dropping mercury electrode at a relatively positive potential. But it does not mean that the present data would directly give an evidence of the reversibility of the system in the sense of thermodynamics.

In order to consider the reversibility of the system, both the reduction wave of D. A. A. and the oxidation wave of A. A. should be studied not only with their limiting current but also with the whole current-voltage curve of the system.

Concerning the problem of this kind, after the previous paper[17] had been published by the present authors, Koutecky[16] reported his mathematically rigorous studies on the system which may coincide with the present one (1) in the case where the latter electrode reaction itself is reversible. He also discussed the character of both the reduction wave of D. A. A. and the oxidation wave of A. A. as an application of his theory.

According to Koutecky, if his theory is valid for the case of the A. A. and D. A. A. system, the height of the reduction wave should take the value to satisfy the relation

$$i_0/i_\infty = 10^{-6.9} \quad (3)$$

where i_0 and i_∞ correspond to the limiting currents of D. A. A. and A. A. of the same concentration, respectively. The above relation may be derived by substituting the experimentally obtained potential shift of the $\pi_{1/2}$ of the oxidation wave from the π_0 of the system, into his equation; the potential shift is usually observed to be about 200 mV. Also the half-wave potential of the reduction wave should be identical with that of the oxidation wave.

In spite of his above conclusion, the discrepancies between the present experimental results and the above theoretically deduced value are quite large; the actual reduction wave is greater by the order of 10^4 and its half-wave potential is about 0.5 V. more negative than that theoretically expected.

Therefore Koutecky's theory may not be said to be applicable to the present problem as he already pointed out. Nevertheless, it seems also interesting to consider the causes from which the above disagreements should arise. In this respect, the assumption of the reversibility of the electrode reaction should be first reconsidered.

If the electrode reaction itself is more or less irreversible, the above phenomena will be more readily understood, though their quantitative analysis may hardly be possible. Also the fact that many investigators remarked the slow establishment of the equilibrium potential of the A. A.

38) J. Koutecky and R. Brdicka, *Coll. Czech. Chem. Communs.*, **12**, 337 (1947).
39) J. Koutecky, ibid., **18**, 597 (1953).

and D. A. A. system[40], when they investigated it potentiometrically, may remind us of the possibility of the polarographically irreversible electrode reaction.

Consequently the reversible character of the oxidation wave should be reinvestigated. Even the experimental results of the half-wave potential dependence on drop time of mercury obtained by Kern[15] do not seem to be in good agreement with his own theory in which he also derived an equation for the oxidation wave which differs from Koutecky's only in the numerical factors.

Summary

L-Ascorbic acid (A. A.) shows an oxidation wave at pH less than 8 and two in a more alkaline range. After standing of A. A. in alkaline solution, the third oxidation wave has been observed.

Dehydro-L-ascorbic acid (D. A. A.) has been also tested in alkaline solution. The mechanism of the electrode oxidation of A. A. and its decomposition in alkaline solution are discussed. The reduction wave of D. A. A. has been obtained at pH 2 to 5, in which the half-wave potential is about −0.3 to −0.5 V. (vs. N. C. E.).

The wave height is about 1/1000 of its expected diffusion current at room temperature. The wave has all the typical characteristics of the kinetic current. The wave height is roughly proportional to the concentration and is not appreciably influenced by pH and the components of the buffer solution, but the shape of the wave is strongly deformed by adding small amounts of surface active substance such as gelatin.

The reduction product of D. A. A. at the dropping mercury electrode has been polarographically proved to be A. A.

Discussions are made on the configuration of the inactive form of D. A. A. and the reversibility of the A. A. and D. A. A. system.

The authors wish to express their thanks to Professor Isamu Tachi of Kyoto University and Assistant Professor Shinji Koide of Mukogawa Women's University for their kind advice and encouragement.

Laboratory of Biophysical Chemistry
College of Agriculture
University of Osaka Prefecture, Sakai

40) See for example E. G. Ball's report[4].

Polarographic Investigations of Vitamin C. II. On the Reduction Waves of Some Conjugated Tricarbonyl Compounds as Related Compounds of Dehydro-L-ascorbic Acid

By Sôzaburo ONO, Masanosuke TAKAGI and Tamotsu WASA

(Received September 24, 1957)

In the previous papers[1,2], it has been reported that dehydro-L-ascorbic acid (D.A.A.) shows a reduction wave which has the character as a kinetic current and the reduction product at the dropping mercury electrode is L-ascorbic acid (A.A.), and discussions were made on the inactive form of D.A.A. in aqueous solution and the hydration of carbonyl group was considered.

Since the possibility of the hydration in D.A.A. was proposed to be due to its conjugated three carbonyl groups, there must be seen also the same kind of kinetic current in other conjugated tricarbonyl compounds and it seems also interesting to study their behavior as kinetic current, in relation to their molecular configuration.

In the present investigations, following three conjugated tricarbonyl compounds were thus taken up.

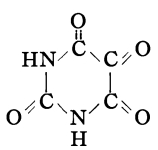

Alloxan
(I)

1) S. Ono, M. Takagi and T. Wasa, *J. Am. Chem. Soc.*, **75**, 4369 (1953).
2) S. Ono, M. Takagi and T. Wasa, This Bulletin, **31**, 356 (1958).

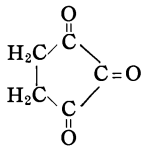

Dehyro-reductic acid
(II)

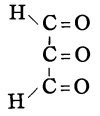

Mesoxalaldehyde
(III)

Of these three substances, the reduction wave of alloxan was already studied by Sartori and Liberti[3], but they do not seem to have paid any attention on its behavior as a kinetic current. Concerning other two substances, though their reduced forms i.e. reductic acid[4] and triose-reductone[5] have been polarographically studied, the reduction waves of dehydro-reductic acid and mesoxalaldehyde have not been hitherto believed to be available.

In the present paper, it will be therefore emphasized that each of the above three substances shows a reduction wave which has a similar behavior to that of D.A.A. and discussions will be developed on some correlations between the characteristics of the waves of these four substances including D.A.A. and their oxidation-reduction potentials.

Experimental

Materials.—L-Ascorbic acid was the same specimen as used in the previous works[1,2]. Triose-reductone was kindly given to us by Professor Hans von Euler of Stockholm University and later it was also prepared in our laboratory according to his method[6].

Reductic acid was prepared by Reichstein and Oppennauer's method[7].

Alloxan monohydrate was a product from Eastman Kodak Co.

Of the above four substances, alloxan could be directly used in aqueous solution for the purpose of the present experiments, while other three substances needed to be oxidized, in order to obtain their dehydro-forms. For that, various oxidizing reagents e.g. iodine, silver acetate and quinone were tried, since it would not be interesting if the polarograms should be unfavorably influenced by the oxidizing reagent used. The oxidation method finally used was as follows.

Each of the above substances, whose amount is weighed to produce 10 or 25 ml. of 0.1 mol./l. solution, is taken in a 10 or 25 ml. volumetric flask and dissolved with a small amount of the four times redistilled water (usually 2 or 5 ml.). Silver nitrate in aqueous solution, whose amount is so weighed as to be bimolar of the sample, is added into the same volumetric flask. After the oxidation has been completed, sodium acetate is added and then the whole solution is filled up with distilled water. The amount of the sodium acetate is taken according to the components of the acetate buffer so that the pH of the resulting solution is to be about 3.5. The solution is then filtered and the filtrate is immediately used as polarographic solution, in which the dehydro-form of 0.1 mol./l., sodium nitrate of 0.2 mol./l. and the components of the acetate buffer are included. In order to prepare the solutions of the dehydro-form whose concentrations are less than 0.1 mol./l., sodium nitrate and components of the acetate buffer are added into the preparation before filling up so that the resulting solutions contain the same concentrations of sodium nitrate and buffer components as above.

Alloxan was directly dissolved into the acetate buffer with sodium nitrate.

The final pH of the polarographic solutions was checked with a glass electrode. McIlvaine's buffer solutions were sometimes used instead of the distilled water to fill up the solutions of samples, and pH's were randomly changed in a limited range between 2.2 and 4.0.

Procedure and Apparatus.—The polarograph was the same one as used in the previous work[1,2]. The maximum galvanometer sensitivity was 1.72×10^{-9} A. The characteristics of the capillary used were $m=0.908$ mg./sec. and $t=4.21$ sec./drop in the buffer solution (pH 3.4) when the height of the mercury reservoir was 60 cm. and the applied potential was -0.4 V. (vs. N.C.E.) at 25°C. For the temperature control, the same cell fitted with a jacket as used in the previous work, was employed. Polarograms were taken from 10°C to 50°C at 5°C intervals. The accuracy of the temperature control was ±0.05°C. As the reference electrode, a normal calomel electrode was used.

Controlled Potential Electrolysis.—The controlled potential electrolysis of alloxan was carried out by means of the same apparatus as described in the previous paper[2].

Results and Discussion

The polarograms of alloxan, dehydro-reductic acid and mesoxalaldehyde are presented in Figs. 1, 2 and 3, respectively. As immediately seen from the above figures, the temperature coefficient of the wave height of each substance is so great as in the case of D.A.A. The wave height was also found to be independent of the height of the mercury reservoir. Therefore it may be said that all the three substances show the character as kinetic currents which are similar to that of D.A.A.

The relationship between the wave height of each substance and the temperature

3) G. Sartori and A. Liberti, *Ricerca sci.*, **16**, 313 (1946).
4) F. Santavy and B. Bitter, *Coll. Czech. Chem. Communs.*, **15**, 112 (1950).
5) R. Brdicka and P. Zuman, ibid., **15**, 766 (1950).
6) H. v. Euler and H. Hasselquist, "Reduktone", Stuttgart, Enke (1950).
7) T. Reichstein and R. Oppennauer, *Helv. Chim. Acta*, **16**, 988 (1933).

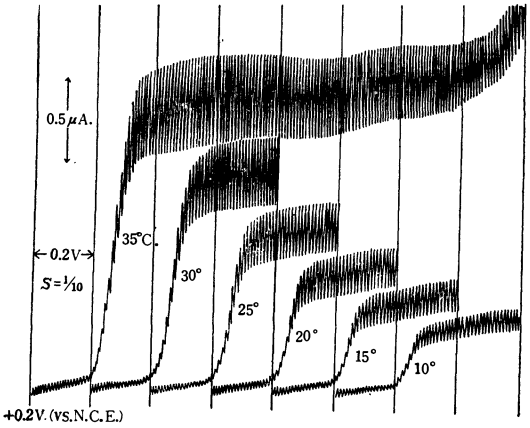

Fig. 1. Temperature dependence of the wave height of alloxan. Concn. of Alloxan=5×10^{-3} mol./l., pH 3.6, Hg 60 cm.

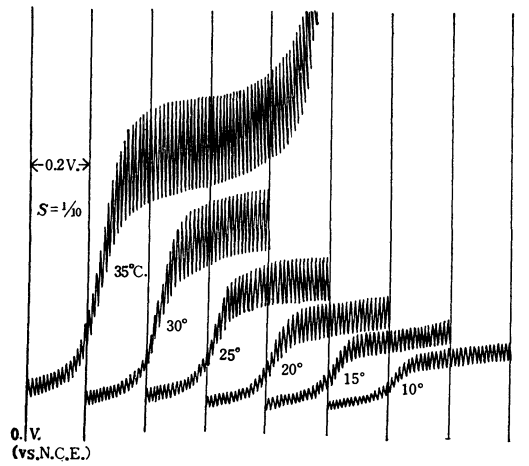

Fig. 2. Temperature dependence of the wave height of Dehydro-reductic acid. Concn. of dehydro-reductic acid=0.05 mol./l., pH 2.8, Hg 60 cm.

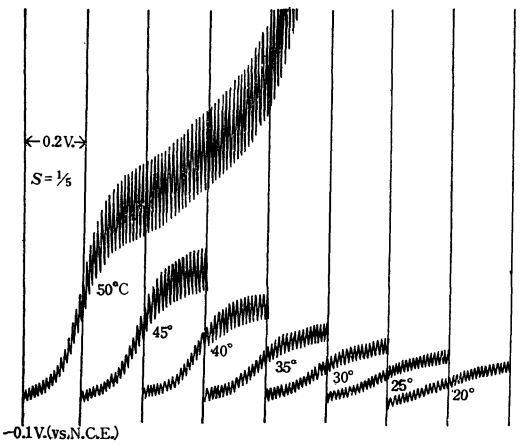

Fig. 3. Temperature dependence of the wave height of Mesoxalaldehyde. Concn. of mesoxalaldehyde = 0.1 mol./l., pH ≒3.0, Hg 60 cm.

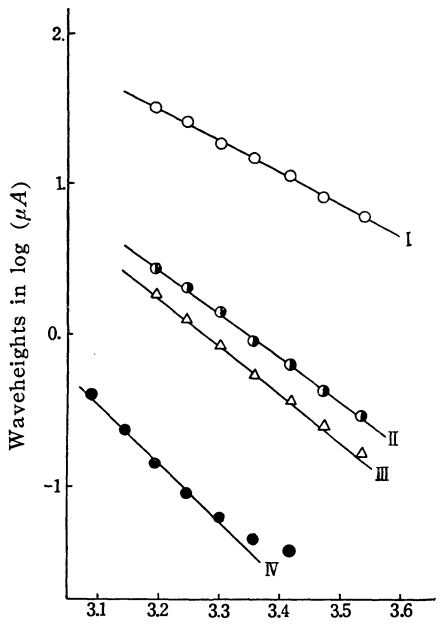

Fig. 4. Plot of logarithm of the reduction wave height against reciprocal absolute temperature.
I Alloxan
II Dehydro-reductic acid
III Dehydroascorbic acid
IV Mesoxalaldehyde
Concn. of each substance = 0.1 mol./l., pH 3.5, Hg 60 cm.

is shown in Fig. 4, where the logarithm of the wave height is plotted against the reciprocal absolute temperature. Since the wave height of each substance, including D.A.A., was found to be roughly proportional to its concentration at a given temperature, the wave heights of the substances of 0.1 mol./l. were in some cases recalculated from the experimental values obtained with more dilute concentrations. Although it was not strictly examined whether the relationship presented in Fig. 4 is valid for a wider pH range, no appreciable change in the wave height has been observed, in a range between pH 2.2 and 4.0.

Since all the substances are not stable enough in aqueous solution, the experiments with changing pH were not made in the outer range other than above mentioned. The half-wave potentials of these substances in pH 3.5 are listed in Table I.

It seems to be difficult to find any correlation between the wave height and the half-wave potential from Fig. 4 and Table I, while it may be of interest to consider

TABLE I

$\pi_{1/2}$ in pH 3.5	Alloxan	Dehydro-reductic acid	Dehydroascorbic acid	Mesoxalaldehyde
V(vs. N.C.E.)	−0.05	−0.27	−0.42	−0.35

TABLE II

$\pi_0-\pi_{1/2}$ of the reduced form	Dialuric[8] acid, Alloxan	<	Reductic acid,[9] Dehydro-reductic acid	<	Ascorbic acid,[10] Dehydro-ascorbic acid	< Triose-reductone,[11] Mesoxalaldehyde
Height of the reduction wave	Alloxan	>	Dehydro-reductic acid	>	Dehydro-ascorbic acid	> Mesoxalaldehyde
Temp. coeff. of the reduction wave	Alloxan	<	Dehydro-reductic acid	<	Dehydro-ascorbic acid	< Mesoxalaldehyde

the present results in connection with the standard oxidation-reduction potential π_0 of the corresponding system and the half-wave potential $\pi_{1/2}$ of the anodic wave of the reduced form.

As Brdicka and Zuman pointed out[5], each of the reduced forms of the above substances (i.e. dialuric acid, reductic acid, triose-reductone and D.A.A.), shows a considerable shift of the $\pi_{1/2}$ of the anodic wave from its corresponding π_0 to a more positive potential. Therefore, they described this fact as a characteristic of endiol group. In their paper, however, no further considerations on these potential shifts were made.

In Table II, these four substances are arranged in the order of magnitude of the above stated potential shift, the reduction wave height and its temperature coefficient, respectively. It may be said, of these four oxidation-reduction systems, that the smaller the height of the reduction wave, the larger both the shift of $\pi_{1/2}$ of the anodic wave from the corresponding π_0 and the temperature coefficient of the reduction wave height.

In the previous paper[2], discussions were made on the problem of the reversibility of the A.A. and D.A.A. system, on the basis of the experimental results, referring to the theoretical studies made by Koutecky[12]. Considerable disagreements between the experimental values and Koutecky's theoretical ones were found when the electrode reaction of the system was assumed to be reversible. Then, as a cause of these disagreements, the irreversible electrode reaction was assumed by the present authors. However, the correlation between the height of the reduction wave and $\pi_0-\pi_{1/2}$ of the anodic wave, presented in Table II, may suggest that although the electrode reaction itself is not reversible, the inactivation of the oxidized form in aqueous solution must be one of the most important factors which may cause both the potential shift and the kinetic current. The inactivation may be due to the hydration at the central carbonyl group among the conjugated three, as it was in the case of D.A.A.

As for the effort to interpret the above disagreements from different standpoint, though Zuman suggested the possibility of the opening of the lactone ring in the case of D.A.A.[13], such may not be taken into consideration, since the above three substances other than D. A. A. have different configurations and still show quite similar behavior of the kinetic current to that of D.A.A. Despite of that, there remains another kind of possibility, that the reducible form which causes the kinetic current is not the completely dehydrated one as shown in I, II and III, but the one in which hydration is still maintained at either one of the two carbonyl groups except the central.

Let us now consider again the reversibility of the above four oxidation-reduction systems. It is obviously seen that the $\pi_{1/2}$ of the reduction waves of D.A.A., dehydro-reductic acid and mesoxalaldehyde do not coincide with those of the corresponding oxidation waves, but in contrast with them, alloxan was expected to give the coincidence of the potentials in this respect, since the $\pi_{1/2}$ of alloxan is considerably more positive than those of the other three; also Sartori and Liberti[3] reported the reversible character of the dialuric acid and alloxan system,

8) G. M. Richardson and R. K. Cannan, *Biochem. J.*, **23**, 68 (1929).
9) N. Mayer, *J. chim. phys.*, **34**, 107 (1937).
10) G. Ball, *J. Biol. Chem.*, **118**, 219 (1937).
11) R. Wurmser, N. Mayer and O. Crepy, *J. chim. phys.*, **33**, 101 (1936).
12) J. Koutecký, *Coll. Czech. Chem. Communs.*, **20**, 116 (1955).
13) P. Zuman, A private communication to the authors. See also M. Brezina and P. Zuman, "Die Polarographie in der Medizin, Biochemie und Pharmazie" Akademische Verlagsgesellschaft, Leipzig, (1956), p. 423.

though they do not seem to have paid any attention on the characteristics of alloxan as a kinetic current.

As seen in Fig. 5, a practically perfect coincidence of the $\pi_{1/2}$ of the reduction wave with that of the oxidation wave, which is due to dialuric acid formed by

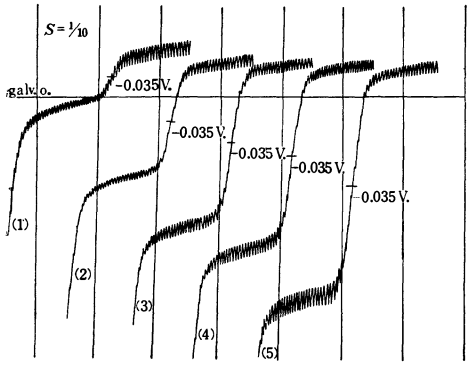

Fig. 5. Controlled potential electrolysis of alloxan at −0.2 V. (vs. N.C.E.). Polarograms were taken at 45 min. intervals. Conc. of alloxan $=1\times10^{-3}$ mol./l., pH 3.09, temp. 35°C, Hg 60 cm.

the electrolysis, has been observed. It may be readily understood that the height of the oxidation wave becomes larger than that of the initial reduction wave as the electrolysis proceeds, since the former is a diffusion current, while the latter a kinetic one.

From these observations, it may be said that the theory derived by Koutecky is at least applicable to the case of alloxan.

In order to solve the question why the electrode reaction is reversible only with the dialuric acid and alloxan system and irreversible with the other three systems, the investigations will be further developed.

Summary

Alloxan, dehydro-reductic acid and mesoxalaldehyde show reduction waves which are similar to that of dehydro-L-ascorbic acid. The half-wave potentials of alloxan, dehydro-reductic acid, dehydro-L-ascorbic acid and mesoxalaldehyde in pH 3.5 are −0.05, −0.27, −0.42 and −0.35 V. (vs. N.C.E.), respectively.

Of these four substances, the lower the height of the reduction wave, the greater both the shift of the half-wave potential of the anodic wave of the corresponding reduced form from the standard oxidation-reduction potential of the system and the temperature coefficient of the height of the reduction wave.

Inactive forms of these substances at the electrode reaction may be the hydrated ones as proposed in the case of dehydro-L-ascorbic acid.

Alloxan has been proved to be polarographically reversible by the controlled potential electrolysis and the half-wave potential of the reduction wave coincides with that of the oxidation wave of dialuric acid, while no such observations have been made with the other three.

The authors would like to express their sincere thanks to Professor Hans von Euler and his coworkers for their kindness that they have given them a specimen of pure triose-reductone.

Laboratory of Biophysical Chemistry
College of Agriculture, University
of Osaka Prefecture, Sakai

Determination of Small Quantities of Acetone in Methyl Methacrylate Monomer

By Yuzi TAKAYAMA* and Fumikazu TOKIWA**

(Received May 24, 1957)

At the present time for the determination of acetone in methyl methacrylate monomer (simply M-MM), hydroxylamine hydrochloride method has been used, but the method is common to both ketones and aldehydes, so that it can not determine acetone only.

Many studies on the determination of acetone are reported and each of them has its own characteristics. Especially, salicylaldehyde method generally is not applicable to the determination of acetone in M-MM on account of coloration of M-MM itself. One of the best is J. Messinger's[1] iodo titration method by iodoform reaction and some of the reported modifications of Messinger's[1] technique indicate the widespread utility of this procedure. But iodometry has generally too low an accuracy for the determination of small quantities of acetone. Absorption method in the ultraviolet region has been well studied including the work of Barthauer[2], Nogare[3], Stolyarov[4], Andreev[5], Etienner[6] and Shchukarev[7]. Nogare's method may be considered as surpassing the others in easiness of obtaining the reagents, and in relative simplicity of the method; it seems also to be comparatively sensitive, but its application is, limited in determination of acetone in either aqueous solution or non-aqueous solvent which is miscible with water. In this report the application of Nogare's method was investigated for determination of small quantities of acetone in a medium which is immiscible with water to establish a method superior to those previously used.

Iodoform has a strong absorption in the ultraviolet region from 400 to 250 mμ. This is characterized by three defined maxima occurring at 274, 307 and 347 mμ, in chloroform as shown in Fig. 1. Therefore, acetone in sample M-MM is caused to react in an alkaline solution with sodium hypoiodite by vigorous shaking. The absorbancy of resulting iodoform is measured at 347 mμ.

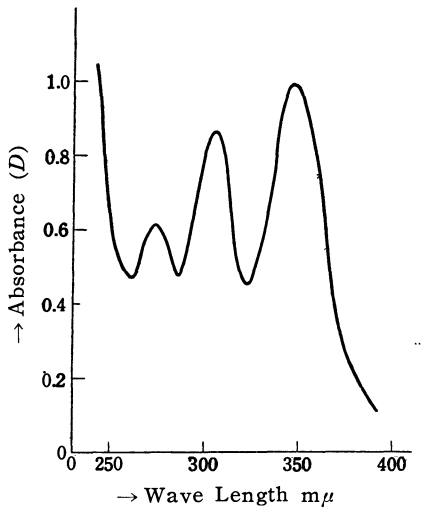

Fig. 1. Iodoform absorption spectrum.

Experimental

Apparatus.—Shimadzu's photoelectric spectrophotometer with glass cells of 10 mm. thickness and a tungsten lamp was used for absorbancy measurement.

Reagents.—Sodium hydroxide solution: 25% aqueous solution.

Iodine solution: 4 g. of potassium iodide and 20 g. of iodine in 80 ml. of water.

Sodium thiosulfate solution: 5% aqueous solution.

Anhydrous sodium sulfate: First grade reagent.

Chloroform: First grade reagent.

Procedure.—Place 7 ml. of 20% iodine solution in a 100 ml. separatory funnel and add 2 ml. of 25% sodium hydroxide solution. Mix by swirling. When the resulting solution is not distinctly orange-yellow, add iodine solution drop by drop. To this hypoiodite solution add 1 ml. of the sample containing no more than 400 γ acetone, and mix immediately. Shake for 5 minutes at

* Mitsubishi Rayon Co., Ltd., Kyobashi, Tokyo.
** Tokyo Scientific College, Shinjuku-ku, Tokyo.

1) J. Messinger, *Ber.*, **21**, 3366 (1888).
2) G. L. Barthauer, F. V. Jones and A. V. Metler, *Ind. Eng. Chem., Anal. Ed.*, **18**, 354 (1946).
3) S. D. Nogare, T. O. Narris and J. Mitchell, *Anal. Chem.*, **23**, 1473 (1951).
4) K. P. Stolyarov and I. A. Stolyarova, *Zhur. Anal. Khim.*, **8**, 33 (1953).
5) S. N. Andreev and R. I. Gindina, *Zhur. Priklad. Khim.*, **26**, 104 (1953).
6) H. Etienne, *Ind. Chem. Belge.*, **17**, 455 (1952).
7) S. A. Shchukarev, S. N. Andreev and O. V. Sapozhnikava, *Zhur. Anal. Khim.*, **9**, 193 (1954).

room temperature continuously to keep the mixture apparently homogeneous. When the orange-yellow color gradually fades, add more iodine solution dropwise until the color is restored.

After reaction, discharge the iodine color with a few drops of 5% sodium thiosulfate. Add 14 ml. of chloroform from a burette and extract the produced iodoform by shaking. Let stand until the phases are separated and transfer the chloroform layer to another 100 mm. separatory funnel containing approximately an equal volume of water. Shake vigorously, and transfer the chloroform layer to a 10 ml. glass cell, through a funnel containing a thin bed of anhydrous sodium sulfate supported on a glass wool as shown in Fig. 2. Measure the absorbancy of this chloroform extract against water in a 10 mm. glass cell. Calculate the amount of acetone using the calibration curve, shown in Fig. 3, obtained by the following procedure.

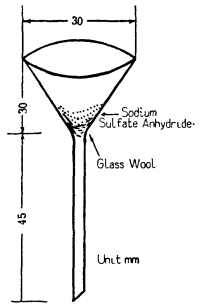

Fig. 2. Drying funnel

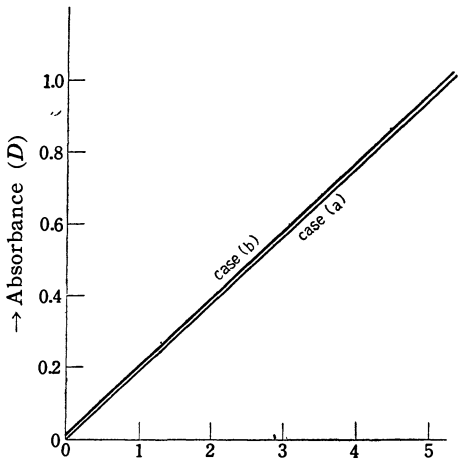

Fig. 3. Working curve for acetone.

Preparation of the calibration curve. Prepare the sodium hypoiodite solution similarly, to which less than 5 ml. of standard solution containing 79.6 γ of acetone in 1 ml. of water is added. Treat this similarly and extract the iodoform with 15 ml. of chloroform; wash the chloroform extract with water. The calibration curve obtained with pure acetone is shown in Fig. 3.

Discussion

(i) *On the calibration curve*:—On drawing the calibration curve employing 1 ml. of M-MM, the iodoform is extracted with 14 ml. of chloroform, as M-MM transfers to chloroform layer. When the M-MM is refined as shown in the following a), the calibration curve is in good agreement with that in Fig. 3; in the case of following b), it deviates higher than in the case of Fig. 3 by 0.1 in the absorbancy scale. This is due to the very small quantity of impurities, the presence of M-MM not affecting this analytical procedue.

(a) After washing M-MM with 10% sodium hydroxide, wash it with water five times, remove the water with calcium chloride, and collect the middle fraction 46°C, 100 mmHg, by vacuum distillation with cuprous chloride as stabilizer. Repeat this operation.

(b) After washing M-MM with 10% sodium hydroxide, wash it twice with water, remove the water with calcium chloride, and then collect the middle fraction similarly.

(ii) *Reaction conditions*:—The critical studies made by Hatcher and Mueller[8] and Nogare[3] showed that both the concentration and the order of addition of reagents determined the yield of the iodoform obtained. It was confirmed that the highest conversion from acetone into iodoform is effected by adding in the order iodine solution, sodium hydroxide solution, on the sample. Concerning the concentration of the reagents, the optimum condition is indicated by the orange-yellow color of the solution obtained by mixing 20% iodine solution and 25% sodium hydroxide. This experiment also exhibits that an insufficient or an excessive iodine relative to sodium hydroxide results in lower conversion into iodoform. Namely it is important to make the sample react in an orange-yellow solution and to maintain this orange-yellow by dropwise addition of iodine solution, when this color is discharged during reaction.

The effect of time on iodoform reaction under the optimum conditions is shown in Table I. Five minutes suffice; no marked change was observed with increasing reaction time up to 7 minutes. No significant difference was observed with the reaction temperature in this experiment but a low-temperature is desirable in order to avoid evaporation of M-MM. After reaction, the excess of iodine in the hypoiodite mixture can also be removed with sodium

8) W. H. Hatcher and W. H. Mueller, *Trans. Roy. Soc. Can.*, **23**, Sect. 3, 35 (1929).

TABLE I

EFFECT OF TIME ON IODOFORM REACTION

Sample	Acetone, mg.	Reaction time, min.	Absorbancy
A	0.232	2	0.465
	0.232	3	0.505
	0.232	4	0.540
	0.232	5	0.550
	0.232	6	0.550
	0.232	7	0.550
B	0.256	2	0.530
	0.256	3	0.590
	0.256	4	0.605
	0.256	5	0.610
	0.256	6	0.610
	0.256	7	0.610

sulfite or additional sodium hydroxide without sodium thiosulfate.

(iii) *On the volume of the sample*:—When more than one ml. of the sample is taken, the absorbancy becomes lower than that calculated or the results are not reproducible, as shown in Table II. The

TABLE II

RELATION BETWEEN THE VOLUME OF THE SAMPLE M-MM AND ABSORBANCY

Sample	Volume		
	1 ml.	2 ml.	3 ml.
D	0.095	0.169 obs.	0.210 obs.
		0.190 calcd.	0.285 calcd.
E	0.286	0.535 obs.	0.810 obs.
		0.572 calcd.	0.845 calcd.
F	0.317	0.555 obs.	0.835 obs.
		0.630 calcd.	0.940 calcd.

calcd.: Absorbance at sampling volume 1 ml. × sampling volume.

reason may be considered as follows. The M-MM layer and the aqueous layer should be mixed well by shaking and acetone in the M-MM layer should be transfered to the aqueous layer, since acetone reacts with sodium hypoiodite in the aqueous layer. On taking more than 1 ml. of the sample, the M-MM and the aqueous layer do not mix perfectly, as M-MM is very easily separated from water.

(iv) *On iodoform*:—The intensity of the absorption in chloroform-M-MM layer was not affected by temperature from 15°C to 30°C. It was observed that iodoform slowly decomposed to liberate iodine in chloroform to decrease the absorbancy; it did not decompose, however when M-MM was present in the chloroform and maintained the absorbancy unchanged for more than one hour.

Ultraviolet absorption spectrum of the chloroform extract, using commercial M-MM as a sample showed complete agreement with that by the use of a mixture of aqueous acetone solution and refined M-MM. It can be ascertained that the product of the reaction is iodoform.

(v) *Effect of coexisting substance*:—Interference will be encountered from compounds which give iodoform by reaction with sodium hypoiodite. Possible interfering compounds are acetaldehyde, ethanol and methyl ethyl ketone, but in this method conversion of acetaldehyde and ethanol into iodoform is, respectively, 58 and 0.3%[3]. In many cases carbonyl compounds which interfere with the absorption at 347 mμ can be washed away from the chloroform extract with aqueous hydroxylamine hydrochloride.

Effect of methanol, formaldehyde, hydroquinone and peroxides which possibly coexist with M-MM is shown in Table III. Small quantities of methanol and formaldehyde do not affect this method.

TABLE III

EFFECT OF COEXISTING SUBSTANCE

Acetone mg.	Coexisting substance	(%)	Absorbancy
0.256	M-M only		0.610
0.256	Methanol*	(0.5)	0.615
	〃	(0.2)	0.610
0.256	Formaldehyde	(0.1)	0.610
	〃	(0.05)	0.610
0.256	Hydroquinone	(0.04)	0.520
	〃	(0.02)	
0.256	Hydrogen Peroxide	(0.06)	0.505
	〃	(0.04)	0.610

* Large quantities of methanol cause white precipitate.

(vi) *Example of analysis*:—A commercial M-MM (90 ml.) was used as the sample of unknown concentration of acetone; this was submitted to single distillation and 5 ml. fractions were collected from forerun fraction in order. These fractions were, respectively named sample No. A_1,

TABLE IV

EXAMPLE OF ANALYSIS OF ACETONE IN M-MM FRACTION

Sample No.	Acetone content mg./ml.
A_1*	0.656
A_2*	0.608
A_3*	0.504
A_4	0.364
A_5	0.268

* Measured after twice dilution.

A_2,……, A_5 and the acetone in these fraction determined by the procedure mentioned above. Table IV shows an example of the results.

Summary

The method described here is based on the utilization of the iodoform reaction. The essential point of this method consists in the complete shaking of the methyl methacrylate monomer with sodium hypoiodate solution. The methyl methacrylate monomer is water-insoluble and iodoform reaction proceeds in an aqueous medium. As a result, it was confirmed that methyl methacrylate monomer does not affect this reaction substantially and one ml. sample makes it possible to determine small quantities (0.001%) of acetone in the sample monomer. This method is more sensitive than the hydroxylamine hydrochloride method previously used.

Institute of Techno-Analytical Chemistry
Faculty of Engineering, Tokyo
University, Hongo, Tokyo

Ion-Exchange Separation of Fission Products[*1]

By Eiiti MINAMI, Masatake HONDA and Yukiyoshi SASAKI

(Received May 27, 1957)

Ion-exchange methods were studied for fission product separation in order to find a suitable separation procedure to prepare pure carrier-free radioactive isotopes and for radiochemical assay purpose. In this field we can refer to the prominent works which were performed during the War by American scientists. Their method, published in 1947[1] and 1948[2], consisted of the application of a cation-exchange chromatography. They used oxalic acid as the eluent for zirconium and niobium, and alkaline earths. Ruthenium, iodine and tellurium were grouped in the filtrate of sample solutions passed through hydrogen-form (HR) cation exchanger. The extension of this method, however, has not much been reported, in spite of recent considerable development of ion-exchange separation techniques[3].

The purpose of our studies was to find a systematic separation method for the fission product mixture, taking into account the minor constituents which are distributed in so-called "trough" region on the curve of the fission yield vs. mass number. For this purpose, both cation- and anion-exchange experiments were carried out using individual radioactive isotopes of these elements. Our interest was especially directed to the change of the exchange behavior caused by the formation of different oxidation states or of different ionic species.

The preliminary experiments showed that an anion-exchange method is not practical for the extraction of the transition elements, antimony and tellurium in the form of chloride complexes from the mixture. It owed to the complex behavior of ruthenium which is usually one of the main constituents in gross fission products. Then in this study a cation exchange was applied to the first step of group separation and various eluents were tested for fractional elution of cesium, rare earths and alkaline earths. However, characteristic behavior of antimony, tellurium and some transition elements to anion exchanger was found to be useful for their mutual isolation.

Measurement of Radioactivity

In this work the behavior of the elements was observed in their carrier-free state whenever possible. The counting device was G-M counter with ordinary scaler or with a self-recording rate meter. The effluents from the ion-exchange column were either collected and evaporated on a glass plate for counting, or led directly under

*1 This communication was presented at the XVth Congress of International Union of Pure and Applied Chemistry held on 13th of September, 1956 at Lisbon.

1) E. R. Tompkins, J. X. Khym and W. E. Cohn, *J. Am. Chem. Soc.*, **69**, 2769 (1947).

2) W. E. Cohn, G. W. Parker and E. R. Tompkins, *Nucleonics*, **3**, No. 5, 22 (1948).

3) K. A. Kraus and F. Nelson, Report presented at the International Conference on the Peaceful Uses of Atomic Energy (Genève, 1955), A/CONF 8/P/837.

the mica end-window of the counting tube through a spiraled vinyl tube.

Ion-exchange Behavior of Individual Element

Ruthenium:—The solution chemistry of ruthenium is fairly complex. We have performed some experiments with carrier-free ruthenium using a cation exchanger, Dowex 50, and several kinds of anion exchanger, Dowex 1, Dowex 3, Amberlite IRA-400, Amberlite IRA-411 and Amberlite IR-4B. The gross fission products*2 were imported from the United States, Atomic Energy Commission (US, AEC).

Ruthenium-106 was presented in the stock solution (4 M nitric acid solution) and was found to be fractionated into the following three groups according to the behavior towards the ion exchangers (Table I).

TABLE I

BEHAVIOR OF CARRIER-FREE RUTHENIUM ON ION-EXCHANGE RESINS

Species	Content	Ion-exchange behavior
Neutral part	26%	Passed through a mixed bed of anion- and cation-exchangers (RCl+HR).
Anionic part	20%	Adsorbed on anion exchanger (RCl or RNO_3).
Cationic part	54% (by difference)	Adsorbed on HR from dilute acid solution.

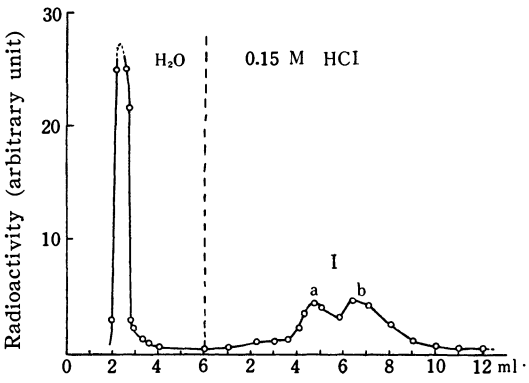

Fig. 1. Elution curve of cationic ruthenium.
Column: Dowex 50-X10, 3 ml. (HR form)

*2 The sample used in this experiment was sufficiently aged, so that its composition was rather simple, i. e. it consisted of chiefly rare earths, strontium-90, cesium-137, ruthenium-106 and their daughters. Antimony-125 was found in the filtrate of the cation exchanger through which the sample solution had passed. The activity was ca. 0.1% of total. The data as far as obtained suggest the sample being cooled for 3~4 years[4].

4) M. Honda, Y. Sasaki and H. Natsume, *Japan Analyst, (Bunseki Kagaku)*, **4**, 240 (1955).

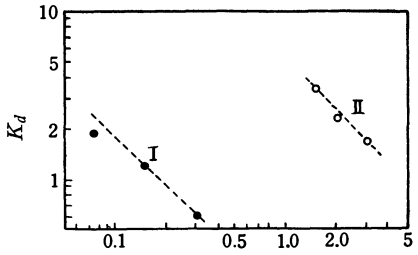

Fig. 2. Cation exchange of cationic ruthenium in $HClO_4$ solutions.
I: weakly retained species.
II: strongly retained species.
K_d's (ml./g.) were calculated from column experiment by

$$K_d = (V - I)/M$$

where V: volume of effluents flowed until the elution of the peak,
I: void volume of the column,
M: weight of dry resin (g.).

The major part of the cationic ruthenium, adsorbed on a cation exchanger, was easily eluted with hydrochloric acid solution stronger than 0.1 M. The elution curve showed two reproducible peaks (Fig. 1). But a small percentage of cationic ruthenium was adsorbed rather strongly, and a more concentrated mineral acid was needed for its rapid elution.

The affinites, distribution coefficients (K_d), of these two cationic species to a cation exchanger are shown with reference to hydrogen-ion concentration (Fig. 2). The inclination of two linear curve suggests that both species are probably univalent cations.

When the stock solution of fission products was treated with concentrated hydrochloric acid, evaporated to dryness and then dissolved in dilute hydrochloric acid solution, all the ruthenium was converted into an anionic species which passes through the column of cation exchanger. After being kept standing more than one week, however, two cationic species were found again from this solution.

This phenomenon might be attributed to the hydrolysis of the anionic chloro-complex formed by the treatment with concentrated hydrochloric acid. In this case, two peaks which could be refered to weakly retained cationic ruthenium were not resolved into separate peaks. This fact is in contrast to the experiments (Fig. 1) using original stock solution of the gross fission products.

The anionic part of ruthenium was

strongly adsorbed from acid solution on strongly basic anion exchangers such as Dowex 1, Dowex 2, Amberlite IRA-400 and Amberlite IRA-411. It was eluted out with 12 M hydrochloric acid in two broad peaks. On the other hand, it was noticed that the weakly basic anion exchangers, Dowex 3 and Amberlite IR-4B, react irreversibly with ruthenium in hydrochloric acid solutions.

Detection of rhodium-106, the short lived daughter of ruthenium-106, was easily performed from this anionic part of ruthenium. Rhodium was found in the effluents of 6~12 M hydrochloric acid passed through with a high flow rate. The decay curve of the activities of rhodium was drawn

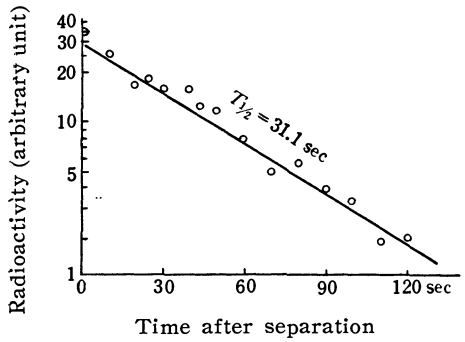

Fig. 3. Decay curve of rhodium-106 isolated by anion exchange.

with an automatic recording rate-meter and it showed $T_{1/2} = 31.1$ seconds (Fig. 3).

Antimony:—The tracer used was antimony-124 imported from the U.S., AEC. It contained 20 microgram Sb/ml. as a carrier, and was stocked in 6 M hydrochloric acid. Appreciable volatility of the activity was noticed during the evaporation of the solution. Then, if necessary, a few milligrams of antimony, Sb(V), were added and the activity was precipitated as antimony(III) sulfide.

Cation exchange. Antimony(V) was passed quantitatively through a cation exchanger in dilute acid solution. On the other hand, antimony(III) which was obtained by reduction with sulfur dioxide was adsorbed completely.

The adsorbability of antimony(III) by cation exchanger indicated the presence of univalent cation, possiblity SbO^+. That is, the plot of log K_d vs. log (HCl) has the slope of about one in the range of 0.05~0.3 M HCl (Fig. 4). These two species of antimony, Sb(V) and Sb(III), were separated from each other by a simple procedure (Fig. 5). Antimony(III) was also

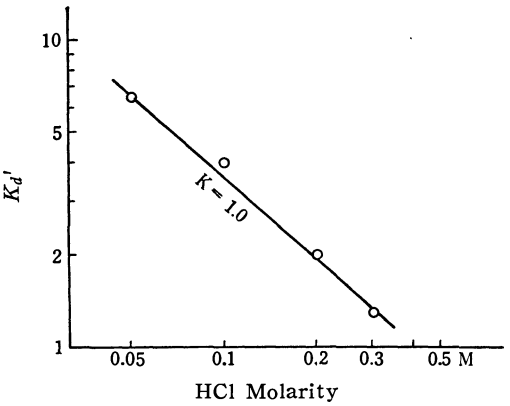

Fig. 4. Cation exchange of antimony(III) in HCl soln.
Exchanger: Dowex 50-X1
K_d': volume distribution coefficient corrected for swelling and measured by column method (Fig. 2).
(adsorption amount/ml. resin)/(concn. in soln.).
K: selectivity coefficient, {SbOR/(SbO)}/HR/(H)}.

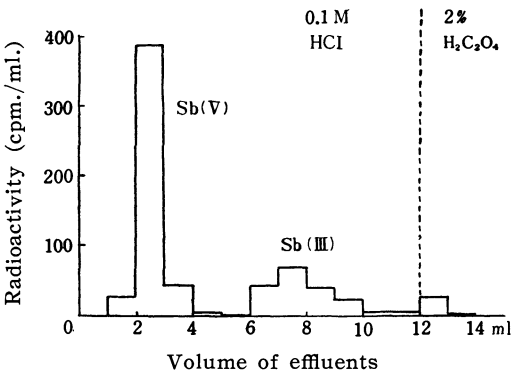

Fig. 5. Separation of Sb(V) and Sb(III).
Column: Dowex 50-X1, 5.5 ml. (capacity 2.10 meq.).

easily eluted out with dilute solution of oxalic acid from cation exchangers.

Anion exchange. High reproducibility was obtained by anion exchange using antimony(V) in hydrochloric acid solution, whereas antimony(III) showed quite complicated behavior. Reproducible results with anion exchangers who obtained by a preliminary treatment with hydrochloric acid solution containing free bromine. This treatment was necessary and effective to eliminate any irreversible reactions in the column. Bromine was retained in the resin phase as Br_3^- or Br_2Cl^-, and kept the proper oxidation state of antimony throughout the procedure. Elution constants are tabulated in Table II.

TABLE II
ELUTION CONSTANTS AND HCl CONCENTRATION IN ANION EXCHANGE[5]
Exchanger: Dowex 1-X4
Concentration of HCl (M)

	0.1	1	2	3	4	6
Sn(IV)	1.3*	<0.1	<0.1	<0.1	<0.1	<0.1
Te(IV)		1.3	0.1	<0.1	<0.1	<0.1
Sb(V)		1.3	1.3	1.0	0.3	<0.1
In(III)	1.3	0.5	—	0.3	—	0.3

* Maximum value of elution constant, 1.3, corresponds to no adsorption to anion exchanger. Elution constant $= v/(I+M\cdot K_d)$, v: column volume (see Fig. 2).

Tellurium:—The carrier-free tellurium-127 was obtained from the gross fission products, which were cooled for about three months, according to the processes described later. If necessary, a few milligrams of inactive tellurium were added in the form of chloride, and the activity was isolated in metallic tellurium precipitated with sulfur dioxide.

Cation exchange[6,7]. Tellurium(IV) was adsorbed by a cation exchanger and eluted out with dilute mineral acid. It behaves as a univalent cation such as $Te(OH)_3^+$ or $TeOOH^+$ in dilute perchloric acid solution. On the other hand telluium(VI) has no affinity towards cation exchangers.

Anion exchange[5,8]. The anion-exchange properties of tellurium(IV) in hydrochloric acid solution were studied using a few milligrams of tellurium tagged with tellurium-127. The results are tabulated in Table II. It was confirmed by some preliminary experiments that the carrier-free behavior was the same as the weighable amount of tellurium(IV) in both cation- and anion-exchange. The affinity of tellurium(VI) to anion exchanger is also negligibly small in acid solution.

Other minor constituents:—Some preliminary experiments were performed using the radioactive isotopes of cadmium, indium and tin (Fig. 6; Table II).

By cation exchange, using 0.5~1 M hydrochloric acid solution as an eluent, one can separate these elements, Cd, Sn(IV), Sb(III) and Te(IV), in one group from the gross fission products. By the following treatment with anion exchanger, cadmium and tin would be separated from antimony and from tellurium.

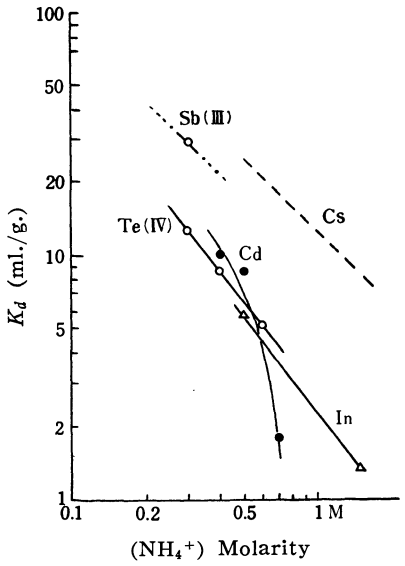

Fig. 6. Cation exchange of Cd, In and Te(IV) in HCl soln.
Exchanger: Dowex 50-X8.

Cesium, rare earths and alkaline earths:—The cation-exchange properties of cesium, rare earths and alkaline earths are rather well known. Some considerations, however, might be needed for the selection of the eluent for the separation of these elements which are adsorbed on the top of HR-form cation-exchange column.

In general, complexing reagent is most effective to remove rare earths from cation exchangers. But every complexing reagent, as far as the solution of its ammonium salt is used, elutes not only rare earths but also cesium from a column of HR-form cation-exchange resin with slightly different rates (Figs. 7 and 8). Therefore in this experiment cesium was eluted beforehand with ca. 1 M hydrochloric acid or 0.5 M ammonium salt of a mineral acid. The identification of the nuclide is possible from the position of the peak in the elution curves.

Detection of barium-137m, the daughter of cesium-137, was performed by cation-exchange separation. Cesium fraction was adsorbed again on the top of a cation-exchange column (NH_4R form), and barium activity was eluted out with ammoniacal 0.01 M EDTA solution. The effluents were directly led under the mica window of a counter tube through a vinyl tube, and the half-life of 2.60 min. was measured repeatedly with the same sample.

Acetate and EDTA were applied for the elution of rare earths and alkaline earths

5) Y. Sasaki, This Bulletin, **28**, 615 (1955).
6) F. Aoki, ibid., **26**, 480 (1953).
7) Y. Sasaki, *Japan Analyst* (*Bunseki Kagaku*), **4**, 637 (1955).
8) Y. Sasaki, This Bulletin, **28**, 89 (1955).

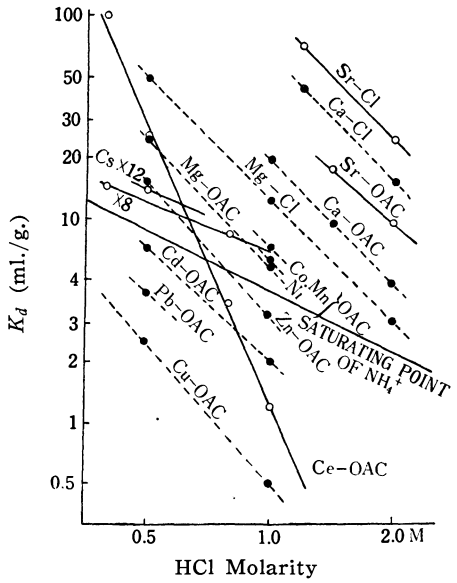

Fig. 7. Cation exchange of several elements in ammonium salt solutions.
Cs and Me—Cl: in NH_4Cl solutions.
OAc: NH_4OAc+HOAc (pH 4.6).
Exchangers: Colloidal Dowex 50 (for alkaline earths); Dowex 50-X8 (for others).

from the cation-exchange column. Ammonium acetate has been used as a fractionating eluent by changing the concentration for the group of rare earths, some transition elements[9] and alkaline earths[10,11]. This eluent has an advantage over any other organic reagent in that it can easily be removed by simple evaporation. Therefore this eluent is not only useful for the titrimetric determination of carrier metals by complexometric method which enables us to compare the elution curves of carriers and activities, but also convenient for the counting of carrier-free nuclides without the difficulty arising from self-absorption.

EDTA is a valuable reagent for the separation of rare earths and alkaline earths, especially for the separation into individual elements by the careful control of the pH. The smaller solubility of the free acid, however, prevents the direct use of HR-form column. For the elution of alkaline earths the mixture containing 0.01 M EDTA and 0.1 M ammonium acetate could be used at the pH between 7 and 9 to separate each member successively.

9) M. Honda. *Japan Analyst (Bunseki Kagaku)*, **4**, 384 (1955).
10) M. Honda, ibid., **3**, 132 (1954).
11) K. Kimura, E. Minami, M. Honda and others, ibid., **3**, 335 (1954).

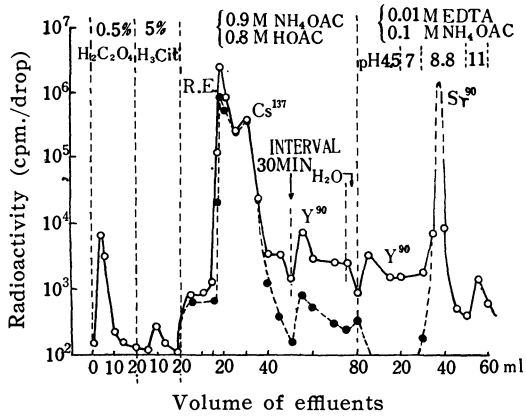

Fig. 8. Group separation with cation exchanger[4].
Sample: the fission products (Batch No. 19) (Oak Ridge Natl. Lab.) ca. 4 mc. in 4 M HNO_3 solution.
-o-o- measured just after the elution.
-•-•- measured after 2 months.
Column: Dowex 50-X8, 5 ml.

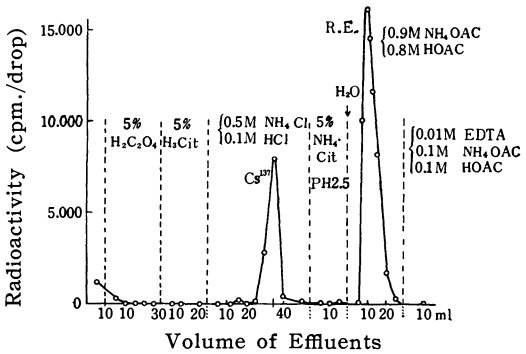

Fig. 9. Separation of cesium and rare earths[4]. (See Fig. 8)
Sample: 10~30 ml. fraction of NH_4OAc effluents in Fig. 8.
Column: Dowex 50-X8, 5 ml.

Systematic Separation Process

The properties of the elements described above could be applied to the systematic ion-exchange separation process for fission-product mixture. The possible scheme of such a process is outlined in Fig. 10. The sample of gross fission products free from heavy metals, is treated with concentrated hydrochloric acid, evaporated to dryness, and dissolved in a few milliliters of 0.1~0.2 M hydrochloric acid solution which contains free bromine. By these procedures, ruthenium is converted into anionic complexes, and bromine will oxidize antimony to its quinquevalent state. This solution is slowly passed through a small cation-exchange column (HR form),

and the column is washed with water. All ruthenium and antimony will be found in the effluents. The latter is treated with sulfur dioxide and passed through another cation-exchange column, which will take up antimony reduced to tervalent state. Oxalic acid (1%) or dilute hydrochloric acid (1 M) could be used for the elution of this element.

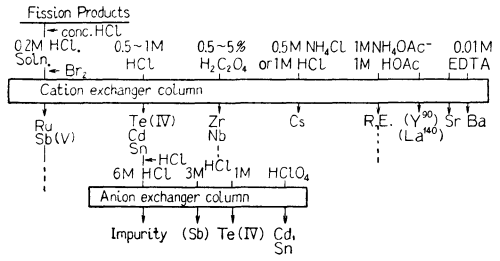

Fig. 10. Method of systematic separation of fission product mixture.

Tellurium(IV), cadmium and tin(IV) are eluted rapidly with 0.5~1 M hydrochloric acid from the former column. To the effluents, concentrated hydrochloric acid is added and the concentration of the acid is adjusted to 6 M. The impurities will be removed from this fraction by passing it through an anion-exchange column, Dowex 1-X4 (pretreated with 6 M HCl), and washing it with 6 M hydrochloric acid. Then carrier-free tellurium is eluted with 1 M hydrochloric acid. Finally, minor constituents, cadmium and tin, would be eluted out with perchloric acid or nitric acid.

After the elution of tellurium and others, zirconium and niobium will be eluted with 0.5~5% oxalic acid from the cation-exchange column. Cesium, rare earths and alkaline earths are then treated as illustrated in Figs. 8 and 9. If the addition of ammonium chloride is not favorable, the use of NH_4R-form cation exchanger and ca. 1 M ammonium acetate solution which is buffered with acetic acid can be recommended to separate rare earths from cesium. In this case, rare earths appear in the effluent with the added eluent and can be separated from cesium which has the elution peak at the same position as in the case in which HR-form resin is used.

In Figs. 8 and 9, citrate and oxalate were used to remove possible heavy-metal impurities.

Department of Chemistry
Faculty of Science
The University of Tokyo
Hongo, Tokyo

SHORT COMMUNICATIONS

New Colorimetric Method for the Determination of Uranium with Neo-thorone

By Shozo SHIBATA and
Teiichi MATSUMAE

(Received February 10, 1958)

In order to determine a microgram amount of uranium, a new colorimetric method has been developed that is based upon the stable blue colored uranium complex of Neo-thorone[1] (*o*-arsonophenyl-azo-chromothropic acid[2]) in an aqueous solution.

Absorption spectra of the reagent and of the complex with uranium are respectively presented in Fig. 1a and 1b. These curves were measured in a buffered solution of pH 6.0. The blue colored complex of uranium was formed by adding several micrograms of uranium (as $UO_2(NO_3)_2$) and 1.0 ml. of 0.1% reagent solution to a 25 ml. volumetric flask and diluting to the mark with a buffered solution. Color was developed for five minutes and its stability was found to be quite adequate for the determination of uranium, the absorbance being proportional to uranium concentration in the range from 1 μg. to at least 40 μg. At 600 mμ, the molar extinction coefficient is about 25,000. or 0.0095 μg. U/cm^2 corresponding to $\log I_0/I=0.001$. Thus this

1) M. Ishibashi and S. Higashi, *Japan Analyst (Bunseki Kagaku)*, **4**, 14 (1955); **5**, 135 (1956).
2) V. I. Kuznetsov, *Compt. rend. acad. sci. U.S.S.R.*, **31**, 898 (1941).

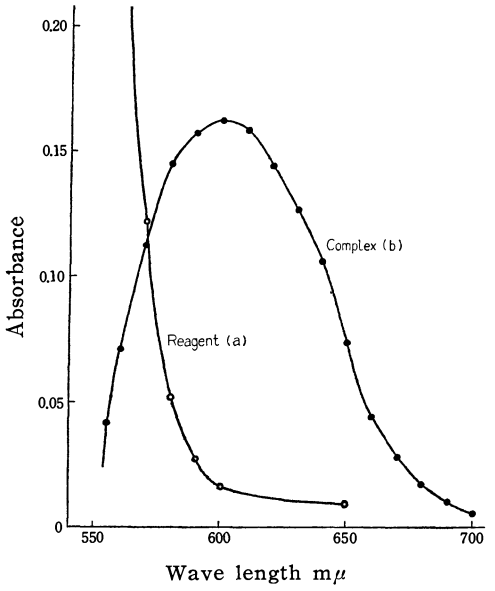

Fig. 1. Absorption spectra of reagent and its complex.

method appears to offer a good basis for the colorimetric determination of a microgram amount of uranium.

Details of the study will be published later.

Government Industrial Research Institute
Nagoya, Kita-ku, Nagoya

The Relationship between the Conformation of Epimeric 6-Substituted 4-ene-3-Ketosteroids and their Ultraviolet and Infrared Absorption Spectra

By Ken-ichi MORITA

(Received January 25, 1958)

In the previous paper[1] an empirical rule has been presented for the absorption spectra of C_6-substituted 4-ene-3-ketosteroids. Namely, 6β-isomers have lower K-band intensities in the ultraviolet absorption spectra than the corresponding 6α-isomers. The effect was ascribed to the greater steric hindrance involved in 6β-isomers in which 6β-substituents have 1:3-X:C_{10}Me and 1:3-X:C_8H interactions[2].

Both α and β substituents in the system cause only the small wavelength displacements ($\pm\Delta\lambda\simeq 5$ mμ) accompanied by decreases in ε. Hence, the type of spectral effects arising from the steric hindrance in the system may be associated with transitions between non-planar ground states and planar or near-planar excited states[3]. Thus the angles θ between the C_3 carbonyl groups and 4,5-unsaturated linkages in the ground state may be calculated from an equation $\cos^2\theta=\varepsilon/\varepsilon_0$, presented by Braude and Sondheimer[3], where ε_0 is the value for the unhindered compound in which $\theta=0$, if it is assumed that the 4-ene-3-keto system of 4-cholesten-3-one has uniplanar conformation. The values of θ derived in this way are given in Table I.

TABLE I

ULTRAVIOLET SPECTRA OF EPIMERIC 6-SUBSTITUTED 4-CHOLESTEN-3-ONE[4]

Compound	λ_{max}^{alc} (mμ)	ε	$\varepsilon/\varepsilon_0$	θ°
4-cholesten-3-one	241	18,000[5]	1.	0
6α-hydroxy-	240	17,080	0.95	13
6β-hydroxy-	237	14,500	0.80	27
6α-acetoxy-	238	15,800	0.88	20
6β-acetoxy-	237	13,200	0.73	31
6α-chloro-	239	17,500	0.97	10
6β-chloro-	241	15,100	0.84	23
6α-bromo-	238	15,800	0.88	20
6β-bromo-	246	13,500	0.75	30
6α-methyl-	241	16,650	0.92	16
6β-methyl-	241	15,100	0.84	23

The greater values in the interplanar angles for the 6β-substituted 4-ene-3-ketosteroids, deduced from the difference in ultraviolet absorption, may be reflected in the infrared spectra. Unfortunately, only a limited number of the infrared spectra of these compounds have been reported[6,7,8]. In the infrared spectra of epimeric 6-acetoxy-4-cholesten-3-one[6] the location of the carbonyl band for 6β-isomer approaches that of saturated ketone more than that for 6α-isomer. A rough linear relationship[9] appears to exist between the interplanar angle θ deduced from difference in ultraviolet and $\Delta\nu/\Delta\nu_0$ where $\Delta\nu$ refers to the shift with respect to an unconjugated ketone (taken as 1713 cm.$^{-1}$) and $\Delta\nu_0$ refers to the shift in the 4-cholesten-3-one (Table II).

TABLE II

INFRARED SPECTRA OF EPIMERIC 6-ACETOXY-4-CHOLESTEN-3-ONE IN CAREON DISULFIDE[4]

Compound	$\nu_{C=O}$(cm.$^{-1}$)	$\Delta\nu/\Delta\nu_0$	$\nu_{C=C}$(cm.$^{-1}$)
4-cholesten-3-one	1684	1.	1626
6α-acetoxy-	1692	0.72	1631
6β-acetoxy-	1698	0.52	—

Sugiyama Chemical Research Institute
Mure, Mitaka, Tokyo

1) K. Morita, *J. Chem. Soc. Japan, Pure Chem. Sec. (Nippon Kagaku Zassi)*, **78**, 1581 (1957).
2) D. H. R. Barton, *J. Chem. Soc.*, **1953**, 1027; D. H. R. Barton and R. C. Cookson, *Quart. Rev.*, **10**, 44 (1956).
3) E. A. Braude and F. Sondheimer, *J. Chem. Soc.*, **1955**, 3754.
4) See Table I of ref. 1 and literatures cited there.
5) L. Dorfman, *Chem. Rev.*, **53**, 47 (1953). cf. D. H. R. Barton and E. R. H. Jones, *J. Chem. Soc.*, **1943**, 602.
6) L. F. Fieser, *J. Am. Chem. Soc.*, **75**, 4377 (1953).
7) K. Dobriner, E. R. Katzenellenbogen and R. N. Jones, "Infrared Absorption Spectra of Steroids", Chart 203, (1953).
8) R. N. Jones and F. Herling, *J. Org. Chem.*, **19**, 1252 (1954).
9) E. A. Braude and C. J. Timmons, *J. Chem. Soc.*, **1955**, 3766.

A Method for the Fractionation of Oligopeptides Based on their Molecular Sizes

By Kozo NARITA, Sadao FUJIWARA and Shimako MURASAWA

(Received June 6, 1957)

Amino-acid sequence studies of proteins are of interest for the elucidation of mechanism of their biological activities. In any such study, a large number of peptides produced by partial hydrolysis of protein must first be separated from one another. Although several methods of their fractionation, such as ion exchange chromatography, ionophoresis based on their electrochemical properties, counter-current distribution utilizing the difference of their partition coefficients between two immissible solvents and adsorption chromatography, are available, no method based on their molecular size is known.

Partridge[1] has suggested the molecular sieve effect of ion exchange resins as a tool for the fractionation of a series of various substances which have only different molecular sizes, and Thompson[2] showed that C-terminal leucine liberated from lysozyme by the action of carboxypeptidase could be separated from the remaining large protein fragment with the aid of strongly acidic ion exchange resin. Further, Deuel et al.[3] found that polygalacturonic, polymannuronic and polymetaphosphoric acid could be separated by such a method from their low molecular components. Richardson[4] has used ion exchange resin for the purification of crude dyestuffs which contained low molecular coupling substances. Kressman[5] has studied fundamental problems of the separation of various dyestuffs based on their ionic sizes.

The present authors attempted to establish a general method to fractionate various oligopeptides based on their hydrated molecular sizes by the molecular sieve of ion exchange resin.

It is a well-known fact that various amino acids are adsorbed on the hydrogen form of sulfonic acid type ion exchangers from neutral or slightly acidic solutions. In general, polystyrene type ion exchange resin has a three dimensional network structure corresponding to the extent of cross-linkage which is attributed to its divinylbenzene content. In order to be exchanged and adsorbed on the resin, the solute has to possess suitable polar group(s), and it has to be able to penetrate into the resin molecule and to react with it. Consequently large molecules, such as proteins, can not diffuse into highly cross-linked ion exchange resin and no adsorption will result, because the network is too small even though suitable dissociable groups are present in the solute molecules. On the contrary, small molecules will be adsorbed easily. On such a principle, when a solution of a peptide mixture is put on the top of the highly cross-linked ion exchange column which is assembled in series with stepwise decreasingly cross-linked resin columns, peptides will be adsorbed separately on the resins which possess the proper pore size respectively.

In the present study Dowex 50-X 16, X 12, X 8, X 4, X 2 and X 1 were used in order to study the behavior of some amino acids, synthetic peptides and the partial hydrolysates of modified silk fibroin[6] and casein towards ion exchange resins of various cross-linkages; it appears that this method was useful for the preliminary separation of peptides based on the difference of their molecular sizes.

Experimental

Materials.—Dowex 50-X 16 (20-50 mesh, lot 5754), X 12 (20-50 mesh, lot 8106), X 6 (20-50 mesh, lot 181), X 4 (50-100 mesh, lot 3458-40), X 2 (50-100 mesh, lot 3458-42) and X 1 (50-100 mesh, lot no. unknown) were used in the hydrogen form after several cycles from sodium to hydrogen forms have been performed.

The oxidative degradation product of silk fibroin, which was prepared by the reaction with hydrogen peroxide as described in earlier papers[6], contains only glycine, alanine and serine in

1) S. M. Partridge, *Nature*, **169**, 496 (1952).
2) A. R. Thompson, ibid., **169**, 495 (1952).
3) H. Deuel, J. Solms and L. Anayas-Weisz, *Helv. Chim. Acta*, **33**, 2171 (1950).
4) R. W. Richardson, *Nature*, **164**, 916 (1949); *J. Chem. Soc.*, **1951**, 910.
5) T. R. E. Kressman, *J. Phys. Chem.*, **56**, 118 (1952).
6) K. Narita, *J. Chem. Soc. Japan, Pure Chem. Sec.* (*Nippon Kagaku Zassi*), **75**, 487 (1954); S. Akabori, K. Satake and K. Narita, *Proc. Japan Acad.*, **25**, 206 (1949).

molar ratio of about 5 : 4 : 1 as constituent amino acids.

Enzymatic digests of casein were kindly supplied by Daigo Nutritive Chemicals, and in this case a mixture of bovine pancreas enzymes was used as a hydrolytic agent. Whale insulin was also supplied by Shimizu Pharmaceutical Co. and various authentic amino acids were supplied by Ajinomoto Co. Ltd.

A part of synthetic peptides (DL-leucylglycylglycine and DL-alanylglycylglycine) was supplied by Professor H. Tani of Osaka University and other peptides were synthesized by one of the authors (K. Narita). To confirm the purity of peptides, these were checked with paper chromatography by the use of several solvents and it was found that these were homogeneous.

Procedure.—*Multicolumn of Dowex 50.* Six columns (inner diameter 0.9 cm.) containing, from top to bottom, Dowex 50-X 16, X 12, X 8, X 4, X 2 and X 1 respectively were assembled in series. To fractionate peptides or to investigate on which column a single peptide was mainly adsorbed, 10 ml. of sample solution was put on the top column (X 16 column), and, after the solution sank under the resin surface, the developer (water or diluted hydrochloric acid) was added with a flow rate of 0.2 ml. per min. at the lowest column (X 1 column) until the effluent amounted to 250 ml.

Water, 0.1 and 0.3% hydrochloric acid were used as solvent for peptide solutions. Prior to the addition of the peptide solution, all columns were equilibrated with the solvent by passing it through them overnight. The effluent was concentrated at 40°C in vacuo to 15 ml., transferred to a 25 ml. volumetric flask and filled with water to the marked level. After the disassembly of the multicolumn system, adsorbed peptides were eluted from each column with 2 N sodium hydroxide using the same flow rate as for the development. It was necessary to use 1.5 fold excess of the sodium ion over the total exchange capacity of the resin, in order to displace the peptide completely under the given conditions; the column was then washed with water. The eluate was collected in a 25 ml. or 50 ml. volumetric flask. Aliquots were used for total and α-amino nitrogen determinations. The analyses were performed by the micro Kjeldahl and the manometric van Slyke method respectively and the average peptide length (number of amino acids in the peptide) in the eluate was represented as follows.

$$\text{average peptide length} = \frac{\text{total nitrogen}}{\alpha\text{-amino nitrogen}}$$

When preparative fractionation of peptides in mixture is attempted, it is preferable to use 10% aqueous ammonia solution instead of sodium hydroxide solution as the eluting solvent, to avoid the trouble of desalting. The total exchange capacities of each resin column were listed in the tables. The amount of sample to be fractionated is preferably equivalent to 1/5 to 1/20 of the total exchange capacity of each resin column.

Batch method.—To get the knowledge about the maximum adsorption amount of some amino acids and peptides on the resins, a batch method was used. Into 30 ml. of the solution containing about 150 mg. of amino acid or peptide, the resin was added in an amount corresponding to the theoretical for the exchange of the entire solute, stirred occasionally, kept to stand over-night and an aliquot of the supernatant was pipetted. The amount of unadsorbed solute was estimated by ninhydrin method using color yield of each solute to leucine and the adsorbed quantity was calculated. In Table VIII the ratios of adsorbed amounts of amino acids or peptides to the sodium ion (exchange capacity) are shown.

Results and Discussion

As mentioned already, chemically modified silk fibroin contained only the neutral amino acids of small molecule, glycine, alanine and serine[6]. Consequently, in order to test the possibility of the success of fractionation of peptides based on their hydrated molecular sizes with the aid of a molecular sieve, it seemed suitable to use the partial hydrolysate of this protein. The peptide mixture obtained by hydrolysis of the sample (500 mg.) with 25 ml. of concentrated hydrochloric acid at 40°C for 2 hours was concentrated in vacuo at 40°C to 15 ml. The concentrate was diluted with four volumes of water and treated with free form of Amberlite IR-45 column to remove the remaining hydrochloric acid. The effluent was concentrated in vacuo to 30 ml. An aliquot of this concentrate was diluted with water to 20 ml. and another aliquot was adjusted to 0.1% hydrochloric acid concentration by adding diluted acid to 20 ml. Both samples were fractionated separately with the Dowex 50 multi-column system as described in the experimental section. As listed in Table I, these results satisfied the authors' expectation.

When the tendencies of adsorption of petidpes from water are compared in Table I with those from 0.1% hydrochloric acid solution, one can find that larger peptides are much more adsorbed from water than from acid solution on the same resin column. This fact suggests that the pore size in the resin molecule decreases in hydrochloric acid. It is a generally well-known fact that ion exchange resins shrink to some extent in the presence of electrolytes and that the degree of shrinkage depends upon the concentration of electrolyte in the surrounding medium. The shrinkage of low cross-linked resin is so particularly

TABLE I

THE FRACTIONATION OF PEPTIDES IN THE PARTIAL ACID HYDROLYSATE OF MODIFIED SILK FIBROIN BY MOLECULAR SIEVE

Developer*		H_2O			0.1 % HCl**		
Cross-linkage	Total exchange capacity of column meq.	Total N mg	α-NH_2 N mg	Average peptide length	Total N mg	α-NH_2 N mg	Average peptide length
X 16	9.4	16.2	6.92	2.4	5.77	2.28	2.6
12	8.6	1.85	0.58	3.2	4.18	1.65	2.4
8	9.5	1.50	0.28	5.4	5.00	1.73	3.4
4	6.1	1.50	0.17	8.8	6.23	1.11	5.6
2	3.8	0.69	0.03	23	1.67	0.26	6.4
1	1.8	0.40	0.01	40	0.71	0.08	8.4
Effluent	—	5.17	0.10	52	3.20	0.15	21.4
Total		27.3	8.09	—	26.8	7.11	—
Charged mixture		29.7	8.25	3.6	29.7	8.25	3.6
Recovery		92.7%	89.1%	3.4***	89.9%	86.1%	3.8***

* Flow rate, 0.2 ml./min.
** pH 1.7
*** The value was calculated from the analytical results.

TABLE II

THE EFFECT OF THE DEVELOPER TO THE ADSORBABILITY OF DL-ALANYLGLYCYLGLYCINE ON DOWEX 50

Developer*		H_2O		0.1 % HCl**		0.3 % HCl**	
Concentration of inflow		0.403 mM		0.314 mM		0.396 mM	
Cross-linkage	Total exchange Capacity of column meq.	Amount adsorbed mM	Per cent. adsorbed %	Amount adsorbed mM	Per cent. adsorbed %	Amount adsorbed mM	Per cent. adsorbed %
X 16	7.2	0.400	99.2	0.124	39.6	0.015	3.8
12	6.2	0	0	0.176	56.2	0.090	22.8
8	6.0	0	0	0	0	0.219	55.5
4	4.5	0	0	0	0	0.071	18.0
2	2.9	0	0	0	0	0	0
1	1.5	0	0	0	0	0	0
Total		0.400	99.2	0.300	95.8	0.395	99.8

* Flow rate, 0.2 ml./min.
** pH 1.7
*** pH 1.3

remarkable that it sometimes shrinks to about half of its initial volume. A natural consequence of the decreasing resin volume is that the pore size of network structure of the resin is decreased. Therefore, when hydrochloric acid concentration is increased, it is expected that the pore size of the resin becomes much smaller. In this respect, the behavior of DL-alanylglycylglycine in water, 0.1 and 0.3 % hydrochloric acid solutions towards resin was studied. As shown in Table II, it is possible to change the pore size of the resin artificially, but to increase the acid concentration above 0.3 % is not practicable because the dissociation of sulfonic acid groups of the resin will be suppressed. However, when organic acids, such as formic or acetic, are used, this defect will be avoided. The extent of the change of the pore size was remarkable in proportion to the decrease of divinylbenzene content as shown in Table I. As an alternate explanation of the above mentioned facts, one can not exclude the change of the shape and the size of the peptide in the presence of the electrolyte. However it appears probable that the change in the pore size of the resin is more important than that of the shape and the size of peptide in this case. On the other hand one must consider that the suppression of the dissociation of sulfonic acid groups in the resin molecule may cause the decrease in adsorption quantity of peptide in the acidic solution.

TABLE III
EXCHANGE CAPACITIES* OF DOWEX 50-X 16, X 12 AND X 8** IN WATER AND DILUTED HYDROCHLORIC ACID

Dowex 50	H_2O		0.1% HCl***		0.3% HCl****	
	meq.	%	meq.	%	meq.	%
X 16	3.95	(100.0)	3.82	(96.7)	3.82	(96.7)
12	3.15	(100.0)	3.07	(97.5)	3.03	(96.2)
8	3.65	(100.0)	3.51	(96.2)	3.45	(94.5)

* These were measured by batch method and the values were expressed for Na ion.
** The resins used were dried at 80°C in the hydrogen form for 10 hours.
*** pH 1.7
**** pH 1.3

But this possibility was excluded because of the finding of no marked differences between exchange capacities of the resins for the sodium ion in water and diluted hydrochloric acid as shown in Table III.

Table IV and V show various kinds of behavior of some amino acids in 0.3% hydrochloric acid towards the resin columns. Although the molecular size of L-leucine should be greater than that of L-alanine, the former was much more adsorbed on X 16 resin than the latter contrary to the authors' expectation as illustrated in Table IV. Similar phenomena were also found by the batch method

TABLE IV
ADSORPTION OF SOME AMINO ACIDS ON DOWEX 50 MULTICOLUMN SYSTEM FROM 0.3% HYDROCHLORIC ACID* SOLUTION

Amino acid		Glycine		L-Alanine		L-Leucine		L-Aspartic acid		L-Lysine	
Concentration of inflow		0.563 mM		0.503 mM		0.416 mM		0.396 mM		0.482 mM	
Cross-linkage	Total exchange capacity	A**	B***	A**	B***	A**	B***	A**	B***	A**	B***
	meq.	mM	%	mM	%	mM	%	mM	%	mM	%
X 16	7.2	0.468	6.5	0.124	1.7	0.335	4.7	0.015	0.21	0.387	5.4
12	6.2	0.093	1.5	0.388	6.3	0.065	1.0	0.018	0.29	0.020	0.34
8	6.0	0	0	0	0	0	0	0.288	4.8	0	0
4	4.5	0	0	0	0	0	0	0.041	0.91	0	0
2	2.9	0	0	0	0	0	0	0	0	0	0
1	1.5	0	0	0	0	0	0	0	0	0	0
Total		0.561		0.512		0.400		0.362		0.407	
Recovery		99.6%		101.7%		96.2%		91.4%		84.6%	

* Flow rate, 0.2 ml./min.; pH 1.3.
** Amount adsorbed.
*** Ratio of adsorption of amino acid to the Na ion.

TABLE V
ADSORPTION OF SOME PEPTIDES ON DOWEX 50 MULTICOLUMN SYSTEM FROM 0.3% HYDROCHLORIC ACID* SOLUTION

Peptide		Gly-L-Leu		DL-Leu-Gly		Gly-L-Leu-Gly		Gly-L-Leu-L-Leu		DL-Leu-Gly-Gly		DL-Ala-Gly-Gly	
Concentration of inflow		0.365 mM		0.422 mM		0.361 mM		0.230 mM		0.292 mM		0.396 mM	
Cross-linkage	Total exchange capacity	A**	B***	A**	B***	A**	B***	A**	B***	A**	B***	A**	B***
	meq.	mM	%	mM	%	mM	%	mM	%	mM	%	mM	%
X 16	7.2	0.086	1.2	0.060	0.83	0.049	0.68	0.041	0.57	0.013	0.18	0.015	0.21
12	6.2	0.241	3.9	0.210	3.4	0.227	3.7	0.148	2.4	0.080	1.3	0.090	1.4
8	6.0	0.036	0.6	0.122	2.0	0.027	0.45	0.035	0.58	0.189	3.2	0.219	3.6
4	4.5	0	0	0	0	0	0	0	0	0.011	0.24	0.071	1.6
2	2.9	0	0	0	0	0	0	0	0	0	0	0	0
1	1.5	0	0	0	0	0	0	0	0	0	0	0	0
Total		0.363		0.392		0.303		0.224		0.293		0.395	
Recovery		99.6%		93.1%		83.9%		97.5%		100.3%		99.8%	

* Flow rate, 0.2 ml./min.; pH 1.3.
** Amount adsorbed.
*** Ratio of adsorption of peptide to Na ion.

(Table VIII). To explain this fact one must consider that the hydrated molecular size of L-alanine is much larger than that of L-leucine in acid solution. In the case of L-aspartic acid, Table IV suggests that the effect of side chain carboxyl group can not be ignored under these conditions.

When the adsorption quantities of glycyl-L-leucine and DL-leucylglycine are compared with one another, it is clear that the effect of the size of the N-terminal amino acid is greater than that of the C-terminal one, as expected. The results of the tripeptides listed in Table V also satisfy the authors' expectation; namely the larger the molecular size of the peptide, the more the decrease in the adsorption quantity of peptide on the resins.

TABLE VI

THE BEHAVIOR OF WHALE INSULIN IN 0.1% HYDROCHLORIC ACID* TOWARDS DOWEX 50 MULTICOLUMN SYSTEM

Concentration of inflow		5.48 mg N	
Cross-linkage	Total exchange capacity meq.	Amount adsorbed mg N	Per cent adsorbed %
X 16	7.2	>0.011	>0.2
12	6.2	>0.025	>0.5
8	6.0	>0.020	>0.4
4	4.5	0.431	7.9
2	2.9	0.683	12.6
1	1.5	1.11	20.3
Effluent	—	2.74	50.0
Total		5.01	91.4

* pH 1.7, flow rate, 0.2 ml./min.

As shown in Table VI, whale insulin was hardly ever adsorbed from 0.1% hydrochloric acid solution on high cross-linked resins. In such an acid solution, it will be considered that insulin is dissociated to monomer molecules (molecular weight 6,000). If the insulin molecule were spherical, the hydrated particle diameter could be calculated as roughly 27Å[7] from the data of Fredericq et al.[8] Thus it seems that Dowex 50-X 16, X 12 and X 8 do not have the pore of diameter of above 27Å in 0.1% hydrochloric acid solution.

In a further experiment, the authors attempted to separate the synthetic mixture of glycine, DL-leucylglycine and DL-alanylglycine in 0.3% hydrochloric acid solution from one another by the molecular sieve. After the elution of adsorbed materials with 2 N sodium hydroxide, the desalting and then one dimensional chromatography in phenol-water system, it was found that glycine was adsorbed on X 16 resin and a part on X 12 resin, DL-leucylglycine was adsorbed mostly on X 12 resin and partly on X 8 resin, and most of the tripeptide was adsorbed on X 8 and a small amount of X 4 resin.

In Table VII, two examples of the result which was obtained by the treatment of enzymatic digests of casein with molecular sieve column are listed. Digest I represents an almost completely digested mixture with an average peptide length of 1.78, while Digest II represents a partial digest mixture of average peptide length of 4.66. These data seem to show that the peptides are poorly separated. However, when the behavior of L-aspartic acid shown in Table IV is considered, one can suppose that the behavior of acidic amino acids and their peptides is not necessarily controlled only by their molecular sizes. It is a well-known fact that casein contains a large amount of acidic amino acids and especially strongly acidic phosphoserine residues. In fact, large quantities of phosphoric acid, serine, proline, aspartic and glutamic acid, leucine and alanine were detected in the complete hydrolysate of the effluent fraction which passed through the whole column system. This fact seems to indicate that the phosphopeptides in casein digests contain these amino acids, and that they are resistant to enzymatic attack as the average peptide length in the effluent fraction is quite great.

Moreover, the maximum adsorption quantities of some amino acids and peptides on resins were measured by the batch method (Table VIII). Comparing these figures with those of Table IV and V, one can see that the adsorption quantities of the solutes in column method are only 7 to 15% of those in the batch method. These facts indicate that the adsorption equilibrium is not reached at the flow rate of 0.2 ml. per min. in the column method and that for the solute to react completely with the resin a much slower rate is required. Table VIII shows that there is only a slight difference between maximum adsorption quantities of DL-leucylglycine and DL-alanylglycylglycine in 0.3% hydrochloric acid solution, but in the column method both peptides

7) The calculation was done by Dr. Y. Kawade of the Virus Research Institute, Kyoto University and the authors express their thanks to him.

8) E. Fredericq and H. Neurath, *J. Am. Chem. Soc.*, **72**, 2684 (1950).

TABLE VII
THE FRACTIONATION OF PEPTIDES IN ENZYMATIC DIGEST OF CASEIN*

Sample: Cross-linkage	Total exchange capacity	Digest I: Total N	Digest I: α-N_2H N	Digest I: Average peptide length	Digest II: Total N	Digest II: α-N_2H N	Digest II: Average peptide length
		mg	mg		mg	mg	
		22.98	12.90	1.78	80.24	17.24	4.66
	meq.	mg	mg		mg	mg	
X 16	7.2	7.19	5.20	1.38**	12.34	4.73	2.51**
12	6.2	4.94	4.26	1.16	5.71	1.78	3.21
8	6.0	2.89	2.76	1.05	10.41	2.89	3.60
4	4.5	1.10	0.95	1.16	25.98	6.34	4.10
2	2.9	0.31	0.31	1.00	4.44	0.97	4.57
1	1.5	0.0	0.0	—	1.50	0.32	4.69
Effluent	—	4.20	0.30	14.0	6.95	0.22	31.58
Total		20.63	13.78		67.33	17.25	
Recovery		89.8%	106.8%	1.49***	83.9%	100.0%	4.90***

* Developed with 0.3% hydrochloric acid, pH 1.3, at flow rate of 0.2 ml./min.
** In this fraction, basic amino acids are also contained.
*** The value was calculated from the analytical results.

TABLE VIII
MAXIMUM ADSORPTION QUANTITIES OF SOME AMINO ACIDS AND PEPTIDES ON DOWEX 50
(Figures show adsorbed solutes in percentages of exchange capacities in water.)

	Cross-linkage	H_2O	0.1% HCl*	0.3% HCl**
		%	%	%
Glycine	X 16	85.2	85.5	55.3
	12	86.9	87.7	58.0
	8	87.2	86.6	54.5
L-Alanine	X 16	—	—	32.8
	12	—	—	40.0
	8	—	—	36.1
L-Leucine	X 16	—	—	38.8
	12	—	—	48.5
	8	—	—	41.8
L-Aspartic acid	X 16	39.8	—	13.4
	12	—	—	21.4
	8	—	—	24.4
L-Lysine	X 16	—	—	37.6
	12	—	—	39.9
	8	—	—	37.1
DL-Leu-Gly	X 16	58.5	34.1	14.0
	12	78.8	46.8	22.8
	8	88.5	53.7	29.8
DL-Ala-Gly-Gly	X 16	62.4	20.2	13.8
	12	78.2	28.3	20.2
	8	85.5	35.6	24.8

* pH 1.7
** pH 1.3

are successfully separated from each other (also see Table V). This fact indicates the adsorption velocity of DL-alanylglycylglycine is lower than that of DL-leucylglycine. Contrary to the authors' expectation, this concept, unfortunately, was incompatible with experimental results

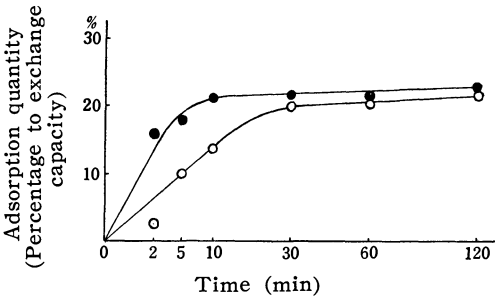

Fig. 1. The rates of adsorption of DL-alanylglycylglycine and DL-leucylglycine on Dowex 50-X 12 from 0.3 per cent. hydrochloric acid solutions.
●—● DL-Alanylglycylglycine
○—○ DL-Leucylglycine

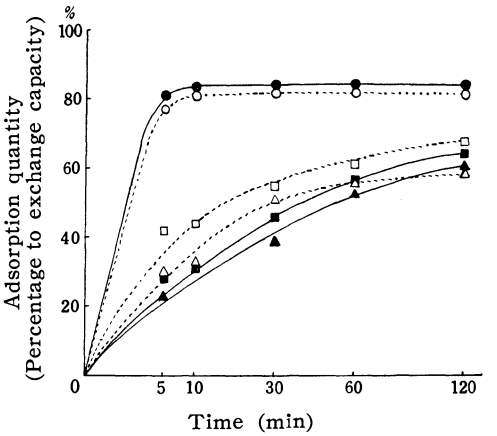

Fig. 2. The rates of adsorption of glycine, L-phenylalanine and DL-alanylglycylglycine on Dowex 50-X 16 from water. The black and the white marks show results obtained at room temperature and at 50°C respectively.
—●···○ Glycine
—■···□ L-Phenylalanine
—▲···△ DL-Alanylglycylglycine

shown in Fig. 1.

The adsorption velocities of glycine, L-phenylalanine and DL-alanylglycylglycine in aqueous solutions were also studied at room temperature (25°C) and 50°C (Fig. 2). No appreciable difference was found between velocities of low molecular glycine at either of the temperatures, while a slight difference was observed between those of L-phenylalanine and DL-alanylglycylglycine. Besides the ion exchange reaction, L-phenylalanine is adsorbed on the resin by van der Waals' force which is reduced at a high temperature, and thus aromatic amino acids may diffuse into a resin molecule easily at a higher temperature and their adsorption velocities will be increased. Generally speaking, the diffusion of solutes into the resin particles is favored by an elevated temperature. Consequently, so far as the solutes are not decomposed at high temperatures in contact with the resin, the fractionation of peptides in the column system will be much more favorable at a high temperature than at room temperature.

In the fractionation of peptides by molecular sieve, it is most important to use resins the size of whose particle is large as possible in order to reduce the surface area of the resin particle[1]; otherwise large peptides will be also adsorbed on the surface of high cross-linked resin as well as small molecular peptides. Another necessary condition is a problem of flow rate. When the flow rate is too great, the solute can not diffuse into properly cross-linked resin particles and then fractionation will be unsuccessful. By this method, not only sulfonic acid-type resins but also those of othe types may be used for peptides and another substances.

Summary

A method to fractionate peptides based on their hydrated molecular sizes by the molecular sieve effect of sulfonic-acid type ion exchange resins, Dowex 50, is described. The behavior of some amino acids, peptides and partial protein hydrolysates towards molecular sieve is also studied. Various factors which control the fractionation of solutes by molecular sieve are discussed.

Department of Chemistry, Faculty of Science, Ochanomizu University, Bunkyoku, Tokyo

Beckmann Rearrangement in Liquid Sulfur Dioxide. III. Rearrangement by Chlorine with Various Salts

By Ritsuro TADA and Niichiro TOKURA

(Received August 28, 1957)

In a previous work[1], it was shown that the Beckmann rearrangement may be carried out by bromine only or by chlorine with a small quantity of bromine at room temperature in liquid sulfur dioxide and a possible mechanism was discussed. When chlorine was used without a catalytic amount of bromine, the rearrangement could not be induced at all. This result led the authors to examine the effect of various inorganic substances, and it now has been found that the addition of small amounts of such substances to chlorine may effect the Beckmann rearrangement in liquid sulfur dioxide.

Four groups of compounds were examined.

(1) The bromine compounds (potassium bromide, *N*-bromosuccinimide and hydrogen bromide) were the most effective, yielding 75.6, 75.2 and 67.6% of the acid amide, respectively. (2) The chlorine derivatives were the least effective. (3) Red phosphorus, sulfur and iron powder gave a moderate yield of products. (4) The effect of potassium nitrate, nitrite and cyanide was similar to that of the chlorine compounds.

The rearrangement of cyclohexanone oxime in liquid sulfur dioxide was studied at 20°C. The molar ratio of chlorine to

1) N. Tokura, R. Asami and R. Tada, *J. Am. Chem. Soc.*, **79**, 3135 (1957).

the promoter was 1 to 0.1. The results are listed in Table 1.

When compounds not easily soluble in liquid sulfur dioxide, such as phosphorus, were used, the reaction mixtures were occasionally shaken during the reaction. In the case of the bromine compounds, it was probable that the bromine liberated by the exchange reaction between chlorine and the bromine compounds promoted the rearrangement as in the previous case. The chlorine compounds were also likely to initiate the rearrangement but the yields of lactam were smaller than in the case of bromine compounds.

TABLE I

EFFECT OF CHLORINE AND INORGANIC MATERIALS OR SALTS ON THE REARRANGEMENT OF CYCLOHEXANONE OXIME IN LIQUID SULFUR DIOXIDE

Chlorine with	Yield of ε-caprolactam	
	g.	%
HBr	16.9	67.6
NaBr	6.9	27.6
KBr	18.9	75.6
N-bromosuccinimide	18.8	75.2
KI	4.1	16.4
KCl	3.2	12.8
PCl_5	5.5	22.0
S_2Cl_2	7.9	31.6
$SOCl_2$	2.9	11.6
$AlCl_3$	5.0	20.0
$FeCl_3$	2.9	11.6
$SnCl_4$	1.8	7.2
Phosphorus (red)	11.2	44.8
Sulfur	8.0	32.0
Iron powder	4.5	18.0
KNO_3	2.9	11.6
KNO_2	3.8	15.2
KCN	3.1	12.4

Cyclohexanone oxime, 25 g. (0.22 mole), liq. SO_2 200 ml., mole ratio of oxime: chlorine: salt=1 : 1 : 0.1, reaction temp. 20°C, reaction time, one hour.

Although the solubilities in liquid sulfur dioxide were very small, sulfur and iron powder gave 32.0 and 18.0% yields, respectively. These results well coincided with 31.6 and 11.6% obtained with sulfur chloride and ferric chloride, respectively, whereas it was expected that in liquid sulfur dioxide, sulfur and chlorine might combine to form sulfur chloride and iron and chlorine to form ferric chloride. The initiation of the rearrangement by chlorine and phosphorus was explicable by the formation of phosphorus chloride followed by the decomposition of the latter to phosphorus oxychloride and thionyl chloride in liquid sulfur dioxide.

The mixture of the oxime, chlorine and an added promoter salt in liquid sulfur dioxide turned blue or bluish green in color, indicating the formation of a chloro-nitroso compound, while, hydrogen bromide, potassium bromide, *N*-bromosuccinimide, sulfur chloride or sulfur gave a reaction mixture reddish brown to orange in color, showing the absence of the chloro-nitroso radical, and the rearrangement was more profound than in the cases using a salt. The rearrangement was not improved by the addition of potassium nitrate, nitrite or cyanide.

Experimental

Reagents.—Cyclohexanone oxime was prepared according to the description of "Organic Syntheses"[2], m.p. 89.5—90.5°C. The salts and the inorganic materials were of the commercial purest grade, and used without further purification. Commercial chlorine from a cylinder was treated with concentrated sulfuric acid and distilled. Liquid sulfur dioxide was dehydrated with concentrated sulfuric acid, but it brought about no difference upon the results whether it was dehydrated or not.

Apparatus and the general procedure.—Glass pressure bottles, 300 ml. capacity, were used. Liquid sulfur dioxide (100 ml.) was added to the oxime (25 g., 0.22 mole) with cooling and a solution (100 ml.) containing chlorine (15.8 g., 0.22 mole) with a small definite amount (0.022 mole) of a promoter (one of the inorganic substances) was added. In experiments with a sparingly soluble material such as sulfur or sodium bromide, the cyclohexanone oxime solution was added to the chlorine solution. The mixture was allowed to stand, with occasional shaking when the mixture was not homogeneous or the reagent was difficultly soluble, for one hour at 20°C. Then the mixture was added to water with cooling and the solvent was allowed to evaporate. The residue was neutralized with diluted sodium hydroxide solution and the products were extracted with chloroform. After removal of the solvent, the residue was distilled under a reduced pressure to yield cyclohexanone (b.p. 55~65°C/35~36 mm.), unchanged oxime (b.p. 95~115°C/10~11 mm.) and ε-caprolactam (b.p. 120~130°C/7~8 mm.). The ε-caprolactam was recrystallized from ether, m.p. 67~68°C. It was identified as ε-benzoylamino-caproic acid, m.p. and mixed m.p. 80~80.5°C.

Rearrangement by chlorine with various reagents.—*Hydrogen bromide.* Liquid sulfur dioxide solution of anhydrous hydrogen bromide (0.022 mole) was prepared by separating the upper layer of the reaction mixture from 1.8 g. (0.011

2) E. W. Bonsquet, "Org. Synth.", **11**, 56 (1931).

mole) of bromine, 0.4 g. (0.022 mole) of water and 100 ml. of liquid sulfur dioxide. When chlorine mixed with the solution was added to the oxime solution, the reddish-orange reaction mixture produced 16.9 g. of ε-caprolactam. Yield 67.6% of the theory.

Sodium bromide. To a mixture of 15.8 g. of chlorine and 2.3 g. of sodium bromide in liquid sulfur dioxide a solution of cyclohexanone oxime in liquid sulfur dioxide was added. The reaction mixture turned blue in color and an insoluble powder precipitated. Treatment as described above gave 6.9 g. of ε-caprolactam. Yield 27.6%.

Potassium bromide. Chlorine and 2.7 g. of potassium bromide in liquid sulfur dioxide afforded 18.9 g. of ε-caprolactam (75.6%). The sulfur dioxide solution was reddish orange in color with fine fibrous precipitates.

N-Bromosuccinimide. This reagent (4.0 g.) gave a transparent solution pale reddish-orange in color with fine white precipitates, which afforded 18.8 g. of ε-caprolactam. Yield 75.2%.

Potassium iodide. ε-Caprolactam (4.1 g., 16.4%) was obtained from the reaction mixture of green emulsion by using 3.7 g. of potassium iodide.

Potassium chloride. By the use of 1.7 g of potassium chloride the reaction mixture became blue in color and gave a small amount of a powder and yielded 3.2 g. (12.8%) of ε-caprolactam.

Phosphorus pentachloride. From the blue reaction mixture from 4.7 g. of phosphorus pentachloride, 5.5 g. of ε-caprolactam (22.0%) was obtatined.

Sulfur chloride. By the use of 3.0 g. of sulfur chloride, the pale blue, turbid, reaction mixture afforded 7.9 g. of ε-caprolactam (31.6%).

Thionyl chloride. To the solution of the oxime in liquid sulfur dioxide, chlorine with 2.7 g. of thionyl chloride in liquid sulfur dioxide was added and the resulting pale blue reaction mixture gave 2.9 g. (11.6%) of ε-caprolactam.

Aluminum chloride. By the use of 3.0 g. of aluminum chloride, the blue reaction mixture afforded 5.0 g. of ε-caprolactam. Yield 20.0%.

Ferric chloride. The pale green reaction mixture from 3.7 g. of ferric chloride produced 2.9 g. of ε-caprolactam, yield 11.6%.

Stannic chloride. From a pale blue reaction mixture from 5.8 g. of stannic chloride and chlorine, 1.8 g. (7.2%) of ε-caprolactam was obtained.

Phosphorus. The pale blue reaction mixture, in which 2.8 g. of red phosphorus had been added in suspension, gave 11.2 g. (44.8%) of ε-caprolactam.

Sulfur. A dark reddish brown reaction mixture was obtained from 5.7 g. of sulfur which was difficultly soluble and afforded 8.0 g. of ε-caprolactam in 32.0% yield.

Iron. Iron powder (1.3 g.) was mixed and occasionally shaken with the reaction mixture to afford 4.5 g. (18.0%) of ε-caprolactam.

Potassium nitrate. When 2.5 g. of potassium nitrate was used, 2.9 g. (11.6%) of ε-caprolactam was obtained from the blue reaction mixture with a small white precipitate.

Potassium nitrite. ε-Caprolactam 3.8 g., 15.2% was obtained from the pale blue reaction mixture with chlorine and 2.4g. of potassium nitrite.

Potassium cyanide. By the use of 1.5 g. of potassium cyanide, the bluish green reaction mixture gave 3.1 g. of ε-caprolactam, yield 12.4%.

The present investigation was supported by a grant from the Ministry of Education. Liquid sulfur dioxide was supplied by the Befu Chemical Industries Co., Ltd. The assistance, in both cases is gratefully acknowledged.

Chemical Research Institute of Non-aqueous Solutions, Tohoku University. Sendai

Reactions of Active Methylene Compounds. II. Ester Condensation of Methyl 2-Methoxybenzoate with Phenylacetonitrile, and of each Methoxy Substitute; a New Synthetic Route to 2-Hydroxyphenyl Benzyl Ketones

By Yoshiyuki KAWASE

(Received October 14, 1957)

In the synthesis of isoflavones, 2-hydroxyphenyl benzyl ketones (2-hydroxydeoxybenzoins) have often been used for the starting materials. The preparation of these ketones is usually carried out by the condensation of phenols with phenylacetonitriles (Hoesch reaction), or with phenylacetic acids (Nencki reaction), or with phenylacetyl chlorides (Friedel-Crafts reaction), and further by the rearrangement of phenyl phenylacetates (Fries reaction). The position of the acyl group entering in the phenol nucleus is restricted by the effects of substitutes, and in some cases another preparative method is desirable for this reason and others.

Here, a different route to make the ketones is studied, and the preparation of 2-hydroxyphenyl benzyl ketone and its methoxy substitutes (VII) is described, which involves ester condensation of methyl 2-methoxybenzoate with phenylacetonitrile and of each methoxy substitutes (I, II) followed by hydrolysis.

The ester condensation of unsubstituted methyl benzoate with unsubstituted phenylacetonitrile to produce benzoylphenylacetonitrile was reported long ago[1,2]. Concerning the condensation between substituted ones, however, only benzoyl-2-methoxyphenylacetonitrile was reported[3]. This reaction seems to be reversible, so it was carried out in benzene by distilling off, with the latter, the ethanol produced in the course of the reaction. 2-Methoxybenzoyl-phenylacetonitrile and its methoxy substitutes (IIIa, b, c, d) were obtained in good yield by means of sodium ethoxide or hydride. Ethyl 2-methoxybenzoyl-phenylacetate and its methoxy substitutes (IVa, b, c, d) were prepared from these nitriles by the action of hydrogen chloride in ethanol following the method similar to that reported for unsubstituted nitrile[2-4]. In the case of nitrile IIIa, 2-methoxybenzoyl-phenylacetamide (V) was obtained as by-product in poor yield. The nitriles III and the esters IV were hydrolized to the desired ketones VII by heating them with hydrochloric acid in acetic acid. In the case of hydrolysis of nitrile IIIa, the product was 2-methoxyphenyl benzyl ketone (VI), and 2-hydroxyphenyl benzyl ketone (VIIa) could be obtained under much more drastic conditions. On the other hand, hydrolysis of nitriles III by 10% aqueous sodium carbonate, and of esters IV by 10% aqueous sodium hydroxide, gave 2-methoxy- or 2,4-dimethoxybenzoic acid.

Experimental[5]

Preparation of the Nitriles III.—Sodium ethoxide prepared from 0.4~2.3 g. of sodium and 20 cc. of absolute ethanol was dried up in vacuo at 150°. To a suspension of this dried sodium ethoxide in 100 cc. of absolute benzene, a mixture of methyl methoxybenzoate and phenylacetonitrile was added and heated at 95~100° on an oil-bath for four hours, during which most of benzene was driven off together with the ethanol produced. Water was added to the well-cooled residue and the mixture was extracted with ether. The gummy product separated by acidification of the aqueous layer was washed with aqueous sodium bicarbonate and then crystallized from ethanol. In some cases, sodium hydride was employed instead of dry sodium ethoxide. The following nitriles were prepared in this way unless otherwise noted.

2-Methoxybenzoyl-phenylacetonitrile (*IIIa*).—Colorless needles from dilute ethanol, m.p. 108~9°;

1) R. Walther and P. G. Schickler, *J. prakt. Chem.*, (2) **55**, 308 (1897); F. Bodroux, *Bull, soc. chim.*, (4). **9**, 651 (1911); B. N. Ghosh, *J. Am. Chem. Soc.*, **109**, 117 (1916).
2) W. Wislicenus, H. Eichert and M. Marquart, *Ann.*, **436**, 92 (1925); B. W. Howk and S. M. McElvain, *J. Am. Chem. Soc.*, **54**, 286 (1932).
3) J. N. Chatterjea, *J. Indian Chem. Soc.*, **33**, 447 (1956).
4) E. P. Kohler, *J. Am. Chem. Soc.*, **46**, 1743 (1924).
5) Melting and boiling points are uncorrected.

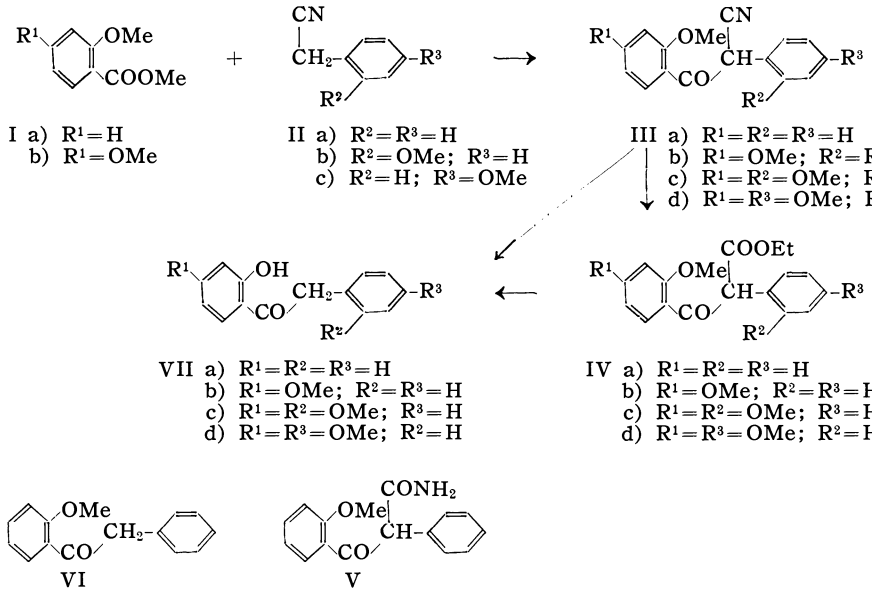

I a) $R^1=H$
b) $R^1=OMe$

II a) $R^2=R^3=H$
b) $R^2=OMe$; $R^3=H$
c) $R^2=H$; $R^3=OMe$

III a) $R^1=R^2=R^3=H$
b) $R^1=OMe$; $R^2=R^3=H$
c) $R^1=R^2=OMe$; $R^3=H$
d) $R^1=R^3=OMe$; $R^2=H$

VII a) $R^1=R^2=R^3=H$
b) $R^1=OMe$; $R^2=R^3=H$
c) $R^1=R^2=OMe$; $R^3=H$
d) $R^1=R^3=OMe$; $R^2=H$

IV a) $R^1=R^2=R^3=H$
b) $R^1=OMe$; $R^2=R^3=H$
c) $R^1=R^2=OMe$; $R^3=H$
d) $R^1=R^3=OMe$; $R^2=H$

VI

V

TABLE

Product	from	reagent	reac. temp. and hr.	m.p. °C	yield %
IIIa	Ia+IIa	1 m. NaOEt	in EtOH, reflux, 4	108~9	8.
〃	〃	〃	in C_6H_6, distill., 4	〃	40.
〃	〃	2 m. NaOEt	〃	〃	70.
IIIb	Ib+IIa	1 m. NaOEt	〃	108~9	67.
〃	〃	2 m. NaH	〃	105~7	61.
IIIc	Ib+IIb	1.2 m. NaOEt	〃	114~5	42.5
〃	〃	1.7 m. NaH	〃	114~5.5	69.
IIId	Ib+IIc	1 m. NaOEt	〃	105~6	59.
IVa	IIIa	HCl—EtOH	room temp., 3 days	63~5	24.
IVa+V	〃	+1 m. H_2O	〃	67~8	56.2
IVb	IIIb	HCl—EtOH	〃	69~72	16.
〃	〃	+1 m. H_2O	〃	76~7	69.
IVc	IIIc	〃	〃	94~6	69.
IVd	IIId	〃	〃	48~50	43.5
VI	IIIa	AcOH—HCl	steam-bath, 15	oil	56.
VIIa	VI	AcOH—HBr	steam-bath, 10	56~7	61.
〃	〃	$AlCl_3$	steam-bath, 1	51~3	35.5
〃	IIIa	AcOH—HCl	steam-bath, 20	oil	47.5
〃	〃	AcOH—HBr	steam-bath, 10	53~5	34.
〃	IVa	AcOH—HCl	steam-bath, 15	oil	35.
VIIb	IIIb	〃	〃	86~7	46.5
〃	IVb	〃	〃	88~9	68.
VIIc	IIIc	〃	〃	90~1	43.
〃	IVc	〃	〃	88~9	39.5
VIId	IIId	〃	〃	100~0.5	38.
〃	IVd	〃	〃	99~100.5	33.

of anhydrous aluminum chloride in 5 cc. of nitrobenzene on steam-bath for one hour. M.p. 51~3°, yield 0.2 g. (35.5%).

(ii) By hydrochloric acid.—A solution of 1.5 g. of nitrile IIIa in 15 cc. of acetic acid containing 10 cc. of concentrated hydrochloric acid was heated for twenty hours with addition of 5 cc. of concentrated hydrochloric acid at the intermediate time. Faintly yellow colored oil, b.p. 150~5°/0.004 mm., yield 0.6 g. (47.5%); 2,4-dinitrophenylhydrazone, m.p. 214~5°.

(iii) By hydrobromic acid.—A solution of 0.7 g. of nitrile IIIa in 8 cc. acetic acid containing 2 cc. of 47% hydrobromic acid was heated for ten hours. Colorless needles, m.p. 53~5°, yield 0.2 g. (34%).

(*b*) *From ester IVa.*—Faintly yellow colored oil, b.p. 145~150°/0.001 mm.; 0.1 g. of the compound (35% yield) was obtained from 0.4 g. of ester IVa by general method, 2,4-dinitrophenylhydrazone, m.p. 217~8°.

2-Hydroxy-4-methoxyphenyl Benzyl Ketone (VIIb).—(*a*) *From nitrile IIIb.*—Colorless needles from methanol, m.p. 86~7°, b.p. 155~165°/0.001 mm. (one distillation); 0.8 g. of the compound (46.5% yield) was obtained from 2 g. of nitrile IIIb; identical with the authentic sample (reported m.p. 90°[8]).

Anal. Found: C, 74.09; H, 5.77. Calcd. for $C_{15}H_{14}O_3$: C, 74.36; H, 5.83%.

(*b*) *From ester IVb.*—Colorless needles, m.p. 88~9°; 0.5 g. of the compound (68% yield) was obtained from 1 g. of ester IVb.

2-Hydroxy-4-methoxyphenyl 2-Methoxybenzyl Ketone (VIIc).—(*a*) *From nitrile IIIc.*—Colorless needles from ethanol, m.p. 90~1°, b.p. 180°/0.001 mm. (one distillation); 0.3 g. of the compound (43% yield) was obtained from 0.8 g. of nitrile IIIc. Reported m.p. of this ketone is 93~4°[9].

Anal. Found: C, 71.15; H, 6.40. Calcd. for $C_{16}H_{16}O_4$: C, 70.57; H, 5.92%.

(*b*) *From ester IVc.*—Colorless needles, m.p. 88~9°, 0.15 g. of the compound (39.5% yield) was obtained from 0.5 g. of ester IVc.

2-Hydroxy-4-methoxyphenyl 4-Methoxybenzyl Ketone (VIId).—(*a*) *From nitrile IIId.*—Recrystallization from ethanol and then from benzene yielded colorless needles, m.p. 100~100.5°, b.p. 190°/0.001 mm. (one distillation); 0.5 g. of the compound (38% yield) was obtained from 1.5 g. of nitrile IIId. Reported m.p. of this ketone is 104°[10].

Anal. Found: C, 70.84; H, 6.48. Calcd. for $C_{16}H_{16}O_4$: C, 70.57; H, 5.92%.

(*b*) *From ester IVd.*—Colorless needles, m.p. 99~100.5°; 0.2 g. of the compound (33% yield) was obtained from 0.8 g. of ester IVd.

The author wishes to express his hearty thanks to Professor K. Fukui for his helpful advice and encouragement, and to Professor Y. Yukawa of Osaka University for his valuable discussion during the course of this work, and to the members of the Agricultural Department of Kyoto University for microanalyses.

Faculty of Literature and Science
Toyama University
Toyama

8) W. Baker and R. Robinson, ibid., **1929**, 160.

9) P. K. Grover and T. R. Seshadri, *Proc. Indian Acad. Sci.*, **38A**, 122 (1953); W. B. Whalley, *J. Chem. Soc.*, **1953**, 3366.

10) F. Wessely and F. Lechner, *Monatsh.*, **57**, 395 (1931).

Fractionation of Ribonuclease-resistant Fraction on ECTEOLA-cellulose

By Kentaro TANAKA

(Received November 25, 1957)

The smaller products of ribonuclease (RNase) digestion of yeast ribonucleic acid (RNA) were fractionated by Volkin and Cohn[1] using ion exchange resin and by Markham and Smith[2] using paper electrophoresis and paper chromatography. For the larger products of the digestion, however, these methods could offer little advantage for the purpose of fractionation. Recently, Bendich et al.[3] suggested the possibility of fractionating RNA fragments which remained after treatment with RNase by ECTEOLA-cellulose columns.

In the investigation to be reported in this paper, the RNase-resistant material

1) E. Volkin and W. E. Cohn, *J. Biol. Chem.*, **205**, 767 (1953).

2) R. Markham and J. D. Smith, *Biochem. J.*, **52**, 558, 565 (1952).

3) A. Bendich, J. R. Fresco, H. S. Rosenkranz and S. M. Beiser, *J. Am. Chem. Soc.*, **77**, 3671 (1955).

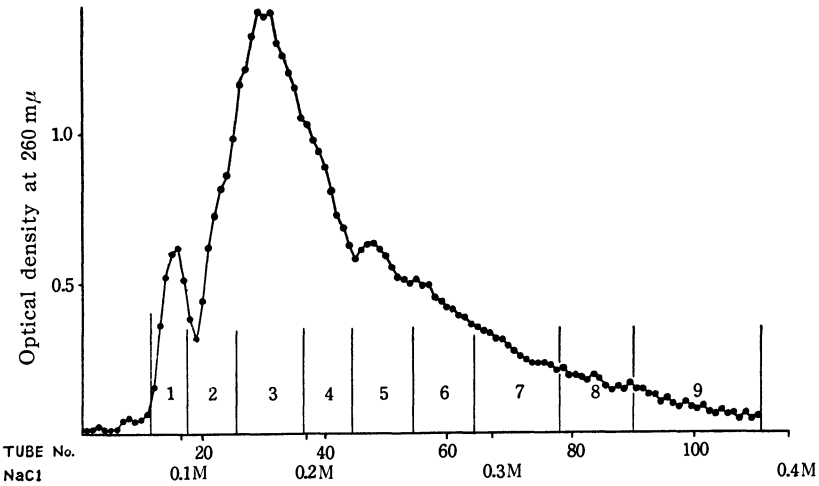

Fig. 1. Fractionation of RNase-resistant fraction of yeast RNA on ECTEOLA-cellulose by continuous gradient elution.
Exchanger: ECTEOLA-cellulose 20 g., 2.8 cm. in diameter.
Sorbed material: 200 mg. of Core 2.
Each tube contained 10 ml. of eluate. The optical density was measured after 20-fold dilution of the eluate in a 1 cm. cell. The fractions indicated with the mark | | were used for the determination of base ratio.

(Core) obtained from yeast RNA was shown to be successfully fractionated on an ECTEOLA-cellulose column. The relative molar ratio of the bases found in each fraction obtained was then measured by paper chromatography. It was thus found that oligonucelotides of larger molecular weight in the RNase-resistant material are remarkably rich in guanylic acid.

Experimental

Yeast RNA.—Commercial yeast RNA (sodium salt, Schwarz; P, 8.3%).

Pancreatic RNase.—The enzyme used in the study was a crystalline preparation obtained from Worthington Biochemical Sales Corporation.

ECTEOLA-cellulose—The sample was prepared by Peterson and Sober's method[4] from Carl Schleicher and Schüll cellulose-powder No. 123 for column chromatography. Nitrogen content of the used sample was 0.28 meq./g. (0.39%).

Core 1.—Fifty grams of sodium salt of yeast RNA were dissolved in 500 ml. of distilled water and deproteinized by chloroform gel formation and dialyzed exhaustively. The concentrated dialyzate (250 ml.) was digested with 8.5 mg. of crystalline RNase for 18 hours at 37°C with frequent addition of sodium hydroxide solution to maintain the pH 7.2. After incubation, the reaction mixture was exhaustively dialyzed in a cellophane tubing against distilled water and then lyophilized (yield 38%). The dried material was dialyzed again in a colodium bag against distilled water and lyophilized (yield about 10%; P, 8.1%).

Core 2.—Fifty grams of sodium salt of yeast RNA were deproteinized by chloroform-gel formation, dialyzed in a cellophane tubing against distilled water, and then lyophilized (yield 52%; P, 8.2%). Fifteen grams of the dried sample were dissolved in 150 ml. of distilled water and digested with 15 mg. of crystalline RNase for 40 hours at 37°C in the presence of chloroform with frequent addition of sodium hydroxide solution to maintain the pH at 7.2. After incubation, the reaction mixture was dialyzed in a cellophane tubing against distilled water, and lyophilized (yield 11%). One gram of the dried sample was dissolved in 50 ml. of distilled water and precipitated by the addition of N hydrochloric acid to pH 1.2. The precipitate was collected by centrifuge and washed twice with 50% acetone and then with pure acetone once (yield 5.8%).

Chromatography on ECTEOLA-cellulose.—The fractionation was carried out with a column (2.8 cm. in diameter) containing 20 g. of ECTEOLA-cellulose or a column (1.2 cm. in diameter) containing 10 g. of ECTEOLA-cellulose. The column was successively washed with 1.0 N sodium hydroxide, 1.0 M dipotassium monohydrogen phosphate and 0.01 M neutral phosphate buffer before each run. The column was charged and eluted under pressure at flow rate of about 0.3 ml./cm^2/min. The oligonucleotides were eluted by sodium chloride solution (in 0.01 M neutral phosphate); the concentration of sodium chloride being either continuously or stepwise increased. The continuous gradient was established in the usual way by introducing buffer containing high concentration of sodium chloride (0.5 M) into a constant volume (725 ml.) mixing chamber originally filled with the buffer. The concentration of sodium chloride in the eluate was calculated

4) E. A. Peterson and H. A. Sober, ibid., **78**, 751 (1956).

from a theoretical equation[5]. The eluates were collected in an automatic fraction collector and the amount of the oligonucleotide in each tube was determined by measuring the absorption at 260 mμ in a Beckman model DU spectrophotometer. Each peak in the elution curve was collected (as indicated in figures), dialyzed in a cellophane tubing, lyophilized and used for the determination of molar ratio of bases.

Determination of relative molar ratio of bases.—The lyophilized sample described above was hydrolyzed with 1 N hydrochloric acid at 100°C for 1 hour. The hydrolyzate was chromatographed on Tōyō 51 A filter paper with *tert*-butanol-hydrochloric acid-water as solvent. The spots were located by an ultraviolet germicidal lamp with a Kaken Ultraviolet Filter 2537*. The spots and the corresponding blanks were cut out and eluted by 0.1 N hydrochloric acid. As molar extinction coefficients for pyrimidine nucleotides and purine bases, the values published by Smith and Markham[6] were employed.

Results and Discussion

In Fig. 1 is shown the elution diagram of Core 2 when the salt concentration of the solvent was continuously increased. As can be seen from the figure, separation of the oligonucleotides in this case was not satisfactory. Nevertheless, as shown in Table I, the base ratios in fractions (indicated in Fig. 1) showed considerable changes with the progress of elution.

TABLE I

MOLAR BASE RATIOS OF THE FRACTIONS OBTAINED BY GRADIENT DEVELOPMENT CHROMATOGRAPHY ON ECTEOLA-CELLULOSE COLUMN

Sample	Base ratio*				Pu/Py
	A	G	U	C	
Core 2	10	13.7	1.7	2.6	5.5
Fraction No.**					
1	10	10.5	3.0	5.2	2.5
2	10	9.2	2.1	3.6	3.4
3	10	8.5	2.0	2.2	4.4
4	10	9.2	1.6	1.6	6.0
5	10	14.9	2.5	1.9	5.7
7	10	28.5	3.2	4.5	5.0
9	10	33.8	5.9	3.1	4.9

* A: Adenine, G: Guanine, U: Uracil, C: Cytosine

** Ref. Fig. 1

5) R. M. Bock and N. S. Ling, *Anal. Chem.*, **26**, 1543 (1954).

6) J. P. Smith and R. Markham, *Biochem. J.*, **46**, 509 (1950).

* The author is indebted to Dr. E. Iwase for his kind gift of this filter.

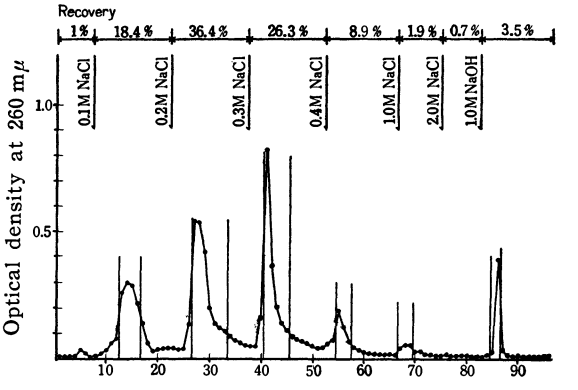

Fig. 2. Fractionation of RNase-resistant fraction of yeast RNA on ECTEOLA-cellulose by discontinuous gradient elution.
Exchanger: ECTEOLA-cellulose 20 g., 2.8 cm. in diameter.
Sorbed material: 100 mg. of Core 1.
Each tube contained ca. 13.3 ml. The volume was directly measured to calculate the recovery. The optical density was measured after 20-fold dilution of the eluate in a 1 cm. cell. The peaks indicated with the mark | | were used for the determination of base ratio.

TABLE II

MOLAR BASE RATIOS OF THE FRACTIONS ELUTED FROM ECTEOLA-CELLULOSE COLUMN BY DISCONTINUOUS GRADIENT ELÜTION

Sample Exp. 1**	Base Ratio*				Pu/Py
	A	G	U	C	
Core 1	10	17.8	4.2	4.4	3.2
Fraction eluted with					
0.1 M NaCl	10	11.4	5.3	6.4	1.8
0.2 M NaCl	10	9.9	2.9	2.9	3.4
0.3 M NaCl	10	28.8	3.9	4.5	4.6
0.4 M NaCl	10	32.7	4.2	3.9	5.3
1.0 M NaCl	10	28.6	—	—	—
N- NaOH	10	30.0	3.4	2.5	6.8
Exp. 2					
0.1 M NaCl	10	11.7	5.1	5.9	2.0
0.2 M NaCl	10	12.3	2.8	3.6	3.5
After rechromatography					
	10	9.8	2.5	2.4	4.0
0.3 M NaCl	10	30.2	3.5	4.2	5.2
After rechromatography					
	10	30.2	5.0	3.6	4.7
0.4 M NaCl	10	31.8	4.0	3.5	5.6
0.5 M NaCl	10	31.8	4.9	3.4	5.0

* A: Adenine, G: Guanine, U: Uracil, C: Cytosine

** Ref. Fig. 2

Further studies were carried out by means of the stepwise elution procedure. In Fig. 2 is presented one of the elution diagrams of Core 1 which was eluted by sodium chloride solutions of successively increassing concentration (in 0.01 M neutral phosphate).

As shown in Fig. 2, about 90% of the ultraviolet absorbing substance was present in the eluates of 0.1, 0.2, 0.3, 0.4 and 1.0 M sodium chloride concentration. The rest was eluted by 1.0 M sodium hydroxide.

In order to determine whether satisfactory fractionations had occurred, selected fractions were dialyzed at 4°C against distilled water, lyophilized, and rechromatographed. As shown in Fig. 3 as an example, it was found that the main peak in the elution diagram reappears in the salt concentration at which the fraction was originally eluted. The base ratios of the fractions indicated in Fig. 2 were given in Table II.

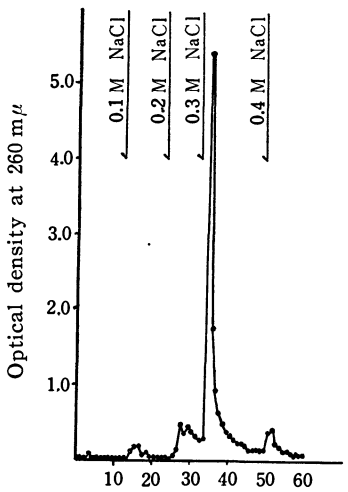

Fig. 3. Rechromatography of the fraction eluted with 0.3 M NaCl.
Exchanger: ECTEOLA-cellulose 10 g., 1.2 cm. in diameter.
Sorbed material: 0.3 M NaCl fraction of the first run. Ref. Fig. 2 (Exp. 1).
Each tube contained 10 ml. of eluate.

Pancreatic ribonuclease appears to be a highly specific phosphodiesterase which hydrolyzes secondary phosphate ester of pyrimidine ribonucleoside 3′-phosphate[7-10]. Consequently, the greater part of the oligonucleotides in RNase reistant core have only one pyrimidine nucleotide per molecule at the terminal position[1,2,8]. Thus the results presented in the Table I and II showed that as the sodium chloride concentration increases the eluate contains the larger molecular oligonucleotides as suggested by larger ratios of purine to pyrimidine. It has been shown that the whole RNase-resistant core of yeast RNA has a higher guanylic acid content than the original RNA[11,12]. The data presented here indicated that the larger molecular oligonucelotides in RNase core of yeast RNA contain increasing amounts of guanylic acid. Thus the results presented in this paper permit us to consider quite naturally that guanylic acid is not equally distributed in yeast RNA and at least some of the guanylic acid residues in the RNA are arranged in rather high molecular oligoguanylic acid structures.

Summary

RNase-resistant material obtained from yeast RNA was fractionated on an ECTEOLA-cellulose column. The elution was performed with sodium chloride-neutral phosphate buffer as solvent, the concentration of sodium chloride being increased by either gradient or stepwise procedure. Separation of oligonucleotides seemed to be affected by their molecular size. The products of larger molecular weight present in pancreatic-RNase digests of yeast RNA were very rich in guanylic acid.

The author wishes to thank Professor Fujio Egami for his encouragement and valuable suggestions. This work was supported by a grant from the Scientific Research Fund of the Ministry of Education.

*Laboratory of Biochemistry, Department of Chemistry, Faculty of Science, Nagoya University, Chikusa-ku, Nagoya**

7) J. E. Bacher and F. W. Allen, *J. Biol. Chem.*, **183**, 633 (1950).
8) G. Schmidt, R. Cubiles, N. Zöllner, L. Hecht, N. Strickler, K. Seraidarian and S. J. Thannhauser, ibid. **192**, 715 (1951).
9) D. M. Brown, and A. R. Todd, *J. Chem. Soc.*, **1953**, 2040.
10) D. M. Browm, C. A. Dekker and A. R. Todd, ibid., **1952**, 2715.
11) S. E. Kerr, K. Seraidarian and M. Wargon, *J. Biol. Chem.*, **181**, 773 (1949).
12) B. Magasanik and E. Chargaff, *Biochem. et Biophys, Acta.*, **7**, 396 (1951).

* Present adress; Shionogi Research Laboratory Shionogi & Co., Ltd., 192 Imafuku, Amagasaki-shi, Hyogo Prefecture.

Synthesen und Konfigurationsermittlung in Rotenoid-Reihe. III. Über die Reaktion der α,β-ungesättigten Säuren mit Resorcin bzw. Phloroglucin; eine Neue Synthese des Chromanon-Rings und ein Versuch zur Synthese des Rotenons

Von Masateru MIYANO und Masanao MATSUI

(Eingegangen am 20. Dezember, 1957)

Die Kondensation von Tubanol(II) mit Toxicarsäure(III) ist, wenn es möglich wäre, wahrscheinlich das schlichteste Aufbauschema für die Synthese des Rotenons(I). Es dürfte sich bei der Kondensation um eine Synthese des Chromanon-Rings handeln.

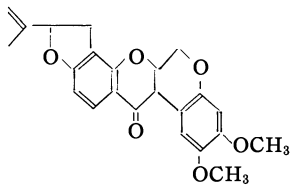

(I)

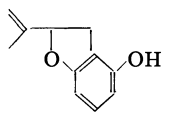

(II)

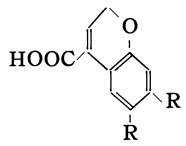

(III)

Die bisher schon bekannten Reaktionen zur Synthese von Chromanon-Ringen sind:

(1) 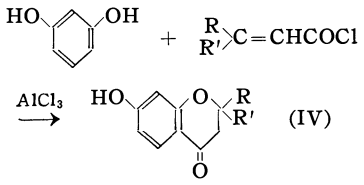

(IV)

(2) 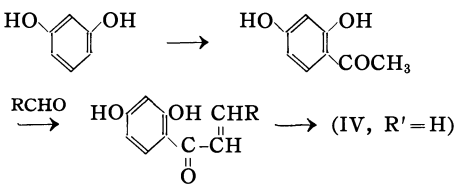

(IV, R'=H)

(3) 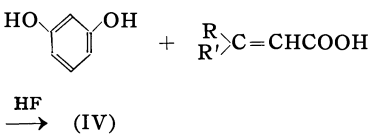

(IV)

Durch die oben beschriebenen drei Methoden vielleicht gelingt es nicht die Synthese des Rotenons. Da Δ^3-Chromen-4-carbonsäure (III, R=H) in das entsprechende Säurechlorid nicht übergeführt wurde[1], muss die Darstellung des Toxicarsäure fast unmöglich sein, umso schwerer, als uns die wenigen Mengen derjenigen Säure zur Verfügung stellen. Daher ist die Reaktion(1) aussichtlos. Es ist selbstverständlich, dass die Reaktion(2) nicht verwendbar sei, insofern man die Toxicarsäure als Ausgangsmaterial braucht. Da das Rotenon gegen Säure so empfindlich ist, bei der für die Reaktion(3) notwendigen Behandlung (einstündiges Erhitzen auf 100°C in Rohr oder 7-tägiges Stehen bei Zimmertemperatur) kann die Doppelbindung von Seitenkette umlagern, um *iso*-Rotenon(V) zu liefern. Löst man das Rotenon in konzentrierte Schwefelsäure bei Zimmertemperatur geht es in *iso*-Rotenon über[2]. Kocht man das Rotenon (10 g) 5 Minuten lang mit Schwefelsäure (30 g) in Eisessig (60 g), erhält man 8.5g von reinem *iso*-Rotenon[3]. Der Vorgang beruht auf der Umlagerung der reaktionsfähigen Doppelbindung in den Hydrofuran-Ring.

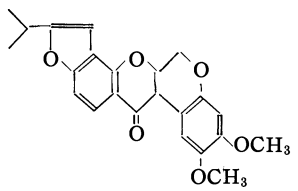

(V)

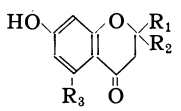

(VI)

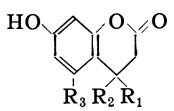

(VII)

1) H. A. Offe und W. Barkow, *Chem. Ber.*, **80**, 458(1947).
2) S. Takei, *Biochem. Z.*, **157**, 1 (1925).
3) S. Takei, M. Koide und S. Miyajima, *Ber.*, **62**, 508 (1930).

α,β-ungesättigte Carbonsäuren treten mit Phenolen unter dem Einfluss von wasserfreiem Aluminiumchlorid oder konzentrierter. Schwefelsäure nicht zu Chromanonen(VI), sondern vielmehr Dihydrocumalinen(VII) zusammen[4]. Um das Rotenon darzustellen, handelt es sich nun in erster Linie um die Möglichkeit, die auf unstabilen Verbindungen verwendbare Chromanon-Synthese aufzustellen.

Als nun wir die Kondensation der α,β-ungesättigten Carbonsäuren mit Resorcin bzw. Phloroglucin unter der Einwirkung von Antimon(III)-chlorid ausgeführt haben, in den gewissen Fällen sind die Chromanone in guter Ausbeute entstanden. Dieselbe Reaktion läuft ab, wenn auch weniger sauber, mit anderen Kondensationsmitteln wie z.B. Zinkchlorid oder Zinn(II)-chlorid.

Resorcin und die gleichen molekularen Mengen von β,β-Dimethylacrylsäure liefern beim Erhitzen auf 150°C in Gegenwart von Antimontrichlorid (oder Zinkchlorid, Zinn(II)-chlorid) 2,2-Dimethyl-7-oxy-chromanon(VI, $R_1=R_2=CH_3$, $R_3=H$) vom Schmp. 169°C(Literatur[5] zeigt 172°), das als Monoacetat vom Schmp. 91°C (identisch mit der Literatur) und 2,4-Dinitrophenylhyrazon identifiziert wird. Antimontrichlorid zeigt sich das Beste sowohl als das Kondensationsmittel auch als das Lösungsmittel (Schmp. 73°C). Arbeitet man aber mit einer ziemlich überschüssigen Menge von Dimethylacrylsäure, neben dem Chromanone entsteht ein Keton vom Schmp. 216~7°C, welches ein 2,4-Dinitrophenylhydrazon und ein Acetat vom Schmp. 113~4°C liefert. Aus dem IR-Spektrum ist es geschlossen, dass das Keton freie Oxygruppe und konjugierte Carbonyl-gruppe hat und keine unkonjugierte C=O Gruppe. Bei der Kondensation von Resorcin mit Crotonsäure, wie zu erwarten, entsteht 2-Methyl-7-oxy-chromanon (VI, $R_1=CH_3$, $R_2=R_3=H$) vom Schmp. 167~8°C, welches in das entsprechende 2,4-Dinitrophenylhydrazon übergeführt wird. In gleicher Weise umgesetzt, reagiert Phloroglucin unter der Einwirkung von Antimon(III)-chlorid mit β,β-Dimethylacrylsäure und liefert 2,2-Dimethyl-5,7-dioxy-chromanon (VI, $R_1=R_2=CH_3$, $R_3=OH$) vom Schmp. 197°C (Literatur[6] 198°C), welches in das zugehörige 2,4-Dinitrophenylhydrazon übergeführt wird.

In den oben erwähnten Fällen, ist nur die Chromanon-Ring-Verbindung isoliert worden und ausser den Ausgangsmaterialien konnten wir nichts anderer Produkte wie z.B. Dihydrocumalin (VII) aus der Mutterlauge erhalten. Bei der Reaktion von Resorcin bzw. Phloroglucin mit Zimtsäure konnten wir dagegen das Chromanon nicht erhalten. Bargellini[7] berichtete, dass beim Erhitzen von Resorcin und Zimtsäure in Gegenwart von Zinkchlorid 2',4'-Dioxy-chalkon(VIII) vom Schmp. 175°C erhalten wurde, aber Stephen[8] und Ellison[9] konnten nach dem von Bargellini angegebenen Verfahren das Chalkon nicht wieder erhalten. Wir konnten auch nichts kristallinisches Produkt isolieren bei der Kondensation mittels Zinkchlorids. Behandelt man Resorcin und Zimtsäure mit Antimon(III)-chlorid, ist farbloses Nädelchen vom Schmp. 129~130°C entstanden. Es stimmt in den Analysenzahlen mit dem Chromanon (VI, $R_1=C_6H_5$, $R_2=R_3=H$; nämlich 7-Oxyflavanon; Schmp. 240°C) oder dem Dihydrocumalin (VIII, $R_1=C_6H_5$, $R_2=R_3=H$; Schmp. 137°) über, aber aus dem IR-Spektrum ist zu entnehmen, dass es sich um den Zimtsäure-ester von Resorcin(IX) handeln dürfte. Dementsprechend wurde diese Verbindung durch alkoholische Kalilauge zur Zimtsäure verseift. Phloroglucin liefert beim Erhitzen mit Zimtsäure in Gegenwart von Antimon(III)-chlorid farbloses Nädelchen vom Schmp. 204~5°C, dessen IR-Spektrum (s. Abb. 1) nur konsequent mit dem Dihydrocumalin (VII, $R_1=C_6H_5$, $R_2=H$, $R_3=OH$) ist.

Mit der Absicht, das Rotenon darzustellen, haben wir die Kondensation von Toxicarsäure mit Tubanol unter der Einwirkung von Antimon(III)-chlorid versucht. Das Kondensationsprodukt wurde in der äthanol-löslichen (Hauptbestandteil) und äthanol-unlöslichen (Nebenprodukt, auch in Benzol unlöslich) Fraktionen abgeteilt. Aus der ersten Fraktion haben wir ein Produkt vom Schmp. 105~110°C (nicht kristallinisch) erhalten. Das IR-Spektrum

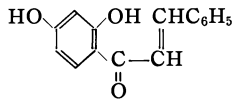

(VIII)

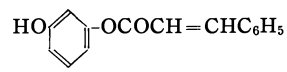

(IX)

4) H. A. Offe und W. Barkow, *Chem. Ber.*, **80**, 474(1947).
5) W. Bridge, A. J. Crocker, T. Cubin und A. Robertson, *J. Chem. Soc.*, **1937**, 1530.
6) W. Bridge, R. G. Heyes und A. Robertson, ebenda, **1937**, 279.
7) G. Bargellini, *Atti R. Accad. Lincei*, [v], **17**, ii, 119 (1908).
8) H. Stephen, *J. Chem. Soc.*, **117**, 1530 (1920).
9) T. E. Ellison, ebenda, **1927**, 1721.

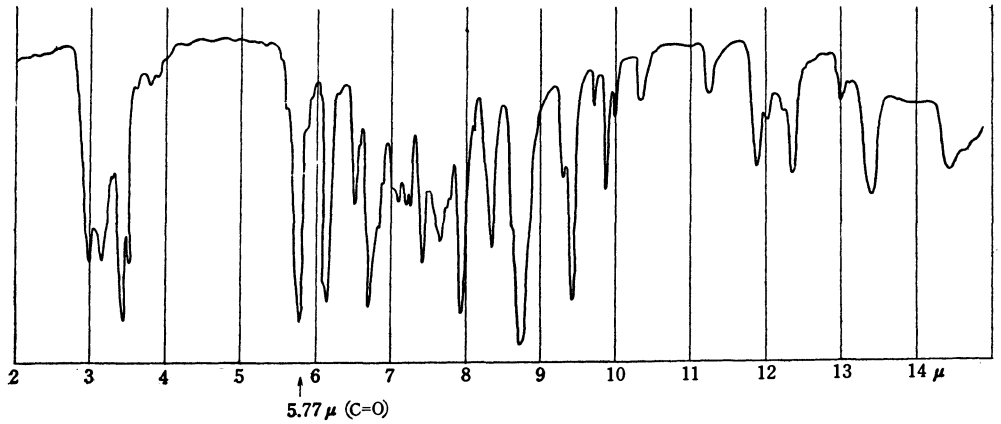

Abb. 1 4-Phenyl-5,7-dioxy-3,4-dihydro-cumalin (VII, $R_1=C_6H_5$, $R_2=H$, $R_3=OH$) in Nujol Paste.

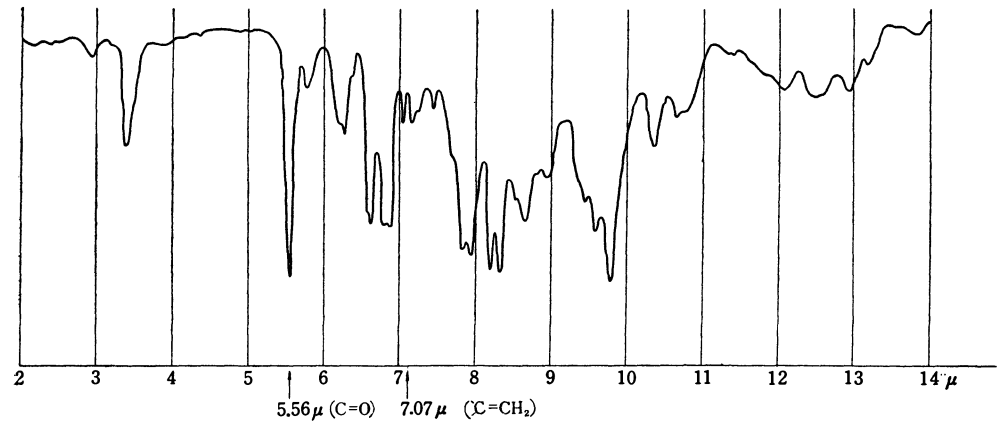

Abb. 2 Die Verbindung (X) oder (XI) oder ihre Mischung fest in KBr gepresst.

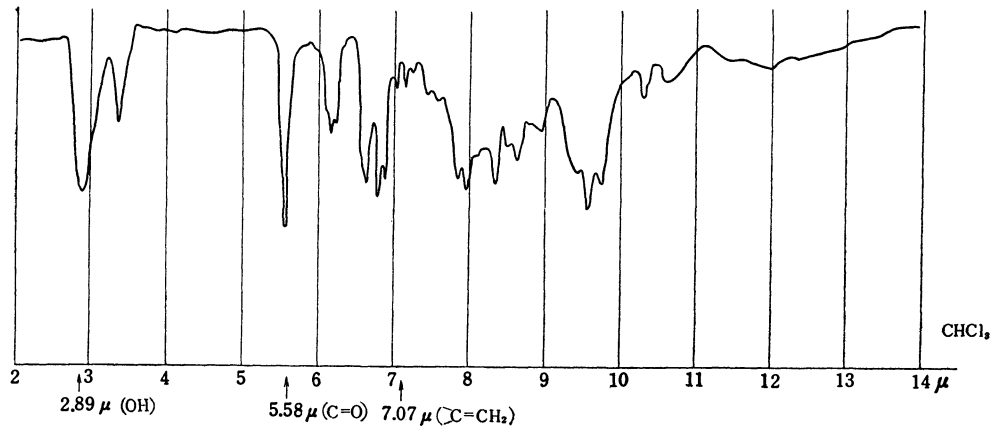

Abb. 3 Das in dem Alkohol unlösliche Nebenprodukt in Chloroformlösung.

macht die Anwesenheit eines β,γ-ungesättigten γ-Lactons (starke C=O Band in 5.56μ, s. Abb.2) sicher, dessen C=O Doppelbindung mit anderer Doppelbindung bzw. aromatischem Ringe nicht konjugieren kann. Ein mässiges Absorptionsband in 7.07μ (entspricht 7.04μ Band des Rotenons) deutet die Anwesenheit der >C=CH_2 Gruppe hin, obgleich die charakteristische Absorption dieser Gruppe in 11.2μ nicht vorhanden ist. Das Produkt hat keine Oxy-gruppe (sehr schwache Absorption

neben 2.9μ stammt vielleicht von wenigen Mengen Begleitstoffs). Ebenso fehlen, wie das IR-Spektrum zeigt, konjugierte Carbonyl-, Ester-, Lacton-gruppe. Ausgehend von der Überlegung von Konstitution der Ausgangsmaterialien sowie von Analysenzahlen, liegt es nahe, dass um alle bisherige Befunde befriedigend zu deuten nur die in den Formeln X und XI angegebene Struktur widerspruchlos seien. Das erhaltene Produkt besteht wohl aus beiden Verbindungen. Durch die chromatographische Reinigung konnten wir reines kristallines Material nicht erhalten. Die in der Formel XII angegebene Struktur ist nicht darum ganz unmöglich, weil es kein β,γ-ungesättigtes Lacton trägt. In der ersten Stufe vielleicht entsteht der Toxicarsäure-ester(XIII). Das aus der äthanol-unlöslichen Fraktion isolierte amorphe Produkt vom Schmp. 195~200°C bezeigt das analoge IR-Spektrum ausgenommen 2.89μ Band (OH, s. Abb. 3), daher ist es zu schliessen, dass eine oder zwei Methoxy-gruppe in dieser Verbindung durch Oxy-gruppe ersetzt werde. Gegen Bartgrundel (loach, dojô) wirken diese Produkte nicht giftig.

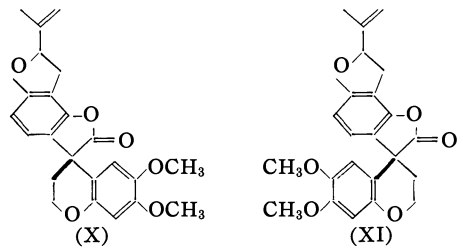

(X)

(XI)

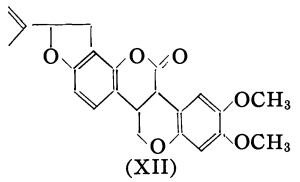

(XII)

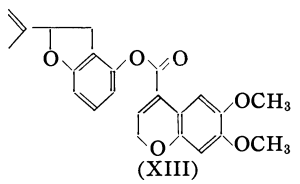

(XIII)

Beschreibung der Versuche

2,2-Dimethyl-7-oxy-chromanon (VI, $R_1=R_2=CH_3$, $R_3=H$)—*a) mittels Antimon(III)-chlorids*—Eine Mischung von 5.5 g Resorcin, 5 g β,β-Dimethylacrylsäure und 5 g Antimon(III)-chlorid wird 15 Minuten auf 140° Cerhitzt. Nach dem Erkalten nimmt man das organische Produkt mit Äther auf und wäscht die ätherische Schicht mit verd. Salzsäure (dreimal), Wasser, Bicarbonat-Lösung, schliesslich mit Wasser, dann trocknet über Natriumsulfat. Nach dem Eindampfen des Lösungsmittels erhält man 8.2 g Chromanon. Die aus heissem wässerigem Alkohol umkristallisiertten Blättchen schmelzen bei 169°C.*

Anal. Gef.: C, 68.8; H, 6.3. Ber. für $C_{11}H_{12}O_3$: C, 68.7; H, 6.3%.

Acetat—Man versetzt 1 g Chromanon in 12 ccm Pyridin mit 2 ccm Acetanhydrid und lässt 3 Tage bei Zimmertemperatur bleiben. Die Mischung wird in verd. Salzsäure gegossen, mit Äther extrahiert, mitWasser,wässeriger Kaliumcarbonatlösung, wieder mit Wasser gewaschen, nud mit Natriumsulfat getrocknet. Die beim Eindampfen des Äthers erhaltenen Kristallen werden abfiltriert, gewaschen mit Cyclohexan. Schmp. 90~91°C.

Anal. Gef.: C, 66.6; H, 6.1; Ber. für $C_{13}H_{14}O_4$: C, 66.65; H, 6.0%.

2,4-Dinitrophenylhydrazon — Das wird beim gewöhnlichen Verfahren erhalten und schmilzt nicht bis auf 250°C (umkristallisiert aus heissem Äthanol—Essigester(1:1). Das ist unlöslich in heissem Äthanol.

Anal. Gef.: C, 54.5; H, 4.6; N, 14.6. Ber. für $C_{17}H_{16}O_6N_4$: C, 54.8; H, 4.3; N, 15.05%.

b) mittels Zinkchlorids in Gegenwart von überschüssiger Dimethylacrylsäure—Ein Gemisch von 17 g β,β-Dimethylacrylsäure, 10 g Resorcin und 14 g Zinkchlorid wird 20 Minuten auf 150~160°C erhitzt. Nach dem Erkalten wird die Mischung mit Essigester und verd. Salzsäure geschüttelt, dann mit Ammoniumchlorid-lösung, Natriumbicarbonat-Lösung und Wasser gewaschen. Die Ester-lösung wird durch 1000 ccm 5-proz. Natronlauge extrahiert. Die gelben Blättchen, welche beim 40-stündigem Aufbewahren bei Zimmertemperatur ausgeschieden sind, werden nun abfiltriert und mit Wasser gewaschen. Das Rohprodukt (2.5 g vom Schmp. ca. 211°C) wird aus wässerigem Äthanol umkristallisiert, Schmp. 216~7°C.

Anal. Gef.: C, 72.6~8; H, 8.1~7. Ber. für $C_{27}H_{28}O_6$: C, 72.30; H, 6.29%.

Die wässerige Mutterlauge wird mit verd. Salzsäure angesauert und ausgeschiedene Kristalle werden abgesaugt, mit Wasser gewaschen. Das Rohprodukt (8.5 g vom Schmp. ca. 160°C) wird durch Umlösen aus wässerigem Alkohol gereinigt, Schmp. 168~9°C, das ist identisch mit dem in a) beschriebenen Chromanon.

2,4-Dinitrophenylhydrazon des Ketons vom Schmp. 216~7°C—Das wird bei der gewöhnlichen Behandlung erhalten und schmilzt nicht bis auf 250°C (umkristallisiert aus heissem Alkohol).. Das ist leicht löslich in heissem Alkohol gegenüber dem 2,4-Dinitrophenylhydrazon des 2,2-Dimethyl-7-oxy-chromanon.

Anal. Gef.: C, 57.5; H, 6.5~8; N, 12.3~7. Ber. für $C_{39}H_{34}O_{12}N_8$: C, 58.2; H, 4.2; N, 13.9%.

Acetat des Ketons vom Schmp. 216~7°C — Obgleich das Keton aus alkalischer Lösung kristallisiert ist (s. oben), doch hat es freie Oxy-gruppe und liefert das Acetat. Zu einer

* Alle Schmpp. sind unkorrigiert.

Lösung des 1 g Ketons in 12 ccm Pyridin fügt man 2 ccm Acetanhydrid und 3 Tage bei Zimmertemperatur aufbewahrt. Die Mischung wird in verd. Salzsäure gegossen, mit Äther aufgenommen, mit Wasser, Kaliumcarbonat, schliesslich mit Wasser gewaschen, über Natriumsulfat getrocknet. Man vertreibt den Äther und erhält die farblosen Blättchen, welche mit wenig Cyclohexan gewaschen werden. Schmp. 113~4°C.

Anal. Gef.: C, 70.2; H, 7.1. Ber. für $C_{31}H_{32}O_8$: C, 69.9; H, 6.1%.

c) mittels Zinn(II)-chlorids—Durch Erhitzen (15 Minuten, 145°C) eines Gemisches von 5.5 g Resorcin, 5g β,β-Dimethylacrylsäure, 10g Zinn(II)-chlorid-dihydrat und die dem schon oben beschriebenen Verfahren analoge nachfolgende Behandlung erhält man 3.0 g Rohprodukt, welches nach dem Umlösen aus wässerigem Alkohol bei 169°C (0.8 g) schmilzt.

2-Methyl-7-oxy-chromanon (VI, $R_1=CH_3$, $R_2=R_3=H$)—Eine Mischung von 12 g Crotonsäure, 7 g Resorcin, 10 g Zinkchlorid wird 30 Minuten auf 170~180°C erhitzt. Nach dem Erkalten wird die erhaltene Mischung mit Äther und verd. Salzsäure stark geschüttelt, und unlösliche rote Körperchen werden abfiltriert. Die ätherische Schicht des Filtrats wird mit Ammoniumchloridlösung, Natriumbicarbonat-lösung und Wasser gewaschen, und mit Natriumsulfat getrocknet. Nach dem Umkristallisieren aus wässerigem Alkohol dann aus wässerigem Methanol erhält man farblose Blättchen vom Schmp. 167~8°C.

Anal. Gef.: C, 67.0; H, 5.9. Ber. für $C_{10}H_{10}O_3$: C, 67.4; H, 5.7%.

Das durch das gewöhnliche Verfahren erhaltene 2,4-Dinitrophenylhydrazon schmilzt nicht bis auf 250°C.

Anal. Gef.: C, 53.6; H, 4.0; N, 15.5. Ber. für $C_{16}H_{14}O_6N_4$: C, 53.6; H, 3.9; N, 15.6%.

2,2-Dimethyl-5,7-dioxy-chromanon (VI, $R_1=R_2=CH_3$, $R_3=OH$) — *a) mittels Antimon(III)-chlorids*—Eine Mischung von 1.6 g Phloroglucin (Dihydrat), 1.0 g β,β-Dimethylacrylsäure und 3 g Antimon(III)-chlorid wird 15 Minuten auf 140~145°C erhitzt. Nach dem Erkalten wird die Mischung mit Äther und verd. Salzsäure geschüttelt und die ätherische Schicht wird mit verd. Salzsäure (zweimal), Wasser, Natriumbicarbonat-lösung und wieder mit Wasser gewaschen, und mit Natriumsulfat getrocknet. Nach dem Eindampfen des Lösungsmittels und Umkristallisieren aus wässerigem Alkohol unter Aktivkohlezusatz erhält man 0.8 g Chromanon vom Schmp. 196~7°C.

Anal. Gef.: C, 63.4; H, 6.0. Ber. für $C_{11}H_{12}O_4$: C, 63.45; H, 5.8%.

2,4-Dinitrophenylhydrazon — Das wird durch gewöhnliches Verfahren erhalten und schmilzt nicht bis auf 250°.

Anal, Gef.: C, 52.8; H,4.3; N, 13.5. Ber. für $C_{17}H_{16}O_7N_4$: C, 52.6; H, 41.5; N, 14.4%

b) *mittels Zinkchlorids* — Man erhält das Chromanon (1.6 g, Schmp. 195°C) durch Erhitzen (15 Minuten, 150~160°C) und nachfolgende Behandlung aus einer Mischung von 3.2 g Phloroglucin (Dihydrat), 2.0 g Dimethylacrylsäure und 2.0 g Zinkchlorid, welches identisch mit dem durch das in a) erwähnten Verfahren erhaltenen Chromanon ist.

Kondensation von Resorcin mit Zimtsäure—Eine Mischung von 5.5 g Resorcin, 7.5 g Zimtsäure und 7.0 g Antimon (III)-chlorid wird 15 Minuten auf 140~148°C erhitzt. Nach dem Erkalten wird das erhaltene Produkt mit Äther und verd. Salzsäure stark geschüttelt und die ätherische Schicht wird mit verd. Salzsäure (zweimal), Wasser, Bicarbonat-lösung, wieder mit Wasser gewaschen, dann über Natriumsulfat getrocknet. Man vertreibt den Äther und löst das zurückbleibende Öl in wenig Benzol. Die farblosen langen Nadeln scheiden langsam aus, welche abfiltriert und aus heissem Cyclohexan umkristallisiert werden. 2.1 g, Schmp. 129~130°C.

Anal. Gef.: C, 74.0; H, 5.0. Ber. für $C_{15}H_{12}O_3$: C, 75.0; H, 5.0%.

Diese Nadeln lieferten kein 2,4-Dinitrophenylhydrazon durch gewöhnliches Verfahren. Dieses Kondensationsprodukt (0.05 g) wird in 10 ccm 10 proz. warmer alkoholischer Kalilauge gelöst und lässt sich 2 Tage bei Zimmertemperatur stehen. Nach dem Eindampfen des Alkohols sauert man es mit verd. Schwefelsäure an. Die ausgeschiedenen weissen Kristalle schmelzen bei 131~2°C (wenn gemischt mit Zimtsäure 132~3°).

Kondensation von Phloroglucin mit Zimtsäure—Eine Mischung von 1.5 g Phloroglucin (Dihydrat), 1.5 g Zimtsäure und 5.5 g Antimon (III)-chlorid wird 15 Minuten auf 140°C erhitzt. Nach dem Erkalten wird das erhaltene Produkt mit Äther und verd. Salzsäure geschüttelt und die ätherische Schicht wird mit verd. Salzsäure (zweimal), Wasser, Bicarbonat-lösung, wieder mit Wasser gewaschen, mit Natriumsulfat getrocknet. Das Lösungsmittel wird vertrieben und das zurückbleibende Öl wird mit wenig Chloroform digeriert. Die farblosen Nadeln werden aus Äther-Chloroform umkristallisiert. 0.4 g, Schmp. 204~5°C.

Anal. Gef.: C, 69.8; H, 4.7. Ber. für $C_{15}H_{12}O_4$: C, 70.3; H, 4.7%.

Die Nadeln lieferten kein 2,4-Dinitrophenylhydrazon beim gewöhnlichen Verfahren. Dieses Produkt wird durch 10 ccm 10 proz. alkoholischer Kalilauge bei Zimmertemperatur (2 Tage) verseift. Man vertreibt das Lösungsmittel und sauert mit verd. Schwefelsäure an. Das Ausgangsmaterial wird zurückerhalten.

Kondensation von Tubanol mit Toxicarsäure: Ein Versuch zur Synthese des Rotenons—Zu einer Mischung von 0.8 g Tubanol und 1.3 g Toxicarsäure in 3 ccm Dioxan fügt man 5.0 g Antimon(III)-chlorid. Man erhitzt diese Mischung 15 Minuten auf 150~160°C, während des Erhitzens dampft das Dioxan ein. Das Reaktionsprodukt wird mit Äther und verd. Salzsäure geschüttelt, mit verd. Salzsäure (zweimal), Wasser, Bicarbonat-lösung, schliesslich mit Wasser gewaschen, über Natriumsulfat getrocknet. Das Lösungsmittel wird vertrieben und das zurückbleibende Öl wird in 20 ccm heissen Äthanol gelöst und unter Aktivkohlezusatz abgesaugt. Beim 3-tägigem Stehen bei

Zimmertemperatur scheidet die alkoholische Lösung wenig Öl. Die in Alkohol lösliche Fraktion wird unter vermindertem Druck konzentriert. Zu dem zurückbleibenden festen Körper fügt man 15 ccm Benzol und die wenigen in Benzol unlöslichen Körperchen abfiltriert. Das benzolische Filtrat wird unter vermindertem Druck konzentriert. Man erhält 1.0 g kristall-ähnliche Körperchen vom Schmp. 105~110°C.

Anal. Gef.: C, 69.9; H, 5.7; -OCH_3, 12.5*. Ber. für $C_{23}H_{22}O_6$: C, 70.0; H, 5.6; -OCH_3, 15.8%.

Die Chromatographische Reinigung war effektivlos. Das aus dem Alkohol abgetrennte Öl lieferte beim Trocknen fast farblose non-kristallinische Körperchen vom Schmp. 195~200°C.

* Da diese Verbindung bei der Mikro-OCH_3-Analyse klumpig wurde, war die Entstehung des Methyliodids unvollständig, daher sind diese OCH_3-Werte etwas nieder.

Anal. Gef.: C, 67.36; H, 5.5; -OCH_3, 8.9*. Ber. für $C_{22}H_{20}O_6$: C, 69.5; H, 5.30; -OCH_3, 8.2%.

Herren Professor Dr. R. Yamamoto, Professor Dr. Y. Sumiki und Dr. S. Tamura danken wir herzlich für die Unterstützung und Förderung dieser Arbeit. Wir sind Herrn K. Aizawa für die Aufnahme der IR-Spektren und Frau K. Satô, Fräulein M. Suzuki und Fräulein I. Isobe für Mikroanalysen zu bestem Dank verpflichtet.

Organisch-Chemisches Laboratorium
Abteilung der Agrikulturchemie
Universitätzu Tokyo
Hongo, Tokyo

Dielectric Constant of Liquid Consisting of Anisotropic Molecules

By Masasi YASUMI, Hideo OKABAYASHI and Hitoshi KOMOOKA

(Received November 11, 1957)

Recently we have derived a formula for the internal field of polar liquid consisting of isotropic spherical molecules[1].

Our idea is based upon the classical electrostatics of continuous medium. Accordingly, the internal field is expressed as follows:

$$\vec{F}=\vec{E}-\vec{E}_s \tag{1}$$

where $\vec{F}$ is the internal field, $\vec{E}$ the electric field and $\vec{E}_s$ the self-field of a molecule. If the self-field is assumed to be dipolar,

$$\vec{E}_s=-\frac{4\pi}{3}\vec{p} \tag{2}$$

where $\vec{p}$ is the dipolar density.

We have assumed that p is the momentary dipolar density, i.e.;

$$\vec{p}=\frac{\vec{\mu}}{v} \tag{3}$$

where $\vec{\mu}$ is the momentary electric moment of the molecule, and v is the volume of the molecule.

1) M. Yasumi and H. Komooka, This Bulletin, **29**, 407 (1956).

$$\vec{\mu}=\vec{\mu}_0+\alpha\vec{F} \tag{4}$$

$\vec{\mu}_0$ is the permanent moment and α is the polarizability of the molecule.

For the liquid consisting of isotropic spherical molecules, the final expression for the internal field is as follows:

$$\vec{F}=\frac{n^2+2}{3}\left(\frac{\vec{\mu}_0}{a^3}+\vec{E}\right) \tag{5}$$

n denotes the (isotropic) refractive index and a is the radius of the spherical molecule.

On the other hand, Debye's internal field is readily obtained from Eqs. 1 and 2, if we assume that the dipolar density is the macroscopic one; i.e.,

$$\vec{p}=\frac{\varepsilon-1}{4\pi}\vec{E} \tag{6}$$

Using (6) and (2), Debye's internal field has the following expression.

$$\vec{F}=\frac{\varepsilon+2}{3}\vec{E} \tag{7}$$

It is our opinion that in calculating the internal field the dipolar density must be taken as the momentary one and not to be taken as the statistical one, because according to the definition the concept of the internal

field is referred to the molecule in the momentary state and is not referred to the molecule in the statistical state.

Assuming our expression for the internal field, the formula for the dielectric constant of polar liquid is readily derived and has the following expression:

$$\varepsilon-n^2=\frac{4\pi}{V}\left(\frac{n^2+2}{3}\right)^3\frac{\mu_0^2}{3kT} \tag{8}$$

This relation is closely related to the empirical relation of Wyman[2].

In spite of the simplified assumption, our equation 8 can fairly explain the experimental facts.

However, if we compare the experimental data with our equation 8 in detail, we can see that the degree of coincidence seems to depend on the chemical structure of the molecule forming a liquid.

On the other hand, most of the real molecules, especially polar molecules are not to be assumed to have spherical shapes and isotropic polarizabilities in general.

In this paper, we extend our previous theory to the case when a molecule has the shape of an ellipsoid and an anisotropic polarizability.

Formula for the Internal Field and the Dielectric Constant

We assume that the molecule forming a liquid has an anisotropic polarizability and a shape of ellipsoid.

We assume that the directions of the three principal axes of the ellipsoid are coincident with the directions of the coordinate axes (x_1, x_2, x_3).

The directions of the principal axes of the polarizability ellipsoid are not the same as those of the ellipsoid determining the molecular shape in general. However, we assume that these two sets of directions are coincident.

Let the lengths of the principal axes of the ellipsoid be $2a_1$, $2a_2$ and $2a_3$ respectively.

The dipolar density $\vec{p}$ of the liquid is represented as follows:

$$\vec{p}=\frac{\vec{\mu}}{v}=\frac{\vec{\mu}}{\frac{4\pi}{3}a_1a_2a_3} \tag{9}$$

The electride field $\vec{E}$ at a point of the liquid is resolved into two parts, i.e. the internal field $\vec{F}$ and the self-field $\vec{E_s}$.

2) J. Wyman, *J. Am. Chem. Soc.*, **58**, 1482 (1936).

$$\vec{E}=\vec{F}+\vec{E_s} \tag{10}$$

The component of the self-field of the ellipsoid along the direction of a principal axis x_i is expressed as[3];

$$E_{si}=-\varphi_i p_i \tag{11}$$

where

$$\varphi_i=2\pi a_1a_2a_3\int_0^\infty\frac{du}{(a_i^2+u)\sqrt{(a_1^2+u)(a_2^2+u)(a_3^2+u)}} \tag{12}$$

Accordingly, the component of the internal field $\vec{F}$ is represented as:

$$F_i=E_i+\varphi_i p_i \tag{13}$$

On the other hand, the total dipole moment of the molecule consists of the permanent dipole moment and the induced dipole moment.

$$\mu_i=\mu_{0i}+\alpha_i F_i \tag{14}$$

where α_i stands for the component of the polarizability tensor along the direction of the principal axis x_i[4].

From the Eqs. 9, 13 and 14,

$$F_i=\left(1-\frac{\varphi_i\alpha_i}{v}\right)^{-1}\left(E_i+\frac{\varphi_i\mu_{0i}}{v}\right) \tag{15}$$

If the number of the molecules in 1 cc. of the liquid is denoted by N_c, then

$$1=N_cv \tag{16}$$

and

$$\begin{aligned}F_i&=(1-N_c\varphi_i\alpha_i)^{-1}(E_i+N_c\varphi_i\mu_{0i})\\&=\gamma_i(E_i+N_c\varphi_i\mu_{0i})\end{aligned} \tag{17}$$

The component of the total dipole moment of the molecule is expressed as:

$$\mu_i=\gamma_i(\alpha_iE_i+\mu_{0i}) \tag{18}$$

The component of $\vec{\mu}$ along the direcion of $\vec{E}$ is denoted by μ_E, and the statistical mean value of μ_E is denoted by $<\mu_E>$. Assuming Boltzmann statistics, we have

$$<\mu_E>=\int\mu_E\cdot e^{-U/kT}d\Omega\Big/\int e^{-U/kT}d\Omega \tag{19}$$

where U is the potential energy of the dipole under the influence of the electric field and $d\Omega$ is an elementary solid angle.

U has the following expression;

$$U=-\left\{\frac{1}{2}\Sigma\alpha_iF_i^2+\Sigma\mu_{0i}F_i\right\} \tag{20}$$

3) e. g. Stratton, "Electromagnetic Theory", McGraw-Hill Book Company, Inc., 1st Ed. (1941), pp. 207-213, 257.

4) φ and α are tensor quantities. However, in our case when they are diagonalized, only diagonal elements (φ_1, φ_2, φ_3) (α_1, α_2, α_3) are necessary.

and

$$\mu_E=\sum\mu_i\frac{E_i}{E}=\sum\gamma_i(\alpha_iE_i+\mu_{0i})\frac{E_i}{E} \quad (21)$$

Inserting 20 and 21 in 19 and making a simple calculation, we have;

$$<\mu_E>=\left\{\frac{\sum\alpha_i\gamma_i}{3}+\frac{\sum\mu_{0i}^2\gamma_i^3}{3kT}\right\}E \quad (22)$$

In this calculation $e^{-U/kT}$ is expanded in the power series of E_i, and only the terms proportional to E_i are retained.

The dielectric constant ε is related to $<\mu_E>$ by the following equation:

$$(\varepsilon-1)E=4\pi N_c<\mu_E> \quad (23)$$

Accordingly, we have

$$\varepsilon-1=4\pi N_c\left\{\frac{\sum\alpha_i\gamma_i}{3}+\frac{\sum\mu_{0i}^2\gamma_i^3}{3kT}\right\} \quad (24)$$

Consider, for a while, a non-polar liquid.

The refractive index of the liquid may be denoted by n. Then

$$n^2-1=4\pi N_c\frac{\sum\alpha_i\gamma_i}{3} \quad (25)$$

We define the quantity n_i by the following equation;

$$n_i^2-1=4\pi N_c\alpha_i\gamma_i \quad (26)$$

n_i may represent the refractive index of the molecule along the direction of the principal axis x_i.

From the Eqs. 25 and 26, we obtain

$$n^2=\frac{1}{3}\sum n_i^2 \quad (27)$$

It must be noticed that according to Lorentz-Lorenz field,

$$\frac{n^2-1}{n^2+2}=\frac{1}{3}\sum\frac{n_i^2-1}{n_i^2+2} \quad (28)$$

in contrast to our equation (27).

The equation 24 is transformed to the following form;

$$\varepsilon=\frac{\sum n_i^2}{3}+4\pi N_c\frac{\sum\mu_{0i}^2\gamma_i^3}{3kT} \quad (29)$$

In the cases of simple molecules, it may be assumed that the direction of the dipole moment coincides with one of the directions of the principal axes of the molecular ellipsoid. We choose the direction of the axis a_1, as the direction of the dipole moment.

In this case, the equation 29 reduces to

$$\varepsilon=\frac{\sum n_i^2}{3}+4\pi N_c\frac{\gamma_1^3\mu_0^2}{3kT} \quad (30)$$

According to J. Wyman[2] we define the quantity $\bar{p}$ by the following equation[5]:

$$\bar{p}=\frac{4\pi}{3}N_c\left\{\frac{\sum\alpha_i}{3}+\frac{\mu_0^2}{3kT}\right\} \quad (31)$$

then

$$\varepsilon+\frac{4\pi N_c}{3}\left\{\sum\alpha_i(\gamma_i^3-\gamma_i)\right\}-1=3\gamma_1^3\bar{p} \quad (32)$$

The equation 32 corresponds to Wyman's empirical relation[2]

$$\varepsilon+1=K_w\bar{p} \quad (33)$$

K_w represents a constant, amounting to 8.5 for most of normal liquids.

The quantity $3\gamma_1^3$ in our equation 32 which corresponds to K_w is slightly dependent on temperature, but practically is constant in the limited range of temperature[1].

Our present theory can treat the gaseous state if we take v appearing in the equation 9 as the volume portioned to one molecule. The form of the space occupied by this volume is assumed to be an ellipsoid confocal to the molecular ellipsoid.

In the gaseous state $N_c\alpha_i$ is much less than unity so the value of γ_i approaches to 1.

The equation (32) reduces to

$$\varepsilon-1=4\pi N_c\left\{\frac{\sum\alpha_i}{3}+\frac{\mu_0^2}{3kT}\right\} \quad (34)$$

The equation 34 coincides with the Debye's equation in the limiting case of $\varepsilon-1\ll1$.

Comparison of Our Formula with Experiments

In order to compare the value calculated with our theoretical formula the Eq. 29 or the Eq. 30 with the experimental value, we must know the value of permanent dipole moment, that of the component of polarizability and that of the molecular dimension.

a) The value of the permanent dipole moment. We take as the value of the permanent dipole moment, the value determined by the experiment of Stark effect in micro-wave spectroscopy.

However, in the case when this value is not available, the value determined by the measurement of the dielectric constant in the gaseous state is used.

b) The value of the component of polarizability. Two factors contribute to

5) In our previous paper[1], we define

$$\bar{p}=\frac{4\pi}{3}N_c\frac{\mu_0^2}{3kT}$$

However in the Wyman's original paper[3], $\bar{p}$ is defined as in this paper.

the polarizability of a molecule, i. e., the electronic polarization and the atomic polarization.

To determine the value of the component of polarizability, the experimental result of refraction, that of depolarization of polarized light, and that of Kerr effect, should be known.

The latter phenomenon concerns both the electronic polarization and the atomic polarization. On the other hand, the two other phenomena concern only the electronic polarization.

We use as the value of component of polarizability the value referred to in the literature of Stuart for the gaseous state[6] and that of Le Fèvre for the solution[7], when the datum for the gaseous state is not available.

This value does not include the contribution from the atomic polarization.

c) Moreover, we need the value of the molecular dimension. We use as the values of the interatomic distances and the values of valence bond angles the values determined by the experiments of electron diffraction or of micro-wave spectroscopy.

As the dimension of atomic size we use the usual van der Waals' radii[8].

From these values we construct a molecular model. Then we approximate a molecule as an ellipsoid, and determine the lengths of the principal axes. They are denoted by $2a_1$, $2a_2$ and $2a_3$, respectively. The direction of axis a_1 is assumed to be the same as that of the dipole moment.

A symmetrical top molecule can be approximated as a spheroid. In this case the parameter which determines the shape of the spheroid is only one. (i. e., the ratio of axes $a_2/a_1=a_3/a_1$).

We choose the value of the parameter in order to fit the experimental values of dielectric constant, and compare this value with the obtained from the geometrical configuration.

In some cases, we also calculate the value of dielectric constant with our formula taking as the value of axial ratio the value determined with the molecular model.

In the case of a general ellipsoid two parameters (i. e. a_2/a_1 and a_3/a_1) are necessary. In this case we use the values of the parameters determined from the geometrical configuration. We calculate the value of dielectric constant with our equation using these values and compare them with the experimental one.

Our assumption that a molecule may be approximated as an ellipsoid may not hold strictly.

In our calculation, we assume that the ratio of the lengths of the axes of the ellipsoid is independent of the temperature. Strictly saying, this assumption is not correct.

However, in the limited range of temperature, at which the liquid state exists, this assumption may be used without serious error.

For about thirty substances, the value of dielectric constant calculated with our formula is compared with the experimental one. As shown in the following tables the coincidence is strikingly excellent.

For most of the symmetrical top molecules the error is within a small percentage and for most of the asymmetrical top molecules the error is within 10 per cent.

The exceptions are revealed in the cases of methyl fluoride, nitromethane, nitrobenzene and diethyl ether.

In the following, some remarks are made on the individual cases.

1) Non-polar Liquid

For the non-polar liquid, our formula becomes coincident with Lorentz-Lorenz formula, provided that the molecule has a spherical shape and an isotropic polarizability[1]. However, if the molecule forming a liquid has an ellipsoidal shape and an anisotropic polarizability, our equation 25 does not coincide with that of Lorentz and Lorenz.

For benzene and carbon dioxide, we can not determine whether the Lorentz-Lorenz formula or our formula fit the experimental results.

For carbon disulfide it is recognized that the better agreement between the experimental value and the theoretical value is achieved if we calculate with our formula instead of the Lorentz-Lorenz formula.

Moreover the value of the ratio of the axes ($a_2/a_1=a_3/a_1$) obtained with our formla using the experimental results, is 0.5 which is in agreement with the geometrical value 0.54.

The considerable discrepancy between the experimental value and the theoretical

6) H. A. Stuart, Landolt-Börnstein Tabellen, I. Band (1951) 510, 512.

7) C. G. Le Fèvre and R. J. W. Le Fèvre, *Reviews of Pure and Applied Chemistry*, 5, 261-318 (1955).

8) L. Pauling, "The Nature of the Chemical Bond", Cornell Univ. Press 1st. ed. (1939).

value calculated with Lorentz-Lorenz formula exists for the liquid state under high pressure. Moreover, the discrepancy is systematic (i.e., the higher the pressure, the greater the discrepancy).

It is striking that in this case the value calculated with our formula is in excellent agreement with the experimental one.

2) Symmetrical Top Molecule

a) Derivatives of methane

For methyl chloride and methyl bromide the theoretical value is fairly in agreement with the experimental one. The assumed ratio of the axes for methyl chloride is 0.75 (if the Stuart's data for Kerr effect are used) or 0.85 (if the Le Fèvre's data are used). The geometrical value is 0.71.

For methyl bromide the same order of agreement is recognized.

For methyl iodide a somewhat smaller value for the ratio of axes (0.45) is assumed in order to fit the experimental result. The value of the ratio of the axes obtained with the molecular model is 0.64.

For methyl fluoride the value of dielectric constant in the liquid state under high pressure is compared with the value calculated with our formula. If we assume 1.7 as the value of the ratio of the axes which corresponds to an oblate spheroid, the calculated value is in excellent agreement with the experimental one over the wide range of temperature. On the other hand, methyl fluoride has a shape of a prolate spheroid whose axial ratio is 0.85.

The reason why the value of the axial ratio calculated from the value of dielectric constant is inconsistent with the value calculated with the molecualr model is as yet obscure.

b) Other symmetrical top molecules

In the case of acetonitrile, *tert*-butyl chloride and chloroform our theory may be regarded as satisfactory.

3) Asymmetrical Top Molecule

As stated above, as the value of the axial ratio the value determined with the molecular model is used.

a) Nitromethane

The calculated value of dielectric constant is considerably smaller than the experimental one.

b) Methylene chloride.

The agreement is satisfactory.

c) Diethyl ether

The molecular shape of diethyl ether is as yet not determined completely. In table 16 the values of dielectric constant calculated with our formula using various values of axial ratio are shown, and compared with the experimental value.

The planar zig-zag form does not fit. The oblate spheroid whose axial ratio is 0.5 fit to the experimental results very well[9].

d) Other ethers

For dimethyl ether our theory can explain the experimental results quite satisfactorily if we use as the values of axial ratios the values determined with the molecular model.

For *n*-propyl ether, it seems that the zig-zag model is suitable. However, the lack of complete data prevents us from furfher discussion.

e) Paraldehyde

The molecular model is assumed to be the chair-form. This substance has the great atomic polarization. Accordingly we have taken into account the atomic polarization[10].

f) Acetone

The agreement of theoretical value with the experimental one is fairly satisfactory if we use as the value of the axial ratio the ratio determined with the molecular model.

g) Other ketones

In these cases, the value of dipole moment is assumed to be the same as that of acetone. The molecular forms are assumed to be planar zig-zag forms. If other suitable molecular models are assumed, better agreements would be obtained.

h) Derivatives of benzene, pyridine and quinoline

Except nitrobenzene, the calculated value of the dielectric constant is considerably in agreement with the experimental one, if we use as the values of the axial ratios the values determined with the molecular model. Nitrobenzene is assumed to have a coplanar molecular shape.

For nitrobenzene, the calculated value is considerably smaller than the experimental one, as in the case of nitromethane.

Appendix

Evaluation of φ_i. Let the lengths of three

9) On the other hand, the zig-zag model fits the experimental result of the Kerr effect when our internal field is used. Detailed discussion will appear in the following paper.

10) We define the quantity f as follows;

$$\frac{P_E+P_A}{P_E}=\frac{45.2}{33.1}=f$$

where P_E and P_A stand for the electronic and the atomic polarization respectively. In the calculation of the dielectric constant, $f\alpha_i$ is used instead of α_i.

principal axes of an ellipsoid be 2a, 2b and 2c respectively, and $a \geqq b \geqq c$.

φ_i's are represented as follows:[11]

$$\varphi_a = \frac{4\pi \frac{b}{a}\frac{c}{a}}{\left\{1-\left(\frac{c}{a}\right)^2\right\}^{3/2}} \frac{F(k,\rho)-E(k,\rho)}{k^2}$$

$$\varphi_b = \frac{4\pi \frac{b}{a}\frac{c}{a}}{\left\{1-\left(\frac{c}{a}\right)^2\right\}^{3/2}} \frac{1}{k'^2}\left\{\frac{E(k,\rho)-k'^2F(k,\rho)}{k^2} - \frac{\frac{c}{a}\sqrt{1-\left(\frac{c}{a}\right)^2}}{\frac{b}{a}}\right\}$$

$$\varphi_c = \frac{4\pi \frac{b}{a}\frac{c}{a}}{\left\{1-\left(\frac{c}{a}\right)^2\right\}^{3/2}} \frac{1}{k'^2}\left\{\frac{b}{a}\tan\rho - E(k,\rho)\right\}$$

where

$$k^2 = \frac{1-\left(\frac{b}{a}\right)^2}{1-\left(\frac{c}{a}\right)^2}$$

$$k'^2 = 1-k^2$$

$$\sin^2\rho = 1-\left(\frac{c}{a}\right)^2$$

$$F(k,\rho) = \int_0^\rho \frac{d\theta}{\sqrt{1-k^2\sin^2\theta}}$$

$$E(k,\rho) = \int_0^\rho \sqrt{1-k^2\sin^2\theta}\, d\theta$$

i. e., $F(k,\rho)$ and $E(k,\rho)$ represent the elliptic integral of first kind and that of second kind respectively. The numerical values of each are shown in the numerical tables[12].

In the case of sphere,

$$\varphi_a = \varphi_b = \varphi_c = \frac{4\pi}{3}$$

In the case of spheroid:

i) $a = b > c$

if we define as:

$$e^2 = 1-\left(\frac{c}{a}\right)^2$$

then

$$\frac{\varphi_c}{4\pi} = \frac{1}{e^2} - \frac{(1-e^2)^{1/2}\sin^{-1}e}{e^3}$$

and

$$\varphi_a = \varphi_b = 2\pi(1-\varphi_c)$$

ii) $a > b = c$

if we define as:

$$e^2 = 1-\left(\frac{b}{a}\right)^2$$

then

$$\varphi_a = 4\pi\left(\frac{1}{e^2}-1\right)\left(\frac{1}{2e}\ln\frac{1+e}{1-e}-1\right)$$

and

$$\varphi_b = \varphi_c = 2\pi(1-\varphi_a)$$

11) W. Magnus and F. Oberbethinger, "Formel und Sätze für die Speziellen Funktionen der Mathematischen Physik", (1948) Springer-Verlag. p. 136.

12) Marcell Boll, "Tables Numeriques Universelles", 1947.

Summary

Our previous theory of dielectric constant of liquid consisting of spherical molecules having an isotropic polarizability is extended to the case when the molecule has an ellipsoidal shape and an anisotropic polarizability.

The theory is compared with experimental results for about thirty substances. The coincidence is quite satisfactory with few exceptions. For non-polar substance, better agreement between the experimental value and the theoretical value is achieved if we use our formula instead of the Lorentz-Lorenz formula.

We are grateful to Professor San-ichiro Mizushima for his kind encouragement throughout this work and to Professor Akira Kotera for his kind advice. Our thanks are also due to the Ministry of Education for a grant in aid of this research.

Institute of Science and Technology
University of Tokyo
Meguro-ku, Tokyo

Phase Relationship in the System $3CaO \cdot P_2O_5$—$MgO \cdot SiO_2$—SiO_2

By Toshiyuki SATA

(Received November 11, 1957)

The ternary system $3CaO \cdot P_2O_5$—$MgO \cdot SiO_2$—SiO_2 is of great importance in considering the compositions of the calcium-magnesium phosphatic fertilizer (or fused phosphatic fertilizer), and of bone ash magnesia porcelain. The author studied this equilibrium as a partial system of the ternary system $3CaO \cdot P_2O_5$—MgO—SiO_2. The equilibrium phase diagrams in this system have never before been presented.

Kiyoura and Sata[1,2] presented in 1953 the softening and melting diagrams of the system phosphate rocks-dunite-quartzite, and showed the most suitable composition for the fused phosphatic fertilizer as the one with the lowest softening and melting temperature regions in these diagrams. This equilibrium study is an extension of these investigations.

Experimental Procedure

Batches of selected compositions in the system $3CaO \cdot P_2O_5$—$MgO \cdot SiO_2$—SiO_2 were held at constant temperatures and quenched in water. Thenceforth the equilibrium phases found therein were determined by microscopic and X-ray examination.

Tricalcium phosphate ($3CaO \cdot P_2O_5$), magnesium metasilicate ($MgO \cdot SiO_2$) and silica (SiO_2) were used as raw materials. The first was prepared by the reaction of calcium carbonate with phosphoric acid or dicalcium phosphate ($2CaO \cdot P_2O_5$) with calcium carbonate at 1350°C. The second was prepared by calcining the mixture of magnesia and silica at 1300°C. The silica gel fired at 1200°C was used as SiO_2 raw material. After weighing, the batches were thoroughly mixed in an agate mortar with some methyl alcohol until they were dried, and calcined in a platinum crucible at 1200°C. The sample was crushed and mixed again and then heated on a platinum plate at 1200—1500°C, followed by rapid cooling in air.

Two silicon carbide resistor furnaces were used for this equilibrium study, the one with an inner diameter of 40 mm. (up to 1450°C) and the other 25 mm. (up to 1550°C).

The samples in platinum envelopes (8×8 mm.) were suspended by platinum wire (0.5 mm., 200 mm. long) in the center of the furnace and quenched together with this wire in water after being held at a constant temperature (±1°C). A thermocouple of platinum-platinum rhodium (10%) was used, and calibrated against the melting point of silver, copper and diopside.

Quenched samples were powdered and examined by a polarization microscope in the usual way and by X-ray diffractometer. X-ray examinations were carried out adding silicon metal (99.9%) to the samples as the standard material with a scanning speed 2θ 1°/min. The accuracy in reading patterns was decided to be ±0.04° using pure magnesia, quartz and silicon.

Results

The System $3CaO \cdot P_2O_5$—SiO_2.—Three reports have been already published on this system, as listed in Table I.

TABLE I
PREVIOUS RESULTS ON THE SYSTEM $3CaO \cdot P_2O_5$—SiO_2

Investigater	Eutectic temp. °C	Eutectic composition SiO_2 %	Max. solid solubility of SiO_2 in C_3P* %
Trömel[3] (1948)	1540	10	5
Pierre[4] (1956)	1555	6—8	4
Wojciechowska[5] (1956)	1535	7.5	2.5

* Abbreviations used throughout this paper; $C_3P = 3CaO \cdot P_2O_5$, $S = SiO_2$, $M = MgO$, $MS = MgO \cdot SiO_2$, $M_2S = 2MgO \cdot SiO_2$.

The present experiments were intended to check the above observations, particularly the presence of the solid solution of SiO_2 in α or β modification of $3CaO \cdot P_2O_5$ by X-ray diffraction method. The results are shown in Table II.

These facts probably show the difficulty of the transition from α to β form of tricalcium phosphate in slow cooling and no variance of its transition temperature.

1) R. Kiyoura and T. Sata, *J. Chem. Soc. Japan, Ind. Chem. Sec.* (*Kogyo Kagaku Zassi*), **54**, 756 (1951).
2) R. Kiyoura and T. Sata, ibid., **56**, 666-8 (1953).
3) G. Trömel, H. J. Harkort and W. Hotop, *Z. anorg. allg. Chem.*, **256**, 253-72 (1948).
4) P. D. S. St Pierre, *J. Amer. Cer. Soc.*, **37**, (6) 243 (1954); **39**, (4) 147 (1956).
5) J. Wojciechowska, J. Berak and W. Trzebiatowskii, *Roczniki Chem.*, **30**, 743-56 (1956): *Chem. Abst.*, **51**. 2373a (1957).

TABLE II

QUENCHING DATA IN THE SYSTEM $3CaO \cdot P_2O_5$—SiO_2

No.	SiO_2 %	Temp. °C	Time hr.	Condition	Phases present by X-ray exam.		
					α-C_3P	β-C_3P	Cristbalite
185	2	1550	—	slow-cooled	very large	very small	—
		1530	1	quenched	α only	none	—
		1250	5	quenched	large	small	—
		1100	5	quenched	small	large	—
186	5	1550	—	slow-cooled	very large	very small	—
		1530	1	quenched	α only	none	—
		1250	5	quenched	large	small	—
		1200	5	quenched	small	large	—
194	10	1530	1	quenched	large	none	none
		1450	1	slow-cooled	large	none	small
23	40	1530	1	quenched	large	none	large
		1200	—	slow-cooled	large	small	large

TABLE III

QUENCHING DATA IN THE SYSTEM $3CaO \cdot P_2O_5$—$MgO \cdot SiO_2$

No.	Composition		Holding		Phases present
	C_3P wt. %	MS	Temp. °C	Time min.	
6	75.5	24.5	1407	50	glass
			1317	30	β-C_3P, glass
			1282	60	β-C_3P, M_2S, glass
			1222	60	β-C_3P, M_2S, clinoenstatite
25	67.3	32.7	1337	60	glass
			1326	60	β-C_3P, glass
			1305	60	β-C_3P, M_2S, glass
26	64.0	36.0	1337	60	glass
			1323	60	M_2S, glass
			1260	80	β-C_3P, M_2S, glass
			1244	60	β-C_3P, M_2S, clinoenst.
15	60.7	39.3	1348	60	very small M_2S, glass
			1332	60	M_2S, glass
			1314	60	M_2S, (clinoenst.), glass
			1292	60	β-C_3P, M_2S, (clinoenst.) glass
			1267	60	β-C_3P, M_2S, (clinoenst.) small glass
			1240	50	all crystal
4	50.8	49.2	1407	80	small M_2S, glass
			1287	60	M_2S, glass
			1272	60	small C_3P, M_2S, glass
			1252	60	C_3P, M_2S, small glass
36	47.0	53.0	1274	60	M_2S, glass
			1258	60	C_3P, M_2S, glass
31	43.6	56.4	1289	60	M_2S, glass
			1262	60	β-C_3P, M_2S, glass
			1247	50	β-C_3P, M_2S, clinoenst.

The X-ray diffraction patterns of α and β tricalcium phosphate in fired specimens indicated no change from their original patterns, as given in Fig. 1. Therefore the solid solubility of silica in tricalcium phosphate $3CaO \cdot P_2O_5$ mentioned by preceding authors is thought to be doubtful by these X-ray examinations.

The System $3CaO \cdot P_2O_5$—$MgO \cdot SiO_2$.— The quenching runs for this binary system are listed in Table III. Fig. 2 shows the equilibrium diagram obtained from the quenching data. The eutectic of this pseudo-binary system is at 40% $3CaO \cdot P_2O_5$ and 60% $MgO \cdot SiO_2$, and 1246±3°C, these data being obtained in connection with

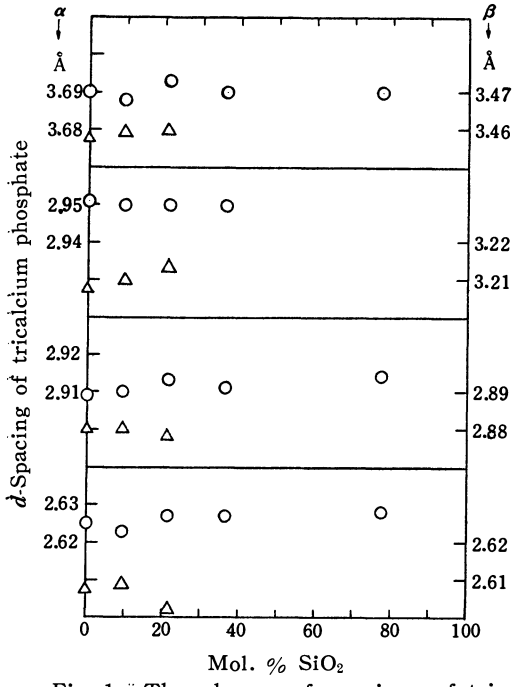

Fig. 1. The change of spacings of tricalcium phosphate.
○; α-$3CaO \cdot P_2O_5$, quenched from 1530°C.
△; β-$3CaO \cdot P_2O_5$, quenched from 1250°C.

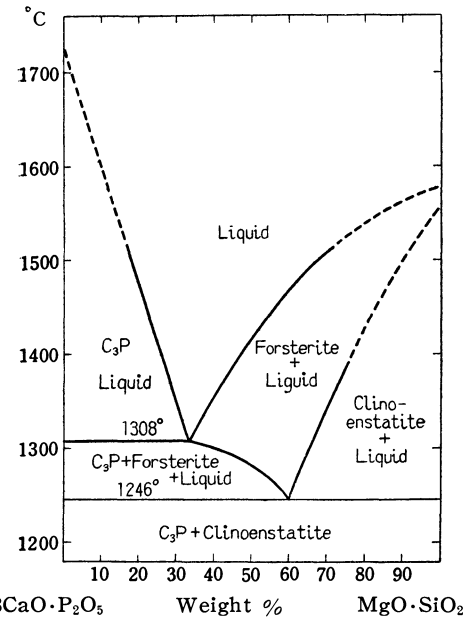

Fig. 2. The system tricalcium phosphate-magnesium metasilicate.

the result of the ternary system $3CaO \cdot P_2O_5$—$MgO \cdot SiO_2$—SiO_2. A minimum of the liquidus in the range from $3CaO \cdot P_2O_5$ to $2MgO \cdot SiO_2$ is at 33.5% $MgO \cdot SiO_2$ and at 1308°C.

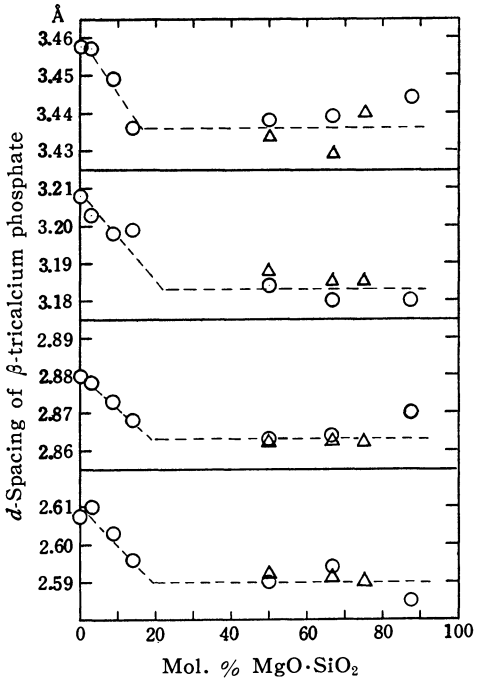

Fig. 3. The change of spacings of β-tricalcium phosphate.
○; quenched from 1250°C.
△; slow-cooled.

The presence of the pyroxene ($MgO \cdot SiO_2$) in quenched sample was chiefly determined by the microscopic examination of the powdered sample, however the X-ray diffraction patterns showed only β-tricalcium phosphate and forsterite, and no pyroxene line was found. It may owe to the difficulty of the equilibrium crystallization of magnesium metasilicate from this system. Only the β-modification, not α, of tricalcium phosphate appeared on X-ray diffraction patterns of all quenched samples at various temperatures, and there was no transition peak on the differential thermal analysis curves up to 1400°C. Thus it is to be concluded that β-tricalcium phosphate seemed to be stabilized at higher temperature over the transition point (1180°C) of pure tricalcium phosphate. The variation of the diffraction patterns of these β-form is indicated in Fig. 3, which shows the apparent solid solubility of 7±2 wt.% (19 mol.%) magnesium metasilicate in β-tricalcium phosphate at 1250°C. Nevertheless it is not yet clear whether tricalcium phosphate just dissolves magnesium metasilicate.

The System $3CaO \cdot P_2O_5$–$MgO \cdot SiO_2$–SiO_2. —The quenching data for this system are listed in Table IV, and the compositions of the mixtures are plotted in Fig. 4.

TABLE IV

QUENCHING DATA IN THE SYSTEM $3CaO \cdot P_2O_5$—$MgO \cdot SiO_2$—SiO_2

No.			Composition			Holding		Phases present
			C_3P	MgO wt. %	SiO_2	Temp. °C	Time min.	
	No. 25	No. 23						
29	85	15	66.2	11.1	22.7	1332	60	C_3P, glass
						1232	45	C_3P, glass
						1208	60	C_3P, clinoenst., very small glass
37	80	20	65.8	10.5	23.7	1292	60	C_3P, glass
						1272	60	C_3P, small cristbl., glass
						1252	60	C_3P, cristbl., glass
27	70	30	65.1	9.2	25.7	1447	60	small cristbl., glass
						1352	60	cristbl., glass
						1324	60	cristbl., C_3P, glass
						1262	60	cristbl., C_3P, small glass
						1217	60	cristbl., C_3P, clinoenst.
	No. 15	No. 23						
48	90	10	60.6	14.2	25.2	1312	60	glass
						1282	50	small C_3P, glass
38	80	20	60.6	12.6	26.8	1312	60	glass
						1287	60	small C_3P, glass
32	70	30	60.5	11.0	28.5	1362	60	cristbl., glass
						1340	60	cristbl., tridymite, glass
						1290	60	cristbl., C_3P, glass
						1244	60	cristbl., C_3P, pyroxene*, glass
						1198	60	cristbl., C_3P, clinoenst.
	No. 4	No. 23						
44	80	20	52.6	15.8	31.6	1272	60	glass
						1264	60	M_2S, glass
						1255	50	C_3P, M_2S, glass
						1252	60	C_3P, M_2S, small glass
						1247	60	almost crystal
46	75	25	53.1	14.8	32.1	1252	60	small C_3P pyroxene* glass
45	70	30	53.5	13.8	32.7	1312	60	very small cristbl., glass
						1272	60	cristbl., glass
						1232	60	C_3P, cristbl., clinoenst.
	No. 31	No. 23						
42	90	10	45.3	20.3	34.4	1262	60	M_2S, small C_3P, glass
39	80	20	47.0	18.0	35.0	1282	60	very small M_2S, glass
						1262	60	M_2S, clinoenst., glass
						1254	60	almost crystal
47	75	25	47.7	17.0	35.3	1254	60	glass
						1247	60	clinoenst., glass
						1240	60	clinoenst., glass
						1232	60	clinoenst., C_3P, glass
						1224	60	all crystal
40	70	30	48.5	15.8	35.7	1272	60	glass
						1262	60	clinoenst., cristbl., glass
						1256	60	clinoenst., cristbl., glass
						1232	60	clinoenst., cristbl., C_3P
43	65	35	49.3	14.7	36.0	1447	60	glass
						1392	60	very small cristbl., glass
						1272	60	cristbl., glass
						1252	60	cristbl., clinoenst., glass
						1242	60	cristbl., clinoenst., C_3P, glass

41	60	40	50.2	13.6	36.2	1447	60	small cristbl., glass
						1332	60	cristbl., tridymite, glass
						1277	60	cristbl., tridymite, glass
						1262	40	cristbl., C_3P, clinoenst., glass
						1228	50	clinoenst., C_3P, cristbl.

* diopsidic pyroxene

Abbreviations; $C_3P=\beta$-$3CaO\cdot P_2O_5$, M_2S=Forsterite, Cristbl.=Cristobalite, Clinoenst.=Clinoenstatite.

These compositions are on the four lines joining No. 23 (60 C_3P—40 SiO_2) with No. 25, 15, 4, or 31 along the C_3P—MS. Fig. 4 was obtained as the phase diagram of this system in which two quintuple points occur, the one at 49% C_3P, 17% M, 34% S and 1246±3°C (alteration point), and the other at 50.5% C_3P, 15% M, 34.5% S and 1230±4°C (the ternary eutectic of the system C_3P—MS—S). It is to be noted that the tie line C_3P—MS may not intersect the boundary curve (alteration curve) between the clinoenstatite and forsterite fields. X-ray examinations of samples No. 42 and No. 47, quenched from 1200°C, gave the β-tricalcium phosphate and clinoenstatite patterns with faint forsterite in the case of the former.

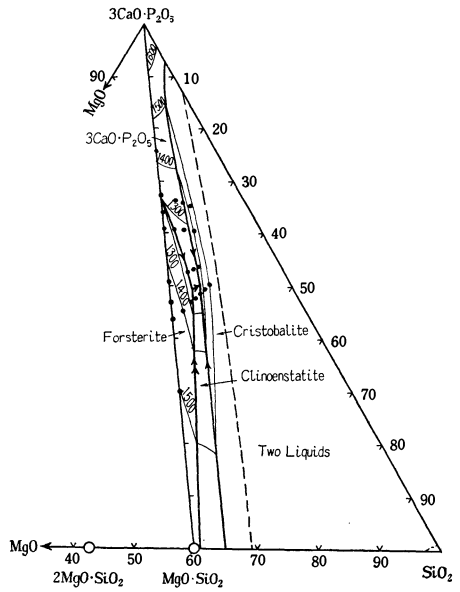

Fig. 4. The system tricalcium phosphate-magnesium metasilicate-silica.

Summary

The phase relationship in the system $3CaO\cdot P_2O_5$—$MgO\cdot SiO_2$—SiO_2 was investigated by the usual quenching method. In the partial system $3CaO\cdot P_2O_5$—SiO_2, the existence of solid solution and the change of the transition temperature of α—β tricalcium phosphate were not found by X-ray examinations.

The partial system $3CaO\cdot P_2O_5$—$MgO\cdot SiO_2$ is pseudo-binary, whose eutectic is at 1246°C and 40% $3CaO\cdot P_2O_5$. In this system, β-$3CaO\cdot P_2O_5$, always appeared in quenched samples, has a maximum solid solubility of 7±2% $MgO\cdot SiO_2$.

The system $3CaO\cdot P_2O_5$—$MgO\cdot SiO_2$—SiO_2 has two quintuple points, the one an alteration point and the other a ternary eutectic at 50.5% $3CaO\cdot P_2O_5$, 15.0% MgO, 34.5%SiO_2 that melts at 1230±4°C.

This system is of great importance to the manufacture of the fused phosphatic fertilizer and the bone ash magnesia porcelain. For instance, in this system, the lower liquidus groove lies at higher silica side along $3CaO\cdot P_2O_5$—$MgO\cdot SiO_2$, in accord with the results of cone fusion and melting point measurements already obtained by Kiyoura and Sata[1,2].

The author acknowledges the constant help and encouragement given by Professor Dr. R. Kiyoura, Tokyo Institute of Technology, and also much helpful advice supplied by Professor, Dr. H. Yamada and Assistant Professor S. Kawakubo, Tokyo Institute of Technology. This work was conducted as a part of a program to investigate the corrosion problems of various refractory bricks in the manufacture of fused phosphatic fertilizer.

Research Laboratory for Ceramics
Tokyo Institute of Technology
Meguro-ku, Tokyo

Polarographic Studies of Metallic Complexes. II.[1] *Isothiocyanato-ammine and Related Complexes of Chromium (III)*[2]

By Nobufumi MAKI, Yoichi SHIMURA and Ryutaro TSUCHIDA

(Received December 14, 1957)

There have been few reports on the relation between the half-wave potentials of chromium (III) complexes and their chemical structures, while some studies have been reported for the cobalt(III) complexes by several authors[1,3-6].

The present paper deals with the polarography of isothiocyanato-ammine series of chromium(III) complexes and the related compounds such as $[Cr\ en_3]Cl_3$, $[Cr\ en_2(NCS)_2]Cl$, or $[Cr\ en_2Cl_2]Cl$. The main purpose of this study is to examine the relationship between the polarographic stabilities of these complexes and their chemical structures. Furthermore, some examples of polarographic behavior of Reinecke's salt and *cis*-$[Cr\ en_2(NCS)_2]^+$ will be reported and discussed. These two salts are quite different from the other members of the chromium(III) isothiocyanato-ammine series from the viewpoint of their catalytic influences on the double wave of the oxygen dissolved in solution.

Experimental

Apparatus—A Heyrovsky-Shikata type polarograph, similar to that previously described[1], was employed to take the polarograms. An H-cell with a saturated calomel electrode was used. Two kinds of capillary were employed for measurements. One of them had an *m*-value of 5.828 mg./sec. and a drop time of 4.00 sec./drop and the other had an *m*-value of 33.661 mg./sec. and a drop time of 5.275 sec./drop. These characteristics of capillaries were measured in distilled water at the mercury height of 65 cm. with an open circuit. The cell temperature was maintained at 25±0.1°C by means of a water thermostat. The half-wave potentials were determined from the enlarged polarograms by "plotting method". The potential values were corrected for *iR*-drop by making use of the minimum value of the cell resistance. The reversibilities of the electrode reaction were tested by determining the slopes of $\log i/(i_d-i)$ vs. potential. Slopes of the log-plots indicated irreversible reduction throughout.

Material—The complex compounds studied were prepared by the methods described in literature[7-11] (the references are given in Tables I—II).

Each solution for the electrolysis was made freshly from the dry crystalline chromium(III) complexes before use and polarographic measurements were made as soon as possible after the removal of oxygen. The concentration of the solution was 0.001 F complex ion per litre. In order to remove the dissolved oxygen, a stream of nitrogen, which was purified from oxygen by means of an alkaline solution of pyrogallol, was bubbled through the cell solution for an hour prior to each electrolysis, preventing the evaporation. For the complexes which aquate easily in solution, such as *cis*-$[Cr\ en_2Cl_2]^+$, nitrogen was bubbled only half an hour and the polarographic runs were completed within ten minutes after the removal of oxygen. No maximum suppressor was used for the purpose of comparing the half-wave potentials of the complexes with one another. The presence of the maximum suppressor causes the lowering of the diffusion current and the shift of the half-wave potential to negative direction. The supporting electrolytes used were 0.1 F potassium chloride and 0.1 F or 1 F potassium thiocyanate.

Results and Discussion

The half-wave potentials of the isothiocyanato-ammine series of chromium(III) complexes are given in Table I. In the neutral and unbuffered solutions of 0.1 F potassium chloride and 0.1 F or 1 F potassium thiocyanate, all the compounds are reduced irreversibly in two steps at the dropping mercury electrode. As is shown in Table I, the half-wave potential

1) Part 1 of this series: N. Maki, Y. Shimura and R. Tsuchida, This Bulletin, **30**, 909 (1957).
2) Presented at the Symposium on Co-ordination Compounds, Nagoya, November 17, 1957.
3) H. F. Holtzclaw, Jr., *J. Am. Chem. Soc.*, **73**, 1821 (1951).
4) H. F. Holtzclaw, Jr., and D. P. Sheetz, ibid., **75**, 3053 (1953).
5) J. Brigando, *Compt. rend.*, **236**, 708 (1953).
6) H. F. Holtzclaw, Jr., *J. Phys. Chem.*, **59**, 300 (1955).
7) M. Mori, *J. Chem. Soc. Japan, Pure Chem. Sec.* (*Nippon Kagaku Zassi*), **74**, 253 (1953).
8) A. Werner and J. von Halban, *Ber.*, **39**, 2668 (1906); R. Tsuchida, *J. Chem. Soc. Japan, Pure Chem. Sec.* (*Nippon Kagaku Zassi*), **59**, 592 (1938).
9) P. Pfeiffer and M. Tilgner, *Z. anorg. Chem.*, **55**, 361 (1907).
10) H. D. Dakin, "Organic Syntheses", Vol. 15, p. 74 (1935).
11) J. Roesler, *Ann.*, **141**, 185 (1867).

TABLE I

HALF-WAVE POTENTIALS OF ISOTHIOCYANATO-AMMINE SERIES OF CHROMIUM(III) COMPLEXES

Complex	SUPPORTING ELECTROLYTE 0.1 F KCl		0.1 F KNCS		1 F KNCS	
	$E_{1/2}$ of 1st Wave	$E_{1/2}$ of 2nd Wave	$E_{1/2}$ of 1st Wave	$E_{1/2}$ of 2nd Wave	$E_{1/2}$ of 1st Wave	$E_{1/2}$ of 2nd Wave
$[Cr(NH_3)_6]Cl_3$[7]	−1.41	−1.65	——	——	——	——
$[Cr(NH_3)_5NCS](NCS)_2$[8]	−1.37	−1.65	−1.37	−1.64	−1.38	——*
$[Cr(NH_3)_4(NCS)_2]NCS$[9]	−1.34	−1.65	−1.34	−1.65	−1.34	——*
$NH_4[Cr(NH_3)_2(NCS)_4]$[10]	−1.31	−1.61	−1.07	——*	−1.23	——*
$K_3[Cr(NCS)_6]$[11]	——	——*	−0.74	——*	−0.79	——*

1) The concentration of the complexes: 0.001 F.
2) The characteristics of capillaries used: $m=5.828$ mg./sec., $t=4.00$ sec./drop.
3) * Maximum wave
4) Applied potential: V. vs. S.C.E.
5) Temperature: 25°C

TABLE II.

HALF-WAVE POTENTIALS OF THE CHROMIUM(III) COMPLEXES

Complex	$E_{1/2}$ of 1st Wave	$E_{1/2}$ of Aquated Complexes	$E_{1/2}$ of 2nd Wave
$[Cr(NH_3)_6]Cl_3$[7]	−1.41	No wave	——*
$[Cr\ en_3]Cl_3 \cdot 3.5\ H_2O$[14]	−1.38	No wave	——*
trans-$[Cr\ en_2(NCS)_2]Cl$[15]	−1.00	−1.30	——*
cis-$[Cr\ en_2(NCS)_2]Cl$[14]	−0.96	−1.30	——*
cis-$[Cr\ en_2Cl_2]Cl$[15]	−0.76	−1.28	——*

(V. vs. S.C.E.).

Supporting electrolyte: 0.1 F KCl.
Characteristics of capillaries used: $m=33.661$ mg./sec., $t=5.275$ sec./drop.
*Maximum wave.

of the first wave shifts to the direction of the more positive potential when the ammonia molecules of $[Cr(NH_3)_6]^{3+}$ are replaced by isothiocyanate ligands. While the half-wave potential of the second wave is always in close proximity to that of $[Cr(OH_2)_6]^{2+}$ ion ($E_{1/2}=-1.63$ V. vs. S.C.E. in 1 F potassium sulfate solution)[12]. Judging from these facts the first wave apparently represents the reduction of chromium(III) complexes to chromium (II) state, and the second represents the reduction to metallic state.

The height of the second wave is significantly greater than twice that of the first wave. The ratio of the wave heights increases with the decreasing concentration of the chromium(III) complexes. Therefore, the second wave is likely to include the "hydrolysis current" which was thoroughly studied by J. J. Lingane and R. L. Pecsok[13]. Thus the hydrogen ion from the hydrolysis of the complexes may contribute to the second diffusion current.

In the supporting electrolyte of 1 F potassium thiocyanate the second wave of these chromium(III) complexes have the maxima, which can not be suppressed in the presence of the high concentration of the usual surface active agents such as gelatin, methyl red, Triton-X 100* or Tween-80**.

The process of the reduction of $[Cr(NH_3)_6]^{3+}$ is considered as follows:

$$[Cr(NH_3)_6]^{3+} + e^- \rightarrow [Cr(NH_3)_6]^{2+}$$
$$[Cr(NH_3)_6]^{2+} + 6H_2O \rightarrow [Cr(OH_2)_6]^{2+} + 6NH_3$$
$$[Cr(OH_2)_6]^{2+} + 2e^- \rightarrow Cr + 6H_2O.$$

Similar mechanisms are applicable to the other chromium(III) complexes here studied. Table II shows the half-wave potentials of some chromium(III) complexes other than the isothiocyanato-ammine series.

For the complexes of $[Cr\ en_2X_2]^+$ type it is expected that they are easily aquated in solution. In fact, these complexes gave rise to the two distinct polarographic waves for the reduction step of chromium

12) J. B. Willis, *J. Proc. Roy. Soc. N. S. Wales*, **78**, 239 (1946).
13) J. J. Lingane and R. L. Pecsok, *J. Am.* Chem. Soc. **71**, 425 (1949).
14) P. Pfeiffer, P. Koch, G. Lando and A. Trieschmann, *Ber.*, **37**, 4255 (1904).
15) C. L. Rollinson, J. C. Bailar, Jr. and J. P. McReynolds, "Inorganic Syntheses", Vol. 2, p. 200 (1946).
* Alkylated aryl polyether alcohol (Rohm & Haas Co. in U. S. A.).
** Polyoxyethylene sorbitan mono-oleate(Atlas Powder Co. in U. S. A.).

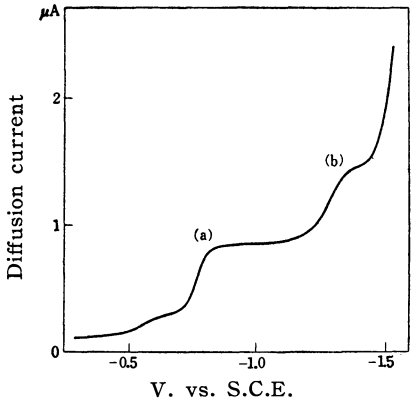

Fig. 1. The polarogram of *cis*-[Cr en_2Cl_2]Cl in 0.1 F KCl.
The concentration of the complex: 0.001 F.
a) The reduction wave of *cis*-[Cr en_2Cl_2]$^+$ to Cr(II) state.
b) The reduction wave of the aquated Cr(III) complexes to Cr(II) state.

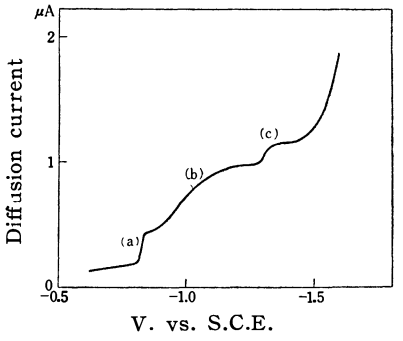

Fig. 2. The polarogram of *cis*-[Cr $en_2(NCS)_2$]Cl in 0.1 F KCl.
The concentration of the complex: 0.001 F.
a) The oxygen wave. (It was impossible to diminish the wave.)
b) The reduction wave of *cis*-[Cr $en_2(NCS)_2$]$^+$ to Cr(II) state.
c) The reduction wave of the aquated Cr(III) complexes to Cr(II) state.

(III)→chromium(II). Figs. 1 and 2 show the typical polarograms. This double wave is thought to be due to an aquation of the complexes. In the process of the aquation one or two of the coordinated negative radicals are replaced by water molecules, resulting in an equilibrium mixture of the aquated and the originial species. For instance,

trans-[Cr $en_2(NCS)_2$]$^+$ + H_2O →*trans*-[Cr $en_2(OH_2)NCS$]$^{2+}$ + NCS^-,

trans-[Cr $en_2(OH_2)NCS$]$^{2+}$ + H_2O →*trans*-[Cr $en_2(OH_2)_2$]$^{3+}$ + NCS^-.

Thus the first wave of the double wave represents the reduction of the original complex and the second that of the aquated species. This postulate is advanced for the following reason. For the *cis* and *trans* isomer of [Cr $en_2(NCS)_2$]$^+$, the half-wave potentials of the second of the double wave have the same values of −1.30 V. vs. S.C.E. within the experimental errors.

The diffusion current of the second waves increased with time. This evidently owes to the formation of the aquo-complexes. For instance, forty minutes after the preparation of the solution, the height of the second wave of [Cr en_2Cl_2]$^+$ is approximately three times as high as that of the second wave of *cis*- or *trans*-[Cr $en_2(NCS)_2$]$^+$. This means that *cis*-[Cr en_2Cl_2]$^+$ aquates more rapidly than *cis*- or *trans*-[Cr $en_2(NCS)_2$]$^+$.

For the benefit of comparing the half-wave potentials of the first wave with

TABLE III
THE HALF-WAVE POTENTIAL OF THE FIRST WAVE OF THE RELATED COMPLEXES OF Cr(III) AND Co(III)[a,1)]

Cr(III) Complex	$E_{1/2}$
$[Cr(NH_3)_6]^{3+}$	−1.41
$[Cr\ en_3]^{3+}$	−1.38
$[Cr(NH_3)_4(NCS)_2]^+$	−1.34
cis-$[Cr\ en_2(NCS)_2]^+$	−0.94
trans-$[Cr\ en_2(NCS)_2]^+$	−1.00
Co(III) Complex[b)]	$E_{1/2}$
$[Co(NH_3)_6]^{3+}$	−0.24
$[Co\ en_3]^{3+}$	−0.43

(V. vs. S.C.E.)

a) The supporting electrolyte: 0.1 F KCl.
b) The experimental conditions are almost the same as for the Cr(III) complexes except the temperature and the characteristics of the capillaries.

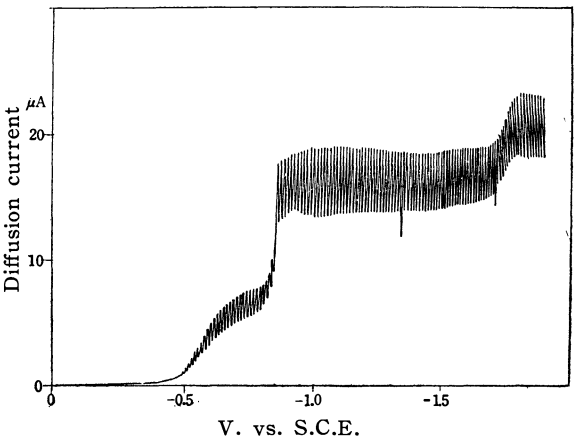

Fig. 3. The polarogram of the double wave of oxygen in the presence of 0.001 F $NH_4[Cr(NH_3)_2(NCS)_4]$ and 0.1 F KCl.

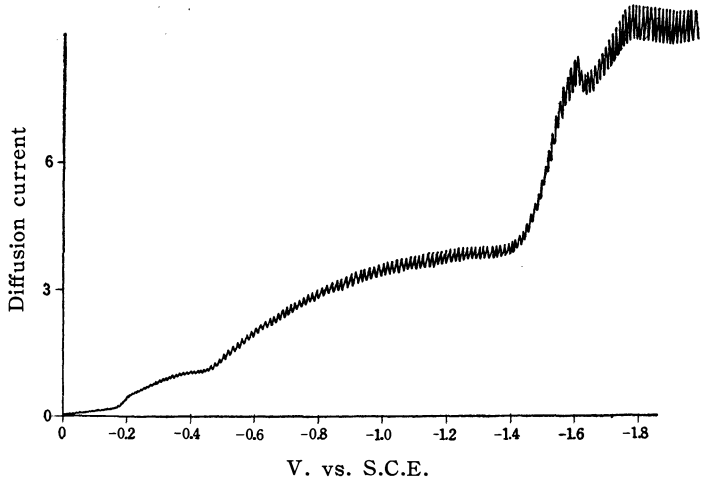

Fig. 4. The polarogram of 0.001 F $K_3[Cr(NCS)_6]$ in 0.1 F KCl. This polarogram was taken immediately after bubbling nitrogen through the solution for an hour.

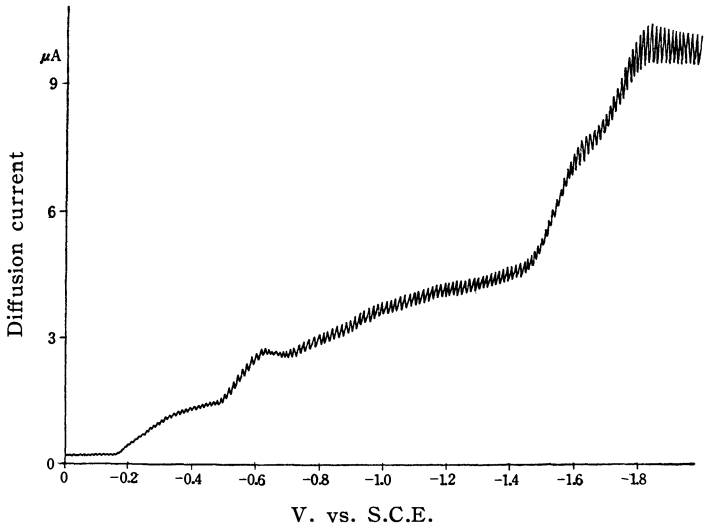

Fig. 5. The polarogram of 0.001 F $K_3[Cr(NCS)_6]$ in 0.1 F KCl. This polarogram was taken ten minutes after the polarographic run of Fig. 5 being completed. It was impossible to determine the half-wave potential of $K_3[Cr(NCS)_6]$ in 0.1 F KCl owing to the interference of the double wave of oxygen.

one another, a part of the data is picked up again here in Table III.

From the comparison of the half-wave potentials for the reduction step of chromium(III)→chromium(II) in the Tables I, II and III, it was found that the polarographic stabilities of the chromium(III) complexes increase in the following order of the ligands:

$$Cl^- < NCS^- < en < NH_3$$

In this series it should be noted that the order of ethylenediamine and ammonia is quite contrary to the order of these ligands for cobalt(III) complexes.

The fact that the *trans* isomer of $[Cr en_2(NCS)_2]^+$ has a slightly more negative half-wave potential than that of the corresponding *cis* isomer agrees with the results obtained by Holtzclaw et al.[3] in the several pairs of *cis* and *trans* isomers of cobalt(III) complexes.

The Peculiar Polarographic Behaviors of *cis*-$[Cr\ en_2(NCS)_2]Cl$ and Reinecke's Salt, $NH_4[Cr(NH_3)_2(NCS)_4]H_2O$. In the presence of 0.001 F $NH_4[Cr(NH_3)_2(NCS)_4]$ in 0.1 F potassium chloride solution, the first wave of oxygen dissolved in the solution shifted to the direction of negative potential and the wave forms of both the first and the second of the oxygen

double wave were extraordinarily modified. Fig. 3 shows the typical polarogram of the dissolved oxygen in the presence of Reinecke's salt. This polarogram was taken after bubbling oxygen into the solution for an hour. It seemed that the limiting current of the oxygen wave depends upon the concentration of oxygen dissolved in the solution. In open air the current value changed from 0.95μA at 25°C after expelling the dissolved oxygen to 8.10μA after saturating oxygen at 25°C. The half-wave potential of the first wave is −0.50 V. (vs. S.C.E.) and that of the second is −0.85 V. (vs. S.C.E) for the solution saturated with oxygen in the air (25°C).

Hexaisothiocyanato chromium(III) complex, $[Cr(NCS)_6]^{3-}$, also shows such kinds of polarographic behavior, though slightly. In the solution of 0.1 F potassium chloride the half-wave potential of the first wave of $[Cr(NCS)_6]^{3-}$ is near to that of the second wave of oxygen double wave and the two waves overlap with each other (Figs. 4 and 5).

No catalytic effects on the double wave of oxygen have been found in the other members of the isothiocyanato-ammine series of chromium(III) complexes. Fig. 6 shows the typical polarogam of the dissolved oxygen in the presence of

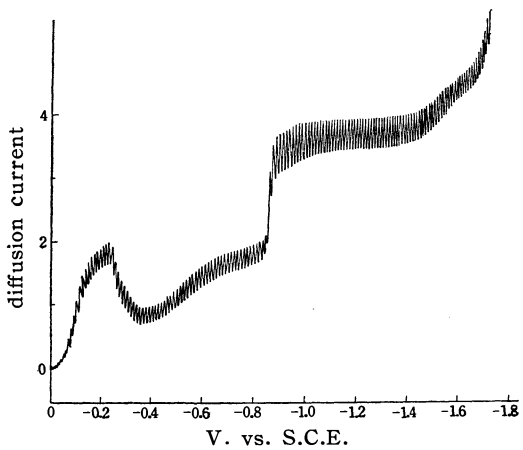

Fig. 6. The polarogram of the double wave of oxygen in the presence of 0.001 F *cis*-$[Cr\,en_2(NCS)_2]Cl$ and 0.1 F KCl.

0.001 F *cis*-$[Cr\,en_2(NCS)_2]Cl$ and of 0.1 F potassium chloride. The first wave of the oxygen double wave has a maximum and the second has the same wave-form and the same half-wave potential (−0.85 V. vs. S. C. E.) as in the case of the Reinecke's salt. The corresponding *trans* isomer, *trans*-$[Cr\,en_2(NCS)_2]Cl$, has never shown the catalytic effects on the oxygen waves.

It should be noted here that all the complexes which show the catalytic effects on the double wave of oxygen have two isothiocyanate ligands on *cis* positions in the coordinated sphere. Therefore, the fact that $[Cr(NH_3)_4(NCS)_2]^+$ did not show such polarographic behavior might be considered as a proof for the *trans* structure of the ion.

Summary

1. In neutral and unbuffered solution of 0.1 F potassium chloride, 0.1 F potassium thiocyanate, or 1 F potassium thiocyanate, the complex ion, $[Cr(NH_3)_n(NCS)_{6-n}]^{n-3}$ and $[Cr\,en_3]^{3+}$ were all reduced irreversibly in two steps at the dropping mercury electrode. The first diffusion current corresponds to the reduction, chromium(III) →chromium(II), and the second to the reduction, chromium(II)→chromium(0).

2. In the solution of 0.1 F potassium chloride, the polarograms of $[Cr\,en_2X_2]^+$ type complexes show three waves. Each of the first two waves, corresponding to a gain of one electron, represents the reduction of chromium(III) to chromium(II) and the last wave, corresponding to a gain of two electrons, represents the reduction to the metallic state. As regards the first two waves, the former wave represents the reduction of the original chromium(III) complexes to chromium(II) state and the latter represents the reduction of the aquated chromium(III) complexes to chromium(II) state.

3. In agreement with the results obtained for cobalt(III) complexes by Holtzclaw et al., the *trans* isomer of $[Cr\,en_2(NCS)_2]^+$ has a little more negative half-wave potential than the corresponding *cis*-form.

4. The polarographic stabilities of chromium(III) complexes increase in the following order of the ligands:

$$Cl^- < NCS^- < en < NH_3$$

5. The catalytic effects on the double wave of oxygen have been found for $[Cr(NH_3)_2(NCS)_4]^-$, $[Cr(NCS)_6]^{3-}$, or *cis*-$[Cr\,en_2(NCS)_2]^+$. Such special polarographic behavior was not found in the other chromium(III) complexes.

Part of the cost of this study was defrayed from a Grant of the Ministry of Education.

Department of Chemistry, Faculty of Science, Osaka University
Kit i-ku, Osaka

Studies on Seven-Membered Heterocyclic Compounds Containing Nitrogen. II. An Improved Synthesis of 1-Azacycloheptan-4-one and Its Related Compounds

By Shiro MOROSAWA

(Received January 30, 1958)

It was reported in the former paper[1] that 1-azacycloheptan-4-one (XI) was synthesized from ethyl *N*-benzyl-γ-(β-carbethoxyethylamino)-butyrate[2] by the Dieckmann condensation. The preparation of the butyrate, however, was so troublesome that the author tried to obtain XI by ring enlargement of 1-benzyl-4-piperidone (X) which prepared from *N*,*N*-bis-(β-carbethoxyethyl)-benzylamine (I) by the Dieckmann condensation.

The method of G. Stork and S. M. McElvain[3] was applied to the preparation of I, and a fraction of b. p. 200~210°C/0.5 mm. was obtained. The author tried at first to prepare azacycloheptane dione (III)

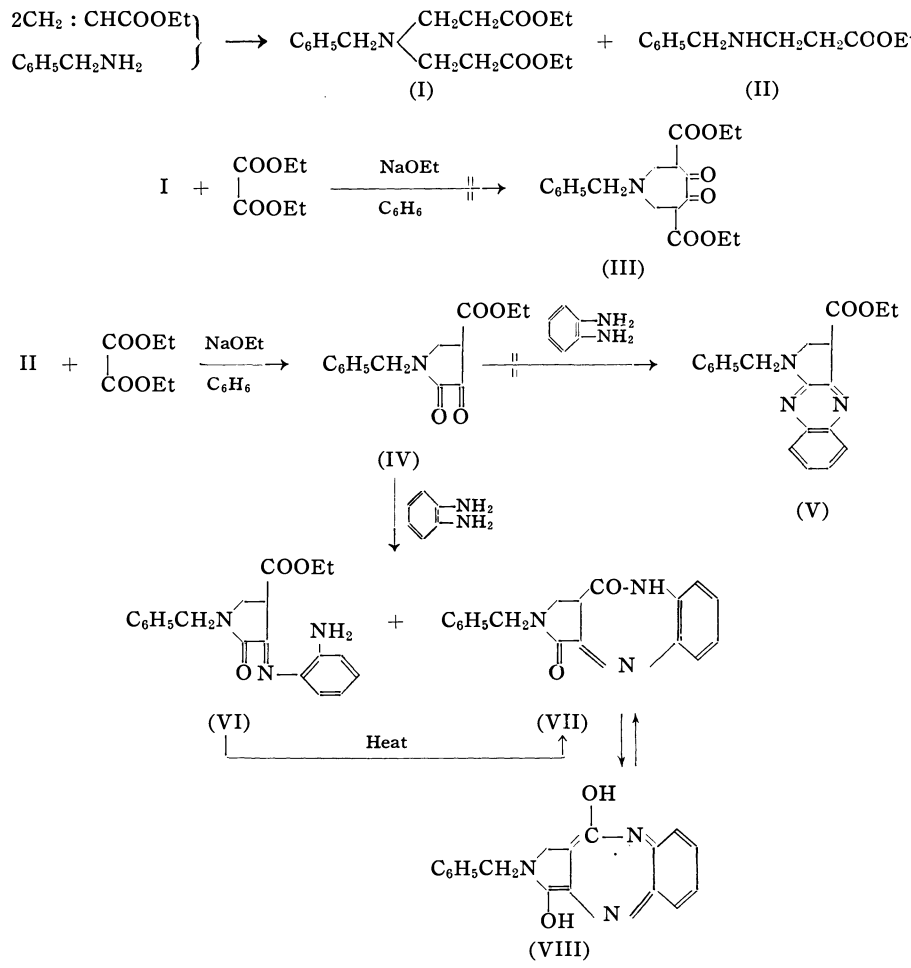

1) A. Yokoo and S. Morosawa, This Bulletin, **29**, 631 (1956).

2) A. Yokoo and S. Morosawa, *J. Chem. Soc. Japan, Pure Chem. Sec.* (*Nippon Kagaku Zassi*), **77**, 599 (1956).

3) G. Stork and S. M. McElvain, *J. Am. Chem. Soc.*, **69**, 971 (1947).

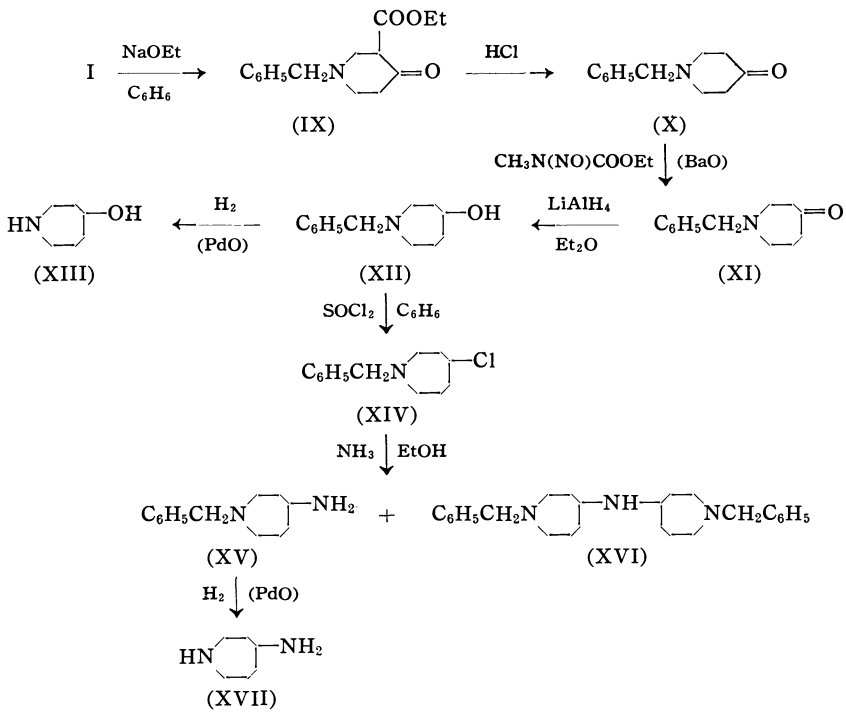

from I and ethyl oxalate, and the fraction was heated with ethyl oxalate in the presence of sodium ethoxide in benzene. But unexpectedly, azacyclopentane dione (IV) was formed. IV was also obtained from ethyl oxalate and pure ethyl β-benzylaminopropionate (II)[3] which was prepared by the Stork and McElvain's method. It was assumed that possibly ethyl oxalate condensed with II which was previously contained in the fraction, or formed by decomposition of I during the heating. With *o*-phenylenediamine IV did not afford a compound of phenazine type (V) but two kinds of crystal; one was light yellow of m. p. 127~8°C and the other orange of m. p. 265~270°C (decomp.). They were revealed from their elementary analyses to have formulae VI and VII (or VIII), respectively. Infrared absorption spectrum of the latter crystals showed the absence of an ester and the primary amine, but because of a wide absorption band (1630~1680 cm.$^{-1}$) near the carbonyl and enol, it was not clearly determined which structure, VII or VIII, is preferable. VI was converted into VII by heating.

Some different boiling points have been reported for I[3,4], but as a result of the present study it was distilled out at 200~210°C/0.5 mm. along with ethyl acrylate which was detected by its faint odor; nitrosoation test with sodium nitrite for the distillate indicated the presence of a secondary amine II. On pyrolysis, the distillate began to decompose at about 197°C to yield ethanol and ethyl acrylate, leaving a residue which was distilled out at 165~210°C/0.65 mm. without indicating a constant boiling point.

From these experiments, it is obvious that I is apt to be affected by heating and can not be refined even by vacuum distillation. In the present study, therefore, the tertiary amine I was separated from the reaction mixture by removing the secondary amine II as a nitroso compound, in 65.5% yield. I thus obtained was possibly considered to be pure from its nitrogen analysis, and was also decomposed at about 197°C on pyrolysis. On heating with an equivalent amount of sodium ethoxide in dry benzene, I was converted into hydrochloride of 1-benzyl-3-carbethoxypiperid-4-one (IX)[4] of m.p. 175°C (decomp.) as colorless prisms in 82.5% yield, which by decarboxylation with hydrochloric acid gave 1-benzylpiperid-4-one (X)[5] as a colorless oil of b. p. 143~6°C/5 mm.

The ring enlargement of X was performed by the C. G. Overberger and A.

4) J. R. Thayer and S. M. McElvain, ibid., **49**, 2862 (1927).

5) G. Stork and S. M. McElvain, ibid., **68**, 1053 (1946).

Katchmann's method[6] who prepared 4-oxo-thiaepane from tetrahydro-1,4-thiapyrone and nitrosomethylurethane in the presence of barium oxide. In order to purify the crude product, this was dissolved in dry ether, and dry hydrogen chloride was passed through to precipitate it as a hydrochloride, which was recrystallized from methanol and ether. The melting point of the hydrochloride was not depressed on admixture with the one described in the former paper. Free base XI was regenerated from the hydrochloride with potassium carbonate, and gave 2,4-dinitrophenylhydrazone hydrochloride, which was also identified as the former one by mixed fusion.

Lithium aluminum hydride reduction of XI afforded 1-benzyl-1-azacycloheptan-4-ol (XII) as a colorless oil of b.p. 129°C/0.5 mm. in 95.5% yield, which on catalytic reduction with palladous oxide yielded 1-azacycloheptan-4-ol (XIII) as a hygroscopic colorless viscous oil of b.p. 82°C/0.5 mm. in 56.2% yield. XIII gave a picrolonate of m.p. 225°C (decomp.). With thionyl chloride, XII afforded 1-benzyl-4-chloro-1-azacycloheptane (XIV) as a hygroscopic colorless liquid of b.p. 104~5°C/0.3 mm. in 67.3% yield, which on standing gradually crystallized. Heating a mixture of XIV and absolute ethanol, saturated with ammonia at 0°C, in a sealed tube gave 4-amino-1-benzyl-1-azacycloheptane (XV) as a colorless oil of b.p. 105~6°C/0.4 mm. in 71% yield. Bis-(4-benzyl-4-azacycloheptyl)-amine (XVI) was also thereby obtained as a higher-boiling, light yellow viscous oil of b.p. 219~221°C/0.3 mm., which gave a picrolonate of m.p. 213°C (decomp.). XV gave a chloroaurate as yellow micro plates of m.p. 194°C (decomp.). Catalytic reduction of XV in the presence of palladous oxide as a catalyst afforded 4-amino-1-azacycloheptane (XVII) as a hygroscopic colorless oil of b.p. 80°C/10 mm., which on standing in the atmosphere gradually deposited white crystalline precipitates under fuming. XVII gave a chloroaurate of m.p. 209°C (decomp.) and a picrate of m.p. 224°C (decomp.).

Experimental

***N,N*-Bis-(β-carbethoxyethyl)-benzylamine (I).**—A mixture of 80 g. of benzylamine and 190 g. of ethyl acrylate was refluxed in an oil bath for 20 hr. After cooling, a mixture of 200 cc. of concentrated hydrochloric acid and 300 cc. of water was added and cooled to below 5°C in an ice-water bath, followed by the addition of 90 g. of solid sodium nitrite in small portions under agitation. After further agitation for 30 min., the mixture was extracted with a mixture of 200 cc. of benzene and 100 cc. of ether. The organic layer was extracted 8 times with each 200 cc. portion of 3 N hydrochloric acid and discarded. Aqueous layers were united and made alkaline by adding 650 g. of anhydrous sodium carbonate and extracted with a mixture of 200 cc. of benzene and 200 cc. of ether, then with that of 100 cc. of benzene and 100 cc. of ether. The extracts were united and washed with a diluted solution of sodium carbonate, and water and dried over calcium chloride. The solvent was distilled off on a water bath; the residue is further heated under reduced pressure until nothing had been distilled out. After that, the reduced pressure was held under heating on a water bath for another one hour, leaving 150 g. (65.5%) of an oily substance. (Found: N, 4.63%).

1-Benzyl-4-carbethoxy-1-azacyclopenta-2,3-dione (IV).—To a suspension of 3.1 g. of powdered sodium in 150 cc. of dry benzene was added 6 g. of absolute ethanol and heated with stirring to convert the sodium into sodium ethoxide. After cooling, a mixture of 13.8 g. of II (b.p. 133~5°C/2 mm.) and 10 g. of ethyl oxalate was added and allowed to stand overnight. In order to distill out 100 cc. of the azeotropic mixture of ethanol and benzene, the resulting mixture was heated in a water bath with stirring. The mixture in the reaction flask was washed with water and 2 N hydrochloric acid until the washing became acidic. The benzene solution was evaporated to a small volume. Crystals formed on standing were filtered, washed with water and recrystallized from ethanol to give 8 g. (46%) of colorless crystals, m.p. 133~4°C.

Anal. Found: C, 64.13; H, 5.86; N, 5.19. Calcd. for $C_{14}H_{15}O_4N$: C, 64.3; H, 5.76; N, 5.37%.

Compounds VI and VII.—A mixture of 1 g. of IV, 1 g. of *o*-phenylenediamine and 10 cc. of ethanol was refluxed on a water bath for 7 hr. Orange crystals formed were filtered and recrystallized from a large amount of ethanol to give 0.2 g. of orange plates (VII), m.p. 265~270°C (decomp.).

Anal. Found: C, 70.85; H, 5.19; N, 13.49. Calcd. for $C_{18}H_{15}O_2N_3$: C, 70.8; H, 4.93; N, 13.76%.

The filtrate of VII was evaporated and allowed to stand. Crystals formed were recrystallized twice from ethanol to yield 1.2 g. of light yellow crystals (VI), m.p. 127~8°C.

Anal. Found: C, 68.28; H, 6.27; N, 11.81. Calcd. for $C_{20}H_{21}O_3N_3$: C, 68.3; H, 5.98; N, 11.95%.

VII by heating VI.—After heating 0.5 g. of VI at 155~165°C in an oil bath for 5 hr., a small amount of ethanol was added, heated and decanted repeatedly. Remaining crystals were recrystallized from a large amount of benzene to

6) C. G. Overberger and A. Katchmann, ibid., **78**, 1967 (1956).

give 0.3 g. of orange crystals (VII).

1-Benzyl-3-carbethoxypiperid-4-one (IX) hydrochloride.—To a suspension of 7.5 g. of powdered sodium in 30 cc. of dry xylene were added 300 cc. of dry benzene and 17 cc. of absolute ethanol, and heated under stirring to convert the sodium into sodium ethoxide. After cooling, a solution of 100 g. of I in 180 cc. of dry benzene was added within 5 min. with stirring. After about 10~20 min., the resulting mixture became gel-like and could not be stirred; it was allowed to stand overnight. About 200 cc. of the solvent was distilled out by heating the mixture for 4 hr. After cooling, 100 cc. of water and 100 cc. of concentrated hydrochloric acid were added to deposit an oily matter, which gradually crystallized. After standing for 2 hr., the crystals were filtered, recrystallized from 40 cc. of ethanol and washed with a mixture of 25 cc. of ethanol and 25 cc. of ether to give 80 g. (82.5%) of IX hydrochloride as colorless prisms, m.p. 175°C (decomp.). (Found: C, 60.77; H, 7.02; N, 4.33%).

1-Benzylpiperid-4-one (X).— A mixture of 120 g. of IX hydrochloride, 400 cc. of concentrated hydrochloric acid and 350 cc. of water was refluxed for 3 hr. After cooling, the solution was evaporated to dryness under reduced pressure. The residue was dissolved in 50 cc. of water, and 100 g. of anhydrous potassium carbonate was added. Liberated oil was extracted 4 times with ether (100 cc., 100 cc., 50 cc. and 50 cc. respectively), and the combined ether extract was dried over potassium carbonate. Ether was removed and vacuum distillation gave 61 g. (70%) of a colorless oil, b. p. 143~6°C/5 mm. (Found: N, 7.24%).

X gave 2, 4-dinitrophenylhydrazone hydrochloride as yellow prisms of m. p. 223°C (decomp.).

Anal. Found: N, 17.26. Calcd. for $C_{18}H_{19}O_4N_5 \cdot HCl$: N, 17.63%.

1-Benzyl-1-azacycloheptan-4-one (XI) by ring enlargement.—In a three-necked, round-bottomed flask, fitted with a Hershberg stirrer and a dropping funnel, 61 g. of X and 100 cc. of methanol were placed and cooled to −15°C in an ice-salt mixture. The stirring was started, and 45 g. of nitrosomethylurethane was added dropwise within 9 hr. During that time, 2 g. of barium oxide was added in small portions, and the temperature in the flask indicated about −5°C. After being kept overnight in the ice-salt mixture, the reaction mixture was filtered from any solid present, and the methanol was expelled under reduced pressure. The residue was dissolved in 400 cc. of ether and the undissolved polymethylene polymers were filtered off. Dry hydrogen chloride was passed through the ether to give a precipitate, which was separated by decantation, dried, recrystallized from 40 cc. of methanol and 20 cc. of ether and washed thrice with a mixture of 15 cc. of methanol and 15 cc. of ether to yield 28.3 g. of XI hydrochloride, m. p. 184~5°C (decomp.). Evaporation of the filtrate gave a further crop of crystals, which was recrystallized as before to give 3 g. of the substance, m. p. 184~5°C (decomp.). The total yield was 43.6%. The melting point of this hydrochloride was not depressed on admixture with that described in the former paper.

The hydrochloride was dissolved in 15 cc. of water and 40 g. of potassium carbonate was added. Oil thereby liberated was taken up in ether and dried over potassium carbonate. After removal of ether, vacuum distillation gave 24.8 g. (37.8%, based on X) of free base as a colorless oil, b. p. 129°C/0.5 mm.

2, 4-Dinitrophenylhydrazone hydrochloride of m. p. 214°C (decomp.) derived from XI did not either depress the m. p. of the former one on mixed fusion. (Found: N, 16.60%).

1-Benzyl-1-azacycloheptan-4-ol (XII).— A solution of 11.1 g. of XI in 150 cc. of dry ether was added dropwise to 1.05 g. of lithium aluminum hydride suspended in 100 cc. of dry ether without cooling during 1 hr. under stirring, which was continued for 15 min. The excessive hydride was then decomposed by adding dropwise 19 cc. of water with stirring. Ether was decanted, dried over magnesium sulfate and removed by distillation. The residue was distilled to yield 10.7 g. (95.5%) of a colorless oil, b. p. 129°C/0.5 mm.

Anal. Found: C, 74.90; H, 9.46; N, 6.70. Calcd. for $C_{13}H_{19}ON$: C, 76.05; H, 9.33; N, 6.82%.

1-Azacycloheptan-4-ol (XIII).—A solution of 4.6 g. of XII in 150 cc. of water containing 2 cc. (a slight excess) of concentrated hydrochloric acid was shaken with 0.2 g. of palladous oxide under an atmosphere of hydrogen at room temperature until the theoretical amount of hydrogen had been absorbed. After removal of the catalyst by filtration, water was evaporated under reduced pressure. To the remainder was added 2 cc. of 50% of potassium carbonate solution, followed by further addition of solid potassium carbonate. This mixture was well agitated to remove water. Ether was then added, agitated well and decanted. This procedure was repeated several times. Ethereal portions were collected and, after drying over potassium carbonate, ether was removed on a water bath to leave a residue. Vacuum distillation of the residue gave 1.45 g. (56.2%) of a quite hygroscopic colorless viscous oil, b. p. 82°C/0.5 mm.

Anal. Found: C, 62.13; H, 11.80; N, 11.64. Calcd. for $C_6H_{13}ON$: C, 62.57; H, 11.38; N, 12.16%.

Picrolonate:—A mixture of 0.1 g. of XIII and 1 g. of picrolonic acid in 40 cc. of ethanol was heated on a water bath for a few min. and allowed to cool. The crystals were recrystallized from ethanol to brownish yellow prisms of m. p. 225°C (decomp.), 0.26 g.

Anal. Found: N, 18.33. Calcd. for $C_6H_{13}ON \cdot C_{10}H_8O_5N_4$: N, 18.46%.

1-Benzyl-4-chloro-1-azacycloheptane (XIV).—To a solution of 5.3 g. of XII in 50 cc. of dry benzene, was added dropwise under cooling in an ice-water bath a solution of 4 cc. of thionyl chloride in 5 cc. of dry benzene with stirring. The solvent was removed under reduced pressure, leaving a dark red residue. The residue was dissolved in a little water and

made alkaline with solid potassium carbonate. The oily substance was taken up in benzene and dried over potassium carbonate. After removal of benzene, vacuum distillation yielded 3.9 g. (67.3%) of a highly hygroscopic colorless liquid, b. p. 104~5°C/0.3 mm. which, on standing, gradually crystallized and showed the presence of halogen by Beilstein test.

Anal. Found: N, 6.10. Calcd. for $C_{13}H_{18}NCl$: N, 6.26%.

4-Amino-1-benzyl-1-azacycloheptane (XV) and bis-(4-benzyl-4-azacycloheptyl)-amine (XVI).—A mixture of 3.4 g. of XIV and 20 cc. of absolute ethanol saturated with ammonia at 0°C was heated in a sealed tube at 100°C for 3 hr. After cooling, the solvent was removed under reduced pressure, and the residue was dissolved in a little water and made alkaline with solid potassium carbonate. The liberated oil was extracted with benzene and dried over potassium carbonate. After removal of benzene, the residue was vacuum-distilled to yield 2.2 g. (71%) of a hygroscopic colorless oil (XV) of b. p. 105~6°C/0.4 mm. and 0.6 g. of a light yellow viscous oil (XVI) of b. p. 219~221°C/0.3 mm.

Anal. Found: N, 13.56. Calcd. for $C_{13}H_{20}N_2$ (XV): N, 13.71%. Found: C, 79.71; H, 9.46; N, 10.46. Calcd for $C_{26}H_{37}N_3$ (XVI): C, 79.74; H, 9.52; N, 10.73%.

XV on mixing with chloroauric acid produced a chloroaurate, which was recrystallized from water to give yellow micro plates, m. p. 194°C (decomp.).

Anal. Found: N, 3.13. Calcd. for $C_{13}H_{20}N_2 \cdot (HAuCl_4)_2$: N, 3.17%.

XVI gave a picrolonate by adding an ethanolic solution of picrolonic acid, which was recrystallized from a large amount of water to give yellow crystals, m. p. 213°C (decomp.).

Anal. Found: N, 16.45. Calcd. for $C_{26}H_{37}N_3 \cdot (C_{10}H_8O_5N_4)_2$: N, 16.75%.

4-Amino-1-azacycloheptane (XVII).— A solution of 2 g. of XV in 80 cc. of water was shaken with hydrogen in the presence of 0.2 g. of palladous oxide at room temperature until the theoretical amount of hydrogen had been absorbed. The catalyst was filtered off, and water was evaporated under reduced pressure. Vacuum distillation of the residue gave 0.55 g. (50%) of a highly hygroscopic colorless oil, b. p. 79~80°C/10 mm. When the distillate is allowed to stand in the atmosphere, white crystalline precipitates appeared in the oil under fuming, possibly because of absorption of carbon dioxide in the atmosphere. So the nitrogen content could not be determined.

On mixing with chloroauric acid, XVII gave a chloroaurate, which was recrystallized from water to yield yellow prisms, m. p. 209°C (decomp.).

Anal. Found: C, 9.18; H, 2.46; N, 3.47; Au, 48.9. Calcd. for $C_6H_{14}O_2 \cdot (HAuCl_4)_2$: C, 9.08; H, 2.03; N, 3.53; Au, 49.63%.

XVII and a saturated ethanolic solution of picric acid formed a picrate, which was recrystallized from ethanol to yield yellow prisms, m. p. 224°C (decomp.).

Anal. Found: N, 19.35. Calcd. for $C_6H_{14}N_2 \cdot (C_6H_3O_7N_3)_2$: N, 19.57%.

The author gratefully acknowledges many helpful discussions with Professor A. Yokoo (this laboratory), and thanks Mr. A. Kondo (The Department of Organic Chemistry of Tokyo Institute of Technology) for carrying out the carbon and hydrogen micro-analyses. Part of the expenses for these experiments was defrayed by a Grant in Aid for Scientific Research provided by the Ministry of Education, which is gratefully acknowledged.

Chemical Institute, Faculty of Science
Okayama University
Tsushima, Okayama

The Centrifugal Distortion and the l-Type Doubling Constants in Linear XYZ-Type Molecules. The Determination of Force Field by These Constants

By Yonezo MORINO and Eizi HIROTA

(Received January 16, 1958)

I

It is usually impossible to determine the set of force constants for a molecule only through vibrational frequencies, unless isotopic substitution is made. Assumptions have frequently been made to reduce the number of unknown constants; one may mention examples of central force field, valence force field[1] or Urey-Bradley field[2]. It is, however, possible to use other experimental data than vibrational frequencies for obtaining the force constants. Wilson and Kivelson[3,4] showed that the centrifugal distortion constants of asymmetric top molecules can be used for the determination of the force constants in general force field. However, their results on sulfur dioxide[4] showed a discrepancy with those of infrared absorption spectra[5] based upon the isotopic substitution. An experimental error or other sources might contribute to this discrepancy, so that it is worth while to discuss about these points in a simpler system such as linear XYZ-type molecules.

The linear XYZ-type molecule has three fundamental modes: two of them are stretching vibrations along the molecular axis (parallel vibrations) and the other is a degenerate bending mode (perpendicular one). The force constant for the latter vibration can be determined by the value of frequency alone, but two observed frequencies are insufficient to determine three force constants associated with the former two modes. The centrifugal distortion constant will give additional information about the parallel vibrations. One may, however, note that there is another constant available: the *l*-type doubling constant. The Coriolis force lifts the degeneracy of the bending vibration and the separation between the two resulting energy states can accurately be measured by the microwave spectroscopy[6]. Since the centrifugal distortion and the *l*-type doubling constants give independent information, one can test the experimental error or the validity of the underlying assumption made in the theory. A sum rule is found to be useful for such a test.

II

The centrifugal force reduces the effective rotational constant and hence the rotational energy. The quantum mechanical expression for the energy decrease by centrifugal distortion is given by

$$\mathbf{H}_D=(1/2)(\mu_{xx}\mathbf{P}^2_x+\mu_{yy}\mathbf{P}^2_y) -(1/2)(\mu^e_{xx}\mathbf{P}^2_x+\mu^e_{yy}\mathbf{P}^2_y) \quad (1)$$

where $\mathbf{P}_x$ and $\mathbf{P}_y$ denote angular momentum operators, μ_{xx} and μ_{yy} inverses of moment of inertia, and the superscript e of μ refers to the equilibrium. Now μ_{xx} and μ_{yy} can be expanded as power series of the internal coordinates, ΔR_{XY} and ΔR_{YZ}, but the moment of inertia is usually defined in terms of Cartesian coordinates of individual atoms. The Cartesian coordinates of composing atoms are bound to each other by the complicated Eckart condition, and it is somewhat difficult to obtain the expansion of the moment of inertia in terms of internal coordinates. Hence it is very desirable to derive in general a relation between the normal coordinates and the Cartesian coordinates. The process using the **B**-matrix has already been discussed by the authors.[7] The relation is given by

1) G. Herzberg, "Molecular Spectra and Molecular Structure," Vol. II, D. Van Nostrand Co., New York, 1949.
2) H. C. Urey and C. A. Bradley, *Phys. Rev.* **38**, 1969 (1931).
3) D. Kivelson and E. B. Wilson, Jr., *J. Chem. Phys.* **20** 1575 (1952); **21**, 1229 (1953).
4) D. Kivelson, ibid. **22**, 904 (1954); L. Pierce, ibid. **24**, 139 (1956).
5) S. Polo and M. K. Wilson, ibid. **22**, 900 (1954).
6) R. G. Shulman and C. H. Townes, *Phys. Rev.* **77**, 421 (1950).
7) Y. Morino and E. Hirota, *J. Chem. Phys.* **23**, 737 (1955).

$$\mathbf{X}=\mathbf{M}^{-1}\mathbf{B}'\mathbf{U}'(\mathfrak{L}^{-1})'\mathbf{Q} \quad (2a)$$

$$=\mathbf{M}^{-1}\mathbf{B}'(\mathbf{L}^{-1})'\mathbf{Q} \quad (2b)$$

where $\mathbf{X}$ and $\mathbf{Q}$ denote the Cartesian coordinates and the normal coordinates matrices. $\mathbf{L}^{-1}$ is easily replaced by $\mathbf{L}$ through the relation $\mathbf{LL}'=\mathbf{G}$, or $\mathbf{L}^{-1}=\mathbf{L}'\mathbf{G}^{-1}$. [Cf. Eq. 20]

The expression of the $\mathbf{B}$-matrix is particularly simple in the present case; then it sufficices to consider only the Cartesian coordinates along the molecular axis (z-axis):

$$\mathbf{B}=\begin{pmatrix}1 & -1 & 0\\ 0 & 1 & -1\end{pmatrix} \quad (3)$$

Hence Eq. 2b becomes

$$\begin{pmatrix}\Delta z_X\\ \Delta z_Y\\ \Delta z_Z\end{pmatrix}=\begin{pmatrix}\dfrac{(m_Y+m_Z)L_{11}+m_ZL_{31}}{m_X+m_Y+m_Z} & \dfrac{(m_Y+m_Z)L_{13}+m_ZL_{33}}{m_X+m_Y+m_Z}\\ \dfrac{-m_XL_{11}+m_ZL_{31}}{m_X+m_Y+m_Z} & \dfrac{-m_XL_{13}+m_ZL_{33}}{m_X+m_Y+m_Z}\\ \dfrac{-m_XL_{11}-(m_X+m_Y)L_{31}}{m_X+m_Y+m_Z} & \dfrac{-m_XL_{13}-(m_X+m_Y)L_{33}}{m_X+m_Y+m_Z}\end{pmatrix}\begin{pmatrix}Q_1\\ Q_3\end{pmatrix} \quad (4)$$

The moment of inertia I_{xx} is given by

$$I_{xx}=\sum_i m_i(y_i^2+z_i^2)\cong\sum_i m_iz_i^{e2}+2\sum_i m_iz^e{}_i\Delta z_i \quad (5)$$

where $y_i=\Delta y_i$ and $z_i=z^e{}_i+\Delta z_i$. The same expression holds for I_{yy}. Thus the inverse of the moment of inertia $\mu_{xx}=1/I_{xx}$ becomes

$$\mu_{xx}=(1/I^e{}_{xx})(1-2\sum_i m_iz^e{}_i\Delta z_i/I^e{}_{xx}+\cdots\cdots), \quad (6)$$

where the equilibrium positions of individual atoms $z^e{}_i$ can readily be calculated

$$z^e{}_X=[(m_Y+m_Z)R_{XY}+m_ZR_{YZ}]/(m_X+m_Y+m_Z), \quad (7a)$$

$$z^e{}_Y=[-m_XR_{XY}+m_ZR_{YZ}]/(m_X+m_Y+m_Z), \quad (7b)$$

and

$$z^e{}_Z=[-m_XR_{XY}-(m_X+m_Y)R_{YZ}]/(m_X+m_Y+m_Z). \quad (7c)$$

If one uses the relations Eqs. 4 and 7 in Eq. 6 the expansion of the inverse of the moment of inertia in normal coordinates is obtained:*

$$\mu_{xx}=\mu_{yy}=(1/I^e{}_{xx})(1-2(bQ_1+aQ_3)/(I^e{}_{xx})^{1/2}+\cdots). \quad (8)$$

a and b are constants including the force constants and given by

$$a=\frac{m_X(m_Y+m_Z)R_{XY}+m_Xm_ZR_{YZ}}{(m_X+m_Y+m_Z)(I^e{}_{xx})^{1/2}}L_{13}+\frac{m_Xm_ZR_{XY}+(m_X+m_Y)m_ZR_{YZ}}{(m_X+m_Y+m_Z)(I^e{}_{xx})^{1/2}}L_{33}, \quad (9a)$$

and

$$b=\frac{m_X(m_Y+m_Z)R_{XY}+m_Xm_ZR_{YZ}}{(m_X+m_Y+m_Z)(I^e{}_{xx})^{1/2}}L_{11}+\frac{m_Xm_ZR_{XY}+(m_X+m_Y)m_ZR_{YZ}}{(m_X+m_Y+m_Z)(I^e{}_{xx})^{1/2}}L_{31}, \quad (9b)$$

and between them there exists a useful relation noted by Nielsen:[8]

$$a^2+b^2=1 \quad (10)$$

When Eq. 8 is inserted into Eq. 1 and terms of the order of $Q^2{}_i$ are neglected,

$$\mathbf{H}_D=-\frac{bQ_1+aQ_3}{(I^e{}_{xx})^{3/2}}(\mathbf{P}^2{}_x+\mathbf{P}^2{}_y). \quad (11)$$

when the average of this term is taken over the vibrational state $(v_1, v^l{}_2, v_3)$, the first order energy $(v_1v^l{}_2v_3|\mathbf{H}_D|v_1v^l{}_2v_3)$ is equal to zero, but the second order perturbation gives

$$E_D=\frac{|(v_1v^l{}_2v_3|\mathbf{H}_D|v_1\pm1v^l{}_2v_3)|^2}{\mp h\nu_1}+\frac{|(v_1v^l{}_2v_3|\mathbf{H}_D|v_1v^l{}_2v_3\pm1)|^2}{\mp h\nu_3}=-4B^3{}_e\left[\frac{b^2}{(h\nu_1)^2}+\frac{a^2}{(h\nu_3)^2}\right][J(J+1)-1]^2. \quad (12)$$

Here $B_e=\hbar^2/2I^e{}_{xx}$ is the equilibrium rotational constant, and ν_1 and ν_3 are vibrational frequencies. Thus the centrifugal distortion constant D_e is given by

$$D_e=4B^3{}_e\left[\frac{b^2}{(h\nu_1)^2}+\frac{a^2}{(h\nu_3)^2}\right]. \quad (13)$$

The l-type doubling originates from the fact that the Coriolis interaction lifts the degeneracy of the bending vibration. This effect corresponds to an operator:[9]

$$\mathbf{H}_C=-\mathbf{h}_x\mathbf{P}_x-\mathbf{h}_y\mathbf{P}_y, \quad (14)$$

where

* μ_{xy} is equal to zero. It is to be noted that μ_{xx} and μ_{yy} are independent of the bending coordinates, Q_{2x} and Q_{2y}. (Cf. ref. 9)

8) H. H. Nielsen, *Revs. Modern Phys.* **23**, 90 (1951).
9) E. B. Wilson, Jr., and J. B. Howard, *J. Chem. Phys.* **4**, 260 (1936).

$$\mathbf{h}_x=\frac{1}{2}[2\mu_{xx}\mathbf{p}_x+(\mathbf{p}_x\mu_{xx})+\mu_{xx}\mu^{1/2}(\mathbf{p}_x\mu^{-1/2})] \tag{15a}$$

and

$$\mathbf{h}_y=\frac{1}{2}[2\mu_{yy}\mathbf{p}_y+(\mathbf{p}_y\mu_{yy})+\mu_{yy}\mu^{1/2}(\mathbf{p}_y\mu^{-1/2})]. \tag{15b}$$

$\mathbf{p}_x$ and $\mathbf{p}_y$, vibrational angular momenta, are

$$\mathbf{p}_x=aQ_{2y}\mathbf{p}_1+bQ_{2y}\mathbf{p}_3-(aQ_1+bQ_3)\mathbf{p}_{2y} \tag{16a}$$

and

$$\mathbf{p}_y=-aQ_{2x}\mathbf{p}_1-bQ_{2y}\mathbf{p}_3+(aQ_1+bQ_3)\mathbf{p}_{2x}, \tag{16b}$$

respectively. The determinant of (μ_{xx}), μ, is simply $\mu^2{}_{xx}$, because, $\mu_{xx}=\mu_{yy}$ and $\mu_{xy}=0$. Since direct calculation shows that the second and the third term of Eq. 15 cancel each other, Eq. 14 becomes

$$\begin{aligned}\mathbf{H}_C=&\frac{a}{I^e{}_{xx}}(Q_{2x}\mathbf{P}_y-Q_{2y}\mathbf{P}_x)\mathbf{p}_1\\&-\frac{a}{I^e{}_{xx}}(\mathbf{p}_{2x}\mathbf{P}_y-\mathbf{p}_{2y}\mathbf{P}_x)Q_1\\&+\frac{b}{I^e{}_{xx}}(Q_{2x}\mathbf{P}_y-Q_{2y}\mathbf{P}_x)\mathbf{p}_3\\&-\frac{b}{I^e{}_{xx}}(\mathbf{p}_{2x}\mathbf{P}_y-\mathbf{p}_{2y}\mathbf{P}_x)Q_3,\end{aligned} \tag{17}$$

where μ_{xx} is approximated by $(I^e{}_{xx})^{-1}$ [see Eq. 8]. For taking average of Eq. 17, it must be noted that Q_{2x} and Q_{2y} belong to a degenerate state, and hence the perturbation theory for a degenerate case should be applied. Here the first order perturbation energy also vanishes while the second order one is finite. When the two degenerate states are designated by $(v_1l^{+1}v_3)$ and $(v_1l^{-1}v_3)$,** according to their positive and negative angular momenta along the molecular axis, only an element $(v_1l^{+1}v_3|\,v_1l^{-1}v_3)$ plays an essential role for the separation of these states: it is calculated as follows:

$$\begin{aligned}&\sum_{v'_1v'_2v'_3}\frac{(v_1l^{+1}v_3|\mathbf{H}_C|v'_1v'^{l}_2v'_3)(v'_1v'^{l}_2v'_3|\mathbf{H}_C|v_1l^{-1}v_3)}{E(v_1l^{+1}v_3)-E(v'_1v'^{l}_2v'_3)}\\&=\frac{B^2{}_e}{h\nu_2}\left(1+4a^2\frac{\nu^2{}_2}{\nu^2{}_1-\nu^2{}_2}+4b^2\frac{\nu^2{}_2}{\nu^2{}_3-\nu^2{}_2}\right)J(J+1).\end{aligned} \tag{18}$$

Here $v'_1=v_1\pm1$, $v'_3=v_3\pm1$, and $v'_2=0^0$ and 2^0. Thus the l-type doubling constant q_e is given by

$$q_e=\frac{2B^2{}_e}{h\nu_2}\left(1+4a^2\frac{\nu^2{}_2}{\nu^2{}_1-\nu^2{}_2}+4b^2\frac{\nu^2{}_2}{\nu^2{}_3-\nu^2{}_2}\right). \tag{19}$$

Eqs. 13 and 19 for the centrifugal distortion and for the l-type doubling constant coincide with those given by Nielsen and others[8,10,11] though they are derived in slightly different manners.

III

Now the force constants to be obtained are implicitly included in the **L**-matrices and accordingly in the constants a^2 and b^2 defined by Eq. 9. On the other hand a^2 and b^2 are connected to each other by the sum rule, Eq. 10, and are given by the two observables, D_e and q_e, through Eqs. 13 and 19. Two of the three equations may be used for determining a^2 and b^2, and the other is available for testing possible errors in D_e and q_e or for confirming the approximation made in deriving Eqs. 13 and 19; that is the harmonic approximation. Table I gives the results of such calculations on several linear molecules of the XYZ-type. Some molecules, such as chlorine cyanide (ClCN) give reasonable values for a^2 and b^2, but others do not. One of the most definite inconsistency is the case of iodine cyanide; its D_e is probably in a considerable error.

D_e is really a correction term for the rotational energy and hence it cannot be obtained very accurately. On the other hand the measurement of q_e is easier, particularly in cases when the direct transition is possible to be observed as in hydrogen cyanide (HCN).[6]*** Since in Eq. 19 the second and the third term of q_e are useful in the calculation of the force constants and they are only about twenty percent of the total q_e, the error of q_e is exaggerated about six times in a^2 and b^2.

According to Eq. 9, b^2 (or a^2) thus determined gives a relation between L_{11} and L_{31} (or between L_{13} and L_{33}). In addition to this, another relation $\mathbf{LL}'=\mathbf{G}$, i.e.

$$\begin{aligned}&L^2{}_{11}+L^2{}_{13}=G_{11}=1/m_X+1/m_Y,\\&L^2{}_{31}+L^2{}_{33}=G_{33}=1/m_Y+1/m_Z,\\&L_{11}L_{31}+L_{13}L_{33}=G_{13}=G_{31}=-1/m_Y,\end{aligned} \tag{20}$$

determines the **L**-matrix, which gives the **F**-matrix by the relation $\mathbf{F}=(\mathbf{L}^{-1})'\Delta\mathbf{L}^{-1}$. Though the signs of the **L**-elements are not fixed in solving Eqs. 20, it does not

** Only $v_2=1$ state is interested here, so that $l=\pm1$.

10) G. Herzberg, *Revs. Modern Phys.* **14**, 219 (1942)

11) A. H. Nielsen, *J. Chem. Phys.* **11**, 160 (1943).

*** Recently direct l-type doubling transitions in ClCN were observed by L. Yarmus, (*Phys. Rev.* **105**, 928 (1957)).

TABLE I

a^2 AND b^2, AND EXPERIMENTAL DATA NECESSARY TO CALCULATE THEM.

Compound	$q+D$			q+sum rule		D+sum rule	
	b^2	a^2	a^2+b^2	b^2	a^2	b^2	a^2
HCN	0.9984	0.0501	1.0485	0.9218	0.0782	1.0305	−0.0305
^{35}ClCN	0.9246	0.0722	0.9968	0.9286	0.0714	0.9242	0.0758
^{79}BrCN	0.9511	0.0592	1.0103	0.9397	0.0603	0.9519	0.0481
^{127}ICN	1.2668	0.0301	1.2969	0.9613	0.0387	1.2816	−0.2816
OC^{32}S	0.9272	0.0460	0.9732	0.9576	0.0424	0.9217	0.0783
N_2O	1.0024	0.0398	1.0422	0.9436	0.0564	1.0235	−0.0235

Compound	(cm^{-1}) [a]			B_0(Mc/s)	q(Mc/s)	D(Mc/s)
	$\tilde{\nu}^0_1$	$\tilde{\nu}^0_2$	$\tilde{\nu}^0_3$			
HCN	2089	712	3312	44315.97[c]	224.478[d]	0.09040[b]
^{35}ClCN	729	397	2201	5970.831[b]	7.459[b]	0.001663[b]
^{79}BrCN	580	368	2187	4120.221[b]	3.915[b]	0.0008844[b]
I^{127}CN	470	321	2158	3255.578[c]	2.69[c]	0.00088[c]
OC^{32}S	859	527	2079	6081.494[c]	6.39[c]	0.00127[c]
N_2O	1285	589	2224	12561.639[b]	23.736[b]	0.005359[b]

a) G. Herzberg, "Molecular Spectra and Molecular Structure", p. 174.
b) C. A. Burrus and W. Gordy, *Phys. Rev.* **101**, 599 (1956).
c) W. Gordy, W. V. Smith, and R. Trambarulo, "Microwave Spectroscopy", Table A4.
d) A. Miyahara, H. Hirakawa, and K. Shimoda, *J. Phys. Soc. Japan*, **11**, 335 (1956).
Values of b^2 with underline are used to calculate force constants.

TABLE II

FORCE CONSTANTS. (10^5 dynes/cm)

Compound	b^2	Present result			Herzberg[a]		Isotopic method[b]		
		F_{XY}	F_{YZ}	F'	F_{XY}	F_{YZ}	F_{XY}	F_{YZ}	F'
HCN	0.9218	5.90	16.93	0.36	5.8	17.9	6.257	18·68	−0.1907
^{35}ClCN	0.9246	4.74	18.35	1.31	5.2	16.7	4.7∼5.0	16.8∼18.2	0∼1
^{79}BrCN	0.9511	3.96	16.00	0.92	4.2	16.9			
OC^{32}S	0.9272	17.84	6.60	2.34	14.2	8.0			
N_2O	0.9436	18.34	11.06	1.63	13.7	14.6	17.88	11.39	1.36

a) G. Herzberg, "Molecular Spectra and Molecular Structure", p. 174
b) H. C. Allen, Jr., E. D. Tidwell and E. K. Plyler, *J. Chem. Phys.* **25**, 302 (1956) (HCN); W. S. Richardson and E. B. Wilson, Jr., ibid. **18**, 155, 694 (1950). (ClCN, N_2O).

influence the resulting F-matrix, and other solutions than those in Table II are not physically reasonable and can readily be rejected.

It must be noted that in the calculation described above $\tilde{\nu}^0_i$ and B_0 are respectively used instead of the quantities $\tilde{\nu}^e_i$ and B_e which should be used in the rigorous sense.

IV

In Table II the values of the force constants thus determined are compared with those from other sources, so far as available. The constants cited in Herzberg's book[1] are of central field type, the cross term being ignored. The diagonal terms show a little difference from the present ones. Richardson and Wilson[12] used isotopic molecules, ^{35}Cl^{13}CN and ^{15}N^{14}NO, to obtain the three force force constants for chlorine cyanide and nitrous oxide. As was stated by them, the cross term F' plays an important role for nitrous oxide molecule: if one uses only two constants, F_{XY} and F_{YZ} to explain the observed $\tilde{\nu}^0_1$ and $\tilde{\nu}^0_3$ (rather than the zeroth order $\tilde{\nu}^e_1$ and $\tilde{\nu}^e_3$), then imaginary constants are resulted. They arrived at well-defined sets of force constants: $F_{XY}=17.88\pm0.7$, $F_{YZ}=11.39\pm0.3$, and $F'=1.36\pm0.3$, which are in close agreement with the values obtained above: $F_{XY}=18.34$, $F_{YZ}=11.06$, and $F'=1.63$. The substitution of ^{13}C for ^{12}C was found to be rather ineffective for determining the force constants of chlorine cyanide, so that only allowed ranges were reported for the three constants: $F_{XY}=4.7$ ∼5.0, $F_{YZ}=16.8\sim18.2$, and $F'=0\sim1$, which

12) W. S. Richardson and E. B. Wilson, Jr., *J. Chem. Phys.* **18**, 155, 694 (1950).

are favorably compared with ours: $F_{XY}=4.74$, $F_{YZ}=18.35$, and $F'=1.31$.

For hydrogen cyanide molecules, a rather complete analysis of vibration-rotation interaction was carried out together with that of DCN,[13,14] so that much more accurate values of force constants are available. As the l-type splitting is large for this molecule, it is possible to measure by the microwave spectroscopy[15] a direct transition between these doublets. With these data much more reliable values are expected in this molecule than in chlorine cyanide and nitrous oxide. However, the comparison made in Table II shows that the agreement for hydrogen cyanide is not better than those for chlorine cyanide and nitrous oxide. One of the reasons for this discrepancy may be considered to be the use of $\tilde{\nu}^0_i$ rather than $\tilde{\nu}^e_i$ in obtaining b^2. In fact, if $\tilde{\nu}^e_i$ is used ($\tilde{\nu}^e_1=2127.63\,cm^{-1}$, $\tilde{\nu}^e_3=3442.81\,cm^{-1}$ for hydrogen cyanide and $\tilde{\nu}^e_1=1953.18\,cm^{-1}$, $\tilde{\nu}^e_3=2702.94\,cm^{-1}$ for DCN)[14], b^2 changes to 0.8368 (q_e is used), but $F_{XY}=6.65$, $F_{YZ}=18.22$, and $F'=2.25$, thus the agreement of F' becomes worse.

If conversely the l-type doubling constant and the centrifugal distortion constant are calculated by using the force constants given in reference 14, they are 215.68 Mc and 0.08406 Mc, respectively, which are compared with the observed, 224.478 Mc[15] and 0.9040 Mc.[16] These differences (8.80 Mc or 3.9% for the l-type doubling constant and 0.00634 Mc or 7.0% for the centrifugal distortion constant) are definitely larger than the errors involved in the observed values. The higher order effects such as anharmonicity of vibrations or higher terms in the expansion of μ_{xx} can produce this order of discrepancy for the two constants. According to the measurement of Douglas and Sharma[13] α/B is about 0.007 and $\omega_e x_e/\omega_e$ about 0.015. Exact expression for the higher order effect has been given only for the centrifugal distortion constant of diatomic molecule, but for polyatomic molecules it would be too complicated to be calculated exactly. One way to avoid the difficulty is to use in Eqs. 13 and 19 B_0 instead of B_e and $\tilde{\nu}^0_i$ for $\tilde{\nu}^e_i$: the l-type doubling constant of hydrogen cyanide increases to 221.45 Mc and the centrifugal distortion constant to 0.08722 Mc, though an exact agreement is not obtained.

For molecules including no hydrogen atom these higher order effects are not very critical, α/B and $\omega_e x_e/\omega_e$ being smaller (e.g. α/B of chlorine cyanide is 0.0027). Fairly good coincidence obtained for cases of chlorine cyanide and nitrous oxide can, therefore, be understood.

13) A. E. Douglas and D. Sharma, ibid. **21**, 448 (1953).
14) H. C. Allen, Jr., E. D. Tidwell and E. K. Plyler, ibid. **25**, 302 (1956).
15) See, for example, A. Miyahara, H. Hirakawa and K. Shimoda, *J. Phys. Soc. Japan*, **11**, 335 (1956).
16) C. A. Burrus and W. Gordy, *Phys. Rev.* **101**, 599 (1956).

Note added in proof.

Recently Wilson gave an expression for the centrifugal distortion constant of linear molecules. [E. Bright Wilson, Jr., *J. Chem. Phys.* **27**, 986 (1957)] The result obtained in the present paper [Eq. 13] can be shown to be in complete agreement with his formula, by some minor transformations.

Department of Chemistry
Faculty of Science
The University of Tokyo
Hongo, Tokyo

Isolation of Agarobiose Derivative from the Mucilage of Gloiopeltis Furcata

By Susumu HIRASE, Choji ARAKI and Toshiya ITO

(Received December 23, 1957)

The mucilage of a red seaweed *Gloiopeltis furcata** resembles carrageenin (the mucilage of *Chondrus* algae) in the respect that it has a high content of sulfate residues as well as that it forms on dissolution in water a highly viscous solution. But our recent report has pointed out the chemical difference that the *Gloiopeltis* mucilage is chiefly composed of D-galactose and 3,6-anhydro-L-galactose as in the case of agar[1], while that carrageenin is composed of D-galactose and the anhydro-D-sugar, an enantiomorph of the above one[2]. Thus the complete methanolysis of the former mucilage afforded methyl D-galactoside and 3,6-anhydro-L-galactose dimethylacetal together with a small amount of a L-galactose derivative[1]. On the other hand, partial methanolysis of agar led to the isolation of crystalline agarobiose dimethylacetal (4-*O*-β-D-galactopyranosyl-3,6-anhydro-L-galactose dimethylacetal) in a good yield[3] and also of crystalline 4-*O*-(4,6-*O*-1′-carboxyethylidene-β-D-galactopyranosyl)-3,6-anhydro-L-galactose dimethylacetal as an acidic product in a slight yield[4]. With this in mind, the *Gloiopeltis* mucilage has been subjected to partial methanolysis, the results being reported herein.

The partial methanolysis has been conducted by refluxing the suspension of the mucilage in 0.5% methanolic hydrogen chloride for two hours as in the case of agar[3]. The methanolysate was treated with a barium hydroxide solution to effect saponification and then with cation- and anion-exchange resin in succession. An acidic substance, which was adsorbed by the anion-exchange resin, was eluted therefrom by displacement with excess of sulfuric acid and isolated as a barium salt. The salt has proved to be entirely barium methylsulfate, derived from sulfate residues present in the mucilage molecule. No evidence was obtained to indicate the presence of pyruvic acid[5] or any other carboxylic acid.

The neutral methanolysate, which passed through the resins without being retained, was subjected to charcoal chromatography[6], which led to the isolation of methyl D-galactoside (6%), a mixture of 3,6-anhydro-L-galactose dimethylacetal (4%) and methyl D-xyloside (2%), and agarobiose dimethylacetal (55%), the yields being based on the neutral methanolysate by weight.

The mixture of 3,6-anhydro-L-galactose dimethylacetal and methyl D-xyloside was further resolved into the components by chromatography on a powdered filter paper column. The methyl D-xyloside, obtained as a syrup, was hydrolyzed to give the free sugar, which was then identified as crystalline di-*O*-benzylidene-D-xylose dimethylacetal after Breddy and Jones[7]. This has been the first report as to the identification of D-xylose as far as the *Gloiopeltis* mucilage is concerned. But the yield was so low that the sugar might be possibly derived from a contaminating xylan.

Agarobiose dimethylacetal has been isolated as crystals, the physical constants of which are identical with those of the sample isolated previously from agar by two of the present writers[3]. The dimethylacetal was hydrolyzed and subsequently converted into agarobiose phenylosazone, which again agreed well with an authentic sample. On acetylation the dimethylacetal yielded hexa-acetate melting at 136~137°C, the value being in disagreement with the melting point 87~88°C reported previously by two of the writers[3], but in agreement with the melting point 137.5~138.5°C reported recently by Clingman, Nunn and Stephen[8]. The experiment

* Japanese name is "Fukuro-funori".

1) S. Hirase, C. Araki and T. Itô, This Bulletin, **29**, 985 (1956).
2) C. Araki and S. Hirase, ibid., **29**, 770 (1956); A. N. O'Neill, *J. Am. Chem. Soc.*, **77**, 2837, 6324 (1955).
3) C. Araki and S. Hirase, This Bulletin, **27**, 109 (1954).
4) S. Hirase, ibid., **30**, 70, 75 (1957).
5) S. Hirase, ibid., **30**, 68 (1957).
6) R. L. Whistler and D. F. Durso, *J. Am. Chem. Soc.*, **72**, 677 (1950).
7) L. J. Breddy and J. K. N. Jones, *J. Chem. Soc.*, **1945**, 738.
8) A. L. Clingman, J. R. Nunn and A. M. Stephen, ibid., **1957**, 197.

was repeated, but the acetate melting at 87~88°C could be prepared neither from the dimethylacetal of a *Gloiopeltis* origin nor from that of an agar origin.

It necessarily follows from the isolation of the agarobiose derivative that D-galactopyranose residues are connected through β-galactoside links with the 4-positions of 3,6-anhydro-L-galactose residues to form agarobiose residues in the mucilage molecule, and that if sulfate residues are left out of consideration, the disaccharide represents the repeating unit in the molecule of the mucilage as in that of agarose, a principal polysaccharide of agar[9].

Experimental

Evaporation and concentration of solutions were carried out under reduced pressure below 40°C. The melting points are uncorrected.

Partial Methanolysis of the Mucilage. — The mucilage preparation used in this study was the same one as that used in the previous work[1]. The mucilage (10 g., moisture 9.33%), after being soaked in 0.5% methanolic hydrogen chloride (100 cc.) overnight at room temperature, was heated under reflux for two hours, and then undissolved material (1.8 g.) was filtered off, washed with methanol and dried in vacuo. The filtrate and washings were combined, neutralized with silver carbonate, refiltered and evaporated to a syrup (9.0 g.). It was then heated with 0.3 N barium hydroxide solution (80 cc.) at 60°C for two hours to effect saponification, excess of the barium hydroxide removed by neutralization with carbon dioxide and subsequent filtration, and the filtrate was concentrated to a syrup, which was dried by repeated dissolution in methanol followed by evaporation; yield 7.3 g.; $[\alpha]_D^{13}$ −9.6° (*c* 0.83 in water).

Barium Methylsulfate.—The syrup obtained above was dissolved in water, the resulting solution allowed to pass through columns of the cation-exchange resin Amberlite IR-120 (100 cc) and the anion-exchange resin Amberlite IR-4B (100 cc.) in succession, and the columns were washed with water (1.3 *l.*). The combined effluents and washings were evaporated to recover the neutral methanolysate, which formed a syrup; yield 4.3 g. (59% of the consumed mucilage on the moisture-free basis); $[\alpha]_D^{13}$ −10.7° (*c* 0.75 in water).

The IR-4B resin, which adsorbed an acidic substance, was transferred to a beaker and stirred with 2 N sulfuric acid (100 cc.) under ice-cooling for a brief period of time. The resin was retransferred to a glass tube to form a column, excess of the liquid allowed to drain, and the column was washed with additional 100 cc. of 2 N sulfuric acid and water in succession. All the effluents were combined, neutralized immediately with a hot saturated barium hydroxide solution, filtered and evaporated, the residue being obtained as a colorless solid; yield 3.5 g.; $[\alpha]_D^{13}\pm0°$ (*c* 1.0 in water). Paper chromatographic examination showed the absence of any carbohydrate compound. Determination of the ash content proved that the solid obtained above was barium methylsulfate;

Anal. Found: Ash (as barium sulfate), 83.2. Calcd. for $(CH_3SO_4)_2Ba\cdot H_2O$: $BaSO_4$, 83.3%.

Chromatography of the Neutral Methanolysate. — The neutral methanolysate (4.3 g.), obtained above from the effluent which passed through the ion exchangers, was dissolved in water (100 cc.), and the solution was soaked into the top of a charcoal*-Celite column (5.0×20 cm.), which was then developed successively with water, 2%, 5%, 7.5%, 15% and 30% ethanol in water. The effluents were separately evaporated to dryness, and the resultant residues were weighed, measured for specific rotation, and examined on paper chromatograms[6], which were irrigated with *n*-butanol-ethanol-water (4 : 1 : 2 v/v) and which were sprayed with *o*-aminophenol reagent[10]. The results are given in Table I.

Experiments described below enabled the following identification: fraction I as methyl D-galactoside, fraction II as a mixture of 3,6-anhydro-L-galactose dimethylacetal and methyl D-xyloside, and fraction IV as agarobiose dimethylacetal. From the paper chromatographic examination, there was also obtained an indicative evidence to show that fraction III was a mixture of 3,6-anhydro-L-galactose dimethylacetal and agarobiose dimethylacetal, and that fractions V, VI and VII were mixtures of higher oligosaccharide derivatives. But these fractions were not studied.

Identification of Methyl D-Galactoside. — Fraction I was dissolved in 95% ethanol and the solution left in a refrigerator, when methyl D-galactoside was obtained as crude crystals of monohydrate; yield 0.06 g.; m. p. and mixed m. p. 95~98°; $[\alpha]_D^{12}$ +172° (*c* 0.57 in water); OCH_3, found 14.69% (calculated for $C_6H_{11}O_5(OCH_3)\cdot H_2O$: 14.62%).

The mother liquor was concentrated to a syrup (0.18 g.), which was then subjected to hydrolysis with 1N sulfuric acid in the usual manner, affording D-galactose; yield 0.15 g.; m. p. and mixed m. p. 160°C; $[\alpha]_D^{12}$ +81.3° (an equilibrium value, *c* 0.64 in water).

Separation and Identification of 3,6-Anhydro-L-galactose Dimethylacetal and Methyl D-Xyloside. — Fraction II showed two distinct spots on a paper chromatogram; one was yellowish brown in color, corresponding to 3,6-anhydro-L-galactose dimethylacetal, and the other blue in color, corresponding to methyl D-xyloside. The mixture (0.38 g.) was separated on a column of powdered filter paper, *n*-butanol-water (6 : 1 v/v)

9) C. Araki, This Bulletin, **29**, 543 (1956); *Mem. Fac. Ind. Arts, Kyoto Tech. Univ.*, **5**, 21 (1956).

10) S. Hirase, C. Araki and S. Nakanishi, This Bulletin, **26**, 183 (1953).

* Charcoal used was "Shirasagi", manufactured by Takeda Pharmaceutical Industries, Ltd., Osaka.

TABLE I
CHROMATOGRAPHIC SEPARATION OF THE NEUTRAL METHANOLYSATE

Fraction	I	II	III	IV	V	VI	VII
Developer	W	2% E	5% E	5% E	7.5% E	15% E	30% E
〃 (*l.*)	3.0	3.6	0.7	9.3	3.0	4.0	3.0
Yield (g.)	0.26	0.38	0.10	2.37	0.13	0.62	0.57
$[\alpha]_D$ (° in W)	+98	+17	−22	−27	−10	−4	−19

W: Water E: Ethanol

being used as a mobile phase. The effluents (7 cc. per fraction) were examined on paper chromatograms and the fractions showing the same contents were combined and evaporated to dryness, two main components being recovered as colorless syrups, respectively.

The faster-moving component was proved to be 3,6-anhydro-L-galactose dimethylacetal; yield 0.19 g.; $[\alpha]_D^{12}$ −26.0° (*c* 0.50 in water); OCH_3, found: 28.72% (calculated for $C_6H_{10}O_4(OCH_3)_2$: 29.81%). When hydrolyzed with 0.02 N sulfuric acid in a boiling water bath for two hours, it afforded 3,6-anhydro-L-galactose (0.12 g.) in a syrupy form. The sugar was identified by its conversion into the phenylosazone in the usual manner[11]; m. p. and mixed m. p. 217°C; $[\alpha]_D^{13}$ −52.0° (*c* 0.50 in pyridine-methanol (2 : 3)).

The slower moving component was proved to be methyl D-xyloside; yield 0.10 g.; $[\alpha]_D^{18}$ +28.0° (*c* 0.50 in water). On hydrolysis with N sulfuric acid in the usual manner, it afforded D-xylose in a sirupy form; yield 0.06 g.; $[\alpha]_D^{18}$ +18.8° (*c* 1.28 in water). The sugar was dissolved in one cc. of Breddy and Jones' reagent[7] which consisted of benzaldehyde (4 cc.) and 0.36 N methanolic hydrogen chloride (14 cc.), and the resulting solution was let stand for a week at room temperature. The di-*O*-benzylidene-D-xylose dimethylacetal which formed was filtered off, washed with water and methanol in succession, and dried at 100°C; yield 0.05 g.; m. p. 207～208°C. Recrystallization from chloroform-ligroin afforded needles; m. p. 208～209°C; $[\alpha]_D^{18}$ −10° (*c* 1.0 in chloroform). Admixture with an authentic sample showed no depression of the melting point.

Anal. Found: C, 66.98; H, 6.51. Calcd. for $C_{21}H_{24}O_6$: C, 67.73; H, 6.50%.

Identification of Agarobiose Dimethylacetal.—Fraction IV of the charcoal chromatography was dissolved in ethanol (5 cc.), acetone (5 cc.) added, and the resulting solution was left in a refrigerator. Crystals of agarobiose dimethylacetal were filtered off, washed with ethanol and dried; yield 1.91 g.; m. p. 162～163°C. Recrystallization was best effected by dissolving the crude crystals in hot methanol, adding a double volumes of acetone, filtering the resulting solution while it was hot, and allowing the filtrate to cool. Pure agarobiose dimethylacetal formed colorless prisms; m. p. 165～166°C; $[\alpha]_D^{10}$ −29.3° (*c* 1.50 in water); $[\alpha]_D^{10}$ −38.7° (*c* 1.50 in methanol). Two of the writers report m. p. 162～164°C, $[\alpha]_D$ −29.1° (in water) and $[\alpha]_D$ −37.4° (in methanol)[3], and Clingman, Nunn and Stephen report m. p. 163～166°C and $[\alpha]_D$ −36° (in methanol)[8]. Admixture with an authentic sample showed no depression of the melting point.

Anal. Found: C, 45.20; H, 7.23; OCH_3, 16.74. Calcd. for $C_{12}H_{20}O_9(OCH_3)_2$: C, 45.40; H, 7.07; OCH_3, 16.76%.

Agarobiose Phenylosazone.—Agarobiose dimethylacetal obtained above was heated in 0.02 N sulfuric acid in a boiling water bath for two hours to effect hydrolysis, and the resulting agarobiose was converted into its phenylosazone in the usual manner. The crude osazone obtained was purified by recrystallization from ethanol, forming yellow crystals; m. p. 219～220°C; $[\alpha]_D^{10}$ −136.6° (an initial value, *c* 0.41 in pyridine-ethanol (2 : 3)) → −107.3° (after forty-eight hours). The values reported from this laboratory are m. p. 218～219°C[12], 220～221°C[13] and 221～222°C[13], and $[\alpha]_D$ −108.8°[3] and −110.8°[13] in pyridine-ethanol (2 : 3). Clingman and others report m. p. 222～223.5°C and $[\alpha]_D$ −115° in the same solvent mixture[8]. Admixture with an authentic sample showed no depression of the melting point.

Hexa-*O*-acetylagarobiose Dimethylacetal.—Agarobiose dimethylacetal (0.5 g.) obtained above was acethylated with acetic anhydride (5 cc.) and pyridine (5 cc.) for two days at room temperature. When the reaction solution was poured into a mixture of ice and water with stirring, the hexaacetate was precipitated as fine powders, which were then filtered off, washed with water and dried in vacuo; yield 0.7 g.; m. p. 136～137°C. The crude crystals were recrystallized from methanol-water (1 : 2), affording the pure acetate in stout needles; m. p. 136～137°C; $[\alpha]_D^{10}$ −5.8° (*c* 1.20 in chloroform) and $[\alpha]_D^{10}$ −12.5° (*c* 1.20 in benzene). Two of the writers reported m. p. 87～88°C, $[\alpha]_D$ −5.8° (in chloroform) and −12.5° (in benzene)[3], and Clingman and others report m. p. 137.5～138.5°C and $[\alpha]_D$ −13.5° (in benzene)[8].

Anal. Found: C, 50.11; H, 6.28; OCH_3, 9.66; $COCH_3$, 41.57. Calcd. for $C_{12}H_{14}O_9(COCH_3)_6(OCH_3)_2$: C, 50.16; H, 6.15; OCH_3, 9.97; $COCH_3$, 41.57%.

Since the observed melting point was in disagreement with that reported by two of the writers, acetylation was re-examined for agarobiose dimethylacetal isolated from agar, but the result was exactly the same as that described above. The reason for the discrepancy is obscure.

11) C. Araki, *J. Chem. Soc. Japan*, (*Nippon Kagaku Kaishi*), **65**, 725 (1944).

12) C. Araki, ibid., **65**, 533 (1944).

13) S. Hirase and C. Araki, This Bulletin, **27**, 105 (1954).

Summary

1. The mucilage of *Gloiopeltis furcata* has been subjected to partial methanolysis, which resulted in the isolation of methyl D-galactoside, 3, 6-anhydro-L-galactose dimethylacetal, methyl D-xyloside and agarobiose dimethylacetal.

2. Since the agarobiose derivative was obtained in a good yield, it has been concluded that the disaccharide represents the chief repeating unit of the mucilage molecule, if the sulfate residues present in the mucilage are left out of consideration.

3. Xylose has been identified for the first place so far as the *Gloiopeltis* mucilage is concerned. But the yield was so low that the sugar might be possibly derived from a contaminating xylan.

One of the present writers (S. H.) is obliged for a Grant in Aid for the Miscellaneous Scientific Research from the Ministry of Education for the year 1956—1957.

Institute of Chemistry, Faculty of Industrial Arts, Kyoto Technical University, Matsugasaki, Kyoto

The Determination and the Solubility of Water in Liquid Sulfur Dioxide

By Daisaburo MURAKAMI and Niichiro TOKURA

(Received December 27, 1957)

Liquid sulfur dioxide has been used in a large scale as a selective solvent for separation of aromatic hydrocarbons in petroleum or as bleaching, fumigating, antiseptic, or refrigerating agent. Recently it has been used as a non-aqueous solvent frequently in inorganic and organic synthetic reactions just like liquid ammonia. But it has a defect as a solvent owing to the presence of a small quantity of water. The corrosion of industrial equipments is largely due to minute amount of water contained in it. The amount was therefore defined to be below 50 p.p.m. by the Sulfur Dioxide Committee[1] in U.S.A. in 1933, the required accuracy for the analytical method being 1~2 p.p.m..

It is also anticipated that the reaction process and the rate are largely affected by a minunte amount of water in sulfur dioxide in case of organic ionic reactions. The determination of water in sulfur dioxide was studied for the first time in 1931.[2,3] The method was consisted of a dehydration of water in liquid sulfur dioxide with phosphorus pentoxide. A titration method using the Karl Fischer (abridged as K.F.) reagent was proposed by Karl Fischer in 1935[4] and lately reformed by Dicaprio[5] to make the analysis of water in liquid sulfur dioxide easier. In the dehydration method[2,3] the liquid sulfur dioxide to be analyzed was evaporated, passed through a tube containing phosphorus pentoxide and the water absorbed in the tube was determined. In this method, it was pointed out by Zavarov[3] that an intolerable amount of water yet remained in the dioxide when more than 0.01% of water was contained in the original sample.

In the Dicaprios method[5], it is difficult to pick up the sample accurately, the manipulation is inconvenient as it required a low-and constant temperature room and the K.F. reagent changes in quality by the lapse of the storing time.

The writers have devised a simple and accurate measuring method of water in liquid sulfur dioxide, improving the method of the K.F. titration.

On application of the new method, the solubility curve of water in liquid

1) F. A. Eustass, *Ind. Eng. Chem., Anal. Ed.*, **5**, 77 (1933).
2) A. Scribner, *Ind. Eng. Chem., Anal. Ed.*, **3**, 255 (1931).
3) G. V. Zavarov, *Zavodskaya. Lab.*, **5**, 1314 (1936); J. Mitchell and D.M. Smith, "Aquametry", Interscience Publishers, Inc., New York. p. 236 (1948).
4) K. Fischer, *Angew. Chem.*, **48**, 394 (1935).
5) B. R. Dicaprio, *Anal. Chem.*, **19**, 1010 (1947).

sulfur dioxide at ordinarily adopted temperatures has been traced. Also a convenient method for drying liquid sulfur dioxide is discussed by estimating the residual water in the dried liquid sulfur dioxide by the present analytical procedure. Two points of improvement are involved in this method as shown in the following.

Firstly, as sulfur dioxide constitutes a component of the K.F. reagent, there is no need to use the so called K.F. reagent. It is satisfactory only to add a mixture of iodine and pyridine in methanol (abridged as iodine mixture) to the sample (liquid sulfur dioxide).

Secondly, to avoid the operative difficulties and the loss due to evaporation in sampling, weighing and titration it has been devised to take up the sample in a small glass pressure bottle to be weighed and put into a titration flask, chilled to about −40°C by dry ice.

A K.F. reagent is prepared instantly and caused to react with the water in the sample at the same moment when a definite amount of the iodine mixture is added to the titration flask. The excess of the iodine mixture is back-titrated by an aqueous methanol, of a known water-equivalent value. The iodine mixture can be kept for a long time without change. Accuracy is also raised by the direct weighing of the sample in the pressure bottle before and after the charge into the flask.

As this method is very convenient in its manipulation, it may be used as a rapid routine analysis in factories. The accuracy of this method was found to be satisfactory. The differences between added water (5 to 30 mg.) in the sample and the water found by this procedure were zero to ±0.06 mg.

In the titration flask, the following series of reaction is occurring and, even at −40°C, the K.F. reaction has been proved to proceed quantitatively[6].

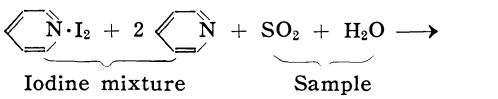

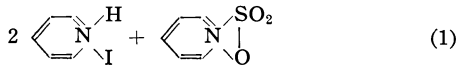

(1)

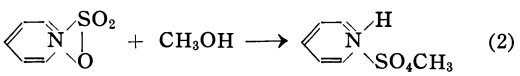

(2)

The solubility of water in liquid sulfur dioxide was measured by Wickert[7] only at 22°C and no other study at different temperatures has been reported. We have measured the solubility of water in liquid sulfur dioxide at various temperatures utilizing the above-mentioned method. (cf. Table I.)

TABLE I
SOLUBILITY OF WATER IN LIQUID SULFUR DIOXIDE

Temp. °C	Solubility g. H_2O/100 g. liq. SO_2
30	2.68
22	2.29
15	1.88
5	1.50
0	1.20
−10	0.81
−20	0.55
−30	0.37
−50	0.22

One part of liquid sulfur dioxide in equilibrium with water in a pressure bottle at a definite temperature was introduced into a small pressure bottle and the water in it was determined by the above described method. Thus the solubility of water in liquid sulfur dioxide in the range between −50°C and +30°C was measured. The solubility at 22°C (2.29 g. H_2O/100 g. liq. SO_2) was well conformed with the Wickert's result (2.3 g. H_2O/100 g. liq. SO_2)[7].

From the solubility value obtained as above, a linear plot of the logarithm of the solubility as a function of the reciprocal

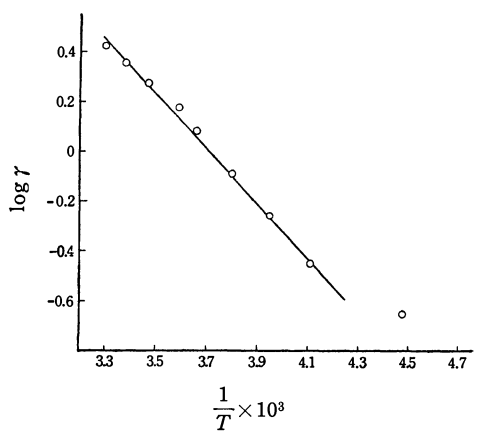

Fig. 1. Solubility of water in liquid sulfur dioxide as a function of temperature.
$\log \gamma = Q/RT + C$ (1), where, Q: heat of solution, γ: solubility, T: absolute temperature, R: gas constant and C: a constant.

6) G. Toennies and M. Elliott, *J. Am. Chem. Soc.*, **59**, 902 (1937).
7) K. Wickert, *Z. anorg. allgem. Chem.*, **239**, 89 (1938).

of the absolute temperature is given in Fig. 1, using the following thermodynamic equation (1): the heat of solution of water in liquid sulfur dioxide is found to be 5.04 kcal./mole (endothermic) for the range between −50°C and +30°C (Table II.).

TABLE II
HEAT OF SOLUTION OF WATER IN LIQ. SO_2
C=4.095 in eq. (1)

Temp. °C	Heat of Soln. Q kcal./mole
30	5.08
22	5.05
15	5.03
5	4.99
0	5.01
−10	5.03
−20	5.04
−30	5.09

Mean Q=5.04 kcal./mole.

Method of the Measurement

(1) Reagents.—Pyridine was dehydrated with potassium hydroxide and distilled. Methanol was dried with metallic magnesium and distilled. Liquid sulfur dioxide was purified and dehydrated with concentrated sulfuric acid and distilled.

The iodine mixture was prepared by mixing the above three materials so that the molar ratio of iodine, pyridine and methanol was to be 1 : 10 : 40. It may be better to increase the quantity of methanol when the water content in the sample was very small. The methanol-water mixture to be used for the back titration was prepared by mixing 1 mole of water with 100 moles of methanol. The water-equivalent value of the iodine mixture and the content of water in aqueous methanol should be previously determined by a standard Karl Fischer's method[4].

(2) Titration apparatus and manipulation.—An ordinary K. F. titration apparatus with conductometrical titrating device was used except that the titrating flask was equipped with a inlet glass tube with a stop cock to connect a small cylindrical pressure bottle (10 cm. long and 2.5 cm. inner diameter) with a valve or cock on its top, containing the sample (Fig. 2).

The flask and the pressure bottle were connected tightly by a couple of jointing screw pieces made of stainless steel. Liquid sulfur dioxide was condensed into this small pressure bottle with cooling and closed. After weighing, the pressure bottle was connected to the titrating flask. Space in the flask was previously replaced with perfectly dried air. The flask was cooled to −40°C with dry ice and ethanol, and the cock of the flask and the valve of the pressure bottle were carefully opened to let the sample flow into the flask. Then the valve and the cock were closed. The pressure bottle was disconnected from the flask and the weight of the empty bottle was

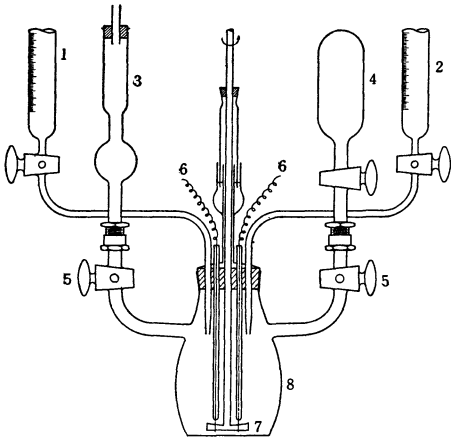

Fig. 2. Titration assembly.
1: Iodine mixture
2: Standard aqueous methanol
3: Drying tube
4: Glass pressure bottle
5: Stainless steel joint
6: Platinum electrode
7: Glass stirrer
8: Titrating flask

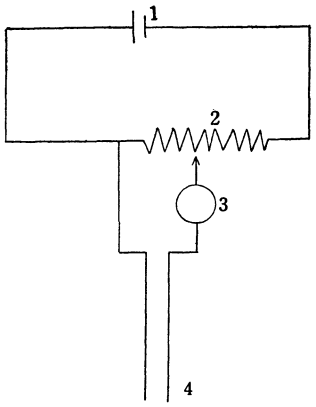

Fig. 3. Circuit diagram.
1: Battery
2: Rheostat
3: Galvanometer
4: Platinum wire electrode.

again examined. When necessary, the sample was diluted with some more liquid sulfur dioxide of a known water content.

As the path between the cock of the flask and the valve or cock of the pressure bottle is very short and made of a thin capillary, the loss due to the wetting or the vaporization of sulfur dioxide is small. The sample was taken to make the water amount about 10 mg. After the sample had been taken up in the titration flask, known amount of iodine mixture was slowly introduced into the flask with stirring and cooling, and its excess was back-titrated with aqueous methanol. The end-point was indicated by applying the dead-stop method (initial E. M. F., 10 mV.) according

to Foulk and Bawden[8,9], a rheostat, a galvanometer, a cell and two platinum electrodes being arranged as shown in Fig. 3.

(3) **Calculation.**—Water content x (g. H_2O/g. liq. SO_2 or 10^{-6} p. p. m. of liq. SO_2) is calculated by the following equation:

$$x = (\alpha A - \beta B)/G,$$

Here A, amount of iodine mixture used (cc.); α, water-equivalent of the iodine mixture (g. H_2O/cc.); B, amount of the aqueous methanol consumed for the back titration (cc.); β, water content of the aqueous methanol (g. H_2O/cc.); G, weight of the sample (g.).

Results and Discussion

(1) **Accuracy.**—To examine the accuracy of the present method, a slight amount of water (5 to 30 mg.) dissolved in methanol was titrated. The result was satisfactory as described above. The difference between the added and the found was less than ± 0.06 mg.

(2) **Solubility of water in liquid sulfur dioxide.**—After equilibrium is reached by heeping a mixture of purified liquid sulfur dioxide and distilled water for four hours in a thermostat maintained at a given temperature, a part of the liquid sulfur dioxide (lower layer) was introduced into another small pressure vessel. The water was then determined by the present method. The equilibrium was obtained within three hours. The fluctuation in temperature was less than ± 0.05°C at above zero degree and ± 0.5°C below zero degree.

The results are shown in Table I, showing an increase in solublility as the temperature increases.

(3) **Heat of solution of water in liquid sulfur dioxide.**—A plot of $\log \gamma$ vs. T^{-1} (Fig. 1) was given as a straight line. The value of C in eq. 1 was determined as 4.095 from the plot. The heat of solution was calculated from equation 1 as 5.04 kcal./mole.

(4) **Comparison of the efficiency of various dehydrating agents for liquid sulfur dioxide.**—Liquid sulfur dioxide was dehydrated using a pressure bottle with various dehydrating agents. Namely, liquid sulfur dioxide (water content: 0.16g./100 g. SO_2) was tapped into pressure bottles filled with a definite amount of concentrated sulfuric acid, phosphorus pentoxide, active alumina, drierite and silica gel, respectively and was allowed to stand for 12 hours for dehydration.

Then the samples were taken up into measuring pressure-bottles and titrated by the present method, the results being as the following: (Table III).

TABLE III

MEASUREMENT OF WATER IN LIQUID SULFUR DIOXIDE DEHYDRATED WITH VARIOUS DRYING AGENTS

Desiccant	Added g.	Liq. SO_2 g.	H_2O p. p. m.
Sulfuric acid	30	180	110
Phosphorus pentoxide	30	180	48
Active alumina	30	180	80
Drierite	30	180	82
Silica gel	30	180	98

It was observed that phosphorus pentoxide had the most powerful dehydrating ability for liquid sulfur dioxide. In the former experiment[10], about one-meter tube filled with phosphorus pentoxide was used for the dehydration of liquid sulfur dioxide which can be replaced by phosphorus pentoxide in a pressure bottle for easier handling with satisfactory result.

A part of the expense used in the present study was defrayed by the Scientific Research Fund of the Ministry of Education. Liquid sulfur dioxde was donated by the Befu Chemical Industries Co., Ltd. Reagents used for this investigation were given by Mr. M. Nuiya, the Reagent Manufacturing Division of the Mitsubishi Chemical Industries Co., Ltd. together with encouraging suggestions. The authors wish to express their sincere thanks to these helps and donations.

Research Institute of Non-aqueous Solutions, Tohoku University, Katahira-cho Sendai

8) C. W. Foulk and A. T. Bawden, *J. Am. Chem. Soc.*, **48**, 2045 (1926).

9) G. Wernimont and F. J. Hopkinson, *Ind. Eng. Chem., Anal. Ed.*, **15**, 272 (1943).

10) K. Ziegler and H. Wollschitt, *Ann.*, **477**, 90 (1930).

Studies on the Proton Transfer in Organic Salts by the Dipole Moment Measurements

By Hiroshi TSUBOMURA

(Received December 21, 1957)

Kraus et al.[1] and Maryott[2] measured independently dipole moments of picrates of alkylamines in benzene and in dioxane solutions, and reported that the dipole moments measured lie between 12 and 13 *D*. As they recognized, these large dipole moments can be explained by assuming that the acid AH and the base B form an ion pair such as $A^-...H-B^+$.

Such a proton transfer from acid to base in non-polar solvents may arise in systems composed of strong acid and strong base. On the other hand, a weak acid such as phenol and a weak proton acceptor such as acetone are known to combine by the usual hydrogen bond A-H...B. In the latter case, the dipole moment usually increases only slightly because of the inductive effect or other intermolecular forces[3]. Hence we can expect the possibility of determining whether an acid-base pair is an ion pair or a hydrogen bonded complex by measuring its dipole moment. Such an investigation will be important for studying the strengths of acids and bases in non-polar solutions.

Customarily, the dissociation constants of acids and bases in aqueous solutions are respectively used as the measure of the acid and the base strength. But they are very complex in their nature, including not only the proton affinities of molecules (namely, the dissociation energies in vacuum) but also the heats of hydration and the entropy terms. On the other hand, in non-polar solvents, the energy and entropy of solvation for the ion pair formation are so small that they may be neglected in the first approximation.

Ultraviolet[4] and infrared[5] absorption measurements have also been used successfully by some authors for the study of acid-base equilibria in non-polar solvents. However, these spectroscopic methods can be applied only to compounds having absorption bands which are easily measurable and vastly affected by the formation of the ion pair. The method of dipole moment measurement has no such limitations and may give in some cases a stronger evidence of the ion-par formation.

Experimental

Measurements of the dielectric constants were made with both the resonance method and the heterodyne beat method. The apparatuses used are described elsewhere[6,7]. Densities were measured with a picnometer.

Preparation and Purification of Materials. —Pyridinium picrate was prepared by mixing the methanol solutions of purified pyridine* and picric acid, followed by recrystallization from methanol, and dried in a vacuum desiccator. Anilinium picrate was prepared from the benzene solutions of aniline and picric acid by a similar method to that described above. Phenol was purified by fractional crystallization, then fused, dried with calcium chloride and distilled under a reduced pressure. Hexamethylenetetramine was recrystallized from ethanol and dried in a vacuum desiccator. Capric acid was purified by distillation. *p*-Nitrophenol was recrystallized from a ethanol-methanol mixture and dried. Triethylamine (the reagent of the Eastman Organic Chemicals Department) was dried with sodium hydroxide and distilled. Acetic acid and trichloroacetic acid are both the guaranteed reagent of the Wako Pure Chemical Industried Ltd. The former was dried with phosphorous pentoxide and distilled, while the latter was used without further purification. Monochloroacetic acid and dichloroacetic acid were purified by distillation under a reduced pressure. Dioxane, benzene and

1) C. A. Kraus, *J. Phys. Chem.*, **60**, 129 (1956); G. S. Hooper and C. A. Kraus, *J. Am. Chem. Soc.*, **56**, 2265 (1934); J. A. Geddes and C. A. Kraus, *Trans. Faraday Soc.*, **32**, 585 (1936).

2) A. A. Maryott, *J. Res. Nat. Bur. St.*, **41**, 1, 7 (1948).

3) H. Baba and S. Nagakura, *J. Chem. Soc. Japan, Pure Chem. Sec. (Nippon Kagaku Zassi)*, **72**, 3 (1951).

4) A. Nisonoff, L. P. Kuhn and R. W. Gurney, *J. Chem. Phys.*, **20**, 985 (1952); M. M. Davies and H. B. Hetzer, *J. Res. Nat. Bur. St.*, **48**, 387 (1952); M. M. Davis and E. A. McDonald, ibid., **42**, 595 (1949).

5) G. M. Barrow and E. A. Yerger, *J. Am. Chem. Soc.*, **76**, 5211, 5248 (1954); **77**, 4474, 6206 (1955); **78**, 5802 (1956).

6) S. Nagakura and A. Kuboyama, *Repts. Inst. Sci. Technol. Univ. Tokyo*, **4**, 242 (1950).

7) K. Kozima and T. Yoshino, *J. Am. Chem. Soc.*, **75**, 166 (1953).

* This was kindly offered by Dr. T. Tamura of this Laboratory.

carbon tetrachloride were dried with sodium, phosphorous pentoxide and calcium chloride, respectively, and distilled.

Experimental Results and Method of Calculation

The results of the measurements are given in Tables I–IX, where n_a and n_b are concentrations of acids and bases in unit of mole/g. of the solution, ε is the dielectric constant and v the specific volume. x_c in Table I denotes the concentration of the salt in unit of mole fraction. For the calculation of the dipole moments, the stoichiometric formation of the acid-base complex was assumed, irrespective of whether it is an ion pair or a hydrogen bond complex, because it is known that the equilibrium constant for the hydrogen-bond formation between acid and base molecules is very great[4,8]. As for the solution where the base is present excessively, therefore, the concentration of the free base was taken as equal to $n_b - n_a$**. For the hexamethylenetetramine-phenol system only, the dissociation is not small enough to be neglected. In this case, the concentration of the complex was calculated by use of the dissociation constant of the system determined by the previous infrared spectroscopic measurement[8].

If we assume that, in dilute solutions, the distances between dipoles are so large that their interactions are negligibly small, the polarization of the solution per one gram of the solution may be expressed as follows:

$$p = (\varepsilon - 1)v/(\varepsilon + 2) = \sum_j n_j P_j \qquad (1)$$

TABLE I
PYRIDINIUM PICRATE
Solvent: dioxane. at 15°C

$x_c \times 10^4$	v	ε
0.000	0.96321	2.239
2.376	0.96256	2.277
4.340	0.96182	2.305
6.824	0.96098	2.355

$\varepsilon = 2.237 + 167.9\, x_c$
$v = 0.96326 - 3.31\, x_c$
$P_c = 2380$, $\mu = 10.43D$

TABLE II
ANILINIUM PICRATE
Solvent: dioxane. at 23°C

$n_c \times 10^5$	v	ε	P_c
0.000	0.97134	2.2265	
1.343	0.97025	2.3030	980
2.696	0.96890	2.4262	1218

P_c(average) = 1099 $\mu = 7.0D$

TABLE III
TRICHLOROACETIC ACID-TRIETHYLAMINE
Solvent: dioxane. at 20°C

$n_a \times 10^5$	$n_b \times 10^5$	v	ε	P_c
0.000	0.000	0.96771	2.2253	
0.5739	2.283	0.96818	2.3003	2130
1.856	4.774	0.96804	2.4329	1784

P_c(average) = 1957 $\mu = 9.6D$

TABLE IV
DICHLOROACETIC ACID-TRIETHYLAMINE
Solvent: dioxane. at 25°C

$n_a \times 10^5$	$n_b \times 10^5$	v	ε	P_c
0.000	0.000	0.97360	2.2258	
1.293	8.318	0.97619	2.3286	1290
2.261	14.548	0.97791	2.3953	1201
4.019	25.86	0.98124	2.5191	1375

P_c(average) = 1289 $\mu = 7.76D$

TABLE V
MONOCHLOROACETIC ACID-TRIETHYLAMINE
Solvent: dioxane (the same material as used in the above system). at 25°C

$n_a \times 10^5$	$n_b \times 10^5$	v	ε	P_c
1.714	9.800	0.97654	2.3461	1134
2.748	16.95	0.97900	2.4173	1110
4.959	34.23	0.98498	2.5610	1049

P_c(average) = 1098 $\mu = 7.15D$

TABLE VI
ACETIC ACID-TRIETHYLAMINE
Solvent: benzene. at 25°C

$n_a \times 10^5$	$n_b \times 10^5$	v	ε	P_c
0.000	0.000	1.14427	2.2724	
0.5453	1.784	1.14445	2.2826	388
1.336	3.761	1.14467	2.2943	349
2.780	8.790	1.14505	2.3206	360

P_c(average) = 366 $\mu = 3.96D$

8) H. Tsubomura *J. Chem. Phys.*, **23**, 2130 (1955).

** Barrow et al. have proposed, by the measurements of the infrared spectra of carboxylic acid-amine systems in non-polar solvents, that in the solution there are two molecular species, I and II, which have the composition of $(Acid)_2 \cdot Amine$ and $Acid \cdot Amine$, respectively. In this paper, the dipole moment of the carboxylic acid-amine complex was calculated under the assumption that all the acid molecules in the solution are converted into species II. For the dioxane solutions of triethylammonium salts of mono-, di- and tri-chloroacetic acids, this assumption seems to be valid because it is known that many carboxylic acids exist as monomers in dioxane solution[9], and under such a condition the formation of I is considered to be impossible. As for the case of acetic acid-triethylamine-benzene system, the validity of the assumption is not quite sure. In carrying out the measurement of this system, therefore, we made the concentration of triethylamine many times greater than that of acetic acid in order to increase the concentration of species II. Hence, even if the species I exists in the solution, its concentration will be small compared with the total acid concentration, and it is considered that the conclusion given later is essentially unaltered.

9) R. J. W. Le Fèvre and H. Vine, *J. Chem. Soc.*, **1938**, 1795.

TABLE VII

p-NITROPHENOL-TRIETHYLAMINE

Solvent: dioxane. at 20°C

$n_a\times10^5$	$n_b\times10^5$	v	ε	P_c
0.000	0.000	0.96825	2.2299	
0.9517	1.3826	0.96836	2.2689	721
1.1935	1.7125	0.96843	2.2786	720

P_c(average) = 721 $\mu = 5.57D$

TABLE VIII

PHENOL-HEXAMETHYLENETETRAMINE

Solvent: carbon tetrachloride. at 27°C

$n_a\times10^5$	$n_b\times10^5$	$1/v$	ε	P_c
0.000	0.000	1.58062	2.2179	
2.721	0.000	1.57852	2.2310	77.3*
2.711	2.535	1.57791	2.2402	158
2.727	1.661	1.57475	2.2364	151

P_c(average) = 155 $\mu = 2.05D$

* Molecular polarization of phenol. From it the dipole moment of phenol is calculated to be 1.55*D*.

TABLE IX

CAPRIC ACID-HEXAMETHYLENETETRAMINE

Solvent: carbon tetrachloride (the same material as used in the above system). at 27°C

$n_a\times10^5$	$n_b\times10^5$	$1/v$	ε	P_c
1.820	2.271	1.57475	2.2256	136

$\mu = 1.50D$

TABLE X

	P_E+P_A	μ
pricric acid[a]	43.0	1.55
phenol	28.0	1.55
p-nitrophenol[b]	37.2	5.0
acetic acid[c]	12.8	1.7
monochloroacetic acid[9]	17.9	2.6[d]
dichloroacetic acid[9]	23.0	2.6[d]
trichloroacetic acid[9]	28.1	2.6[d]
capric acid[e]	49.6	1.7
hexamethylenetetramine[11]	41.0	0.0
triethylamine[10]	33.7	0.8
pyridine[f]	24.0	2.2
aniline[g]	32.0	1.9

a The P_E+P_A of this compound is estimated from those of *p*-nitrobenzene, and *p*-nitrophenol. The dipole moment is taken equal to that of phenol.

b Donle and Gehrckens, *Z. phys. Chem.*, **B18**, 316 (1932).

c C. T. Zahn, *Phys. Rev.*, **37**, 1516 (1931); Wilson and Wenzke, *J. Chem. Phys.*, **2**, 546 (1934).

d Taken as equal to the moment of the ethyl ester.

e The P_E+P_A of this compound is calculated by use of the polarizations of atoms. The moment is assumed as equal to that of acetic acid.

f Leis and Curran, *J. Am. Chem. Soc.*, **67**, 79 (1945).

g Kumler and Halverstadt, ibid., **63**, 2182 (1941).

TABLE XI

Acid	Base	(Debye units) μ_{obs}	μ_s	$\Delta\mu$
picric acid	pyridine	10.43	3.4	7
picric acid	aniline	7.0	1.8	6
trichloroacetic acid	triethylamine	9.6	3.0	8
dichloroacetic acid	triethylamine	7.76	3	7
monochloroacetic acid	triethylamine	7.15	3	6.5
acetic acid	triethylamine	3.96	2.2	3
p-nitrophenol	triethylamine	5.57	5.4	0.3
capric acid	H. M. T.*	2.05	1.55	0.5
phenol	H. M. T.	1.50	1.70	−0.2

* Hexamethylenetetramine

where n_j denotes the n value of each component, and P_j is its molecular polarization. In general, there are four components in the solution: the solvent, the free acid, the free base and the complex. From Eq. 1, the molecular polarization of the complex, P_c, can be calculated, when the polarizations of the other components are known. The polarization of the solvent is derived from the measurement of the pure solvent. The P_j values of the free acid and base need not be very accurate, because their concentrations in the solution are very small. The P_j value of triethylamine was set equal to 46.6 cc. for the benzene solution[10], and to 47.2 cc. in the dioxane solution. The latter value was obtained from the measurement of ε and v of the dioxane solutions of triethylamine. For the system composed of hexamethylenetetramine and phenol, the polarization of the former was taken as

10) K. Higasi, *Sci. Pap. Inst. Phys. Chem. Res.*, **31**, 311 (1937).

41.0 cc.[11] and that of the latter was experimentally obtained with the present sample of phenol (Table VIII).

Kraus et al.[1] stated that, for solutions of some salts with large dipole moments, the measured molecular polarization of the salt decreases rapidly with increasing concentration even in the range of the concentration of 10^{-4} mole fraction. They attributed this as due to the association of the polar salts. Maryott[2] observed, however, that the molecular polarizations of similar salts are nearly constant up to more concentrated solutions, when dioxane is used as the solvent. Also, in the present measurement with the pyridinium picrate solutions, it was found that the P_c values obtained from each solution by use of Eq. 1 agree well with that derived by the method of Halverstadt and Kumler[12]. From these facts, it may be inferred that the effect of association is negligibly small in the dioxane solutions with the range of concentration of the present measurements. In the present investigation, salts with large dipole moments are measured in the dioxane solutions, while other salts (or hydrogen bonded complexes) with smaller dipole moments, where the effect of association will be small, are measured in benzene or carbon tetrachloride solutions. The P_c values obtained by use of Eq. 1 are, therefore, considered to be a good approximation to the true P_c values. They are listed in Table II–IX. The P_c value given in Table I is that obtained by Halverstadt and Kumler's method.

The orientation polarization of the salt was calculated by subtracting from P_c the electronic and atomic polarization of the complex, which were assumed as equal to the sum of those of the free acid and base. The values used were taken from literatures and reproduced in Table X, where the dipole moments of free acids and bases are also listed. The dipole moments of the acid-base complex calculated from the orientation polarizations thus obtained are given in Table I–IX.

Discussion

If the dipole moments of the acid and base in the complex remain the same as those of the free acid and base, the dipole moment of the complex will be given by the vector sum of these two moments. Let it be called the structure moment and denoted by μ_s. Now, if the observed dipole moment of an acid-base complex is very large compared with its structure moment, the complex is conceivably an ion pair. In order to calculate the structure moments, it is assumed that none of the acid and base molecules changes the structure on the complex formation, and that the OH.....N group is on a straight line. The direction of the dipole-moment vectors of the polar molecules are estimated on the basis of the bond moment data and the consideration of the resonance moments. Based on these assumptions, the structure moments are obtained as shown in Table XI. It is readily seen that the first five systems given in Table XI have the form of the ion pair, and that the last three systems are essentially hydrogen bonded complexes.

From the theoretical point of view, the dipole moment produced by the proton transfer can be estimated by assuming the electronic structure of the ion pair as follows:

$$O^-.....H—N^+$$

where the H—N^+ bond is purely covalent. The O.....N distance may be taken as 2.6 Å, because the lengths of the OH.....N hydrogen bonds are in general about 2.8Å, and a slight contraction is expected in the case of the ion pair. Hence, if we assume, as a first approximation, that the positive and the negative charge are, respectively, centered at the nitrogen and the oxygen nucleus, the dipole moment arising from this proton transfer is calculated as $4.80\times10^{-10}\times2.6\times10^{-8}=12.5D$. Actually, even in the case of a complete proton transfer, the dipole moment due to the proton transfer is conceivable somewhat smaller than this value, because the electronic cloud of the two molecules would be distorted so as to decrease the strong field of the dipole produced by the transfer.

Thus we have seen that there is a large dipole moment in the ion pair directed along the OH.....N straight line with the positive end on the nitrogen atom. In Table XI, $\Delta\mu$ represents the dipole moment with the above-mentioned direction, whose magnitude is so determined that the vector sum of this and μ_s is equal to the observed moment of the complex. For the tri-*n*-butylammonium picrate, the

11) R. J. W. Le Fèvre and G. J. Rayner, *J. Chem. Soc.* **1938**, 1921.
12) I. F. Halverstadt and W. D. Kumler, *J. Am. Chem. Soc.*, **64**, 2988 (1942).

dipole moment of which was determined by Maryott as 11.9 D, the $\Delta\mu$ value is calculated to be 9.6 D. If one assumes that this complex is a pure ion pair, then, by inspection of the $\Delta\mu$ values in Table XI, it may be confimed that pyridinium picrate, trichloroacetic acid-triethylamine complex, and dichloroacetic acid-triethylamine complex are almost complete ion pairs. As for the two systems, anilinium picrate, and monochloroacetic acid-triethylamine complex, it is recognized that the $\Delta\mu$ values are a little smaller than those for the above mentioned complexes. In regard to the arbitrariness of the calculated $\Delta\mu$ values, however, it will be rather safe to make no distinction between these five systems***.

Among the remaining four systems, acetic acid-triethylamine has an appreciable $\Delta\mu$ value. It seems that in this complex there is an "incomplete proton transfer" that may be explained by either of the following two theories. The one is that the ground state of such a complex may be represented by the resonance,

$$\text{O—H.....N} \rightleftarrows \text{O}^-\text{.....H—N}^+$$

in which the contributions of the two resonance structures have the same order of magnitude. This occurs in the cases where the potential curve for the proton in the complex has a single minimum near the center of the O.....N straight line. Another explanation is that there is a tautomeric equilibrium between the ion pair and the hydrogen bonded complex. In this case, the potential curve has two minima: one near the oxygen atom and the other near the nitrogen atom, and the proton oscillates between them. At the moment, it is difficult to decide which is the correct theory. Anyway, it may be inferred from the dipole moment that acetic acid-triethylamine complex is more like a hydrogen bonded complex than an ion pair.

Relation between the Dipole Moment and the Proton Affinity.—The energy required for the proton transfer reaction, $AH+B=A^-.....H—B^+$, in vacuo, is generally expressed as follows,

$$E=PA(A^-)-PA(B)+E_{i.p.} \qquad (2)$$

where $PA(A^-)$ is the energy required to remove proton from the acid AH, that is, the proton affinity of the anion A^-, and $PA(B)$ is that of the base B. $E_{i.p.}$ is the energy necessary for bringing the anion and cation from infinite separation to the position which they occupy in the ion pair. In the non-polar solvents, where solvation energy is small, the above formula may be applied approximately with no alteration. Assuming that $E_{i.p.}$ is constant for all the acid-base pairs that have the common O...H...N groups, the energy to produce an ion pair becomes the smaller, the smaller $\{PA(A^-)-PA(B)\}$ is. $PA(A^-)$ and $PA(B)$ are, respectively, related to the acid and base strength, and, therefore, it may be interesting to compare the ability of the ion-pair formation and the dissociation constants of acid and base in aqueous solutions.

Fig. 1 was drawn under this supposition, where the two axes indicate $-\log K_a$ and $-\log K_b$ of the acid and the base of a given complex. The systems which are concluded to have the structure of the ion pair are denoted by a small circle and those which are concluded to have the structure of the hydrogen bonded complex are denoted by the symbol ×. Acetic acid-triethylamine complex is regarded to be in the intermediate state. It can be seen that there is certainly a relation

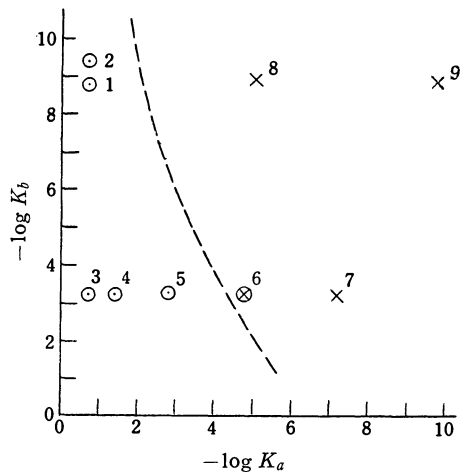

Fig. 1. Relation between the structure of acid-base complexes and the acid and base strength of their component molecules.
1. picric acid-pyridine
2. picric acid-aniline
3. trichloroacetic acid-triethylamine
4. dichloroacetic acid-triethylamine
5. monochloroacetic acid-triethylamine
6. acetic acid-triethylamine
7. *p*-nitrophenol-triethylamine
8. capric acid-hexamethylenetetramine
9. phenol-hexamethylenetetramine

*** For the case of mono- and dichloroacetic acid, the results of calculation of $\Delta\mu$ become more ambiguous owing to the possible existence of the rotational isomers.

between the ability to form ion pairs and the pK values. And the curve drawn in the figure may show roughly the limit of the pK's of acids and bases to produce ion pairs.

Shirai[13] has recently measured dipole moments of salts of dodecylamine with various carboxylic acids of the general formula $C_nH_{2n+1}COOH$ in benzene solution. The obtained values range between 1.5*D* and 2.2*D*. These values are much smaller than the dipole moment of acetic acid-triethylamine complex obtained in the present measurement, showing that the dodecylamine-carboxylic acid complexes are essentially hydrogen bonded complexes. This result may be interpreted as showing that dodecylamine is less basic than triethylamine, a result that is reasonable from the electronic theory.

In the polar solvents, the proton transfer is very much facilitated because of the large solvation energy. In the present investigation, it was observed that the dioxane solution of *p*-nitrophenol and triethylamine, which does not form the ion pair and has a faint yellow color, becomes very intensely yellow when diluted with methanol. This shows that the acid-base pair will become the ion pair or solvated ions in the more polar solvent, methanol.

The author wishes to express his sincere thanks to Professor S. Nagakura for his encouragement and helpful advice.

The Institute for Solid State Physics
University of Tokyo
Komaba, Meguro-ku, Tokyo

13) M. Shirai, *Sci. Pap. Coll. Gen. Educ., Univ. Tokyo*, **6**, 147 (1956).

Reactions of Active Methylene Compounds. III. A New Synthesis of 4-Hydroxy-3-phenylcoumarins

By Yoshiyuki KAWASE

(Received January 13, 1958)

In a previous paper[1], the author reported a preparation of 2-methoxybenzoyl-phenylacetonitriles (I), ethyl 2-methoxybenzoyl-phenylacetates (II), and 2-hydroxyphenyl benzyl ketones by ester condensation and subsequent ethanolysis and hydrolysis. In connection with it, a new synthesis of 3-aryl-4-hydroxycoumarins has been developed, and the preparation of 4-hydroxy-3-phenyl-coumarin (IVa) and its 7-methoxy-derivative (IVb) is reported in this paper.

4-Hydroxy-3-phenylcoumarins have hitherto been prepared by the following four methods:

(A) The cyclization of *o*-phenylacetoxy-derivatives of the benzoic ester with sodium at a high temperature[2].

(B) The interaction of phenols with diethyl phenylmalonate[3] or the cyclization of phenyl phenylmalonates[4] at a high temperature.

(C) The interaction of *o*-acetoxybenzoyl chloride with ethyl sodio-phenylacetate and subsequent hydrolysis[5].

(D) The cyclization of 2-hydroxyphenyl benzyl ketones by carbethoxylation with ethyl carbonate or ethyl chloroformate[6].

In the present work, the action of anhydrous aluminum chloride on the nitriles I in nitrobenzene caused demethylation and subsequent cyclization to give 4-hydroxy-3-phenylcoumarin-2-imides (III), which were also obtained by ester condensation of methyl 2-hydroxybenzoates with phenylacetonitrile. These imides III were soluble in hydrochloric acid, and seemed to be keto-forms because of their negative ferric reaction in ethanol and of their insolubility in cold aqueous alkali. The imides III

1) Y. Kawase, This Bulletin, **31**, 336 (1958).

2) a) H. Pauly and K. Lockemann, *Ber.*, **48**, 32 (1915). b) M. A. Stahmann, I. Wolff and K. L. Link, *J. Am. Chem. Soc.*, **65**, 2285 (1943).

3) G. Urbain and C. Mentzer, *Bull. soc. chim.*, **11**, 171 (1944); C. Mentzer, D. Molho, and P. Vercier, *Bull. soc. chim. France*, **1949**, 749; P. Vercier, D. Molho and C. Mentzer, ibid., **1950**, 12480.

4) E. Ziegler and H. Junek, *Monatsh.*, **86**, 29 (1955): **87**, 217, 789 (1956).

5) B. S. Wildi, *J. Org. Chem.*, **16**, 407 (1951).

6) J. Boyd and A. Robertson, *J. Chem. Soc.*, **1948**, 174: A. H. Gilbert, A. McGookin and A. Robertson, ibid., **1957**, 3740.

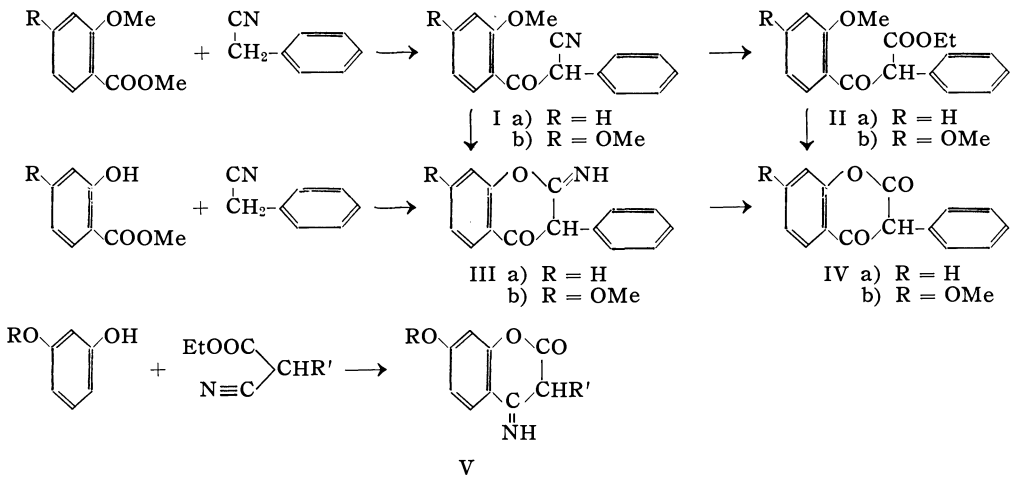

V

gave 4-hydroxy-3-phenylcoumarins (IV)' when hydrolyzed with hydrochloric acid, and while salicylic acid and its 4-methoxy-derivative with aqueous sodium hydroxide. These coumarins IV were also obtained from ethyl 2-methoxybenzoyl-phenylacetates II by the action of anhydrous aluminum chloride in nitrobenzene; they were soluble in aqueous sodium carbonate, and supposed to be in keto-forms from their negative ferric reaction in ethanol.

It had been reported that the condensation of ethyl cyanoacetate with phenols according to the method of Hoesch gives 4-hydroxycoumarin-4-imides[7] (V, R=R'=H). So an attempt was made to prepare 4-hydroxy-3-phenylcoumarin-4-imides (V, R'=Ph), isomers of the imides III, from ethyl phenylcyanoacetate and resorcinol or resorcinol monomethyl ether by the Hoesch reaction, but it resulted in a failure, giving only a small amount of phenylmalonmonoamide ethyl ester[8].

Experimental[9]

4-Hydroxy-3-phenylcoumarin-2-imide(IIIa). (*a*) *From nitrile I a.* — A mixture of 0.7 g. of nitrile I a[1] and 1.5 g. of anhydrous aluminum chloride in 5 cc. of nitrobenzene was heated for two hours on a steam bath. The cooled solution was treated with water, and nitrobenzene was driven off by steam distillation. The residual aqueous mixture was extracted with ether, and the ethereal solution was then extracted with dilute hydrochloric acid. The acid aqueous solution was made alkaline with sodium bicarbonate, and the solid product which separated was recrystallized from ethanol. Colorless microcrystals, m. p. 219.5~220.5°. Yield 0.2 g., identical with the other sample from (b).

(*b*) *By ester condensation.* — To a suspension of dry sodium ethoxide (from 2 g. of sodium) in 50 cc. of absolute benzene, a mixture of 6.5 g. of methyl 2-hydroxybenzoate and 5 g. of phenylacetonitrile was added, and the mixture was heated at about 100° on an oil bath for four hours while most of benzene was driven off with the ethanol produced. Dilute hydrochloric acid was added to the well-cooled resulting mixture, which was extracted with ether. Ether and the unchanged starting materials were driven off by steam distillation. The residual aqueous mixture was treated as before to give the product, colorless microcrystals, m. p. 223~4°, yield 1.5 g.

Anal. Found: C, 76.03; H, 4.97; N, 5.40. Calcd. for $C_{15}H_{11}O_2N$: C, 75.93; H, 4.67; N, 5.90%.

When 2 g. of sodium hydride was used instead of dry sodium ethoxide, the yield was 1.3 g., m. p. 219~220°, from 5 g. of methyl salicylate and 4 g. of phenylacetonitrile.

4-Hydroxy-3-phenylcoumarin (IVa). (*a*) *From imide III a*—A solution of 0.5 g. of imide III a in 10 cc. of dilute hydrochloric acid (1 : 1) was heated for three hours on a steam bath. A crystalline product separated from the warm solution was collected and recrystallized from ethanol to give the product in colorless needles, m. p. 231~2°, yield 0.25 g. The reported melting point is 230°[4], 234~5°[2b], 236°[2a], 237~8°[5], and 240°C[3].

Anal. Found: C, 75.41; H, 4.43. Calcd. for $C_{15}H_{10}O_3$: C, 75.62; H, 4.23%.

(*b*) *From ester II a.*—A mixture of 0.9 g. of ester II a[1] and 2 g. of anhydrous aluminum chloride in 5 cc. of nitrobenzene was heated for one and a half hours on a steam bath. Water was added to the cooled solution, and nitrobenzene was driven off by steam distillation. The residual aqueous mixture was extracted with ether, and the ethereal solution was then extracted with aqueous sodium hydroxide. The soild product separated from the alkaline solution by acidification was purified from ethanol. Colorless needles,

7) A. Sonn, *Ber.*, **50**, 1292 (1917); K. H. Bauer and F. Schoder, *Arch. Pharm.*, **259**, 53 (1921); cf. E. Ziegler, G. Wildtgrube and M. Junek, *Monatsh.*, **88**, 164 (1957).

8) W. Wislicenus and K. Goldstein, *Ber.*, **29**, 2602 (1896).

9) All melting points are uncorrected.

m. p. 229~230°, yield 0.5g., identical with the other sample from (a).

4-Hydroxy-7-methoxy-3-phenylcoumarin-2-imide (III b). (*a*) *From nitrile I b.*—From 1 g. of nitrile I b[1] and 1.9 g. of anhydrous aluminum chloride in 5 cc. of nitrobenzene, 0.2 g. of the compound was obtained by the same operation described before, colorless microcrystals, m. p. 232~232.5° (from ethanol).

Anal. Found: C, 71.52; H, 5.04; N, 5.42. Calcd. for $C_{16}H_{13}O_3N$: C, 71.90; H, 4.90; N, 5.24%.

(*b*) *By ester condensation.*—To a suspension of dry sodium ethoxide (from 0.6 g. of sodium) in 50 cc. of absolute benzene, a mixture of 2 g. of methyl 2-hydroxy-4-methoxybenzoate and 1.4 g. of phenylacetonitrile was added, and the mixture was treated as before to give 0.2 g. of the product, m. p. 230~1°, identical with the other sample from (a). When 0.3 g. of sodium hydride was used instead of dry sodium ethoxide, the yield was 0.1 g., m. p. 229~230°, from 1.2 g. of ester and 0.8 g. of nitrile.

4-Hydroxy-7-methoxy-3-phenylcoumarin (IV b). (*a*) *From imide III b.*—From 0.1 g. of imide III b, 40mg. of the compound was obtained by the same operation described before, colorless microcrystals, m. p. 196~7° (form dilute ethanol), identical with the other sample from (b).

(*b*) *From ester II b.*—From 0.4 g. of ester II b[1] and 0.9 g. of anhydrous aluminum chloride, 50 mg. of the compound was obtained by the same operation described before, m. p. 196~7°. The reported melting point is 202°[3] and 204°[6].

Anal. Found: C, 71.33; H, 4.62. Calcd. for $C_{16}H_{12}O_4$: C, 71.63; H, 4.51%.

The author wishes to express his hearty thanks to Professor K. Fukui for his helpful advice and encouragement, and to the members of the Agricultural Department of Kyoto University for microanalyses.

Faculty of Literature and Science
Toyama University, Toyama

A New Viscosity Relationship in a Wide Concentration Range of Aqueous Solutions of Potassium Chloride

By C. V. SURYANARAYANA and V. K. VENKATESAN*

(Received December 14, 1957)

Viscosity of strong electrolytes in dilute solutions conformed to an equation given on experimental basis by Jones and Dole[1] and Joy and Wolfenden[2]. This equation fails at higher concentrations. So far no equation satisfactorily explained the quantitative relationship between viscosity and concentration in the entire range from infinite dilution up to saturation. In a recent[3] systematic study by us, of electrical conductance of highly concentrated solutions of strong electrolytes up to saturation, we have derived a new concept of concentration and a modified viscosity term. In brief, the following is the basis of the new formulations.

A new concept of concentration.—Let

$$P = f(X) \qquad (1)$$

represent the physical property of a solution at a given temperature for a given solvent as a function of 'X', the mole fraction concentration of the solute. When we compare the physical property 'P' of solutions of different solutes in the same solvent, it is clear that in equation (1) 'X' can not have all possible values from zero to unity. For each electrolyte 'X' can vary from the common zero limit in all cases to the saturation limit at which the mole-fraction of the solute is not unity. Further the mole-fraction concentration at saturation is different for different electrolytes in the same solvent. If 'X' values vary in an identical range, the 'P' values of different salt solutions will be comparable at the same temperature. In other words, in the extreme limit of saturation, for different salt solutions the 'X' values must be such that they tend to an identical limit at which the 'P' values in their limit will be comparable even though they will not be identical. Therefore there is need for a new concept

* Present Address: Central Electrochemical Research Institute, Karaikudi, India.

1) G. Jones and M. Dole, *J. Am. Chem. Soc.*, **51**, 2950 (1929).

2) W. E. Joy and J. H. Wolfenden, *Proc. Roy. Soc.* (London), **A134**, 413 (1931).

3) C. V. Suryanarayana and V. K. Venkatesan, *Nature*, **178**, 1461 (1956).

of concentration (X^1) such that, at a given temperature, its value varies between the same limits for different electrolyte solutions. We may write

$$P = f(X^1) \qquad (2)$$

such that 'X^1' is the ratio of the mole-fraction of the solute at any given molal concentration to that at saturation at the same temperature. Such a ratio should tend to unity at saturation for all solutions at all temperatures irrespective of the nature of the solute and the solvent. This ratio of mole-fractions, was called by us the "concentration potential" (C_p). Now it is clear that a given physical property of a solution plotted against its "concentration potential" will be a curve worthy of comparison with similar ones for different electrolytes in a given solvent. The concentration potential newly conceived herein is a truly thermodynamic concept of concentration dependent only on the initial and final states of stability of a solution and independent of any arbitrary scale of concentration or the nature of both the solvent and the solute.

A new concept of viscosity.—So far in literature the relative viscosity of a solution has been relative to the solvent and our modification consists in making it relative to that at saturation at the same temperature. This modified viscosity term (η_p), as with the concentration potential, will tend to a maximum of unity at saturation for all electrolyte solutions.

Some previous workers[4~20] collected viscosity data for potassium chloride solutions in different ranges of concentrations at a few temperatures. We have measured viscosity of potassium chloride solutions from 1.00 molal to saturation, at temperatures of 30 to 55°C.

Experimental

All solutions were made by weighing water and the required amount of solute to make a certain wanted molal concentration. A 100 cc. pyrex beaker was weighed and the process repeated after adding about 50 cc. of water. Exactly the required amount of a salt was weighed into the beaker. After gentle stirring of the solution the whole of it was transferred and kept in a well-stoppered 250 cc. pyrex bottle. This solution was used for finding the viscosity and density. All solutions except at saturation were thus made so that the concentration was independent of volume. The potassium chloride used was of guaranteed quality. Viscosity measurements were made using an Ostwald viscometer kept in a Gallenkamp b-12210 thermostat provided with a glass tank and giving an accuracy ±0.05°C. At saturation, viscosity determination required great care and repeated verification. A pyrex beaker containing the saturated solution in equilibrium with the undissolved salt was kept stirred continuously by a mechanical stirrer. After attainment of equilibrium an aliquot amount of the saturated solution was sucked through a tube plugged with cotton wool and attached to a pipet. The pipet itself was kept at the same temperature of the thermostat to avoid crystallization of the saturated solution. Soon after withdrawing into the pipet the glass-tube stuffed with cotton wool was quickly disconnected and the solution was transferred into the viscometer. After sufficient repetitions the whole technique could be mastered.

Density determination.—Density was determined in each case using the density bottle whose volume was ascertained by knowing the weight of water filling it at a known temperature and making use of exact density of water at the same temperature from tables given in Lange[21]. The density of the saturated solution was determined by weighing the volume of solution transferred by a calibrated pipet.

Solubility data of each salt at different temperatures were obtained from Seidell's "Solubilities of Organic and Inorganic Compounds"[22]. Results obtained are given in Table I.

Discussion

Figs. 1 and 2 show plots of $\log \eta_p$ vs. C_p at each temperature. At temperatures of 35, 40, 45, 50 and 55°C the plots are straight lines. Only at 30°C the plot though not a straight line, is made up of

4) J. Wagner, *Z. Phys. Chem.*, **5**, 31 (1890).
5) R. Reyer, ibid.. **2**, 744 (1888).
6) H. Brückner, *Wied. Ann.* **42**, 294 (1891).
7) R. Hoskings, *Phil. Mag.*, (6), **17**, 502 (1909).
8) A. Sprung. *Pogg. Ann.* **159**, 1 (1876).
9) W. Herz, *Z. anorg. Chem.*, **86**, 338-40 (1914).
10) K. Hrynakowski, *Iszy zjazd chemikow Polskich*, **1923**, 16-7.
11) H. N. Desai. D. B. Naik and B. N. Desai, *J. Univ. Bombay*, **3**, 109-20 (1934).
12) H N. Desai, D. B. Naik and B. N. Desai, *Curr. Sci.*, **2**, 206 (1933).
13) W. J. Sulston, *Proc. Phys. Soc.*, **47**, 657 (1935).
14) G. Jones and S. K. Talley, *J. Am. Chem. Soc.*, **55**, 624 (1933).
15) J. D. Ranade and G. Paranjpe, *J. Univ. Bombay*, **7**, Pt. 3, 41 (1938).
16) G. Ajon, *Chim. ind. agr. biol.* **17**, 474 (1941); *Chem. Zent.*, **1942**, I, 2856.
17) A. S. Chakravarti, *J. Indian Chem. Soc.*, **20**, 41 (1943).
18) T. Okaya and R. Takeuchi, *Proc. Phys. Math. Soc. Japan*, **25**, 639 (1943).
19) C. Drucker, *Arkiv kemi, Mineral Geol.*, **A22**, No. 21, 17 pp. (1946) (in English).
20) G. Ajon, *Ann. regiastaz. sper. frutticolt. eagrumicolt. Acireale*, **17**, 15 (1948).
21) N. A. Lange, "Handbook of Chemistry", Handbook Publishers, Inc., Sandusky, Ohio (1949).
22) A. Seidell, "Solubilities of Organic and Inorganic Compounds", Van Nostrand Co., New York, Vol. I (1940).

TABLE I

Temp. °C	Molality	C_p	Relative viscosity water=1	η_p	Temp. °C	Molality	C_p	Relative viscosity water=1	η_p
30	1.00	0.2156	1.010	0.8814	45	1.000	0.1950	1.024	0.8307
	1.50	0.3206	1.021	0.8910		1.500	0.2900	1.046	0.8484
	2.00	0.4236	1.028	0.8973		2.000	0.3832	1.058	0.8582
	2.50	0.5249	1.035	0.9033		2.500	0.4747	1.086	0.8810
	3.00	0.6244	1.046	0.9128		3.000	0.5650	1.104	0.8954
	3.50	0.7226	1.064	0.9285		3.500	0.6536	1.125	0.9124
	4.00	0.8189	1.079	0.9417		4.000	0.7406	1.148	0.9311
	4.50	0.9128	1.093	0.9539		4.500	0.8624	1.170	0.9491
	4.963	1.0000	1.145	1.0000		5.540	1.0000	1.233	1.0000
35	1.00	0.2079	1.014	0.9419	50	1.00	0.1895	1.034	0.8136
	1.50	0.3091	1.020	0.8800		1.50	0.2819	1.059	0.8333
	2.00	0.4088	1.022	0.8816		2.00	0.3727	1.076	0.8468
	2.50	0.5064	1.049	0.9048		2.50	0.4617	1.104	0.8686
	3.00	0.6027	1.060	0.9145		3.00	0.5494	1.122	0.8828
	3.50	0.6971	1.077	0.9315		3.50	0.6357	1.147	0.9024
	4.00	0.7900	1.103	0.9515		4.00	0.7202	1.173	0.9230
	4.50	0.8812	1.119	0.9651		4.50	0.8035	1.195	0.9404
	5.164	1.0000	1.159	1.0000		5.714	1.0000	1.271	1.0000
40	1.00	0.2005	1.018	0.8486	55	1.00	0.1841	1.039	0.7943
	1.50	0.2985	1.039	0.8662		1.50	0.2738	1.059	0.8098
	2.00	0.3945	1.044	0.8706		2.00	0.3617	1.081	0.8266
	2.50	0.4889	1.074	0.8958		2.50	0.4483	1.114	0.8517
	3.00	0.5817	1.089	0.9082		3.00	0.5335	1.135	0.8680
	3.50	0.6730	1.105	0.9212		3.50	0.6172	1.161	0.8880
	4.00	0.7628	1.130	0.9423		4.00	0.6993	1.188	0.9086
	4.50	0.8507	1.148	0.9572		4.50	0.7803	1.214	0.9283
	5.365	1.0000	1.199	1.0000		5.902	1.0000	1.308	1.0000

TABLE II

Temp. °C	Cons. A			Const. B
	Expt.	Extra-polated	% deviation	
30	0.8736	0.8710 (Ist line)	−0.3	0.03390
		0.8426 (IInd line)	—	0.05881
35	0.8630	0.8670	+0.4	0.07138
40	0.8339	0.8189	−1.8	0.07922
45	0.8112	0.8128	+0.2	0.09072
50	0.7868	0.7769	−1.27	0.10380
55	0.7647	0.7516	−1.7	0.11880

two non-collinear straight lines intersecting at a point corresponding to 2.336 molal. Therefore, in general the variation of η_p with concentration potential may be represented by the exponential equation

$$\eta_p = A\, e^{BC_p} \qquad (3)$$

the constants A and B being dependent upon temperature. At 30°C and below potassium chloride solutions are known to exhibit negative viscosity. Even then, the above exponential equation is applicable at 30°C, the non-colliner straight lines signifying only variations in constants A and B of the above equation.

It is clear from equation (3) that at infinite dilution C_p is zero and η_p equals to A. In other words A is the ratio of the viscosity of water to that of the solution when saturated with potassium chloride at a given temperature. This value of A

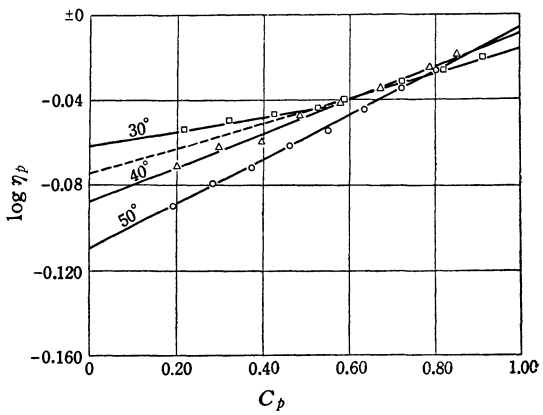

Fig. 1.

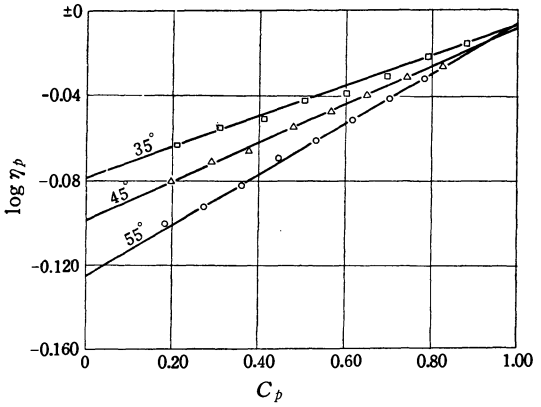

Fig. 2.

could be easily found from the experimental determination of the viscosity of the solution at saturation. Also by plotting at each temperature $\log \eta_p$ against C_p, by extrapolating $C_p = 0$ and by a small mathematical transformation of the value of the intercept we can obtain the value of 'A'. Thus in Table II in addition to the constant B at different temperatures the extrapolated and the experimentally determined values of 'A' are compared side by side. The percentage deviation between the extrapolated and the calculated values ranges from 0.2 to 1.80. Considering the difficulties involved in precision measurements of viscosity of saturated solutions and errors involved in extrapolation of values quite small in magnitude, the agreement is quite within limits. The constant 'B' may be probably related to the properties of the solute and requires further elucidation in furture.

Summary

A systematic investigation of viscosity from 1.00 m. to saturation of aqueous solutions of potassium chloride at temperatures of 30, 35, 40, 45, 50 and 55°C has been made. New concepts of concentration and viscosity have been defined. At a given molal concentration the ratio of the mole-fraction at that concentration to that at saturation at the same temperature has been called concentration potential C_p. The newly defined viscosity term η_p is the ratio of the viscosity at a given concentration to that at saturation at the same temperature. Using these two quantities the variation of viscosity with concentration could be expressed for potassium chloride solutions by a simple exponential equation:

$$\eta_p = A\, e^{BC_p}$$

where A and B are constants.

Physico-Chemical Laboratory
Annamalai University
Annamalainagar
South India

*Ion Exchange in Concentrated Solutions. III. Magnesium Chloride-Hydrochloric Acid and Aluminum Chloride-Hydrochloric Acid Systems**

By Hitoshi OHTAKI and Kazuo YAMASAKI

(Received January 6, 1958)

The ion-exchange equilibria in sodium chloride-hydrochloric acid[1], lithium chloride-hydrochloric acid[1] and beryllium chloride-hydrochloric acid[2] systems were studied in the previous reports. In the present report, the equilibria in magnesium chloride-hydrochloric acid and aluminum chloride-hydrochloric acid systems are investigated.

Experimental

The Resin.—The resin used was Dowex 50-X8 (hydrogen form) of mesh size 30~80 obtained by wet screening. It was dried at 40°C. The water content of the resin used was determined from

* Read before the 10th Annual Meeting of the Chemical Society of Japan held at Tokyo in April, 1957.

1) H. Kakihana, N. Maruichi and K. Yamasaki. *J. Phys. Chem.*, **60**, 36 (1956).

2) H. Ohtaki and K. Yamasaki, This Bulletin, **31**, 6 (1958).

the weight decrease on drying at 110°C. It was about 16.58~20.62%, i. e., 0.20~0.23 ml. per gram resin used for magnesium chloride-hydrochloric acid system and 9.82%, i. e., 0.11 ml. for that used for aluminum chloride-hydrochloric acid system. The amount of the resin used in one batch experiment was 3.6 g. The exchange capacity of the resin used was determined in each series of experiments.

Reagents.—Magnesium chloride of reagent grade was used without purification. Aluminum chloride was dissolved in water to prepare a concentrated solution. After adding hydrochloric acid, the concentrated solution was cooled by the freezing mixture and the stream of dried hydrogen chloride was passed through it. White crystals of aluminum chloride precipitated. After filtration the crystals were washed with cold concentrated hydrochloric acid and then dissolved in water containing a small amount of hydrochloric acid to prevent hydrolysis. This solution was mixed with hydrochloric acid to prepare sample solutions.

Procedure. — All the procedures used for determination of the adsorbed water are similar to those used in the previous studies[1,2]. Mixtures of 0.1~5 N magnesium chloride and 0~11 N hydrochloric acid and those of 0.2~0.9 N aluminum chloride and 0.5~11 N hydrochloric acid were used. In the concentration range lower than 0.5 N of hydrochloric acid the hydrolysis of aluminum chloride occurred, while too much presence of hydrochloric acid caused to crystallize some part of aluminum chloride. Therefore the concentration of hydrochloric acid was maintained lower than 3 N when that of aluminum chloride was 0.9 N.

The concentration of the magnesium ion was determined by titration with 0.02 and 0.001M ethylenediaminetetraacetate solution using Eriochrome Black T as indicator[3]. The concentration of the aluminum ion was titrated by 0.03 M ethylenediaminetetraacetate solution with Chrome Azurol S as indicator[4]. Hydrogen ion concentrations of these solutions were determined by titration with 0.1 N barium hydroxide. Brom Cresol Purple (pH of the color change: 5.2~6.8) was used as indicator for the magnesium chloride-hydrochloric acid system, while Methyl Yellow (pH of the color change: 2.9~4.0) was used for the aluminum chloride-hydrochloric acid system, because aluminum chloride was hydrolyzed in higher pH range.

Results and Discussion

1) Water in the Resin. — The amount of water adsorbed by the resin which was in contact with the external solution was estimated indirectly by measuring the amounts of the hydrogen ion before and after the ion-exchange equilibrium and using the following equation[1,2]:

$$A' = \frac{(H^+)_S \cdot V + [H^+]_Q + [H^+]_R - [H^+]_O - E}{(H^+)_S} \quad (1)$$

In equation (1), A' denotes the adsorbed water in the resin at equilibrium and round and square brackets denote the concentration and the amount of ions, respectively. V represents the volume of the original solution taken up in one batch experiment (30 ml.); subscripts S, Q, R and O denote the external solution at equilibrium, the quasi-exchange phase*, the resin phase at equilibrium and the original solution, respectively[1,2]; E represents the total exchange capacity of the resin used. When the original water content of the resin used is represented by A'', the total amount of the water in the resin is

$$A = A' + A''. \quad (2)$$

Amounts of the water per gram of dried resin thus determined are given in Tables I and II together with other data. As clearly shown in these tables values of the water in the resin for the aluminum chloride-hydrochloric acid system are generally smaller than those for beryllium chloride-hydrochloric acid[2] and magnesium chloride-hydrochloric acid systems. It is known that the larger the charge of the ion exchanged in the resin phase is, the more the resin shrinks. The experimental data shown in Tables I and II are consistent with this fact.

2) Ionic Species in the External Solution and the Resin.—As shown in Tables I and II, the sum of the amounts of hydrogen ion, $[H^+]_R$ and metal ion $[Mg^{2+}]_R$ or $[Al^{3+}]_R$ in the resin phase is larger than the total exchange capacity of the resin used. These discrepancies are supposed to have been caused by the formation of complexes* such as $MgCl^+$, $AlCl^{2+}$ or $AlCl_2^+$ which exchange with hydrogen ions. The existence of such complexes containing chlorine in the resin phase is verified by the detection of a minute amount of chloride ion in the solution eluted from the resin by sodium nitrate even after washing the resin thoroughly with water.

3) G. Schwarzenbach, "Die komplexometrische Titration", F. Enke Stuttgart, 2nd Ed. p. 54 (1956).
4) M. Theis, *Z. anal. Chem.*, **114**, 106 (1955).

* This phase consists of two kinds of solution: one is the solution which adheres to the surface of resin particles and the other is the solution which penetrates into the resin without being exchanged at the time of the exchange equilibrium. See References 1 and 2.

TABLE I

A PART OF THE DATA FOR THE $MgCl_2$-HCl SYSTEM.

(1) Concentration of the original solution of $MgCl_2$, $(Mg^{2+})_O = 0.11$ N; total exchange capacity of the resin, $E = 15.00$ meq.

$(H^+)_O$	0.32	0.65	1.09	1.93	4.31	8.76	N
$(H^+)_S$	0.41	0.75	1.21	2.04	4.44	8.82	N
$(Mg^{2+})_S$	0.00_8	0.02_1	0.04	0.07	0.09	0.09	N
$[H^+]_Q$	0.24	0.56	1.08	1.56	5.11	11.42	meq.
$[Mg^{2+}]_Q$	0.09	0.10	0.04	0.02	0.02	0.06	meq.
$[H^+]_R$	12.89	13.50	13.86	14.30	14.72	14.89	meq.
$[Mg^{2+}]_R$	3.45	2.75	2.37	1.40	0.75	0.43	meq.
$[H^+]_R+[Mg^{2+}]_R$	16.34	16.25	16.23	15.70	15.47	15.32	meq.
water in the resin, A.	0.90	1.12	1.13	0.89	0.84	0.69	ml./g. dry resin.

(2) $(Mg^{2+})_O = 0.29$ N, $E = 15.00$ meq.

$(H^+)_O$	0.00	0.61	2.06	3.09	5.12	8.18	N
$(H^+)_S$	0.20	0.79	2.24	3.23	5.24	8.25	N
$(Mg^{2+})_S$	0.00_9	0.11	0.23	0.26	0.28	0.28	N
$[H^+]_Q$	0.19	0.70	2.06	3.72	5.81	11.96	meq.
$[Mg^{2+}]_Q$	0.01	0.01	0.03	0.02	0.02	0.08	meq.
$[H^+]_R$	9.48	11.08	13.40	14.05	14.37	14.52	meq.
$[Mg^{2+}]_R$	9.03	6.53	2.86	2.01	1.08	0.98	meq.
$[H^+]_R+[Mg^{2+}]_R$	18.51	17.61	16.26	16.06	15.45	15.50	meq.
water in the resin, A.	1.27	1.12	1.10	0.93	0.76	0.74	ml./g. dry resin.

(3) $(Mg^{2+})_O = 0.50$ N, $E = 14.08$ meq.

$(H^+)_O$	0.00	1.02	3.04	5.11	8.17	10.78	N
$(H^+)_S$	0.29	1.21	3.17	5.21	8.15	10.51	N
$(Mg^{2+})_S$	0.07	0.31	0.45	0.48	0.48	0.47	N
$[H^+]_Q$	0.19	1.09	3.44	7.31	10.73	14.01	meq.
$[Mg^{2+}]_Q$	0.01	0.03	0.04	0.11	0.20	0.24	meq.
$[H^+]_R$	5.95	10.15	12.63	13.27	13.60	13.59	meq.
$[Mg^{2+}]_R$	13.13	6.91	2.63	1.86	1.39	1.42	meq.
$[H^+]_R+[Mg^{2+}]_R$	19.08	17.06	15.26	15.13	14.99	15.01	meq.
water in the resin, A.	1.05	1.04	0.92	0.91	0.66	0.43	ml./g. dry resin.

(4) $(Mg^{2+})_O = 1.00$ N, $E = 14.08$ meq.

$(H^+)_O$	0.00	1.02	3.02	5.17	8.24	10.37	N
$(H^+)_S$	0.36	1.29	3.20	5.29	8.25	10.13	N
$(Mg^{2+})_S$	0.48	0.74	0.91	0.96	0.97	0.99	N
$[H^+]_Q$	0.52	1.62	4.37	8.01	13.46	14.01	meq.
$[Mg^{2+}]_Q$	0.05	0.07	0.08	0.30	0.63	0.58	meq.
$[H^+]_R$	3.54	8.11	11.36	12.53	13.02	13.05	meq.
$[Mg^{2+}]$	16.96	10.00	4.90	3.14	2.51	2.51	meq.
$[H^+]_R+[Mg^{2+}]_R$	20.50	18.11	16.26	15.67	15.53	15.56	meq.
water in the resin, A.	1.09	1.06	1.01	0.86	0.86	0.46	ml./g. dry resin.

(5) $(Mg^{2+})_O = 2.99$ N, $E = 14.08$ meq.

$(H^+)_O$	0.27	0.80	2.53	7.09	N
$(H^+)_S$	0.66	1.14	2.77	7.13	N
$(Mg^{2+})_S$	2.55	2.65	2·81	2.90	N
$[H^+]_Q$	1.92	2.80	5.75	13.20	meq.
$[Mg^{2+}]_Q$	1.09	0.69	0.48	1.98	meq.
$[H^+]_R$	2.33	3.96	7.34	10.66	meq.
$[Mg^{2+}]_R$	18.67	16.47	11.36	6.26	meq.
$[H^+]_R+[Mg^{2+}]_R$	21.00	20.43	18.70	16.92	meq.
water in the resin, A.	1.16	1.12	1.06	0.79	ml./g. dry resin.

(6) $(Mg^{2+})_O = 4.96$ N, $E = 14.08$ meq.

$(H^+)_O$	0.00	0.80	5.13	N
$(H^+)_S$	0.41	1.14	5.26	N
$(Mg^{2+})_S$	4.58	4.72	4.92	N
$[H^+]_Q$	1.39	3.60	10.69	meq.
$[Mg^{2+}]_Q$	3.62	3.15	2.71	meq.
$[H^+]_R$	1.30	2.91	8.11	meq.
$[Mg^{2+}]_R$	20.48	18.02	9.98	meq.
$[H^+]_R+[Mg^{2+}]_R$	21.78	20.93	18.09	meq.
water in the resin, A.	1.06	1.17	0.82	ml./g. dry resin.

TABLE II

A PART OF THE DATA FOR THE $AlCl_3$-HCl SYSTEM.*

(1) Concentration of the original solution of $AlCl_3$, $(Al^{3+})_O = 0.18$ N; total exchange capacity of the resin, $E = 16.69$ meq.

$(H^+)_O$	1.07	2.17	3.23	5.30	8.47	11.65	N
$(H^+)_S$	1.25	2.37	3.37	5.44	8.53	11.43	N
$(Al^{3+})_S$	0.03	0.07	0.12	0.14	0.14	0.15	N
$[H^+]_Q$	1.13	2.84	4.69	8.33	16.19	20.26	meq.
$[H^+]_R$	13.49	14.61	15.17	15.54	15.68	15.70	meq.
$[Al^{3+}]_R$	3.99	2.66	2.41	1.28	1.33	1.28	meq.
$[H^+]_R+[Al^{3+}]_R$	17.48	17.27	17.58	16.82	17.01	16.98	meq.
water in the resin, A.	0.95	0.85	0.78	0.76	0.72	0.52	ml./g. dry resin.

(2) $(Al^{3+})_O = 0.52$ N, $E = 16.69$ meq.

$(H^+)_O$	0.38	0.65	1.12	2.17	5.01	10.66	N
$(H^+)_S$	0.72	0.98	1.41	2.42	5.20	10.59	N
$(Al^{3+})_S$	0.12	0.14	0.26	0.39	0.49	0.39	N
$[H^+]_Q$	0.74	1.13	1.49	3.38	8.66	18.80	meq.
$[H^+]_R$	7.87	8.77	10.30	12.80	14.78	15.19	meq.
$[Al^{3+}]_R$	14.23	11.76	9.35	5.18	2.03	1.25	meq.
$[H^+]_R+[Al^{3+}]_R$	22.10	20.53	19.65	17.98	16.81	16.44	meq.
water in the resin, A.	0.89	0.92	0.83	0.86	0.74	0.43	ml./g. dry resin.

(3) $(Al^{3+})_O = 0.77$ N, $E = 16.69$ meq.

$(H^+)_O$	0.45	1.17	2.16	7.41	N
$(H^+)_S$	0.82	1.44	2.39	7.64	N
$(Al^{3+})_S$	0.29	0.51	0.66	0.68	N
$[H^+]_Q$	1.07	2.30	3.87	13.47	meq.
$[H^+]_R$	6.62	9.34	11.96	14.80	meq.
$[Al^{3+}]_R$	14.59	11.36	7.07	1.59	meq.
$[H^+]_R+[Al^{3+}]_R$	21.21	20.70	19.03	16.39	meq.
water in the resin, A.	1.23	0.73	0.87	0.84	ml./g. dry resin.

(4) $(Al^{3+})_O = 0.90$ N, $E = 16.69$ meq.

$(H^+)_O$	0.79	1.26	2.21	N
$(H^+)_S$	1.14	1.58	2.48	N
$(Al^{3+})_S$	0.58	0.76	0.78	N
$[H^+]_Q$	1.50	2.06	3.39	meq.
$[H^+]_R$	6.99	8.89	11.29	meq.
$[Al^{3+}]_R$	15.50	12.10	7.88	meq.
$[H^+]_R+[Al^{3+}]_R$	22.49	20.99	19.17	meq.
water in the resin, A.	1.04	0.87	0.88	ml./g. dry resin.

* The amount of Al^{3+} ion in the quasi-exchange phase is too small to be determined in all cases. Therefore values of $[Al^{3+}]_Q$ are not given in this table.

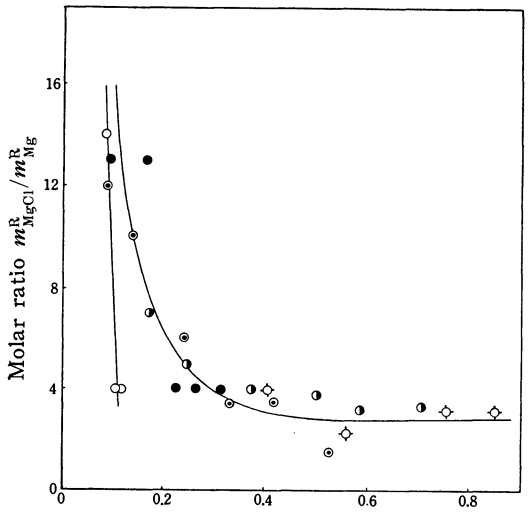

The apparent molar fraction of Mg ion in the resin

Fig. 1. Relation between molar ratio of $MgCl^+$ to Mg^{2+} in the resin and the apparent molar fraction of Mg ion in the resin.
○ 0.1 ● 0.3 ⊙ 0.5 ◑ 1.0
◇ 5.0 N $MgCl_2$

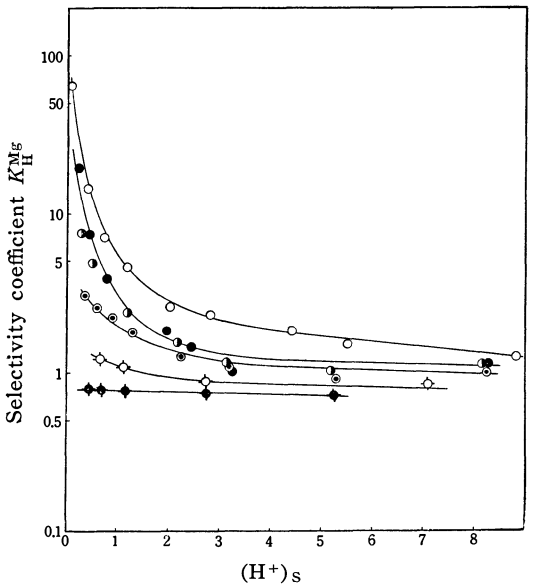

Hydrogen ion concentration in the external solution at equilibrium

Fig. 2. Selectivity coefficients of $MgCl_2$ −HCl system plotted against $(H^+)_S$.
○ 0.1 ● 0.3 ◑ 0.5 ⊙ 1.0
◇ 3.0 ◆ 5.0 N $MgCl_2$

Amounts of Mg^{2+} and $MgCl^+$ ions in the resin phase can be readily calculated from the values of E, $[H^+]_R$ and $[Mg^{2+}]_R$ provided that no other complexes are

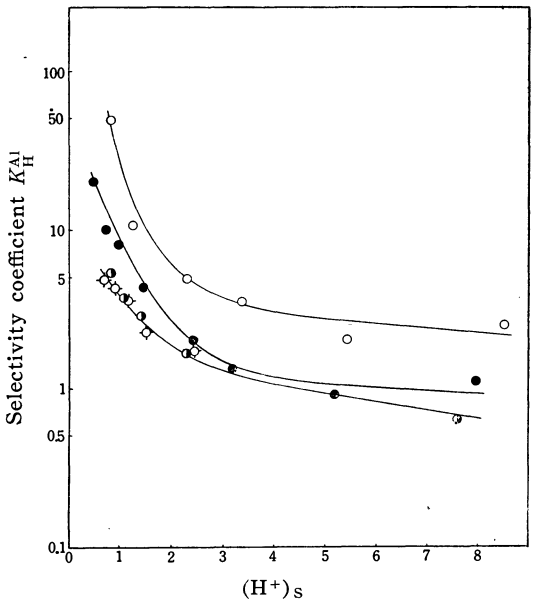

Hydrogen ion concentration in the external solution at equilibrium

Fig. 3. Selectivity coefficients of $AlCl_3$ −HCl system plotted against $(H^+)_S$.
○ 0.18 ● 0.53 ◑ 0.77
◇ 0.90 N $AlCl_3$

formed. In Fig. 1 values of the molar ratio of $MgCl^+$ to Mg^{2+} ion in the resin m^R_{MgCl}/m^R_{Mg} are plotted against the apparent molar fraction of magnesium ion in the resin, X_{Mg}*. The molar ratio increases as X_{Mg} decreases. Thus, in the range of lower concentration of magnesium chloride and at the same time of higher concentration of hydrochloric acid, magnesium in the resin phase consists almost entirely of $MgCl^+$, and it is possible that a large part of magnesium present in the external solution also forms the chloro-complex $MgCl^+$.

In Fig. 2 values of selectivity coefficient of magnesium calculated after the formula

$$K^{Mg}_H = \frac{(H^+)_S\{[Mg^{2+}]_Q + [Mg^{2+}]_R\}}{(Mg^{2+})_S\{[H^+]_Q + [H^+]_R\}} \quad (3)$$

are plotted against $(H^+)_S$, the hydrogen ion concentration of the external solution. In the range of higher values of $(H^+)_S$, as already described, the ionic species predominant is considered to be $MgCl^+$. Consequently the selectivity coefficient thus calculated represents that of the exchange

* Hydroxo-complexes are formed with difficulty in such a strong acidic system as the resin phase concerned. Actually water may be coordinated to these ions in forming $[Mg(OH_2)_5Cl]^{2+}$, $[Al(OH_2)_5Cl]^{2+}$, $[Al(OH_2)_4Cl_2]^+$.

* $X_{Mg} = \frac{1}{2}[Mg^{2+}]_R/\{[H^+]_R + \frac{1}{2}[Mg^{2+}]_R\}$

system of $MgCl^+$—H^+ rather than that of Mg^{2+}—H^+ system.

The selectivity coefficient of the aluminum chloride-hydrochloric acid system was calculated by the similar formula as (3):

$$K_H^{Al} = \frac{(H^+)_S\{[Al^{3+}]_Q + [Al^{3+}]_R\}}{(Al^{3+})_S\{[H^+]_Q + [H^+]_R\}} \quad (4)$$

These data are plotted against $(H^+)_S$ in Fig. 3. In this system it is difficult to estimate the amount of individual species of aluminum like Al^{3+}, $AlCl^{2+}$ or $AlCl_2^+$ in the similar way as in the magnesium chloride-hydrochloric acid system.

Summary

Ion-exchange equilibria in the concentrated solutions of magnesium chloride-hydrochloric acid and aluminum chloride-hydrochloric acid system were studied. Amounts of the water present in the resin at equilibrium were estimated for these systems. In the magnesium chloride-hydrochloric acid system a large part of magnesium in the resin exists as $MgCl^+$ at equilibrium when the concentration of hydrochloric acid is high. Selectivity coefficients of magnesium chloride-hydrochloric acid and of aluminum cholride-hydrochloric acid systems were calculated.

A part of of the expenses of the present study was defrayed by Grant-in-Aid for Fundamental Scientific Research from Ministry of Education.

Chemical Institute, Faculty of Science, Nagoya University
Chikusa-ku, Nagoya

Selective Oxidation of Allylic Alcohols with Active N-Halogen Compounds. I. Synthesis of Testosterone and of 4-Pregnen-20β-ol-3-one[1]

By Ken-ichi MORITA

(Received January 9, 1958)

Treatment of allylic, propargylic and benzylic alcohol with manganese dioxide at room temperature has been shown to be an effective method for the selective oxidation of these alcohols[2]. It seems necessary, however, to search other reagents for the reactions, since recent studies indicate that in some cases even under mild conditions the oxidation of saturated primary and secondary alcohols may occur[3].

Lecompte and his colleagues[4] reported the oxidation reactions of a large number of alcohols containing benzene rings with *N*-bromoacetamide. It should be noted that hydroxyl groups in positions adjacent to the aromatic systems in the alcohols are easily oxidized to carbonyl groups, whereas hydroxyl groups in other positions are unaffected under similar conditions. Thus, 1-hydroxy-1, 2, 3, 4-tetrahydronaphthalene[4a], benzhydrol and benzyl alcohol[4b] are easily oxidized to corresponding carbonyl compounds, while the oxidation of 2-hydroxy-1,2,3,4-tetrahydronaphthalene[4a], 1,3-diphenyl-2-propanol and 2-phenylethanol[4b] does not occur. Lieberman and Fukushima[5] reported that the reaction of 5-cholestene-3β, 4β, 7α-trial 3-monoacetate with *N*-bromoacetamide gave 5-cholestene-3β,4β-diol-7-one 3-monoacetate in a quantitative yield*. These observations suggest that the active *N*-halogen compounds such as *N*-bromoacetamide may be effective

1) Steroids Part XXII; Part XXI, This Bulletin, **31**, 347 (1958).

2) G. Rosenkranz et al., *J. Chem. Soc.*, **1954**, 1226, 2189; *J. Am. Chem. Soc.*, **75**, 5930, 5932 (1953) and literatures cited there.

3) H. Bruderer, D. Arigoni and O. Jeger, *Helv. Chim. Acta*, **39**, 858 (1956) and literatures cited there.

4) a) J. Lecomte and C. Dufour, *Compt. rend.*, **234**, 1887 (1952); b) J. Lecomte and H. Gault, ibid., **238**, 2538 (1954).

5) S. Lieberman and D. K. Fukushima, *J. Am. Chem. Soc.*, **72**, 5211 (1950).

* Cf. M. A. Romero, *J. Org. Chem.*, **22**, 1267 (1957).

TABLE I

SYNTHESIS OF TESTOSTERONE FROM A MIXTURE OF 4-ANDROSTENE-3α,17β- AND -3β,17β-DIOLS BY TREATMENT WITH ACTIVE *N*-HALOGEN COMPOUNDS

No.	androstenediol (mg.)	*N*-hlogene compounds (mg.) (equiv.)	solvents (ml.)	conditions (°C) (hr.)	yields of testosterone (wt.%)
1	147.6	NBA, (76.2) (1.09)	Bu, 10; Py, 0.5; W, 0.3	20~21, 17	45
2	151.1	NBA, (77.1) (1.07)	Bu, 10; Py, 1; W, 1	15~17, 19	52
3	151.4	NBA, (77.5) (1.08)	Bu, 1; Py, 0.5	20~21, 17	71
4	152.0	NBA, (78.6) (1.09)	Bu, 0.5; Py, 1	20~21, 17	69
5	152.8	NBA, (75.9) (1.05)	Bu, 10; Py, 1	15~17, 19	68
6	151.5	NBA, (79.5) (1.10)	Bz, 2; Py, 1	20~21, 17	74
7	152.9	NBA, (76.4) (1.05)	Bz, 3; Py, 0.5	16~18, 41	57
8	151.9	NBA, (75.9) (1.05)	Bz, 8; Py, 0.1	16~18, 23	45
9	151.1	NBA, (76.0) (1.06)	Chf, 2; Py, 1	20~21, 17	47
10	152.6	NBA, (74.0) (1.02)	E, 4; Me, 10; Py, 0.3; W, 0.3	15~17, 19	38
11	152.2	NBS, (97.1) (1.03)	Bu, 0.5; Py, 1	15~17, 19	56
12	148.3	NBS, (100.1) (1.1)	E, 4; Me, 10; Py, 0.3; W, 0.3	15~17, 19	39
13	250.7*	NBS, (163.0) (1.06)	E, 5; Me, 1; 3%$KHCO_3$aq., 0.3	29 18	33
14	151.0	62% ICB, (116.8) (1.14)	Bz, 5; Py, 2	49~51, 1	71
15	155.5	62% ICB, (103.0) (0.98)	Bz, 10; Py, 0.3	50~52, 1	55
16	149.4	72% ICB, (91.3) (1.05)	Bu, 2; Py, 2	60~63, 1	73
17	175.6*	83% ICB, (98.6) (1.1)	Bu, 2; Py, 0.3; W, 0.3	60~65, 1	64

Bu=*tert*-Butanol, Py=Pyridine, W=Water, Bz=Benzene, Chf=Chloroform, E=Ether, Me=Methanol, NBA=*N*-Bromoacetamide, NBS=*N*-Bromosuccinimide, ICB=Isocyanur bromide.

* Eight grams of alumina were used.

reagents for selective oxidation of allylic alcohols.

The reduction of 4-androstene-3, 17-dione (I) with sodium borohydride gave a mixture of 4-androstene-3α, 17β-diol and the corresponding 3β, 17β-diol. The mixture, m.p. 95~145°C[6], was oxidized with about 1.05 equivalents of *N*-bromoacetamide, *N*-bromosuccinimide or isocyanur bromide[10] in various solvents, and the products were separated by chromatography. The results are shown in Table I. It is clear that (1) water disturbs* this reaction especially when used with *N*-bromosuccinimide or *N*-bromoacetamide, (2) *N*-bromoacetamide and isocyanur bromide are superior to *N*-bromosuccinimide as the reagents of this reaction. In the best conditions testosterone (III) was obtained in 70~74% overall yield from 4-androstene-3, 17-dione (I). (No. 3, 4, 6, 14 and 16)

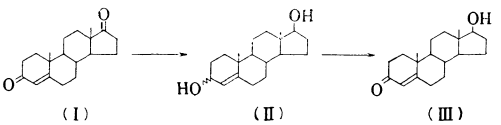

(I) (II) (III)

Progesterone (IV) was reduced with sodium borohydride to give a mixture of 4-pregnene-3α, 20β-diol and the corresponding 3β, 20β-diol. The mixture, m. p. 147~168°C[11], was oxidized with *N*-bromoacetamide in benzene-pyridine. 4-Pregnen-20β-ol-3-one (VI) was obtained in

6) Sondheimer et al.[7] reported that the reduction of compound I with lithium aluminum hydride furnished a mixture of the 3α, 17β-diol and the 3β, 17β-diol and the mixture melted at 165~171°C. Presumably the difference in the melting points of both mixtures is due to difference in the proportions of 3α and 3β alcohols[8], since the C_{17} carbonyl group was exclusively reduced to the β-hydroxyl group on reduction with sodium borohydride[9].

7) F. Sondheimer, C. Amendolla and G. Rosenkranz, *J. Am. Chem. Soc.*, **75**, 5930 (1953).

8) For sodium borohydride reduction of 4-ene-3-ketosteroids see, W. W. Zorbach, ibid., **75**, 6344 (1953); B. Camerino and C. G. Alberti, *Gazz. chim. ital.*, **85**, 51 (1955); S. Bernstein, S. M. Stolar and M. Heller, *J. Org. Chem.*, **22**, 472 (1957).

9) H. J. Ringold, B. Loeken, G. Rosenkranz and F. Sondheimer, *J. Am. Chem. Soc.*, **78**, 816 (1956); K. Miescher and C. Meystre, U. S. Pat. 2,679,502; *Chem. Abst.*, **49**, 6325^i (1955).

10) K. Morita, This Bulletin, **31**, 347 (1958).

11) Reduction of progesterone with lithium aluminum hydride gives a mixture with m. p. 162~172°C[7].

76% overall yield from progesterone (IV). The 20β configuration was deduced from α_D values of compound VI, +85°, and of its acetate, +130°, which were quite similar to the reported[7,12-14]. Sondheimer et al.[7] reported that the reduction of progesterone (IV) with lithium aluminum

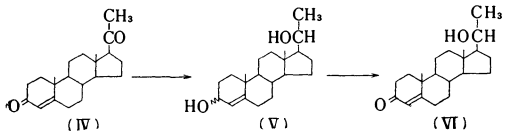

(IV) (V) (VI)

hydride and the succeeding oxidation of the resulted diols with manganese dioxide yielded compound VI in 66% overall yield.

Manganese dioxide attacks preferably unhindered hydroxyl groups such as primary[3] or equatorial hydroxyl[15]. On the other hand, active *N*-halogen compounds attack rather hindered hydroxyl groups[16,17]. The rate-determining step of the latter reaction is known to be the abstraction of the hydrogen atom bonded to the carbinol carbon. *N*-Halogen compounds might be serviceable for selective oxidation of polyhydroxyl compounds carrying primary or equatorial and allylic hydroxyl groups to α,β-unsaturated ketones with unaffected primary or equatorial hydroxyl groups. Such selective oxidation is probably difficult[3] when manganese dioxide is employed. Examples will be reported soon.

Experimental[18]

General Procedure of Synthesis of Testosterone (III) from 4-Androstene-3,17-dione (I).—A mixture of 1 g. of 4-Androstene-3,17-dione (I) with m.p. 165~169°C in 10 ml. of methanol and 1 g. of sodium borohydride in 1 ml. of water was heated under reflux for 1 hour. After cooling, the suspension was poured into dilute hydrochloric acid. Solid was collected by filtration and well washed with water. It melted at 95~145°C, and was presumably essentially a mixture of 4-androstene-3α,17β- and 3β,17β-diols and gave no 2,4-dinitrophenylhydrazone.

A weighed sample from the above solid in a mixed solvent as described in Table I was treated with *N*-bromoacetamide, *N*-bromosuccinimide or isocyanur bromide in the dark. When a solid appeared, it was filtered off. The solution or filtrate was diluted with a mixture of 30 ml. of ether and 10 ml. of benzene and washed successively with 10% aqueous sodium bisulfite, with 10% aqueous sodium hydroxide, with water, with dilute sulfuric acid and again with water, and dried over anhydrous sodium sulfate. The solvent was evaporated under a reduced pressure. The oily or crystalline residue was dissolved in 10 ml. of benzene and adsorbed on a column of alumina (5 g.).

The elution of products was carried out with the following solvent systems[19].

Fraction No.	benzene (ml.)	ether (ml.)
1	12	2
2	14	4
3	6	4
	4	6
4	6	14
5	4	16
6	2	18
7	0	20
	aceton (ml.)	ether (ml.)
8	2	18
9	4	16
10	6	14
11	8	12
12	methanol 30 ml.	

The earlier fractions gave 4-androstene-3,17-dione (I) or an oil. The dione, collected from all the experiments and recrystallized from acetone-*n*-hexane, exhibited m.p. 168~169°C, λ_{max} 240mμ, log ε 4.23. Identity was established by a mixed melting point determination.

From middle fractions testosterone (III) with m.p. 148~153°C and mixed m.p. above 149°C was obtained in yields shown in Table I. Testosterone from all the experiments was brought together and recrystallized from acetone-*n*-hexane to show m.p. 152~153°C; $[\alpha]_D^{19}$ +102 (c, 1.40 in dioxan); λ_{max} 241 mμ, log ε 4.21.

From later fractions the starting material or an oil was obtained. Some oily fractions showed positive Beilstein test. Such oily fractions increased when water and/or *N*-bromosuccinimide was used.

4-Pregnene-20β-ol-3-one (VI) from Progesterone (IV).—A mixture of 1.5 g. of progesterone with m.p. 125~127°C in 30 ml. of methanol and 1 g. of sodium borohydride in 1.5 ml. of water was heated under reflux for one hour. After

12) P. Wieland and K. Miescher, *Helv. Chim. Acta*, **32**, 1922 (1949).
13) J. Romo, M. Romo, C. Djerassi and G. Rosenkranz, *J. Am. Chem. Soc.*, **73**, 1528 (1951).
14) R. B. Turner and D. M. Voitle, ibid., **73**, 2283 (1951).
15) C. Amendolla, G. Rosenkranz and F. Sondheimer, *J. Chem. Soc.*, **1954**, 1226; also see footnote 16 of Ref. 3.
16) The oxidation of primary alcohols with *N*-bromoacetamide is difficult. Cf. R. E. Jones and F. W. Kocher, *J. Am. Chem. Soc.*, **76**, 3682 (1954); T. H. Krichevsky, D. L. Garmaise and T. F. G. Gallagher, ibid., **74**, 483 (1952).
17) Axial hydroxyl groups are more easily oxidized to carbonyl than equatorial ones. Cf. W. Klyne, "Progress in Stereochemistry" **1**, Butterworths Scientific Publications, London (1954), p. 63.
18) All melting points are uncorrected. Ultraviolet absorption spectra were measured in 95% ethanol solution with a Hitachi Photoelectric Spectrophotometer Model EPU-2.
19) The chromatographic separations were carried out in part by Mr. T. Iwama to whom author's thanks are due.

cooling a few drops of acetic acid were added and the solution was poured into an excess of water. The solid was collected by filtration and well washed with water. The mixture of 4-pregnene-3α,20β- and 3β,20β-diols melted at 147~168°C. Yield 1.5 g.

A solution of 499.1 mg. of above solid in 3 ml. of benzene and 5 ml. of pyridine was treated with 265.7 mg. of *N*-bromoacetamide (1.22 equiv.) at 18~19°C for two hours. After treated as usual, the crystalline residue was dissolved in 15 ml. of benzene and adsorbed on a column of alumina (3 g.). The elution with benzene-ether (1 : 1) and recrystallization from ether-*n*-hexean gave needles with m. p. 169~171°C, $[\alpha]_D^{19}$+85 (c, 1.05 in chloroform), λ_{max}242 mμ, log ε 4.22. Yield 378 mg. or 76 % of the theoretical. Identity was established by a mixed[7] melting point determination. Reported m. p. 171~172°C, $[\alpha]_D$+84[12]; m. p. 169~171°C, $[\alpha]_D$+83, λ_{max}242 mμ, log ε 4.31[13]; m. p. 174~175°C, $[\alpha]_D$+90[14]; m. p. 174~175°C, $[\alpha]_D$+86, λ_{max}240 mμ, log ε 4.23[7].

The acetate, recrystallized from acetone-*n*-hexane, exhibited m. p. 159~160°C, $[\alpha]_D^{18}$+130 (*c*, 0.368 in chloroform). Reported m. p. 159~160°C, $[\alpha]_D$+140[12], m. p. 159~161°C, $[\alpha]_D$+137[13], m. p. 161~162°C, $[\alpha]_D$+129[14], m. p. 161~162°C, $[\alpha]_D$+134[7].

The author wishes to express his grateful appreciation to Dr. M. Nakamura, Director of the Institute, for his permission of publishing this work. The author also indebted to Professor S. Mori of Tokyo Metropolitan University and Mr. R. Mamine of the Institute for their encouragement throughout this work.

Sugiyama Chemical Reseach Institute
Mure, Mitaka-shi, Tokyo

Electronic Structure and Spectra of s-Tetrazine

By Noboru MATAGA

(Received December 18, 1957)

Recently, we have studied the electronic structure and the spectra of some nitrogen heterocycles using a semiempirical LCAO SCF MO method[1]. Our investigation has given a theoretical ground to the classification of the spectra of nitrogen heterocycles which has been made by Zanker[2] in analogy to the spectra of aromatic hydrocarbons. The cause of the intensification of ^1L_b band in a nitrogen heterocycle compared with the corresponding aromatic hydrocarbon, was ascribed by some authors[3,4], for example, in the case of pyridine and benzene, to the mixing of unperturbed $^1B_{2u}$ state to which transition from the ground state is virtually forbidden, with some contribution from $^1E_{1u}$ state to which transition is strongly allowed. Tsubomura[5] has studied the same problem, using an antisymmetrized product of naive MO. He has examined the above described possibility and also another possibility that, in pyridine, the lowering of molecular symmetry compared with benzene, may cause the perturbation on MO in the direction of C_{2v} axis, and this perturbation may also lead to the intensification of ^1L_b band. His conclusion is, however, that the latter effect may be small compared with the former. We have confirmed[1] that the latter effect is negligibly small compared with the former, on the basis of SCF MO. In the present paper, we shall report the results obtained for *s*-tetrazine, a typical nitrogen heterocycle, comparing them with the results for some nitrogen heterobenzenes such as pyridine and pyrazine, and discuss the nature of electonic transition in the *s*-tetrazine molecule.

Theoretical Method[1]

The present section is devoted to a brief description of the main ideas and approximations in the theory.

A) Formulation. — The theoretical method is based on the framework of the LCAO SCF MO method developed by

1) N. Mataga and K. Nishimoto, *Z. physik. Chem., N. F.*, **13**, 140 (1957).
2) V. Zanker, ibid., **2**, 52 (1954).
3) W. Moffitt, *J. Chem. Phys.*, **22**, 320 (1954).
4) N. Mataga et al., This Bulletin, **29**, 373 (1956).
5) H. Tsubomura, *J. Chem. Soc. Japan, Pure. Chem. Sec.* (*Nippon Kagaku Zassi*), **78**, 293 (1957).

Roothaan[6] and Hall[7], with only the π-electrons considered explicitly. Its computation procedure is similar to that of Pople[8] and Ooshika[9]. The wave function for the π-electron in the ground state was taken as a Slater determinant built up from orthonormal moleculer orbitals which are themselves linear combinations of $2p\pi$ atomic orbitals $\phi_1 \cdots\cdots \phi_{2m}$ of carbon or nitrogen,

$$\psi_i = \sum_\mu c_{i\mu}\phi_\mu \tag{1}$$

The coefficients $c_{i\mu}$ are chosen to minimize the electronic energy,

$$E = \int \chi_0 \mathbf{H} \chi_0 d\tau \tag{2}$$

where $\mathbf{H}$ is the complete electronic Hamiltonian

$$\mathbf{H} = \sum_i H_i^{core} + \sum_{i<j}^{2m} (e^2/_{ij}) \tag{3}$$

The general set of equations for $c_{i\mu}$ which has been given by Roothaan[6] can be reduced to the following eigenvalue equations, by some simplifying approximations about the integrals that arise[8-10].

$$\sum_\nu F_{\mu\nu} c_{i\nu} = \varepsilon_i c_{i\mu} \tag{4}$$

where

$$F_{\mu\mu} = H_{\mu\mu} + \frac{1}{2} P_{\mu\mu}\gamma_{\mu\mu} + \sum_{\kappa(\neq\mu)} P_{\kappa\kappa}\gamma_{\kappa\mu} \tag{5}$$

$$F_{\mu\nu} = H_{\mu\nu} - \frac{1}{2} P_{\mu\nu}\gamma_{\mu\nu} \tag{6}$$

$$P_{\mu\nu} = 2\sum_{j=1}^{m} c_{i\mu} c_{i\nu} \tag{7}$$

$\gamma_{\mu\nu}$ is the interelectronic Coulomb repulsion integral

$$\gamma_{\mu\nu} = \int \phi_\mu^*(1)\phi_\nu^*(2)\frac{e^2}{r_{12}}\phi_\mu(1)\phi_\nu(2)\mathrm{d}v_1\mathrm{d}v_2 \tag{8}$$

$H_{\mu\mu}$ are the diagonal matrix elements of the core Hamiltonian for all atoms,

$$\begin{aligned} H_{\mu\mu} &= \int \phi_\mu^* \left\{ -\frac{1}{2}\nabla^2 - \sum_\kappa V_\kappa \right\} \phi_\mu \mathrm{d}v \\ &= \int \phi_\mu^* \left\{ -\frac{1}{2}\nabla^2 - V_\mu \right\} \phi_\mu \mathrm{d}v \\ &\quad - \sum_{\kappa(\neq\mu)} \int \phi_\mu^* V_\kappa \phi_\mu \mathrm{d}v \\ &= \alpha_\mu - \sum_{\kappa(\neq\mu)} \gamma_{\kappa\mu}' \end{aligned} \tag{9}$$

where

$$\alpha_\mu = \int \phi_\mu^* \left\{ -\frac{1}{2}\nabla^2 - V_\mu \right\} \phi_\mu \mathrm{d}v \tag{10}$$

$$\gamma_{\kappa\mu}' = \int \phi_\mu^* V_\kappa \phi_\mu \mathrm{d}v \tag{11}$$

α_μ may be regarded as a quantity characteristic to μ atom in an appropriate valence state and for our purpose, it may be satisfactory to assume, $\gamma_{\kappa\mu}' = \gamma_{\kappa\mu}$[8].

We denote $H_{\mu\nu}$, the off-diagonal matrix elements of the core Homiltonian, as $\beta_{\mu\nu}$,

$$\beta_{\mu\nu} = \int \phi_\mu^* \left\{ -\frac{1}{2}\nabla^2 - \sum_\kappa V_\kappa \right\} \phi_\nu \mathrm{d}v \gamma_{\kappa\mu} \tag{12}$$

then the matrix elements of the ground state Fock Hamiltonian may be written as follows, using the approximations described above,

$$F_{\mu\mu} = \alpha_\mu + 1/2 P_{\mu\mu}\gamma_{\mu\mu} + \sum_{\kappa(\neq\mu)} (P_{\kappa\kappa} - 1) \tag{13}$$

$$F_{\mu\nu} = \beta_{\mu\nu} - 1/2 P_{\mu\nu}\gamma_{\mu\nu} \tag{14}$$

When the self-consistent problem for the ground state has been solved by a cyclic process, the unoccupied orbitals $\phi_{m+1} \cdots\cdots \phi_{2m}$ can be used to construct configurational wave functions for excited states. We shall write ${}^1\chi_{i\to k}$ for the singlet configurational wave function in which one electron is excited from an occupied orbital ϕ_i to an unoccupied orbital ϕ_k. The corresponding triplet wave function will be written ${}^3\chi_{i\to k}$, and $({}^1\chi_{i\to k}|\mathbf{H}|{}^1\chi_{j\to l})$ and $({}^3\chi_{i\to k}|\mathbf{H}|{}^3\chi_{j\to})$ represent the matrix elements of total Hamilton $\mathbf{H}$ by these wave functions. Then the excitation energies corresponding to the transition $i\to k$ are expressed as follows for singlet and triplet respectively :

$$\begin{aligned} E({}^1\chi_{i\to k}) &= ({}^1\chi_{i\to k}|\mathbf{H}|{}^1\chi_{i\to k}) - (\chi_0|\mathbf{H}|\chi_0) \\ &= \varepsilon_k - \varepsilon_i - (ik|G|ik) + 2(ik|G|ki) \end{aligned} \tag{15}$$

$$\begin{aligned} E({}^3\chi_{i\to k}) &= ({}^3\chi_{i\to k}|\mathbf{H}|{}^3\chi_{i\to k}) - (\chi_0|\mathbf{H}|\chi_0) \\ &= \varepsilon_k - \varepsilon_i - (ik|G|ik) \end{aligned} \tag{16}$$

where

$$(pq|G|rs) = \int \psi_p^*(1)\phi_q^*(2)\frac{e^2}{r_{12}}\phi_r(1)\phi_s(2)\mathrm{d}v_1\mathrm{d}v_2 \tag{17}$$

The interconfigurational matrix elements may be written in a similar way

$$({}^1\chi_{i\to k}|\mathbf{H}|{}^1\chi_{i\to k}) = 2(jk|G|li) - (jk|G|il) \tag{18}$$

$$({}^3\chi_{i\to k}|\mathbf{H}|{}^3\chi_{i\to k}) = -(jk|G|il) \tag{19}$$

An excited state wave function Ψ_α is approximated by a linear combination of singly excited configuration functions $\chi_{i\to k}$'s.

6) C. C. J. Roothaan, *Rev. Mod. Phys.*, **23**, 61 (1951).
7) G. G. Hall, *Proc. Roy. Soc.*, **A205**, 541 (1951).
8) J. A. Pople, *Proc. Phys. Soc.*, **A68**, 81 (1955).
9) Y. Ooshika, *J. Phys. Soc. Japan*, **12**, 1238 (1957)
10) J. A. Pople, *Trans. Faraday. Soc.*, **49**, 1357 (1953).

The oscillator strength, f, is calculated by the method described by Mulliken and Rieke,

$$f=1.085\times10^{11}\omega_{0\alpha}\sum_{r=x,y,z}[Q_{0\alpha}{}^{r}]^2 \qquad (20)$$

where $\omega_{0\alpha}$ is the frequency of the $\chi_0\rightarrow\Psi_\alpha$ transition in cm^{-1}.

B) Semiempirical Evaluation of Integrals.—Molecular integrals appeared in Eqs. 13 and 16 are evaluated by semiempirical procedure analogous to, but somewhat different from those given by Pariser and Parr[11], Ooshika[9] and Pople[10].

B1. The value of α_μ was taken to be equal to $-I_\mu$, where I_μ is the ionization potential of μ atom in the appropriate atomic valence state[12]. $\beta_{\mu\nu}$ for C-N and N-N were taken from Pariser and Parr[11] and Paoloni[13], respectively, for nearest neighbours and neglected for more distant neighbors:

$$\beta_{CN}=-2.576\ e.v.,\quad \beta_{NN}=-2.35\ e.v.*$$

B2. To estimate the two center Coulomb repulsion integrals of the type $\gamma_{\mu\nu}$, we used the following approximation,

$$\gamma_{\mu\nu}=e^2/R_{\mu\nu} \qquad (21)$$

$$R_{\mu\nu}=a+r_{\mu\nu} \qquad (22)$$

where $r_{\mu\nu}$ is the interatomic distance between μ and ν atoms. a is a parameter, which is determined in the following way, using valence state ionization potential I_μ and electron affinity A_μ in the same valence state. For homonuclear two centers, we put

$$\gamma_{\mu\mu}=e^2/R_{\mu\mu}=e^2/a=I_\mu-A_\mu \qquad (23)$$

In the case of heteronuclear two centers, i.e. carbon and nitrogen, we take as $e^2/R_{\mu\mu}$, simple arithmetic mean of $e^2/R_{\mu\mu}$'s for carbon and nitrogen. The values of a thus evaluted are, $a_{CC}=1.328$Å, $a_{CN}=1.212$Å and $a_{NN}=1.115$ Å. The geometrical structure of *s*-tetrazine has been determined by Bertinotti, Giacomello and Liquori[14], by means of X-ray diffraction. The values of $r_{\mu\nu}$'s necessary for the evaluation of $\gamma_{\mu\nu}$'s and oscillator strength were taken from this work.

Results and Discussion

As pointed out previously[1], the replacement of —CH= with —N= can be regarded as a small perturbation, and the SCF MO's of nitrogen hetrocycles are nearly close to the naive MO's obtained by ordinary procedure, assuming the Coulomb integral at nitrogen atom, α_N, to be equal to $\alpha+0.5\beta$.

We have chosen the naive MO's of *s*-tetrazine obtained in this way as a starting MO's for the SCF calculation. Thus the self-consistent problem for *s*-tetrazine has been solved and the resulting SCF MO's and MO energies are collected in Table I.

TABLE I
SCF MO'S AND MO ENERGIES OF *s*-TETRAZINE

Symmetry	ε_i(e.v.)	
b_{2u}	−15.531	$\phi_1=0.4277\sigma_1+0.3667\sigma_2$
b_{1g}	−12.759	$\phi_2=0.5000\sigma_3$
b_{3g}	−11.973	$\phi_3=0.3256\sigma_4+0.5365\sigma_5$
a_{1u}	− 2.899	$\phi_4=0.5000\sigma_6$
b_{2u}	− 1.573	$\phi_5=0.2592\sigma_1-0.6046\sigma_2$
b_{3g}	0.975	$\phi_6=0.4374\sigma_4-0.3424\sigma_5$

$\sigma_1=(\phi_2+\phi_3+\phi_5-\phi_6)$, $\sigma_3=(\phi_1+\phi_4)$, $\sigma_5=(\phi_2+\phi_3-\phi_5-\phi_6)$

$\sigma_2=(\phi_2-\phi_3-\phi_5+\phi_6)$, $\sigma_4=(\phi_1-\phi_4)$, $\sigma_6=(\phi_2-\phi_3+\phi_5-\phi_6)$

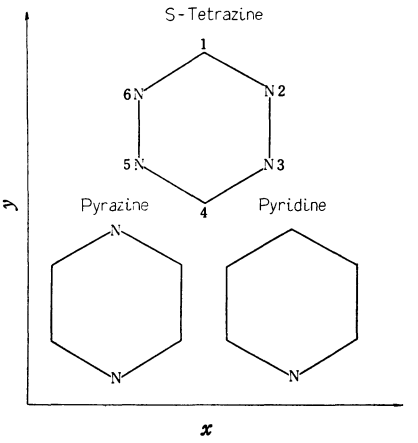

Fig. 1. The numbering of atoms and the coordinate of symmetry operation.

11) R. Pariser and R. G. Parr, (a) *J. Chem. Phys.*, **21**, 466 (1953); (b) ibid., **21**, 767 (1953); (c) ibid., **23**, 711 (1955); (d) R. Pariser, ibid., **24**, 250 (1956).

12) The values of ionization potentials and electron affinities in the valence state are taken from: H. O. Pritchard and H. A. Skinner, *Chem. Rev.*, **55**, 745 (1955).

13) L. Paoloni, *J. Chem. Phys.*, **25**, 1277 (1956).

*) Note added in proof: Paoloni has used the ASMOCI method. Although he has employed the value −2.34 e.v. in ref. 13), he has pointed out in another place§ that β_{NN} could be as low as −1 e.v. if one invokes the configuration interaction among χ_0, $\chi_{2\rightarrow6}$ and $\chi_{1\rightarrow4}$. However, in our present theory which takes into consideration only a limited amount of configuration interaction, the best choise of β_{NN} value seems to be the one employed here. The author is grateful to Dr. L. Paoloni of Rome University for illuminating discussions on this point.

§ L. Paoloni, Gazz. chim. ital., **87**, 313 (1957).

14) F. Bertinotti, G. Giacomello and A. M. Liquori, *Acta Cryst.*, **8**, 513 (1955); ibid., **9**, 510 (1956).

TABLE II
THE ENERGIES OF CONFIGURATIONS AND THE VALUES OF INTERCONFIGURATIONAL MATRIX ELEMENTS*

$\Psi(^1B_{3u}^-) = 0.8691\,{}^1\chi_{3\to4} - 0.4945\,{}^1\chi_{2\to5}$ $E(^1\chi_{3\to4}) = 5.7479$
$\Psi(^1B_{3u}^+) = 0.4945\,{}^1\chi_{3\to4} + 0.8691\,{}^1\chi_{2\to5}$ $E(^1\chi_{2\to5}) = 7.2810$
$(^1\chi_{3\to4} \mid \mathbf{H} \mid {}^1\chi_{2\to5}) = 1.2901$
$\Psi(^3B_{3u}^-) = 0.2181\,{}^3\chi_{3\to4} - 0.9759\,{}^3\chi_{2\to5}$ $E(^3\chi_{3\to4}) = 3.4231$
$\Psi(^3B_{3u}^+) = 0.9759\,{}^3\chi_{3\to4} + 0.2181\,{}^3\chi_{2\to5}$ $E(^3\chi_{2\to5}) = 5.8077$
$(^3\chi_{3\to4} \mid \mathbf{H} \mid {}^3\chi_{2\to5}) = -0.5607$
$(34 \mid G \mid 34) = 5.6509$, $(34 \mid G \mid 43) = 1.1624$,
$(25 \mid G \mid 25) = 5.3782$, $(25 \mid G \mid 52) = 0.7366$
$\Psi(^1B_{1u}^-) = 0.0927\,{}^1\chi_{2\to4} - 0.9957\,{}^1\chi_{3\to5}$ $E(^1\chi_{2\to4}) = 6.8708$
$\Psi(^1B_{1u}^+) = 0.9957\,{}^1\chi_{2\to4} + 0.0927\,{}^1\chi_{3\to5}$ $E(^1\chi_{3\to5}) = 9.9633$
$(^1\chi_{2\to4} \mid \mathbf{H} \mid {}^1\chi_{3\to5}) = -0.2899$
$\Psi(^3B_{1u}^-) = 0.1598\,{}^3\chi_{2\to4} - 0.9871\,{}^3\chi_{3\to5}$ $E(^3\chi_{2\to4}) = 3.1924$
$\Psi(^3B_{1u}^+) = 0.9871\,{}^3\chi_{2\to4} + 0.1598\,{}^3\chi_{3\to5}$ $E(^3\chi_{3\to5}) = 6.5663$
$(^3\chi_{2\to4} \mid \mathbf{H} \mid {}^3\chi_{3\to5}) = -0.5607$
$(24 \mid G \mid 24) = 6.6683$, $(24 \mid G \mid 42) = 1.8392$,
$(35 \mid G \mid 35) = 3.8329$, $(35 \mid G \mid 53) = 1.6985$

* The energies are in unit of *e.v.*

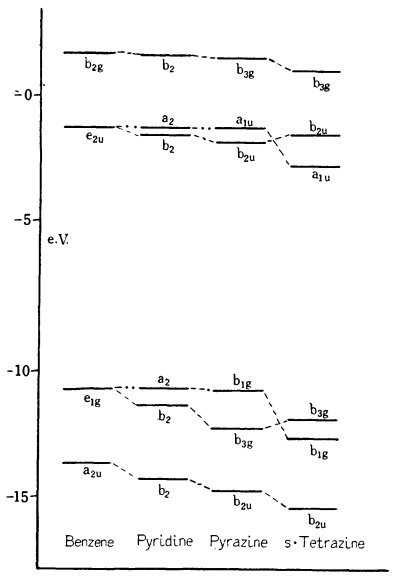

Fig. 2. SCFMO energies of benzene, pyridine, pyrazine and *s*-tetrazine.

The numbering of atoms and the coordinate for the symmetry operation are shown in Fig. 1. For the purpose of comparison, the SCF MO energies are indicated in Fig. 2 together with those of benzene, pyridine and pyrazine[1].

It is evident from Fig. 2 that both of the doubly degenerate benzene MO's e_{1g} and e_{2u} are split into two MO's with different energies in pyridine, pyrazine and *s*-tetrazine owing to the lowering of molecular symmetry. In pyrazine, b_{1g} is higher than b_{3g} in the occupied MO's, and in the vacant MO's a_{1u} is higher than b_{2u}. When molecular symmetry is reduced from D_{2h} in pyrazine to C_{2v} in pyridine, a_{1u} and b_{1g} become a_2, and b_{2u} together with b_{3g} become b_2. In addition, the former is higher than the latter, in the case of pyridine, both in the occupied and the vacant MO's. In the case of *s*-tetrazine, the relative order of the coresponding levels is reversed. The cause of this reversal may plausibly be attributed to the strengthening of the core potential, resulting from the increase of the number of nitrogen atoms. The excited state wave functions, energies of configarations and the values of interconfigurational matrix elements are given in Table II.

The calculated excitation energies and oscillator strengths are collected in Table III, in comparison with the observed values. Unfortunately, the experimental

TABLE III
EXCITATION ENERGIES AND OSCILLATOR STRENGTHS

Symmetry		Excitation energy (*e.v.*)		Oscillator strength	
Group theory	Platt	calc.	obs.	calc.	obs.
$^1B_{3u}^-$	^1L_b	5.013	4.96[a]	0.11	—
$^1B_{1u}^+$	^1L_a	6.842	—	0.43	—
$^1B_{3u}^+$	^1B_b	8.015	—	1.35	—
$^1B_{1u}^-$	^3L_a	9.990	—	0.73	—
$^3B_{1u}^+$	^3L_a	3.101	—	0	—
$^3B_{3u}^+$	^3B_b	3.298	—	0	—
$^3B_{3u}^-$	^3L_b	5.933	—	0	—
$^3B_{1u}^-$	^3B_a	6.657	—	0	—

a) Ref. 15)

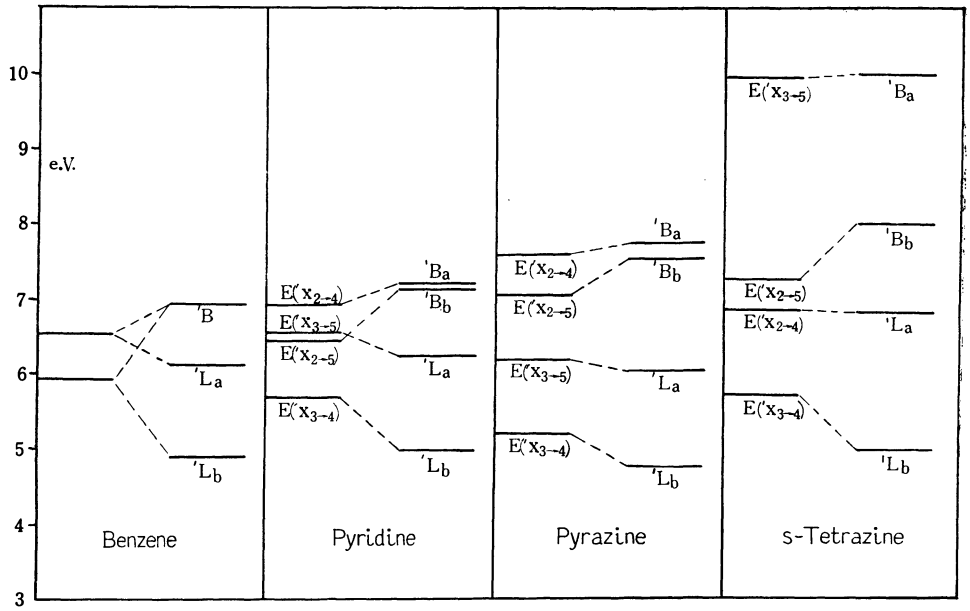

Fig. 3. Interactions between lower excited singlet configurations.

data are not sufficient, and only the value of excitation energy for the lowest singlet $\pi\to\pi$ transition is available[15]. For this transition, the calculated excitation energy agrees satisfactorily with the observed one.

The configuration integration between the singlet excited configurations are illustrated in Fig. 3 together with results[1] for benzene, pyridine, for the purpose of comparison. It is clear, from the results given in Fig. 3, that the configuration interaction plays a very important role for the determination of the spectra. Let us consider, for example, the case of the lowest singlet excited state, $^1B_{3u}$. The two configurations, $^1\chi_{3\to4}$ and $^1\chi_{2\to5}$ are degenerate in benzene, and the degree of splitting due to configuration interaction is very large. The two configurations are no longer degenerate in pyridine, *s*-tetrazine and pyrazine, and the energy difference between the two configurations becomes larger in this order. The magnitude of the splitting is, however, the smaller, the larger is the energy difference between the two configurations. Thus the relative hight of $^1B^-{}_{3u}$ state in this series of nitrogen heterocycles is approximately unchanged, and almost the same as that in benzene. This circumstance of the configuration interaction in nitrogen heterocycles has already been discussed qulitatively by Tsubomura[5], and his conclusion is confirmed by our quantitative study described above. It may be a very interesting problem whether such an argument is still applicable to the electronic spectra of pyridinium ion, the lowest excited state of which has almost the same excitation energy as that of pyridine*.

As mentioned above, we have pointed out previously[1], that the perturbation on MO by hetro-replacement may have only small influence on the oscillator strength, and almost all the part of the latter may arise from the inequality of a and b in Eq. 24.

$$\Psi(\Gamma)=a\chi_1+b\chi_2 \qquad (24)$$

where $\Psi(\Gamma)$ is an excited-state wave function and χ_1 and χ_2 are two configurations interacting upon each other.

That the same circumstance prevails also in the case of *s*-tetrazine is evident from the following analysis. Let us put $a=b$ in Eq. 24, then the oscillator strengths of *s*-tetrazine become as follows.

Γ	f
$^1B^-{}_{3u}$	0.01
$^1B^+{}_{1u}$	0.008

In fact, these values of f are very small compared with the actual values of

15) A. M. Liquori and A. Vaciago, *Ric. Scient.*, **26**, 181 (1956); *Gazz. chim. ital.*, **86**, 759 (1956).

* In this respect, the present author, in collaboration with Miss S. Tsuno, is now working out the electronic structure of pyridinium ion.

calculated oscillator strength and are almost negligible.

Now let us refer to the polarizations of transitions in this molecule, though there are no such experimental data available at present.

With the results and reasonings described hitherto, the polarization of transition to the lowest excited state may be polarized in x direction of Fig. 1, where, in addition to *s*-tetrazine, pyridine and pyrazine are pictured for the convenience of comparison, their corresponding transitions being polarized also in x direction of the figure. The transition to the second excited state, however, is polarized in y direction in *s*-tetrazine as well as in pyridine and pyrazine.

Eventually, the spectral similarity of *s*-tetrazine with the parent hydrocarbon and the other nitrogen heterocycles such as pyridine and pyrazine originates from the close correspondence of the MO's of the former with those of the latter, though the MO energies of *s*-tetrazine are considerably different from those of the others. Whereas the relative order of b_{1g} and b_{3g} or a_{1u} and b_{2u} orbitals in energy scale is reversed in *s*-tetration compared with those in pyrazine or pyridine, the result of configuration interaction gives the excitation energy of the transition to the lowest excited state which is almost the same as those of pyrazine, pyridine and benzene, in good agreement with the experimental observation.

Summary

(1) π-Electronic structure and the nature of the electronic transitions in the *s*-tetrazine molecule has been elucidated using the semiempirical LCAO SCF MO method.

(2) There is satisfactory agreement between the calculated and the observed values of the excitation energy for the transition to the lowest excited state.

(3) Tsubomura's qualitive argument concerning the influence of configuration interaction on the lowest energy transition of nitrogen heterocycles has been confirmed by the quantitative calculation.

(4) The cause of the intensification of ^1L_b band compared with the parent hydrocarbon has been analysed by the same method employed previously[1], and it has been confirmed that, also in the case of *s*-tetrazine the perturbation on MO by hetero-replacement has only a small influence on the oscillator strength.

(5) The spectral simirarity of nitrogen heterocycles with the parent hydrocarbon has been ascribed to the fact that their MO's correspond closely each other, and it has been pointed out that the configuration interaction plays a very important role in the determination of spectra, which is also a cause for the spectral similarity.

The autor expresses his gratitude to Professor S. Mizushima of Tokyo University for his encouragement. He also expresses his cordial thanks to Professor R. Fujishiro for his interest and encouragement during the present study. He is grateful to Dr. S. Nagakura of Tokyo University and Dr. H. Tsubomura of Tokyo University for their illuminating discussions. He also express his hearty thanks to Mr. K. Nishimoto and Miss S. Tsuno for their helpful discussions.

Institute of Polytechnics
Osaka City University
Kita-ku, Osaka

Electronic Spectra of Quinoline and Isoquinoline and the Mechanism of Fluorescence Quenching in These Molecules

By Noboru MATAGA

(Received December 18, 1957)

In the previous papers[1,2] we have reported detailed theoretical studies on the electronic structure and the nature of electronic transitions of some nitrogen heterocycles, using the semiempirical SCF method. The detailed Hartree-Fock SCF study has been made only for nitrogen heterobenzenes, and some semiquantitative extentions to larger molecules such as acridine and phenazine have been made on the basis of the results obtained for nitrogen heterobenzenes. Even by the latter very approximate method, the general feature of the electronic spectra is fairly well comprehended. In the present report and also in following one, we shall employ a more rigorous method and give a more detailed interpretation and reasoning on the nature of the electronic transitions in some two and three ring-nitrogen heterocycles such as quinoline, isoquinoline, acridine and phenazine.

Method

The Hartree-Fock self-consistent field method applied to molecules in terms of MO's, determines the best MO's for approximate ground state, and these MO's may also be satisfactory in describing the excited states[3]. As pointed out by McWeeny[4], however, it may be possible that other choices of MO's may give a comparable result for the interpretation of electronic spectra. From such a viewpoint, rather than pursuing a laborious iterative calculation of SCF, we have assumed that SCF MO's of the parent hydrocarbon[5], naphthalene, may be a satisfactory approximation to the MO's of quinoline and isoquinoline for the description of the excited states. Then the orbital energy of the i-th orbital, ε_i, and the excitation energy of the $i\rightarrow k$ transition, $E(\chi_{i\rightarrow k})$ may be calculated by the following equation[1,2].

$$\varepsilon_i=\int\psi_i^*F\psi_i dv=\sum_{\mu,\nu}c^*_{i\mu}c_{i\nu}F_{\mu\nu} \tag{1}$$

where F is the Fock's Hamiltonian and ψ_i is the LCAO MO of the parent hydrocarbon,

$$\psi_i=\sum_\mu c_{i\mu}\phi_\mu \tag{2}$$

$$F_{\mu\mu}=\alpha_\mu+\frac{1}{2}P_{\mu\mu}\gamma_{\mu\mu}+\sum_{\kappa(\neq\mu)}(P_{\kappa\kappa}-1)\gamma_{\mu\kappa} \tag{3}$$

$$F_{\mu\nu}=\beta_{\mu\nu}-\frac{1}{2}P_{\mu\nu}\gamma_{\mu\nu} \tag{4}$$

The last term in the right hand side of Eq. 3 vanishes because of the uniform charge density, $P_{\kappa\kappa}=1$, in the parent hydrocarbon.

$$F_{\mu\mu}=\alpha_\mu+\frac{1}{2}P_{\mu\mu}\gamma_{\mu\mu} \tag{3'}$$

$$E(^1\chi_{i\rightarrow k})=\varepsilon_k-\varepsilon_i-(ik\,|\,G\,|\,ik)+2(ik\,|\,G\,|\,ki), \tag{5}$$

$$E(^3\chi_{i\rightarrow k})=E(^1\chi_{i\rightarrow k})-2(ik\,|\,G\,|\,ki) \tag{6}$$

where,

$$(ik\,|\,G\,|\,ik)=\int\psi_i^*(1)\psi_k^*(2)\frac{e^2}{r_{12}}\psi_i(1)\psi_k(2)\,dv_1dv_2 \tag{7}$$

$$(ik\,|\,G\,|\,ki)=\int\psi_i^*(1)\psi_k^*(2)\frac{e^2}{r_{12}}\psi_k(1)\psi_i(2)\,dv_1dv_2 \tag{8}$$

Expanding ψ_i's in terms of AO's, and neglecting the differential overlap, Eqs. 7 and 8 become as follows,

$$(ik\mid G\mid ik)=\sum_{\mu,\nu}c^*_{i\mu}c_{i\mu}c^*_{k\nu}c_{k\nu}\gamma_{\mu\nu}\,, \tag{9}$$

$$(ik\mid G\mid ki)=\sum_{\mu,\nu}c^*_{i\mu}c_{k\mu}c^*_{k\nu}c_{i\nu}\gamma_{\mu\nu}\,. \tag{10}$$

ε_i and $E(\chi_{i\rightarrow k})$ thus calculated for nitrogen heterocycles may be different from the corresponding quantities of the parent hydrocarbon by small amounts $\delta\varepsilon_i$ and $\delta E(\chi_{i\rightarrow k})$, because of slight changes in the core potential and electronic repulsion energies due to the hetero-replacement.

The expressions for $\delta\varepsilon_i$ and $\delta E(\chi_{i\rightarrow k})$ may be written as follows

$$\delta\varepsilon_i=\sum_{\mu,\nu}c^*_{i\mu}c_{i\nu}(\delta F_{\mu\nu}) \tag{11}$$

$$\delta F_{\mu\mu}=\delta\alpha_\mu+\frac{1}{2}P_{\mu\mu}(\delta\gamma_{\mu\mu}) \tag{12}$$

$$\delta F_{\mu\nu}=\delta\beta_{\mu\nu}-\frac{1}{2}P_{\mu\nu}(\delta\gamma_{\mu\nu}) \tag{13}$$

$$\delta E(^1\chi_{i\rightarrow k})=\delta\varepsilon_k-\delta\varepsilon_i-\sum_{\mu,\nu}c^*_{i\mu}c_{i\mu}c^*_{k\nu}c_{k\kappa}(\delta\gamma_{\mu\nu})+2\sum_{\mu,\nu}c^*_{i\mu}c_{k\mu}c^*_{k\nu}c_{i\nu}(\delta\gamma_{\mu\nu}) \tag{14}$$

1) N. Mataga and K. Nishimoto, *Z. physik. Chem.*, N. F. in press.
2) N. Mataga, This Bulletin **31**, 453 (1958).
3) C. C. J. Roothaan, *Rev. Mod. Phys.*, **23**, 61 (1951).
4) R. McWeeny, *Proc. Phys. Soc.*, **A70**, 593 (1957).
5) We have calculated the electronic spectra of some unsaturated hydrocarbons by the self-consistent field method, using our semiempirical parameters described in refs. 1) and 2). N. Mataga and K. Nishimoto, to be published elsewhere.

$$\delta E(^3\chi_{i\to k}) = \delta E(^1\chi_{i\to k}) - 2\sum_{\mu,\nu} c^*_{i\mu}c_{k\mu}c^*_{k\nu}c_{i\nu}(\delta\gamma_{\mu\nu}) \quad (15)$$

In addition, we have taken into consideration some amount of configuration intereactions, which is restricted only to those invoked in the calculation of parent hydrocarbon.

The interconfigurational matrix elements may be expressed as follows.

$$(^1\chi_{i\to k}|\mathbf{H}|^1\chi_{j\to l}) = -(jk|G|il) + 2(jk|G|li) \quad (16)$$

$$(^3\chi_{i\to k}|\mathbf{H}|^3\chi_{j\to l}) = (^1\chi_{i\to k}|\mathbf{H}|^1\chi_{j\to l}) - 2(jk|G|li) \quad (17)$$

where,
$$(jk \mid G \mid il) = \sum_{\mu,\nu} c^*_{j\mu}c_{i\mu}c^*_{k\nu}c_{l\nu}\gamma_{\mu\nu}\,, \quad (18)$$

$$(jk \mid G \mid li) = \sum_{\nu,\nu} c^*_{j\mu}c_{l\mu}c^*_{k\nu}c_{i\nu}\gamma_{\mu\nu}\,. \quad (19)$$

The difference between these quantities and the corresponding ones of the parent hydrocarbon may be written as

$$\delta(^1\chi_{i\to k} \mid \mathbf{H} \mid {}^1\chi_{j\to l}) = -\sum_{\mu,\nu} c^*_{j\mu}c_{i\mu}c^*_{k\nu}c_{l\nu}(\delta\gamma_{\mu\nu}) + 2\sum_{\mu,\nu} c^*_{j\mu}c_{l\mu}c^*_{k\nu}c_{i\nu}(\delta\gamma_{\mu\nu}) \quad (20)$$

$$\delta(^3\chi_{i\to k} \mid \mathbf{H} \mid {}^3\chi_{j\to l}) = \delta(^1\chi_{i\to k} \mid \mathbf{H} \mid {}^1\chi_{j\to l}) - 2\sum_{\mu,\nu} c^*_{j\mu}c_{l\mu}c^*_{k\nu}c_{i\nu}(\delta\gamma_{\mu\nu}) \quad (21)$$

It will be shown in the next paragraph that $\delta\varepsilon_i$, $\delta E(_{i\to k})$ and $\delta(\chi_{i\to k} \mid \mathbf{H} \mid \chi_{j\to l})$ are really very small and only a small percent of ε_i, $E(\chi_{i\to k})$ and $(\chi_{i\to k} \mid \mathbf{H} \mid \chi_{j\to l})$, respectively.

Therefore, our present treatment may be regarded also as a kind of perturbation theory*.

Previously, Pariser and Parr[6] calculated the electronic spectra of some nitrogen heterobenzenes by their semiempirical ASMO method including configuration interaction, using, however, MO's of benzene.

Our procedure described above may be equivalent to theirs, but ours is in terms of Hartree-Fock SCF theory, involving configuration interaction. In view of the approximate nature of our treatment and also for lack of experimental data, values of $\gamma_{\mu\nu}$ necessary for the evalution of electronic repulsion integrals $\gamma_{\mu\nu}$ and oscillator strengths are taken from those of naphthalene. The method of the semiempirical evalution of $r_{\mu\nu}$ and the calculation of oscillator strength are the same as in the previous reports[1,2].

Results and Discussions

In Table I, the orbital energies of highest and second highest occupied levels and lowest and second lowest vacant levels which are responsible for transitions to lower excited states, are given together with their $\delta\varepsilon_i$.

In the case of isoquinoline, all levels are more or less depressed; in the case of quinoline, however, fourth and sixth levels are depressed on the one hand and fifth and seventh levels are lifted on the other hand. The perturbation caused by the hetero-replacement on α-position is different from that on β-position, in this way.

TABLE I*
(in unit of *e.v.*)

	Quinoline		Isoquinoline	
i	ε_i	$\delta\varepsilon_i$	ε_i	$\delta\varepsilon_i$
4	−10.791	−0.205	−11.196	−0.611
5	− 9.494	0.120	− 9.767	−0.153
6	− 2.734	−0.348	− 2.518	−0.133
7	− 1.209	0.205	− 1.442	−0.027

* $\delta\varepsilon_i = \varepsilon_i - \varepsilon^0{}_i$, where $\varepsilon^0{}_i$ is the corresponding orbital energy of naphtalene.

In the following, we shall give a detailed account only about the transition to the lowest excited singlet state, the intensity of which is most remarkably influenced by the hetero-replacement. We shall also give some arguments on the corresponding triplet state, i. e. ^3L_b, in relation to the mechanism of fluorescence quenching in quinoline.

The excited state wave functions, energies of configurations and the values of interconfigulational matrix elements as well as their differences from the corresponding quantities of the parent hydrocarbon are given in Table II.

In Table III, the calculated excitation energies and oscillator strengths indicated in comparison with the observed values.

The calculated values of excitation energies are in a satisfactory agreement with observed ones and the slight difference between the observed spectra of quinoline and isoquinoline is well interpreted, i. e., the theory predicts that the excitation energy of isoquinoline is slightly smaller than that of quinoline, in agreement with the observation.

The experimental values of oscillator strengths of these molecules are uncertain, and only the values of log ε_{max} are given in Table III.

By an inspection of this table, the observed intensity of quinoline seems almost the same as that of isoquinoline. The ^1L_b band of quinoline, however, is strongly superposed by ^1L_b band, the intensity of which may be scarcely affected by the hetero-replacement*, in contradistinction to the case of isoquinoline, where the superposition is not so much remarkable

* The present writer is now pursuing a calculation on the electronic structure of nitrogen heterocycles, which is based on stadard method of the perturbation theory.

6) R. Pariser and R. G. Parr, *J. Chem. Phys.*, **21**, 767 (1953).

* The results for ^1L_a state together with those for ^1B_b and ^1B_a states will be published shortly.

TABLE II

(in units of *e.v.*)

Quinoline

$$\Psi(^1L_b) = 0.757\,{}^1\chi_{4\to6} - 0.652\,{}^1\chi_{5\to7}, \qquad E(^1\chi_{4\to6}) = 4.864, \quad E(^1\chi_{5\to7}) = 5.092$$

$$\Psi(^3L_b) = 0.537\,{}^3\chi_{4\to6} - 0.843\,{}^3\chi_{5\to7}, \qquad E(^3\chi_{4\to6}) = 3.857, \quad E(^3\chi_{5\to7}) = 4.085$$

$$(^1\chi_{4\to6} \mid \mathbf{H} \mid {}^1\chi_{5\to7}) = 0.763, \quad (^3\chi_{5\to6} \mid \mathbf{H} \mid {}^3\chi_{5\to7}) = -0.244.$$

$$\sum_{\mu,\nu} c^*_{4\mu}c_{4\mu}c^*_{6\nu}c_{6\nu}\gamma_{\mu\nu} = \sum_{\mu,\nu} c^*_{5\mu}c_{5\mu}c^*_{7\nu}c_{7\nu}\gamma_{\mu\nu} = 4.199,$$

$$\sum_{\mu,\nu} c^*_{4\mu}c_{6\mu}c^*_{6\nu}c_{4\nu}\gamma_{\mu\nu} = \sum_{\mu,\nu} c^*_{5\mu}c_{7\mu}c^*_{7\nu}c_{5\nu}\gamma_{\mu\nu} = 0.503.$$

$$\sum_{\mu,\nu} c^*_{4\mu}c_{6\mu}c^*_{7\nu}c_{5\nu}\gamma_{\mu\nu} = \sum_{\mu,\nu} c^*_{5\mu}c_{7\mu}c^*_{7\nu}c_{5\nu}\gamma_{\mu\nu}, \qquad \sum_{\mu,\nu} c^*_{4\mu}c_{5\mu}c^*_{7\nu}c_{6\nu}\gamma_{\mu\nu} = 0.244.$$

$$\delta E(^1\chi_{4\to6}) = -0.176, \qquad \delta E(^1\chi_{5\to7}) = 0.052, \qquad \delta(^1\chi_{4\to6} \mid \mathbf{H} \mid {}^1\chi_{5\to7}) = 0.000,$$

$$\delta E(^3\chi_{4\to6}) = -0.149, \qquad \delta E(^3\chi_{5\to7}) = 0.079, \qquad \delta(^2\chi_{4\to6} \mid \mathbf{H} \mid {}^3\chi_{5\to7}) = 0.003.$$

$$\sum_{\mu,\nu} c^*_{4\mu}c_{4\mu}c^*_{6\nu}c_{6\nu}(\delta\gamma_{\mu\nu}) = \sum_{\mu,\nu} c^*_{5\mu}c_{5\mu}c^*_{7\nu}c_{7\nu}(\delta\gamma_{\mu\nu}) = 0.033.$$

$$\sum_{\mu,\nu} c^*_{4\mu}c_{6\mu}c^*_{6\nu}c_{4\nu}(\delta\gamma_{\mu\nu}) = \sum_{\mu,\nu} c^*_{5\mu}c_{7\mu}c^*_{7\nu}c_{5\nu}(\delta\gamma_{\mu\nu}) = 0.000.$$

$$\sum_{\mu,\nu} c^*_{4\mu}c_{5\mu}c^*_{7\nu}c_{6\nu}(\delta\gamma_{\mu\nu}) = 0.000.$$

Isoquinoline

$$\Psi(^1L_b) = 0.410\,{}^1\chi_{4\to6} - 0.911\,{}^1\chi_{5\to7}, \qquad E(^1\chi_{4\to6}) = 5.513, \quad E(^1\chi_{5\to7}) = 4.101$$

$$\Psi(^3L_b) = 0.883\,{}^3\chi_{4\to6} - 0.469\,{}^3\chi_{5\to7}, \qquad E(^3\chi_{4\to6}) = 4.454, \quad E(^3\chi_{5\to7}) = 3.043$$

$$(^1\chi_{4\to6} \mid \mathbf{H} \mid {}^1\chi_{5\to7}) = 0.798, \quad (^3\chi_{4\to6} \mid \mathbf{H} \mid {}^3\chi_{5\to7}) - 0.260.$$

$$\sum_{\mu,\nu} c^*_{4\mu}c_{4\mu}c^*_{6\nu}c_{6\nu}\gamma_{\mu\nu} = \sum_{\mu,\nu} c^*_{5\mu}c_{5\mu}c^*_{7\nu}c_{7\nu}\gamma_{\mu\nu} = 4.224.$$

$$\sum_{\mu,\nu} c^*_{4\mu}c_{6\mu}c^*_{6\nu}c_{4\nu}\gamma_{\mu\nu} = \sum_{\mu,\nu} c^*_{5\mu}c_{7\mu}c^*_{7\nu}c_{5\nu}\gamma_{\mu\nu} = 0.529.$$

$$\sum_{\mu,\nu} c^*_{4\mu}c_{6\mu}c^*_{7\nu}c_{5\nu}\gamma_{\mu\nu} = \sum_{\mu,\nu} c^*_{5\mu}c_{7\mu}c^*_{7\nu}c_{5\nu}\gamma_{\mu\nu}, \qquad \sum_{\mu,\nu} c^*_{4\mu}c_{5\mu}c^*_{7\nu}c_{6\nu}\gamma_{\mu\nu} = 0.260.$$

$$\delta E(^1\chi_{4\to6}) = 0.473, \qquad \delta E(^1\chi_{5\to7}) = -0.393, \qquad \delta(^1\chi_{4\to6} \mid \mathbf{H} \mid {}^1\chi_{5\to7}) = 0.035.$$

$$\delta E(^3\chi_{4\to6}) = 0.448, \qquad \delta E(^3\chi_{5\to7}) = 0.095, \qquad \delta(^3\chi_{4\to6} \mid \mathbf{H} \mid {}^3\chi_{5\to7}) = -0.013.$$

$$\sum_{\mu,\nu} c^*_{4\mu}c_{4\mu}c^*_{6\nu}c_{6\nu}(\delta\gamma_{\mu\nu}) = \sum_{\mu,\nu} c^*_{5\mu}c_{5\mu}c^*_{7\nu}c_{7\nu}(\delta\gamma_{\mu\nu}) = 0.058.$$

$$\sum_{\mu,\nu} c^*_{4\mu}c_{6\mu}c^*_{6\nu}c_{4\nu}(\delta\gamma_{\mu\nu}) = \sum_{\mu,\nu} c^*_{5\mu}c_{7\mu}c^*_{7\nu}c_{5\nu}(\delta\gamma_{\mu\nu}) = 0.026.$$

$$\sum_{\mu,\nu} c^*_{4\mu}c_{5\mu}c^*_{7\nu}c_{6\nu}(\delta\gamma_{\mu\nu}) = 0.016.$$

TABLE III

	Excitation Energy (*e.v.*)		Oscillator Strength	
	Calcd.	Obsd.[a,b]	Calcd.	Obsd.[a] ($\log \varepsilon_{max}$)
	Quinoline			
^1L_b	4.207	3.96	0.01	3.4
^3L_b	4.240	—	0.00	—
	Isoquinoline			
^1L_b	3.742	3.86	0.16	3.6
^3L_b	4.592	—	0.00	—

a) R. A. Friedel and M. Orchin, "Ultraviolet Spectra of Aromatic Compounds", John Wiley and Sons, 1951.

b) J. R. Platt, *J. Chem. Phys.*, **19**, 101 (1951).

because ^1L_a band is shifted to a somewhat shorter wave length side and ^1L_b band to a longer wave length side in some degree compared with those of quinoline.

Therefore, in reality, the oscillator strength of quinoline may be far smaller than that of isoquinoline, in qualitative agreement with the theoretical prediction. Now, some considerations on the mechanism of the fluorescence quenching in nitrogen heterocycles will be given on the basis of the present theoretical calculation. Previously, we have studied the hydrogen bonding effect on the fluorescence of quinoline and acridine in non-polar solvent mixed with various proton donors, in order to elucidate the mechanism of inner quenching in these molecules[7]. The results were as follows. The larger the relative fluorescence yields of hydrogen bonded nitrogen heterocycles become, the stronger the donating powers of proton donors are, and from this fact, it has become clear that the cause of the remarkable inner quenching in these molecules compared with the parent aromatic hydrocarbons may be attributable to the interaction between n- and π-electrons in the

7) N. Mataga and S. Tsuno, This Bulletin, **30**, 368 (1957).

excited state, which may probably induce the radiationless transition to the ground state, directly or indirectly.

Moreover, we have found an interesting fact that the difference in the emitting π-electronic state leads to the different behavior of these nirogen heterocycles in fluorescene quenching by a halogen atom.

Although the increase in fluorescence yields of quinoline and acridine by hydrogen bonding with ethanol or by proton addition in aqueous solution is almost the same, the fluorescence yield of quinoline hydrogen bonded with trichloracetic acid is rather small compared with the fluorescence yield in ethanol solution, in contradistinction to the fact that the fluorescence yield of acridine is greatly enhanced by hydrogen bonding with trichloracetic acid. This distinction in these two molecules was ascribsd to the difference of emitting π-electronic state as follows[7].

In aromatic hydrocarbons, such as benzene, naphthalene and anthracene, there exists ^3L_b state which has the same energy as ^1L_b, but for ^1L_a, there exists no such circumstance, the energy of ^3L_a state being considerably different from that of ^1L_a[5,8,9]. If the lowest singlet excited state is ^1L_b, the phosphorescence transition occurs with relative ease probably by the process, $^1L_b \dashrightarrow {}^3L_b \dashrightarrow {}^3L_a \dashrightarrow$ ground state. However, when the lowest singlet excited state is ^1L_a, phosphorescence transition may be very difficult. We have assumed[7] that the analogous situation probably prevails also in these heterocyclic molecules, because of the close similarity of the electronic spectra of the latter with those of isoelectronic aromatic hydrocarbons. Now, as shown in Table III, the results of the present calculation clearly indicate that, at least in the case of quinoline, there exists ^3L_b state which has almost the same energy as ^1L_b. Thus, on the basis of the present results, it is confirmed that, at least in the case of quinoline, the near-by existence of a halogen atom may easily accelerate $^1L_b \dashrightarrow {}^3L_b$ process owing to the spin orbital perturbation, but it may be difficult for such a situation to be realized in acridine*. The circumstance in the case of isoqunoline may be somewhat different from the situation described above, because ^3L_b is somewhat higher than ^1L_b. Unfortunately, such an experimental observation for the case of isoquinoline is not yet available. After all, the close spectral similarity of quinoline and isoquinoline with naphthalene and also the intensification of ^1L_b band due to heteroreplacement are well comprehended by the present perturbation method. Moreover, the assumed effect of emitting π-electronic state on the quenching phenomenon, has been confirmed on the theoretical ground.

Summary

1. A pertubation theory based on the Hartree-Fock SCF theory including a limited number of configuration interactions was applied to quinoline and isoquinoline.

2. The theory satisfactorily interprets the excitation energies and oscillator strengths of ^1L_b bands of these nitrogen heterocycles.

3. The previous assumption concerning the effect of π-electronic state on the fluorescence quenching in nitrogen heterocycles due to the near-by existence of a halogen atom, was confirmed for the case of quinoline, on the basis of the theoretical calculation.

The present author expresses his sincere gratitude to Professor S. Mizushima of Tokyo University for his encouragement. He is also gratful to Professor R. Fujishiro for his encouragement. He expresses his cordial thanks to Dr. S. Nagakura of Tokyo University, Dr. H. Tsubomura of Tokyo University and Dr. H. Baba of Hokkaido University for their fruitful discussions. He also is glad to express his appreciation to Mr. K. Nishimoto and Miss S. Tsuno for their helpful discussions.

Institute of Polytechnics
Osaka City University
Kita-ku, Osaka

8) R. Pariser, *J. Chem. Phys.*, **24**, 250 (1956).
9) J. A. Pople, *Proc. Phys, Soc.*, **68A**, 81 (1955).

* Detailed discussions on acridine will be given in a following paper.

Electronic Spectra of Acridine and Phenazine

By Noboru MATAGA

(Received December 18, 1957)

In the first papar[1] of our studies on the electronic structure and spectra of nitrogen heterocycles, some semiquantitative treatments on the electronic spectra of acridine and phenazine have been given, on the basis of the results obtained for nitrogen heterobenzenes employing the Hartree-Fock SCF theory including the limited amount of configuration interactions. In the present report, we shall apply the perturbation method developed in the third paper[2] to these three-ring nitrogen heterocycles, and give more detailed and quantitative interpretations on the electronic structure and spectra of these molecules.

Electronic Spectra of Anthracene as a Basis of the Perturbation Calculation

As a first step, we have regarded the naive MO's of anthracene as a good approximation to the MO's of these three ring nitrogen heterocycles. As pointed out by Dewar and Longuet-Higgins[3] in their semiquantitative discussions on the general feature of aromatic hydrocarbon spectra, the naive MO's of these aromatic hydrocarbons may be good approximate solutions of the Hartree-Fock self-consistent field equations or close to the best MO's available for constructing the excited state wave functions, owing to the uniformity of electron distribution in these molecules.

In our theoretical work[4] on the electronic spectra of some unsaturated hydrocarbons, it has been clearly indicated, that, for example, employing our semi-empirical parameters,[1,5] the naive MO's of naphthalene interpret the experimental spectra almost equally well as the Hartree-Fock self-consistent field MO's and also the approximate self-consistent field MO's obtained by neglecting the non-diagonal matrix elements of Fock's Hamiltonian in terms of AO's, $F_{\mu\nu}$, when μ and ν are apart each other further than the nearest neighbor. Thus, in this case, naive MO's are very satisfactory for the description of electronic spectra, although they give a wrong prediction about the bond orders in the ground state.

The naive MO's of anthracene also give a satisfactory explanation of the experimental spectra as in the following cases.

In view of the approximate nature of our treatment, the geometrical structure of the molecule has been assumed to be a condensed regular hexagon, the nearest neighbor bond distance of which has been taken as 1.402_7 Å. This value is a weighted mean of five different bond distances determined by X-ray diffraction[6]. The same geometrical structure as anthracence, has been assumed also for acridine and phenazine treated in a latter paragraph.

The MO's and MO energies of anthra-

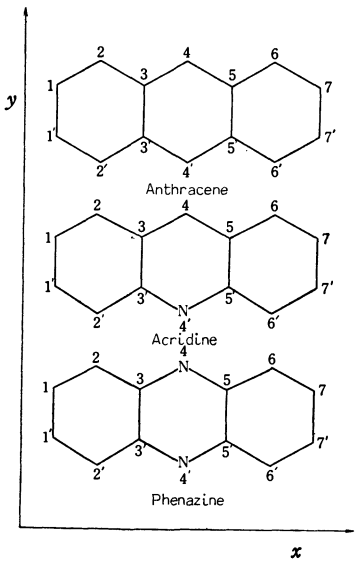

Fig. 1. The numbering of atoms and the coordinate of symmetry operation.

1) N. Mataga and K. Nishimoto, *Z. Phys. Chem.* N. F., in press.
2) N. Mataga, to be published in this Bulletin.
3) M. J. S. Dewar and H. C. Longuet-Higgins, *Proc. Phys. Soc.*, **67A**, 795 (1954).
4) N. Mataga and K. Nishimoto, to be published elsewhere.
5) N. Mataga, to be published in this Bulletin.
6) J. M. Robertson, "Organic Crystals and Molecules", Cornell University Press, 1953.

TABLE I

MO's AND MO ENERGIES OF ANTHRACENE

Symmetry	ε_i(*e.v.*)	
b_{1g}	-10.4865	$\psi_6=0.3535\sigma_6+0.3535\sigma_7$
b_{3g}	-8.8987	$\psi_7=0.3109\sigma_8+0.2199\sigma_9+0.0911\sigma_{10}-0.4397\sigma_{11}$
b_{2u}	-3.1013	$\psi_8=0.3109\sigma_1-0.2199\sigma_2+0.0911\sigma_3-0.4397\sigma_4$
a_{1u}	-1.5135	$\psi_9=-0.3535\sigma_{13}+0.3535\sigma_{14}$

$\sigma_1=(\phi_6+\phi_{6'}+\phi_2+\phi_{2'})$, $\sigma_2=(\phi_7+\phi_{7'}+\phi_{1'}+\phi_1)$, $\sigma_3=(\phi_{3'}+\phi_3+\phi_5+\phi_{5'})$, $\sigma_4=(\phi_4+\phi_{4'})$

$\sigma_8=(\phi_6-\phi_{6'}+\phi_2-\phi_{2'})$, $\sigma_6=(\phi_7+\phi_{7'}-\phi_{1'}-\phi_1)$, $\sigma_7=(\phi_{3'}+\phi_3-\phi_5-\phi_{5'})$, $\sigma_{11}=(\phi_4-\phi_{4'})$

$\sigma_9=(\phi_7-\phi_{7'}-\phi_{1'}+\phi_1)$, $\sigma_{10}=(\phi_{3'}-\phi_3-\phi_5+\phi_{5'})$,

$\sigma_{13}=(\phi_7-\phi_{7'}+\phi_{1'}-\phi_1)$, $\sigma_{14}=(\phi_{3'}-\phi_3+\phi_5-\phi_{5'})$,

TABLE II*

THE EXCITED STATE WAVE FUNCTIONS, ENERGIES OF CONFIGURATIONS AND THE VALUES OF INTERCONFIGURATIONAL MATRIX ELEMENTS OF ANTHRACENE

$\Psi(^1B^+_{1u})=0.9875\,{}^1\chi_{7\to8}+0.1576\,{}^1\chi_{6\to9}$, $E(^1\chi_{7\to8})=3.5549$,

$\Psi(^1B^-_{1u})=0.1576\,{}^1\chi_{7\to8}-0.9875\,{}^1\chi_{6\to9}$, $E(^1\chi_{6\to9})=6.3681$,

$\Psi(^3B^+_{1u})=0.9986\,{}^3\chi_{7\to8}+0.0516\,{}^3\chi_{6\to9}$, $E(^3\chi_{7\to8})=1.6999$,

$\Psi(^3B^-_{1u})=0.0516\,{}^3\chi_{7\to8}-0.9986\,{}^3\chi_{6\to9}$, $E(^3\chi_{6\to9})=4.8158$.

$(78\mid G\mid 78)=4.0975$, $(78\mid G\mid 87)=0.9275$, $(68\mid G\mid 79)=0.1616$,

$(69\mid G\mid 69)=4.1572$, $(69\mid G\mid 96)-0.7761$, $(68\mid G\mid 97)=-0.1496$.

$$\Psi(^1B^+_{3u})=\frac{1}{\sqrt{2}}(^1\chi_{6\to8}+{}^1\chi_{7\to9}),\qquad E(^1\chi_{6\to8})=E(^1\chi_{7\to9})=4.5470$$

$$\Psi(^1B^-_{3u})=\frac{1}{\sqrt{2}}(^1\chi_{6\to8}-{}^1\chi_{7\to9}),$$

$$\Psi(^3B^+_{3u})=\frac{1}{\sqrt{2}}(^3\chi_{6\to8}+{}^3\chi_{7\to9}),\qquad E(^3\chi_{6\to8})=E(^3\chi_{7\to9})=3.7472$$

$$\Psi(^3B^-_{3u})=\frac{1}{\sqrt{2}}(^3\chi_{6\to8}-{}^3\chi_{7\to9}),$$

$(68\mid G\mid 68)=(79\mid G\mid 79)=3.6380$, $(68\mid G\mid 86)=(79\mid G\mid 97)=0.3999$,

$(78\mid G\mid 69)=(68\mid G\mid 79)$, $(78\mid G\mid 96)=(68\mid G\mid 86)$.

$(^1\chi_{7\to8}\mid \mathbf{H}\mid {}^1\chi_{6\to9})=(^1\chi_{6\to8}\mid \mathbf{H}\mid {}^1\chi_{7\to9})=-0.4608$.

$(^3\chi_{7\to8}\mid \mathbf{H}\mid {}^3\chi_{6\to9})=(^3\chi_{6\to8}\mid \mathbf{H}\mid {}^3\chi_{7\to9})=-0.1616$.

* in units of *e.v.*

cene, which concern the electronic transitions to lower excited states are given in Table I.

The numbering of atoms and the coordinate of symmetry operation are shown in Fig. 1. In the approximation of naive MO theory, $\psi_6(b_{1g})$ and $\psi_5(a_{1u})$ are degenerate accidentally in the occupied orbitals as well as $\psi_9(a_{1u})$ and $\psi_{10}(b_{1g})$ in the vacant orbitals. The inclusion of electron interaction, however, removes this accidental degeneracy, and a_{1u} is the lower both in occupied and vacant orbitals. The excited state wave functions, energies of configurations and the values of interconfigurational matrix elements are given in Table II.

The calculated excitation energies and oscillator strengths are collected in Table III, in comparison with the observed values. By an inspection of this table, one may be allowed to say that the theoretical predictions are in very good agreement with the experimental observation, in view of the approximate nature of our calculation.

TABLE III

CALCULATED AND OBSERVED EXCITATION ENERGIES AND OSCILLATOR STRENGTHS OF ANTHRACENE

Symmetry		Excitation Energy (*e.v.*)		Oscillator Strength	
Group theory	Platt	Calcd.	Obsd.	Calcd.	Obsd.[a]
$^1B^+_{1u}$	^1L_a	3.4813	3.30[a]	0.39	~0.1
$^1B^-_{3u}$	^1L_b	3.9087	3.50[a]	0.00	~0
$^1B^+_{3u}$	^1B_b	5.1853	4.80[a]	3.00	2.20
$^1B^-_{1u}$	^1B_a	6.4416	5.64[a]	0.81	0.65
$^3B^+_{1u}$	^3L_a	1.6915	1.8[b]	0.00	—
$^3B^+_{3u}$	^3B_b	3.5856	—	0.00	—
$^3B^-_{3u}$	^3L_b	3.9087	—	0.00	—
$^3B^-_{1u}$	^3B_a	4.8241	—	0.00	—

a) H. B. Klevens and J. R. Platt, *J. Chem. Phys.* **17**, 470 (1949).

b) G. N. Lewis and M. Kasha, *J. Am. Chem. Soc.*, **66**, 2100 (1944); McGlynn, Padhye and Kasha, *J. Chem. Phys.*, **23**, 593 (1955).

Now, let us examine the spectra of heterocycles, on the basis of these results.

Acridine and Phenazine

The orbital energies for acridine and phenazine are collected in Table IV, and Tables V and VI correspond to Tables II and III of the preceding paragraph respectively.

TABLE IV.
ORBITAL ENERGIES OF ACRIDINE AND PHENAZINE

i	ε_i(e.v.)	
	acridine	phenazine
6	−10.4865	−10.4865
7	− 9.3459	− 9.7924
8	− 3.9069	− 3.7815
9	− 1.5135	− 1.5135

The agreement between the calculated and the observed values of excitation energies and oscillator strengths is fairly good in general, although the error between calculated and observed energies of ^1L_a band of phenazine is considerable. About this inconsistency, a more detailed treatment is given in the latter part of this paper. The behavior of ^1L_b band, however, is well comprehended with the above results.

The cause of the intensification of ^1L_b band has been ascribed to the inequality of the coefficients a and b in Eq. 1, in the case of nitrogen heterobenzenes[1,5] and monoazanaphthalenes[2].

$$\Psi(^1L_b) = a^1\chi_{i\to k} + b^1\chi_{j\to l} \tag{1}$$

The ratio of the coefficients in Eq. 1 is correlated to the energies of configurations and the interconfigurational matrix element by

$$\frac{a}{b} = \frac{2(^1\chi_{i\to k} \mid \mathbf{H} \mid {}^1\chi_{j\to l})}{[\{E(^1\chi_{i\to k}) - E(^1\chi_{j\to l})\}^2 + 4(^1\chi_{i\to k} \mid \mathbf{H} \mid {}^1\chi_{j\to l})^2]^{1/2} - \{E(^1\chi_{i\to k}) - E(^1\chi_{j\to l})\}} \tag{2}$$

TABLE V*

THE EXCITED STATE WAVE FUNCTIONS, ENERGIES OF CONFIGURATIONS AND THE VALUES OF INTERCONFIGURATIONAL MATRIX ELEMENTS OF ACRIDINE AND PHENAZINE

$\Psi(^1A^+_1) = 0.9892^1\chi_{7\to8} + 0.1461^1\chi_{6\to9}$, $E(^1\chi_{7\to8}) = 3.2367$,
$\Psi(^1A^-_1) = 0.1461^1\chi_{7\to8} - 0.9892^1\chi_{6\to9}$, $E(^1\chi_{6\to9}) = 6.3681$,
$\Psi(^3A^+_1) = 0.9990^3\chi_{7\to8} + 0.0450^3\chi_{6\to9}$, $E(^3\chi_{7\to8}) = 1.2357$,
$\Psi(^3A^-_1) = 0.0450^3\chi_{7\to8} - 0.9990^3\chi_{6\to9}$, $E(^3\chi_{6\to9}) = 4.8158$.
$(78 \mid G \mid 78) = 4.2033$, $(78 \mid G \mid 87) = 1.0005$, $(68 \mid G \mid 79) = 0.1616$,
$(69 \mid G \mid 69) = 4.1572$, $(69 \mid G \mid 96) = 0.7761$, $(68 \mid G \mid 97) = -0.1556$.
$(^1\chi_{7\to8} \mid \mathbf{H} \mid {}^1\chi_{6\to9}) = -0.4728$, $(^3\chi_{7\to8} \mid \mathbf{H} \mid {}^3\chi_{6\to9}) = -0.1616$.
$\Psi(^1B^+_1) = 0.3870^1\chi_{6\to8} + 0.9221^1\chi_{7\to9}$, $E(^1\chi_{6\to8}) = 3.7182$,
$\Psi(^1B^-_1) = 0.9221^1\chi_{6\to8} - 0.3870^1\chi_{7\to9}$, $E(^1\chi_{7\to9}) = 4.6170$,
$\Psi(^3B^+_1) = 0.9920^3\chi_{6\to8} + 0.1259^3\chi_{7\to9}$, $E(^3\chi_{6\to8}) = 2.9184$,
$\Psi(^3B^-_1) = 0.1259^3\chi_{6\to8} - 0.9920^3\chi_{7\to9}$, $E(^3\chi_{7\to9}) = 4.1712$.
$(68 \mid G \mid 68) = (79 \mid G \mid 79) = 3.6612$, $(78 \mid G \mid 96) = (68 \mid G \mid 86)$,
$(68 \mid G \mid 86) = (79 \mid G \mid 97) = 0.3999$, $(78 \mid G \mid 69) = (68 \mid G \mid 79)$.
$(^1\chi_{6\to8} \mid \mathbf{H} \mid {}^1\chi_{7\to9}) = 0.6382$, $((^3\chi_{6\to8} \mid \mathbf{H} \mid {}^3\chi_{7\to9}) = -0.1616$.

Phenazine

$\Psi(^1B^+_{1u}) = 0{\cdot}9831^1\chi_{7\to8} + 0.1828^1\chi_{6\to9}$, $E(^1\chi_{7\to8}) = 3.8507$,
$\Psi(^1B^-_{1u}) = 0.1828^1\chi_{7\to8} - 0.9831^1\chi_{6\to9}$, $E(^1\chi_{6\to9}) = 6.3681$,
$\Psi(^3B^+_{1u}) = 0.9986^3\chi_{7\to8} + 0.0517^3\chi_{6\to9}$, $E(^3\chi_{7\to8}) = 1.7025$,
$\Psi(^3B^-_{1u}) = 0.0517^3\chi_{7\to8} - 0.9986^3\chi_{6\to9}$, $E(^3\chi_{6\to9}) = 4.8158$.
$(78 \mid G \mid 78) = 4.3084$, $(78 \mid G \mid 87) = 1.0741$, $(68 \mid G \mid 79) = 0.1616$,
$(69 \mid G \mid 69) = 4.1572$, $(69 \mid G \mid 96) = 0.7761$, $(68 \mid G \mid 97) = -0.1616$.
$(^1\chi_{7\to8} \mid \mathbf{H} \mid {}^1\chi_{6\to9}) = -0.4849$, $(^3\chi_{7\to8} \mid \mathbf{H} \mid {}^3\chi_{6\to9}) = -0.1616$.
$\Psi(^1B^+_{3u}) = 0.3341^1\chi_{6\to8} + 0.9425^1\chi_{7\to9}$, $E(^1\chi_{6\to8}) = 3.8205$,
$\Psi(^1B^-_{3u}) = 0.9425^1\chi_{6\to8} - 0.3341^1\chi_{7\to9}$, $E(^1\chi_{7\to9}) = 5.3944$,
$\Psi(^3B^+_{3u}) = 0.9949^3\chi_{6\to8} + 0.1011^3\chi_{7\to9}$, $E(^3\chi_{6\to8}) = 3.0207$,
$\Psi(^3B^-_{3u}) = 0.1011^3\chi_{6\to8} - 0.9949^3\chi_{7\to9}$, $E(^3\chi_{7\to9}) = 4.5946$.
$(68 \mid G \mid 68) = (79 \mid G \mid 79) = 3.6843$, $(78 \mid G \mid 96) = (68 \mid G \mid 86)$,
$(68 \mid G \mid 86) = (79 \mid G \mid 97) = 0.3999$, $(78 \mid G \mid 69) = (68 \mid G \mid 79)$.
$(^1\chi_{6\to8} \mid \mathbf{H} \mid {}^1\chi_{7\to9}) = 0.6382$, $(^3\chi_{6\to8} \mid \mathbf{H} \mid {}^3\chi_{7\to9}) = -0.1616$.

* in units of *e.v.*

TABLE VI
CALCULATED AND OBSERVED EXCITATION ENERGIES AND OSCILLATOR STRENGTHS OF ACRIDINE AND PHENAZINE

Symmetry		Excitation Energy (*e.v.*)		Oscillator Strength	
Group throry	Platt	Calcd.	Obsd.	Calcd.	Obsd.
		Acridine			
$^1A^+_1$	^1L_a	3.1669	3.18[a)]	0.36	*
$^1B^-_1$	^1L_b	3.4504	3.50[a)]	0.29	*
$^1B^+_1$	^1B_b	5.2389	4.96[a)]	2.61	*
$^1A^-_1$	^1B_a	6.4379	5.82[a)]	0.79	*
$^3A^+_1$	^3L_a	1.2284	—	0.00	—
$^3B^+_1$	^3B_b	2.8979	—	0.00	—
$^3B^-_1$	^3L_b	4.1917	—	0.00	—
$^3A^-_1$	^3B_a	4.8231	—	0.00	—
		Phenazine			
$^1B^+_{1u}$	^1L_a	3.7605	3.09[b)]	0.39	*
$^1B^-_{3u}$	^1L_b	3.5942	3.40[b)]	0.38	*
$^1B^+_{3u}$	^1B_b	5.6206	4.95[b)]	2.66	*
$^1B^-_{1u}$	^1B_a	6.4583	5.88[b)]	0.85	*
$^3B^+_{1u}$	^3L_a	1.6941	—	0.00	—
$^3B^+_{3u}$	^3B_b	3.0043	—	0.00	—
$^3B^-_{3u}$	^3L_b	4.6110	—	0.00	—
$^3B^-_{1u}$	^3B_a	4.8241	—	0.00	—

a) V. Zanker, *Z. physikal. Chem.* N. F., **2**, 52 (1954).

b) H. H. Perkampus, ibid., **6**, 18 (1956) and N. Mataga, unpublished.

* The oscillator strengths of these molecules are uncertain. The intensification of ^1L_b band due to hetero-replacement is remarkable, and the oscillator stength of ^1L_b band may be almost equal to that of ^1L_a band, in its order of magnitude, and the oscillator strengths of ^1B_b and ^1B_a bands are approximately equal to those of anthracene, respectively.

When $(^1\chi_{i\to k} \mid \mathbf{H} \mid {}^1\chi_{j\to l})$ is constant, the inequality of a and b becomes more remarkable, the larger the difference of $E(^1\chi_{i\to k})$ and $E(^1\chi_{j\to l})$. This was the case in the series of benzene, pyridine and pyrazine[1], the inequality being increased in this order. Moreover, it is characteristic that, the larger the difference between $(\varepsilon_k-\varepsilon_i)$ and $(\varepsilon_l-\varepsilon_j)$, the greater is the $\{E(^1\chi_{j\to l})-E(^1\chi_{j\to l})\}$, viz., $2(ik \mid G \mid ki)-(ik \mid G \mid ik)$ is nearly equal to $2(jl|G|lj)-(jl|G|jl)$. It was assumed that, this circumstance in nitrogen heterobenzenes might also prevail in the ^1L_b bands of anthracene, acridine and phenazine. On this assumption, the observed intensities of ^1L_b bands in this series of molecules were discussed qualitatively.[1]

From Tables II, V and VI, it is evident that, our previous assumption is almost exactly valid in the approximation of the present calculation, and accordingly the observed intensities are well comprehended by such a consideration. In contradistinction to ^1L_a band, which suffers the red shift by the heteroreplacement, the position of ^1L_b band is almost invariable in this series of molecules. This situation can be interpreted similarly to the case of nitrogen heterobenzenes.[1,5] The two configurations $^1\chi_{6\to8}$ and $^1\chi_{7\to9}$ are degenerate in anthracene, although they are split in the case of acridine and phenazine, the degree of splitting being larger in phenazine. As shown in Tables II, III, V and VI, however, the energy depression due to the configuration interaction is most remarkable in the case of anthracene and it becomes smaller in acridine and phenazine in this order causing the approximate invariance of the excitation energy of ^1L_b band in this series of molecules. Thus, the observed excitation energy and oscillator strength of ^1L_b band in these molecules are well interpreted by the present calculation. Now, the cause of the reversal of the relative order in the calculated energy of ^1L_a and ^1L_b states, in the case of phenazine, may probably be attributable to the inadequacy of the MO's used.

As is pointed out previously,[1,5] the Hartree-Fock self-consistent field MO's of nitrogen heterobenzenes are fairly close to the naive MO's obtained by putting α_N, the Coulomb integral at the nitrogen atom, to be equal to $\alpha+0.5\beta$. Extending this result to the present case, we have calculated the naive MO's of phenazine as shown in Table VII, where only the MO's concerning the lower excited states are indicated.

In terms of these MO's, the excitation

TABLE VII*
MO's AND MO ENERGIES OF PHENAZINE ($\alpha_N=\alpha+0.5\beta$)

Symmetry	ε_i (*e.v.*)	
b_{1g}	−10.6821	$\psi_6=0.3535\sigma_6+0.3535\sigma_7$
b_{3g}	− 9.5282	$\psi_7=0.3557\sigma_8+0.2244\sigma_9+0.0162\sigma_{10}-0.3816\sigma_{11}$
b_{2u}	− 3.6398	$\psi_8=0.2636\sigma_1-0.2182\sigma_2+0.1632\sigma_3-0.4609\sigma_4$
a_{1u}	− 1.7233	$\psi_9=-0.3535\sigma_{13}+0.3535\sigma_{14}$

* The definitions of σ's are the same as those of anthracene.

energies, and oscillator strengths have been computed. The results are collected in Table VIII.

TABLE VIII
CALCULATED EXCITATION ENERGIES AND OSCILLATOR STRENGTHS OF PHENAZINE
(MO's: $\alpha_N=\alpha+0.5\beta$)

Symmetry		Excitation Energy (*e.v.*)	Oscillator Strength
Group theory	Platt		
$^1B^+_{1u}$	^1L_a	3.5142	0.34
$^1B^-_{3u}$	^1L_b	3.9122	0.20
$^1B^+_{3u}$	^1B_b	5.2439	2.84
$^1B^-_{1u}$	^1B_a	6.4294	0.80
$^3B^+_{1u}$	^3L_a	1.6958	0.00
$^3B^+_{3u}$	^3B_b	3.2523	0.00
$^3B^-_{3u}$	^3L_b	4.2029	0.00
$^3B^-_{1u}$	^3B_a	4.8087	0.00

As indicated in Table VIII, ^1L_a and ^1L_b bands are put in their right order, thus making the agreement with the experimental observation more satisfactory.

Eventually, the electronic spectra of acridine and phenazine, as well as those of quinoline and isoquinoline in the previous report[2], are well interpreted by our perturbation calculation, and the assignment of the spectra of three-ring nitrogen heterocycles, which was made in the first paper, has been given a more rigorous basis.

Summary

The electronic spectra of three-ring nitrogen heterocycles have been calculated by the perturbation method based on the Hartree-Fock self-consistent field theory. There is a satisfactory agreement in general between the calculated the and observed excitation energies and oscillator strengths, and the mechanism of the electronic transitions in these molecules has been discussed in detail.

The author is grateful to Professor S. Mizushima of Tokyo University for his encouragement. He is also indebted to Dr. S. Nagakura of Tokyo University, Dr. H. Tsubomura of Tokyo University and Dr. H. Baba of Hokkaido University for their valuable discussions. He expresses his appreciation to Professor R. Fujishiro for his encouragement, and also to Mr. K. Nishimoto and Miss S. Tsuno for their helpful discussions. He is also thankful to Miss S. Wada for typewriting this paper.

Institute of Polytechnics,
Osaka City University,
Kita-ku, Osaka

A Study on the Micellar Solutions of Sodium Oleate and Elaidate

By Bun-ichi TAMAMUSHI, Michio SHIRAI and Kunio TAMAKI

(Received December 17, 1957)

Oleic and elaidic acid, which are known as geometrical isomers, have a certain difference in their physical and chemical properties such as their melting points. It is expected that the soaps of these isomers will behave themselves differently as regards the formation of micelles in solution. The examination of this probable difference will supply useful knowledge regarding the structure of micelles. There are already a good many data for the aqueous solutions of oleic acid salts but scarcely any for those of elaidic acid salts. The object of this work is to examine the effect of the geometrical isomerism on the formation and the structure of micelles by measuring the electrical conductivity, the interaction with a dye, the degree of hydrolysis, and the solubilizing power of aqueous solutions of sodium oleate (*cis* form) and elaidate (*trans* form). The dielectric polarization of *n*-heptane solutions of oleic and elaidic acid will also be determined in order to get information on the molecular association of these isomers.

Experimental

Procedure—The electrical conductivity was measured with the audio-frequency bridge of

Yokogawa & Co. using a frequency of 1000 cycles/sec., and the absorption spectrum with the spectrophotometer of Hitachi & Co.

For the measurement of pH of the solutions a glass electrode pH-meter was used.

The measurement of the dielectric constant was carried out by the method described in our previous paper[1].

Materials—Oleic acid was purified from the sample supplied by Armour & Co., U.S.A. by vacuum distillation. b.p. 202~203°C/5 mmHg. Elaidic acid was prepared by isomerization of oleic acid using nitrogen oxides as catalyst[2], and then extracted with petroleum ether. The product was recrystallized several times from ethanol.

Sodium oleate and elaidate were prepared by adding these acids to the ethanol solution of sodium hydroxide; the amount of the acids was taken slightly less than the amount calculated, the adjustment to neutrality being made with phenolphthalein as an external indicator. The neutral solutions obtained were evaporated under reduced pressure and the products were recrystallized from ethanol and dried in a vacuum desiccator.

Pinacyanol iodide was a pure sample supplied by Nezu Chemical Laboratory.

Benzene was washed with concentrated sulfuric acid, water, dilute sodium hydroxide solution and again with water. After distilling over calcium chloride, it was dried over metallic sodium, and then redistilled. *n*-Heptane was purified in the same way as benzene.

Results and Discussion

1) Electrical conductivity — In Table I and Fig. 1 are given the values of equivalent conductivity (Λ) as a function of the square root of molarity for sodium oleate and elaidate in water. The curves for these two salts are similar to each other as shown in Fig. 1. The result for sodium oleate is in good agreement with that obtained by Flockhart et al.[3] As seen in this figure, Λ increases steadily with decreasing concentration in a very low concentration range. Such a behavior has not been found with other paraffin-chain salts such as salts of higher alkyl sulfonic acids. The position of the breaking point is not clear, which may owe to the hydrolysis as found by Ekwall[4] and Preston[5]. But if we observe carefully the $\Lambda-\sqrt{C}$ curve in Fig. 1, we can detect a slight breaking point. Regarding this point as the critical point, the critical micelle concentration of sodium oleate and elaidate are 2.7×10^{-3} and 2.5×10^{-3} mole/l., respectively. Beyond such a critical point, the equivalent conductivity decreases with increasing concentration just as in the case of other paraffin-chain salts.

In Table I are shown the values of equivalent conductivity in aqueous ethanol of 2 mole/l. and 4 mole/l. For aqueous ethanol of 2 mole/l. the equivalent conductivity decreases slowly and the critical

TABLE I
EQUIVALENT CONDUCTIVITY

concn.	in water		in aq. ethanol of 2 mole/l.	in aq. ethanol of 4 mole/l.
	40°C	60°C	40°C	40°C
	sodium oleate			
0.0001	164	205	108.8	73.0
0.0002	150	194	102.0	71.2
0.0004	135	180	97.6	69.0
0.0007	123	167	93.6	68.0
0.001	113	157	92.3	68.0
0.0012	108	151	—	—
0.0015	104	149	90.0	68.5
0.0017	102	146	—	—
0.002	98.4	142	85.6	69.0
0.0025	95.6	137	80.0	69.5
0.003	91.7	132	76.4	69.2
0.004	—	—	72.4	67.4
0.005	75.4	112	—	—
0.006	—	—	65.6	65.2
0.008	—	—	59.5	63.0
0.01	61.9	89.6	56.0	61.6
0.02	53.6	73.6	48.0	54.8
0.05	46.3	67.4	41.8	45.6
0.1	43.2	63.6	—	—
	sodium elaidate			
0.0001	144	188	102.0	71.0
0.0002	132	180	99.0	68.7
0.0004	120	168	94.0	66.2
0.0007	113	159	91.4	66.8
0.001	110	155	89.5	67.5
0.0012	108	151	—	—
0.0015	106	148	84.1	68.0
0.0017	105	146	—	—
0.002	102	144	79.9	69.0
0.0025	97.2	142	76.0	69.5
0.003	89.3	131	72.5	68.6
0.004	—	—	69.0	67.0
0.005	71.0	102	65.9	—
0.006	—	—	62.5	63.3
0.008	—	—	57.4	60.6
0.01	54.7	80.4	53.9	58.3
0.02	46.4	67.6	45.8	49.5
0.05	39.9	55.8	35.4	42.3
0.1	38.0	53.9	—	—

1) M. Shirai and B. Tamamushi, This Bulletin, **30**, 542 (1957).
2) K. Fuse and B. Tamamushi, *J. Chem. Soc. Japan, Pure Chem. Sec.*, (*Nippon Kagaku Zassi*), **64**, 338 (1953).
3) B. D. Flockhart and H. Graham, *J. Colloid Sci.*, **8**, 105 (1953).
4) P. Ekwall, *Z. physik. Chem.*, **A161**, 198 (1932).
5) W. C. Preston, *J. Phys. & Colloid Chem.*, **52**, 84 (1948).

point is slightly shifted towards lower concentrations than in water, as shown in Fig. 2. For aqueous ethanol of 4 mole/l. the critical point becomes indistinct, the micelle formation being probably inhibited on account of the affinity of the solvent medium for the hydrocarbon chains of the soap molecules.

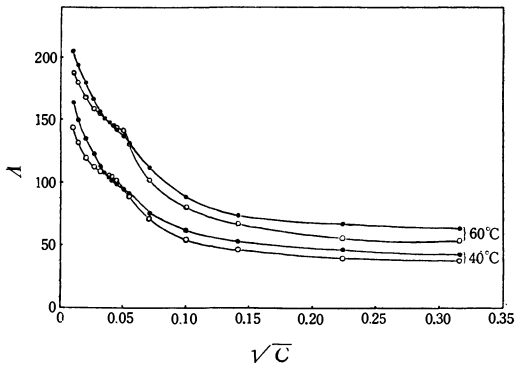

Fig. 1. Electrical conductivity in water. ●, sodium oleate; ○, sodium elaidate.

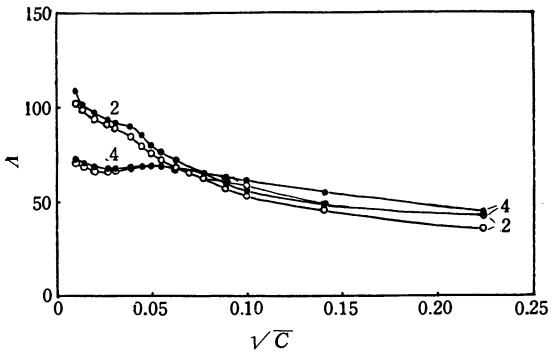

Fig. 2. Electrical conductivity in aqueous ethanol. Numbers on curves refer to the molarity of ethanol. ●, sodium oleate; ○, sodium elaidate.

In pure water the equivalent conductivity of sodium oleate is slightly greater than that of sodium elaidate at concentrations both below and beyond the critical micelle concentration except near that concentration, while in aqueous ethanol of 4 mole/l., where hydrolysis is reduced and the micelle formation is greatly inhibited, the equivalent conductivities of the two salts almost agree with each other. Therefore, it is conceivable that the smaller value of the equivalent conductivity of sodium elaidate is due to its greater power of micelle formation.

2) **Interaction with dye**—Sheppard and Geddes[6] found that, when pinacyanol salt is added to the solutions of surface active agents, its absorption spectrum changes at the critical micelle concentration. This experimental fact serves as a method of measurement of the critical micelle concentration[7]. Fig. 3 shows the optical density of solutions of pinacyanol iodide in sodium oleate and elaidate solution at an absorption maximum near 615 mμ as a function of the concentration of the salts. The critical rise of the optical density has been considered to be due to micelle formation, but the appearance of a minimum below the rise is yet unknown. From this figure we obtain 1×10^{-3} mole/l. as the critical micelle concentration for sodium oleate as well as for elaidate. However, as the concentration of the added dye appropriate for spectroscopic measurement is the same order of magnitude as those of the fatty acid salts, a considerable salt effect on the critical micelle concentration should be expected. Thus, the above obtained values of the critical micelle concentration must be considerably smaller than the true ones.

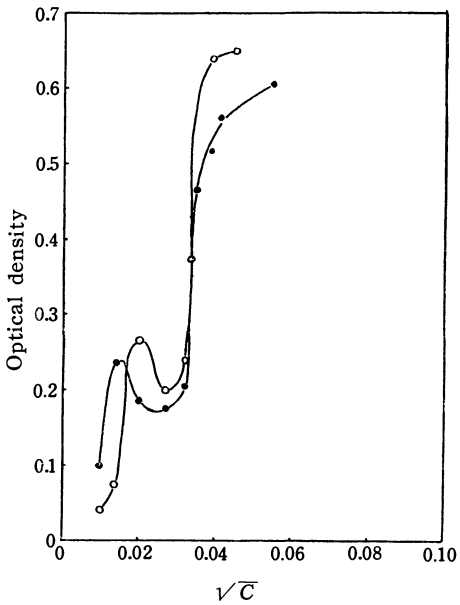

Fig. 3. Optical density of γ band of soap-pinacyanol iodide. ●, sodium oleate; ○, sodium elaidate.

3) **Hydrolysis**—The degree of hydrolysis (β), which is defined as the ratio of the concentration of hydroxyl ion generated by hydrolysis to that of total soap concentration, can be calculated from pH values. In Table II and Fig. 4 is indicated

6) S. E. Sheppard and A. L Geddes, *J. Chem. Phys.*, **13**, 63 (1945).

7) M. L. Corrin, H. B. Klevens and W. D. Harkins, ibid., **14**, 216 (1946).

TABLE II
DEGREE OF HYDROLYSIS

concn.	in water		in aq. ethanol of 2 mole/l.		in aq. ethanol of 4 mole/l.	
	pH	β (%)	pH	β (%)	pH	β (%)
			sodium oleate			
0.0001	7.56	1.10	7.30	0.60	7.25	0.54
0.0002	7.83	1.02	7.65	0.63	7.49	0.47
0.0004	8.10	0.95	8.08	0.91	7.65	0.34
0.0006	8.31	1.03	—	—	—	—
0.0007	—	—	8.43	1.15	7.80	0.27
0.0008	8.60	1.28	—	—	—	—
0.001	8.85	2.14	8.62	1.26	7.99	0.30
0·0015	—	—	8.85	1·43	8.12	0.27
0.002	9.40	3.80	8.97	1.42	8.32	0.32
0.0025	—	—	9.07	1.42	8.48	0.36
0.003	—	—	9.13	1.36	8.52	0.33
0.004	9.60	3.02	9.17	1.12	8.67	0.35
0.006	6.71	2.58	9.32	1.05	8.92	0.42
0.008	9.81	2.44	9.39	0.93	9.02	0.40
0.01	9.85	2.15	9.47	0.89	9.12	0.40
0.02	10.00	1.51	9.52	0.50	9.35	0.34
0.05	10.03	0.65	9.65	0.23	9.48	0.18
			sodium elaidate			
0.0001	7.80	1.90	—	—	7.65	1.14
0.0002	8.08	1.82	7.82	1.00	7.70	1.28
0.0004	8.42	1.99	8.35	1.21	7.75	0.91
0.0006	8.69	2.47	—	—	—	—
0.0007	—	—	8.52	1.43	7.80	0.64
0.0008	8.89	2.90	—	—	—	—
0.001	9.06	3.47	8.86	2.19	7.97	0.65
0.0015	—	—	9.08	2.40	8.27	0.58
0.002	9.67	7.05	9.21	2.45	8.40	0.47
0.0025	—	—	9.30	2.41	8.60	0.48
0.003	—	—	9.38	2.40	8.67	0.47
0.004	9.95	6.75	9.49	2.35	8.75	0.43
0.006	10.00	5.03	9.62	2.10	9.02	0.53
0.008	9.06	4.35	9.68	1.81	9.02	0.40
0.01	10.10	3.80	9.70	1.51	9.05	0.40
0.02	10.02	1.58	9.82	1.00	9.18	0.23
0.05	10.10	0.76	9.88	0.46	9.42	0.16

the result of the pH measurement, together with the degree of hydrolysis calculated therefrom. As shown in Fig. 4 the value of β decreases with increasing concentration and shows a minimum at some concentration below the critical micelle concentration. Then, it rises and reaches the maximum near the critical micelle concentration. Beyond that concentration it decreases gradually. The fact that a minimum and a maximum appear in $\beta-\sqrt{C}$ curve, has been explained by Stainsby and Alexander[8], and Cook[9] in relation to the micelle formation. They supposed that even below the critical micelle concentration submicelles could be formed. By submicelles are meant particles smaller than the well-recognized micelles but containing at least two molecules or ions per particle. The free acid molecules produced by hydrolysis will condense to submicelles, and accordingly, hydrolysis will go on further. With further increase in concentration of salts the counter ion association will take place and the micelle will be formed. At such concentrations the unhydrolyzed ions will condense to micelles too, and consequently, hydrolysis goes on no longer.

As is seen in Fig. 4 the concentrations

8) G. Stainsby and A. E. Alexander, *Trans. Faraday Soc.*, **45**, 585 (1949).
9) M. A. Cook, *J. Phys. & Colloid Chem.*, **55**, 383 (1951).

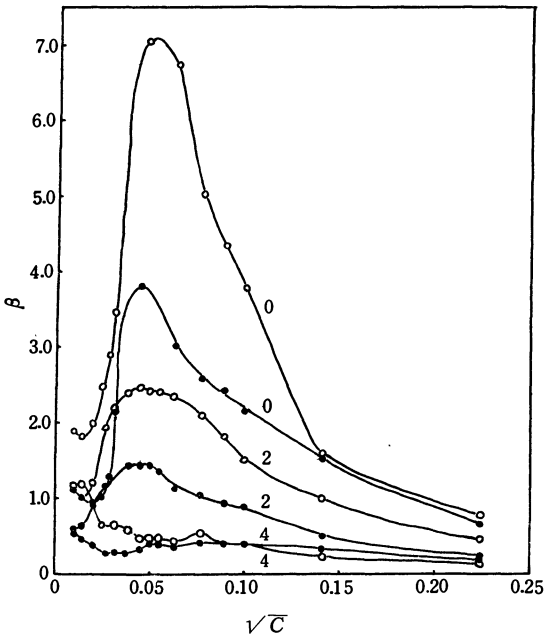

Fig. 4. Degree of hydrolysis in water and aqueous ethanol. Numbers on curves refer to the molarity of ethanol.
●, sodium oleate; ○, sodium elaidate.

where minimum and maximum of β appear for sodium oleate are nearly the same as for elaidate, while the value of β is much greater for sodium elaidate than for sodium oleate except at very large concentrations. This result is presumably due to the fact that sodium elaidate has a greater micelle forming power as well as a greater solubilization power for free acid than sodium oleate. Beyond the critical micelle concentration, β for each salt falls on nearly the same value.

In aqueous ethanol the maximum of β which is caused by hydrolysis and promoted by the submicelle formation becomes smaller. In aqueous ethanol of 4 mole/l., where the critical micelle concentration is not recognized by $\Lambda-\sqrt{C}$ curve, the maximum of β is almost diminished and β decreases monotonously with increasing concentration as in the case of ordinary electrolytes. These results obtained for the aqueous solutions and aqueous ethanol solutions correspond to the conductivity behavior of the salts, and support the view that the hydrolysis of the salts has a close relation with the micelle formation.

4) **Solubilization**—In Table III is given the experimental result of solubilization of benzene in terms of moles of solubilized benzene per mole of soap. It is shown that sodium elaidate has a greater solubilization power for benzene than sodium oleate, which is consistent with the result of pH measurement.

TABLE III
SOLUBILIZATION

substance	concn. of salt (mole/l.)	moles of benzene / mole of salt
sodium oleate	0.02	7.5
sodium elaidate	0.02	9.0
sodium oleate	0.1	12.5
sodium elaidate	0.1	15.0

5) **Dielectric polarization in nonpolar solvent.**—The experimental result of the measurement of dielectric polarization in *n*-heptane is shown in Table IV and Fig. 5, where x is the mole fraction, ε the dielectric constant, d the density, P_2 the molecular polarization of the solute, and μ the dipole moment. The electronic polarization P_E is computed from the atomic refraction and the atomic polarization P_A is assumed to be 5% of the electronic polarization. The molecular polarization decreases considerably with increasing concentration both for oleic and elaidic acid, but this decrease is slightly greater for elaidic acid than for oleic acid. This experimental fact shows that elaidic acid has a greater tendency towards association than oleic acid in a non-polar solvent. On the other hand, the molecular polarization at infinite dilution is nearly the same for both acids, and consequently, the dipole moment calculated

TABLE IV
DIELECTRIC POLARIZATION
n-heptane solution temp. 40°C

oleic acid

x	ε	d	P_2(cc.)
0.000000	1.9213	0.6709	(144.0)
0.003509	1.9272	0.6719	133.1
0.005808	1.9300	0.6726	126.2
0.009164	1.9325	0.6736	118.8
0.013354	1.9350	0.6750	112.7
0.018383	1.9377	0.6763	109.3

$P_E+P_A=90.7$ cc. $\mu=1.65$

elaidic acid

x	ε	d	P_2(cc.)
0.000000	1.9213	0.6709	(143.0)
0.002772	1.9262	0.6722	131.1
0.006295	1.9308	0.6736	120.5
0.009259	1.9335	0.6749	114.4
0.011743	1.9350	0.6757	111.4
0.016467	1.9386	0.6784	105.6

$P_E+P_A=90.7$ cc. $\mu=1.64$

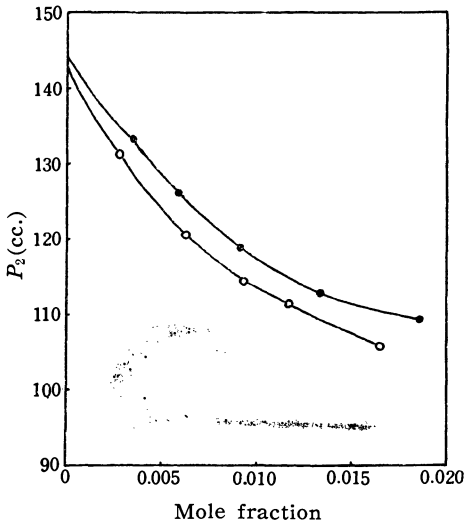

Fig. 5. Molecular polarization in *n*-heptane. ●, oleic acid; ○, elaidic acid.

from them is also nearly the same for both acids.

From these experimental results it is concluded that sodium elaidate has a slightly greater tendency towards association into micelles and a greater solubilization power for hydrocarbons, and accordingly has a greater degree of hydrolysis than sodium oleate.

Summary

The electrical conductivity, the interaction with pinacyanol iodide, the degree of hydrolysis, and solubilization power for benzene have been measured for sodium oleate and elaidate.

The conductivity behavior of these salts is consistent with the experimental result for hydrolysis and the latter result is also consistent with that of solubilization measurement. The result of dielectric polarization is also compatible with other results.

All these experimental results show that sodium elaidate has a slightly greater tendency towards micelle formation than sodium oleate.

We are indebted to the Ministry of Education for a reseach grant.

Chemical Institute, College of General Education, and Institute of Science and Technology, The University of Tokyo, Meguro-ku, Tokyo

*A New Analytical Method of Electroconductivity Data of Surfactant Solutions. III**

By Kenjiro MEGURO, Tamotsu KONDO and Noriaki OHBA

(Received February 1, 1958)

In previous papers[1,2] we have described that $(\Lambda_0-\Lambda)/\sqrt{c}$ vs. $\sqrt{c}$ diagram is better than Λ vs. $\sqrt{c}$ diagram to analyze the critical phenomena of a surfactant solution. In $(\Lambda_0-\Lambda)/\sqrt{c}$ vs. $\sqrt{c}$ diagram we were able to define two concentrations, C_{min} and C_{max}, which characterize the critical phenomena. We also discussed various effects—such as the effect of alkyl chain length,—on them. On the other hand, we found that the values of $(\Lambda_0-\Lambda)/\sqrt{c}$ at C_{min}, C_{max} and the gradient of $(\Lambda_0-\Lambda)/\sqrt{c}$ vs. $\sqrt{c}$ curve between C_{min} and C_{max}, were very useful for analysis. These values were denoted by H_{min}, H_{max} and B.

In this paper we consider the meaning of these constants.

The meaning of C_{min} and C_{max}

Hartley and his associates[3] found the occurrence of a maximum equivalent conductivity in the aqueous solution of cetyl pyridonium chloride in a very high electric field. The C_{max} determined by our method in the case of cetyl pyridonium bromide corresponds to the concentration

* Presented at the 9th Annual Meeting of the Chemical Society of Japan held in Kyoto, April, 1956.

1) K. Meguro et al., This Bulletin **30**, 760 (1957).

2) K. Meguro et al., ibid., **30**, 905 (1957).

3) J. Malsh and G.S. Hartley, *Z. physik. Chem.*, **A140**, 321 (1934).

TABLE I

COMPARISON OF C_{min} AND C_{max} WITH THE TRANSPORT NUMBER DATA

Substance	C_{min}	Breaking pt. in Transport number vs. $\sqrt{c}$ curve	C_{max}	Level off pt. in Transport number vs. $\sqrt{c}$ curve
$C_9H_{17}NH_3Cl$	—	423	—	525
$C_{10}H_{21}NH_3Cl$	15.4	22.5	108	96
$C_{12}H_{25}NH_3Cl$	12.1	12.7	44.1	40.0
$C_{14}H_{20}NH_3Cl$	3.6	5.0	15.8	15.6
$C_{16}H_{33}NH_3Cl$	0.62	1.4	4.9	5.6
$C_{18}H_{37}NH_3Cl$	0.40	0.35	1.7	1.4

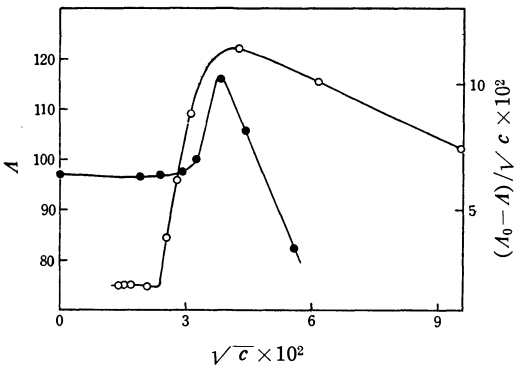

Fig. 1. Comparison of Λ vs. $\sqrt{c}$ curve for cetyl pyridonium chloride solution in high electric field (200 kV) with $(\Lambda_0-\Lambda)/\sqrt{c}$ vs. $\sqrt{c}$ curve for cetyl pyridonium bromide solution:
● Λ vs. $\sqrt{c}$ curve and ○ $(\Lambda_0-\Lambda)/\sqrt{c}$ vs. $\sqrt{c}$ curve.

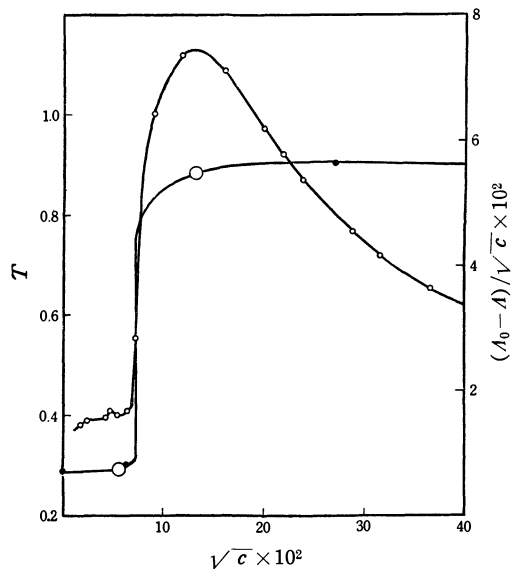

Fig. 2. Comparison of transport number diagram with $(\Lambda_0-\Lambda)/\sqrt{c}$ vs. $\sqrt{c}$ diagram for tetradecyl ammonium chloride:
• and ○ transport number, and
◦ $(\Lambda_0-\Lambda)/\sqrt{c}$ vs. $\sqrt{c}$ diagram.

of the maximum found by Hartley, as shown in Fig. 1.

Hartley made the following explanation for the occurrence of the maximum. At the concentration of surfactant near usual *C.M.C.*, the gegenions fixed on micelles are dissociated by applying high electric field; therefore, the gegenions and multicharged micelles come to contribute to the electroconductivity, and this contribution increases anomalously. At a more concentrated region, the fixed gegenions can not dissociate even in such a strong field; then the conductivity begins to fall again.

The C_{max} may be considered to show the concentration at which the fixation of gegenions on micellar surface is completed.

Furthermore, the data of transport number support this consideration. Ralston[4] found that the curve of transport number against the square root of normality shows a breaking point at a low concentration corresponding to the *C.M.C.*, and rises sharply to an anomalously high value with the increase of concentration, and then levels off. The concentration at which the value of transport number attains this anomalously high value is in good agreement with C_{max}, as shown in Fig. 2. After attaining this value, the transport number keeps a constant level in ordinary concentration, which means that the electrical charge of micelle becomes constant if the equal size of micelle is assumed. That is, the fixation of gegenions on micellar surface may be considered to be completed at this point.

Table I shows the correspondence between this concentration and C_{max} of some alkyl amine hydrochlorides.

On the other hand, it may be supposed that C_{min} indicates the concentration at which the fixation of gegenions begins.

4) A. W. Ralston, C. W. Hoerr and E. J. Hoffman, *J. Am. Chem. Soc.*, **64**, 97 (1942).

TABLE II

Cmin, Cmax, Hmin, Hmax AND B VALUES OF OCTADECYL PYRIDONIUM SALTS WITH REFERENCE TO THEIR GEGENIONS

Substance		Cmin	Cmax	Hmin	Hmax	B
$C_{18}H_{37}$-N	NO_3	(1.14)	0.42	(1.20)	19.6	4300
	Cl	0.24	1.09	0.30	11.0	1530
	IO_3	0.48	4.90	−3.85	2.80	374

The steepest region between Cmin and Cmax will be considered the region in which the gegenions are fixed. By this assumption, it is reasonable to suppose that the great change in electroconductivity takes place at the region between Cmin and Cmax.

The meaning of Hmax

To consider the meaning of Hmax, the effect of gegenions on the maximum point is very suggestive. It was recognized by Hartley[3] and others[5-7] that the gegenions of ionic surfactant play an important role in the formation of micelles and that the *C.M.C.* of surfactant depends on the degree of hydration of gegenions.

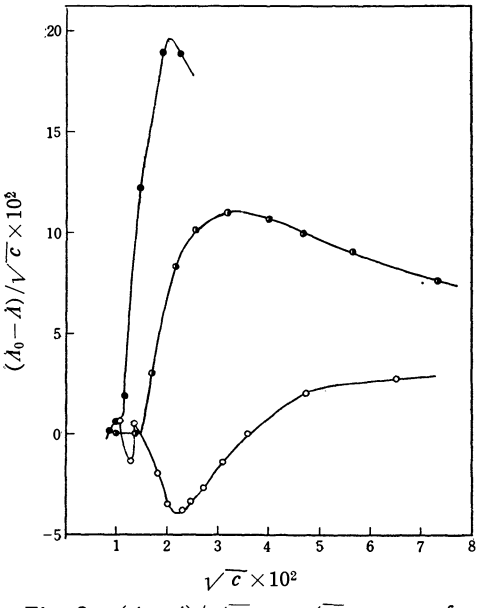

Fig. 3. $(\Lambda_0-\Lambda)/\sqrt{c}$ vs. $\sqrt{c}$ curves for the aqueous solutions of octadecyl pyridonium ● nitrate, ◑ chloride and ○ iodate at 25°C.

To see the relation between the degree of hydration of gegenions and Cmax, Hmax, etc., our method was applied to octadecyl pyridonium nitrate, chloride and iodate, and the results obtained are illustrated in Fig. 3 and Table II, in which it must be noted that there is good correspondence between Cmax or Hmax and lyotropic series of gegenions as below:

(a) The lyotropic number increases in the order:

$$\underset{6.2}{IO_3} < \underset{10.0}{Cl} < \underset{11.6}{NO_3}$$

(b) The value of Cmax decreases in the order:

$$\underset{4.9}{IO_3} > \underset{1.09}{Cl} > \underset{0.42}{NO_3}$$

(c) The value of Hmax increases in the order:

$$\underset{2.8}{IO_3} < \underset{11.0}{Cl} < \underset{19.6}{NO_3}$$

The adsorption (fixation) of gegenions on the surface of micelles is important for the explanation of the above relations. Considering the work of Wo. Ostwald[8] and Y. Osaka[9] on the adsorption of salts on charcoal, we have reached the following conclusion.

(a) The larger the degree of hydration of ion, the higher the concentration, at which the adsorption attains saturation.

(b) The higher the degree of hydration, the larger the quantity of adsorbed ions at saturation.

It may be considered from the relation (a) that the adsorption of gegenions on the micelle surface is saturated as in the above order.

On the other hand, it may be assumed that Hmax depends on the quantity of ions adsorbed at saturation. If the quantity of gegenions adsorbed on micelle at saturation is large, the variation of electroconductivity also becomes large; then, Hmax becomes large.

5) P. F. Grieger and C. A. Kraus, ibid., **70**, 3803 (1948).
6) G. L. Brown, P. F. Grieger and C. A. Kraus, ibid., **71**, 95 (1949).
7) K. Meguro, T. Kondo et al., *J. Chem. Soc. Japan, Pure Chem. Sec.* (*Nippon Kagaku Zassi*), **77**, 1236 (1956).
8) Wo. Ostwald, *Kolloid-Z.*, **87**, 128 (1939).
9) Y. Osaka, *J. Tokyo. Chem. Soc.*, **37**, 241 (1916).
10) Wo. Pauli and L. Sternbach, *Kolloid-Z.*, **84**, 291 (1938).

A new concept for the mechanism of micelle formation

In the above considerations, some doubts still remain as to whether the micelle formation precedes the fixation of gegenions or fixation of gegenions and micelle formation occur simultaneouly; that is, the fixation causes the micelle formation.

Some suggestion on this problem can be obtained in the correspondence between surfactant solution and polyelectrolyte solution.

Pauli,[10] Seiyama[11] and Takahashi[12] found the following Λ vs. $\sqrt{c}$ diagram for sodium alginate solution (Fig. 4.), which is very similar to the one of surfactant solution.

Furthermore, Koizumi and Mataga[13] found the disappearance of fluorescence of Rhodamine 6G by addition of a small amount of potassium polyvinyl sulfate: they also found the recovering of fluorescence in concentrated solution of this polyelectrolyte. The same phenomenon can be found in the case of sodium dodecyl sulfate and Rhodamine 6G system; that is, when the concentration of surfactant is lower than its *C.M.C.*, the fluorescence disappears, while it recovers when the concentration is over the *C.M.C.*

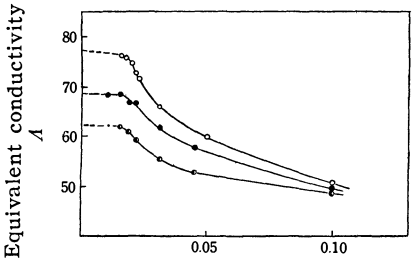

Fig. 4. Λ vs. $\sqrt{c}$ diagram for sodium alginate solution. (taken from Takahashi).

Degree of polymerization of Na alginate ○ 11 ● 35 ◐ 97

If we assume that a molecule of polyelectrolyte corresponds to a micelle of surfactant it will be reasonable to assume the fall of Λ in Λ vs. $\sqrt{c}$ diagram and of the recovering of fluorescence of dye would not be caused by the formation of micelles but by the fact that the number of micelles reaches some definite amount.

According to the theory of Osawa and Kagawa[14], many phenomena for polyelectrolyte solution will be explained by the fixation of gegenions on polyelectrolyte ion; then the dropping of Λ and the recovering of fluorescence in surfactant solution will also be explained as follows;

(1) Owing to the amphipathic properties of surfactant, loose micelles exist in more dilute solution than usual *C.M.C.*.

(2) When the concentration of these loose micelles reaches a definite value, the gegenions are fixed on them; then the charges on micellar surface decrease, decreasing the repulsion among surfactant ions which form micelles, and the micelles become compact. That is to say, the usual *C.M.C.* indicates the concentration at which the compact micelles begin to form.

It should be considered that the micelles of non-ionic surfactants are formed on account of their amphipathic properties; therefore, in this case only the loose micelles can be produced. This fact will be ascertained by the obscurity of critical phenomena in nonionic surfactant solution.

If we consider two types (loose and compact) of micelle, it is necessary to take into account the following facts regarding the discussion of effects on critical phenomena of surfactant solution.

(I) The effects which alter the concentration where the compact micelles appear.

(II) The effects which alter the ability of forming micelles.

The solvent effect and the salt effect on critical phenomena will be ascribed mainly to the effect mentioned in I, but the effect mentioned in II is not well known.

We found the effect which will be regarded as the one mentioned in II in the system of non-ionic and ionic surfactant mixture.

The effect of the addition of polyoxyethylene dodecyl ether on the conductivity of sodium dodecyl sulfate solution was measured.[15] As a result, the following Λ vs. $\sqrt{c}$ diagram was obtained (Fig. 5), which is charaterized by the facts that the breaking point of sodium dodecyl sulfate corresponding to its *C.M.C.* in the usual sense becomes less pronounced with

11) T. Seiyama, *J. Chem. Soc. Japan, Ind. Chem. Sec.* (*Kogyo Kagaku Zassi*), **53**, 122 (1950).
12) T. Takahashi, K. Kimoto and Y. Takano, *J. Chem. Soc. Japan, Pure Chem. Sec.* (*Nippon Kagaku Zassi*), **72**, 292 (1951).
13) M. Koizumi and N. Mataga, ibid., **75**, 273 (1954).
14) F. Osawa, N. Imai and I. Kagawa, *J. Polymer Sci.*, **13**. 93 (1954).
15) O. Yoda, K. Meguro, T. Kondo and T. Ino, *J. Chem. Soc. Japan, Pure Chem. Sec.* (*Nippon Kagaku Zassi*), **77**, 905 (1956).

increasing concentration of the non-ionic surfactant and almost disappears at 10^{-2} M of non-ionic surfactant without a shift of the breaking point toward either side of concentration. This phenomenon is really new, and usually the additions of salt, solvent and solubilizate are accompanied by shifts of the breaking point.

The $(\Lambda_0-\Lambda)/\sqrt{c}$ vs. $\sqrt{c}$ diagram based on the same data is shown in Fig. 6, in which it is noticed that the C_{min} gradually disappears without a shift as the amount of added non-ionic surfactant increases, and that the H_{max} becomes lower and the slope turns less steep with increasing concentration of non-ionic surfactant. Because H_{max} is proportional to the amount of gegenions adsorbed on micelle surface, and because C_{min} shows the concentration at which the compact micelle begins to form by the fixation of gegenions, we can consider that the addition of non-ionic surfactant prevents the formation of compact micelles. This consideration will be supported by the following experiment.

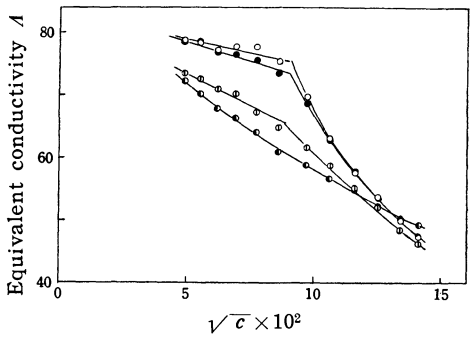

Fig. 5. Λ vs. $\sqrt{c}$ curves for sodium dodecyl sulfate in the aqueous solutions of polyoxyethylene dodecyl alcohol ether:
○ in water, ● 10^{-4}, ① 10^{-3} and ◐ 10^{-2} mole/l.

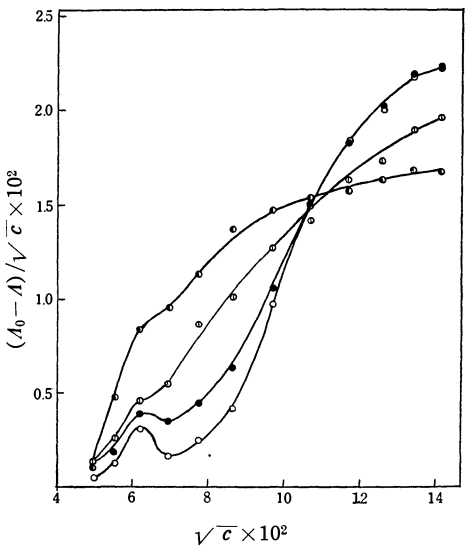

Fig. 6. $(\Lambda_0-\Lambda)/\sqrt{c}$ vs. $\sqrt{c}$ curves for sodium dodecyl sulfate in the aqueous solution of polyoxyethylene dodecyl alcohol ether:
○ in water, 10^{-4}, ① 10^{-3} and ◐ 10^{-2} mole/l.

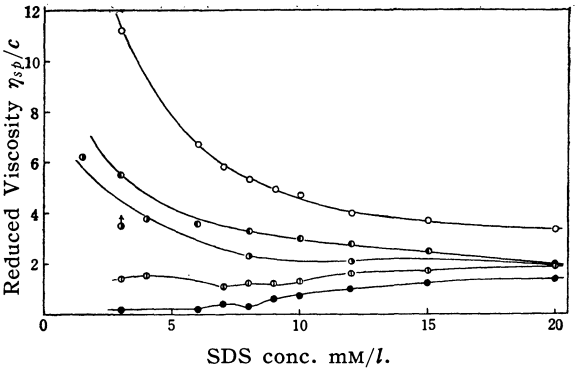

Fig. 7. η_{sp}/c vs. c diagram for sodium dodecyl sulfate in the aqueous solution of polyoxyethylene dodecyl alcohol ether:
● in water, ① 1×10^{-3}, ◑ 2.5×10^{-3}, ◐ 5×10^{-3} and ○ 1×10^{-2} mole/l.

Sata and Tyuzyo[16] found the minimum of η_{sp}/c in the diagram of η_{sp}/c vs. c for the solution of ionic surfactant. We found that the small addition of non-ionic surfactant cancels this minimum, and the curve of η_{sp}/c vs. c approaches to that of polyelectrolyte solution rather than that of surfactant solution (Fig. 7). This fact can be considered that the non-ionic surfactant (molecular or loose micellar) adsorbs ionic surfactant on its lyophobic groups and therefore the micelle formation of ionic surfactant is prevented.

It seems necessary to discuss the various effects on critical phenomena from the two standpoints mentioned above, and these considerations are very useful to obtain the real feature of various effects.

In above explanation our discussion was mainly focused on the compact micelles. Now we should consider the formation of loose micelles, but it is impossible to consider its formation because of the lack of exact data of electroconductivity in very dilute surfactant solution.

Nedzu Chemical Laboratory, Musashi University, Nerima, Tokyo

16) N. Sata and K. Tyuzyo, This Bulletin, **26**, 177 (1953).

Colloid Chemical Studies on Starching Materials. II. Intrinsic Viscosity of Polyvinyl Alcohol in Soap Solutions

By Masayuki NAKAGAKI and Hiroko NISHIBAYASHI*

(Received December 9, 1957)

In the preceding paper[1], the structural viscosity of aqueous solutions of polyvinyl alcohol was studied. In this paper, some results will be reported on the viscometric behavior of polyvinyl alcohol in soap solutions. This study has been made in order to see whether there exists any interaction between polyvinyl alcohol and soap. The interaction of non-ionic high polymer molecules and anionic detergent molecules will be of some interest in the field of both polymer and surface chemistry. It may, further, be of some interest in the field of textile industry, since experiments of this kind will give some fundamental information on the process of removing starching material from the surface of textile fibers.

Experimental

Polyvinyl alcohol.—Two materials provided by Nippon Gosei Kagaku Kogyo K. K., Gohsenol NM-14 and GM-14, were used[2]. The degree of polymerization of both NM and GM is about 1400. The degree of saponification of NM is 99~100%, while that of GM is 90±2%. Two grams of the polymer was dissolved in water by heating at 90°C for 15 min. After being cooled, it was transferred into a volumetric flask and made up to 100 cc. in a thermostat at 40°C. This solution, to be used after volumetric dilution, was prepared on the day when measurements were made, because the viscosity would slightly increase day by day. The method of dissolving the polymer affects the viscosity of the solution as discussed in the preceding paper. Heating for 15 min. is not long enough so that the molecules are probably not fully extended in the solution. This is one of the reasons for the increase of viscosity by aging. The above described method was, however, adopted considering the practical method of preparation of starching solution. Water used throughout the experiments was for the electric conductivity measurement.

Soap.—Sodium laurate was used. Lauric acid (m. p., 44.95°C) was neutralized with sodium hydroxide (extra pure reagent grade, rods) in conductivity water at 90°C. Sodium hydroxide was always used in 2% excess, in order to prevent the hydrolysis of the soap.

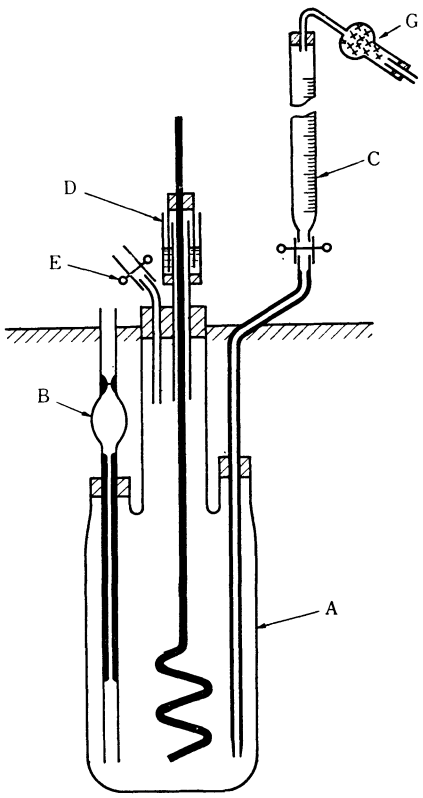

Fig. 1. Viscometer

Viscometer.—A viscometer illustrated in Fig. 1 was used. This is a flask of cylindrical shape (A) with three openings, equipped with a viscometer (B), a burette (C) with a soda lime tube (G), a stirrer (D) and a glass and rubber tubing closed with a pinchcock (E). In the flask (A), 50 cc. of soap solution containing or not containing polyvinyl alcohol was placed and a solution of the same soap concentration and of a different polyvinyl alcohol concentration was added from the burette. After being stirred with D, viscosity was measured with B, with E opened during the measurement. Thus the viscosity of the solution of various concentration of polyvinyl alcohol in a certain soap concentration was measured. The time for distilled water to flow down the viscometer was measured in advance for each

* Present address of H. Nishibayashi: Takase Senkojo, Miyakojima-ku, Osaka.

1) M. Nakagaki and A. Shimazaki, This Bulletin, **29**, 60 (1956).

2) Gohsenol contains a small amount (probably less than 1%) of sodium acetate, but the writers do not believe this affects the results essentially.

amount of water in the flask, on the basis of which the viscosity of the solution relative to distilled water was calculated. Dividing this by the relative viscosity of the soap solution of the same concentration, the viscosity of the solution relative to the soap solution as the solvent was calculated and designated by η_r. All experiments were made in a thermostat at 40°C.

Results and Discussions

Treatment of the Experimental Values.—On treating the experimental values there are several points to be considered. At first, the effect of velocity gradient should be taken into account. Solutions of Gohsenol usually show structural viscosity. The apparent viscosity is, then, a function of the rate of flow, Q(cc./sec.), as shown in the preceding paper[1]. The quantity Q or $1/Q$ is, however, not very adequate to compare the effect of velocity gradient in two capillaries of different radius. On the basis of Poiseuille's law, the largest velocity gradient, G_m, that is the velocity gradient on the wall of the capillary, is

$$G_m = (4/\pi a^3)Q \qquad (1)$$

The average velocity gradient, $\bar{G}$, defined by

$$\bar{G} = \int_0^a G(r)2\pi r\,dr/\pi a^2 \qquad (2)$$

is related to the largest velocity gradient by

$$\bar{G} = (2/3)G_m \qquad (3)$$

where a is the radius of the capillary and r is the distance between the axis of the capillary and the point where the velocity gradient is being considered. Either G_m or $\bar{G}$ may be used to discuss the effect of velocity gradient.

In the present experiments, the value of G_m was in the range between 1000 to 4000 (sec.$^{-1}$), which corresponds to the range of $(1/Q)$-value between 8 and 35 for the viscometer used in the preceding paper. Because of this low value of $1/Q$, it is clear according to the results of the preceding paper[1] that the viscosity data in the present paper is very close to the value of η_N, that is the viscosity value extrapolated to zero of $1/Q$. Therefore, the effect of the velocity gradient may be neglected in the present experiments.

The viscometer used in this experiment is suitable to study the concentration dependence of the viscosity. However, the data should be extrapolated to zero concentration in order to obtain the value of the intrinsic viscosity. There are two well known equations for this purpose, that is Huggins' equation,

$$\eta_{sp}/c = [\eta] + k_1[\eta]^2c \qquad (4)$$

and Staudinger's equation,

$$\ln \eta_r/c = [\eta] - k_2[\eta]^2c \qquad (5)$$

where c is the concentration of polymer. It was pointed out by Heller[3] that the simultaneous use of these two equations can appreciably reduce the arbitrariness in the extrapolation. For this purpose, both η_{sp}/c and $\ln \eta_r/c$ are expressed by $f(c)$ and plotted on the same figure. Three typical pairs of curves thus obtained are shown in Fig. 2. The upper curve of a pair corresponds to η_{sp}/c and the lower to $\ln \eta_r/c$.

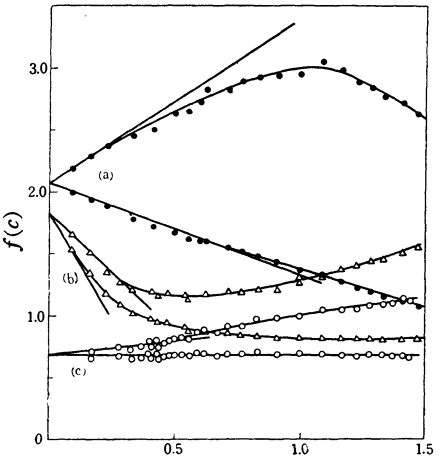

Fig. 2. Three types of $f(c)$-plot.
(a) Gohsenol NM in 0.1 N soap
(b) Gohsenol GM in 0.025 N soap
(c) Gohsenol NM in water

Experimental Results.—The value of the intrinsic viscosity, $[\eta]$, and the limiting slope of $f(c)$ curves, $k_1[\eta]^2$ and $k_2[\eta]^2$, are shown in Table I. In this experiment, the concentration of soap, c_s, shown in the first column is kept constant and the concentration of polymer, c, was changed.

At first, experiments were made using Gohsenol NM. As shown in Table I, the intrinsic viscosity increases when the soap concentration exceeds 0.025 N, which is close to the critical micelle concentration of sodium laurate[4]. This agrees with the experimental observation by Saito[5] that the viscosity of polyvinyl

3) W. Heller, *J. Colloid Sci.*, **9**, 547 (1954).
4) On the critical micelle concentration of sodium laurate, many investigators gave values between 0.02 and 0.028 N, the most probable value being 0.0255 N.
5) S. Saito, *Kolloid-Z.*, **133**, 12 (1953).

alcohol solution increases by addition of sodium oleate or some other detergents. The detailed behavior of the system in soap solutions near the critical micelle concentration will, therefore, be of some interest. This was studied by using Gohsenol GM, which is a little easier to handle than NM.

TABLE I
CONSTANTS IN HUGGINS' AND STAUDINGER'S EQUATIONS

Soap concn.	Gohsenol NM			Gohsenol GM		
c_s(N)	$[\eta]$	$k_1[\eta]^2$	$k_2[\eta]^2$	$[\eta]$	$k_1[\eta]^2$	$k_2[\eta]^2$
0	0.68	0.22	0	0.71	0.24	0
0.005	0.70	0.27	0	—	—	—
0.01	0.68	0.22	0	0.73	0.27	0
0.02	—	—	—	0.71	0.26	0
0.025	0.73	0.27	0	1.16	−0.62	1.24
0.03	—	—	—	1.82	−1.90	3.40
0.04	—	—	—	2.24	−0.84	3.13
0.05	1.62	0.55	0.76	1.98	0.99	0.94
0.1	1.80	0.88	0.69	2.07	1.33	0.84
0.15	1.76	0.81	0.71	—	—	—

The results are also shown in Table I. In this concentration range, the intrinsic viscosity has a maximum.

In a soap solution of low concentration, $\ln \eta_r/c$ is almost constant in the range of the polymer concentration studied here, as an example of the case is shown in Fig. 2 (c). Therefore, $k_2[\eta]^2$ is equal to zero. In a soap solution of high concentration, η_{sp}/c increases and $\ln \eta_r/c$ decreases with polymer concentration, c, at the range of low values of c. An example is shown in Fig. 2 by curve a. In this case, both $k_1[\eta]^2$ and $k_2[\eta]^2$ are positive. In a soap solution of intermediate concentration, both η_{sp}/c and $\ln \eta_r/c$ increases when the concentration of polymer approaches to zero. An example of this type of curves is shown by curve b in Fig. 2. In this case, $k_1[\eta]^2$ is negative and $k_2[\eta]^2$ is positive.

Examination of k_1 and k_2.—The values of k_1 and k_2 were calculated from data given in Table I and shown in Fig. 3, together with the value of $[\eta]$, as a function of the soap concentration c_s. The short vertical lines at c_s=0.025 N show the critical micelle concentration of the soap. At about this soap concentration, the intrinsic viscosity and k_2 increase while k_1 decreases abruptly. The curve of $[\eta]$ and k_2 has a maximum and the curve of k_1 has a minimum.

The relation between k_1 and k_2 is shown in Fig. 4. The straight line shows the well known relation,

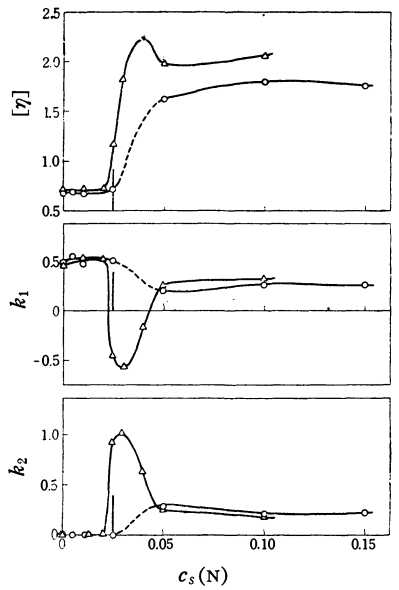

Fig. 3. The c_s dependence of $[\eta]$, k_1 and k_2. ○ Gohsenol NM; △ Gohsenol GM.

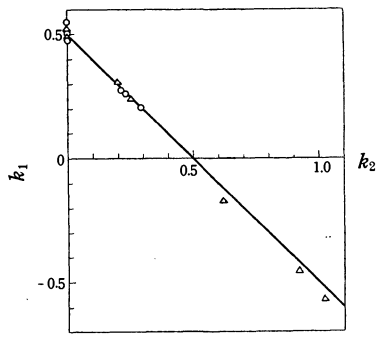

Fig. 4. Relation between k_1 and k_2.

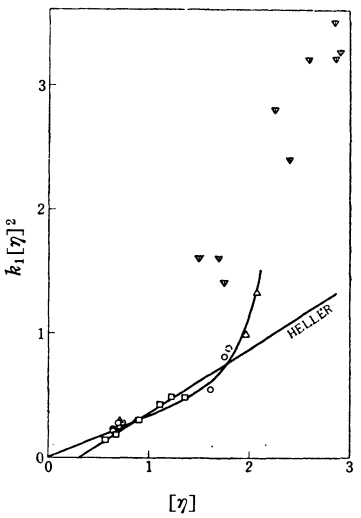

Fig. 5. Relation between $k_1[\eta]^2$ and $[\eta]$.
○ and △: Gohsenol
□ and ▽: Polystyrene

$$k_1 + k_2 = 0.5 \quad (6)$$

which had been pointed out by Ewart[6]. Fig. 4 shows that this relation can be extended to the negative values of k_1. This is a natural consequence because Ewart's relation can be derived mathematically from Eqs. 4 and 5.

The relation between $k_1[\eta]^2$ and $[\eta]$ is shown in Fig. 5. Eirich and Riseman[7] proposed an empirical relation,

$$k_1[\eta]^2 = \alpha + \sigma[\eta] \quad (7)$$

where α and σ are constants. Using data by Streeter and Boyer[8] on polystyrene ($\overline{M}_w=3.7\times10^5$) in various organic solvents, values $\sigma=0.50_7$ and $\alpha=-0.14_6$ were obtained by Heller[3]. This relation is shown in Fig. 5 by a straight line and individual data by □. On the other hand, the present data were plotted for Gohsenol NM by ○ and GM by △, except for three points of negative k_1 values. According to these data, $k_1[\eta]^2$ increases more rapidly than the straight line by Heller at large $[\eta]$ values. This is, however, not strange if we refer to the values given by Cragg[9], which are based on data by Bawn et al. on polystyrene ($M=1.6\times10^6$) in various organic solvents and shown in Fig. 5 by ▽. Therefore, the relation between $k_1[\eta]^2$ and $[\eta]$ of polyvinyl alcohol-soap-water system studied in this paper follows the same tendency as that of polystyrene in organic solvents, except the case for which k_1 is negative.

Interaction between Polyvinyl Alcohol and Soap.—On the basis of the experimental observations described above, polyvinyl alcohol is being dissolved in soap solution in three different states depending on the concentration of soap.

(1) In a soap solution at the concentration lower than its critical micelle concentration, polyvinyl alcohol behaves as it does in water. It is therefore concluded that the effect of soap is negligible at this low concentration. Here, $[\eta]$ is small, k_1 nearly equal to 0.5 and k_2 is nearly equal to zero. This is the usual behavior of polyvinyl alcohol in water, or more generally, of nonionic polymer in a rather poor solvent.

(2) In a soap solution near the critical micelle concentration $[\eta]$ is large, k_1 is negative and k_2 is larger than 0.5. The negative value of k_1, or a rapid increase of η_{sp}/c with decreasing polymer concentration, is usually observed on aqueous solutions of polyelectrolytes. In this range of soap concentration, therefore, polyvinyl alcohol molecules are supposed to be combined with soap molecules, and to behave like polyelectrolyte molecules because of the electrical charges due to the soap ions. The combination of polyvinyl alcohol and soap occurs near the critical micelle concentration of the soap, but the formation of micelle does not seem to be very important to this combination, because at the critical micelle concentration (0.025 N) the intrinsic viscosity of Gohsenol NM is still low while that of Gohsenol GM is already large. This may suggest that the combination of soap with polyvinyl alcohol is due to the aggregation of the hydrophobic part of the soap molecule with the hydrophobic part of the polymer molecule. This will explain the fact that the combination occurs near the critical micelle concentration, because the micelle formation of soap is also due to the aggregation of hydrophobic part of soap molecules. This will, further, explain that Gohsenol GM combines with soap at lower soap concentration than Gohsenol NM does, because GM retains about 10% of acetyl groups so that it is more hydrophobic than NM, the latter being saponified completely.

(3) In a soap solution of high concentration, $[\eta]$ is large and both k_1 and k_2 are positive. This is the usual behavior of nonionic polymer in a good solvent. This will mean that the electric charges of soap molecules combined with the polymer are shielded completely by the ion atmosphere of the counter ion (sodium ion) at this high soap concentration, so that the polymer behaves like a nonionic polymer. The high value of the intrinsic viscosity may be due to the following several reasons. a) The carboxyl group of soap combined with the polymer adds hydrophilic property. A polymer molecule is usually the more extended, the higher the affinity of the polymer to solvent. b) As far as the intermolecular interaction of polymer molecules are concerned, it has been assumed that the electric charge of soap combined with the polymer is completely shielded by counter ions. However, the shielding is probably not perfect inside the molecule. The electric repulsion between segments in a polymer molecule will extend the polymer. c) The soap

6) R. H. Ewart, *Advances in Colloid Sci.*, **2**, 211 (1946).
7) F. Eirich and J. Riseman, *J. Polymer Sci.*, **4**, 417 (1949).
8) D. J. Streeter and R. F. Boyer, *Ind. Eng. Chem.*, **43**, 1790 (1951)
9) L. H. Cragg, *Chem. & Ind.*, **1952**, 623.

molecules combined with the polymer will occupy its own volume. This will make the polymer molecule expanded. d) By the combination with soap molecules, polymer molecules become stiff and lose flexibility to some extent. This will also result the extension of the polymer molecules. The extension of polymer molecules by these reasons will increase the intrinsic viscosity.

Summary

The concentration dependence of the viscosity of polyvinyl alcohol in solutions of constant soap concentration is studied. At the soap concentration lower than its critical micelle concentration, the effect of soap on the viscosity of polyvinyl alcohol is very little. At the soap concentration near the critical micelle concentration, soap molecules are combined with the polymer, the latter behaving like a polyelectrolyte. At high soap concentration, the polymer behaves like a non-ionic polymer in a very good solvent.

The authors wish to thank Nippon Gosei Kagaku Kogyo Co. Ltd. from whom Gohsenols were provided.

Faculty of Living Science
Osaka City University
Nishi-ku, Osaka

Solvent Effects on the Fluorescence of Some π-Electron Systems Naphthylamine and Naphthol

By Noboru MATAGA

(Received December 18, 1957)

Heretofore, in a series of investigations[1-5], we have examined some aspects of solvent effects on the fluorescence of π-electron systems, especially concerning the hydrogen bonding effect.

a) Firstly, a general formula for the difference of solvent shifts of fluorescence and absorption spectra in the approximation of long range dipolar interaction was derived using Ooshika's theory[6] of light absorption in solution. Measurements of fluorescence and absorption spectra of some naphthalene derivatives in various organic solvents were undertaken, and the experimental data were analyzed by the theoretical formula. The formula reproduces the experimental data satisfactorily, and from this fact it was concluded that the most predominant factor which determines the difference of solvent shifts of fluorescence and absorption spectra of these molecules is the interaction energy between solute and solvent molecules due to orientation polarization. The incremental values of dipole moments in the excited state were estimated, and those for α, β-naphthols and β-naphthyl methylether were interpreted as due to the increase of electron migration from the substituent in the excited state.

b) Secondly, the question whether a new and different equilibrium of the hydrogen bond formation is reached during the lifetime of the excited state, was examined using the solutions of α- and β-naphthol as fluorescers and proton donors in non-polar solvent mixed with various proton acceptors.

By quantitative treatment of the experimental results, it was confirmed that β-naphthol in the excited state has a greater tendency toward hydrogen bonding, a new equilibrium being attained during its lifetime.

c) Thirdly, the effect of hydrogen bond formation on the fluorescence yield of the mother substance was investigated, from which some facts of the mechanism of non-radiative degradation of excited state

1) N. Mataga, Y. Kaifu and M. Koizumi, This Bulletin, **28**, 690 (1955); **29**, 465 (1956).
2) N, Mataga, Y. Kaifu and M. Koizumi, *Nature*, **175**, 731 (1955); This Bulletin, **29**, 116 (1955).
3) N. Mataga and S. Tsuno, ibid., **30**, 368 (1957).
4) N. Mataga and S. Tsuno, *Naturwiss.*, **44**. 304 (1957).
5) N. Mataga and S. Tsuno, This Bulletin, **30**, 711 (1957).
6) Y. Ooshika, *J. Phys. Soc. Japan*, **9**, 594 (1954).

due to inter- or intra-molecular processes, were obtained. The role of non-bonding electrons in the inner quenching of some nitrogen heterocycles, and the effect of π-electronic state on the fluorescence quenching caused by the near-by existence of halogen atoms, were studied. The cause of the inner quenching in nitrogen heterocycles was attributed to the n-π interaction in the excited state. The difference between quinoline and acridine in their fluorescence quenching caused by the existence of a halogen atom was ascribed to the different emitting states in these molecules (^1L_b in quinoline, ^1L_a in acridine), and some considerations were made assuming a close similarity of the electronic states of nitrogen heterocycles to those of the parent hydrocarbons. This assumption has been confirmed by some quantum mechanical calculations[7,8].

Fluorescence quenching caused by the hydrogen bond formation between nitrogen heterocycles as proton acceptors and fluorescers, and proton donors such as phenol, naphthol, aniline and pyrrole which are capable of making hydrogen bond intimately related with π-electron systems, was investigated, and interpreted as due to the delocalization of π-electrons through the hydrogen bond, in the excited state.

In the present paper, we shall report other examples of the solvent effect on fluorescence spectra, the shift of the hydrogen bonding equilibrium in the excited state, and the fluorescence quenching due to hydrogen bond formation, in which naphthylamine and naphthol are used as fluorescers and proton donors, and pyridine and acetic acid esters as proton acceptors.

Experimental

Apparatus:—Absorption spectra were measured with a Beckman Spectrophotometer model DU. Fluorescence spectra were photographed with small-type glass prism spectrograph. The fluorometer was the same as described previously[2]. Filters used for naphthol are the same as before[2], and for naphthylamine, they are as follows: for exciting light, Matsuda color filter UV-DI which takes out 365 mμ line of mercury lamp, and for fluorescent light, the yellow filter, attached to Beckman photometer for fluorescence analysis, the transmittance of which is nearly 90% in all the visible spectral region longer than 410 mμ, were used.

Reagent:—β-Naphthol and β-naphthylmethyl ether were the same samples as used before[2]. Chemical-pure grade α- and β-naphthylamine were purified by repeated recrystallization from ligroin. Extra-pure grade N, N-dimethyl-β-naphthylamine was purified by repeated distillation in vacuo. Acetic acid esters[2] and trichloroacetic acid[3] were the same samples as described previously. Extra-pure grade pyridine was dried over sodium hydroxide and distilled carefully. Benzene was the same as described elsewhere[5].

Experimental Results and Discussion

When acetic acid esters are added to the solution of naphthylamine in benzene, the features of phenomena are similar to the case of naphthol. When hydrogen bonded with acetic acid esters, enhancement of fluorescence intensity compared with free molecules is observed, and the excited molecules have greater tendency to form hydrogen bonds, a new equilibrium being reached during the lifetime of the excited state.

When hydrogen bonded with pyridine, however, fluorescence is almost completely quenched, and it is also the case for naphthol. This quenching phenomenon is similar to the previously reported one[5] of non-radiative degradation caused by hydrogen bonding, but the fluorescer and the quencher have exchanged their roles as proton acceptor and donor, with each other.

A. Changes of Absorption Spectrum Caused by Hydrogen Bonding.—Absorption spectra are somewhat strengthened and shifted to red by hydrogen bonding. Some examples of these changes are shown

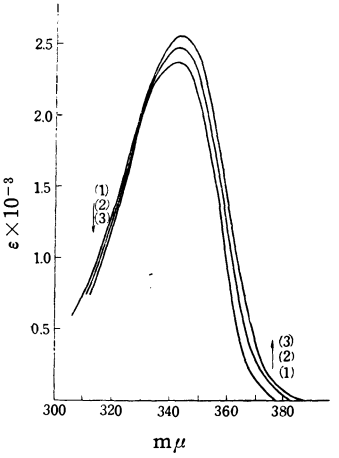

Fig. 1. Change of absorption spectrum of β-naphthylamine in benzene produced by added pyridine.
Concentration of pyridine: (1) 0, (2) 4.96×10^{-1} mole/l., (3) 1.24 mole/l.

7) N. Mataga, to be published in this Bulletin.
8) N. Mataga, to be published in this Bulletin.

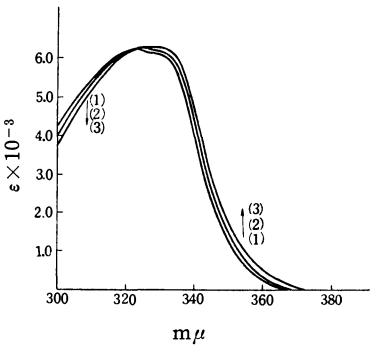

Fig. 2. Change of absorption spectrum of α-naphthylamine in benzene produced by added butyl acetate.
Concentration of butyl acetate: (1) 0, (2) 1.23 mole/l., (3) 2.76 mole/l.

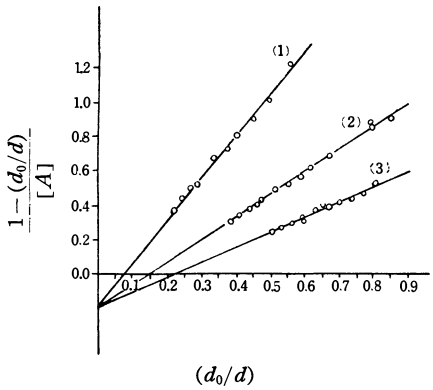

Fig. 3. $\frac{1-(d_0/d)}{[A]}$ vs. (d_0/d) relation for β-naphthylamine-pyridine-benzene system at several wave lengths: (1) 370 mμ, (2) 365 mμ, (3) 362 mμ.

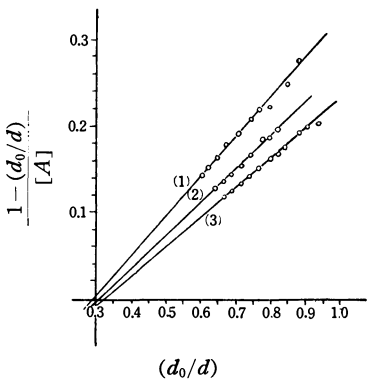

Fig. 4. $\frac{1-(d_0/d)}{[A]}$ vs. (d_0/d) relation for α-naphthylamine-butyl acetate-benzene system at several wave lengths: (1) 365mμ, (2) 354 mμ, (3) 352 mμ.

in Figs. 1 and 2. The change of optical density at a definite wave length is well reproduced by Eq. 1[3]

$$\frac{(1-d_0/d)}{[A]} = -K^{(g)} + (\varepsilon'/\varepsilon)\cdot K^{(g)}\cdot(d_0/d) \quad (1)$$

The equilibrium constants $K^{(g)}$'s of hydrogen bond formation obtained by means of this formula, at several wave lengths, nearly coincide with each other. Some examples of these analyses are shown in Figs. 3 and 4.

B. Change of Relative Fluorescence Intensity Caused by Addition of Proton Acceptor.—Some examples of the enhancement or quenching of fluorescence of β-naphthylamine in benzene caused by the addition of proton acceptors are shown in Fig. 5. The features of these changes are also the same in the case of α-naphthylamine and of β-naphthol. If we use for these cases the following Eqs. 2[3] and 3*,

$$\frac{1-(f_0/f_m)(d_m/d_0)}{[A]} = -K^{(e)} + \alpha(d_m/d_0)K^{(e)}(f_0/f_m) \quad (2)$$

$$(f_m/f_0)(d_0/d_m) = \frac{1}{1+K^{(e)}[A]} \quad (3)$$

the experimental results are well satisfied by these equations, and the equilibrium constants $K^{(e)}$'s of hydrogen bond formation in the excited state are evaluated**. Some examples of these analyses are shown in Figs. 6 and 7. The equilibrium constants $K^{(e)}$'s obtained in this way are remarkably large compared with those evaluated from absorption spectra, as shown in Table I.

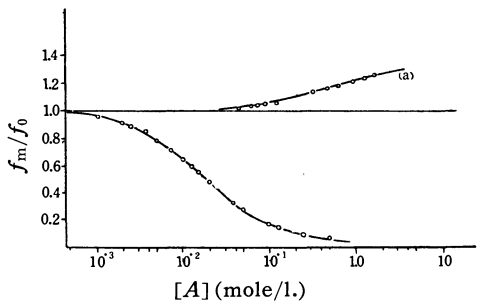

Fig. 5. Change of relative fluorescence intensity, f_m/f_0, of β-naphthylamine produced by added proton acceptors. Acceptors: (a) butyl acetate, (b) pyridine.

* Eq. 3 is obtained putting $\alpha=0$ in Eq. 2 which is the case for naphthylamines or naphthol-pyridine-benzene systems.

** Shifts of fluorescnce spectra of naphthylamines produced by the addition of acetic acid esters is very small in benzene, therefore we may be allowed to neglect the difference of phototube sensitivity for the fluorescence of free and hydrogen bonded naphthylamines.

TABLE I

acceptor	donor		
	α-naphthylamine	β-naphthylamine	β-naphthol
pyridine	$K^{(g)}_{285}$: $0.15K^{(e)}_{286}$: 53	$K^{(g)}_{286}$: 0.2 $K^{(e)}_{286}$: 60	$K^{(g)}_{287}$: $41K^{(e)}_{287}$: ~84
$CH_3CO_2C_4H_9$	$K^{(g)}_{283}$: $0.13K^{(e)}_{285}$: ~1	$K^{(g)}_{287}$: 0.1 $K^{(e)}_{287}$: ~1.8	
$CH_3CO_2C_2H_5$	$K^{(g)}_{287}$: $0.26K^{(e)}_{285}$: ~1	$K^{(g)}_{287}$: ~$0.26K^{(e)}_{287}$: ~1.8	

$K^{(g)}_T$ or $K^{(e)}_T$: T is the temperature (in unit of °K) at which the measurement was made.

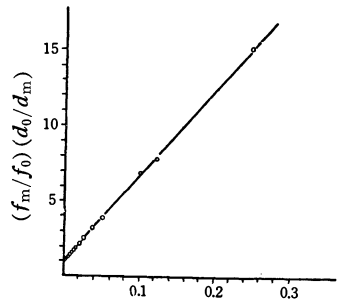

Fig. 6. $(f_0/f_m)(d_m/d_0)$ vs. $[A]$ relation for β-naphthylamine-pyridine-benzene system.

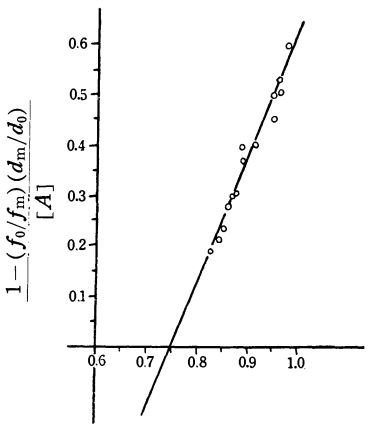

Fig. 7. $\frac{1\sim(f_0/f_m)(d_m/d_0)}{[A]}$ vs. $(f_0/f_m)(d_m/d_0)$ relation for β-naphthylamine-butyl acetate-benzene system.

When pyridine and acetic acid esters are added to the solutions of *N,N*-dimethyl-α-naphthylamine and β-naphthylmethyl ether in benzene, not even a slight change of fluorescence intensity has been observed throughout the whole range of acceptor concentration from ca. 10^{-3} to 1 mole/l.

Therefore, in the present case, the fluorescence quenching or enhancement may probably be wholly attributable to the hydrogen bond formation, and the equilibrium somewhat shifts to the side of association during the lifetime of the excited molecule. We can confirm further, whether the hydrogen bonding equilibrium in the excited state is really concerned with the fluorescence quenching or enhancement, as follows.

Let us examine the case in which the association equilibrium in the ground state is maintained in the excited state, the naphthylamines hydrogen-bonded with pyridine being completely non-fluorescent, and in which there is superposed the ordinary collisional quenching by pyridine. This is equivalent to assuming that, at the time of collision, pyridine affects specially the fluorescence of naphthylamines but not *N, N*-dimethylnaphthlamines. Then the deduction about the fluorescence intensity may be made according to the following scheme, were D and A are proton donor (fluorescer) and proton acceptor (quencher), respectively, and * denotes the excited state.

	rate or equilibrium
$D+A \rightleftarrows DA$	$K^{(g)}=[DA]/[D][A]$
$D+h\nu_a \rightarrow D^*$	$I_0\varepsilon[D]$
	$[D]=[D]_0/(1+K[A])$
$DA+h\nu_a \rightarrow DA^*$	$I_0\varepsilon'[DA]$
	$[DA]=K[A][D]_0/(1+K[A])$
$D^* \rightarrow D+h\nu_f$	$k_f[D^*]$
$D^* \rightarrow D$	$k_i[D^*]$
$DA^* \rightarrow DA$	$k_i'[DA^*]$
$D^*+A \rightarrow D+A$	$k_q[A][D^*]$

I_0: intensity of exciting light.

ε, ε': extinction coefficients of D and DA, respectively, at the wave length of exciting light.

By means of this scheme, the following formula for the relative fluorescence intensity is easily derived.

$$f_0/f_m = 1+(n_q+K^{(g)})[A]+n_qK^{(g)}[A]^2 \quad (4)$$

$$n_q = k_q/(k_f+k_i)$$

Now, let us assume that $K^{(e)}$ obtained by Eq. 3 is almost entirely contributed by n_q of Eq. 4, and plot f_0/f_m as a function of $[A]$.

As shown in Fig. 8, it is evident that the experimental results can not be reproduced by Eq. 4. Therefore, the possibility of the collisional quenching is rejected, and it is almost certain that the hydrogen

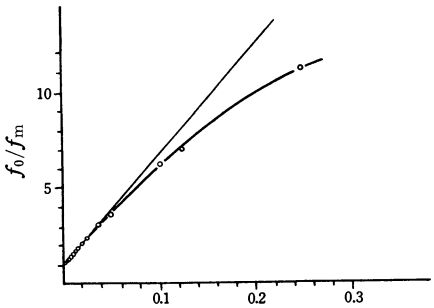

Fig. 8. f_0/f_m vs. [A] relation for β-naphthylamine-pyridine-benzene system.

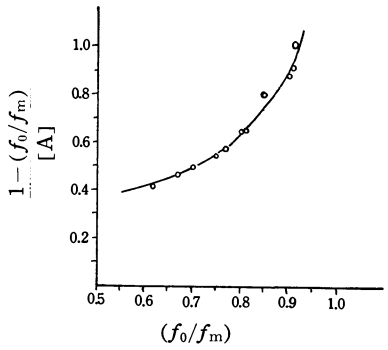

Fig. 9. $\frac{1-(f_0/f_m)}{[A]}$ vs. (f_0/f_m) relationf or β-naphtylamine-butyl acetate-benzene system.

bonding equilibrium shifts remarkably to the side of association during the lifetime of the excited state. For the case of enhancement of fluorescence intensity by acetic acid esters, the shift of equilibrium may be almost certain because Eq. 2 is satisfactorily reproduced by experimental results and the fluorescence of *N,N*-dimethyl-α-naphthylamine solution is not affected by the addition of the esters. If we use Eq. 5[3] which assumes that the equilibrium in the ground state is maintained in the course of fluorescence, instead of Eq. 2, we can see no agreement with experimental results, as shown in Fig. 9.

$$\frac{1-(f_0/f_m)}{[A]} = -K^{(g)} + \alpha(\varepsilon'/\varepsilon)K^{(g)}(f_0/f_m) \quad (5)$$

Further, let us examine, for this case, another possibility that the excited naphthylamine molecule is stabilized specifically by collision with acetic acid ester molecule, provoking the increase in fluorescence yield, though such an effect is very improbable in solution*. Now, let us assume the following scheme involving the equilibrium in the ground state, where the notations are the same as described above and s refers to the fluorescer molecule stabilized by collision.

	rate or equilibrium
$D+A \rightleftarrows DA$	$K^{(g)}=[DA]/[D][A]$
$D+h\nu_a \rightarrow D^*$	$I_0\varepsilon[D]$
$DA+h\nu_a \rightarrow DA^*$	$I_0\varepsilon'[DA]$
$D^* \rightarrow D+h\nu_f$	$k_f[D^*]$
$DA^* \rightarrow DA+h\nu_f'$	$k_f'[DA^*]$
$D^*+A \rightarrow D^{*s}+A$	$k_c[D^*][A]$
$D^{*s} \rightarrow D+h\nu_f$	$k_f^s[D^{*s}]$
$DA^* \rightarrow DA$	$k_i'[DA^*]$
$D^{*s} \rightarrow D$	$k_i^s[D^{*s}]$
$D^* \rightarrow D$	$k_i[D^*]$

According to this scheme, Eq. 6 is easily derived.

$$\frac{1-(f_0/f_m)}{[A]} = -(n_c+K^{(g)}+n_cK^{(g)}[A]) + \frac{(\Phi_0^s\varepsilon n_c+\Phi_0'\varepsilon'K^{(g)}+\Phi_0'\varepsilon'n_cK^{(g)}[A])}{\Phi_0\varepsilon} \times (f_0/f_m), \quad (6)$$

where

$$n_c=k_c/(k_f+k_i), \quad \Phi_0=k_f/(k_f+k_i),$$
$$\Phi_0'=k_f'/(k_f'+k_i'), \quad \Phi_0^s=k_f^s/(k_f^s+k_i^s)$$

Comparing this formula with Fig. 9, it is clear that the former is in essential disagreement with the latter. The possibility of collisional stabilization is thus completely neglected. The rather large difference of observed $K^{(g)}$ and $K^{(e)}$ of naphthylamines compared with that of naphthols may be partially comprehended as due to the difference of ionization potential of non-bonding electrons in the substituent (—OH: 10.95 eV., —NH_2: 9.41 eV.**,[9]). The degree of electron migration from the substituent and accordingly, also the difference of stabilization energy

* The increase in fluorescence yield of β-naphthylamine vapor in the presence of foreign gases was reported by Neporent[a]. Some aspects of his work on this molecule were confirmed by Curme and Rollefson[b] and detailed kinetical study was made by Boudart and Dubois[c].

a) B. S. Neporent, *Zhur. Fiz. Khim.*, **21**, 111 (1947): **24**, 1219 (1950). b) H. G. Curme and G. K. Rollefson, *J. Am. Chem. Soc.*, **74**, 28 (1952). c) M. Boudart and J. T. Dubois, *J. Chem. Phys.*, **23**, 223 (1955).

** These values are the ionization potentials of methanol and methylamine, respectively.

9) J. D. Morrison and A. J. C. Nicholson, *J. Chem. Phys.*, **20**, 1021 (1952).

in the excited and ground state become larger, as the ionization potential of the substituent[10] becomes smaller.

Therefore, in the case of naphthylamines, the difference of the proton donating power in the excited and the ground state may be rather great, although the absolute value of proton donating power in the ground state may be small. In this respect, we have measured the solvent shifts of fluorescence and absorption spectra of naphthylamines in various organic solvents, and the results have been analyzed by Eq. 7[1,11]

$$-hc(\sigma_f^m-\sigma_a^m)\cong\text{Const.}+\left[\frac{2(D-1)}{2D+1}-\frac{2(n^2-1)}{2n^2+1}\right]\frac{(\vec{\mu}_e-\vec{\mu}_g)^2}{a^3} \quad (7)$$

where, σ_f^m and σ_a^m are wave numbers of peaks of fluorescence and absorption spectra, respectively, D and n dielectric constant and refractive index of the solvent, $\vec{\mu}_e$ and $\vec{\mu}_g$ dipole moment of solute molecule in the excited and the ground state, respectively and a is the cavity radius in Onsager's theory of reaction field.

Although we can not make a quantitative discussion because of the broadness of the spectra, it may be certain that the increments of dipole moments of naphthylamines in the excited state are not smaller than those of naphthols in the order of magnitude. In addition we refer to the fact that, Förster has estimated the difference of pK value in the excited and ground states of β-naphthylamine, in the case of the dissociation of the type, $-NH_2 \rightarrow -NH^- + H^+$, to be about 8 units[12], the excited state being very acidic compared with the ground state.

Now, as pointed out in the earlier part of this paragraph, the fluorescence quenching caused by hydrogen bonding with pyridine is analogous to the quenching phenomenon in the case of nitrogen heterocycles hydrogen bonded with phenols and aniline[5]. Accordingly, we may be allowed to say that the quenching in the present case also originates from the interaction between the π-electron systems via the hydrogen bond, in the excited state, although the fluorescer and quencher have reversed their roles as the proton acceptor and donor.

10) A. L. Sklar, ibid., **7**, 984 (1939); K. F. Herzfeld, *Chem. Revs.*, **41**, 233 (1947).
11) E. Lippert, *Z. Naturforsch.*, **109**, 541 (1955); *Z. physik. Chem.*, N. F., **6**, 125 (1956).
12) Th. Förster, *Z. Elektrochem.*, **54**, 531 (1950).

Summary

The enhancement or quenching of fluorescence intensity of naphthylamines and naphthol caused by hydrogen bonding with acetic acid esters or pyridine has been measured. By means of detailed analyses of the experimental results, it has been established that the shift of hydrogen bonding equilbrium toward the side of association is realized during the lifetime of excited state.

The cause of the shift has been interpreted on the basis of the theory of electron migration, and an evidence supporting the interpretation has been provided by measuring the solvent shift of fluorescence spectra. The mechanism of the fluorescence quenching has been discussed as due to the delocalization of π-electrons through the hydrogen bond.

The author expresses his gratitude to Professer S. Mizushima of Tokyo University for his encouragement. He is also grateful to Professor M. Koizumi of Tohoku University for his interest in this investigation. His thanks are especially due to Miss S. Tsuno for her experimental assistance throughout the present study. He is also thankful to Miss S. Wada for typewriting this paper.

Institute of Polytechnics
Osaka City University
Kita-ku, Osaka

Fluorescence Quenching due to the Interactions between π-Electron Systems in the Excited State and Acid-Base Relation: Nitrogen Heterocycles, Naphthylamine and Naphthol in Aqueous and Alcoholic Solution

By Noboru MATAGA

(Received December 18, 1957)

In an earlier paper[1], we have reported the results of our investigation about the hydrogen bonding effect on the fluorescence of acridine, 3,6-diaminoacridine (DAA) and 3,6-bisdimethylaminoacridine (BDAA) in non-polar solvent mixed with proton donor such as phenol, naphthol, aniline and pyrrole. In these cases in which the hydrogen bond is capable of conjugating with the π-election system of proton donor, the fluorescence yields decrease as the result of hydrogen bonding formation in contrast to the case of donors such as benzylalcohol and β-phenylethylalcohol[2] in which the hydrogen bond is isolated by σ-bond from π-electron system, and with which hydrogen bonding leads to the enhancement of fluorescence yield. From the fact that no viscosity dependence of quenching has been observed, the possibility of the participation of diffusion-controlled dynamical process in the non-radiative degradation of excited state has been excluded. Moreover, we have also examined the case of naphthylamines and naphthol, hydrogen-bonded with pyridine where a remarkable fluorescence quenching has been observed[3]. Then the cause of the non-radiative degradation of excited state by means of hydrogen bonding has been attributed to the interaction between two π-electron systems via the hydrogen bond, viz., the delocalization of π-electrons through the hydrogen bond, especially in the excited state.

Hitherto, the ordinary experimental studies of the fluorescence quenching in the case of complex molecules, has been mainly carried out in aqueous or alcoholic solution, and the real nature of this phenomenon is not very clear up to now.

We have attempted to touch the real nature of the fluorescence quenching, in our series of investigation[1-7], mainly concerning with the case of hydrogen bond formation between fluorescer and quencher (or promoter) in non-polar solvent. The above mentioned case of fluorescence quenching due to the hydrogen bonding between the π-electron systems[1,3] may plausibly provide a more clear-cut example in relation to the mechanism of fluorescence quenching, and, in fact, it may be a new type of fluorescence quenching studied in a systematic manner. As an extention of our investigations, we have examined the behavior of the fluorescers and quenchers in aqueous and alcoholic solutions. We have found that, in this case, there exists some regularity in relation to the ability of a molecule as quencher or an approximate parallelism with the case of fluorescence quenching in non-polar solvent. This fact may probably suggest a somewhat analogous mechanism of quenching to the case of non-polar solvents, although, contrary to the case of the latter, the dynamical mechanism may be predominant in the present case. Moreover, the remarkable difference between aqueous and alcoholic solutions in this quenching phenomenon has become clear. In the present paper we shall report these facts with some discussions on the characterization of the quenchers and the influence of liquid structures of solvents on the fluorescence quenching.

Experimental

Apparatus: Absorption spectra were measured with Beckman Spectrophotometer model

1) N. Mataga and S. Tsuno, This Bulletin, **30**, 711 (1957).
2) N. Mataga and S. Tsuno, ibid., **30**, 368 (1957).
3) N. Mataga, to be published in this Bulletin.
4) N. Mataga, Y. Kaifu and M. Koizumi, *Nature*, **175**, 731 (1955); This Bulletin, **29**, 115 (1956).
5) N. Mataga and S. Tsuno. *Naturwiss.*, **44**, 304 (1957).
6) N. Mataga, to be published in this Bulletin.
7) N. Mataga, to be published in this Bulletin.

DU. Fluorometer was the same as described before[4]. A high pressure mercury lamp with appropriate filters was used as an exciting light source. Filters for quinoline, acridine[8] and DAA[1] are the same as used before. The filters used for β-naphthylmethyl ether and the ultraviolet fluorescence[9] of β-naphthol were the same as those of quinoline. For the blue fluorescence[9], the saturated solutions of nickel- and cobalt-sulfate and 0.2 g./l. potassium chromate solution each of which has 1 cm. thickness, were used as exciting light filters, taking out only 310 mμ line of mercury lamp, on the one hand, and yellow filter of Beckman photometer[3] was used for fluorescent light on the other hand. The filters used for β-naphthylamine and *N,N*-dimethyl-α-naphtylamine were the same as used before[3].

Reagent: All fluorescers and quenchers are the same samples as used before[1-5,8]. In order to control the pH of aqueous solution, citrate, phosphates and glycine were used. The reagents were of extra-pure grade, and used without further purification.

Experimental Results

In the following, the results for each fluorescer are described separately, and some of the data are collected in tables* in the latter part of this section. The concentrations of fluorescers are as follows; quinoline, β-naphthol, β-naphthylamine, β-naphylmethyl ether and *N,N*-dimethyl-α-naphthylamine, $\sim 10^{-4}$ mole/l.; acridine, 5×10^{-5} mole/l.; DAA, $\sim 10^{-5}$ mole/l.

In all cases described here, the absorption spectra showed no change caused by the addition of quenchers.

a) Quinoline: Only the quenching action of phenol and pyridine in aqueous solutions of appropriate pH values where the fluorescer exists exclusively as quinolinium ion, was examined quantitatively. The quenching curves in the case of phenol, are well reproduced by Stern-Volmer** equation, and the quenching constant becomes larger, with decrease in the pH value. The fluorescence is quenched also by pyrrole, almost completely disappearing at the quencher concentration, $\sim 10^{-1}$ mole/l. No quenching by pyridine, however, has been observed.

b) Acridine: The quenching actions of phenol, aniline pyrrole, and pyridine were examined mainly in aqueous solutions of various pH values. In the case of phenol, the dependence of quenching constant on the pH value is similar to the case of quinoline. Contrary to this, in the case of aniline, the quenching constant at pH 1 is the smallest. The quencher exists at this pH value, however, as anilinium cation. In contradistinction to the quenching in aqueous solution, the efficiency of phenol in ethanol solution is very poor, and, in practice, there occurs almost no quenching. The efficiencies of aniline and pyrrole in alcoholic solution, however, are not smaller than those in aqueous solution. Moreover, pyridine has no quenching effect on the fluorescence of acridine either in aqueous or alcoholic solutions. The anomalous behavior of phenol as quencher in alcoholic solution compared with the remarkable quenching in aqueous solution, has been studied in detail for the case of DAA.

c) DAA: Mainly the effect of solvent on the fluorescence quenching by phenol, aniline and pyrrole, has been examined in detail. The pH dependence of the quenching by phenol in aqueous solution is analogous to the case of acridine, although practically no quenching occurs at pH 13. In the case of aniline and pyrrole in aqueous solution, measurement was made only at pH 5. The remarkable difference between aqueous and alcoholic solutions is as follows. Although the quenching constants in the case of aniline and pyrrole in various alcoholic solvents are in approximately the same order of magnitude as those in aqueous solution, and the quenching in alcoholic solutions shows a normal dependence on the viscosity of solvent, all values of quenching constants in the case of phenol in alcoholic solutions are ca. 0.1 (l./mole), i.e., practically no quenching occurs in this case. Here also, pyridine shows no quenching effect on the fluorescence either in aqueous or alcoholic solutions.

d) β-Naphthol: In aqueous solution some of the excited naphthol molecules dissociate into ions during the lifetime of excited molecules[9]. Therefore, in this case, the fluorescence of molecule (ultraviolet) and that of ion (blue) should be measured separately. The formula representing the relative fluorescence intensities of molecule and ion, respectively are derived easily employing the following scheme.

8) N. Mataga, Y. Kaifu and M. Koizumi, This Bulletin, **29**, 373 (1956).

9) Th. Förster, *Z. Elektrochem.*, **54**, 42, 531 (1950); A. Weller, ibid., **56**, 662 (1952); *Z. physik. Chem.*, N. F., **3**, 238 (1955).

* In these tables, when the quenching curves show some deviations from Stern-Volmer equation, the values of quenching constants are extrapolated from the regions of dilute quencher concentrations.

** Hereafter, abbreviation "S.-V. equation" will be used.

TABLE I

NITROGEN HETEROCYCLES

Quencher	Solvent (pH)	Quenching Constant (l./mole)*	c_h** (mole/l.)***	t(°C)****
		Quinoline		
	H_2O (1)	65	1.5×10^{-2}	~17
	H_2O (2.97)	32	3.1×10^{-2}	〃
		Acridine		
phenol	H_2O (2.97)	130 ($<2\times10^{-2}$)	7.7×10^{-5}	~20
	H_2O (6.81)	110 ($<3\times10^{-2}$)	9.7×10^{-3}	〃
	H_2O (7.73)	8 ($<4\times10^{-2}$)	1.5×10^{-2}	〃
	H_2O (11.3)	30 ($<4\times10^{-2}$)	3.6×10^{-2}	〃
	H_2O (12.9)	37 ($<5\times10^{-2}$)	3.0×10^{-2}	〃
aniline	H_2O (1.04)	10.6	9.4×10^{-2}	~14
	H_2O (7.17)	94.4	1.05×10^{-2}	〃
	H_2O (13)	32.3	3.09×10^{-2}	〃
pyrrole	H_2O (5)	77	1.3×10^{-2}	~14
		DAA		
phenol	H_2O (2.97)	21.6	4.6×10^{-2}	~21
	H_2O (4.96)	20.8	4.8×10^{-2}	〃
	H_2O (12.9)	no quenching		〃
	MeOH	0.13	(8.0)	~13
	EtOH	0.11	(9.0)	〃
	BuOH	0.12	(8.4)	〃
aniline	H_2O (5)	8	1.2×10^{-1}	~14
	MeOH	32	3.2×10^{-2}	〃
	EtOH	18	5.7×10^{-2}	〃
	BuOH	11.4	8.7×10^{-2}	〃
pyrrole	H_2O (5)	19	5.4×10^{-2}	~14
	MeOH	21	4.7×10^{-2}	〃
	EtOH	6.1	1.6×10^{-1}	〃
	BuOH	3.5	2.8×10^{-1}	〃

* An extrapolation was made in the range of the quencher concentration smaller than this value.

** The concentration of quencher at which f becomes $f_0/2$.

*** Extrapolated value in the case of very small quenching constant.

**** Temperature at which the measurement was made.

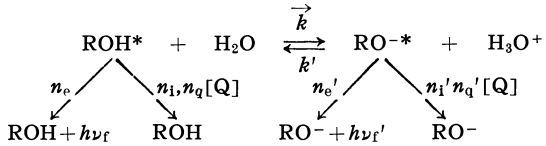

where $k'=\overleftarrow{k}[H_3O^+]$.

Then, for molecule,

$$f/f_0 = \frac{1+\alpha'[Q]}{1+\alpha[Q]+\beta[Q]^2}$$

and for ion,

$$f'/f_0' = \frac{1}{1+\alpha[Q]+\beta[Q]^2}$$

where Q represent quencher.

Therefore, $\left(\frac{f/f_0}{f'/f_0'}\right)=1+\alpha'[Q]$.

The meanings of constants α, α' and β are as follows,

$$\alpha=\frac{n\tau_q(1+k'\tau')+n_q'\tau'(1+\vec{k}\tau)}{1+\vec{k}\tau+k'\tau'},\quad \alpha'=\frac{n_q'\tau'}{1+k'\tau'}$$

$$\beta=\frac{n_q n_q'\tau\tau'}{1+\vec{k}\tau+k'\tau'}$$

where τ and τ' are the mean lifetimes of excited molecule and ion, respectively. When $k'\sim0$, i.e., $[H_3O^+]$ is small, above equations become as follows.

$$f/f_0=\frac{1}{1+\{n\tau/(1+\vec{k}\tau)\}[Q]}$$

$$\left(\frac{f/f_0}{f'/f_0'}\right)=1+n_q'\tau'[Q]$$

These equations are well satisfied by the experimental observations. Using the experimentally datermined values of $\vec{k}$, τ and τ'[9], n_q and n'_q are evaluated. The values of n_q and n'_q are almost the same, although the latter is slightly larger than the former. The dependence of n_q and n'_q on the pH values of the solution is analogous to the case of nitrogen heterocycles as fluorescers and phenol as quencher, i.e., the n_q and n'_q values become larger, the smaller the pH value is. Moreover, also in this case, the quenching efficiency in alcoholic solution is very poor compared with that in aqueous solution.

e) β-Naphthylamine: Remarkable quenching by pyridine occurs in both aqueous and methanol solution, although the quenching constant in the latter solution is somewhat less prominent. The quenching curves are well satisfied by S.-V. equation. Contrary to this, phenol does not show any quenching effect, and the efficiency of aniline as quencher is negligibly small.

f) β-Naphthylmethyl ether: In a preceding paper[3], we have reported that, no quenching effect by pyridine in benzene solution on the fluorescence of this molecule has been observed. Here it is confirmed that also in cyclohexane and acetic acid esters, the same situation prevails. In aqueous and alcoholic solutions, however, there occurs considerable quenching, respectively, almost comparable with the corresponding cases of β-naphthol molecule.

g) *N, N*-Dimethyl-α-naphthylamine: The circumstance is analogous to the case of β-naphthylmethyl ether. In benzene solution, the fluorescence of this molecule is not influenced by pyridine[3]. In aqueous solution, however, the fluorescence is quenched by pyridine considerably.

TABLE II

β-NAPHTHOL-PYRIDINE

Solvent (pH)	n_q	n'_q	t(°C)
H_2O (3.95)	3.6×10^9	4.2×10^9	~16
H_2O (7.17)	1.7×10^9	3.1×10^9	〃

TABLE III

β-NAPHTHYLAMINE-PYRIDINE

Quencher	Solvent	Quenching Constant	t(°C)
pyridine	H_2O*	63	~16
	MeOH	26	〃

*pH is not controlled by buffer.

Discussion and Concluding Remarks

In previous papers[2,6,7], we have reported the fact that, in the case of nitrogen heterocycles, the difference in the emitting π-electronic state leads to the different behavior of these nitrogen heterocycles in fluorescence quenching by the near-by existence of halogen atoms. Some qualitative considerations by means of analogy to the π-electronic structures of parent hydrocarbons were given[2], and a quantitative argument has been given on the basis of a theoretical computation[6,7]. In the present case, however, no such effect of emitting π-electonic state on the fluorescence quenching is observed, and phenol quenches the fluorescence of quinoline as well as acridine and DAA almost equally well. Therefore, with the present type of fluorescence quenching which is caused by the interaction between π-electron systems in the excited state, ^3L_b state may not concern so severely, although the detailed microscopic mechanism of the quenching is not so clear. Now, in the following, some arguments will be given from two standpoints, i.e., the most effective combination of fluorescer and quencher, on the one hand, and the effects of solvents on the quenching efficiency, on the other hand.

A. Fluorescence Quenching and Acid-Base Relation. Phenol, aniline and pyrrole quench severely the fluorescence of nitrogen heterocycles such as quinoline, acridine and DAA. Contrary to this, pyridine does not show any quenching effect on the fluorescence of the nitrogen heterocycles.

Moreover, the fluorescence of naphthol as well as naphthylamine is quenched by pyridine effectively. Phenol and aniline, however, scarcely quench the fluorescence of these naphthalene derivatives at all. Thus, it is evident that the most efficient fluorescer-quencher pair is in acid-base or proton donor-acceptor relation, and roughly speaking, there exists a parallelism between the fluorescence quenching due to hydrogen bonding in non-polar solvent and the present case.

From this fact, we might be allowed to suppose that some analogous mechanism to the case of fluorescence quenching due to hydrogen bonding in non-polar solvent[1],

may prevail also in the quenching of present type, although the circumstance is more complicated.

B. Effects of Solvents on the Efficiency of Fluorescence Quenching. Pyridine does not quench the fluorescence of β-naphthylmethyl ether as well as *N,N*-dimethyl-α-naphthylamine, in benzene, cyclohexane and acetic acid esters. In aqueous and alcoholic solutions where the hydrogen bond between solvent molecules and also between solvent and solute molecules exist, however, the fluorescence of these molecules is quenched remarkably to almost the same extent as in the case of naphthol and naphthylamine, respectively. The important role of hydrogen bonding in the fluorescence quenching of this case is implicit in the fact that, only in the associating liquids such as water and alcohol, the fluorescence is quenched efficiently.

Another remarkable example of the solvent effects is that the behavior of the phenol-nitrogen heterocycles or pyridine-naphthol system in alcoholic solution is very different from that in aqueous solution.

In contradistinction to the severe quenching in aqueous solution, the quenching in alcoholic solution is very slight. Although the cause of this remarkable difference is not clear, we can not but ascribe it to the difference in the liquid structure, viz., the very extensive hydrogen bonding in water on the one hand and the less extensive hydrogen bonding in alcohol on the other hand might have some connection with this phenomenon.

Summary

The acid-base relation in the fluorescence quenching in aqueous and alcoholic solutions, due to the interaction between π-electron systems in the excited state, has been pointed out. Roughly speaking, this is parallel with the fluorescence quenching due to hydrogen bonding between the π-electronic fluorescer and quencher in non-polar solvent. Remarkable solvent effects on the quenching efficiency have been found and some important roles of hydrogen bonding in this phenomenon have been suggested.

The author expresses his sincere gratitude to Professor S. Mizushima of Tokyo University for his encouragement. He is also grateful to Professor M. Koizumi of Tohoku University for his interest in the present work. He expresses his thanks to Professor R. Fujishiro for his encouragement during this investigation. He also expresses his appreciation to Dr. S. Nagakura of Tokyo University and Dr. H. Tsubomura of Tokyo University for their discussions. His thanks are especially due to Miss S. Tsuno for her experimental assistance throughout this investigation. His thanks are also due to Miss S. Wada for typewriting this paper.

Institute of Polytechnics
Osaka City University
Kita-ku, Osaka

*On the Constitution of Myoporone** (*Natural Furan Derivatives. II.***)

By Takashi KUBOTA and Teruo MATSUURA

(Received December 14, 1957)

The essential oil of the genus *Myoporum*, endemic to Australia and New Zealand, was examined by several investigators. McDowall[1] first isolated ngaione from the volatile oil of *Myoporum laetum* Forst. in 1925. Subsequently Birch, Massy-Westropp and Wright[2] isolated the same substance and 3-furoic acid from a specimen of *M. acuminatum*. They also examined the volatile oil of two other specimens of *M. acuminatum* and found that these oil contained at most traces of

* T. Kubota and T. Matsuura, *Chemistry and Industry*, **1957**, 491.

** Part I. T. Matsuura, This Bulletin, **30**, 430 (1957).

1) F. H. McDowall, *J. Chem. Soc.*, **1925**, 2200.

2) A. J. Birch, R. A. Massy-Westropp and S. E. Wright, *Australian J. Chem. Soc.*, **6**, 385 (1953).

ngaione and an α,β-unsaturated furanoketone, $C_{15}H_{20}O_2$.

Ngaione was extensively investigated by several workers[3], but no complete formula has yet been put forward. Recently, we have succeeded in demonstrating that ngaione has the structure I[4], namely the enantiomorph of (+)-ipomeamarone, the toxic bitter principle of black rotten sweet potato. In connection with these works we have recently examined the essential oil from the Japanese *M. Bontioides* A. Gray (the only *Myoporum* found in Japan), and have found that ngaion is contained only in a small amount and the major constitutent is a new terpene ketone (the yield from undried leaves, ca. 0.2%). This ketone has been designated myoporone and the elucidation of its structure will be reported herewith. The essential oil contained also an unsaturated hydrocarbon, C_nH_{2n} of m. p. 63~64°C.

Myoporone (b. p. 117~119°C/10^{-2} mm.; n_D^{21} 1.4770) is a pale yellow oil with a slightly bitter taste, and shows no optical rotation, at D line, but its 2,4-dinitrophenylhydrazone (α-form, see below) has $[\alpha]_D^{23}$ −28.2°***.

It gives a purple coloration with Ehrlich's reagent, a pale brown coloration with concentrated hydrochloric acid, decolorized potassium permanganate, and yield a dark red Liebermann reaction. The molecular formula is $C_{15}H_{22}O_3$, and two bis-2,4-dinitrophenylhydrazones, $C_{27}H_{30}O_9N_8$ are obtained. The α-form has red color and melts at 193°C, while β-form is orange-yellow and turns into red at 143~145°C and melts at 193°C. These substances seem to be dimorphous[5]. Infrared absorptions of myoporone in Nujol are shown at 3.19 (furan), 5.88 (ketone), 5.95 (conjugated ketone), 6.41 (furan), 6.63 (furan) and 11.45 μ (furan).

Oxidative degradation of myoporone ozonide followed by esterification of the acidic fraction yielded a methyl ester, b. p. 88~90°/10^{-2} mm., n_D^{18} 1.4378, λ_{max}^{nujol} 5.77 and 5.84 μ. Conversion of this ester into semicarbazone and subsequent hydrolysis gave a semicarbazone of ketonic acid, m. p. 139~140°C ($[\alpha]_D^{18}$ −9.18), which was found to be identical with the previously synthesized semicarbazone of dihydroanhydroipomic acid (III)[6] by the infrared absorption spectra in Nujol. These facts lead to structure II for myoporone and this has been confirmed by sythesis.

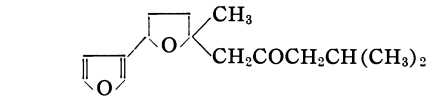

(I)

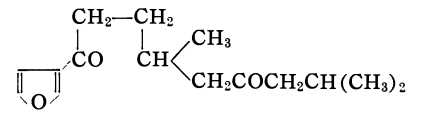

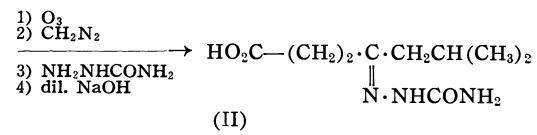

(II)

The synthesis of (±)-myoporone was started from the previously synthesized 2-methyl-4-(3'-furoyl)-1-butene-1-carboxylic acid (IV)[7] and effected according to the following sequence.

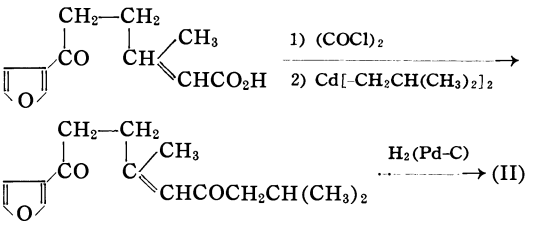

The melting point of the 2,4-dinitrophenylhydrazone (red, α-form) of the synthetic (±)-myoporone was 208~210°C, but its infrared absorption spectrum in Nujol was completely in agreement with that of α-form of 2,4-dinitrophenylhydrazone of the natural product.

Myoporone may probably be produced in vivo through intramolecular oxido-reductive cleavage of the tetrahydrofuran ring of ngaione (I). The isolation of ngaione ((−)-ipomeamarone), myoporone and 3-furoic acid[2] from the essential oil of *Myoporum*, and the isolation of (+)-ipomeamarone (I), batatic acid[8] (VI) ipomeanine[9] (VII) and 3-furoic acid

3) F. H. McDowall, *J. Chem. Soc.*, **1927**, 731; **1928**, 1324; C. W. Brandt and D. J. Ross, ibid., **1949**, 2778; A. J. Birch, R. A. Massy-Westropp, S. E. Wright, T. Kubota and T. Matsuura, *Chemistry & Industry*, **1954**, 175.

4) T. Kubota and T. Matsuura, ibid., **1956**, 521.

*** In the preliminary paper (T. Kubota and T. Matsuura, ibid., **1957**, 491), we reported that natural myoporone is in racemic form, because of its lack of optical activity at D line. This measurement was performed by the courtesy of Professor Y. Hirata, Nagoya University.

5) W. Dirscherl and H. Nahm, *Ber.*, **73**, 448 (1940).

6) T. Kubota and T. Matsuura, *J. Chem. Soc. Japan, Pure Chem. Sec.*, (*Nippon Kagaku Zassi*), **74**, 105 (1953).

7) T. Kubota and T. Matsuura, *Chemistry & Industry*, **1956**, 521; T. Matsuura, *J. Chem. Soc. Japan, Pure Chem. Sec.* (*Nippon Kagaku Zassi*), **77**, 248 (1956).

8) T. Kubota and K. Naya, ibid., **77**, 86, 252 (1956).

9) T. Kubota and N. Ichikawa, ibid., **75**, 450 (1954).

(VIII)[10] from black rotten sweet potatoes is quite interesting in relation to the metabolism of terpenes and β-substituted furan derivatives in plant.

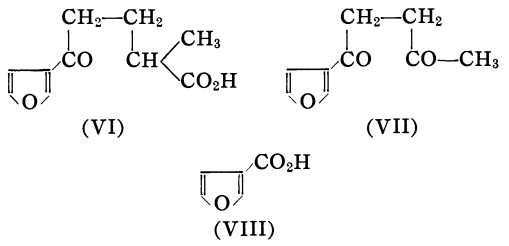

(VI) (VII)

(VIII)

Experimental

Isolation of Myoporone.—Leaves (10.06 kg.) of *Myoporum bontioides* A. Gray, which were collected at fructifying time in Tanegasima Island, Kagoshima Prefecture, Japan, were roughly cut and digested in methanol (15 l.) for about three months. After distilling off the solvent, water was added, and the liquor was extracted with ether (500 cc.×4). The ethereal solution was concentrated to a small volume and was shaken with sodium bicarbonate solution. From the bicarbonate solution, a small amount of the acidic matter was obtained. Evaporation of the ethereal solution left a brownish green liquid (45.5 g.). Vacuum-distillation of the liquid gave a yellow liquid (A; 27.1 g.), b. p. 90~150°C/10^{-2} mm. and n_D^{23} 1.4750, which was fractionally distilled as shown in Table I.

TABLE I

	Fraction	b. p./10^{-2} mm.	Yield	n_D^{23}	Color
A	-I	<121°	1.8 g.	1.4812	yellow
	-II	121 ~125°	23.4 g.	1.4752	yellow
	-III	125°<	1.1 g.	1.4718	yellow
	Fraction	b. p./10^{-2} mm.	Yield	$n_D^{23.5}$	Color
II	-I′	<113°	1.7 g.	1.4780	yellow
	-II′	113 ~116°	20.5 g.	1.4733	yellow
	-III′	116°<	0.8 g.	1.4685	yellow
	Fraction	b. p./10^{-2} mm.	Yield	n_D^{21}	Color
II′	-I″	<117°	1.4 g.	1.4776	pale yellow
	-II″	117 ~119°	13.8 g.	1.4770	pale yellow
	-III″	119°<	3.2 g.	1.4760	pale yellow

The fraction (II″) consists of almost pure myoporone.

Extraction of leaves, which were collected at flowering time, gave the same results as described above.

Isolation of C_nH_{2n}-hydrocarbon. — Dried leaves (430 g.) of *Myoporum bontioides* A. Gray were digested with ether (4 l.). Evaporation of the ethereal solution gave a brownish green semi-solid (14 g.). When the semi-solid was well mixed with ethanol (60 cc.) and filtered, there were obtained crystals (3.7 g.) which crystallized from ethanol in wax-like colorless plates, m. p. 63~65°C.

Anal. Found: C, 85.85; H, 14.71%. Calcd. for C_nH_{2n}: C, 85.63; H, 14.37%.

Distillation of the liquid part of the extract gave a liquid (1.0 g.), b. p. 105~120°C/10^{-2} mm. and n_D^{17} 1.4890. It showed a positive reaction with the Ehrlich's reagent and its infrared spectrum showed the presence of furan ring (3.18, 6.41, 6.65 and 11.42 μ), hydroxyl group (2.85 μ), and two carbonyl groups (5.88 and 5.98 μ) in the molecule, but its semicarbazone could not be obtained in crystalline state.

Detection of Ngaione. — The fraction II″ (0.5 g.), semicarbazide hydrochloride (0.5 g.), and potassium acetate (0.5 g.) were dissolved in dilute ethanol and the whole was kept overnight. Water was added and the resulting sticky mass (0.7 g.) was collected and dried. It was dissolved in benzene (20 cc.) and was purified by chromatography with alumina. From the benzene eluate, a small amount of crystal was obtained. It was recrystallized from benzene and light petroleum as colorless plates, m. p. 130~132°C, which showed no depression on admixture with the semicarbazone of ngaione, kindly supplied by Professor A. J. Birch, m. p. 132~133°C. The further elution with benzene-ethanol gave a semicarbazone as a syrup, which did not crystallize.

Bis-2,4-dinitrophenylhydrazones of Myoporone. — When the fraction II″ (0.4 g.) was mixed with a solution of 2,4-dinitrophenylhydrazine (1.0 g.) in concentrated sulfuric acid (1 cc.) and ethanol (100 cc.), orange red precipitates made their appearance in a few minutes. After standing for 2 hr., the precipitates were filtered. Yield 0.5 g. Repeated treating of the precipitates with ethyl acetate gave red crystals, which was slightly soluble in ethyl acetate. They were recrystallized from benzene to afford red prisms, m. p. 193°C, which were designated as α-bis-2,4-dinitrophenylhydrazone $[\alpha]_D^{23}$ −28.2 (Chloroform, C=0.18).

Anal. Found: C, 53.20; H, 4.92; N, 18.89%. Calcd. for $C_{27}H_{30}O_9N_8$: C, 53.2; H, 4.92; N, 18.33%.

From the mother liquor of the above recrystallization, a mixture of the red α-bis-2,4-dinitrophenylhydrazone and yellow needles separated, and the latter were collected mechanically, which was designated as β-bis-2,4-dinitrophenylhydrazone. It melted at 193°C after changing to red color at 143~145°C. Recrystallization of β-compound from benzene gave α-compound and its mother liquor deposited a mixture of α- and β-compounds.

Anal. Found: N, 18.64%. Calcd. for $C_{27}H_{30}O_9N_8$: N, 18.33%.

Ozonization of Myoporone. — Myoporone (2.0 g.) in chloroform (30 cc.) was saturated with ozone and the solvent was evaporated under reduced pressure. The resulting ozonide was decomposed under ice-cooling with a bichromate

10) T. Kubota, H. Yamaguchi, K. Naya and T. Matsuura, ibid., **73**, 897 (1952).

mixture, the latter being composed of the admixture of potassium bichromate (3.2 g.), concentrated sulfuric acid (2 cc.), and water (20 cc.). After two days' standing the mixture was extracted with ether. The ethereal solution was extracted with a bicarbonate solution. The acidic substance, obtained from the bicarbonate extract, was methylated with diazomethane in ether. Distillation of the methyl ester gave a colorless liquid, b. p. 88~90°C/10^{-2} mm. and n_D^{18}1.4378. Its refractive index coincides with that of synthetic methyl dihydroanhydroipomate, $n_D^{17.5}$ 1.4390[6]. IR-spectrum: 5.77 μ (ester) and 5.84 μ (ketone).

This methyl ester (0.25 g.), semicarbazide hydrochloride (0.2 g.), and potassium acetate (0.2 g.) were dissolved in dilute ethanol and, after standing overnight, water was added. The precipitates, which had separated in the meanwhile, were collected through decantation and then hydrolyzed with 1 N sodium hydroxide (2 cc.). Acidification of the hydrolysate gave white precipitates, which were recrystallized from ethanol. Colorless plates, m. p. 139~141°C. This substance was identical with the synthetic dihydroanhydroipomic acid semicarbazone, i. e. 3,7-dimethyl-5-keto-octane-1-carboxylic acid semicarbazone, m. p. 140~141°C in infrared spectrum. No remarkable depression of melting point was recognized on admixture of both samples.

Synthesis of Myoporone

1-Isovaleryl-2-methyl-4-(3'-furoyl)-1-butene (V). — 2-Mtheyl-4-(3'-furoyl)-1-butene-1-carboxylic acid (IV), m. p. 103~104°C[11], was converted into the acid chloride with oxalyl chloride, according to the method of Barkley et al.[12] The acid (4.2 g.) was dissolved in absolute methanol (20 cc.) and neutralized with 1 N sodium methoxide solution in methanol. After the solvent was evaporated in vacuo, dry benzene was added and evaporated again to dryness in vacuo. The resulting sodium salt was suspended in dry benzene (25 cc.) and oxalyl chloride (4 g.) in benzene (10 cc.) was added in portions under ice-cooling. After the mixture was kept at 40°C for 20 min., benzene and excess of oxalyl chloride were distilled off under reduced pressure. The acid chloride, which was obtained as brown liquid, was dissolved in benzene (20 cc.).

To a Grignard solution, which was prepared from isobutyl bromide (5.5 g.), magnesium (1.0 g.), and absolute ether (30 cc.), dried cadmium chloride (4.0 g.) was added under ice-cooling, and the mixture was refluxed until a Gilman-Schulz test was negative. After distillation of ether, benzene (30 cc.) was added.

To the stirred diisobutyl cadmium solution thus obtained, the acid chloride solution in benzene was rapidly added with constant refluxing. The mixture was refluxed for 30 min. or more and then was decomposed with dilute hydrochloric acid under ice-cooling. The organic layer was separated, washed with a bicarbonate solution, dried and evaporated. Twice distillations of the resulting dark brownish liquid (3.0 g.) gave a pale yellow liquid (1.2 g.), b. p. 119~122°C/10^{-2}mm. and n_D^{12} 1.4925, and its color changed to brownish yellow on standing. IR-spectrum: 3.18 (furan), 5.96 (furyl ketone and α,β-conjugated ketone), 6.08 (double bond), 6.41 (furan), 6.63 (furan), and 11.44 μ (furan).

1-Isovaleryl-2-methyl-4-(3'-furoyl)-butane. (Myoporone).—The above obtained liquid (0.28 g.) was dissolved in ethanol (10 cc.) and hydrogenated in the presence of 5% palladium-charcoal (0.1 g.). After 1.1 moles of hydrogen were absorbed (about one hr.), the catalyst was filtered off. To the filtrate 2,4-dinitrophenylhydrazine (0.4 g.) in ethanol was added in the presence of sulfuric acid. Twice recrystallizations of the resulting precipitates from ethyl acetate gave a red prism, m. p. 208~210°C, which showed no depression on admixture with α-bis-2,4-dinitrophenylhydrazone of myoporone, m. p. 193°C and was identical with α-compound in infrared spectrum.

The writers wish to express their thanks to Professor S. Miki, Department of Biology, Osaka City University, for collection and identification of *Myoporum Bontioides* A. Gray. Cordial thanks are also due to Mr. T. Kurokawa, Kagoshima Prefectural Industrial Research Institute and Mr. T. Uehara, Tanegashima Branch of the Kyushu Goverment Agriculture Experiment Station, for gathering the same plants.

Institute of Polytechnics
Osaka City University
Kita-ku, Osaka

11) T. Matsuura, ibid., **78**, 389 (1957).
12) L. Barkley et al., *J. Am. Chem. Soc.*, **76**, 5017 (1954).

SHORT COMMUNICATIONS

*Fractionation of Sulfur Isotopes during Oxidation**

By Iwaji IWASAKI, Hiroshi FUKUTOMI and Hikaru SHIMOJIMA

(Received February 10, 1958)

Many studies[1] on the abundance of sulfur isotopes in natural sulfur compounds have been already carried out and it was learned that the heavy isotope, sulfur-34 is generally enriched in the compounds of higher oxidation state. When the difference of oxidation state between two compounds is greater, the fractionation of isotopes is more prominent.

An experiment was carried out to make clear the process of the fractionation of sulfur isotopes during oxidation and to explain the distribution of sulfur isotopes in nature using radioisotope, sulfur-35 as tracer. In these experiments radioactive zinc sulfide was prepared by introduction of hydrogen sulfide labelled with ^{35}S into zinc acetate solution. The precipitate of zinc sulfide was filtered and washed with ammonium acetate solution and suspended in ammoniacal solution. A part of the suspended sulfide, about one tenth of the total, was first oxidized to sulfate by adding carefully a definite volume of bromine water into the solution. The residual sulfide was filtered off, and the sulfate in the filtrate was precipitated as barium sulfate. The care against the fractional precipitation of sulfur isotopes, that had been described by the authors[2], was also taken in this case. The residual sulfide precipitate was again suspended in ammoniacal ammonium acetate solution and partly oxidized with bromine water by the same manner as described above. The experiment was carried out sucessively till all the sulfide was consumed. About ten samples of barium sulfate for the determination of the radioactivity were obtained.

Their radioactivities were measured by the infinite-thickness method. Some of the experimental results obtained are shown in Fig. 1. If the fractionation of sulfur isotopes had not taken place during these processes, these samples should have had the same specific activity. However, there is a considerable and regular variation in their radioactivity and the earlier barium sulfate obtained in one series of fractional oxidation from one suspension has remarkably larger specific activity than that of the later. These variations are evidently beyond the possible experimental error. It might be too early to give definite conclusions on the mechanism of fractionation of sulfur isotopes from these results, but the isotope effect will be considered as the most important factor for the explanation of these phenomena and the fractionation of sulfur isotopes

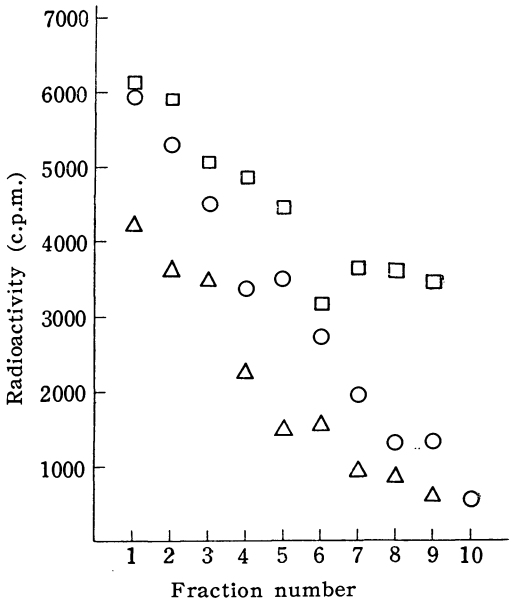

Fig. 1. Variation in radioactivity of barium sulfate obtained in succession from one suspension of zinc sulfide by fractional oxidation.
○ at 4°C △ at 25°C □ at 65°C

* This report was presented at the 1st Symposium of Radiochemistry sponsored by The Chemical Society of Japan, December, 1957.

1) H. G. Thode et al., *Can. J. Research*, **B27**, 361 (1949); **B28**, 567 (1950); A. P. Vinogradov et al., *Geokhimia*, **1**, 96 (1956); H. Sakai, *Geochim. et Cosmochim. Acta*, **12**, 150 (1957).

2) I. Iwasaki, S. Ikeda, H. Shimojima, H. Fukutomi and H. Sugano, *Annual Report of the Radioisotopes in Japan*, **3**, 1 (1956).

during oxidation seems to be one of the most important factors on the enrichment of the heavy sulfur isotope into the compounds of high oxidation state.

Laboratory of Analytical Chemistry and Geochemistry, Tokyo Institute of Technology, Ookayama Meguro-ku, Tokyo

*Fractionation of Sulfur Isotopes during Reduction**

By Iwaji IWASAKI, Hikaru SHIMOJIMA and Hiroshi FUKUTOMI

(Received February 10, 1958)

The experimental and the theoretical studies are being made by the present authors on the natural abundance and their variation of stable isotopes of sulfur. In the previous report[1] a great fractionation of the heavy isotope (^{35}S) during oxidation of sulfide was reported. The present experiment has been carried out to make clear the fractionation of sulfur isotopes during reduction using sulfur-35 as tracer.

Barium sulfate labelled with sulfur-35 was reduced in a carbon dioxide stream with tin(II)—strong phosphoric acid reagent[2]. Hydrogen sulfide evolved from the reaction mixture was taken out of the reaction system with carbon dioxide. This gas was led to two absorbing cells in series. In the first cell, was placed an accurate, known amount of aqueous zinc acetate solution just enough to make precipitate of zinc sulfide for the radioactivity measurement. In the second cell, alkaline suspension of basic cadmium carbonate was put in to absorb and detect the rest of hydrogen sulfide which comes out from the first cell. The detection of hydrogen sulfide coming in the second cell was easily made by observing the formation of yellow cadmium sulfide. When sufficient zinc sulfide was obtained, the gas-flow of hydrogen sulfide and carbon dioxide from reaction system was switched to another set of two absorbing cells using a three-way stopcock.

In this way, many fractions of small and equal amount of zinc sulfide were obtained. The specific counting rate of each sample was measured by the infinite-thickness method. In order to be sure to detect a small variation in the specific counting rate, hydrogen sulfide evolved in the very beginning of the reaction was carefully sampled, and sixty fractions were obtained during a run of reduction experiment. Some of the results obtained are shown in Fig. 1. There found a regular and remarkable variation in their specific counting rate and the earlier

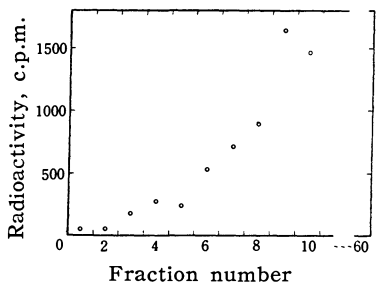

Fig. 1. Variation in radioactivity of each fraction of zinc sulfide obtained in succession from one barium sulfate sample by fractional reduction.

sulfide obtained in a series of a fractional reduction from barium sulfate has remarkably smaller specific counting rate than that in the later stage over the possible experimental error.

The fractionation of sulfur isotopes during oxidation was previously reported[1]. In this case, the radioactive sulfur isotope (^{35}S) was enriched in the products of earlier stage of oxidation. Thus the result agrees with the conclusion shown in the present report.

As the fractionation of radioactivity is quite remarkable in both reduction and oxidation, it would be possible to apply successfully in a larger scale to the purpose of enriching stable isotopes as well as radioactive ones. An experiment is planned to determine the extent of the differentiation between the stable isotopes of sulfur-32, 34 and 36 in the same sort of treatment of sulfur compounds.

Laboratory of Analytical Chemistry and Geochemistry, Tokyo Instiute of Technology, Ookayama Meguro-ku, Tokyo

* Presented by H. Shimojima before the 8th Annual Meeting of the Chemical Society of Japan on April 3, 1955.

1) I. Iwasaki, H. Fukutomi and H. Shimojima, This Bulletin. **31**, 495 (1958).
2) T. Kiba and I. Kishi, ibid. **30**, 44 (1957).

The Solubilization of Benzene in Aqueous Soap-Alcohol Solution

By Kōzō Shinoda and Hideo Akamatu*

(Received January 6, 1958)

One of the most outstanding properties of detergent solution is its ability to solubilize polar or non-polar oil above the critical micelle concentration[1,2]. Klevens[3,4] investigated the effect of added alcohols, salts and the other additives on the solubilization of *n*-heptane in potassium tetradecanoate solution and found a very marked increase in the solubilization of *n*-heptane.

The present paper reports the effect of added alcohols and salts on the solubilization of benzene in potassium dodecanoate solution at 25°C.

Experimental.—The solubilization end point was determined by transmission measurements with the same procedure described by Stearns et al.[1] Butanol, *iso*-pentanol, hexanol, cyclohexanol and octanol were purified materials[5]. Dodecanoic acid was purified by vacuum distillation. The solubilization of benzene in aqueous potassium dodecanoate was the same with that reported by Stearns et al.[1]

Results and Discussion.—*The Effect of Added Alcohols on the Solubilization.* The effect of added alcohols on the solubilization of benzene in aqueous potassium dodecanoate was plotted in Fig. 1.

It is evident that 1) the amount of benzene solubilized markedly increased by the addition of alcohols, 2) the longer chain alcohol is much more effective than shorter chain alcohol in promoting solubilization and 3) the effect of added alcohol is greater than that of corresponding fatty acid soaps. This suggests that the penetrated long-chain alcohol increases the micellar size and that by decreasing the electrical repulsive force of micelle-forming ion the aggregation number of micelle forming ion also increases, causing a marked increase in micellar size and solubilizing power. In the case of cyclo-hexanol and *iso*-pentanol the amount of benzene solubilized showed

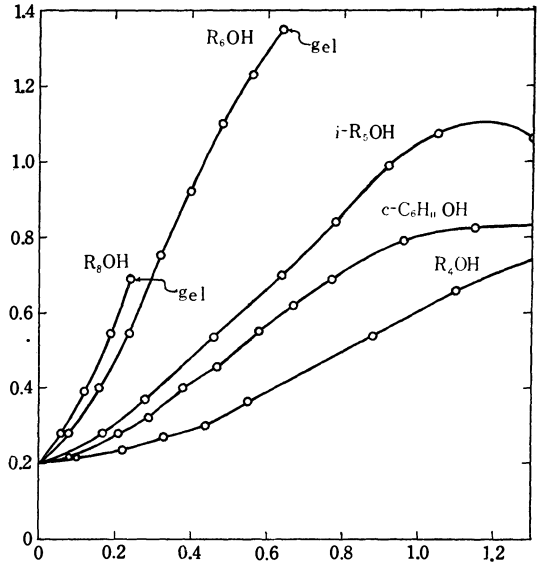

Fig. 1. The effect of added alcohols on the solubilization of benzene in potassium dodecanoate, 0.285 mole/l., solution ordinate: moles of benzene per 1000 cc. of solution.
R_4OH, butanol; i-R_5OH, *iso*-pentanol; R_6OH; hexanol; R_8OH, Octanol; C-$C_6H_{11}OH$, Cyclohexanol.

maximum and then gradual decrease. In the case of hexanol and octanol, gel formation occurred at a relatively low alcohol concentration, therefore the solubilization was determined only at the lower concentration.

Estimation of the Micellar Charge from the Solubilization Measurements. The effect of soap concentration on the solubilization of benzene per mole of micellar potassium dodecanoate was determined and plotted in Fig. 2[6]. The effect of potassium chloride on the solubilization of benzene in aqueous potassium dodecanoate, 0.192 mole/l., was also determined and plotted in Fig. 2.

It is supposed that the increase of solubilization of benzene per mole of soap is essentially the same phenomenon in both systems. Namely, the increase in the counter-ion concentration, due to the increase in soap concentration or added salts, decreases the electrical potential on the micelle surface and tends to increase

* Department of Chemistry, Faculty of Science, the University of Tokyo, Hongo, Tokyo.

1) R. S. Stearns, H. Oppenheimer, E. Simon and W. D. Harkins, *J. Chem. Phys.*, **15**, 496 (1947).
2) M. E.L. McBain and E. Hutchinson,"Solubilization", Academic Press Inc., New York, 1955.
3) H. B. Klevens, *J. Chem. Phys.*, **17**, 1004 (1949).
4) H. B. Klevens, *J. Am. Chem. Soc.*, **72**, 3581. 3780 (1950).
5) K. Shinoda, *J. Phys. Chem.*, **58**, 1136 (1954),

6) The concentration of micellar soap was calculated, subtracting the single ion concentration from the stoichiometric concentration. The solubility of benzene in water was subtracted from the total amount of benzene solubilized to calculate the actual amount of benzene solubilized in the micelle.

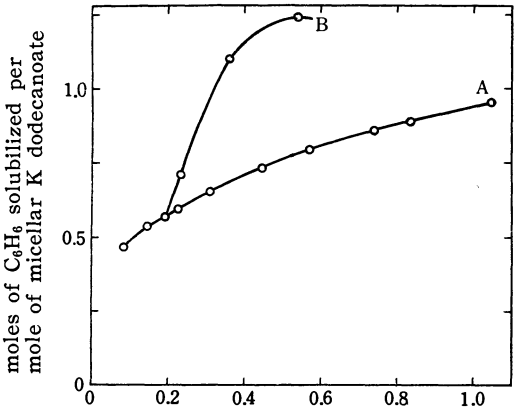

Fig. 2. A. the effect of soap concentration and B. the effect of counterion concentration on the solubilization of benzene in potassium dodecanoate solution at 25°C.

the aggregation number. If the micelles become larger, the amount of non-polar oil solubilized per micelle forming ion may increase. In a soap solution, the free counter-ion does not increase as expected from its stoichiometric concentration, since the counter-ion mostly adheres on the micelle surface. If we assume that the inter-micellar force is negligible, the amount of benzene solubilized per mole of micellar soap depends only on the concentration of counter-ion. From the comparison between curves A and B, we see that the amount of benzene solubilized per mole of micellar soap increases as slowly as about one-fifth times in curve A, therefore it can be concluded that about 80% of the counter-ion is fixed on the micelle surface, i.e., the degree of "ionization" of micelle is about 0.2 at about 0.2~0.3 mole/l. Recalculating Klevens's[4] and Stearn's[1] results with the same procedure, the degree of ionization of micelle was evaluated as 0.25 in the case of potassium tetradecanoate at about 0.5 mole/l.

Department of Chemistry, Faculty of Engineering, Yokohama National University, Minami-ku, Yokohama

E. M. F. Change in the Thermo Cell due to Soret Effect

By Kazuo Sasaki and Shigeo Nagaura

(Received November 25, 1957)

Thermo cell is defined as a cell in which two identical electrodes are kept at different temperatures so as to form a steady temperature gradient in the electrolyte solution. In such a cell, it has long been realized that the electro-motive force (emf) should change as thermal diffusion proceeds and, at a stationary state, should reach a steady value E_∞ corresponding to Soret equilibrium. Although many experimental investigations have been reported about thermo-cell emf, almost all the data refer to the initial emf (E_0), which is the emf of a cell of uniform concentration; that is the state at which no change in concentration due to thermal diffusion has yet been appreciable.

Non-stationary change of thermo-cell emf was first confirmed by Agar and Breck[1] by an ingenious method using amalgam electrode; however, the measurements were restricted only to some special ions which were rather unfamiliar in this field of investigation.

We have long been interested in this problem and engaged in solving it; lately we observed a similar example of the phenomenon using silver-silverchrolide electrode with which most of the previous investigators have been concerned.

The emf change due to Soret effect can not be detected by an ordinary cell construction, which is used to measure the initial emf; because the large volume of the bulk solution in the electrode chamber makes the small change in composition indistinctive. Thus following precautions were taken into account for cell design;

1) the electrodes must be placed directly in the diffusion path,

2) the length of the diffusion path, i.e. the inter-electrode distance should be so determined that the time required for the establishment of the diffusion equilibrium (steady state) will accord with the restriction of the actual measurement,

3) temperature gradient must be linear throughout the diffusion path.

Along these requirements we designed

1) J. Agar and W. Breck, *Trans. Faraday Soc.*, **53**, 167 (1957).

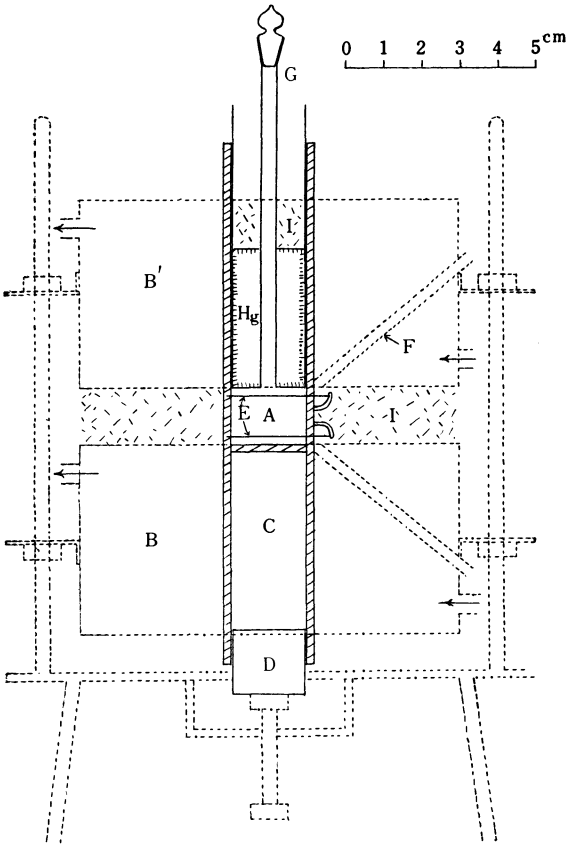

Fig. 1. Cell assembly

E Electrode; A Diffusion path; B, B' Water jacket;
C Heat conducting space (water is enclosed);
Hg Heat conducting space (containing mercury);
D Rubber stopper; F Thermocouple pocket;
G Filling tube; I Insulator.

several types of cells and tested their usefulness. A very simple cell, which is schematically shown in Fig. 1, has eventually revealed itself to be quite useful. Its detailed information will be reported in the succeeding paper.

The temperature gradient was set up by means of two jackets fitted tightly to the body of a cylindrical cell; water of a given temperature could be circulated through them.

As the first step of the present investigation, we took hydrochloric acid in different concentrations as a test solution. The fundamental feature of emf change with time is graphically shown in Fig. 2. In the figure the temperature change in the cell is also drawn, which was obtained by means of differential thermocouple. As

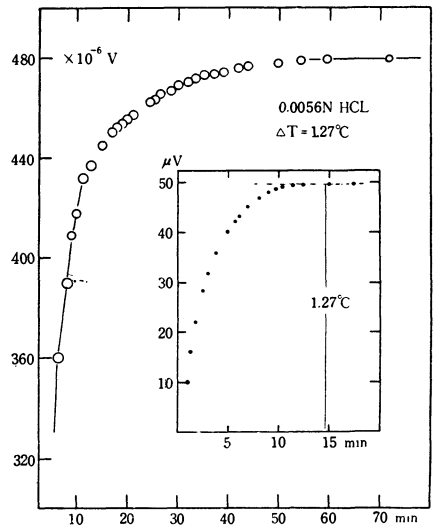

Fig. 2. Emf change with time (min.).
Empty circle: Emf of the cell,
Full circle: Thermocouple reading

is clearly seen from the figure, the emf changes rapidly at the first stage, in which a steady temperature gradient is established. After the temperature gradient has come stationary, the emf increases continuously, although not so rapid as before, exhibiting exponential diffusion behavior and reaches a steady value at a finite period of time. This behavior accords well with the theoretical expectation derived by Bierlein[2]: when the emf is plotted against $\sqrt{t}$ for the initial stage of thermal diffusion (not to be confused with the stage at which the heat conduction is not yet stationary), a straight line is obtained with a good approximation, whilst for the final stage log $(E_\infty - E_t)$ has a linear dependency upon t. These relationships are drawn in Figs. 3 and 4. In contrast to Agar and Breck's result, the reverse curve, which can be obtained

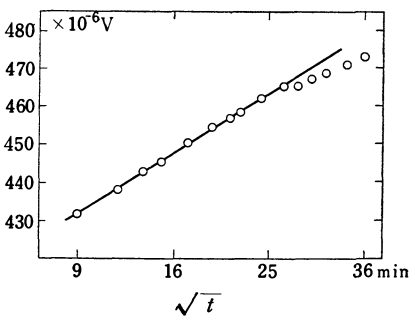

Fig. 3. Emf against $\sqrt{t}$

2) J. Bierlein, *J. Chem. Phys.*, **23**, 10 (1955).

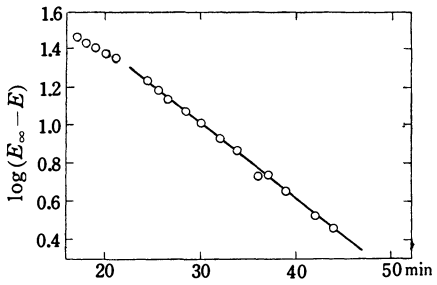

Fig. 4. Log (E_∞—E) against t.

when the temperature gradient is cut off, does not show the symmetric form against the curve of non-isothermal change but is somewhat erroneous. This problem, however, is left for further study.

A similar relation was observed for hydrochloric acid solution of various concentrations. Detailed information and theoretical explanation will successively appear.

Institute of Polytechnics
Osaka City University
Kita-ku, Osaka

The Ultraviolet Absorption Spectra of the Molten and Solidified Mixed Salt Systems $NaNO_2$–$NaNO_3$, $NaCl$–$CdCl_2$

By Kaoru Sakai

(Received February 22, 1958)

According to the previous researches[1-3], it was found that the position of absorption edges of aqueous solutions which contain two component salts is shifted toward longer wave length than that of solutions each containing one of the components alone, provided that the two component salts react with each other and produce some kind of complex. Therefore we tried to find out the same phenomena[4,5] in the case of complex formation of the molten salt systems.

The experimental method is the same as that published by the present author previously[6], and the data are shown in Fig. 1 ($NaNO_2$–$NaNO_3$), and Fig. 2 ($NaCl$–$CdCl_2$), where are given the isotherms showing the relationship between the position of absorption edge and the component.

The phase diagram[7] of the $NaNO_2$–$NaNO_3$ system indicates solid solution over almost the entire range of composition, and the isotherms of its electrical

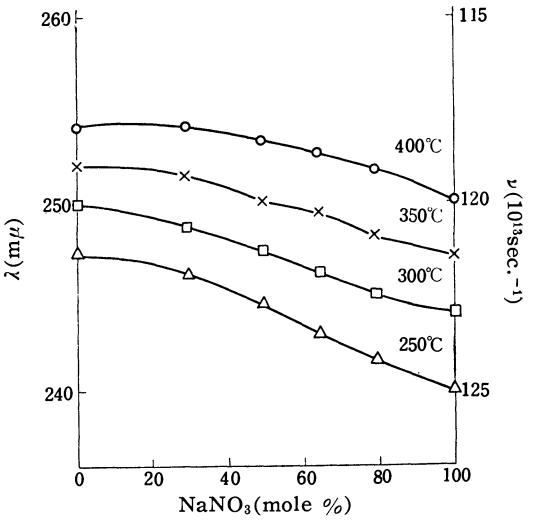

Fig. 1. Isotherms of absorption edges of the $NaNO_2$—$NaNO_3$ system.

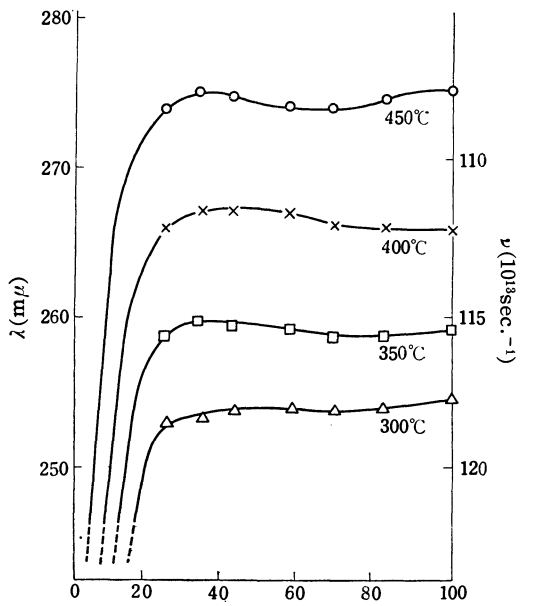

Fig. 2*. Isotherms of absorption edges of the NaCl—$CdCl_2$ system.

1) Y. Shibata, B. Inoue and Y. Nakatsuka, *J. Chem. Soc. Japan, Pure Chem. Sec.* (*Nippon Kagaku Kaishi*), **42**, 983 (1921); Y. Shibata, and B. Inoue, ibid., **43**, 722 (1922).
2) P. Job, *Compt. rend.*, **180**, 928 (1925); **182**, 1622 (1926); *Ann. chim.*, **9**, 143 (1927).
3) R. Tsuchida, This Bulletin, **10**, 27 (1936).
4) K. Sakai, *J. Chem. Soc. Japan, Pure Chem. Sec.* (*Nippon Kagaku Zassi*), **78**, 1108 (1957).
5) K. Sakai, ibid., **78**, 1257 (1957).
6) K. Sakai, ibid., **77**, 1731 (1956).

conductance[7] do not exhibit any appreciable change, i. e., there is no evidence of complex formation. On the other hand, the phase diagram[8] of the $NaCl$-$CdCl_2$ system shows the formation of one incongruently melting compound $2NaCl \cdot CdCl_2$, and also shows the negative deviation in the neighborhood of 30~40 mole % cadmium chloride from additivity of electrical conductance[8], i. e., this system may be considered to exhibit the formation of complex ion $[CdCl_4]^{2-}$.

According to our experimental data shown in Figs. 1 and 2*, the isotherms of absorption edges of the former system show the small deviation from additivity toward longer wave length, but those of the latter system show a large deviation, especially at the neighborhood of 30~40 mole % cadmium chloride.

This fact shows that in the case of the latter system there is some evidence of complex-ion formation $[CdCl_4]^{2-}$, but not in the former system. In the case of the $NaCl$-$CdCl_2$ system, the deviation of isotherms of absorption edges toward longer wave length is not so distinct as that of the KBr-$CdBr_2$ system[5] even in the neighborhood of 30~40 mole % cadmium chloride. This fact may be explained as that the deviation of absorption edges due to the presence of complex ion $[CdCl_4]^{2-}$ is masked by the deviation of absorption edges caused by cadmium chloride which is itself a kind of associated complex[5].

The author wishes to express his hearty thanks to Professor Ryutaro Tsuchida and Professor Kozo Hirota (Osaka University) for their kind guidance and encouragement throughout this work.

Department of Chemistry
Hitachi Research Laboratory
Hitachi, Ibaragi Prefecture

7) H. Bloom, I. W. Knaggs, J. J. Molly and D. Welch, *Trans. Faraday Soc.*, **49**, 1458 (1953).

8) H. Bloom and E. Heymann, *Proc. Roy. Soc. London*, **A188**, 392 (1947).

* Fig. 2 gives no data below 20% cadmium chloride because of the experimental difficulty, i. e., the melting point of samples below 20% cadmium chloride is so high that the cell is occasionally broken and the position of absorption edges of sodium chloride is shifted toward shorter wave length than that of the other component salts of the $NaCl$-$CdCl_2$ system by the previous data (H. Fesefeldt, *Z. Phys.* **64**, 741 (1930).).

Redetermination of the Crystal Structure of Calcium Cyanamide

By Yuzo Yamamoto, Kyoji Kinoshita, Kenzi Tamaru and Teruko Yamanaka

(Received December 3, 1957)

The crystal structure of calcium cyanamide has been studied by Dehlinger and Hanawalt, and later by Bredig[1]. Bredig reached the conclusion from his Debye-Scherrer X-ray analysis that the crystal structure of calcium cyanamide is based upon a rhombohedral lattice with $a_{rh}=5.40$ Å and $\alpha=39°55'$, which correspond to the following values for a hexagonal lattice; $a=3.67$ Å, $c=14.85$ Å. This crystal structure is similar to that of sodium azide.

The specimen used by Bredig, however, was obtained by treating calcium carbide with nitrogen. By this preparation the purity of the product can usually be reached about 70 % at the highest, always containing an appreciable amount of such impurities as calcium oxide (or hydroxide) and carbon. Accordingly, the question naturally arises as to whether pure calcium cyanamide would have the same crystal structure. For this reason the X-ray diffraction patterns of calcium cyanamide of high purity were examined.

The specimen used in this experiment was prepared from dicyandiamide and calcium carbonate according to the method enunciated by Inoue and Kanaji[2]. Dicyandiamide used was obtained by a repeated recrystallization of a commercial sample, and calcium carbonate was obtained from ammonium carbonate and calcium acetate in the presence of ammonia. A mixture of 1.5 g. of calcium carbonate and 30 g. of dicyandiamide was heated up to 770°C for 15 min. The product, white powder, was analyzed by Volhard's method[3], which revealed the product to be calcium cyanamide of 98.5% purity. X-ray diffraction patterns of this specimen were taken using an X-ray diffractometer. The experimental conditions were as follows; filtered copper radiation (Cu K_α, 1.5418 Å); 40 kV; 20 mA; scanning speed, 1/2° 2θ per min.; time con-

1) Bredig, *J. Am. Chem. Soc.*, **64**, 1730 (1942).
2) Y. Inoue and Y. Kanaji, *J. Chem. Soc., Japan, Ind. Chem. Sec.* (*Kogyo. Kagaku Zassi,*), **56**, 524 (1953).
3) I. M. Kolthoff and E. B. Sandell, "Textbook of Quantitative Inorganic Analysis" (third edition), p. 456, MacMillan & Co. Ltd., N.Y. (1952).

stant, 4 sec.; receiving slit, 0.4 mm.; angular aperture, 1°. The mean values of the results are summarized in the Table.

TABLE

No.	2θ	d_{obs}	d_{calc}	hkl	I_{obs}	I_{calc}
1	18.05	4.91	4.90	003	0.37	0.32
2	30.43	2.94	2.94	102	1.00	1.00
3	36.55	2.458	2.45	006	0.03	0.03
4	37.20	2.417	2.417	014	0.16	0.20
5	41.62	2.168	2.166	105	0.23	0.30
6	49.28	1.849	1.849	110	0.28	0.31
7	51.92	1.762	1.757	017	0.08	0.14
8	52.91	1.730	1.731	113	0.09	0.06
9	57.77	1.596	1.593	201	0.03	0.01
10	59.06	1.564	1.565	022	0.08	0.13
11	63.19	1.471	1.469	204	0.03	0.04

Using the chart of Hull and Davey, it was possible to assign indices (hKl) to all of the observed spectra referring to a hexagonal lattice $a=3.70$ Å and $c=14.70$ Å. The calculated values for spacings from these parameters are also listed in the Table as d_{calc}.

The density of the specimen was determined by a pycnometer using benzene, which gave a value 2.36 g. per cc at 25°. From the density and the lattice constants the number of chemical units contained in the unit cell was calculated as three, the calculated density being 2.19 g. per cc.

As the indices given in Column 5 are only those of such kind as $h-k+1=3n$, the translational lattice should be rhombohedral, so that the unit cell can be given as $a_{rh}=5.35$ Å and $\alpha=40°28'$. The probable space group is one of C_{3i}^2—R$\bar{3}$, D_3^7—R32 and D_{3d}^5—R3m. These space groups give the following positions for the calcium, carbon and nitrogen atoms, referring to the rhombohedral lattice,

1Ca: 000,
1C: 1/2 1/2 1/2,
2N: xxx, $\bar{x}\bar{x}\bar{x}$.

Thus we have confirmed that the structure reported by Bredig is essentially correct. The positional parameter x for the nitrogen atoms was further refined by the trial-and-error method, the final value being 0.415. The calculated relative intensities are given in Column 7, which show a satisfactory agreement with the observed ones. It follows that the interatomic distances are C—N=1.25 Å and Ca·····N=2.45 Å.

Institute of Carbide Chemistry, Faculty of Engineering, Yokohama National University, Minami-ku, Yokohama

*Analysis of the Hardening Reaction of Furfurylalcohol Resin**

By Shigehiko YAMADA and Shigeo HAYASHI

(Received January 13, 1958)

Measurement of electric resistivity of thermosetting resins during their hardening stage along with the several other methods[1] provides information on their curing degree. The methods, however, can be done only with difficulty with the common instruments readily at hand, because of the higher resistance value of resins.

In the earlier part of the resinification, mechanism of the accelerator's** action, unobtainable by chemical analysis[2], was easily pictured by this method[3], since the accelerator reduced the resistance of the reactant.

Addition of electro-conductive filler, which may similarly reduce the resistance, was considered to clarify almost the whole curing degree by employing common instruments. In this article, graphite powder was added to furfurylalcohol(FA) resin—one of graphite-cement systems—and Kohlrausch bridge-and drop-method were employed, which exhibited the activation energy of the final cure together with that of the apparent cure.

Experimental

Materials.—Resin—A neutralized initial condensate of FA. Viscosity—31.3 poise at 20°C. Mean Mol. Wt.—220 (Calculated from the freezing point depression of its dioxane solutions.)

Filler—Artificial graphite powder as shown in Table I.

Accelerator—*p*-Toluenesulfonyl chloride (I) and its sulfonic acid (II), reagents of G. R. Grade.

Solvent—Dioxane (G. R. Grade) was used only when the filler was not added, in order to keep the reaction temperature constant.

Mixture of filler and accelerator—One hundred g. of I or 30.0 g. of II was mixed with 1000 g. of filler for more than 45 min. in a mixer at room temperature.

TABLE I
CHARACTERISTICS OF GRAPHITE POWDER

Moisture		0.25%
Volatile Matter		0.84%
Ash		0.09%
Density$^{30}_{4}$		2.073
Distribution of Particle size	<80 meshes	0%
	80～120	1%
	120～160	19%
	160～200	22%
	200～250	3%
	>250	55%

Method.—*1. Determination of resistivity (ρ_d, ρ_a) and apparent resistance (R).* (1) In the case where copper electrode was employed: more than 20 of the similar electrodes $5\phi \times 100$ mm. copper, which were polished prior to use, held by the epoxy resin plate* at intervals of 14.0 mm. were set in equal depths of the cement. Seventy g. of the resin and the same amount of filler containing I or II were mixed in a tall beaker ($45\phi \times 85$ mm., for 100 cc.) for 5 min. A thermometer was inserted in the center of the reactant. The beaker was placed in a thermostat. The plate*, connecting electrodes, was sealed to the beaker with hard clay. Apparent resistance (R) was measured by Kohlrausch bridge from the beginning of resinification to the final cure.

When the filler was not used, solutions containing 1.0 g. of I or 0.2 g. of II as well as 7.0 g. of dioxane and 30.0 g. of resin were prepared, R of which was determined uniformly by Wheatstone bridge instead of Kohlrausch bridge.

Hereafter, experiments, where I is used, will be called A-series and those with II, B-series.

(2) After gel-time the resin (130 g.) and the same amount of the filler containing I or II were mixed and hardened in the beaker, exactly parallel with the above mentioned system. Samples immediately after gel-time were rapidly cut out in approximate sizes $10 \times 10 \times 20$ mm., which were closely held between copper films and their resistivity was measured by the drop method (D. C. employed), and further by Kohlrausch bridge. These will be called ρ_d and ρ_a, respectively.

2. Measurement of adhesion power (F). At the same time that the graphite cement was prepared as mentioned, above "impervious

* Presented at the 10th Annual Meeting of the Chemical Society of Japan held in Tokyo, April, 1957.

** *p*-Toluenesulfonyl chloride, which may react with the monomer or the initial condensate of the resin[3].

1) E. Barr, *Ind. Eng. Chem.*, **48**, 72 (1956).
2) S. Yamada and S. Hayashi, *J. Chem. Soc. Japan, Ind. Chem. Sec.* (*Kogyo Kagaku Zassi*), **61**, 342 (1958).
3) S. Yamada; This Bulletin, **27**, 479 (1954).

* Araldite D, cured with accelerator No. 951, resistance of which was infinitive between electrodes by 500 V. megger.

graphite"* pieces, cut out as large as 10×10×20 mm., were joined with the cement at the 10×10 plane under the same pressure. They were settled in the thermostat, being placed in a glass vessel with a stopper.

Adhesion power (F) was measured as the transverse strength at the joined plane, several values of which were averaged every time.

3. Acetone extraction. At the same time, when samples for measuring ρ_d and ρ_a were taken off, small cubes (10×10×10 mm. in size) were cut out at every curing temperature. Three pieces were held in the thermostat (30±0.1°C) with 25.0 cc. of acetone and weighed after 16 hr.

4. Other measurements.—Shrinkage** of samples employed for the determination of resistivity, filler added, was measured with a micrometer, which gave an exactness of 0.2% to the completely cured cement pieces.

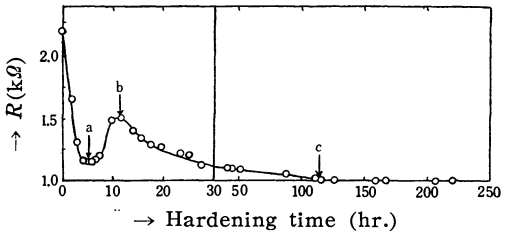

Fig. 1. An example of change in apparent resistance, filler employed.

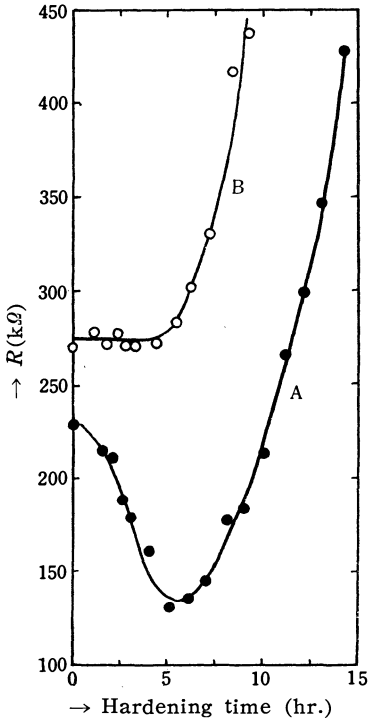

Fig. 2. An example of change in apparent resistance (R), without filler at the earlier stage.

* "Impervious graphite" is made by impregnating a thermosetting resin.

Hardness** was measured with Shore tester complementally.

5. Hardening temperature. 20, 30, 40 and 50, ±1°C were adopted.

Examples of data.—*1. Change in apparent resistance, R.* For instance, data in the case of B-series with filler at 20°C are given in Fig. 1. Reproducibility of the point a, b and c was excellent. Change in R of the reactants without filler at 40°C is shown as an example in Figs. 2 and 3.

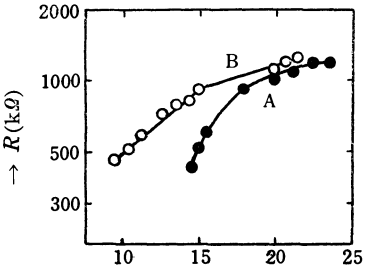

Fig. 3. An example of change in apparent resistance (R), without filler at the final stage.

2. Change in adhesion power, F and hardness H. Data at 30°C are given in Fig. 4 for example.

3. Change in resistivity, ρ_d, ρ_a. Data at 30°C are given in Fig. 5 for example.

4. Change in acetone extract. Data at 40°C are shown in Table II for example.

TABLE II

AN EXAMPLE OF CHANGE IN ACETONE EXTRACT

Series	Reaction time (hr.)	Average (%)	Range (%)
A	51	7.60	0.55
	75	1.73	0.05
	99	2.50	0.35
	118	2.74	0.08
B	51	5.60	1.40
	75	3.30	1.70
	99	1.35	0.02
	118	1.85	0.10

5. Change in shrinkage. Data at 50°C are shown as an example in Table III.

Discussion

1. Change in R, ρ_d and ρ_a.—Elements of change in R may be assumed as R_h, R_w, R_a and R_g. For example; $-dR_h/dt = K_h \cdot V_h$, $-dR_w/dt = K_w \cdot V_w$ etc. Increasing and decreasing velocity of R_h, R_w etc. may be considered to be proportional to that of hardening and dehydrating process.

** Samples were held in a glass vessel set in the thermostat, and at the stopper and the bottom of the vessel dry granules of calcium chloride were placed.

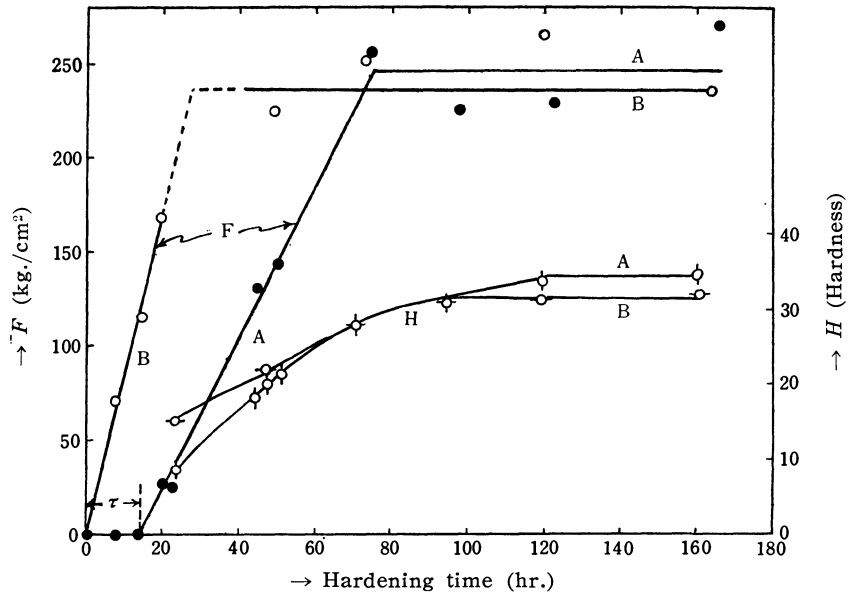

Fig. 4. An example of change in adhesion force (F) and hardness (H).

TABLE III

AN EXAMPLE OF CHANGE IN SHRINKAGE

Series	Reaction time (hr.)	10×10×20 mm.			10×10×10 mm.			10×10×10 mm.		
A	26	9.98	9.95	20.04	9.90	9.96	9.92	9.95	9.90	9.88
	50	−0.01	−0.03	−0.05	−0.01	−0.01	−0.03	−0.01	−0.01	−0.01
	74	〃	〃	〃	〃	−0.02	−0.02	−0.01	−0.02	−0.02
	94	0.00	−0.02	−0.04	0.00	〃	−0.03	0.00	0.00	0.00
B	26	9.91	9.91	20.02	9.93	9.99	9.95	9.99	9.91	9.91
	50	0.00	0.00	−0.02	−0.02	−0.01	−0.02	0.00	−0.01	−0.02
	74	−0.01	−0.01	−0.03	−0.03	−0.02	−0.03	−0.01	〃	−0.03
	94	〃	〃	−0.04	〃	−0.01	−0.04	〃	〃	−0.04

TABLE IV

COMPLEMENTARY DATA TO EXPLAIN THE SETTLING DOWN TENDENCY OF RESISTANCE

Particle size of graphite powder (meshes)	Molding pressure (kg./cm.²)	Comparison[a] between ρ_1, resistivity of sample immediately after molding and, ρ_2, that after curing up to 200°C	Resin
24—32	40	$\rho_1 > \rho_2$ ($\alpha = 1\%$[b])	Initial condensate of FA[c]
32—50	〃	$\rho_1 = \rho_2$ (〃)	〃
50—80	〃	$\rho_1 < \rho_2$ (〃)	〃
50	100, 200, 300, 400, 500, 600.	$\rho_1 = \rho_2$ (〃)	Phenollic

a) Tested by analysis of variance in three-way layout.
b) Risk.
c) In the case where the ratios of the resin added to filler change, ρ_2 decreases to a ratio (12% to filler) and then increases starting from the ratio, as the amount of resin increases.

R_a and R_d correspond to the activation of I[3] and orientation of graphite filler respectively. Values of change in R, dR/dt may be plus, zero or minus depending on the value of each element. It is assumed that V_w and V_a contribute in the early stage and V_h and V_g in the final stage. Change in R, ρ_d, and ρ_a indicated in Figs. 1 and 5, for example, are observed to be of a settling down tendency in the final stage.

On the contrary, the system without

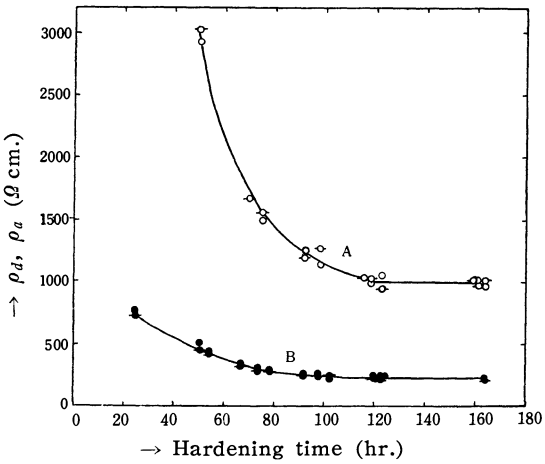

Fig. 5. An example of change in resistivity (ρ_d, ρ_a).

○ ●: ρ_d } These can be considered to
○ ●: ρ_a } be in an approximate agreement.

graphite filler indicates a reasonable increasing tendency as shown in Fig. 3 for example. This fact amply suggests that the effect of filler, $-dR_g/dt$, governs the hardening degree in final stage. Experimental facts from another view as shown in Table IV give a hint to the phenomenon, which may be derived from the following interpretation.

Data in Table IV indicate that the effect of graphite powder on the resistivity directly relates to its particle size and molding pressure. In this article, meshes smaller than 120 of graphite powder and the normal pressure were employed. The facts given in Table IV are summarized as follows.

(a) In the case where coarse particles were used, resistivity decreases with hardening and increase in resin content under a relatively low pressure.

(b) In the case where particle size is reduced, resistivity does not change or increase under the pressure.

(c) In the case of use of fine particles, resistivity does not change under pressure.

Accordingly, the phenomenon of the decreasing tendency even in the case of fine particles used under the normal pressure in these experiments may not be contradictory to this fact. Namely, it is understood that the orientation time of the filler in the resin depends on the hardening velocity, amount and particle size of added filler, and the operating pressure.

From b to c in Fig. 1, the effect of the orientation is predominant, while the effect of hardening is observed from a to b.

Now that the settling time of resistivity can be assumed as the end point of hardening, its activation energy from this time, S_ρ, was calculated to 7 kcal./mol. in A-series*, 6 kcal./mol. in B-series as shown in Fig. 6. Such values can not be obtained from changes in acetone extract given in Table II. under similar conditions.

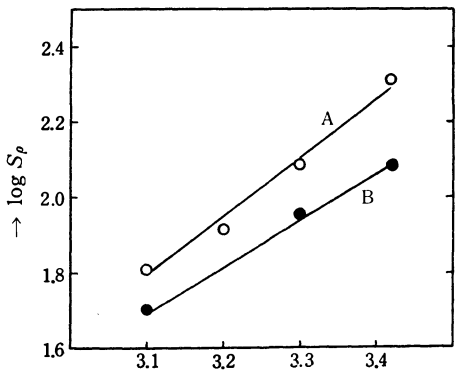

Fig. 6. Relation between log S_ρ and $1/T$.

Besides, the activation energy calculated from the time up to a certain R in Fig. 3 for example (no filler) was 12 kcal./mol.

Cell constant of the cell used, K=9 cm. was obtained by employing saturated aqueous solution of sodium chloride. The resistivity of the cut piece, ρ_a, was however found to be different from that calculated from R (with filler).

This proves that the mixing of resin and filler containing accelerator could not be uniformly processed even in such a small scale, which may be a point to take in consideration in applied use. Large variance in acetone extract as given in Table II may depend upon the same fact.

2. Change in adhesion power, *F*.—In A-series, the induction period τ for the increase of F was observed as shown for example in Fig. 4. This may be assumed to correspond with the activation velocity of I and gives activation energy of the process, 12 kcal./mol., as shown in Fig. 7.

Now further data in a previous paper[3] the relation between the decrease of the velocity of resistance in FA monomer and I, k_r—corresponds with the activation velocity of I—and the reaction temperature

* In A-series, accelerator concentration in the system is considered to increase because of formation of II and hydrochloric acid as I reacts with the resin[3]. Accordingly the energy is only an apparent value differing from that in B-series.

was investigated as shown in Fig. 8. which gave the activation energy, 10 kcal./mol. It may be considered to be closely related to the above value, 12 kcal./mol., in the case

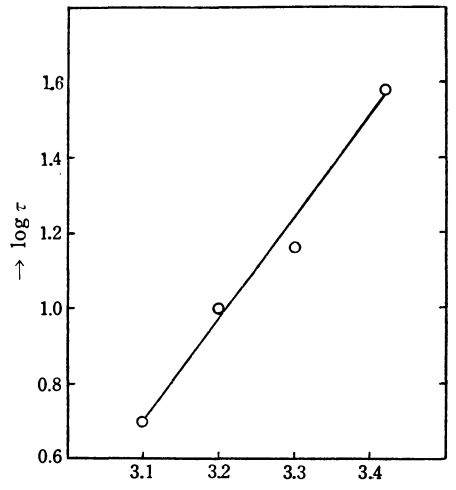

Fig. 7. Relation between $\log \tau$ and $1/T$.

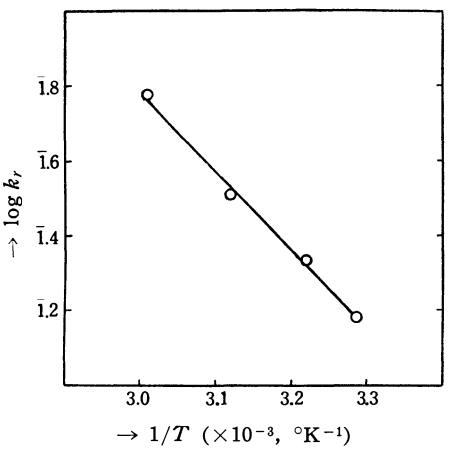

Fig. 8. Relation between $\log k_r$ and $1/T$.

where filler and initial condensate are employed. It is interesting that these values are relatively similar in spite of the difference both in the calculation method and of the reaction system.

Approximate saturation time of F, S_F, in B-series (catalyst concentration is constant), gave, as shown in Fig. 4, the activation energy, 16 kcal./mol., which may be assumed as that for the apparent end point of the hardening process. In this determination, saturated value of F was obtained by averaging arithmetically, such a variance which was inevitable in such a case and similar variances are noted in many reference papers[4].

3. Other problems. — The saturation time of H was greater than that of F in each case as given for example in Fig. 4, which suggests that the saturation time of the F above mentioned gives only an apparent end point of the hardening process.

Change in shrinkage was in the limit of experimental error in almost all cases, which may explain that the settling down phenomenon of resistivity does not depend on the apparent shrinkage.

Summary

Decreasing tendency of resistance in the system consisting of furfurylalcohol resin, graphite filler and accelerator was observed and analysed, and this observation gave an activation energy of the final cure, together with that of the apparent cure calculated from the saturation time of adhesion power. Besides, activation of sulfonylchloride accelerator was investigated taking account of the adhesion power increase and resistance decrease.

These considerations may be full of suggestions for the practical use of such a cement system.

The authors wish to express their thanks to Professor H. Sobue, of Tokyo University for his valuable suggestions, to Mr. G. Sakurai, factory chief of Tokai Electrode Mfg. Co., for his instructive advice and encouragement, and to the authorities of Tôkai Electrode Mfg. Co., for the publication of this article and also to Mr. S. Takata and Mr. H. Matsumoto for their assistance.

Chigasaki Factory
Tôkai Electrode Mfg. Co.
Chigasaki, Kanagawa Prefecture

4) e. g., E. O. Hausman, A. E. Parkinson and G. H. Mains, *Modern Plastics*, **22**, 151—154, 190—198 (1944).

Hydrothermal Treatment of Fluor-phlogopite.—Hydrothermal Treatment of Agglomerate Mass of Synthetic Mica Crystals to Facilitate Separation of Individual Crystals

By Tokiti NODA*, Hajime SAITO**, Isao TATE**, Tsutomu FUKASAWA**, Masahiko FUKASE*** and Eiji SEKINE***

(Received December 23, 1957)

The method now used to produce synthetic mica is to cool a melt having a chemical composition of fluor-phlogopite with small amounts of fluorides and silicates. The cooled mass thus obtained is composed of crystals of fluor-phlogopite with small amounts of glassy substance and fluorides between the mica crystals[1]. The glassy substance binds mica crystals together and makes them difficult to separate from one another.

Further, a thin glass film adhering to the crystals makes them harder and less flexible than natural mica. The quality of mica crystals is often damaged when crystals are separated forcibly.

In order to separate the individual mica crystals more easily and to obtain soft and flexible crystals, agglomerates of synthetic fluor-phlogopite were treated hydrothermally with electrolyte solutions.

Experimental

Samples used were agglomerates of crystals obtained by cooling melts having the following chemical compositions:

I. $3.59\,MgO,\ 0.60\,Al_2O_3,\ 3.00\,SiO_2,\ 0.70\,K_2SiF_6$
$=K_{1.17}Mg_{3.00}Al_{1.00}Si_{3.09}O_{9.52}F_{3.51}$
$=1.14KMg_3AlSi_3O_{10}F_2+0.13K_2SiF_6+0.16MgSiF_6$
$+0.01MgF_2+0.06AlF_3$

II. $0.50K_2O,\ 1.88MgO,\ 1.13MgF_2,\ 0.50Al_2O_3,$
$3.00SiO_2$
$=KMg_3AlSi_3O_{9.88}F_{2.24}$
$=0.80KMg_3AlSi_3O_{10}F_2+0.15MgF_2$
$+0.05KAlSi_3O_8$ (POM2)[1]

All of these agglomerates contained small amounts of glassy substance and fluorides.

Small pieces of the agglomerate mass, together with an aqueous solution of electrolyte, were placed in an autoclave and heated for one or two days at a temperature within the range 150 to 350°C. The ease of separating individual crystals and the flexibility of separated crystals were tested qualitatively. The fluorine content of the original and treated samples was determined and the weight decrease at various temperatures was measured by a thermobalance. The ease of separation is evaluated by grades A_0, A, B and C. Grade A means that the separation is as easy as that of natural muscovite; grade C is the same as that of untreated agglomerate; grade B is between A and C, and A_0 is better than A.

Results

1) Treatment with sodium hydroxide solution.—(*a*) *Effects of concentration of solution and of period of treatment.*—Results of experiments are given in Table I.

TABLE I

Sample No. 1—fluorine content 13.9%, Temperature of treatment: 350°C.

Experiment	No. 1	No. 2	No. 3	No. 4	No. 5
Condition for treatment					
Concn. of NaOH solution (N)	0	0.5	1.0	2.0	2.0
Period (hr.)	24	24	24	24	48
Properties of the product					
Ease of separation	C	B	B	A	A
F content (%)	13.5	13.7	13.0	11.2	8.6
Percentage decrease of F	3	1	7	19	38
W. loss between 600° and 850°C (%)	0.0_7	0.1_0	0.1_1	0.1_8	0.3_1

Sample No. 1 contained free fluorides and had a larger fluorine content than that of pure fluor-phlogopite with the theoretical content of 9.04%. Treatment with tap water for 24 hr. at 350°C had no effect of making separation easier. Treatment with

* Department of Applied Chemistry, Faculty of Engineering, Nagoya University, Chikusa-ku, Nagoya.
** Department of Applied Chemistry, Faculty of Engineering, Yamanashi University, Kofu.
*** The Electro-communication Laboratory, Nippon Telegraph and Telephone Public Corporation, Musashino, Tokyo.

1) a) T. Noda and S. Sugiyama, *J. Chem. Soc. Japan, Ind. Chem. Sec.* (*Kogyo Kagaku Zassi*), **46**, 1082 (1943).
b) T. Noda, *J. Am. Ceram. Soc.*, **38**, 147 (1955).

TABLE II

Sample No. 1—fluorine content 13.9%, Temperature: 350°C, Period: 48 hr.

Experiment	No. 5	No. 6	No. 7	No. 8
Treating solution	2N NaOH	0.95 mol. NaF / 1·2N NaOH	5.1 mol. $KF \cdot 2H_2O$ / 1·2N NaOH $\left(=\frac{\text{4.3 mol. KF}}{\text{1·1.7N NaOH}}\right)$	0.27 mol. Na_2SiF_6 / 1·2N NaOH
Properties of product				
Ease of separation	A	A	A_0	A
F content (%)	8.6	11.2	10.0	12.7
Percentage decrease of F	38	19	28	9
W. loss between 600° and 850°C(%)	0.3_1	—	0.1_9	0.2_5

0.5 N sodium hydroxide had a weak effect, and that with a more concentrated solution had a stronger effect. Products of experiments Nos. 4 and 5 separated easily and the separated crystals were flexible. The more concentrated the solution and the longer the period of treatment, the greater the decrease of the fluorine content in the product. Temperature-weight loss

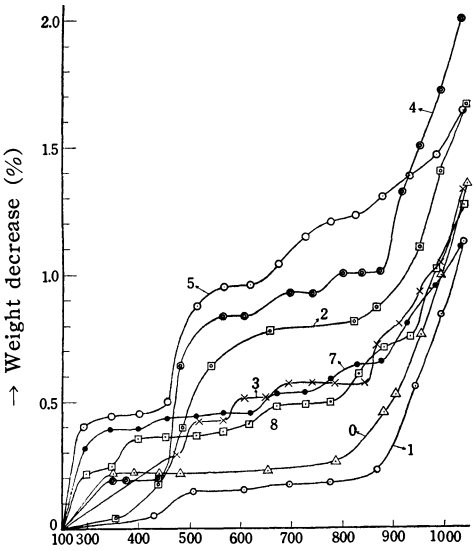

Fig. 1.

curves of these products are given in Fig. 1. The curve for the untreated mass is designated No. 0. In these curves, four stages of weight decrease can be observed, i. e. between 100° and 300°C, between 450° and 550°C, between 600° and 850°C and above 850°C. An agglomerate mass of fluor-phlogopite often occludes gas and carbon. The weight decrease between 100° and 300°C may be due to the evolution of gas and the combustion of carbon. Fluor-phlogopite gradually decomposes and liberates fluorine when heated to above 850°C[2]. These phenomena were verified by the steps of weight decrease observed in the curve of the untreated mass. The glassy substance and fluorides may be changed into hydroxides by these hydrothermal treatments and therefore the weight decrease between 450°C and 550°C is probably due to the decomposition of hydroxides. The weight decrease between 600° and 850°C is related to the dehydration of hydroxyl-phlogopite[3]. It can therefore be concluded that hydrothermal treatments at 350°C with sodium hydroxide solution did produce hydroxides and only the long treatment (No. 5) with concentrated solution changed a part of the fluor-phlogopite into hydroxyl-phlogopite[4].

(*b*) *Effects of addition of fluoride to treating solution.*—As described above, the hydrothermal treatment with sodium hydroxide solution resulted in the change of fluor-phlogopite into hydroxyl-phlogopite. If some equilibrium exists between alkali hydroxide and fluor-phlogopite, such as

$$\text{F-phlogopite} + 2OH^- \rightleftarrows \text{OH-phlogopite} + 2F^-,$$

the hydration of fluor-phlogopite may be suppressed or decreased by the addition of the fluoride ion to the treating solution. Experiments carried out on these lines are given in Table II.

That an addition of fluoride to the solution decreases the percentage decrease of fluorine content of the treated product seems reasonable. The observed decrease in fluorine content of treated products may be due to dissolution of fluoride

2) a) T. Noda and K. Aoki. *J. Chem. Soc. Japan, Ind. Chem. Sec.* (*Kogyo Kagaku Zassi*), **51**, 7 (1948).
b) T. Noda and T. Matsushita, ibid., **51**, 83 (1948).
3) H. S. Yoder and H. P. Eugster, *Geochim. Cosmochim. Acta*, **6**, 157 (1954).
4) T. Noda and Rustum Roy, *Am. Mineral.*, **41**, 929 (1956).

TABLE III

Experiment	No. 9	No. 10	No. 11	No. 12	No. 13	No. 14
Conditions for treatment						
Treating soln.	2N KOH	2N KOH	$\frac{5.31\text{mol. } KF\cdot 2H_2O}{1\cdot 2N \text{ KOH}}$ $\left(=\frac{4.46 \text{ mol. KF}}{1\cdot 1.68N \text{ KOH}}\right)$	$\frac{3.19\text{mol. } KF\cdot 2H_2O}{1\cdot 2N \text{ KOH}}$ $\left(=\frac{2.86 \text{ mol. KF}}{1\cdot 1.80N \text{ KOH}}\right)$	$\frac{2.13\text{mol. } KF\cdot 2H_2O}{1\cdot 2N \text{ KOH}}$ $\left(=\frac{1.98 \text{ mol. KF}}{1\cdot 1.86N \text{ KOH}}\right)$	$\frac{1.06\text{mol. } KF\cdot 2H_2O}{1\cdot 2N \text{ KOH}}$ $\left(=\frac{1.02 \text{ mol. KF}}{1\cdot 1.93N \text{ KOH}}\right)$
Period of treatment (hr.)	12	24	24	24	24	24
Properties of product						
Ease of separation	A	A	A	A	A	A
F content (%)	8.2	7.7	9.2	9.3	9.3	8.7
Percentage decrease of F	41	45	34	33	33	37
W. loss between 600° and 850°C(%)	—	0.1_6	—	—	0.1_4	0.1_0

originally occluded in agglomerate mass. Product No. 7 which was treated with a solution containing 1.7 mol. sodium hydroxide and 4.3 mol. potassium fluoride per liter gave the greatest ease of separation (grade A_0) even though fluor-phlogopite crystals of the product were not changed into hydroxyl-phlogopite.

2) Treatment with potassium hydroxide solution.—(*a*) *Optimum concentration of potassium fluoride.*—Sample No. 1 having a fluorine content of 13.9 % was used. It seems probable that sodium ion replaces some potassium ion of fluor-phlogopite when sodium hydroxide solution is used as a treating solution. Therefore, the use of potassium hydroxide is prefer able to sodium hydroxide as a treating solution. Treatment with 2 N solution of sodium hydroxide gave the best results for easing separation, but for the reason already given, 2 N solution of potassium hydroxide was used in the following experiments. Experimental results obtained in using 2 N potassium hydroxide with the addition of various amounts of potassium fluoride are given in Table III.

It can be seen in Table III that the effect of potassium hydroxide solution was stronger than that of sodium hydroxide solution. Fluorine contents of the products of experiments Nos. 11, 12 and 13 were nearly equal to the theoretical value of 9.04 %, but those of experiments Nos. 9, 10 and 14 were less than this value. Temperature-weight loss curves of these products are shown in Fig. 2. The product of experiment No. 10 gave 0.40 % of the weight decrease between 450° and 550°C

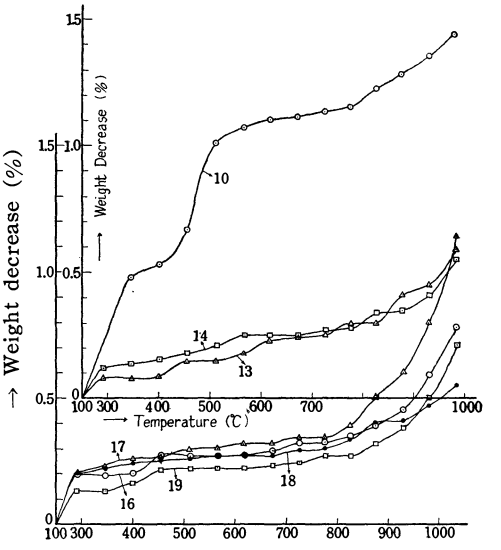

→ Temperature (°C)

Fig. 2.

which corresponds to the decomposition of hydroxides, whereas the products of experiments Nos. 13 and 14, in which potassium fluoride was added to the treating solution, gave a negligible decrease of weight in the same temperature range. The weight decrease between 600° and 850°C was 0.16 % for the product of experiment No. 10 and that of the products of experiments Nos. 13 and 14 was about 0.1 %. These results indicate that both the formation of hydroxides and the hydration of fluor-phlogopite with hydrothermal treatment were suppressed by the addition of fluoride to the treating solution. The concentration of 1.5 to 2mol.

TABLE IV

Concn. of KF: 2.1 mol. per liter, Temp. of treatment: 350°C, Period of treatment: 24 hr.

Experiment	No. 15	No. 16	No. 17	No. 18	No. 19	No. 20
Concn. of KOH(N)	2	1	0.5	0.25	0.125	0
Properties of product						
Ease of separation	A	A	A	A	B	B
F content (%)	9.4	12.2	12.5	9.3	10.2	10.7
Percentage decrease of F	33	12	10	33	27	23
W. loss between 600° and 850°C(%)	—	0.1_0	0.1_3	0.1_0	0.0_8	—

potassium fluoride per liter was necessary in order to suppress the hydration of fluor-phlogopite in the treatment with 2 N potassium hydroxide.

(*b*) *Optimum concentration of potassium hydroxide.*—Sample No. 1 having a fluorine content of 13.9 % was used. In the experiments described above the concentration of potassium hydroxide was fixed at 2 N. Table IV shows the results of experiments carried out with potassium hydroxide solution of various concentrations, 2.1 mol. potassium fluoride being added per liter to every treating solution.

A solution containing 2.1 mol. potassium fluoride and no potassium hydroxide had some effect and a concentration of 0.5 N potassium hydroxide with 2.1 mol. potassium fluoride per liter was sufficient to facilitate separation. Curves shown in Fig. 2 indicate no hydration of fluor-phlogopite for these experiments.

(*c*) *Effect of temperature.*—All experiments hitherto described were carried out at 350°C. When the temperature of treatment is high, the working pressure is consequently high and from a practical standpoint, it is desirable to work with as low temperatures and under as low pressures as possible for the accomplishment of easy separation. Results of experiments using a dilute solution 0.5 N and a concentrated solution (10 N) are given in Table V.

Experiments with 0.5 N potassium hydroxide gave an effect of easing separation when they were carried out at 300°C or above, while in experiments using 10 N potassium hydroxide, treatment at 250°C or above was sufficient to give a good effect. Therefore, the temperature of treatment was fixed at 300°C and the effect of concentration was investigated in experiments given in Table VI.

TABLE V

Period of treatment: 24 hr.
Sample No. 2 having a fluorine content of 9.3% was used.

Temperature of treatment (°C)	350	300	250	200	150
Concn. of KOH					
0.5 N	B	B	C	C	C
10 N	A_0	A	A	C	C

It was found that a solution of 0.25 N potassium hydroxide with 2.1 mol. potassium fluoride per liter was sufficiently strong for easy separation with the treatment at 300°C, as it was with treatment at 350°C.

3) Treatment with acid and salt solutions.—Effects of using acids and some salt solutions as treating solutions for hydrothermal treatment of fluor-phlogopite were investigated because Saito, one of the present authors, had found that hydrothermal treatment of synthetic asbestos with solutions of acids, alkalies or some salts gave easy separation of fiber crystals. Experimental results are given in Table VII.

Treatments with 10 N potassium carbonate solution or with more concentrated solutions gave good results, those with less concentrated solutions had less effect and that with 1 N solution had no effect. Treatments with mixed solutions of 8.4 N potassium carbonate and various concentrations of potassium hydroxide gave the same results as those with mixed solutions of 2.1 N potassium fluoride and various concentrations of potassium hydroxide, as given in Table VI, i. e. treatments with 0.25N potassium hydroxide or more concentrated solutions gave good results. This means that in both cases potassium hydroxide played the main role.

Treatments with hydrochloric acid gave good results when 0.125 N or more concentrated solutions were used. Treatment with potassium hydrogen sulfate gave the best results among those with bisulfate, bicarbonate and biphosphate of potassium.

Fluorides were found to have a suppressing effect on hydration of fluor-phlogopite, and experiments Nos. 27′ to 31′ show that

TABLE VI

Sample No. 1 having a fluorine content of 13.9% was used.
Temp. of treatment: 300°C, Concn. of KF: 2.1 mol. per liter, Period of treatment: 24 hr.

Experiment	No. 21	No. 22	No. 23	No. 24	No. 25	No. 26
Concn. of KOH(N)	2	1	0.5	0.25	0.125	0.0625
Properties of product						
Ease of separation	A	A	A	A	B	B
F content (%)	9.5	13.7	11.0	10.8	10.4	11.7
Percentage decrease of F	32	1	21	23	25	16
W. loss between 600° and 850°C(%)	0.0_7	0.0_5	0.1_7	0.0_6	0.0_8	0.0_7

TABLE VII

Condition I: Temp.: 250°C, Period: 24 hr., except on special notice.
Condition II: Temp.: 350°C, Period: 48 hr.

Experiment	Condition	Treating soln.	Ease of separation
No. 1′	I	11.6N K_2CO_3	A_0
2′	I	10.0N K_2CO_3	A
3′	I	8.4N K_2CO_3	B
4′	I	4.7N K_2CO_3	B
5′	I	1.0N K_2CO_3	C
6′	I	3.0N KOH 8.4N K_2CO_3	A
7′	I	2.0N KOH 8.4N K_2CO_3	A
8′	I	1.0N KOH 8.4N K_2CO_3	A
9′	I	0.5N KOH 8.4N K_2CO_3	A
10′	I	0.25N KOH 8.4N K_2CO_3	A
11′	I	0.125N KOH 8.4N K_2CO_3	C
12′	I	0.0625N KOH 8.4N K_2CO_3	B
13′	I	0.25N HCl	A
14′	I	0.125N HCl	A
15′	I(12 hr.)	0.125N HCl	C
16′	I	0.0625N HCl	B
17′	I	0.0312N HCl	B
18′	I	0.0156N HCl	B
19′	I	0.0078N HCl	C
20′	I	0.125N HCl 4.7N KCl	B
21′	I	0.125N HCl 2.35N KCl	B
22′	I	2.2N $KHSO_4$	A_0
23′	I	1.5N $KHSO_4$	C
24′	I	0.7N $KHSO_4$	C
25′	I	3.0N $KHCO_3$	B
26′	I	2.9N KH_2PO_4	B
27′	I	7.4N KF	A
28′	I(12 hr.)	7.4N KF	B
29′	I	6.2N KF	C
30′	I	5.0N KF	C
31′	II	2.4N KF	A_0
32′	II	H_2O	C

potassium fluoride itself can ease separation of mica crystals.

Crystals treated with acid solutions were found to be harder and less flexible than those treated with alkaline solutions. It seems that the difference in these physical properties of products depends on the different actions of acid and alkali on glassy substance in the agglomerate mass. Alkali reacts on glass to make the silicic acid component of the glass soluble or to accelerate devitrification of the glass, thus decreasing the strength of the glass to bind mica crystals. The dissolution and the devitrification of the glass help the treating solution to penetrate further into the agglomerate mass and react on glass in deep places of the mass. The milk-white substance produced by devitrification of glass which exists between mica crystals in treated agglomerates, was separated easily when the crystals were split from the mass.

Acid reacts on glass to dissolve basic components of glass and leaves the silicic acid component undissolved. The silicic acid skeleton thus produced may prevent penetration of the treating solution into shallow spaces, such as interstices between cleavage planes of mica crystals. This

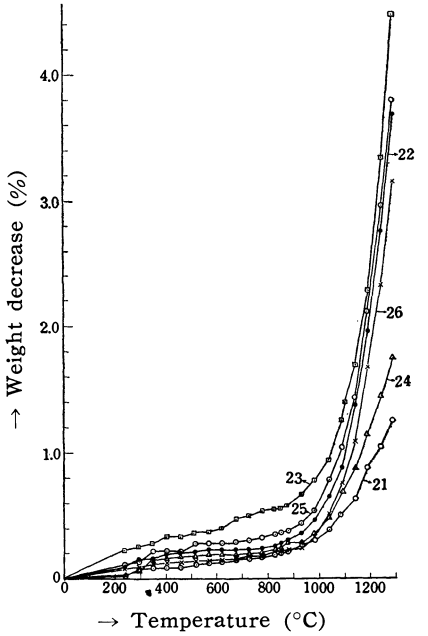

Fig. 3.

makes separation of glassy substance in the acid-treated mass more difficult than separation of glass in the alkali-treated mass and the split crystals from the acid-treated mass are somewhat harder and less flexible than those from the alkali-treated mass.

Hydrothermal treatment for easy separation was much more effective on agglomerates of well developed crystals than on those of small crystals because treating solution penetrates much more easily into the mass along plate crystals than through the mass of irregularly arranged small crystals.

Percentage decreases of fluorine content of the mass treated with potassium carbonate, potassium hydrogen sulfate or hydrochloric acid were found to be smaller than those of the mass treated with alkali by the measurement of fluorine content and temperature-weight loss curve of these products.

4) Investigation on treated mica crystals. — (*a*) *Vacuum test.* — Vacuum characteristics of split mica crystals of untreated synthetic fluor-phlogopite, of products of experiments Nos. 1 to 8 and natural phlogopite were measured. Specimens used for the measurement were washed with ethylalcohol, rinsed with distilled water and dried at 120°C for 1 hr. The specimens were placed in a silica glass tube pumped to a pressure of 1×10^{-5} mmHg. Then the specimens were put into a hot place in the vessel maintained at a definite temperature, and the change of pressure of the vessel was measured. Fig. 4a shows the volume of gas evolved from the specimens when heated. Results of the measurements on specimens which were first outgassed by heating in a high vacuum (1×10^{-5} mmHg) are shown in Fig. 4b. The glassy substance adhering to untreated crystals contains minute amounts of carbon and gas. Hydrothermal treatment decreases the amount of glass adhered. This is why treated crystals evolved smaller amounts of gas than the untreated crystals at temperatures lower than 800°C. Specimen No. 5, which was treated with 2 N sodium hydroxide for 48 hr. and was expected to contain hydroxyl-phlogopite, increased the gas evolution rapidly at about 950°C in the same way as natural phlogopite did. It is worthy of note that specimen No. 7, which was treated with 1.7 N sodium hydroxide in the presence of 4.3 mol. potassium fluoride per liter, evolved the smallest amount of gas among specimens tested.

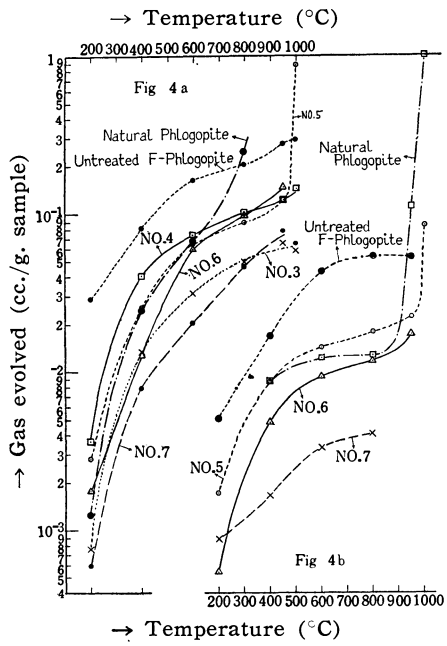

Fig. 4.

(*b*) *X-ray powder diagram.*—It can be said from the experimental results described above that the main part of the original fluor-phlogopite remained unchanged by hydrothermal treatment, although a small part of the mica changed to hydroxyl-phlogopite. X-ray powder photographs taken by using a camera of 114.6 mm. diameter gave no difference between untreated and treated micas. However, by using a Norelco X-ray Geiger counter goniometer, weak extra peaks adjacent to (00*l*) of fluor-phlogopite were detected in the X-ray powder diagram of treated mica which was found to have a weight loss between 600° and 850°C. This means that a small amount of hydroxyl-phlogopite exists in the specimen because these extra peaks correspond to (00*l*) of hydroxyl-phlogopite[4].

Summary and Conclusion

Agglomerates of synthetic mica crystals were treated hydrothermally with alkali, acid and salt solutions in order to ease the separation of mica crystals which are bonded together by glassy substance.

(1) Among treatments with sodium hydroxide solutions of the concentration from 0.5 to 2 N at 350°C for 24 hr., that with 2 N sodium hydroxide facilitated greatly the separation of mica crystals.

A small amount of fluor-phlogopite probably changed to hydroxyl-phlogopite and hydroxides were produced by the hydrothermal treatment.

(2) The hydration of fluor-phlogopite and the formation of hydroxide were suppressed by the addition of fluorides in the treating solution. It was found that the presence of 1.5 mol. potassium fluoride per liter of treating solution was effective for the suppression.

(3) Among treatments with potassium hydroxide solution in the presence of 2 mol. potassium fluoride per liter solution at 350°C for 24 hr., that with 0.25 N or more concentrated solution of potassium hydroxide was effective for easing separation of mica crystals. Potassium fluoride itself was found to be effective for easy separation.

(4) It was necessary to keep the temperature at 250°C or above in the treatment with 10 N potassium hydroxide and 300°C or above in the treatment with 0.5 N potassium hydroxide in order to obtain a good result.

(5) Treatments with potassium hydroxide solution in the presence of 2 mol. potassium fluoride per liter solution at 300°C for 24 hr. were as effective as those with the same solution at 350°C.

(6) Among treatments with solutions of various concentrations of potassium carbonate or potassium carbonate and potassium hydroxide at 250°C for 24 hr., 10 N or more concentrated potassium carbonate solution was effective as a treating solution and in a mixed solution of potassium carbonate and potassium hydroxide the latter played the main role.

(7) Among treatments with solutions of various concentrations of hydrochloric acid or hydrochloric acid and potassium chloride at 250°C for 24 hr., 0.125 N or more concentrated hydrochloric acid solution was effective as a treating solution and the presence of potassium chloride had no effect.

(8) Among treatments with potassium hydrogen sulfate, potassium hydrogen carbonate and potassium dihydrogen phosphate, that with potassium hydrogen sulfate was most effective and the smallest necessary concentration of the treating solution was 2 N.

(9) A solution of 7 N potassium fluoride or a more concentrated one was effective as a treating solution at 250°C for 24 hr.

(10) Split crystals from the mass treated with alkali and potassium fluoride solutions were flexible and those treated with acid were harder and less flexible than the former. The difference of the effects of acid and alkali was interpreted as the difference of their action on binding glass.

(11) Hydrothermal treatment for easy separation was much more effective on agglomerates of well developed crystals than on those of small crystals because the treating solution penetrates easily into the mass along plate crystals.

(12) Investigation of X-ray powder diagram of treated products revealed that the main part of fluor-phlogopite crystals remained unchanged and only a small amount of original mica changed to hydroxyl-phlogopite by treatments with strong alkali solutions. This observation was in good agreement with the experimental results deduced from the observed decreases of fluorine contents and temperature-weight loss curves of treated products.

(13) It was found that split crystals from a treated mass evolved less gas than those from an untreated mass because of the low content of adhering glass in the former. Split crystals which contained a small amount of hydroxyl-phlogopite began to evolve gas at about 950°C.

Department of Applied Chemistry
Faculty of Engineering
Nagoya University
Chikusa-ku, Nagoya

Studies on Explosive Reaction of Ethylene Mixed with Oxygen or Air. I. Explosion Limit at Low Pressure

By Masao SUGA

(Received January 13, 1958)

The explosion and the combustion phenomenon of lower hydrocarbons have been studied extensively[1-3], but there are few investigations about ethylene. The explosion of gas has generally very complex mechanism, and various methods have been taken for the determination of the explosion limit[1,4]. The present author, considering conveniently that the spontaneous ignition was the explosion, investigated systematically on the phenomena of spontaneous ignition of ethylene-oxygen or -air mixture at lower pressures than atomospheric. The explosion limit was determinated by so-called "admission method", in which the gas mixture with a certain definite composition was admitted into the reaction vessel evacuated and heated at a definite temperature. The limit was not only decided by some parameters such as temperature, pressure or composition, but was affected considerably by the nature of the surface of the reaction vessel etc. Thus a standard procedure was adopted for convenience in order to determine the limit, and the effects were briefly discussed.

Experimental

Materials.—The ethylene employed in this experiment was prepared by the dehydration of absolute alcohol by the action of phosphoric acid and purified by the action of concentrated aqueous solution of sodium hydroxide, concentrated sulfuric acid, silica gel and phosphorus pentoxide. About 99% of the gas so treated was absorbed by fuming sulfuric acid. The oxygen employed was obtained from a commercial cylinder (purity: 99.4%). The oxygen and the air were used after being passed through a train consisting of two bottles containing a concentrated aqueous solution of sodium hydroxide, concentrated sulfuric acid and phosphorus pentoxide.

Apparatus and Procedure.—The diagram of the apparatus is shown in Fig. 1. The apparatus was partly screened with wire netting for the prevention of explosion. The inlet tube connecting the reaction vessel to the cock C_1 and the manometer M_1 was used as capillary to decrease dead space, also to prevent danger. The explosion limit was determined by the following procedures:

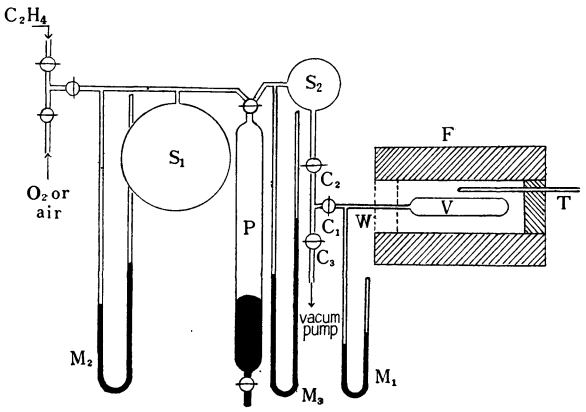

Fig. 1. The apparatus of admission method for determining the explosion limit.
S_1, S_2: Gas storages.
C_1, C_2, C_3: Stop cocks.
M_1, M_2, M_3: Mercury manometers.
P: Toepler pump.
V: Reaction vessel.
F: Electric farnace.
T: Thermocouple.
W: Window.

(1) The gas mixture of the desired composition for the test was prepared in storage S_1 (1 l.), the partial pressures of gases being measured by the manometer M_2, and stored for more than twelve hours in order to be thoroughly mixed.

(2) Then, a part of sample gas in storage S_1 was removed into storage S_2 (ca. 200 cc.) at any desired pressure by the aid of Toepler pump P.

(3) The reaction vessel V (usually 3 cm. diameter and 10 cm. length in order to examine the effect of diameter on the limit, 2 cm. or 1 cm. diameter and equal length) which consisted of a quartz cylinder was placed in a horizontal electric furnace F. The highest temperature in furnace F was measured by an alumel-chromel thermocouple T inserted into furnace F. On this occasion, the reaction vessel was maintained at a definite temperature and

1) B. Lewis and N. von Elbe, "Combustion, Flames and Explosions of Gases", Academic Press Inc., New York, (1951).
2) M. Prettre, "Third Symposium on Combustion, Flame and Explosion Phenomena", The Williams and Wilkins Co., Baltimore, (1949), p. 397.
3) K. Spence and D.T.A. Townend, ibid., p. 404.
4) F. S. Dainton, "Chain Reaction", Methuen Co., London, (1956) p. 23.

thoroughly evacuated (10^{-3} mmHg) in thirty minutes.

(4) The sample gas in storage S_2 was rapidly admitted to pre-evacuated reaction vessel V to give some previously decided initial pressure by operating cocks C_1 and C_2.

(5) The determination of the occurence of explosion or otherwise was made directly by sight through the window W made of mica on one side of the furnace and subsidiarily by the pressure change with the aid of mercury manometer M_1 for thirty minutes.

The induction period, which is the time-lag from the moment of admission of the sample gas to the occurrence of the explosion, was measured by the aid of a stopwatch. Isochors (pressure-temperature diagram) of the explosion limit were determined by the repetition of these procedures 2—5, at the temperature range between 300 and 700°C, and at the pressure range lower than atomospheric pressure for various compositions. Then, these were used to derive isotherms and isobars.

Results and Consideration

Observation.—The results of observation are classified as the following.

(1) After the lapse of various induction periods (usually less than 30 sec.) luminous flames were normally preceded by a glow which rapidly built up into a bright flash filling the vessel and accompanied by a vigorous pulse and sound.

(2) After the lapse of the relatively long induction periods, pale blue flames were observed in the dark room with a mild pressure pulse which was measured with much difficulty by mercury manometer M_1.

(3) After a considerable time interval (the so-called induction period of slow reaction), the pressure gradually rose, and the maximum pressure was maintained for an appreciable period before slowly falling off. But ignition flames were not able to be found even in the dark room.

(4) No change was observed.

Case 1 and 2 are considered to be the explosions.

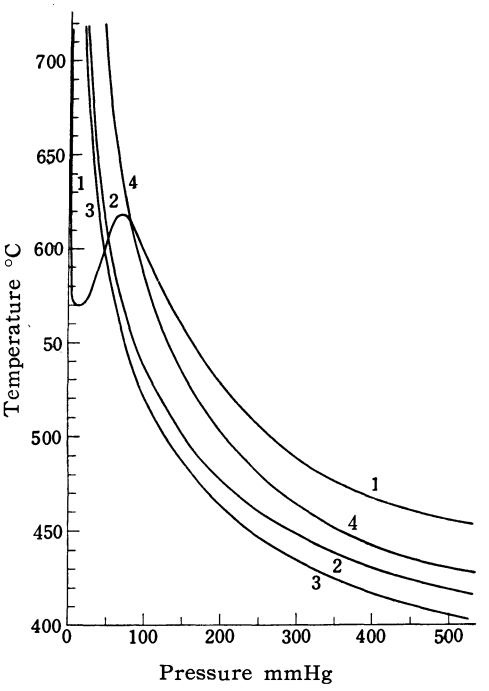

Fig. 2. Isochors for explosion limit of ethylene-oxygen mixtures. curve 1= 20%, 2=40%, 3=60%, 4=80% ethylene.

The Explosion Limit of Ethylene-Oxygen Mixtures.—Isochors were determined for the mixture of the various compositions. Only a certain number of isochors are shown in Fig. 2. Only the

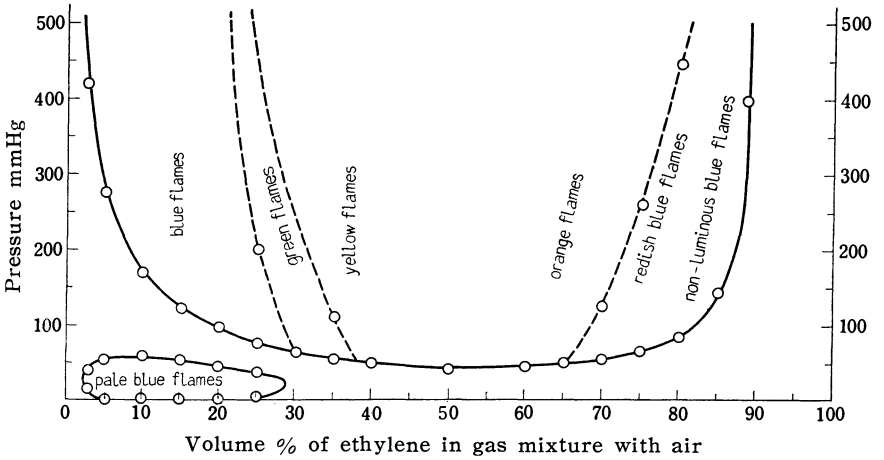

Fig. 3. Isotherm for explosion limit of ethylene-oxygen mixtures at 600°C.

600°C isotherm is shown Fig. 3. The curves shown in these figures exhibit the minima at the composition of about 50% ethylene and are situated about 2.5~90% ethylene. The explosion limit peninsula as indicated in Fig. 2 (curve 1) is found on the definite temperature and pressure condition in the mixture range 2.5~30% ethylene as indicated in the lower closed curve in Fig. 3.

a) Non-luminous blue flames are the flames observed in the ignition of the mixture of more than 70% ethylene. The pressure pulses are relatively mild in company with the flames, and no propagating flames are observed.

b) Luminous blue flames are the flames observed in the ignition of the mixture of less than 30% ethylene. Even at a lower pressure region, the pressure pulses are relatively violent with the flames and propagating flames are often observed.

c) Luminous yellow flames are the flames observed in the ignition of the mixture of 20~80% ethylene. The flames are propagated into the inlet tube of the reaction vessel, with vigorous pulses.

d) Luminous green flames are the flames observed in the ignition of the mixture of about 35% ethylene.

As a whole, the color of ignition flames, as shown in Fig. 3, changes in the order of blue, yellow, green and blue, with decrease of the percentage of ethylene.

Morever, as a remarkable phenomenon, in the mixture range 60~80% ethylene, reddish blue flames are often observed and a small quantity of deposited carbon is found on the wall of the reaction vessel V and capillary inlet tube connecting the reaction vessel V to cock C_1 and manometer M_1. The flames in the explosion peninsula are very faintly visible after the longer induction periods (10 sec.~20 min.) as described in 2). The boundary between the second and the third (thermal)

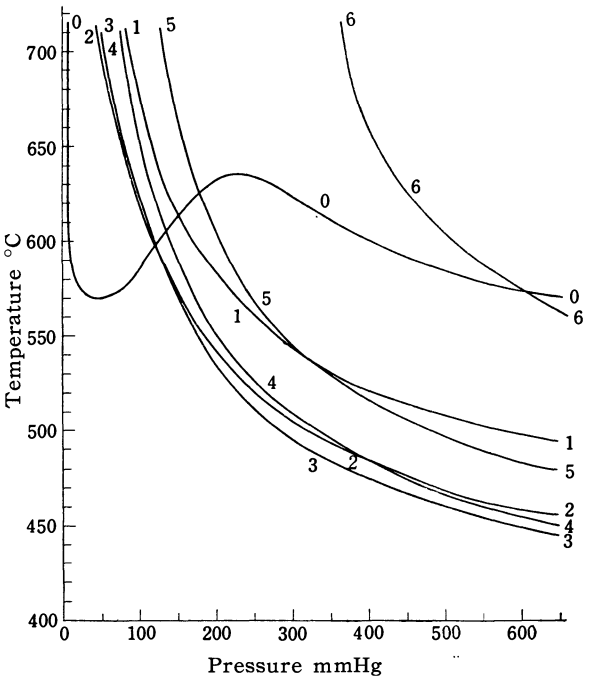

Fig. 4. Isochors for explosion limit of ethylene-air mixtures. curve 0=5%, 1=10%, 2=20%, 3=30%, 4=40%, 5=50%, 6=60% ethylene.

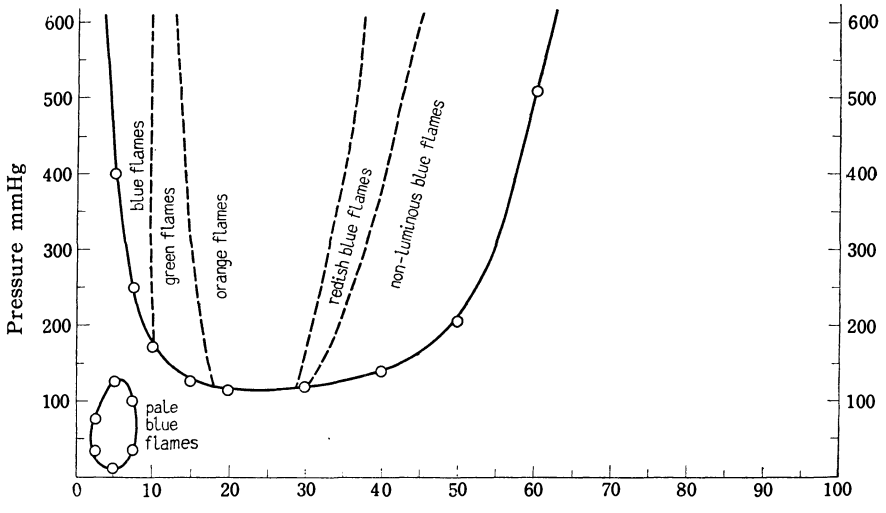

Fig. 5. Isotherm for explosion limit of ethylene-air mixtures at 600°C.

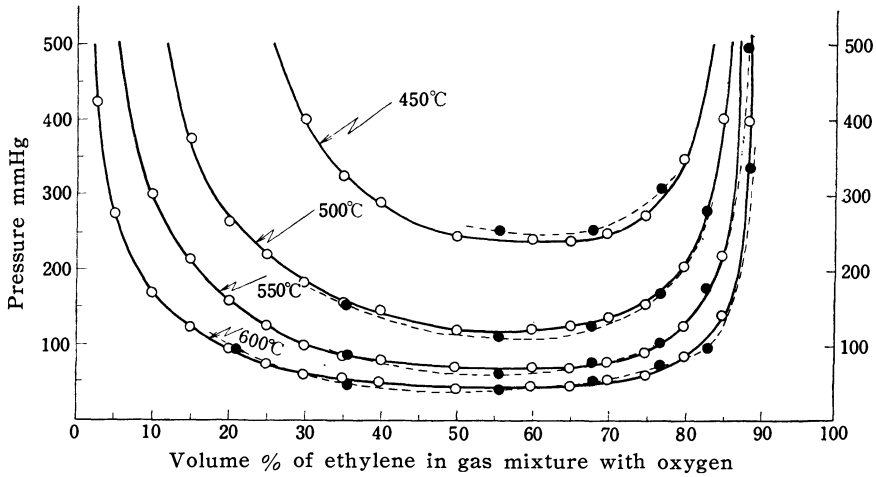

Fig. 6. Relationship between isotherms for explosion limit of ethylene-oxygen and ethylene-air. (Broken lines represent the data calculated from the limit of ethylene-air mixtures, illustrated in considerations.)

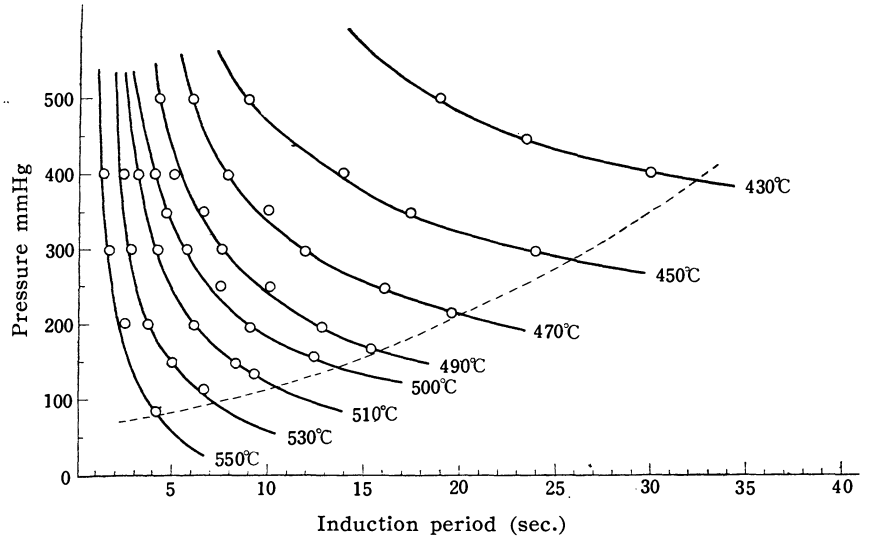

Fig. 7. Relationship between explosion limit pressure and induction period at a definite temperature.

limit was accurately determined with difficulty in the present experimental method.

The Explosion Limit of Ethylene-Air Mixtures.—Isochors of the explosion limit at the compositions of 5, 10, 20, 30, 40, 50 and 60% ethylene with air can be obtained by the same method described as with oxygen and shown in Fig. 4. Also the 600°C isotherm is shown Fig. 5.

In order to elucidate the effect of the foreign gas, N_2, the limiting pressures and composition of ethylen-air mixtures at temperatures of 600, 550, 500 and 450°C are converted in to those of ethylene-oxygen mixtures by calculation, subtracting the partial pressure of nitrogen. These calculations give the broken lines in Fig. 6 which shift little from the corresponding full lines except the second pressure limit. A further investigation of the second pressure limit is now in progress. In addition, the ignition flames are the same as ethylene with oxygen, and may lead to the conclusion that the effect of nitrogen on the first and the third pressure limit should be negligible.

The Explosion Limit and Induction Period.—The results of the experiment with regard to the induction period are shown in Fig. 7. Generally, the higher the admission pressure, the shorter the

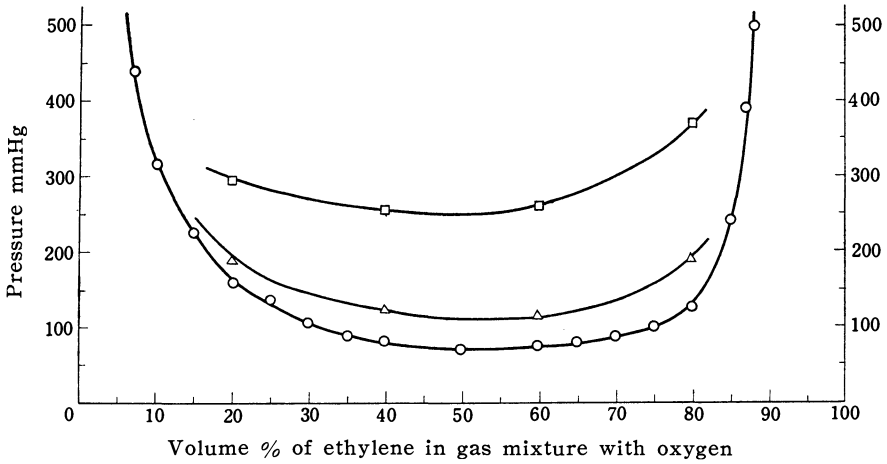

Fig. 8. (a) Effect of reaction vessels diameter for the isotherms at 550°C.
Diameter: □, 1 cm; △, 2 cm; ○, 3 cm.

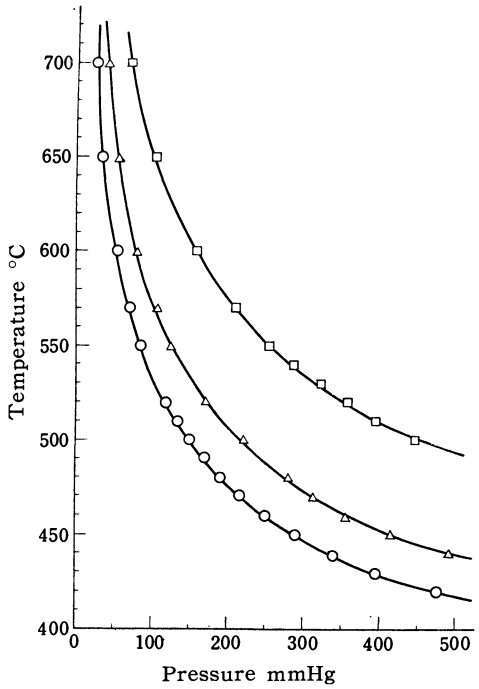

Fig. 8. (b) Effect of reaction vessel diameter for the isochors of 40% ethylene.
Diameter: □, 1 cm; △, 20 cm; ○, 3 cm.

induction period. The influence of temperature is greater than that of pressure.

In consequence, the induction periods, over 650°C, became less than one second and accordingly can not be measured with a stopwatch with accuracy. Slow reactions also had the induction periods which were longer than those of explosions, but the quantitative relationship could not be described in the present experiment. Also as a remarkable phenomenon, preceding the ignition, the pressure changes which anticipated the explosion were often observed by mercury manometer M_1.

The Effect of Reaction Vessel.—The reaction vessels used were usually quartz cylinders of 3 cm. in diameter and 10 cm. in length. Quartz cylinders of 2 cm. or 1 cm. in diameter of the same length were also employed in order to examine the effect of the diameter of reaction vessels. The result is indicated in Fig. 8. The decrease of the vessel diameter serves invariably to retard the explosion. The quantitative relationship can not be discussed in detail. Furthermore it was found that the result varied with previous history of the reaction vessel (e.g. the quality and time of pumping during evacuation of the vessel between experimental runs), and that the induction period was greatly influenced. But these effects were not reproducible, so the present authors adopted the standard procedure as follows.

After the previous runs, the reaction vessel was heated to 600°C and evacuated to 10^{-3} mm Hg (tested by Gaisler tube) for thirty minutes. The virgin vessels were employed after explosive runs. It is confirmed that the experiments with these precaution are reproducible and the results are probably always reliable.

The Activation Energy of the Reaction. — In Fig. 9 is shown the relationship between $\log_{10} p/T$ and $1/T$ for the third limit of Fig. 2. Those graphs are essentially linear at a lower temperature than 600°C and adhere to the relationship $\log_{10} p/T = A/T + B$. If the ignition limit is thermal in character, the gradient of

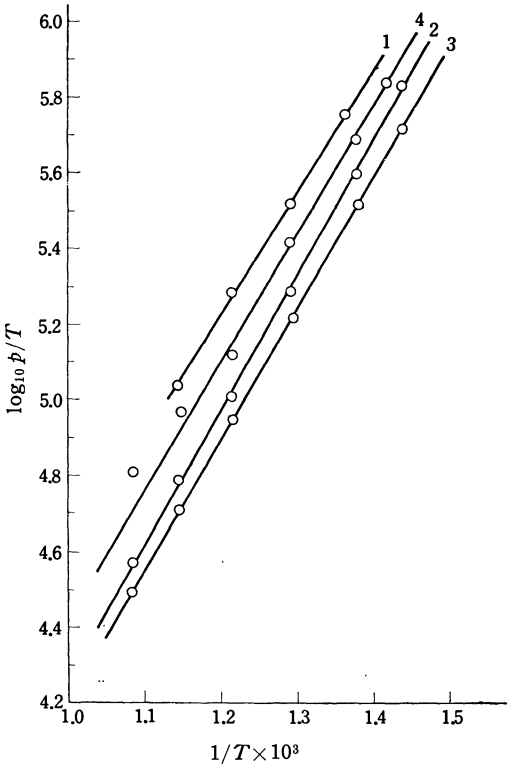

Fig. 9. $\text{Log}_{10}\, p/T$ against $1/T$ curves for the explosion limit of ethylene-oxygen mixtures. curve 1=20%, 2=40%, 3=60%, 4=80% ethylene.

these lines A will be equal to $E/2.303\times 2\times R$.[5,6] Thus values for E, the apparent activation energy, may be calculated as in Table I.

TABLE I
ACTIVATION ENERGIES ESTIMATED FROM SPONTANEOUS IGNITION LIMITS OF ETHYLENE-OXYGEN MIXTURES

C_2H_4%	A	$E=2.303\times2\times1.987\times A$ (kcal./mol.)
80	3.18	29.10
60	3.74	34.23
40	3.47	31.76
20	3.37	30.84

On the other hand, in Fig. 10 is shown the relationship between $\log_{10}\tau=A'/T+B'$. There will be only an in direct meaning of the kinetics, but the gradient of these lines A' is thought to be equal to $E/2.303\times R$.[7] Thus values for E', the apparent activation energy, may be as in Table II.

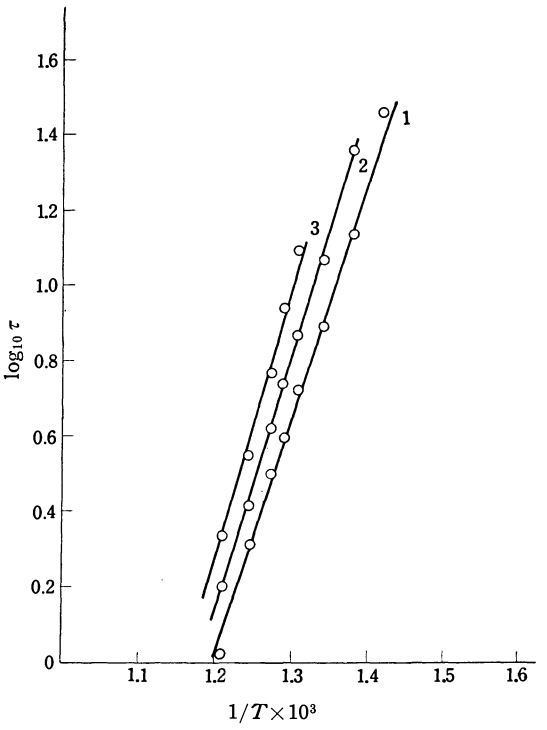

Fig. 10. $\text{Log}_{10}\,\tau$ against $1/T$ curves for the explosion of 40% ethylene-oxygen mixture. curve 1=400, 2=300, 3=200 mmHg.

TABLE II
ACTIVATION ENERGIES ESTIMATED FROM THE INDUCTION PERIODS

Admission pressure (mmHg)	A'	$E=2.303\times1.987\times A'$ (kcal./mol.)
400	6.05	27.69
300	6.52	29.84
200	7.12	32.58

The explosive reactions of ethylene with oxygen or air may be considered to be thermal in apparent character in the present experimental ranges.

Summary

The explosion limit of ethylene mixed with oxygen or air was determined at lower pressure than atomospheric pressure by the statical constant volume method known as the "admission method". Isochors, isotherms and isobars of the explosion limit have been shown. The colors of ignition flames change in the order of blue, yellow and blue with the decrease in the percentage of ethylene. In addition, the explosion peninsula was recognized at a definite condition in the mixture range 2.5~30% ethylene in

5) K. Semenoff, *Z. Physik.*, **48**, 57 (1928).
6) K. Posthmus, *Rev. Trav. Chim.*, **49**, 309 (1930).
7) B. P. Mullins; "Spontaneous Ignition of Liquid Fuels", Butter Worths Sci. Pub., London, (1955).

oxygen. The results of ethylene with oxygen and ethylene with air were equivalent to each other, so far as the partial pressure of nitrogen was neglected. Induction periods were also taken into consideration and the apparent activation energy was estimated to be about 30 kcal./mol.

The author wishes to thank the late Professor R. Kiyama and Dr. Z. Ôsugi of the Kyôto University and Professor T. Kôzu for their kind advice and encouragement throughout this work. He is also grateful to Mr. K. Ochi, Mr. T. Ogura and Mr. M. Siga for the assistance of observations done partly in the present experiment.

Department of Chemistry, Faculty of Science and Literature, Ehime University, Matsuyama

Colorimetric Determination of Bivalent Copper Using Sodium Alizarin-3-Sulfonate as a Reagent

By Anil K. MUKHERJI* and Arun K. DEY

(Received October 1, 1957)

Sodium alizarin-3-sulfonate, commonly known as the dye Alizarin Red S (abbreviated as ARS), has been widely used in the determination of aluminum[1], and has also found application in the analysis of zirconium and hafnium[2]. Raghava Rao and coworkers[3] have suggested the use of the reagent in the colorimetric determination of uranium and thorium and Rinehart[4] for the estimation of rare earths. In a recent communication Mukherji and Dey[5] reported the formation of colored lakes of various metals with Alizarin Red S and suggested that the reagent might be of use in other determinations as well.

In further communications Mukherji and Dey have reported the spectrophotometric study of alizarin sulfonate chelates of cupric[6] and lead[7] and have also discussed the structure of alizarin sulfonate chelates of bivalent metals[8]. It has been found that copper forms a 1:1 chelate with sodium alizarin-3-sulfonate with λ_{max} at 500 mμ. In this paper we are reporting our observations on the possibility of using the reagent for the colorimetric determination of bivalent copper on a micro-scale.

Experimental

Solutions of cupric sulfate (BDH Analar) and of Alizarin Red S (BDH Indicator) were prepared in carbon-dioxide free water and standardised as usual. The spectrophotometric measurements were carried out in an air conditioned room maintaining a constant temperature of 25°C.

Absorption spectra of the chelate.—The absorption spectra of the reagent using 0.0002 M solution and the chelate (1:1 mixture of the reagent and cupric sulfate of the same concentration) were studied at different wave lengths. The optical densities were measured with an SP 500 spectrophotometer, manufactured by Unicam Instruments Ltd. The thickness of the solution was 1 cm. in glass cells supplied with the instrument. pH of both solutions was 4.3. The results are plotted in Fig. 1.

Conformity to Beer's law.—To fixed volumes of ARS solution were added varying volumes of

* Present address: Coates Chemical Laboratory, Louisiana State University, Baton Rouge-3, La., U. S. A.

1) J. H. Yoe, "Photometric Chemical Analysis", Wiley, New York (1928); F. D. Snell and C. T. Snell, "Colorimetric Methods of Analysis", Van Norstand, New York, (1928); "B. D. H. Book of Organic Reagents", Poole (1949).

2) D. E. Green, *Anal. Chem.*, **20**, 370 (1948); J. C. Griess, Jr., U. S. Atomic Energy Comm. Rept., KAPL, 305 (1950); A. Mayer and G. Bradshaw, *Analyst*, **77**, 476 (1952); G. B. Wengert, *Anal. Chem.*, **24**, 1449 (1952); D. L. Manning and D. C. White, ibid., **27**, 1389 (1955).

3) K. S. Venkataswarlu and Bh. S. V. Raghava Rao, *Anal. Chim. Acta*, **13**, 79 (1955); D. V. N. Sarma and Bh. S. V. Raghava Rao, ibid., **13**, 142. (1955).

4) R. W. Rinehart, *Anal. Chem.*, **26**, 1820 (1954).

5) A. K. Mukherji and A. K. Dey, *Proc. Natl. Acad. Sci., India*, **27A**, 2421 (1957).

6) Idem., *J. Ind. Chem. Soc.*, **34**, 461 (1957).

7) Idem., *Proc. Natl. Acad. Sci., India*, **27A**, 20 (1957).

8) Idem., *Vi jñāna Pari. Anu. Patrikā*, **1**, 23 (1958).

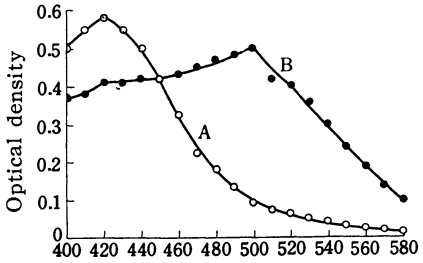

Fig. 1. Absorption spectra studies.
Curve A: Sodium alizarin-3-sulfonate 0.0002 M; Curve B: 1 : 1 mixture of sodium alizarin-3-sulfonate and cupric sulfate (0.0002 M).

cupric sulfate solution, keeping in view that the amount of the chromophoric agent remained in large excess as compared to cupric sulfate. The total volume was kept constant by the addition of water. The optical densities of 1 cm. thickness of the solutions were measured with the spectrophotometer. The observations were repeated at three wave lengths as noted in Table I:

TABLE I

Concn. of Cupric Sulfate $=1.0\times10^{-4}$ M
Concn. of ARS $=1.0\times10^{-3}$ M
Volume of ARS taken $=10$ ml.
Total Volume $=50$ ml.

Volume of $CuSO_4$ ml.	Optical density		
	450 mμ	500 mμ	550 mμ
0	0.410	0.080	0.025
2	0.420	0.140	0.065
4	0.425	0.186	0.095
6	0.430	0.215	0.105
8	0.430	0.245	0.125
10	0.435	0.280	0.145
12	0.440	0.300	0.155
14	0.440	0.340	0.170
16	0.445	0.350	0.185
18	0.445	0.360	0.195
20	0.450	0.380	0.200

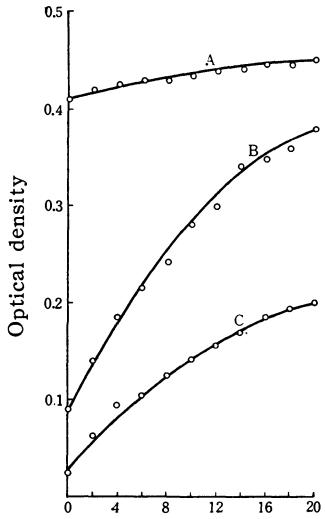

Fig. 2. Conformity to Beer's law.
Curve A, 450 mμ; Curve B, 500 mμ; Curve C, 550 mμ.

The results in Table I are represented graphically in Fig. 2. It may be seen that the calibration curves have a curvature, which is probably due to the colloidal nature of the reagent[9].

Stability of the color at room temperature.—A mixture of solutions of 0.0002 M of cupric sulfate and 0.001 M of ARS (pH of mixture 4.0) gave the same optical density even after 72 hours of standing at room temperature, showing that the color is stable enough for colorimetric measurements.

Influence of temperature.—The color intensity remains constant over a temperature range 20° to 35°C, as may been in Table II:

Influence of pH.—The intensity of color is stable between pH 3.20 to 7.50, as may be seen in Table III:

Sensitivity of the reagent.—The smallest amount of cupric ion that can be detected with Alizarin Red S is 6.4 p. p. m., when absorbance measurements are done in 1 cm. cells.

TABLE II

Concn. of cupric sulfate $=0.0002$ M
Concn. of ARS $=0.001$ M
pH of mixture $=4.00$

Temperature °C	20	25	30	35	40	45
Optical density per cm. (500 mμ)	0.680	0.680	0.680	0.680	0.685	0.685

TABLE III

Concn. of cupric sulfate $=0.00005$ M
Concn. of ARS $=0.0002$ M
Temperature $=25$°C

pH	2.80	3.20	4.00	5.30	6.20	7.50	8.10
Optical density per cm. (500 mμ)	0.420	0.740	0.740	0.740	0.740	0.740	0.440

9) Idem., *Kolloid-Z.*, in press.

TABLE IV

Concn. of cupric sulfate = 0.0002 M (12.7 p. p. m.)
Concn. of ARS = 0.001 M
pH of the mixture = 4.00±0.50
Temperature = 25°C

Ion	Added as	Concn. of ion p. p. m.	Observed change in optical density %	Tolerance limit p. p. m.
Ag^+	$AgNO_3$	9	+ 5	0
Tl^+	Tl_2SO_4	96 32	+ 3 + 1	32
Pb^{2+}	$Pb(NO_3)_2$	16	+20	0
Hg_2^{2+}	$Hg_2(NO_3)_2$	32 2	−11 − 1	2
Hg^{2+}	$HgCl_2$	16 6	− 3 − 1.5	6
Bi^{3+}	Bi-oxalate	80	Turbid	0
Cd^{2+}	$CdCl_2$	45 30	+ 3 + 2	30
AsO_3^{3-}	H_3AsO_3	82 41	− 4 − 2	41
Sb^{3+}	$Sb_2(SO_4)_3$	76	Turbid	0
Fe^{3+}	$FeCl_3$	Interferes at all concn.		0
Fe^{2+}	Ferrous ammonium sulfate	Interferes at all concn.		0
Al^{3+}	$Al(NO_3)_3$	Interferes at all concn.		0
Cr^{3+}	$CrCl_3$	16 8	+ 3 + 1.5	8
Mn^{2+}	$MnSO_4$	80 40	+ 4 + 2	40
Zn^{2+}	$ZnSO_4$	11 6	+ 3 + 2	6
Ni^{2+}	$NiSO_4$	80 40	+ 4 + 2	40
Co^{2+}	$CoSO_4$	50 30	+ 3 + 2	30
Ba^{2+}	$BaCl_2$	55	+20	0
Sr^{2+}	$SrCl_2$	21 10	+ 3 + 2	10
Ca^{2+}	$Ca(NO_3)_2$	32 18	+ 3 + 2	18
Mg^{2+}	$MgSO_4$	10 6	+ 3 + 2	6
Be^{2+}	$BeSO_4$	20 8	+ 4 + 2	8
Zr^{4+}	$ZrO(NO_3)_2$	Interferes at all concn.		0
UO_2^{2+}	UO_2SO_4	Interferes at all concn.		0
Th^{4+}	$ThCl_4$	19 10	+ 3 + 2	10
Ce^{3+}	Cerous ammonium sulfate	22 11	− 3 − 1.5	11
Ce^{4+}	$Ce(SO_4)_2$	12 2	− 4 − 1	2

Ion	Added as	Concn. of ion p. p. m.	Observed change in opitcal density %	Tolerance limit p. p. m.
WO_4^{2-}	Na_2WO_4	20	−11	0
MoO_4^{2-}	$(NH_4)_2MoO_4$	Interferes at all concn.		0
VO_3^-	NH_4VO_3	Interferes at all concn.		0
SeO_4^{2-}	K_2SeO_4	12 6	− 3 − 2	6
TeO_3^{2-}	K_2TeO_3	Interferes at all concn.		0
CO_3^{2-}	Na_2CO_3	20 5	+ 3 + 1	5
SO_4^{2-}	K_2SO_4	152	− 0.5	Large excess
Cl^-	KCl	100	− 1	Large excess
Br^-	KBr	128 64	− 3 − 2	64
I^-	KI	50 30	− 3 − 2	30
ClO_3^-	$KClO_3$	34 20	− 3 − 2	20
BrO_3^-	$KBrO_3$	51 16	− 3 − 1	16
IO_3^-	KIO_3	70 20	+ 3 + 1	20
F^-	NaF	8	− 6	0
SiO_3^{2-}	Na_2SiO_3	31 20	− 3 − 2	20
Citrate	Sodium citrate	76 40	− 3 − 2	40
Tartrate	Potassium tartrate	60 20	− 5 − 2	20
Oxalate	Ammonium oxalate	34 9	− 4 − 1	9
NO_3^-	KNO_3	80 60	− 2.5 − 1.5	60
CNS^-	KCNS	48 24	− 3 − 1.5	24
PO_4^{-3}	Na_2HPO_4	38 8	+ 8 + 2	8
$S_2O_8^{-2}$	$K_2S_2O_8$	80 60	− 3 − 2	60
HCO_3^-	$NaHCO_3$	10 4	− 2.5 − 1	4
$S_2O_3^{2-}$	$Na_2S_2O_3$	45 25	− 3 − 2	25
Acetate	Sodium acetate	Interferes at all concn.		0
$B_4O_7^{2-}$	$Na_2B_4O_7$	13	+ 8	0

Influence of foreign ions.—The effect of a large number of cations and anions on the color intensity was studied with the help of the spectrophotometer. The tolerance limits were quantitatively determined. The tolerance limit represents the concentration of a foreign ion, which would affect the optical density of the solution under investigation by less than ±2%. The results are given in Table IV.

Recommended Procedure

For the determination of copper, a solution is prepared and treated to separate the interfering substances as usual[1,10]. The pure copper salt solution thus obtained, is treated directly or with an aliquot portion with a ten-fold molar excess of a freshly prepared aqueous solution, of the reagent. The pH of the solution is adjusted between 4 and 6. The optical density of the solution is then read at 500 mμ, in an absorption cell of suitable thickness. The color intensity can also be measured with a photoelectric colorimeter with an appropriate filter. The temperature of observation should preferably be 20~30°C.

10) E. B. Sandell, "Colorimetric Determination of Traces of Metals", 2nd Ed., Interscience Publishers, Inc., New York (1950), 295.

Summary

The formation of a 1:1 copper chelate with sodium alizarin-3-sulfonate, having λ_{max} at 500 mμ has been reported. The color formation has been applied to the colorimetric determination of copper on a micro-scale. The color has been found to be stable between pH 3.20 and 7.50, at temperatures 20~30°C. The sensitivity of the reagent is 6.4 p.p.m. of the copper ion. The interference by a large number of cations and anions has been studied and the tolerance limits are quantitatively determined spectrophotometrically. It has been recommended that the reagent is suitable for the colorimetric determination of copper(II) on a micro-scale and the conditions have been prescribed.

Chemical Laboratories
University of Allahabad
Allahabad, India

Further Notes on the Ideal Mixture Law for Viscosity

By Tetsuya ISHIKAWA

(Received January, 23, 1958)

Six years ago the author published a paper[1] on the same subject as the above. The previous paper treated the comparison of the validity among the viscosity formulae of Kendall, Macleod, Drucker and Kassel, and Ishikawa with four examples of binary mixtures of the same crystal forms, three being the systems of AgBr-AgCl, $CdCl_2$-$CdBr_2$, and $PbBr_2$-$PbCl_2$, and one being Na-K system, but the present author has thrown some doubt since then on the result of the last pair whose K (Ishikawa's characteristic constant) takes a unique but abnormally greater value, 2.54, throughout the wide temperature range from 103.7 to 192.8°C than the values not so much different from unity for ordinary mixtures composed of like liquids. This paper is intended as a supplementary report on this subject.

Relation between the Formulae—In order to carry on further study, we must consider the relationship between these formulae. For convenience, sake we adopt the following symbols: η_1, η_2 and η signify the viscosities of component 1, 2, and the mixture respectively, φ_1, φ_2 and φ the fluidities of components 1, 2, and the mixture respectively; x_1, x_2, and x so called Macleod's free spaces of 1 cc. of components 1, 2 and the mixture respectively; a_1, a_2 and a the association degrees of component 1, 2 and the mixture respectively and z, z_m and z_v the weight, molar, and volume fraction of component 2 respectively before mixing.

1) T. Ishikawa, This Bulletin, **25**, 38 (1952).

Macleod's formula for ideal mixtures[2]:

$$\left.\begin{aligned}\eta&=\eta_1(1-z_m)\frac{x_1}{x}+\eta_2 z_m\frac{x_2}{x}\\ x&=x_1(1-z_v)+x_2z_v\end{aligned}\right\}\qquad(1)$$

Drucker and Kassel's formula[3]:

$$\varphi=\varphi_1(1-z)+\varphi_2 z\qquad(2)$$

This formula can also be obtained from Macleod's relation, $\eta=K_{\mathrm{M}}Ma/x$ (M is the molecular weight and K_{M} so called "a universal constant" according to his theory[4], and another assumable relation which becomes identical with Macleod's relation for x in Formula 1 in the case of gaseous state where $z_v=z_m$, and $a_1=a_2=a=1$:

$$\frac{x}{a}=\frac{x_1}{a_1}(1-z_m)+\frac{x_2}{a_2}z_m\qquad(3)$$

Ishikawa's formula for ideal mixtures[5]:

$$\eta=\eta_1\frac{k_1a_1(1-z_m)}{k_1a_1(1-z_m)+k_2a_2z_m}+\eta_2\frac{k_2a_2z_m}{k_1a_1(1-z_m)+k_2a_2z_m}\qquad(4)$$

where k_1 and k_2 denote so-called "field constants" of component 1 and 2 respectively according to his theory.

Now if we transform Formula 2 and 4 into hyperbolic forms, we obtain for Drucker and Kassel's formula, remembering $(1-z)/z=(1-z_m)M_1/z_mM_2$,

$$\frac{(1-z_m)(\eta-\eta_1)}{z_m(\eta_2-\eta)}=\frac{\varphi_2M_2}{\varphi_1M_1}\qquad(5)$$

and for Ishikawa's formula,

$$\frac{(1-z_m)(\eta-\eta_1)}{z_m(\eta_2-\eta)}=\frac{k_2a_2}{k_1a_1}=K\qquad(6)$$

Among 63 kinds of liquid pair which satisfy Formula 6[6], there occur four cases, for which Formula 5 holds good with nearly equal values of $\varphi_2M_2/\varphi_1M_1$ and K: trichloroethylene–pentachloroethane, ethyl propionate–propylacetate, toluene–bromobenzene and *m*-cresol–*p*-cresol (see Table I in which parentheses denote the association degrees quoted from Bingham and Spooner's table[7]).

Since each of these pairs consists of the liquids having nearly equal association degrees, i.e., $a_1=a_2$, there may undoubtedly exist the following relation, comparing Formula 6 with Formula 5:

$$\frac{k_2}{k_1}=\frac{\varphi_2M_2}{\varphi_1M_1},\quad\text{or}\quad K=\frac{\varphi_2M_2a_2}{\varphi_1M_1a_1}\qquad(7)$$

From relation 7, it may easily be understood that the fundamental additive law for viscosity with respect to molar fraction:

$$\eta=\eta_1(1-z_m)+\eta_2z_m\qquad(8)$$

is valid only for such pairs where Gartenmeister's relation, $\eta=k_{\mathrm{G}}M$, k_{G} being a constant[8], holds good and at the same time the condition, $a_1=a_2$, is satisfied

A New Method for evaluating Association Degrees—As regards the evaluation of the association degrees of liquids, a few methods have been proposed by several investigators[9-12]. They are individually no other than deviation factors from a statistically deduced constant in some physico-chemical relation which fits normal liquids, so that for the values of highly associated liquids, there is no means among themselves for confirming whether they are probable values or not.

On the other hand, if relation 7 is applied to evaluate the association degrees of liquids, it is convenient to ascertain their values, since for three ideal mixtures, A—B, B—C, and C—A, there exists the known relation:

$$\frac{k_{\mathrm{A}}a_{\mathrm{A}}}{k_{\mathrm{B}}a_{\mathrm{B}}}=\frac{k_{\mathrm{A}}a_{\mathrm{A}}}{k_{\mathrm{C}}a_{\mathrm{C}}}\cdot\frac{k_{\mathrm{C}}a_{\mathrm{C}}}{k_{\mathrm{B}}a_{\mathrm{B}}},\quad\text{hence}$$

$$\frac{\varphi_{\mathrm{A}}M_{\mathrm{A}}a_{\mathrm{A}}}{\varphi_{\mathrm{B}}M_{\mathrm{B}}a_{\mathrm{B}}}=\frac{\varphi_{\mathrm{A}}M_{\mathrm{A}}a_{\mathrm{A}}}{\varphi_{\mathrm{C}}M_{\mathrm{C}}a_{\mathrm{C}}}\cdot\frac{\varphi_{\mathrm{C}}M_{\mathrm{C}}a_{\mathrm{C}}}{\varphi_{\mathrm{B}}M_{\mathrm{B}}a_{\mathrm{B}}}.$$

Macleod assigned *n*-octane as a standard liquid having $a=1$ to determine K_{M}, and with thus obtained $K_{\mathrm{M}}=4.62\times10^{-6}$, he evaluated the association degrees of 28 kinds of liquid. However, the values of highly associated liquids such as *iso*-propyl, *n*-butyl, and *iso*-butyl alcohol seem to be doubtful. Macleod at first proposed a relation, $\eta x^A=$a constant[13], but replaced it two years later with the above quoted relation, $\eta=K_{\mathrm{M}}Ma/x$. Since A in the former relationship depends mainly upon the amount of molecular association, A being nearly unity for most of the normal

2) D. B. Macleod, *Trans. Faraday Soc.*, **20**, 348 (1924).
3) K. Drucker and R. Kassel, *Z. physik. Chem.*, **76**, 367 (1911).
4) D. B. Macleod, *Trans. Faraday Soc.*, **21**, 162 (1925).
5) T. Ishikawa, This Bulletin, **4**, 5 (1929).
6) T. Ishikawa and T. Baba, This Bulletin, **11**, 64 (1936).
7) E. C. Bingham and L. W. Spooner, *Physics*, **4**, 387 (1933).
8) R. Gartenmeister, *Z. physik. Chem.*, **6**, 524 (1890).
9) W. Ramsay and J. Shields, *J. Chem. Soc.*, **63**, 1089 (1893); *Phil. Trans.*, A. **184**, 647 (1893); *Z. physik. Chem.*, **12**, 433 (1893).
10) J. Traube, *Ber.*, **28**, 3292 (1895): **30**, 273 (1897).
11) D. B. Macleod, *Trans. Faraday Soc.*, **20**, 348 (1924): **21**, 162 (1925).
12) E. C. Bingham and J. P. Harrison, *Z. physik. Chem.*, **66**, 1 (1909); E. C. Bingham and L. W. Spooner, *Physics*, **4**, 387 (1933).
13) D. B. Macleod, *Trans. Faraday Soc.*, **19**, 6 (1923).

TABLE I

CASES OF EQUAL MAGNITUDE OF K AND $\varphi_2M_2/\varphi_1M_1$

Component 1	Component 2	t°C	K	$\varphi_2M_2/\varphi_1M_1$	Observers
C_2Cl_3H (0.99～1.02)	C_2Cl_5H (1.02～1.05)	25	0.40	0.389	Herz and Rathman (1913)
$C_2H_5COOC_2H_5$ (1.13～1.20)	$CH_3COOC_3H_7$ (1.16～1.21)	20 40	0.87 0.98	0.922 0.934	Unkovskaja and Volova (1925)
$C_6H_5CH_3$ (1.16～1.14)	C_6H_5Br (1.19～1.05)	20 35	0.86 0.85	0.866 0.878	Yajnik, Bhalla, Talwar and Soofi (1925)
m-$CH_3C_6H_4OH$ (1.81～1.60)	p-$CH_3C_6H_4OH$ (1.82～1.62)	25	0.90	0.910	Kendall and Beaver (1921)

TABLE II

COMPARISON OF TWO VALUES OF ASSOCIATION DEGREES DUE TO MACLEOD

Substance	x(0°C)	A	x^A	$(x)_{A=1}$	a'	a	a'/a
CH_3OH	0.1037	1.5595	0.0291	0.0580	1.99	3.20	0.62
C_2H_5OH	0.09215	1.948	0.00961	0.0450	4.68	3.75	1.25
n-C_3H_7OH	0.0333	1.3237	0.0110	0.0233	2.12	3.26	0.65
iso-C_3H_7OH	0.0559	2.104	0.00231	0.0252	10.9	4.14	2.63
n-C_4H_9OH	0.0563	2.085	0.00248	0.0248	10.0	3.77	2.65
iso-C_4H_9OH	0.0964	3.405	0.000347	0.0243	70.0	5.71	12.26

liquids, there may exist the equality: $x^A=(x)_{A=1}/a'$, where a' is the association degree when x^A can fortunately be reduced to $(x)_{A=1}$. The actual estimation of $(x)_{A=1}$ appears to be too difficult to obtain concordant values of a' with his obtained values of a, as clearly recognized from a'/a in Table II.

The present author, taking the association degrees of n-hexane and carbon tetrachloride as unity, has calculated those of 27 kinds of liquid, each being taken as a possible mean value as stated above (see Table III in which the values obtained by other investigators are also tabullated for reference).

Interpretation for the Abnormal Value of Na—K System—Quite recently Sakai[14] made experiments on the absorption spectra of mixed fused salts and led to the supposition that the great shift of absorption edge to long wave-length side with the rise of temperature may be the degradation of molecular association of component salts in the systems of $PbCl_2$—$PbBr_2$, $CdBr_2$—CdI_2, $CdCl_2$—CdI_2, and $PbCl_2$—$CdCl_2$.

Now we shall return to the pairs $PbBr_2$—$PbCl_2$, $CdCl_2$—$CdBr_2$ AgBr—AgCl, and Na—K.

For $PbBr_2(1)$—$PbCl_2(2)$ system at 510°C, $K=0.33$ and

$$\frac{\varphi_2M_2}{\varphi_1M_1}=\frac{\eta_1M_2}{\eta_2M_1}=\frac{0.0354\times278.12}{0.0495\times367.04}=0.542,$$

$$\therefore\quad \frac{a_1}{a_2}=\frac{0.542}{0.33}=1.64.$$

N.B. The melting points and latent heats of fusion of $PbBr_2$ and $PbCl_2$ are 490°C and 4.530 kcal./g-mol., and 498°C and 5.136 kcal./g-mol. respectively.[15]

For $CdCl_2(1)$—$CdBr_2(2)$ system at 600°C, $K=0.82$ and

$$\frac{\varphi_2M_2}{\varphi_1M_1}=\frac{0.0232\times272.24}{0.0258\times183.32}=1.348,$$

$$\therefore\quad \frac{a_1}{a_2}=\frac{1.348}{0.82}=1.64.$$

For AgBr(1)—AgCl(2) system at 500°C, $K=1.21$ and

$$\frac{\varphi_2M_2}{\varphi_1M_1}=\frac{0.0284\times143.34}{0.0207\times187.80}=1.047,$$

$$\therefore\quad \frac{a_2}{a_1}=\frac{1.21}{1.047}=1.16.$$

N.B. The melting points and latent heats of fusion of AgBr and AgCl are 430°C and 2.365 kcal./g-mol., and 455°C and 3.058 kcal./g-mol. respectively.[15]

For Na(1)—K(2) system at 103.7～192.8°C, K and $\varphi_2M_2/\varphi_1M_1$ are as follows:

°C	103.7	121.5	147.0	167.4	192.8	mean
K	2.61	2.54	2.45	2.51	2.55	2.54
$\varphi_2M_2/\varphi_1M_1$	2.724	2.678	2.638	2.599	2.581	2.644
a_1/a_2	1.043	1.054	1.077	1.035	1.012	1.04

N.B. The melting points and latent heats of fusion of Na and K are 97.7°C and 0.621 kcal/g-atom, and 63°C and 0.508 kcal./g-atom respectively[16].

14) K. Sakai, *J. Chem. Soc. Japan, Pure Chem. Sec*, (*Nippon Kagaku Zassi*), **78**, 1108 (1957).

15) Quoted from International Critical Tables, V. pp. 131—135.

16) Quoted from F. Henning, Wärmetechnische Richtwerte, pp. 14—15.

TABLE III
ASSOCIATION DEGREES OF LIQUIDS

Substance	Ramsay and Shields (16～46°C)	Traube (15°C)	Macleod (0°C)	Bingham and Spooner	This author (20～60°C)
n-C_6H_{14}	—	1.00	0.99	1.03～1.02	1.00
$CHCl_3$	0.92	1.00	1.19	1.02～1.06	1.00
CCl_4	1.01	1.00	1.12	1.09～1.00	1.00
CH_3I	—	1.30	0.90	0.98～1.05	1.00
C_2H_5I	1.01	1.19	0.92	0.99～1.04	1.24
CS_2	1.07	—	1.50	0.93～1.02	1.10 2.10
C_2H_5SH	1.04	—	—	1.05～1.10	1.29
CH_3COCH_3	1.26	1.53	1.66	1.28～1.31	1.74
C_6H_6	1.01	1.18 (16°C)	1.45	1.32～1.22	1.48
$C_6H_5CH_3$	—	1.08	1.15	1.16～1.14	1.40
C_6H_5Cl	1.03	1.00 (20°C)	—	1.10～1.12	1.84
$HCONH_2$	6.18(20～30°C)* 4.85(45～60°C)*	—	—	2.00～3.40	4.93
$C_6H_5NO_2$	0.93	1.47 (20°C)	—	1.23～1.77	1.38
$C_6H_5NH_2$	1.05	1.35 (20°C)	—	1.62～2.03	2.93
C_9H_7N (Quinoline)	0.81	—	—	1.33～1.58	2.32
$C_2H_5OC_2H_5$	0.99	1.00	1.04	1.02～1.06	1.27
CH_3COOCH_3	—	1.48 (0°C)	1.35	1.23～1.33	1.99
$CH_3COOC_2H_5$	0.99	1.25	1.16	1.20～1.25	1.85
CH_3COOH	3.62 2.13(20°C)**	1.56	2.53	1.71～1.95	3.01
H_2O	3.44(20～30°C) 1.64(20°C)**	3.06	—	—	6.79
CH_3OH	3.43 2.32(20°C)**	1.79	3.20	1.93～1.89	2.22
C_2H_5OH	2.74 1.65(20°C)**	1.67	3.75	1.98～1.90	2.44
n-C_3H_7OH	2.25	1.66	3.26	1.92～1.78	2.87
iso-C_3H_7OH	2.86	1.53	4.14	2.01～1.72	2.77
n-C_4H_9OH	1.94	—	3.77	1.85～1.63	2.57
iso-C_4H_9OH	1.95	1.54	5.61	1.95～1.63	2.25
C_6H_5OH	—	1.43 (20°C)	—	1.89～1.71	3.33

* W. E. S. Turner, E. W. Merry, *J. Chem. Soc.*, **1910**, 2069.
** W. Ramsay, *Z. physik. Chem.*, **15**, 111 (1894).

TABLE IV
K AND $\varphi_2M_2/\varphi_1M_1$ VALUES OF ISOMORPHIC COMPOUNDS

Component 1	Component 2	t°C	K	$\varphi_2M_2/\varphi_1M_1$
Stilbene ($C_6H_5CH{:}CHC_6H_5$)	Azobenzene ($C_6H_5N{:}NC_6H_5$)	125	0.862±0.013	1.831
Stilbene	Dibenzyl ($C_6H_5CH_2CH_2C_6H_5$)	125	0.951±0.006	2.361
Stilbene	Benzalaniline ($C_6H_5CH{:}NC_6H_5$)	125	0.902±0.009	2.516
Azobenzene	Dibenzyl	75	1.03 ±0.09	1.290
Azobenzene	Benzalaniline	75	1.03 ±0.02	1.372
Benzalaniline	Benzylaniline ($C_6H_5CH_2NHC_6H_5$)	75	0.992±0.006	1.531

TABLE V
ASSOCIATION DEGREES OF ISOMORPHIC COMPOUNDS AT 125°C

Compound	m.p. °C	Heat of fusion kcal./g-mol.[15]	Association degree at 125°C estimated	calculated from Eq. (1)	Eq. (2)
Benzylaniline	32	4.002	1.00	(1.25)	1.02
Benzalaniline	49	—	1.54	1.56	1.52
Dibenzyl	52	5.649	1.64	1.62	I.61
Azobenzene	68	5.280	2.05	2.02	2.07
Stilbene	124	7.215	4.24	4.27	(3.70)

As judged from Sakai's first and second experimental results summarized in two figures on single salts[17], the temperature variation of absorption edge of $PbBr_2$ is greater than that of $PbCl_2$, and that of $CdCl_2$ is greater than that of $CdBr_2$. These facts run parallel with the here-obtained association degrees, that is, the association degrees, of $PbBr_2$ and $CdCl_2$ are 1.6 times greater than those of $PbCl_2$ and $CdBr_2$ respectively.

Before entering into the study on Na—K system, we shall add two more systems of molten metals of different crystal forms, lead—tin and lead—bismuth[18].

For both cases, Ishikawa's formula holds strictly good (deviations are at most ±1 in the last cipher of absolute viscosity values), giving for Pb(1)—Sn(2) system $K=1.15$(400°C) and 1.03(500°C), $\varphi_2M_2/\varphi_1M_1=0.926$(400°C) and 0.897(500°C); and for Pb(1)—Bi(2) system $K=2.60$(400°C) and 1.58(500°C), $\varphi_2M_2/\varphi_1M_1=1.323$(400°C) and 1.263(500°C), whence we obtain $a_2/a_1=1.24$ (400°C) and 1.16(500°C) for the former pair, and $a_2/a_1=1.97$(400°C) and 1.25(500°C) for the latter pair.

N.B. The melting points and latent heats of fusion of lead, tin, and bismuth are 327.4°C and 1.18 kcal./g·atom, 231.9°C and 1.66 kcal./g·atom, and 271.0°C and 2.72 kcal/g·atom respectively.[16]

In regards to metals, the atomic complexity of bismuth degrades greatly from 1.97 to 1.25; that of tin degrades slightly from 1.24 to 1.16 both for 100° temperature interval, whereas sodium and potassium, judging from the constancy of a_1/a_2 throughout the temperature range, 103.7~192.8°C, may undoubtedly be monoatomic, or else greatly similar in atomic complexity against temperature change, and hence the constant, $K=2.54$ for the pair composed of these metals, is not abnormal, but is typically normal just as the pair of pentachloroethane(1)—trichloroethylene(2) ($K=1/0.40=2.5$) in Table I.

Examples for elucidating the Degradation of Molecular Complexity—The six cases of ideal mixtures[19] composed of isomorphic and greatly similar compounds in chemical constitution as shown in Table IV are those which nearly satisfy the additive law, i.e., $K=1$, but their corresponding $\varphi_2M_2/\varphi_1M_1$ takes something other than unity. This discrepancy, however, would be elucidated in the following way.

From K values of five pairs except the last, the already mentioned condition for three ideal mixtures composed of three kinds of liquids are calculated as follows:

$$0.862\times\frac{1}{0.951}\times1.03=0.933,$$

$$0.902\times\frac{1}{0.862}\times\frac{1}{1.03}=1.016.$$

These values approach nearer to unity, if we take the probable errors of K into account, and therefore the condition is fairly satisfied in spite of a wide temperature difference, 50°, taken in the viscosity measurements.

Since these isomorphic compounds have, according to the observer, equal viscosity values at the temperature of 1° above their melting points (viscosity values relative to that of water at 4°C are 1.3909±0.0037 or ±0.265% deviations from the mean), the molten state at their melting points should be in equal molecular association. Assuming then that the association degree of benzylaniline having the lowest melting point among them is unity at 75°C, the association values of benzalaniline, dibenzyl, and azobenzene have been found from the pairs at 75°C to be 1.54, 1.64, and 2.05 respectively, and by applying these values to the pairs at 125°C the association degree of stilbene has been estimated to be 4.35, 4.07, 4.30 or the mean 4.24.

17) K. Sakai, *J. Chem. Soc. Japan, Pure Chem. Sec.* (*Nippon Kagaku Zassi*), **78**, 138, 306 (1957).
18) R. Arpi, *Z. Metallographie*, **5**, 142 (1914).
19) K. Beck, *Z. physik. Chem.*, **48**, 652 (1904).

These values in the reverse order in Table V are presumably regarded to be the association degrees of any one of these compounds at temperatures of 1°, 57°, 73°, 76°, and 93° above its melting point (temperature differences of each melting point from 125°C). If it be really so, there should exist some simple functional relationship between the association values and their corresponding temperature differences. Taking logarithms of the association values, a, as ordinate and the temperature differences, Δt, as abscissas, we can easily find that a linear relaiton

$$\log a = 0.6365 - 0.00582\,\Delta t \qquad \text{(i)}$$

nearly holds except the lowest value. Next taking a as ordinate and Δt as abscissa, the following simplest relation

$$a = 3.73 - 0.0291\,\Delta t \qquad \text{(ii)}$$

holds except the highest value. Judging from these two trials, it is highly probable that the molecular association of these compounds degrades at first rapidly (logarithmically) in the neighborhood of the melting point, but then gradually with the rise of temperature.

Summary

In the previous paper on the same subject the author made an erroneous explanation on the result of Na—K system.

Comparison of Ishikawa's formula with Drucker and Kassel's formula leads to the new relation, $K = \varphi_2 M_2 a_2 / \varphi_1 M_1 a_1$, from which the association degrees of 27 kinds of liquid have been evaluated.

By the use of this relation, the abnormally high value of K of Na—K system has been proved to be normal.

Two systems of different crystal forms, Pb—Sn and Pb—Bi, and six systems composed of isomorphic compounds, benzylaniline, benzalaniline, dibenzyl, azobenzene, and stilbene are added for elucidating the degradation of atomic or molecular complexity with rise of temperature.

Junior College of Commerce
Nagasaki University
Nagasaki

Resolution of Amino Acids. I. Resolution of Racemic Phenylalanine and γ-Phenyl-α-aminobutyric Acid by Leucine Aminopeptidase

By Atsushi TANAKA* and Nobuo IZUMIYA

(Received February 22, 1958)

Several methods have been described for the resolution of racemic phenylalanine[1,2] and phenylaminobutyric acid[3], but no method involving the asymmetric hydrolysis of the amides of these two racemic amino acids by aminopeptidase has yet been shown. As Smith[4] has reported that the highly active leucine aminopeptidase was prepared easily from swine kidney and found to hydrolyze L-phenylalaninamide at a moderate rate, we tried in the present work to resolve racemic phenylalaninamide and phenylaminobutyric acid amide by making use of the enzyme.

We prepared a partially purified leucine aminopeptidase of Step 4 according to Smith[4] by which phenylaminobutyric acid amide was also found to be hydrolyzed at a higher rate than that for L-phenylalaninamide. For the resolution, the initial substrate concentration was set at 0.1 mol. for DL-phenylalaninamide and 0.05 mol. for DL-phenylaminobutyric acid amide, the course of hydrolysis was followed by measurements of evolved ammonia, and the digest was allowed to stand beyond the point at which analysis reveals the theoretical 50% hydrolysis. In the course of the digestion of phenylaminobutyric

* Present address, Department of Medical Chemistry, Faculty of Medicine, Kyushu University, Fukuoka.

1) J. P. Greenstein, *Advances in Protein Chem.*, **9**, 121 (1954).

2) K. Michi and H. Tsuda, *J. Jap. Biochem. Soc.*, (*Seikagaku*) **29**, 646 (1957).

3) V. du Vigneaud and O. J. Irish, *J. Biol. Chem.*, **122**, 349 (1938).

4) E. L. Smith, "Methods in Enzymology", vol. 2, edited by S. P. Colowick and N. O. Kaplan, Academic Press Inc., New York, (1956), p. 88; D. H. Spackman, E. L. Smith and D. M. Brown, *J. Biol. Chem.*, **212**, 255 (1955).

acid amide, the L-isomer which is remarkably insoluble in water was partly precipitated.

The products of the reaction were separated in two ways: namely, by differential solubility and the use of ion-exchange resin. It was found that the former way is conveniently applied for the separation of the products from DL-phenylaminobutyric acid amide and the latter way is for that of DL-phenylalaninamide.

For the resolution of phenylaminobutyric acid, only one method has been reported by du Vigneaud and Irish[3], which is based on the fractional crystallization of the brucine salt of the racemic formyl derivative. They assigned the L optical configuration to the isomer of $[\alpha]_D^{30}$ +48.8° (in 1 N hydrochloric acid) according to the Lutz-Jirgensons rule and on the basis of the animal feeding experiment. Since the enzyme employed here was completely inactive toward D-leucinamide, and since no D-leucine aminopeptidases have yet been found in animal tissues, it was assumed that the susceptible isomer was L in optical configuration. The digest contained, therefore, L-amino acid and D-amino acid amide at the end of the incubation. L-Phenylaminobutyric acid obtained here possessed $[\alpha]_D^9$ of +48.1° in 1 N hydrochloric acid, which coincides with the results of du Vigneaud and Irish[3].

Experimental

Preparation of leucine aminopeptidase. A partially purified enzyme solution (Step 4 of Smith) was prepared as described[4]. Table I shows the proteolytic coefficients (C_1) of L-amino acid amides. The C_1 of L-leucinamide is included for comparison. The rate of enzyme action on the amides was followed by measurement of the extent of ammonia liberation in Conway micro-diffusion vessels[5]. The rate of hydrolysis ($C_1 \times$ substrate concentration) of phenylalaninamide and phenylaminobutyric acid amide with the enzyme preparation slightly increased with increase in concentration of the substrates.

TABLE I

PROTEOLYTIC COEFFICIENT (C_1) OF AMINO ACID AMIDES BY PARTIALLY PURIFIED LEUCINE AMINOPEPTIDASE*

Substrates	C_1 at different concn. of substrates**		
	0.01 M	0.025 M	0.05 M
L-Leucinamide	5.5	3.6	2.2
DL-Phenylalaninamide	2.4	1.0	0.5
DL-Phenylaminobutyric acid amide***	8.2	3.4	2.1

* Enzyme was preincubated in 0.1 M Tris buffer of pH 8.0 with 0.008 M manganous chloride for one hour at 38°C. Assays were conducted in 0.1 M Tris buffer of pH 8.0 at 38°C with preincubated enzyme added. $C_1 = \log[100/(100-\%\text{ hydrolysis})]/(\text{min.} \times \text{mg. protein } N \text{ per ml. test solution})$.

** Concentrations of L form of substrates.

*** Crystals of L-amino acid appeared after 50~70% hydrolysis.

The effect of various manganous ion concentrations on hydrolysis of the substrates under the same conditions of the resolution was examined. In the presence of manganous ions (0.0005~0.008 M), the apparent increase of hydrolysis was observed in the case of phenylalaninamide, while little effect of the presence of manganous ions was shown with phenylaminobutyric acid amide.

Substrates. *1. DL-Phenylalaninamide hydrochloride.*—This was synthesized from DL-phenylalanine ethyl ester hydrochloride by the same procedure as that for the L form[6]; yield 95%; m. p. 234~236°C (decomp.).

Anal. Found: N, 13.80. Calcd. for $C_9H_{13}ON_2Cl$: N, 13.96%.

2. DL-γ-Phenyl-α-aminobutyric acid.—Procedure[7] Rothstein and Miller's was slightly modified, the yield being remarkably improved. After refluxing the mixture of ethyl acetamidocyanoacetate, sodium and β-phenylethyl bromide in ethanol, the precipitated salt was filtered off and a small amount of acetic acid was added as described in Rothstein and Miller's paper. The filtrate was then evaporated in vacuo to an oil which was changed to crystals by the addition of water. The crystals were collected and washed with water. A part of the crude crystals was recrystallized from ethanol-water; m. p. 116°C. This is ethyl acetamidocyanophenylbutyrate.

Anal. Found: N, 10.36. Calcd. for $C_{15}H_{18}O_3N_2$: N, 10.21%.

The main part of the crude crystals was refluxed with concentrated hydrochloric acid and turned to phenylaminobutyric acid in the usual manner; yield 66% (based on ethyl acetamidocyanoacetate); m. p. 300~302°C (decomp.). The reported melting point is 305~306°C[3].

3. DL-γ-Phenyl-α-aminobutyric acid ethyl ester hydrochloride.—DL-Phenylaminobutyric acid (81g.) was suspended in ethanol (1.5 l.), dry hydrogen chloride was introduced to saturation at room temperature, and the solution was refluxed for one hour. Removal of the solvent in vacuo and treatment of the residue with dry ether yielded crystals. This was recrystallized from ethanol-ether; yield 98 g. (88%); m. p. 135~136°C.

Anal. Found: N, 5.69. Calcd. for $C_{12}H_{18}O_2NCl$: N, 5.75%.

4. DL-γ-Phenyl-α-aminobutyric acid amide hydrochloride.—This was prepared from DL-phenylaminobutyric acid ethyl ester hydrochloride in

5) R. B. Johnston, M. J. Mycek and J. S. Fruton, ibid. **185**, 629 (1950).

6) E. L. Smith and D. H. Spackman, ibid. **212**, 271 (1955).

7) M. Rothstein and L. L. Miller, ibid. **199**, 209 (1952).

the same way as that for the L-phenylalaninamide hydrochloride[6] and recrystallized from methanol-ether; yield 91%; m. p. 214~217°C (decomp.).

Anal. Found: N, 13.21. Calcd. for $C_{10}H_{15}ON_2Cl$: N, 13.05%.

Resolution of DL-phenylalaninamide. *A. Separation method involving ion-exchange chromatography. 1. D-Phenylalaninamide hydrochloride.*—DL-Phenylalaninamide hydrochloride (45.2 g.) was dissolved in water (1.5 l.) containing manganese chloride tetrahydrate (0.224 g.). The pH was adjusted to 7.5 with 1 N aqueous ammonia (about 180 ml.), the enzyme solution containing the equivalent of 2.25 mg. of protein nitrogen was added, and the volume was made up to 2.25 l. After forty hours' incubation at 38°C, the results of ammonia determination indicated complete hydrolysis of the susceptible L-isomer, when the pH of solution was found to be 8.5. The course of a typical hydrolysis is shown in Fig. 1.

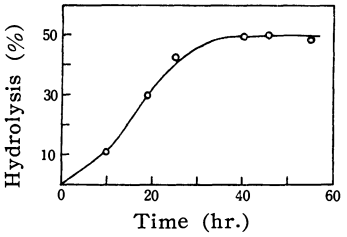

Fig. 1. Time-course of hydrolysis of DL-phenylalaninamide.

The solution that remained clear was passed through a column of Amberlite IRA-400* in the alkaline phase (5 cm.×40 cm.) and water (8 l.) was added to the top of the column. Detection of the amide and ammonia in the fractions was accomplished by means of the Nessler's reagent or the ninhydrin spot test on paper. The fractions were combined and evaporated to dryness in vacuo. The evaporation was repeated several times with addition of ethanol, and the remaining oil was crystallized after being kept in a desiccator for two to three days. The crystals were dissolved in 0.5 N methanolic hydrochloric acid (225 ml.)**. The solution was evaporated to small volume and ether was added. The resulting crystals were collected and recrystallized from methanol-ether; yield 18.6 g. (82%); m. p. 235~237°C (decomp.); $[\alpha]_D^{12}$ −20.4° (c 2, in water).

Anal. Found: C, 53.65; H, 6.55; N, 13.81. Calcd. for $C_9H_{13}ON_2Cl$: C, 53.87; H, 6.53; N, 13.96%.

The reported values for L-phenylalaninamide hydrochloride are $[\alpha]_D^{25}$ +20.7° and m. p. 246°C[6].

2. L-Phenylalanine.—Elution of the L-amino acid from the column was accomplished with 2 N hydrochloric acid (10 l.). Detection of the fractions was accomplished by means of the paper chromatography. The fractions were evaporated to dryness in vacuo three times to remove the excess of hydrochloric acid. The residue was dissolved in water and neutralized with triethylamine. The crystals were recrystallized from hot water-ethanol; yield 17.3 g. (93%); m. p. 270~273°C (decomp.); $[\alpha]_D^{12}$ −34.1° (c 2, in water).

Anal. Found: C, 65.61; H, 6.59; N, 8.26. Calcd. for $C_9H_{11}O_2N$: C, 65.44; H, 6.71; N, 8.48%.

The reported values are $[\alpha]_D^{25}$ −33.35° and m. p. 273~275°C[8].

3. D-Phenylalanine.—D-Phenylalaninamide hydrochloride (4.0 g.) was refluxed with 2 N hydrochloric acid (60 ml.) for five hours and D-phenylalanine was obtained in the usual manner; yield 3.0 g. (91%); m. p. 271~274°C (decomp.); $[\alpha]_D^{9}$ +33.8° (c 2, in water).

Anal. Found: N, 8.41. Calcd. for $C_9H_{11}O_2H$: N, 8.48%.

B. Separation method involving fractional crystallization. 1. L-Phenylalanine.—DL-Phenylalaninamide was resolved as described above. The incubation mixture was evaporated to a small volume and ethanol was added. The resulting crystals were collected and recrystallized from hot water-ethanol; yield 51~55%; $[\alpha]_D^{12}$ −35.1° (c 2, in water).

Anal. Found: N, 8.31. Calcd. for $C_9H_{11}O_2N$: N, 8.48%.

2. D-Phenylalaninamide hydrochloride.—The filtrate and washings from L-amino acid were evaporated to dryness in vacuo and the residue was treated as described later in the preparation of D-phenylaminobutyric acid amide hydrochloride; yield 77~81%; m. p. 234~237°C (decomp.); $[\alpha]_D^{12}$ −20.1° (c 2, in water).

Anal. Found: N, 14.21. Calcd. for $C_9H_{13}ON_2Cl$: N, 13.96%.

Resolution of DL-γ-phenyl-α-aminobutyric acid amide. *1. L-γ-Phenyl-α-aminobutyric acid.*—To DL-phenylaminobutyric acid amide hydrochloride (64.5 g.) dissolved in water, pH being brought to 7.5 with aqueous ammonia, was added the enzyme equivalent to 0.9 mg. of nitrogen. The mixture was made up to 6 l. with water and incubated at 38°C. After about thirty hours beautiful crystals appeared, and after another twenty hours the mixture was cooled for the complete precipitation. The crystals were collected and washed thoroughly with cold water; yield 15.6 g. The filtrate and washings were combined, the additional enzyme equivalent to 0.6 mg. of nitrogen was introduced, and the volume was adjusted to 9 l. After another twenty hours' incubation at 38°C, the results of ammonia determinations indicated complete hydrolysis, no crystals appearing this time. The incubation was continued for another fifteen hours. The course of hydrolysis is shown in Fig. 2. The solution was evaporated to about 150 ml., and the

* In another run, Amberlite IRC-50 in the acid phase, a weak cation-exchange resin, was applied to the separation, but the eluate of the digest contained total amount of L-amino acid with parts of D-amide and ammonia even though a large amount of resin was used.

** The paper chromatography of this solution showed only one spot by means of the ninhydrin test with several solvent systems.

8) S. Sakurai, *J. Biochem.*, **43**, 851 (1956).

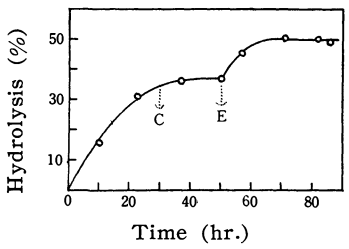

Fig. 2. Time-course of hydrolysis of DL-phenylaminobutyric acid amide. At the point of C, crystals appeared. At the point of E, additional enzyme was added.

resulting crystals were collected; yield 10.5 g. (combined filtrate and washings saved for the D-amide). The combined crystals (26.1 g.) were recrystallized from hot dilute hydrochloric acid-aqueous ammonia; yield 24.5 g. (91%); m. p. 310~313°C (decomp.); $[\alpha]_D^9$ +48.1° (c 1, in 1 N hydrochloric acid).

Anal. Found: C, 66.84; H, 7.44; N, 7.72. Calcd. for $C_{10}H_{13}O_2N$: C, 67.02; H, 7.31; N, 7.82%.

The reported value is $[\alpha]_D^{30}$ +48.8°[3].

2. D-γ-Phenyl-α-aminobutyric acid amide hydrochloride.—The combined filtrate and washings from L-amino acid were evaporated to dryness in vacuo and 5 N sodium hydroxide (75 ml.) was added thereto under cooling. The solution was extracted three times with 3 l. (total volume) of chlorofom. Chloroform solution was dried over sodium sulfate and evaporated to dryness in vacuo. The oily residue was dissolved in 0.5 N methanolic hydrochloric acid (300 ml.), solution was evaporated to small volume, and ether was added. The resulting crystals were collected and recrystallized from methanol-ether; yield 27.2 g. (84%); m. p. 253~254°C (decomp.); $[\alpha]_D^9$ −23.7° (c 2, in water).

Anal. Found: C, 56.12; H, 7.21; N, 12.96. Calcd. for $C_{10}H_{15}ON_2Cl$: C, 55.94; H, 7.04; N, 13.05%.

3. D-γ-Phenyl-α-aminobutyric acid. — This was obtained from D-amide hydrochloride by the same procedure as that for D-phenylalanine; yield 96%; m. p. 308~311°C (decomp.); $[\alpha]_D^9$ −48.7° (c 1, in 1 N hydrochloric acid).

Anal. Found: N, 7.86. Calcd. for $C_{10}H_{13}O_2N$: N, 7.82%.

The reported values are $[\alpha]_D^{30}$ −47.0° and m. p. 323~325°C[3].

Summary

DL-Phenylalaninamide and DL-phenylaminobutyric acid amide were resolved to L-amino acids and D-amino acid amides by the partially purified leucine aminopeptidase preparation.

The products in the digests were separated conveniently by the use of ion-exchange resin, Amberlite IRA-400, in the case of DL-phenylalaninamide, while by the differential solubility in the case of DL-phenylaminobutyric acid amide.

The parts of D-amino acid amide hydrochlorides obtained were changed to D-amino acids by acid hydrolysis.

We wish to express our thanks to Professors S. Shibuya and Y. Yamamura of Kyushu University for their continued interest in this work.

Laboratory of Biochemistry, Faculty of Science, Kyushu University
Fukuoka

The Study of the Adsorption of Detergents at a Solution-Air Interface by Radiotracer Method. I. Adsorption Isotherm for the Solution of Sodium Alkyl Sulfates

By Ryohei MATUURA, Hideo KIMIZUKA, Shigeru MIYAMOTO and Ryosuke SHIMOZAWA

(Received February 6, 1958)

The surface tension lowering properties of detergent solutions are well known and, of course, associated with the adsorption of the detergent at the solution-air interface. The adsorption isotherm is usually discussed on the basis of the Gibbs adsorption equation. However, the Gibbs equation is an ideal, limited equation and it is a problem whether the equation is actually valid for the adsorption of the surface active electrolytes. In the case of an anionic detergent, RNa, the Gibbs

equation may be written as

$$d\gamma = -RT\Gamma_{Na^+} d\ln C_{Na^+} - RT\Gamma_{R^-} d\ln C_{R^-} - RT\Gamma_{H^+} d\ln C_{H^+} \quad (1)$$

where γ is the surface tension of the solution; Γ_{Na^+}, Γ_{R^-} and Γ_{H^+} are amounts of adsorption of sodium ion, detergent anion and hydrogen ion, respectively; and C_{Na^+}, C_{R^-} and C_{H^+} are concentrations of each specified ion. When the concentration of hydrogen ion is kept constant, the equation may be

$$d\gamma = -RT\Gamma_{Na^+} d\ln C_{Na^+} - RT\Gamma_{R^-} d\ln C_{R^-} \quad (2)$$

Without excessive salts or alkali and with a small concentration of the detergent, assuming that $\Gamma_{Na^+}=0$, $\Gamma_{H^+}=\Gamma_{R^-}=\Gamma_{RH}$ and $C_{Na^+}=C_{R^-}=C_{NaR}$, the Eq. 2 becomes

$$\Gamma_{RH} = -\frac{1}{RT}\frac{d\gamma}{d\ln C_{RNa}}. \quad (3)$$

As the concentration of the detergent becomes higher, hydrogen ion may be replaced by sodium ion in the surface layer; hence, assuming that $\Gamma_{H^+}=0$, $\Gamma_{Na^+}=\Gamma_{R^-}=\Gamma_{NaR}$ and $C_{Na^+}=C_{R^-}=C_{NaR}$, the Eq. 2 results in

$$\Gamma_{NaR} = -\frac{1}{2RT}\frac{d\gamma}{d\ln C_{NaR}}. \quad (4)$$

In discussing on the basis of the Gibbs equation the adsorption of the detergent solution without excess salts or alkali, either Eq. 3 or Eq. 4 should be applied if either of the above assumption is satisfied. The problem is to measure the adsorbed amount directly and to compare the result with that calculated from the surface tension data using Eq. 3 or Eq. 4.

Recently the possibility of using radiotracers for the direct measurement of adsorption of detergents at the solution-air interface was developed by Dixon et al.[1], Aniansson and Lamm[2] and Hutchinson[3]. The method in general consists, though in detail some differences exist among the authors, in measuring the difference between radioactivity of tagged surface active agents in the surface adsorbed layer plus bulk solution and that in bulk solution alone. Since then, the method has actually been applied by some authors to the adsorption of respective detergent from the solutions of di-*n*-octyl sodium sulfosuccinate (Aerosol OTN)[4], potassium palmitate[5] and sodium dodecyl sulfate (abbreviated as SDS)[6-8]. The method has proved very successful for the study of adsorption of a detergent from mixtures, for example, the adsorption of Aerosol OTN from the solution of mixture of Aerosol OTN and Aerosol OT (di-2-ethylhexyl sodium sulfosuccinate) has been measured by Judson et al.[9] by tagging Aerosol OTN. Similar measurements have been made on the adsorption of sodium hexadecyl sulfate (abbreviated as SHS)[10,11] and of sodium tetradecyl sulfate (abbreviated as STS)[12] both in the presence of excess SDS, by tagging the former detergents. Nilsson has measured the adsorption of tritiated SDS and dodecanol in the presence of STS and SDS respectively[8].

The radiotracer method has also been applied to the investigation of gegen-ion adsorption from the detergent solutions, as, for example, the adsorption of the sulfate ion in solutions of some cationic, anionic and non-ionic surface active agents[13,14] and of sodium ion in solutions of SDS[3] and Aerosol OTN[15]. Further, the co-adsorption of metal ions with surface active agents has been studied by Aniansson and Steiger by making use of α-recoil atoms[16,17].

All these works have given us some interesting information which could not have been directly obtained before, as to the nature of the adsorption of detergents at the solution-air interface. Especially the validity of the Gibbs adsorption equation has been checked by a couple of authors. Salley et al.[4], Roe and Brass[5] and Ruyssen[6] obtained in the case of Aerosol OTN, potassium palmitate and SDS, respectively, the results that the adsorption

1) J. K. Dixon, A. J. Weith, Jr., A. A. Argyle and D. J. Salley, *Nature*, **163**, 845 (1949).
2) G. Aniansson and O. Lamm, ibid. **165**, 357 (1950).
3) E. Hutchinson, *J. Colloid Sci.*, **4**, 599 (1949).
4) D. J. Salley, A. J. Weith, Jr., A. A. Argyle and J. K. Dixon, *Proc. Roy. Soc.* (London), **A203**, 42 (1950).
5) C. P. Roe and P. D. Brass, *J. Am. Chem. Soc.*, **76**, 4703 (1954).
6) R. Ruyssen, *Bull. soc. chim. Belges*, **62**, 97 (1953).
7) R. Ruyssen and J. Maebe, *Mededel. Koninkl. Vlamm. Acad. Wetenschap, Belg. Kl. Wetenschap.*, **15**, No. 4, 15 (1953).
8) G. Nilsson, *J. Phys. Chem.*, **61**, 1135 (1957).
9) C. M. Judson, A. A. Argle, J. K. Dixon and D. J. Salley, *J. Chem. Phys.*, **18**, 1302 (1950).
10) G. Aniansson, *J. Phys. Chem.*, **55**, 1286 (1951).
11) R. Loos, *Mededel. Koninkl. Vlamm. Acad. Wetenschap, Belg. Kl. Wetenschap.*, **13**, 3 (1951).
12) G. Nilsson and O. Lamm, *Acta Chem. Scand.*, **6**, 1175 (1952).
13) C. M. Judson, A. A. Argyle, J. K. Dixon and D. J. Salley, *J. Chem. Phys.*, **19**, 378 (1951).
14) C. M. Judson, A. A. Lerew, J. K. Dixon and D. J. Salley, *J. Phys. Chem.*, **57**, 916 (1953).
15) C. M. Judson, A. A. Lerew, J. K. Dixon and D. J. Salley, *J. Chem. Phys.*, **20**, 519 (1952).
16) G. Aniansson and N. H. Steiger, ibid. **21**, 1299 (1953).
17) N. H. Steiger and G. Aniansson, *J. Phys. Chem.*, **58**, 228 (1954).

of the detergent at the solution-air interface takes place in accordance with the Eq. 3, provided the solution is dilute. However, the problem has not been treated for a series of surface active agents which have a similar structure but different surface activity. The investigation of the adsorption isotherm of various detergents at the solution-air interface in relation to their surface activity is an important problem in elucidating the nature of surface active agents. So we started to study the problem with application of the radiotracer method to the adsorption of a series of sodium alkyl sulfates at the solution-air interface. The present paper describes the results of the study of the adsorption isotherm for the aqueous solutions of SDS, STS and SHS.

Experimental

Materials.—The alkyl sulfates used were synthesized from corresponding fatty alcohols and concentrated sulfuric acid according to the method written in the text of Sisley[18]. The monoester was neutralized with alkali. The sodium alkyl sulfate thus produced was extracted several times with butanol[19]. By heating the butanol extract, water was removed, and the precipitated inorganic salts were separated from the solution by filtration. Then the sodium alkyl sulfate was recrystallized from the filtrate. The crystal was washed with a large amount of ether several times to remove unsulfated alcohol[20]. The result of elementary analysis verified the purity of the sodium alkyl sulfates within an experimental error. The surface tension-concentration curves for three detergents are shown in Fig. 8, which shows no minima and the values of cmc observed are in good agreement with those in literature[21].

Pure fatty alcohols were prepared by fractional distillation of commercial ones in vacuum, followed by redistillation of the fraction with conditions as shown in Table I.

TABLE I

CONDITIONS FOR THE DISTILLATION AND THE MELTING POINT OF ALCOHOLS

Alcohol	Pressure (mmHg)	Distillation temp. (°C)	m. p. (°C)
Dodecyl alcohol	20	149.6~149.8	23.5~24.5
Tetradecyl alcohol	15	167~168	37.5~38.5
Hexadecyl alcohol	17	192~193	48.5~49.5

Butanol and ether used for extraction and recrystallization were purified by redistillation of pure commercial ones, and concentrated sulfuric acid and alkali were extra pure reagents.

The sulfur-35 was obtained from the Radiochemical Center, England, as a carrier-free sodium sulfate solution. It was converted into sulfuric acid by ion-exchange resin and was isotopically diluted by a small amount of sulfuric acid. This was concentrated and used for synthesis of radioactive sodium alkyl sulfates in the manner as stated above. The specific radioactivity of the labeled sodium alkyl sulfates thus prepared was ca. 10 mc. per millimole for SDS and SHS and 2 mc. per millimole for STS.

Method.—The procedure used for measurement of surface excess of a radioactive detergent in aqueous solutions was essentially similar to that described by Aniansson[10]. The apparatus used in the present experiment is shown in Fig. 1. A lucite cuve A, 5.6 cm. in inner diameter and 0.2 cm. in depth, filled exactly to the brim with the radioactive solution, is fitted exactly to the brass table B, 5.6 cm. in diameter, as shown in the figure. The thickness of the wall of A was all 0.2 cm. The Geiger-Müller tube C (GM-132, an end window type of special use for soft β-ray) is supported by a brass cylinder D with

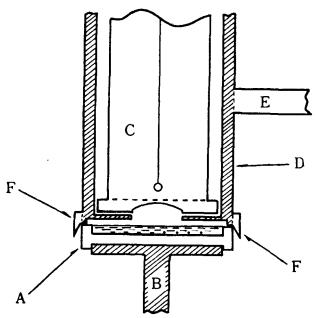

Fig. 1. The measuring apparatus.

an arm E which is fixed to a universal stand. This enables us to move the Geiger-Müller tube up and down precisely. A brass ring F, 6.0 cm. in inner diameter which is identical with the outer diameter of the cuve A, is fixed to D so that tight fitting of the arrangement and reproducibility of the geometric condition can be realized with ease. The distance between the surface of the solution and the Geiger-Müller tube window is 0.15 cm. This small distance enables us to give a low gas volume over the surface. Since the counting of the radioactive sulfuric acid solution was shown to be constant within an experimental error, 5%, over a period of several hours, the evaporation effect may be ignored during the time interval of the present experiment. The whole arrangement was set in an air thermostat to maintain a constant temperature during the experiment. The fresh

18) J. P. Sisley. "Encyclopedia of Surface Active Agents", translated from the French and revised by P. J. Wood, Chem. Pub. Co. Inc., New York, N. Y. (1952).
19) E. E. Dreger, G. I. Keim, G. D. Miles, L. Shedlovsky and J. Ross, *Ind. Eng. Chem.*, **36**, 610 (1944).
20) G. D Miles and L. Shedlovsky, *J. Phys. Chem.*, **48**, 57 (1944).
21) T. Powney and C. C. Addison, *Trans. Faraday Soc.*, **33**, 1243 (1937); **34**, 372 (1938); L. Shedlovsky, J. Ross and C. W. Jacob, *J. Colloid Sci.*, **4**, 25 (1949); G. D. Miles, *J. Phys. Chem.*, **49**, 71 (1945); A. P. Brady, ibid., **53**, 56 (1949).

and plane free surface of the solution in the cuve was easily obtained by sweeping away the surface of the solution with a glass plate, about 7 cm. in width and 8 cm. in length. Both the lucite cuve and the glass plate were coated with a thin layer of paraffin to avoid wetting by the solution, and before use they were rinsed with tap water for a few hours, followed by final washing with distilled water. After the plane-free surface was formed, the Geiger-Müller tube was put down into the measuring arrangement and the intensity of radiation from the solution was measured.

The surface excess, Γ (in mole per cm^2), is calculated according to the equation

$$\Gamma = \frac{I_d - I_i}{SA}, \tag{5}$$

where I_d is the intensity (count per min.) of radiation due to the detergent solution; I_i, that (count per min.) due to the sulfuric acid solution which is the same in both specific activity and molar concentration as the detergent solution; S, the specific activity of the detergent in count per min. per mole, and A, the surface area of the solution in cm^2.

Of these quantities, S was obtained by means of the procedure as reported by Aniansson[10]. A solution of sodium alkyl sulfate was used for the determination of S. Evaporating about 2×10^{-3} cc. of a solution of radioactive sodium alkyl sulfate dropped as a point at the center of a polished lucite plate, it was then placed in the same position as the surface of the solution under the Geiger-Müller tube and counted. The volume of the dropped solution was accurately known by using a micropipette. The lucite plate was used for the measurement of S to avoid the error resulting from the difference in back-scattering effect of water and the material of the plate[10]. Sodium alkyl sulfate dropped was 6×10^{-7} g., so that the error due to the self-absorption could be negligible. The plate was placed at the same distance from the window as the solution surface. First the point source was located at the center line of the Geiger-Müller tube and the radiation was counted (S_0). Then the plate was moved horizontally so that the point source would have a distance r from the center line and counted (S_r). The relative counting efficiency η_r may be given by S_r/S_0. In Fig. 2 the $\eta_r \sim r$ curve is plotted. Now the overall counting efficiency, η, relative to that of the center can be computed by the following equation

$$\eta = \frac{\int_0^R 2\pi r \eta_r dr}{\int_0^R 2\pi r dr}, \tag{6}$$

where R is the radius of the surface of the solution, 2.8 cm. in the present apparatus. The value of η can be determined by graphical integration using the Fig. 2. It was found that η was 0.2237 in the present experiment. The specific activity S is given by $S_0\eta$. The values of S thus calculated for the three detergents were 7.730×10^{10} counts per min. per mole for SDS, 3.075×10^{10} counts per min. per mole for STS and 10.96×10^{10} counts per min. per mole for SHS at the given geometry in the present experiment. In Fig. 3 I_i is plotted as a function of the concentration of sulfuric acid used for the determination of I_i. This figure shows that over a range of concentration studied I_i can be expressed by an equation

$$I_i = I_0 C, \tag{7}$$

where C is the concentration of sulfuric acid and I_0 is the intensity of radiation due to 1 M sulfuric acid. Using the relation I_i of sulfuric acid of any concentration can be obtained.

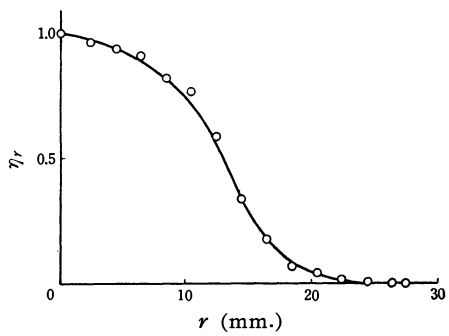

Fig. 2. The counting efficiency relative to that of the center.

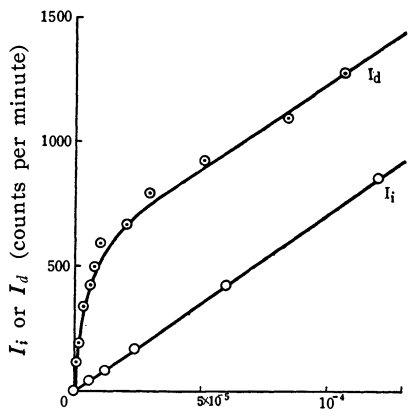

Fig. 3. The surface counts vs. concentration curves. I_i, sulfuric acid solution and, I_d, SHS solution, 28±1°C.

I_d for SHS, as an example, is also shown in Fig. 3, for comparison with I_i, as a function of the concentration of the detergent solution. Since the surface adsorption of the detergent increases with time, I_d is a function of time. I_d plotted in Fig. 3 is the value after the adsorption equilibrium has been attained. Using this figure, I_d—I_i for the same concentration is read off easily and then, knowing S as stated above, the surface excess Γ can be calculated by the Eq. 5. The

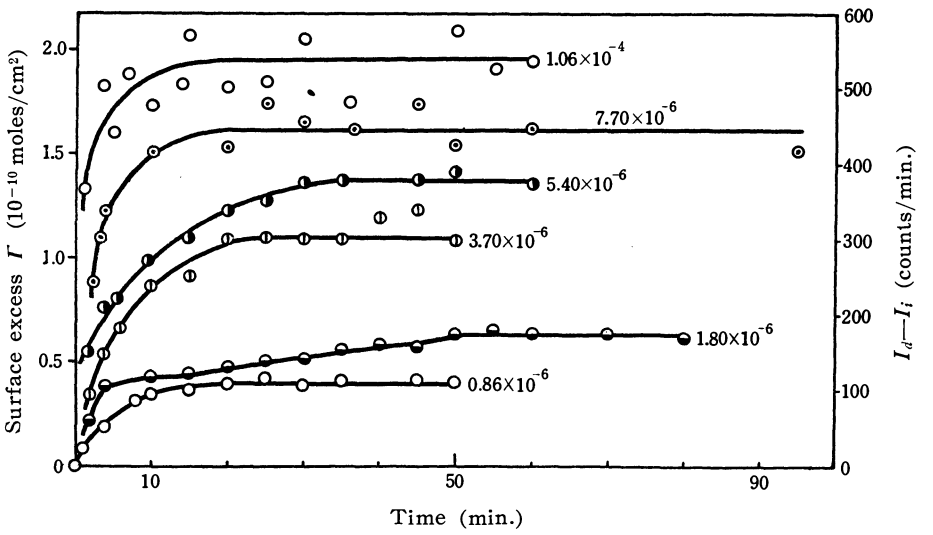

Fig. 4. Surface excess vs. time curves of SHS solution, 28±1°C. Numericals in this figure show the concentration (moles/l.) of the detergent.

same treatment can be done for the other detergents. In this case $I_d - I_i$ should be considerably greater than the statistical error of the value of I_i or I_d; otherwise the reliable value of the surface excess could not be obtained. As the concentration of the detergent solution becoms higher, the ambiguity of this source is introduced and the measurement of an accurate value of the surface excess becomes increasingly difficult. Actually in the case of SDS solution this was the case, and no data of sufficient accuracy could be obtained for this detergent at higher concentrations.

The surface tension of the detergent solution was measured by the Wilhelmy plate method. The plate was of a thin glass and mounted on a Langmuir trough assembly.

Results and Discussion

The surface adsorption of the sodium alkyl sulfates studied in the present experiment reached the equilibrium within about an hour in every case. As an example, the surface excess of SHS is plotted against time in Fig. 4. The equilibrium is reached faster, as the concentration of the solution is higher.

The equilibrium surface excess is plotted against logarithmic concentration for SDS, STS and SHS solutions in Figs. 5, 6 and 7, respectively. The results of the measurement of Γ at different temperatures are also plotted in these figures, which indicate that the effect of temperature is not so appreciable over the range studied in the present experiment. It is seen from these figures that the surface excess has a tendency of taking a saturation value

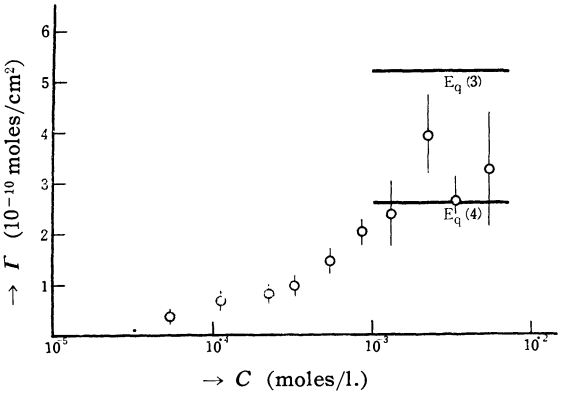

Fig. 5. Surface excess vs. concentration of SDS. 28±1°C. Full lines represent calculated relations from $\gamma \sim \log C$ curves by using Eq. 3 and Eq. 4 at 28°C.

below cmc for every detergent solution.

The surface tension *vs.* logarithmic concentration data on aqueous solutions of sodium alkyl sulfates are represented graphically in Fig. 8, in which surface tension observed are those of the surface of the solution aged for an hour. It is shown that an approximately linear relation exists between γ and $\log C$ below cmc for each detergent solution. The linear portion of the $\gamma \sim \log C$ relation corresponds, although approximately, to the saturation of the surface excess obtained in the present experiment. The values of Γ calculated for this region by using Eq. 3 and Eq. 4 are shown in Figs. 5—7 for the three detergents studied. It is seen that the experimental data lie between

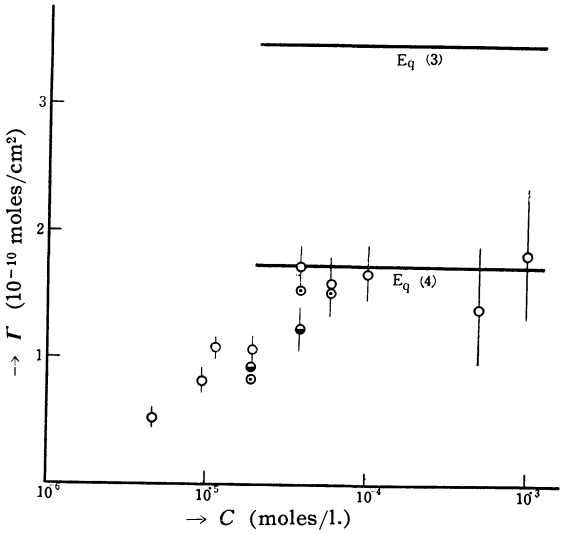

Fig. 6. Surface excess vs. concentration of STS. ○ 28±1°C; ⊙ 40±1°C; ◒ 22±1°C. Full lines represent calculated relations from $\gamma \sim \log C$ curves by using Eq. 3 and Eq. 4 at 28°C.

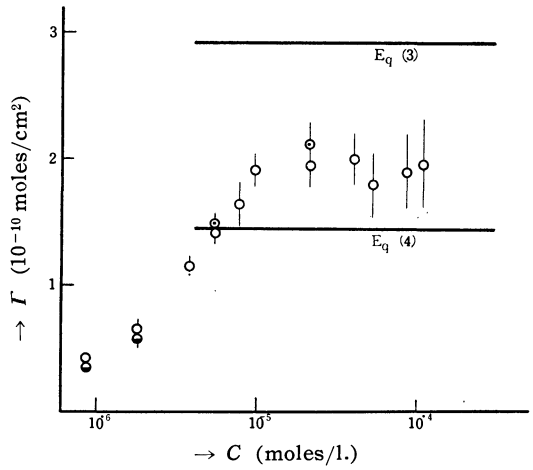

Fig. 7. Surface excess vs. concentration of SHS. ○ 28±1°C; ⊙ 40±1°C; ◒ 22±1°C. Full lines represent calculated relations from $\gamma \sim \log C$ curves by using Eq. (3) and Eq. (4) at 28°C.

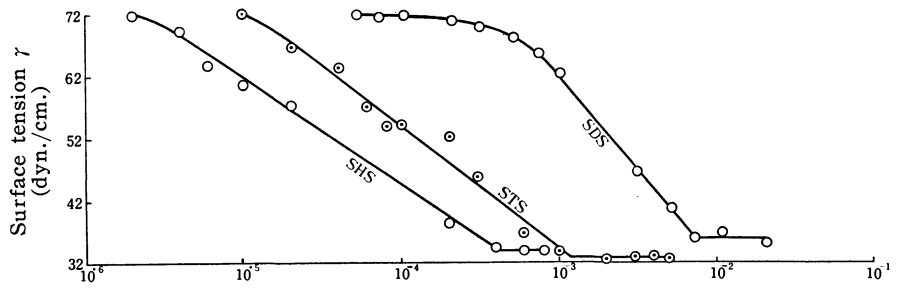

Fig. 8. Surface tension vs. concentration curves, 28±1°C.

the values of Eq. 3 and those of Eq. 4. It is to be noticed that Eq. 3 and Eq. 4 are ideal equations which are valid only if the conditions assumed in the derivation of each equation are perfectly fulfilled. The present results may show that the conditions are not so complete as to permit strict application of Eq. 3 or Eq. 4. It could be said, however, that, as a whole, the experimental points are near the values of Eq. 4 rather than those of Eq. 3 over the concentration range near cmc. Further discussion and the definite conclusion will be postponed until the accuracy of the measurements of both adsorption and surface tension at higher concentration region is improved much more.

By comparing the data of adsorption of three detergents, it is evident that the bulk concentration corresponding to the same surface excess, below the saturation of the adsorption, is lowered as the chain length of the detergent molecule increases. This is what should be expected from the surface tension lowering properties of the three detergents as shown in Fig. 8.

Summary

The adsorption of the three alkyl sulfates, SDS, STS and SHS, at the solution-air interface has been measured directly by means of the radiotracer method. It has been proved that the surface adsorption increases with increase in the concentration and has a tendency to be saturated

at concentrations near cmc for each detergent solution. The results have shown that the adsorption increases with increasing chain length. The Gibbs adsorption equation has been cheked and discussed.

Department of Chemistry, Faculty of Science, Kyushu University
Hakozaki, Fukuoka

*On the Nature of the Red Adduct of Styrene with Sodium**

By Kozo HIROTA, Keiji KUWATA and Kazuo MORIGAKI

(Received February 13, 1958)

As shown independently by Szwarc et al.[1] and by Meshitsuka and Okada[2], the red complexes or adducts formed between styrene and sodium have an interesting property as chain initiators; i. e., in some suitable solvents, the adducts produce living polymers which can grow when a monomer is added. According to Szwarc, the living polymers result from the dimerized styrene anions with both ends "living":

$$(A)\quad (:CHX—CH_2—CH_2—CHX:)^{=} \quad (X=C_6H_5)$$

this bivalent anion is formed by dimerization of univalent monomer anions,

$$(A')\quad (:CHX—CH_2\cdot)^- \text{ or}$$

$$(A'')\quad (\cdot CHX—CH_2:)^-$$

which are produced by the electron transfer process from naphthalene anions:

$$\text{Naphthalene}^- + \text{Styrene} \rightarrow \text{Naphthalene} + \text{Styrene}^-. \qquad (1)$$

However, the proposed formula A as the initiator of the chain polymerization seems to lack firm experimental evidences.

Recently[3] two of the present authors found that there exist two other modifications in styrene adducts, blue and yellow, besides the familiar red one. Comparing the absorption spectra of these adducts with those of α-methylstyrene and *p*-divinylbenzene, not only as a dissolved state but also as a filmy state, they reached some conclusions as to the nature of styrene adducts. The adducts which were used in the research mentioned above were, however, slightly different from those of Szwarc et al. in two points; (a) the adducts** are prepared directly from styrene and metallic sodium immersed in solvents, and (b) the solvents may be non-polar ones, e. g., benzene and toluene as well as polar solvents hitherto reported (dimethylether, tetrahydrofuran, etc.).

In the above paper it is one of the conclusions that the adducts, which dissociate into sodium ions and such anions as shown by the structure A' or A'', constitute one of the stable red adducts whose absorption maximum is 510 mμ as reported already[2]. It is the object of the present paper to reinforce the conclusion further with the paramagnetic resonance absorption measurement.

Experimental Method

Samples.—The apparatus, as shown in Fig. 1, is used to prepare most of the samples. The details of the operations will be omitted, as it has already been described[4]. Thus it was made possible generally to produce the pure adduct of aromatic hydrocarbons, e. g., styrene which was used in the present paper.

Measurement of the Paramagnetic Resonance Absorption. — The conventional apparatus which was constructed by Professor J. Itoh of Osaka University was used. The details of the measurement will be published elsewhere.

* The third report of "The research on the adduct of styrene with alkali metals": I., ref. 4, II., ref. 3.

1) M. Szwarc, M. Levy and R. Milkovitch, *J. Am. Chem. Soc.*, **78**, 2656 (1956); M. Szwarc, *Nature*, **178**, 1168 (1956), etc.

2) G. Meshitsuka and Y. Okada, *Chemistry of High Polymers*, (*Kobunshikagaku*), **14**, 33, 37, 123 (1957).

3) K. Hirota, K. Kuwata, H. Togawa and S. Ishida, *J. Chem. Soc. Japan, Pure Chem. Sec.* (*Nippon Kagaku Zassi*), **79**, 602 (1958).

** According to the present method, the sample is free from other substance, when compared with the samples prepared indirectly by the electron transfer method, such as by Eq. 1.

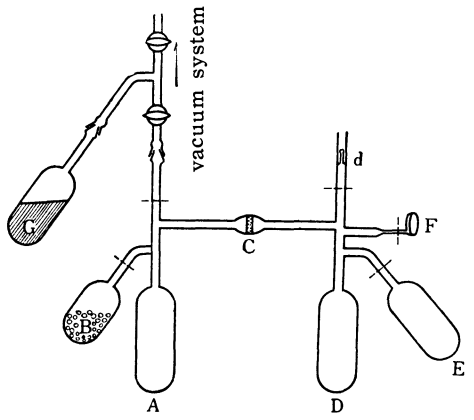

Fig. 1. Apparatus for preparation of samples
A: Reaction vessel, B: Sodium which will be vacuum-distilled into A, C: Glass filter, D: Storage vessel, E: Vessel for waste product, F: Sample cell for P. S. R. measurements, G: Styrene or toluene which will be vacuum-distilled into A, d: Breakable joint.

Results and Discussion

In the previous report[3], the structure A′ or A″ was assigned to the red adduct of styrene rather than the Szwarc's structure A from the results of absorption spectrometry. Now there will be another method of decision of this problem. Because there exists an unpaired electron in the structure A′ or A″, the paramagnetic resonance absorption may be observed if it is true, while the absorption will not be observed if the structure A is true. The measurement carried out at 9400mc by the present writers in tetrahydrofuran solution at the concentration of 10^{-2} molar could confirm the above presumption*. One of the absorption curves is shown in Fig. 2. The Szwarc's structure A, therefore, will not be justified. In sharp contrast with naphthalene anion having seventeen or twenty-three hyperfine splitting[5], the hyperfine

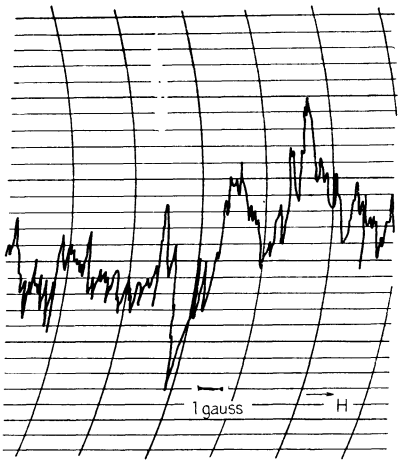

Fig. 2. Paramagnetic Resonance Absorption curve.

structure of the styrene anions seemed to consist of two lines with small intervals, but the decision which is more probable of the two structures, A′ or A″, could not be reached owing to the poor sensitivity of the apparatus. As the problem is very important in structural chemistry, further research is going on with an improved apparatus**.

Summary

Paramagnetic resonance absorption could be observed on the solution of the pure red adduct, which was prepared according to the method reported by the present writers. The adduct, therefore, produces a radical anion consisting of odd electrons by dissociation. The proposition on the structure of the red adduct in the previous report was thus confirmed.

The writers express sincere thanks to Professor Junkichi Itoh of Osaka University who made the measurement of the paramagnetic resonance absorption possible.

Faculty of Science, Osaka University
Kita-ku, Osaka

4) K. Hirota and K. Kuwata, ibid., **78**, 1421 (1957).
5) T. R. Tuttle, Jr., R. L. Ward, and S. I. Weissman, *J. Chem. Phys.*, **25**, 189 (1956), (17 splitting). S. I. Weissman, T. R. Tuttle and E. de Boer, *J. Phys. Chem.*, **61**, 28 (1957).
6) D. E. Paul, D. Lipkin and S. I. Weissman, *J. Am. Chem. Soc.*, **78**, 116 (1956).
* It might be necessary to refer to the Weissman's answer in discussion (*J. Phys. Chem.*, **57**, 507 (1953)) that "the paramagnetic absorption in styrene as it is undergoing polymerization initiated by metallic sodium" is not reproducible.

** Moreover the absorption may occur owing to the interaction with the proton at para-position, but such a probability will be neglected owing to the reactivity of that position.
Note added in proof: It is found that much more hyperfine structure lines can be observed in the samples made under different experimental conditions.
June 13, 1958.

Polymerization of Olefins with Trialkylboron Catalysts. II. Polymerization of Styrene

By Nobuyuki ASHIKARI

(Received February 22, 1958)

The previous work[1] in these series has shown the polymerization of vinyl chloride and acrylonitrile with trialkylboron catalysts. In the present paper the polymerization of styrene with the same catalysts is studied.

The rate of polymerization of styrene is rather smaller, in bulk system, than that of vinyl chloride or acrylonitrile. But in the emulsion system, the rate of polymerization was large and also the molecular weight of the polymer was very high.

Generally, in the polymerization of vinyl compounds with trialkylboron catalyst, it was considered that the reaction velocity and the yield of the polymer were influenced a good deal by an amount of oxygen in the reaction vessel. The degree of the influence, of course, will vary according to the sort of olefin. In this respect, the influence of oxygen in the polymerization of styrene was considered to be not very large. But, by way of precaution, the experiments in this paper were done under nitrogen stream or in a sealed tube in which the air was replaced by nitrogen. Some properties of the polymer prepared with tri-*iso*-propylboron were studied.

Experimental and Results

Preparation of the catalysts.—In a previous paper[1], the detail of the preparation of triethylboron was reported. Here, the detail of the preparation of tri-*iso*-butylboron is explained chiefly. In the cases of tri-*iso*-butyl- and tri-*iso*-propylboron, the preparations were done according to the general method, i. e., the reaction of Grignard reagent and borontrifluoride, as well as the case of triethylboron.

Triisobutylboron.—To ethereal solution of *iso*-butylmagnesiumbromide prepared by the reaction of 24 g. (1 mol.) of magnesium piece and 137 g. (1 mol.) of *iso*-butylbromide in 500 cc. three necked flask, 40 g. (0.28 mol.) of borontrifluoride etherate was dropped slowly under cooling. After the dropping was over the stirring was continued for twenty minutes.

The ethereal solution was cooled and decanted into a distilling flask. The residue consisting of magnesium halide and unchanged *iso*-butylmagnesiumbromide was treated with unhydrous ether, and the trialkylboron involved was extracted. The ethereal solution was added to the first ethereal solution, and the solvent was distilled off. The distillate of b. p. 188~195°C was collected. Thus, 34 g. of tri-*iso*-butylboron was obtained, corresponding to 56.6% yield from magnesium.

Tri-iso-propylboron. — Tri-*iso*-propylboron was prepared, by the same method, by dropping borontrifluoride etherate to isopropylmagnesiumbromide in ether.

Comparison of the rate of polymerization in bulk- and emulsion system.—The rate of polymerization in bulk- and emulsion system was compared in the following experiments. In these experiments the ratio of catalyst to monomer is constant, that is, 80 g. of monomer, and 0.296 g. of tri-*iso*-butylboron were used. Therefore, the ratio of catalyst to monomer is 0.21%.

The reactions were caused to proceed at 40°C under nitrogen stream which was purified by passing through an aqueous pyrogallol-alkali solution and drying over calcium chloride. A certain weight of monomer or a certain weight of monomer and water, was placed in a four-necked flask which was dipped in a constant-temperature bath.

A stirrer, a stopper, and a passage of nitrogen gas were connected to the flask. When the temperature of the contents reached 40°C, the catalyst was added.

After a certain interval of reaction, 10 g. of the sample was taken out from the reaction vessel, and poured into methanol. And then, the polymer contained in the sample was separated from styrene monomer, filtered, dried under reduced pressure at 50°C, and weighed. In the case of emulsion system, the sample taken out was treated with 5% aqueous sodium chloride solution, and the polymer was separated. Then, the polymer was washed fully with water, dried, and weighed.

Fig. 1 represents the relation between the conversion and the reaction time.

1) N. Ashikari, This Bulletin **31**, 229 (1958).

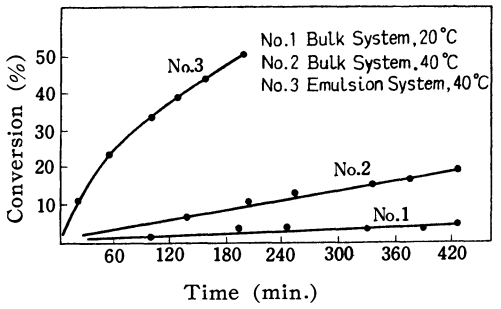

Fig. 1. The rate of polymerization in bulk- and emulsion-system.

In Fig. 1, No. 1 and No. 2 are the cases of bulk-system and No. 3 is the case of emulsion system. From Fig. 1, it is clear that the rate of polymerization in emulsion system is larger than that in bulk system. Especially, in No. 3, 80 g. of aqueous solution which contained 5% of emulsifier was used, so that the ratio of catalyst to the whole solution was very small.

The relation between the conversion and the concentration of catalyst.— A certain weight of monomer (18 g.) and a certain weight of tri-*iso*-propylboron were sealed in a nitrogen-replaced tube, and the polymerization was caused to proceed at 40°C. After ten hours reaction, each sealed tube was opened and the contents were poured into methanol. Thus, the polymer contained was separated from the monomer, filtered, dried under reduced pressure at 50°C, and weighed. The results are shown in Table 1.

TABLE I
THE RELATION BETWEEN THE CONVERSION AND THE CONCENTRATION OF CATALYST

Expt. No.	4	5	6	7	8
catalyst (%)[a]	0.0835	0.1670	0.2505	0.3340	0.4175
polymer (g.)	3.553	4.245	4.540	4.712	4.500
conversion (%)	19.74	23.58	25.22	26.18	25.00

a: catalyst/monomer mol ratio.

Molecular weight of polystyrene.— Each sample in Table 1 was dissolved in pure toluene and the viscosity was measured at 30°C with Ubbelohde viscometer. The intrinsic viscosity, $[\eta]$, was obtained from Fig. 2, in which is plotted η_{sp}/C against concentration (C), where η_{sp} represents a specific viscosity.

The molecular weight was calculated from the intrinsic viscosity with Alfrey's equation[2]; $[\eta]=0.55\times10^{-4}\,M^{0.81}$. The intrinsic viscosities and the molecular weight of the samples polymerized in bulk- and emulsion system were shown in Table II.

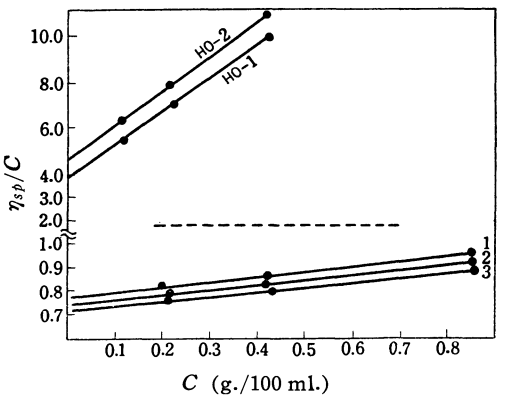

Fig. 2. Viscosity η_{sp}/C vs. C curves for polystyrene

TABLE II
THE INTRINSIC VISCOSITY AND MOLECULAR WEIGHT OF POLYSTYRENE

Exp. No.	4	5	6	HO-1	HO-2
intrinsic viscosity	0.78	0.75	0.72	3.75	4.50
mol. wt. ($\times10^{-3}$)	133	127	121	927	1160

In Fig. 2, the samples of HO-1 and HO-2 were prepared in the emulsion system. In the case of HO-1, 18 g. of monomer, 0.07 g. of tri-*iso*-butylboron, and 18 g. of aqueous solution containing 5% emulsifier were sealed in a glass tube. The reaction was caused to proceed at 40°C for five hours. The polymer was treated by the same method as mentioned on p. 540. Thus, 14 g. of the polymer was obtained. The conversion is 77%.

Similarly, in the case of HO-2, 25 g. of monomer, 0.1 g. of tri-*iso*-butylboron, and 25 g. of aqueous solution containing 5% emulsifier were used. Other conditions, i. e., temperature, time, and treatment of the polymer, were the same as in the case of HO-1. Thus, 18 g. of the polymer was obtained (72% conversion).

Generally, the molecular weight of the polymer prepared in a bulk system was $1\sim2\times10^5$, and in the case of emulsion system, the molecular weight was $1\sim2\times10^6$.

Properties of polystyrene polymerized with tri-*iso*-propylboron in bulk system.

2) T. Alfrey and A. Bartovics, *J. Am. Chem. Soc.*, **65**, 2319 (1943).

—Some properties of polystyrene polymerized with tri-*iso*-propylboron were studied.

The infrared spectra. — The infra-red spectrum of the polymer was compared with that of a polymer prepared with the ordinary catalyst such as radical type. Each film of which the thickness was about 0.01 mm. was prepared by evaporation of toluene used as a solvent of the polymer on a glass plate floated on mercury. The infrared spectrum of the polymer prepared with this catalyst almost exactly resembles that of ordinary polymer, so that only one spectrum is shown in Fig. 3.

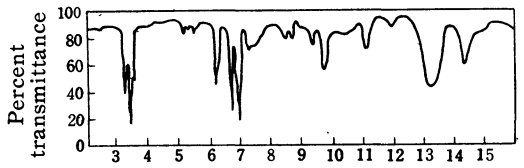

Fig. 3. Infrared spectrum of polystyrene prepared with tri-*iso*-propylboron in bulk system.

X-ray diffraction patterns.—The X-ray diffraction patterns of two samples, i. e., the ordinary polymer and the polymer prepared with this catalyst, were compared as well as the case of infra-red spectra. The specimens having 3 mm. of thickness were made by press at 150°C for ten minutes. Fig. 4-1 is a pattern of ordinary polymer and Fig 4-2 is that of the polymer described in this paper.

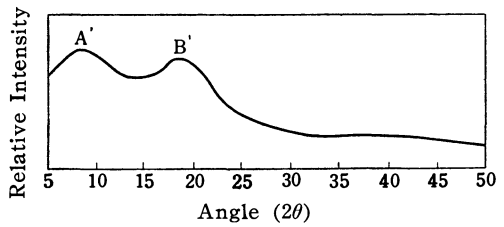

Fig. 4-1. Diffraction pattern of polystyrene prepared with peroxide catalyst.

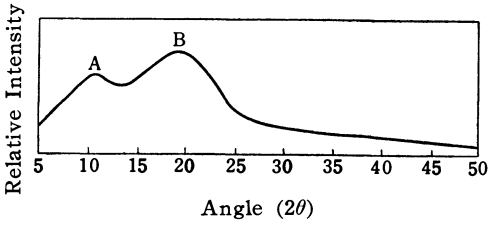

Fig. 4-2. Diffraction pattern of polystyrene prepared with tri-*iso*-propylboron.

Figs. 4-1 and 4-2 represent relative values. From these patterns, it is obvious that the relative intensities between peak A and B in Fig. 4-2 differ from those of peak A′ and B′ in Fig. 4-1.

Solubility in methyl-ethyl-ketone. — The polymer whose molecular weight was 1.2×10^5 was treated with methyl ethyl ketone for two days at room temperature. The polymer perfectly dissolved in this solvent. If the polymer is a crystalline one, it must be insoluble[3].

Softening point.—The softening point of the polymer which was the same kind as the sample used above was measured similarly by the measuring the melting point. In this case, a small piece whose size was about 0.5 mm. × 1 mm. × 20 mm. was used instead of powder in a case measuring melting point, and the temperature of deformation of the piece was observed. The softening point was about 100°C.

Summary

Styrene was polymerized with tri-*iso*-propylboron and tri-*iso*-butylboron prepared by the reaction of Grignard reagents and borontrifluorides. In regard to the rate of polymerization in bulk- and emulsion system, that in the latter was much larger than that in the former. Moreover, in the emulsion system, a very highly polymerized product was easily obtained.

Some properties of the polymer prepared with tri-*iso*-propylboron were studied in comparison with ordinary polymer. The solubility in methyl-ethyl-ketone and the infrared spectrum closely resembled those of ordinary polymers. On the X-ray diffraction pattern, a little difference was observed. But, it is not evident whether the crystalline structure exists or not.

I wish to express my sincere thanks to Mr. H. Matsuo in this laboratory who observed the infrared spectra, and to Mr. S. Ōwaki who observed the X-ray patterns.

The Electrical Communication Laboratory
Nippon Telegraph and Telephone
Public Corporation
Musashino, Tokyo

3) F. Danusso and G. Moraglis, *J. Polymer Sci.*, **24**, 161 (1957)

Structure of Croconic Acid

By Kiyoyuki YAMADA, Nobuhisa MIZUNO and Yoshimasa HIRATA

(Received March 3, 1958)

Croconic acid, $C_5H_2O_5$, is a yellow substance which has been known for a long time. It has a strong acidity and is sensitive to the sun light. However, there has been some ambiguity as regards its structure. So far, two structural formulas I[1] and II[2] have been forwarded; further it was suggested that there was an equilibrium involving the formula III[3] in an aqueous solution.

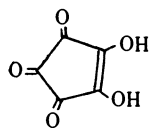

(I)

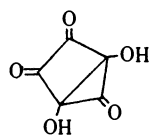

(II)

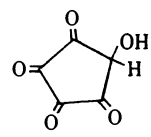

(III)

According to polarographic studies[4] of croconic acid which were done in recent years, it showed properties somewhat different from the typical enediolic compounds studied at the same time.

The properties of croconic acid were examined in order to elucidate its structure, and during the course of studies many interesting observations were obtained. Its ultraviolet spectrum differed from that expected from either structure I or II, the infrared spectrum showed a strong hydrogen bond, and its dipole moment was unusually large.

Methylation.—Since the two hydrogen atoms would naturally be expected to play a unique and important role in the characteristic properties of this acid, a methylation was first carried out. Treatment of the silver salt of the acid with methyl iodide yielded the dimethyl derivative, $C_5O_5(CH_3)_2$.

Ultraviolet spectrum.—Figs. 1—4 show the ultraviolet spectra of the croconic acid and dimethyl croconate. The solvent and the pH of the solution exert a strong influence on the spectra of croconic acid.

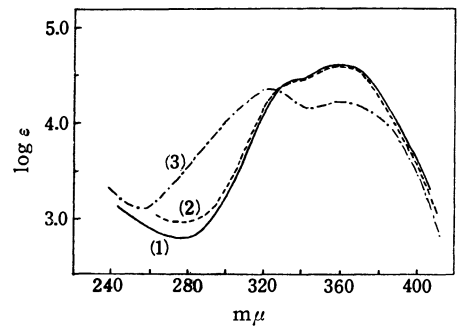

Fig. 1. Croconic acid in water.
(1): neutral; (2): 0.1 N NaOH;
(3): 0.1 N HCl.

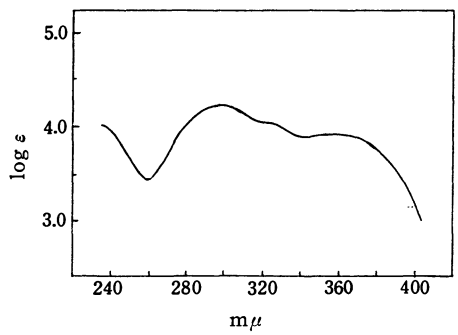

Fig. 2. Croconic acid in ethanol.

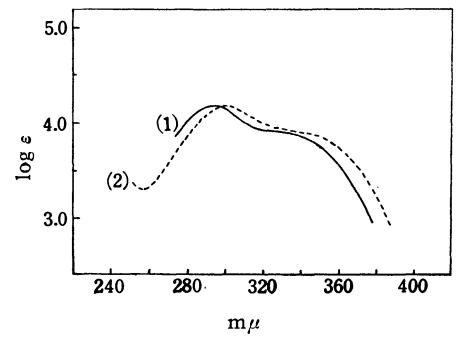

Fig. 3. Croconic acid.
(1): dioxane solution
(2): aqueous solution (9 N HCl)

In the first place, paying attention to the changes of the spectra caused by varying the solvent, we find that the spectrum in an aqueous solution substantially agrees with that in methanol,

1) R. Malachowski, *Chem. Ber.*, **71**, 2246 (1938).
2) R. Nietzki et al., ibid., **18**, 510, 1833 (1885). G. E. Carpéni, *Compt. rend.*, **206**, 601 (1938).
3) Y. Hirata et al., *J. Chem. Soc. Japan, Pure Chem. Sec.* (*Nippon Kagaku Zassi*) **69**, 63 (1948).
4) F. Petuely et al., *Monatsh.*, **83**, 80 (1952). F. Arcamone et al., *Bull. soc. chim. France*, **1953**, 891.

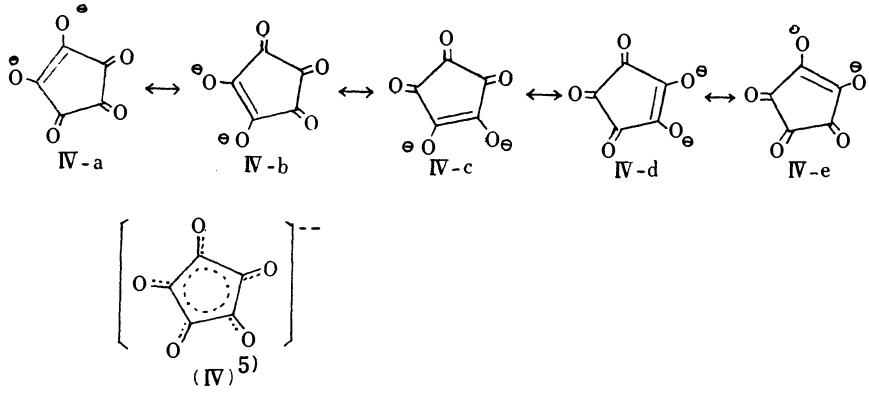

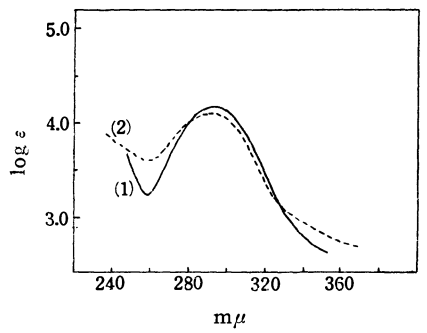

Fig. 4. (1): croconic acid in HCl gas saturated methanol
(2): dimethyl croconate in methanol

but that in ethanol there appears a new absorption in the short wave length region, and the intensity of the band common to aqueous and methanolic solution is lowered. Second, changes in pH lead to the following results; i. e., the spectra taken in a neutral and an alkaline solution are almost the same. On the other hand, when the solution is acidified, a new short wave length band appears. This new absorption is clearly different from the one observed in ethanol solution. Third, the two spectra taken in strong acidic aqueous solution (9 N hydrochloric acid) and in the non-polar dioxane agree with each other fairly well, but a general bathochromic shift of 8~10 mμ is apparent in the former solvent. Finally, though the spectrum of the dimethyl croconate taken in neutral methanol differed from that of the free acid taken in the same solvent, it showed a close similarity when the latter was taken in acidic methanol (compare Figs. 1 and 4).

This spectral behavior may be interpreted as follows. The intensities of the absorptions in Figs. 1—3, are strong enough to exclude the possibility that the absorptions originate from the assumed structures II or III, and, moreover, the absorptions in Figs. 1 and 2 can not be attributed to the enediolic keto form I.

At first, it may be noted that the two curves in Fig. 4, namely, the absorption of the acid in strong acidic methanol, and that of its dimethyl derivative in the neutral methanol show a close resemblance (the difference of two $\lambda_{max.}$ is 3 mμ). Then, considering the positions and the intensities, it is reasonable to conclude that these two absorptions are due to I, or, in other words, due to the chromophore of the enediolic keto structure. We next turn to the absorption maxima in the long wave length region. On account of the strong acidity of croconic acid, it should be almost completely dissociated in water or in methanol to give the dianion, the "croconate ion", which presumably exists in a highly resonating state IV[5], receiving contributions from the structures IVa to IVe. Accordingly, the absorption near 295 mμ due to structure I disappears and, instead, the characteristic absorption of the croconate ion appears around 365 mμ.

In the last place, Fig. 3 will be examined. As mentioned before, the two absorptions are quite similar except the fact that one is shifted by 8~10 mμ as compared to the other. The dipole moment[6] of the acid in dioxane supports structure I with the two hydroxyl groups lying in the plane of the five membered ring. The inference from the observation is that the acid is in an undissociated state in strongly acidic

5) The dotted lines in structure IV simply denote that the two electrons are distributed throughout the entire molecule, and certainly does not denote that the molecule is mesoionic.

6) M. Washino et al., This Bulletin, **31**, 520 (1958).

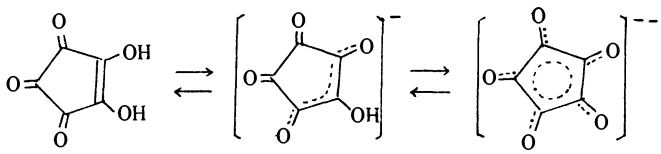

(I) (V) (IV)

aqueous solutions and takes the form of I[7]. The details of the spectra in ethanol and weakly acidic aqueous solution are illustrated in the experimental part.

Acidity.—As is apparent from the synthetic method, croconic acid is a strongly acidic compound and for this reason its purification is not easy. Since this strong acidity had already been well known qualitatively, the spectrophotometric method was applied for the measurement of pK_a.

Since two isosbestic points are present, as shown in Fig. 5, it may be inferred that two equilibrium systems exist; one is I $\rightleftarrows$ V in the low pH range, and the other is V $\rightleftarrows$ IV in the high pH range.

But from the facts that the first isosbestic point (305 mμ) is incomplete and that there exist several absorption curves at intermediate pH's which deviate from both points, it can be deduced that the dissociations do not proceed stepwise and that the croconate ion IV is formed already in the range of low pH. The nature of the monoanion V will be considered next. The monoanion as well as the dianion is stabilized by resonance (Va, Vb); however, the extent of stabilization is smaller with the monoanion.

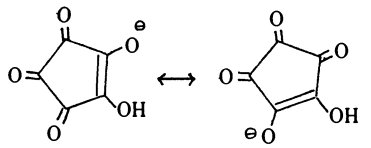

V-a V-b

Based on this consideration, one may account for the experimental facts as follows; the second dissociation occurs to produce the more stable croconate ion before the neutral acid molecule I is completely dissociated into the monoanion. When measuring pK_a values spectrophotometrically, the ultraviolet spectrum of each molecular species must be known[8,9]. For example, with the β-diketone compounds studied by B. Eistert et al.[8], the pK_{a1} and pK_{a2} were determined from the spectra of the three species, i.e., the enol oxonium cation, the neutral enol and the enol anion. In the case of croconic acid, the dissociations are not stepwise, and it is impossible to obtain the absorption curve of the monoanion. Furthermore, the curve of the undissociated acid can not be obtained under the conditions studied.

Thus the values of pK_{a1} and pK_{a2} in aqueous solution can not be measured, but it may be deduced that the first and the second dissociations both occur in the region below pH 2[10].

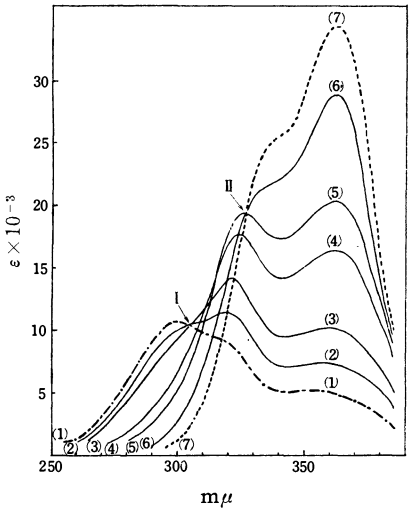

Fig. 5. Isosbestic points.
I: 305 mμ (ε=10400),
II: 327 mμ (ε=19300).
pH: (1) 0.2, (2) 0.3, (3) 0.5, (4) 1.0, (5) 1.3, (6) 2.0, (7) ca. 6.0.

7) The following is worthy of notice; although the acid has the structure I both in strongly acidic aqueous solution and in acidic methanolic solution, the absorptions in these two solutions are different from each other (Fig. 3-(2), Fig. 4-(1)). One possible interpretation of this phenomenon is that in the acidic aqueous solution the lone pair electrons of the hydroxyl groups are able to conjugate with the annular π-electrons, whereas this is not the case in the acidic methanolic solution. However, the exact nature of the role played by solvents is not clear.

8) B. Eistert et al., *Chem. Ber.*, **87**, 108, 1513 (1954).

9) J. E. DeVries et al., *J. Am. Chem. Soc.*, **76**, 1008 (1954).

10) The pK_a can be obtained by plotting the absorbance against the pH at a suitable wave length (315 mμ). The curve obtained is distorted from the usual sigmoid shape on accout of the abnormal dissociations, and the estimation of the acidities is difficult. However, it is roughly estimated that the first dissociation occurs below pH 1 and the second one between pH 1~2.

Dipole moment.—The dipole moment of croconic acid is 9 to 10 D in dioxane. This large value is explicable only on the assumption that it has structure I. The dimethyl croconate has a dipole moment of 5.7~6.0 D and this is also illustrated on the basis of structure I. For further details, see following report on dipole moment measurements.

Infrared spectrum.—(i) The infrared spectra of croconic acid are shown in Fig. 6-(1) and -(2). A broad band is observed around 3000 cm^{-1}, which is located at a higher frequency (3500 cm^{-1}) in potassium bromide than in Nujol (2600 $cm.^{-1}$); this band disappears when the wet method of potassium bromide is applied. In the region of 1500~1800 $cm.^{-1}$, the bands taken in Nujol are somewhat different from those in potassium bromide, and their relative intensities are also different in both cases. The main bands are as follows: 1755, 1720 (w), 1655, 1630, 1540 (in Nujol); 1755, 1720, 1665, 1640, 1600, 1560 (shoulder), (in potassium bromide).

In the finger-print region, the spectra in potassium bromide and in Nujol have little resemblance. It is worth while to

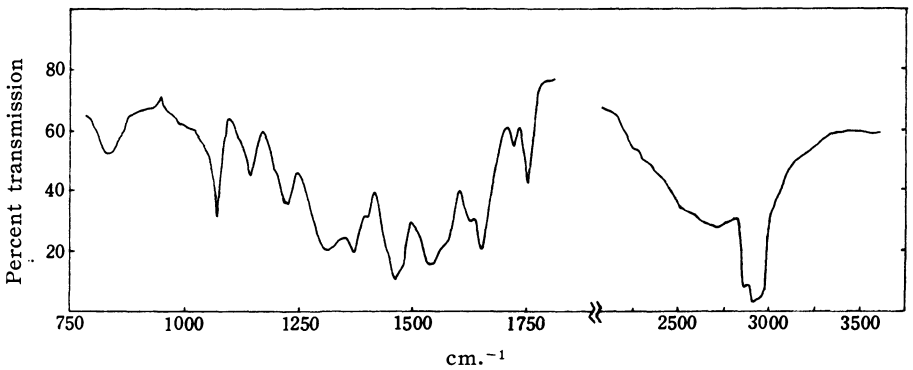

Fig. 6-(1). Croconic Acid (Nujol).

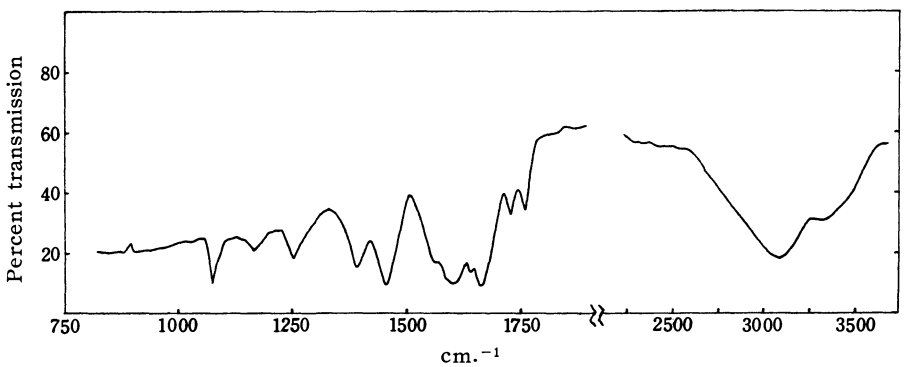

Fig. 6-(2). Croconic Acid (KBr).

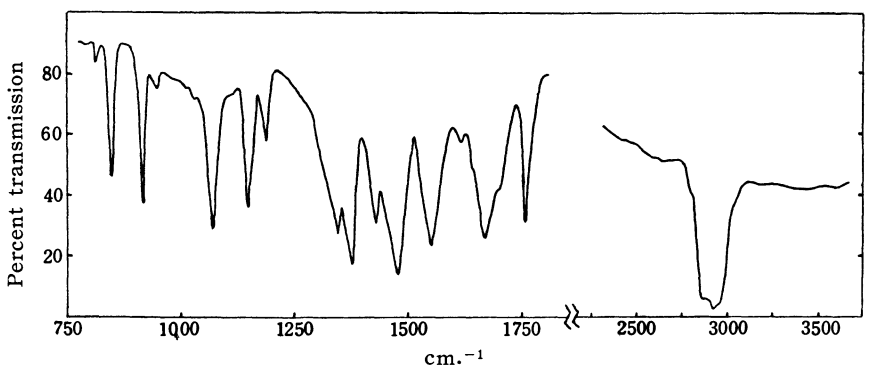

Fig. 7. Dimethyl croconate (Nujol).

notice the sharp band at 1075 cm^{-1}. This band is observed not only in the acid, but in the dimethyl derivative in Fig. 7.

(ii) As expected, there is no absorption band near 3000 cm^{-1} in the spectrum of the dimethyl derivative (Fig. 7). The main bands in the 1500~1800 cm^{-1} region are as follows: 1757, 1695 (shoulder), 1655, 1610, 1550. All the bands are sharp in comparison with those of the acid, and in the finger-print region, there is no band corresponding to the band of the acid except the band at 1075 cm^{-1} described before.

(iii) The spectra of the various metallic salts of the acid were measured (Fig. 8), in order to examine croconic acid in the ionic state. A strong broad band in the region of 1300~1700 cm^{-1} was common to all samples, and besides this, a few weak bands were observed. The bands in the finger-print region are small in number and weak.

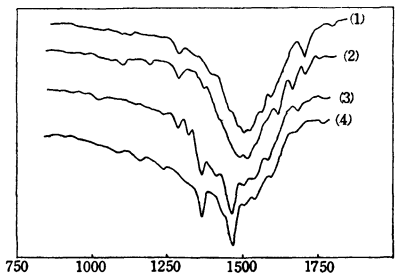

Fig. 8. Metallic salts of croconic acid.
(1) K (2) Ba (KBr)
(3) Ag (4) Cu (Nujol)

(iv) Some of the deductions from these spectra are as follows. Since the molecule is a compact system of conjugated groups in which intense coupling is expected to be present, the assignment of bands to specific groups is almost impossible. Nevertheless, assignments to a limited extent are possible. The band at 1755 cm^{-1} observed in both the acid and the dimethyl croconate is considered to originate from the $\rangle C{=}O$ groups. From the position of this band, the possibility is excluded that the acid might have the three-membered ketonic structure II. A four-membered ring ketone[11] absorbs at 1775 cm^{-1}, and if II is the actual case, the absorption would be expected to be even higher. Because of the broad bands of the acid, an exact comparison of the bands between the acid and the dimethyl croconate is difficult. However, approximate correspondences in their positions and intensities are observed, when the bands in the carbonyl region are compared.

The structure of the dimethyl croconate is believed to be VI, (see the section of ultraviolet spectrum and the report[6] on dipole moment measurement), and the similarity of the bands in the carbonyl region of the two compounds leads to the inference that the acid has structure I in its crystalline state.

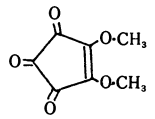

(VI)

The broad band[12] near 3000 cm^{-1} is considered to be one due to a strong hydrogen bond. The band position of the hydrogen bond changes when the spectrum is taken in Nujol and in potassium bromide. The position of the hydrogen-bonded $\nu_{O\text{-}H}$ band suggests a stronger bond in the sample mulled in Nujol.

The metallic salts show besides the very strong and broad band near 1500 cm^{-1} only several weak absorptions. This experimental result is explained by consideration of a symmetric structure IV for the croconate ion. In this structure, all bonds exist in a state more or less intermediate between that of single and double bonds, and the strong broad band at 1500 cm^{-1} is presumably a summation of the absorptions arising from these intermediate $\rangle C{\cdots}O$ bonds. It is well known that the absorptions of simple compounds with highly symmetrical structures are simple, i. e., the tropylium ion[13], and this interpretation is probably applicable to the present case also.

11) Whiffen et al., *J. Chem. Soc.*, **1946**, 1005.

12) In carboxylic dimers, bands at ≃1400 and ≃1300 have been assigned to the coupling of in plane O-H bending and C-O stretching vibrations, and a band at ≃940 to the out of plane O-H bending vibration (Sheppard and Hadži). Similar sets of bands are present in the spectra of dimedone and 2-hydroxy-1, 4-naphthoquinone, and accordingly it is presumed that somewhat analogous strong dimer rings are present in these two compounds. Croconic acid shows bands at 1455, 1245 and 800 cm^{-1} (in potassium bromide), and 1462, 1235 and 820 cm^{-1} (in Nujol), whereas these bands are absent in the spectrum of the dimethyl croconate (the band at 1430 cm^{-1} is probably due to $-CH_3$). It would be intriguing to assume the presence of a similar dimerization (intermolecular hydrogen bond) tentatively in the case of croconic acid.

13) W. v. E. Doering et al., *J. Am. Chem. Soc*, **76**, 3203 (1954).

Results

(A) State in solution.—In solution, croconic acid takes three different forms; the undissociated molecule I, the monoanion V and the dianion IV. The position of the equilibrium depends on the pH and the solvent used, as summarized roughly in Table I.

TABLE I
CROCONIC ACID IN SOLUTION

	Alkaline	Neutral	Acidic	Strong Acidic
Water	IV	IV	I, IV, V	I
Methanol	IV	IV	I, IV, V	I
Ethanol	IV	I, IV, V	I, IV, V	I

The undissociated molecule, the structure of which turned out to be I on the basis of the ultraviolet spectrum of dimethyl croconate VI exists only in strongly acidic solution. There seem to be two types of ultraviolet spectra corresponding to the undissociated molecule and this seems to suggest some effect of the lone pair belonging to the oxygen atoms of hydroxyl groups (Figs. 3-(2) and 4-(1)). Little is known about the monoanion V, existence of which is noticed from the ultraviolet spectrum. Finally, the croconate ion IV is a stable and highly symmetrical dianion, and absorbs strongly at a higher wave length than the undissociated molecule in the ultraviolet spectrum[14]. A similar bathochromic shift in the symmetric ion is observed in the β-diketone system. Namely, the absorption of the highly symmetrical enolate ion occurs at a wave length higher than that of less symmetrical enol[8]. The great stability of the croconate ion accounts for the strong acidity of the two hydroxyl groups.

It is presumed that the keto-form III, if it exists at all, is contained only to a negligible extent.

(B) Solid state.—The dipole moment and the ultraviolet spectrum of the dimethyl croconate support structure VI for this compound. Moreover, structure I for the free acid becomes favorable from the similarity of infrared spectra of the acid and the dimethyl croconate. The characteristic feature of the infrared spectrum of the acid is the strong hydrogen-bonded band and a set of bands similar to those observed with dimeric carboxylic acids, which disappear upon methylation. The three-membered ketonic structure II is excluded from the C=O band at 1755 cm^{-1}. The croconate ion is formed in the metallic salt, and only a few bands are observed because of the symmetrical structure of this ion.

Experimental

The ultraviolet spectra were measured with a Hitachi Spectrophotometer. Infrared spectra were measured with a Hilger H 800 Model, equipped with rock-salt prisms.

Croconic acid.—Glyoxal was used as the starting material, and the sample was recrystallized twice (for details of synthesis, see the following paper[15]).

Ultraviolet spectra of croconic acid.—Table II shows the positions and intensities of the absorptions of croconic acid and its dimethyl derivative. The dimethyl croconate, easily hydrolyzed even in the air, was weighed as rapidly as qossible and dissolved in methanol; once in solution, it is stable. When the solution was placed under the sun light, the intensity of the whole absorption was somewhat weakened, but the extent was not as considerable as in the case of croconic acid (croconic acid is decomposed rapidly by the sun light). The solvent methanol used for the dimethyl croconate was free from water (using metallic calcium) and distilled.

TABLE II

Solvent	Neutral		Alkaline		Acidic		Strong acidic	
	λ_{max}	log ε	λ_{max}	log ε	λ_{max}	log ε	λ_{max}	log ε
	(mμ)		(Croconic acid)					
Water	365	4.6	365	4.6	323 363	4.3 4.2	300	4.2
Ethanol	365	4.6	363	4.6	—	—	296	4.16
Methanol	298 360	4.2 3.9	—	—	—	—	—	—
Dioxane	295	4.16	—	—	—	—	—	—
			(Dimethyl croconate)					
Methanol	292	4.1	—	—	—	—	—	—

14) The calculation[6] based on the molecular orbital method agrees with this experimental fact.
15) K. Yamada et al., This Bulletin, **31**, 550 (1958).
16) B. O. Heston et al., *J. Am. Chem. Soc.*, **56**, 1462 (1954).

Two absorption peaks are clearly present in the weakly acidic aqueous solution and the ethanol solution of the croconic acid. These absorption curves differ from that of the croconate ion measured in water or in methanol. Croconic acid is presumed to exist as an equilibrium mixture among the neutral molecule and the ions (mono- or di-ion). The "solvent basicity" increases in the sequence of ethanol, methanol, and water[16], and thus the equilibrium is shifted towards the ions to a greater extent in the same order. The curves in Figs. 1-(3) and 2 are a composite of the three species.

Isosbestic point of croconic acid.—A stock solution containing 3.638 mg. of croconic acid in 50 ml. of water was prepared. Various solutions having different pH (about 0.1~2.5) were prepared as follows. One normal solution of hydrochloric acid was diluted suitably to make a solution having the desired pH. The ionic strength of every solution was adjusted to that of 1 N hydrochloric acid by adding the proper quantity of 1 M sodium chloride solution. The stock solution (1 ml.) was exactly added to 9 ml. of the solution prepared as noted above. The curve 7 in Fig. 5 was measured in 1 M sodium chloride solution. The absorption curve at pH 2.4, though not shown in Fig. 5, almost coincides with that in the neutral solution. As described previously in this paper, the isosbestic point at 305 mμ (ε=10400) is incomplete and the curves at pH 0.2, 0.3, 0.5, do not intersect at one point strictly. The absorption curves taken in the pH range of 0.6~1.2 pass neither of the isosbestic points. There thus exists an eqilibrium of three components in this pH region.

Metallic salts of croconic acids.—Various metallic salts were obtained easily from croconic acid. Potassium salt and barium salt were obtained during the synthetic process, or adding potassium hydroxide or barium hydroxide (or chloride) to the aqueous solution of croconic acid. The potassium salt loses the crystal water (2 moles) in a desiccator (yellow crystal), but this is easily absorbed again when placed in the air (orange crystal). Cupric salt, lead salt, etc., were obtained from the chloride or nitrate of the metal and the aqueous solution of croconic acid. The silver salt was prepared from silver nitrate. On account of the strong reducing property of croconic acid, the silver nitrate was partly reduced, and metallic silver was deposited. The silver salt was filtered at once under protection from the sun light.

Summary

The structure of croconic acid in solution and in the solid state has been studied. The undissociated molecule is represented by structure I and the ion by structure IV.

The authors are greatly indebted to Assistant Professor K. Nakanishi and Mr. T. Goto for the many helpful discussions we have had during the course of this work. The authors also express their gratitude to Professor M. Kubo for his guidance and interest in this research, and to Mr. O. Shimomura and Mr. M. Miyazaki for their excellent technical assistance. Our thanks are also due to the Ministry of Education for financial support of this research.

Department of Chemistry
Faculty of Science
Nagoya University
Chikusa-ku, Nagoya

Ring Enlargement of Croconic Acid

By Kiyoyuki YAMADA and Yoshimasa HIRATA

(Received March 3, 1958)

The structures I[1], II[2] and III[3] (III, as a tautomer of I in an aqueous solution) have been so far presented for croconic acid.

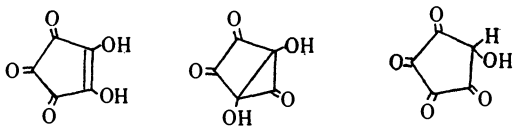

(I) (II) (III)

With the intention of clarifying the structure, various properties of the acid itself and its derivatives have been studied, and it has been concluded that the acid has the structure I and that a strong hydrogen bond is present[4].

In 1938, R. Malachowski prepared various derivatives of croconic acid, and examination of its structure by chemical methods finally led to the formula I. In his research, treatment of the diethyl acetal of croconic acid with diazomethane yielded its dimethyl derivative (liquid).

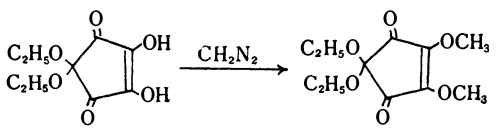

On the other hand, during the course of our studies, it was noticed that the reaction between the acid and ethereal diazomethane yielded orange needles. On the basis of its properties and analyses, this reaction product appeared to be trimethoxy-*p*-benzoquinone resulting from ring enlargement of the acid and successive methylation. Accordingly, this quinone was synthesized from pyrogallol through a route which left no doubt as to the correctness of the structure of the synthetic product[5]. Comparison of infrared and ultraviolet spectra and a mixed melting point test showed the two specimens to be identical. Since croconic acid is insoluble in ether, the reaction is heterogeneous. The quinone is presumably formed by the following mechanism.

Though there are many cases in which the normal product is also produced in anomalous diazomethane reactions, careful scrutiny of the product showed that no dimethyl derivative of croconic acid had been formed. It is interesting that the abnormal reaction takes place in case of croconic acid itself, but does not in case of the acetal derivative.

For the purpose of comparison, the dimethyl ether of the acid was prepared by treating the silver salt with methyl iodide in absolute ether. The compound is, of course, different from the product obtained in the case of the reaction described above. It was, as expected from its structure, easily hydrolyzed to croconic acid even by the moisture in the air.

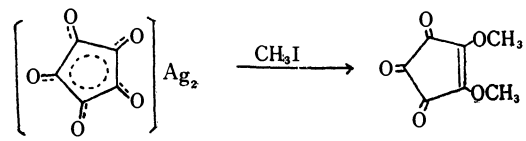

Experimental

Croconic acid.—Croconic acid is usually prepared by oxidation of an alkaline (potassium carbonate) solution of diaminotetrahydroxybenzene with manganese dioxide, or by treatment

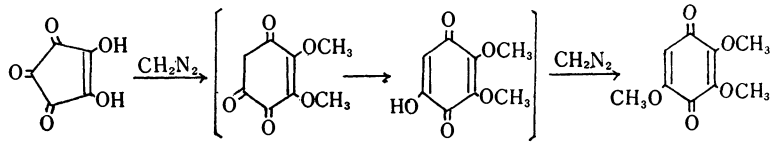

1) R. Malachowski, *Ber.*, **71**, 2246 (1938).
2) R. Nietzki et al., ibid. **18**, 510, 1833 (1885), **19**, 294, 301, 772 (1886), **20**, 1617, 2118 (1887); G. E. Carpéni, *Compt. rend.*, **206**, 601 (1938).
3) Y. Hirata et al., *J. Chem. Soc. Japan, Pure Chem. Sec.* (*Nippon Kagaku Zassi*), **69**, 63 (1948).
4) K. Yamada et al., This Bulletin. **31**, 532 (1958).
5) H. O. Huisman, *Rec. trav. chim.*, **69**, 1145 (1950).

of sodium rhodizonate with an excess of alkali (R. Nietzki)[6]. With the former route the preparation of the diaminotetrahydroxybenzene is troublesome; with the latter route the yield is poor. In the present studies, sodium rhodizonate, easily obtainable from glyoxal[7], was oxidized with manganese dioxide to give potassium croconate in fairly good yield. Namely, to a solution of 7 g. of sodium rhodizonate in 350 ml. of water were added 30 g. of potassium carbonate and 20 g. of manganese dioxide which was freshly prepared from potassium permanganate. After the suspension was refluxed with shaking for one hour, it was filtered at once, and the potassium croconate appeared in the filtrate after cooling. The filtrate containing crystalline potassium croconate was acidified with hydrochloric acid, when the crystals disappeared. The addition of the barium chloride solution to this acidic solution gave 7.6 g. (ca. 85%) of golden barium croconate.

An excessive amount of barium croconate was added to a solution of sulfuric acid (3 N), and the mixture was warmed for about one hour. Excess barium croconate was filtered and the yellow filtrate was concentrated at 40° under reduced pressure, to give crude croconic acid.

The purification was carried out as follows. A saturated solution of crude croconic acid in warm water or alcohol (50°~60°) was cooled in an ice box, upon which there was obtained a small amount of crystals. The remaining solution was concentrated in a desiccator, when the second crop of crystals were obtained in the form of needles or plates. Croconic acid has no melting point, but becomes brown near 150°, and gradually decomposes.

Anal. Found: C, 42.16; H, 1.80. Calcd. for $C_5H_2O_5$: C, 42.25; H, 1.41%.

Reaction product of croconic acid with diazomethane.—A dry ethereal solution (15 ml.) of diazomethane prepared from nitrosomethylurea (containing CH_2N_2 0.007~0.009 M) was placed in a small flask with cooling, and to this 100 mg. (0.0007 M) of croconic acid was added. At first, the reaction occurred on the surface of the acid and the acid gradually dissolved. After thirty minutes, the reaction ceased. The solution became orange, and was left for a while. The orange crystals appearing on the surface of the flask were filtered. The filtrate was concentrated but this only gave an oily residue. The orange crystals were recrystallized from methanol, m. p. 157~158° (quinone prepared from pyrogallol, m.p. 158~160°), yield, 40 mg. Ultraviolet absorption maximum $\lambda_{max.}$ 288 mμ (log ε 4.08 in ethanol).

Anal. Found: C, 54.59; H, 5.49. O-CH_3 (Zeisel): 45.9% (1.96 groups). Calcd. for $C_9H_{10}O_5$: C, 54.55; H, 5.09%.

Purification of the oily material was undertaken, in order to examine the existence of another product, but nothing could be detected except that a further small amount of the above quinone was obtained. When a methanolic solution of croconic acid was added to the ethereal diazomethane, the yield was poor and the amount of the oily product increased.

Dimethyl croconate[1].—It was necessary that all the solvent and the reagents should be quite free from water and that the flask provided with a calcium chloride tube should be used. Since the reaction was heterogeneous, it was necessary to stir occasionally. The reaction was complete after one day at room temperature (10~15°). The product was recrystallized from benzene. Orange prism, m. p. 113~114°.

Anal. Found: C, 48.96; H, 3.65. Calcd. for $C_7H_6O_5$: C, 49.42; H, 3.56%.

The analytical data do not quite agree with the calculated values, probably owing to the hydrolysis of the sample in the air. When placed in dilute hydrochloric acid, the dimethyl croconate was at first insoluble, but after several seconds it started to dissolve fairly rapidly. The aqueous solution was warmed for thirty minutes, and upon evaporation of the solvent there was obtained free croconic acid. The free croconic acid itself is very soluble in water.

Summary

The reaction of croconic acid with diazomethane gives instead of its simple methylated product, a compound with an enlarged ring. Trimethoxy-*p*-benzoquinone was synthesized from pyrogallol, and was identified with the compound obtained from croconic acid.

The authors wish to make grateful acknowledgements to Mr. S. Senoh, Osaka City University, for microanalyses. They also express their gratitude to the Ministry of Education for financial support of this research.

Department of Chemistry, Faculty of Science, Nagoya University
Chikusa-ku, Nagoya

6) R. Nietzki et al., *Ber.*, **18**, 1842 (1885), **19**, 293 (1886).
7) B. Homolka, *Ber.*, **54**, 1393 (1921).

The Dipole Moments and Molecular Structures of Croconic Acid and Dimethyl Croconate

By Masamitsu WASHINO, Kiyoyuki YAMADA and Yukio KURITA

(Received March 3, 1958)

One of the present authors (K. Y.) and his co-workers have carried out extensive studies on the chemical properties of croconic acid and determined its structure to be cyclopentene-1-diol-1,2-trione-3,4,5[1]. They have measured the dipole moments of croconic acid and dimethyl croconate. Comparing the observed moments with those calculated by the method of molecular orbitals, they have undertaken to determine the electronic structures of these molecules as well as the geometrical arrangements of hydroxyl and methoxyl groups.

Experimental

Croconic acid and dimethyl croconate were synthesized and purified by one of them (K. Y.)[1]. Since these compounds were hygroscopic and the latter compound was readily hydrolyzed and gave the former, solvents were dried carefully. The dielectric constants and densities were measured of the solutions in dioxane or benzene. Because of the small solubilities, the measurements could not be extended to solutions of concentrations above 0.1 weight per cent. Therefore, it was difficult to determine the dipole moment very accurately.

The apparatus and the method of measurements were the same as used in our earlier works[2] except that a silvered cell of Sayce-Briscoe type[3] was used for the benzene solutions of dimethyl croconate. The Halverstadt-Kumler's method was employed. The dependence of the dielectric constants of the solutions of croconic acid in dioxane upon concentration was abnormal, the value of $\Delta\varepsilon/w$ increasing sharply with the decrease in concentrations. This fact suggests association or dissociation taking place. The results are shown in Tables I and II, where the same notations are used as in the previous reports[2].

TABLE I
DIELECTRIC CONSTANT AND DENSITY INCREMENTS OF SOLUTIONS OF CROCONIC ACID AND DIMETHYL CROCONATE

	Temp.	$w\times10^6$	$\Delta\varepsilon\times10^4$	$\Delta d\times10^5$
Croconic acid	25°C	80	68	—
in dioxane		233	156	—
		527	273	28
		1233	454	101
	35°C	140	91	0
		269	151	0
		507	220	0.3
		761	254	1.3
		937	264	2.8
Dimethyl croconate	30°C	306	53	—
in benzene		448	92	1.7
		645	134	—
		926	182	3.5
		1271	273	5.1

Discussion

The dipole moments of croconic acid and dimethyl croconate are high*. This indicates an appreciable contribution of polar structures to the ground state. The difference between the moments of the two compounds is as large as about 3~4 D. Since the group moment of C—OH is nearly the same as that of C—OCH_3 in its magnitude and also in its direction, the moments of the two compounds should be of the same order, unless an appreciable difference exists between the electronic and/or geometrical structures of the two compounds.

In calculating the moments of these compounds, one must take into account rotations about C—O single bonds. The moments were calculated for four conceivable configurations shown in Fig. 1. In the case of planar configurations, A and B, in which two OH or two OCH_3 groups lie in the ring plane, the two lone pairs belonging to the oxygen atoms conjugate with the rest of the molecule, so that twelve π-electrons are distributed

1) K. Yamada, N. Mizuno and Y. Hirata, This Bulletin, **31**, 543 (1958).

* Accordingly, the structures having small moments, such as II or III in our previous report,[1] are not conceivable.

2) Y. Kurita, T. Nozoe and M. Kubo, ibid., **26**, 242 (1953).

3) M. Kobayashi, Y. Kurita and M. Kubo, *Chemistry and Chemical Industry* (*Kagaku to Kogyo*), **10**, 138 (1957).

TABLE II

MOLECULAR POLARIZATION AND DIPOLE MOMENTS

Compounds	Solvent	Temp.	ε_1	d_1 (g./cc.)	α	β (g./cc.)	$P_{2\infty}$ (cc.)	P_{A+E} (cc.)	μ(D)
Croconic acid	dioxane	25°C	2.2084	1.02755	80	0.86	1880	31	9.5 ±0.5
		35°C	2.1888	1.01565	76	0.00	1817	31	9.3 ±0.3
Dimethyl croconate	benzene	30°C	2.2625	0.86695	21	0.39	726	35	5.85±0.15

TABLE III

MOLECULAR ORBITAL ENERGIES AND WAVE FUNCTIONS[b]

Planar configuration

Symmetry[c]	ω[a]	c_1	c_2	c_3	c_4	c_5	c_6
S	−3.8480	0.0929	0.1213	0.1677	0.1283	0.3426	0.5713
A	−3.4960	0	0	0.1060	0.1003	0.2290	0.6529
S	−3.1358	0.5255	0.4220	0.2901	0.3612	−0.0231	−0.2400
A	−2.7504	0	0	0.3230	0.6088	0.0275	−0.1556
S	−2.5196	0.6784	0.2493	−0.1656	−0.4507	−0.0292	0.0858
S	−0.7605	0.2686	−0.2355	−0.2795	0.3189	−0.4280	0.2703
S	0.1648	0.3738	−0.5723	−0.2172	0.1419	0.4074	−0.1819
A	0.2037	0	0	0.4995	−0.3206	0.3516	−0.1553
A	2.0427	0	0	0.3673	−0.1285	−0.5685	0.1595
S	2.0989	0.2076	−0.6017	0.4847	−0.1672	−0.1791	0.0498

Perpendicular configuration

S	−3.2515	0.4750	0.4204	0.3476	0.3927	0.1543	
A	−2.7913	0	0	0.3425	0.6120	0.0903	
S	−2.5447	0.7222	0.2782	−0.1568	−0.4070	−0.1015	
S	−1.2804	0.1606	−0.0817	−0.1659	0.3260	−0.5916	
S	0	0.4264	−0.6030	−0.3015	0.2132	0.3015	
A	0	0	0	0.4472	−0.3162	0.4472	
A	1.7913	0	0	0.4275	−0.1595	−0.5402	
S	2.0766	0.2126	−0.6129	0.4860	−0.1686	−0.1580	

a) $\omega=(\alpha-E)/\beta$.

b) E: the energy of molecular orbital $\phi=\sum_r c_r\chi_r$. χ_r: atomic orbital of an r-th atom. As to numbering of atoms, see Fig. 1. Parameters used are as follows: Coulomb integrals are α, $\alpha+2\beta$, and $\alpha+3\beta$ for carbon atoms, carbonyl oxygen atoms and oxygen atoms of OH and OCH_3, respectively. Resonance integrals are β and $\sqrt{2}\beta$ for C-C and C-O bonds, respectively.

c) The suffixes S and A denote the symmetry properties of the molecular orbitals. For symmetric molecular orbitals, $c_7=c_3$, $c_8=c_4$, $c_9=c_5$ and $c_{10}=c_6$. For antisymmetric molecular orbitals, $c_7=-c_3$, $c_8=-c_4$, $c_9=-c_5$ and $c_{10}=-c_6$.

among ten atoms. On the other hand, for the perpendicular configurations, C and D, in which two OH or two OCH_3 groups lie in the plane perpendicular to the ring, the conjugation decreases to its minimum. Then, it can be treated as a system of eight π-electrons distributed among eight atoms.

It is difficult to calculate adequately the moment of a molecule conjugated to such an extent as in croconic acid or dimethyl croconate from the vector addition of relevant bond moments. It is generally accepted that the simple method of molecular orbitals, which neglects mutual re-

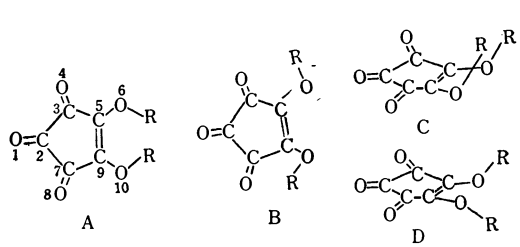

Fig. 1. Croconic acid (R=H) and dimethyl croconate ($R=CH_3$).

pulsion between electrons, always gives too high values for the theoretical moments. Orgel and his co-workers[4] presented an equation to calculate a total moment with due regard to mutual repulsion between electrons.

$$\vec{\mu}_T = \vec{\mu}_\sigma + \vec{\mu}_\pi / 1.6 \qquad (1)$$

They applied this equation to eighteen conjugate heterocyclic compounds and obtained theoretical moments in agreement with the observed ones within 0.30 D in magnitudes and 10° in directions. Following their procedure, we calculated the dipole moments.

In Table III are shown the energies and the coefficients of atomic orbitals in molecular orbitals constructed from π-orbitals belonging to atoms participating in conjugation. Ten and eight atoms are involved in the planar and perpendicular configurations, respectively. In Fig. 2 are shown the corresponding molecular diagrams accommodated with twelve or eight

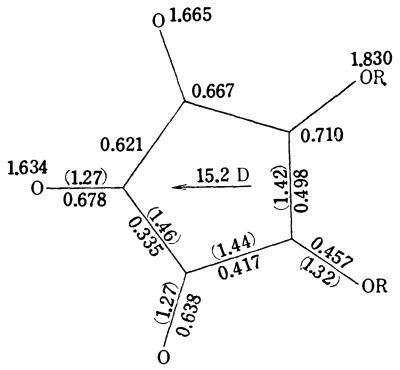

Planar configuration

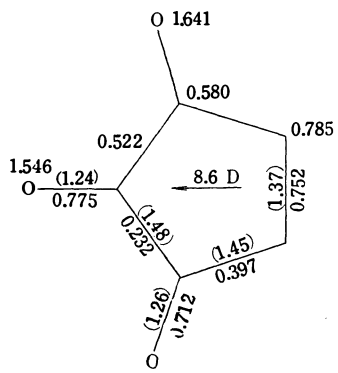

Perpendicular configuration

Fig. 2. Molecular diagrams: π-electron densities, bond orders, bond lengths (in parentheses), and μ_π.

4) L. E. Orgel, T. L. Cottrell, W. Dick and L. E. Sutton, *Trans. Faraday Soc.*, **47**, 113 (1951).

π-electrons allotted to the molecular orbitals of low energies. The bond lengths were calculated from bond orders using the relation described in a preceding report[5]. In each diagram, the estimated μ_π is shown, which was obtained by assuming that the pentagon ring is approximately regular, that the carbon-oxygen bonds lie along the lines from the center of the ring to the respective carbon atoms, and that the bond distances are as given above. On the other hand, μ_σ was calculated with the assumption that the bond moments of OH and OCH_3 were equal to 1.5 D and 1.2 D, respectively, and that the valency angles $\angle COH$ and $\angle COCH_3$ were 105° and 110°, respectively. The total moments calculated from equation 1 are shown in Table IV, together with the observed moments.

TABLE IV
DIPOLE MOMENTS (D)

Configuration		Croconic acid	Dimethyl croconate
Planar	A	8.4	8.8
	B	10.4	10.3
Perpendicular	C	6.7	6.5
	D	6.0	6.0
Observed		9~10	5.7~6.0

The moment of dimethyl croconate can adequately be explained by the perpendicular configurations. The planar configurations are unlikely in view of the steric hindrance acting between the methyl groups or between the methyl group and the carbonyl oxygen atom. The observed moment of croconic acid is in good agreement with those of the planar configurations. In these configurations, the conjugation within the molecule can attain its maximum possible extent. Moreover, a hydrogen bond can be formed between the OH group and carbonyl oxygen or between the OH groups. The hydrogen bond formation stabilizes the molecule and increases the trend of electron attraction of carbonyl oxygen.

The first excitation energy associated with π-electron was calculated as 0.925β, 1.280β and 0.813β* for the planar and perpendicular configurations and for a croconate ion $C_5O_5^{--}$, respectively. This energy level can be shown to be capable of accounting for the spectral features of

5) Y. Kurita and M. Kubo, This Bulletin, **24**, 13 (1951).

* It was calculated with the assumption that croconate ion is planar and symmetrical and the Coulomb integral of oxygen atom is $\alpha + 2.4\beta$.

the acid and its dimethyl ester as well as the changes in their spectra with solvents[1].

Summary

The dipole moments of croconic acid and dimethyl croconate were measured in dioxane and benzene solutions, respectively, as 9~10 D and 5.7~6.0 D. The moments of these molecules were calculated theoretically for several conceivable configurations by the method of molecular orbitals. The results confirm the structure presumed from evidences in organic syntheses. The accumulation of π-electrons on carbonyl oxygen is chiefly responsible for the large dipole moments, the effect being stronger in the acid. The hydroxyl groups of croconic acid lie in the ring plane, whereas the methoxyl groups are out of the ring plane to minimize the steric hindrance.

The authors wish to express their cordial thanks to Professors M. Kubo and Y. Hirata for their guidance and encouragement. Their thanks are also due to the Ministry of Education for financial support of this research.

Department of Chemistry, Faculty of Science, Nagoya University
Chikusa-ku, Nagoya

*Formation and Aging of Precipitates. VII. Habit of Crystals in Vanadium Pentoxide Sols by Electron Microdiffraction Method**

By Kazuyoshi TAKIYAMA

(Received November 21, 1957)

Morphological studies on the crystals in three kinds of vanadium pentoxide sol, such as Biltz-, Müller-, and ion-exchange sols, were reported in a previous paper[1]. Watson, Heller and Wojtowicz[2] indicated the electron diffraction patterns of the crystals in Biltz sol and showed that the patterns verified the crystal growth. This paper describes the identification of crystals in three kinds of sol and the crystal habit of the Biltz sol crystals.

Experiments and Results

Identification of Crystals in Various Sols by Electron Diffraction Method.— Electron diffraction patterns obtained from the crystals in Biltz-, Müller- and ion-exchange sols, reported in the previous paper[1], are shown in Fig. 1. From these patterns the interplanar spacings of each crystal were calculated and the diagrams

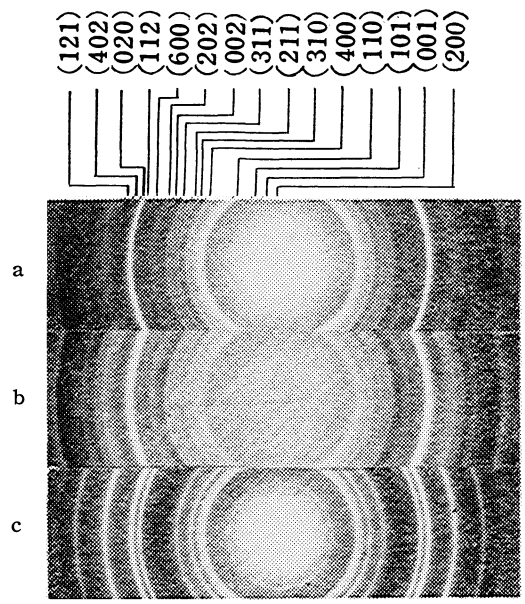

Fig. 1. Electron diffraction patterns of crystals in various sols.
a. Biltz sol
b. Müller sol
c. Ion-exchange sol

* Some parts of this experiment were published in *Proc. Japan Acad.*, **30**, 752 (1954) and were read in advance at the First Regional Conference on Electron Microscopy in Asia and Oceania on October 27, 1956.

1) K. Takiyama, This Bulletin, **31**, 329 (1958).

2) J. H. L. Watson, W. Heller and W. Wojtowicz, *Science*, **109**, 274 (1949).

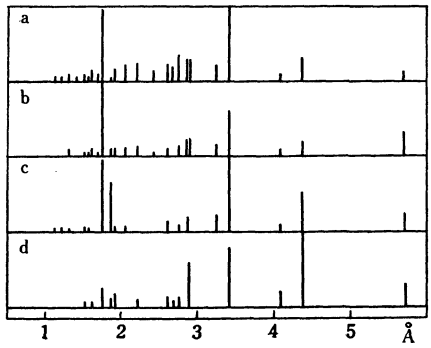

Fig. 2. Diagrams of electron diffraction patterns obtained from crystals in various sols.
a. Biltz sol
b. Müller sol
c. Ion-exchange sol
d. Vanadium pentoxide crystal by means of X-ray diffraction method

of the patterns are shown in Fig. 2. The interplanar spacings of the crystals in every sol agree with those of vanadium pentoxide crystal determined by X-ray diffraction method[3], so that all of the crystals in the sols were identified with vanadium pentoxide.

The Habit of Crystals in Biltz Sol.— The crystals in Biltz sol grew like long fibers upon aging as described in the previous paper[1]. When an aged sol was mounted onto a specimen holder for electron microscopy by the usual method, the photograph was obtained which showed the network of fiber-like crystals as shown in Fig. 3a in the previous paper[1] and its electron diffraction pattern obtained by means of the selected area electron diffraction technique (electron microdiffraction method) was that of Debye-Scherrer rings as shown in Fig. 3a, in which interplanar spacings agreed with those of vanadium pentoxide. The tiny film formed on the surface of the aged sol contained tactoid as shown in Fig. 3b in the previous paper[1], in which the fibrous crystals were oriented parallel to one another. As the direction of the specimen, accordingly that of the fiber axis, was perpendicular to the electron beam, the electron diffraction pattern obtained from the tactoid was a typical fiber pattern as shown in Fig. 3b. Space indices of each reflection point are indicated in Fig. 4. As indicated in Fig. 4, the layer lines are $k=0, \pm1, \pm2, \cdots\cdots$, and the reflection points of (020) and (040) appear on the meridian. By measuring the distance of each layer line from the equatorial line, the fiber period can be calculated by the following equation

$$c = nL\lambda/r_n,$$

where c is the fiber period, L camera

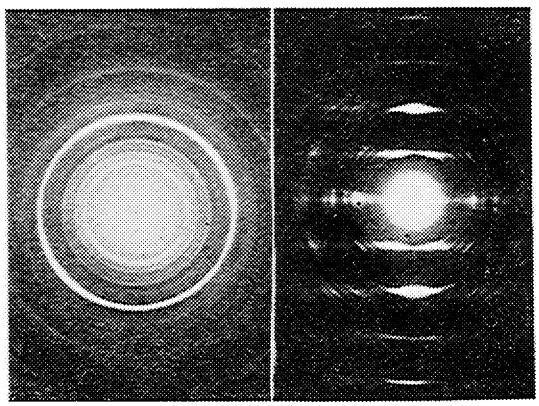

(a) (b)

Fig. 3. Electron diffraction patterns obtained from the two types of crystals in one year old Biltz sol by the selected area electron diffraction technique.
a. Electron diffraction pattern obtained from the part of the network structure.
b. Electron diffraction pattern obtained from the part of the tactoid.

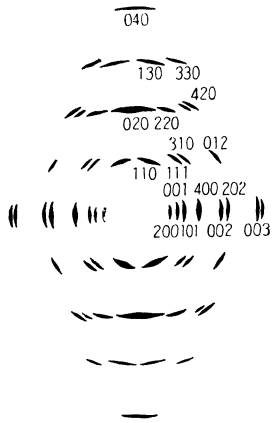

Fig. 4. Space indices of fiber pattern shown in Fig. 3b.

3) J. D. Hanawalt, H. W. Rinn and L. K. Frevel, *Ind. Eng. Chem., Anal. Ed.*, **10**, 510 (1938).

length, λ wave length of the electron beam and r_n distance of the n-th layer line from the equatorial line. The value of $L\lambda$ was calculated from the Debye-Scherrer ring pattern obtained from an evaporated aluminum film used as a standard. The fiber period was calculated from 17 electron diffraction patterns as 3.56±0.011 Å which was in accord with the lattice constant of b-axis of vanadium pentoxide, that is b_0= 3.564Å[4]. So the fiber axis, the direction of the crystal growth, was also clearly confirmed as b-axis.

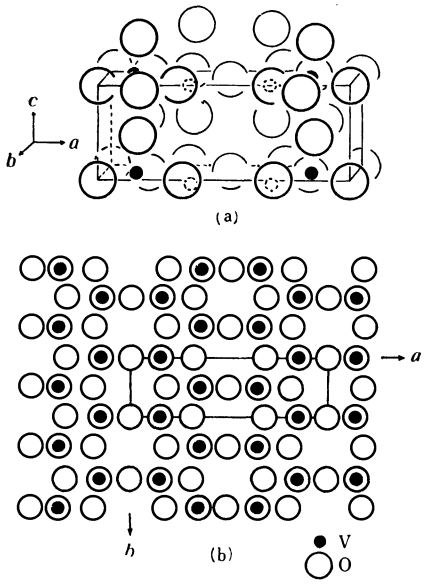

Fig. 5. a: Configuration of vanadium pentoxide crystal.
b: Projection of the structure of vanadium pentoxide crystal on (001).

The fibrous crystals in Biltz sol grew along the b-axis and no growth along the a- and c-axis occurred. The configuration of vanadium pentoxide crystal[4] and the structure projection on (001) of it are given in Fig. 5 a and b. The distribution of vanadium and oxygen atoms along the b-axis is denser than that along other axes. The direction of the growth of the fibrous crystals in Biltz sol agrees with the direction of the dense distribution of atoms.

Summary

The crystals in Biltz-, Müller-, and ion-exchange sols were all identified with vanadium pentoxide by the electron diffraction method.

The crystals in aged Biltz sol were fiber-like. The specimen prepared ordinarily gave rise to the Debye-Scherrer pattern and that of the tactoid corresponded to the fiber pattern. The fiber axis of the fibrous crystal was decided to be the b-axis.

The author wishes to express his sincere thanks to Professor Eiji Suito of Kyoto University for his guidance and discussion. The author particularly wishes to express his deep gratitude to Professor Masayoshi Ishibashi of Kyoto University for his discussion and encouragement during this work and is also indebted to Dr. Ryoichi Kiriyama of Osaka University for his advice.

Institute for Chemical Research
Kyoto University
Takatsuki, Osaka

4) A. J. C. Wilson, "Structure Report", International Union of Crystallography, N.V.A. Oosthoek's Uitgevers, MIJ, Utrecht (1950), p. 232.

Molecular Rotations of Glucides in Relation to their Structures. V. The Internal Conformation of C^6—O Bond in D-Galactopyranose in the Aqueous Solution and the Direction of the Optical Axis of Methylol Group

By Shukichi YAMANA

(Received December 26, 1957)

On the basis of Kirkwood's polarizability theory, the author explained the physical meaning of the empirical rule which had been found by Hudson about isorotation among anomers of aldoses[1]. In this explanation, the author used a simple molecular model of hypothetically ideal shape for simplification of calculation and also assumed that the orientation of OH group of $(CH_2OH)^{5\beta}$ as regards the aldopyranose-ring is definite and similar in D-galactopyranose, D-glucopyranose and D-mannopyranose*1. But strictly speaking, the orientation of OH group in $(CH_2OH)^{5\beta}$ is affected by the neighboring atoms and accordingly it may not always be equal in the molecule of D-galactopyranose and D-glucopyranose in aqueous solution[4]. On the other hand, Kirkwood expected that C*-atom with which C_2H_5 group combines in *sec*-butyl alcohol would have a marked effect on the optical axis of C_2H_5 and consequently this axis would be supposed to be placed on the plane of C*-atom and C—C bond in C_2H_5 group, and this axis would be inclined to this C—C bond at the angle between 0° and 54°44′ (one half the tetrahedral angle)[6]. By this conception, the optical axis of $(CH_2OH)^{5\beta}$ in an aldopyranose-molecule is expected to be on the plane of C^5-atom and C^6—O bond and this axis would incline to the C^6—O bond at an angle of θ*2. (Fig. 1)

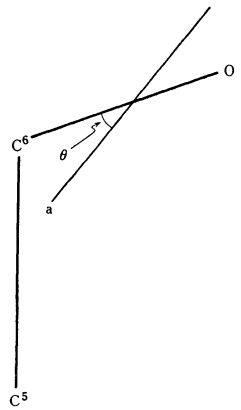

Fig. 1. Direction of the optical axis of $(CH_2OH)^{5\beta}$
a……optical axis.

According to this presumption, the author tried in this article, to calculate the values of the anomeric differences*3 in molecular models of aldopyranoses*4.

Molecular Model and Data Used

In the present calculation, Mc Donald

1) S. Yamana, This Bulletin, **30**, 207 (1957).

*1 By this treatment, $[\mu]^{20}_{D\text{calcd}}$, caused by the dynamical coupling effect of $(CH_2OH)^{5\beta}$ disappeared. Moreover, in order to simplify the calculations, the author assumed also in the previous papers[1-4] that, indifferently to its orientation, OH group has an optical axis of cylindrical symmetry directed along its bond to C atom with which it combines at resting state. In this case, OH group is treated as a single particle, like so-called pseudo-atom (ref. 5) of atomic weight, 17.008, indifferently to the position of H atom in this group. This state of OH group was called "isotropic" in the previous papers (1) (2). But, it never means that OH group is "optically isotropic".

2) S. Yamana, ibid., **30**, 203 (1957).

3) S. Yamana, ibid., **30**, 916 (1957).

4) S. Yamana, ibid., **30**, 920 (1957).

5) C. A. Coulson, *Quart. Rev.*, **1**, 144 (1947).

6) J. G. Kirkwood, *J. Chem. Phys.*, **5**, 479 (1937).

*2 The value of this angle θ may be expected to lie between 0° and 54°44′ (one half the tetrahedral angle).

*3 Ref. *2 in the previous paper 1. The anomeric difference is abbreviated to An. Diff., hereafter.

*4 Then, it became possible to presume the internal conformation of C^6-O bond in D-galactopyranose in aqueous solution and the angle of inclination of the optical axis, θ, of $(CH_2OH)^{5\beta}$.

TABLE I

Name	Unit Groups	$[M]_D^{20}$(W)	Ref.*10
α-D-glucose	[$(OH)^{1\alpha}$, $(OH)^{2\alpha}$, $(OH)^{3\beta}$, $(OH)^{4\alpha}$, $(CH_2OH)^{5\beta.ma}$*10, Ring]	202.1°	a)
β-D-glucose	[$(OH)^{1\beta}$, $(OH)^{2\alpha}$, $(OH)^{3\beta}$, $(OH)^{4\alpha}$, $(CH_2OH)^{5\beta.ma}$, Ring]	33.7°	a)
α-D-mannose	[$(OH)^{1\alpha}$, $(OH)^{2\beta}$, $(OH)^{3\beta}$, $(OH)^{4\alpha}$, $(CH_2OH)^{5\beta.ma}$, Ring]	52.8°	a)
β-D-mannose	[$(OH)^{1\beta}$, $(OH)^{2\beta}$, $(OH)^{3\beta}$, $(OH)^{4\alpha}$, $(CH_2OH)^{5\beta.ma}$, Ring]	−30.6°	a)
α-D-galactose	[$(OH)^{1\alpha}$, $(OH)^{2\alpha}$, $(OH)^{3\beta}$, $(OH)^{4\beta}$, $(CH_2OH)^{5\beta.ga}$*11, Ring]	271.5°	a)
β-D-galactose	[$(OH)^{1\beta}$, $(OH)^{2\alpha}$, $(OH)^{3\beta}$, $(OH)^{4\beta}$, $(CH_2OH)^{5\beta.ga}$, Ring]	95.1°	a)
β-L-arabinose	[$(OH)^{1\alpha}$, $(OH)^{2\alpha}$, $(OH)^{3\beta}$, $(OH)^{4\beta}$, Ring]	286.1°	a)
α-L-arabinose	[$(OH)^{1\beta}$, $(OH)^{2\alpha}$, $(OH)^{3\beta}$, $(OH)^{4\beta}$, Ring]	115.6°*12	a)

and Beevers' molecular model*5 was used. Unit groups in the molecules of several aldopyranoses and corresponding values of molecular rotations are shown in Table I*7,*8.

Except the position of their optical centers, the optical data for OH group and H atom in the previous paper 2, are used again without any correction. Values of mean polarizability α and of anisotropy ratio β of CH_2OH group are 2.87×10^{-24} (cc)[c] and 0.35[d] respectively. It is supposed that CH_2OH group has its optical axis of cylindrical symmetry which is placed on the plane of C^5-atom and its C^6—O bond, and this axis inclines to the C^6—O bond at an angle θ*2 (cf. Fig. 1). It is also supposed that the optical center of OH group which combines with C atom is located at the center of mass of C—(OH) bond, and the optical center of $(CH_2OH)^{5\beta}$ is at C^6-atom*13. The refractive indices

*5 Ref. *4 in the previous paper 4. This model seems to show the molecule-shape of an aldopyranose in aqueous solution more accurately than the ideal model*6 does.

*6 Ref. "Molecular Model and Data Used." in the previous papers 4 and 1.

*7 Isbell and Pigman observed $[M]_D^{20}$(W) of aldopyranoses in details when studying the mutarotation-curves. In this paper, Isbell and Pigman's data were used. By using their data, it became apparent that An. Diff. of D-galactopyranose is not exactly but approximately equal to that of D-glucopyranose.

*8 As it has not been confirmed that D-talopyranose has C 1 conformation in its aqueous solution, this sugar is not treated in this paper. If D-talopyranose has C 1 conformation, the following data would be used for α- and β-isomers.

Name	Unit Groups	$[M]_D^{20}$(W)	Ref.
α-D-talose	[$(OH)^{1\alpha}$, $(OH)^{2\beta}$, $(OH)^{3\beta}$, $(OH)^{4\beta}$, $(CH_2OH)^{5\beta.ga}$*9, Ring]	122.5°	a)*10
β-D-talose	[$(OH)^{1\beta}$, $(OH)^{2\beta}$, $(OH)^{3\beta}$, $(OH)^{4\beta}$, $(CH_2OH)^{5\beta.ga}$, Ring]	23.8°	a)

*9 Ref. *11 in this article. When the orientation of $(OH)^2$ of D-galactopyranose changes from α to β, D-talopyranose is obtained. But, the distance between the O atom in $(OH)^2$ and that in C^6-O bond in $(CH_2OH)^{5\beta.ga}$ is too large to give rise to any influence of the orientation-change of $(OH)^2$ on the internal conformation of C^6-O bond. Therefore, the orientation of OH group in $(CH_2OH)^{5\beta}$ as regards the aldopyranose-ring may be definite and similar in these two sugars in aqueous solutions.

*10 "ma" means the internal conformation concerning $(CH_2OH)^{5\beta}$ in the molecule of D-mannopyranose in aqueous solution. Accordingly, $(CH_2OH)^{5\beta.ma}$ means CH_2OH group which combines with 5-position of the aldopyranose-ring in β-orientation, and at the same time, the internal conformation of the C^6-O bond in this CH_2OH group is of mostly *trans* type and sometimes *gauche* II type. (There exists an equilibrium between these two types). Concerning this information, refer to the previous paper 4.

a) F. J. Bates and associates, "Polarimetry, Saccharimetry and the Sugars", United States Government Printing Office, Washington (1942), p. 762.—"Isbell and Pigman Table of Optical Rotation and Mutarotation of the Reducing Sugars."

*11 "ga" means the internal conformation concerning $(CH_2OH)^{5\beta}$ in the molecule of D-galactopyranose in aqueous solution (cf. *10).

*12 This is $[M]_D^{20}$(W) of α-L-arabinose·$CaCl_2$·$4H_2O$ and not of the pure α-L-arabinose (ref. a)). In order to avoid this defect, it is advisable to use Hudson's data (ref. b)) subsidiarily. ($[M]_D^{20}$(W) of β-L-arabinose=303.3°; $[M]_D^{20}$(W) of α-L-arabinose =133.6°. By using these Hudson's data, An. Diff. of L-arabinose is (303.3−133.6=169.7). This is very consistent with that, obtained by using Isbell and Pigman's data, (286.1−115.6=170.5).

b) E. Montogomery and C. S. Hudson, *J. Am. Chem. Soc.*, **56**, 2074 (1934).

c) Landolt-Börnstein, Physikalisch-Chemische Tabellen, Hw. II. p. 985.

d) Values obtained by Ramakrishna-Rao; see Landolt-Börnstein, Physikalisch-Chemische Tabellen, 5th Ed., Eg. II. p. 91.

*13 As the rotatory parameter, g, in the theoretical formula (ref. *14) contains the term, $1/R^3_{ik}$, the former is very sensitive to the magnitude of R_{ik}. In other words, a small deviation in the position of the optical center of a unit group causes a great deviation in $[\mu]^{20}_{D\text{calcd}}$, with which this unit group is concerned. Then, concerning the position of the optical

of the aqueous solutions of aldopyranoses under question are presumed to be nearly equal (1.34)*16.

Method Proposed

Recently, the author proposed a possible method of estimating the approximate value of the molecular rotation $[M]_D^{20}$(W) of a glucide. The principle of this method is to calculate the partial molecular rotation, $[\mu]_{D\text{calcd}}^{20}$ (or $[\mu]_{D\text{calcd}}^{20}(3/n^2+2)$, for convenience), according to Kirkwood's polarizability theory at first, and next, to multiply this calculated value with a definite coefficient which can be obtained by using experimental data of some glucides, to get the true partial molecular rotation, $[\mu]_{D\text{obs}}^{20}$. By summing up all of these possible $[\mu]_{D\text{obs}}^{20}$ in a molecule, we can get the calculated value of $[M]_D^{20}$(W) of this substance*17. This method has its ground on the following equation

$$[\mu]_{D\text{obs}}^{20} = \kappa[\mu]_{D\text{calcd}}^{20}, \quad (1)$$

where κ is a proportionality-constant and is always positive, and Eq. 1 is derived from the formerly presented equation

$$[M]_{D\text{obs}}^{20} = \kappa[M]_{D\text{calcd}}^{20}*18$$

At any rate*19, a multiplying coefficient κ was found important to perform the semi-empirical application of Kirkwood's theory. But now, it seems appropriate to use a new auxiliary coefficient ζ*21, as below; In the case of the dynamical coupling between two unit groups, A and B, it is assumed that κ is the product of two coefficients, ζ_A and ζ_B, which are derived from the groups *A* and *B*, respectively. This is expressed in the following equation

$$\kappa = \zeta_A\zeta_B*22,*23. \quad (2)$$

Then, from Eqs. 1 and 2,

$$[\mu]_{D\text{obs}}^{20} = \zeta_A\zeta_B[\mu]_{D\text{calcd}}^{20} \quad (3)*24$$

---

center, a special precaution should be taken. In some of his calculations, Kirkwood located the optical center of a unit group at its center of mass. This manner of treatment was used even in the case of CH_3 group which combines with the three-membered ring in 2,3-epoxybutane (ref. 7). On the other hand, from the standpoint of bond-interaction, Murakami located the optical center of a bond at its center of mass (ref. 8). According to Murakami's treatment, OH group which combines with the aldopyranose-ring is to be divided into ^{r}C—O*15 and O—H bonds. But, on account of lack of data for these two bonds, we were forced to treat OH group as a single particle (ref. *11 in the previous paper 2 and *1 in this article). However, the contribution of ^{r}C—O bond (strictly speaking, σ orbitals of ^{r}C- and O-atoms in this bond) to the degree of polarization of ^{r}C—O—H system, is far greater than that of O—H bond. Then, it may be appropriate to locate the optical center of this system (generally speaking, the optical center of OH group) between ^{r}C- and O-atoms (or at the center of mass of ^{r}C—(OH) bond, for convenience). Analogously, the optical center of $(CH_2OH)^{5\beta}$ is to be placed at the weighed center of the system of C^5—C^6, C^6—(OH), and two C^6—H bonds, that is to say, in the vicinity of C^6-atom.

*14 Ref. "Theoretical Formulae" in the previous paper 2.

7) W. W. Wood, W. Fickett and J. G. Kirkwood, *J. Chem. Phys.*, **20**, 561 (1952).

8) H. Murakami, This Bulletin, **27**, 246 (1954); **28**, 583 (1955).

*15 ^{r}C-atom means the C atom which constitutes the aldopyranose-ring.

*16 Ref. *8 in the previous paper 1.

*17 Ref. "Method Proposed." in the previous paper 3. This method is called "Polarizability-Multiplying method (or abbreviated to PM-method)" by the author, hereafter.

*18 Eq. 4 in the previous paper 2.

*19 It has already been demonstrated that, in the calculation of the optical rotatory power by Kirkwood's polarizability theory, a small deviation in atomic distance or in valency angles causes only a small deviation in the calculated value of optical rotatory power. (ref. *7 in the previous paper 2). Then, the comparatively large value of κ, $(12.37/n^2+2)$*20, can not be due to the imperfectness of the molecular model, used for calculation. It may be due either to the inadequate location of the optical center of OH group, or to the changes of the values of $\alpha_i\beta_i$ or $\alpha_k\beta_k$ in the theoretical formula (ref. *14) which are caused by solvation (ref. *13 in the previous paper 2).

*20 Ref. "Method Proposed" in the previous paper 1.

*21 The author chose ζ, a Greek letter which corresponds to *z*, to represent the new coefficient. Thus, the notations in PM-method, X, $\bar{X}$ and ζ were suggested by x, y and *z*. (ref. *10 in the previous paper 3).

*22 From the viewpoint of its physical meaning, ζ should be always positive.

*23 The proportionality constant κ was suggested by the Murakami's report (8) on the study of polypeptides of alanine. But here, κ loses its original physical meaning, and the physical meaning of κ is specified in such a way that its value changes when one of two unit groups, A or B, changes.

*24 As was already described in the previous paper 3, the following equation is given in the case of the dynamical coupling of two OH groups,

$$[\mu]_{D\text{obs}}^{20} = 4.123[\mu]_{D\text{calcd}}^{20}(3/n^2+2)$$

In this case,

$$\kappa = \zeta_{OH}^2 = 4.123(3/n^2+2)$$
$$\therefore \quad \zeta_{OH} = 2.0305(3/n^2+2)^{1/2}$$

TABLE II

$[\mu]^{20}_{D\text{calcd}}(3/n^2+2)$, CAUSED BY THE DYNAMICAL COUPLING EFFECT BETWEEN ANY TWO MEMBERS OF UNIT GROUPS (EXCEPT $(CH_2OH)^{5\beta}$ AND RING) IN MC DONALD AND BEEVERS' MOLECULAR MODEL

	4β	4α	3β	3α	2β	2α
1α	−0.06 (−0.13)	−0.05 (−0.03)	2.23 (1.76)	0.52 (0.45)	1.31 (0.68)	10.62 (5.96)
1β	−0.29 (−0.20)	0.25 (0.14)	0.21 (0.10)	−2.33 (−1.85)	11.86 (6.81)	−12.97 (−7.59)
2α	1.48 (1.38)	0.51 (0.27)	12.47 (7.23)	−10.11 (−5.59)		
2β	0.17 (0.17)	−2.04 (−1.66)	−11.96 (−7.04)	−1.26 (−0.64)		
3α	0.93 (0.48)	10.76 (5.83)				
3β	11.58 (6.59)	−11.97 (−6.57)				

The values, calculated by supposing that the optical center of OH group is located at its O atom, are given in parentheses.

TABLE III

$[\mu]^{20}_{D\text{calcd}}(3/n^2+2)$, CAUSED BY THE DYNAMICAL COUPLING EFFECT OF $(OH)^1$ IN D-GLUCOPYRANOSE

	2α	3β	4α	5β.ma	R
1α	10.62	2.23	−0.05	$(1\alpha)\times(5\beta.\text{ma})$*26	$(1\alpha)\times R$
1β	−12.97	0.21	0.25	$(1\beta)\times(5\beta.\text{ma})$	$(1\beta)\times R$

TABLE IV

$[\mu]^{20}_{D\text{obs}}(3/n^2+2)$, CAUSED BY THE DYNAMICAL COUPLING EFFECT OF $(OH)^1$ IN D-GLUCOPYRANOSE

	2α	3β	4α	5β.ma	R
1α	$10.62\zeta^2_{OH}$*27	$2.23\zeta^2_{OH}$	$-0.05\zeta^2_{OH}$	$\{(1\alpha)\times(5\beta.\text{ma})\}\zeta_{OH}\zeta_{CH_2OH}$	$\{(1\alpha)\times R\}\zeta_{OH}\zeta_R$
1β	$-12.97\zeta^2_{OH}$	$0.21\zeta^2_{OH}$	$0.25\zeta^2_{OH}$	$\{(1\beta)\times(5\beta.\text{ma})\}\zeta_{OH}\zeta_{CH_2OH}$	$\{(1\beta)\times R\}\zeta_{OH}\zeta_R$

On the other hand, $[\mu]^{20}_{D\text{calcd}}$, caused by the dynamical coupling effect between any two members of unit groups (except $(CH_2OH)^{5\beta}$ and ring) in the aldopyranose-molecule, can be calculated by using the theoretical formulae*14. The results of calculation are shown in Table II.

Then, $[\mu]^{20}_{D\text{calcd}}(3/n^2+2)$ and $[\mu]^{20}_{D\text{obs}}(3/n^2+2)$, caused by the dynamical coupling effects between $(OH)^1$*25 and the other unit groups in D-glucopyranose are as shown in Tables III and IV, respectively. Now, $[\mu]^{20}_{D\text{obs}}$ of An. Diff.*3 of D-glucopyranose is as follows;

$$\begin{aligned}&[10.62\zeta^2_{OH}+2.23\zeta^2_{OH}-0.05\zeta^2_{OH}\\&\quad+\{(1\alpha)\times(5\beta.\text{ma})\}\zeta_{OH}\zeta_{CH_2OH}\\&\quad+\{(1\alpha)\times R\}\zeta_{OH}\zeta_R](n^2+2/3)\\&\quad-[-12.97\zeta^2_{OH}+0.21\zeta^2_{OH}+0.25\zeta^2_{OH}\\&\quad+\{(1\beta)\times(5\beta.\text{ma})\}\zeta_{OH}\zeta_{CH_2OH}\\&\quad+\{(1\beta)\times R\}\zeta_{OH}\zeta_R](n^2+2/3)\\&\quad=(25.31\zeta^2_{OH}+A+B)(n^2+2/3)\end{aligned}$$

where

$$A\equiv\{(1\alpha)\times(5\beta.\text{ma})-(1\beta)\times(5\beta.\text{ma})\}\zeta_{OH}\zeta_{CH_2OH} \quad (4)$$

$$B\equiv\{(1\alpha)\times R-(1\beta)\times R\}\zeta_{OH}\zeta_R \quad (5)$$

The corresponding observed value is given by, $\{[M]^{20}_D(W)$ of α-D-glucose$\}$ minus $\{[M]^{20}_D(W)$ of β-D-glucose$\}$. This is $(202.1-33.7)$*28$=168.4$. Of course, this observed value should be equal to its corresponding $[\mu]^{20}_{D\text{obs}}$. Then,

$$168.4=(25.31\zeta^2_{OH}+A+B)(n^2+2/3) \quad (6)$$

By using the method like that mentioned above, three other equations are obtained. From D-mannopyranose,

$$83.4=(-8.83\zeta^2_{OH}+A+B)(n^2+2/3) \quad (7)$$

This is ζ-coefficient of OH group in the aldopyranose-molecule of C 1 conformation in aqueous solution, calculated by using the ideal model and Riiber's data of $[M]^{20}_D(W)$, supposing that the optical center of (OH) group is located at its O atom. This value of ζ_{OH} is nearly equal to that, obtained by using Mc Donald and Beevers' model and Isbell and Pigman's data of $[M]^{20}_D(W)$, supposing that the optical center of OH group is at its O atom. (ref. *44 in this article.)

*25 $(OH)^1$ means OH group, which combines with 1-position of the ring, and so on.

*26 $(5\beta.\text{ma})$ is an abbreviated symbol of $(CH_2OH)^{5\beta.\text{ma}}$, and so on.

*27 Eq. 3 is used, here.

*28 Ref. Table 1 in this article.

From D-galactopyranose,

$$176.4 = (25.84\zeta_{OH}^2 + A' + B)(n^2+2/3) \quad (8)$$

and from L-arabinopyranose,

$$170.5 = (25.84\zeta_{OH}^2 + B)(n^2+2/3) \quad (9)^{*29}$$

where

$$A' \equiv \{(1\alpha)\times(5\beta.\mathrm{ga}) - (1\beta)\times(5\beta.\mathrm{ga})\}\zeta_{OH}\zeta_{CH_2OH} \quad (10)$$

From Eq. 6 minus 7,

$$85.0 = 34.14\zeta_{OH}^2(n^2+2/3)$$

$$\therefore \quad \zeta_{OH}^2 = 2.4897(3/n^2+2) \quad (11)$$

$$\text{or} \quad \zeta_{OH} = 1.5779(3/n^2+2)^{1/2} \quad ^{*22,*30} \quad (12)$$

From Eqs. 6 and 11,

$$106.2 = B(n^2+2/3)$$
$$= \{(1\alpha)\times R - (1\beta)\times R\}\zeta_{OH}\zeta_R(n^2+2/3)^{*31}$$
$$= (1\alpha)\,\bar{\times}\,R - (1\beta)\,\bar{\times}\,R \quad (13)^{*32,*29}$$

from Eqs. 6, 11 and 13,

$$-0.8 = A(n^2+2/3)$$
$$= \{(1\alpha)\times(5\beta.\mathrm{ma}) - (1\beta)\times(5\beta.\mathrm{ma})\}\zeta_{OH}\zeta_{CH_2OH}(n^2+2/3)^{*33,*35}$$

$$\therefore \quad \zeta_{OH}\zeta_{CH_2OH}(n^2+2/3) = -0.8/\{(1\alpha)\times(5\beta.\mathrm{ma}) - (1\beta)\times(5\beta.\mathrm{ma})\} \quad (14)$$

and from Eq. 8 minus 9,

$$5.9 = A'(n^2+2/3)$$
$$= \{(1\alpha)\times(5\beta.\mathrm{ga}) - (1\beta)\times(5\beta.\mathrm{ga})\}\zeta_{OH}\zeta_{CH_2OH}(n^2+2/3)\}^{*34}$$

$$\therefore \quad \zeta_{OH}\zeta_{CH_2OH}(n^2+2/3) = 5.9/\{(1\alpha)\times(5\beta.\mathrm{ga}) - (1\beta)\times(5\beta.\mathrm{ga})\} \quad (15)$$

As each of ζ_{OH}, ζ_{CH_2OH} and $(n^2+2/3)$ in Eqs. 14 and 15 is always positive (ref. *22), the following two inequalities are obtained. From Eq. 14,

$$\{(1\alpha)\times(5\beta\cdot\mathrm{ma}) - (1\beta)\times(5\beta\cdot\mathrm{ma})\} < 0 \quad \text{(Ineq. 1)}$$

From Eq. 15,

$$\{(1\alpha)\times(5\beta\cdot\mathrm{ga}) - (1\beta)\times(5\beta\cdot\mathrm{ga})\} > 0 \quad \text{(Ineq. 2)}$$

The left-hand side of Eq. 14 is equal to that of Eq. 15, then the right-hand sides of these two equations should be equal to each other,

$$-0.8/\{(1\alpha)\times(5\beta.\mathrm{ma}) - (1\beta)\times(5\beta.\mathrm{ma})\} = 5.9/\{(1\alpha)\times(5\beta.\mathrm{ga}) - (1\beta)\times(5\beta.\mathrm{ga})\}$$

$$\therefore \quad \{(1\alpha)\times(5\beta.\mathrm{ga}) - (1\beta)\times(5\beta.\mathrm{ga})\} / \{(1\alpha)\times(5\beta.\mathrm{ma}) - (1\beta)\times(5\beta.\mathrm{ma})\} = -7.38 \quad (16)$$

Eq. 16 indicates that

$$\{(1\alpha)\times(5\beta.\mathrm{ga}) - (1\beta)\times(5\beta.\mathrm{ga})\} \neq \{(1\alpha)\times(5\beta.\mathrm{ma}) - (1\beta)\times(5\beta.\mathrm{ma})\}$$

$$\therefore \quad 5\beta.\mathrm{ga} \neq 5\beta.\mathrm{ma} \quad (17)^{*36}$$

Now, in order to simplify the following calculations, two simplifications are made as below;

(Simp. I) The internal conformation of C^6—O bond in D-mannopyranose in aqueous solution is only of *trans* type. (ref. *10). Shortly speaking,

$$5\beta.\mathrm{ma} = 5\beta.t^{*37}$$

(Simp. II) The internal conformation of C^6—O bond in D-galactopyranose in aqueous solution is one of the *trans*, *gauche* I or *gauche* II types[*38], and this type is represented by x. Then,

$$5\beta\cdot\mathrm{ga} = 5\beta\cdot\mathrm{x}$$

*29 Cf. *35 in this article.

*30 If D-talopyranose has C 1 conformation (ref. *8), it is possible to calculate ζ_{OH} by using $[M]_D^{20}(W)$ of D-galactose and of D-talose. The calculated value of ζ_{OH} in this case, is 1.5086 $(3/n^2+2)^{1/2}$. This is nearly equal to the value in Eq. 12.

*31 Eq. 5 is used, here.

*32 When the partial molecular rotation is caused by the dynamical coupling effect between unit groups A and B,

$$[\mu]_{D\mathrm{obs}}^{20} = \zeta_A\zeta_B[\mu]_{D\mathrm{calcd}}^{20}$$

(Eq. 3 in this article),
where

$$[\mu]_{D\mathrm{obs}}^{20} = (A)\,\bar{\times}\,(B)$$

(ref. *10 in the previous paper 3), and

$$[\mu]_{D\mathrm{calcd}}^{20} = \{(A)\times(B)\}(n^2+2/3)$$

(ref. *14 in the previous paper 2).
Then,

$$(A)\,\bar{\times}\,(B) = \{(A)\times(B)\}\zeta_A\zeta_B(n^2+2/3). \quad (32)$$

*33 Eq. 4 is used, here.

*34 Eq. 10 is used, here.

*35 When using Hudson's data of L-arabinoses (ref. *12 in this article),

$$169.7 = (25.84\zeta_{OH}^2 + B)(n^2+2/3) \quad (9)^*$$
$$105.4 = (1\alpha)\,\bar{\times}\,R - (1\beta)\,\bar{\times}\,R \quad (13)^*$$
$$\{(1\alpha)\times(5\beta.\mathrm{ma}) - (1\beta)\times 5\beta.\mathrm{ma})\}\zeta_{OH}\zeta_{CH_2OH}(n^2+2/3) = 0$$
$$\text{or} \quad (1\alpha)\times(5\beta.\mathrm{ma}) - (1\beta)\times(5\beta.\mathrm{ma}) = 0 \quad (14)^*$$

*36 Strictly speaking, as each of 5β.ga and 5β.ma seems to be the mixture of two types of internal conformation of C^6—O bond (ref. *10), Eq. 17 shows that the quantitative ratio of two types of internal conformation of C^6—O bond is entirely different in D-galactopyranose and in D-mannopyranose in their aqueous solutions.

*37 5β.*t* is an abbreviated symbol of 5β.*trans*.

*38 cf. Fig. 2 in the previous paper 4.

By using these two simplifications, the following two inequalities and two equations are obtained.

From Ineq. 1,

$$\{(1\alpha)\times(5\beta.t)-(1\beta)\times(5\beta.t)\}<0 \quad \text{(Ineq. 1')}$$

From (Ineq. 2),

$$\{(1\alpha)\times(5\beta.\mathrm{x})-(1\beta)\times(5\beta.\mathrm{x})\}>0 \quad \text{(Ineq. 2')}$$

From Eq. 17,

$$5\beta\cdot\mathrm{x}\neq 5\beta\cdot t \qquad (17')^{*39}$$

and from Eq. 16,

$$\{(1\alpha)\times(5\beta.\mathrm{x})-(1\beta)\times(5\beta.\mathrm{x})\}/\{(1\alpha)\times(5\beta.t)-(1\beta)\times(5\beta.t)\}=-7.38 \qquad (16')$$

Next, the value of $\{(1\alpha)\times(5\beta.t)-(1\beta)\times(5\beta.t)\}$ was calculated as a function of the angle θ*2 which defines the direction of the optical axis of CH_2OH group. The results of calculation are given in the second column of Table V.

TABLE V

$[\mu]^{20}_{\mathrm{D\,calcd}}(3/n^2+2)$-DIFFERENCE AS A FUNCTION OF θ, CALCULATED BY USING MC DONALD AND BEEVERS' MODEL

θ	Diff(t)	Diff(gI)	Diff(gII)	Diff(gII)/Diff(t)
0°	9.90			
10°	8.21			
20°	5.80			
30°	2.95			
36°	1.18			
40°	0.02			
40°05′	−0.01	−16.54	4.72	−472.00
40°10′	−0.03	−16.52	4.69	−156.33
41°	−0.27	−16.33	4.42	−16.37
41°50′	−0.51	−16.11	4.16	−8.16
42°	−0.55	−16.07	4.09	−7.44
42°10′	−0.60	−16.02	4.04	−6.73
43°	−0.82	−15.79	3.77	−4.60
50°	−2.65	−13.51	1.21	−0.46
54°44′	−3.73	−11.61	−0.66	0.18

Diff(t) ·····$\{(1\alpha)\times(5\beta\cdot t)-(1\beta)\times(5\beta\cdot t)\}$
Diff(g I)·····$\{(1\alpha)\times(5\beta\cdot g\,\mathrm{I})-(1\beta)\times(5\beta\cdot g\,\mathrm{I})\}$
Diff(g II) ···$\{(1\alpha)\times(5\beta\cdot g\,\mathrm{II})-(1\beta)\times(5\beta\cdot g\,\mathrm{II})\}$

Combining these values with (Ineq. 1'), the following conclusion is obtained,

$$40°05' \leqq \theta \leqq 54°44'$$

In order to examine *gauche* I type, the value of $\{(1\alpha)\times(5\beta.g\,\mathrm{I})^{*40}-(1\beta)\times(5\beta.g\,\mathrm{I})\}$ was calculated as a function of θ which lies between 40°05′ and 54°44′. The results of calculation are given in the third column in Table V. But these values of $\{(1\alpha)\times(5\beta.g\ 1)-(1\beta)\times(5\beta.g\ 1)\}$ are all negative. Then, by referring Ineq. 2′, it is concluded that

$$5\beta.g\,1\neq 5\beta.\mathrm{x} \qquad (18)^{*41}$$

Combining Eqs. 17′ and 18 with (Simp. II),

$$5\beta\cdot\mathrm{ga}=5\beta\cdot\mathrm{x}=5\beta\cdot g\,\mathrm{II} \qquad (19)$$

Consequently, the internal conformation of C^6—O bond in D-galactopyranose in aqueous solution is of *gauche* II type*42. Then, Eq. 16′ becomes as below;

$$\{(1\alpha)\times(5\beta.g\,\mathrm{II})-(1\beta)\times(5\beta.g\,\mathrm{II})\}/\{(1\alpha)\times(5\beta.t)-(1\beta)\times(5\beta.t)\}=-7.38. \qquad (16'')$$

In order to find the suitable value of θ which satisfies Eq. 16″, the value of the left side of this equation was calculated as a function of θ. The results of the calculation are given in the fifth column of Table V, and the value, −7.38, of

$$\{(1\alpha)\times(5\beta.g\,\mathrm{II})-(1\beta)\times(5\beta.g\,\mathrm{II})\}/\{(1\alpha)\times(5\beta.t)-(1\beta)\times(5\beta.t)\}$$

can be found at $\theta\simeq 42°$*43.

It is also apparent in Table V that the value of $\{(1\alpha)\times(5\beta.g\,\mathrm{II})-(1\beta)\times(5\beta.g\,\mathrm{II})\}$ which corresponds to the above-found value of θ is 4.09. When this value, Eqs.

*39 Concretely speaking, the internal conformation of C^6—O bond in D-galactopyranose in aqueous solution is not of *trans* type.

*40 $5\beta.g$I is an abbreviated symbol of $5\beta.$*gauche* I, and so on.

*41 Concretely speaking, the internal conformation of C^6—O bond in D-galactopyranose in aqueous solution is not of *gauche* I type.

*42 This conclusion coincides with that obtained from the viewpoint of the atomic distances between the O atom in $(CH_2OH)^{5\beta}$ (i. e. O^6-atom) and the neighboring atoms. (ref. "Discussion on the Results." in the previous paper 4). The distance between O^6- and $O^{4\beta}$-atoms in D-galactopyranose are as below; *trans* (3.49 Å), *gauche* I (4.16 Å), *gauche* II (2.69 Å) Then, the distance between O^6- and $O^{4\beta}$-atoms in *gauche* II form is the shortest and is equal to the length of a hydrogen bond. Therefore, the movable atom O^6 would be attracted by $O^{4\beta}$-atom and be forced to rest at *gauche* II position.

*43 The value, 0, of

$$\{(1\alpha)\times(5\beta.\mathrm{ma})-(1\beta)\times(5\beta.\mathrm{ma})\}=\mathrm{Diff}(t),$$

(ref. Eq. 14* in *35) is found at $\theta\simeq 40°05'$ in Table V, and its corresponding Diff(g II) is 4.72. Accordingly,

$$\zeta_{CH_2OH}=0.7922(3/n^2+2)^{1/2} \qquad (20)^*$$

These are the values concerning $(CH_2OH)^{5\beta}$, calculated by using Hudson's data of L-arabinoses. (ref. *12).

19 and 12 are used, Eq. 15 becomes as below;

$$1.5779(3/n^2+2)^{1/2}\zeta_{CH_2OH}(n^2+2/3)=5.9/4.09$$
$$\therefore\ \zeta_{CH_2OH}=0.9142(3/n^2+2)^{1/2}\ *43,*44 \qquad (20)$$

Conclusion

The results of calculation in this paper are as follows:

(1) If the internal conformation of C^6—O bond in D-galactopyranose in aqueous solution is only one of the *trans*, *gauche* I or *gauche* II types, it should be of *gauche* II type.

(2) It is expected that the optical axis of $(CH_2OH)^{5\beta}$ is placed on the plane of C^5-atom and its C^6—O bond, and this optical axis inclines to the C^6—O bond at 42°*43.

(3) ζ-coefficients of OH and CH_2OH groups, in this case, are $1.5779(3/n^2+2)^{1/2}$ and $0.9142(3/n^2+2)^{1/2}$ *43, respectively.

The author wishes to express his sincere thanks to Professor S. Tanaka of Kyoto University for his valuable discussion and encouragement throughout the course of this study. Also the author wants to express his great thanks to the members of the Editorial Board of this Bulletin for their helpful suggestion concerning the importance of the position of the optical center of the unit group.

Department of Chemistry
Kyoto Gakugei University
Fusimi-ku, Kyoto

*44 For comparison, the values, calculated by supposing that the optical center of OH group is located at O atom and that of CH_2OH group is at its center of mass (ref. *13), are given here;

	Isbell and Pigman's data of L-arabinoses	Hudson's data of L-arabinoses
ζ_{OH}	$2.0782(3/n^2+2)^{1/2}$	$2.0782(3/n^2+2)^{1/2}$
ζ_{CH_2OH}	$3.5049(3/n^2+2)^{1/2}$	$3.3936(3/n^2+2)^{1/2}$
θ	34°50′	34°20′

Molecular Rotations of Glucides in Relation to their Structures. VI. Optical Superposition in Methyl Pentoses.[*1] *Presumption of Two Unknown* $[M]_D^0$(W)

Shukichi YAMANA

(Received December 26, 1957)

Recently, the author discussed $[M]_D^{20}$(W) of pentoses by using PM-method[*2], and concluded that the principle of optical superposition of Kirkwood's idea exists in this group[2]. In this paper, the author tries to investigate whether this principle exists in methyl pentoses by using the same method.

Molecular Model and Data Used

The names of pentoses and methyl pentoses to which the calculations were applied, with groups in their molecules, and their corresponding molecular rotations are tabulated in Table I.

These pentoses and methyl pentoses except α-D- and β-D-isorhamnoses were concluded to have C 1 conformation by Reeves' experiments of cuprammonium-glycoside complexes[3][*4]. It is presumed

*1 Only the glucides which have the six-membered (pyranose) ring in their molecules, are treated in this article, and so the suffix "-pyranose" of their names is omitted, here.

*2 Ref.*17 in the previous paper 1.

1) S. Yamana, This Bulletin, **31**, 558 (1958).

2) S. Yamana, ibid. **30**, 916 (1957).

*3 Hudson's data is 303.3° (ref. *12 in the previous paper 1).

a) F. J. Bates and Associates, "Polarimetry, Saccharimentry and the Sugars", United States Government Printing Office, Washington (1942), p. 762.

b) ibid. p. 750.

c) ibid. p. 726.

3) R. E. Reeves, *J. Am. Chem. Soc.*, **72**, 1499 (1950).

TABLE I

Name	Unit Groups	$[M]_D^{20}$(W)	Lit.
α-D-xylose	[$(OH)^{1\alpha}$, $(OH)^{2\alpha}$, $(OH)^{3\beta}$, $(OH)^{4\alpha}$, Ring]	140.5°	(a)
β-L-arabinose	[$(OH)^{1\alpha}$, $(OH)^{2\alpha}$, $(OH)^{3\beta}$, $(OH)^{4\beta}$, Ring]	286.1°*3	(a)
α-D-rhamnose	[$(OH)^{1\alpha}$, $(OH)^{2\beta}$, $(OH)^{3\beta}$, $(OH)^{4\alpha}$, $(CH_3)^{5\beta}$, Ring]	15.7°	(a)
β-D-rhamnose	[$(OH)^{1\beta}$, $(OH)^{2\beta}$, $(OH)^{3\beta}$, $(OH)^{4\alpha}$, $(CH_3)^{5\beta}$, Ring]	−63.0°	(b)
α-D-isorhamnose	[$(OH)^{1\alpha}$, $(OH)^{2\alpha}$, $(OH)^{3\beta}$, $(OH)^{4\alpha}$, $(CH_3)^{5\beta}$, Ring]	120.3°	(c)
β-D-isorhamnose	[$(OH)^{1\beta}$, $(OH)^{2\alpha}$, $(OH)^{3\beta}$, $(OH)^{4\alpha}$, $(CH_3)^{5\beta}$, Ring]		
α-D-fucose	[$(OH)^{1\alpha}$, $(OH)^{2\alpha}$, $(OH)^{3\beta}$, $(OH)^{4\beta}$, $(CH_3)^{5\beta}$, Ring]	251.0°	(a)
β-D-fucose	[$(OH)^{1\beta}$, $(OH)^{2\alpha}$, $(OH)^{3\beta}$, $(OH)^{4\beta}$, $(CH_3)^{5\beta}$, Ring]		

TABLE II

$[\mu]_{D\,obs}^{20}$, CAUSED BY THE DYNAMICAL COUPLING EFFECT BETWEEN ANY TWO MEMBERS OF UNIT GROUPS (EXCEPT RING) IN McDONALD AND BEEVERS' MOLECULAR MODEL (WHEN THE OPTICAL CENTER OF (OH) GROUP IS LOCATED AT THE CENTER OF MASS OF ^{r}C—(OH) BOND, AND THAT OF $(CH_3)^{5\beta}$ GROUP IS AT THE CENTER OF MASS OF C^5—$(CH_3)^{5\beta}$ BOND)

	$(CH_3)^{5\beta}$	4β	4α	3β	3α	2β	2α
1α	−2.0 (−4.2)	−0.1	−0.1	5.6	1.3	3.3	26.4
1β	0.4 (0.8)	−0.7	0.6	0.5	−5.8	29.5	−32.3
2α	−0.3 (−0.5)	3.7	1.3	31.0	−25.2		
2β	0.2 (0.4)	0.4	−5.1	−29.8	−3.1		
3α	1.5 (3.2)	2.3	26.8				
3β	−0.6 (−1.2)	28.8	−29.8				
4α	7.3 (15.7)						
4β	−7.6 (−16.4)						

Note: The values of $[\mu]_{D\,obs}^{20}$ concerning $(CH_3)^{5\beta}$, calculated from Hudson's data of β-L-arabinose (ref. *3), are given in parentheses.

TABLE III

$[\mu]_{D\,obs}^{20}$, CAUSED BY THE DYNAMICAL COUPLING EFFECT BETWEEN ANY TWO MEMBERS OF UNIT GROUPS (EXCEPT RING) IN McDONALD AND BEEVERS' MOLECULAR MODEL (WHEN THE OPTICAL CENTER OF (OH) GROUP IS LOCATED AT O ATOM, AND THAT OF $(CH_3)^{5\beta}$ GROUP IS AT C ATOM)

	$(CH_3)^{5\beta}$	4β	4α	3β	3α	2β	2α
1α	−2.7 (−5.7)	−0.6	−0.1	7.6	1.9	2.9	25.7
1β	0.4 (0.8)	−0.9	0.6	0.4	−8.0	29.4	−32.8
2α	−0.3 (−0.6)	6.0	1.2	31.2	−24.1		
2β	0.2 (0.5)	0.7	−7.2	−30.4	−2.8		
3α	2.0 (4.4)	2.1	25.2				
3β	−0.5 (−1.1)	28.5	−28.4				
4α	7.3 (15.7)						
4β	−7.6 (−16.4)						

Note: The values of $[\mu]_{D\,obs}^{20}$ concerning $(CH_3)^{5\beta}$, calculated from Hudson's data of β-L-arabinose (ref. *3), are given in parentheses.

that α-D- and β-D-isorhamnoses have also C 1 conformation because their corresponding aldohexoses(α-D- and β-D-glucoses) were determined to have C 1 conformation. McDonald and Beevers' molecular model, used in the previous papers 1 and 4, is used again in this article. The optical data for OH group and H atom, used in the previous paper 1, are also employed without any correction. It is supposed that CH_3 group has its optical axis of cylindrical symmetry directed along its bond to the atom with which it combines*5 and the optical center of $(CH_3)^{5\beta}$ group is located at the center of mass of C^5—$(CH_3)^{5\beta}$ bond*6. Values of mean polarizability α and of anisotropy ratio β of CH_3 group are 2.27×10^{-24}(cc)[d] and 0.35[e] respectively. The refractive indices of the aqueous solutions of pentoses and methyl pentoses under question are presumed to be nearly equal (1.34)*7.

Method Proposed

If the orientation of $(OH)^4$ in α-D-fucose changes from β to α, α-D-isorhamnose is obtained*8,*9. Therefore, it is appropriate to treat $[M]_D^{20}$(W)-change, caused by the orientation-change of $(OH)^4$*10 in these two sugars at first. The unit groups which can couple with $(OH)^4$ dynamically in α-D-fucose, are $(OH)^{1\alpha}$, $(OH)^{2\alpha}$, $(OH)^{3\beta}$, $(CH_3)^{5\beta}$ and Ring*8. Then, $\sum[\mu]^{20}_{Dobs}$, caused by the dynamical coupling effect of $(OH)^4$ in α-D-fucose, is given by the following equation,

$$(4\beta)\,\lambda\{(1\alpha)+(2\alpha)+(3\beta)+(CH_3)^{5\beta}+R\}^{*11}$$
$$=(4\beta)\,\lambda\,(1\alpha)+(4\beta)\,\lambda\,(2\alpha)+(4\beta)\,\lambda\,(3\beta)$$
$$+(4\beta)\,\lambda\,(CH_3)^{5\beta}+(4\beta)\,\lambda R\equiv E$$

In the same way, the value in α-D-isorhamnose is as below,

$$(4\alpha)\,\lambda\{(1\alpha)+(2\alpha)+(3\beta)+(CH_3)^{5\beta}+R\}$$
$$=(4\alpha)\,\lambda\,(1\alpha)+(4\alpha)\,\lambda\,(2\alpha)+(4\alpha)\,\lambda\,(3\beta)$$
$$+(4\alpha)\,\lambda\,(CH_3)^{5\beta}+(4\alpha)\,\lambda R\equiv F$$

Accordingly, $[\mu]^{20}_{Dobs}$-change, caused by the orientation-change of $(OH)^4$ in α-D-fucose from β to α (that is to say, $[\mu]^{20}_{Dobs}$ of Yo. Diff. among α-D-isorhamnose and α-D-fucose), is $(F-E)$. The corresponding observed value is given by, {$[M]^{20}_D$(W) of α-D-isorhamnose} minus {$[M]^{20}_D$(W) of α-D-fucose}.

This is $(120.3-251.0)^{*8}=-130.7$. As these two values should be equal to each other,

$$-130.7=\text{Yo. Diff.}=(F-E)=\{(4\alpha)\,\lambda\,(1\alpha)$$
$$+(4\alpha)\,\lambda\,(2\alpha)+(4\alpha)\,\lambda\,(3\beta)+(4\alpha)\,\lambda\,(CH_3)^{5\beta}$$
$$+(4\alpha)\,\lambda R\}-\{(4\beta)\,\lambda\,(1\alpha)+(4\beta)\,\lambda\,(2\alpha)$$
$$+(4\beta)\,\lambda\,(3\beta)+(4\beta)\,\lambda\,(CH_3)^{5\beta}+(4\beta)\,\lambda R\}$$
$$(1)^{*12}$$

By using the method similar to that mentioned above, the following equation is obtained from Yo. Diff. among α-D-xylose and β-L-arabinose.

$$\{(4\alpha)-(4\beta)\}\,\lambda\{(1\alpha)+(2\alpha)+(3\beta)+R\}$$
$$=\{(4\alpha)\,\lambda\,(1\alpha)+(4\alpha)\,\lambda\,(2\alpha)+(4\alpha)\,\lambda\,(3\beta)$$
$$+(4\alpha)\,\lambda R\}-\{(4\beta)\,\lambda\,(1\alpha)+(4\beta)\,\lambda\,(2\alpha)$$

*4 There are sixteen kinds of methyl pentose of D-series and the conformations of α-D- and β-D-rhamnoses and of α-D- and β-D-fucoses have been decided. But, the rest of them have not yet been determined.

4) S. Yamana, This Bulletin, **30**, 920 (1957).

*5 This is C^5-atom, in this case (ref. Fig. 1 in the previous paper 4).

*6 cf. *13 in the previous paper 1.

d) Landolt-Börnstein,"Physikalisch-Chemische Tabellen", Hw. II, p. 985.

e) Values obtained by Cabannes and Granier; see Landolt-Börnstein, "Physikalisch-Chemische Tabellen", 5th Ed. Eg. II, p. 90.

*7 Ref. *8 in the previous paper 5.

5) S. Yamana, This Bulletin, **30**, 207 (1957).

*8 Ref. Table I in this article.

*9 Generally, the diastereomer at C^1-atom is called "anomer" and that at C^2-atom is called "epimer" (ref. 6). Now, the author proposes to use the names of "miner [mi:mə]" and "yomer [jɔ:mə]" to represent the diastereomers at C^3- and C^4-atoms, respectively. "mi-" and "yo-" mean 3 and 4 in Japanese, respectively. The reason for using the oriental language and not European in this case, is to avoid their confusion with the names of polymers ("trimer" etc.). Then, it can be said that α-D-fucose and α-D-isorhamnose are "yomer" to each other.

6) Tollens-Elsner, "Kurzes Handbuch der Kohlenhydrate", Johann Ambrosius Barth, Verlag Leipzig (1935), p. 16, 20.

*10 This is called "yomeric difference (or abbreviated to Yo. Diff.)" by the author (ref. *9 in this article cf. *3 in the previous paper 1).

*11 Ref. *10 in the previous paper 2.

*12 The right side of Eq. 1 can be rewritten as below,

$$\{(4\alpha)\,\lambda\,(1\alpha)+(4\alpha)\,\lambda\,(2\alpha)+(4\alpha)\,\lambda\,(3\beta)$$
$$+(4\alpha)\,\lambda\,(CH_3)^{5\beta}+(4\alpha)\,\lambda R\}-\{(4\beta)\,\lambda\,(1\alpha)$$
$$+(4\beta)\,\lambda\,(2\alpha)+(4\beta)\,\lambda\,(3\beta)+(4\beta)\,\lambda\,(CH_3)^{5\beta}$$
$$+(4\beta)\,\lambda R\}=(4\alpha)\,\lambda\{(1\alpha)+(2\alpha)+(3\beta)$$
$$+(CH_3)^{5\beta}+R\}-(4\beta)\,\lambda\{(1\alpha)+(2\alpha)+(3\beta)$$
$$+(CH_3)^{5\beta}+R\}=\{(4\alpha)-(4\beta)\}\,\lambda\{(1\alpha)+(2\alpha)$$
$$+(3\beta)+(CH_3)^{5\beta}+R\}$$

(∵ the notation λ can be treated in the same way as the multiplication-symbol × of the algebra.) Then, it can be said that $\{(4\alpha)-(4\beta)\}$ λ{……} is a formula of $[\mu]^{20}_{Dobs}$ of Yo. Diff.

$$+(4\beta)\,\Lambda\,(3\beta)+(4\beta)\,\Lambda\,\mathrm{R}\}=-145.6^{*13} \quad (2)$$

From Eq. 1 minus 2,

$$(4\alpha)\,\Lambda\,(CH_3)^{5\beta}-(4\beta)\,\Lambda\,(CH_3)^{5\beta}=14.9$$

This equation can be rewritten as below*14,

$$\{(4\alpha)\times(CH_3)^{5\beta}-(4\beta)\times(CH_3)^{5\beta}\}\zeta_{OH}\zeta_{CH_3}(n^2+2/3)=14.9 \quad (3)^{*13}$$

On the other hand, the value of $(4\alpha)\times(CH_3)^{5\beta}$ and $(4\beta)\times(CH_3)^{5\beta}$ in Eq. 3 can be calculated by using the theoretical formulae*15 as 23.58 and -24.54 respectively. By using these values in Eq. 3,

$$\zeta_{OH}\zeta_{CH_3}=0.3096\ (3/n^2+2) \quad (4)^{*13}$$

But, ζ_{OH} was already calculated and its value is 1.5779 $(3/n^2+2)^{1/2}$*16. Then

$$\zeta_{CH_3}=0.3096(3/n^2+2)/1.5779(3/n^2+2)^{1/2}=0.1962(3/n^2+2)^{1/2} \quad (5)^{*17,*18}$$

Thus, ζ-coefficient of CH_3 group which is indispensable in calculation of $[\mu]^{20}_{D\mathrm{obs}}$ concerning CH_3 group, can be obtained quasi-empirically. Next, an attempt has been made to examine whether this value of ζ_{CH_3} is suitable or not, as follows; at first, by combining these values of ζ_{CH_3} and ζ_{OH} with Table II of the previous paper 1, the tables of $[\mu]^{20}_{D\mathrm{obs}}$ in the methyl pentose-molecule can be made*19. They are Tables II and III.

The unit groups which can couple with $(OH)^1$ dynamically in D-rhamnose, are $(OH)^{2\beta}$, $(OH)^{3\beta}$, $(OH)^{4\alpha}$, $(CH_3)^{5\beta}$ and Ring*8. Then, $\Sigma[\mu]^{20}_{D\mathrm{obs}}$-change, caused by the orientation-change of $(OH)^1$ in this sugar from β to α (that is to say $[\mu]^{20}_{D\mathrm{obs}}$ of An. Diff.*20 of D-rhamnose), is represented as below,

$$\{(1\alpha)-(1\beta)\}\Lambda\{(2\beta)+(3\beta)+(4\alpha)+(CH_3)^{5\beta}+\mathrm{R}\}^{*21}=\{(1\alpha)\,\Lambda\,(2\beta)+(1\alpha)\,\Lambda\,(3\beta)+(1\alpha)\,\Lambda\,(4\alpha)+(1\alpha)\,\Lambda\,(CH_3)^{5\beta}+(1\alpha)\,\Lambda\,\mathrm{R}\}-\{(1\beta)\,\Lambda\,(2\beta)+(1\beta)\,\Lambda\,(3\beta)+(1\beta)\,\Lambda\,(4\alpha)+(1\beta)\,\Lambda\,(CH_3)^{5\beta}+(1\beta)\,\Lambda\,\mathrm{R}\}=\{3.3+5.6-0.1-2.0+(1\alpha)\,\Lambda\,\mathrm{R}\}-\{29.5+0.5+0.6+0.4+(1\beta)\,\Lambda\,\mathrm{R}\}^{*22}=-24.2+(1\alpha)\,\Lambda\,\mathrm{R}-(1\beta)\,\Lambda\,\mathrm{R}=82.0^{*23,*24}$$

The corresponding observed value is given by, $\{[M]^{20}_{D}(\mathrm{W})$ of α-D-rhamnose$\}$ minus $\{[M]^{20}_{D}(\mathrm{W})$ of β-D-rhamnose$\}$. This is, $15.7-(-63.0)=78.7$.

This observed value is almost consistent with the above calculated value, 82.0. This fact indicates that there exists the principle of optical superposition of Kirkwood's idea in methyl pentoses, and also that the values in Table II are all suitable and accordingly the value of ζ_{CH_3} in Eq. 5 is almost satisfactory. Next, the unknown $[M]^{20}_{D}(\mathrm{W})$ of β-D-fucose is presumed by using the method, similar to that mentioned above.

$[\mu]^{20}_{D\mathrm{obs}}$ of An. Diff. of D-fucose is given by the following equation.

$$\{(1\alpha)-(1\beta)\}\Lambda\{(2\alpha)+(3\beta)+(4\beta)+(CH_3)^{5\beta}+\mathrm{R}\}^{*21}=\{(1\alpha)\,\Lambda\,(2\alpha)+(1\alpha)\,\Lambda\,(3\beta)+(1\alpha)\,\Lambda\,(4\beta)+(1\alpha)\,\Lambda\,(CH_3)^{5\beta}+(1\alpha)\,\Lambda\,\mathrm{R}\}-\{(1\beta)\,\Lambda\,(2\alpha)+(1\beta)\,\Lambda\,(3\beta)+(1\beta)\,\Lambda\,(4\beta)+(1\beta)\,\Lambda\,(CH_3)^{5\beta}+(1\beta)\,\Lambda\,\mathrm{R}\}=\{26.4+5.6-0.1-2.0+(1\alpha)\,\Lambda\,\mathrm{R}\}-\{-32.3+0.5-0.7+0.4+(1\beta)\,\Lambda\,\mathrm{R}\}=62.0+(1\alpha)\,\Lambda\,\mathrm{R}-(1\beta)\,\Lambda\,\mathrm{R}=168.2^{*23}$$

The corresponding observed value is obtained by, $\{[M]^{20}_{D}(\mathrm{W})$ of α-D-fucose$\}$ minus $\{[M]^{20}_{D}(\mathrm{W})$ of β-D-fucose$\}$. Then, if $[M]^{20}_{D}(\mathrm{W})$ of β-D-fucose, now unknown, is x,

---

*13 cf. *17 in this article.

*14 Ref. Eq. 32 in *32 in the previous paper 1.

*15 Ref. "Theoretical Formulae" in the previous paper 7.

7) S. Yamana, This Bulletin, **30**, 203 (1957).

*16 Eq. 12 in the previous paper 1.

*17 By using Hudson's data of β-L-arabinose (ref. *3),

$$\{(4\alpha)-(4\beta)\}\Lambda\{(1\alpha)+(2\alpha)+(3\beta)+\mathrm{R}\}=-162.8 \quad (2)^*$$

$$\{(4\alpha)\mathrm{X}(CH_3)^{5\beta}-(4\beta)\mathrm{X}(CH_3)^{5\beta}\}\zeta_{OH}\zeta_{CH_3}(n^2+2/3)=32.1 \quad (3)^*$$

$$\zeta_{OH}\zeta_{CH_3}=0.6671\ (3/n^2+2) \quad (4)^*$$

$$\zeta_{CH_3}=0.4228\ (3/n^2+2)^{1/2} \quad (5)^*$$

*18 It is apparent here that $\zeta_{OH}>\zeta_{CH_2OH}>\zeta_{CH_3}$ (ref. Eq. 20 in the previous paper 1). This fact coincides with the assumption that the magnitude of ζ-coefficient depends mostly upon the degree of change of $\alpha_i\beta_i$ of an unit group by solvation (ref. *19 in the previous paper 1). In other words, the magnitude of ζ indicates roughly the degree of solvation of an unit group. Moreover it is interesting that, when Hudson's data of L-arabinoses are used, $\zeta_{OH}\zeta_{CH_3}$ (this is 0.6671 $(3/n^2+2)$) is nearly equal to $\zeta^2_{CH_2OH}$ (this is 0.6276 $(3/n^2+2)$). (ref. *17 in this article and *43 in the previous paper 1).

*19 Concerning the procedure of making the table of $[\mu]^{20}_{D\mathrm{obs}}$, refer to Eq. 3 in the previous paper 1. The values of ζ_{OH} and ζ_{CH_3} which are used for Table III, are given in *44 in the previous paper 1 and *31 in this article.

*20 Ref. *3 in the previous paper 1.

*21 It can be said that $\{(1\alpha)-(1\beta)\}\Lambda\{\cdots\cdots\}$ is a formula of $[\mu]^{20}_{D\mathrm{obs}}$ of An. Diff. (cf. *12).

*22 The values in Table II are used.

*23 Eq. 13 in the previous paper 1 is used here.

*24 cf. *30.

the observed value of An. Diff. of D-fucose is $(251.0-x)$. This value should be equal to the above calculated $[\mu]^{20}_{D\text{obs.}}$ Then $251.0-x=168.2$ hence $x=82.8$*24

By using the same method, $[M]^{20}_{D}$(W) of β-D-isorhamnose, now unknown, is calculated as -46.6*24.

Discussion on the Results

In the previous paper[4], the author presumed the internal conformation of C^6—O bond in D-mannose molecule in aqueous solution by a new method, devised by the author, and the obtained result satisfied the conditions which were required from the viewpoint of the atomic distances in the molecule of D-mannose. By the calculation in reversing the order of this method, it becomes possible to find another method*25 of presuming the unknown $[M]^{20}_{D}$(W), as below; according to the previous paper 1, the internal conformation of C^6—O bond in D-galactose in aqueous solution seems to be mostly of *gauche* II type. Then, the unit groups which can couple with $(OH)^1$ dynamically in this sugar are $(OH)^{2\alpha}$, $(OH)^{3\beta}$, $(OH)^{4\beta}$, $(CH_2OH)^{5\beta\cdot g\mathrm{II}}$ and Ring*26. Therefore, $[\mu]^{20}_{D\text{obs}}$ of An. Diff. of D-galactose is given by,

$$\{(1\alpha)-(1\beta)\}\lambda\{(2\alpha)+(3\beta)+(4\beta)+(5\beta.g\mathrm{II})+\mathrm{R}\}^{*21}=\{(1\alpha)-(1\beta)\}\lambda\{(2\alpha)+(3\beta)+(4\beta)+\mathrm{R}\}+\{(1\alpha)-(1\beta)\}\lambda(5\beta.g\mathrm{II})\equiv G$$

Whereas, $[\mu]^{20}_{D\text{obs}}$ of An. Diff. of D-fucose has already been given by,

$$\{(1\alpha)-(1\beta)\}\lambda\{(2\alpha)+(3\beta)+(4\beta)+(CH_3)^{5\beta}+\mathrm{R}\}=\{(1\alpha)-(1\beta)\}\lambda\{(2\alpha)+(3\beta)+(4\beta)+\mathrm{R}\}+\{(1\alpha)-(1\beta)\}\lambda(CH_3)^{5\beta}\equiv H$$

Then, the difference between these two $[\mu]^{20}_{D\text{obs}}$, (G and H), is as follows;

$$G-H=\{(1\alpha)-(1\beta)\}\lambda(5\beta.g\mathrm{II})-\{(1\alpha)-(1\beta)\}\lambda(CH_3)^{5\beta}=\{(1\alpha)\lambda(5\beta.g\mathrm{II})-(1\beta)\lambda(5\beta.g\mathrm{II})\}-\{(1\alpha)\lambda(CH_3)^{5\beta}-(1\beta)\lambda(CH_3)^{5\beta}\}\simeq(1\alpha)\lambda(OH)^{6\cdot g\mathrm{II}*27}-(1\beta)\lambda(OH)^{6\cdot g\mathrm{II}}=7.3^{*28}$$

The corresponding observed value is given by, $(271.5-95.1)^{*26}-(251.0-x)^{*28}=x-74.6$.

As these two values should be equal to each other,

$$7.3=x-74.6 \quad \therefore \quad x=81.9$$

This is the presumed value of $[M]^{20}_{D}$(W) of β-D-fucose, by the new method without using ζ_{CH_3}. By using the same method*29, $[M]^{20}_{D}$(W) of β-D-isorhamnose can be calculated to be -43.4*24. These presumed values are not exactly but approximately consistent with those, calculated by using ζ_{CH_3} in "Method Proposed" of this article, (82.8 and -46.6), respectively.

Comparing these calculated values by two different methods with each other,

*25 In this method, ζ_{CH_3} is needless.

*26 Ref. Table I in the previous paper 1.

*27 $(OH)^{6\cdot g\mathrm{II}}$ means OH group which combines with C^6-atom in *gauche* II conformation (i.e. OH group in $(CH_2OH)^{5\beta\cdot g\mathrm{II}}$), and so on.

*28 Concerning the process of this simplification, refer to "Method Proposed" in the previous paper 4. And here, the optical center of OH group is located at the center of mass of C—(OH) bond.

*29 {$[\mu]^{20}_{D\text{obs}}$ of An. Diff. of D-mannose} minus {$[\mu]^{20}_{D\text{obs}}$ of An. Diff. of D-rhamnose} $\simeq(1\alpha)\lambda(OH)^{6\cdot ma}-(1\beta)\lambda(OH)^{6\cdot ma}$*28; {$[\mu]^{20}_{D\text{obs}}$ of An. Diff. of D-glucose} minus {$[\mu]^{20}_{D\text{obs}}$ of An. Diff. of D-isorhamnose} $\simeq(1\alpha)\lambda(OH)^{6\cdot ma}-(1\beta)\lambda(OH)^{6\cdot ma}$*28 $\therefore$ {$[\mu]^{20}_{D\text{obs}}$ of An. Diff. of D-mannose} minus {$[\mu]^{20}_{D\text{obs}}$ of An. Diff. of D-rhamnose} = {$[\mu]^{20}_{D\text{obs}}$ of An. Diff. of D-glucose} minus {$[\mu]^{20}_{D\text{obs}}$ of An. Diff. of D-isorhamnose}. This equation can be rewritten by using the corresponding observed values, as below; {$[M]^{20}_{D}$(W) of An. Diff. of D-mannose} minus {$[M]^{20}_{D}$(W) of An. Diff. of D-rhamnose} = {$[M]^{20}_{D}$(W) of An. Diff. of D-glucose} minus {$[M]^{20}_{D}$(W) of An. Diff. of D-isorhamnose}; $\{52.8-(-30.6)\}-\{15.7-(-63.0)\}=\{202.1-33.7\}-\{120.3-x\}$*3,*24,*26 or $x=-43.4$.

*30 When using Hudson's data of L-arabinoses (ref. *17 in this article), $[\mu]^{20}_{D\text{obs}}$ of An. Diff. of D-rhamnose is 78.6 (Eq. 13* in *35 of the previous paper 1 is used here). (This is just equal to its corresponding observed value, 78.7). The presumed values of $[M]^{20}_{D}$(W), in this case, are as below; β-D-fucose (86.2) (This is somewhat greater than that, calculated in "Method Proposed" and "Discussion on the Results" in this article.); β-D-isorhamnose (-43.2).

*31 For comparison, the calculated values by supposing that the optical centers of OH and CH_3 groups are located at their respective O and C atoms, are given here (cf. *44 in the previous paper 1),

	Isbell and Pigman's data of L-arabinoses	Hudson's data of L-arabinoses
ζ_{CH_3}	0.2880 $(3/n^2+2)^{1/2}$	0.6206 $(3/n^2+2)^{1/2}$
$[M]^{20}_{D}$(W) of β-D-fucose	83.6	87.8
$[M]^{20}_{D}$(W) of β-D-isorhamnose	-46.1	-41.9

$[M]_D^{20}$(W) of β-D-fucose, and β-D-isorhamnose are presumed to be about 81.9～82.8 and −46.6～−43.4 respectively*[31].

Summary

It was concluded by PM-method that the principle of optical superposition of Kirkwood's idea exists in methyl pentoses, and two $[M]_D^{20}$(W), formerly unknown, were presumed.

The author wishes to express his deepest thanks to Professor S. Tanaka (Kyoto University) for his valuable discussion and encouragement throughout the course of this study.

Department of Chemistry
Kyoto Gakugei University
Fushimi-ku, Kyoto

The Synthesis of Carvone from α-Terpinyl Acetate

By Takayuki SUGA

(Received February 22, 1958)

Up to the present, the synthesis of *l*-carvone from *d*-limonene has been attained through the intermediates of *d*-limonene nitrosochloride and *l*-carvoxime[1,2]. In these cases the conversion of limonene into carvone resulted in relatively high yields (35% and 56~60%, respectively), but it was necessary to use toxic nitrosylchloride gas. Recently, two alterative methods[3] of the conversion of *d*-limonene into *l*-carvone have been reported. The first involves conversion of limonene monoxide into limonene glycol, oxidation of the glycol to a keto alcohol with *tert*-butyl chromate, and dehydration of the keto alcohol to *l*-carvone. In the second, the oxide is first converted into limonene glycol diacetate, which is in turn pyrolyzed to carveol acetate, saponified to carveol, and then oxidized to carvone. The overall yields of *l*-carvone from *d*-limonene in these cases do not exceed 9.2% and 7%, respectively.

Oppenauer and Oberrauch[4] previously found that *tert*-butyl chromate, described by Wienhaus and Treibs[5], is useful as an oxidant, and that *tert*-butyl chromate dissolved in a non-polar solvent with addition of a small amount of an organic acid oxidizes the methylene group adjacent to a double bond to the ketonic group without attacking the double bond.

The oxidation of terpene compounds with *tert*-butyl chromate has been investigated in this laboratory, and it has been reported that the oxidation of α-pinene[6] gives mainly verbenone and a little verbenyl acetate, and the oxidation of carvomenthene[7] produces carvotanacetone. It has been also described by Dupont et al.[8] that, on oxidation with *tert*-butyl chromate, carvomenthene yields carvotanacetone and piperitone, both α- and β-pinenes give verbenone only, and camphene remains unchanged. Thus it is evident that when a terpene hydrocarbon containing an isolated double bond is treated with *tert*-butyl chromate, the methylene group in the α-position to an ethylenic linkage in the ring is oxidized to a ketonic group.

Oxidation of α-terpineol with tert-butyl chromate[9]. The author considered that, if the methylene group adjacent to the ethylenic linkage of α-terpineol (I_a) was oxidized to a ketonic group with *tert*-butyl chromate as in the cases of terpene hydrocarbons and if 8-hydroxycarvotanacetone (II_a) was thus obtained in a high

1) C. Bordenca, F. K. Allison and P. H. Dirstine, *Ind. Eng. Chem.*, **43**, 1196 (1951).
2) E. E. Royals and S. E. Horne, Jr., *J. Am. Chem. Soc.*, **73**, 5856 (1951).
3) S. M. Linder and F. P. Greenspan, *J. Org. Chem.*, **22**, 949 (1957).
4) R. V. Oppenauer and H. Oberrauch, *Anales Asoc. Quim. Argentina*, **37**, 246 (1949).
5) H. Wienhaus and W. Treibs, *Ber.*, **56**, 1648 (1923).
6) T. Matsuura and K. Fujita, *J. Sci. Hiroshima Univ.*, **A16**, 173 (1952).
7) K. Fujita and T. Matsuura, ibid., **A18**, 455 (1955).
8) G. Dupont, R. Dulou and O. Mondou, *Bull. soc. chim. France*, **1953**, 60.
9) T. Matsuura and T. Suga, *J. Chem. Soc. Japan, Pure Chem. Sec.* (*Nippon Kagaku Zassi*), **78**, 1117 (1957).

TABLE I
CONDITIONS AND RESULTS IN OXIDATION OF *dl*-α-TERPINEOL

Expt.	Conditions			Reaction Products**		
	Sample/Chromic acid (mole ratio)	Temp. (°C)	Time*	8-Hydroxy-carvotan-acetone (%)	8-Hydroxy-piperitone (%)	Homoterpenyl methyl ketone (%)
1	I:5	50	36 hr., then 4 days at R.T.	8	5	22
2	1:2.5	35	36 hr., then 12 hr., at R.T.	I5	7	20
3	1:2.5	20	10 days at R.T.	14	7	18

* R.T.: Room temperature.
** Yields represent wt.% for α-terpineol used.

yield, it would be possible to convert the latter into carvone by dehydration to form an isopropenyl group from the hydroxy-isopropyl group. Then, an attempt was first made to study the action of *tert*-butyl chromate on *dl*-α-terpineol. A benzene solution of *tert*-butyl chromate containing glacial acetic acid and acetic anhydride was used as an oxidizing agent, and the oxidation was carried out in a current of carbon dioxide under three different conditions as shown in Table I. From the results (Table I) it was found that the reaction products consisted of 8-hydroxycarvotanacetone (II_a), 8-hydroxy-piperitone (III_a), a new compound, and

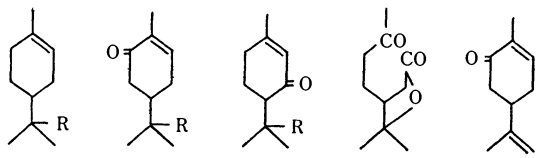

a, R=OH
b, R=OAc

homoterpenyl methyl ketone (IV), but in all cases unchanged α-terpineol was recovered in amounts ranging from 32% to 44%.

Considerable amounts of homoterpenyl methyl ketone were produced from α-terpineol by oxidative fission of the double bond in the ring. Such cleavage occurred scarcely ever or only a little in the oxidation of α-pinene, carvomenthene and limonene (to be described later). It was difficult to suppress the cleavage of the ethylenic bond even by using milder conditions, viz., a small amount of the oxidant at a low temperature (e.g., Expt. 3).

Oxidation of α-terpinyl acetate with tert-butyl chromate[10]. Accordingly it is of interest to attempt an oxidation of *dl*-α-terpinyl acetate (I_b) to see whether, by acetylating the hydroxyl group of α-terpineol, it is possible to suppress the cleavage reaction of the ethylenic linkage in the ring*.

A benzene solution of *tert*-butyl chromate (three moles of chromic anhydride to one mole of α-terpinyl acetate) containing glacial acetic acid and acetic anhydride was used as in the case of α-terpineol. Treatment of α-terpinyl acetate with this oxidant at room temperature (the average temperature was 20°C) for fifteen days in a current of carbon dioxide led to the formation of 8-acetoxycarvotanacetone (II_b) (the yield was 23% to α-terpinyl acetate), which had not yet been described, and homoterpenyl methyl ketone (15%), but in this case no product resulting from the oxidation of the methylene group in the $C_{(3)}$ position of α-terpinyl acetate was detected. The oxidation of a large amount of α-terpinyl acetate, however, gave a small amount (ca. 3%) of a new compound, 8-acetoxypiperitone (III_b), in which the methylene group in the $C_{(3)}$ position was changed into a ketonic group, while the yields of 8-acetoxycarvotanacetone and homoterpenyl methyl ketone were

10) T. Matsuura, T. Suga and K. Suga, *J. Chem. Soc. Japan, Pure Chem. Sec.* (*Nippon Kagaku Zassi*), **78**, 1122 (1957).

* It is interpreted by J. L. Simonsen ("The Terpenes", University Press, Cambridge, 1947, Vol. 1, p. 259) that on oxidation of α-terpineol, homoterpenyl methyl ketone is formed by loss of water from a γ-hydroxyacid (VI).

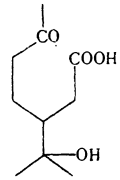

(VI)

26% and 10%, respectively. A respectable amount of α-terpinyl acetate (26% and 43%, respectively) was recovered unchanged.

Thus it was made quite clear that, on action of *tert*-butyl chromate on α-terpinyl acetate, the oxidation of the methylene group in the $C_{(6)}$ position in the ring to a ketonic group (to give 8-acetoxycarvotanacetone) proceeds prominently, while both the oxidation of the $C_{(3)}$ position (to 8-acetoxypiperitone) and the cleavage of the double bond (to homoterpenyl methyl ketone) are restrained.

Dehydroacetoxylation of 8-acetoxycarvotanacetone[11]. There have been a great deal of works showing that the pyrolysis of esters is an excellent method for the introduction of the unsaturated linkage, and it has frequently been used for the syntheses of olefins. Bailley et al.[12] have recently shown that the vapor phase pyrolysis of acetates of secondary and tertiary alcohols proceeds selectively with the formation of the least alkylated olefin, and the direction of elimination is always such that the hydrogen is abstracted in the order: primary>secondary >tertiary. It has also been reported by Aratani and Matsuura[13] that the pyrolysis of terpin diacetate produced β-terpinyl acetate in 57% yield.

It is of interest, therefore, to study the pyrolysis of 8-acetoxycarvotanacetone (II_b) to produce carvone (V) by the elimination of acetic acid.

The pyrolysis was carried out by the distillation through a Vigreux column under an atmospheric pressure in an air-bath, the temperature of which was raised gradually from the room temperature to 340°C during the operation. Acetic acid was liberated in an amount of 92% of the theoretical and the pyrolysate which distilled out was 91% of the starting material. The pyrolysate freed from acetic acid gave a neutral oil (66%), which contained 72% (or 59% of the theoretical amount to the starting material) of the desired ketone, *dl*-carvone, and the undesired substances, carvacrol (7%) and piperitenone (13%). It was sure that piperitenone was formed through the dehydroacetoxylation of 8-acetoxypiperitone which existed as a contaminate in 8-acetoxycarvotanacetone. A small amount (ca. 7%) of 8-acetoxycarvotanacetone was recovered.

Thus, it has been established that when 8-acetoxycarvotanacetone is pyrolyzed in the liquid phase, the dehydroacetoxylation takes place in the direction of a primary hydrogen atom to form an isopropenyl group and gives a relatively high yield of *dl*-carvone.

Selection of the conditions in the oxidation of α-terpinyl acetate. As mentioned above, the pyrolysis of 8-acetoxycarvotanacetone proceeds in a highly selective manner to give the prominent yield of carvone, but the conversion of α-terpinyl acetate into 8-acetoxycarvotanacetone is unsatisfactory in respect of the yield under the employed circumstances.

An extensive study was then made in order to develop a satisfactory procedure for the conversion of α-terpinyl acetate into 8-acetoxycarvotanacetone and to accumulate, in addition, fundamental data for the *tert*-butyl chromate oxidation. The effects of the solvent, (acetic acid), and the reaction temperature, and the catalytic action of benzoyl peroxide, on the yield of the reaction products from oxidation of α-terpinyl acetate, particularly the desired α,β-unsaturated ketone, were studied.

The relative yields of crude 8-acetoxycarvotanacetone in the reaction mixtures were determined by measuring the absorption at the maximum 235 mμ, specific to the α,β-unsaturated ketone, and the yields were estimated by weighing the desired ketone isolated by fractional distillation.

To examine the effect of the solvent on the yield, *n*-hexane, carbon tetrachloride, and benzene, were compared under the identical conditions (Expt. 1, 2 and 3 in Table II), and benzene was found the best. Therefore, benzene was henceforward used as the solvent for *tert*-butyl chromate.

Next, the influence of aeration was examined. The experiments showed that the yield of the α,β-unsaturated ketone in the acidic oxidation (Expt. 3 and 4) was greater in the current of air than in the current of carbon dioxide, but such was not the case in the neutral oxidation (Expt. 5 and 6). The results were similar irrespective of the amounts of the oxidant (Expt. 7 and 8) and of the acid (Expt. 9 and 10). The increase in the yield, however, seems not to be concerned with a simple autoxidation, because α-terpinyl acetate was fairly indifferent to air in

11) T. Suga and T. Matsuura, ibid., **78**, 1089 (1957).
12) W. J. Bailey, et al., *J. Am. Chem. Soc.*, **77**, 75, 357 (1955).
13) T. Aratani and T. Matsuura, *J. Sci. Hiroshima Univ.*, **A20**. 191 (1957).

the same medium and under the same conditions as in the acidic oxidation (Expt. 11), infrared absorption (Fig. 1) showing that α-terpinyl acetate was not changed by air.

Further, in the acidic oxidation in the current of either carbon dioxide or air, the yield of α,β-unsaturated ketone increased with the addition of increasing quantities of acetic acid. However, the increase in the acid made difficult the separation of the benzene layer from the aqueous layer in the treatment of the reaction mixture with water.

The effect of the temperature on the yield of the products was studies with the results as follows. In the oxidation with the acidic oxidant in the air-stream, elevation of the temperature from 30°C to 50°C* brought a significant increase in the yield of the α,β-unsaturated ketone even when the amount of acetic acid was small (Expt. 12). The yield of the ketone was somewhat greater when more acid was used (Expt. 13), reaching 45% to α-terpinyl acetate used.

Thus it was established that the desired α,β-unsaturated ketone is produced in 45% yield to α-terpinyl acetate when the oxidation using the fixed quantity of the benzene solution of *tert*-butyl chromate (the mole ratio of α-terpinyl acetate to chromic anhydride is 1 : 2.7) is carried out with the addition of ca. 9% acetic acid at 50°C for one hundred hours in the current of air.

Then, in the acidic oxidation in the current of carbon dioxide, the effect of benzoyl peroxide, which has been frequently used as an initiator of radical reactions, was examined (Expt. 14 and 15). The acidic oxidation in the presence of benzoyl peroxide was carried out at 55°C, since it has been reported[14,15] that the catalytic ability of benzoyl peroxide increases with the elevation of the temperature, and results in an increase in the yield of the α,β-unsaturated ketone, compared with the oxidation in the absence of the peroxide.

Though not yet examined, a larger excess of the oxidant with benzoyl peroxide and air may increase more remarkably the yield of the desired ketone.

It was thus established that the conversion of *dl*-α-terpinyl acetate into *dl*-carvone through 8-acetoxycarvotanacetone is effected by means of the combined procedure of the *tert*-butyl chromate oxidation and the pyrolysis, giving an overall yield of 28 mole%.

In conclusion, it may be added that Fujita[16] of this laboratory treated *d*-limonene with a benzene solution of *tert*-butyl chromate containing acetic acid and acetic anhydride at 50°C for a period of thirty-six hours and obtained chiefly *dl*-carvone in a yield of 20% to limonene along with *d*-isopiperitenone (13%) and piperitenone (3%).

Experimental

Oxidation of *dl*-α-Terpineol—Expt. 2 (Table I) is described below in details. Expt. 1 and 3 followed in the wake of Expt. 2.

dl-α-Terpineol[17], b.p.$_2$ 79~80°C, n_D^{25} 1.4814, d_4^{25} 0.9310, was prepared by refluxing terpin hydrate with 0.5% aqueous solution of oxalic acid for 5 hr. and by rectifying the crude product.

tert-Butyl chromate[4] was prepared by adding 163 g. of chromic anhydride in small portions to 325 g. of *tert*-butyl alcohol with ice-cooling, diluting the resultant with 1000 g. of benzene, drying the resulted benzene solution over anhydrous sodium sulfate, and concentrating it to 75 vol.% in vacuo. To the solution were added 55 g. of glacial acetic acid and 75 g. of acetic anhydride just prior to the oxidation.

Oxidation and treatment of reaction products.—To 100 g. of α-terpineol in 150 g. of dry benzene was added dropwise the above oxidant in a period of 4 hr. with agitation at 35°C, and then the mixture was maintained at the same temperature for 32 hr. with stirring in an atmosphere of carbon dioxide, and left to stand at the room temperature for 12 hr. When the reaction was over, the whole reaction mixture was treated with 500 cc. of water and 290 g. of hydrated oxalic acid with vigorous stirring. The mixture was separated into two layers and the aqueous solution was repeatedly extracted with benzene. The combined benzene solution was treated with aqueous alkali and with water successively and dried. After removal of the solvent, 78.5 g. of a neutral oil was obtained (Product A). The alkaline solution was repeatedly extracted with ether and chloroform in succession. From the both extracts 4.5 g. of a brown viscous oil was obtained (Product B).

Identification of products.—Distillation of Product A at 7 mmHg gave the following four fractions: (A) b.p.$_7$ 82~86°C, n_D^{25} 1.4775~1.4792, d_4^{25} 0.9445~0.9516, yield 43.9 g.; (B) b.p.$_7$ 111~121°C, n_D^{25} 1.4832~1.4850, d_4^{25} 1.0182~1.0202, yield 6.6 g.;

* It is described[4] that *tert*-butyl chromate explodes when heated above 60°C.

14) S. Kamenskaya and S. Medvedev, *Acta Physicochim.*, **13**, 565 (1940); *Chem. Abst.*, **35**, 2400 (1941).

15) M. F. R. Mulcahy and I. C. Watt, *J. Chem. Soc.*, **1954**, 2971.

16) K. Fujita, *J. Chem. Soc. Japan, Pure Chem. Sec.* (*Nippon Kagaku Zassi*), **78**, 1112 (1957).

17) K. Ono and Z. Taketa, *Reports of Saisei Shôno Co.*, **1**, 11 (1924).

(C) b.p.$_7$ 146~151°C, n_D^{25} 1.4914, d_4^{25} 1.0325, yield 14.9 g.; (D) b.p.$_7$ 166~170°C, yield 16.2 g.

(1) 8-Hydroxypiperitone (III$_a$). Ultraviolet absorption spectrum of fraction B gave λ_{max}^{alc}: 235mμ (strong), which corresponded to the *K*-band of the α,β-unsaturated ketone[18], and 276mμ (very weak). The chromatogram on Kirchner's chromatostrip[19], developed with 45 vol.% ethyl acetate in *n*-hexane and sprayed with 2,4-dinitrophenylhydrazine—hydrochloric acid, gave two spots. One, R_f value=0.20, was large and distinct, while the other, R_f value=0.73, was small and faint. Accordingly, the weak band at 276mμ seemed to be attributable to the impurity which gave the spot, R_f value=0.73. The heating of 3.3 g. of fraction B with 0.4 g. of palladium charcoal[20] (palladium: 30%) at 240~245°C for 9 hr. in the current of carbon dioxide gave 2.1 g. of thymol. This fact was established by the following procedures: (a) Ultraviolet absorption spectrum of the oil obtained exhibited the same λ_{max}^{alc} 277mμ (ε: 1870) as λ_{max}^{alc} 277mμ (ε: 2400) of thymol. (b) On heating with phthalic anhydride in presence of conc. sulfuric acid, thymolphthalein was obtained. (c) An alkaline solution of monochloroacetic acid[21] gave thymoxyacetic acid, m.p. and mixed m.p. 149~149.5°C.

Next, a mixture of 0.89 g. of fraction B, 0.90 g. of xylene and 0.09 g. of anhydrous zinc chloride was heated at 140°C for 0.5 hr. with agitation. This treatment gave 0.57 g. of piperitenone. This fact was confirmed by the following procedures: (a) Ultraviolet absorption spectrum exhibited λ_{max}^{alc} 242mμ (ε: 4760) and 276mμ (ε: 3180) identical with the *K*-band of the cross conjugated dienone chromophore in piperitenone[22]. (b) The chromatogram on chromatostrip did not give a spot of R_f value 0.20 corresponding to the original ketone but gave a spot of R_f value 0.73 corresponding to piperitenone. (c) A warm solution of 2,4-dinitrophenylhydrazine in alcoholic hydrochloric acid gave an isomeric mixture of piperitenone 2,4-dinitrophenylhydrazone. The separation by chromatography on silica—plaster of Paris (4:1) with benzene—petroleum ether (1:1) gave two isomers*, m.p. 152~153°C (67%) and m.p. 183.5~184°C (33%), of the 2,4-dinitrophenylhydrazone. Each showed no depression on admixture with the known specimens.

The results are schematically summarized as follows:

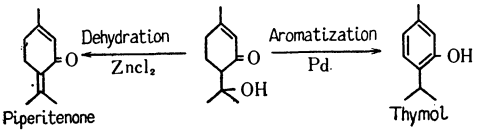

Thus, it was evident that fraction B consisted of 8-hydroxypiperitone.

(2) 8-Hydroxycarvotanacetone. (II$_a$) The chromatostrip—chromatogram of fraction C by the same method as above gave a single spot, R_f value=0.33. Ultraviolet absorption spectrum exhibited λ_{max}^{alc} 235mμ.

Treatment of a part of this fraction with palladium charcoal gave carvacrol, which was identified as the phenylurethane, m.p. and mixed m.p. 134.8~135°C.

Fraction C gave a semicarbazone, m.p. 175~176°C, and an oxime, m.p. 133~134°C. These were identified as the derivatives of 8-hydroxycarvotanacetone by mixing with known samples. By the treatment with a warm solution of 2,4-dinitrophenylhydrazine in alcoholic hydrochloric acid, 2,4-dinitrophenylhydrazone, m.p. 201~201.5°C (*Anal.* Found: N, 16.23. Calcd. for $C_{16}H_{20}O_5N_4$: N, 16.08%), was obtained.

Thus, it was established that fraction C consisted of 8-hydroxycarvotanacetone.

Ultraviolet absorption spectra of the derivatives: semicarbazone, λ_{max}^{alc} 264mμ (ε: 24000); oxime, λ_{max}^{alc} 234mμ (ε: 16300); 2,4-dinitrophenylhydrazone, λ_{max}^{alc} (the principal band) 378mμ (ε: 26650).

2,4-Dinitrophenylhydrazone of 8-hydroxycarvotanacetone, and ultraviolet absorption spectra of the ketone and its derivatives, have not yet been described in the literatures.

(3) Homoterpenyl methyl ketone (IV). Fraction D solidified. The crystalline product had m.p. 62~63°C. Its semicarbazone had m.p. 205~206°C. Product B (described above), after being distilled (b.p.$_4$ 154~160°C), also gave a semicarbazone, m.p. 204.5~205°C. These were identified as homoterpenyl methyl ketone and its semicarbazone by mixing with the genuine specimens. From fraction D, 2,4-dinitrophenylhydrazone, m.p. 164~164.5°C (*Anal.* Found: N, 15.53. Calcd. for $C_{16}H_{20}O_6N_4$: N, 15.38%) was quantitatively prepared.

(4) Unchanged α-terpineol (I$_a$). Fraction A gave *dl*-α-terpinyl phenylurethane, m.p. and mixed m.p. 112~113°C, and nitrosochloride, m.p. and mixed m.p. 112~113°C.

Further, from the recovered benzene solution, a small amount of acetone was isolated as the semicarbazone, m.p. and mixed m.p. 187~188°C.

Oxidation of *dl*-α-Terpinyl Acetate—*dl*-α-*Terpinyl acetate*, b.p.$_{15}$ 112~113.5°C, n_D^{25} 1.4638, d_4^{25} 0.9563, ester value 286.4 (calcd. for $C_{12}H_{20}O_2$: 285.9), was prepared by refluxing *dl*-α-terpineol with acetic anhydride and anhydrous sodium acetate in xylene and by rectifying the product.

I. Identification of the Reaction Products.—To 90 g. of α-terpinyl acetate was added dropwise a benzene solution of *tert*-butyl chromate, which was prepared from 255 g. of *tert*-butyl alcohol, 138 g. of chromic anhydride, 560 g. of benzene,

18) R. B. Woodward, *J. Am. Chem. Soc.*, **63**, 1123 (1941); L. K. Evans and A. E. Gillam, *J. Chem. Soc.*, **1941**, 815; ibid., **1943**, 565.

19) J. G. Kirchner, J. M. Miller and G. J. Keller, *Anal. Chem.*, **23**, 420 (1951); J. M. Miller and J. G. Kirchner, ibid., **25**, 1107 (1953).

* Y. R. Naves[22] isolated the three isomers, m. p. 132~133°C, m. p. 152~153° and m. p. 183.5~184°C. We could also isolate these three isomers in another part of the experiments (described later).

20) R. P. Linstead, K. O. A. Michaelis and S. L. S. Thomas, *J. Chem. Soc.*, **1940**, 1139.

21) F. Koelsch, *J. Am. Chem. Soc.*, **53**, 304 (1931).

22) Y. R. Naves, *Bull. soc. chim. France*, **1951**, 370.

100 g. of acetic acid and 100 g. of acetic anhyride, in a period of 6.5 hr. with stirring and cooling in ice, and then the mixture was maintained at the room temperature (20°C averaged) for 15 days with occasional agitation. Treated in the same way as in the case of α-terpineol, the benzene solution gave 59.5 g. of a neutral oily product and the alkaline aqueous solution gave 10.0 g. of a viscous oil (b.p.$_{12}$ 180~184°C).

Distillation of the neutral oily product at 7mmHg gave the following three fractions: (A) b.p.$_7$ 93~98°C, n_D^{25} 1.4592, d_4^{25} 0.9718, yield 23.1 g.; (B) b.p.$_7$ 139~142°C, n_D^{25} 1.4706, d_4^{25} 1.0498, yield 17.9 g.; (C) b.p.$_7$ 145~160°C, n_D^{25} 1.4737, d_4^{25} 1.0495, yield 6.2 g.

(1) 8-Acetoxycarvotanacetone (II_b). Ester value of fraction B was 263.6 (calcd. for $C_{12}H_{18}O_3$: 266.3). The λ_{max}^{alc} 235mμ in ultraviolet spectrum and the wave number of 1672 cm.$^{-1}$ (liquid film) in infrared spectrum indicated the presence of a ketonic group conjugated with a double bond. In the infrared spectrum, wave numbers 1729 cm.$^{-1}$ and 1246 cm.$^{-1}$, characteristic of acetate, were also observed. The saponified product gave 8-hydroxycarvotanacetone semicarbazone and oxime.

These results established that fraction B consisted of 8-acetoxycarvotanacetone.

The derivatives of 8-acetoxycarvotanacetone and their ultraviolet absorption spectra were as follows:

Semicarbazone, m.p. 191.5~192°C, λ_{max}^{alc} 264mμ (ε: 23710).

Anal. Found: C, 58.23; H, 7.91; N, 15.85. Calcd. for $C_{13}H_{21}O_3N_3$: C, 58.41; H, 7.92; N, 15.72%.

Oxime, m.p. 107.2~107.5°C, λ_{max}^{alc} 233mμ (ε: 15870).

Anal. Found: C, 64.16; H, 8.36; N, 6.51. Calcd. for $C_{12}H_{19}O_3N$: C, 63.98; H, 8.50; N, 6.22%.

2,4-Dinitrophenylhydrazone, m.p. 217.8~218°C, λ_{max}^{alc} (a principal band) 376mμ (ε: 27580).

Anal. Found: N, 14.64. Calcd. for $C_{18}H_{22}O_6N_4$: N, 14.35%.

(2) Homoterpenyl methyl ketone (IV). Fraction C (6.2 g.) was saponified with alkali and extracted with ether. From the ethereal solution 3.0 g. of 8-hydroxycarvotanacetone was isolated as the semicarbazone. The residual alkaline solution, after being acidified with dilute sulfuric acid and extracted with chloroform, gave 3.2 g. of homoterpenyl methyl ketone. The viscous oil (10.0 g.), b.p.$_{12}$ 180~184°C, from alkaline aqueous solution (vide ante) was also homoterpenyl methyl ketone.

(3) Unchanged α-terpinyl acetate (I_b). Ester value of fraction A was 283.2 (calcd. for $C_{12}H_{20}O_2$: 285.9). The saponified product gave *dl*-α-terpinyl phenylurethane and nitrosochloride.

(4) 8-Acetoxypiperitone (III_b). When 280 g. of α-terpinyl acetate was oxidized with *tert*-butyl chromate, prepared from 852 g. of *tert*-butyl alcohol, 426 g. of chromic anhydride, 3360 g. of benzene, 420 g. of acetic acid and 320 g. of acetic anhydride, at 50°C for 36 hr. and then at the room temperature for 3 days, 249 g. of the neutral oxidation product was obtained.

The product gave unchanged α-terpinyl acetate (43% to α-terpinyl acetate used), 8-acetoxycarvotanacetone (26%), homoterpenyl methyl ketone (10%) and a fraction of b.p.$_{3.5}$ 100~120°C, n_D^{25} 1.4670, d_4^{25} 1.0100, yield 7.3 g. (ca. 3%), which was the intermediate fraction between α-terpinyl acetate and 8-acetoxycarvotanacetone.

Ultraviolet absorption spectrum of this fraction exhibited λ_{max}^{alc} 235mμ (very strong) and 277mμ (very weak). In the chromatogram on chromatostrip, developed with 30 vol. % ethyl acetate in *n*-hexane and sprayed with 2,4-dinitrophenylhydrazine—hydrochloric acid, the major portion (λ_{mcx}^{alc} 235mμ) gave a large spot, R_f value=0.38 and the weak 277mμ band seemed to be attributable to an impurity which gave a faint spot, R_f value=0.62.

2,4-Dinitrophenylhydrazone, after being chromatographed on silica—plaster of Paris (4:1) with benzene—petroleum ether (1:1) and recrystallized from ethyl acetate, had m.p. 166~166.5°C and λ_{max}^{alc} 378mμ (ε: 30650) in the ultraviolet absorption spectrum. This absorption band and the λ_{mx}^{alc} 235mμ of the original ketone support that the ketonic group is conjugated with a double bond. The analysis of the hydrazone, C, 55.36; H, 5.74; N, 14.42%, agreed with the calculated values for $C_{18}H_{22}O_6N_4$ (8-acetoxypiperitone 2,4-dinitrophenylhydrazone): C, 55.38; H, 5.68; N, 14.35%.

Treatment of the fraction with palladium charcoal in the same manner as in the case of 8-hydroxypiperitone gave thymol and acetic acid (identified by paper-chromatography of the hydroxamic acid prepared[23]). The fraction (3.5 g.) was gently heated from 200°C to 300°C in an air-bath for 1.5 hr., and a distillate, b.p. 110~231°C, was collected. The distillate gave 0.91 g. (91% of the theoretical) of acetic acid and 1.2 g. of piperitenone. The identity of the piperitenone was established by the same way as in the case of 8-hydroxypiperitone.

The establishment of 8-acetoxypiperitone was schematically summarized as follows:

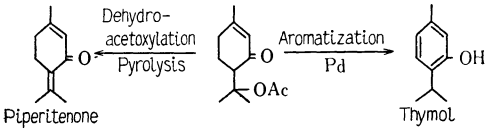

Acetone was also isolated as the semicarbazone from the recovered benzene solution in a very small amount.

II. Selection of the Conditions of the Oxidation.—Oxidation was carried out in a flask equipped with a reflux condenser, a mechanical stirrer, a thermometer and a gas inlet tube opening directly beneath the stirrer. The flask was held in a constant-temperature bath which could be regulated to ±1°C. Air, dried with conc. sulfuric

23) Y. Inoue and M. Noda, *J. Agr. Chem. Soc. Japan*, (*Nippon Nôgei-Kagaku Kaishi*) **23**, 294 (1950): **24**, 291 (1951).

TABLE II
THE CONDITIONS OF OXIDATION AND THE YIELDS OF CRUDE 8-ACETOXYCARVOTANACETONE

Expt.	Sample	Conditions of oxidation							Product
	α-Terpinyl acetate (g.)	Terpinyl acetate/Chromic acid (mole ratio)	Sol-* vent	Acetic acid (g.)	Acetic anhydride (g.)	Gas** passed	Temp. (°C)	Time (hr.)	Crude*** 8-acetoxycarvotanacetone (%)
1	50	1:2.7	H	20	50	C	30	100	10.9
2	50	1:2.7	C	20	50	C	30	100	11.7
3	50	1:2.7	B	20	50	C	30	100	15.6
4	50	1:2.7	B	20	50	A	30	100	23.0
5	50	1:2.7	B	—	—	C	30	100	7.4
6	50	1:2.7	B	—	—	A	30	100	7.5
7	50	1:0.4	B	2.4	4.0	C	30	60	8.0
8	50	1:0.4	B	2.4	4.0	A	30	60	12.0
9	50	1:2.7	B	200	100	C	30	100	26.3
10	50	1:2.7	B	200	100	A	30	100	40.0
11	50	—	B	20	50	A	30	100	—
12	50	1:2.7	B	20	50	A	50	100	41.2
13	50	1:2.7	B	100	50	A	50	100	44.8
14	50	1:2.7	B	100	50	C	55	100	43.0
15****	50	1:2.7	B	100	50	C	55	100	53.2

* H: *n*-Hexane. C: Carbon tetrachloride. B: Benzene.
** C: Carbon dioxide. A: Air.
*** Yields represent wt.% for α-terpinyl acetate used.
**** The oxidant contains benzoyl peroxide.

acid and calcium chloride, was passed in at 350 cc. per min.

In all experiments listed in Table II except Expt. 7 and 8, *tert*-butyl chromate was prepared from 138 g. of *tert*-butyl alcohol, 69 g. of chromic anhydride and 1060 cc. of the solvent in the same way as above. In Expt. 7 and 8, 20.4 g. of *tert*-butyl alcohol, 10.2 g. of chromic anhydride and 114 cc. of benzene were used. Acetic acid and acetic anhyride were added as shown in Table II. In Expt. 15 benzoyl peroxide, which corresponded to 2 mole % for α-terpinyl acetate, was further added to the acidic oxidant just prior to the oxidation.

In all cases, the oxidant was added at a time to 50 g. of α-terpinyl acetate dissolved in 57 cc. of the solvent. When oxidation was over, the same treatment of the oxidation mixture as above gave a neutral reaction mixture. The relative yield of α,β-unsaturated ketone in each reaction mixture was determined by measuring ultraviolet absorption spectrum at 235mμ (in ethyl alcohol). Then, the reaction mixture was fractionally distilled under the reduced pressure of carbon dioxide. The fractions were separated into the unchanged and the changed parts by the chromatostrip color test and the yield of crude 8-acetoxycarvotanacetone was determined.

The conditions employed and the results obtained are summarized in Table II.

In Fig. 1 the infrared spectra (liquid film) of the reaction mixture in Expt. 11 and of *dl*-α-terpinyl acetate used were compared in the 2000～750 cm.$^{-1}$ range. Agreement between these spectra showed that in Expt. 11, *dl*-α-terpinyl acetate was not at all attacked by air.

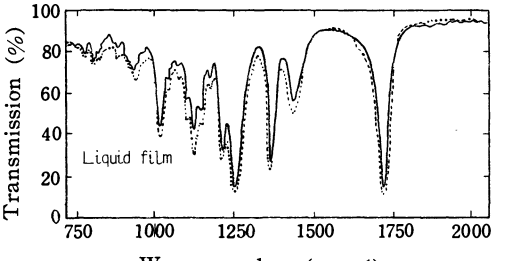

Fig. 1. Infrared spectra of the reaction mixture in Expt. 11 and of *dl*-α-terpinyl acetate used.
——: the reaction mixture in Expt. 11.
……: *dl*-α-terpinyl acetate used.

In Expt. 15 (the oxidation catalyzed by benzoyl peroxide) the same reaction products were also obtained as in Expts. 1～14.

Dehydroacetoxylation of 8-Acetoxycarvotanacetone—*8-Acetoxycarvotanacetone*, b.p.$_2$ 129～131°C, n_D^{25} 1.4820, d_4^{25} 1.0434, ester value 269.5 (calcd. for $C_{12}H_{18}O_3$: 266.8), was prepared by oxidation of *dl*-α-terpinyl acetate with *tert*-butyl chromate. The chromatogram on chromatostrip indicated that this ketone was contaminated by a small amount of 8-acetoxypiperitone.

Dehydroacetoxylation. — 8-Acetoxycarvotanace-

tone (35.7 g.) was distilled under an atmospheric pressure in a distilling flask equipped with a Vigreux column, the temperature of the air-bath being raised slowly to 340°C in a period of 4 hr. Dehydroacetoxylation took place actively at bath temperature 220~280°C (the reaction mixture 200~240°C). A pyrolysate (32.3 g., 91% to 8-acetoxycarvotanacetone), b.p. 114~245.5°C, distilled out leaving 2.8 g. (8%) of a polymer. Acid value of the pyrolysate was 271.0, corresponding to 9.4 g. (92% of the theoretical) of acetic acid.

Treatment and identification of the pyrolysate.— The pyrolysate was shaken with a dilute sodium bicarbonate solution to remove acetic acid, which was identified as *p*-acetotoluide. The solution of the neutral oil in petroleum ether was quickly shaken with a 5% sodium hydroxide solution. The alkaline solution was repeatedly extracted with ether. The ethereal solution gave 1.1 g. of carvacrol, which was characterized as the phenylurethane, m.p. and mixed m.p. 134.5~135.5°C. The petroleum ether solution gave 21.2 g. of a neutral oil.

Distillation of the oil at 5 mmHg gave the following three fractions: (A) b.p.$_5$ 85~90°C, n_D^{25} 1.4978~1.4985, d_4^{25} 0.9569~0.9571, yield 14.9 g.; (B) b.p.$_5$ 90~122°C, n_D^{25} 1.5200~1.5232, d_4^{25} 0.9746~0.9829, yield 5.6 g.; (C) b.p.$_5$ 122~126°C, yield 0.6 g.

(1) *dl*-Carvone (V). Ultraviolet absorption spectrum of fraction A exhibited λ_{max}^{alc} 235mμ identical with that of carvone[24]. The chromatogram on chromatostrip, developed with 30 vol. % ethyl acetate in *n*-hexane and sprayed with 2,4-dinitrophenylhydrazine — hydrochloric acid, gave a single spot. This fraction yielded *dl*-carvone semicarbazone, m.p. and mixed m.p. 155~156°C, *dl*-carvoxime, m.p. and mixed m.p. 92~92.5°C, and 2,4-dinitrophenylhydrazone, m.p. 187~187.2°C[25] (*Anal.* Found: N, 17.03. Calcd. for $C_{16}H_{18}O_4N_4$: N, 16.96%). These showed that this fraction consisted of *dl*-carvone only.

(2) Piperitenone. Ultraviolet absorption spectrum of fraction B showed λ_{max}^{alc} 243mμ and 277mμ, and the chromatogram on the chromatostrip developed as above gave three spots which possessed R_f value 0.75, 0.62 and 0.51, respectively. Then, 1.0 g. of fraction B was separated into these fractions by the elution-chromatography on silica (20 g.) with *n*-hexane—ether (3:2).

The fraction, yield 36%, which gave a spot of R_f value 0.75, consisted of *dl*-carvone (77%) and carvacrol (23%).

The fraction, yield 59%, which gave a spot of R_f value 0.62, consisted of piperitenone. This was established as follows: (a) Ultraviolet absorption spectrum exhibited λ_{max}^{alc} 243mμ (ε: 9930) and 277mμ (ε: 7250) characteristic of piperitenone[22]. (b) Treatment of 0.20 g. of this fraction with palladium charcoal gave 0.18 g. of thymol. (c) Ozonolysis of the fraction in ethyl acetate—acetic acid gave levulinic acid (semicarbazone, m.p. and mixed m.p. 183.2~184°C) and acetone (2,4-dinitrophenylhydrazone, m.p. and mixed m.p. 123~125°C). (d) The separation of 2,4-dinitrophenylhydrazone by chromatography on silica—plaster of Paris with benzene—petroleum ether and recrystallization gave three isomers, (i) m.p. 151~152°C, λ_{max}^{alc} 387mμ (ε: 29780), (*Anal.* Found: C, 58.30; H, 5.96; N, 16.94%). (ii) m.p. 132~133°C, λ_{max}^{alc} 388mμ (ε: 29700). (iii) m.p. 183.8~184.5°C, λ_{max}^{alc} 389mμ (ε: 27520). (*Anal.* Found: C, 58.23; H, 5.66; N, 17.39. Calcd. for $C_{16}H_{18}O_4N_4$: C, 58.17; H, 5.49; N, 16.96%). These were identical with the three isomers of piperitenone 2,4-dinitrophenylhydrazone reported by Naves[22], respectively.

The fraction, yield 5%, which gave a spot of R_f value 0.51, yielded 2,4-dinitrophenylhydrazone in reddish violet needles, m.p. 171~171.5°C, λ_{max}^{alc} 392mμ. The fraction was so small that it was not investigated further.

(3) Unchanged 8-acetoxycarvotanacetone. 2,4-Dinitrophenylhydrazone of fraction C, chromatographed on alumina with benzene, melted at 215~216°C. It was identified as 8-acetoxycarvotanacetone 2,4-dinitrophenylhydrazone.

Summary

(1) Oxidation of *dl*-α-terpineol with *tert*-butyl chromate yielded 8-hydroxypiperitone, which has not previously been described, 8-hydroxycarvotanacetone and homoterpenyl methyl ketone. In this case the oxidative fission of the double bond in the ring took place to a remarkable extent.

(2) Oxidation of *dl*-α-terpinyl acetate with *tert*-butyl chromate gave 8-acetoxypiperitone, 8-acetoxycarvotanacetone (neither have previously been described) and homoterpenyl methyl ketone. In this oxidation the cleavage of the ethylenic linkage was suppressed, and the yield of 8-acetoxycarvotanacetone was relatively good.

Moreover, the effects of the solvent, acetic acid, benzoyl peroxide, air, and the reaction temperature, on the yield of 8-acetoxycarvotanacetone were investigated.

(3) 8-Acetoxycarvotanacetone was converted into *dl*-carvone when acetic acid was eliminated by pyrolysis.

(4) The synthesis of carvone from α-terpinyl acetate was attained through the intermediate of 8-acetoxycarvotanacetone. The overall yield of carvone from α-terpinyl acetate was 28 mole%.

The author wishes to express his hearty gratitude to Professor Tamon Matsuura for his guidance and encouragement, to

24) R. G. Cooke and A. K. Macbeth, *J. Chem. Soc.*, **1938**, 1408.

25) A. Kergomard [*Ann. chim.* (*Paris*), **8**, 193 (1953)] has reported m.p. of *dl*-carvone 2,4-dinitrophenylhydrazone to be 185~186°C.

Assistant Professor Syûichi Hayashi for his advice, and to Mr. Tadami Sakoda, Miss Miyoko Sakai and Mrs. Kiyoko Suga who assisted in a part of the experiment. This research was aided by a grant from the Ministry of Education.

Department of Chemistry
Faculty of Science
Hiroshima University
Hiroshima

The Mechanical Behavior of Swollen Polymethyl Acrylate Gels. I. The Determination of Polymer-Solvent Interaction Parameter μ by the Mechanical Measurement

By Kazuyoshi OGINO

(Received January 20, 1958)

When a slightly cross-linked linear chain polymer is in contact with a solvent, it absorbs the solvent and expands to a limited volume, attaining the so-called swollen gel state. In this case, the interaction forces between the polymer and the solvent are considered to be one of the important factors which determine the degree of swelling of this system. A parameter which is called the polymer-solvent interaction patameter μ is employed to express the power of solvation. Mullin[1] showed that this parameter could be determined mechanically by the measurement of initial stress-strain relations using a gel of vulcanized natural rubber swollen in an organic solvent.

In this paper, the author determined this parameter μ of slightly cross-linked polymethyl acrylate gels swollen in several organic solvents, following the same method reported by Mullin.

Theory

The force f required to strain a gel to an extension ratio λ is given by[2]

$$f=2A_0(\lambda-\lambda^{-2})v_r^{-1/3}(\partial W/\partial I_1+\lambda^{-1}\partial W/\partial I_2) \tag{1}$$

where A_0 is the unstrained area of cross section, v_r the volume fraction of polymer at swelling equilibrium, W the free energy of deformation per unit volume, called as the stored energy function, and I_1 and I_2 are strain invariants which are defined as follows;

$$I_1=\lambda_1^2+\lambda_2^2+\lambda_3^2$$
$$I_2=\lambda_1^{-2}+\lambda_2^{-2}+\lambda_3^{-2}$$

where λ_1, λ_2 and λ_3 are the principal extension ratios.

This relation can also be expressed as follows[1]

$$f=2A_0(\lambda-\lambda^{-2})v_r^{-1/3}(C_1+\lambda^{-1}C_2) \tag{2}$$

In this relation, C_1 and C_2 are constants, and are obtained experimentally. Since the value of C_2 decreases to zero at a high degree of swelling ($v_r \leqq 0.25$), the equation 1 or 2 is reduced to the form predicted by the kinetic theory, if

$$C_1(\text{swollen})=\frac{1}{2}\cdot\rho\cdot\boldsymbol{R}\cdot T\cdot M_c^{-1} \tag{3}$$

where ρ is the density of pure solvent, and M_c a parameter, which can be assumed as the average molecular weight between junction points.

On the other hand, at swelling equilibrium with solvent, the following equation is obtained from statistical consideration[3],

$$\ln(1-v_r)+v_r+\mu v_r^2=-\rho V_0 v_r^{1/3}/M_c \tag{4}$$

Or, from equation 3

$$-\ln(1-v_r)-v_r-\mu v_r^2=2V_0C_1v_r^{1/3}/\boldsymbol{RT} \tag{5}$$

In practice, the value of C_1 for a swollen gel can be obtained either by direct measurements of a high degree of swelling or by plotting the results of the simple extension measurement as

1) L. Mullin, *J. Polym. Sci.*, **19**, 225 (1956).
2) S. M. Gumbrell, L. Mullin and R. S. Rivlin, *Trans. Faraday Soc.*, **49**, 1495 (1953).
3) P. J. Flory and J. Rehner, *J. Chem. Phys.*, **11**, 512 (1943); M. L. Huggins, *J. Am. Chem. Soc.*, **64**, 1712 (1942).

$f\{2A_0(\lambda-\lambda^{-2})\}^{-1}v_r^{1/3}$ against λ^{-1} and extrapolating the curve to $\lambda^{-1}=0$.

With the value of C_1 thus obtained, the parameter μ can be determined by the equation 5.

Experimental

Sample — Commercial methyl acrylate was purified by shaking with aqueous alkaline solution, and was redistilled under reduced pressure. Diallyl adipate which was used as cross-linking agent was synthesized by esterification of allyl alcohol with adipic acid in the presence of *p*-toluene sulfonic acid as catalyst, and purified by fractional distillation under reduced pressure.

α-α'-azodi-*iso*-butyronitrile, used as initiator, was prepared according to Thiele and Heuser[4], and was recrystalized from ether.

About 8 cc. of methyl acrylate monomer which contains one drop (about 3 mg.) of the cross-linking agent and about 30 mg. of the initiator was polymerized in bulk in a sealed glass tube. The polymer rod was then cut into several pieces, about 1 cm. in length, and immersed into the solvent to be tested.

Organic solvents used in this experiment are chloroform, benzene, toluene and carbon tetrachloride. They were purified in the usual way.

Apparatus.—The apparatus used in this experiment is shown in Fig. 1[5,6]*.

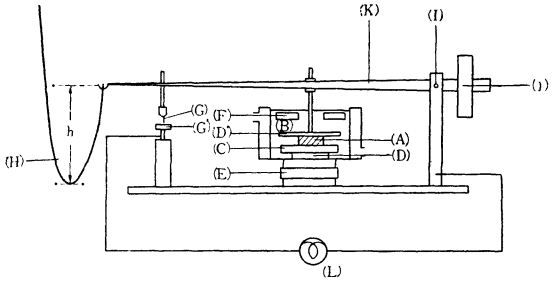

Fig. 1. The apparatus used in this experiment.
A: Specimen. B: Solvent. C: Iris of microscope. D: Brass block. D': Pressure plate. E: Screw gauge. F: Desiccating agent. G and G': Contacts. H: Chain. I: Fulcrum. J: Balancing weight. K: Beam.

Specimen A in the swelling equilibrium with a solvent B was placed between a flat brass block D and a pressure plate D', and was strained to a definite extent by rotating the screw E which was graduated to 0.01 mm., and the stress was measured by the chain H with the known linear density.

Force f in equation 2 at each strain can be calculated by the following equation

$$f=(bdhg)/a$$

where d is the linear density of the chain, h the vertical component of the chain length suspended from the beam, b the distance from the fulcrum to the chain, a the distance from the fulcrum to the center of the pressure plate and g the acceleration of gravity. In this experiment, $b/a\approx 4.3$, and d was 0.80 or 0.39 g/cm.

The temperature of the sample was controlled by circulation of water from a water bath kept at 25±0.5°C, and was read directly by a thermometer inserted in the solvent.

Results and Discussion

When W_b and W_a are the weights of the polymer before and after swelling, ρ_1 and ρ_2 are the densities of the solvent and of the polymer, respectively, the volume fraction v_r of the polymer after swelling can be given by the following equation[7];

$$v_r=\frac{1}{1+\frac{\rho_2}{\rho_1}\left(\frac{W_a}{W_b}\right)-\frac{\rho_2}{\rho_1}}$$

The results are shown in Table I. The solvent, in which a gel has a small value

TABLE I
THE VALUES OF VOLUME FRACTION OF POLYMER, v_r, AND μ AT 25°C.

Solvent	v_r	$1/v_r$	$\mu_{25°C}$
Chloroform	0.035_5	28.2	0.49
Benzene	0.065_9	15.2	0.51
Toluene	0.192_5	5.2	0.54
Carbon Tetrachloride	0.501_0	2.0	0.69

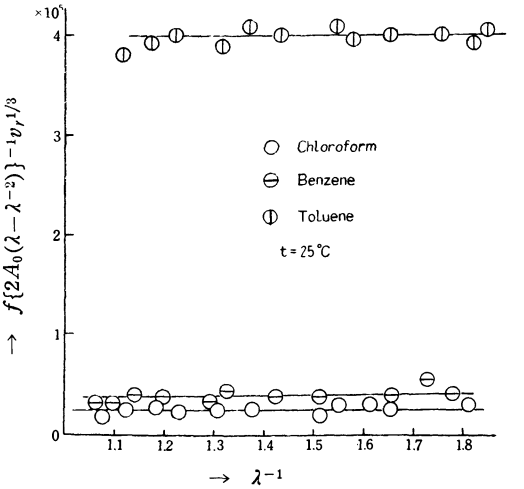

Fig. 2. The plot of $f\{2A_0(\lambda-\lambda^{-2})\}^{-1}v_r^{1/3}$ against λ^{-1} at 25°C.

* This apparatus has been designed for the measurement of stress relaxation.

4) J. Thiele and K. Heuser, *Ann.*, **290** (1896).
5) S. L. Dart and E. Guth, *J. Appl. Phys.*, **17**, 314 (1946).
6) H. Fujita, K. Ninomiya and T. Homma, This Bulletin, **25**, 374 (1952).
7) P. Doty and H. S. Zable, *J. Polym. Sci.*, **1**, 90 (1946).

of v_r, may be considered approximately to be a good solvent, because polymer-solvent contacts are attained sufficiently in it. From this table, we can assume that the solvent becomes poorer in the order of chloroform, benzene, toleuene and carbon tetrachloride.

An example for the plot of $f\{2A_0(\lambda-\lambda^{-2})\}^{-1}v_r^{1/3}$ against λ^{-1} is shown in Fig. 2. There is a good linear relationship between these two quantities. Extrapolation of the curve to $\lambda^{-1}=0$ gives C_1. The value of μ can be determined with the use of these values of C_1 and v_r. The results are shown in Table I. These values are about 0.50 except for carbon tetrachloride, and decrease in the order, toluene>benzene>chloroform. We can say that chloroform is the best solvent for polymethyl acrylate in these four solvents, and carbon tetrachloride is the poorest solvent.

The gradient of the lines in Fig. 2 is identified with C_2, and this can be regarded as zero from this figure. The value of C_2 can be considered to show the degree of the restriction to the possible configuration of the molecular chain, and therefore those solvents, in which the interaction forces between long chain molecules can be considered to be fairly loosen, are good.

Doty and Zable[7] showed that $\mu=0.55$ is the border-line between poor solvent and non-solvent. Huggins[8] showed that $\mu=0.50$ is the border-line between poor and good solvent. Further, in the case of gel, μ depends upon the concentration of cross-linking agent[9]. On the other hand, the different values of μ for the same polymer-solvent system are reported by the different workers, even if the values are determined mechanically by the same method[2].

In this experiment, from the considerations on the values of v_r, μ or C_2, the author has assumed that chloroform, benzene and toluene are good solvents and carbon tetrachloride is a poor solvent. The values of μ obtained at 31, 25 and 15°C seem to show, also, that benzene is a good solvent**.

From the accuracy in the determination of μ, especially from its temperature dependency, the results obtained in this experiment are not enough to be discussed in detail. There are also some questions concerning the effect of cross-linking agent as mentioned above. However, the values of μ obtained here seem to be not so unreasonable compared with the other workers' results.

The author is indebted to Professor H. Akamatu and Assistant Professor T. Nakagawa for their interest in and support of this experiment.

Department of Chemistry
Faculty of Science
The University of Tokyo
Hongo, Tokyo

8) M. L. Huggins, *Ann. N. Y. Acad. Sci.*, **44**, 431 (1943).
9) R. F. Boyer and R. S. Spencer, *J. Polym. Sci.*, **3**, 97 (1948).
** These values are; $\mu_{31}=0.51_6$; $\mu_{25}=0.51_3$; $\mu_{15}=0.50_9$.

The Mechanical Behavior of Swollen Polymethyl Acrylate Gels. II. The Stress Relaxation in Organic Solvents

By Kazuyoshi OGINO

(Received February 4, 1958)

In the previous paper[1] the interaction parameter μ between polymer and solvent has been determined for slightly cross-linked polymethyl acrylate gels in equilibrium with several organic solvents, from their initial stress-strain relations. Although these gels respond purely elastically to a rapid deformation, it is observed that the stress relaxes with time under a constant deformation. The stress relaxation and its dependency upon the degree of swelling of these gels are investigated in the present paper.

The stress-strain behavior of a visco-elastic body may be expressed by the Maxwell equation, or by generalizing the Maxwell theory in consideration of a distribution of relaxation times.

If the distribution of relaxation times is continuous, the rate of strain, ds/dt, is expressed as,

$$\frac{ds}{dt}=\frac{1}{E(\tau)}\cdot\frac{df(\tau,t)}{dt}+\frac{1}{\tau\cdot E(\tau)}\cdot f(\tau,t)$$

where $f(\tau,t)$ and $E(\tau)$ are the distribution functions of the stress and the elastic modulus respectively. Total stress is expressed as,

$$f(t)=\int_0^\infty f(\tau,t)\,d\tau.$$

Then, at a constant strain s_0, the decay of stress with time can be expressed as follows:

$$f(t)=\int_0^\infty s_0\cdot E(\tau)\cdot\exp\cdot(-t/\tau)\cdot d\tau$$
$$=s_0E(t) \qquad (1)$$

where $E(t)$ is the relaxation elastic modulus, which can be determined by the experiment. $E(\tau)$, which is the distribution function of elastic modulus, is a fundamental measure of the mechanical behavior of a substance. Several methods have been proposed to obtain this function approximately from the experimental curves[2].

As a first approximation we can replace the function $\exp.(-t/\tau)$ in equation 1 by step function $K(t,\tau)$, which is defined as follows:

$$K(\tau,t)=\begin{cases}1 & \cdots\cdots\ t<\tau\\ 0 & \cdots\cdots\ t>\tau\end{cases}$$

Then equation 1 turns out to be

$$E(t)=\int_t^\infty E(\tau)\cdot d\tau$$

then,

$$E(\tau)=-dE(t)/dt$$

Using the latter relation, we can obtain the distribution function of elastic modulus among the various relaxation times experimentally from the negative slope of the observed relaxation curve.

On the other hand, Tobolsky et al. found that[3] the shape of the relaxation curve for a given polymer is the same at different temperatures, when plotted as reduced stress* against logarithmic time, but a change in temperature essentially shifts the position of the curve along the logarithmic time scale.

Experimental

Sample. — Cross-linked polymethyl acrylate used in this experiment is the same as described in the previous paper[1]. Samples are brought to the swelling equilibrium with chloroform, benzene, toluene, carbon tetrachloride and methanol.

Apparatus. — The specimen is vertically compressed to a given height, and the stress which corresponds to the strain is recorded continuously by means of a chainomatic balance (the same one as was used in the previous work[1]) which is equipped with an automatically balancing system. This is shown in Fig. 1. The apparatus is the same as originally used by Guth[4] for the measurement of stress relaxation of cork, and recently improved by Fujita et al.[5].

1) K. Ogino, This Bulletin, **31**, 577 (1958).
2) H. Fujita, *Busseiron Kenkyu*, **63**, 48 (1953), (*in Japanese*)

* The stress is arbitrarily reduced to 25°C. The reduced stress g_{25} is calculated by multiplying the actual experimental stress value, f, by $298/T$, where T is absolute temperature.

3) A. V. Tobolsky et al., *J. Polym. Sci.*, **3**, 669 (1948).
4) S. L. Dart and E. Guth, *J. Apply Phys.*, **17**, 314 (1946).
5) H. Fujita, K. Ninomiya and T. Homma, This Bulletin, **25**, 274 (1952).

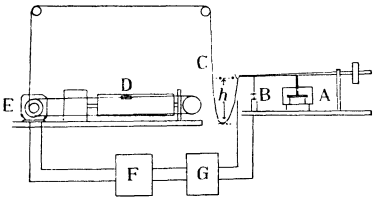

Fig. 1. The apparatus for the measurement of stress relaxation.
(A): Specimen (B): Contact
(C): Chain (D): Pencil for recording
(E): Balancing motor (F): Relay
(G): Amplifier circuit

In Fig. 1, (A) is the specimen at a given constant strain, and the stress is measured by the suspended length of a chain (C), which is controlled by the reversible motor (E) through the relay (F) and the amplifier circuit (G).

The reduced stress g_{25} at t°C can be expressed as follows

$$g_{25}=\frac{h\cdot d\cdot G\cdot n}{A_0}\cdot\frac{298}{t+273}\ \text{dyne/cm}^2$$

where, h the vertical component of the chain length from the arm, d the linear density of the chain, n the magnification of the arm, that is the ratio of the distances to the hook and to the pressure plate from the fulcrum, A_0 the cross-sectional area of the sample, t the temperature of the sample, and G is the acceleration of gravity. In this apparatus, n is about 4.3. The experimental curves of reduced stress against logarithmic time scale obtained by this method are shown in Fig. 2.

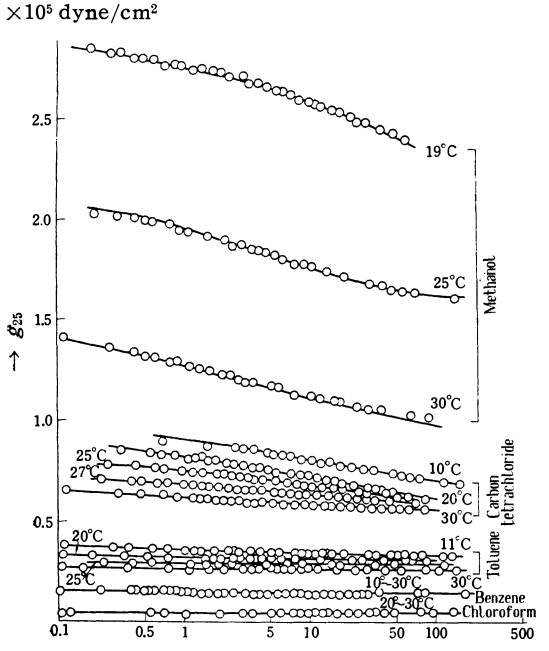

Fig. 2. The curves of reduced stress g_{25} against logarithmic time.

Results and Discussion

It is obvious from Fig. 2 that the smaller degree of swelling corresponds to the larger magnitude of stress, and to the larger degree of stress relaxation. For the good solvents, such as benzene or chloroform, relaxation curves at different temperatures expressed in reduced stress nearly overlap with each other. The slight dependency upon temperature means the small activation energy in relaxation.

Stress relaxation corresponds primarily to the breakage of some sort of linkage, such as secondary bonds or entanglement which are formed in the gel structures. As weak linkages may exist hardly at all in the well-swollen gels, only some strong linkages remain unbroken. As the weak linkages which are present at lower temperatures would be broken at higher temperatures, the degree of relaxation at higher temperatures is less remarkable than at lower temperatures. The greater temperature dependency, i. e., the greater activation energy, is expected for a poor solvent than for a good solvent. (Tobolsky has calculated this apparent activation energy for relaxation process[3,6]. But in this work, its calculation was not carried out, considering the large error involved in the data of the initial stress.) When the curves in Fig. 2 are superposed upon each other by sliding along the logarithmic time scale, master curves as shown in Fig. 3 are obtained. The slope of the master curve is large for the small degree of swelling, and for the high degree

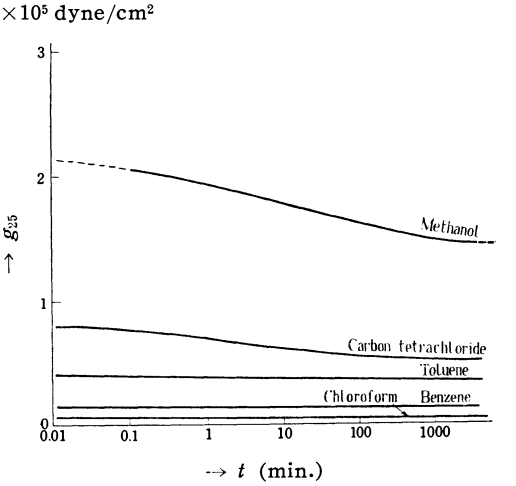

Fig. 3. The master curve of gels for each solvent.

6) G. M. Brown and A. V. Tobolsky, *J Polym. Sci.*, **6**, 165 (1951).

of swelling, a constant slope over the wide range of the time scale is observed. This means that the height of distribution function $E(\tau)$ becomes higher, while its width is restricted, when the degree of swelling is small.

For the actual relaxation phenomena, the continuous distribution of relaxation times must be taken into account as mentioned above. However, how these phenomena can be expressed by the spring-dashpot model is now considered, applying the four-element system as shown in Fig. 4. To determine the magnitude of each parameter in this system, from actual relaxation data, the following method has been proposed[7].

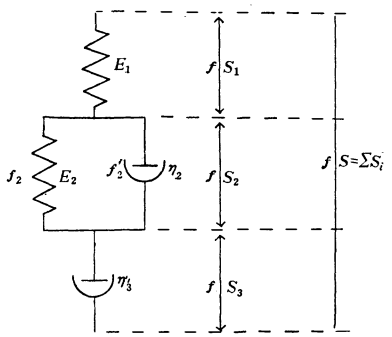

Fig. 4. The four-element model.

In the model shown in Fig. 4, the total strain $s=\sum_j s_j$, and f is the reactant stress.

Thus the following equations are obtained:

$$f/s_1=E_1$$
$$f_2/s_2=E_2 \quad : \quad f'_2/\dot{s}_2=\eta_2 \quad : \quad f_2+f'_2=f$$
$$f/\dot{s}_3=\eta_3$$

From these relations, we obtain at a constant strain,

$$\ddot{f}+\left\{E_1\left(\frac{1}{\eta_2}+\frac{1}{\eta_3}\right)+\frac{E_2}{\eta_2}\right\}\dot{f}+\frac{E_1E_2}{\eta_2\eta_3}\cdot f=0 \qquad (1)$$

The solution of equation 1 can be expessed as follows

$$f=Ae^{-\alpha t}+Be^{-\beta t} \qquad (2)$$

where,

$$\begin{cases} 2\alpha=\left[\dfrac{E_1}{\eta_3}+\dfrac{E_2}{\eta_2}+\dfrac{E_1}{\eta_2}\right] \\ \qquad -\sqrt{\left[\dfrac{E_1}{\eta_3}+\dfrac{E_2}{\eta_2}+\dfrac{E_1}{\eta_2}\right]^2-4\dfrac{E_1E_2}{\eta_2\eta_3}} \\ 2\beta=\left[\dfrac{E_1}{\eta_3}+\dfrac{E_2}{\eta_2}+\dfrac{E_1}{\eta_2}\right] \\ \qquad +\sqrt{\left[\dfrac{E_1}{\eta_3}+\dfrac{E_2}{\eta_2}+\dfrac{E_1}{\eta_2}\right]^2-4\dfrac{E_1E_1}{\eta_2\eta_3}} \end{cases} \qquad (2')$$

If a rapid strain $s=s_0$ was given at $t=0$, from equation 2,

$$\begin{cases} A=\dfrac{-\beta f_{t=0}-\dot{f}_{t=0}}{\alpha-\beta} \\ B=f_{t=0}-A \end{cases} \qquad (3)$$

and,

$$\begin{cases} E_1\cdot s_0=f_{t=0} \\ \dfrac{\dot{f}_{t=0}}{E_1}=-\dfrac{f_{t=0}}{\eta_2}-\dfrac{f_{t=0}}{\eta_3} \quad \text{or} \quad \dfrac{1}{\eta_2}+\dfrac{1}{\eta_3}=-\dfrac{s_0\cdot\dot{f}_{t=0}}{f^2{}_{t=0}} \end{cases} \qquad (3')$$

From these general relations, we can determine the values of four parameters.

For simplicity, we calculate for the case when $\alpha \ll \beta$. For the large value of $t=t_l$, we can neglect the second term in equation 2 and,

$$\alpha=-\dot{f}_{t=t_l}/f_{t=t_l} \qquad (4)$$

$$A=\frac{f_{t=t_l}}{e^{(\dot{f}t=tl/ft=tl)\cdot t_l}} \qquad (5)$$

From equation 3, 4 and 5, we obtain

$$B=f_{t=0}-\frac{f_{t=t_l}}{e^{(\dot{f}t=tl/ft=tl)\cdot t_l}} \qquad (6)$$

$$\beta=(-\dot{f}_{t=0}-\alpha A)/B \qquad (7)$$

and from equation 2′

$$\alpha+\beta=(E_1/\eta_3+E_2/\eta_2+E_1/\eta_2) \qquad (8)$$

$$\alpha\beta=E_1E_2/\eta_2\eta_3 \qquad (9)$$

From 4—7, we obtain α, β, A and B, and with these values, from 8 and 9, we obtain two equations for parameters. Combining these equations with equation 3′, we can calculate four parameters. These parameters at 25°C calculated by this method are listed in Table I.

These results show that at the small degree of swelling, or at the large value of v_r, the values of each parameter become larger. This is naturally expected from the fact that the small degree of swelling means the large concentration of the polymer substance in gel.

E_1 is the so-called instantaneous elasticity, and has a large value for the small degree of swelling. This may be due to the presence of many remaining secondary bonds besides the strong primary bonds for the small degree of swelling**. η_3 is the viscosity coefficient for the flow after the attainment of the stationary flow, and

7) T. Alffey, "Mechanical Behavior of High Polymers", Interscience Pub., Inc., N.Y. (1948) p. 181.

** From the theory of rubber elasticity, for instance, the stress is inversely proportional to the average molecular weight, M_c, between the junction points.

TABLE I
THE VALUS OF EACH PARAMETER FOR FOUR-ELEMENT MODEL

Solvent	Parameter						
	v_r	E_1 dyne/cm².	E_2 dyne/cm².	η_2 poise	η_3 poise	η_2/E_2 sec.	η_3/E_1 sec.
Methanol	0.68	0.98×10^6	5.2×10^6	1.5×10^9	9.6×10^{11}	3.0×10^2	1.0×10^6
Carbon tetrachloride	0.50	$3.9_7\times10^5$	8.4×10^5	2.9×10^8	1.1×10^{11}	3.5×10^2	2.6×10^5
Toluene	0.19	2.0×10^5	1.6×10^6	6.5×10^7	4.2×10^{10}	4.0×10^1	2.1×10^5
Chloroform	0.036	$3.4_5\times10^4$	5.1×10^5	2.3×10^7	$8.9_7\times10^9$	4.0×10^1	2.5×10^5

has also a large value for the small degree of swelling. Such a flow may have originated from the squeezing out of solvent which is contained between networks, or from the breaking of many junction points. These inferences are consistent with the order of the degree of swelling and the value of η_3. η_2 and E_2 characterize the part which expresses the transient state from instantaneous deformation to final steady flow, which occurs in a comparatively short time after the strain is imposed ($10^1\sim10^2$ sec., expected from η_2/E_2 in Table I), and may reflect the change of the inner structures. η_2 and E_2 have always larger values as the degree of swelling is lower. Taking account of the fact that η_2 and E_2 large, it seems that the weaker bond would be broken faster after the strain is imposed, or the solvent which can be pushed out more easily from the network would be squeezed out more readily.

In chloroform or benzene, polymer swells to a large extent, so that the greater part of the gel is occupied by solvent. The appearance of this gel is very soft. The mechanical behavior of these gels can be expressed by a simple Maxwell model as shown in Fig. 5 ($\ln f/f_0$ plotted against t). The slope of this curve gives $-1/\tau$, where τ is relaxation time. The relaxation time obtained from this method is approximately in agreement with the value η_3/E_1 of the four element model.

Chain molecules in these gels are fixed

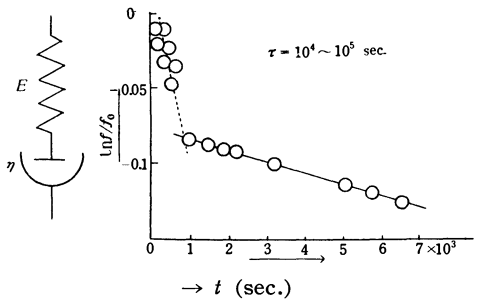

Fig 5. The curve plotted $\ln f/f_0$ against t for benzen.

at several junction points by cross-linking, and the interaction between these chains is considered to be stronger than in an ordinary polymer solution. The effect of this interaction appeared in the difference of dependency of stress relaxation upon the degree of swelling. The more detailed discussion must be expected from thermodynamic consideration of elasticity.

The author is particulary indebted to Professor H. Akamatu and Assistant Professor T. Nakagawa for their discussion and encouragement during this investigation, and to Mr. H. Arakawa, the University of Shizuoka, especially for his suggestion about the analysis by a four-element model.

Department of Chemistry, Faculty of Science, The University of Tokyo
Hongo, Tokyo

The Mechanical Behavior of Swollen Polymethyl Acrylate Gels. III. Thermoelastic Properties of Swollen Gels

By Kazuyoshi OGINO

(Received February 4, 1958)

When a gel is in equilibrium with a solvent, the degree of swelling and its mechanical properties depend upon the intermolecular interaction. This is shown in the preceding paper[1] for the phenomena of stress relaxation.

Gee investigated the effect of several kinds of solvent upon the elasticity of rubber[2], and pointed out that the elasticity observed in his experiment does not always coincide with the result expected from statistical theories proposed by Flory, or James and Guth[3].

Continuing from the preceding paper, the author has observed the temperature dependence of the elastic behavior of polymethyl acrylate gel in two kinds of solvent which have different powers for the polymer.

The external force of extension f is expressed as

$$f=(\partial G/\partial l)_T$$

when the volume dose not change during the deformation, where G is free energy and l is the length of the body.

As the entropy S is $S=-(\partial G/\partial T)_l$, one may write $(\partial S/\partial l)_T=-(\partial f/\partial T)_l$.

The thermodynamical relation can be expressed as,

$$(\partial G/\partial l)_T=(\partial H/\partial l)_T+T(\partial f/\partial T)_l$$

or

$$(\partial H/\partial l)_T=f-T(\partial f/\partial T)_l$$

where H is the enthalpy.

Using the extension ratio $\alpha=l/l_0$, where l_0 is the initial length, the following relation can be deduced.

$$(\partial G/\partial \alpha)_T=fl_0 \quad (1)$$

$$(\partial H/\partial \alpha)_T=fl_0-Tl_0(\partial f/\partial T)_\alpha \quad (2)$$

$$T(\partial S/\partial \alpha)_T=(\partial H/\partial \alpha)_T-(\partial G/\partial \alpha)_T \quad (3)$$

The equation 1 gives the relation between free energy change and extension ratio α when the force under the various extensions at a constant temperature is measured for a sample which has the initial length l_0; the equation 2 gives the relation to obtain the enthalpy change from the temperature dependence of force at a constant extension ratio and the values of fl_0. From equation 3 combined with equation 1 and 2, we obtain the entropy change.

Experimental

The apparatus to observe the change in force with extension is the same one as used in the previous paper[4] (cf. Fig. 1 in the reference 4). Sample is polymethyl acrylate gel, cross-linked diallyl adipate and swollen in carbon tetrachloride and benzene; the former is a poor and the latter is a good solvent as reported in the previous papers[1,4]. The stress-strain relations observed at constant temperatures are shown in Fig. 1 or Fig. 2, where the strain means the compression and the stress is the initial stress. These curves are drawn connecting the observed points by a smooth line. Some deviations of these points from the smooth curve were observed. Gee supposed that these deviations may be due to the stress relaxation in the sample[2].

It must be noticed that the initial length l_0 itself changes with variation of temperature. To give the *same* extension ratio to the sample at different temperatures, the amount of compression for the sample must be changed corresponding to each temperature. In practice, the contact (G and G' in the Fig. 1 of the reference 4) is adjusted for each run to touch slightly, and therefore the change of stress which originated from the change of initial length, l_0, by thermal expansion is cancelled by this operation, then some definite compression which is determined from the initial length of the sample at the standard temperature (30°C) is given, and the corresponding stress is measured. It seems to be more correct to assume that the value of the strain imposed on the sample is adjusted according to the linear thermal expansion of the sample. But it has not been taken into account to perform this calibration in the present experiment, because, owing to the change in the length accompanying the temperature change, precise determination of the dimension of the sample is not possible*.

1) K. Ogino, This Bulletin, **31**, 580 (1958).
2) G. Gee, *Trans. Faraday Soc.*, **42**, 585 (1946).
3) P. J. Flory, *J. Chem. Phys.*, **11**, 521 (1943). H. M. James and E. Guth, ibid. **11**, 455 (1943).
4) K. Ogino, This Bulletin, **31**, 577 (1958).

* Physical meaning of this thermal expansion is discussed in reference 2.

The temperature dependency of the stress is determined from the values at several strains on each curve in Fig. 1 or Fig. 2. The results are shown in Fig. 3 and Fig. 4.

$(\partial f/\partial T)_\alpha$ is calculated by multiplying the slopes of each curve in Fig. 3 or Fig. 4 by the cross sectional area of the specimen. Also we obtain $(\partial G/\partial\alpha)_T$ from f and l_0 for each extension ratio at constant temperature. $(\partial H/\partial\alpha)_T$ and $T(\partial S/\partial\alpha)_T$ can be calculated from these values with equations 2 and 3. $(\partial G/\partial\alpha)_T$, $(\partial H/\partial\alpha)_T$ and $T(\partial S/\partial\alpha)_T$ per cubic centimeter can be obtained by dividing these values by the volumes of each specimen.

Results and Discussion

Fig. 5 and Fig. 6 are the curves which show the calculated values of $(\partial G/\partial\alpha)$, $(\partial H/\partial\alpha)$ and $T(\partial S/\partial\alpha)$ at 30°C in these two solvents. In practice, $T(\partial S/\partial\alpha)$ is obtained graphically from the difference between $(\partial G/\partial\alpha)$ and $(\partial H/\partial\alpha)$. Free energy change at constant temperature and pressure equals the external work, and enthalpy change at constant pressure equals the change of internal energy when no volume change occurs. Fig. 5 and Fig. 6 show the direction of the change of G, H and S when strain, or α, increases.

Carbon tetrachloride is not a good solvent for polymethyl acrylate considering the degree of swelling or other experimental results, as reported in the previous papers. In this solvent, $(\partial S/\partial\alpha)$ has a positive value for increasing of α, and so the

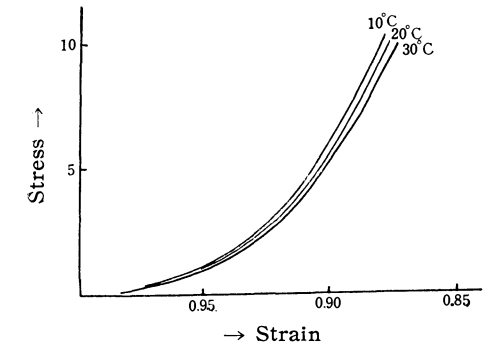

Fig. 1. The stress-strain curves for carbon tetrachloride.

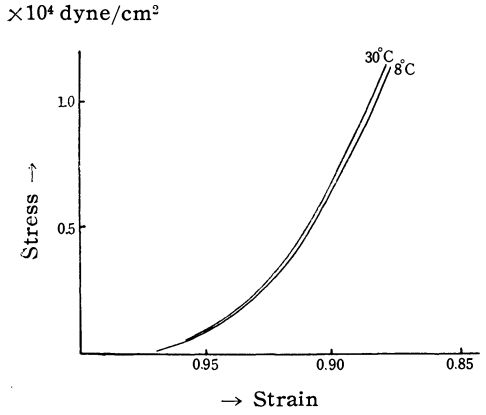

Fig. 2. The stress-strain curves for benzene.

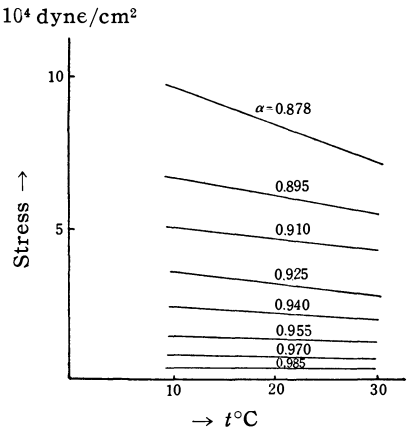

Fig. 3. The stress-temperature curves for carbon tetrachloride.

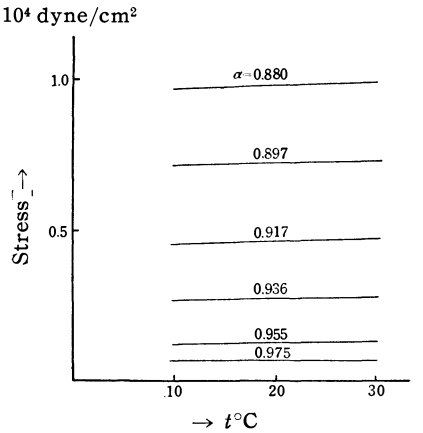

Fig. 4. The stress-temperature curves for benzene.

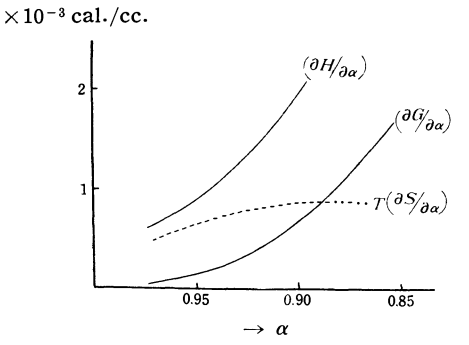

Fig. 5. Thermodynamics of compression for carbon tetrachloride.

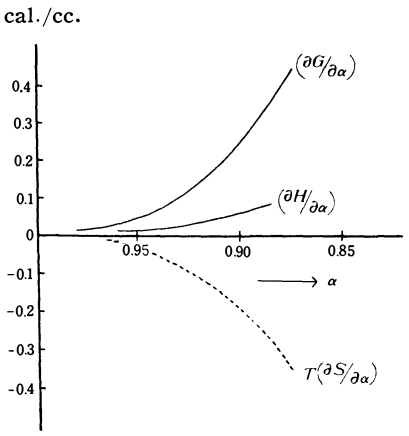

Fig. 6. Thermodynamics of compression for benzene.

magnitude of this entropy change increases with the increase of strain. Enthalpy change $(\partial H/\partial \alpha)$ is also positive, thus the change of internal energy increases with the increase of strain.

On the contrary, in benzene, polymer swells to a great extent, and in this case, with the increase of strain, the degree of the change of internal energy (positive, in this case) is not so large, and $(\partial S/\partial \alpha)$ is negative; i. e., the magnitude of entropy change decreases with increase of strain.

The increase of internal energy with extension would correspond to the fact that the external work is stored as potential energy between molecules.

In a poor solvent, like carbon tetrachloride, intermolecular interaction exists to a considerable degree, as expected from the above results. In this case, external force may loose to some extent the cohesion between molecules, and the increase of randomness of polymer molecules or the releasing of solvent molecules fixed around the polymer chains contributes to the increase of entropy of the system. These aspects seem to be acceptable from the fact that the degree of stress relaxation is more remarkable in a poor solvent, and that each parameter in four-element model is larger compared with the values obtained for a good solvent.

In the case of benzene, which is a good solvent, the decrease in entropy change is much higher than the increase in internal energy change. This may originate from the fact that the restriction for free rotation or flexion of chain molecules is removed by the high degree of swelling, and that the freedom of chain molecules is expected to decrease with the increase of strain.

Acknowledgement is made to Professor H. Akamatu and Assistant Professor T. Nakagawa for their support and advice in this experiment.

Department of Chemistry, Faculty of Science, The University of Tokyo
Hongo, Tokyo

Correction for the Intensities of Infrared Absorption Bands

By Kenji KURATANI and Atsuko MINEGISHI

(Received January 13, 1958)

The serious disadvantage of infrared absorption spectroscopy is the fact that the band shapes and the peak intensities measured in liquids or in solutions are markedly affected by the spectral slit widths of the spectrometers. Therefore it is desirable to find the method of correction of the apparent peak intensities and the band half widths to the true intensities and half widths, respectively, and to express them with the universal values. A number of authors[1-4] have discussed this problem. In the present work we have compared the methods established by these authors from the view points of the spectral slit width, the slit function, and the shape of the absorption band, and have proposed improved methods.

In the last section of this paper, the improved correction method was applied.

1) D. A. Ramsay, *J. Am. Chem Soc.*, **74**, 72 (1952).
2) A. C. Hardy and F. M. Young, *J. Opt. Soc. Am.*, **39**, 265 (1949).
3) R. A. Russell and H. W. Thompson, *Spectrochim. Acta*, **9**, 133 (1957).
4) E. B. Wilson, Jr. and A. J. Wells, *J. Chem. Phys.*, **14**, 578 (1946).

to the C=O stretching vibration bands of fifteen esters in carbon tetrachloride solutions, and the values of the true molecular extinction coefficient were determined. The true integrated absorption intensities per one C=O group were also obtained by the extrapolation method. These values are dispensable for the group type analysis of esters.

Correction for the Peak Intensity. Method I.—For monochromatic radiation, the well known absorption law,

$$I=I_0e^{-\alpha ct} \tag{1}$$

applies, and the true molecular extinction coefficient at the absorption maximum is described as*

$$E_{\max}=\frac{1}{ct}\log_{10}(I_0/I)_{\max} \tag{2}$$

However, in the actual spectrometer, due to the use of finite slit widths, the radiation is not monochromatic, and the energy from the exit slit of a spectrometer set at a frequency ν' may be expressed by an energy distribution function $g(\nu,\nu')$**. Accordingly when the spectrometer is set at frequency ν', the apparent intensities of the incident and transmitted radiation are described as

$$\begin{aligned} T_0&=\int I_0(\nu)g(\nu,\nu')\mathrm{d}\nu \\ T&=\int I(\nu)g(\nu,\nu')\mathrm{d}\nu \end{aligned} \tag{3}$$

and the apparent molecular extinction coefficient is given by

$$E^a{}_{\max}=\frac{1}{ct}\log_{10}(T_0/T)_{\max} \tag{4}$$

In the actual prism spectrometer, the observed absorbances $[\log_{10}(T_0/T)=D]$ at the band peaks are markedly affected by the spectral slit widths and are very different from the true values $[\log_{10}(I_0/I)]$.

One of the well known method to correct the apparent absorbance at the band maximum for the true absorbance is proposed by Ramsay[1]. Under the following assumptions as,

i) the slit function may be represented by a triangle whose base length is equal to the twice the spectral slit width s,

ii) spectral slit width s is the sum of the term s_1 represents the contribution from the finite mechanical slit width and the term s_2 responsible for the finite resolving power of the prism, and the values of each term are evaluated by the equation given by Williams[5],

iii) the true band shape may be represented by a Lorentz curve,

$$\log_e(I/I_0)=\frac{a}{(\nu-\nu_0)^2+b^2} \tag{5}$$

Ramsay has computed the apparent band absorbance

$$\log_{10}(T_0/T)_\nu=\log_{10}\int g(\nu,\nu')\mathrm{d}\nu$$
$$-\log_{10}\int g(\nu,\nu')\cdot\exp\left(\frac{-a}{(\nu-\nu_0)^2+b^2}\right)\mathrm{d}\nu \tag{6}$$

and obtained the relationships between the ratio of the true and apparent peak intensities and the ratio of the spectral slit widths to the band half widths.

However, Ramsay's assumption is not applicable to every case, and it is necessary to reexamine it. Ignoring the diffraction by a prism, the slit function for a perfectly aligned spectrometer with an equal entrance and exit slit width may be represented by a triangle as described by Ramsay. But owing to the mismatching of the curved image of the entrance slit with the exit slit curvature, the misfocusing of the collimator mirror, etc., for the spectrometer which we actually used, the slit widths of the entrance and exit slits are not equal, and therefore the shape of the slit function may be approximated more closely to trapezoid than to triangle.

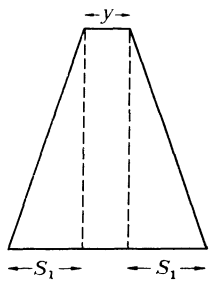

Fig. 1. Trapezoidal slit function.

Then the spectral slit width itself is rewritten as

$$s=s_1+s_2+s_3 \tag{7}$$

where s_1 and s_2 are the same as defined by Ramsay and s_3 is the term represents the contribution from opical misalignment. The details of the trapezoidal slit function illustrated in Fig. 1 are

* In this equation c is expressed moles per liter of solution and t is the cell length in cm.

** This function is defined as the slit function.

5) V. Z. Williams, *Rev. Sci. Instrumensts*, **19**, 151 (1948).

TABLE I-1

VALUES OF $\log_{10}(I_0/I)_{max}/\log_{10}(T_0/T)_{max}$ FOR THE VARIOUS VALUES OF y IN TERMS OF THE RATIO OF $s_1+y/\Delta\nu^a{}_{1/2}$*

$\log_{10}(I_0/I)_{max}/\log_{10}(T_0/T)_{max}$

$s_1+y/\Delta\nu^a{}_{1/2}$	0.15	0.20	0.25	0.30	0.35	0.40	0.45	0.50	0.55	0.60
for $y'=0.000$**	1.016	1.028	1.046	1.066	1.095	1.131	1.176	1.229	1.308	1.416
for $y'=0.025$	1.013	1.025	1.041	1.061	1.088	1.124	1.167	1.220	1.295	1.396
for $y'=0.050$	1.011	1.022	1.037	1.057	1.082	1.116	1.158	1.210	1.283	1.378
for $y'=0.075$	1.011	1.019	1.033	1.052	1.076	1.108	1.150	1.200	1.270	1.364
for $y'=0.100$	1.009	1.017	1.030	1.049	1.072	1.102	1.139	1.188	1.255	1.345
for $y'=0.125$	1.009	1.016	1.028	1.045	1.066	1.095	1.133	1.180	1.245	1.330

* This Table can be applied to the values of $\log_{10}(T_0/T)_{max}$ from 0.2 to 0.4.

** The value of y' is defined as $y/\Delta\nu^t{}_{1/2}$.

TABLE I-2

VALUES OF $\Delta\nu^a{}_{1/2}/\Delta\nu^t{}_{1/2}$ FOR THE VARIOUS VALUES OF y IN TERMS OF $\log_{10}(T_0/T)_{max}=D_{max}$ AND THE RATIO OF $s_1+y/\Delta\nu^a{}_{1/2}$

$\Delta\nu^a{}_{1/2}/\Delta\nu^t{}_{1/2}$

$s_1+y/\Delta\nu^a{}_{1/2}$	0.15	0.20	0.25	0.30	0.35	0.40	0.45	0.50	0.55	0.60
for $y'=0.000$										
$D_{max}=0.2$	1.021	1.038	1.060	1.091	1.131	1.180	1.242	1.320	1.422	1.550
$=0.3$	1.020	1.036	1.058	1.087	1.125	1.172	1.228	1.302	1.398	1.525
$=0.4$	1.020	1.035	1.056	1.084	1.120	1.165	1.218	1.284	1.372	1.485
for $y'=0.025$										
$D_{max}=0.2$	1.018	1.034	1.054	1.084	1.122	1.168	1.229	1.304	1.402	1.528
$=0.3$	1.018	1.032	1.053	1.081	1.117	1.162	1.216	1.287	1.380	1.502
$=0.4$	1.018	1.031	1.051	1.078	1.112	1.154	1.206	1.272	1.358	1.472
for $y'=0.050$										
$D_{max}=0.2$	1.015	1.030	1.050	1.078	1.113	1.159	1.216	1.290	1.384	1.510
$=0.3$	1.015	1.029	1.047	1.074	1.108	1.152	1.204	1.273	1.362	1.482
$=0.4$	1.015	1.027	1.045	1.071	1.103	1.144	1.195	1.258	1.343	1.452
for $y'=0.075$										
$D_{max}=0.2$	1.013	1.027	1.047	1.074	1.106	1.149	1.204	1.274	1.365	1.490
$=0.3$	1.013	1.026	1.045	1.070	1.102	1.142	1.193	1.259	1.348	1.465
$=0.4$	1.013	1.025	1.043	1.067	1.097	1.134	1.181	1.246	1.330	1.437
for $y'=0.100$										
$D_{max}=0.2$	1.012	1.024	1.042	1.066	1.098	1.138	1.191	1.262	1.348	1.472
$=0.3$	1.012	1.023	1.040	1.063	1.094	1.132	1.182	1.246	1.332	1.445
$=0.4$	1.012	1.022	1.039	1.061	1.090	1.128	1.175	1.234	1.314	1.415
for $y'=0.125$										
$D_{max}=0.2$	1.010	1.022	1.039	1.063	1.094	1.134	1.182	1.248	1.332	1.445
$=0.3$	1.010	1.021	1.037	1.059	1.088	1.124	1.172	1.233	1.314	1.425
$=0.4$	1.010	1.020	1.035	1.056	1.083	1.118	1.162	1.220	1.296	1.395

defined as follows. The length of the upper side is equal to the sum of s_2+s_3 and denoted as y, and the lower base length is equal to $2s_1+y$. This slit function is regarded as the combination of the triangular slit function whose base length is equal to twice the term which represents the contribution from the finite mechanical slit width, and the rectangular slit function whose base length is equal to the term which is responsibie for the prism diffraction and the optics misalignment.

Using the trapezoidal slit function as defined above, Eq. 6 was evaluated by numerical integration, for the various values of a, b, and the slit widths s_1 and y. For the stepwise increment of the value of y, the ratios of $\log_{10}(I_0/I)_{max}/\log_{10}(T_0/T)_{max}$ and $\Delta\nu^a{}_{1/2}/\Delta\nu^t{}_{1/2}$ were represented as functions of the apparent intensities

and of the ratio $s/\Delta\nu^{a}_{1/2}$. The results are given in Table I, and the rows for $y=0$ are the same as given by Ramsay.

With this Table we can correct the observed intensities and band half widths to true ones, but it is necessary to determine the value of y experimentally, since the value of y is not known a priori. For this purpose, the absorption measurements of the same sample are made with the various mechanical slit widths, and one set of observed values for the peak intensities and band half widths are obtained. Then assuming an arbitrary y value, the spectral slit width s is determined, and the correction factor for the peak intensities observed by that slit width is found from Table I-1. Using the same y value, the similar processes are tried for the values observed with the other mechanical slit widths. If we assume an unsuitable y value, the corrected peak intensities for the various mechanical slit widths should not agree, and the similar calculations with the another y values must be repeated until we get the satisfactory agreement among the corrected intensities. The corrected peak intensities which finally agree may be considered as the true peak intensities. For the observed band half widths, the similar treatments should be made by the use of Table I-2, and the band half widths are also corrected.

This method is applied to the C=O stretching vibration bands of ethyl capronate measured in carbon tetrachloride solution, and illustrated in Table II. The corrected peak intensities show always good agreement, when we assume the value of y to be ca. 1.6 cm^{-1}. (In Table I, the correction factors are represented as the functions of $y'=y/\Delta\nu^{t}_{1/2}$ and in this case $\Delta\nu^{t}_{1/2}$ is nearly equal to 16 cm^{-1}, therefore, we get a good agreement with the value of $y'=0.1$). Therefore, when the intensity measurement in the 1700 $cm.^{-1}$ region is made with the same spectrometer under the same condition of alignment, the value of y should be always assigned to ca. 1.6 cm^{-1}*, but the value of y' should be altered according to the band half widths. In Table II, the result obtained from Ramsay's method is compared with the result of ours. The more excellent agreement among the corrected intensities is obtained with our method. The reliability of our method is also proved from the agreement between the observed resolution and the spectral slit width, and the equality between the corrected intensities and the intensities measured with a grating spectrometer under the higher resolution.

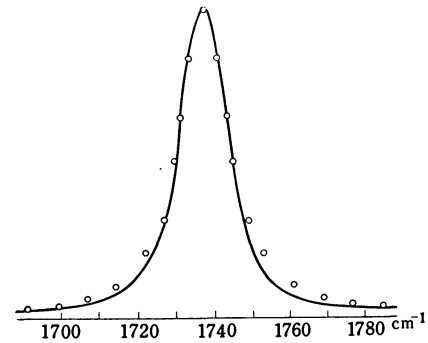

Fig. 2. Comparison between the observed and the calculated absorbance.

The aforementioned correction method is derived from the Lorentz curve approximation for the true band shape. To examine this assumption, the results of numerical integration of Eq. 6 are compared with the observed absorption curves of ethyl capronate in carbon tetrachloride solution. The results are shown in Fig. 2, where the full line represents the observed absorbance curve and the dots represent the calculated values.

The agreement between these curves is well in the central region of the bands and in the band wings, but in the middle of these regions, comparatively large differences are observed. An exponential curve, which is used by Philpotts[6] for the band shape, is also examined, but the calculated points markedly deviate from the observed curves except in the narrow central region of the bands. Therefore, for the correction of the observed peak intensities and the band half widths, it is considered to be reasonable to assume Lorentz curve for the true band shape.

Correction for the Peak Intensity. Method II.—Koana[7] and Hardy[2] showed the other correction method. For the symmetrical bands, the corrected absorbance at the band maximum (D^{0}_{max}) is represented as a first approximation by the

* The value of s_3 which represents the contribution from the misalignment of optics is nearly equal to 1.2 cm^{-1} (=1.6–0.4 cm^{-1}). This value is surprisingly large, but after the readjustment of optics, the value of s_3 was diminished to ca. 0.4 cm^{-1}.

6) A. R. Philpotts, W. Thain and P. G. Smith, *Anal. Chem.*, **23**, 268 (1951).

7) K. Koana, et al., *Proc. Phys.-Math. Soc. Japan*, (*Nippon Sugaku-Butsuri Gakkaishi*) **22**, 940 (1940).

TABLE II

CORRECTION FOR THE INTENSITIES (METHOD I) ETHYL CAPRONATE IN CARBON TETRACHLORIDE CONCENTRATION 0.044 mol./l. PATH LENGTH 0.124 mm. BAND AT 1737 cm^{-1}

mechanical slit width mm.	0.13	0.17	0.23	0.29	0.225*
s_1 cm^{-1}	1.43	1.87	2.53	3.19	1.0 *
observed D_{max}	0.327	0.326	0.324	0.318	0.332*
$\Delta\nu^a_{1/2}$ cm^{-1}	15.6	15.7	16.0	16.2	15.5 *
for $y/2b_0=0.025$					
s_1+y cm^{-1}	1.82	2.26	2.92	3.58	
corrected D_{max}	0.330	0.330	0.331	0.328	
for $y/2b_0=0.05$					
s_1+y cm^{-1}	2.21	2.65	3.31	3.97	
corrected D_{max}	0.330	0.331	0.332	0.329	
for $y/2b_0=0.075$					
s_1+y cm^{-1}	2.58	3.02	3.68	4.34	
corrected D_{max}	0.332	0.332	0.333	0.331	
for $y/2b_0=0.10$					
s_1+y cm^{-1}	2.96	3.40	4.06	4.72	
corrected D_{max}	0.332	0.333	0.334	0.332	
for $y/2b_0=0.125$					
s_1+y cm^{-1}	3.33	3.77	4.43	5.09	
corrected D_{max}	0.334	0.335	0.336	0.335	
for $y/2b_0=0.0$					
$s_1+0.4$** cm^{-1}	1.83	2.27	2.93	3.59	
corrected D_{max}	0.331	0.331	0.332	0.329	

* These values are measured with a P-E. 112G grating spectrometer.

** These values are obtained using a triangular slit function, the term s_2 responsible for the finite resolving power of the prism is equal to 0.4 cm^{-1}.

TABLE III

CORRECTION FOR THE PEAK INTENSITIES (METHOD II) ETHYL CAPRONATE IN CARBON TETRACHLORIDE. CONCENTRATION 0.044 mol./l. PATH LENGTH 0.124 mm. BAND AT 1737 cm^{-1}

mechanical slit width mm.	0.13	0.17	0.23	0.29
s_1 cm^{-1}	1.43	1.87	2.53	3.19
observed D_{max}	0.327	0.326	0.324	0.318
observed D''_{max}	−0.009	−0.009	-0.008_5	-0.008_5
for $y=0.0\ cm^{-1}$*				
coefficient a_2	0.279	0.428	0.715	1.074
corrected D_{max}	0.330	0.330	0.330	0.327
for $y=1.2\ cm^{-1}$				
coefficient a_2	0.373	0.539	0.847	1.226
corrected D_{max}	0.330	0.331	0.331	0.328
for $y=1.6\ cm^{-1}$				
coefficient a_2	0.468	0.648	0.978	1.380
corrected D_{max}	0.331	0.332	0.332	0.330
for $y=2.0\ cm^{-1}$				
coefficient a_2	0.575	0.770	1.123	1.545
corrected D_{max}	0.332	0.333	0.334	0.331

* These values are obtained using a triangular slit function, the term s_2 responsible for the finite resolving power of the prism is equal to 0.4 cm^{-1}.

TABLE IV
ESTER C=O BANDS IN CARBON TETRACHLORIDE SOLUTION

Compounds	ν_{max} (cm^{-1})	E_{max} (l/mol. cm.)	$\Delta\nu^{1}_{1/2}$ (cm^{-1})	$A\times10^{8}$ (cm^2/molecule. sec.)
methyl formate	1735	730	10.5	142
methyl acetate	1748	715	12.6	143
ethyl acetate	1742	732	12.7	149
n-butyl acetate	1741	590	15.9	151
isoamyl acetate	1742	605	15.7	156
ethyl propionate	1739	560	15.6	137
ethyl capronate	1737	615	15.6	147
dimethyl oxalate	1752	1050	9.5	268
	1781	570	9.8	
diethyl oxalate	1747	1010	11.6	291
	1773	540	12.5	
diethyl malonate	1739	825	15.6	302
	1756	630	16.7	
diethyl succinate	1739	1180	15.7	285
di-2-ethylhexyl adipate	1737	1090	17.5	307
di-2-ethylhexyl azelate	1736	1130	17.2	325
di-2-ethylhexyl sebacate	1736	1130	17.0	297
diethyl maleate	1735	1000	20.0	302

observed absorbance and its second derivative, i. e.,

$$D^{0}_{max}=D_{max}-a_2(d^2D/d\nu^2)_{max} \qquad (8)$$

where a_2 is a coefficient determined by the slit function, and given by

$$a_2=\frac{\int g(\nu,\nu')\nu^2 d\nu}{\int g(\nu,\nu')d\nu} \qquad (9)$$

The a_2 values* are represented for the cases of a triangular slit function whose base length is equal to twice the spectral slit width s as $s^2/12$, and for a trapezoidal slit function whose details are defined in the preceding section as $[(s_1+y/2)^4-(y/2)^4]/12s_1(s_1+y)$.

To obtain the true corrected intensity, the trial and error examination of the value of y should be made in a similar manner as described in the preceding section. An example of this process is carried out for the C=O stretching band of ethyl capronate, and shown in Table III, where the third and fourth rows show the observed peak intensities and their second derivatives, respectively. The good agreement among the corrected intensities is obtained when we assume the value of y to be ca. 1.6 cm^{-1}.

This method is attractive, because of the non-existence of the assumption on the band shape, but the process to obtain the second derivatives of absorbances is troublesome. Moreover, Eq. 8 is only a first approximation, and for the large values of absorbances, Eq. 8 should be extended to the fourth derivative. These two disadvantages are too serious, and in the last section of this paper this method is not adopted.

True Integrated Absorption Intensity.—As regards the integrated intensities, there are few to be discussed, and the extrapolation method proposed by Wilson and Wells[3] can be applied to the actual cases. Namely, true integrated intensity A is obtained as the limiting value of the intensity B, i. e.,

$$A=\lim_{ct\to0} B=\lim_{ct\to0}\frac{1}{ct}\int\log_e(T_0/T)d\nu \qquad (10)$$

where c is the concentration of the solute in molecules per $cm.^3$ of solution, t is the cell length in cm., and ν is the frequency in cycles per second. Integration of the band is carried out over the frequency interval of the four times the apparent band half width on either sides of the band center. Special correction for the residual area under the wings is ignored.

Results on the C=O Band of Esters.—Table IV gives the frequencies of the band maxima, the true molecular extinction coefficients at the peak, the true band half widths, and the true integrated absorption intensities of C=O stretching vibration bands of fifteen esters as measured in carbon tetrachloride solutions. These results show good agreement with the

* In the original paper[2], a_2 is determined experimentally. But this procedure is quite erroneous, and here a_2 is calculated from the assumed slit function.

values obtained by the other authors[8-10].

The mean values and their standard deviations of the peak and area intensities per one C=O group are computed for the seven monoesters as

$$(E_{group})_{max}=647\pm73 \quad l.mol.^{-1}cm.^{-1},$$

$$A_{group}=146.4\pm6.3\times10^{-8} \quad cm^2\,molecule^{-1}\,sec.^{-1},$$

and the mean value of area intensities per one C=O group for the fifteen mono- and di-esters is given by

$$A_{group}=147.5\pm6.2\times10^{-8} \quad cm^2\,molecule^{-1}\,sec.^{-1}$$

The mean values of area intensities per one C=O group are similar for the mono- and di-esters, and in both cases, the standard deviations of area intensities are quite small. This fact is valuable for the group type analysis of esters.

8) R. R. Hampton and J. E. Newell, *Anal. Chem.*, **21**, 914 (1949).
9) G. M. Barrow, *J. Chem. Phys.*, **21**, 2008 (1953).
10) S. A. Francis, ibid. **19**, 942 (1951).

Experimental

A Perkin-Elmer Model 112 spectrometer with calcium fluoride prism and a cell of 0.124 mm. thickness, determined by the interference method, was employed. All of the esters were purified by the ordinary method and distilled. The boiling points of the purified materials were in good agreement with the literature values.

We wish to express our sincere thanks to Professor S. Mizushima and Assistant Professor T. Shimanouchi who permitted us to use the grating spectrometer.

The cost of this work has been partly defrayed by a grant from the Ministry of Education.

Institute of Science and Technology
University of Tokyo
Meguro-ku, Tokyo

Über die Einwirkung des Bromwasserstoffs und des Sauerstoffs auf α, β-ungesättigte Ketone. II. Bildung eines α-Diketons aus dem ungesättigten α-Bromketon durch Sauerstoffeffekt[1]

Von Hazime KASIWAGI

(Eingegangen am 3. März, 1958)

Die α, β-ungesättigten Arylketone sind allgemein sehr schwierig den Sauerstoffeffekt zu erleiden, während derselbe Effekt bei ihren α-bromsubstituierten deutlich bemerkt worden ist, was die Bildung der aromatischen Carbonsäure durch die Abspaltung an der Kohlenstoffkette dieser letzteren zur Folge hat. Einige Beispiele davon sind im vorigen Bericht[2] hingewiesen, bzw. bildet Benzoesäure sich durch diese Zersetzung des α-Bromchalkons und *p*-Toluylsäure aus 4'-Methyl-α-bromchalkon. Hier gehört es notwendig zur Frage, die Struktur der mit der aromatischen Carbonsäure paarweise gebildeten Verbindung oder ihrer Umwandlungsprodukte zu ermitteln, was aber unglücklicherweise dem Verfasser nicht gelungen ist. Da aber man ein α-Diketon als Reaktionsprodukt unter Versuchsbedingungen, worin der Sauerstoffeffekt sich beteiligt, erhalten konnte, hier sollen Betrachtungen über das Resultat der Versuche und den darauf begründeten Reaktionsmechanismus angestellt werden.

Man lässt den Bromwasserstoff auf die stark verdünnte Petroleumätherlösung des α - Bromchalkons (ω - Brom - ω - benzylidenazetophenons I) oder α-Brom-4'-methylchalkons (ω-Brom - 4-methyl-ω-benzylidenazetophenons II) unter heftigem Sauerstoffstrom reagieren. Nach der Reaktion wäscht man die eine kleine Menge von Wasser abscheidende, gelbe Lösung mit Bicarbonatlösung, trocknet und dampft den Petroleumäther unter vermindertem Druck ab. Die gelbe Lösung scheidet den braungelben, öligen Rückstand ab, der beim Stehen allmählich schwarzgrün wird.

1) Eingebracht in der vierten Jahresversammlung der Japanischen Chemischen Gesellschaft, Tokyo, 1951.
2) Dieses Bulletin, **26**, 355 (1953).

Beim Keton II, d. h. 4'-methylsubstituierten vom Keton I ist das Schwarzwerden durch Zersetzung nicht auffallender als beim ersteren und in den meisten Fällen kristallisiert die ölige Substanz sich zum Teil. Durch mehrmalige Umkristallisation mit wässrigem Alkohol wird diese Substanz gereinigt und kommt den bei 83.0~84.5°C schmelzenden, gelben Kristall zu geben. Der ermittelten Zahlen seines Molekulargewichts, Bromgehalts und seiner Reaktion nach, wodurch diese Verbindung unter Isolierung des Jods durch Einwirkung der Jodwasserstoffsäure reduziert wird, er zeigt sich als ein α-Diketon und zwar wird als *p*-Tolyl-ω-brombenzylglyoxal ($C_6H_5CHBrCOCOC_6H_4$-*p*-CH_3) (III) angesehen.

Um die Annahme zu versichern, dass die Struktur dieses gelben Kristalls wirklich der oben angedeuteten entspricht, hat man einen synthetischen Beweis ausführt, indem man den nach Beschreibung Jorländers[3] hergestellten *p*-Tolyl-benzylglyoxal mit Brom behandelt hat. Aus der Eisessiglösung der Reaktionsprodukte erhält man nach ihrer wiederholten Umkristallisation mittels wässriges Äthanols, einen gelben Kristall von Schmelzpunkt 84~85°C. Da jener gelbe Kristall mit dieser dargestellten Verbindung zusammengeschmolzen, keine Schmelzpunktserniederung zeigt, kann man annehmen, dass der erhaltene, gelbe Kristall mit dem bromsubstituierten vom *p*-Tolyl-benzylglyoxal übereinstimmt. Ungeachtet seiner Struktur als α-Diketon bildet der bromierte *p*-Tolyl-benzylglyoxal, mit *o*-Phenylendiamin behandelt, sich kein Chinoxalinderivat. Aber der nicht substituierte *p*-Tolyl-benzylglyoxal selbst gibt das Chinoxalin, das den von Jorländer angedeutete Schmelzpunkt und den der Theorie entsprechenden N-Gehalt hat. Angenommen, es bei der Frage nicht stehe, dass das Reaktionsprodukt mit der durch Einwirkung des Broms auf das oben erwähnte Glyoxal entstandenen Verbindung identisch sei, muss man aber darauf Aufmerksamkeit lenken, ob die Bromierung wirklich sich an α-Methylengruppe des Diketons vollzieht oder nicht. Jorländer nahm dem bromierten α-Diketon die Struktur von der oben genannten Formel III[4] an. Dieses Umstands und der Reduzierbarkeit des Reaktionsprodukts durch Jodwasserstoffsäure nach kann man mit Bestimmtheit annehmen, dass es zwar die Struktur III hätte. Das entsprechende α-Diketon konnte man aus den Reaktionsprodukten des nicht 4-methylierten, ungesättigten Bromketons I nicht erhalten, da der aus der Reaktionsflüssigkeit durch Abdampfen des Lösungsmittels unter vermindertem Druck hintergebliebene Rückstand durch Zersetzung merkwürdigerweise schwarz wird und die unverkennbare Substanz nicht gibt. Aber die von den sauren Stoffen durch Ausschütteln mit Bicarbonat befreite Lösung nimmt eine dem α-Diketon eigentümliche gelbe Farbe an.

Unter Umständen erhielt man einen anderen Kristall aus den Umwandlungsprodukten des nicht 4-methylierten Ketons I. Mit wiederholter Umkristallisation mittels wässriges Äthanols wird der Kristall weiss und allmählich schwerer löslich in Äthanol, und erweist sich als das Dibromid des Phenylstyrylketons, und zwar als das von tieferem Schmelzpunkt. In manchen Fällen wurde das entsprechende Dibromid auch bei der Reaktion betreffs des ungesättigten Bromketons II durch das ähnliche Verfahren erhalten. Bei dem Falle aber, worunter man das Dibromid empfangte, wurde es nicht gelungen, α-Diketon zu isolieren.

Diese Tatsache zusammengenommen, kann man schliessen, dass das ungesättigte Bromketon I oder II unter den Bedingungen, die für den Sauerstoffeffekt seinen Auftritt verantwortlich sind, die saure Substanz und den augenreizenden Stoff von unbekannter Struktur, wie gesagt im vorigen Bericht, gleichzeitig mit dem α-Diketon oder andernfalls dem Ketondibromid gäbe. Solche Ketondibromide jedoch auch für die normalen Additionsprodukte des Bromwasserstoffs zum Keton I und II gelten, weist die Beweisführung ihrer Bildung allein die Mitwirkung eines Mechanismus von der anomalen Addition nicht auf.

Aber wenn eine von dem Sauerstoffeffekt herrührende Reaktion wirklich stattfinden könnte, würde das Keton als sich mit dem Bromatom zuerst ein organische, freie Radikal zu bilden, vermutet, folgendermassen;

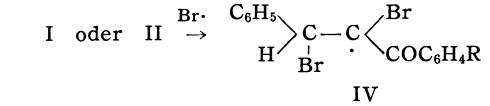

IV

Als die alternierende Form des freien Radikals kommt es zwar in Betracht eine von der Struktur, worin das Bromatom

3) *Ber.*, **50**, 418 (1917).
4) Jorländer, loc. cit..

sich an das α-ständigen, ungesättigten Kohlenstoffatom addieren könne, aber darf solche Struktur im Vergleich mit den oben angestellten von ihrer minderen Beständigkeit aus wohl als die geeignetere Form nicht angesehen werden[5]. Das einmal gebildete Radikal IV, der Einwirkung des Sauerstoffs und des Bromwasserstoffs ausgesetzt, geht in ein Hydroperoxyd V über.

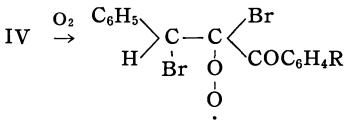

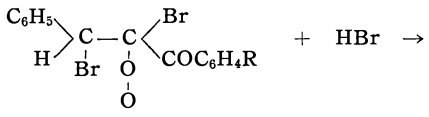

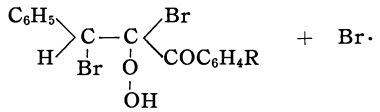

Obwohl man hier bezüglich der Bildungsweise des Hydroperoxyds vermutete, dass das Wasserstoffatom, das von Peroxydradikal empfangt wird und in die Zusammensetzung eingeht, seinen Ursprung ausschliesslich im reagierenden Bromwasserstoff hätte, wenn die freien Radikale das aktive Wasserstoffatom enthalten, auch dieses letzteren könnte an die Bildung des Hydroperoxyds teilnehmen. So kann man als das dafür geltende Beispiel betrachten, dass das bei der genannten Reaktion der Zimtsäure gebildete Peroxydradikal einen aktiven Carboxylwasserstoff enthält und die intramolekulare Umlagerung ihm als möglich angesehen wird[6]. Das Wasserstoffatom der verzweigten Methylgruppe von Dimethylstilben bediene sich auch als solches. In diesem Falle kann wahrscheinlich seine intermolekulare Austausch stattfinden[7].

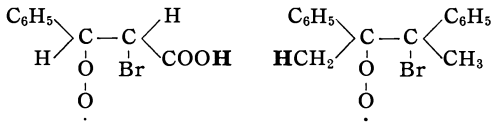

Das unbeständige Hydroperoxyd gibt durch Zersetzung das freie Hydroxylradikal und ein anderes sauerstoffhaltige Radikal VI. Dieses Radikal, die Einwirkung des Bromwasserstoffs erleidet, gibt das Hydroxyd VII unter Wiederherstellung des Bromatoms. Daher bietet auch diese Stufe von Reaktion die der Fortpflanzung der Reaktionskette dar. Das Hydroxyd mag auch durch unmittelbare Vereinigung des eigentlichen, freien Radikals IV mit dem Hydroxyl gebildet werden.

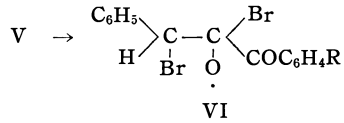

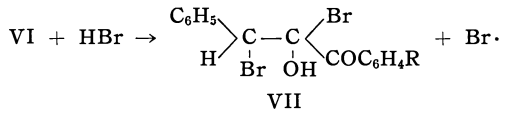

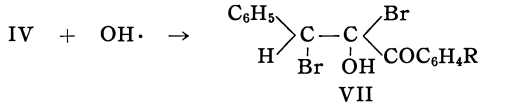

Im Radikal VI übrigens befindet seine Bindung zwischen den Atomen des Carbonylkohlenstoffs und seines α-ständigen wegen der grossen Elektronenaffinität des Sauerstoffs, sich in einem schwächerem Zustand, was ihr Auflösen zur Bildung der aromatischen Säure und nicht identifizierter Stoffe von augenreizender Eigenschaft zur Folge haben kann.

Die Bildung α-Diketons beruht auf der Abspaltung des Bromwasserstoffs aus dem Hydroxyd VII, da hier dieses als recht unbeständig angesehen wird, um es in einem selbständigen Zustand zu erkennen.

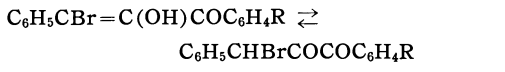

Die der Form VII entsprechende Hydroxylverbindung sei nicht immer unbeständig, so ist es in gewissen Fällen gelungen worden, die zuständige Hydroxylverbindung als solche wirklich zu identifizieren. Dafür gilt die Isolierung der α-Hydroxy-β-brombuttersäure aus den Reaktionsprodukten der Krotonsäure mit dem Bromwasserstoff und dem Sauerstoff[8].

Die andere Möglichkeit von der Formation α-Diketons, die hier in Betracht kommen müsste, wäre die Anhäufung des Broms an die Doppelbindung des eigentlichen, ungesättigten Ketons und die nachherige Verseifung des so entstandenen Tribromids.

Zur Prüfung dieser Bildungsweise α-Diketons stellt man das Tribromid durch

5) F. R. Mayo und C. Walling, *Chem. Revs.*, **27**, 373 (1940).
6) O. Simamura und M. Takahashi, Dieses Bulletin, **22**, 60 (1949).
7) H. Suzuki, O. Simamura und T. Ichihashi, ebenda, **27**, 234 (1954).
8) O. Simamura, ebenda, **17**, 327 (1942).

Addition des Broms zum Keton II. Das so erhaltene Tribromketon bietet einen bei 104.5~106°C schmelzende, weissen Kristall dar und ist zwar genügend beständig, mit Wasser oder Alkali behandelt, keine Veränderung zu erleiden. Freilich kann man eine Schmelzpunktserniederung beobachten. Bezüglich des Ketons I wird das entsprechende Tribromketon als der bei 202~4°C schmelzende, ebenfalls weisse Kristall erhalten. Daraus kann man ersehen, dass α-Diketon die Ursache seiner Bildung über das Tribromketon der Verseifung dieses letzteren nicht zugeschrieben wird.

Die Gelegenheit für das erste Radikal IV, mit dem Bromwasserstoff zu begegnen, bildet eine andere Fortpflanzungsstufe der Reaktionskette, die Formation des Dibromketons vom tieferen Schmelzpunkt verursacht, das übrigens auch als gebildet durch elektrophile Addition des Bromwasserstoffs auf das ungesättigte Bromketon betrachten werden könne.

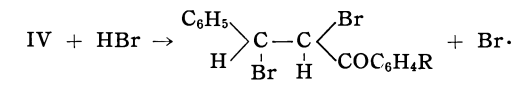

Wie erwähnt im vorigen Bericht, bei der Reaktion α-Bromchalkons ist der Ertrag der aromatischen Säure ungefähr dreimal soviel als bei seinem 4′-Methylderivat. Die Ursache davon sei vielleicht dem Umstand zuzuschreiben, dass bei dem 4′-Methylderivat das sauerstoffhaltige Radikal VI infolge seiner Stabilisierung durch die Vergrösserung seiner Delokalisierungsenergie, damit die Gegenwart der 4′-Methylgruppe wegen ihrer Hyperkonjugierung mit dem Benzolkern zustandekommt, sich im beständigeren Zustand im Vergleich mit dem aus nicht substituierten Bromketon entstandenen Radikal befindet, was dem Radikal VI das Hydroxyd, die Muttersubstanz α-Diketons zu bilden hilft. Daraus kann man ersehen, dass der verminderte Ertrag der aromatischen Säure durch Zersetzung des Radikals VI im Falle von der Reaktion des 4′-Methylderivats der leichten Isolierbarkeit α-Diketons entspreche.

Beschreibung der Versuche

Ungesättigte Bromketone I und II. — Ihre Darstellung; schon erwähnt im vorigen Bericht[2].

Isolierung des gelben Kristalls.—Löst man 2.00 g ω-Brom-4′-methyl-ω-benzylidenazetophenon in bei 75~90°C siedendem Petroleumäther auf und leitet den Bromwasserstoff und den Sauerstoff ein. Die Lösung wird nach der Reaktion zur Beseitigung der sauren Stoffe mit Carbonatlösung ausgeschüttelt, mit wasserfreiem Natronsulfat getrocknet und dann das Lösungsmittel unter vermindertem Druck abdampfen lassen. Der Rückstand beträgt 2.5 g und ist ein gelbe, ölige Stoff von stürmisch augenreizendem Geruch, der durch Abspaltung von Bromwasserstoff allmählich schwarzgrün wird. Dieser ölige Körper ist in Petroleumäther leichter löslich. Wenn man diesem öligen Stoff mit wenig Äthanol versetzt und ihn unter Kühlung mittels Eiswassers stehen lässt, so kristallisiert es sich allmählich aus. Das erhaltene Produkt ist der bei 78~81°C schmelzende, weisse Kristall, der 1.10 g beträgt. Der Schmelzpunkt desselben steigt auf nach dreimaliger Umkristallisation mittels Äthanols bis auf 83.0~84.5°C. Es riecht augenreizend keineswegs mehr. Die Anwesenheit des Halogens lässt durch Beilsteinsche Prüfung erkennen. Mol. Gew. nach Rast und Br%: 315, 25.05; ber. für $C_{16}H_{13}O_2Br$ 317, 25.23.

Reaktion mit o-Phenylendiamin. Wenn man zur 3 ccm Äthanollösung von 0.1 g des Kristalls mit 0.3 g *o*-Phenylendiamin versetzt, so färbt sich die Lösung sofort rot und, gibt, mit Wasser verdünnt, ein rote Öl, das, mit Äthanol oder Benzol-Ligroin behandelt, sich nicht kristallisieren kann.

Darstellung des p-Tolyl-ω-brombenzylglyoxals. Um die Übereinstimmung des aus der Reaktionsflüssigkeit erhaltenen mit dem *p*-Tolyl-ω-brombenzylglyoxal zu versichern, stellt man zuerst den nicht bromierten Glyoxal dar, indem man den Benzaldehyd mit dem Methylphenazylchlorid durch Natriumäthylat kondensieren lässt, dann das so erhaltene Oxydäthan mit Natronlauge in Äthanol und nachher mit Salzsäure behandelt, lautet es wie folgt:

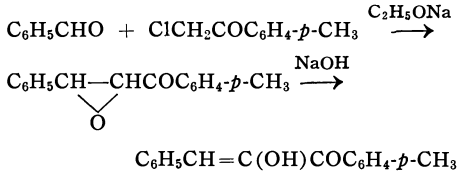

Das rohe Glyoxal, aus wässrigem Methanol auskristallisiert, bietet einen bei 89°C schmelzenden, schwachgelb gefärbten Kristall dar. Löst man sodann 0.71g dieses Kristalls in 4ccm Methanol auf und versetzt mit 0.32 g *o*-Phenylendiamin, so färbt die Lösung rot. Wird die durch Hinzufügen mit wenig Wasser weiss getrübte Reaktionsflüssigkeit solange auf dem Wasserbad erhitzt, bis sie klar gemacht wird, und stehen zum Abkühlen lassen, so scheidet das Chinoxalin als weisser Kristall sich von der Lösung ab. Der Kristall, dreimal mit wässrigem Äthanol umkristallisiert, schmilzt bei 112.0~112.5°C. N%: Beob. 9.08; ber, für $C_{22}H_{18}N_2$ 8.92. Man lässt 1 Mol. Äquiv. Broms (1.2 g) unter Kühlung mit Eis in die Lösung allmählich eintropfen. Wird das Ganze ins Wasser eingegossen, so sinkt das Reaktionsprodukt als rote, ölige Tropfen auf den Boden. Wenn man es mit Äther aufnimmt,

zuerst mit Bicarbonatlösung, dann mit Wasser auswäscht, trocknet und das nach dem Wegdampfen des Lösungsmittels nachgebliebene Öl mit Kältemischung stark abkühlt, so kristallisiert es sich langsam. Das so erhaltene Reaktionsprodukt ist ein gelbe, bei 82.5～84.0°C schmelzende Kristall, der 1.7 g beträgt. Dieser Kristall, mit wässrigem Methanol umkristallisiert, kommt bei 84～5°C zu schmelzen, und mit dem oben erwähnten aus der Reaktionspetroleumätherlösung erhaltenen, ebenfalls gelben Kristall zusammengeschmolzen, zeigt keine Schmelzpunktserniederung, d. h. schmilzt bei 84～5°C. Wenn man ferner einen Teil desselben nimmt und zu seiner Äthanollösung mit der kleinen Menge von Kaliumjodidlösung versetzt, so scheidet das Jod nach Ansäuerung der Lösung sich von derselben ab, was man aus der Entfärbung durch Einwirkung des Natriumthiosulfatlösung erkennt. Daraus kann man schliessen, dass sowohl die Bromierung am α-Kohlenstoffatom des p-Tolyl-ω-benzylglyoxals stattfindet wie das eine von der unter den Bedingungen, die für den Auftritt des Sauerstoffeffekts verantwortlich sind, aus dem ungesättigten Bromketon II entstandenen Produkten mit dem p-Tolyl-ω-brombenzylglyoxal übereinstimmt.

Die Einwirkung des Broms auf die α-Bromketon I und II. — Man löst 1.10 g Bromketon II in 5 ccm Chloroform auf und lässt 0.59 g Brom in die Lösung hinzufügen. Während des Eintropfens verschwindet die Farbe des Broms nicht, wird aber die Reaktion unter Entfärbung der Lösung hervorgerufen, wenn man die Lösung auf dem Wasserbad erwärmt. Nach dem Abdampfen des Lösungsmittels löst man das Produkt im ein wenig Chloroform hinzugefügten Äthanol auf und lässt die Lösung eiskalt stehen. Auf solche Weise gewinnt man 1.0 g einen farblosen Kristall. Der Schmelzpunkt desselben, wenn es mit dem genannten Lösungsmittel wieder umkristallisiert, wird zu 104.5～106°C. Obwohl man zu diesem Produkt aus den ermittelten Zahlen durch Elementaranalyse (beob.: C, 41.15; H, 2.53; Br, 51.87. ber. für $C_{16}H_{13}OBr_3$: C, 41.65; H, 2.82; Br, 52.03%) die dem Dibromid vom ungesättigten α-Bromketon entsprechenden Zusammensetzung zuschreiben mag, sollte man das von diesem Tribromketon sekundär durch Alkali verwandelte Produkt nicht ansehen, weil dieser Kristall, mit Sodalösung geschüttelt, keine Veränderung erleidet. Die gleiche Additionsreaktion ist auch bei dem ungesättigten Bromketon I durchzuführen. D. h. wenn man dieselbe Reaktion des 0.77 g Ketons mit 0.45 g Brom in Chloroformlösung vollzieht, so erhält man den 0.72 g bei 102～4°C schmelzenden, farblosen Kristall (Br: Beob. 53.94; ber. für $C_{15}H_{11}OBr_3$, 53.66%). Auch wird dieser Stoff durch schwachem Alkali nicht angegriffen.

Hydrobromide der Ausgangsketone.— Unter den gleichen Bedingungen, als man betreffs der Isolierung des gelben Kristalls von α-Diketon am Anfang dieser Beschreibung angestellt hat, andernfalls wird aber das Hydrobromid des eigentlichen, ungesättigten Bromketons als ein Reaktionsprodukt aus der Reaktionsflüssigkeit isoliert. Hierbei ist die Ursache nicht klar, was für ein Zustand die Unbestimmtheit des isolierten Produkts veranlassen soll. Ein Beispiel wie folgt: Löst man 3.68 g Keton I in 145 ccm bei 62～75°C siedendem Petroleumäther auf und lässt darauf den Bromwasserstoff unter Durchleitung des heftigen Sauerstoffstroms eiskalt für 3.5 Std reagieren. Nach der Reaktion die Lösung, durch Bicarbonatlösung von den sauren Stoffen befreit, nimmt eine auffallende, gelbe Farbe an. Man nimmt einen kleineren Teil davon, lässt das Lösungsmittel unter vermindertem Druck abdestillieren und den nachgebliebenen Rückstand in Eiskasten stehen. Der Kristall ist in Äthanol recht schwer löslich, wird durch Umkristallisation aus demselben Lösungsmittel gereinigt und kommt bei 116～120°C zu schmelzen. Dieser Stoff ergibt aus der Mischprobe sich als das Dibromid des ω-Benzylidenazetophenons von tieferem Schmelzpunkt, d. h. das bei 120～1°C schmelzenden. In ähnlicher Weise kann man aus 2.0 g Bromketon II 1.2 g des weissen Kristalls erhalten, der, mit dem bei 156.5～157.5°C schmelzenden Dibromid des 4-Methyl-ω-benzylidenazetophenons[9] zusammengeschmolzen, keine Schmelzpunktserniederung zeigt. Bei diesem Falle aber, abweichend von dem Falle, worin das α-Diketon isoliertworden ist, tritt ein merkwürdigeres Schwarzwerden der Reaktionsflüssigkeit während ihrer Behandlung auf.

Zusammenfassung

Aus der Untersuchung über die Einwirkung des Bromwasserstoffs und des Sauerstoffs auf α-Brom-α, β-ungesättigten Arylketone ergeben sich auch das α-Diketon und die Hydrobromide der Ausgangsketone neben den im vorigen Bericht mitgeteilten, aromatischen Säuren als die Reaktionsprodukte. So erhält man aus ω-Brom-ω-benzylidenazetophenon und ω-Brom-4-methyl-ω-benzylidenazetophenon ihr Hydrobromid und aus dem letzteren auch ein α-Diketon, bzw. p-Tolyl-ω-brombenzylglyoxal. Darauf hin kann man annehmen, dass die Reaktion einem durch die freien Radikale hervorgebrachten Kettenmechanismus gemäss läuft. Von solchen freien Radikalen werden sowohl das aus dem Ausgangsstoff unter Vereinigung desselben mit Bromatom gebildeten Radikal $C_6H_5CHBr\dot{C}BrCOC_6H_4R$ als das aus ihm über das Hydroperoxyd durch die Abspaltung des freien OH· verwandelten, sauerstoffhaltigen Radikal $C_6H_5CHBrCBr(O\cdot)COC_6H_4R$ für besonders wichtig angesehen, weil sie als die Zwischenstoffe der Reaktion die Natur der Produkte bestimmen.

9) C. Weygaand und A. Matthes, *Ber.*, **59**, 2247 (1926); siehe auch die Mitteil. I, S. 356, Anm. 7.

Hinzufügen ist dazu, dass die Ertragsverminderung der durch die dem Sauerstoffeffekt zugeschriebene Zersetzung der Kohlenstoffkette der Ketone abgespaltenen, aromatischen Säuren bei der Strukturabänderung des Substrats von α-Bromketon I zu seinem 4'-methylierten(II) wahrscheinlich in Folge der Stabilisierung des oben angestellten, sauerstoffhaltigen Radikal durch die Gegenwart des letztgenannten Substituenten mit seinem Hyperkonjugierungseffekt hervorgerufen werde.

Zum Schluss muss der Verfasser den Herren Professor Y. Urushibara und Professor O. Simamura an der Universität zu Tokyo für ihre freundlichen Leitungen den herzlichen Dank aussprechen.

Chemisches Laboratorium
Abteilung der allgemeinen Bildungen
Universität zu Nagoya
Mizuho-ku, Nagoya

*The Separation of Polythionates with Anion-Exchange Resins**

By Akira IGUCHI

(Received March 14, 1958)

The separation of di-, tri-, tetra- and penta-thionates is very difficult by an ordinary analytical method. In the present study, the author applied the anion-exchange chromatography to this separation. First, the distribution coefficients, K_d, of polythionates to the anion-exchange resin were measured and, by the use of these results, polythionates were separated with satisfactory results.

Experimental

Materials. — Anion-exchange resin, Dowex 1-X2, X4 and X8 of mesh size 50~100 were used in air dried state and in chloride form.

The following polythionates were synthesized by the usual methods described in text books[1,2].

Sodium dithionate was prepared by the reaction of sodium sulfite with silver nitrate[3].

Sodium trithionate was obtained by passing sulfur dioxide into a solution containing both sodium thiosulfate and bisulfite with a small amount of sodium arsenite. Potassium salt was obtained by the double decomposition of sodium salt with potassium acetate[4].

Sodium tetrathionate was prepared by mixing sodium thiosulfate with iodine in the granular state[5].

Potassium pentathionate was prepared by the reaction of concentrated hydrochloric acid with a solution containing sodium thiosulfate and a small amount of sodium arsenite at $-10°C$[6].

Procedure. *Analysis of polythionates.*—Sodium dithionate was oxidized by potassium bromate in acidic solution and the formed sulfate ion was determined by the usual gravimetric method. The purity of this salt was also determined by heating and decomposing it into sodium sulfate. The sodium sulfate was determined gravimetrically[7,8].

Potassium trithionate was titrated with potassium iodate[9]. Its purity was also determined from the decrease of weight on conversion into potassium sulfate by heating[10].

Sodium tetrathionate and potassium pentathionate were titrated with potassium iodate as in the case of trithionate[9]. The purity of these salts was also determined through the reaction with sodium sulfite. The thiosulfate ion thus formed was determined by iodimetric titration after masking the residual sulfite ion with formalin[11].

The results of these analyses showed that these salts were pure enough for the purpose of this study.

Measurement of Distribution Coefficients in Various Concentrations of Hydrochloric

* This paper was presented before the Autumn Meeting of the Chemical Society of Japan held on Nov. 23, 1957 in Tokyo.

1) W. G. Palmer, "Experimental Inorganic Chemistry", Cambridge Univ. Press, England (1954), p. 365.

2) T. Inouye, "Inorganic Preparative Experiments" (Mukikagaku Seizojikken), Shokabo, Tokyo (1956), p. 96.

3) H. Baubigny, *Ann. chim. phys.*, (VIII), **20**, 5 (1910).

4) A. Kurtenäcker and K. Matejka, *Z. anorg. allgem. Chem.*, **193**, 367 (1930).

5) N. v. Klobukow, *Ber.*, **8**, 1871 (1885).

6) A. Kurtenäcker and W. Fluss, *Z. anorg. allgem. Chem.*, **210**, 125 (1933).

7) C. Mayr and I. Szentpaly-Peyfuss, ibid., **131**, 203 (1924).

8) W. C. de Baat, *Rec. trav. chim., Pays-Bas*, **45**, 237 (1926); *Chem. Zentr.*, **97**, (I) 3133 (1926).

9) A. Kurtenäcker et al., *Z. anorg. allgem. Chem.*, **224**, 399 (1935).

10) H. Stamm, K. Goejring and U. Feldmann, ibid., **250**, 226 (1942).

11) F. Forster and K. Centner, ibid., **157**, 45 (1926).

Acid.—The measurement of distribution coefficients K_d was carried out by the column method. The K_d values of the ions were calculated from the volume of the eluant, using the following equation:

$$K_d = (V-i)/M$$ [12]

where K_d (cc./g.) is the distribution coefficient, V (cc.) the volume of eluant passed through the column until the concentration of solute in the effluent becomes maximum, i (cc.) the interstitial volume of the column and M (g.) the weight of the resin.

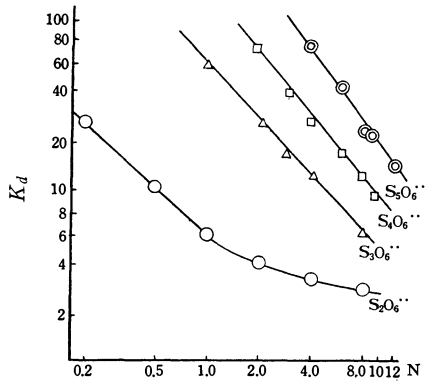

Fig. 1. Relationship between K_d and the concentration of hydrochloric acid in the eluant.

Each column contains 0.5~2.0 g. of the resin, Dowex 1-X2 in chloride form. The flow rate is adjusted to less than 0.1 cc./min. The relation between K_d and the concentration of hydrochloric acid (C) in the eluant is shown in Fig. 1. A nearly linear relationship between $\log K_d$ and $\log C$ is recognized. The values of K_d of polythionate ions for the same concentration of hydrochloric acid increase with the increase of the numbers of sulfur atom in the ion. The curves for these polythionates were almost parallel to one another. The gradient of these curves was not so great as two, but almost unity; hence as was studied by M. Honda[13], these polythionate ions may exist in these acidic solutions as $HS_nO_6^-$, n being 2~5.

Results and Discussion

The Effect of pH and the Pore-size of Ion-Exchange Resins on the Distribution Coefficient. — i) *pH.* — By using sodium chloride solution, or sodium chloride solution containing ammonia as an eluant in place of hydrochloric acid, the values of K_d in different pH** were measured. The concentrations of sodium chloride used were 0.5 mol./l. for dithionate and 4.0 mol./l. for other polythionates. The results are shown in Fig. 2. The K_d was almost independent of pH.

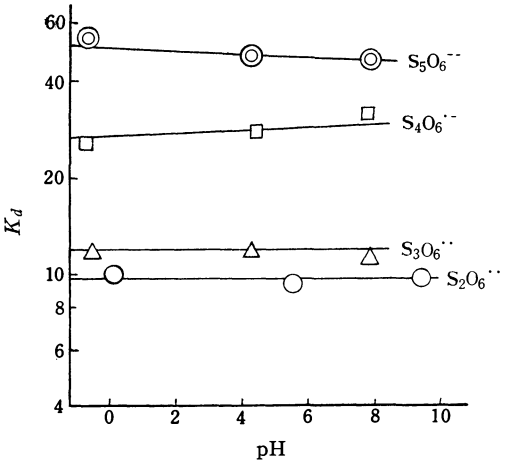

Fig. 2. Relationship between K_d and the pH of eluant. The concentration of hydrochloric acid used as the eluant was 0.5 N for dithionate and 4 N for tri-, tetra- and penta-thionates.

ii) *Pore-size.*—The resins of different X numbers were employed in place of X2 resin to observe the effect of pore-size. The K_d values for dithionate in 1.0 N hydrochloric acid, trithionate in 3.0 N hydrochloric acid, tetrathionate in 6.0 N hydrochloric acid and pentathionate in 9.0 N hydrochloric acid were measured by the elution method using Dowex 1-X2, -X4 and -X8 resins. The results are shown in

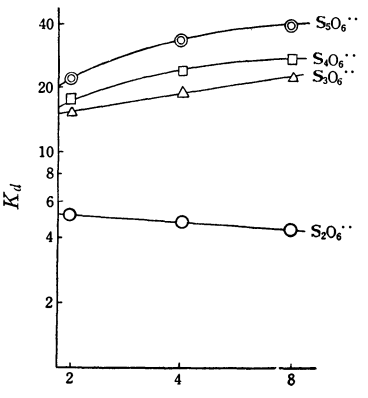

Fig. 3. Relationship between K_d and the X numbers of resins. The concentration of hydrochloric acid used as the eluant was 1 N for dithionate, 3 N for trithionate, 6 N for tetrathionate and 9 N for pentathionate.

12) M. Honda, *Japan Analyst (Bunseki Kagaku)*, **2**, 155 (1953).
13) M. Honda, *J. Chem. Soc. Japan, Pure Chem. Sec. (Nippon Kagaku Zassi)*, **72**, 361 (1951).
** pH of the solution was measured with a glass electrode pH-meter, Type 43, made by Iio Denki Co..

TABLE I
THE ANALYSIS OF MIXED SAMPLES

Thionates	Sample 1 Added millimole	Sample 1 Observed millimole	Sample 1 Observed %	Sample 2 Added millimole	Sample 2 Observed millimole	Sample 2 Observed %
Dithionate	0.124	0.122	98.6±2.0	0.100	0.0987	98.7±2.0
Trithionate	0.0584	0.0560	96.0±5.0	0.0707	0.0690	97.4±4.0
Tetrathionate	0.0650	0.0650	100 ± 2.6	0.0336	0.0328	97.7±2.3
Pentathionate	0.0339	0.0343	101 ± 2.8	0.0338	0.0333	98.6±2.3

TABLE II
THE ANALYSIS OF WACKENRODER'S LIQUID

	Sample A Observed value millimole	Sample A Mol. %	Sample B Observed value millimole	Sample B Mol. %
Sulfide, Sulfite, Thiosulfate	0.00	0.00	0.00	0.00
Sulfate	6.77×10^{-2}	23.2	4.90×10^{-2}	20.5
Dithionate	2.58×10^{-3}	0.89	3.75×10^{-3}	1.57
Trithionate	5.82×10^{-2}	19.9	5.63×10^{-2}	23.7
Tetrathionate	9.12×10^{-2}	31.2	4.83×10^{-2}	32.9
Pentathionate	5.40×10^{-2}	18.5	4.59×10^{-2}	19.2
Higher thionates	7.70×10^{-3}	2.63	4.87×10^{-3}	2.04

Fig. 3. Slight increase of K_d with the increase of X number was recognized in cases of tri-, tetra-, and penta-thionates, though the difference is not so great. In the case of higher polythionates, elongation of the tail part was observed in the elution process.

Separation of Polythinonates by the Column Method.—The polythionates may be separable because they show different K_d values as shown in Fig. 1. The used column contains 2.16 g. of Dowex 1-X2 and the size of the column is about 0.90 cm. in diameter and about 11 cm. in length. First the dithionate is eluted with 1 N hydrochloric acid. When any other oxy-acids of sulfur than polythionates are contaminated in the sampe to be analyzed, they are eluted out at this stage before the dithionate appears in the eluant. Then trithionate was eluted with 3 N hydrochloric acid, tetrathionate with 6 N and pentathionate with 9 N hydrochloric acid successively.

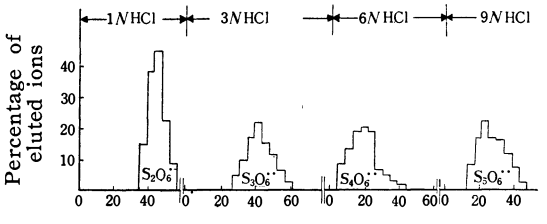

Fig. 4. Elution curve of a mixed sample. The flow rate was 0.5 cc./sec.

The amount of eluted dithionate is determined by gravimetric method and tri-, tetra- and penta-thionates are by the titration with standard potassium iodate solution as described in the experimental part.

One of the typical clean-cut separation of mixed sample is shown in Fig. 4.

Analysis of Mixed Samples. — The method of separation, described above, was applied to the mixture of the known amounts of polythionates and the results are shown in Table I, the mean values of the triplicate experiments being given.

When the sample contains other oxy-acids of sulfur, (e.g., sulfate, sulfite, etc.), they are eluted prior to the elution of dithionate, and are determined separately.

Analysis of Wackenroder's Liquid[14,15]**.** —This method of separation was applied to the determination of the composition of Wackenroder's liquid. The composition of the liquid, however, may change owing to the preparation method, and further, it contains a large amount of suspended sulfur which interferes with the analytical process. Two samples made by the following methods were analyzed.

i) *Sample A.* — This sample was prepared by dissolving hydrogen sulfide into

14) H. W. F. Wackenroder, *Ann. chim. phys.*, (III), **20**, 144. (1847).
15) H. Debus, *Ann.*, **244**, 76, (1888).

saturated aqueous solution of sulfur dioxide at 0°C. Hydrogen sulfide was passed twice after an interval of 48 hours, and the solution was left standing 38 days at room temperature (20~15°C). Then the suspended sulfur in the liquid was caused to coagulate by the addition of an equal volume of 1.00 M ammonium chloride solution and filtered off. A portion of the filtrate was titrated with standard iodine solution after being acidified with acetic acid, but the presence of sulfide, sulfite or thiosulfate was not recognized. With another portion of the filtrate, the content of sulfate was determined by the gravimetric method in the form of barium sulfate.

The ion-exchange chromatographic method used for the analysis of Wackenroder's liquid is the same as that used for the known mixed sample, but after the elution of pentathionate with 9 N hydrochloric acid, there remained only a small amount of polythionate which could be eluted only by 12 N hydrochloric acid. Although it was difficult to determine this species, the values in Table II were calculated on the assumption that this species would be hexathionate.

The quantity of dithionate was calculated from the difference between the amount of barium sulfate obtained from the first effluent after oxidation and the amount of the barium sulfate directly from the original sample solution.

ii) *Sample B.*—Sample B was prepared by the same method as that for Sample A, but the solution was left standing only 11 days after passage of hydrogen sulfide. As the suspended sulfur coagulates with difficulty, 1.5 times (by volume) of 1.00 M ammonium chloride solution was mixed before filtration of the sulfur.

The results of the analysis of 1 cc. of the original Wackenroder's liquid are given in Table II.

Summary

1) The distribution coefficient of di-, tri-, tetra-, and penta-thionates between anion-exchange resins and hydrochloric acid solution was measured. The adsorbability of the polythionates increases with the number of sulfur atoms in the ion, i. e. pentathionate>tetrathionate>trithionate>dithionate.

2) The separation of polythionates was accomplished by the anion-exchange chromatography by the use of hydrochloric acid in various concentrations as the eluant.

3) The application of anion-exchange chromatography to the analysis of Wackenroder's liquid was studied.

The author expresses his gratitude to Professor T. Shirai, Dr. Y. Yoshino and to his colleagues in the laboratory for their suggestions throughout the work.

Institute of Chemistry
College of General Education
University of Tokyo
Meguro-ku, Tokyo

*The Separation of Sulfate, Sulfite, Thiosulfate and Sulfide Ions with Anion-Exchange Resins**

By Akira IGUCHI

(Received March 14, 1958)

Several methods of analysis of the mixture of sulfite, thiosulfate and sulfide ions have been reported by some researchers[1], most of which are based on the method of titration without separation of these components. In this study the author has applied the anion-exchange chromatography to the mutual separation of the above-mentioned oxy-acids of sulfur and sulfide, obtaining satisfactory results.

* This paper was presented before the 6th Annual Meeting of Japan Society for Analytical Chemistry held on Oct. 19, 1957 in Kyoto.

1) For example, A. Kurtenäcker et al., *Z. anorg. allgem. Chem.*, **161**, 201 (1927).

Experimental

Materials. — *Anion-exchange resins.* — Diaion SA ♯100, a strongly basic type resin (polystyrene-

divinyl benzene quaternary amine) prepared by Mitsubishi Kasei Co. was used. It is of mesh size 100~200 in beads (nitrate form).

Sodium thiosulfate.—The guaranteed reagent of Junsei Chemicals Co. was used. The iodometric titration showed that this sample did not contain impurities which would interfere with the experiment.

Sodium sulfate.— The guaranteed reagent of Junsei Chemicals Co. was used. The result of gravimetric analysis showed that this sample was sufficiently pure for the purpose of this study.

Sodium sulfite and sodium sulfide.—Aqueous solutions of both salts are oxidized easily, but the decrease of the concentration was found to be less than about 1% for sulfite, and less than 2% for sulfide during the process of separation (about 6~10 hours). The quantity of sulfate in the original sulfite solution was determined from the difference between the quantity of sulfite titrated iodometrically and that of sulfate plus sulfite which was weighed gravimetrically in the form of barium sulfate after oxidizing the sulfite into sulfate. The amount of impurity contained in the sulfide solution newly prepared was found to be negligible.

Procedure.—*Measurement of distribution coefficient.*—For the separation of these readily oxidizable anions, it is not desirable to use resins in the nitrate form, as the nitrate acts as an oxidant. On the other hand, the chloride solution is not suitable for the elution of these anions, as the tail part of the elution curve becomes long. Solution of sodium or ammonium nitrate plus ammonia was found to be an excellent eluant, the oxidizing effect not appearing in these conditions. In a neutral solution, a slight decomposition of sulfite and sulfide was recognized, especially in contact with resins in nitrate form. This decomposition may be due to the catalytic action of resins.

The measurement of distribution coefficient, K_d, was made by the column method. The K_d values of the ion were calculated from the volume of eluant by using the following equation:

$$K_d = (V - i)/M$$ [2]

where K_d(cc./g.) is the distribution coefficient, V (cc.) the volume of eluant passed through the column until the concentration of solution in the effluent becomes maximum, i(cc.) the interstitial volume of the column and M(g.) the weight of the resin.

Each resin column contains 1 to 3 g. of Diaion SA #100. The size of the column is 7.0 mm. in diameter. The flow rate is less than 0.1 cc./min.. The eluant was aqueous solution of sodium nitrate, but the solution of ammonium nitrate containing ammonia was also used for sulfite ion.

2) M. Honda, *Japan Analyst (Bunseki Kagaku)*, **2**, 155 (1953).
3) M. Honda, *J. Chem. Soc. Japan, Pure Chem. Sec. (Nippon Kagaku Zassi)*, **72**, 361 (1951).

Results and Discussion

Relations Between the Distribution Coefficient and the Concentration of Nitrate Ion in the Eluant.—The mean values of the distribution coefficient of triplicate experiments are shown in Fig. 1. From these data a linear relationship between $\log K_d$ and the concentration of nitrate ($\log C$) is recognized, especially in the region of low concentration. The curves for sulfite, thiosulfate and sulfate ions are nearly parallel, and the slope is about 2 at 0.1~0.2 mol./l., hence, as Honda discovered and reported[3], they must be doubly charged ions. In the case of sulfide, the slope of the line is nearly unity, suggesting the probable presence of HS^- ion even in a neutral solution. From the data in Fig. 1, thiosulfate, sulfate and sulfite may be separable using 0.1 mol./l. nitrate solution as an eluant.

The Relation between pH and Distribution Coefficients. — The distribution coefficient K_d of ions of polybasic acids may change with the variation of pH. Accordingly the relationship between pH and K_d was checked in the range of pH 7~11. The buffer solution, prepared by

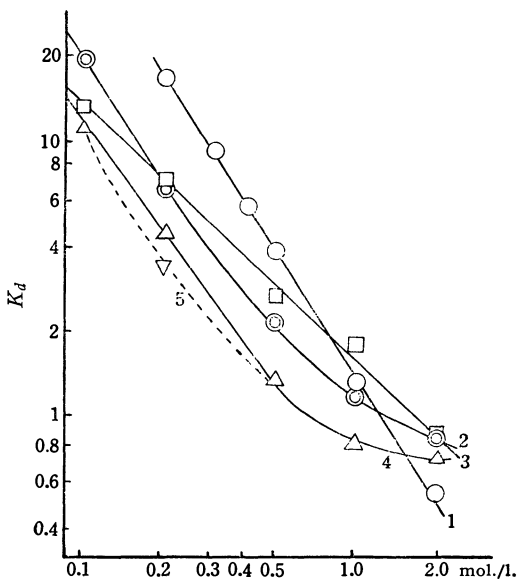

Fig. 1. Relationship between K_d and the concentration of nitrate ions in eluants.
1: Sodium thiosulfate. 2: Sodium sulfate. 3: Sodium sulfide. 4: Sodium sulfite by neutral eluant. 5: Sodium sulfite by an alkaline eluant of pH≒9.7.

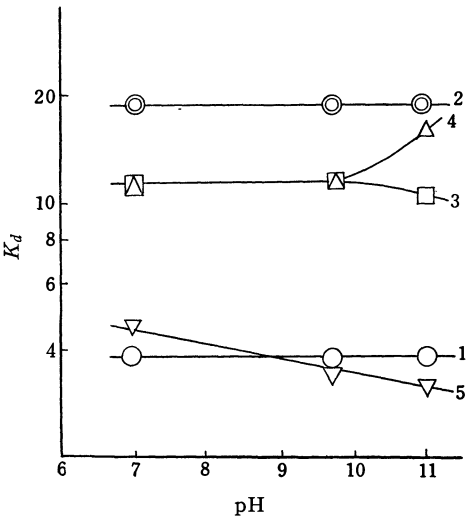

Fig. 2. Relationship between K_d and the pH of eluant.

1: Sodium thiosulfate eluted by 0.5 mol./l. nitrate solution. 2: sodium sulfate eluted by 0.1 mol./l. nitrate solution. 3: sodium sulfide eluted by 0.1 mol./l. nitrate solution. 4: Sodium sulfite eluted by 0.1 mol./l. nitrate solution. 5: Sodium sulfite eluted by 0.2 mol./l. nitrate solution.

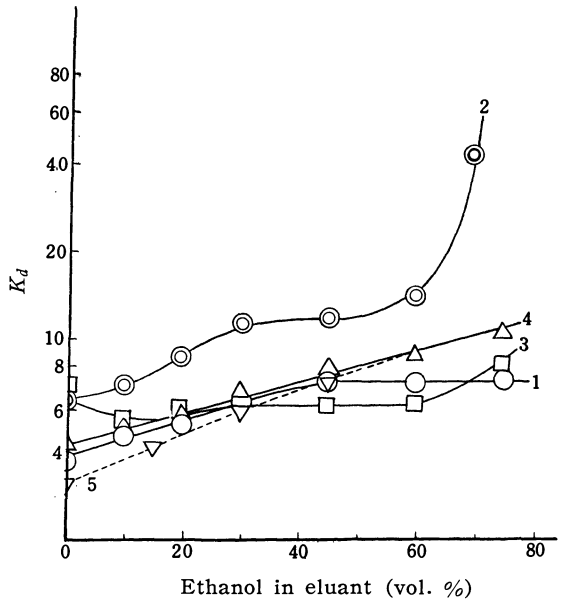

Fig. 4A. Relationship between K_d and the volume percentage of organic solvent in eluant.

1: Sodium thiosulfate. 2: Sodium sulfate. 3: Sodium sulfide. 4: Sodium sulfite eluted by neutral eluant. 5: Sodium sulfite eluted by alkaline eluant of pH≒9.7. The concentration of nitrate ion used as the eluant was 0.5 mol./l. for thiosulfate, and 0.2 mol./l. for the other salts.

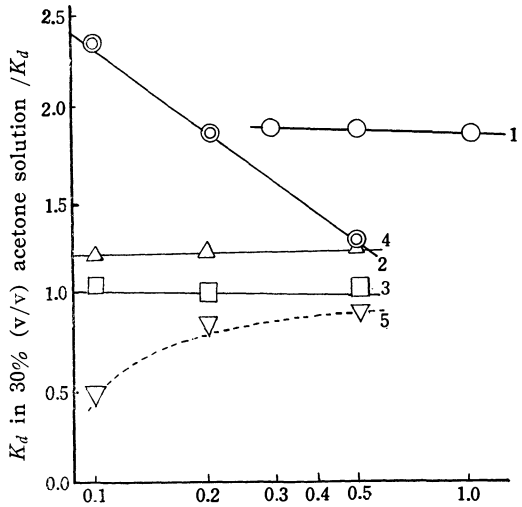

Fig. 3. Relationship between K_d in 30% (v/v) acetone solution /K_d in aqueous solution and the concentration of nitrate ion in eluant.

1: Sodium thiosulfate. 2: Sodium sulfate. 3: Sodium sulfide. 4: Sodium sulfite eluted by neutral eluant 5: Sodium sulfite eluted by alkaline eluant of pH≒9.7.

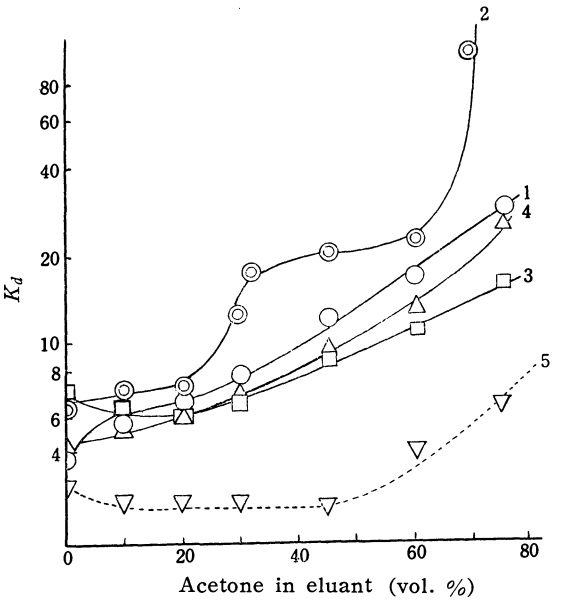

Fig. 4B. Relationship between Kd and the volume percentage of organic solvent in eluant. The same legend as Fig. 4A. stands for Fig. 4B.

mixing ammonium nitrate, sodium nitrate and ammonia, was used. The pH was checked by a glass electrode pH meter (Type 43, made by Iio Denki Co.). The results are shown in Fig. 2. There is no remarkable change of K_d in this pH region, though the K_d of sulfite and sulfide eluted with 0.1 mol./l. nitrate solution showed a slight deviation with increase in pH at about pH 9~11.

The Effect of Organic Solvent on the Distribution Coefficient.—When the eluant which contained 30% (by volume) of acetone was employed together with various quantities of nitrate in place of aqueous solution, the value of the distribution coefficient showed deviation. The relation between the ratio of the K_d values thus determined in 30% (by volume) acetone solution to the K_d values of the original aqueous solution of the nitrate ion and the concentration of eluant was shown in Fig. 3. In the case of sulfide, the K_d in 30% (by volume) acetone solution is not affected by the addition of acetone, while the K_d values of thiosulfate and sulfite in 30% (by volume) acetone solution become 1.9 and 1.1 times greater than the values of K_d determined in the original aqueous solution, respectively. The concentration of nitrate does not affect the ratio K_d in 30% (by volume) acetone solution and that in aqueous solution. In the case of sulfate, this ratio increased with the decrease of the concentration of nitrate. Generally the increase of K_d in 30% acetone solution by the addition of organic solvent may be caused by the stripping off of the hydrated water molecules surrounding the anion of oxy-acid of sulfur. In the case of sulfite in alkaline solution, however, a decrease of K_d was recognized in 30% acetone solution.

In the next place, in order to clarify the effect of organic solvent on the adsorbability of these anions, the relationship between K_d and concentration of ethanol or acetone was examined, the concentration of nitrate being kept constant (0.5 mol./l. for thiosulfate and 0.2 mol./l. for other anions). The results were shown in Figs. 4A and 4B.

Experimental results showed a remarkakle increase of K_d values with the percentage of organic solvent. In general, the increase of K_d values by the addition of acetone is greater than that by the addition of the same percentage of ethanol. But exceptions were recognized in cases of sulfite by acetone, and of sulfide by ethanol. In these cases the K_d values decrease until they reach constant in spite of the increase in amount of organic solvent (even up to 40~60% by volume). From this result, the method of separation of sulfite, sulfide and sulfate is suggested, that is, the use of eluant which contains 30% (by volume) of actone and 0.1 mol./l. of nitrate, with pH adjusted to 9.7 by ammonia.

In addition to these measurements of K_d values using Diaion SA #100, the measurements by the use of Amberlite IRA-410 were also carried out. But the K_d values for the latter resin almost exactly coincided with those for the former resin within the range of experimental error.

Discussion on the Variation of Distribution Coefficients.—Judging from the slopes of the curves shown in Figs. 1 and 2, sulfate and thiosulfate may exist in the form of doubly charged anion, and their adsorbability does not change in the range of pH 7~11. The effect of organic solvent upon thiosulfate and sulfate is shown in Figs. 4A and 4B. In these data, an inflexion point is recognized at about 10% (by volume) in acetone for thiosulfate and at about 30% for sulfate. These facts may be attributed to some discontinuous dehydration grade of these anions. In the case of sulfide, as is shown in Fig. 1, the HS^- ion may be a predominant species as is expected from the slope of the curve. The effect of adding ethanol, as is shown in Fig. 4A, keeps the K_d constant even up to 60%, while the increase of K_d by acetone appeared even at 30%. These phenomena may be caused by a special interaction between ethanol and sulfide, ions. In the case of sulfite, the formation of a compound between sulfite ions and acetone is expected,[4] whereas, as is shown in Figs. 4A and 4B, the K_d in a neutral solution shows no special change compared with the other oxy-acid ions; in other words, only a monotonous increase of K_d with the increase of the content of organic solvent was observed. But, in the case of alkaline solution, the K_d decreases and then remains constant even up to 45% of acetone. This fact can perhaps be ascribed to the formation of special compounds between acetone and sulfite or between acetone, ammonia

4) G. Gabrielson and O. Samuelon, *Svensk. Kem. Tid.*, **62**, 214 (1950).

TABLE I
THE ANALYSIS OF MIXED SAMPLES OF SULFITE, SULFATE, AND THIOSULFATE

		Sulfite	Sulfate	Thiosulfate
Added.	mg.	6.39	19.4	20.0
Observed.	mg.	6.32±0.064	19.0±0.41	20.0±0.20
	%	99.0±1.0	98.0±2.0	100.0±1.0

TABLE II
THE ANALYSIS OF MIXED SAMPLE OF SULFITE, SULFATE, SULFIDE AND THIOSULFATE

		Sulfite	Sulfide	Sulfate	Thiosulfate
Added	mg.	7.00	2.96	19.3	21.98
Observed.	mg.	6.93±0.69	2.78±0.16	18.58±0.30	22.20±0.22
	%	99.0±1.0	94.1 ±5.5	96.3 ±1.5	101.1 ±1.0

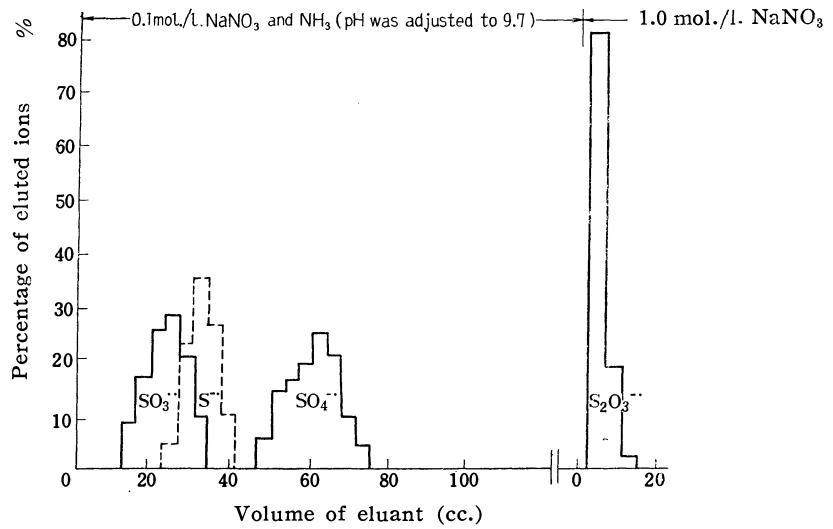

Fig. 5A. Elution curve of a mixed sample. The flow rate was 0.3 cc./min.

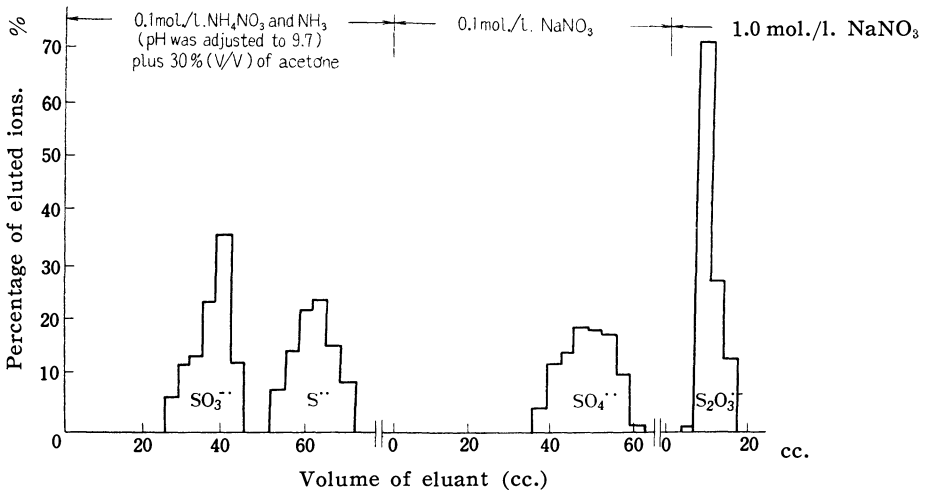

Fig. 5B. Elution curve of a mixed sample. The flow rate was 0.1 cc./min.

and sulfite[5]. In alkaline solution without acetone the K_d of the sulfite ion shows only slight deviation from the K_d of sulfite ion in a neutral solution as shown in Fig. 1, from which it is inferred that this phenomenon is due neither to the change in the form of the sulfite ion only, nor to the reaction between the ammonia and the sulfite ion before the addition of acetone.

The Chromatographic Separation of Sulfate, Sulfite and Thiosulfate.—When sulfide does not coexist with the other three, the result shown in Fig. 1 may be applicable to their separation. By using 0.1 mol./l. of nitrate solution, first sulfite, and next sulfate were eluted; then thiosulfate was eluted by 1.0 mol./l. of nitrate solution. But, when the neutral nitrate solution was used as an eluant, recovery of sulfite did not reach 100%, and accordingly it was necessary to use an alkaline eluant. The 0.1 mol./l. ammonium nitrate solution with the pH adjusted to 9.7 by ammonia was most suitable. The ion-exchange resin Diaion SA #100 of analytical grade mounted in a column of 0.7 cm. in diameter and 17 cm. in length was employed. The amount of the resin used was 4.9 g. The results are shown in Fig. 5A. The collected sulfite and thiosulfate were titrated with the standard solution of iodine, while the quantity of sulfate was determined gravimetrically in the form of barium sulfate.

The analysis by this method is simpler than the method which is shown in the next paragraph, because the flow rate is kept relatively great and the quantity of sulfite is determined by titration.

The recovery percentage of oxy-acid ions of the known composition shown in Table I was calculated from the data of the experiments repeated five times.

The Chromatographic Separation of Sulfate, Thiosulfate, Sulfite and Sulfide.—When sulfide is present, sulfide and sulfite are not separable by an elution with simple nitrate solution. The nitrate solution containing acetone can be employed for this purpose, as was expected from the data shown in Fig. 4B. The resin column is the same as that used in the experiment shown in Fig. 5A.

Sulfite and sulfide are first eluted successively by the eluant containing 30% (by volume) of acetone, 0.1 mol./l. of ammonium nitrate, with its pH adjusted to 9.7 by ammonia; second, sulfate is eluted with 0.1 mol./l. sodium nitrate, and finally thiosulfate by 1.0 mol./l. sodium nitrate. A typical run of such experiments is illustrated in Fig. 5B.

The quantity of collected sulfite is determined gravimetrically in the form of barium sulfate after oxidation by sodium peroxide in alkaline solution. Sulfide is titrated by standard iodine solution.

A example of recovery of each salt by this method, with the percentage calculated from the experiments repeated twelve times is shown in Table II.

From the results of these experiments it was found that this method can be used for the analysis of these salts. In the results shown in Table II, however, the recovery of sulfide is slightly less than the theoretical value. This defect may be remedied by improving the acceptor of the effluent so as to protect hydrogen sulfide from escaping.

Summary

1. The distribution coefficients of sulfate, thiosulfate, sulfite and sulfide in the nitrate solution were measured.

2. By the addition of ethanol or acetone to the neutral eluant solution, the adsorbability of sulfate, sulfite, thiosulfate and sulfide was increased, while that of sulfite in alkaline acetone solution showed a marked decrease.

3. By the use of these results a mutual separation of sulfate, thiosulfate, sulfite and sulfide was effected by the anion-exchange chromatography.

The author desires to express his gratitude to Professor T. Shirai, Dr. Y. Yoshino and to his colleagues in the laboratory for their suggestions and for the discussion helpful in publishing this paper.

Institute of Chemistry, College of General Education, University of Tokyo, Meguro-ku, Tokyo

5) For example, G. Palmer, "Experimental Inorganic Chemistry" Cambridge Univ. Press, England, p. 330 (1954).

*On the Determination of Fine Structure of Cellulosic Fibers**

By Taketoshi KŌSHIRO, Kazuo YAGAMI, Eiichiro SHIRATSUCHI and Toshikazu FUJIMURA

(Received October 7, 1957)

It is well known that the mechanical properties of cellulosic fibers depend on their fine structure. P. H. Herrent and A. Lude suggested double net-work structure, in which the crystalline regions constitute the knots[1]. Therefore, it seems significant to clarify the nature of crystalline regions. The mean crystallinity determined by existing methods is insufficient to elucidate the mechanical properties, then it is desirable to estimate the distribution of order and of size. W. A. Sisson and J. A. Howsmon have proposed "lateral order" $\overline{O}$ which was defined by the equation,

$$\overline{O}=(\mathrm{OH})_c/(\mathrm{OH})_t$$

Where $(\mathrm{OH})_c$ is the total number of hydrogen bonds in the region and $(\mathrm{OH})_t$ is the total possible number of hydrogen bonds if all the molecules are perfectly crystallized. This value is dependent on the choice of the volume element. If this volume is too large, the curves as depicted become single sharp peak at $\overline{O}$ corresponding to an average order; if too small, the curves split into two sharp peaks at zero order and perfect order[2]. To measure the lateral order distribution, Maeda and Yurugi applied fractional solution of hydrolyzed cellulose[3] and the methods which determine the moisture regain or levelling-off degree of polymerization after mercerization, were suggested[4]. These methods are based on the thermodynamic properties and do not have direct relation to the fine structure.

Recently, the distribution of crystallite sizes is estimated by means of X-ray diffraction[5] or electron microscopy[6].

In the present paper, on the assumption that the length of crystalline residue corresponds to the length of hydrogen-bond train along cellulose molecule chain, we have undertaken to determine its distribution by the molecular weight fractionation of the residue which is freed from the amorphous region by hydrolysis or its modification. Since recrystallization has been found to occur during acid hydrolysis[7,8], the following methods were tried to avoid it.

(1) Ordinary aqueous acid hydrolysis after partial acetylation or partial oxidation with lead tetra-acetate, which may prevent the recrystallization by steric hindrance due to the modification in amorphous region.

(2) Methanolysis, which is carried out in non-aqueous medium to prevent additional forming of hydrogen-bond.

(3) Oxidizing hydrolysis with sulfuric acid containing potassium dichromate. It is effective in removing the amorphous chain ends produced by chain cleavage, before recrystallization takes place. The residues after these treatments were nitrated and fractionated, and the chain length distribution curves were obtained. The availability of these methods and the fine structure of rayon staple were discussed.

Experimental

Materials. Commercial viscose rayon staple (Bright regular 1.5 D) was steeped in water and then the water was replaced with reaction medium.

Methods. *a) Apparent total crystallinity.*—It was given as a weight per-cent yield of the residue after the hydrolysis or its modified treatments.

b) Average degree of polymerization ($\overline{DP}$).—It was determined from the viscosity of cuprammonium solutions, or that of acetone solution of

* Presented at the 10th Annual Meeting of the Chemical Society of Japan, Tokyo, April 1957.

1) P. H. Herrent and A. Lude, *Textiel Research J.*, **21**, 137 (1951).

2) Otto-Spurlin "Cellulose and Cellulose Derivatives", Interscience Publishers, New York, Vol. I, (1954) p. 252.

3) H. Maeda, *J. Soc. Textile Cellulose Ind. (Japan)*, (*Sen-i Gakkaishi*) **12**, 6 (1956); T. Yurugi, *J. Chem. Soc. Japan, Ind. Chem. Sec.* (*Kôgyô Kagaku Zassi*) **58**, 27 (1955).

4) L. Jörgensen, *Acta Chem. Scand.*, **3**, 790 (1949); **4**, 185, 658 (1950); O. A. Battista et al. *Ind. Eng. Chem.*, **48**, 333 (1956).

5) K. Kobayashi, presented at the 10th Annual Meeting of the Chemical Society of Japan, Tokyo, April 1957.

6) E. A. Immergut and B. G. Rånby, *Ind. Eng. Chem.*, **48**, 1183 (1956).

7) H. Mark, F. C. Brenner and V. Frilette, *J. Am. Chem. Soc.*, **70**, 877 (1948).

8) P. H. Hermans and A. Weidinger, *J. Polymer Sci.*, **4**, 315 (1949).

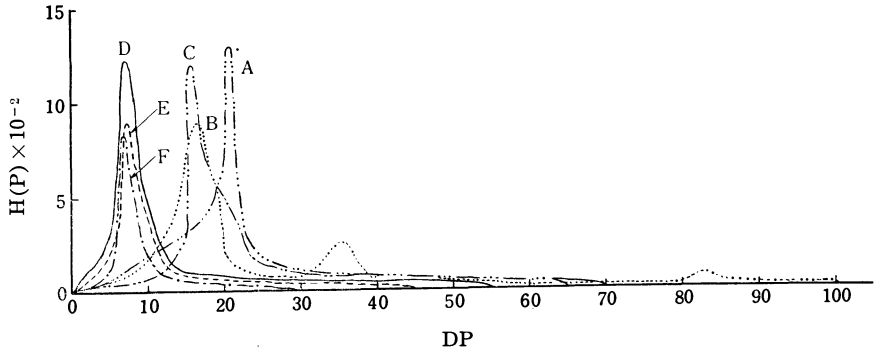

Fig. 1. Chain-length distribution of hydrolyzed cellulose.

A —·····—	Maeda's method	D ———	4 N HCl 1 hr.
B ·····	1 N HCl 1/6 hr.	E ------	4 N HCl 4 hr.
C —··—	1 N HCl 1 hr.	F —·—	4 N HCl 6 hr.

the nitratde products. An Ostwald viscometer was employed and the intrinsic viscosity was calculated by Schulz-Blaschke's Formula.

c) Chain-length distribution.—The sample was nitrated with Mitchel's mixed acid[9] and dissolved in acetone and fractionated using water as the precipitant.

d) Accessibility. — Iodine sorption method of Hessler and Power[10] was employed. Concentration of sodium sulfate was 200 g./l. and the sorption was carried out at 20±0.1°C for an hour.

e) Partial acetylation pretreatment.—The rayon staple swollen with glacial acetic acid was treated at 50°C for twelve hours with the mixture, which consists of 6 volumes pyridine, 8 volumes acetic acid and 60 volumes benzene.

f) Partial oxidation pretreatment.—The samples swollen with glacial acetic acid were treated at 50°C for twenty hours with the glacial acetic acid solution which contains 0.077 M lead tetra-acetate. The lead tetra-acetate used was prepared according to Colson's method[11].

g) Hydrolysis.—Samples were refluxed at 100°C with hydrolyzing agents. After the pre-determined reaction time, the residue was filtered off with a glass filter and washed with water to neutral. Then its moisture was exchanged with absolute alcohol, and it was dried in vacuo at 50°C for five hours and weighed.

h) Methanolysis.—Samples were first refluxed at 68°C with methanol, saturated with dry hydrogen chloride gas, and then the residue was washed to neutral with absolute alcohol and dried in vacuo.

i) Oxidizing-hydrolysis.—A similar procedure to hydrolysis was used except that the hydrolyzing mixture, consisted of 1 N sulfuric acid and 0.017 M potassium dichromate.

Results

A) Ordinary Acid Hydrolysis. — The effects of acidity, reaction time and substrate on the yield and the $\overline{DP}$ of the residue are shown in Table I. The levelling-off degree of polymerization (LODP) of these samples was obtained by the treatment with 1 N hydrochloric acid for an hour.

TABLE I

DEGREE OF POLIMERIZATION AND YIELD OF RESIDUE AFTER ORDINARY HYDROLYSIS

Conditions of Hydrolysis			Residue	
Acidity of HCl N (aq.)	Temp. °C	Time hr.	Yield wt. %	$\overline{DP}$ (Nitrate)
1	100	1/6	98.8	26
		1	90.0	22
4	100	1	72.4	22
		2	57.5	22
		4	43.9	22
		6	37.0	22
Maeda's Method*	80	6	98.1	23

* Mixture of 5 parts 3.5 N HCl and 95 parts ethanol.

As shown in Fig. 1, the peak of distribution curve shifts to lower DP regions with the increase of acidity or reaction time, but after the peak has attained a definite DP, only the height of the peak decreases.

TABLE II

DEGREE OF POLIMERIZATION AND YIELD OF HYDROLYZED RESIDUE AFTER PRETREATMENT

(Conditions of Hydrolysis: 1 N HCl, 100°C, 25 hr.)

Pretreatment method	Degree of Substitution (M/C_6 unit)	Residue	
		Yield wt. %	$\overline{DP}$ (Cupram.)
Acetylation	0.331	58.8	17.5
Oxidation	0.157	25.2	
No Treatment	0	65.5	25.4

9) R. L. Mitchel, *Ind. Eng. Chem.*, **38**, 843 (1946).
10) L. E. Hessler and R. E. Power, *Textile Research J.*, **24**, 822 (1954).
11) A. Colson, *Compt. rend.*, **136**, 1, 676, 892 (1903).

B) Effect of Pretreatment. — The weight loss and $\overline{DP}$ of the hydrolyzed residue after pretreatment are shown in Table II. Generally speaking, pretreatments caused severe degradation. The chain length distributions of the above residues are shown in Fig. 2.

C) Methanolysis.—The effects of acidity in methanolysis are shown in Table III. The reaction is accelerated by the increase of acidity and the yield of residue decreases. However, little decrease in LODP and accessibility was observed.

The reaction rate of methanolysis is retarded by the addition of water, and the yield and the $\overline{DP}$ of the residue decreases with the increase in water content. Hydrochloric acid in the reagent is consumed very rapidly in the absence of water, but little at 100% aqueous medium, as shown in Fig. 3. The methanolysis gives higher ultimate yields of residue than the hydrolysis, although methanolysis proceeds initially at higher rates.

The results of fractional solution in which caustic soda solutions up to 8% are used as solvents and by which the residual amorphous portions may be dissolved owing to the probable imperfect removal, are shown in Fig. 4. Fig. 5 gives the chain-length distribution of methanolyzed

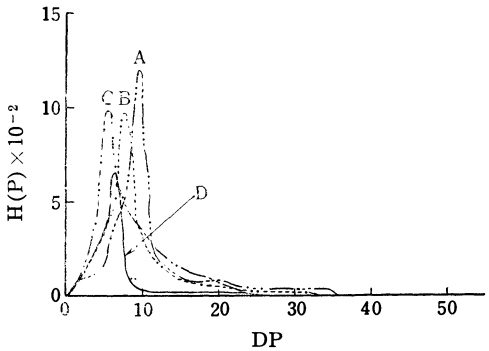

Fig. 2. Chain-length distribution of hydrolyzed cellulose after pretreatment.

Pretreatment		Hydrolysis: Acidity of HCl	Hydrolysis: Time hr.
A	None	1 N	25
B	None	4 N	2
C	Acetylation	1 N	25
D	Oxidation	1 N	25

TABLE III

DEGREE OF POLYMERIZATION, ACCESSIBILITY AND YIELD OF RESIDUE AFTER METHANOLYSIS

(Temp. of Methanolysis, 67±1°C)

Condition: Acidity N	Condition: Time hr.	Residue: Yield wt. %	Residue: $\overline{DP}$ (Cupram.)	Residue: Accessibility %
2.5	0	100.0	293.5	
	1/3	93.0		
	1	90.0		33.9
	3	87.0	30.0	
	8	83.5	27.9	25.8
	24	78.9	27.0	24.3
4	2	75.6	30.6	28.2
	6	74.7	28.4	25.3
	12	73.0	26.2	24.8
6	2	71.7	29.0	23.6
	6	67.7	27.4	24.3
	12	64.6	26.2	22.9
8	12	58.3	26.2	19.5

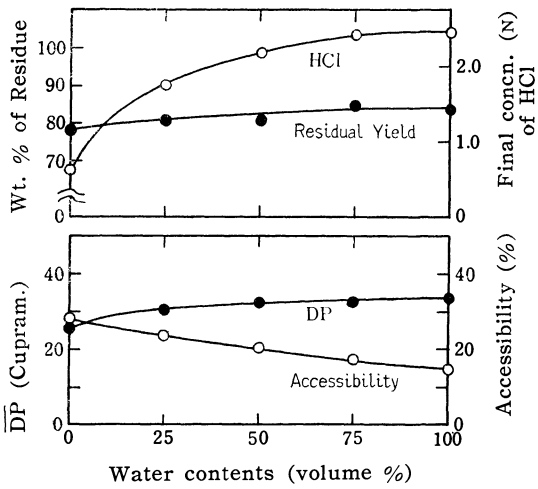

Fig. 3. Effects of water in methanolysis reagent. Methanolysis, 2.5 N HCl, at 68°C, 24 hr.

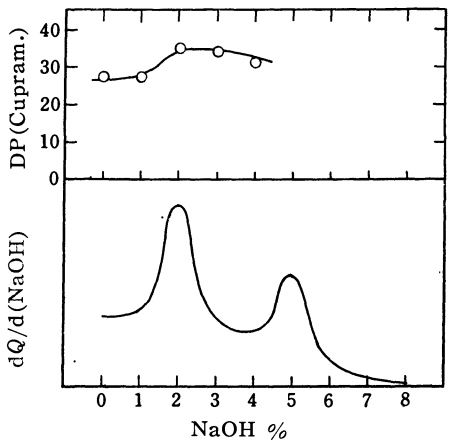

Fig. 4. Alkali extraction of methanolyzed cellulose. Methanolysis 1 N HCl, 68°C, 24 hrs. alkali extraction 20°C, 1 hr. Q: weight loss of alkali extraction.

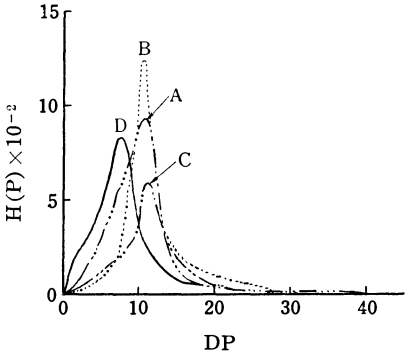

Fig. 5. Chain-length distribution of methanolyzed, and its alkali-extracted cellulose.
A —····— 2.5 N HCl in MeOH 24 hr.
B ····· 2% alkali-extracted residue of A.
C —·—· 4% alkali-extracted residue of A.
D ——— 8 N HCl in MeOH 12 hr.

TABLE IV
DEGREE OF POLYMERIZATION, ACCESSIBILITY AND YIELD OF RESIDUE AFTER OXIDIZING-HYDROLYSIS
(Conditions of solvolysis: 100°C, 0.017 M $K_2Cr_2O_7$, 1 N H_2SO_4)

Reaction Time hr.	Residue Yield wt. %	$\overline{DP}$ (Cupram.)	Accessibility %
0	100.0	293.5	51.8
1	73.1	27.7	11.8
3	65.7	26.5	11.6
5	61.5	24.6	11.5
8	59.0	24.4	11.4
12	57.0	23.9	11.4

residue and its alkali-extracted residue.

D) Oxidizing-Hydrolysis. — Samples were oxidized and simultaneously hydrolyzed with the mixture of potassium dichromate and sulfuric acid, and the effect of the reaction time on the yield, DP and the accessibility of the residue are shown in Table IV.

It is very characteristic that the accessibility of the residue obtained from the oxidizing hydrolysis, levels off rapidly and exhibits relatively lower values than those of the other degradation residues.

The residue from the oxidizing hydrolysis is wholly dispersed in 2% caustic soda solution. Fig. 6 gives the chain-length distribution of this residue at various reaction times.

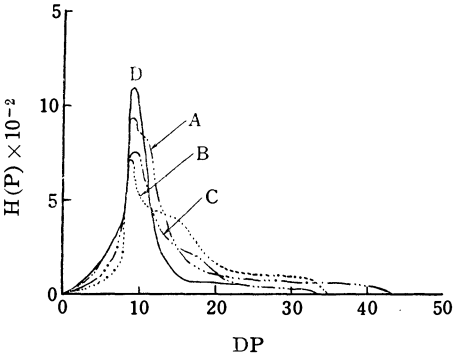

Fig. 6. Chain-length distribution of oxidizing-hydrolyzed cellulose.
A —····— 0.017 M $K_2Cr_2O_7$ + 1 N H_2SO_4 3 hrs.
B ····· 〃 〃 5 hrs.
C —·—· 〃 〃 8 hrs.
D ——— 〃 〃 12 hrs.

Discussion

Ordinary Hydrolysis Process. — The results that the peak of chain-length distribution curves of hydrolyzed residue moves initially to lower DP as the hydrolysis proceeds and then after it has attained a definite limit, only the height of the peak decreases, is in agreement with the observation by electronmicroscope that during the hydrolysis process the distribution of crystalline length remains almost constant and the distribution of crystalline width shifts to a more narrow side[6].

TABLE V
COMPARISON OF VARIOUS METHODS

Method	Conditions Concn.	Time hr.	Residue Yield wt. %	Accessibility %	$\overline{DP}$	Mode of DP
Ordinary hydrolysis	4 N	2	52.9	12.6	29	7
Hydrolysis after acetylation	1 N	25	58.5			6
Hydrolysis after oxidation	1 N	25	25.2			7
Oxidizing-hydrolysis	0.017 M + 1 N	8	61.8	11.4	24	9.5
Methanolysis	8 N	12	58.3	19.5	26	7.5
Alkali extraction after methanolysis	4% + 2.5 N	24	31.3	14.0	31	12

Comparison of Various Methods for Removal of the Amorphous Region.— The results of various methods are summarized in Table. V.

In the case of the methanolysis with 8 N hydrochloric acid, the peak of chain-length distribution is located at a somewhat lower DP. However, its residue which is controlled to give similar yield to other methods, exhibits high levelling-off accessibility, high partial solubility in 4% caustic soda solution and somewhat higher DP. These results suggest that the methanolyzed cellulose contains considerable amorphous regions. In our experiment with methanol-water systems, the yield of residue and its DP increase, and its accessibility decreases with the increase in water content. From these results, it may be concluded that water increases the probability of recrystallization and methanol has the reverse effect. However, Nelson et al. have described recently that the methanolysis prevented the reversion of cellulose III to cellulose I but appeared not to avoid the recrystallization[12]. Therefore, methanolysis or hydrolysis is not suitable for our object.

The chain-length distribution of hydrolyzed residue seems to shift its peak to lower DP regions on oxidation pretreatments. Therefore, the pretreatment may hinder the growth of the crystallites, but the low yield may be derived from the destruction of the crystallite, especially by the severe action of lead tetra-acetate. The chain-length distribution of the hydrolyzed residue from acetylation pretreatment has a similar width of DP range, but its peak exists at a slightly lower DP, compared with ordinary hydrolysis. The degree and the distribution of degradation may be influenced by the heterogeneity of the acetylation pretreatment. From the above reason and the troublesome operation which requires a long time, pretreatment methods are not so desirable.

In order to remove the amorphous region which remains around the end of the crystallites during hydrolysis, the oxidizing-hydrolysis method was carried out with dichromic acid whch is considered not likely to penetrate into the crystalline region. The results that the peak of chain-length distribution shifts to slightly higher DP, but the shoulder on the higher DP side disappears and the DP decrease, seem to disprove the recrystallization. Since oxidizing-hydrolysis gives lower levelling-off accessibility than ordinary hydrolysis, the residue of oxidizing-hydrolysis may show probably the original crystalline state. However, since its residue is easily soluble in dilute alkaline solution, the carboxyl groups formed by the oxidation may be responsible for its solubility in alkaline solution and for the poorer iodine sorption which results apparently in lower accessibility.

Although further study by means of X-ray diffraction, infrared absorption analysis etc. is necessary, oxidizing-hydrolysis may be the most hopeful.

Fine Structure of Rayon Staple.—From the above results, it is estimated that the length of crystalline region distributes within the range up to approximately the DP of 40 (ca. 200 Å) and its distribution has one peak between 6 and 10.

Relation between the Lateral Order and the Chain-Length Distribution of Solvolyzed Residue. — Maeda determined "lateral order", based on the solubility of hydrolyzed residue in alkaline solution, C, which is given by the following equation,

$$C = A \exp(-PE/RT)$$

where P is the degree of polymerization, E transition energy of solution per glucose unit, R gas constant, T absolute temperature, because E can be substituted for "lateral order"[13]. However, even an intensively degraded sample has so wide a chain-length distribution that the solubility in alkaline solution would depend not only on E, but also on P, as the lower DP region of methanolyzed residue is more soluble in alkaline solution.

If the chain-length of suitably degraded residue coincides with the length of the crystallite formed by hydrogen bond without gap, this length may indicate the fine structure of cellulosic fiber more clearly than the so-called "lateral order", which depends theoretically on the volume in consideration. But the solubility of the methanolyzed residue or the residue from the oxidizing hydrolysis in alkaline solution suggests the possibility of cracks in hydrogen-bonded crystallite.

Summary

In order to clarify the fine structure of

12) M. L. Nelson, L. Segal, T. Mares and J J. Creely, *J. Polymer Sci.*, **20**, 29 (1956).

13) H. Maeda, *J. Soc. Textile Cellulose Ind. Japan, (Sen-i Gakkaishi)* **12**, 6 (1956).

rayon staple, it may be necessary to estimate not only the total crystallinity but also the distribution of crystalline size and quality. For this purpose, various methods which seemed to remove the amorphous region without recrystallization, were studied.

Methanolysis is affected by water content in the mixture and its residue may still contain an amorphous region because of its high accessibility. The recrystallization may be possible during not only hydrolysis but also methanolysis.

The hydrolysis after pretreatment is not very effective to prevent recrystallization and may destroy crystalline region. Moreover, its procedure is troublesome.

The oxidizing-hydrolysis, which shifts the crystalline length distribution toward slightly higher DP region diminishing the shoulder on higher DP side and gives the lowest levelling-off accessibility, holds out considerable promise for the elucidation of the original crystalline structure. But its high solubility in alkaline solution may be derived from a carboxyl group formed during oxidation or from the cracks in a hydrogen-bond train of crystallites. Therefore, problems to study still remain.

The crystalline region of viscose rayon staple seems to have the chain-length distribution, which extends to a DP of ca. 40 and shows one maximum between the DP of 6 and 10.

Research Department, Yatsushiro Mill
Kōkoku Rayon and Pulp Co. Ltd.
Yatsushiro, Kumamoto

Crystal Structure of Quinhydrone, $C_{12}H_{10}O_4$

By Haruo MATSUDA,* Kenji OSAKI and Isamu NITTA

(Received March 17, 1958)

The peculiar properties of some aromatic molecular compounds and the question as to the forces responsible for their formation have been attracting the attention of a number of authors. Anderson[1] investigated a series of molecular compounds containing quinone, or its derivatives, and concluded that in all these compounds the component molecules are alternately stacked plane to plane, and that the most probable mechanism for the binding is effected by the interaction between strongly polar groups and by the highly anisotropic and polarizable aromatic systems. Such a type of parallel stacking was also found in *p*-iodoaniline-*s*-trinitrobenzene[2] which was the first example fully analyzed among the aromatic molecular compounds. For the discussion of the nature of intermolecular attraction, however, it is very desirable to obtain more data on inter- and intra-molecular distances and bond angles in these aromatic molecular compounds.**

Quinhydrone, or benzoquinhydrone, is the simplest of the series of molecular compounds containing quinones. It is highly desirable to determine its structure in detail, though there have been published a few papers which describe the general arrangement of molecules in this crystal.

Palacios and Foz reported in their first paper[3] that the monoclinic unit cell ($\beta=90°$) of quinhydrone contains one formula unit $C_{12}H_{10}O_4$ and the molecules are linked in endless chains by symmetrical hydrogen bonding. This structure in which both the molecules of quinone and hydroquinone are placed in the same equivalent positions, so that they are not distinguishable, was however revised by the same authors[4].

* Deceased 1950. This work, especially the most laborious part of it, was almost completed by H. Matsuda. It was continued and written up after his death.

1) J. S. Anderson, *Nature*, **140**, 583 (1937).

2) H. M. Powell, G. Huse and P. W. Cooke, *J. Chem. Soc.*, **1943**, 153.

** When the present work was almost completed, Dr. Wallwork was so kind as to inform us of his detailed analysis of phenoquinone. See S. C. Wallwork and T. T. Harding, *Nature*, **171**, 40; T. T. Harding and S. C. Wallwork, *Acta Cryst.*, **6**, 791 (1953); **8**, 787 (1955).

3) O. R. Foz and J. Palacios, *Anales Soc. Españ. Fis. Quim.*, **30**, 421 (1932).

4) J. Palacios and O. R. Foz., *Anales Soc. Españ. Fis. Quim.*, **33**, 627 (1935); **34**, 779 (1936).

They observed weak superstructure reflections requiring doubled a and c axes, and they ascribed the observed subperiodicity to the discrete existence of quinoid and quinoloid units in the structure. This view is in accord with that of Anderson quoted above.[1)]

Preliminary Investigations.—Most of the well-defined, apparently single crystals grown from acetone solutions have the appearance of hexagonal prisms. Laue photographs showed, however, that they are twins, and that the axial angle β was not exactly equal to 90° as has been reported. The deviation was estimated from the separation of Laue spots to be about 45′. Single crystals were easily obtained by splitting these twins with the aid of a razor blade and were used for subsequent works.

Lattice constants, derived from a series of symmetrical back reflection photographs, are

$$a=7.674\pm0.001\text{Å}, \quad b=6.001\pm0.001\text{Å}$$
$$c=21.788\pm0.002\text{Å}, \quad \beta=90°38'\pm3'.$$

Four $C_{12}H_{10}O_4$ units are contained in this lattice and the calculated density is 1.444 g./cm^3 as compared with the observed value 1.401 at 20°C. Systematic extinctions were observed in (hkl) when $h+l$ is odd, in $(0k0)$ when k is odd and in $(h0l)$ when $h-l$ is not multiple of 4. The only space group which conforms to these rules is $C_{2h}^5-B2_1/d$ with the glide translation $(a-c)/4$ for the above set of axes. The symmetry elements of this space group are shown in Fig. 1, and general and special point positions are listed in Table I. This lattice can be reduced to another having $a=7.647$ Å, $b=6.001$ Å, $c'=11.590$ Å and $\beta'=109°58'$ expressed in terms of $P2_1/c$, if we take the c'-axis as indicated in Fig. 1. Although this expression is more common, the former one ($\beta\approx90°$) was adopted throughout this work for the sake of convenience.

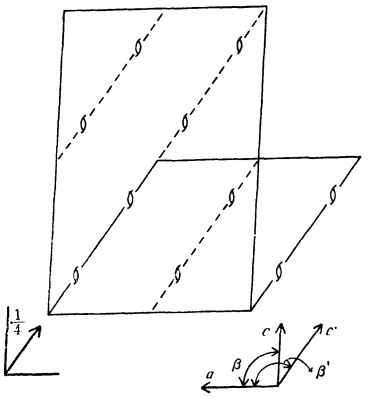

Fig. 1. Unit cell and symmetry elements of $B2_1/d$ and its reduction to $P2_1/c$.

Determination of the Averaged Structure.—A characteristic feature of the X-ray pattern of quinhydrone, as has been reported by Palacios and Foz, is that all the reflections with h, l odd are very weak, compared with those with h, l even. If we construct a Fourier representation of such a structure using even reflections alone, we shall obtain a hypothetical averaged structure repeating with lattice dimensions (1/2) a, b and (1/2) c. This averaged structure will be a fairly good approximation to the "true" structure, since reflections with h, l odd are all weak and will not contribute much to the Fourier representation of the true structure. Therefore first we determined this averaged structure and then proceeded to the true one.

The hypothetical averaged structure introduced above contains only one sort

TABLE I

GENERAL AND SPECIAL POINT POSITIONS FOR THE ADOPTED SPACE GROUP $B2_1/d$

8-fold general positions

$$8\ (e):\ \pm\left[\begin{array}{ccc} x,\ y,\ z & ; & \frac{1}{2}+x,\ y,\ \frac{1}{2}+z \\ \frac{1}{4}+x,\ \frac{1}{2}-y,\ \frac{3}{4}+z & ; & \frac{3}{4}+x,\ \frac{1}{2}-y,\ \frac{1}{4}+z. \end{array}\right]$$

4-fold symmetry centers

$$4\ (a):\ 0\,0\,0,\ \frac{1}{2}0\frac{1}{2},\ \frac{1}{4}\frac{1}{2}\frac{3}{4},\ \frac{3}{4}\frac{1}{2}\frac{1}{4}. \quad (H)$$

$$4\ (b):\ \frac{1}{2}0\,0,\ 0\,0\frac{1}{2},\ \frac{1}{4}\frac{1}{2}\frac{1}{4},\ \frac{3}{4}\frac{1}{2}\frac{3}{4}. \quad (Q)$$

$$4\ (c):\ 0\frac{1}{2}0,\ \frac{1}{2}\frac{1}{2}\frac{1}{2},\ \frac{1}{4}0\frac{3}{4},\ \frac{3}{4}0\frac{1}{4}.$$

$$4\ (d):\ \frac{1}{2}\frac{1}{2}0,\ 0\frac{1}{2}\frac{1}{2},\ \frac{1}{4}0\frac{1}{4},\ \frac{3}{4}0\frac{3}{4}.$$

of averaged molecule $1/2(C_{12}H_{10}O_4)$ lying on two of the centers of symmetry in a lattice of space group $P2_1/n$, and corresponds to the structure given in the first paper of Foz and and Palacios.[3] The

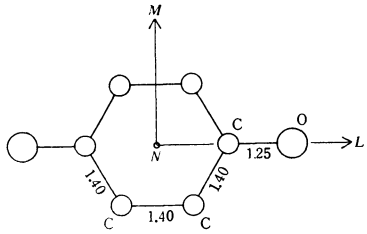

Fig. 2. Molecular model used in calculating the Fourier transform. The weight of the oxygen atom was taken to be 4/3 times that of the carbon. Axis N points up and is perpendicular to both L and M.

orientation of the molecular axes was determined easily by the method of Fourier transform[5] using the reflections $(0k0)$ and $(00l)$. In calculating this transform, a hypothetical molecular model shown in Fig. 2 was adopted. Atomic parameters thus obtained were refined through repeated $\rho(yz)$ syntheses and structure-factor calculations $(0kl)$.

The averaged structure obtained here was in striking accordance with that suggested by Banerjee[6] from magnetic data. According to our results, the normal to the averaged molecular plane, when projected upon (010), makes an angle 15.0° with the a axis, which accords well with the angle 15.1° between the a axis and the direction of maximum susceptibility reported by Banerjee. This fact alone will support Banerjee's view that the crystal of quinhydrone consists of molecules of quinone and hydroquinone.

Determination of x and z Parameters. —Since there are four $C_{12}H_{10}O_4$ units in the unit cell having eight-fold general positions, two types of structure are possible; one of which consists of two different kinds of molecules, corresponding to quinone and hydroquinone, each lying on one of the four-fold centers of symmetry, say 4(a) and 4(b) (Table I.); and the other consists of only one kind of molecule (semiquinone type) which are situated around (1/4 0 0), etc. Since the former type consisting of quinone and hydroquinone seemed to be more plausible in view of the work of Anderson[1] and that of Banerjee[6], we studied mainly on this line. We also examined the semiquinone type structure, which we shall later mention briefly.

In order to find out how and to what extent these two sorts of component molecule deviate in shape and orientation from the hypothetical averaged molecule, we performed trial-and-error calculations on $(h0l)$ reflections with h and l odd, using scaled structure factor maps.

After sufficient agreement was obtained between calculated and observed F-values, we prepared an electron density projection $\rho(xz)$ using almost all $(h0l)$ reflections. Parameters thus found, when combined with $\rho(yz)$ already obtained, led us to a group of structures in which the benzene ring of the hydroquinone molecule was somewhat deformed. Thus we performed two series of extensive trial-and-error calculations in order to be sure whether this deformation was real or not. In one series of the calculation we always assumed a regular hexagon with sides 1.39Å for hydroquinone, while in the other no such assumption was made. The best model we obtained in each of the two series gave the values of reliability indices 0.158 and 0.154 respectively, both including the contribution of hydrogen atoms. The signs of F-values calculated from these two models differed only in two weak reflections out of 67 observed values, and the change in $\sum |F(h0l)|$ is only 0.6% if we neglect them. Hence we proceeded to the next stage omitting these two reflections.

The next step was to obtain the final x and z parameters for all the atoms. To do this we used the method of differential synthesis and applied the corrections for series-termination. This step was repeated twice. Carbon atom C_{IV}, which is linked to oxygen O_{II} to form a quinone molecule, was not resolved in $\rho(xz)$ projection (Fig. 3), so that x and z parameters for C_{IV} were obtained by least squares calculations treating only these two parameters as variables, after other atoms were all fixed.

The reliability index R obtained for $F(h0l)$ was reduced to 0.124 including the contributions of hydrogen atoms.

Determination of y Parameters—The determination of y parameters was much more troublesome. Although we had obtained by this stage (R=0.139 for $(0kl)$ including hydrogen atoms) fairly good parameters for all the atoms from trial-

5) G. Knott, *Proc. Phys. Soc.*, **52**, 229 (1940).
6) S. Banerjee, *Z. Krist.*, **100**, 316 (1939).

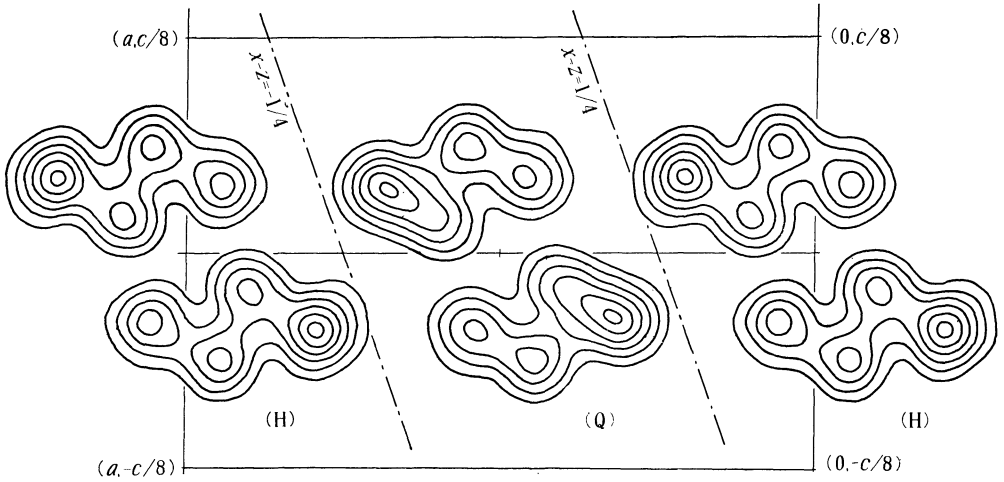

Fig. 3. Electron density projection $\rho(xz)$. Limiting planes for the bounded projections are also indicated by chain lines (see text).

and-error method, the refinement seemed to be hopeless when we used (0*kl*) reflections only, even by way of least squares calculations, since the component molecules overlap atom to atom almost completely in the projection along [100] (Fig. 4). However, we were able to overcome this difficulty using the method of bounded projection. This method was especially convenient in this structure, because, if we choose suitable limiting planes, we need only (*hkl*) intensities with h and l odd, which are all weak, and appropriate values for them can be estimated without too much difficulty. Actually, we prepared bounded projections in a modified form so as to separate quinone and hydroquinone completely. The projection was made along [100] axis, with the limiting planes at,

$$x-z=1/4 \text{ and } x-z=-1/4,$$

as indicated in Fig. 3. The expressions for these bounded projections are as follows:

$$B_I=\frac{2a}{V}\sum_{-k}^{k}\sum_{0}^{l}\sum_{-h}^{h}\int_{x=-\frac{1}{4}+z}^{x=\frac{1}{4}+z}F_{hkl}\cos 2\pi(hx+ky+lz)\,dx$$

$$=B_0+B_h$$

$$B_{II}=\frac{2a}{V}\sum_{-k}^{k}\sum_{0}^{l}\sum_{-h}^{h}\int_{x=-\frac{1}{4}+z}^{x=\frac{3}{4}+z}F_{hkl}\cos 2\pi(hx+ky+lz)\,dx$$

$$=B_0-B_h$$

where

$$B_0=\frac{a}{V}\sum_{-k}^{k}\sum_{0}^{l}F_{0kl}\cos 2\pi(ky+lz)$$

$$B_h=\frac{2a}{V}\sum_{-k}^{k}\sum_{1}^{l}\left[\sum_{\substack{-h\\(h\neq 0)}}^{h}\left(\frac{1}{\pi h}\sin\frac{\pi h}{2}\right)F_{hkl}\right]\times\cos 2\pi\{ky+(l+h)z\}$$

The intensities for (*hkl*) with $h=3$, 1, $\bar{1}$ and $\bar{3}$ collected from oscillation photographs were utilized after the application of necessary corrections. No effort was made to obtain data with h higher than these, as they did not seem to effect the results seriously. Signs of $F(hkl)$ were derived from calculated values using the best set of parameters obtained at that stage, contributions from hydrogen atoms being neglected. The first projection was calculated using x and z parameters which were obtained by differential Fourier syntheses, and the third and last one was calculated only along b axis through the atomic positions, after x and z parameters were all fixed. Termination corrections were also applied. y parameters thus obtained were listed in Table II together with the x and z parameters obtained in the previous section. Calculated and

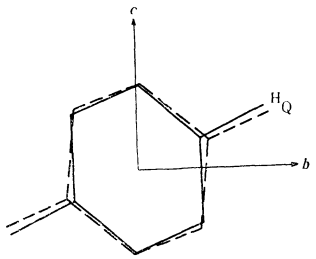

Fig. 4. Projection of the two component molecules along the a axis.
H: hydroquinone, Q: quinone.

TABLE II

FINAL ATOMIC CO-ORDINATES

	x	y	z		x	y	z
C_I	0.1039	0.1640	0.0216	C_V	0.5523	0.0121	0.0621
C_{II}	0.0518	0.0077	0.0610	C_{VI}	0.5439	0.1632	−0.0453
C_{III}	0.0549	0.1695	−0.0412	O_I	0.2128	0.3355	0.0440
C_{IV}	0.6021	0.1854	0.0195	O_{II}	0.6849	0.3496	0.0374

TABLE III

OBSERVED AND CALCULATED F-VALUES FOR ZONAL REFLECTIONS

$0k$ l	$\lvert F_{obs}\rvert$	F_{calc}	$0k$ l	$\lvert F_{obs}\rvert$	F_{calc}	$h0$ l	$\lvert F_{obs}\rvert$	F_{calc}	$h0$ l	$\lvert F_{obs}\rvert$	F_{calc}
00. 4	122	142	01. 2	54	−63	10. 1	12	−13	$\bar{1}$0. 3	5	− 1
8	82	−85	4	37	−45	5	8	− 5	7	3	− 1
12	72	83	6	29	−17	9	9	9	11	11	−11
16	15	−12	8	47	−60	13	12	12	15	10	−10
20	6	6	10	13	− 5	17	2	3	19	0	− 1
24	3	0	12	31	−31	21	5	− 5	23	6	6
			14	20	19	25	7	− 5			
02. 0	32	−37	16	10	−12						
2	39	41	18	15	8	20. 2	24	−22	$\bar{2}$0. 2	92	79
4	47	−52	20	7	− 4	6	92	−85	6	35	39
6	59	73	22	14	−17	10	42	−34	10	26	32
8	23	−17	24	0	3	14	9	11	14	33	31
10	16	17	26	14	−15	18	4	− 4	18	32	26
12	26	25				22	19	−14	22	0	3
14	39	−41	03. 2	13	17						
16	34	33	4	13	−14	30. 3	21	21	$\bar{3}$0. 1	0	2
18	38	−45	6	36	−40	7	22	21	5	8	− 7
20	3	1	8	0	− 3	11	0	0	9	4	− 3
22	15	−15	10	35	−33	15	12	−13	13	5	− 1
24	15	−13	12	4	− 5	19	6	−10	17	5	− 4
26	12	10	14	15	8				21	0	− 2
			16	0	5	40. 0	0	2			
04. 0	16	−22	18	24	16	4	21	22	$\bar{4}$0. 4	42	−39
2	22	23	20	0	2	8	13	11	8	63	−71
4	30	−28	22	0	3	12	5	− 6	12	25	−24
6	32	34	24	3	1	16	23	−26	16	40	42
8	10	− 8				20	20	−19	20	50	48
10	3	3	05. 2	29	27						
12	28	24	4	7	8	50. 1	8	− 8	$\bar{5}$0. 3	7	8
14	33	33	6	0	− 3	5	17	−19	7	11	11
16	24	26	8	17	17	9	6	− 8	11	10	13
18	25	27	10	5	−10	13	9	8	15	0	− 1
20	4	−19	12	15	17	17	10	13	19	0	0
22	9	7	14	3	4						
24	12	12	16	5	6	60. 2	37	28	$\bar{6}$0. 2	8	− 4
			18	0	3	6	8	−11	6	0	5
06. 0	42	56	20	0	− 2	10	19	18	10	21	−16
2	9	− 7				14	12	13	14	18	−19
4	22	25	07. 2	4	5	18	0	− 1	18	2	0
6	11	−11	4	7	− 7						
8	22	−20	6	8	− 5	70. 3	0	− 2	$\bar{7}$0. 1	10	−11
10	4	− 3	8	7	− 6	7	9	10	5	8	− 8
12	22	−22	10	5	− 4	11	10	13	9	0	1
14	0	1	12	4	− 4	15	4	4	13	0	4
16	4	− 3									
						80. 0	21	−24	$\bar{8}$0. 4	16	−16
						4	6	5	8	0	2
						8	33	36			

TABLE IV
OBSERVED AND CALCULATED F-VALUES FOR hkl REFLECTIONS

hk	l	$\lvert F_{obs}\rvert$	F_{calc}	hk	l	$\lvert F_{obs}\rvert$	F_{calc}	hk	l	$\lvert F_{obs}\rvert$	F_{calc}	hk	l	$\lvert F_{obs}\rvert$	F_{calc}
11.	1	6	− 4	$\bar{1}$1.	1	5	8	15.	1	5	4	$\bar{1}$5.	1	5	− 5
	3	9	8		3	4	3		3	0	3		3	2	1
	5	7	11		5	7	9		5	0	2		5	8	− 9
	7	3	0		7	2	− 3		7	4	5		7	2	3
	9	18	20		9	7	7		9	4	− 3		9	4	− 7
	11	10	−10		11	2	0		11	0	1		11	0	0
	13	11	8		13	0	1		13	0	− 1		13	0	− 2
	15	12	−10		15	8	6		15	0	− 2		15	2	− 2
	17	5	− 4		17	5	− 4		17	4	4		17	2	2
	19	0	− 3		19	4	4								
	21	9	− 8		21	3	− 4	16.	1	0	0	$\bar{1}$6.	1	5	− 5
	23	2	3		23	0	0		3	10	11		3	2	3
	25	5	− 4		25	2	2		5	0	− 2		5	0	3
	27	3	4		27	3	− 2		7	6	8		7	2	3
									9	0	0		9	4	5
12.	1	6	6	$\bar{1}$2.	1	0	2		11	0	2		11	2	− 2
	3	10	−12		3	0	− 1		13	2	2		13	5	5
	5	6	15		5	0	0		15	0	− 1		15	5	− 4
	7	17	−18		7	0	1								
	9	4	0		9	0	0	17.	1	2	− 2	$\bar{1}$7.	1	5	5
	11	5	− 5		11	6	6		3	6	2		3	6	2
	13	9	− 5		13	3	− 5		5	0	1		5	8	7
	15	11	9		15	7	6		7	0	1		7	0	0
	17	0	− 3		17	9	− 8		9	0	4		9	6	6
	19	11	11		19	4	3								
	21	2	0		21	6	− 5	31.	1	10	−13	$\bar{3}$1.	1	10	−15
	23	2	3		23	0	− 2		3	1	1		3	0	− 2
									5	13	−13		5	7	− 6
13.	1	3	5	$\bar{1}$3.	1	3	− 3		7	14	−14		7	6	5
	3	10	− 8		3	0	− 2		9	3	− 1		9	1	1
	5	0	− 1		5	0	0		11	11	−12		11	0	3
	7	5	− 4		7	0	0		13	8	9		13	0	− 2
	9	7	− 7		9	7	− 4		15	3	2		15	5	1
	11	8	9		11	2	2		17	9	8		17	2	− 5
	13	6	− 7		13	6	− 3		19	9	9		19	2	2
	15	15	13		15	0	0		21	3	0		21	0	− 3
	17	2	− 3		17	6	4		23	5	4		23	5	2
	19	10	7		19	0	− 2								
	21	0	0		21	9	7	32.	1	13	−11	$\bar{3}$2.	1	0	3
	23	2	− 4		23	2	− 3		3	9	− 9		3	13	13
									5	0	3		5	6	7
14.	1	0	1	$\bar{1}$4.	1	4	6		7	12	−14		7	7	6
	3	2	− 1		3	0	0		9	16	17		9	3	4
	5	2	− 2		5	0	0		11	5	− 6		11	2	1
	7	6	3		7	0	− 2		13	17	16		13	0	0
	9	7	− 7		9	8	− 6		15	6	4		15	0	− 1
	11	0	0		11	0	− 2		17	4	3		17	0	1
	13	6	− 4		13	2	− 3		19	6	6		19	2	− 3
	15	7	− 4		15	0	− 1		21	8	− 7		21	4	3
	17	3	4		17	3	3		23	0	0		23	6	− 4
	19	7	− 5		19	0	0								
	21	8	7		21	5	4								

hk	l	$\lvert F_{obs}\rvert$	F_{calc}	hk	l	$\lvert F_{obs}\rvert$	F_{calc}	hk	l	$\lvert F_{obs}\rvert$	F_{calc}	hk	l	$\lvert F_{obs}\rvert$	F_{calc}
33.	1	12	12	$\bar{3}3.$	1	1	3	34	17	0	− 2	$\bar{3}4$	17	0	0
	3	3	− 8		3	0	− 1		19	8	5		19	0	0
	5	14	14		5	0	0								
	7	4	− 8		7	3	− 5	35.	1	0	4	$\bar{3}5.$	1	0	0
	9	0	− 1		9	0	− 1		3	4	5		3	0	4
	11	0	− 2		11	0	− 1		5	0	1		5	0	2
	13	13	−12		13	0	0		7	8	8		7	0	− 1
	15	0	4		15	0	1		9	0	0		9	0	− 1
	17	7	− 8		17	0	1		11	7	4		11	5	− 6
	19	2	5		19	0	− 1		13	4	2		13	0	− 1
	21	0	0		21	0	1		15	4	− 3		15	7	− 6
									17	0	3		17	1	2
34.	1	8	9	$\bar{3}4.$	1	0	− 3								
	3	2	− 2		3	2	− 3	36.	1	0	2	$\bar{3}6.$	1	0	− 1
	5	4	2		5	2	− 3		3	4	3		3	2	− 5
	7	0	1		7	3	5		5	0	− 1		5	2	− 2
	9	10	−10		9	0	− 3		7	3	4		7	6	− 6
	11	2	6		11	0	4		9	0	− 2		9	0	0
	13	9	−11		13	0	− 2		11	0	1		11	6	− 6
	15	8	8		15	0	0								

observed F-values are given in Tables III and IV.

Tests on the Semiquinone-type structure.—Another type of structure consisting of semiquinone-type molecules was also checked by trial calculations followed by differential Fourier syntheses. After two steps of approximations we were able to obtain a parameter set with reliability index $R=0.24$ for $(h0l)$ reflections neglecting the contributions of hydrogen atoms, while that for the correct structure was 0.15. If we devide F-values into groups of even and odd reflections we find for the semiquinone type (excluding hydrogen atoms) $R(\text{even})=0.19$ and $R(\text{odd})=0.55$, as compared with those of the other (excluding hydrogen atoms) $R(\text{even})=0.15$ and $R(\text{odd})=0.16$. The R-value for the reflections with h odd is exceedingly large in the case of semiquinone-type. It may be considered as an indication that the structure of this type is wrong as to the structural features especially responsible for these reflections, that is, as to the deviations from the averaged structure.

Collection of intensity data.—Most of the intensity data were collected from two sets of oscillation photographs about a and b axes. In order to obtain good intensity estimates even for weaker reflections with h and l odd, we prepared, for each range of oscillation, a photograph of very long exposure in addition to a usual one. A rotation photograph was taken about the a axis using multiple-film technique. This provided further confirmation and gave measurable intensities even for very strong reflections. All these data were combined and served for most part of the present work.

During the course of analysis, however, it was found that the specimen showed a strong extinction. Additional sets of oscillation photographs were then prepared for both a and b axes using a tiny crystal dipped into liquid air several times. The disagreement between calculated and observed F-values for strongest reflections became less remarkable, but we were unable to eliminate the effect of extinction completely.

All the photographs were prepared using Cu-K radiations, with or without a nickel filter, and the intensities were estimated by comparing them visually with a series of standard intensity scales, except in measuring rotation photographs where a recording microphotometer was used. The number of reflections actually observed as compared with what were possible is listed below:

type of reflections		number of reflections: observed	possible
$0kl$		74	83
$h0l$	h and l even	39	44
	odd	33	42
$1kl$, $\bar{1}kl$	$(k=0)$	100	142
$3kl$, $\bar{3}kl$		73	120

Description and Discussion of the Structure

The structure of quinhydrone obtained here consists of two sorts of molecules, quinone and hydroquinone, of which the latter appears to be deformed to some extent as is shown in Fig. 5. The average plane of six carbon atoms of quinone with its center at 1/4, 0, 0 is given by the equation

$$-0.836(ax-3.837)+0.507by+0.210cz'=0,$$

where the z' axis was taken perpendicular to x and the oxygen O_{II} comes by 0.055Å

outside of the plane. The difference between the two C-C(H) bond lengths adjacent to the C=O group is scarcely significant and the mean value 1.465Å is rather short in comparison with 1.50 Å reported for *p*-benzoquinone[7]. This is probably related to the observed elongation of $C_V=C_{VI}'$ bond from the standard value 1.32 Å to 1.335 Å, though the difference is hardly significant. C=O bond length 1.234Å observed is a value commonly found for the carboxyl group forming a hydrogen bond, though somewhat shorter value 1.15Å is reported for *p*-benzoquinone. The average plane containing six carbon atoms of the hydroquinone molecule with its center at the origin is given by

$$-0.811ax+0.542by+0.219\,cz'=0$$

The oxygen atom O_I calculated to be only 0.014Å outside the plane may well be considered to be almost coplanar with the benzene ring. The observed C-O(H) distance 1.409Å is considerably larger than the usual 1.36Å for a phenolic C-O, which may possibly be related to the deformation of the benzenoid ring described below.

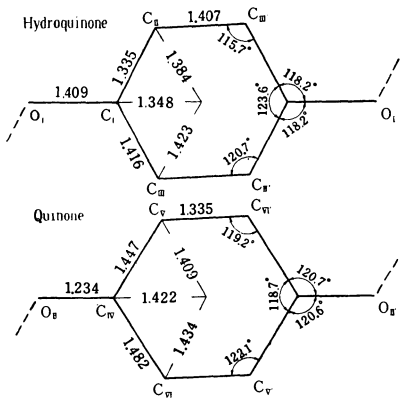

Fig. 5. Shape of the component molecules. Hydrogen bonds are indicated by broken lines.

A rather striking feature is the deformation of the benzenoid ring of the hydroquinone molecule. In fact, the bond length C_I-C_{II} is contracted to 1.335Å, while C_I-C_{III} and $C_{II}-C_{III}'$ are 1.416 and 1.407Å respectively, and they seem to be elongated somewhat. Further, the angle $C_I-C_{III}-C_{II}'$ is found to be 115.7° and as a result of these changes, the benzenoid ring rather resembles a quinoid ring. Although the cause of this deformation is not yet clear, it will be interesting to add here that the C_I-C_{II} bond, which appears shorter than C_I-C_{III}, is nearly parallel to the hydrogen bond O-H···O which will be described in the next paragraph. A similar deformation was also reported in the case of 1, 4-dimethoxybenzene (Fig. 6) by Robertson and others[8] although they did not try to explain it. We may mention in this connection that Tomiie[9] pointed out once that the lone-pair electrons at the oxygen atom may possibly influence the benzenoid ring to stabilize one of the resonance forms.

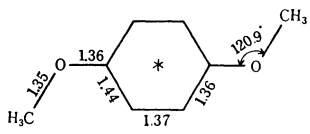

Fig. 6. Shape of 1,4-dimethoxybenzene after Robertson.

The two sorts of molecules, quinone and hydroquinone, are linked alternately through O-H···O hydrogen bonds of moderate length (2.71Å) to form a zigzag chain which is extended throughout the crystal*. Fig. 7 (a) is a part of the structure at $z=0$ and shows that these chains are running along [120]. Planes of molecules of the same sort are all parallel within a single chain, since they correspond to some translation of the crystal lattice, while those of one sort are tilted slightly (about 2°30′) with respect to those of the other. Fig. 7 (b) shows a part of the similar sheet at $z=1/4$, but in this case, the chains are seen to be running along [$\bar{1}$20]

Fig. 7 (a) also shows how these chains are stacked side by side to form a molecular sheet parallel to (001). These sheets are again piled up into a sort of layer lattice. A perspective view of a part of the structure is given in Fig. 8.

Between the neighboring sheets, the nearest approach distances are those between non-bonded carbon and oxygen atoms of lengths 3.31~3.83Å as shown in Fig. 8. These values are comparable with 3.4Å reported by Robertson in *p*-benzoquinone[7]

7) J. M. Robertson, *Proc. Roy. Soc.*, **A150**, 106 (1953).

8) T. H. Goodwin, M. Przybylska and J. M. Robertson, *Acta Cryst.*, **3**, 279 (1950).

9) Y. Tomiie, informal discussion.

* Such a chain-like structure is often accompanied by marked thermal motion of the molecular plane, which was actually observed in the present case as strong diffuse scattering on both Laue and oscillation photographs.

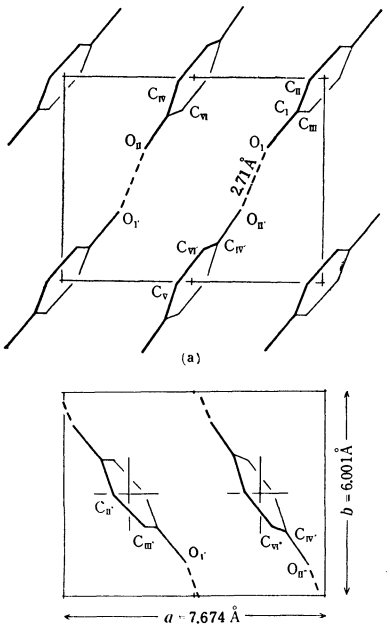

Fig. 7. Part of the molecular sheet at $z=0$ (a) and $z=1/4$ (b).

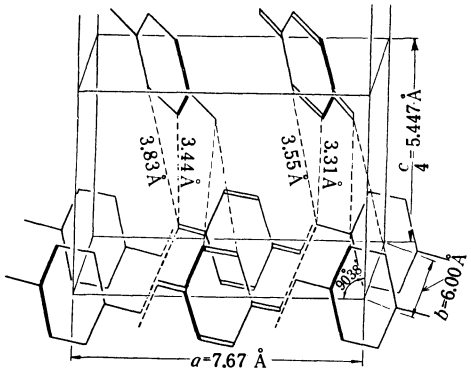

Fig. 8. Perspective view of a part of the structure of quinhydrone.

and with 3.24 and 3.39Å given by Abrahams in *p*-dinitrobenzene.[10] Similar values are often found between aromatic carbon and oxygen atoms and do not seem to be exceptionally short. Only it will be interesting to notice here that the oxygen atom of one sort of molecule always has the carbon atoms of the other as its neighbors. No C···C or O···O distances are shorter than 4Å between the neighboring sheets.

Hitherto we have seen that the crystal of quinhydrone is a sort of layer structure containing hydrogen bonds. Suzuki and Seki[11] determined the heat of formation of crystalline quinhydrone and estimated that the hydrogen-bond energy seems to contribute to a considerable part to it. But the remarkably compact structure, suggested by the observed density 1.401 in comparison with those of hydroquinone 1.33 and quinone 1.32, and the characteristic coloring of quinhydrone are not explained by hydrogen bonds.

Another type of interaction also seems to be taking place within the molecular sheet. We have already mentioned that the two component molecules are piled up alternately along the *a* axis, and overlap atom to atom almost completely when projected along this axis (Fig. 4). The planes of adjacent molecules are nearly parallel (inclination about 2°30′) and the perpendicular distance between the averaged molecular plane is measured to be 3.16Å. This value is remarkably short for an interplanar distance of aromatic molecules which is usually found to be larger than 3.4Å and may not have been realized without a considerable attraction between these molecules, if the repulsive forces are assumed to be the same. We may thus consider that these component molecules are linked in some way along the *a* axis and make up a sort of molecular column of alternating quinone and hydroquinone molecules along this direction. Or we may even look upon the structure of quinhydrone as consisting of such columns linked side by side through hydrogen bonds to form a sheet. Similar columns are also found in the molecular compound analyzed by Powell et al.[2] which does not contain hydrogen bonds. So that the existence of such columns may be looked upon to be a characteristic feature of these types of molecular compounds.

Now let us look into the detailed structure of the molecular column in quinhydrone. Fig. 9 is the projection of two

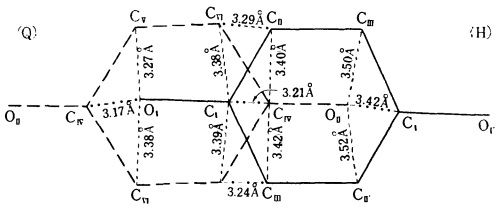

Fig 9. Perpendicular projection of two neighboring molecules within a column.

10) S. C. Abrahams, *Acta Cryst.*, **3**, 194 (1950); F. J. Llwellyn, *J. Chem. Soc.*, **1947**, 884.

11) K. Suzuki and S. Seki, This Bulletin, **26**, 372 (1953).

succeeding molecules within a column upon the mean molecular plane and shows the relative positions of the stacking molecule more clearly. Here, it must be born in mind that each molecule lies on the center of symmetry, so that each component molecule is sandwiched between molecules of the other component on both sides. Atomic distances between the molecules are also given in the figure. C···O distances found here are not very different from those between the molecular sheets. But the intermolecular C···C distances so short as those given here do not seem to have been reported before except in 3 : 4-benzophenanthrene.[12]

Nakamoto[13] investigated the optical dichroism of quinhydrone and some other molecular compounds of similar type and concluded that, in these substances, π-electrons are more mobile in the direction perpendicular to the plane than in the plane of the molecule, contrary to the case of ordinary aromatic compounds, where π-electrons are more mobile along the molecular plane. This result, as was pointed out by himself, will be explained qualitatively if we assume that the characteristic absorption in quinhydrone is due to a stable complex which is made up from quinone and hydroquinone through the mechanism of charge-transfer proposed by Mulliken.[14] Also the observed short intermolecular distance will be explained by this concept.

But why, then, is an unusually stable complex formed in the case of quinhydrone? A theoretical treatment by Suzuki[15] seems to answer the essential points of this question. He extended the treatment of Mulliken to the case of an infinite chain and calculated the electronic state of quinhydrone to the Bloch approximation and concluded that in the excited state most of the mobile electrons are transferred from hydroquinone to quinone molecule, so that the observed spectra (maximum approximately at 550 and 380 mμ) correspond to the intermolecular charge-transfer spectra. In other words, he concludes that the attraction between the two components in quinhydrone may be due to the interaction between the highest occupied molecular orbital level of hydroquinone and the lowest unoccupied one of the quinone molecule, and that the very strong interaction in this case may probably be attributed to the fact that the molecular orbitals of quinone and hydroquinone have the same symmetry and, at the same time, their energy difference is small.

Thus, we have in quinhydrone a remarkable example of a series of molecular compounds of which combined investigations of the crystal structure and of physical properties seem to be worth performing.

The authors would like to express their sincere thanks to Professor Akabori of Osaka University for his interest and constant encouragement especially of one of them (H. M.). Their thanks are also due to the Ministry of Education, to which they owe a part of the cost of this work.

Department of Chemistry, Faculty of Science, Osaka University
Kita-ku, Osaka

12) F. H. Herbstein and G. M. Schmidt, *J. Chem. Soc.*, **1954**, 3302.
13) K. Nakamoto, *J. Am. Chem. Soc.*, **74**, 1739 (1952).
14) R. S. Mulliken, ibid., **74**, 811 (1952).
15) K. Suzuki, *Busseironkenkyu*, No. **102**, p. 5 (1956), (in Japanese).

Refining of Low Temperature Cresol No. 1

By Keisho YAMADA

(Received November 18, 1957)

The low temperature cresol No. 1 has an offensive smell and a strong tendency of spontaneous coloration. According to Funakubo et al.[1], coloration of tar-acid oil occurs in the presence of acetic and formic acids, and more rapidly when the oil is exposed to the sunlight or contains a trace of iron together with acetic and formic acids. It has been stated by Lunge[2] that coloration of phenol has its origin in ferric benzoate formed from benzoic acid in the tar-acid oil and iron from distilling equipments, and he referred to indene as another source. According to Ueda et al.[3], coloration of tar-acid oil is caused chiefly by pyrrol, and in the case of low-temperature tar, catechol also partakes of its cause. Jaeger[4] said that coloration of tar occurs chiefly by oxygen in the air and basic oil promotes the coloration.

Egloff et al.[5] reports that spontaneous coloration of gasoline is due to free sulfur and alkyl disulfides, and when both are present, remarkable coloration takes place. According to Suzuki et al.[6], an offensive smell of low temperature tar is due to thiophenols.

The investigations of impurities in the coal tar products have become the topics of interest in recent years. However, only a little literature has been published on the inquiries of impurities in the low temperature cresol No. 1 which may cause the offensive smell and coloration.

The present paper is the report on the researches of the impurities which may deteriorate the quality of low temperature cresol No. 1, and on the suitable method for removing them.

This study revealed about thirty substances as impurities in the low temperature cresol No. 1, including those which have not been certified in coal tar up to the present. Several of them showed remarkable spontaneous coloration and strong peculiar smells, and these substances together with other unstable materials, which may cause the disgusting smell and coloration, were successfully removed by oxidation and active-clay treatment. The impurities in this refined cresol were investigated, and it was found that most of them were removed.

The author has reported the results of his inspections of the impurities in the low temperature cresol No. 1 in the Journal of the Chem. Soc. of Japan, Ind. Chem. Sec. from part 1 to 7, and in this paper the results have been summarized and discussed further.

Experimental Results

(1) Preparation and Properties of Low Temperature Cresol No. 1—At the Nitrogen Factory of Ube Industries, Ltd., the low temperature cresol No. 1 is prepared by the way shown in Tables I and II. The low temperature cresol No. 1 has an offensive smell and a dark brown color, and its specific gravity is 1.036 at 24°C. Engler's distillation curve is shown in Fig. 1.

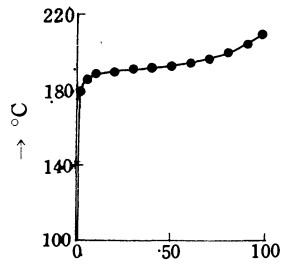

Fig. 1. Engler's distillation curve.

Immediately after distillation, the low temperature cresol No. 1 is a colorless and transparent oil, but gradually it begins to color on storage in the open air, and finally becomes an opaque black brown oil. In a dark place, however, its color turns only a light yellowish red in thirty days after distillation, which is lighter than the coloration caused by leaving the distillate

1) E. Funakubo and G. Kawasaki, unpublished data.
2) G. Lunge, "Coal-Tar and Ammonia" Part I, Gurney and Jackson, London, (1916), p. 266.
3) T. Ueda and H. Matsuda, Japanese Patent No. 199, 897.
4) A. Jaeger, *Brenn. Chem.*, **1**, 257 (1923).
5) G. Egloff, J. C. Morrell, W. L. Benedict and C. Wirth, U. O. P. Booklet No. 35, Universal Oil products Company, Chicago, (1938).
6) M. Suzuki, F. Kitahara and M. Koga, *J. Chem. Soc. Japan, Ind. Chem. Sec.*, (*Kogyo Kagaku Zassi*), **55**, 28 (1952).

TABLE I
SEPARATION OF CRUDE ACID OIL FROM LOW-TEMPERATURE TAR

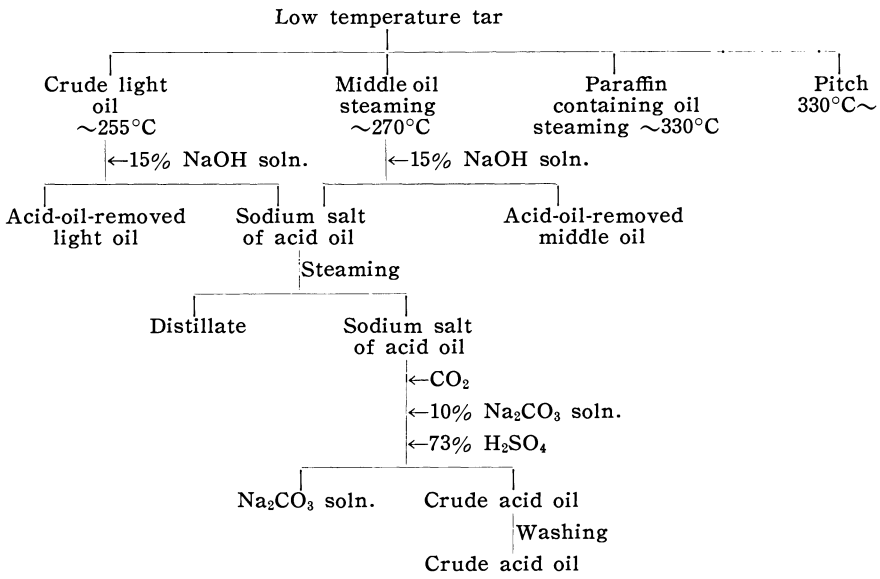

TABLE II
PREPARATION OF LOW TEMPERATURE CRESOL No. 1

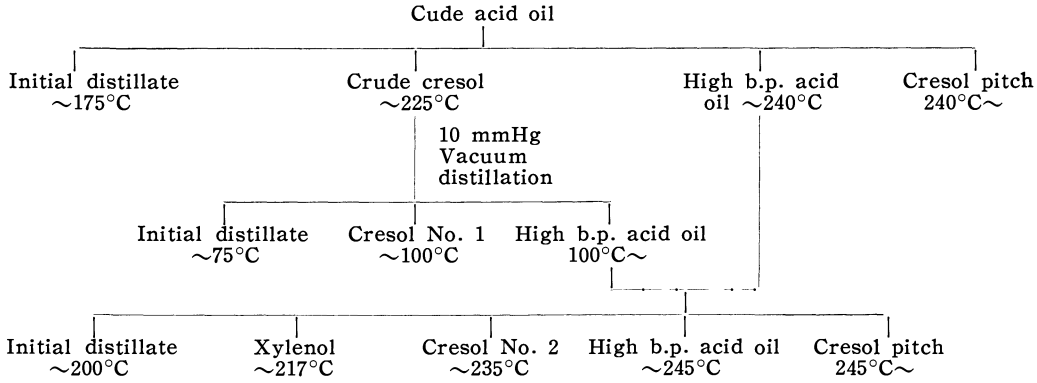

in the air for one day. When the low temperature cresol No. 1. is distilled under a stream of nitrogen or carbon dioxide, and the distillate is stored in a glass bottle, containing nitrogen or carbon dioxide, the coloration does not develop in thirty days after distillation, and the distillate remains colorless and transparent just as it is immediate after distillation. On the other hand, the low temperature cresol No. 1 absorbs a considerable amount of oxygen, and the coloration is nearly proportional to the amount of absorbed oxygen[7].

In the case of lack of either light or oxygen, the low temperature cresol No. 1 is stable enough against coloration. So, it is clear that the remarkable coloration occurs only when both light and oxygen are present.

According to Amemiya et al.[8], for example, the components of low temperature cresol No. 1 are: 23 weight% of phenol, 8 of *o*-cresol, 22 of *m*-cresol, 11 of *p*-cresol and 31 of xylenols and the higher homologs, (including 5% operation loss). The impurities in the low temperature cresol No. 1 were determined by the method listed in Tables III and IV. The composition was 0.217 volume % of strong acid oil, 0.367 of weak acid oil, 0.733 of neutral oil and 0.033 of basic oil, and the total impurities were 1.350 volume %. The 176~210°C fraction of normal acid oil obtained by removing these impurities from the low temperature cresol No. 1, did not color even when it was left in the open air[9], and had no more offensive smell. Thus it is indicated that the materials included in these impurities cause an offensive smell and spontaneous coloration.

(2) Identification of the Constituents of

7) K. Yamada, ibid., **60**, 1319 (1957).
8) J. Amemiya, E. Tunetomi and T. Nagazawa, *J. Japan Tar Ind. Association*, **4**, 104 (1952).
9) K. Yamada, *J. Chem. Soc. Japan, Ind. Chem. Sec.*, (*Kogyo Kagaku Zassi*), **60**, 591 (1957).
10) K. Yamada, ibid., **60**, 921 (1957).

TABLE III

SEPARATION OF STRONG ACID OIL, NORMAL ACID OIL

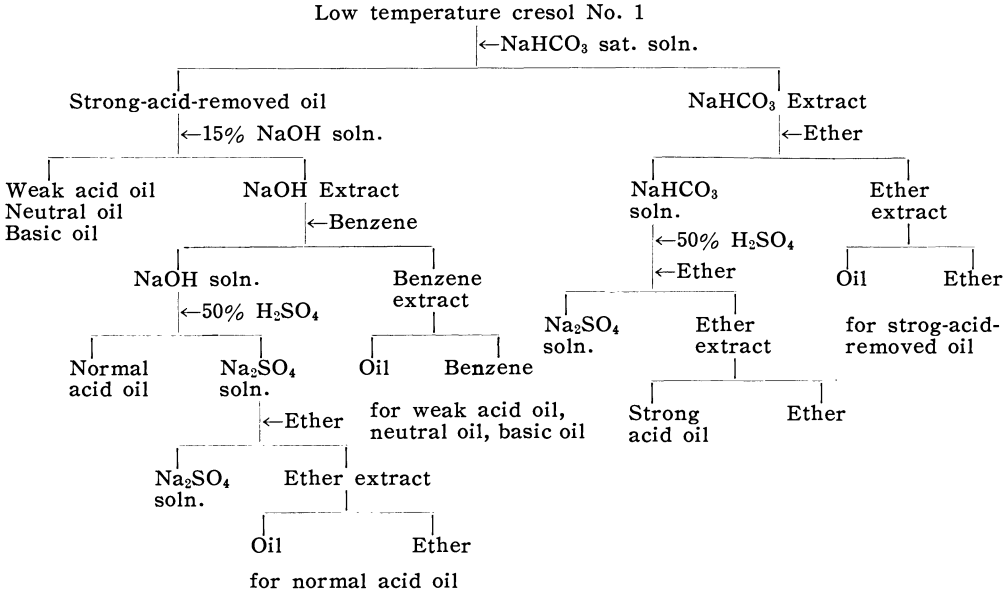

TABLE IV

SEPARATION OF WEAK ACID OIL, NEUTRAL OIL, BASIC OIL FROM BENZENE EXTRACT

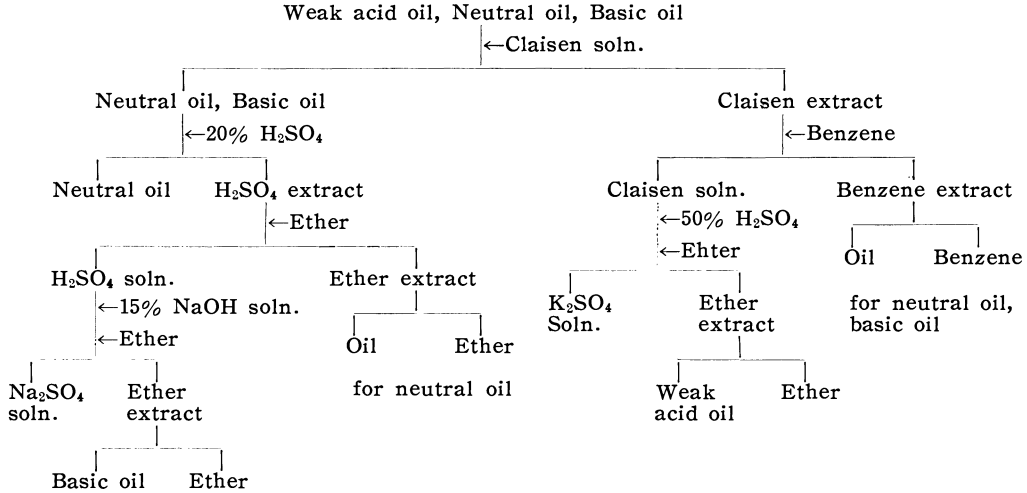

TABLE V

SULFUR CONTENT IN SEVERAL SAMPLES (wt. %)

Sample	(1) Low temperature cresol No. 1	(2) Lower boiling fraction	(3) Medium fraction	(4) Residue
Total S (A)	0.0427	0.0183	0.0160	0.0792
Hydrogen sulfide S	0.0003	0.0004	0.0001	0.0000
Elementary S	0.0070	0.0059	0.0054	0.0059
Mercaptan S	0.0061	0.0045	0.0036	0.0032
Disulfide S	0.0012	0.0010	0.0008	0.0010
Sulfide S	0.0004	0.0005	0.0004	0.0005
Thiophene S	0.0010	0.0005	0.0004	0.0010
Sum up (B)	0.0160	0.0128	0.0107	0.0116
Total S in Residue (A−B)	0.0267	0.0055	0.0053	0.0676
B/A	37.4	69.9	66.8	14.7

the Impurities.—*a*) *Strong Acid Oil.*—The distillation curve of the strong acid oil is similar to that of the low temperature cresol No. 1, but the former is contained chiefly in the lower boiling fraction of the low temperature cresol No. 1.[10] Strong acid oil has an offensive and stimulative smell like rancid butter.

Several acidic impurities such as propionic, *iso*-butyric, *n*-butyric, *iso*-valeric, *n*-valeric acids and catechol were detected in the strong acid oil by means of rectification, specific gravity, refractive index, neutralization value, bromine number, paper chromatography, melting point of the corresponding derivatives (amides), mixed-melting point test with the corresponding authentic samples, ultraviolet absorption spectra and infrared absorption spectra of each fraction[10].

The iodine number of the carboxylic acid fraction isolated by esterification, hydrolysis and extraction, was 110.2. On heating, the strong acid oil forms polymeric material; this fact suggests the presence of unsaturated acids.

b) *Weak Acid Oil.*—Weak acid oil in impurities was rectified, and the specific gravity, the refractive index, the boiling point, the average molecular weight and the hydroxyl value of each fraction were determined; furthermore qualitative test (ferric chloride test), melting-point test of the derivatives (phenoxy acetic acids) and mixed-melting point test with the corresponding authentic samples were also made. Upon these experiments, the presence of *p*-cresol, 2,4- and 2,5-dimethylphenols was noticed[11].

It seems that *p*-cresol, because of its small dissociation constant, intrudes into weak acid oil in the course of separation based on the said method. The rest of the components of the weak acid oil are supposed to be higher boiling phenols such as dimethylphenols, trimethylphenols, ethylphenols and methylethylphenols.

c) *Neutral Oil.*—The distillation curve of the neutral oil shows that fractions below 176°C, as well as fractions above 210°C and residue, occupy a considerable amount of the total distillate, and that medium fractions (176~210°C) take a much smaller part, though this temperature range corresponds to the main fraction of the low temperature cresol No. 1[11].

So it is possible to say that a considerable amount of unstable materials which polymerize easily by heating, is included in the neutral oil. The neutral oil was rectified and the specific gravity, the refractive index, the sulfur content, the absorption loss by sulfuric acid and the iodine number of each fraction were determined. There was a great deal of absorption loss by both 80 and 98% sulfuric acid; especially the lower boiling fractions were absorbed more by 80% sulfuric acid, and showed high iodine numbers[11,12].

Every fraction was distinctly positive to silver mirror test and Schiff's reagent test. Carbonyl compounds in the neutral oil were investigated, through melting-point check of the derivatives (2,4-dinitrophenylhydrazones or semicarbazones) and mixed-melting point test with the corresponding authentic samples. Thus *n*-propyl methyl ketone, mesityl oxide, *n*-amyl methyl ketone, *iso*-butyl methyl ketone, *o*-hydroxybenzaldehyde, benzaldehyde, 4-methylcyclohexanone and acetophenone were detected in the neutral oil[11,12].

By the same research tests, aromatic hydrocarbons in the neutral oil were identified as *p*-xylene (*O*-aroyl tetrachlorobenzoic acid), mesitylene (*O*-aroyl benzoic acid) and naphthalene[11] (picrate).

d) *Basic Oil.*—Forty nine volume per cent of the basic oil runs out below 150°C and 71% below 176°C in contrast to the case of the low temperature cresol No. 1 which gives a little distillate below 176°C[13].

Through several tests as described in the previous sections and of derivatives (mercuric chloride complexes and picrates), 2-, 3-, 4-methylpyridines, 2,3-, 2,4-, 2,5-, 2,6-, 3,4-dimethylpyridines, 4-ethylpyridine and 2,4,6-trimethylpyridine were identified in the basic oil[13].

e) *Sulfur Compounds.*—The low temperature cresol No. 1 contains 0.0427 weight % of sulfur. Concerning spontaneous coloration, each fraction of the low temperature cresol No. 1 and classified impurities were studied. On the other hand, sulfur content was measured in each sample. As a result it was found that the degree of coloration is nearly parallel to sulfur content[14]. Sulfur contents measured in conformity with their chemical forms are shown in Table V. Four samples were checked: (1) low temperature cresol No. 1, (2) its lower boiling fraction (15 volume %), (3) medium fraction (50%), (4) residue (33%) (water 1 %, loss 1%).

According to Table V, it is understood that all of them contain free sulfur and mercaptans as predominant constituents, alkyldisulfides as next, and a little of hydrogen sulfide, alkyl sulfides and thiophenes are also contained.

(3) Purification by Oxydation.—*a*) *Spontaneous Coloration of the Refined Cresol.*—As stated above, the coloration of the low temperature cresol No. 1 hardly ever occurs in the absence of oxygen, even if it is exposed to the sunlight. It absorbs a considerable amount of oxygen and the relation between coloration and absorbed oxygen is almost proportional. These facts led to the idea that the impurities which bring about spontaneous coloration by absorbing oxygen, are to be removed by the use of enough amount of oxidizing agent, followed by adsorption of the products on active clay.

As the oxidizing agent, potassium cyanoferrate or sodium bichromate was used. Adopting one of the oxidizing agents only, or active clay only, or both substances, purification by oxidation was carried out in several cases. The most preferable result was obtained when the low temperature cresol No. 1 was treated with 0.2% of potassium cyanoferrate together with 5% of

11) K. Yamada, ibid., **60**, 1314 (1957).
12) K. Yamada, ibid., **61**, 269 (1958).
13) K. Yamada, ibid., **60**, 1310 (1957).
14) K. Yamada, ibid., **60**, 925 (1957).

active clay, and, after filtration, the distillate of 176~210°C (90 volume % of yield) was collected[7]. The product was named "Refined Cresol".

Hourly change of color was examined on four samples. They are: (1) above-mentioned refined cresol, (2) 176~210°C distillate of the low temperature cresol No. 1, (3) medium 50% of the distillate (25~75 volume %) of the first class *m*-cresol (97 % of this was distilled at 201~202°C), (4) 176~210°C distillate of the normal acid oil which was prepared by removing strong acid oil, weak acid oil, neutral oil and basic oil from the low temperature cresol No. 1.

Using spectrophotometer, transmissions at wave lengths 420, 470, 520, 580, 620 and 700 mμ were measured, and by their mean value, the degree of coloration was represented. Fig. 2 shows the results obtained when the samples were placed by the window to be exposed to the sunlight and Fig. 3 shows that obtained when they were exposed to the ultraviolet rays.

As the refined cresol and the normal acid oil free from the impurities gave nearly equal results, the description of the latter was omitted.

Figs. 2 and 3 indicate that the coloration of the refined cresol advances very little. Therefore, most of the impurities which influence the spontaneous coloration of the low temperature cresol No. 1 seem to be eliminated by this operation.

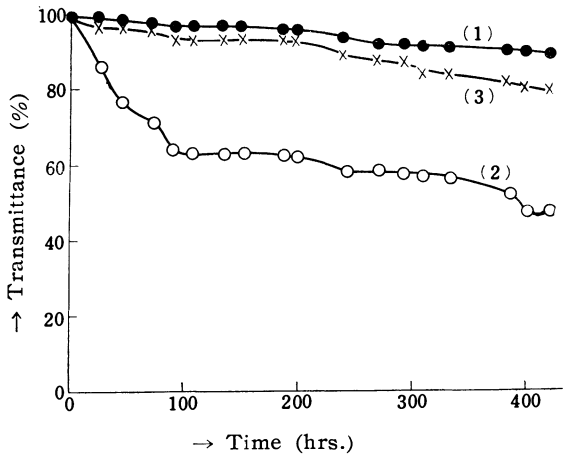

Fig. 2. Spontaneous coloration by the sunlight.
(1) ● Refined cresol
(2) ○ Low temperature cresol No. 1
(3) × *m*-cresol

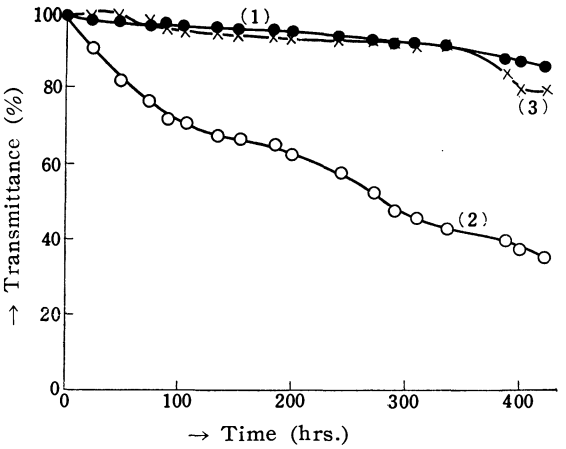

Fig. 3. Spontaneous coloration by the ultraviolet rays.
(1) ● Refined cresol
(2) ○ Low temperature cresol No. 1
(3) × *m*-cresol

TABLE VI
IMPURITIES IN THE REFINED CRESOL (vol. %)

	Low temperature cresol No. 1	Refined cresol
Strong acid oil	0.217	0.154
Normal acid oil	95.133	95.749
Weak acid oil	0.367	0.403
Neutral oil	0.733	0.411
Basic oil	0.033	0
Total impurities	1.350	0.968
Sum up	96.483	96.717
(Loss)	(3.517)	(3.283)

TABLE VII
SULFUR CONTENT IN THE REFINED CRESOL
(wt. %)

Sample	Low temperature cresol No. 1	Refined cresol
Total S (A)	0.0427	0.0151
Hydrogen sulfide S	0.0003	0.0001
Elementary S	0.0070	0.0042
Mercaptan S	0.0061	0.0026
Disulfide S	0.0012	0.0007
Sulfide S	0.0004	0.0002
Thiophene S	0.0010	0.0005
Sum up (B)	0.0160	0.0083
Total S in Residue (A−B)	0.0267	0.0068
B/A	37.4	55.0

b) Impurities in the Refined Cresol.—Impurities and sulfur compounds in the refined cresol are shown in Tables VI and VII.

Results and Discussion

(1) Formation of the Impurities.—As shown in Tables I and II, sodium salts of the strong acid oil are formed by adding 15% sodium hydroxide solution to the crude light oil and the middle oil. When carbon dioxide is introduced to the sodium salts, normal acid oil is separated as an oil layer, but owing to weak acidity of carbon dioxide the sodium salts of the strong acid oil remain in the same form in aqueous layer and are rejected together with the waste liquor of the sodium carbonate.

A small amount of sodium salts of the

strong acid oil still remaining is removed by washing with 10% sodium carbonate aqueous solution, but a portion of the sodium salts remains in the crude acid oil. These sodium salts change to the strong acid oil at the time of 73% sulfuric acid washing, and they form strong acidic impurities in the normal acid oil.

Weak acid oil is accompanied by the normal acid oil as it has the same chemical properties except for possessing slightly higher boiling point than that of the normal acid oil.

Neutral oil which comes through dissolution or mixing into the sodium salts of the acid oil, is removed at the steaming of the sodium salt, but their portion remains through dissolution and become neutral impurities in the normal acid oil.

A typical composition of the crude light oil shown in Table I is 47.5 volume % of acid oil, 2.0 of basic oil and 50.5 of neutral oil; of this neutral oil, 12.2 and 46.3 volume% are the parts absorbed by 80 and 98% sulfuric acid respectively, so that 41.5 volume% of the neutral oil is the unabsorbed part by 98% sulfuric acid. On the other hand the typical composition of the oil (distillate in Table I) which has been distilled off by the steaming of the sodium salts of acid oil is 42% of acid oil, 11 of basic oil and 47 of neutral oil; the absorption diminutions of this neutral oil by 80 and 98% sulfuric acid are 51.5 and 44.0 % respectively. Thus the portion unabsorbed by 98% sulfuric acid is only 4.5%.

Neutral oil in the low temperature cresol No. 1 is also absorbed largely by 80 and 98% sulfuric acid, and the unabsorbed is about 2%. Therefore the neutral oil which enters into the sodium salt of the acid oil through dissolution or mingling, is such a peculiar oil as to be absorbed in 80 and 98% sulfuric acid.

Basic oil forms particular compounds with acid oil[15], and a large amount of the former is removed by sulfuric acid washing, but through dissolution its portion remains, similar to the case of the neutral oil, in the sodium salts of acid oil, forming the impurities in the normal acid oil.

On this account, not only by the above mentioned manufacturing process but also by the improved process where the sodium salts of acid oil are washed with benzene, more or less impurities, including weak acid, strong acid and neutral and even basic oil, get inevitably mixed with the low temperature cresol No. 1.

(2) **Decrease of the Impurities by Refining.**—As shown in Table VI the impurities in the refined cresol have considerably decreased in contrast to those in the low temperature cresol No. 1. According to a qualitative test the presence of catechol is indicated in the strong acid oil of the low temperature cresol No. 1, but not in the refined cresol. The iodine number of the strong acid oil in the low temperature cresol No. 1 and that of the strong acid oil in the refined cresol is 180.8 and 73.9 respectively. Diminution of iodine number seems to indicate the decrease of unsaturated acids, the content of the weak acid oil having scarcely changed.

The presence of carbonyl compounds is shown by a qualitative test in the neutral oil of the low temperature cresol No. 1, but not in the refined cresol. The iodine number of the neutral oil in the low temperature cresol No. 1 and that of the neutral oil in the refined cresol are 59.2 and 24.2 respectively, and this diminution seems to indicate the decrease of unsaturated compounds.

As to the neutral oil of the low temperature cresol No. 1 and that of the refined cresol, the absorption diminutions by 80% sulfuric acid are 24.0 and 9.4 volume % respectively; by 98% sulfuric acid they are 73.5 and 86.0%, unabsorbed part being 2.5 and 4.6%.

As the yield of the refined cresol is 90%, the decrease of the neutral oil contained in 100 cc. of the low temperature cresol No. 1 by this refining process is calculated as follows: the absorption diminution 0.176 cc. by 80% sulfuric acid is decreased to 0.035 cc., the absorption diminution 0.539 cc. by 98% sulfuric acid is decreased to 0.318 cc., and unabsorbed oil 0.018 cc. is decreased to 0.017 cc..

Since carbonyl compounds are well absorbed by 80% sulfuric acid and easily react with iodine, it may be said that carbonyl impurities are especially cut down by this refining process. Almost all basic oil is removed by this process. As shown in Table VII, the content of sulfur compounds decreases considerably by this purification.

Summary

Low temperature cresol No. 1 has an offensive smell, and its spontaneous

15) Y. Ohshima and K. Ishibashi, ibid., **29**, 445 (1925).

coloration is remarkable. It was treated with an oxidizing agent and active clay for the purpose of refining, and then washed with sodium bicarbonate solution in order to remove carboxylic acids which give a strong peculiar smell. Refined cresol which has no more offensive smell and shows a little spontaneous coloration, was obtained.

The impurities in the low temperature cresol No. 1 and in the refined cresol were measured, and it was found that in the refined cresol every impurity was decreased; especially unsaturated carboxylic acids, carbonyl compounds and basic oil were diminished. In the strong acid oil were detected, propionic, *iso*-butyric, *n*-butyric, *iso*-valeric, *n*-valeric acids and catechol, in the weak acid oil, *p*-cresol, 2, 4- and 2, 5-dimethylphenols, in the neutral oil, *n*-propyl methyl ketone, mesityl oxide, *n*-amyl methyl ketone, *iso*-butyl methyl ketone, *o*-hydroxybenzaldehyde, benzaldehyde, 4-methylcyclohexanone, acetophenone, *p*-xylene, mesitylene and naphthalene and in the basic oil, 2-, 3-, 4-methylpyridines, 2,3-, 2,4-, 2,5-, 2,6-, 3,4-dimethylpyridines, 4-ethylpyridine and 2,4,6--trimethylpyridine, respectively.

Sulfur compounds were measured in accordance with chemical forms, and it was found that free sulfur and mercaptans are contained as the predominant components, and alkyl disulfides as the next; a little hydrogen sulfide, alkyl sulfides and thiophenes are also present.

Coal tar contains many components, and two hundred and eighty-two[16], or three hundred and ninety-four components[17] have already been reported in the literature of the subject.

But *n*-propyl methyl ketone, mesityl oxide, *n*-amyl methyl ketone, *iso*-butyl methyl ketone, *o*-hydroxybenzaldehyde, benzaldehyde and 4-methylcyclohexanone, that have been identified in this study, are not found in literature. Among those substances listed above, many have strong peculiar smell, and exhibit spontaneous coloration.

The refined cresol, which was treated with the oxidizing agent, active clay and sodium bicarbonate solution, scarcely has any offensive smell and exhibits only a slight spontaneous coloration. Measurement of the impurities in the refined cresol shows that almost all the above mentioned substances have been removed. Thus it is concluded that an offensive smell and spontaneous coloration of the low temperature cresol No. 1 arise, at least partially, from these substances.

The author wishes to express his sincerest gratitude to Dr. K. Ohyama of Ube Industries, Ltd., Dr. B. Masumoto and Dr. T. Matsuura of Hiroshima University for their kind and constant guidance in the course of this work and also to Mr. M. Kishida, Mr. S. Nagai, Mr. S. Mori, Mr. Y. Kawaguchi and others of Ube Industries, Ltd. for their kind assistance.

Central Research Laboratory
Ube Industries, Ltd.
Ube, Yamaguchi

16) O. Krubber, A. Raeithel and G. Grigoleit, *Erdöl und Kohle*, **8**, 637 (1955).

17) The Coal Data Book (Loose-Leaf), Section A-4 "List of compounds identified in and isolated from coal tar", The Coal Tar Research Association, Oxford Road, Gomersal, Nr. Leeds. (1956).

On the Cooking Mechanism of Wood. XVII. Further Investigations on the Conductometric Titrations of Lignin Models with Phenolic Hydroxyl Groups and a Brief Theory of the Conductometric Titration of Phenols

By Hiroshi MIKAWA and Koichiro SATO

(Received March 4, 1958)

Conductometrically Untitratable *o*-Substituted Phenolic Hydroxyl Group.— In part XIII of this series[1], it was reported that although simple guaiacol-type phenolic hydroxyl group (I) was conductometrically titratable, having a very clear "break" (the neutralization point), non-guaiacyl phenolic hydroxyl group of the model sulfonic acid (III) was conductometrically untitratable. Assuming in general that the phenolic hydroxyl groups belonging to type-II are conductometrically untitratable, a method of the separate estimation of both type-I and -II phenolic hydroxyl groups of lignosulfonic acid was wroked out with the aid of the ultraviolet absorption spectra taken simultaneously with the conductometric titration. It seems, therefore, to be quite important to make further confirmation of the non-titratability of such phenolic hydroxyl group, with other model compounds.

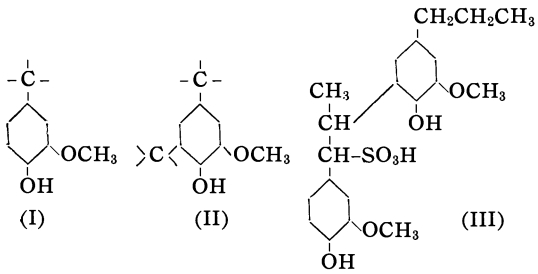

(I) (II) (III)

Four model compounds IV-VII, all containing type-II phenolic hydroxyl groups, were therefore conductometrically titrated and it was confirmed that such phenolic hydroxyl groups were not conductometrically titratable.

As shown in Figs.1—3, conductometrically titratable groups of the model compound IV are its carboxyl group and one of its two phenolic hydroxyl groups, one phenolic hydroxyl, possibly that of type II, remaining untitrated.

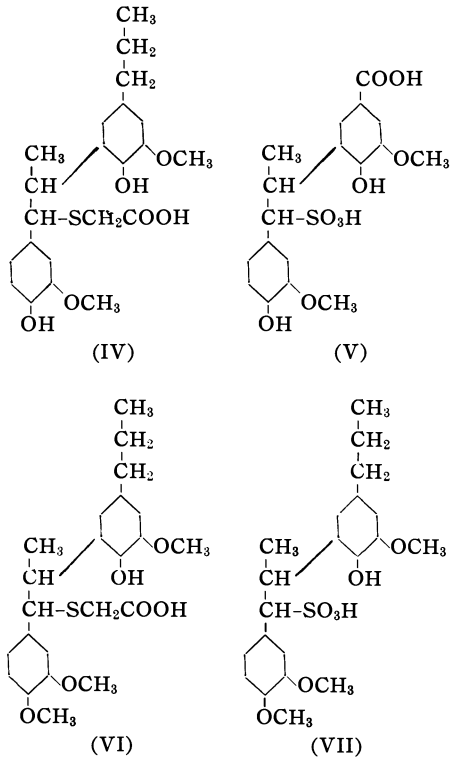

(IV) (V) (VI) (VII)

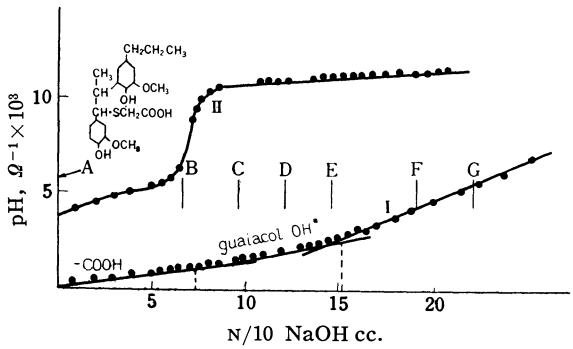

Fig. 1. Conductometric(I) and potentiometric(II) titrations of the model compound IV.

1) H. Mikawa, K. Sato, C. Takasaki and K. Ebisawa, This Bulletin **29**, 245 (1956).

Fig. 4 shows that the titratable groups of the model compound V are as expected the sulfonic acid group, the carboxyl group and only one of its two phenolic hydroxyl groups, the ratio of the strongly acidic part and the weakly acidic part of the titration curve being 1 : 2. No perceptible "break" existed in the weakly

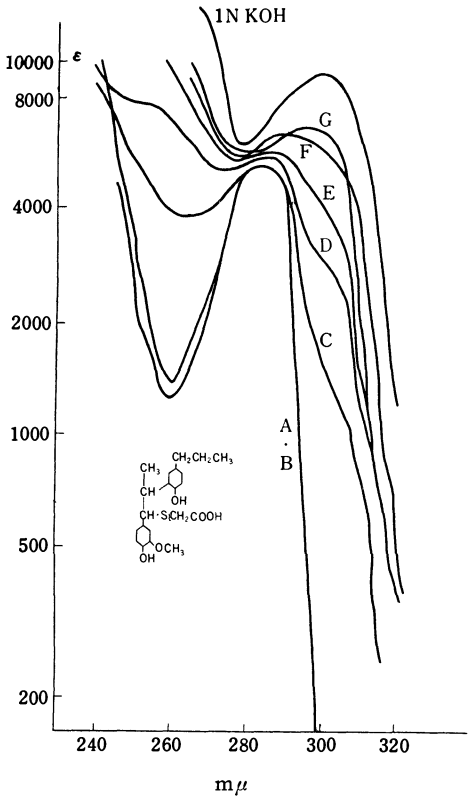

Fig. 2. Change of the UV-absorption spectrum observed during the titration of the compound IV.

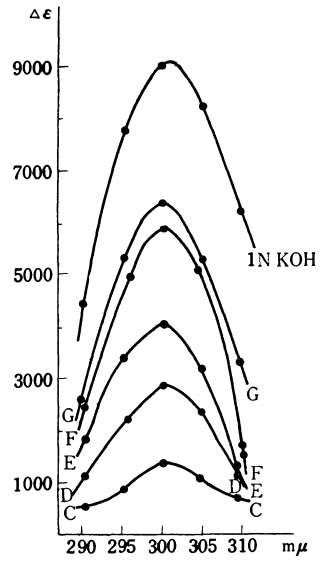

Fig. 3. $\Delta\varepsilon$-curves obtained at point C—G of the conductmetric titration curve of the compound IV shown in Figs. 1 and 2.

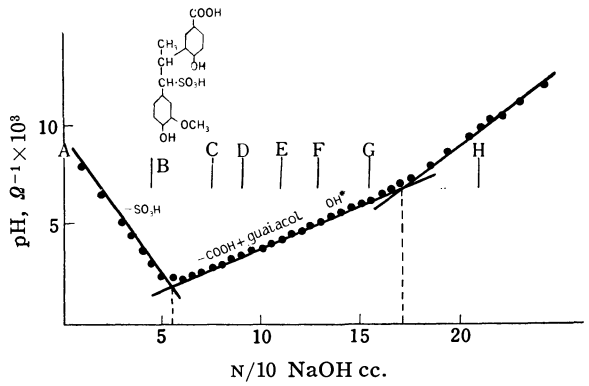

Fig. 4. Conductmetric titration curve of model compound V.

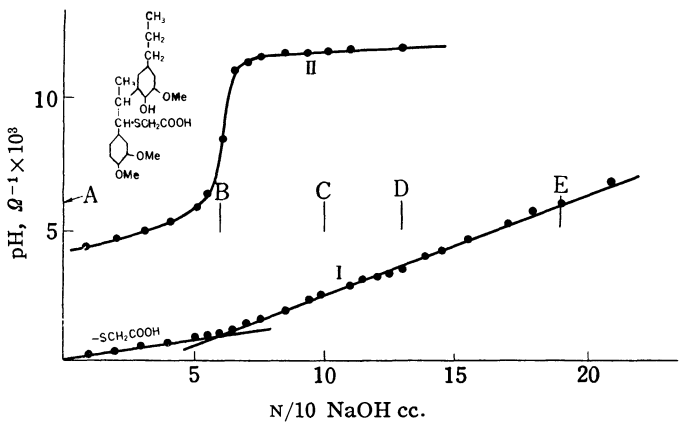

Fig. 5. Conductmetric(I) and potentiometric(II) titrations of the model compound VI.

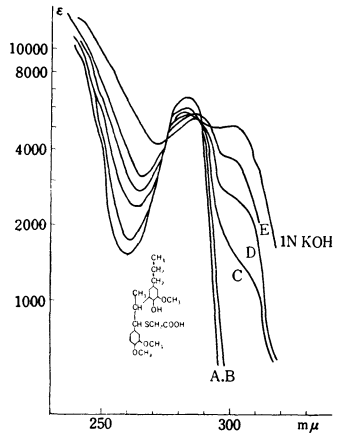

Fig. 6. Change of the UV-absorption spectrum observed during the titration of the compound VI.

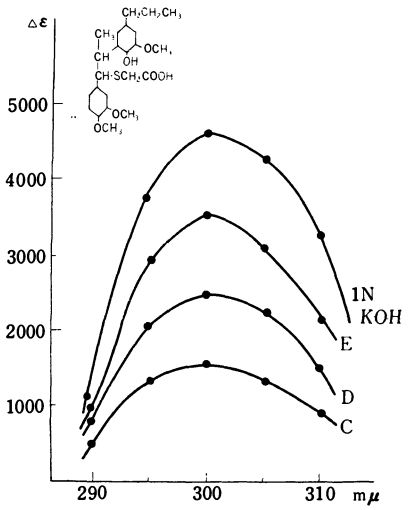

Fig. 7. $\Delta\varepsilon$-curves obtained at point C~E of the conductometric titration curve of the compound VI shown in Figs. 5 and 6.

acidic part just as in the case of lignosulfonic acid. Thus, the separation of carboxyl group and the conductometrically-titratable phenolic hydroxyl group seems to be impossible even in the case of the model compound.

Model compound VI demonstrates, as shown in Figs. 5—7, most clearly that type-II phenolic hydroxyl group is not conductometrically titratable. The titratable group is only its carboxyl group in this case, type-II phenolic hydroxyl of this compound having no effect on the titration curve.

The same is true again in the case of the model compound VII, as shown in Figs. 8—9. Type-II phenolic hydroxyl of this

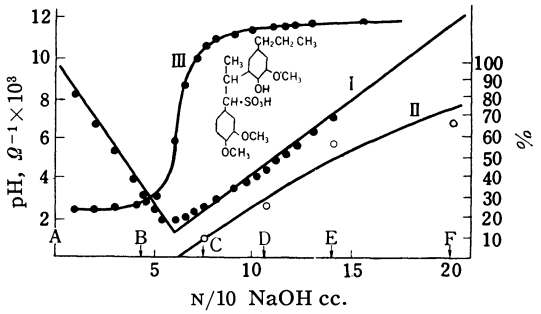

Fig. 8. Conductometric(I) and potentiometric(III) titrations of the model compound VII and the percentage of the phenolic hydroxyl group ionized during the titration (II).

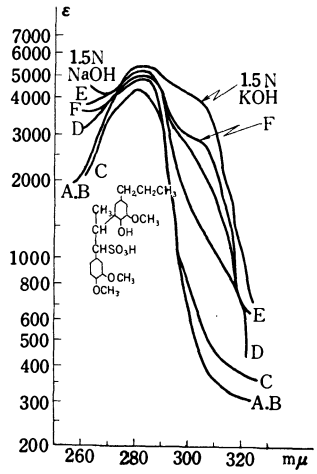

Fig. 9. Change of the UV-absorption curve observed during the titration of the compound VII shown in Fig. 8.

compound was not titrated.

From the above findings it will now safely be concluded that type-II phenolic hydroxyl group of at least III-VII type may be in general definitely conductometrically untitratable. A method of the separate estimation of both type I and type II phenolic hydroxyl groups, worked out in the previous communication, may therefore be valid in general.

Conductometric Titration of *o, o'*-Diphenol-Type Phenolic Hydroxyl Groups.—We have now considerable accumulation of the facts supporting the existence of *o, o'*-diphenol type phenolic hydroxyl groups in lignin. Among others according to the recent view of the biosynthesis of lignin, the formation of such *o, o'*-diphenol type linkage is expected during the dehydrogenative condensation of coniferyl alcohol or other monomeric

phenolic lignin precursors[2], as the phenols, without double bond conjugated with benzene nucleus in its para position, dimerize easily resulting in the formation of *o*, *o'*-diphenol structure by dehydrogenation[3]. The results of the nitrobenzene oxidation of lignin and lignin-model compounds support also the existence of such structure in lignin, as degradation products having such *o*, *o'*-diphenol-type linkage are obtained only from lignin but not from model compounds with simple guaiacol type nucleus[4,5].

Three water-soluble model compounds VIII—X were prepared and titrated conductometrically and the results are summarized in Fig. 10.

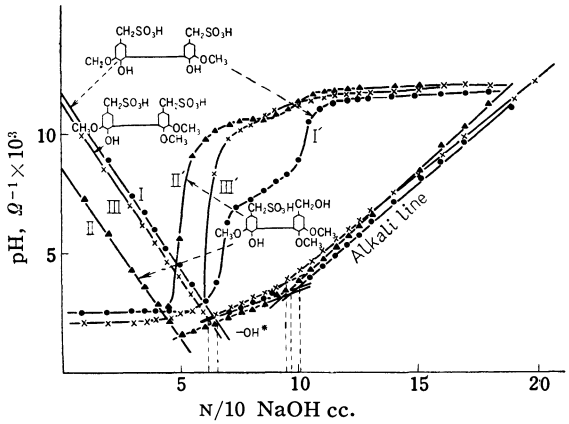

Fig. 10. Conductometric and potentiometric titrations of the model compounds VIII—X.

Only one of the two phenolic hydroxyl groups of the compound VIII was found to be titratable as shown by curves I and I' of the same figure. Phenolic hydroxyl groups of the compounds IX and X were conductometrically titratable (cf. curves II, II'; III and III'). That the phenolic hydroxyl group of the compound XI was conductometrically titratable by back titration in aqueous alcohol solution, as it was already reported in part XIII of this series[1].

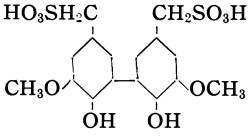

(VIII)

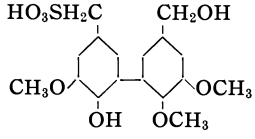

(IX)

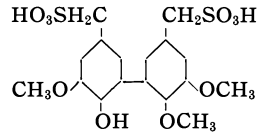

(X)

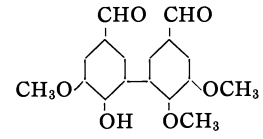

(XI)

According to G. Aulin-Erdtman one of the phenolic hydroxyl groups, which belong to *o*, *o'*-diphenol is very strongs, on the other hand, the remaining one is extremely weak[6]. It has been assumed that, owing to the formation of hydrogen bonding between two hydroxyl groups, a proton belonging to any one of these two hydroxyl groups acquires very strong tendency for ionization, although the remaining one is held firmly by net negative charge left after the ionization of one phenolic hydroxyl group, resulting in weakening of the acidity of this second hydroxyl group. As the phenolic hydroxyl groups of monomethyl ethers IX—XI are conductometrically titratable, there seems to exist no strong hydrogen bonding between phenolic hydroxyl group and methoxyl group in these structures.

We shall now be able to summarize the limitations of our method of the separate estimation of type-I and II phenolic hydroxyl groups as follows. If lignosulfonic acid contains *o*, *o'*-diphenol type structure or its monoether structure like those of VIII—XI, (i) one phenolic hydroxyl group may be estimated per such structure as conductometrically titratable type-I hydroxyl group; (ii) one very weak phenolic hydroxyl group of *o*, *o'*-diphenol structure will be missed completely in so far as the total amount of phenolic hydroxyl groups is estimated spectroscopically. The type-I phenolic hydroxyl group estimated by our method may, therefore, contain half of the phenolic hydroxyl groups belonging to *o*, *o'*-diphenol structure and that belonging to *o*, *o'*-diphenol monoether structure if any.

Brief Theory of the Conductometric Titration of Very Weak Phenols.—As stated above, the behavior of type-I and II phenolic hydroxyl groups in conductometric titration is very different, the former being titratable while the latter is completely untitratable. As it is easily expected that the difference between the two types of phenols is due to the difference of dissociation constants of both types of phenolic hydroxyl groups, it

2) K. Freudenberg and Hubner, *Chem. Ber.*, **85**, 1181 (1952).
K. Freudenberg and H. Dietrich, ibid, **86**, 4 (1953).
K. Freudenberg and W. Fuche, ibid., **87**, 1824(1954).
3) H. Erdtman, *Biochem. Z.*, **258**, 172 (1933).
4) I. A. Pearl, *J. Am. Chem. Soc.*, **72**, 2309 (1950).
5) J. C. Pew, ibid., **77**, 2831 (1955).
6) G. Aulin-Erdtman, *Svensk Papperstid.*, **57**, 745 (1954).

must be interesting to make a brief theoretical discussion on the conductometric titration of phenols having different dissociation constants.

Assume that a strong base BOH is added to a solution of a weak acid (phenol) HA of concentration [S] and the total volume of the solution remains constant. Applying the mass law to the dissociation of the acid:

$$[H^+] = K_a[HA]/[A^-] \quad (1)$$

where K_a is the dissociation constant of the acid HA. From the principle of electroneutrality of the solution it follows that:

$$[A^-] + [OH^-] = [B^+] + [H^+] \quad (2)$$

Since the total amount of the acid HA used is [S]:

$$[HA] = [S] - [A^-] \quad (3)$$

Substituting 2 and 3 into 1 to eliminate both $[A^-]$ and [HA], one finds that:

$$[H^+] = K_a \frac{1 - [\alpha_t + ([H^+] - [OH^-])/[S]]}{\alpha_t + ([H^+] - [OH^-])/[S]} \quad (4)$$

where $\alpha_t = [B^+]/[S]$ represents the ratio of the amount of the added base BOH to the total amount of the acid. Since the pH of the solution is in alkaline side throughout the titration, the hydrogen ion concentration is negligibly small in comparison to that of hydroxyl ion:

$$[H^+] \ll [OH^-]$$

Hence from equation 4 it follows that:

$$[H^+] = K_a\left[1 - \alpha_t + \frac{[OH^-]}{[S]}\right]\Big/\left[\alpha_t - \frac{[OH^-]}{[S]}\right] \quad (5)$$

Eliminating $[H^+]$ by using ion-product of water $K_w = [H^+][OH^-]$, $[OH^-]$ can be calculated:

$$[OH^-] = -\frac{1}{2}\left[\left([S] - [S]\alpha_t - \frac{K_w}{K_a}\right) + \sqrt{\left([S] - [S]\alpha_t - \frac{K_w}{K_a}\right)^2 - 4\frac{K_w}{K_a}[S]\alpha_t}\right]$$

This equation gives the concentration of hydroxide ion $[OH^-]$ of the solution of weak acid HA of concentration [S] when titrated with strong base BOH until α_t of the equivalent point. When the concentration [S] is assumed to be 0.01 normal, the concentration of the hydroxide ion increases during the titration for phenols having different pK values 9 to 12, as shown in Fig. 11.

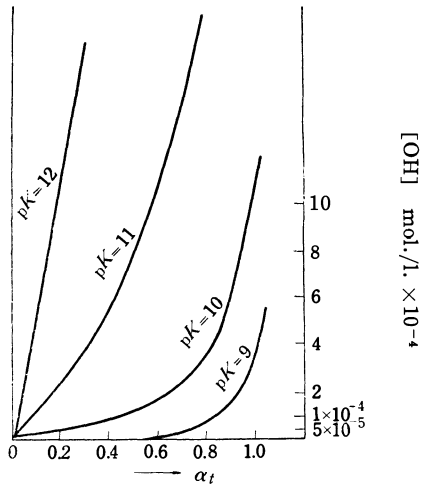

Fig. 11. The increase of the concentration of the hydroxide ion during the titration of phenols having various pK values.

Next, the specific conductivity of this solution is the summation of the products of the mobilities and one thousandth of the concentrations of the ions, as the concentration is expressed by mol./liter, that is

$$\kappa \cdot 10^3 = L_{H^+}[H^+] + L_{OH^-}[OH^-] + L_{A^-}[A^-] + L_{B^+}[B^+] \quad (6)$$

where L_{H^+}, L_{OH^-}.....are the mobilities of the ions. As L_{H^+} and L_{OH^-} are of the same order of magnitude and $[H^+] \ll [OH^-]$, $L_{H^+}[H^+]$ is negligible when compared to $L_{OH^-}[OH^-]$. Although of course $[A^-]$ and $[B^+]$ are not equal because of the hydrolysis, for simplicity we may be able to assume $[A^-] \fallingdotseq [B^+]$, as the value of L_{A^-} is, as expected, not very large. Then

$$\kappa \cdot 10^3 = L_{OH^-}[OH^-] + (L_{A^-} + L_{B^+})0.01\alpha_t$$

Here, $L_{OH^-} = 174$ and $L_{Na^+} = 43$. The value of L_{A^-} is of course not known but as the mobility of large organic anion is not expected to be so large as that of, for example, sodium ion, L_{A^-} is assumed for simplicity to be 10 in the above equation. Then,

$$\kappa \cdot 10^3 \fallingdotseq 174[OH^-] + 0.53\alpha_t \quad (7)$$

This equation 7 represents the conductometric titration curve. It is clearly shown that because of hydrolysis the measured conductivity lies higher by $174[OH^-]$ over the salt line $0.53\alpha_t$. Relations between κ and α_t calculated for various pK phenols having different pK values are shown in Fig. 12.

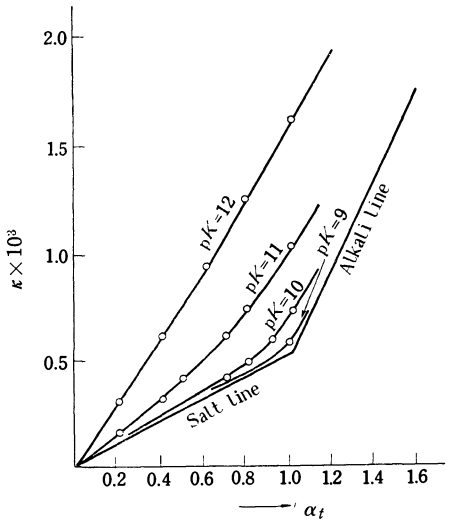

Fig. 12. Theoretically obtained conductometric titration curves of phenols having various pK values.

It is clearly demonstrated in this figure that one can calculate the equivalent point in so far as the pK values of the acids are smaller than 10, it being however quite impossible to find out the equivalent point when pK values are larger than 10. The difference of only about one unit in the pK values near pK 9~11 definitely decide whether the phenol in question is conductometrically titratable or not. As the calculated titration curve for pK 12 is nearly linear, it is expected that the pK value of phenolic hydroxyl group of type II may be 12 or larger.

Experimental

Model Compounds IV, V and VI.—Compounds IV and VI were synthesized as reported previously[7]. Compound V was prepared according to Richtzenhain[8]. The sulfonic acid was separated as its benzylthiuronium salt was not crystallizable.

Anal. Found: C, 54.14; H, 5.58. Calcd. for $C_{26}H_{30}O_9N_2S_2$: C, 54.08; H, 5.58%.

Synthesis of α-(3, 4-Dimethoxyphenyl)-β-(2-hydroxy-3-methoxy-5-propylphenyl)-*n*-propanesulfonic Acid (VII).—Dihydrodehydro-di-isoeugenol methyl ether (5 g.) was dissolved in 500 ml. of cooking acid (to 25 g. of sodium hydroxide in one liter of 50% alcohol was added 30 g. of sulfur dioxide after having been neutralized to pH 6 with sulfur dioxide) and heated in a vigorously rotating stainless autoclave for 20 hours at 135°C with a little amount of copper powder. After filtration, excessive sulfur dioxide was expelled in vacuo, sulfuric acid added, sulfur dioxide expelled and the solution was set aside over-night in order to decompose thiosulfate if any, after having adjusted the concentration of excess sulfuric acid to one normal. Sodium was removed by ion exchange, and the solution was concentrated, neutralized with barium carbonate, filtered, concentrated to dryness and extracted with water. A concentrated solution of benzylthiuronium hydrochloride was added to the extract thus obtained and the viscous precipitate of benzylthiuronium salt was washed with water, dissolved in a little amount of alcohol and reprecipitated with water. After having been purified twice by reprecipitation, the precipitate was rubbed with ice water. The powder thus obtained was not crystallizable.

Anal. Found: C, 58.98; H, 6.51; N, 5.11. Calcd. for $C_{29}H_{38}O_7N_2S_2$: C, 58.9; H, 6.49; N, 4.75%.

As the material was not obtained as crystals, the analytical values obtained did not agree well with the calculated values. Conductometrically the sulfonic acid group amounted to 92.5% of the theoretical amount. Without further purification the material was used for our purpose.

Synthesis of Dehydro-divanillyl Sulfonic Acid (VIII).—Although this compound is already known[9], no details are published as yet. Dehydro-divanillin was synthesized according to Elbs and Lerch[10]. It was found that dehydro-divanillin was very easily purified via its mono sodium salt. The crude product was dissolved in hot sodium hydroxide solution, which, upon cooling, separates beautiful crystals of mono sodium salt, which was recrystallized from aqueous alcohol.

Anal. Found: C, 59.21; H, 4.54; Na, 6.83. Calcd. for $C_{16}H_{13}O_6Na$: C, 59.3; H, 4.08; Na, 7.10%.

Dehydro-divanillin was dissolved in the least amount of dilute alkali, reduced with an exess of sodium borohydride until free from aldehyde color-reaction, acidified with carbon dioxide and the separated crystalline dehydro-divanillyl alcohol was filtered, m. p. 190°C.

Anal. Found: C, 62.51; H, 6.06; OCH_3, 20.32. Calcd. for $C_{16}H_{18}O_6$: C, 62.8; H, 5.89; OCH_3, 20.26%.

Dehydro-divanillyl alcohol thus obtained (2 g.) was shaken at 100°C for two hours in a sodium-base sulfite cooking acid of pH 1.8 (100 ml.). Dehydro-divanillyl sulfonic acid was separated as barium salt just as in the case of vanillyl sulfonic acid.

Anal. Found: C, 31.54; H, 3.58; S, 10.5; Ba, 22.42; OCH_3, 10.69. Calcd. for $C_{16}H_{16}O_{10}S_2Ba$: C, 33.7; H, 2.81; S, 11.2; Ba, 24.1; OCH_3, 10.69%.

Synthesis of Dehydro-divanillyl Alcohol Monomethyl Ether. Monosulfonic Acid (IX) and Disulfonic Acid (X) of the Monoether.—Dehydro-divanillin monomethyl ether[11]

7) H. Mikawa et al., This Bulletin, **29**, 245 (1956).
8) Richtzenhain and Alfredsson, *Acta Chem. Scand.*, **8**, 1519 (1954).
9) E. Adler and S. Hernestam, ibid., **9**, 319 (1955).
10) K. Hlbs and H. Lerch, *J. prakt. Chem.*, **93**, 1 (1916).

was dissolved in a calculated amount of sodium hydroxide, reduced with excessive sodium boron-hydride over-night until free from aldehyde color-reaction, neutralized with diluted hydrochloric acid and extracted exhaustively with chloroform. The oily product thus obtained in nearly theoretical yield was not crystallizable.

The oily dehydro-divanillyl alcohol monomethyl ether obtained was sulfonated at pH 1.9 for four hours at 100°C by sodium-base sulfite cooking acid. The crystalline barium salt separated as usual was not analyzed, however the strong acidic group amounting to 112% of the sulfonic acid group calculated from the formula IX was conductometrically titrated. This crystalline barium salt may, therefore, be contaminated a little by disulfonic acid X.

In order to prepare disulfonic acid X dehydro-divanillyl monomethyl ether was sulfonated at 135°C for five hours with the same cooking acid as above. As usual the disulfonic acid was isolated as barium salt. Conductometric titration of the acid revealed the existence of a strong acidic group amounting to 98.8% of the calculated amount.

Summary

1. Conductometric titrations of the model compounds IV, V, VI and VII provided reconfirmation of the previously reported[1] findings that simple guaiacol-type phenolic hydroxyl group I was conductometrically titratable, while non-guaiacyl phenolic hydroxyl group belonging to type II was conductometrically untitratable.

2. It was thus further confirmed, that the separate estimation of both type-I and -II phenolic hydroxyl groups of lignosulfonic acid by the method of conductometric titration is possible in combination with the ultraviolet absorption spectra taken simultaneously with the conductometric titration without any dilution of the solution.

3. As we have now considerable accumulation of facts supporting the existence of *o*, *o'*-diphenol type phenolic hydroxyl group in lignin, three water-soluble model compounds VIII, IX and X were titrated conductometrically. Phenolic hydroxyl groups of IX and X were found to be conductometrically titratable. Of the two phenolic hydroxyl groups of the model compound VIII only one was found to be titratable.

4. A brief theoretical consideration of the conductometric titration of extremely weak acid (phenol) having pK values larger than 9 were made. As is evident from Fig. 12, which shows theoretical conductometric titration curves of phenols having pK values 9~12, one can calculate the equivalence-point in so far as the pK values of the phenols are smaller than 10; it is, however, impossible to find the equivalence-point when pK values are larger than 10. As the calculated titration curve for pK 12 is nearly linear, it is expected that the pK value of phenolic hydroxyl group of type II is 12 or larger.

The authors wish to express their gratitude to Dr. H. Okada, the head of the laboratory, and Miss S. Suehiro for their encouragement.

Research Laboratory of the Kokusaku Pulp Ind. Co., Ltd.
Kamiochiai, Shinjuku-ku, Tokyo

Capture of Radioactive Cesium onto a Phosphomolybdate Precipitate Layer and its Determination

By Tadashi HARA

(Received January 28, 1958)

The object of this research was to find a simple, rapid and accurate method for the determination of radioactive cesium in solutions which are extremely dilute or contain various substances. In the conventional method[1] for the determination of radioactive cesium, the coprecipitation method using a suitable carrier has been mainly adopted. However, that method is incomplete and unsuitable for such sample solutions as mentioned above.

Therefore, a new method is here presented which is based on filtering a sample solution through a precipitate layer of thallium phosphomolybdate and directly measuring the radioactivity of the precipitate on the layer after washing and drying. In this method, the coexistence of various substances scarcely ever interferes with the determination of radioactive cesium and moreover the cesium, even in 2 liters of a solution, is almost completely recovered.

Experimental

Apparatus and Chemicals. — The Shimadzu D-55 type GM-counter, a specially designed glass-filter and a holder as indicated in Fig. 1 were used for the measurement of the radioactivity. Phosphomolybdic acid was prepared by Brauer's method[2] and a 2% solution in 2% nitric acid was used. The thallium solution which contained 1 mg. thallium per 1 ml. of 2% nitric acid was prepared by dissolving metallic thallium in nitric acid. Sodium cobaltinitrite reagent was prepared by Ishibashi's method[3]. Processed cesium-137, thallium-204 and strontium-90 were obtained and diluted to about 1 μC/ml.

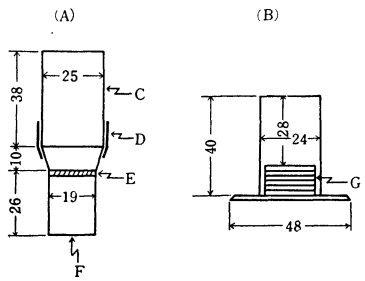

Fig. 1. Glass-filter and holder (unit; mm.)
(A) Glass-filter, separable to C and F
(B) Holder
C; Glass-cylinder
D; Gum
E; Filter-plate
F; Glass-filter, used for the measurement of radioactivity
G; Metallic-plates

Procedure.—Fifty ml. of thallium solution, 4 ml. of concentrated nitric acid and 126 ml. of water were placed in a 300 ml. beaker. Then, 20 ml. of phosphomolybdic acid was added to it. After being concentrated to about 7 ml., the contents were transferred into a glass-filter as shown in Fig. 1, filtered and washed with 2% nitric acid. The washing was continued until only a small amount of washing solution remained on the precipitate layer. Then, the sample solution which was a 2% nitric acid solution containing radioactive cesium was filtered through the previous glass-filter at the rate of 2 drops every 3 seconds or more. At the end of the filteration, the precipitate layer was washed with 2% nitric acid followed by concentrated acetic acid and dried at 120°C for about an hour. Finally, the activity on the precipitate layer was measured by using a holder as shown in Fig. 1 and GM-counter.

Results and Discussion

Reproducibility.—The results obtained

TABLE I
REPRODUCIBILITY OF MEASUREMENTS

No. of sample	Counts per min.
1	3017
2	3032
3	2928
4	2975
5	3071
6	3033
7	2957
Mean value	=3002
Max. error	=+2.5%

1) For example, B. Kahn, D. K. Smith and C. P. Straub, *Anal. Chem.*, **29**, 1210 (1957).

2) G. Brauer, "Handbuch der Präparativen Anorganishen Chemie", Ferdinand Enke Verlag, Stuttgart (1954), p. 1278.

3) M. Ishibashi, "Qualitative Analysis", Shōkabō, Tōkyo (1947), p. 25.

with regard to seven samples are shown in Table I. The values for each sample correlate within an error of ±2.5%. Therefore it is believed that the present method can be used adequately for the quantitative determination of radioactive cesium.

Proportionality. — Portions of 0.2, 0.5, 0.8, 1.1, 1.4, 1.7, 2.0 and 2.5 ml. of each radioactive cesium solution were diluted to a 100 ml. of 2% nitric acid solution with nitric acid and water. The results obtained with these samples are indicated in Fig. 2. It is clear that a linear relationship holds between the amount of radioactive cesium in a sample solution and the strength of the activity on the precipitate layer, and the maximum error involved is 8.3% when this calibration curve is used.

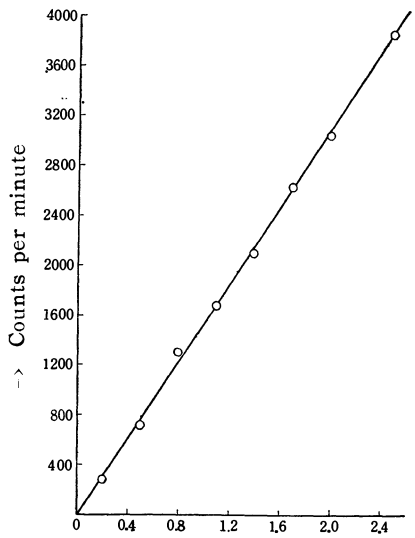

Fig. 2. Calibration curve

Volume of Sample Solution.—Portions of 25, 50, 100, 400, 600, 1000 and 2000 ml. of each sample solution were used in a 2% nitric acid solution which contained about 1 μC of cesium. The results in Table II indicate that the recovery of radioactive cesium is almost complete. Therefore, all the sample solutions in the following experiments will be diluted to 100 ml.

TABLE II
VOLUME OF SAMPLE SOLUTIONS

Volume (ml.)	Counts per min.
25	2974
50	3051
100	2962
400	2985
600	2958
1000	2974
2000	2992

Amount of the Precipitate.—Table III shows the relationship between the amount of the precipitate and the activity of the precipitate for the case where a definite amount of radioactive cesium is used. It is seen from the table that the activity gradually increases in accordance with an increasing amount of the precipitate. Therefore, the amount of the precipitate had better be as definite as possible for accurate measurements.

TABLE III
AMOUNTS OF THE PRECIPITATE

Tl soln. (ml.)	Wt. of ppt. (mg.)	Counts per min.
2	13.6	2548
5	25.8	2669
10	39.5	2712
20	69.1	2762
30	90.5	2849
50	156.7	2986
75	204.3	3113
100	275.0	3123

Concentration of Nitric Acid. — The relationship between the concentration of nitric acid in the sample solution and the activity of the precipitate is shown in Table 4. The data indicate that the activity slowly increases with an increase in the concentration of the nitric acid. However for convenience and economy, in view of the small difference all sample solution were prepared as 2% nitric acid solution.

TABLE IV
CONCENTRATION OF NITRIC ACID IN SAMPLE SOLUTIONS

Concn. of HNO_3 (%)	Counts per min.
0.0	2917
0.5	2957
1.0	2945
2.0	2967
4.0	3013
8.0	3068
16.0	3113

Rate of Filtration. — The relationship between the rate of filtration and the activity of the precipitate is shown in Table V. The results indicate that radioactive cesium is completely captured on

the precipitate, when 100 ml. of sample solution is passed as uniformly as possible through the precipitate layer for more than 27 minutes.

TABLE V
VELOCITY OF FILTRATION

Time (min.)	Counts per min.
8	2812
18	2937
27	2997
60	3013
120	3058

Capturing Capacity of Cesium on the Precipitate.—This experiment was made to determine what amount of cesium is captured on a definite amount of the precipitate. The results obtained are shown in Table VI and indicate that an amount of cesium chloride less than 500 μg. is almost completely captured on about 156 mg. of thallium phosphomolybdate.

TABLE VI
CAPTURING CAPACITY OF CESIUM ON THE PRECIPITATE

CsCl taken g.	Activity (cpm)		Wt. of ppt. mg.
	Ppt.	Filt.	
5	3017	0	—
10	2997	0	—
25	3091	0	—
50	3021	0	—
100	3059	0	—
200	2978	0	—
500	3085	0	—
1000	2856	0	157.3
2000	2514	11	157.5
5000	1710	368	156.3
10000	1068	1228	155.4

The radioactive cesium in the filtrate was determined by the cobaltinitrite method using potassium as a carrier. The results obtained in the preliminary experiment are shown in Table VII.

TABLE VII
PRELIMINARY EXPERIMENT BY COBALTINITRITE METHOD

Cesium-137 soln.	K_2SO_4 taken	Counts per min.
0.5 ml.	20 mg.	608
1.0 〃	〃	1206
2.0 〃	〃	2393

Distribution of Cesium on the Precipitate Layer. — This experiment was made to determine how the radioactive cesium was distributed on the precipitate layer. Three different procedures were tested with the same amount of radioactive cesium and the results obtained are shown in Table VIII.

TABLE VIII
DISTRIBUTION OF CESIUM ON THE PRECIPITATE LAYER

Exp. No.	Counts per min.
1	2381
2	3061
3	2405

Exp. 1; Cesium-137 was coprecipitated with thallium phosphomolybdate.
Exp. 2; The present method.
Exp. 3; The precipitate followed by the present method was homogenized.

Judging from the self-absorption by the precipitate and the results indicated in Table VIII, it is inferred that the radioactive cesium dose not uniformly distribute itself in the precipitate layer, but is captured more in the upper layer than in the lower of the precipitate. Moreover, a measurment of the activity by the present method is more sensitive than that by the coprecipitation method. Therefore, the present method is superior to the conventional coprecipitation method.

Solubility of the Precipitate. — This experiment was made to investigate how much precipitate is dissolved when 100 ml. of 2% nitric acid solution is passed through the precipitate layer. The solubility was radiometrically determined by the use of radioactive thallium-204 as a tracer. The results obtained are shown in Table IX and the solubility was found to be 0.18 mg. per 100 ml. of the filtrate at 20.5°C.

TABLE IX
SOLUBILITY OF THE PRECIPITATE

	Ppt. layer	100 ml. of filt.
Wt.	157.6 mg.	?*
cpm	9630	11

* Thallium-204 in the filtrate was precipitated by using the same amount of thallium as that in the precipitate layer.

Mechanism of Cesium Capturing.— These experiments were made to clarify the mechanism by which cesium was captured on the precipitate. 1.47×10^{-4} moles of thallium phosphomolybdate labelled with radioactive thallium-204 was used as the precipitate layer and potassium, rubidium and cesium chloride solution each of which contained 2.94×10^{-4}

moles in 100 ml. of 2% nitric acid, were used as sample solutions, After a sample solution is filtered through the precipitate layer, the radioactive thallium in the filtrate was coprecipitated by adding 25 ml. of 4% potassium iodide solution and 10 ml. of the standard thallium solution to it. Then the radioactivity of the precipitate was measured after filtration, washing and drying. Judging from the results shown in Table X and the other results obtained previously, the radioactive cesium in a sample solution seems to be captured by means of the ion exchange phenomenon. However it is not possible to conclude that all the cesium captured on the precipitate layer depends upon the ion exchange phenomenon.

TABLE X
MECHANISM OF CESIUM CAPTURING

Sample soln.	Radioactivity (cpm)	
	Ppt. layer	filt.
Blank	9454	11
K^+	9457	12
Rb^+	9228	349
Cs^+	8919	590

Influence of Potassium Sulfate. — The relationship between the amount of potassium sulfate and the strength of the activity is shown in Table XI. It is found that less than 1 g. of potassium sulfate in 100 ml. solution does not affect the strength of the activity on the precipitate layer.

TABLE XI
INFLUENCE OF THE POTASSIUM ION

K_2SO_4 (g./100 ml.)	Counts per min.
0.2	3068
0.5	3044
1.0	2974
2.0	2891
4.0	2751
8.0	2518
ca. 12 (Sat. soln.)	1862

Influence of Ammonium Chloride.—The relationship between the amount of ammonium chloride and the intensity of the activity is shown in Table XII. From

TABLE XII
INFLUENCE OF THE AMMONIUM ION

NH_4Cl (g./100 ml.)	Counts per min.
0.1	3008
0.2	2986
0.4	2776
0.8	2448
1.2	2011
2.5	1366
5.0	683

TABLE XIII
INFLUENCE OF THE RUBIDIUM ION

RbCl (mg./100 ml.)	Counts per min.
1	3059
2	3015
4	3016
8	2935
16	2868
32	2561
64	2228

TABLE XIV

Compounds	Wt./100 ml.	Counts per min.
LiCl	2 g.	2984
Na_2SO_4	2 〃	3017
〃	5 〃	2857
$Mg(NO_3)_2$	5 〃	3014
$CaCl_2$	5 〃	3008
$Sr(NO_3)_2$	5 〃	3013
$Ba(NO_3)_2$	5 〃	3008
$Al(NO_3)_3$	5 〃	2889
$Cu(NO_3)_2$	1 〃	2996
$AgNO_3$	1 〃	3017
$Zn(NO_3)_2$	1 〃	3045
$Cd(NO_3)_2$	1 〃	2970
$Hg(NO_3)_2$	1 〃	2999
H_3BO_3	1 〃	3020
$Pb(NO_3)_2$	1 〃	2951
$Fe(NO_3)_3$	1 〃	2912
$Co(NO_3)_2$	1 〃	3081
$Ni(NO_3)_2$	1 〃	2968
NaH_2PO_4	1 〃	3030
$Bi(NO_3)_3$	1 〃	2976
$SnCl_4$	1 〃	3052
$Cr(NO_3)_3$	1 〃	2847
Na_2WO_4	1 〃	1361
$Mn(NO_3)_2$	1 〃	2930
$Th(NO_3)_4$	0.5〃	3008
$P_2O_5 \cdot 18MoO_3 \cdot aq$	0.5〃	2985
NaCl	1 〃	3092
KBr	1 〃	3088
KI	1 〃	3075
K_2CrO_4	1 〃	3015
Na_2SO_3	1 〃	2962
$KClO_3$	1 〃	2920
$NaNO_2$	1 〃	1677
$H_2C_2O_4$	1 〃	3058
conc. HCl	5 ml.	2992
conc. H_2SO_4	5 〃	2942
conc. H_3PO_4	5 〃	2969
conc. CH_3COOH	5 〃	2880
$BeSO_4$	50 mg.	2982
$TlNO_3$	2.6〃	2939
〃	13.0〃	1113
〃	32.5〃	373

the table, it is seen that less than 0.2 g. of ammonium chloride in a 100 ml. solution does not affect the activity on the precipitate.

Influence of Rubidium Chloride.—The results obtained in the presence of rubidium chloride are shown in Table XIII. They indicate that less than 8 mg. of rubidium chloride in 100 ml. solution does not affect the activity on the precipitate.

Influence of Other Substances.—The results obtained in the presence of various other substances are shown in Table XIV. For the most part, the substances do not interfere with the determination of radioactive cesium, but the following substances do; thallium, sodium tungstate and sodium nitrite.

Recovery in the Presence of Other Radioactive Elements.—The rare earth nuclides used in this experiment were prepared from a fission products by Yamatera's method[4] in which the fission products were easily divided into ruthenium, cesium, strontium and the rare earth group by use of mineral acids and the ion exchange resin, Dowex-50 (×8). According to the above mentioned method, about 3% of the radioactive strontium and 11% of the radioactive rare earth nuclides were captured on the precipitate layer. However, their interference with the determination of cesium was prevented by the following pretreatment. To the sample solution which contains radioactive cesium and other nuclides were added 5 mg. of ferric iron, 10 mg. of calcium ion and 50 ml. of 1% sodium carbonate solution. After filtration the filtrate was diluted to produce 100 ml. of 2% nitric acid solution. This solution was treated by the same procedure as before.

The results obtained are shown in Table XV. As can be seen from the table, the radioactive cesium is quantitatively recovered by this method in the presence of strontium-90 and rare earth nuclides which are commonly encountered in an aged fission product.

TABLE XV
INFLUENCE OF OTHER RADIOACTIVE NUCLIDES

Sample	Counts per min.
Blank	3014
R. E. N.+Cs	2989
Sr+Cs	2919
R. E. N.+Cs+Sr	2941
F. P.	472
F. P.+Cs	3464

R. E. N.; Rare Earth Nuclides
F. P.; Fission Products

Recovery of Radioactive Cesium from Natural Waters.—This experiment was made to investigate what percentage of cesium was recovered in the case of using one liter of natural water as a sample solution. One liter each of river and sea water were acidified to produce 2% nitric acid solution and filtered through a filter-paper, Tōyō-Roshi No. 5A, after a definite amount of the radioactive cesium was added to it. The same procedure as mentioned above was followed. The results obtained are shown in Table XVI and indicate that about 93% of the radioactive cesium was recovered from one liter of either river or sea water by this method.

TABLE XVI
RECOVERY OF CESIUM-137 FROM NATURAL WATERS

Sample	Counts per min.	Recovery (%)
Blank	3069	100
River water	2842	92.6
Sea water	2864	93.3

Other Results.—In these experiments, the same glass-filters were repeatedly used, but no adverse effects resulted when they were twice boiled with 2N-aqueous ammonia and dilute nitric acid for about an hour.

Summary

(1) Up to 500 μg. cesium dissolved in less than 2 liters of solution is quantitatively captured on the precipitate layer by filtering the cesium solution through it.

(2) The activity on the precipitate is proportional to the amount of cesium-137 present in the solution and consequently, the quantity of cesium-137 is easily determined.

(3) The mechanism of capturing cesium on the precipitate layer is believed to be due to the ion exchange phenomenon.

(4) Determination of the radioactive cesium by this method is not interfered with by the presence of a large amount of various substances except rubidium, cesium, thallium, tungstate and nitrite. Radioactive strontium and rare earth elements also interfere, but their interference may be prevented by pretreatment.

4) H. Yamatera, A paper read before the 10th Annual Congress, Chem. Soc. of Japan, April, 1957.

(5) Recovery of the radioactive cesium dissolved in one liter of either river or sea water are about 93%.

The author wishes to express his deep gratitude to Professor Dr. M. Ishibashi of Kyoto University and Mr. H. Yamatera of Osaka City University for their encouragement and advice. The author also expresses his sincere thanks to Mr. K. Nishimoto of Doshisha University for his valuable assistance in this research.

Department of Chemistry
Faculty of Engineering
Doshisha University
Kamikyo-ku, Kyoto

The Formic Acid Rearrangement of 2-Cyclohexyl-3-butyn-2-ol

By Tatsuo TAKESHIMA, Kazuo WAKAMATSU and Akira FURUHASHI

(Received April 14, 1958)

The present work, as well as the several reports from this laboratory[1,3], was directed to exploring the effect of the structure of tertiary ethynylcarbinols on the course of Rupe reaction.

Here, 2-cyclohexyl-3-butyn-2-ol (II) was chosen for another model carbinol in which R_1 (or R_2; R_1, R_2=alkyl; I) is secondary and, at the same time, R_2 (or R_1) is not primary.

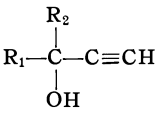

(I)

It was previously shown[1] that the tertiary ethynylcarbinols may be classified into two groups in relation to Rupe reaction. One group involves the carbinols in which R_1 or R_2 is primary or secondary. They are capable of undergoing dehydration followed by hydration (at the ethynyl group), and afford chiefly ketones as the reaction product; the formation of aldehydes is generally of a small quantity.

The other group consists of the carbinols in which both R_1 and R_2 are neither primary nor secondary. They undergo mainly Meyer-Schuster rearrangement to yield aldehydes. Seemingly, the methyl group which is adjacent to the carbon atom attached to the hydroxyl group plays a role somewhat similar to the tertiary alkyl viewed from the several instances already reported[2]; the dehydration between the methyl group and the neighboring hydroxyl group seems to occur actually, however the formation of ketones is inconsiderable.

Though the carbinols such as II belong to the first group, they have only one hydrogen atom on the concerned carbon atom (adjacent to the carbon atom attached to the hydroxyl group). The question whether such a carbinol has, to a certain degree, a tendency suitable for yielding aldehydes besides ketones is now under investigation. Of course, such a trend may not necessarily result only from the above structure, however it was observed on the two model carbinols of this type. One is 3, 4-dimethyl-1-hexyn-3-ol, from the reaction products of which 3, 4-dimethyl-2-hexenal was easily isolated by simple distillation[3] (ca. 3% yield, a small but significant quantity). The other is II in the present experiment, which gave 3-cyclohexyl-2-butenal(IV) in ca. 12% yield in addition to 3-cyclohexylidene-2-butanone(III) (ca. 28% yield). That such a considerable amount of the aldehyde could easily be isolated, may be noteworthy compared with other carbinols which are capable of undergoing the usual Rupe reaction. There are of course some reports[4] regarding the isolation of aldehydes (up to ca. 10%) from the reaction products

1) T. Takeshima, *J. Sci. Research Inst.*, **45**, 211 (1951); ibid., **47**, 237 (1953); ibid., **48**, 103, 113 (1954); *J. Am. Chem. Soc.*, **75**, 4107 (1953).
2) C. D. Hurd and W. D. McPhee, ibid., **71**, 398 (1949); T. Takeshima, *J. Sci. Research Inst.*, **48**, 113 (1954).
3) T. Takeshima, *J. Am. Chem. Soc.*, **75**, 3309 (1953).
4) F. G. Fischer and K. Löwenberg, *Ann.*, **475**, 183 (1929); J. D. Chanley, *J. Am. Chem. Soc.*, **70**, 244 (1948).

TABLE I

REACTION PRODUCTS FROM II

Fraction	B. p., °C (30 mm.)	Yield, g., from 20 g. of II	Constituent
1	75~80	ca. 2.5	Cyclohexanone and possibly 3-cyclohexylidene-1-butyne
2	81~95 (81~85)*	ca. 3.2	III and possibly 3-cyclohexylidene-1-butyne
3	ca. 100~130 (ca. 105~110)*	ca. 5.5	III predominating
4	132~138 (ca. 135)*	ca. 2.3	IV

* The boiling point enclosed with parentheses shows the one at which the greater part of the fraction distilled out.

DERIVATIVES OF THE CARBONYL COMPOUNDS

Original compd.	2,4-Dinitrophenylhydrazone		Semicarbazone	
	M. p., °C	Appearance	M. p., °C	Appearance
III	123~124	Deep yellow crystals	174~175	Colorless needles
IV	199~200	Light red long plates	183~184 (slow heating) ca. 196 (rapid heating)	Colorless long plates
V	125~127	Deep yellow crystals	139~140	Colorless plates

	Dimedone Derivative	
	M. p., °C	Appearance
IV	160~161	Colorless crystals

of the carbinols which have secondary carbon atom in the concerned position.

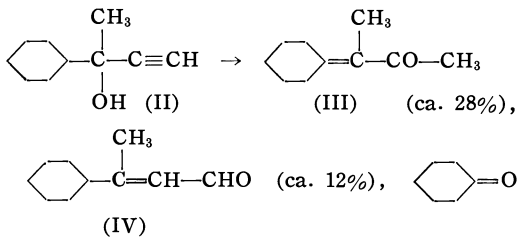

(II) (III) (ca. 28%), (ca. 12%),

(IV)

The present experiment is outlined as follows. II was refluxed with ca. 80% formic acid and treated in the usual manner. The reaction products were distilled and four fractions were collected (consult Table I). The low-boiling fraction (fraction 1) contained a considerable amount of cyclohexanone, which, considering the fact mentioned below, seemed to owe its origin to the acid hydrolysis of III. The greater part of fraction 3 consisted of a carbonyl compound III which gave the ketonic derivatives shown in Table I. III, one of the two main products in this reaction, was practically indifferent toward Schiff reagent, had unsaturated nature, and gave pyrazoline derivative. Further, III on hydrolysis by acid gave cyclohexanone and methyl ethyl ketone as their 2,4-dinitrophenylhydrazone. Thus III proved to be 3-cyclohexylidene-2-butanone. Though the boiling point of III corresponded to the one reported by Thakur[5], the melting point of its semicarbazone was quite different from the one obtained by him.

Fraction 4, which had a pleasant smell, proved to consist of a carbonyl compound IV of formula $C_{10}H_{16}O$ of which derivatives are shown in Table I. The compound had an unsaturated aldehydic nature. On treatment with phenylhydrazine, it readily gave an oily product which had a pyrazoline reaction of a coloration different from that of III. Further, ozonolysis gave glyoxal as the 2,4-dinitrophenylosazone. Hydrogenation afforded the corresponding saturated compound V which had an intensely positive test with Schiff reagent. Thus structure IV, 3-cyclohexyl-2-butenal, and V, 3-cyclohexylbutyraldehyde, were assigned to these two compounds, respectively.

Finally, fraction 1 seemed to contain, besides cyclohexanone, a non-ketonic substance of unsaturated nature. Likewise, fraction 2, in which some quantity of cyclohexanone and III was detected as

5) R. S. Thakur, *J. Chem. Soc.*, **1933**, 1481. He obtained the ketone by a different route, and reported three melting points of somewhat indefinite nature for its semicarbazone, one distinct melting point being obtained after fractional recrystallization. The one in the present experiment was believed to be of the single compound.

their 2,4-dinitrophenylhydrazones, also contained the same substance. It was inferred from the behavior of these two fractions (see experimental part) that the compound is possibly 3-cyclohexylidene-1-butyne.

Experimental

2-Cyclohexyl-3-butyn-2-ol. — The carbinol was prepared by ethynation of acetylcyclohexane in the usual manner[1] using sodium amide as the reagent. Yield ca. 83%, b. p. 104~106° (18 mm.) (reported b. p. 106~110° (23 mm.)[6]); practically no ketonic compound was detected in this fraction by the 2,4-dinitrophenylhydrazine test. Fairly good yield could be thus obtained without depending on the liquid ammonia method[6]; in the present preparation acetylene was passed through for ca. 12 hr. at ca. −7° and the reaction mixture was then left overnight in an ice-box.

The original **acetylcyclohexane** was prepared by hydrogenating 1-acetylcyclohexene with palladium; b. p. 178~180°, yield 86%.

1-Acetylcyclohexene was prepared from 1-ethynylcyclohexanol with the aid of its acid rearrangement[7]; 130 g. of the carbinol was treated with a mixture of 12 g. of sulfuric acid, 280 g. of acetic acid and 2 g. of water. On heating, a vigorous spontaneous reaction was initiated; a large reflux condenser was preferably fitted; the heating must be stopped immediately after the initiation and the reaction, if needed, was moderated by cooling with water. The pure ketone could be obtained by this method, which contained practically no aldehyde; b. p. 110~111° (50 mm.), yield 65%.

The Formic Acid Rearrangement of 2-Cyclohexyl-3-butyn-2-ol (II). — Twenty grams of II was gently refluxed with 160 g. of ca. 80% formic acid for ca. 1 hr.; the heating was interrupted during the spontaneous boiling at the beginning. The reaction mixture was left to be cooled, and then neutralized with a concentrated solution of potassium carbonate, extracted with ether, dried by potassium carbonate, the ether driven off, and distilled collecting the following fractions. (1) b. p. 75~80° (30 mm.), ca. 2.5 g.; (2) b. p. 81~95° (30 mm.), ca. 3.2 g. (the greater part distilled out at 81~85° (30 mm.)); (3) b. p. ca. 100~130° (30 mm.), ca. 5.5 g. (ca. 28%; the greater part distilled out at ca. 105~110° (30mm.)); (4) b. p. 132~138° (30 mm.), ca. 2.3 g. (ca. 12%; the greater part distilled out at ca. 135° (30mm.)); Distillation residue, tarry material

All these fractions were colorless, scarcely soluble in water, easily soluble in common organic solvents, and had a smaller density than water at room temperature.

Fraction 1 gave considerable quantity of cyclohexanone 2,4-dinitrophenylhydrazone, which on recrystallization from hot ethanol melted at 158~160° and did not depress the melting point of an authentic sample (Found: C, 51.72; H, 5.08; N, 19.81%). Another 2,4-dinitrophenylhydrazone obtained from this fraction, perhaps that of III, was only of a small quantity; it was difficult to obtain any derivative from the same fraction by treating it, as it is, with semicarbazide reagent. It, as it is or as the ethanolic solution, readily decolorized bromine water; II apparently had much more inertia toward this reaction, and had a much higher boiling point than this fraction. Further, it gave some precipitates with ammoniacal silver nitrate (fraction 3 and 4 gave practically no precipitates), gave red halochromism with sulfuric acid, and turned yellowish on a few hour's standing and also turned viscous on long standing. Analyses and molecular weight measurement of this fraction gave intermediate values between cyclohexanone and 3-cyclohexylidene-1-butyne.

Anal. Found: C, 81.07; H, 9.95; mol. wt., (Rast), 130. Calcd. for $C_6H_{10}O$ (cyclohexanone): C, 73.43; H, 10.27; mol. wt., 98.1. Calcd. for $C_{10}H_{14}$ (3-cyclohexylidene-1-butyne); C, 89.49; H, 10.51; mol. wt., 134.2. Calcd. for $C_{10}H_{16}O$ (III): C, 78.90; H, 10.60%; mol. wt., 152.2.

Fraction 2 had properties similar to those of fraction 1; the quantity obtained of cyclohexanone 2,4-dinitrophenylhydrazone was less than that from the latter, and, in addition, some amount of 2,4-dinitrophenylhydrazone of III was obtained.

Fraction 3 (III).—The fraction was redistilled, collecting ca. 3 g. of a fraction boiling at 105~110° (30 mm.). Most part of it consisted of 3-cyclohexylidene-2-butanone (III), which was ascertained from the quantity obtained of the 2,4-dinitrophenylhydrazone. It was only weakly positive toward Schiff reagent, readily decolorized bromine water, gave practically no precipitates with ammoniacal silver nitrate, and did not reduce Fehling solution. It gave a positive test for methyl ketone[8], fuchsine-red color being produced on heating with potassium hypobromite solution and pyridine. On refluxing the same fraction for ca. 1.5 hr. with a solution of phenylhydrazine hydrochloride in ethanolic acetic acid, colorless crystals were produced, which gave a pyrazoline reaction of wine-red coloration with sulfuric acid and sodium nitrite; the crystals were very easily soluble in aqueous methanol.

2,4-Dinitrophenylhydrazone of III was recrystallized from methanolic pyridine, deep yellow needles or crystals, easily soluble in pyridine, m. p. 123~124°.

Anal. Found: C, 57.53; H, 5.82; N, 16.83. Calcd. for $C_{16}H_{20}O_4N_4$: C, 57.82; H, 6.07; N, 16.86%.

Semicarbazone of III was recrystallized from methanol, colorless needles somewhat soluble in the same solvent, m. p. 174~175° (indefinite melting points reported[5] are: 180~184°, 155~160°, 160~163° in different preparations; the least soluble semicarbazone in the case of the fractional crystallization, m. p. 192~193° rapid heating), 187° (slow heating)).

6) Domenick Papa, Frank J. Villanits and Helen F. Ginsberg, *Arch. Biochem. Biophys.*, **33**, 482 (1951).
7) T. Takeshima, *J. Sci. Research Inst.*, **48**, 103 (1954).
8) J. Adachi, *Anal. Chem.*, **23**, 1491 (1951).

Anal. Found: N, 19.93. Calcd. for $C_{11}H_{19}ON_3$: N, 20.08%.

On adding 2,4-dinitrophenylhydrazine reagent directly to the semicarbazone, the corresponding 2,4-dinitrophenylhydrazone was obtained, which was identical with that of III mentioned above.

Hydrolysis of Fraction 3 (III).—A mixture of 0.5 g. of the above redistilled portion of fraction 3 and 3 cc. of ca. 80% formic acid and 0.5 cc. of 50% sulfuric acid, was boiled under reflux for ca. 3 hr. The reaction mixture was neutralized with a solution of potassium carbonate, extracted with ether, dried with potassium carbonate and distilled. A distillate up to ca. 40°, which consisted almost entirely of the solvent, was rejected. Next ethereal distillate, on treatment with 2,4-dinitrophenylhydrazine reagent, yielded yellow needles which melted at ca. 115°; the melting point was not depressed on admixture with an authentic sample of methyl ethyl ketone 2,4-dinitrophenylhydrazone. The higher boiling distillate, which amounted to a considerable quantity, was converted to cyclohexanone 2,4-dinitrophenylhydrazone which melted at 158~159°; the melting point was not depressed on admixture with the authentic sample.

Fraction 4, b. p. 132~138° (30 mm.), consisted almost only of 3-cyclohexyl-2-butenal (IV), which was ascertained from the quantity obtained of the 2,4-dinitrophenylhydrazone mentioned below. The fraction had a pleasant smell, gave positive test with Schiff reagent (violet color was gradually produced, which was accompanied with a formation of some dregs), reduced ammoniacal silver nitrate, decolorized bromine water, and gave a halochromic coloration with sulfuric acid; a trace of the aldehyde on contact with sulfuric acid turned into deep red and the whole became golden yellow when it was made uniform by shaking; the behavior was somewhat similar to that of III. It, on heating, merely turned Fehling solution into turbid bluish green and the oil became reddish, which seemed to be caused by fine particles of perhaps copper or cuprous oxide; the behavior resembled those of β-methylcrotonaldehyde and 3,4-dimethyl-2-hexenal[9].

It was slightly positive toward methyl ketone test[8], which may be due to contamination with III.

On heating with phenylhydrazine hydrochloride in ethanolic acetic acid, it gave an oily product which had a pyrazoline reaction of dark violet or bluish violet color quite different from that in the case of III.

2,4-Dinitrophenylhydrazone of IV. — The derivative of fraction 4 was recrystallized from pyridine. light red needles or long plates, m. p. 199~200°, easily soluble in hot pyridine and sparingly soluble in cold ethanol.

Anal. Found: C, 57.84; H, 5.91; N, 16.83. Calcd. for $C_{16}H_{20}O_4N_4$: C, 57.82; H, 6.07; N, 16.86%.

Semicarbazone of IV. — The semicarbazone of fraction 4 was recrystallized from methanol, colorless long plates or needles, m. p. 183~184° (slow heating), ca. 196° (rapid heating), easily soluble in hot ethanol.

Anal. Found: N, 20.05. Calcd. for $C_{11}H_{19}ON_3$: N, 20.08%.

The above 2,4-dinitrophenylhydrazone of IV was obtained also from this semicarbazone.

Dimedone Derivative of IV.—To a solution of ca. 0.1 g. of fraction 4 in ca. 4 cc. of 50% ethanol was added ca. 0.6 g. of dimedone and one drop of piperidine, and the mixture then was gently boiled for a while. After being cooled, a small quantity of water was added to the reaction mixture, and the resulting precipitates were collected, recrystallized from aqueous ethanol and then from methanol. Colorless crystals, m. p. 160~161°, fairly soluble in 50% ethanol.

Anal. Found: C, 75.11; H, 9.15. Calcd. for $C_{26}H_{38}O_4$: C, 75.32; H, 9.24%.

Ozonolysis of Fraction 4 (IV).—A solution of 0.5 g. of the fraction in ca. 16 g. of carbon tetrachloride was cooled with ice and ozonized oxygen was passed through for ca. 2 hr., and then the solvent was removed on a water-bath. The viscous product was shaken with aqueous methanol and the oily portion was treated with 2,4-dinitrophenylhydrazine reagent. The dark reddish brown viscous oil produced was recrystallized from methanolic pyridine to yield orange yellow fine needles, m. p. ca. 310°. Reported melting points of glyoxal 2,4-dinitrophenylosazone are: 311~312°[10], 326~328°[11], 318°[12].

Hydrogenation of Fraction 4 (IV). — The fraction was hydrogenated using palladium-kieselguhr catalyst. The greater part of the product distilled out at 112~115° (30 mm.), a colorless liquid which had a camphoraceous odor and produced deep pink color with Schiff reagent. It was considered to be 3-cyclohexylbutyraldehyde (V) and gave the derivatives mentioned below.

2,4-Dinitrophenylhydrazone of V. — It was recrystallized from methanolic pyridine to give deep yellow (tinged with orange) crystals, m. p. 125~127°; mixed melting point with 2,4-dinitrophenylhydrazone of III was 95~103°.

Anal. Found: C, 57.36; H, 6.46; N, 16.66. Calcd. for $C_{16}H_{22}O_4N_4$: C, 57.47; H, 6.63; N, 16.76%.

Semicarbazone of V. — It was recrystallized from methanol, colorless plates, m. p. 139~140°.

Anal. Found: C, 62.40; H, 9.69; N, 20.09. Calcd. for $C_{11}H_{21}ON_3$: C, 62.52; H, 10.02; N, 19.89%.

2,4-Dinitrophenylhydrazone of V was obtained also from the above semicarbazone.

Summary

The formic acid rearrangement of ethynylcarbinols has been extended to 2-cyclo-

9) T. Takeshima, *J. Sci. Research Inst.*, **45**, 103 (1951); *J. Am. Chem. Soc.*, **75**, 3309 (1953).

10) T. L. Jacobs and W. J. Whitcher, ibid., **64**, 2635 (1942).

11) H. H. Strain, ibid., **57**, 758 (1935).

12) C. Neuberg and E. Simon, *Biochem. Z.*, **256**, 488 (1932); J. Meisenheimer and W. Schmidt, *Ann.*, **475**, 181 (1929).

hexyl-3-butyn-2-ol(II), a model carbinol in which the tertiary carbon atom and the methyl group are adjacent to the carbon atom attached to the hydroxyl group. The major rearrangement product consisted of a mixture of 3-cyclohexylidene-2-butanone (III) (ca. 28% yield) and a new aldehyde, 3-cyclohexyl-2-butenal(IV) (ca. 12% yield). The latter was hydrogenated to give 3-cyclohexylbutyraldehyde (V). These compounds were isolated and characterized.

We wish to express our heartfelt thanks to Dr. T. Ukaji for his care kindly extended to us. Thanks are also due to Messrs M. Otsuka and N. Maejima for their kind assistance.

Department of Chemistry
Faculty of Science
Ibaraki University, Mito

Magnetochemical Study of Cyanuric Acid, Melamine, and Some Derivatives

By Yoshio MATSUNAGA and Shiro MORITA*

(Received March 28, 1958)

The structure of highly symmetrical heterocyclic rings which appear in cyanuric acid and melamine has been the subject of much interest. Their structures in the solid state were established from X-ray studies. The former molecule[1] was found to be in the carbonyl form II and the latter[2] in the amide form V. Magnetic susceptibilities and anisotropies of cyanuric ring compounds have been examined by several investigators, but their conclusions as to the structure of cyanuric acid were conflicting. Pascal[3] concluded that the magnitude of the diamagnetic susceptibility favors form I, however, Maruha[4] suggested that its structure is a resonance hybrid of form II and the zwitter-ionic forms III and IV. On the other hand, Lonsdale[5] found that the cyanuric acid molecule has anisotropy of the same order as those of melamine and cyanuric triazide and she favored form I. Besides, the recorded values for cyanuric acid disagreed considerably as shown in Table I. Therefore, a more detailed examination of the diamagnetic susceptibilities of cyanuric acid and melamine, including also their derivatives which have no tautomeric forms, was undertaken.

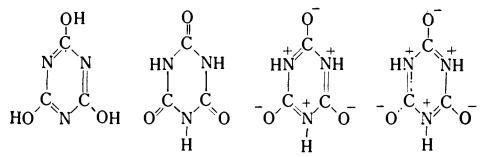

(I) (II) (III) (IV)

Experimental

Materials.—Cyanuric chloride, commercial product, recrystallized from benzene, m.p. 146°C. Trimethyl cyanurate[6c], m.p. 135°C. Triphenyl cyanurate[6d], m.p. 230~231°C. Hexaethylmelamine[6b], b.p. 147~148°C/2.5 mmHg. Melamine, commercial product, recrystallized from water and sublimed in vacuo. Trimethylolmelamine, commercial product, dried in vacuo. 2,4-Dianilino-6-chloro-*s*-triazine[6a], sublimed in vacuo, m.p. 199°C. 2,4-Dianilino-6-methoxy-*s*-triazine[6c] sublimed in vacuo, m.p. 168°C. Melamine hydrochloride, prepared by dehydration in vacuo from hemihydrate. Cyanuric acid, supplied by Nippon Carbide Ind. Co., recrystallized from water repeatedly and sublimed in vacuo.

Magnetic measurements — The susceptibility measurements were carried out using a Gouy balance as previously described[7].

Results and Discussion

In Table I specific and molar susceptibilities together with other recorded values of the latter quantity are presented for

* Present address, Research Laboratory, Mitsubishi Chemical Industries Ltd., Kawasaki, Kanagawa.

1) E. H. Wiebenga, *J. Am. Chem. Soc.*, **74**, 6156 (1952).
2) E. W. Hughes, ibid., **63**, 1737 (1941).
3) P. Pascal, *Compt. rend.*, **176**, 1887 (1923).
4) J. Maruha, *J. Chem. Soc. Japan, Pure Chem. Sec.* (*Nippon Kagaku Zassi*), **71**, 627 (1950).
5) K. Lonsdale, *Proc. Roy. Soc.*, **A177**, 272 (1941).
6) J. T. Thurston et al., *J. Am. Chem. Soc.*, **73**, 2981, 2984, 2986, 2990 (1951).
7) H. Akamatu and Y. Matsunaga, This Bulletin, **26**, 364 (1953).

TABLE I

DIAMAGNETIC SUSCEPTIBILITIES OF CYANURIC ACID, MELAMINE, AND THEIR DERIVATIVES

	Substance	Suscept. $(-\chi)$	Molar Suscept. $(-\chi_M)$ Obs.	Calc.	Lit.
I	Cyanuric chloride	0.435	80.2	82.1	81.1[10]
	Trimethyl cyanurate	0.525	89.9	89.9	—
	Triphenyl cyanurate	0.576	205.9	205.1	—
	Hexaethylmelamine	0.675	198.8	197.9	—
II	Melamine	0.502	63.3	60.8	65.2[11], 61.7[12]
	Trimethylolmelamine	0.519	112.2	110.2	—
	2,4-Dianilino-6-chloro-*s*-triazine	0.558	166.7	165.8	—
	2,4-Dianilino-6-methoxy-*s*-triazine	0.586	172.5	168.5	—
	Melamine hydrochloride	0.538	87.5	84.9	—
	Cyanuric acid	0.422	54.5	52.6	63.2[3], 50.5[4], 61.5[13]

ten compounds. The first group consists of four compounds which have no tautomeric form. On the basis of these experimental values we estimated the constant for unsubstituted triazine at -36.5[8] on the assumption that the magnetic contribution of substituents is just the same as in the case of derivatives of benzene. The molar susceptibilities in the fourth column were evaluated on the same assumption. Pascal[3] gave -36.5 for the contribution of the triazine ring and -1.85 for the correction term. Our values which must be compared with these two are -27.7 and $+6.95$. It must be noted that our values are in serious disagreement with Pascal's, but our correction term is close to those for the pyrimidine ring ($+6.5$) and for the pyrazine ring ($+9$) given by Pacault[9].

The agreement between the experimental and the calculated values in the case of the first group is satisfactory; however, it should be noted that in the second group the former values are appreciably and consistently more diamagnetic. The substances in the latter group have the amino nitrogen on which one or two hydrogen atoms remain, so they have the possibility of being in another form, the imide structure (for example, the form VIII of melamine). But from X-ray and spectroscopic studies[14,15], it seems to be unreasonable that the increase of diamagnetism is due to the structural change to the imide form.

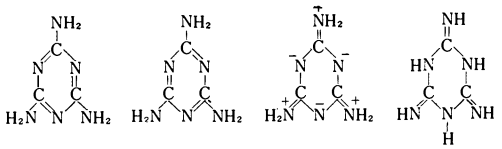

(V) (VI) (VII) (VIII)

The contribution of the zwitter-ionic forms seems to be rather important in the melamine molecule. To explain the C-N bond lengths the three structures V, VI and VII must contribute nearly equally[2]. The conjugation between amino group and aromatic nucleus diminishes considerably in the derivatives of benzene, when the hydrogen atoms attached to the amino nitrogen are completely substituted by alkyl groups[16]. By analogy, it would seem that the increase of diamagnetism appearing in the substances in the second group relates to the extraordinarily large contribution of ionic structures.

We shall examine more quantitatively the magnitude of molar susceptibilities of these heterocyclic compounds. The value for the Kekulé-like form of unsubstituted triazine is estimated at -19.6 by Gray and Cruickshank's method[17]. If this value is equal to the isotropic contribution of the ring as is usual in aromatic nuclei, the molar anisotropy must be about -50. This is too large if we compare it with -30 reported by Lonsdale[18] for the molar anisotropy of

8) All values of susceptibility are in c. g. s. units and are multiplied by 10^6 throughout this paper.
9) A. Pacault, *Ann. chim.*, (12), **1**, 527 (1946).
10) J. Farquharson, *Trans. Faraday Soc.*, **32**, 219 (1936).
11) I. E. Knaggs and K. Lonsdale, *Proc. Roy. Soc.*, **A177**, 140 (1940).
12) J. Ploquin and C. Vergneau-Souvray, *Compt. rend.*, **234**, 97 (1952).
13) S. K. Siddhanta and P. Ray, *J. Indian Chem. Soc.*, **20**, 359 (1943).
14) I. M. Klotz and T. Askounis, *J. Am. Chem. Soc.*, **69**, 801 (1947).
15) M. J. S. Dewar and L. Paoloni, *Trans. Faraday Soc.*, **53**, 261 (1957).
16) G. W. Wheland, "Resonance in Organic Chemistry", John Wiley & Sons, Inc., New York, (1955), p. 99-100.
17) F. W. Gray and J. H. Cruickshank, *Trans. Faraday Soc.*, **31**, 1491 (1935).
18) K. Lonsdale, *Z. Krist.*, **95**, 471 (1936).

cyanuric chloride. Such a discrepancy becomes more remarkable in the case of melamine. The calculated value for the form V or VI is −45.6 and the anisotropy given by the combination with the experimental molar susceptibility is equal to −53. On the other hand, Knaggs and Lonsdale's observed values are −58.1 for the isotropic contribution and −21 for the anisotropy. These disagreements suggest that the real isotropic contribution of a triazine ring is more diamagnetic than the calculated one and the resonance with the zwitter-ionic form brings about a marked increase of the isotropic diamagnetism.

As to cyanuric acid, the calculated value, obtained by assuming the presence of a triazine ring, is near the experimental one. However, this agreement cannot be considered as conclusive evidence for form I since we can say that the value of the molar susceptibility also favors the carbonyl form as discussed in the following paragraph.

The structure of urea is closely similar to part of the carbonyl form of cyanuric acid. With this compound the resonance energy is relatively large. This fact suggests that resonance with the zwitter-ionic structures is important in this case too. The diamagnetism of urea was examined in detail by Clow[19]. The experimental values are in serious disagreement with the calculated ones for the carbamide structure especially in the case of urea itself and the monosubstituted derivatives. Therefore, it is no wonder that Gray and Cruickshank's method gives such unreasonable estimates as −39.3 for the isotropic contribution of the carbonyl form of cyanuric acid and −45.6 for the molar anisotropy.

Since Pascal determined his first constants, it has been well known that the magnetic contributions of oxygen and nitrogen atoms depend markedly on their surroundings. He gave many group constants in his second system of the additivity rule[20]. Some of them are cited in Table II. Using the constant for the amide group with substituent, we obtain −47.5 for the isotropic diamagnetism of the carbonyl form II and −21 for the molar anisotropy. The latter value is in good agreement with −24 given by Lonsdale[5]. The molecule of cyanuric acid contains a triazine ring only in the zwitter-ionic forms III and IV; hence the large anisotropy suggests that the contribution of these structures to a resonance hybrid is very important. This view is consistent with the evidence from other sources.

TABLE II
PASCAL'S CONSTANTS IN HIS SECOND SYSTEM

Group		Constant ($-\chi_M$)
C=O		8.1
		15.15
	(amide without substituent)	15.70
	(amide with substituent)	13.83
	(urea)	25.5

Recently Sato[21] measured the susceptibilities of barbituric acid (IX) and its many derivatives. Using the constants for the oxygen atoms in alcohol (−4.61) or the carboxyl group (−3.36) instead of that in ketone (+1.72), his calculated values were found to be in rather good agreement with the experimental ones. However, if we apply his procedure to cyanuric acid, the calculated values are −51.7 to −55.5 for the isotropic contribution of the carbonyl form and nearly zero to −8.4 for the molar anisotropy. This estimated anisotropy is in poor agreement with that reported by Lonsdale. The procedure which was applied successfully to the case of barbituric acid seems to be unreliable for cyanuric acid.

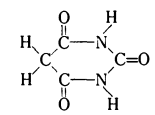 (IX)

Summary

The magnetic susceptibilities of melamine, cyanuric acid, and eight of their derivatives were measured by the Gouy method. On the basis of the molar susceptibilities of the four compounds which have no tautomeric form, the constant for triazine was estimated at −36.5. It appeared that Gray and

19) A. Clow, *Trans. Faraday Soc.*, **33**, 381 (1937): **34**, 457 (1938).
20) J. Hoarau, A. Pacault and P. Pascal, *Cahier de physique*, No. 74, p. 30 (1955).
21) Y. Sato, *Bull. Res. Inst. Non-Aqueous Solns. Tohoku Univ.*, **6**, 1 (1956).

Cruickshank's method gives too small an estimate for the isotropic part of the molar susceptibility in all cases and resonance with the zwitter-ionic structures brings about an increase of the isotropic diamagnetic contribution. With regard to cyanuric acid, the magnitude of the molar susceptibility seemed to be not inconsistent with the form containing a triazine ring. However, using Pascal's second additivity rule we found that both the magnitude of the isotropic diamagnetism and that of the molar anisotropy favor the carbonyl form.

Department of Chemisrty, Faculty of Science, The University of Tokyo
Hongo, Tokyo

A Theoretical Consideration of Simple Catalytic Reactions. Decomposition of Gaseous Hydrides

By Kenzi TAMARU

(Received February 11, 1958)

The thermal decomposition of gaseous hydrides on their own constituent elements to produce hydrogen gas is one of the simplest catalytic reactions. During the reaction, the surfaces of the elements are always renewed by the continuous deposition of fresh elements and only two elements are involved including the catalyst. The kinetics of such reactions are summarized in Table I. A similar reaction, the decomposition of nickel carbonyl, was also listed in the Table. The reason why the kinetics of these similar reactions are so different is to be treated here in a semi a priori fashion.

TABLE I

Kind of reaction	Kinetics of decomp.	Apparent activation energy
AsH_3 on As[1]	$v=kP_{AsH_3}$	23.2 kcal./mol·
SnH_4 on Sn[2]	$v=kP_{SnH_4}$	9.1
H_2Se on Se[3]	$v=kP_{H_2Se}$	
SbH_3 on Sb[4,5]	$v=kP_{SbH_3}^{0.6\sim1.0}$	8.8 at $P_{SbH_3}=40$cm.
CH_4 on C[6]	$v=\frac{kP_{CH_4}}{1+bP_{H_2}}$	53.4
$Ni(CO)_4$ on Ni[7,8]	$v=\frac{kP_{Ni(CO)_4}}{1+bP_{CO}}$	10.3, 12.0
GeH_4 on Ge[9]	$v=k$	41.2

As to the other gaseous hydrides, the decompositions of silane, SiH_4[10], and diborane, B_2H_6[11,12] have also been studied, but these decompositions were found to be homogeneous reactions. In the cases of methane[6,13,14], germane[9] and nickel carbonyl[9], both heterogeneous and homogeneous reaction take place under ordinary circumstances at their decomposition temperatures, but the heterogeneous reaction only is taken into account in Table I.

In the case of germane decomposition it has been shown in previous papers[9,15-17] that (1) the decomposition on germanium is a zero order reaction, and (2) during the decomposition the whole surface of the germanium is practically covered by chemisorbed hydrogen atoms the number of which is approximately equal to that of surface germanium atoms. (3) No hydrogen deuteride is formed by the decomposition of germane in the presence of an

1) K. Tamaru, *J. Phys. Chem.*, **59**, 777 (1955).
2) K. Tamaru, ibid., **60**, 610 (1956).
3) M. Bodenstein, *Z. physik. Chem.*, **29**, 429 (1899).
4) A. Stock et al., *Ber.*, **37**, 901 (1904); **40**, 532 (1907); **41**, 1309 (1908)
5) K. Tamaru, *J. Phys. Chem.*, **59**, 1084 (1955).
6) R. M. Barrer, *Proc. Roy. Soc.*, **A149**, 253 (1935).
7) A. P. Garratt and W. H. Thompson, *J. Chem. Soc.*, **1934**, 1882.
8) C. E. H. Bawn, *Trans. Faraday Soc.*, **31**, 440 (1935).
9) K. Tamaru, M. Boudart and H. Taylor, *J. Phys. Chem.*, **59**, 801 (1955).
10) T. R. Hogness et al., *J. Am. Chem. Soc.*, **58**, 108 (1936).
11) R. P. Clarke and R. N. Pease, ibid., **73**, 2132 (1951).
12) J. K. Bragg et al., ibid., **73**, 2134 (1951).
13) L. S. Kassel, ibid., **54**, 3949 (1932).
14) H. H. Storch, ibid., **54**, 4188 (1932).
15) P. J. Fensham, K. Tamaru, M. Boudart and H. Taylor, *J. Phys. Chem.*, **59**, 806 (1955).
16) K. Tamaru and M. Boudart, "Advances in Catalysis", Vol. IX, Academic Press Inc., N. Y. (1957), p. 699.
17) K. Tamaru, *J. Phys. Chem.*, **61**, 647 (1957).

excess of deuterium. (4) When the mixture of germanium hydride and deuteride are decomposed together, abundant quantities of equilibrated deuteride are produced. (5) No exchange takes place between the two kinds of germane. (6) The desorption rate of the chemisorbed hydrogen on germanium at full coverage is equal to the decomposition rate of germanium hydride. (7) The ratio of the decomposition rates of germane and deuterogermane is 1.8 to 1.

The zero-order kinetics and the observation 2 exclude the Eley-Rideal mechanism, i. e., involving collisions of germane molecules in the gas phase, or those in the van der Waals' adsorption layer with the chemisorbed species on the surface. The observations 2 and 3 exclude the possibility of hydrogen molecules splitting off from the germanium hydrides on the surface, such as, for example, $GeH_4(a) \rightarrow GeH_2(a) + H_2(g)$, throughout the decomposition, because this process will not give so much hydrogen deuteride as has been found in the product, bearing in mind that no exchange reaction between hydrogen and deutrium molecules takes place while germane is being decomposed.

The following mechanism for the decomposition is consistent with all the data;

$$GeH_4(g) \rightarrow GeH_3(a) + H(a) \quad (A)$$

$$GeH_3(a) \rightarrow GeH_2(a) + H(a) \quad (B)$$

$$GeH_2(a) \rightarrow GeH(a) + H(a) \quad (C)$$

$$2H(a) \text{ or } 2GeH(a) \rightarrow H_2(g) \quad (D)$$

and the last step, the desorption of hydrogen atoms to form hydrogen molecules, is a rate-determining step for the reaction. As the chemisorbed hydrogen covers the surface during the decomposition, the chemisorption of the germane, as will be shown later, is suppressed by the chemisorbed hydrogen and accordingly it appears most probable that as soon as the hydrogen desorbs, the step A takes place to keep the saturation of the surface, which results in the observation 5, no exchange between GeH_4 and GeD_4 being detected during the reaction.

For most of the other hydrides, the chemisorption step onto the surface could be considered as rate-determining from their kinetics. By making some assumptions we can expect to treat this kind of reaction with a statistical mechanical method to estimate the rate of each elementary step of the reaction and hence the order of reaction.

The rate of the heterogeneous elementary reaction V per unit surface area of catalyst surface is given by the following equation[18].

$$V = \frac{kT}{h} Gq^* \frac{N_a}{F_a^\circ} Q_{C^*(0)} \quad (1)$$

where G is the number of sites for the activated complex a^* per cm^2., q^* is the partition function of a^* and N_a is the concentration of initial reactant a in the gas phase, F_a° is the partition function of a per unit volume and $Q_{C^*(0)}$ is the probability that the sites for the activated complexes are vacant.

The following assumptions are used for the calculation of the rate of each elementary step of the decompositions.

(1) The bond energies between a hydrogenated element and the hydrogen atoms are the same for all the hydrogen atoms in the hydride molecule and are independent of the number of hydrogen atoms remaining within the hydride fragment.

(2) The translational, rotational and vibrational partition functions of the activated complexes of each elementary reaction and those of the chemisorbed radicals or molecules are taken as unity.

(3) All the elementary reactions other than the rate-determining step are rapid enough to be considered in equilibrium in the stationary state of the reaction.

(4) Each hydrogen atom of hydrides is assumed to split off one by one, as has been shown in the case of germane decomposition, and as each successive removal of a hydrogen atom accompanies an M–H bond cutting to form a M–M bond and an adjacent H(a), it is assumed that the true activation energy in each step is almost the same except the last step.

N_a in the Eqation 1 can be replaced by P_a/kT and T by $T_m e^{1-\frac{T_m}{T}}$, where T_m is the median of the reaction temperature range[18,19]. Thus

$$V = \frac{kT_m eG}{h} \frac{P_a}{F_a} Q_{C^*(0)} \exp\left(-\frac{\Delta^* E}{RT}\right) \quad (2)$$

where $F_a = \frac{kT_m}{B} F_a^\circ(T_m)\ e^{n+1}$ and n is the sum of the exponents of T in the translational and rotational partition functions, B, conversion factor from mmHg into

18) J. Horiuti, *Catalyst*, Inst. Catalyst Res., Hokkaido Univ., Sapporo. **2**, 1 (1947); **7**, 107 (1951).

19) T. Kwan, "Advances in Catalysis", Vol. VI Academic Press Inc., N. Y. (1954), p. 67.

c.g.s. unit, P_a, the pressure of a in mmHg, $F_a^\circ(T_m)$, translational, rotational and vibrasional partition functions of a at T_m, and Δ^*E is the difference of potential energy between the initial reactant a and the activated complex a^*. The values of F_a are listed in Table II.

TABLE II

T	a	F_a(mm.$^{-1}$)	a	F_a(mm.$^{-1}$)
551°K	AsH_3	3.2×10^{15}	H_2	4.2×10^{10}
350	SnH_4	1.1×10^{15}	H_2	8.6×10^{9}
573	H_2Se	2.8×10^{15}	H_2	4.8×10^{10}
308	SbH_3	0.9×10^{15}	H_2	5.5×10^{9}
1000	CH_4	5.0×10^{14}	H_2	3.4×10^{11}
381	$Ni(CO)_4$	6.5×10^{17}	CO	3.4×10^{13}
551	GeH_4	2.4×10^{15}	H_2	4.2×10^{10}

When a part of the catalyst surface is covered by the adsorption of a^*, etc., $Q_{C^*(0)}$ is expressed as follows;

$$Q_{C^*(0)}=\{Q_{C(a)}F_a\exp(-\Delta E(a)/RT)/P_a\}^\alpha \quad (3)$$

where $Q_{C(a)}$ is the probability that the sites for the adsorption are occupied by a, $\Delta E(a)$, the heat of adsorption of a, and α, the ratio of the number of lattice points for the activated complex over that for a, which is usually assumed to be unity.

Decomposition of Stibine on Antimony Surface.—The heat of the reaction is 34.8 kcal./mol.[20] and hydrogen does not chemisorb on an antimony surface[21]. The rate of each elementary reaction at 35° can be expressed as follows,

$$V_A=S(P_{SbH_3}/F_{SbH_3})Q_{C^*(0)}\exp(-\Delta^*E_A/RT)$$
$$=1.1\times10^{-15}SP_{SbH_3}\exp(-\Delta^*E_A/RT) \quad (4)$$

$$V_B=S(P_{SbH_3}/F_{SbH_3})(F_{H_2}/P_{H_2})^{\frac{1}{2}}\times\exp(-\Delta^*E_B/RT)Q_{C^*(0)}$$
$$=1.4\times10^{-2}S\frac{P_{SbH_3}}{\sqrt{P_{H_2}}}\times\frac{\exp(-\Delta^*E_A/RT)}{(1+1.4\times10^{-2}P_{SbH_3}/P_{H_2}^{\frac{1}{2}})} \quad (5)$$

$$V_C=\frac{2}{3}S\left(\frac{P_{SbH_3}}{F_{SbH_3}}\right)^{\frac{2}{3}}\exp(-\Delta^*E_C/RT)Q_{C^*(0)}$$
$$=0.6\times10^{-10}S(P_{SbH_3})^{\frac{2}{3}}\exp(-\Delta^*E_C/RT) \quad (6)$$

where V_A, V_B and V_C are the rates of the following elementary reactions, respectively,

$$SbH_3(g)\rightarrow SbH_2(a)+H(a) \quad (A)$$
$$SbH_2(a)\rightarrow SbH(a)+H(a) \quad (B)$$
$$2SbH(a)\text{ or }2H(a)\rightarrow H_2(g) \quad (C)$$

and S is $kTGe/h$ and Δ^*E_A, Δ^*E_B and Δ^*E_C are the activation energies for the steps, A, B and C, respectively.

The temperature, T_e, at which V_A and V_C are equal can be obtained by putting $V_A=V_C$.

$$T_e=\frac{\Delta^*E_C-\Delta^*E_A}{2.30R[(1/3)\log(F_{SbH_3}/P_{SbH_3})+\log(2/3)]}$$
$$=(\Delta^*E_C-\Delta^*E_A)/(21.6-1.52\log P_{SbH_3}) \quad (7)$$

Above this temperature V_A controls the overall rate and below this temperature V_C controls the rate, provided Δ^*E_C is larger than Δ^*E_A. In other words, at higher temperatures the decomposition is of first order, while at lower temperatures it is proportional to 2/3 power of the stibine pressure, being independent of hydrogen pressure. In the transition region of the two, at higher stibine pressures the activation energy becomes larger, as V_C controls the rate more predominantly, and at lower pressures vise versa from the Equation 7.

As shown in a previous paper[5] the observed activation energy for this reaction is dependent upon the partial pressure of stibine and decreases as the pressure decreases, and the order of the reaction increases as the reaction temperature becomes higher from a fractional order to a first order. Hence the experimental results seem to support those theoretical conclusions, if it is tentatively assumed that the difference between Δ^*E_C and Δ^*E_A is around 6 kcal./mol. provided that all the other assumptions are valid.

Another explanation of the experimental results is the interpretation of the fractional order on the basis of the Langmuir concept, assuming that the adsorption of SbH_3(a) is appreciable. As has been discussed in the previous paper[5], however, this explanation seems to have little physical meaning according to Boudart[22].

Decomposition of Arsine on an Arsenic Surface at 278C°.—The heat of the reaction at 551°K is 38.6 kcal./mol. from the value at standard temperature and the

20) "Handbook of Chemistry and Physics", 35th Edition, by C. D. Hodgman et al., Chemical Rubber Publishing Co., Ohio. (1953).
21) B. M. W. Trapnell, "Advances in Catalysis," Vol. IX., Academic Press Inc., N. Y., (1957), p. 238.
22) M. Boudart, "Structure and Properties of Solid Surfaces", edited by G. R. Gomer and C. S. Smith, University of Chicago Press Chicago, Illinois, (1953) p. 400.

heat capacities of the gases[23], the followings are the results of a similar calculation for the decomposition.

$$V_A=3.1\times10^{-16}SP\exp(-\Delta^*E_A/RT) \quad (8)$$

$$V_B=8.3\times10^{-6}S(P_{AsH_3}/P_{H_2}^{\frac{1}{2}})\times\exp(-\Delta^*E_A/RT) \quad (9)$$

$$V_C=3.1\times10^{-11}SP_{AsH_3}^{\frac{2}{3}}\exp(-\Delta^*E_C/RT) \quad (10)$$

where Δ^*E_C in the Equation 10 is the true activation energy for the step C. The overall reaction is first order as is shown by the experiments, step A being rate-determining, provided that $\Delta^*E_C-\Delta^*E_A<10$ kcal. If this is the case and all the other assumptions are valid, T_e, where V_A equals to V_C, becomes lower than 200°C at 100 mm. of arsine pressure from the similar calculations and above this temperature the decomposition will be first order, which is the case in the experiments.

Decomposition of Methane on Carbon Surface.—The decomposition of methane on a carbon surface at 1000°K can be treated in the same way. The change of the heat content in this decomposition, ΔH, is 21.6 kcal. per mole at this temperature, as ΔH at 25°C is 17.89 kcal./mol.[23] and $\Delta C_p=9.18-5.96\times10^{-3}T-0.051\times10^5T^{-2}$[24].

According to Barrer[6], the heat of adsorption of hydrogen on carbon is about 50 kcal./mol. being independent of its coverage. The results of the calculation are as follows, if we use the same suffixes for V_A, V_B, V_C and V_D as in the germane decomposition.

$$V_A=S(P_{CH_4}/F_{CH_4})\exp(-\Delta^*E_A/RT)Q_{C^*(0)}=2.0\times10^{-15}S\frac{P_{CH_4}\exp(-\Delta^*E_A/RT)}{1+0.24P_{H_2}} \quad (11)$$

if it is noted that the step A takes place on the unsaturated carbon bonds on the surface and hence

$$Q_{C^*(0)}=\frac{1}{1+(P_{H_2}/F_{H_2})\exp(50{,}000/RT)}$$

and

$$V_B=S\frac{P_{CH_4}}{F_{CH_4}}\left(\frac{F_{H_2}}{P_{H_2}}\right)^{\frac{1}{2}}Q_{C^*(0)}\exp(-\Delta^*E_B/RT)=2.1\times10^{-9}S\frac{P_{CH_4}}{P_{H_2}^{\frac{1}{2}}}\frac{\exp(-\Delta^*E_A/RT)}{1+0.23P_{H_2}} \quad (12)$$

$$V_C=S\frac{P_{CH_4}}{F_{CH_4}}\frac{F_{H_2}}{P_{H_2}}Q_{C^*(0)}\exp(-\Delta^*E_C/RT)=2.1\times10^{-2}S\frac{P_{CH_4}}{P_{H_2}}\frac{\exp(-\Delta^*E_A/RT)}{1+0.23P_{H_2}} \quad (13)$$

as Δ^*E_B and Δ^*E_C are equal to $\Delta^*E_A-\frac{1}{3}(25{,}000-21{,}600)$ and $\Delta^*E_A-\frac{2}{3}(25{,}000-21{,}600)$, respectively and the coverage of CH(a), $Q_{C^*(CH(a))}$, of $H_2(g)\rightleftarrows2H(a)$, are appreciable according to the calculation. On the other hand,

$$V_D=8.0\,S\frac{P_{CH_4}^{\frac{1}{2}}\exp(-\Delta^*E_{0D}/RT)}{(1+4.0P_{CH_4}^{\frac{1}{4}})^2}\fallingdotseq\frac{S}{2}\exp(-\Delta^*E_{0D}/RT) \quad (14)$$

which is obtained from the following equations,

$$V_D=\frac{S}{2}\left(\frac{P_{CH_4}}{F_{CH_4}}\right)^{\frac{1}{2}}Q_{C^*(0)}\exp(-\Delta^*E_D/RT)$$

$$\theta_H/(1-\theta_H)=(P_{CH_4}/F_{CH_4})^{\frac{1}{4}}\times\exp\left(\frac{-25{,}000\times4+21{,}600}{4RT}\right)=4.0\times P_{CH_4}^{\frac{1}{4}}$$

$$Q_{C^*(0)}=(1-\theta_H)^2$$

$$\Delta^*E_D=\Delta^*E_{0D}-\frac{1}{2}(25{,}000\times4-21{,}600)$$

where $\Delta^*{}_0E_D$ is the true activation energy for the step D.

The observed activation energy for this reaction is 53.4 kcal. and $\exp(70{,}000/RT)$ is equal to 2.0×10^{15}. Hence the step A is rate-determining, if Δ^*E_{0D} is less than 120 kcal./mol., which is most probably the case.

Barrer found that a kinetic expression,

$$V=\frac{kP_{CH_4}}{1+0.022P_{H_2}}$$

is applicable to this reaction, which is in fair agreement with the theoretical equation 11, if the ambiguity of the heat of adsorption of hydrogen on carbon is taken into account. As $\exp(30{,}000/RT)$ is equal to 3.6×10^6, the assumption 4 of the equal activation energies can be adjusted to nearly 30 kcal. for the step B, if all the other assumptions are valid.

Decomposition of Germane on a Germanium Surface at 302°C.—The results of a similar calculation are as follows, as the heat of adsorption of hydrogen on

23) F. D. Rossini and D. D. Wagman, "The Selected Values of Chemical Thermodynamic Properties," U. S. Government Printing Office (1952).
24) Kelley, Bull. of Bur. of Mines, No. 407 (1937).

germanium is 23.5 kcal./mol. at low coverages[17].

$$V_A = S \frac{P_{GeH_4}}{2.4\times10^{15}} \left(\frac{1}{1+0.23\sqrt{P_{H_2}}}\right)^2 \times \exp\left(-\Delta^* E_A/RT\right) \quad (15)$$

$$V_B = S \frac{P_{GeH_4}}{F_{GeH_4}} \left(\frac{F_{H_2}}{P_{H_2}}\right)^{\frac{1}{2}} \times \exp\left[-\left(\Delta^* E_A - \frac{1}{3}(q+11{,}800)\right)\Big/ RT\right] Q_{C^*(0)}$$

$$= \frac{3.1\times10^{-10} S P_{GeH_4} \exp\left[-(\Delta^* E_A - q/3)/RT\right]}{(1+0.23 P_{H_2}^{\frac{1}{2}})^2 P_{H_2}^{\frac{1}{2}}} \quad (16)$$

$$V_C = \frac{2.3\times10^{-2} S P_{GeH_4} \exp\left[-(\Delta^* E_A - 2q/3)/RT\right]}{P\left[1+0.23 P_{H_2}^{\frac{1}{2}} + 0.023 \frac{P_{GeH_4}}{P_{H_2}} \exp\left(\frac{2q}{3RT}\right)\right]^2} \quad (17)$$

$$V_D = \frac{S}{2} \exp\left(-\Delta^* E_{0D}/RT\right) \quad (18)$$

where q is the heat of the reaction and $\Delta^* E_{0D}$ is the true activation energy for the step D. As the decomposition is probably exothermic, either V_A or V_D is the rate-determining step.

The experimental results show that the step D is the rate-determining step and the observed activation energy is 41.2kcal./mol. As $\exp(41{,}200/RT)$ is equal to 2.2×10^{16} at 302°C, V_D can be slower than V_A by 10^2 at the slowest at 10 cm. pressure of germane if $\Delta^* E_A$ is small enough. As will be shown later the observed reaction rate agrees satisfactorily with the calculated V_D. In the cases of the decompositions of tin hydride, arsine, etc., on the other hand, in which the step A is rate-determining, the partition functions of the activated complexes of V_A are usually not unity, but have fairly large values, which is probably the case in V_A of the Equation 15. This is probably one of the reasons why the step D is rate-determining, and, consequently, at much higher temperatures it can be expected that the reaction becomes first order in respect to germane, V_A being rate-determining, as the apparent activation enenrgy of V_A is smaller than $\Delta^* E_{0D}$.

The fact that no exchange between GeD_4 and GeH_4 to form GeH_xD_y is observed during the reaction is explained by the slow rate of chemisorption of germane on the germanium surface, as the rate of chemisorption is retarded by the chemisorbed hydrogen atoms which cover the surface. If the desorption of hydrogen is assumed to be the only rate-determining step, the adsorption rate of germane onto the surface is so retarded by the chemisorbed hydrogen that it turns out slower than the desorption rate from the calculation. This implies that the adsorption rate is so retarded by the chemisorbed hydrogen atoms that another potential energy cascade appears at this adsorption step besides the desorption step, while the germanium surface is still almost saturated in this case.

Decomposition of Other Hydrides and Nickel Carbonyl.—The decomposition of tin hydride on tin surfaces can be treated in the similar way. It can be shown that the step A is rate-determining and the reaction is first order as in Table I, provided that the heat of the reaction is between 40 and −40 kcal./mol. and $\Delta^* E_{0D}$ is not larger than 20 kcal./mol.

In the case of the decomposition of hydrogen selenide, a similar calculation shows that it should be of first order in respect to hydrogen selenide.

The decomposition of nickel carbonyl on nickel surface can be treated in a similar way, though the nature of the chemical bonds between CO and nickel atom are different from those in the hydrides. The heat of the decomposition was given by Fischer et al.[25] The results of the calculation showed that the chemisorption of nickel carbonyl on nickel surface is rate-determining, having the kinetic expression of $v = kP_{Ni(CO)_4}/(1+bP_{CO})$ as Bawn has observed. The value of b in the expression was also computed with a reasonable agreement.

The observed and the calculated reaction rates are shown in Table III, where the unit of pressure, P, is mmHg. and the activation energy at 10 cm. stibine pressure is used for stibine decomposition; the tin and germanium surface are considered to be smooth. In these calculations the number of the sites for the reactions per cm.^{2}, G, is taken as 10^{15}. The discrepancies between the observed and

TABLE III

	Temp.	Observed rate	Calculated rate
GeH_4	302°C	5.2×10^{13}	0.5×10^{13} mol./sec. cm.^{2}
AsH_3	278	7.9×10^{9} P	6.0×10^{3} P
SbH_3	35	8.2×10^{10} P	3.6×10^{8} P
SnH_4	77	2.3×10^{13} P	3.7×10^{7} P

25) A.K. Fischer et al., *J. Am. Chem. Soc.*, **79**, 2044 (1957).

the calculated values are probably due to the large values of the partition functions of the activated complexes, not being unity.

The number of collisions of gas molecules on unit surface area per second (n_c) and that of reacted molecules (n_r) are shown in Table IV, where Δ^*E is the observed activation energy for the reaction. In the case of germane decomposition it is shown that $n_c \exp(-\Delta^*E/RT)$ is much smaller than n_r, which suggests that the rate-determining step is not the chemisorption step on bare surface.

TABLE IV

	Temp.	n_c	$n_c \exp\left(\frac{-\Delta^*E}{RT}\right)$	n_r
GeH_4	302°C	1.7×10^{20} P	3.7×10^{4} P	5.2×10^{13}
AsH_3	278	1.7×10^{20} P	1.1×10^{11} P	0.8×10^{10} P
SbH_3	35	1.8×10^{20} P	3.3×10^{15} P	0.8×10^{11} P
SnH_4	77	1.7×10^{20} P	3.5×10^{14} P	2.3×10^{13} P

A tin surface, for instance, does not chemisorb hydrogen[26], nevertheless it chemisorbs tin hydride to decompose it to tin and hydrogen. This chemisorption depends upon the bond strength between the chemisorbed species and the element, and if the total strength of the dissociative adsorption is strong enough to chemisorb, the chemisorption takes place to decompose the hydride. Thus hydrogen from hydride might be chemisorbed on the elements on which hydrogen gas is not chemisorbed. The fact that arsine can be decomposed on antimony more rapidly than on an arsenic surface[1], or that ammonia can be decomposed on germanium[27] might be explained on this basis.

Summary

The decomposition of arsine, stibine, tin hydride, methane, germane, hydrogen selenide and nickel carbonyl on the surface of the corresponding elements have been discussed from the statistical mechanical view-point. As these decompositions are catalytic reactions of the simplest type, several reasonable assumptions enable us to calculate the rates of each elementary step of each reaction and hence to decide the rate-determining step in a semi a priori fashion. It is shown that the calculations impose definite limitations to the possible mode of decompositions of this kind.

The author wishes to express his thanks to Dean Hugh Taylor and Professor W. J. Kauzmann of Princeton University and also to Professor J. Horiuti, Professor T. Kwan and Professor K. Miyahara of Hokkaido University for their valuable suggestions and encouragement.

Department of Chemical Industry
Yokohama National University
Minami-ku, Yokohama

26) B. M. W. Trapnell, *Proc. Roy. Soc.*, **A218**, 566 (1953).

27) K. Tamaru, *J. Phys. Chem.*, **60**, 612 (1956).

Studies of Aggregation of Dodecylammonium Carboxylates in Carbon Tetrachloride by Infrared Absorption Spectra and Thermistors

By Ayao KITAHARA

(Received March 15, 1958)

It was reported that the phenomenon of solubilization by some detergents takes place in carbon tetrachloride solutions as happens in other non-polar solvents[1], though Palit et al.[2] had reported the occurrence of erratic behavior in carbon tetrachloride. Hence, it is considered necessary to investigate micelle formation or aggregation in carbon tetrachloride solutions of detergents by some direct method.

For the present purpose, studies by infrared spectroscopy and on the vapor pressure depression by the use of a couple of thermistors were carried out at varying concentrations. Results obtained by both of these independent methods were compared.

Experimental

Materials. — Dodecylammonium butyrate and dodecylammonium caprylate, the preparation of which had been described previously[1], were employed as detergents. Carbon tetrachloride was distilled after drying over calcium chloride or phosphorus pentoxide and the constant boiling center cut used.

Measurements. — Infrared spectra were obtained using a Perkin-Elmer 21 instrument with rock salt optics. Cells of 1 and 0.5 mm. thickness were used. Room temperature was controlled to about 20°C. Measurements of vapor pressure depressions using a couple of matched thermistors made it possible to calculate the apparent mean aggregation number (Z) which is evaluated involving the monomer present. The apparatus and the method were the same as those described in the previous paper[3]. The temperature of thermostat was controlled to 19.7 ± 0.0005°C. The calibration curve of the thermistor resistance vs. concentration was made using carbon tetrabromide as solute, because it will be safely said that solutions of carbon tetrabromide in carbon tetrachloride are ideal. Measurements by thermistors were made in triplicate or quadruplicate at each concentration and the average value was adopted for the calculation of Z.

1) A. Kitahara, *J. Colloid Sci.*, **12**, 342 (1957).
2) S. R. Palit and V. Venkateswarlu, *Proc. Roy. Soc.*, **A208**, 542 (1951).
3) A. Kitahara, This Bulletin, **31**, 288 (1958).

Results and Discussion

Assignment of Infrared Spectra.—The infrared spectra of detergents in carbon tetrachloride were depicted in Fig. 1 ranging from 1600 to 1750 cm^{-1} at varying concentrations. Absorption bands which become remarkable with increasing concentration are found at 1640 cm^{-1} in both spectra of dodecylammonium butyrate and

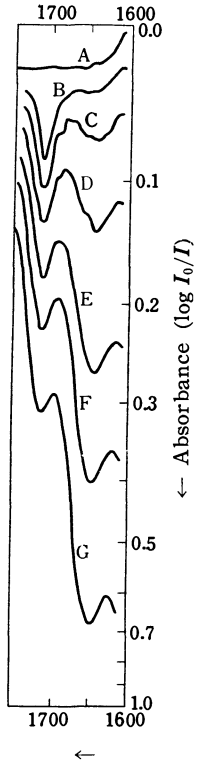

Fig. 1 (a). Change in infrared spectra of dodecylammonium butyrate with varying concentration. (A) pure solvent; (B) 0.0025mole/l.; (C) 0.0050 mole/l.; (D) 0.010 mole/l.; (E) 0.020 mole/l.; (F) 0.030 mole/l.; (G) 0.050 mole/l. Cell length: 1 mm.

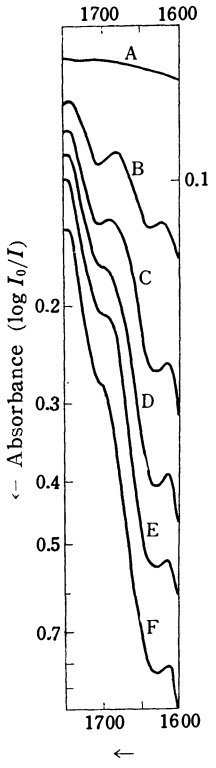

Fig. 1 (b). Change in infrared spectra of dodecylammonium caprylate with varying concentration. (A) pure solvent; (B) 0.018 mole/l.; (C) 0.036 mole/l.; (D) 0.055 mole/l.; (E) 0.073 mole/l.; (F) 0.112 mole/l. Cell length: 0.5 mm.

caprylate. On the other hand, it is seen that the absorption bands of 1710 cm^{-1} in neither of these spectra are sensitively variable with increasing concentration. Yeager and Barrow[4] have shown from infrared spectra of the reaction products of acetic acid and *n*-butylamine, diethylamine or triethylamine that the absorption bands of 1712 and 1630 cm^{-1} are assigned to the carbonyl group forming a hydrogen bonds with the same or another molecule and to the NH_2^+ or NH_3^+ group of the ammonium salt, respectively. The absorption band of "Amino-Acid I" which falls within the narrow range of 1640~1610 cm^{-1} for many monoamino-monocarboxylic acids has been assigned to NH_3^+ by many authors[5]. Hence, it may be concluded that the absorption bands of 1710 and 1640 cm^{-1} belong to the molecules of following formulae A and A_1, respectively:

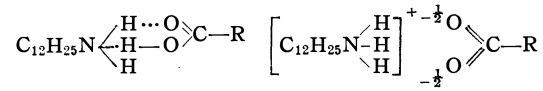

(A) (A_1)

It will be thought that the molecule of A_1 aggregates to λ-mer in a non-polar solvent by virtue of ionic parts. Then the following equilibrium will exist in the carbon tetrachloride solutions:

$$A \rightleftarrows A_1 \rightleftarrows 1/\lambda A_\lambda \qquad (1)$$

where A_λ represents a λ-mer molecule. It is safely assumed that aggregation does not affect the absorption band, because aggregation will not be so strong as to affect chemical bonding, and that the greater part of molecules of A_1 exists in the aggregated state instead of the monomeric form because of the highly polar part. Hence, the equilibrium 1 can be rewritten as follows:

$$\lambda A \rightleftarrows A_\lambda \qquad (2)$$

The absorption bands of 1710 and 1640 cm^{-1} are characteristic for the molecule existing as monomer and the one taking part in aggregation, respectively. This assignment is consistent with the fact that the infrared spectra of these detergents by the potassium chloride disc method which represent the absorption band in the solid state show the more intense absorption at the 1640 cm^{-1} than those of the relatively concentrated solutions and show no absorption at the 1710 cm^{-1}. The absorbances (log I_0/I) of each absorption band, which are shown in Table I, were obtained using the base-line method and the peak-intensity method from Fig. 1.

Analysis of Absorbance Data.—Aggregation equilibrium of a detergent in a non-polar solvent can be described by the Equation 2. The true aggregation number λ is evaluated by excluding the monomer present in the solution. It may be assumed that the aggregates are approximately monodisperse in a non-polar solution of the detergents[3]. No shift in the absorption band of 1640 cm^{-1} which is characteristic for the aggregate is evident from Fig. 1. This fact may be considered as an evidence of forming a single kind of aggregation[6]. The equilibrium constant is represented using molar concentration instead of activity, which is valid

4) E. A. Yeager and G. M. Barrow, *J. Am. Chem. Soc.*, **76**, 5211 (1954); **77**, 4474, 6206 (1955).
5) L. T. Bellamy, "The Infrared Spectra of Complex Molecules", Methuen and Co., London, (1954), p. 204.
6) N. D. Coggeshall and E. L. Saier, *J. Am. Chem. Soc.*, **73**, 5414 (1951).

TABLE I

THE VALUES OF ABSORBANCE (cell thickness: 1 mm.)

Dodecylammonium Butyrate					Dodecylammonium Caprylate				
	Absorbance					Absorbance			
Concentration (mole/l.)	D_a		D_1		Concentration (mole/l.)	D_a		D_1	
	B. L.*	P. I.*	B. L.	P. I.		B. L.	P. I.	B. L.	P. I.
0.0025	0.010	0.018	0.047	0.060	0.018	0.034	0.20_8	0.050	0.13_7
0.0050	0.016	0.050	0.053	0.082	0.036	0.080	0.47_2	0.050	0.23
0.010	0.035	0.11_5	0.055	0.11	0.055	0.18	0.76_4	0.060	0.29
0.020	0.070	0.24_5	0.065	0.15_5	0.073	0.24	1.02	0.060	0.36_4
0.030	0.12	0.38	0.075	0.21	0.112	0.42	1.62	0.070	0.50_4
0.050	0.23	0.65_7	0.085	0.28_5					

* B. L. ...Base line method, P. I. ...Peak intensity method

for the dilute concentration range under consideration. That is,

$$C_\lambda / C_1{}^\lambda = K \tag{3}$$

where C_λ and C_1 are the molar concentration of λ-mer and monomer, respectively. Beer's law of absorption is approximately obeyed for absorption bands of the monomer and of the detergent molecule taking part in aggregation in these dilute concentration ranges. Hence,

$$\left.\begin{aligned}(\log I_0/I)_1 &= k_1 C_1 l = D_1 \\ (\log I_0/I)_a &= k_a C_a l = D_a\end{aligned}\right\} \tag{4}$$

where k, C and l are the extinction coefficient, the molar concentration in monomer unit and a length of the cell, respectively. The subscripts of 1 and a represent a coexisting monomer and a detergent molecule taking part in aggregation, respectively. By definition,

$$C_a = \lambda C_\lambda \tag{5}$$

The following equation is deduced from the Equations 3, 4 and 5:

$$\lambda \log D_1 - \log D_a + k' = 0 \tag{6}$$

where $k' = \log\{\lambda k_a l K / (k_1 l)^\lambda\}$

As it has been assumed that λ is constant, k' is constant. The values of λ and k' can be calculated by means of the Equation 6 using the data of Table I. The values of λ calculated by means of the least square are given in the 2nd and 3rd columns of Table II.

TABLE II

THE VALUES OF TRUE AGGREGATION NUMBER (λ)

	Spectral method		Thermistor method
	Base line	Peak intensity	
Dodecylammonium butyrate	2.7	2.4	2.8
Dodecylammonium caprylate	3.3	2	3.0

In order to ascertain the result obtained above, the absolute intensity method was employed for comparison. Integrated densities (D_A) of absorption bands were calculated from the values of measurements for both bands of 1640 and 1710 cm^{-1} at a few concentrations of these detergents in carbon tetrachloride. These measurements* were carried out by means of a Perkin-Elmer 112 instrument with calcium fluoride prism. Room temperature was 25±1°C. Integrated density is represented by the following form[7]:

$$D_A = K \ln (I_0/I)_{\nu_{max}} \Delta\nu_{1/2}$$

where $\ln (I_0/I)_{\nu_{max}}$ is the apparent peak intensity, $\Delta\nu_{1/2}$ the apparent half-intensity band width and K the constant which is determined by $\ln (I_0/I)_{\nu_{max}}$ and $S/\Delta\nu_{1/2}$ (S is the slit width). The λ's were calculated from the Equation 6 using the values of D_A instead of the absorbances in Table I. The λ's obtained thus were approximately equal to 2 for both detergents. The agreement between those values and those from the peak intensity in Table II is satisfactory. The difference between the values from the absolute intensity and those from the base line is not serious, since it is sufficient only if we confirm the agreement of the order of magnitude of aggregation.

Analysis of Data by Thermistor.—The apparent mean aggregation numbers Z obtained by the thermistor method are shown in Table III. The fraction of the solute

* These measurements were carried out in cooperation with Mr. Suetaka by suggestion of Professor K. Kojima of Tokyo Institute of Technology, to whom the author wishes to express his sincere gratitude.

7) D. A. Ramsey, ibid., **74**, 72 (1952): J. Wenograd and R. T. Spurr, ibid., **79**, 5844 (1957).

TABLE III
THE VALUES OF Z, α, C_1 AND λ

	Concentration (C) (mole/l.)	Z	α	C_1 (mole/l.)	λ
Dodecylammonium butyrate	0.085_5	1.8	0.32	0.026	2.8
	0.050	1.5_5	0.43_5	0.022	2.6
	0.035	1.6	0.47_5	0.016_5	3.6
	0.017	1.2	0.71	0.012	2.1
	0.009	≈1.0	≈1.0	—	—
Dodecylammonium caprylate	0.111	2.0	0.24	0.027	3.0
	0.073	1.7_5	0.31	0.023	2.7
	0.055	1.7_5	0.35_5	0.020	3.0
	0.036_5	1.6_5	0.43	0.016	3.2
	0.018	≈1.0	≈1.0	—	—

present as the monomer (α) which is equal to C_1/C can be calculated by means of the following Kreuzer's equation[8]:

$$\ln(1/\alpha)=(Z-1)/Z+\int_0^C\{(Z-1)/ZC\}dC \quad (7)$$

where C is the total concentration of the solute. The values of C_1 are, therefore, calculated at each total concentration. The values of α and C_1 are given in the 4th and 5th columns of Table III. The following relations are deduced for the equilibrium 2 under an assumption that λ and K are constant[8,9]:

$$C-\lambda C/Z=-(\lambda-1)C_1$$

or

$$\lambda=(1-\alpha)/(1/Z-\alpha). \quad (8)$$

The values of the true aggregation number λ calculated using the Equation 8 are given in the last colum of Table III. The mean values of λ are given in the 4th column of Table II.

It is evident from Table II that the agreement between the values of λ obtained by both spectral and thermistor methods is satisfactory as for the order of magnitude of aggregation. This gives us an evidence to an assumption made in the derivation of the Equation 8. The true aggregation numbers λ of these detergents in carbon tetrachloride solutions are relatively smaller than those in cyclohexane solutions[3]. This fact corresponds qualitatively to the solubilizing power in carbon tetrachloride which is smaller than that in cyclohexane[1].

The Critical Micelle Concentration.— These aggregates may be regarded as small micelles. It has been shown experimentally[10] and theoretically[11] that formation of small micelles gradually takes place over an extended range of concentration. Hence, the critical micelle concentration (cmc) may not be sharply determined. The values of the cmc were tentatively evaluated by plotting C_1 in Table III vs. C and extrapolating to $C_1=C$. These cmc's are 0.010±0.001 and 0.013±0.001 mole/l. for dodecylammonium butyrate and caprylate, respectively. The plot of absorbance (D_1 and D_a) from base line method vs. total concentration (C) was depicted in Fig. 2.

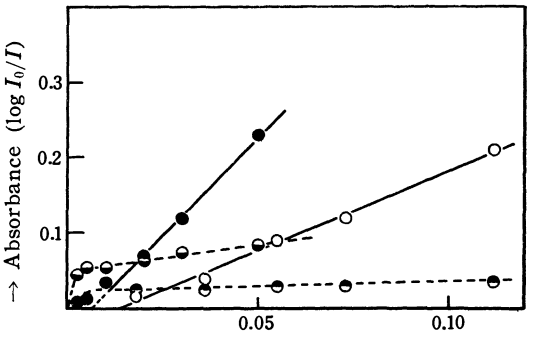

Fig. 2. Plots of absorbance (log I_0/I) versus concentration.

- ○ Plot for absorption at 1640 cm^{-1} of dodecylammonium caprylate
- ◓ Plot for absorption at 1710 cm^{-1} of dodecylammonium caprylate

Cell length, 0.5 mm.

- ● Plot for absorption at 1640 cm^{-1} of dodecylammonium butyrate
- ◒ Plot for absorption at 1710 cm^{-1} of dodecylammonium butyrate

Cell length, 1 mm.

It is evident from Fig. 2 that the relation between D_a and C is approximately linear excepting the range of lower concentra-

8) J. Kreuzer, *Z. physik. Chem.*, **B53**, 213 (1943).
9) I. Prigogine and R. Defay, "Chemical Thermodynamics", Longmans Green and Co., London, (1954), p. 422.
10) E. F. Williams, N. T. Woodberry and J. K. Dixon, *J. Colloid Sci.*, **12**, 452 (1957).
11) J. Stauff, *Z. Elektrochemie*, **59**, 246 (1995).

tions in the case of dodecylammonium butyrate where the experimental error is appreciable. It will be reasonable to assume that extrapolation of the $D_a \sim C$ line to zero concentration shows the cmc. These cmc's are 0.007 ± 0.001 and 0.013 ± 0.002 mole/l. for dodecylammonium butyrate and caprylate, respectively. The values obtained using the peak intensity by a similar way were 0.002 ± 0.001 and 0.006 ± 0.002mole/l., respectively. The agreement between the cmc's obtained by spectral and thermistor method is satisfactory as for the order of magnitude. On the other hand, these cmc's do not show good concordance with values obtained by solubilization of water which were 0.016 ± 0.002 and 0.035 ± 0.005 mole/l.*, respectively. This may be considered to indicate that the cmc has an extended range of concentration or that the cmc may be affected by the presence of water.

Solubilization which takes place in these solutions may be a type similar to that by adsorption on polar groups of small micelles by McBain et al.[12], though polar groups will be properly present in the interior of the aggregate in these non-polar solutions.

Summary

Measurements of infrared absorption spectra and of vapor pressure depressions using a couple of matched thermistors were carried out with carbon tetrachloride solutions of dodecylammonium carboxylates at varying concentrations. The absorption bands at 1710 and 1640 cm^{-1} were assigned to the carbonyl group of the monomer molecule which is formed by hydrogen bonding between amine and acid, and to the NH_3^+ group of ammonium salt resulting from the aggregation, respectively. The equation which was derived from the Beer's law and the aggregation equilibrium made it possible to calculate the true aggregation number λ using the values of absorbance at each absorption band.

Alternatively, the λ was calculated by means of the Kreuzer's equation from the apparent mean aggregation number Z which was obtained using thermistors. The agreement between the λ's obtained by the spectral and thermistor methods was satisfactory as for the order of magnitude. The cmc was tentatively estimated by both spectral and thermistor method. The agreement between the cmc's obtained by these independent methods was good. But these cmc's did not show good agreement with those obtained from solubilization.

The author wishes to express his thanks to Dr. Yukio Mikawa for the measurement of infrared spectra, to Dr. Hiroshi Tubomura for his suggestions with the infrared analysis and to Professor Hideo Akamatu for his continuing interest in this study.

Department of Chemistry
Toho University
Narashino, Chiba

* These values are those at 18 ± 2°C instead of those at 26°C in Ref. 1.

12) J. W. McBain and H. McHan, *J. Am. Chem. Soc.*, **70**, 3838 (1948).

Aconite Alkaloids.—On Pyrolytic Products of Aconitine, Oxonitine, and their Derivatives

By Takeo SHIMA and Takashi AMIYA

(Received March 17, 1958)

It is well known that the pyrolysis of aconitine I ($C_{34}H_{47}O_{11}N$) at or above its melting point results in the internal loss of a molecule of acetic acid whereupon pyraconitine II ($C_{32}H_{43}O_9N$) is formed. Little is known, however, about the mode of elimination of acetic acid. Stern[1] mentioned that epoxide-formation occurred between the acetoxy group and an adjacent hydroxyl group or that a new ethylenic

1) R. H. F. Manske and H. L. Holmes, "The Alkaloids", Vol. IV, Academic Press Inc. New York, (1954), p. 292.

kage was introduced by this pyrolysis. cently on the ground of the observation the infrared spectra Schneider[2] sug- ested that a new ethylenic linkage was ntroduced in the conjugated position to an inert ethylenic linkage initially present in compound I during pyrolysis of compound I by abstraction of a molecule of acetic acid between the acetoxy group and a hydrogen atom from a neighboring carbon atom. This mechanism was supported by Nath and Dasgupta[3,3a] although it had been previously denied by Edwards and Marion[4]. Attempts were made therefore to re-investigate pyrolytic reactions of compound I, oxonitine, and their derivatives by means of an examination of both ultraviolet and infrared spectra.

Thus, it was found that on pyrolysis of each of these alkaloids a new carbonyl group was formed by the splitting of a molecule of acetic acid between the acetoxy group and the hydroxyl group on a carbon atom near the acetoxy group.

Results were as follows:

Pyraconitine hydroperchlorate (III) ($C_{32}H_{43}O_9N \cdot HClO_4 \cdot H_2O$)[5,*]: infrared spectrum (nujol), >C=O and ester carbonyl 5.83 μ**; OH 3.01 μ: ultraviolet spectrum (methanol), λ_{max} 230 mμ, log ε 4.15; λ_{max} 275 mμ, log ε 3.03***.

Diacetyl pyraconitine (IV) ($C_{36}H_{47}O_{11}N \cdot C_2H_5OH$)[6,*]: infrared spectrum (nujol), >C=O 5.85 μ; ester carbonyl 5.76 μ; no-OH.

Pyroxonitine(V) ($C_{30}H_{37}O_{10}N$)[1]: infrared spectrum (nujol), lactam carbonyl 6.06 μ; >C=O and ester carbonyl 5.83 μ**; OH 3.01 μ: ultraviolet spectrum (methanol), λ_{max} 230 mμ, log ε 4.26; λ_{max} 275 mμ, log ε 3.03.

Diacetyl pyroxonitine(VI) ($C_{34}H_{41}O_{12}N \cdot C_2H_5OH \cdot H_2O$)[7,*]: infrared spectrum (nujol), lactam carbonyl 5.98 μ; >C=O 5.88 μ; ester carbonyl 5.80 μ; no-OH.

Pyraconine(VII) ($C_{25}H_{39}O_8N$)[8,****]: infrared spectrum (nujol), >C=O 5.88 μ; OH 2.94 μ: ultraviolet spectrum(methanol), λ_{max} 275 mμ, log ε 1.66.

Pyraconine hydrochloride(VIII) ($C_{25}H_{39}O_8N \cdot HCl \cdot 2.5H_2O$)*****[,8]: infrared spectrum (nujol), >C=O 5.94 μ; OH 2.94, 2.89, 2.87 μ: ultraviolet spectrum (methanol), λ_{max} 320 mμ, log ε 1.64.

Pyraconine hydroiodide(IX) ($C_{25}H_{39}O_8N \cdot HI \cdot H_2O$)[6]: infrared spectrum (nujol), >C=O 5.94 μ; OH 3.01, 2.88, 2.80 μ: ultraviolet spectrum (methanol), λ_{max} 220 mμ, log ε 4.11; λ_{max} 310 mμ, log ε 1.99.

Aconine(X) ($C_{25}H_{41}O_9N$)[8,****]: infrared spectrum (nujol), OH 2.88 μ: ultraviolet spectrum (methanol), no λ_{max} at wave lengths 210~350 mμ.

Aconine hydrochloride(XI) ($C_{25}H_{41}O_9N \cdot HCl \cdot 2H_2O$)[8,****]: infrared spectrum (nujol), H_2O 6.08 μ; OH 2.98 μ: ultraviolet spectrum (methanol), no λ_{max} at wave lengths 210~350 mμ.

Pyroxonine(XII) ($C_{23}H_{33}O_9N$)[1]: infrared spectrum (nujol), lactam carbonyl 6.08 μ, >C=O 5.87 μ; OH 3.01, 2.91 μ: ultraviolet spectrum (methanol), λ_{max} 305 mμ, log ε 1.64.

Oxonine(XIII) ($C_{23}H_{35}O_{10}N$)[1]: infrared spectrum (nujol), lactam carbonyl 6.02~6.07 μ; OH 2.9 μ.

Pyrodesmethanol aconitinone hydroperchlorate(XIV) ($C_{31}H_{37}O_8N \cdot HClO_4 \cdot H_2O$)[8]: ultraviolet spectrum (methanol), λ_{max} 233 mμ, log ε 4.39*.

Desmethanol aconitinone(XV) ($C_{33}H_{41}O_{10}N$)[8]: ultraviolet spectrum (methanol), λ_{max} 233 mμ, log ε 4.38[3a].

According to the above data there are marked differences between the absorption bands of compounds VII and VIII and those of compounds X and XI in the ultraviolet spectra and the infrared spectra. Also there was a marked difference in the infrared spectrum between the absorption bands of compound XII and those of compound XIII. Thus compounds VII, VIII and XII are believed to possess carbonyl groups newly formed by pyrolyses. Compounds IV and VI showed no bands at wave length 2.6~3.2 μ characteristic of hydroxyl group. This fact sug-

2) W. Schneider, *Ber.*, **89**, 768 (1956).
3) B. Nath, *J. Sci. Ind. Res., India*, **16, B**, 159 (1957).
3a) S. Dasgupta and B. Nath, *J. Ind. Chem. Soc.*, **34**, 204 (1957).
4) O. E. Edwards and L. Marion, *Can. J. Chem.*, **30**, 627 (1952).
5) H. Schulze and A. Liebner, *Arch. Pharm.*, **251**, 453 (1913).
* The infrared absorption spectra of these compounds were determined after drying in vacuo.
** This absorption band is broad.
*** The ultraviolet spectrum of compound III is nearly identical with that of pyraconitine.
6) H. Schulze and A. Liebner, *Arch. Pharm.*, **254**, 567 (1916).
7) K. Tamura, *Ann.*, **533**, 183 (1938).
8) T. A. Henry, "The Plant Alkaloids", J. & A. Churchill Ltd., London, (1949), p. 673.

**** Compounds VII, X and XI consume one mole each of periodic acid respectively. This fact suggests that the α-glycol of aconine X is not concerned in the pyrolytic reaction.
***** When aconine hydrochloride XI was heated at 180°C for 10 minutes pyraconine hydrochloride VIII was obtained. This compound VIII, which was crystallized from water, was identical with pyraconine hydrochloride which was prepared from pyraconitine by hydrolysis[1] (m. p. and analysis). *Anal.* Found: C, 54.01; H, 8.16. Calcd. for $C_{25}H_{45}O_{10\cdot5}NCl$: C, 54.01; H, 8.18%.
* The ultraviolet spectrum of compound XIV was nearly identical with that of pyrodesmethanol aconitinone.

gests that a new carbonyl group was introduced by abstraction of a molecule of acetic acid between the acetoxy group and the hydroxyl group on a carbon atom near the acetoxy group. On the other hand there was no marked difference between the ultraviolet spectrum of compound III and that[9] of compound I at wave lengths 210~280 mμ. Hence, just as the former investigators[4] stated, no conjugated unsaturation results from pyrolysis. Reduction of compound VII with lithium aluminum hydride gave an amorphous base which the present workers named "pyraconiol". This base formed a hydroiodide which crystallized from water. Pyroconinol hydroiodide XVI ($C_{25}H_{41}O_8N \cdot HI \cdot 1.5H_2O$) showed m. p. 185°C (*Anal.* Found: C, 47.33; H, 7.23; H_2O, 4.25. Calc. for $C_{25}H_{45}O_{9.5}NI$: C, 47.20; H, 7.10; H_2O, 4.25%). The infrared absorption spectrum of compound XVI lacks the band corresponding to that (5.94 μ) of compound IX in the carbonyl region. Also the ultraviolet spectrum of compound XVI (λ_{max} 220 mμ, log ε 4.03) in methanol lacks a maximum corresponding to that (310 mμ) of compound IX in the carbonyl region. From the above data, it is suggested that the carbonyl group does not exist in compound XVI. The ultraviolet spectra of compound XIV and compound XV were rather similar at wave lengths 210~280 mμ. This fact suggests that the carbonyl group newly formed by pyrolysis in compound XIV is not conjugated to the α, β-unsaturated ketone which has been present in compound XV.

The authors are grateful to Professor Harusada Suginome, President of Hokkaido University, for his unfailing kindness in encouraging this work, and to Messrs. M. Yamaguchi and A. Fujino, Institute of Polytechnics, Osaka City University, for their kindness in the determination of the infrared spectra.

Department of Chemistry,
Faculty of Science,
Hokkaido University, Sapporo

9) E. Ochiai, T. Okamoto and S. Sakai, *J. Pharm. Soc. Japan* (*Yakugaku Zasshi*), **75**, 545 (1955).

SHORT COMMUNICATIONS

On the Extraction of Residual Lignin in the Unbleached Sulfite Pulp

By Koichiro SATO, Kiyo EBISAWA and Hiroshi MIKAWA

(Received March 4, 1958)

Generally lignin can not be removed completely by ordinary pulping process. In order to elucidate the bleaching mechanism, it is desirable to make clear the nature of the residual lignin (R.L.) in the unbleached pulp. Mainly because of the difficulties of separation of this lignin, almost nothing is known about it. As the reasons for this difficulty, one or several of the following facts will be considered in the case of sulpfite process. Residual lignin 1) is not sulfonated sufficiently, 2) is combined to carbohydrate firmly, 3) goes into solution with difficulty, because of morphological reasons of fiber, and 4) is condensed to other lignin unit during the digestion.

We have found that the resolution of residual lignin is effected with drastic beating in water, which causes fibrillation of the fiber and is expected to diminish morphological hindrance of the dissolution of R.L.

Commercial unbleached sulfite pulp (air dry, 540 g.) prepared from spruce (*Picea jezoensis*) was suspended in water (21 l) and beaten with NIAGARA-TYPE 1 to 1/2 pound BEATER (TAPPI-STANDARD T200m-45) for 20 hr.

Fig. 1 shows the course of treatment.

Curve I shows the increase of freeness. Freeness levels off at about SR 96 after 12 hr. no further increase being observed. Specific surface (curve II) measured with

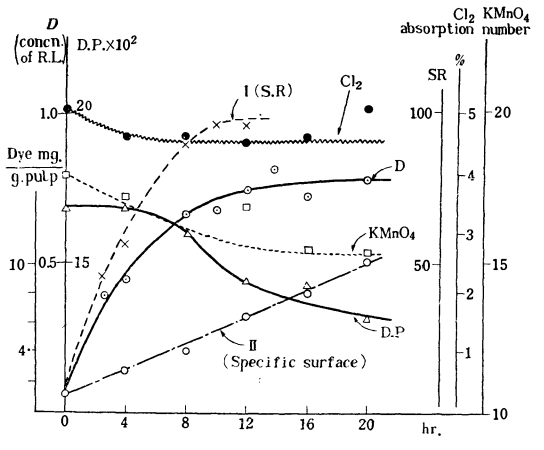

dye (Benzo Fast Scarlet 4BS) adsorption[1], increased linearly, and this shows that the fibrillation was progressing yet after beating 20 hr. On the other hand, the curves representing the permanganate number and the chlorine absorption of the beaten pulp have a slightly downward tendency.

The dissolution of R.L., measured by the ultraviolet absorption spectra of the filtrate of the beaten pulp which was diluted three times with water, reached maximum at 12 hr. After 8 hr., the D.P. of pulp began to decrease slowly. In this treatment the amount of the dissolved lignosulfonic acid does not exceed one-fifth of the total amount of R.L. Further dissolution of the remaining lignosulfonic acid in the beaten pulp is now under investigation.

The sulfonation degree of this lignin thus obtained is as low as that of the so-called "low-sulfonated lignosulfonic acid." Analytical data of R.L., low-sulfonated lignosulfonic acid (LSLA)[2] and ordinary lignosulfonic acid (L.S.A.)[3] are compared in the following table.

R.L.	$C_9H_{9.43}O_{3.90}(OCH_3)_{0.88}$
	$(SO_3Ba/2)_{0.27}S^{neut}_{0.938}\ B^{excess}_{a_{0.014}}$
L.S.L.A.	$C_9H_{9.80}O_{3.76}(OCH_3)_{1.05}$
	$(SO_3Ba/2)_{0.23}S^{neut}_{0.03}\ B^{excess}_{a_{0.028}}$
L.S.A.	$C_9H_{10.7}O_{3.2}(OCH_3)_{1.05}$
	$(SO_3Ba/2)_{0.51}S^{neut}_{0.08}\ B^{excess}_{a_{0.04}}$

The amount of the total phenolic hydroxyl group of R.L. measured by the G.A.-Erdtman's method[4] is 0.17~0.21 per methoxyl, being the same with that of L.S.A. In the case of R.L. the phenolic hydroxyl group belonging to type I[5] is only 20% of the total, the remaining 80% being expected to be type II.

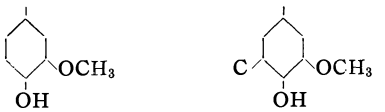

Type I Type II

Along with the dissolution of R.L., some amount of hemicellulose goes also into solution.

Research Laboratory of the Kokusaku Pulp Co., Kamiochiai Shinjuku-ku, Tokyo

1) E. F. Thode, J. W. Bedmesderfer and A. J. Chase: TAPPI **35** No. 8, 379 (1952); Sumikawa and Yoshino: unpublished data.
2) H. Mikawa, K. Sato, T. Takasaki and K. Ebisawa: unpublished data.
3) H. Mikawa, K. Sato, T. Takasaki and K. Ebisawa: This Bulletin **28** 653 (1955).
4) G. A. Erdtman: *Svensk Papperstidn* **56** (1953) 287.
5) H. Mikawa, K. Sato, T. Takasaki and K. Ebisawa: This Bulletin **29** 245 (1956).

Pure Quadrupole Spectrum of Trithiazyl Trichloride

By Hisao NEGITA and Ziro HIRANO

(Received March 18, 1958)

So far we have studied pure quadrupole spectra of some heterocyclic compounds. In this connection, trithiazyl trichloride $(SNCl)_3$ was prepared[1] by chlorinating sulfur nitride $(SN)_4$. It is very unstable and reacts with moisture so easily that some precaution must be taken to preserve it. The spectrum due to ^{35}Cl was observed by the frequency-modulated super-regenerative spectrometer, and only one weak absorption line 29.842 megacycle/sec. was found at 285°K.

This result is evidently different from that of cyanuric chloride $(CNCl)_3$ which shows two adjacent lines[2], although trithiazyl trichloride might be benzene-like heterocyclic compound as well. It crystallizes in hexagonal prisms or needles, which should be closely related to the above fact. However, its crystal structure

1) A. Meuwsen, *Ber.*, **64**, 2311 (1931).
2) H. Negita and S. Satou, This Bulletin, **29**, 426 (1956).

has not yet been established.

On the other hand, it will be seen that the line situates in the neighborhood of those of thionyl chloride $SOCl_2$. This reminds us of the case of phosphonitrile chloride $(PNCl_2)_3$, where the lines are found at almost the same region as those of phosphorus oxychloride $POCl_3$. In the same way, those of cyanuric chloride are near to those of phosgene $COCl_2$. These results are summarized in Table I. When many lines are found in a compound, they are shown on an average for convenience.

TABLE I

COMPARISON OF ^{35}Cl RESONANCE ABSORPTION FREQUENCIES (ν) OF VARIOUS COMPOUNDS

Compd.	ν (Mc./sec.) at room temp.	Compd.	ν (Mc./sec.) at 77°K
$(SNCl)_3$	29.8	SO_2Cl_2	37.7[4]
		$SOCl_2$	31.9[5]
		PCl_5	32.4[6]
$(PNCl_2)_3$	27.8[2]	$POCl_3$	28.6[5]
		PCl_3	26.2[7]
$(CNCl)_3$	36.3[3]	CCl_4	40.6[7]
		$COCl_2$	35.7[7]

In this table, our data are concerned with the value at room temperature, and they should have about 1 megacycle/sec. added to them to compare with those of the compounds at 77°K. As seen from the table, there is a close relation between the valence state of the central atom, e.g., sulfur and the resonance frequency of the chlorine attached to it.

It would be difficult to explain the difference between the frequencies of sulfur and carbon compounds cited above in view of electronegativities of the composed atoms, because both sulfur and carbon atoms have the same negativity 2.5, according to Pauling. Of course, it is more difficult to interpret the slight frequency shifts between the ring compounds and the corresponding oxychlorides.

However, the frequency decrease of phosgene in comparison with cyanuric chloride might be attributed to its resonance structure $\overset{+}{O}\equiv CC\overset{-}{Cl}Cl$ which may be deduced from the shorter distance 1.18A[8] between the carbon and oxygen than the normal double bond length 1.21A. The corresponding triple bond structure would hardly contribute anything to cyanuric chloride, and this may be the case also in both trithiazyl trichloride and thionyl chloride which is low pyramid structure[9].

The authors wish to express their thanks to Professor T. Ichikawa and Dr. H. Yamamura for their encouragement throughout this work.

Department of Chemistry, Faculty of Science, Hiroshima University
Hiroshima

3) H. Negita, S. Satou, T. Yonezawa and K. Fukui, This Bulletin, **30**, 721 (1957).
4) P. J. Bray, *J. Chem. Phys.*, **23**, 703 (1955).
5) R. Livingston, *Phys. Rev.*, **82**, 289 (1951).
6) D. W. McCall and H. S. Guttowsky, *J. Chem. Phys.*, **21**, 1300 (1953).
7) R. Livingston, *J. Phys. Chem.*, **57**, 496 (1953).
8) T. L. Cottrell and L. E. Sutton, *Quart. Rev.*, **2**, 260 (1948).
9) K. J. Palmer, *I. Am. Chem. Soc.*, **60**, 2360 (1938).

The Visible and Ultraviolet Absorption Spectra of Cellulose- and Amylose-Iodine Complexes

By Takehiro Abe

(Received April 16, 1958)

The structure of the amylose-iodine complex has been established, by Rundle and his co-workers[1], as a helical α-amylose chain in which the iodine molecules are arranged in a linear array, parallel to the helical axis. On the other hand, it has been described in a few books[2,3] that cellulose, structurally related to amylose, also gives a blue color on treatment with iodine. So, an attempt has been made, in the present work, to compare the cellulose-iodine complex with the amylose complex by means of their absorption spectra.

A solution of cellulose was obtained by dissolving a filter paper (the Toyo filter paper, No. 1 with a diameter of 12.5 cm.) into about 100 ml. of aqueous solution of commercial guaranteed zinc chloride. By adding a drop of solution of iodine and potassium iodide into this cellulose solution a deep blue color yields at once and numerous blue fibers precipitate. This blue color disappears at about 80°C by warming and re-appears by cooling.

1) R. E. Rundle and D. French, *J. Am. Chem. Soc.*, **65**, 1707 (1943); **69**, 1769 (1947).
2) Y. Kondo, "Experiments in Microchemistry of Cellulose Fibers", Bosekizashi, Osaka (1939), p. 5.
3) Y. Tsuzuki, "Simple Experiments in Organic Chemistry" Shokabo, Tokyo (1949), p. 58.

The visible absorption band of amylose-iodine complex has been found to shift toward the shorter wavelengths with increasing iodide concentration[4]. Thus, in the present measurement, a saturated iodine water was used to avoid an effect of iodide. The solution of cellulose-iodine complex to be measured was obtained after removing the blue fibers from the solution by a centrifuge.

α-Amylose was fractionated from an alkaline solution of potato starch as a complex with n-butanol[5]. The complex was crystallized three times from butanol. After washing it with ethanol it was dried by a vacuum pump for four hours and α-amylose was obtained. By adding a little iodine water into a solution of amylose and zinc chloride the sample of amylose-iodine complex was prepared. The absorption measurement was carried out with Hitachi Quartz Spectrophotometer Model EPU-2 at room temperature.

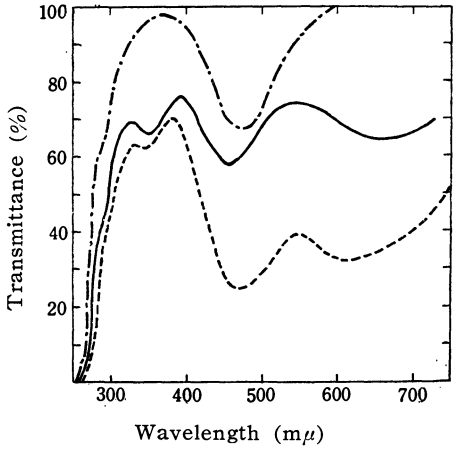

Fig. 1. Absorption spectra of cellulose-iodine complex (——), amylose-iodine complex (- - - -), and iodine in zinc chloride solution (—·—·).

The results in Fig. 1 show that the absorption spectrum of cellulose-iodine complex in solution of zinc chloride is closely analogous to that of amylose-iodine. The absorption band at about 470 mμ seems to be attributed to iodine, because the spectrum of iodine in aqueous zinc chloride is observed at the same region. It is well known that a blue color of starch-iodine is decolorized by warming and is regenerated by cooling. As described above, the color of cellulose-iodine is found to behave like starch-iodine towards change in temperature. In the present experiments the cellulose-iodine complex is, thus, analogous to amylose-iodine. This fact leads to the suggestion that the cellulose-iodine complex is able to yield the blue color by the same mechanism as that by which the amylose-iodine does; in other words the iodine molecules may be arranged in the helical cellulose chain.

If a little of the iodine iodide solution is droped on a filter paper immersed in a solution of sodium hydroxide (of a concentration above several per cent.) for half an hour at room temperature and the paper is washed with water, a blue color can be seen distinctly on it. It has been found that the β-amylose is transformed to the helical α-amylose on treatment with a solution of sodium hydroxide[6]. It seems, therefore, possible that by sodium hydroxide cellulose is also transformed to a helical state giving a blue color with iodine.

The author is particularly indebted to Professor Y. Nomura for discussions and encouragement. The author also thanks Assistant Professor S. Maeda for use of the spectrophotometer.

Department of Chemistry
Defense Academy
Yokosuka, Kanagawa

4) S. Ono, S. Tsuchihashi and T. Kuge, *J. Am. Chem. Soc.*, **75**, 3600 (1953).
5) H. Azumi and T. Nakajima, *Sci. Rep. Tohoku Univ.*, 1, **36**, 282 (1952).
6) J. R. Katz and J. C. Derkson, *Z. phys. Chem.*, **A150**, 81 (1930).

On the Radioactive Deposits of Thoron

By Hirotoshi SANO

(Received April 22, 1958)

Numerous reports have been published of the disintegration products of thoron or radon collected on a metal surface[1]. However, it seems to the present author that little information is available on the decay curve of such deposits collected on materials other than metals. To study

1) G. B. Cook and J. F. Duncan: "Modern Radiochemical Practice", Oxford, Clarendon Press, p. 14, (1952).

this problem, an experiment was performed in this laboratory. Copper plate, polyethylene film, and also the surface of water were used as collecting surface in this experiment. For not less than fifty hours, a collecting surface was exposed to a gas containing thoron, without application of electric field. The thoron was in equilibrium with thorium-X produced in crystalline thorium nitrate. As soon as the collecting surface was taken out from the gaseous medium, the radioactivity of the deposits was measured with a G-M counter. The geometry was kept as constant as possible for the counting of the activity of deposits on both copper plate and polyethylene film. Corrections were made for the coincidence loss on all the data obtained. It has been found that the amount of the radioactivity per unit area of collecting surface is roughly equal for different kinds of surface material, but the shape of the decay curve of the collected products depends on the kind of material. From the experimental results, the decay curves of the radioactive deposits were partly illustrated in Fig. 1. In Fig. 1, the decay curve A of the radioactive deposits collected on a copper plate constitutes almost a straight-line in semilogarithmic scale, showing the half-life of ThB (10.6 hr.). On the other hand, the decay curve B of the deposits collected on a polyethylene film shows some deviation from the straight-line at the initial stage of decay. Then it turned to a straight-line showing the half-life of ThB. For the measurement of the deposits collected on the surface of water, the water was evaporated up in a stainless steel dish and the radioactivity of the invisible residue was measured. The decay curve C obtained for the deposite on water has an intermediate shape between the cases of copper plate and polyethylene film. The total amount of the deposits collected on the surface of water is, however, smaller than that on the copper plate or polyethylene film because of the different surface area as well as the different geometry for the deposition. These results were always reproducible. The shapes of the decay curves indicate that there is some difference between the deposition velocity of ThB and ThC, and that the ratio of deposition velocity of ThC to ThB is greater for the collection on a copper plate than on a polyethylene film or the surface of water. To date, the phenomenon and the mechanism of the preferential deposition of some daughter disintegration products from thoron on different surface materials have not been described. Detailed results and probable explanation of the phenomenon will be reported elsewhere.

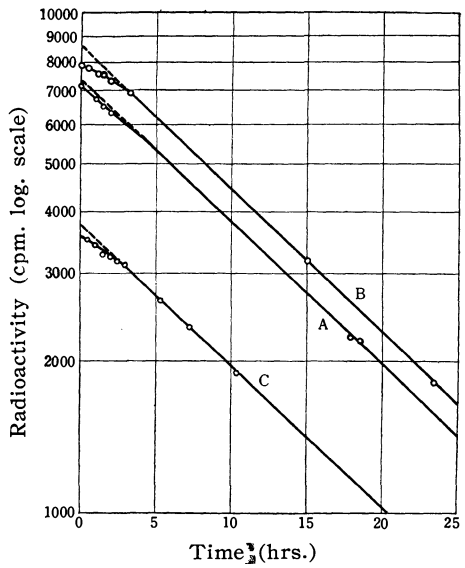

Fig. 1. Curve A: Copper plate.
Curve B: Polyethylene film.
Curve C: Surface of water.

The author acknowledges with thanks the interest and encouragement of Dr. Nobufusa Saito, Professor of this laboratory.

Department of Chemistry
Faculty of Science
The University of Tokyo
Hongo, Tokyo

The Polyaddition of Diphenylsilane to Difunctional Unsaturated Compounds

By Kuniharu KOJIMA

(Received April 25, 1958)

Since about 1947, it has been known that trichlorosilane adds to olefinic double bonds, under the influence of peroxide catalysts[1], azo catalysts[2], and platinum

1) L. H. Sommer et al., *J. Am. Chem. Soc.*, **69**, 188 (1947); **70**, 484 (1948); C. A. Burkhard et al., ibid., **69**, 2687 (1947): R. H. Krieble, U. S. Pat., 2,524,529. (1950).
2) R. V. Lipscomb, U. S. Pat., 2,570,462 (1951).

catalysts[3,4]. Methyldichlorosilane[5], phenylsilane[6], diphenylsilane[6] and phenylmethylsilane[6] also have been added to olefins, by the same method. Tribromosilane has been added to olefins, under the influence of ultraviolet light[7] and also at elevated temperatures[8].

Recently, platinum catalyzed additions of some chloro- and ethoxysilanes to a variety of vinyl[9], allyl[9] and methacrylic monomers[10] have been reported to give polymeric products in good yield under mild conditions.

I have now carried addition reaction between difunctional unsaturated compounds (divinyltetramethyldisiloxane or diallyl phthalate etc.) and diphenylsilane. In this case, the polyaddition products were obtained as resinous solid or viscous oily liquids.

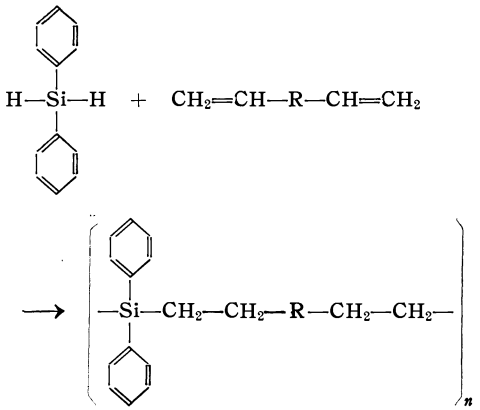

Diallyl phthalate (4.92 g., 0.02 mol.), diphenylsilane (3.68 g., 0.02 mol.) and platinum black catalyst (0.03 g.) were placed in a glass tube and it was sealed in a stream of nitrogen. The tube was heated at 110~120°C in an air oven for 50 hours. The reaction product was dissolved in benzene (100 c.c.) and reprecipitated with methanol (200 c.c.). The precipitate was separated and dried in a vacuum desiccator at 50°C for 7 days and analyzed for silicon and the molecular weight was determined by cryoscopic method in benzene.

Anal. Found: Si, 5.34. Calcd. for $C_{26}H_{26}O_4Si$: Si, 5.83 %. Mol. Wt., 2390. Yield, 76 %.

Divinyltetramethyldisiloxane (3.72 g., 0.02 mol.), diphenylsilane (3.68 g.) and platinum black (0.03 g.) were placed in a glass sealed tube. The tube was heated at 110~120°C in an air oven for 50 hours. The reaction product was dissolved in benzene and reprecipitated with methanol. The product was dried in a vacuum desiccator at 50°C, for 7 days, analyzed for silicon, and the molecular weight was determined.

Anal. Found: Si, 22.46. Calcd. for $C_{20}H_{30}OSi_3$: Si, 22.70 %. Mol. Wt., 2160. Yield, 78 %.

Further study is in progress.

Tokyo Medical and Dental University
Yushima, Bunkyo-ku, Tokyo

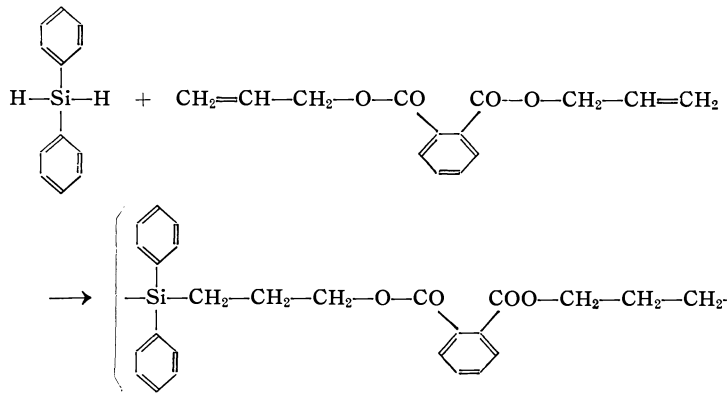

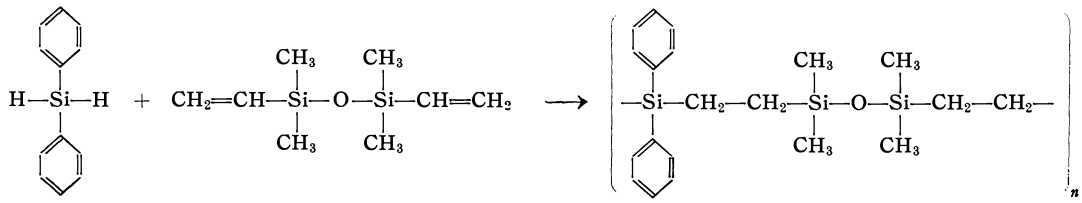

3) G. H. Wagner, Brit. Pat., 670,617 (1952), U.S. Pat., 2,632,013., 2,637,738 (1953).
4) J. L. Speier et al., *J. Am. Chem. Soc.*, **79**, 974 (1957).
5) E. T. McBee et al., ibid., **79**, 2326,2329 (1957).
6) J. L. Speier et al., ibid., **78**, 2278 (1956).
7) A. J. Topchiev et al., *Doklady Akad. Nauk.* S.S.S.R., **86**, 965 (1952).
8) A. J. Barry et al., U. S. Pat., 2626,271 (1953).
9) L. Goodman et al., *J. Am. Chem. Soc.*, **79**, 3073 (1957).
10) L. H. Sommer et al., ibid., **79**, 2768 (1957).

The Isomerization of 2,4-Dinitrophenylhydrazones of α-Keto Acids

By Hirohiko KATSUKI, Koichiro SUMIZU, Tarumi MORIWAKI and Shozo TANAKA

(Received May, 20, 1958)

Most of 2, 4-dinitrophenylhydrazones of α-keto acids derived from monocarboxylic amino acids have been observed to give two spots on the paper chromatogram except dimethylpyruvic acid (DMPA) and methylethylpyruvic acid[1]. Because of the confirmation of the presence of *cis*- and *trans*-isomers in 2, 4-dinitrophenylhydrazones of pyruvic acid (PA), a representative of α-keto acid giving two spots on the paper chromatogram, we have ascribed these two spots to geometrical isomers of the hydrazones[2]. Furthermore we have recognized that DMPA, a representative of α-keto acid giving one spot on the paper chromatogram, gave only one isomer in some conditions on account of rapid isomerization velocity[3]. Since then in our laboratory the isomerization of these hydrazones had been studied and it was found that the directions of the isomerization were determined by the polarity of solvent.

Each component in the isomeric mixtures of the hydrazones of PA was determined by Hayashi's method[4] based on the fact that only the *cis*-form is extracted by ethyl acetate-ether mixture (3 : 1) from 0.1 % sodium carbonate solution containing 10 % sodium chloride. In less-polar solvent such as ethyl acetate, acetone or ether, the isomerization did not occur but in a polar solvent such as water or glacial acetic acid, the *cis*-form converted into the *trans*-form and a part of the hydrazone decomposed. But the inversion in the opposite direction was not observed. Both isomerization and decomposition were greatly accelerated by hydrogen ions. The rates of isomerization and decomposition of the *cis*-form in 0.3 N hydrochloric acid at 18°C for 5 hours, for example, were 30 % and 60 % respectively. On the other hand, in a less-polar solvent, hydrogen ions accerelated the interconversion in either direction and an equilibrium state was estabilshed, the composition of which being determined by the kind of solvent used, by the water content of the solvent and by temperature. For example, when standing in ethyl acetate saturated with 6 N hydrochloric acid for 30 min. at 18°C, the equilibrium mixture consisted of 46 % of the *cis*-form and 47 % of the *trans*-form. Seven per cent was proved to decompose.

In the case of the hydrazone of DMPA, the isomerization is so rapid that the equilibrium state is attained as soon as the isomer is dissolved in a solvent, and the simultaneous measurements of spectra of both isomers in the same solvent is impossible. For this reason the paper chromatogram gives only one spot. The α-isomer, m. p. 198°C (decomp.) is stable in anhydrous less-polar solvent, whereas the β-isomer, m. p. 188°C (decomp.) is stable in polar solvent. In absolute alcohol, the absorption maximum of the α-isomer in visible region lay at 365 mμ but with the increase of water content of the solvent it shifted to a longer wave length until it reached 380 mμ where the component consisted of β-isomer. The same results were obtained when formamide was used instead of water. That the rearrangement of the configuration of the hydrazone of DMPA occurred very easily was shown as follows: the freshly precipitated hydrazone in hydrochloric acid for the most part, consisted of the α-form but changed to the β-form within a few hours. Furthermore, when the sodium salt of the β-form was acidified with dilute hydrochloric acid precipitated free hydrazone at first was found to be the α-form. The structures of two isomers of the hydrazones of DMPA, at present, are not fully elucidated and will be discussed elsewhere.

Department of Chemistry, Faculty of Science, Kyoto University
Sakyo-ku, Kyoto

1) D. E. Metzler, J. Olivard and E. E. Snell, *J. Am. Chem. Soc.*, **76**, 644 (1954).
2) T. Moriwaki, H. Katsuki, and S. Tanaka, *J. Chem. Soc. Japan, Pure Chem. Sec.* (*Nippon Kagaku Zassi*) **76**, 1367 (1955); F. A. Isherwood, and R. H. Johnes, *Nature*, **175**, 419 (1955); H. Katsuki, K. Sumizu, T. Moriwaki, S. Tanaka and I. Hayashi, *Nature*, **181**, 639 (1958).
3) H. Katsuki, *J. Am. Chem. Soc.*, **77**, 4686 (1955).
4) I. Hayashi, private communication. Our sincere thanks are offered to him for his suggestion and continuous interest.

Adsorption Measurements during Surface Catalysis

By Kenzi TAMARU

(Received May 20, 1958)

It is one of the most fundamental problems in the field of surface catalysis to estimate the area of active part on catalyst surface. Since Taylor suggested his "active center theory" in 1925, many discussions have been presented from various view-points on the problem. Taylor emphasized that certain centers on the catalyst surface were responsible for most of the catalytic activity. These centers were tentatively identified as the corners and edges of the crystals in the surface. Other interpretations associated them with the existence of a number of different crystalline faces on the catalyst, each face having its own specific catalytic activity. The area of these active regions should accordingly be all extremes between the case in which all the atoms on the surface are active and that in which relatively few are active.

This short note is to emphasize a new approach to elucidate the mechanism of the catalytic reaction as well as the number of active atoms on the catalyst surface, measuring the adsorption during surface catalysis.

Recently it has been shown[1-4] that during the catalytic decomposition of germane (GeH_4) on germanium surface, which is a zero order reaction, the germanium surface is mostly saturated with chemisorbed hydrogen atoms. On the other hand it was also shown that the adsorption of hydrogen on germanium is an activated, reversible, dissociative and immobile adsorption, and also that if the chemisorbed hydrogen is supplied from the ambient hydrogen gas, the coverage of the surface in the adsorption equilibrium should be less than 0.6 under the experimental condition of the decomposition. From other data such as, for instance, obtained with deuterium and germanium deuteride, it was concluded that the desorption of chemisorbed hydrogen from the germanium surface is a rate-determining step of the overall decomposition reaction. All the evidence[1,3,5] seemed to indicate that the clean surface of germanium laid down by the decomposition of the hydride appeared to behave homogeneously energetic as to sites in the decomposition of the hydride, the major part of the germanium atoms on the surface participating in the catalysis.

It was thus suggested that the adsorption measurements during catalytic reaction would associate not only with the elucidation of the reaction mechanism, but also with the approximate estimation of active area of the catalyst surface, especially in the case of immobile adsorption.

When we study the kinetics of gas reaction on a solid catalyst, we elucidate the reaction mechanism, in most cases, on the basis of Langmuir-Hinshelwood, or sometimes, of Eley-Rideal mechanism, tacitly assuming that the elementary steps other than the rate-determining steps are all in equilibrium. The coverage of the surface to be guessed from the kinetics is that on the active part of the catalyst surface where the catalysis is actually taking place, and these coverages are not always the same with those derived from the adsorption equilibrium with the ambient gases, but are dependent upon the mechanism of the reaction, or the rate-determining step of the reaction, because of the free energy change accompanied by the reaction. This is the reason why the germanium surface is saturated with the chemisorbed hydrogen during the decomposition reaction, while the hydrogen adsorption equilibrium only covers less than sixty per-cent of the surface under the pressure.

If the adsorption on catalyst surface could be measured during reaction and the results were far from that on the active part which have been guessed from the kinetics, then we might consider that the active part on the catalyst surface which participates in the catalysis is a minor part of the surface. For instance, if a reaction is exactly zero order, it suggests that the active part of the catalyst surface is saturated with such things as reactants, products or intermediate compounds, the adsorption being independent of the ambient gas pressures. When the adsorption measurements during the reac-

1) K. Tamaru, M. Boudart and Hugh Taylor, *J. Phys. Chem.*, **59**, 801 (1955).
2) P. J. Fensham, K. Tamaru, M. Boudart and Hugh Taylor, ibid. 806 (1955).
3) K. Tamaru and M. Boudart, "Advances in Catalysis," Vol. IX Academic Press Inc., N.Y., p. 699 (1957).
4) K. Tamaru, *J. Phys. Chem.*, **61**, 647 (1957).
5) K. Tamaru, ibid., **60**, 612 (1956).

tion, however, would show the adsorption appreciably dependent upon the ambient gas pressure, it suggests that the active region is a minor part of the surface, and from the pressure-independent adsorption we could not only guess the area which participates in the catalysis, but also determine what actually saturates the active part, which suggests the rate-determining step of the overall reaction. On the other hand, if the adsorption is immobile and all the surface is saturated throughout the reaction, it suggests that all the surface is taking part in the catalysis, when the saturation does not result from the adsorption equilibrium of any of the ambient gases, as in the case of germane decomposition.

If the chemisorption of A in the catalytic reaction, $A+B \rightarrow C$, is rate-determining, the adsorption of A will not be observed during the reaction except the physical adsorption and the back-adsorption from C such as $C \rightleftarrows B(ads.)+A(ads.)$. The ammonia synthesis would be an example of this kind, as the chemisorption of nitrogen on the synthesis catalyst is generally accepted to be rate-determining.

Thus the new approach to measure the adsorption during catalytic reaction in addition to the separate measurements of each gas might enable us to attain a much better understanding of the mechanism of catalytic reaction as well as the nature of the catalyst surface. In most discussions of surfact catalysis it is tacitly assumed that the equilibrium case applies except the rate-determining step. We can also find with this new approach whether it is the case.

The adsorption measurements during reaction can be carried out in a closed circulating system in a similar way to those of the mixed adsorption. From the amount of the reactant introduced in the system and the pressure and the composition of the circulating gas, we can calculate the adsorbed amount of gases on the catalyst surface. The amount of catalyst is preferably large for accurate measurements and the adsorption should be measured under such conditions that the reaction takes place very slowly; otherwise the composition of the circulating gas will not be practically the same throughout the system and it might be affected by the heat of the reaction in the reactor.

The author wishes to express his gratitude to Sir Dean Hugh Taylor of Princeton University and Professor J. Horiuti and Professor T. Kwan of Hokkaido University for their valuable discussions and encouragement.

Department of Chemical Industry
Facluty of Engineering
Yokohama National University
Minami-ku, Yokohama

Surface Areas of Sulfated Detergents

By Maresuke KASHIWAGI

(Received June 4, 1958)

The following report is concerned with surface films of some organic salts of lauryl sulfate. Apart from surface films of insoluble materials, relatively few data are available on the spread monolayers of soluble detergents. These soluble materials can not be spread under ordinary conditions, but by using a sufficiently high concentration of salts in the substrate, they can be expected to spread at the air-water interface. As for surface films of sodium lauryl sulfate (SLS), very useful studies[1-3] have been made since the early works of Bull[4] and Brady[5]. The present writer attemps here to investigate the spread surface films of morphorin, triethanolamine and pyridine salts of lauryl sulfate.

These three specimens are synthesized from lauryl alcohol and obviously they differ from one another only in end group attached to the same dodecyl sulfate portion of the molecule. It is therefore expected that the dodecyl sulfate portion with these heavy organic groups at the end would exhibit effects different from SLS, but it is found experimentally that they occupy the identical surface area with SLS.

Experimental

Materials.—A general synthetic method is as follows; thirty seven grams of lauryl alcohol distilled at 142~144°C/15 mmHg is sulfated in

1) B. A. Petheica, *Trans. Faraday Soc.*, **50**, 413 (1954).
2) J. T. Davis, *J. Colloid. Sci.*, **11**, 377 (1956).
3) G. Nilsson, *J. Phys. Chem.*, **61**, 1135 (1957).
4) H. B. Bull, *J. Am. Chem. Soc.*, **67**, 10 (1945).
5) A. P. Brady, *J. Colloid Sci.*, 4, 417 (1949).

hexane with 33 g. of pure chlorosulfonic acid at around 0°C over the period of 4 hours. After the completion of the reaction, the product is poured dropwise into 200 cc. of 10% aquous morpholin solution with stirring at the temperature below 5°C. The whole material is then shaken twice with petroleum ether to remove unreacted alcohol. The water portion is dried over the hot water bath and finally in a vacuum desiccator. The product is recrystalized repeatedly from ethylacetate or ethanol.

The chemical structure and nitrogen analysis are shown in Table I.

TABLE I
ANALYSIS OF LAURYL SULFATE

	N calcd.	Analysis found %
Morpholin	3.97	3.90
Triethanolamine	3.37	3.50
Pyridine	4.05	4.08

Measurements.—Surface pressure (F) is measured with a surface balance of Wilhelmy type. The detergent is spread from its *iso*-propanol (40% by volume)—water solution over the substrate containing 25% ammonium sulfate. After 10 minutes, the film is compressed to a desired area for the measurements.

Results.—Fig. 1 shows surface pressure changes of morpholin, triethanolamine and pyridine salt of lauryl sulfate on 25% ammonium sulfate at 18°C, respectively.

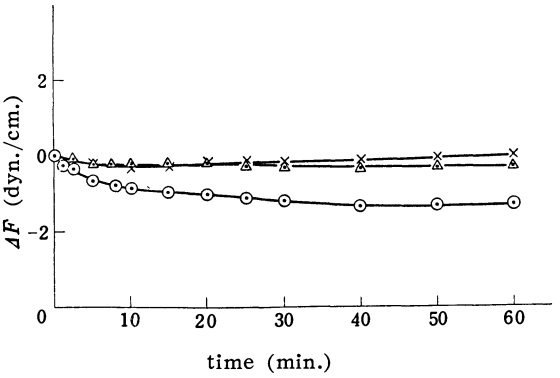

Fig. 1. Surface pressure changes with time (Substrate 25% $(NH_4)_2SO_4$)
Const. area
⊙ Morpholin 50.1 Å²/mol.
△ triethanolamine 50.7
× pyridine 47.7

These $F-t$ curves indicate[6] that F does not decrease considerably and they make fairly stable monolayers inspite of heavy soluble organic group attached. Fig. 2 represents $F-A$ diagrams of these sulfated detergents on the same substrate. It appears that $F-A$ curves of these three specimens are approximately identical.

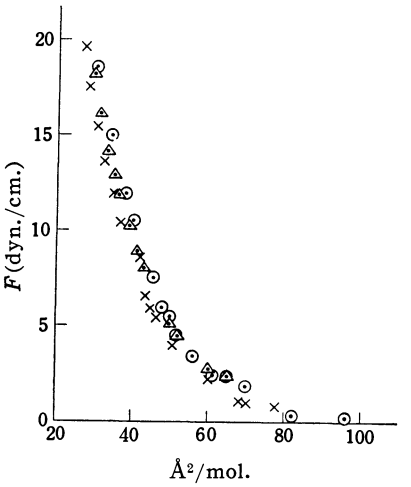

Fig. 2. Surface pressure-area diagrams (Substrate 25% $(NH_4)_2SO_4$)
⊙ Morpholin
△ triethanolamine
× pyridine

Discussion

It is known that spread and adsorbed monolayers of SLS are of the same character[1]. Although added salt condenses the monolayer as would be expected[7], Petheica has shown that all the monolayers obey the relation $F(A-A_0)=nkT$ where A_0 is a coarea term for an uncohering film, T the absolute temperature, k Boltzmann constant and n a constant.

The whole part of curves in Fig. 2 is slightly more expanded than SLS[1], but it obeys the above equation within graphical and experimental error. A_0 is thus calculated to be about 34 Å²/mol. between areas of 40 Å²/mol. and 70 Å²/mol. for all organic salts, and 40 Å²/mol., A_0 decreases to about 18 Å²/mol., which corresponds to the cross sectional area of hydrocarbon chain of the detergent molecule. It is interesting to note that these values of A_0 are in good agreement with surface areas of SLS calculated from the above equation of state or by other methods[1-3].

The writer wishes to express thanks to Professor Ryohei Matsuura of Kyushu University for his kind advice.

Mitsuwa Chemical Laboratory
Marumiya Co. Ltd.
Terajima-machi, Sumida-ku, Tokyo

6) M. Kashiwagi, This Bulletin, **30**, 176 (1958).

7) J. T. Davis, *Proc. Roy. Soc.*, **208**, 224 (1951).

Additions and Corrections

Volume 31, 1958

Dielectric Constant of Liquid Consisting of Anisotropic Molecules

By Masasi YASUMI, Hideo OKABAYASHI and Hitoshi KOMOOKA

The following tables are added. (Vol. 31, No. 4, p. 402).

TABLE I

DIELECTRIC CONSTANT OF BENZENE

(Å)		(10^{-25} cc.)
$a_1=7.1$	$a_2/a_1=1.00$	$\alpha_1=123.1$[1]
$a_2=7.1$		$\alpha_2=123.1$
$a_3=3.7$	$a_3/a_1=0.52$	$\alpha_3=63.5$

temp. (°C)	ε (Ob.)[2]	ε (L-L)[3]	ε (Cal.) (0.52)[4]
10	2.302	2.266	2.204
20	2.283	2.244	2.185
30	2.263	2.223	2.165
40	2.243	2.203	2.147
55	2.213	2.170	2.117
65	2.194	2.150	2.099

1) Stuart; loc. cit.
2) Observed values are refered in the following paper. R. J. W. Le Fèvre; *Trans. Faraday Soc.*, **34**, 1127 (1938).
3) Calculated value with Lorentz-Lorenz formula.
4) Calculated value with our formula assuming as the axial ratio 0.52.

TABLE II

DIELECTRIC CONSTANT OF CARBON DIOXIDE UNDER HIGH PRESSURE

(Å)		(10^{-25} cc.)
$a_1=5.3$	$a_2/a_1=0.52$	$\alpha_1=44.9$[1]
$a_2=3.0$		$\alpha_2=21.4$
$a_3=5.3$	$a_3/a_1=0.52$	$\alpha_3=21.4$

temp. = 50°C

d_{amagat}	ε (Ob.)[2]	ε (L-L)	ε (Cal.) (0.6)
24.28	1.02486	1.02433	1.02436
61.20	1.06343	1.06216	1.06202
116.87	1.12444	1.1208	1.1205
231.23	1.25991	1.2487	1.2477
350.40	1.41189	1.3943	1.3898
470.70	1.57801	1.5546	1.5456
549.90	1.69318	1.6684	1.6562
595.89	1.76244	1.7380	1.7232

1) Stuart; loc. cit.
2) Michels and Kleerekoper; Physica, **6**, 586 (1939).

TABLE III

DIELECTRIC CONSTANT OF CARBON DISULFIDE

(Å)			(10^{-25} cc.)
$a_1=6.8$	$a_2/a_1=0.54$		$\alpha_1=151.4$[1]
$a_2=3.7$			$\alpha_2=55.4$
$a_3=3.7$	$a_3/a_1=0.54$		$\alpha_3=55.4$

temp. (°C)	ε (Ob.) (Z.I.)[2]	ε (Ob.) (Fè)[3]	ε (Ob.) (G)[4]	n^2 (L.W.)[5]	ε (L-L)	ε (Cal.) (0.5)
40		2.603			2.671	2.545
25		2.625			2.716	2.584
20	2.626	2.632	2.635	2.650	2.732	2.600
15			2.648			
10	2.657	2.644		2.673	2.765	2.625
0	2.688	2.658	2.661	2.699	2.799	2.655
− 20	2.740	2.686	2.739	2.752	2.861	2.708
− 40	2.792		2.794	2.806	2.928	2.762
− 60	2.839		2.850	2.859	2.993	2.819
− 80	2.885		2.904	2.914	3.063	2.876
−100	2.954		2.961	2.969	3.137	2.935
−110	2.988			2.996	3.172	2.966

1) Stuart; loc. cit.
2) A. A. Zuehke and L. R. Ingersoll; *J. Opt. Soc. Amer.*, **27**, 314 (1937).
3) R. J. W. Le Fèvre; *Trans. Faraday Soc.*, **34**, 1127 (1938).
4) M. R. Guillerin; *Compt. rend*, **206**, 1001 (1938).
5) N. Lyon and F. Wolfram; *Ann. d. Physik*, **63**, 739 (1920).

TABLE IV
DIELECTRIC CONSTANT OF CARBON DISULFIDE UNDER HIGH PRESSURE

temp.=30°C

Press.(Atm.)	ε(Ob.)[1]	ε(L-L)	ε(Cal.) (0.5)
1	2.61	2.67	2.56
500	2.74	2.79	2.66
1000	2.82	2.88	2.73
2000	2.94	3.03	2.85
4000	3.11	3.27	3.05
6000	3.23	3.45	3.19
8000	3.33	3.60	3.29
12000	3.52	3.87	3.52

1) W. E. Danforth; *Phys. Rev.*, **38**, 1224 (1931).

TABLE V
DIELECTRIC CONSTANT OF METHYL FLUORIDE UNDER HIGH PRESSURE

(Å)		(10^{-25} cc.)*
$a_1=4.7$	$a_2/a_1=0.85$	$\alpha_1=31.6$[1]
$a_2=4.0$		$\alpha_2=23.2$
$a_3=4.0$	$a_3/a_1=0.85$	$\alpha_3=23.2$

$\mu_0=1.79$ D (Stark effect)[2]

temp.=50°C

Press.(Int. Atm.)	ε(Ob.)[3]	ε(Cal.) (1.7)[4]
21.706	1.218	1.207
29.919	1.333	1.316
41.373	1.551	1.517
49.400	1.783	1.729
55.683	2.067	1.982
60.819	2.496	2.38
63.630	3.001	2.84
65.468	3.811	3.63
66.190	4.210	4.08
67.287	4.726	4.62
69.052	5.214	5.15
71.724	5.659	5.68
74.993	5.992	6.06
81.402	6.422	6.54

1) C. G. Le Fèvre and R. J. W. Le Fèvre; loc. cit.
2) S. N. Ghosh, R. Trambarulo and W. Gordy; *J. Chem. Phys.*, **21**, 308 (1953).
3) H. G. David, S. D. Hamann and J. F. Pearse; *J. Chem. Phys.*, **20**, 969 (1952).
4) Calculated value with our formula assuming as the axial ratio 1.7.
* In the literature of C. G. Le Fèvre and R. J. W. Le Fèvre, the authors assume that $P_E+P_A=9$ cc. and $P_E=6.6$ cc.. However, we assume that $P_A=0$, $P_E=9$ cc.. Using this value we calculate the values of the components of polarizability.

TABLE VI
DIELECTRIC CONSTANT OF METHYL CHLORIDE

(Å)		(10^{-25} cc.)
$a_1=5.6$	$a_2/a_1=0.71$	$\alpha_1=54.2$[1]
$a_2=4.0$		$\alpha_2=41.4$
$a_3=4.0$	$a_3/a_1=0.71$	$\alpha_3=41.4$

$\mu_0=1.87$ D (Stark effect)[2]

temp. (°C)	ε(Ob.)[3] (M.L.)	ε(Ob.) (Fevre)[4]	ε(Cal.) (0.71)	ε(Cal.) (0.75)
−20	12.61	12.6	11.90	12.22
−30	13.26	13.22	12.61	12.91
−40	14.02	14.07	13.38	13.75
−50	14.88	15.00	14.21	14.66
−60	15.84	15.95	15.19	15.64
−70	16.88	16.92	16.23	16.75
−80	18.02		17.44	18.03
−90	19.27		18.76	19.45

1) Stuart; loc. cit.
2) R. G. Shulman, C. H. Towres and B. P. Dailey; *Phys. Rev.*, **78**, 145 (1950).
3) S. C. Morgan and H. H. Lowry; *J. Phys. Chem.*, **34**, 3285 (1930).
4) R. J. W. Le Fèvre; *Trans. Faraday Soc.*, **34**, 1127 (1938).

TABLE VII
DIELECTRIC CONSTANT OF METHYL BROMIDE

(Å)		(10^{-25} cc.)
$a_1=5.9$	$a_2/a_1=0.68$	$\alpha_1=68.5$[1]
$a_2=4.0$		$\alpha_2=49.0$
$a_3=4.0$	$a_3/a_1=0.68$	$\alpha_3=49.0$

$\mu_0=1.80$ D (Stark effect)[2]

temp. (°C)	ε(Ob.) (M.L.)[3]	ε(Cal.) (0.68)	ε(Cal.) (0.6)
0	9.97	10.50	9.67
−10	10.42	11.05	10.17
−20	10.91	11.69	10.73
−30	11.43	12.39	11.32
−40	12.00	13.13	11.99
−50	12.63	13.95	12.73
−60	13.32	14.85	13.50
−70	14.07	15.86	14.39
−80	14.96	16.96	15.35
−90	16.02	18.18	16.41
−100	17.4	19.61	17.66

1) Stuart; loc. cit.
2) R. G. Schulman, C. H. Townes and B. P. Dailey; *Phys. Rev.*, **78**, 145 (1950).
3) S. O. Morgan and H. H. Lowry; *J. Phys. Chem.*, **34**, 3285 (1930).

TABLE VIII
DIELECTRIC CONSTANT OF METHYL IODIDE

(Å)		(10^{-25} c.c.)
$a_1=6.3$	$a_2/a_1=0.64$	$\alpha_1=87.2$[1]
$a_2=4.0$		$\alpha_2=65.7$
$a_3=4.0$	$a_3/a_1=0.64$	$\alpha_3=65.7$

$\mu_0=1.65$ D (Stark effect)[2]

temp. (°C)	ε(Ob.) (M.L.)[3]	ε(Cal.) (0.60)	ε(Cal.) (0.45)
40	6.50	7.33	6.35

30	6.75	7.65	6.60
20	7.00	8.00	6.86
10	7.26	8.36	7.14
0	7.53	8.76	7.45
−10	7.81	9.17	7.77
−20	8.13	9.64	8.12
−30	8.48	10.14	8.50
−40	8.87	10.68	8.91
−50	9.28	11.29	9.37
−60	9.74	11.91	9.85
−70	10.33	12.63	10.39

1) Le Fèvre; loc. cit.
2) R. G. Shulman, C. H. Townes and B. P. Dailey; *Phys. Rev.*, **78**, 145 (1950).
3) S. O. Morgan and H. H. Lowry; *J. Phys. Chem.*, **34**, 3285 (1930).

TABLE IX

DIELECTRIC CONSTANT OF ACETONITRILE

(Å)		(10^{-25} cc.)
$a_1=6.2$	$a_2/a_1=0.64$	$\alpha_1=54.3$[1]
$a_2=4.0$		$\alpha_2=37.0$
$a_3=4.0$	$a_3/a_1=0.64$	$\alpha_3=37.0$

$\mu_0=3.92$ D (Stark effect)[2]

temp. (°C)	ε(Ob.)[3] (U.N)	ε(Ob.) (G.P.)[4]	ε(Ob.) (T)	ε(Cal.) (0.7)
15	38.3			37.4
20	37.5		37.45	36.4
25	36.7			35.4
82		26.2		26.3

1) Le Fèvre; loc. cit.
2) S. N. Ghosh, R. Trambarulo and W. Gardy: *J. Chem. Phys.*, **21**, 308 (1953).
3) H. Ulich and W. Nespital; *Z. Physik. Chem.*, **B16**, 221 (1932).
4) F. V. Grimm and W. A. Patrick; *J. Am. Chem. Soc.*, **45**, 2794 (1923).
5) J. Timmermans, A. M. Piette and R. Phillipe; *Bull. Soc. Chim. Belges*, **64**, 5 (1955).

TABLE X

DIELECTRIC CONSTANT OF TERT-BUTYL CHLORIDE

(Å)		(10^{-25} cc.)
$a_1=6.2$	$a_2/a_1=1.11$	$\alpha_1=109.2$[1]
$a_2=6.9$		$\alpha_2=92.6$
$a_3=6.9$	$a_3/a_1=1.11$	$\alpha_3=92.6$

$\mu_0=2.13$ D (Vapour)[2]

temp.(°C)	ε(Ob.) (S)[3]	ε(Cal.) (1.33)
−20	12.2	12.32
−10	11.5	11.58
0	10.95	10.90
10	10.4	10.29
15		10.00
20		9.73
30	9.37	9.19

1) Le Fèvre; loc. cit.
2) B. H. Wismall and C. P. Smyth; *J. Chem. Phys.*, **9**, 356 (1941).
3) W. O. Baker and C. P. Smyth; *J. Am. Chem. Soc.*, **61**, 2798 (1939).

TABLE XI

DIELECTRIC CONSTANT OF CHLOROFORM

(Å)		(10^{-25} cc.)
$a_1=4.6$	$a_2/a_1=1.54$	$\alpha_1=66.8$[1]
$a_2=7.1$		$\alpha_2=90.1$
$a_3=7.1$	$a_3/a_1=1.54$	$\alpha_3=90.1$

$\mu_0=1.05$ D (Vapour)[2]

temp. (°C)	ε(Ob.) (M.L.)[3]	ε(Ob.) (F)[4]	ε(Ob.) (C)[5]	ε(Cal.) (1.54)	ε(Cal.) (1.82)
60	4.12			3.80	4.03
50	4.29	4.31		3.95	4.19
40	4.47	4.47		4.09	4.35
30	4.65	4.64		4.24	4.53
20	4.84	4.81	4.785	4.40	4.71
10	5.02	5.00		4.57	4.90
0	5.22	5.19	5.172	4.74	5.10
−10	5.43	5.40		4.94	5.34
−20	5.65	5.51	5.601	5.15	5.58
−30	5.89			5.38	5.85
−40	6.16		6.095	5.62	6.14
−50	6.45			5.91	6.47
−60	6.79		6.772	6.21	6.83

1) Stuart; loc. cit.
2) S. C. Sircar; *Indian J. Phys.*, **3**, 197.
3) S. C. Morgan and H. H. Lowry; *J. Phys. Chem.*, **34**, 3285 (1930).
4) R. J. W. D. Fèvre; *Trans. Faraday Soc.*, **34**, 1127 (1938).
5) I. E. Coop; *Trans. Faraday Soc.*, **33**, 583 (1937).

TABLE XII

DIELECTRIC CONSTANT OF NITROMETHANE

(Å)		(10^{-25} cc.)
$a_1=5.5$	$a_2/a_1=0.94$	$\alpha_1=51.8$[1]
$a_2=5.2$		$\alpha_2=71.7$
$a_3=4.0$	$a_3/a_1=0.73$	$\alpha_3=18.3$

$\mu_0=3.46$ D (Stark effect)[2]

temp. (°C)	ε(Ob.) (B.M.)[3]	ε(Ob.) (T.P.P.)[4]	ε(Cal.)[5]
10	39.1		31.3
20		38.57	
30	35.9		28.3
50	32.9		25.5
70	30.1		23.1
90	27.6		20.9

1) Le Fèvre; loc. cit.
2) E. Tannenbaum, R. J. Myers and W. D. Gwinn; *J. Chem. Phys.*, **25**, 42 (1956).
3) F. Buckley and A. A. Maryott; Jour. of Research of National Bureau of Standards, **53**, 229 (1954).
4) J. Timmermans, A. M. Piette and R. Phillipe; *Bull. soc. chim. Belges*, **64**, 5 (1955).
5) For asymmetric top molecules the value of dielectric constant is calculated with our formula using as the value of the axial ratio, the value determined with the molecular model.

TABLE XV

DIELECTRIC CONSTANT OF DIETHYL ETHER

(Å) (10^{-25} cc.)

$a_1 = 4.9$[1] $a_2/a_1 = 1.80$ $\alpha_1 = 78.7$[2]

$a_2 = 8.8$ $\alpha_2 = 112.6$

$a_3 = 4.0$ $a_3/a_1 = 0.82$ $\alpha_3 = 70.7$

$\mu_0 = 1.17$ D (Vapour)[3]

temp. (°C)	ε(Ob.) (S)[4]	ε(Ob.) (F)[5]	ε(Ob.) (C)[6]	ε(Ob.) (T)[7]	ε(Ob.) (L.L)[8]	ε(Cal.) (E)[9]	ε(Cal.) (O.S.)[10]
−116	10.42					6.43	9.21
−101	9.05					5.87	8.28
− 80			7.541			5.24	7.18
− 75	7.25					5.11	6.93
− 60	6.55		6.545			4.79	6.37
− 40		5.91	5.791			4.36	5.67
− 30	5.45	5.60				4.18	5.38
− 20		5.325	5.180			4.01	5.09
− 10	4.96	5.066				3.86	4.86
0	4.75	4.803	4.706			3.71	4.64
10		4.575				3.58	4.43
15		4.480				3.52	4.33
18				4.360		3.48	4.28
20	4.29	4.376	4.300			3.46	4.23
25		4.265				3.40	4.13
30		4.152				3.34	4.04
40				3.966		3.22	3.88
60				3.652		3.02	3.57
80				3.375		2.84	3.29
100				3.122		2.65	3.02
120				2.890		2.47	2.78
128					2.716	2.41	2.67
140				2.658		2.30	2.54
143					2.557	2.28	2.50
158					2.392	2.15	2.33
160				2.408		2.13	2.30
168					2.270	2.05	2.20
180				2.124	2.081	1.905	2.02
190				1.885	1.878	1.738	1.814
193				1.533	1.798	1.648	1.702

1) This structure corresponds to the planar zig-zag form.
2) Stuart; loc. cit.
3) L. G. Groves and S. Sudgen; *J. Chem. Soc.*, 1779 (1935).
4) S. A. McNeight and C. P. Smyth; *J. Am. Chem. Soc.*, **58**, 1718 (1936).
5) R. J. W. Le Fèvre; *Trans. Faraday Soc.*, **34**, 1127 (1938).
6) I. E. Coop; *Trans. Faraday Soc.*, **33**, 583 (1937).
7) Karl Tangl; *Ann. d. Physik*; **10**, 748 (1903).
8) N. Litrinoff and W. Litrinoff; *Z. Physik*; **57**, 134 (1929).
9) The value calculated with our formula assuming the value of the axial ratio the value corresponding to the planar zig-zag form.
10) Molecular model is assumed to be the oblate spheroid whose axial ratio is 0.5 : 1 : 1.

TABLE XIII

DIELECTRIC CONSTANT OF METHYLENE CHLORIDE

(Å)		(10^{-25} cc.)
$a_1=4.4$	$a_2/a_1=1.50$	$\alpha_1=59.6$[1]
$a_2=6.6$		$\alpha_2=84.7$
$a_3=4.0$	$a_3/a_1=0.91$	$\alpha_3=50.2$

$\mu_0=1.62$ D (Stark effect)[2]

temp.(°C)	ε(Ob.) (M.L.)[3]	ε(Cal.)
40	8.29	7.57
30	8.71	7.93
20	9.14	8.31
10	9.58	8.72
0	10.02	9.19
−10	10.51	9.62
−20	11.00	10.22
−30	11.56	10.82
−40	12.14	11.46
−50	12.77	12.17
−60	13.49	12.94
−70	14.23	13.78
−80	15.05	14.74
−90	15.97	15.79
−100	16.98	16.94

1) Stuart; loc. cit.
2) R. J. Myers and W. D. Gwinn; *J. Chem. Phys.*, **20**, 1420 (1952.)
3) S. O. Margan and H. H. Lowry; *J. Phys. Chem.*, **34**, 3285 (1930).

TABLE XIV

DIELECTRIC CONSTANT OF DIMETHYL ETHER

(Å)		(10^{-35} cc.)
$a_1=4.3$	$a_2/a_1=1.47$	$\alpha_1=48.6$[1]
$a_2=6.3$		$\alpha_2=63.0$
$a_3=4.0$	$a_3/a_1=0.93$	$\alpha_3=43.1$

$\mu_0=1.30$ D (Vapour)[2]

temp.(°K)	ε(Ob.)[3]	ε(Cal.)
298	5.02	4.45
318	4.54	4.01
338	4.07	3.62
358	3.59	3.22
378	3.12	2.79
398	2.37	2.15

1) Stuart; loc. cit.
2) L. G. Groves and S. Sudgen; *J. Chem. Soc.*, 1779 (1937). K. L. Ramaswamy; *Proc. Indian Acad. Sci.*, **A4**, 108 (1936).
3) J. Marsden and O. Maass; *Can. J. Research*; **B13**, 296 (1935).

TABLE XVI

DIELECTRIC CONSTANT OF *n*-PROPYL ETHER

(Å)		(10^{-25} cc.)
$a_1=4.9$[1]	$a_2/a_1=2.41$	$\alpha_1=117.0$[2]
$a_2=11.8$		$\alpha_2=137.0$
$a_3=4.0$	$a_3/a_1=0.82$	$\alpha_3=122.0$

$\mu_0=1.18$ D (Vapour)[3]

temp.(°C)	ε(Ob.)[4]	ε(Cal.)
26	3.39	3.36

1) These values correspond to the planar zig-zag form.
2) Stuart; loc. cit.
3) G. A. Barclay and R. J. W. Le Fèvre; *J. Chem. Soc.*, 1643 (1952).
4) Pyle; *Phys. Rev.*, **38**, 1057 (1931).

TABLE XVII

DIELECTRIC CONSTANT OF PARALDEHYDE

(Å)		(10^{-25} cc.)
$a_1=4.0$	$a_2/a_1=2.05$	$\alpha_1=116.2$[1]
$a_2=8.2$		$\alpha_2=129.2$
$a_3=8.2$	$a_3/a_1=2.05$	$\alpha_3=129.2$

$\mu_0=1.43$ D (Vapour)[2]

temp.(°C)	ε(Ob.)[3]	ε(Cal.)[4]
20	14.70	11.62
40	12.25	10.23
60	10.30	9.04
80	8.70	8.03
100	7.46	7.14
120	6.42	6.38

1) Le Fèvre; loc. cit.
2) R. J. W. Le Fèvre, J. W. Mulley and B. M. Smyth; *J. Chem. Soc.*, 291 (1950).
3) R. C. Miller and C. P. Smyth; *J. Phys. Chem.*, **60**, 1354 (1956).
4) We assume that the polarizability effective for the dielectric constant is $(P_A+P_E)/P_E$ times the value estimated by Le Fèvre.

TABLE XVIII

DIELECTRIC CONSTANT OF ACETONE

(Å)		(10^{-25} cc.)
$a_1=5.4$	$a_2/a_1=1.24$	$\alpha_1=69.6$[1]
$a_2=6.7$		$\alpha_2=72.2$
$a_3=4.0$	$a_3/a_1=0.74$	$\alpha_3=48.2$

$\mu_0=2.87$ D[2] (Vapour)

temp.(°C)	ε(Ob.) (C.)[3]	ε(Ob.) (E.)[4]	ε(Cal.)
−80	34.5		33.3
−59	31.31		28.6
−40	28.42		25.2
−20	25.91		22.3
0	23.65	21.58	19.8
10		20.49	18.6
15		19.99	18.1
20	21.54	19.54	17.6
25		19.10	17.2
30		18.68	16.6
40	19.38	17.82	15.8
50		17.00	14.9

1) Stuart assumes that the value of the dipole moment is 2.7 D. But we recalculate the values of components of polarizability assuming that $\mu_0=2.87$ D.
2) K. L. Ramaswamy; *Proc. Indian Acad. Sci.*, **A4**, 108 (1936).
3) R. H. Cole; *J. Chem. Phys.*, **9**, 251 (1941).
4) R. J. W. Le Fèvre; *Trans. Faraday Soc.*, **34**, 1127 (1938).

TABLE XIX

DIELECTRIC CONSTANT OF METHYL-ETHYL KETONE

(Å)		(10^{-25} cc.)
$a_1=5.4$[1]	$a_2/a_1=1.50$	$\alpha_1=85.5$[2]
$a_2=8.1$		$\alpha_2=98.3$
$a_3=4.0$	$a_3/a_1=0.74$	$\alpha_3=60.2$

$\mu_0=2.87$ D[3]

temp.(°C)	ε(Ob.)(C.)[4]	ε(Ob.)(F.)[5]	ε(Cal.)
0	20.30		16.8
5		20.35	16.3
10		19.83	15.9
15		19.33	15.5
20	18.51	18.85	15.1
25		18.41	14.7
40	16.80		13.6
60	15.29		12.3
80	13.89		11.2

1) This assumed structure is the planar zig-zag form.
2) Stuart; loc. cit.
3) We assume that the value of the dipole moment has the same value as that of acetone.
4) R. H. Cole; *J. Chem. Phys.*, **9**, 251 (1941).
5) R. J. W. Le Fèvre; *Trans. Faraday Soc.*, **34**, 1127 (1938).

TABLE XX

DIELECTRIC CONSTANT OF DIETHYL KETONE

(Å)		(10^{-25} cc.)
$a_1=5.4$[1]	$a_2/a_1=1.67$	$\alpha_1=100.1$[2]
$a_2=9.0$		$\alpha_2=126.4$
$a_3=4.0$	$a_3/a_1=0.74$	$\alpha_3=71.5$

$\mu_0=2.87$ D[3]

temp.(°C)	ε(Ob.)(C.)[4]	ε(Cal.)
−40	19.77	18.5
−20	19.37	16.4
0	18.90	14.7
20	17.00	13.2
40	15.31	11.9
60	15.83	10.9
80	12.52	9.91
100	11.49	9.08

1) The structure corresponds to the planar zig-zag form.
2) Stuart; loc. cit.
3) We assume that the value of the dipole moment has the same as for acetone.
4) R. H. Cole; *J. Chem. Phys.*, **9**, 251 (1941).

TABLE XXI

DIELECTRIC CONSTANT OF TOLUENE

(Å)		(10^{-25} cc.)
$a_1=8.5$	$a_2/a_1=0.76$	$\alpha_1=156.4$[1]
$a_2=6.5$		$\alpha_2=136.6$
$a_3=4.0$	$a_3/a_1=0.47$	$\alpha_3=74.8$

$\mu_0=0.37$ D (Vapour)[2]

temp.(°C)	ε(Ob.)[3]	ε(Cal.)
−50	2.5889	2.563
−33	2.5336	2.504
−15	2.4785	2.450
0	2.4350	2.406
10	2.4065	2.377
25	2.3661	2.337
35	2.3421	2.312
45	2.3196	2.286
60	2.2846	2.252
80	2.2449	2.205
100	2.2061	2.159
110	2.1901	2.139

1) Stuart; loc. cit.
2) J. W. Baker and L. G. Groves; *J. Chem. Soc.*, 1144 (1939).
3) R. J. W. Le Fèvre; *Trans. Faraday Soc.*, **34**, 1127 (1938).

TABLE XXII

DIELECTRIC CONSTANT OF *o*-XYLENE

(Å)		(10^{-25} cc.)
$a_1=7.8$	$a_2/a_1=0.92$	$\alpha_1=163.9$[1]
$a_2=7.1$		$\alpha_2=135.2$
$a_3=4.0$	$a_3/a_1=0.51$	$\alpha_3=107.5$

$\mu_0=0.62$ D (Vapour)[2]

temp.(°C)	ε(Ob.)[3]	ε(Cal.)
−20	2.701	2.768
0	2.648	2.679
20	2.594	2.599
40	2.541	2.526
60	2.488	2.459
80	2.434	2.399
100	2.381	2.341
120	2.328	2.287
130	2.302	2.258

1) Le Fèvre; loc. cit.
2) E. C. Hurdis, and C. P. Smyth; *J. Am. Chem. Soc.*, **64**, 2212 (1942).
3) L. M. Heil; *Phys. Rev.*, **39**, 666 (1932).

TABLE XXIII

DIELECTRIC CONSTANT OF CHLOROBENZENE

(Å)		(10^{-25} cc.)
$a_1=8.5$	$a_2/a_1=0.76$	$\alpha_1=155.1$[1]
$a_2=6.5$		$\alpha_2=138.2$
$a_3=3.7$	$a_3/a_1=0.44$	$\alpha_3=74.2$

$\mu_0=1.70$ D[2] (Vapour)

temp. (°C)	ε(Ob.)(F.)[3]	ε(Ob.)(S.)[4]	ε(Ob.)(C.)[5]	ε(Cal.)
−50		7.28		7.88
−40			6.872	7.54
−30		6.76		7.20
−20			6.401	6.92
−10		6.26		6.64
0			5.982	6.40
10		5.82		6.15
20			5.605	5.95
21	5.670			5.93

25	5.612		5.84
30		5.46	5.75
40	5.372		5.55
48			5.41
50		5.15	5.38
70	4.886	4.89	5.04
80	4.768		4.90
96.2	4.521		4.66
100		4.52	4.61
106	4.435		4.53
115	4.314		4.42
130		4.17	4.24
131	4.144		4.23

1) Stuart assumes that the dipole moment has the value of 1.60 D. However we recalculate the polarizability value assuming $\mu_0=1.70$ D.
2) L. G. Groves and S. Sudgen; *J. Chem. Soc.*, 1094 (1934).
3) R. J. W. Le Fèvre; *Trans. Faraday Soc.*, **34**, 1127 (1938).
4) C. P. Smyth and S. O. Morgan; *J. Am. Chem. Soc.*, **50**, 1547 (1928).
5) I. E. Coop; *Trans. Faraday Soc.*, **33**, 583 (1937).

TABLE XXIV
DIELECTRIC CONSTANT OF BROMOBENZENE

(Å)		(10^{-25} cc.)
$a_1=8.8$	$a_2/a_1=0.74$	$\alpha_1=168.4$[1]
$a_2=6.5$		$\alpha_2=121.3$
$a_3=3.9$	$a_3/a_1=0.44$	$\alpha_3=95.6$

$\mu_0=1.64$ D[2] (Vapour)

temp.(°C)	ε(Ob.)[3]	ε(Cal.)
1	5.74	6.37
25	5.39	5.84
40	5.18	5.58
55	4.96	53.0

1) Le Fèvre; loc. cit.
2) R. J. W. Le Fèvre and Narayana Rao; *Australian J. Chem.*, **8**, 140 (1955).
3) W. A. Hestone, E. T. Hennelly and C. P. Smyth; *J. Am. Chem. Soc.*, **72**, 2071 (1950).

TABLE XXV
DIELECTRIC CONSTANT OF FLUOROBENZENE

(Å)		(10^{-25} cc.)
$a_1=7.6$	$a_2/a_1=0.85$	$\alpha_1=112.6$[1]
$a_2=6.5$		$\alpha_2=110.6$
$a_3=3.7$	$a_3/a_1=0.49$	$\alpha_3=71.1$

$\mu_0=1.57$ D[2] (Vapour)

temp.(°C)	ε(Ob.)[3]	ε(Cal.)
25	5.42	5.18
60	4.76	4.58

1) Le Fèvre; loc. cit.
2) K. B. McAlpine and C. P. Smyth; *J. Chem. Phys.*, **3**, 55 (1935).
3) A. A. Maryott and E. R. Smyth; "Table of Dielectric Constants of Pure Liquid." NBS Circular 514 (1951).

TABLE XXVI
DIELECTRIC CONSTANT OF IODOBENZENE

(Å)		(10^{-25} cc.)
$a_1=9.2$	$a_2/a_1=0.71$	$\alpha_1=198.4$[1]
$a_2=6.5$		$\alpha_2=140.7$
$a_3=4.3$	$a_3/a_1=0.47$	$\alpha_3=113.6$

$\mu_0=1.70$ D[2] (Vapour)

temp.(°C)	ε(Ob.)[3]	ε(Cal.)
20	4.625	5.48

1) Le Fèvre; loc. cit.
2) E. C. Hurdis and C. P. Smyth; *J. Am. Chem. Soc.*, **64**, 2212 (1942). R. J. W. Le Fèvre and Narayana Rao; *Australian J. Chem.*, **8**, 140 (1955).
3) A. Audsley and Goss; *J. Chem. Soc.*, 497 (1942).

TABLE XXVII
DIELECTRIC CONSTANT OF *o*-DICHLOROBENZENE

(Å)		(10^{-25} cc.)
$a_1=7.7$	$a_2/a_1=0.92$	$\alpha_1=176.8$[1]
$a_2=7.1$		$\alpha_2=158.5$
$a_3=4.3$	$a_3/a_1=0.55$	$\alpha_3=89.7$

$\mu_0=2.50$ D[2] (Vapour)

temp.(°C)	ε(Ob.)[3]	ε(Cal.)
0	11.130	13.0
25	9.930	11.6
50	8.900	10.4

1) Stuart assumes that the value of the dipole moment is 2.25 D. But we recalculate the values of the components of polarizability assuming that $\mu_0=2.50$ D.
2) E. M. Moore and M. E. Hobbs; *J. Am. Chem. Soc.*, **71**, 411 (1949). E. C. Hurdis and C. P. Smyth; *J. Am. Chem. Soc.*, **64**, 2212 (1942).
3) C. P. Smyth and S. P. Morgan; *J. Am. Chem. Soc.*, **50**, 411 (1928).

TABLE XXVIII
DIELECTRIC CONSTANT OF *m*-DICHLOROBENZENE

(Å)		(10^{-25} cc.)
$a_1=7.1$	$a_2/a_1=1.28$	$\alpha_1=158.2$[1]
$a_2=9.1$		$\alpha_2=178.4$
$a_3=3.7$	$a_3/a_1=0.52$	$\alpha_3=90.4$

$\mu_0=1.72$ D (Vapour)[2]

temp.(°C)	ε(Ob.)[3]	ε(Cal.)
0	5.403	6.97
25	5.039	6.34
50	4.703	5.82

1) Stuart assumes that the value of dipole moment is 1.48 D. But we recalculate the values of the components of polarizability assuming that $\mu_0=1.72$ D.
2) L. G. Groves and S. Sudgen; *J. Chem. Soc.*, 1782 (1937).
3) C. P. Smyth and S. O. Morgan; *J. Am. Chem. Soc.*, **50**, 1547 (1928).

TABLE XXIX

DIELECTRIC CONSTANT OF BENZONITRILE

(Å)		(10^{-25} cc.)
$a_1=9.2$	$a_2/a_1=0.71$	$\alpha_1=163.8$[1]
$a_2=6.5$		$\alpha_2=121.1$
$a_3=3.7$	$a_3/a_1=0.41$	$\alpha_3=84.9$

$\mu_0=4.14$ D (Stark effect)[2]

temp.(°C)	ε(Ob.)(M.)[3]	ε(Ob.)(T.)[4]	ε(Cal.)
0	27.6		26.7
18	25.85		24.6
20		25.58	24.2
25	25.2		23.7
30			23.2
40	24.0		22.2
50			21.3
50.3	23.28		21.2
60	22.7		20.3
70	22.1		19.5

1) Le Fèvre; loc. cit.
2) Lide; *J. Chem. Phys.*, **22**, 1577 (1954).
3) A. R. Martin; *Trans. Faraday Soc.*, **33**, 191 (1938).
4) J. Timmermans; A. M. Piette and R. Phillippe; *Bull. soc. chim. Belges*, **64**, 5 (1955).

TABLE XXX

DIELECTRIC CONSTANT OF NITROBENZENF

(Å)		(10^{-25} cc.)
$a_1=8.5$	$a_2/a_1=0.76$	$\alpha_1=171.6$[2]
$a_2=6.5$		$\alpha_2=141.9$
$a_3=3.7$	$a_3/a_1=0.44$	$\alpha_3=74.1$

$\mu_0=4.19$ D (Vapour)[3]

temp.(°C)	ε(Ob.)[4]	ε(Cal.)
10	37.85	28.0
25	34.89	26.1
30	33.97	25.5
40	32.26	24.4
50		23.4
60	29.08	22.4
70		21.4
90	24.88	19.8
110	22.68	18.3
130	20.79	16.9
150	19.27	15.8
170	18.15	14.6
200	15.95	13.1
211	15.61	12.7

1) The structure corresponds to the planar form.
2) Stuart assumes that the value of the dipole moment is 3.92 D. However we recalculate the value of polarizability assuming $\mu_0=4.19$ D.
3) K. B. McAlpine and C. P. Smyth; *J. Chem. Phys.*, **55**, (1935).
4) R. J. W. Le Fèvre; *Trans. Faraday Soc.*, **34**, 1127 (1938).

TABLE XXXI

DIELECTRIC CONSTANT OF PYRIDINE

(Å)		(10^{-25} cc.)
$a_1=6.6$	$a_2/a_1=0.98$	$\alpha_1=108.4$[1]
$a_2=6.5$		$\alpha_2=118.8$
$a_3=3.7$	$a_3/a_1=0.56$	$\alpha_3=57.8$

$\mu_0=2.15$ D[2] (Stark effect)

temp.(°C)	ε(Ob.)[3]	ε(Cal.)
1	14.65	12.0
20	13.55	11.0
40	12.45	10.1
60	11.44	9.26

1) Stuart; loc. cit.
2) B. B. De More, W. S. Wilcox and J. H. Goldstein; *J. Chem. Phys.*, **22**, 876 (1954).
3) Russel, Holland and C. P. Smyth; *J. Phys. Chem.*, **59**, 1088 (1955).

TABLE XXXII

DIELECTRIC CONSTANT OF QUINOLINE

(Å)		(10^{-25} cc.)
$a_1=7.1$	$a_2/a_1=1.25$	$\alpha_1=165$[1]
$a_2=8.9$		$\alpha_2=224$
$a_3=3.7$	$a_3/a_2=0.52$	$\alpha_3=79.5$

$\mu_0=2.29$ D[2] (Vapour)

temp.(°C)	ε(Ob.)[3]	ε(Cal.)
1	9.70	10.19
20	9.03	9.44
40	8.40	8.77
90	7.81	8.19

1) Le Fèvre; loc. cit.
2) A. D. Buckinghas, J. Y. H. Chan, H. C. Freeman, R. J. W. Le Fèvre, D. A. A. S. Narayana Rao and J. Tardif; *J. Chem. Soc.*, 1405 (1956).
3) Russell, Holland and C. P. Smyth; *J. Phys. Chem.*, **59**, (1955).

Mercury Photosensitized Reaction of Cyclo-octatetraene and the Comparison with the Direct Photochemical Reaction

By Hideo YAMAZAKI

(Received December 28, 1957)

Both experimental and theoretical investigations on cyclo-octatetraene have been made in our laboratory[1-6]. Among them the experiment of the direct photochemical reaction[3,6], the spectroscopic studies[1,4] and the calculation of energy levels[2] relate closely to the present work.

Cyclo-octatetraene has two singlet excited states near 2800 Å and 2000 Å[1,4], through which the direct photochemical reaction takes place[3,6]. According to the calculation of the molecular orbitals, however, several triplet states are expected to exist in the vicinity of these singlet states[2,7]. In view of the spin correlation rule, cyclo-octatetraene may react via the triplet states in the mercury photosensitized reaction[8]. In order to distinguish between these two processes, the mercury photosensitized reaction has been compared experimentally with the direct photochemical reaction, because even in the latter the reaction mechanism has not yet been clarified in the preceding works[3,6]. The experiment was carried out in vapor phase in the presence or the absence of mercury vapor, using mercury resonance line, λ2537, under both flow and static conditions, and the preliminary study on the decomposition reactions has already been reported[9]. In the present study, to elucidate the whole reaction mechanism, decomposition, isomerization and polymerization processes have been investigated quantitatively.

Experimental

Static Method. — The apparatus ordinarily used is shown in Fig. 1. The light source is a quartz mercury resonance lamp wound in the form of a spiral. The lamp was operated from the secondary of a transformer which maintained a current of 100 mA through the lamp and provided a starting potential of 1000 V. In its operation the potential drop across the lamp was 500 V. The lamp emits a small amount of radiation at 1849 Å, which is absorbed by oxygen in the light-path of 15 cm. in length. The light from the lamp was collimated by a quartz lens, in order to make the light nearly parallel at the reaction cell. The absolute light intensity was measured by a uranyl actinometer[10], which was placed behind the reaction cell. The light intensity at 2537 Å was approximately 3.7×10^{16} photons/sec.

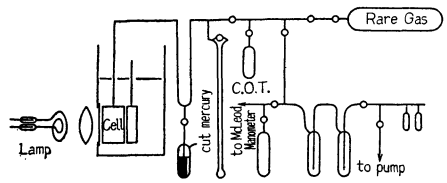

Fig. 1. Apparatus of static system.

Before starting an experiment, the fused-quartz reaction cell (4 cm. long and 5 cm. in diameter) was removed from the system, cleaned with hot chromic acid solution and flamed out. Adding small droplets of distilled mercury, the reaction cell was then attached to the system using de Khotinski cement on the standard taper joint. The de Khotinski cement was chosen because cyclo-octatetraene is insoluble in it. The reaction cell was immersed in a distilled water bath, thermostated at 20.0°C. A definite amount of cyclo-octatetraene vapor was then introduced into the cell and isolated by a mercury cut which served also as a manometer.

At the end of an experiment, the lamp was turned off and the condensable products in the reaction cell were frozen in a trap with liquid nitrogen. The noncondensable gas at dry ice temperature was transferred into a trap with liquid nitrogen through another trap with dry-ice in methanol. After the distillation was completed, the pressure in this part of the system was measured by a small McLeod gauge. The gas mixtures which were noncondensable at dry-ice temperature were analyzed by a mass spectrometer. A Beckman spectrophotometer model

1) I. Tanaka and S. Shida, This Bulletin, **23**, 54 (1950).
2) Y. Mori, I. Tanaka and S. Shida, ibid., **23**, 168 (1950).
3) I. Tanaka, S. Miyakawa and S. Shida, ibid., **24**, 119 (1951).
4) S. Miyakawa, I. Tanaka and T. Uemura, ibid., **24**, 136 (1951).
5) S. Shida and S. Fujii, ibid., **24**, 173 (1951).
6) I. Tanaka and M. Okuda, *J. Chem. Phys.*, **23**, 1780 (1955).
7) P. Schiess and Mme. A. Pulman, *J. chim. phys.*, **53**, 101 (1956).
8) K. J. Laidler "The Chemical Kinetics of Excited States", Clarendon Press, Oxford (1955), p. 32.
9) H. Yamazaki and S. Shida, *J. Chem. Phys.*, **24**, 1278 (1956).
10) J. N. Pitts et al., *J. Am. Chem. Soc.*, **77**, 5499 (1955).

D. U. and Hilger E2 type spectrograph were used for the analysis of the products which were condensable at dry-ice temperature.

In the case of the direct photochemical reaction, the absence of mercury vapor has to be fully checked, since the same reaction system is used for those two kind of experiment. The detection of mercury vapor was made by the mercury photosensitized reduction of tungsten oxide in the presence of hydrogen. The greenish tungsten oxide powder turned black for a few minutes of irradiation in the presence of a small amount of mercury vapor. In its absence, however, there was no appreciable change in color even after two hours' irradiation.

In the case of the direct photochemical reaction, oil manometers were used in place of mercury manometers. The small amount of mercury vapor, when left in the system, was trapped with liquid nitrogen. In addition, gold and indium foils, placed in the side tube of the reaction vessel, were used for the removal.

For avoiding the mercury photosensitization, another supplementary experiment was made using the reversed resonance line. The light source was a hot mercury lamp operated by 100 V. D. C. The broadened resonance line was then filtered by a quartz cell containing mercury vapor and hydrogen as quencher.

Flow Method.—The light source was a low-pressure mercury-rare-gas lamp of U-type, which was operated at nearly the same power supply as that for the spiral-type lamp in the static method described before. The dimension of the reaction tube was 20 cm. long and 2.5 cm. in diameter.

In a typical experiment, cyclo-octatetraene was introduced into the reaction system at a linear flow rate, which was controlled by the two cocks placed at both ends of the reaction cell. The cyclo-octatetraene pressure in the reaction tube was measured by a mercury or an oil manometer. During an experiment the product was condensed into the trap immersed in liquid nitrogen. The lamp current was adjusted to a fixed value. At the end of the irradiation, the lamp and the cyclo-octatetraene stream were shut off and the condensable gas in the system was frozen in the trap. The analysis of the products is similar to that in the static method.

Effect of the Addition of Rare Gases.—Since these reactions are supposed to proceed through the excited state of cyclo-octatetraene, the investigation on the deactivation of excited cyclo-octatetraene is of interest. Rare gases are chosen as the quenchers, because of their negligibly small quenching cross section towards the excited mercury atom relative to that of cyclo-octatetraene, and the result is compared with that of ethylene.

The experiment was made in the static system. A definite amount of cyclo-octatetraene was introduced into the reaction cell and condensed with dry-ice. Then a definite amount of the rare gas was added. The system was allowed to stand for four hours for mixing before irradiation. After the reaction was completed the rare gas was gradually pumped off through a trap with liquid nitrogen, in which the acetylene produced was trapped. The amount of acetylene was determined by a method already described. The rare gases which were spectroscopically pure were commercially obtained, and cyclo-octatetraene furnished by the Mitsubishi Kasei Co., was purified by repeating the recrystalization and vacuum distillation.

Result

Decomposition Reaction. — Both in the mercury photosensitized reaction and the direct photochemical reaction, no gas noncondensable at the liquid nitrogen temperature, such as hydrogen and methane, was detected, and the noncondensable at the dry-ice temperature was acetylene. Since acetylene and benzene were produced in the same amount in the mercury photosensitized reaction as well as in the direct photochemical reaction, their appearance seems to be the result of the molecular decomposition. The rate and the quantum yield of the decomposition reaction as a function of cyclo-octatetraene pressure were shown in Fig. 2 and Fig. 3 respectively, in which the rate of the decomposition reaction is that measured by the acetylene produced. In the case of mercury photosensitized reaction, quantum yield of decomposition as a function of cyclo-octatetraene pressure has a maximum; it may be considered that below this pressure the quantum yield decreases on account of the incomplete

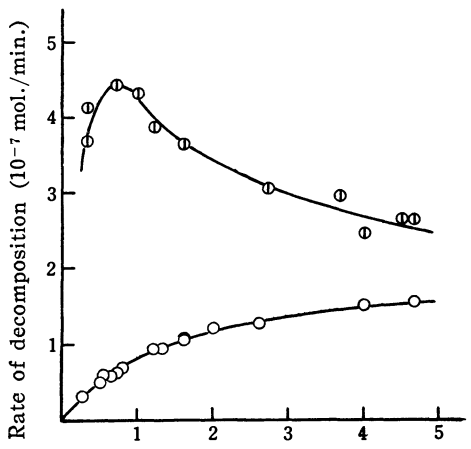

Fig. 2. Rate of decomposition as a function of C.O.T. pressure.
◑: Mercury photosensitized reaction
○: Direct photochemical reaction

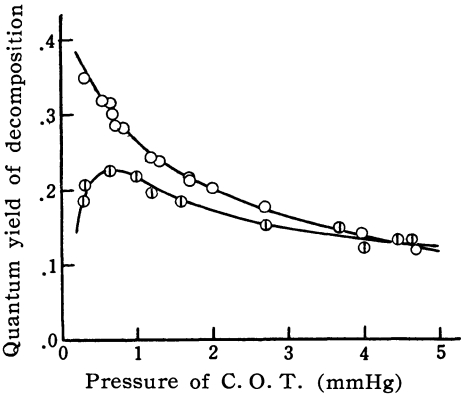

Fig. 3. Quantum yield of decomposition as a function of C. O. T. pressure.
⦶: Mercury photosensitized reaction
○: Direct photochemical reatcion

quenching of the excited mercury atom by cyclo-octatetraene molecule and, above this pressure, the quantum yield also decreases on account of the collisional deactivation of the excited cyclo-octatetraene molecule by the normal cyclo-octatetraene. Such a type of behavior has previously been observed with ethylene. In the case of the direct photochemical reaction, however, the quantum yield of decomposition decreases monotonically as increasing cyclo-octatetraene pressure by the collisional deactivation. Plotting the reciprocal of the quantum yield, ϕ_d, of the decomposition reaction against the pressure of cyclo-octatetraene, straight lines were obtained, which are shown in Fig. 4. From the intercept of the ordinate by these lines, the limiting quantum yield of decomposition can be estimated as 0.3 and 0.4 for the mercury photosensitized reaction and the direct photochemical reaction, respectively.

In the experiment with the reversed light source, the rate of the decomposition reaction as a function of pressure of cyclo-octatetraene is shown in Fig. 5. This is similar to the result in the direct photochemical reaction in absence of mercury vapor.

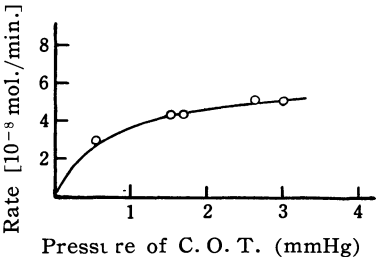

Fig. 5. Rate of decomposition as a function of C. O. T. pressure.
(A filter containing mercury vapor and hydrogen gas was used.)

Polymerization and Isomerization Reaction.—As the reaction proceeds, a thin yellowish film deposits in front of the reaction cell, which seems to owe to the polymerization of cycro-octatetraene. To examine the polymerization reaction, the total pressure change and the amount of acetylene produced were measured in the course of reaction in the complete quenching region of cyclo-octatetraene pressure for the excited mercury atom. The result of the experiment was shown in Fig.

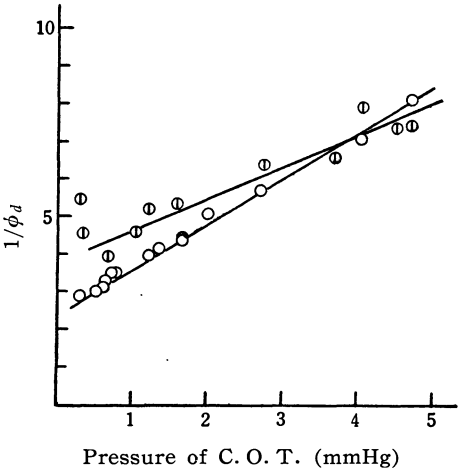

Fig. 4. Plots of $1/\phi_d$ as a function of C. O. T. pressure.
⦶: Mercury photosensitized reaction
○: Direct photochemical reaction

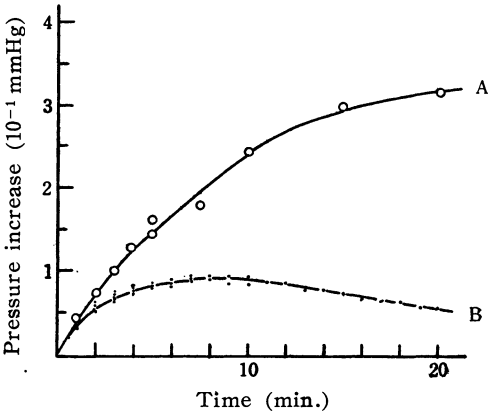

Fig. 6. Total pressure increase and acetylene production in the course of reaction.
A: Acetylene production
B: Total pressure change

6, in which the total pressure initially increased, reaching a maximum after about seven minutes' irradiation and then began to decrease slowly; the production of acetylene on the other hand increased monotonically except that the rate of production gradually decreased on account of the filtering effect by the polymeric clinging to the front of the reaction cell. In this experiment the amount of acetylene produced was measured after the reaction was complete in each run. By removing acetylene produced, no change was observed in the behavior of the total pressure variation in the course of the reaction. Therefore it may be considered that acetylene does not act as an intermediate of the polymerization reaction and furthermore the secondary effect of acetylene is ignored in this reaction. After irradiation, absorption spectra of the mixture of reaction products and cyclo-octatetraene were measured in methanol solution. The result was shown in Fig. 7, in which there

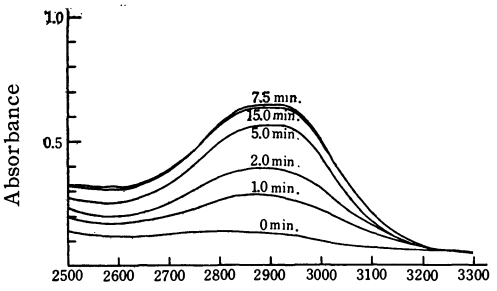

Fig. 7. Change of absorption spectrum in the course of reaction.

is seen a marked increase in absorption spectra at the wave length near 2900 Å. The product shows orange color due to the fact that the foot of this absorption is in a visible region. This absorption spectrum shows also the band structure at 3050, 3005, 2912 and 2820 Å in the gas phase spectrogram. The absorption spectra gradually increased and reached a maximum value after about seven minutes' irradiation as observed for the total pressure change in Fig. 6.

The spectra of unirradiated cyclo-octatetraene, that obtained after 20 minutes' irradiation and that preserved for a week in vacuo are shown together in Fig. 8. The orange colored liquid, which seems to be an isomer of cyclo-octatetraene, is unstable and during the presservation in vacuo for a week, a yellowish plastic substance was obtained which is

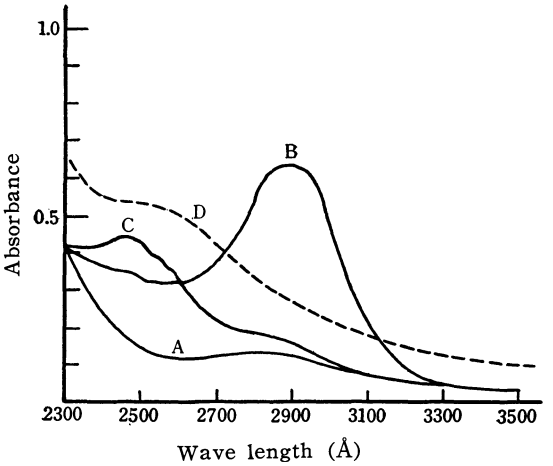

Fig. 8. A: Before the run. B: After the run. C: After the run and a week stored in vacuo. D: Polymer film dipositted in front of the reaction cell.

partially soluble in hexane and shows an absorption near 2600 Å. In this polymerizing process there is no evidence that noncondensable gases in dry-ice temperature such as acetylene and hydrogen are produced. The orange colored liquid may be polymerized without decomposition.

In an attempt to examine the initial stage of the reaction just described more precisely, a series of runs was made under the flow condition. The relative amount of the orange-colored liquid produced was measured by the absorption at 5000 Å using the pure cyclo-octatetraene as the reference. An experiment has been made on the pressure dependence of the production of orange-colored liquid in comparison with that of acetylene production, only in the mercury photosensitized reaction. The result, as shown in

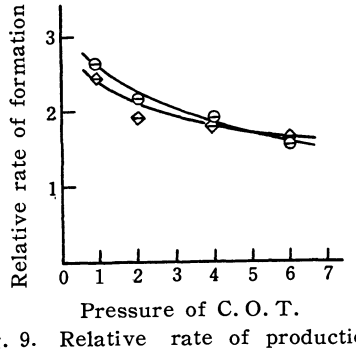

Fig. 9. Relative rate of production of acetylene and orange-colored substance in mercury photosensitized reaction. ⊖ Acetylene ◇ Orange-colored substance (Different scales were used for two kinds of products).

Fig. 9, almost coincides with that of acetylene production.

The relative amount of acetylene and orange-colored liquid has been investigated both in the mercury photosensitized reaction and the direct photochemical reaction. The plots against the time of the relative amount of these products were shown in Fig. 10. The ratio of the production of orange-colored liquid to that of acetylene

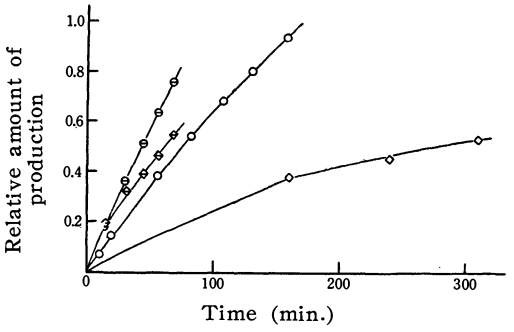

Fig. 10. Relative amounts of production of acetylene and orange-colored substance. ⊖ Acetylene ◈ Orange-colored substance (mercury photosensitized reaction); ○ Acetylene ◇ Orange-colored substance (direct photochemical reaction) (different scales were used for two kinds of products).

is twice as great in the photosensitized reaction as in the direct photochemical reaction. Assuming the extinction coefficient of the orange-colored liquid at 2900 Å as 10^4, the ratio of orange-colored liquid to acetylene is about 2:1 and 1:1 in the mercury photosensitized reaction and the direct photochemical reaction, respectively. In the forgoing experiment, as the limiting quantum yield of decomposition was 0.3 and 0.4 for the mercury photosensitized reaction and the direct photochemical reaction, respectively, it may be considered that the whole excited cyclo-octatetraene molecules would undergo either the decomposition reaction or the isomerization giving orange-colored liquid in the limiting case in which the pressure of cyclo-octatetraene is zero.

Styrene Formation.—In the case of the mercury photosensitized reaction, for over 20 minutes' irradiation, new absorption spectral lines at 2800 Å and 2880 Å appeared in the gas phase spectrogram of the reaction products, which coincide with that of styrene. The amount of styrene produced was about one-tenth of benzene and therefore we performed no further quantitative experiment on this product, because this seems to make little contribution to the elucidation of the reaction mechanism.

Effect of the Addition of Rare Gases.—As shown in Fig. 2 and Fig. 9, the rate of the decomposition reaction and that of the formation of orange-colored liquid decrease with increase in the pressure of cyclo-octatetraene. Then it may be considered that the excited cyclo-octatetraene molecule is deactivated by cyclo-octatetraene itself. The collisional deactivation of excited cyclo-octatetraene was also investigated, measuring the change in the quantum yield of the decomposition reaction by mixing rare gases.

The reciprocal of the quantum yield of decomposition measured by the amount of acetylene produced is plotted against the pressure of rare gases in Fig. 11, in which there is seen a fairly well linear relationship between these two quantities.

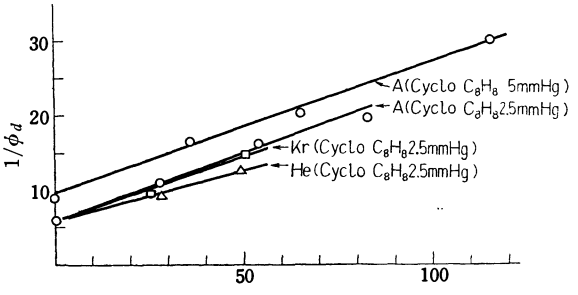

Fig. 11. Plot of the reciprocal of the quantum yield of decomposition as a function of rare gas pressure.

Discussion

In an attempt to explain the experimental result, the reaction will be discussed in terms of a sequence of reactions which is somewhat similar to the one proposed for ethylene; however, in addition the discussion includes the reactions producing orange-colored liquid (presumably bicyclo form of C_8H_8) and polymer. The reaction mechanism is as follows:

$$Hg + h\nu \rightarrow Hg^* \quad (a)$$

$$Hg^* \rightarrow Hg + h\nu \quad (b)$$

$$C_8H_8 + Hg^* \rightarrow C_8H_8^*(\text{triplet}) + Hg \quad (1)$$

$$C_8H_8^*(\text{triplet}) + C_8H_8 \rightarrow 2C_8H_8 \quad (2)$$

$$C_8H_8^*(\text{triplet}) \rightarrow C_2H_2 + C_6H_6 \quad (3)$$

$$C_8H_8^*(\text{triplet}) \rightarrow \text{bicyclo } C_8H_8 \quad (4)$$

bicyclo $C_8H_8+Hg^* \rightarrow$ bicyclo $C_8H_8^*+Hg$ (5)

bicyclo $C_8H_8^*+$wall $\rightarrow$ polymer (6)

For the direct photochemical reaction in place of step 1 the following two processes may be considered,

$C_8H_8+h\nu \rightarrow C_8H_8^*$(singlet) (1a)

$C_8H_8^*$(singlet) $\rightarrow C_8H_8^*$(triplet) (1b)

Even in the case of mercury photosensitized reaction, it will be possible for the direct light absorption by cyclo-octatetraene molecules to occur. The absorption coefficient of mercury vapor at room temperature for mercury resonance line is about 3 $cm.^{-1}$ [11], while the absorption coefficient for several mmHg of cyclo-octatetraene is 0.1 $cm.^{-1}$, the extinction coefficient of the latter at 2537 Å being 300 l./mol. cm.[1,4] Hence the mercury resonance line was selectively absorbed by mercury vapor under the condition studied; the reaction 1a will be ignored in comparison with reaction 1.

Making use of the usual stationaly state assumption, we find the concentration of of Hg^* and $C_8H_8^*$ to be

$$[C_8H_8^*]=k_1[C_8H_8][Hg^*]/(k_2[C_8H_8]+k_3+k_4) \quad (1)$$

$$[Hg^*]=I_{abs}/(k_b+k_1[C_8H_8]) \quad (2)$$

The rate of acetylene production is given by

$$d[C_2H_2]/dt=k_3[C_8H_8^*] \quad (3)$$

Eqs. 1 and 2 are introduced into Eq. 3 to give the quantum yield of decomposition, ϕ_d, as a function of cyclo-octatetraene,

$$\phi_d=k_1k_3[C_8H_8]/(k_1[C_8H_8]+k_b)(k_2[C_8H_8]+k_3+k_5) \quad (4)$$

Similarly in the case of the direct photochemical reaction we have

$$\phi_d'=k_3'/(k_2'[C_8H_8]+k_3'+k_4') \quad (5)$$

The pressure dependence of the quantum yield of the decomposition can be interpreted by the formulae 4 and 5 in the pressure range studied; thus in the mercury photosensitized reaction the quantum yield of decomposition has a maximum, while in the case of the direct photochemical reaction the quantum yield of decomposition monotonically decreases as cyclo-octatetraene pressure increases.

The reaction rate constants in the sequence of reactions can be estimated from the formulae mentioned above: k_b, the reciprocal of the life time of the excited mercury atom, $Hg(6^3P_1)$, is 10^7 $sec.^{-1}$ [12], and from the slope of the straight line in Fig. 4 the value of k_2/k_3 is 2.1×10^7 cc./mol., and as we have described (Result, polymerization and isomerization reaction) k_3/k_4, the ratio of formation of acetylene to the orange-colored liquid, is 0.5. If the excited cyclo-octatetraene molecule is deactivated by one collision with the normal cyclo-octatetraene molecule, then assuming the collisional diameter as 6 Å, the life time of the excited cyclo-octatetraene molecule is calculated to be 10^{-8} sec.

Similarly in the case of the direct photochemical reaction the ratio of the reaction constants can be estimated from Fig. 4 as $k_2'/k_3'=2.5\times10^7$ cc./mol. and $k_3'/k_4'=1$, which is the same order of magnitude as those of the mercury photosensitized reaction.

Differentiating Eq. 4 with respect to $[C_8H_8]$ and putting it to be zero, then the following expression is obtained:

$$k_1=(k_3+k_4)k_b/k_2P_0^2 \quad (6)$$

where P_0 is the pressure of cyclo-octatetraene corresponding to the maximum ϕ_d.

Introducing the reaction rate constants estimated before into Eq. 6, k_1 becomes 10^{15} cc./sec. mol., from which the quenching cross section of the excited mercury atom by cyclo-octatetraene is to be 10^2 $Å^2$, which is of reasonable magnitude.

The collisional deactivation of the excited cyclo-octatetraene molecule may be explained by the following reaction in addition to the above sequence,

$$C_8H_8^*(\text{triplet})+M \rightarrow C_8H_8+M \quad (7)$$

where M is rare gas.

The quantum yield of decomposition is then represented by the following equation,

$$\phi_d=k_1k_3[C_8H_8]/(k_1[C_8H_8]+k_b)\times(k_2[C_8H_8]+k_7[M]+k_3+k_4) \quad (7)$$

which can be reduced, under the condition for the complete quenching of the excited mercury atom, to

$$\phi_d^{-1}=k_7[M]/k_3+\text{const.} \quad (8)$$

The relative efficiencies of deactivation calculated from the slope of the lines in Fig. 11 are 0.13, 0.19 and 0.17 for helium, argon and krypton respectively, taking the efficiency of cyclo-octatetraene as unity.

The deactivation cross section calculated

11) A. C. G. Mitchell and M. W. Zemansky, "Resonance Radiation and Excited Atoms", Cambridge Univ. Press, Cambridge (1934) p. 203.

12) see reference 11) p. 147.

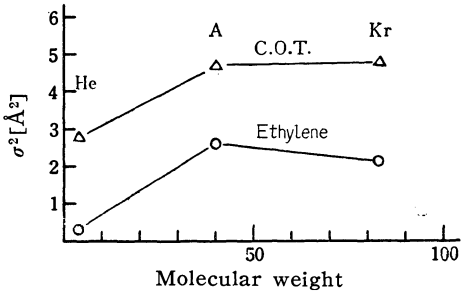

Fig. 12. Quenching cross section of excited C. O. T. and ethylene molecule by rare gases.

from these values were shown in Fig. 12 together with those of ethylene[13], where the cross section for self-deactivation were taken as 30 Å^2 and 11 Å^2 for cyclo-octatetraene and ethylene respectively by considering the geometrical dimension. There is seen a parallel dependence of the cross section on the molecular weight of the deactivating gases.

The estimation of the rate constants can also be made on the isomerization and the polymerization path,

$$\begin{aligned} &d[\text{bicyclo } C_8H_8]/dt \\ &=k_4[C_8H_8^*]-k_5[\text{bicyclo } C_8H_8][Hg^*] \\ &=k_1k_4[C_8H_8][Hg^*]/(k_2[C_8H_8]+k_3+k_4) \\ &\quad -k_5[\text{bicyclo } C_8H_8][Hg^*] \end{aligned} \tag{9}$$

Integrating Eq. 9 [bicyclo C_8H_8] is given as a function of time:

$$[\text{bicyclo } C_8H_8]=A\{1-\exp(-Bt)\} \tag{10}$$

where the constants A and B are given by

$$A=k_1k_4[C_8H_8]/k_5(k_2[C_8H_8]+k_3+k_4) \tag{11}$$

and

$$B=k_5I_{abs}/(k_1[C_8H_8]+k_b) \tag{12}$$

For the formation of the polymer, the following equation will be obtained,

$$d[P]/dt=k_5[\text{bicyclo } C_8H_8][Hg^*] \tag{13}$$

Integrating the equation, the amount of polymer produced is given by

$$[P]=ABt+A\{\exp(-Bt)-1\} \tag{14}$$

The experimental result shown in Fig. 7, that the amount of orange-colored liquid increases reaching a saturation value after seven minutes' irradiation, may be explained by the formula 10. Using this formula the parameter was estimated as follows; B is 5×10^{-2} sec.$^{-1}$, then k_5 calculated from Eq. 12, is 10^{14} cc./mol. sec. which is a reasonable value considering that the polymerization proceeds with a small amount of activation energy.

In Fig. 6, if we consider that the difference between the production of acetylene and the total pressure-increase is equal to the production of polymer, then the rate of production is zero at the beginning of the irradiation and becomes constant after a sufficient time later. This trend of polymer production can be quantitatively explained by Eq. 14.

The electronic states of mercury atom and cyclo-octatetraene molecule are shown in Fig. 13, in which the singlet states are

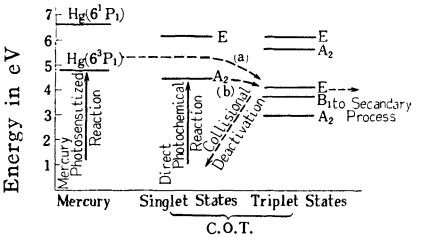

Fig. 13. Electronic states of mercury and C. O. T.

inferred from the spectroscopic data[1,4]. For the triplet states, the values from the molecular orbital calculation were used because of lack of the experimental data[2,7]. Some ambiguity is involved, however, in the determination of the assignment of those states.

In the case of the mercury photosensitized reaction, it may be considered that the reaction proceeds by path a); on the other hand in the case of the direct photochemical reaction, by path b). From the similarity of the reaction products and of the quantum yield, it may be considered that there is a cross between these states through which the reaction takes place.

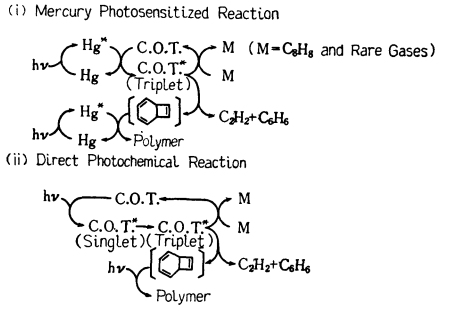

Fig. 14. Schematic representation of the mercury photosensitized and direct photochemical reactions of cyclo-octatetraene.

13) A. B. Callear and J. C. Robb, *Discussion Faraday Soc.*, No. **17**, 21 (1954).

The whole process of the reactions, mercury photosensitized as well as direct photochemical, are schematically represented in Fig. 14. Both the reactions involve the same kinds of process, i. e. the excitation of cyclo-octatetraene, the deactivation and the decomposition of the excited cyclo-octatetraene, and the polymerization process through the orange-colored liquid as intermediate.

Although the bicyclo form as an isomer of cyclo-octatetraene has not been isolated, the bicyclo forms of several derivatives of cyclo-octatetraene show ultraviolet spectra similar to those of the present orange-colored liquid[14], and this variation has been used by Reppe as an intermediate of the reaction of cyclo-octatetraene[15].

Further discussion on the present problem, however, would be largely speculative and would require much more detailed experimental result.

Summary

The reaction products of both the mercury photosensitized reaction and the direct photochemical reaction are the same, i. e. acetylene, benzene, orange-colored liquid (presumably bicyclo form of C_8H_8), polymer and a trace of styrene; the non-condensable products at liquid nitrogen temperature such as hydrogen and methane were not detected.

A quantitative experiment has been made on the decomposition reaction, in which cyclo-octatetraene shows a similar behavior to ethylene in the pressure dependence of the quantum yield. The quantum yields of the decomposition are of the same magnitude in both the mercury photosensitized and the direct photochemical reaction. The result shows that the two reactions proceed via the same excited state (probably triplet), directly or indirectly.

An investigation has also been made on the polymerization reaction, for which the total pressure change and the absorption spectrum of the reaction products have been examined in the course of the reaction. It is concluded that the polymerization takes the place via orange-colored liquid as an intermediate.

In the study of the reaction of hydrocarbons with $Hg(6^3P_1)$ atom a great deal of evidence has now been accumulated which shows the fact that the reaction always accompanies hydrogen production. The mercury photosensitized reaction of cyclo-octatetraene is one of the rare exceptions in this generality.

Thanks are due to Professor S. Shida, Tokyo Institute of Technology, for his guidance throughout this work, also to Dr. I. Tanaka, Dr. Z. Kuri and Mr. Y. Mori for their helpful discussion, and to Mr. K. Matsuzawa and Mr. R. Matsuura, Mitsubishi Kasei Co., who have furnished the sample of cyclo-octatetraene.

Laboratory of Physical Chemistry
Tokyo Institute of Technology
Meguro-ku, Tokyo

14) A. C. Cope and M. Burg, *J. Am. Chem. Soc.*, **74**, 168 (1952).
15) W. Reppe et al., *Ann. Chem.*, **560**, 1 (1948).

Polymerization of Methyl Methacrylate Initiated by a Combined Action of Trichloroacetic Acid and Dimethylaniline

By Ryoichi UEHARA

(Received May 27, 1958)

The author[1] preliminarily reported that polymerization of methyl methacrylate could be initiated, even at room temperature, by a combined action of trichloroacetic acid and dimethylaniline. Neither trichloroacetic acid nor dimethylaniline alone was responsible for the initiation, but, when they were dissolved together in methyl methacrylate, the polymerization was initiated. Recently, Lal[2] and others, in their paper concerning initiating actions of saccharine amine salts for polymerization of vinyl monomers, have reported that some combinations of carboxylic acids and dimethylaniline act as initiators for methyl methacrylate. But, in their report, only a brief mention of per cent yields of polymethyl methacrylate after 1 hr., at 58.6°C, was given.

This paper presents the results of experiments about the dependence of the initial rate of polymerization of methyl methacrylate upon the concentrations of both trichloroacetic acid and dimethylaniline, and a bimolecular reaction between trichloroacetic acid and dimethylaniline to form radicals is suggested as the initial reaction of the polymerization.

Experimental

Materials.—Methyl methacrylate was washed with 5% aqueous sodium carbonate and water, then distilled with steam, dried over anhydrous sodium sulfate, and carefully distilled in oxygen-free nitrogen under reduced pressure through a fractionating column. A fraction boiling at 46°C/12 mmHg was used immediately after the distillation. Dimethylaniline was distilled under nitrogen and a fraction boiling at 110°C/12 mmHg was used. Trichloroacetic acid was prepared from chloral and nitric acid, and a fraction boiling at 196°~197°C was employed. Thiophene-free benzene was dried over anhydrous sodium sulfate and distilled. Hydroquinone was dissolved in ether, decolorized by means of active carbon, and then precipitated by adding dry benzene, m.p. 174°C.

Determination of Initial Rate of Polymerization.—Polymerization of methyl methacrylate was carried out in sealed test tubes which were 15 mm. in diameter and 10 cm. in height and made of hard glass. The test tubes were cleaned by immersing them in 1% aqueous hydrofluoric acid for 12 hr., then washed with pure water and steam, and dried. Trichloroacetic acid and dimethylaniline were dissolved separately in methyl methacrylate. Both solutions were cooled in a methanol-dry ice bath, and measured amounts of both solutions were placed in a test tube and mixed. When hydroquinone was used, it was dissolved in methyl methacrylate together with dimethylaniline. In case of solution-polymerization, benzene was added to test tubes from a burette. The volume of the contents of one test tube was limited, not to exceed 5 cc. The test tubes were flashed for 10 minutes with dry nitrogen, which had been deoxygenated according to the procedure described by Fieser[3], then evacuated to 1 mmHg, and sealed. They were kept in a cooling bath for 30 minutes in order to ensure uniformity of temperature. The polymerization was effected by shaking the test tubes in a thermostat. The time of polymerization was measured from the beginning of the shaking. The yields of the polymer were measured at intervals of 15 minutes. Two tubes were picked up for one measurement, chilled in a cooling bath, and then opened. The contents of the tube were diluted with 5 cc. of acetone and taken out. The tube was then washed with 5 cc. of acetone. The contents and the washing were combined, and poured into 200 cc. of methanol so as to precipitate the polymer formed. The precipitated polymer was collected on a glass filter, washed three times with 10 cc. of methanol, then dried to a constant weight at 50°C under reduced pressure. The average weight of the samples of polymer from the two test tubes was taken as its yield. The initial rate of polymerization was determined from a linear part of the time-conversion curve in the initial stage of the polymerization, and expressed in a unit of per cent per minute.

Results and Discussion

Fig. 1 shows the relation between the initial rate of polymerization (R) and the concentration of trichloroacetic acid ([TCA]). In this case the equimolar

1) R. Uehara, Kagaku-no-Ryoiki, **7**, 295 (1953).
2) J. Lal et al., *J. Polymer Sci.*, **24**, 81 (1957).
3) L. Fieser, "Experiments in Organic Chemistry", D. C. Heath Co., New York (1941) p. 395.

amounts of trichloroacetic acid and dimethylaniline were used. So, the dependence of the initial rate of polymerization upon the concentration of dimethylaniline ([DMA]) was the same as that of Fig. 1. From Fig. 1, it can be seen that the initial rate is linearly dependent upon the concentration of trichloroacetic acid at temperatures of 25°, 35° and 55°C, respectively.

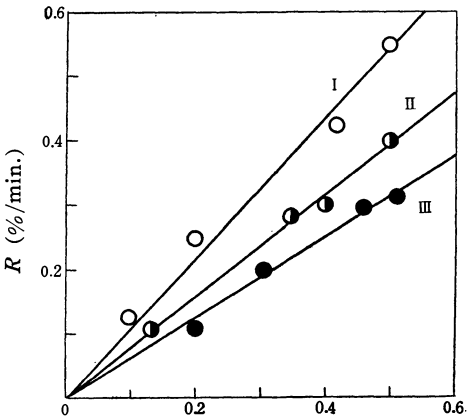

Fig. 1. Relation between R and [TCA] ([TCA]=[DMA]) I, at 55°; II, at 35°; III, at 25°C.

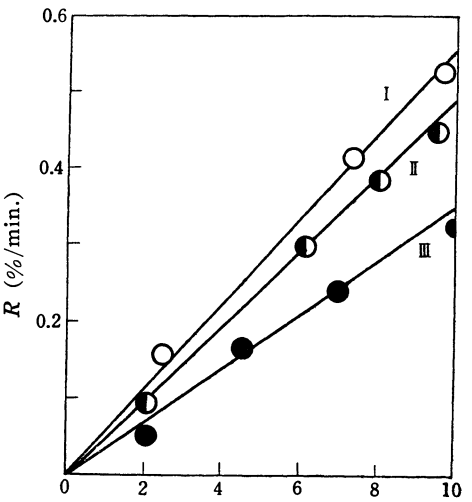

Fig. 2. Correlation of R with square-root of [DMA] at 35°C, I, [TCA]=0.50; II, [TCA]=0.42; III, [TCA]=0.21 mol./l.

When the concentration of trichloroacetic acid was held constant and that of dimethylaniline was varied, the initial rate of polymerization was linearly dependent upon the square root of the concentration of dimethylaniline, i. e., the so-called square-root dependence was observed as shown in Fig. 2. From this figure, the square-root dependence can be seen to hold for each case, in which 0.21, 0.42 and 0.50 mol./l., respectively, of trichloroacetic acid was used at 35°C. The fact that each of the straight lines in Fig. 2 is brought to a focus at the origin shows that trichloroacetic acid alone is not responsible for the initiation of polymerization.

In Fig. 3, initial rates of polymerization

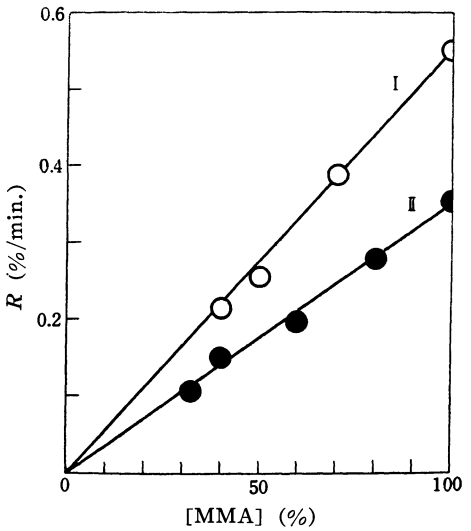

Fig. 3. Correlation of R with [MMA] at 55°C ([TCA]=[DMA]).
I, 0.50 mol./l. of TCA
II, 0.34 mol./l. of TCA

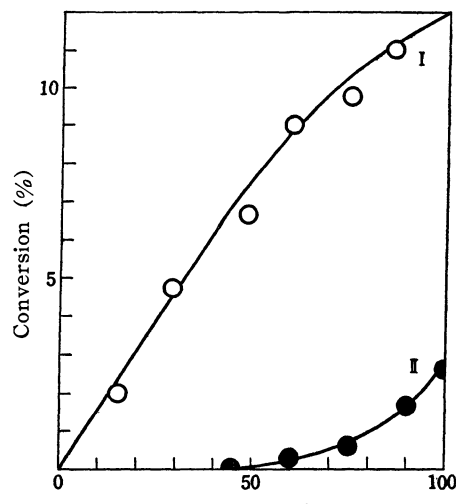

Fig. 4. Time conversion curves of bulk polymerization at 35°C ([TCA]=[DMA] =0.20 mol./l.).
I, without hydroquinone
II, with 0.026 mol./l. of hydroquinone

in benzene are plotted against the concentration of methyl methacrylate ([MMA]). Two cases, in which 0.34 and 0.50 mol./l. of trichloroacetic acid with equimolar amounts of dimethylaniline were used, are shown. The initial rate of polymerization was proportional to the concentration of methyl methacrylate.

In Fig. 4, the time-conversion curves for the bulk polymerization at 35°C, in which 0.20 mol./l. of each of trichloroacetic acid and dimethylaniline were used with or without hydroquinone, are shown. In the presence of 0.025 mol./l. of hydroquinone, a considerably long induction period was observed, therefore, it was clear that hydroquinone acted as an inhibitor for this reaction.

The relation between the initial rate and the concentration shown in Figs. 1, 2 and 3, can be represented by the following equation:

$$R=k[\mathrm{TCA}]^{1/2}[\mathrm{DMA}]^{1/2}[\mathrm{MMA}] \quad (1)$$

where k is a constant. This equation suggests a bimolecular reaction between trichloroacetic acid and dimethylaniline to form radicals as the initial reaction of the polymerization:

$$\mathrm{TCA}+\mathrm{DMA} \xrightarrow{k_1} \mathrm{R}\cdot \quad (2)$$

where k_1 is the rate constant and R· represents the radical, the chemical identity of which will be the subject for further investigation. Reaction 2 is followed by the usual series of reactions of polymerization, i. e., initiation, propagation and termination:

$$\mathrm{TCA}+\mathrm{DMA} \xrightarrow{k_1} \mathrm{R}\cdot$$

$$\mathrm{R}\cdot+\mathrm{M} \xrightarrow{k_2} \mathrm{P}_1\cdot$$

$$\mathrm{P}_m\cdot+\mathrm{M} \xrightarrow{k_3} \mathrm{P}_{m+1}\cdot$$

$$\mathrm{P}_m\cdot+\mathrm{P}_n\cdot \xrightarrow{k_4} \mathrm{P}_{m+n} \text{ or } \mathrm{P}_m+\mathrm{P}_n$$

where $\mathrm{P}_1\cdot$, $\mathrm{P}_m\cdot$, $\mathrm{P}_n\cdot$ and $\mathrm{P}_{m+1}\cdot$ represent polymer radicals, P_m, P_n and P_{m+n} polymer molecules, M is MMA, and k_2, k_3 and k_4 are rate constants, respectively, for initiation, propagation and termination. By assuming a stationary state for each of R· and P·, the following equation can be deduced for the initial rate of polymerization:

$$R=k_3(k_1/k_4)^{1/2}[\mathrm{TCA}]^{1/2}[\mathrm{DMA}]^{1/2}[\mathrm{M}] \quad (3)$$

Although the chemical identity of R· is unknown at present, equation 3 perfectly coincides with equation 1.

The rate-concentration relation represented by equation 1 or 3 is quite similar to that of Imoto[4] and others for the polymerization of vinyl monomers initiated by a combined action of benzoyl peroxide and dimethylaniline. They also postulated a bimolecular reaction between benzoyl peroxide and dimethylaniline for the initial reaction of the polymerization.

Summary

The polymerization of methyl methacrylate is initiated even at room temperature by a combined action of trichloroacetic acid and dimethylaniline. In case of bulk polymerization, the initial rate of polymerization is proportional to each of the square roots of the concentrations of trichloroacetic acid and dimethylaniline. In case of polymerization in benzene, the initial rate depends upon the concentration of methyl methacrylate. These relationships can be reasonably explained by assuming a bimolecular reaction between trichloroacetic acid and dimethylaniline to form radicals as the initial reaction of the polymerization. Hydroquinone acts as an inhibitor for this reaction.

The author thanks Professor Osamu Simamura of University of Tokyo for his kind guidance and also Mr. Tsurahide Cho, the President of Tama Kagaku Kogyo Co., for permission to undertake this work.

Tama Kagaku Kogyo Co.
2-28 Minamirokugo
Ota-ku, Tokyo

4) M. Imoto and K. Takemoto, *Chem. High Polymers (Kobunsi Kagaku)*, **12**, 120 (1955).

Synthetic Studies on the Benzofuran Derivatives. Part III. Reaction of 7-Hydroxy-8-formyl-2-methylisoflavone with Ethyl Bromomalonate and Synthesis of Furano(2',3':7,8)-2-methylisoflavone

By Takashi MATSUMOTO, Yoshiyuki KAWASE, Mutsumu NANBU and Kenji FUKUI

(Received April 16, 1958)

In previous papers of this series[1], it has been found that 2-carbethoxybenzofuran derivatives (I) or 2,2-dicarbethoxy-3-hydroxy-2,3-dihydrobenzofuran derivatives (II) were obtained by interaction of 7-hydroxy-8-formyl-flavone derivatives or *o*-hydroxybenzaldehyde derivatives with ethyl bromomalonate by means of Tanaka's method[2] for benzofuran synthesis. The present investigation was undertaken to examine a reaction of 7-hydroxy-8-formyl-2-methylisoflavone (III) with ethyl bromomalonate and to derive furano-(2',3':7,8)-2-methylisoflavone (VIII) from the condensation product (IV).

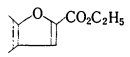
(I)

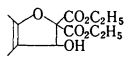
(II)

III and ethyl bromomalonate were refluxed in methyl ethyl ketone or acetone in the presence of potassium carbonate. The resulting condensation product, m.p. 171~172°C, was assigned structure IV (5'-carbethoxy-furano(2',3':7,8)-2-methylisoflavone) on the basis of the following facts. The compound IV was hydrolyzed with methanolic potassium hydroxide to yield the corresponding acid V, m.p. 295~297°C (decomp.). Esterification of V with ethanol gave a compound, m.p. 171~172°C, which was identical with IV. It is of interest that the condensation reaction is analogous to the conversion of *o*-hydroxybenzaldehyde derivatives into I[1]. On hydrolytic fission with aqueous sodium hydroxide, IV gave an acid VI, m.p. 256~257°C, which had a dark violet ferric reaction; it may be benzyl 2-carboxy-4-hydroxy-5-benzofuranyl ketone. VI was esterified with ethanol to give the ester VII, m.p. 166~166.5°C, which was different from IV; it seemed to be benzyl 2-carbethoxy-4-hydroxy-5-benzofuranyl ketone, the ester of VI. The acid V was decarboxylated at 180~190° (bath temperature) into the isoflavone VIII, m.p. 187~188°C, which was thought to be furano(2',3':7,8)-2-methylisoflavone. Ramachandra Row and Seshadri[3] obtained, by an alternate route, 5'-carbethoxy-furano (2',3':7,8)-2-methylisoflavone, 5'-carboxy-furano(2',3':7,8)-2-methylisoflavone and furano(2',3':7,8)-2-methylisoflavone; the melting points of these compounds, however, differed markedly from those of the present products (IV, V and VIII) (see Table I).

TABLE I
THE MELTING POINTS OF SYNTHETIC PRODUCTS

	Our results	Results of Ramachandra Row et al.
5'-carbethoxy-furano(2',3':7,8)-2-methylisoflavone (IV)	171~172°C	225~227°C
5'-carboxy-furano(2',3':7,8)-2-methylisoflavone (V)	295~297°C (decomp.)	253~255°C (decomp.)
furano(2',3':7,8)-2-methylisoflavone (VIII)	187~188°C	95~ 96°C

To confirm the structure of IV, V and VIII, alkaline hydrolysis of VIII was carried out to give acetic acid and a substance (IX) of colorless needles, m.p. 86~87°C, which gave a dark blue ferric reaction in ethanol. On boiling IX with a mixture of sodium acetate and acetic anhydride, an isoflavone derivative, m.p. 187~188°C, was obtained, which was identical with VIII. On oxidation with hydrogen peroxide IX gave phenylacetic acid (X), m.p. 76°C, and furan-2,3-dicarboxylic acid (XI), m.p. 220~221°C(decomp.); thus

1) Y. Kawase, T. Matsumoto and K. Fukui, This Bulletin, **28**, 273 (1955); T. Matsumoto and K. Fukui, ibid., **30**, 3 (1957).
2) S. Tanaka, *J. Am. Chem. Soc.*, **73**, 872 (1951).
3) L. Ramachandra Row and T. R. Seshadri, *Proc. Indian Acad. Sci.*, **34A**, 187 (1951).

IX was considered to be benzyl 4-hydroxy-5-benzofuranyl ketone. To further confirm the structure of IX, its methyl ether XII, m.p. 61.5~62°C, was derived. This ether was conveniently compared with a ketone prepared from the acid chloride of karanjic acid methyl ether and dibenzyl-

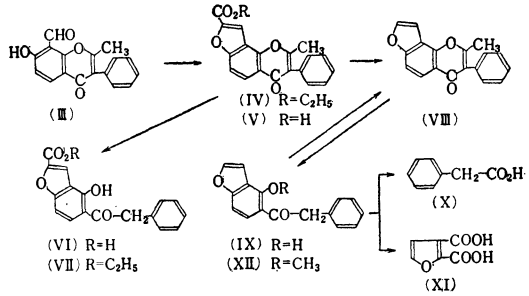

cadmium (m.p. 63~63.5°C). The mixed melting point was undepressed*. VIII, IV and V were thus assigned furano(2',3':7,8)-2-methylisoflavone and 5'-carbethoxy-furano(2',3':7,8)-2-methylisoflavone and 5'-carboxy-furano(2',3':7,8)-2-methylisoflavone, respectively.

Experimental**

7-Hydroxy-8-formyl-2-methylisoflavone (III).—The aldehyde was prepared from 7-hydroxy-2-methylisoflavone by the hexamine method[3].

5'-Carbethoxy-furano(2',3':7,8)-2-methylisoflavone (IV).—A mixture of 6.5 g. of the aldehyde III, 6.1 g. of ethyl bromomalonate, 12 g. of anhydrous potassium carbonate and 230 cc. of methyl ethyl ketone was refluxed with stirring for 10 hr. in a steam-bath. After being cooled, the mixture was filtered and evaporated to dryness. Recrystallization from ethanol yielded colorless needles, which gave a negative ferric reaction (in ethanol) and also gave no 2,4-dinitrophenylhydrazone; yield 4.8 g., m.p. 171~172°C.

Anal. Found: C, 72.43; H, 4.38. Calcd. for $C_{21}H_{16}O_5$: C, 72.40; H, 4.63%.

Acetone was favorably substituted for the methyl ethyl ketone.

5'-Carboxy-furano(2',3':7,8)-2-methylisoflavone (V).—A mixture of 2.0 g. of the ester IV, 1.0 g. of potassium hydroxide and 80 cc. of methanol was heated under reflux for 1 hr. in a steam-bath. The reaction mixture was acidified with dilute sulfuric acid. After the solvent was distilled off, the residual solids were collected, washed with water and recrystallized from methanol in colorless needles, m.p. 295~297°C (decomp.), which gave a negative ferric reaction (in ethanol) and was soluble in 5% aqueous sodium hydrogen carbonate; yield 1.7 g.

Anal. Found: C, 71.23; H, 3.90. Calcd. for $C_{19}H_{12}O_5$: C, 71.25; H, 3.78%.

Esterification of V.—A mixture of 0.5 g. of the acid V, 1 cc. of concentrated sulfuric acid and 35 cc. of absolute ethanol was refluxed for 8 hr. The reaction mixture was treated in the usual manner and recrystallized from ethanol to give 0.4 g. of colorless needles, m.p. 171~172°C; the melting point was undepressed on admixture with the above sample IV, m.p. 171~172°C.

Anal. Found: C, 72.28; H, 4.82. Calcd. for $C_{21}H_{16}O_5$: C, 72.40; H, 4.63%.

Fission of IV.—A mixture of 2.3 g. of the ester IV and 150 cc. of 5% aqueous sodium hydroxide was heated in a steam-bath with occasional shaking for 3 hr. After the reaction mixture was filtered and acidified with sulfuric acid, the precipitates were collected and washed with water. Recrystallization from methanol yielded benzyl 2-carboxy-4-hydroxy-5-benzofuranyl ketone VI, m.p. 256~257°C in colorless needles, which gave a dark violet ferric reaction (in ethanol); yield 1.3 g.

Anal. Found: C, 69.21; H, 4.06. Calcd. for $C_{17}H_{12}O_5$: C, 68.91; H, 4.08%.

A mixture of 0.5 g. of VI, 1 cc. of concentrated sulfuric acid and 35 cc. of absolute ethanol was refluxed for 8 hr. The reaction mixture was worked up in the usual manner and recrystallized from ethanol to give colorless needles of benzyl 2-carbethoxy-4-hydroxy-5-benzofuranyl ketone (VII), which had a brown ferric reaction (in ethanol); yield 0.4 g., m.p. 166~166.5°C.

Anal. Found: C, 70.23; H, 5.04. Calcd. for $C_{19}H_{16}O_5$: C, 70.36; H, 4.98%.

Furano(2',3':7,8)-2-methylisoflavone(VIII).—A mixture of 6.0 g. of V, 3.5 g. of copper powder and 180 cc. of quinoline was heated with stirring in an atmosphere of nitrogen for ca. 30 min. at 180~190° (bath temperature) until evolution of carbon dioxide ceased. After being cooled, the copper powder was filtered off, and the solution was acidified with dilute sulfuric acid. The precipitates thus formed were collected, washed with aqueous sodium hydrogen carbonate and then with water. Recrystallization from ethyl acetate gave colorless needles, which had a negative ferric reaction (in ethanol); yield 3.4 g., m.p. 187~188°C.

Anal. Found: C, 78.44; H, 4.46. Calcd. for $C_{18}H_{12}O_3$: C, 78.25; H, 4.38%.

Fission of VIII.—A mixture of 2.0 g. of VIII, 4.0 g. of potassium hydroxide and 110 cc. of ethanol was heated for 4 hr. in a steam-bath. After the solvent was evaporated, the residue was mixed with water and acidified with dilute sulfuric acid. The resulting precipitates were collected, washed with water and recrystallized from ethanol as colorless needles of benzyl 4-hydroxy-5-benzofuranyl ketone (IX), which had a dark blue ferric reaction (in ethanol); yield 1.6 g., m.p. 86~87°C.

Anal. Found: C, 76.23; H, 5.02. Calcd. for $C_{16}H_{12}O_3$: C, 76.18; H, 4.80%.

The mother liquor, which was freed from the above precipitates, was steam-distilled and the

* The details of the synthesis of this ketone (XII) will be given in the following paper.

** All the melting points were uncorrected.

distillate was neutralized with 0.1 N sodium hydroxide solution. A part of the neutralized solution (0.0025 mole) was concentrated to ca. 2 cc. in vacuo, and mixed with 0.7 g. of a solution of *p*-bromophenacyl bromide in 100 cc. of ethanol. The mixture was refluxed for 1 hr. in a steam-bath, the solvent, removed, and water was added. The precipitates obtained were collected, washed with water and recrystallized from aqueous ethanol to form colorless plates; yield 0.3 g., m.p., 84~85°C. The melting point was undepressed on admixture with an authentic sample of *p*-bromophenacyl ester of acetic acid, m.p. 84~85°C.

Anal. Found: C, 46.99; H, 3.79. Calcd. for $C_{10}H_9O_3Br$: C, 46.72; H, 3.53%.

Reactions of Benzyl 4-Hydroxy-5-benzofuranyl Ketone (IX).—*a*).—A mixture of 0.35 g. of the ketone IX, 2.0 g. of anhydrous sodium acetate and 10 cc. of acetic anhydride was refluxed for 12 hr. in an oil bath. The excessive acetic anhydride was removed in vacuo, the residue was made alkaline with 5% aqueous sodium hydroxide and then extracted with ether. The ethereal solution was washed with 5% aqueous sodium hydroxide, then with water, dried over anhydrous sodium sulfate and evaporated. The crude residue was recrystallized from ethyl acetate in colorless needles, which had a negative ferric reaction (in ethanol); yield 0.15 g., m.p. 187~188°C (alone or mixed with VIII).

b) *Oxidation.*—On a steam-bath 1.0 g. of IX was heated with 200 cc. of 2.5% aqueous potassium hydroxide until a clear solution was obtained, which was cooled to room temperature, and 50 cc. of hydrogen peroxide solution (8%) was added slowly. Then the reaction mixture was kept for 18 hr. at room temperature and then heated for 6 hr. in a steam-bath to decompose the excessive hydrogen peroxide. The solution was acidified with dilute hydrochloric acid and evaporated in vacuo to dryness and then extracted continuously with ether for 17 hr. The ethereal solution was extracted with 5% aqueous sodium hydrogen carbonate. This solution was made slightly acidic with dilute hydrochloric acid and then made slightly alkaline with dilute aqueous ammonia solution, then a solution of 1.0 g. of calcium chloride was added and the precipitates formed were filtered off. The filtrate was acidified with dilute hydrochloric acid and evaporated to ca. 20 cc. in vacuo. After cooling, the crude phenylacetic acid was removed by filtration. The mother liquor was continuously extracted with ether for 17 hr. The ethereal extracts, upon evaporation, yielded a mixture of phenylacetic acid and furan-2,3-dicarboxylic acid (XI), which were separated by trituration with cold chloroform. The suspended solid was collected. Recrystallization from acetic acid gave XI in colorless needles, m.p. 220~221°C (decomp.) which had a negative ferric reaction (in ethanol); yield 0.1 g. This product did not depress the melting point of authentic furan-2,3-dicarboxylic acid[4] made from karanjic acid.

Anal. Found: C, 46.26; H, 2.90. Calcd. for $C_6H_4O_5$: C, 46.17; H, 2.58%.

Evaporation of the chloroform layer yielded crude phenylacetic acid. The combined crude phenylacetic acid was recrystallized from water in colorless plates; yield 0.15 g., m.p. 76°C. The melting point was undepressed on admixture with an authentic sample of phenylacetic acid, m.p. 76°C.

c) *Methylation.*—A mixture of 1.0 g. of IX, 1.0 g. of anhydrous potassium carbonate and a solution of 1 cc. of dimethyl sulfate in 20 cc. of anhydrous acetone was refluxed for ca. 20 hr. in a steam-bath. The precipitates were filtered off, the acetone was removed and the residue washed with 5% dilute sodium hydroxide and then with water. Recrystallization from ethanol gave colorless plates, m.p. 61.5~62°C, which had a negative ferric reaction (in ethanol); yield 0.7 g. The melting point of this compound was undepressed on admixture with synthetic sample m.p. 63~63.5°C, which was obtained from the acid chloride of karanjic acid methyl ether and dibenzylcadmium.*

Anal. Found: C, 76.98; H, 5.88. Calcd. for $C_{17}H_{14}O_3$: C, 76.67; H, 5.30%.

Summary

5'-Carbethoxy-furano(2',3' : 7,8)-2-methylisoflavone (IV) was obtained from 7-hydroxy-8-formyl-2-methylisoflavone (III) and ethyl bromomalonate by Tanaka's method for benzofuran synthesis. The condensation product IV was hydrolyzed to give the free acid V, which was decarboxylated in quinoline with copper powder to yield furano(2',3' : 7,8)-2-methylisoflavon (VIII). The structures of the condensation product and its derivatives were discussed.

We are grateful to the Institute of Agricultural Chemistry, Faculty of Agriculture, Kyoto University for microanalyses.

Faculty of Literature and Science
Toyama University, Toyama

4) B. L. Manjunath, A. Seetharamiath and S. Siddappa, *Ber.*, **72B**, 93 (1939).

Synthetic Studies on the Benzofuran Derivatives. Part IV. A New Synthesis of Benzyl 2-Methoxyphenyl Ketones and a Synthesis of Benzyl 4-Methoxy-5-benzofuranyl Ketone (Benzyl O-Methyl-karanjyl Ketone)

By Yoshiyuki KAWASE, Teruo FUJIMOTO and Kenji FUKUI

(Received April 16, 1958)

In the preceding paper[1] of this series, the preparation of furano (2′, 3′ : 7, 8)-2-methylisoflavone (I), m.p. 187~188°C, was described, but as mentioned already, the melting points of it and the related compounds were quite different from those of the compounds reported by Row et al.[2]

Now, to further confirm the structure of the expected benzyl 4-hydroxy-5-benzofuranyl ketone (benzyl karanjyl ketone) (II) which was obtained by alkaline hydrolysis[1] of I, a synthesis of II or its methyl ether III by a different method from that of Row et al. 's[2] was attempted; III was prepared by the interaction of 4-methoxy-5-benzofuranoyl chloride (*O*-methyl-karanjic acid chloride) (IV) and dibenzylcadmium.

The usual preparative methods of benzyl 2-hydroxyphenyl ketones are: a) the interaction of phenols with phenylacetonitriles or phenylacetic acids or phenylacetyl chlorides, according to the Hoesch, Nencki, and Friedel-Crafts reaction, respectively; b) the rearrangement of phenyl phenylacetates according to the Fries reaction. In these reactions, however, the position of the phenylacetyl group which enters into the phenol nucleus is restricted, and thus the preparation of the hydroxyketone II from 4-hydroxybenzofuran (karanjol) by these methods is unsuccessful[3].

A new synthetic route to benzyl 2-hydroxyphenyl ketones was recently reported by one of the authors[4], which involves the ester condensation of methyl 2-methoxybenzoates with phenylacetonitriles followed by hydrolysis. But an attempted synthesis, by this method, of II from methyl 4-methoxy-5-benzofuranoate (methyl *O*-methyl-karanjate) and phenylacetonitrile resulted in failure because of the abortive ester condensation.

The preparation of benzyl 2-methoxyphenyl ketones has been described by Tiffeneau et al.[5], but this method which involves the Grignard reaction and the Tiffeneau rearrangement is unfavorable in the present case.

Therefore, another method of synthesis for benzyl 2-methoxyphenyl ketones was explored. By this means it was found that a reaction of 2-methoxybenzoyl chlorides with dibenzylcadmium in anhydrous benzene was feasible. A reaction of benzoyl chloride or 2-methoxybenzoyl chloride or 2,4-dimethoxybenzoyl chloride with dibenzylcadmium gave phenyl benzyl ketone (deoxybenzoin) (V), benzyl 2-methoxyphenyl ketone (VI), and benzyl 2,4-dimethoxyphenyl ketone (VII), respectively. A small amount of 1,2-diphenyl ethane was obtained as a by-product from the forerun of the distillates.

By the interaction of IV and dibenzylcadmium in anhydrous benzene, the desired methoxy-ketone (III) was obtained in colorless crystals, m.p. 63~63.5°C, which was identical with the sample reported in the preceding paper.

Experimental[6]

Phenyl Benzyl Ketone (Deoxybenzoin) (V). —The following reaction was carried out under a stream of dry nitrogen gas with stirring. To a solution of Grignard reagent prepared from 4.2 g. of freshly distilled benzyl bromide and 0.6 g. of magnesium in 100 cc. of anhydrous ether was carefully added 2.4 g. of powdered anhydrous cadmium chloride at room temperature, and the mixture was refluxed for 1 hr. Most of the ether was distilled off, 100 cc. of anhydrous benzene

1) Part III by T. Matsumoto, Y. Kawase, M. Nanbu and K. Fukui, This Bulletin, **31**, 688 (1958).
2) L. R. Row and T. R. Seshadri, *Proc. Indian Acad. Sci.*, **34A**, 187 (1951); *Chem. Abstr.*, **47**, 12374 (1953).
3) B. L. Manjunath, A. Seetharamiah and S. Siddappa, *Ber.*, **72**, 93 (1939); S. H. Harper, *J. Chem. Soc.*, **1942**, 593; A. Seetharamiah, ibid., **1948**, 894.
4) Y. Kawase, This Bulletin, **31**, 390 (1958).
5) J. Lévy and R. Pernot, *Bull. soc. chim.*, **49**, 1730 (1931); M. Tiffeneau, A. Oryékhov and M. Roger, ibid., **49**, 1757 (1931).
6) Melting and boiling points are uncorrected.

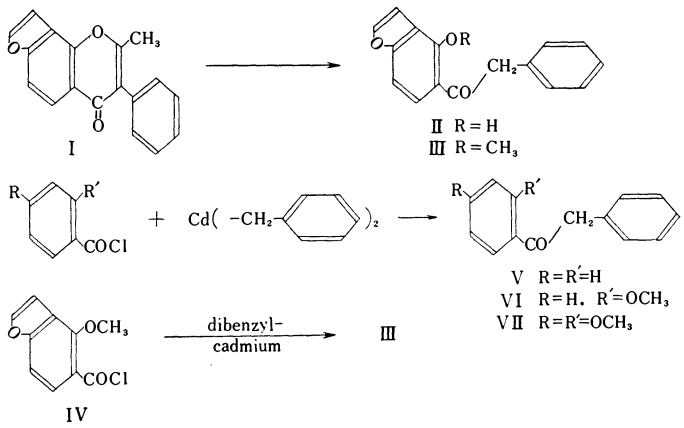

was added, and the remaining ether was distilled off. Then a solution of 5 g. of benzoyl chloride in 50 cc. of anhydrous benzene was added slowly at room temperature, and the mixture was refluxed for ca. 4 hr. The cooled reaction mixture was shaken with 200 cc. of dilute sulfuric acid, the organic portion separated, washed with water, and then warmed with 5% aqueous sodium hydroxide with shaking for a while to decompose the excess of chloride. The benzene solution which had separated was washed with water, dried, and the solvent was distilled off. The residual oily product was distilled, b.p. 120~180°C/4 mm. (bath temperature); yield 2.3 g. A sample of V for analysis was obtained from a higher-boiling fraction by crystallization from ethanol in colorless needles, m.p. 52~53°C, which was identical with an authentic sample[7]. V which was contained in the distillate was confirmed through its 2,4-dinitrophenylhydrazone, m.p. 197~197.5°C, identical with an authentic sample, m.p. 197~198°C; reported b.p. 160°C/5 mm., m.p. 55~56°C[7] and m. p. of 2, 4-dinitrophenylhydrazone 202~204°C[8].

Anal. of V. Found: C, 85.41; H, 6.35. Calcd. for $C_{14}H_{12}O$: C, 85.68; H, 6.16%.

From the mother liquor of 2,4-dinitrophenylhydrazone, 1,2-diphenylethane was obtained by distillation. Crystallization from ethanol gave colorless crystals, m.p. 51~52°C, which was identical with an authentic sample[9]; yield 0.4 g.; reported b.p. 158°C/10 mm. and m.p. 51°C[9].

Benzyl 2-Methoxyphenyl Ketone (VI).— By the procedure described before, dibenzylcadmium was prepared from 2.3 g. of cadmium chloride and benzylmagnesium bromide (from 3.5 g. of benzyl bromide and 0.5 g. of magnesium) in 100 cc. of anhydrous benzene. The reagent was allowed to react with a solution of 5 g. of 2-methoxybenzoyl chloride in 50 cc. of benzene; the chloride was prepared from 2-methoxybenzoic acid and excessive thionyl chloride, b.p. 145~146°C/25 mm. After the same treatment as described before, two fractions were obtained by distillation: (a) b.p. 90~150°C/4 mm., yield 0.5 g.; (b) b.p. 163~164°C/4 mm., yield 1.5 g. The lower boiling fraction became solid on standing, which on recrystallization from ethanol yielded a compound, m.p. 50~51°C, identical with an authentic sample of 1,2-diphenylethane. The higher boiling fraction which remained unsolidified consisted of VI, which was ascertained from its 2,4-dinitrophenylhydrazone, m.p. 162~163°C (from ethanol), identical with the other sample[4]. Reported boiling points of VI are 202~204°C/14 mm.[5], 198~202°C/14 mm.[5] and 130~131°C/0.001 mm.[4], and the melting point of the 2,4-dinitrophenylhydrazone 163~164°C[4].

Benzyl 2,4-Dimethoxyphenyl Ketone (VII).—The preparation followed the same method as in the above case. 2,4-Dimethoxybenzoyl chloride was employed in place of 2-methoxybenzoyl chloride; the chloride was prepared by heating an excess of thionyl chloride with 7 g. of 2,4-dimethoxybenzoic acid at 50° for twenty minutes, the excess of thionyl chloride removed in vacuo, and the crude chloride was used. The product was distilled at 160~180°C/4 mm. (bath temperature) to give colorless oil, yield 2 g., which was crystallized from ethanol in colorless needles, m.p. 46.5~47°C, identical with an authentic sample prepared by methylation of benzyl 2,4-dihydroxyphenyl ketone. The 2,4-dinitrophenylhydrazone, m.p. 194~195°C (from ethanol-ethyl acetate), was identical with an authentic sample; reported m.p. of VII 47~48°C[5].

Anal. of VII. Found: C, 74.90; H, 6.40. Calcd. for $C_{16}H_{16}O_3$: C, 74.96; H, 6.30%.

From the forerun in the case of the distillation (0.5 g.), 1,2-diphenylethane was obtained, m.p. 52~53°C.

Benzyl 4-Methoxy-5-benzofuranyl Ketone (III). — *O*-Methyl-karanjic acid (4-methoxy-5-benzofuranoic acid)[10] was prepared from karanjic

7) C. F. H. Allen and W. E. Barker, *Org. Synth.*, Coll. Vol. II, 156 (1943).
8) M. S. Newman and W. M. Edwards, *J. Am. Chem. Soc.*, **76**, 1840 (1954).
9) T. Reichstein and R. Oppenauer, *Helv. Chim. Acta*, **16**, 1377 (1933).
10) T. R. Seshadri and V. Venkateswalu, *Proc. Indian Acad. Sci.*, **13A**, 404 (1941), *Chem. Abstr.*, **35**, 7961 (1941); B. L. Manjunath and A. Seetharamiah, *J. Mysore Univ.*, Sec. B. 2, 3, 19 (1941), *Chem. Abstr.*, **36**, 1935 (1942).

acid[11] by refluxing it with dimethyl sulfate and potassium carbonate in acetone for 15 hr. The product was subjected to alkaline hydrolysis, and the acid obtained (3 g.) was warmed with excessive thionyl chloride at 50°C for 20 min., and the excessive thionyl chloride was removed in vacuo. Benzene (50 cc.) was added to the residue, and the traces of thionyl chloride, together with benzene, were removed by warming to dryness in vacuo. A solution of the crude chloride IV[10] in 50 cc. of anhydrous benzene was added to a suspension of dibenzylcadmium (prepared from 2 g. of cadmium chloride and benzylmagnesium bromide (from 2.7 g. of benzyl bromide and 0.4 g. of magnesium)) in 100 cc. of anhydrous benzene. After the same treatment as described before, the product was distilled at 150~180°C/0.003 mm. (bath temperature) to give colorless oil, yield 1.1 g., which was crystallized from ethanol in colorless crystals, m.p. 63~63.5°C, and identical with the sample reported in the preceding paper. It gave 2,4-dinitrophenylhydrazone of m.p. 227~228°C (from ethanol-ethyl acetate).

Anal. of III. Found: C, 76.23; H, 5.41. Calcd. for $C_{17}H_{14}O_3$: C, 76.66; H, 5.30%.

From the forerun in the case of the distillation (0.3 g.), 1,2-diphenylethane was obtained, m.p. 51~52°C.

We are grateful to the Institute of Agricultural Chemistry, Faculty of Agriculture, Kyoto University for microanalyses.

Faculty of Literature and Science
Toyama University, Toyama

11) R. T. Foster and A. Robertson, *J. Chem. Soc.*, **1948**, 115.

Synthetic Studies on the Benzofuran Derivatives. Part V. Synthesis of Furano(2′, 3′ : 7, 8)-isoflavone

By Kenji FUKUI and Yoshiyuki KAWASE

(Received April 16, 1958)

In a previous paper[1], furano (2′, 3′ : 7, 8)-2-methylisoflavone (I) was obtained by Tanaka's method[2] for benzofuran synthesis. It is of interest to prepare some furano-isoflavone derivatives and compare their behavior with that of the 2-methyl compounds in a number of reactions.

The present paper describes the synthesis of furano(2′, 3′ : 7, 8)-isoflavone (III). For this purpose two possible methods have been explored. The first method was to complete the isoflavone structure using a suitable coumarone derivative, benzyl 4-hydroxy-5-benzofuranyl ketone (II), as the starting material. The second one consisted in the introduction of a furan nucleus into an isoflavone skeleton (Tanaka's method[2]).

By means of the first method, II[1] (benzyl karanjyl ketone), which was fairly easily obtained as the product of hydrolysis of I, led to III, m.p. 152~152.5°C, on condensation with ethyl orthoformate in pyridine containing a little piperidine (method of Sathe and Venkataraman[3]).

As regards the second method, the application to the present case presented more difficulties than in the case of the synthesis of the 2-methyl derivative (I). The starting material was 7-hydroxyisoflavone (IV) which readily yielded the corresponding 8-aldehyde (V) by the hexamine method. The next step which involved the condensation with bromomalonic ester to 5′-carbethoxy-furano-(2′, 3′ : 7, 8)-isoflavone (VI) also proceeded smoothly.

The reaction of VI with hot aqueous sodium hydroxide brought about a conversion into benzyl 2-carboxy-4-hydroxy-5-benzofuranyl ketone (VIII), which was identical with the sample obtained[1] by hydrolysis of 5′-carbethoxy-furano(2′, 3′ : 7, 8)-2-methylisoflavone (X). By the action of ethanolic sodium hydroxide, 5′-carboxy-furano(2′, 3′ : 7, 8)-isoflavone (VII) could be obtained together with a small quantity of benzyl 2-carbethoxy-4-hydroxy-5-benzofuranyl ketone (IX), which was identical with the sample produced[1] by esterification

1) T. Matsumoto, Y. Kawase, M. Nanbu and K. Fukui, This Bulletin, **31**, 688 (1958).
2) S. Tanaka, *J. Am. Chem. Soc.*, **73**, 872 (1951).
3) V. R. Sathe and K. Venkataraman, *Current Sci. (India)*, **18**, 378 (1949), *Chem. Abst.*, **44**, 8916 (1950).

of VIII. When VI was refluxed with aqueous sodium carbonate in acetone, VII was also obtained together with a small quantity of VIII. While X gave corresponding acid XI in a satisfactory yield[1], saponification of the ester VI to VII was of lower yield. This difference may be due possibly to the greater reactivity of an isoflavone ring owing to the absence of the 2-methyl group. VII was decarboxylated into III, m.p. 151~151.5°C, which was identical with the isoflavone prepared by the ethyl orthoformate method. The ultraviolet spectrum of III almost agreed with that of I (Fig. 1). Hydrolytic decomposition of III gave II, which was identical with the sample obtained[1] from I.

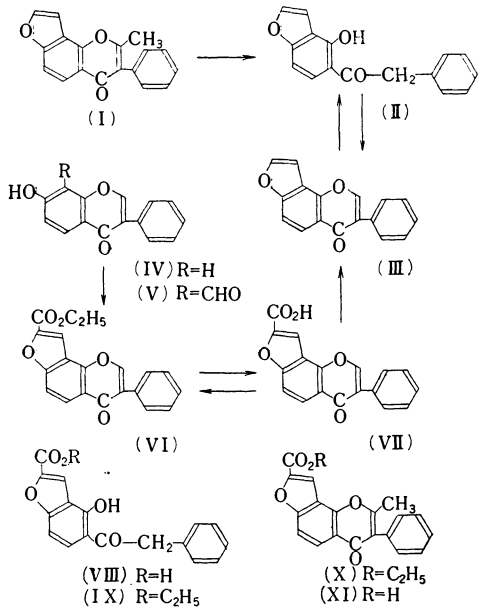

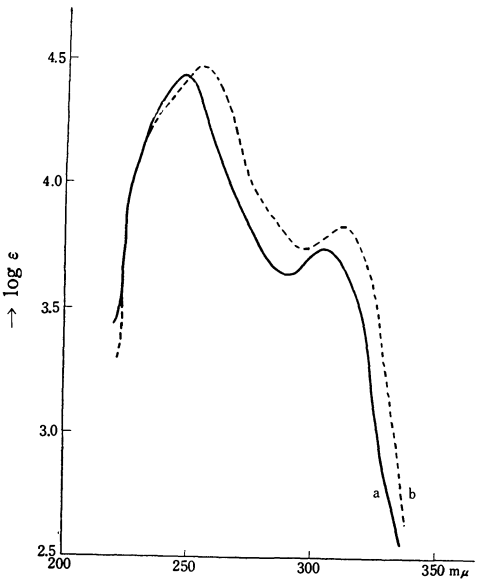

→ Wave length

Fig. 1. Ultraviolet absorption of the isoflavone in ethanol.
(a) Furano(2', 3':7, 8)-2-methylisoflavone(I)
(b) Furano(2', 3':7, 8)-isoflavone(III)

Experimental*

7-Hydroxy-8-formyl-isoflavone(V).—A mixture of 7-hydroxy-isoflavone (IV) (1.5 g.), hexamine (8 g.) and glacial acetic acid (25 cc.) was heated in a steam-bath for 6 hr. The resulting hot reddish brown liquid was treated with hydrochloric acid (1:1, 24 cc.) and again heated in a steam-bath for ca. 5 min. After dilution with water (40 cc.) it was allowed to stand overnight. The yellow precipitates were collected, washed with water and dried. The dry solids were extracted twice with hot benzene (25 cc.) and the residue rejected. The benzene solution was evaporated, leaving V which, on repeated purification from ethanol, formed colorless needles, m.p. 197~198°C, which gave a red ferric reaction (in ethanol); yield 0.6 g.

Anal. Found: C, 72.01; H, 4.01. Calcd. for $C_{16}H_{10}O_4$: C, 72.18; H, 3.79%.

5'-Carbethoxy-furano(2', 3' : 7,8)-isoflavone (VI).—V (3 g.) was treated with ethyl bromomalonate (3.3 g.) and anhydrous potassium carbonate (13.5g.) in anhydrous acetone (150cc.). After being refluxed for 10.5 hr., the mixture was filtered and evaporated to dryness. The residue was collected, and washed with water. Recrystallization from ethanol gave colorless needles, which had a negative ferric reaction (in ethanol); yield 2.5 g., m.p. 172~173°C.

Anal. Found: C, 71.48; H, 4.31. Calcd. for $C_{20}H_{14}O_5$: C, 71.85; H, 4.22%.

Hydrolysis of 5'-Carbethoxy-furano(2', 3' : 7,8)-isoflavone (VI).—*a) Hydrolysis by aqueous sodium hydroxide.*—A mixture of VI (0.6 g.) and 5% aqueous sodium hydroxide (50 cc.) was heated in a steam-bath for 3 hr. After the reaction mixture was acidified with dilute sulfuric acid, the precipitates were collected, washed with water and crystallized from ethanol to yield colorless needles (0.5 g.), m.p. 256~257°C, which gave a dark violet ferric reaction in ethanol and was soluble in 5% aqueous sodium hydrogen carbonate. The mixed melting point test showed the identity of the above compound with benzyl 2-carboxy-4-hydroxy-5-benzofuranyl ketone (VIII), m.p. 256~257°C, obtained[1] from 5'-carbethoxy-furano (2', 3':7, 8)-2-methylisoflavone (X).

b) Hydrolysis by aqueous sodium carbonate-acetone.—A mixture of VI (0.5 g.), acetone (20 cc.) and 5% aqueous sodium carbonate (20 cc.) was heated under reflux in a steam-bath for

* All the melting points were uncorrected.

4 hr.; a great amount of the precipitates was formed during the reaction. Acetone was evaporated in vacuo, the reaction mixture was diluted with water (20 cc.) and filtered. The precipitates, perhaps sodium salt of the acid VII, were heated with dilute hydrochloric acid for a few minutes; the deposits were collected and washed with water. Recrystallization from glacial acetic acid gave 5'-carboxy-furano(2', 3':7, 8)-isoflavone (VII) in microcrystals. This had a negative ferric reaction in ethanol and produced carbon dioxide and sparingly soluble sodium salt with 5% aqueous sodium hydrogen carbonate; yield 0.2 g., m.p. 283°C (decomp.). The analytical sample was further dried at 120°C over phosphoruspentoxide for 4 hr. in vacuo.

Anal. Found: C, 66.77; H, 3.63. Calcd. for $C_{18}H_{10}O_5 \cdot H_2O$: C, 66.67; H, 3.70%.

VII afforded VI on esterification with ethanol in the presence of sulfuric acid, m.p. and mixed m.p. 172~173°C. VII was converted into VIII, m.p. 252~253°C, by further hydrolysis with aqueous sodium hydroxide.

The mother liquor of the sodium salt of VII was acidified with dilute hydrochloric acid and the precipitates obtained were crystallized from ethanol to yield VIII (0.1 g.), m.p. 251°C. This gave a dark violet ferric reaction (in ethanol).

c) Hydrolysis by ethanolic sodium hydroxide.—A hot solution of VI (0.5 g.) in ethanol (50 cc.) was added to a hot solution of sodium hydroxide (0.1 g.) in ethanol (20 cc.) and refluxed for 1 hr. After being cooled, the white precipitates were collected and treated with hot dilute hydrochloric acid. Recrystallization from glacial acetic acid gave microcrystals, which had a negative ferric reaction (in ethanol); yield 0.25 g., m.p. 280°C (decomp.). The mixed melting point test proved the compound to be identical with VII.

The filtrate, which was separated from the above precipitates, was acidified with diluted hydrochloric acid and diluted with water until it became turbid. The deposits were collected and recrystallized from ethanol to give colorless needles, which had a brown ferric reaction in ethanol and were insoluble in 5% aqueous sodium hydrogen carbonate; yield 0.1 g., m.p. 163~164°C.

Anal. Found: C, 70.35; H, 4.83. Calcd. for $C_{19}H_{16}O_5$: C, 70.36; H, 4.98%.

The mixed melting point test proved the compound to be identical with benzyl 2-carbethoxy-4-hydroxy-5-benzofuranyl ketone (IX), m.p. 166~166.5°C, which was obtained[1] by esterification of VIII. IX produced the acid VIII, m.p. 250~252°C, on further hydrolysis with aqueous sodium hydroxide.

Furano (2', 3' : 7, 8) - isoflavone (III). — *a)* Benzyl 4-hydroxy-5-benzofuranyl ketone (II) (0.7 g.), which was prepared from furano(2', 3':7, 8)-2-methylisoflavone[1], was heated under reflux with freshly distillated ethyl orthoformate (2 g.) in anhydrous pyridine (8 cc.) containing one drop of piperidine for 8 hr. After the solution was cooled and acidified with dilute sulfuric acid, the precipitates were collected, washed with 5% aqueous sodium hydroxide and then with water. Recrystallization from ethanol gave colorless needles, which had a negative ferric reaction (in ethanol); yield 0.3 g., m.p. 152~152.5°C.

Anal. Found: C, 77.64; H, 4.10. Calcd. for $C_{17}H_{10}O_3$: C, 77.85; H, 3.84%.

b) A mixture of VII (0.8 g.), copper powder (0.5 g.) and quinoline (35 cc.) was heated while stirred in an atmosphere of nitrogen for ca. 40 min. at 180~190°C (bath temperature) until evolution of carbon dioxide ceased. After being cooled and freed from copper powder, quinoline was removed by steam distillation. Dilute sulfuric acid was poured into the remainder and the precipitates were collected. After being treated with 5% aqueous sodium hydrogen carbonate and washed with water, the solids were recrystallized from ethyl acetate and then ethanol to give the isoflavone (III) (0.5 g.) in colorless needles, m.p. 151~151.5°C. This had a negative ferric reaction (in ethanol). The melting point was undepressed on admixture with the sample in the case *a*).

Hydrolytic Fission of the Isoflavone (III) to II.—A mixture of III (1 g.), potassium hydroxide (1.8 g.) and ethanol (70 cc.) was heated under reflux for 3 hr. in a steam-bath. After the solvent was evaporated, the residue was mixed with water (50 cc.) and acidified with dilute sulfuric acid. The precipitates were collected and washed with water. Recrystallization from ethanol gave colorless needles which had a dark blue ferric reaction (in ethanol); yield 0.8 g., m.p. 85~86°. The melting point was undepressed on admixture with II, m.p. 86~87°C, which was obtained[1] from furano(2', 3':7, 8)-2-methylisoflavone (I).

Summary

1) Furano(2', 3' : 7,8)-isoflavone (III) was prepared from benzyl 4-hydroxy-5-benzofuranyl ketone (II) and ethyl orthoformate.

2) 7-Hydroxy-8-formyl-isoflavone (V) was obtained from 7-hydroxy-isoflavone (IV) by the hexamine method. 5'-Carbethoxy-furano(2', 3' : 7, 8)-isoflavone (VI) was prepared from 7-hydroxy-8-formylisoflavone (V) and ethyl bromomalonate by Tanaka's method for benzofuran synthesis. The ester VI was hydrolyzed to the free acid VII and then decarboxylated in quinoline with copper powder to the isoflavone III.

We are grateful to the Institute of Agricultural Chemistry, Faculty of Agriculture, Kyoto University, for microanalyses and to Miss M. Fukushima for her helpful assistance.

Faculty of Literature and Science
Toyama University, Toyama

*Studies on Organic Peroxides. IV. Polymerization of Vinyl Acetate in Benzoyl Peroxide-Fe(II)-Benzoin Redox System**

By Shigeo HASEGAWA, Nishio HIRAI, Norio NISHIMURA and Tsugio KAWANO

(Received May 21, 1958)

Polymerization of vinyl monomers in the redox systems of non-aqueous solution has been widely studied by W. Kern et al.[1]. According to them, in the redox system which consists of ferrous ion, benzoin and benzoyl peroxide, the following reactions take place by the Haber-Weiss one-electron transfer mechanism[2], in which the ferric ion is reduced to the ferrous by benzoin acting as reductant:

$$P+Fe^{2+} \xrightarrow{k_1} RCOO\cdot+RCOO^-+Fe^{3+} \quad (1)$$

$$BzH_2+2Fe^{3+} \xrightarrow{k_2} 2Fe^{2+}+Bz+2H^+ \quad (2)$$

where P, BzH_2, Bz and RCOO· represent benzoyl peroxide, benzoin, benzil and benzoate radical, respectively; k_1 and k_2 are the rate constants of the reactions 1 and 2, respectively.

Ukida[3] has ascertained the reaction 2 polarographically, and has also found that the rate of polymerization of vinyl acetate in this redox system was appreciably affected by the amount of ferrous salt added. The reaction 2 may reasonably be assumed to take place in two steps as follows:

$$BzH_2+Fe^{3+} \xrightarrow{k_2} Fe^{2+}+BzH\cdot+H^+$$

$$BzH\cdot+Fe^{3+} \xrightarrow{\text{rapid}} Fe^{2+}+Bz+H^+ \quad (2')$$

No kinetic considerations seem, however, to have been proposed about the redox polymerization in this system.

In this paper, the dependence of the rate and the extent of polymerization of vinyl acetate on the initial concentration of the ferrous ion which was added was studied by following the course of the rate of polymerization dilatometrically, to make clear the mechanism of the ferrous-ion catalysed decomposition of benzoyl peroxide in ethanol.

Experimental

Reagents. — In order to remove aldehydes, commercial vinyl acetate was washed with 5% sodium bisulfite solution, followed by washing with water, then the monomer was dried with calcium chloride, and stored in the dark after distillation. Just before use, the monomer was distilled once more and the fraction at 71.5~73°C was used. Ferrous chloride ($FeCl_2 \cdot 4H_2O$) was crystallized from iron powder and hydrochloric acid, and stored in carbon dioxide atomosphere to prevent oxidation. Ethanol was repeatedly distilled with calcium oxide to remove water. Benzoyl peroxide and benzoin were prepared and recrystallized in the usual manner.

Procedure. — Ethanolic solution of ferrous chloride and vinyl acetate solution containing benzoyl peroxide and benzoin were mixed, and then introduced into a cylindrical glass dilatometer which consists of a reaction vessel, 1.3 cm. in diameter and 15 cm. in length with a capillary tube of 25 cm. After removing the gas dissolved in the solution under reduced pressure and below −50°C, the dilatometer was sealed off and held in a thermostat at 50°C.

The initial concentration of benzoyl peroxide and benzoin was 10^{-2} mol. both per liter. The decrease in volume of the solution was followed by a travelling microscope. As the extent of conversion is directly proportional to the extent of decrease in volume of the solution, the former can be calculated by measuring the latter. In order to find the ratio of the extent of conversion to that of decrease in volume, five dilatometers containing polymerized solution were taken at random and each polymer was dried under reduced pressure and weighed. The mean value of the ratio was found to be 3.63 which is very close to the value, 3.65, reported by Starckweather et al.[4].

The temperature in the dilatometer increases somewhat owing to the inefficient dissipation of the heat of reaction; however, as the increment was at most 0.5°C, the temperature might be taken as constant during the polymerization.

* Presented at the Chugoku-Shikoku Local Meeting of the Chemical Society of Japan, Niihama, October 19 (1956).

1) W. Kern, *Makromol. Chem.*, **1**, 209, 246 (1947); W. Kern, R. Schulz and J. Stallmann, ibid., **6**, 216 (1951); W. Kern and R. Schulz, ibid., **13**, 210 (1954).

2) F. Haber and P. Weiss, *Proc. Roy. Soc. London*, A **147**, 332 (1934).

3) J. Ukida, *Chem. High Polymers* (*Kobunshi Kagaku*), **10**, 358 (1953).

4) H. G. Starckweather and G. B. Taylor, *J. Am. Chem. Soc.*, **52**, 4708(1930).

Results and Discussion

The extent of conversion, y, can be defined as a fraction of monomer converted into polymer, i. e. $1-[M]/[M]_0$, where $[M]$ and $[M]_0$ are the concentrations of the monomer at $t=t$ and $t=0$, respectively. The plots of y against t for various initial concentrations of the ferrous ion, x, in the case of the polymerizations of vinyl acetate containing 20% ethanol are shown in Fig. 1.

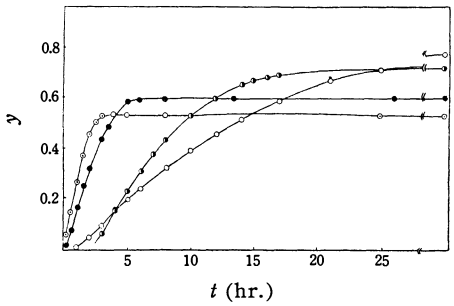

Fig. 1. Polymerization of vinyl acetate in 20% ethanol at 50°C.
$x \cdot 10^4$ (mol./l.):
○ 0, ◑ 1.0, ● 5.0, ⊙ 10.0

As seen in Fig. 1, the rate of conversion depends on the amount of ferrous salt added. In the case of rapid polymerization, the increasing viscosity of the solution at high conversion causes distortion of the meniscus and makes accurate reading difficult. Considerably sharp curvatures shown in Fig. 1 would be due to this reason.

TABLE I
DEPENDENCE OF MOLE RATIO AND FERROUS ION CONCENTRATION ON THE INITIAL RATE OF CONVERSION, THE EXTENT OF CONVERSION AND INDUCTION PERIOD

r	$x \cdot 10^4$ (mol./l.)	$(dy/dt)_0^2 \cdot 10^2$ (hr.$^{-2}$)	y_∞	Z	ind. period (hr.)
0.63	0.0	0.14	0.740	0.55	—
	2.5	0.16	0.649	0.91	4.0
	5.0	0.20	0.649	0.91	1.5
	10.0	0.25	0.597	1.20	1.5
1.89	0.0	0.12	0.791	0.41	7.5
	1.0	0.42	0.709	0.66	1.5
	5.0	1.00	0.600	1.18	1.5
	10.0	1.96	0.547	1.61	1.0
2.52	0.0	0.25	0.773	0.45	1.0
	1.0	0.96	0.715	0.63	2.5
	5.0	2.90	0.595	1.23	0.2
	10.0	6.76	0.523	1.82	—
5.67	0.0	0.25	0.825	0.33	1.0
	1.0	0.80	0.792	0.41	—
	5.0	4.00	0.737	0.56	—
	10.0	9.00	0.655	0.94	—

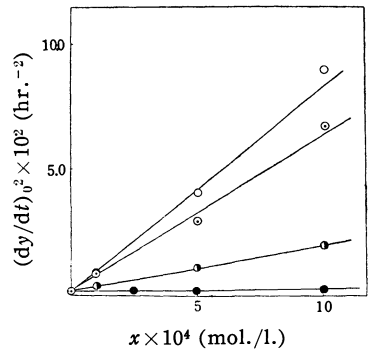

Fig. 2. Dependence of the rate of conversion on x for various values of mole ratio r.
r: ● 0.63, ◑ 1.89, ⊙ 2.52, ○ 5.67

The square of the initial rate of conversion, $(dy/dt)_0^2$, the extent of conversion when no more polymerization proceeds, y_∞, and the value of induction period are listed in Table I. For each value of mole ratio, r, of the initial concentration of the monomer to that of ethanol, the plot of the square of $(dt/dy)_0$ against x, gives a straight line shown in Fig. 2. This relation may be derived kinetically in the following manner.

The polymerization of vinyl acetate is initiated by the radicals produced from the decomposition of benzoyl peroxide. Assuming a stationary state with benzoate radicals, the rate of polymerization can be expressed as follows:

$$-d[M]/dt = (k_p/k_t^{1/2}) \times (k_d + k_1[Fe^{2+}])^{1/2}[P]^{1/2}[M] \quad (3)$$

where $[M]$ and $[Fe^{2+}]$ are the concentrations of the monomer and the ferrous ion, respectively, and k_p, k_t and k_d are the rate constants of chain growth, chain termination and apparent spontaneous decomposition of benzoyl peroxide, respectively.

The thermal decomposition of benzoyl peroxide in ethanol is of the first order with respect to the concentration of benzoyl peroxide and the rate of decomposition is the sum of a spontaneous cleavage and a radical induced chain reaction[5]. The following expression for the ferrous ion concentration may be derived from reactions 1 and 2:

$$k_1[P][Fe^{2+}] = 2k_2[BzH_2][Fe^{3+}] \quad (4)$$

5) S. Kato and F. Mashio, *J. Chem. Soc. Japan, Ind. Chem. Sec.* (*Kôgyô Kagaku Zassi*), **59**, 380 (1956).

The rate of reaction 2 may be appreciably slower than that of 1[3], therefore, the rate determining step of this redox system may be involved in 2. As mentioned above, the initial concentrations of benzoyl peroxide and benzoin have been chosen as the same and they are much greater than that of the ferrous ion. In this case, the ferrous-ion concentration can be expressed as

$$[Fe^{2+}] = (2k_2/k_1)x \qquad (5)$$

Therefore, the concentration of ferrous ion in the polymerizing solution may be directly proportional to that of ferrous ion added. From Eqs. 3 and 5, the following expression for the initial rate of conversion can be derived:

$$(dy/dt)_0^2 = (k_p^2/k_t)[P]_0(k_d+2k_2x) \qquad (6)$$

This equation corresponds to the curves in Fig. 2.

The initial rate of polymerization is, however, greatly affected by the mole ratio, r, as shown in Table I. In deriving Eq. 6, ethanol was assumed to be an ideal solvent which would not affect $(dy/dt)_0$; however, if a new radical which is produced from a molecule of ethanol attacked by a growing radical, is not so active as to initiate a new chain, ethanol will act as inhibitor or retarder. However, this reason may be invalidated by the fact that $(dy/dt)_0$ was approximately constant and independent of the ratio, r, in the absence of ferrous ion. The dependence of the rate of conversion on the ratio r, therefore, would be ascribed to the changes of the rate constants k_1 and k_2, which would be affected by the composition of the solution.

From the curves in Fig. 2, the ratio k_2/k_d can be calculated; for example, k_2/k_d is about 12,000 for $r=2.52$, showing that a small amount of ferrous chloride accelerates efficiently the rate of polymerization in this redox system.

The concentration of benzoyl peroxide at time t may be expressed as

$$[P] = [P]_0 \exp\{-(k_d+2k_2x)t\} \qquad (7)$$

in the early stage of polymerization.

Substituting Eq. 7 into Eq. 3, and integrating from $t=0$ to $t=t$, it follows:

$$\ln(1-y) = (2k_p/k_t^{1/2})[P]_0^{1/2}(k_d+2k_2x)^{-1/2} \times [\exp\{-(k_d+2k_2x)t/2\}-1] \qquad (8)$$

The concentration of benzoyl peroxide, however, will be reduced more rapidly than that of benzoin, for the former decomposes not only in the reaction 1, but it will also decompose thermally. The concentration of ferrous ion, therefore, will be increased gradually. But assuming the concentration of ferrous ion to be constant, the extent of conversion at sufficient time of duration, y_∞, can be expressed as:

$$Z \equiv \{1/\ln(1-y_\infty)\}^2 = (k_t/4k_p^2[P]_0)(k_d+2k_2x) \qquad (9)$$

The values of Z are listed in Table I. From Eq. 9, it is expected that a plot of Z against x would give a straight line. Fig. 3 shows the relation between Z and x, and it is seen that the extent of conversion decreases with increasing ferrous ion concentration for each value of r. The abnormal decrease of Z with monomer concentration 90%, may be ascribed to the decrease of k_t due to the increased viscosity at a high conversion[6].

Eq. 9 has been introduced on the assumption that none of the velocity constants nor the ferrous ion concentration vary through the polymerization processes. But, these would actually vary with the change in the composition of the solution. However, it is possible, in principle, to calculate the value of x that makes the extent of conversion at any time t maximum.

If the right-hand side of Eq. 8 is differentiated with respect to x and the result equated to zero, the condition for the minimum of $\ln(1-y)$ and hence the maximum of y may be obtained. The relationship found is

$$\exp(k_d+2k_2x)t/2 = 1+(k_d+2k_2x)t \qquad (10)$$

Two solutions of this equation may be obtained graphically, i. e.,

$$(k_d+k_2x)t/2 = 0 \qquad (11)$$

$$k_d+2k_2x \cong 2.5/t \qquad (12)$$

Since neither k_d nor k_2 is zero, Eq. 11 has no physical meaning. It may be said that Eq. 12 is the relation between x and the time t when the extent of conversion y with the initial ferrous ion concentration x becomes of greater value than any other one.

The rate constants k_d and k_2 can be calculated from Figs. 2 and 3 which correspond to Eqs. 6 and 9, respectively, though it is very doubtful whether each rate constant in Eq. 9 has kept up its original meaning.

The values of k_d and k_2 thus obtained

6) G. V. Schulz and G. Harborth, *Makromol. Chem.*, **1**, 106 (1947).

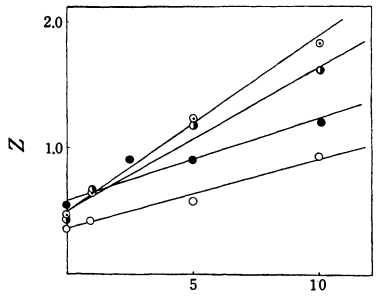

Fig. 3. Relation between Z and x for each value of r.
r: ● 0.63, ◑ 1.89, ⊙ 2.52, ○ 5.67

were 0.07 $hr.^{-1}$ and 300 $l.\,mol.^{-1}\,hr.^{-1}$, respectively, and the ratio k_2/k_d was about 4,300 which was much less than that obtained only from Eq. 6. The cause of this discrepancy may be ascribed to the reason mentioned above.

It is of interest, however, to test Eq. 11. Substitution of those numerical values into Eq. 12 leads to Eq. 13, i. e.,

$$0.07+600x\cong 2.5/t \qquad (13)$$

For a series of x, the corresponding time was calculated from Eq. 13 and compared with one obtained experimentally from Fig. 1.

It is noted, as seen in Table II, that the values of t calculated are in fairly good agreement with those obtained experimentally.

Table II
Comparison of calculated values of t with those observed

$x \cdot 10^4$ (mol. l^{-1})	t (calcd.) (hr.)	t (obsd.) (hr.)
10	4	~ 4
5	7	4~12
1	18	12~25
0	36	25~

Summary

Polymerization of vinyl acetate in the benzoyl peroxide-iron-(II)-benzoin redox-system was studied in ethanol. From the extent of decrease in volume, the rate of conversion was calculated. It was found that the square of the initial rate of conversion was proportional to the initial concentration of ferrous ion and that the extent of conversion at the time when the polymerization was finished, decreased with increasing amount of ferrous ion which was added.

The initial rate of conversion in this redox system was found to depend also on the mole ratio of the monomer to ethanol. The reason might be ascribed to the change in the rate constant.

Department of Chemistry, Faculty of Science, Okayama University
Tsushima, Okayama

Behavior of Zirconium-95 and Niobium-95 in Dilute Hydrochloric Acid toward Cation Exchange Resin

By Seishi YAJIMA

(Received February 26, 1958)

Zirconium and niobium nuclides contained in fission products are ^{95}Zr—^{95}Nb and ^{97}Zr—^{97}Nb. The abundance of short-lived ^{97}Zr—^{97}Nb becomes negligibly small in a cooling period of about 10 days, while that of comparatively long-lived ^{95}Zr—^{95}Nb increases to the maximum after a longer period of about 200 days. Even after a few years, its abundance is still remarkable[1].

Zirconium-95 and niobium-95 in a mineral acid solution are present as radiocolloids[2] and the chemical behavior of these colloids is very complicated. Although many investigations[3] have been made regarding the chemical separation of ^{95}Nb from ^{95}Zr, the behavior of these nuclides toward the

1) H. F. Hunter and N. E. Ballow, *Nucleonics*, **9**, No. 11, C-2(1951).

2) J. Schubert and E. E. Cohn, ibid., **4**, No. 6, 2 (1949); J. Schubert and J. W. Richter, *J. Colloid Sci.*, **5**, 376 (1949).

3) K. A. Kraus and G. E. Moore, *J. Am. Chem. Soc.*, **73**, 2900 (1951); **73**, 9 (1951); R. E. Wacker and W. H. Baldwin, AEC report, *ORNL*, 637 (1950).

cation exchange resin has not been thoroughly investigated. The author has made a study of the difference in the adsorbability of ^{95}Zr and ^{95}Nb to the cation exchange resin and also the effects of conditions of preparing solutions on the adsorbability.

Experimental

Material.—Zirconium-95 was obtained as oxalate complex from U.S.A.E.C.. Since it has been allowed to stand for about one year, ^{95}Zr and its daughter, ^{95}Nb, must be in transient equilibrium. The activity of this material was about 100 μC. To this, 10 ml. of concentrated sulfuric acid was added and heated slowly to almost dryness. After repeating this step twice more, the residue was heated with 200 ml. of 0.2 N hydrochloric acid to be dissolved. An aliquot of this solution, having an activity of about 1 μC, was used as a sample. The aliquot contained about 10^{-13} mole each of ^{95}Zr and ^{95}Nb, thus corresponding to about 5×10^{-11} mol./l., respectively.

Procedures.—After slurring the cation exchange resin Dowex 50-X8 (100 to 200 mesh) was placed in a glass tube, the resin was washed with 3 N hydrochloric acid to convert it into the hydrogen form and further washed completely with demineralized water. After complete washing, the interstitial water was replaced by 0.2 N hydrochloric acid. The resin bed was 0.7 cm. in diameter, 6.5 cm. in length and its volume was 2.5 ml.. A 2 ml. aliquot of the 0.2 N hydrochloric acid solution of ^{95}Zr—^{95}Nb mixture was diluted to 20 ml. with 0.2 N hydrochloric acid and poured into the column. Then 70 ml. of 0.2 N hydrochloric acid, 20 ml. of demineralized water, and 40 ml. of 0.5% oxalic acid solution or 3 N hydrochloric acid were poured successively. The flow rate was 0.5 ml. per minute. The 2 ml. fractions of the effluent were poured successively into the glass dishes which were 2.5 cm. in diameter and 0.6 cm. in height, and then heated with an infrared lamp to dryness. The activity in the dishes was measured by a G.M. counter whose window was 2.5 mg./cm^2 in thickness. The distance between the test sample and the window was 1.5 cm. and about 8% of the total activily was counted.

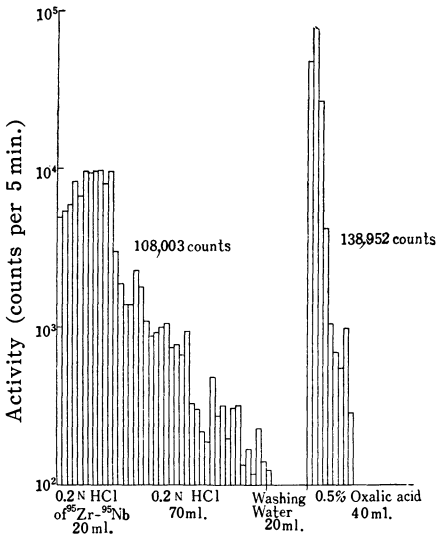

Fig. 1. Elution of a ^{95}Zr—^{95}Nb mixture. effluent fraction: 2 ml.

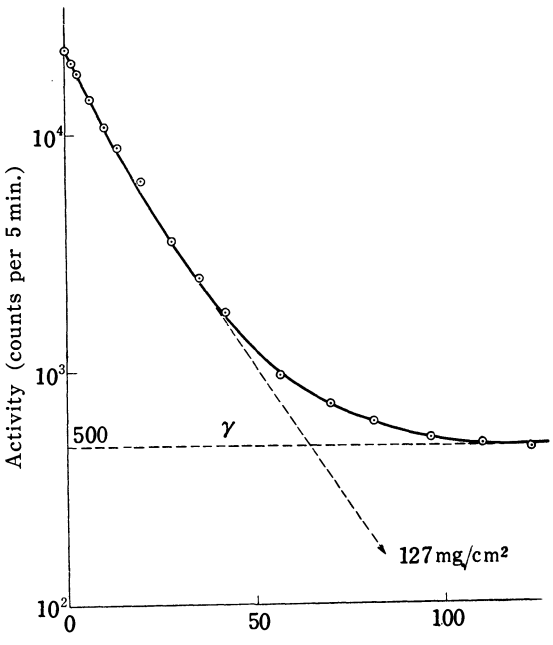

Fig. 2. Aluminum absorption curve of 0.5% oxalic acid fraction.

Results

Difference in Adsorbability of ^{95}Zr and ^{95}Nb.—The results obtained by the above mentioned procedures are shown in Fig. 1. It will be seen that ^{95}Zr—^{95}Nb mixture could be separated into two fractions; the one eluted by 0.2 N hydrochloric acid and the other by 0.5% oxalic acid. To identify ^{95}Zr and ^{95}Nb in these fractions, the maximum β-energy of the fraction activity was determined using a set of aluminum abosorbers. Instead of measuring the maximum β-energy of activities on all dishes, suitable aliquots of two fractions of 0.2 N hydrochloric acid and 0.5% oxalic acid were evaporated to dryness and the β-energy was measured. The results are shown in Figs. 2 and 3. The values of maximum range in Figs. 2 and 3, converted into MeV., agree with those for ^{95}Zr—β and ^{95}Nb—β in Table I. As shown

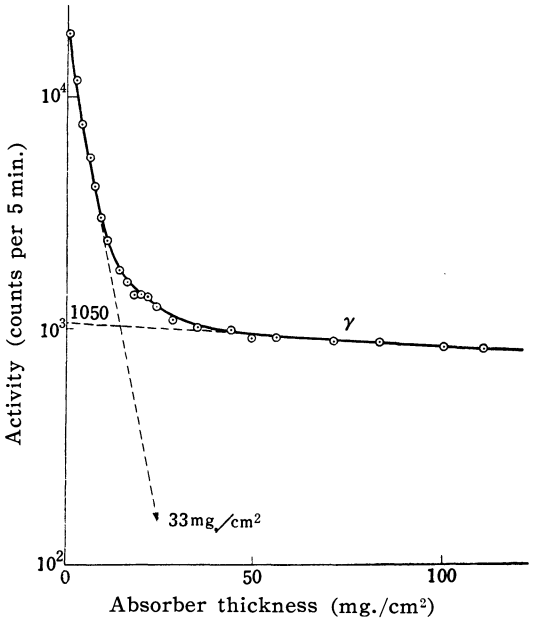

Fig. 3. Aluminum absorption curve of 0.2 N HCl fraction.

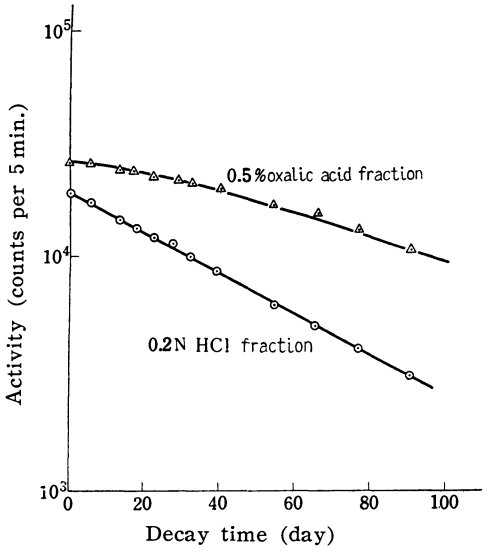

Fig. 4. Decay curves of two fractions.

TABLE I.

Nuclide	Half-life (day)	λ(day^{-1})	β(MeV)	γ(MeV)
^{95}Zr	65	0.01066	0.364	0.754
^{95}Nb	35	0.0198	0.165	0.76

in Fig. 4, the decay curve of the 0.5% oxalic acid fraction shows the production of ^{95}Nb from ^{95}Zr. After 26 days, the curve shows a half-life of 65 days. On the other hand, the activity of the 0.2 N hydrochloric acid fraction decayed with a half-life of 35 days. These half-life values coincide with those of ^{95}Zr and ^{95}Nb shown in Table I.

From the measurement of the maximum β-energy and the half-life, it was found that the 0.2 N hydrochloric-acid fraction contained mainly ^{95}Nb and the 0.5% oxalic-acid fraction mainly ^{95}Zr.

Relation between Time of Preserving the Solution of ^{95}Zr—^{95}Nb and the Adsorbability of ^{95}Zr.—Since ^{95}Zr and ^{95}Nb in a mineral acid solution are present as radiocolloids, it was thought probable that there might be an appreciable difference in adsorbability toward a cation exchanger between a fresh solution and an aged solution of ^{95}Zr—^{95}Nb.

After storage of the fresh sample solutions which were prepared as described before for 3, 7, 10 and 15 days, the experiments were carried out similarly. The results are shown in Fig. 5. It is obvious

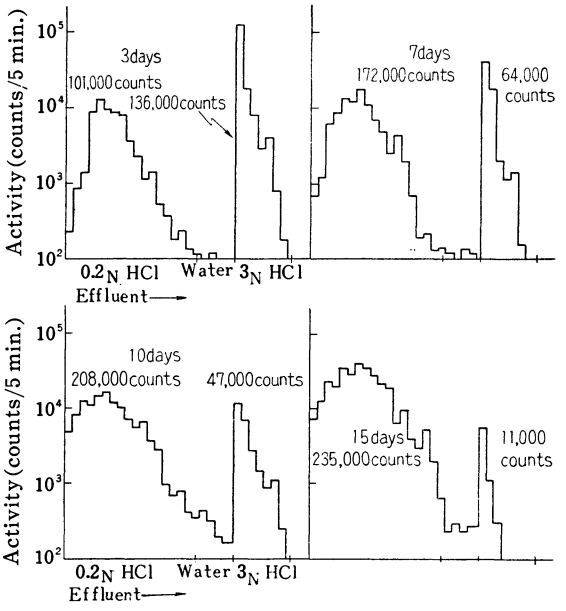

Fig. 5. Time of keeping solution of ^{95}Zr and ^{95}Nb and adsorbability of ^{95}Zr.

that the amount of ^{95}Zr retained on the resinbed decreases as time passes. when thesolution is 10 days old, ^{95}Nb and a considerable amount of ^{95}Zr are eluted in the same fraction. This phenomenon may be related to the characteristics of ^{95}Zr, the pH, other ions and dust in the solution, the wall of the vessel, etc., but can not be defined quantitatively.

Variation in Adsorbability of ^{95}Zr and ^{95}Nb with the Concentration of Hydrochloric Acid.—Two fractions of ^{95}Zr and

^{95}Nb were obtained by the procedure described above, and each fraction was converted into 0.2 N hydrochloric acid solution. To 0.1 ml. aliquots of these solutions 25 ml. of hydrochloric acid having the following concentrations was added respectively: 0.01, 0.02, 0.04, 0.06, 0.1, 0.15, 0.2, 0.3, 0.4, 0.5, 1.0, 1.9, 2.85 and 3.8 N. The addition of the small volumes of ^{95}Zr or ^{95}Nb solution did not appreciably change the hydrochloric acid concentrations of the resultant solutions. The activities of ^{95}Zr or ^{95}Nb in these solutions were about 0.5 μC corresponding to 10^{-13} mole (5×10^{-12} mol./l.).

These solutions were transferred to glass-stoppered flasks containing one gram each of air-dried Dowex 50—X8 (100 to 200 mesh) which had been treated with hydrochloric acid, and were agitated for five hours, at 25°C. Five-hour agitation was sufficient to give constant adsorption values. After the resin had settled the aliquots of the supernatant solution were transferred to glass dishes, evaporated to dryness, and their activities were measured. Also the entire procedure was run without the addition of the resin. Fig. 6 shows the relation between the adsorbability (%) of ^{95}Zr and ^{95}Nb and the concentration of hydrochloric acid. The adsorbability is defined by the ratio of the difference in activity between the aliquot obtained without resin and that with resin to the activity of the aliquot obtained without resin.

Fig. 6 indicates that about 0.2 N hydrochloric acid is suitable for the separation of ^{95}Zr from ^{95}Nb. As mentioned already,

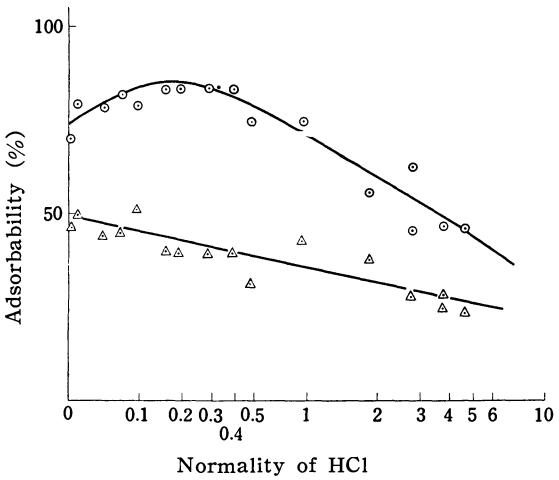

Fig. 6. Effect of hydrochloric-acid concentration on the absorbability of ^{95}Zr and ^{95}Nb.

the adsorption of neither nuclide is due to the ion exchange. Consequently the complete separation of ^{95}Zr from ^{95}Nb is difficult even though there is a difference in adsorbability of both nuclides. Nevertheless by repeating the procedures a complete separation will be possible. It is also indicated that 3 N hydrochloric acid may be used as an eluent for ^{95}Zr instead of 0.5% oxalic acid. This was later confirmed experimentally.

Effect of Concentrations of Zr and Nb. —It was thought desirable to investigate the separation of larger amounts of ^{95}Zr and ^{95}Nb than 0.5 μC. Because of the limited amounts of these nuclides, non-active isotopes were used as carriers. For this purpose a solution of reagent grade zirconium oxychloride ($ZrOCl_2\cdot8H_2O$) and an oxalic acid solution of niobium pentoxide previously fused with potassium bisulfate were prepared. From these solutions, four solutions containing 10^{-9}, 10^{-8}, 10^{-7}, and 10^{-6} mol./l. each of zirconium and niobium were prepared, and 10^{-13} mol./l. each of ^{95}Zr and ^{95}Nb was added as tracers. These four solutions were then treated with concentrated sulfuric acid, and processed as mentioned above. As a result, in all the cases tested, the degree of separation of ^{95}Nb from ^{95}Zr was the same as that with 0.5×10^{-11} mol./l. It may be concluded that the separation of ^{95}Nb from ^{95}Zr is possible under the conditions described in the experimental part, in the concentration range 10^{-12} to 10^{-6} mol./l.

Effect of Strontium. — Schubert[2] reported that the state of tracer amounts of ^{95}Zr and ^{95}Nb in dilute mineral acid was radiocolloid and the adsorbability of these nuclides to a cation exchanger increased with the concentration of other cations. In the group-separation of fission products with a cation exchange resin, it is often the case that the complicated behavior of ^{95}Zr—^{95}Nb makes their complete separation impossible[4,5]. As a large amount of strontium is found in fission products, the effect of this ion on the adsorbability of ^{95}Zr and ^{95}Nb was investigated to solve this problem. The sample solution contained about 2 μC of ^{95}Zr—^{95}Nb (about 10^{-12} mol.) in a volume

4) E. R. Tompkins, J. X. Khym and W. E. Chon, *J. Am. Chem. Soc.*, **69**, 2769 (1947); W. E. Cohn, G. W. Parker and E. R. Tompkins; *Nucleonics*, **3**, No. 5, 22 (1948).

5) T. Shiokawa, T. Ozaki, T. Kambara and M. Yagi, *The 1st Atomic Energy Symposium*. (1957), Tokyo. Japan, Section: Material and Chemistry, B-33.

of 20 ml. of 0.2 N hydrochloric acid. To a series of this solution, 1 mg. (0.571×10^{-3} mol./l.), 2 mg. (1.141×10^{-3} mol./l.), 3 mg. (1.712×10^{-3} mol./l.), and 4 mg. (2.282×10^{-3} mol./l.) of strontium (as chloride) were added respectively. After passing 20 ml. of the sample solution through the same resin column as described before, elution was done successively with 50 ml. of 0.2 N hydrochloric acid, 30 ml. of washing water, and 50 ml. of 3 N hydrochloric acid. The results are shown in Figs. 7, 8, 9 and 10. It is pointed out that, when the strontium concentration is 2.282×10^{-3} mol./l., ^{95}Nb is eluted with difficulty with 0.2 N hydrochloric acid (Fig. 10). In other words, separation of ^{95}Nb from ^{95}Zr becomes impossible under such a condition.

In the group separation of ^{95}Zr and ^{95}Nb from fission products using a cation exchange resin, a good recovery may be obtained when 0.2 N hydrochloric acid

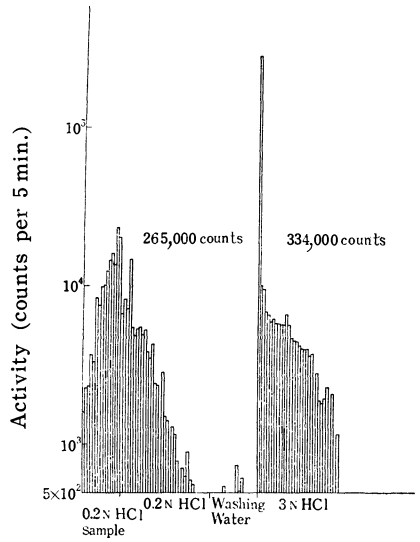

Effluent fraction: 1.5 ml.

Fig. 7. Effect of 1 mg. Sr^{2+}.
Sample solution: 20 ml.

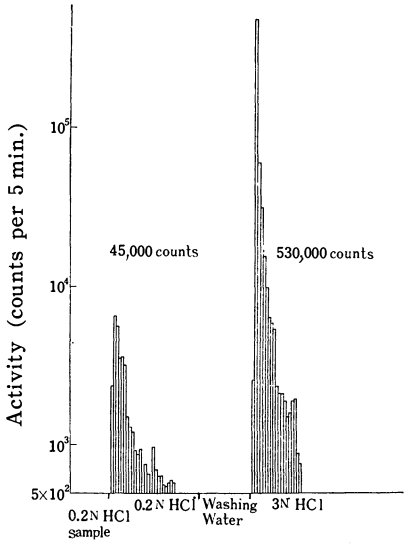

Effluent fraction: 1.5 ml.

Fig. 9. Effect of 3 mg. Sr^{2+}.
Sample solution: 20 ml.

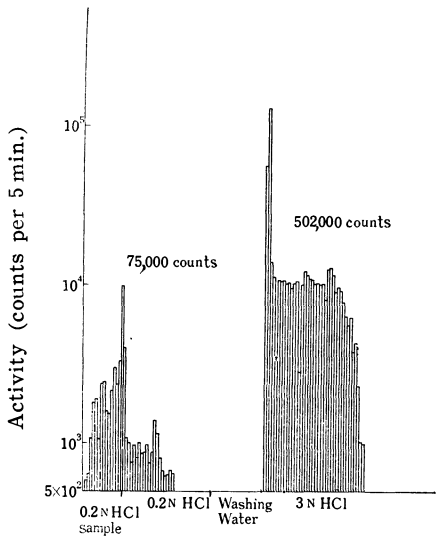

Effluent fraction: 1.5 ml.

Fig. 8. Effect of 2 mg. Sr^{2+}.
Sample solution: 20 ml.

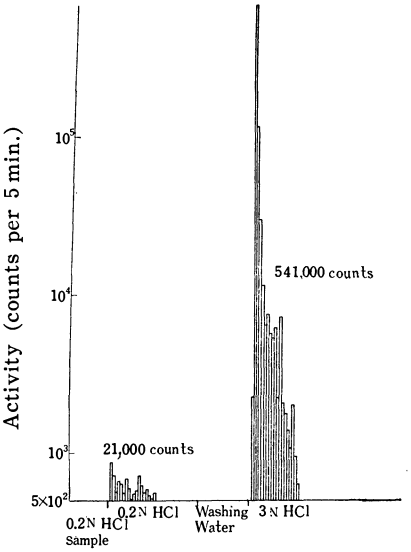

Effluent fraction: 1.5 ml.

Fig. 10. Effect of 4 mg. Sr^{2+}.
Sample solution: 20 ml.

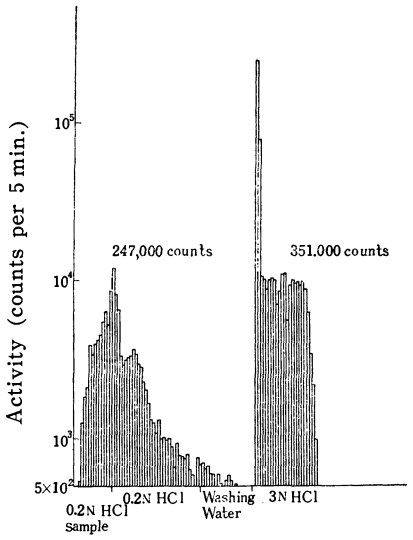

Effluent fraction: 1.5 ml.

Fig. 11. Effect of 2 mg. Sr^{2+} previously adsorbed.

solution of ^{95}Zr and ^{95}Nb containing a large amount of strontium is passed through the resin and the elution of two nuclides is made with 0.5% oxalic acid.

When 2 mg. of strontium was first adsorbed to the resin column and then a solution of ^{95}Zr—^{95}Nb was poured into the column, the result shown in Fig. 11 was obtained. By comparing Fig. 8 with Fig. 11, it is seen that the activity of ^{95}Nb in the effluent is greater in the latter. It is believed that this is due to the change in the state of ^{95}Nb rather than to the variation of the resin surface. The effect of the cations other than the strontium ion will be studied in future.

Separation of ^{95}Zr and ^{95}Nb Using Other Cation Exchangers.—According to Schallert[6], ^{95}Zr and ^{95}Nb were strongly adsorbed by Amberlite IR-1 and IR-100. As these resins were no more available, experiments were carried out with Amberlite IR-120 and Diaion SK. The results were the same as those with Dowex 50-X8.

Adsorption of ^{95}Zr and ^{95}Nb to a Glass Vessel.—It is said that the tracer amounts of ^{95}Zr and ^{95}Nb in dilute mineral acid were adsorbed on a glass vessel[7]. In the present work, a solution of ^{95}Zr that had been kept in a soft-glass bottle for 30 days did not show any appreciable loss due to the adsorption. On the other hand, about 0.5% of ^{95}Nb activity was lost when 0.2 N hydrochloric acid solution of ^{95}Nb had been kept in a glass bottle for 3 days, and considerable activity was lost when this solution had been kept for 30 days.

Summary

By passing 0.2 N hydrochloric acid solution of tracer amounts of ^{95}Zr and ^{95}Nb (about 10^{-11} mol./l., 10^{-13} mol., or 1 μC, with respect to each nuclide) through a cation exchange resin column (Dowex 50—X8, Amberlite IR-120, or Diaion SK) and eluting with 0.2 N hydrochloric acid, a fraction containing mainly ^{95}Nb was obtained. A fraction containing mainly ^{95}Zr was then obtained by eluting with 0.5% oxalic acid or 3 N hydrochloric acid. With higher concentrations of non-active zirconium and niobium (about 10^{-6} mol./l. each), similar results were also obtained.

As the 0.2 N hydrochloric acid solution of ^{95}Zr—^{95}Nb became aged, the adsorbability of ^{95}Zr decreased. Effect of hydrochloric acid concentration on the adsorbability of ^{95}Zr and ^{95}Nb was studied and the concentration range 0.1 to 0.3 N was found to be suitable for separation.

The adsorbability of ^{95}Nb increased with an increase in the concentration of strontium ion.

This work has been done in the laboratories of the Government Chemical Industrial Research Institute, Tokyo. The author wishes to express his thanks to Dr. Toshio Nakai for helpful suggestions and guidance in the course of this work. Thanks are also due to Dr. Kenjiro Kimura for his advice and encouragement. The helpful suggestions of Mr. Hiroshi Onishi in the preparation of this manuscript are also acknowledged.

Chemistry Division, Japan Atomic Energy Research Institute, Tokai, Ibaraki

6) P. O. Schallert, AEC report, *ORNL*-1144, (1952).

7) A. G. Maddock and W. Pugh, *J. Inorganic and Nuclear Chem.*, **2**, 144 (1956).

Investigation on Dissolving Pulp. XIV. Some Behavior of Wood Pulp and Cotton Linters in Phosphoric Acid

By Tokumi KOSHIZAWA

(Received march 19, 1958)

In a previous paper[1], the author investigated the solubility of various kinds of cellulose into phosphoric acid to know the details of mechanism of the phosphoric-acid swelling which was observed in Heide's test for cellulose reactivity[2], and pointed out the influence of other factors than the degree of polymerization as shown by a Ekenstam[3] on the solubility of various kinds of cellulose into phosphoric acid.

In this paper, the dissolved part of cellulose (sulfite pulp, prehydrolyzed sulfate pulp and cotton linters) in phosphoric acid of various concentrations was studied with regard to the average degree of polymerization, and the rates of hydrolysis in 70% phosphoric acid at 20°C. The rates of hydrolysis of the insoluble residues, swelled to various degrees were also determined.

Experimental

1) Solubility of Cellulose into Phosphoric Acid and Average Degree of Polymerization of Dissolved Part. — First cellulose samples were pretreated with 73.3% phosphoric acid for 10 min. at 20°C, then the proper amount of 82, 86 or 90% phosphoric acid was added drop by drop to get the required concentration under costant stirring, at the constant temperature, 20°C. After 20 minutes, 58% phosphoric acid was added to dilute the solution to 70% Ten minutes after the dilution, the solution was centrifuged and the supernatants were filtered through a glass filter (1G-3). The filtrate was diluted properly and its viscosity was determined in Ostwald's viscometer. The change of viscosity with time in 70% phosphoric acid at 20°C was plotted and the extrapolated value of viscosity to time 0 was determined graphically. Intrinsic viscosity $[\eta]$ was determined by the usual method to plot η_r against various concentrations of the solute. The solubility of cellulose was determined by the oxidation with potassium bichromate and iodometry.

2) The Average Degree of Polymerization of Insoluble Residue.—Insoluble residue in 1 was poured into a large quantity of ice-cold water, washed repeatedly with distilled water, and dried. The cellulose residue was dissolved into cupro-ammonium solution and its viscosity was determined to know the average degree of polymerization. The sample was also dissolved into 85% or 90% phosphoric acid after pretreatment with 73.3% phosphoric acid. After complete dissolution—it takes about 30~60 min.—, to the solution was added 58% phosphoric acid until the concentration of the solution became 70% and the intrinsic viscosity in 70% phosphoric acid was determined by the extrapolation of the viscosity curves to the zero time. The constant K_m of cellulose in 70% phosphoric acid was calculated from the $[\eta]$ and the K_m constant (5×10^{-4}) in cupro-ammonium solution, and $[\eta]$ in the phosphoric acid solution. The value in 70% phosphoric acid thus obtained is about 13×10^{-4}. But this value is not exact and serves only to know the relative change of DP.

Results and Discussion

(1) Average Degree of Polymerization of Dissolved Part.—The solubility curves of sulfite pulp, prehydrolyzed sulphate pulp, and cotton linters were shown in Fig. 1. The average degrees of polymerization of cellulose dissolved into the acid of various concentrations were shown in

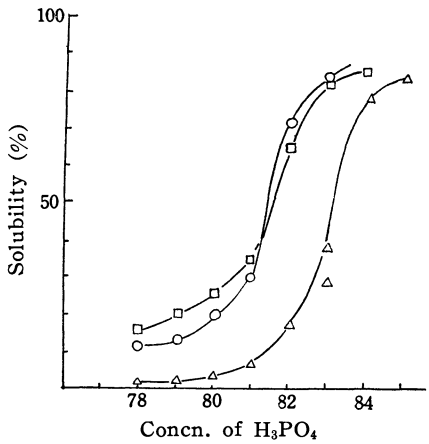

Fig. 1. Solubility of cellulose into phosphoric acid.
△: Cotton linters, ○: Sulfite pulp,
□: Prehydrolyzed sulfate pulp

1) T. Koshizawa, *J. Soc. Textile and Cellulose Ind., Japan (Sen-i Gakkaishi)*, in press (Part XII of this paper).
2) K. Heid, *Faserforsch. u. Textil Techn.*, **3**, 486 (1952).
3) Alf af Ekenstam, *Svensk papperstidn*, **45**, 81 (1942).

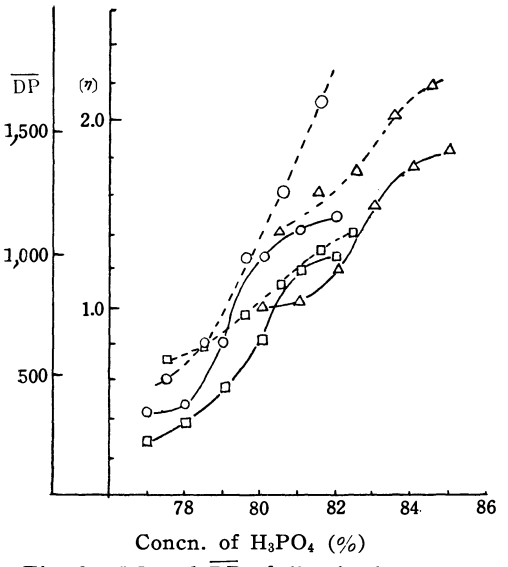

Fig. 2. [η] and $\overline{DP}$ of dissolved part.
△: Cotton linters, ○: Sulfite pulp,
□: prehydrolyzed sulfate pulp.
——: [η] and $\overline{DP}$ of dissolved part,
----: [η] and $\overline{DP}$ of dissolved part corresponding to 1% increase in phosphoric acid concn.

Fig. 2. The degree of polymerization was calculated from [η] using the K_m 13×10^{-4}. Although the K_m constant derived from the comparison of [η] in cupro-ammonium solution and [η] in phosphoric acid solution might not be an exact value, it would be sufficient to discuss the relative difference, as in the present case. The dotted lines in Fig. 2 are the average degree of polymerization of the dissolved part corresponding to the increase in the concentration of phosphoric acid by 1%. The values were calculated from the curves in Fig. 1 and unbroken lines in Fig. 2. In the calculation the assumption that the viscosity shows the weight average of degree of polymerization was taken. The degree of polymerization of newly dissolved part corresponding to the increase in phosphoric acid concentration by a% is calculated from the following relationship,

$$P_{c+a}\times W_{c+a}=P_c\times W_c+P_a\times W_a$$

or $$P_a=(P_{c+a}\times W_{c+a}-P_c\times W_c)/W_a$$

where W_c, W_{c+a} and W_a are weight % of dissolved parts in c%, $c+a$% and a% phosphoric acid, and P_c, P_{c+a} and P_a are their average DP, respectively. Although the above stated assumption might not be strictly valid as we have to consider the distribution of molecular weight or other factors, the curves show us the approximate trends. As seen in the dotted lines in Fig. 2 the average DP of newly dissolved pulp which correspond to the increase in the concentration of phosphoric acid, clearly differ according to the kind of cellulose sample. Namely the increase in concentration of phosphoric acid accompanies a marked increase in the DP of dissolved part in sulfite pulp, while it accompanies a slight increase in the DP in the case of prehydrolyzed sulfate pulp and cotton linters. So the abrupt increase in solubility at a certain concentration of phosphoric acid as shown in Fig. 1 cannot be ascribed solely to the factor of DP as stated by af Ekenstam[3] and suggests the influence of a fine structure such as lateral order upon the solubility of cellulose into phosphoric acid. Needless to say the increase in DP proportional to the increase in concentration of the acid shows the effect of DP, and a relatively large increase in DP with the increase in acid concentration in the case of sulfite pulp may be caused by the wide spread of distribution of DP. The existence of molecules with small DP among large molecules gives much influence upon the solubility or swellability and the fact may be correlated to the lowering of swellability or the hornification caused by cold alkali treatment.

(2) **Decrease in Degree of Polymerization in Dissolved and Insoluble Part.** —The change of 1/DP of the dissolved part with the time of hydrolysis is shown

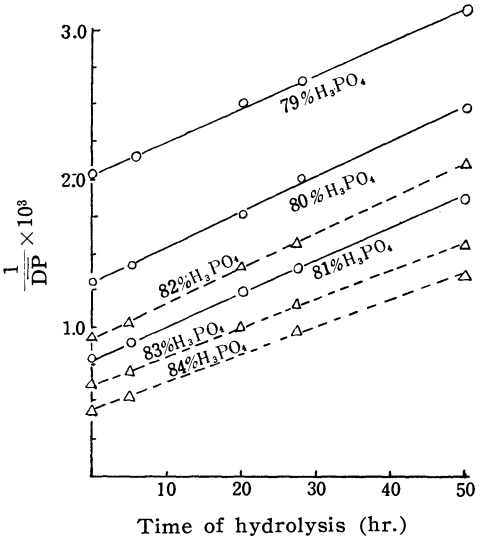

Fig. 3. Degradation of dissolved part in 70% H_3PO_4 at 20°C.
△: Cotton linters, ○: Sulfite pulp.

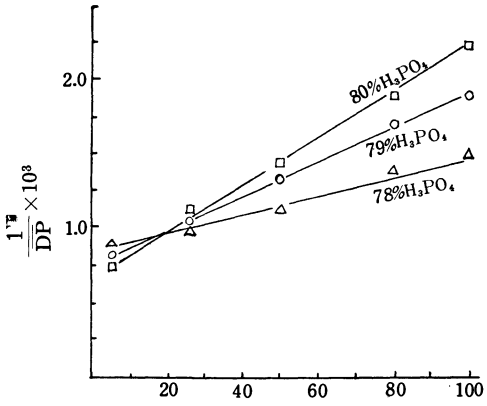

Fig. 4-1. Degradation of insoluble residue in 70% H_3PO_4 at 20°C. (Sulfite pulp)

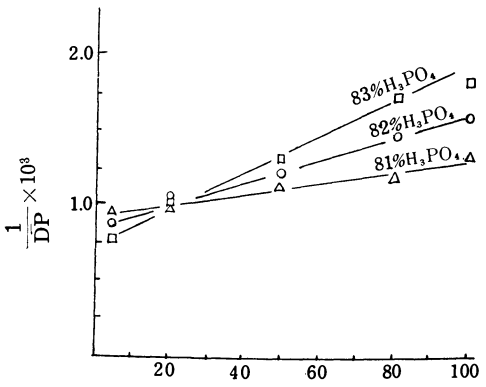

Fig. 4-2. Degradation of insoluble residue in 70% H_3PO_4 at 20°C. (Cotton linters)

in Fig. 3 in which the DP is calculated from $[\eta]$ in 70% phosphoric acid, assuming the constant, K_m 13×10^{-4}. Figs. 4-1, and 4-2 shows that of insoluble residues. The rate constant for the hydrolysis can be derived from the following equation

$$K=1/t\cdot\frac{(1-1/DP_0)}{(1-1/DP_t)}$$

where DP_0 and DP_t are the average DP of the cellulose at zero time and time t, respectively. Expansion of the right side of the equation to an infinite series and neglect of all of the terms other than the first gives the following equation,

$$K=1/t(1/DP_t-1/DP_0)$$

Many investigations[4,5] found the validity of this equation in the initial stage of hydrolysis. The tangents of the curves in Figs. 3 and 4 correspond to the rate

4) O. A. Battista, *Ind. Eng. Chem.*, **42**, 502 (1950).
5) Alf af Ekenstam, *Ber.*, **69B**, 549 (1936).

TABLE I

RATE CONSTANT OF HYDROLYSIS OF DISSOLVED PART IN 70% PHOSPHORIC ACID AT 20°C

	Cotton linters	
Concn. of H_3PO_4	82%	$K=3.8\times10^{-7}\,min^{-1}$
	83%	$K=3.0\times10^{-7}\,min^{-1}$
	84%	$K=3.2\times10^{-7}\,min^{-1}$
	Sulfite pulp	
Concn. of H_3PO_4	79%	$K=4.0\times10^{-7}\,min^{-1}$
	80%	$K=4.0\times10^{-7}\,min^{-1}$
	81%	$K=4.0\times10^{-7}\,min^{-1}$

TABLE II

RATE CONSTANT OF HYDROLYSIS OF INSOLUBLE RESIDUE IN 70% PHOSPHORIC ACID AT 20°C

	Cotton linters	
Concn. of H_3PO_4	81%	$K=0.56\times10^{-7}\,min^{-1}$
	82%	$K=1.3\times10^{-7}\,min^{-1}$
	83%	$K=1.7\times10^{-7}\,min^{-1}$
	Sulfite pulp	
Concn. of H_3PO_4	78%	$K=0.85\times10^{-7}\,min^{-1}$
	79%	$K=1.5\times10^{-7}\,min^{-1}$
	80%	$K=2.5\times10^{-7}\,min^{-1}$

constants of hydrolysis which are given in Tables I and II. The rate constant of hydrolysis of dissolved part does not vary in either case of linters or sulfite pulp. On the other hand that of insoluble residue changes with the concentration of phosphoric acid before the dilution to 70%. Namely the rate of hydrolysis depends on the degree of swelling in the solution. Thus we may conclude that the rate of inhomogeneous degradation of cellulose is greatly influenced by the state of molecular orientation. This fact also makes easy the test on swellability of cellulose in phosphoric acid which is proposed by Heide[1] or the test modified by us[1] to determine the transparency or turbidity of the cellulose suspension in phosphoric acid because, on the one hand, the swelled part dissolves into the solution with the lapse of time because of the greater rate of hydrolysis, and, on the other hand, the insoluble residue such as the constricted part in balloon-like swelling remains unchanged, even after a long time because of the lower rate of hydrolysis.

Summary

The average DP of cellulose dissolved into phosphoric acid of various concentrations has been determined by viscometry. The relations of average DP of dissolved

part to the concentration of phosphoric acid are not the same in the three samples — dissolving sulfite pulp, prehydrolyzed sulfate pulp and cotton linters. The fact may be ascribed to the factors such as lateral order other than the degree of polymerization.

The rate of hydrolysis of cellulose in 70% phosphoric acid at 20°C was also determined as to both cases of dissolved part and insoluble residue. The rate of hydrolysis of the dissolved part is almost independent of the kind of cellulose, while that of the insoluble residue greatly depends on the degree of swelling in the solution.

The author wishes to express his hearty thanks to Professor Hiroshi Sobue, Faculty of Engineering, University of Tokyo, for his kind directions. The author also thanks Mr. Toshio Ōba, Kokoku Rayon and Pulp Co. Ltd., for his kind co-operation throughout this work.

Research Division
Kōkoku Rayon and Pulp Co., Ltd.
1, 1-chome Shiba-Tamura-cho
Minato-ku, Tokyo

Effect of Substitution on Dipole Moments of Molecules

By Hayami YONEDA

(Received October 26, 1957)

When hydrogen in a molecule RH is replaced by a substituent X, the polarities of the RH and RX bonds will generally differ. Therefore R in RX will be either more positive or more negative than R in RH. This polarity effect is called the inductive effect. Substituents which induce a negative charge on an adjacent atom when they replace hydrogen, are called anionoid inductive (or $-I$) substituents, and those which induce a positive charge, cationoid inductive (or $+I$) substituents. Alkyls belong to the former group, and amino, hydroxyl and halogens to the latter group. Thus, when substituents including hydrogen are arranged in the order of $+I$ effect we obtain a series; halogens> hydroxyl> amino> hydrogen> alkyls. Although the inductive effect was postulated by organic chemists in order to understand various chemical properties of organic compounds (e.g. acid strength), still it should be supported by the experimental data of dipole moments. In fact, measurements of dipole moments have confirmed in many cases the existence and the sign of the electron displacement which organic chemists had postulated. For example, the dipole moments of a series of hydrogen halides and the dipole moments of a series of alkyl halides have the same tendency of variation of dipole moments from chloride to iodide; hydrogen chloride > hydrogen bromide > hydrogen iodide and methyl chloride> methyl bromide> methyl iodide. The similar tendency is observed between the two series, methyl chloride> methyl alcohol> methylamine and ethyl chloride> ethyl alcohol> ethylamine.

However, when we examine the data of dipole moments more carefully, we will find out several series of compounds which make us doubt the existence of the definite inductive effect. For example, in a series of water, methyl alcohol and dimethyl ether, the dipole moment should increase in the order water, methyl alcohol and dimethyl ether, as methyl is a $-I$ substituent. The actual order is, however, quite reverse. The purpose of this paper is to find out such anomalous series of compounds which apparently seem to contradict the inductive effect and to establish a general rule which holds good in every case.

Discussion

Data of dipole moments which form the basis of discussion in the present paper are listed in Table I. First, we will consider the series of alkyl halides whose observed dipole moments suggest the existence of the definite inductive effect. From Table I it is easily seen that except in the case of fluorides, the dipole moment increases in the order hydrogen halide,

methyl halide, ethyl halide, etc. and reaches fairly rapidly a definite value in all series of chlorides, bromides and iodides. This tendency can be easily explained when we consider the inductive effect. If hydrogen in methyl is replaced by another methyl, the second methyl induces a negative charge on the carbon of the original methyl and lowers its electron affinity and hence increases its $-I$ activity. Therefore ethyl should be a more active $-I$ group than methyl. Similarly *n*-propyl should be a more active $-I$ group than ethyl, and *n*-butyl should be a more active $-I$ group than *n*-propyl and so on. This second order relayed inductive effect dies away, however, down the chain. Therefore the polarity of the RX bond will be expected to increase from methyl halide to ethyl halide, from ethyl halide to propyl halide, etc. and to reach a certain definite limit. Since the polarity of alkyl itself can be neglected, the bond polarity of the RX bond corresponds directly to the observed dipole moment. Thus the data of dipole moments can be understood simply by the concept of the inductive effect.

TABLE I

DIPOLE MOMENTS* (in Debye unit)

Alcohols	
H_2O	1.85[1]
CH_3OH	1.69[2]
CH_3CH_2OH	1.67[2]
$CH_3CH_2CH_2OH$	1.657[3]
$CH_3CH_2CH_2CH_2OH$	1.63[2]
Ethers	
CH_3OCH_3	1.29[4]
$CH_3CH_2OCH_2CH_3$	1.17[4]
$CH_3CH_2CH_2OCH_2CH_2CH_3$	1.18[4]
Sulfur Compounds	
H_2S	1.1[5]
CH_3CH_2SH	1.39[5]
CH_3SCH_3	1.40[5]
$CH_3CH_2SCH_2CH_3$	1.58[5]
Fluorides	
HF	1.91[6]
CH_3F	1.808[7]
CH_3CH_2F	1.92[7]
Chlorides	
HCl	1.034[8]
CH_3Cl	1.83[9]
CH_3CH_2Cl	1.98[10]
$CH_3CH_2CH_2Cl$	2.04[9]
$CH_3CH_2CH_2CH_2Cl$	2.11[9]
Bromides	
HBr	0.79[9]
CH_3Br	1.79[11]
CH_3CH_2Br	2.01[11]
$CH_3CH_2CH_2Br$	2.15[11]
$CH_3CH_2CH_2CH_2Br$	2.15[11]
Iodides	
HI	0.38[8]
CH_3I	1.64[11]
CH_3CH_2I	1.87[11]
$CH_3CH_2CH_2I$	2.01[11]
$CH_3CH_2CH_2CH_2I$	2.08[11]
Amines	
NH_3	1.466[12]
CH_3NH_2	1.32[4]
$(CH_3)_2NH$	1.02[13]
$(CH_3)_3N$	0.65[4]
$CH_3CH_2NH_2$	0.99[13]
$(CH_3CH_2)_2NH$	0.90[13]
$(CH_3CH_2)_3N$	0.82[13]
Phosphorus Compounds	
PH_3	0.55[14]
$CH_3CH_2PH_2$	1.17[14]
$(CH_3CH_2)_2PH$	1.4[14]
$(CH_3CH_2)_3P$	1.45[14]

* Except for sulfur and phosphorus compounds, all the data were obtained for the vapor state.

1) L. G. Groves and S. Sugden, *J. Chem. Soc.*, **1935**, 971.
2) M. Kubo, *Sci. Papers Inst. Phys. Chem. Res.* (Tokyo), **27**, 65 (1935).
3) J. B. Miles, Jr., *Phys. Rev.*, **34**, 964 (1929).
4) L.G. Groves and S. Sugden, *J. Chem. Soc.*, **1937**, 1779.
5) Clark, "The Fine Structure of Matter", Vol. II, Part II, "Molecular Polarisation", John Wiley & Sons, Inc., New York, (1938), p. 405.
6) N. B. Hannay and C. P. Smyth, *J. Am. Chem. Soc.*, **68**, 171 (1946).
7) C. P. Smyth and K. B. McAlpine, *J. Chem. Phys.*, **2**, 499 (1934).
8) C. T. Zahn, *Phys. Rev.*, **24**, 400 (1924).
9) P. C. Mahanti, *Phil. Mag.*, (7) **20**, 274 (1935).
10) K. Higasi, "Bunshi-kozoron no Kiso", "Table of Dipole Moments", Kawade-shobo, Tokyo, (1952), p. 172.
11) L. G. Groves and S. Sugden, *J. Chem. Soc.*, **1937**, 158.
12) J. M. A. de Bruyne and C. P. Smyth, *J. Am. Chem. Soc.*, **57**, 1203 (1935).
13) P. N. Ghosh and T. P. Chatterjee, *Phys. Rev.*, **37**, 427 (1931).
14) J. C. Bailar, Jr., "The Chemistry of the Coordination Compounds", Chap. 3, Reinhold Publishing Corporation, New York, (1956), p.129.

As the order of the inductive activities of substituents must be constant in every series of compounds, a similar situation should be expected also in the case of a series of alcohols. That is, it is expected that the dipole moment increases in the order water, methyl alcohol, ethyl alcohol, etc. But this is not the case. As is seen in Table I, the dipole moment decreases in the order water, methyl alcohol, ethyl alcohol, etc. A similar anomaly is also seen in a series of amines. The dipole moment decreases in the order ammonia, methylamine, ethylamine, etc. These two cases are related with variation of dipole moments which is caused by the second-order inductive effect. If such an anomaly is not caused by chance but comes from the definite origin, it can be expected to be seen more clearly in cases where the first-order inductive effect is related, because the first-order effect is stronger than the second-order one. Indeed this expectation is realized. As is seen in Fig. 1 the dipole moment decreases stepwise when hydrogen atoms of water and ammonia are replaced successively by alkyl groups.

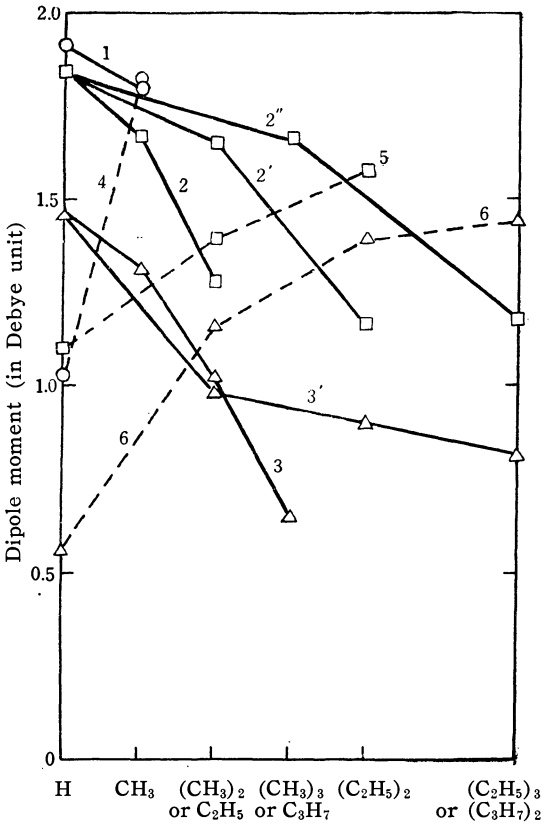

Fig. 1. Variation of dipole moments of various hydrides with successive alkyl substitution.

1 -○—○- HF and CH_3F
2 -□—□- H_2O, CH_3OH and $(CH_3)_2O$
2′ -□—□- H_2O, C_2H_5OH and $(C_2H_5)_2O$
2″ -□—□- H_2O, C_3H_7OH and $(C_3H_7)_2O$
3 -△—△- NH_3, CH_3NH_2, $(CH_3)_2NH$ and $(CH_3)_3N$
3′ -△—△- NH_3, $C_2H_5NH_2$, $(C_2H_5)_2NH$ and $(C_2H_5)_3N$
4 -○—○- HCl and CH_3Cl
5 -□—□- H_2S, C_2H_5SH and $(C_2H_5)_2S$
6 -△—△- PH_3, $C_2H_5PH_2$, $(C_2H_5)_2PH$ and $(C_2H_5)_3P$

In Fig. 1 the variations of dipole moments of a series of hydrogen sulfide, ethyl mercaptan, diethyl sulfide and of a series of phosphine, ethyl phosphine, diethyl phosphine, triethyl phosphine are also plotted. Both series indicate the existence of the normal inductive effect. In Fig. 1 the dipole moments of hydrogen fluoride, methyl fluoride and hydrogen chloride, methyl chloride are also plotted. The variation of the dipole moment from hydrogen chloride to methyl chloride is normal, while the variation of the dipole moment from hydrogen fluoride to methyl fluoride is abnormal. Here it must be noticed that such an anomaly appears only in hydrogen fluoride, water, ammonia and their alkyl derivatives. That is, the anomaly appears only in the hydrides and their alkyl derivatives of elements in the second period in the periodic table. Here it must be stated that such an anomaly was not discovered suddenly by the present author, but that its discovery was due to the works of Sidgwick[15] and of Parry[16]. Sidgwick suggested a very interesting empirical rule about the coordinating ability of various donor groups. In the series of alkyl derivatives of water and ammonia, the affinity of a donor group toward a metal ion decreases rapidly in the order water, methyl alcohol, dimethyl ether and ammonia, methylamine, dimethylamine and trimethylamine, while in a series of alkyl derivatives of hydrogen sulfide the affinity toward a metal ion increases with increasing alkyl substitution. As in his article no further discussion was given about the origin of this empirical rule, it hardly attracted the attention of other chemists at all. Recently, however, the same problem was taken up again by Parry and Keller, who noticed

15) N. V. Sidgwick, *J. Chem. Soc.*, **1941**, 433.
16) J. C. Bailar, Jr., "The Chemistry of the Coordination Compounds", Chap. 3, R. W. Parry and R. N. Keller, "The Electronic Theory of Coordination Compounds", Reinhold Publishing Corporation, New York, (1956), p. 129.

a parallel relation between the coordinating ability of a donor group and its dipole moment and showed that Sidgwick's rule could be easily understood when the increasing or decreasing order of dipole moment of donor groups was taken into consideration. At the same time they showed that alkyl substitution caused a quite reverse effect on the magnitude of dipole moment between a series of hydrides of oxygen and nitrogen and a series of hydrides of sulfur and phosphorus, and they pointed out that the coordinating ability of phosphine derivatives increases in the order phosphine, ethyl phosphine, diethyl phosphine and triethyl phosphine,

Now let us turn our attention to the origin of the anomaly. The anomaly can not be explained by the variation of the valence angles of nitrogen and oxygen. For, the valence angle of nitrogen is nearly equal to 110° in ammonia[17], dimethylamine[19] and trimethylamine[20], and hence the valence angle in monomethylamine is presumed also to be nearly equal to 110°. Similarly, the valence angle of oxygen is nearly equal to 110° in water[17] and in dimethyl ether[21], and hence the valence angle of oxygen in alcohol is also supposed to be nearly equal to 110°. Besides, the anomaly appears also in the case of fluorides, where no valence angle can be considered. Accodingly we must consider another kind of origin. As the inductive effect is a very useful concept in understanding various chemical properties of organic compounds, the complete abandonment of this concept may only cause confusion. Far from abandonment, we must rather conclude that this anomaly has a close relation to the inductive effect, because the order of the magnitudes of dipole moments in a series is not irregular but strictly reverse to that which is expected from the consideration of the inductive effect. Therefore we take the view that the inductive effect exists in every kind of molecule. Consequently there should be the bond polarity induced by the inductive effect even in alcohols and amines, and this bond polarity should increase with successive alkyl substitution. Therefore, besides the bond polarity, we should assume another kind of component of the dipole moment which decreases reversely to the bond polarity with successive alkyl substitution. Frank[22] and Higasi[23] independently noticed this and attributed the variation of the dipole moment in a homologous series to the induction of alkyl groups by the primary dipole. They successfully gave the following interpretation to the systematic increase or decrease of the dipole moment in a homologous series with increasing alkyl substitution: Put the angle between the direction of the primary dipole and the line joining the center of the polarisable alkyl group and the center of the primary dipole θ. When the angle θ is below 60°, the secondary dipole is induced in the same sense as that of the primary one, and as a result the whole dipole moment increases with increasing alkyl substitution. On the contrary, when the angle θ exceeds 60°, the induced dipole has an opposite sense to the primary dipole, and hence the whole dipole moment decrease with increasing alkyl substitution. The series of alkyl chlorides, bromides and iodides belong to the former case, and the series of alcohols and amines to the latter case. This interpretation seems to be obviously reasonable. However, when we examine the data carefully, we meet several difficulties which can be by no means overcome by the theory of such a simple induction. In the first place, let us compare the data for three homologous series of alkyl chlorides, bromides and iodides. If the variation of the dipole moment in a homologous series were mainly due to the simple induction in the growing chain by the primary dipole between the carbon and halogen atoms, these three series should all show the same effect. That is, as the dipole moment of methyl halides rises in the order iodide, bromide and chloride, the dipole moment of ethyl, propyl and butyl halides should rise in the same order. The actual order is, however, iodide, chloride and bromide in these cases. In addition, as is seen in Table I, while methyl substitution in hydrogen chloride, bromide and iodide causes a marked increase in the dipole moment, the same substitution in hydrogen fluoride causes reversely the decrease in the dipole moment. The theory of induction can not give any reasonable suggestion to the

17) G. Herzberg, "Infrared and Raman Spectra of Polyatomic Molecules", D. van Nostrand Co. Inc., New York (1945), p. 439.
18) ibid., p. 489.
19) S. H. Bauer, *J. Am. Chem. Soc.*, **60**, 524 (1938).
20) L. O. Brockway and H. O. Jenkins, *J. Am. Chem. Soc.*, **58**, 2036 (1936).
21) H. A. Stuart, *Z. Physik.*, **59**, 13 (1929).
22) H. Frank, *Proc. Roy. Soc.*, **A152**, 171 (1935).
23) K. Higasi, *Sci. Papers Inst. Phys. Chem. Res.* (Tokyo), **28**, 284 (1936).

interpretation of this fact. Further, let us compare the two cases of methylamine and ethylamine series. As the secondary dipole moment induced in the ethyl group should be larger than that induced in the methyl group in every case, and as such a secondary dipole should have an opposite sense to the primary dipole in an amine molecule, all methylamines should have a larger dipole moment than the corresponding ethylamines. This expectation is fulfilled in the cases of primary and secondary amines; the dipole moments of monomethylamine and dimethylamine are both larger than those of the corresponding monoethylamine and diethylamine. However, the dipole moment of trimethyl amine is smaller than that of triethylamine. This fact can not be explained by the theory of induction.

Therefore, in order to overcome these difficulties, we must seek for a component of the dipole moment quite different from the above-mentioned induced dipole moment. Such a component should be rather predominant in an anomalous series of compounds and decrease reversely to the bond polarity with the increasing $-I$ substitution. The atom dipole moment may be regarded as such a component. According to Coulson's calculation[24], the main part of the dipole moments of water and ammonia comes from "the atom dipole moment" produced by localization of electronic clouds which is caused by *s-p* hybridization of non-bonding electrons of oxygen and nitrogen, and the bond polarity contributes a little to the whole dipole moment. Thus we may assume the whole dipole moment μ_m consists of the bond polarity μ_b and the atom dipole moment μ_a;

$$\mu_m = \mu_a + \mu_b$$

Such an *s-p* hybridization of non-bonding electrons is considered to take place to a considerable extent especially in the hydrides of nitrogen, oxygen and fluorine and their derivatives. This may be presumed from the fact that the valence angle of nitrogen and oxygen is nearly equal to 110°. On the contrary, in compounds of elements below the third period in the periodic table such an *s-p* hybridization hardly ever takes place. This is presumed from the fact that the valence angles of sulfur[18] and phosphorus[25] are both near to 90°.

Now let us apply the above interpretation to methylamine and ethylamine series. Since the $-I$ effect of ethyl is greater than that of methyl, the bond polarity of monoethylamine is greater than that of monomethylamine. The actual moment is, however, smaller in ethylamine than in methylamine. Further, compare the case of monoethylamine with that of dimethylamine. As the bond polarity of a secondary amine is much greater than that of a primary amine, we must assume that the atom dipole moment of primary amine is much greater than that of secondary amine, in order to explain the nearly equal dipole moments of monoethylamine and dimethylamine.

Thus we have obtained the following conclusion. *The more $-I$ active a substituent is, the more the degree of s-p hybridization decreases, and hence the more the contribution of the atom dipole moment to the whole dipole moment decreases.* In addition, it must be noted that such a decrease of hybridization may have its own limit. As already stated, the dipole moment of monoethylamine is much smaller than that of monomethylamine. This suggests that the decrease of the degree of hybridization takes place to a much greater extent in the case of methyl substitution. But the introduction of the second and third ethyl groups no longer causes a great decrease of the whole dipole moment, and in this respect an ethylamine series forms a contrast to a methylamine series. This change of dipole moments in an ethylamine series may be explained as follows. In an ethylamine series, as a result of a considerably great decrease of the degree of hybridization by the introduction of the first ethyl group, the introduction of the further ethyl groups brings about the increase of the bond polarity rather than the decrease of the degree of hybridization. Consequently no marked stepwise decrease of the dipole moment which appears in a methylamine series, is observed. Similarly in the case of fluorides, the decrease of the degree of hybridization approaches to its limit at the change from hydrogen fluoride to methyl fluoride, and the further $-I$ substitution brings about the increase of the bond polarity rather than the decrease of the atom dipole moment, so that the dipole moment of ethyl fluoride rises again from that of methyl fluoride. This interpretation is illustrated in Fig. 2.

Thus we have established the rule that

24) C. A. Coulson, *Proc. Roy. Soc.*, **A 207**, 63 (1951).
25) D. P. Stevenson, *J. Chem. Phys.*, **8**, 285 (1940).

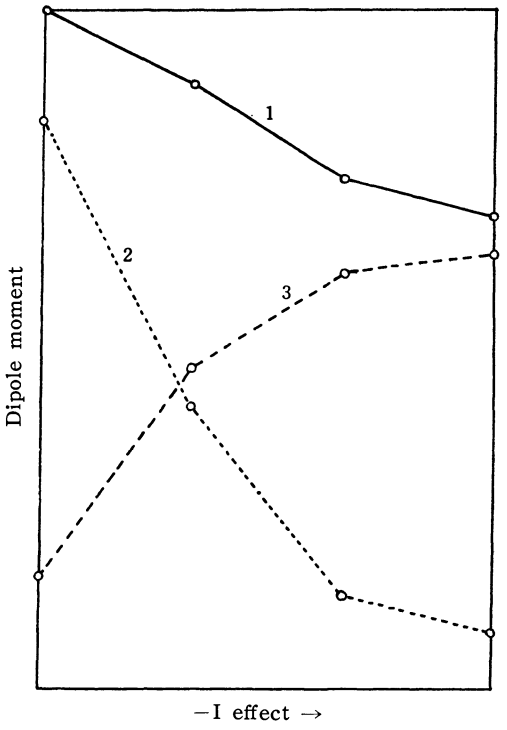

Fig. 2. Illustration of variation of the components of the dipole moment with successive −I substitution.
1 —— whole dipole moment
2 ····· atom dipole moment
3 - - - bond dipole moment

the introduction of the −I substituent prevents *s-p* hybridization of non-bonding electrons. If this rule is true, it should hold well not only for alkyl substitution, but also for any kind of substitution. Consequently, the introduction of the +I substituent should promote the *s-p* hybridization and hence increase the atom dipole moment. Therefore we can expect a large atom-dipole moment in hydrazine and hydroxylamine. But the problem is complicated in these cases. Because, these molecules consist of two parts which contribute equally or nearly equally to the whole dipole moment. These two parts make the restricted oscillation[26] near the trans positions, so that there occurs the compensation of the dipole moments of these two parts. This compensation is complete when the two parts are in the trans positions and becomes partial as they go away from the trans positions. Therefore unless the potential energy of oscillation is determined, we can not estimate the dipole moment of each part from the observed dipole moment. Therefore at present we can not prove directly the validity of the present view. With respect to the strong interaction between these molecules and metal ions, we have following evidences. Previously amine complexes of nickel(II), platinum(II) and cobalt(III) having various amines as ligands, were studied spectrochemically by the present author[27]. The result obtained shows that the affinity of amines toward these metal ions increases in the following order; ethylamine, methylamine, ethanolamine, ammonia and hydroxylamine. This series is the same as the order of the inductive effect of substituents, and the position of hydroxylamine in this series means the strong affinity toward metal ions, which indicates the large atom dipole moment of nitrogen in hydroxylamine. Further, according to Schwarzenbach's measurement[28] the consecutive formation constants of hexahydrazine nickel(II) complex are much larger than the corresponding consecutive formation constants of hexammine nickel(II) complex. This fact suggests that the atom dipole moment of nitrogen is much greater in hydrazine than in ammonia.

In addition, we can give a quite new interpretation to the unusal stability of ethylenediamine complexes. They have a great stability which can by no means be explained by the fact that they have a small probability with which a chelating agent leaves simultaneously two coordination positions. Further it must be noted that the characteristic absorption bands of ethylenediamine complexes of nickel(II), copper(II), cobalt(III), platinum(II) etc. lie in the wavelength shorter than those of the corresponding ammonia- and methylamine complexes. According to the crystal field theory[29], such characteristic absorption bands of transition metal complexes are due to the energy transitions between the split *d*-levels. As the energy intervals between the split d-levels increase with the increase of the electrostatic field set up by the ligands, it can be concluded that the stronger the field by the ligand is, the more the absorption bands of the complex appear in the shorter wavelength. Accordingly,

26) S. Mizushima, K. Higasi and Y. Morino, *Sci. Papers Inst. Phys. Chem. Res.* (Tokyo), **25**, 159 (1934); *Phys. Z.*, **35**, 905 (1934).

27) H. Yoneda, This Bulletin, **30**, 130 (1957); **30**, 924 (1957).

28) G. Schwarzenbach and A. Zobrist, *Helv. Chim. Acta*, **35**, 1291 (1952).

29) For example, L. E. Orgel, *J. Chem. Phys.*, **23**, 1004 (1955).

the above-mentioned fact indicates that the electric field toward the *d*-electrons which is produced by the ligands is stronger in ethylenediamine complexes than in ammonia- and methylamine complexes, and that the atom dipole moment of ethylenediamine is greater than that of ammonia and methylamine. Such an increased atom dipole moment of ethylenediamine can be explained as being due to a result of the mutual +I effect of the two amino groups within the molecule. The difference of the coordinating abilities between mono- and poly-alcohols[30] can also be explained in the same way.

Summary

As a result of the examination of dipole moments of hydrides of various elements and their alkyl derivatives the following regularity was found. Hydrides of elements below the third period in the periodic table show the normal variation of dipole moments with successive alkyl substitution. That is, the dipole moment increases with successive alkyl substitution, which is expected from the consideration of the inductive effect of substituents. On the other hand, hydrides of elements in the second period in the periodic table show the abnormal variation of dipole moments with successive alkyl substitution, which apparently seems to contradict the existence of the inductive effect. That is, the dipole moment decreases with successive alkyl substitution. This fact was connected with the concept of *s-p* hybridization of non-bonding electrons, and the following rule was drawn. The more −I active a substituent is, the more the degree of *s-p* hybridization of non-bonding electrons decreases, and hence the more the contribution of the atom dipole moment to the whole dipole moment decreases. Some applications of this rule to the chemistry of coordination compounds were also presented.

The author wishes to express his sincere thanks to Dr. M. Mashima of Saga University for his valuable discussions.

Department of Chemistry
Wakayama University
Masago-cho, Wakayama

30) For example, M. Kubota, *J. Chem. Soc. Japan* (*Nippon Kagaku Kaisi*), **61**, 1182 (1940).

*The Structure of Kainic Acid, the Most Active Component of Digenea Simplex Ag. II. The Molecular and Crystal Structure of Kainic Acid Monohydrate**

By Hideo WATASE, Yujiro TOMIIE and Isamu NITTA

(Received April 16, 1958)

As reported in the general survey[1] of our studies on the structures of kainic acid and its isomer, investigations based on X-ray crystal analysis were carried out. In the preceding paper[2] of this series, we already concluded that the structure of kainic acid, $C_{10}H_{15}O_4N$, was 2-carboxy-3-carboxymethyl-4-isopropenylpyrrolidine, and also determined the stereochemical configuration of the molecule from the structure of the kainate anion in the zinc salt.

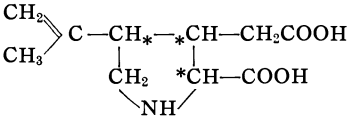

However, it will be of still greater interest to determine the molecular structure of kainic acid in its own crystal, and thus to know how the molecular structures in the crystals of the salt and the free acid are related to each other.

The structure of the kainic acid crystal has been examined by two-dimensional

* Part of this paper was presented at the Autumnal Joint Meeting of Chemical Societies in Japan, Tokyo, 1956.

1) I. Nitta, H. Watase and Y. Tomiie, *Nature*, **181**, 761 (1958).

2) H. Watase and I. Nitta, This Bulletin, **30**, 889 (1957).

X-ray procedure. The electron-density projections along the three principal crystal axes were derived by the trial method, and the structure was determined. In this account, moreover, some general remarks on X-ray crystal analysis are added.

Experimental

Kainic acid crystallizes with one water molecule from its aqueous solution. Crystalline kainic acid monohydrate ($C_{10}H_{15}O_4N \cdot H_2O$) is composed of colorless thin needles elongated along a principal crystal axis (monoclinic b axis).

Oscillation-, Sauter- and Weissenberg-photographs, were taken about the three principal crystal axes, using Cu K_α radiation. The specimens used had the following cross-sections at right angles to the axis of rotation; 0.08×0.30 mm. for the b axis rotation, 0.15×0.6 mm. for the c axis and 0.4×0.5 mm. for the a axis**.

The intensity data for ($h0l$), ($hk0$) and ($0kl$) used in the two-dimensional analyses were taken from the integrated Weissenberg photographs for each zone. By comparing them with a calibrated scale, the intensities of the reflections were estimated visually, multiple-film technique being used for accurate measurements of strong reflections. The corrections for polarization and Lorentz factors were made in the usual way. The corrections for absorption and the form of the specimen were made only for ($hk0$) in an approximate way, the linear absorption coefficient for Cu K_α radiation being $\mu = 10.4$/cm***.

Relative structure factors were then deduced from these intensity data by the ordinary process.

Results and Discussion

Unit Cell and Space Group.—It was found from the X-ray examinations that the crystal belongs to the monoclinic system, and the dimensions of the unit cell are as follows;

$$a = 12.07 \pm 0.03 \text{ Å}$$
$$b = 5.86 \pm 0.02 \text{ Å}$$
$$c = 8.19 \pm 0.03 \text{ Å}$$
$$\beta = 94.7° \pm 0.2°.$$

Systematic absence of reflections being only ($0k0$) with k odd, the space group may be either $C_2^2 - P2_1$ or $C_{2h}^2 - P2_1/m$. However, since kainic acid is of an optically active compound, the space group is uniquely determined to be $C_2^2 - P2_1$ with no centers of symmetry. Judging from the cell size and the symmetry element of the crystal, it is clear that the unit cell contains two formula units of $C_{10}H_{15}O_4N \cdot H_2O$.

The axial period of b is short enough for a projection to provide useful information about the structure. Moreover, the two-fold screw axis lying parallel to this axis, the b axis projection is effectively centro-symmetrical. Therefore the determination of the structure was approached from the b axis projection.

Determination of the Structure. — As will be described in the last section of this paper, neither did the inequality method bring success in the present case, nor did the Patterson method give any information about the structure. On the other hand, we analyzed the zinc salt[2] and gave kainic acid the structure as mentioned previously (2-carboxy-3-carboxymethyl-4-isopropenylpyrrolidine). Adopting this structure, the trial method making use of the structure-factor maps for all the possible reflections of ($h0l$) was applied to locate all the atoms in the projection along the b axis.

Considering the packing, the probable position of the isopropenyl group could be roughly determined. Considering the various possible structures conceivable in connection with the position of the isopropenyl group, the signs of the structure factors of the lowest order except for those of small F values could be determined, and it was known that the absolute structure-factor values are close to those which are obtained from Wilson's method[3]. Then, determining the signs of the structure factors, the quantitative trial was carried on step by step from the lower to the higher orders so as to obtain a good agreement between the calculated and the observed F values, until all the atoms were located satisfactorily to permit the Fourier refinements. The final electron-density projection of Fig. 1 was thus derived, and the atomic positions were further refined from this map. The x and z atomic parameters were thus obtained.

In order to estimate the unknown y parameters, the projection along the c axis was investigated, using the structure-factor data of ($hk0$). Since this projection has no center of symmetry, differing from the case of the centro-symmetrical b axis projection, each structure factor consists of real and imaginary parts. By the trial use of the structure-factor maps for the

** To take the photographs about the a and c axes, the specimens were prepared by cutting the crystals at right angles to the needle axis (b axis).

*** This value comes from the unit cell containing two formula units. (see next section).

3) A. J. C. Wilson, *Acta Cryst.*, **2**, 318 (1949).

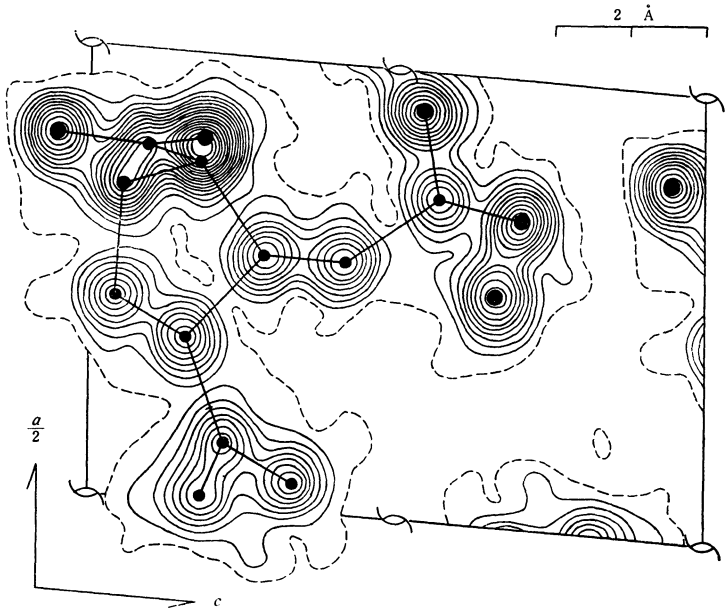

Fig. 1. The final electron-density projection along the *b* axis. Contour lines are at unit electron intervals, the lowest line, broken line, being 1 electron per Å^2. Black circles show the final atomic positions, there being large, intermediate and small circles for oxygen, nitrogen and carbon respectively.

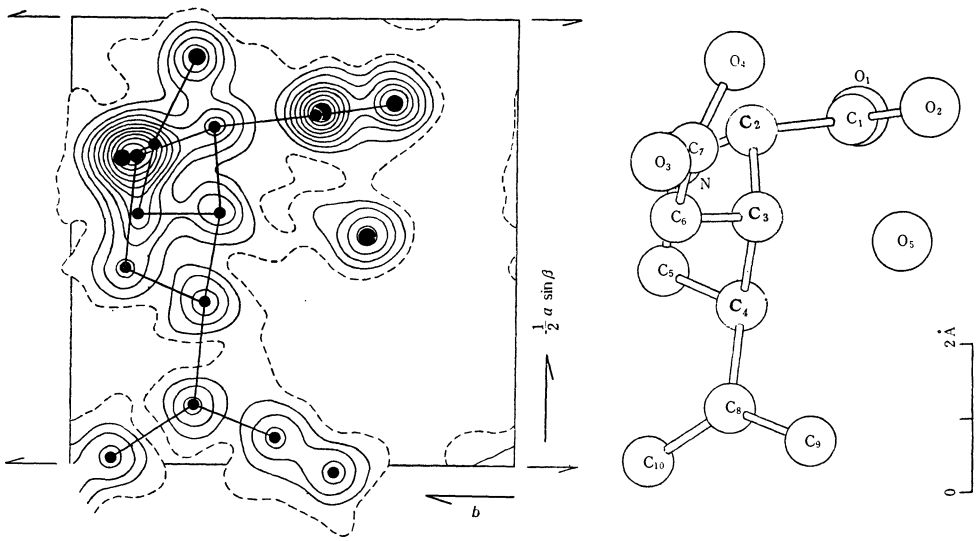

Fig. 2. The final electron-density projection along the *c* axis. Contour lines are at two electrons intervals, the lowest line, broken line, being 2 electrons per Å^2. Black circles show the atomic positions, there being large, intermediate and small circles for oxygen, nitrogen and carbon respectively. The interpretation of the density map is given on the right side.

lower order reflections only, the *y* parameters of all the atoms were easily obtained, and these parameters were further refined by the Fourier refinements. In this trial, since for a weak reflection, both the real and the imaginary part of the structure factor should be small, the structure-factor maps of the weak reflections were most useful. The final electron-density projection along the *c* axis was thus derived as shown in Fig. 2. The final *x*, *y* and *z* atomic parameters are listed in Table I.

The phases of the structure factors for

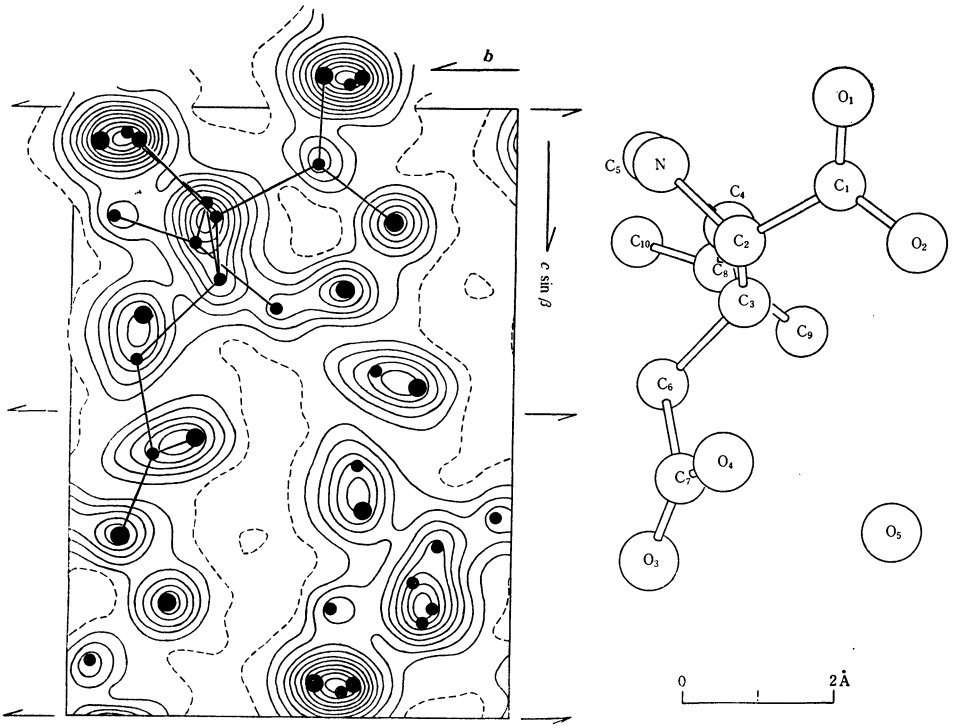

Fig. 3. The final electron-density projection along the *a* axis. Contours and symbols are the same as those of Fig. 2. The interpretation of the density map is given on the right side.

(0*kl*) were calculated from the *y* and *z* atomic parameters, and the electron-density projection along the *a* axis was obtained as shown in Fig. 3.

TABLE I
ATOMIC PARAMETERS

Atom	*x*/*a*	*y*/*b*	*z*/*c*
C_1	0.393	0.451	0.094
C_2	0.379	0.679	0.178
C_3	0.282	0.667	0.282
C_4	0.183	0.698	0.158
C_5	0.222	0.878	0.042
C_6	0.281	0.850	0.415
C_7	0.360	0.815	0.567
C_8	0.069	0.722	0.220
C_9	0.030	0.540	0.332
C_{10}	0.008	0.908	0.182
N	0.347	0.855	0.053
O_1	0.397	0.438	0.943
O_2	0.405	0.277	0.185
O_3	0.344	0.887	0.704
O_4	0.458	0.719	0.540
O_5 (H_2O)	0.257	0.337	0.658

At this stage, the discrepancy indices ($R=\sum||F_o|-|F_c||/\sum|F_o|$) are 0.175 for (*h*0*l*), 0.159 for (*hk*0) and 0.244 for (0*kl*), employing the data up to $\sin\theta/\lambda=0.625$ for (*h*0*l*) and 0.640 for (*hk*0) and (0*kl*), assuming the values of the unobserved structure factors to be precisely zero and neglecting the contributions from hydrogen atoms. In the structure-factor calculations, the effect of thermal motion was taken into account, the value of $B=3.0$ Å^2 being used for each zone as the temperature factor common to all the atoms. The atomic scattering factors were taken from McWeeny's paper[4]; for oxygen $\bar{f}_0=1/3(f^{\parallel}+2f^{\perp})$ and for carbon the values for 'valence states'.

The observed and the calculated structure factors for (*h*0*l*) are listed in Table II, and those for (*hk*0) and (0*kl*) in Table III.

Molecular Structure.—The bond lengths and bond angles, calculated from the atomic parameters of Table I, are shown in Fig. 4. It may be said that the bond lengths will be correct to ±0.03Å and the bond angles to ±3°. As a result, it was confirmed that the structure of kainic acid is 2-carboxy-3-carboxymethyl-4-isopropenylpyrrolidine in agreement with the structure determined from that of the

4) R. McWeeny, *Acta Cryst.*, **4**, 513 (1951).

TABLE II

OBSERVED AND CALCULATED STRUCTURE FACTORS $F(h0l)$

$h\ k\ l$	$1/2F_o$	$1/2F_c$	$h\ k\ l$	$1/2F_o$	$1/2F_c$	$h\ k\ l$	$1/2F_o$	$1/2F_c$	$h\ k\ l$	$1/2F_o$	$1/2F_c$
0 0 0	—	124	1 0 4	2.8	4.4	4 0 9	1.0	1.0	13 0 $\bar{4}$	—	0.6
1 0 0	20.0	−23.1	2 0 4	—	−1.0	5 0 9	—	0.4	14 0 $\bar{4}$	2.1	2.9
2 0 0	5.2	− 5.2	3 0 4	2.7	2.7	6 0 9	2.3	− 1.9	1 0 $\bar{5}$	2.6	4.6
3 0 0	29.8	29.8	4 0 4	2.1	−2.0	0 0 10	1.0	− 1.1	2 0 $\bar{5}$	7.2	6.7
4 0 0	3.2	− 5.4	5 0 4	4.4	−4.3	1 0 10	—	1.0	3 0 $\bar{5}$	12.1	−12.6
5 0 0	15.8	15.6	6 0 4	2.4	3.2	2 0 10	1.3	− 1.0	4 0 $\bar{5}$	5.6	6.9
6 0 0	5.0	− 4.6	7 0 4	6.8	−7.4	1 0 $\bar{1}$	11.2	10.1	5 0 $\bar{5}$	3.4	4.8
7 0 0	2.5	− 1.9	8 0 4	2.7	2.8	2 0 $\bar{1}$	2.6	4.2	6 0 $\bar{5}$	4.7	−4.8
8 0 0	3.2	5.1	9 0 4	1.9	−0.7	3 0 $\bar{1}$	13.3	13.5	7 0 $\bar{5}$	1.8	−2.0
9 0 0	3.5	− 3.9	10 0 4	2.9	−2.9	4 0 $\bar{1}$	16.0	−15.8	8 0 $\bar{5}$	2.3	−1.9
10 0 0	0.8	− 0.5	11 0 4	—	−0.7	5 0 $\bar{1}$	24.1	22.4	9 0 $\bar{5}$	—	−1.2
11 0 0	3.3	3.3	12 0 4	1.9	−1.2	6 0 $\bar{1}$	3.7	3.9	10 0 $\bar{5}$	2.3	2.6
12 0 0	—	− 0.3	13 0 4	2.3	2.8	7 0 $\bar{1}$	4.4	− 3.8	11 0 $\bar{5}$	2.1	−2.6
13 0 0	—	− 0.2	0 0 5	—	0.5	8 0 $\bar{1}$	11.1	10.2	12 0 $\bar{5}$	—	0.4
14 0 0	—	− 0.2	1 0 5	—	1.0	9 0 $\bar{1}$	5.3	− 6.3	13 0 $\bar{5}$	—	0.0
15 0 0	1.5	2.3	2 0 5	1.9	−2.3	10 0 $\bar{1}$	3.2	4.2	1 0 $\bar{6}$	6.7	6.7
0 0 1	7.7	7.7	3 0 5	8.5	9.4	11 0 $\bar{1}$	—	0.2	2 0 $\bar{6}$	2.7	−1.7
1 0 1	13.2	−12.6	4 0 5	6.1	−5.9	12 0 $\bar{1}$	1.9	1.1	3 0 $\bar{6}$	2.8	2.9
2 0 1	1.0	− 2.6	5 0 5	—	0.3	13 0 $\bar{1}$	1.2	1.4	4 0 $\bar{6}$	4.0	4.2
3 0 1	9.6	− 8.5	6 0 5	1.8	0.7	14 0 $\bar{1}$	—	0.1	5 0 $\bar{6}$	1.8	2.6
4 0 1	14.3	−14.7	7 0 5	2.3	2.7	15 0 $\bar{1}$	1.3	1.6	6 0 $\bar{6}$	3.0	3.1
5 0 1	13.1	11.5	8 0 5	2.3	1.8	1 0 $\bar{2}$	5.4	5.7	7 0 $\bar{6}$	3.3	4.4
6 0 1	6.6	− 8.0	9 0 5	1.3	−0.8	2 0 $\bar{2}$	14.1	−13.5	8 0 $\bar{6}$	5.4	−5.0
7 0 1	3.7	− 4.1	10 0 5	1.2	1.3	3 0 $\bar{2}$	0.7	− 1.9	9 0 $\bar{6}$	3.2	3.1
8 0 1	5.7	− 6.0	11 0 5	2.5	2.8	4 0 $\bar{2}$	12.2	− 9.4	10 0 $\bar{6}$	1.2	0.9
9 0 1	2.8	3.1	12 0 5	—	0.3	5 0 $\bar{2}$	1.8	− 2.5	11 0 $\bar{6}$	1.9	−1.9
10 0 1	7.0	7.4	0 0 6	1.2	2.6	6 0 $\bar{2}$	9.5	6.9	12 0 $\bar{6}$	—	1.4
11 0 1	6.6	− 8.0	1 0 6	0.8	−0.5	7 0 $\bar{2}$	4.3	− 4.0	1 0 $\bar{7}$	1.0	−0.8
12 0 1	2.2	2.4	2 0 6	4.7	4.2	8 0 $\bar{2}$	3.7	− 4.9	2 0 $\bar{7}$	1.0	−1.3
13 0 1	1.2	1.8	3 0 6	5.4	−4.6	9 0 $\bar{2}$	5.6	5.6	3 0 $\bar{7}$	—	0.4
14 0 1	—	− 0.9	4 0 6	2.3	2.3	10 0 $\bar{2}$	2.3	− 2.6	4 0 $\bar{7}$	1.0	0.0
0 0 2	4.7	− 5.6	5 0 6	3.3	4.0	11 0 $\bar{2}$	1.9	− 2.7	5 0 $\bar{7}$	3.3	−4.0
1 0 2	34.5	−35.9	6 0 6	—	−1.0	12 0 $\bar{2}$	2.3	− 2.1	6 0 $\bar{7}$	6.6	7.6
2 0 2	9.9	12.0	7 0 6	1.3	−1.4	13 0 $\bar{2}$	2.1	2.4	7 0 $\bar{7}$	1.9	1.3
3 0 2	15.9	−15.0	8 0 6	5.7	5.4	14 0 $\bar{2}$	—	− 0.8	8 0 $\bar{7}$	—	−0.6
4 0 2	5.3	3.4	9 0 6	—	−0.8	15 0 $\bar{2}$	1.6	− 1.3	9 0 $\bar{7}$	—	0.3
5 0 2	6.2	4.6	10 0 6	—	−0.9	1 0 $\bar{3}$	3.7	3.9	10 0 $\bar{7}$	—	1.5
6 0 2	7.5	− 6.6	11 0 6	1.2	1.5	2 0 $\bar{3}$	14.2	−14.3	11 0 $\bar{7}$	2.9	2.9
7 0 2	1.6	− 0.5	0 0 7	—	−0.7	3 0 $\bar{3}$	1.7	− 2.2	1 0 $\bar{8}$	7.0	5.9
8 0 2	5.4	5.1	1 0 7	—	−0.9	4 0 $\bar{3}$	10.6	10.0	2 0 $\bar{8}$	—	−0.8
9 0 2	0.8	0.5	2 0 7	4.8	−4.1	5 0 $\bar{3}$	13.6	−13.6	3 0 $\bar{8}$	10.2	−8.2
10 0 2	0.8	0.6	3 0 7	1.0	−0.4	6 0 $\bar{3}$	1.5	1.0	4 0 $\bar{8}$	1.3	0.3
11 0 2	1.9	2.0	4 0 7	1.0	0.6	7 0 $\bar{3}$	1.6	− 0.2	5 0 $\bar{8}$	1.0	−1.5
12 0 2	1.8	− 2.4	5 0 7	1.0	−0.7	8 0 $\bar{3}$	0.8	− 0.1	6 0 $\bar{8}$	3.0	−3.2
13 0 2	—	0.1	6 0 7	—	−0.5	9 0 $\bar{3}$	1.8	1.9	7 0 $\bar{8}$	1.7	0.7
14 0 2	—	0.0	7 0 7	1.2	−0.3	10 0 $\bar{3}$	1.9	− 1.4	8 0 $\bar{8}$	2.2	−2.0
0 0 3	1.5	0.4	8 0 7	1.1	−1.2	11 0 $\bar{3}$	2.7	− 2.5	9 0 $\bar{8}$	—	0.2
1 0 3	1.3	0.9	9 0 7	—	0.3	12 0 $\bar{3}$	—	1.5	10 0 $\bar{8}$	0.8	−1.4
2 0 3	17.0	−15.4	10 0 7	1.1	−2.0	13 0 $\bar{3}$	2.0	− 2.8	1 0 $\bar{9}$	—	0.8
3 0 3	17.8	17.0	0 0 8	9.7	−7.8	14 0 $\bar{3}$	—	0.2	2 0 $\bar{9}$	3.8	3.3
4 0 3	1.9	2.1	1 0 8	1.3	0.1	1 0 $\bar{4}$	9.8	− 8.5	3 0 $\bar{9}$	2.3	−1.9
5 0 3	1.4	0.0	2 0 8	—	−0.5	2 0 $\bar{4}$	6.5	6.9	4 0 $\bar{9}$	1.6	2.3
6 0 3	1.6	− 1.5	3 0 8	—	0.3	3 0 $\bar{4}$	3.3	− 3.1	5 0 $\bar{9}$	3.7	−4.0
7 0 3	2.9	− 3.3	4 0 8	4.3	3.6	4 0 $\bar{4}$	—	− 0.6	6 0 $\bar{9}$	—	0.0
8 0 3	3.6	4.8	5 0 8	4.2	−4.5	5 0 $\bar{4}$	2.2	− 2.8	7 0 $\bar{9}$	1.3	1.1
9 0 3	1.9	1.1	6 0 8	2.2	1.7	6 0 $\bar{4}$	3.0	− 2.0	8 0 $\bar{9}$	3.2	−2.7
10 0 3	5.2	− 5.6	7 0 8	—	0.6	7 0 $\bar{4}$	3.0	3.6	1 0 $\bar{10}$	—	−0.7
11 0 3	1.8	− 1.2	8 0 8	1.2	−1.6	8 0 $\bar{4}$	6.3	− 8.5	2 0 $\bar{10}$	1.7	2.1
12 0 3	—	− 0.4	0 0 9	2.0	−1.6	9 0 $\bar{4}$	6.5	6.4	3 0 $\bar{10}$	1.2	1.2
13 0 3	2.5	− 2.7	1 0 9	2.0	2.1	10 0 $\bar{4}$	—	0.5	4 0 $\bar{10}$	—	−0.1
14 0 3	1.3	0.8	2 0 9	—	0.5	11 0 $\bar{4}$	—	0.2			
0 0 4	0.9	− 0.3	3 0 9	—	0.3	12 0 $\bar{4}$	1.2	0.6			

TABLE III

OBSERVED AND CALCULATED STRUCTURE FACTORS FOR ($hk0$) AND ($0kl$)

The values for ($h00$) and ($00l$) are listed in Table II.

h k l	$1/2F_o$	$1/2F_c$	h k l	$1/2F_o$	$1/2F_c$	h k l	$1/2F_o$	$1/2F_c$	h k l	$1/2F_o$	$1/2F_c$
1 1 0	22.1	23.2	6 3 0	2.8	4.6	1 6 0	1.5	2.2	0 3 2	3.8	5.7
2 1 0	3.2	4.8	7 3 0	1.9	2.3	2 6 0	4.1	4.2	0 3 3	9.3	10.5
3 1 0	9.6	12.1	8 3 0	2.8	2.6	3 6 0	1.1	0.8	0 3 4	5.8	5.9
4 1 0	10.9	11.8	9 3 0	2.0	2.1	4 6 0	2.8	2.7	0 3 5	2.1	2.8
5 1 0	10.6	9.8	10 3 0	3.9	5.2	5 6 0	2.2	2.2	0 3 6	4.4	3.5
6 1 0	1.9	2.5	11 3 0	1.5	0.5	6 6 0	2.1	2.0	0 3 7	4.0	4.1
7 1 0	13.8	13.8	12 3 0	2.2	1.9	7 6 0	1.9	1.4	0 3 8	1.0	2.4
8 1 0	13.2	12.7	13 3 0	1.4	0.8	8 6 0	0.9	1.5	0 3 9	1.3	0.6
9 1 0	4.1	3.8	14 3 0	1.2	0.4	9 6 0	1.3	1.9	0 4 1	3.5	6.0
10 1 0	5.8	4.4	0 4 0	7.3	6.2	1 7 0	3.0	2.2	0 4 2	4.3	0.8
11 1 0	2.3	3.1	1 4 0	2.3	2.0	2 7 0	2.2	1.5	0 4 3	5.3	7.5
12 1 0	3.4	3.9	2 4 0	8.8	9.1	3 7 0	2.0	2.1	0 4 4	0.6	2.2
13 1 0	3.9	4.2	3 4 0	5.3	5.4	4 7 0	1.2	1.0	0 4 5	1.6	1.9
14 1 0	1.0	1.0	4 4 0	2.9	3.3	5 7 0	1.2	0.6	0 4 6	1.0	0.7
15 1 0	2.0	2.5	5 4 0	3.0	3.5	0 1 1	17.3	17.5	0 4 7	1.4	1.2
0 2 0	26.9	28.3	6 4 0	3.1	2.8	0 1 2	9.5	8.9	0 4 8	1.4	1.1
1 2 0	14.3	13.4	7 4 0	2.0	1.2	0 1 3	10.5	10.8	0 5 1	5.1	4.6
2 2 0	8.3	11.0	8 4 0	3.6	3.0	0 1 4	7.3	8.2	0 5 2	1.9	4.9
3 2 0	15.1	15.2	9 4 0	3.0	2.5	0 1 5	5.5	5.4	0 5 3	0.6	2.2
4 2 0	1.9	3.5	10 4 0	2.8	3.0	0 1 6	10.8	9.5	0 5 4	1.5	2.7
5 2 0	5.0	6.2	11 4 0	1.7	1.4	0 1 7	1.1	2.1	0 5 5	0.6	0.5
6 2 0	2.6	3.1	12 4 0	1.8	0.9	0 1 8	3.4	2.1	0 5 6	1.6	2.6
7 2 0	3.4	2.9	13 4 0	1.2	2.5	0 1 9	2.1	1.5	0 5 7	2.3	1.4
8 2 0	7.2	6.4	1 5 0	6.3	7.4	0 1 10	0.4	0.3	0 6 1	1.0	2.1
9 2 0	3.2	3.0	2 5 0	6.7	7.0	0 2 1	6.7	11.0	0 6 2	0.6	0.8
10 2 0	1.7	2.5	3 5 0	1.3	2.0	0 2 2	13.1	9.3	0 6 3	0.7	1.6
11 2 0	2.9	3.2	4 5 0	—	1.0	0 2 3	16.8	15.1	0 6 4	0.6	1.4
12 2 0	2.2	2.6	5 5 0	3.1	4.4	0 2 4	4.3	2.7	0 6 5	1.1	0.1
13 2 0	1.1	1.1	6 5 0	2.9	2.2	0 2 5	6.8	5.4	0 6 6	0.4	1.3
14 2 0	1.9	1.3	7 5 0	4.3	3.3	0 2 6	3.2	2.9	0 7 1	1.9	2.4
1 3 0	0.9	0.9	8 5 0	2.7	1.1	0 2 7	1.2	2.1	0 7 2	1.4	1.2
2 3 0	4.1	4.9	9 5 0	2.3	1.3	0 2 8	3.1	3.6	0 7 3	1.2	1.2
3 3 0	3.7	6.1	10 5 0	1.9	0.9	0 2 9	0.6	0.8			
4 3 0	5.4	7.0	11 5 0	1.7	1.3	0 2 10	1.0	0.6			
5 3 0	5.6	7.0	0 6 0	2.2	3.8	0 3 1	5.8	4.4			

kainate anion in the zinc salt[2] and also with the conclusion deduced from the chemical evidences[5].

The observed lengths of the bonds except for the C—O distances are in agreement within ±0.03 Å with those of the corresponding bonds in the kainate anion, the differences being not definitely significant, if the errors be taken into consideration, while some of the bond angles are fairly different from those of the kainate anion.

The C—O distances of the carboxymethyl group of C_3 are found to be 1.23 Å for C_7—O_3 and 1.34 Å for C_7—O_4, owing presumably to the formations of the hydrogen bonds involved (Fig. 9). The oxygen O_4 is of the hydroxyl group (OH). The C—O distances of the carboxyl group of C_2 are 1.24 Å for C_1—O_1 and 1.27 Å for C_1—O_2, being also due to hydrogen bond formations. The dimensions of this group are in good agreement with those of the CH_2COO^- group in the kainate anion (1.24 and 1.28 Å) or with those of the COO^- groups in similar hydrogen-bonded cases; hydroxyproline (1.25 and 1.27 Å)[6] and hexamethylene-diammonium adipate (1.24 and 1.28 Å)[7].

5) M. Miyasaki, *J. Pharm. Soc. Japan* (Yakugaku Zasshi), **75**, 695 (1955); Y. Ueno, H. Nawa, J. Ueyanagi, H. Morimoto, R. Nakamori and T. Matsuoka, ibid., **75**, 840 (1955); S. Murakami, T. Takemoto, Z. Tei and K. Daigo, ibid., **75**, 869 (1955).

6) J. Zussman, *Acta Cryst.*, **4**, 493 (1951); J. Donohue and K. N. Trueblood, ibid., **5**, 419 (1952).

7) S. Hirokawa, T. Ohashi and I. Nitta, *Acta Cryst.*, **7**, 87 (1954).

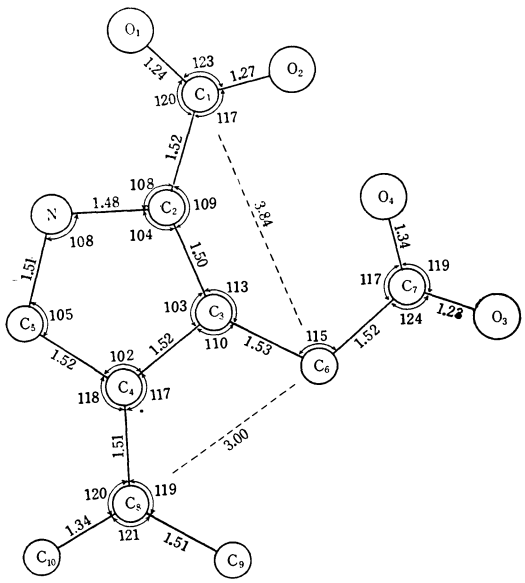

Fig. 4. Bond lengths (Å) and bond angles (°).

Judging from the dimensions of the carboxyl group of C_2 and the consideration about the observed hydrogen bonds (Fig. 9), at least in crystalline state, the kainic acid molecule is considered to be of the 'zwitter ion' structure in which the carboxyl group of C_2 is of COO^- and the nitrogen is of N^+H_2, although the positions of no hydrogen atoms are located in the present work. The infrared spectrum of this crystal also suggests the existence of the ionized carboxyl group, showing the absorption at 6.20 μ[8].

The stereochemical relations of the atoms in kainic acid molecule are in agreement with those of the kainate anion. Namely, the carboxyl group of C_2 and the carboxymethyl group of C_3 take the *trans*-configuration relative to the ring, and the latter group and the isopropenyl group of C_4 are in the *cis*-configuration. This fact supports the reasoning based on chemical evidences[9]. In the isopropenyl group, the double bond C_8—C_{10} is so located as to be more close to the ring than the single bond C_8—C_9 as in the case of the kainate anion. The stereochemical configuration of the molecule is shown in Fig. 5.

Owing mainly to the *cis*-configuration of the two side-chains attached to the neighboring C_3 and C_4, the five-membered pyrrolidine ring (N, C_2, C_3, C_4, C_5) is considerably distorted from the planar form as it is in the case of the kainate anion, their valence angles being remarkably deviated from the ordinary values. The distance between C_6 and C_8 is found to be 3.00 Å, a value similar to 2.96 Å in the kainate anion. As seen clearly in Fig. 3, the four atoms N, C_2, C_4 and C_5 of the pyrrolidine ring are approximately lying on one plane, and the carbon atom C_3 is shifted from the plane of the other four by about 0.6 Å, much greater than about 0.4 Å of the similar displacement in hydroxyproline[6]. The mode of the deformation of the pyrrolidine ring is different in the kainate anion due presumably to the difference of crystalline field, the pyrrolidine ring being thus found to be fairly flexible. In the case of the kainate anion, the carbon atom C_5 is displaced much farther from the mean plane than the other four.

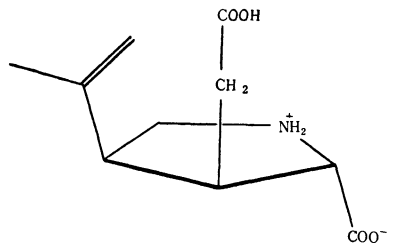

Fig. 5. Stereochemical configuration.

Finally, in Fig. 6, the molecule of kainic acid is indicated by the model which is derived from the atomic parameters of the present X-ray analysis, viewed along the *b* axis.

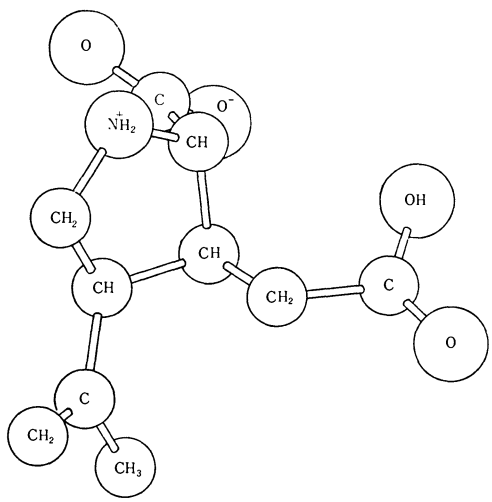

Fig. 6. The arrangement of the atoms in kainic acid, viewed along the *b* axis.

8) Y. Ueno, H. Nawa, J. Ueyanagi, H. Morimoto, R. Nakamori and T. Matsuoka, *J. Pharm. Soc. Japan* (Yakugaku Zasshi), **75**, 807 (1955).

9) H. Morimoto and R. Nakamori, *J. Pharm. Soc. Japan* (Yakugaku Zasshi), **76**, 294 (1956); *Proc. Japan Acad.*, **32**, 41 (1956); T. Takemoto, Z. Tei and K. Daigo, *J. Pharm. Soc. Japan* (Yakugaku Zasshi), **76**, 298 (1956).

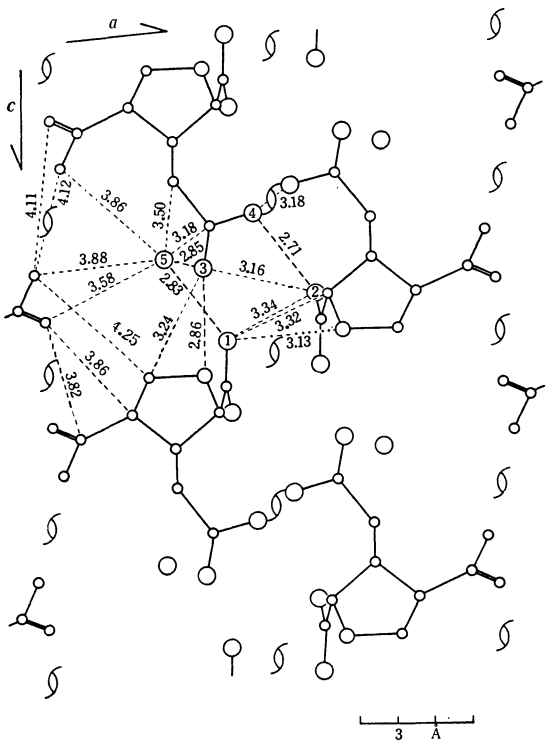

Fig. 7. View of the crystal structure along the *b* axis. The intermolecular distances are shown in Å. Large circles represent oxygens, intermediate nitrogens and small carbons.

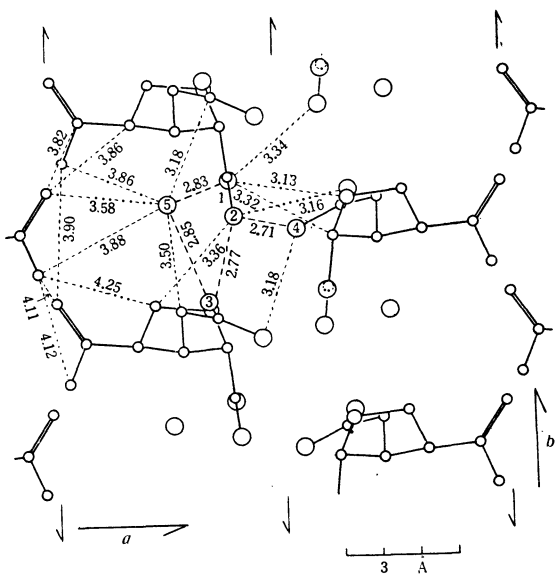

Fig. 8. View of the crystal structure along the *c* axis. The intermolecular distances are shown in Å. Symbols are the same as those of Fig. 7.

Crystal Structure. — The views of the crystal structure along the *b*, *c* and *a* axes are illustrated in Figs. 7, 8 and 9 respectively, giving the intermolecular distances. The space group being C_2^2—$P2_1$, the crystal has only two-fold screw axes parallel to the *b* axis as the symmetry element. The unit cell contains two molecules of kainic acid and two waters, the kainic acid molecule being the zwitter ion of which the account is given in the last section. As a whole, the crystal structure is a layered one, like those of the zinc salt[2] or allokainic acid[10].

There are five kinds of short intermolecular distance of 2.71~2.86 Å between oxygens or oxygen and nitrogen, and the intermolecular hydrogen bonds are considered to be formed there. The two hydrogens of N^+H_2 form the intermolecular hydrogen bonds between the nitrogen and the oxygen O_2 of the carboxyl group $(COO)^-$ or the oxygen O_3 of the carboxymethyl group. These hydrogen bond distances are 2.77 Å for N—H···O_2 and 2.86 Å for N—H···O_3. The hydrogen attached to the oxygen O_4 of the carboxymethyl group also forms the hydrogen bond between the molecules, its O_4—H···O_2 distance being 2.71 Å. The water which is packed into the crystal to fill the space links one molecule to another by forming two hydrogen-bridges between the water oxygen O_5 and two molecules. They are O_5—H···O_1 of 2.83 Å and O_5—H···O_3 of 2.85 Å. The hydrogen bond angles are given in Fig. 9.

The projection along the *a* axis (Fig. 9) shows well how one molecule is linked to others by the hydrogen bonds. By these hydrogen bonds, the molecules and the waters are linked to each other infinitely, forming a double layered structure parallel to the (100) plane. In the projections along the *b* and *c* axes (Figs. 7 and 8), it is clearly seen that between the double layers the nonpolar groups or atoms are in contact with each other, the distances of the closest approach being 3.82 Å for C_8···C_{10}, 3.86 Å for C_4···C_{10}, 4.11 Å for C_9···C_{10} and 4.12 Å for C_9···C_9. This is compatible with the observed cleavage parallel to the (100) plane.

Some Remarks on X-ray Crystal Analysis

In order to derive the *b* axis electron-density projection, the analysis based on

10) H. Watase, to be published.

TABLE IV
SIGN RELATIONS AND CORRECT SIGNS (+OR−)

ξ	(3 0 0) +	(1 0 $\bar{4}$)*−		$-ad\xi$	(3 0 6) −	
η	(8 0 $\bar{1}$) +			acd	(2 0 $\bar{6}$) −	
$\xi\eta$	(5 0 $\bar{1}$) +	(3 0 $\bar{5}$) −		$acd\eta$	(4 0 1)*−	
a	(0 0 8) −	(2 0 $\bar{4}$) +	(8 0 2) +	$acd\xi\eta$	(1 0 1) −	(3 0 5) +
$a\xi$	(3 0 $\bar{8}$) −			ae	(6 0 $\bar{6}$) +	
$a\eta$	(2 0 7) −	(8 0 $\bar{9}$) −		$b\xi$	(5 0 0) +	
$a\xi\eta$	(3 0 3) +	(5 0 $\bar{9}$) −		$c\xi$	(1 0 $\bar{8}$) +	(3 0 $\bar{4}$) −
ab	(8 0 $\bar{8}$) −			$c\eta$	(2 0 3) −	
$ab\xi$	(5 0 8) −			$cd\xi\eta$	(5 0 1) +	(5 0 $\bar{3}$)*−
$ac\xi$	(1 0 0) −			d	(2 0 $\bar{10}$) +	(4 0 $\bar{6}$) +
$ac\eta$	(4 0 $\bar{1}$) −			$d\xi$	(1 0 $\bar{6}$) +	
ad	(2 0 $\bar{2}$) −	(4 0 2) +		$d\eta$	(4 0 5) −	(6 0 $\bar{7}$) +
$ad\xi$	(1 0 2) −	(9 0 $\bar{4}$) +		$e\xi$	(3 0 2) −	
$ad\eta$	(4 0 3) +	(6 0 1) −		−	(4 0 8) +	
$ad\xi\eta$	(3 0 1) −			+	(8 0 $\bar{6}$) −	

* These were determined by Sayre's method.

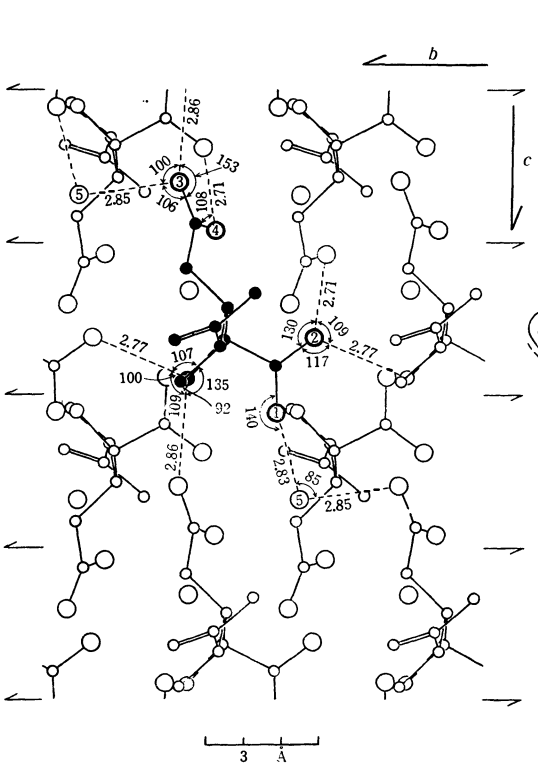

Fig. 9. View of the crystal structure along the a axis. The hydrogen bonds about one molecule are shown by broken lines, their distances (Å) and angles (°) being given. Symbols are the same as those of Fig. 7.

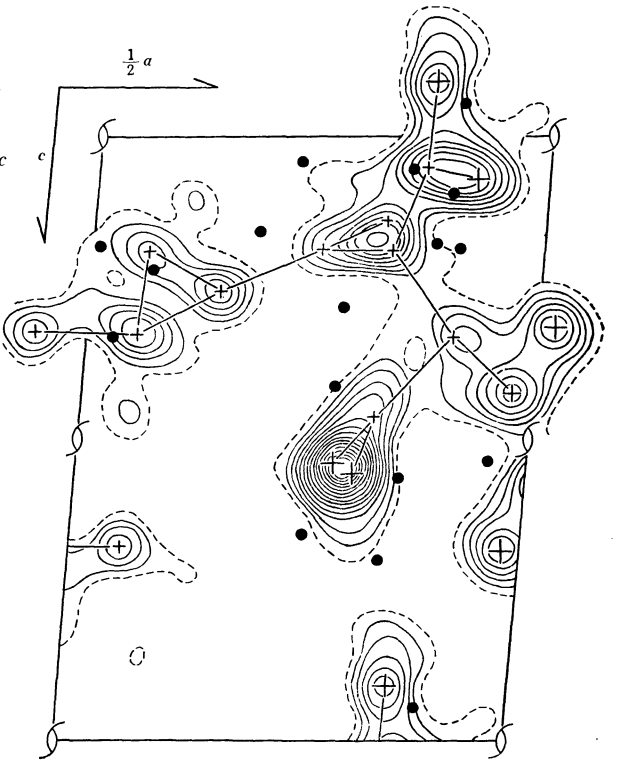

Fig. 10. Projection of incorrect electron-density on (010). Contours are drawn at equal intervals on an arbitrary scale, the lowest contour, broken line, being drawn at zero level of Fourier summations. Cross-symbols indicate the incorrect atomic positions considered from this map, there being large, intermediate and small symbols for oxygen, nitrogen and carbon respectively. The correct atomic positions are shown by black circles. An incorrect structure considered from this map is indicated by interatomic bonds.

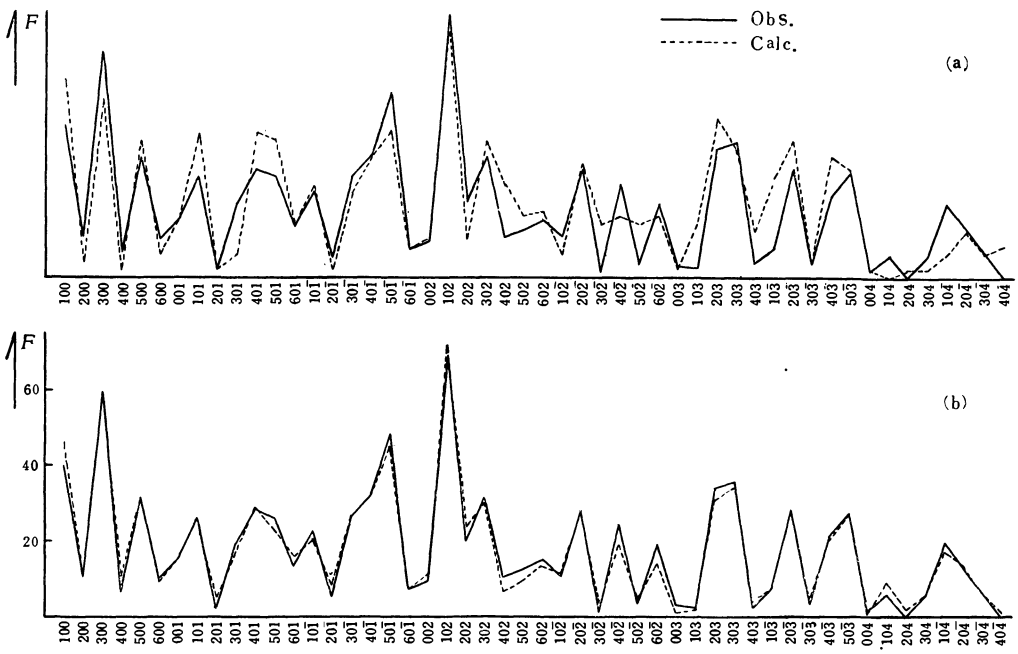

Fig. 11. F-values, (a) for the incorrect structure of Fig. 10, (b) for the correct structure of Fig. 1. The values for only fifty reflections of lower orders ($\sin\theta/\lambda < 0.29$) are shown.

direct methods was first attempted, because the crystal of kainic acid contains no heavy atom, and, furthermore, the chemical structure was entirely unknown when this work began.

The Harker-Kasper inequalities[11] was applied to obtain the sign relations of the structure factors for ($h0l$), using Sakurai's chart[12]. Unitary structure factors $U(h0l)$ were calculated from the relative structure factors $F'(h0l)$, as follows:

$$U(h0l),\ K=|F'(h0l)|\exp B(\sin\theta/\lambda)^2/\sum f_i$$

where f_i is the atomic scattering factor[13] of the ith atom. The scale factor K and the temperature factor B were obtained by Wilson's method[3].

However, since by this procedure sign relations could not be given because of low magnitudes of the unitary structure factors, an attempt was made to determine sign relations of some terms as in the case of the analysis of sodium tropolonate[14]. Namely, the unitary structure factors were multiplied by an artificial constant of about 1.3, and the sign relations of 44 terms were then obtained without contradiction by the Harker-Kasper inequalities. In addition, these relations were also checked by Sayre's method[15]. These sign relations together with the correct signs for the structure of Fig. 1 are listed in Table IV, where ξ and η are arbitrary parameters[16].

By the Fourier method based on these signs and further trial-and-error, an electron-density map was derived as shown in Fig. 10, the sign relations of Table IV being satisfied except for only four reflections with small F value. From this map a structure might be guessed by connecting reasonably with the peaks found as indicated also in Fig. 10. However, the R index calculated on this structure was about 40%, and it seemed impossible to decrease the R value satisfactorily by the further refinement of this map. Moreover, even in the lower order, some of the calculated structure factors showed considerable discrepancy from their observed values as shown in Fig. 11 (a); for example (301), (402), (10$\bar{3}$), (10$\bar{4}$), etc. We gave up this map, Fig. 10, considering that it was wrong, being of a 'false structure'. When

11) D. Harker and J. S. Kasper, *Acta Cryst.*, **1**, 70 (1948).
12) K. Sakurai, ibid., **5**, 546 (1952).
13) "Internationale Tabellen zur Bestimmung von Kristallstrukturen", Bornträger, Berlin (1935).
14) Y. Sasada and I. Nitta, *Acta Cryst.*, **9**, 205 (1956).
15) D. M. Sayre, ibid., **5**, 60 (1952).
16) Y. Okaya and I. Nitta, ibid., **5**, 564 (1952).

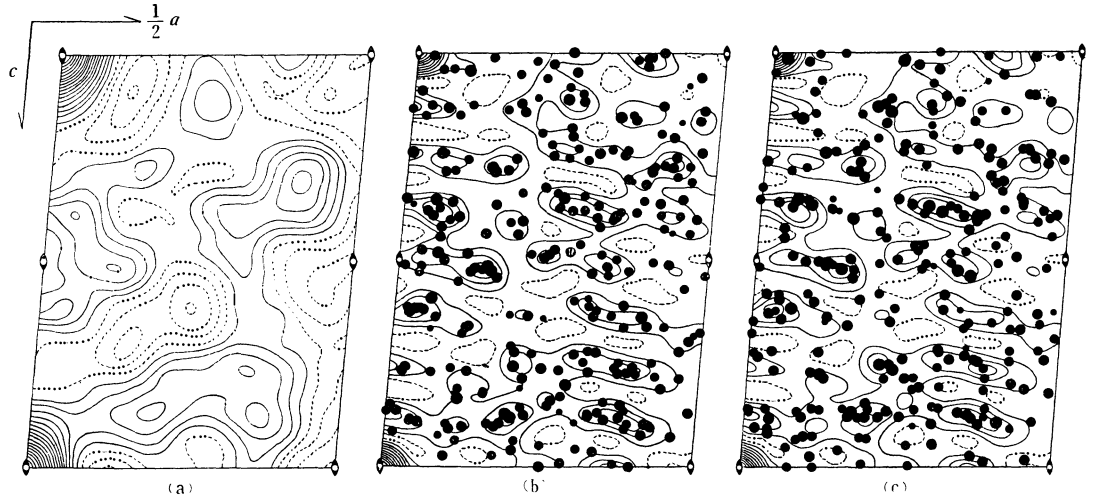

Fig. 12. The Patterson function projected on (010), a) ordinary function, b) and c) modified function to obtain sharp peaks. Contours of each map are drawn at equal intervals on an arbitrary scale, the lowest solid line being drawn at zero level of Fourier summations. Black circles of the maps b) and c) show the positions of the Patterson peaks, b) derived from the correct structure of Fig. 1, c) derived from the incorrect structure of Fig. 10. The area of each black circle is approximately proportional to the weight of the peak.

the correct structure was next determined, it was revealed that the sign relations obtained above were quite random ones, as shown in Table IV, though the above inequalities gave apparently consistent relations.

In the present case, thirty-two atoms are in the unit cell excluding hydrogen atoms, and, generally speaking, this number of atoms per unit cell is too many for the inequality method to be applied. A successful application of the inequality method to tropolone hydrochloride[17] has been reported, the unit cell of which contains forty atoms. However, there are four heavy chlorine atoms which are distinguishable from others, and the signs obtained by this method coincide with those of the contributions from the chlorine atoms except for only one structure factor with a small F value.

Although there is the fortunate case of sodium tropolonate, it must be borne in mind that the sign relations obtained by raising artificially the scale of unitary structure factors may not necessarily correspond to the true structure and even may lead to a false structure as in the present case. It generally seems that the more atoms are contained in a unit cell, the more various false structures will be possible.

As for the application of the Patterson method, the ordinary Patterson function $P(x, z)$ was first calculated, and further to obtain sharp peaks a modified Patterson function $P'(x, z)$ was also calculated as follows:

$$P'(x, z) = k \sum_h \sum_l U(h0l)^2 \cos 2\pi(hx + lz)$$

where k is the scale factor. Both projection maps are shown in Fig. 12. However, no useful information about the structure was provided from these maps. Even in such a case, this function may be applicable as a method to check whether or not a derived structure is correct, as seen from a comparison between the maps b and c of Fig. 12. If a structure derived by any other method is correct, the Patterson map should be quantitatively interpreted as shown in the map b of Fig. 12.

We wish to express our thanks to Professor-Emeritus S. Murakami, Dr. T. Takemoto and their collaborators of this University and Drs. S. Kuwada, S. Tatsuoka, Y. Ueno and their collaborators of the Research Laboratory of Takeda Pharmaceutical Industry, Ltd. for supplying the specimens and kindly discussing problems with us. Thanks are also due to Dr. H. Tani, Mr. Y. Sasada and Mr. T. Shiba of this University for helpful advice and continued interest. Appreciation is

17) Y. Sasada, K. Osaki and I. Nitta, ibid., 7, 113 (1954).

also expressed to Messrs. S. Sakakibara, M. Okumiya and Miss K. Koike of this University for their help in micro-analyses.

Department of Chemistry
Faculty of Science
Osaka University
Kita-ku, Osaka

A Study of Tin Oxides by X-Ray Diffraction Method

By Kichizo NIWA, Iwao YAMAI and Tsuguyasu WADA

(Received March 31, 1958)

There are various reports available for the occurrence and stability of tin oxides: stannous oxide, β-stannous oxide, tritin tetroxide and stannic oxide. Most of these reports are in accord with one another on the point that stannous oxide decomposes into tin and stannic oxide at higher temperatures, though various temperatures have been reported for the decomposition such as 400°C[1], 510°C[2], 385°C[3] and 300°C.[4] Weiser and Milligan[5], however, showed that heating of stannous oxide in vacuo at 500°C gives a product which is neither stannous oxide, nor tin and stannic oxide and which they called β-stannous oxide.

According to Spandau and Kohlmeyer[6,7] stannous oxide decomposes into tin and tritin tetroxide over the temperature range from about 400°C to 1040°C, the melting point of stannous oxide. On the other hand, Platteeuw and Meyer[4] have recently reported that stannous oxide on heating in vacuo at 300°C and 550°C completely decomposed into tin and stannic oxide.

Owing to the results of the measurements on equilibria of $Sn—SnO_2—CO—CO_2$[8] and $Sn—SnO_2—H_2—H_2O$[9] the existence of β-stannous oxide and tritin tetroxide as stable compounds is improbable in the temperature range about 550°C to 850°C. But Fraenkel and Snipischski[2] deduced from an equilibrium measurement that some compound other than stannous oxide and stannic oxide existed above 900°C.

The thermodynamic data obtained by Veselovsky[10] indicate that stannous oxide (solid) is stable only within temperature range about 300° to 600°K. But recent calorimetric determination of the heat of formation of the tin oxides performed by Humphrey and O'Brien[11] indicates that stannous oxide (solid) is unstable over all temperature ranges.

In this work, a change of stannous oxide by heating, observed by X-ray diffraction methods, is reported and discussion is offered as to the existence of β-stannous oxide or tritin tetroxide and the decomposition of stannous oxide.

Experimental

Materials.—Stannous oxide was prepared by adding sodium hydroxide solution to a hydrochloric acid solution of stannous chloride until the solution became slightly alkaline and by boiling the resulting mixture until the precipitate turned black. The black stannous oxide precipitate was decanted until it became free from chloride; then it was dried at 110°C for eighteen hours. Stannic oxide was prepared by drying and calcining the white metastannic acid obtained by the reaction of concentrated nitric acid with metallic tin. X-ray diffraction patterns obtained from these two oxides were in agreement with the previous data, and no other impurities were observed.

Heating of stannous oxide, and tin-

1) M. Staumanis and C. Strek, *Z. anorg. u. allgem. Chem.*, **213**, 310 (1933).
2) W. Fraenkel and K. Snipischski, ibid., **125**, 235 (1922).
3) C. G. Fink and C. L. Mantel, *J. Phys. Chem.*, **32**, 103 (1928).
4) J. C. Platteeuw and G. Meyer, *Trans. Faraday Soc.*, **52**, 1066 (1956).
5) H. B. Weiser and W. O. Milligan, *J. Phys. Chem.*, **36**, 3039 (1932).
6) H. Spandau and E. G. Kohlmeyer, *Z. anorg. u. allgem. Chem.*, **254**, 65 (1947).
7) H. Spandau, *Z. angew. Chem.*, **A/60**, 73 (1948).
8) E. D. Eastman and R. Robinson, *J. Am. Chem. Soc.*, **50**, 1106 (1928).
9) P. H. Emmett and J. F. Shultz, ibid., **55**, 1390 (1933).
10) B. K. Veselovsky, *J. Appl. Chem.* (U. S. S. R.), **16**, No. 9/10, 397 (1943); *Chem. Abst.*, **38**, 6148 (1944).
11) G. L. Humphrey and C. J. O'Brien, *J. Am. Chem. Soc.*, **75**, 2805 (1953).

stannic oxide mixture.—One- to two-tenths grams of sample were sealed in Pyrex tube in vacuo at 100°C or in nitrogen gas at 1/3 atmosphere. Each tube was heated in an electric furnace for a given time, then quenched to room temperature and cut for opening. The contents were examined by X-ray diffraction method, using Cu$K\alpha$ ray in a Debye-Scherrer camera of 90 mm. diameter.

High temperature X-ray diffraction.—A high temperature camera (Rigaku-Denki Co.) was used to obtain the patterns at elevated temperature by using Cu$K\alpha$-ray. The samples were sealed in a Pyrex capillary in vacuo.

Results

The diffraction patterns obtained from the quenched samples are illustrated in Fig. 1, A—C, corresponding to No. 6—8 in Table I. In Table I, the results of analysis of patterns, which were obtained from the sample quenched after treatment at various temperatures (column 3) and durations (column 4), are listed. No other compounds than tin, stannous oxide and stannic oxide were observed. Results of heating in nitrogen agree with those in vacuo.

TABLE I
RESULTS OF HEATING OF SnO AND A MIXTURE OF Sn AND SnO_2

Sample No.	Initial Sample	Temperature °C	Time min.	Detected Substances SnO	Sn	SnO_2
1	SnO	550	3	−	##	##
2	〃	〃	10	−	##	##
3	〃	〃	75	−	##	##
4	〃	〃	180	−	##	##
5	Sn+SnO_2	〃	75	−	##	##
6	SnO	500	5	##	+	+
7	〃	〃	10	+	+	+
8	〃	〃	15	−	##	##
9	〃	450	60	+	##	##
10	〃	〃	120	−	##	##
11	〃	400	600	##	+	+
12	Sn+SnO_2	〃	〃	−	##	##

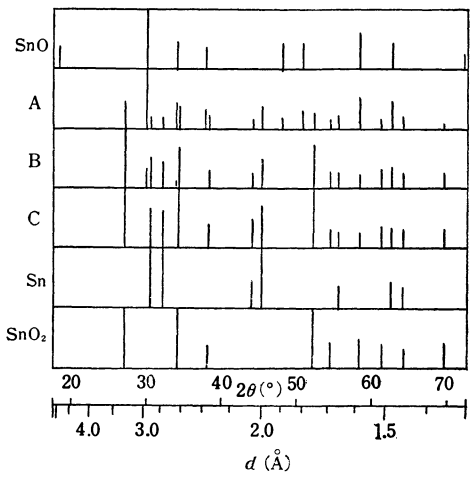

Fig. 1. X-ray powder diagrams of SnO heated at 500°C.

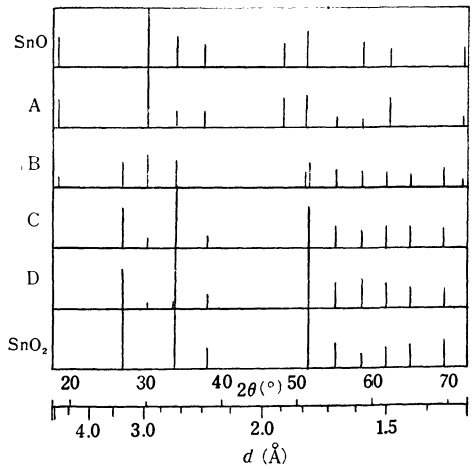

Fig. 2. X-ray powder diagrams of SnO heated at 445°C and 500°C, obtained by high temperature camera.

The patterns obtained by the high temperature camera are shown in Fig. 2. Fig. 2-D gives schematic pattern for thirty minutes of exposure at 500°C, where the material was ascertained only as stannic oxide. Fig. 2-A, -B and -C are patterns which were obtained step-by-step at 445°C. At each step forty minutes of exposure are needed. The pattern 2-A reveals the presence of monoxide and a small amount of dioxide; 2-B, monoxide and a comparable amount of dioxide; and 2-C, dioxide and a very small amount of monoxide, respectively.

Discussion

When stannous oxide is heated at 550°C in vacuo, the decomposition reaction,

$$2SnO \rightarrow Sn + SnO_2$$

is completed in a relatively short time. The reaction is also completed in the same manner at 500°C and 450°C, though the reaction time is prolonged. At 400°C, a certain small amount of stannous oxide still remains even after a considerably long time of heating. But reverse reaction started from tin and stannic oxide does not proceed at all. From these facts, it is deduced that the decomposition reaction may be completed even at 400°C, though the reaction velocity is very slow.

TABLE II

COMPARISON BETWEEN β-SnO* AND A MIXTURE OF Sn, SnO_2 AND SnO

β-SnO*		Sn		SnO_2		SnO		Corresponding
d	*I*	*d*	*I*	*d*	*I*	*d*	*I*	Substance
						(4.81	1)	
3.38	10	—	—	3.34	10	—	—	SnO_2
2.99	5	—	—	—	—	2.97	4	SnO
2.92	5	2.91	7	—	—	—	—	Sn
2.88	9	2.80	5	—	—	—	—	Sn ?
2.66	9	—	—	2.64	7	2.66	1	SnO_2
				(2.36	2)	(2.39	f)	
2.08	1	2.05	2	—	—	—	—	Sn
2.02	4	2.01	5	—	—	—	—	Sn
						(1.89	f)	
1.77	8	—	—	1.75	7	1.79	1	SnO_2
1.67	2	1.65	2	1.67	2	—	—	Sn & SnO_2
1.59	2	—	—	1.58	1	1.59	2	SnO_2 & SnO

* Obtained by Weiser and Milligan.

d: Spacing *I*: Intensity f: Faint

The patterns obtained by the high temperature X-ray diffraction camera show that the quenched samples sufficiently represent the high temperature state. In this temperature tin exists in liquid phase and hence gives no lines.

The conclusion is that, in the temperature range from 550°C to 400°C stannous oxide is thermodynamically unstable and decomposes into tin and stannic oxide.

As shown in Table II, the pattern of β-stannous oxide which was obtained by Weiser and Milligan is very similar to that of a mixture of tin, stannous oxide and stannic oxide except for minor disagreements. However, the pattern of stannous oxide reported by the same authors is found to be slightly inconsistent with the other authors' data. Further, Weiser and Milligan found the color of β-stannous oxide to be gray. This color is the same as that of the mixture of tin, stannous oxide and stannic oxide, but does not agree with the deep orange color of β-stannous oxide, which was prepared by two different methods by Partington and Moser[12]. It is presumed, therefore, that β-stannous oxide observed by Weiser and Milligan was not a new phase, but substantially a mixture of tin, stannous oxide and stannic oxide.

The existence of tritin tetroxide in equilibrium, which was deduced by Spandau at high temperatures, is rather open to question, since stannous oxide completely decomposes into tin and stannic oxide at high temperatures. Since patterns other than those of stannous oxide and stannic oxide were observed and no change in lattice-spacings was detected in the patterns obtained by a high temperature camera, it is clear that the coexistence of tin, stannous oxide and stannic oxide is not stable, and that they form neither a new phase nor a solid solution. The experiments by Spandau were carried out in a nitrogen-gas stream. But it is hardly probable that nitrogen has any influence on the decomposition, since the results of heating of stannous oxide in nitrogen agree with those in vacuo.

Department of Chemistry
Faculty of Science
Hokkaido University, Sapporo

12) J. R. Partington and W. Moser, *Nature*, **154**, 643 (1944).

Electronic States of p-Benzoquinone. III. Calculation of the Out-of-plane Vibrational Frequencies in the Ground Electronic State

By Tosinobu ANNO and Akira SADÔ*

(Received March 31, 1958)

In the first[1] and the second[2] part of this series the present authors, in collaboration with Matubara, have calculated the energy levels of *p*-benzoquinone using the semiempirical molecular orbital method proposed by Pariser and Parr[3], taking account of non-bonding electrons explicitly as well as π electrons. Experimental checking of the theoretical results requires the vibrational analysis of the electronic band spectrum of this molecule. To this end, the assignment of fundamental frequencies to modes of vibrations in the ground electronic state should be made at first.

Although the calculation of the fundamental frequencies using the force constants carried over from similar molecules would help those assignments using infrared and Raman data, the force constants to be carried over for *p*-benzoquinone are nearly unknown, since the normal coordinate treatments of quinones have not been performed yet.

In a recent paper[4] by one of the present authors, a method of obtaining some of the out-of-plane force constants in conjugated hydrocarbons from bond orders and of borrowing the remaining kinds of these constants from similar molecules was described. In the present paper the result of calculation of the non-planar frequencies of *p*-benzoquinone using this method will be reported.

Group-Theoretical Considerations

The molecular structure of *p*-benzoquinone has been studied by both the X-ray and electron-diffraction[6] experiments and it is known that this molecule belongs to the point group V_h. We take the axis connecting the two oxygen atoms as y axis and the molecular plane as xy plane. Then, the symmetry notations are the same as those given by Herzberg[7].

The fundamental vibrations of this molecule are distributed among symmetry species as follows; $6A_g+5B_{1g}+1B_{2g}+3B_{3g}+2A_u+3B_{1u}+5B_{2u}+5B_{3u}$. Vibrations in species B_{2g}, B_{3g}, A_u and B_{1u} are non-planar ones and the remaining vibrations are of planar modes.

Internal Coordinates and G Matrix

Notations for internal and symmetry coordinates are chosen to be as consistent as possible with those of benzene[8,9].

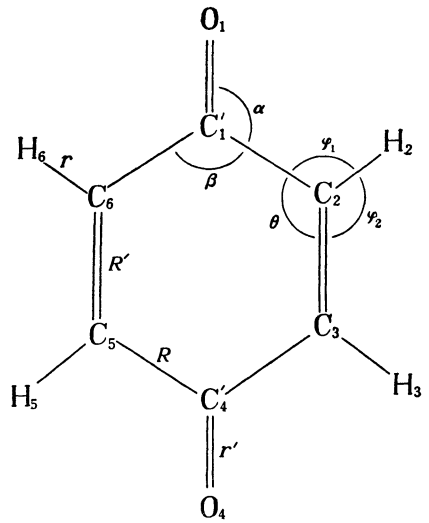

Fig. 1. Notations expressing bond angles and bond distances and the numbering of atoms for *p*-benzoquinone.

* Present address; Department of Chemistry, Faculty of Science, Kyushu University, Hakozaki, Fukuoka.

1) T. Anno, I. Matubara and A. Sadô, This Bulletin, **30**, 168 (1957).
2) T. Anno, A. Sadô and I. Matubara, *J. Chem. Phys.*, **26**, 967 (1957).
3) R. Pariser and R. G. Parr, ibid., **21**, 466, 767 (1953).
4) T. Anno, ibid., **28**, 944 (1958).
5) J. M. Robertson, *Proc. Roy. Soc.* (London), **A150**, 106 (1935).
6) S. M. Swingle, *J. Am. Chem. Soc.*, **76**, 1409 (1954).
7) G. Herzberg, "Infrared and Raman Spectra of Polyatomic Molecules", D. van Nostrand Co., New York (1945), p. 108.
8) F. A. Miller and B. L. Crawford, Jr., *J. Chem. Phys.*, **14**, 282 (1946).
9) Y. Kakiuti and T. Shimanouchi, ibid., **25**, 1252 (1956).

Thus, as shown in Fig. 1 the carbon atoms are numbered consecutively, and the oxygen and the hydrogen atoms are numbered altogether consecutively. The carbon atom to which an oxygen atom attaches is distinguished by being primed. Equilibrium internuclear distances are represented by: $C_1'O_1=r'$, $C_2H_2=r$, $C_1'C_2=R$, and $C_2C_3=R'$, as also shown in Fig. 1, together with the notations for bond angles. The internal coordinates used are chosen as follows: the perpendicular displacement of the ith hydrogen(oxygen) atom out of the plane defined by the three nearest carbon atoms is termed $r\gamma_i$ ($r'\gamma_i'$); the out-of-plane ring bendings are regarded as torsions around carbon-carbon bonds; carbon atoms 1, 2, and 3 define one plane and carbon atoms 2, 3, and 4 define another; these planes intersect along the C_2C_3 bond; the angle between them is designated δ_2', prime denoting that the angle refers to a nominal double bond; for the corresponding quantities referring to a "single bond" the prime is dropped.

Table I contains symmetry coordinates formed from internal coordinates described above. In benzene, symmetry coordinates corresponding to S_A, S_B, and S_C are redundant. In the case of *p*-benzoquinone, however, S_A and S_C are not redundant by themselves. Therefore, we retain them in the following calculation and a frequency of zero is found in each of the cases of species A_u and B_{3g}.

Following Wilson's[10] procedure we obtain the factorized **G** matrix whose elements are given in Table II. Although **G**-matrix elements given in Table II are expressed as generally as possible in conformity with V_h structure, we need the internuclear distances and bond angles in order to calculate the numerical values of these elements. The following values are used: $r=1.08$ Å, $r'=1.23$ Å, $R=1.461$ Å, $R'=1.349$ Å, $\alpha=\theta=122°$, and $\beta=116°$. These are the values determined by electron-diffraction experiment[6] except R, R', and r. The values of CC distances are those calculated from bond order rather than experimental values, because when we later estimate the frequencies in the excited electronic states, the CC length will also be obtained from bond order. The CH distance assumed is taken from benzene[11]. Moreover, the C_2H_2 bond, for example, is assumed to bisect the external angle between bonds $C_1'C_2$ and C_2C_3. Therefore, it follows $\varphi_1=\varphi_2=119°$. The values of bond orders used are those calculated by a semiempirical MO method taking CI into account. Just as in the case of the calculation of the energy levels[2] not only the singly-excited configurations but also the doubly-excited configurations were considered, although only the "more important configurations" were taken into the secular equation and the neglected configurations were considered by the second-order perturbation theory. Bond orders obtained are:

$$p_{C_1'C_2}=0.226 \text{ and } p_{C_2C_3}=0.945.$$

Potential Function

Notations for valence force constants are also chosen as consistently as possible with those for benzene[8,9]. Fig. 2 shows **F** matrix in terms of internal coordinates.

	$r'\gamma_1'$	$r\gamma_2$	$r\gamma_3$	$r'\gamma_4'$	$r\gamma_5$	$r\gamma_6$	$R\delta_1$	$R'\delta_2'$	$R\delta_3$	$R\delta_4$	$R'\delta_5'$	$R\delta_6$
$r'\gamma_1'$	A''	a_o'	a_m'	a_p''	a_m'	a_o'	c_o'	c_m''	c_p'	$-c_p'$	$-c_m''$	$-c_o'$
$r\gamma_2$		A	a_o	a_m'	a_p	a_m	$-c_o$	$\bar{c}_o$	$c_m{}^d$	c_p	$-\bar{c}_p$	$-c_m{}^s$
$r\gamma_3$			A	a_o'	a_m	a_p	$-c_m{}^d$	$-\bar{c}_o$	c_o	$c_m{}^s$	$\bar{c}_p$	$-c_p$
$r'\gamma_4'$				A''	a_o'	a_m'	$-c_p'$	$-c_m''$	$-c_o'$	c_o'	c_m''	c_p'
$r\gamma_5$					A	a_o	c_p	$-\bar{c}_p$	$-c_m{}^s$	$-c_o$	$\bar{c}_o$	$c_m{}^d$
rr_6						A	$c_m{}^s$	$\bar{c}_p$	$-c_p$	$-c_m{}^d$	$-\bar{c}_o$	c_o
$R\delta_1$							B	b_o'	b_m	b_p	b_m'	b_o
$R'\delta_2'$		(Symmetric)						B''	b_o'	b_m'	b_p''	b_m'
$R\delta_3$									B	b_o	b_m'	b_p
$R\delta_4$										B	b_o'	b_m
$R'\delta_5'$											B''	b_o'
$R\delta_6$												B

Fig. 2. **F** matrix in terms of internal coordinate.

10) E. B. Wilson, Jr., ibid., **7**, 1047 (1939); **9**, 76 (1941).

11) P. W. Allen and L. E. Sutton, *Acta Cryst.*, **3**, 46 (1950).

TABLE
SYMMETRY COORDINATES IN TERMS

S_{16a}							
S_{17a}			$-1/2$	$1/2$		$-1/2$	$1/2$
S_A							
S_{11}		$1/\sqrt{6}$	$1/\sqrt{6}$	$1/\sqrt{6}$	$1/\sqrt{6}$	$1/\sqrt{6}$	$1/\sqrt{6}$
S_{16b}							
S_{17b}	=	$-2/\sqrt{12}$	$1/\sqrt{12}$	$1/\sqrt{12}$	$-2/\sqrt{12}$	$1/\sqrt{12}$	$1/\sqrt{12}$
S_{10a}			$1/2$	$1/2$		$-1/2$	$-1/2$
S_B							
S_4							
S_5		$1/\sqrt{6}$	$-1/\sqrt{6}$	$1/\sqrt{6}$	$-1/\sqrt{6}$	$1/\sqrt{6}$	$-1/\sqrt{6}$
S_{10b}		$-2/\sqrt{12}$	$-1/\sqrt{12}$	$1/\sqrt{12}$	$2/\sqrt{12}$	$1/\sqrt{12}$	$-1/\sqrt{12}$
S_G							

TABLE II

G-MATRIX ELEMENTS FOR THE OUT-OF-PLANE VIBRATIONS OF *p*-BENZOQUINONE

(Species A_u)

$G_{16a,16a}=(4\mu_C/3)(D+E-2F)^2$

$G_{17a,17a}=\mu_H+\mu_C(1+B+2C)^2$

$G_{A,A}=(2\mu_C/3)(D-2E-2F)^2$

$G_{16a,17a}=(2\sqrt{3}\,\mu_C/3)(D+E-2F)(1+B+2C)$

$G_{16a,A}=(2\sqrt{2}\,\mu_C/3)(D+E-2F)(D-2E-2F)$

$G_{17a,A}=(\sqrt{6}\,\mu_C/3)(1+B+2C)(D-2E-2F)$

(Species B_{1u})

$G_{11\ 11}=(\mu_O/3)+(2\mu_H/3)+(\mu_C/3)[(1+2A-2B)^2+2(1+B-A)^2]$

$G_{16b,16b}=3\mu_C(F+G-H)^2$

$G_{17b,17b}=(2\mu_O/3)+(\mu_H/3)+\mu_C(1+2A+B)^2$

$G_{11,16b}=(\sqrt{6}\,\mu_C)(F+G-H)(A-B)$

$G_{11,17b}=(\sqrt{2}/3)(\mu_H-\mu)_O-(\sqrt{2}\,\mu_C)(1+2A+B)(A-B)$

$G_{16b,17b}=-(\sqrt{3}\,\mu_C)(1+2A+B)(F+G-H)$

(Species B_{2g})

$G_{10a,10a}=\mu_H+\mu_C(1+B)^2$

$G_{B,B}=\mu_C(F+G+H)^2=0$

$G_{10a,B}=-\mu_C(1+B)(F+G+H)=0$

(Species B_{3g})

$G_{4,4}=(2\mu_C/3)[2(D-F-G+H)^2+(-D-2E+3F+G-H)^2]$

$G_{5,5}=(\mu_O/3)+(2\mu_H/3)+(\mu_C/3)[(1+2A+2B)^2+2(1+A+B+2C)^2]$

$G_{10b,10b}=(2\mu_O/3)+(\mu_H/3)+(\mu_C/3)[2(1+2A-B)^2+(1-2A+B+2C)^2]$

$G_{G,G}=(\mu_C/3)[2(H-G-F-2D)^2+(2D-2E-3F+G-H)^2]$

$G_{4,5}=(2\mu_C/3)[(D-F-G+H)(-1-2A-2B)+(-D-2E+3F+G-H)(1+A+B+2C)]$

$G_{4,10b}=(\sqrt{2}\,\mu_C/3)[2(D-F-G+H)(1+2A-B)+(-D-2E+G+3F-H)(1-2A+B+2C)]$

$G_{4,G}=(\sqrt{2}\,\mu_C/3)[2(D-F-G+H)(-2D-F-G+H)$
$+(-D-2E+3F+G-H)(2D-2E-3F+G-H)]$

$G_{5,10b}=(\sqrt{2}/3)(\mu_H-\mu_O)+(\sqrt{2}\,\mu_C/3)[(1-2A-2B)(1+2A-B)$
$+(1+A+B+2C)(1-2A+B+2C)]$

$G_{5,G}=(\sqrt{2}\,\mu_C/3)[(1+2A+2B)(2D+F+G-H)+(1+A+B+2C)(2D-2E-3F+G-H)]$

$G_{10b,G}=(\mu_C/3)[2(1+2A-B)(-2D-F-G+H)+(1-2A+B+2C)(2D-2E-3F+G-H)]$

$A=(r'\sin\alpha/R\sin\beta)$ $B=(r\sin\varphi_2/R\sin\theta)$ $C=(r\sin\varphi_1/R'\sin\theta)$ $D=R'/R\sin\theta$
$E=R/R'\sin\theta$ $F=\cos\theta/\sin\theta$ $G=\cos\beta/\sin\beta$ $H=1/\sin\beta$

μ_H, μ_C and μ_O are the reciprocal masses of the hydrogen, the carbon and the oxygen atom, respectively.

I

OF INTERNAL COORDINATES

$-1/\sqrt{12}$	$2/\sqrt{12}$	$-1/\sqrt{12}$	$-1/\sqrt{12}$	$2/\sqrt{12}$	$-1/\sqrt{12}$	$r'\gamma_1'$
						$r\gamma_2$
$1/\sqrt{6}$	$1/\sqrt{6}$	$1/\sqrt{6}$	$1/\sqrt{6}$	$1/\sqrt{6}$	$1/\sqrt{6}$	$r\gamma_3$
						$r'\gamma_4'$
$1/2$		$-1/2$	$1/2$		$-1/2$	$r\gamma_5$
						$r\gamma_6$
						$R\delta_1$
$1/2$		$-1/2$	$-1/2$		$1/2$	$R'\delta_2'$
$1/\sqrt{6}$	$-1/\sqrt{6}$	$1/\sqrt{6}$	$-1/\sqrt{6}$	$1/\sqrt{6}$	$-1/\sqrt{6}$	$R\delta_3$
						$R\delta_4$
						$R'\delta_5'$
$1/\sqrt{12}$	$2/\sqrt{12}$	$1/\sqrt{12}$	$-1/\sqrt{12}$	$-2/\sqrt{12}$	$-1/\sqrt{12}$	$R\delta_6$

TABLE III

FACTORIZED **F**-MATRIX ELEMENTS

(Species A_u)

$F_{16a,16a}=(1/3)(B+2B''-4b_o'+b_o-4b_m'+b_m+2b_p''+b_p)$

$F_{17a,17a}=A-a_o-a_m+a_p$

$F_{A,A}=(1/3)[2B+B''+2(b_o+2b_o')+2(b_m+2b_m')+2b_p+b_p'']$

$F_{16a,17a}=(1/\sqrt{3})(-c_o-2\bar{c}_o+c_m{}^d-c_m{}^s+c_p+2\bar{c}_p)$

$F_{16a,A}=(\sqrt{2}/3)(B''-B+b_o'-b_o+b_m'-b_m+b_p''-b_p)$

$F_{17a,A}=\sqrt{2/3}\,(c_o-\bar{c}_o-c_m{}^d+c_m{}^s-c_p+\bar{c}_p)$

(Species B_{1u})

$F_{11,11}=(1/3)[A''+2A+2(2a_o'+a_o)+2(2a_m'+a_m)+a_p''+2a_p]$

$F_{16b,16b}=B-b_o-b_m+b_p$

$F_{17b,17b}=(1/3)(2A''+A+a_o-4a_o'+a_m-4a_m'+a_p+2a_p'')$

$F_{11,16b}=\sqrt{2/3}\,(c_0'-c_o+c_m{}^s-c_m{}^d+c_p-c_p')$

$F_{11,17b}=(\sqrt{2}/3)(A-A''+a_o-a_o'+a_m-a_m'+a_p-a_p'')$

$F_{16b\ 17b}=(1/\sqrt{3})(-2c_o'-c_o-c_m{}^d+c_m{}^s+2c_p'+c_p)$

(Species B_{2g})

$F_{10a,10a}=A+a_o-a_m-a_p$

(Species B_{3g})

$F_{4,4}=(1/3)[2B+B''-2(2b_o'+b_o)+2(2b_m'+b_m)-(2b_p+b_p'')]$

$F_{5,5}=(1/3)[A''+2A-2(2a_o'+a_o)+2(2a_m'+a_m)-(a_p''+2a_p)]$

$F_{10b,10b}=(1/3)(2A''+A+4a_o'-a_o-4a_m'+a_m-2a_p''-a_p)$

$F_{C,C}=(1/3)(B+2B''+4b_o'-b_o-4b_m'+b_m-b_p-2b_p'')$

$F_{4,5}=(2/3)[(c_o'+c_o+\bar{c}_o)-(c_m''+c_m{}^d+c_m{}^s)+(c_p'+c_p+\bar{c}_p)]$

$F_{4,10b}=(\sqrt{2}/3)[(c_o+\bar{c}_o-2c_o')-(c_m{}^d+c_m{}^s-2c_m'')+(c_p+\bar{c}_p-2c_p')]$

$F_{4,C}=(\sqrt{2}/3)(B-B''+b_o'-b_o-b_m'+b_m+b_p''-b_p)$

$F_{5,10b}=(\sqrt{2}/3)(A-A''+a_o'-a_o-a_m'+a_m+a_p''-a_p)$

$F_{5,C}=(\sqrt{2}/3)[(c_o'+c_o-2\bar{c}_o)-(c_m{}^d+c_m{}^s-2c_m'')+(c_p'+c_p-2\bar{c}_p)]$

$F_{10b,C}=(1/3)[(-2c_o'-2\bar{c}_o+c_o)-(c_m{}^d+c_m{}^s+4c_m'')-(2c_p'-c_p+2\bar{c}_p)]$

The transformation from internal to symmetry coordinates yields the factorized **F** matrix whose elements are shown in Table III. Following the work on benzene by Kakiuti and Shimanouchi[9] only the interaction constants referring to such internal coordinates that are "ortho" with each other are considered in the actual calculation. Moreover, interaction constants referring to the wagging motion of C=O bonds are also neglected because of difficulties in their estimation. Descriptions

will be made of the retained force constants in succession.

Force constants for the torsions around CC bonds are obtained using the relation proposed in a previous paper[4]. Bond orders used were explained above. Overlap integrals used correspond to the CC distances obtained from bond orders. Using these torsional constants interaction constants c_o and $\bar{c}_o$ are obtained using the method which has also been described in a previous paper[4]. Potential constants A, a_o, b_o and b_o' are taken from benzene.

The remaining constant A'' is determined in such a way that the calculated value of the lowest B_{3g} fundamental coincides with the smallest Raman shift of 243 cm^{-1} which can be assigned to the B_{3g} mode of lowest frequency, as will be discussed in a subsequent paper[12]. A summary of the value of force constants is given in Table IV.

TABLE IV

VALUES OF FORCE CONSTANTS

(in 10^5 dyn./cm.)

$A''=$ 0.201	$c_o=+0.038$
$A=$ 0.402	$\bar{c}_o=+0.205$
$a_o=-0.073$	$c_o'=$ 0
$a_o'=$ 0	$B=$ 0.048
$b_o'=-0.012$	$B''=$ 0.287
$b_o=-0.011$	

Calculation of the Frequencies and Discussions

Now that all the necessary values of potential constants are determined, it is possible to calculate the frequencies. The calculated values are shown in Table V.

TABLE V

CALCULATED AND OBSERVED FREQUENCIES OF OUT-OF-PLANE VIBRATIONS OF *p*-BENZOQUINONE (cm^{-1})

mode	A_u		B_{1u}		B_{2g}		B_{3g}	
	calc.	obs.	calc.	obs.	calc.	obs.	calc.	obs.
C=O bending			533	—			(243)	243
C-H bending	962	—	871	876	839	794	959	932
ring bending	403	533	98	99			790	—

In this table experimental frequencies are also given for comparison. All the experimental frequencies, except those belonging to species A_u, are obtained from the analysis of the infrared and Raman data as will be discussed in part IV[12] of this series. Of the two vibrations belonging to species A_u experimental frequency is available only for the lower one (hereafter denoted as $\nu_2(A_u)$) and this frequency is obtained from the vibrational analysis of the electronic spectrum of *p*-benzoquinone vapor.

The agreement between calculated and observed frequencies is fairly good except for $\nu_2(A_u)$. Since the potential constants (both the diagonal and the interaction constants) referring to the wagging of C=O bond do not appear in the **F** matrix for species A_u, the neglect of or the inadequate values of these constants are not the reasons why the calculated $\nu_2(A_u)$ does not agree with the experiment.

In the vibrational analysis of the electronic spectrum lying around 4500 Å to be discussed in a separate article, two bands assigned to vibronic transitions in which $\nu_2(A_u)$ is superimposed by one quantum on the forbidden 0, 0 transition in the ground and the excited state, respectively, are found 1066 cm^{-1} apart from each other. This separation should represent the sum of ground- and excited-state value of $\nu_2(A_u)$. On the other hand it is found in a calculation of the non-planar frequencies for the excited state using the scheme similar to that used for the ground state that $\nu_2(A_u)$ is almost completely insensitive to the electronic excitation concerned. Therefore, one-half of the above-mentioned separation may be considered to represent the value of $\nu_2(A_u)$ in the ground state. Hence, we take 533 cm^{-1} as the "experimental" value of $\nu_2(A_u)$ in the ground state. It is to be noted that the bond angles assumed for the calculation of upper-state frequencies are the same as those used for the ground state, although the change of bond length and torsional force constants are taken into consideration from the bond order. As can been seen in Eq. 20 of reference 4, c_o and $\bar{c}_o$ depend on the bond angles which may be changed by the electronic excitation. Therefore, the reason for the disagreement between calculated and "experimental" values of $\nu_2(A_u)$ should be searched for not only in the calculated but also on the "experimental" side. This point will be discussed more fully in a later paper.

The authors express their sincere thanks to Professor S. Imanishi and to Dr. Y.

12) T. Anno and A. Sadô, This Bulletin, **31**, 734 (1958).

TABLE VI
L MATRIX[a)]

A_u	$\lambda_1(\nu=962\ cm^{-1})$	$\lambda_2(\nu=403\ cm^{-1})$	$\lambda_3(\nu=0\ cm^{-1})$
S_{16a}	1.169 417	2.717 244	0
S_{17a}	3.210 802	1.251 510	0
S_A	−0.049 317	−0.114 592	0

B_{1u}	$\lambda_1(\nu=871\ cm^{-1})$	$\lambda_2(\nu=533\ cm^{-1})$	$\lambda_3(\nu=98\ cm^{-1})$
S_{11}	1.661 739	1.360 246	−0.182 856
S_{16b}	1.602 491	−2.110 660	−0.659 572
S_{17b}	2.543 457	−1.186 288	0.144 455

B_{2g}	$\lambda(\nu=839\ cm^{-1})$
S_{10a}	2.753 927

B_{3g}	$\lambda_1(\nu=959\ cm^{-1})$	$\lambda_2(\nu=790\ cm^{-1})$	$\lambda_3(\nu=243\ cm^{-1})$	$\lambda_4(\nu=0\ cm^{-1})$
S_4	−1.879 766	4.447 465	−0.998 018	0
S_5	2.914 687	−2.090 424	−0.188 288	0
S_{10b}	1.570 902	0.817 234	0.893 017	0
S_G	−0.019 107	0.045 207	−0.010 144	0

a) Numerical values in these tables are based on the length in 10^{-8} cm. and the mass in 10^{-23} gram.

Kanda for their encouragement throughout this work and their kind suggestions in preparing the manuscript.

Appendix: L Matrix

Following Wilson[10)] **L** matrix is defined as

$$\mathbf{S} = \mathbf{LQ}$$

where **S** and **Q** are the column matrices formed by the internal (or internal symmetry) and the normal coordinates, respectively. Normalization condition is

$$\mathbf{LL}' = \mathbf{G}$$

in which prime denotes the transpose of the matrix.

Since **L** matrix elements may be used to estimate the change of the frequencies owing to some small changes of the various force constants by the perturbation method[13)] we have calculated normalized **L** matrix which is shown in Table VI. Numerical values in this table are based on the length in Å and the mass in 10^{-23} gram.

Chemical Laboratory, General Education Department, Kyushu University, Ootsubo-machi, Fukuoka

13) T. Anno, A. Sadô and I. Matubara, This Bulletin, **29**, 703 (1956).

Electronic States of p-Benzoquinone. IV. Infrared Spectrum and Assignment of Vibrational Frequencies in the Ground Electronic State

By Tosinobu ANNO and Akira SADÔ*

(Received March 31, 1958)

The infrared absorption band due to C=O stretching vibration of the *p*-benzoquinone molecule has been extensively studied by Josien, Fuson et al.[1] together with those of other quinones. Rosenkrantz[2] measured the infrared spectrum of this substance in molten state in 12~2 μ region as one of the basic researches of the analyses of vitamine E and related compounds. Stammreich and Forneris[3] reported the Raman spectrum of *p*-benzoquinone. In spite of these spectroscopic works, however, the assignment of the fundamental frequencies to the modes of vibrations have not yet been reported.

In the present paper the infrared-spectral data of *p*-benzoquinone in carbon disulfide and carbon tetrachloride solutions in rock salt region will be presented and the vibrational analysis will be given utilizing the Raman data of Stammreich and Forneris[3] and the calculated values of the out-of-plane vibrational frequencies reported in a previous paper[4].

Experimental

The sample of *p*-benzoquinone was obtained from a commercial product recrystallizing it several times from ligroin. Solvents used were purified in the usual manner. The infrared spectrum was recorded with Perkin-Elmer model 21 spectrophotometer. The wavelength was calibrated by the spectrum of polystyrene. Wavelengths and relative intensities of observed absorption bands are given in Table I together with Rosenkrantz' data and interpretations discussed below.

Results and Discussion

Normal Coordinate Treatment of Totally Symmetrical Skeleton Vibrations.—In a later part of this series[5], in which the vibrational analysis of the electronic spectrum will be made, the calculation of the frequencies of the totally symmetrical skeleton vibrations in excited electronic state will be reported. The reason for restricting ourselves to totally symmetrical vibrations is that these are the only vibrations which form the vibrational structure of the electronic spectrum prominently. To compare with this later treatment, ground-state frequencies of the totally symmetrical skeleton vibrations were calculated as described in this subsection. This treatment is expected to help to some extent the vibrational assignment in the ground electronic state.

In this calculation the method proposed by the present authors[6] based on the simple valence force field approximation was used. The stretching force constants of the CC bonds were determined in the same way as in a previous article[6] from the bond order described in another paper[4] assuming the hybridization of carbon σ atomic orbital to be sp^2.

As for CO bond, the force constant was determined from the experimental value of CO distance (r_{CO}) 1.23Å[7] in the following manner since the order-length relation is less well established. In formaldehyde r_{CO}=1.21Å[8] and it is determined that the CO stretching force constant (k_{CO}) is equal to 12.286×10^5 dyn./cm. from the CO stretching frequency of this molecule 1744 cm^{-1} [9] treating the CH_2 group in this

* Present address: Department of Chemistry, Faculty of Science, Kyushu University, Hakozaki, Fukuoka.

1) M.-L. Josien, N. Fuson, J.-M. Lebas and T. M. Gregory, *J. Chem. Phys.*, **21**, 331 (1953); M.-L. Josien and N. Fuson. *Bull. soc. chim. France*, **19**, 389 (1952); *Compt.* rend., **234**, 1680 (1952); **236**, 1879 (1953); *J. Am. Chem. Soc.*, **73**, 478 (1951); N. Fuson, M.-L. Josien and E. M. Shelton, ibid. **76**, 2526 (1954); M.-L. Josien and J. Deschamps, *J. chim. phys.*, **52**, 213 (1955); **53**, 885 (1956); *Compt. rend.*, **242**, 3067 (1956); A. Hadni, J. Deschamps and M.-L. Josien, ibid. **242**, 1014 (1956).

2) H. Rosenkrantz, *J. Biol. Chem.*, **173**, 439 (1948).

3) H. Stammreich and R. Forneris, *Z. Naturforsch.*, **7a**, 756 (1952).

4) Part III of this series. T. Anno and A. Sadô, This Bulletin, **31**, 728 (1958).

5) Unpublished.

6) T. Anno, A. Sadô and I. Matubara, ibid. **29**, 703 (1956).

7) S. M. Swingle, *J. Am. Chem. Soc.*, **76**, 1409 (1954).

8) R. B. Lawrence and M. W. P. Strandberg, *Phys. Revs.*, **83**, 363 (1951).

9) G. Herzberg, "Infrared and Raman Spectra of Polyatomic Molecules", D. Van Nostrand Co., Inc., New York (1945), p. 300.

TABLE I

ABSORPTION BANDS OF *p*-BENZOQUINONE IN THE INFRARED REGION TOGETHER WITH INTERPRETATION (cm^{-1})

CS_2 solution	CCl_4 solution	Crystalline melt[a]	Interpretation
3322 mw[b]	3333 mw		$1667+1667=3334$ (B_{2u})
3268 mw	3279 mw		$3049+243=3292$ (B_{1u})
3049 w	3049 w	3058 s	$b_{2u}+b_{3u}$ fundamentals
2681 vw			
2577 vw			$876+1688=2564$ (B_{1u})
2445 vw			$1298+1149=2447$ (B_{2u})
1968 w	1976 w	2008 vw	
1869 w	1880 w	1908 vw	$1064+794=1858$ (B_{1u})
1764 m	1767 m	1761 vw	$99+1667=1766$ (B_{1u})
1715 ms	1721 ms		b_{2u} fundamental
1667 vs	1675 vs		$1064+610=1674$ (B_{2u})
1656 vs	1664 vs	1664 s	b_{2u} fundamental
	1597 ms	1595 s	$1064+540=1604$ (B_{2u})
1355 m	1357 m		b_{3u} fundamental
1323 m	1323 m	1337 s	$876+444=1320$ (B_{1u})
1297 vs	1300 vs	1302 vs	b_{2u} fundamental
1174 vw	1171 w		$730+444=1174$ (B_{2u})
1139 w	1139 w	1135 w	$370+770=1140$ (B_{3u})
1116 vw	1119 w		$876+243=1119$ (B_{2u})
1063 vs, b	1065 vs	1079 m	b_{3u} fundamental
983 mw		1001 w	$370+610=980$ (B_{2u}) / $730+243=973$ (B_{1u})
943 s	945 s	949 s	b_{3u} fundamental
876 vs	883 vs	909 m	b_{1u} fundamental
730 mw, b			b_{2u} fundamental

a) Estimated from absorption curve given in Ref. 2.
b) Abbreviations denoting relative intensities are as follows: vs=very strong, s=strong, ms=medium strong, m=medium, mw=medium weak, w=weak, vw=very weak, b=broad.

molecule as a mass point. Since in Badger's relation[10]

$$r_{CO}=(C/k_{CO})^{1/3}+d_{CO},$$

C is considered to be a universal constant and $C^{1.3}=1.230$[6,10], d_{CO} can be determined from the r_{CO} and k_{CO} values for formaldehyde described above. Then it follows that $d_{CO}=0.677$ Å, which is in good agreement to the value given by Badger[10a]. From the d_{CO} value thus obtained and the experimental value of r_{CO} (1.23 Å) k_{CO} for *p*-benzoquinone is calculated to be 11.004×10^5 dyn./cm. As will be discussed later, it seems to be most appropriate to assign the Raman line reported as 444cm^{-1} to the ring-defomation vibration belonging to a_g. This frequency was used to evaluate the ring-deformation force constant. From these values of force constants the totally symmetrical vibrational frequencies shown in Table II are obtained.

10) (a) R. M. Badger, *J. Chem. Phys.*, **2**, 128 (1934). (b) R. M. Badger, ibid., **3**, 710 (1935).

TABLE II

CALCULATED FREQUENCIES OF TOTALLY SYMMETRICAL SKELETON VIBRATIONS OF *p*-BENZOQUINONE (cm^{-1})

(444)[a]
782
1596
1900

a) The value in parentheses is used to calculate the ring deformation force constant.

Assignment of Fundamental Frequencies.—In this subsection the assignment of the fundamental frequencies will be discussed using the Raman and infrared spectral data as well as the calculated values of frequencies. Group-theoretical considerations for the normal vibrations of *p*-benzoquinone were briefly given in a previous paper[4] and will not be repeated here. As to the planar vibrations the calculation of the frequencies is made only for the totally symmetrical skeleton vibrations, so the comparison with the

TABLE III

COMPARISON OF FUNDAMENTAL FREQUENCIES OF IN-PLANE MODES OF VIBRATION IN MOLECULES OF TYPE X-⬡-X[a]

(Frequencies are given in the unit of cm^{-1})

Modes	Species a_g			Species b_{1g}			Species b_{2u}			Species b_{3u}		
	X=D[b]	F[c]	O	D[b]	F[c]	O	D[b]	F[c]	O	D[b]	F[c]	O
CH stretching	3050(ν_{7a})	3048	3058	3042(ν_{7b})	3080	3058	3060(ν_{13})	3028	3049	3079(ν_{20b})	3088	3049
CX stretching	2280(ν_2)	1245	1667				2275(ν_{20a})	1183	1667			
CC stretching	1587(ν_{8a})	1617	1688	1569(ν_{8b})	1285	610	1469(ν_{19a})	1511	1715	1603(ν_3)	1437	943
CC breathing	978(ν_1)	859	770				992(ν_{12})	737	730	1413(ν_4)	1212	1063
CX bending				909(ν_{9b})	635	[~400]				814(ν_{18b})	350	370
CH bending	1173(ν_{9a})	840	1149	1309(ν_3)	1142	1360	1033(ν_{18a})	1012	1297	1106(ν_{15})	1085	1355
ring bending	597(ν_{6a})	451	444	601(ν_{6b})	507	540						

a) X=D, F and O for *p*-dideuterobenzene, *p*-difluorobenzene and *p*-benzoquinone, respectively.
b) Frequencies taken from Garforth, Ingold and Poole (*J. Chem. Soc.* **1948**, 406) are followed by Wilson's numbering scheme (*Phys. Revs.*, **45**, 706 (1934)).
c) E. E. Ferguson, R. L. Hudson, J. R. Nielsen and D. C. Smith, *J. Chem. Phys.*, **21**, 1457 (1953).

spectral data of similar molecules may be helpful. The data used for comparison are those of *p*-dideuterobenzene[11] and *p*-difluorobenzene[12]. These are listed in Table III together with the assignment to the mode of vibrations.

Raman-active Frequencies.—*Species* a_g. —Although of the Raman-active frequencies those belonging to species a_g give polarized Raman lines, the depolarization factors of the Raman lines of *p*-benzoquinone have not been studied yet. However, it is known that the totally symmetrical vibrations produce, in general, stronger Raman lines in comparison with the other types of vibrations. It will be natural to assign the Raman lines at 3058 cm^{-1} and 1667 cm^{-1} to CH and CO stretching vibrations belonging to a_g, respectively, from the intensities and the magnitudes of so-called group frequencies[13]. The ring bending vibration belonging to a_g in this molecule corresponds to 606 cm^{-1} benzene value. As can be seen in Table III the corresponding frequency in *p*-benzoquinone should be sought around 450 cm^{-1}. It is reporteted that the Raman line at 444 cm^{-1} is a relatively stronger one in its neighborhood[3]. Moreover, in the normal-coordinate treatment of totally symmetrical skeleton vibrational frequencies described above a fairly large change of the ring deformation force constant results, if we change the value of the frequency to be inserted for the determination of this constant a little in the neighborhood of 444 cm^{-1}. These facts suggest that 444 cm^{-1} may be assigned to the a_g ring-bending vibration. As described previously if the ring-bending force constant is determined from this frequency, the calculated values of totally symmetrical skeleton vibrational frequencies shown in Table II are obtained. Of these values the calculated value of 1900 cm^{-1} which may correspond to the experimental value of 1667 cm^{-1} agree with the experiment only poorly. This may be due either to the experimental error of CO bond length or to the fact that the bond length-force constant relation has not been established well. Moreover, from the calculation of **L**-matrix elements[14] it can be shown that this frequency is fairly sensitive to the interaction constants, so use of valence-force field approximation may not be adequate for the calculation of this frequency. On the other hand, since the order-length and the length-force constant relations are established fairly well for CC bonds, it is expected that the agreement between the calculated values and the experimental ones is fairly good for CC breathing and stretching vibrations. Therefore, 770 and 1688 cm^{-1} Raman lines may be assigned to CC breathing and stretching vibrations belonging to a_g from comparison with the calculated values. The remaining vibration belonging to this species is an in-plane bending vibration of the hydrogen atom and is expected to

11) F. M. Garforth, C. K. Ingold and H. G. Poole, *J. Chem. Soc.*, **1948**, 406.
12) E. E. Ferguson, R. L. Hudson, J. R. Nielsen and D. C. Smith, *J. Chem. Phys.*, **21**, 1457 (1953).
13) L. J. Bellamy, "The Infrared Spectra of Complex Molecules", Methuen and Co., Ltd., London (1954).
14) E. B. Wilson, Jr., *J. Chem. Phys.*, **7**, 1047 (1939); **9**, 76 (1941). See also the last section of Ref. 6.

TABLE IV

FUNDAMENTAL FREQUENCIES OF *p*-BENZOQUINONE (GROUND ELECTRONIC STATE) (cm^{-1})[a, b]

	a_g	b_{1g}	b_{2g}	b_{3g}	a_u	b_{1u}	b_{2u}	b_{3u}
C—H stretching	3058	3058					3049	3049
C=O stretching	1667						1667	
C—C stretching	1688	610					1715	944
C—C breathing	770						730	1064
C=O bending		[~400][c]		243 (—)		—(533)		370
C—H bending	1149	1360	794(839)	932(959)	—(962)	876(871)	1298	1356
ring bending	444	540		—(790)	533(403)	99 (98)		

a) Calculated values of non-planar vibrational frequencies are closed in parentheses.
b) Experimental values with underlining are obtained from combination bands or electronic spectral data (see text).
c) Estimated.

appear in the region of 1100~1300 cm^{-1}. From its intensity the Raman line at 1149 cm^{-1} may be assigned to a_g. Therefore it is natural to assign this frequency to the CH in-plane bending vibration belonging to a_g.

Species b_{2g} and b_{3g}.—Before discussing the Raman-active in-plane mode other than those belonging to species a_g the Raman-active out-of-plane species b_{2g} and b_{3g} will be discussed.

Of the C=O out-of-plane bending vibrations the one which is symmetric with respect to inversion belongs to b_{3g}. Although the out-of-plane deviations of the oxygen atom from the molecular plane decreases the overlap of the σ AO of the oxygen atom with the σ AO of the carbon atom to which the oxygen atom in question is attached, the increase of the potential energy thus results will be partially compensated by the increase in the overlap of π AO of the oxygen atom with σ AO of the carbon atom. Compensation of such a kind in the potential energy is not expected in the case of C=O in-plane bending mode. Therefore it is expected that C=O out-of-plane bending frequency is rather low and lower than that of C=O in-plane bending. The Raman line reported at 243 cm^{-1} may represent this vibration. This is the Raman line of lowest frequency reported by Stammreich and Forneris[3] and the Raman line of lowest frequency is assigned to species b_{3g} (in our notation) also in the case of *p*-difluorobenzene[12].

As described in a previous paper[4] if 243 cm^{-1} is used as the b_{3g} C=O out-of-plane bending vibrational frequency in order to determine the force constant of C=O out-of-plane bending motion, the other nonplanar vibrational frequencies of *p*-benzoquinone shown in parentheses in Table IV are obtained. From the comparison with these calculated values Raman lines at 794 and 932 cm^{-1} are assigned to b_{2g} and b_{3g} fundamentals, respectively. The remaining calculated frequency belonging to species b_{3g} is 790 cm^{-1} and has no corresponding Raman line.

Species b_{1g}.—One of the five b_{1g} fundamentals is a hydrogen stretching mode which is assumed to overlap the Raman line at 3058 cm^{-1} assigned to a_g. Raman lines at 540, 610 and 1360 cm^{-1} which have been left unassigned may all be assigned to the b_{1g} fundamentals. The last frequency may be assigned to an in-plane hydrogen bending vibration with considerable certainty, while the other two may be caused by carbon vibrations. It is true that one of the C=O in-plane bending modes is contained in this species and 540 or 610 cm^{-1} Raman line might be assigned to this vibration. However, the C=O in-plane bending frequency belonging to species b_{1g} is expected to lie around 400 cm^{-1} from comparison with the data of *p*-difluorobenzene (see Table III) and with the frequency of another C=O in-plane bending vibration belonging to species b_{3u} of *p*-benzoquinone. Therefore we believe that none of the three Raman frequencies mentioned above correspond to this vibration and there fails the Raman line corresponding to this vibration. We assign 540 cm^{-1} to ring bending mode and 610 cm^{-1} to C—C (single bond) stretching mode. This assignment for 540 cm^{-1} is also consistent with the fact, which may be seen in Table III, that b_{1g} component of 606 cm^{-1} e_g^+ benzene vibration diminishes in frequency only slightly although the a_g component is lowered considerably.

Infrared-active Frequencies.—*Species b_{2u}.*—Infrared bands at 3049 cm^{-1} and 1667 cm^{-1}

may be assigned to two of the five b_{2u} fundamental vibrations, namely the hydrogen and oxygen stretching vibrations, with considerable certainty by comparison with the values of the corresponding symmetric (a_g) vibration. We note here that the double maximum of the latter band (1667 and 1656 cm^{-1} in carbon disulfide) is interpreted to be caused by Fermi resonance between the b_{2u} fundamental and $1064(b_{3u})+610(b_{1g})=1674(B_{2u})cm^{-1}$ combination as shown in Table I. A medium strong band at 1715 cm^{-1}, which can not be explained as a combination, may represent CC stretching vibration. This assignment is consistent with the corresponding values of the frequencies in *p*-dideuterobenzene and *p*-difluorobenzene as shown in Table III. A medium weak and broad band at 730 cm^{-1} may be assigned to the ring-breathing vibration from comparison with the corresponding vibrations in other molecules (see Table III). The remaining vibration of this species is the hydrogen bending vibration. It must be searched for in the region between 1100 and 1400 cm^{-1} from the values of the corresponding Raman-active mode. They must be selected among medium to very strong bands observed at 1355, 1323 and 1297 cm^{-1}, of which the middle one can also be explained as a combination band as shown in Table I. We assign the remaining bands to hydrogen bending vibration, 1355 cm^{-1} and 1297 cm^{-1} being taken as b_{3u} and b_{2u} fundamentals, respectively. It is to be noted that the following sequence results for frequency values of hydrogen bending vibration from this assignment together with the assignment of the Raman-active fundamentals described previously: $b_{1g}>b_{3u}>b_{2u}>a_g$. This sequence also exists in the case of *p*-difluorobenzene[12].

Species b_{3u}.—One of the five b_{3u} fundamental vibrations is the hydrogen stretching mode which is assumed to overlap the band at 3049 cm^{-1} assigned to a b_{2u} fundamental. Mention was made of another fundamental, i. e., the hydrogen bending vibration, which was taken to be 1355 cm^{-1}. Strong or very strong bands at 943 and 1063 cm^{-1} may also be taken as b_{3u} fundamentals. The remaining fundamental vibration is an oxygen in-plane bending mode and this is expected to have a frequency of 400 cm^{-1} from the comparison with the corresponding vibrational frequency of *p*-difluorobenzene. Although this region is outside our measurements, we tentatively assign the value of 370 cm^{-1} to this vibration because this assumption favors the explanation of some of the absorption bands as combinations.

Species b_{1u}—Calculated values of three non-planar frequencies belonging to this species are 98, 533 and 871 cm^{-1}. The highest frequency is realized in the spectrum by the band at 876 cm^{-1}. Although we could not obtain the experimental value of frequency corresponding to the calculated value of 533 cm^{-1} even from the combination bands, we infer the experimental value of the lowest b_{1u} fundamental to be 99 cm^{-1} from the combination band (see Table I).

Inactive Frequencies.—*Species* a_u.—The two vibrations in species a_u are neither active in the Raman nor in the infrared spectra. Calculated values of these vibrational frequencies are 403 and 962 cm^{-1}. Although we infer the "experimental" value corresponding to the former frequency to be 533 cm^{-1} from the vibrational analysis of the electronic spectrum, this value should be considered to be tentative for reasons described briefly in a previous paper[4].

TABLE V
INTERPRETATION OF RAMAN SPECTRUM OF *p*-BENZOQUINONE

$\Delta\nu$ (cm^{-1})[3]	Interpretation
243 (3)	b_{3g} fundamental
444 (4)	a_g fundamental
540 (2)	b_{1g} fundamental
610 (3)	b_{1g} fundamental
770 (2)	a_g fundamental
794 (1)	b_{2g} fundamental
932 (2)	b_{3g} fundamental
1149 (7)	a_g fundamental
1360 (3)	b_{1g} fundamental
1667 (10)	a_g fundamental
1688 (5?)	a_g fundamental
3058 (4)	a_g+b_{1g} fundamentals

Interpretation of Spectra.—Fundamental frequencies assigned are summarized in Table IV. The interpretations of the Raman and infrared spectra are included in Tables V and I, respectively. In interpreting the bands as combinations only the possibilities of binary combinations were considered. In Table IV, underlined values were obtained from the combination bands (lower a_u fundamental was obtained from the electronic spectral data — see above) and the calculated values of non-planar frequencies are given in parentheses. The value of frequency

of C=O bending vibration belonging to species b_{1g} is only an estimated value and is included in brackets.

Summary

The infrared absorption spectra of *p*-benzoquinone in carbon disulfide and carbon tetrachloride solutions in rock salt region are measured and interpreted together with the Raman data reported by Stammreich and Forneris[3]. A complete, although more or less tentative, assignment of the fundamental frequencies to modes of vibrations is proposed.

The authors express their sincere thanks to Professor S. Imanishi and to Dr. Y. Kanda for their encouragement throughout this work and their kind suggestions in preparing the manuscript. Thanks are also due to the Research Department of Toyo Rayon Co., Ltd. for recording infrared spectrum.

Chemical Laboratory, General Education Department, Kyushu University
Ootsubo-machi, Fukuoka

*Renieratene, a New Carotenoid Containing Benzene Rings, Isolated from a Sea Sponge**

By Masaru YAMAGUCHI

(Received March 5, 1958)

With regard to the chemical constitution of renieratene[1], a carotenoid pigment isolated from a sponge "*Reniera japonica*", it has previously been shown from the result of the chromic acid oxidation, by which crocetin dialdehyde has been isolated besides other products, that renieratene is a derivative of tetramethyl-octadeca-nonaene[2]. Shortly afterwards the author has elucidated the chemical constitution of isorenieratene (I), and it has become clear that isorenieral which is the degradation product of the former, has the constitution indicated by II[3]. As isorenieral is also one of the degradation products of renieratene, it is clear that renieratene can be expressed by the partial formula III. Therefore the remaining problem in the chemical constitution of renieratene is the elucidation of R-group in the formula III. From the molecular formula of renieratene, $C_{40}H_{48}$, and the number of double bonds, 15, it can be concluded that the R-group has the formula C_9H_{11}–, and that it contains one ring and three double bonds. Furthermore, it can be inferred from the analogy with another terminal group, that the ring may be a benzene ring.

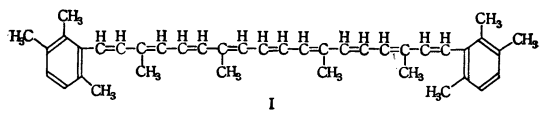

I

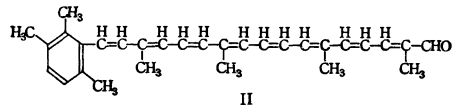

II

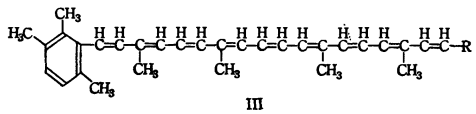

III

In the present paper is described the potassium permanganate oxidation of renieratene, by which whole its constitution has been clarified.

The oxidation products were separated into some neutral and acidic fractions by the ordinary method. From the neutral

* "Pigments of Marine Animals", VI. V of this series, This Bulletin, **31**, 51 (1958).

1) T. Tsumaki, M. Yamaguchi and T. Tsumaki, *J. Chem. Soc. Japan, Pure Chem. Sec.* (*Nippon Kagaku Zassi*), **75**, 297 (1954); M. Yamaguchi, This Bulletin, **30**, 111 (1957).

2) M. Yamaguchi, ibid., **30**, 979 (1957).

3) M. Yamaguchi, ibid., **31**, 51 (1958).

fractions a considerable amount of 2,3,4-trimethylbenzaldehyde (IV) was obtained in the form of semicarbazone. The confirmation was done by the mixed melting point determinations of the semicarbazone and 2,4-dinitrophenylhydrazone with the authentic samples and further by the oxidation into 1,2,3,4-benzene-tetracarboxylic acid. As another neutral constituent, 2,3,6-trimethylbenzaldehyde (V) which was fairly reasonably expected, was obtained in the form of 2,4-dinitrophenylhydrazone by the chromatographic separation, from the mother liquor of the above semicarbazone. From the petroleum ether soluble part of the acidic fraction, a small quantity of 2,3,6-trimethylbenzoic acid (VI) was isolated in the form of its 4-phenylazophenacyl ester. However the main part of the acidic fraction consisted of an acid of m. p. 205~220°, which gave 1,2,3,4-benzene-tetracarboxylic acid, on oxidation. As the acid of m. p. 205~220° could not be purified effectively by recrystallization, it was converted into 4-phenylazophenacyl ester. The main product thus obtained after the chromatographic separation was a di-ester of 2,4-dimethyl-benzene-1,3-dicarboxylic acid (VII).

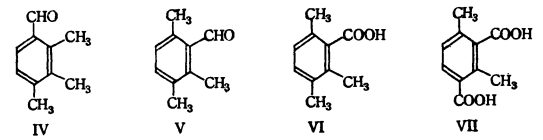

IV V VI VII

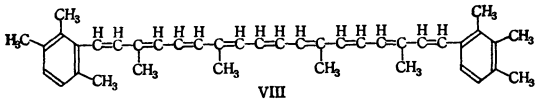

VIII

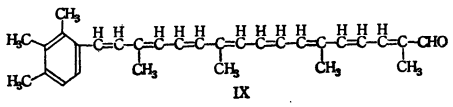

IX

These results decidedly show that besides 2,3,6-trimethylphenyl group as one terminal group, 2,3,4-trimethylphenyl group must exist as another terminal group which has been expressed by R-group in III. Therefore the structural formula of renieratene can be given by VIII. This formula can explain all its properties or behaviors hitherto observed[1,2].

Renieral, which, as well as isorenieral, is a degradation product of the mild oxidation of renieratene[2], can therefore be considered to have a 2,3,4-trimethylphenyl group, and can be expressed by the formula IX.

It has already been pointed out that for the explanation of the spectral properties of isorenieratene, it is necessary to suppose the steric hindrance caused by the two methyl groups which are standing at the two neighboring positions of the polyene chain in benzene ring[3]. In the case of renieratene, the position of the absorption maxima can also be accounted for by the same effect. The difference between the wavelength of the longest wavelength maximum of diphenyltetramethyl-octadeca-nonaene[4], 541 mμ in carbon disulfide, and that of isorenieratene, 520 mμ in the same solvent, is ca. 21 mμ. The effect caused by only one 2,3,6-trimethylphenyl group can therefore be considered to be a half, i.e. about 10 mμ. Renieratene has one 2,3,6-trimethylphenyl group and one 2,3,4-trimethylphenyl group. As the latter possesses only one methyl group at the *o*-position to the polyene chain, the steric effect may be much smaller than that caused by the former. Therefore renieratene will possess the longest wavelength maximum at ca. 10 mμ shorter wavelength position than that of unsubstituted diphenyltetramethyl-octadecanonaene, i.e. at 531 mμ. This value shows good agreement with the observed value, 532 mμ, of renieratene.

Renieratene can be considered to be resolved into isoprene unites. However, as indicated in X, the modes of binding of isoprene residues in the terminal groups of renieratene are considerably different from those in the carotenoids of plant-occurence, in which isoprene residues are arranged top-to-tail. Therefore, in these respect also, renieratene can be regarded as a carotenoid of a new type.

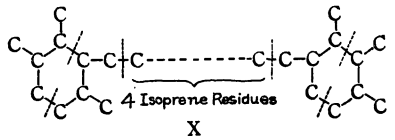

X

Experimental

Renieratene (200 mg.) dissolved in pure benzene (90 cc.) and potassium permanganate (2.7 g.) and sodium carbonate (2.7 g.) dissolved in water (100 cc.) were stirred efficiently at the room temperature. After 8 hours the color of the benzene layer completely disappeared. The excess of permanganate was reduced with the solution of sodium hydrogen sulfite, the precipitates were

4) C. H. Eugster, C. Garbers and P. Karrer, *Helv. Chim. Acta*, **35**, 1179 (1952).

filtered and washed several times with hot benzene and water. The filtrate and washings were combined and treated as below.

2,3,4-Trimethylbenzaldehyde.—The benzene layer of the above product was separated, washed with water, dried with sodium sulfate, and concentrated under diminished pressure. The oily residue was dissolved in ethanol (10 cc.) and treated with the solution of semicarbazide hydrochloride (40 mg.) and sodium acetate (80 mg.) in water (2 cc.). After 24 hours the precipitates were collected, and the recrystallization from ethanol gave 2,3,4-trimethylbenzaldehyde semicarbazone in colorless plates, m. p. 240~242°, (16 mg.).

Anal. Found: C, 64.47; H, 7.43. Calcd. for $C_{11}H_{15}ON_3$: C, 64.36; H, 7.37%.

The semicarbazone (7 mg.), potassium permanganate (45 mg.) and sodium carbonate (45 mg.) were mixed and finely ground, and after the addition of water (3 cc.) heated on the steam bath for 12 hours with occasional additions of a small amount of potassium permanganate. The precipitates were dissolved by the addition of sodium hydrogen sulfite solution and diluted sulfuric acid, and the solution was extracted many times with ether. Ether was evaporated and the residue, recrystallized from water, yielded 1,2,3,4-benzene-tetracarboxylic acid in colorless plates (2 mg.), m. p. 215~236°, which was identified by the light absorption curve and mixed melting point determination with the authentic sample.

The semicarbazone gave 2,4-dinitrophenylhydrazone in red needles, m. p. 227~229°, when treated with 2,4-dinitrophenylhydrazine in ethanolic sulfuric acid. The semicarbazone and the hydrazone exhibited no melting point depression when mixed with the authentic samples derived from the synthetic 2,3,4-trimethylbenzaldehyde. (It was synthesized from 4-bromohemimellithene and ethyl orthoformate by Grignard reaction[5]. Semicarbazone, colorless plates from ethanol, m. p. 240~242°. *Anal.* Found: C, 64.28; H, 7.21. Calcd. for $C_{11}H_{15}ON_3$: C, 64.36; H, 7.37%. 2,4-dinitrophenylhydrazone, red needles from benzene-ethanol, m. p. 229°. *Anal.* Found: C, 58.77; H, 5.09. Calcd. for $C_{16}H_{16}O_4N_4$: C. 58.53; H, 4.91%.)

2,3,6-Trimethylbenzaldehyde.—The mother liquor of the above semicarbazone was treated with 2,4-dinitrophenylhydrazine and sulfuric acid in ethanol. The precipitates (31 mg.) were recrystallized from benzene-ethanol and adsorbed on alumina (column, 2×15 cm.; developer, benzene), forming two main zones. The upper brown zone gave red needles of 2,3,4-trimethylbenzaldehyde-2′,4′-dinitrophenylhydrazone (11 mg.), m. p. 225~228°, when recrystallized from benzene-ethanol.

Anal. Found: C, 58.62; H, 5.18. Calcd. for $C_{16}H_{16}O_4N_4$: C, 58.53; H, 4.91%.

The lower orange zone afforded 2,3,6-trimethyl benzaldehyde-2′,4′-dinitrophenylhydrazone in red needles (13 mg.), m. p. 219°.

Anal. Found: C, 58.88; H, 4.94. Calcd. for $C_{16}H_{16}O_4N_4$: C, 58.53; H, 4.91%.

2,3,6-Trimethylbenzoic Acid.—The aqueous solution separated from benzene layer containing neutral fractions was concentrated under vaccum to ca. 4 cc., acidified with sulfuric acid (20%), and extracted with ether (total, 50 cc.). Ether was evaporated and the residue was extracted with petroleum ether (3 cc.). The petroleum ether solution was evaporated and the oily residue was neutralized with the solution of sodium hydroxide (20.6 cc., 0.0143 N) using phenolphthalein. The indicator was removed by the ether extraction, the solution was evaporated to dryness and the residue was heated under reflux with 4-phenylazophenacyl bromide[6] (80 mg.) in ethanol (3 cc.) for 30 minutes. The product was dissolved in benzene (10 cc.), washed with water, dried, and chromatographed on alumina (column, 2×20 cm.; developer, benzene) giving seven zones. The third orange zone from the top afforded faint red needles (ca. 1 mg.), m. p. 165~169°, when recrystallized from benzene-ethanol. It seemed to be an impure ester of 2,4-dimethylbenzene-1,3-dicarboxylic acid described below. The sixth orange zone afforded red needles of 4′-phenylazophenacyl-2,3,6-trimethylbenzoate (2.3 mg.), m. p., 160~162°, when the residue of the eluate was recrystallized twice from benzene-ethanol. Mixed m. p. 160~162°.

Anal. Found: N, 7.28. Calcd. for $C_{24}H_{22}O_3N_2$: N, 7.25%.

2,4-Dimethylbenzene-1,3-dicarboxylic Acid.—The colorless residue of the above petroleum benzine extraction was recrystallized from water giving colorless solid (12 mg.), m. p. 205~220°. As it was unsuccessful to obtain pure substance by recrystallization, a part of the sample (5 mg.) was oxidized with potassium permanganate (35 mg.) and sodium carbonate (35 mg.) in a way as described in the oxidation of semicarbazone, yielding a small quantity of 1,2,3,4-benzene-tetracarboxylic acid in colorless plates, m. p. 215~230°, mixed m. p. 215~230°.

The remaining part (ca. 6 mg.) was neutralized with a sodium hydroxide solution and after the removal of the indicator the solution was evaporated. The residue was refluxed with 4-phenylazophenacyl bromide (20 mg.) in ethanol (3 cc.) for one hour. When chromatographed on alumina (column, 2×15 cm.; solvent, benzene) the precipitates gave a main orange zone besides several minor zones. The main zone was eluted with benzene containing methanol and the residue of the eluate was recrystallized from benzene-ethanol, yielding di-(4′-phenylazophenacyl)-2,4-dimethylbenzene-1,3-dicarboxylate in fine red needles (5 mg.), m. p. 169~172°.

Anal. Found: C, 71.15; H, 4.75. Calcd. for $C_{38}H_{30}O_6N_4$: C, 71.46; H, 4.74%.

5) The aldehyde has been reported to be synthesized from hemimellithene by Gattermann-Koch's reaction, but no characterizations has been described. H. A. Smith and J. A. Stanfield, *J. Am. Chem. Soc.*, **71**, 81 (1949).

6) S. Masuyama, *J. Chem. Soc. Japan, Pure Chem. Sec.* (*Nippon Kagaku Zassi*), **71**, 402 (1950).

The ester exhibited no melting point depression when mixed with the authentic sample (prepared from synthetic acid[3]; red needles, m. p. 172°. *Anal*: C, 71.12; H, 4.83%.).

The author wishes to express his thanks to Professor Tokuichi Tsumaki for his exceedingly kind directions throughout this work. The author also thanks Mr. Michio Shido and Miss Sachiko Indo for microanalysis. The cost of this work has been partially covered by the Scientific Research Grant of Ministry of Education.

Department of Chemistry
Faculty of Science
Kyushu University
Hakozaki, Fukuoka

Relations between the Substructure and the Rate of the Sluggish Inversion of Quartz Rock

By Taneki TOKUDA

(Received March 31, 1958)

Rate of the Sluggish Inversion from Quartz to Cristobalite. — We have confirmed the fact that all of these quartz specimens were slowly converted into cristobalite when heated at 1000~1600°C in air, carbon monoxide, or steam. Tridymite has never been detected by X-ray diffraction. The rate of the sluggish inversion from quartz to cristobalite was calculated from density measurement using the following formula,

$$X=D_2(D_1-D)/D(D_1-D_2)$$

where X is the fraction converted, D is the apparent density at a given time of firing, D_1 is the apparent density of quartz aggregates, D_2 is the apparent density of cristobalite aggregates (D_1 and D_2 was corrected for irreversible expansion of polycrystal aggregates[1]). It was found that this sluggish inversion is a reaction of the first order although the rates are found to be different for air, steam, or for such a reducing atmosphere as carbon monoxide. The results obtained when heated in air are shown in Fig. 1. Chemical analysis of the quartz rock specimens is shown in Table I.

These specimens are divided into three classes as can be seen in this figure; a) pegmatite quartz, b) recrystallized cherty part or interstitial quartz veinlet part in

TABLE I
CHEMICAL ANALYSIS OF QUARTZ SPECIMENS

Sample No.	3	5	6	9	10	12
Classification	Unmetamorphosed (Radiolarian) red chert	Slightly metamorphosed red chert	Recrystallized part in red-white silica stone	Vein quartz in red-white silica stone	Vien quartz in green-white silica stone	Pegmatite quartz
Locality	Kuroda	Tamba	Tamba	Tamba	Wakasa	Hongū
SiO_2	94.12	95.68	97.23	99.13	99.40	99.72
Al_2O_3	1.87	2.87	0.20	0.01	0.12	0.00
Total iron as Fe_2O_3	1.89		2.12	0.63	0.15	0.14
CaO	0.25	0.81	0.09	0.09	trace	0.10
MgO	0.66	0.24	0.03	0.01	—	0.00
MnO	0.24	—	—	—	—	—
Alkalis	—	—	0.18	0.11	0.10	—
Ig. loss	0.77	0.19	0.09	0.10	0.05	0.00
Total	99.80	99.79	99.99	100.08	99.82	99.96

1) T. Tokuda, This Bulletin, **28**, 435 (1955).

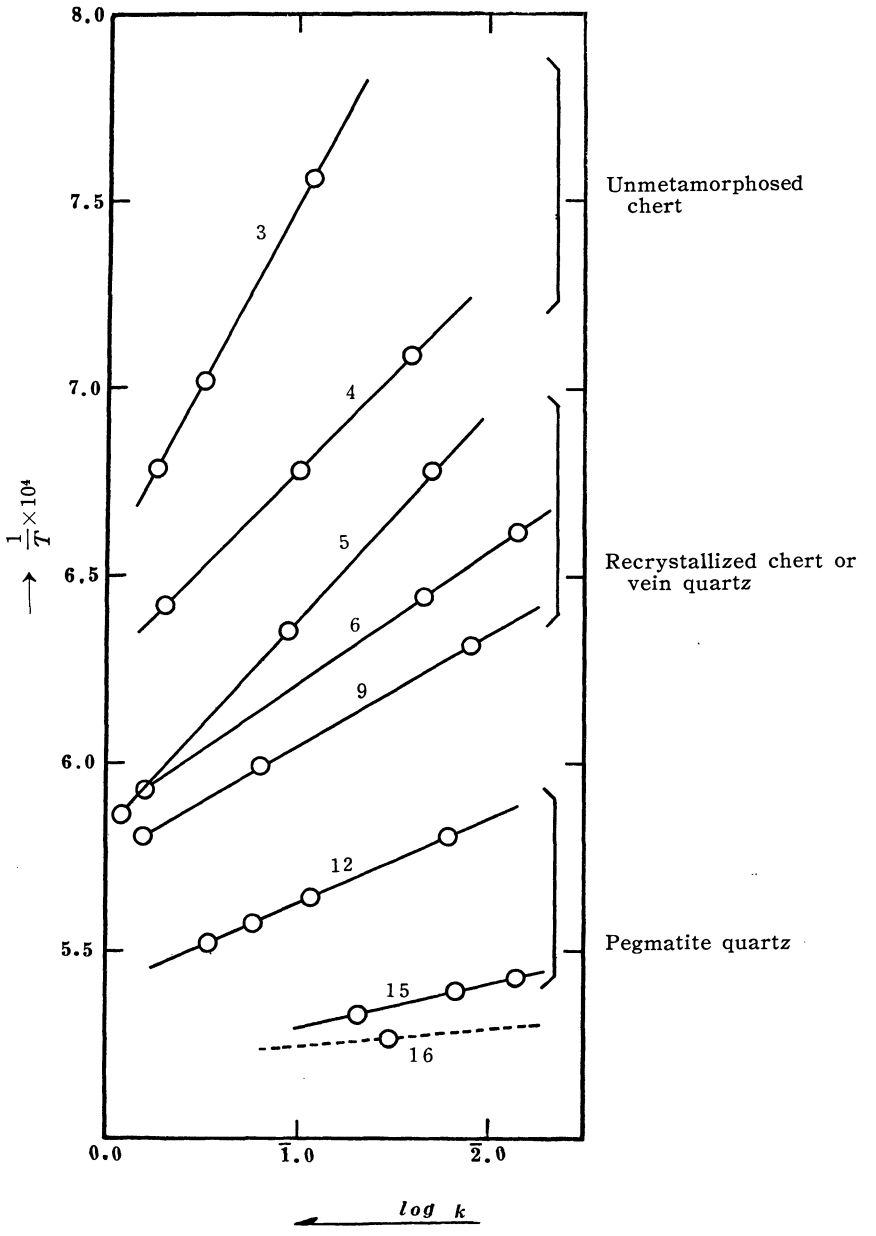

Fig. 1. The rate of the sluggish inversion of several specimens of natural quartz in Japan from quartz to cristobalite (This inversion was a reaction of first order, and k(hr.$^{-1}$) is a rate constant) when heated at a constant temperature (T°K) in an electric furnace. The heating atmosphere was the air. Numbers (1—14) on lines indicate the sample numbers in Table III.

silica stone and c) unmetamorphosed or slightly metamorphosed chert. Quartz occurring as veinlets in the green-white silica stone or red-white silica stone belongs to the same group as recrystallized chert, but not to the pegmatite quartz group.

Variation of Line Breadths.—In order to compare the imperfection of quartz crystals of contrasted geologic origin, the width at half maximum of lines (234)α_1, and (240)α_1 was determined by means of "Norelco" X-ray diffractometer. Filtered copper K-rays were used with the X-ray tube running at 35 kV., 10 mA. The scanning speed of the GM-counter was 1/8° per minute. Operation condition of the rate

meter was, scale factor 4, multiplier 1, and time constant 16 sec. Divergence and scatter slits were 4°, and receiving slit was 0.006 (inches).

TABLE II
GRAIN SIZE OF QUARTZ SPECIMENS VS. INTENSITY AND WIDTH AT HALF MAXIMUM

	Intensity (cps)	width at half maximum (Degree)
<400 mesh	75.0	0.505
<200 mesh	75.6	0.500

Grain size effect was checked with vein quartz specimens (Table II). As shown in the table, the difference of line breadth and intensity obtained from two specimens, the one ground to pass a 200-mesh, screen and the other ground to pass a 400-mesh, was smaller than 1%. Therefore, in the following, all the measurements were made with samples which were ground to pass a 200-mesh screen. The results obtained for $(234)\alpha_1$ are shown in Table III. Those specimens of quartz which contain more impurities and smaller activation energy of sluggish inversion, have larger line breadth.

Lattice Spacing Variation.— Variation of the spacings of quartz specimens has been measured in the back reflection region. Relative values of the spacings (234) and (240) have been determined by mixing silicon powder with the quartz specimens, and measuring the relative positions of the $(642)\beta_1$ reflection of the silicon and the $(240)\alpha_1$ reflection of quartz. The 2θ value of the $(642)\beta_1$ reflection was taken as 147.152° (at 20°C). Results obtained are shown in Table III. As is shown in this table, those quartz specimens which contain more impurities and smaller activation energy of the sluggish inversion, have larger spacings.

These results, obtained by the measurement of variation of line breadth and lattice spacings, suggest that the impurities might be included in the quartz matrix forming a solid solution. Lattice distortion due to the formation of solid solution would be one of the causes which lower the activation energy of the sluggish inversion.

Conclusion

1) The sluggish inversion of quartz rock of different origins, from quartz to cristobalite, was the primary reaction

TABLE III
WIDTH AT HALF MAXIMUM AND SPACING OF $(234)\alpha_1$ (AT 20°C) VS. ACTIVATION ENERGY OF SLUGGISH INVERSION FROM QUARTZ TO CRISTOBALITE ($CuK_{\alpha_1}=1.540501$ Å)

No.	Classification of quartz specimens	Locality	Silica content (%)	Line breadth (Degree)	D (Å)	Diffraction angle (2θ) (Degree)	Spacings (Å)	Energy of activation (kcal.)
1	Siliceous shale	Kamiiso, Japan	—	1.5	230	153.16	0.792	—
2	Hot spring product	Onikōbe, 〃	—	0.8	620	153.17	0.792	—
3	Unmetamorphosed (Radiolarian) red chert	Kuroda, 〃	94.12	0.8	620	153.53	0.79125	48
4	Unmetamorphosed (Radiolarian) grey chert	Kyōto 〃	94.42	0.700	760	153.54	0.79124	88
5	Slightly metamorphosed red chert	Tamba, 〃	95.68	0.650	910	153.55	0.79123	81
6	Recrystallized red chert (Chert part of a breccia)	〃 〃	97.23	0.530	1220	153.57	0.79120	120
7	Recrystallized white chert and vein (A breccia)	Ofuku, 〃	—	0.525	1250	—	—	—
8	Quartzite	Hwang He Do, Korea	—	0.515	1290	153.57	0.79120	—
9	Vein quartz (Vein part of a breccia)	Tamba, Japan	99.13	0.500	1340	153.57	0.79120	145
10	Vein quartz (Vein part of a breccia)	Wakasa, 〃	—	0.455	1670	—	—	—
11	Quartzite	Okuyama, 〃	—	0.447_5	1730	—	—	—
12	Pegmatite quartz	Hongū, 〃	99.72	0.427_5	1930	153.58	0.79119	205
13	Quartzite	Yakeyama, 〃	—	0.412_5	2110	—	—	—
14	〃	Yagen, 〃	—	0.410	2140	—	—	—
15	Pegmatite quartz	Kawamata, 〃	99.75	0.305	6230	—	—	380
16	Rock crystal	Brazil	99.95	0.250	Standard	153.59	0.79117	very large

when fired in air, in steam, or in reducing atmosphere of carbon monoxide.

2) Those specimens of quartz rock which contain more impurities and smaller activation energy of the sluggish inversion, have larger spacings and larger line breadth.

3) The lattice distortion caused by the formation of solid solution would be one of the causes which lower the activation energy of the sluggish inversion.

Institute of Scientific and Industrial Research, Osaka University, Sakai Osaka

Thermal Decomposition of Chromic Anhydride Supported on Alumina

By Yoshio MATSUNAGA

(Received June 9, 1958)

In our previous papers[1,2] we have described the anomalous oxidation of supported chromia associated with its highly dispersed structure and have presented a new method of examining the structure of chromia-alumina and chromia-zinc oxide catalysts. In the infinite two-dimensional dilution of chromium, it has been shown that chromia is oxidized completely to chromic anhydride. This chemical change is in sharp contrast to our knowledge of the thermal decomposition of chromic anhydride to chromia. The anomalous stability of the plus-six oxidation state of chromium in a highly dispersed state has been explained by the relative importance of surface oxidation of chromia. The present work has as its purpose the confirmation of this stabilization of the higher oxidation state by a study of the thermal decomposition of supported chromic anhydride.

Experimental

Gamma-alumina prepared by the method described in the previous paper[1] was chosen as a carrier because of its high surface area and of its lack of reactivity. Samples were prepared by impregnation with chromic acid solution. They were allowed to stand overnight, filtered, and dried at 110°C. Thermal decomposition was carried out in a stream of oxygen for five hours at 300, 350 and 450°C. A part of the sample, heated at 350°C, was reduced in a stream of hydrogen for five hours at 360°C for the purpose of applying the susceptibility-composition isotherm method[3] to the product. The magnetic susceptibility measurements and the determination of the mean oxidation number of chromium were described previously. The alumina used in this work was found to have a susceptibility of -0.36×10^{-6} per gram.

Results and Discussion

Fig. 1 shows the mean oxidation number of chromium, determined by an iodometric titration, plotted against the chromium content. Glemser et al.[4] showed that chromic anhydride begins to decompose in a stream of oxygen above 250°C, the products being $CrO_{2.6}$ in the temperature range from 283 to 314°C, $CrO_{2.4\sim5}$ from 334 to 388°C, and $CrO_{1.6}$ above 400°C. As the chromium content increases, it would be expected that the compositions of the products in the present system would become close to those reported by Glemser provided that samples are heated in the same temperature ranges. We chose 300, 350, and 450°C as the representative conditions of the above-mentioned three temperature ranges. The curves in Fig. 1 indicate clearly that the plus-six oxidation state is stabilized by the dispersed structure and even at 450°C chromic anhydride in the infinite two-dimensional dilution does not decompose at all. On the other hand, in the higher content range of chromium, the compounds $CrO_{2.6}$ and $CrO_{2.4\sim5}$ which appear in the thermal decomposition of massive chromic anhydride, are not found in our samples. These intermediate oxides seem to be insufficiently stable to exist in the dispersed state.

1) Y. Matsunaga, This Bulletin, **30**, 868 (1957).
2) Y. Matsunaga, ibid., **31**, 58 (1958).
3) R. P. Eischens and P. W. Selwood, *J. Am. Chem. Soc.*, **69**, 1590, 2693 (1947).
4) O. Glemser, U. Hauschild and F. Trüpel, *Z. anorg. u. allgem. Chem.*, **277**, 113 (1954).

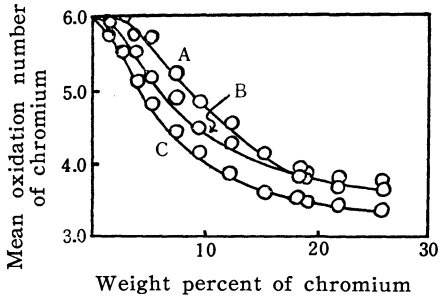

Fig. 1. Relation of oxidation number of chromium supported on gamma-alumina to its content.
A, chromic anhydride was decomposed at 300°C; B, at 350°C; C, at 450°C.

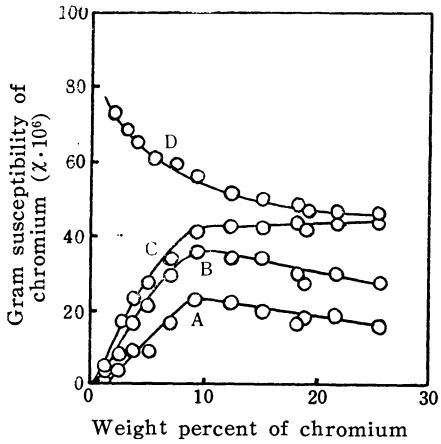

Fig. 2. Susceptibility-composition isotherm for chromium in its oxides supported on gamma-alumina.
A, chromic anhydride was decomposed at 300°C; B, at 350°C; C, at 450°C; D, reduced to chromia.

The gram susceptibility of the chromium ion, calculated on the assumption that the magnetic contributions of the chromium, aluminum, and oxygen ions are additive, is shown in Fig. 2. The chromium in the plus-six oxidation state has no unpaired electron and the estimated susceptibility based on the value for chromic anhydride[5] is 1×10^{-6}, so the decrease of the susceptibility value to almost zero, accompanying the dilution, means an increase of oxidation number to plus-six.

The relationships of the oxidation number and the magnetic susceptibility of chromium to its content in the samples treated at 450°C bear close resemblance to the similar ones shown in the previous paper. It is suggested that the same product is given by the heat-treatment at 450°C regardless of the starting materials; chromic anhydride or chromic oxide. The oxidation number in the series treated at 300 and 350°C are appreciably higher than four in the content range of chromium, less than that corresponding to point *l* in the susceptibility-composition isotherm of the reduced samples. Although we can not find any marked difference between the oxidation numbers of chromium in the samples decomposed at 300 and at 350°C, which contain more than 15% of chromium, the susceptibility values in the series treated at 350°C are significantly larger than thsoe in the series treated at 300°C. Such an increase of susceptibility value without the change of oxidation number suggests the occurrence of a structural change in chromium oxide. The samples containing less than 15% of chromium continue to lose a considerable amount of oxygen between 300 and 350°C.

As shown in Fig. 3, the thermal decomposition of chromic anhydride in the dispersed state occurs continuously, and it seems that the oxidation state of chromium changes from plus-six to plus-three without taking intermediate oxidation states. This view is consistent with the fact that there is only one kind of catalytically-active center for the decomposition of aqueous hydrogen peroxide on the surface of the oxidized chromia-alumina catalysts throughout the range of mean oxidation number of chromium from 3.12 to 5.65[6].

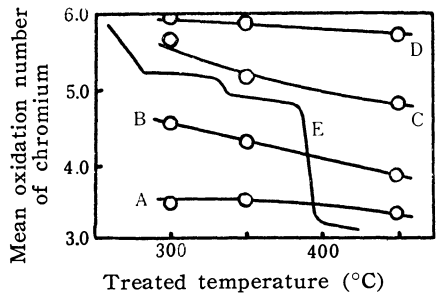

Fig. 3. Relation of oxidation number of chromium to treated temperature in the thermal decomposition of chromic anhydride.
Chromium content A, 27 percent; B, 12.5 percent; C, 5.5 percent; D, 1.8 percent; E, massive chromic anhydride (after Glemser et al.).

Consequently, it appears that the relatively large and thick aggregates of chromic anhydride on the surface of alumina

5) F. W. Gray and J. Dakers, *Phil. Mag.*, **11**, 297 (1931).

6) Y. Matsunaga, This Bulletin, **30**, 984 (1957).

lose the greater part of their active oxygen below 300°C and only a small amount between 350 and 450°C. (cf. curve A in Fig. 3) This anomaly seems to be due to the instability of the intermediate compounds $CrO_{2.6}$ and $CrO_{2.4\sim5}$. There is no loss of oxygen between 300° and 350°C, but the product continues the structural change to chromia in this temperature range and completes it between 350° and 450°C. As described in the previous paper, the surface-accessible sites and some vacant sites due to lattice defects accommodate excess of oxide ions so the apparent oxidation number in the final product is always higher than plus-three. The smaller aggregates of chromium oxide are more defective and have higher surface area, so they have larger accommodation capacity for excess of oxygen. Therefore, the stabilization of the plus-six oxidation state becomes more effective as the chromium content decreases and the size of aggregates becomes smaller. The continuous loss of oxygen throughout the whole temperature range suggests that the product from small aggregates is highly defective and has no definite structure. (cf. curves C and D in Fig. 3)

In the previous paper we showed that the study of the oxidation of the chromia-alumina catalyst system by chemical analysis may be as useful as the susceptibility-composition isotherm method proposed by Selwood. However, the thermal decomposition of chromic anhydride on alumina is a step which takes place practically in the preparation of this catalyst and we can point out easily the position of point *l* in curves B and C in Fig. 1 and curves A, B and C in Fig. 2. Therefore, in the process of preparation, it is possible to get directly the same useful information about the degree of dispersion of chromium as from the oxidation of the final products either by the chemical method or by the magnetic method.

Summary

The thermal decomposition of chromic anhydride supported on gamma-alumina at 300°, 350° and 450°C was examined by chemical analysis and by magnetic susceptibility measurements. The stabilization of the plus-six oxidation state of chromium in a highly dispersed state was confirmed by the present experiments. In addition, by comparing the oxidation number and the magnetic susceptibility of chromium, it was found that the behavior of supported chromic anhydride in large aggregates is also anomalous. Contrary to the case of the thermal decomposition of massive chromic anhydride, the intermediate oxides $CrO_{2.6}$ and $CrO_{2.4\sim5}$ were not found. The large aggregates of chromic anhydride on alumina lose the greater part of their active oxygen at relatively low temperatures and crystallize continuously into chromia with further loss of oxygen.

The author wishes to express his hearty thanks to Professor Akamatu for his kind direction.

Department of Chemistry
Faculty of Science
The University of Tokyo
Hongo, Tokyo

The Separation of Tellurite, Selenite and Sulfite Ions by Anion-Exchange Resins

By Akira IGUCHI

(Received February 14, 1958)

The separation of tellurite, selenite and sulfite is a difficult problem. A few ion-exchange separations of chloro complexes of tellurium and selenium have recently been reported[1,2]. In this paper the behavior of sulfite, selenite and tellurite towards anion exchange resins is studied in alkaline media. The results give a new successful separation of these oxy-acid anions.

Experimental

Materials. — *Anion-exchange resin.* — Air-dried Dowex 1-X8, 100- to 200-mesh, was used in either the hydroxide or the nitrate form.

Sodium tellurite and sodium selenite.—Guaranteed reagents were used without purification. The ordinary gravimetric analysis of these salts[3] showed that they were pure enough for the purpose of this study. The samples dissolved in water could not be kept for a long time, since the state of these salts in the aqueous solution changes with the lapse of time in a neutral solution; in an alkaline stock solution oxidation may occur, when they are kept too long. Hence the sample solution has been kept for 3 days at the longest, in a glass stoppered Erlenmeyer flask kept in a refrigerator.

Sodium sulfite.—The neutral aqueous solution of this salt decomposes only about 0.5% a day right after dissolution. But the rate of decomposition increases when the solution is kept longer. Thus it is desirable to dissolve the salt right before each experiment. On the anion-exchange resin of the hydroxide form, the sulfite ion seems to be more stable than in a neutral solution; the quantity of sulfite ions eluted from the resin is equal to that expected even after two days' keeping on the resin. The quantity of sulfite is estimated by the iodimetric titration.

Procedures. *Analysis of samples.*—The quantity of tellurite in the solution was determined by the titration of thiosulfate proposed by R. A. Johnson and D. R. Fredrickson[4]. The tellurite in the sample was potentiometrically titrated with standard iodine solution after the addition of hydrochloric acid, potassium iodide and a known quantity of thiosulfate. Ammonium salt did not cause interference even when its concentration was as high as 1.5 mol./l. Since a positive error is expected in a more concentrated solution, the effluent was diluted with a suitable amount of water to keep the concentration of ammonium salts less than 1.3 mol./l.

The quantity of selenite in the solution was determined by the titration method which was proposed by J. F. Norris and H. Fay[5], by the use of standard iodine solution, starch and a definite amount of thiosulfate. Of course the end point was also determined potentiometrically as in the case of tellurite.

The quantity of sulfite in the solution was titrated with standard iodine solution, together with acetic acid and glycerin[6].

The measurement of distribution coefficients of tellurite, selenite and sulfite ions in various concentrations of sodium nitrate and sodium hydroxide.—The distribution coefficient, K_d was measured by the column method. The K_d values of the ion were calculated from the volume of the eluant through the following equation,

$$K_d = (V - i)/M \quad [7-9] \qquad (1)$$

where K_d(cc./g.) is the distribution coefficient, V(cc.) the volume of eluant passed through the column until the concentration of the sample in the effluent becomes maximum, i(cc.) the interstitial volume of the column and M(g.) the weight of the resin. The columns were 7.0 mm. in diameter, and contained 1~3 g. of the resin. The flow rate was less than 0.3 cc./min.

Results and Discussion

Relationship between the distribution coefficient of tellurite, selenite and sulfite and the concentration of nitrate or hydroxide ion in the eluant.—The results obtained with the procedure using aqueous solutions of sodium nitrate as eluants are shown in Fig. 1, and those with sodium hydroxide solutions in Fig. 2. The values are the mean values of the two

1) F. Aoki, This Bulletin, **26**, 480 (1953).
2) Y. Sasaki, ibid., **28**, 89 (1955).
3) e.g., F. P. Treadwell and W. T. Hall, "Analytical Chemistry" 8th English Ed., John Wiley & Sons, New York, (1935), Vol II, p. 268.
4) R. A. Johnson and D. R. Fredrickson, *Anal. Chem.*, **24**, 866 (1952).
5) J. F. Norris and H. Fay, *J. Am. Chem. Soc.*, **23**, 119 (1900).
6) A. Kurtenacker and R. Wollak, *Z. anorg. u. allgem. Chem.*, **161**, 201 (1927).
7) M. Honda, "Ion Exchange" (Ion Kokan) (in Japanese), Nankodo, Tokyo, Japan. (1954) p. 95.
8) D. DeVault, *J. Am. Chem. Soc.*, **65**, 532 (1943).
9) J. N. Wilson, ibid., **62**, 1583 (1940).

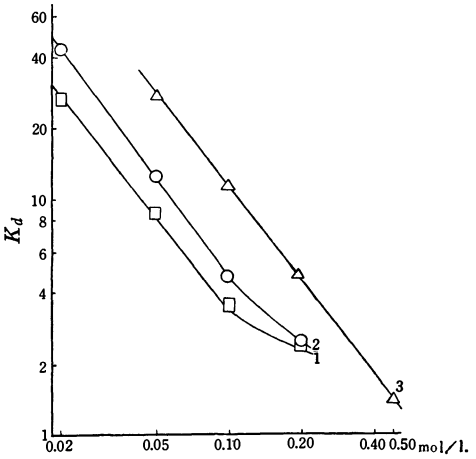

Concentration of sodium nitrate

Fig. 1. Relationship between K_d and the concentration of sodium nitrate in the eluant.
1: Sodium tellurite. 2: Sodium selenite.
3: Sodium sulfite.

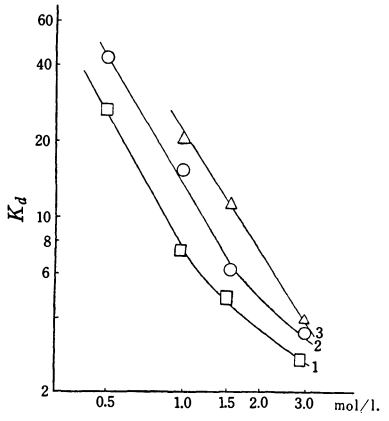

Concentration of sodium hydroxide

Fig. 2. Relationship between K_d and the concentration of sodium hydroxide in the eluant.
1: Sodium tellurite. 2: Sodium selenite.
3: Sodium sulfite.

experimental data and the error is less than about 2%.

When the reaction of the ion with the ion-exchanger is supposed to be

$$\nu RX + A^{\nu-} = R_\nu A + \nu X^-$$

the distribution coefficient K_d is given by the equation,

$$K_d = [R_\nu A]/[A^{\nu-}] \qquad (2)$$

and the equilibrium constant K_{ex} is given by the equation,

$$K_{ex} = [R_\nu A][X^-]^\nu / [RX]^\nu [A^{\nu-}] \qquad (3)$$

From equations 2 and 3 it is seen that

$$K_d = K_{ex} \cdot [RX]^\nu / [X^-]^\nu \fallingdotseq k/[X^-]^\nu \qquad (4)$$

where k is a constant.

So the equations 5 and 6 are obtaind:

$$\log K_d = \log k - \nu \log[X^-] \qquad (5)$$

or $$d \log K_d / d \log[X^-] = -\nu \qquad (6)$$

Consequently from the slope of the curve, it is possible to induce the charge of the exchanged ion.

From Figs. 1 and 2, linear relationships of log K_d towards log C are observed except in the region of high concentrations of the eluants. The linear lines for tellurite, selenite and sulfite in Fig. 1 are almost parallel and their slope is about 1.5 at a low concentration. So they may contain the ions of one negative charge; in other words, $HTeO_3^-$, $HSeO_3^-$ may be present together with anions of two negative charges in these neutral solution.

The straight linesf or these salts in Fig. 2 are also almost parallel and their slope is about 2.0 at a low concentration, so they must exist in the form of anions with two negative charges, that is, TeO_3^{2-}, SeO_3^{2-} and SO_3^{2-} in these strongly alkaline solutions.

As the difference of K_d among these three anions is not very remarkable, and as the tailing part of selenite and tellurite in elution process is not sharp, it is very difficult to separate them by using sodium nitrate or sodium hydroxide solution as an eluant.

The relationship between the concentration of ammonia added and the distribution coefficient.—In the elution process of the column method, these anions are eluted too readily by neutral nitrate solution to be separated from each other, and with too great difficulty by hydroxide solution. Consequently it is necessary to study the intermediate region of pH of the eluant. But aqueous ammonia without salt cannot be used as the eluant, for these anions are not eluted with it in any concentration. Thus the effect of the addition of aqueous ammoia to the eluant containing nitrate or hydroxide was studied. The results are shown in Fig. 3.

By adding ammonia to a nitrate eluant, the values of the distribution coefficients, K_d, for tellurite and selenite increase rapidly, but the difference among the ions becomes smaller; therefore this combination is not suitable for the purpose of

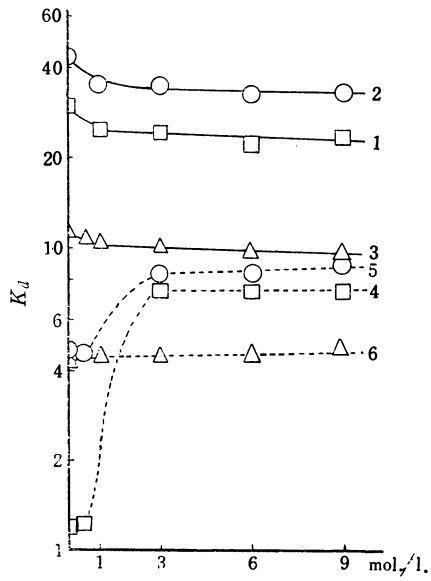

Ammonia in eluant

Fig. 3. Relationship between K_d and the concentration of added ammonia in eluant.
1: Sodium tellurite eluted with 0.4 N sodium hydroxide. 2: Sodium selenite eluted with 0.4 N sodium hydroxide. 3: Sodium sulfite eluted with 1.5 N Sodium hydroxide. 4: Sodium tellurite eluted with 0.1 mol./l. sodium nitrate. 5: Sodium selenite eluted with 0.1 mol./l. sodiumnitrate. 6: Sodium sulfite eluted with 0.2 mol./l. sodium nitrate.

separation. On the contrary, although the addition of ammonia to a hydroxide eluant causes only a small decrease of K_d, the difference of K_d for each anion remains unchanged and fortunately the tailing part of selenite and tellurite in the elution process is much shortened. Therefore the eluant containing 0.5 mol./l. of sodium hydroxide and 3.0 mol./l. of ammonia may be the most suitable for the separation of selenite and tellurite.

The effect of an organic solvent on the distribution coefficient.—In order to study the effect of an organic solvent on the distribution coefficient of these anions, the relationship between K_d and the percentage of added ethanol was examined. The concentration of nitrate and ammonia are kept constant, i.e. 0.1 mol./l. of sodium nitrate and 0.5 mol./l. of ammonia for tellurite and selenite, and 0.2 mol./l. of sodium nitrate and 0.5 mol./l. of ammonia for sulfite. Results are shown in Fig. 4A.

From the results thus obtained considerable differences are recognized among selenite, tellurite and sulfite. The distribution coefficient of sulfite increased with the increase of the concentration of ethanol, while the coefficients of the other two ions remain almost constant even up to 75% of ethanol.

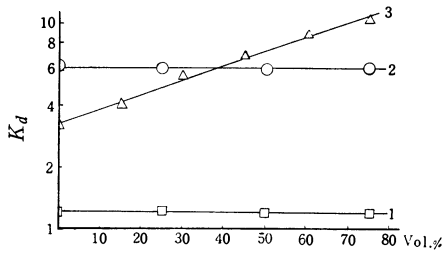

Ethanol in eluant

Fig. 4A. Relationship between K_d and the percentage of added ethanol. The eluants contained also 0.5 mol./l. of ammonia.
1: Sodium tellurite eluted wilh 0.1 mol./l. sodium nitrate. 2: Sodium selenite eluted with 0.1 mol./l. sodium nitrate. 3: Sodium sulfite eluted with 0.2 mol./l. sodium nitrate.

These results seemed to suggest a promising method of separating sulfite from selenite or tellurite, but the tailing part of tellurite or selenite is not sharp in the elution process, and no satisfactory result was obtained even with fairly long columns containing up to 5.0 g. of resins. This separation may be completed, when a much longer column is used.

In case of sodium hydroxide eluants,

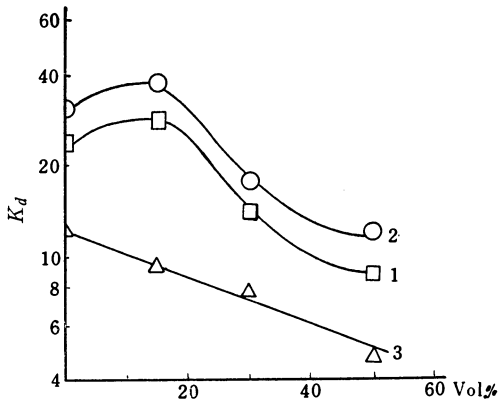

Ethanol in eluant

Fig. 4B. Relationship between K_d and the percentage of added ethanol. The eluant contained also 3.0 mol./l. of ammonia.
1: Sodium tellurite eluted with 0.5 N sodium hydroxide. 2: Sodium selenite eluted with 0.5 N sodium hydroxide. 3: Sodium sulfite eluted with 1.5 N sodium hydroxide.

the relationships between K_d and the percentage of ethanol are shown in Fig. 4B. The concentration of sodium hydroxide is 0.5 mol./l. for the tellurite and selenite, and 1.5 mol./l. for sulfite; the concentration of ammonia is 3.0 mol./l. in both cases.

As shown in Fig. 4B, the distribution coefficient of sulfite decreases as the concentration of ethanol increases, and this is a result in contrast to that of nitrate eluant. This fact may be due to the decrease of the dissociation of HSO_3^- ion.

But in cases of tellurite and selenite, the K_d increased up to 20% of ethanol and beyond this value began to decrease. When 50% of ethanol was added to the eluant, tellurite and selenite were eluted more easily, though the separation of selenite and tellurite is not so clear-cut. Therefore, this method can be used only for separating selenite, or tellurite from sulfite by using 5.0 g of Dowex 1-X8 resin column (in Figs. 5A and 5B).

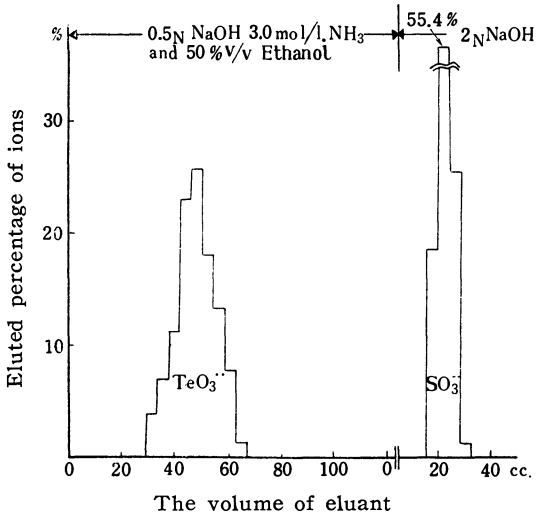

Fig. 5A. Elution curve of mixed sample of tellurite and sulfite. (The flow rate is 0.1 cc./min.)

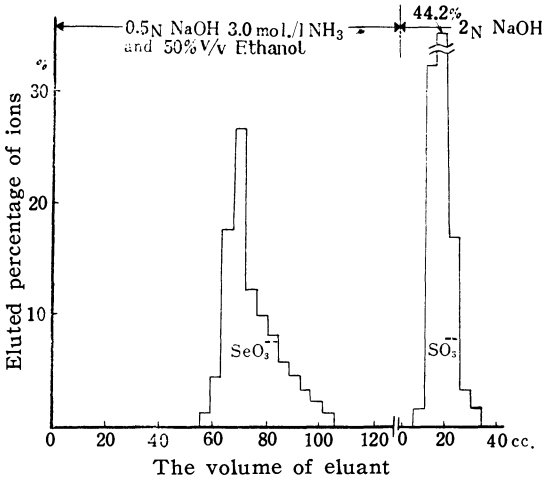

Fig. 5B. Elution curve of mixed sample of selenite and sulfite. (The flow rate is 0.1 cc./min.).

The separation of tellurite, selenite and sulfite.—From the result of Fig. 3, the eluant containing 0.5 mol./l. of sodium hydroxide and 3.0 mol./l. of ammonia is expected to be suitable for separating tellurite from selenite. Then sulfite can be eluted by 2.0 mol./l. of sodium hydroxide solution.

The column of the size 1.0×13.0 cm. containing 5.0 g. of Dowex 1-X8 (analytical grade) was used. One of the typical examples of the perfect separation is shown in Fig. 6. The collected tellurite, selenite and sulfite are titrated by the methods described before.

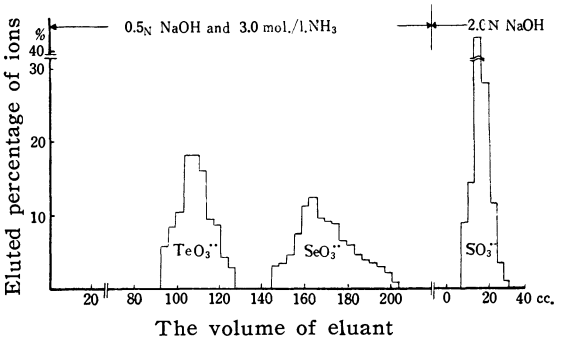

Fig. 6. Elution curve of mixed sample. (The flow rate is 0.1 cc./min.)

The analysis of the mixture of tellurite, selenite and sulfite.—This method of separation was applied to a mixture of known quantities of these salts and the results obtained are shown in Table I. Each value is the mean value of the four repeated experiments.

When the sample solution of tellurite was not fresh or the elution process was too prolonged, the recovery of tellurite was decreased. Therefore, it is desirable to use a newly prepared sample and to shorten the time of analysis. When resins of larger grain size are used, the clear-cut separation is not obtained. Difficulties in handling these intractable materials, for example, the changes of the state in the solution, cause a small discrepancy between the data of recovery and the theoretical values.

TABLE I
THE ANALYSIS OF MIXED SAMPLES

		Sample I		Sample II	
		mmol.	%	mmol.	%
Tellurite	Added values	0.0712_5	100	0.142_5	100
	Observed values	0.0705_5	99.2±0.21	0.141_1	99.0±0.23
Selenite	Added values	0.134_6	100	0.188_5	100
	Observed values	0.123_8	98.0±1.8	0.183_4	97.5±2.5
Sulfite	Added values	0.100_9	100	0.117_8	100
	Observed values	0.0996_9	98.8±1.6	0.116_3	98.7±1.3

Summary

1. The distribution coefficients of tellurite, selenite and sulfite in neutral nitrate solution and alkaline hydroxide solution were measured and the results suggest the presence of an acid salt ion HXO_3^- in neutral solution.

2. By the addition of ammonia to the eluant solution, the distribution coefficient of these salts in nitrate solution was increased, but in hydroxide solution it was decreased.

3. By the addition of ethanol to the eluant solution containing nitrate and ammonia, the distribution coefficient of sulfite increased, but that of tellurite and selenite remained constant even up to 75%. On the contrary, in the addition of ethanol to the hydroxide solution, the distribution coefficient of sulfite decreased, while that of tellurite and selenite increased at first and then decreased.

4. By using these results a complete separation of tellurite, selenite and sulfite was accomplished by the anion exchange chromatographic method using an alkaline eluant.

The author expresses his gratitude to Professor T. Shirai, Dr. Y. Yoshino and his colleagues in the laboratory both for their suggestions and for the discussion helpful in publishing this paper.

Department of Chemistry, College of General Education, University of Tokyo, Meguro-ku, Tokyo

π-Electronic Structures of α-Naphthoquinone and Anthraquinone

By Akira KUBOYAMA*

(Received March 13, 1958)

The *p*-quinone type compounds such as *p*-benzoquinone, α-naphthoquinone, and anthraquinone play an important role as oxidizing reagents in organic chemistry and biochemistry. As for their π-electronic structures, *p*-benzoquinone has already been studied by many workers but the theoretical work on α-naphthoquinone and anthraquinone is scanty[1]. Therefore, the π-electronic structure of α-naphthoquinone and anthraquinone is studied by the simple MO method.

Method of Calculations.—Because of the great discrepancy from the uniform distribution of π-electron density in quinones, which is due to the existence of electronegative oxygen atoms, it is desirable to use the self-consistent method which was used in our previous paper[2] concerning *o*- and *p*-benzoquinones. But the application of this method to α-naphthoquinone and anthraquinone is difficult, since these molecules contain too many π-electrons compared with *p*-benzoquinone.

* Present address, Government Chemical Industrial Research Institute, Tokyo.

1) a) D. Hadzi, *Arkiv. Kem.*, **25**, 33 (1953); b) M. L. Josien and J. Deschamps, *J. chim. phys.*, **52**, 213 (1955); c) J. W. Sidman, *J. Am. Chem. Soc.*, **78**, 4567 (1956).

2) S. Nagakura and A. Kuboyama, *J. Chem. Soc. Japan, Pure Chem. Sec.* (*Nippon Kagaku Zassi*), **74**, 499 (1953); S. Nagakura and A. Kuboyama, *J. Am. Chem. Soc.*, **76**, 1003 (1954).

Now, as is seen in the following X-ray diffraction data[3], the bond lengths of the C=O bond and the adjacent C—C bond are

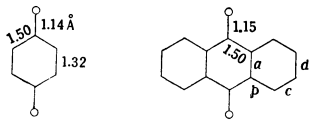

a,b,c,d = 1.38~1.40Å

nearly equal in *p*-benzoquinone and anthraquinone, and the structures of the two six-membered carbon rings of anthraquinone are similar to that of the benzene nucleus. In view of these facts, we assumed the coulomb (α_i) and exchange (β_{ij}) integrals for α-naphthoquinone and anthraquinone as follows:

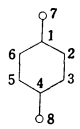

$\alpha_{C_2}=\alpha_{C_3}=\alpha \quad \alpha_O=\alpha+1.3\beta$
$\alpha_{C_1}=\alpha+0.2\beta$
$\beta_{1-7}=\beta \quad \beta_{1-2}=0.8\beta$
$\beta_{2-3}=1.1\beta$

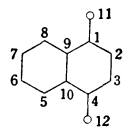

$\alpha_{C_2}=\alpha_{C_{10}}=\alpha_{C_5}=\alpha_{C_6}=\alpha$
$\alpha_O=\alpha+1.3\beta \quad \alpha_{C_1}=\alpha+0.2\beta$
$\beta_{1-11}=\beta_{9-10}=\beta_{10-5}=\beta_{5-6}$
$=\beta_{6-7}=\beta$
$\beta_{1-2}=\beta_{1-9}=0.8\beta \quad \beta_{2-3}=1.1\beta$

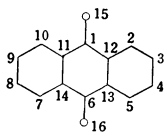

$\alpha_{C_{12}}=\alpha_{C_2}=\alpha_{C_3}=\alpha$
$\alpha_O=\alpha+1.3\beta \quad \alpha_{C_1}=\alpha+0.2\beta$
$\beta_{1-15}=\beta_{12-13}=\beta_{12-2}=\beta_{2-3}$
$=\beta_{3-4}=\beta \quad \beta_{1-12}=0.8\beta$

Among these values, those concerning the quinone nuclei were made equal to the values evaluated for *p*-benzoquinone by the SCF method in the previous paper[2].

Results

The obtained molecular diagrams and the energy levels are given below.

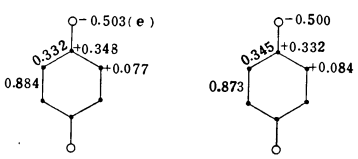

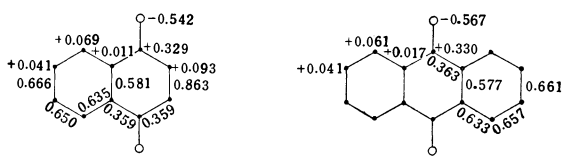

3) For *p*-benzoquinone; J. M. Robertson, *Proc. Roy. Soc.*, **150**, 106 (1935). For anthraquinone; S. N. Sen, *Indian J. Phys.*, **22**, 347 (1948).

The energy levels are classified according to the symmetry properties of the corresponding orbitals in the symmetry group of the molecule (D_{2h} for *p*-benzoquinone and anthraquinone, C_{2v} for α-naphthoquinone), taking the O—O direction as the x-axis and the molecular plane as the xy plane. The energy difference between the orbitals E_5 and E_6 of α-naphthoquinone is 0.003β. The letters x and y attached to the arrow showing the transition between the energy levels denote the directions of the polarization in the allowed transitions. The molecular diagram I for *p*-benzoquinone is the one previously calculated by the SCF method[2] and the diagram II for the same molecule is the one calculated by the present method. The agreement between these two molecular diagrams is satisfactory. Further, the energy levels of *p*-benzoquinone calculated by the two methods mentioned above are also in good agreement with each other. Thus, the results evaluated for α-naphthoquinone and anthraquinone may be thought to be nearly self-consistent.

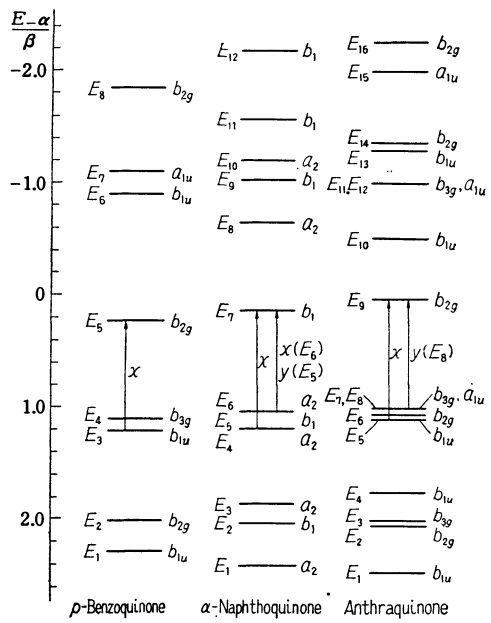

Discussion

Molecular Diagrams. — The molecular diagrams of the three *p*-quinones are similar in many points. As for charge distributions, the negative charges of oxygen atoms slightly increase in the order *p*-benzoquinone, α-naphthoquinone and anthraquinone. The dipole moment (ca. 2.2 D) of α-naphthoqueinone calculated under

the assumption that the angle between the two carbonyl bond axes is 180°, is considerably larger than the measured value[4] (1.30 D) in which the contribution (ca. 0.6 D) of the atomic polarisation[5] characteristic of *p*-quinones is contained. Therefore the calculated dipole moment seems too large, though its value is thought to be considerably affected by the angle between the two carbonyl bond axes.

As for bond orders, the value for the C_2—C_3 bond is nearly equal in α-naphthoquinone and *p*-benzoquinone. Furthermore, the above diagrams show that the six-membered carbon rings of α-naphthoquinone and anthraquinone are properly approximated by the benzene nucleus. The bond orders of the two bonds, C_1—C_2, C_1—C_9 of α-naphthoquinone are equal. B. Pullman and J. Deudel[6] also obtained a similar result in their work on 1,2-benzanthra-3,4-quinone. From these results, it seems probable that the bond orders of the C—C bonds adjacent to the C—O bonds in quinones can hardly be affected by side carbon atom groups.

Energy Levels.—From the energy levels given above, the following two points are worthy of notice. First, the difference between the highest filled and the lowest vacant orbitals is similar in these *p*-quinones. This result explains a similarity among the π—π transition bands of the three *p*-quinones in the long-wavelength region, that is to say, they have a relatively weak band*1 near 300 mμ and a strong band near 250 mμ, respectively. The bands near 250 mμ are assigned as $E_3 \rightarrow E_5$ (*p*-benzoquinone), $E_4 \rightarrow E_7$ (α-naphthoquinone), and $E_5 \rightarrow E_9$ (anthraquinone), and the bands near 300 mμ as $E_4 \rightarrow E_5$ (*p*-benzoquinone), $E_5, E_6 \rightarrow E_7$ (α-naphthoquinone) and $E_6, E_7, E_8 \rightarrow E_9$ (anthraquinone). The fact that the intensity of the band near 300 mμ of *p*-benzoquinone is about ten times weaker than that of α-naphthoquinone and of anthraquinone can be explained with the present result that in *p*-benzoquinone alone, the corresponding transition is forbidden.

Second, the energy levels as a whole are a little elevated as the size of the *p*-quinone molecule becomes larger. This result can be anticipated considering the ratios of the number of electronegative oxygen atoms to that of far less electronegative carbon atoms in each *p*-quinone molecule. As a measure of the elevation of the energy levels, the average value of the highest filled and the lowest vacant orbital energies of each *p*-quinone may be adopted. This value has $\alpha+0.665\beta$, $\alpha+0.577\beta$, and $\alpha+0.514\beta$ for *p*-benzoquinone, α-naphthoquinone, and anthraquinone, respectively. Now, the lone-pair orbital energies of the oxygen atoms in the three *p*-quinones are thought to be nearly equal. Then, it may be expected that the n-π transition energy becomes greater in the order of *p*-benzoquinone, α-naphthoquinone and anthraquinone. The observed phenomenon[1c,2] agrees satisfactorily with this expectation. It seems sure that the same explanation can be applied to the same phenomenon observed in *o*-quinones[1c,2].

The Effect of the Electron-Donating Substituent on the π—π Transition Bands.—In our previous work[7], the effect of the alkyl groups on the near UV absorption bands of *o*- and *p*-benzoquinones are studied using a modified form of Herzfeld-Nagakura-Baba's formula[8]. In a one-electron transition (m orbital $\rightarrow n$ orbital), the shift in wave numbers ($\Delta\nu_{m\rightarrow n,i}$) due to a substitution on the ith carbon atom in a quinone molecule has the value,

$$\Delta\nu_{m\rightarrow n,i} = K_m C_{mi}^2 - K_n C_{ni}^2 \qquad (1)$$

Here, the two conditions are required, that m and n orbitals are non-degenerate and the m orbital energy is higher than the substituent's lone-pair orbital energy. C_{mi} and C_{ni} are the coefficients of the ith atomic orbital in the LCAO MO, m and n, respectively. K_m and K_n are nearly constant if the kind of substituent is fixed, and $K_m < K_n < 0$. So, if $C_{mi}^2 \geq C_{ni}^2$, $\Delta\nu_{m\rightarrow n,i} < 0$. Then, the greater the C_{mi}^2 value is and the smaller the C_{ni}^2 value, the greater the extent of the red-shift of the band is. Thus, considering the C_{mi}^2 and C_{ni}^2 values, the magnitude of the red shift of a band by a substituent can be presumed.

Now, let us apply the above method to α-naphthoquinone and anthraquinone whose data are given in Figs. 1[9], 2[10] and

4) B. Eda, Presented at the Symposium on Structural Chemistry, Sendai (1954).
5) R. J. W. LeFèvre, "Dipole Moments", Methuen & Co. Ltd., London (1948), p. 100.
6) B. Pullman and J. Daudel, *Compt. rend.*, **238**, 964 (1954).
*1 In view of the intensity and the solvent effect, this band is thought to be due to π-π transition.
7) A. Kuboyama *J. Chem. Soc. Japan, Pure Chem. Sec.* (*Nippon Kagaku Zassi*), **77**, 1062 (1956).
8) K. F. Herzfeld, *Chem. Rev.*, **41**, 233 (1947); H. Baba and S. Nagakura, *J. Chem. Soc. Japan, Pure Chem. Sec.* (*Nippon Kagaku Zassi*), **72**, 72 (1951).
9) M. O'L Crowe, *J. Biol. Chem.*, **115**, 479 (1936).
10) R. A. Morton and W. T. Earlam, *J. Chem. Soc.*, **1941**, 159.

Tables I, II. In Figs. 1 and 2, in all cases, the substituent is the hydroxyl group and the solvent ethanol. Since the solvent effect[9] of ethanol on the bands near 250 mμ and 300 mμ of α-naphthoquinone are very small compared with the substitution effect, the former effect may safely be

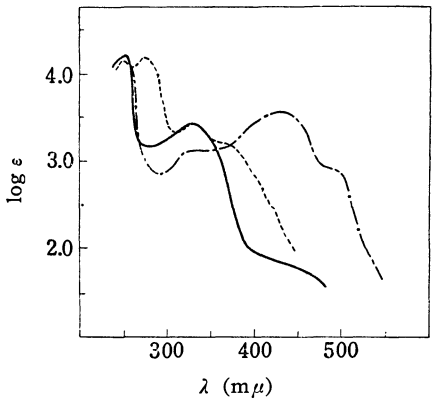

Fig. 1. ——, 1,4 Naphthoquinone;
- - - -, 2-Hydroxy- 〃 ;
— - —, 5-Hydroxy- 〃 ;
Solvent, Ethanol.

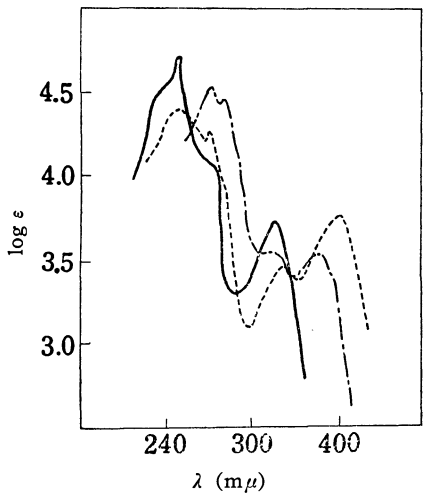

Fig. 2. ——, Anthraquinone;
- - - -, 2-Hydroxy- 〃 ;
— - —, 3-Hydroxy- 〃 ;
Solvent, Ethanol.

TABLE I

THE SQUARE VALUES OF THE COEFFICIENTS IN α-NAPHTHOQUINONE (THE NUMBERS IN THE FIRST ROW DENOTE THE POSITIONS OF THE SUBSTITUTIONS)

	2	5	6
$E_4(a_2)$	0.270	0.001	0.017
$E_5(b_1)$	0.000	0.298	0.073
$E_6(a_2)$	0.085	0.000	0.207
$E_7(b_1)$	0.082	0.036	0.028

TABLE II

THE SQUARE VALUES OF THE COEFFICIENTS IN ANTHRAQUINONE

	2	3
$E_5(b_{1u})$	0.001	0.098
$E_6(b_{2g})$	0.136	0.032
$E_7(b_{3g})$	0.000	0.125
$E_8(a_{1u})$	0.167	0.042
$E_9(b_{2g})$	0.032	0.031

neglected. All the π-orbitals of α-naphthoquinone and anthraquinone are intrinsically non-degenerate and we can reasonably assume that the lone-pair orbital energy of the oxygen atom in the hydroxyl group as a substituent is lower than the E_4(α-naphthoquinone) and E_5(anthraquinone) orbital energies. Thus, the above method can be applied. As the consequence it may be expected that, as for α-naphthoquinone, the band near 250 mμ largely shifts towards longer wave lengths for 2-substitution and remains almost constant for 5-substitution. The data in Table I clearly fit these expectations. On the other hand, the bands near 300 mμ split into the two bands for both 2- and 5-substitutions, and from the data in Table I, the longer-wavelength bands are thought to correspond to the transitions, $E_6 \rightarrow E_7$ (2-substitution) and $E_5 \rightarrow E_7$ (5-substitution), and the shorter wavelength bands to the transitions, $E_5 \rightarrow E_7$ (2-substitution) and $E_6 \rightarrow E_7$ (5-substitution). As for anthraquinone, the band near 250 mμ largely shifts towards longer wavelengths for 3-substitution and scarcely shifts at all for 2-substitution. This fact is clearly explained from eq. (1), and C_{mi}^2 and C_{ni}^2 values given in Table II. It is thought that the band near 300 mμ of unsubstituted anthraquinone is mainly contributed by the transition, $E_8 \rightarrow E_9$, since this transition alone is allowed among the three transitions assigned to this band, but in hydroxy anthraquinone the forbidden transitions come to be allowed to some extent by the perturbation of the substituent group. From the coefficient values in Table 2, it may be induced that the longest wavelength max. of the band near 300 mμ corresponds to the transition $E_8 \rightarrow E_9$ for 2-substitution and $E_7 \rightarrow E_9$ for 3-substitution, respectively. These assignments seem reasonable from the fact that the intensity of the absorption band under consideration is stronger in 2-hydroxy anthraquinone than in 3-hydroxyl derivative (see Fig. 2). Thus, the above theoretical consideration can clearly explain the effect

of the electrondonating substituent on the π—π transition bands in the near UV region of α-naphthoquinone and anthraquinone.

In addition, as for the report[11] that in the α-naphthosemiquinone ion the probability of finding the unpaired electron in a $p_z\pi$ orbital centered on the 2nd carbon atom is ca. ten times greater than that in a $p_z\pi$ orbital centered on the 5th or 6th carbon atoms, the probabilities are thought to be approximately parallel to the C_{7i}^2 values and the result in Table I is unsatisfactory in comparison with the experimental result, but a similar trend is seen for the *o*-benzosemiquinone ion[11b,*2], naphthoquinone and anthraquinone. The calculated dipole moment (2.2 D) of α-naphthoquinone seems too large. As for bond orders, the reasonable results were obtained. Two problems concerning the near UV absorption bands (1. a similarity among the π—π transition bands of the three *p*-quinones, 2. a relative magnitude of the n—π transition energy in the order of *p*-benzoquinone, α-naphthoquinone and anthraquinone) can be clearly explained with the calculated results. Especially, the effect of the electrondonating group on the π—π transition bands of α-naphthoquinone and anthraquinone can also be favourably explained, according to the modified Herzfeld-Nagakura-Baba's formula, with the calculated results. It seems sure that for the *o*-quinone type compounds the similar result can be obtained with the same method as used for the *p*-quinone type compounds.

Summary

Electronic structures of *p*-benzoquinone, α-naphthoquinone, and anthraquinone were studied with the simple MO method, using the same integral values as adopted in the SCF MO calculation for *p*-benzoquinone. As for charge distributions, the negative charges of oxygen atoms slightly increase in the order *p*-benzoquinone, α-

The author wishes to express his sincere thanks to Professor S. Nagakura of the Institute for Solid State Physics, Tokyo University, for his kind guidance.

Faculty of Agriculture
University of Miyazaki
Miyazaki

11) a) J. E. Wertz and J. L. Vivo, *J. Chem. Phys.*, **24**, 479 (1956); b) H. M. McConnell, ibid., **24**, 632 (1956).

*2 In our previous calculation[2], the similar result to 11b) was obtained.

The Action of Hydrogen Bromide and Oxygen on Various Ethenoid Compounds. III. The Steric Effects of the Bromo Free Radicals Produced from Various Ethenoid Compounds on the Reactivities with Oxygen

By Makoto TAKAHASI

(Received March 18, 1958)

The mechanism of the action of hydrogen bromide on various ethenoid compounds in the presence of a large amount of oxygen has been discussed in the preceding papers of this series[1,2], and the fundamental reaction scheme has been assumed as follows:

(1) $\rangle C{=}C\langle + O_2 + HBr \longrightarrow$
$Br\cdot$ (initiation)

(2) $\rangle C{=}C\langle + Br\cdot \longrightarrow$
$\rangle \dot{C}-C\langle$ (propagation)
Br

(3) $\rangle \dot{C}-C\langle + O_2 \longrightarrow$
Br
$\rangle C(\cdot O_2)-C\langle$ (propagation)
Br

1) M. Takahasi, This Bulletin, **29**, 625 (1956).
2) M. Takahasi, ibid., **29**, 973 (1956).

(4) $\rangle C(\cdot O_2)-C(Br)\langle + HBr \longrightarrow$

$\rangle C(HO_2)-C(Br)\langle + Br\cdot$ (propagation)

(5) $\rangle C(HO_2)-C(Br)\langle + HBr \longrightarrow$

oxidation products $+ Br\cdot$ (propagation)

(6) $\rangle C(\cdot)-C(Br)\langle + Br_2 \longrightarrow$

$\rangle C(Br)-C(Br)\langle + Br\cdot$ (propagation)

(7) $Br\cdot + Br\cdot \longrightarrow$

Br_2 (termination)

(8) $\rangle C(\cdot)-C(Br)\langle + Br\cdot \longrightarrow$

$\rangle C(Br)-C(Br)\langle$ (termination)

From the kinetical point of view, it is desirable to establish a complete method to determine the velocity constants of these reactions, but at present it may be difficult to carry out a kinetical study of the reactions of the three component systems. The author attempted to study qualitatively the reactions of bromine with ethenoid compounds, such as β-methylcinnamic acid, cinnamic acid, *p*-methoxycinnamic acid, atropic acid, and diphenylethylene, to compare the intermediate bromo free radicals to be produced from these ethenoid compounds in the reactivity with oxygen, expecting that it may be helpful to elucidating the mechanism of the reactions of hydrogen bromide and oxygen with ethenoid compounds, because the reactions are presumed to include the same reaction processes as 2,3,6,7, and 8 as shown below:

(1′) $Br_2 \longrightarrow$

$2\,Br\cdot$ (compare with process 1)

(2′) $Br\cdot + \rangle C=C\langle \longrightarrow$

$\rangle C(\cdot)-C(Br)\langle$ (same as process 2)

(3′) $\rangle C(\cdot)-C(Br)\langle + O_2 \longrightarrow$

$\rangle C(\cdot O_2)-C(Br)\langle$ (same as process 3)

(4′) $\rangle C(\cdot O_2)-C(Br)\langle +$ hydrogen donor $\longrightarrow$

$\rangle C(HO_2)-C(Br)\langle$ (compare with process 4)

(5′) $\rangle C(HO_2)-C(Br)\langle \xrightarrow{\text{thermal or acid decomposition}}$

oxidation products (compare with process 5)

(6′) $\rangle C(\cdot)-C(Br)\langle + Br_2 \longrightarrow$

$\rangle C(Br)-C(Br)\langle$ (same as process 6)

(7′) $Br\cdot + Br\cdot \longrightarrow$

Br_2 (same as process 7)

(8′) $\rangle C(\cdot)-C(Br)\langle + Br\cdot \longrightarrow$

$\rangle C(Br)-C(Br)\langle$ (same as process 8)

If any hydrogen donor such as hydrogen bromide does not exist, reaction 4′ does not proceed, and no bromohydroperoxide is produced. R. F. Brown and F. Daniels[3] observed the rate of the reaction of cinnamic acid with bromine in the absence of a hydrogen donor is reduced by the presence of oxygen in the light, and O. Simamura[4] observed the same effect of oxygen to occur even in the dark. J. L. Magee and F. Daniels[5] ascribed the inhibitive action of oxygen to the reaction of the bromo free radical with oxygen and to the reaction of the bromohydroperoxide radical thus produced with another bromo free radical, giving a peroxide or further oxidation products with evolution of a large amount of heat.

$C_6H_5-CH(\cdot O_2)-CH(Br)-COOH$ $\longrightarrow$

$C_6H_5-CH(\cdot)-CH(Br)-COOH$

$C_6H_5-CH(O-O\cdot)-CH(Br)-COOH$ $\longrightarrow$ oxidation products such as benzoic acid.

$C_6H_5-CH(O-O-)-CH(Br)-COOH$

The author attempted to identify the reaction products produced by the reactions of ethenoid compounds with bromine in the presence of an excess of oxygen. The ethenoid compounds, except β-methylcinnamic acid and diphenylethylene, did

3) R. F. Brown and F. Daniels, *J. Am. Chem. Soc.*, **62**, 2820 (1940).
4) O. Simamura, This Bulletin, **17**, 274 (1942).
5) J. L. Magee and F. Daniels, *J. Am. Chem. Soc.*, **62**, 2825 (1940).

not give any appreciable amounts of oxidation products other than dibromides by the reactions with bromine in nonpolar solvents in spite of the presence of a large amount of oxygen, and the inhibitive action by oxygen was not remarkable. However, the reaction of β-methylcinnamic acid with bromine in the presence of a large amount of oxygen manifested a remarkable feature, as described below.

When oxygen was passed through a benzene solution of β-methylcinnamic acid in the sunlight with simultaneous addition of a benzene solution of bromine, the color of bromine faded far less rapidly than without introduction of oxygen. The reaction products were found to consist of carbon dioxide, acetophenone, a small amount of β-methylcinnamic acid dibromide, and some unidentified aldehyde.

Further, the reaction of β-methylcinnamic acid with hydrogen bromide and oxygen was carried out, and the reaction products were found to include carbon dioxide, α-bromoacetophenone and *p*-bromophenol, and a large amount of β-methylcinnamic acid was recovered, while β-methylcinnamic acid dibromide could not be detected in the products. It is to be noted that the reaction products in this case do not correspond to those of the reaction of cinnamic acid with hydrogen bromide and oxygen[1]. *p*-Bromophenol formed may inhibit the progress of the reaction of β-methylcinnamic acid with hydrogen bromide and oxygen.

Generally, in the reactions of ethenoid compounds with bromine in the presence of a large amount of oxygen, no hydrogen donor apparently exists. However, if acetophenone is formed in the reaction of β-methylcinnamic acid with oxygen and bromine via a bromohydroperoxide formation, reactions 4′, and 5′, it is necessary to assume the presence of a hydrogen donor. Although no evidence for either an intra- or an inter-molecular hydrogen transfer is available, it seems probable that the hydrogen of the carboxyl group moves to the peroxidic oxygen to give a bromohydroperoxide, considering the relative positions of the carboxyl group and the peroxidic oxygen. The structure of the intermediate was presumed to be

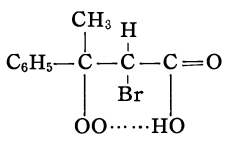

The special reactivity of β-methylcinnamic acid with oxygen, compared with other ethenoid compounds, may be understandable from following consideration.

The yields of oxidation products in the reactions of the ethenoid compounds with oxygen and bromine are not directly related with the structures of the ethenoid compounds themselves, but depend on the reactivity of the bromo free radicals with oxygen. However, the discussions on the ethenoid compounds as described below may be helpful to understanding the reactivity of the bromo free radicals.

H. Suzuki[6], in his study on the absorption spectra of a series of stilbene derivatives, i.e. stilbene, α-methylstilbene, and α, β-dimethylstilbene, found that the absorption maxima of these compounds are shifted progressively in the order towards shorter wave lengths with increasing angles of twist of the phenyl groups out of the plane of the ethylenic linkage caused mainly by the steric repulsion between the methyl group and the phenyl group attached to different carbon atoms of the ethylenic linkage. In parallel with the study of the steric effect on the ultraviolet absorption spectra, H. Suzuki, O. Simamura and T. Ichihashi[7,8] studied the action of the bromine atom and oxygen on stilbene derivatives, and they found that the action of the bromine atom and oxygen on α, β-dimethylstilbene caused an oxidative cleavage of the double bond.

β-Methylcinnamic acid may be in a state of less steric strain than α,β-dimethylstilbene, because in the former the methyl group interacts only with one phenyl group, and the methyl and the phenyl group are attached to the same carbon atom of the ethylenic linkage. In the latter, the both methyl groups interact with the phenyl groups attached to different carbon atoms respectively, so that it may be in a state of a larger steric strain than β-methylcinnamic acid. Notwithstanding, in the series of cinnamic acid, β-methylcinnamic acid, and β-ethylcinnamic acid, the maxima of the absorp tion spectra are also shifted progressively in the order towards shorter wave lengths with decrease in extinction coefficients, as in the series of stilbene derivatives. This fact may indicate existence of a

6) H. Suzuki, This Bulletin, **25**, 145 (1952).
7) H. Suzuki, O. Simamura and T. Ichihashi, ibid., **27**, 235 (1954).
8) O. Simamura and H. Suzuki, ibid., **27**, 231 (1954).

steric repulsion between the methyl group and the phenyl group in β-methylcinnamic acid.

The amount of the steric strain of π-electron system caused by the repulsion between the methyl group and the phenyl group may be of the same order in the intermediate bromo free radical from β-methylcinnamic acid as in β-methylcinnamic acid, because the methyl group and the phenyl group are attached to the same carbon atom. Thus the reactivity of the bromo free radical produced from β-methylcinnamic acid with oxygen may be larger than the reactivity of the bromo free radicals produced from cinnamic acid and any other ethenoid compounds with no steric strain.

β-Methylcinnamic acid, α,β-dimethylcinnamic acid and diphenylethylene and the intermediate free radicals therefrom as well may be subject to a large steric strain. In α-methylcinnamic acid, however, the interaction of the α-methyl group with the β-phenyl group will be released at the stage of the intermediate bromo free radical, so that the reactivity of the bromo free radical produced from α-methylcinnamic acid with oxygen may not be large.

An experiment on the reaction of α-methylcinnamic acid with hydrogen bromide and oxygen was attempted, but no reaction took place. On the other hand, the experiment on the reaction of α,β-dimethylcinnamic acid with hydrogen bromide and oxygen by Simamura, Nomura, and the present author[9], which has not yet been published, showed that it gives α-bromoacetophenone and acetophenone by the reaction with hydrogen bromide and oxygen.

Diphenylethylene gave a large amount of the dibromide and a very small amount of *p*-bromophenol by the reaction with bromine and oxygen. This result is apparently inconsistent with the result discussed above. It is to be noted, however, that diphenylethylene has no reactive hydrogen in the molecule, so that the peroxide radical produced from oxygen and bromo free radical (reaction 4′), cannot give a bromohydroperoxide. In the case of α,β-dimethylstilbene, it may be possible that the methyl groups serve as hydrogen donors for the bromo peroxide radical by either an inter- or an intramolecular mechanism. Although the electronic effect of the methyl groups attached to the carbon atoms of the ethylenic linkage on the reactivity with bromine and oxygen has not been discussed, the present author considers such an effect as mentioned above possible, but at present no experimental evidence for the effect is available.

M. S. Kharasch, A. Fono, and W. Nudenberg[10] reported that diphenylethylene gave phenol and acetophenone by the reaction with hydrogen peroxide in the presence of perchloric acid. The present author also observed a special reactivity of β-methylcinnamic acid with hydrogen peroxide in the presence of perchloric acid. β-Methylcinnamic acid was decomposed to give carbonyl compounds, while cinnamic acid did not give any product under the same conditions. Investigation on the reaction is continued.

Experimental

Materials.—β-Methylcinnamic acid was synthesized by the Reformatsky reaction of acetophenone with ethyl iodoacetate in benzene, and recrystallized from ethyl alcohol, m.p. 104.5°. α-Methylcinnamic acid was synthesized by the Perkin reaction of benzaldehyde with propionic anhydride in the presence of sodium propionate, and recrystallized from ethyl alcohol, m.p. 81～82°C. The preparation of *p*-methoxycinnamic acid, atropic acid, and diphenylethylene, and their purification were described in a previous paper[2].

The Reaction of β-Methylcinnamic acid with Bromine and Oxygen.—β-Methylcinnamic acid (2 g.) was dissolved in 60 ml. of benzene and the solution was divided into equal portions in separate flasks, each being equipped with a small dropping funnel, and one in addition with two glass tubes for introducing oxygen into the solution. The flasks were placed in the strong sunlight, and 20 ml. of a benzene solution containing 1 g. of bromine was dropped into each flask, oxygen being passed simultaneously into one of the solutions. Here the experiment with introduction of oxygen is designated as Expt. 42-a, and the experiment without oxygen as Expt. 42-b. The color of the solution in Expt. 42-b faded in less than five minutes, while that of Expt. 42-a slowly and remained even for four hours. No evolution of hydrogen bromide was observed during the reaction in either case. In Expt. 42-a, after oxygen was passed for about 130 minutes, the solution was kept standing in the diffused daylight for 210 minutes. From the reaction mixture, 0.31 g. of crystalline substance and 0.852 g. of an oil were obtained. The oil

9) O. Simamura, S. Nomura, and M. Takahasi, unpublished work.

10) M. S. Kharasch, A. Fono, and W. Nudenberg, *J. Org. Chem.*, **15**, 748 (1950).

(0.852 g.) was brought to react with 0.5 g. of 2,4-dinitrophenylhydrazine dissolved in 40 ml. of ethyl alcohol with 1 ml. of conc. hydrochloric acid, and about 0.239 g. of a 2,4-dinitrophenylhydrazone, m.p. 220~235°C, was obtained. The chloroform solution of the dinitrophenylhydrazone was passed through a chromatographic column of alumina, giving an orange zone and a dark brown zone. Acetophenone 2,4-dinitrophenylhydrazone, m.p. 248~250°C, was obtained from the latter zone, and identified by the mixed melting point. The orange zone gave a very small amount of an unidentified substance. The crystalline product (0.31 g.) was identified with the dibromide of β-methylcinnamic acid by the mixed melting point.

From Expt. 42-b, about 1.93 g. of β-methylcinnamic acid dibromide, m.p. 128°C, was obtained, but no oily product.

In another experiment similar to Expt. 42-a, 30 ml. of a benzene solution containing 1 g. of β-methylcinnamic acid was treated, in the sunlight for 320 minutes, with oxygen and with 30 ml. of a benzene solution containing 1 g. of bromine simultaneously. The gas from the solution was passed through distilled water and then through an aqueous barium hydroxide solution. The distilled water then gave a positive Schiff test, indicating the formation of a water-soluble aldehyde. When the benzene solution was washed with 10 ml. of distilled water, the aqueous layer gave positive reactions in Schiff test, with 2,4-dinitrophenylhydrazine, and with dimedone. An alcohol solution of dimedone gave a very small amount of a crystalline substance, m.p. 195~200°C, but its identification was unsuccessful. Barium carbonate precipitated from the aqueous barium hydroxide during the reaction weighed 0.707 g. (0.0031 mol.).

The Influence of Oxygen on the Reaction of Other Ethenoid Compounds with Bromine.—To a solution of 4 g. of cinnamic acid in 40 ml. of benzene, 30 ml. of a benzene solution containing 4.7 g. of bromine was added dropwise with passage of oxygen in the sunlight for 125 minutes. The color of bromine disappeared in about one hour. The gas from the solution was passed through distilled water and then through a barium hydroxide solution, but no barium carbonate was formed in the barium hydroxide solution, and neither the bromide ion nor a carbonyl compound was found in the distilled water. From the benzene solution about 5.9 g. of crystalline cinnamic acid dibromide precipitated, and on evaporation of the mother liquor 1 g. of slightly oil-stained crystals of cinnamic acid dibromide were further obtained.

p-Methoxycinnamic acid (1 g.) was dissolved in 60 ml. of carbon tetrachloride, and the solution was divided into two flasks. Into each flask 0.28 g. of bromine dissolved in 20 ml. of carbon tetrachloride was added in the sunlight, oxygen being passed into one of the solutions. The color of bromine faded nearly at the same rate in both solutions, and no remarkable inhibition by oxygen from addition of bromine to the ethenoid compound was observed. Hydrogen bromide was not evolved in the course of reaction, and it was suggested that addition of bromine to the double bond took place more predominantly than nuclear substitution.

The same experimental procedure as above was followed in the case of atropic acid and diphenylethylene. From atropic acid, only atropic acid dibromide, m.p. 115~116°C, was obtained either with or without introduction of oxygen. In the case of diphenylethylene, the reaction mixture was shaken with water and aqueous alkali successively. When a bromine potassium bromide solution was added to the neutral aqueous extract, tribromophenol was precipitated. Moreover, when the alkaline extract was saturated with carbon dioxide and extracted with ether, a very small amount of a phenolic substance was obtained, which showed a positive test of a phenol with ceric ammonium nitrate, and had a melting point, 63.5°C. Diphenylethylene dibromide was obtained from the both carbon tetrachloride solution on removing the solvent by distillation.

Reaction of β-Methylcinnamic Acid with Hydrogen Bromide and Oxygen.—β-Methylcinnamic acid (5.000 g.) was suspended in 70 ml. of carbon tetrachloride, and a mixture of hydrogen bromide and oxygen was passed through the suspension for 485 minutes. Here the treatment was continued longer than in the cases of the other ethenoid compounds, because preliminary experiments showed that the reaction was not completed in spite of a relatively long reaction time. A moderate amount of carbon dioxide was evolved during the whole reaction period, giving 0.608 g. of barium carbonate. About 1.5 g. of brown oil separated from the carbon tetrachloride solution. The carbon tetrachloride solution was shaken three times with 70 ml. of distilled water, and then twice with 30 ml. of 2 N aqueous sodium hydroxide. The sodium hydroxide solution was saturated with carbon dioxide, separating about 3 ml. of an oil, which was extracted with ether. Benzoyl chloride was added to 1 ml. of the oil, and the mixture was heated for some time, and poured into water. The crystalline product, after washed with aqueous sodium carbonate, was recrystallized from ethyl alcohol, giving a white crystalline substance, m.p. 102~104°C. It was identified with *p*-bromophenyl benzoate by the mixed melting point with an authentic specimen. *Anal.* Found: Br, 29.5. Calcd. for $C_{13}H_9O_2Br$: Br, 28.9%. The sodium hydroxide solution, from which the phenolic substance had been separated, was acidified with dil. sulfuric acid, and shaken twice with 100 ml. of ether. Evaporation of the ethereal solution gave about 0.321 g. of a pale yellow oil, which contained only a trace of bromine. It was presumably crude β-methylcinnamic acid, although it could not be brought to crystallization.

In another similar experiment, hydrogen bromide and oxygen were passed into a solution of β-methylcinnamic acid (10 g.) in 80 ml. of benzene for 360 minutes, and 2.2 g. of a precipitate was obtained which was identified with

β-methylcinnamic acid dibromide. Evaporation of the benzene solution gave a yellow oil. When 1.1 g. of the oil was brought to reaction with 2,4-dinitrophenylhydrazine in ethyl alcohol, a small amount of a yellow precipitate was formed. It was separated into parts soluble and insoluble in hot ethyl alcohol. The soluble part was a yellow crystalline substance, which melted at 160~164°C. The insoluble part, which weighed 0.05 g., melted at 210°C, and contained 15.8% of bromine. Further purification was unsuccessful with both substances, but the soluble substance was supposed to be 2,4-dintrophenylhydrazone of formaldehyde or of glyoxylic acid, and the insoluble to be that of α-bromoacetophenone, m.p. 214~215°C.

When hydrogen bromide was passed through a solution of 3 g. of β-methylcinnamic acid in 60 ml. of benzene without introduction of oxygen for 210 minutes, a crystalline substance, m.p. 42~80°C, was obtained, but recrystallization gave β-methylcinnamic acid only.

A reaction of α-methylcinnamic acid with hydrogen bromide and oxygen was attempted in the same way as that of β-methylcinnamic acid. No evolution of carbon dioxide was observed, and the reaction mixture gave no positive tests of a carbonyl compound, and α-methylcinnamic acid was recovered from the solution.

The Reaction of Cinnamic Acid with Hydrogen Peroxide in the Presence of Perchloric Acid.—Cinnamic acid (6.0 g.) was dissolved in 40 ml. of acetic acid, and 6 ml. of 30% hydrogen peroxide and 2 g. of 70% perchloric acid were added. Even after two days, cinnamic acid was recovered almost completely, and no formation of either a carbonyl compound or a phenol was observed. A preliminary experiment on the reaction of β-methylcinnamic acid with hydrogen peroxide in the presence of perchloric acid has shown the formation of acetophenone and glyoxylic acid.

Ultraviolet Absorption Spectra of Cinnamic Acid and its Derivatives.—The measurements of the ultraviolet absorption spectra were carried out with a Beckman type spectrophotometer. The absorption maxima of cinnamic acid, β-methylcinnamic acid and β-ethylcinnamic acid in 94% ethyl alcohol, were 273, 260 and 244 mμ, respectively, and the molecular extinction coefficients were 2.2×10^4, 1.5×10^4 and 1.0×10^4, respectively.

Summary

The action of oxygen and bromine on β-methylcinnamic acid in benzene in the sunlight at room temperature caused an oxidative cleavage of the double bond, giving acetophenone and carbon dioxide, in addition to β-methylcinnamic acid dibromide. Similar experiments with cinnamic acid, atropic acid, *p*-methoxycinnamic acid, gave only dibromides either with or without introduction of oxygen.

Although a complete identification of the reaction products from the reaction of hydrogen bromide and oxygen on β-methylcinnamic acid was unsuccessful, it was found that a phenolic substance and a carbonyl compound were produced and that the formation of the phenol inhibited the progress of the reaction.

On the ground of these and other results which were described in the three preceding papers, the mechanism of the reactions of hydrogen bromide, bromine, and oxygen with ethenoid compounds is discussed.

The author wishes to express his hearty thanks to Professor Y. Urushibara and Professor O. Simamura for their kind guidance and encouragement for the present work.

Department of Chemistry
College of General Education
The University of Tokyo
Meguro-ku, Tokyo

The Infrared Spectra of Methoxy-, Methylmethoxy- and Methoxy Endblocked Dimethyl-polysiloxanes

By Toshio TANAKA

(Received June 3, 1958)

The group frequency assignments have already been given for the infrared spectra of organoalkoxypolysiloxanes, such as alkylalkoxysilanes[1] and ethoxy- and methylethoxy-polysiloxanes[2]. In this paper the infrared spectra of three types of polysiloxanes represented by A, B and C, which contain methoxy and methyl groups in various proportions, will be described.

A_n : $CH_3O[(CH_3O)_2SiO]_nCH_3$ $n=1\sim3$
B_n : $CH_3O[CH_3OSi(CH_3)O]_nCH_3$ $n=1\sim5$
C_n : $CH_3O[Si(CH_3)_2O]_nCH_3$ $n=1\sim6$

These polysiloxanes have simple structural units, and the infrared spectra seem to be explained fairly well. The vibrational spectrum of C_1 (dimethyldimethoxysilane) has been reported[3] and most of the assignments have agreed with the results which would be described in this paper. Referring to the results of this experiment and the infrared spectra of

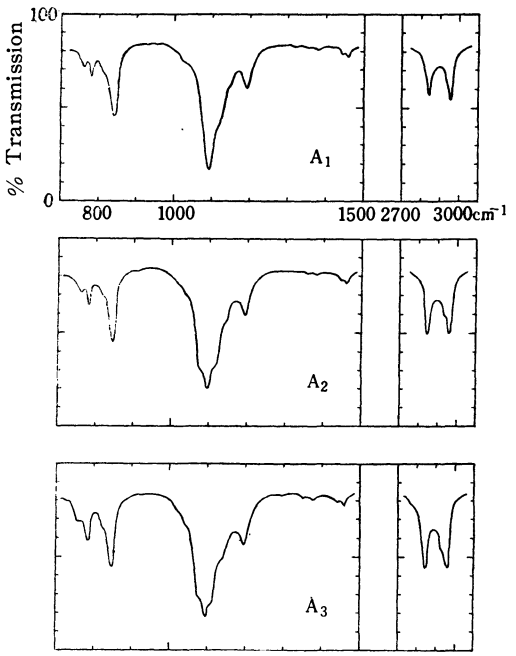

Fig. 1. Infrared spectra of methoxy-polysiloxanes.
A_n: $CH_3O[(CH_3O)_2SiO]_nCH_3$, 2% in CS_2 and CCl_4.

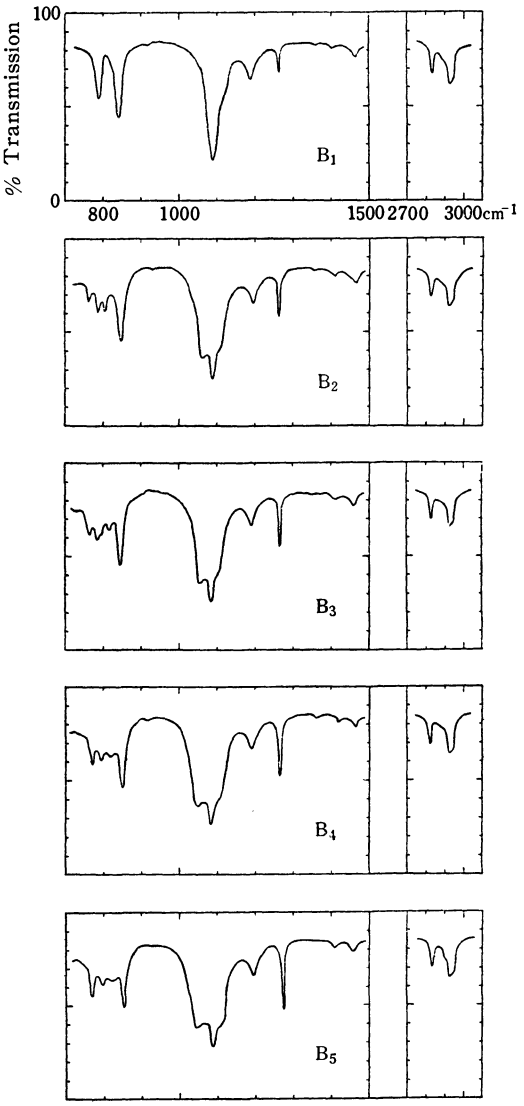

Fig. 2. Infrared spectra of methylmethoxy-polysiloxanes.
B_n: $CH_3O[CH_3OSi(CH_3)O]_nCH_3$, 3% in CS_2 and CCl_4.

1) R. E. Richards and H. W. Thompson, *J. Chem. Soc.*, **1949**, 125.
2) R. Ōkawara, This Bulletin, **31**, 154 (1958).
3) M. Hayashi, *J. Chem. Soc. Japan, Pure Chem. Sec.* (*Nippon Kagaku Zassi*), **79**, 436 (1958).

dimethylpolysiloxanes[4] (represented by D), one would make the explanation of the infrared spectra of the more complicated organoalkoxypolysiloxanes.

D_n : $CH_3[Si(CH_3)_2O]_nSi(CH_3)_3$ $n=1\sim7$

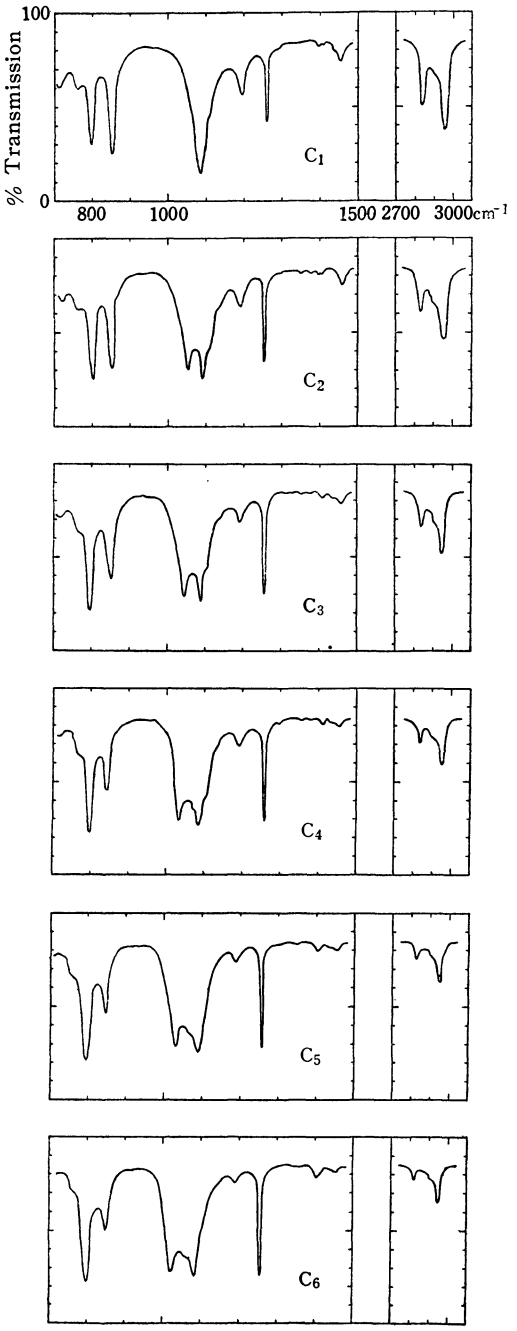

Fig. 3. Infrared spectra of methoxy endblocked dimethylpolysiloxanes.
C_n: $CH_3O[Si(CH_3)_2O]_nCH_3$, 5% in CS_2 and CCl_4.

4) N. Wright and M. J. Hunter, *J. Am. Chem. Soc.*, **69**, 803 (1947).

Experimental

Materials.—The preparations and the properties of the members of A[5], B[6] and C[7] used in this experiment were already reported.

Measurements.—The spectra were obtained by the use of Hilger H-800 infrared spectrophotometer with a rock salt prism. Samples

TABLE I
INFRARED SPECTRA OF METHOXYPOLYSILOXANES: POSITIONS OF BANDS (in cm^{-1})

A_n		
$n=1$	$n=2$	$n=3$
760 w	762 sh	761 sh
784 m	785 m	784 m
840 s	842 s	842 s
1038 sh	1044 sh	1046 sh
—	1078 sh	1080 sh
1094 vs	1095 vs	1095 vs
1112 sh	1112 sh	1112 sh
—	1143 sh	1144 sh
1195 m	1195 m	1196 m
1352 vw	1350 vw	1351 vw
1381 w	1381 w	1381 w
1444 w	1443 w	1443 w
1458 w	1459 w	1459 w
2350 br	2332 br	2321 w
—	—	2361 w
2847 m	2848 m	2848 s
—	2943 sh	2941 sh
2965 m	2968 m	2967 s

TABLE II
INFRARED SPECTRA OF METHYLMETHOXYPOLYSILOXANES: POSITIONS OF BANDS (in cm^{-1})

B_n				
$n=1$	$n=2$	$n=3$	$n=4$	$n=5$
—	767 m	767 m	769 m	769 m
790 m	790 m	790 m	791 w	792 w
—	808 m	818 m	821 w	822 w
845 m	847 m	848 m	850 m	850 m
—	1066 m	1051 m	1045 m	1041 m
1089 s	1088 s	1087 s	1085 s	1086 s
1110 sh	1108 sh	1109 sh	1110 sh	1112 sh
1192 m	1192 m	1193 m	1192 m	1194 m
1267 m	1266 m	1267 m	1267 m	1268 m
1402 vw	1404 vw	1403 vw	1402 vw	1405 vw
1459 w	1458 w	1457 w	1457 w	1458 w
2333 br	2342 br	2343 br	2344 br	2338 br
2825 m	2824 m	2823 m	2823 m	2825 m
2931 m	2930 m	2931 m	2930 m	2932 m
2953 sh	2951 sh	2953 sh	2953 sh	2953 sh

5) T. Tanaka and T. Watase, This Bulletin, **28**, 258 (1955).
6) T. Tanaka, A. Tasaka and R. Ōkawara, *Technol. Repts. Osaka Univ.*, **7**, 193 (1957).
7) T. Tanaka and R. Ōkawara, This Bulletin, **28**, 364 (1955).

TABLE III
INFRARED SPECTRA OF METHOXY ENDBLOCKED DIMETHYLPOLYSILOXANES: POSITIONS OF BANDS (in cm^{-1})

	C_n					
$n=1$*	$n=1$	$n=2$	$n=3$	$n=4$	$n=5$	$n=6$
730 s	713 w	720 w	716 vw	715 vw	—	—
	761 w	761 w	762 sh	761 sh	762 sh	761 sh
797 s	797 s	798 s	799 s	798 s	799 s	798 s
849 vs	855 s	853 s	851 s	847 s	849 m	850 m
998 vw	—	—	—	—	—	—
—	—	1055 s	1045 s	1036 s	1028 s	1021 s
1089 vs	1083 s	1091 s	1092 s	1092 s	1091 s	1092 s
—	—	1112 sh	1113 sh	1115 sh	—	—
1160 sh	—	—	—	—	—	—
1188 m	1190 m	1189 m	1191 w	1190 w	1190 w	1189 w
1258 m	1258 m	1261 s	1263 s	1263 s	1262 s	1262 s
1295 sh	—	1296 vw	1298 sh	1298 vw	—	—
1340 w	1343 vw	1343 vw	1342 vw	—	—	—
1399 sh	1399 w	1403 w	1403 w	1405 w	1405 w	1406 w
—	—	—	—	1435 sh	1439 sh	1443 sh
1456 s	1460 m	1458 m	1459 w	1458 w	1457 vw	1460 vw
—	—	2342 br	2342 br	2333 br	2316 w	2323 w
					2358 sh	2355 w
—	2830 m	2829 m	2827 m	2825 w	2826 w	2821 w
—	—	2906 sh	2906 sh	2907 sh	2906 sh	2908 sh
—	2947 s	2960 s	2956 s	2955 m	2953 m	2953 m

* M. Hayashi, *loc. cit.*[3]

were observed in this experiment both as a solution in carbon disulfide for the range 700 to 1500 cm^{-1} and in carbon tetrachloride from 1250 to 3500 cm^{-1}, and as pure liquid. The concentration of each solution was 2, 3 and 5% for A, B and C, respectively. The celles were 0.03 mm. thick in the case of the solution and less than 0.01 mm. in the case of pure liquids. No appreciable difference was observed between the two cases.

In order to compare the relative intensity approximately, the absorption of the compounds belonging to the same series have been recorded on the same chart, keeping the conditions as similar as possible. The spectra and the positions of the absorption bands obtained are presented in Figs. 1—3 and Tables I—III, respectively.

Discussion of the Results

All the compounds of A, B and C show two absorption peaks in the region 2800~3000 cm^{-1}. The members of A have a kind of methyl group attached to oxygen atom, so the two bands near 2847 and 2965 cm^{-1} are assigned to the symmetric and non-symmetric stretching vibration of (O—)CH_3 group*, respectively. These bands are also observed in B and C; the intensities decrease with the decreasing concentration of methoxy group as the polymer sizes increase, and this behavior is distinct in C. Considering this behavior and fairly weak intensity of C—H stretching band in (Si—)CH_3 group* the bands near 2825 and 2930 cm^{-1} in B and near 2825 and 2955 cm^{-1} in C are attributed to the symmetric and the non-symmetric C—H stretching vibration arising mainly from (O—)CH_3 group, respectively**. Thus the band associated with (O—)CH_3 group appears on the low frequency side of the CH absorption in (C—)CH_3 group, and this fact has been observed by Henbest et al.[8] The shoulders near 2953 cm^{-1} in B and near 2906 cm^{-1} in C would be due to the non-symmetric and symmetric C—H stretching modes of (Si—)CH_3 group in each series, respectively.

In B and C, the band near 1460 cm^{-1} decreases in strength with increasing polymer size, and that near 1400 cm^{-1} has the reverse tendency. Accordingly, the

* Represent the methyl group attached to oxygen atom.

8) H. B. Henbest, G. D. Meakins, B. Nicholls and A. A. Wagland, *J. Chem. Soc.*, **1957**, 1462.

* It has been reported[4] that the intensity of the C-H stretching band in (Si-)CH_3 was the order of one-third to one-fourth that in (C-)CH_3.

** As the concentration of O-CH_3 group is considerably small compared with that of Si-CH_3 group in the comparative higher members of C, the bands near 2925 and 2955 cm^{-1} would not always be due to the C-H stretching mode in (O-)CH_3 group.

former band is attributed to the methyl deformation vibration in O—CH_3 group referring to the wave number of that found in dimethylether (1466 cm^{-1})[9], and the latter to the methyl deformation vibration in Si—CH_3 group as already assigned[3,10].

The sharp intense band near 1260 cm^{-1} in B and C has been known to be the characteristic absorption of Si—CH_3 group. Some different assignments have been made to this band, that is, the rocking vibration[4], symmetrical deformation vibration[11] and γ-(CH) vibration[12] of (Si—)CH_3 group. In this investigation, it could not be decided what kinds of mode give this band, but considering the question from the relation between the position of methyl symmetrical deformation frequency and the electronegativity of atom, to which methyl group attaches*, the band near 1260 cm^{-1} would arise from(Si—)CH_3 symmetrical deformation mode.

The band near 1190 cm^{-1} is observed in all the members of A, B and C, and in the latter its intensity decreases with increasing polymer size. Diethyldimethoxysilane and ethyltrimethoxysilane show this band at 1189 and 1192 cm^{-1}, respectively[1], but no band is found near this wave number in D[4], and alkylalkoxy-silanes[1,3] and -polysiloxanes[2] not having methoxy group**. Therefore, the 1190 cm^{-1} band is clearly associated with O—CH_3 group, and referring to the wave number of methyl rocking vibration in dimethylether (1180 cm^{-1})[9], this band is considered to be the rocking vibration of (O—)CH_3 group. The wave number of the band associated with $Si(OCH_3)_n$ group is an approximately constant one and is larger than that of C—OCH_3 group, and the band in the region of 1189~1196 cm^{-1} is considered to be the characteristic frequency of Si—OCH_3 group.

In A, B and C, a common strong band appears near 1090 cm^{-1} which may be connected with the Si—O—C linkage*. Referring to the infrared spectra of dimethylether**, this band would be associated with $\overrightarrow{Si}—\overleftarrow{O}—\overrightarrow{C}$ stretching vibration†. The common band is also observed as a shoulder in the high-frequency side of the band near 1090 cm^{-1}, except C_1, C_5 and C_6. This band will probably correspond to the band near 1110 cm^{-1} observed in ethoxy- and methylethoxy-polysiloxanes[2].

Except in the case of the first members in each series, other bands having fairly strong intensity are observed at 1080 cm^{-1} in A, 1066~1041 cm^{-1} in B and 1055~1021 cm^{-1} in C. These bands in B and C decrease in wave number with increasing polymer size. This tendency has been observed in D[4] and in methylethoxypolysiloxanes[2], and these bands are clearly connected with Si—O stretching vibration in Si—O—Si linkage. The corresponding band at 1080 cm^{-1} in A would be observed as a shoulder on account of the extremely strong band at 1090 cm^{-1}. Thus, in the compounds except in the case of the first

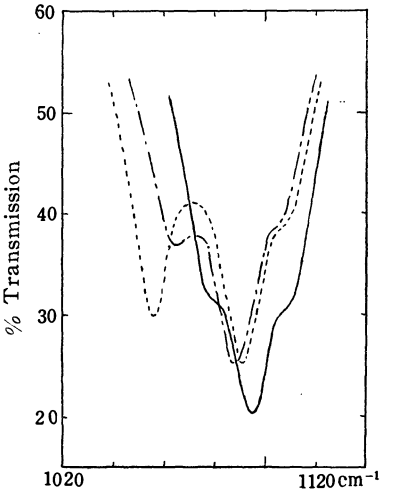

Fig. 4. Spectral sequence corresponding to the structural unit sequence of SiO_4, SiO_3C and SiO_2C_2.
——— $CH_3O[(CH_3O)_2SiO]_2CH_3$
— — — $CH_3O[CH_3OSi(CH_3)O]_2CH_3$
------ $CH_3O[Si(CH_3)_2O]_2CH_3$

9) G. Herzberg, "Molecular Spectra and Molecular Structure II. Infrared and Raman Spectra of Polyatomic Molecules", D. Van Nostrand Company, New York (1949) p. 353.
10) M. Sakiyama, This Bulletin, **31**, 67 (1958).
11) C. Y. Young, J. S. Koehler and D. S. McKinney, *J. Am. Chem. Soc.*, **69**, 1910 (1947).
12) D. H. Rank, B. D. Saksena and E. R. Shull, *Discuss. Farad. Soc.*, **9**, 187 (1950).

* For example, F-CH_3 1475, O-CH_3 1466 (in dimethylether), N-CH_3 1418 (in methylamine), Cl-CH_3 1355, S-CH_3 1323 and P-CH_3 1280 cm^{-1}; L. J. Bellamy, "The Infrared Spectra of Complex Molecules," Methuen & Co. London (1954) p. 24.

** For example, in ethoxypolysiloxanes the corresponding band appears near 1160 cm^{-1}, and has been considered to be the characteristic frequency of Si-OC_2H_5 group[2].

* The band near 1090 cm^{-1} would be also connected with Si-O-Si linkage as later described.

** The band due to the non-symmetric stretching vibration of C-O-C linkage appears at 1110 cm^{-1} [9].

† $\overrightarrow{Si}\text{-}\overleftarrow{O}\text{-}\overrightarrow{C}$ stretching band may be expected to appear in the vicinity of $\overrightarrow{C}\text{-}\overleftarrow{O}\text{-}\overrightarrow{C}$ stretching band, on account of the great force constant of Si-O bond, in spite of the large mass of silicon atom.

members in each series, a spectral sequence corresponding to the structural unit sequence of SiO_4, SiO_3C and SiO_2C_2 is found for the Si—O stretching frequency as shown in Fig. 4.

In D except D_2, the further band connected with Si—O—Si linkage has been found in the region of 1070~1093 cm^{-1} [4]. The corresponding band is expected to appear in A, B and C, but it will probably be comprised in the band due to $\vec{Si}—\overleftarrow{O}—\vec{C}$ stretching. This presumption is considered from the following fact; in C, as the polymer size increases the concentration of Si—O—C linkage decreases rapidly, but the rapid decreasing in strength of 1090 cm^{-1} band is not less noticeable observed.

Some strong bands appear in the region 750~900 cm^{-1}. One of them is observed at approximately constant wave number near 850 cm^{-1} in A, B and C, but is not in D. The intensity of this band decreases with increasing polymer size in B and C, especially in the latter. So there is no doubt that the band is associated with the grouping $Si(OCH_3)_n$ (n=1~4), and is not considered to be due to the rocking vibration of (Si—)CH_3 group which has been reported by Hayashi[3]. Similar behavior to the above has been observed in the 840 cm^{-1} band of ethoxy endblocked dimethylpolysiloxanes[2]. Referring to the spectra of dimethylether*, this band will probably be associated with the $\overleftarrow{Si}—O—\vec{C}$ vibration.

It has been known that the bands near 790 cm^{-1} in B and near 800 cm^{-1} in C have been associated with $SiCH_3$ and $Si(CH_3)_2$ groups, respectively[1,4]. In B except B_1, the absorption bands appear in the frequency on both sides of the 790 cm^{-1} band; the one at the lower wave number increases in strength as well as shifting to the side of less wave number, and the other becomes broader, as the polymer size increases. The band at 795 cm^{-1} in A would be considered to be a harmonics of the deformation vibration band involving Si—O linkage, which has been supported to fall in 770~830 cm^{-1} region by Wright and Hunter[4].

* The band due to the symmetric stretching vibration of C-O-C linkage is observed at 940 cm^{-1} [9].

Summary

1) The infrared spectra of the lower members of methoxy-, methylmethoxy- and methoxy endblocked dimethyl-polysiloxanes have been discussed by comparing them with that of dimethylether, dimethylpolysiloxanes, and so on.

2) The characteristic absorption band of $Si—OCH_3$ group has appeared near 1190 cm^{-1}.

3) Except in the case of the first members of these alkoxysiloxanes, a spectral sequence corresponding to the structural unit sequence of SiO_4, SiO_3C and SiO_2C_2 has been observed in the region of 1000~1100 cm^{-1}.

The author wishes to express his hearty thanks to Professor T. Watase and Dr. R. Ōkawara for their helpful discussion.

Department of Applied Chemistry
Faculty of Engineering
Osaka University
Miyakojima-ku, Osaka

SHORT COMMUNICATIONS

A New Method for Determining the Potential of the Electrocapillary Maximum by the Vibrated Dropping Mercury Electrode

Hideo IMAI, Senkichi INOUYE and Shōkichi CHAKI

(Received May 15, 1958)

The current-voltage curve of the mercuric ion was recorded with a conventional polarograph, using the vibrated dropping mercury electrode (VDME), to which an a. c. electric field is applied (cf. Fig. 1).

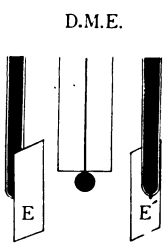

Fig. 1. The vibrated dropping mercury electrode: E, E' are the platinum plate electrodes to which the a. c. voltage is applied.

The a. c. electric field exerts a force as great as qE (q; the surface charge of the DME, E; the intensity of the a. c. electric field) on the DME, and causes the mechanical vibration of the DME. The vibration results in the increase of the limiting current of the electrolytic reduction of the mercuric ion, the convection current being superinduced on the diffusion-controlled one.

In the region of the positive polarization, the vibration gradually retards as the applied potential is shifted toward more negative potentials, corresponding to the decrease of the surface charge, and accordingly, the convection current gradually decreases. At the potential of zero charge, that is, the potential of the electrocapillary maximum, the vibration entirely ceases, and the limiting current is solely controlled by the diffusion. In the region of the negative polarization, the limiting current reincreases as the applied potential is shifted toward more negative potentials, corresponding to the increase of the surface charge. Thus, one can obtain the current-voltage curve which gives a minimum at the potential of the electrocapillary maximum, as is illustrated in Fig. 2. The more intensified is the electric field, the sharper is the "cut-in" of the minimum (cf. Fig. 2 A and B).

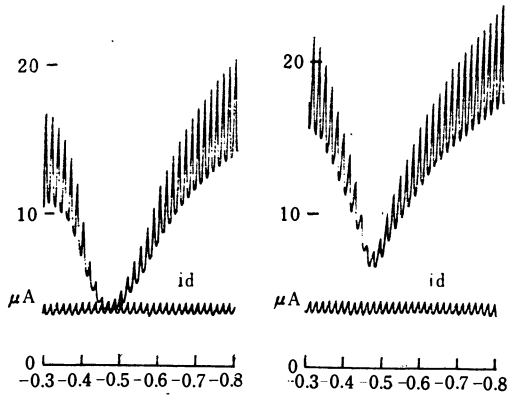

Fig. 2. The VDME current-voltage curve of $1 \cdot 10^{-3}$M Hg^{++} in 0.1 M KCl. The a. c. frequency = 25 c. p. s. The intensity of the a. c. field = 0.55 volts/cm. (Curve A), 0.60 volts/cm. (Curve B). The mercury head = 23.5 cm. The life-time of the DME = 9.9_4 sec. (open circuit). The rate of mercury flow = 0.85_5 mg./sec. Temperature = 25°C.

The potential of the electrocapillary maximum in various solutions was evaluated by this method, and the data gave a good agreement with those given by D. C. Grahame[1]. Among the various methods of measuring the potential of the electrocapillary maximum[2], this VDME method seems to be most promising in point of the ease and rapidness of the recording, of its good reproducibility and

1) D. C. Grahame, *Chem. Revs.*, **41**, 441 (1947).
2) D. C. Grahame, R. P. Larson and M. A. Poth, *J. Am. Chem. Soc.*, **71**, 2978 (1949). T. I. Popova and T. A. Kryukova, *J. physik. Chem.*, **25**, 283 (1951). J. A. V. Butler, "*Electrocapillarity*", Methuen Co. Ltd., London, (1940), p. 56.

accuracy. Moreover, this technique has the potentiality for the sensitization of the polarographic analysis as the rotated dropping mercury electrode[3] is the case.

Laboratory of Chemistry
Minami College
Hiroshima University
Hiroshima

3) G. Charlot, "*Modern Electroanalytical Methods*", Elsevier Pub. Co., Amsterdam, (1958), I. M. Kolthoff and Y. Okinaka, p. 83 and N. Tanaka et al., p. 97.

Nuclear Magnetic Resonance Experiment of Diacetylhydrazine

By Ryuichi Shintani, Hideaki Chihara, Junkichi Itoh and Isamu Nitta

(Received May 26, 1958)

The X-ray difference electron-density contour map (D-map) of anhydrous diacetylhydrazine clearly shows peaks to be ascribed to hydrogen atoms of methyl groups as well as of amide groups[1]. This led us to the study of the proton nuclear magnetic resonance of this crystal in order to examine if the methyl groups really rest in the most stable potential minima or they are reoriented among equivalent positions.

Diacetylhydrazine was purified by repeated fractional sublimation in high vacuum, and powdered specimen was sealed in a thin glass tube in vacuo at above the dehydration temperature 82°C to assure the formation of no hydrate crystals.

The magnetic resonance was recorded with the equipment already reported elsewhere[2]. The results are given in the figures. The second moments (see Fig. 1) of the absorption at room temperature and down to −180°C are nearly constant in rough agreement with the theoretical value based on a rotating methyl group (about its three-fold symmetry axis). At liquid nitrogen temperature the second moment approaches to that corresponding to the rigid-lattice value. Therefore, the hydrogen peaks in the D-map[1] must correspond to reorienting methyl groups. It is inferred that there would be rather severe requirements to be satisfied in order for such peaks to appear in the D-map. The fact that the C–C_{Me} bond length is very short (1.48 Å) for a normal single bond may possibly be responsible for that effect.

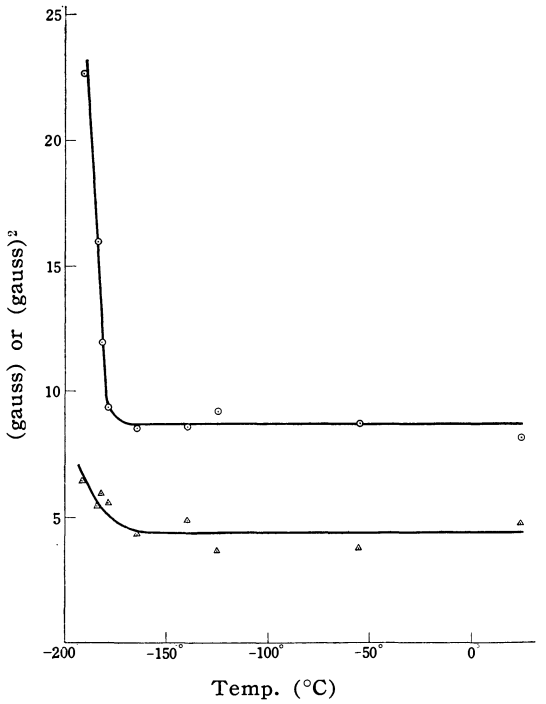

Fig. 1. The second moment and the linewidth of proton nuclear reasonance absorption of diacetylhydrazine crystals.
⊙ Second moment in gauss²
△ Width in gauss

The measurements of the spin-lattice relaxation time T_1 were then made with a hope of obtaining the barrier height hindering the internal rotation of the

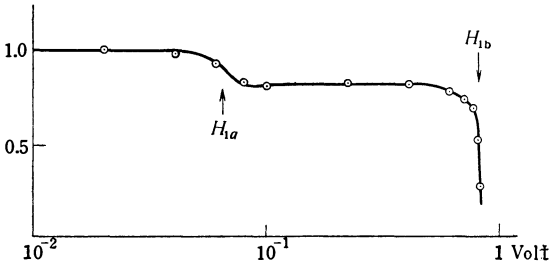

Fig. 2. A typical saturation curve at −110°C. The ordinate is in an arbitrary scale.

1) R. Shintani and I. Nitta, read before the 4th International Congress of Crystallography, July 1957 (Montreal, Canada).
2) T. Yukitoshi, H. Suga, S. Seki and J. Itoh, *J. Phys. Soc. Iaban.* **12**. 506 (1957).

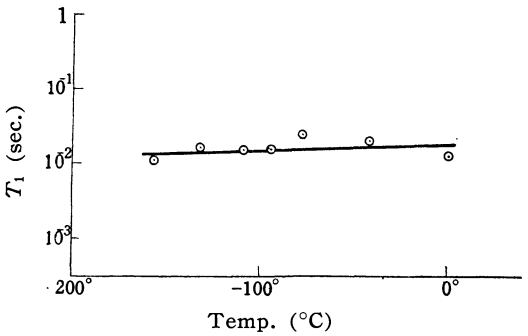

Fig. 3. The temperature dependence of the spin-lattice relaxation time T_1.

methyl groups. One of saturation curves is reproduced in Fig. 2, which has two horizontal portions with two knees at H_{1a} and H_{1b} followed by a monotonous decline. The first knee at H_{1a} was not so distinct at some other temperatures as the one reproduced here, owing to poor signal-to-noise ratio. The temperature dependence of T_1 in Fig. 3, obtained by correlating the oscillator output with the strength of the high-frequency field through calculation based on the coil dimensions and by using the portion of saturation curve at higher field than H_{1a} as the reference, was rather unusual in that T_1 (of the order of magnitude 2×10^{-2} sec.) was almost independent of the change in temperature. Although the magnitude of the T_1 values may be considered as reasonable for this type of crystal, it seems that the invariance of T_1 can hardly be accounted for by reorientation of methyl groups as dominating mechanism of nuclear relaxation. A trial of detecting possibly-present paramagnetic ingredients in the specimen by the electron-spin resonance was not successful[3]. Paramagnetic species does not exist, if any, in a greater concentration than 10^{-5} in mole fraction. Incidentally, it was found that the absorption linewidth, measured by the separation between points of maximum positive and negative slope, also depends on the strength of the high-frequency field as is shown in Fig. 4. This type of experiment was conducted only at −183°C, but its precision was much greater than the measurements of the saturation curves. The absorption narrowed at an oscillator output coinciding approximately with H_{1a}. This means that the component of absorption having larger width is more readily saturated.

3) The authors are grateful to Mr. K. Morigaki of Department of Physics, Osaka University for examination of the electron spin resonance of diacetylhydrazine.

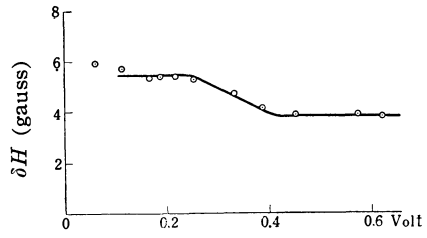

Fig. 4. Change of line-width with the strength of high-frequency field at −183°C.

An explanation was seeked which can account for the entire observation with consistency, but the present data seem to be insufficient to permit it. The role of the amide hydrogen atoms is not quite evident and substitution of deuterium for the hydrogen will provide us with further information. Inasmuch as we have no further attempt to attack this problem, satisfactory elucidation of the mechanism of the nuclear resonance in this crystal will be deferred until more data are accumulated as to the behavior of analogous substances.

Two of us (R. S. and H. C.) wish to thank Mr. Y. Yamagata of Osaka University for suggestions on the experimental details.

Faculty of Science
Osaka University
Kita-ku, Osaka

Intramolecular Interaction between Hydroxyl Group and Aromatic Nucleus in 2-Hydroxy-4- or 4'-nitrobiphenyl

By Michinori Ōki, Hiizu Iwamura and Yoshiyuki Urushibara

(Received June 3, 1958)

In the course of a study on the ultraviolet spectra of biphenyl derivatives, the authors observed a phenomenon[1] possibly interpretable from the intermolecular

1) For example, 2-methyl-4-nitrobiphenyl shows an ultraviolet absorption maximum at a shorter wave length than 2-methyl-4'-nitrobiphenyl does. A paper on this phenomenon was presented at the Eleventh Annual Meeting of this Society, April, 1958, in Tokyo, but no full explanation has been obtained so far.

TABLE I

INFRARED SPECTRA OF 2-HYDROXY-4-NITROBIPHENYL (I) AND 2-HYDROXY-4'-NITROBIPHENYL (II)

Compound	Temp. (°C)	Hydroxyl	ν_{max} (cm^{-1})	$\Delta\nu_{1/2}^{a}$ (cm^{-1})	$A\times10^{-4}$ $mole^{-1}\cdot liter\cdot cm^{-2}$	$\Delta\nu_{max}$ (cm^{-1})
I	26.5	interacted	3553.8	19.4	1.703	44.0
		free	3597.8	19.6	0.233	
II	23.5	interacted	3579.6	17.6	0.765	21.4
		free	3601.0	17.2	0.787	

interaction involving a participation of the aromatic nucleus, which led the authors to study the absorption spectra of 2-hydroxy-4-nitrobiphenyl (I)[2], m.p. 103~105°C, and 4'-nitro-isomer (II)[3], m. p. 123~124°C.

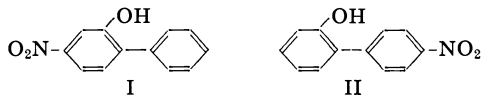

I II

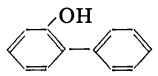

III

Wulf[4] observed two O-H stretching bands in the first overtone region in 2-hydroxybiphenyl (III), attributing them to *cis* and *trans* isomerism. Barnard et al.[5] also observed two bands in 3μ region in cumene α-hydroperoxide. In view of recent studies on the intermolecular interaction between the hydroxyl group and the aromatic nucleus, these phenomena are undoubtedly caused by the intramolecular interaction between the hydroxyl group and the π-electrons of the aromatic nucleus. While the present study was in progress, Trifan and his coworkers[6] reported that they also observed two O-H stretching bands in α-hydroxyethylferrocene and β-phenethyl alcohol.

It can naturally be expected that introduction of a nitro group into compound III will either enhance or suppress the interaction by the electron drawing power of the nitro group and compounds I and II will be the two extremes as far as the positions 4 and 4' concern on the basis of Hammett's σ values.

The infrared absorption was measured with a Perkin Elmer Model 112-G Double Pass High Precision Grating Infrared Spectrometer, the spectral slit width being 0.82 cm^{-1} in this region. Eastman-Kodak spectro grade carbon tetrachloride was used as a solvent without further treatment. A quartz absorption cell of 2 cm. length was used with a ca. 0.001 mol./l. solution. The temperature varied from 25° to 65°C. The integrated intensity was calculated from the equation given by Ramsay[7], four parameters a_1, b_1, c_2 and b_2 being used for the two bands. Examples of the results are shown in Table I.

Energy differences between free and interacted hydroxyl groups calculated from the values at various temperatures are 2.5±0.2 and 0.93±0.03 kcal./mol. for compounds I and II, respectively, and are in good agreement with the expectation. There may exist a relation between ΔE and $\Delta\nu$ or the integrated intensities of free and interacted forms, but we can not comment about this until further examples are studied.

Department of Chemistry, Faculty of Science, The University of Tokyo
Hongo, Tokyo

2) C. Finzi and A. Mangini, *Gazz. chim. ital.*, **62**, 664 (1932); *Chem. Abst.*, **27**, 77 (1933).
3) W. G. Christiansen and S. E. Harris, *J. Am. Pharm. Assoc.*, **22**, 723 (1933); *Chem. Abst.*, **29**, 4382 (1935).
4) O. R. Wulf, *J. Am. Chem. Soc.*, **58**, 2290 (1936).
5) D. Barnard, K. R. Hargrave and G. M. G. Higgins, *J. Chem. Soc.*, **1956**, 2845.
6) D. S. Trifan, J. L. Weinmann and L. P. Kuhn, *J. Am. Chem. Soc.*, **79**, 6566 (1957).
7) D. A. Ramsay, ibid., **74**, 72 (1952).

Gas Chromatographic Separation of Hydrogen Isotopes D_2 and HD

By Sumio Ohkoshi, Yuzaburo Fujita and Takao Kwan

(Received June 12, 1958)

A simple gas adsorption chromatographic apparatus was constructed by us[1] with materials readily available in this physicochemical laboratory. The apparatus had the advantage of operating the adsorption column at any desired temperature and so far was used as a tool for analyses of

1) S. Ohkoshi, Y. Fujita and T. Kwan. *Catalyst*, **15**, 1 (1958).

low boiling gases, however with potential purpose of separating and analyzing hydrogen isotopes D_2, HD and H_2. The latter investigation was now performed and led to a certain satisfactory aspect which will be described below.

Experience[1] has shown that the efficiency of gas chromatographic separation largely depends on the nature of column packings and on the temperature of the column. Experiments were therefore conducted primarily to find out most favorable column packing and temperature. As a result Pyrex glass U-tube of 80 cm. long and 0.3 cm. internal diameter was employed as a column and filled with "molecular sieve 5 A" due to Linde Air Co. New Jersey, the column being immersed, when working, in a liquid nitrogen bath.

Two hydrogen isotope samples were investigated for the purpose; one was pure deuterium (>99.5 %) supplied by Stuart Oxygen Co. San Francisco and the other was prepared by contacting a mixture of pure deuterium and ordinary hydrogen in a ratio of 1.8 : 1.0 with a reduced nickel powder kept at 100°C to reach isotopic exchange equilibrium. Ordinary hydrogen from cylinder was used as a carrier gas, its flow rate being 70 ml. per min. A known amount of the sample gas under reduced pressure was introduced in a manner as described previously[1] into the stream of the carrier from the sample tube of known volume which was connected to sample reservoirs, mercury manometer and then to vacuum line. The thermal conductivity cell with thermistor was used to detect hydrogen isotopes. Now, under such experimental circumstances there appeared two distinct elution peaks, when a mixture sample after equilibration was introduced, which were almost perfectly separated with each other. In Fig. 1 is shown such a chromatogram which was recorded however by a commercial set of the gas chromatography-Shimazu GC-1A, No. 58035* recently furnished in this laboratory.

As shown in Fig. 1, it is apparent that the retention time for pure deuterium is coincident with that of the second peak

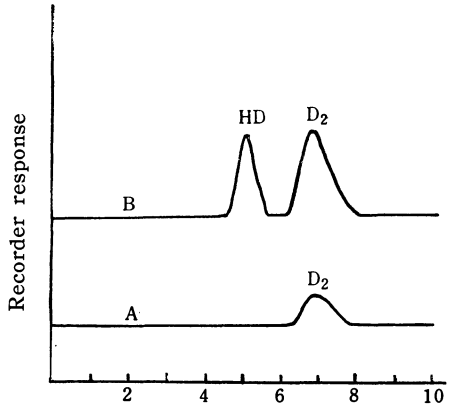

Fig. 1. Chromatogram of hydrogen isotopes. A: Pure deuterium. B: A mixture of D_2, HD and H_2 after equilibration at 100°C.

of the chromatogram for the mixture sample. Since ordinary hydrogen was employed as the carrier gas, H_2 in the mixture should not appear in the chromatogram. The first peak, therefore, should be identified as HD. It is interesting to note that coiled Pyrex column of the same length tended to have a slightly lower efficiency to separate hydrogen isotopes.

Attempts were made by Glueckauf and Kitt[2] to obtain pure deuterium from a mixture of D_2 and H_2 by using a column filled with palladium black-asbestos and kept between 0 and 100°C. Similar investigation was carried out by Tamaru[3] who used palladium-on-Celite as column packing. So far as we are aware, there is no report concerning complete separation of D_2 and HD by means of the gas chromatographic technique. The present finding surely proves the gas chromatography to be a new tool for quantitative as well as qualitative analysis of hydrogen isotopes; it is possible to proceed to determination of the amount of constituents D_2, HD and H_2 for a given volume of the mixture, if appropriate calibration data are beforehand arranged. Experiments are continuing along this line and will soon be published.

Research Institute for Catalysis and Chemistry Department, Hokkaido University, Sappro, Japan

* The function of this instrument is essencially the same with that constructed in our laboratory except that the thermal conductivity cell is equipped with coiled tungsten heater wires. The advantage of the commercial set may be the equipping of a self-recording system which we lack in ours. Its disadvantage, on the other hand, is a certain limitation in operating the column temperature, viz., it is designed primarily for above-room-temperature. The only modification was that the original stainless steel column arranged horizontally had to be replaced by a vertical glass U-tube.

2) E. Glueckauf and G. P. Kitt, "Vapor Phase Chromatography", Butterworths Scientific Publications, London (1957) p. 422

3) K. Tamaru, Private communication.

*Gas Chromatography as a New Tool for Analyses of Hydrogen Isotopes**

By Sumio Ohkoshi, Shoko Tenma, Yuzaburo Fujita and Takao Kwan

(Received July 5, 1958)

A mixture of hydrogen isotopes could completely be separated[1,2] by use of a technique of the gas adsorption chromatography, when the adsorption column was filled with "molecular sieves 5A"** and cooled in a liquid-nitrogen bath. Preliminary experiments were then carried out with special interest in applying the gas chromatography as a new tool for quantitative analyses of these hydrogen molecular species. In the followings a record of these will be presented.

Ordinary hydrogen and pure deuterium*** (>99.5%) were mixed in a ratio of 1.0 : 2.0 and reserved in a glass flask (sample I). A portion of this mixture was brought into contact with platinum-wire catalyst kept at 300°C overnight to reach isotopic exchange equilibrium (sample II). Chromatograms were obtained alternatively on the sample I and II by varying the sample volume. As the amount of deuterium is known in the sample I, the relation between deuterium amounts and peak heights or any other peak feature can be determined. Thus, it was found that a linear relationship, passing through the origin, holds between deuterium amounts and peak heights. The amount of deuterium in the sample II can now be estimated from the observed peak height by use of the calibration line just determined.

The amount of D_2 for a given volume of the sample II was found always smaller, as expected, than that before equilibration. Assuming that this difference in the deuterium content is due to the formation of HD and therefore corresponds to one-half of the amount of HD formed during the equilibration reaction, the amount of HD in the sample II was evaluated. Such a datum for HD is given in the Table I together with that of D_2 calculated according to the calibration line. The amount of H_2 in the sample II must now be equal to the total volume of the sample minus the sum of D_2 and HD.

In view of the rapid chemisorption and desorption of hydrogen on platinum catalyst at 300°C,[3] the hydrogen molecular species D_2, HD and H_2 in the sample II may well be expected to be in complete exchange equilibrium. In the last column of the table is shown the equilibrium constant K of the reaction as estimated from the data illustrated there.

Very slight inaccuracies in the deuterium amount of the sample II do affect the values for HD, H_2 and hence, K in the method of analysis used here. Thus, an error of about ±5% is anticipated for the value of K. The discrepancy between the observed K, 3.79, and the calculated one, 3.69[4] at a temperature of 300°C should therefore be convincing or the agreement is satisfactory.

It is concluded that the gas chromatographic techniques are convenient and powerful to analyze the amount of hydrogen molecular species D_2, HD and H_2 for both qualitative and quantitative purposes. The mass spectrometric method so far used for such purposes may be replaced to a certain extent by the gas chromatographic method.

Research Institute for Catalysis and Chemistry Department Hokkaido University, Sapporo

TABLE I

AMOUNTS OF HYDROGEN MOLECULAR SPECIES D_2, HD and H_2 BEFORE (I) AND AFTER (II) EQUILIBRATION ON PLATINUM AT 300°C.

Run	Isotope sample	Total volume of sample, ml. 20°C	Vol. of components, ml. 20°C			Equilibrium constant
			D_2	HD	H_2	$K=[HD]^2/[H_2][D_2]$
1	I	1.51	1.01	0.0	0.50	
2	II	1.21	0.540	0.532	0.138	3.79
3	I	0.947	0.632	0.0	0.315	

* Presented by T. Kwan before the Meeting of the Japan Society for Analytical Chemistry, Hokkaido on June 28, 1958.

1) S. Ohkoshi, Y. Fujita and T. Kwan, *Catalyst*, **15**, 1 (1958).

2) S. Ohkoshi, Y. Fujita and T. Kwan, This Bulletin, **31**, 770 (1958).

** Linde Air Products Co., New Jersey, U. S. A.

*** Stuart Oxygen Co., San Francisco, U. S. A.

3) T. Kwan, *J. Res. Inst. Catalysis, Hokkaido University*, **2**, 81 (1949); *Advances in Catalysis*, **6**, 67 (1954) (Academic Press. New York).

4) H. C. Urey, *J. Chem. Soc.*, **1947**, 562.

Enrichment of Deuterium by Low Temperature Gas Adsorption Chromatography

By Sumio Ohkoshi, Shoko Tenma, Yuzaburo Fujita and Takao Kwan

(Received August 15, 1958)

In 1934 Taylor et al.[1] found that the separation of hydrogen isotopes H_2, HD and D_2 is effective by the use of the desorption of these molecules from the surface of active charcoal kept at liquid air temperature. Accordingly, the composition of the hydrogen sample desorbed during the last stage showed an increase in the amount of HD and D_2 compared with that of the initial gas. In recent years, Barrer[2] and others have shown that dehydrated zeolite gives rise to efficient adsorption characteristics in many respects. The finding has led to an idea of "molecular sieve" which was now made available by Linde Air Products Co. New Jersey in commercial scale. We employed the molecular sieve as column packing of the gas adsorption chromatography and were able to separate HD and D_2 at a column temperature of liquid nitrogen[3]. Further investigtions by us[4] proved that the gas chromatographic technique is useful for the analyses of H_2, HD and D_2.

In view of the remarkable efficiency with which HD and D_2 are separated chromatographically through a column, filled with molecular sieve 5A and immersed in a liquid nitrogen bath, attempts were made to enrich deuterium by passage of a mixture of hydrogen isotopes such a column. The result, though of preliminary nature as yet, seemed to be noteworthy and will be communicated here.

The apparatus[5] used for the investigation of hydrogenation kinetics was used without any particular modification for the present purpose. A glass flask of ca. 1 liter volume containing 330 mmHg hydrogen isotope mixture was connected to a U-shaped glass column filled with molecular sieve 5A, to a Töpler pump and then to a sample vessel of ca. 10 cc. volume. The column was of 30 cm. in length and 0.6 cm. in internal diameter. Mercury manometers were equipped between the sample flask and the adsorption column as well as between the column and the Töpler pump to read the pressure of hydrogen sample before and after passage through the column.

The experimental procedure was as follows: the apparatus was first evacuated at room temperature and then the column was immersed into a liquid nitrogen bath. A mixture of hydrogen isotopes was introduced, by opening the cock of the flask, into the column. Rapid adsorption of hydrogen on the packing took place with residual pressure of about 30 mmHg. The rate of passage of hydrogen through the column was however not so fast; it took more than 5 minutes to reach a few mmHg in a space between the column and the Töpler pump. The hydrogen once passed through the column was continuously collected by means of the Töpler pump, and a small portion of the collected hydrogen was analysed for the isotopic composition by the gas chromatographic technique developed by us[3].

It was found that the hydrogen sample collected initially contained neither HD nor D_2. The amount of HD, however, increased gradually with increase of the volume of the hydrogen passed, and finally D_2 was found to appear in the sample gas when the liquid nitrogen bath was removed from the column and adsorbed hydrogen sample was collected back into the original flask. The pressure of the hydrogen sample in the flask was 140 mmHg showing that about 60% of the hydrogen sample was passed through the column.

In Table I is shown the composition of hydrogen isotopes H_2, HD and D_2 before and after the passage.

Table I

Enrichment of deuterium by the low temperature gas adsorption chromatography

	Total vol. ml. 20°C	H_2		HD		D_2	
		ml.	%	ml.	%	ml.	%
Isotope sample before passage	435	196	45	100	23	139	32
Isotope sample after passage	184	20	11	32	17	132	72
Isotope sample* passed through	251	176	70	68	27	7	3

* Calculated from the volume of hydrogen sample before and after the passage.

The separation factor f of the hydrogen isotopes H_2 and D_2 is defined as

$$f=\frac{n'_{D2}}{n'_{H2}}\Big/\frac{n_{D2}}{n_{H2}}$$

where (n_{H2}, n_{D2}) and (n'_{H2}, n'_{D2}) are the concentrations of H_2 and D_2 before and

1) A. J. Gould, W. Breakney and H. S. Taylor, *J. Chem. Phys.*, **2**, 362 (1934).
2) R. M. Barrer, ibid., **47**, 82 (1950).
3) S. Ohkoshi, Y. Fujita and T. Kwan, This Bultin, **31**, 770 (1958).
4) S. Ohkoshi, S. Tenma, Y. Fujita and T. Kwan, ibid., **31**, 772 (1958).
5) S. Tenma and T. Kwan, *Catalyst*, **15**, 11 (1958).

after the passage respectively. From the data in the table the separation factor was found to be 92.

It is concluded that the low temperature gas adsorption chromatography is extremely efficient and very simple to enrich deuterium from a mixture of H_2, HD and D_2. Experiments are to be conducted to enrich deuterium from hydrogen isotope mixture of various concentrations including ordinary hydrogen.

Research Institute for Catalysis
and Chemistry Department
Hokkaido University, Sapporo

Magnetic Susceptibilities of Aromatic Compounds Dissolved in Sulfuric Acid

By Yoshio MATSUNAGA

(Received June 9, 1958)

Various authors have reported that a number of aromatic compounds dissolved in concentrated sulfuric acid exhibit electron spin resonance absorption. In the case of bianthraquinon and perylene, the fraction of the radical form has been estimated as ten percent or more[1,2]. On the other hand, the static susceptibility measurement is available only for bianthraquinone, and this result does not support such a high fraction of the radical form[3].

In Table I the molar susceptibilities are presented, observed for ten compounds dissolved in 96% sulfuric acid together with the values in the solid state. The concentration of the compounds in sulfuric acid ranged from four to nine percent. The values for dissolved materials were calculated by the application of Wiedemann's additivity rule. The apparent molar susceptibilities of perylene and bianthraquinone in solution are undoubtedly less than those in the solid state. If we assume that the decrease of molar susceptibility is due to the partial compensation of diamagnetism by the paramagnetic contribution of the radical form and the diamagnetic contribution of the paramagnetic species is equal to that of the diamagnetic molecule, the fraction of the molecules with a single unpaired electron is given by $\Delta\chi \times 10^{-6}/1270 \times 10^{6}$. The estimated fraction for perylene is found to be 13.2 percent. This value is only one third of that given by Yokozawa and Miyashita[2]. As Selwood and Dobres[4] pointed out in the case of triarylmethyl radicals, the disagreement may be due, at least in part, to the enhanced diamagnetic contribution of the radical form. Although Theilacker, Kortüm and Elliehausen[3] could not find any appreciable change in the diamagnetic susceptibility of bianthraquinone, our measurement shows that 4.6 percent of the molecules are in the paramagnetic state. However, our value is still about one half of that estimated by resonance absorption[1]. Anthraquinone and fluorenone were reported to be paramagnetic in sulfuric acid and the fraction of the radical form was estimated as five percent or less[1]. Our results show that the last eight compounds in Table I including anthraquinone and fluorenone do not form any radical or the fraction of the paramagnetic species is less than one percent.

TABLE I
MAGNETIC SUSCEPTIBILITIES OF AROMATIC COMPOUNDS IN SULFURIC ACID AND IN THE SOLID STATE

Substance	Molar Suscept. in H_2SO_4	$(-\chi_M \times 10^6)$ in Solid
Perylene	0± 8*	168[5]
Bianthraquinone	161±11	220[6]
Anthraquinone	103± 6	114[6]
1-Aza-anthraquinone	102± 6	109
Phenanthraquinone	102± 6	105[5]
Anthrone	122± 6	118[6]
Bianthrone	231±11	229[6]
Fluorenone	90± 5	99.4
Benzanthrone	141± 7	143[5]
Bis(anthronylidene)-ethane	232±12	232

* Estimated experimental error.

As to the nature of the paramagnetism, a triplet state[2] and a positive ion[7] were suggested for perylene and conjugated

1) J. M. Hirshon, D. M. Gardner and G. K. Fraenkel, *J. Am. Chem. Soc.*, **75**, 4115 (1953).
2) Y. Yokozawa and I. Miyashita, *J. Chem. Phys.*, **25**, 796 (1956).
3) W. Theilacker, G. Kortüm and H. Elliehausen, *Ber.*, **89**, 2306 (1956).
4) P. W. Selwood and R. M. Dobres, *J. Am. Chem. Soc.*, **72**, 3860 (1950).
5) H. Akamatu and Y. Matsunaga, This Bulletin, **26**, 364 (1953).
6) Y. Matsunaga, ibid., **29**, 582 (1956).
7) S. I. Weissman, E. de Boer and J. J. Conrad, *J. Chem. Phys.*, **26**, 963 (1957).

acid ions[1] for anthraquinone and bianthraquinone etc. These compounds are markedly protonated in solutions of strong acids like sulfuric acid[8,9], however, it has been pointed out that protonation is not sufficient condition for radical formation[10]. As shown in this paper, the fraction of the radical form is not high, so the structure of the paramagnetic species without protonation cannot be excluded. Although we cannotdiscuss in detail the nature of the radical form based on our own data, it must be noted that the appearence of the paramagnetic species in sulfuric acid depends greatly on the structural feature of the aromatic molecule.

Department of Chemistry
Faculty of Science
The University of Tokyo
Hongo, Tokyo

8) R. A. Herbert, M. B. Goren and A. A. Vernon, *J. Am. Chem. Soc.*, **74**, 5779 (1952).
9) T. Handa, This Bulletin, **28**, 483 (1955).
10) C. MacLean and J. H. van der Waals, *J. Chem. Phys.*, **27**, 827 (1957).

Vapor Phase Catalytic Hydrogenation of Organic Compounds Using Stabilized Nickel Catalyst[1]

By Kazuo HATA, Ken-ichi WATANABE and Masaru TANAKA

(Received June 24, 1958)

It has been known for a long time that reduced nickel catalyst prepared by thermal decomposition of nickel formate is effective for hydrogenation of many organic substances. "Stabilized Nickel Catalyst" (a kind of catalyst obtained from nickel formate) has been developed and can be prepared more conveniently for practical use, and it has been reported to show excellent quality with regard to activities and stability[1].

However, investigations in catalytic hydrogenation of organic substances using the nickel catalyst mentioned above were carried out exclusively in liquid phase, and none in vapor phase has been reported. In this paper, a new study applying this catalyst to vapor-phase hydrogenation is introduced.

As a result of experiments in which some typical organic compounds were hydrogenated, it was found that hydrogenation which this catalyst was able to be carried out in vapor phase as well as in liquid phase, and the preparation of this catalyst is simpler than that of any other nickel catalyst.

Experimental Method

The hydrogenation was carried out according to the Sabatier's method[2]. The catalyst was put into a hard-glass tube and was heated up to reaction temperature with an electric furnace, while dry hydrogen was passed through the tube. After a small amount of water from the catalyst was expelled by heating, the vaporized sample together with a large excess of hydrogen was introduced into the reaction tube. The reaction products flowing out of the tube were collected into the receiver through a condenser, and were isolated by suitable methods especially by means of fractional distillation. Then each product was identified by preparing an appropriate derivative respectively.

Results

Representative results of the experiments are summarized in Table I. Styrene and acetophenone were reduced to ethylbenzene each in high yield. Benzene was completely reduced to cyclohexane, phenol to cyclohexanol with some cyclohexanone, and benzaldehyde to benzene and toluene. Nitrobenzene was mostly reduced to aniline, however, a small amount of diphenylamine and white crystals (m. p. 193~197°C) were obtained as secondary products. Benzonitrile was reduced to toluene in good yield at about 250°C, and to benzene and toluene at about 350°C[3].

From these experiments, it is proved that the effectiveness of this nickel catalyst is as good as Sabatier's reduced nickel catalyst, and that the reaction procedure is quite simplified because of the stability of the catalyst.

1) T. Yamanaka and Y. Takagi, *J. Sci. Res. Inst. Tokyo*, **51**, 168 (1957).

2) P. Sabatier, "La Catalyse en Chimie Organique", Ch. Béranger (1913).

3) M. Tanaka, K. Watanabe and K. Hata, *J. Chem. Soc. Japan, Pure Chem. Sec.*, (*Nippon Kagaku Zassi*), **76**, 1392 (1955).

TABLE I

VAPOR PHASE CATALYTIC HYDROGENATION OF ORGANIC COMPOUNDS USING STABILIZED NICKEL CATALYST

Catalyst: a) contains 28% Ni; b) contains 40% Ni, the remainder is kieselguhr

Compound	Wt. of sample (g.)	Wt. of catalyst (g.)	Temp. (°C)	Time (hr.)	Flow velocity of sample (g./min.)	Vol. of H_2 passed (l.)	Wt. of products (g.)	Products and yields (%)
Styrene	5	20[a)]	203	$1\frac{3}{4}$	0.077	12.7	5	Ethylbenzene (98)
Benzene	5	20[b)]	182	$1\frac{1}{2}$	0.073	12.1	4.1	Cyclohexane (77)
Phenol	5	20[a)]	180	2	0.063	16.0	5	Cyclohexanol (77) Cyclohexanone (7)
Benzaldehyde	5	20[b)]	230	$1\frac{1}{6}$	0.122	9.0	3.8	Benzene (25) Toluene (40)
Acetophenone	5	20[a)]	203	2	0.079	14.5	4.95	Ethylbenzene (93)
Nitrobenzene	5	20[a)]	230	$1\frac{1}{2}$	0.091	10.2	4.85	Aniline (66)
Benzonitrile	5	20[a)]	250	2	0.089	11.3	3.3	Toluene (72)
Benzonitrile	6	20[a)]	354	2	0.094	12.6	3.1	Benzene (43) Toluene (18)

The authors are indebted to Dr. Yamanaka of the Scientific Research Institute for his suggestion and offer of "Stabilized Nickel Catalyst".

Department of Chemistry, Faculty of Science, Tokyo Metropolitan University
Setagaya-ku, Tokyo

A New Type of Urushibara Nickel Catalyst

By Kazuo HATA, Shin-ichi TAIRA and Izumi MOTOYAMA

(Received June 24, 1958)

The preparation[1], the application[2] and the characteristics[3] of Urushibara nickel catalyst, prepared from nickel chloride and zinc dust, have already been reported. In this paper the procedure of preparing a new nickel catalyst, prepared from nickel chloride and aluminum grains in place of zinc dust and named Urushibara nickel BA or U-Ni-BA in abbreviation, is presented. Aluminum grains of a proper size must be used to obtain an active catalyst. Commercially available aluminum powder proved to be invalid. Using aluminum grains of 40~80 meshes, a new type of Urushibara nickel was prepared: the precipitated nickel from aqueous nickel chloride solution with such aluminum grains was digested with aqueous caustic alkali, and a new hydrogenating catalyst was obtained. This nickel catalyst proved to be very effective for hydrogenation of various organic compounds. Above all, benzene, aniline and methyl salicylate were respectively hydrogenated under a high pressure to cyclohexane, cyclohexylamine and methyl hexahydrosalicylate, these hydrogenation being unsuccessful with Urushibara nickel B or A.

A procedure for the preparation of the most active catalyst was determined from the results of hydrogenation of acetone under ordinary pressure.

Aluminum grains of 40~80 meshes (10 g.) are washed with water and treated with 50 ml. of 3% sodium hydroxide solution until the mixture becomes hot and vigorously frothy. To this mixture is added water to suppress the frothing and the upper liquor is decanted. The aluminum grains are washed well with water to remove a trace of alkali. They are transferred into a 500 ml. wide-mouthed, round-bottomed flask or beaker and warmed with a little water on a boiling water bath. To this is added 20 ml. of hot aqueous nickel chloride solution which contains 2 g. of nickel. Occasional stirring is continued until the slushy reaction mixture becomes nearly solid. The solids are crushed two or three times with hot water to remove water-soluble products. To a mixture of the solids and a little water is cautiously added with stirring 250 g. of 20% sodium hydroxide solution in several portions. As a addition of the first portion is followed by a violent reaction, good stirring and cooling with ice are necessary to prevent the contents running over. After a half

1) Y. Urushibara, This Bulletin, **25**, 280 (1952); Y. Urushibara et al., ibid., **27**, 480 (1954); Y. Urushibara et al., ibid., **28**, 446 (1955).

2) S. Nishimura, *J. Chem. Soc. Japan, Pure Chem. Sec.* (*Nippon Kagaku Zassi*), **77**, 340 (1956); ibid., **78**, 1741 (1957); ibid., **79**, 56 (1958); K. Hata et al., ibid., **77**, 1405 (1956); ibid., **78**, 186 (1957); This Bulletin, **30**, 431 (1957).

3) Y. Urushibara et al., This Bulletin, **29**, 815 (1956).

part of the alkali is added during about ten minutes, the other half is added at once to the reaction mixture, which is continuously stirred until the generation of hydrogen gas ceases. The temperature of the reaction mixture should be kept below 60°C throughout this operation. After being kept for a few minutes, the upper liquor of the dark reaction mixture is carefully

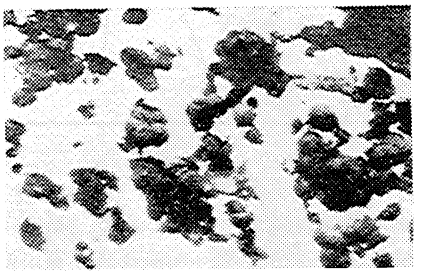

Fig. 1. Micro-photograph of Urushibara nickel BA.

decanted and the residue is washed five times with each 100 ml. of hot water and then thrice with each 50 ml. of ethanol. The solids are transferred into a hydrogenating vessel with the solvent to be used. In these stages contact with air must be avoided as far as possible. Distilled water is used for wash, and every washing is removed by decantation. In this way a very active catalyst containing about 2 g. of nickel, a small amount of aluminum and a trace of alkali is obtained.

A micro-photograph of this catalyst is given. This photograph shows that ion-exchange occurred on the surface of aluminum grains and then inner aluminum was dissolved out by the action of sodium hydroxide solution.

Department of Chemistry, Faculty of Science, Tokyo Metropolitan University, Setagaya-ku, Tokyo

Reduction of p-Nitrosodiethylaniline by Means of Activated Zinc Dust and Ammonium Chloride

By Ryoichi Uehara and Tsurahide Cho

(Received July 11, 1958)

Some reducing agents for preparation of *N*, *N*-diethyl-*p*-phenylenediamine from *p*-nitrosodiethylaniline have been reported, e. g., hydrochloric acid and stannous chloride[1], hydrochloric acid and zinc[2], and hydrochloric acid and iron[3]. Electrolytic reduction[4] and catalytic reduction[5] with Urushibara nickel are also favorable methods for the preparation. It has been found by the present authors that the reduction can be achieved very easily in methanol or ethanol by means of ammonium chloride and zinc dust activated with mercuric chloride. Reduction of nitrobenzene to phenylhydroxylamine with zinc dust and aqueous ammonium chloride is noted, but no application of this reducing agent in non-aqueous media has been reported. For the reduction of *p*-nitrosodiethylaniline, zinc dust and ammonium chloride are not effective either in water or in methanol or ethanol, but, by using zinc dust activated with mercuric chloride, the reduction takes place very smoothly in methanol or ethanol.

The procedure of this reaction is very simple. In a three-necked flask (500 cc.), fitted with a reflux condenser, a stirrer, and a dropping funnel, 40 g. (0.615 atom) of zinc dust and 50 g. (0.28 mole) of *p*-nitrosodiethylaniline are taken, and 300 cc. of methanol and 0.1 g. of mercuric chloride are added. The mixture is heated with stirring until *p*-nitrosodiethylaniline is completely dissolved and an active ebullition takes place. Then heating is stopped and 5 g. of ammonium chloride in 20 cc. of water is added drop by drop into the mixture. An active reaction occurs, and methanol boils owing to the heat of the reaction. Addition of the ammonium chloride solution is controlled so as to keep the methanol boiling gently without applying heat. After the addition of ammonium chloride, the mixture is again heated and refluxed until the original dark brown color turns pale yellow. The change of color indicates the completion of reduction of the nitroso compound to the amino compound. The solution is filtered, and the residue washed with 100 cc. of hot methanol. The filtrate and the washing are combined and evaporated in nitrogen. The residual dark oil is distilled under a reduced pressure to yield 35 g. (75.6 % of the theory) of *N*, *N*-diethyl-*p*-phenylenediamine boiling at 139~140°C/10 mm.Hg, or at 216.5°C/760 mm.Hg. Anal., N, 16.98%.

For a smooth reaction and a good yield, it is necessary to use purified *p*-nitrosodiethylaniline melting at 83~84°C, because resinous impurities in crude *p*-nitrosodiethylaniline decrease the yield of the reduction and mask the color change

1) Gattermann, "Die Praxis des Organischen Chemikers", W. de Gruyter, Berlin (1940), p. 315.
2) G. Wurster, *Ber.*, **12**, 523, 530 (1878).
3) **FIAT No. 1313** Vol. 1, p. 29, 175, 229 (1948).
4) S. Kikuchi and K. Honda, *Seisan-Kenkyu*, **2**, 267 (1950).
5) R. Uehara, unpublished data.

to indicate the end point of the reaction. *N, N*-dimethyl-*p*-phenylenediamine can be obtained from *p*-nitrosodimethylaniline in the same way.

Tama Kagaku Kogyo Co.
2-28, Minamirokugo
Ota-ku, Tokyo

A Study on Anion Exchange Separation of Neptunium from Irradiated Uranium

By Fujio Ichikawa

(Received July 18, 1958)

Phillips and Jenkins[1] reported the removal of plutonium by nitrate-form anion exchanger before the analysis of fission products. According to their study, plutonium (IV) is adsorbed onto an anion exchange resin from 7.5 N nitric acid solution forming nitrate complex, but fission products and uranium pass through the column and are separated from plutonium. This method is used in a separating plant of plutonium fuel[2].

In the present communication, the adsorption of neptunium is studied in a similar way and a good separation of neptunium from fission products and uranium is found. Neptunium-239 obtained by the following way is used as a tracer.

Distribution coefficient (K_d) of neptunium is measured in systems of nitric acid and nitrate-form anion exchanger (Dowex 1, 100~200 mesh) by batch method. Figure 1 shows the acid dependence of the K_d value. In the concentration range from 1 to 10 N nitric acid, K_d value shows a linear relationship toward the concentration of nitric acid on a logarithmic scale. The maximum value is about 10^3 at 10 N nitric acid and beyond this normality the K_d value decreases suddenly.

The separation study is carried out as follows. Uranium nitrate (10 mg. U) is irradiated in J.R.R.-1 Reactor for two hours at a flux of 10^{11} neutrons/cm^2/sec.

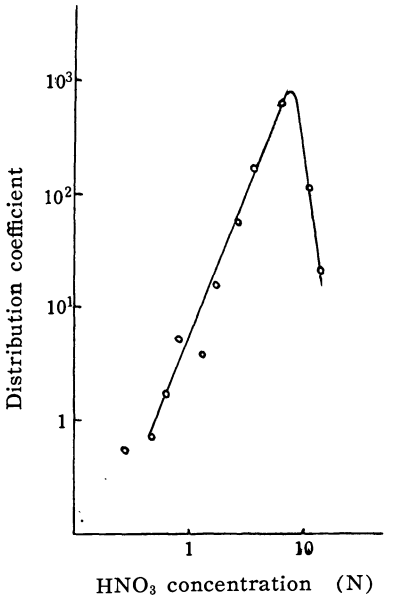

Fig. 1. The acid dependence of the distribution coefficient of Np.

The irradiated sample is dissolved in 1 N hydrochloric acid. A few mg of ascorbic acid is added to the solution in order to keep neptunium at a reduced state. After drying up the solution, the residue is taken up by 7.5 N nitric acid and then neptunium is eluted with 0.7 N nitric acid. Figure 2 shows the elution curve. According to the γ-ray spectrometry, no neptunium is found in 7.5 N nitric acid fraction. On the other hand, a spectrograph of pure ^{239}Np is obtained in 0.7 N nitric acid fraction. When the reduction procedure is omitted, the elution peaks of neptunium and fission products appear very closely in 7.5 N nitric acid and the separation is unsatisfactory.

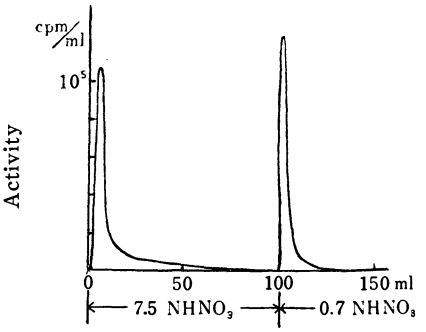

Fig. 2. The elution curve of Neptunium and fission products.

1) G. Phillips and E. N. Jenkins, *J. Inorg. Nucl. Chem.*, 4, 220 (1957).
2) W. M. Campbell, *Nucleonics*, No. 9, 92 (1956).

From these facts, it is likely that neptunium forms a nitrate complex at a lower oxidation state in 7.5 N nitric acid and is adsorbed onto an anion exchanger, but a higher oxidation state the complex formation is very weak.

Chemistry Division, Japan Atomic Energy Research Institute
Tokai, Ibaraki

Selective Reduction of Phospholipids with Lithium Aluminum Hydride I. Ovolecithin

By Chieko URAKAMI and Hirochika OKURA

(Received July 19, 1958)

Recently, Long and Maguire[1] have reported a method of determination of the structure of the phosphatidylcholines, involving a long series of reactions which leads to the formation of L, α-glycerophosphoric acid; Baer and Maurukas[2] have shown another method involving the diazometholysis which is simpler but applicable only to the phosphatidylserines and cephalins. Therefore, it seems desirable to find a new method which is simple in itself to be applicable even when small amounts of phosphatides are available from natural sources.

Since the mechanism of reduction by lithium aluminum hydride is generally considered to be analogous to that of Grignard reaction, the reductive cleavage of the two fatty acid ester linkages in the phosphatidylcholine molecule would take place at an equal rate and with the retention of the configuration. On the other hand, the cleavage of the linkage between the glyceryl or choline and the phosphoryl would not be so easy as the previous case since approach of the nucleophilic reagent to the P^+ to attain a coordination at the transition state may be interfered by the presence of the oxygen atoms with a high electron density around the P^+. The cleavage of the linkage between the phosphoryl and choline may, however, be effected if the mechanism proposed by Gaylord[3] is assumed to be involved. When a group such as —N—C—O is present, a quasi ring is formed by coordination of the nitrogen atom with AlH_3[4] and of the hydrogen atom of the AlH_3 with the electron pair on the oxygen atom. The adjacent carbon atom being positive in character owing to the electrostatic effect of the cationic nitrogen would then react with the hydride ion, H^-, present in the solution[4], resulting in cleavage of the C—O bond. Since a six-membered ring would be equally stable as the five-membered, as illustrated by Gaylord, this mechanism may be applicable to the case of the phosphatidylcholine molecule. In this case however, the reaction would not take place so readily as the cleavage of the fatty acid ester for the following two reasons; firstly, the weakly acidic AlH_3 must overcome the zwitterionic effect in its approach to the nitrogen atom; and secondly, the electrostatic effect would be much weaker on the β-carbon atom. Therefore, under carefully controlled reaction conditions, it may be possible to carry out the cleavages in a stepwise manner to give L, α-glycerophosphorylcholine in the first step and L, α-glycerophosphoric acid in the following. Complicated reactions may, however, occur in the last step, as demonstrated by Karrer and Jucker[5].

The sample of lecithin employed was purified according to the method described by Rhodes and Lea[6] and Hanahan, et. al.[7]

TABLE I

HYDROGENOLYSIS OE OVOLECITHIN WITH LITHIUM ALUMINUM HYDRIDE

Expt. No.	I	II	III
Reaction time (min.)	10	30	60
Temperature (°C)	14	16	16
Mole ratio of L.: $LiAlH_4$	1:2	1:2	1:2
Total choline, calcd.	19.1	17.8	17.8
Total choline[8] in aq. phase	18.0	19.1	19.6
Free choline[9] in aq. phase	0.8	4.1	4.1

L. stands for lecithin.

The reaction was carried out in anhydrous ether. No significant amount of organic phosphorus was found in the ether phase nor inorganic phosphorus in the aqueous phase.

1) C. Long and M. F. Maguire, *Biochem. J.*, **57**, 223 (1954).
2) E. Baer and J. Maurukas, *J. Biol. Chem.*, **212**, 39 (1955).
3) N. G. Gaylord, *Experientia*, **X**, 356 (1954).
4) N. L. Paddock, *Nature*, **167**, 1070 (1951).
5) P. Karrer and E. Jucker, *Helv. Chim. Acta*, **35**, 1586 (1952).
6) D. N. Rhodes and C. H. Lea, *Biochem. J.*, **65**, 526 (1957).
7) D. J. Hanahan, M. S. Turner and M. E. Jayko, ibid., **192**, 623 (1951).
8) D. Glick, *J. Biol. Chem.*, **156**, 643 (1944).
9) G. Schmidt, L. Hecht, P. Fallot, L. Greenbaum and S. J. Thannhauser, ibid., **197**, 601 (1952).

As shown in Table I, glycerophosphorylcholine appears to be formed in 95% yield, accompanied by an insignificant amount of free choline under the conditions of Expt. I. The "free choline" designated in the table, however, should be questioned according to the mechanism discussed above which should give rise to trimethylethylamine. Thus, its structure remains to be investigated.

The product was isolated according to the procedure described by Baer and Kates[10], after passing the aqueous solution through a column of a mixture of IRC—50 and Dowex-3. Since only a limited amount of the product was available, a concentrated solution of the aqueous phase was used for the following determinations: P: choline, 1.0:1.02; absorption of a periodate solution, 97% of theory; and $(\alpha)_D^{24}$ -2.96 ± 0.2(in water), $(\alpha)_D^{23}$ -2.85 ± 0.1[10]. On drying the crystalline cadmium complex of the product, two moles of water was found to be lost.

Anal. Found(amorphous): P, 5.24. Calcd. for $(C_8H_{22}O_7NP)_2(CdCl_2)_3$: P, 5.62.
Found (crystalline): C, 19.66; H, 5.32. Calcd. for $(C_8H_{22}O_7NP) \cdot CdCl_2 \cdot 2H_2O$: C, 19.46; H, 5.30.
Found (dehydrated crystals): C, 21.56; H, 4.80. Calcd. for $C_8H_{22}O_7NP \cdot CdCl_2$: C, 20.97; H, 4.84.

These results show that the glycerophosphorylcholine isolated has the L, α-configuration. It also suggests that the method can be utilized in obtaining L, α-glycerophosphoric acid from phosphatidic acids, and this is now under investigation.

Faculty of the Science of Living
Osaka City University
Nishi-ku, Osaka

10) E. Baer and M. Kates, *J. Am. Chem. Soc.*, **70**, 1394 (1948).

On the State of Formic Acid Adsorbed on Dehydrated Silica

By Kozo Hirota, Kenji Fueki, Yasuo Nakai and Kotaro Shindo

(Received July 21, 1958)

It has been found recently by the kinetic method[1] and by the infrared absorption method[2] in our laboratory that formic acid is chemisorbed as the ion on some metallic powders. However, from the fact that activity of metal as an adsorbent differs from that of silica[3] it is inferred that the acid may be adsorbed on the latter in a different state. To settle the problem some physico-chemical studies were undertaken. A combined method of infrared absorption and proton magnetic resonance was adopted and some conclusions on the chemisorbed state were obtained.

Sample. — The formic acid used in the experiment was dehydrated with anhydrous copper sulfate after repeated distillations. The amorphous silica adsorbent was prepared by dehydrating commercial silica gel at 300°C over a week, and it was confirmed by X-ray analysis that the amorphous structure of silica did not change before and after the dehydration. The specific surface area of silica gel was found to be 520 m^2/g. by the BET method (adsorbate : nitrogen) and formic acid was adsorbed on silica by an amount less than that necessary to form a monolayer*.

Measurement. — The infrared spectra were obtained with the same spectrometer as used in the previous report (Hilger H 800)[2], and a paste method, in which mulling was done with Nujol, was adopted in the present research. The proton resonance spectra were obtained with a high resolution spectrometer (Varian V-4310 C) at a fixed frequency of 40 Mc/sec. Both measurements were made at room temperature.

Results and Discussion.—The infrared spectrum of formic acid adsorbed on silica is quite different from those of formic acid adsorbed on metallic adsorbents which are supported on silica, From the present results shown in Fig. 1, three conclusions may be derived. First, a broad band appears at 3537 cm^{-1}, ranging

1) K. Hirota and T. Otaki, *J. Chem. Soc. Japan, Pure Chem. Sect.* (*Nippon Kagaku Zasshi*), in Press.
2) K. Hirota, K. Kuwata and Y. Nakai, This Bulletin, in press (1958).
3) G. M. Schwab et al., *J. Am. Chem. Soc.*, **71**, 1806 (1949).
* The cross section of the formic acid molecule was assumed to be 17 A^2.

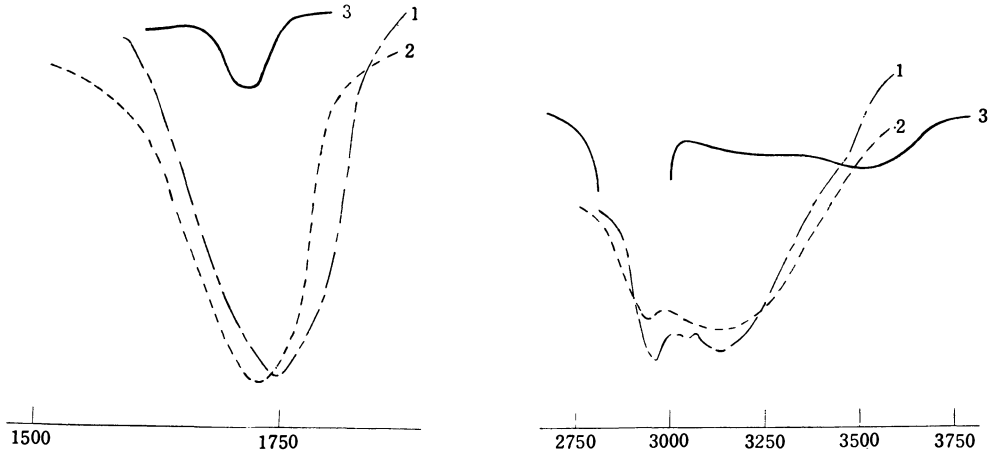

Fig. 1. Infrared spectrum of formic acid in various states.
1: vapour, 2: liquid, 3: adsorbed on silica.

from 3010 to 3765 cm^{-1}*. Such a band did not appear in the cases of formic acid adsorbed on metallic adsorbents and formic acid in the liquid state. According to Bonner and Hofstadter[4] and Wilmshurst[5], associated dimer of formic acid has a broad band near 3080 cm^{-1} which is ascribed to the formation of hydrogen bond, while monomeric formic acid has a sharp band near 3570 cm^{-1}. The band obtained in the present experiment is more similar in frequency to that of monomer than that of associated dimer, but it is broader, probably owing to the interaction between formic acid and silica.

Secondly, the antisymmetric band (ν_4) near 1580 cm^{-1}, which could be assigned to the formate ion $HCOO^-$ in the previous paper[2], is not observed in the present research. This result conforms the above suggestion that formic acid does not dissociate on the silica surface, but exists as a monomeric state. Thirdly, it is found that the C=O stretching band, whose center is at 1717 cm^{-1}, exists in lower frequency than that of monomeric formic acid[5].

The above conclusions can also be given by the proton magnetic resonance method, when the spectrum of the adsorbed formic acid is compared with that of liquid. As shown in Fig. 2, the proton resonance spectrum of liquid formic acid gives two proton signals in a lower field relative to that of water. The shift of one signal is

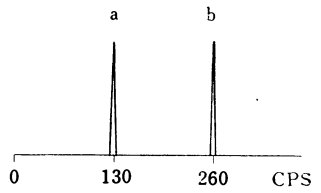

← Magnetic field H increasing
a: ^1H bonded to C. Zero of reference: H_2O
b: ^1H bonded to O.

Fig. 2. Proton resonance spectrum of formic acid.

130 cps, while that of the other is 260 cps, both intensities being the same, as is expected from the structure of the formic acid molecule.

It may be assigned from the studies on similar compounds that the former is due to the hydrogen atom bonded to the carbon atom, while the latter to the hydrogen atom bonded to the oxygen atom. To make sure of it, the proton resonance spectrum of deuteroformic acid HCOOD (90% in mol.) was measured. As shown in Fig. 3, the latter signal diminished to one tenth of the former in intensity.

However, the proton resonance spectrum of formic acid adsorbed on silica (Fig. 4)

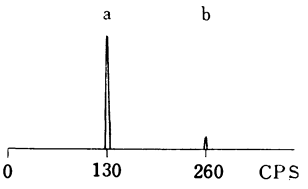

← H increasing

Fig. 3. Proton resonance spectrum of deuteroformic acid HCOOD (90% in mole).

* This band is obtained by subtracting absorption intensity of silica alone from that of the system of formic acid-silica.

4) L. G. Bonner and R. Hofstadter, *J. Chem. Phys.*, **6**, 531 (1938).

5) J. K. Wilmshurst, ibid., **25**, 478 (1956).

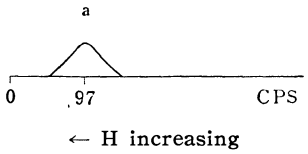

Fig. 4. Proton resonance spectrum of formic acid adsorbed on silica.

is quite different from that in liquid state; i. e., only one signal corresponding to the hydrogen atom bonded to the carbon atom appears as a broad one, its position, moreover, shifting by 33 cps to a higher field. Thus it can be concluded that the motion of hydrogen in the carboxyl group is fixed by adsorption, i. e., its free motion is hindered markedly*. Such a conclusion is in accord with the result that the OH stretching band found in the infrared spectrum becomes broad and shifts to higher frequency. It is supposed that the hydrogen bonds formed in associated formic acid decrease in number as a result of dissociation, caused by the strong adsorption of hydrogen atoms on the silica surface.

It can also be said, from the shift of the signal observed in the proton resonance spectrum of formic acid adsorbed on silica, that the electron density of the hydrogen atom bonded to the carbon atom is increased by adsorption. Detailed discussion on this result will be published later.

The authors express their sincere thanks to Professor Junkichi Itoh and Mr. Shiro Sato who measured the proton resonance spectra, and also to Mr. Tadaaki Otaki who gave them the sample of formic acid.

Department of Chemistry
Faculty of Science
Osaka University
Kita-ku, Osaka

* Recently the proton resonance spectrum of acetic acid, propionic acid etc. adsorbed on amorphous silica was reported (The 11th Annual Meeting of the Chemical Society of Japan, April 6, 1958) by M. Shimizu, T. Ikegami and I. Higuchi. Their conclusion on the adsorbed state is similar to the present one.

The Synthesis of Nootkatin, a Sesquiterpenoid Tropolone[1]

By Yoshio KITAHARA and Makoto FUNAMIZU

(Received July 31, 1958)

Nootkatin, the only known sesquiterpenoid tropolone, was isolated by Erdtman and his collaborators from the heart-wood of *Chamaecyparis nootkatensis* (Alaskan yellow ceder)[2]. The structure has been demonstrated as 4-isopropyl-5-(γ-methyl but-β-enyl) tropolone (I) by chemical reaction[2] and X-ray analysis[3]. As far as the authors are aware, the synthesis of nootkatin has not been attained as yet. This paper deals with the synthesis of nootkatin by a simple method.

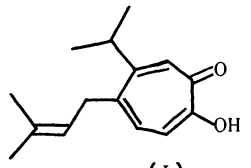

(I)

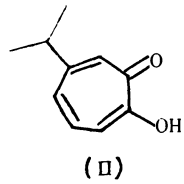

(II)

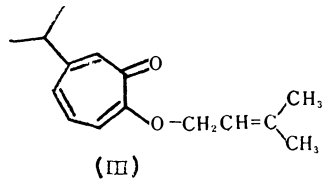

(III)

4-Isopropyltropolone (II) has been chosen as a starting material since (II) was synthesized before[4]. The procedure initiated from 5-substituted 4-isopropyltropolones, i. e. 5-cyano and 5-formyl derivatives derived from 5-amino-4-isopropyltropolone, was fruitless.

The Claisen rearrangement reaction has been applied to the synthesis of I. Preliminary work on the rearrangements of tropolone allyl ether and 3,7-dibromotropolone allyl ether resulted in the formation of 3-allyltropolone (80% yield) and in recovery of a small amount of 3,7-dibromotropolone, respectively, and no *p*(5)-rearrangement product was observed.

1) Presented at the 11th Annual Meeting of the Chemical Society of Japan in Tokyo, April 3, 1958. This investigation was supported in part by a donation of the Sankyo Co., Tokyo.

2) B. Carlsson, H. Erdtman, A. Frank and W. E. Harvey, *Acta Chem. Scand.*, **6**, 690 (1952); H. Erdtman and W. E. Harvey, *Chem. and Ind.*, **1952**, 1267; S. R. Duff and H. Erdtman, ibid., **1954**, 432.

3) R. B. Campbell and J. M. Robertson, ibid., **1952**. 1266.

4) T. Nozoe et al., *Proc. Japan Acad.*, **26**. No. 7, 43 (1950).

However, it seemed to us that a steric effect of dimethyl group in the cyclic intermediate of rearrangement of 4-isopropyltropolone γ: γ-dimethylallyl ether (III) might bring about a possibility of p-rearrangement to give nootkatin.

The reaction of silver salt[5] of II with γ: γ-dimethylallyl bromide in anhydrous ether gave an oily mixture of III and its isomer. On refluxing the mixture in xylene for three hours and treating the resulting reaction mixture with aqueous sodium bicarbonate-, sodium carbonate- and then with sodium hydroxide solution, nootkatin, m. p. 95° was obtained in 7% yield from a soluble part in aqueous sodium hydroxide solution.

Anal. Found; C, 77.61; H, 8.36. Calcd. for $C_{15}H_{20}O_2$: C, 77.55; H, 8.68%.

The identity with an authentic specimen of natural nootkatin was established by mixed melting point determination, infrared and nuclear magnetic resonance spectral comparisons.

The authors express their thanks to Professor T. Nozoe and to Professor T. Toriumi for their interest and encouragement, to Professor J. D. Roberts of the California Institute of Technology, U. S. A., for a supply of isoprene as a starting material and to Professor H. Erdtman of the Royal Institute of Technology, Sweden for a gift of natural nootkatin.

The Chemical Research Institute of Non-Aqueous Solutions
Tohoku University, Katahira-cho, Sendai

5) H. Iinuma, *J. Chem. Soc. Japan, Pure Chem. Sec.* (*Nippon Kagaku Zassi*), **64**, 742 (1943).

Determination of Aluminum in True Solution in the Presence of Colloidal Hydrated Alumina

By Katsumi Goto, Hiroshi Ochi and Takeshi Okura

(Received August 4, 1958)

For lack of a cenvenient method of determining small amounts of aluminum, few attempts have been made to differentiate between the aluminum in true solution and that in the colloidal form (or better, large hydroxoaquoaluminum ions[1]), except Tanaka's work[2], who separated ionic aluminum from waters containing colloidal hydrated alumina, using an ion-exchange technique.

On the other hand, a simple and accurate method, involving a chloroform extraction of aluminum as 8-hydroxyquinolate and subsequent determination of the absorbance of the extract, was recently developed by Gentry and Sherrington[3] and also by other workers.[4,5] This method was later modified by Motojima[6] to be used for the simultaneous determination of iron and aluminum, and by Goto[7,8] to prevent iron from being extracted.

It has been reported by Motojima[6] that while the extraction of aluminum 8-hydroxyquinolate is complete at pH 4.5 to 9.5, the recovery of aluminum is low when the pH of the sample is adjusted prior to the addition of 8-hydroxyquinoline. This statement seems to indicate the applicability of the above extraction method to the differentiation between the two forms of aluminum in water.

The extraction method was somewhat modified in the present investigation and actually applied to the determination of aluminum in true solution.

Method. *Reagents.—8-Hydroxyquinoline (oxine) solution.*—Dissolve 2 g. of pure 8-hydroxyquinoline in 5 ml. of glacial acetic acid and dilute to 200 ml. with distilled water. *Sodium acetate solution,* 1 M. *Chloroform. Sodium sulfate, anhydrous.*—Purest grade of commercial product often contains substances which produce a considerable blank color. Purify by recrystallization from water.

Procedure.—Take approximately 10 ml. of distilled water in a separatory funnel. Add to this 2 ml. of 8-hydroxyquinoline solution and 2 ml. of sodium acetate solution, and mix well. Pour slowly from a buret 10.0 ml. of chloroform into the separatory funnel. Do not shake at this step. Add, as rapidly as possible, 20 ml. of sample (containing less than 4 mg./l. of extractable aluminum) to the separatory funnel. The pH value must be within the range 4.5 to 9.5. Shake vigorously for about 10 sec., and allow the mixture to separate into two layers. Stable emulsions will be produced in the presence of colloidal form of hydrated alumina. It is important in

1) See H. Tanabe, *J. Pharm. Soc. Japan (Yakugaku Zasshi)*, **74**, 253, 866 (1954); **77**, 33, 37 (1957).
2) M. Tanaka, This Bulletin, **27**, 98 (1954).
3) C. H. R. Gentry and L. G. Sherrington, *Analyst*, **71**, 432 (1946).
4) S. E. Wiberley and A. G. Bassett, *Anal. Chem.*, **21**, 609 (1949).
5) J. L. Kassner and K. A. Ozier, ibid., **23**, 1453 (1951).
6) K. Motojima, *J. Chem. Soc. Japan, Pure Chem. Sec. (Nippon Kagaku Zassi)*, **76**, 903 (1955).
7) K. Goto, *Chem. and Ind.*, **1957**, 329.
8) T. Okura, K. Goto and H. Suzuki, *Industrial Water (Kogyo Yosui)* **2**, 338 (1956).

such a case that the emulsions are broken with a glass rod. Run the chloroform layer into a test tube containing a small amount of anhydrous sodium sulfate, which serves to remove droplets of water in the chloroform. Measure the absorbancy at 420 mμ.

Discussion.—In the usual procedure, 8-hydroxyquinoline, sodium acetate and chloroform are added to the sample in this order, and then the mixture is skaken to extract aluminum 8-hydroxyquinolate into the chloroform layer. The usual procedure can not be applied when the sample contains colloidal hydrated alumina of a very low degree of polymerization, since such colloidal hydrated alumina is also extracted to a considerable extent into the chloroform layer because of its rather rapid depolymerization. This interference from colloidal alumina, however, will be minimized by carrying out the extraction very rapidly. The procedure described in the present paper may meet this requirement. A 10 second's shaking is sufficient for the complete extraction of aluminum in a true solution at 20°C, as will be clear from Table I.

The form of aluminum available for the present method is not known strictly. However, it may be ionic or, if not, of a very low degree of polymerization, since a clear solution containing much unextractable aluminum can be easily obtained.

It has been shown by the above method that when an acidic solution of the aluminum ion is neutralized to a pH between 5 and 8, the concentration of extractable aluminum approaches the solubility very rapidly (Fig. 1) while the solution remains clear for more than 30 min. No other methods may be able to determine such a rapidly dercreasing concentration of aluminum in a true solution. Total aluminum can be determined after decomposing colloidal alumina by boiling with a small amount of hydrochloric acid. A larger amount of sodium acetate is required in this case to obtain a suitable extraction pH.

TABLE I
EFFECT OF SHAKING TIME ON THE EXTRACTION OF ALUMINUM AT 20°C
(Concn. of Al^{3+}: 2.55 mg./l.)

Shaking time (sec.)	Recovery of Al (%)
5	102
10	99
20	99
30	99
60	100

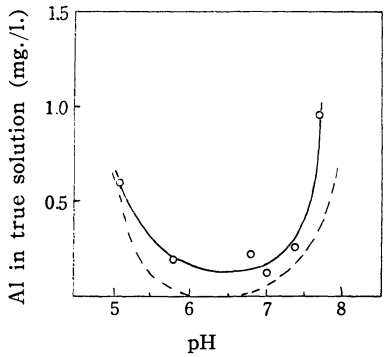

Fig. 1. Very rapid disappearance of Al^{3+} at various pH values. (25.0°; pH adjusted with NaOH)

-o-o- Al in true solution 1 min. after neutralization.
----- Solubility (see Ref. 8)
Initial concentration of Al^{3+}: 2.42 mg/l

Faculty of Engineering
Hokkaido University
Sapporo

Synthesis and Use of L-Histidine Benzylester

By Shiro Akabori, Shumpei Sakakibara and Sumiko Shiina

(Received August 5, 1958)

Up to the present, histidine methylester[1] has been known to be an only actual example of the histidine esters. Izumiya[2] attempted the synthesis of histidine benzylester, but the benzylester in a pure form was not obtained by his procedure.

In this communication, crystalline histidine benzylester di-*p*-toluene sulfonate(I) was prepared in a good yield. A suspension of powdered L-histidine hydrochloride monohydrate (20 g.), *p*-toluene sulfonic acid monohydrate(44 g.) and benzyl alcohol (100 ml.) in chloroform (500 ml.) was refluxed for about 30 hr. in Wieland's[3] apparatus, in which silica gel and anhydrous sodium carbonate were used as desiccants. Distillation of chloroform, followed by addition of dry ether (350 ml.),

1) E. Fischer und L. H. Cone, *Ann.*, **363**, 107 (1908).
2) N. Izumiya and K. Makisumi, *J. Chem. Soc. Japan, Pure Chem. Sec.* (*Nippon Kagaku Zassi*), **78**, 662 (1957).
3) T. Wieland, G. Ohnacker und W. Ziegler, *Ber.*, **90**, 194 (1957).

TABLE I

PEPTIDE-DERIVATIVES SYNTHESIZED FROM HISTIDINE BENZYLESTER

Substance	Solubility in dil. HCl	Yield (%)	Melting point (°C)	$[\alpha]_D^{30}$	Anal. (%) Calcd. C	Calcd. H	Calcd. N	Found C	Found H	Found N
Cbzo-Gly-L-His-OBz[a]	+	77.9	99～100.2	−6.8°[g]	63.29	5.54	12.84	63.01	5.73	12.43
〃 [b]		82.5	98.5～99.2	−5.5°[g]						
〃 [c]		45.8	99～99.5	−6.3°[g]						
Cbzo-L-Thr-L-His-OBz[b]	+++	66.5	137～137.5	−16.4°[h]	62.48	5.87	11.66	62.48	6.19	11.80
Cbzo-L-Phe-L-His-OBz[a]	−	68.5	118～118.5	−17.3°[h]	68.42	5.74	10.64	68.44	5.95	10.76
〃 [b]		53.3	117～118.5	−22.4°[h]						
Isovaleryl-L-His-OBz[d]	+	7.6	144	−23.6°[h]	65.63	7.04	12.76	65.79	7.29	12.72
H-Gly-L-His-OH HCl[e]		80.0	174～175 (dec.)[f]	+28.5°[i]						

(a), Mixed anhydride method (isovaleryl); (b), dicyclohexylcarbodiimide method; (c), azide method; (d), this substance was obtained as a byproduct from the dil. HCl extract of the reaction mixture of Cbzo-Phe-His-OBz (mixed anhydride method); (e), dried at 135° in vacuo; (f), corrected value; M. Hunt[5] reported m. p. 175° (corr.); (g), c 2, ethanol; (h), c 1, ethanol; (i), c 1, water; M. Hunt[5] reported $[\alpha]_D^{26}$ +25° (c 1, water).

Cbzo..... Carbobenzoxy, Bz..... benzyl.

gave a syrupy mass which was reprecipitated from chloroform and dry ether. The product was then crystallized gradually from a mixture of dry dioxane and dry acetone (1 : 2); colorless fine needles, weight 48～51 g. (85～90%), $[\alpha]_D^{30}$ −2.4° (c 4.7, water). This substance I was obtained in a hydrated state on recrystallization from a dioxane-acetone mixture containing a small amount of water. The hydrated crystals could be handled more conveniently than the anhydrous because the hydrated crystals were not so hygroscopic as the anhydrous ones. Almost all of the crystallization water, if necessary, could be dried off over phosphorous pentoxide in vacuo at 30°. These properties of the hydrated crystals, however, made difficult the quantitative determination of the crystallization water. This substance I sintered at 82～85° and decomposed at 225° after dryness in vacuo at ordinary temperature, and melted at 146～149° after dryness in vacuo at 135°.

Anal. Found (dried at 135°): C, 54.95; H, 5.48; N, 7.37. Found (hydrated crystals, dried in vacuo at 30°): C, 54.90; H, 5.46; N, 6.72. Calcd. for $C_{27}H_{31}O_8N_3S_2$: C, 54.99; H, 5.30; N, 7.13%.

Histidine methylester di-hydrochloride is hard to dissolve in usual organic solvents other than methanol or ethanol; and aqueous strong alkali or sodium methoxide is required for preparing the free methylester. On the other hand, the benzylester sulfonate I was considerably soluble in dry chloroform, and a solution of I and a calculated amount of triethylamine in chloroform could be used as a free benzylester solution for peptide synthesis. For example, carbobenzoxy glycyl histidine benzylester (II) was prepared as follows. A solution of mixed anhydride, which was prepared from carbobenzoxy glycine (1.05 g.), isovaleryl chloride (0.6 g.) and triethylamine (0.7 ml.) according to Vaughan and Osato's procedure[4], was allowed to react overnight with a mixture of I (3.54 g.) and triethylamine (1.70 ml.) in chloroform (15 ml.), and after usual treatment of the reaction mixture, the substance II was obtained in a yield of 1.7 g. The substance II was then hydrogenated in the presence of Palladium charcoal into glycyl histidine hydrochloride, and it was confirmed that the product obtained here was superior in specific optical rotation to the reported one[5] which was prepared from carbobenzoxy glycyl histidine methylester. The peptide-derivatives synthesized from the histidine benzylester are listed in Table I.

Department of Chemistry, Faculty of Science
Osaka University, Kita-ku, Osaka
Institute for Protein Research,
Osaka University, Kita-ku, Osaka

4) J. R. Vaughan Jr., and R. L. Osato, *J. Am. Chem. Soc.*, **73**, 5553 (1951).
5) M. Hunt and V. du Vigneaud, *J. Biol. Chem.*, **127**, 46 (1939).

*Proton Resonance in Sulfamic Acid**

By Shizuo FUJIWARA and Ichiro YAMAGUCHI**

(Received August 5, 1958)

Structural investigations on sulfamic acid by X-ray diffraction[1] and infrared absorption[2] measurements have shown the results to suggest the zwitter-ion form of $NH_3^+SO_3^-$ in crystal. Since nuclear magnetic resonance method is very straight-forward to distinguish two-proton system[3] from three-proton one[4], we have applied this method to the crystal of sulfamic acid. Evidences of zwitter-ion form will be shown here as well as the informations on the intramolecular rotation as the results of the measurements of line shape and widths.

Experimental.—The sample studied is crystalline powder with a purity of 99.95%. The proton resonance is observed at about 20 megacycles. The temperature range of the experiment is between −180°C and +60°C. The apparatus used is of the autodyne-detector type which has been described elsewhere[5]. Though efforts to make measurements below the temperature of liquid nitrogen were made, reliable record was not obtained as the sample was saturated.

The resonance curve has a shoulder over all the temperature range of the experiment and, furthermore, the second shoulder appears below −170°C outside of the first shoulder. Fig. 1 presents the half of the derivative of the resonance curves at several temperature ranges. With decreasing temperature, the line shape becomes of three-peaked form, the evidence of three-proton system[4]. This suggests that the zwitter-ion form can be taken plausible as the molecular configuration at this temperature range.

Fig. 2 shows the temperature dependence of the second moment of the resonance absorption curve. A constant value of about 6±0.5 gauss[2] is taken throughout the temperature range of the experiment higher than −170°C. It begins to increase in the range below −170°C, taking a value of about 12 gauss[2] at −180°C. This change in the second moments will suggest that the molecule begins to freeze at this temperature range.

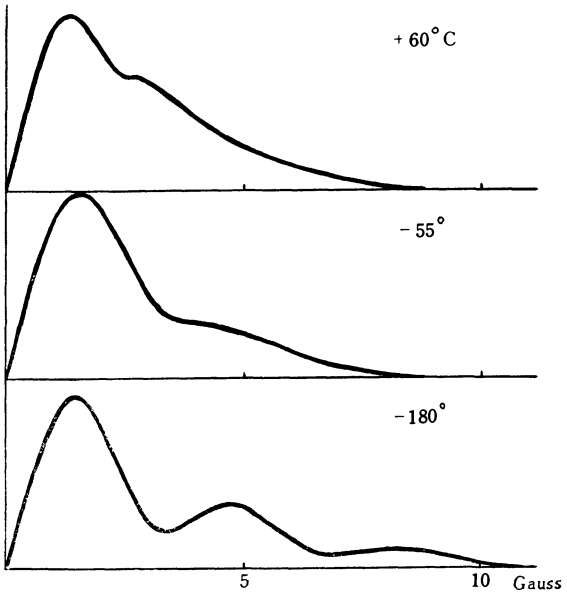

Fig. 1. Derivative of the proton resonance absorption curves for sulfamic acid at various temperatures.

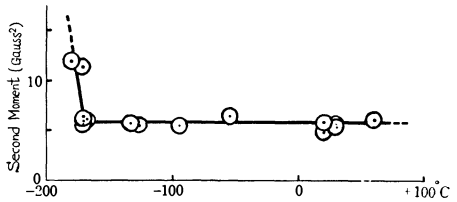

Fig. 2. Temperature dependence of the second moment.

Discussion of the Results. — Second moments are calculated for various models of the molecular structure: a) 30.7 gauss[2] for the model suggested by X-ray diffraction[1] where three protons in NH_3 group are taken equivalent, and b) 15~20 gauss[2] for the model of NH_2SO_3H having the same structure as a) with respect to the skeleton of heavy atoms. When NH_3 group in the model a) rotates freely about N-S bond axis, the second moment is expected to be reduced to 7.5 gauss[2].

According to the results shown above, we assume that the molecule takes zwitter-ion structure in crystal and reorientates about N-S bond axis in the temperature range higher than −170°C. Sano[6] reported a value of the second moment at room temperature almost the same as that obtained by the present authors. He

* Presented at the Autumnal Meeting of the Chemical Society of Japan, held in Tokyo, November, 1957.

** Present address: Japan Atomic Energy Research Institute, Tokai, Ibaraki.

1) F. A. Kanda and A. J. King, *J. Am. Chem. Soc.*, **73**, 2315 (1951).
2) A. M. Vugguat and E. L. Wagner, *J. Chem. Phys.*, **26**, 77 (1957).
3) G. E. Pake, ibid., **16**, 327 (1948).
4) E. R. Andrew and R. Bersohn, ibid., **18**, 159 (1950).
5) S. Fujiwara and S. Hayashi, *Reports of the University of Electro-Communications*, No. 8, 95 (1956).
6) K. Sano, *Reports of the Faculty of Liberal Arts, Yamanashi University*, **7**, 143 (1556).

explained this value by taking a model where molecules were rigid with the zwitter-ion form and N-H bonds in NH_3 groups were unusually elongated. This seems unplausible, however, since such an unreasonably deformed structure will show temperature dependence in the second moment values and, moreover, such a model can not explain the increasing tendency at around $-180°C$.

Another comment will be added here with respect to the zwitter-ion structure: asymmetrical derivative curve was obtained when the sample was moist. We assume that this curve is superposition of a narrow line and a broad one being different in resonance center. Since the intensity of the central narrow line is humidity dependent, it is attributed to the water molecules adsorbed by the sample. The asymmetrical curve was decomposed to show that the resonance center for the adsorbed water was shifted to the field higher than that for the broad line by 10^{-5}; in another words, proton in sulfamic acid is electronically less shielded than in water molecules. The asymmetrical figure of the derivative curve is not due to the saturation effect since the same result has been obtained when the polarity of the bias field is reversed.

A similar result of large positive shift has been reported with formamide[7], which is also considered to form zwitter-ion, and, therefore, the finding presented here may be taken as the characteristic nature of protons forming zwitter-ions.

Authors' thanks are due to Mr. K. Nukada of Government Chemical Industrial Research Institute and to Dr. M. Kobayashi of Tokyo University who supplied the samples for the experiments. They are also indebted to Dr. T. Sugawara of Tohoku University who made the measurements at liquid hydrogen temperature.

University of Electro-Communications, Chofu, Tokyo

7) L. H. Meyer, A. Saika and H. S. Gutowsky, *J. Am. Chem. Soc.*, **75**, 4567 (1953).

Particle Size Dependence of Heat of Transition of Crystalline Trimethylamine Sulfurtrioxide, $(CH_3)_3N \cdot SO_3$

By Hiroshi Suga*, Kunio Nakatsuka** and Syûzô Seki

(Received August 9, 1958)

The crystal structure of trimethylamine sulfurtrioxide at room temperature (hexagonal) has been determined by Shimizu and MacLachlan[1] who revealed the presence of rotational disorder of $(CH_3)_3N$ and SO_3 groups about the N-S axis. This result implies that a kind of order-disorder phase transition due to disappearance of such a disordered state will take place when the crystal is cooled.

The present material was prepard by a new method by adding chlorosulfonic acid (SO_3ClH) to a chloroform solution of trimethylamine. The sample thus obtained was identified by the m. p. determination and by Norelco X-ray diffractometer. The specimens used for the measurements were recrystallized from aqueous solution and then ground to about 0.1~0.01 mm in diameter; m. p. 241~243°C (decomp.).

As we expected, the differential thermal analysis has really confirmed that the crystal undergoes a phase transition at about −30°C in the cooling and at about +20°C in the heating directions, showing an anomalously marked hysteresis phenomenon. Quite unusually, however, the magnitude of heat effect associated with the phase transition changes from specimen ot specimen to a considerable extent depending on their particle sizes.

To examine this effect quantitatively, the heat capacities were measured with the following specimens; specimen A, the mean particle diameter of 0.0075~0.03 mm, specimen B 0.11~0.15 mm and specimen C 0.25~0.36 mm. In the C_p-T curves of these specimens measured immediately after cooling there appears always a broad maximum (about +17°C) followed by irregular heat evolution and absorption (see Fig. 1). This irregular thermal anomaly, however, disappeared when the

* Present address: Department of Physics, Faculty of Science Osaka, University.

** Present address: Kanzakigawa Factory, Takeda Pharmaceutical Industries, Ltd., Higashiyodogawa-Ku, Osaka.

1) H. Shimizu and Dan MacLachlan, *J. Am. Chem. Soc.*, **75**, 4352 (1953).

TABLE I

PARTICLE SIZE DEPENDENCE OF THE HEAT OF TRANSITION

Specimen	Mean diameter (in mm)	Method of preparation*	$T_{tr.}$ (°C)	ΔH (cal./mole)	ΔS (e. u.)
A	0.0075~0.03	sublimation	+18 (heating) −38 (cooling)	80	—
B	0.11~0.15	grinding, separated by sieve set	+16 (heating) −30 (cooling)	230 230	0.80 0.98
C	0.25~0.36	〃	+16 (heating) −28 (cooling)	300	—

* The identification of the crystalline modification of the samples prepared by different methods was made by their m. p. and the Norelco X-ray diffraction patterns.

specimens were cooled down very slowly to −80°C with taking several days (see Fig. 2). After this treatment of each specimen, we carried out the measurement. It was found that the greater the particle size, the greater difficulty was encountered for obtaining the equilibrium curve.

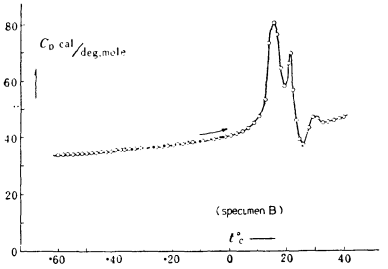

Fig. 1. Heat capacity vs. temperature curve of $(CH_3)_3N \cdot SO_3$ before the treatment.

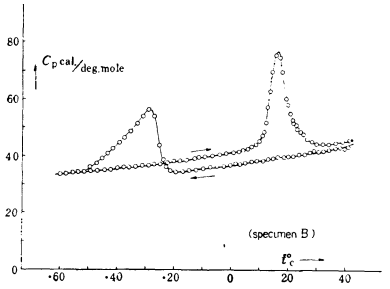

Fig. 2. Heat capacity vs. temperature curve of $(CH_3)_3N \cdot SO_3$ after the treatment.

Table I lists enthalpy changes at transition point of three different specimens. Although an effort was made to obtain true equilibrium (heating rate : 1 deg./6 min.), the values reported here are of approximate nature owing to the unusually sluggish velocity of this phase transition. Such a remarkable dependence of the enthalpy of the transition on particle size has never been reported as far as we are aware of. It is supposed that the observed heat of transition arises from at least two origins; one is the enthalpy difference between the bulk enthalpies of the two phases and the other the difference in enthalpies which come from the formation of micro-structure, such as a domain structure or submicro-region[2], on passing through the transition point.

We are now investigating the above-mentioned phenomenon by use of dilatometry, X-ray and other available methods. The detailed discussion on the present results will be reported elsewhere.

The authors wish to express their sincere thanks to Professor I. Nitta for his continued interest in the present study.

Department of Chemistry
Faculty of Science
Osaka University. Kita-ku, Osaka

2) A. R. Ubbelohde, *Brit. J. Appl. Phys.*, **7**, 313 (1956); *Quart. Revs. (London)*, **11**, 246 (1957).

The Structure of Stipitatonic Acid, a Mould Metabolite from Penicillium[1)]

By Kôzo Doi and Yoshio Kitahara

(Received August 9, 1958)

Stipitatonic acid, a mould tropolone, $C_9H_4O_6$, m. p. 237~237.5° (decomp.) has been isolated from *Penicillium Stipitatum*

1) The paper was presented before the Local Meeting of the Chemical Society of Japan in Yonezawa, June 23, 1958. This work was supported in part by a donation of the Sankyo Co., Tokyo.

Thom. by Segal and the structure A has been assigned to it rather than the alternative isomer B[2]. We now wish to show evidence which permits the assignment of structure B to stipitatonic acid contrary to that proposed before[2].

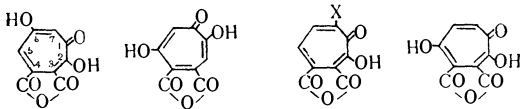

6-Hydroxytropolone-3,4-dicarboxylic anhydride(A) and its two isomers concerning with hydroxyl group were synthesized by the following methods and these anhydrides were compared with stipitatonic acid.

Bromination of tropolone-3,4-dicarboxylic anhydride (C:X=H), an oxidation product of purpurogallin[3] gave 7-bromo compound (C:X=Br), m. p. 198°C[4]. It has been reported[5] that liquid phase hydrolysis of 3-bromotropolone afforded 4-hydroxytropolone, and a minute amount of 3-hydroxytropolone. Application of this reaction to the 7-bromo compound (C:X=Br) gave 7-hydroxy compound (C:X=OH) in 40% yield and a hydroxytropolone-3,4-dicarboxylic anhydride, m. p. 237°C (*not decomp.*), yellow needles, in 6% yield.

Anal. Found: C, 51.94; H, 1.86. Calcd. for $C_9H_4O_6$: C, 51.93; H, 1.94%. Ultraviolet maxima, $m\mu(\log \varepsilon)$ in methanol: 272(4.46), 345(3.90), 363 (3.92).

The latter anhydride, m. p. 237°C underwent decarboxylation to give stipitatic acid, m. p. 279 ~280°C[6] whose identity was confirmed by ultraviolet and infrared spectra,

Anal. Found: C, 52.43; H, 3.47. Calcd. for $C_8H_6O_5$; C, 52.75; H, 3.32%. Therefore the structure of the anhydride, m. p. 237°C. also has to be the structure A. Persulfate oxidation of the anhydride (C:X=H) gave 7- and 5-hydroxy compounds (C:X=OH and D).

Anal. Found: (5-hydroxy compound, m. p. 250°C): C, 51.79; H, 1.68%. The structure of the 5-hydroxy compound was supported by the decarboxylation to give 5-hydroxytropolone, m. p. 250°C (decomp.)[7].

Any hydroxy compound of the tropolone-3,4-dicarboxylic anhydride mentioned above was not identical with natural stipitatonic acid which was kindly spared by Dr. Segal. The proof to support the structure A for stipitatonic acid rather than the structure B has been based on the submission to azo-coupling but no detail on the azo compound is mentioned[2]. It seems to us that unless a true azo-coupling compound is produced, the test for the vacant *p*-position can be misleading because even *p*-substituted tropolones show red coloration with aryl diazonium salts.

The difference, $\Delta\nu$ between two carbonyl frequencies of anhydride group of almost all derivatives of tropolone-3,4-dicarboxylic anhydride in infrared spectra in 60±2 cm^{-1}, while $\Delta\nu$ of stipitatonic acid is 78 cm^{-1} [2].

Therefore the above results and evidence that decarboxylation of stipitatonic acid gave stipitatic acid[2] suggest that *the structure of stipitatonic acid is not A but B.*

When this manuscript was completed, one of us (Y. K.) received a letter from Dr. Segal on August 6, in which he described that his observation on a potash fusion of stipitatonic acid was in complete agreement with our belief regarding the structure.

The authors wish to thank Professor T. Toriumi of this Institute for his encouragement and Dr. W. Segal for a supply of stipitatonic acid.

The Chemical Research Institute of Non-Aqueous Solutions
Tohoku University
Katahira-cho, Sendai

2) W. Segal, *Chem. and Industry*, **1957**, 1040.
3) W. D. Crow, R. D. Haworth and P. R. Jefferies, *J. Chem. Soc.*, **1952**, 3705.
4) T. Nozoe, K. Doi and T. Hashimoto, to be published.
5) Y. Kitahara, *Science. Repts. Tôhoku Univ., First Ser.*, **39**, 258 (1956).
The mechanism may be explained by benzyne* type process (dehydrotropolone).
* J. D. Roberts, H. E. Simmons, Jr., L. A. Carlsmith and C. W. Vanghan, *J. Am. Chem. Soc.*, **75**, 3290 (1953) and subsequent papers.
6) R. B. Johns, A. W. Johnson and M. Tišler, *J. Chem. Soc.*, **1954**, 4605.
7) T. Nozoe, S. Seto, S. Ito, M. Sato and T. Katono, *Science Repts. Tôhoku Univ., First Ser.*, **37**, 191 (1953).

Chemical State of Uranium-239 in Neutron-Irradiated Uranium(IV) and Uranyl(VI) Sulfate Solutions

By Nobufusa Saito and Tatsuya Sekine

(Received August 14, 1958)

Very few investigations have been devoted to study the chemical state of ^{239}U in neutron-irradiated uranium compounds. In 1939, Irvine[1] reported probable

1) J. Irvine, Jr., *Phys. Rev.*, **55**, 1105 (1939).

formation of quadrivalent ^{239}U in neutron-irradiated ammonium uranyl acetate solution and its enrichment with respect to ^{238}U in the first fraction of a hydrolytic precipitation by a factor of the order of ten. On the other hand, Aten, Beers and De Groot[2] reported that quadrivalent and sexivalent uranium isolated from U_3O_8 irradiated with slow neutrons have the same specific activity of ^{239}U. The following experiments have been carried out by the present authors to study the chemical state of ^{239}U in neutron-irradiated uranium(IV) and uranyl(VI) sulfate solutions.

TABLE I

COMPOSITION OF THE SOLUTIONS (in moles)

	U(VI)	U(IV)	SO_4^{--}*	H^+
Soln. A**	0.02	—	1.9	2.8
Soln. B	0.02	0.02	1.9	2.8
Soln. C	—	0.02	1.9	2.8

* SO_4^{2-} was supplied as sulfuric acid and sodium sulfate.

** Nitrogen gas was passed through the Soln. A.

Three kinds of target solution were made up as shown in Table I, and 100 ml. of each solution in a glass vessel was exposed for one hour to a neutron flux of $\sim 10^7/cm^2/sec$. During irradiation, the container of the solution was covered with a black paper to keep the whole system in the dark. In addition, it was cooled with ice to reduce the velocity of isotopic exchange reaction between uranium(IV) and uranium(VI)[3]. After irradiation, either uranyl(VI)- or uranium(IV) sulfate was added to the solutions A and C, so that the solutions became 0.02 M in both uranyl(VI)- and uranium(IV) sulfate. The separation of uranium(IV) from uranium(VI) was carried out with portions of the resulting solution within 30 minutes after the end of irradiation. The uranium(IV) fraction was extracted with chloroform as cupferronate. After the solvent and the excess of cupferron were removed from the chloroform layer, the residue was dissolved in nitric acid. To the resulting solution containing uranium(VI) were added ammonia water to precipitate ammonium diuranate. The precipitate was dissolved in a hot mixture of acetic and nitric acids; finally sodium uranyl acetate was precipitated from the solution. The uranium(VI) fraction in the aqueous layer after the chloroform extration was treated in a similar way as above to precipitate sodium uranyl acetate. All precipitates of sodium uranyl acetate were dried, mounted on a stainless-steel dish and submitted to counting with a thin end-window Geiger-Müller counter. The decay of the activity was followed for more than three half-lives of ^{239}U, and the distribution of ^{239}U in uranium(VI) and uranium(IV) fractions was calculated. The results are shown in Table II.

TABLE II

RADIOACTIVITY OF ^{239}U IN EACH FRACTION

	^{239}U in U(VI) fraction		^{239}U in U(IV) fraction	
	c.p.m.	%	c.p.m.	%
Soln. A	7200	97	250	3
Soln. B	9750	75	3280	25
Soln. C	4630	61	2930	39

Remarks: Decay correction was made for each fraction. If U(III) were formed, it should be air-oxidized to U(IV) state during the separation procedure and counted as U(IV) fraction.

In another experiment with the solution C, it was found that ^{239}U is enriched in the uranium(VI) fraction by a factor of approximately 50. From those data, the following conclusions can be drawn.

i) Most part of ^{239}U in the neutron-irradiated uranyl(IV) sulfate solution is in the sexavalent state.

ii) More than half of ^{239}U in the neutron-irradiated uranium(IV) sulfate solution is not in the quadrivalent state, but in the sexavalent state.

iii) Hot-atom effect plays an important role in the formation of ^{239}U in the sexivalent state, since ^{239}U is enriched in the uranium(VI) fraction separated from the neutron-irradiated uranium(IV) sulfate solution.

The details of this work will be reported elsewhere.

Department of Chemistry
Faculty of Science
The University of Tokyo
Hongo, Tokyo

2) A. Aten, Jr., M. Beers and D. De Groot, *J. Inorg. Nucl. Chem.*, **5**, 159 (1958).

3) R. Betts, *Can. J. Research*, **26B**, 702 (1948).

The Viscosity of Ideal Solutions

By Tetsuya ISHIKAWA

(Received April 14, 1958)

The viscosity determination of artificially ideal solutions of glass spheres in a suspending medium with density equal to that of the solids in order to preclude sedimentation, done by Vand[1] and by his followers, Sweeny and Geckler[2], gave a decisive confirmation of Einstein's viscosity equation for infinite dilution

$$\eta_r = 1 + k\phi \text{ with } k = 2.5$$

where η_r is the relative viscosity and ϕ is the volume fraction occupied by N spheres of radius a in a volume V, $\phi = \frac{4}{3}\pi a^3 N/V$

The extention of Einstein's equation to a suspension of finite concentration proposed by Mooney[3],

$$\ln \eta_r = 2.303 \log \eta_r = 2.5\, z_v/(1-\lambda z_v)$$

where λ is a constant, the self-crowding factor, predicted only approximately by Mooney's theory, and z_v is the volume fraction of spheres, fits Vand's data as well as Sweeny and Geckler's data. It is noted here that since $z_v = \phi/(1+\phi)$, z_v becomes ϕ at infinite dilution where Mooney's equation tends to Einstein's equation. For actually ideal solutions, however, Einstein's equation fails and Arrhenius' equation[4] is frequently used:

$$\ln \eta_r = 2.303 \log \eta_r = A z_v$$

where A is a constant determined by the extrapolation of $\ln \eta_r/z_v$ at $z_v = 0$. Its determination, however, is difficult because the limit of precision of viscosity determination is reached. A general viscosity equation for infinite dilution derived later in this paper is

$$\eta_r = 1 + K_v(\eta_2/\eta_1) z_v$$

where η_2/η_1 is the viscosity ratio of the solute 2 to the solvent 1, and K_v is a constant throughout the concentration, determined easily as an arithmetic mean of the values $(1-z_v)(\eta-\eta_1)/z_v(\eta_2-\eta)$ at several finite concentrations, η being the viscosity of the solution at concentration z_v, so that K_v is accurate and trustworthy. The constant $K_v(\eta_2/\eta_1)$ has been found always to have a smaller value than 2.5 for the solute of low viscosity ratio, but its value comes near to 2 or more as the viscosity ratio becomes high.

In a case where the viscosity ratio is high and K_v keep constancy no longer against concentration, Mooney's equation having $(K_v)_0(\eta_2/\eta_1)$ in place of 2.5, namely:

$$\ln \eta_r = 2.303 \log \eta_r = (K_v)_0(\eta_2/\eta_1) z_v/(1-\lambda z_v)$$

where $(K_v)_0$ is the limiting value of K_v at $z_v = 0$, has been proved to be valid for the whole range of concentration.

Derivation of a New Equation at Infinite Dilution.—The hyperbolic form of the present author's fundamental formula for binary mixtures[5] is

$$\frac{(1-z_m)(\eta-\eta_1)}{z_m(\eta_2-\eta)} = \frac{k_2 a_2}{k_1 a_1} = K$$

where z_m is the molar fraction of component 2, a_1 and a_2 are the association degrees of components 1 and 2 respectively, k_1 and k_2 are the characteristic constants of components 1 and 2 respectively and K keeps constancy so long as no change occurs in the molecular association of either or both of components.

Now, between the molar fraction z_m and volume fraction z_v, there is the following relationship:

$$\frac{(1-z_m)M_1}{z_m M_2} = \frac{(1-z_v)d_1}{z_v d_2}$$

in which M_1 and M_2 are the molecular weights of components 1 and 2 respectively, and d_1 and d_2 are the densities of components 1 and 2 respectively, and therefore the similar hyperbolic form with respect to z_v:

$$\frac{(1-z_v)(\eta-\eta_1)}{z_v(\eta_2-\eta)} = K\frac{M_1 d_2}{M_2 d_1} = \text{a constant, say } K_v$$

is valid as well.

At very low concentration where z_v is small enough to be neglected as compared

1) V. Vand, *J. Phys.* and *Colloid Chem.*, **52**, 300 (1948).
2) K. H. Sweeny and R. D. Geckler, *J. Appl. Phys.*, **25**, 1135 (1954).
3) M. Mooney, *J. Colloid Sci.*, **6**, 162 (1951).
4) S. Arrhenius, *Z. Phys. Chem.* **1**, 285 (1887).
5) T. Ishikawa, This Bulletin, **4**, 5 (1929).

to 1, the above formula can be reduced to

$$\frac{\eta-\eta_1}{z_v(\eta_2-\eta)}=K_v$$

from which it follows:

$$\frac{\eta}{\eta_1}=\frac{1+K_v(\eta_2/\eta_1)z_v}{1+K_v z_v}$$

Since K_v has been found to be always less than or very rarely equal to unity in cases where the component having higher viscosity between the two is taken as component 2 (see Table I), the second term of the denominator can be neglected as compared to 1, hence the following general equation results:

$$\frac{\eta}{\eta_1}=\eta_r=1+K_v(\eta_2/\eta_1)z_v$$

In Table I are shown K_v, (η_2/η_1) and $K_v(\eta_2/\eta_1)$ of 18 kinds of ideal mixture quoted from as many viscosity data with respect to z_v as are found in the literature. Each K_v is an arithmetic mean of these at all the concentrations determined. Out of these pairs three cases, the one having the lowest viscosity ratio, benzene-carbon tetrachloride, and the other two having the highest viscosity ratios, toluene-ethyl benzoate and toluene-diphenyl, are exemplified in Tables II, III and IV.

The solutions of naphthalene and of diphenyl in benzene and in toluene have often been used as typical ideal solutions since Kendall and Monroe[6] made the viscosity measurements on these solutions in order to test their own cube-root formula[7], $\eta^{1/3}=(1-z_m)\eta_1^{1/3}+z_m\eta_2^{1/3}$ but they obtained different values 0.0225 and 0.0183 for the solutional viscosity of naphthalene in benzene and in toluene respectively, and 0.0344 and 0.0282 for that of diphenyl in these solvents respectively. The present author[8], by using his own formula described above, obtained concordant values in both solvents, 0.02653 for naphthalene and 0.05413 (revised value 0.05509) for diphenyl. Van der Wyk[9] reported that he had obtained concordant values in both

TABLE I

K_v, (η_2/η_1) AND $K_v(\eta_2/\eta_1)$ VALUES OF IDEAL SOLUTIONS

Component 1	Component 2	t°C	η_1	η_2	η_2/η_1	K_v	$K_v\times(\eta_2/\eta_1)$	Observer
Benzene	Carbon tetrachloride	60	0.00391	0.00582	1.488	0.737	1.097	Thorpe and Rodger[10]
Benzene	Bromobenzene	18.2	0.00654	0.01129	1.726	0.926	1.598	Yajnik et al[11]
Benzene	Ethyl benzoate	25	0.006051	0.01991	3.290	0.430	1.415	Kendall and Monroe[7]
Benzene	Naphthalene	25	0.006048	(0.02653)	4.387	0.347	1.522	Kendall and Monroe[6]
Benzene	Diphenyl	25	0.006051	(0.05509)	9.104	0.172	1.566	Kendall and Monroe[6]
Toluene	Chlorobenzene	20	0.00447	0.00709	1.586	1.063	1.681	Yajnik et al[11]
Toluene	Bromobenzene	25	0.00447	0.00880	1.969	0.877	1.725	Yajnik et al[11]
Toluene	Ethyl benzoate	25	0.005520	0.01990	3.605	0.446	1.609	Kendall and Monroe[7]
Toluene	Naphthalene	25	0.005526	(0.02653)	4.716	0.322	1.519	Kendall and Monroe[6]
Toluene	Diphenyl	25	0.005520	(0.05509)	9.980	0.168	1.677	Kendall and Monroe[6]
Ethyl ether	Benzene	25	0.00230	0.00599	2.604	0.494	1.287	Linebarger[12]
Acetone	Benzene	25	0.00315	0.005758	1.823	0.486	0.886	Fischler[13]
Ethyl alcohol	*iso*-propyl alcohol	25	0.01080	0.02048	1.896	0.595	1.128	Parks and Kelley[14]
Methyl alcohol	Nitrobenzene	25	0.005608	0.018126	3.232	0.303	0.979	Fischler[13]
Cyclohexane	Decaline	25	0.009287	0.02171	2.338	0.539	1.259	MacFarlane and Wright[15]
Ethylene chloride	Ethylene bromide	25	0.007812	0.01613	2.065	0.646	1.334	MacFarlane and Wright[15]
Benzene	Benzyl benzoate	25	0.006044	0.08454	13.99	0.132 ~0.225	1.847	Kendall and Monroe[7]
Toluene	Benzyl benzoate	25	0.005520	0.08450	15.31	0.124 ~0.215	1.898	Kendall and Monroe[7]

6) J. Kendall and K. P. Monroe, *J. Am. Chem. Soc.*, **43**, 115 (1921).
7) J. Kendall and K. P. Monroe, ibid., **39**, 1787 (1917).
8) T. Ishikawa, This Bulletin, **5**, 47 (1930).
9) A. J. A. van der Wyk, *Nature*, **138**, 845 (1936).
10) T. E. Thorpe and M. D. Rodger, *J. Chem. Soc.*, **71**, 360 (1897).
11) N. A. Yajnik, M. D. Bhalla, R. C. Talwar and M. A. Soofi, *Z. phys. Chem.*, **118**, 305 (1925).
12) C. E. Linebarger, *Am. J. Sci.*, [4] **2**, 331 (1896).
13) J. Fischler. *Z. Elektrochem.*, **19**, 126 (1913).
14) G. S. Parks and K. K. Kelley, *J. Phys. Chem.*, **29**, 727 (1925).
15) W. MacFarlane and R. Wright, *J. Chem. Soc.*, **1933**, 114.

TABLE II

BENZENE(1)-CARBON TETRACHLORIDE(2), 60°C

z_v	z_m	η_{obs}	K_v	η_{calc}	S_v	λ
0.000	0.0000	0.003905				
0.208	0.1949	0.00422	0.738	0.00422	1.11	−9.33
0.414	0.3944	0.00456	0.730	0.00456	1.12	−4.66
0.656	0.6377	0.00503	0.743	0.00503	1.10	−2.81
1,000	1.0000	0.005835	0.737		1.11	

N. B. $K_v(\eta_2/\eta_1)=1.097$, $2.303\log(\eta_2/\eta_1)/S_v=0.358$

TABLE III

TOLUENE(1)-ETHYL BENZOATE(2), 25°C

z_v	z_m	η_{obs}	K_v	η_{calc}	S_v	λ
0.0000	0.0000	0.005520				
0.1951	0.1524	0.006845	(0.4187)	0.006924	1.202	−2.35
0.4256	0.3546	0.009076	0.4434	0.009094	1.170	−0.89
0.6964	0.6299	0.01279	0.4448	0.01279	1.207	−0.48
0.7890	0.7349	0.01452	0.4474	0.01451	1.219	−0.40
0.8798	0.8442	0.01655	0.4498	0.01653	1.229	−0.33
1.0000	1.0000	0.01990	0.4464		1.205	

N. B. $K_v(\eta_2/\eta_1)=1.609$, $2.303\log(\eta_2/\eta_1)/S_v=1.064$

TABLE IV

TOLUENE(1)-DIPHENYL(2), 25°C

z_v	z_m	η_{obs}	K_v	η_{calc} Ishikawa $\eta_2=0.05509$	Kendall $\eta_2=0.0282$	van der Wyk $\eta_2=0.0374$, $\eta_{12}=0.0154$	S_v	λ
0.000	0.0000	0.005520						
0.186	0.1398	0.007335	0.166	0.007353	0.007369	0.007334	1.62	−0.52
0.282	0.2197	0.008587	0.168	0.008588	0.008584	0.008547	1.65	−0.25
0.348	0.2761	0.009627	0.169	0.009599	0.009528	0.009552	1.67	−0.14
			0.168				1.65	

N. B. $K_v(\eta_2/\eta_1)=1.677$, $2.303\log(\eta_2/\eta_1)/S_v=1.395$

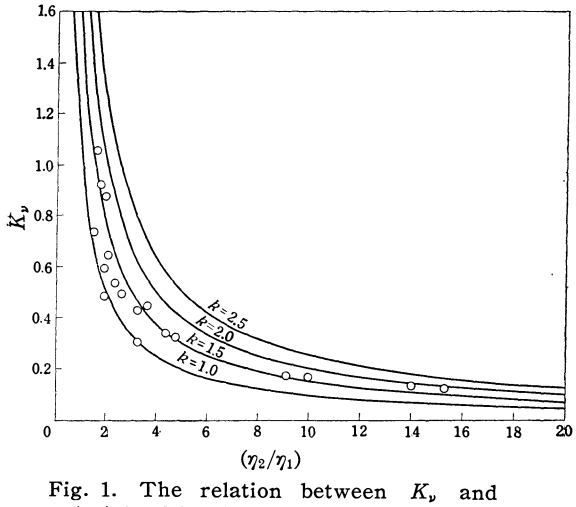

Fig. 1. The relation between K_v and (η_2/η_1) of ideal solutions.

solvents, 0.0219~0.0224 for naphthalene and 0.03740 for diphenyl by the use of his formula

$$\log\eta=(1-z_m)^2\log\eta_1+2z_m(1-z_m)\log\eta_{12}+z_m^2\log\eta_2$$

In Table IV are also shown for reference the calculated viscosity values due to Kendall and Monroe's formula and van der Wyk's formula.

Fig. 1 shows a plot of K_v against (η_2/η_1) for the results given in Table I. Let the product $K_v(\eta_2/\eta_1)$ be denoted by k as the same signature as the above, mixtures or solutions having the same values as k will take positions on a hyperbolic curve $K_v(\eta_2/\eta_1)=k$. In Fig. 1 solid lines represent $k=1.0$, 1.5, 2.0 and 2.5. As seen from the positions of the points, it appears that the higher (η_2/η_1) becomes, the less K_v decreases, and that this tendency undoubtedly signifies the approach of k to 2 or more, yet its limit can not be determined by this method of deduction.

Cases where K_v varies with Concentration. — Kendall and Monroe[7] took the

following four systems: benzene-ethyl benzoate, toluene-ethyl benzoate, benzene-benzyl benzoate, and toluene-benzyl benzoate, as chemically indifferent mixtures having great differences in viscosities and molecular weights of both components, and ascertained the validity of their cube-root formula with good result for the first two mixtures, but with bad result for toluene-benzyl benzoate contrary to their presupposition that this system was regarded to be a normal mixture as judged from the fact of there being no appreciable thermal effect and volume change on mixing.

Since then the data of this system have been used for the verification of ideal viscosity formulas. The present author[16] considered, however, that if component 2 suffers molecular dissociation in solution, K of his formula keeps no more constancy, and that if observed K values lie on a straight line, the extrapolation values at $z_m=0$, and $z_m=1$ can be obtained with ease and accuracy, and he obtained for this mixture 0.250 at $z_m=0$, and 0.390 at $z_m=1$. Lederer[17] proposed an ideal viscosity formula in the form

$$\log\eta=\frac{(1-z_m)\log\eta_1}{1-z_m+z_m/S}+\frac{z_m\log\eta_2/S}{1-z_m+z_m/S}$$

where S is the ratio of association degrees of component 2 to that of component 1. His idea of an association molecule of liquids is a molecule similar to a chemically fast-combined molecule. This is quite different from the present author's idea expressing an associated molecule as a group of single molecules interchangable with singly existing molecules, which is in accord with an idea of a cybotactic group proposed a short time later by Stewart[18]. The value of S obtained by Lederer for this mixture is 1.197[19] which is an arithmetic mean of 1.250, 1.217, 1.190, 1.166 and 1.160 at respective concentrations in their order in Table V. Van der Wyk[9] also treated this mixture with his formula, and obtained, by putting $\eta_{12}=0.0275$, fairly concordant values with experimental data (see columns 9 and 10 in Table V).

As stated above, K for this mixture varies linearly with z_m, so K_v varies with z_v and is found to be expressible by a linear equation with $(K_v)_0=0.124$ and $(K_v)_1=0.215$. Similarly for benzene-benzyl benzoate mixture we get $(K_v)_0=0.132$ and $(K_v)_1=0.225$. These values are tabulated in Table I, and the accuracy of these values can be acknowledged from η calculated from thus obtained K_v in column 6 in Tables V and VI.

If there be among the dissociated molecules the crowding effect postulated by Mooney's theory, the following modified form of his equation having $(K_v)_0(\eta_2/\eta_1)$ in place of 2.5 would be valid for these cases:

$$\ln\eta_r=2.303\log\eta_r=(K_v)_0(\eta_2/\eta_1)z_v/(1-\lambda z_v)$$

A few trials have given satisfactory results to this presumption: $(K_v)_0(\eta_2/\eta_1)=1.898$ and $\lambda=0.300$ for toluene-benzyl benzoate, and $(K_v)_0(\eta_2/\eta_1)=1.847$ and $\lambda=0.296$ for benzene-benzyl benzoate, and the calculated viscosity values by making use of these equations are tabulated in column 7 in Tables V and VI.

A severe test which must be made here is the viscosity data of the system, petroleum-non-plastic asphalt ($\eta_2/\eta_1=10^6$ at 15°C), observed by Saal and Koens and studied by Cragoe[20] for the confirmation of the latter's formula for ideal mixtures:

$$L_m=(1-z)L_1+zL_2$$

where z is the weight fraction of component 2, L with suffixes 1, 2 and m (the mixture) are defined by $\eta=Ae^{\frac{B}{L}}$, and A and B are constants, $A=5\times10^4$ and $B=1000\ln 20$. Cragoe applied his formula with success not only to mixtures of viscosity ratios less than 100, but also to this system, for which other formulas such as those of Arrhenius[4], Bingham ($1/\eta=(1-z_v)/\eta_1+z_v/\eta_2$)[21], and Kendall and Monroe[7] failed.

For this mixture the variation of K_v values displays a strongly sagged curve not to be satisfactorily expressed by any simple functional form, so we obtain at first 5.45 as the extrapolation value of the usual form η_{sp} (specific viscosity)$=kz_v$, by assuming a straight line to pass the values at two low concentrations, $z_v=0.224$ and 0.464, and then put this or a near value in the modified Mooney's equation to find λ to have a constant against z_v. By a few trials the following equation has been found to fit the observed values:

$$\ln\eta_r=2.303\log\eta_r=5.40z_v/(1-0.608z_v)$$

16) T. Ishikawa, This Bulletin, **4**, 288 (1929).
17) E. L. Lederer, *Proc. World Petroleum Congress, London*, **2**, F. 526 (1933).
18) G. W. Stewart, *Rev. Mod. Phys.*, **2**, 116 (1930); *Koll. Z.*, **67**, 130 (1934).
19) E. L. Lederer, *Nature*, **139**, 27 (1937).
20) C. S. Cragoe, *Proc. World Petroleum Congress, London*, **2**, F. 529 (1933).
21) E. C. Bingham, *Am. Chem. J.*, **35**, 195 (1906).

TABLE V

TOLUENE(1)-BENZYL BENZOATE(2), 25°C

z_v	z_m	η_{obs}	K_v	$(K_v)_{calc}$	Ishikawa eq. with $(K_v)_{calc}$	Modified Mooney eq. $\lambda=0.300$	Lederer eq. $S=1.197$	Van der Wyk eq. $\eta_{12}=0.0275$	S_v
0.0000	0.0000	0.005520		(0.124)					
0.3558	0.2367	0.01183	0.157	0.156	0.01179	0.01175	0.01154	0.0115	1.686
0.5693	0.4261	0.02015	0.172	0.176	0.02043	0.02031	0.01993	0.0201	1.463
0.7682	0.6502	0.03614	0.191	0.194	0.03642	0.03670	0.03624	0.0364	1.498
0.8694	0.7890	0.05080	0.202	0.203	0.05070	0.05143	0.05104	0.0515	1.526
0.9416	0.9002	0.06660	0.212	0.210	0.06650	0.06660	0.06707	0.0667	1.541
1.0000	1.0000	0.08450		(0.215)					1.507

N. B. $(K_v)_0(\eta_2/\eta_1)=1.898$, $2.303\log(\eta_2/\eta_1)/S_v=1.811$

TABLE VI

BENZENE(1)-BENZYL BENZOATE(2), 25°C

z_v	z_m	η_{obs}	K_v	$(K_v)_{calc}$	Ishikawa eq. with $(K_v)_{calc}$	Modified Mooney eq. $\lambda=0.296$	S_v
0.0000	0.0000	0.006044		(0.132)			
0.3308	0.1886	0.01196	0.165	0.163	0.01190	0.01190	1.416
0.5991	0.4124	0.02301	0.185	0.188	0.02326	0.02319	1.455
0.7484	0.5832	0.03584	0.205	0.202	0.03550	0.03567	1.434
0.8844	0.7827	0.05478	0.214	0.214	0.05477	0.05523	1.506
0.9478	0.8952	0.06883	0.220	0.220	0.06885	0.06884	1.535
1.0000	1.0000	0.08454		(0.225)			1.467

N. B. $(K_v)_0(\eta_2/\eta_1)=1.847$, $2.303\log(\eta_2/\eta_1)/S_v=1.755$

TABLE VII

PETROLEUM(1)-NON-PLASTIC ASPHALT(2), 15°C

z	z_v	η_{obs}	$(\eta_r)_{obs}$	K_v	$(\eta_r)_{calc}$: Modified Mooney eq. $\lambda=0.608$	$(\eta_r)_{calc}$: Lederer eq. $S_v=2.52$	$(\eta_r)_{calc}$: Cragoe eq.	S_v
0.00	0.000	1.31	1.000					
0.25	0.224	5.30	4.046	1.097×10^{-5}	4.055	4.122	4.450	2.56
0.50	0.464	39.6	30.23	5.564×10^{-5}	32.77	33.94	39.54	2.63
0.75	0.724	1850	1412	56.01×10^{-5}	1078	1133	1328	2.36
1.00	1.000	1.26×10^6	9.618×10^5		9.582×10^5	9.670×10^5		2.52

N. B. $(K_v)_0(\eta_2/\eta_1)=5.40$, $2.303\log(\eta_2/\eta_1)/S_v=5.47$

the calculated values being tabulated in column 6 in Table VII with reference to Cragoe's results. $(K_v)_0=0.561\times10^{-5}$ obtained by putting $(K_v)_0(\eta_2/\eta_1)=5.40$ may be an acceptable value as supposed from a plot of K_v against concentration. Furthermore, $\lambda=0.608$ is quite coincident with the hydrodynamic interaction constant 0.609 derived by Vand[22].

It is noted that another method of finding the shape factor k and the crowding factor λ is the proposition recommended by Maron et al.[23] that a graph $z_v/\log\eta_r$ *vs* z_v should be linear.

Applicability of Modified Mooney's Equation.—Since Lederer's formula is analogous in form to the author's formula, it can be transformed into the following hyperbolic form with respect to z_v:

$$\frac{(1-z_v)(\log\eta-\log\eta_1)}{z_v(\log\eta_2-\log\eta)} = \text{a constant, say } 1/S_v$$

or

$$\log\eta_r=\frac{\{\log(\eta_2/\eta_1)/S_v\}z_v}{1-(1-1/S_v)z_v}$$

and therefore

$$\ln\eta_r=2.303\log\eta_r=\frac{2.303\{\log(\eta_2/\eta_1)/S_v\}z_v}{1-(1-1/S_v)z_v}$$

This transformed formula, when it is applied to the above taken petroleum-non-plastic asphalt system with constant

22) V. Vand, *J. Phys.* and *Colloid Chem.*, **52**, 277 (1948).
23) S. H. Maron. B. P. Madow and I. M. Krieger, *J. Colloid Sci.*, **6**, 584 (1951).

$S_\nu=2.52$, is found to be available with accuracy equal to the modified Mooney's equation (see column 7 in Table VII), so that these two equations appear to be identical. If the identity is generally true, the numerical values of the corresponding factors $2.303\log(\eta_2/\eta_1)/S_\nu$ and $(K_\nu)_0(\eta_2/\eta_1)$ should coincide with each other, and to such solutions only the applicability of the modified Mooney's equation should be restricted, because its application to solutions of low viscosity ratios (K_ν=constant) gives λ negative inconstant values as seen from λ values in Tables II, III and IV.

Examinations of all the data taken in this paper lead us to the conclusions (1) that for solutions of low viscosity ratios (K_ν=constant) e.g., benzene-carbon tetrachloride, toluene-ethyl benzoate, and toluene-diphenyl (see N. B. in Tables II, III and IV), $2.303\log(\eta_2/\eta_1)/S_\nu$ is always less than $(K_\nu)_0(\eta_2/\eta_1)$, (2) that for solutions of appreciably high viscosity ratios in which slight molecular dissociation occurs e.g., benzene-benzyl benzoate and toluene-benzyl benzoate (see N. B. in Tables V and VI), the constancy of S_ν is not favorable and, if we take the mean of such S_ν values, $2.303\log(\eta_2/\eta_1)/S_\nu$ becomes slightly less than $(K_\nu)_0(\eta_2/\eta_1)$ to make the validity of Ledere's formula inferior to the modified Mooney's equation, and (3) that for solutions of extemely high viscosity ratios where the molecular dissociation follows and consequently geometric crowding action and hydrodynamic interaction occur among the dissociated molecules, e. g., petroleum-non-plastic asphalt (see N. B. in Table VII), these two factors coincide with each other and $(1-1/S_\nu)$ will tend to λ in consequence.

From what has been discussed above a modified form of Mooney's equation with $(K_\nu)_0(\eta_2/\eta_1)$ in place of 2.5:

$$\ln\eta_T=2.303\ln\eta_T=(K_\nu)_0(\eta_2/\eta_1)z_\nu/(1-\lambda z_\nu)$$

may be regarded as a viscosity formula for ideal solutions of high viscosity ratios.

Junior College of Commerce
Nagasaki University
Nagasaki

The Two Stable Isomers of Chlorocyclohexane

By Kunio KOZIMA and Kiyoshi SAKASHITA*

(Received May 28, 1958)

Twenty years ago Canals et al.[1] studied the Raman spectra of chlorocyclohexane and found the two bands which may be assigned to the C-Cl stretching vibration. As it is now well established that the structure of cyclohexane ring is the chair form, it can be easily understood that the two bands are due to the two isomers which may be represented by the usual symbols e and a. Hassell and Viervoll[2] concluded from their electron diffraction data that the molecules of chlorocyclohexane are almost all of the e-form in the vapor state. Larnaudie[3], however, pointed out the coexistence of the e- and the a-form in the vapor as well as in the liquid state, since the two characteristic bands for the C-Cl stretching vibration were observed in both states in his infrared investigations. It seems likely to be interesting to determine the form of the more stable isomer and the energy difference between these two isomers. For these purposes we carried out the following researches.

Experimental

Preparation and Purification of Chlorocyclohexane. — According to Markownikoff[4] cyclohexanol was heated at 100°C in a sealed glass tube with concentrated hydrochloric acid solution for five hours. The oily substance which had separated in the tube was distilled with

* Present adress: Hitachi Research Laboratory, Hitachi Ltd., Hitachi, Ibaragi.

1) E. Canals, M. Mousseron, R. Granger and J. Gastaud, *Bull. soc. chim. France*, **4**, 2048 (1937).

2) O. Hassel and H. Viervoll, *Tids. Kjemi, Bergvesen Met.*, **5**, 35 (1943).

3) M. Larnaudie, *Compt. rend.*, **235**, 154 (1952); *J. phys. radium*, **15**, 650 (1954).

4) W. Markownikoff, *Ann.*, **302**, 19 (1898).

TABLE I

VIBRATIONAL SPECTRA OF CHLOROCYCLOHEXANE

Raman*		Infrared**		Configuration
liquid (cm^{-1})	solid (cm^{-1})	liquid (cm^{-1})	solid (cm^{-1})	
200 (1)				
259 (1)				
339 (9)	340 (3)			e
437 (3)	435 (1)	435.2(w)		e
		472.4(w)		
509 (3)	508 (0)	512 (m)	510.5(s)	e
560 (6)		559 (m)		a
			628 (vw)	e
686 (4)		684.5(s)		a
			711.7(w)	e
734 (8)	726 (4)	731 (vvs)	728 (vvs)	e
		789 (vw)	790 (w)	e
808 (5)		807 (m)		a
822 (5)	821 (2)	817 (vs)	817 (vs)	e
			~845 (w)sh	e
852 (5)	851 (2)	852 (m)	850.5(m)	e
		858 (m)		a
		863 (m)		a
		~868 (m)		a
890 (2)		889 (s)	888.5(vs)	e
		920 (w)	920.5(w)	e
		972 (vw)	972 (vw)	e
992 (6)	993 (3)	993 (vs)	994 (s)	e
		1014 (m)		a
1027 (6)	1027 (2)	1029 (w)	1025 (w), 1031 (w)	e
1051 (2)	1053 (1)	1051 (vw)	1050 (w)	e
		1070 (vw)	1068 (vw), 1075 (vw)	e
		1089 (vw)	1088 (w)	e
		1098 (w)		a
		1132 (w)	1134 (m)	e
		1145 (w)		a
		1184 (w)	1186 (w)	e
1215 (2)	1216 (0)	1215 (s)	1216 (s)	e
1263 (6)	1261 (1)	1258 (m), 1267 (s)	1256 (s), 1267 (m)	e, e
1297 (0)		1301 (vw)	1300 (w)	e
1337 (2)		1340 (m)	1323 (m), 1332 (m), 1339 (m)	e, e, e
1447 (7)	1443 (2)	1448 (vs)	1446 (s)	
2865 (10b)		2617 (vw)		
2904 (9b)		2675 (w)	2670 (s)	
2951 (10b)	2945 (2b)	2860 (vs)	2860 (s)	
		2930 (vs)	2930 (vs)	

* For the Raman spectra the numbers shown in the brackets are the visually estimated relative intensities.

** The infrared spectra were not investigated below 430 cm^{-1} in the liquid and below 500 cm^{-1} in the solid. The letters shown in the brackets mean the relative intensities. v=very, s=strong, m=medium and w=weak. sh=shoulder.

TABLE II

INFRARED SPECTRA OF THE VAPOR OF CHLOROCYCLOHEXANE

wave number	configuration	wave number	configuration	wave number	configuration
~502		864 (m)	a	1160 (vw)	
510.0(m)	e				
516		872 (m)	a	1180 (vw)	
~566 (m,b)	a	887 (s)	e	1183 (vw)	
		893			
682.6				1214	
690.2(m)	a	992		1220 (m)	e
697.0		997 (s)	e	1225	
		1001			
734.4				1265 (s)	
740.3(vs)	e	1017 (m)	a	1269 (s)	
745.8				1273 (s)	
		1024 (m)		1280 (s)	
~796 (vw)	e			1352 (m)	
		1079 (w)		1459 (vs)	
814.5					
820 (s)	e	1094		2176 (vw)	
826		1103 (w)	a	2510 (vw)	
		1111		2680 (w)	
854 (m)	e			2890 (vs)	
		1129		2950 (vs)	
		1140 (w)	e		

steam, washed with water, and dried over calcium chloride. The product was further purified by fractional distillation. (b.p. 142.0~142.3°C).

Vibrational Spectra.—The Raman spectra of this compound were observed for the liquid and the solid state with the same spectrograph as in our earlier works[5]. The infrared spectra were obtained for the vapor (ca. 120°C), liquid, and solid states, by use of a Perkin-Elmer Spectrometer Model 112 equipped with sodium chloride and potassium bromide prisms. The wave number readings for both spectra are shown in Tables I and II.

The Raman spectra of the liquid obtained by Kohlrausch et al.[6] agree with our data, except the doublets at 808 and 822 cm^{-1} and some additional weak bands. The data obtained by Canals et al.[1] are incomplete and disagree with our results at several points.

Measurements of the Integrated Intensities in the Vapor State.—The integrated intensities of the two bands at 689 cm^{-1} and 741 cm^{-1} were obtained with a potassium bromide prism. The slit width used was 0.280 mm and the spectral slit widths were 3.3cm^{-1} at 700cm^{-1} and 4.0cm^{-1} at 750cm^{-1}. The gas absorption cell was made of a glass cylinder with two potassium bromide windows and was heated electrically by a nichrome wire. In order to avoid the condensation of the vapor on the windows short glass cylinders heated electrically were attached in front of the windows. The path length of the cell was 6 cm.

Measurements were made at the two temperatures 117°C and 200°C*. Atmospheric carbon dioxide was removed from the optical path as far as possible. Such a high temperature, at which the measurements were made, causes emission bands of the compound with noticeable intensities. The radiation intensity I_b of the high temperature cell and the intensity I_d of the emission band of the sample at frequency ν were measured by placing a non-reflecting shutter made of a piece of glass and a sheet of black paper behind the cell. For the evaluation of the absorbance $\log_{10} I_0/I$, and I_0 and I should be

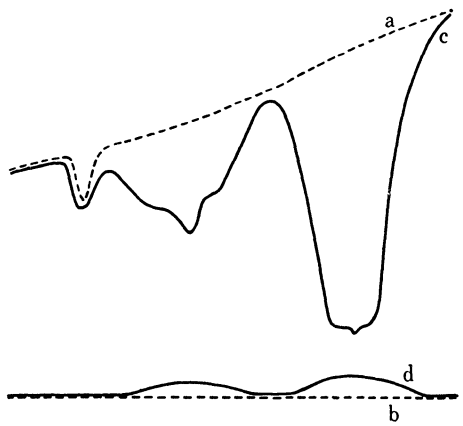

Fig. 1. The absorption curves a, b, c and d are used for obtaining I_a, I_b, I_c, and I_d, respectively.

5) a) K. Kozima and T. Yoshino, *J. Am. Chem. Soc.*, **75**, 166 (1953); b) K. Kozima, K. Sakashita and S. Maeda, ibid., **76**, 1965 (1954).

6) K. W. F. Kohlrausch and W. Stockmair, *Z. physik. Chem.*, **B31**, 382 (1936).

* Above 250°C the shapes of the bands change gradually and new bands appear.

TABLE III
RATIO OF INTEGRATED INTENSITIES (VAPOR)

	No. of Experiments	$\bar{\nu}_{max}$	Ratio of integrated intensities obtained by weighing
$t=117°C$	1	689.5 cm^{-1} 741.5	0.347
	2	690.0 741.2	0.347
	3	689.7 741.3	0.349
	Mean	689.7 741.3	0.348
$t=200°C$	1	689.0 740.6	0.376
	2	689.5 740.0	0.380
	3	689.3 739.7	0.371
	Mean	689.3 740.1	0.376

taken as

$$I_0=I_a-I_b,\ I=I_c-I_d$$

where I_0 and I have their usual meanings, and I_a and I_c are the monochromatic intensities of radiation after passage through the vacant cell and the cell containing the sample at a high temperature, respectively. The absorption curves obtained are shown in Fig. 1.

The area-intensities were obtained by the graphical integration of the absorbances over the frequency interval from 641 cm^{-1} to 790 cm^{-1}, which sufficiently covers the range of about four times the half intensity width for each band. The integration outside this interval may be neglected without noticeable influences on the evaluation of the relative intensities, because the absorption on the wings of the band decreases rather rapidly; that is to say, for the band near 689 cm^{-1} its absorbance at 641 cm^{-1} is smaller than 1/20 of that at the peak and for the other band near 741 cm^{-1} the decrement of that at 790 cm^{-1} is more serious. The absorption curve near 710 cm^{-1}, which consists of the two bands overlapping each other at their wings, was divided into the original bands, so that the bands have the most reasonable shapes. The band near 741 cm^{-1} overlaps slightly with that near 820 cm^{-1}, which includes a very weak band near 796 cm^{-1}. This overlapping was also treated by the same method as described above. The correction for finite slit widths may be neglected, because of the broadness of the bands. The results obtained are shown in Table III.

Measurements of the Integrated Intensities in the Solution.—The integrated intensities of the two bands near 685 cm^{-1} and 732 cm^{-1} were obtained at 25°C in the solution, carbon disulfide and methyl acetate being used as solvents. The prism and the slit width were the same as those employed in the above intensity measurement. The thickness of the cell used was 0.2 mm. There were no remarkable differences between the ratios of the integrated intensities obtained by the graphical integration and those obtained by Ramsay's method[7] of direct integration corrected for finite slit widths. The results are listed in Table IV.

Discussion

As shown in Table I the vibrational spectra in the solid state differ clearly from those in the liquid state; viz., some of the relatively strong bands observed in the liquid spectra disappear in the solid spectra.

For the C-Cl stretching vibration two characteristic bands were observed at 684.5 and 731 cm^{-1} in the liquid state, while in the solid state the former disappeared and the latter persisted. Therefore, it is concluded that the dynamic equilibrium of the two isomers, which exists in the liquid state, breaks down in the course of the crystalization of the compound and only one isomer persists in the solid state. On the other hand the infrared spectra in the vapor state, shown in Table II, correspond well with those in the liquid state.

7) D. A. Ramsay, *J. Am. Chem. Soc.*, **74**, 72 (1952).

TABLE IV
THE RATIOS OF INTEGRATED INTENSITIES (SOLUTION)

temperature: 25°C
solvent: carbon disulfide

No. of experiments	mol./l.	$\bar{\nu}$ cm^{-1}	$\log_e(T_0/T)$	$\Delta\bar{\nu}^a_{1/2}$ cm^{-1}	A	A_a/A_e	A'_a/A'_e (graphical)
1	0.36	685.8 733.2	0.504 1.52	6.5 7.2	4.8_5 $17._1$	0.28	0.34
2	0.32	686.0 733.5	0.445 1.39	7.0 7.4	4.6_4 $16._1$	0.29	0.33
	mean	685.9 733.4				0.29	0.34
solvent:	methyl acetate						
1	0.55	684.8 731.8	0.532 1.94	8.1 8.6	6.5_1 $26._4$	0.25	0.26
2	0.40	684.6 731.5	0.445 1.64	8.0 8.4	5.3_8 $21._7$	0.25	0.25
	mean	684.7 731.7				0.25	0.26

The cell thickness for both solvents is 1.96×10^{-2} cm. The slit widths are 3.1 cm^{-1} at 686 cm^{-1}, 3.8 cm^{-1} at 733.5 cm^{-1} and 3.7 cm^{-1} at 731.5 cm^{-1}. A is the true integrated absorption intensity given by

$$A = K\log_e(T_0/T)_{\nu(\max)}\cdot\Delta\bar{\nu}^a_{1/2}$$

where the letters have their usual meanings. A_a/A_e shown in the table denotes the intensity ratio thus obtained and A'_a/A'_e the same ratio obtained by graphical integration. As for the carbon disulfide solution, agreements of the results obtained by both methods are not quite satisfactory, but the difference does not seriously alter the value of ΔE. ΔE for this solvent given in Table V is the mean value for both methods.

Therefore, the two isomers also coexist in the vapor state as pointed out by Larnaudie[3].

As has been shown by Larnaudie, the two C-Cl bands observed in the vapor state can confidently be identified with the e- and the a-form by the consideration of their band envelopes, respectively, based on the results obtained by Badger and Zumwalt[8]. The band at 740.3 cm^{-1} is assigned to the e-form and that at 690.2 cm^{-1} to the a-form. Since the band at 740.3 cm^{-1} in the vapor state corresponds to that at 728 cm^{-1} in the solid state, the isomer which persists in the solid state is the e-form. Among the relatively strong bands which appeared in the liquid and the vapor spectrum, the bands which persist in the solid state are assigned to the e-form and the other bands to the a-form as shown in Tables I and II.

It is possible to determine the energy difference between the two isomers by the measurement of the ratio of the integrated intensities of the two bands exhibited by the a- and the e-form, respectively, by use of the following formula:

$$A_a/A_e = \alpha_a N_a/\alpha_e N_e = (\alpha_a/\alpha_e)(f_a/f_e) \times\exp.(-\Delta E/RT)$$

where $A=\int\log_e(I_0/I)\,d\nu$ is the integrated intensity, $\Delta E = E_a - E_e$ the energy difference, α the molecular absorption coefficient, N the number of molecules, f the partition function, and the suffixes a and e refer to the a- and the e-form, respectively. In order to eliminate the unknown quantity $(f_a/f_e)(\alpha_a/\alpha_e)$, the measurements must be made at two temperatures at least. The ratio of the partition functions f_a/f_e is taken to be constant, because of the narrow range of temperature. The band at 740 cm^{-1} of the e-form and that at 690 cm^{-1} of the a-form are adequate for the purpose.

The results obtained for the vapor state at the temperatures 117° and 200°C are shown in Table III, and the energy difference thus obtained is about 0.34 kcal./mole, the e-form being the more stable isomer.

The energy differences in the dilute solutions can be estimated from the ratios of the integrated intensities shown in Table IV, if the values of (α_a/α_e) and (f_a/f_e) in the solution are assumed to be the same as those in the vapor state. The energy differences obtained for the solutions of carbon disulfide and methyl acetate are shown in Table IV. In these

8) R. M. Badger and L. R. Zumwalt, *J. Chem. Phys.*, **6**, 711 (1938).

solutions the e-form is also the more stable isomer.

As has been reported in our previous article[5b], the two mutually convertible isomers of *trans*-1,2-dichlorocyclohexane represented by the usual symbols as (e,e) and (a,a) are in a dynamic equilibrium for the various states, except for the solid state. By the studies on the electric dipole moment of the compound the energy difference between the isomers has been determined. For the reason mentioned below the energy difference between the isomers for both compounds should be determined for the same state. Therefore, the difference between the energy of the (e,e)-form and that of the (a,a)-form, $E_{ee}-E_{aa}$, was determined for the vapor, carbon disulfide solution and methyl acetate solution, by use of the same method as that used for the monochloro derivative. The results are listed in Table V.

TABLE V
THE ENERGY DIFFERENCES BETWEEN TWO MUTUALLY CONVERTIBLE ISOMERS
(inverted isomers)

State	$\Delta E=E_a-E_e$ chlorocyclohexane kcal./mole	$\Delta E=E_{ee}-E_{aa}$ *trans*-1,2-dichlorocyclohexane kcal./mole
vapor	0.34	0.61
CS_2 soln.	0.33	0.17
CH_3COOCH_3 soln.	0.44	−0.43

The energy difference between the mutually convertible isomers in the vapor state may be due to the difference between the intramolecular potential energies which are taken to be the sums of the potential energies of various pairs of non-bonded atoms.

Based upon this point of view, the following relation is obtained:

$$E_{ee}-E_{aa}+2(E_a-E_e)=E_g-E_t$$

where $E_{ee}-E_{aa}$ and E_a-E_e have the meanings mentioned above and E_g-E_t is the energy difference between the *gauche* and the *trans* form of 1,2-dichloroethane. The derivation of this formula will be given in an Appendix.

With this formula and the values for the vapor state listed in Table V, we find that $E_g-E_t=1.29$ kcal./mole. The value is in good agreement with that directly determined for the vapor state of 1,2-dichloroethane[9]. By use of the values for the solutions shown in the table, we find that $E_g-E_t=0.83$ kcal./mole for the dilute carbon disulfide solution and $E_g-E_t=0.45$ kcal./mole for the dilute methyl acetate solution.

These values, compared with the experimental data[10], seem to be reasonable, when taking into account the assumption made for the measurement in the solution. The reasons why the formula is available for the solution may be attributed to the facts that the variations of $E_{ee}-E_{aa}$ and E_g-E_t with the solvents are approximately the same and E_a-E_e does not appreciably change with the solvents.

It should be pointed out that at first sight the energy difference E_a-E_e may be expected to be about half of that between the (a,a)-form and the (e,e)-form of *trans*-1,4-dichlorocyclohexane[5a], but this is not actually the case.

While the present paper was in preparation, an interesting paper by Klæboe et al.[11], which concerned a part of our investigations, appeared. Their results are in accord with ours.

Appendix

By numbering the carbon atoms of cyclohexane ring from one to six in turn and using the symbols of e and a, we shall represent the potential energies between non-bonded atoms in the molecule of cyclohexane derivative. As for chlorocyclohexane, for instance, the energy between the chlorine atom attached to 1a and the carbon atom of 3 is represented as $V_{1a\,3}$ and that between the same chlorine atom and the hydrogen atom attached to 2e is $V'_{1a\,2e}$.

By the use of these symbols the potential energies, E_a and E_e, of the a- and the e-form of chlorocyclohexane can be represented as follows, respectively;

$$\begin{aligned}E_a=&2V_{1a\,3}+V_{1a\,4}+2V'_{1a\,3a}+2V'_{1a\,3e}+V'_{1a\,4a}\\&+V'_{1a\,4e}+2V'_{1a\,2a}+2U_{1e\,3}+U_{1e\,4}+2U'_{1e\,3a}\\&+2U'_{1e\,3e}+U'_{1e\,4a}+U'_{1e\,4e}+2U'_{1e\,2a}+\Psi \qquad (1)\end{aligned}$$

$$\begin{aligned}E_e=&2V_{1e\,3}+V_{1e\,4}+2V'_{1e\,3a}+2V'_{1e\,3e}+V'_{1e\,4a}\\&+V'_{1e\,4e}+2V'_{1e\,2a}+2U_{1a\,3}+U_{1a\,4}+2U'_{1a\,3a}\\&+2U'_{1a\,3e}+U'_{1a\,4a}+U'_{1a\,4e}+2U'_{1a\,2a}+\Psi \qquad (2)\end{aligned}$$

where V denotes the potential energy between the chlorine and the carbon atom, V' that between the chlorine and the hydrogen atom, U that between the hydrogen and the carbon atom, U' that between the hydrogen atoms attached to the different carbon atoms and Ψ contains all the terms of the potential energies which do not vary by changing the position of the chlorine

9) S. Mizushima, "Structure of Molecules and Internal Rotation", Academic Press Inc., New York, (1954), p. 41.
10) A. Wada, *J. Chem. Phys.*, **22**, 200 (1954).
11) P. Klæboe, J. J. Lothe and K. Lunde, *Acta Chem. Scand.*, **10**, 1465 (1956).

atom from la to le, and vice versa. As for these equations the equivalent terms are represented by one of them; for instance, as $V_{1e\,3}$ is equal to $V_{1e\,5}$ for Eq. 2, $V_{1e\,3}$ is multiplied by 2.

The potential energies, E_{aa} and E_{ee} of the (a,a)- and the (e,e)-form of *trans*-1,2-dichlorocyclohexane can be similarly represented as follows;

$$\begin{aligned}E_{aa}=&4V_{1a\,3}+2V_{1a\,4}+4V'_{1a\,3a}+4V'_{1a\,3e}\\&+2V'_{1a\,4a}+2V'_{1a\,4e}+2V'_{1a\,2a}+\Phi_{1a\,2a}\\&+4U_{1e\,3}+2U_{1e\,4}+3U'_{1e\,2e}+4U'_{1e\,3a}\\&+4U'_{1e\,3e}+2U'_{1e\,4a}+2U'_{1e\,4e}+\Psi \qquad (3)\\E_{ee}=&4V_{1e\,3}+2V_{1e\,4}+4V'_{1e\,3a}+4V'_{1e\,3e}\\&+2V'_{1e\,4a}+2V'_{1e\,4e}+2V'_{1e\,2e}+\Phi_{1e\,2e}\\&+4U_{1a\,3}+2U_{1a\,4}+3U'_{1a\,2a}+4U'_{1a\,3a}\\&+4U'_{1a\,3e}+2U'_{1a\,4a}+2U'_{1a\,4e}+\Psi \qquad (4)\end{aligned}$$

where Φ denotes the potential energy between the chlorine atoms attached to the carbon atoms of 1 and 2 and the other symbols have the same meanings as in Eqs. 1 and 2.

By use of Eqs. 1, 2, 3 and 4 and assuming that these terms do not change from molecule to molecule, we can obtain the following equation;

$$(E_{aa}-E_{ee})-2(E_a-E_e)=E_t-E_g.$$

This relation should also be available for the other derivatives in the same way as for the chlorine derivatives.

The authors wish to thank the Ministry of Education for a grant.

Tokyo Institute of Technology
Ookayama, Meguro-ku, Tokyo

*Synthesis of Poly-(L-prolyl-L-leucyl-glycyl). An Attempted Synthesis of Model Collagen**

By Hidetoshi KITAOKA, Shumpei SAKAKIBARA and Hisaya TANI

(Received March 11, 1958)

The presence of proline residues in a polypeptide chain has two important influences upon its chain configuration. Firstly, the lack of hydrogen atom on the pyrrolidine imide nitrogen makes it impossible to form the hydrogen linkage in the molecule. Secondly, the presence of pyrrolidine rings in the polypeptide chain reduces the degree of freedom of its internal rotation. These effects are supposed to be primarily responsible for the special chain configuration of collagen, gelatin and proline-rich fibrous proteins.

The structural investigations of collagen have been continued by many workers. On the basis of the amino acid analysis[1], it seems to be reasonable that collagen may consist of the polypeptide containing statistically a repeating unit of (glycyl-L-prolyl (or hydroxyprolyl)-X), where X represents any one of amino acid residues other than glycine and proline (or hydroxyproline). Furthermore, the presence of scattering units corresponding to the three amino acid residues in natural collagen was confirmed by X-ray analysis[2]. Following the above considerations, it seems most reasonable to regard the polypeptide with a regular repeating unit of (glycyl-L-prolyl-X) as a simplified model of collagen. Berger et al.[3], prepared poly-L-proline by the *N*-carboxy anhydride method, and the chain configuration of the polypeptide was determined by Cowan and McGavin[4] through X-ray analysis. This polyproline, however, is far from the model collagen.

In principle, the synthesis of high molecular weight polypeptide with a regular repeating unit of two or more amino acid residues is not impossible by the polymerization of tri- or higher membered peptide. For example, tri- or tetrapeptide ester[5], azide[6], thioester[7], mixed anhy-

* Presented in part at the Symposium of Protein Chemistry, Fukuoka, October, 1956.

1) J. H. Bowes and R. H. Kenten, *Biochem. J.*, **43**, 358 (1948); W. A. Schroeder et al,. *J. Am. Chem. Soc.*, **76**, 3556 (1954).

2) M. L. Huggins, ibid., **76**, 4045 (1954).

3) A. Berger, J. Kurtz and E. Katchalski, ibid., **76**, 5552 (1954).

4) P. M. Cowan and S. McGavin, *Nature*, **176**, 501 (1955).

5) E. Pacsu and E. J. Wilson, Jr., *J. Org. Chem.*, **7**, 117, 126 (1942).

6) M. Z. Magee and K. Hofmann, *J. Am. Chem. Soc.*, **71**, 1515 (1949); M. Winitz and J. S. Fruton, ibid., **75**, 3041 (1953).

7) T. Wieland and H. Bernhard, *Ann.*, **582**, 218 (1953).

dride[8], carbothiophenyl derivative[9] and so on are polymerizable into polypeptides and tri- or higher-membered free peptides are polymerizable by the action of some peptide linkage forming reagents such as tetraethyl pyrophosphite[10] and dicyclohexyl carbodiimide[11]. However, these methods contain the hazard of forming ring peptides besides the main product of polypeptides. Then, the optimum condition for high molecular weight polymerization must be investigated in each case where the starting material may be different in solubility and reactivity.

In this paper, the synthesis of poly-(L-prolyl-L-leucyl-glycyl) was attempted in several ways. Firstly, the tripeptide, L-prolyl-L-leucylglycine(IV), and its derivatives were prepared, and the relative efficiencies of polycondensation methods involving dicyclohexyl carbodiimide, tetraethyl pyrophosphite and *p*-nitrothiophenylester methods were compared. Secondly, the relative reactivity for polycondensation was compared between L-prolyl-L-leucylglycine (IV) and glycyl-L-prolyl-L-leucine (X). Although two tripeptides, IV and X, differ in the position of proline residue in the molecule, it must be expected that they should give polypeptides with the same amino acid sequence with the only exception of both *N*- and *C*-terminal amino acid residues.

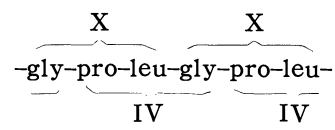

Synthesis of tripeptides and their derivatives. — Carbobenzoxy-L-prolyl-L-leucylglycine (III) was prepared according to the description of Ressler and du Vigneaud[12], and the protecting group was removed by hydrogenation in the presence of palladium-charcoal.

The tripeptide thioester, L-prolyl-L-leucylglycine *p*-nitrophenylthioester hydrobromide, was prepared by the procedure of Schwyzer[13]. Such a peptide *p*-nitrophenyl thioester was used for the preparation of the cyclic peptide by kenner[14].

The synthesis of ethyl carbobenzoxyglycyl-L-prolyl-L-leucinate (VIII) was accomplished by coupling carbobenzoxyglycyl-L-proline with ethyl L-leucinate through both mixed anhydride[15] and carbodiimide procedures[16]. After saponification of the product, the carbobenzoxy tripeptide (IX) was hydrogenated into glycyl-L-prolyl-L-leucine (X) similarly. On the formation of the peptide linkage, dicyclohexyl carbodiimide gave generally good results, but in the course of saponification of ethyl carbobenzoxyglycyl-L-prolyl-L-leucinate (VIII), a small amount of non-saponifiable substance remained. This material may be the addition product of carbodiimide with carbobenzoxy peptide, as was reported by other workers[16,17].

Carbobenzoxyglycyl-L-prolyl-L-leucine (IX) was hard to dissolve in most usual organic solvents and exhibited a marked contrast to the great solubility of carbobenzoxy-L-prolyl-L-leucylglycine (III). Both the free tripeptides, L-prolyl-L-leucylglycine (IV) and glycyl-L-prolyl-L-leucine (X), were easily soluble in glacial acetic acid and water, sparingly soluble in hot methanol containing some water and in hot dimethylformamide, and insoluble in other usual organic solvents. These solubility behaviors rather limited the experimental conditions for polycondensation. The tripeptide, glycyl-L-prolyl-L-leucine (X), contained one molecule of firmly bound crystallization water, and it could not be removed by heating over phosphorus pentoxide at 135°C(2 mmHg) for six hours. The significance of this water will be discussed in a later section.

Polycondensation of tripeptides. — In the polycondensation of L-prolyl-L-leucylglycine (IV) by the carbodiimide and the tetraethyl pyrophosphite procedures or in the polycondensation of its *p*-nitrothiophenylester, the most promising result was obtained by pyrophosphite. The most favorable molar ratio of this reagent to the tripeptide was about 1.5~2, the amount of consumption of the reagent by inevitable contamination of water being taken into consideration, and excess or insufficiency of reagent reduced the molecular

8) R. A. Boissonas and I. Schumann, *Helv. Chim. Acta*, **35**, 2229 (1952).
9) J. Noguchi and T. Hayakawa, *J. Am. Chem. Soc.*, **76**, 2846 (1954).
10) S. G. Waley, *J. Chem. Soc.*, **1955**, 517.
11) V. Bruckner, M. Szekerke and J. Kovács, *Naturwiss.*, **43**, 107 (1956).
12) C. Ressler and V. du Vigneaud, *J. Am. Chem. Soc.*, **76**, 3107 (1954).
13) R. Schwyzer, B. Iselin, W. Rittel and P. Sieber, *Helv. Chim. Acta*, **39**, 872 (1956).
14) G. W. Kenner and J. M. Turner, *Chem. and Ind.*, **1955**, 602.
15) J. R. Vaughan, Jr. and R. L. Osato, *J. Am. Chem. Soc.*, **73**, 5553 (1951).
16) J. C. Sheehan and G. P. Hess, ibid., **77**, 1067 (1955); ibid., **78**, 1367 (1956).
17) H. Zahn and J. F. Diehl, *Angew. Chem.*, **69**, 135 (1957).

weight of polypeptide formed. Tetraethyl pyrophosphite is very sensitive to moisture and the estimation of its purity was difficult, hence, the reproducibility of the result was rather inadequate.

The use of carbodiimide for polycondensation of L-prolyl-L-leucylglycine (IV) was limited by the low solubility of the tripeptide in inert solvents such as dimethylformamide at room temperature. At higher temperature, although the tripeptide dissolved in dimethylformamide, none of the free carboxyl group was detected in the product, where the addition reaction of the reagent to the end-carboxyl group may proceed in the course of polycondensation.

The *p*-nitrophenyl thioester procedure for polycondensation was also limited by the lack of available solvent, quite different from the method of Kenner[14] for cyclic peptides. In this reaction, it was considered to be reasonable that anhydrous organic solvents were preferred to water, because water would not be expected to dissolve the high molecular-weight polypeptide. Equivalent triethylamine was used for the separation of hydrogen bromide, but the reacting solution became colored markedly and the difficulty of separation of sulfur-containing compound from the product gave an undesirable result.

The polycondensation reaction by the pyrophosphite procedure was carried out at 100°, so it was supposed that the thermal side reaction might occur in the process and that equilibrium might exist between peptide linkages of the polycondensate. If the peptide-bond exchange or chain degradation occurs to any appreciable degree, the sequence of amino acid residues in the polypeptide chain would no longer retain that of the starting tripeptide. In order to clarify these questions, the nature of end amino acid residues and the content of phosphorus were determined on the products from the tripeptide(IV). After the complete hydrolysis of the polypeptide, proline, leucine and glycine were determined by paper chromatography. No appreciable amount of phosphorus was detected. From the amino nitrogen determination by the manometric van Slyke method, the free NH_2 group could not be detected either, so the *N*-terminal residue was assumed to be wholly L-proline. Determination of *C*-terminal amino acid residue of this polypeptide by hydrazinolysis[18] gave only DNP-glycine. All of these results indicated that no change in the sequence of amino acid residues has occurred during the course of the polycondensation by tetraethyl pyrophosphite.

The position of prolyl residue in tripeptide should have some influences on the peptide chain configuration which would affect the reactivity of either or both end groups in the polycondensation process. This factor must also depend upon the nature of end amino acid residues. To see these effects, the polycondensation reactions of both the tripeptides, L-prolyl-L-leucylglycine (IV) and glycyl-L-prolyl-L-leucine (X), were compared in parallel runs under the same conditions by the tetraethyl pyrophosphite procedure. The comparison indicated that the former gave a higher molecular weight product. This result differs from the expectation that the *N*-terminal glycyl residue on the tripeptide (IV) would be more reactive than the *N*-terminal prolyl residue on the tripeptide (X). Taking into consideration the results of Rydon[19], the latter peptide may be oriented in a rather rigid chain configuration.

Poly-(glycyl-L-prolyl-L-leucyl), prepared from both the tripeptides, IV and X, contained very firmly bound water, the amount of which was one mole per tripeptide unit. The tripeptide, glycyl-L-prolyl-L-leucine (X), also contained one molecule of crystallization water, as mentioned above. In addition, many other workers[19,20] have also reported the presence of crystallization water in the oligopeptides containing glycyl-prolyl residues. These facts suggest that the glycyl-prolyl linkage always has an ability to fix water molecule very firmly. If this hydration ability is general, this factor also may play a major role in the configuration of polypeptide chain of gelatin and collagen in addition to the other effects described in the first section.

The highest molecular weight fraction of the products by the pyrophosphite procedure had a molecular weight of about 6000, and this material was rather brittle and all efforts to make it into film or fiber form failed. This material showed three peaks (12.0; 6.6; 4.0 Å) in the X-ray diffraction chart by using Norelco diffractometer.

18) S. Akabori et al., This Bulletin, **29**, 507 (1956).
19) H. N. Rydon and P. W. G. Smith, *J. Chem. Soc.*, **1956**, 3642.
20) J. R. Vaughan and J. A. Eichler, *J. Am. Chem. Soc.*, **76**, 2474 (1954); N. C. Davis and E. L. Smith, *J. Biol. Chem.*, **200**, 373 (1953).

Experimental

Ethyl carbobenzoxy-L-leucylglycinate (I).—To a solution of 2.65 g. of carbobenzoxy-L-leucine[21] and 2.3 g. of dicyclohexyl-carbodiimide[22] in 20 ml. of tetrahydrofuran was added a solution of 1.67 g. of ethyl glycinate hydrochloride and 1.25 g. of triethyl amine in 10 ml. of tetrahydrofuran. The mixture was allowed to stand at room temperature for 4 hours. A small amount of acetic acid was added to the reaction mixture and after 30 minutes, the separated urea derivative was filtered off. The mother liquor was evaporated to dryness under reduced pressure and the residue was dissolved in ethyl acetate. The solution was washed with three portions of sodium bicarbonate solution, one portion of 0.2 N hydrochloric acid and water successively, and dried over magnesium sulfate. Evaporation of the solvent gave a viscous syrup, from which crystals separated out immediately on the addition of some petroleum ether. The colorless needles obtained were recrystallized from aqueous ethanol; m.p. 102~103°C and $[\alpha]_D^{18}$ −26.94° (c 5.01, ethanol). The yield was 2.65 g. (75%). Anderson et al.[23] reported a yield of 80%, m.p. 104~105°C and $[\alpha]_D^{25}$ −26.4°, and also yield of 65%, m.p. 102~103°C and $[\alpha]_D^{25}$ −27.2°. Bergmann[24] reported m. p. 103~104°C.

Ethyl carbobenzoxy-L-prolyl-L-leucylglycinate (II).—This substance was prepared from carbobenzoxy-L-proline[3] and I according to the description of du Vigneaud et al.[12] by the mixed anhydride procedure using isovaleryl chloride in 92% yield; m. p. 147~148°C, $[\alpha]_D^{18}$ −80° (c 2.5, ethanol). These values were identical with those reported previously[12].

Carbobenzoxy-L-prolyl-L-leucylglycine (III).—This substance was prepared from II according to the description of du Vigneaud et al.[12] in 91.5% yield; m. p. 163~164°C, $[\alpha]_D^{22.5}$ −85.0° (c 3.23, ethanol). These values were identical with those reported previously[12].

L-Prolyl-L-leucylglycine (IV).—To a solution of 6 g. of III in 150 ml. of methanol containing a small amount of glacial acetic acid was added 4 g. of palladium-charcoal, and hydrogen was introduced into the suspension for three hours under stirring. The catalyst was filtered off and washed thoroughly with distilled water, and then the combined filtrate was concentrated under reduced pressure. The residual syrup was dried by the addition of benzene followed by evaporation under reduced pressure. The remaining white powdery mass was dissolved in 10% methanolic acetic acid and reprecipitated with hot ethyl acetate. The yield of the colorless needles which were obtained was 3.5g. (84.5%); m.p. 220°C (decomp.), $[\alpha]_D^{20}$ −83.7° (c 3.43, glacial acetic acid).

Anal. Found: C, 54.54; H, 8.01; N, 14.80; mol. wt. 290*. Calcd. for $C_{13}H_{23}O_4N_3$: C, 54.75; H, 8.13; N, 14.73%; mol. wt. 285.3.

Paper chromatography showed this tripeptide to have only one spot, which turned yellow with ninhydrin, with an R_f value of 0.74 in *n*-butanol: water: acetic acid (4:1:1). The *p*K' values, 4.0 and 9.5, of the tripeptide were determined by the method of Parke and Davis[25].

Carbobenzoxy-L-prolyl-L-leucylglycine *p*-nitrophenyl-thioester (V).—A solution of 1.85 g. of III in 5 ml. of dimethylformamide was mixed with a solution of 0.45 g. of triethylamine in 5 ml. of ethylacetate and the mixture was cooled to −5°C. A solution of 0.48 g. of ethyl chlorocarbonate in ethyl acetate was then added dropwise into the reaction mixture at −5°C under stirring. After ten minutes a solution of 0.69 g. of *p*-nitrothiophenol and 0.45 g. of triethylamine in 10 ml. of ethyl acetate was added into the reaction mixture, which was allowed to stand for one hour at room temperature, when the dark red color of the mixture vanished gradually. The reacted solution was washed with dilute hydrochloric acid and dried over magnesium sulfate. Evaporation of the solvent followed by addition of petroleum ether, gave colorless crystals. The yield was 2.22 g. (90%). After recrystallization from aqueous ethanol, this substance melted at 137~138.5°C; wt. 1.9 g.

Anal. Found: C, 58.13; H, 5.99; N, 9.99. Calcd. for $C_{27}H_{32}O_7N_4S$: C, 58.25; H, 5.75; N, 10.08%.

L-Prolyl-L-leucylglycine *p*-nitrophenyl-thioester hydrobromide (VI).—A solution of 1.75 g. of V in 5 ml. of glacial acetic acid was saturated with dry hydrogen bromide. After one hour at room temperature, the solution was concentrated under reduced pressure and the residual syrupy mass was reprecipitated from glacial acetic acid by the addition of dry ether. The yield of the white powder was 1.57 g. (97%); m. p. 170°C (decomp.). This material was very hygroscopic and its aqueous alkaline solution was dark red. Analytical value of bromine determined by the Volhard method was 94% of the theoretical, but further purification of the substance was unsuccessful.

Carbobenzoxyglycyl-L-proline (VII).—This substance was prepared from carbobenzoxyglycyl chloride and L-proline according to the description of Bergmann et al.[26] in 77% yield; m. p. 155°C. Rydon[19] reported m.p. 155°C and Bergmann reported m. p. 156°C.

Ethyl carbobenzoxyglycyl-L-prolyl-L-leucinate (VIII).—This substance was prepared both

21) M. Bergmann, L. Zervas and J. S. Fruton, *J. Biol. Chem.*, **115**, 593 (1936).
22) E. Schmidt, F. Hitzler and E. Lahde, *Ber.*, **71**, 1933 (1938).
23) G. W. Anderson et al., *J. Am. Chem. Soc.*, **74**, 5307, 5309 (1952).
24) M. Bergmann, L. Zervas and J. S. Fruton, *J. Biol. Chem.*, **111**, 225 (1935).

* The molecular weight was determined by the end-carboxyl titration using sodium methoxide in dimethylformamide: J. S. Fritz and N. M. Lisicki, *Anal. Chem.*, **23**, 589 (1951); M. Sela and A. Berger, *J. Am. Chem. Soc.*, **77**, 1893 (1955).
25) T. V. Parke and W. W. Davis, *Anal. Chem.*, **26**, 642 (1954).
26) M. Bergmann et al., *Ber.*, **65**, 1192 (1932); *Z. physiol. Chem.*, **212**, 72 (1932).

by carbodiimide and by mixed anhydride procedures, but all efforts for crystallization failed in every case. (a) Carbodiimide procedure. To a solution of 9.3 g. of VII and 6.8 g. of dicyclohexyl-carbodiimide in 70 ml, of tetrahydrofuran was added a suspension of 7.5 g. of ethyl L-leucinate hydrochloride and 3.82 g. of triethylamine in 50 ml. of tetrahydrofuran, and the mixture was allowed to stand overnight. The reacted mixture was treated in the same manner as in the case of I and 13 g. of syrupy mass was obtained. (b) Mixed anhydride procedure. Two grams of VII, 0.7 g. of isovaleryl chloride and 1.3 g. of ethyl L-leucinate were treated in the same manner as in the case of II in tetrahydrofuran and 2.3 g. of the syrupy mass was obtained.

Carbobenzoxyglycyl-L-prolyl-L-leucine (IX).—To a solution of 13 g. of VIIIa in 40 ml. of acetone was added 16 ml. (1.1 equivalent) of 2 N sodium hydroxide. After 2.5 hours at room temperature (10°C) the solution was acidified and the separated oil was extracted with ethyl acetate. The ethyl acetate solution was extracted again with aqueous sodium bicarbonate, and the aqueous layer was acidified. A white crystalline solid separated, which was filtered off. After recrystallization from a large amount of aqueous methanol this solid gave 8.4 g. (66% based on VII) of the colorless plates; m. p. 201~202°C, $[\alpha]_D^{13}$ −62.7° (c 1.4, dimethyl formamide).

Anal. Found: C, 60.51; H, 6.75; N, 10.08. Calcd. for $C_{21}H_{29}O_6N_3$; C, 60.13; H, 6.97; N, 10.02%.

Glycyl-L-prolyl-L-leucine (X).—To a solution of 2.7 g. of IX in 100 ml. of methanol containing a small amount of glacial acetic acid was added 2 g. of palladium-charcoal, and hydrogen was introduced into the suspension for two hours under stirring. Then, the catalyst was filtered off and washed with water. The combined filtrate was concentrated to dryness under reduced pressure, and colorless needles of 1.55 g. were obtained in 85% yield. After recrystallization from aqueous methanol, the substance decomposed at 180~190°C; $[\alpha]_D^{9.5}$ −124° (c. 2.16, glacial acetic acid), $[\alpha]_D^{20.5}$ −125.1° (c 3.1, water).

Anal. Found*: C, 52.43; H, 8.15; N, 13.53. Calcd. for $C_{13}H_{23}O_4N_3 \cdot H_2O$: C, 51.47; H, 8.37; N, 13.85%. Found**: C, 54.61; H, 7.18; N, 15.00. Calcd. for $C_{13}H_{23}O_4N_3$: C, 54.75; H, 8.13; N, 14.73%. Paper chromatography showed this tripeptide to have only one spot, which turned yellow with ninhydrin, with an Rf value of 0.72 in *n*-butanol: water: acetic acid (4 : 1 : 1).

Polycondensation of L-prolyl-L-leucylglycine by the pyrophosphite procedure.—The suspension of 2.74 g. of IV and 4.0 g. of tetraethylpyrophosphite (1.5 equivalent against IV) in 7 ml. of diethylphosphite was sealed in a glass tube and heated in a boiling water bath. After about 5 minutes the tripeptide dissolved clearly in the solvent, and after about half an hour another slight precipitate appeared. The heating was continued for another hour, but no increase was observed in the amount of the precipitate. After cooling to room temperature 2 ml. of water was added into the reaction mixture in order to hydrolyse the excess reagent and active centers in the product. Removal of the diethylphosphite and water under reduced pressure left the polycondensation product as a white amorphous solid, which was treated with ethanol and ether for pulverization. This product was soluble in hot ethanol and partially soluble in hot methanol. After the hot methanol-soluble part was extracted out, the residue was dissolved in hot ethanol and fractionated with ether into three parts; namely, the first precipitate (Fr-1), the second precipitate (Fr-2) from the first mother liquor, and the residual part (Fr-3) which was obtained from the second mother liquor after removal of the solvent and the treatment with ether. The hot methanol extract was concentrated to dryness and the residue was pulverized by adding ether (Fr-4). The first fraction (Fr-1) was further fractionated in two parts, (Fr-1A) and (Fr-1B), using dimethylformamide and ether. The yields and the molecular weights of these fractions are given in Table I.

TABLE I

YIELD OF EACH FRACTION AND ITS MOLECULAR WEIGHT OF THE POLYCONDENSATE OF L-PROLYL-L-LEUCYLGLYCINE BY THE PYROPHOSPHITE PROCEDURE

Fraction number	Yield (mg.)	Mol. wt.*
Fr-1	480	—
Fr-1A	90	6600
Fr-1B	340	4200
Fr-2	450	3000
Fr-3	440	2000
Fr-4	615	1200
Total	1,985 mg. (77% based on IV)	

* These values were determined by the end-carboxyl titration using sodium methoxide in dimethylformamide: M. Sela and A. Berger, *J. Am. Chem. Soc.*, **77**, 1893 (1955).

The polypeptide (Fr-1B) was soluble in glacial acetic acid, pyridine, dimethylformamide and hot ethanol, and insoluble in water, benzene, chloroform and ethyl acetate; m. p. 190°C (decomp), $[\alpha]_D^{20}$ −104° (c 5.3, dimethylformamide). This material showed no biuret reaction.

Anal. Found: C, 54.81; H, 7.82; N, 14.70. Calcd. for $(C_{13}H_{21}O_3N_3 \cdot H_2O)_n$: C, 54.75; H, 8.13; N, 14.73%.

The phosphorus content of this material was determined by the method of Fiske[27], but it was only less than 0.01%. No amino nitrogen was detected by the manometric van Slyke method. This material was hydrazinolysed[18] with

* This substance was dried at 118°C (2 mm.) for 6 hours.

** This substance was dried at 138°C (2 mm.) for 6 hours. In this state it was strongly hygroscopic and easily returned to the initial state by being carelessly allowed to stand in the air.

27) C. H. Fiske and Y. Subbarow, *J. Biol. Chem.*, **66**, 375 (1925).

anhydrous hydrazine for 12 hours and the reaction mixture was dinitrophenylated. Thus, only one spot corresponding to DNP-glycine was detected by paper chromatography[28] from the acidic part of the reaction mixture, in which all the *C*-terminal amino acid of the polypeptide must be included.

The lower molecular weight fractions (Fr-3, Fr-4) were treated once more with tetraethyl-pyrophosphite in the same manner as described above, but no molecular weight increase was observed.

Polycondensation of L-prolyl-L-leucylglycine by the carbodiimide procedure.—One gram of dicyclohexylcarbodiimide and 1.07 g. of IV were suspended in 5 ml. of dimethylformamide and the suspension was sealed in a glass tube, but no change in the appearance of this suspension was observed at room temperature. When the mixture was heated at 70°, it changed to a clear solution. After 3 hours the solution was cooled to room temperature and the dimethylformamide was removed under reduced pressure. The residual syrup was treated with ethanol and ether, and 1.0 g. of crystalline product was obtained. However, the separation of polypeptide from the product was unsuccessful and no free carboxyl group was detected in this material by the sodium methoxide titration.

Polycondensation of L-prolyl-L-leucylglycine *p*-nitrophenylthioester.—The solution of 500 mg. of VI and an equivalent of triethylamine in 2 ml. of dimethylformamide was sealed in a glass tube and heated at 60° for 15 minutes. After standing at room temperature for 18 hours the resulting dark red solution changed to light yellow on the addition of a small amount of hydrochloric acid, and then excess of water was added to the solution. The precipitate formed was filtered off and dissolved in glacial acetic acid. Some hydrogen peroxide was added to the solution and the crystals which separated were filtered off. The mother liquor was concentrated under reduced pressure, and then the residual mass was extracted with hot ethanol. The extract was concentrated to dryness and the residue was treated twice in the same way as described above. The last amorphous residue was purified with dimethylformamide and ether, and about 100 mg. of white powdery substance was obtained. The molecular weight of this fraction (1150) was determined by end-carboxyl titration, but no analytical data were determined.

Parallel runs of the polycondensation reaction of L-prolyl-L-leucylglycine (IV) and of glycyl-L-prolyl-L-leucine (X).—The tripeptides IV and anhydrous X were treated in parallel runs under the same condition by the pyrophosphite procedure. The results are listed in Table II.

TABLE II

COMPARISON OF THE POLYCONDENSATION PRODUCTS OF THE TWO TRIPEPTIDES IV AND X

Tripeptide	mg.	Diethyl-phosphite ml.	Tetraethyl-pyrophosphite mg.	Yield mg.	Yield %	Mol. wt.
IV	400	3.0	700	250	60	3000
X	400	3.0	700	130	35	1900
IV	400	2.5	1300	300	80	550
X	400	2.5	1300	170	45	500

Summary

The two tripeptides, L-prolyl-L-leucylglycine (IV) and glycyl-L-prolyl-L-leucine (X), were synthesized, and IV was subjected to polymerization by the tetraethyl pyrophosphite, carbodiimide and *p*-nitrophenyl thioester methods, in which the most promising result was obtained by the pyrophosphite method. The highest molecular weight of the polypeptide which was obtained was about 6000 and the repetition of the original tripeptide unit in the polypeptide was confirmed by the end groups determination. The polycondensation reactions of both the tripeptides, IV and X, were compared in parallel runs by the tetraethyl pyrophosphite procedure, and the comparison showed that IV gave a better yield and a higher molecular weight product than X. X and poly-(L-prolyl-L-leucyl-glycyl), which was obtained from IV, contained firmly bound water in spite of the fact that IV contained no crystallization water.

The authors should like to express their thanks to Dr. M. L. Huggins for suggesting this problem and encouraging them constantly during his stay here.

Department of Chemistry
Faculty of Science
Osaka University
Kita-ku, Osaka

28) A. L. Levy, *Nature*, **174**, 126 (1954).

Synthetic Amphoteric Polypeptide. III. A Water-Soluble Amphoteric Polypeptide

By Heimei YUKI, Kenji OKAWA and Hisaya TANI

(Received March 13, 1958)

In the preceding paper[1] it was reported that the synthetic polypeptides, copoly-1 : 1 : 3-(DL-glutamic acid, DL-lysine, DL-phenylalanine) and copoly-1 : 1 : 1.9-(L-glutamic acid, L-lysine, L-leucine), are insoluble in water in the neutral pH region. On the other hand, in view of the great solubility of polyserine[2] in water, it may be considered that the water-solubility of a number of proteins, such as albumins, should be contributed largely by the serine and threonine residues in these proteins. To confirm this, it is desired to obtain an amphoteric polypeptide which contains any amount of serine residue as a component and is soluble in water over a whole pH range. In order to know how many serine residues are required to make the polypeptide freely soluble in water, four copolymers composed of various compositions of L-glutamic acid and DL-serine were synthesized and their solubilities were tested. While α-poly-L-glutamic acid is sparingly soluble in water in its free acid form, it was found that the copoly-(L-glutamic acid, DL-serine) was freely soluble in water, if the content of serine residue becomes more than about 50 mole per cent; hence the synthesis of copoly-1 : 1 : 2-(L-glutamic acid, L-lysine, DL-serine), as a water-soluble amphoteric polypeptide, was investigated.

The four copolymers composed of L-glutamic acid and DL-serine, the molar ratios of which were 4 : 1, 3 : 2, 2 : 3 and 1 : 4, and copoly-1 : 1 : 2-(L-glutamic acid, L-lysine, DL-serine) were obtained from four corresponding copoly-(γ-benzyl L-glutamate, *O*-benzyl-DL-serine) and copoly-1 : 1 : 2-(γ-benzyl L-glutamate, ε-*N*-carbobenzoxy-L-lysine, *O*-benzyl-DL-serine), respectively, which were prepared by the *N*-carboxy anhydride method as described in the preceding paper[1]. In the debenzylation reaction of these copolymers some attention should be paid to the occurrence of side reaction, because in most cases some degree of ester linkages may be formed during the reaction between hydroxyl group of serine residue and carboxyl group of either glutamic acid residue or of an acid used as solvent.

The debenzylation of copoly-(γ-benzyl L-glutamate, *O*-benzyl-DL-serine) was carried out in dioxane with dry hydrogen bromide, and in acetic acid with phosphonium iodide. The reaction with hydrogen bromide in dioxane gave the products in theoretical amount all insoluble, but swellable, even in hot aqueous potassium hydrogen carbonate. Poly-L-glutamic acid and poly-DL-serine, prepared under similar conditions from poly-γ-benzyl-L-glutamate and poly-*O*-benzyl-DL-serine, were readily soluble in aqueous potassium hydrogen carbonate and in water respectively. Those insoluble products obtained from the copolymers could be converted into soluble forms by treating with aqueous triethylamine (pH 10) at room temperature overnight. Under this condition, no change in the content of amino-nitrogen of poly-DL-serine and in the value of specific rotation of poly-L-glutamic acid was observed. These results indicate clearly that the inter- and/or intra-chain ester linkages were broken by a fairly mild condition, such as aqueous triethylamine, without accompanying any hydrolysis of the peptide bond or racemization.

The reaction of phosphonium iodide on the four copolymers in glacial acetic acid gave the products, the yields of which somewhat exceeded the theoretical amounts, partly insoluble in aqueous potassium hydrogen carbonate. These products could also be converted into perfectly soluble forms by treating with aqueous triethylamine, and may be considered as polymers the hydroxyl groups of which had been partly esterified both by acetic acid used as solvent and by the carboxyl groups of glutamic acid residues.

The final products obtained by these

1) H. Yuki, S. Sakakibara and H. Tani, This Bulletin, **29**, 654 (1956).
2) K. Okawa and H. Tani, *J. Chem. Soc. Japan, Pure Chem. Sec.* (*Nippon Kagaku Zassi*), **75**, 1199 (1954).

two different processes were all soluble in aqueous potassium hydrogen carbonate and copoly-2 : 3- and copoly-1 : 4-(L-glutamic acid, DL-serine) were soluble even in water. When dried in vacuo at an elevated temperature, these polypeptides showed a slight tendency to become insoluble in aqueous potassium hydrogen carbonate, but could readily be returned soluble by heating in this medium.

It was found that a pyrrolidone ring may be formed by the ring-closure of glutamyl residue, existing at the amino-end of these polymer molecules, because no free amino-nitrogen was detected in poly-L-glutamic acid prepared by this method.

The optical rotations of these copoly-(L-glutamic acid, DL-serine) were measured in their anionic forms and the intrinsic rotation of L-glutamic acid residue was calculated for each polypeptide, as the serine residues might be regarded to have no contribution to the optical rotation of the polymer since they were racemic. These values were almost constant ($-50°$ to $-57°$) and differed from that of poly-L-glutamic acid ($-88°$).

When the debenzylation of copoly-1 : 1 : 2-(γ-benzyl L-glutamate, ε-*N*-carbobenzoxy-L-lysine, *O*-benzyl-DL-serine) was carried out in glacial acetic acid with phosphonium iodide, it gave a cross-linked product insoluble, but swellable, in various aqueous and organic media, and this product could not be turned soluble by treating with triethylamine. The debenzylation of this copolymer was effected in dichloroacetic acid by using the theoretical amount of phosphonium iodide satisfactorily without formation of any cross-linkage. From the resulting polypeptide hydriodide, free copoly-1 : 1 : 2-(L-glutamic acid, L-lysine, DL-serine) was obtained by treating repeatedly with triethylamine.

This amphoteric polypeptide was found to be soluble in water over the whole pH range. Intrinsic viscosity of its solution in water was 0.04, and such small $[\eta]$ value may reflect rather low molecular weight. In view of the known lability of serine peptide to acid, the molecular weight depression, if any, might be due to the action of hydrogen iodide during the debenzylation process.

Dependence of specific viscosity on pH is shown in Fig. 1. The viscosity was minimum at the isoelectric point (pH 7), and increased gradually on both sides. This behavior is typical of amphoteric polyelectrolyte.

Dependence of specific rotation on pH was shown in Fig. 2. The specific rotation was *laevo*-rotatory over whole pH range; the value was constant ($-32°$) from pH 3.6 to pH 11.3, and increased rapidly on both sides. This specific rotation *vs* pH curve is very similar to that of serum albumin[3] and of ovalbumin[4].

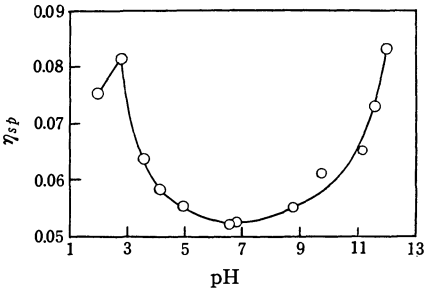

Fig. 1. Relation between specific viscosity of copoly-1:1:2-(L-glutamic acid, L-lysine, DL-serine) and pH.

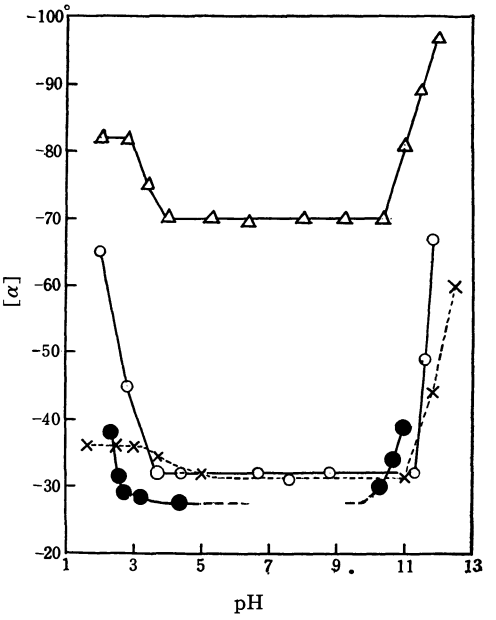

Fig. 2. Relation between specific rotation and pH.
○, Copoly-1:1:2-(L-glutamic acid, L-lysine, DL-serine); ●, Copoly-1:1:1.9-(L-glutamic acid, L-lysine, L-leucine)[1]; △, Serum albumin[3]; ×, Ovalbumin[4].

The optical rotatory behavior of synthetic polypeptide was discussed recently

3) M. A. Colub and E. E. Pickett, *J. Polymer Sci.*, **13**, 427 (1954).
4) J. T. Edsall and J. F. Foster, *J. Am. Chem. Soc.*, **70**, 1860 (1948).

both theoretically[5] and experimentally[6-8], and the workers concerned concluded that the chain configuration of the polymer contributes a great deal to this behavior. In the polypeptides obtained here, serine residue is DL-form and hence the problem of chain configuration would be rather complex[9], but it is very interesting that the behavior concerning optical rotation of this synthetic amphoteric polypeptide is quite similar to that of albumins; their specific rotations are *laevo*-rotatory in the whole pH range and have minimum constant values over wide ranges of pH around their isoelectric points. This behavior may correspond to the observation of P. Doty and his collaborators[8], who found that the specific rotation of poly-L-glutamic acid is constant until about 40% of the side-chain carboxyl group are dissociated. The reason for the very interesting result that the intrinsic rotation of glutamic acid residue in copoly-(L-glutamic acid, DL-serine) is almost constant in spite of the great difference of glutamic acid content and differs from that of poly-L-glutamic acid, remained obscure.

Although the viscosity and optical rotation could be measured on copoly-1 : 1 : 1.9-(L-glutamic acid, L-lysine, L-leucine)[1] only at both sides of the neutral pH region, because of its water-insolubility in the neutral pH region, the object of the measurements of these properties could now be attained completely on copoly-1 : 1 : 2-(L-glutamic acid, L-lysine, DL-serine) over the whole pH range. Some physicochemical properties of these synthetic amphoteric polypeptides are very similar to those of some natural proteins, and the latter, copoly-1 : 1 : 2-L-glutamic acid, L-lysine, DL-serine), may be regarded as the first member of 'model albumin', if the former, copoly-1 : 1 : 1.9-(L-glutamic acid, L-lysine, L-leucine)[1], together with copoly-1 : 1 : 3-(DL-glutamic acid, DL-lysine, DL-phenylalanine)[1], might be called 'model globulin'.

Experimental

Poly-γ-benzyl L-glutamate, poly-*O*-benzyl-DL-serine, and copoly-(γ-benzyl L-glutamate, *O*-benzyl-DL-serine).—Six different mixtures of *N*-carboxy-γ-benzyl L-glutamate anhydride[1] and *N*-carboxy-*O*-benzyl-DL-serine anhydride[2] were prepared: their molar ratios were 1:0, 4:1, 3:2, 2:3, 1:4 and 0:1, and the total amount was 10 m mol. in each mixture. Ten percent solution of each mixture in chlorobenzene was heated in a sealed glass tube for 2 hours at 90°C and then for one week at 40°C. The polymer mas precipitated by adding petroleum ether, washed with methanol and ether and dried. The results are shown in Table I.

Polymer G was soluble in dioxane, tetrahydrofurane, chloroform, nitrobenzene, pyridine and dichloroacetic acid, and was insoluble in water, ethanol and glacial acetic acid. While the solubility of polymer I was similar to that of polymer G polymer, II was soluble only in dichloroacetic acid and in hot dioxane, and polymer III, IV and S were soluble only in dichloroacetic acid.

TABLE I

Polymer	Molar ratio A/B	Appearance of polymerizing solution	Yield %		Anal. % C	H	N	Formula*
G	1 : 0	viscous solution	97	Calcd.			6.5	$[A]_n$
				Found			6.4	
I	4 : 1	viscous solution	97	Calcd.	66.1	6.0	6.6	$[4A, B]_n$
				Found	65.7	6.4	6.6	
II	3 : 2	transparent gel	93	Calcd.	66.4	6.1	6.9	$[3A, 2B]_n$
				Found	65.9	6.4	7.0	
III	2 : 3	opalescent gel	94	Calcd.	66.8	6.1	7.2	$[2A, 3B]_n$
				Found	65.8	6.2	7.2	
IV	1 : 4	opalescent gel	92	Calcd.	67.3	6.2	7.6	$[A, 4B]_n$
				Found	66.4	6.2	7.6	
S	0 : 1	opalescent gel	91	Calcd.			7.9	$[B]_n$
				Found			8.0	

*A: γ-Benzyl L-glutamate residue, $C_{12}H_{13}NO_3$.
B: *O*-Benzyl-DL-serine residue, $C_{10}H_{11}NO_2$.

5) D. D. Fitts and J. G. Kirkwood, ibid., **78**, 2650 (1950); *Proc. Natl. Acad. Sci.*, **42**, 33 (1956).
6) E. R. Blout and M. Idelson, *J. Am. Chem. Soc.*, **78**, 497 (1956).
7) P. Doty and J. T. Yang, ibid., **78**, 500 (1956).
8) P. Doty, A. Wada, J. T. Yang and E. R. Blout, *J. Polymer Sci.*, **23**, 851 (1957).
9) A. Elliott, W. R. Hanby and B. R. Malcolm, *Nature*, **178**, 1170 (1956); E. R. Blout, P. Doty and J. T. Yang, *J. Am. Chem. Soc.*, **79**, 759 (1957).

TABLE II

Product	Reaction condition: Polymer/Dioxane mg./ml.	Reaction time* min.	Yield** %		Anal.** % C	H	N	Formula***
G′	500/15	60	101	Found			10.5	$[A']_n$
				Calcd.			10.9	
I′	400/15	25	100	Found	44.5	5.9	11.3	$[4A', B']_n$
				Calcd.	45.8	5.5	11.6	
II′	180/12	20	106	Found	41.3	5.8	11.8	$[3A', 2B']_n$
				Calcd.	44.9	5.6	12.5	
III′	300/13	15	100	Found	41.2	6.0	12.7	$[2A', 3B']_n$
				Calcd.	43.9	5.6	13.5	
IV′	400/15	25	101	Found	40.0	5.5	13.7	$[A', 4B']_n$
				Calcd.	42.8	5.7	14.7	
S′	400/10	20	94	Found			15.2	$[B']_n$
				Calcd.			16.1	

* The time hydrogen bromide passed through; during this period the polymer was completely precipitated.

** Each sample was dried over phosphorus pentoxide at 108°C/2 mmHg for five hours, but the data show that even after this treatment, the polymer may contain about 3～6% of water.

*** A′; Glutamic acid residue, $C_5H_7O_3N$. B′: Serine residue, $C_3H_5O_2N$.

TABLE III

Polypeptide	Intrinsic rotation of glutamic acid residue $[\alpha_{glu}]_D$	Insoluble pH range	Amino-nitrogen %
G′	−88°* (at pH 8.3, 10.4)	below 3.9	0.00
I′	−50° (at pH 9.6)	below 3.5	0.04
II′	−56° (at pH 9.8)	below 1.1	0.18
III′	−57° (at pH 9.8)	none	0.21
IV′	−51° (at pH 10.1)	none	0.18
S′	0°	none	0.19 (at pH 6 and 10.1)

* Reported value[6]: −83°.

Poly-L-glutamic acid, poly-DL-serine and copoly-(L-glutamic acid, DL-serine).—(*a*) *Debenzylation with hydrogen bromide in dioxane.* To a mixture of the polymer and dioxane, dry hydrogen bromide was passed at room temperature, the solvent was distilled off in vacuo, and the residue was washed successively with anhydrous ether, methanol, and ether. After drying, white powder was obtained. The results are shown in Table II.

While polypeptide G′ was soluble in aqueous potassium hydrogen carbonate and polypeptide S′ was soluble in water, the others were insoluble but swellable in aqueous potassium hydrogen carbonate. A suspension of each insoluble copolymer in water containing an equivalent amount of potassium hydrogen carbonate was changed to a clear solution by adding a few drops of triethylamine and on standing overnight at room temperature. The optical rotation, pH and amino-nitrogen value were determined on each solution. No change in these values was observed even after standing the solution for two weeks. In Table III the value of $[\alpha_{glu}]_D$, the intrinsic rotation of L-glutamic acid residue, was calculated based on the cencentration of glutamic acid residue contained in the solution, but not on the concentration of polymer itself.

(*b*) *Debenzylation with phosphonium iodide in glacial acetic acid.* — About 1.4 g. of weighed polymer sample (I, II, III or IV) was suspended in 75 ml. of glacial acetic acid. To this mixture 4～5 g. phosphonium iodide was added in portions at 65～65°C during 4.5 hours with passing through dry hydrogen. The solvent was evaporated in vacuo under a stream of dry hydrogen, and the remaining precipitate was washed thoroughly with dry ether and ethanol, and dried. A white powder was obtained on each polymer, the yield of which was 106% for I″; 117% for II″, 117% for III″, and 138% for IV″, where I″, II″, III″ and IV″ are the corresponding products from the polymers I, II, III and IV, respectively. These were all insoluble in water and in methanol, and I″ and IV″ are mostly, while II″ and III‴ are partly soluble in aqueous potassium hydrogen carbonate. After dissolution was attained by standing in aqueous triethylamine for several hours, each solution was concentrated in a vacuum desiccator over conc. sulfuric acid. To

the syrups thus obtained, acetone and a few drops of acetic acid were added and the precipitated polymers were washed with acetone, methanol and ether. After drying, the purified polymers were obtained in 85~95% of the theoretical yields. The final products of I'' and II'' were insoluble in water and soluble in aqueous potassium hydrogen carbonate, and III'' and IV'' were soluble in water. All the solutions gave strong positive biuret reactions. After drying at 108°C/2 mm.Hg over phosphorus pentoxide for five hours, the samples became insoluble, but could readily be turned soluble by heating in aqueous potassium hydrogen carbonate. The observed analytical data were as follows—I'': C, 44.5; H, 5.9; N, 11.3. II'': C, 43.7; H, 6.3; N, 12.1. III'': C, 43.2; H, 6.4; N, 13.2. IV'': C, 44.8; H, 5.7; N, 14.5%.

Copoly-1 : 1 : 2-(γ-benzyl L-glutamate, ε-N-carbobenzoxy-L-lysine, O-benzyl-DL-serine) (V).—A mixture of 1.315 g. (5 m mol.) or γ-benzyl N-carboxy-L-glutamate anhydride, 1.530 g. (5 m mol.) of α-*N*-carboxy-ε-*N*-carbobenzoxy-L-lysine anhydride and 2.210 g. (10 m mol.) of *N*-carboxy-*O*-benzyl-DL-serine anhydride in a mixture of 47 ml. of chlorobenzene and 3 ml. of pyridine was sealed in a glass tube. The mixture was heated at 100°C until dissolved, and then allowed to stand for several days at 40°C. The solution gradually increased in viscosity and finally became opalescent gel. The polymer, precipitated on addition of petroleum ether, was thoroughly washed with methanol. After being reprecipitated from chloroform and methanol, the polymer was obtained as a white powder. Yield 3.85 g. (92% of the theor.)

Anal. Found: C, 65.4; H, 6.6; N, 8.3. Calcd. for $[(C_{12}H_{13}NO_3), (C_{14}H_{18}N_2O_3), 2(C_{10}H_{11}NO_2)]_n$: C, 66.1; H, 6.4; N, 8.4%.

The polymer was soluble in chloroform, dioxane, tetrahydrofuran, pyridine and dichloroacetic acid, partially soluble in acetone, and was insoluble in alcohol, ether, petroleum ether and water. It was partially soluble, with swelling, in hot acetic acid.

Copoly-1 : 1 : 2-(L-glutamic acid, L-lysine, DL-serine).—A solution of 3.00 g. of polymer V in 24 ml. of dichloroacetic acid was treated with 5 g. of phosphonium iodide. The reaction product was precipitated by the addition of about 100 ml. of dry ether, and the precipitate was washed repeatedly with dry ether, and then 2.4 g. of a yellowish powder was obtained. This powder was dissolved in methanol and a small amount of insoluble orange-brownish precipitate, included in the product, was almost all removed by centrifugation, and further, the trace of this matter remaing in the solution was precipitated by the addition of a small amount of ether. To the almost colorless clear solution, thus obtained, was added a solution of 0.9 g. of triethylamine in methanol; the resulting precipitate was washed repeatedly with methanol containing a small amount of triethylamine until no iodide ion was detected in the polymer by Beilstein test and by Volhardt method. The free polypeptide was obtained as a white powder. Yield 1.07 g. (68% of the theor.)

Anal. Found: C, 46.4; H, 6.1; N, 15.4; Amino-N, 3.0. Calcd. for $[(C_5H_7NO_3), (C_6H_{12}N_2O), 2(C_3H_5NO_2)]_n$: C, 47.3; H, 6.8; N, 16.2; Amino-N, 3.2%.

This free polypeptide was soluble in water, dilute mineral acids and glacial acetic acid, slightly soluble in methanol and ethanol, and insoluble in acetone and ether. The aqueous solution showed a strong biuret reaction. The viscosities at 25°C and the optical rotations were measured on the solutions having the same concentration of polymers, i.e. 0.464 g./100 ml., and various pH values made by appropriate amounts of hydrochloric acid or sodium hydroxide.

Summary

1. Preparation of four copoly-(L-glutamic acid, DL-serine), the molar ratios of the two amino acid residues were 4 : 1, 3 : 2, 2 : 3 and 1 : 4, by debenzylation of the corresponding four copoly-(γ-benzyl L-glutamate, *O*-benzyl DL-serine), was attempted.

2. The inter- and/or intra-molecular ester-linkages, formed during the debenzylation reaction between hydroxyl group of serine residue and carboxyl group of glutamic acid residue, was broken by treating with aqueous triethylamine without accompanying racemisation or hydrolysis of the peptide bond.

3. Copoly-(L-glutamic acid, DL-serine) became freely soluble in water when the content of serine residue was more than about 50 mole per cent.

4. Copoly-1 : 1 : 2-(L-glutamic acid, L-lysine, DL-serine), prepared by debenzylation from the parent copolymer, was soluble in water over a whole pH range, and the pH dependence of viscosity and of optical rotation was measured on its solutions. It was found that these properties are very similar to those of natural albumins.

The authors express their hearty thanks to Professor S. Akabori and Professor S. Murahashi for their interest and encouragement throughout the work. This research was financially supported by the Ministry of Education and The Fiber Research Institute.

Department of Chemistry
Faculty of Science
Osaka University
Kita-ku, Osaka

Spectrochemical Study of Microscopic Crystals. XVIII[1]. *The Color and the Structure of Compounds of a Magnus Green Salt Type*

By Shoichiro YAMADA and Ryutaro TSUCHIDA

(Received May 13, 1958)

Magnus green salt having an empirical formula of $[Pt(NH_3)_4][PtCl_4]$ is peculiar in that the salt in the crystalline state is colored green, whereas the separate component complex-ions in solution are colorless and red, respectively. In order to elucidate the peculiarity, the present authors[2] formerly determined the dichroism of the compound, and concluded that the unusually deep color of Magnus green salt might be due to the possible interaction between platinum atoms which are arranged in a straight line.

When the ammonia molecules in Magnus green salt are replaced by molecules of an alkylamine, the condition around the platinum atoms is supposed to change electronically as well as sterically. Therfore, it seemed to be interesting to see what change would occur in the structure of compounds of a Magnus green salt type with several alkylamines. This paper presents the results obtained concerning the above problem on the basis of dichroism measurements in the visible and ultraviolet region.

Experimental

Materials.—Tetrakis-(methylamine)-platinum-(II) chloride was prepared in colorless crystals from potassium tetrachloroplatinate(II) and an excess of methylamine.

Tetrakis-(ethylamine)-platinum(II), tetrakis-(*n*-propylamine)-platinum(II) and tetrakis-(*n*-butylamine)-platinum(II) chloride were prepared in colorless crystals by the same method as in the case of methylamine. The reaction in every case proceeded in quite a similar way. The crystals were purified by repeated recrystallization from hot water. The solubility of the complex compounds in water seems to decrease as the number of carbon atom increases. All the amines used in the present work were of reagent grade.

Compounds of a Magnus green salt type, $[Pt(amine)_4][PtCl_4]$, were prepared by adding a solution of a tetramine-platinum(II) compound into a solution of potassium tetrachloroplatinate-(II). The crystals of the compounds precipitated at once when the solutions of the two compounds were mixed together.

$[Pt(methylamine)_4][PtCl_4]$ forms green, needle-like crystals. The crystals show a marked dichroism on the prism face; they are dark green with polarized light having its electric vector along the needle-axis, and pale green with the electric vector perpendicular to the axis. The dichroism measurements were made on the prism face with the electric vectors along the two directions.

$[Pt(ethylamine)_4][PtCl_4]$ forms pink, needle-like crystals, which show a straight extinction and are dichroic. They are pink with the electric vector perpendicular to the needle-axis, and very pale pink with the electric vector along the needle-axis. The dichroism measurements were carried out with the electric vectors along the two directions.

$[Pt(n\text{-propylamine})_4][PtCl_4]$ and $[Pt(n\text{-butylamine})_4][PtCl_4]$ form pink, microcrystalline aggregates. The crystals obtained were so small that the dichroism measurements were not made.

Measurements.—The dichroism measurements in the visible and near-ultraviolet region of the crystals were carried out by Tsuchida-Kobayashi's microscopic method[3], as in the former papers of this series. The measurements were also made with a newly constructed apparatus, which consists in principle of a monochromator, a reflecting microscope and a photo-electric detector with a photomultiplier. Most of the parts were made by the Olympus Co.[4] The detailed description of the apparatus will be presented elsewhere.

The *c*- and *a*- absorption in the figures represent the absorption with the electric vector along and perpendicular to the needle-axis of the crystal, respectively.

Results and Discussion

The results of the measurements are shown in Fig. 1 and Fig. 2. It is seen that $[Pt(methylamine)_4][PtCl_4]$ in the crystalline state absorbs the light in a wavelength region much longer than the component complex-ions in solution (Fig. 1).

1) Paper XVII of this series, S. Yamada, H. Nakamura and R. Tsuchida, This Bulletin, **31**, 303 (1958).

2) S. Yamada and R. Tsuchida, *J. Chem. Soc. Japan, Pure Chem. Sec.* (*Nippon Kagaku Zassi*), **70**, 142 (1949); S. Yamada, *J. Am. Chem. Soc.*, **73**, 1579 (1951).

3) R. Tsuchida and M. Kobayashi, "The Color and the Structure of Metallic Compounds," Zoshindo, Osaka, 1944, p. 180.

4) R. Tsuchida and S. Yamada, to be published later. The apparatus was constructed in co-operation with the staffs of Olympus Co., to whom we are greatly indebted.

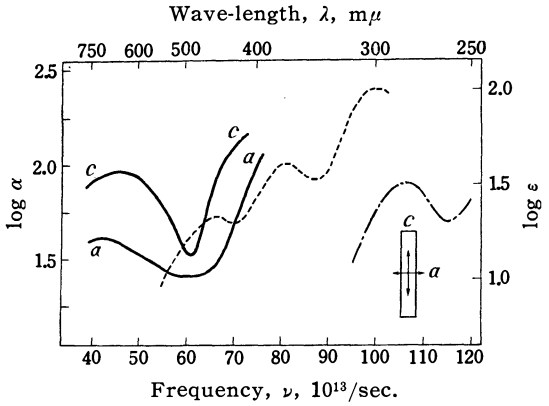

Fig. 1. Absorption spectra of [Pt(methylamine)$_4$][PtCl$_4$] in the crystalline state (——), [Pt(methylamine)$_4$]Cl$_2$ (— — —) and K$_2$[PtCl$_4$] (-----) in aqueous solution. The latter two curves are taken from H. Yoneda, This Bulletin, **30**, 130 (1957) and ref. 6, respectively.

Thus the Magnus green salt type compound of methylamine shows a band at 46.6× 10^{13}/sec. (644 mμ), whereas the separate component ions are transparent in this region. It is presumed, therefore, that the complex-ions in the crystal of [Pt(methylamine)$_4$][PtCl$_4$] are under an effect, which is much stronger than that due to the crystalline field of ordinary compounds. The crystal structure analysis of the methylamine Magnus salt is not available for the present. The nature of the effect, however, may be judged from comparison of the dichroism of the compound with the dichroism of Magnus green salt, [Pt(NH$_3$)$_4$][PtCl$_4$][2]. The comparison reveals that the dichroism of the former is quite similar to that of the latter. Therefore, the state of the component complex ions in both the compounds may be almost the same.

It would be appropriate to recall the results with the latter[2], in the crystal of which the planar complex-ions were determined with X-rays to be arranged parallel to each other with platinum atoms disposed at an equal distance along a straight line. The crystal of [Pt(NH$_3$)$_4$][PtCl$_4$] was found to show in the longer wave-length region an absorption band of a new sort, which was not shown by either of the separate component complex-ions alone. For the new absorption band, the absorption is considerably stronger in the direction perpendicular to the planar complex-ions than along the complex-ions. This relationship, combined with the crystal structure analyses[5], led us to the conclusion that in the crystal of Magnus green salt there would be a direct type of interaction between the platinum atoms along the direction perpendicular to the complex-plane.

Based on this result and on the close similarity in the dichroism between the two compounds, the dichroism of [Pt(methylamine)$_4$][PtCl$_4$] in the crystalline state, as has been determined in the present work, may be readily understood, when it is assumed that the *c*-absorption corresponds to the absorption with the electric vector perpendicular to the complex-plane and the *a*-absorption to the absorption with the electric vector along the complex-plane. Thus it may be most likely that the planar complex-ions in the crystal of this compound are arranged in such a way that they are piled one just above and one below another with their planes parallel to each other, and that there would exist a direct type of interaction between platinum atoms in the direction along the needle-axis.

On the contrary, the absorption spectra of [Pt(ethylamine)$_4$][PtCl$_4$] in the crystalline state may be understood in terms of the absorption spectra of the separate component ions undergoing no extraordinary effect. It is seen in Fig. 2 that the

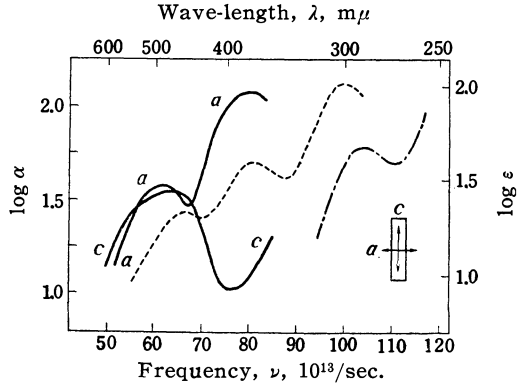

Fig. 2. Absorption spectra of [Pt(ethylamine)$_4$][PtCl$_4$] in the crystalline state (——), [Pt(ethylamine)$_4$]Cl$_2$ (-----) and K$_2$[PtCl$_4$] (----) in aqueous solution. The last two curves are taken from the references cited in Fig. 1.

ethylamine Magnus salt does not show an absorption band in the region of longer wave-length than the region where either of the separate complex-ions alone absorbs

5) E. G. Cox, F. W. Pinkard, W. Wardlaw and G. H. Preston, *J. Chem. Soc.*, **1932**, 2527; M. Atoji, J. W. Richardson and R. E. Rundle, *J. Am. Chem. Soc.*, **79**, 3017 (1957).

in solution. Moreover, the dichroism as well as the absorption spectrum of the crystal closely resembles that of $K_2[PtCl_4]$ in the crystalline state[6]. Thus it may be assumed that the *c*-absorption of the former represents the feature of the $\perp$-absorption and the *a*-absorption the $\parallel$-absorption of the latter, where the $\parallel$- and the $\perp$-absorption denote the absorption with the electric vector parallel and perpendicular to the plane of the complexion. The crystal structure analysis has not yet been reported with this salt. The above consideration indicates, however, that between platinum atoms in the crystal of $[Pt(ethylamine)_4][PtCl_4]$ there is no interaction of such a sort as exists in the crystal of Magnus green salt and the corresponding compound of methylamine.

Summarizing the results obtained in the present and former reports, we may derive the following presumption. *The compound of a Magnus salt type, which is represented by* $[Pt(amine)_4][PtCl_4]$, *may be classified into two kinds. One is colored green, involving a direct type of metal-to-metal interaction. The other is pink and involves no interaction of the above kind.*

The above conclusion may be used for differentiating the two types. In fact, this criterion has been applied in the present work to the case of higher alkylamines. The Magnus salt type compound of *n*-propylamine is obtained in pink microcrystals by the same method as in the case of Magnus green salt. Thus a difficultly soluble precipitate of $[Pt(n\text{-propylamine})_4][PtCl_4]$ is formed at once, when an aqueous solution of $[Pt(n\text{-propylamine})_4]Cl_2$ is added to a solution of $K_2[PtCl_4]$. The pink color of the salt may be regarded on the basis of the above-mentioned criterion as showing that the compound involves no metal-to-metal interaction. It is concluded in a similar way that no metal-to-metal interaction is operative in the crystal of $[Pt(n\text{-butylamine})_4][PtCl_4]$.

It may well be presumed further that *no metal-to-metal interaction would be present in the crystals of the compounds of a Magnus salt type with higher homologues of alkylamines.* The conclusion which has been obtained up to the present is shown in Table I. It is worth noting that the drastic change from methylamine to ethylamine or higher alkylamines is found.

TABLE I

THE METAL-TO-METAL INTERACTION IN THE COMPOUNDS OF A MAGNUS SALT TYPE, $[Pt(amine)_4][PtCl_4]$

Amine	Color	Pt-to-Pt interaction
NH_3	green	present
CH_3NH_2	green	present
$C_2H_5NH_2$	pink	absent
$n\text{-}C_3H_7NH_2$	pink	absent
$n\text{-}C_4H_9NH_2$	pink	absent

This result may be explained tentatively in terms of the following two effects. One is due to the change in the inductive effect of the alkyl-group upon the nitrogen atom, and the other to the change in the steric condition around the platinum atom.

The inductive effect, on the one hand, seems to be inadequate for explaining the transition as mentioned above. The tendency of the alkyl-group to push the electronic density toward the nitrogen atom becomes greater as we go from methyl- to higher alkyl-groups. Since higher electronic density on the platinum atom would be favorable for the metal-to-metal interaction, the tendency, as is observed in Table I, can not be explained as due to the inductive effect of the alkyl-group.

On the other hand, the steric condition is considered to become less favorable for the suitable arrangement of the planar complexes, as the alkyl-groups become more bulky. Although increasing number of carbon atoms would not absolutely prevent the platinum atoms from approaching each other so closely that the metal-to-metal interaction might result, it would certainly make difficult the formation of the crystal lattice consisting of series of platinum atoms which are arranged along straight lines.

We have also found that the direct type of interaction between platinum atoms is not present in the crystals of $[Pt\,en_2][PtCl_4]$ or $[Pt(pyridine)_4][PtCl_4]$[7]. This conclusion may be understood in terms of the steric factor, similarly to the case of alkylamines.

Summary

The color and the structure of the compounds of a Magnus green salt type, $[Pt(amine)_4][PtCl_4]$, have been studied. The dichroism with crystals of $[Pt(methylamine)_4][PtCl_4]$ and $[Pt(ethylamine)_4][PtCl_4]$ has been quantitatively determined

6) S. Yamada, H. Yoneda and R. Tsuchida, *J. Chem. Soc. Japan, Pure Chem. Sec.* (*Nippon Kagaku Zassi*), **69**, 145 (1948).

7) S. Yamada and R. Tsuchida, to be published later.

at room temperature in the visible and ultraviolet region by the microscopic method. From the measurements, the unusually deep color of the former has been shown to be ascribed to a direct type of interaction between platinum atoms. No interaction of this sort is present in the crystal of the latter, which is pink in color.

It is suggested that the compounds having a formula of $[Pt(alkylamine)_4][PtCl_4]$ may generally be classified into two kinds, one being colored green and the other pink. In the crystals of the former there is a direct type of interaction between platinum atoms at the center of the planar complexes, but no interaction of such a sort is operative in the crystals of the latter.

We wish to thank the Ministry of Education for a grant, which enabled us to purchase the reflecting microscope and accessories. We also thank Dr. Miyata, Dr. Noma and other members of the staff of the Olympus Co. for their co-operation in setting up the apparatus.

Department of Chemistry, Faculty of Science, Osaka University
Kita-ku, Osaka

The Ignition of Hydrogen-Oxygen Mixture by Shock Wave. I. The Condition for Shock Ignition for Hydrogen-Oxygen Mixture

By Momotaro SUZUKI, Hajime MIYAMA and Shiro FUJIMOTO

(Received April 10, 1958)

Although the ignition of hydrogen-oxygen mixture by shock wave has been investigated by several authors[1-3], there are not complete data about the shock ignition under various pressures of a gaseous mixture. Therefore, a series of experiments was carried out by the authors of this paper to determine the limit concentration for the gaseous hydrogen-oxygen mixture of various pressures in a shock tube.

The experimental method and procedure are almost the same as in the previous report[4]. Commercial oxygen and hydrogen in cylinders were mixed to a desired composition, and the mixture was kept in a tank over 24 hours, to make the mixing complete.

Results and Discussion

We have carried out a series of experiments on ignition by shock wave against certain gaseous mixtures of definite composition and pressure. The lowest pressure necessary for the ignition is called minimum ignition pressure P_1 for the gaseous mixture of a definite composition

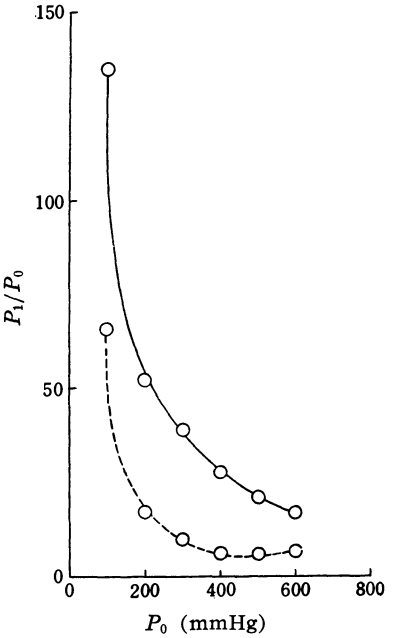

Fig. 1. Variation of P_1/P_0 with P_0, in the case of 80.2% H_2.
——, plane end; ------, conical end.

1) J. A. Fay, "Fourth Symposium on Combustion", The Williams Wilkins Co., Baltimore (1953), p. 501.
2) D. J. Berets, E. F. Greene and G. B. Kistiakowsky, *J. Am. Chem. Soc.*, **72**, 1086 (1950).
3) M. Steinberg and W. E. Kaskan, "Fifth Symposium on Combustion", The Williams and Wilkins Co., Baltimore (1955), p. 664.
4) M. Suzuki, H. Miyama and S. Fujimoto, This Bulletin, **31**, 232 (1958).

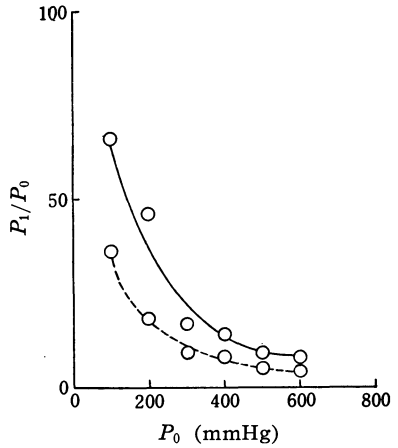

Fig. 2. Variation of P_1/P_0 with P_0, in the case of 66.8% H_2.
——, plane end; ------, conical end.

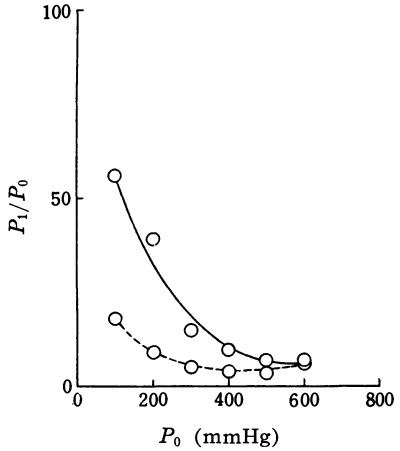

Fig. 3. Variation of P_1/P_0 with P_0, in the case of 48.9% H_2.
——, plane end; ------, conical end.

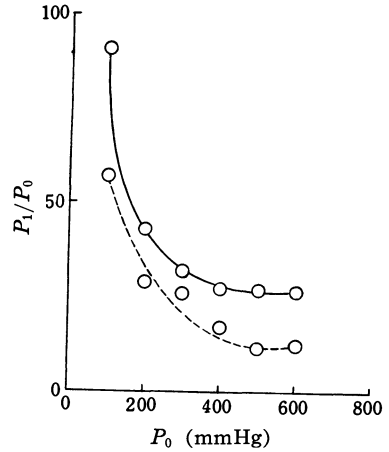

Fig. 4. Variation of P_1/P_0 with P_0, in the case of 10.4% H_2.
——, plane end; ------, conical end.

and a definite pressure P_0. In Figs. 1—4 the ratio P_1/P_0 is plotted against various pressures P_0 of the gaseous mixture of a definite composition. The thick curves correspond to the experiment in which a plane bottom is used in the test chamber and on the other hand the dotted ones for a conical bottom having a vertical angle of 90°, respectively. As shown in these figures, it will be deduced that the higher the pressure P_0, the easier the ignition, and that the ignition is easier in the case of a conical bottom than by the use of a plane bottom.

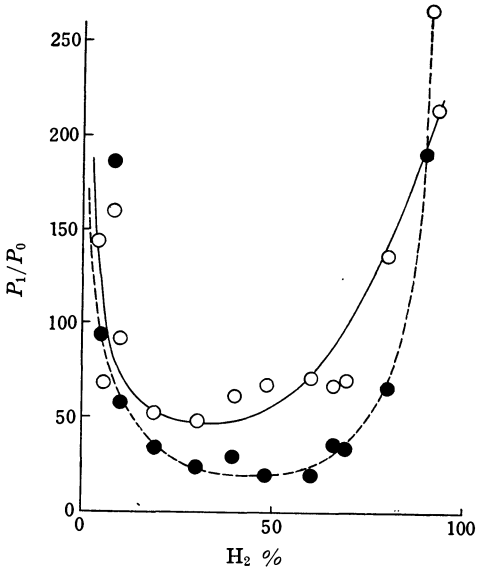

Fig. 5. Variation of P_1/P_0 with the concentration of H_2, when $P_0=100$ mmHg.
——, plane end; ------, conical end.

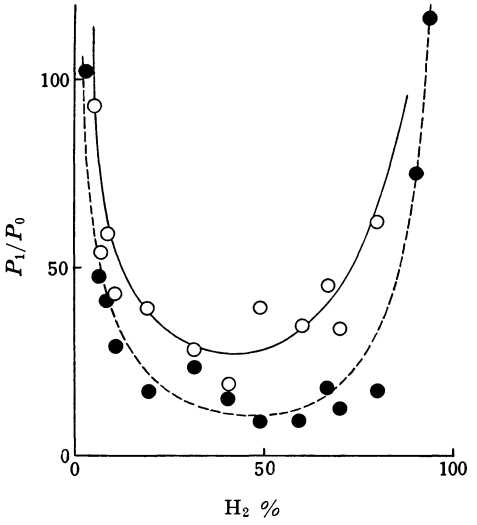

Fig. 6. Variation of P_1/P_0 with the concentration of H_2, when $P_0=200$ mmHg.
——, plane end; ------, conical end.

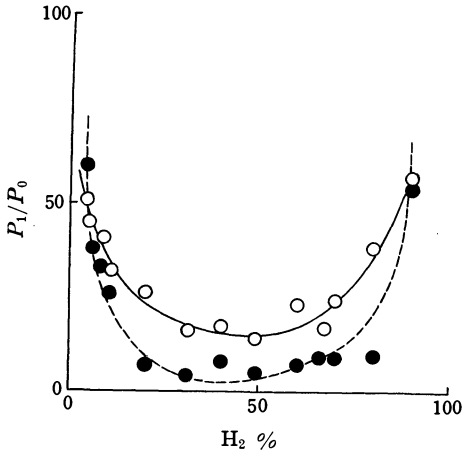

Fig. 7. Variation of P_1/P_0, with the concentration of H_2, when $P_0=300$ mmHg. ——, plane end; ------, conical end.

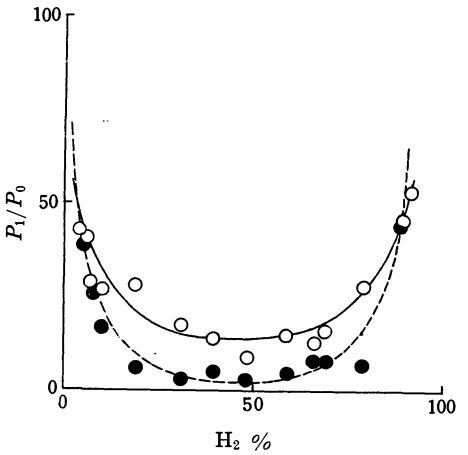

Fig. 8. Variation of P_1/P_0 with the concentration of H_2, when $P_0=400$ mmHg. ——, plane end; ------, conical end.

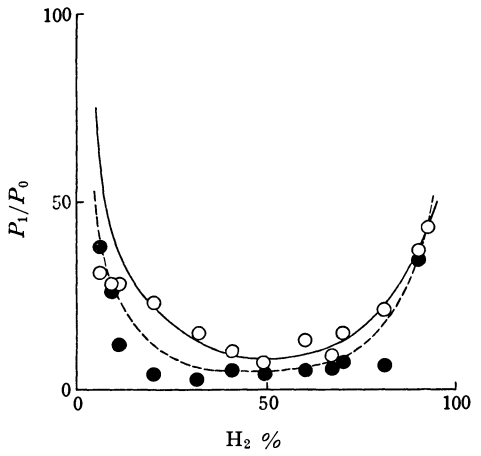

Fig. 9. Variation of P_1/P_0 with the concentration of H_2, when $P_0=500$ mmHg. ——, plane end; ------, conical end.

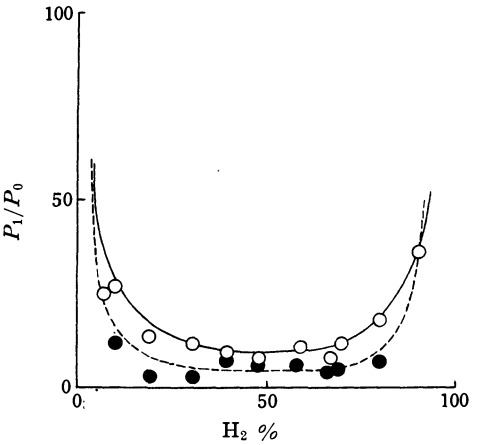

Fig. 10. Variation of P_1/P_0 with the concentration of H_2, when $P_0=600$ mmHg. ——, plane end; ------, conical end.

In Figs. 5—10, the ratio P_1/P_0 is plotted against various compositions of hydrogen and oxygen of definite pressure P_0. For all the diagrams except the case of $P_0=$ 100 mmHg, the minimum ignition point observed corresponds to the gaseous mixture of about 40~50% hydrogen. The limit of explosion of the gaseous mixture, so far as it can be measured, seems to lie in the region from 4 to 94% hydrogen.

Since the reproducibility of the experimental values of the minimum ignition pressure P_1 is not very good, the accuracy of the experimental values is ca. ±10%. These errors seem to cause the irregularity of the measured values of P_1/P_0 in Figs. 5—10.

In our experiments, the ignition temperatures have not been determined directly. Although they may be estimated by means of the same calculations which were described in the previous paper[4], we will postpone the discussion about this problem until the results of further investigation can be obtained using a shock tube equipped with pick-ups, which can be used for measuring the pressure and the velocity of the shock or detonation wave.

Summary

Using the shock tube, the authors measured the minimum ignition pressure P_1 of the reservoir for the hydrogen-oxygen mixture of various pressures (P_0) and various compositions, and obtained the following results.

1) The higher the value of P_0, the easier the ignition.

2) The concentration range of hydrogen in the gaseous mixture for shock ignition is 4~94%, and the minimum value of P_1/P_0 was found in the gaseous mixture of about 40~50% hydrogen, when P_0 is over 200 mmHg.

3) The ignition is easier by the use of a shock tube with a conical end rather than that with a plane end.

Department of Chemistry
Defence Academy
Yokosuka

The Ignition of Hydrogen-Oxygen Mixture by Shock Wave. II. Measurement of the Pressure and the Velocity of Shock or Detonation Wave

By Momotaro SUZUKI, Hajime MIYAMA and Shiro FUJIMOTO

(Received April 15, 1958)

In the previous paper[1] of this series, we described the results on the shock ignition of hydrogen-oxygen mixture using a shock tube of rather simple construction. Further investigation with a more complex device will be preferred to get more detailed knowledge. In this report some investigations were made to get fundamental information on the shock ignition of this mixture with a shock tube, equipped with pick-ups of barium titanate for the sake of measurements of pressure as well as of velocity of shock or detonation wave.

Experimental

A brief scheme of the measuring system is given in Fig. 1. As is shown in the figure, the shock tube made from mild steel has a square cross section with an inside lateral of 5 cm. The tube is divided into two portions, the reservoir chamber of A of 60 cm. length and the ignition test chamber C of 180 cm. length respectively. The chambers A and C are separated by several sheets of cellophane films, which can be punctured by the needle N through a side tube attached obliquely to the central axis of the shock tube.

For the measurement of pressures, five checking stations which are denoted by P_1, P_2, P_3, P_4 and P_5, are located on the wall of the test chamber. These stations are placed at a distance of 20 cm. from each other. The measuring equipment of each station is a pick-up (Fig. 2) consisting of ceramics of barium titanate whose natural frequency is something over 10 kc. A pick-up at P_0, placed near the membrane, is used for starting the sweep of the oscillograph.

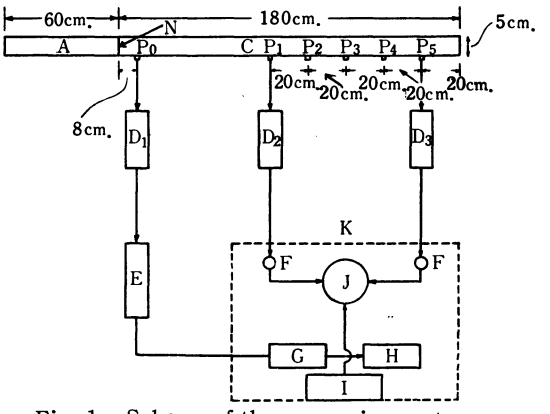

Fig. 1. Scheme of the measuring system.
A, Reservoir chamber;
C, Test chamber;
D_1, D_2 and D_3, Pre-amplifiers;
E, Trigger amplifier;
F, Signal input;
G, Sweep trigger;
H, Sweep oscillator:
I, Time-mark-oscillator;
J, Cathode-ray tube;
K, Two-element-oscillograph;
N, Needle;
P_0~P_5; Pick-up stations.

Just as the shock wave starts at the puncturing of the diaphragm, the pick-up at P_0 operates, and accordingly the signal from this pick-up will be transmitted through the pre-amplifier D_1 to the trigger amplifier E which operates the sweep-trigger G. Then the sweep-oscillator H of the oscillograph K will start and will give a horizontal time axis on the oscillogram. As the wave further propagates and passes the pick-up stations P_1 etc., the pressure change which is caused by the wave passing there will register on the pick-ups and this transient pressure change will

1) M. Suzuki, H. Miyama and S. Fujimoto, This Bulletin, **31**, 816 (1958).

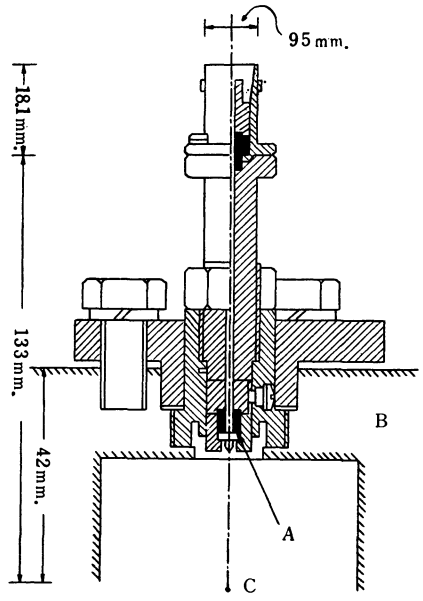

Fig. 2. Pick-up.
A, Barium titanate;
B, Wall of the shock tube;
C, Center of a cross section of the shock tube.

show itself as a displacement along the vertical axis of the oscillogram whose height gives the value of the pressure change. As we have a synchronous time marking by means of oscillator I in each oscillogram, we can evaluate the time delay of these successful pressure signals and then estimate the average velocity of the wave between two subsequent stations accordingly.

The characteristics of the apparatus used are given below. The pre-amplifiers have input-impedance 5 MΩ, output-impedance 100 kΩ, gain 53 db, maxium deviation of gain −2 db between 2c./s. and 20 kc./sec., and noise ratio less than −60 db. The trigger amplifier has output-impedance 100 kΩ, gain 40 db, maximum deviation of gain −2 db between 1 kc./sec. and 20 kc./sec., trigger-output 75 V_{p-p}, trigger-delay 0.6 msec.∼1.3 msec. which on requirement can be reduced to less than 2μsec. by cutting off the circuit of the trigger-delay. The scale of the time-mark oscillator can be varied in four steps i.e. 10 msec., 1 msec., 100 μsec. and 10 μsec., and the error of scale is less than 5%. The two-element oscillograph has the following characteristics. Cathode-ray tube is the type 130 SB11 (Toshiba). The amplifier has an input-impedance ca. 2 MΩ, gain ca. 70 db, maximum deviation of gain ±3 db between DC and 500 kc./sec., input-level about 1 mV∼100 V, and continuous variable attenuator 1:1 to 1000:1. The sweep-trigger and sweep-oscillator have input-level ca. 10 mV_{p-p}, and time of duration for a single-sweep 100 msec./cm.∼10 μsec./cm.

The pick-up used for measurement was calibrated by means of the device shown in Fig. 3. The procedure of calibration is as follows. The

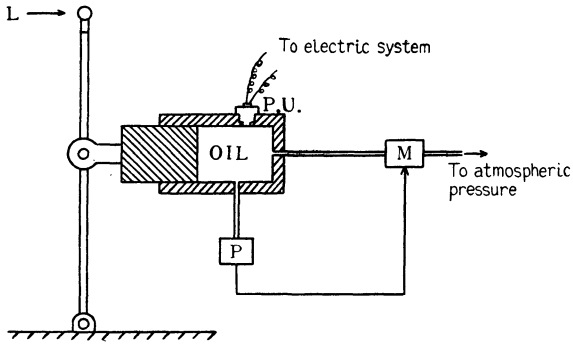

Fig. 3. Apparatus for calibrating pick-up.
P, Pressure switch;
M, Electro-magnetic valve;
L, Lever

pressure of the vessel, which is filled with low viscosity oil, will increase by pushing the lever L. When the pressure attains a certain definite value on which the pressure switch P is adjusted, electrically operate the valve M, which is suddenly opened. Accordingly, the pressure inside the vessel is reduced to atmospheric pressure during a very short period, and this pressure change is recorded through the pick-up in the oscillogram. We can calibrate the displacement of the oscillogram at a certain value of pressure by comparing this with the scale of the pressure switch which is previously standardized by an absolute manometer.

Other details about the experiment which are not described in this paper will be found in our previous papers[1,2] or elsewhere.[3]

Results and Discussion

A picture of an oscillogram of a propagating shock wave in the test chamber, which is filled only with air, is shown in Fig. 4. The picture was taken for the sake of visualizing the real behavior of a shock wave propagating in a tube filled with air without initiating any chemical reaction. The variation of the pressure P and the velocity of the shock wave with P_1/P_0 is obtained from many such pictures as this and shown in Figs. 5 and 6, where P_1 and P_0 are the pressures of the reservoir and the test chambers respectively. The values of P_0 are always atmospheric pressure. The experimental values of P are rather greater than the theoretical

2) M. Suzuki, H. Miyama and S. Fujimoto, This Bulletin, **31**, 232 (1958).

3) R. B. Morrison, "A Shock-Tube Investigation of Detonative Combustion", Engineering Research Institute, Univ. of Michigan, Ann Arbor (1955); P. F. W. Geiger and C. W. Mautz. "The Shock Tube as an Instrument for the Investigation of Transonic and Supersonic Flow Patterns", Engineering Research Institute, Univ. of Michigan, Ann Arbor (1949): P. M. Steinberg and W. E. Kaskan, "Fifth Symposium on Combustion", The Williams and Wilkins Co., Baltimore (1953), p. 664.

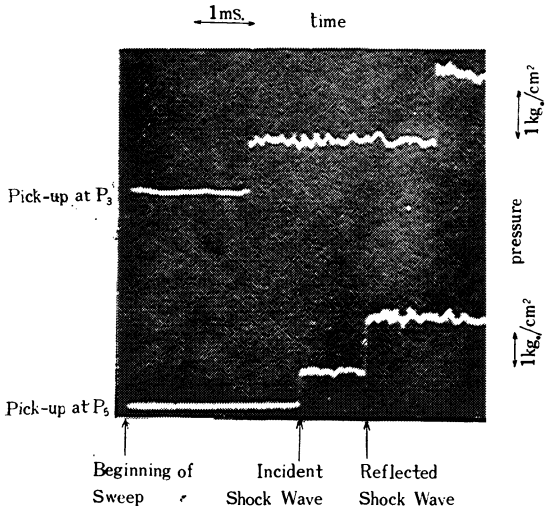

Fig. 4. A picture of oscillogram, when the test chamber is filled with air. $P_0=760$ mmHg, $P_1/P_0=5$.

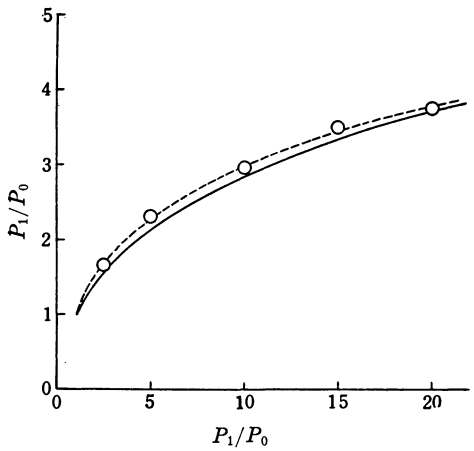

Fig. 5. Variation of the pressure of the incident shock wave with P_1/P_0
------ experimental value;
—— theoretical value.

values as shown in Fig. 5. The discrepancies probably lie within the limit of characteristic error of the pick-up used. As may be seen in Fig. 6, the experimental values of the velocity of shock wave are smaller than those expected from the theoretical considerations, and this tendency looks more reasonable when compared with the results of any other author.[4]

In the next experiment we have carried on a series of measurements using the

4) R. E. Duff, "The Use of Real Gases in a Shock Tube" Engineering Research Institute, Univ. of Michigan, Ann Arbor (1951).

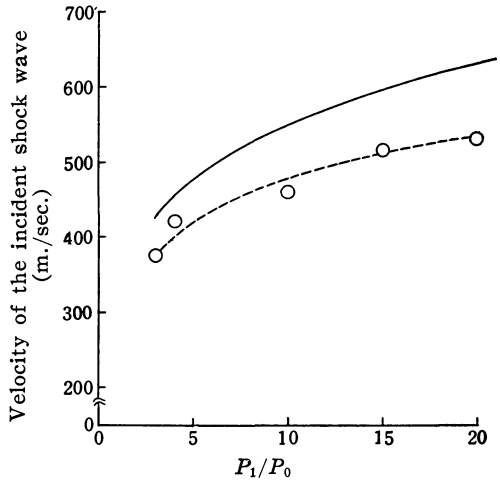

Fig. 6. Variation of the velocity of the incident shock wave with P_1/P_0.
------ experimental value;
——theoretical value.

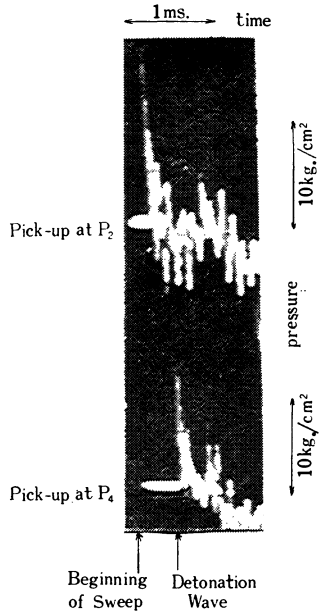

Fig. 7. A picture of oscillogram, when the test chamber is filled with $2H_2+O_2$. $P_0=200$ mmHg, $P_1/P_0=10.1$.

gaseous mixture $2H_2+O_2$ in the test chamber. Compared with the former case[1], the ignition was easier, i.e., the ignition pressure P_1 is lower, but the critical value of this pressure was more ambiguous. These results probably occur because the cross-section of this shock tube is larger, the number of sheets of cellophane films under the same pressure-difference, is more, and therefore the effect of puncturing the membrane upon the detonable

gaseous mixture is greater than in the previous shock tube.[1].

A typical oscillogram of pick-up pressures in a series of detonation experiments where the pressure of the detonable gas mixture in the test chamber is more than 200 mmHg, is shown in Fig. 7. In this figure, the pressure of the shock wave is not observable, but only the pressure of the detonation wave can be observed. The same features are observed in oscillograms of all pick-up stations and therefore it is concluded that the detonation was initiated between the membrane and the first pick-up P_1 and that the detonation of the gaseous mixture became stable before the detonation wave arrived at the pick-up P_1.

Under a pressure of 100 mmHg, the detonation took place somewhere along the test chamber. This detonation was initiated by an incident shock wave in some cases and by a reflected one in other cases. The distinction as to whether the cause of initiation is due to the incident or the reflected shock wave, can be told from the relative position of the detonation sign and the shock sign in the oscillograms of the pick-up stations (Figs. 8 and 9).

These differences of the oscillograms between points at high pressure and at

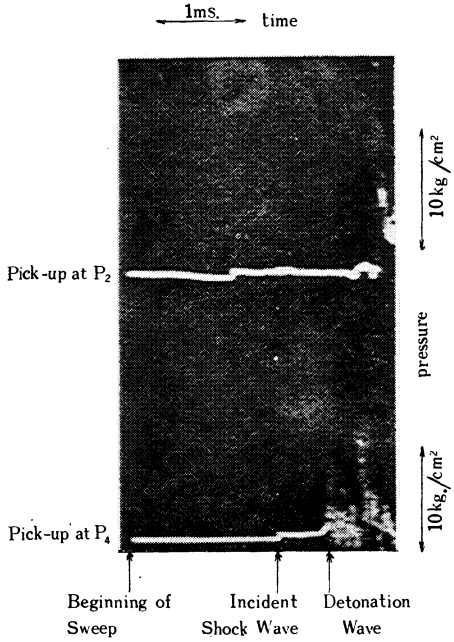

Fig. 8. A picture of oscillogram, when the test chamber is filled with $2H_2+O_2$. $P_0=100$ mmHg, $P_1/P_0=57.0$.

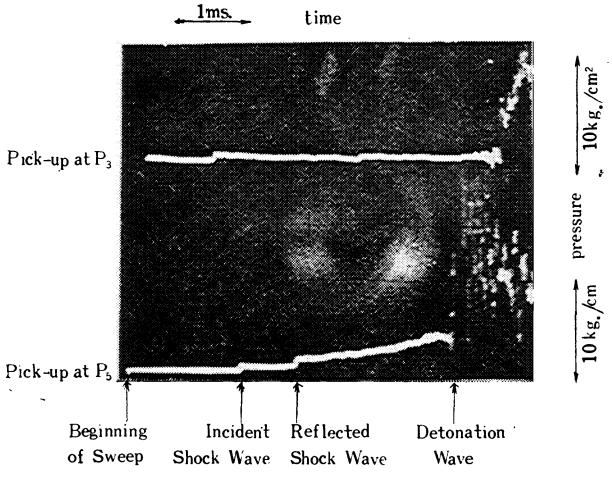

Fig. 9. A picture of oscillogram, when the test chamber is filled with $2H_2+O_2$. $P_0=100$ mmHg, $P_1/P_0=55.8$

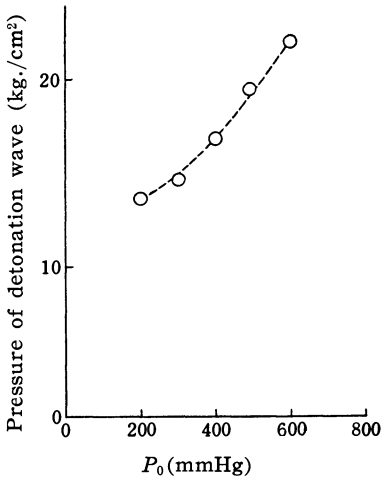

Fig. 10. Variation of the pressure of detonation wave with P_0.

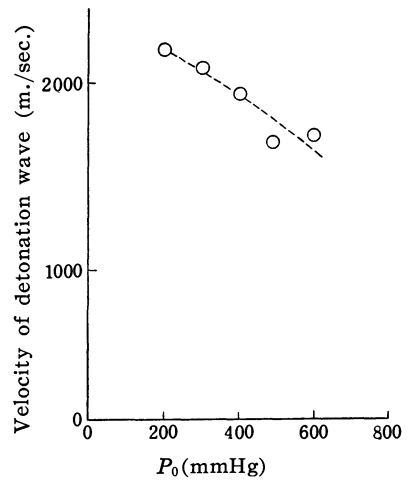

Fig. 11. Variation of the velocity of detonation wave with P_0.

low pressure is perhaps because of the difference of the disturbing effect of fractured membrane fragments in both cases. Although this effect seems to be very little in the latter case, it must be verified by a further investigation.

The variation of the pressure and the velocity of detonation wave with the pressure of the detonable gas mixture, P_0, calculated from the oscillograms, are shown in Figs. 10 and 11. These figures correspond to the cases where P_0 is higher than 200 mmHg. It will be concluded from the results of these experiments that the pressure of the detonation waves increases along with the increase of the pressure P_0, but on the other hand the velocity of waves decreases as the pressure P_0 increases.

Summary

We have carried on a series of experiments on the shock ignition of a gaseous mixture $2H_2+O_2$ by using a shock tube equipped with pick-ups, which can be used for measuring the pressure and the velocity of shock or detonation waves. The results are summarized as follows:

1) When the pressure P_0 of a gaseous mixture is higher than 200 mmHg, the ignition starts between the membrane and the first pick-up along the test chamber and the detonation becomes stable before the detonation wave arrives at the first pick-up.

2) In case P_0 is 100 mmHg, the detonation is initiated by an incident shock wave in some cases and by a reflected one in other cases.

3) When P_0 is higher than 200 mmHg, the pressure of the detonation wave initiated by shock ignition increases along with the increase of P_0 but its velocity decreases with a similar increase.

The authors wish to express their thanks to Dr. Martin Steinberg of the Armour Research Foundation of Illinois Institute of Technology for his helpful advice in constructing our apparatus, and to Mr. Y. Iwai and his staff of Tokyo Shibaura Electric Co. for the construction of our shock tube.

Department of Chemistry
Defense Academy
Yokosuka

The Formation of Stable Semiquinone of Methylene Blue by the Irradiation of Visible Light and γ-Rays.

By Masao KOIZUMI and Hiroshi OBATA

(Received May 15, 1958)

According to a recent paper of A. J. Swallow[1], stable semiquinone radical is formed when a deaerated solution of methylene blue in 22.9 N sulfuric acid containing a small quantity of ethanol is irradiated by γ-rays. He considered that methylene blue, in this case, is reduced while ethanol is oxidized.

In connection with Swallow's results, we have taken up the following three questions.

1) Is it not possible to form semiquinone by the irradiation of Swallow's system with the visible light?

According to Swallow's view, ethanol is to be oxidized into aldehyde by OH radical produced from the radiolysis of water, hence semiquinone should remain unaffected by the existing aldehyde. Now it is well known that when alcoholic solution of methylene blue is irradiated by the visible light in vacuo, the dehydrogenation of alcohol by dye-ion takes place, the dye being transformed into the leuco compound. Therefore it is very natural to expect that the visible-light irradiation of Swallow's system will produce a stable semiquinone.

2) Is benzoic acid which is dissolved in concentrated sulfuric acid as a protonated form, more effective than alcohol for preparing semiquinone radical?

1) A. J. Swallow, *J. Chem. Soc.*, **1957**, 1553.

If ethanol acts as OH scavenger as Swallow seemingly supposed, benzoic acid, which is a strong OH scavenger in neutral or alkaline solution, is expected to be so in the case of strong acidic solution. In addition it would be interesting to examine the concentration effect of ethanol from the above viewpoint.

3) Which reaction will predominate when the solution of methylene blue in 22.9 N sulfuric acid but containing no ethanol is irradiated by γ-rays, the formation of semiquinone or the decomposition of methylene blue by OH radical? Or alternatively, does the reaction proceed in quite a different manner?

In case of a neutral solution of methylene blue, decomposition of dye and the formation of leuco compound take place simultaneously, the former being suppressed by the addition of OH scavenger. It therefore seems worth while to examine the case of strong acidic solution.

In order to examine these problems the following experiments were undertaken using a similar system to that of Swallow.

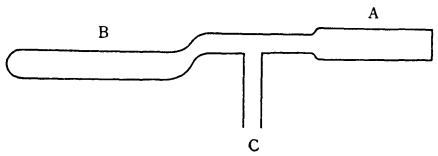

Fig. 1. Reaction cell.
Part A. Thickness 10 mm. plane parallel.
Part B. Diameter ca. 12 mm. (painted with black enamel).

Experimental

The reaction cells used are shown in Fig. 1. The solution is irradiated in Part B, the outside wall of which is painted with black enamel to interrupt the visible light. The absorption spectra of the solution is observed in Part A with the use of Hitachi Spectrophotometer. The solution, when necessary, is evacuated, transferred into B through C, and then the cell is fused off at C.

The irradiation of γ-rays was performed at the Department of Radiology in Tohoku University. Twenty Curie ^{60}Co injecting source was placed 25 cm. away from the samples and all the samples were irradiated for about 15 hours. The dose of γ-rays entering the solution during this period is estimated to be about 21000 Rentgen.

The irradiation of visible light was done by a projection lamp (75 V, 500 W) which was used at 55 V, and placed 4.5 cm. away from the cell.

The procedure for sampling was as follows. The solution of methylene blue 1×10^{-4}M in sulfuric acid (22.9 N) containing 0.001~0.6 M ethanol, for example, was prepared by mixing 0.25 cc. of 2×10^{-3}M aqueous methylene blue solution, 3.18 cc. of pure sulfuric acid and 1.57cc. of an aqueous alcoholic solution of appropriate concentration. The volume contraction during the mixing was disregarded. No special attention was paid to the formation of ester[2].

Below will be given the experimental results and discussions about the afore-mentioned three questions.

Results and Discussion

1) Photochemical Formation of Semiquinone. — The results obtained for the

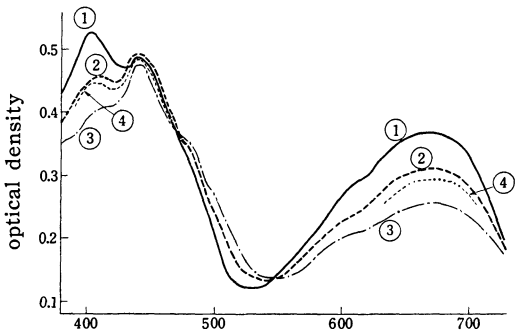

Fig. 2. Change of absorption spectra (visible light irradiation).
Methylene blue ca. 4×10^{-5}M
H_2SO_4 22.9 N
Alcohol 3.38 M
①—— initial
②- - - after 3.5 hr.' irradiation
③—·— after 8 hr.' irradiation
④····· exposed to oxygen after irradiation

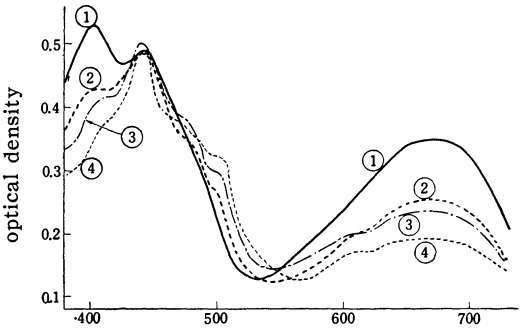

Fig. 3. Change of absorption spectra (visible light irradiation).
Methylene blue ca. 4×10^{-5}M
H_2SO_4 22.9 N
Alcohol 4.96 M
①—— initial
②- - - after 1 hr. irradiation
③—·— after 2.5 hr.' irradiation
④····· after 5.5 hr.' irradiation

2) D. J. Clark and G. Williams, ibid., **1957**, 4218.

following two deaerated solutions are shown in Fig. 2 and Fig. 3.

a) Methylene blue ca. 4×10^{-5}M; sulfuric acid, 22.9 N; ethanol 4.96 M.

b) Methylene blue ca. 4×10^{-5}M; sulfuric acid, 22.9 N; ethanol 3.38 M.

The absorption curves of the illuminated solutions are quite similar to those reported by Swallow and in view of the investigation of Michaelis et al.[3], it can safely be concluded that the stable radical is very easily produced by the photochemical reaction. Perhaps the photochemical method would be a better one for preparing a stable free radical than that employing high energy radiation, since the reaction in the former case would be far more simple than in the latter.

2) Formation of Semiquinone by γ-ray Irradiation.—In Fig. 4 to Fig. 6 are shown the typical results obtained when the deaerated solutions of methylene blue in 22.9 N sulfuric acid containing ethanol of various concentrations or benzoic acid instead of ethanol are irradiated by γ-rays.

As to the effect of the concentration of ethanol, there exists scarcely any difference from 0.1 M up to 0.5 M. Below 0.01 M, the quantity of semiquinone formation seems somewhat smaller, but the reproducibility being not so good, an exact comparison is difficult. Roughly speaking, the effect of concentration is rather small from 0.001 to 0.5 M. The use of benzoic acid in place of ethanol is very effective

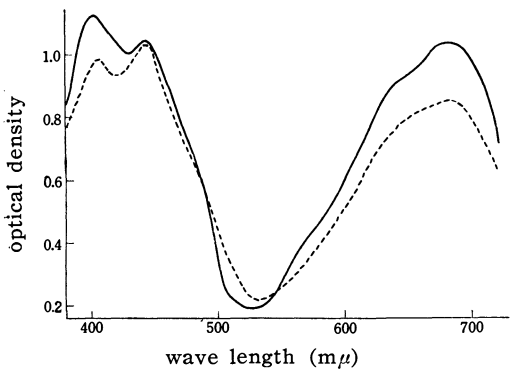

Fig. 4. Change of absorption spectra (γ-rays irradiation, 15 hr.)
Methylene blue 1×10^{-4}M
H_2SO_4 22.9 N
Alcohol 0.01 M
—— initial
····· after irradiation

3) L. Michaelis, M. P. Schubert and S. Granick, *J. Am. Chem. Soc.*, **62**, 204 (1948).

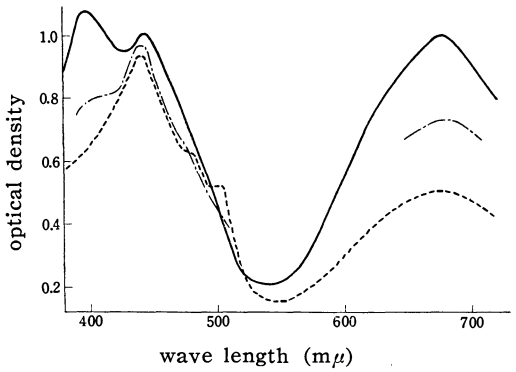

Fig. 5. Change of absorption spectra (γ-rays irradiation, 15 hr.)
Methylene blue 1×10^{-4}M
H_2SO_4 22.9 N
Alcohol 0.5 M
—— initial
····· after irradiation
– – – exposed to oxygen after irradiation

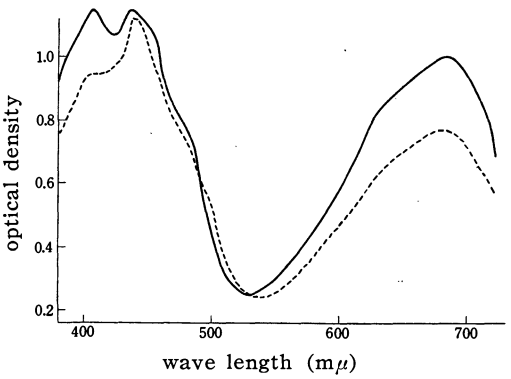

Fig. 6. Change of absorption spectra (γ-rays irradiation 15 hr.)
Methylene blue 1×10^{-4}M
Benzoic Acid 0.005 M
H_2SO_4 22.9 N
—— initial
····· after irradiation

for producing semiquinone and 0.005 M of the acid gives quite a similar result as that of 0.15 M or more of ethanol. Thus it is certain that benzoic acid which in this case must be dissolved as $C_6H_5COOH_2^+$ acts as a good OH-scavenger.

The above results support the view that ethanol acts as a pure OH-scavenger and the necessary condition for the formation of semiquinone is perhaps the existence of OH-scavenger in a certain amount.

3) The Results when no OH-scavenger is added. — When the deaerated solution of methylene blue in 22.9 N sulfuric acid is irradiated by γ-rays, practically no

change is perceived in the original absorption curve. But the solutions of methylene blue in 22.9 N sulfuric acid not deaerated, when irradiated by γ-rays, show a small but definite decrease of absorption throughout the whole visible region as shown in Fig. 7 and Fig. 8, whether it contains 0.1 M ethanol or not. This decrease must undoubtedly be attributed to the destruction of some dye molecules.

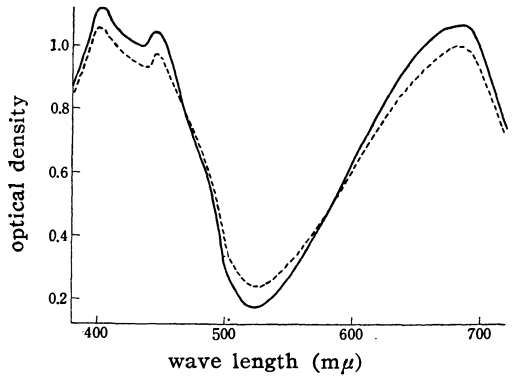

Fig. 7. Change of absorption spectra (γ-rays irradiation, 15 hr., in the presence of oxygen).
Methylene blue 1×10^{-4}M
H_2SO_4 22.9 N
Alcohol 0.1 M
—— initial
····· after irradiation

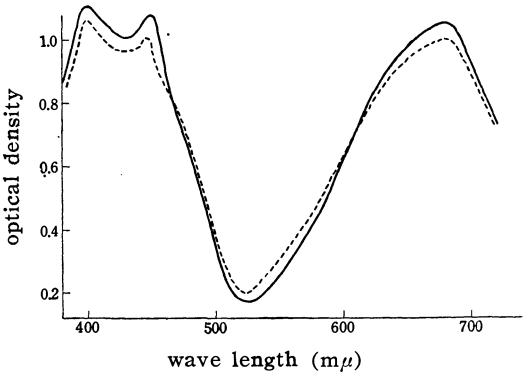

Fig. 8. Change of absorption spectra (γ-rays irradiation, 15 hr., in the presence of oxygen).
Methylene blue 1×10^{-5}M
H_2SO_4 22.9 N
Alcohol not added
—— initial
····· after irradiation

These results are in sharp contrast with those for neutral solutions of methylene blue where the decomposition of dye and the formation of leuco-compound go hand in hand in vacuo. These noteworthy results would be interpreted as follows.

Let us take up the case of the deaerated system at first. If the attack of hydrogen atom and that of OH radical upon dye molecules take place simultaneously, both the formation of semiquinone and the irreversible destruction of dye molecules should occur as is the case in neutral solution. This contradicts the experimental results and the interpretation must be as follows. Hydrogen atom produced by the radiolysis of water first attacks the methylene blue molecule, converting it into semiquinone radical, and following this step, the attack of OH on the latter takes place recovering the original dye molecule. It seems worth while to note that OH attacks the semiquinone radical preferentially and in such a way as to reproduce the original dye, since this behavior is quite different from that of the neutral solution where dye molecules are believed to be attacked at various points by OH radical. In the presence of oxygen, the semiquinone radical intermediately produced would be reoxidized by OH radical (in case of no ethanol) or O_2 molecule (when ethanol exists), and the irreversible destruction would perhaps occur in a common way in the existent oxygen.

The above interpretation that hydrogen first attacks the dye molecule and then the produced semiquinone reacts with OH, seems at first rather curious. But the following consideration will make it very plausible.

The production of H and OH from water is generally believed to occur by the following processes.

$$H_2O \rightsquigarrow H_2O^+ + e \qquad (1)$$

$$\left.\begin{array}{ll} e + H_2O \rightarrow H + OH^- & (a) \\ e + H^+aq. \rightarrow H + aq. & (b) \end{array}\right\} \qquad (2)$$

$$H_2O^+ + aq. \rightarrow OH + H^+aq. \qquad (3)$$

In the case of strong acidic solution, the hydrogen atom should be easily produced via 1 and 2b, but the existence of $H^+aq.$ in large quantity would inhibit the reaction 3. Or it may be said that when the reaction 3 takes place, the reverse reaction would at once recover H_2O^+ again. Thus the oxidative radical that exists is not OH but H_2O^+ and this is expected to be removed by ethanol, but the dye ion which exists as a polyvalent cation would not be attacked by H_2O^+ owing to a strong electrostatic repulsion. This causes the reduction by hydrogen atom to proceed and H_2O^+ only attacks the semiquinone

radical and by depriving its labile hydrogen atom stabilizes as H_3O^+. Such would perhaps be a correct interpretation for the fact that the dye is scarcely affected at all when OH scavenger does not exist.

Thus our results can be comprehended very well along Stein's general view[4] for the radiolysis of the aqueous solution.

Summray

In connection with Swallow's observation that methylene blue in 22.9 N sulfuric acid aqueous solution containing a small amount of alcohol is reduced to a stable semiquinone when irradiated with γ-rays in vacuo, some experiments were done to investigate the role of alcohol.

It was elucidated that alcohol acts most certainly as an OH scavenger. Benzoic acid was found to be an effective OH scavenger in this case just as in usual solutions.

In the absence of alcohol either the formation of semiquinone or the irreversible decomposition of dye scarcely ever takes place in vacuo while in the aerated solution, only the latter reaction slowly proceeds. A plausible interpretation of these results was given.

It was further found that the formation of stable semiquinone can easily occur on irradiation of Swallow's system with the visible light.

The authors express their thanks to Dr. Y. Koga, Professor of the Department of Radiology, Tohoku University, for permitting them to use the ^{60}Co injection source.

The cost of the present research has been partly defrayed by the Scientific Grant from the Ministry of Education.

Department of Chemistry, Faculty of Science, Tohoku University
Katahira-cho, Sendai

4) G. Stein, *Discussions Faraday Soc.*, **12**, 227 (1952).

Polarographic and Coulometric Studies of Tropolone

By Nobuyuki TANAKA, Tetsuo NOZOE, Tsutomu TAKAMURA and Sadako KITAHARA

(Received April 21, 1958)

Polarographic behavior of tropolone and its derivatives has been studied by several authors[1-5]. James and Speakman[2] studied the polarographic behavior of tropolone, but they used a supporting electrolyte which contained borate ions. It has been confirmed that borate ions form complexes with tropolone. Neish and Müller[3] studied the polarographic behavior of β-methyltropolone and the related compounds and discussed the reduction mechanism, but they did not include tropolone itself in their study. Moreover, no coulometric analysis has been made as far as tropolone and the related compounds are concerned. The mechanisms of the electrode processes of tropolone so far proposed were analogized from those of benzaldehyde.

It seems worth-while, this being the case, to reinvestigate the polarographic behavior of tropolone in buffer solutions containing no borate ion and to determine the number of electron involved in the reduction from the coulometric analysis.

Experimental

Materials.—Tropolone was purified by recrystallization from mixed solvent of petroleum ether and benzene and by successive sublimation. A white needle-like crystalline compound of a melting point of 51°C (uncorrected) was obtained. The buffer solutions used in this study are listed in Table I. All electrolytic solutions contained

1) F. Šantavý, *Collection Czechoslov. Chem. Communs.*, **14**, 145 (1949).
2) J. C. James and J. C. Speakman, *Trans. Faraday Soc.*, **48**, 474 (1952).
3) W. J. P. Neish and O. H. Müller, *Rec. trav. chim.*, **72**, 301 (1953).
4) T. Murayama, Presented at the 7th Annual Meetings of Chem. Soc. Japan in Tokyo (1954).
5) F. Šantavý, B. Jámbor, A. Němečkova, J. Mollin and J. Bartek, *Collection Czechoslov. Chem. Communs.*, **22**, 1655 (1957).

TABLE I
BUFFER SOLUTIONS USED

pH	Buffer solutions
2.2～ 8.0	Citric acid—disodium phosphate
8.9～11.4	Sodium carbonate —sodium bicarbonate
11.0～12.0	Sodium hydroxide —disodium phosphate
13.0	0.1 M Potassium hydroxide

0.1 M of potassium nitrate as an indifferent electrolyte and also contained 0.01% of gelatin as a maximum suppressor. Commercial guaranteed reagents were used for the buffer and supporting electrolyte without further purification.

pH measurements.—The pH of the solution was measured before and after the measurements with a Hitachi pH meter Model EHP-1 with a glass electrode.

Polarography.—Current-voltage curves were recorded with a Shimadzu photo-recording polarograph Model SH-UI and with a Yanagimoto pen-recording Galvarecorder Model 2 with an automatically scanning applying potentiometer attached.

The dropping mercury electrode used had an m value of 0.893 mg./sec. and a drop time t of 3.94 sec., being measured in 0.1 M potassium chloride solution at 55 cm. of mercury height at 25°C with open circuit. An H-type cell with a saturated calomel electrode was used. Pure nitrogen gas was bubbled through the solution for about 30 minutes to remove oxygen dissolved in the solution. All measurements were carried out in a thermostat of 25.0±0.1°C.

Coulometry.—For the coulometric measurements[6], the solutions whose constituents were the same as those subjected to the polarographic measurement were employed. The potentials of the working electrode were controlled against a saturated calomel electrode during the electrolysis with a Yanagimoto automatic potentiostat. The electrolytic current was recorded with a Yanagimoto pen-recording Galvarecorder Model 2 connected to the circuit in series. The potentials of the working electrode were adjusted to be −1.15 volts vs. S.C.E. at pH 3.0, −1.35 volts at pH 5.35 and −1.55 volts at pH 8.0.

The electrolysis cell was of a beaker type, the diameter being 4.8 cm. and the height, 5.5 cm., which is shown in Fig. 1b. A mercury pool was used for the working electrode and a spiral platinum wire whose effective area was approximately 1 cm^2 was used for the auxiliary anode. The latter was connected to the electrolytic solution through a Hickling-type salt bridge of potassium nitrate. The dropping mercury electrode was also placed in the electrolysis cell, which made it possible to measure the current-voltage curve at any moment during the controlled potential electrolysis. The electrical circuit of the equipment was designed for the purpose, as shown in Fig. 1a. The electrolytic solution was stirred by bubbling pure nitrogen gas and by means of a magnetic stirrer.

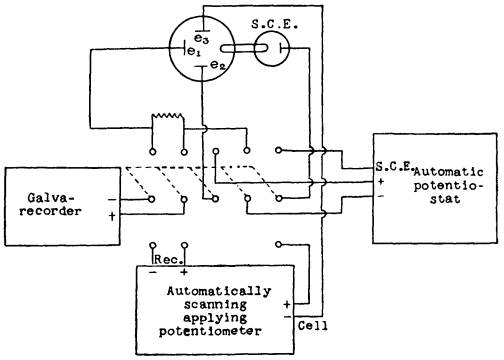

Fig. 1a. Schematical diagram of the circuit for the electrolysis: e_1, working electrode (Hg pool); e_2, auxiliary anode (Pt wire); e_3, dropping mercury electrode.

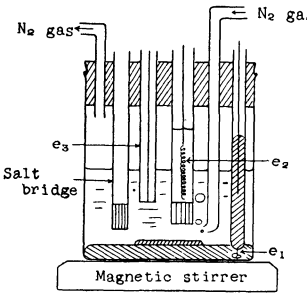

Fig. 1b. Electrolysis cell: e_1, e_2 and e_3, the same as in Fig. 1a.

The concentration of tropolone was varied in the range from 2×10^{-4} M to 1×10^{-3} M. The temperature of the solution was kept at 20°C. The maximum current in the coulometry was 5 milliamperes.

Results

Current-voltage curves.—The current-voltage curves obtained with the solution containing 1×10^{-3} M of tropolone at various pH's are shown in Fig. 2. One wave was observed in the media of pH lower than 4.0, two waves in the pH range from 5 to 7 and one wave in the pH range from 8 to 10. Only an indistinct wave was observed in the pH region higher than 11.

The half-wave potentials of all waves except the second wave at the intermediate pH's were observed to shift to negative potential with the increase of pH. The wave height except that of the second wave decreased with the increase of pH. The half-wave potential and the wave height of the second wave were observed

6) J. J. Lingane, "Electroanalytical Chemistry", Interscience Publishers, Inc., New York (1953), p. 347.

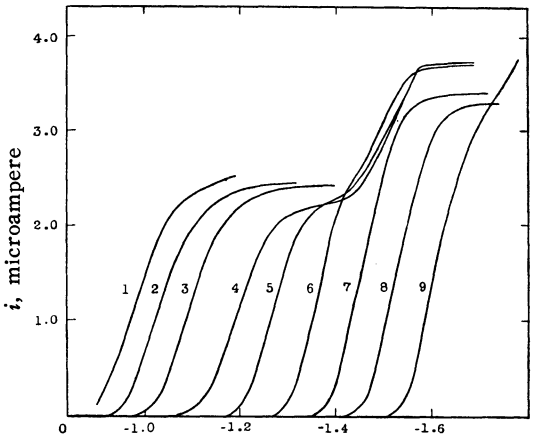

Fig. 2. Current-voltage curves of 1×10^{-3} M tropolone obtained with dropping mercury electrode: 1, pH 2.2; 2, pH 3.0; 3, pH 4.0; 4, pH 5.0; 5, pH 6.0; 6, pH 7.0; 7, pH 8.0; 8, pH 9.0; 9, pH 10.0.

to be almost independent of pH. The variation of half-wave potential $E_{1/2}$ of the first wave with pH was given by

$$E_{1/2}=-0.837-0.07\ \text{pH}$$

volt vs. S.C.E. at 25°C.

As seen in Fig. 3, a linear relation was obtained between the concentration and the wave height of the first wave in the pH region of 3.0 to 6.0.

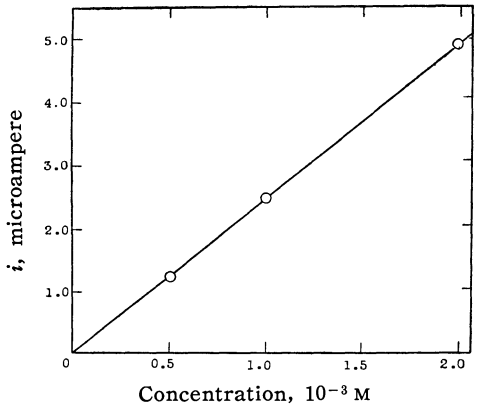

Fig. 3. Relation between the concentration of tropolone and the limiting current obtained at pH 4.0 at 25°C.

Provided that the limiting current is controlled by diffusion, it must be proportional to the square root of the effective height of mercury. The relation was examined with the first and the second waves at three different mercury heights, i. e., 55 cm., 45 cm. and 40 cm. in the pH range of 3.0 to 7.0. The results obtained are listed in Table II, which indicate that the ratio, $i_l/h_{eff.}^{1/2}$, is nearly constant and that the limiting current is of diffusion control.

TABLE II
RELATION BETWEEN THE LIMITING CURRENT AND THE MERCURY HEIGHT

pH	Mercury height*	$i_l/h_{eff.}^{1/2}$ μ amp. cm$^{-1/2}$ 1st wave	2nd wave
	I	0.346	
3.0	II	0.344	
	III	0.347	
	I	0.337	
4.0	II	0.330	
	III	0.332	
	I	0.302	0.213
5.0	II	0.320	0.227
	III	0.341	0.206
	I	0.330	0.209
6.0	II	0.335	0.214
	III	0.341	0.202
	I	0.519	
7.0	II	0.478	
	III	0.456	

* I, $h=55$ cm.; II, $h=45$ cm.; III, $h=40$ cm. The concentration of tropolone was 1×10^{-3} M.

Coulometric measurements. — Before and after the electrolysis, the polarograms were recorded with the sample solution, so that the initial and the final concentration of tropolone could be estimated from the wave heights. However, the polarogram which was recorded when a half quantity of tropolone was reduced showed two new waves appearing at the potentials more positive than that of the reduction wave of tropolone. A typical example of the polarograms is given in Fig. 4. The first wave is anodic and the second is cathodic, the latter appearing at somewhat more positive potentials than the reduction wave of tropolone. The third wave is consipered to be the wave of tropolone because the potentials are identical with those of tropolone.

The height of the first wave was observed to decrease with the lapse of time; it decreased to nearly a half of the original height after some twenty minutes. The height of the second wave, on the other hand, increased with the lapse of time. This was observed with all solutions whose pH's were between 3 and 8. The half-wave potentials of those new waves were found to depend on pH of the

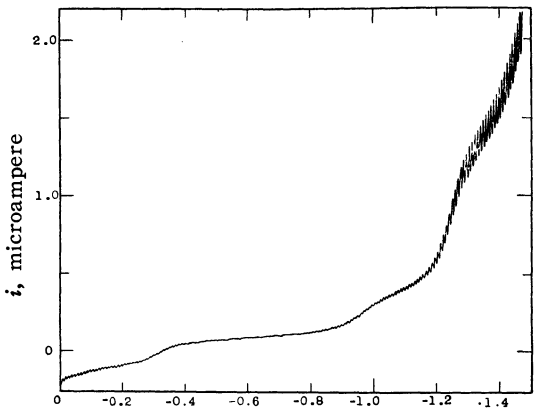

Fig. 4. Current-voltage curve recorded at pH 5.35, at 20°C, with the solution in which a half of tropolone was reduced by controlled potential electrolysis. The initial concentration of tropolone was 3.53×10^{-4} M.

solution and both waves shifted to more negative potentials by 40 to 80 mV. with the increase of one unit of pH.

The quantity of electricity required in the controlled potential electrolysis was determined by integrating graphically the recorded current-time curve. The quantity due to the residual current which was measured separately with the same procedure was subtracted. The values thus obtained naturally included the electricity that was consumed in the reduction of the substance which had been produced as a result of the electro-reduction of tropolone followed by the chemical conversion, because the substance is easily reduced at the potential where tropolone is reduced. Moreover, the concentration of tropolone after a certain period of the electrolysis could not be determined accurately from the polarogram, because of the occurrence of the ill-defined reduction wave whose potentials are close to those of the reduction wave of tropolone. On account of those two unavoidable causes of error, the electricity required for the reduction of the unit concentration of tropolone could not be determined accurately in the usual way.

From the careful observation of the current-voltage curves obtained after the controlled potential electrolysis, it was found that the rate of formation of the new reducible substance was not extremely great. This indicates that a shorter period of electrolysis is more favorable for determining the quantity of electricity required for the reduction of tropolone itself. In an extreme case, at a zero time, only tropolone must be reduced. In the present investigation, therefore, the following procedure was employed. The controlled potential electrolyses were carried out in varied electrolysis periods with the solutions in which the initial concentration of tropolone and the pH were the same. The quantity of electricity was obtained from each current-time curve recorded. With the same solution as was subjected to the electrolysis the limiting current was measured, before and immediately after the electrolysis, with the dropping mercury electrode at potential where tropolone gives the diffusion current. The apparent amount of tropolone which was reduced in the given period was calculated from the difference of the limiting current by assuming the limiting current obtained immediately after the electrolysis to be caused by tropolone only. The apparent number of electrons required in the reduction was calculated by dividing the quantity of electricity with the product of the Faraday constant and the apparent molar amount of tropolone reduced in the period. The apparent numbers of electrons thus obtained for various electrolysis periods were found to have the tendency to decrease with the decrease of the electrolysis period. Thus, the true value of n could be obtained by plotting the apparent value of n against the electrolysis period and by extrapolating the curve to a zero time. An example of such a plotting is given in Fig. 5. The values

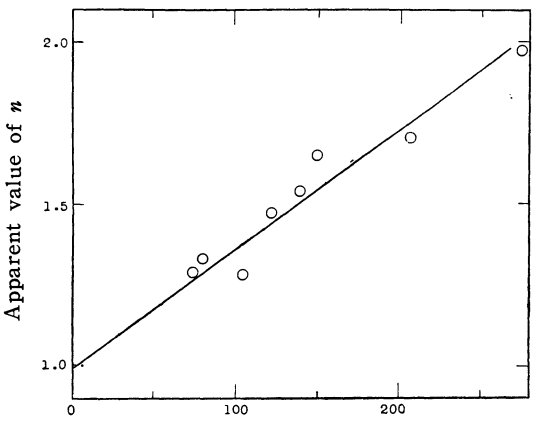

Fig. 5. Plot of apparent number of electrons involved in the reduction of tropolone against electrolysis period, measured at pH 5.35 at 20°C. The initial concentration of tropolone was 3.53×10^{-4} M.

of n obtained are given in the third column of Table III. Using the revised Ilkovič equation[7], the diffusion coefficients of tropolone were calculated from the limiting currents obtained at various pH's, which are given in the fourth column of Table III.

TABLE III
NUMBER OF ELECTRONS REQUIRED IN THE REDUCTION OF TROPOLONE AND DIFFUSION COEFFICIENT AT 25°C

pH	Wave used in the calculation	n	D, cm²/sec.
3.0	1st wave	1.0	9.0×10^{-6}
5.0	〃	1.0	7.6×10^{-6}
8.0		2.0	5.0×10^{-6}

Discussion

The diffusion coefficient of organic compounds can be evaluated with the aid of Oeholm's law[8],

$$M^{1/2}D \doteqdot 7 \quad \text{(at 20°C)}$$

where M is molecular weight and D, the diffusion coefficient expressed in cm²/day. The value calculated for tropolone is 0.63 cm²/day, i. e., 7.4×10^{-6} cm²/sec. The diffusion coefficient of benzoic acid which is the isomer of tropolone was observed to be 9.2×10^{-6} cm²/sec. at 25°C[9] and is calculated to be 8.7×10^{-6} cm²/sec. at 25°C from the conductance data[10,11]. Comparing with those referred values, the diffusion coefficients of tropolone obtained in this study (Table III) seem to be reasonable.

Tropolone molecules dissociate to form anions in an alkaline medium, the dissociation constant being 1.2×10^{-7} at 25°C[12]. Since the degree of interaction between the anion and the solvent molecules would be greater than that between undissociated tropolone and solvent molecules, the diffusion coefficient of the former is expected to be smaller than that of the latter, and, therefore, a smaller coefficient is expected in an alkaline medium. The experimental results given in Table III coincide with the above expectation.

As already indicated, one anodic wave and two cathodic waves were observed on the polarogram which was recorded with the solution subjected to the controlled potential electrolysis. The first wave which was anodic decreased with the lapse of time and the second which was cathodic increased. This showed that an oxidizable substance which is produced upon the electro-reduction of tropolone to give the anodic wave is unstable and converted gradually into a reducible substance which gives a cathodic wave at potentials more positive than tropolone.

The mechanism of the electro-reduction of tropolones has been inferred from that of benzaldehyde[2,3]. Neish and Müller[3] gave the following to the first wave in the acid region:

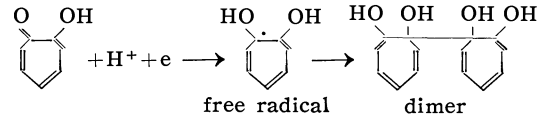

The double wave in the intermediate pH region was assumed to appear according to the mechanism[3],

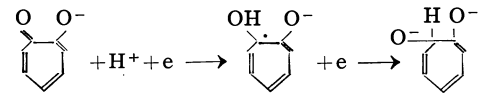

Recently Šantavý et al.[5] proposed the following processes for the reduction of tropolone and its ethers:

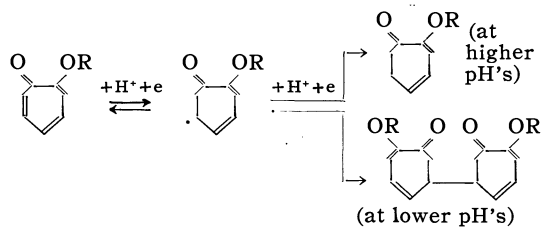

One-electron reduction followed by the dimerization was assumed at lower pH's, while two-electron reduction was assumed at higher pH's. In both cases the reduction of tropone nucleus was assumed.

In this study, the number of electrons involved in the electro-reduction of tropolone was determined from the coulometric measurement at constant potential. One-electron reduction at lower pH's and two-electron reduction at higher pH's were confirmed. This supports partly the reduction mechanism of tropolone previously proposed. However, the observation of current-voltage curves which were obtained with the solution preliminarily subjected to the controlled potential electrolysis strongly suggests that the chemical

7) M. von Stackelberg, *Z. Elektrochem.*, **57**, 338 (1953); etc.
8) L. W. Oeholm, *Z. physik. Chem.*, **70**, 378 (1910).
9) H. Freundlich and D. Krüger. *Biochem. Z.*, **205**, 186 (1929).
10) F. G. Brockman and M. Kilpatrick, *J. Am. Chem. Soc.*, **56**, 1483 (1934).
11) B. Saxton and H. F. Meiner, ibid., **56**, 1918 (1934).
12) N. Yui, *Sci. Repts. Tohoku Univ. First Ser.*, **40**, 102 (1956).

processes following on the electro-reduction are not so simple as has been proposed. The half-life period of the substance which formed upon the controlled potential electrolysis and gave the anodic wave would not indicate this substance to be the free radical described above, but a secondary substance produced therefrom. It is also unlikely that the dimer which Šantavý et al. assumed in their mechanism corresponds to the substance which gives the anodic wave, because the dimer seems not to be easily oxidizable. However, the difficulty in preparation of the substance because of chemical conversion, at present, seems to make it impossible to identify the substance. It would be desirable to carry out more elaborate studies for the precise explanation of the reduction mechnism.

Summary

The current-voltage curves of tropolone were recorded at the dropping mercury electrode in buffer solutions of various pH's containing no borate. One reduction wave was observed in the pH region of 2.2 to 4.0, two waves with nearly equal heights, in the pH region of 5 to 6 and one wave, in the solution of pH higher than 8. All waves except the second in the intermediate pH region were found to shift to negative potentials with the increase of pH of the solution by approximately 70 mV./pH. The number of electrons involved in the reduction was determined by the controlled potential coulometric method. One-electron reduction was confirmed for the first wave at lower pH's, two-electron reduction for the two-step waves at the intermediate pH region and two-electron reduction for the wave at higher pH's. The current-voltage curves which were recorded with the solution preliminarily subjected to the controlled potential electrolysis gave two new waves; one is anodic and the other, cathodic. The former decreased with time and the latter increased. This indicates that the reduction product of tropolone is unstable and changed gradually to the substance which gives the reduction wave. The diffusion coefficients of tropolone were calculated from the limiting current using the revised Ilkovič equation.

The authors thank the Ministry of Education for the financial support granted for this research.

Department of Chemistry
Faculty of Science
Tohoku University
Katahira-cho, Sendai

Dipole Moments and Nuclear Quadrupole Coupling Constants of Alkyl Halides

By Hidekazu HAMANO

(Received September 25, 1957)

The relation between nuclear quadrupole coupling constants of molecules and the nature of chemical bonds has been discussed by Townes and Dailey[1]. Miyagawa[2] pointed out a parallelism between the nuclear quadrupole coupling constant and the apparent C—Cl bond moment of various chlorides.

It has been known that the dipole moment of alkyl halide increases with the increasing number of carbon atoms. The data are listed in Table I. This fact has hitherto been interpreted by an inductive effect[3], which, however, has not always given a satisfactory interpretation to it. At the same time, the values of nuclear quadrupole coupling constants of these molecules in the solid state decrease zigzag with the increasing number of carbon

1) C. H. Townes and B. P. Dailey, *J. Chem. Phys.*, **17**, 782 (1949).

2) I. Miyagawa, *J. Chem. Soc. Japan, Pure Chem. Sec.* (*Nippon Kagaku Zassi*), **75**, 1061 (1954).

3) K. Higashi, *J. Chem. Soc. Japan* (*Nippon Kagaku Kaisi*). **57**, 1006 (1936); L. G. Groves and S. Sugden, *J. Chem. Soc.*, **1937**, 158.

TABLE I

DIPOLE MOMENTS* OF ALKYL HALIDE (DEBYE UNITS)

CH_3Cl	1.869[a]	CH_3Br	1.797[a]	CH_3I	1.647[a]
C_2H_5Cl	1.98[b]	C_2H_5Br	1.99[c]	C_2H_5I	1.93[c]
	2.00[c]		2.01[d]		1.87[d]
n-C_3H_7Cl	2.04[c]	*n*-C_3H_7Br	2.01[c]	*n*-C_3H_7I	1.97[c]
			2.15[d]		2.01[d]
n-C_4H_9Cl	2.11[d]	*n*-C_4H_9Br	2.15[d]	*n*-C_4H_9I	2.08[d]
	2.04[f]				
tert-C_4H_9Cl	2.13[g]				

* The observed values in the gaseous state.

a) W. Gordy, W. V. Smith and R. F. Trambarulo, "Microwave Spectroscopy", John Wiley and Sons, Inc., New York, N. Y., (1953), p. 361.

b) J. C. Jelatis, *Tech. Rep.*, **7**, O. N. R. Contract N5 ori—78 T. O. I. Lab. Ins. Res., Mass. Inst. Tech. (1947).

c) P. C. Mahanti, *Phil. Mag.*, (7) **20**, 274 (1935).

d) L. G. Groves and S. Sugden, *J. Chem. Soc.*, **1937**, 158.

e) R. Sanger, O. Steiger and K. Gachter, *Helv. Phys. Acta*, **5**, 200 (1932).

f) C. P. Smyth and K. B. McAlpine, *J. Chem. Phys.*, **3**, 347 (1935).

g) R. H. Wiswall and C. P. Smyth, ibid., **9**, 356 (1941).

TABLE II

NUCLEAR QUADRUPOLE COUPLING CONSTANTS OF ALKYL HALIDE (Mc)

Alkyl chloride (^{35}Cl)[a]		Alkyl bromide (^{79}Br)[b]		Alkyl iodide (^{127}I)[b]	
CH_3Cl	68.40	CH_3Br	528.9	CH_3I	1753
C_2H_5Cl	66.0	C_2H_5Br	497.0	C_2H_5I	1647
n-C_3H_7Cl	66.4	*n*-C_3H_7Br	503.0	*n*-C_3H_7I	1672
n-C_4H_9Cl	—	*n*-C_4H_9Br	499.9	*n*-C_4H_9I	1660
tert-C_4H_9Cl	62.3				

a) See foot-note a) appendix under Table I.

b) S. Kojima, K. Tsukada, S. Ogawa and A. Shimauchi, *J. Chem. Phys.*, **21**, 1415(1953).

atoms as shown in Table II. To throw light on these facts, the correlation among the electronic properties of the carbon-halogen bonds in alkyl halide molecules and the nuclear quadrupole coupling constants and the dipole moments of the molcules has been studied. A valence bond theory is developed to get the dependences of dipole moments and of nuclear quadrupole coupling constants on the ionicity of the carbon-halogen bond. The method used here is similar to that developed by Baughan, Evans and Polanyi[4].

Calculation and Results

The bonding wave function for a C—X (X=halogen) bond of an alkyl halide molecule can be constructed as follows:

$$\psi_{bCX} = (2+2S^2_{CX}+4\lambda S_{CX}+\lambda^2)^{-1/2} [\psi_X(1)\psi_C(2)+\psi_X(2)\psi_C(1)+\lambda\psi_X(1)\psi_X(2)] \quad (1)$$

where

$$\psi_X = a\psi_{ns}+b\psi_{np}$$
$$\psi_C = 1/2\psi_{2s}+\sqrt{3}/2\,\psi_{2p} \quad (2)$$

$n=3$, 4 and 5 for Cl, Br and I, respectively, and S_{CX} is the overlap integral defined by

$$S_{CX} = \int \psi_X(1)\psi_C(1)d\tau_{(1)}$$

The non-bonding hybrid orbital of the halogen atom is given by

$$\psi_{nb} = c\psi_{ns}+d\psi_{np}$$

From the orthogonality and normalization conditions for ψ_X and ψ_{nb}, we have

$$\left.\begin{aligned} a^2+b^2 &= 1 \\ c^2+d^2 &= 1 \\ ac+bd &= 0 \end{aligned}\right\} \quad (3)$$

The C—H bonds in methyl halide molecules are assumed to be pure covalent bonds, so that the wave functions for the bonds can be described as

$$\psi_{bCH} = (2+2S^2_{CH})^{-1/2} \times [\psi_C(1)\psi_H(2)+\psi_C(2)\psi_H(1)] \quad (4)$$

4) E. C. Baughan, M. G. Evans and M. Polanyi, *Trans. Faraday Soc.*, **37**, 377 (1941).

where

$$S_{CH} = \int \psi_C(1)\psi_H(1)d\tau_{(1)}$$

ψ_H is the 1s orbital of hydrogen atom, and ψ_C is assumed to be the tetrahedral hybrid orbital given by Eq. 2.

On the assumption of the orthogonality relationship between ψ_{bCX} and ψ_{bCH} the dipole moment of methyl halide is given by

$$\vec{\mu} = 3\vec{\mu}_{CH} + \vec{\mu}_{bCX} + \vec{\mu}_{nb}$$

where

$$\vec{\mu}_{CH} = e(2\overline{Z}_{CH} - R_{CH})$$
$$\vec{\mu}_{bCX} = e(2\overline{Z}_{CX} - R_{CX})$$
$$\vec{\mu}_{nb} = 2e\overline{Z}_{nb}$$

e is the electronic charge; R_{CH} and R_{CX} are the C—H and the C—X bond distances, respectively; the z-axis is taken along each bond direction with the carbon atom at the origin; $\overline{Z}_{CH}$, $\overline{Z}_{CX}$ and $\overline{Z}_{nb}$ are the average values of the z coordinates of the bonding electrons for the C—H and C—X bonds, and the non-bonding electrons of the halogen atom, respectively. The explicit expressions for $\overline{Z}_{CH}$, $\overline{Z}_{CX}$ and $\overline{Z}_{nb}$ are well known, so that they are not described here.

A nuclear quadrupole coupling constant is usually expressed by eQq, where e is the electronic charge, Q is the nuclear quadrupole moment and q is the electric field gradient at the nucleus of the coupled atom with reference to the charge symmetric axis z, that is

$$q = e\sum_i \int \psi_i^*[(3\cos^2\theta_i - 1)/r_i^3]\psi_i d\tau_i \ .$$

where the subscript i refers to the i-th electron, ψ_i is the wave function of the i-th one, r_i is the distance from the nucleus of the coupled atom, and θ_i is the angle between the r direction and the z axis. In the present work, only the valence electrons of the halogen atom are taken into account; the contributions from the others in the molecule are ignored, because the electrons on other atoms are too far away and the inner-shell clouds of the halogen atom have the symmetry to make the contribution to q insignificant. In this approximation, we obtain

$$q = 2q_{bCX} + 2q_{npx} + 2q_{npy} + 2q_{nb} \qquad (5)$$

where

$$q_\psi = e\int \psi^*[(3\cos^2\theta - 1)/r^3]\psi d\tau$$

Now since q equals to naught for a completely filled p-shell, it can be easily be seen that

$$q_{npx} = q_{npy} = -\frac{1}{2}q_{npz} \qquad (6)$$

In consideration of Eqs. 3, 5 and 6, q is expressed as

$$q = [-b^2(1+2S^2_{CX}+2\lambda S_{CX})q_{npz} + 2(S_{CX}+\lambda) \times q_{CX} - q_C]/(1+S^2_{CX}+2\lambda S_{CX}+\lambda^2/2)$$

where

$$q_{CX} = e\int \psi_C[(3\cos^2\theta - 1)/r^3]\psi_X d\tau$$

In this case, q_C is very small compared with other terms, so the halogen quadrupole coupling constant may be written as

$$eQq = [-b^2(1+2S^2_{CX}+2\lambda S_{CX})eQq_{npz} + 2(S_{CX}+\lambda)eQq_{CX}]/(1+S^2_{CX} + 2\lambda S_{CX}+\lambda^2/2)$$

The atomic orbitals used in the calculation are the following hydrogen-like ones in which the screening constants were determined by Pauling and Sherman[5]: Cl(Z_{3s}=8.3, Z_{3p}=6.5), Br(Z_{4s}=11.3, Z_{4p}=8.8), I(Z_{5s}=14.5, Z_{5p}=11.7), C(Z_{2s}=3.96, Z_{2p}=3.09), H(Z_{1s}=1.00). The bond distances are taken to be R_{CH}=1.10 Å, R_{CCl}=1.78 Å, R_{CBr}=1.94Å, and R_{CI}=2.14 Å throughout the series of these alkyl halides.

The q_{npz} values calculated by use of these atomic orbitals, are shown in Table III. The results are in poor agreement

TABLE III

	q_{np_z} values	
	$q_{calc.}$ (10^{15}e.s.u.)	$q_{obs.}$* (10^{15}e.s.u.)
$q^{Cl}_{3p_z}$	6.06	9.59
$q^{Br}_{4p_z}$	6.34	15.9
$q^{I}_{5p_z}$	7.63	~45

* These values were obtained by using the experimental quadrupole coupling constants[6] of atomic halogen and the quadrupole moments[a] of the halogen nucleus.

a) See foot-note a) appendix under Table I.

with the accurate values. This means that such a theoretical procedure does not give satisfactory results because of the inaccuracy of the wave functions, especially in the part closer to the nucleus. In this work, therefore, the values of eQq_{npz} are taken from the experimental quadrupole coupling constants of atomic halogen;

5) L. Pauling and J. Sherman, *Z. Krist.*, **81**, 1 (1932).

$eQq^{Cl}_{3p_z}=109.74$Mc,[6] $eQq^{Br}_{4p_z}=-769.62$Mc[6] and $eQq^{I}_{5p_z}=2292.44$Mc,[6] respectively.

The exchange term eQq_{CX} is evaluated by means of Löwdin's approximation[7] in which eQq_C is disregarded. In this procedure, μ and eQq are represented as the functions of λ and b^2, so that these values are determined by the experimental values of μ and eQq for methyl halide. For this purpose, the experimental values* for these gaseous molecules ($eQq_{CH_3Cl}=-75.3$Mc[3], $eQq_{CH_3Br}=577.3$Mc[3] and $eQq_{CH_3I}=-1934$Mc[3]) are used. The values of λ and b^2 so obtained are given in Table IV.

TABLE IV

	CH_3Cl	CH_3Br	CH_3I
λ	1.0209	0.9134	0.6056
b^2	0.9749	0.9661	0.9456
$\mu_{bCX}(C^+X^-)$ (a.u.)	1.0321	0.7544	0.3107
μ_{nb}(a.u.)	0.6035	0.8516	1.2359

The determination of λ for the R—X bonds in alkyl halides (R=ethyl, *n*-propyl, *n*-butyl, *tert*-butyl) other than methyl halide is made by using the following process.

We obtain the following relation for the R—X bond from Eq. 1

$$\lambda^2/(2+2S^2_{CX}) = R_{ic}/(H_{ii}-E) \qquad (7)$$

where R_{ic} is the ionic-convalent resonance energy for the R—X bond, H_{ii} is the energy of the pure ionic structure R^+X^-, and E is the dissociation energy of the R—X bond.

Based on the assumption that the value of the factor b^2 is the same as that in methyl halide in the series of R-X bonds, the same value of overlap integral S_{CX} can be used for all R—X bonds. Thus, from Eq. 7, the value of λ can be determined if the values for R_{ic}, H_{ii} and E are known. The method is similar to that of Baughan, Evans and Polanyi[4]. They made an interesting application of the theory of ionic-covalent resonance to their correlation of changes in dipole moment and to bond energy along the series of alkyl derivatives R—X, in which R is methyl, ethyl, *n*-propyl or *tert*-butyl. They drew attention to the following trends along these series.

(1) The R—H bond energy decreases markedly.

(2) The R—X (X≠H) bond energy decreases less rapidly than the R—H bond energy.

(3) The dipole moment of the C—I bond increases parallel to the decrease in the R—I bond energy.

The data for the bond energy E(R—X) are shown in Table V. The interpretation has been given that the decrease in E(R—H) was attributed solely to the increasing resonance energy in alkyl radicals R_r, because the C—H bond was considered to be approximately a pure covalent bond. Hence

$$E(R—H) = E(CH_3—H) - R_r \qquad (8)$$

TABLE V

E(R-X) values*

R	E(C-H)[a]	E(C-Cl)[b]	E(C-Br)[a]	E(C-I)[b]
methyl	102.5	80.5	68.5	54.0
ethyl	97.5	79.4	67.0	52.0
n-propyl	95.0	77.4	64.5	50.0
n-butyl	94.0	—	63.5	49.0
tert-butyl	86.0	74.7	—	—

* All the E values are given in kcal. mole^{-1}.

a) E. T. Butler and M. Polanyi, *Trans. Faraday Soc.*, **39**, 19 (1943).

b) J. S. Roberts and H. A. Skinner, ibid., **45**, 339 (1959).

In the case of R—X bonds (X≠H), the ionic-covalent resonance energy in the R—X molecule increases along the series, due to the increased stability of the R^+X^- ion pair. Accordingly, there is the radical resonance energy R_r, which, as with R—H bonds, tends to decrease the bond energy, and there is an increase in ionic-covalent resonance energy R_{ic}, in the molecules, tending to increase the bonding energy. That is

$$E(R—X) = E(CH_3—X) - R_r + \Delta R_{ic} \qquad (9)$$

where

$$\Delta R_{ic} = R_{ic}(R—X) - R_{ic}(CH_3—X) \qquad (10)$$

The E(R—X) values in Table V are used in the present calculation and the R_r values are obtained by Eq. 8. By use of Eqs. 9 and 10, the R_{ic}(R—X) values can be evaluated, when we know the $R_{ic}(CH_3—X)$ values. These values are obtained from Eq. 7, using the λ, S_{CX} and $H_{ii}(CH_3—X)$ values. The $H_{ii}(CH_3—X)$ values are evaluated by using the Born-Meyer formula[8]

$$H_{ii} = e^2[-1/R_{CX} + \rho/R_i^2 \times \exp\{(R_i - R_{CX})/\rho\}] + I_C - E_X$$

6) H. Robinson, H. G. Dehmelt and W. Gordy, *J. Chem. Phys.*, **22**, 511 (1954).

7) P. O. Löwdin, ibid., **21**, 374 (1953).

* The dipole moment values used here are taken from those in Table I.

8) M. Born and J. E. Meyer, *Z. Physik.*, **75**, 1 (1932); E. Warhurst, *Trans. Faraday Soc.*, **45**, 461 (1949).

TABLE VI

Molecules	λ	μ_{bCCl} (a.u.)	$\Delta\mu_{bCCl}$ (D)	$\Delta\mu_{obs.}$* (D)	$\lvert eQq\rvert$ (Mc)	$\Delta eQq_{calc.}$ (Mc)	$\Delta eQq_{obs.}$ (Mc)
CH_3Cl	1.021	1.032	0	0	75.3	0	0
C_2H_5Cl	1.076	1.067	0.09	0.11 0.13	73.7	1.6	2.4
n-C_3H_7Cl	1.098	1.081	0.12	0.17	73.0	2.3	2.0
t-C_4H_9Cl	1.205	1.146	0.29	0.26	70.1	5.2	6.1
Molecules	λ	μ_{bCBr} (a.u.)	$\Delta\mu_{bCBr}$ (D)	$\Delta\mu_{obs.}$* (D)	$\lvert eQq\rvert$ (Mc)	$\Delta eQq_{calc.}$ (Mc)	$\Delta eQq_{obs.}$ (Mc)
CH_3Br	0.913	0.754	0	0	577.3	0	0
C_2H_5Br	0.971	0.797	0.11	0.19 0.21	564.7	12.6	31.9
n-C_3H_7Br	0.990	0.811	0.14	0.19 0.33	560.5	16.8	25.9
n-C_4H_9Br	0.998	0.817	0.16	0.33	558.8	18.5	29.0
Molecules	λ	μ_{bCI} (a.u.)	$\Delta\mu_{bCI}$ (D)	$\Delta\mu_{obs.}$* (D)	$\lvert eQq\rvert$ (Mc)	$\Delta eQq_{calc.}$ (Mc)	$\Delta eQq_{obs.}$ (Mc)
CH_3I	0.606	0.311	0	0	1934	0	0
C_2H_5I	0.666	0.365	0.14	0.22 0.28	1889	45	106
n-C_3H_7I	0.686	0.382	0.18	0.36 0.32	1875	59	81
n-C_4H_9I	0.692	0.387	0.19	0.43	1870	64	93

* These values are obtained from the data in Tables I and II.

where e is the electronic charge, ρ is given the value $\rho=0.345$ Å,[8] R_i is the equilibrium distance of R^+X^- ion pair, I_C is the ionization potential of carbon atom and E_X is the electron affinity of the halogen atom. The values of the quantities employed here are R_i(C—Cl)=2.17 Å[9], R_i(C—Br)=2.30 Å[9], R_i(C—I)=2.48 Å[9], I_C=11.42 eV[10], E_{Cl}=3.82 eV[10], E_{Br}=3.69 eV[10] and E_I=3.55 eV[10].

The H_{ii} values for R^+X^- ion pair are evaluated from $H_{ii}(CH_3—X)$ according to the following assumption by Baughan, Evans and Polanyi.

$$H_{ii}(R—X) \approx H_{ii}(CH_3—X) - R_r$$

Thus, using Eq. 7, we can calculate the λ values for the R—X bonds. The values of λ obtained and those of μ_{bCX} and eQq consequently obtained are shown in Table VI.

The variations of dipole moments and quadrupole coupling constants along the series of these molecules are interesting for us, so the quantities $\Delta\mu$, $\Delta\mu_{bCX}$ and ΔeQq defined as follows are introduced for comparisons between the observed values and the calculated ones.

$$\Delta\mu = \mu(R—X) - \mu(CH_3—X)$$

$$\Delta\mu_{bCX} = \mu_{bCX}(R—X) - \mu_{bCX}(CH_3—X)$$

$$\Delta eQq = eQq(R—X) - eQq(CH_3—X)$$

These values are listed in Table VI.

Discussion and Conclusion

In this calculation, the exchange terms eQq_{CX} are evaluated by Löwdin's approximation. Both Mulliken's approximation[11] and the neglect of the exchange terms have not always been sufficient for determining of b^2 and λ for all methyl halides. Usually these terms[1] have been evaluated as about a few percent or less of eQq_{np_z}. The values of these terms calculated here, however, are 19 percent of eQq_{3p_z} for the C—Cl bond, 14 percent of eQq_{4p_z} for the C—Br bond and 9 percent of eQq_{5p_z} for the C—I bond, respectively.

The b^2 values obtained here are greater than the values[1] estimated hitherto for Cl,

9) E. C. Baughan and M. Polanyi, ibid., **37**, 648 (1941).
10) H. O. Pritchard and H. A. Skinner, *Chem. Revs.*, **55**, 745 (1955).
11) R. S. Mulliken, *J. chim. phys.*, **46**, 500, 521 (1949).

less than those[1] for bromine and iodine though their accurate values have not yet been known. These greater values indicate the small amount of *s* character in the halogen bonding orbitals. It should be noted, however, that the so-called atomic dipole is considerably great, as seen in Table IV.

The magnitude of μ of alkyl halide depends to a great extent on those of μ_{bCX} and μ_{nb}, though it is not determined by them alone. It is seen from the results in Table VI that the variations of the C—X bond moments $\Delta\mu_{bCX}$ give a considerable contribution to those of molecule $\Delta\mu$. Furthermore, these results can be improved by taking account of the increasing *s* character in the halogen bonding orbitals along the series of these molecules, which means the elimination of the assumption that b^2 is constant along the series of these molecules, because it results in the increasing values of $\Delta(\mu_{bCX}+\mu_{nb})$* and of ΔeQq. They show that the variations of dipole moments along the series of these molecules should be interpreted by those of μ_{bCX} or $(\mu_{bCX}+\mu_{nb})$ instead of by an inductive effect.

The variations of dipole moments $\Delta\mu$ of the corresponding alkyl halides listed in Table VI increase in the sequence R—Cl, R—Br and R—I. This fact is not interpreted by an inductive effect. The present results suggest a qualitative explanation for this.

From these results, we can expect the values of eQq to decrease smoothly with the increasing carbon number. On the other hand, these values in the solid state fall zigzag as described above. This correlation is similar to the relations between the boiling points and the melting points of these molecules. It may be, therefore, reasonable that the zigzag of the eQq values in the solid state comes from the same reason as the one on which the irregularity between the melting points and the number of carbon is based.

In view of the present calculations, it seems highly probable that the eQq values of these molecules in the gaseous state will decrease smoothly with the increasing carbon number, though those in the solid state decrease zigzag with the increasing carbon number and that the ionic character of the C—X bonds in alkyl halide molecules increase with the increasing carbon number.

The author wishes to thank Professor K. Kozima for his kind criticism and Dr. J. Higuchi for his helpful advice and discussion.

Chemical Laboratory
Tokyo Gakugei University
Setagaya-ku, Tokyo

* The quantity is given the same definition as $\Delta\mu_{bCX}$ and so on.

Dielectric Contribution to Miscibility in the Ternary System 1-Propanol-Water-Toluene

By K. M. SOMASUNDARAM and C. V. SURYANARAYANA

(Received May 13, 1958)

When a third component miscible with each of the two liquids is added, to two layers of either immiscible or partially miscible liquids, the added component distributes between the two layers. Progressive additions of the third component results in a corresponding variation of the physico-chemical properties in the two layers till at the miscibility point they tend to reach a limit at which the interphase just disappears, forming a homogeneous system. Just at the point of disappearance of the interphase we may expect a quantitative relationship between the value of dielectric constant of the solution and those of the three pure components. The ternary of system 1-propanol, water and toluene has been studied from the above point of view. Incidentally the physico-chemical properties of different percentage compositions of the two binary systems 1-propanol-water and 1-propanol-toluene were also studied.

Experimental

Preparation of Solutions.—In clean dry 100 ml. Pyrex conical flasks different ratios of the two immiscible components, water and toluene, of the ternary system under study were taken by weight in such a way that the variation was progressive in the range of 10 to 90%. The third component, 1-propanol was added at a constant temperature of 35°C from a burette as in a usual titration and shaken thoroughly after each addition till a perceptible cloudiness appeared with no distinction between the two layers. Just a little more of the component from the burette was added cautiously in drops just till the cloudiness disappeared. Now the conical flask was weighed with its contents. From this, the weight of the added 1-propanol could be easily computed. From the weights of the individual components, the mole fractions of the constituents in the ternary mixture could be computed.

Measurement of Dielectric Constant, Density and Viscosity.—For measuring the dielectric constant of the homogeneous solution "Dekameter type DKO3" of Wissenschaftlich-Technische Werkstätten was used at a fixed frequency of 1.8 Mc/sec. with Hoppler's ultra thermostat. The homogeneous solution was put into the cell, allowed to attain the temperature of 35°C and then measurement was made.

Viscosity was measured as usual with an Ostwald viscometer using Gallenkamp's glass-walled thermostat b-12210. Density was determined using the density bottle, whose volume was determined by weighing it filled with water and dividing the weight of the water by the density at 35°C, which was looked up in Lange's[1] "Hand Book of Chemistry."

Purification of the Components.—E. Merck's Purest 1-propanol[2] was dried with anhydrous potassium carbonate and distilled. The fraction boiling between 97~98°C was collected and further dried with magnesium activated with iodine. The product was then distilled with exclusion of moisture and the distillate boiling at 97.2°C was collected and preserved in a Pyrex bottle. Baker's analysed toluene meeting the American Chemical Society specifications was dried over anhydrous calcium chloride, filtered and distilled. The distillate boiling at 110.6°C was collected and preserved in a Pyrex bottle. Conductivity water was distilled once more in a Pyrex outfit and this was preserved free from carbon dioxide and used. A dielectric constant check was made now and then. This water was used throughout the investigation.

Results obtained are detailed in the following tables.

Discussion

The equation for the molar polarization of a mixture

$$P_{1,2\cdots k}=\frac{\varepsilon_{1,2,\cdots k}-1}{\varepsilon_{1,2,\cdots k}+2}\frac{M_1x_1+M_2x_2+\cdots M_kx_k}{\rho_{1,2\cdots k}} \quad (1)$$

holds strictly for solutions of zero volume of mixing. Therefore, in normal practice, apart from many other factors that influence the dielectric constant of a solution the occurrence of the density factor in equation 1 limits its rigorous application.

Van Arkel and Snoek[3] adopt the equation

$$L_{1,2}=L_1v_1+L_2v_2 \quad (2)$$

where v is the volume concentration and L the volume polarization. Sugden[4] found

1) N. A. Lange, "Hand Book of Chemistry", Hand Book Publishers, Inc., Sandusky, Ohio (1949) p. 1385
2) A. I. Vogel, "Practical Organic Chemistry", Longmans, London, 2nd ed., (1951), p. 168.
3) A. E. van Arkel and J. L. Snoek, *Trans. Faraday Soc.*, **30**, 710 (1934).
4) S. Sugden, *Nature*, **133**, 415 (1934).

that when P_2 is plotted against volume polarization for solutions of benzo nitrile, nitrobenzene and chlorobenzene in a number of non-polar solvents, all the points for each substance lie near a straight line through the entire range of solutions to the pure liquid. For the change in polarization of the solute in concentrated solution Sugden[5] found a very simple relation ship

$$ {}_cP_2 = A - B\frac{\varepsilon_c - 1}{\varepsilon_c + 2} \qquad (3) $$

where A and B are constants. From these considerations it is clear that volume polarization seems to be more fundamental than molar polarization.

Böttcher[6] derives the equation

$$ \frac{\varepsilon - 1}{\varepsilon + 2} = \sum_k \varphi_k \cdot \frac{\varepsilon_k - 1}{\varepsilon_k + 2} \qquad (4) $$

which is the same as

$$ L_{1,2\cdots k} = L_1V_1 + L_2V_2 \cdots L_kV_k \qquad (5) $$

where $\frac{\varepsilon - 1}{\varepsilon + 2} = L_{1,2\cdots k}$ = volume polarization of the mixture, $\varphi_k = V_k$ = volume fraction of the component k, and $\frac{\varepsilon_k - 1}{\varepsilon_k + 2} = L_k$ = volume polarization of the component k.

In equation 5 V_k is the ratio of the volume v_k of component k to the total volume $v_1 + v_2 \cdots v_k$ in the mixture. Let $n_1, n_2 \cdots n_k$ be the actual number of molecules contained in $v_1, v_2 \cdots v_k$ cc. respectively. Therefore the volume fraction V_k equals effectually $n_k / \sum n_k$ which is the same as the mole fraction x_k. The total volume polarization $L_{1,2\cdots k}$ of the mixture as measured will be due to the sum of total contribution of $\sum n_k$ molecules. Hence we may write,

$$ \sum_k L_k x_k = L_{1,2\cdots k} \qquad (6) $$

Equation 6 is clearly independent of the volume of mixing. Volume polarization L is a dimensionless function and depends only on the number of molecules present in unit volume and their polarisabilities.

Data obtained in the above investigations have been used to compare equation 6 with the well known equation

$$ \sum_k P_k x_k = P_{1,2\cdots k} \qquad (7) $$

Table I records the data obtained for the ternary system. Table II brings out a comparison of the equations 6 and 7. It is quite clear that percentage deviation from the mean value is almost negligible with equation 6, whereas deviations are considerable with equation 7.

Akerlöf[7] determined the dielectric constant of mixtures of 1-propanol and water at 25°C. Table III gives the data on density, viscosity and dielectric constant of mixtures of 1-propanol and water at 35°C as determined in this laboratory.

Plots of molar polarization and volume polarization against mole percent of 1-propanol (not given) show a linear variation. The plot of dielectric constant against mole percent of alcohol (not given) falls off rapidly with increasing mole percent of alcohol. The viscosity curve (not given) shows a maximum at about 28 mole percent of 1-propanol. The last column of Table III shows that at about 26 mole percent of 1-propanol, the volume contraction is maximum. If from viscosity and volume contraction data we have to conclude any molecular combination involving solute-solvent interaction we must expect with Hassel and Uhl[8] anomalously high molecular polarization about 28 mole percent of 1-propanol which is obviously not true here. It is also known[9,10] that the effect of association on the dielectric constant depends on the sizes and shapes of the participating dipoles. As a result of a greater electrostatic moment of a polymerized molecule than the simple one the dielectric constant of the solvent will be greater in its associated state. Deassociation in some solutions is indicated by the lowering of the dielectric constant of that component in solution. Conversely when dipole-dipole interaction occurs, the forces holding the electric charge will be weakened as a result of probable increase of the electrostatic moment of the molecule and the dielectric constant of a component becomes greater in solutions than in its pure state. In this context merely from the viscosity peak, it is rather unsafe particularly in the absence of absorption and Raman spectra, to conclude the existence of a compound of whatever composition between 1-propanol-water. Further investigations are required to solve this

5) S. Sugden, *Trans. Faraday Soc.*, **30**, 720 (1934).
6) C. J. F. Böttcher, "Theory of Electric Polarisation", Elsevier, Amsterdam, (1952), p. 203.
7) G. Akerlöf, *J. Am. Chem. Soc.*, **54**, 4125 (1932).
8) O. Hassel and A. H. Uhl, *Naturwissenschaften*, **18**, 247 (1930).
9) R. N. Kerr, *J. Chem. Soc.*, **1926**, 2796.
10) J. W. Williams and I. J. Krchma, *J. Am. Chem. Soc.*, **48**, 1886 (1926).

TABLE I
(1-Propanol-water-toluene).

Mole fraction			Density	Viscosity in centipoises	Dielectric constant	Volume contraction in ml. per 1000 ml. of solution
1-Propanol x_1	Water x_2	Toluene x_3				
0.5042	0.2793	0.2166	0.8326	0.8804	12.70	4.861
0.4888	0.3351	0.1761	0.8355	0.9553	14.49	8.557
0.4645	0.3996	0.1359	0.8399	1.0360	16.50	8.971
0.4138	0.4976	0.0886	0.8487	1.1840	20.35	10.720
0.3657	0.5778	0.0565	0.8588	1.3160	25.00	12.650
0.3191	0.6400	0.0409	0.8694	1.3910	28.48	14.700
0.2754	0.6928	0.0318	0.8794	1.4740	32.00	15.770
0.2197	0.7603	0.0200	0.8936	1.5620	37.53	10.840
0.1389	0.8501	0.0110	0.9169	1.7000	46.80	7.316

TABLE II

$\sum_{k=1,2,3} P_k x_k$	$P_{1,2,3}$	% deviation from the mean value	$\sum_{k=1,2,3} L_k x_k$	$L_{1,2,3}$	% deviation from the mean value
44.885	52.85	8.149	0.7672	0.7960	1.843
43.500	50.56	7.506	0.7952	0.8181	1.419
41.702	47.51	6.510	0.8239	0.8377	0.831
38.529	42.83	5.286	0.8600	0.8658	0.336
35.738	38.91	4.251	0.8857	0.8888	0.175
33.257	35.76	3.659	0.9011	0.9018	0.042
31.033	33.15	3.301	0.9115	0.9118	0.014
28.198	29.73	2.644	0.9251	0.9243	0.043
24.111	25.27	2.347	0.9395	0.9387	0.043

TABLE III
(1-Propanol-water)

Mole fraction		Density	Viscosity in centipoises	Dielectric constant	Volume contraction in ml. per 1000 ml. of solution
1-Propanol x_1	Water x_2				
—	1.0000	0.9941	0.723	74.94	—
0.0243	0.9757	0.9815	0.849	69.75	6.69
0.0599	0.9400	0.9661	1.038	64.37	14.91
0.1044	0.8956	0.9454	1.232	58.50	17.46
0.1392	0.8608	0.9305	1.348	51.38	19.75
0.2072	0.7928	0.9063	1.472	43.30	19.36
0.2629	0.7371	0.8902	1.519	38.75	20.16
0.3383	0.6617	0.8722	1.523	34.00	18.68
0.4273	0.5727	0.8553	1.494	29.71	17.44
0.5839	0.4161	0.8326	1.406	25.00	13.08
0.8250	0.1750	0.8085	1.290	20.95	8.40
1.0000	—	0.7918	1.614	18.90	—

question.

Data of dielectric constant, density and viscosity of mixtures of 1-propanol and toluene, are given in table V. Table VI shows that both the equations 6 and 7 fail with the system.

Plots of molar polarization and volume polarization (not given) against percentage composition of 1-propanol show a continuous increase with a tendency for a maximum in the former about 75 mole percent of the alcohol. The dielectric constant and viscosity (curves not given) vary with mole percent of 1-propanol in a similar way, increasing rapidly and continuously with increase of alcohol.

Several other binary systems worked recently in this laboratory show that both equations 6 and 7 are valid in polar-polar binary mixtures and definitely fail in the case of polar-nonpolar mixtures. It is rather difficult to explain this fact.

TABLE IV

$\sum_{k=1,2} P_k x_k$	$P_{1,2}$	% deviation from the mean value	$\sum_{k=1,2} L_k x_k$	$L_{1,2}$	% deviation from the mean value
—	17.42	—	—	0.9610	—
18.568	18.59	0.0592	0.9582	0.9583	0.0052
20.254	20.28	0.0641	0.9543	0.9548	0.0262
22.387	22.53	0.3111	0.9500	0.9504	0.0211
24.041	24.23	0.3914	0.9463	0.9441	0.1163
27.280	27.55	0.4922	0.9392	0.9337	0.2936
29.940	30.27	0.5480	0.9337	0.9264	0.3924
35.520	33.88	0.5342	0.9254	0.9166	0.4889
37.754	38.11	0.4953	0.9164	0.9055	0.5955
45.207	45.48	0.3010	0.9000	0.8890	0.6151
56.670	56.69	0.0176	0.8747	0.8694	0.3039
—	65.01	—	—	0.8566	—

TABLE V
(1-Propanol-toluene)

Mole fraction		Density	Viscosity in centipoises	Dielectric constant	Volume contraction in ml. per 1000 ml. of solution
1-Propanol x_1	Toluene x_2				
—	1.000	0.8528	0.5474	2.34	—
0.1148	0.8852	0.8459	0.5495	2.82	0.825
0.2642	0.7358	0.8393	0.5691	4.00	−2.248
0.3860	0.6140	0.8335	0.6002	5.09	−0.224
0.5022	0.4978	0.8272	0.6466	6.90	−0.223
0.6123	0.3877	0.8215	0.7062	9.25	1.045
0.7121	0.2879	0.8157	0.7902	11.50	2.396
0.8095	0.1905	0.8097	0.8888	14.05	2.840
0.9353	0.0647	0.8005	1.0880	17.43	3.186
1.0000	—	0.7918	1.6140	18.90	—

TABLE VI

$\sum_{k=1\ 2} P_k x_k$	$P_{1,2}$	% deviation from the mean value	$\sum_{k=1,2} L_k x_k$	$L_{1,2}$	% deviation from the mean value
—	33.42	—	—	0.3092	—
37.056	39.51	3.205	0.37217	0.3777	0.738
41.760	49.83	8.918	0.45380	0.5000	4.848
45.610	55.25	9.557	0.52060	0.5772	5.156
49.270	60.94	10.590	0.58400	0.6630	6.336
52.760	64.74	10.200	0.64450	0.7335	6.604
55.935	66.13	8.345	0.69926	0.7778	5.318
58.986	66.48	5.973	0.75231	0.8130	3.877
62.962	65.63	2.075	0.82111	0.8455	1.462
—	65.01	—	—	0.8566	—

Tables I, III and V show that in all cases there is involved some volume contraction. Equation 6 holds excellently in the ternary system. Equation 6 cannot be claimed, therefore, to have set right the error due to volume of mixing inherent in equation 1. On the other hand as observed recently with several other ternary systems in this laboratory, equation 6 may be considered to give tentatively a quantitative condition involving a dielectric contribution of the components to miscibility. In other words, just at the point wherein two phases disappear to give a homogeneous system, equation 6 seems to apply excellently.

Summary

In place of the familiar equation $\sum_k P_k x_k = P_{1,2\cdots k}$, which does not hold good in many cases, we have formulated alternatively

the equation $\sum_k L_k x_k = L_{1,2\cdots k}$ where L is volume polarization. This equation has been applied to the ternary system 1-propanol-water and toluene just at the point of miscibility, when to a given ratio of toluene and water addition of an optimum amount of 1-propanol results in the disappearance of the two phases. Also the new equation has been applied to two fully miscible binary systems 1-propanol-water and 1-propanol-toluene. It has been concluded that the new equation gives a condition concerning the dielectric contribution of the components to miscibility in the ternary system.

Physico-Chemical Laboratory, Annamalai University, Annamalainagar South India

Stress Relaxation of Non-electrolytic Thermo-reversible Gels.— Concentration Dependence of Distribution Function of Relaxation Times. Polyvinyl Alcohol-Glycerin-Water Gels*

By Kiyoshi ARAKAWA

(Received January 28, 1958)

According to the reversibility of sol-gel transition with temperature, gels are classified into two groups, thermo-reversible and thermo-irreversible. As typical thermo-reversible gels we have agar, gelatine, etc. But most of these are polyelectrolytes, rheological properties of which are complicated by charge effects. In the present work the rheological property of non-electrolytic thermo-reversible gels was examined. A system consisting of polyvinyl alcohol, glycerin, and water was used as an example of such a gel. The elastic behavior of the gel has been studied previously by N. Hirai[1], but the distribution function of relaxation times was not obtained for this gel. Such a function has been determined from stress relaxation of the gel and discussed here briefly.

Experimental

Apparatus.—A chainomatic balance relaxometer shown in Fig. 1 was used to measure Young's modulus of a sample under constant strain. The relaxometer is of similar type with those used by S. L. Dart and E. Guth[2] for the study of stress relaxation in cork, and recently by several workers in studies of polymers[2].

In this relaxometer a sample is strained by compression betweeen two plates, the upper of which is attached to the horizontal bar of chainomatic balance. The lower plate is connected with a screw gauge. The stress produced by the constant strain is balanced with a chain, whose unfixed end is moved by a balancing motor. The

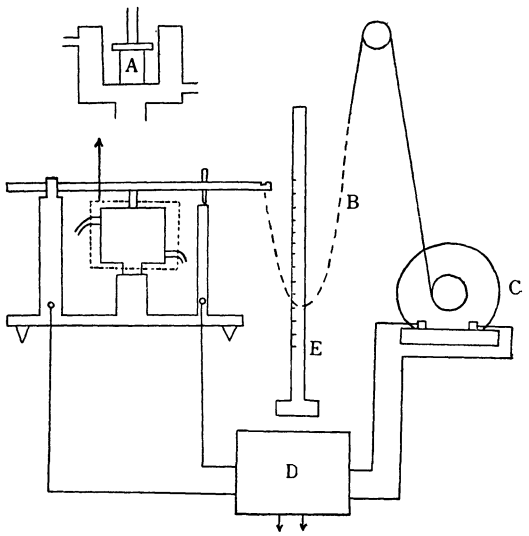

Fig. 1. Schematic diagram of chainomatic balance relaxometer.
A: specimen
B: chain
C: balancing motor
D: relay circuit
E: scale

* Presented in part at the 10th Annual Meeting of the Chemical Society of Japan held in Tokyo, April 1957.

1) N. Hirai, *J. Chem. Soc. Japan, Pure Chem. Sec.*, (*Nippon Kagaku Zassi*), **74**, 235 (1953): ibid., **74**, 259 (1953).

2) S. L. Dart and E. Guth, *J. Appl. Phys.*, **17**, 314 (1946): H. Fujita and K. Ninomiya, *J. Polymer Sci.*, **24**, 233 (1957); This Bulletin, **26**, 24 (1953): K. Ogino, the 9th Annual Meeting of Chem. Soc. Japan (1956).

motor is driven through a relay circuit which is connected with a point contact attached to the bar. From the suspended length of the chain the stress is calculated and Young's modulus of the sample under constant strain can be obtained. The temperature of the sample is controlled by water circulated from a thermostat into a double jacket which contains the sample.

Materials.—In the present study a commercial polyvinyl alcohol was used throughout. The amount of residual ester groups in the sample was 2% by mole. The intrinsic viscosity $[\eta]_{20}$ of this unfractionated sample was 0.27, which was determined by means of a capillary viscometer of Ostwald type. The viscosity average molecular weight M_V was 1.1×10^4 according to the formula by H. Staudinger and H. Warth[3].* As solvent a mixture of glycerin and water was used with a mixing ratio of 4:1 by volume.

The preparation of testing specimens was as follows. A definite quantity of polyvinyl alcohol powder was mixed with glycerin and water in a conical beaker. Being covered with liquid paraffin, the powder was dissolved slowly by heating in an oil bath kept at 125±5°C. In adjusting of the mixing ratio 4:1 of glycerin and water the presence of adsorbed water in polyvinyl alcohol powder, the amount of which was determined before each preparation, was taken into account. After the polyvinyl alcohol powder was dissolved completely, the solution was poured into a mould and kept at about 90°C for about thirty minutes. It was then cooled down slowly to about 50°C in four hours, and was aged at room temperature. Gels of three different concentrations, 8.3%, 9.9% and 12.1 % by weight were prepared.

Results and Discussion

Stress Relaxation Data.—The data of stress relaxation of gels of three different concentrations are plotted in the form $\log(298E_r/T)$ vs. $\log t$, where E_r is Young's relaxation modulus and t time, in Fig. 2 a, b and c**.

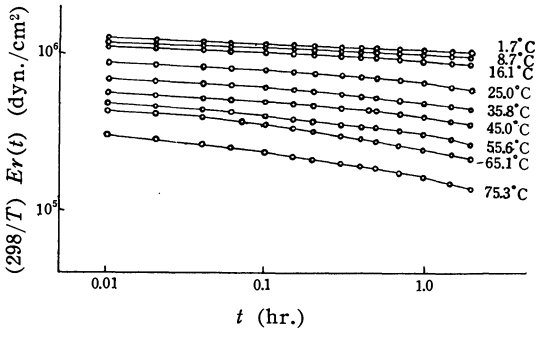

Fig. 2 (a). Reduced Young's relaxation modulus $\frac{298}{T}E_r(t)$ of 8.3% gel.

These data are reduced to 25°C by multipling E_r by a factor $298/T$. The multiplication by this factor is often subjected to objection, but in the present work the stress relaxation experiment was made in rubbery region mainly, and therefore this reduction is thought to be reasonable.

According to the time temperature superposition principle[4] a master relaxation curve at 25°C for each concentration may be composed by shifting these relaxation curves along the $\log t$ axis. The master relaxation curves for each concentration, thus obtained, are plotted in Fig. 3.

The amounts of the shift along the $\log t$ axis at various temperatures, $\log a_T$, are plotted against $1/T$ in Fig. 4. They give a nearly straight line. The apparent

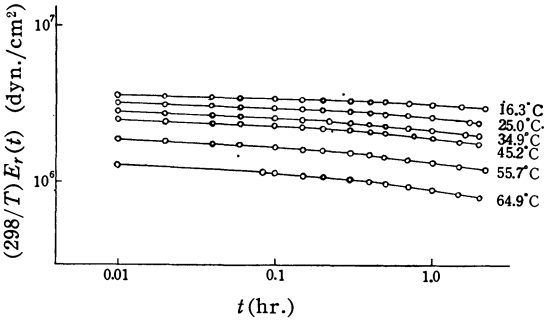

Fig. 2 (b) Reduced Young's relaxation modulus $\frac{298}{T}Er(t)$ of 9.9% gel.

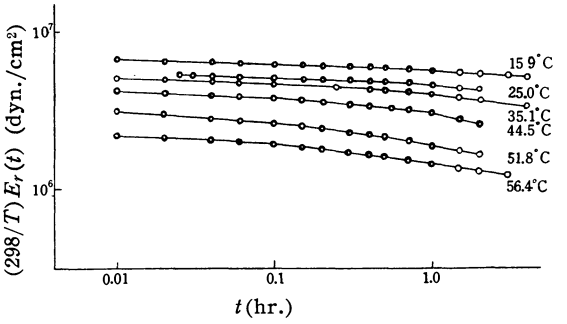

Fig. 2 (c). Reduced Young's relaxation modulus $\frac{298}{T}E_r(t)$ of 12.1% gel.

3) H. Staudinger and H. Warth, *J. Prakt. Chem.*, **155**, 261 (1944).

* In application of this formula, the effect of the residual ester groups was ignored.

4) A. V. Tobolsky and R. D. Andrews, *J. Chem. Phys.*, **11**, 125 (1943); R. D. Andrews, N. Hofman-Bang and A. V. Tobolsky, *J. Polymer Sci.*, **3**, 669 (1948); J. D. Ferry, *J. Am. Chem. Soc.*, **72**, 3746 (1950); F. Schwarzl and A. J. Staverman, *J. Appl. Phys.*, **23**, 838 (1952); C. A. Dahlquist and M. R. Hatfield, *J. Colloid Sci.*, **7**, 253 (1952).

** Compressions applied in the present experiment were 3% in 12.1% and 9.9% gels, and 5% in 8.3% gel. In this range of compressions the linear relation between stress and strain was almost maintained.

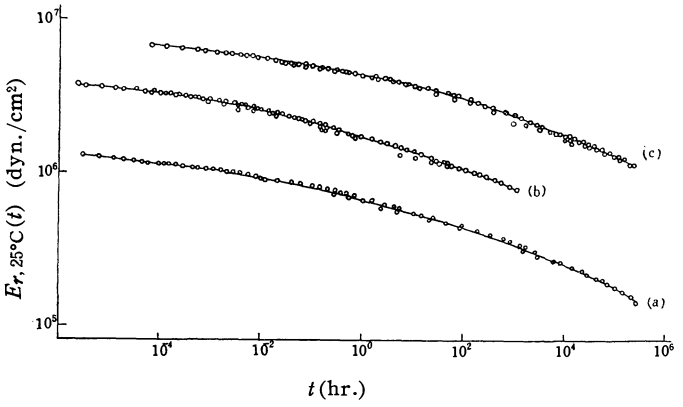

Fig. 3. Master relaxation curves at 25°C.
(a) 8.3%, (b) 9.9%, (c) 12.1%

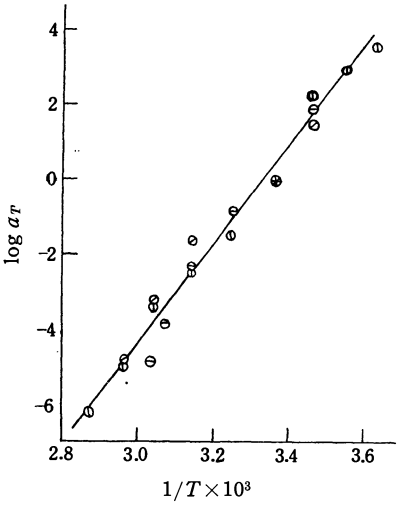

Fig. 4. Log a_T versus $1/T$ relation.

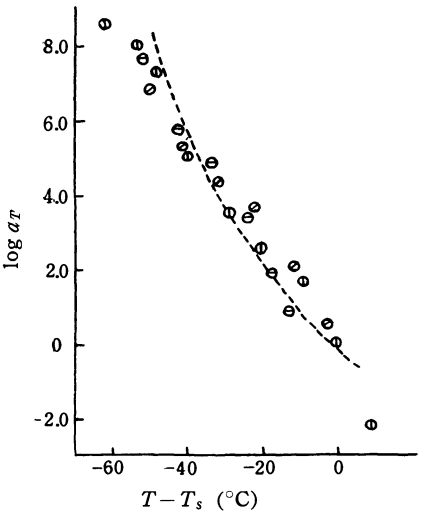

Fig. 5. Log a_T versus $T-T_s$ relation.
⓪ 8.3%, ⓪ 9.9%, ⊖ 12.1%
T_s: 338°K for 8.3%
340°K for 9.9%
342°K for 12.1%
------ equation of WLF form[5]
$C_1=8.86$, $C_2=101.6$

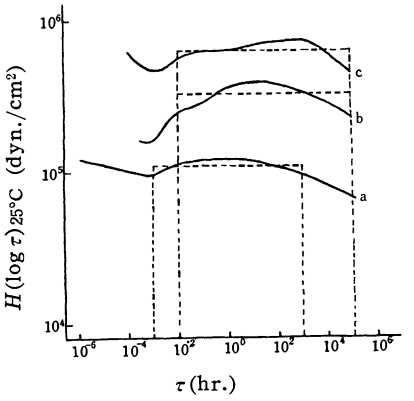

Fig. 6. Distribution functions of relaxation times.
(a) 8.3%, (b) 9.9%, (c) 12.1%

activation energy H_a, defined as $R\partial\ln a_T/\partial(1/T)$ is 60 kcal./mole, which is nearly kept constant over the temperature- and concentration-range in the present work. As for the temperature dependence of the factor a_T a function on the log a_T vs. $T-T_s$ relation has been proposed recently by M. L. Williams, R. F. Landel and J. D. Ferry[5], where T_s is a reference temperature. The coincidence between the values of a_T obtained in this work and the function is fairly good in the range of $T-T_s$, $-40\sim0$°C, but outside this range they deviate from the curve, as seen in Fig. 5.

Distribution Functions of Relaxation Times.—A distribution function of relaxation times $H(\log\tau)$ may be determined from a master curve, using the following first order approximation[6]

$$H(\log\tau)=-2.303[E_r\mathrm{d}\log E_r/\mathrm{d}\log t]_{t=\tau} \quad (1)$$

It was found that the difference between the first and the second order approximation was small enough in the calculated values to be ignored. Therefore the former was used throughout.

Logarithms of $H(\log\tau)$, thus obtained, are plotted against $\log\tau$ in Fig. 6.

5) M. L. Williams, R. F. Landel and J. D. Ferry, *J. Am. Chem. Soc.*, **77**, 3701 (1955).

6) R. D. Andrews, *Ind. Eng. Chem.*, **44**, 707 (1952): F. Schwarzl, *Physica*, **17**, 830, 865 (1951).

TABLE I

VALUES OF PARAMETERS OF BOX-TYPE DISTRIBUTION

Concn. (wt. %)	τ_1 (hr.)	τ_2 (hr.)	$\overline{H}\times10^{-5}$ (dyn./cm^2)	τ_m (hr.)	$H_m\times10^{-5}$ (dyn./cm^2)
8.3	10^{-3}	10^{3}	1.1	10^{0}	1.2
9.9	10^{-2}	10^{5}	3.3	$10^{1.5}$	4.0
12.1	10^{-2}	10^{5}	6.3	10^{3}	7.1

Concentration Dependence of Master Relaxation Curve and Relaxation Spectrum.—It is seen in Fig. 3 that the master curve shifts upwards and to the longer time side with increase of concentration. But, when seen in details, the concentration dependence of the master curve is fairly complicated. Therefore, it is impossible to reduce the curves for different concentrations to a composite curve, as carried out by T.W. DeWitt et al.[7] on the decalin solution of polyisobutylene and previously by J. D. Ferry et al.[7]

Also, in Fig. 6 we can see that the relaxation spectrum exhibits a fairly complicated nature on the concentration dependence. Simple approximations of box type for each spectrum are shown by dotted lines. Three parameters characterizing a box type distribution, two abscissae τ_1 and τ_2 ($\tau_1<\tau_2$), corresponding to two vertical sides, and the height $\overline{H}$ of the box are tabulated in Table I, together with the maximum value of $H(\log\tau)$, H_m and the abscissa τ_m at the maximum point. The value of $\overline{H}$ is taken to be an average value of $H(\log\tau)$ between τ_1 and τ_2. As seen in Fig. 6 and Table I, the maximum point in the region shifts upwards and to the longer time side with increase of concentration. The relation between $\overline{H}$ and concentration seems to be complicated. To draw any conclusion on this relation, further studies are required. Also it is evident that the shift of the spectrum due to the change of concentration is not uniform over the region covered in the present study. Concerning the shift along the $\log\tau$ axis, the minimum point which appears in the short time region nearly retains its position, while the maximum point shifts to the longer-time side, as the concentration increases. From this non-uniformity of the shift it is tentatively supposed that the relaxation mechanism in this region consists of two or more groups of mechanisms, which exhibit the different dependence on the concentration of polyvinyl alcohol.

7) T. W. DeWitt, H. Markovitz, F. J. Padden and L. J. Zapas, *J. Colloid Sci.*, **10**, 174 (1955); J. D. Ferry, *J. Am. Chem. Soc.*, **72**, 3746 (1950); W. M. Sawyer and J. D. Ferry. ibid., **72**, 5030 (1950).

Summary

From a stress relaxation experiment by means of a chainomatic balance relaxometer the stress relaxation curves were obtained for the gel of polyvinyl alcohol-glycerin-water system, which was taken as an example of non-electrolytic thermo-reversible gel. Gels of 8.3%, 9.9% and 12.1% were used. The temperature of the samples was changed between about 2°C and 75°C. Master relaxation curves were obtained for each concentration over the range of time, $10^{-4}\sim10^{5}$ hours, using the time temperature superposition principle. According to Alfrey's approximation, relaxation spectra were calculated.

The following results were obtained.

1) The master relaxation curves exhibit a fairly complicated nature on concentration dependence.

2) The $\log a_T$ vs. $T-T_s$ relation obeys approximately the formula by Williams, Landel and Ferry in the range of $T-T_s$, $-40\sim0$°C, but outside the range deviates fairly from it.

3) The apparent activation energy is 60 kcal./mole, which is nearly kept constant over the temperature- and concentration-range in the present work.

4) The shift of the relaxation spectrum due to the change of concentration is not uniform over the region of box type. The maximum point in that region shifts upwards and to the longer-time side with increase of concentration.

The author wishes to express his gratitude to Mr. K. Ogino of Tokyo University for his helpful advice in designing the relaxometer, and Dr. T. Nakagawa of Tokyo University for his encouragement throughout this work.

Department of Chemistry, Faculty of Engineering, Shizuoka University
Oiwake, Hamamatsu

On the Bromination Reaction of Tropone and its Bromine Compounds[1]

By Toshio MUKAI

(Received April 21, 1958)

On bromination, tropone is not directly subject to replacement with bromine but intermediately forms a bromine addition product and subsequently forms the true bromine-substitution product by its dehydrobromination and debromination[2,3]. This fact gives a new observation regarding the aromaticity of tropone and is one of the experimental facts that indicate highly unsaturated characteristic of tropone compared to tropolone. It has been noticed, however, that tropones show different modes in the bromine addition according to their structures. For example, bromination of 2-phenyltropone chiefly gave a tetrabromide (I) and indicated that the C_2-C_3 double bond of I was fairly resistant to further bromination owing to the steric hindrance by the phenyl group at C_2 position[3]. Tropone itself was also brominated to form the tetrabromide (II) but its dehydrobromination gave 2,7-dibromotropone and this indicated that the C_4-C_5 double bond of II was resistant to bromine addition[2]. In addition, bromination of 2-bromotropone also afforded 2,7-dibromotropone via the addition product, and this dibromotropone was not further brominated even on application of an excess of bromine in chloroform or acetic acid with heating[2]. These facts also indicated that the C_4-C_5 double bond in tropone ring was inactive to bromine addition or substitution. In 1951, Brown[4] suggested that the C_2 (or C_7) position on the tropone ring will be most easily submitted to electrophilic substitution from his calculation by the molecular orbital method, and this is rather interesting when the above facts are considered.

In the present paper, further bromination reaction of tropone and its various bromine-substituted derivatives is reviewed and examinations are made on whether the double bond at C_4-C_5 of II is entirely inactive to bromine addition. Also what effect the bromine atoms present in the tropone ring have on this addition reaction is described.

Tropone invariably affords 2,7-dibromotropone, on causing an excess of bromine to react under heating and it is known to give the tetrabromide (II) when cold[2]. Therefore, different reaction conditions were adopted. Tropone was dissolved in glacial acetic acid or chloroform, an excess of bromine was added, and the mixture was allowed to stand for a long period. The oily addition product obtained by this reaction differs from II and its analytical value agrees with that for a hexabromide. Its dehydrobromination with sodium acetate was found to give chiefly 2,4,7-tribromotropone, though accompanied with 2,7-dibromotropone. It has become clear through this experiment that the addition product obtained here has the structure of III and that the double bond at C_4-C_5 submits to bromine addition under the above conditions. The ultraviolet spectrum of the addition product III is shown in Fig. 1 and there is no marked absorption maximum. Its infrared spectrum[5] has no

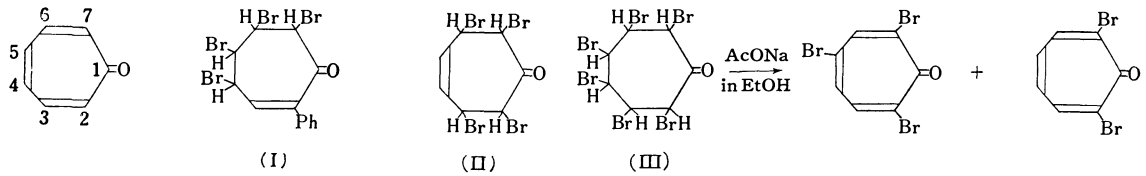

(I) (II) (III)

1) This paper was read before the 9th Annual Meeting of the Chemial Society of Japan held in Kyoto on April 5, 1956.

2) T. Nozoe, T. Mukai and K. Takase, *Science Repts. Tohoku Univ.*, **1**, **39**, 164 (1956).

3) T. Mukai, ibid., **1**, **38**, 281 (1954).

4) R. D. Brown, *J. Chem. Soc.*, **1951**, 2670.

5) Infrared spectrum was measured with Perkin-Elmer Model 21 double beam spectrophotometer by Mr. Yusaku Ikegami of the Chemical Research Institute of Non-aqueous Solutions, to whom the author's deep gratitude is hereby expressed.

marked absorption in the C=C region either. These facts support the conclusion that the addition compound has the saturated ketone structure of III. The absorption of C=O in III appears as two bands* at 1735 and 1706 cm^{-1}. Toda and Kitahara[6] have found that the equatorial

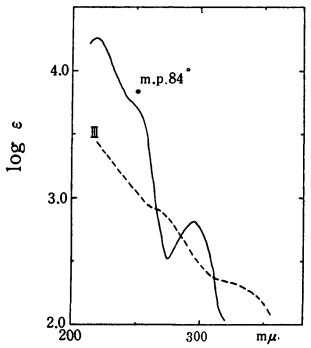

Fig. 1. U. V. absorption spectra of addition product III in cyclohexane and of compound melted at 84°C in methanol.

α-bromine atom of bromosuberones shifts its carbonyl band to the higher frequency by 17 cm^{-1} than that of suberone at 1701 cm^{-1}. The absorption at 1735 cm^{-1} is higher in frequency by 34 cm^{-1} than that of suberone, so this is thought to indicate the fact that the two α-bromine atoms of III are in equatorial to C=O.

The addition product III was dissolved in glacial acetic acid and refluxed or heated in an oil bath to 140~150°C without a solvent[7]. In this case, hydrogen bromide and bromine were evolved and in both cases, only 2,7-dibromotropone was obtained and not the 2,4,7-tribromo compound.

Similarly, when 2-bromotropone[8] and bromine in glacial acetic acid solution are allowed to stand over a long period of time, a pentabromo-compound is obtained. Dehydrobromination of this addition product by heating in ethanol, in the presence of sodium acetate, easily affords 2,4,7-tribromotropone, from which it is certain that this addition product has the structure shown by IV. It is known from this that the bromine addition occurs not at the C_2-C_3 double bond but at C_4-C_5 double bond. Decomposition of IV by heating in acetic acid results in evolution of hydrogen bromide and bromine, and 2,7-dibromotropone alone is obtained, while its decompostition by heating without a solvent chiefly gives 2,7-dibromotropone accompanied by a small amount of 2,4,7-tribromotropone. It should be noted that in these cases also elimination of free bromine has occurred at C_4-C_5 bond.

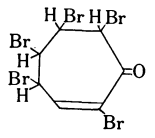

(IV)

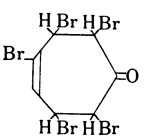

(V)

Bromination of tropone and 2-bomotropone under heating affords 2,7-dibromotropone, as mentioned earlier, and there is a possibility that the dibromo compound is formed through the addition products, III and IV. In order to confirm this point, sodium acetate was added in this bromination but the 2,7-dibromotropone was invariably obtained and not the 2,4,7-tribromotropone. Therefore, it may be concluded that bromination with heating does not form addition products like III and IV.

Application of an excess of bromine to acetic acid solution of 4-bromotropone[9] results in direct substitution reaction and 2,4,7-tribromotropone is obtained, the bromine addition compounds being obtained with difficulty. In this case, the use of chloroform in place of acetic acid as a solvent affords pentabromo compound as the addition product and this addition product invariably forms 2,4,7-tribromotropone, either by heating in ethanol with sodium acetate or by heating without a solvent or in acetic acid solution. These facts support the structure of V for the addition compound. Decomposition of V in ethanol in the presence of sodium acetate gives, besides 2,4,7-tribromotropone, colorless crystal melting at 84°. This latter substance is stable and neutral and its ultraviolet and infrared spectra are shown respectively in Figs. 1 and 2. From this ultraviolet spectrum, it is seen that the substance no longer retains a tropone ring[10] but its structure remains unsolved.

* It may owe to the presence of two conformationally different isomers.

6) T. Toda. and Y. Kitahara, to be published. (From the dissertation of T. Toda, Tohoku University) cf. E. J. Corey, *J. Am. Chem. Soc.*, **75**, 2301 (1953).

7) These reaction conditions were taken in order to compare them with that used in the troponization (bromination-dehydrobromination) of suberone. cf. T. Nozoe, Y. Kitahara, T. Ando, S. Masamune and H. Abe, *Science Repts. Tohoku Univ.*, **1**, **36**, 166 (1952): *Proc. Japan Acad.*, **27**, 415 (1951).

8) T. Nozoe, S. Seto and S. Matsumura, *Proc. Japan Acad.*, **28**, 483 (1952).

9) T. Nozoe, T. Mukai, Y. Ikegami and T. Toda, *Chem. & Ind.*, **1955**, 66.

10) M. Tsuboi, This Bulletin, **25**, 369 (1952).

The infrared spectrum of V exhibits an absorption band of C=C at 1605 cm^{-1} and of C=O group at 1738 cm^{-1}. The latter band is 37 cm^{-1} higher in frequency than C=O band of suberone at 1701 cm^{-1} and this will indicate the fact that the two α-bromine atoms of V are located in the equatorial position[6].

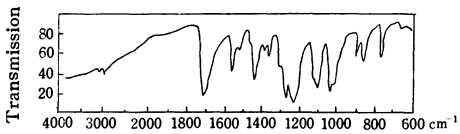

Fig. 2. I. R. absorption spectrum of compound melting at 84°C in KBr.

The behavior of 2,5-dibromotropone[9] toward bromination is similar to that of 4-bromotropone, that is, it forms 2,4,7-tribromotropone on standing with bromine in acetic acid solution at room temperature. However, the use of chloroform as a solvent also affords the tetrabromo-compound. This addition compound always forms 2,4,7-tribromotropone, either on dehydrobromination with sodium acetate or on heating alone or in acetic acid solution.

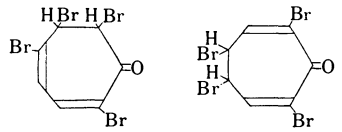

(VI) (VII)

From these facts, the structure represented by VI is given to this addition compound, and also, in this case the double bond with the bromine is found to be resistant to bromine addition. The infrared spectrum of VI exhibits absorptions at 1658 cm^{-1} for C=O and at 1613 cm^{-1} for C=C, and these values seem approximately as suitable as those for such a conjugated, unsaturated ketone. The bromine addition compound of tropones having bromine atom at C_4 or C_5 position, as in V and VI, tends to decompose and the ultraviolet spectra of V and VI in a polar solvent like methanol exhibit absorption similar to that of 2,4,7-tribromotropone resulting from the decomposition. It is assumed that the failure to obtain addition compounds from the bromination of 4-bromo- and 2,5-dibromotropone in acetic acid solution may be related to this instability.

When 2,7-dibromotropone[8] is allowed to stand with an excess of bromine in acetic acid solution at room temperature for a long period, a tetrabromo compound crystallizes out. Heating with sodium acetate in ethanol solution, affords 2,4,7-tribromotropone together with 2,7-dibromotropone. This proves that the structure of the addition compound is correctly represented by VII. The infrared spectrum of VII has absorptions for conjugated C=O and C=C respectively at 1656 and 1613 cm^{-1}. Heating VII alone or in acetic acid solution results in evolution of bromine and only 2,7-dibromotropone is formed and this also indicates that bromine is easily eliminated from C_4–C_5 bond.

The foregoing bromination reaction of tropones may be summarized as follows: 1) Bromine addition of tropone seems to proceed in a stepwise manner, the addition being facile up to two moles, but addition to the C_4–C_5 double bond requires a long period. This is thought to be due to the increased repulsion between the bromine atoms and between the carbonyl group and bromine atom by the formation of hexabromo compound (III) by the third mole of bromine. 2) Further addition of bromine to bromotropones does not occur in the double bond carrying the bromine atom and this is probably due to increased repulsion between bromine atoms by the formation of a geminated dibromo-structure[11]. 3) The bromine atoms attached to the C_4–C_5 positions tends to be easily liberated as bromine, while those bonded to C_2–C_3 and C_6–C_7 positions are liberated as hydrogen bromide. 4) It is difficult to derive tropone, 2-bromotropone, and 2,7-dibromotropone by bromination into 2,4,7-tribromotropone without going through the addition compounds.

The important point in connection with the foregoing bromination reaction of tropone is the troponization of suberone by the action of bromine[7]. This is one of the fundamental reactions in the preparation of tropones but, because the reaction is so complicated, its reaction mechanism has not been clarified as yet. Therefore, several polybromosuberones that form as intermediates during this reaction have been isolated and their troponization reaction has been examined[12]. The bromine addition compounds formed in the present series of experiments may also be regarded as allied substances of polybromo compounds of suberone, but

11) The addition compound having geminated two bromine atoms was obtained on the bromination of 2-phenyltropone. cf. Ref. 3.

12) Paper presented at the Local Meeting of Tohoku district of the Chemical Society of Japan held in Yamagata on June 28, 1954.

it should be noted that there is a fair difference between the compounds of these two series as to the position and configuration of the bromine atom. It is interesting that troponization of suberone by bromination affords 2,4,7-tribromo-, 2,5-dibromo-, and 4-bromotropones[9], and not 2-bromo- or 2,7-dibromotropones, while the bromine addition compounds obtained by the bromination of tropone invariably are 2-bromo-[2] and 2,7-dibromotropone rather than 2,4,7-tribromotropone.

Experimental[13]

Bromination of Tropone.— *a) In carbon tetrachloride solution.*—To a solution of 150 mg. of tropone dissolved in 3 cc. of carbon tetrachloride, 950 mg. (4.2 mol. equiv.) of bromine was added, by which reddish orange oil separated out and later crystallized. This mixture was allowed to stand in a sealed vessel at room temperature and the crystal again changed to an oil. After about 3 weeks, the mixture containing oil was dried in a vacuum desiccator over potassium hydroxide and paraffin to get constant weight, and 800 mg. of hexabromo compound (III) was obtained as yellowish orange syrup, which was submitted to elemental analyses and ultraviolet and infrared spectral measurements.

Anal. Found: C, 14.95; H, 1.25. Calcd. for $C_7H_6OBr_6$: C, 14.36; H, 1.02%. I.R. Spectrum: $\tilde{\nu}$ (C=O) 1735, 1706 cm^{-1}, (C=C) very weak band (without solvent).

b) In acetic acid solution.—A mixture of 100 mg. of tropone dissolved in 1.5 cc. of acetic acid and 950 mg. (6.3 mol. equiv.) of bromine was allowed to stand for 10 days at room temperature and treated as in a), from which 600 mg. of yellowish orange oil was obtained. The analytical values of this oil did not agree with those for the hexabromo compound (Found: C, 17.74; H, 1.83) but its decomposition with sodium acetate afforded 2,4,7-tribromotropone and thermal decomposition gave 2,7-dibromotropone, exactly as in the case of III (q.v.).

c) Bromination in the presence of sodium acetate under heating.—A mixture of 30 mg. of tropone, 230 mg. of bromine (5 mol. equiv.) and 70 mg. of sodium acetate in 1.5 cc. of acetic acid was heated for 3 hours on a water bath. At the end of this period, some bromine still remained. Acetic acid was removed and residual crystals were washed with ethanol and water, affording 60 mg. of pale greenish yellow crystals, m. p. 145~160°C. Recrystallization from ethanol-benzene mixture gave 40 mg. of crystals melting at 167~169°C, undepressed on admixture with 2,7-dibromotropone, m. p. 170°C.

Bromination of 2-Bromotropone.— *a) In acetic acid solution.*—To a solution of 150 mg. of 2-bromotropone dissolved in 2 cc. of acetic acid, 640 mg. (5 mol. equiv.) of bromine was added and the mixture was allowed to stand in a sealed vessel for one month at room temperature. Crystals began to separate out from the tenth day. The crystals were collected by filtration to give 320 mg. of colorless crystals, m. p. 115°C (decomp. with efferv.). Recrystallization from ethanol gave colorless needles IV, m. p. 135°C (decomp. with efferv.).

Anal. Found: C, 15.92; H, 1.09. Calcd. for $C_7H_5OBr_5$: C, 16.61; H, 1.00%. U.V. Spectrum: $\lambda_{max}^{cyclohexane}$ mμ (log ε): 280(4.35). I.R. Spectrum: $\tilde{\nu}$ (C=O, C=C) 1736, 1704, 1607 cm^{-1} (in KBr disk).

b) Bromination in the presence of sodium acetate under heating.—A mixture of 50 mg. of 2-bromotropone and 80 mg. of sodium acetate in 2 cc. of acetic acid containing 170 mg. (4 mol. equiv.) of bromine was heated on a water bath for 3 hours. Acetic acid was removed, and the residue was washed with water. Filtration afforded 70 mg. of pale brown crystals, m. p. 130~150°C. Washing with ethanol gave 40 mg. of crystals melting at 162~166°C, and recrystallization from ethanol-benzene mixture gave pale yellow plates, m. p. 169~170°C. This was found to be 2,7-dibromotropone by mixed fusion.

Bromination of 4-Bromotropone.— *a) In acetic acid solution.*—To a solution of 400 mg. of 4-bromotropone dissolved in 10 cc. of acetic acid, 1.73 g. (5 mol. equiv.) of bromine was added and the mixture was allowed to stand in a sealed vessel at room temperature. After about one month, some needle crystals crystallized out but the mixture was allowed to stand for a total of 3 months and the crystals were collected. The first crop of crystals was 450 mg. of pale yellow needles, m. p. 183°C. The mother liquor was allowed to stand over potassium hydroxide in a vacuum desiccator and a second crop of 15 mg. of crystals, m. p. 175~179°C, and a third crop of 15 mg. of crystals, m. p. 173~175°C, were obtained. All these crystals showed no depression of the melting point on admixture with 2,4,7-tribromotropone, m. p. 183°C. The final residual oil decomposed on heating, evolving bromine and afforded 90 mg. of 2,4,7-tribromotropone, m. p. 177~179°C.

b) In chloroform solution.—To a solution of 150 mg. of 4-bromotropone dissolved in 3 cc. of chloroform, 390 mg. (3 mol. equiv.) of bromine was added, and the mixture was allowed to stand in a sealed vessel for one month. This was then dried to constant weight over potassium hydroxide and paraffin in a vacuum desiccator and 410 mg. of reddish orange viscous oil V was obtained. This oil began to crystallize after a few days but showed such a tendency to decompose that the oil itself was submitted to analyses and spectral measurements.

Anal. Found: C, 16.54; H, 1.38. Calcd. for $C_7H_5OBr_3$: C, 16.61; H, 1.00%. I.R. Spectrum: $\tilde{\nu}$ (C=O, C=C) 1738, 1675, 1605 cm^{-1} (without solvent).

On washing with benzene, the crystals which melted at ca. 85°C with decomposition were obtained but after standing, they showed m. p. 125~140°C.

13) m.p. are uncorrected. The microanalyses were carried out by Mr. Shin-ichi Ohyama to whom the author's sincere acknowledgements are hereby extended.

Bromination of 2,5-Dibromotropone. — *a*) *In acetic acid solution.*—One gram (3 mol. equiv.) of bromine was added to a solution of 550 mg. of 2,5-dibromotropone dissolved in 6 cc. of acetic acid and the mixture was allowed to stand in a sealed vessel at room temperature. Needle crystals began to crystallize out after one month and the crystals were collected after a total of two months. The first crop of 100 mg. of pale yellow needle crystals, m. p. 183~184°C, were collected and the filtrate was dried over potassium hydroxide, affording a second crop of 220 mg. of crystals, m. p. 180~181°C. Both were identified with 2,4,7-tribromotropone by mixed fusion. The final mother liquor also began to crystallize but was dissolved in chloroform and passed through a short column of alumina. Removal of the solvent from the effluent afforded 220 mg. of crystals which melted at 80~120°C with decomposition. It probably contained some addition products but recrystallization from benzene gave only 50 mg. of 2,4,7-tribromotropone, m. p. 178~180°C, and the residue could not be purified further.

b) *In chloroform solution.*—To a solution of 280 mg. of 2,5-dibromotropone dissolved in chloroform, 510 mg. (3 mol. equiv.) of bromine was added and the mixture was allowed to stand in a sealed vessel for 2 weeks. This was dried to a constant weight over paraffin and potassium hydroxide in a vacuum desiccator to remove the chloroform and 460 mg. of reddish orange oil VI was obtained. This oil was submitted to analyses and spectral measurements as it had a tendency to undergo decompostition.

Anal. Found: C, 19.97; H, 1.16. Calcd. for $C_7H_4OBr_4$: C, 19.83; H, 0.95%. I.R. Spectrum: $\tilde{\nu}$ (C=O, C=C) 1658, 1613 cm^{-1}.

After about 2 days, the oil crystallized and melted at 60~65°C with decomposition, but recrystallization from ethanol afforded crystals melting at 165~173°C, and indicated that the majority had changed to 2,4,7-tribromotropone.

Bromination of 2,7-Dibromotropone. — *a*) *In acetic acid solution.*—Three hundred milligrams (3.3 mol. equiv.) of bromine was added to a solution of 150 mg. of 2,7-dibromotropone dissolved in 15 cc. of acetic acid and the mixture was allowed to stand for one month at room temperature. This mixture was dried over potassium hydroxide in a vacuum desiccator to give 200 mg. of pale yellow crystals, m. p. 155°C (decomp.), which was recrystallized from benzene and afforded pale yellow prisms VII, m. p. 156~157°C (decomp.).

Anal. Found: C, 20.45; H, 1.61. Calcd. for $C_7H_4OBr_4$: C, 19.83; H, 0.95%. U.V. Spectrum: $\lambda_{max}^{cyclohexane}$ mμ (log ε): 230(3.95), 295(3.73). I.R. Spectrum: $\tilde{\nu}$ (C=O, C=C) 1656, 1613 cm^{-1}. (in KBr disk).

In another experiment by the same procedure, some crystals other than VII were obtained, which partially melted at 105°C and melted with decomposition at 130°C (Anal. Found: C, 16.55; H, 0.94%).

b) *Bromination under heating.*—A solution of 70 mg. of 2,7-dibromotropone dissolved in 3 cc. of acetic acid containing 130 mg. (3 mol. equiv.) of bromine was sealed in a tube and heated in a boiling water bath for 6 hours. The mixture was dried over potassium hydroxide in a vacuum desiccator and 70 mg. of pale yellow plates, m. p. 167~169°C, were obtained. This was the recovered starting material.

c) *Bromination in the presence of sodium acetate under heating.*—A mixture of 50 mg. of 2,7-dibromotropone and 50 mg. of sodium acetate dissolved in 2 cc. of acetic acid containing 90 mg. (3 mol. equiv.) of bromine was heated for 3 hours. Treatment as above afforded 50 mg. of plae yellow crystals, m. p. 145~163°C, which on recrystallization from ethanol-benzene mixture gave 30 mg. of crystals melting at 168~169°C and 5mg. of those melting at 160~163°C. Both were found to be 2,7-dibromotropone by admixing.

Reaction of Various Bromine Addition Compounds with Sodium Acetate in Ethanol Solution. — *a*) *2, 3, 4, 5, 6, 7-Hexabromocycloheptanone (III).*—A solution of 300 mg. of III and 200 mg. of sodium acetate dissolved in 5 cc. of ethanol was refluxed on a water bath for 30 minutes. The ethanol was evaporated off from the mixture and a small amount of water was added to the residual solution by which 100 mg. of pale yellow needles, m. p. 180~181°C, was obtained. The mixed melting point proved it to be 2,4,7-tribromotropone. This mother liquor, was diluted with water, extracted with chloroform and the extract was passed through a column of alumina. The alumina was eluted with ethanol and evaporation of ethanol from the effluent left 100 mg. of colorless crystals, m. p. 157~162°C, which showed no depression on admixture with 2,7-dibromotropone but the mixed melting point was depressed on fusion with 2,4,7-tribromotropone. Therefore, this was assumed roughly to be 2,7-dibromotropone.

b) *2, 4, 5, 6, 7-Pentabromo-2-cyclohepten-1-one (IV).*—To a solution of 80 mg. of IV dissolved in 5 cc. of ethanol, 100 mg. of sodium acetate was added and the mixture was heated on a water bath for 50 minutes. Evaporation of ethanol left 30 mg. of pale yellow needles, m. p. 178~180°C, and the melting point was raised to 180~181°C on recrystallization from benzene, undepressed on admixture with 2,4,7-tribromotropone.

c) *2, 3, 4, 6, 7-Pentabromo-4-cyclohepten-1-one (V).*—A mixture of 200 mg. of V and 100 mg. of sodium acetate in 4 cc. of ethanol was refluxed on a water bath for 30 minutes and thereafter treated as in a), from which 90 mg. of crystals, m. p. 110~155°C (sint. 80°C), was obtained. Recrystallization from ethanol afforded 30 mg. of pale yellow crystals, m. p. 173~175°C, whose mother liquor will be designated as (A). The melting point of these crystals was raised to 179~180°C by recrystallization from benzene and admixed melting point test identified them to be 2,4,7-tribromotropone.

Ethanol was evaporated off from the mother liquor (A), the residue was dissolved in chloroform, and the solution was passed through a short alumina column. Evaporation of chloroform

from the effluent gave 50 mg. of crystals melting at 70~80°C. The crystals were dissolved in carbon tetrachloride and again passed through a short alumina column. Crystals obtained from the effluent were recrystallized from ethanol and afforded 30 mg. of colorless plates, m. p. 83~84°C. (*Anal.* Found: C, 33.59; H, 2.53%.)

d) 2,5,6,7-Tetrabromo-2,4-cycloheptadien-1-one (VI).—A solution of 130 mg. of oily VI and 70 mg. of sodium acetate dissolved in 2.5 cc. of ethanol was heated on a water bath for 30 minutes, water was added to the mixture, and crystals that separated out were collected by filtration to give 90 mg. of yellowish needles, m. p. 179~180°C, undepressed on admixing with 2, 4, 7-tribromotropone.

e) 2,4,5,7-Tetrabromo-2,6-cycloheptadien-1-one (VII).—A mixture of 100 mg. of VII and 100 mg. of sodium acetate in 2.5 cc. of ethanol was refluxed on a water bath for 30 minutes, ethanol was evaporated, and water was added to the residue by which 70 mg. of pale yellow silky crystals, m. p. 155~170°C, were obtained. Recrystallization from benzene first afforded 30 mg. of crystals melting at 182~183°C, identified by admixture with 2, 4, 7-tribromotropone. Concentration of this recrystallization mother liquor gave another crop of crystals, m. p. 160~173°C, which were dissolved in chloroform and passed through an alumina column. Elution with ethanol afforded 20 mg. of crystals, m. p. 169~170°C, showing no depression on admixture with 2, 7-dibromotropone.

Thermal Decomposition of Various Bromine Addition Compounds in Acetic Acid Solution.—*a) 2, 3, 4, 5, 6, 7-Hexabromocycloheptanone (III).*—A solution of 120 mg. of III dissolved in 2 cc. of acetic acid was refluxed in an oil bath for 3 hours, during which the evolution of hydrogen bromide (blue coloration of Congo-red paper) and bromine (blue coloration of iodine-starch paper) was observed. Acetic acid was then evaporated from the solution, and the residue was washed with ethanol, affording 40 mg. of pale yellow crystals, m. p. 150~161°C. The crystals were dissolved in chloroform and the solution was passed through a short alumina column. Evaporation of chloroform from the effluent left crystals melting at 160~165°C, which were recrystallized from ethanol-benzene mixture, giving 25 mg. of pale yellow plates, m. p. 170~171°C, identified as 2, 7-dibromotropone by mixed fusion.

b) 2, 4, 5, 6, 7-Pentabromo-2-cyclohepten-1-one (IV).—A solution of 80 mg. of IV dissolved in 2 cc. of acetic acid was refluxed on a water bath for 3 hours, acetic acid was evaporated, and the crystalline residue was washed with ethanol, affording 30 mg. of colorless plates, m. p. 169~170°C, undepressed on admixture with 2, 7-dibromotropone.

c) 2, 3, 4, 6, 7-Pentabromo-4-cyclohepten-1-one (V).—A solution of 80 mg. of V dissolved in 2cc. of acetic acid was refluxed for 3 hours and thereafter treated as in b), affording 45 mg. of crystals melting at 125~140°C. Recrystallization from ethanol gave 20 mg. of pale yellow needles, m. p. 178~180°C, identified as 2, 4, 7-tribromotropone by mixed fusion.

Ethanol was evaporated from the recrystallization mother liquor, the residue was dissolved in chloroform, and passed through an alumina column. This effluent gave 10 mg. of pale yellow crystals, m. p. 120~135°C, which were not identified.

d) 2, 5, 6, 7-Tetrabromo-2, 4-cycloheptadien-1-one (VI).—A solution of 90 mg. of VI dissolved in 2 cc. of acetic acid was refluxed for 3 hours and thereafter treated as in b), affording 30 mg. of dark brownish crystals, m. p. 165~175°C. The crystals were dissolved in benzene and passed through an alumina column, and evaporation of the solvent left yellow needles, m. p. 172~176°C, undepressed on admixing with 2,4,7-tribromotropone.

e) 2,4,5,7-Tetrabromo-2,6-cycloheptadien-1-one (VII).—A solution of 60 mg. of VII dissolved in 2 cc. of acetic acid was refluxed in an oil bath for 3 hours and thereafter treated as in b), affording 40 mg. of pale yellow plates, m. p. 169~170°C, identified with 2, 7-dibromotropone by mixed fusion.

Thermal Decomposition of Various Bromine Addition Compound.—*a) 2,3,4,5,6,7-Hexabromocycloheptanone (III).*—One hundred milligrams of III was placed in a small test tube and dipped in an oil bath at 145~150°C by which the compound melted and decomposed, with evolution of hydrogen bromide and bromine. The contents were heated at this temperature for 20 minutes, cooled, and the crystalline residue was washed out with ethanol, affording 40 mg. of dark brown crystals, m. p. 140~150°C. The crystals were dissolved in benzene, passed through a column of alumina, and the column was eluted with chloroform. The benzene eluate gave a few mg. of crystals, m. p. 140~150°C, and the chloroform effluent gave 25 mg. of colorless crystals, m. p. 169~170°C. Mixed fusion proved the latter to be 2, 7-dibromotropone.

b) 2, 4, 5, 6, 7-Pentabromo-2-cyclohepten-1-one (IV).—One hundred milligrams of IV was heated and decomposed in a small test tube as in a) and 50 mg. of colorless crystals, m. p. 145~150°C, were obtained. Recrystallization from ethanol afforded colorless plates, m.p. 150~157°C. These crystals were dissolved in chloroform, passed through an alumina column, and eluted with ethanol. Chloroform effluent afforded a few mg. of colorless crystals, m. p. 170~172°C, and ethanol eluate afforded 30 mg. of colorless plates, m. p. 167~169°C. By mixed fusion, the former was identified with 2, 4, 7-tribromotropone and the latter with 2, 7-dibromotropone.

c) 2, 3, 4, 6, 7-Pentabromo-4-cyclohepten-1-one (V).—Thermal decomposition of 120 mg. of V in a small test tube as in a) afforded 60 mg. of pale brown crystals, m. p. 177~179°C, which were recrystallized from ethanol to pale yellow needles, m. p. 182~183°C and identified with 2, 4, 7-tribromotropone by admixture with an authentic sample.

d) *2, 5, 6, 7-Tetrabromo-2, 4-cycloheptadien-1-one* (*VI*).—Thermal decomposition of 120 mg. of VI in a small test tube as in a) afforded 70 mg. of pale yellow crystals, m. p. 179~181°C, which showed no depression on admixing with 2, 4, 7-tribromotropone.

e) *2, 4, 5, 7-Tetrabromo-2, 6-cycloheptadien-1-one* (*VII*).—Thirty milligrams of VII was placed in a small test tube and heated for 20 minutes in an oil bath at 160°C. After cooling, the crystalline residue was sublimed at 5 mm. Hg in a bath at 140°C and afforded 15 mg. of crystals melting at 163~166°C. Recrystallization from benzene raised the melting point to 167~169°C, undepressed on admixing with 2, 7-dibromotropone.

The author takes this opportunity to express his sincere gratitude to Professor Tetsuo Nozoe for his kind guidance throughout the course of this work and to Professor Shuichi Seto and Assistant Professor Yoshio Kitahara for much helpful advice.

Department of Chemistry, Faculty of Science, Tohoku University, Katahira-cho, Sendai

Reaction of Troponoids and Organometallic Compounds. III[1,2]. *Synthesis and Reaction of 2,7- and 2,3-Diphenyltropone*[3]

By Toshio MUKAI

(Received April 21, 1958)

In the reaction of 2-phenyltropone and phenylmagnesium bromide, two compounds with the composition $C_{19}H_{14}O$, m. p. 87°C and 130°C, were obtained[4]. From their analytical values and ultraviolet and infrared spectra, one of these was assumed to be 2,7-diphenyltropone but there still remained a doubt about this structure for the following reasons. The first is the fact that this reaction would be substitution of a ring hydrogen with phenyl, which would be very unlikely to occur. The second is that 2,7-diphenyltropone is an unknown compound and it would probably have properties fairly different from tropones due to a hindered carbonyl group.

The present paper deals with the synthesis of 2,7-diphenyltropone by an unequivocal process, establishing the structure of the foregoing products from the Grignard reaction, and at the same time, examinations are made on the properties of tropones substituted in the 2- and 7-positions[5].

2,7-Diphenyltropone was synthesized by the reaction of 3-phenyltropolone and phenyllithium. Doering and Hisky[6] had already obtained 2-phenyltropone by the reaction of tropolone and phenyllithium. Later Haworth and Tinker[7] proved that although an abnormal substitution occurred in the Grignard reaction of 4-methyltropolone methyl ethers, the reaction of the copper complex of 4-methyltropolone and phenyllithium resulted in the normal substitution, affording 6-methyl-2-phenyltropone. Since the reaction of tropolones and phenyllithium results firstly in the formation of the lithium salt of tropolones, it may be assumed that it would result in the normal substitution, as in the case of the copper complex, to form 2-phenyltropones.

Actually, the reaction of 3-phenyltropolone and phenyllithium afforded two kinds of compound, one of m. p. 132°C (I) and the other of m. p. 147°C (II).

These were assumed to be the corresponding diphenyltropones from their analytical values and the infrared absorption

1) Part I: T. Nozoe, T. Mukai, J. Minegishi and T. Fujisawa, *Science Repts. Tohoku Univ.*, **1**, **37**, 388 (1953).

2) Part II: K. Kikuchi, *J. Chem. Soc. Japan, Pure Chem. Sec.* (*Nippon Kagaku Zassi*), **77**, 1439 (1956).

3) This paper was read before the Local Meeting of Tohoku District of the Chem. Soc. Japan held in Hirosaki on September 27, 1956.

4) T. Nozoe, T. Mukai and others, unpublished work.

5) A number of 2,7-dibenzyltropones were synthesized, of which the chemical behavior has not been much described. N. J. Leonard, L. A. Miller and J. W. Berry, *J. Am. Chem. Soc.*, **79**, 1482 (1957).

6) W. von E. Doering and C. F. Hisky, ibid., **74**, 5688 (1952).

7) R. D. Haworth and P. B. Tinker, *J. Chem. Soc.* **1955**, 911.

spectra[8] shown in Fig. 1. As will be shown later, II was identified as 2, 3-diphenyltropone by its conversion into 2, 3-diphenylbenzoic acid. I was identified with one of the products, of m. p. 130°C, from the foregoing reaction of 2-phenyltropone and phenylmagnesium bromide as expected. From the course of these two reactions, it may be concluded that I is 2, 7-diphenyltropone. It follows, therefore, that the reaction of tropolone and phenyllithium results in the normal substitution.

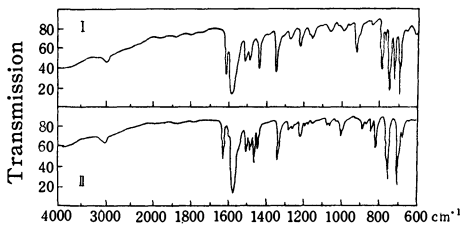

Fig. 1. I. R. absorption spectra of 2, 7-diphenyl-(I) and 2, 3-diphenyltropone (II) in KBr.

The reaction of tropolone methyl ether and methylmagnesium iodide does not give 2-methyltropone[9], but, since 2-alkyltropones are obtained by the reaction of tropolone and methyllithium[10] or *n*-butyllithium[6], it may be assumed that a lithium compound convenient for the formation of tropones is formed as an intermediate. This may be illustrated as shown below with the reaction of 3-phenyltropolone and phenyllithium as an example. This reaction is rather interesting when compared with the fact that a ketone and not a carbinol is formed in the reaction of free carboxylic acid and an organolithium compound[11].

The ultraviolet spectra of 2, 3- (II) and 2, 7-diphenyltropone (I) are shown in Fig. 2. The absorption of I is very similar to that of 2-phenyltropone[1,12] but is shifted slightly to a longer wave length region. On the contrary, the absorption of II is shifted to a much shorter wave length region than that of I and indicates that the phenyl groups in the 2- and 3-positions have a fair amount of steric strain.

Both I and II have weak basicity and do not form picrates. Passage of hydrogen chloride gas through the benzene solution of I or II only precipitates a part of the hydrochloride.

Since the two reactive sites, 2- and 7-positions, in I are blocked, the reactivity of 2, 7-diphenyltropone is of interest. I is extremely stable to alkalis and amines, and it remains unchanged on heating with dilute alkali or *p*-toluidine in ethanol solution[1,13]. Heating with hydroxylamine or hydrazine fails to effect amination of the ring[1,13]. I does not react with ketonic reagents such as 2, 4-dinitrophenylhydrazine[1,13]. These facts indicate that the substitution of 2- and 7-positions of the tropone ring with a bulky group like phenyl results in an extremely great increase in stability and the above reactions characteristic to tropones in general are not observed.

In contrast to the stability of I, 2, 3-diphenyltropone (II) is labile to alkali and on heating with dilute alkali in ethanolic solution, it forms an acid substance as colorless crystals, m. p. 178°C. The ultraviolet spectrum of this substance is shown in Fig. 2, which indicates that it does not contain the tropone ring[12]. Since alkaline rearrangement of 2-phenyltropone results in the formation of diphenyl-2-carboxylic

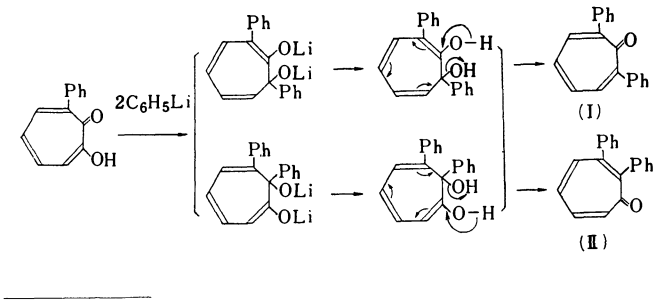

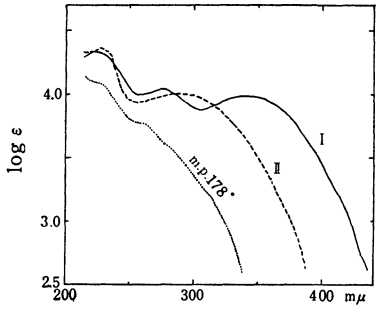

Fig. 2. U. V. absorption spectra of 2, 7-diphenyl-(I), 2, 3-diphenyltropone (II) and a compound melted at 178°C in methanol.

8) I. R. spectra are measured using Perkin-Elmer Model 21 double beam spectrophotometer by Mr. Yusaku Ikegami of the Chemical Research Institute Non-aqueous Solutions, to whom the author is deeply indebted.

9) T. Nozoe, T. Mukai and J. Minegishi, *Proc. Japan Acad.*, **27**, 419 (1951).

10) T. Mukai, to be published.

11) H. F. Bluhm, H. V. Donn and H. D. Zook, *J. Am. Chem. Soc.*, **77**, 4406 (1955).

12) M. Tsuboi, This Bulletin, **25**, 369 (1952).

13) T. Nozoe, T. Mukai and K. Takase, *Science Repts. Tohoku Univ.*, **I**, **39**, 164 (1956).

acid[1], the rearrangement product of II was assumed to be 2, 3-diphenylbenzoic acid but mixed fusion with 2, 3-diphenylbenzoic acid resulted in depression of the melting point. The reaction must have been quite specific and examination is still in progress as to the structure of this rearrangement product.

II easily forms a 2, 4-dinitrophenylhydrazone and gives 2-amino-6,7-diphenyltropone (III) by reaction with hydrazine[1,13]. Alkali hydrolysis of III affords 3, 4-diphenyltropolone (IV) which shows the coloration with ferric chloride characteristic of tropolone. The ultraviolet spectrum of IV, shown in Fig. 3, exhibits the

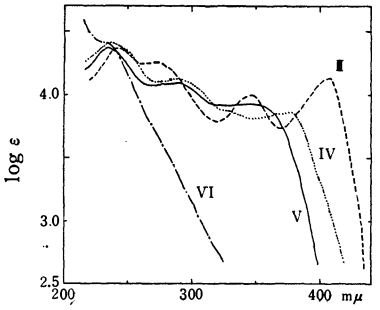

Fig. 3. U. V. absorption spectra of 2-amino-6, 7-diphenyltropone (III), 3, 4-diphenyltropolone (IV), methyl ether of IV (V) and 2, 3-diphenylbenzoic acid (VI) in methanol.

maximum absorptions at 323 and 374 mμ, which is a tropolone type[14], but it seems to be different from that of 3-phenyltropolone[1] since there is a maximum at 285mμ. IV forms a methyl ether (probably V[15]) on the application of diazomethane and reaction of the methyl ether with sodium methoxide in absolute methanol, followed by hydrolysis gives compound VI of m. p. 162°C. 2, 3-Diphenylbenzoic acid had already been synthesized by K. Alder et al.[16], who reported the compound to melt at 161°C, so that VI must be identical with it. From the series of reactions of II to VI, the structure of II was established as 2, 3-diphenyltropone. Fig. 3 gives the ultraviolet spectra of V and VI.

Next, bromination of these two diphenyltropones was carried out. Application of

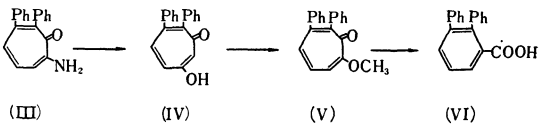

an excess of bromine to I in acetic acid first afforded a dibromide VII which, on treatment with sodium acetate, formed a monobromo compound VIII. Ultraviolet absorption spectra of VII and VIII are shown in Fig. 4. From the result of

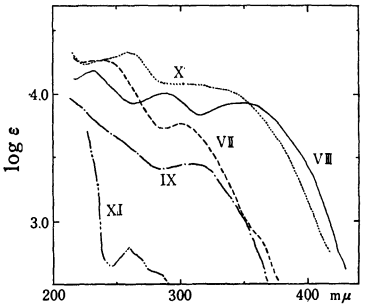

Fig. 4. U. V. absorption spectra of brominated compounds of I (VII and VIII), of II (IX and X) and 2, 7-diphenylsuberone (XI) in methanol.

dehydrobromination of VII and the fact that the ultraviolet spectrum of VII is shifted to a shorter wave-length region, it is assumed that VII is a bromine addition product. On the other hand, the absorption curve of VIII is similar to that of I, shifted slightly to a longer wavelength region, which indicates that VIII may be considered to be a bromine substituted compound. Experiments to determine the position of the bromine were not carried out but it has been pointed out that bromine addition does not take place at the double bond with the phenyl group in the bromination of 2-phenyltropone[17]. It follows, therefore, that VII would be the compound with bromine addition in C_4—C_5 positions and VIII is most probably 4-bromo-2, 7-diphenyltropone. In the ultraviolet spectrum of VII there is a certain amount of absorption in a region near 300 mμ, so that an unsaturated ketonic structure like VII seems to be most appropriate.

Bromination of II in acetic acid also results in the formation of a tetrabromide IX whose treatment with sodium acetate to effect dehydrobromination affords a dibromo compound X. Since there are two phenyl substituents in C_2 and C_3 position of II, it follows that bromine addition

14) T. Nozoe, *Fortshr. Chem. Org. Naturst.*, **13**, 232 (1956).
15) There are two isomers of methyl ether of 3-phenyltropolone, of which the ether corresponding to V was more easily isolated than another isomer. (cf. Ref. 1).
16) K. Alder, J. Haydn, K. Heimbach and K. Neufang, *Ann.*, **586**, 110 (1954).

must take place in C_4—C_5 and C_6—C_7 double bond[17]. Ultraviolet spectra of IX and X, indicated in Fig. 4, show that the absorption of IX is low in intensity and there is a good probability that it is an addition product, while the absorption of X is shifted to a longer wave-length region than that of II and it is probably safe to conclude that X is a bromine substituted compound.

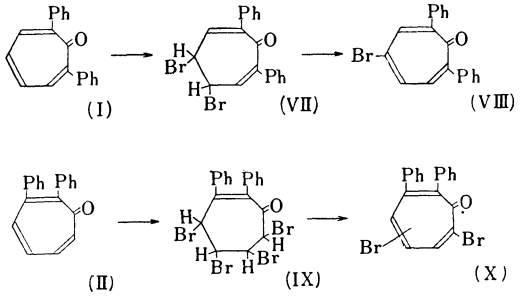

Hydrogenation of I with palladium-charcoal as a catalyst resulted in facile absorption of hydrogen and 2, 7-diphenylsuberone (XI) was formed. The ultraviolet spectrum of XI in Fig. 4 shows the absorption of two phenyl at groups 259mμ[18], while its infrared spectrum in Fig. 5 shows absorptions for C=O at 1706 for C=C of phenyl at 1603 and for CH_2 at 2935 and

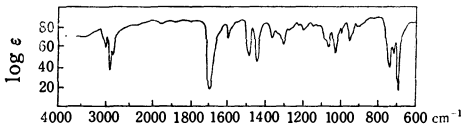

Fig. 5. I. R. absorption spectrum of 2,7-diphenylsuberone (XI) in KBr.

2860 cm^{-1}, which support the structure of XI. In connection with the examination of unsaturated characters, both I and II were heated with maleic anhydride in xylene but no addition products were obtained.

Experimental[19]

Reaction of 3-Phenyltropolone and Phenyllithium. — To a solution of phenyllithium, obtained from 0.42 g. (0.06 g. at.) of lithium, 4.7 g. (0.03 mole) of bromobenzene, and 18 cc. of ether, a solution of 1.00 g. (0.005 mole) of 3-phenyltropolone in 18 cc. of ether and 18 cc. of benzene was added dropwise in a nitrogen stream, when a slight generation of heat was observed. The mixture was stirred for 2 hours at room temperature and dilute sulfuric acid was then added under ice-cooling to effect decomposition. The organic solvent layer was separated, washed with water, and dried over anhydrous sodium sulfate. Evaporation of the solvent left 1.2 g. of dark reddish brown oil which was dissolved in benzene, saturated with hydrogen chloride gas, and the oily hydrochloride that separated out was collected by decantation. This was decomposed with water, extracted with carbon tetrachloride, and the solution was passed through an alumina column. Evaporation of the solvent from the initial carbon tetrachloride eluate afforded 180 mg. of colorless crystals I, m. p. 130~132°C. Recrystallization from ethanol gave colorless microplates, m. p. 133°C.

Anal. Found: C, 87.97; H, 5.65. Calcd. for $C_{19}H_{14}O$: C, 88.34; H, 5.46%. λ_{max}^{MeOH} mμ (log ε): 226(4.37), 279(4.06), 340(4.01).

The alumina column was then eluted with benzene and evaporation of benzene from the effluent left 130 mg. of colorless crystals II, m. p. 146°C. Recrystallization from ethanol afforded colorless plates, m. p. 147°C.

Anal. Found: C, 88.40; H, 5.47. Calcd. for $C_{19}H_{14}O$: C, 88.34; H, 5.46%. λ_{max}^{MeOH} mμ (log ε): 227(4.39), 292(4.03).

The benzene solution obtained after removal of the oily hydrochloride was washed with water and then passed through an alumina column. Initial effluent afforded 60 mg. of I, m. p. 132°C, and the latter eluate afforded further 110 mg. of II, m. p. 146°C. By mixed fusion, I was identified with the compound, m. p. 130°C, obtained from the reaction of 2-phenyltropone and phenylmagnesium bromide[4].

Addition of ethanolic solution of picric acid to the ethanolic solution of I or II failed to afford any crystalline picrate.

2, 4-Dinitrophenylhydrazone of II was obtained as dark red crystals, m. p. 208°C (decomp.).

Anal. Found: N, 12.24. Calcd. for $C_{25}H_{18}O_4N_4$: N, 12.87%. λ_{max}^{MeOH} mμ (log ε): 400(4.36).

On the other hand, application of 2, 4-dinitrophenylhydrazine to I in ethanol, in the presence of a trace of hydrochloric acid, with heating resulted in the recovery of I.

Behavior of the Diphenyltropones (I and II) to Alkali. — To a mixed solution of 1 cc. of ethanol and 1 cc. of 2N potassium hydroxide, 20 mg. of II was added and the mixture was refluxed on a water bath for 1.5 hours, when the solution turned brown in color and a small amount of resinous solid separated out. Ethanol was then evaporated from the mixture, water was added, and solid matter was filtered off. The filtrate was acidified and extracted with chloroform, from which 10 mg. of a pale yellow oil was obtained.

17) T. Mukai, *Science Repts. Tohoku Univ.*, **I**, **38**, 280 (1954).

18) In the series of Ph-$(CH_2)_n$-Ph (n>1), the absorption band is situated near 260 mμ and is not so intense (ε< 3000). cf. A. E. Gillam and E. S. Stern "An Introduction to Electronic Absorption Spectroscopy in Organic Chemistry" Edward Arnold Ltd., London (1955), p. 64.

19) m.p. are uncorrected. The microanalyses were carried out by Mr. Shinichi Ohyama and Miss Ayako Iwanaga, to whom the author's deep gratitude is hereby expressed.

Trituration of this oil with cyclohexane effected crystallization and colorless crystals which sintered at 170°C and melted at 175~178°C were obtained. This substance showed depression of the melting point on admixture with 2, 3-diphenylbenzoic acid (VI), m. p. 162°C, described later.

On the other hand, the same treatment of 20 mg. of I with ethanolic potassium hydroxide solution by refluxing for 4 hours afforded 20 mg. of crystals melting at 124~126°C, indicating the complete recovery of I.

Reaction of the Diphenyltropones (I and II) with Hydrazine or Hydroxylamine. — *a*) To a solution of 40 mg. of II dissolved in 0.2 cc of ethanol, 0.10 cc. of 80% hydrazine hydrate was added and the mixture was heated on a water bath for a few minutes, from which 30 mg. of 2-amino compound was obtained as yellow crystals of m. p. 253~258°C. Recrystallization from ethanol afforded gold colored scales III, m. p. 260°C.

Anal. Found: C, 83.36; H, 5.67; N, 5.92. Calcd. for $C_{19}H_{15}ON$: C, 83.49; H, 5.53; N, 5.13%. λ_{max}^{MeOH} mμ (log ε): 242(4.35), 270(4.25), 346(4.00), 406(4.14).

I is recovered on reacting with hydrazine in the same manner. Application of hydrazine to a mixture of I and II results in amination of II alone and I remains inactive. This is a convenient method for the separation of I and II.

b) A mixture of 30 mg. of II, 30 mg. of hydroxylamine hydrochloride, 0.5 cc. of absolute ethanol, and 0.5 cc. of pyridine was refluxed on a water bath for 2 hours. The solvent was evaporated from the mixture and water was added, from which 25 mg. of yellow crystals, m.p. 210~213°C, separated out. Recrystallization from ethanol raised the melting point to 212~213°C.

Anal. Found: N, 4.80. Calcd. for $C_{19}H_{15}ON$: N, 5.13%. λ_{max}^{MeOH} mμ (log ε): 237(4.30), 345(3.70), 403(3.72).

From the color of this substance and its ultraviolet spectrum, it is still doubtful that the substance is an oxime and probable occulusion of III may be considered.

I is completely recovered on similar reaction with hydroxylamine.

Formation of 3, 4-Diphenyltropolone (IV). —A solution of 120 mg. of III dissolved in a mixture of 6 cc. of ethanol and 2 cc. of 6N potassium hydroxide was refluxed for 12 hours on a water bath, ethanol was evaporated, and the residue was diluted with water. The solution was neutralized to weak acidity, extracted with benzene, and evaporation of benzene left 110 mg. of pale brown crystals, m. p. 160~165°C. Recrystallization from ethanol afforded 100 mg. of colorless crystals (IV), m. p. 173°C.

Anal. Found: C, 83.08; H, 5.41. Calcd. for $C_{19}H_{14}O_2$: C, 83.20; H, 5.15%. λ_{max}^{MeOH} mμ (log ε): 235(4.39), 285(4.11), 323(3.87), 365(3.83), 374(3.85).

Formation of 3, 4-Diphenyltropolone Methyl Ether (V) and Aromatization Rearrangement of V.—To 2cc. of 2.8% ethereal solution of diazomethane, 70 mg. of IV was added and the mixture was allowed to stand in a cool place overnight. Evaporation of ether left 70 mg. of pale yellow needles, m. p. 140~144°C. Recrystallization from benzene-cyclohexane mixture gave V melting at 147°C.

Anal. Found: C, 83.31; H, 5.39. Calcd. for $C_{20}H_{16}O$: C, 83.31; H, 5.59%. λ_{max}^{MeOH} mμ (log ε): 235(4.37), 287(4.09), 355(3.89).

A solution of 60 mg. of the methyl ether V dissolved in 3 cc. of absolute ethanol containing 10 mg. of sodium was refluxed for 30 hours, 5 cc. of water was added, and the mixture was heated again for 3 hours. Ethanol was evaporated, the residue diluted with water, and the solution extracted with ether to remove any neutral substance. The aqueous layer was neutralized until the acidity was weak, extracted with benzene, and benzene residue gave 20 mg. of colorless crystals. Recrystallization from benzene-cyclohexane mixture afforded colorless crystals, m. p. 162°C. Reported m. p. for 2, 3-diphenylbenzoic acid is 161°C[16].

Bromination of 2, 7-Diphenyltropone (I).— A mixture of 200mg. of I and 300mg. (5mol. equiv.) of bromine in 7 cc. of acetic acid was warmed, sealed in a vessel, and allowed to stand for 6 days. Evaporation of acetic acid over potassium hydroxide in a vacuum desiccator left 100 mg. of pale yellow crystals, m. p. 115°C (decomp.). The filtrate obtained after removal of these crystals was evaporated and 150 mg. of orange solid obtained.

Its treatment with ethanol and benzene afforded 60mg. of pale yellow crystals, m.p. 123°C (decomp.).

Recrystallization of the former from ethanol and benzene gave 80 mg. of pale yellow needles VII, m. p. 120°C (decomp.), which were identified with the later-obtained crystals by mixed fusion.

Anal. Found: C, 54.58; H, 3.41. Calcd. for $C_{19}H_{14}OBr_2$: C, 54.78; H, 3.34%. λ_{max}^{MeOH} mμ (log ε): 227(4.28).

Dehydrobromination of the Bromine Adduct VII.—A mixture of 60 mg. of VII and 50 mg. of sodium acetate in 2 cc. of ethanol and 1 cc. of benzene was refluxed for 2 hours, the solvent was evaporated, and the residue was diluted with water. Extraction with benzene and evaporation of solvent afforded 50 mg. of orange yellow oil which solidified to crystals of m. p. 75~80°C. The carbon tetrachloride solution of this substance was passed through an alumina column and the crystals obtained therefrom were recrystallized from ethanol to pale yellow needles VIII, m. p. 92°C.

Anal. Found: C, 68.01; H, 3.91. Calcd. for $C_{19}H_{13}OBr$: C, 67.60; H, 3.89%. λ_{max}^{MeOH} mμ (log ε): 229(4.20), 285(4.01), 347(3.94).

Bromination of 2, 3-Diphenyltropone (II). —To a solution of 50 mg. of II dissolved in 3 cc. of acetic acid, 130 mg. (4.5 mol. equiv.) of bromine was added and the mixture was allowed to stand for 3 days at room temperature. Acetic acid was evaporated over potassium hydroxide and 100 mg. of orange crystals, m. p. 123~130°C, was obtained. Recrystallization from benzene-cyclohexane mixture afforded pale yellow plates IX, m. p. 131°C (decomp.).

Anal. Found: C, 40.35; H, 2.74. Calcd. for $C_{19}H_{14}OBr_4$: C, 39.41; H, 2.41%. λ_{max}^{MeOH} mμ (log ε): 305(3.43).

Dehydrobromination of Bromine Adduct IX.—To a solution of 60 mg. of IX dissolved in 2 cc. of ethanol, 30 mg. of sodium acetate was added and the mixture was refluxed on a water bath for 3 hours. Ethanol was evaporated from the mixture, the residue was dissolved in carbon tetrachloride, and the solution was passed through an alumina column. The column was eluted with benzene, and evaporation of the solvent from both eluates left 30 mg. of pale yellow crystals, m. p. 135~160°C, which recrystallized from ethanol to pale yellow needles X, m. p. 167°C.

Anal. Found: C, 55.19; H, 3.01. Calcd. for $C_{19}H_{12}OBr_2$: C, 54.81; H, 2.88%. λ_{max}^{MeOH} mμ (log ε): 258(4.33), 295(4.10).

Catalytic Reduction of 2, 7-Diphenyltropone (I).—To a solution of 50 mg. of I dissolved in 10 cc. of methanol, 10 mg. of 5% palladium-charcoal was added and the mixture was hydrogenated at ordinary temperature and pressure. The absorption of hydrogen ceased after 14.2 cc. (3 mol. equiv.) of hydrogen had been absorbed. The filtrate obtained after removal of the catalyst was evaporated and the colorless crystalline residue was recrystallized from methanol to 40 mg. of colorless needles XI, m. p. 143°C.

Anal. Found: C, 86.72; H, 7.11. Calcd. for $C_{19}H_{20}O$: C, 86.32; H, 7.63%. λ_{max}^{MeOH} mμ (log ε): 259(2.79).

Diels-Alder Reaction of the Diphenyltropones (I and II).—A solution of 50 mg. of I and 40 mg. of maleic anhydride dissolved in absolute xylene was refluxed for 4 hours and the residue obtained on evaporation of the solvent was recrystallized from ethanol to 40 mg. of pale yellow crystals, m. p. 132°C, identified with I by mixed fusion.

The same treatment of II with maleic anhydride also resulted in its recovery but the amount recovered was smaller. However, no addition product was obtained even in this case.

The author takes this opportunity to express his sincere gratitude to Professor Tetsuo Nozoe for his kind guidance throughout the course of this work, to Professor Shuichi Seto for much helpful advice and to Mr. Mutsuo Ishii for his cooperation in carrying out the experiments.

Department of Chemistry, Faculty of Science, Tohoku University, Katahira-cho, Sendai

Synthesis of α-Substituted Glutarimides via Michael Condensation

By Tetsuji KAMETANI[1], William TAUB and David GINSBURG

(Received May 10, 1958)

A useful approach to the synthesis of certain α-substituted glutarimides required as intermediates in the synthesis of potential hypnotic compounds appeared to be the Michael condensation of appropriate donors to various nitrogen containing acceptors.

Cyanoethylation of dibenzyl methyl malonate in the presence of sodium hydride gave the appropriate Michael condensation adduct I whose conversion into α-methylglutarimide(III) proved inefficient. However, it was found that when acrylamide was used as acceptor, a glutarimide derivative II was isolated directly upon workup of the Michael reaction mixture. The α-methyl-α-carbobenzoxy-glutarimide (II) thus obtained could be debenzylated either by catalytic hydrogenolysis using palladized carbon or by treatment with hydrogen bromide in acetic acid[2], affording α-methyl-glutarimide (III). The structure of the latter was proven by hydrolysis to yield the known α-methylglutaric acid and by lithium aluminium hydride reduction to yield the known 3-methylpiperidine. These reactions are summarized in reaction scheme 1.

Similarly, cyanoethylation of diphenylacetonitrile in the presence of methanolic potassium hydroxide gave α,α-diphenylglutarodinitrile (IV). The transformations of this product into α,α-diphenylglutarimide (V) and intermediate products are summarized in reaction scheme 2.

1) Present Address, Pharm. Faculty, the University of Osaka, Hotarugaike, Toyonaka, Osaka.

2) D. Ben-Ishai and A. Berger, *J. Org. Chem.*, **17**, 1564 (1952).

Reaction Scheme 1.

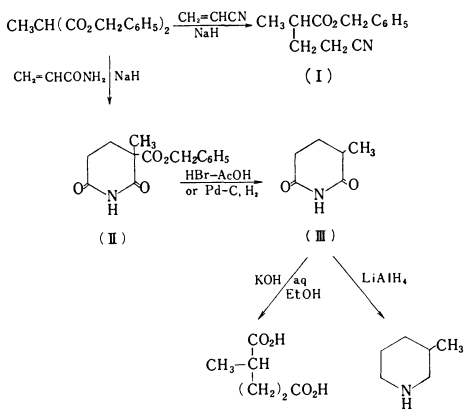

Reaction Scheme 2.

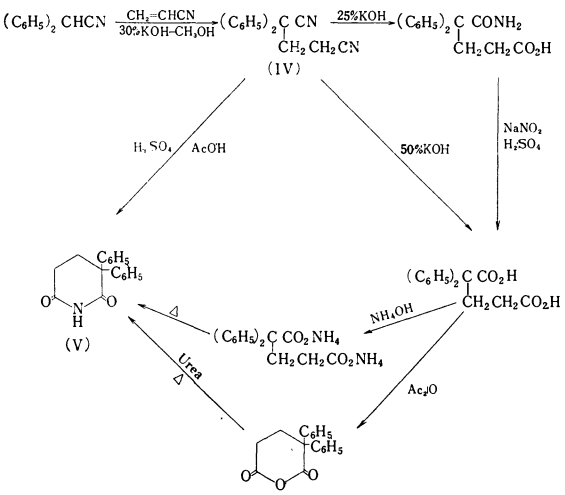

Experimental

Dibenzyl methylmalonate.—This was prepared analogously to the preparation of dibenzyl malonate[3] by transesterification of diethyl methylmalonate[4] (58 g.; 0.33 mole) with benzyl alcohol (72 g.; 0.67 mole) in dry benzene (660 ml.) in the presence of sodium methoxide (1.7 g.). The ester had b. p. 164~167°C/0.04 mm.Hg (71 g.; 72%).

Benzyl α-(2'-cyanoethyl)-propionate (I).—The sodio-derivative was prepared by heating under reflux dibenzyl methylmalonate (37 g.) and sodium hydride (3.8 g.) in dry benzene (300 ml.) for 6 hr. The reaction mixture was cooled and a solution of acrylonitrile (8 g.) in dry benzene (50 ml.) was added and the whole was again refluxed for 6 hr. The benzene was removed at the water pump and the residue was poured into water containing sufficient acetic acid for neutralization. The oily precipitate was extracted with ethyl acetate, the extract was dried, and the solvent was evaporated. Ether was added to the residue (46 g.) and the extract was filtered to remove yellow polymeric material. The ether-soluble material (33 g.) solidified after long standing and was recrystallized from benzene-petroleum ether, m. p. 79~80°C.

Anal. Found: C, 76.85; H, 6.37; N, 4.43. Calcd. for $C_{13}H_{15}O_2N \cdot C_6H_6$: C, 77.28; H, 7.11; N, 4.74%.

3-Carbobenzoxy-3-methylglutarimide (II).—A mixture of dibenzyl methylmalonate (4 g.), sodium hydride (0.33 g.) and dry benzene was refluxed for 2 hr. After cooling, acrylamide[5] (0.33 g.) was added and the mixture was refluxed for 4~5 hr. A clear solution was finally obtained. The benzene was removed under reduced pressure and the residue was poured into ice water containing the calculated quantity of acetic acid required for neutralization. Scratching the precipitated oil after the addition of a small amount of ethanol induced crystallization. The crude solid (3 g.) was filtered, m. p. 93~94°C (from aqueous ethanol).

Anal. Found: C, 64.53; H, 5.61; N, 5.10. Calcd. for $C_{14}H_{15}O_4N$: C, 64.36; H, 5.79; N, 4.36%.

3-Methylglutarimide (III).—*a*) The imide-ester II (36.9 g.) was refluxed with 30% hydrogen bromide in acetic acid (200 ml.) for 6 hr. After evaporation to dryness, the residue was treated with aqueous sodium bicarbonate and ether. The ether layer was evaporated in vacuo to remove the solvent and benzyl bromide. A small amount of imide (0.6 g.) crystallized in the residue. The bicarbonate solution was acidified with dilute hydrochloric acid. The imide was extracted with ether and afforded more crystalline material on evaporation (4.1 g.). Continuous extraction of the acidified solution with ether afforded more of the imide (6.7 g.). Total yield, 62%, m. p. 101~102°C (from ethanol-ether). The imide can be sublimed in a vacuum.

Anal. Found: C, 56.40; H, 7.24; N, 11.10. Calcd. for $C_6H_9O_2N$: C, 56.68; H, 7.14; N, 11.02%.

b) The imide can also be obtained by hydrogenolysis of the imide-ester II (5 g.) in ethyl acetate (100 ml.) in the presence of 10% palladized carbon (0.5 g.) at an initial pressure of 48 lbs./sq. in metric system. Hydrogen uptake (1 mole) was complete within 30 min. The catalyst was removed by filtration and the solvent was removed by distillation. The residue soon solidified, m. p. 94~95°C. Recrystallization from ethanol-ether gave the imide III, m. p. 101~102°C, identical with that described above.

Proof of Structure of 3-Methylglutarimide.—*a*) The imide III (100 mg.) was saponified by refluxing for 7 hr. with potassium hydroxide (0.52 g.) in 50% ethanol (4.5 ml.). Ammonia was evolved. The mixture was evaporated to dryness and the residue was taken up in a little water and the solution was acidified and extracted with ether. The ether was removed from the

3) D. Ginsburg and R. Pappo, *J. Am. Chem. Soc.*, **75**, 1094 (1953).

4) "Organic Syntheses", Coll. Vol. II, Wiley, New York, (1946), p. 279.

5) Cf. D. Elad and D. Ginsburg, *J. Chem. Soc.*, **1953**, 4137.

extract and the residual oil which soon solidified (100 mg.) was recrystallized from benzene-petroleum ether, m. p. 75°C. Lit.[6] m. p. 77~80°C for α-methylglutaric acid.

b) A solution of the imide III (1.27 g.) in dry dioxan (20 ml.) was added to a solution of lithium aluminium hydride (0.27 g.) in dry ether (30 ml.) during 20 min. The mixture was refluxed for 90 min. and was cooled and decomposed slowly with hydrochloric acid (10%). The mixture was evaporated to dryness under reduced pressure. Aqueous potassium hydroxide (50%) was added and the mixture was extracted with ether. Removal of the ether gave an oil (0.3 g.) of piperidine-like odor. The hydrochloride was prepared and had m. p. 171~172°C (from ether-benzene). Lit.[7] m. p. 171~172°C for 3-methylpiperidine.

α,α-Diphenylglutaronitrile (IV).—To a solution of diphenylacetonitrile (77.5 g.) in *tert*-butanol (120 ml.) and dioxan (30 ml.) was added methanolic potassium hydroxide (30%; 3 ml.). A solution of acrylonitrile (21.2 g.) in *tert*-butanol (200 ml.) was then added with stirring at 10~25°C during 30 min. Stirring at room temperature was continued for 2 hr. The emulsion deposited much crystalline material. The mixture was poured into ice-water and the solid was filtered and recrystallized from dilute methanol, m. p. 69~70°C (87 g.). The product depressed the m. p. of diphenylacetonitrile.

Anal. Found: C, 82.82; H, 5.72; N, 11.06. Calcd. for $C_{17}H_{14}N_2$: C, 82.90; H, 5.73; N, 11.37%.

γ-Carboxamido-γ,γ-diphenylbutyric acid.—This was obtained by refluxing the dinitrile (2.46 g.) with potassium hydroxide (2.46 g.) in aqueous (10 ml.) ethanol (10 ml.) for 17 hr. followed by the addition of more potassium hydroxide (5 g.) and continued reflux for 23 hr. longer. The ethanol was evaporated, dilute hydrochloric acid was added and the precipitate was recrystallized first from methanol, then from benzene, m. p. 153~154°C (1.19 g.).

Anal. Found: C, 72.13; H, 5.97; N, 5.04. Calcd. for $C_{17}H_{17}O_3N$: C, 72.06; H, 6.05; N, 4.94%.

α,α-Diphenylglutaric acid.—*a*) The dinitrile (2.46 g.) was saponified by refluxing with aqueous potassium hydroxide (50%; 5.6 g.) for 4 hr. After dilution with water and hydrochloric acid the resinous solid which separated was recrystallized from aqueous methanol, m. p. 187~188°C (1.77 g.).

Anal. Found: C, 72.35; H, 6.15. Calcd. for $C_{17}H_{16}O_4$: C, 71.82; H, 5.67%.

b) The above amido-acid (0.14 g.) was dissolved in concentrated sulfuric acid (0.6 g.) and a saturated solution of sodium nitrite (0.4 g.) was added beneath the surface of the yellow acid solution. The mixture was warmed on the steam bath for 1 hr. It was poured into ice water and the precipitate was filtered. Recrystallization from aqueous methanol gave α,α-diphenylglutaric acid (30 mg.) identical with that described above.

α,α-Diphenylglutaric anhydride.—A solution of the above diacid (4.26 g.) and acetic anhydride (25 ml.) was refluxed for 90 min. The solvents were removed under reduced pressure and the residue was recrystallized from benzene-petroleum ether (3 g.; 2 crops), m. p. 134°C.

Anal. Found: C, 76.99; H, 5.38. Calcd. for $C_{17}H_{14}O_3$: C, 76.67; H, 5.30%.

α,α-Diphenylglutarimide.—*a*) A mixture of the dinitrile IV (24.6 g.), concentrated sulfuric acid (50 g.), acetic acid (35 g.) and water (15 ml.) was refluxed for 3 hr. It was poured into ice-water and the viscous solid was triturated with a little methanol and then washed with a little water and filtered (18.2 g.), m. p. 169~170°C (sinters 160°C) (from methanol). The imide is soluble in potassium hydroxide solution, but not in sodium bicarbonate solution.

Anal. Found: C, 77.02; H, 5.76; N, 5.39. Calcd. for $C_{17}H_{15}O_2N$: C, 76.96; H, 5.70; N, 5.28%.

b) A mixture of the above anhydride (1.33 g.) and urea (3 g.) formed a clear melt when heated to 140~150°C in an oil bath. The temperature was raised to 200~210°C and the contents solidified after 1 hr. at this temperature. After cooling and extraction with water to remove excess urea, the undissolved residue was recrystallized from aqueous methanol, m. p. 169°C (sinters 161°C) (0.76 g.). This product was identical with the imide described above.

c) α,α-Diphenylglutaric acid was dissolved in excess ammonium hydroxide and the viscous ammonium salt (1.67 g.) was obtained by evaporation to dryness. This was heated in a distillation flask with a free flame and some material distilled at 190°C. Ether was added to the distillate and petroleum ether was then added, inducing crystallization of the imide (0.1 g.) identical with that described above, m. p. 168~169°C.

Summary

A method for the synthesis of α-monosubstituted and α,α-disubstituted glutarimides by Michael addition of active methylene and methine compounds to acrylonitrile or acrylamide, is described.

One of the authors (T. K.) thanks Calanda Foundation for the award of Fellowship.

Department of Chemistry
Israel Institute of Technology
Haifa, Israel

6) A. Franke and M. Kohn, *Monatsh.*, **23**, 740 (1920).
7) A. Franke and M. Kohn, ibid., **23**, 884 (1902).

Synthesis of 3,3-Disubstituted-2-Piperazinones

By Tetsuji KAMETANI[1], William TAUB and David GINSBURG

(Received May 10, 1958)

It was believed that 2-piperazinones containing a quaternary carbon atom adjacent to the carbonyl group might exhibit hypnotic activity. Several 3,3-disubstituted-2-piperazinones were therefore synthesized essentially by the method of Aspinall[2] although with some modification (see experimental section). Although the desired activity was present in several of the compounds, it did not appear sufficient for further extention.

The 3-methyl-3-*sec*-butyl compound Ia was prepared

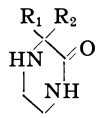

(I) a. R=Me; R_2=*sec*-Bu
b. $R_1=R_2$=Ph
c. R_1=Ph; R_2=Et

in accordance with the reaction scheme.

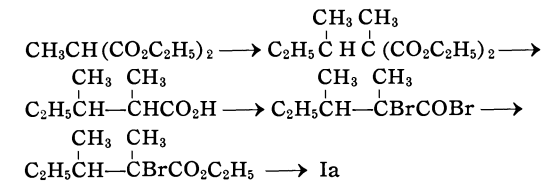

The 3,3-diphenyl derivative Ib was prepared by treatment of methyl α-bromodiphenylacetate resulting from treatment of methyl diphenylacetate with *N*-bromosuccinimide, with ethylene diamine.

The 3-phenyl-3-ethyl derivative (Ic) was prepared by bromination of methyl α-ethyl phenylacetate with *N*-bromo-succinimide followed by treatment of the resulting bromo-ester with ethylene diamine.

Experimental

Diethyl methyl-*sec*-butylmalonate was prepared in 73% yield by alkylation of diethyl methylmalonate[3] with 2-bromobutane, in the presence of sodium ethoxide. The ester boils at 110~123°C/19 mmHg.

α-*sec*-Butylpropionic acid was prepared in 66% yield by refluxing the above ester with 20% aqueous ethanolic potassium hydroxide for 3 hrs., acidification with 10% hydrochloric acid, ether extraction and decarboxylation of the crude malonic acid at 200°C.

α-Bromo-α-*sec*-butylpropionyl bromide was obtained in 86% yield[4] by treating the above acid (6.8 g.) in the usual way with red phosphorus (0.68 g.) and bromine (6.8 ml.), b. p. 114~121°C/40 mmHg.

Ethyl α-bromo-α-*sec*-butylpropionate was prepared in 68% yield by the usual procedure from the freshly distilled acid bromide (25.5 g.) and dry ethanol (4.4 g.), b. p. 116°C/33 mmHg.

3-Methyl-3-*sec*-butyl-2-piperazinone (Ia).— A solution of ethyl α-bromo-α-*sec*-butylpropionate (15.4 g.) in dry ethanol (100 ml.) was added dropwith with stirring at roon temperature during 3 hr. to a solution of ethylene diamine (50 g.) in dry ethanol (150 ml.). After 2 hr. longer at reflux temperature, a solution of sodium ethoxide (1.51 g.) of sodium in dry ethanol (30 ml.) was added to the boiling solution during 30 min. Refluxing was continued for two additional hours. Excess ethanol and ethylene diamine were removed at the water pump. Acetone was added to the residue and the colorless precipitate was filtered. The mother liquor was evaporated and acetone was again added and the residue was distilled in 0.2 mm. It crystallized on standing, m.p. 58~61°C (from petroleum ether).

Anal. Found: C, 63.35; H, 10.62; N, 17.13. Calcd. for $C_{19}H_{18}ON_2$: C, 63.49; H, 10.66; N, 16.46%. The hydrobromide had m.p. 203~206°C (from absolute ethanol-ether).

When an ether solution of the α-bromo-acid bromide was added to a solution of excess ethylene diamine in chloroform at 0°C, a colorless precipitate was formed. After refluxing for 3 hrs. a brown insoluble oil was obtained and this solidified on standing. Recrystallization from benzene gave a product, m.p. 172~174°C which was insoluble in water and gave a negative test with aqueous silver nitrate. Its analysis was unsatisfactory but there is indication that this product is the α,α-dibromo-bis-amide, $[CH_3C(Br)(sec\text{-}C_4H_9)\text{-}CONHCH_2]_2$.

Anal. Found: C, 44.30; H, 6.84; N, 7.13; Br, 34.73. Calcd. for $C_{16}H_{30}O_2N_2Br_2$: C, 43.44; H, 6.78; N, 6.35; Br, 36.19%.

Methyl diphenylacetate was prepared from

1) Present Adress, Pharm. Faculty, the University of Osaka, Hotarugaike, Toyonaka, Osaka.

2) S. R. Aspinall, *J. Am. Chem. Soc.*, **62**, 1202 (1940). *cf.* R. L. Hodgson, I. R. C. Bick and D. J. Cram, ibid., **76**, 1138 (1954).

3) "Organic Syntheses", Coll. Vol. **II**, Wiley, New York, (1946), p. 279.

4) Ibid., Vol. 33, Wiley, New York, (1953), p. 29.

diphenylacetic acid (25 g.), methanol (500 ml.) and concentrated sulfuric acid (25 ml.). The mixture was refluxed for 3 hrs., most of the methanol was removed at the water pump and the residue was poured into ice-water. The oil which soon solidified was recrystallized from aqueous ethanol, m.p. 60°C (24.8 g.). Lit.[5] m.p. 60.°C.

Methyl α-bromodiphenylacetate.—A mixture of the above methyl ester (2.26 g.), carbon tetrachloride (15 ml.) and *N*-bromosuccinimide (1.82 g.) was refluxed for 6 hrs. After the usual workup the bromo-ester was obtained (2.77 g.; 91%) as an oil which was used in its crude form.

3,3-Diphenylpiperazinone (Ib).—A mixture of the crude bromoester (2.5 g.), ethylene diamine (1.2 g.) and dry chloroform (10 ml.) was refluxed for 4 hrs. After standing overnight the red oil which had separated solidified and appeared to be the hydrobromide of ethylene diamine. The chloroform solution was evaporated to dryness and the glassy residue was triturated with benzene, affording colorless crystals (2.3 g.; 96%), m.p. 163°C (from dry benzene; sinters 155~156°). The product gives a picrate, m.p. 248~249°C (from ethanol).

Anal. Found: C, 76.20; H, 6.488; N, 11.18. Calcd. for $C_{16}H_{16}ON_2$: C, 76.16; H, 6.39; N, 11.10%.

Methyl α-phenylethylate was obtained in 91% yield by esterification of the acid as described above for methyl diphenylacetate. It had b.p. 225~228°C. Lit.[6] b.p. 225~226°C.

Methyl α-bromo-α-phenylethylacetate was obtained by bromination of the above ester (17.8 g.) with *N*-bromosuccinmide (20.8 g.) in carbon tetrachloride (100 ml.) during 4 hr. After the usual workup the crude ester (94% yield) was used in order to avoid dehydrobromination during distillation at a relatively high temperature.

3-Ethyl-3-phenylpiperazinone (Ic). — This was prepared in poor yield from the crude bromo-ester and ethylene diamine as described for the preparation of Ia. It was an oil, b.p. 140~160°C/0.4 mmHg. (1g. from 9.7g. bromo-ester).

Anal. Found: N, 14.01. Calcd. for $C_{12}H_{16}ON_2$: N, 13.72%.

Summary

Several 3, 3-disubstituted-2-piperazinones have been synthesized for pharmacological testing as potential hypnotics.

One of the authors (T. K.) thanks Calanda Foundation for the award of Fellowship.

Department of Chemistry
Israel Institute of Technology
Haifa, Israel

5) P. Fritsch and F. Feldmann, *Ann.*, **306**, 81 (1899).

6) M. M. Rising and T. W. Zee, *J. Am. Chem. Soc.*, **50**, 1211 (1928).

Infrared Studies of Formic Acid, Chemisorbed on Copper, Nickel and Zinc

By Kozo HIROTA, Keiji KUWATA and Yasuo NAKAI

(Received March 25, 1958)

The catalytic decomposition of formic acid into hydrogen and carbon dioxide, $HCOOH \rightarrow H_2 + CO_2$, has been studied kinetically by many researchers, and the mechanisms of the decomposition were often suggested in recent years[1]. However, it may be admitted that these mechanisms are established on the kinetic data without any exact knowledge of the adsorbed state of formic acid. Considering such situations, the present authors attempted to solve the problem by the infrared absorption technique which had been explored by Eischens et al.[2], i. e., the infrared spectra of formic acid adsorbed on metal surface were measured, and were compared with those of gaseous formic acid and solid formates.

Experimental

The catalysts studied were copper, nickel and zinc, each being dispersed in the extra fine powder of silica. Each metal catalyst was prepared by the thermal decomposition of the corresponding formate, followed by its reduction

1) a) G. M. Schwab and E. Schwab-Agallidis, *J. Am. Chem. Soc.*, **71**, 1806 (1949). b) D. A. Dowden et al., *Trans. Faraday Soc.*, **42**, 680 (1948). c) G. Rienäcker and N. Hansen, *Z. Elektrochem.*, **60**, 887 (1956).

2) R. P. Eischens, S. A. Francis and W. A. Pliskin, *J. Phys. Chem.*, **60**, 194 (1956).

with hydrogen at 200°C. The spectrum was measured at room temperature with Hilger H-800 spectrometer. The cell, which was constructed so as to be heated from the outside to reduce the catalyst enclosed, was laid horizontally before the slit of the spectrometer. The cell was made of pyrex glass and was similar to that described by Eischens. The windows of the cell and the thin plate supporting the catalysts were made of sodium chloride. It was ascertained previously that all the metal-silica-catalysts had no absorption bands in the spectral region concerned, and also that there was no absorption band caused by the interaction of formic acid with the windows and plates of sodium chloride in the same region.

Results

The absorption spectra of chemisorbed formic acid could be obtained from the bands which remained when the excess of free formic acid was desorbed by evacuating the cell until the strongest absorption band of free formic acid at 1740 cm^{-1} disappeared. These bands of chemisorbed formic acid, as shown in Table I, do not coincide with those of gaseous formic acid (1740 cm^{-1} and 1380 cm^{-1}). Typical spectra of formic acid chemisorbed on copper and zinc are shown in Fig. 1 and Fig. 2, where the pressure of gaseous formic acid is reduced successively in the order a, b and c. It is found generally that the absorption intensity of these bands increases in comparison with those of gaseous formic acid, according as its pressure decreases.

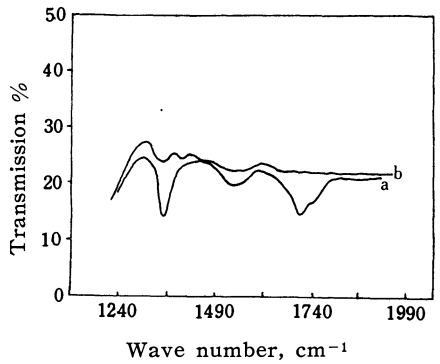

Fig. 1. Absorption spectrum of formic acid chemisorbed on copper catalyst.

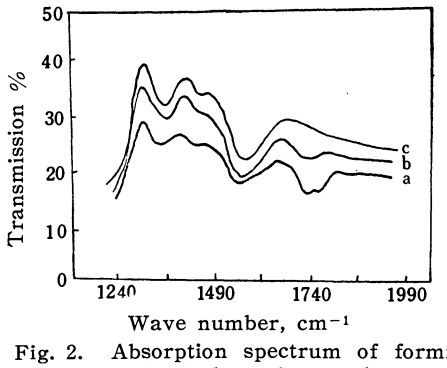

Fig. 2. Absorption spectrum of formic acid chemisorbed on zinc catalyst.

TABLE I

INFRARED ABSORPTION BANDS OF FORMIC ACID CHEMISORBED ON COPPER, NICKEL AND ZINC, OF THE CORRESPONDING SOLID METAL FORMATES AND OF FORMATE ION

(cm^{-1})

Modes of vibration	Formic acid chemisorbed on			Metal formates of			Formate ion[3]
	Cu	Ni	Zn	Cu	Ni	Zn	
ν_4	1560	1600	1590	1580	1570	1580	1585
ν_5	1400	1380	1360(?)	1400	1400	1400	1385
ν_2	1360	(?)		.....[a]	.....[a]	.....[a]	1351

a) As Nujol oil was used, these bands were masked.

In the table, the bands of metal formates $(HCOO)_2Cu \cdot 2H_2O$, $(HCOO)_2Ni \cdot 2H_2O$ and $(HCOO_2)Zn \cdot xH_2O$ obtained are shown for the sake of reference. The spectra of these formates coincide fairly well with those of several formates in the literature[4]. Since the accuracy in measuring wave number of the maximum absorption was low, predominantly owing to weakness of the absorption, the last figures in the table were round figures.

Discussion

In each catalyst, two or three bands were observed. In Table I they are given the notations of the ν_4, ν_5 and ν_2 vibrations, because they seem to correspond to the antisymmetric ν_4 and ν_5 vibrations and to the symmetric ν_2 vibration of formate ion*, respectively. However, the other two symmetric vibrations, designated as ν_1 and ν_3, which will appear near 2825 cm^{-1} (ν_1) and 775 cm^{-1} (ν_3), were not observed. The ν_1 vibration would be masked by the strong and broad absorption bands of silica, while the ν_3 vibration would be hard to detect because of the small transmission of the sample in this region, even if there is. Moreover, it is noteworthy

3) Landolt-Börnstein, "Zahlenwerte und Funkionen", **1**, 2 Teil, p. 237 (1951).

* Theoretical assignment of the vibrations of formate ion was given by T. Miyazawa, *J. Chem. Soc. Japan, Pure Chem. Sec.*, (*Nippon Kagaku Zassi*), **77**, 381 (1956).

4) Ll. Puval, H. Gerding et J. Lecomte, *Rec.Trav. Chim.*, **69**, 391 (1950).

that the ν_4, ν_5 and ν_2 vibrations are similar to those of the corresponding metal formates as shown in the table and also to those observed in the liquid solution[4]. Therefore the new bands caused by the adsorbed formic acid may be ascribed to the formate ion present on the surface of the catalysts.

According to the X-ray analysis of these crystals[5] and the spectrochemical studies of their microcrystals[6], a carbon atom combines with a metal atom via an oxygen atom in those crystals which are composed of formate groups (HCOO), metal atoms and water molecules. If the above structure can be extended to such surface complexes, it will be reasonable to assume that the formic acid is not physically adsorbed, but is chemisorbed, dissociating into the hydrogen atom and the formate group. Considering the structure of the metal formates[5], it is possible that the formate ion forms a bridged bond with two metal atoms on the surface. However, the ionic degree of the bond between the oxygen atom and the catalyst cannot be estimated in the present state of experimental accuracy.

It must be pointed out that the ν_5 vibration of formic acid chemisorbed on zinc is a little different from that of formate ion (1385 cm^{-1}), the difference being 75 cm^{-1}. It was supposed that it might owe to the imperfect reduction of the catalyst. However, as the difference decreased to 55 cm^{-1} when an amount of oxygen was chemisorbed, the deviation may be ascribed to some causes other than the chemisorption of oxygen, e. g., the mutual interaction between the chemisorbed chemical species, as pointed out by Eischens[2] and Yang[7]. Concerning this point, further research is required.

The above conclusion supports the "dissociation mechanism" of the Rienäcker[1c], i. e.,

$$HCOOH + H^+ + 2e \rightarrow H_2 + HCOO^- \quad (1a)$$

$$HCOO^- + [Met] \rightarrow CO_2 + [Met]^- + H \quad (1b)$$

but rejects the "monomolecular-mechanism", the essential feature of which is depicted in Fig. 3: i. e.,

$$HCOOH \rightarrow H_2 + CO_2 \quad (2)$$

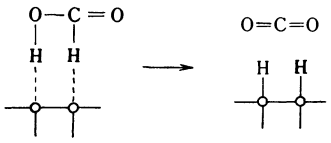

Fig. 3. Eley's Mechanism.

This latter mechanism, which was first proposed for the oxide catalysts by Schwab et al.[1a], was also proposed by Eley et al.[8] in the case of gold-palladium catalysts. Besides the above-mentioned reason, there is another one against Eley's mechanism from the standpoint of the structure of formic acid molecule[3,9], because the chemisorbed formic acid molecule would require higher potential energy to keep such a distorted structure.

It is interesting to mention that the kinetic studies[10] on the decomposition of formic acid on silver catalyst performed by one of the present authors (K. H.) also support the dissociation mechanism; i. e. in the intermediate state of the decomposition at the pressure of 2~3 cm Hg, more hydrogen was always found to exist than carbon dioxide at the temperature between 80~130°C, the maximum deviation of the ratio H_2/CO_2 being ca. 30%. If the decomposition had proceeded monomolecularly in one step as shown in Eq. 2, such a result would surely not have been found, because the decomposition was carried out on the condition that the adsorption of carbon dioxide was negligibly small and the addition of carbon dioxide in the original gas had no effect on the progress of the decomposition.

Therefore, for the several reasons cited above it seems that the dissociation mechanism is better than that of Eley, at least in the case of the metal catalysts. However, Schwab's mechanism may be justified in the case of the oxide catalysts which can act partly as dehydrogenation catalysts and partly as dehydration catalysts. Of course, it can not be asserted from the present experimental data that the free formate ion, $HCOO^-$, as described in Rienäcker's paper, exists on the metal surface.

5) R. Kiriyama, H. Ibamoto and K. Matsuo, *Acta Cryst.*, **2**, 482 (1954).
6) S. Yamada, H. Nakamura and R. Tsuchida, This Bulletin, **30**, 953 (1957).
7) A. C. Yang and C. W. Garland, *J. Phys. Chem.*, **61**, 1504 (1957).
8) D. D. Eley and P. Lucky, *Trans. Faraday Soc.*, **51**, 1483 (1957).
9) S. H. Bauer and R. M. Badger, *J. Chem. Phys.*, **5**, 852 (1937).
10) K. Hirota and T. Otaki, *J. Chem. Soc. Japan, Pure Chem. Sec.* (*Nippon Kagaku Zassi*), to be published (Accepted March 25,1958).

Conclusion

By the use of the infrared absorption technique, it can be concluded that formic acid, chemisorbed on copper, nickel and zinc, dissociates into two groups as HCOO and H at room temperature. Such a conclusion conforms with Rienäcker's mechanism on the dehydrogenation of formic acid. However, it can not be determined at the present state of the study whether or not these groups are linked to the metal atoms by ionic or covalent bonds.

The detailed discussion will be published in near future in addition to the data of kinetic research.

A part of the expense for the present experiment has been defrayed from a grant given by the Ministry of Education, to which the authors' thanks are due.

Department of Chemistry,
Faculty of Science,
Osaka University,
Kita-ku, Osaka

Studies on the Interaction of Surface Films with Solute in Solution. I. Potentiometric Titration of Aqueous Dye Solution and Calculation of Ionization Constant of Dye

By Mitsuo MURAMATSU

(Received April 30, 1958)

Up to the present, work has been accumulated on the interaction of substances in aqueous solution with surface films of amphipathic compounds spread upon it[1]. Among these, the effect of solute in a substrate solution on monolayers spread on it was extensively studied and many interesting results were obtained. For instance, a remarkable expansion and solidification have been reported for surface film such as stearic acid or octadecylamine due to such a substance cobalt, aluminum, thorium, or alginate ion dissolved in the substrate upon which the film was spread[2,3]. Marked increase in film thickness and wettability were also reported when a built-up film of stearic acid was immersed in solutions containing these ions[4].

All these phenomena seem to show that the nature of the film is profoundly affected by ions which interlink with each other and are taken up by the film. To confirm this, further contributions will be made from the study of interaction between mono- or multilayers of amphipathic compounds and aqueous solutions of dyes, since the latter compounds have a tendency to form micelles or aggregates in an aqueous medium[5] and, as a result, they behave sometimes as if they were macromolecular electrolyte. It will be presumed, however, that the association of molecules is dominantly affected by the degree of ionization of dissociating groups in the dye molecule, which can be calculated from their respective ionization constants and pH of the medium. In spite of such a significance of ionization constant, little was successfully attempted to determine it for usual dyes. This may be due to the failure of the application of simple method of pK determination[6], while a more rigorous method gives values of low reliability in spite of an elaborate calculation as in

1) A general review, cf. M. Muramatsu, T. Sasaki and R. Matuura, *Reports, Kyūshū Univ., Chem. Sect.*, **2**, 47 (1955).

2) T. Sasaki and R. Matuura, This Bulletin, **24**, 274 (1951); T. Sasaki and M.Muramatsu, ibid., **29**, 35 (1956); J. H. Schulman et al., *Trans. Faraday Soc.*, **46**, 475 (1950); **50**, 1128, 1131, 1139 (1954), etc.

3) E. G. Cockbain and J. H. Schulman, *Trans. Faraday Soc.*, **35**, 716 (1939); T. Sasaki and M. Muramatsu, This Bulletin, **26**, 96 (1953).

4) M. Muramatsu and T. Sasaki, This Bulletin, **25**, 21, 25 (1952); A. Inaba, ibid., **26**, 43 (1953).

5) E. L. Valko, "Colloid Chemistry" edited by J. Alexander, Vol. 6, Reinhold Publ. Corp., New York, (1946), p. 594; see also W. Pauli and F. Lang, *Monath. Chem.*, **67**, 159 (1936).

6) e. g., L. Michaelis, Physical Method of Organic Chemistry, Part II, in "Technique of Organic Chemistry", edited by A. Weissberger, Interscience Publ., Inc., New York, (1949), p. 1712.

the case of polybasic acid[7].

The present paper describes an improved method of evaluating the dissociation constant of polybasic acid and polyacidic base, as well as the results obtained for several dyes.

Method of Calculation

The following three assumptions are made for calculating ionization constants of ionizable groups in the dye molecule.

(i) Dye, OH^-, Cl^-, Na^+, etc., in the titration mixture are so dilute that the concentration instead of the activity is used in calculation.

(ii) Volume of titration mixture is the sum of the volume of the solution of dye and of titrating acid or alkali.

(iii) As for the concentration of the carbonate ion, the effect due to the second ionization constant is small enough to be neglected in the pH region of the present experiment.

Now we show the case of titrating a solution of chrysoidine, one of the diacidic bases, with a solution of sodium hydroxide or hydrochloric acid. Ionization constants, K_1 and K_2, for this dye are defined by

$$\left.\begin{aligned} R^{2+} &\rightleftarrows R^+ + H^+ : \quad K_1 = [H^+][R^+]/[R^{2+}] \\ R^+ &\rightleftarrows R + H^+ : \quad K_2 = [H^+][R]/[R^+] \end{aligned}\right\} \quad (1)$$

where R, R^+, and R^{2+} are the dye molecules possessing zero, one, and two ionized amino groups, respectively, and [ ] denotes the concentration of inscribed species. Total concentration, C, of the dye is then expressed by

$$C = [R] + [R^+] + [R^{2+}] \quad (2)$$

We now introduce a parameter f different from Schwarzenbach's[7], defined by

$$f = 2[R^{2+}] + [R^+] \quad (3)$$

Then, from the condition of electrical neutrality

$$f = [Cl^-] + [OH^-] + [HCO_3^-] - [Na^+] - [H^+] \quad (4)$$

Substituting 1 and 3 into 2 we obtain

$$\left(\frac{f}{C}\right) + \left(\frac{f}{C} - 1\right)\frac{[H^+]}{K_2} + \left(\frac{f}{C} - 2\right)\frac{[H^+]^2}{K_1K_2} = 0 \quad (5)$$

In the case of aluminon, one of the acidic dyes, the following relations result;

$$\left.\begin{aligned} K_1 &= [H^+][R^-]/[R] \\ K_2 &= [H^+][R^{2-}]/[R^-] \\ K_3 &= [H^+][R^{3-}]/[R^{2-}] \end{aligned}\right\} \quad (6)$$

$$C = [R] + [R^-] + [R^{2-}] + [R^{3-}] \quad (7)$$

The solution of this dye is titrated with hydrochloric acid, so the parameter f is given by

$$f = -3[R^{3-}] - 2[R^{2-}] - [R^-] = [Cl^-] + [OH^-] + [HCO_3^-] - [NH_4^+] - [H^+] \quad (8)$$

Substituting 6 and 8 into 7 we have

$$\left(\frac{f}{C} + 3\right) + \left(\frac{f}{C} + 2\right)\frac{[H^+]}{K_3} + \left(\frac{f}{C} + 1\right)\frac{[H^+]^2}{K_2K_3} + \left(\frac{f}{C}\right)\frac{[H^+]^3}{K_1K_2K_3} = 0 \quad (9)$$

For the titration of a solution of such an amphoteric dye as methyl orange or tropäolin OO with hydrochloric acid solution, we obtain eventually

$$\left(\frac{f}{C} + 1\right) + \left(\frac{f}{C}\right)\frac{[H^+]}{K_2} + \left(\frac{f}{C} - 1\right)\frac{[H^+]^2}{K_1K_2} = 0 \quad (10)$$

with f being given by the equation 4 and K_1 and K_2 by

$$\left.\begin{aligned} K_1 &= [H^+][R^\pm]/[R^+], \text{ for sulfonic group} \\ K_2 &= [H^+][R^-]/[R^\pm], \text{ for basic group} \end{aligned}\right\} \quad (11)$$

where $R^\pm$ denotes the zwitterion form of dye molecule.

Similar treatment applied to Congo red, possessing two amino and two sulfonic groups in a molecule, leads us to the expression

$$\left(\frac{f}{C} + 2\right) + \left(\frac{f}{C} + 1\right)\frac{[H^+]}{K_4} + \left(\frac{f}{C}\right)\frac{[H^+]^2}{K_3K_4} + \left(\frac{f}{C} - 1\right)\frac{[H^+]^3}{K_2K_3K_4} + \left(\frac{f}{C} - 2\right)\frac{[H^+]^4}{K_1K_2K_3K_4} = 0 \quad (12)$$

with the parameter f determined by 4 and K's by

$$\left.\begin{aligned} K_1 &= [H^+][R^{\pm+}]/[R^{2+}], \text{ for first sulfonic group} \\ K_2 &= [H^+][R^{2\pm}]/[R^{\pm+}], \text{ for second sulfonic group} \\ K_3 &= [H^+][R^{\pm-}]/[R^{2\pm}], \text{ for first amino group} \\ K_4 &= [H^+][R^{2-}]/[R^{\pm-}], \text{ for second amino group} \end{aligned}\right\} \quad (13)$$

7) G. Schwarzenbach et al., *Helv. Chim. Acta*, **30**, 1303, 1798 (1947); **32**, 1175 (1949).

From the assumption (ii), $[Cl^-]$, $[Na^+]$ or $[NH_4^+]$ in equation 4 or 8 can be calculated from the initial concentration, C_0, and volume, V_0, of dye solution, as well as initial concentration, C_0', and the volume, V_t, of the solution of acid or alkali added. Further, from the assumption iii

$$[HCO_3^-] = (K_c + [H^+]_0)([H^+]_0 - [OH^-]_0)/K_c$$

and we have also

$$[OH^-] = K_w/[H^+]$$

where K_w and K_c are the ionic product of water and first dissociation constant of carbonic acid, respectively, and $[H^+]_0$ and $[OH^-]_0$ are the concentration of H^+ and OH^-, respectively, in conductivity water into which dye is dissolved. Therefore we can calculate the parameter f from equations 4 or 8. C in equations 5, 9, 10 or 12 can also be calculated from the initial concentration of dye used. Thus, putting the numerical value of f/C for given $[H^+]$ into the equations 5, 9, 10 or 12 enables the evaluation of K's for each dye.

Experimental

Material.—Dyes used were of chemically pure grade and were further purified by a special method, e. g., salting-out[8] for Congo red and methyl orange and reduction-precipitation[9] for aluminon, as the case requires. Although dye suffered hydrolysis occasionally during purification, the purification was continued until the titration curve became unaltered by the subsequent recrystallization. Actually, the successive recrystallization proved able to shift the titration curve of aminazobenzene hydrochloride, as shown in Fig. 1. Color of the solution also changed gradually from red to yellowish-red with the repeated recrystallization. These facts clearly show a detachment of hydrogen chloride from dye base. Assuming no impurity contained in dye, the amount of the acid detached can be calculated from the elemental analysis of the dye. Table I

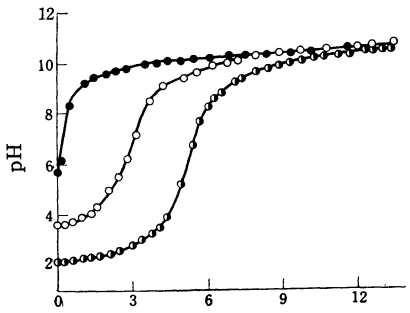

Fig. 1. Effect of recrystallization of aminazobenzene hydrochloride upon the titration curve: $[NaOH] = 1.25 \times 10^{-3}$ mol./l.; $[dye] = 2.0 \times 10^{-4}$ mol./l.; volume of dye solution = 50.00 cc.
◑ recrystallized 3 times
○ recrystallized 6 times
● recrystallized 9 times

TABLE I
MOST PROBABLE COMPOSITION OF DYES USED

Name	Constitution	Type	Occurence, %	Type	Occurence, %
Chrysoidine	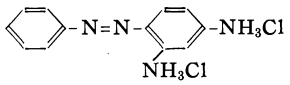	R^+Cl^-	98.06	$R^{2+}2Cl^-$	1.94
Aluminon	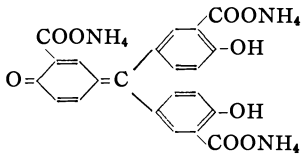	$R^{3-}3NH_4^+$	26.84	$R^{2-}2NH_4^+$	73.16
Methyl orange	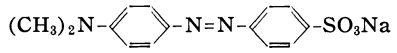	R^-Na^+	80.97	$R^\pm$	19.03
Tropäolin OO	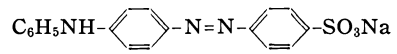	R^-Na^+	78.31	$R^\pm$	21.69
Congo red	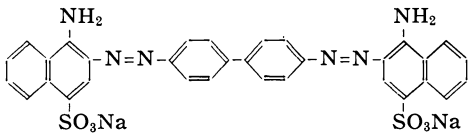	$R^{2-}2Na^+$	46.03	$R^\pm{-}Na^+$	53.97

8) C. Robinson and H. A. T. Mills, *Proc. Roy. Soc.*, **A131**, 576 (1931).

9) N. Caro, *Ber.*, **25**, 939 (1892).

shows the most probable degree of detachment of such an acid or a base for samples used in the experiment. The calculation of composition in the table is based on the elemental analysis of carbon, hydrogen, nitrogen and sodium (for amphoteric dyes) or chlorine (for basic dye). The molar concentration of dye solution was calculated taking into account this detachment of acid or base.

Hydrochloric acid, twice distilled in an all-grand glass apparatus, and sodium hydroxide purified by alcohol were used as titratingagents and standardized with perchloric acid solution. Conductivity water to be used often suffered a slight lowering of pH presumably owing to the dissolution of carbon dioxide, the content of which was calculated as mentioned in the previous section.

Procedure. — Exactly 50 cc. of ca. 2×10^{-4} mol./l. of dye solution was titrated with hydrochloride acid or sodium hydroxide of ca. 1.25×10^{-3} mol./l. under mechanical stirring of 400 rpm and pH change was traced by means of pH meter (Shimadzu Model GU, using GL-6 glass electrode), which was calibrated with buffer solutions of two different pH values. The error introduced in the measurement of pH was estimated to be within ±0.02. Reading of pH was taken after equilibrium was attained for successive titration which was completed within 10 hrs. after the preparation of dye solution. It was confirmed in the preliminary experiment that the effect of aging of dye solution upon the titration curve could be eliminated by leaving it alone for at least 24 hrs.

All experiments were carried out at room temperature of 20 ± 5°C.

Results

Fig. 2 shows the value of pH of the solution of methyl orange titrated with hydrochloride acid. The concentration of each ion species, except for dye ions, in the solution could be calculated from these pH values and from given conditions of $[Na^+]=1.64\times10^{-4}$ g. ion/l. at $V_t=0$,

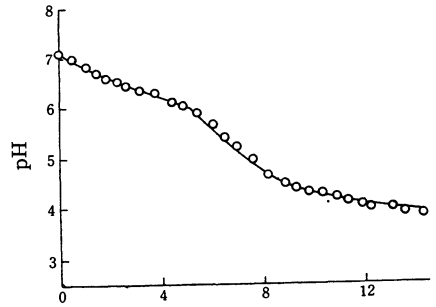

Fig. 2. V_t~pH relationship for methyl orange: $C_0=2.03\times10^{-4}$ mol./l.; $C_0'=1.25\times10^{-3}$ mol./l.; $V_0=50.00$ cc.; ○, observed; ——, calculated by Eq. 10 assuming $K_1=2.75\times10^{-4}$ and $K_2=3.22\times10^{-7}$.

$[Cl^-]=1.25\times10^{-3}$ g.ion/l. for the initial concentration of titrating solution, $[H^+]_0=2.29\times10^{-7}$ ($pH_0=6.64$), $K_w=1.02\times10^{-14}$, and $K_c=3.5\times10^{-7}$. Table II shows the typical examples of these terms and f/C with varying V_t.

In applying these data to 10, we were hardly able to evaluate simultaneously K_1 and K_2 successfully from the graphical plotting of $\left(\frac{f}{C}\right)[H^+]\Big/\left(\frac{f}{C}+1\right)$ against $-\left(\frac{f}{C}-1\right)[H^+]^2\Big/\left(\frac{f}{C}+1\right)$. This was mainly due to the fact that $[H^+]$ changed widely from 10^{-7} to 10^{-4}, as V_t changed from 1 to 13 cc. Therefore a conventional approximation was made to determine K's. Since it was roughly estimated from Fig. 2 that K_2 was nearly of the order of 10^{-7} while K_1 was larger than 10^{-5}, the last term of left side of (10) was considered to be negligible in the region of $[H^+]\approx10^{-7}$. That is, we can safely ignore the reaction

TABLE II
CONCENTRATION OF VARIOUS ION SPECIES IN THE SOLUTION AND f/C FOR THE TITRATION OF METHYL ORANGE

V_t	C	$[H^+]$	$[Na^+]$	$[Cl^-]$	$[OH^-]$	$[HCO_3^-]$	f	f/C
1.0	1.99×10^{-4}	1.45×10^{-7}	1.61×10^{-4}	2.45×10^{-5}	0.69×10^{-7}	2.15×10^{-7}	-1.38×10^{-4}	−0.694
2.0	1.95 〃	2.63 〃	1.58 〃	4.81 〃	0.38 〃	1.73 〃	−1.10 〃	−0.565
3.0	1.91 〃	4.27 〃	1.55 〃	7.02 〃	0.23 〃	1.37 〃	−0.85 〃	−0.445
4.0	1.88 〃	6.61 〃	1.52 〃	9.62 〃	0.15 〃	1.06 〃	−0.56 〃	−0.298
5.0	1.85 〃	1.07×10^{-6}	1.49 〃	1.14×10^{-4}	0.10 〃	0.75 〃	−0.36 〃	−0.194
6.0	1.81 〃	1.95 〃	1.46 〃	1.34 〃	0.05 〃	0.46 〃	−0.14 〃	−0.0774
7.0	1.78 〃	6.03 〃	1.44 〃	1.55 〃	0.02 〃	0.17 〃	+0.05 〃	+0.0281
8.0	1.75 〃	1.66×10^{-5}	1.41 〃	1.72 〃	0.00 〃	0.06 〃	+0.14 〃	+0.0800
9.0	1.72 〃	3.47 〃	1.39 〃	1.91 〃	0.00 〃	0.00 〃	+0.17 〃	+0.0988
10.0	1.69 〃	4.90 〃	1.37 〃	2.08 〃	0.00 〃	0.00 〃	+0.22 〃	+0.130
11.0	1.66 〃	7.08 〃	1.34 〃	2.26 〃	0.00 〃	0.00 〃	+0.21 〃	+0.127

$R^{\pm}+H^+ \rightarrow R^+$ in this region, since $f=[R^+]-[R^-]$ is negative in this region. Thus we have a linear relationship between $-(f/C)[H^+]$ and $(f/C)+1$ in the region of $[H^+] \lesssim 5\times10^{-7}$ as shown in Fig. 3, from which we obtain $K_2=3.30\times10^{-7}$. Putting this value into 10 and plotting

$$-\left(\frac{f}{C}-1\right)\frac{[H^+]^2}{K_2} \text{ against } \left(\frac{f}{C}+1\right)+\left(\frac{f}{C}\right)\frac{[H^+]}{K_2},$$

as shown in Fig. 4, we obtain $K_1=2.73\times10^{-4}$. Successive approximation not neglecting the last term gave limiting values

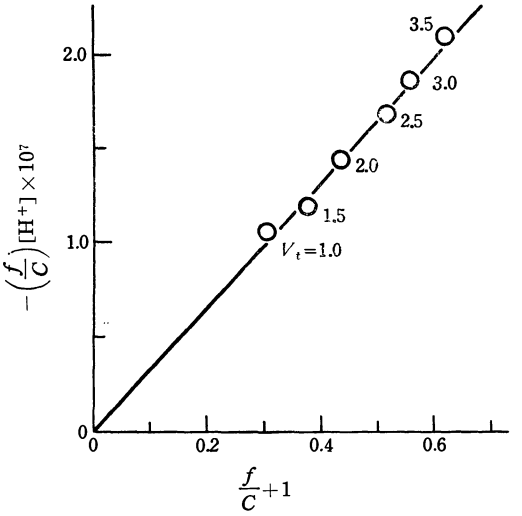

Fig. 3. $-\left(\frac{f}{C}\right)[H^+]$ vs. $\left(\frac{f}{C}+1\right)$ for methyl orange.

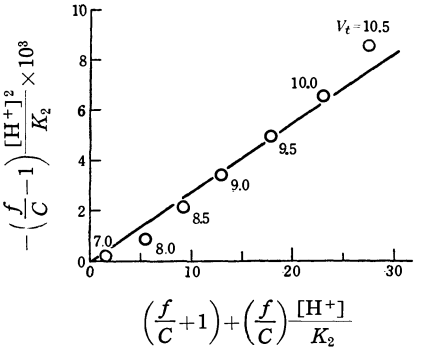

Fig. 4. $-\left(\frac{f}{C}-1\right)\frac{[H^+]^2}{K_2}$ vs. $\left(\frac{f}{C}+1\right)+\left(\frac{f}{C}\right)\frac{[H^+]}{K_2}$ for methyl orange.

of $K_1=2.75\times10^{-4}$ and $K_2=3.22\times10^{-7}$. Substitutions of these values back into 10 give f/C for given $[H^+]$ which in turn gives V_t. V_t~pH relationship thus obtained is expressed as a full line in Fig. 2. A fairly good coincidence is seen between observed and calculated values in this figure.

The open circles in Fig. 5 denote the observed values of pH of the solution of tropäolin OO titrated with hydrochloric acid. Similarly to the case of methyl orange, we obtained the dissociation constants, K_1 and K_2, defined by 11. The final values were $K_1=5.60\times10^{-4}$ and $K_2=2.98\times10^{-7}$. Again, the dependence of pH upon V_t is reproduced by putting these values into 10. The full curve in Fig. 5 represents the V_t~pH relationship thus obtained.

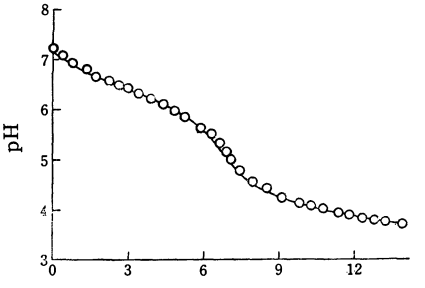

Fig. 5. V_t~pH relationship for tropäolin OO: $C_0=2.08\times10^{-4}$ mol./l., $C_0'=1.25\times10^{-3}$ mol./l., $V_0=50.00$ cc; ○, observed; ——, calculated by Eq. 10 assuming $K_1=5.60\times10^{-4}$ and $K_2=2.98\times10^{-7}$.

Solution of chrysoidine was titrated separately with the solutions of hydrochloric acid and sodium hydroxide, since the greater part of starting sample of dye is of R^+ form. The result is shown in Fig. 6. Putting the experimental data into equation 5, we obtained $K_1=4.84\times10^{-4}$ and $K_2=7.09\times10^{-6}$. V_t~pH relationship reproduced from these values of K's is shown as a full curve in Fig. 6.

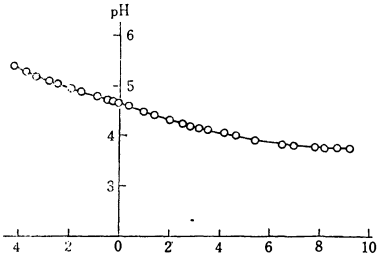

Fig. 6. Titration curve for chrysoidine: $C_0=2.01\times10^{-4}$ mol./l., C_0' of HCl$=1.25\times10^{-3}$ mol./l., C_0' of NaOH$=1.58\times10^{-3}$ mol./l., $V_0=50.00$ cc.; ○, observed; ——, calculated by Eq. 5 assuming $K_1=4.84\times10^{-4}$ and $K_2=7.09\times10^{-6}$.

Fig. 7 shows the titration curve of aluminon. When we followed the method of calculation mentioned above to equation 9, $K_3=6.08\times10^{-8}$ and $K_2=1.595\times10^{-5}$ were obtained. In calculation of K_1, however, plotting of (f/C) $[H^+]^3/K_2K_3$ against

$$\left(\frac{f}{C}+3\right)+\left(\frac{f}{C}+2\right)\frac{[H^+]}{K_3}+\left(\frac{f}{C}+1\right)\frac{[H^+]^2}{K_2K_3}$$

was unsuccessful, owing to considerable fluctuation of the plot. If we reproduce the V_t~pH relationship assuming $K_2=1.595\times10^{-5}$, $K_3=6.08\times10^{-8}$ and K_1 being

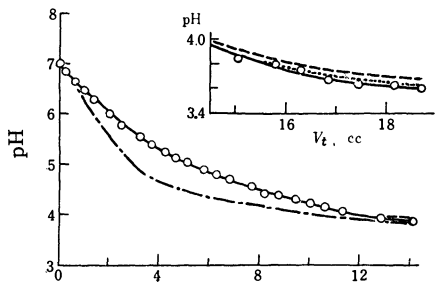

Added HCl, V_t, cc.

Fig. 7. Titration curve for aluminon: $C_0=2.06\times10^{-4}$mol./l., $C_0'=1.44\times10^{-3}$mol./l., $V_0=50.00$ cc.; ○, observed; curves, calculated by Eq. 9 assuming $K_2=1.595\times10^{-5}$, $K_3=6.08\times10^{-8}$ and $K_1\approx1$ (——), 10^{-2} (------) or 10^{-3} (– – –); semidotted curve, based on high-molecular electrolyte.

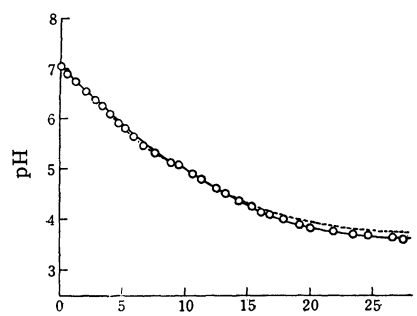

Added HCl, V_t, cc.

Fig. 8. Titration curve for Congo red: $C_0=2.03\times10^{-4}$ mol./l., $C_0'=1.25\times10^{-3}$ mol./l., $V_0=50.00$cc.; ○, observed; -----, calculated by Eq. 12; ——, calculated by Eq. 16.

either of 1, 10^{-2} or 10^{-3}, we obtain three corresponding curves differing from one another in the tail parts of titration curves reproduced, as seen in the figure inserted in Fig. 7. Thus, when we take into account the experimental error in determining pH, we can say no more than $K_1=10^{-2}$ or larger.

Titration curve for Congo red is shown in Fig. 8. From these data we obtained the following values of K's using equation 12;

$$K_4=9.59\times10^{-8}$$
$$K_3=7.19\times10^{-6}$$
$$K_2=1.82\times10^{-4}$$

Again, we failed to plot and calculate the value of K_1, similar to the case of aluminon. Therefore we could merely evaluate K_1 to be 10^{-1} or larger. In Fig. 8 the dotted curve represents the calculated values of V_t for given pH using these experimental values for K's. We can see some deviations between calculated and observed values of pH for given V_t at the tail part of the titration curve.

Discussion

In Table III are summarized the values of pK's determined for each ionizable group in the dye used, except for Congo red. It should be noticed that the ionization constants are defined by 1, 6 or 11 and, therefore, that the stronger acid is of the smaller pK, while the stronger base is of the larger pK.

TABLE III

pK'S OF IONIZABLE GROUPS IN THE DYE

Dye	Acid group	Basic group
Chrysoidine	——	$pK_1=3.32$ $pK_2=5.21$
Aluminon	$pK_1\lesssim2$, $pK_2=4.80$ $pK_3=7.22$	——
Methyl orange	$pK_1=3.56$	$pK_2=6.49$
Tropäolin OO	$pK_1=3.25$	$pK_2=6.53$

It is well known that, when the second acid group of the same kind is introduced in the molecule having one acid group, the ionization constant of the former becomes smaller than that of the latter, while the value of the latter is slightly affected by the addition of the former. A typical example of this is seen in the case of dicarboxylic acids[10]. When we apply this principle to the dibasic dye, the pK values of chrysoidine are explained as those expected from the ionization constant, $pK=2.91$ as defined by 1, for aminazobenzene[11]. By means of the

10) B. Adell, "Über die Elektrolytische Dissoziation von Dicarbonsäuren in Alkalichloridlösungen", Lund, (1938).

11) R. C. Farmer and F. J. Warth, *J. Chem. Soc.*, **85**, 1726 (1904).

methods of titration and spectrophotometry, Woislawaski[12] has also reported $pK_2=5.3$ for an amino group in chrysoidine in aqueous solution.

Substitution of amino group by sulfonic group makes little difference in pK_2 between chrysoidine and methyl orange or tropäolin OO. It is hardly believed that the ionization constant of an amino group in the dye is remarkably affected by dimethylation or phenylation, both of which show little effect upon the ionization constant of aniline[13]. It is further noted that pK_1 of methyl orange or tropäolin OO is of nearly the same value as that, $pK=3.28$ at 20°C, for sulfanilic acid[14].

It seems to be premature to ascribe the deviation of calculated pH value from the observed one at the tail part of the titration curve of Congo red, as seen in Fig. 8, to a mere experimental error. Actually the deviation is larger than that due to the pH measurement and exhibits a systematic tendency; namely, the calculated value is always larger than the observed one. Now, let us make a tentative explanation of this deviation which is ascribed to the special nature of Congo red in aqueous solution. If we assume two sulfonic groups, not distinguishable from each other with regard to their ionization, in the molecule, then we can treat Congo red similarly to a high-polymer electrolyte. We can safely assume this, since two sulfonic groups are both strongly ionizing and are far apart from each other. At least, such a consideration would be valid for the region where titrating hydrochloric acid reacts with these acid groups. The high-molecular or micellar nature of Congo red, suggested by the data of ultracentrifuge[15] and diffusion[5], in aqueous medium would also support this consideration.

From this standpoint we shall take the following K's, instead of those defined by 13, for Congo red as a high polymer-like substance;

$$\left.\begin{aligned} &K_1=K_2=[H^+][R^{2\pm}{}_{1/2}]/[R^{2+}{}_{1/2}] \\ &[R^{\pm}{}_{1/2}]=2[R^{2\pm}] \\ &K_3=[H^+][R^{\pm-}]/[R^{2\pm}] \\ &K_4=[H^+][R^{2-}]/[R^{\pm-}] \end{aligned}\right\} \quad (14)$$

where $R^{2\pm}{}_{1/2}$ and $R^{2+}{}_{1/2}$ express the unit segments in ionizing molecule, as appears in

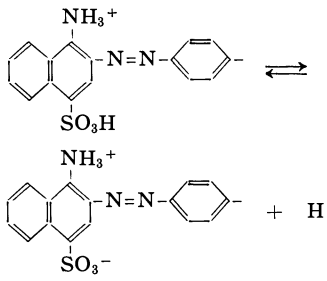

Consequently

$$\left.\begin{aligned} C&=[R^{2-}]+[R^{\pm-}]+[R^{2\pm}]+1/2[R^{2+}{}_{1/2}] \\ f&=[R^{2+}{}_{1/2}]-[R^{\pm-}]-2[R^{2-}] \\ &=[Cl^-]+[OH^-]+[HCO_3{}^-] \\ &\quad -[Na^+]-[H^+] \end{aligned}\right\} \quad (15)$$

Substituting 15 into 14 we obtain eventually,

$$\left(\frac{f}{C}+2\right)+\left(\frac{f}{C}+1\right)\frac{[H^+]}{K_4}+\left(\frac{f}{C}\right)\frac{[H^+]^2}{K_3K_4} +\left(\frac{f}{C}-2\right)\frac{[H^+]^3}{K_2K_3K_4}=0 \quad (16)$$

Application of the successive approximation to 16 leads us to the following result;

$$K_4=1.252\times10^{-7}$$
$$K_3=4.75\times10^{-6}$$
$$K_1=K_2=1.83\times10^{-3}$$

Table IV shows pK values of respective ionizing groups in Congo red for two equations on which the calculation is based.

TABLE IV
pK VALUES FOR CONGO RED

Equation used	Acid group	Basic group
(12)	$pK_1\lesssim1$ $pK_2=3.74$	$pK_3=5.14$ $pK_4=7.02$
(16)	$pK_1=pK_2=2.74$	$pK_3=5.32$ $pK_4=6.90$

In Fig. 8 the full and dotted curves express the $V_t\sim$pH relationship reproduced using equations 16 and 12, respectively. A better coincidence of equation 16 shows the validity of the above treatment. Applying a similar treatment to aluminon, we obtained $K_1=K_2=2.5\times10^{-4}$ and $K_3=6.18\times10^{-8}$ for this dye but we failed to confirm the coincidence between observed and calculated values in the range of $V_t>$

12) S. Woislawski, *Proc. Soc. Exp. Biol. Med.*, **79**, 390 (1952); *J. Am. Chem. Soc.*, **75**, 5201 (1953).
13) Landolt-Börnstein, "Physikalisch-Chemische Tabellen", 5th ed., **2**, 1159, second suppl., 1093 (1923).
14) R. O. MacLaren and D. F. Swinehardt, *J. Am. Chem. Soc.*, **73**, 1822 (1951).
15) T. Svedberg and K. O. Pedersen, "The Ultracentrifuge," Clarendon press, Oxford, (1940), p. 310.

12 cc., as shown as semi-dotted curve in Fig. 7.

Various methods have been presented to determine the ionization constant. Of the methods, spectrophotometry seems hardly applicable for a polyionizing substance. In contrast with this, the potentiometric method is, in principle, applicable to any substance. However, we must solve a rather complicated equation which is liable to produce an appreciable error for a larger ionization constant appearing in the higher-order term of the equation[7]. In order to minimize the error and to facilitate the calculation, it is important to adopt a suitable parameter. The present method of successive approximation is convenient in evaluating the ionization constants of a polyionizing acid or base.

Summary

Change of pH of aqueous dye solution was traced by titrating with the solution of hydrochloric acid or sodium hydroxide. From these data, ionization constants for each ionizing group in chrysoidine, methyl orange, tropäolin OO and aluminon were calculated, making use of equations based on the law of mass action with a specially-selected parameter. The validity of the ionization constants thus determined were confirmed by reasonable coincidence of the titration curves obtained by calculation using these data with those observed, over the wide range of pH.

In the case of Congo red, however, it seemed better to treat it as a high-molecular electrolyte. Ionization constants calculated by an equation based on such a treatment explain the experimental result better than those based on the treatment similar to the case of other simple dyes.

In conclusion, the author wishes to express his sincere thanks to Professor T. Sasaki for his guidance and encouragement during this experiment. A part of the cost of this research has been defrayed from the Scientific Research Expenditure of the Ministry of Education.

Department of Chemistry, Faculty of Science
Tokyo Metropolitan University
Setagaya-ku, Tokyo

Studies on the Interaction of Surface Films with Solute in Solution. II. Sorption of Dye on the Built-up Film of Stearic Acid and Barium Stearate

By Mitsuo MURAMATSU

(Received April 30, 1958)

Knowledge of the surface interaction between amphipathic compounds in the film state and dyes in aqueous solutions contributes considerably not only to the understanding of the mechanism of the dying processes of fiber, the solubilization of dye, the physiological action of bile and other living dye, etc., but also to the knowledge of the substance in its two-dimensional state. From this standpoint the effect of aqueous dye solution on the monolayer of stearic acid[1], cetyl acetate, synthetic fibers, and other polar-nonpolar compounds[2] were studied. Sobotka[3], studying the adsorption of physiologically active substance including porphyrin derivatives upon the built-up film of stearic acid and protein, pointed out an important role of molecular structure of adsorbate in increasing the film thickness and affecting the wettability. It should be further noticed in the case of dye substance that such a type of interaction may be affected

1) R. Matuura, This Bulletin, **24**, 282 (1951).

2) M. M. Allingham, C. H. Giles and E. L. Neustädter, *Discussion Faraday Soc.*, No. **16**, 92 (194).

3) Sobotka, "Recent Advances in Surface Chemistry and Chemical Physics", Science Press Printing Co., Lancaster, (1939), p. 54.

considerably by the nature of dye ions, especially by the balance of anionic and cationic charges, as was pointed out for the interaction of a number of dyes and anionic and cationic detergents in an aqueous medium[4].

In connection with these, the present author intends to study the action of dye ion upon the built-up film of stearic acid and related substances, under varying pH of aqueous dye solution. It may be expected furthermore that such a study may contribute to the knowledge of surface interaction between metal ion and fatty acid, which was reported by Sasaki and Matuura[5], Schulman et al.[6], and Sasaki and the present author[7,8].

Experimental

Reagent.—The stearic acid was the same as that used in a preceding experiment[7]. The dyes were all Takeda's or Merck's reagent grade, except for benzoazurin G (C. I. No. 502)* and benzopurpurin 4B which were kindly supplied by Mr. M. Fujimoto of Mitsubishi Kasei Co. Of the dyes used Congo red, methyl orange and crystal violet were thoroughly purified by repeated recrystallization[9]. Other dyes were used without any special purification, since it was confirmed in the preliminary experiments that the successive purification of Congo red and crystal violet resulted in little change in the sorbed amounts of dyes.

Method.—Monolayer of stearic acid spread on a substrate of pH 4 was successively transferred by means of Langmuir-Blodgett technique[10] onto a highly polished slide of stainless steel, so as to obtain a base echelon. Then a half part of it was immersed for thirty seconds into an aqueous solution of the dye 10^{-4} mol./l. varying in its pH, while the other half was immersed into a control solution of the same pH without dye. The surface of dye or control solution was swept by two barriers prior to immersion. After washing the film with distilled water the changes in thickness of both parts of the echelon were measured by means of the simplified optical method[11], assuming the refractive index of dye to be the same as that of the base material. Calculation was based on the fact that spacing and refractive index of stearic acid in the multilayer were 22.9 Å and 1.482, respectively[10]. The difference, Δ, in changes of thickness thus calculated between two halves of the slide was taken for the sorbed amount. In the case of the solution of crystal violet, night blue (C. I. No. 731), benzoazurin G, or phloxine (C. I. No. 778), each of them forming an elastic film, the down- and up-trip of slide sometimes resulted in the building-up of an adsorbed layer at the air-solution interface. For such a dye, therefore, all experiments were carried out for different times of immersion during thirty seconds, against which the amount of Δ was plotted. A typical example is shown in Fig. 1. True values of the sorbed amount were assumed to be obtained by extrapolation of the curves to zero time of immersion.

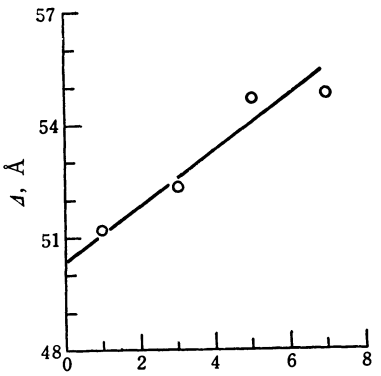

Fig. 1. Effect of immersion upon the apparent amount, Δ, of sorption of crystal violet: pH 6.5.

Experiments were also carried out using the echelon of barium stearate, instead of stearic acid, for the interaction with Congo red and crystal violet. In this case the built-up film was obtained by transferring the monolayer of stearic acid spread on an aqueous substrate containing barium chloride onto the slide. Spacing and refractive index were assumed to be 24.4 Å and 1.462[10], respectively, for this case. All experiments were carried out for 10^{-4} mol./l. of dye solutions, pH of which was varied merely using redistilled hydrochloric acid and aqueous ammonia solution and its value was determined using Beckman's glass electrode.

Results

Acid Dyes.—Fig. 2 shows the effects of pH of dye solution on the amount of aluminon (triammonium aurintricarboxylate) sorbed on the built-up film of stearic acid and on the degree of ionization of three carboxyl groups in the dye molecule. The latter values were calculated using $pK_1 \lesssim 2$, $pK_2 = 4.80$ and $pK_3 = 7.22$ for each

4) G. S. Hartley, *Trans. Faraday Soc.*, **30**, 444 (1934).
5) T. Sasaki and R. Matuura, This Bulletin, **24**, 274 (1951); R. Matuura, ibid., **24**, 277 (1951).
6) J. H. Schulman et al., *Trans. Faraday Soc.*, **46**, 475 (1950); **50**, 1128, 1131, 1139 (1954); *Discussion Faraday Soc.*, No. **16**, 158 (1954).
7) M. Muramatsu and T. Sasaki, This Bulletin, **25**, 21, 25 (1952).
8) T. Sasaki and M. Muramatsu, ibid., **29**, 35 (1956).
9) C. Robinson and H. A. T. Mills, *Proc. Roy Soc.*, **A131**, 576 (1931).
* Abbreviation according to "Color Index", edited by F. M. Rowe, Society of Dyers and Colourisis, Bradford, First edition, (1924).
10) K. B. Blogett and I. Langmuir, *Phys. Rev.*, **51**, 964 (1937), etc.
11) T. Tachibana, *J. of Japanese Biochem. Soc.*, (*Seikagaku*), **20**, 8 (1948).

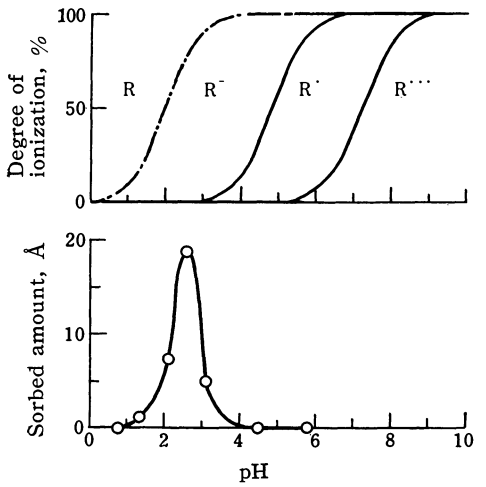

Fig. 2. Effect of pH on the degree of ionization of aluminon and on its amount sorbed on the built-up film of stearic acid.
Semi-dotted curve represents the lower limit of degree of ionization for a given pH, with regard to the reaction, $R \rightleftarrows R^- + H^+$.

groups[12]. They decreased with decreasing pH of the solution, while a maximum sorption was observed at pH from 2 to 3, where the majority of dye molecules were of singly ionized carboxylic acid.

The pH dependence of the amount of phloxine, scarlet red and benzoazurin G sorbed is shown in Fig. 3. All these dyes showed a large amount of sorption in an acidic medium, though there exist some differences in details. Phloxine, one of the triphenylmethane dyes having one carboxyl and one phenolic group, showed a maximum amount of sorption in the range of pH from 3 to 4, where we usually observed a faint turbidity in the bulk and a remarkable rigidity in the surface of the dye solution. Precipitation of dye was evident when pH decreased beyond this range. In the case of benzoazurin G, neither the maximum point of sorption nor the precipitation of dye was observed throughout pH range investigated. The amount sorbed on the film proved to increase with decreasing pH for benzoazurin G. Scarlet red, having both one phenolic and one sulfonic group in the molecule corresponding to a split-in-half structure of benzoazurin G, showed a small amount of sorption at pH less than 3.

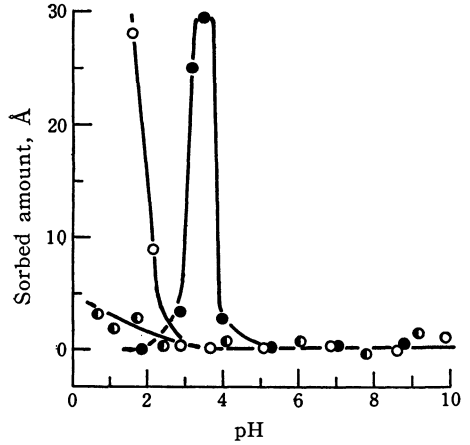

Fig. 3. pH vs. sorbed amount of phloxine (●), scarlet red (◐) and benzoazurin G (○).

Basic Dyes.—In Fig. 4 full curves represent the pH dependence of the amount

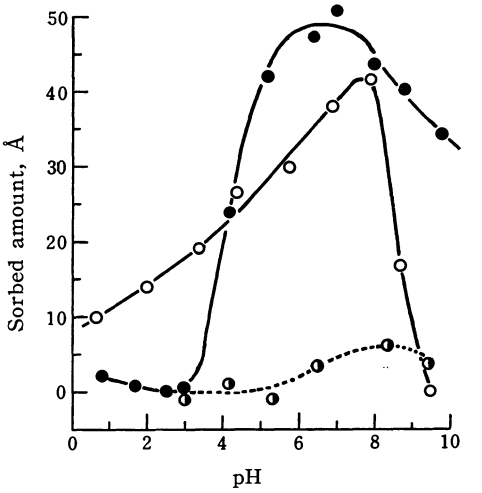

Fig. 4. Effect of pH upon the amount of dye sorbed on the built-up film: ○, night blue on stearic acid; ● crystal violet on stearic acid; ◑, crystal violet on barium stearate.

of crystal violet and night blue sorbed on the built-up film of stearic acid. Maximum sorption was observed in the range of pH from 6 to 8 for both dyes where we often experienced a remarkable wetting of a paraffined wall of the tray by a heavily foaming solution of dye. In the same figure the dotted curve shows the effect of pH upon the amount of crystal violet sorbed on the built-up film of barium stearate. When we compare this curve with the corresponding full curve, it is evident that the use of barium stearate instead of stearic acid resulted in a remarkable diminution of interaction with dye.

12) M. Muramatsu, This Bulletin, **31**, 864 (1958).

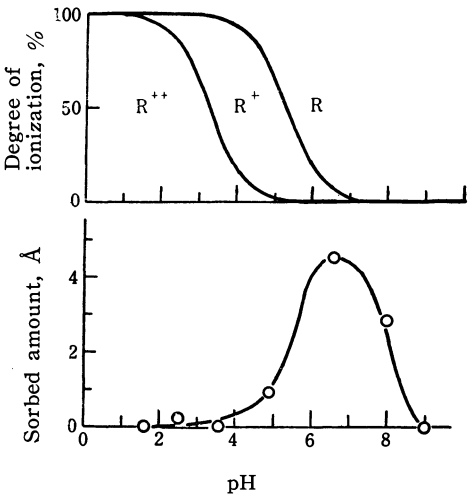

Fig. 5. pH dependence of degree of ionization and of amount of chrysoidine sorbed on the built-up film of stearic acid.

Curves for ionization and sorption of chrysoidine are shown in Fig. 5. The former curves were obtained assuming $pK_1=3.32$ and $pK_2=5.21$[12]. It can be seen in the figure that the maximum of sorption lies in the range of pH from 6 to 7 where one of the amino groups is ionized to the extent of less than 20% while the other is in an entirely non-ionized state.

Amphoteric Dyes.—In Figs. 6 to 8 are shown the results for the dyes possessing both the acidic and the basic groups. Ionization curves for acid and basic groups in

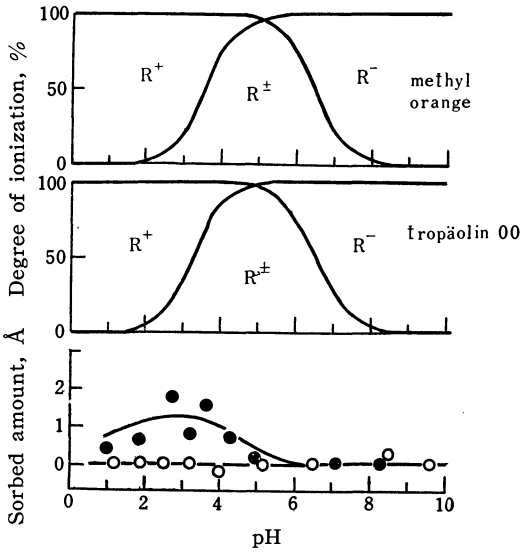

Fig. 6. pH dependence of degree of ionization and of sorbed amount of tropäolin OO (●) and methyl orange (○).

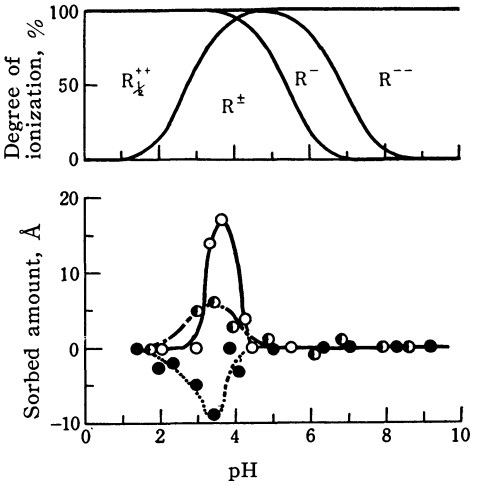

Fig. 7. pH dependence of degree of ionization and of amount of Congo red sorbed on the built-up film of stearic acid (○) and of barium stearate, with (◐) or without (●) the conditioning by the solution of aluminum chloride.

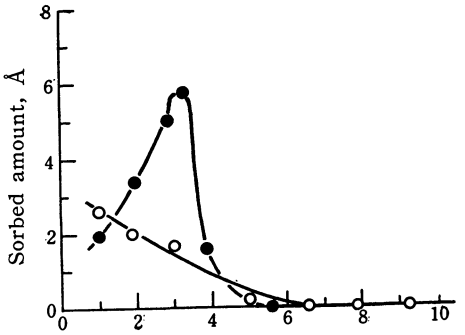

Fig. 8. pH vs. sorbed amount of benzopurpurin 4B (●) and trypan red (○).

methyl orange, tropäolin OO (C. I. No. 143) and Congo red are calculated from all pK values which have been reported in the preceding paper[12].

Of the dyes investigated, tropäolin OO, Congo red and benzopurpurin 4B showed a maximum of sorption on the film of stearic acid in pH range characteristic of each substance, while no measurable sorption was observed for methyl orange in the pH range from 1 to 10. It can be seen furthermore in Figs. 6 and 7 that pH ranges for maximum sorption of tropäolin OO and Congo red were roughly in agreement with the isoelectric region where the majority of dye molecules were in zwitterion form.

Striking results were obtained for the interaction of Congo red with barium

stearate in the film. When the echelon was immersed in an aqueous solution of dye, the pH of which was in the range of 2 to 4, we recorded the decrease in thickness of the echelon, which is shown as a dotted curve in Fig. 7. This might be ascribed to the dissolution of molecules of barium stearate into the solution of dye, which could be seen as the indication of the interaction between the dye and stearate. Similar phenomena have been reported in the case of interaction between serum protein and built-up film of stearic acid[13] or barium stearate[14]. In the other pH range, however, no change was observed in the thickness of the echelon. On the other hand, whenever the film was once conditioned with an aqueous solution of aluminum chloride, the subsequent immersion in the dye solution of pH 2 to 4 always resulted in an increase in the thickness of the film, as is shown by a brokenline in the same figure.

It is seen in Fig. 8 that benzopurpurin 4B has a maximum in pH range for sorption on the built-up film of stearic acid. In contrast with this, trypan red (C. I. No. 438) seemed to be increasingly sorbed with decreasing pH of the solution, this behavior being observed in the case of an acid dye such as benzoazurin G or scarlet red.

Discussion

In our former reports[7], the sorption of metal ion on the built-up film of stearic acid could be explained by the ionic interaction. This has been confirmed[8] by the experiments using radioactive $^{89(90)}Sr$ and ^{60}Co. It was pointed out, however, in the case of the monolayer of octadecylamine[15] that the behavior of the surface film depended markedly upon the molecular structure of the solute in aqueous subphase, so that we should take account not only of the ion-ion interaction but also such an interacting force as ion-dipole, dipole-dipole, hydrogen-bonding and/or van der Waals' attraction when the molecule of solute was complicated in structure. From such a point of view, Matuura[1] explained the expansion of the monolayer of stearic acid spread on aqueous solution of dye by an attraction between the dye and the stearic acid, involving ionic and van der Waals' forces.

In the present experiment the action of acid dyes on the built-up film seems to show that van der Waals' attraction plays an important role in the marked adsorption. It would be likely that the decreasing negative charges of both acid dye and stearic acid with decreasing pH of the medium may weaken the repulsive force acting between the dye molecules themselves as well as between the molecules of dyes and stearic acid. On the other hand dipole-dipole and van der Waals' attraction are considered to be largely independent of the pH of the medium. Thus the decreasing repulsion may cause the increasing sorption of dyes on the built-up film. These are the cases with benzoazurin G and scarlet red. The fact that the sorbed amount of the former is much greater than that of the latter, as shown in Fig. 3, may suggest a large contribution of van der Waals' attraction to the amount of sorption, since the latter is of the split-in-half structure compared with the former.

If, however, ionic repulsion is reduced too much, we can expect such a large aggregates that they are removed from the region of the interfacial film. It is therefore probable that the maximum amount of sorption is observed, if the molecular weight of dye is sufficiently great and the pH of the medium is in a range where the molecules of dye retain an appropriate amount of charge. Fig. 2 offers a typical example for such an effect of ionization upon the sorbed amount of aluminon, the molecular weight of which has the order of magnitude of 800. Dye is presumably in a colloidal state when the pH of the solution is in the range of optimum sorption. Such an explanation would also be made for the case of phloxine, the molecular weight of which is of the same order of magnitude as that of aluminon. From the studies on the velocity of ultrasonic wave in the bulk solution[16] and on the rheological properties of the surface[17] of aqueous solution of phloxine, it has been pointed out that dye molecules are presumably in a state of colloidal aggregate at the pH regions beyond which they precipitate. It may be reasonable therefore to ascribe the appearance of maximum

13) I. H. Sher and H. Sobotka, *J. Collold Sci.*, **10**, 125 (1955).
14) T. Tachibana. K. Fukuda and K. Hamaguchi, This Bulletin, **24**, 155 (1951).
15) E. G. Cockbain and J. H. Schuman, *Trans. Faraday Soc.*, **35**, 716 (1939); T. Sasaki and M. Muramatsu, This Bulletin **26**, 96 (1953).
16) T. Yasunaga and T. Sasaki, To be published in future.
17) H. Kimizuka, This Bulletin, **26**, 33 (1953).

sorption to the formation of colloidal aggregates resulting from the balance between attractive force and ionic repulsion.

A similar explanation can be made for the interaction of basic dyes with stearic acid in the film, results of which are shown in Figs. 4 and 5. A large contribution of van der Waals' force to the interaction may be suggested when we consider the pH dependence of the degree of ionization together with that of the amount of chrysoidine sorbed on the film. It should be noticed, however, that chrysoidine retains still a small amount of positive charge even at pH 6.5 where the maximum interaction is observed, while stearic acid is considered to have a slight negative charge when it is in the state of monolayer spread on distilled water of the same acidity[18]. Therefore the ionic attraction between dye and stearic acid which may exaggerate the sorption should not be neglected. A similar explanation was made for the interaction between stearic acid in the built-up film and metal ion in aqueous solution[7]. Remarkable solidification of the surface film of fatty acid spread on an aqueous crystal violet[1,19] could also be explained from this point of view. This idea is further supported by the fact that the built-up film of barium stearate takes up a smaller amount of crystal violet than that of stearic acid does.

Somewhat complicated results are obtained in the case of amphoteric dyes, which are shown in Figs. 6 to 8. It can be seen in general that the maximum sorption is observed near the isoelectric region of dye. This is indeed the case for tropäolin OO and Congo red. The isoelectric region of benzopurpurin 4B may presumably be around pH 3, where the built-up film of stearic acid takes up the maximum amount of dye from the solution. The exceptional behavior of trypan red would be caused by its negative charge due to five sulfonic groups overwhelming the positive charge due to two amino groups. It might be expected therefore that the maximum sorption could be attained if the solution was rendered much more acidic than in the present experiment.

The majority of molecules of amphoteric dye are considered to be in zwitterion form in the isoelectric region, so that they might exist as colloidal aggregates or micelles differing in size and shape, according to their physico-chemical properties[20]. The molecules in the aggregates would be bound to each other by dipolar attraction, hydrogen-bonding and/or van der Waals' force. In the other pH region the ionic repulsion due to the same sign of charge would suppress the association of dye molecules. Such a presumption may be valid from the results of rheological study on the surface of aqueous dye solution[12], in which it was seen that a film was most coherent for an amphoteric dye when a solution is in an isoelectric region. Such a mechanism for the interaction between dye molecules themselves may also serve to explain the attraction between the built-up film and the aggregate of dye. This presumption is supported by a greater amount of sorption in a respective isoelectric pH range for a larger molecule of dye. Non-sorption of methyl orange may be explained by the smallest molecular weight. An exception is observed however in the relation between Congo red and benzopurpurin 4B. As would be seen in Figs. 7 and 8, the built-up film of stearic acid takes up less benzopurpurin 4B than Congo red, in spite of the molecule being larger by two methoxy groups in the case of the former dye. This may come from the less favorable conditions of forming the aggregate for the latter, presumably owing to the steric hindrance by methoxy groups facing each other in the diphenyl group in the molecule. From the measurement of diffusion velocity of dye, it has been reported[21] that the former dye showed a degree of association of about 9 in 0.01 M sodium chloride solution while the latter had a degree of association of only 6 in the same medium.

It is well known[7,10] that the nonpolar surface of built-up film of barium stearate is rendered polar when it is conditioned by the solution of such cations as copper, aluminum and thorium. This has been explained by the overturning of the molecules in the outermost layer of the film. In connection with this, it is of interest that Congo red interacts with the built-up film of either stearic acid or barium stearate, irrespective of the pre-treatment by the solution of aluminum chloride.

18) J. Glazer and M. Z. Dogan, *Trans. Faraday Soc.*, **49**, 448 (1953).
19) E. Heymann and A. Yoffe, ibid., **38**, 408 (1942).
20) W. Pauli and F. Lang, *Monatsh. Chem.*, **67**, 159 (1936).
21) E. L. Valko, "Colloid Chemistry", edited by J. Alexander, Vol. 6, Reinhold Publ. Corp., New York, (1946), p. 601.

Similar results were obtained for the wettability of the surfaces of various substances including pure paraffin when they were immersed into the solution of Congo red[22]. Again, van der Waals' attraction plays an important role in such a type of interaction. Precisely speaking, however, the possibility of dipolar attraction interacting between dye and film molecules seems to be open to discussion. This is supposed from the fact that the optimum pH range shifts to a more acid position than the pH region where the molecules of dye are almost in zwitterion form, as shown in Fig. 7. At any rate, it would be reasonably deduced that the same attractive force by which the dye molecules are bound to each other is also mainly responsible for the interaction between dye and built-up film molecules, and thus for the change in thickness of the film.

Summary

The amounts of dyes sorbed on the built-up films of stearic acid and of barium stearate were measured, under varying pH of the dye solutions into which the films were immersed. It has been observed in general that the amount of sorption was greater when the molecular weight of dye became greater. Nonionic attraction such as van der Waals' force, which is considered to be a cause of interaction between dye molecules themselves, and aggregate formation among them may also be responsible for the interaction between dye and built-up film. Such an interaction may be favored by the decreasing ionic charges of the same sign existing on dye molecule and film.

Acid dyes proved to be increasingly sorbed with decreasing pH until the aggregates of dye grew so large that they fell from the interface as a precipitate. The difference in detailed behaviors for sorption of several acid dyes could be explained by the difference in the strength of repulsive force of dye ions, suppressing the attraction, as well as of van der Waals' force which was considered to be largely affected by molecular weight.

In the case of basic dyes, ionic attraction is additionally taken into account to explain their sorption on the film of stearic acid. This has been suggested by the correlation between the degree of ionization and sorbed amount of chrysoidine, and supported by the fact that the built-up film of barium stearate took up less crystal violet than that of stearic acid did.

In the case of the sorption of amphoteric dyes, a maximum was observed in general in a pH range which is roughly in agreement with an isoelectric region of dye. Tentative explanations have been made for this phenomenon, taking account of a change in the dissolved state of dyes.

The author expresses his hearty thanks to Professor T. Sasaki for his kind guidance in the course of this study and also to Professor R. Matuura of Kyūshū University for his discussion on this work.
The cost of this research has been defrayed from the Scientific Research Expenditure of the Ministry of Education given to Professor Sasaki.

Department of Chemistry, Faculty of Science,
Tokyo Metropolitan University,
Setagaya-ku, Tokyo

22) A. Inaba, unpublished work.

Studies on the Interaction of Surface Films with Solute in Solution. III. Effect of Dissolved Dyes upon the Monolayer of Octadecylamine

By Mitsuo MURAMATSU

(Received June 24, 1958)

In a preceding paper[1] the action of dissolved dye on the built-up film of stearic acid and barium stearate was reported. There it has been shown that the maximum amount of solute taken up by the film was observed for dye solution in a specific pH range where the remarkable change of dissolved state in bulk[2], as well as the change of rheological properties in surface[3], was observed for dye solution. Various kinds of behavior in such a type of interaction could be explained chiefly by the balance of the attractive and repulsive forces acting between film materials and dyes, when we take account of their ionized as well as dissolved state. This was in general accord with the experimental results on the effect of the aqueous dye solutions not only upon the nature of the monolayer of stearic acid[4] but also upon the wettability of its solid surface[5].

In order to check the validity of such reasoning it has been attempted in the present work to investigate the interaction between several dyes in aqueous solution and octadecylamine monolayer spread on it.

Experimental

Of the samples of dyes used in the preceding work[1], chrysoidine, crystal violet, scarlet red, phloxine (C. I. No. 778*), trypan red (C. I. No. 438), and benzoazurin G (C. I. No. 502) were chosen also for the present experiment, because of the typical behavior of each in the interaction with stearic acid. Each of these dyes was dissolved in water and a stock solution of 10^{-2}mol./l. was made, which was diluted to 10^{-4}mol./l. prior to use as a substrate solution of the monolayer. To minimize the disturbing effects of coexisting ions for dye, pH of the solution was controlled simply by the solutions of hydrochloric acid and ammonia, both of which are twice distilled in an all-ground glass apparatus. The hydrogen ion concentration of this solution was determined using Beckman's glass electrode.

The octadecylamine was the same as that used in a former experiment[6]. It was spread from benzene solution onto the aqueous solution of dye. As we actually used bicarbonate of amine, calculation of the cross-sectional area, A, per molecule was based on the nitrogen content of material which was determined for original samples by micro Dumas method. Surface pressure, F, was measured by means of the modified hanging-plate method[7].

All experiments were carried out at room temperature.

Results

Effect of pH of Substrate Water upon the Monolayer of Amine Spread on It.— It was pointed out by the present author[6] that poor reproducibility was observed for the $F\sim A$ curves of the monolayers of octadecylamine when they were spread on the surface of distilled water. This could be ascribed chiefly, in agreement with the opinion of the other investigators[8,9], to differences in the content of carbon dioxide in water, aging of the film, the velocity of compression, etc. Such an effect was observed also in the present experiment in which pH of substrate water was widely changed over the range of 1 to 10. But $F\sim A$ curve of the monolayer fluctuated only within the hatched zone shown in Fig. 1, though the solution was rendered sufficiently acidic.

In Fig. 2 open circles represent the area, A_0, of octadecylamine molecule at $F=2$ dyn./cm. for varying substrate pH. If we take account of the ambiguity mentioned above, we could not express the $A_0\sim$pH relationship more precisely than as a hatched zone shown in the figure. In

1) M. Muramatsu, This Bulletin, **31**, 871 (1958).
2) T. Sasaki and T. Yasunaga, to be published.
3) H. Kimizuka, This Bulletin, **26**, 33 (1953).
4) R. Matuura, ibid., **24**, 282 (1951).
5) A. Inaba, unpublished work.
* Abbreviation according to "Color Index" edited by F. M. Rowe, First edition, (1924).
6) T. Sasaki and M. Muramatsu, This Bulletin, **26**, 96 (1953).
7) T. Sasaki, *J. Chem. Soc. Japan, Pure Chem. Sec.* (*Nippon Kagaku Zassi*), **62**, 796 (1941).
8) J. Marsden and J. H. Schulman, *Trans. Faraday Soc.*, **34**, 748 (1938).
9) W. C. Bigelow, E. Glass and W. A. Zisman, *J. Colloid Sci.*, **2**, 563 (1947); E. J. Hoffman, G. E. Boyd and A. W. Ralston, *J. Am. Chem. Soc.*, **64**, 498 (1942).

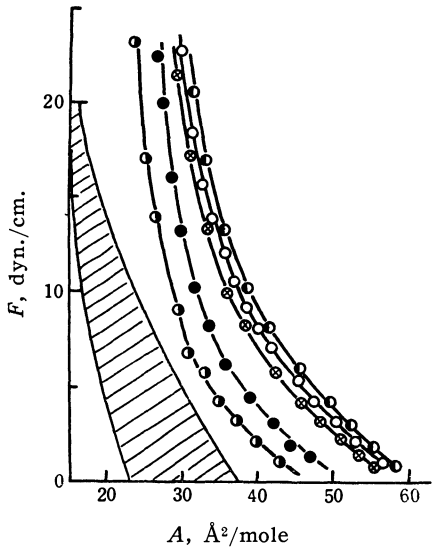

Fig. 1. $F\sim A$ curves for monolayers of octadecylamine spread on aqueous solution of crystal violet under varying substrate pH: hatched zone expresses the limit of fluctuation of $F\sim A$ curves in the control (without dye) experiments for varying substrate pH.

- ◑ pH 2.9
- ● 5.5
- ⊗ 6.1
- ◐ 7.1
- ○ 9.8

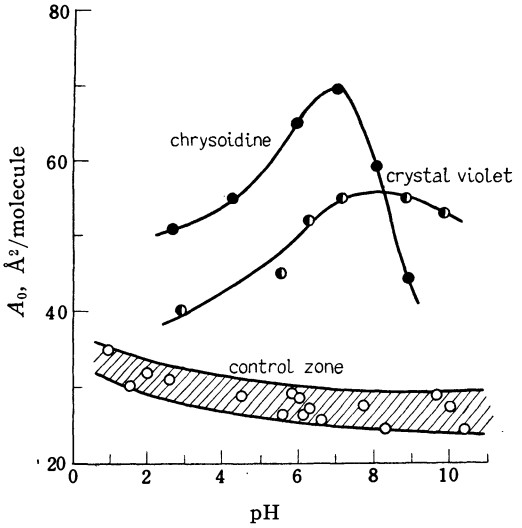

Fig. 2. Effect of substrate pH upon A_0 of octadecylamine spread on aqueous solution of basic dye and on distilled water (control experiment).

general the monolayer showed a tendency of expansion on an acidic substrate. This made a contrast with the case of stearic acid spread on an alkaline substrate[10] and, as assumed by the other authors[8,10], might be attributed to the ionic repulsion due to the ionization of the monolayer.

Monolayer of Amine on the Solution of Basic Dye.—In Fig. 1 are shown the $F\sim A$ curves for the monolayers of octadecylamine spread on the solutions of crystal violet of varying acidity. It is seen in the figure that the $F\sim A$ curve shifts gradually towards right, showing the increasing expansion of the monolayer with increasing pH of substrate. Such an effect of pH upon the nature of the monolayer is reproduced in Fig. 2, in which pH dependence of A_0 of octadecylamine is shown for the cases of crystal violet and chrysoidine. For both dyes we observed characteristic pH ranges for maximum expansion of the monolayer.

Monolayer of Amine on the Solution of Acid Dye.—In the presence of phloxine in the substrate, we observed a marked effect of pH upon F—A curve for the monolayer of octadecylamine, as illustrated in Fig. 3. It can be seen in the figure that the remarkable expansion and increase in compressibility of the film were observed when pH of the substrate was

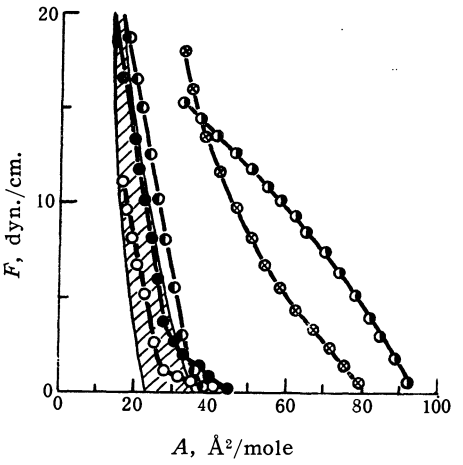

Fig. 3. $F\sim A$ curves for monolayers of octadecylamine spread on aqueous solutions of phloxine, under varying pH: hatched zone expresses the limit of fluctuation of $F\sim A$ curves for the control experiments.

- ◐ pH 1.7
- ◑ 2.9
- ⊗ 3.5
- ● 4.1
- ○ 7.9

10) N. K. Adam, "The Physics and Chemistry of Surfaces", Oxford University Press, London, (1937), p. 71.

around 3~3.5. In the case of scarlet red, however, little change was observed in the cross-sectional area of amine even if pH of the substrate solution was small. The compressibility of the monolayer of amine was not affected by the presence of this dye. Fig. 4 shows the A_0~pH

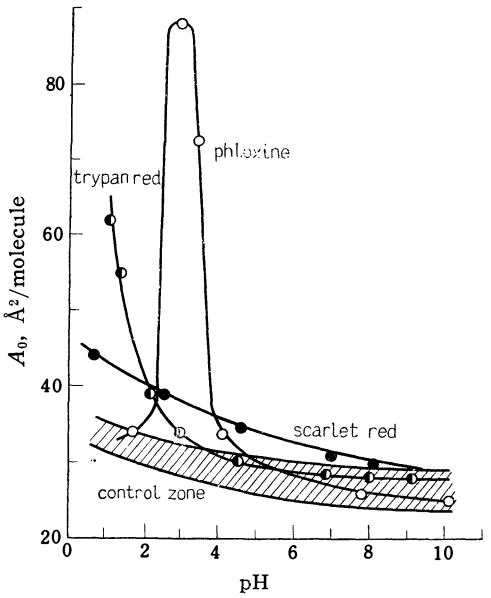

Fig. 4. Effect of substrate pH upon A_0 of octadecylamine on aqueous solution of acid dye.

relation for these dyes, together with for trypan red which made the monolayer expand at pH less than 4 but did not affect its compressibility throughout the whole pH range investigated. It has been pointed out in a preceding paper[1] that trypan red, in spite of its molecule containing five sulfonic and two amino groups, should be regarded rather as an acid dye from the viewpoint of pH dependence of the dye solution.

A somewhat different feature was observed in the case of benzoazurin G. When a fresh surface of a solution of pH 1.7 was compressed by barriers, we recorded a remarkable increase in surface pressure, F, owing to its adsorption to the surface of its own. Though the value of F fluctuated considerably for a given area, σ, of the surface bounded by two barriers, F~σ curve lies always in the zone A in Fig. 5. A more exaggerated feature of F~σ relationship was observed for the monolayer of octadecylamine spread on this solution. In Fig. 5, the hatched zone B and C express the limit of fluctuation in F~σ relationship for the monolayer of

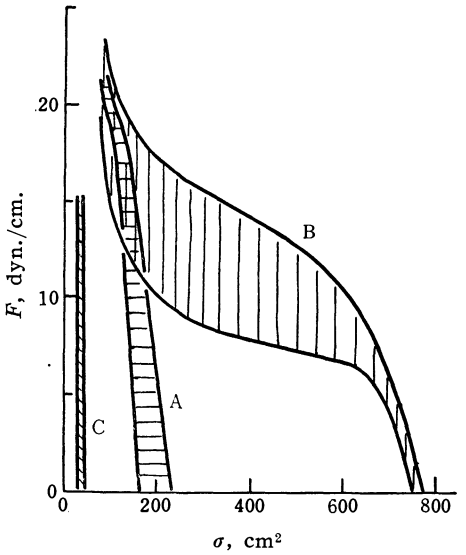

Fig. 5. Limit of fluctuation of F~σ curves: (A) for the surface of solution of benzoazurin G, (B) for the monolayer of 1.29×10^{16} molecules of octadecylamine spread on the substrate containing and (C) lacking the dye. Substrate pH 1.7.

1.29×10^{16} molecules of octadecylamine spread on a substrate of the same pH, containing or lacking benzoazurin G. As is seen in the figure, behavior in the low pressure region exhibited a typical example of the profound effect of benzoazurin G upon the monolayer of amine spread on it. Now, let us compare the surface area, σ_0, at F=2 dyn./cm. for

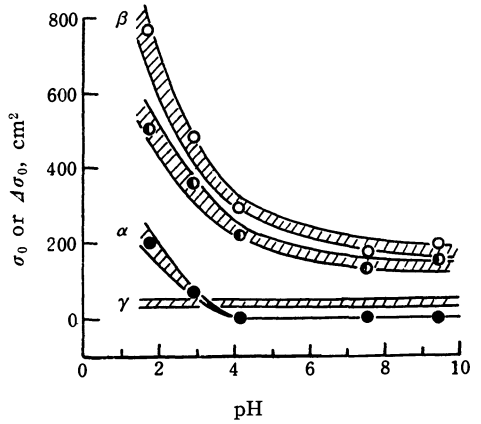

Fig. 6. pH dependence of σ_0 and of $\Delta\sigma_0$ at F=2 dyn./cm.: zone α, pH dependence of σ_0 for adsorbed dye film of its own; β and γ, for the monolayer of 1.29×10^{16} molecules of octadecylamine spread on the substrate containing or lacking, respectively, this dye.

zone B with those for A and C. A similar procedure was applied also for the experiment, varying pH of substrate. The results are illustrated in Fig. 6 in which the velues of σ_0's are plotted against pH. It can be seen that the amounts of σ_0 for zone β (amine+dye) are generally far greater than the sum of those for zone α (amine alone) and γ (dye alone). Such behavior is favorably expessed in terms of the deviation, $\Delta\sigma_0$, from the additivity in σ_0 of the monolayers of amine and the adsorbed dye film of its own and it is plotted against substrate pH in the same figure. It is surprising that the amount of $\Delta\sigma_0$ for around pH 1.7 was evaluated to be 500 cm.^{2}, the figure corresponding to 380 Å^2/molecule of amine. Again, we can see a similar effect as observed in the case of scarlet red or trypan red.

Discussion

It would be reasonable to assume that in the present results an expansion of the monolayer of octadecylamine spread on an aqueous solution of dye comes from an interaction between the monolayer and the dye. Then, the more profoundly the interaction arises between octadecylamine and a certain dye, the more remarkably the monolayer would be expected to expand, apart from the quantitative discussion on the amount of expansion.

Adam[11] observed an expansion of the monolayer of octadecylamine spread on a solution of simple organic acid and explained the phenomenon by ion—ion attraction between the amine and the acid. Such a consideration was verified by means of the mono- and multilayer techniques applied for the interaction between octadecylamine in film state and such simple acids as oxalic, malonic, succinic and adipic acid in an aqueous solution[6]. It has been shown[12], however, that we should also take account of an additional contribution of van der Waals' attraction to the expansion of monolayer of amine, which interacts with organic compound of large molecular weight such as thapsic acid or *pp'*-dihydroxydibenzyl in an aqueous substrate. Because of the dye molecule being larger than these compounds, the present results can hardly be explained at all unless we take account of various forces of interaction. Actually, the behavior of basic dye in alkaline region, as shown in Fig. 2, can not be explained by ion—ion attraction. In this case, ionic repulsions between dye molecules themselves and between the molecules of amine and the dye are considered to decrease with increasing pH of the substrate. Therefore increase of substrate pH may cause an increasing tendency of dye to be bound to the monolayer of amine by the attraction different from ion—ion interaction. This would be valid for the region of pH not large enough to form an aggregate of dye, due to the perfect disappearance of the repulsion. Such a consideration has also been made to explain the action of dissolved acid dye upon the mono-[4] or multilayer[1] of stearic acid.

It has been pointed out in a preceding paper[1] that the conditions favorable for the formation of aggregate of dye are generally in accord with those for the enhancement of the surface interaction. Chrysoidine makes the monolayer of amine expand most remarkably, when it was dissolved in the substrate of pH 7 in which the molecules of dye have little ionic charge, as expected from its pK values, i. e., $pK_1=3.32$ and $pK_2=5.21$[13]. In contrast with this, the maximum amount of aluminon, one of the acid dyes, sorbed on the built-up film of stearic acid was observed when pH of the dye solution was around 2~3 where we can expect the effect of ionic repulsion due to the remaining charge[1]. The difference in the molecular weight between chrysoidine (M. W. =250) and aluminon (M. W.=480) may be responsible for the difference in the contribution of van der Waals' attraction to the interaction between dye molecules themselves by which the difference in easiness of aggregation can also be accounted for. However, it should be noticed that the molecules of amine in the monolayer were considered to be in perfectly ionized state as presumed from the experimental data of surface potential[14]. In this case, therefore, we can expect the possibility of an additional contribution of ion—dipole attraction to the expansion of the monolayer.

A similar explanation can also be made for the effect of acid dye upon A_0 or alternatively $\Delta\sigma_0$ of octadecylamine which is shown in Fig. 4 or 6, respectively; namely, decreasing charge of dye with

11) N. K. Adam, *Proc. Roy. Soc.*, **A126**, 526 (1930).
12) E. G. Cockbain and J. H. Schulman, *Trans. Faraday Soc.*, **35**, 716 (1939).
13) M. Muramatsu, This Bulletin, **31**, 864 (1958).
14) J. Glazer and M. Z. Dogan, *Trans. Faraday Soc.*, **49**, 448 (1953).

decreasing pH of the substrate will cause the formation of aggregate of dye with which octadecylamine interacts. If we confine ourselves to this point of view, the expansion of a monolayer may be accounted for by such attractions as dipolar and van der Waals' forces. However, it has been pointed out by means of mono-[4] and multilayer[1] technique, that the effect of basic dye dissolved in alkaline medium upon the surface film of stearic acid was due to the strong interaction being of complex nature, involving not only dipolar and van der Waals' force but also ionic attraction. For the present results, therefore, we had better take into consideration ionic attraction in addition to dipolar or van der Waals' force. At least we can find no objection to such a reasoning for the expansion of octadecylamine monolayer by scarlet red, trypan red and benzoazurin G. Since small pK values are expected for sulfonic groups in the molecules of these dyes[15], an electrostatic attraction may contribute throughout a wide range of substrate pH to the expansion of the monolayer of octadecylamine, the pK of which is reported to be 8.5[14].

It has been shown[2,3] that acid dye formed colloidal aggregates when it was dissolved in aqueous solution of pH being slightly larger than that for distinct precipitation. A typical example was observed in the case of phloxine dissolved in aqueous medium. Actually we observed faint turbidity in this solution when pH was less than 3. Thus the remarkable expansion of the monolayer on substrate of pH 3 can be accounted for by the interaction between the molecules of octadecylamine and the colloidal aggregates of dye. In connection with this, it is interesting to note that the more the monolayer of octadecylamine expands, the more it becomes compressible. This behavior is shown in Fig. 3. The same type of $F\sim A$ curve was observed also for the interaction between stearic acid in the monolayer and cobalt ion in the substrate[16]. This has been explained by the ionized monolayer of stearic acid with which the colloidal aggregate of cobalt ion interacts. Studies on the dissolved state of cobalt ion[17] seemed to support this explanation.

15) N. Andō, "Senryō Kōshitsugaku (Chemistry of Dye Stuffs in Japanese)," Shōkabō, Tokyo, (1948), p. 44.

16) T. Sasaki and M. Muramatsu, This Bulletin, **29**, 35 (1956).

17) R. Matuura and H. Kimizuka, This Bulletin, **28**, 668 (1955); T. Sasaki and K. Izawa, unpublished work.

Summary

The interaction between octadecylamine in monolayer and various dyes in aqueous substrate under varying pH was studied. Such a basic dye as chrysodine or crystal violet remarkably expanded the monolayer when pH of the solution was in a certain range on alkaline side. This has been attributed to the interactions between the molecules of dye themselves and that between dye and octadecylamine. Thus, it is mainly dipolar and van der Waals' attraction, which was considered to be overshadowed by ionic repulsion when substrate pH was in the other region. Additional possibility of ion-dipole attraction due to the remaining charge of the monolayer was discussed in connection with the ionizations of octadecylamine and basic dyes.

In contrast with this, the monolayer expanded remarkably when it was spread on an acidic solution of acid dye. The behavior could be accounted for by the sum of ionic, dipolar and van der Waals' attraction. The possibility of the formation of colloidal aggregate of dye with which octadecylamine interacts has been discussed, in connection with the effect of metal ion in the substrate upon the monolayer of stearic acid.

The author wishes to express his hearty thanks to Professor T. Sasaki for his kind guidance and encouragement throughout this research. His thanks are also due to the Ministry of Education for the Scientific Research Expenditure.

Department of Chemistry, Faculty of Science, Tokyo Metropolitan University, Setagaya-ku, Tokyo

Untersuchungen über die Bildung der Proteinase aus einem Aspergillus awamori-Stamm. I. Faktoren mit Einflüssen über die Bildung der Proteinase

Von Jiro HOSHINO

(Eingegagen am 1. Mai, 1958)

Die proteolytischen Enzyme werden bekanntlich von verschiedenartige Schimmelpilzen in die Nährlösung sezerniert, die deswegen von alters her in den orientalischen Ländern zur Gärungsindustrie verwendet worden sind. Über den gründlichen Bildungsmechanismus der Proteinase aus dem Schimmelpilz ist aber wenig untersucht worden. Es ist daher dem Verfasser ein besonderes Interesse, solche Probleme mittels eines Pilzes *Aspergillus awamori* aufzuklären, das vom Verfasser aus der Erde isoliert wurde und ein starkes Vermögen zur Bildung der "sauren" Proteinasen bietet, von denen der Verfasser eine enzymatische Natur angegeben hat[1].

Die Bildung der Proteinase unter den verschiedenen Züchtungsbedingungen durch das Oberflächenverfahren hat der Verfasser näher studiert[2,3], aber infolge der Mycelentwicklung ist das Versuchssystem in diesem Falle etwas kompliziert und damit wird der wesentliche Bildungsmechanismus des Enzyms schwer aufzuklären.

Verwendet man dagegen das ausgewaschene Schüttelmycel in einem stickstofffreien Milieu, so kann man die oben erwähnte Schwierigkeit leicht beseitigen.

In den letzten Jahren wurden die Bildungsmechanismen der Enzyme von mehreren Forschern, wie z. B. dasselbe der Amylase aus *Bacillus subtilis* von J. Fukuomoto et al.[4] und von M. Nomura[5], der Amylase aus *Asp. oryzae* von O. Tanabe et al.[6] und der Proteinase aus *Asp. oryzae* von H. Shiota et al.[7], mittels des ausgewaschenen schüttelmycels oder der Zellen mitgeteilt.

Um weitere Kenntnisse über den Bildungsmechanismus der "sauren" Proteinase zu erkennen, hat der Verfasser in den vorliegenden Arbeiten das ausgewaschene Schüttelmycel als Versuchsmaterial zur Prüfung unterworfen.

Arbeitsmethode

Gewinnung des ausgewaschenen Schüttelmycels.—Einige Anzahl der Schüttelkolben von 500 ccm Inhalt wurden mit je 80 ccm Nährlösung beschickt, die 10% Rohrzucker, 0.2% Ammoniumnitrat und Monokaliumphosphat, 0.025 % Magnesiumsulfatheptahydrat, 0.002% Mangansulfattetrahydrat, 0.0025% Eisen(III)-chloridhexahydrat und 0.03% Gelatine als Nährsubstrat enthält. Nach dem üblichen Sterilisieren wurden jede Kolben von den etwa 5~10 Tagen Würzeagarkulturen mit Conidiosporen von Stamm Nr. 82—2 geimpft, und danach wurden die Kulturen 72 Stunden lang auf einer Schüttelmaschine mit 130 Hin- und Herbewegungen pro Minute bei 30°C behandelt. Das so sich entwickelnde Mycel wurde dann unter sterilen Bedingungen gemeinsam auf einem groben Filter gesammelt. Das gut abgesaugte und ausgewaschene Mycel wurde in kleine Stücke (1.0 g feuchtes: etwa 0.2 g Trockengewicht) zerschnitten, welche zur Untersuchungen der Bildung der Proteinase in den 50 ccm Versuchslösungen wieder suspensiert, und bei 30°C weiter geschüttelt wurden.

Bestimmung der proteolytischen Aktivität.—Zur Ermittelung der proteolytischen Aktivität hat der Verfasser die Caseinverdauung mittels des Folinschen Reagens nach B. Hagiwara[8] kolorimetrisch bestimmt, wobei die enzymatische Reaktion unter den Bedingungen von 1% Casein, pH=3.2, bei 55°C eine Stunde lang geprüft wurde. Der Wert der proteolytischen Aktivität wurde

1) J. Hoshino und N. Taketomi, *Waseda Applied Chem. Soc. Bull.* (*Waseda Ōyokagakukaihō*), **24**, No. 65 9 (1957).
2) J. Hoshino, *Synopses of Eng. Graduate School of Sci. and Eng. Waseda Univ.* (*Waseda Daigaku Kōgaku Kenkyu Ihō*), **6**, 64 (1957).
3) J. Hoshino, *Memoirs of College of Sci. and Eng., Waseda Univ.* (*Waseda Daigaku Rikogakubu Kiyō*), (im Drucke).
4) J. Fukumoto, T. Yamamoto und D. Tsuru, *J. Agr. Chem. Soc. Japan* (*Nippon Nogei Kagaku Kaishi*), **31**, 421, 429, 506, 510, 545 (1957).
5) M. Nomura et al., *J. Biochem*, **43**, 251, 841 (1956), **44**, 87 (1957).
6) O. Tanabe et al., *J. Agr. Chem. Soc. Japan* (*Nippon Nogei Kagaku Kaishi*), **30**. 596 (1956), **28**, 227 (1954).
7) H. Shiota et al., ebenda, **30**, 724 (1956), **31**, 173 (1957).
8) B. Hagiwara, *Ann. Rep. Fac. Sci. Osaka Univ.*, **2**, 35 (1954).

mit dem Absorptionskoeffizient pro Gramm trockenen Mycels pro 50 ccm Versuchslösung derjenigen mit dem Folinschen Reagens sich färbenden und 0.2 M Trichloroessigsäure löslichen Stoffen, die unter den obigen Bedingungen aus Casein bilden, bei der Wellenlänge von 660 mμ ausgedrückt.

Ergebnisse

1. Bildungsverlauf der Proteinase.— Der Bildungsverlauf der Proteinase aus dem Schüttelmycel wurde unter Verwendung von M/30 KH_2PO_4 (pH=4.8) und des destillierten Wassers als Versuchslösung beobachtet. Die Ergebnisse sind in der Figur 1 dargestellt.

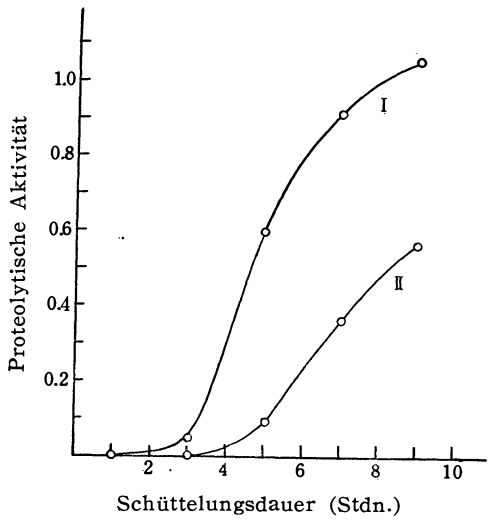

Fig. 1. Bildungsverlauf der Proteinase. Versuchslösung:
Kurve I, M/30 KH_2PO_4 (pH=4.8)
Kurve II, Destilliertes Wasser

Das Mycel fängt an, wie aus der Figur ersichtlich ist, beim Schütteln mit der stickstofffreien Phosphatlösung nach einer Weile Proteinase reichlich zu sezernieren.

Weiter ist es auch der Fall mit dem Wasser Proteinase zu bilden. Hierbei bleibt aber die Frage noch offen, ob die Proteinase durch das Mycel wirklich *de novo* synthetisch hergestellt wurde oder die innere Proteinase durch das Schütteln ausgelassen wurde. Um diese Frage zu beantworten, hat der Verfasser die Mycelhomogenate und den Auszug des Acetonpulvers des Mycels zur Ermittelung der proteolytischen Aktivität herangezogen. Keine proteolytischen Aktivität wurde darin bestätigt (Tabelle I). Einige metabolischen Inhibitoren, wie Kaliumcyanid, 2, 4-Dinitrophenol und Toluol haben die Bildung der Proteinase verhindert (Tabelle II). Durch die oben angegebenen Tatbestände wurde es festgestellt, dass die Bildung der Proteinase sich nicht das Auslassen der inneren Proteinase, sondern echte Biosynthese durch einen von den genannten metabolischen Inhibitoren verhinderten Prozess stattfindet.

TABELLE I
PROTEOLYTISCHE AKTIVITÄT DES MYCELHOMOGENATES UND DES AUSZUGS

Reaktionsdauer (Min.)*	15	30	60	120
Mycelhomogenate	0	0	0	0
Auszug	0	0	0	0
Kontrolle**	0.39	0.52	0.64	0.71

* Enzymatische Reaktionen wurden unter den Bedingungen von 1% Casein, pH=3.2 bei 55°C ausgeführt.

** Zum Kontrollversuch wurde die Versuchslösung herangezogen, nachdem sie mit dem ausgewaschenen Mycel 20 Stunden lang geschüttelt worden war.

TABELLE II
EINWIRKUNGEN DER METABOLISCHEN INHIBITOREN AUF DIE PROTEINASEBILDUNG

Inhibitoren	Konz.	Proteolytische Aktivität der Versuchslösung, Schüttelungsdauer (Stdn.) 3	5	24
Toluol	10% V/V	0	0	0.06
KCN	1×10^{-2} M	0	0	0.27
	1×10^{-3} M	0	0	2.94
2, 4-DNP*	1×10^{-2} M	0	0	0.09
	1×10^{-3} M	0	0	0.95
Kontrolle	1×10^{-3} M	0	0.24	3.16

* 2, 4-Dinitrophenol

2. Bildung der Proteinase bei der Züchtung und durch das Schütteln des dabei sich entwickelten Mycels.—Als einzelne C-Quelle zur Entwicklung des Pilzes wurden je 10% Saccharose, Glucose, Fructose und Lactose in der Nährlösung zugesetzt und die Anhäufung der Proteinase in der Kulturflüssigkeit nach 3 Tagen und das Bildungsvermögen derselben des so sich entwickelten Mycels beobachtet.

Die Versuche mit dem ausgewaschenen Mycel wurden mittels derjenigen Versuchslösung ausgeführt, die aus M/5-Phosphatpuffergemisch (pH=6.1) und 1% Glucose besteht. Die Resultate sind in der Tabelle III zusammengestellt. Dabei hat es sich ergeben, dass das ausgewaschene Schüttelmycel ein grösseres Vermögen zur Proteinasebildung unter dem Mangel an den

TABELLE III

PROTEINASEBILDUNG DURCH DAS AUSGEWASCHENE MYCEL UND DURCH DAS ENTWICKLUNGSVERFAHREN

	C-Quelle im Nährboden	Oberflächenverfahren	Schüttelverfahren	
		Entwicklungszüchtung* 7 Tage	Entwicklungszüchtung* 3 Tage	Dabei entwickeltes ausgewaschene Mycel** 24 Stunden
Proteinasebildung (Prot. Akt.)	Saccharose	0.31	0.39	5.29
	Fructose	6.65	0.20	6.53
	Glucose	0.08	0.06	9.70
	Lactose	—	0.82	10.57
Entwicklung (Gewicht des Mycels in mg)	Saccharose	91	560	
	Fructose	913	562	
	Glucose	81	540	
	Lactose	—	116	

* Die Entwicklungsnährlösung steht im Text geschrieben, aber ohne Gelatine für Oberflächenverfahren.

** Die Versuchslösung besteht aus 0.2 M Phosphatpufferlösung und 1% Glucose.

Nährsubstrate als des sich entwickelten Mycels erweist.

3. Proteinasebildungsvermögen des Mycels in den verschiedenen Entwicklungsphasen.—Es ist bekannt, dass sich die physiologische oder biochemische Aktivität der Zellen mit der Dauer der Züchtung ändert. Hinsichtlich dieses Tatbestandes hat der Verfasser das Proteinasebildungsvermögen des Schüttelmycels in den verschiedenen Entwicklungsphasen ermittelt und seine Beziehung zum Gehalt des Mycels an den freien Aminosäuren näher studiert. Die Ergebnisse sind in der Figur 2 illustriert.

Die Anhäufung der Proteinase nach dem zwanzigstündigen Schütteln des Mycels in der 1% glucosehaltigen M/5-Phosphatpufferlösung wurde zur Bestimmung des Proteinasebildungsvermögen ermittelt.

Wie aus der Figur 2 ersichtlich ist, fand eine beträchtliche Änderung des Vermögens des Mycels während seiner Entwicklung statt: je jünger das Mycel ist, desto grösser ist das Vermögen. Dementsprechend sind die reichlichere Mengen der wasserlöslichen Eiweissstoffen und des totalen Stickstoffes im solchen Mycel enthalten. Wenn das Mycel sich kräftig entwickelt, vermindert sich allmählich sein Proteinasebildungsvermögen. Es deutet an, dass es zwischen dem anabolischen Stoffwechsel des sich entwickelnden Mycels und demselben des ruhenden Mycels ein grosser Unterschied gibt, wie von M. Nomura[5] schon darauf hingewiesen wurde.

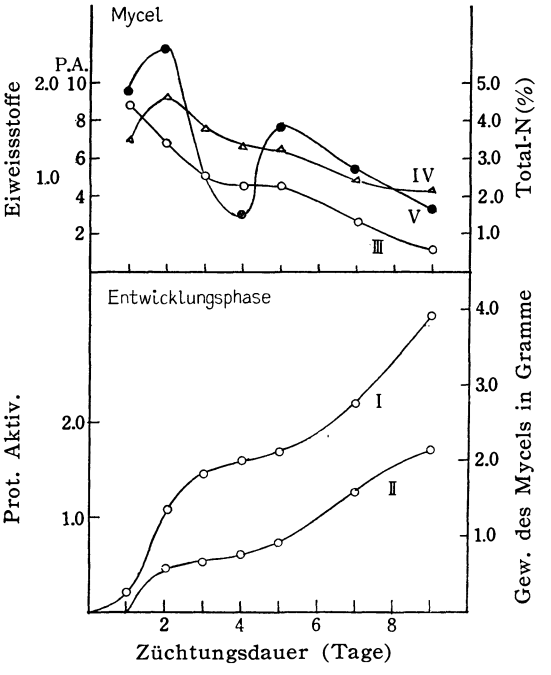

Fig. 2. Änderung des Proteinasebildungsvermögens des Mycels mit der Züchtungsdauer.

Kurve I: Mycelentwicklung
II: Proteinasebildung bei der Züchtung
III: Proteinasebildungsvermögen des Mycels (P. A.)
IV: Stickstoffgehalt des Mycels
V: Wasserlösliche Eiweissstoffe*

* Ausgewaschenes Mycel wurde unter Rückflüsskühler mit Wasser 10 min. dreimal extrahiert, Eiweissstoffe im Extrakt wurden mittels des Folinschen Reagens kolorimetrisch ermittelt.

TABELLE IV
EINFLUSS DER ANAEROBEN BEDINGUNGEN AUF DIE PROTEINASEBILDUNG

	Kontrolle				Anaerobenschütteln								
	Wattebausch				Gummistöpsel				N_2-Einfüllung				Vakuum
0.2 M-Phosphatpuffer	−	−	+	+	−	−	+	+	−	−	+	+	+
1% Glucose	−	+	−	+	−	+	−	+	−	+	−	+	+
Schluss pH	5.6	1.4	5.9	5.4	5.6	1.8	5.9	5.6	5.6	2.2	5.9	5.8	5.8
Proteolytische Aktivität	4.3	0.7	4.0	4.2	4.0	0.9	3.8	4.4	0.6	1.4	0.8	1.2	0

4. Einfluss des pH auf die Proteinasebildung.—Um den Einfluss des pH auf die Bildung der "sauren" Proteinase zu erkennen, hat der Verfasser die Pufferlösungen von N/10-Phosphat und N/10-Acetat als Versuchslösungen unter den variierenden pH verwendet. Die Ergebnisse sind in der Figur 3 illustriert.

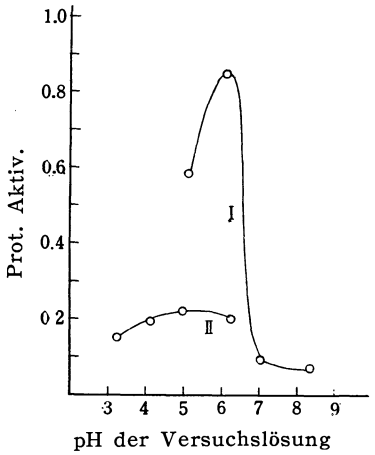

Fig. 3. pH-Abhängigkeit der Proteinasebildung.
Versuchslösung; I, N/10 Phosphatpuffer
II, N/10 Acetatpuffer

Bei den Versuche mit den Phosphatpufferlösungen ergab es sich, dass die Bildung der Proteinase gegen die Änderung des pH äusserst empfindlich ist, deren Optimum bei pH=6.1 liegt. Demgegenüber bleibt die Acetatpufferlösung auf die Bildung der Proteinase ohne Wirkung, die daher durch das Phosphat gar nicht ersetzlich ist. Daraus wurde es festgestellt, dass das Phosphat nicht nur als ein Puffer, sondern auch als ein Hilfsmittel auf die Biosynthese der Proteinase wesentlich einwirkt.

5. Einfluss der Phosphatkonzentration.—Wie im vorigen Paragraph beschrieben, übt die Anwesenheit des Phosphates auf die Bildung der Proteinase eine vorzügliche Wirkung aus, die aber dem Acetat ganz fehlt.

In Berücksichtigung dieser wichtigen Tatsache hat der Verfasser den Einfluss der Phosphatkonzentration der Versuchslösung auf die Proteinasebildung mit dem Anfangswert von pH=6.1 näher studiert. In der Figur 4 sind die Ergebnisse wiedergegeben. Hierbei ist es gezeigt, dass die Änderung der Phosphatkonzentration sehr einflussreich ist und ihr Optimum bei M/30 liegt.

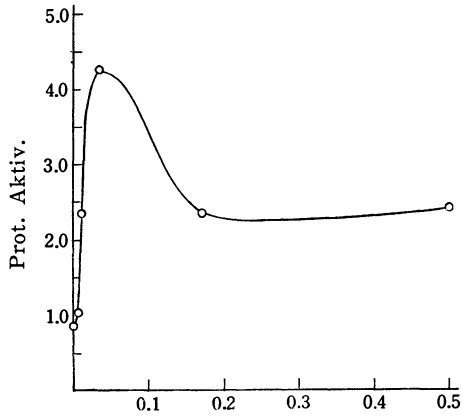

Fig. 4. Einfluss der Phosphatkonzentration.

6. Bedürfnis des Sauerstoffs.—Es wurde von H. Shiota[7] veröffentlicht, dass die Proteinasebildung aus dem ausgewaschenen Mycel des *Asp. oryzae*-Stammes stark gehemmt wird, wenn die Luft in den Schüttelkolben durch Kohlendioxyd, Stickstoff und Wasserstoff ersetzt wird. Identischer Tatbestand hat J. Fukumoto[9] bei den Versuche über die Amylasebildung aus *Bacillus subtilis* wahrgenommen.

Um den Effekt der anaeroben Bedingung bei meinem System in Anbetracht dessen zu erkennen, hat der Verfasser das Mycel je in den Kolben mit dem Gummistöpsel, in der Stickstoffatmosphäre und im Vakuum zum Vergleich mit dem Versuch mit dem Wattebausch geschüttelt. Die Ergebnisse finden sich in der Tabelle IV..

9) J. Fukumoto und T. Yamamoto, *J. Agr. Chem. Soc. Japan* (*Nippon Nogei Kagaku Kaishi*), **31**, 421 (1957).

Diese zeigen, dass Sauerstoff auf die Bildung der Proteinase unentbehrlich einwirkt, dessen Menge aber mit ein wenig genügend ist.

Schlusswort

Es wurde über die Bildungsfaktoren der "sauren" Proteinase aus den ausgewaschenen Schüttelmycel eines Schimmelpilzes *Aspergillus awamori*, das vom Verfasser neulich isoliert wurde und durch das starken Vermögen zur Bildung der "sauren" Proteinese charakteristisch ist, und auf ihre Beeinflussbarkeit durch einige Schüttelbedingungen untersucht.

Zusammenfassend darf es festgestellt werden, dass das Mycel durch einen synthetischen Prozess aus den Aminosäuren die Proteinase bildet, für das die Zusammenwirkung von Sauerstoff und der Energiequelle sowie Phosphat unentbehrlich zu sein scheint. Die pH-Abhängigkeit der Bildung dieses Enzyms ist so bemerkenswert, dass man für die reichliche Bildung mit der konzentrierten Pufferlösung günstigen pH-Wert festhalten muss. Das Optimum liegt bei pH=6.1. Diesbezüglich ist diese Proteinasebildung von derselben bei der Entwicklungszüchtung sehr verschieden, wobei sie im mehr sauren Bereich am günstigsten stattfand, während es noch nicht imstande ist, diesen Unterschied aufzuklären.

Es ist mir ein Bedürfnis, Herrn Professor Dr. N. Taketomi für seine Anregung und stetige Leitung bei dieser Arbeit meinen besten Dank auszusprechen.

Institut der Angewandten Chemie
Fakultät der Naturwissenschaft und Technik
Waseda Universität
Shinjuku-ku, Tokyo

SHORT COMMUNICATIONS

*Chronopotentiometry at Varying Current Density with the Use of Current Controlled Dropping Mercury Electrode**

By Masayoshi Ishibashi and Taitiro Fujinaga

(Received May 26, 1958)

The authors have previously introduced a new method for obtaining the polarogram at the dropping mercury electrode with controlled current[1], whose phenomena were mathematically revised by Senda et al.[2] In connection with this study, potential-time curves have been investigated and many interesting phenomena were observed with several electrode reactions. From the stand point of analytical chemistry, it is expected that, with proper control of current, the wave of a more cathodically reducible substance is recorded alone on the chronopotentiogram (potential-time curve), independently, in the presence of large quantities of less cathodically reducible substances. For instance, with a solution of cadmium in hydrochloric acid, a very negative potential corresponding to that of hydrogen deposition is expected at the beginning of the drop growth and then it moves to a positive potential of the cadmium ion—cadmium amalgam system with the decrease in current density due to the increase in surface area, so that a chronopotentiogram of inversed shape to that in the ordinary chronopotentiometry is recorded even in the presence of less cathodically reducible substances e.g. the lead ions. Apparently this characteristic is more effective than any other voltammetric methods hitherto used in trace analysis. Therefore a preliminary report is presented here.

The chronopotentiogram was recorded by the x-y recorder made by Shimadzu Mfg. Co. (Pen speed: 0.8 sec./25 cm.,

1) M. Ishibashi and T. Fujinaga, *J. Electrochem. Soc. Japan (Denki-kagaku)*, **24**, 375, 525 (1956): *Anal. Chim. Acta*, **18**, 112 (1958).

2) M. Senda, T. Kambara and Y. Takemori, *J. Phys. Chem.*, **61**, 965 (1957).

* Presented at the Symposium on Instrumental Methods of Chemical Analysis at Himeji in 1958 sponsored by the Chemical Society of Japan.

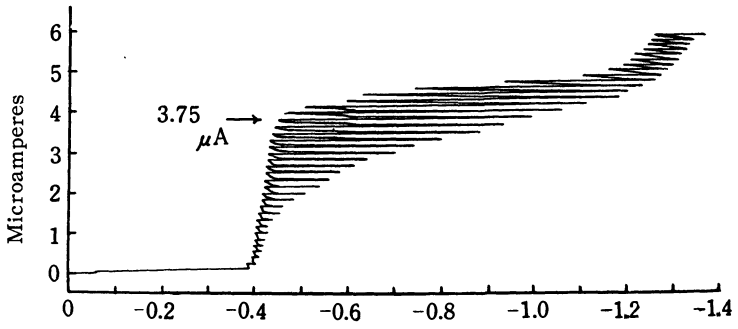

Volt vs. S. C. E.

Fig. 1. Current scanning polarogram.
(4×10^{-5}M-Cd^{2+}, 1×10^{-3}M-Pb^{2+}, 0.01%-Polyacrylamide and 0.1 N-HCl)

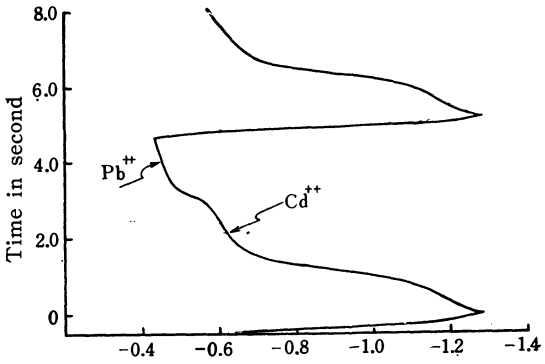

Volt vs. S. C. E.

Fig. 2. Chronopotentiogram.
(Solution: same as Fig. 1, t=5.26 sec. at i=3.75 μA)

maximum sensitivity: 10 mV./25 cm. and maximum chart speed: 2.0 sec./35 cm.), to which were attached a pre-amplifier of increasing the input impedance for the x-axis and a voltage scanner of changeable velocity for the y-axis. The controlled current was supplied from a DC source composed of a high voltage and a high resistance used in a previous paper[1].

Fig. 1 shows a current scanning polarogram of cadmium ions in the presence of 25 times as many lead ions. Fig. 2 is the corresponding chronopotentiogram for cadmium wave at the current of 3.75 microamperes.

Besides the use of the ordinary dropping mercury electrode for the change of current density, combination of the dropping mercury electrode with extremely slow drop rate (ca. 60 sec./drop) and the potentiometer-recorder for ordinary chronopotentiometry was investigated. Also an ordinary chronopotentiometry with stationary electrode but with decreasing current scan was studied. These methods show a similar effect to that of the present method described above. Therefore these three methods, all employing varying current density, would give potential values for analytical instrumentation. The detailed discussion will be presented later.

The authors gratefully acknowledge to Professor I. M. Kolthoff of the University of Minnesota for his kind interest and suggestion on the subject at the time of the International Symposium on Modern Electrochemical Methods of Analysis held at Paris in 1957. The authors also wish to thank Mr. A. Saito for his cooperation in this work.

Laboratory of Analytical Chemistry
Faculty of Science
University of Kyoto
Kyoto

A New Colorimetric Method for the Determina tion of Beryllium with Neo-thorone

By Shozo Shibata, Fukuo Takeuchi and Teiichi Matsumae

(Received August 22, 1958)

In order to determine a few micrograms of beryllium, a new colorimetric method has been developed based upon the stable violet-colored beryllium complex of Neothorone[1] (*o*-arsonophenylazo-chromothropic acid)[2] in an aqueous solution.

1) S. Shibata and T. Matsumae, This Bulletin, **31**, 377 (1958).
2) V. Kuznetsov, *Compt. rend. acad. Sci. U. S. S. R.*, **31**, 898 (1941).

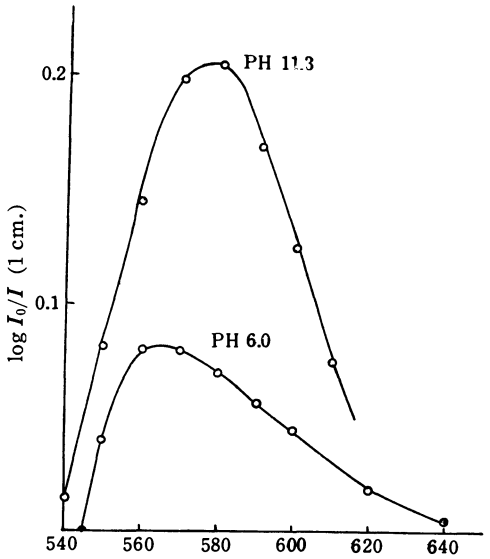

Fig. 1. Absorption spectra of Neo-thorone-beryllium complex at pH 6.0 and 11.3.

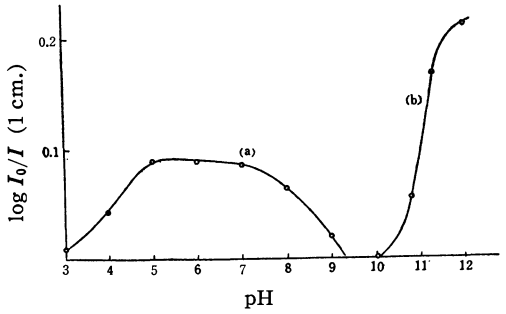

Fig. 2. The effect of pH on the absorbance (a, at 570 mμ; b, at 580 mμ).

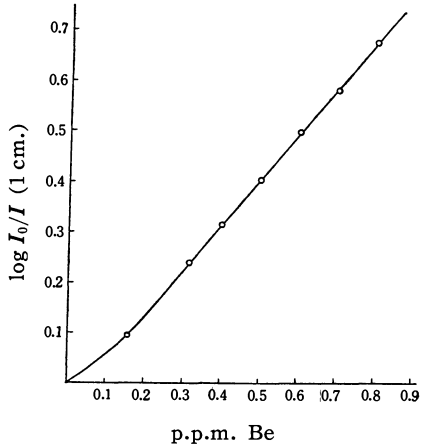

Fig. 3. Absorbance-concentration curve of beryllium (570 mμ, pH 6.0).

Absorption spectra of the complex are presented in Fig. 1. These curves were measured in a buffered solution of pH 6.0 and 11.3 respectively. The violet colored complex of beryllium was formed by adding several micrograms of beryllium and 1.0 ml. of 0.1% reagent solution to a 25 ml. volumetric flask and diluting to the mark with a buffered solution of pH 6.0. Color was developed within five minutes and its stability was found to be quite adequate for the determination of beryllium, the absorbance being proportional to beryllium concentration in the range from 0.15 p.p.m. to at least 1 p.p.m. (Fig. 3). At 570 mμ, the molar extinction coefficient is about 7,160, the sensitivity being 0.03 μg. Be/cm^2 corresponding to log I_0/I=0.001.

In a strong alkaline solution (pH 11.0~12.0), the absorbance becomes very high. The relationship between absorbance and pH of solution is shown in Fig. 2. The results given in Fig. 2 indicate the presence of two species of neo-thorone-beryllium complex. At pH 11.3, the absorbance is proportional to beryllium concentration in the range from 0 to 0.15 p.p.m. (Fig. 4). At

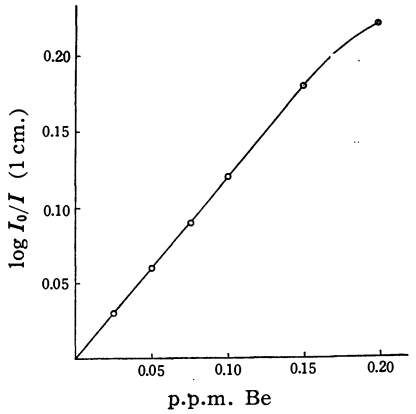

Fig. 4. Absorbance-concentration curve of beryllium (580 mμ, pH 11.3).

580 mμ, the molar extinction coefficient is about 10,000, the sensitivity being 0.002 μg. Be/cm^2 corresponding to log I_0/I=0.001.

Thus these two methods appear to offer a good basis for the colorimetric determination of microgram amounts of beryllium. Details of the study will be published later.

Government Industrial Research Institute Nagoya
Kita-Ku, Nagoya

On the First Ionization Energies of Heterocyclic Molecules

By Kogoro MAEDA

(Received August 23, 1958)

In the present note the author wishes to show some results of semi-empirical estimation of the first ionization energies of π-electrons in heterocyclic molecules. The evaluation of these values was carried out according to Hush and Pople's method[1] in which electron interaction was taken into account explicitly.

The values of the integrals, resonance β_{pq}, one center electron repulsion $(pp|pp)$, and two center electron repulsion $(pp|qq)$, were taken from Pariser and Parr's paper[2], those of the first integrals for non-neighboring atoms p and q being neglected; it was assumed that Coulomb integral α_{cp} and resonance integral β_{pq} were identical for all carbon atoms and carbon-carbon bonds in the different molecules (see Table I) respectively. The interatomic distances in the molecules considered here were taken from electron diffraction data by Schomaker and Pauling[3].

With respect to the molecular orbitals, those obtained by the Hückel method were used as approximations, because in practice it is rather tedious to solve the self-consistent equation completely. The parameters of energy integrals in the Hückel method were chosen from Orgel et al.[4], except for all carbon atoms and the sulfur atom in thiophene. For the carbon the common value was taken (so-called α_c), and for the sulfur Longuet-Higgins' idea was employed. Furthermore electron densities of the carbon atoms were assumed to have equal values of those in alternant hydrocarbons, and the Coulomb integral was chosen to make the ionization energy computed for benzene equal to the experimental value.

In Table I are given the results, which are in good agreement with experiment, although many approximations were necessary through the calculation. It has been proposed that in pyridine and pyrazine the ionization energies of these compounds are largely determined by the non-bonding electrons on the nitrogen atom, from the studies of their methyl derivatives by electron impact method[6] and from the results of self-consistent calculation on these electrons[7]. The energy interval of bombarding electrons, however, should be examined in the electron bombarding study, especially when the highest-occupied π-level may exist near nonbonding σ-levels. Details will be further discussed in subsequent publications.

TABLE I

RESULTS OBTAINED OF THE FIRST IONIZATION ENERGIES OF π-ELECTRONS, eV.

	calc.	obs.
benzene	9.24	9.24[8]
pyridine	9.45	9.76±0.05[9], 9.23[10]
pyrazine	9.90	10.01±0.02[6]
pyrrole	9.03	8.97±0.05[9]
furan	8.94	9.00±0.10[9], 8.89[10]
thiophene	9.34	9.1±0.2[9]

Electrotechnical Laboratory
Tanashi P. O., Tokyo

1) N. S. Hush and J. A. Pople, *Trans. Faraday Soc.*, **51**, 600 (1955).
2) R. Pariser and R. G. Parr, *J. Chem. Phys.*, **21**, 767 (1953).
3) V. Schomaker and L. Pauling, *J. Am. Chem. Soc.*, **61**, 1769 (1939).
4) L. E. Orgel, T. L. Cottrell, W. Dick and L. E. Sutton, *Trans. Faraday Soc.*, **47**, 113 (1951).
5) H. C. Longuet-Higgins, ibid., **45**, 173 (1949).
6) I. Omura et al., This Bulletin, **30**, 633 (1957).
7) T. Nakajima and A. Pullman, *Compt. rend.*, **246**, 1047 (1958).
8) In the present report, this value was adopted as the most probable one; cf. J. D. Morrison, *J. Chem. Phys.*, **22**, 1219 (1954), K. Watanabe, ibid., **22**, 543 (1954).
9) H. Baba et al., This Bulletin, **29**, 521 (1956).
10) K. Watanabe, *J. Chem. Phys.*, **26**, 542 (1957).

Solubility of Ethylenediaminetetraacetic Acid in Some Aqueous Solutions

By Yukichi Yoshino, Akira Iguchi, Masuo Kojima and Kunihiko Mizumachi*

(Received September 9, 1958)

In the course of study on the use of ethylenediaminetetraacetic acid as eluant for ion-exchange chromatography, it was found necessary to investigate its solubility behavior. No such data being available**, the authors measured the solubility of free acid, H_4Y, under various conditions.

The free acid was recrystallized thrice from an ammoniacal solution by adding dilute hydrochloric acid and then dried at 110°C for several hours. Chemical analysis by titration with standard zinc solution using Eriochrome Black T as indicator proved the sample was pure enough for this purpose. The free acid thus obtained was shaken with various media in a thermostat until equilibrium was attained. Then a portion of the saturated solution was taken by means of a pipette attached with cotton filter and the concentration of the free acid was determined by titration with 0.005 M standard zinc solution at pH 10 using the same indicator. All other chemicals were of guaranteed grade and were purified by distillation or recrystallization, if necessary.

* Department of Chemistry, Faculty of Science, The University of Tokyo, Hongo, Tokyo.

** Solubility of disodium salt was reported by N. J. Blaedel and H. T. Knight, *Anal. Chem.*, **26**, 743 (1954).

TABLE I

TEMPERATURE VARIATION OF THE SOLUBILITY OF ETHYLENEDIAMINETETRAACETIC ACID IN WATER

Temperature (°C)	Concentration of EDTA (H_4Y) (10^{-3}mol./l.)
2.7	0.566*
25.0	1.153
30.0	1.372
35.0	1.660
40.0	1.990
45.0	2.350
100	32.1

* Preliminary data of less accuracy.

Table I shows the temperature dependence of the solubility of ethylenediaminetetraacetic acid in water. Within the range of temperature between 25°C and 45°C the plot of the logarithm of solubility against the reciprocal of absolute temperature gave straight line and from its slope the heat of solution was found to be 6.76 kcal./mol. (endothermic) in the temperature range of our experiment.

TABLE II

SOLUBILITY OF ETHYLENEDIAMINETETRAACETIC ACID IN POTASSIUM CHLORIDE SOLUTIONS AT 30°C

Concentration of potassium chloride (mol./l.)	Concentration of EDTA (H_4Y) (10^{-3}mol./l.)
0.00	1.372
0.01	1.509
0.04	1.636
0.09	1.781
0.16	1.901
0.20	1.990
0.50	2.330
1.00	2.650

The effect of the ionic strength on the solubility of the acid was determined in solutions of varying concentration of potassium chloride. The results are given in Table II. As is expected from the amphoteric nature of ethylenediaminetetraacetic acid, the solubility curve plotted against hydrochloric acid concentration passed through a minimum which is illustrated in Fig. 1.

The solubility of the acid in water-ethanol mixture was decreased with increasing of ethanol contents, as was shown in Fig. 2.

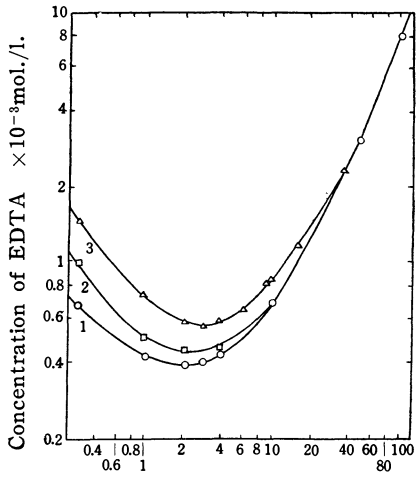

Fig. 1. Relationship between the solubility of EDTA (H_4Y) and the molarity of HCl at 30°C.
1. The aqueous solution of HCl.
2. The aqueous solution of HCl-KCl. ($\mu=0.10$)
3. The aqueous solution of HCl-KCl. ($\mu=0.50$)

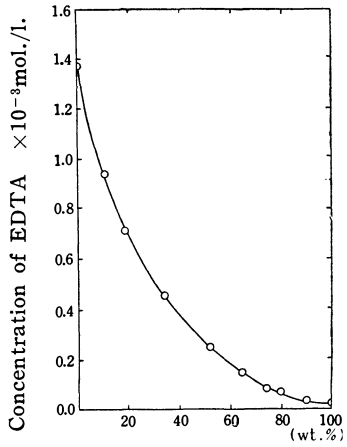

Fig. 2. Solubility of EDTA (H_4Y) in ethanol-water mixtures (at 30°C).

Details of the experiment will be reported elsewhere.

A part of the expense of this study was defrayed by a grant-in-aid from the Ministry of Education.

College of General Education
The University of Tokyo
Meguro-ku, Tokyo

Estimation of Specific Surface Area of Particles in Colloidal Silica Sols From the Rate of Dissolution

By Katsumi GOTO

(Received May 12, 1958)

The performance of colloidal silica in many of its applications largely depends on particle size or specific surface area. However, the application of currently available methods[1-7] for the determination of this property encounters difficulty in many cases, and a more rapid and simple method is urgently needed. An attempt has been made in the present investigation to determine the specific surface area of colloidal silica from the rate of dissolution of particles in a solution containing sodium fluoride and hydrochloric acid.

1) G. B. Alexander, *J. Am. Chem. Soc.*, **75**, 2887 (1953).
2) G. B. Alexander, ibid., **76**, 2094 (1954).
3) G. B. Alexander and R. K. Iler, *J. Phys. Chem.*, **57**, 932 (1953).
4) P. V. Nauman and P. Debye, *J. Phys. & Colloid Chem.*, **55**, 1 (1951).
5) M. F. Bechtold, *J. Phys. Chem.*, **59**, 532 (1955).
6) R. K. Iler, "The Colloid Chemistry of Silica and Silicates," Cornell Univ. Press, New York (1955), p. 100.
7) G. W. Sears, Jr., *Anal. Chem.*, **28**, 1981 (1956).

Experimental

Materials.—*Colloidal silica.*—Sols of colloidal silica were prepared by allowing to stand the mixture of the solution of sodium metasilicate and the solution of silicic acid prepared from sodium metasilicate by ion exchange. Colloidal silica having a small specific surface area was prepared by aging at higher temperatures.

Aluminum chloride solution.—Two hundred and seventy g. of aluminum chloride hexahydrate was dissolved in distilled water and made up to 1 l. One mililitre of this solution contains about 30 mg. of aluminum ions.

Ammonium molybdate solution. — Ten % (w/v) aqueous solution.

Concentrated hydrochloric acid solution

All reagents were of purest grade commercial products and used without further purification.

Apparatus.—A photoelectric colorimeter equipped with a glass prism and a barrier layer cell was employed for the colorimetric determination of molecularly-dispersed form of silica. The dissolution reaction was conducted in polyethylene

bottles to avoid contamination from glass vessels.

Measurements of dissolution rate.—Colloidal silica is dissolved in a medium prepared fulfilling the conditions given in Table I. Ten mililitre portions of the solution in which the colloidal silica sample is being dissolved are taken at definite intervals in beakers containing 0.5 ml. of aluminum chloride solution, the dissolution reaction being stopped by this procedure. To each beaker 0.5 ml. of ammonium molybdate solution is then added and the absorbancy is measured after 6 or 8 min. at wave-length of 430 mμ. The amount of conecntration of a molecularly-dispersed form of silica is calculated from the color intensity and is plotted against the time of sampling. Since, as is discussed later, the plot was a straight line over a wide range of time, the dissolution rate, which is expressed by the ratio of the initial rate of increase in the concentration of molecularly-dispersed silica (mg./l./min.) to the initial concentration of colloidal silica (mg./l.), could be easily obtained from the slope.

TABLE I
CONDITIONS EMPLOYED FOR THE DISSOLUTION REACTION

Concentration of sodium fluoride	300 mg./l. with respect to F^-
Concentration of hydrochloric acid	0.12 N
Temperature	25.0±0.1°C
Concentration of colloidal silica sample	around 20 mg./l. with respect to SiO_2

Results

Fig. 1 shows the dissolution rate as a function of the specific surface area as determined by the titration procedure developed by Sears[7]. Correction was made, in the titration, for molecularly-dispersed silica which exists in equilibrium with colloidal silica and also reacts with the titrant. For sols of higher degrees of secondary aggregation, the dissolution rate is generally higher than is expected from the titration. This may be due to the gelation taking place during the titration of such sols, giving rise to difficulty in reaching equilibrium between the silica particles and the titrant.

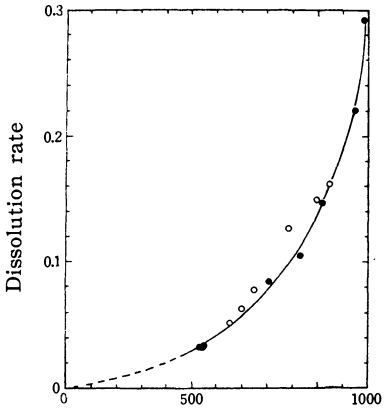

Fig. 1. Correlation of dissolution rate with specific surface area. ● indicates that gelation did not take place during titration.

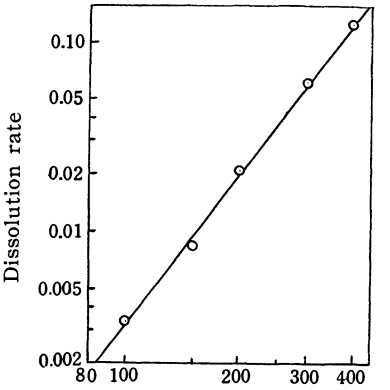

Fig. 2. Fffect of fluoride ion concentration on the dissolution rate.

The effect of fluoride ion concentration on the dissolution rate is shown on logarithmic scale in Fig. 2, from which it is apparent that the dissolution rate is roughly proportional to the 2.6th power of fluoride concentration.

The concentration of hydrochloric acid in the range 0.09 to 0.14 N has little effect on the dissolution rate, as is shown in Table II.

TABLE II
EFFECT OF THE CONCENTRATION OF HYDROCHLORIC ACID ON THE DISSOLUTION RATE

Normality of HCl	Dissolution rate
0.03	0.050
0.06	0.039
0.09	0.0314
0.12	0.0320
0.14	0.0315

The fact that, as is shown in Table III, the aluminum ion greatly reduces the dissolution rate at high concentrations permits the use of aluminum salt to stop the dissolution reaction. Although 600 mg./l. of the aluminum ion is sufficient for this purpose, an aluminum-ion concentration of about 1500 mg./l. was used in the present investigation. It is shown in Table

TABLE III
EFFECT OF ALUMINUM ION (a)

Concentration of Al (mg./l.)	Dissolution rate
0	0.0675
150	0.0025
300	ca. 8×10^{-5}
600	ca. 2×10^{-5}
0, in the absence of fluoride	ca. 1×10^{-5}

TABLE IV
EFFECT OF ALUMINUM ION (b)

Concentration of Al (mg./l.)	Dissolution rate
0	0.0300
0.2	0.0315
0.4	0.0280
0.6	0.0278
0.8	0.0264

TABLE V
EFFECT OF THE CONCENTRATION OF COLLOIDAL SILICA SAMPLE

Concentration (mg. SiO_2/l.)	Dissolution rate
10.8	0.068
20.0	0.065
32.0	0.062
40.5	0.053

IV, however, that small amounts of aluminum, which is the most common among the impurities in colloidal silica, have little effect on the dissolution rate.

The concentration of a colloidal silica sample in a dissolution medium also affects the dissolution rate as shown in Table V. It is essential, therefore, to measure the dissolution rate at about a constant concentration of colloidal silica.

Discussion

The foregoing results indicate a possibility of estimating the specific surface area of colloidal silica particles from the measurement of dissolution rate in an acid solution of sodium fluoride under carefully controlled conditions.

It is very interesting to note in Fig. 1 that the surface of a smaller particle is more reactive than that of a larger one: the dissolution rate per unit surface area increases with decreasing particle size. Since, therefore, the decrease in surface area during dissolution is compensated by the increasing rate of dissolution per unit surface area, the concentration of molecularly-dispersed silica increases linearly with time over an unexpectedly wide range, permitting an easy graphical determination of the initial rate of dissolution.

The dissolution reaction may be of first order with respect to colloidal silica, since the dissolution rate given in Table V is about the same for varying silica concentrations. It is interesting to note that the dissolution reaction is of the order between 2 and 3 with respect to the fluoride concentration and that it is more rapid at lower acidities. Further discussion of the reaction mechanism, however, is not described here since it is beyond the scope of this paper.

The variation of the rate of dissolution per unit surface area with particle size, however, prevents the accurate determination of a specific surface area of colloidal silica in polydisperse systems. It is also a serious question associated with this method whether the dissolution rate is the same or not for sols prepared under different conditions. However, since the sols used in the present investigation were prepared under alkaline conditions, where silica particles of uniform size can be formed[8], the method may be applicable at least to alkaline sols, including the active silica used in water purification.[9]

Sears' titration procedure[7] is applicable only to sols containing more than 10 g./l. of silica since it deals with 150 ml. of sols containing 1.5 g of silica. On the other hand, only a few mg. of silica is sufficient for the present method, which may therefore be applicable also to extremely dilute sols. This may well offset the disadvantage discussed above.

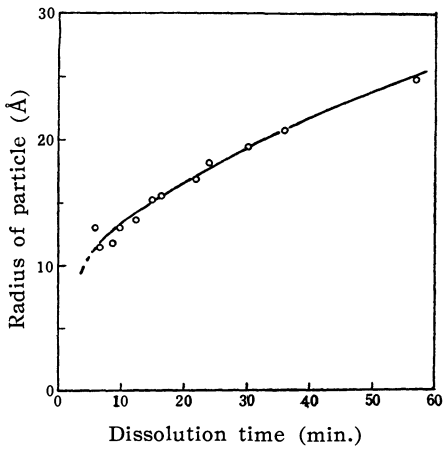

Fig. 3. Relation between particle size and dissolution time.

8) R. K. Iler and R. L. Dalton, *J. Phys. Chem.*, **60**, 955 (1956).
9) Ref. 6 p. 119

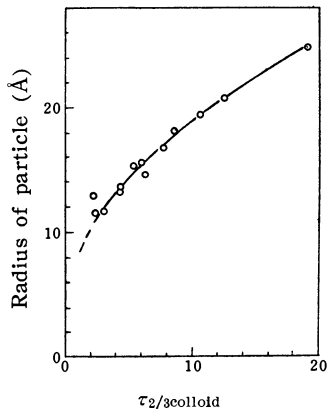

Fig. 4. Relation between the particle size and the time required for the dissolution of two thirds of colloidal silica.

It is essential, in determining a specific surface area from Fig. 1, to observe as strictly as possible the conditions given in Table I, since the reduction in the concentration of available fluoride during the dissolution reaction was not taken into account in the present investigation.

Molecularly-dispersed silica, when present in large amounts, may interfere with the method by reducing the concentration of available fluoride. This, however, may be removed by passing through a column containing a mixture of cation- and anion-exchange (strongly basic type) resins.

In our earlier report[10], dissolution time was used as a measure of particle size. It is the time required for the complete dissolution of particles and was determined by plotting the cube root of the concentration of colloidal silica versus time and extrapolating the plot to the abscissa, based on the assumption that the rate of dissolution per unit surface area remains constant during the process of dissolution. Though such an assumption has been proved to be incorrect, the dissolution time may still be a rough measure of the particle size, and is shown in Fig. 3 as a function of the particle size calculated from the result of titration on the assumption that the particles are spheres with a specific gravity of 2.2[11].

The reactivity toward alkaline solutions was also used in earlier works[12,13] as a measure of particle size. The reaction with alkali, however, is greatly retarded by traces of aluminum[14] and thus may be applicable only to sols prepared with special precautions.

It is also desirable to use the time, $\tau_{2/3\text{colloid}}$, required for particles to lose two thirds of their initial masses under conditions given in Table I. As the concentration of remaining colloidal silica decreases linearly with time at least up to this point, the $\tau_{2/3\text{colloid}}$ can be easily determined graphically. In Fig. 4 is shown the relation between $\tau_{2/3\text{colloid}}$ and particle size.

The author wishes to express his thanks to Professors G. Okamoto and T. Okura for their valuable advice and suggestion. The author is also indebted to the Asahi Glass Foundation for the Promotion of Researches in Chemical Industries for the financial support of this work.

Faculty of Engineering, Hokkaido University, Sapporo

10) T. Okura, K. Goto and T. Komatsu, This Bulletin, **31**, 139 (1958).

11) Ref. 6 p. 135.
12) K. Goto, *J. Phys. Chem.*, **60**, 1007 (1956).
13) K. Goto, *J. Chem. Soc. Japan, Pure Chem. Sec.*, (*Nippon Kagaku Zassi*), **77**, 957 (1956).
14) G. Okamoto, T. Okura, and K. Goto, *Geochim. et Cosmochim. Acta*, **12**, 123 (1957).

Ultraviolet Absorption Spectra of Nitro-, Dinitro- and Trinitro-substituted Benzenes

By Takehiro ABE

(Received May 28, 1958)

The near ultraviolet absorption spectrum of nitrobenzene shows an intense band at 260 mμ and two shoulders at about 290 and 340 mμ[1-3]. The maximum absorption band at 260 mμ, which has been measured in various solvents[4,5], has been interpreted by Doub and Vandenbelt[6] and later by Wenzel[7] to correspond to the 200 mμ band of benzene but has been interpreted by Nagakura and Tanaka[8] in terms of the strong electron-attracting nature of the nitro group. The hidden transition near 290 mμ and the weak band at 340 mμ have been shown by Wenzel to be related to the 256 mμ transition of benzene and to be due to the nitro group, respectively.

In the present paper, an attempt is made to investigate the influence of the number of nitro groups on the spectra of polynitrobenzenes in various solvents, together with the solvent effects upon their spectra. The ultraviolet absorption spectra of nitrobenzene (NB), *m*-dinitrobenzene (DNB), 1, 3, 5-trinitrobenzene (TNB) and 2,4,6-trinitrotoluene (TNT) have been measured in solvents like water, water-hydrochloric acid, water-sodium hydroxide, ethanol, benzene and acetone.

Experimental

Materials. — Nitro compounds of commercial extra pure grade were purified by distillation or by recrystallization several times. NB: b. p. 210°C, DNB: m. p. 90.4°C, TNB: m. p. 123.1°C, TNT: m. p. 81.3°C. Commercial guaranteed solvents were fractionally distilled after usual treatments.

Spectra. — The spectra of the solutions were measured with a Hitachi quartz spectrophotometer, Model EPU-2 at room temperature. The path length of absorption cells was 1 cm.

Results

The Spectra of Nitro Compounds in Some Solvents.—*In ethanol* (Fig. 1).—In Table I progressive blue shifts of the 260 mμ band of nitrobenzene for the nitro compounds are seen in the following order: NB, DNB, TNT and TNB. Their molar extinction coefficients also increase in the same order. It is obvious that these blue shifts are attributed to the numbers of nitro groups attached to a benzene nucleus.

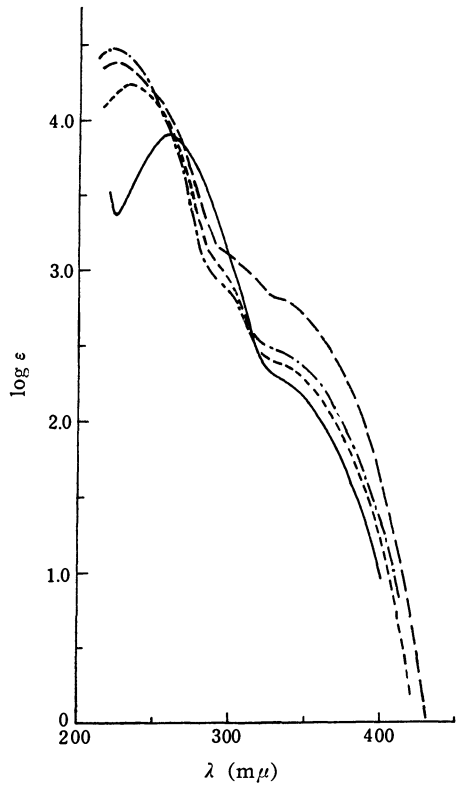

Fig. 1. Absorption spectra of NB (——), DNB (- - -), TNB (—·—) and TNT (— —), all in ethanol.

1) Landolt-Börnstein, "Physikalish-chemishe Tabellen", Springer, Berlin, 1951, 6th ed., Part 3 (II), p. 267.
2) G. S. Hammond and F. Modie, *J. Am. Chem. Soc.*, **75**, 1385 (1953).
3) H. Ungnade, ibid., **75**, 432 (1953).
4) N. S. Bayliss and E. G. McRae, *J. Phys. Chem.*, **58**, 1006 (1954).
5) W. M. Schubert, J. Robins and J. L. Haun, *J. Am. Chem. Soc.*, **79**, 910 (1957).
6) L. Doub and J. M. Vandenbelt, ibid., **69**, 2714 (1947).
7) A. Wenzel, *J. Chem. Phys.*, **22**, 1623 (1954).
8) S. Nagakura and J. Tanaka, ibid **22**, 236 (1954).

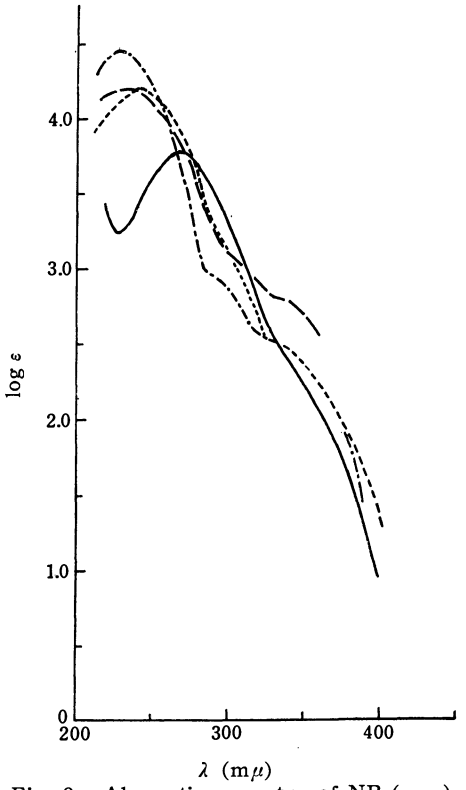

Fig. 2. Absorption spectra of NB (——), DNB (- - -), TNB (—·—) and TNT (— —), all in water.

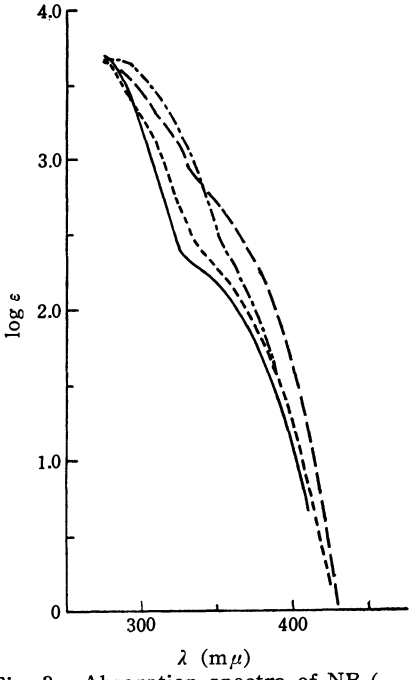

Fig. 3. Absorption spectra of NB (——), DNB (- - -), TNB (—·—) and TNT (— —), all in benzene.

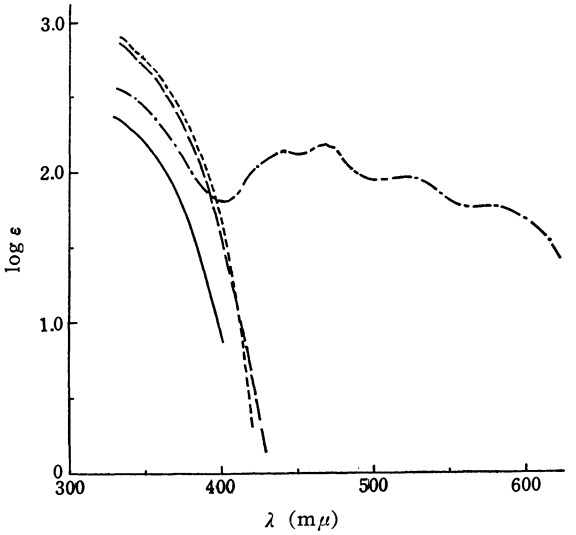

Fig. 4. Absorption spectra of NB (——), DNB (- - -), TNB (—·—) and TNT (— —), all in acetone.

TABLE I
VALUES OF THE ABSORPTION MAXIMA OF NITRO COMPOUNDS IN ETHANOL AND IN WATER

Compound	Solvent: Ethanol a) λ_{max} (mμ)	Ethanol ε	Water b) λ_{max} (mμ)	Water ε	b)-a) (mμ)
NB	260	8,140	267	6,910	7
DNB	233	17,200	244	15,400	11
TNB	223	29,700	229	28,100	6
TNT	225	22,900	233	15,800	8

λ: Wavelength.
ε: Molar extinction coefficient.

Let us consider an electron migration between the benzene nucleus and the nitro groups in each nitro compound. By substituting nitro groups for hydrogen atoms in the nucleus, the π-electron density at the nucleus decreases owing to their strong electron-attracting nature as illustrated in Fig. 5. The positive charges of the nuclei of the nitro compounds increase in the order of the increasing numbers of nitro groups:

$$NB < DNB < TNT < TNB \quad (1)$$

Here the charge of TNB is more positive than that of TNT, because the σ-electron of the methyl group can migrate to some extent, through hyperconjugation, toward the nucleus of TNT. The order in Eq. 1 is in good agreement with that of the blue shifts in Table I. Consequently, it is

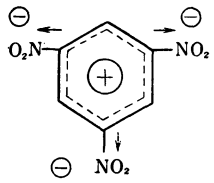

Fig. 5. Charge distribution of TNB.

noticed that the absorption maxima of the nitro compounds shift to the blue, as the electron densities of their nuclei decrease by the action of the nitro groups.

The shoulders near 290 mμ are more distinct with increasing number of nitro groups. Owing to the influence of methyl group in TNT, the molar extinction coefficient of the absorption maximum of TNT is smaller than that of TNB, but the coefficient of the 340 mμ shoulder of the former is greater than that of the latter.

In water (Fig. 2).—There are similar blue shifts as in ethanol. In Table I it is also found that the maximum absorption bands of the respective nitro compounds are to a great extent shifted to the blue in ethanol as compared with those in water and that their molar extinction coefficients are greater in ethanol than in water.

In benzene (Fig. 3). — The shoulder at about 340 mμ becomes indistinct with the increasing number of nitro group. In all the spectra, a small shoulder can be observed at about 280 mμ.

In acetone (Fig. 4).—All the nitro compounds show absorption shoulders at about 340 mμ. There is no correlation between their intensities and the numbers of nitro groups. Only TNB shows weak absorption bands in the visible range as given in Table II.

TABLE II
THE VISIBLE ABSORPTION BANDS OF TNB IN ACETONE

λ(mμ)	441	469	524	575
ε	135	148	93	58

Effects of Acid and Alkali in Water (Fig. 6).—The positions of the absorption maxima of nitro compounds have not been found to be influenced by hydrochloric acid in water. In Fig. 6 it is seen that in an aqueous solution of sodium hydroxide the nitro compounds show intense absorption bands at longer wavelengths in the order of increasing number of nitro groups. In these regions no absorption bands are observed in ethanol. The trinitro compounds give red colors with alkali. These colors are reversively decolorized by addition of acids. DNB and NB give yellow colors on treatment with a concentrated solution of sodium hydroxide. These yellow colorations are very slow, but become faster by warming.

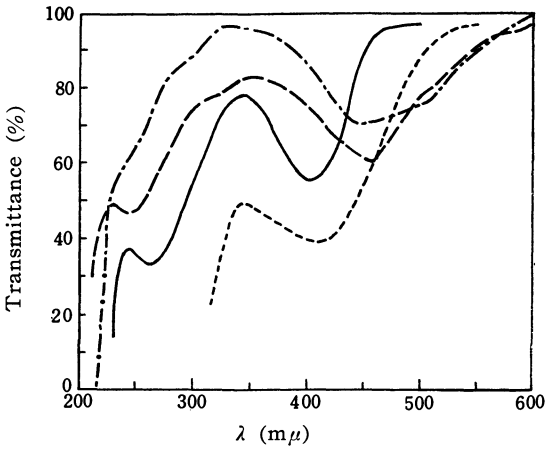

Fig. 6. Absorption spectra of NB (——), DNB (- - -), TNB (—·—) and TNT (— —), all in H_2O+NaOH.

Analogous color reactions of sodium ethoxide with TNT and TNB in ethanol have been, by Caldin and his co-workers[9,10], interpreted in terms of a proton-transfer reaction for TNT and in terms of an addition reaction for TNB. The color of the nitro compounds with sodium hydroxide seems to be also produced by the formation of complexes between the compounds and the hydroxide ion, because the compounds give the same color with other alkalies and the position of the absorption maxima of nitro compounds in water is not influenced by hydrochloric acid.

Solvent Effects on the Spectra of the Respective Nitro Compounds (Figs. 1-4).—The intensity of the 340 mμ band of DNB is very strong only in acetone. At wavelengths longer than 260 mμ the spectra of the trinitro compounds in ethanol are close to those in water.

The trinitro compounds show absorption bands near 280 mμ in benzene, probably owing to the formation of molecular complexes between the compounds and benzene. In this region Briegleb and Czekalla[11]

9) E. F. Caldin and G. Long, *Proc. Roy. Soc.*, **A228**, 263 (1955).
10) J. B. Ainscough and E. F. Caldin, *J. Chem. Soc.*, **1956**, 2528, 2540, 2546.
11) G. Briegleb and J. Czekalla, *Z. Elektrochem.*, **59**, 184 (1955).

have already found an absorption band of a molecular complex between TNB and benzene. The corresponding bands in the spectra of DNB and NB can not be determined owing to the presence of other absorption bands near 280 mμ, although DNB seems to show the band at 280 mμ. The formation of a complex between NB and benzene has been reported by Cheshko and Tavadze[12].

Summary

1) In ethanol and in water the progressive blue shifts of the 260 mμ band of nitrobenzene for the nitro compounds are observed in the order of increasing number of nitro groups.

2) Only TNB shows visible weak absorption bands in acetone.

3) In an aqueous solution of sodium hydroxide these nitro compounds show intense absorption bands at longer wavelengths as the number of nitro group increases.

The author is particularly indebted to Professor Y. Nomura for his suggestion and encouragement through this work. Thanks are also due to Assistant Professor S. Maeda for the use of the spectrophotometer.

Department of Chemistry
Defense Academy
Yokosuka, Kanagawa

12) F. F. Cheshko and N. Sh. Tavadze, *Doklady Akad. Nauk S. S. S. R.*, **95**, 833 (1954).

Studies on Polymerization and Depolymerization of ε-Caprolactam Polymer. V. On the Reaction Mechanism of the Catalytic Polymerization of ε-Caprolactam by Alkali Metal***

By Hirosuke YUMOTO and Naoya OGATA

(Received may 9, 1958)

The rapid polymerization of ε-caprolactam catalyzed by alkali metal behaves in a manner quite different from the polymerization by water, acids or amino acids. W. Griehl[1,2] found that the molecular weight distribution of poly-ε-capramide obtained in the presence of alkali metal or its salt is very sharp just after reaching the ring-chain equilibrium and then gradually changes into Flory's distribution. O. Wichterle[3] and D. Heikens[4] proposed the mechanism of ε-caprolactam polymerization catalyzed by alkali metal salt.

Experimental

(1) The Initial Reaction between ε-Caprolactam and Alkali Metal.—The Mixture of equal moles of ε-caprolactam and alkali metal was heated together at 100°C. The generated gas was brought to copper oxide heated at 400°C with a stream of nitrogen. It was found as shown in Table I that 1/2 mole of hydrogen molecule to 1 mole of alkali metal is produced.

TABLE I
THE REACTION DEGREE OF SODIUM TO ε-CAPROLACTAM AT 100°C

Sodium (mole)	Produced water (mole)	Molar ratio of hydrogen to sodium
1.34×10^{-2}	6.1×10^{-3}	2.2
1.58 〃	7.2 〃	2.2
1.49 〃	9.7 〃	1.6

The infrared spectrum of the reaction product is shown in Fig. 1. The absorption bands of =NH group at 3.16 μ and 3.28 μ is very weak. After the product was exposed in the atmosphere for only 5 minutes, the spectrum came to be similar to that of ε-caprolactam (Fig. 2). Therefore the reaction product is thought to react easily with water moisture in the atmosphere and to change into ε-caprolactam. By dissolving the reaction product in the heavy water, the solution

* IV. *Makromolekulare Chem.*, **25**, 91 (1958).
** Presented at the 3rd Autumn Meeting of the Chemical Society of Japan in Tokyo, Nov. 24, 1957.
1) W. Griehl, *Faserforsch. u. Textiltech.*, **6**, 260 (1955).
2) W. Griehl, ibid., **7**, 207 (1956).
3) O. Wichterle, ibid., **6**, 237 (1955).
4) D. Heikens, *Makromolekulare Chem.*, **18**, 62 (1956).

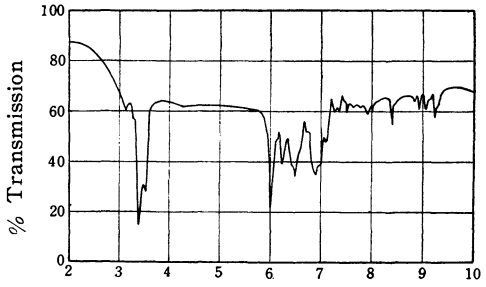

Fig. 1. The infrared spectrum of the reaction product of ε-caprolactam and sodium.

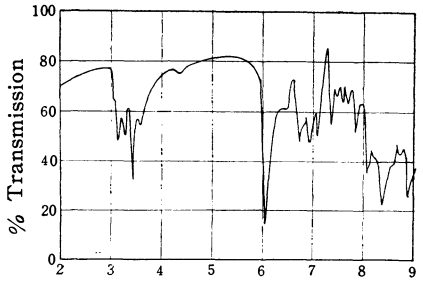

Fig. 2. The infrared spectrum of ε-caprolactam.

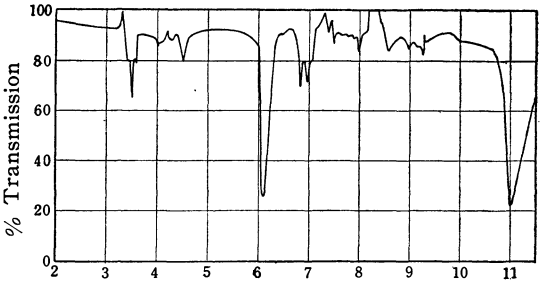

Fig. 3. The infrared spectrum of the product in the lower layer of the heavy water solution.

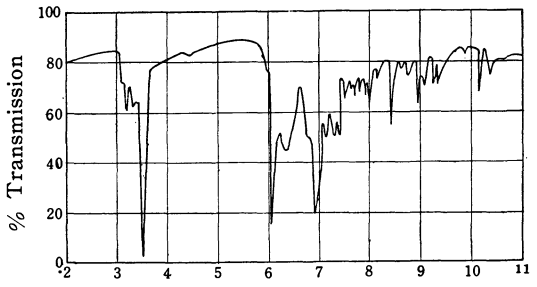

Fig. 4. The infrared spectrum of the reaction product of ε-caprolactam and lithium.

was separated into two layers. The substance extracted in chloroform from the lower layer has the absorption band of =N—D group at 4.46 μ as shown in Fig. 3 and that from the upper layer has both absorption bands of =N—H and =N—D. It was ascertained in an experiment that the hydrogen of the amide group in ε-caprolactam cannot be substituted by deutrium, when it was only dissolved in the heavy water. It is concluded that the following reactions take place:

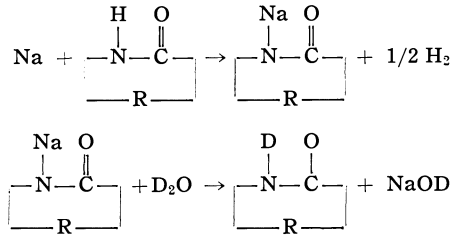

The reaction product of equal moles of ε-caprolactam and lithium has absorption bands at 8.75 μ and 9.05 μ (Fig. 4), which are expected to be assigned to =N—Li.

(2) The Rate of Polymerization. — The mixture of sodium and dried ε-caprolactam (water content of 0.01% or less) at the molar ratio of 1/25, 1/50, 1/100 or 1/200, was heated in a sealed glass tube at 232°C and the quantity of ε-caprolactam in product was determined from the soluble fraction in chloroform. The result is shown in Table II and Fig. 5. Similar experiments using lithium were carried on and the

TABLE II

THE RATES OF POLYMERIZATION OF ε-CAPROLACTAM WITH SODIUM

Sodium (mole/mole)	Time (min.)	Quantity of ε-caprolactam (%)	$[\eta]^{25°C}_{cresol}$ of polymer
1/25	2.5	40.0	
	5	14.6	
	10	8.9	
	15	9.1	
	20	7.5	
	30	6.4	0.602
1/50	5	61.3	
	10	9.0	
	15	7.8	
	20	5.0	
	30	4.9	0.809
1/100	5	84.4	
	10	13.6	
	15	10.5	
	20	5.0	
	30	4.7	1.085
1/200	5	91.4	
	10	81.0	
	15	55.9	
	20	30.8	
	30	5.3	1.435

TABLE III
THE RATE OF POLYMERIZATION OF ε-CAPROLACTAM WITH LITHIUM

Lithium (mole/mole)	Time (min.)	Quantity of ε-caprolactam (%)	$[\eta]^{25°C}_{cresol}$ of polymer
1/50	1	94.5	
	2	89.3	
	3	68.4	
	6	4.3	
	9	4.8	0.824
1/100	2	90.7	
	3	83.1	
	4	48.5	
	5	32.2	
	6	6.1	2.110
1/200	2	98.4	
	4	86.0	
	5	72.3	
	6	49.6	
	10	5.6	2.210

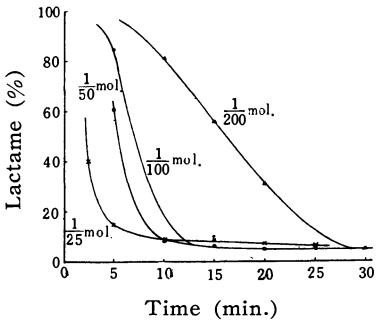

Fig. 5. The rate of polymerization of ε-caprolactam with sodium at 232°C.

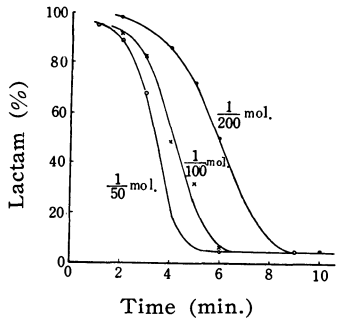

Fig. 6. The rate of polymerization of ε-caprolactam with lithium at 232°C

result is shown in Table III and Fig. 6. The catalytic effect is greater in case of lithium than sodium. Induction periods for the polymerization appear in both cases. The rate of polymerization increases with the quantity of catalyser as shown in Fig. 7.

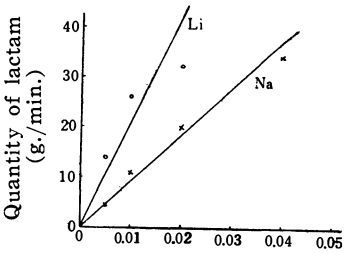

Fig. 7. The rates of polymerization at various quantities of catalyst.

A mixture of 0.041 g. of sodium and 5 g. of ε-caprolactam was heated at 280°, 255°, 238° or 230°C for 10 minutes and then 95 g. of dry ε-caprolactam heated previously at the same temperature was mixed to polymerize. The rate of polymerization is given in Table IV. The induction period disappears in such a case.

TABLE IV
THE RATE OF POLYMERIZATION OF ε-CAPROLACTAM WITH 1/200 MOLES OF SODIUM AT VARIOUS TEMPERATURES

Temp. (°C)	Time (min.)	Quantity of ε-caprolactam (%)
280	1	6.8
	5	7.6
255	0.3	86.2
	1.5	54.9
	1.75	51.9
	3.5	6.4
238	1	78.7
	2	65.0
	2.5	59.2
	2.75	54.7
	3.5	45.2
	4.5	31.0
	10.0	5.7
230	0.5	91.0
	1.5	85.3
	2.5	81.2
	3.5	73.1
	4.0	67.5
	4.5	63.6
	5.0	55.8
	5.5	54.5
	7.0	44.7
	8.0	34.4
	9.0	22.8
	11.0	21.0
	15.0	15.0
	30.0	5.4

The rate of polymerization decreases with the increase in the water content as shown in Fig. 8. When the water content is less than 0.01%,

its influence on polymerization can be assumed to be negligible. The acidic substance in trace makes the polymerization retard. The ε-caprolactam used in experiments, therefore, was once distilled in the presence of 0.1% of sodium hydroxide to remove volatile acidic substances.

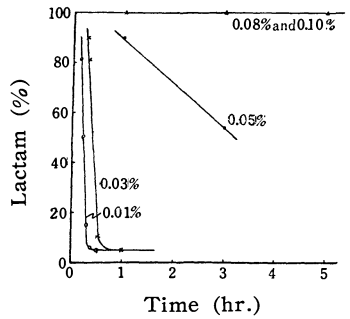

Fig. 8. The rate of polymerization at various water contents.

(3) Electric Conductivities. — The change of electric conductivity during polymerization was measured. The results are shown in Figs. 9 and 10. It increases to maximum and then

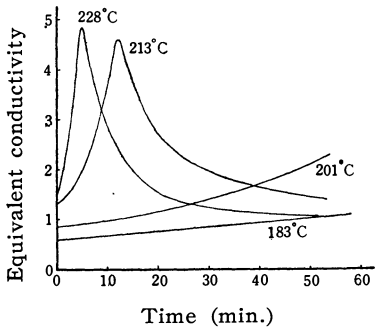

Fig. 9. The electric conductivities of ε-caprolactam during the polymerization in the presence of 0.5 mole % of sodium.

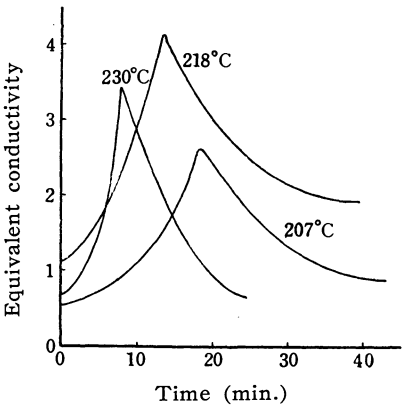

Fig. 10. The electric conductivities of ε-caprolactam during the polymerization in the presence of 0.5 mole % of lithium.

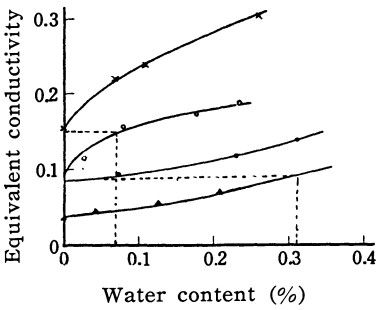

Fig. 11. The electric conductivity of ε-caprolactam at 100°C.
× 0.2 mole % of sodium hydroxide
○ 0.2 mole % of sodium
● 2 mole % of sodium hydroxide
△ 2 mole % sodium

decreases to the equilibrium. It is seen in Fig. 11 that the electric conductivity of ε-caprolactam containing 0.5 or 2 mole percents of sodium and water together is almost the same as that of

TABLE V
ANALYTICAL VALUES OF POLYMER OBTAINED BY HEATING ε-CAPROLACTAM WITH 1/4 MOLES OF SODIUM

Time of polymerization (min.)	Mole of added sodium (mole/mole)	Condition of extraction	Quantity of alkali in water (mole/mole)	Number of acidic groups (mole/113 g.)	Number of basic groups (mole/113 g.)	Quantities of water-soluble chain oligomers (%)	Quantities of ring monomer (%)	Quantities of ring oligomers (%)
5	0.252	25°C, 2 hrs.	0.268	4.0×10^{-2}	9.90×10^{-2}	—	—	
		100°C, 2 hrs.	0.262	2.99 〃	8.65 〃	—	—	
10	0.218	25°C, 2 hrs.	0.210	3.90×10^{-2}	9.92×10^{-2}	12.7	28.8	0
		100°C, 2 hrs.	0.191	2.20 〃	8.65 〃	—	—	—
20	0.247	25°C, 2 hrs.	0.273	3.24×10^{-2}	11.2×10^{-2}	9.7	13.7	1.2
		100°C, 2 hrs.	0.246	3.28 〃	9.1 〃	—	—	—
		25°C, 5 hrs.	0.244	3.40 〃	11.3 〃	—	—	—
		100°C, 5 hrs.	0.245	3.11 〃	10.5 〃	—	—	—

ε-caprolactam containing 0.5 or 2 mole percent of sodium hydroxide. It is expected in the presence of water, therefore, that sodium transforms into its hydroxide before it reacts with ε-caprolactam and loses the catalytic effect. Sodium hydroxide has only a catalytic effect on the ε-caprolactam polymerization in a boiling[3,5] state.

(4) Quantitative and Qualitative Determination of End Groups of polymer.—The polymer was steeped in water and then the number of acidic and basic groups were measured[6]. The quantities of alkali, water-soluble chain-oligomers, ring-monomer and oligomers were determined from the analyses of water extracts. The results are shown in Table V. Sodium bonded to polymer is dissolved easily in water. The number of acidic groups of polymer is hardly changed by the polymerization time and the condition of water steeping. It is always about one-third of the number of basic groups.

As concerns the polymer heated in 0.2 N sodium hydroxide solution at 70°C, the number of acidic groups did not change at all as shown in Table VI. The polmer was steeped in absolute methanol, aqueous ammonia solution or isopropyl amine, for 5 hours at room temperature and then washed repeatedly with methanol and water until the washing did not show alkaline. The results are given in Table VII. The number of acidic groups in case of isopropyl amine was very small and isopropyl amine was found on the hydrolysis.

The polymer and its water extract were colorized reddish yellow by the diazo reaction and grey by the Nessler's reagent, while ε-aminocaproic acid was not. On the paperchromatogram of the water extract, a spot having the same Rf value as that of 6-aminohexanol appear as shown in Table VIII, besides those corresponding to ε-aminocaproic acid, di- and tri-ε-aminocaproic acids. In the infrared spectrum of the water extract, the absorption bands of hydroxyl and free =N—H group appear at 2.8 μ and 2.98 μ.

TABLE VI

THE NUMBER OF ACIDIC GROUPS IN POLYMER BEFORE AND AFTER HYDROLYSIS BY 0.2 N SODIUM HYDROXIDE

Time of polymerization (min.)	Number of acidic groups before hydrolysis (mole/113 g.)	Number of acidic groups after hydrolysis (mole/113 g.)
5	4.00×10^{-2}	3.87×10^{-2}
10	3.00 〃	3.32 〃
20	3.24 〃	3.12 〃

TABLE VII

THE NUMBER OF ACIDIC AND BASIC GROUPS IN POLYMERS STEEPED IN VARIOUS SOLUTIONS

Time of polymerization (min.)	Kind of solution	Number of acidic groups (mole/113 g.)	Number of basic groups (mole/113 g.)
10	Water	2.28×10^{-2}	10.1×10^{-2}
	Methanol	—	—
	Ammonia	1.70×10^{-2}	10.4×10^{-2}
	Isopropyl amine	0.40 〃	10.5 〃
20	Water	1.96 〃	12.4 〃
	Methanol	0.10 〃	12.7 〃
	Ammonia	0.25 〃	10.8 〃
	Isopropyl amine	0.36 〃	11.1 〃

TABLE VIII

R_f VALUES OF PRODUCTS OBTAINED BY EXTRACTION OF POLYMER WITH WATER

Sample	R_f values of spots				
Product	0.19	0.37	0.46	0.54	0.94
ε-Aminocaproic acid	0.19				
Di-ε-aminocaproic acid		0.37			
Tri-ε-aminocaproic acid			0.46		
6-Aminohexanol					0.94

The polymer, of which basic groups had previously been acetylated, was steeped in 1% alkaline solution of potassium permanganate for 2 hours at room temperature. The number of acidic groups increases to the number of basic groups as shown in Table IX.

TABLE IX

THE NUMBER OF END GROUPS OF POLYMER OXIDIZED BY 1% ALKALINE POTASSIUM PERMANGANATE SOLUTION

Sample	Number of carboxyl groups (mole/113 g.)	Number of amino groups (mole/113 g.)
Polymer at first	2.50×10^{-2}	10.2×10^{-2}
Acetylated polymer	3.50 〃	0
Oxidized polymer	7.50 〃	0

From these experimental results, it is expected that the end groups of polymer steeped in water are carboxyl, amino and hydroxyl groups. The third is probably produced by the reduction. No decarboxylation occures because neither carbon monoxide nore dioxide was found during the polymerization.

Discussion

It is expected that the catalytic polymerization of ε-caprolactam by alkali metal is an ionic reaction and the reaction proceeds through the following mechanism:

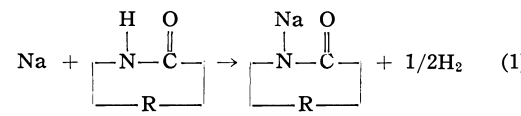

(1)

5) H. Yumoto and N. Ogata, to This Bulletin, **31**, 913 (1958).

6) J. E. Walz and G. B. Taylor, *Anal. Chem.*, **91**, 448 (1947).

7) H. Zahn and H. Wolf, *Melliand Textilber.*, **32**, 317 (1951).

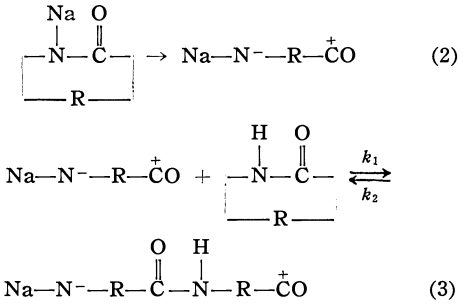

(2)

(3)

As the number of amino groups is about 40 percent of the mole number of added sodium, the reactions between chain molecules may also occur as shown below;

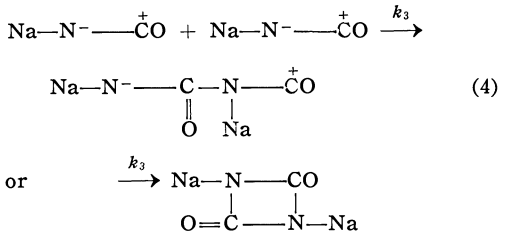

(4)

or

If the following termination reaction occured, the number of carboxyl groups should be increased by boiling the polymer in the aqueous solution of acid or base,

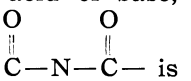

because the bond such as —C—N—C— is easily hydrolyzed. The number of carboxyl groups was scarely changed. It is expected therefore that the termination reaction such as shown in equation 5 does not occur.

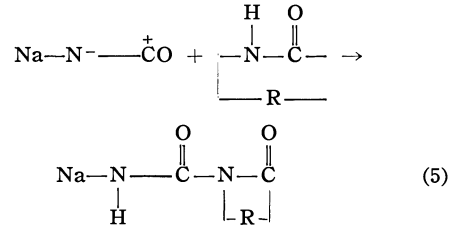

(5)

Sodium combined to polymer dissolves in water because the bond >N—Na is affected by water and amino groups are formed. On the other hand carbonyl cations react with water to form carboxyl groups. When polymer is steeped in an amine, carbonyl cations are changed into acid amides.

When dry ε-caprolactam is added to the molten polymer catalyzed by sodium, reactions 3 and 4 may occur and the following equations can be derived, where $[\sum M_1]$ and $[L]$ are chain molecule and lactam monomer and k_1, k_2 and k_3 are rate constants of reactions shown by arrows and A is the mole number of the Brownian motion unit in whole reaction phase[8].

$$d[L/A]/dt = k_2([\sum M_{i+1}]/A) - k_1([\sum M_i][L]/A^2) \quad (6)$$

$$-d[\sum M_i/A]/dt = k_3([\sum M_i]^2/A^2) \quad (7)$$

Suppose $d[L/A]/dt=0$ at equilibrium and $[\sum M_i] \fallingdotseq [\sum M_{i+1}]$ in high polymeric system, then

$$k_2 = k_1([L_\infty]/A) \quad (8)$$

where $[L_\infty]$ represents $[L]$ at equilibrium. Substituting Eq. 8 into Eq. 6, the following equation is obtained;

$$d[L/A]/dt = k_1([\sum M_i]/A^2)([L_\infty]-[L]) \quad (9)$$

Integreating Eq. 7 under the conditions that $[\sum M_i]$ is $[\sum M_i^0]$ at $t=0$ and A is invariable.

$$[\sum M_i]/A = [\sum M_i^0]/(k_3[\sum M_i^0]t + A) \quad (10)$$

Substituting Eq. 10 into Eq. 9 and integrating it under the condition that $[L]$ is $[L^0]$ at $t=0$:

$$\begin{aligned}\ln\{([L_\infty]-[L^0])/([L_\infty]-[L])\} &= (k_1/k_3)\ln\{(k_3[\sum M_i^0]t/A)+1\} \\ &= (k_1/k_3)\{k_3[\sum M_i^0]t/A - (1/2)(k_3/A[\sum M_i^0])^2t^2+\cdots\} \\ &= k_1[\sum M_i^0]t/A - (k_1/k_3/2)([\sum M_i^0]/A)^2t^2+\cdots \quad (11)\end{aligned}$$

When $\ln\{([L_\infty]-[L^0])/([L_\infty]-[L])\}$ are plotted against t a linear relation is obtained from the data of Table IV (Fig. 12). Therefore, the rest below the second term can be assumed to be negligible. Then

$$\ln([L_\infty]-[L^0])/([L_\infty]-[L]) \fallingdotseq k_1[\sum M_i^0]t/A \quad (12)$$

The value of $k_1[\sum M_i^0]/A$ can be determined from Fig. 12, as shown in Table X.

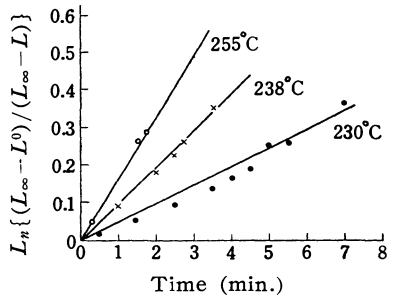

Fig. 12. The relation between $L_n\{(L_\infty - L^0)/(L_\infty - L)$ and time.

8) H. Yumoto, This Bulletin, **28**, 101 (1955).

TABLE X

Temp. (°C)	$k_1\sum M_i^0/A$ (mole/mol, min.)	L_∞ (%)	K/A
230	0.14	5.4	18.4
238	0.27	—	—
255	0.38	6.4	15.6
280	—	7.2	13.9

The logarithm of $k_1[\sum M_i^0]A$ is plotted against the reciprocal of the absolute temperature in which $\Delta E_{act.}$ of about 22 kcal./mole is estimated. This value is greater than the activation energy of 8.7 kcal./mole for the polymerization of ε-caprolactam in the presence[7] of water.

Summary

When alkali metal reacts with ε-caprolactam, it was found experimentally that hydrogen and *N*-alkali metal ε-caprolactam are produced at first. The rate of polymerization of ε-caprolactam in the presence of *N*-alkali metal derivative was studied. The change in the electric conductivity during polymerization was also measured. In this case the polymerization is expected to proceed by an ionized molecule.

The authors wish to thank to Dr. K. Hoshino and Dr. H. Kobayashi who instructed them in these studies and permitted this publication and Mr. M. Ishikawa et al. who collaborated with them on experiments.

Research Department of Toyo Rayon Co. Ltd.
Minato-ku, Nagoya,

Studies on Polymerization and Depolymerization of ε-Caprolactam Polymer VI. On the Reaction Mechanism of the ε-Caprolactam Polymerization by Alkali Metal Compound.***

By Hirosuke YUMOTO and Naoya OGATA

(Received on June 2, 1958)

It is well known that[1,2,3] alkali metal compounds cause the polymerization of ε-caprolactam and the high polymer can be obtained in several minutes. The mechanism of the reaction has been also studied[2]. It is the main object of this paper to elucidate the reaction mechanism and to find the method for giving reproducible results.

Experimental

1. The Reaction Product of ε-Caprolactam and Alkali Metal Compound.—The mixtures of dry ε-caprolactam and sodium hydroxide or sodium carbonate were heated at 270°C for 30 minutes in a nitrogen stream. In this case a stream of nitrogen was passed through a calcium chloride tube or aqueous barium hydroxide solution in order to detect the generated volatile compound. Water in case of sodium hydroxide or water and carbon dioxide in case of sodium carbonate were detected. Since the mixed components were not dissolved completely, the molar ratio of the product to the added sodium hydroxide or carbonate was smaller than 1 as shown in Tables I and II.

TABLE I

MOLAR RATIO OF WATER TO SODIUM HYDROXIDE (270°C)

Molar ratio of NaOH to lactam	reaction time (min.)	Molar ratio of water to NaOH
1	25	0.191
1	45	0.251
1/2	60	0.664
1/2	50	0.588
1/2	20	0.368

TABLE II

MOLAR RATIO OF CARBON DIOXIDE TO SODIUM CARBONATE (270°C)

Molar ratio of Na_2CO_3 to lactam	Reaction time (min.)	Molar ratio of CO_2 to Na_2CO_3
1	60	0.102
1	60	0.250

* V, This Bulltin, **31**, 907 (1958).

** Presented at the 11 th Annual Meeting of the Chemical Society of Japan in Tokyo on April 5, 1958.

1) BIOS Final Reports, No. 1472, p. 14.

2) O. Wichterle, *Faserforsch. und Textiltech.*, **6**, 237 (1955).

3) W. Griehl, ibid., **7**, 207, (1956).

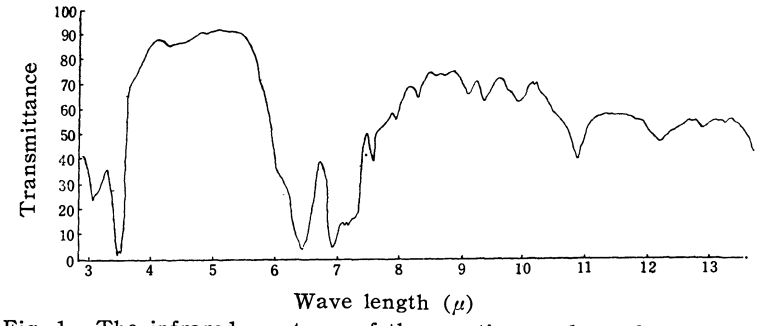

Fig. 1. The infrared spectrum of the reaction product of equal mole of sodium hydroxide and ε-caprolactam (270°C, 30 min.)

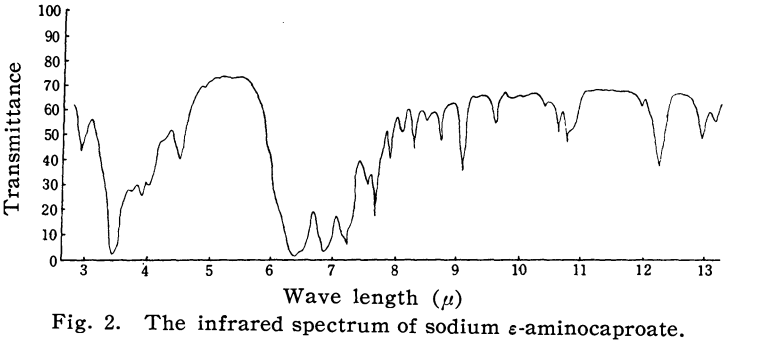

Fig. 2. The infrared spectrum of sodium ε-aminocaproate.

The reaction product of equal moles of sodium hydroxide and ε-caprolactam resembles sodium ε-aminocaproate in the infrared spectrum as shown in Figs. 1 and 2. The quantities of sodium ε-aminocaproate, ε-caprolactam-monomer and -oligomers in the product were analyzed[4,5]. The results are given in Table III.

TABLE III
ANALYSIS OF REACTION PRODUCT OF EQUAL MOLES OF ε-CAPROLACTAM AND SODIUM HYDROXIDE

Product	Yield (%)
Sodium ε-aminocaproate	85
Lactam monomer	15
Lactam oligomers	0

2. Polymerization of ε-Caprolactam by Alkali Metal Compounds.—The alkali metal compound must be added to the boiling ε-caprolactam for the polymerization. ε-Caprolactam was kept boiling at 290°C previously and 0.5 mole percent of sodium -hydroxide, -carbonate, -cyanate, -acetate, -formate, -ε-aminocaproate, potassium -hydroxide or -carbonate, was added subsequently. The rate of polymerization is given in Fig. 3.

When alkali metal compound is mixed previously in ε-caprolactam and then the mixture is boiled, it is difficult to polymerize and the rate of the reaction is not reproducible. When an alcoholic solution of alkali metal hydroxide is added to the boiling ε-caprolactam, the polymerization hardly ever occurs either. It may be said, therefore, that the solid surface must be considered for the catalytic effect.

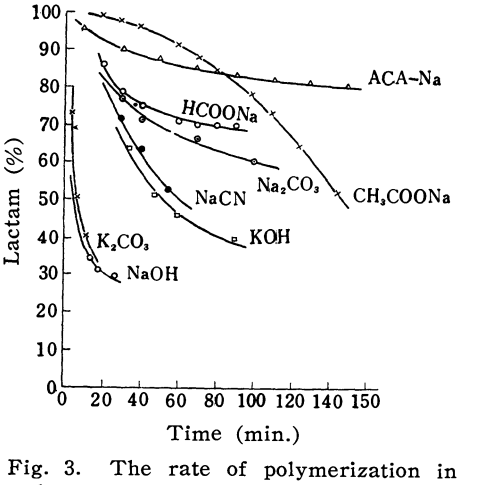

Fig. 3. The rate of polymerization in the presence of various alkali compounds.

In case of the polymerization of pyrolidone (γ-butyrolactam), *N*-acetyl pyrolidone is the promotor in the presence of potassium hydroxide[6]. ε-Caprolactam was heated at 290°C in the presence of 0.5 mole percent of sodium hydroxide and various mole percents of *N*-acetyl-ε-caprolactam.

4) H. Zahn and H. Wolf, *Melliand Textilber.*, **32**, 317 (1951).
5) P. H. Hermans, *J. Appl. Chem.*, **5**, 493 (1955).
6) W. O. Ney et al., U. S. *Atomic Energy Comm. Nuclear Soc. Abstr.*, 2,739,959 (1956).

TABLE IV

THE RATE OF POLYMERIZATION OF ε-CAPROLACTAM BY COLLOIDAL SODIUM CARBONATE

Na_2CO_3 (mole %)	Time (min.)	Water-soluble component (%)	$\eta_{rel}^{98\%\ H_2SO_4}$	25°C $[\eta]_{cresol}$
0.5	30	15.0	2.10	0.754
0.25	2	98.2	—	
	3	37.2	4.47	
	4	16.5	4.68	2.017
	10	13.5	3.35	
	30	14.0	2.85	
0.10	2.5	19.8	8.69	2·850
	5	21.4	5.35	2.210
	10	17.7	4.56	
	30	13.6	3.09	1.172
0.05	6	49.5	7.45	
	10	38.5	7.77	
	15	22.9	3.92	
	30	29.8	4.18	
0.025	60	68.2	—	

TABLE V

ANALYSES OF POLYMERS OBTAINED BY HEATING ε-caprolactam at 250°C UNDER REDUCED PRESSURE OF 250 mmHg WITH COLLOIDAL SODIUM CARBONATE

Na_2CO_3 (mole %)	Time (min.)	Water-soluble component (%)	$\eta_{rel}^{98\%\ H_2SO_4}$	25°C $[\eta]_{cresol}$
0.1	30	11.0	11.2	3.27
0.05	30	76.9	—	—

TABLE VI

ANALYSES OF POLYMERS OBTAINED BY HEATING ε-CAPROLACTAM WITH 0.1 MOLE % OF COLLOIDAL SODIUM CARBONATE AT VARIOUS CONDITIONS

Polymerization condition	Temp. (°C)	Time (min.)	Water-soluble component (%)	$\eta_{rel}^{98\%\ H_2SO_4}$
with 10% tetralin	290	10	17.3	6.27
with 10% toluene	290	10	14.9	5.69
with 20% xylene	250	120	64.0	2.84
with 30% xylene	250	60	43.7	6.55
with 20% toluene	250	60	100.0	—
with 30% toluene	250	60	41.3	6.59
with 30% xylene	230	60	100.0	—
with 30% toluene	230	60	100.0	—
with blowing dry	250	60	13.5	6.69
nitrogen into	250	60	17.6	8.80
ε-caprolactam	250	37	16.4	—
	230	60	100.0	

TABLE VII

THE RATE OF POLYMERIZATION OF ε-CAPROLACTAM BY COLLOIDAL POTASSIUM CARBONATE (290°C)

K_2CO_3 (mole %)	Time (min.)	Water-soluble component (%)	25°C $[\eta]_{cresol}$
0.2	3	13.5	4.52
	5	14.3	4.18
	10	16.8	3.84
	30	14.4	2.88
0.1	3	25.7	7.57
	5	35.4	5.93
	11.5	20.4	4.78
	30	29.3	3.16
0.05	10	68.8	—
	30	57.4	4.77

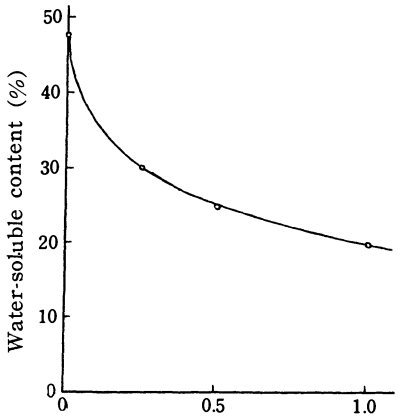

Fig. 4. The quantity of water-soluble content in the polymer in the presence of various mole percents of *N*-acetyl-ε-caprolactam (290°C, 1 hr.)

The quantities of water-soluble contents in the products are shown in Fig. 4.

Since the alkali metal compound is assumed to have great catalytic effect at its surface as stated above, it is expected that the greater effect can be obtained in case of dispersing the alkali metal compound colloidally in ε-caprolactam in order to increase the solid surface. Sodium hydroxide is dissolved previously in ε-caprolactam at 100°C and then carbon dioxide is bubbled for about 30 min. to 1 hour. The stable colloidal dispersion of sodium carbonate is obtained. The diameter of sodium carbonate is less than 0.1 μ. ε-Caprolactam containing 0.5 to 0.025 mole percent of colloidal sodium carbonate was boiled at 290°C. The rate of polymerization is given in Table IV. In case of 0.25 to 0.1 mole percent it took 3 to 4 minutes to polymerize. The reaction is reproducible. The degree of polymerization reaches maximum after 2 to 5 minutes and then decreases gradually. Even if sodium carbonate is pulverized finely in a mortar and added to the boiling ε-caprolactam, such a high rate of reaction can not be obtained. When ε-caprolactam was boiled at 250°C under the reduced pressure of 250 mmHg in the presence of the colloidal sodium carbonate, the decrease in the polymerization degree after the maximum is slower than at 290°C as shown in Table V.

When the solvent of low boiling point is dissolved in ε-caprolactam, the boiling can occur under the boiling temperature of ε-caprolactam (263°C). As shown in Table VI, ε-caprolactam containing 0.1 mole percent of colloidal sodium carbonate, polymerizes in the presence of 30% of xylene or toluene for about 20 minutes at 250°C.

When dry nitrogen was bubbled, polymerization also occurred under the boiling temperature as shown in Table VI. The polymerization by the colloidal potassium carbonate is slower than that by sodium carbonate, as shown in Table VII.

Discussion

At first sodium hydroxide or carbonate may react with ε-caprolactam into *N*-sodium ε-caprolactam as follows:

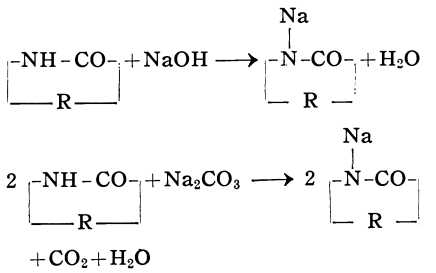

Water or carbon dioxide is analysed as mentioned above. Sodium ε-aminocaproate is also found in the reaction product practically. It can be assumed that sodium ε-caprolactam is hydrolyzed easily into sodium ε-aminocaproate in the presence of water. The reason why boiling is necessary for the polymerization seems to be ascribed to rapid removal of water or carbon dioxide from the reaction phase. Therefore the salt such as sodium stearate or adipate which yields non-volatile acid can not cause the polymerization. It has been reported that -COONa does not cause the reaction[7].

N-Acetyl ε-caprolactam functions slighlty as a promotor in the presence of alkali metal hydroxide. After *N*-alkali metal ε-caprolactam is formed, the reaction mechanism can be assumed to be similar to that of polymerization in the presence of alkali metal[8]. The catalytic effect of alkali metal compound is expected to be eminent at its solid surface, because the colloidal dispersion is much more effective than the pulverized solid. The degree of polymerization is very large in case of using colloidal alkali metal compound. The polymer has a rubber-like elasticity in a molten state.

Summary

The basic compound of alkali metal reacts with ε-caprolactam and gives at first *N*-alkali metal ε-caprolactam. It can cause the polymerization of ε-caprolactam. The boiling of the reaction phase is necessary for making the reaction proceed. The polymerization is especially rapid and reproducible in case of dispersing alkali

7) H.Yumoto and N. Ogata, *Makromolekulare Chem.*, **25**, 91 (1958).
8) H. Yumoto and N. Ogata, This Bulletin, **31**, 907 (1958).

metal compound colloidally in ε-caprolactam. It is supposed, therefore, that the solid surface of the catalyser is a very important factor in the polymerization.

The authors wish to thank to Dr. K. Hoshino and Dr. H. Kobayashi who instructed them and permitted the publication of this study and Mr. S. Yamauchi et al. who collaborated with them on experiments.

Research Department of Toyo Rayon Co., Ltd., Minato-ku, Nagoya

The Determination of Boron in Glass Using Radium-Beryllium Neutron Source (Neutron Absorption Technique)

By Yuzuru KUSAKA

(Received February 10, 1958)

When a substance containing an element with a high absorption cross section for neutron is placed in a flux of neutrons, a reduction of the flux is caused. When the neutron absorption of other elements in the sample is negligibly small, the reduction degree of the neutron flux can be used as a measure of the quantity of the neutron-absorbing elements.

Such a neutron absorption method has been utilized as a means of determining the boron content of various substances[1-4], because of the high cross section of boron for thermal neutrons ($\sigma_{abs.}=755$ barn), of which the nuclear reaction is $^{10}B(n.\alpha)^{7}Li$. The author has applied this neutron absorption technique to the determination of boron in borosilicate glass with some interesting results.

Experimental and Discussion

The activation source consisted of a mixture of 84.2 mg. of radium bromide (49.3 mg. as radium element) with beryllium, which was sealed in a platinum tube (length: 40.0 mm., diameter: 5.0 mm., wall-thickness: 0.5 mm.). The source was surrounded by paraffin to moderate the fast neutrons to thermal velocities and to reflect these neutrons.

Studies on the Arrangements of Paraffin. —In order to obtain as much thermal neutron flux as possible, the following experiments were tried. In these experiments, the neutron detector was a silver plate (silver content, 75%; diameter, 23 mm.; weight, 4.6 g.). The time of neutron irradiation was 20 minutes and, after an interval of 30 seconds, the induced radioactivity (^{110}Ag [24.2 sec.], ^{108}Ag[2.3 min.]) was measured for 5 minutes by means of an end-window G. M. counter (thickness of mica window: 1.96 mg./cm^2) at a fixed position.

When a cadmium filter (thickness: 0.6 mm.) which absorbs all the neutrons with energies less than 0.4 eV. is used, the radioactivity produced by thermal neutrons only is given by the following equation.

$$I_{thermal}=I_0-I_{Cd}$$

$I_{thermal}$: the radioactivity obtained by thermal neutrons.

I_0: the radioactivity obtained without cadmium filter.

I_{Cd}: the radioactivity obtained with cadmium filter*.

In the first experiment the relationship between the thermal neutron density at the center of an upper surface of paraffin and its distance from the neutron source was studied. The maximum neutron flux was obtained at 2.5 cm. from the source as is shown Fig. 1.

In the second experiment, a cylindrical hole (diameter: 4.2 cm.) was bored through the paraffin block above the neutron source, as is shown by the dotted line in Fig. 2, and the relationship between the thermal neutron density at the outlet of the hole and the hole length was investigated.

The results obtained are shown in Fig. 3.

1) P. Süe and J. Martelly, *Bull. Soc. Chim. France*, **1946**, 103, 410.
2) J. Govaerts, *Exper.* **6**, 459 (1950).
3) M. Green and G. R. Martin, *Trans. Faraday Soc.* **48**, 416 (1950).
4) R. P. Hamlen and W. S. Koski, *Anal. Chem.* **28**, 1631 (1956).

* As shown on Fig. 2, a cadmium plate is put on the silver detector at every I_0 and I_{Cd} measurement to shut out thermal neutrons from the upper side of the detector. In the case of I_{Cd} measurement, two Cadmium plates must be put separately on and beneath the silver detector to shut out thermal neutrons from each side of the detector.

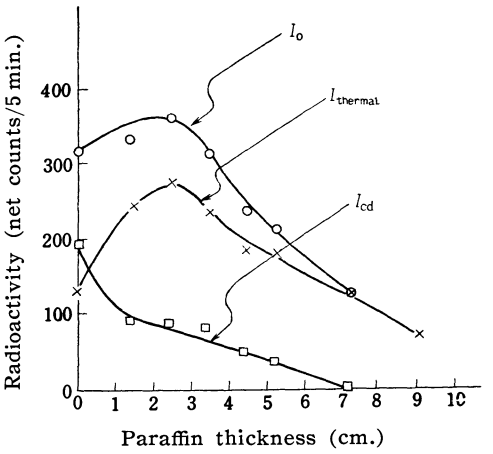

Fig. 1. Relationship between paraffin thickness and radioactivity induced in silver plate.

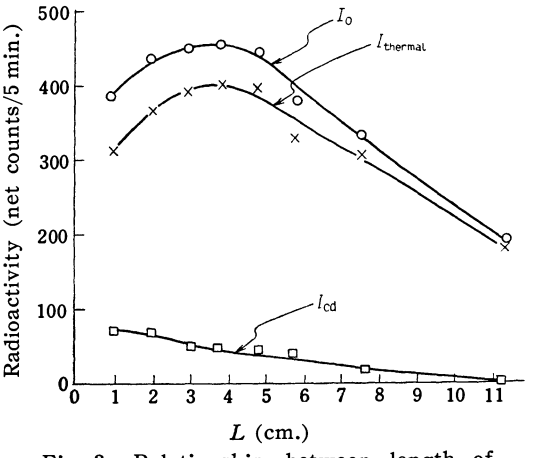

Fig. 3. Relationship between length of hole in paraffin ("L" in Fig. 2) and radioactivity induced in silver plate.

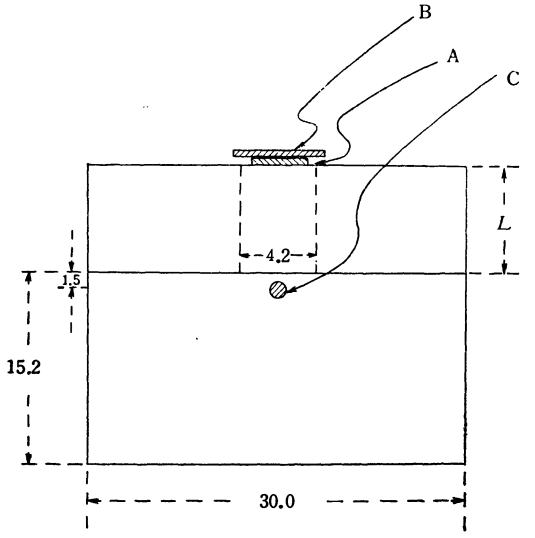

Fig. 2. Irradiation geometry (Dimensions in cm.)
A=silver plate. B=cadmium plate.
C=radium+beryllium neutron source.

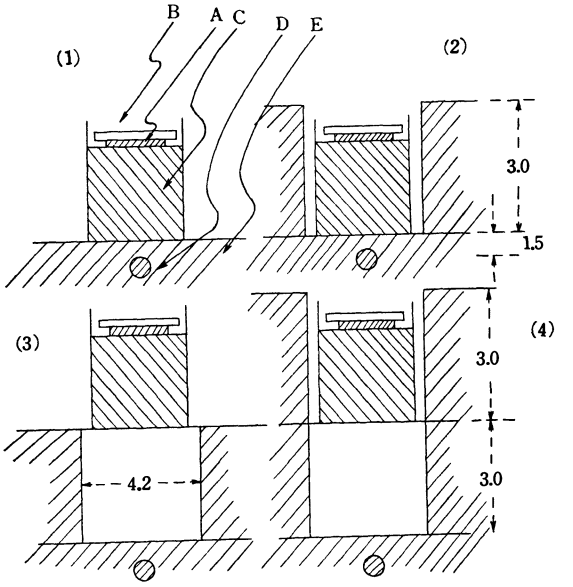

Fig. 4. Experiments for evaluating irradiation geometry. (Dimensions in cm.)
A=silver plate. B=cadmium plate.
C=sample powder. D=radium+beryllium neutron source. E=paraffin.

From these experimental results it is observed that a remarkable increase in neutron flux is caused by the use of a paraffin block with a hole in its centre. For example, the thermal neutron density at 5 cm. from the neutron source is about 2.2 times as great as that obtained by the use of a paraffin block without a hole. This phenomenon must be due to the "howitzer effect"[5,6], by which the collimation of neutrons is caused.

This effect was also observed in the following experiment. Ten grams of silicic oxide power (sieved through a 100 mesh screen) was placed in an aluminum cup (diameter: 3.0 cm., thickness: 0.05 cm.) and was irradiated with neutrons as shown in Fig. 4. The radioactivities of the silver detector in each case are shown in Table I. Then, in order to obtain stronger thermal

TABLE I
TESTS FOR IRRADIATION GEOMETRY

Geometry No. (in Fig. 4)	$I_{thermal}$ (net counts/5 min.)
1	82
2	477
3	90
4	439

5) F. L. Hopwood and T. A. Chalmers, *Nature*, **135**, 341 (1935).
6) G. A. Fink, *Phys. Rev.*, **50**, 738 (1936).

neutron flux, such geometrical arrangement as 2 or 4 in Fig. 4 would be more advantageous for neutron absorption analysis.

Studies on the Determination of Boron Content in Borosilicate Glass.—Relative cross section values of the various components in three practical examples of borosilicate glass were calculated[7] and summarized in Table II. As is shown in the table, the greater part of the cross section values (about 99% in σ_{abs} and about 95% in σ_t) in borosilicate glass is attributed to boron in the sample. Therefore it would be possible to apply the neutron absorption technique effectively to boron analysis of such samples.

TABLE II
RELATIVE CROSS SECTION VALUES OF VARIOUS COMPONENTS IN GLASS

Example 1
(Mean value of borosilicate glass[8])

Component	Composition (%)	σ_{abs} (%)	σ_t (%)
SiO_2	80	0.06	4.23
Na_2O	4	0.02	0.26
B_2O_3	14	99.92	95.41
Al_2O_3	2	—	0.10

Example 2

Component	Composition (%)	σ_{abs} (%)	σ_t (%)
SiO_2	68.60	0.03	2.37
Na_2O	3.84	0.01	0.17
K_2O	5.41	0.05	0.13
Al_2O_3	0.34	—	0.01
B_2O_3	21.81	99.91	97.32

Example 3
(BK-7 glass)

Component	Composition (%)	σ_{abs} (%)	σ_t (%)
SiO_2	69.58	0.07	5.09
Na_2O	8.44	0.06	0.77
K_2O	8.32	0.16	0.42
MgO	0.08	—	0.01
CaO	0.10	—	0.01
BaO	2.55	0.01	0.10
B_2O_3	9.91	99.69	93.54
Al_2O_3	0.44	—	0.03
As_2O_3	0.31	0.01	0.02

The geometrical arrangement of the paraffin, the analyzed sample and the neutron source in the experiments is shown in Fig. 5. In these cases, a round

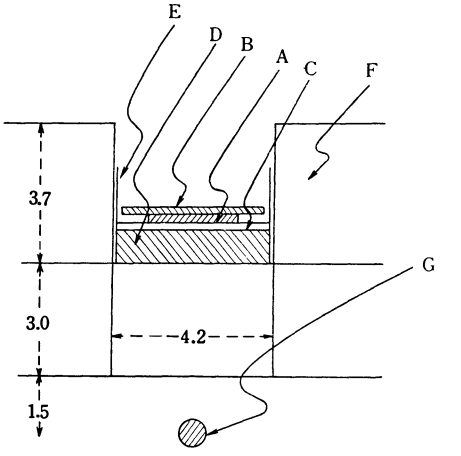

Fig. 5. Irradiation geometry for analysis (Dimensions in cm.)
A=indium plate. B=cadmium plate. C=plastic plate (thickness: 0.1 cm.). D=sample powder. E=plastic sample container. F=paraffin. G=radium+beryllium neutron source.

metallic plate of indium (diameter, 22 mm.; weight, 2.1 g.) was used as neutron detector. The irradiation samples were the mixed powder (100 mesh) of glass and aluminum oxide as the diluent (weight ratio=1:1.5). Ten grams of it were irradiated for 2.0 hours, in which case the saturation factor of ^{116m}In is 0.78. After an interval of one minute, the induced radioactivity of the indium detector was measured for 20 minutes. The method of determining the thermal neutron density is similar to that illustrated above.

By using a calibration curve, as shown

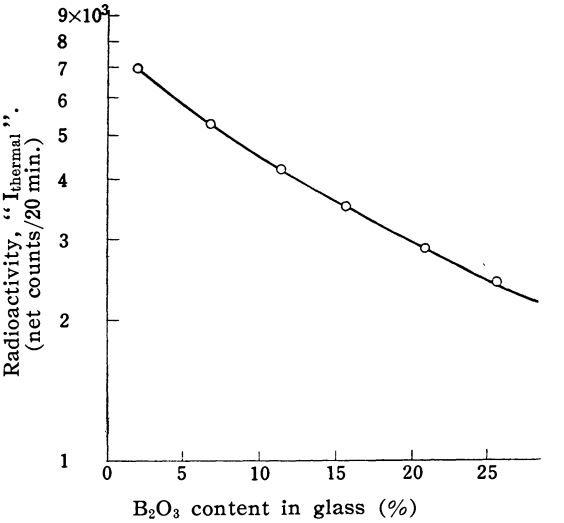

Fig. 6. Calibration curve in boron analysis.

7) The values in Table II were calculated from D. J. Hughes and J. A. Harvey's, "Neutron Cross Section", BNL 325 (1955), (U. S. A. E. C).
8) "Encyclopedia of Chemical Technology" Vol 7, Interscience Encyclopedia Inc., New York, p 181.

TABLE III
BORON ANALYSIS BY THIS METHOD AND COMPARISION WITH CHEMICAL METHOD

Sample*	Induced radioactivity (net counts/20 min.)				B_2O_3 content (%)	
	I_0.	I_{cd}.	$I_{thermal}$	Probable error	Neutron method	Chemical method
1	8159	2081	6078	68	4.3±0.2	4.44
2	6457	1994	4463	62	10.1±0.3	9.91
3	5593	1861	3732	58	14.4±0.4	13.15
4	5544	1930	3614	58	15.2±0.4	15.91
5	4390	1817	2573	53	23.9±0.6	23.28

* The samples used for this study were as follows;
No. 1: Optical glass containing BaO (19.7%), ZnO (11.9%) and PbO (3.2%), called as BaK-4.
No. 2: Optical glass containing BaO (2.5%), called as BK-7.
No. 3 and No. 4.: Commercial borosilicate glasses.

in Fig. 6, which is obtained from measurements on the glass of known boron content, it is possible to determine the boron content in any borosilicate glass.

Some experimental results by this method and the comparisons with the chemical method[9] are summarized in Table III.

The results given in Table III indicate the validity of the neutron absorption method. Fig. 7 shows the plots of the probable error in analysis versus the content of boric oxide in glass. This graph represents the degree of accuracy that can be expected from the method.

The most striking error involved in this method is due to the statistical uncertainty during the radioactivity measurement.

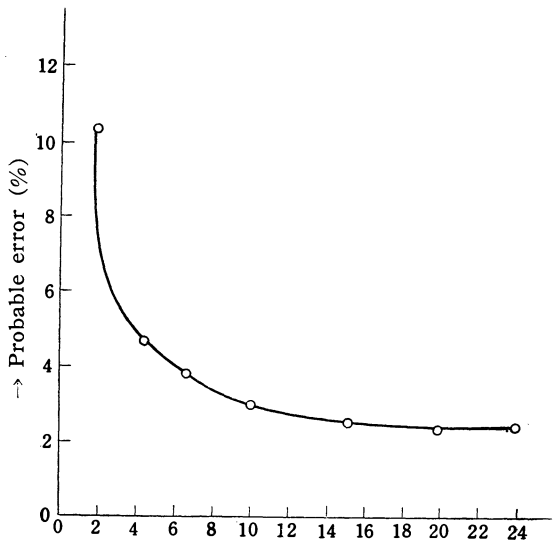

Fig. 7. Statistical error in boron analysis.

9) W. F. Hillebrand and G. E. F. Lundell, "Applied Inorg. Analysis", Wiley, New York, (1929), p 611.

Summary

The neutron absorption technique using radium-beryllium neutron source has been shown to be useful for rapid assay of boron in the samples containing other low cross-section elements. This method may also be useful for the analyses of other high cross-section elements.

The writer wishes to express his hearty thanks to Professor Masayoshi Ishibashi of Kyoto University and President Bunsaku Arakatsu and other members of the Chemical and Physical Laboratory of Kōnan University for their kind guidance and valuable advice through this study, to Professor Shoji Tsuchihashi of Kōbe University for furnishing glass samples, and to Mr. Haruo Tsuji for considerable help in repeating and checking the procedures in many of the experiments.

Department of Chemistry, Faculty of Science, Kōnan University, Higashinada-ku, Kōbe

Rotatory Dispersion of Metallic Co-ordination Compounds. I. Rotatory Dispersion in the First and the Second Absorption Bands of Cobaltic Compounds[1,2]

By Jinsai HIDAKA, Shoichiro YAMADA and Ryutaro TSUCHIDA

(Received June 11, 1958)

In order to understand the nature of absorption bands, analyses of rotatory dispersion curves are considered to be of importance. In fact, there are a number of reports available concerning the rotatory dispersion of cobaltic complexes with ethylenediamine[3-7] but many of these studies are confined within a comparatively narrow wave-length region. Rotatory dispersion measurements over wider wave-length regions have been reported in some of the compounds, but only a very few of them have been precisely analyzed. In these circumstances, it was thought to be desirable to study more systematically the rotatory dispersion of metallic complexes on the basis of measurements in wider wave-length regions.

This paper presents rotatory dispersion measurements of optically active *cis*-dichloro-bis-(ethylenediamine)-cobalt(III) chloride and *cis*-chloronitro-bis-(ethylenediamine)-cobalt(III) chloride in the visible and ultraviolet region, and discusses the results of the measurements in relation to their absorption spectra.

Experimental

Measurements.—A Rudolph photoelectric polarimeter 200S-80 was employed in the rotatory dispersion measurement.

The measurements were made at room temperature in the region from 666 mμ to 312 mμ using mainly the lines of the mercury spectrum: 58×10^{13}/sec. (577 mμ), 55×10^{13}/sec. (546 mμ), 68.8×10^{13}/sec. (436 mμ), 74×10^{13}/sec. (405 mμ), 82×10^{13}/sec. (365 mμ) and 89.8×10^{13}/sec. (334 mμ). A xenon-or a tungsten lamp was used occasionally.

The solvent employed was methyl alcohol for *cis*-dichloro-bis-(ethylenediamine)-cobalt(III) chloride and 50% hydrochloric acid for *cis*-chloronitro-bis-(ethylenediamine)-cobalt(III) chloride.

In the measurements with *cis*-dichloro-bis-(ethylenediamine)-cobalt(III) chloride, its solution was alternated with a new one at times. As *cis*-chloronitro-bis-(ethylenediamine)-cobalt (III) chloride is so unstable in solution that it is liable to undergo aquotization[8]. Therefore, its freshly prepared solution was used in each measurement. The measurements were made as rapidly as possible after preparation of the solution to keep the reactions of the complex with water at a minimum.

The concentrations for the measurements of *cis*-dichloro-bis-(ethylenediamine)-cobalt(III) chloride were $1/3\times10^3$ F, $1/6\times10^3$ F and $1/8\times10^3$ F, and the cell lengths 20, 10 and 2 cm. For *cis*-chloronitro-bis-(ethylenediamine)-cobalt(III) chloride, the concentrations used were $1/3\times10^3$ F, $1/6\times10^3$ F and $1/8\times10^3$ F, and the cell lengths 20, 10 and 2 cm.

Material. — Racemic *cis*-dichloro-bis-(ethylenediamine)-cobalt(III) chloride was prepared in violet crystals by the method of Werner[8] and resolved by the method of Bailar et al[9]. The preparation and the resolution of racemic *cis*-chloronitro-bis-(ethylenediamine)-cobalt(III) chloride were made according to the directions of Werner[10].

Both the optically active compounds, which were precipitated as more insoluble salts with *d*-α-bromocamphorsulphonic acid, gave positive values of optical rotation in sodium D line. According to Bailar, *cis*-dichloro-bis-(ethylenediamine)-cobalt(III) chloride was a levo-salt and gave a negative value in sodium D line, but our and Douglas's experiments[11] have given a positive one. Thus the reagents employed in the present study may be regarded as *cis*-dextro-$[Co\ en_2Cl_2]Cl$ and *cis*-dextro-$[Co\ en_2ClNO_2]Cl$.

1) R. Tsuchida, S. Yamada and J. Hidaka, Presented before the Symposium on Metallic Co-ordination Compounds, Nagoya, October, 1957.

2) Abstracted in part from a thesis submitted by J. Hidaka to the Faculty of Science of Osaka University in partial fulfillment of the requirements for the degree of Master of Science, 1958.

3) R. Tsuchida, *J. Chem. Soc. Japan, (Nippon Kwagaku Kwaisi)*, **58**, 621 (1937); M. Kobayashi, ibid., **64**, 684 (1943).

4) W. Kuhn and K. Bein, *Z. physik. Chem.*, **B24**, 355 (1934).

5) J. P. Mathieu, *Bull. soc. chim. France*, (5) **6**, 873 (1939).

6) J. P. Mathieu, ibid., (5) **3**, 476 (1936).

7) J. P. Mathieu, *J. chim. phys.*, **83**, 78 (1936).

8) A. Werner, *Ann.*, **386**, 48, 107 (1912).

9) J. C. Bailar, Jr. and R. W. Auten, *J. Am. Chem. Soc.*, **56**, 774 (1934).

10) A. Werner, *Ber.*, **44**, 3276 (1911); *Ann.*, **386**, 284 (1912).

11) B. E. Douglas and W. C. Erdman, *J. Am. Chem. Soc.*, **79**, 3012 (1954).

Analyses

***Cis*-dichloro-bis-(ethylenediamine)-cobalt(III) chloride.**—The rotatory dispersion of D-*cis*-[Co en_2Cl_2]Cl in the wave-length region from 450 mμ to 680 mμ, which has been reported by Mathieu[12], coincides with our result in this wave-length region. The first rotatory inversion in the longer wave-length side involves a positive value of the Cotton effect. Thus the molar rotations change from negative to positive values at about 636 mμ. On the other hand, the second inversion appears at about 520 mμ, and shows a negative Cotton effect.

The dispersion curve in the shorter wave-length side, as determined in the present work, was analyzed as follows. It is assumed that the observed curve is the superposition of partial rotations in the visible region and the tail of a large partial rotation which has its inversion centre in the far ultraviolet region. In the analysis of the curve, the method of trial and error was employed. The result of the analysis is shown in Fig. 1.

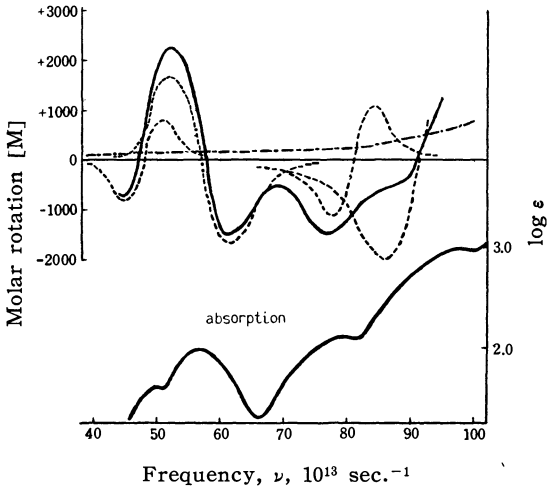

Fig. 1. Rotatory dispersion of D-*cis*-[Co en_2Cl_2]Cl in methanol: —— observed curve, ------ partial rotation obtained through analysis.

According to this result, the rotatory inversion with its centre at about 370 mμ shows a negative value of rotation in the longer wave-length side, its magnitude being almost equal to the rotatory inversion in the wave-length region of the "first absorption band". The rotatory inversion with its center at about 330 mμ is seen to give a negative value of rotation in the longer wave-length side.

***Cis*-chloronitro-bis-(ethylenediamine)-cobalt(III) chloride.**—In the wave-length region of the "first absorption band", the rotatory inversion with its center at about 544 mμ, which gives a positive value in the longer wave-length side, coincides with Mathieu's results[13] on the whole.

As the observed curve indicates, the maximal value of molar rotation in the region of the "first absorption band" is greater in the shorter wave-length side than in the longer wave-length side and the total dispersion curve is apparently displaced to the negative side. Therefore, it is assumed in the analysis of the curve that the observed curve is the superposition of the partial rotations under consideration in the visible region and the tail of a large partial rotation which has its inversion center in the far ultraviolet region. The curve was analyzed in the same way as in the former. The result of the analysis is shown in Fig. 2.

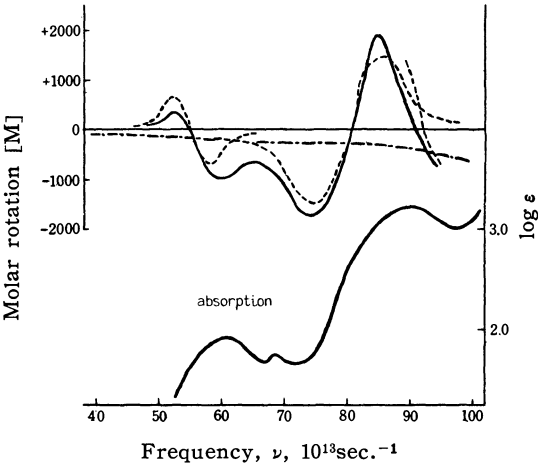

Fig. 2. Rotatory dispersion of D-*cis*-[Co en_2ClNO_2]Cl in 50% hydrochloric acid: —— observed curve, ------ partial rotation obtained through analysis.

Discussion

As described in the preceding part, the dextro-rotatory *cis*-dichloro-bis-(ethylenediamine)-cobalt(III) chloride shows, in the wave-length region of the "first absorption band", two inversive rotatory dispersions. One of them has a positive value for the Cotton effect and the other

12) J. P. Mathieu, *Bull. soc. chim. France*, (5) **3**, 483 (1936).

13) J. P. Mathieu, ibid., (5) **3**, 485 (1936).

a negative value. These may be regarded as corresponding to the two component absorptions resulting from the splitting of an original "first absorption band". In fact, the dichroism as determined in the crystalline state indicates that the violeo-salt shows two absorption bands at 51×10^{13}/sec. (588 mμ) and 57×10^{13}/sec. (527 mμ) which correspond to the component absorptions of the "first absorption band"[14]. This result is found to be in good agreement with the above described result of the present measurement.

In the wave-length region of the "first absorption band", dextro-rotatory *cis*-chloronitro - bis - (ethylenediamine) - cobalt (III) chloride shows a rotatory inversion with its center at about 55.5×10^{13}/sec. (541 mμ), a rotatory dispersion which is quite different from that of the violeo-salt. Judging from the symmetry of the complex ion, however, it is presumed that the chloronitro-salt shows separate absorption maxima corresponding to the components of the "first absorption band". In fact, the dichroism measurement indicates that the *cis*-chloronitro chloride in the crystalline state shows absorption bands at 54×10^{13}/sec. (551 mμ) and 58×10^{13}/sec. (517 mμ)[14], which may be regarded as corresponding to the first absorption band.

On the basis of the above consideration, the present observation that only one rotatory inversion appears in the wave-length region of the "first absorption band" might be understood in the following way. There would be actually two or more "rotatory inversions" which are superposed upon each other. The component absorptions are so close together that the superposition of the "rotatory inversions" gives the curve that has been experimentally determined.

A rotatory inversion at 81×10^{13}/sec. (370 mμ) for the violeo-salt and a similar sort of a rotatory inversion at about 81×10^{13}/sec. (370 mμ) for the chloronitro-salt may originate from the transitions closely related with the second absorption band. The magnitudes of both the inversive dispersions are found to be of an equal order. It is to be noted that such a type of rotatory inversion, as had previously been reported for the "first band", was observed for the "second band" as well.

Another inversive dispersion showing a Cotton effect with a negative sign is observed at about 91×10^{13}/sec. (330 mμ) for the violeo-salt. A rotatory inversion with a Cotton effect of a positive sign is also observed at an almost identical wave-length in the *cis*-chloronitro-complex. These inversions may be regarded as originating from the "specific absorption band" due to the chloride or nitro group in co-ordination with the metal.

Summarizing the results obtained in the present study, we may be able to derive the following conclusion (Table I and II.)

In the wave-length region of the "first absorption band", there appear two "inversive dispersions" due to the component absorptions, the sign of the Cotton effect for one being reverse to that for the other.

In the wave-length region of the "second absorption band", only one "inversive dispersion" is observed, its magnitude being of an identical order with that for the "first absorption band". An inversive rotatory dispersion is also observed in the wave-length region of the "specific absorption band", its magnitude being greater than that for the "first or the second absorption band".

General Discussion

As has been described in the preceding part of the present paper, optically active complex-ions such as *cis*-$[Co\ en_2X_2]^+$ and *cis*-$[Co\ en_2XY]^+$ show rotatory inversions corresponding to the component absorptions of the "first absorption band". Reexamining formerly reported data on the basis of the above result, complex ions may be divided into the following two groups from the nature of rotatory dispersion in the wave-length region of the "first absorption band". (1) In the first group, the sign of the Cotton effect for one component differs from that for the other, the examples of this type being *cis*-$[Co\ en_2Cl_2]^+$ and *cis*-$[Co\ en_2ClNCS]^+$. (2) In the second group, the sign of the Cotton effect is the same for the two components, the examples being *cis*-$[Co\ en_2NH_3OH_2]^{3+}$, *cis*-$[Co\ en_2NH_3Br]^{2+}$ and *cis*-$[Co\ en_2NH_3Cl]^{2+}$.

Typical curves for the two types are shown in Fig. 3. The absolute configuration of optically active complexes has not been determined except for the tris-(ethylenediamine)-cobalt(III) ion[15].

14) S. Yamada and R. Tsuchida, to be published later.

15) N. Nakatsu, Y. Saito and H. Kuroya, This Bulletin, **29**, 428 (1956).

TABLE I

ROTATORY DISPERSION AND UV ABSORPTION SPECTRA OF D-*cis*-[Co en_2Cl_2]Cl

		First band		Second band	Specific band
Absorption band ν_{max}	solution	49.5	57.5	79	98
	crystal	51	57		
Inverted dispersion	ν	48	57	81	91
	sign of Cotton effect	−	+	−	−
	$[M]_{max}$	750	1650	1150	

[M]: molar rotation, ν: frequency, 10^{13} sec.$^{-1}$

TABLE II

ROTATORY DISPERSION AND UV ABSORPTION SPECTRA OF D-*cis*-[Co en_2ClNO_2]Cl

		First band			Second band	Specific band
Absorption band ν_{max}	solution		60	68		89.5
	crystal	54.5	58	71		
Inverted dispersion	ν	55			81	91
	sign of Cotton effect	−			−	+
	$[M]_{max}$	600			1500	

[M]: molar rotation, ν: frequency, 10^{13} sec.$^{-1}$

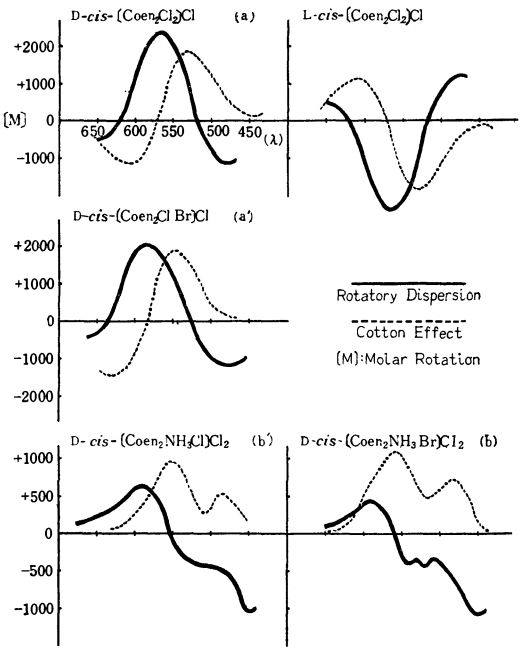

Fig. 3. Relationship between rotatory dispersion and Cotton effect. Data are taken from J. P. Mathieu, *Bull. soc. chim. France*, **3**, 476 (1936).

Making measurements of rotatory disperpersion in the longer wave-length range, Mathieu[16] suggested a possibility of determining the absolute configuration from the rotatory dispersion curves in the long wave-length range. This possibility, however, has not been fully examined up to the present. In the following, we will discuss this possibility by using the results obtained in the present study.

It has been shown in the present work that the "first absorption band" of *cis*-disubstituted-bis-(ethylenediamine)-complexes splits itself into components, each of which gives rise to a rotatory inversion of its own. If these components correspond to the same type of electronic transition in the optically active complex under consideration, the sign of the Cotton effect for these components should depend only upon the absolute configuration. Therefore, the Cotton effect may be used as a criterion for determining the absolute configuration of metallic complexes if precautions are taken.

In other words, if a comparison is made among compounds which are closely similar in the linkage involved, and consequently in the stability order of energy states of the metallic complex, we may assume that the compounds with the same type of absolute configuration would show the same sign of the Cotton effect and the same type of the rotatory inversion.

Now, if we choose complexes resembling each other in the linkage from the complexes in the group 1 or in the group 2, their absolute configuration may be determined on the basis of the sign of the Cotton effect. Thus, in the case of *cis*-[Co en_2Cl_2]$^+$ and *cis*-[Co en_2ClBr]$^+$, in which the above-mentioned requirements are satisfied, it seems possible to determine the absolute configuration.

It is seen in Fig. 3 that the diastereomer of *cis*-[Co en_2ClBr]$^+$, which forms a more

16) J. P. Mathieu, *J. chim. phys.*, **33**, 78 (1936).

insoluble compound with *d*-α-bromocamphorsulfonate than does the other diastereomer, shows a rotatory dispersion curve represented by the curve (a′) in Fig. 3. If we tentatively define a D-form of *cis*-[Co en_2Cl_2]$^+$ to be the optically active form[17] related with the curve (a) in Fig. 3, it may be reasonable to assume that the former diastereomer of *cis*-[Co en_2ClBr]$^+$ belongs to the D-series.

A similar consideration applies to the components classified as the group 2. Thus *cis*-[Co en_2NH_3Br]$^{2+}$, *cis*-[Co en_2NH_3Cl]$^{2+}$ and *cis*-[Co $en_2NH_3OH_2$]$^{3+}$, all showing the rotatory dispersion of the type 2, closely resemble one another in the respect of the linkage involved.

It is seen in Fig. 3 that the diastereomer of *cis*-[Co en_2NH_3Br]$^{2+}$, which forms with *d*-α-bromocamphorsulfonate a more insoluble salt than does the corresponding salt of the other diastereomer, has the same sign for the Cotton effect as the sign possessed by the optically active form related with the curve b in Fig. 3.

If we tentatively assume that the curve b in Fig. 3 refers to the salt of the D-series, then the curve b′ may also be regarded as corresponding to the D-series.

So far, we have taken account of the rotatory behavior in the wave-length region of the "first absorption band" alone. The above discussion may be expected to become more reliable when due account is taken of the Cotton effect in the region covering the "second absorption band" as well. The discussion on this phase of the problem will be made in the succeeding papers of this series.

17) a diastereomer which forms with ammonium *d*-α-bromocamphorsulfonate a less easily soluble compound than does the other diastereomer of the complex salt.

Summary

Rotatory dispersions in the visible and the ultraviolet region have been determined with *cis*-[Co en_2Cl_2]Cl and *cis*-[Co en_2ClNO_2]Cl, and dispersion curves have been analyzed by the method of successive approximation.

Both the complexes show two inversive dispersions in the wave-length region of the "first absorption band", and only one dispersion in the region of the "second absorption band".

The magnitude of those dispersions was found to be of the same order.

An inversive dispersion was also observed in the region of the "specific absorption band".

In the wave-length region of the "first absorption band", there appear two inversive dispersions due to the component absorptions, in accordance with the dichroism measurement. As for the inversive dispersions in the region of the "first absorption band", the sign of the Cotton effect for the one is reverse to that for the other in the violeo-salt, but in the *cis*-chloronitro-salt, the Cotton effect is the same for the two components.

A possibility of determining the absolute configuration was suggested from the rotatory dispersion curve in the wave-length region of the "first absorption band".

The present authors wish to thank the Ministry of Education for a grant-in-aid.

Department of Chemistry, Faculty of Science
Osaka University, Kita-ku, Osaka

*Synthesis of Histidyl Peptides**

By Fumio SAKIYAMA, Kenji OKAWA, Tsuneo YAMAKAWA and Shiro AKABORI

(Received June 18, 1958)

Peptides containing L-histidine have frequently been obtained from biologically active substances such as ribonuclease[1], insulin[2], bacitracin[3] and strepogenin[4], and it has recently been suggested that the histidyl residue constitutes an essential part of the active sites of α-chymotrypsin, cholinesterase, lysozyme[5], and so on. Despite these findings indicating the importance of histidyl peptides in biochemistry, no satisfactory methods have so far been worked out for their convenient synthesis. This appears to be due mainly to the fact that there have been no successful procedures available to protect the imidazole nucleus of histidine.

Even when the α-amino group of histidine is masked with an acyl group, the molecule still behaves as a zwitter-ion owing to the presence of the imidazole ring, and this character affords unavoidable difficulties to the subsequent reactions. First of all, the presence of unprotected imidazole residue in the molecule often leads to various undesirable side reactions during the peptide synthesis. Furthermore, restricted solubility in organic solvents of the acylated derivative, e. g., *N*-α-carbobenzyloxyhistidine, is not favorable for their coupling with amino acid esters. The use of *N*-α-carbobenzyloxyhistidine is also impractical in view of the poor yield obtainable in its synthesis from histidine by the direct carbobenzyloxylation method[6].

Theodropoulos[7] has synthesized histidyl peptides using *N-Im*-benzyl-L-histidine prepared by the procedure of du Vigneaud[8]. Although this method is free from most of the defects mentioned above, it is not suitable for practical purpose because of the fact that the benzyl derivative is not easily accessible. Of late, Amiard et al. reported the preparation of the ditrityl histidine through which some of the histidyl peptides were synthesized[9]. The trityl method was valuable for the limited instance as it was rather tedious.

Holley and Sondheimer[10] have prepared a number of histidyl peptides employing the azide procedure in which the imino group of the imiazole ring was not protected. This method, though widely used as the only practical means for the synthesis of histidyl peptides[11], could not be regarded as a very excellent one because of the difficulty associated with the preparation of the intermediate *N*-α-carbobenzyloxyhistidine azide and its instability.

In the present paper the authors wish to report the preparation of dicarbobenzyloxy-L-histidine and its availability for the synthesis of histidyl peptides.

Preparation and Properties of Dicarbobenzyloxyhistidine. — Using sodium carbonate in place of sodium hydroxide, the authors succeeded in the percarbobenzyloxylation of L-histidine and obtained the α, *Im*-dicarbobenzyloxy derivative in 81% yield. Sodium hydroxide was also effective under limited conditions, but the yield in this case was relatively low.

The dicarbobenzyloxy compound thus obtained was found to be rather unstable

* A part of this investigation has been reported in "*Nature*", **181**, 772 (1958).

1) C. H. W. Hirs, *Fed. Proc.*, **16**, 196 (1957); R. R. Redfield and C. B. Anfinsen, *J. Biol. Chem.*, **221**, 385 (1956).

2) H. Brown, F. Sanger and R. Kitai, *Biochem. J.*, **60**, 556 (1956).

3) J. Porath, *Nature*, **172**, 871 (1953); I. M. Lockhart and E. P. Abraham, *Biochem. J.*, **58**, 633 (1954); L. C. Craig et al., *J. Am. Chem. Soc.*, **77**, 731 (1955).

4) R. B. Merrifield and D. W. Woolley, ibid., **78**, 358 (1956).

5) The late Dr. C. Fromageot suggested in the discussion that the histidyl residue might be the active site of lysozyme. (International Symposium on Enzyme Chemistry. Tokyo, Oct., 1957).

6) M. Bergmann and L. Zervas, *Ber.*, **65**, 1199 (1932).

7) D. Theodropoulos, *J. Org. Chem.*, **21**, 1550 (1956).

8) V. du Vigneaud and O. K. Behlens, *J. Biol. Chem.*, **117**, 27 (1937).

9) G. Amiard, R. Heymes and L. Velluz, *Bull. soc. chim. France*, 191 (1956).

10) R. Holley and E. Sondheimer, *J. Am. Chem. Soc.*, **76**, 1326 (1954).

11) R. F. Fischer et al., ibid., **76**, 5076 (1954); R. A. Boissonas et al., *Experientia*, **12**, 446 (1956); D. W. Woolley, et al., *J. Am. Chem. Soc.*, **78**, 4646 (1956); K. Hofmann et al., ibid., **76**, 1641 (1957); R. Schwyzer, et al., *Helv. chim. Acta*, **40**, 614 (1957).

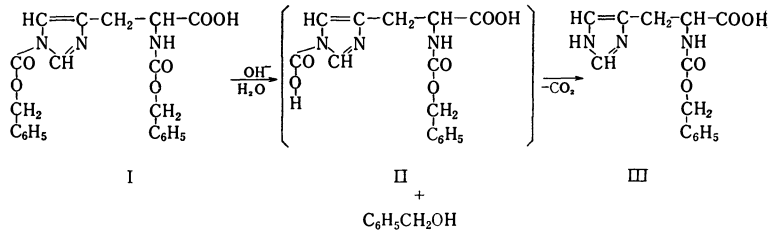

Fig. 1. Decomposition of dicarbobenzyloxy histidine in alkaline media.

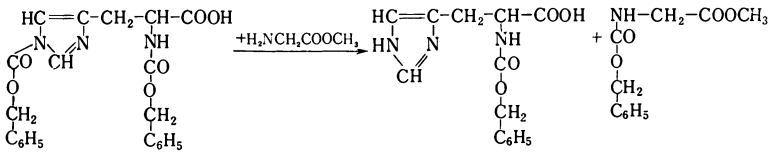

Fig. 2. The transfer of the carbobenzyloxy group.

in alkaline media. The compound was convertible into *N*-α-carbobenzyloxyhistidine with elimination of the imidazole-linked carbobenzyloxy group (Fig. 1). It was thought that, in alkaline solution, dicarbobenzyloxyhistidine (I) was partly split into an intermediate II and benzyl alcohol by the action of hydroxyl ions. Then, II might spontaneously changed to form the *N*-α-carbobenzyloxy derivative (III) and carbon dioxide. The low yield of the dicarbobenzyloxy compound encountered in the presence of sodium hydroxide may have been due to such instability of the product in alkaline reaction.

In non-aqueous basic media the carbobenzyloxy residue linked to imidazole appeared to act as an active acyl group. When the dicarbobenzyloxy derivative and glycine methyl ester were incubated in dioxane at 50~60°C for one hour, a gelatinous precipitate of silky lustre was formed. Carbobenzyloxy glycine methyl ester and *N*-α-carbobenzyloxy histidine were isolated and identified from the precipitate. These compounds must have been formed by the transcarbobenzyloxylation reaction as illustrated in Fig. 2. This mechanism received some support from the fact that no transfer reaction but the decomposition took place in basic media if an acceptor compound was absent in the reaction mixture. Bergmann[12] and Wieland[13] have already observed that acetyl or amino acyl groups linked to the imidazole nucleus can be transfered to suitable acceptors under mild conditions.

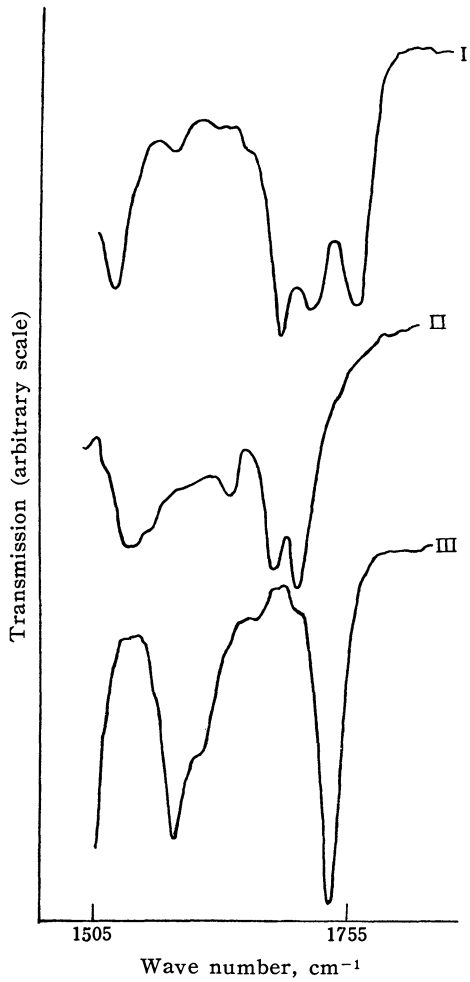

Fig. 3. Infrared absorption spectra of carbobenzyloxy derivatives of L-histidine. I, DCH; II, α-MCH; III, *Im*-MCH. (Rock salt, Hilger H800)

12) M. Bergmann and L. Zervas, *Z. physiol. Chem.*, **175**, 154 (1928).
13) Th. Wieland and G. Schneider, *Ann.*, **580**, 159 (1953).

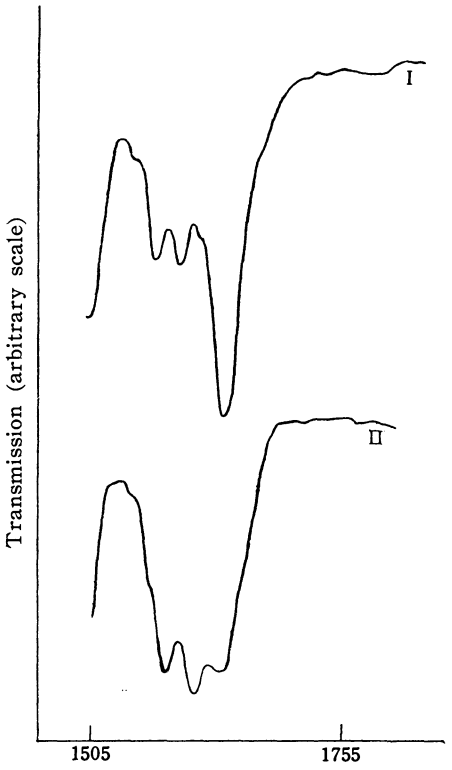

Fig. 4. Infrared absorption spectra of L-histidine (I) and its hydrochloride hydrate (II). (Rock salt, Hilger H800)

As a by-product, a small amount of monocarbobenzyloxy-L-histidine was isolated from the crude dicarbobenzyloxy derivative which was obtained by the reaction between L-histidine and the equivalent mole of carbobenzyloxychloride. It melted at 194~195°C with decomposition and gave a positive ninhydrin and a negative Pauly's reaction. These facts, together with the result of the infrared absorption analysis, were utilized to identify the compound as *N-Im*-carbobenzyloxyhistidine.

Infrared absorption spectra of dicarbobenzyloxy-L-histidine (DCH), α-carbobenzyloxy-L-histidine (α-MCH) and *Im*-carbobenzyloxy-L-histidine (*Im*-MCH) are shown in Fig. 3. Those of L-histidine and its hydrochloride hydrate are also shown in Fig. 4 for comparison. The band at 1759 cm^{-1} and that at 1733 cm^{-1} were assumed to correspond to the —CO—N= grouping which was formed by the combination of the imidazole nucleus with the carbobenzyloxy group.

These findings might be in good agreement with Otting's observation[14] that those characteristic absorption maxima of several acyl imidazoles appeared in the region of 1744~1748 cm^{-1}.

Synthesis of the Histidyl Peptide.— Several peptide derivatives of L-histidine, methyl ester of dicarbobenzyloxy-L-histidylglycine, -L-leucine, -L-threonine, -L-methionine, -*O*-benzyl-L-serine and -L-glutamic acid** were synthesized from dicarbobenzyloxy-L-histidine monohydrate and the respective amino acid ester with the aid of *N, N'*-dicyclohexylcarbodiimide[15]. Dicarbobenzyloxy-L-histidine was superior to the monocarbobenzyloxy compound as a starting material in respect to the higher solubility, the easier preparations and less possibility of undergoing some side reactions.

Dicarbobenzyloxy-L-histidyl glycine methyl ester was converted into the α-monocarbobenzyloxy dipeptide by alkaline hydrolysis in dimethylformamide[16]. L-Histidyl-L-leucine was prepared from the corresponding dipeptide ester by treatment with concentrated hydrochloric acid at 37°C[17]. The resulting product possessed properties identical with those reported by Holley and Sondheimer[10].

The synthesis of the L-histidyl-L-threonyl-L-valyl-L-glutamic acid derivative, the sequence of which was found in a heme-linked peptide obtained from cytochrome c[18], was explored by the following route. This involved the condensation of dicarbobenzyloxy-L-histidine and the tripeptide ester which was prepared from its carbobenzyloxy derivative by the action of hydrogen bromide in dioxane[19]. The coupling by the Sheehan's reagent proceeded smoothly as in the case of the dipeptide derivative, giving an yield of 50%.

N-Carbobenzyloxy-L-threonine was prepared using sodium carbonate in place of sodium bicarbonate[20] or sodium hydroxide, and was isolated as fine crystals, the yield of which was quite satisfactory. The tripeptide derivative, carbobenzyloxy-L-threonyl-L-valyl-L-glutamic acid dimethyl

14) W. Otting, *Ber.*, **89**, 1940 (1956).
15) J. C. Sheehan and G. P. Hess, *J. Am. Chem. Soc.*, **77**, 1067 (1955).
** The diethyl ester was exceptionally used for the peptide synthesis.
16) G. Weitzel, F. Schneider and A-M. Fretzdorff, *Z. physiol. Chem.*, **307**, 23 (1957).
17) R.B. Merrifield and D. W. Woolley, *J. Am. Chem. Soc.*, **78**, 4646 (1956).
18) H. Tuppy and S. Paleus, *Acta chim. Scand.*, **9**, 353 (1955).
19) K. Okawa, This Bulletin, **30**, 977 (1957).
20) G. Riley, J. H. Turnbull and W. Wilson, *J. Chem. Soc.*, **1957**, 1373.

ester, was derived from the above compound and L-valyl-L-glutamic acid ester in 78% yield by the carbodiimide method.

In a preliminary experiment, it was observed that both the two carbobenzyloxy groups in dicarbobenzyloxy-L-histidyl-L-threonine methyl ester were quantitatively removed by the action of hydrogen bromide in dioxane as in the case of dicarbobenzyloxy-L-histidine. Then the dipeptide ester produced was coupled with carbobenzyloxy-*S*-benzyl-L-cysteine by carbodiimide and the carbobenzyloxy tripeptide ester was produced (m. p. 114~115°C). Elementary analysis of the product was in good agreement with carbobenzyloxy-*S*-benzyl-L-cysteinyl-L-histidyl-L-threonine methyl ester ($C_{29}H_{35}O_7N_5S$). Furthermore, dicarbobenzyloxy-L-histidyl-L-threonine methyl ester was subjected to the reaction with 80% hydrazine hydrate and the hydrazide of the monocarbobenzyloxy dipeptide, containing one molecule of water, was obtained in a moderate yield (m. p. 186°C). This substance may also be utilized for the synthesis of the L-histidyl-L-threonyl peptide through the azide.

It could be concluded from the results of the present investigation that dicarbobenzyloxy histidine can be utilized for the synthesis of the histidyl peptides by the Sheehan's method though no general procedure for the hydrolysis of dicarbobenzyloxy peptide derivatives has been established.

At the end of this investigation, we had a chance to read the paper by Dr. E. Katchalski[21] on the carbobenzyloxy derivative of histidine, in which he reported the synthesis by a somewhat different method of dicarbobenzyloxy histidine and its chemical properties. It was found that the dicarbobenzyloxy histidine obtained by us showed coincidence with his product in all respects.

Experimental

N*-α, *N*-*Im*-Dicarbobenzyloxy-L-histidine.**— L-Histidine monohydrochloride monohydrate (10 g.) was dissolved in 48 ml. of 2 N sodium hydroxide solution and after addition of 2 N sodium carbonate solution (75 ml.), carbobenzyloxychloride (17.2 g.) was portion-wise dropped into the above solution under vigorous stirring and cooling for about half an hour. It was about five minutes until the white precipitates began to appear. Stirring was continued for 20 to 30 min. at room temperature and the solution was acidified to Congo red with 6 N hydrochloric acid under cooling. The gelatinous mass produced was separated from the supernatant by decantation. The product was first dissolved and then gradually crystallized out when it was triturated with ethanol. The white crystals were collected and washed with a small amount of ethanol. The yield was about 17g. (81%), m.p. 95~98°C (decomp.). Recrystallization from acetone-cold water gave white needles of dicarbobenzyloxy-L-histidine monohydrate (14g. 66%). m.p. 103~105°C (decomp.). $[\alpha]_D^{14}$ +34.01 (c. 28.99 mg. in 1 ml. of ethyl acetate).

Anal. Found: C, 59.86; H, 5.11; N, 9.46. Calcd. for $C_{22}H_{21}O_6N_3 \cdot H_2O$: C, 59.64; H, 5.25; N, 9.52%. Crystallization water: Found: 4.19; Calcd. 4.08%

When the dicarbobenzyloxy derivative was recrystallized from methanol, it was found that the compound, which melted at 105~107°C with decomposition, had one molecule of alcohol in place of water.

Anal. Found: C, 60.70; H, 5.50; N, 9.18. Calcd. for $C_{22}H_{21}O_6N_3 \cdot CH_3OH$: C, 60.65; H, 5.53; N, 9.23%.

The product is readily soluble in acetone, dioxane, tetrahydrofuran, chloroform and dimethylformamide, moderately soluble in warm methanol and ethanol, slightly soluble in benzene****, ethyl acetate and ether, and insoluble in petroleum ether and water. The negative Pauly's reaction was given at 0°C, but the solution turned to deep red color at room temperature as it elapsed. It was unstable to moisture and heat, and it decomposed to a material with some oily product, both when it was exposed to the atmosphere and when it was kept in the Abderhalden's apparatus (acetone in jacket) to dry the sample for analysis. This gelatinous substance washed with acetone and ethyl acetate gave hygroscopic powder, from which *N*-α-carbobenzyloxyhistidine was isolated in 70~80% yield by recrystallization from ethanol. Although little decomposition was encountered when it was kept over phosphorous pentoxide, it seemed preferable for the peptide synthesis to use freshly prepared crystals than the stored one. Both the carbobenzyloxy groups were quantitatively removed by the Ben-Ishai's procedure and the paper chromatography in the system of *n*-butanol-acetic acid-water (4 : 1 : 1 by volume) showed no spots except one corresponding to histidine.

The reaction of dicarbobenzyloxy-L-histidine with glycine methyl ester. — Dicarbobenzyloxy-L-histidine monohydrate (2.2 g.) and glycine methyl ester (prepared from its hydrochloride (1.3 g.) and ammonia-chloroform solution) were dissolved in 20 ml. of absolute dioxane and the mixture was kept at 50~60°C for 3 hours. The white precipitate produced was separated

21) A. Patchornik, A. Berger and E. Katchalski, *J. Am. Chem. Soc.* **79**, 6416 (1957).

*** Vigorous shaking of the vessel containing the mixture of histidine, alkali and acylchloride also gave the dicarbobenzyloxy derivative in the same yield.

**** Though, in a preliminary paper published in "Nature", it was reported that the dicarbobenzyloxy derivative of histidine was soluble in benzene, ethyl acetate and ether, further invesitigation on the solubility showed that the derivative in pure state had the least solubility in those solvents.

from the supernatant by decantation and was washed with ethyl acetate. The resulting white crystals were recrystallized from ethanol and identified to be *N*-α-carbobenzyloxy-L-histidine, which gave the positive Pauly's reaction. m. p. 165~166°C $[\alpha]_D^{25}$ −24.56 (c. 11.7 mg. in 1 ml. of 6 N hydrochloric acid).

Anal. Found: N, 14.50: Calcd. for $C_{14}H_{15}O_4N_3$: N, 14.50%.

On the paper chromatogram it showed an Rf. 0.64 in the system of *n*-butanol-acetic acid-water (4 : 1 : 5 by volume) and an Rf. 0.79 in that of the same solvents (4 : 1 : 1 by volume). Carbobenzyloxy glycine was obtained from the supernatant and washing by concentration and hydrolysis. When dicarbobenzyloxyhistidine was subjected to the reaction with twice equivalent mole of triethylamine under the same condition except the absence of any primary amine, it partly decomposed to give *N*-α-carbobenzyloxy-L-histidine.

***N-Im*-Carbobenzyloxy-L-histidine.**—From L-histidine monohydrochloride monohydrate (5.1 g. 0.025 M), 2 N sodium carbonate and an equivalent mole of carbobenzyloxychloride (5.1 g. 0.03 M), the crude material was obtained by the same procedure as the preparation of the dicarbobenzyloxy derivative. The crystals of this compound happened to separate from the solution when the crude carbobenzyloxy derivative, most of which was composed of the dicarbobenzyloxy derivatives, was recrystallized from the mixture of acetone-water (3 : 1 by volume). The yield was very poor. It was slightly soluble in water and in organic solvents. m. p. 193~194°C (decomp.).

Anal. Found: N, 14.44. Calcd. for $C_{14}H_{15}O_4N_3$: N, 14.53%.

Dicarbobenzyloxy-L-histidyl amino acid esters.—The same procedure as in the synthesis of dicarbobenzyloxy-L-histidyl-L-threonine methyl ester was applied to other histidyl peptide derivatives.

Dicarbobenzyloxy-L-histidyl-L-threonine methyl ester.—Freshly prepared dicarbobenzyloxy-L-histidine monohydrate (4.4 g.) was dissolved in 33 ml. of absolute chloroform and the solution was added to the chloroform solution containing L-threonine methyl ester (prepared from its hydrochloride (2.5 g.) and 1.5 N ammonia-chloroform solution (14 ml.) and *N*, *N'*-dicyclohexylcarbodiimide (2.1 g.). Dicyclohexylurea was precipitated after a few minutes with evolution of heat. The solution was cooled with water for several minutes and allowed to stand overnight at room temperature. About 1 ml. of glacial acetic acid was added and the precipitate produced was filtered off after an hour. The filtrate was washed with 0.2 N hydrochloric acid, 1% sodium bicarbonate and water successively, dried over anhydrous sodium sulfate and concentrated in vacuo to a paste-like mass. The residue was triturated with ether and the resulting crystals were collected. White needles of dicarbobenzyloxy-L-histidyl-L-threonine methyl ester (4.25 g.) were obtained in 78.8% yield. m. p. 140~144°C. After recrystallization from ethyl acetate-petroleum ether, the melting point was raised to 149~150°C. $[\alpha]_D^{14}$ +12.74 (c. 30.5 mg. in 1 ml. of glacial acetic acid).

Anal. Found: C, 59.61; H, 5.77; N, 10.21. Calcd. for $C_{27}H_{30}O_8N_4$: C, 60.21; H, 5.61; N. 10.40%.

Dicarbobenzyloxy-L-histidyl glycine methyl ester.—By the same procedure, fine crystals (3.4 g.) were obtained in 68% yield from dicarbobenzyloxy-L-histidine (4.4 g.) and glycine methyl ester. The dicarbobenzyloxy dipeptide ester was recrystallized from ethyl acetate. m. p. 68~70°C. $[\alpha]_D^{10}$ +10.47 (c. 19.4 mg. in 1 ml. of methanol).

Anal. Found: C, 59.75; H. 5.68; N, 10.23. Calcd. for $C_{25}H_{26}O_4N_7 \cdot CH_3OH$: C, 59.31; H, 5.74; N, 10.64%.

Dicarbobenzyloxy-L-histidyl-L-leucine methyl ester.—L-Leucine methyl ester, prepared from its hydrochloride (2.4 g.), was coupled with dicarbobenzyloxy-L-histidine monohydrate (2.8 g.) by carbodiimide. Dicarbobenzyloxy-L-histidyl-L-leucine methyl ester (2.4 g.) was obtained as a white precipitate in 68% yield. Recrystallization from ethyl acetate-petroleum ether gave fine crystals. m. p. 101~103°C. $[\alpha]_D^{14}$ +21.44° (c. 29.0 mg. in 1 ml. of ethyl acetate).

Anal. Found: C, 63.14; H, 6.31; N, 10.44. Calcd. for $C_{29}H_{34}O_7N_4$: C, 63.26; H, 6.22; N, 10.18%.

Dicarbobenzyloxy-L-histidyl-L-glutamic acid diethyl ester.—From dicarbobenzyloxy-L-histidine monohydrate (1.4 g.) and L-glutamic acid diethyl ester was prepared dicarbobenzyloxy-L-histidyl-L-glutamic acid diethyl ester (1.25 g. 70%), melting at 78~80°C. $[\alpha]_D^{14}$ +0.21 (c. 28.5 mg. in 1 ml. of ethyl acetate).

Anal. Found: C, 60.42; H, 5.92; N, 9.06; Calcd. for $C_{31}H_{36}O_9N_4$: C, 61.17; H, 5.96; N, 9.19%.

Dicarbobenzyloxy-L-histidyl-*O*-benzyl-L-serine methyl ester. — The coupling reaction between dicarbobenzyloxy-L-histidine monohydrate (1.4 g.) and *O*-benzyl-L-serine methyl ester by the carbodiimide procedure gave 1.5 g. of dicarbobenzyloxy-L-histidyl-*O*-benzyl-L-serine methyl ester: yield 81%. m. p. 113~115°C. $[\alpha]_D^{14}$ +19.80 (c. 29.6 mg. in 1 ml. of ethyl acetate).

Anal. Found: C, 64.75; H, 5.57; N, 9.54. Calcd. for $C_{33}H_{34}O_8N_4$: C, 64.48; H, 5.58; N, 9.12%.

Dicarbobenzyloxy-L-histidyl-L-methionine methyl ester.—White crystals (1.5 g.) of dicarbobenzyloxy-L-histidyl-L-methionine methyl ester were prepared from dicarbobenzyloxy-L-histidine monohydrate (1.3 g.) and L-methionine methyl ester. The dipeptide derivative (m. p. 110~113°C) was recrystallized from chloroform-petroleum ether. $[\alpha]_D^{22}$ +9.07 (c. 28.0 mg. in 1 ml. of glacial acetic acid).

Anal. Found: C, 59.10; H, 5.55: N, 9.72. Calcd. for $C_{28}H_{32}O_7N_4S$: C, 59.14; H, 5.67; N, 9.85%.

Carbobenzyloxy-L-histidyl glycine. — The dimethylformamide solution (2 ml.) containing the dicarbobenzyloxy dipeptide ester (2 g.) was adjusted to pH 9.0~9.2 with 2 N sodium hydroxide solution under cooling. The solution was kept for 30 min. at room temperature and then acidified to pH 5.0 with 1 N hydrochloric acid. By concentration and addition of acetone a swollen

material (1 g.) was obtained. m. p. 140~145°C Recrystallization from methyl alcohol gave the carbobenzyloxy dipeptide (0.5 g.) melting at 237~238°C.

Anal. Found: C, 54.40; H, 5.47; N, 15.79. Calcd. for $C_{16}H_{18}O_6N_4$: C, 55.48; H, 5.24; N, 16.17%.

Carbobenzyloxy-L-threonyl-L-valyl-L-glutamic acid dimethyl ester.—Carbobenzyloxy-L-threonine (2.5 g.) was dissolved in 5 ml. of chloroform and the solution was added to the chloroform solution containing *N, N'*-dicyclohexylcarbodiimide (2.1 g.) and L-valyl-L-glutamic acid dimethyl ester (prepared from its hydrobromide (4.3 g.) and triethylamine). As the reaction proceeded with evolution of heat, the resulting dicyclohexylurea was precipitated. After 3 hours the precipitate was filtered off, a few drops of glacial acetic acid was added to the filtrate and the solution was kept overnight at 5°C. The filtrate liberated from dicyclohexylurea (0.3 g.) was washed with 0.2 N hydrochloric acid, 0.25 N sodium carbonate and water successively, and dried. By concentration and dilution with petroleum ether, white crystals (3.9 g.) were obtained. From the filtrate an additional 0.1 g. of the product was obtained. The two crops were combined and recrystallized from ethyl acetate-petroleum ether. The yield was 3.6 g. (72%). m. p. 172~174°C. (sintered at 145~150°C). It gave the positive biuret reaction. $[\alpha]_D^{10}$ −56.5 (c. 23 mg. in 1 ml. of methanol).

Anal. Found: C, 56.70; H, 7.33; N, 8.47. Calcd. for $C_{24}H_{35}O_9N_3$: C, 56.57; H, 6.92; N, 8.25%.

Dicarbobenzyloxy-L-histidyl-L-threonyl-L-valyl-L-glutamic acid dimethyl ester. — Into the dimethylformamide solution containing L-threonyl-L-valyl-L-glutamic acid dimethyl ester (1.4 g.) and *N, N'*-dicyclohexylcarbodiimide (0.7 g.) was added the dimethylformamide solution (3 ml.) of dicarbobenzyloxy-L-histidine monohydrate (1.4 g.) under stirring. The resulting dicyclohexylurea appeared within 5 minutes and was filtered off after 30 minutes. The filtrate was allowed to stand overnight at 5°C. A small amount of dicyclohexylurea precipitated was filtered and the solvent of the filtrate was replaced by chloroform (20 ml.). Then it was washed with 0.2 N hydrochloric acid and water, successively, and dried over anhydrous sodium sulfate. The fluffy precipitate appeared when twice the volume of petroleum ether was added to the above solution. Additional material was obtained from the mother liquor by dilution with petroleum ether for the total of 1.2 g. (50%) of white powders. m. p. 95~98°C. $[\alpha]_D^{10}$ +20.1 (c. 16.4 mg. in 1 ml. of chloroform).

Anal. Found: C, 57.53; H, 6.71; N, 10.65. Calcd. for $C_{38}H_{48}N_6O_{12}\cdot H_2O$: C, 57.13; H, 6.31; N, 10.72%.

The dicarbobenzyloxy tetrapeptide ester was positive to the biuret reaction and its acid hydrolysate gave all the constitutional amino acids on the paper chromatogram.

Carbobenzyloxy-L-valyl-L-glutamic acid dimethyl ester.—From the syrupy carbobenzyloxy-L-valine (15 g.), glutamic acid dimethyl ester (prepared from its hydrochloride (17 g.)) and *N, N'*-dicyclohexylcarbodiimide (12 g.) was obtained the carbobenzyloxy dipeptide ester in 80% yield using dioxane as a reaction solvent. m. p. 117~120°C (sintered at 102~103°C). A sample for the analysis was twice recrystallized from ethyl acetate-petroleum ether. m. p. 122~123°C (sintered at 115~116°C). $[\alpha]_D^{10}$ −130.7 (c. 16 mg. in 1 ml. of methanol).

Anal. Found: C, 59.24; H, 7.08; N, 6.76. Calcd. for $C_{20}H_{28}O_7N_2$: C, 59.10; H, 6.94; N, 6.89%.

L-Threonyl-L-valyl-L-glutamic acid dimethyl ester and L-valyl-L-glutamic acid dimethyl ester were quantitatively obtained by decarbobenzyloxylation with hydrogen bromide in dioxane from the respective carbobenzyloxy derivative.

***N*-Carbobenzyloxy-L-threonine.**—To the cold solution of 2 N sodium hydroxide (25 ml.) containing L-threonine (6 g.) was added 2 N sodium carbonate (38 ml.) and carbobenzyloxychloride (8.5 g.). The mixture was shaken vigorously for 15 minutes at room temperature. Excess of carbobenzyloxychloride precipitated was removed into ether and the aqueous layer was acidified to Congo red with 6 N hydrochloric acid. Then the oily product precipitated was extracted into ethyl acetate (30 ml. three times) and the united extracts were dried over anhydrous sodium sulfate. Concentration, followed by addition of petroleum ether, afforded silky crystals (12 g. 95%). m. p. 95~98°C. Recrystallization from ethyl acetate-petroleum ether gave white needles. m. p. 103~105°C. $[\alpha]_D^{25}$ −2.4 (c. 11.7 mg. in 1 ml. of ethanol).

Anal. Found: C, 57.50; H, 6.25; N, 5.67. Calcd. for $C_{12}H_{15}O_5N$: C, 56.91; H, 5.97; N, 5.53%.

L-Histidyl-L-leucine. — Dicarbobenzyloxy-L-histidyl-L-leucine methyl ester (2.4 g.) was suspended in 20 ml. of concentrated hydrochloric acid and was kept at 37°C for 50 minutes. The opaque solution was spread on a glass plate and evaporated to dryness over concentrated sulfuric acid under reduced pressure. The residue was dissolved in a small amount of 99% ethanol and triethyl amine was added after the removal of insoluble substance. A fluffy material precipitated was collected. Yield 0.5 g. (42%). The dipeptide was recrystallized from 33% ethanol. m. p. 212~214°C (decomp.) $[\alpha]_D^{14}$ −43.5 (c. 10 mg. in 1 ml. of 0.1 N sodium hydroxide) (lit.[9] $[\alpha]_D^{22}$ −43.5 (c. 1.0, 0.1 N sodium hydroxide)).

Anal. Found: N, 20.54. Calcd. for $C_{12}H_{20}O_3N_4$: N, 20.88%.

Summary

N-α,*N*-*Im*-Dicarbobenzyloxyhistidine was prepared in good yield using sodium carbonate, and some histidyl peptide derivatives were synthesized by Sheehan's method using the compound as a starting material.

Grateful acknowledgement is due to Ajinomoto Company for supplying materials of amino acids.

Department of Chemistry
Faculty of Science, and
Institute for Protein Research
Osaka Universiy
Kita-ku, Osaka

*The Molecular and Crystal Structure of Allokainic Acid**

By Hideo WATASE

(Received June 4, 1958)

As parts of our studies[1] on the structures of kainic acid and its isomer, we reported in the previous papers the X-ray investigations on zinc kainate[2] and kainic acid[3], which determined the three-dimensional structure of kainic acid $C_{10}H_{15}O_4N$, the most active component of *Digenea simplex* Agardh. *Digenea simplex* Agardh contains also an isomer of kainic acid, allokainic acid[4], in a very small proportion. Allokainic acid $C_{10}H_{15}O_4N$ is an acidic and optically active** compound of m. p. 237°(decomp.), and is said to have a very weak anthelmintic effect if any. It is of interest to elucidate the relationship between the structures of the two isomers of which the physiological nature (anthelmintic effect) of one is very different from that of the other.

According to the reports[5] based on organic chemistry, the chemical behavior of one of the two isomers is similar to that of the other, and the structural formula of allokainic acid is concluded to be the same as that of kainic acid, 2-carboxy-3-carboxymethyl-4-isopropenylpyrrolidine.

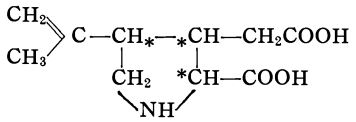

To confirm this conclusion and to determine moreover the stereochemical configuration of the molecule, the structure of allokainic acid has been investigated by means of X-ray crystal analysis. The electron-density projections along the two principal crystal axes were derived by the trial method, and the three-dimensional structure of the molecule was determined quantitatively.

In this paper is described the structure determination of allokainic acid in detail.

Experimental

Allokainic acid crystallizes with no molecules of water from its aqueous solution. Crystalline allokainic acid is of a colorless prism elongated along a principal crystal axis chosen as the *b* axis, having a plane of cleavage perpendicular to another principal axis (*a* axis).

Oscillation and Weissenberg photographs were taken about two principal crystal axes (*b* and *c* axes), using filtered Cu K_α radiation. The specimens used had the following cross-sections at right angles to the axis of rotation; 0.15×0.2 mm. for the *b* axis rotation and 0.2×0.4 mm. for the *c* axis***.

The intensity data of (*h* 0 *l*) and (*h k* 0) used in the two-dimensional analyses were prepared from the integrated Weissenberg photographs. By comparing them with a calibrated scale, the intensities of the reflections were estimated visually, multiple-film technique being used for accurate measurements of strong reflections. The corrections for polarization and Lorentz factors were made in the usual way, and the effects of absorption were neglected, the linear absorption coefficient for Cu K_α radiation being $\mu = 10.1/\text{cm}$****.

Relative structure factors were then deduced from these intensity data by the ordinary process.

* Part of this paper was presented at the autumnal joint meeting of chemical societies of Japan, Tokyo, 1956.

1) I. Nitta, H. Watase and Y. Tomiie, *Nature*, **181**, 761 (1958).

2) H. Watase and I. Nitta, This Bulletin, **30**, 889 (1957).

3) H. Watase, Y. Tomiie and I. Nitta, This Bulletin, **31**, 714 (1958).

** $[\alpha]_D^{10}: +8.0°$ (H_2O).

4) S. Murakami, T. Takemoto, Z. Tei, K. Daigo and S. Takagi, *J. Pharm. Soc. Japan* (*Yakugaku Zasshi*), **75**, 766 (1955).

5) H. Morimoto, ibid., **75**, 937 (1955); S. Murakami, K. Daigo, S. Takagi, T. Takemoto and Z. Tei, ibid., **75**, 1252 (1955).

*** The specimen used for the *c* axis rotation was prepared by cutting the crystal at right angle to the elongated *b* axis.

**** This value comes from the unit cell containing four molecules (see next section).

Results and Discussion

Unit Cell and Space Group.—From the X-ray examinations, the crystal is found to belong to the orthorhombic system, and the dimensions of the unit cell are as follows;

$$a = 26.08 \pm 0.07 \text{ Å}$$
$$b = 5.83 \pm 0.02 \text{ Å}$$
$$c = 6.95 \pm 0.03 \text{ Å}$$

Systematic absence of reflections being recognized only in (h 0 0), (0 k 0) and (0 0 l) when h, k and l are odd respectively, the space group is uniquely determined to be D_2^4-$P2_12_12_1$. The unit cell with this crystal symmetry has four-fold general positions[6]. Judging from the cell size, in the present case, four formula units of $C_{10}H_{15}O_4N$ are expected to be contained in the unit cell, an asymmetric unit being unimolecular.

The axial periods of the b and c axes seemed to be short enough to permit a good resolution of many of the atoms, while the a axis is very long, and the projections along the b and c axes were tried to obtain the atomic parameters.

Determination of the Structure. — As already given, the space group involved is D_2^4-$P2_12_12_1$, and each two-dimensional projection was treated separately with the origin lying on the two-fold screw axis so that the origin is a center of symmetry in the projection, as in the analysis of zinc kainate dihydrate[2] with the same space group. However, the atomic parameters (Table I), the final electron-density projections (Figs. 2 and 3) and the projections of the crystal structure (Figs. 6 and 7) are described returning to the customary space group origin.

The structure-factor maps (see Fig. 1 given below) for all the possible reflections of (h 0 l) and (h k 0) were prepared in order to locate all the atoms by the trial method in the projections along the b and c axes. By assuming the structure of allokainic acid to be 2-carboxy-3-carboxymethyl-4-isopropenylpyrrolidine, the b axis projection was investigated in the first place.

The sign of (6 0 1) with a large F value was defined to be negative. Considering

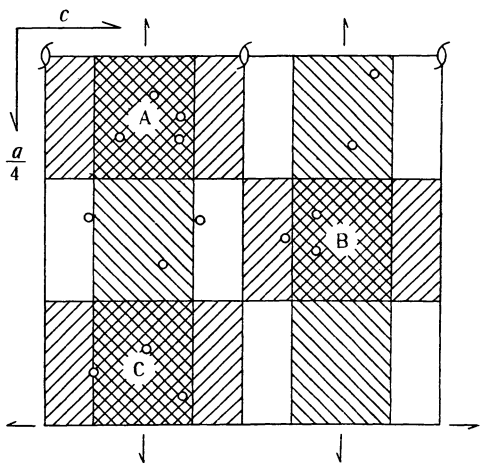

Fig. 1. Superposed structure-factor maps for (6 0 1) with negative sign and (0 0 2) with negative sign, the positive areas being shaded. The F values of these reflections being large, the regions **A**, **B** and **C** are strongly positive. Circles show the final atomic positions. Origin is on the projection of a two-fold screw.

the various structures compatible with the structure factors for the lower order reflections, the absolute values of the structure factors were roughly known, and the sign of (0 0 2) with the largest F value was determined to be negative. Fig. 1 shows the structure-factor map by superposing those for (6 0 1) and (0 0 2), in which the positive areas are shaded. The regions around **A**, **B** and **C** of Fig. 1 being strongly positive, it seems probable that most of the atoms will be found in these regions, and it might be considered at this stage that each of the three side-chains of allokainic acid has its location in each of these regions; the carboxyl group in the region **A** or **C**, the carboxyl group of the carboxymethyl group in the region **B** and the isopropenyl group in the region **A** or **C**.

There was an ambiguous point about the probable positions of the carboxyl and the isopropenyl group. Since packing consideration of the isopropenyl group was found helpful for the further analysis, the trial was carried out, using the structure-factor maps only for the reflections with h even because the $|F|$ values of these reflections are estimated independently of the above ambiguity. All the atoms were then roughly located, leaving the ambiguity about the choice of the origin of the projection out of the

6) "Internationale Tabellen zur Bestimmung von Kristallstrukturen", Bornträger, Berlin (1935); "International Tables for X-ray Crystallography", Kynoch Press, Birmingham (1952).

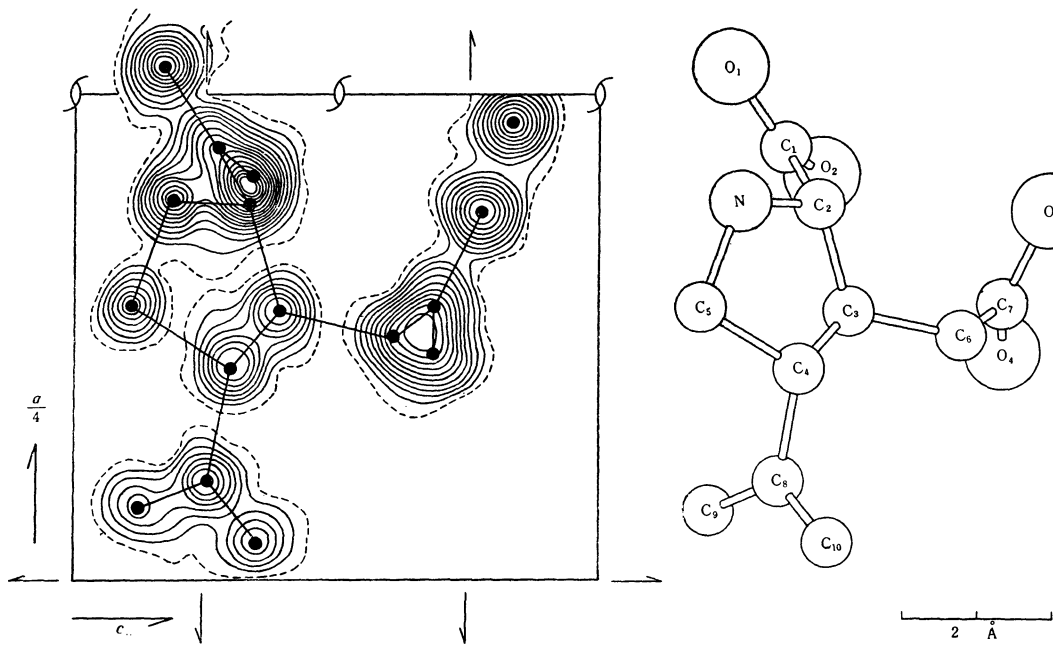

Fig. 2. Electron-density projection along the *b* axis. Contour lines at unit electron intervals, the lowest line, broken line, being 2 electron per Å^2. Black circles show the atomic positions. The interpretation of the density map is given on the right side.

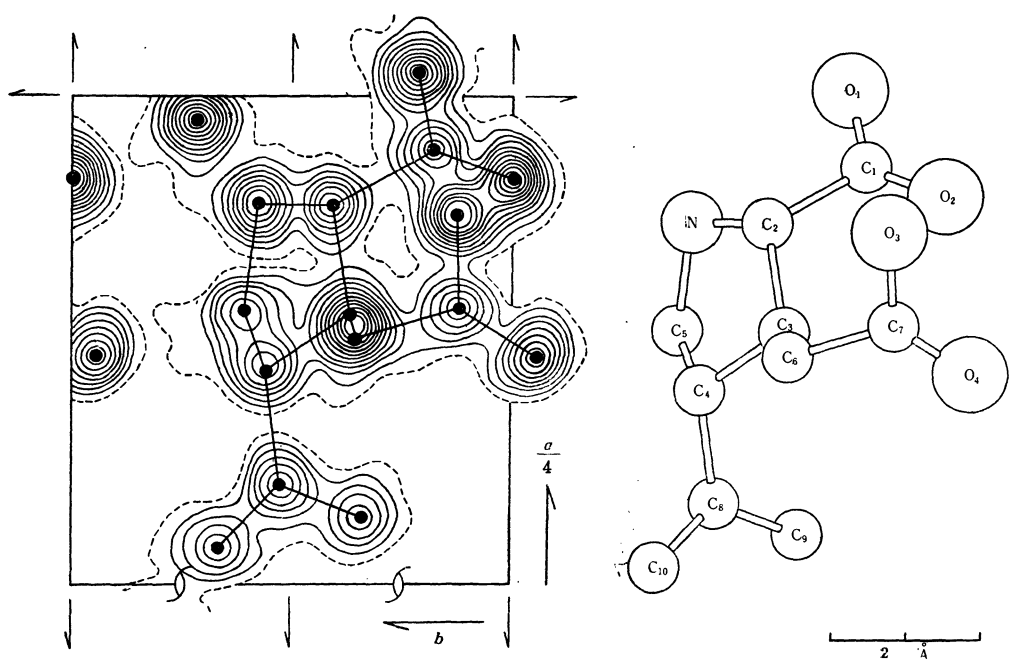

Fig. 3. Electron-density projection along the *c* axis. Contours and symbols are the same as those of Fig. 2. The interpretation of the density map is given on the right side.

question, and in order to be compatible with the F values of (5 0 2) and (7 0 2) it was determined that the carboxyl group is in the region **A** and the isopropenyl group in the region **C**. In this trial (12 0 0) could be used powerfully. The observed structure factors were reduced from the relative values nearly to those in the absolute scale.

Determining the signs of the structure factors, the quantitative trial was carried on step by step from the lower to the higher orders so as to obtain a good agreement between the calculated and the observed F values, until all the atoms were located satisfactorily to permit the Fourier refinements. In this way the electron-density projection along the b axis was derived.

On the basis of the x parameters obtained from the b axis projection, the electron-density projection along the c axis was derived in the same way. Figs. 2 and 3 show the final electron-density projections along the b and c axes respectively. In these maps, each peak has a reasonable height, the peaks of oxygen or nitrogen being higher than those of carbon. The final atomic parameters referred to the customary space group origin are listed in Table I.

TABLE I
ATOMIC PARAMETERS

Atom	x/a	y/b	z/c
C_1	0.222_9	0.183	0.273
C_2	0.194_2	0.402	0.339
C_3	0.138_8	0.363	0.393
C_4	0.109_2	0.558	0.298
C_5	0.140_8	0.608	0.115
C_6	0.126_6	0.353	0.607
C_7	0.142_2	0.117	0.683
C_8	0.051_7	0.525	0.260
C_9	0.035_8	0.337	0.123
C_{10}	0.020_0	0.663	0.350
N	0.195_1	0.578	0.184
O_1	0.237_1	0.718	0.828
O_2	0.208_3	0.998	0.340
O_3	0.190_0	0.127	0.773
O_4	0.117_5	0.942	0.683

At this stage, the discrepancy indices ($R=\sum||F_o|-|F_c||/\sum|F_o|$) are 0.178 for ($h$ 0 l) and 0.192 for (h k 0), employing the data up to sin $\theta/\lambda=0.640$ for (h 0 l) and 0.642 for (h k 0), assuming the values of the unobserved structure factors to be precisely zero and neglecting the contributions from hydrogen atoms. In the structure-factor calculations, the value of $B=4.0$ Å^2 was used for each zone as the temperature factor common to all the atoms. The atomic scattering factors were taken from McWeeny's paper[7]; for oxygen $\bar{f}_o=1/3(f^{\parallel}+2f^{\perp})$ and for carbon the values for 'valence states'.

The observed and the calculated structure factors for (h 0 l) and (h k 0) are listed in Tables II and III respectively, in which the signs of the calculated structure factors are given as those for the coordinates used in the analysis for each projection.

Molecular Structure.—The bond lengths and bond angles, calculated from the atomic parameters of Table I, are shown in Fig. 4. It may be said that the bond lengths will be correct to ±0.03 Å and the bond angles to ±3°. As a result, it is confirmed that allokainic acid is a stereoisomer of kainic acid, its structure being 2-carboxy-3-carboxymethyl-4-isopropenylpyrrolidine. Namely, the five-membered ring (N, C_2, C_3, C_4, C_5) is of pyrrolidine, and the side-chains C_2–(C_1–O_1, O_2), C_3–(C_6–C_7–O_3, O_4) and C_4–(C_8–C_9, C_{10}) are the carboxyl, the carboxymethyl and the isopropenyl group respectively. In the isopropenyl group, the C_8–C_{10} bond of the length 1.31 Å is its double bond.

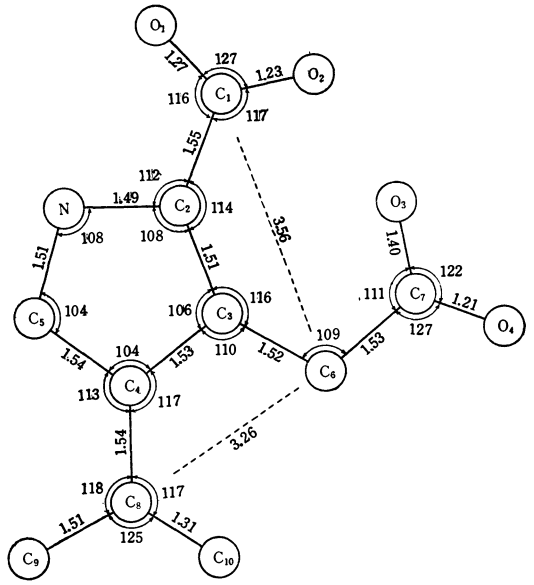

Fig. 4. Bond lengths (Å) and bond angles (°).

The observed bond lengths except for the C_7···O_3 distance are in agreement within ±0.03 Å with those of the corresponding

7) R. McWeeny, *Acta Cryst.*, **4**, 513 (1951).

TABLE II

OBSERVED AND CALCULATED STRUCTURE FACTORS $F(h\ 0\ l)$
THE VALUES FOR $(h\ 0\ 0)$ ARE LISTED IN TABLE III

$h\ k\ l$	$1/4F_o$	$1/4F_c$	$h\ k\ l$	$1/4F_o$	$1/4F_c$	$h\ k\ l$	$1/4F_o$	$1/4F_c$	$h\ k\ l$	$1/4F_o$	$1/4F_c$
1 0 1	6.6	− 8.1	21 0 2	—	0.6	11 0 4	—	− 0.2	8 0 6	0.7	0.7
2 0 1	10.2	− 7.7	22 0 2	—	−0.4	12 0 4	1.6	2.6	9 0 6	—	0.0
3 0 1	7.6	7.0	23 0 2	2.0	2.0	13 0 4	—	− 0.6	10 0 6	2.2	−2.4
4 0 1	0.7	0.5	24 0 2	3.1	1.9	14 0 4	1.8	2.0	11 0 6	—	0.8
5 0 1	8.6	9.4	25 0 2	0.7	−1.0	15 0 4	1.4	− 2.0	12 0 6	—	−0.2
6 0 1	21.4	−21.7	26 0 2	2.2	1.8	16 0 4	0.7	0.8	13 0 6	0.7	−0.6
7 0 1	4.4	− 4.3	27 0 2	1.4	1.4	17 0 4	2.0	− 0.6	14 0 6	1.0	0.5
8 0 1	0.8	0.0	28 0 2	1.0	1.0	18 0 4	4.6	− 3.9	15 0 6	1.2	1.3
9 0 1	—	− 0.3	29 0 2	—	0.1	19 0 4	—	− 0.2	16 0 6	—	0.0
10 0 1	4.4	− 2.8	30 0 2	0.7	−0.7	20 0 4	0.7	0.7	17 0 6	1.6	0.9
11 0 1	7.9	7.5	31 0 2	1.1	0.8	21 0 4	—	− 0.2	18 0 6	1.4	0.8
12 0 1	1.5	1.7	32 0 2	0.7	0.3	22 0 4	—	− 0.5	19 0 6	—	0.1
13 0 1	3.2	4.2	1 0 3	6.4	5.6	23 0 4	0.7	− 0.6	20 0 6	1.0	0.4
14 0 1	3.6	1.6	2 0 3	4.4	−3.9	24 0 4	1.0	− 0.8	21 0 6	—	0.2
15 0 1	1.3	1.0	3 0 3	10.5	−8.8	25 0 4	—	0.1	22 0 6	1.6	1.7
16 0 1	4.3	5.0	4 0 3	5.3	−5.0	26 0 4	1.4	− 0.8	23 0 6	0.8	−0.4
17 0 1	0.8	− 1.4	5 0 3	8.7	−6.9	27 0 4	0.6	− 0.6	24 0 6	—	−0.1
18 0 1	6.5	7.2	6 0 3	2.2	1.0	28 0 4	0.6	− 0.5	1 0 7	0.7	−0.4
19 0 1	1.7	2.3	7 0 3	4.1	3.3	29 0 4	—	0.0	2 0 7	1.0	1.0
20 0 1	2.3	2.6	8 0 3	6.4	5.5	1 0 5	0.9	− 0.2	3 0 7	1.0	−1.2
21 0 1	0.7	− 1.1	9 0 3	1.3	0.9	2 0 5	1.3	1.2	4 0 7	1.4	−1.6
22 0 1	—	− 0.3	10 0 3	—	0.2	3 0 5	2.6	4.0	5 0 7	0.7	0.6
23 0 1	0.7	− 0.5	11 0 3	7.8	−8.5	4 0 5	3.6	3.6	6 0 7	1.7	−1.6
24 0 1	1.4	1.7	12 0 3	0.8	1.5	5 0 5	—	0.2	7 0 7	1.9	2.0
25 0 1	1.0	− 1.1	13 0 3	5.3	−4.2	6 0 5	2.4	4.3	8 0 7	1.9	−1.7
26 0 1	0.8	0.9	14 0 3	—	−0.1	7 0 5	1.5	− 1.4	9 0 7	1.8	1.8
27 0 1	—	− 0.2	15 0 3	2.0	−2.0	8 0 5	1.2	− 0.9	10 0 7	1.9	1.9
28 0 1	0.7	− 0.6	16 0 3	4.1	4.0	9 0 5	1.2	− 1.9	11 0 7	1.0	1.0
29 0 1	—	− 0.1	17 0 3	—	−0.7	10 0 5	1.5	− 1.2	12 0 7	5.6	3.2
30 0 1	—	− 0.2	18 0 3	—	0.0	11 0 5	0.7	1.4	13 0 7	—	−0.2
31 0 1	0.7	− 0.5	19 0 3	1.7	−2.8	12 0 5	5.1	− 4.8	14 0 7	1.8	1.1
32 0 1	1.3	0.7	20 0 3	3.3	−3.3	13 0 5	0.7	0.8	15 0 7	—	0.4
33 0 1	—	0.4	21 0 3	1.7	1.7	14 0 5	1.7	− 1.5	16 0 7	0.6	0.8
0 0 2	37.1	−34.8	22 0 3	1.0	−0.9	15 0 5	0.7	0.9	17 0 7	1.7	−1.5
1 0 2	2.6	− 3.0	23 0 3	0.7	0.9	16 0 5	4.2	− 4.0	18 0 7	—	0.0
2 0 2	13.4	−12.3	24 0 3	0.7	−0.6	17 0 5	3.1	2.9	19 0 7	0.7	−0.4
3 0 2	1.1	− 0.2	25 0 3	1.0	0.9	18 0 5	1.0	− 1.2	20 0 7	0.9	0.9
4 0 2	2.6	− 3.7	26 0 3	1.6	1.3	19 0 5	—	0.7	0 0 8	—	−0.1
5 0 2	14.4	14.4	27 0 3	1.0	0.8	20 0 5	—	0.4	1 0 8	—	0.1
6 0 2	—	− 1.4	28 0 3	—	−0.5	21 0 5	1.6	− 0.5	2 0 8	1.0	−1.3
7 0 2	12.4	12.6	29 0 3	0.9	0.8	22 0 5	—	0.2	3 0 8	—	−0.3
8 0 2	4.6	4.4	30 0 3	1.2	−1.0	23 0 5	—	− 0.3	4 0 8	—	0.4
9 0 2	5.7	5.2	31 0 3	0.7	0.6	24 0 5	1.1	0.8	5 0 8	0.8	0.9
10 0 2	7.7	6.9	0 0 4	6.7	−6.7	25 0 5	0.6	0.4	6 0 8	—	−0.5
11 0 2	2.2	− 3.1	1 0 4	1.2	−1.3	26 0 5	0.5	− 0.3	7 0 8	—	0.0
12 0 2	6.5	6.9	2 0 4	—	0.5	27 0 5	0.7	− 0.7	8 0 8	—	−0.3
13 0 2	2.6	4.2	3 0 4	1.1	−0.2	0 0 6	2.4	3.0	9 0 8	—	0.4
14 0 2	2.5	− 2.7	4 0 4	2.0	1.7	1 0 6	0.7	1.1	10 0 8	1.8	1.2
15 0 2	2.3	1.7	5 0 4	4.3	−6.2	2 0 6	2.2	2.2	11 0 8	—	0.1
16 0 2	2.7	− 3.2	6 0 4	2.7	2.6	3 0 6	—	0.0	12 0 8	0.7	−0.4
17 0 2	0.9	− 0.1	7 0 4	5.7	−6.0	4 0 6	1.6	1.5	13 0 8	—	0.0
18 0 2	—	0.5	8 0 4	6.5	−5.8	5 0 6	—	− 0.1	14 0 8	0.9	−0.3
19 0 2	0.7	− 0.7	9 0 4	3.4	−2.9	6 0 6	—	0.2			
20 0 2	1.9	− 1.6	10 0 4	2.0	−2.0	7 0 6	1.4	0.9			

TABLE III

OBSERVED AND CALCULATED STRUCTURE FACTORS $F(h\ k\ 0)$

$h\ k\ l$	$1/4F_o$	$1/4F_c$	$h\ k\ l$	$1/4F_o$	$1/4F_c$	$h\ k\ l$	$1/4F_o$	$1/4F_c$	$h\ k\ l$	$1/4F_o$	$1/4F_c$
0 0 0		114	0 2 0	7.3	−8.5	18 3 0	0.4	− 0.8	9 5 0	1.7	1.7
2 0 0	20.1	−21.0	1 2 0	9.2	−9.8	19 3 0	3.2	− 3.1	10 5 0	0.6	0.3
4 0 0	5.5	− 5.7	2 2 0	1.3	0.1	20 3 0	—	0.1	11 5 0	2.0	−2.2
6 0 0	7.6	7.1	3 2 0	7.8	8.6	21 3 0	2.4	2.3	12 5 0	0.9	0.3
8 0 0	8.4	6.9	4 2 0	9.7	10.4	22 3 0	1.2	1.7	13 5 0	2.2	−2.4
10 0 0	5.2	5.4	5 2 0	1.1	−2.3	23 3 0	—	− 0.1	14 5 0	1.2	−1.1
12 0 0	22.2	−21.3	6 2 0	2.4	−2.3	24 3 0	1.1	1.1	15 5 0	0.6	0.5
14 0 0	0.3	− 0.3	7 2 0	3.5	−5.3	25 3 0	0.3	0.1	16 5 0	2.2	2.1
16 0 0	6.3	5.7	8 2 0	8.3	6.6	26 3 0	1.3	− 1.1	17 5 0	0.9	1.3
18 0 0	5.8	− 5.6	9 2 0	3.5	3.6	27 3 0	0.5	− 0.5	18 5 0	1.1	−1.2
20 0 0	1.5	1.7	10 2 0	8.7	−8.3	28 3 0	2.1	1.6	19 5 0	0.7	−0.4
22 0 0	1.3	0.4	11 2 0	0.8	0.9	29 3 0	0.6	0.4	20 5 0	0.6	0.7
24 0 0	3.3	− 2.5	12 2 0	7.4	8.0	30 3 0	1.1	− 0.8	21 5 0	1.1	0.9
26 0 0	1.5	1.6	13 2 0	2.0	−1.8	0 4 0	4.3	− 5.5	22 5 0	0.3	−0.3
28 0 0	1.2	− 0.7	14 2 0	0.5	−1.0	1 4 0	0.7	− 1.3	23 5 0	0.5	−0.1
30 0 0	—	0.0	15 2 0	1.1	−2.8	2 4 0	—	− 0.2	24 5 0	—	0.1
32 0 0	1.6	− 1.0	16 2 0	1·8	−2.3	3 4 0	4.0	3.9	0 6 0	0.4	−0.7
1 1 0	3.6	− 4.1	17 2 0	0.6	−1.4	4 4 0	5.7	5.0	1 6 0	1.0	−0.6
2 1 0	10.6	− 8.2	18 2 0	1.1	−1.6	5 4 0	2.3	− 2.0	2 6 0	0.5	−1.2
3 1 0	9.5	10.4	19 2 0	0.4	1.4	6 4 0	7.3	− 6.2	3 6 0	0.6	0.4
4 1 0	9.5	−10.1	20 2 0	3.8	−3.3	7 4 0	2.3	2.6	4 6 0	1.2	−1.8
5 1 0	1.8	− 3.9	21 2 0	1.7	−1.9	8 4 0	0.4	− 0.8	5 6 0	1.8	−1.7
6 1 0	0.2	− 1.3	22 2 0	2.3	2.1	9 4 0	0.6	− 0.5	6 6 0	0.5	0.0
7 1 0	0.5	− 0.6	23 2 0	3.8	−3.7	10 4 0	0.4	0.2	7 6 0	0.8	0.8
8 1 0	9.3	−10.3	24 2 0	0.5	−0.9	11 4 0	0.4	− 0.2	8 6 0	0.5	0.0
9 1 0	5.4	5.1	25 2 0	2.2	1.7	12 4 0	0.7	1.5	9 6 0	0.6	−0.3
10 1 0	1.4	− 0.2	26 2 0	0.3	0.2	13 4 0	1.0	− 1.5	10 6 0	0.8	0.8
11 1 0	1.8	1.8	27 2 0	0.4	0.4	14 4 0	0.6	− 0.7	11 6 0	0.3	0.3
12 1 0	0.6	− 0.4	28 2 0	0.4	−0.2	15 4 0	0.8	− 0.9	12 6 0	0.7	0.9
13 1 0	2.5	4.1	29 2 0	0.9	−0.4	16 4 0	2.0	− 1.6	13 6 0	0.3	0.1
14 1 0	1.9	0.6	30 2 0	0.9	0.8	17 4 0	0.5	− 0.1	14 6 0	1.4	−0.7
15 1 0	4.9	− 4.7	31 2 0	—	0.0	18 4 0	5.1	4.2	15 6 0	0.3	0.5
16 1 0	—	0.4	32 2 0	0.4	0.5	19 4 0	1.9	− 2.5	16 6 0	1.8	1.2
17 1 0	2.5	3.3	1 3 0	2.2	−2.9	20 4 0	0.4	0.4	17 6 0	0.4	0.7
18 1 0	0.4	− 0.4	2 3 0	4.4	−4.4	21 4 0	0.5	0.2	18 6 0	1.0	−0.4
19 1 0	0.6	0.8	3 3 0	1.4	−1.3	22 4 0	1.9	− 1.6	19 6 0	0.3	−0.3
20 1 0	2.8	3.1	4 3 0	0.5	−0.2	23 4 0	—	0.2	20 6 0	1.2	0.8
21 1 0	0.6	− 0.7	5 3 0	5.6	5.3	24 4 0	1.8	1.7	1 7 0	0.8	−0.7
22 1 0	2.6	− 2.9	6 3 0	1.6	1.1	25 4 0	0.4	0.2	2 7 0	0.5	0.1
23 1 0	3.4	− 3.0	7 3 0	0.5	−0.9	26 4 0	0.3	− 0.5	3 7 0	0.4	0.3
24 1 0	0.5	− 0.1	8 3 0	—	−1.3	27 4 0	0.7	− 0.6	4 7 0	2.2	1.7
25 1 0	0.8	0.8	9 3 0	2.2	−2.5	28 4 0	0.2	− 0.2	5 7 0	—	0.1
26 1 0	0.6	− 0.4	10 3 0	7.1	−7.5	1 5 0	4.5	4.2	6 7 0	2.6	−1.4
27 1 0	1.7	− 1.7	11 3 0	—	−0.3	2 5 0	1.9	0.8	7 7 0	—	−0.2
28 1 0	0.7	0.6	12 3 0	1.3	−0.6	3 5 0	4.9	− 4.3	8 7 0	2.0	1.4
29 1 0	0.3	0.4	13 3 0	2.5	3.1	4 5 0	3.0	− 3.0	9 7 0	0.6	0.2
30 1 0	0.3	0.3	14 3 0	0.5	−0.4	5 5 0	0.6	− 0.9	10 7 0	0.6	0.8
31 1 0	2.0	− 1.5	15 3 0	0.4	0.2	6 5 0	1.2	0.7	11 7 0	1.1	−0.7
32 1 0	1.2	− 0.9	16 3 0	2.5	−2.7	7 5 0	—	− 0.4			
33 1 0	0.4	0.1	17 3 0	1.1	−0.6	8 5 0	2.5	− 2.0			

bonds in kainic acid[3], the differences being not definitely significant, while some of the bond angles are fairly different from the corresponding ones of kainic acid.

The C–O distances of the carboxymethyl group of C_3 are found to be 1.40 Å for C_7–O_3 and 1.21 Å for C_7–O_4, the oxygen O_3 being of the hydroxyl group (OH) and forming a hydrogen bond as will be described in the next section (Figs. 6 and 7). The corresponding distances of kainic acid are found to be 1.34 and 1.23 Å, both the oxygens being linked to others by hydrogen bonds.

The C–O distances of the carboxyl group of C_2 are 1.27 Å for C_1–O_1 and 1.23 Å for C_1–O_2, both forming hydrogen bonds. These values are in good agreement with those of the carboxyl group in kainic acid (1.24 and 1.27 Å), similarly hydrogen bonded.

Judging from the dimensions of the carboxyl group of C_2 and the consideration about the observed hydrogen bonds, as in the case of kainic acid, the allokainic acid molecule is considered to be of the 'zwitter ion' structure in which the carboxyl group of C_2 is of $(COO)^-$ and the nitrogen is of N^+H_2, although the positions of no hydrogen atoms are located in the present work.

As for the stereochemical relations of the atoms in allokainic acid molecule, the carboxyl group of C_2 and the carboxymethyl group of C_3 take the *trans*-configuration relative to the ring. This relation is the same as that in kainic acid. The carboxymethyl group of C_3 and the isopropenyl group of C_4 are in the *trans*-configuration, while in kainic acid it was the *cis*-configuration. This fact supports the reasoning based on chemical evidences[8]. The relationship between the structure of kainic acid and allokainic acid is shown in Fig. 5. It is of interest that the anthelmintic effects of the two isomers are very different from each other due only to the configurations of their isopropenyl groups.

The five-membered pyrrolidine ring being fairly flexible, as found in the case of kainic acid, this ring is in the present case also considerably distorted from the planar form owing presumably to the influences of its side-chains and of the interactions between molecules. Deviations from the ordinary values of the

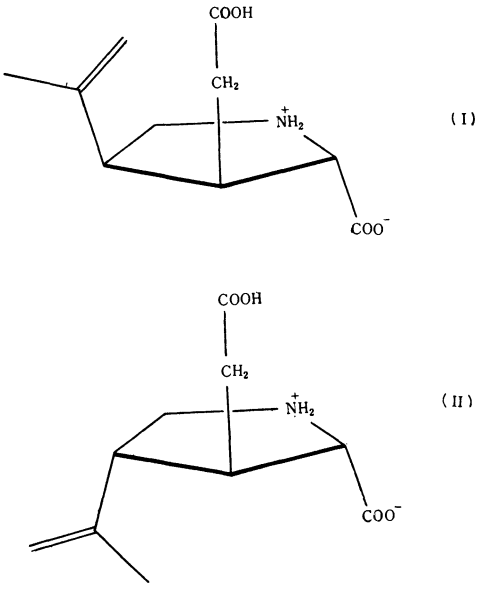

Fig. 5. Stereochemical configuration, (I) kainic acid, (II) allokainic acid.

bond angles of the pyrrolidine ring (108°, 108°, 106°, 104°, 104°) are found to be of the same order as those of hydroxyproline[9] (109°, 105°, 108°, 104°, 105°), the deviations being, however, smaller than those of kainic acid (108°, 104°, 103°, 102°, 105°) or zinc kainate[2] (105°, 110°, 102°, 105°, 102°).

Crystal Structure.—The projections of the crystal structure along the *b* and *c* axes are illustrated in Figs. 6 and 7 respectively, giving the intermolecular distances. The unit cell contains four zwitter ion molecules of allokainic acid. As a whole, the crystal structure resembles that of kainic acid[3].

From the short intermolecular N...O or O...O distances, three kinds of hydrogen bond are considered to be formed among the molecules. The two hydrogens of N^+H_2 form the intermolecular hydrogen bonds between the nitrogen of one molecule and the carboxyl groups $(COO)^-$ of other two molecules. These hydrogen bond distances are 2.82 Å for N—H...O_1 and 2.70 Å for N—H...O_2. The hydrogen of the oxygen O_3 of the carboxymethyl group also forms an intermolecular hydrogen bond between this group and the carboxyl group, its O_3—H...O_1 distance being 2.71 Å. The hydrogen bond angles are as follows:

8) H. Morimoto and R. Nakamori, *J. Pharm. Soc. Japan* (*Yakugaku Zasshi*), **76**, 294 (1956); *Proc. Japan Acad.*, **32**, 41 (1956); T. Takemoto, Z. Tei and K. Daigo, *J. Pharm. Soc. Japan* (*Yakugaku Zasshi*), **76**, 298 (1956).

9) J. Zussman, *Acta Cryst.*, **4**, 493 (1951); J. Donohue and K. N. Trueblood, ibid., **5**, 419 (1952).

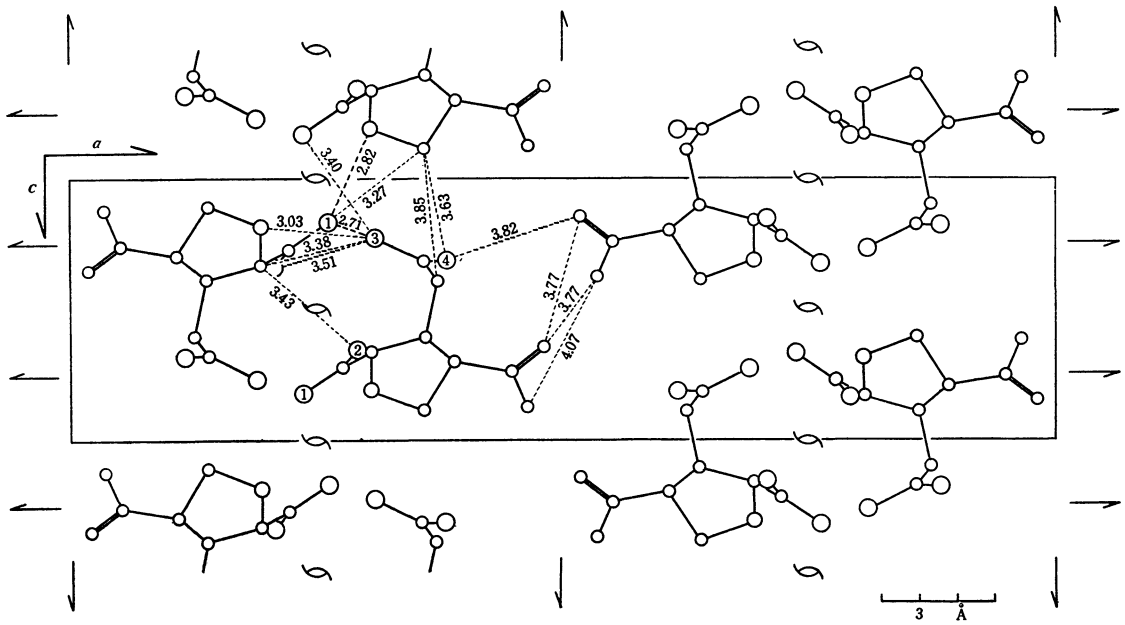

Fig. 6. View of the crystal structure along the *b* axis. The intermolecular distances are shown in Å. Large circles represent oxygens, intermediate nitrogens and small carbons.

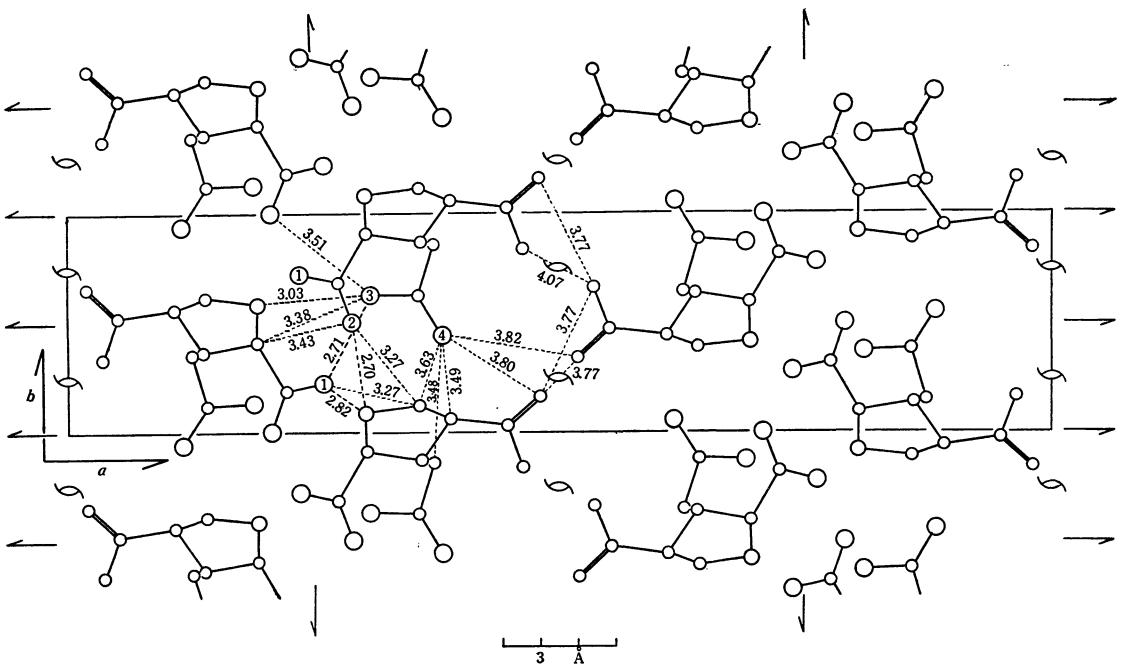

Fig. 7. View of the crystal structure along the *c* axis. The intermolecular distances are shown in Å. Symbols are the same as those of Fig. 6.

C_2—N...O_1=144°	C_2—N...O_2 =110°
C_5—N...O_1= 93°	C_5—N...O_2 = 98°
O_1...N...O_2= 93°	C_1—O_1...O_3=116°
C_1—O_1...N=139°	O_3...O_1...N =102°
C_1—O_2...N=132°	C_7—O_3...O_1=114°

By these hydrogen bonds, the molecules are linked to each other infinitely, forming a layered structure perpendicular to the *a* axis. Between the layers, the isopropenyl groups are in contact with each other, the distances of the closest approach being 3.77 Å for C_9...C'_{10}, 3.77 Å for C_9...C''_{10}, 3.77 Å for C_{10}...C'_{10} and 4.07 Å for C_9...C'_9. It is compatible with the existence of the cleavage along the (1 0 0) plane.

The configuration of the isopropenyl group in allokainic acid being different from that of kainic acid as shown in Fig. 5, crystalline allokainic acid has no sufficient space to contain water of crystallization among molecules, while kainic acid crystallizes with one water molecule which is packed in the space and links the kainic acid molecules by forming the hydrogen bonds in addition to the other hydrogen-bridges such as described above. Corresponding to this difference between the crystal structures, allokainic acid is found to be much more soluble in water than kainic acid. In connection with this fact, it is of interest to note that, although zinc kainate easily crystallizes with two waters, the zinc salt of allokainic acid is too soluble in water to obtain crystals. The crystal structure of zinc kainate[2] being, in a sense, similar to that of kainic acid[3], it seems that in the case of zinc allokainate, water molecules may not be packed so as to link the molecules to form the crystal because of the configuration of the molecule.

The author wishes to express his hearty thanks to Professor I. Nitta for his kind guidance and encouragement throughout this work. He is indebted to Professor-Emeritus S. Murakami, Dr. T. Takemoto and their collaborators of this University for supplying the specimen and kind discussion. Thanks are also due to Dr. Y. Tomiie and Mr. Y. Sasada of this University for helpful advice and continued interest.

Department of Chemistry, Faculty of Science, Osaka University
Kita-ku, Osaka

Studies on the Synthesis of Metal Complexes. IV[1]. *The Cobalt(III) Complexes of Ammoniatriacetic Acid*

By Motoshichi MORI, Muraji SHIBATA, Eishin KYUNO and Yoshito OKUBO

(Received June 26, 1958)

It is commonly known that ammoniatriacetic acid (ATA) acts as a tetradentate donor in combining with metal ions, and this has been proved by Schwarzenbach and his co-workers[2] by the titration of the acid with a base in the presence of a number of metal ions. In the event that one molecule of ATA co-ordinates to a cobalt(III) ion having a co-ordination number six, it is to be expected that two positions around the cobalt ion, not occupied by the chelating agent, are filled by solvent molecules or other donors in the solution. On the other hand, if two molecules of ATA combined with the ion, it would be expected that the two nitrogen atoms and four of the carboxyl groups participate in the bonding, and the remaining two carboxyl groups are uncomplexed. It was the purpose of this investigation to ascertain whether ATA could behave in this way. A few complexes containing only one ammoniatriacetate ion per cobalt(III) as a quadrivalent ligand have been isolated and identified by chemical analysis, thermal decomposition, absorption spectroscopy etc. The attempt to prepare a complex containing

1) Presented at the 10th Annual Meeting of the Chemical Society of Japan, Tokyo, April 6, 1957. For a previous paper in this series see M. Mori, M. Shibata, E. Kyuno and K. Hoshiyama, This Bulletin, **31**, 291 (1958).

2) G. Schwarzenbach et al., *Helv. Chim. Acta*, **28**, 828 (1945); G. Schwarzenbach and W. Biedermann, ibid., **31**, 331 (1948).

TABLE I
ANALYTICAL RESULTS (amounts in %)

	Co		N		K		H_2O	
	calcd.	obsd.	calcd.	obsd.	calcd.	obsd.	calcd.	obsd.
α-K[Co ata(OH)(OH_2)]·$2H_2O$	16.5	16.1	3.86	3.75	10.9	10.4	10.1	10.3
β-K[Co ata(OH)(OH_2)]·$3H_2O$	15.7	16.0	3.75	3.66	10.4	9.8	14.4	14.0
K_2[ataCo$(OH)_2$Co ata]·$6H_2O$	16.5	16.0	3.97	3.89	10.9	10.9	15.2	15.5
K_2[Co ata(CO_3)]·H_2O	14.6	14.2	3.47	3.19	19.3	19.0	4.5	4.7
K_2[Co ata(C_2O_4)]·H_2O	13.6	13.4	3.24	—	18.1	17.9	4.2	4.2

two ammoniatriacetate ions was unsuccessful.

Experimental

Synthesis. — 1) *α-Form of potassium hydroxoammoniatriacetatoaquocobaltate(III)*, α-K[Co ata(OH)(OH_2)]·$2H_2O$*. — To a solution of 4 g. of ATA in 25 ml. of 2.5 N potassium bicarbonate were added 5 g. of cobalt chloride hexahydrate and 1 ml. of 30% hydrogen peroxide, and the mixture was placed in an ice-bath until blue crystals separated out (about 5 hr.). The crystals were filtered, washed several times with a little cold water, dissolved in a little hot water containing potassium acetate and then recrystallized by the usual procedure. The product was washed with ethanol and ether in turn. Yield, about 1 g. This complex will hereafter be referred to as α-form. It is slightly soluble in water and is converted into another variety (β-form) by heating the solution or acidifying it with acetic acid.

2) *β-Form of potassium hydroxoammoniatriacetatoaquocobaltate(III)*, β-K[Co ata(OH)(OH_2)]·$3H_2O$.—This was prepared from a filtrate in 1); after the filtrate was acidified with 6N-acetic acid (about 10 ml.), a large amount of ethanol was added to it, and the solution was kept overnight in a refrigerator. The reddish violet crystals deposited were collected and recrystallized from the cooled solution by the addition of ethanol. The final product was washed with ethanol and ether. Yield, about 2.5 g.

3) *Potassium bis-(ammoniatriacetato)-μ-dioldicobaltate(III)*, K_2[ata Co$(OH)_2$Co ata]·$6H_2O$. — This also was prepared from a separate filtrate in 1); after the filtrate was acidified with 1 N-hydrochloric acid (about 5 ml.), the solution was heated on a boiling water-bath until a pink solution appeared. On cooling, pink precipitates began to appear, which were collected and dissolved in hot water and reprecipitated by cooling and washed with ethanol and ether in turn. Yield, about 2 g.

4) *Potassium carbonatoammoniatriacetatocobaltate(III)*, K_2[Co ata(CO_3)]·H_2O. — Approximately 4 g. of ATA was added to a cold green solution of potassium tricarbonatocobaltate(III) prepared from 20 g. of $KHCO_3$ and 10 g. of $CoCl_2 \cdot 6H_2O$ — 5 ml. of 30% H_2O_2 by the previous method[3]. The mixture was warmed on a water-bath until the green color of the solution changed into violet (about 10 min.). After the solution was cooled, about an equal volume of ethanol was added to it and the whole was kept overnight in a refrigerator. The crystals were recrystallized from water in the hot. They were brilliant violet in color. Yield, about 2.5 g.

5) *Potassium oxalatoammoniatriacetatocobaltate (III)*, K_2[Co ata(C_2O_4)]·H_2O.—About 3.5 g. of the α-form obtained in 1) was dissolved in 25 ml. of 2 N-potassium acetate solution containing 1.3 g. of oxalic acid. The solution was warmed on a water-bath until the color changed to reddish violet, and then cooled and about 12 ml. of ethanol was added, whereupon crystallization of the substance took place. It was recrystallized in the form of bright, reddish-violet needles. This was also obtained by using the β-form or the carbonato-complex obtained in 4).

Determination of the Chemical Formulae. —For this purpose, chemical analysis, thermal decomposition, coagulation of ferric oxide sol and spectroscopic measurement were used in the same manner as described in the previous papers[3,4].

Results and Discussion

Chemical Analysis. — The numerical values are given in Table I. The water of crystallization was estimated from the weight loss in the thermal decomposition. For the determination of cobalt and potassium, the residues from the thermal decompositions of the complexes were used as samples. The nitrogen content was determined by Kjeldahl's method.

Thermal Decomposition. — When a sample was heated with gradual elevation of temperature up to nearly 300°C, decomposition took place in several steps, and finally a residue containing an oxide of cobalt (perhaps, Co_2O_3) and potassium carbonate was left behind. Decomposition curves showing the weight loss per millimole vs. temperature are shown in Fig. 1.

It may be noted that the weight loss of the β-form at 150~190°C corresponds closely to one molecule of water (curve

* "ata" stands for ammoniatriacetate ion.

3) M. Mori et al., This Bulletin, **29**, 883 (1956).

4) M. Mori et al., This Bulletin, **31**, 291 (1958).

2). In fact the product had exactly the same pink color as the diol-complex reported in the previous syntheses. However, the weight loss of the α-form in the same temperature range is too great for one to assume the formation of the diol-complex and it is at present unknown what happens in that stage (curve 1). In the case of the carbonato- and the oxalato-complexes, the weight loss corresponding to removal of a carbonate or an oxalate ion from each of the complexes was observed prior to the final decomposition (curves 4 and 5).

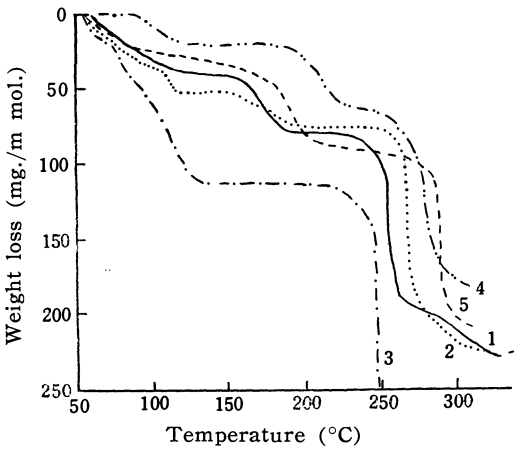

Fig. 1. Thermal decomposition curves of:
1. α-K[Co ata(OH)(OH_2)]·$2H_2O$
2. β-K[Co ata(OH)(OH_2)]·$3H_2O$
3. K_2[ataCo$(OH)_2$Co ata]·$6H_2O$
4. K_2[Co ata(CO_3)]·H_2O
5. K_2[Co ata(C_2O_4)]·H_2O

Coagulation Value.—Nakahara and co-workers[5] have given 6.6 mF and 0.48 mF as the average values for uni- and bivalent complex anions respectively, but the values obtained in the present experiment deviated from the average to a considerable extent. Namely, (i) α-K[Co ata(OH)(OH_2)]...2 mF, (ii) β-K[Co ata(OH)(OH_2)]...0.6 mF, (iii) K_2[Co_2(ata)$_2(OH)_2$]...0.2 mF, (iv) K_2[Co ata(CO_3)]...0.3 mF, (v) K_2[Co ata(C_2O_4)]...0.3 mF.

Among these, the values for the species of the β-form and the diol-salt are too low for a uni- or a bivalent anion respectively, but they may be explained by assuming the following reactions;

$$[\text{Co ata}(OH)(OH_2)]^- \rightleftarrows [\text{Co ata}(OH)_2]^{2-} + H^+$$

$$[\text{ataCo}\langle^{OH}_{OH}\rangle\text{Co ata}]^{2-} \rightleftarrows$$

$$[\text{ataCo}\langle^{OH}_{O}\rangle\text{Co ata}]^{3-} + H^+$$

As an evidence for these equilibria, it was found that the pH values of the β-form and the diol-salt were 5.8 and 3.6 in the M/500 solutions. The coagulation value for the α-form is also lower than the average, but this deviation may be attributed to partial conversion into the β-form, because the sample solution was prepared by heating.

Visible and Ultraviolet Absorption Spectra.—All the absorption curves are shown in Figs. 2 and 3, and the numerical data are given in Table II. As is seen in Fig. 2, the curves 1 and 2 have shoulders at about 100×10^{13}/sec. probably owing to the ligand OH^- in the complex radicals. This is supported by the fact that the shoulder disappears in an acidified solution but remains in an alkaline solution, as are illustrated by the curves 3 and 4.

The curve 1 in Fig. 3 also has a shoulder at nearly the same frequency as the above and this may be considered as a specific band of diol-bond, because a similar band has been found in octammine-μ-diol-dicobalt(III) salt[6].

For the carbonato- and the oxalato-complex, the absorption curves are similar to each other in appearance (Figs. 3-2 and 3). It may be noted that both complexes are perhaps the first examples represented by the general type [$CoNO_5$].

TABLE II
ABSORPTION MAXIMA AND log ε(10^{13}/sec.)

	ν_1	log ε_1	ν_2	log ε_2	ν_s	log ε_s	ν_3	log ε_3
α-K[Co ata(OH)(OH_2)]·$2H_2O$	54.25	2.28	74.62	2.48	ca 100	3.54	132.74	4.21
β-K[Co ata(OH)(OH_2)]·$3H_2O$	55.56	1.72	73.89	1.73	ca 100	2.94	134.53	3.69
K_2[ataCo$(OH)_2$Co ata]·$6H_2O$	58.36	1.65	—	—	ca 100	2.54	—	—
K_2[Co ata(CO_3)]·H_2O	53.19	2.22	77.32	2.18	—	—	123.97	4.09
K_2[Co ata(C_2O_4)]·H_2O	54.55	2.30	77.32	2.29	—	—	127.12	4.33

5) S. Nakahara et al., *J. Chem. Soc. Japan, Pure Chem. Sec.* (*Nippon Kagaku Zassi*), **74**, 488 (1953).

6) Y. Inamura and Y. Kondo, ibid., **74**, 627 (1953).

Fig. 4 is a diagram in which the frequency values for the first band of the complexes belonging to the types $[CoN_5O]$, $[CoN_3O_3]$ and $[CoNO_5]$ are plotted against the number of nitrogen atoms co-ordinated.

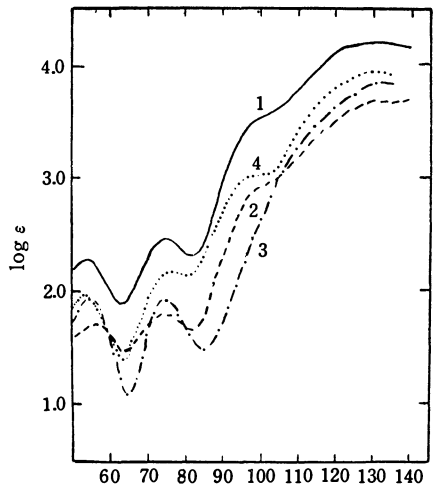

Fig. 2. Absorption spectra of:
1. α-K[Co ata(OH)(OH$_2$)] (aqueous sol.)
2. β-K[Co ata(OH)(OH$_2$)] (aqueous sol.)
3. β-K[Co ata(OH)(OH$_2$)] (at pH 2.6)
4. α-K[Co ata(OH)(OH$_2$)] (at pH 13.3)

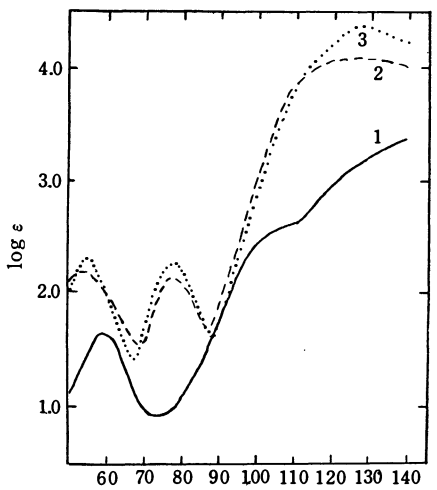

Fig. 3. Absorption spectra of:
1. K$_2$[ataCo(OH)$_2$Co ata]
2. K$_2$[Co ata(CO$_3$)]
3. K$_2$[Co ata(C$_2$O$_4$)]

Infrared Spectra.—These were measured in order to confirm the fact that the three carboxyl groups in the chelate agent were complexed. Strong split bands were observed at 1718 and 1735 cm^{-1} for the free acid. On the other hand, the

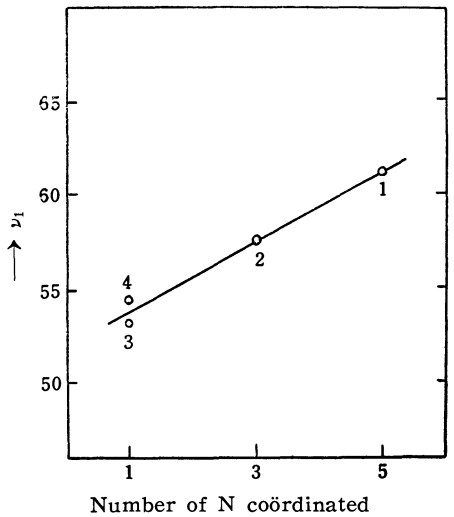

Fig. 4. Frequency position of:
1. [Coen$_2$(gly)]ClO$_4$[7]
2. β-[Co(gly)$_3$][7]
3. K$_2$[Co ata(CO$_3$)]
4. K$_2$[Co ata(C$_2$O$_4$)]

α-form shows bands at 1672 and 1618 cm^{-1}, the β-form at 1667 cm^{-1} and the diol-salt at 1600 cm^{-1}. It is obvious that these bands are due to the co-ordinated carboxyl groups since such an assignment has been best established for the EDTA-complexes[8].

Structure. — The structures of the complexes must be considered on the basis of the above discussion. In the case of the α- and the β-form, a type of isomerism illustrated by formula I and II in Fig. 5 is possible and to the other complexes the structures illustrated by formula III, IV and V may be assigned. It is hard to say conclusively, which of the formulae, I or II, is the α-form and which the β-form, but an assumption is possible based upon the following discussion.

In the previous paper[3], the authors reported that the absorption maximum of the first band for the blue variety of potassium dicarbonatodiamminecobaltate K[Co(NH$_3$)$_2$(CO$_3$)$_2$], shifted to a somewhat longer wave length than that for the corresponding violet variety, and the former variety may be *cis*- and the latter *trans*-form. The same relationship exists in the present case, too; the α-form has a maximum at longer wave length than the β-form (Table II). In addition to this, when the fact that ligands H_2O and NH_3 stand in a near position and ligands OH^- and CO_3^{2-}

7) Y. Shimura and R. Tsuchida, This Bulletin, **28**, 573 (1955).
8) D. H. Bush and J. C. Bailar *J. Am. Chem. Soc.*, **75**, 4574 (1953); **78**, 716 (1956).

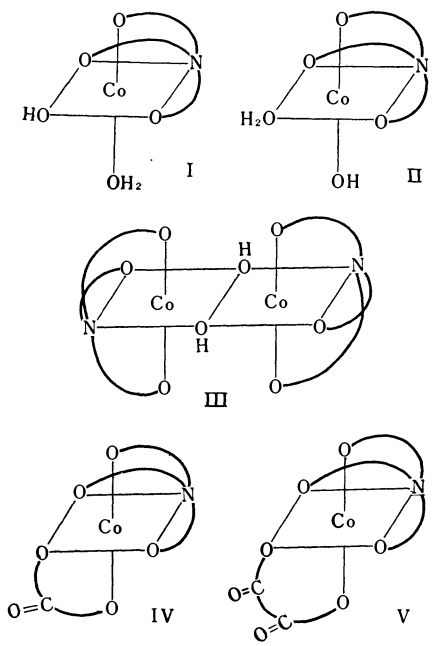

Fig. 5. Structural formulae.

in almost the same position of the spectrochemical series is taken into consideration*, formula I in which ligand H_2O is cis to the co-ordinated nitrogen atom will be assigned to the α-form.

Summary

The cobalt(III) complexes containing ammoniatriacetato group (ata) as a quadridentate ligand are newly prepared:

i) α-K[Co ata(OH)(OH_2)]$\cdot 2H_2O$
ii) β-K[Co ata(OH)(OH_2)]$\cdot 3H_2O$
iii) K_2[ataCo$(OH)_2$Co ata]$\cdot 6H_2O$
iv) K_2[Co ata(CO_3)]$\cdot H_2O$
v) K_2[Co ata(C_2O_4)]$\cdot H_2O$

In order to determine the structural formulae of these complexes, their visible, ultraviolet and infrared spectra were measured, as well as their thermal decomposition and their potency to coagulate ferric oxide sol.

Department of Chemistry, Faculty of Science, Kanazawa University
Kanazawa

---

* NO_2^- SO_3^{2-} en NH_3 ONO^- NCS^- OH_2 $C_2O_4^{2-}$ ONO_2^- OSO_3^{2-} $OCHO^-$ OH^- CO_3^{2-} $OCOR^-$ .....

Formation and Aging of Precipitates. VIII. Formation of Monodisperse Particles (1) Gold Sol Particles by Sodium Citrate Method*

By Kazuyoshi TAKIYAMA

(Received May 23, 1958)

Recently many investigations on the precipitation from homogeneous solution have been made to prepare pure and filterable precipitates. The author prepared a few kinds of monodisperse particle by the homogeneous solution method to study the reaction of precipitation. In this paper the formation of gold sol, containing monodisperse particles, is reported. A great many methods for preparing the gold sol have been investigated, but only the sodium citrate method, reported by Turkevich, Stevenson and Hillier[1], seems to be suitable to produce monodisperse gold particles. The author took advantage of the sodium citrate method to prepare the gold sol, and studied the relationship between the condition of formation and the properties of particles produced, and the growth process of gold particles by electron microscopy.

Experimental

Formation of Gold Sol.—Varying amounts (1, 2, 5, 7.5, 10, 15, 20 and 25 ml.) of chlorauric acid solution (0.10% Au) were taken into Erlenmeyer flasks with two openings and diluted with

* The seventh paper of this series, This Bulletin, **31**, 555 (1958).

1) J. Turkevich, R. C. Stevenson and J. Hillier, *Discuss. Faraday Soc.*, **11**, 55 (1951).

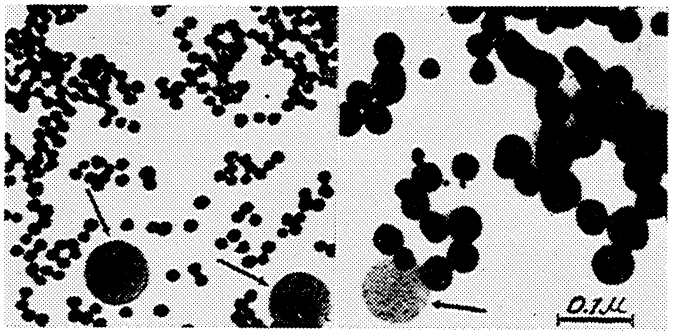

(a) (b) (×100, 000)

Fig. 1. Electron micrographs of gold sol particles.
a: Sodium citrate sol b: Zsigmondy sol
(Larger particles in micrographs (arrow) are polystyrene latex particles (880 Å in diameter) using as calibration standard)

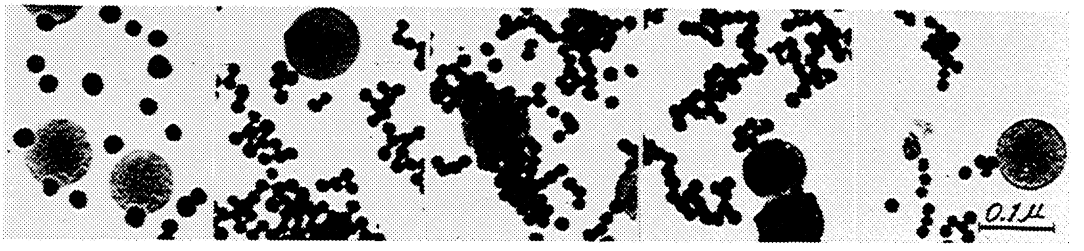

(a) (b) (c) (d) (e)
(×100, 000)

Fig. 4. Electron micrographs of gold particles prepared from the various initial concentrations of auric ion at 80°C.
a : 10.15×10^{-5} moleAu/l. (2 mg.Au/100 ml.)
b : 25.37×10^{-5} moleAu/l. (5 mg.Au/100 ml.)
c : 50.75×10^{-5} moleAu/l. (10 mg.Au/100 ml.)
d : 76.13×10^{-5} moleAu/l. (15 mg.Au/100 ml.)
e : 101.50×10^{-5} moleAu/l. (20 mg.Au/100 ml.)

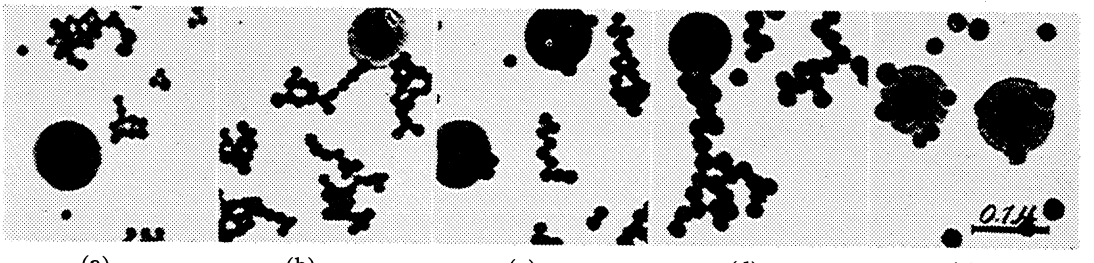

(a) (b) (c) (d) (e)
(×100, 000)

Fig. 6. Electron micrographs of gold particles prepared at various temperatures.
(25.37×10^{-5} moleAu/l.)
a: 50°C b: 60°C c: 70°C d: 80°C e: 100°C

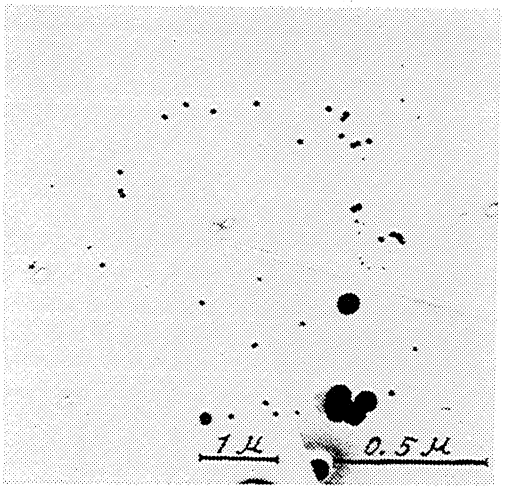

Fig. 8. Electron micrograph of spray mounted drop pattern of gold sol. (Small particles are gold and large particles are polystyrene latex.) (×10,000)
One segment further enlarged. (×40,000)

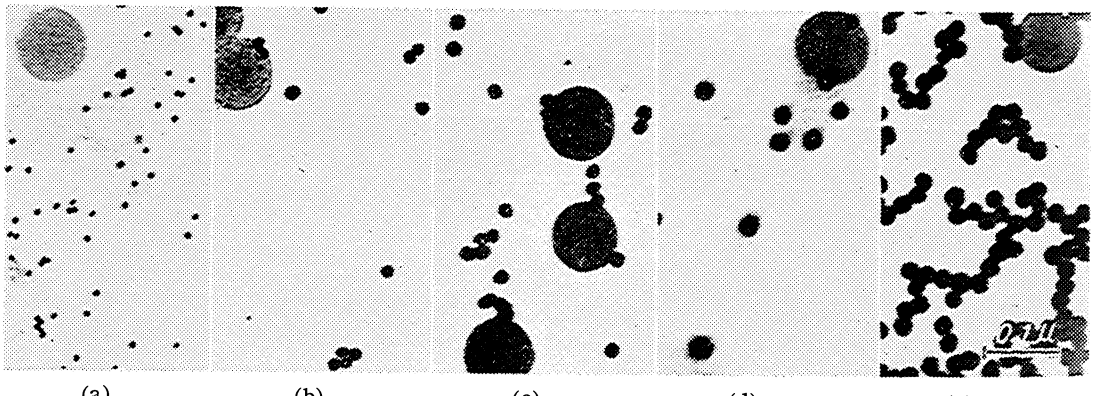

(a) (b) (c) (d) (e)
(×100,000)

Fig. 9. Electron micrographs of gold particles during the growth process.
(25.37×10^{-5} moleAu/1., 80°C)
a: 5 min. b: 10 min. c: 20 min. d: 30 min. e: 60 min.

water to 90 ml. After the solutions were warmed to a desired temperature (50, 60, 70, 80 and 100°C), 10 ml. of sodium citrate solution (1.0%) was added to them, the reaction flask connected with a reflux condenser and a thermometer was held in a thermostatted bath.

Measurement of Size of Gold Particles with Electron Microscope.—The diameter of gold sol particles has been determined by electron microscopy. Particle-diameter measurement was made from micrographs enlarged at ten-fold magnification. The particle-diameter distribution, the mean particle-diameter** and the standard deviation*** were obtained. The monodisperse polystyrene latex, run No. LS-040-A (880 Å in mean diameter)[2], of the Dow Chemical Co., has been used as calibration standard to measure the particle-diameter****. At different intervals during the course of a reaction, a drop of the reaction mixture was taken onto a small Formvar film, and the film with the drop was floated on the surface of cold water. About ten minutes, the drop on the film was allowed for diffusion of mother liquid ions from the drop into the water below. The film was scooped up with a grid for electron microscopy and was mounted with polystyrene latex. The specimen was observed with electron microscope to determine the growth rate of gold particles.

Determination of the Number of Gold Particles by Spray Method[3].—At fixed intervals during the reaction of sol formation, about 10 ml. of the reaction mixture was taken and was poured into a test tube, dipped in an ice bath, to stop the reduction of the auric ion. 5.0 ml. of this sample was mixed thoroughly with 1.0 ml. of polystyrene latex to a definite concentration, and then the mixture was sprayed with a Vaponefrin Nebulizer onto a film made on grid for electron microscopy, which was placed about 20 cm. away from the nozzle of the nebulizer. The specimen was observed with an electron microscope. The number of gold particles during the course of sol formation was estimated by counting the number of gold and polystyrene latex particles in droplet patterns.

Determination of Gold Sol Concentration by Absorption Spectroscopy.—An absorption spectrum of gold sol was measured with Hitachi spectrophotometer, using 1-cm. cell, at intervals of 5 mμ over a range of 350 to 700 mμ and a relation between concentration and absorbance was obtained at the wave length of absorption maximum. Absorption spectra of the reaction mixture during the course of sol formation were also obtained.

Experimental Results

Size of Gold Sol Particles.—*Uniformity of gold sol particles.*—The gold sol particles prepared by sodium citrate method were almost spherical. An electron micrograph of particles in one of the gold sol, which was formed from chlorauric acid solution at the initial concentration of 25.37×10^{-5} mole per liter (5 mg. Au/100 ml.) at 80°C, is shown in Fig. 1 a and the particle-diameter distribution of gold particles is shown in Fig. 2 a. The mean particle-diameter was 172 Å and the standard deviation was 13 Å. To compare the property of the gold sol, an electron micrograph of particles in the Zsigmondy's sol (25.37×10^{-5} mole Au/1.) prepared by the reduction with an alkaline formaldehyde solution is shown in Fig. 1 b, and the particle-diameter distribution is shown in Fig. 2 b. The shape of particles in Zsigmondy's sol was also spherical, but the mean diameter was 417 Å and the standard deviation was 145 Å. Then the particles in Zsigmondy's sol were polydisperse. Larger spherical particles contained in the electron micrographs (arrows) are polystyrene latex particles. The polystyrene latex particles are also contained in every micrograph indicated below. The size of gold sol particles was affected by the condition of formation as described in the next section. An example of the change of standard deviation by the variation of the condition of formation

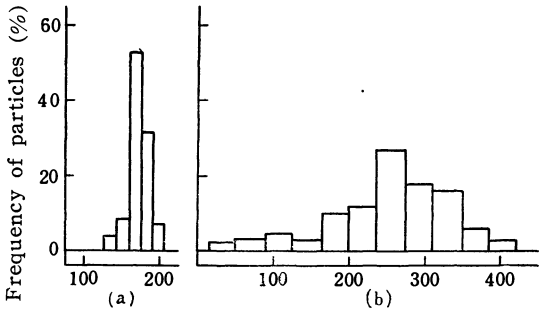

Fig. 2. Particle-diameter distribution of gold sol particles.
a: Sodium citrate sol
b: Zsigmondy sol

2) E. B. Bradford and J. W. Vanderhoff, *J. Appl. Phys.*, **26**, 864 (1955).

** The mean particle-diameter used here is the arithmetic mean obtained by

$$d_0=\frac{\sum n_i d_i}{N}$$

where d_0 is the arithmetic mean particle-diameter, n_i is the frequency of particles having diameter d_i, and N is the total number of particles.

*** The standard deviation, σ, is obtained by

$$\sigma=\sqrt{\frac{\sum(d_i-d_0)^2 n_i}{N}}$$

**** Polystyrene latex used here was sent from Dr. E. B. Bradford of Dow Chemical Co. to whom the author's thanks are due.

3) R. C. Backus and R. C. Williams, *J. Appl. Phys.* **21**, 11 (1950).

TABLE I
THE SIZE OF GOLD PARTICLES PREPARED FROM VARIOUS INITIAL CONCENTRATION OF AURIC ION AT 80°C

Concn. C_0 (moleAu/l.$\times 10^5$)	5.07	10.15	25.37	38.06	50.75	76.13	101.50	126.87
Mean particle dia. d_0 (Å)	149	191	172	173	168	155	140	146
Standard deviation σ (Å)	31.5	9.4	7.5	8.1	8.3	7.1	21.5	28.1
Particle weight $M\times 10^{-5}$	203	430	312	317	290	233	168	191
Particle number* $N\times 10^{-10}$	29	28	97	144	209	390	720	793

* Particle number per ml. of sol. $N=(C_0/\text{mole number of one particle})\times 10^{-3}$

is listed in Table I, and the summarized results are indicated in Fig. 3. For the gold particles in sodium citrate sols prepared over a range of the initial concentration from 20×10^{-5} to 80×10^{-5} mole auric ion per liter and at the reaction temperature above 70°C, the values of standard deviation ranged below 10% of the particle-diameter. Thus the particles are recognized to be monodisperse. The

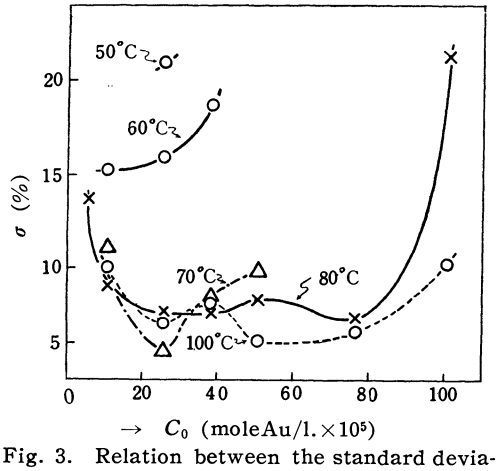

Fig. 3. Relation between the standard deviation of particle-diameter (σ%) and the initial concentration of auric ion (C_0 mole Au/l.$\times 10^5$) of sodium citrate sol.

size distribution of the gold sol particles prepared outside the range of concentration and reaction temperature described above became wide, and the particles were not monodisperse.

Relation between initial concentration of the auric ion and size of gold sol particles.— The size of particles in the gold sols was only affected by the initial concentration of auric ions and was not affected by the concentration of sodium citrate over the range from five-fold to ten-fold mole of the auric ion. As the initial concentration of auric ion was increased, the particles became smaller as indicated in Fig. 4 and in Table I. The size of particles is expressed by the particle weight in molecular weight unit, M, calculated according to the following equation:

$$M=(4/3)\pi(d_0/2)^3\rho A$$

where d_0 is the mean particle diameter (cm.), ρ is the density of gold, and A is Avogadro's number. The logarithm of particle weight of the gold sol particles prepared at 70, 80 and 100°C, log M, was linear with the initial concentration of auric ion, C_0 (mole Au/l.), as shown in Fig. 5. Then the particle weight, M, is represented by

$$M=\alpha e^{-\beta C_0} \qquad (1)$$

where α and β are constants. α is dependent upon the reaction temperature showing the values of 3.63, 4.79 and 6.31×10^{-7} at 70, 80 and 100°C respectively. β is always constant and is 1000.

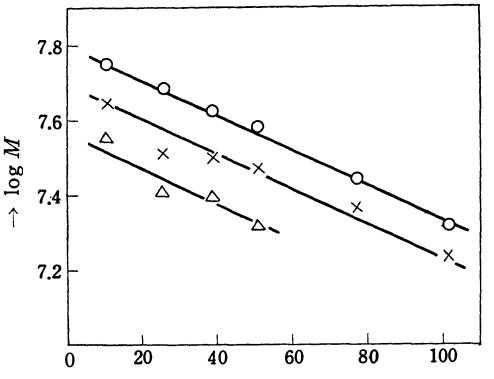

Fig. 5. Relation between the initial concentration of the auric ion and the size of gold particles.
○ 100°C × 80°C △ 70°C

The number of particles per ml. gold sol was related to the size of particles and increased with increasing initial concentration of the auric ion.

Relation between reaction temperature and size of particle. — The size of gold sol particles increased with temperature as shown in Fig. 6. The logarithm of particle weight of gold particles prepared at various concentrations, log M, is linear with the reaction temperature, T (°C),

as shown in Fig. 7. Then the particle weight, M, is represented by

$$M=\gamma e^{\delta T} \quad (2)$$

where γ and δ are constants. γ is a function of initial concentration of the auric ion. They are 9.55, 7.08, 6.76, 6.17, 5.01 and 3.55×10^{6} at 10.15, 25.37, 38.06, 50.75, 76.13 and 101.50×10^{-5} mole Au/l. respectively. δ is always constant and is 0.0184.

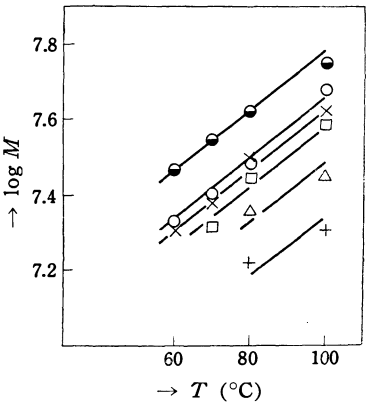

Fig. 7. Relation between the reaction temperature of sol formation and the size of gold particles.
◒ 10.15×10^{-5} moleAu/l.
○ 25.37 〃
× 38.06 〃
□ 50.75 〃
△ 76.13 〃
+101.50 〃

The number of particles per ml. sol prepared at a fixed concentration decreased with the rise of the reaction temperature.

Formation Process of Gold Sol Particle.—*Number of gold particles determined by spray method.*—A spray mounted drop pattern of the reaction mixture during the sol formation is shown in an electron micrograph of Fig. 8. Every droplet sprayed is deposited individually in a circular form and it is possible to determine the number of gold and polystyrene latex particles in each droplet pattern. The relationship between the number of particles of gold and polystyrene latex in the droplet patterns prepared at different times after the commencement of the reaction of the sol formation, is shown in Table II. The polystyrene latex sol used here was the same, so its concentration was unchanged throughout the experiment. The ratio of the number of particles of gold and polystyrene latex in the same run was kept almost constant, and it was recognized that the number of gold particles during the reaction of sol formation was constant over the range of time spent in measuring the number of particles.

Observation of growth process of gold particles with electron microscope.—The growth process of gold particles during the course of sol formation is shown in a series of electron micrographs of Fig. 9. The particles were monodisperse from the initial stage of the reaction. The size of a particle measured at the time t (min.) is expressed by the mole number of one particle, x (mole), calculated from the mean particle-diameter, d (cm.), according to the following equation:

$$x=(4/3)\pi(d/2)^{3}\rho/W$$

TABLE II
THE NUMBER OF PARTICLES OF GOLD AND POLYSTYRENE LATEX IN DROPLET PATTERNS PREPARED BY THE SPRAY METHOD DURING THE FORMATION OF GOLD SOL

No.	Initial concn. of auric ions C_0 (mole Au/l.$\times10^{5}$)	Reaction time t (min.)	Number of gold particles A_n	Number of polystyrene latex particles P_n	$(A_n/P_n)\times100$
1	25.37	5	329	386	85.2
		10	502	579	86.7
		30	1142	1319	86.6
		60	358	417	85.8
2	25.37	5	142	169	84.1
		10	64	73	88.0
		20	231	271	85.0
		30	304	352	86.5
3	50.75	5	193	103	187
		10	130	72	180
		20	429	229	186
		30	152	82	185

where W is the molecular weight of gold. The plot of x vs. t in two runs exhibits S-shaped curve as shown in Fig. 10.

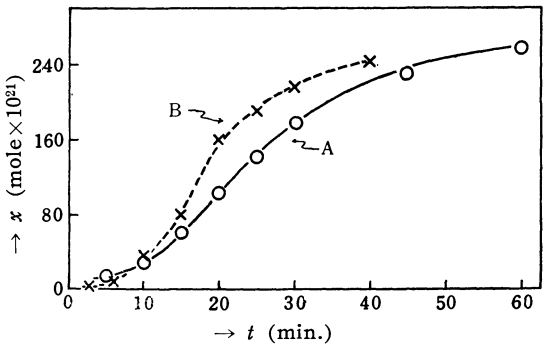

Fig. 10. Growth curve of gold particle measured by electron microscopy.
A: 25.37×10^{-5} mole Au/l.
B: 50.75×10^{-5} mole Au/l.

The rate of growth of a single gold particle is supposed to be expressed by the following equation:

$$dx/dt = kx^{2/3}(x_\infty - x) \qquad (3)$$

where x and x_∞ are the size of particles at time t and after the completion of the sol, respectively; k is the rate constant. The value of $x^{2/3}(x_\infty - x)$ was calculated and dx/dt was obtained from the tangent of the growth curve at time t, and the value of k was calculated from equation 3 and was shown in Fig. 11. The value

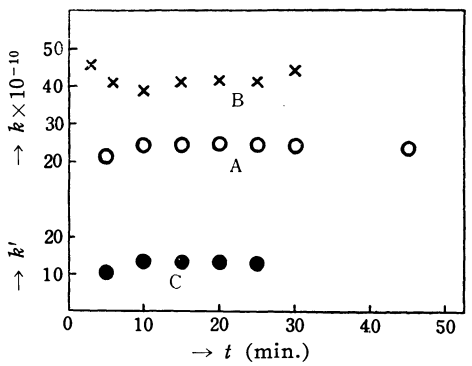

Fig. 11. Constancy of the rate constant.
A: 25.37×10^{-5} mole Au/l. } obtained
B: 50.75×10^{-5} mole Au/l. } from Fig. 10
C: 25.37×10^{-5} mole Au/l. obtained from Fig. 12

of k was constant except the very initial stage of the reaction. Then the rate of growth of a gold particle was proved to obey equation 3.

A study was made of the rate of disappearance of the auric ion during the formation of gold sol in the reaction mixture by withdrawing at definite times aliquot portions and analysing by means of iodometry*. The results of the experiment are given in Fig. 12.

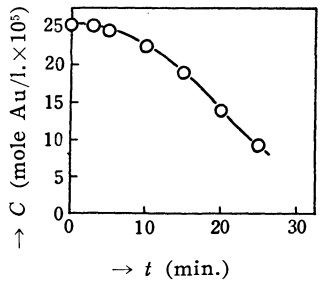

Fig. 12. Reaction rate of gold sol formation measured by the titration.
25.37×10^{-5} mole Au/l.

The rate of disappearance of the auric ion is supposed to be shown by the following equation:

$$-dC/dt = k'(C_0 - C)^{2/3}C \qquad (4)$$

where k' is the rate constant, and C_0 and C are concentrations of auric ion at initial and at time t during the sol formation. k' calculated from the experimental data is constant as shown in Fig. 11, and it is confirmed that equation 4 was proper.

Absorption Spectra of Gold Sol.—The absorption spectra of the reaction mixture

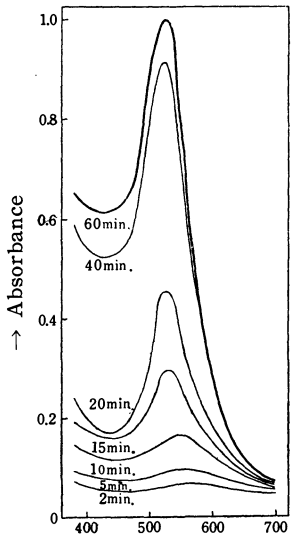

Fig. 13. Absorption spectra of gold sol.
(25.37×10^{-5} mole Au/l., 80°C)

* Iodine liberated by the reduction of Au^{3+} to Au^{+} oxidize gold particles to Au^{+} and the experimental data were obtained from the corrected volume of standard thiosulfate solution.

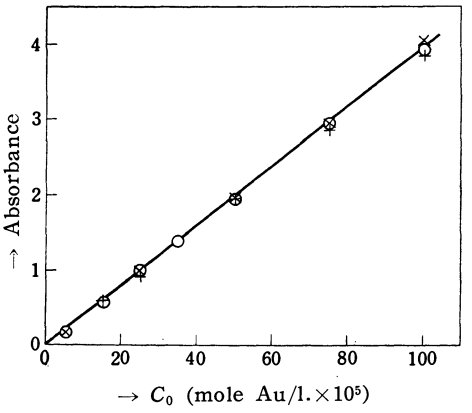

Fig. 14. Calibration curve of gold sol at 525 mμ.

measured at various times after the commencement of the reaction of sol formation are shown in Fig. 13. The maximum absorption shifted slightly toward the shorter wave length as the reaction proceeded. But after the lapse of about one fourth of the total reaction time, the wave length of maximum absorbance was fixed at 525 mμ. The maximum absorbance of gold sol formed under various conditions lay also at 525 mμ. The absorbance of gold sol at 525 mμ was linear with the initial concentration of auric ion as shown in Fig. 14, and the plots of absorbance vs. initial concentration of auric ion of the gold sols prepared above 70°C gave the same straight line.

Discussion

Gold particles in sodium citrate sol were the monodisperse and highly reproducible. Then particles can be used as a calibration standard in the measurement of particle sizes.

The size of particles decreased exponentially with increasing initial concentration of the auric ion. It has been reported that the gold sol particles prepared with various reducing agents in a basic medium increased in size with increasing initial concentration of the auric ion[4] and these phenomena were caused by the auric hydroxide produced as an intermediate. The sodium citrate sol is slightly acidic and the pH value is about 5.5. It is supposed that the auric ion exists as a chloride complex[5] before the reduction, and that free auric ion produced slowly from the complex reacts with citrate. Turkevich, Stevenson and Hillier[1] asserted that acetone dicarboxylate, generated from sodium citrate, reduced chlorauric acid. But as a pure sodium citrate solution was not known to be changed by heating, a certain kind of complex ion may be formed at first between gold and citrate ions, and the complex may be changed to acetone dicarboxylate. It seems that the formation of acetone dicarboxylate is the reaction from homogeneous solution and that the formation of gold sol proceeds homogeneously.

In order to prepare monodisperse particles it is necessary that the nucleation in the formation of gold sol should occur rapidly at the initial stage of the reaction, and that the new particle should not be produced during the growth period of gold particles. It was proved that new particles were not created during the growth process of gold sol particles by the spray method. Turkevich, Stevenson and Hillier[1] studied the rate of nucleation in gold sol. But it seems that at high temperature when a certain quantity of substance (acetone dicarboxylate) is generated homogeneously as described above, nuclei of gold are formed rapidly[6], and after the nucleation the growth of the particles seems to balance the deposition of gold, and the new particles are not formed.

The growth of gold particles after the nucleation is slow in the initial stage, then rapid and finally the size of particles approaches a definite value. The rate of growth is represented by equation 3. The general nature of the growth process is of an autocatalytic type with respect to the surface of gold particles. This process is also proved by equation 4 obtained from the rate of the disappearance of the auric ion.

The absorption maximum of gold sol shifts toward the shorter wave length as the reaction proceeds; that is, as the size of particle is increased and finally to 525 mμ. The relation between the absorbance at 525 mμ of gold sol produced and the initial concentration of auric ions gives the same straight line for every gold sol containing monodisperse particles ranging from 100 to 200 Å in diameter and the relation is not affected by the reaction temperature. This phenomenon is proved by Mie's theory that the absorbance of

4) H. B. Weiser and W. O. Milligan, *J. Phys. Chem.*, **36**, 1950 (1930).
5) H. M. Irving and D. Phil, *Quart. Rev.*, **5**, 200 (1951).
6) V. K. LaMer and R. H. Dinegar, *J. Am. Chem. Soc.*, **73**, 380 (1951).

gold sol containing very fine particles is proportional to the product of the volume of one particle with the number of particles in unit volume. Then the small quantity of gold can be determined by the sodium citrate method using the calibration curve described above.

Summary

Gold sol particles prepared by sodium citrate method were monodisperse. The size of gold particles decreased exponentially with increasing initial concentration of the auric ion, and increased exponentially with the reaction temperature. At the initial stage of the reaction of the gold sol formation, the gold nuclei were formed rapidly. After the nucleation the number of particles was kept constant over the whole period of reaction and the particles grew with the autocatalysis-like reaction at the surface of the particle.

The author acknowledges with thanks the guidance and discussion of Professor Eiji Suito of Kyoto University. He also wishes to express his hearty thanks particularly to Professor Masayoshi Ishibashi of Kyoto University for his discussion and encouragement throughout this investigation. The expense of this study was defrayed in part by a grant from the Ministry of Education.

Institute for Chemical Research
Kyoto University, Takatsuki
Osaka

Formation and Aging of Precipitates. IX. Formation of Monodisperse Particles (2) Barium Sulfate Precipitate by EDTA Method*

By Kazuyoshi TAKIYAMA

(Received June 13, 1958)

Sparingly soluble salts were suitable in the study of the physicochemical properties of precipitates and the precipitation reaction in analytical chemistry. Barium sulfate has been widely used for these purposes. The author previously reported the size and shape of barium sulfate particles precipitated by the direct mixing of ions[1]. In this paper the monodisperse particles of barium sulfate precipitated from a homogeneous solution, are reported. A few methods, e.g. the dimethyl sulfate method[2], and the sulfamic acid method[3] have been investigated to precipitate barium sulfate from a homogeneous solution, but the particles produced by these procedures were almost all polydisperse. The author has produced the monodisperse particles by means of the decomposition of the complex of barium and ethylenediaminetetra-acetate (EDTA) with hydrogen peroxide in the presence of sulfate. The EDTA method was used to precipitate ferric hydroxide by McNevin and Dunton[4] and the present author improved the method of precipitating barium sulfate.

Experimental

Formation of the Precipitate.—Equivalent quantities of barium chloride and EDTA solutions were mixed and an ammonium chloride-ammonia buffer was added to bring the pH of the solution to 10. After addition of ammonium sulfate which was equivalent to barium chloride, the mixed solution was warmed at 80°C and hydrogen peroxide was added to decompose EDTA. The reaction mixture was kept at 80°C during the course of reaction.

Measurement of the Particle Size.—Barium sulfate precipitates produced were observed with

* The eighth paper of this series, This Bulletin, **31**, 944 (1958).

1) E. Suito and K. Takiyama, This Bulletin, **27**, 121, 123 (1954); **28**, 305 (1955).

2) P. J. Elving and R. E. van Atta, *Anal. Chem.*, **22**, 1375 (1950).

3) W. F. Wagner and J. A. Wuellner, ibid., **24**, 1031 (1952).

4) W. M. McNevin and M. L. Dunton, ibid., **26**, 1246 (1954).

TABLE I
PARTICLE SIZES OF BARIUM SULFATE PRECIPITATES

Concn. C (M)	Size of particle: Length of long axis a (mμ)	Standard deviation σ_a (mμ)*	Length of short axis b (mμ)	Standard deviation σ_b (mμ)*	Mole number of particle M (mole)	Number of particle N (per ml.)
0.0022	993	34	298	21	8.89×10^{-16}	2.47×10^{9}
0.0033	1022	63	346	37	1.23×10^{-15}	2.68×10^{9}
0.0044	1066	68	420	44	1.87×10^{-15}	2.35×10^{9}
0.0066	1237	67	473	32	2.79×10^{-15}	2.37×10^{9}
0.0088	1400	58	535	41	4.04×10^{-15}	2.20×10^{9}

Reaction mixture:
- $BaCl_2$ original solution (0.022, 0.22 M)
- EDTA original solution (0.022, 0.22 M)
- $(NH_4)_2SO_4$ original solution (0.022, 0.22 M)

} same volume (3~10 ml.)

- Buffer solution 5 ml.
- H_2O_2 (30%) 20 ml.
- Total volume 100 ml.

* σ_a and σ_b are the standard deviation of a and b respectively.

an electron microscope. All particles were spindle-shaped, and the mean lengths of long and short axes and their standard deviation were determined. Then, the mole number of one particle, M (mole), was calculated according to the following equation:

$$M=(4/3)\pi(a/2)(b/2)^2\rho/W \qquad (1)$$

where a and b are the mean length of long and short axes, ρ and W are the density and the molecular weight of barium sulfate.

Measurement of the Reaction Rate.—The quantity of EDTA present at any given time was determined by titration. At various times during the course of the reaction, 10 ml. samples of the reaction mixture were poured into beakers, which were kept in ice water, and were titrated with 0.010 M zinc sulfate using Eriochrome Black T as indicator in the presence of a large excess of ammonium sulfate.

The growth of the particles was determined by electron microscopy as follows. At various intervals one drop of the reaction mixture was taken onto a tiny Formvar film floating on the surface of cold water. About ten minutes, the product was allowed for the diffusion of mother liquid ions from the drop into the water below. The film was then scooped up with a sample grid for electron microscopy.

Exprimental Results

Relation between the Particle Size and the Concentration of Reagents.—Barium sulfate particles precipitated at various concentrations of the reagents* are shown in Fig. 1 and the sizes of particles determined are listed in Table I. Particles are spindle-shaped and monodisperse over a range of 0.0022 to 0.0088 M

* The concentraton of reagents means the initial concentration of barium ion which is equivalent to that of EDTA or sulfate, and is expressed by mole per liter.

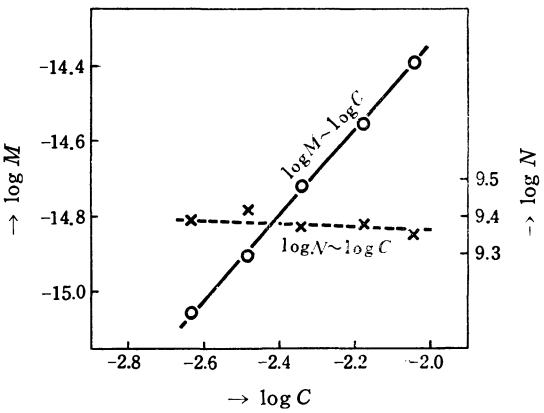

Fig. 2. Relation of the particle size to the concentration of reagents.

of the reagents. The size of particles increased with the increase of concentration of reagents. The logarithm of the mole number of particle, $\log M$, is linear with the logarithm of the concentration, $\log C$, as shown in Fig. 2. Then the relation between M and C is expressed by the following equation:

$$MC^{\alpha}=K \qquad (2)$$

where α and K are constants, being -1.2 and 1.15×10^{-12} respectively. As the number of particles per ml., N, is given as $C/M\times10^{-3}$, $\log N$ is also linear with $\log C$ as shown in Fig. 2. The number of particles per ml. remained almost constant over the range of cocentration listed in Table I.

Growth Process of Particle.—*Reaction rate determined by titration.*—The rate of decomposition of EDTA in two series of experiments, in which the concentrations

of reagents were 0.0022 and 0.0044 M, was expressed by curve (EDTA) in Fig. 3. The decomposition of EDTA was of the first order with respect to EDTA concentration. Barium ion liberated with decomposition of EDTA was expressed by curve (Ba^{2+}) in Fig. 3.

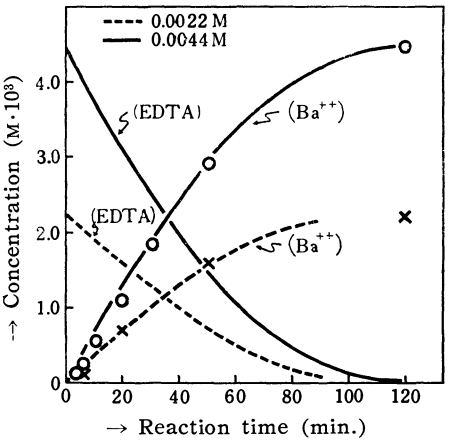

Fig. 3. Rate of formation of barium sulfate precipitate.
(EDTA): Concentration of EDTA in the reaction mixture
(Ba^{2+}): Rate of liberation of barium ion calculated from (EDTA)
○, ×: Quantity of barium sulfate precipitate determined by electron microscopy

Growth rate of particle observed by electron microscopy.—The particles during the course of reaction are shown in Fig. 4. The particles were monodisperse from the initial stage of the reaction. The value obtained by multiplication of the mole number of one particle, x(mole), obtained by electron microscopy at the time listed by the number of particles per liter of suspension, $N\times10^3$, calculated after completion of the reaction is equal to the quantity of barium sulfate precipitated. The values obtained as described above are shown by ○ and × in Fig. 3. It was proved from Fig. 3 that the rate of formation of barium sulfate determined by electron microscopy was almost the same as that of liberation of the barium ion obtained by titration.

Discussion

Barium sulfate precipitates formed at the concentration of reagents over a range from 0.0022 to 0.0088 M by EDTA method contained monodisperse particles. According as the concentration of the barium ion generated by the decomposition of EDTA increased, the ion product $(Ba^{2+})\times(SO_4^{2-})$ increased. It seemed that, when the ion product exceeded a certain critical value, corresponding to the limiting degree of supersaturation reported by LaMer and Dinegar[5], crystal nuclei were formed rapidly and after the nucleation the particles grew according to the liberation of barium ion as discussed later. If the concentration of reagents was too high, the rate of the generation of barium ion was rapid and the new particles were formed even after the nucleation. If the concentration of reagents was too low, the rate of formation of nuclei was slow and the growth of the nuclei previously formed proceeded faster than those formed later. Then in these cases the particles produced were polydisperse.

The relation of the particle size to the concentration of reagents was expressed by equation 2. The value of α in the equation was negative and the size of particles increased with the increase of concentration. The number of particles per unit volume of the suspension formed at various concentrations was almost constant as shown in Fig. 2. Thus a definite number of nuclei was formed over the range of concentration described above. O'Rourke and Johnson[6,7] reported that the number of particles per unit volume of barium sulfate suspension formed by direct mixing of ions over a range of initial concentration of 10^{-3} to 10^{-4} M was almost independent of concentration and the size of particles increased with the increase of initial concentration. These relations were also confirmed by the EDTA method over the range of concentration slightly above that proved by the direct mixing method.

The author previously reported the shape and size of particles of barium sulfate precipitated by direct mixing of ions[1]. Taking the data from that report, the logarithm of the mole number of one particle, $\log M$, and the logarithm of the initial concentration of barium sulfate, $\log C$, were calculated. The relation of $\log M$ to $\log C$ was shown in Fig. 5, and M and C were expressed by equation 2. The value of α was 2.7 and −1.4 at the concentration above and below about

5) V. K. LaMer and R. H. Dinegar, *J. Am. Chem. Soc.*, **73**, 380 (1951).
6) R. A. Johnson and J. D. O'Rourke, ibid., **76**, 2124 (1954).
7) J. D. O'Rourke and R. A. Johnson, *Anal. Chem.*, **27**, 1699 (1955).

(×15,000)

Fig. 1. Electron micrographs of barium sulfate particles produced at various concentrations.
a: 0.0022 M, b: 0.0044 M, c: 0.0066 M, d: 0.0088 M

(×20,000)

Fig. 4. Electron micrographs of barium sulfate particles during the growth process. (C=0.0044 M) a: 3 min., b: 5 min., c: 10 min. d: 40 min.
(Spherical particles shown in b are polystyrene latex used as the calibration standard to measure the particle size.)

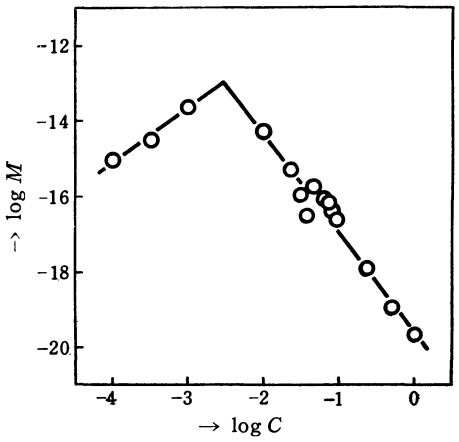

Fig. 5. Relation of the particle size to the initial concentration of barium sulfate formed by direct mixing of ions.

0.002 M respectively. The value of K was always constant and was 2.2×10^{-20}. The number of particles per ml. suspension, which was calculated from the initial concentration and the mean size of particles, increased rapidly with the increase of concentration above about 0.002 M, but was nearly constant at the concentration below about 0.002 M. The induction period of the precipitation appeared over the range of the initial concentration below about 0.002 M, that is, over the range of α being negative. The precipitation by EDTA method was made above 0.0022 M and the concentration was such that the induction period in the direct mixing did not appear. As EDTA method was one of the homogeneous solution methods, the induction period was, of course, found before the precipitation. It seems that when the induction period appears in the case of the precipitation, the size of particles increases with the increase of concentration of reagents.

Generally speaking, it would be plausible that when the nucleation plays a predominant role in the precipitation, the particle size decreases with the increase of initial concentration (Weimarn theory), and that when the growth of particles plays a predominant role, the particle size increases with the increase of initial concentration.

The rate of liberation of the barium ion calculated from the titration of EDTA agreed with that of the formation of barium sulfate precipitate obtained by electron microscopy. Thus the number of particles per unit volume of suspension was kept constant and no new particles were formed during the growth period of particles. Furthermore, the barium sulfate were deposited on each particle immediately after the liberation of barium ion, and the growth of particles was balanced with the liberation of barium ion.

Summary

Monodisperse spindle-shaped particles of barium sulfate were formed by means of the decomposion of barium-EDTA complex with hydrogen peroxide in the presence of sulfate. The logarithm of the size of the particle produced was linear with the logarithm of the concentration of reagents. The particles grew at the same rate of liberation of barium ion from the complex. The number of particles per unit volume of the reaction mixture was kept constant during the growth process of particles.

The author desires to thank Professor Eiji Suito of Kyoto University for his guidance and discussion. He also wishes to express his hearty thanks particularly to Professor Masayoshi Ishibashi of Kyoto University for his continuous advice and encouragement. The expense of this study was defrayed in part by a grant from the Ministry of Education.

Institute for Chemical Research
Kyoto University, Takatsuki
Osaka

Surface Films of Physically and Chemically Treated Ovalbumin (Dynamic Studies on Monolayer. II)

By Maresuke KASHIWAGI

(Received May 2, 1958)

Studies have previously been made of monolayer properties of crystalline ovalbumin in which it has been shown that the monolayer structure can be examined conveniently in its spreading process and this spreading of monolayer at the air-water interface was found to be directly linked with the denaturation[1]. The structural status of the spread monolayer can now be investigated to a certain extent from the measurements of surface pressure or potential changes with time at a constant area of a given substrate.

It appears that relatively few studies have been made on the measurement of surface pressure changes with time. Although important roles of experimental conditions, that of substrate in particular, have been fully emphasized, it must also be pertinent to investigate the effect of physical or chemical treatments on protein prior to spreading. Proteins are known to be denatured both by chemical and physical treatments. The surface denaturation of proteins was studied by Bull and Neurath[2-4]. Kaplan also has extensively studied the effect of physical and chemical treatments on ovalbumin monolayers[5-8].

Since denaturation is essentially an intramolecular phenomenon, involving changes in an unknown structure, it can be investigated and described in terms of these changes, whether physical, chemical or biological. Among others, the effect of heat with infrared irradiation, acid and alkali treatments on the ovalbumin molecule before spreading are investigated and discussed here.

Experimental

Apparatus.—The surface balance used is the same as the one previously described[1]. Wilhelmy's vertical plate type is found to be more convenient than Langmuir and Adam's apparatus for the measurement of pressure changes with time.

Materials.—Ovalbumin was obtained by the usual method as described before[1]. This ovalbumin is treated with heat, acid and alkali, respectively. Except for the treatment with heat, acid and alkali treatments are based partially on MacPherson and Heidelberger's studies[9]. The temperature condition of heat treatment in this case is made somewhat mild. The protein under those conditions is expected to be slightly denatured as indicated by the nitroprusside test[10]. This test was also applied to the untreated native protein with negative result. Conditions adopted hereby are summarized in Table I.

Experimental procedure.—Protein is spread from its aqueous solution by means of a micropipet over a large area (2.5 m^2/mg.) and the film is kept there for exactly 5 minutes before the start of compression for *F-t* curve measurement. To determine pressure-area diagrams, the time allowed for after spreading is 20 minutes instead of 5 minutes. The most commonly used substrate is aqueous 20% ammonium sulfate solution at pH 4.8 since this is one of the best substrates[1].

TABLE I
CONDITIONS OF OVALBUMIN TREATMENTS

Modification	Concn.	Reagent used	Temp.	Time	pH	Nitroprusside test
Acid	0.224 mg./cc.	0.1 N HCl	2~4°C	17 hrs.	2.2	+
Alkali	〃	0.04 N NaOH	2~4°C	17 hrs.	9.6	+
Heat	〃	infrared light 100 V. 250 W	42°C	1/3 hrs.	—	+

1) M. Kashiwagi, This Bulletin, **31**, 176 (1958).
2) H. B. Bull and H. Neurath, *J. Biol. Chem.*, **118**, 163 (1937).
3) H. B. Bull, ibid., **125**, 585 (1938).
4) H. Neurath, *J. Phys. Chem.*, **40**, 361 (1936).
5) J. G. Kaplan, *J. Colloid Sci.*, **7**, 382 (1952).
6) J. G. Kaplan and M. J. Fraser, *Biochim et Biophys. Acta*, **9**, 585 (1952).
7) J. G. Kaplan, D. H. Andrews and M. J. Fraser, *J. Colloid Sci.*, **9**, 203 (1954).
8) J. G. Kaplan and M. J. Fraser, *J. Biol. Chem.*, **210**, 57 (1954).
9) C. F. C. MacPherson and M. Heiderberger, *J. Am. Chem. Soc.*, **67**, 574 (1945).
10) D. Glick, "Methods of Biochemical Analysis", Vol. 1, p. 20 (1954).

Results

Fig. 1 represents measured surface pressure changes ΔF with time of heat-treated ovalbumin monolayers at various surface areas and on the substrate of 0.1 N hydrochloric acid. Pressure-time curves of the same sample on the substrate of 20% ammonium sulfate solution are also shown in Fig. 2. It can be seen from Fig. 1 that F increases with time, but the rate of increase is markedly dependent on surface area, being only slightly noticeable at 1.18 m^2/mg., while it is very pronounced at 0.914 m^2/mg. On the other hand, as shown in Fig. 2, F decreases in the initial stage on ammonium sulfate substrate and then becomes constant at 0.92 m^2/mg., while at larger areas, F seems to increase very slowly but linearly with time. Surface pressures of acid-treated ovalbumin remain practically constant for the whole period of the experiment, or very slightly increase on the substrate of 20% ammonium sulfate (Fig. 3). *F-t*

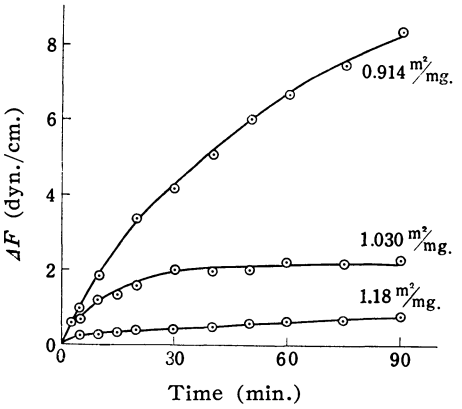

Fig. 1. Surface pressure changes of heat-denatured ovalbumin (Substrate 0.1 N HCl, 14°C).

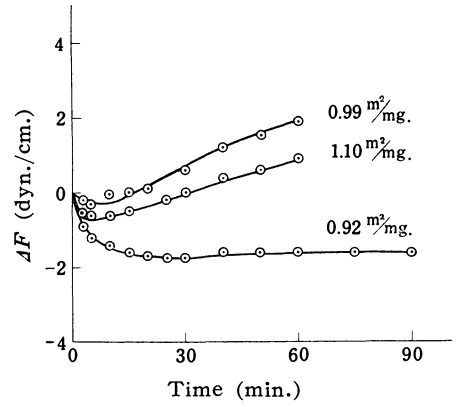

Fig. 2. Surface pressure changes of heat-denatured ovalbumin (Substrate 20% $(NH_4)_2SO_4$, 15°C) pH 4.8.

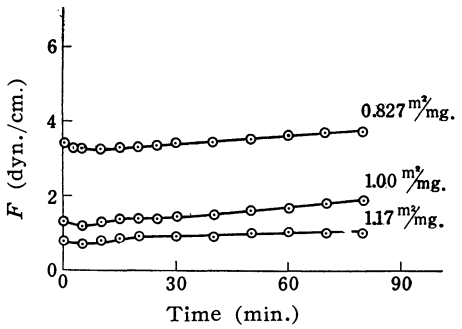

Fig. 3. Surface pressure changes of acid-treated ovalbumin (Substrate 20% $(NH_4)_2SO_4$, pH adjusted 7.1, 19°C).

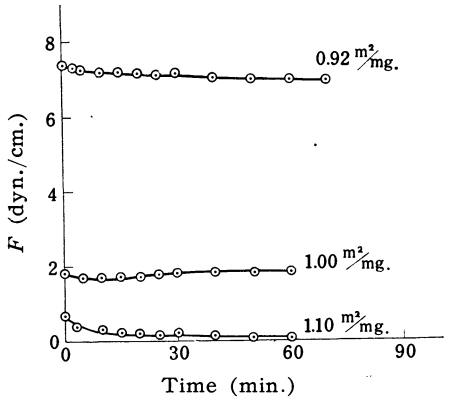

Fig. 4. Surface pressure change of alkali-treated ovalbumin (Substrate 20% $(NH_4)_2SO_4$, 16°C) pH 4.8.

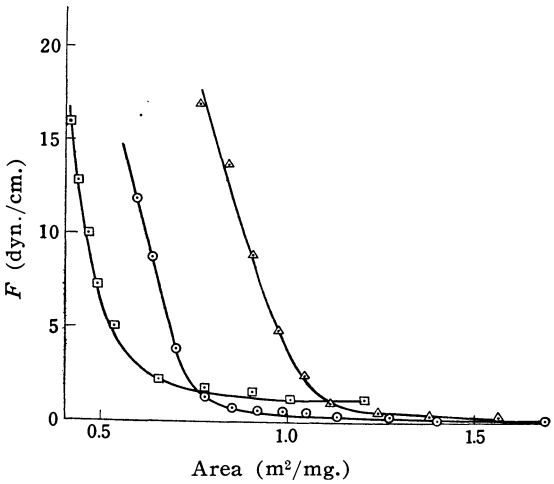

Fig. 5. Pressure-area diagram of heat-treated ovalbumin.
△ 20% $(NH_4)_2SO_4$ Substrate pH 4.8
⊙ 0.1 N HCl Substrate
⊡ untreated ovalbumin on 0.1 N HCl

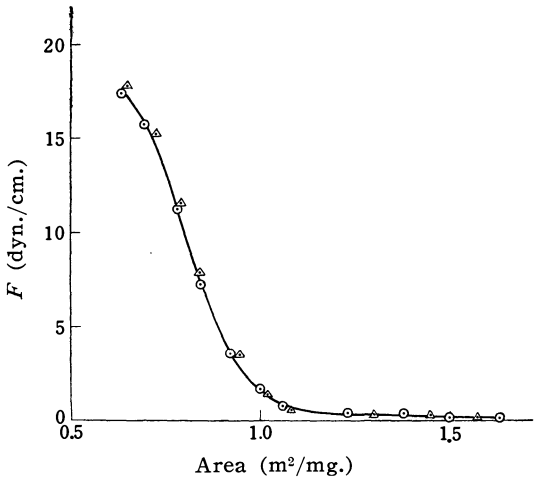

Fig. 6. Pressure-area diagrams of ovalbumin (Substrate 20% $(NH_4)_2SO_4$).
△ alkali-treated
⊙ acid-treated
PH of Substrate
△ 4.8
⊙ 7.1

curves of alkali-treated ovalbumin soon reach a final equlibrium pressure and remain constant (Fig. 4).

All the actual measurements of pressure changes with time are carried out every three minutes at least, but the recording of all points on *F-t* curves are not attempted for convenience' sake. Pressure-area diagrams of these treated ovalbumin monolayers are shown in Figs. 5 and 6, respectively, together with that of untreated native ovalbumin for comparison. *F-A* curves of both acid- and alkali-treated protein are identical within the limit of the present experimental condition, as indicated in Fig. 6.

Discussion

It may be expected that all these treatments applied here would not cause substantial structural change in the protein[9,11]. The present condition of heat treatment was rather milder than in the case of ordinary conditions for denaturation, but it is interesting to note that surface pressure of heat treated ovalbumin increases with time on 0.1 N hydrochloric acid as indicated in Fig. 1, while with the untreated native protein surface pressure decreased with time on the same substrate[1], indicating partial desorption. Pressure-area diagrams of the former also shift obviously from that of the untreated. By heat treatment the intramolecular cohesion forces are lessened to such an extent that the protein spreads to a larger area than they normally occupy[2,8] and the ease of molecular unfolding increased by heat must have retarded the factor to cause desorption from the surface.

The protein denaturation is often followed inevitably by intermolecular aggregation, which makes the interpretation of the denaturation effect very difficult, but ovalbumin molecules under the present condition would not proceed progressively to marked aggregation or dissociation[9,11].

We have seen in Figs. 3 and 4, that under a constant film area, the surface pressure is independent of time, that is

$$\left(\frac{\partial F}{\partial t}\right)_{A_0} = 0$$

where A_0 refers to co-area.

But since we have a general relation

$$\left(\frac{\partial A_0}{\partial t}\right)_F = -\left(\frac{\partial F}{\partial t_0}\right)_{A_0} \Big/ \left(\frac{\partial F}{\partial A_0}\right)_t$$

where $\left(\frac{\partial F}{\partial A_0}\right)_t$ shows a finite value, $\left(\frac{\partial A_0}{\partial t}\right)_F$ vanishes, which means, that A_0 is independent of time. Therefore we can expect that under such a condition, molecules in the film would be fully denatured in accordance with our former report[1].

Summary

Monolayer properties of acid, alkali and heat-treated ovalbumin are investigated from the measurements of surface pressure changes with time and surface pressure-area diagrams.

These treated specimens are found to be characteristically different from the untreated native protein in their surface behavior. The process of surface denaturation is also discussed.

The author wishes to express thanks to Professor Ryohei Matsuura of Kyushu University and Professor Taro Tachibana of Ochanomizu Women's University for their kind discussion of the subject.

Mitsuwa Chemical Laboratory
Marumiya Co., Ltd.
Terashima, Sumida-ku, Tokyo

11) V. A. Belister and T. V. Saenko, *Biokhimiya*, **22**, 274 (1957).

Kinetics of Hydrolytic Reaction Catalyzed by Crystalline Bacterial α-Amylase. I. The Influence of pH

By Sôzaburo ONO, Keitaro HIROMI and Yoshiko YOSHIKAWA

(Received February 24, 1958)

It is well known that enzyme reactions consist of two elementary processes, namely formation of an intermediate enzyme-substrate complex and the subsequent breakdown of the complex into reaction products and free enzyme. These processes are represented kinetically by two parameters, i. e., the Michaelis constant and the rate constant for the breakdown of the complex, respectively. Systematic investigation of the influence of various extrinsic factors such as temperature, pH, ionic strength, dielectric constant of the medium, pressure, inhibitors, etc., upon these parameters, provides a means for elucidating the mechanisms of the enzyme reactions. Recently certain enzyme reactions have been studied along these lines and important information on the mechanisms has been obtained[1-4].

Bacterial amyloclastic α-amylase of *Bac. amyloliquefaciens* Fukumoto has long been studied by Fukumoto and his co-workers, and was crystallized by Hagihara[5]. Although various investigations have been made about this crystalline enzyme[6,7], few kinetic studies have been reported on it[8,9]. In our laboratory the influence of various factors on the rate of reactions catalyzed by this crystalline enzyme has been studied from the kinetic point of view, using substrates as simple and pure as possible. In the present report, the influence of pH on the reaction rate was investigated with the hope of obtaining a certain clue for elucidating the mechanism of the enzyme reaction involved.

1) R. Lumry, E. L. Smith and R. R. Glantz, *J. Am. Chem. Soc.*, **73**, 4330 (1951).
2) R. Lumry and E. L. Smith, *Discussions Faraday Soc.*, No. **20**, 105 (1955).
3) K. J. Laidler, ibid., No. **20**, 83 (1955).
4) A. Stockell and E. L. Smith, *J. Biol. Chem.*, **227**, 1 (1957).
5) B. Hagihara, *Proc. Japan Acad.*, **27**, 346 (1951).
6) T. Yamamoto, *Bull. Agr. Chem. Soc. Japan*, **19**, 121 (1955).
7) T. Yamamoto, ibid., **20**, 188 (1956).
8) J. Osugi, *Rev. Phys. Chem. Japan*, **22**, 66, 71 (1952).
9) J. Osugi and K. Hiromi, ibid., **22**, 76 (1952).

Experimental

Materials. — 1) *Substrate.* — Potato amylose (degree of polymerization ca. 900) manufactured by Nagase Sangyô Co. Ltd. was used. 2) *Enzyme.* —Bacterial amyloclastic α-amylase (six-times recrystallized; molecular weight 45,000) was kindly provided by Professor J. Fukumoto of Osaka City University. The enzyme was dissolved in four-times redistilled water, and the solution was stored in a refrigerator as the stock solution. The enzyme concentration in this solution was determined from the optical density at 280 mμ to be 3.88×10^{-6} M. The enzyme activity in this solution was constant throughout the whole experiment. 3) *Buffer solution.*—A solution of 0.15 M veronal sodium and sodium acetate was mixed with 0.1 N hydrochloric acid in various ratios. This buffer solution was confirmed to have no specific effect on the reaction rate and on the determination of products.

Methods. — A mixture of 10 ml. of amylose solution in 0.5 N sodium hydroxide and 13 ml. of the buffer was neutralized with 5 ml. of 1 N hydrochloric acid in a reaction vessel immersed in a thermostat adjusted to 25°±0.05°C, unless otherwise stated. After equilibrium temperature was reached, 2 ml. of the enzyme solution (containing an appropriate amount of the stock solution in 1/300 M calcium acetate) was added quickly to make the total volume 30 ml. The reaction mixture was stirred mechanically. Two ml. of the reaction mixture was pipetted into 1 ml. of 0.5 N sodium hydroxide to stop the reaction at intervals of one minute during the first four minutes of the reaction.

The reducing end-groups produced as the result of the reaction were determined photometrically with 3, 5-dinitrosalicylate[10]. In lower concentrations of the products (below 1.4×10^{-4} mole of reducing end group per liter), the atomspheric oxygen made the determination impossible because of its oxidizing action. Therefore, the nitrogen was bubbled through the reaction mixture and the reagents used in the analytical procedure before and during the experiment.

The pH of the reaction mixture was measured by means of a quinhydrone electrode at the same temperature as that of the reaction. The error of the measurements was within ±0.01 pH. The concentrations of substrate and products were

10) G. N. Smith and C. Stocker, *Arch. Biochem.*, **21**, 95 (1949).

expressed in mole per liter of the bond hydrolyzable and hydrolyzed, respectively. The initial reaction rate was estimated from the tangent of the reaction-time curve at zero time. The error in this procedure was minimized by choosing appropriate concentrations of enzyme so that the curves would not show any marked curvature.

Results

The initial rate v was in good proportionality with the enzyme concentration [E], as shown in Fig. 1. The plots of the reciprocals of the initial rate v versus substrate concentration [S] were found to fulfil the linear relationship required by the Lineweaver-Burk equation[11],

$$\frac{1}{v} = \frac{\bar{K}_m}{\bar{k}_2[\mathrm{E}]} \cdot \frac{1}{[\mathrm{S}]} + \frac{1}{\bar{k}_2[\mathrm{E}]} \qquad (1)$$

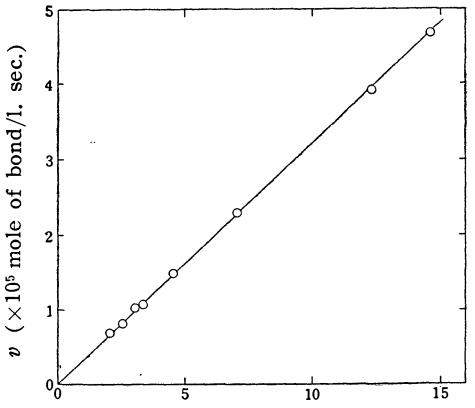

Fig. 1. Plot of initial rate versus enzyme concentration (substrate concentration, 0.0154 mole of bond/l.; 25°C; pH 5.41).

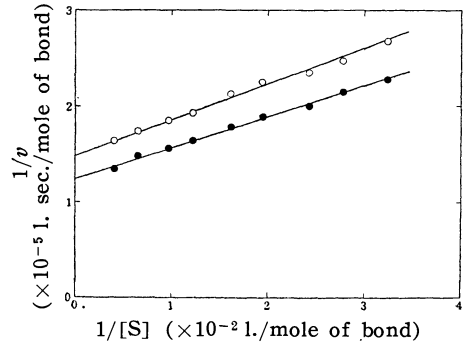

Fig. 2. Plot of $1/v$ versus $1/[S]$ at 25°C. ○ pH 7.51, ● pH 4.84

This relationship holds for any pH studied (see Fig. 2). The concentration of the enzyme [E] being known, the apparent Michaelis constant $\bar{K}_m$, and the apparent rate constant $\bar{k}_2$ for the breakdown of the enzyme-substrate complex, were obtained from the formula. The values of $\bar{K}_m$ and $\bar{k}_2$ at various pH's are summarized in Table I. In Fig. 3, $\log 1/\bar{K}_m$ and $\log \bar{k}_2$ are plotted versus pH. $\bar{K}_m$ is constant over the pH range examined (pH 3.6~8.4), while $\bar{k}_2$ decreases on both the acid and the alkaline side.

TABLE I

VALUES OF $\bar{K}_m$ AND $\bar{k}_2$ AT VARIOUS pH'S AT 25°C

pH	[E] ×10⁹ mole/l.	$\bar{K}_m$ ×10³ mole of bond/l.	$\bar{k}_2$ ×10⁻³ sec.⁻¹
3.59	7.05	2.3±0.4	0.37±0.03
3.73	9.94	2.3±0.3	0.61±0.02
4.16	3.38	2.3±0.2	1.91±0.05
4.84	2.56	2.6±0.2	3.20±0.04
5.60	2.56	2.6±0.2	3.94±0.15
5.95	2.06	1.8±0.2	3.91±0.11
6.25	1.54	2.1±0.2	3.80±0.10
6.92	2.06	2.6±0.1	3.90±0.05
7.51	3.08	2.4±0.2	2.18±0.04
8.23	4.58	2.1±0.3	0.75±0.02
8.40	14.6	2.6±0.2	0.47±0.02

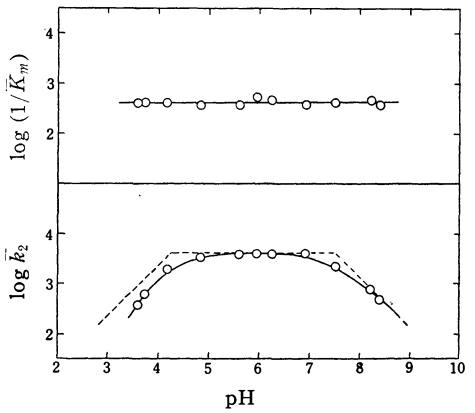

Fig. 3. Plots of log $(1/\bar{K}_m)$ and log $\bar{k}_2$ versus pH at 25°C.

The results of another series of experiments are shown in Fig. 4, in which the ratio of the initial rate v at a given pH, to that v_{max} at the optimum pH, measured at constant substrate and enzyme concentration, was plotted against pH. A nearly symmetrical bell-shaped curve was obtained. Neither the shape nor the position of the curve was affected by varying the substrate concentration. The solid line in Fig. 4 represents the theoretical curve which will be described below. The experimental points satis-

11) H. Lineweaver and D. Burk, *J. Am. Chem. Soc.*, **56**, 658 (1934).

factorily fit the theoretical curve except in the narrow region below pH 4, where the occurrence of a rapid irreversible inactivation of the enzyme was observed. The influence of temperature on the v/v_{max}—pH curve was also investigated, and the results are presented in Table III, which will be discussed below.

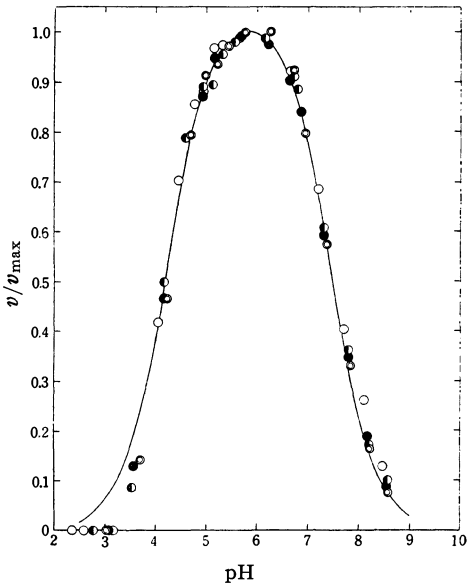

Fig. 4. Plot of v/v_{max} versus pH at various substrate concentrations at 25°C.
○ 0.0247, ◐ 0.0123, ● 0.00617,
◎ 0.00308 mole of bond/l.

Discussion

The results will be analyzed according to the following scheme which has been employed by various authors[12-15]:

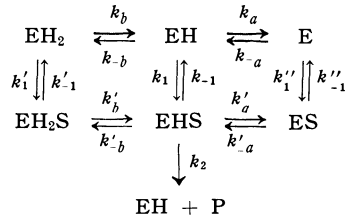

where E represents the enzyme in a particular state of ionization, H a proton, S the substrate and P the products. Of the three forms of enzyme-substrate complexes, only the complex EHS is assumed to break down into the reaction products. The various rate constants k's are indicated above.

The initial rate v can be expressed as follows:

$$v=\frac{k_2[E][S]}{K_m\left(1+\frac{K_a}{[H]}+\frac{[H]}{K_b}\right)+[S]\left(1+\frac{K_a'}{[H]}+\frac{[H]}{K_b'}\right)} \quad (2)^*$$

where

$$K_m=(k_{-1}+k_2)/k_1$$

and

$$K_a=k_a/k_{-a}, \quad K_b=k_b/k_{-b}$$
$$K_a'=k_a'/k_{-a}', \quad K_b'=k_b'/k_{-b}'$$

Thus K_a, K_b, K_a' and K_b' are the ionization constants of the two ionizable groups taken into account in the scheme, in the substrate-free enzyme and enzyme-substrate complex, respectively.

Comparing Eqs. 1 and 2, $\bar{K}_m$ and $\bar{k}_2$ are represented in the following formula;

$$\bar{K}_m=K_m\cdot\frac{1+\frac{K_a}{[H]}+\frac{[H]}{K_b}}{1+\frac{K_a'}{[H]}+\frac{[H]}{K_b'}} \quad (3)$$

$$\bar{k}_2=\frac{k_2}{1+\frac{K_a'}{[H]}+\frac{[H]}{K_b'}} \quad (4)$$

From our results which show that $\bar{K}_m$ is constant over a wide range of pH in which $\bar{k}_2$ varies (see Fig. 3), it is concluded that K_a equals to K_a' and K_b equals to K_b' in Eq. 3; that is to say, the ionization of the two groups considered is not affected by the substrate binding. If these ionizable groups were directly involved in the complex formation, their ionization constants would be changed considerably by the combination of the substrate with the enzyme[16]. Thus it may be most reasonable to conclude that these groups in the enzyme molecule are not directly responsible for the complex formation. The variation of $\bar{k}_2$ with pH is in accordance with the prediction of the theory (see Fig. 3 and Eq. 4) and it is evident that the breakdown of the complex occurs only when group A (whose ionization constant is K_a) is undissociated and group

12) S. G. Waley, *Biochim. et Biophys. Acta*, **10**, 27 (1953).
13) R. A. Alberty and V. Massey, ibid., **13**, 347 (1954).
14) K. J. Laidler, *Trans. Faraday Soc.*, **51**, 528 (1955).
15) A. Takamiya, "Kôso-kenkyûhô", edited by S. Akabori, Asakura Shoten, Tokyo (1955), p. 198.

* The exact steady-state treatment[14] leads to the expression which includes the perturbation term in the denominator of Eq. 2. But this term is reasonably neglected in the present case (see the foot-note** below).
16) K. J. Laidler, *Trans. Faraday Soc.*, **51**, 540 (1955).

B (whose ionization constant is K_b) is dissociated.

When K_a equals to K_a' and K_b equals to K_b', Eq. 2 reduces to a simpler form;

$$v=\frac{k_2[\mathrm{E}][\mathrm{S}]}{\left(1+\frac{K_a}{[\mathrm{H}]}+\frac{[\mathrm{H}]}{K_b}\right)(K_m+[\mathrm{S}])} \tag{5}$$

Let v_{max} denote the initial rate at the optimum hydrogen ion concentration $[\mathrm{H}]_{opt}$ with a given substrate concentration [S]. Then differentiation of Eq. 5 with respect to [H] leads to the following relationships;

$$[\mathrm{H}]_{opt}=\sqrt{K_a K_b} \tag{6}$$

$$v_{max}=\frac{k_2[\mathrm{E}][\mathrm{S}]}{(1+2\sqrt{K_a/K_b})(K_m+[\mathrm{S}])} \tag{7}$$

Consequently,

$$\frac{v}{v_{max}}=\frac{1+2\sqrt{K_a/K_b}}{1+\frac{K_a}{[\mathrm{H}]}+\frac{[\mathrm{H}]}{K_b}} \tag{8}$$

Thus v/v_{max} should be a function independent of the substrate concentration over the whole range of pH. The results shown in Fig. 4 obviously fulfil this requirement, again confirming the validity of the theory.

Moreover, several conclusions of considerable importance can be drawn from the foregoing results. (i) The apparent Michaelis constant $\bar{K}_m$ at any pH is equal to the true Michaelis constant K_m (see Eq. 3). (ii) The constancy of $\bar{K}_m$, as pointed out by Morales[17] and Laidler[16], leads to a reasonable conclusion that $k_2 \ll k_{-1}$**, i. e., there is equilibrium between enzyme, substrate and complex. The Michaelis constant may be regarded as the dissociation constant of the enzyme-substrate complex, i. e., $K_m=k_{-1}/k_1$. (iii) The apparent rate constant $\bar{k}_2$ at the optimum pH is equal to $k_2/(1+2\sqrt{K_a/K_b})$ (compare Eqs. 1 and 7), about 5 per cent less than the true rate constant k_2 at 25°C.

The ionization constants of the groups, K_a and K_b, were evaluated[13,15] according to Eq. 8, using the experimental values shown in Fig. 4. These values expressed in pK at various substrate concentrations at 25°C are presented in Table II. The mean values of these are 7.45 for pK_a and 4.22 for pK_b, from which the optimum pH is found from Eq. 6 to be 5.84, which is in good agreement with the experimental value 5.85. The solid line in Fig. 4 represents the theoretical curve drawn according to Eq. 8 using the mean pK values thus obtained. Except for the narrow region below pH 4, where the irreversible inactivation of the enzyme was detected, the coincidence between the theory and the experiment is remarkable.

TABLE II
THE pK VALUES AT VARIOUS SUBSTRATE CONCENTRATIONS AT 25°C

$[\mathrm{S}]\times10^2$ mole of bond/l.	pK_b	pK_a
2.47	4.18	7.49
1.23	4.20	7.45
0.617	4.24	7.45
0.308	4.27	7.41
Mean	4.22	7.45

TABLE III
TEMPERATURE DEPENDENCE OF pK'S

Temp. °C	pK_b	pK_a
6.0	4.44	7.60
12.0	4.29	7.56
18.0	4.38	7.46
25.0	4.24	7.45
32.0	4.28	7.37

Substrate concentration: 0.00617 mole of bond/l.

The pK values of the groups at various temperatures are summarized in Table III. The heats of ionization of these groups are calculated to be $\Delta H_a=4$ kcal. for group A, and $\Delta H_b=2$ kcal. for group B. From these values of pK and ΔH, one can infer the nature of the ionizing groups under consideration by comparing them with the reported values of various ionizing groups found in proteins[18]. Considering some deviations from these values which might be expected in the actual enzyme molecule, it may be reasonable to conclude that group B, having a pK of 4.22 and a ΔH of 2 kcal. is a carboxyl group, and that group A, having a pK of 7.45 and a ΔH of 4 kcal., may be either an imidazolium or an ammonium group (the ΔH value is in favor of the former possibility). As already stated, these groups are not considered to be involved in the complex formation, but to be essential in the breakdown of the complex into reaction products in the forms, respectively, of COO^- and $\rangle NH^+$ (or $-NH_3^+$).

17) M. F. Morales, *J. Am. Chem. Soc.*, **77**, 4169 (1955).

** This is the condition under which the perturbation term which would appear in the denominator of Eq. 2, can be neglected (see ref. 14).

18) J. T. Edsall, "Proteins, Amino Acids and Peptides", Reinhold Pub. Corp., New York (1943), p. 444.

Yamamoto[6] examined the activity of this enzyme treated with several specific reagents, and concluded that the phenoxyl group of the tyrosine residue is essential. Since the pK value of this group lies outside the pH range in which kinetic studies are feasible (see Fig. 4), it is impossible to determine whether this group is involved in the formation or the breakdown of the complex. The above-stated constancy of $\bar{K}_m$ over the pH range examined (3.6~8.4) implies that no ionizable group having its pK in this range is involved in the complex formation. However, it does not exclude the possibility that some group having its pK outside this region may also participate in the formation and/or breakdown of the complex. His conclusion, therefore, is not incompatible with our findings.

Recently mechanisms of certain hydrolytic enzyme reactions have been considered in terms of bifunctional catalysis, or concerted mechanism[19-21]. It seems likely that the acidic (proton-donating) and basic (proton-accepting) groups of the enzyme function as an acid and a base simultaneously in the enzyme-catalyzed hydrolysis. From this point of view, a tentative scheme on the mechanism of this enzyme reaction is presented in Fig. 5.

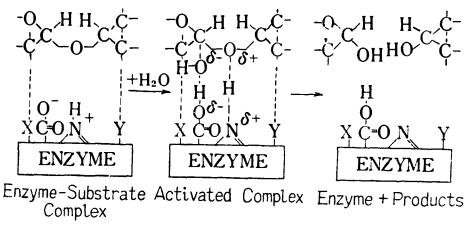

Fig. 5.

In this scheme it is supposed that the imidazolium cation, acting as an acid, attacks the etheric oxygen atom of the glucosidic bond, and simultaneously the carboxylate anion, acting as a base, pulls the proton from the water molecule which is situated between C_1 atom of the glucoside residue at the left and the carboxylate anion. X and Y represent the unknown groups of the enzyme which are responsible for binding the substrate in a geometrically favorable position so that the carboxylate and imidazolium groups will be able to form an activated complex with the substrate. The nature of groups X and Y cannot be determined from the present study. If they are ionizable groups, their pK's must lie either below 3.6 or above 8.4. Another possible mechanism is presented in the scheme[22] shown in Fig. 6.

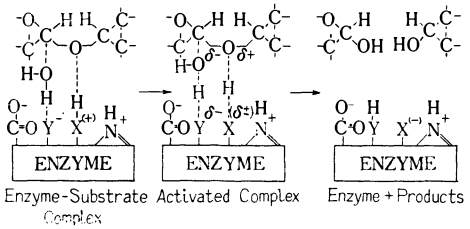

Fig. 6.

The possible charge separation in the activated complex, as depicted in each scheme, can be inferred from the study of the solvent effect upon this enzyme reaction, which will be reported in a later paper.

Summary

The influence of pH on the rate of the hydrolytic reactions of amylose catalyzed by the crystalline bacterial α-amylase of *Bac. amyloliquefaciens* Fukumoto has been examined at various substrate concentrations and temperatures.

The apparent Michaelis constant $\bar{K}_m$ is constant over the pH range examined (3.6~8.4), whereas the apparent rate constant $\bar{k}_2$ for the breakdown of the enzyme-substrate complex into the reaction products and free enzyme decreases on both the acid and the alkaline side of the optimum pH 5.85. The relative rate - pH curves are not affected by the substrate concentration. From these facts, it is concluded that at least two ionizable groups in the enzyme are involved in the breakdown of the complex, although these groups are not directly responsible for the formation of the enzyme-substrate complex.

The ionization constants and the heats of ionization of the two groups involved in the reaction have been determined. From these values, the ionizing groups are inferred to be the carboxyl and imidazole (or amino) groups. The ionized

19) C. G. Swain and J. F. Brown, *J. Am. Chem. Soc.*, **74**, 2534, 2538 (1952).
20) H. Lindley, *Advances in Enzymol.*, **15**, 271 (1954).
21) K. J. Laidler, "Introduction to the Chemistry of Enzymes", McGraw-Hill Book Co., New York (1954), p. 155.
22) S. Ono, K. Hiromi and Y. Yoshikawa, *Symposia on Enzyme Chem. Japan*, **12**, 1, 291 (1957).

form of the former and the positively charged form of the latter are considered to be essential for the breakdown process.

Tentative mechanisms of the reaction are proposed.

The kindness of Professor J. Fukumoto and Dr. T. Yamamoto of Osaka City University in providing the crystalline enzyme is gratefully acknowledged.

Laboratory of Biophysical Chemistry
College of Agriculture
University of Osaka Prefecture
Sakai, Osaka

*Irreversible Photobleaching of the Solutions of Fluorescent Dyes. VI. Photobleaching of Uranin in Alkaline Solutions**

By Masashi IMAMURA

(Received on June 20, 1958)

Previous papers[1-6] in this series have described the photobleaching of two halogenated xanthene dyes, eosin and erythrosin, in aerated and deaerated solutions. Photochemical primary processes of these dyes both in aqueous and in alcoholic solutions have been concluded. Reactivities of the triplet-excited states toward oxygen and alcohol molecules have also been discussed.

The present paper concerns with the photobleaching reactions of uranin, an unhalogenated xanthene dye, in water and in aqueous alcohols in the presence of alkali. Comparative studies on the photoreduction of uranin and its halogenated derivatives have been done by Adelman and Oster[7]. The present study has been performed under aerated and deaerated conditions, and some new facts have been revealed.

Experimental

Uranin (sodium fluoresceinate). — Ishizu Chemicals guaranteed uranin was employed without further purification. Its purity was stated to be greater than 98.5%. (*Anal.* Found: C, 63.02; H, 2.70. Calcd. for $C_{20}H_{10}O_5Na_2$: C, 63.83; H, 2.67.) Maximum molar extinction coefficient (at λ 490 mμ) was reported by several authors to be 7.85×10^4 [8], 7.82×10^4 [9], 7.62×10^4 [10] and 5.46×10^4 (at pH 7)[7]. Under the consideration of a fluorescence error accompanying absorption measurements with Beckman Model DU Spectrophotometer[11-13], real molar extinction coefficient in an alkaline (pH more than 9) aqueous solution was measured to be 7.80×10^4 at λ_{max} 490 mμ.

Other Materials.—Commercial alcohols were purified by the usual methods[14] and were distilled with a fractionating column of a high efficiency. Takeda Chemicals sodium hydroxide (extra pure) and doubly distilled water were used in all mixtures.

Procedures.—Apparatus and technique were essentially identical with those described previously[2]. Matsuda V-B2-photographic Y1 combination, which transmits λ 450~570 mμ with maximum transmission 52% at λ 490 mμ, was used as a filter. Concentration was determined from the optical density at λ_{max} of the solution. Aqueous or aqueous alcoholic solution of uranin exhibits stronger fluorescence than that of eosin or erythrosin. Accordingly, measured optical densities would more or less include the fluorescence error mentioned above. This error was, however, evaluated experimentally to be less than 1.6%, which was within experimental error.

* Presented in part before the 11 th Annual Meeting of the Chemical Society of Japan, Tokyo, April 5, 1958.

1) M. Imamura and M. Koizumi, This Bulletin, **28**, 117 (1955).
2) M. Imamura, *J. Inst. Polytech. Osaka City Univ.*, **5C**, 85 (1956).
3) M. Imamura and M. Koizumi, This Bulletin, **29**, 899 (1956).
4) M. Imamura and M. Koizumi, ibid., **29**, 913 (1956).
5) M. Imamura, ibid., **30**, 249 (1957).
6) M. Imamura, ibid., **31**, 62 (1958).
7) A. H. Adelman and G. Oster, *J. Am. Chem. Soc.*, **78**, 3977 (1956).
8) J. Q. Umberger and V. V. LaMer, ibid., **67**, 1107 (1945).
9) V. L. Levschin, *Z. Phys.*, **72**, 368 (1931).
10) W. R. Orndorff, R. C. Gibbs and C. V. Shapiro, *J. Am. Chem. Soc.*, **50**, 819 (1928).
11) K. S. Gibson and H. J. Keegan, *J. Opt. Soc. Am.*, **28**, 180 (1938); E. A. Braude, J. S. Fawcett and C. J. Timmons, *J. Chem. Soc.*, **1950**, 1019.
12) T. C. J. Ovenston, *P. S. G. Bull.*, No. 6, 132 (1953).
13) J. J. Moran and H. I. Stonehill, *J. Chem. Soc.* **1957**, 779.
14) A. Weissberger and E. S. Proskauer, "Organic Solvents", Interscience, New York (1955).

Observed values of optical density were therefore not calibrated except in the cases where higher precise values were needed. Deviation from Beer's law resulting from re-absorption of fluorescence by the solution[13] was not observed at λ's 450, 470, 490 and 500 mμ in the concentration range $0 \sim 10 \times 10^{-6}$ mole/l.

pH of the solution was determined with Horiba Glass Electrode pH-Meter Model P.

Results

Photobleaching of Aerobic Aqueous Solutions.—*Effect of pH.*—Data on the photobleaching of aerated aqueous solutions to which no alkali was added have been reported[1,2]. Absorption spectrum of aqueous uranin solution below pH 7.5 depends sensitively on pH of the solution, while above pH 7.5 it is independent[15] of it. Over the whole pH-range investigated the simple rate formula, which has been applied to the cases of eosin and erythrosin[3], is applicable:

$$-\frac{dc}{dt} = \frac{k}{d} I_0 (1 - e^{-\alpha c d}) \times 10^3 \qquad (1)$$

Integrated form:

$$\alpha c d + \ln(1 - e^{-\alpha c d}) = -k\alpha I_0 t \cdot 10^3 + [\alpha c_0 d + \ln(1 - e^{-c\alpha_0 d})] \qquad (2)$$

The mean molar absorption coefficient, α, was determined experimentally with a thermopile or by calculation[4].

Quantum yields, k's, which were obtained with the solutions of various alkali concentrations or pH's are listed in Table I. It shows that the quantum yield is constant at least down to pH 7.17, where the absorption spectrum is affected to a certain extent; at pH 5.9, however, k is reduced considerably.

TABLE I.
QUANTUM YIELDS FOR AEROBIC AQUEOUS URANIN SOLUTION. EFFECT OF pH. 30°C

Mean molar absorption coeff. $\alpha \times 10^{-4}$	NaOH concn. N	pH	Quantum yield $k \times 10^4$
2.7	0.0242		1.6
2.7	〃		2.0
2.7	〃		1.7
2.7	0.0121		1.7
2.7	〃		1.7
2.7	0.0024		1.7
2.7	〃		1.7
2.3	—	7.17*	1.7
1.6	—	5.9*	0.8
1.6	—	5.9*	1.1

* Phosphate (1/15 N) buffer solutions.

15) In contrast to uranin, absorption spectra of eosin and erythrosin are quite independent of pH at pH above 5.5 and 6.5, respectively.

Effect of Concentration of Oxygen Dissolved in the Aqueous Solution upon the Quantum Yield.—As already reported[1,2], pure aqueous uranin solution does not photobleach in vacuo and its quantum yield gradually increases with increasing concentration of oxygen dissolved in the solution; with eosin and erythrosin, at a considerably low oxygen concentration, their quantum yields reach the constant values which are equal to those obtained with the aerated solutions. An analogous phenomenon to that in the pure aqueous uranin solution is observed also in the presence of alkali (sodium hydroxide 0.0121 N).

Retarding Effect of Ethanol on the Aerobic Photobleaching.—On addition of ethanol to the aqueous alkaline (sodium hydroxide 0.0121N) solution, photobleaching of uranin is strongly retarded as in the cases of eosin and erythrosin. Rates of reaction for all solutions investigated can be reproduced by Eq. 1 or 2. Since absorption spectra show the shift of $\lambda_{max.}$ for longer wavelengths with increase in ethanol concentration, α was calculated for each solution.

Quantum yield decreases with increasing concentration of ethanol as shown in Fig. 1. Irradiated solutions do not show any shift of $\lambda_{max.}$ compared with the initial ones. In the low concentration range of ethanol, $0 \sim 20$ vol. %, the experimental formula[1,2]

$$\frac{1}{k} = \frac{1}{k^0} + K\frac{[EtOH]}{[H_2O]} \qquad (3)$$

holds well also for the present case (see Fig. 2). Here, k^0 and k are the quantum yields for aqueous and aqueous ethanolic solutions (ethanol concentration: [EtOH]), respectively. From the slope of the straight line of Fig. 2. one obtains

$$K = 1.0_9 \times 10^6 \quad (30°C) \qquad (4)$$

then

$$k^0 K = 185 \qquad (5)$$

Photobleaching of Alkaline Solutions in Aqueous Alcohol in Vacuo.—On the contrary to the aerobic system described above, alkaline (sodium hydroxide 0.0121 N) aqueous solution of uranin, in the absence of air, does not photobleach. With increase in ethanol concentration, however,

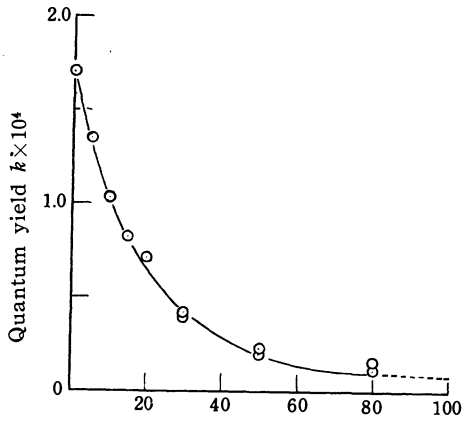

Fig. 1. Variation of k with ethanol concentration. Aerobic, 30°C.

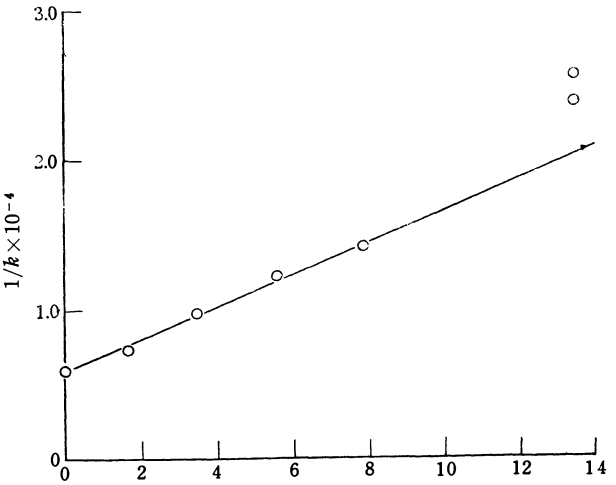

Fig. 2. Dependence of $1/k$ on $[EtOH]/[H_2O]$. (Eq. 3).

the rate of photobleaching becomes appreciable and reaches a constant value after passing through a maximum point, as shown in Fig. 3. An essentially analogous phenomenon is observed in the isopropanol system. In both cases the rates of photobleaching for the solutions of every alcohol concentration are expressed by Eq. 1 or 2.

Similar photobleaching in vacuo to that of alkaline uranin solutions is also observed in the case of eosin or erythrosin. A characteristic feature for the present case is that, at pH above a certain value, photobleaching of uranin is almost reversible. Photobleaching of eosin or erythrosin solution in the absence of alkali and of

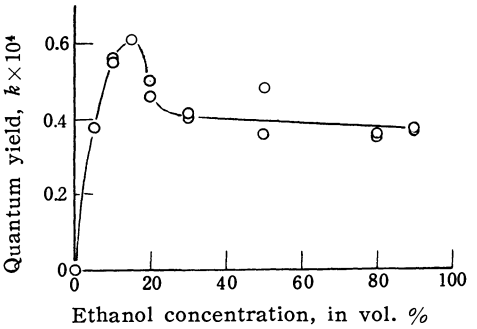

Fig. 3. Variation of the quantum yield with ethanol concentration in vacuo. NaOH, 0.0121 N, 30°C.

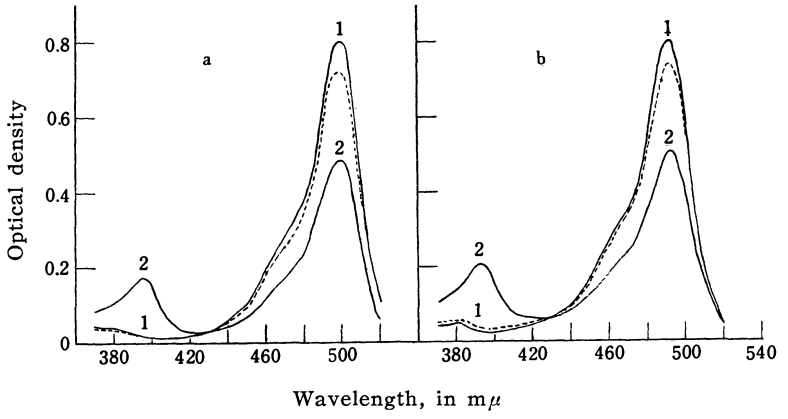

Fig. 4. Spectrum changes on irradiation in vacuo. NaOH, 0.0121 N, 30°C.
a: 80 vol. % aqueous ethanol: 1, initial; 2, 180 min.-irradiation.
b: 10 vol. % aqueous ethanol: 1, initial; 2, 123 min.-irradiation.

uranin solution of a lower alkali-concentration, are, on the other hand, irreversible. A few examples of the spectrum change of uranin resulting from irradiation are illustrated in Figs. 4 and 5. Fig. 4 shows the results obtained with alkaline solutions in aqueous ethanol, and Fig. 5 with an alkaline solution in aqueous isopropanol.

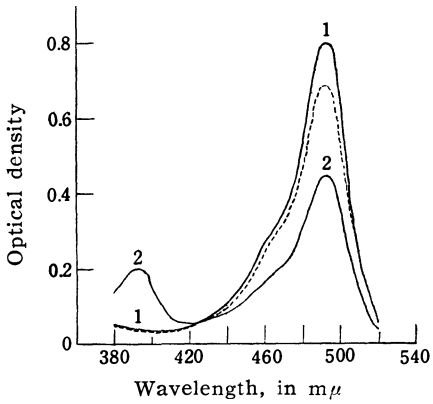

Fig. 5. Spectrum changes on irradiation in vacuo. NaOH, 0.0121 N, 30°C. 20 vol. % aqueous isopropanol: 1, initial; 2, 110 min.-irradiation.

In Figs. 4 and 5 full curves represent absorptions of the solutions unirradiated (1) and those irradiated for a while (2). On introduction of air into the irradiated solutions, their absorption curves 2 are immediately restored to a great extent, which are shown in Figs. 4 and 5 by dotted curves.

A striking feature is that, as shown in Figs. 4 and 5, a new absorption band appears at λ 390~400 mμ by irradiation, which is enhanced with decrease in the optical density at $\lambda_{max.}$ near 490 mμ, and which disappears immediately by introducing air. A distinct isosbestic point is seen in each figure. A quite analogous but very slow restoration of the absorption curve is realized even in vacuo, when an irradiated solution is kept in the dark for a long time. Since it usually takes 20~40 hours to attain the same degree as air-restoration, the slight restoration during absorption measurement which should result in an error on determining concentration could be neglected.

Degree of air-restoration, which is almost 80~90% of the initial height, is almost independent of the alcohol concentration of the solution, no definite relationship between them being able to be found. Two or more cycles of photobleaching with new band formation and restoration in the dark and in vacuo, are possible without appreciable variation of the individual rates.

As mentioned above, such a reversible photobleaching is predominant in the higher pH range, while, in the lower alkali-concentration range, it is almost irreversible. In the case where irreversible photobleaching predominates, the new band formation is hardly observed at all. In Table II are given the results on the pH-dependency of the photobleaching of the alkaline uranin solutions in 20 vol. % aqueous isopropanol performed at 20°C.

In Table II, D^0 and $D_b{}^V$ are the optical densities determined at $\lambda_{max.}$ for the initial and the irradiated (in vacuo 80 min.) solutions, respectively. $D_r{}^V$ and $D_r{}^A$ are for the solutions which are, after irradiation, kept in vacuo and in the dark for 60 min., and for the solutions into which air is introduced (determined immediately after air-introduction), respectively. $\Delta D^V{}_{b395}$ is an increase in optical density at λ 395 mμ by irradiation. All the values of optical density correspond to the 10 mm-path length.

TABLE II

pH-DEPENDENCY OF THE PHOTOBLEACHING OF THE SOLUTIONS IN 20 VOL. % ISOPROPANOL IN VACUO, AT 20°C

$\alpha = 2.7 \times 10^4$ $\lambda_{max.} = 492$ mμ

pH	D^0	$D_b{}^V$ (80 min.)	$D_r{}^V$ (60 min.)	$D_r{}^A$	$\frac{D_r{}^A - D_b{}^V}{D^0 - D_b{}^V}$	$\frac{D_r{}^V - D_b{}^V}{D_r{}^A - D_b{}^V}$	$\frac{\Delta D^V{}_{b395}}{D_r{}^A - D_b{}^V}$	$k \times 10^4$
9.24	0.812	0.500	0.538	0.721	0.708	0.172	0.629	0.57
8.70	.822	.536	.565	.768	.812	.125	.647	.57
8.34	.822	.532	.560	.770	.821	.118	.643	.51
8.00	.826	.545	.607	.785	.854	.258	.613	.54
7.92	.822	.542	.610	.753	.755	.322	.697	.52
7.42	.830	.615	.680	.692	.358	.845	.695	.31
7.30	.820	.645	.700	.702	.326	.965	.175	.27
7.04	.815	.600	.655	.660	.279	.834	.083	.31

Thus, $(D_r^A - D_b^V)/(D^0 - D_b^V)$ represents a fraction of the amount of an intermediate which can be restored by air to that of photobleached dye. It is seen that this fraction increases with increase in pH, having its highest value 0.8~0.9. On the other hand, $(D_r^V - D_b^V)/(D_r^A - D_b^V)$ may give a measure for the stability of the reversible intermediate in vacuo. This value increases with decrease in pH-value, indicating that the reversible intermediate, in vacuo, is relatively unstable at low pH.

In the last column of Table II are given the quantum yields, which may include slight errors resulting from a back reaction. Since the time required for determining optical densities of the irradiated solution is as short as possible, the errors from the dark back reaction may, even in a low pH solution, be considerably small or negligible. Essentially analogous results have been obtained with the solutions in 50 vol. % ethanol in vacuo at 20°C. It is presumable, from these data, that the completely reversible photobleaching would give a quantum yield which is twice that of the completely irreversible one. The molar extinction coefficient of the newly formed intermediate can be estimated from the limiting value of $\Delta D^V_{b395}/(D_r^A - D_b^V)$ to be 6.5×10^4 at λ 395 mμ in alkaline aqueous ethanol and isopropanol.

Discussion

Photobleaching of the Alkaline Solutions in Aqueous Alcohol in Vacuo.—As in the case of uranin at a lower pH, alcoholic eosin and erythrosin solutions into which no alkali is added show an irreversible photobleaching in vacuo[3-6]. It has been concluded experimentally that the primary process in these systems is the dehydrogenation from alcohol molecules by the excited (in the triplet state) dyes. No distinct absorption in the near ultraviolet region as the one observed for the irradiated uranin solutions at higher pH is detected. It has been assumed therefore that the succeeding process is the formation of leuco dye DH_2[16], which have no distinct absorption in near ultraviolet and may decompose into irreversible products under the experimental conditions.

Quite a different result obtained with alcoholic uranin solutions at higher pH in vacuo may be interpreted as assuming the formation of a carbinol base. It is known that triphenylmethane dyes, such as crystalviolet, form their carbinol bases in the presence of alkali[17]. Though it is not the case for xanthene dyes, it may probably be assumed that the presence of sufficient alkali in the reductive condition is preferable to form a carbinol base.

Carbinol bases should reverse to the original dyes not only by oxidation with oxygen (or air) but also by spontaneous separation of water from them. Their stabilities in vacuo and in the dark may probably be more or less higher at higher pH than at lower pH. These expectations are all realized in the present experimental results summarized in Table II, at least qualitatively.

Next, it is noted that the quantum yield at a higher pH is nearly twice those at lower pH. At lower pH, uranin photobleaches preferentially in an irreversible fashion. The situation will be the same as those for eosin and erythrosin, i.e.,

$$D^t + RH \rightarrow DH\cdot + R\cdot \quad \text{(i)}$$

$$DH\cdot + DH\cdot \rightarrow DH_2 + D \quad \text{(ii)}$$

$$DH_2 \rightarrow \text{Products.} \quad \text{(iii)}$$

On the other hand, in the case of higher pH solutions, where the formation of carbinol base is assumed to occur as mentioned above, the succeeding process followed i should be quite a different one:

$$DH\cdot \xrightarrow{OH^-} DH(OH) \quad \text{(iv)}$$

Here DH(OH) represents a carbinol base. From the above schemes it is shown that, in the former case, of one mole of DH· formed by i, one-half should return to the original dye by the disproportionation reaction ii, whereas, in the latter where the reaction ii is almost negligible, such a regeneration of a dye, on neglect of a slow dark back reaction, does not occur. Thus, for limiting conditions of these two cases, it is apparent that the quantum yield of the latter case may reach a value close to twice the value found in the former. Experimental data are, therefore, considered as good evidence for the formation of carbinol base of uranin at higher pH, and it follows therefrom that the appearence of a new absorption at λ 390~395 mμ may be due to this formation.

16) Leuco forms of these dyes are obtained by reduction of their alkaline solutions with zinc powder, which exhibit no absorption in ultraviolet region.

17) a) L, Gattermann, "Die Praxis des organischen Chemikers", Walter de Gruyter, Berlin (1940), p. 328. b) K. Venkataraman, "The Chemistry of Synthetic Dyes", Vol. II, (1952), pp. 705—754.

Primary Process in Alcoholic Solutions and the Reactivity of the Excited Uranin toward Alcohol. — It is clear from the above discussion that the primary process conducted in the deaerated alcoholic solutions should, independently of pH, be given by mechanism i. Excited uranin is assumed to be in the triplet state, in analogy with the cases of eosin and erythrosin. So far as semileuco-dye DH· is assumed to be colorless, the specific rate (quantum yield) of the photobleaching of the deaerated alcoholic solutions is given as

$$k = \varphi_{S\to T}\frac{k_2[\mathrm{RH}]}{k_1{}^S[\mathrm{H_2O}]+k_2{}^S[\mathrm{RH}]} \tag{6}$$

Here, transition probability $\varphi_{S\to T}$ for uranin without substituted halogen atoms may be considered to be lower than those for eosin and erythrosin with substituted halogen atoms[18]. From Eq. 6 one obtains

$$\frac{1}{k}\frac{[\mathrm{RH}]}{[\mathrm{H_2O}]} = \frac{1}{\varphi_{S\to T}}\frac{k_1{}^S}{k_2}+\frac{1}{\varphi_{S\to T}}\frac{k_2{}^S[\mathrm{RH}]}{k_2[\mathrm{H_2O}]} \tag{7}$$

Plotting $[\mathrm{RH}]/k[\mathrm{H_2O}]$ against $[\mathrm{RH}]/[\mathrm{H_2O}]$ using the results obtained with the alkaline (sodium hydroxide 0.0121 N) solutions in aqueous ethanol at 30°C, one obtains a straight line in the relatively low alcohol concentration region, as shown in Fig. 6.

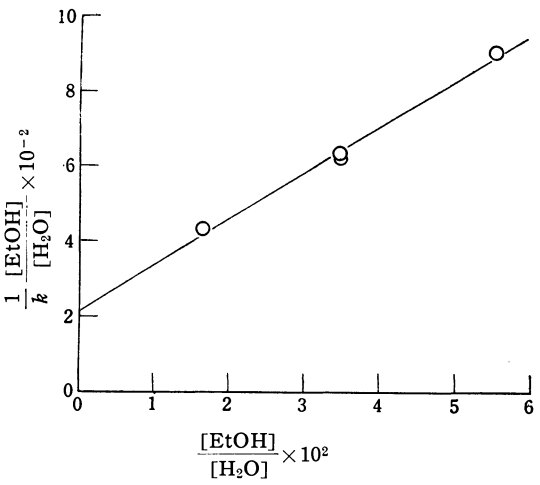

Fig. 6. Dependence of $[\mathrm{EtOH}]/k[\mathrm{H_2O}]$ on $[\mathrm{EtOH}]/[\mathrm{H_2O}]$ in vacuo, 30°C. (Eq. 7).

From the slope and the intercept of this straight line, respectively,

$$\varphi_{S\to T}\frac{k_2}{k_2{}^S} = 0.81\times10^{-4} \tag{8}$$

and

$$\varphi_{S\to T}\frac{k_2}{k_1{}^S} = 4.7\times10^{-3} \tag{9}$$

and from these two values

$$\frac{k_2{}^S}{k_1{}^S} = 57 \tag{10}$$

The last value gives a ratio of the interaction probability of D^t with alcohol to that with water molecules.

Primary Process in Aerobic Aqueous Solution and the Reactivity of the Excited Uranin toward Oxygen.—As to the primary process in the aerobic aqueous solutions, the following two possible mechanisms have been suggested[1,2]:

$$D^t+O_2 \rightarrow D\cdots O_2 \xrightarrow{H_2O} \cdots\mathrm{Prod.}$$

$$D^t+H_2O \rightarrow D\cdots HOH \xrightarrow{O_2} \cdots\mathrm{Prod.}$$

On the kinetic ground, it has been concluded[5] that, if the former mechanism is a correct one,

$$\frac{k_2{}'^S}{k_1{}'^S} = k^0K \tag{11}$$

on the other hand, if the latter is a correct one,

$$\frac{k_2{}^S}{k_1{}^S} = k^0K \tag{12}$$

Though it is difficult to obtain the value of $k_2{}'^S/k_1{}'^S$ experimentally in the present investigation, comparison of the value of k^0K (5) obtained in the aerobic systems with that of $k_2{}^S/k_1{}^S$ (10) in the deaerated systems leads to the conclusion that the primary process of the excited uranin in the aerobic aqueous solutions is expressed by the former mechanism, as in the cases of eosin and erythrosin[5,6].

According to the conclusion obtained above, the specific rate (quantum yield) for the photobleaching of the aqueous solutions should be given as

$$k = \varphi_{S\to T}\frac{k_{O_2}[\mathrm{O_2}]}{k^S{}_{O_2}[\mathrm{O_2}]+k_1{}^S[\mathrm{H_2O}]}\frac{k_1{}'[\mathrm{H_2O}]}{k_1{}'^S[\mathrm{H_2O}]} \tag{13}$$

The fact that the quantum yields of photobleaching of eosin and erythrosin solutions reach, already at the relatively low oxygen concentrations, the corresponding limiting values which are equal to those for the aerobic solutions, indicates that, in Eq. 13 $k_1{}^S[\mathrm{H_2O}]$ can be neglected against $k_{O_2}{}^S[\mathrm{O_2}]$, above a relatively low oxygen concentration, i.e.,

$$k_{O_2}{}^S[\mathrm{O_2}] \gg k_1{}^S[\mathrm{H_2O}] \tag{14}$$

18) D. S. McClure, N. W. Blake and P. L. Hanst, *J. Chem. Phys.*, **22**, 255 (1954).

In the case of uranin, however, such a limiting value is not attained, indicating that, even under the atmospheric air, neglect of $k_1^S[H_2O]$ is unreasonable for the present case. Then, from Eq. 13, one obtains

$$\frac{1}{k}\frac{[O_2]}{[H_2O]} = \frac{k_1'^S}{\varphi_{S\to T}k_1'}\frac{k_1^S}{k_{O_2}} + \frac{k_1'^S}{\varphi_{S\to T}k_1'}\frac{k_{O_2}^S}{k_{O_2}}\frac{[O_2]}{[H_2O]} \quad (15)$$

Application of Eq. 15 to the results previously obtained with the aqueous uranin solutions at 30°C is illustrated in Fig. 7.

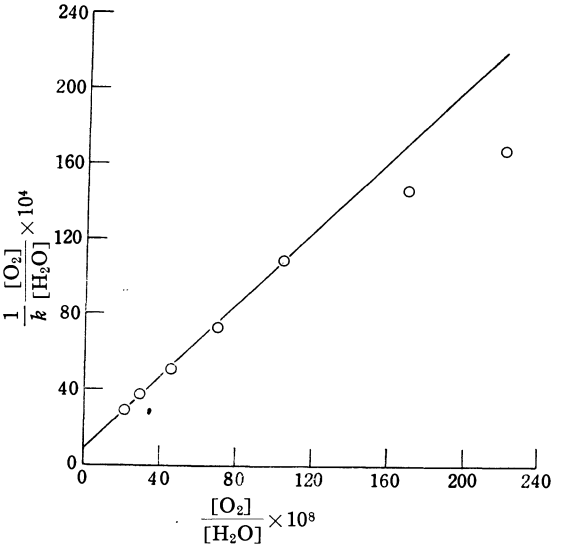

Fig. 7. Dependence of $[O_2]/k[H_2O]$ on $[O_2]/[H_2O]$, 30°C (Eq. 15).

It is shown in Fig. 7 that a linear relation is realized at the oxygen concentration up to 58×10^{-6} mole/l. The intercept and the slope of the line yield, respectively,

$$\frac{k_1'^S k_1^S}{\varphi_{S\to T}k_1'k_{O_2}} = 9\times10^{-4} \quad (16)$$

and

$$\frac{k_1'^S k_{O_2}^S}{\varphi_{S\to T}k_1'k_{O_2}} = 0.96\times10^4 \quad (17)$$

From these values, it follows that

$$\frac{k_{O_2}^S}{k_1^S} = 1\times10^7 \quad (18)$$

which gives the reactivity of D^t toward oxygen relative to that toward water molecules.

If a sufficient amount of oxygen is dissolved in the solution to justify the relation 14, the quantum yield should be given as the reciprocal of the relation 17:

$$\varphi_{S\to T}\frac{k_1'k_{O_2}}{k_1'^S k_{O_2}^S} = 1.0\times10^{-4} \quad (19)$$

Under the atmospheric air, aqueous uranin solution gives a rather higher value (1.3×10^{-4}, at 30°C) than that from Eq. 19. As to the nature of this enhancing effect of oxygen at higher concentrations, it is noteworthy to mind the recent Evans' work[19] on the perturbation of $S\to T$ transitions of organic molecules by oxygen. For eosin and erythrosin such an enhancing effect of oxyen is, at least under the atmospheric air, not observed, and, moreover, the quantum yields at the sufficient oxygen concentrations are quite consistent with those obtained from the slopes of the corresponding plots of Eq. 15. According to the Evans' results, these halogenated dyes may be affected by oxygen far less than the unhalogenated one is. In the case of uranin, the transition probability, $\varphi_{S\to T}$, should depend on oxygen pressure, resulting in an increase in quantum yield with increasing oxygen concentration. This is still in speculation; more quantitative studies must be performed to throw light on this problem.

Comparison between the Reactivities of Excited Xanthene Dyes toward Oxygen and Alcohol.—Reactive species of three xanthene dyes so far investigated are in the excited triplet states, and their primary processes are concluded to be the formation of labile complexes with oxygen molecules in the aerobic aqueous solutions, and to be the dehydrogenation from alcohol molecules in the alcoholic solutions. Relative reactivities of excited eosin and erythrosin have been reported previously[5,6]. In Table III are summarized the relative reactivities of these dyes.

TABLE III
RELATIVE REACTIVITIES OF EOSIN, ERYTHROSIN AND URANIN

	Eosin	Erythrosin	Uranin
$\frac{k_2^S}{k_1^S}$ (ethanol)	19(27°C)	3(27°C)	57(30°C)
$\frac{k_{O_2}^S}{k_1^S}\times10^7$	7.7(30°C)	1.3(30°C)	1.0(30°C)

The values in Table III are reactivities toward ethanol and oxygen (dissolved) relative to those toward water molecules. Though it is difficult to compare exactly their reactivities in absence of the numerical values of k_1^S, it appears possible

19) D. F. Evans, *J. Chem. Soc.*, **1957**, 1351; *Nature*, **178**, 534 (1956).

to say that, in general, halogenated dyes are more reactive toward oxygen than the unhalogenated ones, while toward alcohol vice versa. There seems to be a close relation between such facts and the characteristic pH-dependency of the absorption spectra mentioned before[15].

Summary

Investigation of the photobleaching of uranin solutions has led to the same conclusions as for eosin and erythrosin, concerning the primary processes both in aqueous and in alcoholic media. Strongly alkaline solutions of uranin in aqueous alcohol show an irreversible photobleaching in vacuo. On the reactivities of the excited uranin, and on the comparison of them with those of two other xanthene dyes previously investigated, some discussions have been given.

The author thanks Professor M. Koizumi for his valuable advice throughout this investigation, and Professor R. Fujishir for his interest in this work.

Institute of Polytechnics
Osaka City University
Kitaku, Osaka

Kinetics of the Caro's Acid Oxidation of Dimethylanilines

By Yoshiro OGATA and Iwao TABUSHI

(Received June 21, 1958)

It has been reported that Caro's acid (peroxymonosulfuric acid), presumably contained in a mixture of aqueous sulfuric acid and sodium persulfate, converts aniline (or *N*-monomethylaniline) into phenylhydroxyamine, nitrosobenzene, nitrobenzene and azobenzene[1], while *N*-dimethylaniline (abbreviated as DMA) produces a stable amine oxide on oxidation with Caro's acid[2].

$$\mathrm{Ph{-}N(Me)(Me)} + \mathrm{H_2SO_5} \rightarrow \mathrm{Ph{-}N^{+}(Me)(Me){-}O^{-}} + \mathrm{H_2SO_4}$$

The amine oxide can also be obtained from other tertiary amines, e. g. pyridine, and other oxidizing agents such as hydrogen peroxide[3].

The rate of hydrogen-peroxide oxidation of trimethylamine was measured by Ross[4] only in neutral aqueous solutions. It was found that the rate was proportional to the concentration of the reactants. However, the effects of amine structure and pH of the solution on the rate have not yet been investigated in detail. The present paper describes the data and the probable mechanism of the oxidation of unsubstituted and ring-substituted DMA with Caro's acid in aqueous media.

Experimental

Materials. — DMA was purified by duplicate fractional distillations, b. p. 193°. *p*-Methyl-(b. p. 133°/55 mm.) and *p*-methoxy-dimethylaniline (m. p. 49°) were prepared by the dimethyl-sulfate methylation of *p*-toluidine and *p*-anisidine, respectively[5]. *p*-Chlorodimethylaniline was synthesized by the chlorination of DMA[6], m. p.[7] 35.5°. Caro's acid was prepared by the reaction of potassium persulfate (10 g.) and concentrated sulfuric acid (11 g.) and stored in the form of a dilute solution.

Rate Measurements. — A known amount of acidic aqueous solution of DMA with sulfuric acid or a mixture of potassium hydroxide and borate was mixed in a brown flask and kept at a constant temperature. The solution was mixed with a known amount of aqueous Caro's acid solution maintained at a constant temperature and the reaction was caused to start. Aliquots were taken out at appropriate intervals of time and their peroxide contents were determined iodimetrically. The data of the iodometry were corrected for hydrogen peroxide and peroxydisulfate by another iodometry with cuprous iodide

1) E. Bamberger and F. Tschirner, *Ber.*, **31**, 1675 (1899); E. Bamberger and M. Vuk, ibid., **35**, 703 (1902).
2) E. Bamberger and P. Leyden, ibid., **34**, 12 (1901); E. Bamberger and F. Tschirner, ibid., **32**, 342 (1899).
3) E. Ochiai, *J. Org. Chem.*, **18**, 534 (1953).
4) S. D. Ross, *J. Am. Chem. Soc.*, **68**, 1484 (1946).
5) H. Wieland, *Ber.*, **43**, 712 (1910).
6) D. V. Tischtschenko, *J. Russ. Phys. Chem. Soc.*, **60**, 153 (1928).
7) T. Heidelberg, *Ber.*, **20**, 149 (1887).

as a catalyst[8]. The rate constants were calculated by means of the usual second-order rate equation or pseudo-first-order equation.

The Equilibrium Constants for the Protonation of Substituted DMA.—The equilibrium constant in aqueous solution, $K' = [BH^+]/([B][H^+])$ was determined spectrophotometrically in buffer solutions at various pH's. The spectral data for free and protonated amines were obtained from those in 0.1 N potassium hydroxide and 0.1 N hydrochloric acid, respectively. The used absorption maxima of free and protonated *p*-substituted dimethylanilines were as follows, respectively: MeO, 237 and 223 mμ; Me 237 and below 210 mμ; H, 240 and below 210 mμ; Cl, 250 and 215 mμ.

Since ordinary organic acids showed interference in UV spectra, 0.5 N ammonium chloride solution containing various amounts of ammonium hydroxide, hydrochloric acid or sodium borate was used as a buffer agent. The measurements were carried out at spectral regions of longer wave lengths to avoid the interference of inorganic materials. The results obtained from experiments carried out at more than one kind of wave length agreed well.

The K' values for substituted DMA are listed in Table I. These values are in accord with the Hammett equation. The values are somewhat different from those obtained by Davies[9] probably because of the difference of his solvent, 50% ethanol.

Supplementary Notes. — (1) A method of volumetric analysis of tertiary amine is suggested, in which an excess of Caro's acid is titrated by iodometry after oxidation of the amine sample at an appropriate pH (pH 4~5 for DMA). The method may be suitable for the analysis where acidimetry is difficult, e. g. in a buffer solution.

(2) Hall's pK values[10] for anilines are of most systematic ones, but his datum on dimethylaniline somewhat differs from the present datum and seems to be too small on the basis of the following considerations. The increase of pK by the introduction of a second methyl group into monomethylaniline is unusually small, if compared with that of an ethyl group into monomethylaniline or that of a methyl group into monoethylaniline.

$PhNH_2$	4.62	
PhNHMe	4.85,	$\Delta^0_{Me}=0.23$
$PhNMe_2$	5.06,	$\Delta^{Me}_{Me}=0.21$
PhNHEt	5.11,	$\Delta^0_{Et}=0.49$
$PHNEt_2$	6.26,	$\Delta^{Et}_{Et}=1.15$
PhNMeEt	5.98,	$\Delta^{Et}_{Me}=0.87$
		$\Delta^{Me}_{Et}=1.13$

On the other hand, our datum on dimethylaniline leads to a reasonable increment ($\Delta^{Me}_{Me}=0.52$).

TABLE I

EQUILIBRIUM CONSTANTS FOR THE PROTONATION OF DIMETHYLANILINE

Substituent		pH	K'[a]	pK'	pK[b]
p-MeO		5.21	0.920×10^6	−5.964	
		5.73	1.03×10^6	−6.013	
		6.00	1.01×10^6	−6.004	
	(av.)		0.967×10^6	−5.96	8.04
p-Me		5.50	4.93×10^5	−5.693	
		5.70	5.02×10^5	−5.701	
		5.90	5.06×10^5	−5.705	
	(av.)		5.00×10^5	−5.70	8.30
None		5.41	2.52×10^5	−5.402	
		5.67	2.66×10^5	−5.425	
		5.80	2.39×10^5	−5.378	
	(av.)		2.52×10^5	−5.40	8.60
p-Cl		3.99	4.71×10^4	−4.673	
		4.50	4.82×10^4	−4.683	
	(av.)		4.76×10^4	−4.68	9.32

a) $K' = \dfrac{[BH^+]}{[B][H^+]}$ b) $K = \dfrac{[BH^+][OH^-]}{[B][H_2O]}$

Results

The rate data show that the second-order kinetics are satisfied.

$$dx/dt = k(d-x)(p-x) \qquad (1)$$

Here $(d-x)$ and $(p-x)$ represent the concentrations of dimethylaniline and Caro's acid, respectively. Tables II and III list the effect of initial concentration and acidity on the rate with various substituted DMA's, respectively.

It was reported that some deviation of the apparent rate constant k was observed in the persulfate oxidation in alkaline solution[11] probably owing to the radical reaction, but no indication of the deviation was observed in this case, even if a relatively large excess of DMA was used.

TABLE II

SECOND-ORDER RATE CONSTANT k AT VARIOUS INITIAL CONCENTRATIONS FOR THE CARO'S ACID OXIDATION OF DMA

Temp. 20°C, pH 1.35, Solvent, water

Initial concn. of Caro's acid (M)	Initial concn. of DMA (M)	k(l. mole^{-1} sec.$^{-1}$)
3.93×10^{-3}	0.0167	3.84×10^{-3}
3.67×10^{-3}	0.0308	4.02×10^{-3}
3.76×10^{-3}	0.0600	3.64×10^{-3}
3.96×10^{-3}	0.0800	3.85×10^{-3}

8) M. A. Bodin, *Zavodskaya Lab.*, **7**, 1248 (1938).
9) W. C. Davies and H. W. Bddis, *J. Chem. Soc.*, **1937**, 1622.
10) N. F. Hall and M. R. Spinkle, *J. Am. Chem. Soc.*, **54**, 3469 (1932).
11) L. S. Levitt and E. R. Malinowski, ibid., **77**, 4517 (1955).

TABLE III

SECOND-ORDER RATE CONSTANTS FOR THE CARO'S ACID OXIDATION OF DIMETHYLANILINES

Unsubstituted DMA

pH	Temp. °C	$k\times10^2$ (l. mole^{-1} sec.$^{-1}$)	$k_4=k\cdot[H^+]\cdot K_2$
1.00	25.0	0.241	60.6
1.22	25.0	0.384	58.5
1.40	25.0	0.600	60.0
1.80	25.0	1.73	69.0
1.85	25.0	1.80	64.2
1.98	25.0	2.36[a)]	62.4
2.04	25.0	3.10	71.1
2.29	25.0	4.70	60.5
2.40	25.0	6.05	60.5
2.99	25.0	41.4	
3.70	25.0	346	
4.81	25.0	3200	
6.00	25.0	4250	
7.30	25.0	4360	
8.10	25.0	3780	
9.10	25.0	2700	
9.44	25.0	2220	
10.00	25.0	680	
10.50	25.0	348	
1.70	30.0	2.91	
1.70	20.0	0.980	
1.80	15.0	0.580	
1.80	25.0	1.65[b)]	
1.82	25.0	1.80[c)]	

p-MeO-DMA

1.50	25.0	0.443	135
1.70	25.0	0.590	114
1.70	15.0	0.255	
2.04	25.0	1.20	101
2.28	25.0	2.64	134
3.11	25.0	18.5	139
4.17	25.0	185	121
7.90	25.0	7090	
9.30	25.0	4470	
10.28	25.0	3080	
11.52	25.0	142	
12.20	25.0	22.9	
12.64	25.0	8.79	

p-Me-DMA

pH	Temp. °C	$k\times10^2$ (l. mole^{-1} sec.$^{-1}$)	$k_4=k\cdot[H^+]\cdot K_2$
1.26	25.0	0.403	111
1.36	25.0	0.490	107
1.75	25.0	1.12	105
2.30	25.0	4.16	104
2.42	25.0	5.99	114
3.00	25.0	32.4	162
3.50	25.0	99.6	157
4.00	25.0	368	
4.70	25.0	3260	
7.30	25.0	5280	
8.00	25.0	5040	
8.95	25.0	5720	
9.93	25.0	1980	
10.30	25.0	944	
10.63	25.0	413	
11.60	25.0	59.4	
12.03	25.0	30.3	
12.59	25.0	10.6	
1.90	15.0	0.782	
1.90	25.0	2.15	

p-Cl-DMA

1.38	25.0	2.40	47.6
1.60	25.0	3.22	38.5
2.03	25.0	11.8	52.5
2.50	25.0	36.2	54.3
2.81	25.0	73.6	55.9
3.21	25.0	223	
3.53	25.0	965	
4.32	25.0	3340	
7.13	25.0	4110	
7.80	25.0	4160	
8.81	25.0	3360	
9.40	25.0	2360	
9.95	25.0	969	
11.02	25.0	101	
11.52	25.0	38.7	
11.92	25.0	20.1	
1.89	15.0	1.76	
1.89	25.8	9.25	

a) Na_2SO_4 (100 mg.) was added in 50 ml. of the solution.
b) Benzoyl peroxide (5 mg.) was added in 50 ml. of the solution.
c) Hydroquinone (3 mg.) was added in 50 ml. of the solution.

In strong acid media, the rate constant k increases with increasing pH, the plot of $\log k$ against pH giving a satisfactory straight line with a slope of ca. +1. In the strong acidity the rate constants for substituted DMA at a given pH decrease, in the order: *p*-Cl, *p*-H, *p*-Me and *p*-MeO.

The increase of the k value with decreasing acidity diminishes gradually, and then k reaches a constant value in the neighborhood of the neutrality, where the accurate rate can not be obtained because of its large value together with the spontaneous decomposition of the oxidizing agent.

In weakly alkaline media, k tends to decrease with increasing pH and after reaching a bending point at pH 9.5~10.5 an approximate linear relation is observed between $\log k$ and pH with the slope of

−1. The k values in neutral and an alkaline region decrease with substituents of DMA in the order p-MeO, p-Me, p-H and p-Cl.

The energies of activation for substituted DMA are shown in Table IV.

TABLE IV
TEMPERATURE COEFFICIENT AND ENERGY OF ACTIVATION FOR THE CARO'S ACID OXIDATION OF DIMETHYLANILINES

Substituent	MeO	Me	H	Cl
k_{25}/k_{15}	2.32	2.75	2.98	4.97[a]
E_a(kcal./mole)	14.5	17.4	18.7	25.6

a) $k_{25.8}/k_{15}$

Discussion

The observed second-order kinetics and the effects of acidity and substituents suggest the following mechanism which involves a rate-determining electrophilic attack of neutral molecules of Caro's acid on the free dimethylaniline.

$$ArNMe_2 + H^+ \rightleftarrows Ar\overset{+}{N}Me_2H \text{ (rapid)} \quad (2)$$

$$H_2SO_5 \leftrightarrows HSO_5^- + H^+ \text{ (rapid)} \quad (3)$$

$$ArNMe_2 + H_2SO_5 \rightarrow Ar\overset{+}{N}Me_2OH + HSO_4^- \text{ (slow)} \quad (4)$$

$$Ar\text{—}\overset{+}{N}Me_2\text{—}OH \rightleftarrows Ar\overset{+}{N}Me_2\text{—}O^- + H^+ \text{ (rapid)} \quad (5)$$

From this mechanism, the following relation between the apparent rate constant k and the rate constant of rate-determining step 4 should be expected.

$$k = \frac{1}{K_2[H^+]+1} \cdot \frac{[H^+]}{[H^+]+K_3} k_4 \quad (6)$$

where k and K are rate- and equilibrium constant of the steps.

At relatively high acidity, equation 6 will be to

$$k = \frac{1}{K_2[H^+]} k_4 \quad (7)$$

and in alkaline media where $[H^+]$ is very small, equation 6 is reduced to

$$k = K_3[H^+]k_4 \quad (8)$$

These two equations 7 and 8 satisfy the observed effect of acidity. In alkaline and neutral solutions, almost none the amine molecules are protonated, hence an electron-releasing group in the amine will facilitate the reaction (the substituent affects k_4 alone in eqation 8). But the protonation equilibria 2 become important at high acidity as is obvious from the substituent effect on K_2 in equation 7, and the reverse substituent effect may appear, if the effect on K_2 is larger than that for k_4. These expectations were actually recognized as described previously.

In the acid media the linearity between log k and pH breaks when $K_2[H^+]$ becomes comparable with unity as seen in equation 6. This break (Fig. 1) was actually observed at pH 4∼5 and it depended on the p-substituent of dimethylaniline, i. e.,

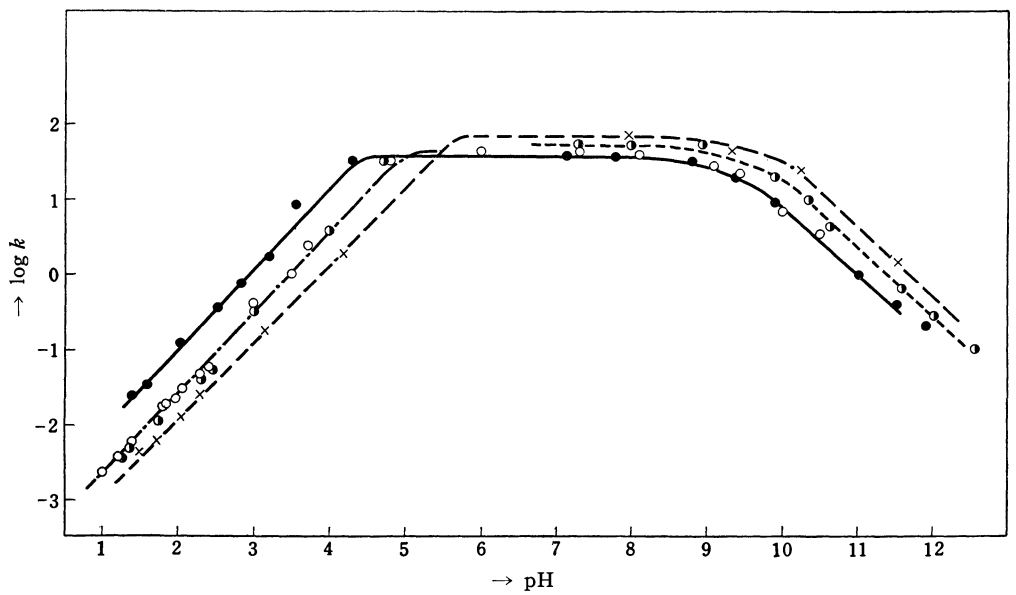

Fig. 1. Plots of log k vs. pH.
—×— p-MeO, ---◑--- p-Me, —○— p-H, —●— p-Cl

the pH value of this break increased in the order: *p*-Cl, *p*-H, *p*-Me and *p*-MeO. This is natural, since the electron-releasing groups increase the K_2 value in equation 6. On the other hand, the break in alkaline media was observed at pH 9.5~10.5 and was independent of *p*-substituent of DMA. This phenomenon seems to be attributable to a decrease of the concentration of H_2SO_5 because of its dissociation.

On the basis of the prevailing electronic theory, the other mechanisms described below are less probable, but they are discussed briefly. Instead of eq. 4, the rate-determining reaction between

(*a*) $\overset{+}{\text{Ar}}\text{NMe}_2\text{H}$ and HSO_5^-

(*b*) ArNMe_2 and HSO_5^-

(*c*) $\overset{+}{\text{Ar}}\text{NMe}_2\text{H}$ and H_2SO_5

leads to the following relation, respectively.

$$(a)\quad k = \frac{K_2[H^+]}{K_2[H]^+ + 1} \cdot \frac{K_3}{[H^+]+K_3} k_4'$$

$$(b)\quad k = \frac{1}{K_2[H^+]+1} \cdot \frac{K_3}{[H^+]+K_3} k_4''$$

$$(c)\quad k = \frac{K_2[H^+]}{K_2[H^+]+1} \cdot \frac{[H^+]}{[H^+]+K_3} k_4'''$$

The observed linearity of $\log k$ vs. pH at high acidity is at least unexplicable by the mechanism *c*, and that of $-\log k$ vs. pH in alkaline media is unexplicable by the mechanism *b*. The concentrations of the reactants in *b*, ArNMe_2 and HSO_5^-, should be much lower in an alkaline solution, hence the possibility of mechanism *b* is inconceivable over the whole pH range. Similarly, the concentrations of reactants, $\overset{+}{\text{Ar}}\text{NMe}_2\text{H}$ and H_2SO_5, should be much lower in an alkaline solution, hence the mechanism *c* is unlikely.

The mechanism *a* leads to the observed effects of acidity and substituents, and is indistinguishable from eq. 4 with kinetics alone; but the mechanism is less probable, since it involves a reaction between a very weak acid (aminium ion) and a very weak base (peroxysulfate ion) and the possible reaction should be the transfer of a proton from the cation to the anion. Furthermore, the fact that added salt (sodium sulfate) has little effect on the rate, favors the reaction between neutral molecules than that between ions.

It has been reported that the neutralizing equivalent of Caro's acid is a half of its oxidizing equivalent[12], thus the dissociation of its second hydrogen atom is inappreciable. Therefore, the mechanism, in which equilibrium 3 is replaced by

$$HSO_5^- \rightleftarrows SO_5^{2-} + H^+$$

and the attacking agent is HSO_5^- instead of H_2SO_5, is unlikely.

Attempts to isolate pure Caro's acid by way of elimination of sulfuric acid with barium hydroxide or ion-exchange resin failed because of its instability.

No appreciable effect on the rate was recognized on addition of a small amount of hydroquinone or benzoyl peroxide, thus showing the absence of radical intermediates in the main reaction course.

Summary

The rates of the Caro's acid oxidation of dimethylaniline and *p*-substituted dimethylanilines were measured in aqueous solutions of various pH's and temperatures. The rates were found to be proportional to the product of the concentrations of both reactants. The effects of pH and *p*-substituents on the rate constant were estimated. The rate constant in acid media increased with increasing electron-withdrawing power of the *p*-substituent of dimethylaniline, while the constant in alkaline media increased with decreasing pH or increasing electron-releasing power of the substituent. A probable mechanism involving a rate-determining attack of neutral Caro's acid molecule on free amine was proposed and discussed.

Department of Industrial Chemistry
Faculty of Engineering
Kyoto University
Sakyo-ku, Kyoto

Studies on Organic Reagents for Inorganic Analysis. IV. Syntheses of New Phenylfluorone Derivatives and their Reactions with Metal Ions

By Hirotoshi SANO

(Received May 13, 1958)

Although numerous investigations have been published on the colorimetric determination of germanium[1-3], tin[4], titanium[5], and zirconium[6] with phenylfluorone (abbreviation for 2,3,7-trihydroxy-9-phenylfluorone), the research for the phenylfluorone derivatives is far from satisfactory. As is well known, phenylfluorone has some excellent properites as a colorimetric reagent. For instance, phenylfluorone has high sensitivity toward germanium, titanium, and zirconium, and germanium phenylfluoronate shows a high stability. However, it has some weak points such as small solubility of its chelates, somewhat low stability of the chelate of zirconium and undesirably high absorbance of the reagent solution at the wavelength used in the determination of germanium. Therefore, it is desirable to find out a new derivative which keeps the advantages and has no such difficulty. For this purpose, only 2,3,7-trihydroxy-9-(4'dimethylaminophenyl)fluorone was synthesized by the author and his coworkers,[7] and it was applied successfully to the colorimetric determination of germanium by Kimura and Asada[8]. Subsequently, some other derivatives, i. e., 2,3,7-trihydroxy-9-(3'-nitrophenyl) fluorone, 2,3,7-trihydroxy-9-(4'-nitrophenyl) fluorone and 2,3,7-trihydroxy-9-(2'-sulfophenyl) fluorone have been synthesized by a similar procedure. These compounds except 3'-nitrophenyl-fluorone[9] have never been described in the literature.

Experimental and Results

Syntheses of Derivatives.—*Reagents Used.*- *m*-Nitrobenzaldehyde, *p*-nitrobenzaldehyde, and benzaldehyde-*p*-sodium sulfonate were first grade reagents prepared by Tokyo Kasei Ind., Co., Japan, and used without further purification. Hydroxyhydroquinone triacetate was synthesized[10] from commercial *p*-benzoquinone, acetic anhydride and concentrated sulfuric acid, and recrystallized twice or thrice from 95% ethanol. Commercial 95% ethanol was used.

Procedures for Syntheses.—For the synthesis of 3'- or 4'-nitro derivative, 20 g. of *m*- or *p*-nitrobenzaldehyde was dissolved in 300 ml. of 20% ethanol in a 500 ml. Erlenmeyer's flask. To the solution were added 100 ml. of ethanolic solution, containing 70 g. of hydroxyhydroquinone triacetate and 10 ml. of concentrated sulfuric acid. A deep red color appeared in the solution by heating it on a steam bath for two or three hours. The solution was allowed to stand for about three weeks. The resulting red crystalline precipitate was filtered, washed with warm 20% ethanol, and suspended in 400 ml. of water at controlled pH of 4. The hydrolyzed precipitate, whose color was deep red, was filtered, washed and dried in a vacuum desiccator.

For 2'-sulfo derivative, the procedure was somewhat different from that described above because of a considerable solubility of the sulfo derivative. Twenty grams of *o*-sulfobenzaldehyde was dissolved in 300 ml. of 20% ethanol in a 500 ml. round-bottom flask. To the solution were added 100 ml. of ethanol containing 70 g. of hydroxyhydroquinone triacetate and 30 ml. of concentrated hydrochloric acid. The solution was heated on a steam bath for two or three hours. Red color appeared in the solution. Even after being allowed to stand for several weeks, no precipitate was formed. The solution was then concentrated on a steam bath by vacuum evaporation. A red precipitate with greenish fluorescence was formed when the volume of the solution was reduced to nearly a half. The crystalline precipitate was filtered, washed with warm 20% ethanol roughly, and suspended in 400 ml. of water at pH 4. The hydrolyzed precipitate, of orange-yellow color which was considered to be sodium-sulfophenylfluorone was filtered, washed and dried. The orange yellow crystalline precipitate was dissolved or suspended in 1 l. of 95% ethanol containing 10 ml. of distilled hydrochloric acid on a steam

1) H. J. Cluley, *Analyst*, **76**, 523 (1951).
2) Y. Oka, T. Kanno and K. Shiba, *Japan Analyst (Bunseki Kagaku)*, **3**, 389 (1954).
3) C. L. Luke and M. E. Campbell, *Anal. Chem.*, **28**, 1273 (1956).
4) C. L. Luke, ibid., **28**, 1276 (1956).
5) H. Sano, *Japan Analyst (Bunseki Kagaku)*, **7**, 235 (1958).
6) K. Kimura and H. Sano, This Bulletin **30**, 80 (1957).
7) K. Kimura, H. Sano and M. Asada, ibid., **29**, 640 (1956).
8) K. Kimura and M. Asada, ibid., **29**, 812 (1956).
9) E. Heintschel, *Ber.*, **38**, 2878 (1905).
10) "Organic Syntheses, Collective Vol. I", John Wiley & Sons Inc., New York (1948), p. 317.

bath. The solution was allowed to stand for one or two days, and an orange red precipitate was obtained. The precipitate was filtered, washed, and dried in a vacuum desiccator.

The author is of the opinion that the following reactions occurred in this procedure.

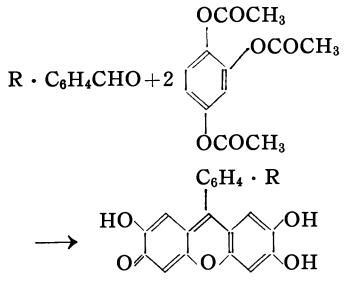

R: *m*-NO_2, *p*-NO_2 or *o*-SO_3H.

in $\begin{cases} H_2O \\ C_2H_5OH \\ H_2SO_4 \text{ or } HCl \end{cases}$

The yields of 3'-nitro, 4'-nitro and 2'-sulfo derivative are 30, 21 and 25% of the theoretical, respectively.

Anal. of the 3'-nitro derivative. Found: C, 60.76; H, 3.70. Calcd. for $C_{19}H_{11}O_7N$: C, 62.47; H, 3.04%.

Anal. of the 4'-nitro derivative. Found: C, 60.25; H, 3.27. Calcd. for $C_{19}H_{11}O_7N$: C, 62.47; H, 3.04%.

Anal. of the 2'-sulfo derivative. Found: C, 56.03; H, 3.35. Calcd. for $C_{19}H_{12}O_8S$: C, 57.01; H, 3.02%.

Properties of the Products.—3'-Nitro derivative: m.p.>310°C, orange-red powder, insoluble in water, sparingly soluble in ethanol. Addition of mineral acid to an ethanolic solution of the compound increases its solubility giving a yellow color. This compound is easily soluble in alkaline solution, giving a faded red-violet color. 4'-Nitro derivative: m.p.>310°C, brownish red powder, insoluble in water, soluble in ethanol with difficulty. The general trend of the effect of acid or alkali on the solubility is similar to the case of 3'-nitro derivative. 2'-Sulfo derivative: m.p.>295°C, orange powder, (its addition compound with hydrochloric acid is composed of brownish needles having green fluorescence.) slightly soluble in water or in ethanol, giving yellow color and weak green fluorescence. The addition of a small amount of mineral acid to the solution increases its solubility slightly. The addition of sodium hydroxide greatly increses the solubility, giving red color and strong green fluorescence. In a strong alkaline solution, the color turns red-violet and the fluorescence disappears.

Absorption Spectra of the Solutions of the Derivatives.—The absorption spectra of the derivatives in an acidic and an alkaline solution are shown in Figs. 1a, b, c, d and e, together with those of phenylfluorone and dimethylamino-phenylfluorone for comparison. The absorption measurements were made with a Uvispek spectrophotometer and Beckman model DU spectrophotometer

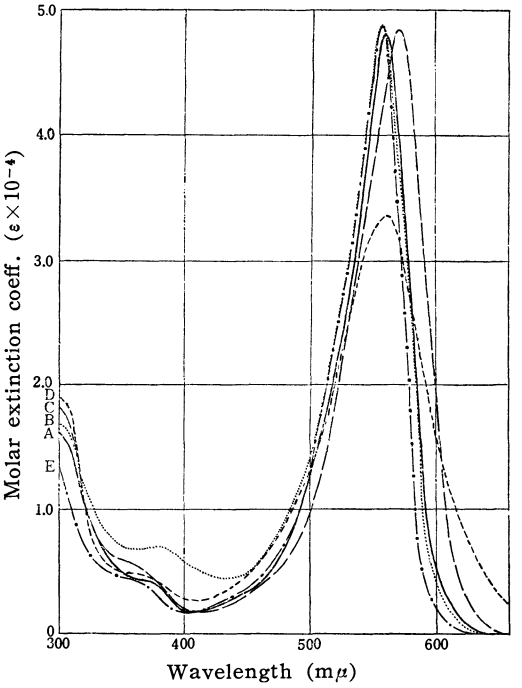

Fig. 1a. Absorption spectra of products in alkaline media.

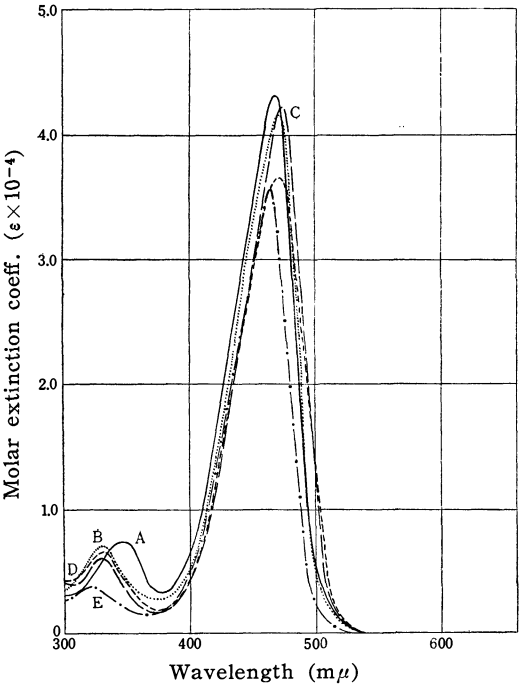

Fig. 1b. Absorption spectra of products in acidic media.

Curve A: Phenylfluorone ———
Curve B: 4'-Dimethylamino- 〃 ·····
Curve C: 3'-Nitro- 〃 – – –
Curve D: 4'-Nitro- 〃 ·····
Curve E: 2'-Sulfo- 〃 — · —

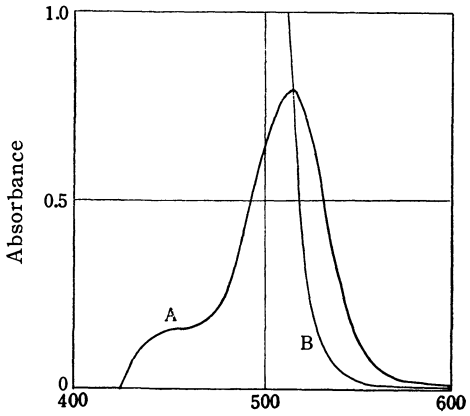

Fig. 2a.
Curve A. Germanium-4'-nitrophenylfluoronate
〃 B. Reagent only (1.0 N HCl solution)

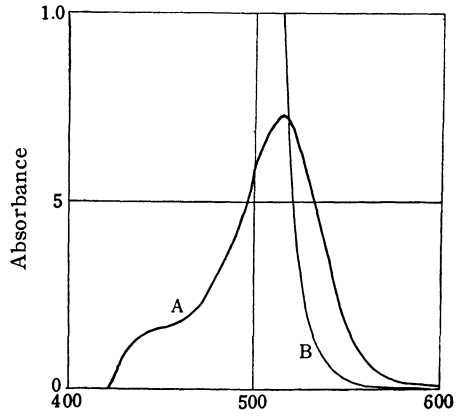

Fig. 2b.
Curve A. Germanium-3'-nitrophenylfluoronate
〃 B. Reagent only (1.0 N HCl solution)

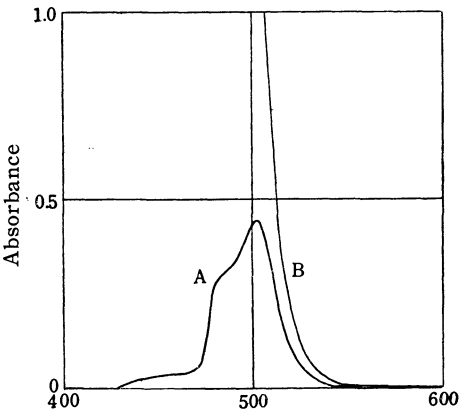

Fig. 2c.
Curve A. Germanium-4'-dimethylaminophenylfluoronate
〃 B. Reagent only (2.0 N HCl solution)

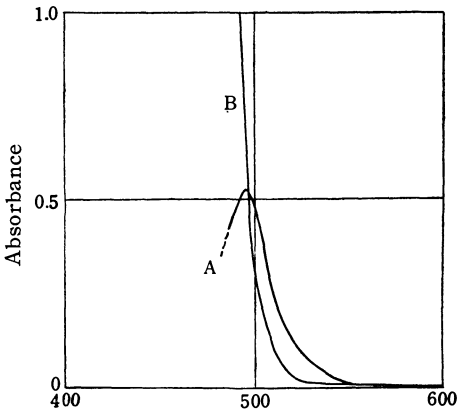

Fig. 2d.
Curve A. Germanium-2'-sulfophenylfluoronate
〃 B. Reagent only (0.1 N HCl solution)

Fig. 2a, b, c and d. Absorption spectra of germanium-fluoronates.

equipped with 1 cm. glass cells. All measurements were made with the blank solution as the reference.

Reaction of the Derivatives with Metal Ions.—*Reagents used.*—Germanium solution was prepared by dissolving water-soluble germanium dioxide (99.9% GeO_2) in hot water, and standardized gravimetrically. Zirconyl chloride solution and titanium chloride solution were prepared by dissolving zirconyl chloride octahydrate (containing 0.5% hafnium) and titanium tetrachloride in 1 N hydrochloric acid. Ethanolic solutions of phenylfluorone and its derivatives were prepared by dissolving 0.120 g. of the dyes* in 150 ml. of warm ethanol containing 1 ml. of 5.0 N hydrochloric acid, and diluting it to 200 ml. with ethanol. Gum arabic solution was prepared by dissolving 0.5 g. of gum arabic in 200 ml. of warm water. The solution was filtered when necessary. Analytical grade cyclohexanol was used without further purification.

Procedure.—Because the metal chelates of 3'- or 4'-nitro derivative are difficultly soluble in many solvents, all the absorbance measurements of the metal chelates were taken in the presence of a suitable stabilizer such as gum arabic or cyclohexanol. The light-scattering effect of the colloidal particle on the absorption spectra is negligible for several hours after the preparation of the solution. The effect of the stabilizer on the absorption maximum of the chelate was also negligibly small. Germanium (15.0 μg.), titanium (60.8 μg.), or zirconium (20.7 μg.) was taken in a 25 ml. volumetric flask. An

* Because the solubility of the sulfo derivative is less than 0.06%, the supersaturated solution of the dye was prepared by dissolving corresponding sodium salt of sulfo derivative similarly. The precipitation of sulfo derivative appeared about two weeks after the preparation.

appropriate volume of hydrochloric acid was added to adjust the acidity of the final solution to desirable strength. Five ml. of ethanol, and 2.5 ml. of gum arabic solution (for germanium) or cyclohexanol (for zirconium) was added. To the solution was added 5 ml. of the phenylfluorone or its derivatives and the final volume of the solution was adjusted to 25 ml. with distilled water. The blank solution was prepared in the same way as that for the sample solution.

Reaction with germanium.—The germanium complexes of 4'- and 3'-nitrophenylfluorone are

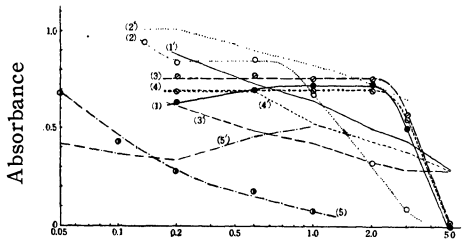

Normality of HCl solution (log. scale)

Fig. 3. Effect of acidity on germanium-fluoronates with germanium concentration fixed**.

Curve (1) Phenylfluorone (510 mμ)
〃 (2) 4'-Dimethylaminophenylfluorone (510 mμ)
〃 (3) 3'-Nitrophenylfluorone (520 mμ)
〃 (4) 4'-Nitrophenylfluorone (520 mμ)
〃 (5) 2'-Sulfophenylfluorone (500 mμ)
〃 (1'), (2'), (3'), (4') and (5') Blank solution, respectively.

almost insoluble in ethanolic solution, whereas that of 2'-sulfophenylfluorone is soluble to the same extent as the 4'- and 3'-nitrophenylfluorone. The last two are almost insoluble in ethanolic solution, whereas germanium complex of 2'-sulfophenylfluorone is soluble to the same extent as that of 4'-dimethylaminophenylfluorone. The absorption spectra of the germanium chelates are shown in Figs. 2a, b, c and d. The absorbance of the solutions of germanium chelates at various acidities is illustrated in Fig. 3, including that of the phenylfluorone and 4'-dimethylaminophenylfluorone, together with that of the blank solutions at the same wavelengths for comparison.

Reaction with zirconium.—The zirconium complexes of 4'- and 3'-nitrophenylfluorone are slightly soluble in cyclohexanol-ethanol solution. Figs. 4a and b show the absorption spectra of the zirconium chelates. The reactivities of the dyes with zirconium at various acidities are illustrated in Fig. 5, together with the absorbance of the blank solutions at the same wavelengths. The colored chelates of 2'-sulfo- and 4'-dimethylaminophenylfluorone are found only in a lower acidity region, so they are excluded from the comparison.

Reaction with titanium.—The titanium complexes of 4'- and 3'-nitrophenylfluorone are fairly

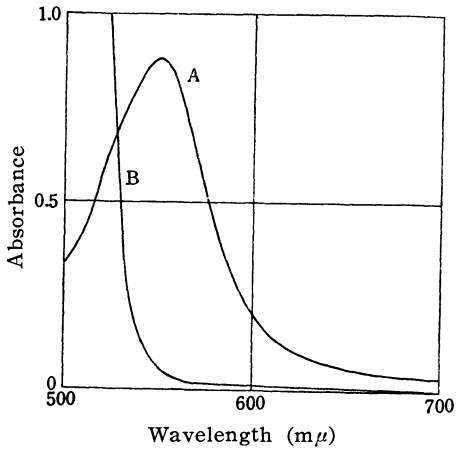

Fig. 4a.

Curve A. Zirconium-3'-nitrophenylfluoronate
〃 B. Reagent only (0.15 N HCl solution)

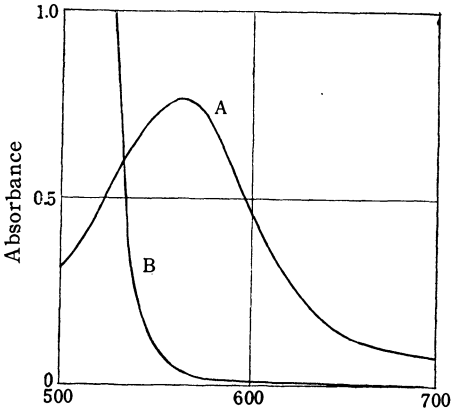

Fig. 4b.

Curve A. Zirconium-4'-nitrophenylfluoronate
〃 B. Reagent only (0.15 N HCl solution)

Fig. 4a and b. Absorption spectra of zirconium-fluoronates.

soluble in cyclohexanol-ethanol. The absorption spectra of the titanium chelates are shown in Figs. 6a and b. The reactivities of the dyes with titanium at various acidities are illustrated in Fig. 7, together with the absorbance of the blank solutions at the same wavelength. The stability of titanium chelates is lower than that of zirconium chelates at the same acidity. Colored chelates of 2'-sulfo- or 4'-dimethylaminophenylfluorone is not formed in the acidity above 0.05 N hydrochloric acid concentration.

Discussion

The process in the syntheses of 3'-nitro, 4'-nitro, and 2'-sulfo derivatives is performed without such a difficulty as was

** The absorbances were measured thirty minutes after the preparation of the solution. They slightly increase with increasing digestion time.

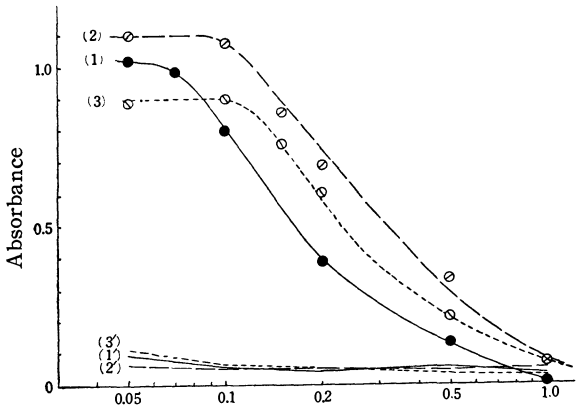

Normality of HCl solution (log. scale)

Fig. 5. Effect of acidity on zirconium-fluoronates with zirconium concentration fixed**.

Curve (1) Phenylfluorone (540 mμ)
〃 (2) 3'-Nitrophenylfluorone (550 mμ)
〃 (3) 4'-Nitrophenylfluorone (560 mμ)
〃 (1'), (2') and (3') Blank solution respectively.

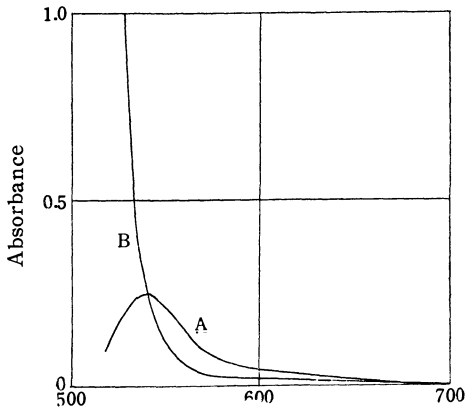

Wavelength (mμ)

Fig. 6a.

Curve A. Titanium-4'-nitrophenylfluoronate
〃 B. Reagent only (0.1 N HCl solution)

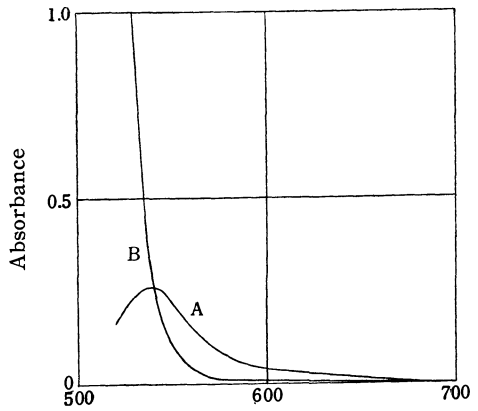

Wavelength (mμ)

Fig. 6b.

Curve A. Titanium-3'-nitrophenylfluoronate
〃 B. Reagent only (0.1 N HCl solution)

Fig. 6a and b. Absorption spectra of titanium-fluoronates.

experienced in the formation of oily polymeried products in the synthesis of phenylfluorone. The absorption spectra of the products resemble closely that of phenylfluorone and 4'-dimethlylaminophenylfluorone. The value of shifts of their absorption maxima with variation of the medium from acidic to alkaline agrees with one another and lies at the range from 90 to 95 mμ. In 3'-nitro and 4'-nitro derivative, the absorption maximum shifts toward a longer wavelength than that of phenylfluorone, as is expected because of the increasing electronegativity of the carbon atom at position 9 caused by the "inductive" or the "mesomeric" effect of the nitro group. On the other hand, the absorption maximum shifts toward the shorter side in 2'-sulfo derivative, suggesting that the effect of the phenyl group is reduced by the steric hindrance of the sulfo group at position 2'. These facts convince the author that the products correspond to the compounds named. The wavelength of absorption maximum in the metal chelate of phenylfluorone derivative can be estimated from the maximum wavelength of the phenylfluorone derivative anion and of the metal phenylfluoronate. As a first approximaton, the estimation was performed as follows:

$$\frac{hc}{\lambda_{max}} = \Delta E = \Delta E_0 + \Delta\varepsilon + \Delta'\varepsilon$$

where ΔE_0 is, the energy difference between the highest ground state and the lowest excited state in phenylfluorone anion,* $\Delta\varepsilon$ the effect of perturbation caused by chelate formation and is calculated from the absorption maximum of the metal phenylfluoronate,* and $\Delta\varepsilon'$ the

** See the foot note in Fig. 3.

* The value, ΔE_0, $\Delta\varepsilon$, or $\Delta\varepsilon'$, is expressed as follows, respectively:
$\Delta E_0 = h^2(N+1)/8mcL^2 = hc/\lambda_{max.}$ phenylfluorone anion,
$\Delta\varepsilon = (1-1/N)V_0 = hc(1/\lambda_{max.}$ metal phenylfluoronate $-1/\lambda_{max.}$ phenylfluorone anion),
$\Delta\varepsilon' = 4V_1a/L = hc(1/\lambda_{max.}$ phenylfluorone anion $-1/\lambda_{max.}$ derivative anion).
For the information on the physical meaning of V_0, V_1 a, etc., see references; H. Kuhn, *J. Chem. Phys.*, **17**, 1198 (1949), *Helv. Chim. Acta*, **34**, 2371 (1951); H. Sano, This Bulletin, **30**, 790 (1957).

TABLE I

ABSORPTION MAXIMUM OF METAL CHELATES (Å)

		(H)	Ti	Ge	Zr	Dye anion
Phenylfluoronate	(obsd.)	4680	5250	5080	5400	5600
3'-Nitro 〃	(obsd.)	4750	5390	5150	5500	5700
	(calcd.)	4750	5338	5162	5487	—
4'-Nitro 〃	(obsd.)	4720	5390	5150	5620	5620
	(calcd.)	4694	5268	5096	5419	—
2'-Sulfo 〃	(obsd.)	4660	—	4950	—	5570
	(calcd.)	4659	—	5056	—	—
4'-Dimethylamino 〃	(obsd.)	4720	—	5030	5200	5570
	(calcd.)	4659	—	5056	5372	—
4'-Hydroxy 〃	(obsd.)*	4590	—	5050	—	—

* This value was given by Dr. Takuji Kanno.

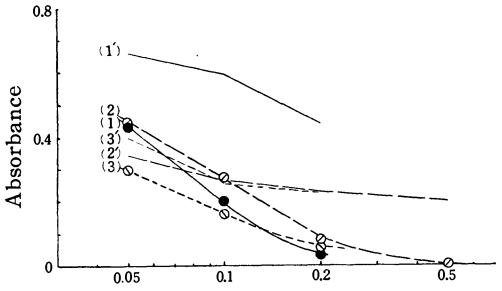

Fig. 7. Effect of acidity on titaniumfluoronates with titanium concentration fixed**.

Curve (1) Phenylfluorone (525 mμ)
〃 (2) 3'-Nitrophenylfluorone (540 mμ)
〃 (3) 4'-Nitrophenylfluorone (540 mμ)
〃 (1'), (2') and (3') Blank solution respectively.

effect of perturbation caused by the substituent introduced into the phenyl group and is calculated from the absorption maximum of derivative anion.* The wavelengths calculated and observed for the chelates are shown in Table I.

Only the 4'-nitro derivative shows a certain anomaly in the absorption maximum of the dye anion, which is expected to be a longer wavelength than the observed from its strong electron-attracting effect, and in the absorption maximum of the metal chelate, which lies at a longer side than that expected. The low value of molar extinction of 4'-nitro derivative and these anomalies may be due to the fact that a mesomeric group is substituted at the 4'-position, and that the interaction between $\Delta\varepsilon$ and $\Delta\varepsilon'$ was neglected in the calculation of the absorption maximum of the chelate.

From the reactivities of the derivatives with metal ions shown in Figs. 3, 5, and 7, it will be seen that the stability of the chelate increases with an increasing "inductive" or "mesomeric" effect of the substituent. The low stability of 2'-sulfophenylfluoronate may be due to the steric hindrance of the 2'-sulfo group. This shows that the stability of the chelate increases with the increasing ionizability of the donor oxygen atom of the dye. The absorbance of the 3'-nitrophenylfluoronate is higher than that of the others, except that of 4'-dimethylaminophenylfluoronate, whereas the absorbance of the blank solution is the lowest and the stability is greater than in the case of the others. This suggests the compound may be excellent as the colorimetric reagent for the determination of metal ions such as germanium or zirconium. It will be expected that the other derivatives, e. g., 3'-sulfo, 4'-sulfo, 3', 4'-disulfo, 3', 3''-dinitro, and 3'-amino derivative will be useful from the results above mentioned. They are under investigation.

Summary

2, 3, 7-Trihydroxy-9-(3'-nitrophenyl) fluorone, 2, 3, 7-trihydroxy-9-(4'-nitrophenyl) fluorone, and 2, 3, 7-trihydroxy-(2'-sulfophenyl)fluorone were synthesized by a comparatively simple procedure, for the purpose of studying the reaction between the colorimetric reagent and metal ions and to search for a useful colorimetric reagent. The effects of the substituents introduced on the absorption maxima of the dyes and the metal chelates formed, and on the reactivities of the dyes with metal ions such as germanium(IV), zirconium(IV), and titanium(IV). 2'-Sulfophenylfluorone metal chelates are soluble in an ethanolic or cyclohexanol-ethanolic solution. 3'-Nitrophenylfluorone is most excellent as the colorimetric reagent for the determination of metal

** See the foot note in Fig. 3.

ions because of the high stability, high sensitivity and low absorbance of the blank solution.

The author is indebted to Mr. Shozo Masuda of this Department for elementary analyses of the products, and to Dr. Kenjiro Kimura, Professor Emeritus, and to Professor Nobufusa Saito, in this laboratory, for their encouragement in carrying out this study. Part of the cost of this study was defrayed from a Grant of the Ministry of Education.

Department of Chemistry
Faculty of Science
The University of Tokyo
Hongo, Tokyo

Optical Properties of Colored Colloidal Systems. I. Theoretical Studies on the Extinction of Light by the System of Small Spherical Particles

By Masayuki NAKAGAKI

(Received May 19, 1958)

Recently the light scattering of colorless systems has been studied quite extensively by many investigators. However, the light scattering of the colloidal systems of colored particles has had little systematic study, although the papers by G. Mie[1] and R. Gans[2] concerned with the optical properties of metal colloids.

In the present paper, theoretical expressions for the extinction, scattering and absorption by a system of colored spherical particles are derived and the numerical values are calculated for systematically varied values of the particle size, refractive index and absorption coefficient of the dispersed phase.

Theoretical Derivations

Definitions.—Consider a system of colored spherical particles dispersed in a colorless medium whose refractive index is μ_1. The refractive index, μ_2, of the colored particle is complex and may be written as follows:

$$\mu_2 = \mu_0(1 - ik) \tag{1}$$

Then, the relative refractive index, m, is

$$m = \mu_2/\mu_1 = m_0 - ik_0 \tag{2}$$

where

$$m_0 = \mu_0/\mu_1 \quad \text{and} \quad k_0 = m_0 k \tag{3}$$

Here the physical meaning of the quantities, μ_0, k and k_0 are as follows. If the homogeneous phase of the material which composes the colloidal particles is considered, the refractive index of the phase is μ_0, and

$$-\ln(I'/I_0')/l' = 4\pi\mu_0 k/\lambda_0 = 4\pi k_0/\lambda \tag{4}$$

where l' is the thickness of the phase, I_0' and I' are the intensity of the incident and transmitted light, respectively, and λ and λ_0 are the wave lengths, in the medium and in vacuum, respectively. Therefore, k and k_0 are both zero if the phase is colorless.

Now consider a colloidal system of thickness l, the unit volume of which contains N particles of radius a. A parameter α defined by

$$\alpha = 2\pi a/\lambda \tag{5}$$

is used in the studies of light scattering. If the density of the particle is ρ_2, the concentration c in g./cc. is

$$c = \alpha^3\lambda^3\rho_2 N/6\pi^2 \tag{6}$$

If the intensities of the incident and transmitted light are I_0 and I, respectively, the quantity E defined by

$$E = -\ln(I/I_0)/l \tag{7}$$

will be called extinction. It is equal to the turbidity, τ, if the particles are colorless, while it is equal to the product of the specific extinction coefficient, ε, and

1) G. Mie, *Ann. Phys.*, (4), **25**, 377 (1908).
2) R. Gans, *Ann. Phys.*, (4), **37**, 881 (1912); **62**, 331 (1920).

the concentration, c, if the particles are colored and the turbidity of the system is small and negligible. In general cases,

$$E/N = R+A \tag{8}$$

where R and A are the energy of light scattered and absorbed, respectively, by one particle par unit time.

Scattering R.—The total of the energy of light scattered in all directions by one particle par unit time, R, is

$$R = 2\pi\int_0^{\pi} J(\gamma)\sin\gamma\,\mathrm{d}\gamma = (\lambda^2/2\pi)\Sigma \tag{9}$$

where $J(\gamma)$ is the intensity of light per unit solid angle[3] scattered in the direction designated by the scattering angle, γ, when the intensity of the incident light is unity, and Σ is a dimensionless quantity defined by[4]

$$\Sigma=\sum_{n=1}^{\infty}(|A_n|^2+|B_n|^2)n^2(n+1)^2/(2n+1) \tag{10}$$

where A_n and B_n are complex functions expressed by combinations of Bessel's functions, as shown by the Mie theory[1]. If α is small compared to unity, A_n and B_n can be expanded as a power series in α and the results are[5]

$$\left.\begin{aligned} A_1&=\frac{m^2-1}{m^2+2}\alpha^3+\frac{3}{5}\frac{(m^2-1)(m^2-2)}{(m^2+2)^2}\alpha^5 \\ &\quad -i\frac{2}{3}\left(\frac{m^2-1}{m^2+2}\right)^2\alpha^6+\cdots \\ B_1&=-\frac{1}{30}(m^2-1)\alpha^5+\cdots \\ A_2&=-\frac{1}{18}\frac{m^2-1}{2m^2+3}\alpha^5\cdots \end{aligned}\right\} \tag{11}$$

Neglecting the term higher than the eighth power of α,

$$\Sigma=\frac{4}{3}\left|\frac{m^2-1}{m^2+2}\right|^2\alpha^6 \tag{12}$$

This is the well known equation by Rayleigh[6].

In the case of $k\ll 1$ (that is $k_0\ll m_0$), Σ can be expanded as a power series in k_0 as follows:

$$\Sigma=\frac{4}{3}\left(\frac{m_0^2-1}{m_0^2+2}\right)^2\alpha^6+8\frac{(3m_0^4+m_0^2+2)}{(m_0^2+2)^4}\alpha^6k_0^2+\cdots \tag{13}$$

The quantity R obtained from Eqs. 9 and 13 is the total scattering by one particle, and RN is the scattering by the unit volume of the colloidal system. It is, however, not adequate to call RN turbidity, because the turbidity is extinction in case of colorless systems. The extinction by a colored system should include the contribution of absorption as well as that of scattering. In order to take the absorption into account, it is not sufficient to use complex refractive index in the Rayleigh equation, because the term of k_0^2 in Eq. 13 is not the term of absorption but is the term which expresses the effect of absorption on the scattering.

Now RN/c is set as κ. Then,

$$\kappa = RN/c = (3\pi/\lambda\rho_2)(\Sigma/\alpha^3) \tag{14}$$

In the case of a colorless system, κ is the specific turbidity (τ/c), which can be determined experimentally by the measurement of transmittancy. In the case of a colored system, however, what is obtained by the measurement of transmittancy is not the turbidity but it containes the effect of absorption as well. Therefore, there exists no handy experimental method to determine the value of κ. It may, however, be worth-while to mention that there should exist, at least principally, an experimental method to determine the value of κ, although the method is very tedious and almost impossible to practice. It will be done by measuring the intensity of scattered light as a function of the angle of observation in all ranges and integrating the results in all possible directions.

According to Eq. 13, R and Σ are zero if k_0 is zero and m_0 is unity. That is, the scattering does not occur in a colorless system if the refractive index of particles and the medium are equal. In the case of a colored system, however, the scattering occurs even when m_0 is equal to unity. Generally, there exists no value of m_0 which makes R equal to zero when k_0 is not equal to zero.

Extinction E. — The extinction by one particle, E/N, can be calculated theoretically by the equation

$$E/N=-(\lambda^2/\pi)I[j_{\perp}(180)] \tag{15}$$

where $I[j_{\perp}(180)]$ indicates the imaginary

3) In order to avoid the use of photometric distance, the intensity is defined here per unit solid angle, instead of per unit area in the usual definiton of the intensity.

4) See, e. g., W. J. Pangonis, W. Heller and A. Jacobson, "Tables of Light Scattering Functions for Spherical Particles", Wayne State Univ. Press, Detroit, U. S. A. (1957).

5) See, e. g., H. C. van de Hulst, "Optics of Spherical Particles", Chapter 4(a), Holland (1946). His notation is different from that used here. A_n and B_n are $(-1)^n ia_n(2n+1)/n(n+1)$ and $(-1)^{n+1}ib_n(2n+1)/n(n+1)$, respectively, in van de Hulst's notation.

6) Lord Rayleigh, *Phil. Mag.*, (5), **47**, 375 (1899).

part of $j_\perp(180)$, and the latter is the quantity which appeared in the expression[7]:

$$J_\perp(\gamma)=(\lambda^2/4\pi^2)|j_\perp(\gamma)|^2 \tag{16}$$

Therefore, $j_\perp(\gamma)$ is proportional to the amplitude of the light scattered at the direction γ and vibrating perpendicularly to the observation plane, the proportionality constant being $(\lambda/2\pi)$. According to the Mie theory,

$$j_\perp(\gamma)=\sum_{n=1}^{\infty}[A_nP_n^1(\cos\gamma)/\sin\gamma + B_n\mathrm{d}P_n^1(\cos\gamma)/\mathrm{d}\gamma] \tag{17}$$

where $P_n^1(\cos\gamma)$ is Legendre's function of the first kind. In the forward direction, or in the case of $\gamma=180$,

$$j_\perp(180)=A_1-B_1-3A_2+\cdots = \frac{m^2-1}{m^2+2}\alpha^3+\left(\frac{m^2-1}{m^2+2}\right)^2\frac{(m^4+27m^2+38)}{15(2m^2+3)}\alpha^5 - i\frac{2}{3}\left(\frac{m^2-1}{m^2+2}\right)^2\alpha^6+\cdots \tag{18}$$

can be obtained using Eq. 11 if $\alpha \ll 1$.

In order to be analogous to the relation between R and $\sum$ in Eq. 9, $\sum_f$ is introduced by

$$E/N=(\lambda^2/2\pi)\sum_f \tag{19}$$

Then,

$$\sum_f=-2I[j_\perp(180)] \tag{20}$$

Using Eq. 18 for $j_\perp(180)$ and expanding it as a power series in k_0,

$$\sum_f=\frac{4}{3}\left(\frac{m_0^2-1}{m_0^2+2}\right)^2\alpha^6+2\left(\frac{6m_0}{(m_0^2+2)^2}\alpha^3+F\alpha^5\right)k_0 + 8\frac{(3m_0^4-11m_0^2+2)}{(m_0^2+2)^4}\alpha^6k_0^2+\cdots \tag{21}$$

where,

$$F=\frac{2m_0}{15}\times\frac{(m_0^2-1)(2m_0^8+20m_0^6+349m_0^4+935m_0^2+674)}{(m_0^2+2)^3(2m_0^2+3)^2} \tag{22}$$

If the particles are colorless and k_0 equals to zero, E/N is equal to R, and E is equal to τ, indicating that the attenuation of the light is due to the scattering only.

By analogy with the colored system of no scattering, the specific extinction coefficient in a wider sense, ε, is defined here by E/c and it is to be understood that this quantity containes the contribution of both scattering and absorption. Then,

$$\varepsilon=E/c=(3\pi/\lambda\rho_2)(\sum_f/\alpha^3) \tag{23}$$

This is the quantity obtained by the measurement of the intensity of transmitted light.

Absorption A.—The absorption by the colored colloidal system can be obtained directly neither by theoretical calculation nor by experimental determination. It is, however, theoretically obvious that the absorption is the difference of extinction and scattering, as already shown by Eq. 8. Thus, the absorption per one particle, A, is given by

$$A=(\lambda^2/2\pi)(\sum_f-\sum) \tag{24}$$

Using Eqs. 13 and 21,

$$\sum_f-\sum=2\left[\frac{6m_0}{(m_0^2+2)^2}\alpha^3+F\alpha^5\right]k_0 - \frac{96m_0}{(m_0^2+2)^4}\alpha^6k_0^2 \tag{25}$$

Then, using the symbol ε_a for the specific extinction coefficient due to the absorption,

$$\varepsilon_a=AN/c=(3\pi/\lambda\rho_2)(\sum_f-\sum)/\alpha^3 \tag{26}$$

or

$$\varepsilon_a=\varepsilon-\kappa \tag{27}$$

For the homogeneous phase of the material which composes the colloidal particles, the value of ε and ε_a obtained from Eq. 4 is

$$\varepsilon(\mathrm{bulk})=\varepsilon_a(\mathrm{bulk})=4\pi k_0/\lambda\rho_2 \tag{28}$$

since no scattering occurs and the concentration in g./cc. is equal to the density, ρ_2, for the bulk phase.

Numerical Computations

The numerical values of ε, κ and ε_a could be calculated if the values of density, ρ_2, and the wave length of light to be used, λ, are assigned. In order to make, however, the results of the computation applicable more widely, the quantities x, y and z are defined by

$$x=(\lambda\rho_2/3\pi)\varepsilon=\sum_f/\alpha^3 \tag{29}$$

$$y=(\lambda\rho_2/3\pi)\kappa=\sum/\alpha^3 \tag{30}$$

and

$$z=(\lambda\rho_2/3\pi)\varepsilon_a=x-y \tag{31}$$

The values of x, y and z for systematically varied values of α, m_0 and k_0 are calculated by using these equations together with Eqs. 13 and 21. For the bulk phase,

7) The derivation of Eq. 15 was shown, e. g., by H. C. van de Hulst (loc. cit.) although his notation is different from that used here. In the case of colorless particles, B. H. Zimm and W. B. Dandliker (*J. Phys. Chem.*, **58**, 644 (1954) have also shown the derivation of a similar equation in which the turbidity was used instead of the extinction E. However, the negative sign was dropped in their equation by a typographical mistake.

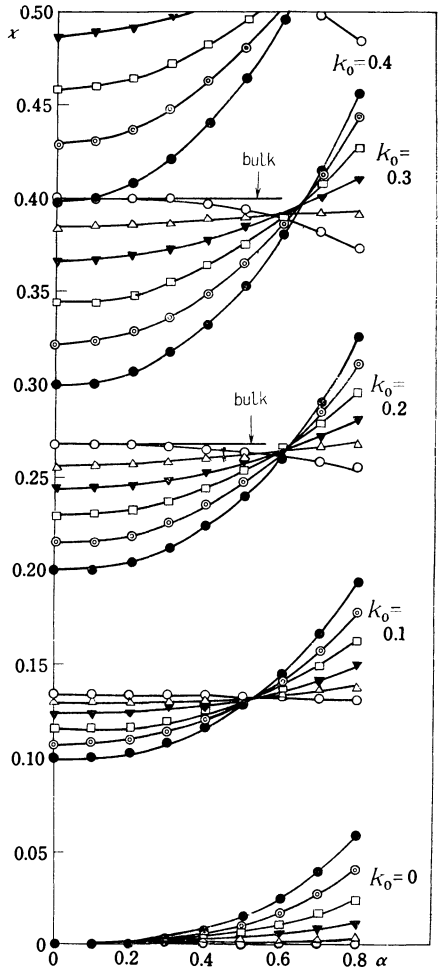

Fig. 1. $x-\alpha$ Relation for m_0=1.0 (○); 1.1 (△); 1.2 (▼); 1.3 (□); 1.4 (◎); 1.5 (●).

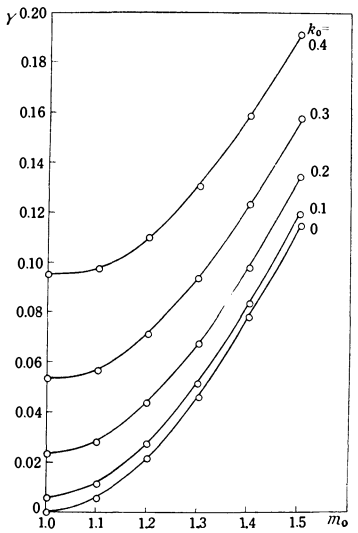

Fig. 2. $Y-m_0$ Relation.

$$\left.\begin{aligned} x(\text{bulk}) &= z(\text{bulk}) = (4/3)k_0 \\ y(\text{bulk}) &= 0 \end{aligned}\right\} \qquad (32)$$

The value of x thus computed as a function of α is shown in Fig. 1, the complex relative refractive index (m_0-ik_0) being the parameter. The rather complicated nature of the curves will be explained as the sum of y and z in the succeeding figures.

As readily understood from Eqs. 30 and 13, the quantity y, a quantity proportional to the specific turbidity in the case of colorless particles, is proportional to α^3. As the consequence, the value of y increases with α so rapidly that it is not convenient to show it in a figure. Therefore, the proportionality constant, Y, in

$$y = Y\alpha^3 \qquad (33)$$

is shown in Fig. 2. The figure shows that

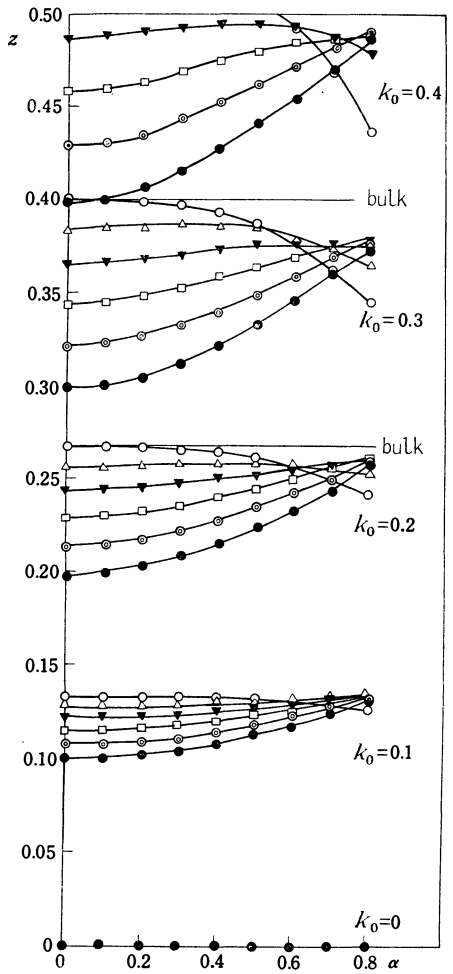

Fig. 3. $z-\alpha$ Relation for m_0=1.0 (○); 1.1 (△); 1.2 (▼); 1.3 (□); 1.4 (◎); 1.5 (●).

the value of Y increases with k_0 as well as with m_0. The value of Y is not equal to zero even when m_0 is equal to 1, if the value of k_0 is not zero. This means that the scattering occurs not only by the difference of refractive index, but also by the absorption.

The value of absorption, z, against α is shown in Fig. 3. The values corresponding to the bulk phase are shown by horizontal lines. It may be worth-while to mention that the value of z is equal to the value of the bulk phase only when m_0 is equal to unity and the particles are very small. If the relative refractive index is not equal to unity, the value of the absorption is, even for very small particles, not equal to the value of the bulk phase but is smaller than the latter. The absorption by colloidal particles is the smaller, the larger the value of m_0. With the increase of the particle size, α, the value of z at first increases and then decreases after passing a maximum. The value of α corresponding to the maximum is zero for m_0 is equals 1 and increases with the value of m_0.

Considering again the value of x, its α-dependence can be understood on the basis of the α-dependence of y and z since x is the sum of them. The value of x decreases with the increase of α if m_0 is small, because the absorption decreases while the scattering is not significant. On the other hand, the value of x increases rapidly if m_0 is large, because both the scattering and the absorption increase.

Check of the Results of Computation

The scattering coefficient of colored particles is considered here. Both the extinction per one particle, (E/N), and the total scattering, R, have the dimension of the area. Therefore, the quantity R is called the scattering cross section, and its ratio to the geometrical cross section is called the scattering coefficient, K. The extinction and the scattering are the same for colorless particles, but they are different for colored particles. The quantity usually measured is the extinction. Therefore, using the word "scattering coefficient" in its wider sense, K may be defined by[8]

$$K = (E/N)/\pi a^2 = 2\sum f/\alpha^2 \qquad (34)$$

8) National Eureau of Standards (U. S. A.), "Tables of Scattering Functions for Spherical Particles", Washington, U. S. A. (1948).

for colored particles.

Now, the people in the National Bureau of Standards of the U. S. A.[8] expanded K as a power series in k_0,

$$K=C_0+C_1k_0+C_2k_0^2+\cdots \qquad (35)$$

and calculated the values of the coefficients, C_0, C_1 and C_2 on the basis of the Mie theory for the m_0-values between 1.44

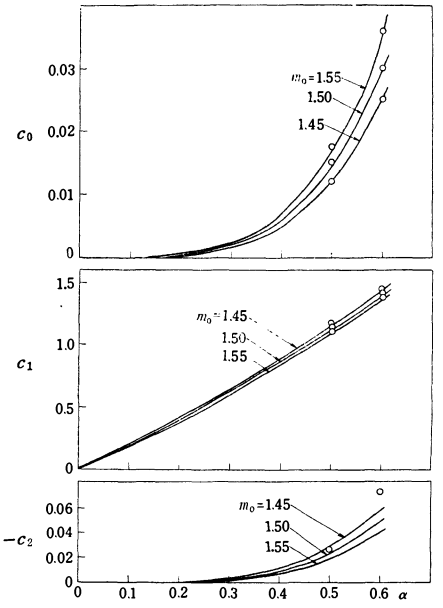

Fig. 4. Comparison with Mie theory.

and 1.55 and for the α-values of 0.5, 0.6, 1.0 and so forth. The values of C_0, C_1 and $-C_2$ by the Mie theory are plotted in Fig. 4 with open circles, while the results by the approximate equations derived in the present paper are shown with solid lines for $m_0=1.45$, 1.50 and 1.55. The agreements are excellent for C_0 and C_1 in the range of α up to 0.6. As for $-C_2$, the computation by the National Bureau of Standards neglected its dependence on m_0, so that the accuracy of their computation is probably rather poor. Taking this into consideration, the agreement between their values and the values by the present paper is sufficient.

Summary

The extinction, scattering and absorption of light by the colored colloidal systems of small spherical particles have been discussed. Approximate equations for these quantities have been derived for a case where the size of particles and the absorption coefficient of the dispersed

phase are relatively small. Using these equations, the numerical values of the quantities have been computed for the systematically varied values of the relative refractive index, (m_0-ik_0), and of α.

It is shown by the results of the computation that the values of the extinction and the absorption by the colloidal systems of small colored spheres (whose α-value is smaller than about 0.5) are the smaller, the greater the value of m_0. On the other hand, the scattering increases with m_0, k_0 and α.

The values of the scattering coefficient calculated by the approximate equations showed sufficient agreement with the values by the Mie theory as far as α is smaller than 0.6.

Faculty of the Science of Living
Osaka City University
Nishi-ku, Osaka

Über die Addition des Bromwasserstoffs auf die Phenylpropiolsäure[1]. *Eine Betrachtung der Reaktion mit Rücksicht auf den Einfluss des in Lösungsmitteln hinzugefügten Brenzkatechins*

von Hazime KASIWAGI

(Eingegangen am 23. Mai, 1958)

Im Vergleich mit den Untersuchungen über die anomale Additionsreaktion, die bei der Anlagerung von Bromwasserstoff an die Äthylenverbindungen auftritt, sind dieselben über die Reaktion bezüglich der ungesättigten Verbindungen mit einer Dreifachbindung nicht so viel angekündigt worden. Die vorliegende Abhandlung bezieht sich auf die Addition des Bromwasserstoffs auf einen Acetylenanalog der Zimtsäure, die Phenylpropiolsäure, worüber einige Untersuchungen früher von Michael und seinem Mitarbeiter und anderen Forschern berichterstattet worden sind[2]. Angenommen, dass die Anlagerung von Bromwasserstoff an die Phenylpropiolsäure vor sich der elektrophilen Reaktion gemäss gehen sollte, so entstände die β-Bromderivate als Reaktionsprodukte wie bei der Zimtsäure[3]. So aber gibt sie bei der in den für nicht polaren angesehenen Lösungsmitteln ausgeführten Reaktion das α-Bromderivat, zwar die *trans*-Verbindung, die α-Bromzimtsäure vornehmlich. Als Lösungsmittel werden die folgenden, die den *trans*-Isomer zu geben als festgestellt betrachtet worden sind, aufgezählt: Benzol, Toluol, Brombenzol, Chloroform, Schwefelkohlenstoff, einschliesslich Tetrachlorkohlenstoffs, der von dem Verfasser neu geprüft worden ist.

Die Bildung der α-Bromzimtsäure in den genannten Lösungsmitteln wird vermutet als erklärt durch den Mechanismus von der durch Wirken des Sauerstoffeffekts hervorgebrachten Radikalkettenreaktion. Ausserdem kann man diejenige Säure aus der *cis*-Verbindung durch ihre Stereomerisierung erhalten[4], und zwar ist diese Isomerisierung als veranlassen durch den Sauerstoffeffekt anerkannt worden[5]. Deshalb, wenn die Anlagerung von der elektrophilen Addition liefe, so mag sich ausschliesslich die α-Brom*allo*zimtsäure unter den Bedingungen bilden, die das Auftreten von Sauerstoffeffekt streng zurückhalten. Hierauf leitet man den getrockneten Bromwasserstoffstrom in die Benzollösung der Phenylpropiolsäure bei Gegenwart des Brenzkatechins von der nicht mehr als 0.02 Mol. Konzentration

1) Eingebracht in der fünften Jahresversammlung der Japanischen Chemischen Gesellschaft, Tokyo, 1952.

2) A. Michael und G. H. Shadinger, *J. Org. Chem.*, **4**, 128 (1939); M. Sudborough und H. Thompson, *J. Chem. Soc.*, **83**, 1152 (1903).

3) Bei der Reaktion jedoch, in deren Lösung eine beträchtliche Menge von Sauerstoff vorhanden ist, sind einige anomale Reaktionsprodukte isoliert worden. O. Simamura und M. Takahashi, Dieses Bulletin, **22**, 60 (1948). Bezüglich der Reaktion bei der Krotonsäure, siehe O. Simamura, ebenda, **17**, 327 (1942).

4) A. Michael und G. H. Shadinger, loc. cit.; R. Stoermer und P. Heymann, *Ber.*, **46**, 1258 (1913).

5) H. Kasiwagi, Dieses Bulletin, **25**, 81 (1952).

ein, so erhält man nur die β-Bromverbindungen. Unter Niederdrücken desselben Effekts also entsteht keine Verbindung von α-Bromreihe, d.h. weder *trans*-Säure noch *cis*-Säure. Daraus kann man annehmen, dass auch die *cis*-Verbindung der α-Bromsäure das aus der Phenylpropiolsäure durch elektrophile Reaktion entstandene Produkt nicht wäre.

Ferner, wenn man den Bromwasserstoff auf die Phenylpropiolsäure unter jeder Anwendung einer Anzahl Lösungsmittel, wie Acetons, Äthers, Nitromethans, Nitrobenzols usw. addieren lässt, so entstehen die Säuren von α-Bromreihe niemals, sondern nur die β-Bromsäuren. Unter den Lösungsmitteln von gleichem Wirken sind weiter noch das Anisol und das als „Antioxidant" das Brenzkatechin enthaltende Benzol aufgezählt zu werden. Das Nitrobenzol gibt immer nur die β-Bromverbindungen ohne Rücksicht auf das Vorhandensein des „Antioxidants". Genauere Beobachtung der Reaktion aber zeigt den feineren Unterschied bei Gegenwart desselben; jedoch wird näheres darüber noch in anderem Zusammenhang erörtert.

Das durch Addition des Bromwasserstoffs erhaltene Produkt ist ein Gemisch von der *cis*- und *trans*-Säure, und hebt gegen die durch das gleiche Verfahren in der Benzollösung gebildete α-Bromsäure, die ausschliesslich von der *trans*-Säure besteht, scharf ab. Dies weicht auch von dem Ergebnisse Michaels usw. ab, wonach nur die β-Bromzimtsäure(*trans*) bei den in oben genannten Lösungsmitteln ausgeführten Reaktionen erhalten worden sei. Ferner sahen diejenige Ankündiger an, dass die aus den Reaktionsprodukten isolierte β-Bromzimtsäure das sekundär von der *cis*-Säure umlagerte Produkt sein mag, da die letztere durch Einwirkung der Mineralsäure in die *trans*-Säure isomerisieren könnte.

Hierauf hat der Verfasser die Meinung Michaels usw. über die durch Bromwasserstoff hervorzubringende Stereomerisierung der β-Brom*allo*zimtsäure geprüft. Als Lösungsmittel wählte man das Benzol und das Nitrobenzol bei An- und Abwesenheit des Brenzkatechins aus und liess den Bromwasserstoff darauf für zwei Tage reagieren. Die Versuche ergaben, dass die Stereomerisierung in Benzol oberhalb 90 Prozent und in Nitrobenzol ungefähr um die Hälfte verlief, während bei Anwesenheit des Brenzkatechins aber die umlagerte Menge sich auf nur eine Spur beschränkte (Tabelle I). Gerade in Bezug auf die *cis-trans*-Isomerisierung der β-Brom*allo*zimtsäure, wobei mehr als um die Hälfte davon auch in Nitrobenzol sich in die *trans*-Form verändert, muss eine Radikalreaktion in demselben Lösungsmittel stattfinden, weil die Reaktion durch die Wirkung des Brenzkatechins stark verhindert wird. D.h. bezüglich der Additionsreaktion tritt die Ionenreaktion sowohl in Nitrobenzol als auch in Brenzkatechin lösendem Benzol auf, und die damit konkurrierende Radikalreaktion wird verzögert. Im Gegensatz dazu, läuft die Isomerisierung durch Wasserstoffion nicht schnell genug, um die durch Bromatom erregte Reaktion[6] auszugleichen, wobei der Effekt des Bromatoms durch Anwendung Nitrobenzols als Lösungsmittel allein nicht, aber erst bei Anwesenheit „Antioxidants" erfolglos werden kann. Sogar da R. Stoermer und P. Heymann die β-Brom*allo*zimtsäure, die Wirkung des in Chloroform gelösten Broms unter Sonnenlicht erleidend, sich isomerisieren bemerkt haben[4], mag ein durch Bromatom hervorgerufenen Radikalkettenmechanismus auch der in Nitrobenzol verlaufenden Stereomerisierung verliehen werden.

TABELLE I

MENGENVERHÄLTNISSE DER DURCH ADDITION DES BROMWASSERSTOFFS AUF DIE PHENYLPROPIOLSÄURE GEBILDETEN ISOMERE VON β-BROMSÄUREN*

Lösungsmittel	Brenzkatechin	Verhältnis (*trans*/*cis*)
Nitrobenzol	−	2.2
Nitrobenzol	−	2.3
Anisol	−	1.4
Nitromethan	−	2.4
Benzol	+	1.2
Benzol	+	1.0
Nitrobenzol	+	1.0

Genau beobachtet, wie später in der Beschreibung der Versuche erörtert, scheint die Menge der isolierten *cis*-Säure gegenüber derselben von der *trans*-Säure, beim Falle von Bildung der β-Bromsäuren durch Addition, einiges Abwechseln dadurch zu erfahren, dass das Brenzkatechin anwesend ist order nicht. Bei Gegenwart desselben bilden sich die beiden Säuren ungefähr um die gleiche Menge ohne Rücksicht auf die Verschiedenheit des

6) Y. Urushibara und O. Simamura, ebenda, **13**, 566 (1938); Y. Urushibara, *J. Chem. Soc. Japan*, (*Nippon Kwagaku Kwaisi*), **60**, 717 (1938).

benutzten Lösungsmittels, aber beträgt die Menge des *trans*-Isomers bei Abwesenheit Brenzkatechins über doppelt so viel als dieselbe des *cis*-Isomers (Tabelle II).

TABELLE II

STEREOMERISIERUNG DER β-BROM*ALLO*ZIMTSÄURE DURCH EINWIRKUNG DES BROMWASSERSTOFFS*.

Lösungsmittel	Brenzkatechin	Isomerisierter Teil der *cis*-Säure %
Benzol	−	92
Nitrobenzol	−	47
Benzol	+	0
Nitrobenzol	+	0

* Umrechnet aus den Tabellen IV und V. Jeder Zahlenwert wird entsprechend der Reihenfolge in jenen Tabellen angeordnet.

Aus dieser Tatsache kann man ersehen, dass es in den Additionsprodukten der Phenylpropiolsäure selbst die beiden Formen der Isomere gäbe, die sich bei der Reaktion ungefähr um die gleiche Menge nebeneinander bilden, und ein Teil des *cis*-Isomers, das Wirken des Bromatoms erleidet, sich in den *trans*-Isomer isomerisieren könnte. Weil das Bromatom, der Radikalkettenträger, solange durch das „Antioxidant" nicht wirklos gemacht würde, sekundär eine partielle Isomerisierung verliefe, mag die erhaltene *trans*-Säure wahrscheinlich aus dem durch Addition unmittelbar gebildeten Teil und dem aus der *cis*-Säure durch ihre Isomerisierung nachher geformten Teil bestehen. Solange es sich um den reinen Ionenmechanismus handelt, fänden die beiden, *cis*- und *trans*-Addition ungefähr um den gleichen Grad statt[7].

Unter den aromatischen Flüssigkeiten, die man für Reaktionen als Lösungsmittel benutzt hat, um ihren Einfluss auf die Reaktion zu prüfen, kann man Benzol, Toluol, Brombenzol, Anisol und Nitrobenzol nennen. Die vorderen drei sind die α-Bromderivate gebenden, dagegen sind die letzteren zwei die β-Bromderivate gebenden Lösungsmittel. Deshalb gäbe es keinen Parallelismus zwischen den Einfluss des Substituenten aromatischer Verbindungen auf die Kernsubstitutionsreaktion und jener Wirkung dieser Verbindungen als Lösungsmittel bei der Addition von Bromwasserstoff. Selbst hat Michael, der sogenannten Lösungsmitteleffekt bei der Additionsreaktion annahm, geschlossen, dass derselbe Effekt mit den physikalischen Grössen, wie den Dissoziations- und Assoziationskonstanten der isomeren Säuren mit Rücksicht auf die Verschiedenheit der Lösungsmittel und den dielektrischen Konstanten von den letztgenannten usw. nicht in unmittelbaren Zusammenhang stände.

Wenn die Molekel des Lösungsmittels das Sauerstoffatom oder dergleichen enthält, durch dessen besondere Solvatationswirkung das Wasserstoffatom des Reagens sich in das Proton verwandelt und zur Molekel des ersteren herangezogen wird, so mag die normale Addition, die als Ionenreaktion anzusehen ist, durch diese Solvatation des Wasserstoffatoms vor sich gehen. Als Beispiele dieser Art vom Lösungsmittel mögen das Nitrobenzol und Anisol genannt werden.

In Lösungsmitteln, wie dem Benzol, den es an derartiger Solvatationswirkung fehlt, mag jetzt die Rolle, die Ionisierung des Reagens auszuführen, ausschliesslich von der eigentlichen ungesättigten Verbindung mit einem Carbonyle oder Carboxyle gespielt werden und die über diese Oxoniumbildung hinaus verlaufende Ionenreaktion mit der anomalen Addition gegenüberstellen lassen. Bei der Reaktion der Zimtsäure, würde Tendenz des Carbonylsauerstoffs, das Proton zu sich heranzuziehen, immer grösser, als die Folge der Verstärkung der Konjugierung der Kohlenstoffdoppelbindung mit dem Carboxyle durch Gegenwart von Benzolkern, und so würde die anomale Addition ganz und gar verzögert ohne Rücksicht auf die Verschiedenheit des Lösungsmittels. In den Fällen von α,β-ungesättigten Ketonen, wie dem Chalkon, verliefe die auf oben geschilderten Umstand zurückzuführende, normale Additionsreaktion allzu geschwind, als dass die anomale Addition damit konkurrieren könnte[8]. Im Gegensatz dazu, sei die Konjugierung der Dreifachbindung mit dem Carboxyle bei der Phenylpropiolsäure nicht so gross, deshalb bei der Reaktion, die in den an der Solvatationswirkung ärmeren oder fehlenden Lösungsmitteln ausgeführt wird, mag der Mechanismus von der anomalen Additionsreaktion, der die Vermöge des

7) Die Anlagerung des Chlorwasserstoffs an die Phenylpropiolsäure, in Eisessig vollgezogen, gibt hauptsächlich die *trans*-β-Chlorzimtsäure nebendem eine kleine Menge des *cis*-Isomers. R Stoermer und P. Heymann, loc. cit. Bezüglich der gleichen Reaktion der Tetrolsäure mit dem Bromwasserstoff, siehe A. Michael und G. H. Shadinger, loc. cit.; R. Mayo und C. Walling, *Chem. Revs.*, **27**, 351 (1940), S. 361, Anm. betreffs Untersuchung Grigorieffs.

8) H. Kasiwagi, Dieses Bulletin, **26**, 355 (1953).

TABELLE III

Phenylpropiolsäure g	Lösungsmittel cc		Temp. °C	Reaktionsdauer Std	Produkt g: Rohes	Produkt g: Getrennter Isomer: α-Bromzimtsäure	Produkt g: Getrennter Isomer: α-Bromallozimtsäure	Unlösliches****
1.0	Benzol	15	15	1, 24**	1.35	1.22	Spur	0.02
7.0	Benzol	200	10	1.5, 48	10.74	10.22	Spur	0.02
3.0	Toluol*	80	8	3, 24	3.93 128～135***	3.85	0.00	—
4.0	CCl_4	80	8	1.5, 24	5.86 128.5～130***	5.01	0.00	—

* Toluol wurde unter vermindertem Druck abdestilliert.

** Die Lösung wird für durch die vordere Ziffer gezeigten Zeitverlauf von Bromwasserstoff durchströmt und lässt auf durch die letztere Ziffer gezeigte Dauer, mit Bromwasserstoff berührend, stehen.

*** Schmelzpunkt des aus Benzol-Ligroin oder Chloroform-Tetrachlorkohlenstoff umkristallisierten Exemplars. Die über das Bariumsalz getrennte α-Bromzimtsäure, mit demselben Lösungsmittel umkristallisiert, schmilzt bei 129～130°C.

**** Dieser Teil ist im Ammoniakwasser nicht gelöst worden.

TABELLE IV

Phenylpropiolsäure g	Lösungsmittel cc		Brenzkatechin g	Temp. °C	Reaktionsdauer Std	Produkt g: Rohes	Produkt g: Getrennter Isomer: β-Bromzimtsäure	Produkt g: Getrennter Isomer: β-Bromallozimtsäure
4.5	Nitrobenzol*	140	Unbenutzt	8	3, 24	5.02 113～122***	3.33	1.54
5.5	Nitrobenzol*	80	Unbenutzt	8	3, 24	6.46** 94～101***	3.55	1.85
						2.03** 124～129***	1.33	0.30
					sämtlich;	8.49	4.88	2.15
3.5	Anisol*	100	Unbenutzt	8	3, 24	3.57 110***	1.97	1.41
2.8	Nitromethan	40	Unbenutzt	8	2, 24	3.35	2.19	0.91
7.0	Benzol	200	0.18	8	1.5, 18	9.10	4.69	4.03
2.0	Benzol	30	0.083	8	1.5, 18	—	1.25	1.22
5.0	Nitrobenzol*	150	0.13	8	3, 24	4.85 113～128***	2.37	2.33

* Das Lösungsmittel wird mit Wasserdampf abdestilliert. Die Produkte, die sich von der zurückgebliebenen Wasserlösung beim Erkalten ausgeschieden sind, mit Äther aufgenommen, getrocknet, dann den Äther wegdampfen lassen.

** Der Niederschlag (6.46 g) wird gesondert von dem in Nitrobenzol aufgelösten Teil (2.03 g) behandelt. Man lässt den ersteren nach Durchschütteln mit Wasser sich sofort sein K-Salz bilden, während man zur Nitrobenzollösung eine grössere Menge von Äther hinzufügt und vereinigte Lösung, nach Waschen mit Wasser und Trocknen, zuerst den Äther, dann das Nitrobenzol unter vermindertem Druck abdestillieren lässt.

*** Schmelzpunkt.

TABELLE V

β-Bromallozimtsäure g	Lösungsmittel cc		Brenzkatechin g	Produkt g: Rohes	Produkt g: β-Bromzimtsäure	Produkt g: Unveränderte β-Bromallozimtsäure
0.20	Benzol	10	Unbenutzt	0.19	0.16	0.015
0.20	Nitrobenzol	7	Unbenutzt	0.16	0.07	0.08
0.30	Benzol	15	0.047	0.27	Spur	0.25
0.30	Nitrobenzol	10	0.049	0.25	Spur	0.23

minderen Grads der Konjugierung verlangsamte Protonbildung des Carbonyls übertrifft, die Hauptrolle spielen. Daraus folgt es, dass das Differenzieren des Reaktionsmechanismus durch die Verschidenheit des Lösungsmittels bei der Reaktion der Phenylpropiolsäure der ärmeren Fähigkeit ihrer Dreifachbindung, mit dem Carboxyle zu konjugieren, zuschreiben könnte. Dieser Umstand besteht auch zwischen der Krotonsäure und der Tetrolsäure und bei der letzteren wird das Differenzieren der Additionsprodukte durch die Art des Lösungsmittels beobachtet[7].

Beschreibung der Versuche

Bildung der α-Bromsäure.—Man lässt die Phenylpropiolsäure (dargestellt und gereinigt, Schmelzpunkt: 136~137°C) in Lösungsmittel suspendieren, und den von Brom befreiten, getrockneten Bromwasserstoff darin einleiten. Während der Reaktion löst sich die Suspension einmal auf, aber bald danach scheidet der Niederschlag von Addukten ab. Nach Beendigung der Durchströmung lässt man die Reaktionsflüssigkeit auf erforderliche Zeit stehen, dann wäscht man dieselbe mit Wasser ab und filtriert den Niederschlag. Der Kristall des Addukten und das Waschwasser werden zusammen mit Äther aufgenommen. Die eigentliche Lösung, mit der Ätherlösung vereinigt, wird mit wasserfreiem Calciumchlorid getrocknet und lässt dann das Lösungsmittel abdestillieren. Zur Trennung beider Isomere, die sich im nachgebliebenen, gelblichen Rückstand vermengt befinden sollen, wird der letztgenannte nach der Methode von Sudborough und Thompson behandelt[9]. Neben dem wesentlichen Teil davon ist das zur Identifizierung beider Isomere angewandte Verfahren auf einer anderen Mitteilung schon erörtert worden[5]. Auf Tabelle III werden die Versuchsbedingungen und das Resultat angegeben.

Bildung der β-Bromsäuren.—Die Additionsreaktion von Bromwasserstoff an die Phenylpropiolsäure wird durch das im wesentlichen gleiche Verfahren mit Ausnahme von der Anwendung entweder des Brenzkatechins oder der alternierenden Lösungsmittel ausgeführt. Wenn man als Lösungsmittel das Benzol oder das Nitromethan benutzt, so werden die Reaktionsflüssigkeiten, getrocknet, auf Wasserbad abdestilliert. Zur Trennung der isomeren β-Bromsäuren hat man den Unterschied ihrer Löslichkeit in der konzentrierten Kaliumacetatlösung[10] ausgenutzt. Zur Identifizierung beider isomeren β-Bromsäuren hat man ihre Exemplar dargestellt, indem man die Phenylpropiolsäure in Wasser suspendieren und den Bromwasserstoff darin unter Erkaltung mit Eiswasser durchströmen liess und dann das erhaltene Säuregemisch durch das oben erwähnte Verfahren getrennt hat. Das mit Benzol oder Benzol-Ligroin umkristallisierte Exemplar der β-Bromzimtsäure schmilzt bei 134~135°C (Br: Beob. 34.9%. Ber. für $C_9H_7O_2Br$ 35.2%) und dasselbe der β-Brom*allo*zimtsäure bei 159~160°C (Br: Beob. 34.8%). Auf Tabelle IV werden die Versuchsbedingungen und die Zusammensetzung der Produkte angegeben.

***Cis-trans*-Isomerisierung der β-Brom*allo*zimtsäure.**—Die Reaktionen werden in Benzol und Nitrobenzol, worin man vorläufig den Bromwasserstoff eingeleitet hat, unter An- und Abwesenheit Brenzkatechins ausgeführt. Nach zweitägigem Stehen wäscht man die Reaktionsflüssigkeit mit Wasser und trocknet. Wenn man als Lösungsmittel das Nitrobenzol anwendet, fügt man das Wasser zum Waschen der Lösung hinzu und nimmt die ganze Flüssigkeit mit Äther auf. Man destilliert das Benzol auf Wasserbad, das Nitrobenzol unter 4 mmHg Druck ab. Der nachgebliebene Rückstand wird mit bezüglich der Additionsreaktionen schon erwähnten Verfahren in beiden Isomere getrennt. Tabelle V erklärt das Resultat.

Zusammenfassung

Wenn man den Bromwasserstoff an die Phenylpropiolsäure addieren lässt, so erhält man nach Verschiedenheit benutzter Lösungsmittel bald die α-Bromsäure, bald die β-Bromsäuren. Die Bildung der α-Bromsäure läuft dem von Brom atom hervorgerufenen Radikalkettenmechanismus gemäss, wird durch Hinzufügen einer kleinsten Menge von Brenzkatechin stark verzögert und hat dabei die Bildung der β-Bromderivate zur Folge. Die erhaltene β-Bromderivate bestehen aus fast gleicher Menge von beiden Isomeren, d.h. β-Brom*allo*zimtsäure(*cis*) und β-Bromzimtsäure(*trans*). Dasselbe Resultat kann auch durch Austausch des Lösungsmittels mit anderem, z.B. mit Nitrobenzol (oder Anisol) erhalten werden, wenn das "Antioxidant" vorhanden ist. In diesem Falle vergrössert aber unter Abwesenheit desselben sich die Menge der *trans*-Säure in den Produkten gegenüber derselben der *cis*-Säure. Anderseits verliefe auch die Stereomerisierung der β-Brom*allo*zimtsäure in ihre *trans*-Isomer durch den Radikalkettenmechanismus. Deshalb unter den durch Hinzufügen Brenzkatechins dem Gang der Radikalreaktion schädlich gemachten Bedingungen, mag sich eine gleiche Menge von beiden Isomeren durch Anlagerung von Bromwasserstoff bilden und im Falle von der Anwendung Nitrobenzols oder Anisols als Lösungsmittel ein Teil der gebildeten β-Brom*allo*zimtsäure in den *trans*-Isomer umlagern. Dabei darf die gesamte Menge des letzteren das sekundär aus *cis*-Isomer verwandelte Produkt nicht angesehen werden.

Ferner dass nur die β-Bromsäuren bezüglich der Zimtsäure bei jedem Falle erhalten werden, mag erklärt werden dadurch, dass eine Ionenreaktion durch verstärkte Konjugierung der Doppelbindung mit dem Carboxyle Vermöge ihres

9) M. Sudborough und H. Thompson, *J. Chem. Soc.*, **83**, 686 (1903).
10) R. Stoermer und P. Heymann, loc. cit.

Benzolkerns beschleunigt würde, was die Verzögerung der damit gegenüberstellenden Radikalreaktion veranlassen hätte. Im Gegensatz dazu träte bei der Phenylpropiolsäure die Radikalreaktion als Folge der Verminderung der oben genannten Konjugierung durch Austausch der Doppelbindung mit Dreifachbindung auf, wenn die Reaktion in den an dem Solvatationseffekt ärmeren oder fehlenden Lösungsmitteln, wie Benzol, Toluol, Tetrachlorkohlenstoff usw. ausgeführt würde.

Also kann man ansehen das bei einer gewissen Klasse von Verbindungen mit Doppelbindung nicht befindliche Differenzieren der Orientation und des Mechanismus von der Anlagerung des Bromwasserstoffs in die zwei Richtungen als eigentümlich den entsprechend gebauten Verbindungen mit Dreifachbindung.

Zum Schluss möchte der Verfasser den Herren Professor Y. Urushibara und Professor O. Simamura an der Universität zu Tokyo für ihre freundlichen Leitungen und guten Räte den herzlichsten Dank aussprechen.

Chemisches Laboratorium
Abteilung der allgemeinen Bildungen
Nagoya Universität
Mizuho-ku, Nagoya

The Reaction of 1,8-Cineole with Acid Solutions

By Tamon MATSUURA, Hisashi KOMAE and Kōzō SAITŌ

(Received April 16, 1958)

On the oxidation of 1,8-cineole with chromic acid in acetic acid[1] or with Beckmann's chromic acid mixture[2], terpin hydrate or α-terpineol has been obtained in a poor yield together with the main reaction products such as homoterpenyl methyl ketone or terpenylic acid. As terpin hydrate and α-terpineol are not oxidation products, it is of interest to clarify the effect of acid solutions on 1,8-cineole.

No work has been reported about the reaction of 1,8-cineole with an aqueous acetic acid solution and only a little attention has been paid to the reaction of cineole with sulfuric acid[3-6]. In 1887, Wallach observed that when cineole and sulfuric acid (sp. gr. 1.64) in alcohol were heated for 5 hours on a water bath, α-terpinene and terpinolene were obtained[3]. Recently Lombard et al. treated this subject somewhat in detail[4]. They studied the problem at various concentrations of sulfuric acid (at 55 and 64% mainly) for various reaction times under stirring at 15°C, and obtained the following compounds: terpin hydrate, *trans*-terpin, α-terpineol and hydrocarbons. Limonene, α-terpineol and terpin hydrate were also studied. Before Lombard's observation, it was reported from this laboratory that when cineole and 21% aqueous sulfuric acid solution were heated at 70°C under stirring, terpin hydrate, α-terpineol, α-terpinene and *p*-cymene were obtained[5]. In this case, it was observed that as the time of contact increases, cineole gives progressively less terpene alcohols and more hydrocarbons.

In this investigation we intended to make clear the actions of acetic acid and sulfuric acid solutions on 1,8-cineole under conditions similar to those described in the foregoing papers[1,2], and to propose a reaction mechanism for the formation of terpins and α-terpineol from 1,8-cineole.

Results and Discussion

1,8-Cineole was treated with an aqueous acetic acid solution (60 wt. %) and an aqueous sulfuric acid solution (21 wt. %) and terpin hydrate was also treated with the same reagents. Further, the reaction of *trans*-terpin with 60% acetic acid solution and that of 1,8-cineole with 0.6% sulfuric acid solution were examined. The reaction conditions and the products

1) T. Matsuura and H. Matsuo, *J. Sci. Hiroshima Univ.*, **A16**, 153 (1952).
2) T. Matsuura and S. Yasuda, ibid., **15**, 273 (1952).
3) O. Wallach, *Ann.*, **239**, 22 (1887).
4) R. Lombard and E. Geiger, *Bull. soc. chim. France*, **1956**, 1564.
5) T. Matsuura and T. Furukawa, *J. Sci. Hiroshima Univ.*, **A18**, 447 (1956).
6) I. Ogura et al., *J. Pharm. Soc. Japan*, (*Yakugaku Zasshi*), **77**, 1355 (1957).

TABLE I

RESULTS OF THE REACTIONS OF CINEOLE AND TERPINS WITH ACID SOLUTIONS AT 70°C

Expt. No.	Reaction condition			Reaction time hr.	Yield of reaction products (wt. percentage to the charged sample)			
		Reagent	Sample		Terpineol	Terpin hydrate	*trans*-Terpin	Hydrocarbons
1	60%	Acetic acid	Cineole	10	0.12	0	0.03	0
2	64%	Acetic acid	Terpin hydrate	10	2.7	—	trace	0
3	60%	Acetic acid	*trans*-Terpin	10	1.8	0	—	0
4	21%	Sulfuric acid	Cineole	3	4.6	0.20	0.12	small
5	21%	Sulfuric acid	Terpin hydrate	0.25	17.8	—	0.20	11
6	0.6%	Sulfuric acid	Cineole	10	0.02	0	0.004	0

are shown in Table I. Among the reaction products, α-terpineol was identified as its phenylurethane and nitrosochloride. Fractional crystallization was employed for the separation of terpin hydrate and *trans*-terpin. For the identification of a small amount of the reaction products, strip-chromatography and I. R. and U. V. absorption spectra were used.

The reaction of cineole (1400 g.) with the acetic acid solution gave *dl*-α-terpineol (0.12% to cineole used) and *trans*-terpin (0.03% to cineole used). Under the same conditions terpin hydrate (90 g.) was converted into *trans*-terpin (trace) and *dl*-α-terpineol (2.7%) which was confirmed to be free from its acetate by the measurement of ester value. In order to compare the action of the acetic acid solution on *trans*-terpin with that on terpin hydrate, the former (4.0 g.) was treated under the same conditions as in the case of the latter. The reaction product was *dl*-α-terpineol (1.8%). The unsuccessful detection of terpin hydrate in the reaction product may result from the small scale of the experiment.

Cineole was attacked more easily by the aqueous sulfuric acid solution (21%) than by the aqueous acetic acid solution (60%), and converted into terpin hydrate, *trans*-terpin, *dl*-α-terpineol and monocyclic hydrocarbons consisting of α-terpinene and *p*-cymene*. In addition, the presence of $\Delta^{2,4(8)}$-*p*-methadiene was confirmed by the U. V. absorption maximum at 244 mμ[7]. The reaction of terpin hydrate with the sulfuric acid solution gave the following products: *dl*-α-terpineol, monocyclic hydrocarbons, *trans*-terpin and 1,8-cineole. The fact that terpin hydrate is attacked more easily than cineole shows that the cleavage of the ether ring in cineole is more difficult than the dehydration of terpin. A remarkable difference between the reaction of cineole with 60% acetic acid solution and that with 21% sulfuric acid solution lies in the point that the latter gives both *cis*- and *trans*-terpins in comparable amounts while the former gives *trans*-terpin predominantly. Since the reaction of cineole with a very dilute aqueous sulfuric acid solution (0.6%), having the same pH value as 60% aqueous acetic acid (pH 1), gives *trans*-terpin predominantly, it seems that the ratio of *cis*-terpin to *trans*-terpin is largely changed by the hydrogen ion concentration of the reagent.

From the above results, the mechanism of the reaction for the formation of the products obtained by the action of aqueous acid solutions on cineole is probably as shown in Fig. 1.

In this mechanism we consider that the main course of the reaction is as follows:

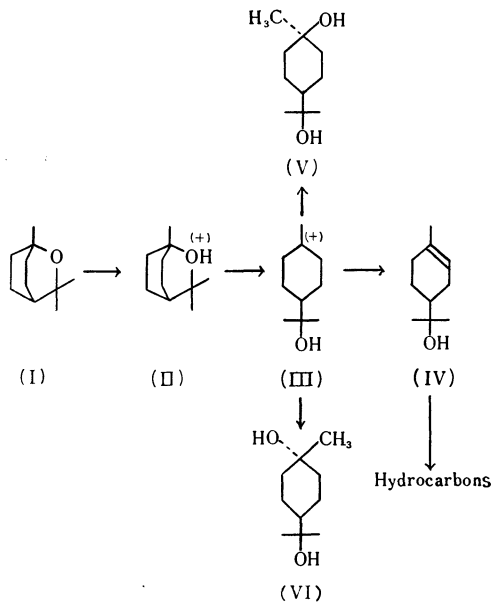

Fig. 1.

* cf. 5).

7) R. T. O'Connor and L. A. Goldblatt, *Anal. Chem.*, **26**, 1726 (1954).

cineole (I)→oxonium ion(II)→carbonium ion(III)→α-terpineol(IV)→hydrocarbons.

The main reaction product of cineole with the acid solutions is *dl*-α-terpineol under the above conditions (Expt. 1,4,6). We see, also, that *cis*- and *trans*-terpins (V and VI) are considerably stable to the action of 60% acetic acid (Expt. 2,3). If terpin were the intermediate in the main reaction course, a considerable amount of terpin should be accumulated as a reaction product. But the yield of terpin is very small in comparison with that of α-terpineol (Expt. 1,4,6). Furthermore, terpin hydrate is converted easily into hydrocarbons by the action of 21% sulfuric acid (Expt. 5), while in the case of cineole this is not true (Expt. 4). Therefore, one may probably assume that *cis*- and *trans*-terpins are not intermediates in the main reaction course but only by-products formed by the hydration of a carbonium ion(III) derived from an oxonium ion(II). The formation of the carbonium ion(III) may be considered on the basis of the presence of both *cis*- and *trans*-terpins in the reaction products.

In the cases of Expt. 1 and 6, where aqueous acetic acid and very dilute sulfuric acid solutions are the reagents, the terpin found in the reaction products is the only *trans* modification. This may be explained by taking into consideration that the stability of the carbonium ion (III) is decreased greatly in Expt. 1 and 6 as compared with in Expt. 4, owing to the difference of the hydrogen ion concentration. Thus in Expt. 1 and 6, the unstable carbonium ion(III) may react very rapidly with water while the departing group $\ddot{O}H—C(CH_3)_2—R$ in the formation of the carbonium ion(III) from the oxonium ion (II) is still partially screening one side of the planar carbonium ion (III).

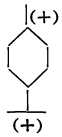

(VII)

Although, Lombard et al. have proposed a carbonium ion(VII) as an intermediate in the hydrolysis of mono- and di-sulfates[5], the above obtained results can be explained by assuming the carbonium ion (III) instead of that of Lombard. In the reaction of 1,8-cineole with acid solutions, the transitory carbonium ion(III) which is derived from the oxonium ion(II) formed by the addition of the hydrogen ion to 1,8-cineole may react with a water molecule to form terpins (S_N 1 type reaction), or may liberate a proton to form α-terpineol (E 1 type reaction). The above S_N 1 and E 1 processes will be competed with each other, but in the E 1 reaction there will not be a steric hindrance which is possibly included in the S_N 1 reaction. Thus it seems probable that the elimination process which results in the formation of α-terpineol is predominating.

If an S_N 2 type reaction proceeded by the attack of an anion such as acetate on the oxonium ion(II) in Expt. 1, there would be a change of the configuration at C_1 atom resulting in a Walden inversion. In this case, however, an ester thus produced would give both *cis*- and *trans*-terpins by a successive hydrolysis*. Also, if the acetate were formed, it would be so stable that the hydrolysis could not occur under our conditions. Thus an S_N 2 type reaction may be left out of consideration in our experiments.

Considering the results of this investigation, in the cases of the oxidation of 1,8-cineole with chromic acid in acetic acid[1] and with Beckmann's chromic acid mixture[2], the reaction seems to proceed in the intermediary formation of α-terpineol by the above mechanism. α-Terpineol thus formed is then oxidized to homoterpenyl methyl ketone (VIII) which in turn goes to terpenylic acid (IX).

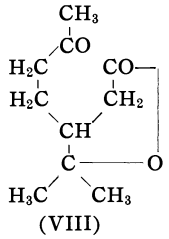

(VIII)

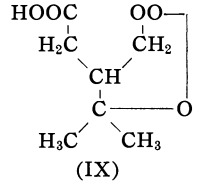

(IX)

Experimental

Reaction of Cineole with Acetic Acid Solution.—Cineole (700 g.) isolated from a comphor white oil according to the method described before[8] (b. p. 173~173.5°C, n_D^{25} 1.4540, d_4^{25} 0.9195) and 60% aqueous acetic acid solution (1309 g.) were mixed in a flask. After the mixture was heated at 70°C for 10 hours under stirring, it separated into two parts, an oil and an aqueous solution, and they were neutralized with sodium

* It has been reported that hydrolysis of tertiary alkyl acetate by acid proceeds in alkyl-oxygen fission (C. K. Ingold et al., *Nature*, **166**, 680 (1950)).

8) S. Hayashi, T. Matsuura and B. Masumoto, *J. Sci. Hiroshima Univ.*, **A15**, 165 (1951).

carbonate. A large amount of sodium acetate was obtained from the aqueous solution. The oil was repeatedly washed with water and dried. The oil (1190 g.) obtained from two runs of the above treatment was distilled under a reduced pressure, b. p.$_{40}$ 80~85°C, n_D^{25} 1.4532, d_4^{25} 0.9196, yield 1173 g. Treatment of this fraction with *o*-cresol gave needle crystals, m. p. 55~56°C, which were identified as cresineol by the mixed melting point determination. Thus, it was confirmed that this fraction consisted of unchanged cineole.

The residue remaining in the flask was a pale yellow oil possessing a fragrant odor. After it was dissolved in ether and stood over night, white needle crystals (Crystal I), m. p. 155~156°C, deposited and were taken up by filtration. From the filtrate (the ether solution) a viscous oil (2.3 g.) was obtained, which on distillation gave the following fractions: (1) b. p.$_{20}$ 69~105°C, n_D^{25} 1.4580, yield 0.1 g.; (2) b. p.$_{20}$ 105~135°C, n_D^{25} 1.4730, d_4^{25} 0.9444, yield 1.7 g.; (3) residue (0.4 g.). Fraction (2) was distilled and the main fraction, (b. p.$_{17.5}$ 103~107°C, n_D^{25} 1.4742, d_4^{25} 0.9388, yield 0.8g.), phenylurethane m. p. 112.5°C, and nitrosochloride m. p. 113~113.5°C, were obtained. This fraction was identified as *dl*-α-terpineol by mixing its derivatives with authentic specimens. The residue (0.4 g.) was washed with a little ether and recrystallized from water-ethanol mixture twice. Colorless needle crystals (Crystal II), m. p. 156~156.5°C, were obtained. A large amount of sodium acetate which was produced by the neutralization of both the aqueous and the oily layers of the reaction mixture was extracted with ethanol. The ethanol extract was evaporated up to dryness and then repeatedly extracted with ether. From the ether extract colorless needle crystals (Crystal III), m. p. 152~154°C, were obtained. The aqueous layer separated from the precipitated sodium acetate was extracted with ether several times and crystals (Crystal IV), m.p. 155.5~156°C, were obtained from the ether extract. Crystals I, II, III and IV, which amounted to 0.427 g. in all, were identified as *trans*-terpin by the mixed melting point determination.

Reaction of Terpin Hydrate with Acetic Acid Solution. — Terpin hydrate, m. p. 119~121°C (90 g.), was heated with 64% aqueous acetic acid solution (132 g.)* at 70°C for 10 hours under stirring. Unchanged terpin hydrate was filtered off and washed with water until the odor of acetic acid vanished. The aqueous layer of the reaction mixture and the water washings were neutralized with sodium carbonate. The precipitated sodium acetate was filtered and washed with a small amount of ether in order to catch the oily product adhering to it and then extracted with ethyl acetate. The aqueous layer separated from sodium acetate was extracted with ether and then evaporated up to dryness. The non-volatile material thus obtained was again extracted with ethyl acetate. The ether extracts gave an oily matter (4.4 g.) which on distillation gave a main fraction, b. p.$_{18}$ 98~103°C, n_D^{25} 1.4759, d_4^{25} 0.9264, E. V. 16.26, yield 2.4 g. Phenylurethane and nitrosochloride of this fraction were identical with those of *dl*-α-terpineol.

Unchanged terpin hydrate (71.6 g.) was recovered. On the other hand crystals, m. p. 154.5~155.5°C, which were identified as *trans*-terpin by the mixed melting point determination, were obtained in a very small amount from the ethyl acetate extracts mentioned above. Furthermore, strip-chromatography of these crystals was tried, and only one spot (Rf 0.45) corresponding to that of *trans*-terpin was found on the chromatogram developed with *n*-butanol-ethyl acetate (1 : 9) mixture[9].

Reaction of *trans*-Terpin with Acetic Acid Solution. — *trans*-Terpin[10], m. p. 156°C (4.0 g.), was heated with 60% aqueous acetic acid solution (6.9 g.) at 70°C for 10 hours under stirring. An oily product (0.07 g.) was separated according to the procedure described in the above section.

A strip-chromatogram of the oil gave one spot (Rf 0.24) corresponding to α-terpineol when the oil was developed with 15% ethyl acetate in *n*-hexane[11].

Unchanged *trans*-terpin, m. p. 155~156°C (3.00 g.), was recovered.

Reaction of Cineole with Sulfuric Acid Solution.—Cineole (100 g.) was heated with 21% aqueous sulfuric acid solution (303 g.) at 70°C for 3 hours under stirring. After the neutralization with sodium carbonate, the reaction mixture was steam-distilled. The oily distillate (97.3 g.) was fractionated into the following fractions under reduced pressure. (1) b. p.$_{28}$ 74°C, n_D^{25} 1.4546, d_4^{25} 0.9175, yield 83.7 g.; (2) b. p.$_{28}$ 74~112°C, n_D^{25} 1.4554, d_4^{25} 0.9163, yield 2.4 g.; (3) b. p.$_{28}$ 112~113°C, n_D^{25} 1.4769, d_4^{25} 0.9276, yield 4.6 g.; (4) residue (1.1 g.). Fractions 1 and 2 were mainly unchanged cineole, because their odors and physical properties were close to those of cineole. But their U. V. absorption spectra (Fig. 2) showed absorption maxima at 244, 265 and 273 mμ corresponding to the characteristic absorption maxima for $\Delta^{2,4(8)}$-*p*-menthadiene, α-terpinene and *p*-cymene, respectively. I. R. spectrum of fraction (3) is shown in Fig. 3. The absorption curve coincides with that of α-terpineol and has no strong bands at 1643 and 885 cm^{-1} such as are characteristic of the end methylene group presented in β-terpineol[12].

When the aqueous solution remained in a flask after the steam-distillation was evaporated up, a solid material including sodium sulfate was obtained. It was extracted thoroughly with ethyl

* In the case of terpin hydrate 64% acetic acid solution was employed under consideration of crystallization water in terpin hydrate.

9) K. Yamamoto and T. Furukawa, *Educational studies* (*J.* Faculty of Education), *Hiroshima Univ.* (2), **4**, 45 (1956).

10) *trans*-Terpin was prepared by the hydrolysis of *trans*-dipentene dihydrochloride with silver oxide and water (R. Lombard and E. Geiger, *Bull. soc. chim. France*, **1953**, 927).

11) J. G. Kirchner, J. M. Miller and G. J. Keller, *Anal. Chem.*, **23**, 420 (1951).

12) T. Aratani and T. Matsuura, *J. Sci. Hiroshima Univ.*, **A20**, 199 (1957).

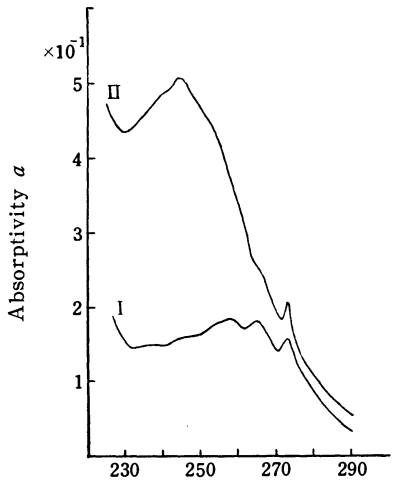

Fig. 2. Ultraviolet absorption spectra of hydrocarbon fractions: I fraction (1), II fraction (2) (in ethanol).

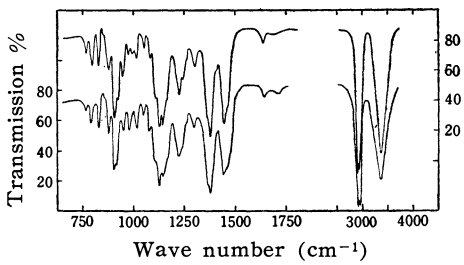

Fig. 3. Upper α-terpineol (liquid film). Lower fraction (3) (liquid film).

acetate. Colorless crystals (0.48 g.), which were obtained from the extract by evaporating the solvent, were recrystallized from water. The crystals, m. p. 117~119°C (0.20 g.), obtained by the repeated recrystallizations were identified as terpin hydrate by mixing with an authentic specimen. Evaporation of the mother liquor of the first recrystallization gave crystals possessing larger solubility in water than that of terpin hydrate. By recrystallization from ethyl acetate, the crystals were purified to colorless ones, m. p. 155~156°C (0.12 g.), which showed no depression of melting point on admixture with *trans*-terpin.

Reaction of Terpin Hydrate with Sulfuric Acid Solution. — Terpin hydrate (50 g.) was heated with 21% aqueous sulfuric acid solution (945 g.)* at 70°C for 15 minutes under stirring. Unlike the result in the case of acetic acid, terpin hydrate disappeared rapidly and was attacked easily. The reaction mixture which consisted of two layers, an oil and an aqueous solution, was neutralized with sodium carbonate under vigorous stirring, and then steam-distilled. The distillate was extracted with ether. After removal of the solvent, an oil (17.8 g.) was obtained, which was fractionated to the following fractions: (1) b.p.$_{50}$ 80~90°C, n_D^{25} 1.4600, d_4^{25} 0.8818, yield 4.4 g.; (2) b. p.$_{50}$ 90~103°C, n_D^{25} 1.4773, d_4^{25} 0.8661, yield 1.6 g.; (3) b. p.$_{50}$ 125~130°C, n_D^{25} 1.4789, d_4^{25} 0.9296, yield 8.9 g.; (4) residue (1.6 g.).

Condensation of fraction (1) with maleic anhydride at 80°C for half an hour was carried out, and the reaction mixture was separated to an unchanged oil and an addition product by distillation. The adduct was treated with a dilute sodium carbonate solution and a dilute aqueous sulfuric acid successively. Thus there were obtained crystals, m. p. 133.5~134°C, undepressed with the free acid of α-terpinene maleic anhydride adduct by the mixed melting point determination. The U. V. absorption curve of fraction (1) shows a λ_{max}^{alc} 265 mμ (*a*: 4.25), characteristic of α-terpinene (Fig. 4). The oil which remained unchanged by the maleic-anhydride treatment was extracted with a saturated resorcine solution. Steam-distillation of the extract gave an oil (0.3 g.) which was identified as 1,8-cineole by the formation of cresineol, m. p. 55~56°C, and by strip-chromatography (Rf 0.48)[11]. After the above treatment of fraction (1) there remained an oil consisting of dipentene and *p*-cymene. The former was characterized by its tetrabromide, m. p. 124~125°C, and the latter was confirmed by the absorption maxima at 258 and 273 mμ characteristic of *p*-cymene in a U. V. absorption spectrum (Fig. 4).

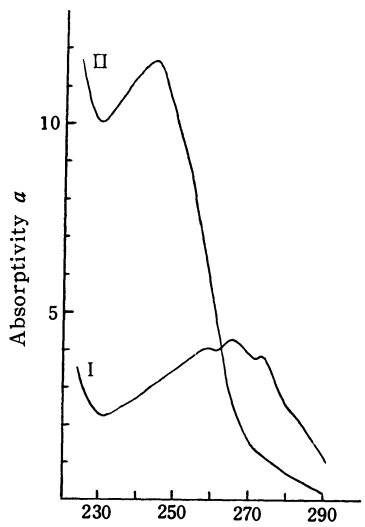

Fig. 4. Ultraviolet absorption spectra of hydrocarbon fractions: I fraction (1), II fraction (2) (in ethanol).

Fraction 2 consisted of dipentene (tetrabromide, m. p. 124~125°C) mainly and of a small amount of $\Delta^{2,4(8)}$-*p*-menthadiene (λ_{max}^{alc} 244 mμ, *a*: 11.67, in U. V. absorption curve in Fig. 4).

Redistillation of fraction (3) gave a main fraction: b. p.$_{20}$ 105~108°C, n_D^{25} 1.4793, d_4^{25} 0.9260,

* In this case the amount of crystallizaton water in terpin hydrate was so small that the concentraton of the acid was practically not changed.

phenylurethane m. p. 112~113°C characteristic of *dl*-α-terpineol.

The aqueous layer containing sodium sulfate was evaporated up on a water bath and the solid matter thus obtained was extracted with the same procedure described in the case of cineole. Unchanged terpin hydrate, m. p. 119.5~120°C (6.8 g. after repeated recrystallizations), was recovered, and *trans*-terpin, m. p. 156°C (0.1 g.), which was identified by mixing with an authentic specimen, was obtained.

Reaction of Cineole with Dilute Sulfuric Acid Solution. — Cineole (1000 g.) was heated with 0.6% aqueous sulfuric acid solution (706 g.) at 70°C for 10 hours under stirring. The acid solution used here showed the pH value (pH 1) equal to 60% aqueous acetic acid solution. After neutralization of the reaction mixture, and steam-distillation, a large amount of oil (952 g.) was obtained. Fractional distillation under reduced pressure gave a main fraction (935 g.) consisting of unchanged cineole and a higher boiling fraction (b. $p._{20}$ 71~96.5°C, n_D^{25} 1.4783, yield 0.2 g.) whose I. R. spectrum agreed with that of α-terpineol.

Terpin was obtained from the aqueous layer according to the method mentioned above. Separation of *cis*- and *trans*-terpins by fractional crystallization was tried, and only *trans*-terpin, m.p. 154.5~155°C (0.04 g.), was obtained.

Summary

The reaction of 1,8-cineole with 60% acetic acid at 70°C for 10 hours under stirring gave *dl*-α-terpineol (0.12%) and *trans*-terpin (0.03%). By the action of 21% sulfuric acid at 70°C for 3 hours, cineole yielded *dl*-α-terpineol (4.6%), terpin hydrate (0.20%), *trans*-terpin (0.12%) and monocyclic hydrocarbons (a small amount). On the other hand, the reaction of cineole with 0.6% sulfuric acid solution at 70°C for 10 hours gave *dl*-α-terpineol and *trans*-terpin in poor yields. In this case the reaction products are the same as in the case of 60% acetic acid.

Next, terpin hydrate was treated with 64% acetic acid at 70°C for 10 hours. The reaction products were *dl*-α-terpineol (2.7%) and *trans*-terpin (trace). By the action of 21% sulfuric acid at 70°C, terpin hydrate was attacked easily, and after 15 minutes it was converted to *dl*-α-terpineol (17.8%), *trans*-terpin (0.20%), 1,8-cineole and monocyclic hydrocarbons (11%). The monocyclic hydrocarbons consisted of α-terpinene, dipentene, $\Delta^{2,4(8)}$-*p*-menthadiene and *p*-cymene. *trans*-Terpin was, also, treated with 60% acetic acid at 70°C for 10 hours, the reaction product being *dl*-α-terpineol (1.8%).

On the basis of the above experiments a reaction mechanism for the action of acid solutions on 1,8-cineole was proposed.

The authors wish to thank Mrs. Michiko Satō for her assistance. This research was financed partly by the Scientific Research Grant of the Ministry of Education.

Department of Chemistry
Faculty of Science
Hiroshima University
Hiroshima

SHORT COMMUNICATIONS

Optimum Sample Position in Radioactivation Analysis Using Radium-Beryllium Neutron Source in Paraffin Moderator

By Fumio Aoki and Minoru Okada

(Received June 3, 1958)

It is known that in the radioactivation of samples by (n, γ) reaction by use of a radium-beryllium neutron source surrounded by a paraffin moderator, the distance between the sample and the neutron source is an important factor affecting the intensity of the radioactivity induced in the sample. However, the optimum distance depends on the size of the sample and the neutron source. In spite of this fact, data for the optimum distance[1-4] have been given without the specification of the size of the sample and the neutron source.

We feel that the size of the sample and the neutron source has some influence on the optimum distance and that, in so far as the problem of the size effect is not solved, it is highly desirable for practical purpose to specify the size of the sample and the neutron source. Therefore, we report in this letter the optimum distance for specified experimental conditions as well as the effect of the orientation of sample surface on induced activity.

The optimum distance was determined on three samples by use of a radium-beryllium neutron source placed in a paraffin moderator. The neutron source had a cylindrical shape (2.2 cm. in diameter and 2.5 cm. in height) and was made of mixture of 1g. of radium and 5 g. of beryllium. The paraffin moderator had a shape of a rectangular parallelepiped, and the minimum distance from the neutron source to the external surface of the moderator was 11 cm. The samples were: a circular plate of silver and flat packages of rhodium and of vanadium powder, their diameter or corresponding size being less than that of the neutron source. The sample position was on the axis of the neutron source cylinder. The nuclides chosen for the measurement of a flux of neutrons which brought about the (n, γ) reaction in the sample were 24.2 sec. ^{110}Ag, 44 sec. ^{104}Rh, and 3.76 min. ^{52}V.

As is shown in Fig. 1, each of the three curves, obtained from the counting rates of the product nuclides, shows a maximum at the same distance of 1.7 ± 0.1 cm. Meanwhile, if the total cross-section curves given by Hughes and Harvey[5], were referred to, it would be difficult to suppose that the relation between the (n, γ) reaction cross-section and the energy of neutrons for one of these elements was quite similar to the relation for the others. Nevertheless, the curves obtained showed very good agreement in the distance. The authors thus feeled that the distance may be valid for many other elements.

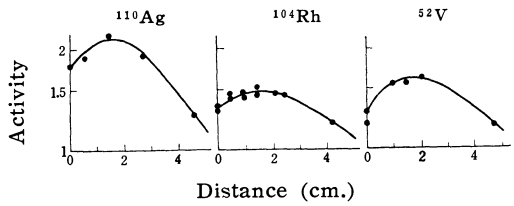

Fig. 1. Activity induced vs. distance from radium-beryllium neutron source.

In the study of the effect of the orientation of sample surface on the induced activity, a strip of silver plate of 0.8 cm. in width was placed at a distance of 2.2 cm. from the same neutron source as above, on the axis of the neutron source cylinder, and irradiated in two orientations: (a) perpendicular to, and (b) parallel to the neutron source axis. The measurements of induced activity for the two cases showed no appreciable difference, the

1) J. E. Hudgens and L. C. Nelson, *Anal. Chem.*, **24**, 1473 (1952).
2) W. W. Meinke and R. E. Anderson, *Anal. Chem.*, **25**, 781 (1953).
3) Y. Kusaka, Report presented at the 10th Annual Meeting of the Chemical Society of Japan, held in Tokyo, April 1957.
4) T. Shiokawa, M. Yagi and N. Yamashiro, Report presented at the 1st Annual Symposium on Radiochemistry, held in Tokyo, Dec. 1957.
5) D. J. Hughes and J. A. Harvey, Neutron Cross Sections (U. S. Atomic Energy Commission) **BNL-325**, 1955.

standard deviation of the observed values of the activity being within ±1% of the absolute values. Thus, it may be said that the orientation of sample surface has no appreciable effect on induced activity, so far as the sample size is less than one-third of the neutron source diameter; although the sample position for this experiment was not at the optimum distance, the same statement will apply to the samples placed at the optimum distance.

We are greatly indebted to Dr. S. Uchida, Professor S. Makishima and Mr. H. Takahashi for their encouragement and helpful suggestions, and to Dr. T. Naito for permission to use laboratory facilities.

Government Chemical Industrial Research Institute
Shibuya-ku, Tokyo

Synthesis of Isoflavono(7′,8′ : 6, 5)-α-pyrones and Formylation of 2,4-Dihydroxyphenyl Benzyl Ketone

By Yoshiyuki KAWASE, Tetsuya SEKIBA and Kenji FUKUI

(Received June 5, 1958)

In previous papers[1,2], the authors reported the preparation of furano(2′,3′ : 7, 8)-isoflavones. In connection with it, the present paper describes the preparation of isoflavono(7′,8′ : 6,5)-α-pyrones (IIa, b).

The synthesis of flavono(7′,8′ : 6,5)-α-pyrones has been carried out by two methods: that is, by α-pyrone-ring formation on 7-hydroxy-8-formyl-flavones[3], and by flavone-ring formation on 5-hydroxy-6-acyl-coumarins[4]. But, so far as the preparation of isoflavono(7′,8′ : 6,5)-α-pyrones is concerned, only the preparation of 2′,4-dimethyl-isoflavono-α-pyrone from 5-hydroxy-4-methyl-6-coumaryl benzyl ketone has been reported[5].

Here, isoflavono(7′,8′ : 6,5)-α-pyrone (IIa) and its 2′-methyl homologue (IIb) were prepared from 7-hydroxy-8-formyl-isoflavones (Ia,b) by the Perkin reaction in the usual way. IIa and IIb were hydrolyzed to a same acid, 2,6-dihydroxy-3-phenyl-acetyl-cinnamic acid (III) (not a lactone of it, namely a coumarin-derivative), which was re-derived into IIb by the action of acetic anhydride and sodium acetate.

It has been reported recently[6] that formylation of 2,4-dihydroxyphenyl benzyl ketone (resbenzylphenone) (IV) by the Hoesch reaction gives isoflavone through the compound formylated in α-methylene group.

In the present work, formylation of IV by the same reaction as above in the presence of anhydrous aluminum chloride gave 2,4-dihydroxy-3-formyl-phenyl benzyl ketone (V), the structure of which was confirmed by deriving it into IIb. (α-Acylresorcinols are usualy substituted in the 3-position in the Hoesch[7] or the

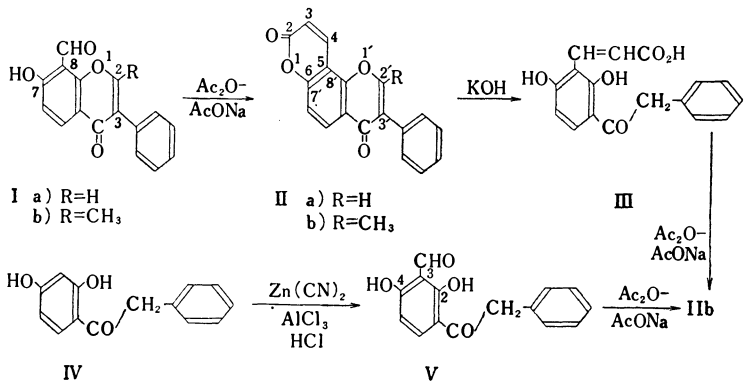

I a) R=H b) R=CH3 II a) R=H b) R=CH3 III IV V

1) T. Matsumoto, Y. Kawase, M. Nanbu and K. Fukui, This Bulletin, **31**, 688 (1958).
2) K. Fukui and Y. Kawase, ibid., **31**, 693 (1958).
3) S. Rangaswami and T. R. Seshadri, *Proc. Indian Acad. Sci.*, **9A**, 7 (1939). [*Chem. Abstr.*, **33**, 4244 (1939)].
4) S. M. Sethna, N. M. Shah and R. C. Shah, *J. Chem. Soc.*. **1938**, 228.
5) C. V. Deliwala and N. M. Shah, ibid., **1939**, 1250.
6) L. Farkas, *Chem. Ber.*, **90**, 2940 (1957).
7) K. Nakazawa, *J. Pharm. Soc. Japan*, (*Yakugaku Zasshi*), **59**, 297 (1939); H. R. Shah and R. C. Shah, *J. Chem. Soc.*, **1939**, 132.
8) S. M. Sethna, N. M. Shah and R. C. Shah, *Current Sci.* (*India*), **6**, 93 (1937) [*Chem. Abstr.*, **32**, 549 (1938)].

Pechmann[4,5,8] reaction in the presence of anhydrous aluminum chloride.)

Experimental[9]

Isoflavono(7', 8' : 6, 5)-α-pyrone (IIa).—A mixture of Ia[2] (0.6 g.) and anhydrous sodium acetate (0.7 g.) in acetic anhydride (4 cc.) was refluxed for 10 hr. The cooled mixture was poured into water, and the solid product was recrystallized from ethyl acetate, colorless needles, m.p. 200~200.5°C; yield 0.3 g. *Anal.* Found: C, 74.18; H, 3.55. Calcd. for $C_{18}H_{10}O_4$: C, 74.48; H, 3.47%.

2, 4-Dihydroxy-3-formyl-phenyl benzyl ketone (V).—A mixture of IV (5 g.), zinc cyanide (6 g.) and anhydrous aluminum chloride (5 g.) in anhydrous ether (100 cc.) was saturated with dry hydrogen chloride with stirring and cooling. By the usual treatment for the Hoesch reaction, the product was obtained in colorless microcrystals, m.p. 108~109°C (from dilute ethanol); yield 3.5 g. *Anal.* Found: C, 70.51; H, 4.85. Calcd. for $C_{15}H_{12}O_4$: C, 70.30; H, 4.72%.

2'-Methyl-isoflavono(7', 8' : 6, 5)-α-pyrone (IIb). (*a*) *From Ib.*—By the same procedure as described for IIa, starting from Ib[10] (1 g.), sodium acetate (1.1 g.) and acetic anhydride (6 cc.) the product IIb was obtained; m.p. 202~203.5°C (from ethyl acetate), yield 0.3 g. *Anal.* Found: C, 75.03; H, 4.05. Calcd. for $C_{19}H_{12}O_4$: C, 74.99; H, 3.97%.

(*b*) *From V.*—By the same treatment asd escribed for (a), starting from V (0.5 g.), sodium acetate (1 g.) and acetic anhyride (7 cc.) the product IIb (0.15 g.) was obtained; m.p. 202~203.5°C, identical with the sample from (a).

Hydrolysis of IIa and IIb to 2, 6-dihydroxyl-3-phenyl-acetyl-cinnamic acid (III).—(*a*) A mixture of IIa (0.1 g.) and 10% aqueous potassium hydroxide (5 cc.) was heated on a steam-bath for 4 hr. After being cooled, the solution was acidified with dilute hydrochloric acid, and the precipitates were collected and recrystallized from ethanol to give III, m.p. 210~211°C (decomp.), which was identical with the sample obtained from IIb. (*b*) A mixture of IIb (0.7 g.) and 10% aqueous potassium hydroxide (15 cc.) was treated similarly as described for a. Colorless microcrystals, m.p. 213~214°C (decomp.). III gave a brown ferric reaction in ethanol, and dissolved slowly in aqueous sodium bicarbonate. III was not converted into a lactone (coumarin-derivative) by heating with dilute hydrochloric acid. *Anal.* Found: C, 67.95; H, 4.73. Calcd. for $C_{17}H_{14}O_5$: C, 68.19; H, 4.74%. The mixture of III (0.1 g.), acetic anhydride (3 cc.) and sodium acetate (0.4 g), when refluxed for 10 hr., furnished IIb, m.p. 197~198°C (from ethyl acetate), which was identical with the sample described before.

An attempted preparation of IIa from III by the ethyl orthoformate-pyridine-piperidine method[11] was unsuccessful.

9) Melting points are uncorrect.
10) L. R. Row and T. R. Seshadri, *Proc. Indian Acad. Sci.*, **34A**, 187 (1951) [*Chem. Abstr.*, **47**, 12374 (1953)].
11) V. R. Sathe and K. Venkataraman, *Current Sci. (India)*, **18**, 378 (1949) [*Chem. Abstr.*, **44**, 8916 (1950)].

We are grateful to the Institute of Agricultural Chemistry, Faculty of Agriculture, Kyoto University for microanalyses.

Faculty of Literature and Science
Toyama University
Hasumachi, Toyama

A New Organic Reagent for the Colorimetric Determination of Iron(III) Ion; Phenothiazine Derivatives

By Masao MARUYAMA, Tomonori MIKI and Shogo UEDA

(Received September 1, 1958)

During the course of examinations on interactions between 2-acetyl-10-(3-dimethylaminopropyl)phenothiazine maleate (I) or 2-chloro-10-(3-dimethylaminopropyl)-phenothiazine hydrochloride (II), and metal ions in aqueous solution, it was found that these phenothiazine derivatives reacted with iron (III) ions to form a

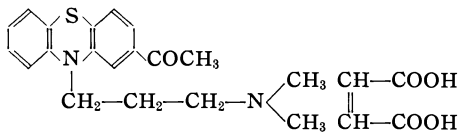

(I)

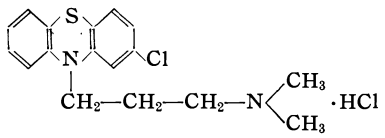

(II)

markedly colored solution. Both I and II react specifically with iron (III) ions and not with other ions such as iron (II), copper, nickel, cobalt, titanium and lead. Qualitatively, this reaction enables the detection of iron (III) ions in a concentration of 0.5 γ/cc., and a determination can be made for iron (III) ions of 1 to 8 γ/cc.

The compound I forms a yellow solution in water so that II is better suited for the determination than I. Aqueous solution of a mixture of iron (III) and the compound II exhibits an absorption spectrum in the visible region, with absorption maximum at 512 mμ, as shown in Fig. 1, and the absorbance depends on the concentration of iron (III) ion and of the compound II. When the concentration

of II is above 0.2%, absorbance depends solely on the concentration of the iron ion.

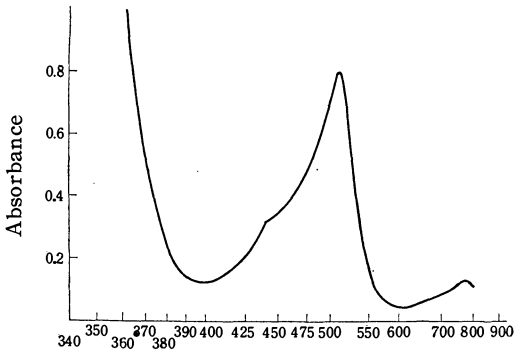

Fig. 1. Absorption spectrum of phenothiazine derivative with iron (III) ion in aqueous solution.
Contration of iron (III); 2.08×10^{-4}M/l.
Contration of the compound II; 4.82×10^{-3} M/l.
pH, 1.0 (H_2SO_4·aq.)

An examination showed that a linearity was established with iron concentrations of 1 to 8 γ/cc.

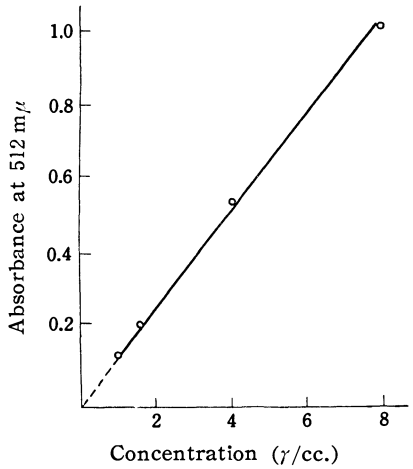

Fig. 2. Relation of iron (III) concentration to absorbance of colored solution.

As for the stability of the color developed, the color faded gradually with time but it was stable for 15 minutes after coloration.

In order to examine the effect of other metal ions, a sample solution containing iron (II), nickel, cobalt, copper, lead, titanium or chromium besides iron (III), in an amount 10 times that of iron (III) ion, was prepared, and caused to react with the compound II. It was found that the effect of these coexisting ions was negligible.

TABLE I
STABILITY OF COLORED SOLUTION
CONCENTRATION OF IRON (III): 4 γ/cc.
CONCENTRATION OF THE COMPOUND II: 2 mg./cc.

Time after coloration (min.)	Absorbance at 512 mμ
0	0.560
15	0.557
30	0.540
60	0.527

TABLE II.
EFFET OF OTHER IONS
CONCENTRATION OF IRON (III): 4 γ/cc.
CONCENTRATION OF THE COMPOUND II: 2 mg./cc.

Other ions (40 γ/cc.)	Absorbance at 512 mμ
—	0.560
Ni	0.551
Co	0.560
Cu	0.550
Cr	0.545
Ti	0.555
Pb	0.558

The presence of ethylenediaminetetraacetate interfered with this reaction.

Examinations are now under way on the effect of anions and on various problems, as well as the structure of the reaction product.

Shinagawa Plant, Sankyo Co., Ltd.
Nishi-shinagawa, Shinagawa-ku, Tokyo

*Isotope Effect of Boron in the Thermal Decomposition of the Boron Trifluoride-Calcium Fluoride Compound**

By Tatsuo MATSUURA
and Hisateru OKUNO

(Received October 8, 1958)

One of the purification methods of boron trifluoride gas for neutron counters involves the thermal decomposition of boron trifluoride-calcium fluoride addition compound[1,2]. In one of the papers describing

* Partly read at the 2nd Symposium of Atomic Energy in Japan, Feb. 1958.

1) A. C. Graves and D. K. Froman, "Miscellaneous Physical and Chemical Techniques of the Los Alamos Project", McGraw-Hill, New York (1952), p. 153.

2) F. Hudswell, J. S. Nairn and K. L. Wilkinson, AERE, C/R 651 (1951).

this process, Hudswell et al.[2] reported the unconfirmed, but apparently not erroneous result that at the earliest stage of the thermal decomposition of the boron trifluoride-calcium fluoride compound the fraction of the boron fluoride gas evolved might be enriched in ^{11}B. The present authors attempted to make sure of this fact and found that there is a considerable isotopic fractionation effect in this reaction, to such an extent that this phenomenon might be of use for the isotope separation of boron-10.

The results obtained are shown in Figs. 1 and 2, in which the percentages of boron trifluoride gas evolved are taken at the abscissa in sequence as the gas was evolved, and the isotopic abundance ratios of boron in each fraction in terms of the ratio $^{11}B/^{10}B$ are taken at the ordinate. The latter was read directly from the height of the peaks of m/e 49 and 48 (due to $^{11}BF_2^+$ and $^{10}BF_2^+$, respectively) in the mass spectrogram.**,*** These ratios can also be estimated by the peaks of m/e 11 and 10, but these peaks are less sensitive than those of 48 and 49, and, as is shown in Fig. 2, the $^{11}B/^{10}B$ values from these lower m/e regions were smaller than those from the higher regions[3].

It is no doubt that a significant isotopic effect occurred in this reaction, and the separation factors calculated schematically reach 1.035 in Batch A and ca. 1.015 in Batch B. As this factor is considered to depend on the speed of evolution of the gas, it was kept as low as possible, i.e., in the case of Batch A, it was ca. (21.)STP/hr, the total gas content in the batch being 0.8 mol. Also, the boron trifluoride is so strongly adsorbed (chemisorbed) on calcium fluoride, that the sampling of the last fraction of the gas, which probably contains ^{10}B most enriched, was sometimes incomplete on account of cracking in the glass vessel by strong heating. Had these

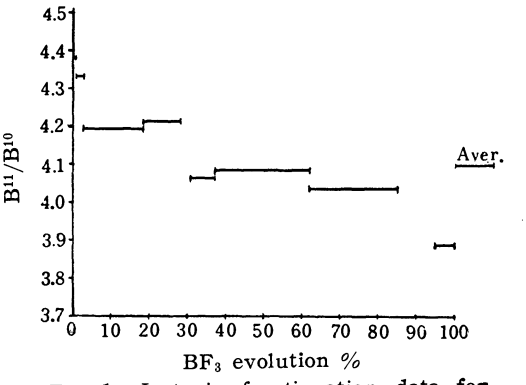

Fig. 1. Isotopic fractionation data for Batch A.†

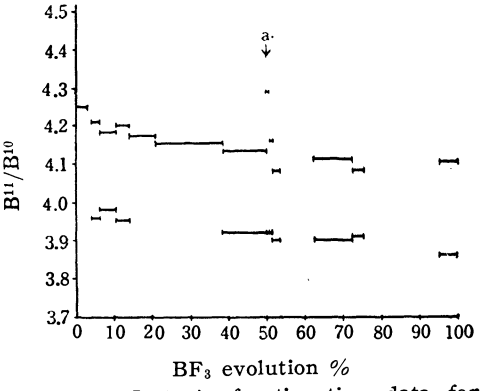

Fig. 2. Isotopic fractionation data for Batch B.†
(The lower group of the plots indicates the values from the peaks of m/e 11 and 10. The point a indicates the interruption of the gas evolution for several days.)

difficulties been avoided, the separation factor might have reached a greater value than this. Nevertheless, this observed separation factor in Batch A ($\alpha=1.035$) shows the largest value hitherto reported on the isotopic separation of ^{10}B using chemical exchange reactions[5].

The boron trifluoride-calcium fluoride compound was prepared by the method of Graves et al.[1] and the original boron trifluoride gas was prepared by Booth's method[6]. The thermal decomposition of

** The mass-spectroscopic measurements were done with a 21-103A Type Mass Spectrometer (Consolidated Electrodynamic Corp.) at the University of Tokyo or with a 103 Type Mass Spectrometer (Scientific Research Institute) at Nagoya University.

*** When the peak of m/e 47 was considerably large, correction was made on the observed values of peaks 48 and 49, on the basis that the whole peak of 47 is due to $^{28}SiF^+$, and that $^{29}SiF^+$ and $^{30}SiF^+$ did contribute to the peaks of 48 and 49 respectively, depending on the natural abundance ratio of ^{28}Si, ^{29}Si, and ^{30}Si[8]. Lately, however, M. Yamane of Hitachi Co., in a personal communication, suggested that the peaks of 46 and 47 are due to $^{10}EF(OH)^+$ and $^{11}BF(OH)^+$. Although this is perhaps true, the tendency of the isotopic fractionation by this process and thus the separation factor do not deviate seriously from the data reported in this paper.

3) W. W. Watson, J. C. Buchanan and F. K. Elder, *Phys. Rev.*, **71**. 887 (1947).

† Batch A was prepared from purified (distilled) boron trifluoride etherate, $BF_3\cdot(C_2H_5)_2O$, and Batch B was from the residue of this etherate distillation. The fact that there is a difference between the average $^{11}B/^{10}B$ ratios of the two batches (Figs. 1 and 2 (upper group)) indicates that the isotopic fractionation effect occurred at the boron trifluoride etherate distillation[4,5].

4) R. Nakane, T. Watanabe and S. Isomura, *Report of Scientific Research Institute*, **33**, 330 (1957).

5) International Symposium on Isotope Separation, Amsterdam, 1957.

6) H. S. Booth and K. S. Willson, *J. Am. Chem. Soc.*, **57**, 2273 (1935).

the compound and the sampling of the gas were done in a closed, evacuated apparatus, in which the gas began to be evolved at about 200°C, and evolution did not completely cease even at about 350°C.

The authors believe that this effect is applicable to the practical separation of boron 10, the scheme of which and some fundamental data for which will be reported later.

In this connection, the authors wish to call attention to the expectation that, in regard to substances which contain the comparatively lighter atomic weight elements such as lithium[7] and boron, their isotopic abundance ratio may possibly change appreciably by a simple procedure, such as vaporization, recrystallization or adsorption. As for boron, its well known indefinite atomic weight due to various geological origins[8] has, without doubt, much connection with this inference.

The authors wish to express their hearty thanks to Dr. S. Araki of the Faculty of Engineering in the University of Tokyo, and to Mr. T. Matsuo of the Department of Earth Science in the University of Nagoya, for their labor and advice in the mass-spectroscopic measurements.

College of Science
Rikkyo University
Toshima-ku, Tokyo

7) A. E. Cameron, *J. Am. Chem. Soc.*, **77**, 2731 (1955); G. Wagner and A. Pelz, *Monatsh*, **86**, 414 (1955) [*Chem., Abstr.* **50**, 692h (1956))], etc.

8) H. G. Thode, J. Macnamara, F. P. Lossing and C. B. Collins, *J. Am. Chem. Soc.*, **70**, 3008 (1948); H. V. A. Briscoe, P. L. Robinson and H. C. Smith, *J. Chem. Soc.*, **1927**, 282, etc.

The Variation of the Dielectric Constant of Phenol with Respect to Temperature

By K. M. Somasundaram and C. V. Suryanarayana

(Received September 19, 1958)

For the temperature variation of dielectric constant Abegg and other workers[1-4] gave the relation

$$D = D_0 e^{-T/190}$$

Later work has shown, however, that the coefficient of T in the exponent is, like D_0, specific for each liquid[5,6]. The equation

$$D = D_0 e^{-LT}$$

seems to hold with considerable accuracy for all the liquids hitherto examined. The second empirical constant L is seen to have the dimension of the reciprocal of temperature.

The above relation is verified with phenol.

Experimental procedure. — "BDH. Analar" variety of phenol was distilled and the fraction boiling at 181.75°C was collected and used. Dielectric constant of phenol was determined at different temperatures ranging from 41.5 to 65.9°C. "Dekameter type DK03" of Wissenschaftlich Technische Werkstätten was used at a fixed frequency of 1.8 MC/sec., controlling the temperature of the cell with Hoppler's ultrathermostat. The results are given in the following table.

t°C	41.5	42.3	49.8	50.6	58.1
D	11.78	11.72	11.10	11.03	10.48
t°C	60.7	64.8	65.4	65.5	65.9
D	10.32	10.03	9.98	9.97	9.95

From the above data a plot of $\log_{10}D$ versus T is a straight line and the variation of dielectric constant with temperature may be represented best by the relation

$$D = D_0^{-LT}$$

where $D_0 = 109.8$ and $L = 0.007094$.

It may be of interest that the data of Smyth and Hitchcock[7] for crystalline phenol has been tried by us to fit into the exponential equation. A plot of $\log_{10}D$ versus T gives a curve tending towards a limiting value. The exponential equation, as pointed by Abegg, is valid only for liquids.

Physico-Chemical Laboratory
Annamalai Universlty
Annamalainagar, South India

1) Abegg, *Ann. Physik.*, **60**, 54 (1897).
2) Abegg and Seitz, *Z. physik. Chem.*, **29**, 242 (1899).
3) Walden, ibid., **70**, 569 (1909).
4) Tangl, *Ann. Physik.*, **26**, 59 (1908).
5) Lowry and Jessop, *Trans. Chem. Soc.*, 782 (1930).
6) Akerlöf, *J. Am. Chem. Soc.*, **54**, 4125 (1932).
7) Smyth and Hitchcock, ibid., **54**, 4631 (1932).

Synthesis of Antimycic Acid Methyl Ester Methyl Ether

By Shigeo Okumura, Mitsuo Masumura, Tokunaru Horie and F. M. Strong*

(Received September 22, 1958)

The structure of antimycic acid was shown to be *N*-(3-aminosalicyloyl)-L-threonine by Strong and co-workers[1,2]. Dembro and Okumura have been trying to synthesize this acid without success[3].

Recently, the synthesis of both L- and DL-antimycic acid methyl ester methyl ether (VIb) has been achieved by us by the following process.

3-Nitrosalicylic acid methyl ether (I), m. p. 195~196°C[4], was prepared by hydrolysis with sodium hydroxide after methylation of 3-nitrosalicylic acid with diazomethane. I was refluxed with thionyl chloride to give the chloride (II) which was condensed with DL-threonine to obtain *N*-(3-nitro-2-methoxybenzoyl)-DL-threonine (IIIa) in 89% yield, m. p. 144.5~145.5°C. (*Anal.* Found: N, 9.38. Calcd. for $C_{12}H_{14}O_7N_2$: N, 9.39%). Prolonged methylation of IIIa with diazomethane gave 87% yield of methyl ester of IIIa, m.p. 92.5~93.5°C. (*Anal.* Found: N, 9.17. Calcd. for $C_{13}H_{16}O_7N_2$: N, 8.98%). IIIa was boild with in acetic anhydride to give 85% yield of *N*-(-3-nitro-2-methoxybenzoyl)-aminocrotonic azlactone (IV), m. p. 175~176°C. (*Anal.* Found: N, 10.70. Calcd. for $C_{12}H_{10}O_5N_2$: N, 10.68%). IIIa was catalyticaly reduced in methanol solution with palladium-carbon to obtaln *N*-(3-amino-2-methoxybenzoyl)-DL-threonine (Va), in 98% yield, m. p. 163~164°C. (*Anal.* Found: N, 10.53. Calcd. for $C_{12}H_{16}O_5N_2$: N, 10.45%). Prolonged methylation of this product with diazomethane gave *N*-(3-amino-2-methoxybenzoyl)-DL-threonine methyl ester (VIa), in 60% yield, m. p. 128.5~129.5°C. (*Anal.* Found: N, 9.92. Calcd. for $C_{13}H_{18}O_5N_2$: N, 9.93%), which was also prepared by catalytic reduction of the methyl ester of IIIa with palladium-carbon in methanol in 91% yield.

II was condensed with L-threonine to obtain the oily *N*-(3-nitro-2-methoxybenzoyl)-L-threonine (IIIb), which gave *N*-(3-amino-2-methoxybenzoyl)-L-threonine, (antimycic acid methyl ether) (Vb) by prolonged catalytic reduction in methanol with palladium-carbon, in 83% yield, m. p. 123.5~124.5°C, $[\alpha]_D^{28°}+14°$ (c 1.82, alcohol). (*Anal.* Found: N, 10.28. Calcd. for $C_{12}H_{16}O_5N_2$: N, 10.45%). Vb was methylated in methanol with diazomethane to obtain 78% yield of *N*-(3-amino-2-methoxybenzoyl)-L-threonine methyl ester, (Antimycic acid methyl ester methyl ether) (VIb) m. p. 155~156°C, $[\alpha]_D^{28°}+10°$ (c 2.05, alcohol). (*Anal.* Found: C, 55.27; H, 6.54; N, 10.09. Calcd. for $C_{13}H_{18}O_5N_2$: C, 55.32; H, 6.43; N, 9.93%).

A sample of antimycic acid methyl ester methyl ether, m. p. 155~156°C, obtained by methylation of natural antimycic acid in methanol with diazomethane, showed no depression of m. p. when mixed with VIb, and neither the infrared nor the ultraviolet spectra showed any significant difference between the two substances. Va or Vb was boiled in acetic anhydride with pyridine to give respectively 84% or 78% yield of *N*-(3-acetamino-2-methoxybenzoyl)-aminocrotonic azlactone (VII), m. p. 136.5 ~ 137.5°C. (*Anal.* Found: N, 10.45. Calcd. for $C_{14}H_{14}N_4O_2$: N, 10.22%), which gave by prolonged hydrolysis with 0.08 N sodium hydroxide 73% yield of *N*-(3-acetamino-2-methoxybenzoyl)-aminocrotonic acid (VIII), m. p. 195.5~196.5°C. (*Anal.* Found: N, 9.66. Calcd. for $C_{14}H_{16}O_5N_2$: N, 9.59%), as described previously for antimycic acid itself by Strong[1,2].

Department of Applied Chemistry
Faculty of Engineering
University of Tokushima
Tokushima

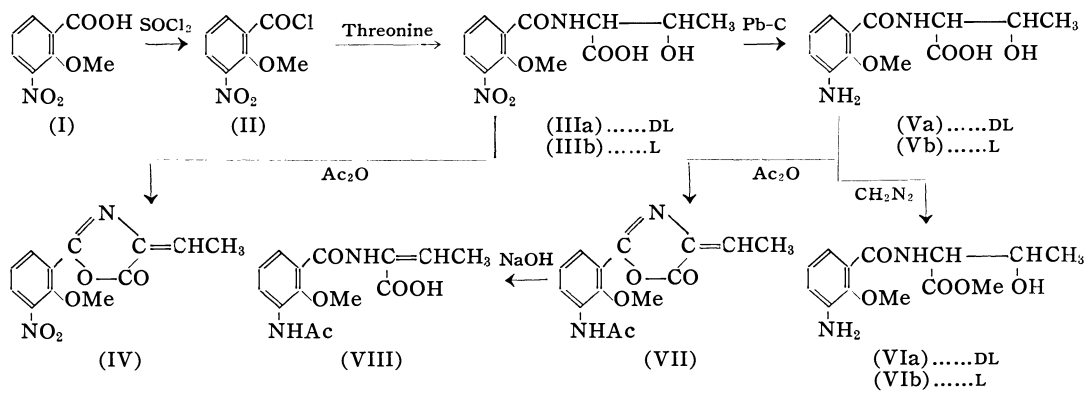

* Present Address, Department of Biochemistry, University of Wisconsin, Medison 6, Wisconsin, U. S. A.

1) G. M. Tener, F. M. Bumpus, B. R. Dunshee and F. M. Strong, *J. Am. Chem. Soc.*, **75**, 1100 (1953).

2) G. M. Tener, E. E. van Tamelen and F. M. Strong, ibid., **75**, 3623 (1953).

3) Unpublished work at Wisconsine University.

4) J. F. Simpnsen and M. G. Rau, *J. Chem. Soc.*, **111**, 220 (1917).

5) Eastman Organic Chemica[s.

TABLE I

SYNTHESES OF 1-METHYL-3, 4-DIHYDROISOQUINOLINE FROM BENZYLACETONE OXIME IN LIQUID SO_2[a, b]

No.	Reagent	Molar ratio of oxime to reagent	Reaction		*N*-Phenethyl acetamide yield (%)	1-Methyl-3, 4-dihydroisoquinoline yield (%)
			temp.(°C)	time(hr.)		
1	P_2O_5	1 : 5	20	6	10.0	4.5[c]
2	P_2O_5	1 : 5	20	12	20.0	trace
3	P_2O_5	1 : 5	−10	12	trace	0
4	P_2O_5	1 : 5	70	6	15.0	15.9
5	$P_2O_5+SOCl_2$	1 : 5 : 5	70	6	trace	0
6	$P_2O_5+POCl_3$	1 : 5 : 10	50	12	40.0	13.6
7	$P_2O_5+POCl_3$	1 : 5 : 10	70	3	36.0	18.1
8	$P_2O_5+POCl_3$	1 : 5 : 10	70	6	24.0	40.9
9	$P_2O_5+POCl_3$	1 : 5 : 10	70	12	4.0	45.4[d]
10	$P_2O_5+POCl_3$	1 : 5 : 10	110	12	0.0	29.5
11	$P_2O_5+POCl_3$	1 : 5 : 10	70	12	10.0	13.6[e]
12	$P_2O_5+POCl_3$	1 : 5 : 10	70	12	6.0	18.1[f]

a) Reactions were caused to proceed with 5 g. (0.03 mole) of the oxime in 70 ml. of liq. SO_2.
b) $POCl_3$, $SOCl_2$, PCl_5, or SO_3, used as the reagent in liquid sulfur dioxide (molar ratio of oxime to reagent was 1 : 5) at 20°C for 12 hr. or at 70°C for 6 hr., caused no reaction.
c) Reaction with shaking.
d) No difference was observed between the reaction with shaking and that without shaking.
e) Reaction was caused to proceed without solvent (liquid SO_2).
f) Tetralin (70 ml.) was added to the reaction mixture.

dioxide by modifying Bradsher and Sinclair's cyclodehydration. It was ascertained that 1-methyl-3, 4-dihydroisoquinoline was obtained in a yield of over 40 per cent. The results and the related facts observed will be reported elsewhere.

From the facts mentioned above, it appeared reasonable to expect that the reaction of the oximes of phenethyl ketones with acidic reagents in liquid sulfur dioxide may well lead to the production of isoquinoline derivatives.

For the purpose of estimating the efficiency of this procedure benzylacetone oxime (V, R=CH_3) seemed suitable and it was subjected to the simultaneous rearrangement and cyclodehydration in liquid sulfur dioxide to obtain 1-methyl-3, 4-dihydroisoquinoline (II, R=CH_3). As shown in Table I, the best result (45.4% yield) was attained by treating the oxime with a mixture of phosphorus pentoxide and phosphorus oxychloride at 70°C in liquid sulfur dioxide.

Among various reagents examined, sulfuric acid, sulfur trioxide, thionyl chloride and phosphorus pentachloride were ineffective and phosphorus pentoxide gave a small quantity of the product. But when a mixture of phosphorus pentoxide and phosphorus oxychloride was used at 70°C for twelve hours, the amount of the product reached the maximum (45.4%). As for the reaction temperature, a better yield was obtained at 70°C rather than below 0°C, which differed somewhat from the experience of Bradsher and Sinclair[9]. Shaking of the reaction vessel resulted only in a slight improvement. Addition of another solvent such as tetralin gave no good effect. Because phosphorus pentoxide was not dissolved but suspended in liquid sulfur dioxide, the addition of a large amount of phosphorus oxychloride served probably to keep the suspension homogeneous.

A considerable amount of acid amide (I, R=CH_3) was found in the reaction mixture. This explains the fact that the cyclodehydration is rather a slow reaction and the first step (the Beckmann rearrangement) proceeds promptly before the cyclodehydration takes place. When benzylideneacetone oxime (VI, R=CH_3) was subjected to this reaction, only a resinous product was produced. This suggests that a vinyl polymerisation occurred in liquid sulfur dioxide.

The preparation of 9-phenylphenanthridine (VIII) in liquid sulfur dioxide was attempted. Smith[6] reported that the yield of this substance from *o*-phenylbenzophenone oxime (VII) by heating with polyphosphoric acid was 17 per cent.

Chart 3.

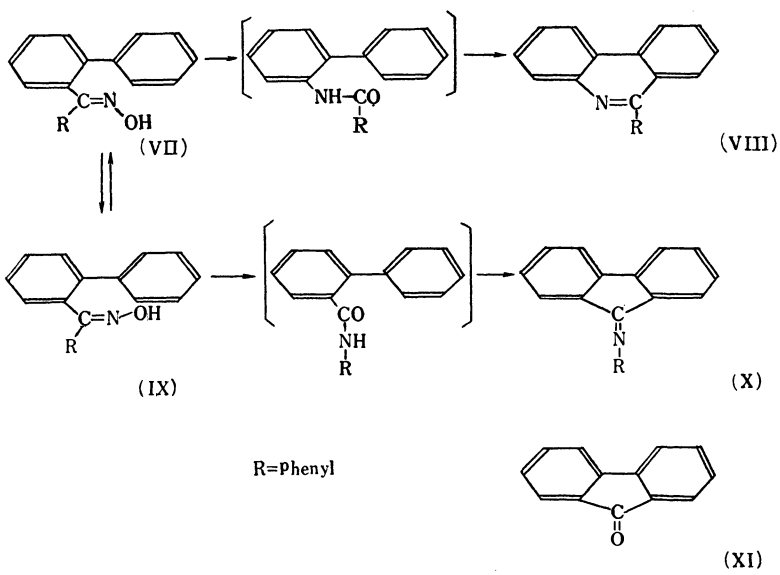

With phosphorus pentoxide and phosphorus oxychloride in liquid sulfur dioxide, 9-phenylphenanthridine (VIII) was obtained in an improved yield of 29.4 per cent. Moreover, fluorenone (XI) was also isolated from the reaction mixture as was reported by Smith.

It is an established fact that a *trans*-migration occurs in the Beckmann rearrangement. When *o*-phenylbenzophenone oxime (VII) takes another geometrical structure IX, it may afford fluorenoneanil (X) as the product. This will produce fluorenone (XI) by hydrolysis in the acidic medium.

The method mentioned above, the simultaneous rearrangement and cyclodehydration in liquid sulfur dioxide under mild conditions, may give excellent syntheses of dihydroisoquinoline, phenanthridine and their derivatives and may be applied extensively with great advantages.

Experimental

Liquid sulfur dioxide.—Commercial sulfur dioxide was dried with sulfuric acid and distilled.

Reagents.—Phosphorus pentoxide, oxychloride, and pentachloride, sulfuric acid, sulfur trioxide and thionyl chloride were of extra pure grade.

Apparatus and general procedure.—Glass pressure vessels (300 ml. capacity) equipped with metal joints and appropriate cocks or valves were used as before[1]. A liquid sulfur dioxide solution of an oxime was added to a mixture or a solution of the dehydrating reagent in the same solvent with ice-cooling. The vessel was kept at a definite temperature during the reaction period for a definite time. If necessary, the vessel was shaken. Then the solvent was evaporated and recovered. The residue was dropped into ice water and the excessive reagent was decomposed. Then the products were separated for their identification.

Synthesis of 1-methyl-3, 4-dihydroisoquinoline from benzylacetone oxime.—*Benzylacetone.*—Essentially the methods of Leuchs[10] and Meerwein[11] were followed. Metallic sodium (42 g.) was dissolved in 500 ml. of absolute ethanol and 500 g. of ethyl acetoacetate was added. To this mixture cooled below 30°C, 246 g. of benzyl chloride was added and the whole was stirred for 1 hour at room temperature. The reaction mixture was further refluxed for 1 hour and filtered. From the filtrate 350 g. of ethyl 2-benzylacetoacetate was obtained as a transparent liquid boiling at 140~145°C (5 mmHg). In an autoclave, a mixture of 350 g. of the ethyl 2-benzylacetoacetate and 200 ml. of water was heated for 30 min. at 250°C. The oily layer and the ethereal extract of the aqueous layer were combined, washed with 50 ml. of 0.1 N sodium hydroxide solution and with water successively, and distilled. Benzylacetone distilled at 105~110°C (10 mmHg). Yield, 160 g.

Benzylacetone oxime.—Prepared by the ordinary method[12], m. p. 84~85°C. From 160 g. of benzylacetone, 134 g. of the oxime was obtained.

1-Methyl-3, 4-dihydroisoquinoline (*II*, $R=CH_3$).—A solution of 5 g. (0.03 mole) of benzylacetone oxime in 20 ml. of liquid sulfur dioxide was added to a mixture of the reagents (molar ratio of oxime, phosphorus pentoxide and phosphorus oxychloride was 1 : 5 : 10) in 50 ml. of the same solvent. After the reaction at 70°C for 12 hours, the solvent (sulfur dioxide) was allowed to

10) H. Leuchs, *Ber.*, **44**, 1510 (1911).
11) H. Meerwein, *Ann.*, **398**, 249 (1913).
12) P. W. Neber and A. Uber, ibid., **467**, 63 (1928).

evaporate from the mixture. The residue was added to ice water and excessive reagents were decomposed. The mixture was extracted with ether. The ethereal solution, after being dried over calcium chloride, was condensed and the residue was distilled in vacuo. The rearranged product, acid amide (I, R=CH_3), was obtained as an oil boiling at 155~157°C (5 mmHg); yield, 0.2 g. (4%). The acid amide was hydrolyzed to phenethylamine with hydrochloric acid, and a picrate of the amine was prepared. The melting point and the mixed melting point with an authentic sample were 167~168°C (reported[13] m. p. 171°C).

The residual aqueous solution was made alkaline with caustic alkali and steam-distilled. The distillate was again made alkaline and extracted with ether. The ether solution, after being dried over magnesium sulfate, was condensed and the residue was distilled in vacuo. A pale yellow oil boiling at 95~105°C (5~6 mmHg) was obtained. This was 1-methyl-3, 4-dihydroisoquinoline. Picrate, yellow needles, m. p. 188~189°C (reported[14] m. p. 188~190°C). No depression of the melting point was observed when mixed with an authentic sample.

Anal. Base: Found; N, 9.74%. Calcd. for $C_{10}H_{11}N$; N, 9.65%. Picrate: Found; N, 15.13%. Calcd. for $C_{16}H_{14}O_7N_4$; N, 14.97%.

Dihydroisoquinoline was not produced with phosphorus oxychloride or with thionyl chloride. Sulfuric acid or sulfur trioxide appeared to produce water soluble substances which could not be separated. The effects of reaction conditions on the yield of 1-methyl-dihydroisoquinoline are listed in Table I.

An attempted synthesis of 1-methyl-isoquinoline from benzylideneacetone oxime (VI, R = CH_3). — Vorländer's[15] recipe was followed. A mixture of 320 g. of acetone, 210 g. of benzaldehyde washed with dilute soda solution, and 200 ml. of water was added to 50 ml. of 10% caustic soda solution in two hours at 10~20°C. The reaction mixture was stirred further for two hours and was allowed to stand for 24 hours at room temperature. The solution was made acidic with hydrochloric acid and the oily layer was separated. The aqueous layer was thoroughly extracted with benzene. The oily layer combined with the benzene extract was washed with water and dried over calcium chloride. After the benzene and the unchanged benzaldehyde were distilled off, a pale yellow oil boiling at 105~110°C (3 mmHg) was obtained. Yield, 180 g. The above benzylideneacetone was mixed with hydroxylamine hydrochloride in methanol. The crystals separated in a few days were recrystallized from 60% ethanol: benzylideneacetone oxime[16], m. p. 114~115°C. Yield, 45 g.

Reaction of benzylideneacetone oxime (VI, R=CH_3).—A solution of 4.8 g. of the oxime in 20 ml. of liquid sulfur dioxide was added to a mixture of reagents (molar ratio of oxime to phosphorus pentoxide and phosphorus oxychloride was 1 : 5 : 10) in 50 ml. of liquid sulfur dioxide. The reaction mixture was treated as described above after 3 hours shaking at 70°C, or 6 hours shaking at room temperature. No significant amount of basic materials was found in the reaction mixture except resinous matters.

Synthesis of 9-phenylphenanthridine (VIII) from *o*-phenylbenzophenone oxime (VII).—*o-phenylbenzophenone.*—This was prepared from fluorene as follows: fluorenone obtained from the oxidation of fluorene[17] was cloven to *o*-phenylbenzoic acid[18] by alkali fusion. *o*-phenylbenzonitrile was prepared from this acid via its acid amide and was treated with phenylmagnesium bromide by Schlenk and Bergmann's[19] method to yield *o*-phenylbenzophenone. From 200 g. of fluorene, 25 g. of the ketone was obtained.

o-Phenylbenzophenone oxime (VII).—This was Prepared by the procedure of Smith[6]. Yield 18.3 g. from 25 g. of the ketone.

9-Phenylphenanthridine (VIII).—A solution of 5.4 g. (0.02 mole) of the oxime (VII) in 20 ml. of liquid sulfur dioxide was added to a mixture of the reagents (mole ratio of oxime: phosphorus pentoxide : phosphorus oxychloride, 1 : 5 : 10) in 50 ml. of liquid sulfur dioxide. After being allowed to stand at 70°C for 3 hours the reaction mixture was treated as described above. The resulting aqueous acidic mixture was made alkaline with ammonia and extracted with benzene. The extract was washed first with dilute, then with conc. hydrochloric acid, and finally with water. Neutralization of the acidic solution precipitated a basic material, which was recrystallized from ethanol to give crystalline 9-phenylphenanthridine. Yield, 1.5 g. (29.4%), m. p. 103~104°C. Picrate: yellow needles, m. p. 247~247.5°C (decomp.) (reported[20] m. p. 242°C (decomp.)). The mixed melting points of the base and of the picrate with the authentic samples respectively showed no depression.

Anal. Base: Found; N, 5.68%. Calcd. for $C_{19}H_{13}N$; N, 5.49%. Picrate: Found; N, 11.94%. Calcd. for $C_{25}H_{16}O_7N_4$; N, 11.57%.

When the benzene solution was condensed, 2.7 g. of dark yellow crystals was obtained. Recrystallization from ligroin (b. p. 60~80°C) gave 2.4 g. of pale yellow plates, m. p. 83~84°C, which showed no depression of the melting point on mixing with fluorenone (m. p. 83~84°C).

When the reaction was conducted at 20°C for 12 hours, 0.2 g. (3.9%) of VIII and 1 g. of XI were obtained. A viscous orange liquid (4.2 g.) was also obtained along with XI from the benzene extracts in this case, the liquid being separated by fractional distillation under a reduced pressure. The liquid which distilled at 190~200°C (1~2 mmHg) contained nitrogen (N, 5.96%), but

13) H. Decker and W. Kropp, *Ber.*, **42**, 2078 (1909).
14) E. Späth, F. Berger and W. Kuntara, ibid., **63**, 137 (1930).
15) D. Vorländer, *Ann.*, **294**, 275 (1897).
16) C. Harries and A. S. de Osa. *Ber.*, **36**, 2998 (1903).
17) J. Schmidt and H. Wagner, ibid., **43**, 1797 (1910).
18) C. Graebe and A. Sc. Rateanu, *Ann.*, **279**, 259 (1894).
19) W. Schlenk and E. Bergmann, ibid., **464**, 34 (1928).
20) A. Pictet and A. Hubert, *Ber.*, **29**, 1188 (1896).

showed no change on refluxing with hydrochloric acid in ethanol.

The authors are indebted to Dr. C. K. Bradsher for his valuable suggestions. The financial support of this project was granted by the Ministry of Education. Liquid sulfur dioxide was donated by the Befu Chemical Industries Co., Ltd., A large quantity of fluorene was kindly given by Dr. T. Yoshida, Yawata Chemical Industries Co., Ltd. The authors are grateful to all.

Research Institute of Non-aqueous Solutions, Tohoku University
Katahira-cho, Sendai

Rapid Separation of Radioactive Strontium by Solvent Extraction with TTA-Hexone

By Toshiyasu KIBA and Shigeru MIZUKAMI

(Received May 30, 1958)

It is an important problem at present to develop a rapid method of separating and estimating radioactive strontium (^{89}Sr, and ^{90}Sr) contained in mixed fission products. Such a method is indispensable for devising a workable procedure for the chemical elimination of strontium from reactor wastes. Previously the authors attempted to separate the fission products into groups by solvent extraction, with TTA (*o*-thenoyl trifluoroacetone)-benzene[1], and cupferron-chloroform[2]. As a result of the experiment, it was found that by the solvent extraction with TTA-benzene at pH 6, and with cupferron-chloroform at pH 4, strontium, cesium, and ruthenium remained in the aqueous phase and the other fission products entered the organic phase. Hence the next problem to be solved is to recover the strontium retained by the aqueous phase after the extraction. The present paper describes an investigation on the separation of strontium from other fission products by liquid-liquid extraction.

TTA (*o*-thenoyl trifluoroacetone), dissolved in benzene, toluene, or xylene, is widely employed as a reagent for solvent extraction of zirconium and cerium from their acidic solutions[3], but there are few papers which treat of the separation from a solution of a given pH value. Khym, Tompkins and Cohen[4] have reported separation of ^{45}Ca, which was produced by Sc(*d*, 2*p*) reaction, by solvent extraction with 0.5 M TTA-benzene from a solution of pH 9. As it seems advantageous to use a reagent-solvent phase of low concentration when the extraction is made, the present authors employed 0.05 M TTA-benzene for the purpose to examine the behavior of strontium. Belonging to the same family with calcium, strontium could not be extracted by the reagent-solvent phase though experiments were conducted over a wide range of pH of the aqueous solution. Afterward, various solvents other than benzene were tried and hexone (methyl isobutylketone) was found to be the best, both because of the high solubility of TTA in it and because of its superior power to effect the separation of strontium. In the following experiments 0.05 M TTA-hexone is always used as the extracting agent for the separation of strontium.

Experimental

Reagents, Materials and Apparatus.—*TTA (o-thenoyl trifluoroacetone)* imported from L. Light & Co. Ltd., England, was dissolved in hexone of extra pure grade to a concentration of 0.05 M. TTA-benzene was prepared by dissolving the reagent in thiophene-free benzene to a concentration of 0.05 M and 0.5 M.

1) T. Kiba, S. Ohashi and K. Yoshizawa, Unpublished paper, read at the 10th Annual Meeting of the Chemical Society of Japan (April, 1957).

2) T. Kiba and M. Kanetani, This Bulletin, **31**, 1013 (1958).

3) G. H. Morrison and H. Freiser, "Solvent Extraction in Analytical Chemistry", John Wiley & Sons, Inc. New York (1957).

4) J. X. Kyhm, P. C. Tompkins and W. E. Cohen, USAEC, **MDDC-1214** (1947).

Radioactive Strontium.—$^{90}Sr(^{90}Y)$ was imported from Oak Ridge National Laboratory, U.S.A. as nitrate in nitric acid solution, a part of which was diluted to 0.02 N nitric acid solution having an activity of about 10,000 cpm. per 0.2 ml. The mixed fission products (Batch No. 35), ^{45}Ca, and ^{106}Ru were imported from the Oak Ridge National Laboratory and used for the comparative investigation of the method.

Buffer Solution.—A system composed of 0.5 M acetic acid, ammonium acetate and aqueous ammonia was used, and its pH was measured by a glass-electrode pH-meter, Horiba Instrument Co., Japan.

Measurement of Radioactivity.—The radioactivity was measured as β-counting by a G-M counting set (No. 131 G-M tube, mica-window: 2.8 mg./cm^2, counting efficiency for $^{90}Sr(^{90}Y)$: 11.7%, "100" scalor, Kobe Kogyo Co. Ltd.).

Separatory Funnel.—The separatory funnel is a spindle-shaped vessel made of hard glass, with a capacity of 30 ml. In order to prevent the mixing of the two phases when being drained, a type with a small bore above the cock and a large bore below was chosen.

Shaking Machine.—Shaking of the content of the separatory funnel was done by means of an electric vertical oscillator performable 230 double strokes per minute. The equipment can handle six funnels at the same time.

Other chemicals were all of pure grade, and the utensils were of ordinary laboratory types.

Procedure.—In a 30 ml. separatory funnel, place 0.2 ml. of the solution of the mixed fission products or the radioactive nuclides, and add the buffer solution of a definite pH to make 6 ml. Then pour 2 ml. of the organic solvent into the vessel, and stopper tightly. Shake the vessel for five minutes with the electric vertical oscillator. After the phases have disengaged, take out the aqueous layer into a second funnel. Re-extract the aqueous phase in the second funnel with 2 ml. of the organic solvent for five minutes. To the organic phase retained in the first funnel, add 5 ml. of the buffer solution and shake for another five minutes. Combine the aqueous phases of the first and the second funnel in a vessel, and the organic phases in another, and evaporate the content in a porcelain counting dish, and measure the radioactivity with the G-M counting set. Plot the decay curve of the activity or draw a Harley plot to identify the nuclide contained in the sample.

1) The experiments were carried out with 0.5 M TTA-benzene, 0.05 M TTA-benzene, and 0.05 M TTA-hexone at different pH of the solution to determine the optimum pH for the separation of strontium.

2) Some experiments with TTA-hexone were carried out with the buffer solution of the optimum pH for the separation of strontium, containing a known amount of barium nitrate, magnesium nitrate, or calcium nitrate, in order to examine the effect of salts present in the solution on the extraction of strontium.

3) The behavior of calcium in the solution was examined using ^{45}Ca as tracer, and was compared in detail with the behavior of strontium.

4) The effect of such agents as EDTA (disodium ethylenediaminetetra-acetate) and ammonium citrate as masking agent on the extraction was examined.

5) For the purpose of rapidly isolating the radioactive strontium from the aged fission products, a two-step extraction was attempted: a solution of the gross fission products was first treated with 0.05 M TTA-benzene at pH 7, and after the organic layer was discarded, the remaining aqueous phase was shaken with 0.05 M TTA-hexone at pH 8. The radioactivity was measured in each case. The radioactive strontium, ^{89}Sr and ^{90}Sr, came out in the last organic phase.

Results and Discussion

The percentage of the material recovered by extraction from the solution of the fission products of different pH by 0.05 M TTA-benzene and 0.05 M TTA-hexone is shown in Fig. 1. The percentage extraction was computed as the ratio between the counting rate of the organic phase to that of the original solution. Before the counting, the organic phase was, of course, evaporated and dried in a counting sample pan, and the original activity taken in the solution was determined for 0.2 ml. of the stock solution of the fission products.

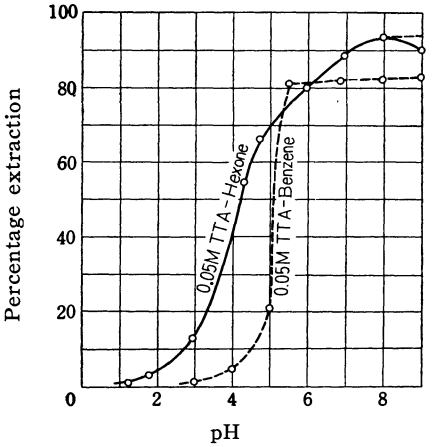

Fig. 1. Effect of pH on the extraction of gross fission products by TTA-benzene and TTA-hexone.

Comparing the results obtained by the extraction with TTA-benzene and TTA-hexone with each other, the amount extracted at pH 8 is greater by the latter than by the former. Since it has been confirmed[1] that after extraction with TTA-benzene at pH 6, strontium, cesium

TABLE I

EXTRACTION OF $^{90}Sr(^{90}Y)$ BY 0.05 M TTA-HEXONE

pH of the solution pH	$^{90}Sr(^{90}Y)$ taken cpm.	Extracted in org. phase cpm.	Retained in aqueous phase cpm.	Extracted %
7	10,050	7,610	2,400	75.8
8	9,220	9,190	30	99.6
9	9,220	9,125	96	98.9

TABLE II

EXTRACTION OF $^{90}Sr(^{90}Y)$ WITH VARIOUS SOLVENTS AT pH 8

Reagent-solvent	$^{90}Sr(^{90}Y)$ taken cpm.	Separation into the phases cpm. (%)	Note: Nuclide and its radiochemical purity
0.5 M TTA-Benzene	8,020	Org. Phase 4,490 (56.0%)	$^{90}Y+^{90}Sr$
		Aq. Phase 3,530	^{90}Sr
0.05 M TTA-Benzene	7,750	Org. Phase 4,290 (55.3%)	^{90}Y (98%)
		Aq. Phase 3,460	^{90}Sr (98~100%)
0.05 M TTA-Hexone	7,540	Org. Phase 7,510	$^{90}Sr+^{90}Y$
		Aq. Phase 30	None

and ruthenium remain in the aqueous phase, the increase in counting rate of TTA-hexone phase should perhaps be attributed to strontium. The following experiment will confirm this supposition.

A solution containing $^{90}Sr(^{90}Y)$ was adjusted to a different pH, and the extraction was carried out with 0.05 M TTA-hexone. The partition of the radioactivity between the aqueous phase and the organic phase was determined as the ratio of their counting rates. As shown in Table I the $^{90}Sr(^{90}Y)$ was completely transferred into the organic phase.

The results of the extractions carried out with 0.05 M TTA-benzene, 0.5 M TTA-benzene, and 0.05 M TTA-hexone, respectively, are illustrated in Table II. By the extraction with TTA-benzene all the ^{90}Y was transferred into the organic phase and the ^{90}Sr remained in the aqueous phase. On the other hand, by the extraction with TTA-hexone both the ^{90}Sr and the ^{90}Y went into the organic phase. When the two-step extraction is performed, that is, when the solution is extracted first with 0.05 M TTA-benzene and then 0.05 M TTA-hexone, the latter organic phase contains ^{90}Sr alone.

The distribution coefficient and the equilibrium constant were measured at 20°C when the extraction of ^{90}Sr with TTA-hexone was performed from aqueous solution of pH 8.05. Writing the formula for TTA as HT, the reaction involved can be described by the following equation:

$$Sr^{2+}_{aq}+2HT_{org}=SrT_{2org}+2H^{+}_{aq}$$

in which subscript *org* refers to organic phase and *aq* to adueous phase. The equilibrium expression may be written as follows,

$$K=[SrT_2]_{org}\cdot[H^+]^2_{aq}/[Sr^{2+}]_{aq}\cdot[HT]^2_{org}$$

In this case the aqueous phase is a buffer solution of pH 8.05, that consists of 0.5 M ammonium acetate and aqueous ammonia, so the hydrogen ion concentration, $[H^+]_{aq}$ could be considered as being kept constant before and after the extraction. Then,

$$K'=[SrA_2]_{org}/[Sr^{2+}]_{aq}\cdot[HT]^2_{org}$$

The distribution coefficient of strontium, q, can be written as

$$q=[SrA_2]_{org}/[Sr^{2+}]_{aq}$$

so

$$K'=q/[HT]^2_{org}$$

$$\log K'=\log q-2\log[HA]_{org}$$

As the concentration of radioactive strontium is far less than that of TTA in the organic phase, $[HA]_{org}$ may be considered as being invariable during the extraction. Before the experiment, ^{90}Sr had been separated from $^{90}Sr(^{90}Y)$ by the extraction with 0.05 M TTA-benzene at pH 7 as described above, and the ^{90}Sr retained in the aqueous solution was used for the purpose. Six ml. of hexone containing TTA of various concentrations was mixed with the same volume of the aqueous solution of pH 8.05, which contained the radioactive strontium. After a separatory funnel was shaken for thirty

TABLE III

DISTRIBUTION OF ^{90}Sr BETWEEN TTA-HEXONE AND BUFFER SOLUTION OF pH 8.05, AT 20°C

Concn. of TTA in hexone M	Activity in aq. phase I_{aq} (cpm.)	Activity in org. phase I_{org} (cpm.)	Distribution coeff. q	$\log_q$	$\log K'$
0.0005	3516	126	0.03583	−1.4458	5.16
0.001	3255	104	0.03195	−1.4955	4.50
0.005	2694	840	0.3118	−0.506	4.10
0.01	2256	1422	0.6303	−0.2005	3.80
0.05	232	3495	15.065	+1.178	3.78
0.1	243	3531	14.531	+1.162	3.16
				avr.	4.08_3

TABLE IV

DISTRIBUTION OF $^{90}Sr(^{90}Y)$ BETWEEN TTA-HEXONE AND BUFFER SOLUTION OF pH 8.05, AT 20°C.

Concn. of TTA in hexone M	Activity in aq. phase. I_{aq} (cpm.)	Activity in org. phase I_{org} (cpm.)	Distribution coeff. q	$\log_q$
0.001	1778	1772	0.997	−0.0015
0.005	1486	2151	1.448	+0.1606
0.01	1156	2418	2.092	+0.3205
0.02	399	2784	6.978	+0.8437
0.04	265	3505	13.226	+1.1214
0.05	105	3364	33.04	+1.5190

minutes and the phases were disengaged, each phase was poured out through the stem and the activity measured in the ordinary way. The results are shown in Table III, from which it is found that the distribution coefficient increases with the concentration of TTA in hexone and that the 0.05 M TTA-hexone is preferable for the extraction of strontium. Table IV shows the results of the same experiments which were carried on ^{90}Sr (^{90}Y) under the same condition.

To examine the effect of the amount of strontium carrier added to the solution, extraction of $^{90}Sr(^{90}Y)$ was performed in the presence of various amounts of strontium nitrate in the buffer solution of pH 8. In this case 2 ml. of 0.05 M TTA-hexone was used as organic solvent, corresponding to 100 μg. equivalent to the chelating agent. More than 98% of the ^{90}Sr went into the organic phase in the presence of up to 1 μg. equivalent (45 μg.) of strontium carrier, and this seemed to be the upper limit of the amount of the strontium carrier that could coexist with ^{90}Sr in this extraction.

On the other hand, the extraction of ^{45}Ca with TTA-hexone was attempted in the presence of calcium carrier by the same procedure in order to obtain some information on the behavior of the metal in the solvent extraction. The calcium could be completely extracted till the amount of the carrier reached 20 μg. equivalent. Calcium seems to be chelated more tightly than strontium with TTA. The results of the above experiments are illustrated together in Fig. 2.

The effect of other alkaline earth metals —calcium, magnesium and barium—that might be present in the solution was investigated as follows. Various amounts of the metallic salt were added to the solution and the extraction of $^{90}Sr(^{90}Y)$ was done at pH 8 by 0.05 M TTA-hexone according to the above procedure. The activity of the $^{90}Sr(^{90}Y)$ separated in the organic phase was measured to find the percentage recovery of the $^{90}Sr(^{90}Y)$ in each case. Fig. 3 illustrates the relation between the amounts of the other coexisting ions and the recovery of the $^{90}Sr(^{90}Y)$. From the figure, it is found that barium and calcium do not affect the extraction till their amounts reach 8 μg. and 4 μg. equivalent, respectively, but magnesium gives a remarkable influence upon the extraction and more than 1 μg. of it should not be present.

To separate the ^{90}Sr selectively into the organic phase from the $^{90}Sr(^{90}Y)$, the solution containing $^{90}Sr(^{90}Y)$ was first adjusted to pH 7, and the extraction was done with 0.05 M TTA-benzene, by which ^{90}Y could be completely transferred out of the solution into the organic phase as shown in Table V. The aqueous phase retained after the extraction was adjusted again to pH 8, and a second extraction was done with 0.05 M TTA-hexone. Thus

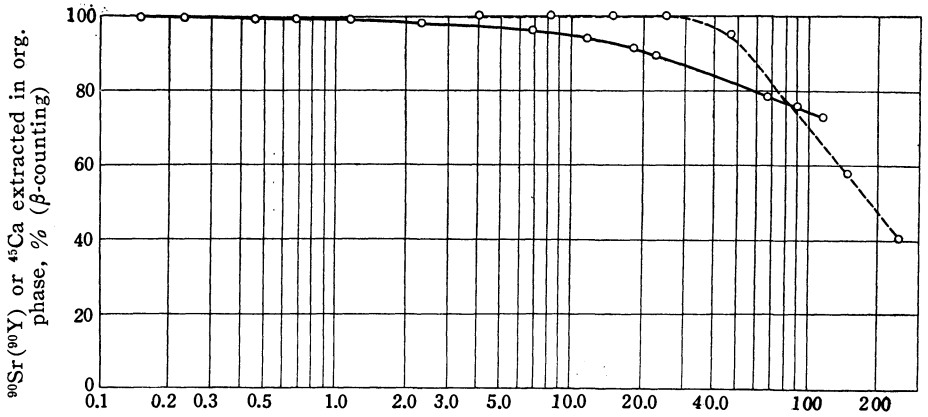

Fig. 2. Effect of strontium carrier on the extraction of ^{90}Sr(^{90}Y) and of calcium carrier on the extraction of ^{45}Ca by TTA-hexone.
—— strontium, ... calcium

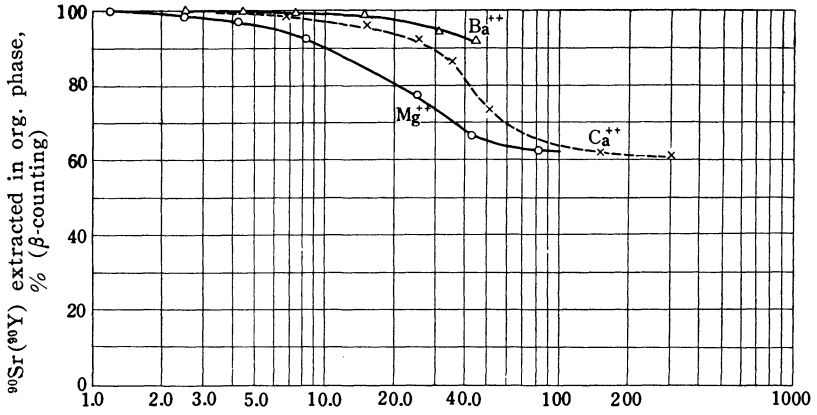

Fig. 3. Effect of the amounts of coexisting alkaline earth metals on the extraction of ^{90}Sr(^{90}Y) by TTA-hexone.

TABLE V
ISOLATION OF ^{90}Sr FROM ^{90}Sr(^{90}Y) BY THE TWO-STEP EXTRACTION

^{90}Sr(^{90}Y) taken cpm.	Taken up by the 1st org. phase (0.05 M TTA-benzene at pH 7) cpm.	Taken up by the 2nd org. phase (0.05 M TTA-hexone at pH 8) cpm.	Retained in aq. phase cpm.
16,590	8,890	7,186	510
17,050	9,440	7,328	280
Radiochemical purity (^{90}Y: 99%)		(^{90}Sr: 100%)	

the strontium could be separated in the last organic phase. Table V shows the excellent results of the extraction.

The presence of a masking agent such as EDTA (disodium ethylenediaminetetra-acetate), and ammonium citrate may probably affect the extraction of ^{90}Sr(^{90}Y).

Investigation was carried out to test this view, and was unsuccessful to keep the calcium in the solution by the masking effect of EDTA and to transfer the strontium into the organic phase; moreover, even the extraction of yttrium into the organic phase was markedly hindered. When a buffer solution consisting of ammonium citrate and aqueous ammonia was used to keep the solution at pH 8, only ^{90}Y could be extracted into the organic phase of TTA-hexone. The results obtained are shown in Table VI.

TABLE VI

EFFECT OF THE MASKING AGENTS ON THE EXTRACTION OF $^{90}Sr(^{90}Y)$ BY TTA-HEXONE

$^{90}Sr(^{90}Y)$ taken cpm.	Ca^{2+} added μg.	EDTA added ml.	Extracted into org. phase %	Nuclide extracted
6,980	2,000	1	4.8_1	^{90}Y
7,040	1,000	1	9.1_2	〃
7,110	800	1	6.2_0	〃
6,890	400	1	2.8_1	〃
7,080	1,000	2	2.6_1	〃
6,650	600	2	1.5_6	〃

Note: One milli liter of EDTA solution corresponds to 566 μg. Ca^{2+}.

$^{90}Sr(^{90}Y)$ taken cpm.	0.1 M Ammonium citrate soln. ml.	Extracted in org. phase %	Nuclide extracted
7,600	5	60.52	^{90}Y
18,800	5	55.67	〃

TABLE VII

ISOLATION OF RADIOACTIVE STRONTIUM BY TWO-STEP EXTRACTION FROM THE MIXED FISSION PRODUCTS

The fission products taken cpm.	Extracted by 0.05 M TTA-benzene cpm.	Extracted by 0.05 M TTA-hexone cpm.	Retained in aq. phase cpm.
57,980	48,640	6,260(10.8%)	3,080
56,980	48,550	5,960(10.4%)	2,470
120,900	102,500	12,370(10.2%)	6,050

In order to separate the radioactive strontium from mixed fission products, the solution of the material was at first adjusted to pH 7 and extracted with 0.05 M TTA-benzene. By this treatment rare earths and yttrium were made go into the organic phase out of the solution, but ruthenium was not. The aqueous phase remaining after the extraction and the removal of the organic phase, was transferred into another separatory funnel, and adjusted to pH 8 with the addition of ammonia, and extracted with 0.05 M TTA-hexone. In this case the radioactive strontium was completely extracted into the organic phase. Only less than 5% of ruthenium presented in the solution was extracted together.

The organic phase containing radioactive strontium was transferred from the funnel into a counting pan and rapidly evaporated to dryness under an infrared lamp, and the activity was measured as usual. The results obtained are shown in Table VII, in which the percentage of the strontium, represented by the activity ratio to the total, coincides well with that obtained by the ion-exchange resin method for the separation of the same material[5].

The Harley plot for the activity of the separated strontium is shown in Fig. 4 with ^{32}P as standard. The plot indicates that the radioactive strontium consists of 64% ^{89}Sr and 36% ^{90}Sr. The above separation process can be performed without spending much time.

The strontium extracted in the organic phase can easily be taken in the solution by the stripping with nitric acid of various concentrations. However, as the evaporation of the organic phase of TTA-hexone proceeds rapidly under an infrared lamp, the stripping of the strontium seems unnecessary for the purpose. Thus, by

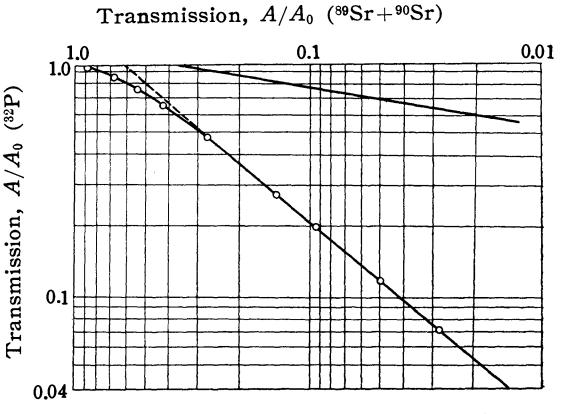

Fig. 4. Harley plot of the radioactive strontium separated in TTA-hexone from the gross fission products.

5) M. Honda, Y. Sasaki and H. Natsume, *Japan Analyst (Bunseki Kagaku)*, 4, 240 (1955).

the two-step extraction method devised by the authors, radioactive strontium could be separated rapidly and efficiently from mixed fission products.

Summary

Radioactive strontium in mixed fission products could be rapidly separated by the two-step extraction deviced by the authors. The solution of the material was first adjusted to pH 7 and extracted with 0.05 M TTA-benzene. By this treatment rare earths and yttrium were made to go into the organic phase out of the solution. The remaining aqueous phase was transferred into another separatory funnel, adjusted to pH 8, and extracted with 0.05 M TTA-hexone. In this case the radioactive strontium was completely extracted into the organic phase. Only less than 5% of ruthenium present in the solution was extracted at the same time. Detailed data of the experiments on the extraction involving the determination of distribution coefficient, and the equilibrium constant were tabullated.

This study was done as a part of the co-operative research on the radiochemical studies of the fission products and a part of the expenses was defrayed by a grant from the Ministry of Education, to which the authors' thanks are due.

Department of Chemistry
Faculty of Science
Kanazawa University
Kanazawa

Separation of Fission Products by Liquid-Liquid Extraction with Cupferron-Chloroform

By Toshiyasu KIBA and Mitsue KANETANI

(Received May 30, 1958)

Workers in various fields of study are looking for methods of rapidly separating radioactive strontium and cesium from solutions containing fission products. Before such separation is attempted, preliminary elimination of other nuclides and non-radioactive ions must be accomplished. When the precipitation method is employed for this purpose, some carrier must be added to the solution and some loss of the radioactive elements in question results from adsorption by the precipitate. Also the method takes a considerable length of time.

The solvent extraction method can be carried out rapidly and simply without any carrier. The aim of the investigation described in this paper was to establish a new method of liquid-liquid extraction by which the radioactive strontium and cesium are retained in the aqueous solution, while other metallic ions are transferred into the organic phase. The strontium and cesium may be further separated conveniently by the TTA-hexone extraction method as described in another paper by the present authors. The extracting agent for this purpose should be a compound which easily combines with various metallic ions, and forms chelated compounds, readily soluble in some organic solvent. Cupferron was chosen for the purpose for this reason.

Cupferron (nitrosophenyl hydroxylamine) is easily obtainable as an ammonium salt, which is a common reagent; it forms chelated compounds with zirconium in strong acids[1], with ter- to quinqui-valent metallic ions in weakly acidified solutions[2], and with rare earths in solutions whose pH is between 3 to 4[3], and produces precipitate when large amounts of these ions are present. Both the reagent and the chelated compounds are soluble in chloroform, with which they are easily removed from the aqueous solution. These characteristics of the

1) N. H. Furman, W. B. Marson and J. S. Pekola, *Anal. Chem.*, **21**, 1355 (1949).
2) D. Dyrssen and V. Dahlberg, *Acta Chim. Scand.*, **7**, 1186 (1953).
3) A. I. Popov and W. W. Wendlandt, *Anal. Chem.*, **26**, 883 (1954).

reagent were found very useful in the treatment of an aqueous solution containing fission products.

Experimental

Reagent and apparatus.—*Cupferron Solution*, 5%.—The reagent of extra pure grade was dissolved in water immediately before use.

Gross Fission Products.—A drop of nitric acid solution of gross fission products, imported from Oak Ridge National Laboratory, U. S. A. (Batch No. 35; cooling period, about three years) was diluted with 0.02 N hydrochloric acid so that 0.2 ml. of the solution possesed an activity of 10,000 cpm.

Other Radioisotopes.—^{90}Sr(^{90}Y), ^{95}Zr(^{95}Nb), ^{137}Cs, ^{106}Ru(^{106}Rh), ^{144}Ce, and ^{147}Pm were used and their behavior during the solvent extraction with cupferron was examined.

Buffer Solution.—0.5 M solution consisting of acetic acid, ammonium acetate, and aqueous ammonia was used, and the pH was measured by a glass electrode pH-meter.

Activity Measurement.—For β-radiation, a counting set made by the Kobe Kogyo Co. Ltd., Japan (No. 131 G-M tube: mica window, 2.2 mg./cm^2, counting efficiency: 11.7% for ^{90}Sr(^{90}Y)) was employed; for γ-radiation, a counting set made by Nuclear Instrumental and Chemical Corp., U. S. A., (sodium iodide scintillation tube, and Model D 47 counting equipment with lead absorber) was used.

Separatory Funnel.—A 30 ml. and a 300 ml. spindle shaped separatory funnel having a big short stem were used for good separation of the two phases.

Shaking Machine.—Shaking was effected by a vertical electric oscillator with 230 double strokes per minute. Up to six separatory funnels can be loaded on the shaker at a time.

Other chemicals used were all of extra pure grade and the utensils were of the ordinary laboratory type.

Procedure.—1) In a 30 ml. separatory funnel place 0.2 ml. of a solution of the gross fission products or radioisotopes, and 5 ml. of 1 to 7 N hydrochloric acid or 5 ml. of the buffer solution, and make up the volume with water to 6 ml. Then, add 1 ml. of the cupferron solution and 2 ml. of chloroform, successively. Shake the contents of the vessel for five minutes. After the phases have disengaged, transfer the organic phase into another funnel and add to it 5 ml. of hydrochloric acid or the buffer solution, and shake with the organic phase for five minutes. To the aqueous phase retained in the first funnel add again 1 ml. of the cupferron solution and 2 ml. of chloroform, and shake for five minutes. Combine the aqueous phases from the first and the second funnel in a centrifuge tube, and the organic phases in another tube and centrifuge them for about two minutes to separate the phases completely from each other. Transfer each phase to a porcelain counting dish and evaporate to dryness under an infrared lamp, and then measure the radioactivity by the counting set. Draw off the decay and the Harley plot of the activity, if necessary, to identify the nuclide isolated.

2) When various metallic ions other than fission products are present, the following procedure was adopted, by which the radioactive strontium and cesium were retained in the solution unaccompanied by other metallic ions.

Put 100 ml. of a solution containing 10 mg. of iron(III), thorium(IV), and uranyl(II) ions and fission products in a 350 ml. separatory funnel, and adjust its acidity to 1 N hydrochloric acid. Add 2 ml. of the cupferron solution and 5 ml. of chloroform, and shake for five minutes. Take out the organic phase from the first funnel and retain the aqueous phase in the vessel. Repeat the same extraction process in the first funnel till further addition of the cupferron solution produces no precipitate and the aqueous phase becomes colorless. The organic phase separated after each extraction should be collected in another funnel and washed with an equal volume of 1 N hydrochloric acid. The washing should be added to the solution in the first funnel. By this process, iron(III) is completely removed from the solution.

After the removal of iron(III), add 3 N hydrochloric acid to restore to 1 N hydrochloric acid the acidity of the solution, which has been lowered by the successive entrainments of the cupferron solution. Add 2 ml. of the cupferron solution and 10 ml. of ethyl acetate, and shake for two or three minutes. Drain the aqueous phase from the first funnel into the second, and repeat the extraction with cupferron and ethyl acetate. Collect the ethyl acetate phase retained in each extraction in the first funnel and wash the contents with an equal volume of hydrochloric acid. Add the washings to the solution in the third funnel. Thorium(IV) is transfered to the ethyl acetate phase by this extraction.

Add 20 ml. of 3% zinc amalgam to the solution in the second or the third separatory funnel, stopper well, and shake vigorously for five minutes to reduce the uranyl ion which does not combine with cupferron to uranium(IV). After removing the amalgam through the stem, add 2 N aqueous ammonia drop by drop till the pH of the solution becomes 1.8. Then add 2 ml. of the cupferron solution and 10 ml. chloroform, and shake the content for five minutes. Repeat the extraction till further addition of cupferron produces no precipitate. By this treatment the uranium is completely removed, going into the organic phase that is discarded after the extraction.

Add 2 N aqueous ammonia to the solution retained in the separatory funnel to adjust the pH to 4. Add again 2 ml. of the cupferron solution and 10 ml. chloroform, and shake for five minutes. By the last extraction rare earths of the fission products and non-radioactive metals are transferred into the chloroform phase. If necessary, repeat the extraction.

The separated aqueous phase which contains the radioactive strontium and cesium and possibly

some unextractable cations, may be given additional treatments of separation, for example, with TTA-hexone.

3) The behavior of the various radioisotopes were examined throughout all the stages of the extraction described above, and the percentages of the nuclides recovered were noted.

Results and Discussion

After the extraction was carried out by Procedure 1 on the aqueous solution of the gross fission products at different pH, the separated organic phase was evaporated to dryness and the radioactivity was measured by means of a G-M β-counting set. The ratio of the counting rate (cpm.) of the organic phase to that of the original solution represents the amount extracted of the gross fission products. As illustrated in Fig. 1, the

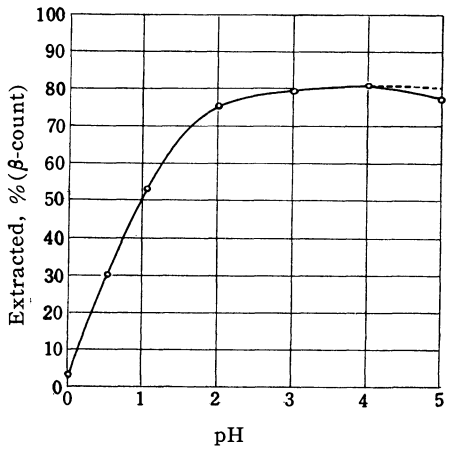

Fig. 1. Effect of pH on the extractability of gross fission products by cupferron-chloroform.

ratio reaches its maximum of 81% at pH 4 and decreases slightly as the pH of the solution increases still further, probably because of formation of radiocolloid in the solution. Evaporation of the chloroform containing cupferron may be readily accomplished with an infrared lamp, and the residue transformed into the oxide by ignition to red heat. Therefore, the stripping of the nuclide from the organic phase was not found necessary.

To find what nuclides could be extracted from the mixed gross fission products into the organic phase, the extraction was done with the solution containing ^{106}Ru, ^{137}Cs, $^{90}Sr(^{90}Y)$, and rare earths that had been separated as a fraction of the fission products by the cation exchange resin method[4]. The results of the experiments for each nuclide is shown in Fig. 2., from which it is found that rare earths and yttrium go into the organic phase at pH 4, and cesium, strontium and ruthenium remain in the solution.

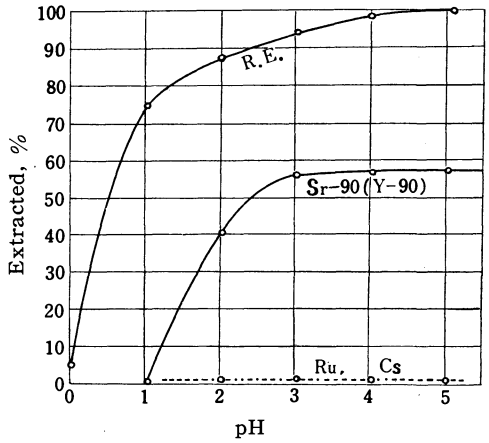

Fig. 2. Effect of pH on the extractability of some nuclides in fission products by cupferron-chloroform.

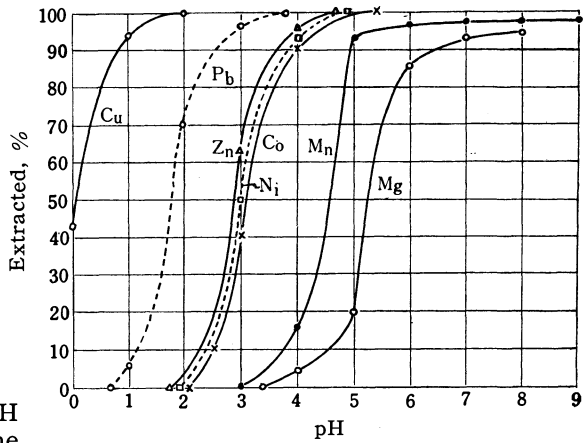

Fig. 3. Effect of pH on the extractability of various metallic ions by cupferron-chloroform.

The extraction of other non-radioactive metallic ions at different pH is shown in Fig. 3. Many ions can be removed into the cupferron-chloroform while the acidity of the solution is higher than pH 4.

One hundred ml. of the solution containing the gross fission products together with iron(III), thorium(IV), and uranyl(II) ions, was treated by successive extractions of Procedure 2. The aqueous phase

4) M. Honda, Y. Sasaki and H. Natsume, *Japan Analyst (Bunseki Kagaku)*, **4**, 240 (1955).

TABLE I

EXTRACTION OF FISSION PRODUCTS AND RADIOISOTOPES BY CUPFERRON-CHLOROFORM

Amounts taken or original radioactivity	Percentage of radioactivity in the last aqueous phase %
Fe(III) : 10 mg. Fission products : 10,000 cpm.	18.05 (^{90}Sr and ^{137}Cs)
Fe(III) : 10 mg. ^{137}Cs : 10,000 cpm.	100. (^{137}Cs)
Fe(III) : 10 mg. ^{90}Sr(^{90}Y) : 10,000 cpm.	42.5 (^{90}Sr)
Fe(III) : 10 mg. U(VI) : 5 mg. Th(IV) : 10 mg. Fission products : 10,000 cpm.	20.3 (^{90}Sr, ^{137}Cs and ^{106}Ru) 15.9 (after the Ru was expeled by distillation)

TABLE II

RESULTS OF TWO-STEP EXTRACTION WITH CUPFERRON-CHLOROFORM AND TTA-HEXONE

Material taken or original radioactivity in original solution	Percentage of radioactivity extracted in TTA-hexone phase %	Percentage of radioactivity retained in the last aq. phase %
Fe(III) : 10 mg. ^{137}Cs : ca. 10,000 cpm.	0.	100.
Fe(III) : 10 mg. ^{90}Sr(^{90}Y) : 10,000 cpm.	42.1 (^{90}Sr)	0.36 (^{90}Sr)
Fe(III) : 10 mg. ^{106}Ru : ca. 10,000 cpm.	1.5 (^{106}Ru)	97.9 (^{106}Ru)

remaining at the end was evaporated and the radioactivity was measured to determine the recovery of the radioactive substances. Very satisfactory results were obtained in each case as shown in Table I.

The aqueous phase remaining after the solvent extraction with cupferron-chloroform was next subjected to treatment with TTA-hexone as described in the following paper, and strontium was extracted into the organic phase. The two-step extraction gave the results shown in Table II, and the strontium in the original solution could be separated rapidly and quantitatively from the gross fission products.

Summary

In order to separate rapidly the radioactive strontium and cesium from the solution containing gross fission products and other non-radioactive metallic ions, cupferron-chloroform extraction was attempted. By changing the acidity of the aqueous solution from 1 N hydrochloric acid to pH 4, and by performing extractions in each stage, the strontium and the cesium could remain in the aqueous phase, while the other could be removed into the organic phase. The radioactive strontium may be extracted in the organic phase by the following extraction with TTA-hexone at pH 8.

A part of the expenses for this study was defrayed by a grant from the Ministry of Education, to which the authors' thanks are due.

Department of Chemistry, Faculty of Science, Kanazawa University
Kanazawa

Metal Complexes with Terdentate Ligands. I. Synthesis of Copper(II) and Nickel(II) Complexes having Salicylaldehydesemicarbazone and Related Compounds as Ligands

By Yoneichiro MUTO

(Received June 6, 1958)

In marked contrast with the extensive studies that have been carried out on the metal complexes with terdentate ligands, those with terdentate ligands have received much less attention. The latters are of particular interest in coordination chemistry because of their steric requirements. A few examples of the terdentate chelating agents of types I and II are shown in Table I. The chelating agents of type III, while satisfying one primary valence of the metal, fill three coordination positions. The examples of type III are comparatively meagre.

It has been reported that a thiosemicarbazide molecule occupies two coordination positions of platinum(II)[1], palladium (II)[1], cobalt(II)[2], copper(II)[2] and nickel[2] ions* and that some thiosemicarbazones coordinate to copper(II)- and nickel ions as a bidentate ligand[3]. Semicarbazide forms complexes having the compositions, $CH_5ON_3CuCl_2$ and $(CH_5ON_3)_2NiSO_4$[4]. It is likely that a semicarbazide molecule occupies two coordination positions of copper(II) and nickel. Therefore, it is expected that semicarbazone or thiosemicarbazone of salicylaldehyde acts as a terdentate ligand of type II (in enol form) or type III (in keto form) and that α-pyridylaldehyde-*o*-hydroxyanil similarly acts as a ligand of type III. The present author synthesized copper(II) and nickel complexes having the ligands shown in Table II.

Salicylaldehydesemicarbazone was treated with copper(II) salts in a boiling ethanol solution. Depending on the kind of copper(II) salt, the copper(II) complexes of two different types were formed in the following way.

From the chemical analysis and the properties of the complex as well as the terdentate nature of the ligand, it seems reasonable to give the formula A to salicylaldehydesemicarbazone copper(II), although no direct evidence has yet been afforded by physical methods such as X-ray analysis. Similarly, the formula B has been presumed for salicylaldehydesemi-

TABLE I

Types	Example	
I. A-A-A[a]	$CH_2(NH_2)$—$CH(NH_2)$—$CH_2(NH_2)$	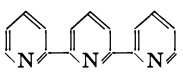
II. HA-A-AH[b]	$HN(CH_2COOH)(CH_2COOH)$	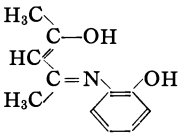
III. HA-A-A	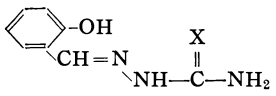 (X: O, S.)	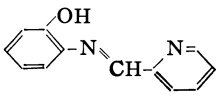

a) A: a donor atom such as N, O and S. b) H: a hydrogen atom replaceable with metal atom. c) the enol form of acetylacetonemono-(2-hydroxyanil). Y. Muto, *J. Chem. Soc. Japan, Pure Chem. Sec.*, (*Nippon Kagaku Zassi*), **76**, 1407 (1955).

1) K. A. Jensen, *Z. anorg. allgem. Chem.*, **221**, 6 (1934).
2) K. A. Jensen and E. Ranke-Madsen, ibid., **219**, 243 (1934).
3) G. Bähr and E. Hess, ibid., **268**, 351 (1952).
4) K. A. Jensen and E. Ranke-Madsen, ibid., **227**, 25 (1936).

TABLE II

	Chelating agents (A)*	Composition of the complex	Solubility of the complex
1.	Salicylaldehydesemicarbazone	Cu(A)	Insol. in H_2O, EtOH, benzene. Sol. in pyridine.
		$Cu(A)NH_3$	Insol. in H_2O, benzene. Sol. in EtOH.
		$Cu(A)Cl\cdot 2H_2O$	Insol. in EtOH, benzene. Sol. in H_2O.
		$Cu(A)NO_3$	the same as the above
		$Ni(A)_2\cdot H_2O$	Insol. in H_2O, EtOH, benzene, pyridine.
2.	5-Bromosalicylaldehydesemicarbazone	Cu(A)	Insol. in H_2O, EtOH, benzene.
		Cu(A)Cl	Insol. in EtOH, benzene. Slightly sol. in H_2O.
3.	Salicylaldehydethiosemicarbazone	Cu(A)	Insol. in H_2O, EtOH, benzene. Sol. in pyridine.
		Cu(A)py	Insol. in H_2O. Slightly sol. in EtOH.
		$Cu(A)Cl\cdot H_2O$	Insol. in EtOH, benzene. Slightly sol. in H_2O.
		Ni(A)py	Insol. in H_2O. Slightly sol. in EtOH.
		$Ni(A)_2\cdot 2H_2O$	Insol. in H_2O, EtOH, benzene. Sol. in pyridine.
4.	α-Pyridylaldehyde-*o*-hydroxyanil	$Cu(A)Cl\cdot 2H_2O$	Sol. in H_2O, EtOH, $CHCl_3$, nitrobenzene.
		$Cu(A)NO_3\cdot 2H_2O$	the same as the above

* " A " denotes a terdentate ligand.

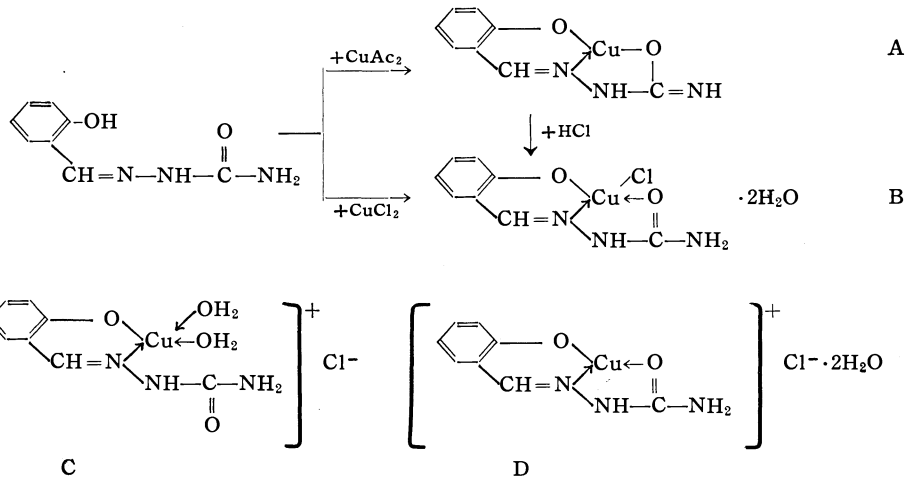

A B C D

carbazone-monochloro copper(II) dihydrate for the following reasons. First, if salicylaldehydesemicarbazone were assumed to act as a bidentate ligand for a copper(II) ion, the chelate compounds with the molar ratio 1:2 of copper(II) to the reagent molecule should be formed just as in the case of Shiff's base prepared from salicylaldehyde and various primary amines. However, the composition of this complex and other copper(II) complexes obtained in this work had the molar ratio 1:1 of copper(II) to the reagent molecule as shown in Table II. Therefore, this reagent must occupy three coordination positions of a copper (II) ion. Secondly, from the fact that the water molecules contained in this complex could easily be removed by drying in a desiccator over calcium chloride at room temperature, it seems very likely

that the water molecules do not coordinate directly to the copper atom. Thirdly, provided that the coordination number of copper(II) is four as usual, another unidentate ligand is required to fill the inner sphere around the copper atom which has already a terdentate ligand combined with it. Furthermore, the electric conductivity of dilute aqueous solutions of this complex was found to be small. Therefore, the chlorine atom is considered as being in the inner sphere around the copper atom, and it seems unlikely that this complex has a salt-like structure as shown in the formula C or D.

Experimental

1) **Salicylaldehydesemicarbazone copper (II).**—A solution of copper acetate monohydrate (0.6 g.) in water (30 ml.) was added to a boiling solution of salicylaldehydesemicarbazone (0.55 g.) in ethanol (50 ml.). Pale green micro crystals immediately precipitated. This precipitate was purified in the following way. The precipitate was dissolved in a mixture of ethanol (20 ml.) and aqueous ammonia (28%, 2 ml.) and then 10 ml. of water was added to it. The greenish solution was allowed to cool at room temperature for about three hours; mean while the addition compound with ammonia crystallized in gray prismatic crystals. The separated crystal was heated at 60~70°C until ammonia was no longer evolved. To ensure the complete removal of ammonia, the residue was boiled in ethanol on a water bath for ten minutes. After being allowed to cool, the precipitate was filtered off and dried at about 80°C.

Anal. Found: C, 39.92; H, 2.93; N, 17.46; Cu, 26.38%. Calcd. for $C_8H_7O_2N_3Cu$: C, 40.01; H, 3.15; N, 17.36; Cu, 26.19%.

The addition compound with ammonia liberates ammonia gradually at room temperature; hence the analysis was performed without delay after preparation.

Anal. Found: N, 21.70; Cu, 24.69; NH_3, 6.44%. Calcd. for $C_8H_7O_2N_3Cu \cdot NH_3$: N, 21.74; Cu, 24.65; NH_3, 6.61%.

2) **Salicylaldehydesemicarbazone - mono chloro copper(II) dihydrate.**—A hot solution of copper(II) chloride dihydrate (0.5 g.) in water (10 ml.) was added to a hot solution of salicylaldehydesemicarbazone (0.5 g.) in ethanol (20 ml.). The greenish solution was allowed to stand overnight at room temperature. The green precipitate formed was washed with ethanol. The pure compound was obtained in deep green prismatic crystals by recrystallization from water. The hydrate lost water gradually in a desiccator over calcium chloride and was completely dry at 50~60°C. The color of the crystals became brown after dehydration.

Anal. Found: C, 30.77; H, 3.79; N, 13.73; Cl, 11.23; Cu, 20.34; H_2O, 11.40%. Calcd. for $C_8H_8O_2N_3ClCu \cdot 2H_2O$: C, 30.68; H, 3.94; N, 13.70; Cl, 11.32; Cu, 20.29; H_2O, 11.50%.

This compound was also obtained by heating the compound prepared in 1) with dilute hydrochloric acid on a water bath.

3) **Salicylaldehydesemicarbazone - mononitrato copper(II).**—This compound was prepared in the same way as the monochloro compound by the reaction between salicylaldehydesemicarbazone and copper(II) nitrate. The green crystals formed were dried in a desiccator over calcium chloride at room temperature.

Anal. Found: N, 18.51; Cu, 20.77%. Calcd. for $C_8H_8O_5N_4Cu$: N, 18.45; Cu, 20.92%.

4) **Bis-salicylaldehydesemicarbazone nickel monohydrate.**—A solution of nickel acetate tetrahydrate (0.5 g.) in water (10 ml.) was added to a boiling solution of salicylaldehydesemicarbazone (0.7 g.) in ethanol (40 ml.). Light green prismatic crystals were immediately precipitated. The separated crystals were washed with hot ethanol, then with pyridine and finally with hot water and they were dried in a vacuum desiccator. The corresponding nickel complex was not formed by the reaction between nickel sulfate and salicylaldehydesemicarbazone although the solutions were mixed in the same way as described above.

Anal. Found: N, 19.31; Ni, 13.7%. Calcd. for $C_{16}H_{16}O_4N_6Ni \cdot H_2O$: N, 19.41; Ni, 13.6%.

5) **5-Bromosalicylaldehydesemicarbazone copper(II).**—This compound was prepared as pale green micro crystals in the same way as the compound described in 1).

Anal. Found: N, 13.38; Cu, 19.92%. Calcd. for $C_8H_6O_2N_3BrCu$: N, 13.15; Cu, 19.88%.

6) **5-Bromosalicylaldehydesemicarbazone-monochloro copper (II).**—This compound was prepared in the same way as the compound described in 2). The gray crystals formed were dried in a desiccator over calcium chloride at room temperature.

Anal. Found: N, 11.86; Cu, 17.80%. Calcd. for $C_8H_7O_2N_3ClBrCu$: N, 11.80; Cu, 17.84%.

7) **Salicylaldehydethiosemicarbazone copper(II).**[5]—This compound was prepared in the same way as the compound described in 1). The brown crystals formed were dried at 60°C.

Anal. Found: C, 37.62; H, 3.10; N, 16.41; Cu, 24.74%. Calcd. for $C_8H_7ON_3SCu$: C, 37.42; H, 2.75; N, 16.36; Cu, 24.75%.

The pyridinate of this copper complex was obtained as pale brown needles by recrystallizing it from pyridine.

Anal. Found: N, 16.71; Cu, 19.02; pyridine, 23.49%. Calcd. for $C_8H_7ON_3SCu \cdot C_5H_5N$: N, 16.68; Cu, 18.92; pyridine, 23.55%.

8) **Salicylaldehydethiosemicarbazone-monochloro copper(II) monohydrate.**—This compound was prepared in the same way as the

5) V. Hovorka and Z. Holzbecher, *Collection Gzechoslov. Chem. Communs.*, **15**, 267 (1950).

* 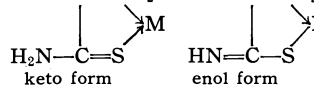

compound described in 2). Green prismatic crystals.

Anal. Found: N, 13.68; Cu, 20.23%. Calcd. for $C_8H_9ON_3SClCu \cdot H_2O$: N, 13.50; Cu, 20.41%.

9) **Monopyridino-salicylaldehydethiosemicarbazone nickel.**—A solution of nickel acetate tetrahydrate (0.5 g.) in water (10 ml.) was added to a boiling solution of salicylaldehydethiosemicarbazone (0.4 g.) in ethanol (30 ml.). Orange crystals were precipitated immediately. The separated precipitate was dissolved in pyridine and filtered. When water was added to the filtrate, the monopyridino compound separated out as brown-red needles.

Anal. Found: N, 16.92; Ni, 17.6; pyridine, 23.12%. Calcd. for $C_8H_7ON_3SNi \cdot C_5H_5N$: N, 16.93; Ni, 17.7; pyridine, 23.90%.

10) **Bis-salicylaldehydethiosemicarbazone nickel dihydrate.**—A hot solution of nickel sulfate heptahydrate (0.3 g.) in water (5 ml.) was added to a boiling solution of salicylaldehydethiosemicarbazone (0.4 g.) in ethanol (50 ml.). Light green crystals were precipitated immediately. The separated precipitate was boiled in ethanol on a water bath, filtered off and washed by hot water. This procedure was repeated two or three times, and then the crystals were dried in a vacuum desiccator.

Anal. Found: N, 17.67; Ni, 12.08%. Calcd. for $C_{16}H_{16}O_2N_6S_2Ni \cdot 2H_2O$: N, 17.40; Ni, 12.10%.

When this compound was recrystallized from pyridine, the monopyridino compound described in 9) was formed.

11) **α-Pyridylaldehyde-o-hydroxyanil-monochloro copper (II) dihydrate.** — This compound was prepared in the same way as the compound described in 2) by the reaction between copper(II) chloride and α-pyridylaldehyde-*o*-hydroxyanil. Brown-black prismatic crystals.

Anal. Found: C, 43.70; H, 4.00; N, 8.22; Cu, 19.07; H_2O, 10.80%. Calcd. for $C_{12}H_9ON_2ClCu \cdot 2H_2O$: C, 43.40; H, 3.95; N, 8.44; Cu, 19.12; H_2O, 10.84%.

12) **α-Pyridylaldehyde-o-hydroxyanil-mononitrato copper (II) dihydrate.** — This compound was prepared in the same way as the compound described in 2) by the reaction between copper nitrate and α-pyridylaldehyde-*o*-hydroxyanil. Brown-black prismatic crystals.

Anal. Found: N, 11.60; Cu, 17.63; H_2O, 10.01%. Calcd. for $C_{12}H_9O_4N_3Cu \cdot 2H_2O$: N, 11.71; Cu, 17.71; H_2O, 10.04%.

13) **Electric conductance of copper (II) complexes.**—The concentration of the solution used for measurement at 15°C was 0.001 M. The results were listed in Table III.

TABLE III

	Compound	Molar conductance (mho)
1.	Salicylaldehydesemicarbazone -monochloro copper(II) dihydrate	30.5
2.	Salicylaldehydesemicarbazone -mononitrato copper(II)	32.5
3.	α-Pyridylaldehyde-*o*-hydroxyanil -monochloro copper(II) dihydrate	30.7
4.	α-Pyridylaldehyde-*o*-hydroxyanil -mononitrato copper(II) dihydrate	30.5

The pH values of these solutions were found to be 5.4~6.3. Therefore, it is possible that these complexes decompose to some extent in water. This accounts for such a low yield as 50% of the recrystallization of these complexes from water.

The author is grateful to Mr. Michio Shido of Kyushu University for carrying out the elementary analysis of the compounds prepared.

Chemical Laboratory, Faculty of Liberal Arts, Saga University
Saga

*Chemical Studies on Wood Hemicelluloses. II. On the Hemicellulose of Ganpi Bast Fibres. I**

By Seishi MACHIDA and Sadanori NISHIKORI**

(Received June 13, 1958)

Wood hemicelluloses, which have generally undesirable influences upon the manufacture and qualities of chemica lfibres, are said to have rather favorable effects on paper-making[1].

Cottrall[2] investigated the bearing of hemicelluloses of wood pulp fibres on paper-making properties, and assented that the excellent character of Japanese hand-made paper could be attributed to the peculiar method of paper-making. The Japanese hand-made paper which has elegant and strong quality, is made in the traditional manner. Bast fibres of certain plants are used as the raw material and the extracted juice of various plant roots and barks are employed as sizing and dispersing agents[3].

The present investigation, therefore, was attempted to explain the behavior of hemicellulose during the processes of Japanese paper-making. The relation between the chemical characteristic of the hemicellulose and the paper-making properties of the fibres was also investigated.

Experimental

1) Sample.—The bast fibres used in the present study were obtained from the Ganpi plant (*Wickstroemia sikokiana* Franch. et Sav.) grown in Simane Prefecture. Ganpi, a species of *Thymelaeaceae*, is a wild shrub growing widely in Japan, and the paper made from it is one of the most typical hand-made papers of Japan. The bast fibres removed from the plant stems were cleaned by removing the upper brown cork tissue and flawed parts, washed sufficiently with water, and dried.

2) Process of paper-making.—The bast fibres thus purified were boiled with a sodium carbonate solution, in which the concentration of sodium carbonate is 20% of that of the pulp, and washed in a stream to remove the meterial formed by the reaction with alkali for two days. In the stream the fibres are also mildly bleached.

Next, the fibres were beaten for about an hour in a beater. The rotation of the beater-roll is about 150 r. p. m.; pulp concentration is about 3%. The degree of beating of the resultant pulp estimated with Schopper-Riegler's tester was 25. The paper was made from the pulp by the hand process in the usual manner of Japanese paper-making, using the mucilage of the Tororo-aoi plant[4] as the dispersing and sizing agent.

3) Chemical constituents of the fibres in the process of paper-making.—The samples from the various stages of the process were analysed in the usual manner[5]. The results obtained are shown in Table I.

4) Hemicellulose of the Ganpi plant.—Hemicellulose fractions were obtained by alkaline extraction of holocelluloses prepared from Ganpi bast fibres. These fibres finely chopped were extracted with benzene-ethanol, filtered and air dried prior to use. From this sample, holocellulose was prepared by Wise's method[6]. Yield was 87.0%. Hemicellulose fractions were extracted from the holocellulose with sodium hydroxide solution. Successive extractions with the 5 and 16% solution for periods of an hour at room temperature yielded two fractions; these hemicellulose fractions were designated "5% extract" and "16% extract", respectively. The solid hemicelluloses were recovered from the alkaline solutions by pouring the latter into 4 volumes of ethanol containing sufficient acetic acid to adjust the pH to about 6.5. The flocculent precipitate was centrifuged, washed with ethanol and ether, and then dried in a desiccator.

The dilute solution viscosity of the water-soluble "5% extract" in distilled water was measured and a plot of the reduced specific viscosity against concentration is represented by the upper curve of Fig. 1. In the $\eta_{sp}/c \sim C$ curve, a significant polyelectrolyte behavior of the hemicellulose is indicated. The lower curves of Fig. 1 are the $\eta_{sp}/c \sim C$ curves for the hemicelluloses in 10% potassium hydroxide solution

* The principal part of this paper was presented at the 11th Annual Meeting of the Chemical Society of Japan on April 5, 1958 at Tokyo.

** Present address: Industrial Experimental Station of Shimane Prefecture, Matsue.

1) M. N. Fineman, *Tappi*, **35**, 320 (1952).

2) L. G. Cottrall, "World's Paper Trade Rev.", 393, 445 (1954).

3) S. Machida and M. Inano, This Bulletin, **28**, 629 (1955).

4) S. Machida and N. Uchino, *Bull. of the Faculty of Textile Fibres, Kyoto Univ. of Ind. Arts & Text. Fibres*, **1**, 116 (1954).

5) S. Machida, M. Inano and Y. Matsumura, This Bulletin, **30**, 201 (1957).

6) L. E. Wise and E. K. Ratliff, *Anal. Chem.*, **19**, 459 (1947).

7) J. O. Thompson and L. E. Wise, *Tappi*, **35**, 331 (1952).

TABLE I
COMPOSITION OF BAST FIBRES OF GANPI PLANT

	Original raw bast fibre	Pulp after alkali-cooking	Pulp after wet beating	Paper
Moisture	13.90%	10.98%	11.39%	11.51%
Ash	1.84〃	1.86〃	1.29〃	1.57〃
Benzene-Ethanol extract	2.11〃	1.71〃	1.62〃	1.85〃
Cold water extract	2.84〃	2.68〃	0.81〃	1.97〃
Hot water extract	6.03〃	3.48〃	1.32〃	2.43〃
0.1% NaOH extract	15.54〃	4.46〃	3.74〃	5.49〃
Lignin	3.30〃	2.77〃	2.80〃	2.89〃
Uronic acid	16.36〃	7.60〃	4.46〃	2.08〃
Total cellulose	61.56〃	81.46〃	82.19〃	84.30〃
α-Cellulose	60.89〃	65.32〃	63.91〃	63.25〃
β-Cellulose	17.47〃	20.56〃	21.84〃	22.48〃
γ-Cellulose	11.64〃	14.12〃	14.25〃	14.27〃
Pentosan	21.62〃	18.37〃	16.02〃	14.15〃
Copper value	1.33	1.16	0.84	0.59
Degree of polymerisation	—	1832	1688	1397

at 30°C. Intrinsic viscosities of the hemicelluloses in 10% aqueous potassium hydroxide were determined from these curves, and the degree of polymerisation was calculated by using the relation[7] $[\eta]=4.4\times10^{-3}\times(\text{D. P.})$. The component

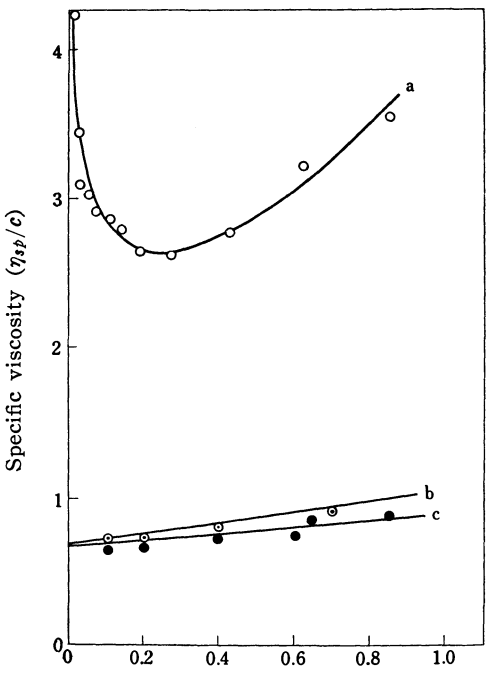

Fig. 1. Plot of viscosity against concentration for 5% extracted hemicellulose in water (a), and 5% and 16% extracted hemicellulose in 10% potassium hydroxide solution (b and c respectively).

sugars of the hemicelluloses were analysed chromatographically in the usual manner, using butanol-pyridine-water (6 : 4 : 3 by volume) as a solvent, and *o*-aminodiphenyl reagent[8] as a spraying reagent. The hemicelluloses were found to be mainly composed of D-xylose and D-glucuronic acid and of small amounts of D-mannose, D-galactose, L-arabinose and L-rhamnose. The chromatogram shows that the uronic acid is partly presented as 4-*O*-methyl-D-glucuronic acid. Data obtained are shown in Table II.

TABLE II
COMPARATIVE DATA FOR HEMICELLULOSE FRACTIONS ISOLATED FROM GANPI HOLOCELLULOSE

Fraction	Yield[a] (%)	Degree of polymerisation[b]	Uronic anhydride[c] (%)	Xylan[c] (%)
5% extract	18.0	157	15.8	80.9
16% extract	7.3	160	13.6	58.1

a) Expressed as percentage of extractive-free bast fibres and corrected for moisture and ash.
b) Calculated as a pentosan.
c) Corrected for moisture and ash.

Discussion

As is shown in Table I, substances other than cellulose are contained in the bast fibres of the Ganpi plant than in wood pulp fibres. In the paper-making processes mentioned above, these substances are still retained without much injury.

Especially, it is noticeable that much hemicellulose is kept in the fibres. The hemicellulose extracted from the bast fibres with aqueous sodium hydroxide is mainly composed of D-xylose and D-glucuronic acid (which may be partly present as 4-*O*-methyl-D-glucuronic acid),

8) T. E. Timell, C. P. J. Glaudemans and A. L. Currie, *Anal. Chem.*, **28**, 1916 (1956).

and it contains also small quantities of D-mannose, D-galactose, L-arabinose and L-rhamnose. The analytical data are interesting with regard to the fact that a polysaccharide containing D-galacturonic acid was found in the water-extract of the Ganpi bast fibres[9]. The polysaccharide is removed in the course of the preparation of holocellulose and hemicellulose. As is shown in Table II, the average degree of polymerisation of each alkali-extracted fraction of hemicellulose calculated as a pentosan is about 160. The fractions contain 15.8% and 13.6% uronic anhydride, which correspond to one carboxyl group for each six and eight pentose sugar units respectively. It is found that the hemicellulose molecule has a linear structure and the uronic groups are present along the polymer chain, because the hemicellulose indicates typical polyelectrolyte behavior in the solution. Although a great part of the uronic residue in the fibres is removed in the paper-making processes, it is found that a few percent of the uronic residue still remains in the hand-made paper.

The contents of total cellulose in the bast fibres increase naturally in each paper-making process. In the beating process, a part of α-cellulose depolymerizes to β-cellulose; this depolymerization of cellulose is also proved from the degree of polymerization. Nevertheless, the degree of polymerisation of the Ganpi cellulose is kept higher not only than wood pulp but also than Mitsumata fibres[10].

It is due to the presence of a great quantity of hemicelluloses that the long bast fibres are rendered so amenable to the wet beating process in a beater, by being fibrillated rather than cut or tangled. The hemicelluloses which are strongly hydrophilic polyuronides make also the fibres and fibrils to be more plastic, and tend to increase the areas of intimate contact between these elements, when they are felted to form a sheet of paper. Further, the hemicelluloses, cooperating with the plant mucilage employed, cause the fibres to be well dispersed in water to accomplish a good distribution of fibres in the fibre mat. Both these effects of the hemicelluloses increase the strength, transparency, density, softness and grease-proofness of the paper produced. This view would be proved, for example, by Leech's experiment[11] in which locust bean gum was employed in the beating of wood pulp for the sake of increasing the strength of the paper made from the pulp. But Jayme[12] assents that the quality as well as quantity of hemicellulose present in the fibres is of importance in attaining strength in paper made from pulp. Limeric and Corey[13] said that the hemicellulose containing many uronic acids is of advantage for the production of strong papers. The hemicellulose molecule of Ganpi bast fibres has comparatively long linear structure, and is strongly hydrophilic on account of the presence of uronic acid residue along the molecular chain. This fact has probably a significant bearing on the character of Japanese hand-made paper. It is considered to be necessary to investigate the question further to find a complete picture of the chemical nature of Ganpi hemicellulose.

9) S. Machida and S. Nishikori, unpublished.
10) A. Sera and R. Goto, *Wood Research (Mokuzai-Kenkyu)*, **No. 14**, 42 (1950).

Summary

The composition of the bast fibres of Ganpi plant (*Wickstroemia sikokiana* Franch. et Sav.) was investigated in the processes of the traditional paper-making of Japan. It was found that hemicelluloses of the bast fibres had significant bearings on the paper-making and the excellent character of Japanese paper.

The hemicellulose isolated from holocellulose of the Ganpi bast fibres by alkaline extraction were found to be composed of 13.6~15.8% of D-glucuronic acid (which is partly present as 4-*O*-methyl-D-glucuronic acid), 58.1~80.9% of D-xylose, and small amounts of D-mannose, D-galactose, L-arabinose, and L-rhamnose. It was shown that the degree of polymerisation of the hemicellulose calculated as a pentosan is about 160, and the molecule has basically a linear structure in which the uronic groups are present along the polymer chain at a ratio of one carboxyl group for each six or eight pentose sugar units.

The authors wish to thank Mr. M. Inano for help in the analysis of component sugars and uronic acid.

Chemical Laboratory of Textile Fibres
Kyoto University of Industrial Arts
and Textile Fibres
Kita-ku, Kyoto

11) H. J. Leech, *Tappi*, **37**, 343 (1954).
12) G. Jayme and E. Lochmüller-Kerler, *Holz. Roh.* ü. *Werkstoff*, **5**, (11), 377 (1942).
13) J. M. Limeric and A. J. Corey, *Pulp Paper Mag. Canada*, **47**, No. 4. 62 (1946).

Synthesis of 2-Alkyl-4H, 1, 3-benzoxazine-4-ones

By Takeyosi HANADA

(Received June 20, 1958)

4*H*,1,3-Benzoxazine-4-one derivatives are expected to show interesting chemical and biological properties, owing to the characteristic structure that the carbonyl group adjacent to N=C double bond is present in them. However, only a few 2-aryl derivatives have been reported[1,2], and no literature has appeared concerning 2-alkyl derivative. Titherley[1] reported the preparation of 2-phenyl-4*H*,1,3-benzoxazine-4-one (I: R=Ph) from *O*- or *N*-benzoylsalicylamide by the action of hydrogen chloride in boiling xylene. But Titherley et al.[3] failed in the preparation of 2-methylbenzoxazinone (Ia) from *O*-acetylsalicylamide (IIa) by the same procedure, and isolated only *N*-acetylsalicylamide (IIIa) produced by O→N acyl rearrangement. They assumed that the abortive isolation of 2-methylbenzoxazinone was due to its decomposition by alkali which was present.

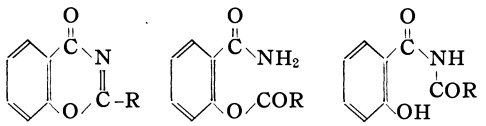

I II III

(a: R=CH_3, b: R=C_2H_5, c: R=C_3H_7)

In the present experiment *O*-acetylsalicylamide (IIa) was treated with hydrogen chloride in boiling xylene according to the procedure of Titherley[1], and without using alkali there were isolated yellow crystals, $C_9H_7O_2N$, m. p. 217°C, together with *N*-acetylsalicylamide (IIIa) produced by the acyl rearrangement. The yellow compound was considered to be 2-methyl-4*H*,1,3-benzoxazine-4-one (Ia). Its infrared spectrum showed carbonyl band at 1680 cm^{-1}, and C=N band at 1645 cm^{-1}, and indicated also the absence of both OH and NH group. This was insoluble in cold dilute aqueous alkali and showed no coloration with ferric chloride in chloroform. It also was produced from *N*-acetylsalicylamide (IIIa) in low yield under similar conditions.

Similarly, 2-ethyl- and 2-propyl-benzoxazinone (Ib and Ic) were synthesized from *O*-propionyl- and *O*-butyrylsalicylamide (IIb and IIc) respectively, though in poor yield. Their chemical and physical properties were very similar to those of the 2-methyl compound. It is noticeable that the infrared spectra of these compounds are essentially identical in the region below 7μ, while the 2-phenyl homologue shows an infrared band of carbonyl group at 1665 cm^{-1} and of C=N group at 1645 cm^{-1}.

2-Methyl-4*H*, 1, 3-benzoxazine-4-one was stable towards acid in contrast with the 2-phenyl homologue, but very sensitive to alkali; it was easily hydrolyzed to salicylamide by boiling with 1 N-sodium hydroxide for a few minutes. When heated with dilute aqueous ammonia it produced an alkali-soluble compound, m. p. 227°C (empirical formula, $C_{18}H_{15}O_3N_3$), of which the structure is now under investigation.

2-Alkyl-benzoxazinone contains a characteristic skeleton, —CO—N=C—, which has not yet been studied well and is assumed to be stabilized by a hydrid among the structures I, IV, V, and VI. It is supposed that the carbon atom at the 2-position is easily attacked by the nucleophilic reagent owing to the influence of the carbonyl group.

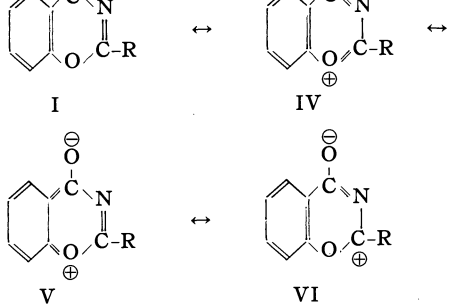

I IV

V VI

1) A. W. Titherley, *J. Chem. Soc.*, **97**, 200 (1910).
2) A. Mustafa and A. E. A. A. Hassan, *J. Am. Chem. Soc.*, **79**, 3846 (1957).
3) A. W. Titherley and W. L. Hicks, *J. Chem. Soc.*, **99**, 866 (1911).

Experimentral

***O*-Acetylsalicylamide (IIa).**—McConnan and Titherley[4] prepared this compound by the action of acetyl chloride on salicylamide in pyridine at −15°C. In the present study it was obtained by the following procedure: a few drops of concentrated sulfuric acid were added to a mixture of 20 g. of salicylamide and 50 ml. of acetic anhydride. After this mixture was kept for about 10 min., 500 ml. of water was added in order to decompose the excess of acetic anhydride. Upon filtration and washing with water, 18.5 g. (71%) of crude product was obtained and used for the next step without further purification. Recrystallization from ethyl acetate gave colorless needles, m. p. 138°C (Reported m. p. 138°C.).

***O*-Propionylsalicylamide (IIb).**—A solution of 10 g. of salicylamide in 20 ml. of pyridine was cooled to −15°C and 6.8 g. of propionyl chloride was added dropwise under vigorous stirring. After the addition, the mixture was kept for 30 min. at the same temperature, and 100 ml. of ether was added under stirring and then the ether was decanted off. To the remaining pasty mixture was added 1 N-sulfuric acid at 0°C, under stirring, in the course of ca. 10 min. The solid was filtered and washed with water. After the above ethereal solution had been allowed to stand for several hours, an additional small quantity of crystals was separated. The combined solids (9.1g.; 65%) were recrystallized from benzene to give colorless needles, m. p. 112~113°C, which showed no coloration with ethanolic ferric chloride.

Anal. Found: C, 62.27; H, 5.93. Calcd. for $C_{10}H_{11}O_3N$: C, 62.16; H, 5.74%.

***N*-Propionylsalicylamide (IIIb).**—When dilute aqueous ammonia was added to IIa, the solid was dissolved gradually and a yellow solution was obtained. By acidification with dilute hydrochloric acid colorless crystals were obtained, m. p. 123~125°C. Recrystallization from benzene gave colorless needles, m. p. 126~127°C, readily soluble in ethanol and ether; they revealed a purple-brown color with ethanolic ferric chloride.

IIIb was also obtained by boiling IIb with water for 30 min.

Anal. Found: C, 62.68; H, 5.92. Calcd. for $C_{10}H_{11}O_3N$: C, 62.16; H, 5.74%.

***O*-Butyrylsalicylamide (IIc).**—To a solution of 10 g. of salicylamide in 20 ml. of pyridine, was added 7.8 g. of butyryl chloride at −15°C following the same procedure as in the case of IIb. A solid thus obtained was crystallized from benzene to yield colorless needles, but the melting point was not sharp (m. p. ca. 90~110°C) because of persistent contamination of IIIc.

Anal. Found: C, 64.02; H, 6.59. Calcd. for $C_{11}H_{13}O_3N$: C, 63.75; H, 6.32%.

***N*-Butyrylsalicylamide (IIIc),**—This material was prepared by the action of dilute aqueous ammonia on IIc, or by boiling IIc with water for 20 min. Recrystallization from benzene gave colorless needles, m. p. 128~129°C, readily soluble in ethanol and ether. They produced an orange brown color with ethanolic ferric chloride.

Anal. Found: C, 63.64; H. 6.55. Calcd. for $C_{11}H_{13}O_3N$: C, 63.75; H, 6.32%.

2-Methyl-4*H*, 1, 3-benzoxazine-4-one (Ia).—a) *From O-Acetylsalicylamide (IIa).*—A mixture of 15 g. of IIa and 200 ml. of xylene was heated in a bath to 145°C, and when the solution became clear, a stream of dry hydrogen chloride was passed through for several min. By gradually raising the temperature of the bath to 155°C, the xylene was allowed to distil out, carrying with it the water formed during the reaction. In order to make up for the loss of hydrogen chloride by distillation, a few bubbles of the gas were passed into the solution at an interval of several minutes. When the greater part of the solvent was distilled off, the residue solidified on cooling. It was treated with warm ethanol to remove IIIa. The remaining yellow solid (7.4g.; 50%) was repeatedly crystallized from benzene to yield yellow needles (Ia), m. p. 217°C. It was insoluble in ethanol and ether, soluble in dioxane, pyridine and chloroform. The infrared spectrum showed bands at 1684 cm^{-1} (C=O) and 1645 cm^{-1} (C=N).

Anal. Found: C, 67.05; H, 4.18; N, 8.74. Calcd. for $C_9H_7O_2N$: C, 67.06; H, 4.35; N, 8.69%.

From the ethanolic solution, by evaporation of the solvent and recrystallization from benzene, colorless needles, m. p. 140~141°C, were obtained. The melting point was not depressed on admixture with IIIa.

b) *From N-Acetylsalicylamide (IIIa).*—A solution of 6.5 g. of IIIa in 25 ml. of dry xylene was heated for ca. 5 hr. under passage of dry hydrogen chloride. After removal of the greater part of the solvent under reduced pressure, yellow crystals deposited on cooling. After recrystallization from benzene, the compound had m. p. 217°C; mixed m. p. with Ia prepared from IIa, 217°C.

2-Ethyl-4*H*, 1, 3,-benzoxazine-4-one (Ib).—A solution of 15 g. of IIb in 200 ml. of dry xylene or toluene was heated in the presence of dry hydrogen chloride following the same procedure as above. The product, after removal of the ethanol-soluble part, was crystallized from benzene to yield yellow needles m. p. 212~213°C, insoluble in ethanol and ether. The infrared spectrum showed bands at 1680 cm^{-1} (C=O) and 1645 cm^{-1} (C=N).

Anal. Found: C, 68.48; H, 5.40; N, 8.23. Calcd. for $C_{10}H_9O_2N$: C, 68.56; H, 5.18; N, 8.00%.

The ethanol extracts obtained above were concentrated to a solid, which on crystallization from benzene gave colorless needles, m. p. 126~127°C, undepressed on admixture with IIIb.

2-Propyl-4*H*, 1, 3-benzoxazine-4-one (Ic).—A solution of 15 g. of IIc in 180 ml. of toluene was heated with dry hydrogen chloride in the same manner as described above. In this case, the residue was wholly soluble in ethanol, but on standing overnight, a small quantity of crystals separated out from the ethanol solution. Recrystallization from benzene gave yellow plates, m.p. 142~143.5°C, soluble in ethanol and benzene.

4) J. McConnan and A. W. Titherley, *J. Chem., Soc.*, **89**, 1333 (1906).

The infrared spectrum showed bands at 1680 cm^{-1} (C=O) and 1645 cm^{-1} (C=N).

Anal. Found: C, 69.77; H, 6.06. Calcd. for $C_{11}H_{11}O_2N$: C, 69.82; H, 5.86%.

Further concentration of ethanolic mother liquor gave crystals which on repeated recrystallizations from benzene had m. p. 124~128°C. The material did not depress the melting point of an authentic sample of IIIc.

Alkaline Hydrolysis of Ia. — When Ia was boiled for a few minutes with 1 N sodium hydroxide, a pale yellow solution was formed. After acidification with diluted hydrochloric acid, the precipitates formed were collected and recrystallized from water to give colorless needles, m. p. 136~137°C. The material was identified as salicylamide on the basis of the mixed melting-point test.

Reaction of Ia with Aqueous Ammonia.— A mixture of 2 g. of Ia, 60 ml. of 3N aqueous ammonia and 60 ml. of ethanol was heated for 30 min. on a steam bath. After cooling the yellow solution was acidified with dilute hydrochloric acid, and the precipitates were collected and recrystallized twice from benzene (once using charcoal) to give colorless needles, m. p. 227°C, in almost quantitative yield. The material was soluble in ether, ethanol and chloroform, and showed no color with ferric chloride in ethanol. It was dissolved in dilute sodium hydroxide solution to give a yellow solution, and was recoverable, as it was, from this solution, after ten minutes' heating in a water bath.

Anal. Found: C, 67.55; H, 4.31; N, 13.09; Mol. wt. (Rast), 323. Calcd. for $C_{18}H_{15}O_3N_3$: C, 67.28; H, 4.71; N, 13.08%; mol. wt., 321.

The infrared spectrum showed bands at 3390 cm^{-1} (OH) and 1640 cm^{-1} (C=O).

Summary

2-Alkyl-4*H*,1,3-benzoxazine-4-ones (Ia, Ib, and Ic) were synthesized from the corresponding *O*-acylsalicylamides (II), and some of the properties of I were studied.

The author wishes to thank Professor T. Irie for his kind guidance and encouragement throughout this work. He is also indebted to Miss N. Fujino for the microanalyses.

Department of Chemistry
Faculty of Science
Hokkaido University
Sapporo

Benzylation of Allylbenzene. Formation of 3,4-Diphenyl-1-butene and 3-Benzyl-3,4-diphenyl-1-butene

By Teisuke ANDO and Niichiro TOKURA

(Received July 2, 1958)

In the preceding papers[1,2] the authors reported the formation of 3, 4-diphenyl-1-butyne (I), 3, 4-diphenyl-1, 2-butadiene (II), and 3-benzyl-3, 4-diphenyl-1-butyne (III) by the reaction of benzyl chloride and sodium acetylide in liquid ammonia.

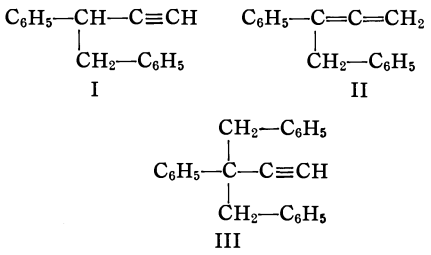

I II III

It is assumed that 3-phenyl-1-propyne (i. e. propargylbenzene) (IV) is formed as an intermediate at the first stage.

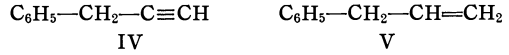

IV V

In 1952, Young, Kosmin, Mixer and Campbell[3] reported on methylation and allylation of allylbenzene (V) in liquid ammonia. More recently, Mixer and Young[4] conducted the same reactions in *n*-pentane. Herbrandson and Mooney[5] reported the isomeric transformation

1) T. Ando and N. Tokura, This Bulletin, **30**, 259 (1957).
2) T. Ando and N. Tokura, ibid., **31**, 351 (1958).
3) W. G. Young, M. Kosmin, R. Y. Mixer and T. W. Campbell, *J. Am. Chem. Soc.*, **74**, 608 (1952).
4) R. Y. Mixer and W. G. Young, ibid., **78**, 3379 (1956).
5) H. F. Herbrandson and D. S. Mooney, ibid., **79**, 5809 (1957).
6) W. v. Miller and G. Rohde, *Ber.*, **25**, 2015 (1892).

between allylbenzene and propenylbenzene in the presence of butyllithium or lithium amide.

Since allylbenzene (i. e. 3-phenyl-1-propene) (V) is closely related to IV in its structure, it was also expected that the benzylation of V in liquid ammonia would afford mono- and di-benzyl derivatives of V, corresponding to I and III in the benzylation of acetylene. The present paper, records the results of the study on the benzylation reaction which was observed to occur as expected. The structures of the products formed in this reaction and the relations among the products from benzylation of allylbenzene, benzyl cyanide and acetylene have been established unequivocally.

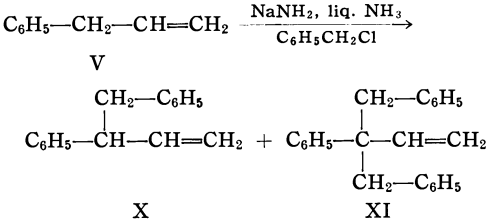

When V was allowed to react with an equi-molecular amount of benzyl chloride in the presence of sodium amide in liquid ammonia, two fractions were obtained, A, b. p. 160~162°C (17 mm.), and B, b. p. 191~192°C(2 mm.).

By oxidizing A with potassium permanganate, a white crystalline substance (VI), m. p. 88~89°C, was obtained. Miller and Rohde[6] reported on the synthesis of 2, 3-diphenylpropionic acid (VII), and it was observed that the substance exists in three isomers, m. p. 82°C, and 95~96°C[7,8]; the present authors prepared 2, 3-diphenylpropionic acid (VII) by hydrolyzing 2, 3-diphenylpropionitrile (VIII), obtained by the reaction of benzyl cyanide with an equi-molecular amount of benzyl chloride in the presence of sodium alcoholate according to the method of Miller and Rohde[6].

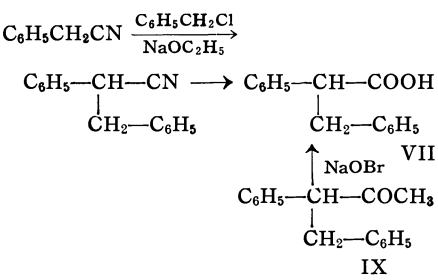

In this case two kinds of crystalline product having melting points 82°C and 88~89°C, respectively, were isolated, but the one having the highest melting point, 95~96°C, was not isolated. A mixture of the crystalline product having m. p. 88~89°C and VI gave no lowering of the melting point. By oxidizing the known compound, 3, 4-diphenyl-2-butanone[9] (IX), with sodium hypobromite, an acid showing an m. p. and a mixed m. p. with VI of 88~89°C was also obtained.

Infrared spectra in potassium bromide disks and carbontetrachloride solution of two specimens of 2, 3-diphenylpropionic acid having m. p. 82~82.5°C and 88~89°C were measured. The spectra in the disks gave different curves, while those in the solution gave the same. (Compare Fig. 1 and the experimental part.).

Thus, the structure of VI being established as 2, 3-diphenylpropionic acid, A is regarded as 3, 4-diphenyl-1-butene (X), which is further supported by the elementary analysis (molecular formula: $C_{16}H_{16}$), and infrared spectrum.

The boiling point, the molecular formula $C_{23}H_{22}$ and the infrared spectrum of B were almost coincident with those of the partially hydrogenated product of III, 3-benzyl-3, 4-diphenyl-1-butene (XI). The structure of XI for B was proved by several reactions as follows. Oxidation of B with potassium permanganate afforded an α-keto acid (XII), m. p. 138.5~139.5°C, which showed no depression of the mixed melting point with an authentic phenyldibenzylpyruvic acid[2]. Furthermore, oxidation of XII with potassium permanganate or hydrogen peroxide gave an acid (XIII), m. p. 122~123°C, a mixture of which with the α-form of 2-benzyl-2, 3-diphenylpropionic acid[2] obtained previously gave no melting point lowering. As was already reported[2], this acid showed a polymorphic transformation and the melting point was raised to 153~154°C after standing for two months.

No material to be considered as derived from propenylbenzene was isolated in this reaction. Therefore, in the metallation of allylbenzene(V) with sodium amide in liquid ammonia, the carbon atom adjacent

7) C. R. Hauser and W. J. Chambers, *J. Am. Chem. Soc.*, **78**, 4942 (1956).

8) N. Campbell and E. Ciganck, *J. Chem. Soc.*, **1956**, 3834.

9) M. M. Tiffeneau and M. J. Levy, *Bull. soc. chim. France*, **33**, 779 (1923).

TABLE I

BENZYLATION OF ACETYLENE, ALLYLBENZENE, AND BENZYL CYANIDE

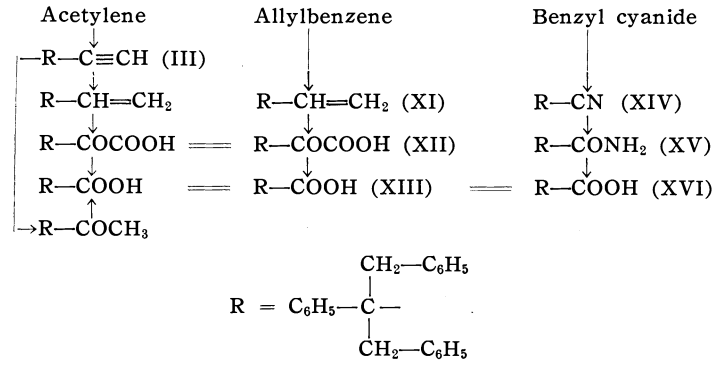

to the benzene ring was metallated, and the action of benzyl chloride afforded the mono- or di-benzyl compounds, 3, 4-diphenyl-1-butene (X) (40 percent) and 3-benzyl-3, 4-diphenyl-1-butene (XI) (30 percent).

Benzylation of allylbenzene, benzyl cyanide and acetylene[1,2], and the relations of the products are schematically represented by Table I.

Experimental[10]

Benzylation of allylbenzene.—Liquid ammonia (700 cc.) was taken in a three-necked flask of 100 cc. capacity equipped with a mechanical agitator, a dry-ice condenser and a dropping funnel, and kept at $-50°\pm5°C$ in a dry-ice-ethanol bath, and 14 g. of metallic sodium was dissolved in the liquid ammonia. After being mixed with a minute amount of ferric nitrate, the content was agitated for about 20 minutes to produce sodium amide. After another 20 minutes' agitation, 60 g. of allylbenzene (b. p. 47°C/12 mm.) was added in 30 minutes. The solution was tinged with reddish brown color. It was further agitated for 20 minutes and 68 g. of benzyl chloride was added drop by drop in 40 minutes. When the addition of the same mole of benzyl chloride was completed, the color of the solution changed to grayish white. The benzylation reaction was exothermic. The dry-ice bath was removed and the flask was left overnight at room temperature, while liquid ammonia was naturally evaporated off. The residue was extracted with ether, and the ethereal solution was washed with water to neutral reaction and dried with dehydrated Glauber's salt. After the ether was distilled off, the residue was fractionated in vacuo to give two fractions: A fraction, boiling at 150~155°C/11 mm., (yield 44.2 g.), which was redistilled to give 38.7 g. of b. p. 160~162°C/17 mm. B fraction, boiling at 175~200°C/2 mm., (yield 24.6 g.), which gave 18.2 g. of b. p. 191~192°C/2 mm. by redistillation.

10) Melting points and boiling points were not corrected.

	Molecular formula	Crude (g.)	Distillate (%)	Theoretical yield based on benzyl chloride (%)
A	$C_{16}H_{16}$	44.2	51	40
B	$C_{23}H_{22}$	24.6	28	30

Anal. Found: C, 92.32; H, 7.77. Calcd. for A or $C_{16}H_{16}$: C, 92.26; H, 7.74%. I. R. ν_{max}: 1635, 1452, 1415, 990, and 910 cm^{-1}. *Anal.* Found: C, 92.61; H, 7.39. Calcd. for B or $C_{23}H_{22}$: C, 92.57; H, 7.43%. I. R. ν_{max}: 1634, 1455, 1415, 1005, and 912 cm^{-1}.

Oxidation of A with potassium permanganate. 2, 3-Diphenylpropionic acid (VI).—A (4.1 g.) was dissolved in 300 cc. of acetone in a three-necked flask of 1000 cc. capacity equipped with an agitator. Powdered potassium permanganate (9 g.) was added to the solution little by little with agitation at the room temperature. After 6 hours' agitation, the mixture was left overnight at room temperature, and then the solvent was distilled off. Water was added to the residue and manganese dioxide was dissolved by passing sulfur dioxide gas into the mixture.

The substance in crystalline suspension was extracted with ether and the ethereal solution was washed with aqueous alkali. The aqueous solution was acidified and extracted with ether. The ethereal solution was washed with water until the solution became neutral. After drying with dehydrated Glauber's salt, the solution was evaporated to give 4 g. (88 %) of a white crystalline substance, m. p. 70~83°C, and recrystallization from petroleum ether (b. p. 60~80°C) gave VI, m. p. 88~89°C. A mixture of VI and 2. 3-diphenylpropionic acid (VII), m. p. 88~89°C, prepared by the method given by Miller and Rohde[6], gave no melting point lowering.

Anal. Found: C, 79.81; H, 6.30. Calcd. for 2, 3-diphenylpropionic acid (VI) or $C_{15}H_{14}O_2$: C, 79.62; H, 6.24%.

2, 3-Diphenylpropionic acid (VII)[6].—Metallic sodium (12 g.) was dissolved in 100 g. of absolute ethanol in a flask of 300 cc. capacity, and 58 g. of benzyl cyanide and 69 g. of benzyl chloride were added and the mixture was refluxed for 4 hours. Sodium chloride was filtered off and

the solution was evaporated. Vacuum distillation of the residue gave 33 g. (48%) of unchanged benzyl cyanide and 10 g. (15.7%) of diphenylpropionitrile, m. p. 57.5~58.5°C (recrystallized from alcohol). The nitrile (1 g.) was heated with 2 cc. of concentrated hydrochloric acid in a sealed tube at 130°C for 5 hours. After the reaction was completed, the product was made alkaline and the unchanged nitrile and the intermediate acid amide were removed with ether. The remaining aqueous solution was acidified and extracted with ether. The crystalline substance from the ethereal solution was recrystallized from petroleum ether (b. p. 60~80°C). Needles, m. p. 82~82.5°C. Recrystallization of the needles from water gave small white plates, m. p. 88~89°C. Melting points of the two crystalline specimens were coincident with those of 2,3-diphenylpropionic acid. 82°C and 88~89°C, given in the literature[6].

Anal. Found: C, 86.75; H, 6.43; N, 6.67. Calcd. for 2,3-diphenylpropionitrile (VIII) or $C_{15}H_{13}N$: C, 86.92; H, 6.32; N, 6.76%. Found: C, 79.74; H, 6.73; N, 6.06. Calcd. for 2,3-diphenylpropionamide or $C_{15}H_{15}ON$: C, 79.97; H, 6.71; N, 6.22%. Found: C, 79.56; H, 6.22. Calcd. for 2,3-diphenylpropionic acid (VII) or $C_{15}H_{14}O_2$: C, 79.62; H, 6.24%.

Crystals having m. p. 82~82.5°C: I. R. crys. ν_{max}: 3300~2300, 1700, 1688, and 940 cm^{-1}, I. R. CCl_4 soln. ν_{max}: 3300~2300 and 1708 cm^{-1}, U. V. λ_{max}: 258 mμ (log ε: 2.76) and 265 mμ (log ε: 2.65).

Crystals having m. p. 88~89°C: I. R. crys. ν_{max}: 3180, 1724, 1677, and 1173 cm^{-1}, I. R. CCl_4 soln. ν_{max}: 3300~2400, and 1705 cm^{-1}, U. V. λ_{max}: 258 mμ (log ε: 2.68), and 265 mμ (log ε: 2.61).

Synthesis and oxidation of 3,4-diphenylbutanone (IX). — According to Tiffeneau and Lévy[9], phenylacetone was metallated with sodium alcoholate and then refluxed with the same mole of benzyl chloride for 2 hours. The product boiled at 188~189°C/20 mm. and melted at 31~32°C after recrystallization from petroleum ether (b. p. 40°C). The same m. p. was given by the literature[9]. Its oxime, m. p. 138~138.5°C. (literature[9]: 134~135°C) semicarbazone, m.p. 169~170°C. (literature[9]: 168°C).

Anal. Found: C, 85.77; H, 6.94. Calcd. for 3,4-diphenyl-2-butanone (IX) or $C_{16}H_{16}O$: C, 85.68; H, 6.84%. I. R. oil ν_{max}: 1700, 1351, 1148, 1088, and 1030 cm^{-1}, U. V. λ_{max}: 268 mμ (log ε: 2.78), 265 mμ (log ε: 2.74) and 288 mμ (log ε: 2.70).

Sodium hypobromite[11] was prepared by adding 5 cc. of bromine to an aqueous solution of 15 g. of sodium hydroxide in 50 cc. water cooled in ice. It was added to a solution of 5 g. of the above substance of m. p. 31~32°C in 50 cc. of 1,4-dioxane with vigorous agitation and the mixture was kept at the room temperature for 2 days. On concentration, the aqueous layer gave a grayish-white semi-solid, from which the unchanged substance was removed with ether. After acidifying with hydrochloric acid, the product was extracted with ether. The ethereal solution gave 1.8 g. (36.4%) of a crystalline substance, m. p. 82~82.5°C. Recrystallization from petroleum ether (b. p. 60~80°C) gave white crystals, m. p. 88~89°C. A mixture of the acid and VI showed no lowering of the melting point.

Oxidation of B with potassium permanganate. — *Phenyldibenzylpyruvic acid (XII).* — B (4.2 g.) was dissolved in 400 cc. of acetone in a three-necked flask of 2 liter capacity equipped with an airtight agitator and a reflux condenser. To the solution 8 g. of potassium permanganate dissolved in 400 cc. of water was added and the mixture was agitated for 48 hours at the room temperature. After removal of acetone, sulfur dioxide gas was introduced into the residue under cooling in ice and then the solution was made alkaline with dilute aqueous caustic soda. The unchanged neutral part was extracted with ether and the remaining alkaline layer was acidified with hydrochloric acid and extracted with ether. The ethereal solution gave 4.3 g. of a crystalline substance, m. p. 138~139.5°C, in a yield of 88%. The melting point of the keto acid (XII) did not change on admixture with phenylbenzylpyruvic acid obtained by oxidation of III.

Anal. Found: C, 79.92; H, 5.98. Calcd. for phenyldibenzylpyruvic acid (XII) or $C_{23}H_{20}O_3$: C, 80.21; H, 5.85%. I. R. ν_{max}: 1722, 1711, and 1370 cm^{-1}.

The α-form of 2-benzyl-2,3-diphenylpropionic acid (XIII). — *a) Oxidation of XII with potassium permanganate.* — XII (0.5 g.) was dissolved in 100 cc. of 2% aqueous sodium hydroxide in a round-bottom flask of 300 cc. capacity, and to the solution 50 cc. of 1% aqueous potassium permanganate was added. The mixture was agitated for 8 hours and left to stand overnight. It was then neutralized with dilute sulfuric acid, treated with sulfur dioxide gas to dissolve manganese dioxide, and extracted with ether. The white crystalline substance from the ethereal solution was recrystallized from ligroin (b. p. 80~100°C). White scales m. p. 121~122°C. (α-form) (XIII). Yield 0.2 g. (43.5%).

b) Reaction of XII with hydrogen peroxide. — In a beaker of 200 cc. capacity, 1.5 g. of XII was mixed with 20 cc. of 10% sodium hydroxide and 30 cc. of 10% sodium hydrogen peroxide and the mixture was allowed to stand overnight in an ice box. Then 10 cc. more of hydrogen peroxide was added to the mixture with agitation. After 8 hours, the mixture was acidified and extracted with ether. The ethereal solution gave 0.4 g. (87%) of fine scales, m. p. 118~120°C, and recrystallized from ligroin (b. p. 80~100°C). White scales (α-form, XIII), m. p. 122~123°C. Yield 3 g. No melting point depression was observed on admixture of the acid (XIII) with α-form of 2-benzyl-2,3-diphenylpropionic acid, obtained by the oxidation of III.

Anal. Found: C, 83.32; H, 6.42. Calcd. for 2-benzyl-2,3-diphenylpropionic acid (XIII) or

11) W. S. Johnson, C. D. Gutsche and R. D. Offenhauer, *J. Am. Chem. Soc.*, **68**, 1648 (1946).

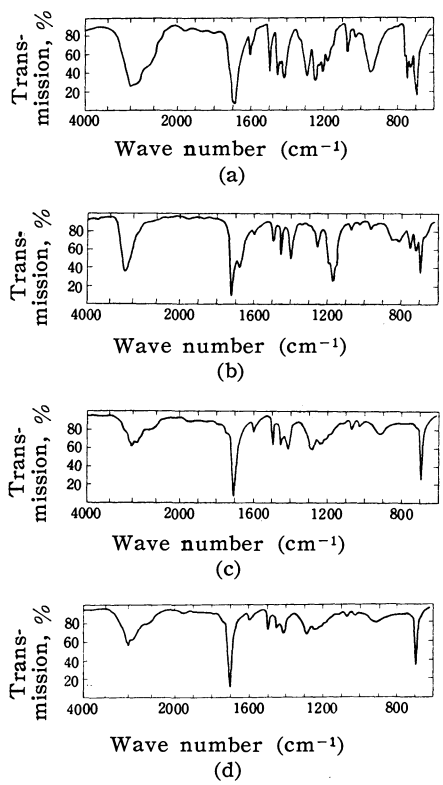

Fig. 1.
(a) KBr disk of the specimen of 2, 3-diphenylpropionic acid melting at 82°C.
(b) KBr disk of specimen of the same compound melting at 88~89°C.
(c) A CCl_4 solution of the specimen of the same compound melting at 82°C.
(d) A CCl_4 solution of the specimen of the same compound melting at 88~89°C.

$C_{22}H_{20}O_2$: C, 83.51; H, 6.37%. I. R. crys. ν_{max}: 3200~2300, and 1702 cm^{-1} I. R. CCl_4 soln. ν_{max}: 3300~2400 and 1700 cm^{-1} U. V. λ_{max}: 258 mμ (log ε: 2.67) and 265 mμ (log ε: 2.56).

On standing for about two months at room temperature, the α-form of XIII, m. p. 122~123°C, was changed to the β-form, m. p. 153~154°C. In I. R. and U. V. spectra of the two forms, not even a slight difference was estimated. A mixture of the β-form, m. p. 153~154°C, and the β-form of 2-benzyl-2, 3-diphenylpropionic acid (XVI), synthesized by the method of Hauser and Brasen[12], gave no melting point lowering.

12) C. R. Hauser and W. R. Brasen, ibid., **78**, 494 (1956).
13) R. H. Baker, ibid., **70**, 3857 (1948).

Benzylation of benzyl cyanide. The β-form of 2-benzyl-2, 3-diphenylpropionic acid (XVI).—According to the method of Hauser et al.[12] and Baker[13], 2-benzyl-2, 3-diphenylpropionitrile (XIV) was obtained in a fairly good yield. The product (XIV), m. p. 81~83°C, b. p. 204~205°C/2 mm., was refluxed with 70% sulfuric acid in glacial acetic acid for 4 days, and gave 2-benzyl-2, 3-diphenylpropionamide (XV), m. p. 122.7~124°C. (Baker[11]: m. p. 111~112°C).

Anal. Found: N, 4.20. Calcd. for 2-benzyl-2, 3-diphenylpropionamide (XV) or $C_{22}H_{21}ON$, 4.44%.

Treatment of the amide (XV) with sodium nitrite gave 2-benzyl-2, 3-diphenylpropionic acid (XVI, β-form). The melting point of the substance and of a mixture with an authentic specimen of the β-form was the same, m. p. 154~154.5°C.

Anal. Found: C, 83.51; H, 6.45. Calcd. for 2-benzyl-2, 3-diphenylpropionic acid (XVI) or $C_{22}H_{20}O_2$: C, 83.51; H, 6.37%. I. R. ν_{max}: 5300~2200 and 1700 cm^{-1}, U. V. λ_{max}: 258 mμ (log ε: 2.67) and 265 mμ (log ε: 2.56).

Summary

When allylbenzene was treated with the same moles of sodium amide and benzyl chloride in liquid ammonia, one or two benzyl radicals were introduced into allylbenzene to produce 3, 4-diphenyl-1-butene and 3-benzyl-1-butene.

The reaction is similar to the well-known reaction[12] of benzyl cyanide and benzyl chloride in liquid ammonia and that[13] of 2-phenyl-1-ethanol and benzyl chloride in benzene.

Two forms of 2, 3-diphenylpropionic acid were isolated and their I. R. spectra were measured. Different curves were obtained in KBr disks, while the identical curves were obtained carbon tetrachloride solution.

Infrared absorption spectra were measured by Professor Kinumaki and his associates of this Institute and the elementary analyses were performed in the laboratory of Shionogi and Company, Ltd., to whom the writers are deeply indebted.

Chemical Research Institute of Non-aqueous Solutions, Tohoku University, Katahira-cho, Sendai

Thermal Effects of Some Kaolin Minerals. I. Kaolinite and Kibushi-clay

By Hiroshi TAKAHASHI

(Received February 25, 1958)

All kaolin minerals are made of aluminosilicate layers in their crystal structures. However, there are imperfections in the mode of stacking of unit layers, and this leads to variety in the structure of kaolin minerals[1]. The different properties which are found among kaolin minerals are due to there being many kinds of characteristic factor in each mineral. Of such factors, the most important one is the structural perfection or imperfection, that is, the degree of crystallinity including the stacking disorder.

It is well known that a kaolinite transforms into mullite through heat-treatment at 950~1000°C[2]. Investigations on the structural change of kaolin minerals with heat-treatment have been made chiefly in a temperature region higher than 950°C. However, little investigation has been done in regard to the effect of heat-treatment in the relatively low temperature region.

The course of the transformation of a kaolinite into mullite involves two major structural changes. One is a structural change due to the loss of the adsorbed water. The other is a structural change caused by the loss of the lattice water. In this paper, the fundamental information regarding the change in the structure of kaolinite with heat-treatment, in the relatively low temperature region, are presented, through X-ray diffraction method, differential thermal analysis and particularly using these together with density measurement.

Experimental

Twenty samples of kaolinte and kaolin mineral of fireclay type were used in this study. In studying these samples continuous disordering was observed among different samples. For the structural changes of kaolinite and kaolin mineral of fireclay type through heat-treatment, the structural changes of the following three samples are generally representative of the whole. Three of the samples mentioned above are as follows; Kaolinite from Mesa Alta, N.M., U.S.A.; Kaolinite from Drybranch, Geor., U.S.A.; Kibushi-clay from Shidare, Gifu, Japan. Two of the kaolinite samples are the API Standard Clay Minerals; Kibushi-clay is a kaolin mineral of fireclay type. The structural characteristics of these samples have been discussed in the previous paper[3]. The original samples were powdered and sieved through 250 mesh. The heat-treatment was made in an electric furnace under the ordinary atmosphere, keeping at a given temperature for an hour.

The X-ray powder diagrams were recorded by the X-ray diffractometer (Geigerflex). Experimental conditions were as follows. Filtered Copper radiation (Cu$K\alpha$:1.5418 Å) at about 35 kV and 15 mA was used; scanning speed was 1° or 1/4° 2θ per minute; time constant was 4 seconds; receiving slit was 0.2 mm or 0.1 mm; angular aperture was 1° or 1/2°.

The differential thermal analysis curves were obtained by the apparatus described by Sudo et al.[4]. Care was taken to pack a specimen into the sample block in the homogeneous manner and also to keep the weight of the specimen constant. The mean heating rate is 12.5°C per minute.

The density of the specimens was measured by a pycnometer in carbon tetrachloride. It was made in the original state after it had been dried at 110°C in order to avoid the effect of the adsorbed or interlayer water.

Results and Discussion

X-ray Diffraction Studies.—X-ray diffractometer traces for heat-treated kaolinite and Kibushi-clay are given in Figs. 1 and 2, respectively.

In the traces of Mesa Alta kaolinite, which are observed in the X-ray diagram before it is heat-treated at 400°C, an increase in the intensity of reflection, particularly (00 l), and the reduction in the line breadth are most remarkable. In the 545°C heat-treated specimen, the intensity of all reflections, particularly (00 l) reflections, sharply decreases. In this specimen,

1) G.W. Brindley and K. Robinson, *Trans, Farad. Soc.*, **42B**, 198 (1946).
2) W. F. Bradley and R. E. Grim, *Am. Mineral.*, **36**, 182 (1951).
W. D. Jones, *Min, Mag.*, **30**, 186 (1953).
H. D. Glass, *Am. Mineral.*, **39**, 193 (1954).
3) H. Takahashi, This Bulletin, **31**, 275 (1958).
4) T. Sudo et al., *J Geol. Soc. Japan* (*Chishitsu-Gaku-Zasshi*), **58**, 116 (1952).

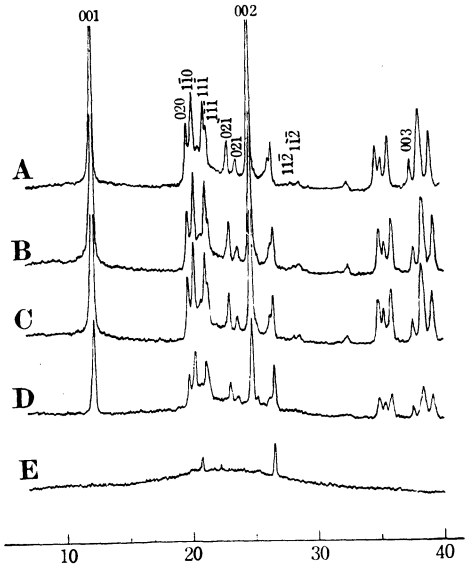

Fig. 1. X-ray diffractometer traces of heat-treated specimens of kaolinite (Mesa Alta, N.M.).
A, original kaolinite
B, treated at 200°C
C, treated at 400°C
D, treated at 545°C
E, treated at 700°C

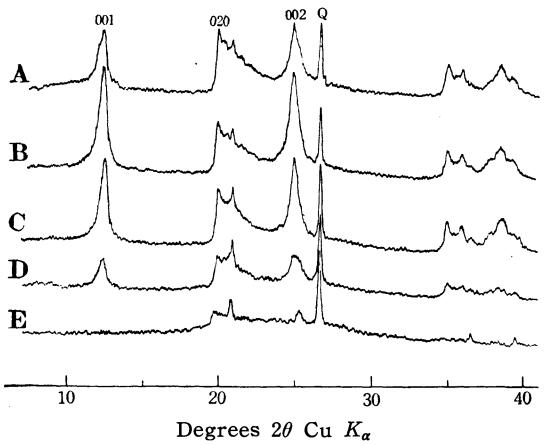

Fig. 2. X-ray diffractometer traces of heat-treated specimens of Kibushi-clay.
A, original clay
B, treated at 200°C
C, treated at 400°C
D, treated at 545°C
E, treated at 700°C

the $(11\bar{2})$ reflection of 3.14 Å spacing, which is weak in the original state, the $(1\bar{1}\bar{2})$ reflection of 3.09 Å spacing disappear, and the $(11\bar{1})$ and the $(1\bar{1}\bar{1})$ reflections are not resolved from each other. In the process up to this stage, the values of the interplanner spacings of all the reflections remain almost unchanged. In the 700°C heat-treated specimen, all reflections disappear, the original regular kaolin structure is entirely broken, and only a very diffuse and weak band is observable.

The structural transformation of Drybranch kaolinite through heat-treatment follows practically the same process as that of Mesa Alta kaolinite. In the 545°C heat-treated specimen, its X-ray diagram indicates that the structure is in remarkably disorder in comparison with the 545°C heat-treated specimen of Mesa Alta kaolinite. The lattice water is lost, in this case, at a lower temperature than in the case of Mesa Alta kaolinite. This fact means that the velocity of the disintegration of the kaolinite structure attending the loss of the lattice water is related to the degree of crystallinity of the original mineral.

In Kibushi-clay, it is revealed in the light of X-ray traces that it has also the two elements of the progress and lowering of crystallinity as in the case of kaolinite. The progress of crystallinity of Kibushi-clay is remarkable up to 400°C heat-treatment. The lowering of crystallinity begins also at a low temperature as compared to that of kaolinite. In Kibushi-clay, its basal spacing slowly decreases with the rising of heat-treatment. This means that it is due to the loss of the inter-layer water which exists sporadically in this clay. In other words, it is because this clay originally contains the inter-layer water in its structure. This proves certainly that Kibushi-clay is low in crystallinity.

Differential Thermal Analysis.—Fig. 3 shows the differential thermal analysis curves in the process of heat-treatment of kaolinite. Table I shows the thermal data obtained from these curves.

In Mesa Alta kaolinite, as can be supposed, no endothermic reaction associated with the loss of the inter-layer water is observed. For the endothermic reaction (E_n) associated with the loss of the lattice water, the reduction in the area under the peak is not so remarkable between its original and 200°C heat-treated specimen; however, a slight reduction due to the loss of the lattice water becomes broad. In the 400°C heat-treated specimen, the area of this reaction reduces a little, and so does its height. In the 545°C heat-treated specimen, the area reduces con-

TABLE I

THERMAL DATA OF HEAT-TREATED SPECIMENS OF KAOLINITE

Sample	Treated temp.	E_n Temp. at peak	E_n Height of peak	E_x Temp. at peak	E_x Height of peak	E_x Breadth of peak
Kaolinite	original	604°C	16	966°C	39	5.1°C
(Mesa Alta,	200°C	598	14	964	41	4.8
N.M.)	400	593	11	964	44	4.2
	545	543	9	962	50	4.7
	700	—	—	962	63	5.0
Kaolinite	original	592	20	964	41	4.8
(Drybranch,	200	588	16	962	44	3.5
Geor.)	400	572	10	962	49	3.4
	545	559	3	963	58	3.9
	700	—	—	960	62	4.1

TABLE II

THERMAL DATA OF HEAT-TREATED SPECIMENS OF KIBUSHI-CLAY

Treated-temperatre	E_{n1} Temp. at peak	E_{n1} Height of peak	E_{n2} Temp. at peak	E_{n2} Height of peak	E_x Temp. at peak	E_x Height of peak	E_x Breadth of peak
original	130°C	1	574°C	14	945°C	13	10.5°C
200°C	120	1	572	12	943	14	10.3
400	120	1	570	12	944	13	10.5
545	—	—	561	5	944	14	10.4
700	—	—	—	—	942	18	9.6

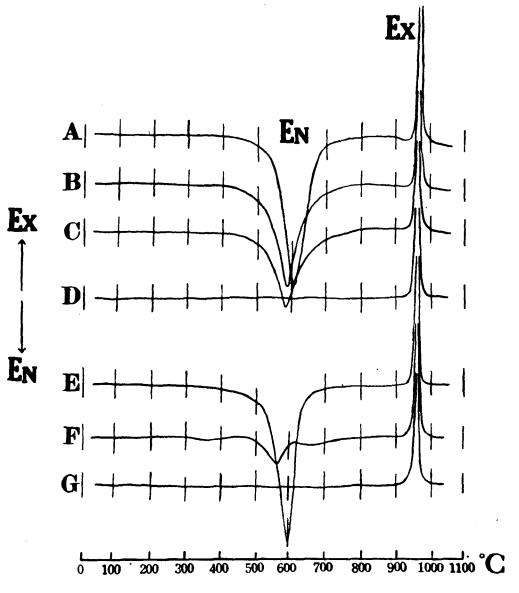

Fig. 3. Differential thermal analysis curves of heat-treated specimens of Mesa Alta and Drybranch kaolinite.
A, original Mesa Alta kaolinite
B, treated at 200°C
C, treated at 545°C
D, treated at 700°C
E, original Drybranch kaolinite
F, treated at 545°C
G, treated at 700°C

siderably. This means that the loss of the lattice water has considerably increased. In the 700°C heat-treated specimen, this endothermic reaction completely disappears.

Drybranch kaolinite behaves in a manner similar to Mesa Alta kaolinite. However, in the 545°C heat-treated specimen, the area of the endothermic reaction is small as compared with the 545°C heat-treated specimen of Mesa Alta kaolinite. This means that the crystallinity of its original sample is slightly lower than that of Mesa Alta kaolinite.

The final exothermic reaction (E_x) is due to the mullite nucleation. It is seen that the peak shifts slightly to the lower temperature side as the treated temperaturerises, and the peak height slowly increases. In the 700°C heat-treated specimen, the peak is considerably higher as compared with that of the original sample. From this fact, in spite of the fact that the X-ray diagram indicates that this state is amorphous, the rearrangement of ions is slowly occurring in the metakaolin matrix for the mullite nucleation. Generally, the breadth the exothermic reaction is defined as the breadth of temperature between the beginning point and the end

point. However, as these points are not so clear, in this study, the breadth at the point of the half value of the peak height is taken as the breadth of the peak. The breadth of the peak thus defined is considered to indicate the sharpness of the mullite nucleation. This breadth slightly reduces as the heat-treatment temperature rises. After reaching the minimum value, it increases again. Any definite conclusion can hardly be made from this phenomenon, however.

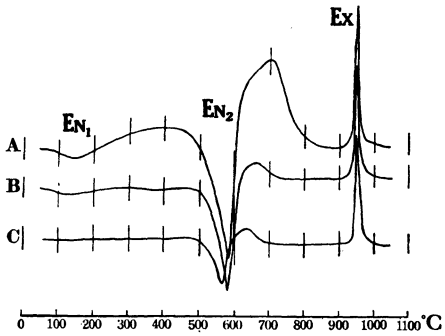

Fig. 4. Differential thermal analysis curves of heat-treated specimens of Kibushi-clay.
A, original clay
B, treated at 400°C
C, treated at 545°C

Fig. 4 shows the differential thermal analysis curves taken in the process of heat-treatment of Kibushi-clay and Table II gives data obtained from these curves. In the original sample, a weak endothermic reaction appears, associated with the loss of adsorbed or inter-layer water. In the 200°C and 400°C heat-treated specimens, the presence of weak but clear endothermic reaction is still observable. This might be due either to the fact that, after the heat-treatment it adsorbs water vapor so rapidly from the atmospheric air, or to the fact that the inter-layer water still remains even after the heat-treatment. The presence of such reactions in the heat-treated Kibushi-clay indicates that the degree of crystallinity of this clay is low. Similar phenomena are also observable in halloysite with a lower degree of crystallinity. For the endothermic and the exothermic reactions, the features in the variation of these reactions are similar to those of kaolinite, but these features are more pronounced.

Density.—The change in the density with the heat-treatment is shown in Fig. 5. The

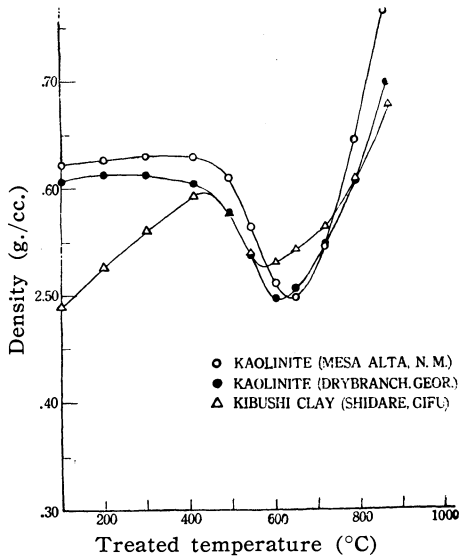

Fig. 5. Curves showing the changes of the density with the treated temperature.

density changes to a maximum through heat-treatment, then it falls and reaches the minimum value at the point where the lattice water is lost, finally it increases again rapidly. It can be seen that the higher the crystallinity is, the lower is the temperature correspoding to the maximum value on the density curve, and the higher is the temperature corresponding to the minimum value. This is correlated with the fact that as the internal degree of crystallinity is lower, the lattice water is lost at a lower temperature. The fact that the density of Kibushi-clay sharply increases in the early stage of heat-treatment is due to the presence of organic substance in it. The organic substance is slowly carbonized and oxidized through heat-treatment, and it is released as carbon dioxide. This corresponds to the fact that size of a broad exothermic reaction which appears just byond 600°C on the differential thermal analysis curve becomes smaller and smaller as the heat-treatment temperature rises.

The minimum value of density where the lattice water is lost, has no relation to the degree of crystallinity in either the kaolinite or the fireclay. Past the minimum point, the density increases almost in a straight line. The curve is steeper as the degree of crystallinity of the original sample is higher. It is evident that the rearrangement of ions is occurring in the lattice of the metakaolin state prior to

the mullite nucleation after the loss of lattice water. It is supposed that the stronger the structure of the original sample is, the faster and more perfect is the rearrangement of ions for the mullite nucleation.

Mechanism of Structural Change of Kaolinite and Kibushi-clay with Heat-Treatment.—The crystallinity of kaolin minerals consists of two elements as described in the previous paper[3], that is the degree of crystallinity in stacking of layers, and the internal degree of crystallinity in each layer. In the heat-treatment process of kaolinite and Kibushi-clay, there are two opposite processes. In the structural change of these clays in the early stage of heat-treatment, a minute water adsorbed on the surface of its crystallite or existing between micelles which is not detectable by th thermal curve, is lost gradually, and from this fact, it can be considered that its apparent crystallite size increases owing to the aggregation of several neighbouring crystallites. The apparent crystallite size becomes larger than that of the original crystallite. This tendency is remarkable particularly along the direction of *c*-axis which is perpendicular to the layer plane. Also the value of the density increases and the progress of the crystallinity is observable. In the next stage, the loss of the lattice water in the kaolin mineral takes place. At the beiginning of this reaction, the kaolin mineral transforms suddenly to metakaolin, and this lead to the amorphous structure in the X-ray diagram. In the metakaolin state which is realized prior to the mullite nucleation from the metakaolin, no observable indication for the structural change can be seen in the X-ray diagram. However, it is evident that, in the metakaolin structure, the rearrangement of ions takes place for the mullite nucleation. The rate of rearrangement depends on the crystallinity of the original sample. The higer the original crystallinity is, the more perfect is the rearrangement, and the more clearly can the mullite nucleation be seen. Compared with Kibushi-clay, in kaolinite the rearrangement proceeds more remarkably.

Summary

The structural change of kaolinite and Kibushi-clay with heat-treatment in the relatively low temperature region has been studied. It has been found that there are generally three processes, and that the structural change depends on the degree of crystallinity of the original samples.

Department of Chemistry
Faculty of Science
The University of Tokyo
Hongo, Tokyo

Electronic Structure of Phenol

By Kichisuke NISHIMOTO and Ryoichi FUJISHIRO

(Received July 5, 1958)

Effects of substituents on the electronic structures of reference hydrocarbons are very important from the standpoint of understanding their molecular properties. Hence, much work has been carried out in this domain. As far as the quantitative interpretation of the electronic spectra is concerned, satisfactory results have not yet been obtained, because of the difficulties in calculating the inter-electronic repulsion integrals.

In the previous papers[2], we studied the electronic structures of nitrogen heterocycles by semi-empirical *SCF* method with satisfactory results. In these cases, the repulsion integrals were approximated by the simplified formula.

In this paper, the semi-empirical calculation is applied to the electronic structure of phenol, assuming some further approximations.

Outline of the Method.—The method used is similar to that of Pariser-Parr[3]. It is based on the framework of the method for antisymmetrized products, in *LCAO* approximation, including configuration interaction, with only $2px$ electrons considered explicitly.

The molecular orbitals (*MO*), φ_i, are expressed in the form

$$\varphi_i = \sum_{\mu} c_{\mu i}\phi_{\mu} \tag{1}$$

where ϕ_{μ} is the μ th $2px$ atomic orbital (*AO*), and $c_{\mu i}$ are the coefficients to be determined by the variational method. We give each electron a molecular spin orbital (*MSO*) which is given by the product of coordinate function φ_i and spin function α or β. The configurational wave functions χ_n, for the system are constructed from the antisymmetrized product, or Slater determinant, of these *MSO*'s. A given electronic state function, ψ_a, is represented by a linear combination of these configurational functions;

$$\psi_a = \sum_n A_{an}\chi_n \tag{2}$$

In the case of excited configuration, χ_n is written as ${}^1\chi_{i\to j}$ or ${}^3\chi_{i\to j}$ which denote a singlet or a triplet excited configuration caused by the excitation of an electron from an occupied orbital φ_i to a vacant orbital φ_j.

The energies of the electronic state are determined by solving a secular determinant

$$\mathrm{Det}\,|H_{mn}-\delta_{mn}E| = 0 \tag{3}$$

and the coefficients A_{an} are obtained by the solution of simultaneous equations

$$\sum_n A_{an}(H_{mn}-\delta_{mn}E) = 0 \tag{4}$$

where

$$H_{mn} = \int \chi_m^* \boldsymbol{H} \chi_n \mathrm{d}v$$

and $\delta_{mn}=1$ if m=n, $=0$ otherwise.

$\boldsymbol{H}$ is the complete electronic Hamiltonian operator determining the motion of the π-electrons, which is expressed in the form

$$\boldsymbol{H} = \sum_i H_{\mathrm{core}}(i) + \frac{1}{2}\sum_{ij}\frac{e^2}{r_{ij}} \tag{5}$$

According to the method described by Mulliken and Rieke[4], oscillator strength, f, associated with a transition between the ground state ψ_0 and an excited state ψ_i is calculated as

$$f = 1.085\times 10^{11} \times \omega_{0i} \sum_{\gamma=x,y,z} (M^{\gamma}{}_{0i})^2 \tag{6}$$

where ω_{0i} is the frequency of the transition in cm^{-1} and $M^{\gamma}{}_{0i}$ is the transition moment defined by

1) G. W. Wheland and L. Pauling; *J. Am. Chem. Soc.*, **57**. 2086 (1935).
A. L. Sklar, *J. Chem. Phys.*, **7**, 984 (1939).
K. F. Herzfeld, *Chem. Revs.*, **41**, 233 (1947).
F. A. Matsen, *J. Am. Chem. Soc.*, **72**, 5243 (1950).
S. Nagakura and J. Tanaka, *J. Chem. Phys.*, **22**, 236 (1954).
F. J. I. López-Vázquez, *An. Soc. Esp. Fis. y Qui.*, (Madrid), **51B**, 203 (1955) etc.

2) K. Nishimoto and N. Mataga, *Z. physik. Chem.* (N. F.) **12**, 335 (1957).
N. Mataga and K. Nishimoto, ibid., **13**, 140 (1957).

3) R. Pariser and R. G. Parr, *J. Chem. Phys.*, **21**, 466, 767 (1953); ibid., **23**, 711 (1955).
R. Pariser, ibid., **24**, 250 (1956).

4) R. S. Mulliken and C. A. Rieke, *Rep. Progr. Phys.*, **8**, 231 (1941).

$$M_{0i} = \int \psi_0^* \sum_t e_t \mathbf{r}_t \psi_i \mathrm{d}v \qquad (7)$$

where e_t and $\mathbf{r}_t$ are the charge and the position vector of the t-th charged particle, respectively.

The π-electronic dipole moment, μ_π, is expressed in a similar form:

$$\mu_\pi = \int \psi_0^* \sum_t e_t \mathbf{r}_t \psi_0 \mathrm{d}v \qquad (8)$$

In our calculation, the following approximations are used.

1) As a set of *LCAO MO*'s, the conventional semi-empirical *MO*'s are chosen.

2) Differential overlap is neglected.

3) Values of some theoretical quantities are estimated by the empirical or semi-empirical procedure.

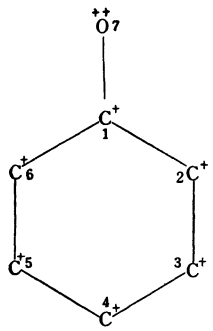

Fig. 1. Core structure of phenol.

4) The core structure of the molecule is shown in Fig. 1. Benzene ring is made up of the hexagone, with all nearest *C–C* distances equal to 1.390 Å. *C–O* distance is taken as 1.460 Å[5] which is the value of methyl acetate.

5) In the calculation of the configuration interaction, only the ground state configuration and the four lowest singly excited configurations are taken into account.

Calculation of Conventional Semi-empirical *MO*'s.—The core field of phenol pictured in Fig. 1 belongs to the symmetry group C_{2v}. It is, therefore, more convenient to express *MO*'s in terms of symmetry orbitals, σ_t, constructed from the *AO*'s according to the symmetry of the molecule;

$$\phi_i = \sum_t c_{ti}\sigma_t$$

σ_t's are written in the form,

$$\sigma_1 = \phi_1 \qquad \sigma_2 = \phi_2 + \phi_6 \qquad \sigma_3 = \phi_3 + \phi_5$$

$$\sigma_4 = \phi_4 \qquad \sigma_5 = \phi_7 \qquad (9)$$

$$\sigma_6 = \phi_2 - \phi_6 \qquad \sigma_7 = \phi_3 - \phi_5 \qquad (10)$$

The orbitals (9) belong to the representation B_1 and the orbitals (10) to A_2. The coefficients, c_{ti}, are determined by minimizing the expression for the energy, ε,

$$\varepsilon = \int \varphi^* H^e \varphi \mathrm{d}v \Big/ \int \varphi^* \varphi \mathrm{d}v$$

where H^e is the total effective Hamiltonian.

The matrix elements are assumed as follows,

i) When μ and ν are both carbon atoms,

$$H^e_{\mu\mu} = \int \phi_\mu^* H^e \phi_\mu \mathrm{d}v = \alpha$$

$$H^e_{\mu\nu} = \int \phi_\mu^* H^e \phi_\nu \mathrm{d}v = \beta \quad (\mu\nu: \text{neighbor})$$

$$H^e_{\mu\nu} = 0 \quad (\mu\nu: \text{non-neighbor})$$

ii) When μ is an oxygen atom,

$$H^e_{77} = \alpha + \delta\beta$$

δ is determined to be 1.5 by the combination of the ionization potentials of CH_3OH and C_6H_6[6], setting the value of β equal to 3 eV[7].

iii) When μ is an oxygen atom and ν a carbon atom located at the position indicated by 1 in Fig. 1.

$$H^e_{71} = k\beta$$

where the value of k is chosen so as to bring the difference between the calculated energies of the highest occupied orbitals for benzene and phenol close to that between the observed ionization potentials[6] for them. Thus the suitable value is found to be 0.7.

The calculated orbital energies and the corresponding *MO*'s, using above mentioned parameters, are given in Table I.

The four *MO*'s, φ_1, φ_2, φ_3, and φ_4, are occupied by two electrons, respectively, and they form closed shells. The other three are vacant orbitals.

Semi-empirical Evaluation of Some Theoretical Quantities.—Molecular integrals appearing in eqs. 3 and 4 are expanded in terms of atomic integrals which are divided into two groups, one of the type of core integrals and one of the type of repulsion integrals. These quantities are adjusted by the empirical or semi-empirical procedure which is similar to that of Pariser-Parr, but somewhat different.

(1) By the assumption of zero differential overlap, only the two electron

5) J. M. O'Gorman, Jr., W. Shand and V. Schomaker, *J. Am. Chem. Soc.*, **72**, 4222 (1950).

6) K. Watanabe, *J. Chem. Phys.*, **26**, 542 (1997).

7) R. S. Mulliken, *Phys. Rev.*, **74**, 736 (1948).

TABLE I
CONVENTIONAL SEMI-EMPIRICAL *MO*'S OF PHENOL

Orbital energies in β	*MO*
2.1754	$\varphi_1=0.4955\sigma_1+0.3592\sigma_2+0.2860\sigma_3+0.2630\sigma_4+0.5134\sigma_5$
1.6266	$\varphi_2=0.1269\sigma_1-0.1423\sigma_2-0.3584\sigma_3-0.4407\sigma_4+0.7016\sigma_5$
1.0000	$\varphi_3=0.5000\sigma_6+0.5000\sigma_7$
0.7869	$\varphi_4=0.4692\sigma_1+0.3458\sigma_2-0.1971\sigma_3-0.5009\sigma_4-0.4606\sigma_5$
−1.0000	$\varphi_5=-0.5000\sigma_6+0.5000\sigma_7$
−1.0642	$\varphi_6=0.5733\sigma_1-0.2503\sigma_2-0.3070\sigma_3+0.5770\sigma_4-0.1566\sigma_5$
−2.0248	$\varphi_7=0.4353\sigma_1-0.4105\sigma_2+0.3958\sigma_3-0.3909\sigma_4-0.0864\sigma_5$

repulsion integrals of the type $(\mu\mu|\nu\nu)$ may be considered. These are assumed to be as follows,

$$(\mu\mu|\nu\nu)=\int\phi_\mu^*(1)\phi_\nu^*(2)e^2/\mathbf{r}_{12}\phi_\mu(1)\phi_\nu(2)\mathrm{d}v$$
$$=e^2/(a+r_{\mu\nu})$$

where $r_{\mu\nu}$ is the interatomic distance between μ and ν atoms. The parameter a is determined in the following way, using the valence state ionization potential, I_μ, and the electron affinity, A_μ, in the same valence state.

(a) For the case of homonuclear two centers, we put

$$e^2/a=(\mu\mu|\mu\mu)=I_\mu-A_\mu$$

(b) For the case of heteronuclear two centers, i. e., for carbon and oxygen, we take as e^2/a, simple arithmetic mean of e^2/a's for carbon and oxygen.

The values of I_μ and A_μ for carbon are found in the paper of Pritchard-Skinner[8]. For the case of oxygen, I_μ and A_μ may be equal to the second and the first ionization potentials, respectively, because as shown in Fig. 1 the oxygen core has doubly positive charges. Unfortunately, the second ionization potential of oxygen in the valence state has not yet been established. Assuming that the promotion energies from the second ionized state and the first ionized state of oxygen to their valence states are the same, $(I_\mu-A_\mu)$ obtained by the spectroscopic method may be equal to that of the valence state values. The spectroscopic values are found in Ref. (9). Using the above assumption, we find

$$a_{CC}=1.328\ \text{Å}$$
$$a_{CO}=0.889\ \text{Å}$$

For the carbon two centers, in order that our expression for $(\mu\mu|\nu\nu)$ may coincide with one computed by Slater's atomic orbital, the effective nuclear charge, Z, must be put equal to 2.036 at $r_{\mu\nu}=0$[10] and decrease with the increase of $r_{\mu\nu}$.

Since the σ-core is not a point charge, but consists of a nucleus and many electrons surrounding it, it stands to reason that Z approaches to unity with the increase of $r_{\mu\nu}$ considering that the screening of the electrons against the nucleus becomes more and more complete with the increase of $r_{\mu\nu}$. In many papers published hitherto, the effect of the variation of effective nuclear charge has been neglected. Treatment taking such an effect into consideration seems to be desirable.

(2) The core integrals, $H_{\mu\nu}^{\text{core}}$, are given by

$$H_{\mu\nu}^{\text{core}}=\int\phi_\mu^*(1)H_{\text{core}}\phi_\nu(1)\mathrm{d}v$$

Pariser-Parr have given the following expressions for $H_{\mu\nu}^{\text{core}}$

$$H_{\mu\mu}^{\text{core}}=-\sum_\nu(\mu\mu|\nu\nu)-A_\mu$$

$$H_{\mu\nu}^{\text{core}}=\beta_{\mu\nu}\qquad(\mu\nu:\text{ neighbor})$$

$$H_{\mu\nu}^{\text{core}}=0\qquad(\mu\nu:\text{ non-neighbor})$$

For the case of an oxygen atom, the value of A_μ is chosen somewhat arbitrarily in the following way. On the calculation of simple *MO*'s, we have taken the value of $\delta=1.5$ for H^e_{77}. $H^e_{\mu\nu}$'s formally correspond to the matrix elements of the Hartree-Fock Hamiltonian, $F_{\mu\nu}$, which are expressed by

$$F_{\mu\nu}=\int\phi_\mu^*\boldsymbol{F}\phi_\nu\mathrm{d}v$$

where $\boldsymbol{F}$ is the Hartree-Fock Hamiltonian which is composed of the core operator, $\boldsymbol{H}$, and an operator concerned with the electron interaction, $\boldsymbol{G}$. If we put $F_{77}=\langle F_{CC}\rangle+1.5\langle F_{12}\rangle$ and calculate, using the approximated formula proposed by

8) H. O. Pritchard and H. A. Skinner, *Chem. Revs.*, **55**, 745 (1955).
9) C. E. Moore, "Atomic Energy Levels" Vol. 1 (1949), The National Bureau of Standards, Washington.
10) R. G. Parr and B. L. Crawford, *J. Chem. Phys.*, **16**, 1049 (1948).

Pople[11], A_μ amounts to 11.649 eV, where $<>$ means the simple arithmetic average about the relating matrix elements. In a similar way, if we put $H_{17}=0.7<F_{12}>$, it is found to be $\beta_{CO}=-2.115$ eV. The value of β_{CC} is the same as in the previous papers.

Results and Discussion

In the calculation of configuration interaction, the four lowest singly excited configurations, $\chi_{4\to5}$, $\chi_{4\to6}$, $\chi_{3\to5}$, and $\chi_{3\to6}$, and ground state χ_0 are taken into account. $\chi_{4\to5}$ and $\chi_{3\to6}$ belong to the irreducible representation B_2 and the other three to A_1. According to the symmetry consideration, the secular determinant of 5th degree is factorized into two determinants, one degree and one of 3rd degree. The computed energies of configurations and the interconfigurational matrix elements, using the above described semi-empirical quantities are given inTable II.

TABLE II
VALUES OF THE ENERGIES OF CONFIGURATIONS AND THE INTERCONFIGURATIONAL MATRIX ELEMENTS IN eV UNITS

$E(\chi_0)$	0	$(^1\chi_{3\to5}\|\boldsymbol{H}\|\chi_0)$	0.020
$E(^1\chi_{3\to5})$	6.556	$(^1\chi_{4\to6}\|\boldsymbol{H}\|\chi_0)$	0.049
$E(^1\chi_{3\to6})$	6.018	$(^1\chi_{3\to5}\|\boldsymbol{H}\|^1\chi_{4\to6})$	−0.313
$E(^1\chi_{4\to5})$	5.264	$(^1\chi_{4\to5}\|\boldsymbol{H}\|^1\chi_{3\to6})$	0.927
$E(^1\chi_{4\to6})$	5.770	$(^3\chi_{3\to5}\|\boldsymbol{H}\|^3\chi_{4\to6})$	−0.375
$E(^3\chi_{3\to5})$	3.610	$(^3\chi_{4\to5}\|\boldsymbol{H}\|^3\chi_{3\to6})$	−0.375
$E(^3\chi_{3\to6})$	4.638		
$E(^3\chi_{4\to5})$	3.914		
$E(^3\chi_{4\to6})$	3.280		

The calculated excitation energies and oscillator strengths are presented in Table III, in comparison with the observed values, and the corresponding electronic state wave functions are collected in Table IV.

TABLE III
CALCULATED AND OBSERVED EXCITATION ENERGIES (IN eV) AND OSCILLATOR STRENGTHS

	Excitation energies		Oscillator Strengths	
	Calcd.	Obsd.	Calcd.	Obsd.
$^1B_2^-$	4.640	4.59[a]	0.022	0.02[b]
$^1A_1$	5.662	5.89[a]	0.251	—
$^1B_2^+$	6.642	—	0.987	—
$^1A_1$	6.667	—	0.971	—
$^3A_1^+$	3.035	—	0	—
$^3B_2^+$	3.755	—	0	—
$^3A_1^-$	3.855	—	0	—
$^3B_2^-$	4.797	—	0	—

a) L. Doub and J. M. Vandenbelt, *J. Am. Chem. Soc.*, **69**, 2714 (1947).
b) R. S. Mulliken, Ref. 4).

As shown in Table III, the agreement between the calculated and the observed values is satisfactory and further improvement will be expected by including other excited configurations and adjusting the core parameters. It may be reasonable to interpret the spectra of phenol in the near-ultraviolet region as those of benzene perturbed by mobile lone pair electrons of the substituent. As shown in our calculation, this correspondence will be explained by considering only four excited configurations. It is interesting to note that in the case of benzene the state energies of $^3B_{2u}^-$ and $^1B_{2u}^-$ which is the radiation emitting state are the same, while in phenol the latter is higher than the former by 0.157 eV which is greater compared with kT. It may be regarded as the principal reason for the appearance of intense fluorescence of phenol, because the radiationless,

TABLE IV
ELECTRONIC STATE WAVE FUNCTIONS AND THEIR ENERGIES

Symmetry	State energy (in eV)	Wave function
A_1	−0.001	$^1\psi_0=\chi_0-0.0092\ ^1\chi_{4\to6}-0.0038\ ^1\chi_{3\to5}$
B_2	4.640	$^1\psi_1=0.8298\ ^1\chi_{4\to5}-0.5581\ ^1\chi_{3\to6}$
A_1	5.661	$^1\psi_2=0.0092\chi_0+0.9439\ ^1\chi_{4\to6}+0.3301\ ^1\chi_{3\to5}$
B_2	6.642	$^1\psi_3=0.5581\ ^1\chi_{4\to5}+0.8298\ ^1\chi_{3\to6}$
A_1	6.666	$^1\psi_4=0.0038\chi_0-0.3301\ ^1\chi_{4\to6}+0.9439\ ^1\chi_{3\to5}$
A_1	3.035	$^3\psi_1=0.8372\ ^3\chi_{4\to6}+0.5469\ ^3\chi_{3\to5}$
B_2	3.755	$^3\psi_2=0.9204\ ^3\chi_{4\to5}+0.3909\ ^3\chi_{3\to6}$
A_1	3.855	$^3\psi_3=0.5469\ ^3\chi_{4\to6}-0.8372\ ^3\chi_{3\to5}$
B_2	4.797	$^3\psi_4=0.3909\ ^3\chi_{4\to5}-0.9204\ ^3\chi_{3\to6}$

11) J. A. Pople, *Proc. Phys. Soc.*, **A68**, 81 (1955).

or thermal, transition is inhibited. The fact that the values of interconfigurational matrix elements among the ground configuration and the excited configurations are small gives us to understand that the calculated conventional semi-empirical *MO*'s are fairly close to the self-consistent field *MO*'s. The π-electronic dipole moment, invoking the assumption of neglect of differential overlap, is calculated as

$$\mu = 1.04\,\mathrm{D}$$

The π-electronic dipole moment should be obtained by subtracting vectorially the σ-electronic dipole moment from the total moment determined experimentally. Unfortunately, the σ-electronic dipole moment has not been estimated, because the information about the σ-electronic states, especially for the substituent, is not enough and, moreover, the σ-core is not rigid, but is affected by the π-electronic state. Hence, we will not discuss this further.

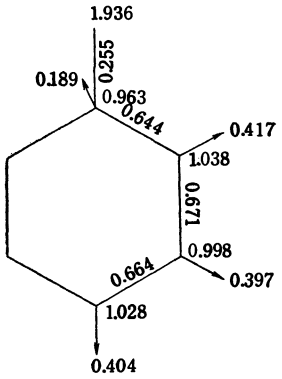

Fig. 2. Molecular diagram of phenol

The molecular diagram calculated by present treatment is shown in Fig. 2. From this diagram it may be expected that;

(i) In the electrophilic reactions, *o-p* substitution takes place.

(ii) The radical reactions take place preferentially at the *o*-positions.

(iii) The C—C bond distances are $C_1—C_2 > C_3—C_4 > C_2—C_3$.

(i) agrees with the experimental facts generally recognized. The information compared with (ii) or (iii) are not available. In the case of anisol which is similar to phenol in the π-electronic configuration, Suehiro[12] reported the order $o > p > m$ in the radical reactivities.

Summary

The electronic structure and spectra of phenol was studied from the semi-empirical point of view, using the *LCAO-ASP-CI-MO* method. The excitation energies and oscillator strengths of transitions to lower excited states were calculated. The agreement between the calculated and the observed values is very good. The charge distribution, bond orders and the π-electronic dipole moment are also calculated.

The authors express their appreciation to Mr. N. Mataga for many valuable discussions.

Institute of Polytechnics
Osaka City University
Kita-ku, Osaka

12) T. Suehiro, *J. Chem. Soc. Japan, Pure Chem. Sec.* (*Nippon Kagaku Zassi*), **72**, 301 (1951).

*Studies on the Thermal Decomposition of Cellulose Nitrate by Means of the Recording Thermal Balance**

By Takehiro ABE, Shōtaro TOBISAWA and Yōkan NOMURA

(Received July 10, 1958)

The products afforded by the thermal decomposition of cellulose nitrate have been investigated by many workers, recently by Wolfrom et al.[1-4] and by others[5,6]. The reaction of thermal decomposition has also been pursued by Will[7,8] and others[9,10] by means of measuring the gases evolved. However, no precise investigation by measuring the decomposition losses in weight has been made, because it is very difficult to measure the losses in weight successively with precision owing to the slow thermal decomposition.

In the present paper, therefore, we have, by means of a recording thermal balance with a high sensitivity, tried to follow the decomposition reaction of cellulose nitrate by raising the temperatures stepwise, after preheating at a low temperature below the decomposition point, or after keeping in reduced pressure.

Experimental

Cellulose nitrate was prepared by immersion of absorbent cotton (5 g.) into a mixed acid (303 cc.) of sulfuric acid (sp. gr.: 1.84, 171 cc.) and nitric acid (sp. gr.: 1.50, 110 cc.) at about 20°C for two hours. The product was washed thoroughly, and boiled with distilled water many times until a litmus paper did not show any trace of acidity on the wet cellulose nitrate. After being squeezed out, the cellulose nitrate was dried under vacuum for a day and kept in a desiccator. The cellulose nitrate contains 10.6% of nitrogen.

A recording magnetic balance devised by Hirone, Maeda and Tsuya[11] was used as our thermal balance without magnetic field. This balance, plotting automatically the loss in weight

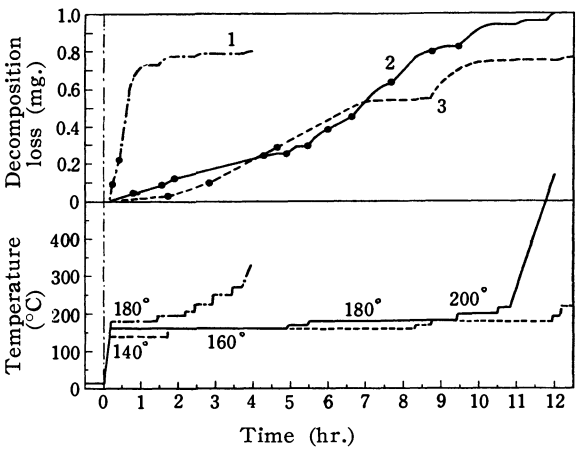

Fig. 1. Thermal decompositions by raising temperatures stepwise.

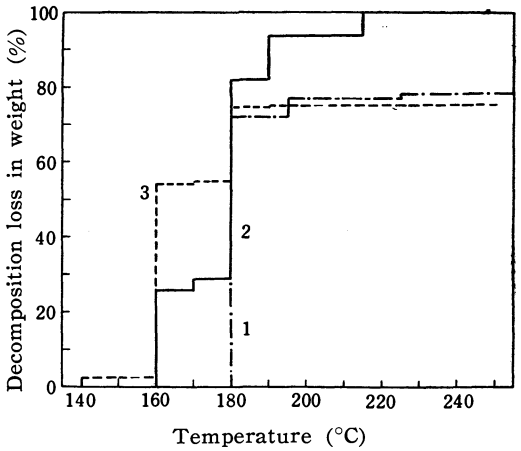

Fig. 2. Relation between the temperature and the decomposition loss in Fig. 1.

* Presented before the 10th Annual Meeting of the Chemical Society of Japan held at Tokyo in April, 1957.

1) M. L. Wolfrom et al., *J. Am. Chem. Soc.*, **77**, 6573 (1955).
2) M. L. Wolfrom et al., ibid., **78**, 4695 (1956).
3) M. L. Wolfrom, A. Chaney and P. McWain, ibid., **80**, 946 (1958).
4) F. Shafizadeh and M. L. Wolfrom, ibid., **80**, 1675 (1958).
5) R. W. Phillips, C. A. Orlick and R. Steinberger, *J. Phys. Chem.*, **59**, 1034 (1955).
6) G. Gelernter, L. C. Browing, S. R. Harris and G. M. Mason, ibid., **60**, 1260 (1956).
7) W. Will, *Fahresbericht der Centralstelle für wissenschaftlich-technische Untersuchungen.* **2** (1900).
8) W. Will, ibid., **3** (1900).
9) T. Hikita, *J. Ind. Explosives Soc., Japan*, **8**, 11 (1947).
10) E. K. Rideal and A. J. B. Robertson, "Third Symposium on Combustion and Flame", Reinhold, Baltimore (1949).
11) T. Hirone, S. Maeda and N. Tsuya, *Rev. Sci. Instr.*, **25**, 516 (1954).

vs. temperature curves of substances, was modulated to be able to indicate distinct differences of 0.02 mg. on a recorded chart. All samples in weight 1.0 mg. were packed in small quartz baskets and thermally decomposed under the pressure of about 50 mmHg, which was necessary for our present instrument.

Results and Discussion

Thermal decomposition by raising temperatures stepwise (Fig. 1).—The cellulose nitrate was decomposed at a constant temperature, and then at a higher temperature after a loss in weight stopped at the former temperature. Temperature was raised in this way. It is remarkable that several breaking points appear on each decomposition curve at constant temperatures. In Fig. 2 it is shown that a greater part of the cellulose nitrate decomposes at 160 and 180°C.

Thermal decomposition at constant temperature (Fig. 3).—As a matter of course, the higher the reaction temperature, the faster becomes the decomposition rate with an increase in the decomposition loss in weight. There appears no breaking point on the decomposition curve at 190°C.

The modes of decomposition at 140 and 150°C, giving only several per cent losses in weight, are different from those above 160°C. The loss in weight below 150°C is, therefore, is not considered to be due to the decomposition of cellulose nitrate itself, but is probably due to the volatilization of absorbed water, as mentioned below. Consequently, the decomposition temperature of the cellulose nitrate may be at about 160°C.

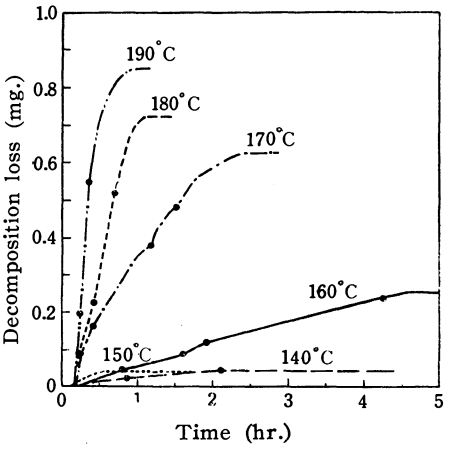

Fig. 3. Thermal decompositions at constant temperatures.

Thermal decomposition after preheating at low temperatures below the decomposition point.—a) In Fig. 4 it is shown that the thermal decomposition at 160°C after preheating at 140 or 150°C for an hour and a half gives a greater loss in weight than that without preheating.

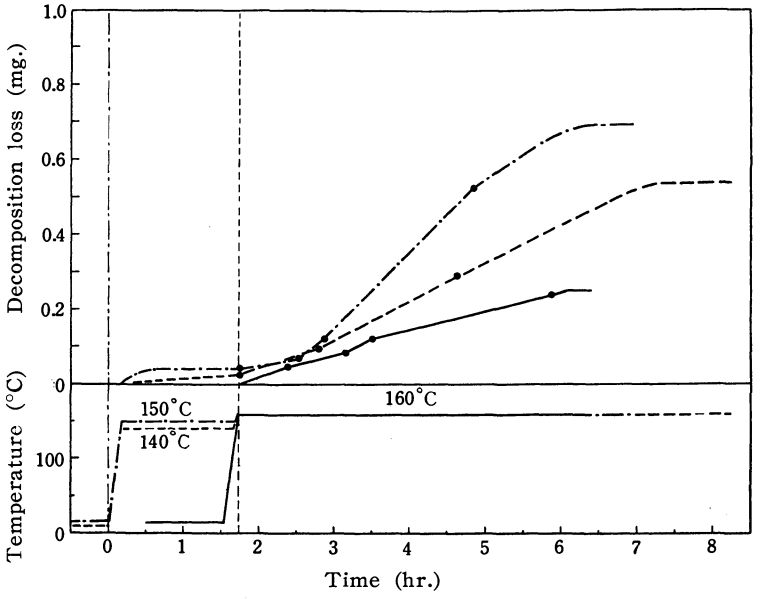

Fig. 4. Thermal decomposition after preheating.
——: not preheated.
------ and —·—: preheated at 140 and 150°C, respectively.

The sample preheated at 150°C decomposes more than that preheated at 140°C.

b) As shown in Fig. 5, the decomposition rate after preheating at 140°C for a long time is slower than that preheated at the same temperature for a short time. Both decompositions give about the same loss in weight.

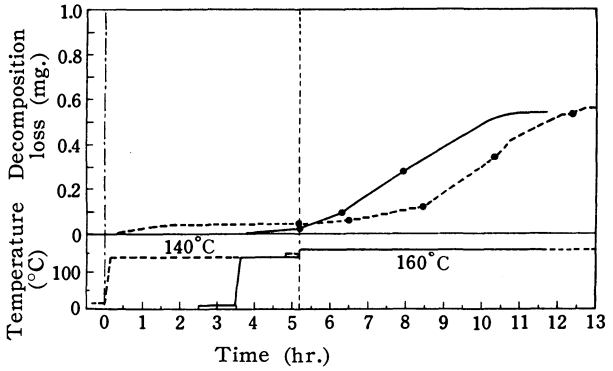

Fig. 5. Thermal decomposition after preheating at 140°C.
——: for a long time.
------: for a short time.

From the above results it is known that a thermal decomposition after preheating at a temperature slightly below the decomposition point for an hour or so results in greater decomposition loss in

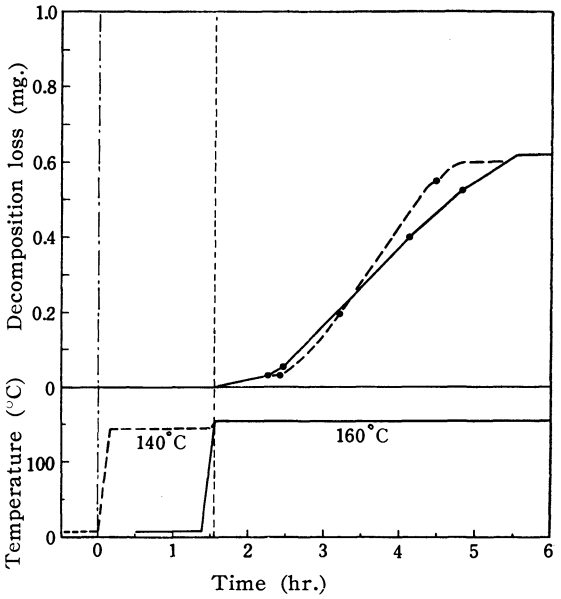

Fig. 6. Thermal decomposition after keeping under a reduced pressure and preheating.
——: not preheated.
------: preheated at 140°C.

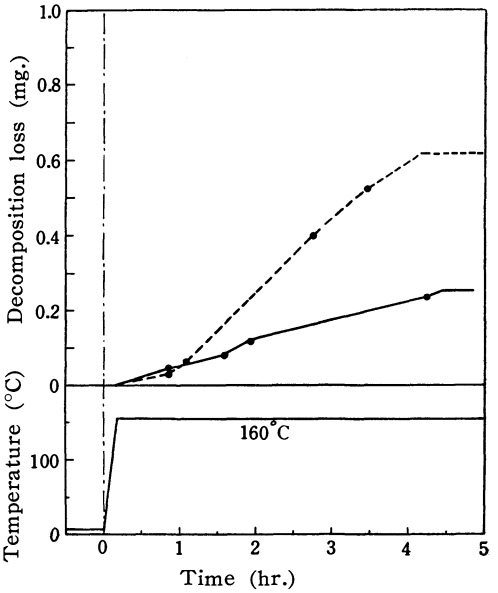

Fig. 7. Thermal decompositions after keeping under a reduced pressure.
——: without this procedure.
------: with this procedure.

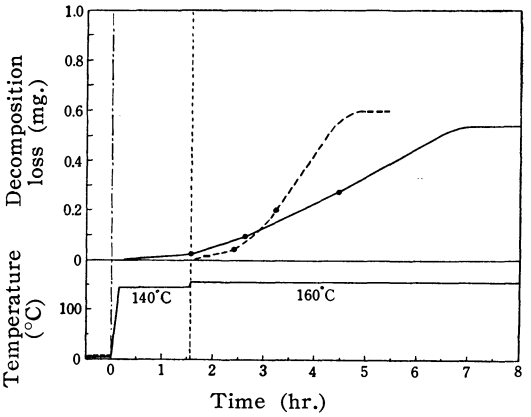

Fig. 8. Thermal decomposition after keeping under a reduced pressure and at 140°C.
——: only preheated.
------: low pressure and preheating.

weight than that without preheating.

Thermal decomposition after keeping a reduced pressure. — After being kept previously under reduced pressure of about 10^{-2} mmHg for four hours in the apparatus, the samples were decomposed under the same condition as measured before.

a) As seen in Fig. 6, the sample kept previously under a reduced pressure of 10^{-2} mmHg and preheated, decomposes rather faster than that kept only under a reduced pressure although both samples yield about the same loss in weight.

Heating the sample at 150°C results in no loss in weight, although the samples, which are not kept previously under a pressure of 10^{-2} mmHg, give several per cent loss in weight, as indicated in Figs. 1, 3, 4 and 5. These loss in weight below 150°C seems to be probably due to the volatilizations of water absorbed strongly by the cellulose nitrate in the air, since they can not be observed by keeping the samples previously under a pressure of 10^{-2} mmHg.

b) It is found from Fig. 7 that the sample kept previously in the reduced pressure yields a greater decomposition loss than that without any treatment.

c) As shown in Fig. 8, the decomposition of the sample kept previously under a reduced pressure and at 140°C, proceeds faster than that of the sample only preheated although there is no great difference between the decomposition losses of the two samples.

Summary

(1) The cellulose nitrate containing 10.6% of nitrogen decomposes above about 160°C. There appear distinct breaking points on the decomposition curves at constant temperatures slightly above the decomposition point. The higher the constant temperature of reaction, the greater becomes the decomposition loss in weight.

(2) The thermal decomposition after preheating at a temperature slightly below the decomposition point for an hour or so gives a greater loss of decomposition than that without preheating.

(3) The cellulose nitrate kept previously under a reduced pressure of about 10^{-2} mmHg yields a greater decomposition loss in weight than that without any treatment.

Department of Chemistry
Defense Academy
Yokosuka, Kanagawa

Ring Cleavage in Liquid Sulfur Dioxide. I. Cleavage of Cyclic 1,2-Diketone Monoximes

By Daisaburo MURAKAMI and Niichiro TOKURA

(Received July 7, 1958)

When a 1,2-diketone 1-monoxime is treated under the conditions of the Beckmann rearrangement, it is cleaved into two fragments, a cyano compound and a carboxylic acid[1,2]. This reaction, designated as the Beckmann rearrangement of the second order[2,3], is distinguished from the normal Beckmann rearrangement in its mechanism.

$$R-\overset{O}{\overset{\|}{C}}-\overset{NOH}{\overset{\|}{C}}-R' \longrightarrow RCOOH+R'CN$$

Usually the reaction is conducted in a basic solvent such as pyridine[2,4] at its refluxing temperature with an aromatic sulfonic acid or its chloride as the reagent[2]. Sulfuric acid, phosphoric acid, hydrochloric acid in acetic acid, and phosphorus compounds are used sometimes as the reagents but their use is limited because of inevitable side reactions. For example, 9,10-phenanthrenequinone 9-monoxime (II) gives a fluorenone derivative[1,3].

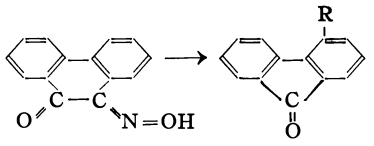

R=CN or $CONH_2$

(II)

Considering the characteristic properties of liquid sulfur dioxide as solvent, the authors studied ring opening reactions of some cyclic 1, 2-dione 1-monoximes in liquid sulfur dioxide, expecting smoother

1) a. E. Beckmann and A. Koster, *Ann.*, **274**, 15 (1893). b. E. Beckmann and O. Liesche, *Ber.*, **56**, 1 (1923). c. E. Beckmann and P. Wegerhoff, *Ann.*, **252**, 14 (1889).
2) A. Werner and A. Piguet, *Ber.*, **37**, 4293 (1904).
3) W. Borsche and W. Sander, ibid., **47**, 2825 (1914).
4) a. M. Gates, *J. Am. Chem. Soc.*, **72**, 228 (1950). b. B. Rapoport and J. Z. Pasky, ibid., **78**, 3788 (1956).

cleavages under milder conditions than in previously reported cases. Three typical diketone monoximes, viz., 1,2-naphthoquinone 1-oxime (I), 9,10-phenanthrenequinone 9-oxime (II) and tetralin-1,2-dione 2-oxime (III), were chosen.

Among various reagents tried, thionyl chloride only was found to effect the ring opening of I to *o*-cyanocinnamic acid (IV) in liquid sulfur dioxide. Toluenesulfonyl chloride and phosphorus pentoxide were slightly effective, but sulfur trioxide, sulfuric acid, phosphorus oxychloride, sulfuryl chloride, phosphorus pentachloride and aluminum chloride gave always resinous matters containing nitrogen.

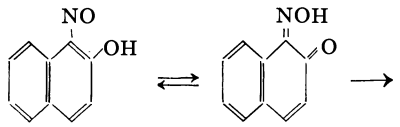

(I)

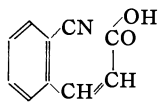

(IV)

Effects of the reaction time and temperature were studied with the results listed in Table 1.

TABLE I

EFFECTS OF REACTION TIME AND TEMPERATURE ON RING OPENING OF 1,2-NAPHTHOQUINONE 1-OXIME IN LIQUID SULFUR DIOXIDE

Expt.	Thionyl chloride/naphthoquinone monoxime (Mole Ratio)	Reaction temp. °C	Reaction time	Yield (%)
1	3	−20	10 days	5
2	1	15	12 hrs.	10
3	1	15	10 days	40
4	1	50	6 hrs.	51
5	1	70	6 hrs.	54
6	2	70	6 hrs.	48
7	1	100	6 hrs.	46

The best yield (54 percent) recorded in Table I is a great improvement if compared with the result obtained by Borsche[3] (1 g. of *o*-cyanocinnamic acid chloride from 17.3 g. of I). The temperature over 100°C caused a decrease in the yield of *o*-cyanocinnamic acid (IV) and an increase in resinous matters in the product.

9,10-Phenanthrenequinone 9-monoxime (II) was treated in the same way. By six hours' reaction at 70°C 2-cyanobiphenyl-2'-carboxylic acid (V) was obtained in a yield (60 percent) much greater than that reported previously[2]. As a by-product, diphenic acid imide (VI) was obtained in a yield of 11 percent. No fluorenone derivative was found in the reaction products[3].

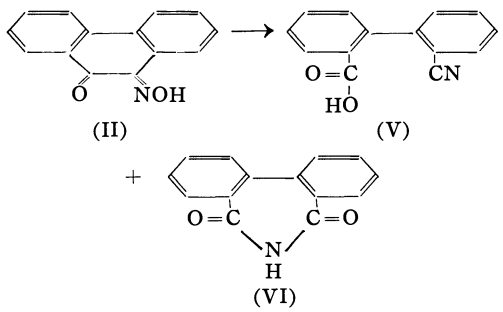

(II) (V)

(VI)

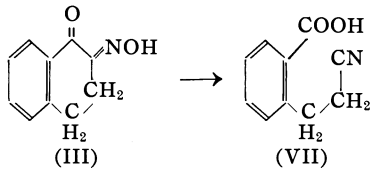

(III) (VII)

No attempt has been reported on the cleavage of tetralin-1,2-dione 2-oxime (III). When the oxime was treated with thionyl chloride at 70°C for six hours in liquid sulfur dioxide, an almost quantitative yield (98%) of *o*-(2-cyanoethyl)benzoic acid (VII) was obtained. The experimental results are summarized in Table II.

The *trans*-migration in the Beckmann rearrangement has long been established[5]. The group in *anti* position to the hydroxyl group may shift to the nitrogen atom by rearrangement, which proceed, as is well recognized, through a nitrogen cation intermediate (IX) and intramolecular migration of the anion R.

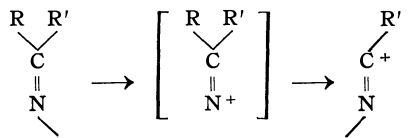

(VIII) (IX) (X)

In such a rearrangement it may not be possible for either a bulky group or a sterically strained group to take part. The carbon atom starred in XI could not migrate[6] owing to its double bond strain

5) B. Jones, *Chem. Revs.*, **35**, 355 (1944).
6) F. J. Donat and A. L. Nelson, *J. Org. Chem.* **22**, 1107 (1957).

TABLE II
RING-OPENING OF 1,2-DIKETONEMONOXIMES WITH THIONYL CHLORIDE IN LIQUID SULFUR DIOXIDE

Compound	React. temp. (°C)	React. time (hr.)	Product	Yield (%)
1,2-naphthoquinone 1-oxime (I)	70	6	*o*-cyanocinnamic acid (IV)	54
9,10-phenanthrene-quinone 9-oxime (II)	70	6	2-cyanobiphenyl-2'-carboxylic acid (V) diphenic acid imide (VI)	60 11
tatralin-1,2-diketone 2-oxime (III)	70	6	*o*-(2-cyanoethyl)-benzoic acid (VII)	98

in a ring. Also ketoximes having bulky groups such as phenyl in XII[7] or *tert*-butyl[8] in XIII could not yield acid amides, and often gave cyano compounds.

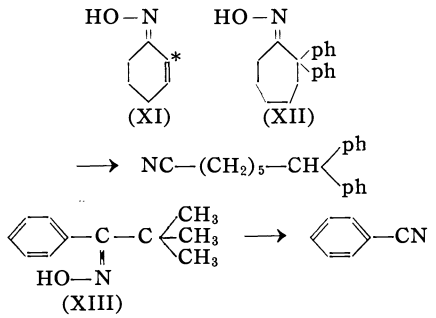

In naphthoquinone monoxime (I), the isonitrosomethylene group is sterically restricted in two ways, namely, by the condensation of a benzene ring and by the ring closure of groups on both its sides. Carbon atom 8a in I is inhibited from taking part in the rearrangement, and it may be impossible for carbon atom 2 to migrate to the nitrogen atom, since a steric interaction may prohibit the hydroxyl group from taking a *syn*-position to the condensed benzene ring, and thus the formation of dicarboxylic acid imide XIV may be improbable.

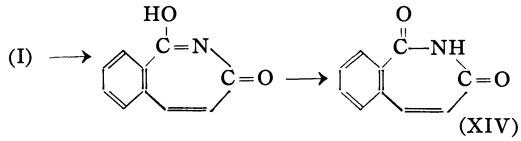

The present authors would not like to consider the dicarboxylic acid imide (XIV) as a precursor or an intermediate to *o*-cyanocinnamic acid (IV), because then one more final product (XV) would be expected from the imide (XIV).

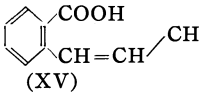

In the present study each cleavage gave only one kind of cyano acid, which resulted from a cleavage between the carbonyl group and the isonitrosomethylene group and a migration of the hydroxyl group. No isonitrile was found in the reaction product.

The only explanation for such a cleavage was presented by Blatt and Barnes[9] in 1934. However, little can be said regarding the mechanism of the cleavage reaction of the cyclic dione monoxime system, except some explanation of the cause which hinders the normal Beckmann rearrangement from taking place.

A superior method for preparing cyanocarboxylic acids by the cleavage in liquid sulfur dioxide may find a wide application in synthetic organic chemistry. Experiments in such a direction are now in progress.

Experimental

Solvent, reagents and apparatus.—Commercial liquid sulfur dioxide was distilled after dehydration with concentrated sulfuric acid[10]. Commercial reagents of pure grade were used. The reaction was carried out in a glass pressure bottle as reported in the preceding papers[11].

1,2-Naphtoquinone 1-oxime (I).—The oxime was synthesized by nitrosation of β-naphthol according to the method of C. S. Marvel and P. K. Porter[12], and recrystallized from ligroin. Brown crystals, m.p. 108°C. Yield 82%.

Ring cleavage of I to *o*-cyanocinnamic acid (IV).—Into a mixture of 5 g. of oxime I (0.03 mole) and 100 ml. of liquid sulfur dioxide, 5 g. of thionyl chloride (0.03 mole) in 30 ml. of

7) R. E. Lyle and J. L. Fielding, ibid., **20**, 623 (1955).
8) R. F. Brawn and N. M. Van Gulick, *J. Am. Chem. Soc.*, **77**, 1094 (1955).
9) A. H. Blatt and R. P. Barnes, ibid., **56**, 1148 (1934).
10) D. Murakami and N. Tokura, This Bulletin,. **31**, 431 (1958).
11) N. Tokura, R. Asami and R. Tada, *Sci. Rep. of Res. Inst., Tohoku Univ.*, **A8**, 149 (1956).
12) C. S. Marvel and P. K. Porter "Organic Syntheses", Coll. Vol. I, p. 403 (1941).

liquid sulfur dioxide was introduced. The mixture was heated on a water bath at 70°C for 6 hours, when it became dark green in color. After the reaction was completed, sulfur dioxide was removed by evaporation. The residue was dissolved in 150 ml. of chloroform, and the acidic substance was extracted with 250 ml. of 1 N sodium bicarbonate solution. The extract was acidified to pH 3 with concentrated hydrochloric acid. *o*-Cyanocinnamic acid (IV), which separated out, was recrystallized from methanol. White plates, m. p. 254~255°C (reported as 254°C by Werner[2]). Yield, 2.7 g. (54%).

Anal. Found: C, 69.36; H, 4.24; N, 8.38. Calcd. for $C_{10}H_7O_2N$: C, 69.36; H, 4.07; N, 8.09%.

The results obtained under various conditions are listed in Table I.

To a mixture of 30 ml. of ethanol and 10 ml. of concentrated sulfuric acid was added 0.5 g. of IV and the solution was refluxed for several hours. Ethyl *o*-cyanocinnamate was obtained from the reaction mixture by treating it as usual. White plates (from ethanol), m. p. 57~57.5°C. Yield, 0.3g.

Anal. Found: N, 7.05. Calcd. for $C_{12}H_{11}O_2N$: N, 6.96%.

9,10-Phenanthrenequinone 9-oxime (II).—The quinone was synthesized by oxidizing phenanthrene with chromic acid[13]. The quinone was then monoximated with hydroxylamine hydrochloride by modifying Pschorr's[14] procedure. Five grams of monoxime II was obtained from 10 g. of the quinone.

Ring cleavage of II to 2-cyanobiphenyl-2'-carboxylic acid (V).—In 100 ml. of liquid sulfur dioxide 3 g. (0.015 mole) of the oxime (II) was dissolved and the solution was treated with 1.8 g. (0.015 mole) of thionyl chloride in 30 ml. of liquid sulfur dioxide at 70°C for 6 hours. After evaporating off the solvent, the residue was dissolved in alcohol. The alcoholic solution was filtered and the filtrate was treated with 1 N sodium bicarbonate solution. By acidifying the solution 2-cyanobiphenyl-2'-carboxylic acid (V) was precipitated, and recrystallized from benzene. White pillars, m. p. 169~171°C, (reported[2] m. p. 171~172°C). Yield, 1.8 g. (60%).

Anal. Found: C, 75.06; H, 4.23; N, 6.05. Calcd. for $C_{14}H_9O_2N$: C, 75.32; H, 4.06; N, 6.28%.

In 10 ml. of methanol 0.3 g. of V was dissolved and hydrogen chloride was introduced into the mixture. By cooling, methyl 2-cyano-biphenyl-2'-carboxylate was precipitated. Recrystallized from 50% ethanol, white pillars, m.p. 79~80°C. (reported[2] m.p., 79~80°C). Yield, 0.2 g.

From the part insoluble in cold ethanol, a white crystalline subtance, m.p., 217~218°C, was obtained by sublimation in a yield of 0.5 g. (11%) and proved to be diphenic acid imide (VI) by the mixed melting point with an authentic specimen[15].

Anal. Found: N, 6.04. Calcd. for $C_{14}H_9O_2N$: N, 6.28%.

When the reaction was conducted at 15°C, the yields of V and VI decreased to 33% and 5%, respectively.

Tetralin-1,2-dione 2-oxime (III).—Tetralone was prepared from tetralin by air oxidation[16] and the ketone was then treated with isoamyl nitrite to give tetralin-1, 2-dione 2-oxime (III) according to the method of Straus and Eckhard[17] with a slight modification. Pale yellow crystals, m.p. 140~142°C. Yield, 45%.

Cleavage of III to *o*-(2-cyanoethyl) benzoic acid (VII).—A mixture of 3 g. (0.017 mole) of III and 2 g. (0.017 mole) of thionyl chloride in 130 ml. of liquid sulfur dioxide was treated for 6 hours at 70°C as stated above. After evaporating off the solvent, the residue was washed with dilute sodium bicarbonate solution and the solution was acidified. Recrystallization of the precipitates from water afforded 2.9 g. (98%) of *o*-(2-cyanoethyl) benzoic acid (VII). White plates, m. p. 111~112°C.

Anal. Found: C, 68.71, H, 5.04, N, 8.15. Calcd. for $C_{10}H_9O_2N$: C, 68.56, H, 5.18, N, 8.00%.

As a proof of the structure of VII, VII was decarboxylated to β-phenylpropionitrile (XVI), which was then hydrolyzed to β-phenylpropionic acid (XVII) in the following way.

Decarboxylation of VII to β-phenylpropionitrile (XVI).—A mixture of 2 g. (0.012 mole) of VII, 1 g. of copper powder and 30 g. of quinoline was refluxed with stirring for four hours. Evolution of carbon dioxide was observed. The mixture was filtered and the filtrate was diluted with 200 ml. of chloroform. The solution was washed with 5 percent hydrochloric acid and with 2 percent aqueous sodium hydroxide solution successively, and dried with anhydrous sodium sulfate. After the evaporation of the solvent (chloroform), the residue was subjected to a distillation in vacuo and β-phenylpropionitrile (XVI) was obtained as a pale yellow liquid of b.p. 115~117°C (7 mm.) (reported[18] b.p., 114~118°C (8 mm.)). Yield, 1.1 g, (73%).

Anal. Found; C, 77.75, H, 6.27, N, 9.19. Calcd. for C_9H_9N; C, 82.40, H, 6.92, N, 10.68%.

XVI was not pure enough for analysis. It was hydrolyzed to β-phenylpropionic acid (XVII).

Hydrolysis of XVI to β-phenylpropionic acid (XVII).—A mixture of 0.5 g. of XVI in 5 ml. of 10 percent alcoholic potash was refluxed for ten hours. Then the reaction mixture was poured onto ice water and extracted with chloroform. The solution was dried and evaporated. The residue was recrystallized from water to obtain 0.3 g. (53%) of XVII as white needles, m. p. and mixed m.p. with an authentic specimen, 48~49°C. (reported[19] m. p. 47.5~48.0°C).

Anal. Found: C, 70.42, H, 6.68. Calcd for $C_9H_{10}O_2$: C, 71.98, H, 6.71%.

13) R. Wendland and J. LaLonde, *Org. Synth.*, **34**, 76 (1954).
14) R. Pschorr, *Ber.* **35**, 2734 (1902).
15) N. Tokura and S. Anazawa, *Sci. Rep. of Res. Inst. Tohoku Univ.*, **A9**, 239 (1957).
16) R. B. Thompson, "Organic Syntheses" Coll. Vol. II, 995 (1943).
17) F. Straus and W. Eckhard, *Ann.*, **444**, 162 (1925).
18) V. Grignard, E. Bellet and Ch. Courtot, *Annales de chimie et de physique*, [9], **4**, 43 (1915).
19) A. W. Ingersoll, "Organic Syntheses", Coll. Vol, I, p. 311 (1941).

Summary

1,2-Diktone monoximes were subjected to treatment with thionyl chloride in liquid sulfur dioxide to obtain cyanocarboxylic acids in good yields.

The authors wish to express their thanks to Befu Chemical Industries Co. Ltd., for the donation of liquid sulfur dioxide, and to Miss Yoko Endo for the microanalyses. The present investigation was supported by a grant from the Ministry of Education.

Chemical Research Institute
of Non-aqueous Solutions
Tohoku University, Sendai

Studies on Meso-ionic Compounds. VIII[1]*. Oxidation of Sydnones*

By Mutsuko HASHIMOTO and Masaki OHTA

(Received June 3, 1958)

Substitution reactions of 3-phenylsydnone and the behavior of 3-phenyl-4-bromosydnone suggest us that the sydnone nucleus is aromatic in character to a considerable extent. As many instances are known where a methyl substituent in aromatic heterocycles is oxidized to a carboxylic group, it seemed possible to oxidize 4-methylsydnones to corresponding 4-carboxylic acid derivatives. Although this was not realized, we found an interesting rearrangement during the oxidation of several sydnones.

The oxidation of 3-phenyl-4-methlsydnone (Ia) with potassium permanganate in acetone did not afford the expected carboxylic acid, but the oxidative cleavage of sydnone ring occurred, affording acetophenone. The same reaction product was also obtained by oxidation of Ia with potassium permanganate in aqueous pyridine or with aqueous hydrogen peroxide in acetic acid. In each case a slight evolution of gas was observed. The results obtained here suggest that the rearrangement of a phenyl group in 3-position of 3-phenyl-4-methylsydnone from nitrogen (3-position) to carbon (4-position) occurred in the course of the oxidation process.

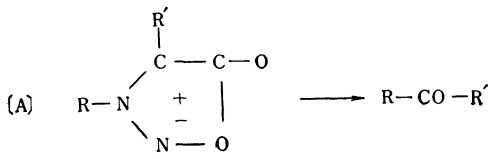

I

Fig. 1.

a; $R=C_6H_5$, $R'=CH_3$
b: $R=C_6H_5$, $R'=H$
c: $R=p\text{-}CH_3\cdot C_6H_4$, $R'=H$
d: $R=R'=C_6H_5$
e: $R=o\text{-}CH_3\cdot C_6H_4$, $R'=H$

A reaction of the same type also occurred when 3-phenylsydnone (Ib) and 3-*p*-tolylsydnone (Ic) were treated with aqueous hydrogen peroxide in acetic acid at room temperature, affording benzaldehyde and *p*-tolualdehyde, respectively.

When the same procedure was applied to 3,4-diphenylsydnone (Id) and 3-*o*-tolylsydnone (Ie), however, the expected ketone or aldehyde was not obtained, but the starting materials were recovered unchanged. When 3, 4-diphenylsydnone was heated with a mixture of hydrogen peroxide and acetic acid, a very small amount of phenol was obtained, which was identified by Liebermann's nitroso test, coloration on addition of ferric chloride and formation of tribromophenol.

The oxidation of 3-phenylsydnone (IIa) with potassium permanganate in acetone gave, quite unexpectedly, 3, 4-diphenylsydnone (IIIa) and benzaldehyde. The 3, 4-diphenylsydnone obtained here was identical with a specimen prepared by the method reported by Baker et al.[2]. The oxidation of 3-*p*-tolylsydnone (IIb)

1) Part VII of this series, H. Kato and M. Ohta, *J. Chem. Soc. Japan, Pure Chem. Sec.*, (*Nippon Kagaku Zassi*), **78**, 1653 (1957).

2) W. Baker, W. D. Ollis and V. D. Poole, *J. Chem. Soc.*, **1949**, 307.

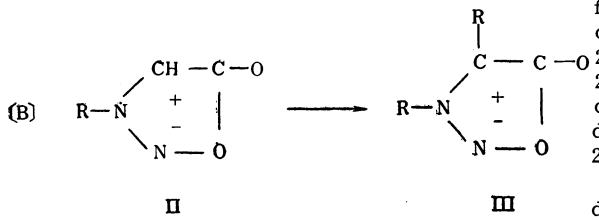

Fig. 2.

a: R=C_6H_5(=Ib) a: R=C_6H_5(=Id)
b: R=p-CH_3·C_6H_4(=Ic) b: R=p-CH_3·C_6H_4

with potassium permanganate also gave 3,4-di-p-tolylsydnone (IIIb).

The results obtained above are not quite sufficient for a deduction concerning the reaction mechanism. However, from a consideration of the result obtained in the case of 3-phenyl-4-methylsydnone, it might be assumed that only 3-arylsydnone which has no substituent in 4-position could give 3, 4-diarylsydnone by the action of potassium permanganate, and that 4-substituted sydnone was oxidized to ketone. On the basis of this fact, it seems reasonable to conclude that the intermolecular rearrangement described above was preceded by the formation of aryl radical by the action of potassium permanganate on sydnone, followed by the attack of the aryl radical on 4-position of the unchanged sydnone. The value of the free valence in 4-position of sydnone lends some support to this consideration; namely, according to Orgel et al.[3], a value of 0.562 is calculated, which corresponds with that of free valence in 9- or 10-position of anthracene where radical substitution occurs readily. For the determination of the mechanism of such reactions, however, a more detailed investigation will probably be required.

Two novel types of the rearrangement reaction presented in this paper, have not yet been observed with heterocyclic compounds.

Experimental

Oxidation of 3-Phenyl-4-methylsydnone (Ia) with Potassium Permanganate.—a) To a solution of 4.4 g. of Ia, prepared by Earl's method[4], in 200 cc. of acetone was added portionwise 7.9 g. of finely powdered potassium permanganate with stirring at room temperature. After being kept overnight, the precipitated manganese dioxide was filtered off and the filtrate was evaporated. From the residue was obtained an oily product boiling at 68°/17 mm., 2,4-dinitrophenylhydrazone of which melted at 239~240°, and did not show any melting point depression on admixture with the authentic 2, 4-dinitrophenylhydrazone of acetophenone (m. p. 238°).

b) In aqueous pyridine, 4.4 g. of Ia was oxidized with 7.9 g. of potassium permanganate at room temperature. After being kept overnight, the precipitated manganese dioxide was filtered off and the filtrate was evaporated under reduced pressure. The residue was extracted with ethanol and the ethanol was removed. The crude reddish brown oil, dissolved in benzene and passed through an alumina column, gave 0.34 g. of Ia and an oily product, 2,4-dinitrophenylhydrazone of which did not show any melting point depression on admixture with the authentic 2,4-dinitrophenylhydrazone of acetophenone.

Oxidation of Ia with Hydrogen Peroxide.—To a solution of 8.8 g. of Ia in 20 cc. of glacial acetic acid was added 8.4 g. of aqueous 30% hydrogen peroxide and this was kept standing at room temperature for 29 hours. The reaction mixture was diluted with 80 cc. of water, neutralized by sodium carbonate and extracted with ether. The extracts were washed with aqueous sodium bicarbonate and dried. An oily product (1.3 g.) gave phenylhydrazone (m. p. 101°) and 2, 4-dinitrophenylhydrazone (m. p. 239°) which did not show any melting point depression on admixture with those of acetophenone, respectively.

Oxidation of 3-Phenylsydnone (Ib) with Hydrogen Peroxide.—a) To a solution of 4 g. of Ib, prepared by our method[5], in 25 cc. of glacial acetic acid was added 4.2 g. of aqueous 30% hydrogen peroxide. After standing at room temperture for 24 hours, the reaction mixture was treated by the same procedure as described above. An oily product obtained gave phenylhydrazone (m. p. 155~156°) and 2, 4-dinitrophenylhydrazone (m. p. 233°), both of which showed no melting point depression on admixture with the authentic samples obtained from benzaldehyde.

b) When Ib was treated by the same procedure as described in a) except that the reaction time was 5 hours, 70% of Ib was recovered.

Oxidation of 3-p-Tolylsydnone (Ic) with Hydrogen Peroxide.—When a mixture of Ic, prepared by Baker's method[2], and 20 cc. of glacial acetic acid and 2.1 g. of aqueous 30% hydrogen peroxide was kept standing at room temperature for 24 hours, and then treated by essentially the same method as described above, p-tolualdehyde was obtained and identified as phenylhydrazone (m. p. 112°) and 2, 4-dinitrophenylhydrazone (m. p. 230°).

3-o-Tolylsydone (Ie).—A suspension of 29 g. of o-tolylglycine, prepared by Steppes' method[6], in 350 cc. of water was treated with 20 cc. of concentrated hydrochloric acid and cooled at 0°. A solution of 13 g. of sodium nitrite in 35 cc. of

3) L. E. Orgel, T. L. Cottrell, W. Dick and L. E. Sutton, *Trans. Faraday Soc.*, **47**, 113 (1951).
4) J. C. Earl and A. W. Mackney, *J. Chem. Soc.*, **1935**, 899.
5) M. Hashimoto and M. Ohta, *J. Chem. Soc. Japan, Pure Chem. Sec.*, (*Nippon Kagaku Zassi*), **78**, 181 (1957).
6) F. Steppes, *J. prakt. Chem.*, [2] **62**, 491 (1900).

water was added dropwise with vigorous stirring. After an hour dark brown viscous oil had separated. The oil was dissolved in ether, washed with water and dried and the ether was evaporated. Reddish brown oil was obtained, giving a positive Liebermann's nitroso test. Yield 37.2 g. In 200 cc. of acetic anhydride was dissolved 37.2 g. of the crude nitroso acid, kept standing for three days at room temperature, and water was then added. The solid which separated out was collected and washed with aqueous sodium carbonate and water. White flakes were obtained, m. p. 86°, yield 6.8 g.. An analytical sample was prepared by recrystallization from water, m. p. 96° (the reported melting point[7] is 89°). *Anal.* Found: N, 15.66. Calcd. for $C_9H_8O_2N_2$: N, 15.90%.

Reaction of 3-*o*-Tolylsydnone (Ie) with Hydrogen Peroxide.—A mixture of 1.1 g. of Ie and 20 cc. of glacial acetic acid and 1.05 g. of aqueous 30% hydrogen peroxide was kept standing at room temperature for 24 hours, and then diluted with water. White crystals separated out (m. p. 96°, 0.57 g.), undepressed on admixture with Ie.

When the filtrate was neutralized with sodium carbonate, and extracted with ether and the ether was evaporated, 0.16 g. of Ie was still recovered.

Reaction of 3,4-Diphenylsydnone (Id) with Hydrogen Peroxide.—When a mixture of 24 g. of Id and 20 cc. of glacial acetic acid and 1.7 g. of aqueous 30% hydrogen peroxide was treated with the same procedure as described above, 2.22 g. of Id was recovered.

b) A mixture of 2.4 g. of Id and 20 cc. of glacial acetic acid and 1.7 g. of aqueous 30% hydrogen peroxide was heated for 5 hours at 90°, and diluted with 100 cc. of water. The crystals which separated out were recrystallized from ethanol, m. p. 181~181.5°, undepressed by admixture with Id. Yield 0.61 g..

The acidic filtrate was neutralized with sodium bicarbonate, and extracted with ether and then the ether was evaporated. A very small amount of oil with a smell of phenol was obtained, giving a positive Liebermann's nitroso test and a red ferric chloride reaction, and afforded a bromoderivative which showed no melting point depression on admixture with the authentic sample of tribromophenol.

Oxidation of 3-Phenylsydnone (IIa) with Potassium Permanganate.—To a solution of 8.1 g. of IIa in 400 cc. of acetone was added portionwise 15.8 g. of finely powdered potassium permanganate with stirring at room temperature. After being kept overnight, the precipitated manganese dioxide was filtered off and the acetone was removed. From the residue light yellow crystals separated out, and were collected and recrystallized from ethanol. Pale yellow prisms, m. p. 183~184.5°, were obtained and did not show any melting point depression on admixture with 3,4-diphenylsydnone (IIIa), prepared by Baker's method[8]. Yield 1.1 g., 22%.

The filtrate (2.1 g.) gave 2,4-dinitrophenylhydrazone, m. p. 233°, undepressed on admixture with the authentic 2,4-dinitrophenylhydrazone of benzaldehyde.

Oxidation of 3-*p*-Tolylsydnone (IIb) with Potassium Permanganate.—To a solution of 5.28 g. of IIb in 240 cc. of acetone was added 9.48 g. of finely powdered potassium permanganate. The reaction mixture was treated by essentially the same method as described above, and the yellow crystals obtained were recrystallized from ethanol. Light yellow flakes, m. p. 156.5~157° (the reported melting point[8] for 3,4-di-*p*-tolylsydnone (IIIb) is 156~157.5°). Yield 0.82 g., 20.6%.

Anal. Found: N 11.01. Calcd. for $C_{16}H_{14}O_2N_2$: N, 10.52%.

The authors are grateful to Mr. Asaji Kondo for carrying out the microanalyses.

Laboratory of Organic Chemistry
Tokyo Institute of Technology
Meguro-ku, Tokyo

7) J. Hadáček et al., *Publs. fac. sci. univ. Masaryk Cišlo*, **357**, 257 (1954).

8) W. Baker, W. D. Ollis and V. D. Poole, *J. Chem. Soc.*, **1950**, 1542.

Electron Diffraction Investigation on Tropone[1]

By Katsumi KIMURA, Satoshi SUZUKI, Masao KIMURA and Masaji KUBO

(Received June 19, 1958)

In recent years, considerable interest has been directed to the determination of the molecular structures of compounds having a seven-membered carbon ring by electron diffraction[2,3] as well as by X-ray crystal analysis[4-6]. However, the investigations that have hitherto been made have dealt with tropolone and its derivatives. Tropone is the simplest compound having a cycloheptatriene ring and for this reason it is most suitable for the determination of the geometric form of this carbon ring. According to the results of dipole moment measurements, this compound is characterized by special resonance stability[7], which is expected to be revealed more directly by the measurements of bond lengths. Recent advances in the experimental technique of electron diffraction by gas molecules have made it possible to obtain the values of structural parameters with high precision. In view of this situation, the present investigation was undertaken in order to determine the structure of tropone by measuring the scattered intensity using the sector-microphotometer method. In this study, it was also possible to determine the magnitudes of vibrational amplitudes of some atom pairs.

Experimental

The electron diffraction photographs of the molecule were taken using a rotating sector. The present studies were made with an r^2-sector provided with a beam trap. The trap was 20 mm. long and 2 mm. in radius[8]. The use of this trap was effective in eliminating extraneous scatterings. The apparatus used was essentially the same as that previously employed[9]. The camera distance was 12 cm. long. The electron beam passing through slits was focused onto a photographic plate, the focused spot being about 0.1 mm. in diameter. The electron wavelength was determined by calibration with a gold foil to be equal to about 0.063 Å.

The sample was kindly furnished by Professor Nozoe of Tohoku University[10]. At room temperature, tropone is a liquid having a low vapor pressure. In order to obtain vapor pressures required for taking good diffraction photographs, it was necessary to use a high-temperature nozzle. Therefore, a number of capillary tubes containing the sample were placed in the furnace. The furnace and the nozzle were maintained at about 100°C during exposures of photographic plates to diffraction beams. The vapor was led through the nozzle and was projected across the electron beam. The pressure of the sample was controlled by regulating the temperature of the reservoir.

In order to apply Karle's method[11] of density-intensity calibration, several sets of two sector photographs were taken, different exposures (about 2 : 1) being employed in each set under otherwise the same conditions. Microphotometric tracings were made on the diffraction patterns using a recording microphotometer. The conversion of the observed densities into intensity curves made after Karle's method[11].

Analysis of Data

Radial Distribution Curve. — In the first place, the structure of the molecule was studied by the radial distribution method, although the correlation method was employed later. The radial distribution curve, $f(r)$ was calculated from the experimental molecular intensity curve according to the equation[12],

1) A part of the results presented here has been reported at a meeting of the Chemical Society of Japan held in Sendai in October 1956. A preliminary report has been published in a short communication: K. Kimura, S. Suzuki, M. Kimura and M. Kubo, *J. Chem. Phys.*, **27**, 320 (1957).

2) E. Heilbronner and K. Hedberg, *J. Am. Chem. Soc.*, **73**, 1386 (1951).

3) M. Kimura and M. Kubo, This Bulletin, **26**, 250 (1953). M. Kubo, M. Kimura and K. Kimura, ibid., **27**, 455 (1954).

4) J. M. Robertson, *J. Chem. Soc.*, **1951**, 1222.

5) Y. Sasada, K. Osaki and I. Nitta, *Acta Cryst.*, **7**, 113 (1954).

6) Y. Sasada and I. Nitta, ibid., **9**, 205 (1956).

7) Y. Kurita, T. Nozoe and M. Kubo, This Bulletin, **24**, 10 (1951). Y. Kurita, S. Seto, T. Nozoe and M. Kubo, ibid., **26**, 272 (1953).

8) S. Shibata, The Eighth Symposium on X-ray and Electron Diffraction, Osaka, November 1956.

9) M. Kimura, K. Kimura and S. Shibata, *J. Chem. Phys.*, **24**, 622 (1956).

10) T. Nozoe, S. Seto, Y. Kitahara, M, Kunori and Y. Nakayama, *Proc. Japan Acad.*, **26**, 38 (1950).

11) I. L. Karle and J. Karle *J. Chem. Phys.*, **17**, 1052 (1949). J. Karle and I. L. Karle, ibid., **18**, 957 (1950).

12) See, for example, P. A. Schaffer, Jr., V. Schomaker and L. Pauling, *J. Chem. Phys.* **14**, 659 (1946).

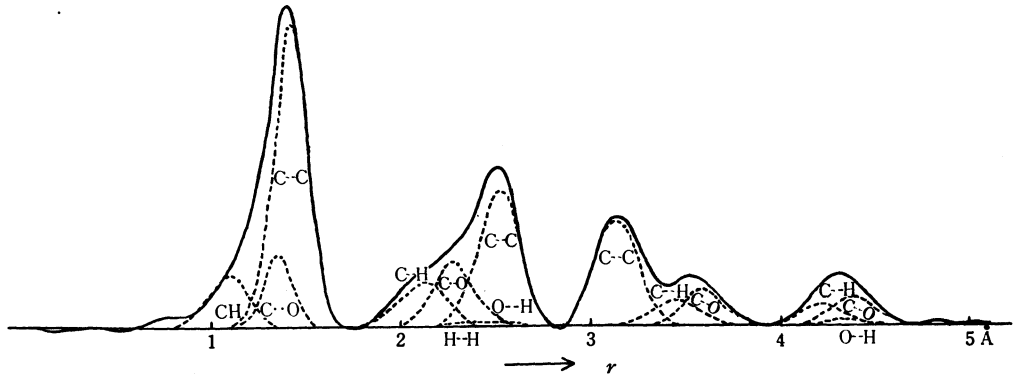

Fig. 1. Radial distribution curve for tropone.

$$f(r) = \sum_{s=0}^{s_{max}} sM(s)\exp(-bs^2)\sin(sr)$$

where $M(s)$ is the molecular scattering intensity and other symbols have their usual significances. The experimental $M(s)$ curve was obtained by dividing the total intensity by the background intensity, corrections being made for the interference arising from non-nuclear scattering[13]. Fig. 1 shows the radial distribution curve computed with an artificial damping factor chosen so as $\exp(-bs_{max}^2)=0.1$.

The values of distance were evaluated by fitting Gaussian peaks to the experimental curve. The first peak at about 1.4 Å is due mainly to seven bonded C-C distances (C_1-C_2, C_2-C_3, etc.) and has some contributions from bonded C=O and C—H distances (C_2—H_2, etc.) appearing on the left-hand side of the prominent peak. Here, the carbon atoms composing the ring and the hydrogen atoms attached to it are numbered as shown in Fig. 2. If

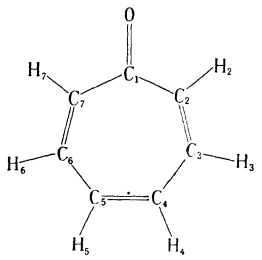

Fig. 2. The numbering of carbon and hydrogen atoms in a tropone molecule.

it is assumed that all the bonded C—C distances are equally long and that C—H distances are also the same, the C-C peak can be located at 1.405 Å and the most probable values for the C—H and C=O distances are 1.09 and 1.26 Å, respectively. The mean amplitude of vibration has been found to be 0.050 Å for the C—C distances. Even if there is some spread in the values of C—C distances, the mean amplitude for each C—C bond will be essentially the same as the above-mentioned value derived on the assumption that all the C-C distances are equally long. However, it is not possible from this analysis to decide whether or not there are small differences among the bonded C-C distances. For example, even if the individual C-C distances were shifted by less than about ±0.01 Å, to give an average distance 1.405 Å, no appreciable change would result in either the position of the C-C peak or in the mean amplitude.

The second peak at about 2.5 Å can be assigned mainly to the short C···C (C_1-C_3, C_2-C_4, etc.), short C···O (C_2-O and C_7-O) and short C···H (C_1-H_2, etc.) distances. Contributions from short O···H and short H···H distances are negligibly small. The second peak was decomposed into three Gaussian peaks in the following way. The analysis of the first peak showed that even if the carbon ring is distorted from a regular heptagon form, the distortion is slight. Therefore, the short C···O and C···H distances were first assumed to be 2.26 and 2.12 Å, respectively, on the basis of the result from the first peak. Then, the corresponding peaks were subtracted from the total curve, the mean amplitudes of 0.070 and 0.100 Å being used for the C···O and C···H peaks, respectively. The subtraction yielded a peak corresponding to the short C···C distance capable of being fitted with a Gaussian peak centered at 2.52 Å. Next, the reverse procedure was followed, the C···C peak

13) L. S. Bartell and L. O. Brockway, ibid., **23**, 1854 (1955).

thus obtained was subtracted from the total curve and then the remaining portion was separated into two peaks, one at 2.28 Å for the C···O distance and the other at 2.10 Å for the C···H distance. The separation was made so that each of these peaks has an area proportional to the number of distances times $z_i z_j / r_{ij}$. Thus the mean amplitude turned out to be 0.066 and 0.110 Å for the C···O and C···H distances, respectively. If the seven-membered carbon ring is assumed to be undistorted from a regular heptagon form, the short nonbonded C···C, C···O and C···H distances are calculated on the basis of the observed C—C and C—H distances to be equal to 2.53, 2.26 and 2.12 Å, respectively, in good agreement with the experimental values.

The third peak at about 3.15 Å is due almost solely to long nonbonded C···C (C_1-C_4, etc.) distances and a weak neighboring peak at about 3.5 Å to long C···O (C_3-O and C_6-O) and long C···H (C_1-H_3, etc.) distances. This composite peak was decomposed in the same manner as for the second peak mentioned above. In this case, the separation of the C···C peak was scarcely affected by the peak corresponding to the long C···O distances. The observed values for these three distances, 3.15, 3.58 and 3.46 Å, are in fair agreement with the respective values, 3.16, 3.60 and 3.45 Å, calculated from the model of a regular heptagon form. The mean amplitudes of the C···C distance is 0.079 Å. The remaining peak at 4.3 Å corresponds for the most part to longer nonbonded C···C (C_4-O and C_5-O) and C···H (C_1-C_4, etc.) distances. The distances for the Gaussian peaks resulting from the proper decomposition of the composite peak are 4.40 and 4.20 Å, while the values calculated on the assumption of the undistorted carbon ring are 4.39 and 4.23 Å, respectively.

TABLE I. COMPARISON OF THE OBSERVED DISTANCES WITH THOSE CALCULATED ON THE BASIS OF A REGULAR HEPTAGON MODEL.*

Bond type	Atom pair	Distance (Å) obs.	Distance (Å) calc.
Bonded distances	C—H	1.09	
	C=O	1.26	
	C—C	1.405	
Short nonbonded distances	C_1···H_2	2.10	2.12
	C_2···O	2.28	2.26
	H_2···H_3	(2.35)	2.35
	O···H_2	(2.43)	2.43
	C_1···C_3	2.52	2.53
Long nonbonded distances	C_1···C_4	3.15	3.16
	C_1···H_3	3.46	3.45
	C_3···O	3.58	3.60
Longer nonbonded distances	C_1···H_4	4.20	4.23
	O···H_3	(4.37)	4.37
	C_4···O	4.40	4.39

* Assumed values are enclosed in parentheses.

Table I shows a comparison of the observed distances from the radial distribution curve with the calculated distances for the molecule having an undistorted regular heptagon ring. It is apparent that the observed and calculated values are in good agreement with each other. In addition, a test for the relative areas of peaks in the radial distribution curve shows an agreement within 5% between the observed and calculated values. Thus, from the analysis of the experimental curve, it was found that the curve could be interpreted adequately on the basis of a coplanar model having a regular heptagon carbon ring. It is important to note that, if the molecule is not planar, some peaks in the radial distribution curve would have appeared in shorter distances than those actually observed. Accordingly, it seems to be adequate to conclude that this molecule is definitely coplanar.

Choice of the Molecular Models.— Before the construction of theoretical curves of molecular intensity is attempted, it is necessary to define the molecular parameters required for the complete description of selected models. The parameters were chosen for the present purpose on the basis of the results obtained from the radial distribution curve. A tropone molecule is presumed to have a plane of symmetry perpendicular to the molecular plane. Consequently, the structure has C_{2v} symmetry and the geometric configuration of heavy atoms can be completely described by giving seven independent parameters, because the carbon ring of the molecule involves four nonequivalent C—C distances. The following seven parameters were chosen in order to determine the structure having the C_{2v} symmetry: C=O, C_1-C_2 (=C_1-C_7), C_2-C_3 (=C_7-C_6), C_3-C_4 (=C_6-C_5) and C_4-C_5 distances along with the x- and y-components of the C_1···C_3 (=C_1···C_6) distance, which determine the positions of C_3 and C_6 atoms relative to C_1 atom. The C_1-C_2 and C_3-C_4 distances will be almost equal to or longer than the C_2-C_3 and C_4-C_5 distances, since it is likely that the latter bonds have a more or less pronounced

double bond character compared with the former. Therefore, two extreme cases were taken up for the C-C distances: First, all the C-C distances are equally long and secondly, C_1-C_2=C_3-C_4=1.43 Å., C_2-C_3=1.38 Å and C_4-C_5=1.37 Å. These distances give an average value that is almost the same as the observed value. As regards the position of the C_3 atom, six points were chosen on a circle of 0.04 Å in radius with its center at the position of the C_3 atom for the regular heptagon ring. The values for the C=O distance were selected at 1.21, 1.26 and 1.31 Å. Since the mean amplitude is an important factor in determining the maxima and minima of intensity curves, various values of mean amplitudes were used for C-C atom pairs as shown in Table II.

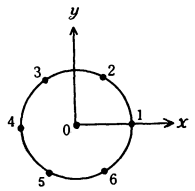

Fig. 3. Various positions of the C_3 atom for "distorted" models. The origin of rectangular coordinates coincides with the position of the C_3 atom in the regular heptagon ring.

TABLE II. VARIOUS SETS OF THE MEAN AMPLITUDES OF C-C ATOM PAIRS IN 10^{-3} Å.

Set	1	2	3	4	5	6	7	8
C—C	50	50	50	50	50	50	50	50
Short C···C	55	55	55	65	65	75	75	85
Long C···C	60	80	100	80	100	80	100	100

Comparison of Theoretical and Experimental Intensity Curves.—In calculating theoretical intensity curves, various atom pairs could be grouped into four different types: (1) C—C, short C···C and long C···C, (2) C=O, short C···O, long C···O and longer C···O, (3) C—H, short C···H, long C···H and longer C···H, and (4) nonbonded O···H and H···H. The distances belonging to types 1 and 2 determine the framework of the molecule. The contributions from the distances of type 1 dominate the greater portion of the intensity curve, i. e., 60~80% of the total intensity depending upon the s values. They practically determine the positions of maxima and minima of the intensity curve. On the other hand, the distances of type 2 affect the form of a number of shelves in the intensity curves in such a remarkable manner that the C=O distance can be evaluated with fair accuracy. The intensity curves are relatively insensitive to changes in the bond lengths and the valency angles involving hydrogen atoms, i. e., to changes in distances belonging to

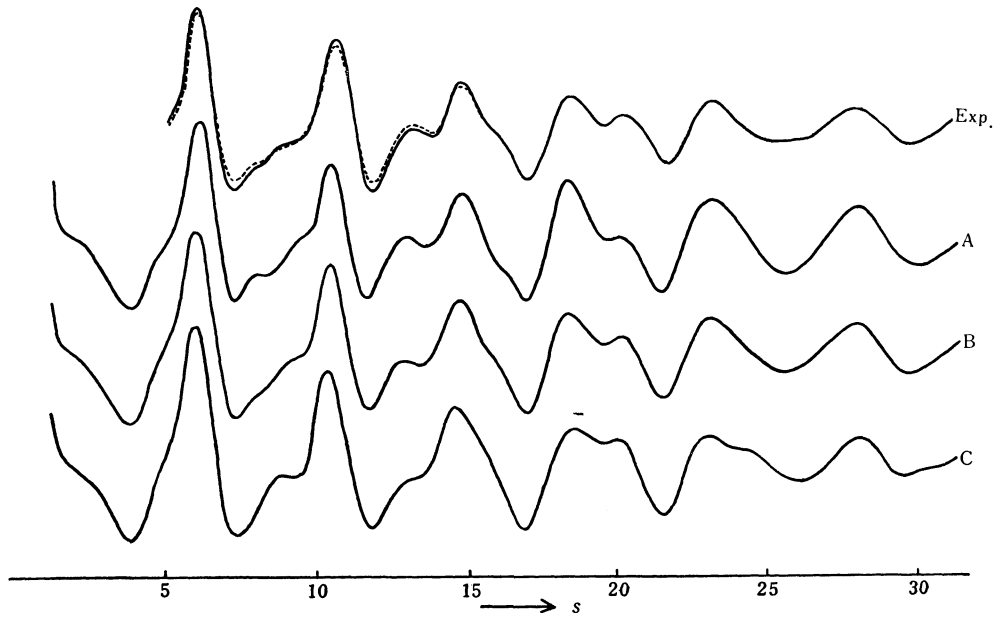

Fig. 4. Comparison between experimental and theoretical intensity curves for tropone. In the experimental curve, the full line represents the intensity curve that was corrected for the constant coefficient[13] and the broken line represents the uncorrected curve.

type 3. The changes of ±0.02 Å in the bonded C—H distances have no appreciable effect on the intensity curves. Therefore, the C—H distance, 1.09 Å, derived from the radial distribution curve was used throughout. The effect of the separations of type 4 is inappreciable. In calculating theoretical intensity curves, all terms of the function[12,13],

$$sM(s)=\sum_{ij}(Z_iZ_j/r_{ij})\exp(-b_{ij}s^2)\sin(sr_{ij})$$

were included. Theoretical curves were calculated using various values for the selected parameters mentioned in the foregoing section and were compared with the observed curve. From this comparison, it became clear that the observed curve could be adequately interpreted in terms of the heptagon model and the C=O distance of 1.26 Å determined from the radial distribution curve was also very satisfactory. An increase or decrease in this distance by 0.05 Å resulted in considerable changes in the intensity curve. Fig. 4 illustrates the experimental curve together with the theoretical curves A, B and C computed for the regular heptagon ring with C=O=1.21, 1.26 and 1.31 Å, respectively. As to the mean amplitudes of the C-C distances, set 4 in Table II was found to give the best values consistent with the experimental curve. As can be seen from Fig. 4, curves A and C show departures from the observed one: for instance, a shelf at about $s=13$ and a maximum at $s=20$ are too high in curve A and too low in curve C. The portion of the experimental curve between $s=7.5$ and 9.4 shows small humps. Curve B well reproduces this feature, whereas curves A and C do not. The value of s/s_{exp} averaged over ten maxima and minima in curve B is 1.000 with an average deviation of 0.0040.

A number of curves for various "distorted" models were also carefully compared with the experimental curve. It was shown that none of the curves for the "distorted" models reproduced the experimental curve better than the heptagon model in regard to the following points. The major points were: First the shape of shelves in the region, $s=7.0\sim9.5$ and at about 14 and 15.5, secondly the shape of the minimum at about $s=19$ and lastly the intensity relations in the region, $s=7\sim24$.

Results and Discussion

The structural results obtained for a tropone molecule are summarized in Table III. Attention should be called to the fact that the experimental radial distribution curve and various features in the experimental intensity curve can be precisely interpreted in terms of a regular heptagon model. Unlike a tropolone molecule, a tropone molecule having only one oxygen atom resonates among a single electronic structure without a formal charge on any atoms of the molecule and various electronic structures of dipolar character. Accordingly, it is likely that the C-C distances are not equally long, but have a more or less pronounced single or double bond character. Therefore, as mentioned above, various "distorted" models were tried. It was found that, provided that the average C-C distance was equal to 1.405 Å, disparities of the order of 0.04 Å in C-C bond lengths as well as of about 10° in ∠CCC valency angles did not lead to models giving theoretical intensity curves very different from that of the "undistorted" model. However, it is of particular interest that the best agreement was obtained between the observed intensity curve and the final theoretical intensity curve for the simple "undistorted" regular heptagon model.

TABLE III. STRUCTURE OF A TROPONE MOLECULE.

Essentially regular heptagon carbon ring
C···C = 1.405±0.005 Å with $\langle l^2\rangle^{1/2}=0.050\pm0.005$ Å
C=C = 1.26±0.02 Å with $\langle l^2\rangle^{1/2}=0.038$ Å
C—H = 1.09±0.03 Å

It is also of interest to observe that the values determined for the C—C and C···H distances in tropone are very close to those reported for benzene[14,15]. The mean C-C distance of 1.405 Å in tropone is almost identical with that in tropolone determined as 1.40 Å[2] and 1.39 Å[3] by the electron diffraction method and with those in various crystalline modifications of tropolone derivatives studied by X-ray analysis, i. e., 1.40 Å[4] in copper(II) tropolonate (=cupric tropolone), 1.40 Å[5] in tropolone hydrochloride and 1.414 Å[6] in sodium tropolonate.

Layton, Kross and Fassel[16] showed that the stretching frequency of carbon-oxygen bonds in carbonyl compounds plotted against the bond length can be represented by a smooth curve. With the aid of this

14) I. L. Karle, ibid., **20**, 65 (1952).
15) A. Almennigen and O. Bastiansen, Research Correspondence, 9 (September 1956).
16) E. M. Layton, R. D. Kross and V. A. Fassel, ibid., **25**, 135 (1956).

relationship, it is possible to estimate the C=O bond length in a tropone molecule by interpolation from the observed vibrational frequency[17] of the C=O bond. The interpolation indicates that the C=O bond distance is about 1.27 Å, in excellent agreement with the value observed in the present work. Further, an approximate method[18] enables one to evaluate the mean amplitude from the vibrational frequency as $<l_{CO}^2>^{1/2}=0.039$ Å, which is also in good agreement with the observed value. In Table IV, the mean amplitudes of C-C atom pairs in tropone are compared with those in benzene.

TABLE IV. COMPARISON OF THE MEAN AMPLITUDES IN Å FOR C-C ATOM PAIRS BETWEEN TROPONE AND BENZENE MOLECULES.*

Atom pair	Tropone	Benzene	
		Karle[14]	Bastiansen[19]
C—C	0.050(1.405)	0.055(1.393)	0.0454
Short C···C	0.066(2.52)	0.067(2.41)	0.054
Long C···C	0.079(3.15)	0.075(2.786)	0.061

* The corresponding equilibrium distances in Å are enclosed in parentheses.

17) E. Kloster-Jensen, N. Tarköy, A. Eschenmoser and E. Heilbronner, *Helv. Chim. Acta*, **39**, 786 (1956).
18) K. Kimura and M. Kimura, *J. Chem. Phys.*, **25**, 362 (1956).
19) O. Bastiansen and S. J. Cyvin, *Nature*, **180**, 980 (1957).

Summary

The electron diffraction photographs of tropone in the gaseous state were taken with an s^2-sector. The data of the scattered intensity was analyzed by means of the radial distribution method as well as by the correlation method. The investigation of the molecule has led to the conclusion that the molecule assumes an essentially co- planar structure having a regular heptagon ring. The most probable values for the bond distances are: C—C=1.405±0.005 Å, C=O=1.26±0.02 Å and C···H=1.09±0.03 Å.

We wish to express our thanks to Professor T. Nozoe for providing us with the sample used in the present investigation, to Professor R. Uyeda for his permission to use a microphotometer and to Mr. H. Morimoto for his help in carrying out microphotometric tracings. We are also to the Ministry of Education for financial assistance.

Chemical Department, Nagoya University
Chikusa-ku, Nagoya

*Über die Kupfer- und Nickelkomplexsalze des Salicylaldehyd-benzoylhydrazons und seiner Oxyderivate**

Von Hiroshi OHTA

(Eingegangen am 12. Juli, 1958)

Seit der Entdeckung der tuberkulostatischen Wirkung von Isonikotinsäurehydrazid, sind verschiedene Säurehydrazide synthetisiert worden. Vor kurzem haben Buu-Hoï und seine Mitarbeiter[1] mitgeteilt, dass die Oxybenzoesäurehydrazide und ihre *N*-Salicyliden-Derivate in vitro ziemlich stark tuberkulostatisch sind, was darauf zurückzuführen sei, dass sie mit Schwermetallen, die für Enzyme nötig sind, Komplexsalze bilden können. Die Komplexsalze dieser Verbindungen sind aber bisher noch nicht beschrieben worden.

In der vorliegenden Mitteilung sollen die Kupfer- und Nickelkomplexsalze einiger Salicylaldehyd-aroylhydrazone berichtet werden. Als Ausgangsstoffe für die Darstellung wurden Salicylaldehyd-benzoylhydrazon, -2-methoxybenzoylhydrazon, -4-oxybenzoylhydrazon, -2-oxybenzoylhydrazon, -2-oxy-4-aminobenzoylhydrazon und

* Organische Metallkomplexsalze. II. Vorgetragen auf der XI. Versammlung der Japanischen Chemischen Gesellschaft in Tokyo, am 4. April, 1958. I. Mitteilung: H. Ohta, *J. Chem. Soc. Japan, Pure Chem. Sec.*, (*Nippon Kagaku Zassi*), **78**, 1608 (1957).

1) Ng. Ph. Buu-Hoï und Mitarbb., *J. Chem. Soc.*, **1953**, 1358.

5-Bromsalicylaldehyd-2-oxybenzoylhydrazon herangezogen, von denen Salicylaldehyd-2-oxy-4-amino-benzoylhydrazon und 5-Bromsalicylaldehyd-2-oxybenzoylhydrazon bisher unbekannt waren.

Reagieren die Salicylaldehyd-aroylhydrazone in der Keto-Form I mit dem Kupfer- oder Nickel-Ion, so sollten sie, wie Salicylaldehyd-phenylhydrazon, Komplexsalze von der Formel II bilden.

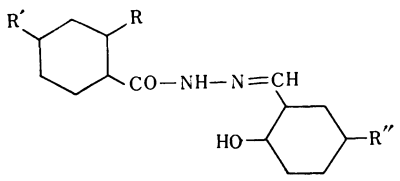

I

(1) R=R'=R''=H.
(2) R=OCH_3, R'=R''=H.
(3) R=R''=H, R'=OH.
(4) R=OH, R'=R''=H.
(5) R=OH, R'=NH_2, R''=H.
(6) R=OH, R'=H_2, R''=Br.

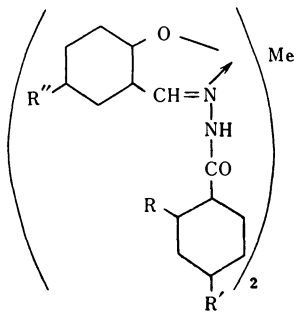

II

Me=Cu oder Ni

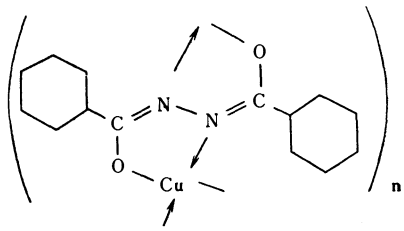

III

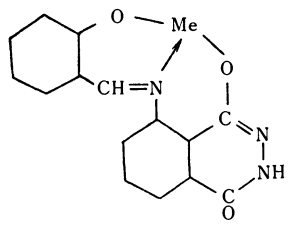

IV

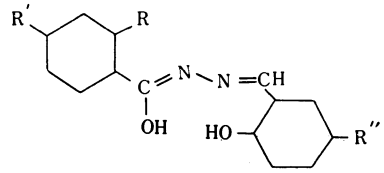

V

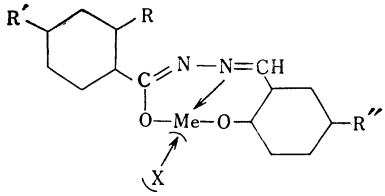

VI

X=NH_3 oder C_5H_5N

Da aber Benrath[2] schon früher ein Kupferkomplexsalz des Dibenzoylhydrazins von der Formel III erhielt, und Tsumaki und seine Mitarbeiter[3] neuerdings Kupfer- und Nickelkomplexsalze des 5-Salicylidenamino-1, 4-dioxo-tetrahydrophthalazins IV darstellten, so ist es zu erwarten, dass die Salicylaldehyd-aroylhydrazone auch in der Enol-Form V reagieren können.

Gehen sie nun in die Enol-Form über, dann können die Atome bzw. Atomgruppen so aufgestellt werden, dass die Bildung der Komplexsalze von der Formel VI sterisch nicht verhindert wird;

$$-C(OH)=N-N=CH-\overset{|}{C}=(OH)C-$$

kann auf einer Ebene liegen und die interatomischen Abstände sind zur Ausbildung von Wasserstoffbrücke begünstigt (Abb. 1). Die der VI analogen Komplexsalze sind schon von mehreren Autoren beschrieben worden, so z. B. die Kupferkomplexsalze des 2-Salicylidenaminophenols[4], 2,2'-Dioxy-azobenzols[4], Salicylaldehyd-thiosemicarbazons[6] und des Salicyliden-salicylamins[6], sowie die Nickelkomplexsalze des 2-Salicylidenaminophenols[4] und des Salicylaldehyd-thiosemicarbazons[5].

2) N. Benrath, *J. prakt. Chem.*, [2] **107**, 223 (1924).
3) T. Tsumaki und Mitarbb., *Reports of the Faculty of Science, Kyushu University, Chem. Sec.*, **1**, 161 (1950).
4) P. Pfeiffer und Mitarbb., *J. parkt. Chem.*, [2] **149**, 217 (1937).
5) V. Hovorka und Mitarbb., *Collection Czechoslov. Chem. Communs.*, **15**, 267 (1950).
6) M. Yamaguchi, *J, Chem. Soc. Japan, Pure Chem. Sec. (Nippon Kagaku Zassi)*, **74**, 261 (1953).

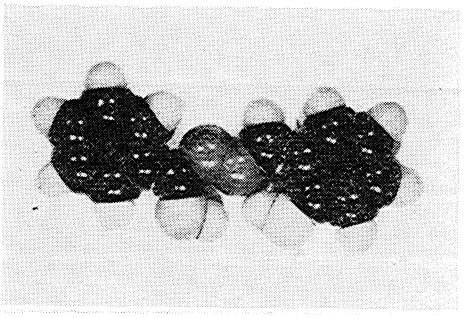

Abb. 1. Kalottenmodell des Salicylaldehydbenzoylhydrazons (Enol-Form).

Die Komplexsalze wurden nach der Beschreibung im Versuchsteile durch Gemischen der Hydrazone und der Metallacetate in Ammoniakwasser oder Ammoniakwasser-Alkohol-Gemische dargestellt. Die Kupfersalze bilden bräunlichgrüne Kristalle, die Nickelsalze orangerote Kristalle. Nach den analytischen Daten kommt ihnen eine allgemeine Formel $C_{14}H_7N_2O_2RR'R''Me \cdot NH_3$ zu (In bezug auf R, R' und R'', siehe Formel I). Das Kupferkomplexsalz von Salicylaldehyd-2-methoxybenzoylhydrazon enthält jedoch kein Ammoniak. Wenn die Komplexsalze in Vakuum erhitzt werden, dann geben die Kupfersalze Ammoniak völlig ab; die Farbe schlägt nach Olivgrün um. Die Nickelsalze dagegen erleiden keinen Gewichtsverlust. Von Interesse sind die Kupferkomplexsalze von Salicylaldehyd-2-oxybenzoylhydrazon und -4-oxybenzoylhydrazon, sowie das Nickelkomplexsalz von Salicylaldehyd-2-oxy-4-aminobenzoylhydrazon; jedes enthält ausser dem Ammoniak auch 1 Mol. Wasser, und, beim Erhitzen in Vakuum geben die Kupfersalze anfangs Wasser dann Ammoniak ab. Das Nickelsalz verliert aber nur das Wasser und verwandelt sich zu orangerotem Pulver. Daher muss das Wasser mit den Molekülen lockerer gebunden sein als das Ammoniak. Die Farbe des wasserfreien Kupfersalzes von Salicylaldehyd-2-oxybenzoylhydrazon ist der des wasserhaltigen ähnlich; diejenige des wasserfreien Kupfersalzes von Salicylaldehyd-4-oxybenzoylhydrazon ist aber deutlich braun. In diesem Falle also könnte sich das Wasser mehr oder weniger an der Koordination beteiligen.

Diese Salze sind alle in Pyridin leicht löslich und können daraus umkristallisiert werden. Die Kupfersalze bilden schwärzlich-braune Kristalle und enthalten an Stelle des Ammoniaks je 1 Mol. Pyridin, das sich beim Erhitzen in Vakuum völlig abspalten lässt. Die pyridinfreien Salze sind olivgrün. Die Nickelsalze bilden zwar bräunlich-rote Kristalle, die aber keine stöchiometrische Menge Pyridin enthalten. Doch ausnahmsweise enthält das Nickelsalz von Salicylaldehyd-2-oxybenzoylhydrazon 3 Mol. Pyridin. Beim Erhitzen in Vakuum werden nur 2 Mol. Pyridin, mit Glanzverlust, aber ohne Farbveränderung der Kristalle abgegeben

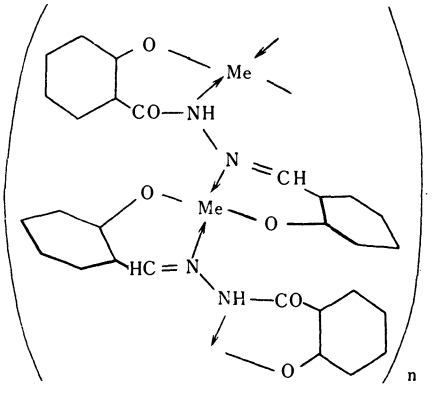

VII

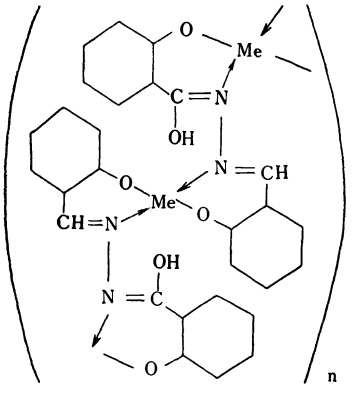

VIII

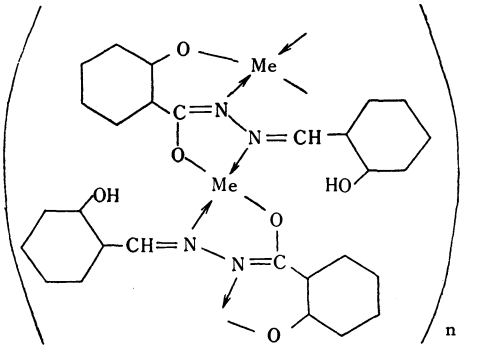

IX

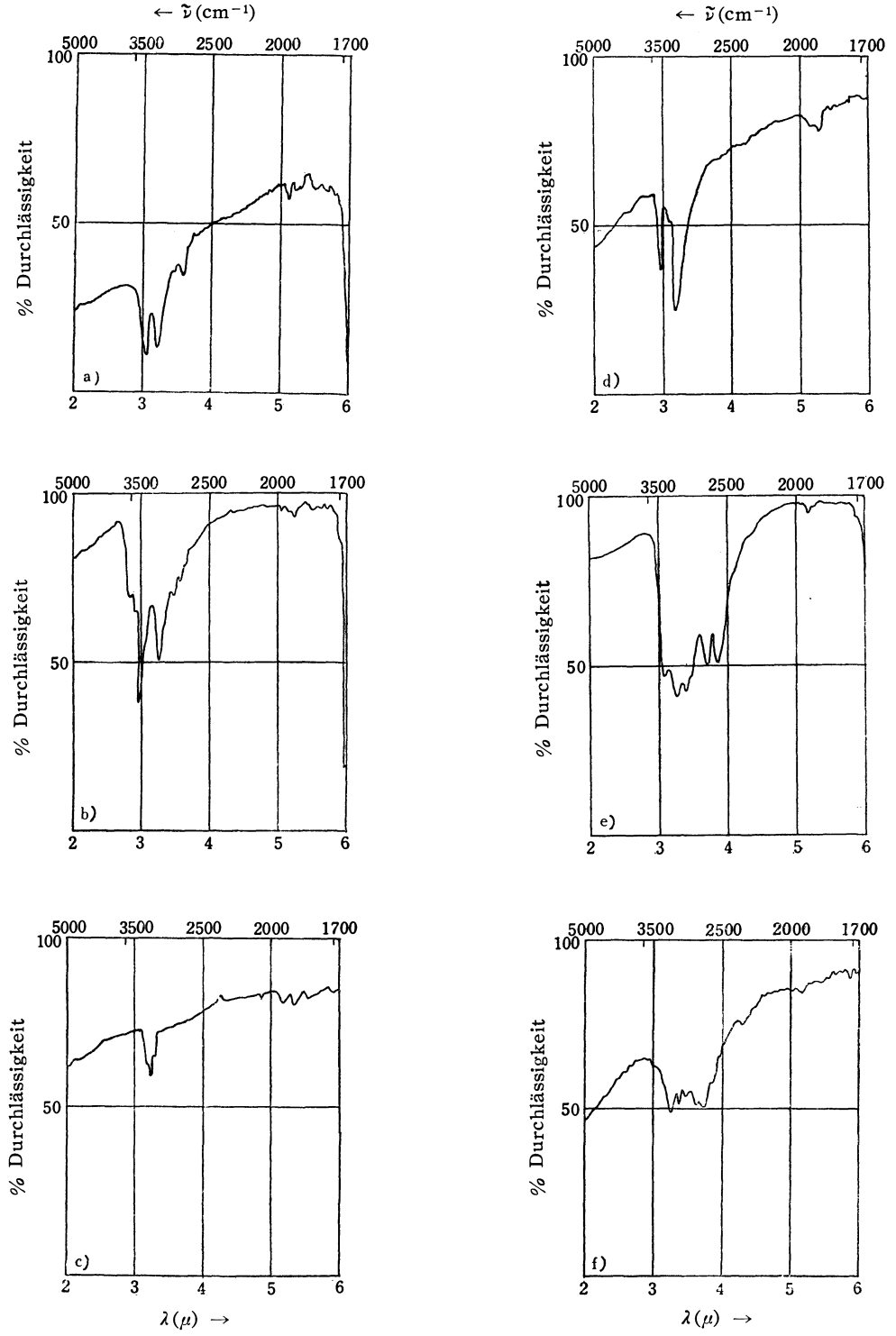

Abb. 2. IR-Spektren. a) Benzaldehyd-benzoylhydrazon; b) Salicylaldehyd-benzoylhydrazon; c) *N*-Salicyliden-*N'*-benzoyl-hydrazino-kupfer (II); d) *N*-Salicyliden-*N'*-benzoyl-hydrazino-monoammin-nickel (II); e) Salicylaldehyd-2-oxybenzoyl-hydrazon; f) *N*-Salicyliden-*N'*-(2-oxybenzoyl)-hydrazino-kupfer (II). (Hexachlorbutadien-Paste).

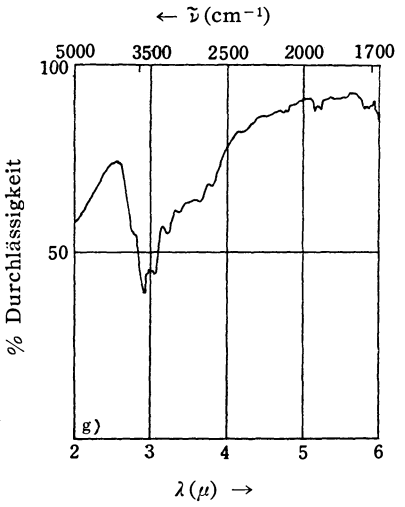

Abb. 2. IR-Spektren. g) *N*-Salicyliden-*N'*-(2-oxybenzoyl)-hydrazino-monoammin-nickel(II). (Hexachlorbutadien-Paste).

(Kristallpyridin); 1 Mol. Pyridin haftet so fest, dass es sich nicht entfernen lässt.

Aus den strukturellen Überlegungen und diesen experimentellen Tatsachen kann man schliessen, dass Ammoniak sowohl als Pyridin (Kristallpyridin ausgenommen) koordinativ mit den Metallatomen gebunden sind, und die Komplexsalze mit VI formuliert werden können. In den ammoniak- bzw. pyridinfreien Kupferkomplexsalzen sind die Kupferatome deshalb koordinativ 3-zählig.

Nach den analytischen Daten allein, könnte man den Komplexsalzen des Salicylaldehyd-2-oxybenzoylhydrazons auch die Formel VII, VIII order IX geben, aber diese drei Formeln werden wohl als unwahrscheinlich ausgeschlossen, weil

1) die hier erhaltenen Komplexsalze schöne Kristalle bilden, während die Salze von der Formel VII, VIII oder IX nur als Pulver erhalten würden,

2) die Ausbildung der Salze von der Formel VIII bzw. IX sterisch nicht oder sehr schwer möglich ist, und schliesslich,

3) die IR-Spektren der Komplexsalze die Anwesenheit chelatisierter Hydroxylgruppen sicher machen; die Salze VII keine Hydroylgruppe, diejenigen von der Formel VIII oder IX nur die nicht chelatisierten Hydroxylgruppen, besitzen sollten.

Einige Vesuche, sie zu methylieren und aus den methylierten Komplexsalzen das Salicylaldehyd-2-methoxybenzoylhydrazon zu isolieren, aber schlugen fehl.

Erhalten wurden, Salicylaldehyd-2-oxy-4-aminobenzoylhydrazon, 5-Bromsalicylaldehyd-2-oxybenzoylhydrazon; *N*-Salicyliden-*N'*-benzoyl-hydrazino-monoammin-kupfer(II)-monohydrat, *N*-Salicyliden-*N'*-benzoyl-hydrazino-monopyridin-kupfer(II), *N*-Salicyliden-*N'*-benzoyl-hydrazino-kupfer-(II), *N*-Salicyliden-*N'*-(2-methoxybenzoyl)-hydrazino-kupfer(II), *N*-Salicyliden-*N'*-(4-oxybenzoyl)-hydrazino-monoammin-kupfer-(II)-monohydrat, *N*-Salicyliden-*N'*-(4-oxybenzoyl)-hydrazino-monoammin-kupfer-(II), *N*-Salicyliden-*N'*-(4-oxybenzoyl)-hydrazino-mono-pyridin-kupfer(II), *N*-Salicyliden-*N'*-(4-oxybenzoyl)-hydrazino-kupfer (II), *N*-Salicyliden-*N'*-(2-oxybenzoyl)-hydrazinomonoammin-kupfer(II)-monohydrat, *N*-Salicyliden-*N'*-(2-oxybenzoyl)-hydrazino-monoammin-kupfer(II), *N*-Salicyliden-*N'*-(2-oxybenzoyl)-hydrazino-monopyridin-kupfer(II), *N*-Salicyliden-*N'*-(2-oxybenzoyl)-hydrazino-kupfer(II), *N*-Salicyliden-*N'*-(2-oxy-4-aminobenzoyl)-hydrazino-kupfer(II), *N*-(5-Bromsalicyliden)-*N'*-(2-oxybenzoyl)-hydrazino-monoammin-kupfer(II), *N*-(5-Bromsalicyliden)-*N'*-(2-oxybenzoyl)-hydrazino-monopyridin-kupfer(II), *N*-(5-Bromsalicyliden)-*N'*-(2-oxybenzoyl)-hydrazino-kupfer(II); *N*-Salicyliden-*N'*-benzoyl-hydrazino-monoammin-nickel(II), *N*-Salicyliden-*N'*-(4-oxybenzoyl)-hydrazino-monoammin-nickel(II), *N*-Salicyliden-*N'*-(2-oxybenzoyl)-hydrazino-monoammin-nickel(II), *N*-Salicyliden-*N'*-(2-oxybenzoyl)-hydrazino-monopyridin-nickel(II)-dipyridinat, *N*-Salicyliden-*N'*-(2-oxybenzoyl)-hydrazino-monopyridin-nickel(II), *N*-Salicyliden-*N'*-(2-oxy-4-aminobenzoyl)-hydrazino-monoammin-nickel(II)-monohydrat, *N*-Salicyliden-*N'*-(2-oxy-4-aminobenzoyl)-hydrazino-monoammin-nickel(II), und *N*-(5-Bromsalicyliden)-*N'*-(2-oxybenzoyl)-hydrazino-monoammin-nickel(II).

Beschreibung der Versuche

Die IR-Spektren wurden mit dem Ōyō-Kōken-Gerät, Modell DS 201 aufgenommen.

Salicylaldehyd-aroylhydrazone.—Sie sind, im allgemeinen, durch Gemischen berechneter Mengen von Salicylaldehyd und Säurehydraziden im Alkohol leicht darstellbar.

Salicylaldehyd-2-oxy-4-aminobenzoylhydrazon.—Man mischt 1.2 g Salicylaldehyd in 25 ccm Ammoniakwasser (28%) und 1.7 g 2-Oxy-4-aminobenzoesäurehydrazid in 15 ccm Ammoniakwasser. Nach einiger Zeit neutralisiert man vorsichtig mit verdünnter Salzsäure und kristallisiert den so entstandenen Niederschlag aus wässrigem Pyridin um. Hellgelbe Platten, die bei 225°C zu zersetzen beginnen und bei 259~260°C (unkorr.) unter Zersetzung schmelzen.

Anal. Gef.: C, 62.00; H, 4.84; N, 15.54. Ber. für $C_{14}H_{13}O_3N_3$: C, 61.98; H, 4.83; N, 15.49%.

5 - Bromsalicylaldehyd - 2 - oxybenzoylhydrazon wurde nach der allgemeinen Methode dargestellt und aus Eisessig umkristallisiert. Hellgelbe Nadeln, die bei 271～272°C (unkorr.) unter Zersetzung schmelzen.

Anal. Gef.: C, 49.97; H, 3.49; N, 8.12. Ber. für $C_{14}H_{11}O_3N_2Br$: C, 50.17; H, 3.31; N, 8.36%.

Kupferkomplexsalze. — *N-Salicyliden-N'-benzoyl-hydrazino-monoammin-kupfer(II)-monohydrat.* —Man gibt zur Lösung von 240 mg Salicylaldehydbenzoylhydrazon in 15 ccm Ammoniakwasser(28%)-Alkohol-Gemische (Volumverhältnis: 2:1), 200 mg Kupferacetat (Monohydrat) gelöst in 5 ccm demselben Gemische. Es entsteht sofort eine grüne Lösung, aus der braune Nadeln nach und nach ausfallen.

Anal. Gef.: C, 50.21; H, 4.58; N, 12.33; H_2O+NH_3, 10.34; Cu, 18.62. Ber. für $C_{14}H_{10}O_2N_2 \cdot NH_3 \cdot Cu \cdot H_2O$: C, 49.92; H, 4.49; N, 12.48; H_2O+NH_3, 10.41; Cu, 18.86%.

N-Salicyliden-N'-benzoyl-hydrazino-monopyridin-kupfer(II).—Man fügt zur Lösung von 240 mg Salicylaldehyd-benzoylhydrazon in 10 ccm Alkohol, eine Lösung von 200 mg Kupferacetat (Monohydrat) in 20 ccm Alkohol zu. Es scheidet sich sofort ein gelblich-grüner Niederschlag ab, der aus Pyridin-Wasser-Gemische umkristallisiert wird. Grünlich-braune Säulen oder grünlich-schwarze Körnchen.

Anal. Gef.: C, 60.09; H, 4.02; N, 11.09; Py., 20.50; Cu, 16.81. Ber. für $C_{14}H_{10}O_2N_2 \cdot C_5H_5N \cdot Cu$: C, 59.91; H, 3.97; N, 11.03; Py., 20.77; Cu, 16.68%.

N - Salicyliden - N'-benzoyl - hydrazino - kupfer(II) wird durch 1- bis 2-stündiges Erhitzen vom Ammin-oder Pyridin-Salze unter vermindertem Drucke (130°C/25 mmHg) erhalten. Die Farbe ist olivgrün.

Anal. Gef.: C, 56.14; H, 3.51; N, 9.09; Cu, 20.82. Ber. für $C_{14}H_{10}O_2N_2Cu$: C, 55.72; H, 3.34; N, 9.28; Cu, 21.05%.

N-Salicyliden-N'-(2-methoxybenzoyl)-hydrazino-kupfer(II).—Man versetzt eine Lösung von 166 mg 2-Methoxybenzoesäurehydrazid in 5 ccm Alkohol mit 122 mg Salicylaldehyd. Eine gelbe Lösung entsteht, zu der man eine Lösung von 200 mg Kupferacetat (Monohydrat) in 5 ccm Ammoniakwasser (28%) gibt. Die so erhaltene, schwarzgrüne klare Lösung engt man auf dem Wasserbade allmählich ein. Dunkelgrüne Nädelchen, die in Pyridin so leicht löslich sind, dass sie sich nicht daraus umkristallisieren lassen.

Anal. Gef.: C, 54.26; H, 3.97; N, 8.32; Cu, 19.18. Ber. für $C_{15}H_{12}O_3N_2Cu$: C, 54.30; H, 3.64; N, 8.44; Cu, 19.15%.

N-Salicyliden-N'-(4-oxybenzoyl)-hydrazino-monoammin-kupfer(II)-monohydrat wird in derselben Weise wie beim *N*-Salicyliden-*N'*-(2-methoxybenzoyl)-hydrazino-kupfer (II), aus 256 mg Salicylaldehyd-4-oxybenzoylhydrazon in 10 ccm Ammoniakwasser (28%) und 200 mg Kupferacetat (Monohydrat) in 5 ccm Ammoniakwasser dargestellt. Dunkelgrüne glänzende Nädelchen oder Prismen.

Anal. Gef.: C, 47.72; H, 4.55; N, 11.71; H_2O, 5.19; Cu, 17.98. Ber für $C_{14}H_{10}O_3N_2 \cdot NH_3 \cdot Cu \cdot H_2O$: C, 47.66; H, 4.28; N, 11.91; N_2O, 5.11; Cu, 18.01%.

N-Salicyliden-N'-(4-oxybenzoyl)-hydrazino-monoammin-kupfer(II) wird durch 1-stündiges Erhitzen des Monohydrates auf 110～120°C/25 mmHg erhalten. Schwärzlich-braune, glänzende Kristalle.

Anal. Gef.: C, 49.81; H, 4.32; N, 12.53; NH_3, 4.92; Cu, 19.15. Ber. für $C_{14}H_{10}O_3N_2 \cdot NH_3 \cdot Cu$: C, 50.22; H, 3.91; N, 12.55; NH_3, 5.09; Cu, 18.98%.

N-Salicyliden-N'-(4-oxybenzoyl)-hydrazino-monopyridin-kupfer(II) wird durch Umkristallisieren von den Ammin-Salzen aus Pyridin dargestellt. Schwarz-violette, glänzende Körnchen.

Anal. Gef.: C, 57.95; H, 4.05; N, 10.67; Py., 19.93; Cu, 15.86. Ber. für $C_{14}H_{10}O_3N_2 \cdot C_5H_5N \cdot Cu$: C, 57.50; H, 3.81; N, 10.59; Py., 19.93; Cu, 16.01%.

N - Salicyliden - N' - (4 - oxybenzoyl) - hydrazino-kupfer(II) wird entweder durch 2-stündiges Erhitzen von den Ammin-Salzen auf 160～170°C/25 mm Hg als dunkelgrünes Pulver, oder durch 7-stündiges Erhitzen vom Pyridin-Salze auf 170°C/25 mmHg als gelb-grünes Pulver erhalten.

Anal. Gef.: C, 52.96; H, 3.44; N, 8.81; Cu, 19.58. Ber. für $C_{14}H_{10}O_3N_2Cu$: C, 52.91; H, 3.17; N, 8.82; Cu, 19.99%.

N-Salicyliden-N'-(2-oxybenzoyl)-hydrazino-monoammin-kupfer(II)-monohydrat. — Man fügt zur Lösung von 256 mg Salicylaldehyd-2-oxybenzoylhydrazon in 15 ccm verdünntem Ammoniakwasser (hergestellt aus 1 Vol. 28%-igem Ammoniakwasser und 1 Vol. Wasser), eine Lösung von 200 mg Kupferacetat (Monohydrat) in 10 ccm verdünntem Ammoniakwasser zu. Es fällt sofort ein hellgrüner Niederschlag ab, den man aus Ammoniakwasser-Alkohol-Gemische (Volumverhältnis: 1:2) umkristallisiert. Bräunlich-grüne Nadeln.

Anal. Gef.: C, 47.85; H, 4.39; N, 11.79; H_2O, 5.40; Cu, 18.22. Ber. für $C_{14}H_{10}O_3N_2 \cdot NH_3 \cdot Cu \cdot H_2O$: C, 47.66; H, 4.28; N, 11.91; H_2O, 5.11; Cu, 18.01%. Erhitzt man das Komplexsalz 1 Stunde auf 80～100°C/25 mmHg, so erhält man das kristallwasserfreie Salz, *N-Salicyliden-N'-(2-oxybenzoyl)-hydrazino-monoammin-kupfer(II)*, in bräunlich-grünen Nadeln.

Anal. Gef.: C, 50.71; H, 3.64; N, 10.85; NH_3, 4.70; Cu, 18.72. Ber. für $C_{14}H_{10}O_3N_2 \cdot NH_3 \cdot Cu$: C, 50.22; H, 3.91; N, 12.55; NH_3, 5.09; Cu, 18.98%.

N-Salicyliden-N'-(2-oxybenzoyl)-hydrazino-monopyridin-kupfer(II).—Man kristallisiert den hellgrünen Niederschlag oder die Ammin-Salze aus Pyridin um. Schwarz-grüne Säulen.

Anal. Gef.: C, 57.39; H, 4.05; N, 10.56; Py., 19.93; Cu, 15.96. Ber. für $C_{14}H_{10}N_2O_3 \cdot C_5H_5N \cdot Cu$: C, 57.50; H, 3.81; N, 10.59; Py., 19.93; Cu, 16.01%.

N - Salicyliden - N' - (2 - oxybenzoyl) - hydrazino-kupfer(II).—Man erhält es entweder durch 2-stündiges Erhitzen von den Ammin-Salzen auf 130～140°C/25 mmHg, oder durch 4-stündiges Erhitzen vom Pyridin-Salz auf 130～140°C/25 mmHg als gelb-grünes Pulver.

Anal. Gef.: C, 52.85: H, 3.09; N, 8.76, Cu, 20.11. Ber. für $C_{14}H_{10}O_3N_2Cu$: C, 52.91; H, 3.17; N, 8.82; Cu, 19.99%.

N-Salicyliden-N'-(2-oxy-4-aminobenzoyl)-hydrazino-kupfer(II).—Man gibt zur Lösung von 271 mg Salicylaldehyd-2-oxy-4-aminobenzoylhydrazon in 10 ccm Ammoniakwasser (28%), eine Lösung von 200 mg Kupferacetat (Monohydrat) in 10 ccm Ammoniakwasser. Der anfangs entstandene grüne

Niederschlag wird, während des Umrührens, bräunlich-grüne Nädelchen, die man aus Pyridin umkristallisiert. Schwarz-violette Säulen, die keine stöchiometrische Menge Pyridin enthalten. Analysiert wurde eine Substanzprobe, die durch 2-stündiges Erhitzen auf 130~140°C/25 mmHg als dunkelgrünes Pulver erhalten worden war.

Anal. Gef.: C, 50.76; H, 3.48; N, 12.39; Cu, 18.81. Ber. für $C_{14}H_{11}O_3N_3Cu$: C, 50.53; H, 3.33; N, 12.63; Cu, 19.09%.

N-(5-Bromsalicyliden)-N'-(2-oxybenzoyl)-hydrazino-monoammin-kupfer(II).—Man gibt zur Lösung von 335 mg 5-Bromsalicylaldehyd-2-oxybenzoylhydrazon in 15 ccm *n*-Propylalkohol-Ammoniakwasser (28%)-Gemische (Volumverhältnis: 2:1), eine Lösung von 200 mg Kupferacetat (Monohydrat) in 15 ccm demselben Gemische. Gelb-grüne Nädelchen.

Anal. Gef.: C, 40.48; H, 3.13; N, 9.72; NH_3, 4.26; Cu, 15.30. Ber. für $C_{14}H_9O_3N_2Br \cdot NH_3 \cdot Cu$: C, 40.64; H, 2.92; N, 10.16; NH_3, 4.12; Cu, 15.36%.

N-(5-Bromsalicyliden)-N'-(2-oxybenzoyl)-hydrazino-monopyridin-kupfer(II). — Man gibt zur Lösung von 335 mg 5-Bromsalicylaldehyd-2-oxybenzoylhydrazon in 10 ccm Ammoniakwasser (28%), eine Lösung von 200 mg Kupferacetat (Monohydrat) in 10 ccm Ammoniakwasser. Es scheidet sich sofort ein dunkelgrüner Niederschlag, der aus Pyridin umkristallisiert wird. Schwarze Säulen. Das Pyridin haftet so fest, dass es durch Erhitzen nur schwer (ca. 20 Stunden, auf 150~160°C/25 mmHg) entfernt werden kann.

Anal. Gef.: C, 48.21; H, 3.06; N, 9.00; Py., 16.67; Cu, 13.06. Ber. für $C_{14}H_9O_3N_2Br \cdot C_5H_5N \cdot Cu$: C, 47.96; H, 2.96; N, 8.83; Py., 16.62; Cu 13.35%.

N-(5-Bromsalicyliden)-N'-(2-oxybenzoyl)-hydrazino-kupfer(II) ist entweder aus dem Ammin- oder dem Pyridin-Salze durch Erhitzen unter vermindertem Drucke darstellbar. Gelb-grünes (aus dem Ammin-Salze) oder olivgrünes (aus dem Pyridin-Salze) Pulver.

Anal. Gef.: C, 42.48: H, 2.32; N, 7.19; Cu, 15.97. Ber. für $C_{14}H_9O_3N_2BrCu$: C, 42.39; H, 2.29; N, 7.06; Cu, 16.02%.

Nickelkomplexsalze. — *N-Salicyliden-N'-benzoylhydrazino-monoammin-nickel(II)*. — Man gibt zur Lösung von 240 mg Salicylaldehyd-benzoylhydrazon in 15 ccm Ammoniakwasser (28%)-Alkohol Gemische (Volumverhältnis: 2:1), eine Lösung von 250 mg Nickelacetat (Tetrahydrat) in 5ccm demselben Gemische. Die enstandene tiefrote Lösung engt man auf dem Wasserbade ein. Es scheiden sich nach dem Erkalten schöne, rote Nadeln aus.

Anal. Gef.: C, 53.62: H, 4.24; N, 13.54; Ni, 18.52. Ber. für $C_{14}H_{10}O_2N_2 \cdot NH_3 \cdot Ni$: C, 53.56; H, 4.17; N, 13.38; Ni, 18.70%.

N-Salicyliden-N'-(4-oxybenzoyl)-hydrazino-monoammin-nickel(II) ist in derselben Weise wie beim *N*-Salicyliden-*N'*-benzoylhydrazino-monoammin-nickel(II), aus 256 mg Salicylaldehyd-4-oxybenzoylhydrazon in 10 ccm Ammoniakwasser (28%) und 250 mg Nickelacetat (Tetrahydrat) in 5 ccm Ammoniakwasser darstellbar. Schöne, rote Nädelchen.

Anal. Gef.: C, 50.89: H, 4.19; N, 12.58; Ni, 17.60. Ber. für $C_{14}H_{10}O_3N_2 \cdot NH_3 \cdot Ni$: C, 50.96; H, 3.97; N, 12.73; Ni, 17.79%.

N-Salicyliden-N'-(2-oxybenzoyl)-hydrazino-monoammin-nickel(II).—Man fügt 250 mg Nickelacetat (Tetrahydrat) gelöst in 10 ccm Ammoniakwasser (28%) zu einer Lösung von 256 mg Salicylaldehyd-2-oxybenzoylhydrazon in 100 ccm Ammoniakwasser zu. Das Gemisch trübt sich. Nach einiger Zeit beginnen hellbraune, glänzende Kristalle sich auszuscheiden, die abgesaugt und mit wenig Ammoniakwasser gewaschen werden. Beim Liegen an der Luft schlägt die Farbe von Hellbraun nach Orangerot um. Orangerote, glänzende Blättchen.

Anal. Gef.: C, % 50.75; H, 4.12; N, 12.22; Ni, 17.91. Ber. für $C_{14}H_{10}O_3N_2 \cdot NH_3 \cdot Ni$: C, 50.96; H, 3.97; N, 12.73; Ni, 17.79%.

N-Salicyliden-N'-(2-oxybenzoyl)-hydrazino-monopyridin-nickel(II)-dipyridinat wird durch Umkristallisieren des Ammin-Salzes aus wässrigem Pyridin dargestellt. Gelblich-braunrote, glänzende, Blätter.

Anal. Gef.: C, 63.45; H, 4.65; N, 12.46; Py, 28.49; Ni, 10.89. Ber. für $C_{14}H_{10}O_3N_2 \cdot C_5H_5N \cdot Ni \cdot 2C_5H_5N$: C, 63.30; H, 4.58; N, 12.73; Py., 28.75; Ni, 10.67%.

N-Salicyliden-N'-(2-oxybenzoyl)-hydrazino-monopyridin-nickel(II).—Man erhitzt das Dipyridinat 1 Stunde auf 110°C/25 mmHg. Braun-rote, glanzlose Blätter.

Anal. Gef.: C, 58.29; H, 4.10; N, 10.68; Ni, 15.12. Ber. für $C_{14}H_{10}O_3N_2 \cdot C_5H_5N \cdot Ni$: C, 58.21; H, 3.86; N, 10.72; Ni, 14.97%.

N-Salicyliden-N'-(2-oxy-4-aminobenzoyl)-hydrazino-monoammin-nickel(II)-monohydrat. — Man gibt zur Lösung von 271 mg Salicylaldehyd-2-oxy-4-aminobenzoylhydrazon in 10 ccm Ammoniakwasser (28%), eine Lösung von 250 mg Nickelacetat (Tetrahydrat) in 10 ccm Ammoniakwasser. Es entsteht eine braunrote, klare Lösung, die man auf dem Wasserbade einengt. Braunrote, glänzende Nadeln, die in Ammoniakwasser leicht löslich sind.

Anal. Gef.: C, 46.59; H, 4.60; N, 15.28; H_2O, 5.11; Ni, 16.00. Ber. für $C_{14}H_{11}O_3N_3 \cdot NH_3 \cdot Ni \cdot H_2O$: C, 46.32; H, 4.44; N, 15.43; H_2O, 4.96; Ni, 16.17%. Erhitzt man das Komplexsalz einige Zeit auf 110~120°C/25 mmHg, so erhält man das kristallwasserfreie Salz, *N-Salicyliden-N'-(2-oxy-4-aminobenzoyl)-hydrazino-monoammin-nickel(II)* als braun-rotes Pulver.

Anal. Gef.: C, 48.53; H, 4.09; N, 16.11; Ni, 17.23. Ber. für $C_{14}H_{11}O_3N_3 \cdot NH_3 \cdot Ni$: C, 48.74; H, 4.09; N, 16.24; Ni, 17.02%.

N-(5-Bromsalicyliden)-N'-(2-oxybenzoyl)-hydrazino-nickel(II).—Man gibt zur Lösung von 335 mg 5-Bromsalicylaldehyd-2-oxybenzoylhydrazon in 10 ccm Ammoniakwasser (28%) - Alkohol - Gemische (Volumverhältnis: 1:1), eine Lösung von 250 mg Nickelacetat (Tetrahydrat) in 10 ccm demselben Gemische. Sofort entsteht eine rot-braune Lösung, aus der, beim gelinden Erwärmen auf dem Wasserbade, rötlich-gelbe Nadeln allmählich auskristallisieren.

Anal. Gef.: C, 41.14; H, 3.09; N, 10.36; Ni,

14.43. Ber. für $C_{14}H_9O_3N_2Br \cdot NH_3 \cdot Ni$: C, 41.12; H, 2.96; N, 10.28; Ni, 14.36%.

Meinem Lehrer, Herrn Professor Dr. Tokuichi Tsumaki danke ich herzlich für die Unterstützung und Förderung dieser Arbeit. Herrn a. o. Prof. Dr. Yo Ueda, Herren Hidetoshi Yoshimura und Hiroshige Yano (Pharmazeutisches Institut, Medizinische Fakultät, Kyushu Universität) bin ich für die Aufnahme der IR-Spektren zu grossem Dank verpflichtet. Herrn Michio Shido und Frl. Sachiko Indo (Laboratorium der Elementaranalyse, Kyushu Universität) verdanke ich die Durchführung der C-, H-, und N-Bestimmungen.

Chemisches Institut, Naturwissenschaftliche Fakultät, Kyushu Universität, Hakozaki Fukuoka

Separation of Radioactive Cesium in Biological Materials

By Noboru YAMAGATA and Toshiko YAMAGATA

(Received July 15, 1958)

A number of procedures for the separation of low concentrations of radioactive cesium in natural materials have been studied by several workers. When the final radioassay is to be achieved by beta counting, the first problem is the decontamination of natural radioactive elements, rubidium and potassium, the second is the removal of the other fission activities, particularly of the long-lived strontium-90 and cerium-144, and the third is the method of elimination of the bulk of other elements including sodium and potassium.

In the earlier work on the determination of cesium-137 in biological materials[1], the authors adopted the usual method of separation of the alkali elements, that consists in the elimination of the sulfate ion with barium chloride followed by the removal of alkaline earth elements as carbonate and oxalate. Those procedures were supposed to carry down other fission activities, although the loss of cesium in the whole process was proved to be very small as already reported[2]. The bulk of the sodium chloride and a part of the potassium chloride were removed by hydrochloric acid—the ethanol method and the elimination of rubidium and potassium were effectively undertaken by the cesium chloroplatinate precipitation method in an aqueous medium[3].

This method is certainly generally useful and suitable but the first half of the procedure is troublesome when dealing with a large number of samples. The present study deals with the examination of the direct precipitation of cesium with ammonium phosphomolybdate and a simple and rapid separation method for cesium-137 is presented.

Principle.—The method is based on two separations involving the selective precipitation of cesium with ammonium phosphomolybdate in an acid medium and the relative solubilities of the alkali chloroplatinates in water.

Because an excess of phosphate ion which is usually present in the processed solution of food, urine or tissues will interfere with the perfect precipitation of cesium with ammonium phosphomolybdate, it must be previously removed by alkalination to form calcium and magnesium phosphates. In this procedure a partial elimination of other fission activities can be attained. The precipitated cesium ammonium phosphomolybdate is dissolved in ammonium hydroxide and after boiling to expel excess of ammonia, the precipitation with chloroplatinic acid is performed. The precipitate is weighed and mounted for beta counting.

Experimental

Special Reagents. — Ammonium molybdate solution, 10% of $(NH_4)_6Mo_7O_{24}\cdot 4H_2O$ in water; Cesium carrier (CsCl), 10mg. of Cs per ml. of water; Chloroplatinic acid, 10% of $H_2PtCl_6\cdot 6H_2O$ in water; Salt solutions, containing 20 g. of K^+,

1) N. Yamagata and T. Yamagata, *Japan Analyst (Bunseki Kagaku)*, **7**, 433 (1958).
2) N. Yamagata and T. Yamagata, ibid., **5**, 37 (1956).
3) N. Yamagata and E. Tajima, This Bulletin, **30**, 674 (1957).

Na^+, and Ca^{2+} respectively, 10 g. of Mg^{2+} and 0.2 g. of Fe^{3+} per liter of water.

Radioactive tracers. — ^{137}Cs (carrier-free), Nitrate in nitric acid solution, from the Radiochemical Center, England; ^{89}Sr (carrier-free), Chloride in hydrochloric acid solution from Oak Ridge National Laboratory Batch No. 229A; ^{144}Ce (carrier-free), Nitrate in nitric acid solution from Oak Ridge National Laboratory Batch No. 50; ^{91}Y (carrier-free), Chloride in hydrochloric acid solution from Oak Ridge National Laboratory Batch No. 76.

To make the conditions of precipitation as close as possible to the actual case, a salt solution containing potassium, sodium, calcium, magnesium and ferric ions was prepared. It was considered to possess a similar elementary composition to food, urine or tissues. A proper quantity of the salt solution was used for the tracer experiments.

Conditions of phosphomolybdate precipitation. — As for the conditions of phosphomolybdate precipitation, above all, for interfering substances, the temperature and the composition of precipitate, many investigations have been reported. As far as only the recovery of cesium is concerned, it matters but little what the composition of the phosphomolybdate precipitate may be. For this reason, the solution containing the phosphate ion was heated to 50~60°C and then ammonium molybdate solution was added. To determine the minimum volume of ammonium molybdate solution necessary to precipitate cesium completely, an experiment was performed of which the results are shown in Table I. Provided that one mole of P_2O_5 combines with 24 moles of MoO_3, 0.68 ml of 10% ammonium molybdate solution is equivalent to 1 mg. of phosphorus. The result of the experiment indicates that about three times or more excess of the reagent solution is needed for the perfect precipitation of cesium.

TABLE I

PRECIPITATION OF CESIUM WITH AMMONIUM PHOSPHOMOLYBDATE

Total volume of soln., 50 ml.; conc. HNO_3, 2 ml.; H_3PO_4 (as P), 1 mg.; Cs carrier, 2 mg.

Soln.		NH_4 molybdate soln. added (ml.)	Cs pptd. (%)
Salt soln.	5 ml.	0.5	0
〃	〃	1.0	3.6
〃	〃	2.0	96.9
〃	〃	3.0	100.1
〃	〃	5.0	99.6
Oak leaf ash (processed)	2 g.	3.0	98.8
Human urine (processed)	50 ml.	3.0	95.7
Bittern	10 ml.	3.0	99.6
〃	30 ml.	3.0	95.9
〃	42 ml.	3.0	85.6

Several samples of natural materials were substituted for the salt solution and the result is satisfactory except in the case of 42 ml. of bittern. Two grams of oak leaf ash contained 0.232 g. of potassium and 50 ml of urine contained about 0.05 g. of potassium and 0.2 g. of sodium.

TABLE II

EFFECT OF SEVERAL IONS ON THE RECOVERY OF CESIUM

Total vol. of soln., 100 ml.; conc. HNO_3, 4 ml.; H_3PO_4 (as P), 2 mg.; ^{137}Cs, carrier-free; NH_4 molybdate soln., 10 ml.

Ions	Concn. (%)	^{137}Cs recovery (%)
NH_4^+ (nitrate)	0	99.2
〃	0.01	98.2
〃	0.1	97.2
〃	1	68.0
〃	5	23.7
K^+ (chloride)	1	99.5
〃	5	87.4
〃	10	79.9
〃	20	53.3
Na^+ (chloride)	1	100
〃	2	98.9
〃	5	99.2
〃	10	98.9

One hundred milliliters of the bittern contained 4.99 g. of potassium chloride, 5.24 g. of sodium chloride, 24.8 g. of magnesium chloride and 8.36 g. of magnesium sulfate and the results of the experiment indicate that milligram quantities of cesium could successfully be precipitated from considerably dense solutions.

Effect of several ions on the recovery of cesium.—The effect of ammonium, potassium and sodium ions on the recovery of carrier-free cesium was examined (Table II). A bulk quantity of those ions which hastened the separation of the precipitate and ammonium ion might decrease the solubility as a result of the common-ion effect. At concentrations above one per cent of ammonium and five per cent of potassium, the precipitate carried no more the cesium tracer completely. Sodium chloride did not interfere with the perfect precipitation at its almost saturated solution.

TABLE III

PRECIPITATION OF VARIOUS AMOUNTS OF CESIUM BY THE PHOSPHOMOLYBDATE METHOD

Total vol. of soln., 100 ml.; conc. HCl, 4 ml.; H_3PO_4 (as P), 2 mg.; NH_4Cl (as NH_4), 100 mg.; Ammonium molybdate soln., 10 ml.; ^{137}Cs activity added, 1750 c.p.m.

Cs taken mg.	Activity carried c. p. m.	Cs recovery %
carrier-free	1718	98.2
0.01	1726	98.6
0.1	1740	99.4
1	1773	101
10	1782	101
100	239	13.6

TABLE IV
CONTAMINATION OF CESIUM AMMONIUM PHOSPHOMOLYBDATE WITH OTHER FISSION ACTIVITIES

Tracer	Carrier	Activity taken c. p. m.	Activity carried c. p. m.	Contamination %	Remarks
^{89}Sr	carrier-free	3.3×10^5	227	0.068	HNO_3 acid
〃	〃	〃	95	0.029	HCl acid
〃	Sr 70 p.p.m.	4.1×10^4	23	0.056	HCl acid
^{144}Ce	carrier-free	5×10^4	80	0.16	HNO_3 acid
〃	〃	〃	86	0.17	HCl acid
^{91}Y	〃	5×10^4	175	0.35	HNO_3 acid
〃	〃	〃	203	0.40	HCl acid

Effect of the amount of carrier cesium.—For the purpose of determining cesium-137 concentrations in natural materials, a definite quantity of carrier cesium is added prior to the separation procedures, and the measured activity must be corrected for the chemical yield of cesium. To determine a preferable amount of the carrier, and to ditermine whether various amounts of cesium could successfully be precipitated with ammonium phosphomolybdate or not, an experiment was carried out. The result is shown in Table III. From tracer concentrations up to 100 p.p.m. of cesium in acid solution could be perfectly precipitated with ammonium phosphomolybdate in the presence of 20 p.p.m. of phosphorus.

Contamination of cesium ammonium phosphomolybdate with other fission activities.—Contamination of cesium ammonium phosphomolybdate with other radioactive nuclides is a matter of concern when a direct precipitation is performed without scavenging pretreatment. Attention has therefore been centered on isotopes of fairly long half-lives, strontium and cerium. Cesium was precipitated from the solution containing each of the following, strontium-89, cerium-144 and yttrium-91, and the precipitate was mounted for counting. The conditions of the precipitation were the same as described in Table I. The result shown in Table IV indicates good decontamination of each of the nuclides in question.

Contamination with potassium and rubidium.—An accurate estimation of cesium-137 by beta counting will be unsuccessful when the precipitate of cesium ammonium phosphomolybdate is contaminated with rubidium and/or potassium. According to the geochemical studies by one of the authors on the rare alkali elements in biological materials[4], the average weight ratio of K : Rb : Cs was about $10^5 : 10^2 : 1$ for natural plants. A preliminary investigation on the cesium-137 concentration indicated that the isotopic ratio of ^{137}Cs : ^{133}Cs in 1957 was $(1\sim10)\times10^{-8}$ for human urine and Japanese food materials. Thus the disintegration ratio of ^{40}K : ^{87}Rb : ^{137}Cs is calculated to be approximately 200 : 5 : (2～20). When the radioactivity of cesium-137 is to be measured with an average error of 10% and the contamination with potassium and/or rubidium must be kept less than 2～3% of the cesium activity, a decontamination factor of 10～100 is necessary for rubidium and $10^3\sim10^4$ is necessary for potassium.

TABLE V
CONTAMINATION OF AMMONIUM PHOSPHOMOLYBDATE PRECIPITATE WITH POTASSIUM AND RUBIDIUM
Total vol. of soln., 100 ml.; conc. HNO_3, 4 ml.; H_3PO_4 (as P), 2 mg.; NH_4 molybdate soln., 10 ml.

Dissolved element mg.		Found in ppt. mg.	Decontamination factor
K	0.1	n. d.	—
〃	1	n. d.	—
〃	10	n. d.	—
〃	10^2	0.1	10^3
〃	10^3	1.1	9×10^2
〃	10^4	7.3	1.4×10^3
Rb	0.01	n. d.	—
〃	0.1	n. d.	—
〃	1	0.5	2
〃	10	4.3	2.3
〃	10^2	13	7.7

Ammonium phosphomolybdate was precipitated from the solutions containing various amounts of potassium and rubidium and analyzed for those elements by a flame photometry. The result shown in Table V suggests that this single separation is insufficient for the necessary decontamination especially for rubidium. Another step of decontamination is desirable. To meet with this demand, the chloroplatinate precipitation method[3] was adopted because of the great difference of solubilities between the alkali elements including ammonium. The potassium chloroplatinate is approximately 90 times, the ammonium salt 60 times, and the rubidium salt 3 times more soluble in water than the cesium chloroplatinate at 20°C[3]. This method was already proposed for the carrier-free separation of cesium by one of the authors.

4) N. Yamagata, *J. Chem. Soc. Japan, Pure Chem. Sec.* (*Nippon Kagaku Zassi*), **72**, 299, 610 (1951).

TABLE VI
PHOSPHATE ELIMINATION BY HOT-WATER EXTRACTION
(200 ml. of human urine)

No.	^{137}Cs			P	
	added c.p.m.	extracted c.p.m.	recovery %	contained mg.	extracted mg.
1	1920	1816	94.6	816	110
2	1948	1853	95.2	827	112
3	1937	1809	93.5	686	92.5
4	2111	2003	94.8	356	48.0

Preliminary removal of excessive phosphate and other fission activities.—Biological material contains a bulk quantity of phosphate and the phosphomolybdate precipitation can not be applied directly, because an excess of phosphate and a shortage of ammonium molybdate reagent results in insufficient precipitation of cesium as shown in Table I. When sufficient quantity of the reagent for the perfect precipitation of phosphate is added, a bulky precipitate is formed and the later treatment will become impracticable.

Dry-ashed biological material was treated with hydrochloric - nitric acid mixture (1 : 1) and heated to dryness to destroy the remaining organic matter. If organic matter remains, it may interfere with the precipitation of ammonium phosphomolybdate. The completely dried residue was repeatedly extracted with hot water. The recovery of cesium by the hot-water extraction was checked by a tracer experiment and the result was satisfactory (93.5~95.2%). By this means, a greater part of phosphate remained insoluble as calcium or magnesium phosphate (Table VI).

The extract was treated with ammonium hydroxide and the phosphates of calcium and magnesium were precipitated. These carried down the tracers of cerium-144 and yttrium-91 almost perfectly and a part of strontium-89. The loss of cesium-137 was only a tenth of one per cent (Table VII).

TABLE VII
REMOVAL OF THE FISSION ACTIVITIES BY PHOSPHATE PRECIPITATION
Total vol. of soln., 150 ml.; Salt soln., 50 ml.; H_3PO_4 (as P), 100 mg.; conc. NH_4OH, 2 ml. excess.

Tracer (carrier-free)	Activity taken c. p. m.	Activity carried c. p. m.	Removal %
^{89}Sr	39853	6703	16.8
^{91}Y	47501	47401	99.8
^{137}Cs	21573	37	0.17
^{144}Ce	64947	64712	99.6

Over-all decontamination and recovery of cesium.—The elimination of other elements and radioactive nuclides by the present method of cesium separation is schematically summarized in Table VIII. The over-all decontamination and the recovery of cesium were determined by an experiment with 75 ml. of salt solution (containing 1.5 g. each of calcium, potassium and sodium, 0.75 g. of magnesium and 0.015 g. of iron). The solution was diluted to about 300 ml. with water after the addition of 10~30 mg. of cesium carrier, 1 mg. of rubidium and a proper quantity of radioactive tracer. Then, it was treated as described in the following paragraph under separation. The precipitate of cesium chloroplatinate was examined for the presence of ammonium, rubidium, and potassium after being weighed and counted.

TABLE VIII
ELIMINATION OF OTHER ELEMENTS AND NUCLIDES BY THE PRESENT METHOD OF CESIUM SEPARATION

Procedure		Eliminated elements and nuclides
1st	Phosphate pptn.	Ca, Mg, Fe, Al, Heavy metals ^{144}Ce, ^{91}Y
2nd	NH_4 phosphomolybdate pptn.	Ca, Mg, K, Na ^{144}Ce, ^{89}Sr, ^{91}Y
3rd	Chloroplatinate pptn.	NH_4^+, ^{87}Rb, ^{40}K

Only a trace of ammonium was found in the precipitate. The contribution of the activity of potassium-40 is less than 0.2 dpm, while that of rubidium-87 is calculated as approximately 1 dpm without regard to self absorption. As the beta energy of rubidium-87 is considerably lower (0.275 Mev) than that of cesium-137 (0.52 Mev), the greater absorption minimizes the contribution of contaminated rubidium activity to the cesium activity[1].

A device for cesium-133 determination.—The precipitation of a trace of cesium with ammonium phosphomolybdate is so effective that it can be applied to the determination of natural cesium in biological materials without the addition of a carrier.

The precipitate of cesium ammonium phosphomolybdate is dissolved in ammonium hydroxide. The ammoniacal solution is passed through an anion-exchange resin column (OH-form. For example, ϕ 8 mm.×150 mm., Diaion SA #200). The effluent solution is free from phosphate and molybdate and contains ammonium hydroxide and cesium. The solution is evaporated to expel excess of ammonia and to reduce the volume. After neutralization with a drop of

TABLE IX

OVER-ALL DECONTAMINATION AND RECOVERY OF CESIUM

Cs carrier added mg.	Cs recovery %	Activity added c.p.m.	Activity carried c.p.m.	Decontamination factor	K carried μg	Rb carried μg
10	80.5	—	—	—	93	26
30	93.1	—	—	—	77	20
20 (Sr 1 mg.)	84.8	^{89}Sr 6.6×10^5	2.1	3×10^5	88	13
20	92.7	^{91}Y 9.2×10^5	6.1	1.5×10^5	99	21
20	90.4	^{144}Ce 2.2×10^6	10.2	2×10^5	72	18

hydrochloric acid, the cesium can be determined without interference of any other elements by a flame spectrophotometric technique.

Proposed Procedure

The following procedure is proposed for the determination of cesium-137 in biological materials and soil samples. It has been designed for samples containing approximately 10 μμc of cesium-137 or 1/2~1/7 g. of potassium[5]. An aliquot of the sample must be taken aside before the addition of cesium carrier when the natural cesium-133 is being determined.

Sample Preparation.—*Urine.*—Add 50ml. of nitric acid and 2 ml. of cesium carrier to 500 ml. of urine in a beaker and evaporate to approximately 50 ml. Transfer the solution into a porcelein dish and heat to dryness. Moisten the residue with hydrochloric-nitric acid mixture (1 : 1) and heat to dryness. Repeat the treatment several times to destroy all of the organic matter. Extract the dried residue with five 50 ml. portions of hot-water and filter. Make up the combined filtrate to approximately 300 ml, and proceed as under separation.

Cereals, Vegetables and Dry Milk.—Dry ash about 300~500 g. of cereals (100~200 g. of dried vegetables, 50 g. of dry milk) at 400~450°C. Extract the ash (or carbonized matter) after the addition of 2 ml. of cesium carrier with five 50 ml. portions of hot hydrochloric acid (1 : 10) and filter. Transfer the combined filtrate into a porcelein dish and evaporate to dryness after the addition of 50 ml. of nitric acid. Extract the dried residue with five 50 ml. portions of hot-water and filter. Make up the combined filtrate to approximately 300 ml, and proceed as under separation.

Soil (N-ammonium acetate extraction).—Add 3 liters of N-ammonium acetate solution (pH 7) to 300 g. of fresh soil in a 5 liter beaker. Stand the mixture for 4~5 days with occasional agitation, and then filter the supernatant. Evaporate the filtrate after the addition of 2 ml. of cesium carrier in a porcelein dish to dryness. Moisten the residue with hydrochloric-nitric acid mixture (1 : 1) and heat to dryness. Repeat the treatment several times to destroy all of the organic matter. Extract the dried residue with five 50 ml. portions of hot-water and filter. Make up the combined filtrate to approximately 300 ml, and proceed as under separation.

Separation.—Add ammonium hydroxide dropwise to the solution derived from sample preparation until a dense precipitate of phosphates appears and then add 2 ml. excess of ammonium hydroxide. Allow to settle and test the supernatant liquid for complete precipitation by the addition of ammonium hydroxide. Filter and wash the precipitate with ammonium hydroxide (1 : 100). Combine the wash solution and the filtrate. Discard the precipitate. Add 20 ml. of nitric acid and 5 mg. of P (as phosphoric acid). Heat the mixture to 50~60°C, then add 20 ml. of 10% ammonium molybdate solution. Agitate vigorously and rub the wall of the beaker with a glass rod to hasten the precipitation. Allow to settle and after cooling filter and wash with 5 portions of nitric acid (2 : 100). Take up the yellow precipitate with ammonium hydroxide (1 : 1) and wash thoroughly with water. Boil the combined filtrate and washings until the odour of ammonia disappears. Dilute to 100 ml. with distilled water and cool with cold water. Add 1 ml. of 10% chloroplatinic acid with stirring. Rub the wall of the beaker with a glass rod until yellow precipitate appears. Stand for several hours. Filter through a weighed one inch filter paper mounted on a Hirsch funnel. Wash with 10 ml. of cold water and 3 portions of ethyl alcohol. Dry the filter paper and precipitate at 110°C and

5) During 1956~57, milk, rice and human urine in different countries showed a general ^{137}Cs concentration of 20~70 μμc ^{137}Cs/g potassium. (U. N. Scientific Committee on the Effects of Atomic Radiation. A/AC.82/R. 65/Add.3 p. 31, 8 May 1958).

weigh to determine the cesium recovery. Mount the precipitate in a measuring dish for counting. Standardize the counter with a known amount of cesium-137 and 20 mg. of cesium carrier precipitated as the chloroplatinate.

Summary

A simple and rapid separation method for cesium-137 in biological materials has been presented. It is composed of three steps, phosphate elimination, ammonium phosphomolybdate precipitation and chloroplatinate precipitation. The over-all yield of cesium is over 85% and the decontamination from other fission activities is more than 10^5 for cerium-144 and strontium-89. The contribution of the activities of rubidium-87 and potassium-40 is negligibly small in the determination of cesium-137 in biological materials by beta counting.

Kiriu College of Technology
Gunma University, Kiriu

*The Formation of Coprostane, 6β-Coprostanol, and 3α,6β-Coprostanediol by the Catalytic Reduction of Epicholesterol β-Oxide**

By Yoshiyuki URUSHIBARA and Kazuko MORI

(Received July 22, 1958)

M. Shiota and one of the authors (K. M.)[1] have previously reported on the reduction of epicholesterol β-oxide with lithium aluminum hydride and with sodium and amyl alcohol. In continuation, the present authors have examined the catalytic reduction of epicholesterol β-oxide (I) with Adams platinum oxide, and obtained coprostane (II), 6β-coprostanol (IIIa), and 3α,6β-coprostanediol (VIa). The 3,6-coprostanediol hitherto known being only the 3β,6β-isomer[2], the authors synthesized the 3α,6β-isomer by another method, and confirmed its structure.

Plattner et al.[3] reduced epicholesterol β-oxide with platinum oxide as the catalyst and obtained 3α-cholestanol besides an oily substance supposed to be a hydrocarbon. The present authors, however, obtained coprostane derivatives only, but no cholestane derivatives.

The products from the catalytic reduction of epicholesterol β-oxide (I) with platinum oxide were acetylated, and a chromatographical separation gave coprostane (II), 6β-coprostanol acetate (IIIb), and 3α,6β-coprostanediol diacetate (VIb). The structure of 6β-coprostanol acetate (IIIb) was determined by hydrolyzing the acetate to the free alcohol, 6β-coprostanol (IIIa), oxidizing the alcohol to the corresponding ketone, 6-coprostanone (IV), and isomerizing the latter to 6-cholestanone (V) by treatment with concentrated hydrochloric acid in acetic acid. The β-configuration of the 6-hydroxyl group comes from the β-configuration of the oxide ring of the starting material, epicholesterol β-oxide. The 6β-coprostanol acetate (IIIb) was also identical with the specimen obtained from 4-cholestene-6β-ol acetate by the method of Shoppee et al.[4].

Hydrolysis of 3α,6β-coprostanediol diacetate (VIb) and oxidation of the free diol (VIa) gave 3,6-coprostanedione (VII). The 3α,6β-coprostanediol diacetate synthesized by another method as described below was identical with the 3α,6β-coprostanediol diacetate (VIb) obtained from the catalytic reduction of epicholesterol β-oxide, and probably with the 3α,6β-coprostanediol diacetate prepared by Shoppee

* Presented at the 8th Annual Meeting of the Chemical Society of Japan held in Tokyo, April, 1955, and at the 9th Annual Meeting of the Chemical Society of Japan held in Kyoto, April, 1956.

1) M. Shiota and K. Mori, *J. Chem. Soc. Japan, Pure Chem. Sec.* (*Nippon Kagaku Zassi*), **76**, 1192 (1955).

2) V. Prelog and E. Tagmann, *Helv. Chim. Acta*, **27**, 1880 (1944).

3) Pl. A. Plattner, A. Fürst, F. Koller and H. H. Kuhn, ibid., **37**, 258 (1954).

4) D. N. Jones, J. R. Lewis, C. W. Shoppee and G. H. R. Summers, *J. Chem. Soc.*, **1955**, 2876.

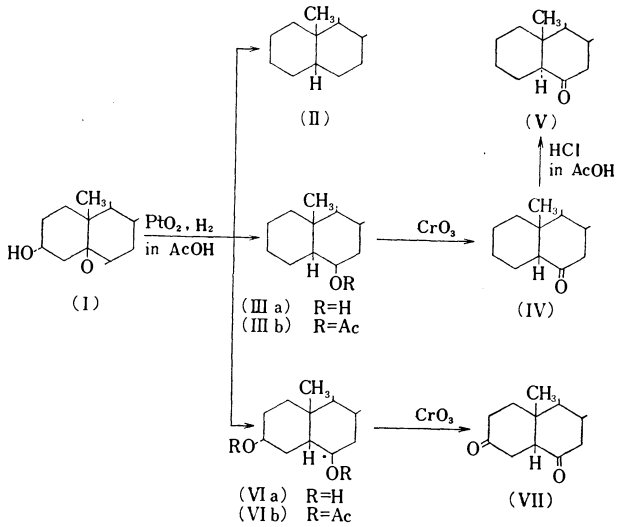

et al.[5] by the reduction of 6β-acetoxy-3-coprostanone followed by acetylation.

Thus it was concluded that the catalytic reduction of epicholesterol β-oxide (I) gave coprostane (II), 6β-coprostanol (IIIa), and 3α,6β-coprostanediol (VIa):

The catalytic reduction of cholesteryl acetate β-oxide with platinum oxide gave cholestane, 3β-cholestanol acetate, and 3β, 6β-cholestanediol 3-acetate but no coprostane derivatives[6,7]. Hence, the formation of the coprostane derivatives in the catalytic reduction of epicholesterol β-oxid may be caused by the effect of the α-configuration of the 3-substituent. Because the 3α-substituent in epicholesterol β-oxide possesses the axial conformation, it may be possible for it to compel the β-face, rather than the normally more easily adsorbed α-face, of the steroid molecule to be adsorbed on the surface of the catalyst, and the subsequent transfer of hydrogen will lead to the formation of coprostane derivatives. Shoppee et al.[8] observed a similar effect of the 3α-substituents on the catalytic reduction of Δ^5-steroids; however, they obtained, besides 3α-coprostanol, about 40% yield of 3α-cholestanol in the case of epicholesterol, and an exclusive yield of coprostane derivatives when the 3α-substituents were greater than the hydroxyl group. The catalytic reduction of epichlesterol β-oxide by the present authors yielded no cholestane derivatives. Shiota et al.[9] observed recently a similar effect of the 3α-substituent on the catalytic reduction of epicholesteryl chloride.

3α,6β-Coprostanediol diacetate (VIb) was synthesized by another route as follows: Treatment of epicholesterol with formic acid and hydrogen peroxide, followed by hydrolysis, acetylation and chromatographic separation, gave 3α,5,6β-cholestanetriol 3,6-diacetate (VIIIc), 3α,5,6β-cholestanetriol 6-acetate (VIIIb), and 3α, 5,6β-cholestanetriol (VIIIa). The structure of 3α,5,6β-cholestanetriol 6-acetate (VIIIb) was determined by oxidizing the 6-acetate to 5,6β-cholestanediol-3-one 6-acetate (X)[10]. 3α,5,6β-Cholestanetriol 3,6-diacetate(VIIIc) and 3α,5,6β-cholestanetriol 6-acetate(VIIIb) are probably identical with the substances obtained by the hydration of epicholesterol α-oxide and β-oxide by Plattner et al.[3]. The authors presume that 3α,5,6β-cholestanetriol 6-acetate (VIIIb) and 3α,5,6β-cholestanetriol (VIIIa) were produced by the hydrolysis of the primary product, 3α, 5,6β-cholestanetriol 3,6-diacetate (VIIIc), on aluminum oxide in chromatographic separation. The 3α,5,6β-cholestanetriol 3,6-diacetate (VIIIc) was dehydrated to 4-cholestene-3α,6β-diol diacetate (IX), and catalytic reduction of the latter gave 3α, 6β-coprostanediol diacetate (VIb), which was identical with the specimen from the catalytic reduction of epicholesterol β-oxide.

5) C. W. Shoppee, R. J. Bridgwater, D. N. Jones and G. H. R. Summers, ibid., **1956**, 2492.
6) M. Chuman, *J. Chem. Soc. Japan, Pure Chem. Sec.* (*Nippon Kagaku Zassi*), **64**, 1486 (1943); Y. Urushibara and M. Chuman, This Bulletin, **22**, 69 (1949).
7) Pl. A. Plattner, Th. Petrzilk and W. Lang, *Helv. Chim. Acta*, **27**, 513 (1944).
8) J. R. Lewis and C. W. Shoppee, *J. Chem. Soc.*, **1955**, 1365.
9) M. Shiota, Y. Kita and T. Sano, Presented at the 11th Annual Meeting of the Chemical Society of Japan held in Tokyo, April, 1958.
10) B. Ellis and V. Petrow, *J. Chem. Soc.*, **1939**, 1078.

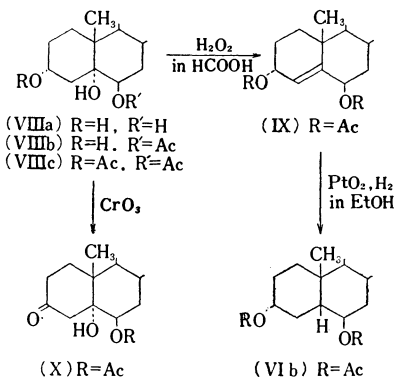

Experimental**

Catalytic Reduction of Epicholesterol β-oxide (I). — A suspension of epicholesterol β-oxide (I) (180 mg.) in acetic acid (18 cc.) was shaken with hydrogen in the presence of Adams platinum oxide (36 mg.) at the ordinary temperature and pressure. The reaction was completed in one hour, one mole and a half of hydrogen being absorbed. Evaporation of acetic acid under a reduced pressure from the solution filtered from the catalyst gave an oily substance (178 mg.). Acetylation of the oil with acetic anhydride and pyridine gave an oily substance (183 mg.). It was chromatographed on a column of aluminum oxide (9 g.) prepared in petroleum ether. Elution with petroleum ether (40 cc.) gave an oily material (13.5 mg.), which was brought to crystallization by dissolving it in methanol and placing the solution in a refrigerator. Recrystallization from acetone gave coprostane (II) in needles, m. p. and mixed m. p. 67~70°C.

Elution with petroleum ether-benzene (9 : 1, 60 cc.) gave another material (27 mg.) which on recrystallization from methanol gave a crystalline product (24 mg.), m. p. 108~109°C. It was identified with 6β-coprostanol acetate (IIIb) as follows. It was dissolved in anhydrous ether (1 cc.), the solution was dropped into a solution of lithium aluminum hydride (10 mg.) in anhydrous ether (1 cc.), and the mixture was boiled under a reflux condenser for one hour. The ethereal solution, after being washed and dried, was evaporated to give an oily substance (19.5 mg.). The substance (6β-coprostanol, IIIa) did not crystallize even when placed in a refrigerator in methanol solution, as it did not in the case of Shoppee et al.[4]. The substance was dissolved in acetic acid (0.2cc.) and the solution was mixed with a solution of chromic anhydride (12.5 mg.) in 90% acetic acid (0.5 cc.). After the mixture was left to stand overnight, a small amount of water was added, when crystals (15 mg.), m. p. 125~131°C, were obtained, which were recrystallized from methanol to yield 6-coprostanone (IV) (12 mg.), m. p. 128~129.5°C. The substance (8 mg.) was dissolved in acetic acid (1 cc.) and the solution was refluxed for 30 minutes after adding one drop of concentrated hydrochloric acid. The product (7 mg.) thus obtained was recrystallized from methanol to give 6-cholestanone (V) (5 mg.), m. p. and mixed m. p. 85°C.

The 6β-coprostanol acetate (IIIb) showed no depression of the m. p. in admixture with 6β-coprostanol acetate prepared by the catalytic reduction of 4-cholestene-6β-ol acetate[4].

Fractions (21.5 mg. in total) eluted with benzene-ether (19 : 1, 60 cc.; 9 : 1, 40 cc.) were combined and brought to crystallization by keeping them in a refrigerator in methanol solution. Repeated recrystallization from methanol gave 3α, 6β-coprostanediol diacetate (VIb) (6.5 mg.) in needles, m. p. 103~106.5°C. The substance showed no depression of the m. p. in admixture with the 3α,6β-coprostanediol diacetate prepared by the catalytic reduction of 4-cholestene-3α,6β-diol diacetate as described below, but a depression of the m. p. with 3α,6β-cholestanediol diacetate. Deacetylation of the 3α,6β-coprostanediol diacetate (VIb) with lithium aluminum hydride gave free 3α,6β-coprostanediol (VIa) in a glassy mass, m. p. 134~136°C. Oxidation of the latter with chromic anhydride in acetic acid gave 3,6-coprostanedione (VII) in needles, m. p. 174~175.5°C, which showed no depression of the m. p. on admixture with an authentic specimen of 3,6-coprostanedione prepared by the oxidation of 3β,6β-coprostanediol[2], but a depression with 3,6-cholestanedione.

3α, 5, 6β-Cholestanetriol 3, 6-diacetate (VIIIc).—A suspension of epicholesterol (1 g.) in 90% formic acid (10 cc.) was heated to 70~80°C with stirring for 5 minutes to form the 3-formate which separated in an oily layer, and the mixture was cooled to 25°C. The solidified 3-formate was shaken occasionally with 30% hydrogen peroxide (1 cc.), the temperature being kept at 40°C. In about 30 minutes the solid dissolved and the solution was allowed to stand overnight at room temperature. The mixture was treated with boiling water (15 cc.), and allowed to cool. The white granular solid material was collected, and dissolved in methanol (30 cc.), and the solution was treated with 25% aqueous sodium hydroxide (1 cc.), warmed on the water-bath for 10 minutes, acidified with hydrochloric acid, diluted with water, and extracted with ether. Isolation in the usual way gave 3α,5,6β-cholestanetriol (VIIIa) in a glassy mass. Acetylation of the 3α,5,6β-cholestanetriol (VIIIa) with acetic anhydride (7 cc.) and pyridine (10 cc.) gave an oily substance (1.2 g.).

This substance was chromatographed on a column of aluminum oxide (30 g.) prepared in petroleum ether. Fractions (450 mg. in total) eluted with petroleum ether-benzene (9 : 1, 2100 cc.; 4 : 1, 2300 cc.) were combined and recrystallized from methanol to give 3α,5,6β-cholestanetriol 3,6-diacetate (VIIIc) (270 mg.), m. p. 86~87°C.

Fractions (190 mg. in total) eluted with petroleum ether-benzene (1 : 1, 300 cc.), benzene (400 cc.) and benzene-ether (99 : 1, 100 cc.; 98 : 2, 100 cc.; 95 : 5, 100 cc.) showed no sharp melting point. The substance is presumed to be a mixture of

** Melting points are uncorrected.

3α, 5, 6β-cholestanetriol 3, 6-diacetate (VIIIc) and 3α, 5, 6β-cholestanetriol 6-acetate (VIIIb), because it gave 3α, 5, 6β-cholestanetriol 3, 6-diacetate (VIIIc) on acetylation.

Fractions (165 mg. in total) eluted with benzene-ether (9 : 1, 200 cc.; 4 : 1, 200 cc.; 1 : 1, 100 cc.) and ether (600 cc.) were recrystallized from methanol to give 3α, 5, 6β-cholestanetriol 6-acetate (VIIIb) (125 mg.), m. p. 177~178°C. The structure of this compound was determined by oxidizing it to a product, m. p. 159~160°C, which showed no depression of the m. p. on admixture with the 5, 6β-cholestanediol-3-one 6-acetate (X), m. p. 163~164°C, prepared by oxidation of 3β, 5, 6β-choletanetriol 6-acetate.

Fractions (170 mg. in total) eluted with ether-acetone (600 cc.) were a gel. The substance is presumed to be a mixture of 3α, 5, 6β-cholestanetriol 6-acetate (VIIIb) and 3α, 5, 6β-cholestriol (VIIIa), for on acetylation it gave 3α, 5, 6β-cholestanetriol 3, 6-diacetate (VIIIc).

4-Cholestene-3α, 6β-diol diacetate (IX). — 3α, 5, 6β-Cholestanetriol 3, 6-diacetate (VIIIc) (165 mg.) was treated with thionyl chloride (2 drops) in pyridine (1 cc.) at 0°C. After 5 minutes the mixture was poured into ice water. Working up in the usual way, it gave a substance and recrystallization from methanol gave 4-cholestene-3α, 6β-diol diacetate (IX) (130 mg.) in needles, m. p. 102.5~103.5°C; $[\alpha]_D^{30}$ +117° (c, 2.20 in chloroform).

Anal. Found: C, 76.30; H, 10.59. Calcd. for $C_{31}H_{50}O_4$: C, 76.50; H, 10.36%.

3α, 6β-Coprostanediol diacetate (VIb). — Platinum oxide (10 mg.) in ethanol (50 cc.) was saturated with hydrogen, and 4-cholestene-3α, 6β-diol diacetate (IX) (47 mg.) was added, and the mixture was shaken with hydrogen at the ordinary temperature and pressure. The reaction was completed in 20 minutes, about one mole of hydrogen being absorbed. Evaporation of ethanol from the filtered solution gave an oil (46 mg.). It was chromatographed on a column of aluminum oxide (1.5 g.) prepared in petroleum ether. Fractions (23 mg. in total) eluted with petroleum ether-benzene (4 : 1, 30 cc.; 7 : 3, 20 cc.; 1 : 1, 20 cc.) were recrystallized from methanol to give 3α, 6β-coprostanediol diacetate (VIb) (18 mg.), m. p. 103~104°C; $[\alpha]_D^{18}$ +56° (c, 1.85 in chloroform).

Anal. Found: C, 76.07; H, 10.79. Calcd. for $C_{31}H_{52}O_4$: C, 76.18; H, 10.72%.

Department of Chemistry
Faculty of Science
The University of Tokyo
Hongo, Tokyo

Electron Diffraction Investigation on the Molecular Structure of 1, 1, 2, 2-Tetrafluoro-1, 2-dichloroethane

By Machio IWASAKI

(Received July 19, 1958)

The molecular structure of some fluorochloroethanes presents two interesting problems. One of them is concerned with rotational isomerism, while the other with the effect of the neighboring halogene atoms on the C–F and C–Cl bond distances. In a previous publication[1], the molecular structure of 1, 2-difluoro-1, 1, 2, 2-tetrachloroethane has been reported. This report presents the results of the determination of the molecular structure of 1,1,2,2-tetrafluoro-1,2-dichloroethane which was undertaken by the sector-microphotometer method of electron diffraction in order to find the effect of substitution with fluorine on the energy difference between isomers and on the bond distances.

The preliminary work[2] on this molecule was carried out merely by the radial distribution method on the assumption of a rather short distance of the C–C bond, 1.46 Å, which had been reported in early investigations on some fluorocarbons[3]. Now, new experimental data obtained by use of an r^3-sector have been analysed by the correlation method as well as the radial distribution method without making any assumption about the C–C bond distance.

Experimental

The sample was prepared by Nagase in this laboratory from hexachloroethane, which was

1) M. Iwasaki, S. Nagase and R. Kojima, This Bulletin, **30**, 230 (1957).

2) M. Iwasaki, S. Nagase and R. Kojima, *J. Chem. Phys.*, **22**, 959 (1954).

3) See Table VII.

fluorinated with antimony trifluoride under a superatmospheric pressure in the presence of antimony pentachloride as a catalyst[4]. The product distilled at 3.8°C. The purity of this sample was tested with an infrared absorption spectrum. It was confirmed that the amount of $CFCl_2$–CF_3, that could not be removed by fractionation, was less than about 1~2 per cent. Hence, its amount was so small as to affect the electron diffraction patterns in an inappreciable manner.

The diffraction patterns were obtained at a room temperature of about 10°C with an apparatus[5] having an r^3-sector, which was rapidly rotated during exposures. The apparatus used was essentially similar to that constructed by Ino[6]. The details will be reported elsewhere. Two nozzle-to-plate distances of 125 mm. and 285 mm. were used: the former was used for large-angle scattering while the latter for small-angle scattering. The extraneous scatterings were prevented by a beam trap fixed at the center of the sector. The wavelength of the electron beam was determined from the Debye rings of a gold foil to be about 0.055 Å. The sample was introduced into the electron beam through a fine nozzle which was surrounded by a trap cooled with liquid air to prevent the sample from spreading throughout the camera chamber. Diffraction photographs were taken on Fuji Process Hard Plates with the consecutive exposures of 30~60 sec. The photographic densities were measured up to a q value of about 100 by a Riken B-type recording microphotometer. In this measuremens, the photographic plate was rapidly rotated about the center of the diffraction pattern in order to average out the inevitable irregularities in the emulsion. The microphotometer traces thus obtained were measured by a coordinate comparator as a function of q. After calibrating the non-linearity of voltage-deflection relation of the electrometer in the microphotometer, the photographic density was converted into the relative intensity by the method similar to that employed by J. Karle and his coworker[7].

The molecular scattering intensity, I_m, was calculated from the total scattering, I_t, and a smooth background, I_b, that was drawn with the aid of the positivity criteria[7] as

$$I_m = I_t/I_b - 1 \qquad (1)$$

The averaged molecular scattering intensity qI_m shown by the top curve in Fig. 4 and Fig. 5 was obtained from several photographs with an average deviation of 4 per cent. of maximum amplitude, and it had an index of resolution of 0.95 to 1.00; that is, the ratio of the amplitude of the molecular scattering terms to the magnitude of the smooth background upon which the molecular terms are superposed is 0.95 to 1.00 times that given by theory for a perfect pattern.

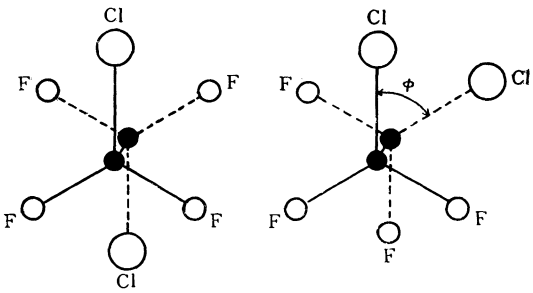

Fig. 1. Stable configurations of CF_2Cl-CF_2Cl.

Analysis

Radial Distribution Curve.—The radial distribution (RD) curve shown in Fig. 2 was calculated by the following equation:

$$f(r) = \sum_{q=0}^{q_{max}} qI_m \exp(-aq^2)\sin(\pi qr/10) \qquad (2)$$

where I_m is the molecular scattering intensity. The artificial damping factor a was chosen so as $\exp(-aq^2)=0.1$ at $q=100$, and $q=(40/\lambda)\sin(\theta/2)$, where θ is the angle of scattering and λ is the wavelength of the electron beam.

In the calculation of the RD curves, a theoretical intensity curve with constant coefficients which was computed for the assumed model was substituted in place of the observed intensity below $q=18$. Several steps of successive approximations were taken in order to make the assumed model selfconsistent with the final RD curve which would satisfy Karle's criteria[7] as closely as possible.

The RD curve has maxima at 1.33_0, 1.74_5, 2.1—3.1, 3.48, 3.90 and 4.29 Å. The first two peaks at 1.33_0 and 1.74_5Å are assigned to C—F and C—Cl bond distances, respectively. The unresolved peak at 2.1—3.1 Å is due to the superposition of various non-bonded distances, while that at 3.48 Å to the *trans* F···F distance.

There are two conceivable configurations, i. e., the *trans* (C_{2h}) and the *gauche* (C_2) form, for this molecule as shown in Fig. 1. The peak at 3.90 Å corresponds to the *trans* F···Cl distance, which is characteristic of the *gauche* form, while the peak at 4.29 Å corresponds to the *trans* Cl···Cl distance which is characteristic of the *trans* form (see Fig. 1). Therefore, these two peaks evidently show the existence of two isomeric forms for this

4) R. Kojima, M. Iwasaki, S. Nagase and H. Baba, *Repts. Govt. Ind. Research Inst., Nagoya (Nagoya Kogyo Gijutsu Shikenjo Hokoku)*.5, 225 (1956).
5) Y. Morino, M. Kimura and M. Iwasaki, Lectured at the Sixth Annual Meeting of the Chemical Society of Japan, April 1953.
6) T. Ino, *J. Phys. Soc. Japan*, **8**, 92 (1953).
7) J. Karle and I. L. Karle, *J. Chem. Phys.*, **18**, 957 (1950).

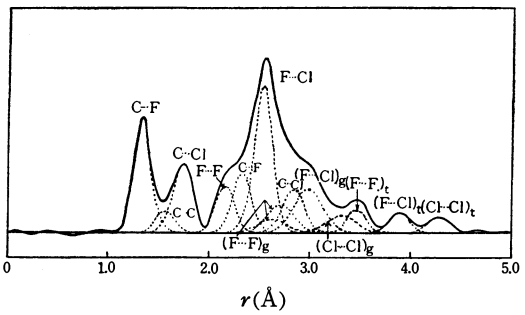

Fig. 2. Radial distribution curve for CF_2Cl-CF_2Cl (the full line). The dotted curves indicate individual peaks for the respective interatomic distances.

molecule. As the area under the RD peak is approximately proportional to Z_iZ_j/r_{ij}, the ratio of the two forms, N_t/N_g, can be calculated from the areas of the two peaks mentioned above by means of the following formula:

$$\frac{N_t}{N_g}=\frac{2Z_{\mathrm{F}}r_{\mathrm{Cl}\cdots\mathrm{Cl}}A_{\mathrm{Cl}\cdots\mathrm{Cl}}}{Z_{\mathrm{Cl}}r_{\mathrm{F}\cdots\mathrm{Cl}}A_{\mathrm{F}\cdots\mathrm{Cl}}} \qquad (3)$$

where Z_{F} and Z_{Cl} are the atomic numbers of fluorine and chlorine, $A_{\mathrm{Cl}\cdots\mathrm{Cl}}$ and $A_{\mathrm{F}\cdots\mathrm{Cl}}$ are the areas of the peaks, and $r_{\mathrm{Cl}\cdots\mathrm{Cl}}$ and $r_{\mathrm{F}\cdots\mathrm{Cl}}$ are *trans* Cl···Cl and *trans* F···Cl distances, respectively.

TABLE I

THE ASSUMED AND THE CALCULATED AMOUNT OF THE *GAUCHE* FORM IN ANALYSING THE RD CURVE

Assumed amount of the *gauche* form (%)	Calcd. amount of the *gauche* form (%)
60	54
50	49
45	46
35	42

In applying this formula, it was necessary to use the following procedure. Because the theoretical intensity with constant coefficients was used in place of the observed intensity below $q=18$ in the calculation of the RD curve, the ratio of the areas was affected by the assumed value of the abundance ratio of the two isomers. In order to see this effect, the RD curves were calculated on the assumption that the amount of the *gauche* form is equal to 60, 50, 45 and 35 per cent. The amount of the *gauche* form obtained from the areas of the RD peaks is shown in Table I for various cases. Table I shows that the self-consistent value was obtained from the RD curve if the amount of the *gauche* form was assumed to be equal to 50~45 per cent. Therefore, the amount of the *gauche* form was estimated as 50~45 per cent. from the RD curve. This value was further tested by the consideration of the theoretical intensity curves described in the next section.

In the range from 1.0 to 2.0 Å of the RD curve, a small peak corresponding to the C—C distance is masked by the skirts of prominent peaks on either side of the C—C peak. It seems to be unlikely that the contribution from the C—C distance affects the left side of the C—F peak as well as the right side of the C—Cl peak. Hence the right side of the former peak and the left side of the latter were fitted with Gaussian functions. The Gaussian curves which were fitted almost exactly to each side of the composite peak were subtracted from the composite peak. The remaining area formed a smooth curve having a maximum at 1.54 Å which was attributable to the C—C distance. The three components of the first peak of the RD curve are illustrated in Fig. 2. The areas of these decomposed peaks can favorably be compared with the theoretical values and fairly good agreement was obtained as shown in Table II.

TABLE II

THE RESULT OF ANALYSIS OF THE RD CURVE (THE REGION OF THE BONDED DISTANCES)

		C-F (Å)	C-C (Å)	C-Cl (Å)
Distance		1.33_0	1.54	1.74_5
Mean amplitude	obs.	0.052	0.045	0.061
	calc.	0.045	0.050	0.054
Peak area	obs.	1.00	0.18	0.70
	calc.	1.00	0.14	0.72

The portion of the RD curve from 2.1 to 3.7 Å corresponds to the superposition of the contributions from twelve interatomic distances in the *trans* as well as in the *gauche* form. This part of the RD curve was so complicated that the values of mean amplitudes and the peak heights could not be taken as unknown parameters in decomposing this part; hence the assumed values listed in Table II were used for the mean amplitudes, while for the peak heights the theoretical values calculated from the atomic numbers and the mean amplitudes were used. The amount of the *gauche* form was assumed to be 50 per cent. in accordance with the result obtained from the areas under peaks at 3.90 Å and 4.29 Å. As the left

side of this peak (2.0~2.4 Å) was composed of the contribution from the non-bonded F···F, C···F and F···Cl distances, these three distances were determined from the analysis of this part of the RD curve by trial and error on the assumption described above. The region from 2.4 Å to 3.0 Å was decomposed in a similar manner into contributions from non-bonded C···Cl, *gauche* F···F and *gauche* F···Cl distances. The remaining portion of the RD curve from 3.0 Å to 3.7 Å which was obtained by subtracting the contributions from the distances below 3 Å was, further, decomposed into contributions from the *gauche* Cl···Cl and *trans* F···F distances. These components lying between 2.0 and 3.7 Å are illustrated in Fig. 2. The molecular model which was constructed so as to satisfy the positions of the decomposed peaks as closely as possible, gave the set of interatomic distances listed in Table III. These interatomic distances are in good agreement with the respective RD peaks within 0.01~0.02 Å. Moreover, the azimuthal angle of two C—Cl bonds of the *gauche* form can be estimated to be 62° from the *gauche* Cl···Cl distance. Although the amount of the *gauche* form was fixed at 50 per cent. in the foregoing analysis, the RD curve was affected, as mentioned above, by the assumed value of the abundance ratio of the isomers in the region for r larger than 2.7 Å. In order to see this effect, a number of theoretical and experimental RD curves were computed for various values of the abundance ratio as shown in Fig. 3. The theoretical RD curve shifts gradually from the full line to the dotted one with varying amounts of the *gauche* form from 30 to 70 per cent. On the other hand, the experimental RD curve falls in the shaded portion even if the assumed amounts of the *gauche* form were varied from 30 to 70 per cent. in calculating the theoretical part of the intensity. The discrepancy between the observed and the theoretical RD curve was minimized, when the amount of the *gauche* form was assumed to be about 50 per cent. This fact coincides with the results obtained from the areas of 3.90 and 4.29 Å peaks.

The mean amplitudes listed in Tables II and III were obtained by fitting the RD peaks with Gaussian functions, no corrections being made for second order effects, such as a sample spread, multiple scatterings and the failure of Born approximation[8]. The observed mean amplitudes are

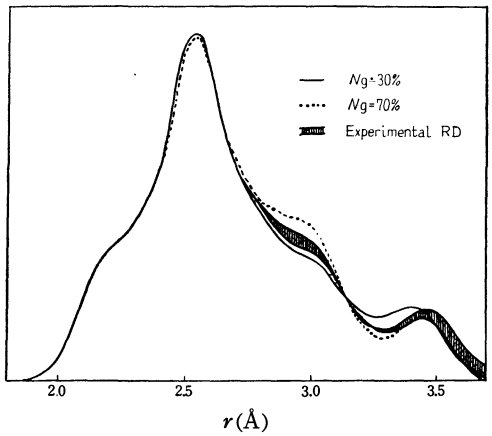

Fig. 3. Theoretical and experimental RD curves. The full line indicates the theoretical RD curve for the amount of the *gauche* form of 30%, and the dotted line for that of 70%. The shaded portion indicates the experimental RD curve, assuming the amount of the *gauche* form ranging from 30 to 70%.

in good agreement with those calculated by Morino et al.[9] from spectroscopic data.

Theoretical Intensity Curves. — The theoretical expression of the molecular scattering intensity obtained experimentally from Eq. 1 is given by the following equation:

$$qI_m(q) = \sum_{i \neq j}\sum (c_{ij}/r_{ij}) \exp(-b_{ij}q^2) \times \sin(\pi q r_{ij}/10) \qquad (4)$$

where r_{ij} denotes the interatomic distance between the i-th and the j-th atom and b_{ij} is the respective temperature factor which is calculated from its mean amplitude listed in Tables II and III. In the region of moderate and large q values, c_{ij} was considered to be constant proportional to Z_iZ_j, while in the region of small q,

$$c_{ij} = (Z_i - f_i)(Z_j - f_j) / \sum (Z_i - f_i)^2 + S_i \qquad (5)$$

was used, where Z_i is the atomic number, and f_i and S_i are the elastic and inelastic atomic scattering factors, respectively. The summations of Eq. 4 were performed by use of punchedcards and a Remington Rand Type-285 Model-2 tabulating machine[10,11]. Though the majority of the

8) R. Glauber and V. Schomaker, *Phys. Rev.*, **89**, 667 (1953); L. S. Bartell and L. O. Brockway, *Nature*, **171**, 978 (1953); J. A. Ibers and J. A. Hoerni, *Acta Cryst.*, **7**, 405 (1954).

9) Y. Morino, K. Kuchitsu, A. Takahashi and K. Maeda, *J. Chem. Phys.*, **21**, 1927 (1953).

10) Y. Morino and K. Kuchitsu, *X-ray* (*X sen*), **8**, 37 (1954).

11) The calculation by use of punched cards was carried out by Mr. K. Kuchitsu and Mr. E. Hirota of the University of Tokyo.

calculated values of the mean amplitudes listed in Tables II and III were those calculated by Morino et al.[9] from spectroscopic data, values for the non-bonded F···Cl and the *trans* F···Cl distances were appropriately taken from other data. The values for the *gauche* F···F and the *gauche* Cl···Cl distances were taken from Karle's experimental data on C_2F_6[12] and C_2Cl_6[13] by ascribing the contribution of torsional oscillation to the over-all vibration. For the *gauche* F···Cl distance, an appropriate value was also assumed using Karle's data.

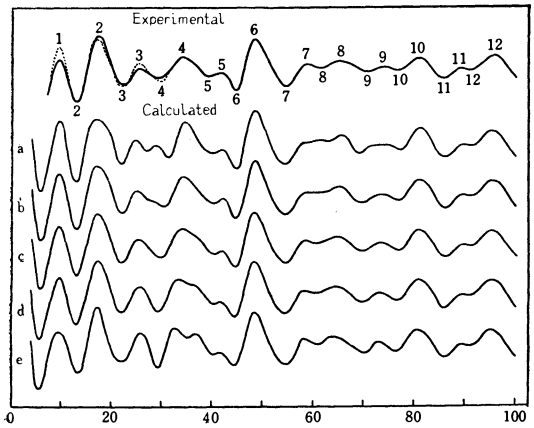

Fig. 4. Experimental and theoretical intensity curves for CF_2Cl-CF_2Cl. In the experimental curve, the dotted line indicates the correction for non-nuclear scatterings. Curves a and e indicate the theoretical intensity curves for the *trans* and the *gauche* form, respectively. Curves b, c and d indicate those for the amount of the *gauche* form of 30, 50 and 70%.

Theoretical intensity curves were computed for the *trans* and the *gauche* form using the values obtained from the RD curve (C—F=1.33$_0$, C—Cl=1.74$_5$, C—C=1.54, ∠CCCl=112°, ∠FCCl=110°, ∠CCF=108° and the azimuthal angle of the *gauche* form=63°) on the assumption that the structural frame of the molecule does not change with rotation about the C—C bond. The curves a and e in Fig. 4 refer to the *trans* and the *gauche* form, respectively. These curves completely disagree with the experimental curve with respect to the features in the region $20<q<40$. The curves b, c and d represent isomeric mixtures, in which the amount of the *gauche* from is 30, 50 and 70 per cent., respectively. The fact that the curve c is in satisfactory agreement with experiments definitely confirms the amount of the *gauche* form estimated above from the RD curve.

In order to determine the range of inaccuracy in various structure parameters, a number of intensity curves were computed for various assumed models which have a C—F distance ranging from 1.31 to 1.38 Å, a C—C distance from 1.46 to 1.58 Å, a C—Cl distance from 1.70 to 1.79 Å, ∠CCF from 106°30′ to 111°, ∠CCCl from 109°30′ to 115°, and ∠ClCF from 104°30′ to 114°30′. Moreover, the azimuthal angle and the amount of the *gauche* form were varied for each assumed model.

In order to determine the limit of one structural parameter, it is desirable to

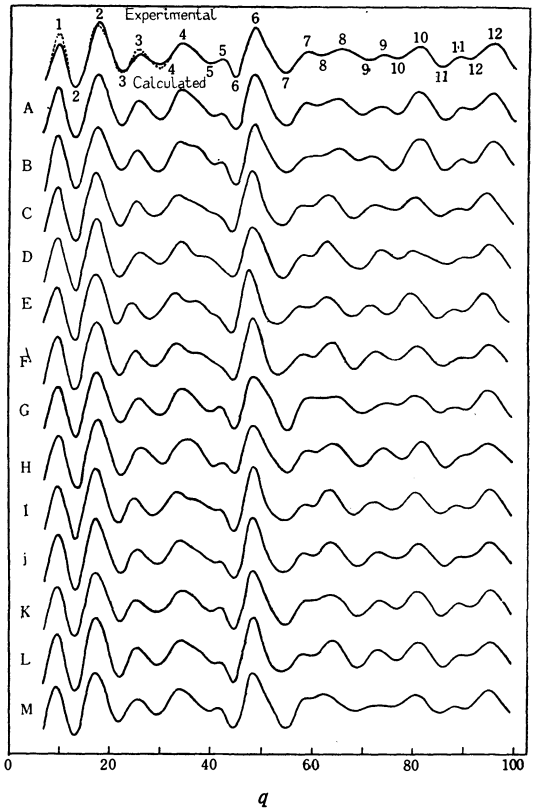

Fig. 5. Experimental and theoretical intensity curves for CF_2Cl-CF_2Cl. In the experimental curve, the dotted line indicates the correction for non-nuclear scattering. The molecular parameters used in the calculation are listed in Table IV.

12) D. A. Swick, I. L. Karle and J. Karle, *J. Chem. Phys.*, **22**, 1242 (1954).
13) D. A. Swick and I. L. Karle, ibid., **23**, 1499 (1955).

TABLE III

THE RESULT OF ANALYSIS OF THE RD CURVE (THE REGION OF NON-BONDED DISTANCE)

						trans form			
		F···F	C···F	F···Cl	C···Cl	$(F\cdots F)_g$	$(F\cdots Cl)_g$	$(F\cdots F)_t$	$(Cl\cdots Cl)_t$
Distance	obs.	2.15	3.33	2.53	2.72	2.72	2.97	3.48	4.29
	calc.	2.16	2.33	2.53	2.73	2.70	2.98	3.46	4.31
Mean amplitude	obs.	—	—	—	—	—	—	—	0.088
	calc.	0.056	0.059	0.065	0.073	0.114	0.120	0.061	0.074

		gauche form					
		$(F\cdots F)_g$	$(F\cdots F)_g$	$(F\cdots Cl)_g$	$(Cl\cdots Cl)_g$	$(F\cdots F)_t$	$(F\cdots Cl)_t$
Distance	obs.	2.62	2.72	2.97	3.30	3.48	3.90
	calc.	2.63	2.71	2.98	3.31	3.46	3.88
Mean amplitude	obs.	—	—	—	—	—	0.062
	calc.	0.114	0.114	0.120	0.125	0.061	0.074

TABLE IV

MOLECULAR PARAMETERS USED IN CALCULATING THE THEORETICAL INTENSITY CURVES SHOWN IN FIG. 5

Model	C—F	C—C	C—Cl	∠CCCl	∠CCF	∠FCCl
A (RD)	1.33_0Å	1.54Å	1.74_5Å	112°	108°	110°
B	1.31	1.54	1.75	112	108	110.5
C	1.35	1.54	1.75	112	108	110.5
D	1.35	1.54	1.73	112	108	110.5
E	1.35	1.54	1.77	112	108	110.5
F	1.34	1.48	1.74	112	108	110.5
G	1.34	1.58	1.74	112	108	110.5
H	1.34	1.54	1.74	112	108	109
I	1.34	1.54	1.74	112	108	111.5
J	1.34	1.54	1.74	111	108	110.5
K	1.34	1.54	1.74	113	108	110.5
L	1.34	1.54	1.74	112	107	110.5
M	1.34	1.54	1.74	112	109	110.5

select the regions in which the intensity curve is unaffected by other parameters. If such regions were not found and the effects of several parameters overlapped, the contribution from other parameters must be considered properly. Some of the computed curves are reproduced in Fig. 5 in order to illustrate the dependence of relative positions and intensities of maxima and minima upon the parameters. The values of the parameters used are listed in Table IV except the amount of the *gauche* form and the azimuthal angle which are kept constant at 50 per cent. and 63°, respectively.

C—F and C—Cl Parameters. — The position of the 6 th maximum and the relative depth of 3 rd and 4 th minima depend mainly upon the C—F and C—Cl parameters[14]. This relation gives the acceptable region in the parameter chart illustrated in Fig. 6. The full lines refer to the position of the 6 th maximum, and the broken lines the relative depth of 3 rd and 4 th minima. The area enclosed by these border lines is the acceptable domain. The positions of dots indicate the parameters of the models for which intensity curves were computed.

C—C Parameter. — The changes of the intensity curves caused by the variation of the C—C parameter, can be improved by the modification of other parameters, because there is no region in which the intensity curve depends solely upon the C—C parameter. In other words, it means that the contribution from the C—C distance is very small. However, the modification of the C—F or the C—Cl parameter makes the position of the 6 th maximum shift out of the limit of the experimental error, because the position of the 6 th maximum does not depend upon the C—C parameter. Although the change in the C—C distance is accompanied by the changes in the interatomic distances

14) The intensity relation between 3 rd and 4 th minima depends also upon the abundance ratio of the isomers but the changes are not serious in the region of the amount of the *gauche* form from 40 to 60 per cent.

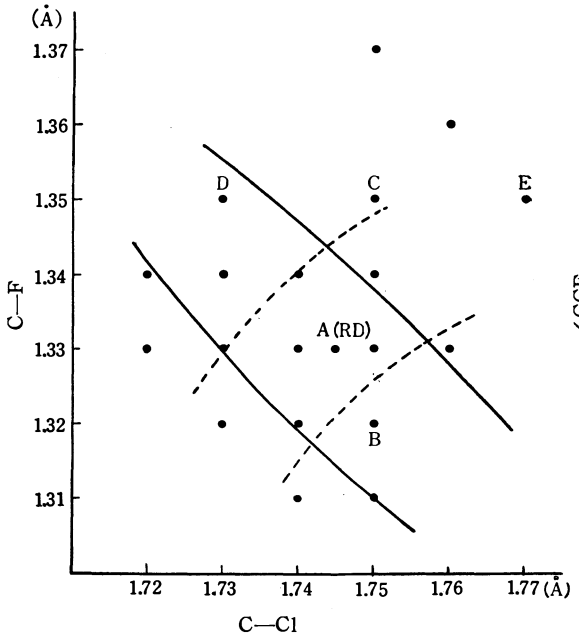

Fig. 6. Parameter chart. The positions of dots indicate the parameters of models for which intensity curves were computed. The positions of letters indicate the parameters of models for which intensity curves are shown in Fig. 5.

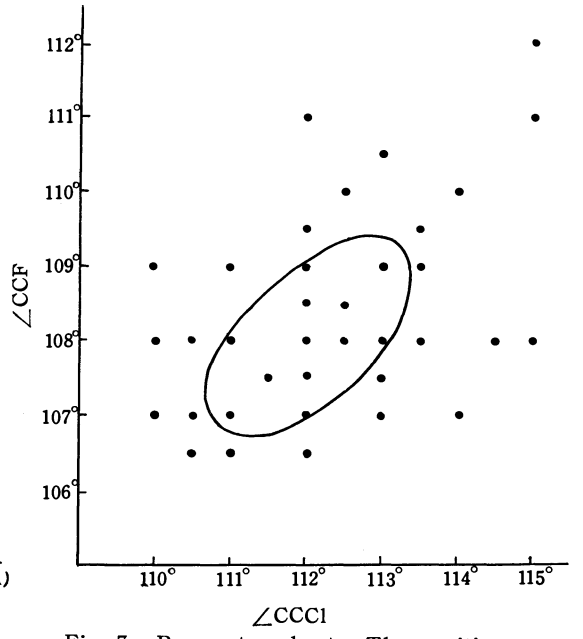

Fig. 7. Parameter chart. The positions of dots indicate the parameters of models for which intensity curves were computed. The area enclosed by the curved line roughly indicates the acceptable region.

TABLE V

COMPARISON BETWEEN EXPERIMENTAL AND THEORETICAL INTENSITY CURVES

Peak		Peak position			Peak height		
min.	max.	q_0	q_c	q_c/q_0	I_0	I_c	I_0/I_c
3		22.0	22.0	1.000	−1.00	−1.12	0.893
	3	25.4	25.4	1.000	+0.42	+0.36	1.167
4		29.5	29.6	1.003	−0.70	−0.82	0.854
	4	33.9	33.9	1.000	+0.86	+1.04	0.827
5		39.5	40.2	1.018	−0.44	−0.56	0.786
	5	41.6	41.8	1.005	−0.29	−0.41	0.707
6		44.5	44.5	1.000	−1.31	−1.42	0.923
	6	48.3	48.3	1.000	+1.87	+2.06	0.908
7		54.7	54.5	0.996	−0.06	−1.11	0.955
	7	58.3	58.3	1.000	+0.46	+0.25	(1.840)
8		61.3	60.6	0.989	+0.05	+0.11	(0.455)
	8	65.0	65.0	1.000	+0.54	+0.50	1.080
9		70.4	69.7	0.990	−0.22	−0.49	(0.449)
	9	74.0	73.5	0.993	+0.11	+0.07	(1.571)
10		76.9	76.7	0.997	−0.13	−0.42	(0.310)
	10	80.8	81.0	1.002	+0.62	+0.94	0.660
11		85.6	86.0	1.005	−0.66	−0.84	0.786
	11	89.1	89.4	1.003	+0.02	−0.05	(——)
12		91.0	91.0	1.000	−0.14	−0.14	(1.000)
	12	95.6	95.4	0.998	+0.78	+0.84	0.929
Average				1.000			0.883
Average deviation				0.003			0.104

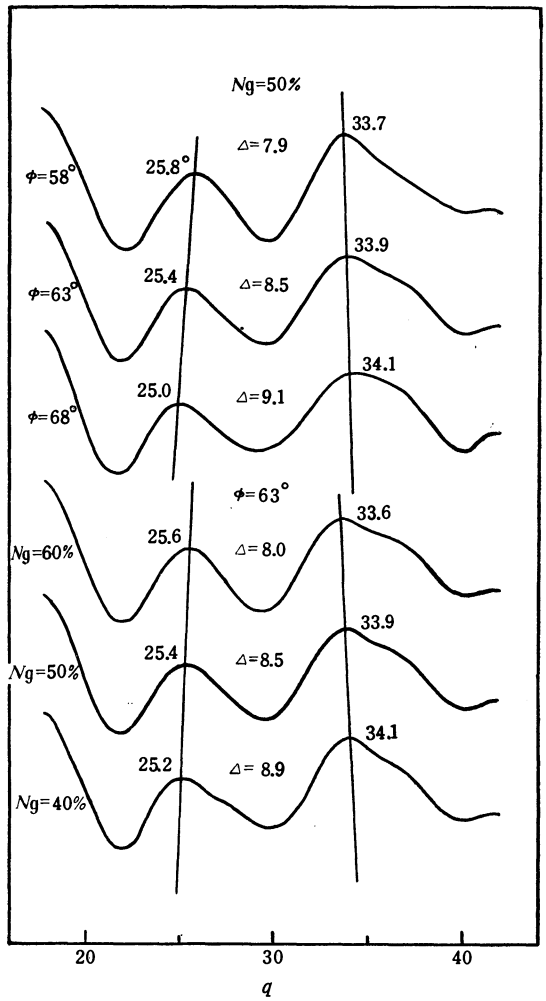

Fig. 8. Changes of the intensity curves with the parameters ϕ and N_g.

between two halves of the molecule, these changes can considerably be compensated by modifying ∠CCF and ∠CCCl parameters. Therefore, the ambiguity of the C—C distance becomes somewhat larger than those of other parameters. The acceptable models could be obtained for the C—C distance ranging from 1.50 to 1.58 Å by means of the suitable combination of other parameters.

∠FCCl Parameter. — This parameter affects sensitively the position of the 9th maximum and the depth of the 6th minimum. The models with ∠FCCl larger than 111° were unacceptable in the position of the 9th maximum, even if various combinations of other parameters, C—Cl or C—C, were considered. The lower limit of ∠FCCl was obtained from the depth of the 6th minimum which depends only upon this parameter. The

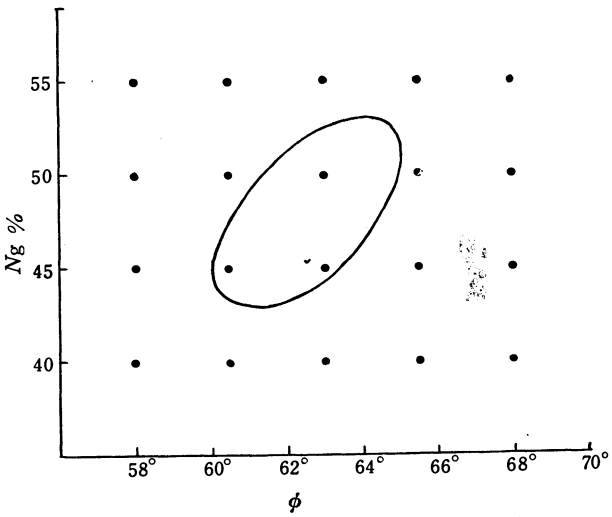

Fig. 9. Parameter chart for the fractional abundance and the azimuthal angle of the *gauche* form. The positions of dots indicate the parameters of models for which intensity curves were computed.

6th minimum is too shallow compared with the experiment for the model with ∠FCCl smaller than 109°. This fault could not be improved by adjusting other parameters.

∠CCF and ∠CCCl Parameters. — As stated above, the effects of ∠CCF and ∠CCCl parameters are compensated by the C—C parameter. Projecting the three dimensional parameter chart composed of the ∠CCF, ∠CCCl and C—C parameters to a ∠CCF—∠CCCl plane, the domain shown in Fig. 7 was obtained as a result of the superposition of a number of domains which are acceptable for various values of the C—C parameter.

The Abundance Ratio and the Azimuthal Angle. — The positions of the 3rd and the 4th maximum depend upon many other parameters, but the interval between these two maxima depends only upon the abundance ratio and the azimuthal angle as shown in Fig. 8. Therefore, this interval can be used to determine the limits of these parameters. Because the positions of the 3rd the 4th maximum can precisely be measured by use of the long camera length, those parameters were determined with considerably little ambiguity, as shown in Fig. 9.

From the analysis described above, the best model and the limits of ambiguity were estimated as follows:

C—F $=1.33_0\pm0.01_5$Å ∠CCF $=108°\pm1°30'$
C—C $=1.54\pm0.04$ Å ∠CCCl $=112°\pm1°30'$
C—Cl $=1.74_5\pm0.01_5$Å ∠FCCl $=110°\pm1°$

The azimuthal angle of the *gauche* form $=62.5\pm3°$

The amount of the *gauche* form $=48\pm5$ per cent. at 10°C.

For the best model the mean value of $q_{calc.}/q_{obs.}$ and $I_{obs.}/I_{calc.}$ for the maxima and the minima are 1.000 and 0.883 with the average deviation of 0.003 and 0.104, respectively. (See Table V.)

Discussion of the Results

It is interesting to compare the C—F and C—Cl bond distances obtained in this investigation with those on other chlorofluorocompounds having different numbers of fluorine atoms. As shown in Table VI, the C—F distance in a CF_2Cl-CF_2Cl molecule lies between the value of 1.32 Å in CF_3-CF_3[12] and that of 1.38 Å in $CFCl_2-CFCl_2$[1]. On the other hand, although the inaccuracy of the data does not permit to draw a definite conclusion, it appears that the C—Cl distance of CF_2Cl-CF_2Cl is shorter than that of C_2Cl_6[15] and $CFCl_2-CFCl_2$[1]. This fact coincides with the results from a number of investigations on the molecular structures of organic fluorine compounds[16] in which the C—F and C—Cl bond distances decrease with the number of the fluorine atoms bonded with the same carbon atom.

TABLE VI
C-F AND C-Cl BOND DISTANCES IN SOME FLUOROCHLOROETHANES

Molecule	C-F (Å)	C-Cl (Å)
CF_3-CF_3	1.32 ± 0.01[12]	
CF_2Cl-CF_2Cl	$1.33_0\pm0.01_5$*	$1.74_5\pm0.01_5$*
$CFCl_2-CFCl_2$	1.38 ± 0.02[1]	1.76 ± 0.01[1]
CCl_3-CCl_3		1.77 ± 0.02[15a] / $1.76_3\pm0.01$[15b]

* Present work.

An abnormal shortening of the C—C bond distance has been reported[17,18] in the early investigations of some organic fluorine compounds as shown in Table VII. However, the recent investigations by Karle[12] and Livingston[19-21] have shown that several fluorine compounds listed in the table have almost normal distances of the C—C bond. Although in the preliminary analysis the abnormally short distance of the C—C bond was assumed, it was found from this more precise analysis that the experimental results could be explained by a normal value of the C—C distance in this molecule. However, because of great inaccuracy of the determination of this distance, a definite conclusion could not be given for the problem of the effect of halogen atoms on the C—C bond distances in organic halides.

TABLE VII
C-C BOND DISTANCES IN SOME FLUOROCARBONS

Molecule	Early results	Recent results
CF_3-CF_3	1.45 ± 0.06[17]	1.56 ± 0.03[12] / 1.51 ± 0.06[19]
CH_3-CF_3	1.45 ± 0.04[17]	1.53 ± 0.04[17] / 1.52 ± 0.04[20]
$CF_3-C_2H_5$	1.49 ± 0.04[18]	
$CF_3-CF_2-CF_3$	1.47 ± 0.03[18]	
CHF_2-CHF_2	1.46 ± 0.05[18]	
$CH_3-CF_2-CH_3$	1.51 ± 0.02[18] / 1.48 ± 0.03[18]	
CF_3-CH_2Cl	1.47 ± 0.03[18]	
CF_3-CCl_3	<1.54[18]	
CF_3CH_2OH		1.52 ± 0.04[21]
CF_2Cl-CF_2Cl		1.54 ± 0.04*

* Present work.

It is to be noted that the value of ∠FCF somewhat smaller than the tetrahedral angle as reported in many organic fluorine compounds except carbon tetrafluoride, seems to be revealed also in this molecule, that is, the value of 108°44′ obtained from other angle parameters is consistent with those in CH_2F_2(108°17′)[22], in CCl_2F_2(109°)[23], and in many other compounds containing a CF_3 group[24].

The problem of the rotational isomerism

15a) Y. Morino and M. Iwasaki, *J. Chem. Phys.*, **17**, 216 (1949).
15b) Y. Morino and E. Hirota, ibid., **28**, 185 (1958).
16) The C—F and the C—Cl distances in many organic fluorine compounds were tabulated in a previous paper. (See ref. 1.)
17) Theae data were quoted from the tabulation compiled by P. W. Allen and L. E. Sutton, *Acta Cryst.*, **3**, 46 (1950).
18) These data were quoted from the tabulation by S. H. Bauer, *U. S. Atomic Energy Com. Report, MDDC* 1494 (1947).
19) J. L. Brandt and R. L. Livingston, *J. Am. Chem. Soc.*, **76**, 2096 (1954).
20) J. L. Brandt and R. L. Livingston, ibid., **78**, 3573 (1956).
21) R. L. Livingston and G. Vanghan, ibid., **78**, 2711 (1956).
22) D. R. Lide, *J. Am. Chem. Soc.*, **74**, 3548 (1952); W. C. Hamilton and K. Hedberg, ibid., **74**, 5529 (1952).
23) L. O. Brockway, *J. Phys. Chem.*, **40**, 747 (1936). According to a recent study by R. L. Livingston and D. H. Lyon (*J. Chem. Phys.*, **24**, 1283 (1956)), the value of 109.5°±3° was obtained. At any rate, because these two values from the visual method of electron diffraction are not free from great uncertainty, more accurate studies by the microwave spectroscopy or the sector—microphotometer method of electron diffraction are desired for the elucidation of the structure of this molecule.
24) Many examples of the data for ∠FCF in the compounds containing a CF_3 group are cited in ref. 20.

in this molecule has previously been studied by several investigators. On the basis of a number of observed Raman lines, Glockler and Sage[25] conculuded that two isomeric forms were present in the liquid state. Simpson and Plyler[26] have studied the infrared spectrum in the vapor state, and carried out a partial assignment on the basis of two isomeric forms. Kagarise[27] has recently studied the dependence of infrared spectra on temperature and state, and concluded that the *trans* isomer persists in the crystalline solid, and is the stable form in the liquid and the vapor state. The energy difference between the isomers in the vapor state was reported to be 500±200 cal./mol.

The energy difference, ΔE, was also obtained from the diffraction data by use of the following formula:

$$\frac{N_g}{N_t}=2\frac{f_g}{f_t}\exp(-\Delta E/\boldsymbol{R}T) \qquad (6)$$

where f_t and f_g are the vibrational and rotational partition functions of the *trans* and the *gauche* molecules. The factor 2 is introduced to account for the double weight of the *gauche* form. The ratio of f_g to f_t is considered to be approximately equal to unity. Therefore, neglecting the difference between f_g and f_t, the value of 440±110 cal./mol. is obtained from the diffraction data. This result is in good agreement with the value of 500±200 cal./mol. obtained by Kagarise in the vapor state from the temperature dependence of the infrared spectra.

The energy difference for the molecule in question is smaller than the value of 1140 cal./mol.[28] for a CH_2Cl—CH_2Cl molecule in contrast to the fact that methyl substitution[29] does not seriously decrease the energy difference. This lowering of the energy difference is probably caused by the fact that the dipole interaction is not much different between the *trans* and the *gauche* position as a result of the substitution of C—H with C—F, the bond moment of which is almost equal to that of a C—Cl bond. This fact is consistent with the conclusion proposed by Mizushima, Morino and Shimanouchi[30] that the steric repulsion plays an important role in determining the potential barrier but the electrostatic force is the important factor in determining the energy difference between the various configurations. Miyagawa[31] and Kreevoy et al.[32] supported this conclusion by a quantitative calculation.

Summary

The molecular structure of 1,1,2,2-tetrafluoro-1,2-dichloroethane was investigated by means of the sector-microphotometer method of electron diffraction. The existence of two isomeric forms, i.e., *trans* and *gauche*, was confirmed, and the amount of the *gauche* form was found to be 48±5 per cent. at 10°C. This corresponds to the energy difference of 440±110 cal./mol., the *trans* form being more stable than the *gauche* form. The interatomic distances and the bond angles were determined as follows:

C—F $=1.33_0\pm0.01_5$ Å ∠CCF $=108°\pm1°30'$
C—C $=1.54\pm0.04$ Å ∠CCCl $=112°\pm1°30'$
C—Cl $=1.74_5\pm0.01_5$ Å ∠FCCl $=110°\pm1°$

and the azimuthal angle of the *gauche* form $=62.5°\pm3°$.

The diffraction patterns and the microphotometer records were taken by using apparatuses in Nagoya University. The author wishes to express his sincere gratitude to Professor M. Kubo, Professor R. Uyeda and Dr. M. Kimura for giving him fascility to use the apparatus and for their valuable advice. Thanks are also due to Mr. S. Shibata, Mr. H. Morimoto and Mr. K. Kimura of Nagoya University for their friendly assistance, and to Mr. K. Kuchitsu and Mr. E. Hirota of the University of Tokyo for their help in calculating the theoretical intensity by means of a punched card machine in the Division of Health and Welfare Statistics, Welfare Minister's Secretariat. Further, the author is much indebted to Professor Y. Morino of the University of Tokyo for his helpful criticism of this investigation.

Government Industrial Research Institute, Nagoya, Hiratemachi, Kitaku, Nagoya

25) G. Glockler and C. Sage, *J. Chem. Phys.*, **9**, 387 (1941).
26) D. Simpson and E. K. Plyler, *J. Research Natl. Bur. Standards*, **50**, 223 (1953).
27) R. E. Kagarise, *J. Chem. Phys.*, **26**, 380 (1957).
28) K. Kuratani, T. Miyazawa, and S. Mizushima, *J. Chem. Phys.*, **21**, 1411 (1953).
29) I. Miyagawa, *J. Chem. Soc. Japan, Pure Chem. Sec.* (*Nippon Kagaku Zassi*), **75**, 1162 (1954).
30) S. Mizusima, Y. Morino and T. Shimanouchi, *J. Phys. Chem.*, **56**, 323 (1952).
31) I. Miyagawa, *J. Chem. Soc. Japan, Pure Chem. Sec.* (*Nippon Kagaku Zassi*), **75**, 1169 (1954).
32) M. M. Kreevoy and E. A. Mason, *J. Am. Chem. Soc.*, **79**, 4851 (1957).

SHORT COMMUNICATIONS

Solubility of Alcohols in Water Determined by the Surface Tension Measurements

By Kyoji KINOSHITA, Hidehiko ISHIKAWA and Kōzō SHINODA

(Received September 11, 1958)

The solubility data of alcohols in water are very important and useful for the study in colloid chemistry. Surface active molecules, like higher alcohols, aliphatic amines or fatty acids, have an habitual tendency to form supersaturated solution and the solubility determination encounters some difficulties by the use of the usual method[1]. However, the surface tension in aqueous solutions of these substances monotonously decreases up to their saturation concentration and then remains constant in the heterogeneous region. Therefore, it is possible to determine the solubility of surface active substance in water from the surface tension —logarism of concentration curve without the disturbance from supersaturation as it is in some other cases. As the surface tensions change over the common range, namely from 74 to 30 dynes/cm., the accuracy of this method is nearly equal for any alcohol of markedly different solubility. This principle of determining the solubility by surface tension method was proposed already by several authors[2-4]. But, there are few reports expect for those by Addison and Hutchinson[3,6] who determined the solubility of alcohols from the measurement of surface tension by vibrating-jet or vertical plate method.

Experimental. — *n*-Butanol, *n*-pentanol, *n*-hexanol, *n*-octanol, *n*-nonanol and *n*-decanol were purified by vacuum distillation through 50~100cm. column. The boiling points were 11°C, 138°C, 155.7~156°C, 96°C at 16 mmHg, 113~114.5°C at 20 mmHg and 101°C at 5 mmHg, respectively. Heptanol was of Kahlbaum pure grade material. Pentanol and nonanol were synthesized from *n*-propanol and nonanoic acid, respectively. Surface tension was measured by the drop weight method, using a tip of 6 mm. in diameter. The measurements were carried out in a water thermostat at 25±0.05°C. From the surface tension—logarism of concentration curves the saturation points are determined as the intersections of the curves with the horizontal straight lines passing through the lowest experimental points[7]. The experimental error by this method is about 4% or less.

Results and Discussion. — The results are summarized in Table I and plotted in Fig. 1.

TABLE I
THE SOLUBILITY OF ALCOHOLS IN WATER DETERMINED BY SURFACE TENSION MEASUREMENT AT 25°C

Substance	moles/l.	weight %	weight %
Butanol	0.97	7.4	7.35[8] 7.3[9]
Pentanol	0.25	2.2	2.2[9]
Hexanol	0.059	0.60	0.62[9]
Heptanol	0.0146	0.17	0.18[9]
Octanol	0.0038	0.049	0.059[9]
Nonanol	0.00097	0.014	—
Decanol	0.000234	0.0037	0.0037[6]*

* Solubility measured at 20°C.

The logarithms of the solubility of *n*-aliphatic alcohols in water as a function of hydrocarbon chain length showed a linear relationship and is expressed as follows,

$$\log C = -1.39m + 5.53 \qquad (1)$$

Here C is the solubility of alcohol in mole per liter and m the number of carbon atoms in the alcohol molecule studied.

We have, however, no reliable data of the temperature dependence of the solubility of alcohols in water. We may estimate the heat term, at least, the difference of heat of solution due to the change in

1) T. Sasaki, "Koshitsugaku Ronso" No. 1, 45 (1943).
2) S. Motylewski, *Z. Anorg. Chem.*, **38**, 410 (1904).
3) A. Taubamann, *Z. Physik. Chem.*, **A161**, 141 (1932).
4) H. K. Zimmermann Jr., *Chem. Rev.*, **51**, 25 (1952).
5) C. C. Addison, *J. Chem. Soc.* **1945**, 98.
6) C. C. Addison and S. K. Hutchinson, ibid., **1949**, 3387.
7) K. Shinoda, T. Yamanaka and K. Kinoshita, *J. Phys. Chem.*, to be published.
8) A. E. Hill and W. M. Walisoff, *J. Am. Chem. Soc.*, **48**, 918 (1926).
9) J. A. V. Butler, D. W. Thomson and W. H. Maclennan, *J. Chem. Soc.*, **1933**, 674.

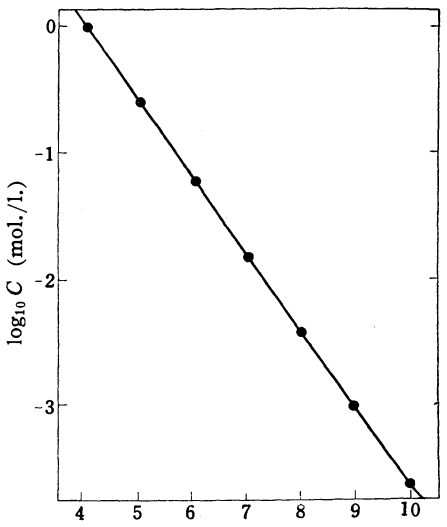

Fig. 1. The relation between the logarithum of the solubility (mole/l.) and the number of carbon atoms in alcohol.

hydrocarbon chain length, by the aid of the following equation[10],

$$0 \cong \ln a_2 = \ln X_2 + \phi_1^2(m\omega + c_2)/kT \qquad (2)$$

Where a_2 is the activity of solute, X_2 the solubility of solute expressed in mole fraction, ϕ_1 the volume fraction of solvent, ω the heat of solution (or the energy) required for passing one methylene group from hydrocarbon medium into water, c_2 the experimental constant, k the Boltzmann constant and T the absolute temperature.

Replacing the solubility values of alcohols in equation 2, we obtain, as the heat of solution, $4.8\,kT$ for R_4OH, $5.6\,kT$ for R_5OH, $6.9\,kT$ for R_6OH, $8.2\,kT$ for R_7OH, $9.6\,kT$ for R_8OH, $11.0\,kT$ for R_9OH and $12.4\,kT$ for $R_{10}OH$. From the difference of these values, the heat (or the energy if there is no volume change) required for passing one methylene group from hydrocarbon medium into water was calculated to be about 811 cal./mole ($1.37\,kT$). (This value is of course very close to the values 823 cal./mole obtained from the slope in Fig. 1, neglecting the change in volume fraction of solute.) This value shows excellent agreement with the value 824 cal./mole obtained by Sasaki and his collaborator[11] for the energy required passing one methylene group from paraffin surface into water.

In connection with this, we draw further attention to the fact that the energy obtained passing one methylene group from water to air-water interface was also determined as 656 cal./mole by the same authors[11]. This value again shows excellent agreement with the value 652~640 cal./mole obtained by Davies[12] and one of us[13,14].

We wish to thank Mr. T. Masumizu for his exploratory work and the Department of Education for the Scientific Research Expenditure.

Department of Chemistry
Faculty of Engineering
Yokohama National University
Minami-ku, Yokohama

10) J. H. Hildebrand and R. L. Scott, "Solubility of Nonelectrolytes", Reinhold Publishing Corporation, (1950), p. 131.

11) T. Sasaki and M. Tsunoda, 11th Annual Meeting of the Chemical Society of Japan (1958).
12) J. T. Davies, *Trans. Faraday Soc.*, **48**, 1052 (1952).
13) K. Shinoda, *J. Phys. Chem.*, **58**, 1136 (1954).
14) K. Shinoda, ibid., **59**, 432 (1955).

*On Lucaconine**

By Takashi AMIYA ane Takeo SHIMA

(Received Septemper 11, 1958)

An alkaloid, lucaconine (I) ($C_{24}H_{39}O_7N$), was first isolated from the roots of *Aconitum luciduscul*um, Nakai by Suginome et al.[1,2] in this Laboratory. Moreover, Furusawa[3] has studied the degradation reactions of compound I. The present authors have further investigated the degradation reactions.

Oxidation of compound I with chromium trioxide-pyridine complex yielded neutral products, oxolucaconine (II)[3] ($C_{24}H_{37}O_8N$. $1^3/_4H_2O$), oxolucaconinone-II (III), m. p. 218°, λ_{max} 298 mμ, log ε 1.9 (*Anal.* Found: C, 62.31; H, 7.64; OCH_3, 18.22. Calcd. for C_{24} $H_{35}O_8N$: C, 61.92; H, 7.58; OCH_3, 19.99%) and oxolucaconinedione (IV)[3] ($C_{24}H_{33}O_8N$). Compound III showed a lactam carbonyl band at 6.15 μ and a six-membered ketone carbonyl band at 5.83 μ in the infrared spectrum**.

---

* Read before the 9th Annual Meeting of the Chemical Society of Japan held in Kyoto, April, 1956 and the Meeting of the Hokkaido Branch of the Chemical Society of Japan held in Muroran, July, 1958. This constitutes a part of a series entitled "The Aconite Alkaloids" by H. Suginome.

1) H. Suginome, S. Kakimoto, J. Sonoda and S. Noguchi, *Rroc. Japan Acad.*, **22**, 122 (1946).

2) H. Suginome and S. Furusawa, in preparation.

3) S. Furusawa, in preparation.

** All infrared spectra were measured in nujol mulls.

To the previously obtained experimental results[3] and the observations so far recorded, the partial formula of I may be extended as follows:

$C_{15}H_{19}$ { $(OCH_3)_3$, $(>COH)_2$, $>CHOH$ (five-membered ring), $>CHOH$ (six-membered ring), $>NC_2H_5$ }

Lucaconine.

Next, oxidation of a naturally occurring base, monoacetyllucaconine (V)[2] ($C_{26}H_{41}O_8N$), with chromium trioxide-pyridine complex, followed by hydrolysis, afforded compound III. This fact shows that an acetylated hydroxyl group in compound V is the secondary one attached to a carbon atom in a five-membered ring.

It was reported that on treatment of each of compound I or its derivatives, except compound IV, with acetyl chloride, one molecule of water was lost and an anhydro-compound was produced[3].

Anhydrodiacetyllucaconine (VI)[3] ($C_{28}H_{41}O_8N$), obtained by the treatment of lucaconine (I) with acetyl chloride, showed carbonyl bands at 5.77 and 5.81 μ due to ester carbonyl groups and a ketone carbonyl group newly formed by dehydration, but no hydroxyl band in the infrared spectrum.

On hydrogenation over platinum in acetic acid, compound VI absorbed one mole of hydrogen and yielded anhydrodihydrodiacetyllucaconine (VII), m. p. 175° (*Anal.* Found: C, 64.42; H, 8.03; OCH_3, 17.54. Calcd. for $C_{28}H_{43}O_8N$: C, 64.47; H, 8.31; OCH_3, 17.85%), showing carbonyl bands at 5.77 and 5.93 μ due to the ester carbonyl groups and the ketone carbonyl group; no hydroxyl band appeared in the infrared spectrum. On hydrolysis, compound VII splits off two moles of acetic acid to give anhyrodihydrolucaconine (VIII), m.p. 210° (*Anal.* Found: C, 65.98; H, 9.11. Calcd, for $C_{24}H_{39}O_6N$: C, 65.87; H, 8.98%). The infrared spectrum of compound VIII showed a band at 5.92 μ characteristic of a ketone carbonyl group. On reduction of compound VIII by lithium aluminum hydride, followed by acetylation with acetic anhydride in pyridine, anhydrodihydrotriacetyllucaconinol (IX) yielded, m. p. 130~133° (*Anal.* Found: C, 64.19; H, 8.62; OCH_3, 19.66; $COCH_3$, 20.18. Calcd. for $C_{30}H_{47}O_9N$: C, 63.69; H, 8.38; OCH_3, 18.23; $COCH_3$, 22.83%) showing neither keton carbonyl band near 5.92 μ nor hydroxyl band in the infrared spectrum. On reduction of compound VI with lithium aluminum hydride, anhydrolucaconinol (X), m.p. 185~190° (*Anal.* Found: C, 66.22; H, 8.74; OCH_3, 20.31. Calcd. for $C_{24}H_{39}O_6N$: C, 65.87; H, 8.98; OCH_3, 21.25%) was given, showing no ketone carbonyl band in the infrared spectrum. On treatment of compound III with acetyl chloride, followed by hydrolysis and further oxidation by chromium trioxide-pyridine complex, anhydrooxolucaconinedione (XI) ($C_{24}H_{31}O_7N$) was produced. This had previously been obtained from VI through two steps[3].

These experiments indicate that in each compound, VI and XI, obtained by treatment with acetyl chloride both a ketone carbonyl group and a double bond were formed with elimination of one mole of water, and, moreover, that this dehydration took place between the two tertiary hydroxyl groups. This dehydration reaction seems to be one of 1—3 cleavages[4] and the following mechanism may be shown.

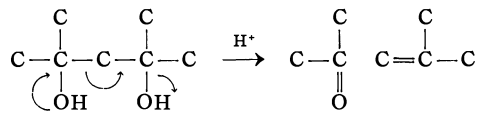

Wolf-Kishner reduction of lucaconinone-I (XII) ($C_{24}H_{37}O_7N$), which was previously prepared[3] and showed a five-membered ketone carbonyl band at 5.72 μ, gave deoxylucaconinone-I (XIII), m. p. 165° (*Anal.* Found: C, 66.16; H, 8.96; OCH_3, 19.25. Calcd. for $C_{24}H_{39}O_6N$: C, 65.87; H, 8.98; OCH_3, 21.27%), showing no band characteristic of the ketone carbonyl group in the infrared spectrum. Treatment of compound XIII with acetyl chloride, followed by hydrogenation over platinum in acetic acid, gave anhydrodihydromonoacetyldeoxylucaconinone-I (XIV), m. p. 84~90° (*Anal.* Found: C, 67.41; H, 9.26; OCH_3, 21.58; $COCH_3$, 10.36. Calcd. for $C_{26}H_{41}O_6N$: C, 67.36; H, 8.91; OCH_3, 20.08; $COCH_3$, 9.28%), showing carbonyl bands at 5.79 and 5.93 μ due to an ester carbonyl and a ketone carbonyl group formed by dehydration but no hydroxyl band in the infrared spectrum.

On the other hand, it was previously shown that treatment of compound I with acetyl chloride gave the anhydro-compound VI with loss of a mole of water, and that, on the contrary, the same treatment of compound IV, gave monoacetyloxolucaconinedione (XV) [$C_{24}H_{32}O_8N(COCH_3)$] without elimination of water[3].

On the basis of the above-mentioned experimental results, it may be shown that whilst on treatment of each of compounds I, III and XIII, which contained no five-membered ketone carbonyl group, with acetyl chloride, a mole of water was lost, on the same treatment of compound IV water was not lost. Accordingly, it may be reasonably concluded that dehydration by acetyl chloride occurs in such a case that a secondary hydroxyl group attached to the carbon atom in the five-membered ring is present or substituted for hydrogen atom, and that dehydration does not occur on

4) S. Archer, T. R. Lewis and B. Zenitz, *J. Am. Chem. Soc.*, **80**, 958 (1958).

the contrary in such a case that the above hydroxyl group is converted into a ketone carbonyl group.

The authors are grateful to Professor Harusada Suginome, President of Hokkaido University, for his unfailing kindness in encouraging this work, and to Messrs. M. Yamaguchi and A. Fujino, Institute of Polytechnics, Osaka City University, for their kindness in the determination of the infrared spectra.

Department of Chemistry
Faculty of Science
Hokkaido University, Sapporo